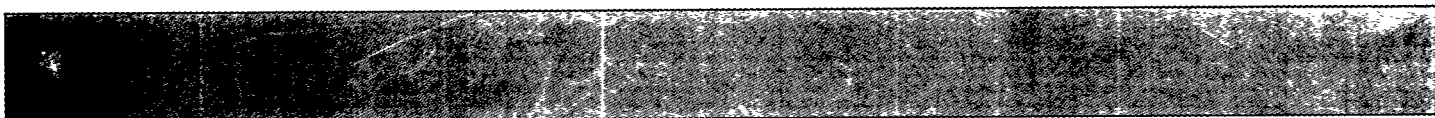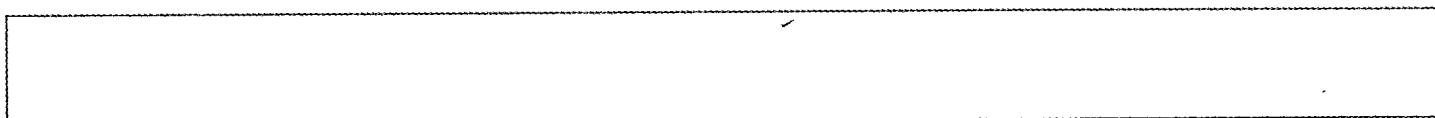# INTERNATIONAL CONTAINMENT TECHNOLOGY CONFERENCE

February 9 - 12, 1997

St. Petersburg, Florida, USA

Conference Proceedings

Sponsoring Organizations:

U.S. Department of Energy

DuPont Company

U.S. Environmental Protection Agency

Co-sponsoring Organizations:

Florida State University

U.S. Air Force, Armstrong Laboratory - Environics

American Society of Civil Engineers (ASCE)

Society of American Military Engineers (SAME)

CONTAINMENT

INTERNATIONAL

TECHNOLOGY

CONFERENCE

February 9 - 12, 1997

St. Petersburg, Florida, USA

Conference Proceedings

Conference Administration

Conference Chairs

Skip Chamberlain
U.S. Department of Energy

Calvin Chien
DuPont Company

Nicholas Lailas
U.S. Environmental Protection Agency

Technical Committee Chairs

George Filz
Virginia Polytechnic Institute and State University

John Heiser
Brookhaven National Laboratory

Joyce Whang
DuPont Company

Technical Committee Members

David Daniel
University of Illinois

Steven Day
Geo-Con, a Woodward-Clyde Company

Annette Esnault
Bachy (France)

Jean-Pierre Giroud
GeoSyntec Consultants

Stephan Jefferis
Golder Associates Ltd. (UK)

Executive Committee

David Daniel
University of Illinois

Annette Esnault
Bachy (France)

Lorne Everett
Geraghty & Miller, Inc.

Hsai-Yang Fang
University of Massachusetts - Lowell

Clyde Frank
U.S. Department of Energy

Bruno Gemmi
Geotechnical Consultant (Italy)

Andrea Hart
MSE Technology Applications, Inc.

John Heiser
Brookhaven National Laboratory

Roy Herndon
Florida State University

Stephan Jefferis
Golder Associates Ltd. (UK)

Michael Katona
U.S. Air Force

John Koutsandreas
Florida State University

Walter Kovalick, Jr.
U.S. Environmental Protection Agency

Stefan Melchior
IGB Hamburg (Germany)

James Mitchell
Virginia Polytechnic Institute and State University

Za-Chieh Moh
Moh and Associates, Inc. (Taiwan)

James Owendoff
U.S. Department of Energy

Phillip Palmer
DuPont Company

Paul Schroeder
U.S. Army Corps of Engineers

Inge-Marie Skovgård
Danish Environmental Protection Agency

Hans-Joachim Stietzel
German Federal Ministry for the Environment

Ramona Trovato
U.S. Environmental Protection Agency

Linda Ward
Geo-Con, a Woodward-Clyde Company

Joseph Welsh
Hayward Baker Inc.

Joyce Whang
DuPont Company

Peter Yen
Bechtel Corporation

Conference Coordinator
Loreen Kollar
Florida State University

Exhibition Coordinator
Eugene Jones
Florida State University

Publications Coordinator
Adieren Roark
Florida State University

DISCLAIMER

Portions of this document may be illegible electronic image products. Images are produced from the best available original document.

Table of Contents

Chapter 1: Plenary Presentations

Chapter 2: Slurry Walls: Materials & QA/QC

Chapter 3: Slurry Walls: Cementitious & Composite

Chapter 4: Slurry Walls: Soil/Bentonite Case Histories

Chapter 5: Vertical Barriers: Sheet Piling & Geomembranes

Chapter 6: Caps: Capillary Barriers

Chapter 7: Caps: Innovative Techniques

Chapter 9: Grouting

Chapter 10: Jet Grouting

Chapter 11: Stabilization/Solidification

Chapter 12: Barrier Materials

Chapter 13: Reactive, Low Permeability Materials

Chapter 14: Permeable Reactive Walls: Materials Development/Characterization

Chapter 15: Permeable Reactive Walls: Zero-Valent Metals

Chapter 16: Permeable Reactive Walls: Field Studies

Chapter 17: Modeling: Groundwater Flow

Chapter 18: Modeling: Transport Through Barriers

Chapter 19: Performance Criteria

Chapter 20: Performance Monitoring

PREFACE

This document contains the manuscripts of the papers and posters presented at the 1997 International Containment Technology Conference and Exhibition. These manuscripts represent a valuable compilation of information and data on the environmental challenges and technology-based solutions associated with containment technologies. The purpose of the conference was to promote the advancement of containment technologies by providing a forum from which participants from related disciplines could meet to exchange ideas and information on recent developments.

More than 500 participants from all over the world participated in this event which initiated a biennial series of conferences on containment and related technologies. Through exhibitions, platform presentations and poster presentations, as well as through personal interactions, the 1997 International Containment Technology Conference and Exhibition was a successful event for the conference participants. This conference was a follow-on activity to the international workshop on containment technology systems conducted in August of 1995 in Baltimore, Maryland. The planning has already been initiated for the 1999 conference and exhibition through a series of workshops which will form the foundation for this conference. The 1999 conference will provide a forum for future discussions on advancements and experiences gained in the application of containment technology systems.

The manuscripts are presented as they were submitted by the authors in the official language of the conference, which was English. Each manuscript was peer-reviewed. Editorial revisions were not made to the manuscripts other than those from the comments the reviewers and session chairs provided to the authors. Questions or comments concerning a particular manuscript should be directed to the authors.

Skip Chamberlain	Calvin Chien	Nick Lailas
U.S. Department of Energy	DuPont Company	U.S. Environmental Protection Agency

EXECUTIVE SUMMARY

The 1997 International Containment Technology Conference and Exhibition was conducted on February 9-12, 1997, in St. Petersburg, Florida. The conference was jointly sponsored by the US Department of Energy, the US Environmental Protection Agency, and the DuPont Company. The focus of the conference was on the application of containment technologies to contaminated sites and landfills. More than 500 professionals from government, industry, and academic institutions, from 22 countries, participated at this event. Participants included engineers, scientists, researchers, designers, regulatory personnel, owners of contaminated sites, educators, construction contractors, and material suppliers. In total, 148 papers were presented, 108 as oral presentations and 40 as poster presentations. The papers covered topics including groundwater flow modeling, contaminant transport modeling, sheet piling, geomembranes, stabilization and solidification, barrier materials, permeation grouting, jet grouting, performance monitoring, performance criteria, permeable reactive walls, low permeability reactive walls, caps, slurry walls, floors, case histories, and quality assurance/quality control (QA/QC) issues. In addition to the technical sessions, the conference included two training seminars, one on barrier emplacement quality assurance and monitoring strategies, and another on quality control for vertical barriers. Thirty-three exhibitors provided information on state-of-the-art equipment, technology, and services in support of waste containment. The opening plenary session included keynote presentations from the primary sponsors as well as two regional presentations on the application of containment technologies in Europe and Australia. The closing plenary session consisted of a panel discussion that provided an opportunity to summarize and synthesize the conference and identify future needs in the area of containment technologies. Finally a site tour of the U.S. DOE Pinellas Plant was provided to over 100 conference participants.

The training seminars were well-attended, and the quality of the course materials and presentations were outstanding. Training Seminar I: Barrier Emplacement Quality Assurance and Monitoring Strategies was organized by Geraghty & Miller, Inc. (Lorne Everett), MSE Technology Applications, Inc. (David Reichhardt) and Heidemij Advies (Ben Viveen). This seminar focused on technologies for verification, monitoring and methods for construction quality assurance/control applied to barriers. A video was presented, followed by a discussion covering the largest construction project ever undertaken in the Netherlands, involving emplacement of a 180 foot barrier at a former gas works facility. Technical presentations on geophysical techniques and their application to subsurface barrier verification and monitoring were also made.

Training Seminar II: Quality Control for Vertical Barriers was organized by Geo-Con, a Woodward-Clyde Company (Steven Day and Linda Ward), Mueser Rutledge Consulting Engineers (Peter Deming) and Cargill Fertilizer, Inc. (Ralph Remmert). This seminar focused on the typical methods, measures and tests performed during construction of both deep soil mixed (DSM) barriers and soil-bentonite slurry cutoff walls (SCOW). Also presented were case studies which highlighted the various project perspectives of the site owner, the design engineer and the engineering contractor. Information was provided on the special advantages of each type of barrier (DSM and SCOW) as well as on installation considerations and elements of QA/QC related to barrier performance, scheduling, applicability to varying site conditions and cost.

The conference demonstrated that substantial improvements and innovations in containment technologies have occurred in recent years. Examples include:

- **Capillary barriers.** New capillary barriers have been developed for use in capping systems at contaminated sites.
- **Combined systems.** Examples include directional drilling combined with jet grouting and geomembranes combined with drains and/or with soil-based or cement-based barrier materials.

- **New applications of existing technologies.** Hydraulic fracturing and multipoint injection are existing technologies that have found new application in contaminant containment.
- **Equipment.** Enhancements to "chain saw" trenchers permit excavations to 35 m depths. Jet-grouting technology now permits creation of up to 8 m diameter columns for use in constructing floors beneath contaminated sites.
- **Material enhancements.** Geomembrane and sheet pile interlocks are now designed to permit inspection. Additives to soil- and cement-based, low hydraulic conductivity barrier materials are being used to treat contaminants and improve physical performance.
- **Permeable reactive walls.** This technology has moved from the concept stage through demonstration projects to full-scale field applications.

Other opportunities for improved understanding and implementation of existing technologies and for development of new and improved containment technologies include the following:

- Field performance tests, sensors, and geophysical techniques;
- Maintenance and repair technologies;
- Technologies for sealing vertical barriers into aquicludes;
- Diffusion of organic contaminants through geomembranes;
- Investigation of existing walls that have been in service for many years;
- Improved understanding of barrier material physical characteristics, such as strength, deformation, shrink-swell, and freeze-thaw responses;
- Collection of feasibility, installation, and performance data;
- Emplacement of barriers under difficult geologic conditions;
- Emplacement of barriers at increasing depths;
- Development of manuals and guidance documents for design, construction, QA/QC, and performance monitoring;
- Improvements in the long-term performance of barriers;
- Use of "no-dig" technologies;
- Metals precipitation and clogging in permeable reactive barriers;
- Use of wastes as barrier materials;
- *In situ* material properties necessary for contaminant transport analyses; and
- Improved cooperation among the various disciplines involved in containment technology development, design, implementation, verification, monitoring, operation, and maintenance.

The strong interest in this conference is partly the result of increased levels of acceptance of containment as a viable waste management alternative within the technical and regulatory communities. This acceptance has been driven primarily by the high ratios of benefits-to-costs that containment technologies can provide. In addition, the push toward risk-based corrective actions is likely to continue to promote containment technologies as highly effective alternatives for many problems.

One of the reasons that the conference was successful was that it brought together contractors, technology developers, academicians, and regulatory personnel and other interested parties into a common forum. The success of this conference has encouraged planning for the 1999 International Containment Technology Conference and Exhibition.

Chapter 1
Plenary Presentations

Containment and DOE's Environmental Management Ten-Year Plan

Dr. Clyde W. Frank
Deputy Assistant Secretary
Office of Science and Technology
U.S. Department of Energy
Washington, D.C., USA

Webster's Dictionary defines the verb "contain" as "to keep within limits." That is exactly the message the American public is sending the Department of Energy (DOE). Previous DOE planning efforts called for more time and more money than the nation thinks is necessary to clean up the former DOE nuclear weapons complex. In July 1996, under Assistant Secretary Al Alm's leadership, a vision of completing as much cleanup as possible within ten years was implemented and the "Ten-Year Planning Process" was set in motion. Each DOE site is preparing a Ten-Year Plan and from these plans, a national plan will be presented for public review on March 31, 1997. The final plan will be completed in September of 1997 after all stakeholder issues have been addressed. Before we proceed, we need to obtain community support—certainly support from the public bodies, the regulatory bodies, and the states.

Since 1989 the mission of the Office of Science and Technology is to develop and implement "better, faster, safer, and cheaper" environmental technologies. Today, we say "reduce cost, reduce risk, and do what can't be done." We have incorporated the basic sciences to help with the "can't-be-done". In light of the Ten-Year Plan, cost reduction is key. Achieving this goal also requires a certain amount of break-through management and a great deal of attention to the efficiency of operations. In pursuing these efficiency goals, let me restate our commitment to listening to stakeholders. We plan to work closely with those most affected by our decisions.

Containment technologies offer the best and fastest opportunities to reduce cost and risk at the same time. As an environmental cleanup solution, containment eliminates the cost of transportation and the risks associated with it. Most of the containment technologies are simple and efficient to implement and also minimize worker exposure. DOE's monitoring capabilities are becoming more reliable and sophisticated, providing long term solutions. Containment, where appropriate, can save millions of dollars when compared to conventional treatment technologies.

It is clear from the initial review of the preliminary Ten-Year Plans submitted that improved containment technology is a common need at all the sites. The Ten-Year Plans list approximately 24 different innovative technologies for containment, stabilization, and in-situ treatment of buried waste and/or contaminants in groundwater and soils. The success of the Ten-Year Plan depends on the timely implementation of these technologies. Many of these technologies are proven and commercially available, and many others are approaching that stage of development.

To reduce the cost and risk of the DOE cleanup, the Ten-Year Plan requires that the Office of Science & Technology refocus its efforts from technology development to the commercialization and widespread deployment of technologies which have already been developed. There are over 300 technologies in the pipeline and available in the Ten-Year Plan. We have identified over 40 technologies that are commercially available and implemented within DOE. That leaves more than 250 additional opportunities for near-term deployment. With aggressive technology deployment, these opportunities can translate to more than $31 billion in savings. The Office of Science and Technology is developing a new investment strategy to focus on accelerating the pace of deployment and broadening the deployment within EM of these proven, available technology solutions.

EM has invested in a suite of containment technologies ranging from robust, mechanically driven technologies, to jet grouting, to low-energy permeation technologies. These technologies apply to varied soils and site conditions.

The Office of Science and Technology has been in the technology deployment business for 8 years. Life-cycle engineering and cost benefit analyses have been employed to evaluate the individual technologies and track their progress toward deployment. Large-scale demonstrations, involving multiple technologies at one site, have been successful and cost effective. Now we need a new integrated approach for cleaning up the weapons complex. We propose a deployment initiative that will identify the best prospects for multi-site use through a competitive bid process. The initiative will reward adoption of improved technology. Deploying technologies more quickly saves in three ways: first, in unit cost savings; second, in mortgage reduction; and third, from the results of reinvesting the savings. So we win both in terms of velocity and acceleration of savings and cleanup.

We cannot accelerate deployment without also accelerating timely regulatory approval. The deployment initiative will continue the investment in regulatory cooperation. Through work with the Interstate Technology Regulatory Cooperation, the Cone Penetrometer has achieved acceptance in 22 states and saved $20 million in permitting fees. The Alternative Landfill Cover Design is also addressing the regulatory acceptance issue by involving the EPA and environmental divisions from the western states in the project. We must continue to work to establish technology performance verification standards and streamline the permitting process.

Over the last three years, the Department of Energy has made significant progress. The system is much more efficient, contract reform is working; there have been substantial reductions in support costs; and we have initiated a privatization program. We now see the possibility in most places, though not in all, to achieve completion of cleanup.

Privatization is a key investment strategy. We need to maximize the effectiveness of privatization. Private industry will not enter the competition for federal cleanup and compliance work alongside traditional contractors unless it has a reasonable chance to profit. Therefore, the Office of Science and Technology will support the generation and application of data to deliver end-product specifications that achieve an appropriate balance of public and private risk and thereby encourage industry to enter the EM market.

Partnering has been a successful strategy within the Office of Science and Technology in the last few years and we will continue to actively reach out to non-EM users within DOE to develop and transfer needed technologies. The result will be greater benefits in terms of greater cost savings across DOE and beyond, including both the domestic industrial sector and the international arena (public and private). Containment is not by any means a unique need of US DOE sites, as evidenced by our industry partners and international colleagues represented here at this conference.

With respect to the achievements of the Ten-Year Plan goals, containment technologies are a critical component because groundwater and soil contamination is a significant and pervasive problem at all of the DOE sites. Containment technologies are being designed to integrate stabilization and in-situ treatment technologies to provide permanent remedial solutions. Some of the technologies in the Subsurface Containment Focus Area include Reactive Barriers that actually assist in the remediation effort and Capillary Barriers, part of the Alternative Landfill Cover Design that are easily constructed and low cost. Since major cost reductions have been identified with these technologies, rapid deployment becomes imperative if we are to realize DOE's cleanup goals.

A prime example of the cost reduction achievable through containment technology is the Alternative Landfill Cover Project. The problem is well known: 90% of conventional landfill covers could allow infiltration and contamination of water. In a study by the EPA of some 163 randomly selected landfills, various problems were discovered at 146 sites, suggesting that the caps are not fulfilling their goal as effective sealers of landfills. Some of the alternative designs emphasize unsaturated hydraulic conductivity, increased water storage potential to allow for eventual evaporation, and increased transpiration through engineered vegetative covers. The alternative covers were designed to take

advantage of local materials to allow for easier construction of the covers at substantial cost savings. The numbers speak for themselves:

Potential EM Savings: $1 billion (by the year 2006)
EM Development Cost: $5 million

This is a cost/benefit ratio of 200:1. With over 2,000 landfill sites under DOE's management, the economic impact of improved containment technology is tremendous.

Close-coupled jet grout barriers are vertical, angled, and horizontal subsurface barriers composed of grouting material that prevent the spread of contamination without disturbing the waste site. Multi-site demand for subsurface barriers is outlined in the field Ten-Year Plans. Three sites—Idaho, Chicago, and Oak Ridge—report combined potential cost savings of $42 million over ten years. This technology is applicable at many sites that pose sufficient long-term risk where existing barrier and cover technology is not adequate.

When this type of *in situ* stabilization technology enables end-users and regulators to support a containment option, rather than an *ex situ* option, the potential cost savings can reach billions of dollars. A recent comparison cost study at Idaho National Engineering Laboratory's Pit 9 (which is typical of DOE's buried waste sites) put the savings upwards of $20,000/yd against the baseline of retrieval followed by thermal treatment and disposal in a repository. Estimated EM development costs for jet grout stabilization will total about $4 million by the end of FY97. This is clearly a good return on investment.

Another new barrier technology is Two Phase Hybrid Thermosyphons, a frozen soil barrier technology based on previous uses in groundwater control and tunnel construction. During FY 1997 there will be a hot cell demonstration at Oak Ridge National Laboratory's Waste Area Group 9 Homogeneous Reactor Experiment Impounding Pond. Artic Foundations, Inc. has been awarded the contract and EPA Superfund Innovative Technology Evaluation Program (SITE) is developing methods to evaluate the barrier's integrity using tracer testing. This is just one of many projects that we co-sponsor with the EPA and other agencies. EPA's close involvement with our technology development and deployment planning has proven time and again to expedite the process toward commercialization.

Innovative characterization and monitoring technologies for containment processes also contribute to the complex-wide cost savings. The Cone Penetrometer is a truck mounted, ground penetration device with push rods used to deploy various sensors and sampling tools for determination of subsurface characteristics, e.g., chemical, physical, and geologic parameters. The device reduces the number of wells required and allows *in situ* contaminant sampling and analysis. The potential EM savings are $72 million, while EM development costs are $4.4 million. This results in a cost/benefit ratio of 16:1.

The Surface Acoustic Wave Sensor (SAWS) is also applicable to many DOE sites. This in-well sensor provides continuous data on contaminants in the water and replaces the need for manual water sampling and lab analysis. By solving this long term monitoring problem, SAWS reduces the mortgage from site surveillance and saves $840 million. With EM development costs of $10 million, that is a cost/benefit ratio of 84:1.

In accordance with the mission of this conference, the Office of Science and Technology projects like the Poland Initiative provide an international perspective. This cooperative effort serves to address mutual environmental management objectives of Poland and the U.S. through subsurface contaminant technologies, including bioremediation and phytoremediation. The international goal of environmental stewardship is, after all, the overriding principle for our work. I am proud to be part of this conference that has had such a successful participatory response. Thank you for your participation and the contributions you have brought this conference.

Containment Technology and the Success of a Joint Initiative
Dr. Hugh J. Campbell, Jr.
DuPont Company
Wilmington, Delaware, USA

It is my pleasure to be one of the three keynote speakers here at the 1997 International Containment Technology Conference and Exhibition. I would like to thank the Executive Committee, the Technical Committee Chairs and Members, and Florida State University for their hard work in organizing this conference. I would also like to thank Skip Chamberlain from the DOE, Nick Lailas from the EPA, and Calvin Chien from DuPont for their leadership in making this conference a reality. In addition, the other three co-sponsoring organizations – the Air Force, American Society of Civil Engineers, and the Society of American Military Engineers -- should be commended for their support.

And last but not least, thank you all for attending and sharing your expertise. This conference is an excellent example of the firm commitment by the DOE, EPA, and DuPont that has allowed us to maintain a three-year cooperative relationship. We are proud of that relationship and this conference. But I can tell you, the next three days will only be a success with your active participation. Your input will help us advance our understanding of containment technologies in environmental applications.

Next I would like to place containment in perspective relative to overall remediation challenges. Ideally, we all want to use innovative technologies that are effective in remediating soil and groundwater to acceptable levels without being excessively complex or costly. However, real life applications of remedial technologies often prove to be technologically ineffective, unfeasible, unaffordable, and often a "force fit." You can probably relate to the frustration of a technology that looks good on paper or in the lab, but just doesn't quite work in the field. Specific factors related to the site or target contaminant can lower a technology's effectiveness or totally preclude it as a viable remediation option. For example, low soil permeability may exclude the use of a technique such as soil vapor extraction or a technology that works well for one contaminant may be ineffective with another. Bioremediation, for instance, has been found in many cases to effectively clean up chlorinated solvents, but it naturally won't be effective, or as effective, in addressing lead or mercury contamination.

It is in these situations where containment can play an important role. Containment, by its very definition, prevents contaminants from migrating beyond a designated area. It can be used in an emergency situation, as a temporary measure, or as a permanent solution. It can, in some cases, provide a cost-effective means of sufficiently reducing risk to an acceptable level without resorting to cleanup technologies that have relatively high costs or that may not reduce the risk effectively.

I will now provide information on DuPont's remediation challenge and approach. At DuPont, we have chosen to approach the challenge of protecting human health and the environment at over 60 major and diversified sites worldwide by using the same tool that has served us so well throughout our corporate history of nearly 200 years: that is, technology. DuPont is a technology based company. We believe in the potential of technology to improve the quality of life and to solve problems. – You have no doubt heard of our slogan "Better Things for Better Living"? So it was natural for us to put our top scientists and engineers to work on our past contamination situations. Our goal has been and will continue to be to find or develop the technologies that enable us to meet our environmental responsibilities while using our resources wisely. What we discovered from our experience in remediation since the mid-80s was that there are very few "on-the-shelf" technologies that we can readily apply to highly variable and often unique remediation challenges. What we found instead were existing technologies that need to be improved in effectiveness or made more cost-effective, or innovative technologies that need to be proven. Unfortunately, in many instances, there are no "treatment" technologies available for certain remediation situations.

To tackle these problems and focus our remediation program, DuPont formed five technology teams: Soil Processing, Pump and Treat, *In Situ* Treatment, Bioremediation, and, finally, Containment and Transport Modeling. We formed these teams around technology areas associated with specific DuPont needs. Each team developed its own mission depending on the status of the technology. This morning I will focus only on the Containment and Transport Modeling Team for obvious reasons. This team was formed five years ago and is led by Calvin Chien, who, by no coincidence, represents DuPont as one of this symposium's co-chairs. His team has been one of our most productive teams, forging partnerships with academia, the government, and global experts to advance the understanding of containment technologies.

To demonstrate its commitment and direction, Dr. Chien's team developed a mission which is focused on containment technology. It was and still is to review and evaluate existing containment technologies, identify technology weaknesses and gaps, thereby facilitating practical and meaningful technology developments that will make containment technologies more economical, technically reliable, and readily accepted by regulatory agencies and the public as a remedial alternative. With that mission clearly defined, the team went to work under Dr. Chien's leadership.

The first order of business for the team was to review and evaluate all existing containment technologies. With this huge task ahead, Calvin's team enlisted the help of academia. Experts in the field helped us determine where we were with each technology. The result was an internal summary report that presented an overview of available containment technologies. When the report was completed it was published commercially by John Wiley and includes chapters on contaminant transport, walls, floors, and caps. To demonstrate our corporate environmental commitment, DuPont has donated all of the proceeds from this book to an environmental conservation organization.

Even with this book in hand, we knew it was only the first step and that there was still much more to do. Advancing the understanding of containment technology is a major effort, especially considering its multi-disciplinary nature. There are limits on the resources that any one organization can commit and still stay in business. There are also limits on the resources society as a whole can commit and still deal with other important priorities. Let me be very clear that this does not negate or in any way lessen our obligation to protect human health and the environment, it simply means that we have to be wise about how we do it. And, in this case, I think we can take credit for being wise. Knowing that three heads are better than one, DuPont, the DOE, and the EPA joined forces in the effort to assess containment technology and its potential uses. After all, each of us brings a different but equally important perspective to the table.

DuPont and the DOE share the challenge of protecting human health and the environment at a great many sites nationwide and overseas. The DOE alone has over 3,700 contaminated landfill sites, possibly requiring billions of dollars for remediation. The EPA's stake is just as high – overseeing the nation's environmental agenda, ensuring that environmentally sound solutions are used, and helping to communicate these solutions to the public. But because DuPont is a business, we bring a unique perspective: we must integrate environmental responsibilities into our overall business plan. Like the rest of industry in the United States, we must work to improve and protect the environment, build upon our credible corporate image, and, at the same time, maintain our position in a fiercely competitive global marketplace. I am proud to say that we are succeeding.

DuPont recently was presented the Keystone Center Award in recognition of our ambitious environmental goal of zero wastes and emissions. In addition, the EPA recognized DuPont as one of the companies in the "early-achiever" category for making substantial progress toward the goal of a 50% reduction of releases and transfers of 17 high-priority chemicals identified by the EPA. The so called 33/50 program was a voluntary program with over 1,200 companies committing to a 33% reduction of releases and transfers of these chemicals by the end of 1992 and a 50% reduction by the end of 1995.

When attempting to apply containment at specific sites, all of us have received public resistance. This is in part due to the lack of understanding about the technology – how it works and its value. Essentially, containment was thought of as a "do nothing" approach that was a cheap and easy way to claim you were environmentally responsible. Slowly but surely this perception is changing. By sharing experiences and bringing together our own experts as well as those from academia and other countries, the DOE, EPA, and DuPont have been working together to improve the understanding of the technology and fill many technological information gaps to make containment a more reliable, acceptable, and cost-effective remedial technology.

Knowing that the government had mutual interests and similar needs, DuPont joined forces with the DOE and EPA to sponsor and organize the First International Containment Technology Workshop, held two years ago in Baltimore, MD. The workshop brought together over 100 experts in containment from eight countries and focused on the applicability and reliability of various containment technologies. Barriers, caps, and walls were just some of the topics discussed. Ten small working sessions allowed participants to share information, exchange opinions, and hammer out ideas to achieve a consensus on what was known, what was not known, and what was needed to apply containment technologies in real-life remedial applications.

The result of these extensive discussions and debates is a follow-up to the first book that furthers our understanding of containment, entitled: "Assessment of Barrier Containment Technologies." This book gives a detailed account of where we are today in applying various containment technologies for environmental applications. Consultants and government and industry members are already finding it an invaluable tool for increasing the understanding of the technology and determining if containment is applicable and appropriate at a particular site and ultimately that is the final proof or value in this program. Containment should not be used because it sounds like the easiest or cheapest thing to do. Rather, it should be used because it is based on sound science and engineering and because it is the sensible choice at certain sites for reliably and cost-effectively reducing risks to human health and the environment.

The workshop generated great interest in containment technologies worldwide. So, the DOE, EPA, and DuPont decided to provide additional technical forums to allow experts to continue exchanging ideas and information. And here we are at the First Biennial International Containment Conference! And there are high expectations that this gathering will result in another productive step to advance our knowledge of various containment approaches and their practical applications.

This conference is the latest step in our journey. Only by working together can we further the understanding of containment technologies and, eventually, their proper place in remediation. Cooperative agreements such as those between the DOE, the EPA, and DuPont are win-win-win propositions and allow the sharing of knowledge and resources unique to each organization for the common good of all.

But getting together and merely discussing containment technologies is not enough. We decided to take these partnerships one step further and actually field test technologies. Armed with all of the information we had gathered and organized around containment, our trio joined forces again; this time, the U.S. Air Force joined in. The project is in its beginning stages and is a demonstration of the use of high-pressure jet grouting to create thin diaphragm walls. Work has begun at the Groundwater Remediation Field Laboratory National Test Site at Dover Air Force Base, which is designed to provide a testbed and infrastructure for evaluating technologies. The project is a three-phase effort: Phase I is aimed at developing site-specific jetting parameters and investigating nondestructive verification techniques and innovative monitoring methods. Phase II will involve emplacing a double-walled coffer dam. The scope of Phase III is in the conceptual stage, but is intended to test the coffer dam and its ability to contain specific types of contaminants. This technique, if proven, could serve as a cost-effective containment technology. In the meantime, experts from each organization are working together to ensure that the program is conducted in a streamlined manner, integrating tasks and

coordinating efforts to save time and money. Joint efforts such as this have helped in the advancement of various containment technologies. By testing specific technologies, containment is becoming more recognized and accepted as a viable alternative to costly remedial treatment options.

But our partnerships can't stop at our nation's boundaries. After all, environmental challenges are not unique to the United States. The DOE and EPA have sponsored many conferences in Europe in recent years, some of which have addressed containment as an environmental technology. In an effort to learn what other countries are doing, Dr. Chien's Containment Team is talking to European research institutes, and we plan to collaborate on projects in the future. Today, we welcome the experts from 23 countries located in Europe, Canada, and Asia-Pacific who are here to share what has been learned about how to improve existing technologies and their applications. We need to compare and cross-reference innovations and methods with U.S. approaches.

In summary, the process of developing a technology to the point where it is both understandable to the public, workable, and affordable to apply requires a tremendous commitment of resources. That is one reason DuPont is committed to cooperative endeavors such as this conference and the other efforts I mentioned earlier. They enable us to pool our resources in a way that brings together the best scientists and engineers from a variety of organizations globally to tackle our shared problems. We look forward to learning more about containment through these collaborative efforts.

Priorities for In-situ Remediation Research
E. Timothy Oppelt
U.S. EPA National Risk Management Research Laboratory
Cincinnati, Ohio, USA

The following is a summary of the keynote address made by E. Timothy Oppelt at the 1997 International Containment Technology Conference and Exhibition which was conducted 9-12 February 1997 in St. Petersburg, Florida, USA. Mr. Oppelt is the Director of the National Risk Management Research Laboratory (NRMRL) of the U.S. Environmental Protection Agency (Cincinnati, Ohio). Much of the research conducted by the U.S. EPA related to containment technology is conducted at the NRMRL. Mr. Oppelt provided an overview of the efforts at the NRMRL associated with containment technology systems in the context of the U.S. EPA's Superfund Innovative Technology Evaluation (SITE) Program and other related initiatives.

Mr. Oppelt began his presentation by summarizing the U.S. EPA's programs related to site remediation and waste management. In terms of site remediation activities at the NRMRL, the following are the current priorities:

- groundwater modeling;

- clean-up of contaminated soils, primarily using ex-situ extraction; and

- technical support provided for SITE demonstrations.

Regarding waste management activities at the NRMRL, the current emphases have been on the development of more effective waste combustion and containment technology systems. It is in this context that the NRMRL is involved with the general area containment technologies. Mr. Oppelt indicated that research initiatives at the NRMRL are designed to influence the following objectives:

- reducing the "high" cost of site clean-up;

- increasing the pace of site clean-up activities in the United States;

- addressing critical aspects related to the reauthorization of the Superfund Program;

- addressing issues related to "Brownfields" in the United States; and

- to disseminate information on completed SITE demonstrations so as to increase the effectiveness of ongoing and planned site remediation activities throughout the country.

Some of the major outcomes of research conducted by the NRMRL have lead to the following more obvious conclusions:

- effective site remediation approaches include the use of properly designed containment technology systems;

- also included among effective site remediation approaches is the use of "natural attenuation" and

- when feasible, in-situ remediation approaches can be effective as well as significantly cost-effective when compared with ex-situ approaches for addressing contaminated soils and groundwater.

Mr. Oppelt identified the following areas of research as priorities as related to groundwater contamination:

- permeable reactive barriers;

- modeling;

- Non-Aqueous Phase Liquids (NAPLs) extraction;

- natural attenuation;

- bioremediation; and

- containment technology systems.

Regarding soil contamination, Mr. Oppelt identified the following areas of research as priorities at the NRMRL:

- bioremediation;

- phytoremediation;

- metals stabilization; and

- facilitating the use of "enabling technologies".

Data were provided on 259 completed innovative technology demonstrations which were conducted in North America. These data are show that approximately 25% of all projects (65 projects) involved the use of a biologically-related treatment technology. The other projects involved the use of either physical, chemical, or thermal treatment technologies.

Data were also provided on 139 in-situ innovative technology demonstrations conducted in North America. These data indicated that for contaminated soils, 40% of the projects involved the use of physical/chemical methods, 20% utilized biological methods and 14% utilized thermal methods. For contaminated groundwater, 17% of the projects utilized physical/chemical methods while 9% of the projects utilized biological methods.

Mr. Oppelt summarized the application of technologies used for completed technology demonstrations (86 projects) associated with the U.S. EPA's SITE Program. These data indicate that the following distribution of technologies were used for these demonstration projects:

- physical/chemical treatment methods - 41 projects

- biological treatment methods - 14 projects

- thermal treatment methods - 10 projects

- desorption treatment methods - 8 projects

- radioactive waste handling methods - 3 projects

- solidification/stabilization methods - 7 projects

- materials handling methods - 3 projects

Data were also provided on the distribution of SITE demonstration projects between the use of in-situ vs. ex-situ approaches. For completed demonstration projects (of which there are 86 projects), 58 (67%) were conducted using an ex-situ approach while 28 (33%) were conducted using an in-situ approach. While for either on-going or planned projects (of which there are 28 projects), the distribution was 15 (54%) ex-situ and 13 (46%) in-situ. The trend is increasingly toward the use of less costly, in-situ remediation approaches, and often these approaches are utilizing containment technology systems in combination with other site remediation technologies.

(The transparencies utilized by Mr. Oppelt for his keynote address follow.)

11

Priorities for *In-situ* Remediation Research

E. Timothy Oppelt

U.S. EPA National Risk Management

Research Laboratory

Cincinnati, Ohio

Remediation/Waste Management Program

○ Remediation

* Groundwater modeling & remediation

* Soil remediation

Ex-situ extraction

* Demonstrations (SITE)

Technical support

○ Waste Management

* Combustion

* Containment systems

Remediation Research Priorities

○ Influences

- High cost of clean-up

- Pace of clean-up

- Reauthorization of Superfund

- Brownfields

- Completed demonstrations

○ Possible Outcomes

- Alternate clean-up endpoints

- Natural attenuation

- Containment

- In-situ technologies

Research Priorities - Groundwater

- Modeling
- Permeable reactive barriers
- NAPL extraction
- Natural attenuation
- Bioremediation
- Containment

Research Priorities - Soils

- Alternate endpoints

- Bioremediation

- Phytoremediation

- Metal stabilization

- Enabling technologies

Research Priorities – Waste Containment

○ Long-term performances (GCLs)

○ Improved guidance – covers

○ Landfill bioreactors

Research Priorities - SITE Demonstrations

- Problem-driven
- *In-situ*
- Containment
- Low-cost/Low-tech
- Know-how based

Completed N. American Innovative Technology Demonstrations (259)

Soil Vapor Extraction 13%

Air Stripping 9%

Other Biological Proc. 2%

Bioslurry 2%

Bioreactor 2%

Biodegradation 13%

Solvent Extraction 3%

Other Thermal Processes 1%

Bioventing 6%

Soil Washing 9%

Vitrification 1%

Stabilization/Solidification 9%

Thermal Enhanced Extraction 2%

Incineration 4%

Oxidation 5%

Thermal Desorption 5%

Precipitation/Filtration 4%

Radio/Electric Heating 5%

Other Physical Processes 5%
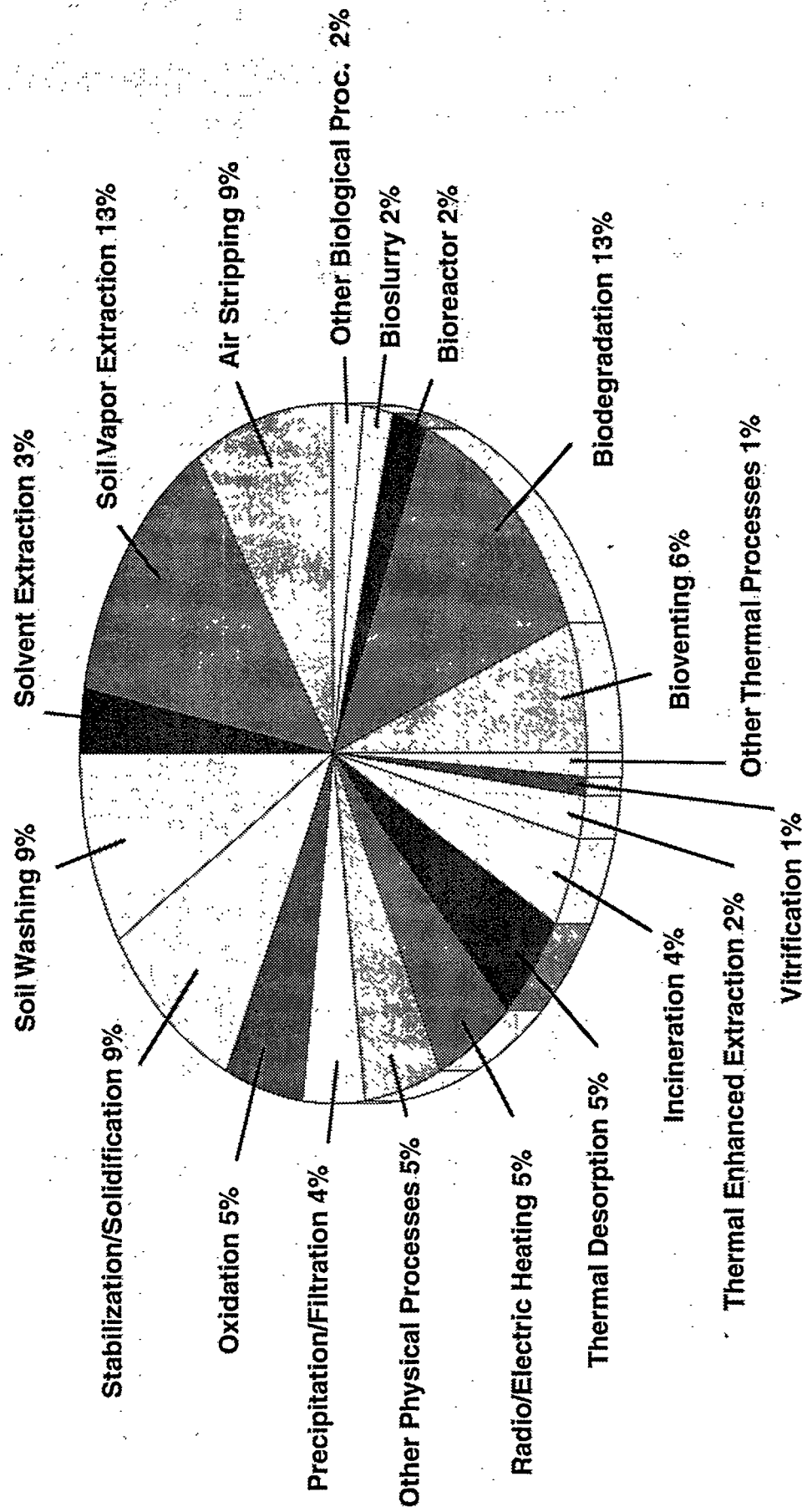
Completed N. American Innovative Technology Demonstrations (In-situ/139)

Groundwater Biological 9%

Soil Thermal 14%

Groundwater Physical/Chemical 17%

Soil Physical/Chemical 40%

Soil Biological 20%
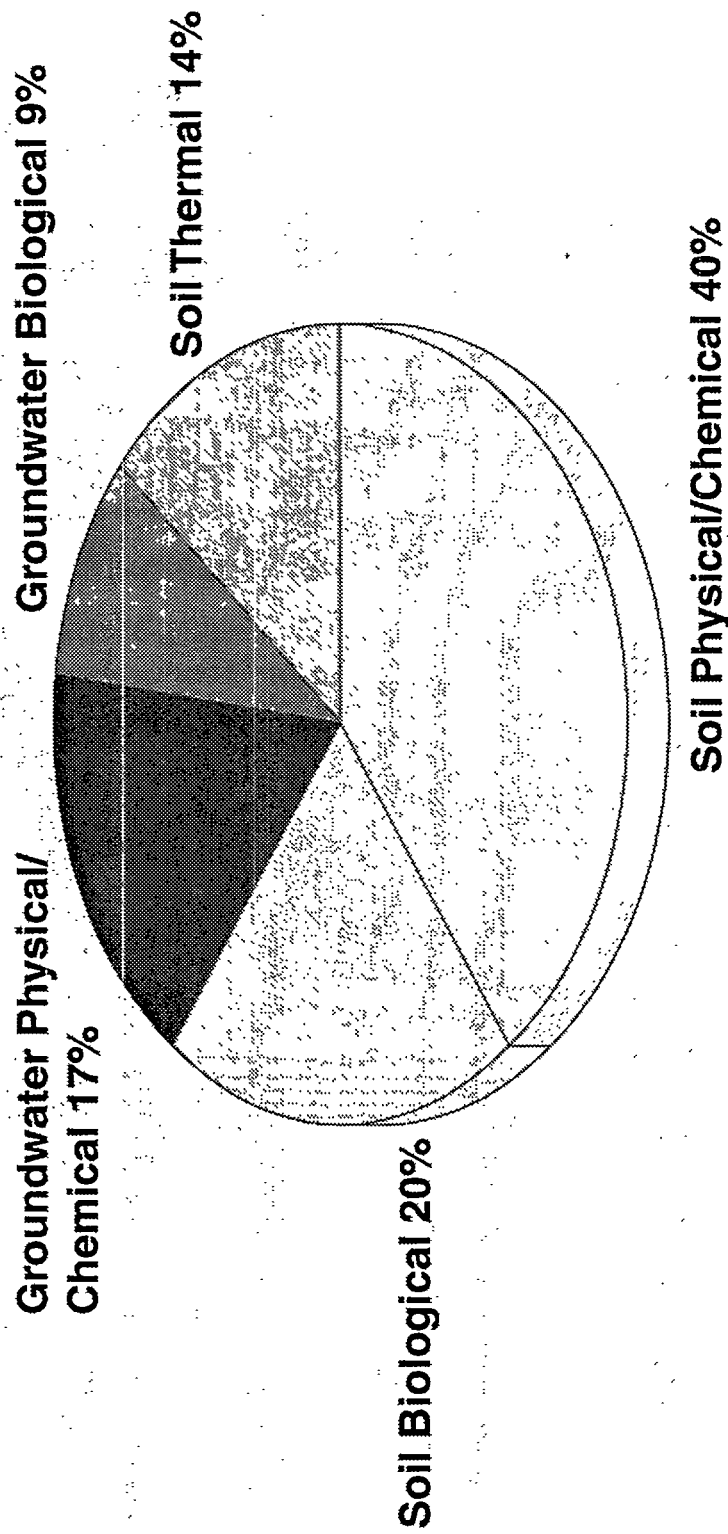
In-situ/Ex-situ Distribution of SITE Demonstration Projects

Completed 86
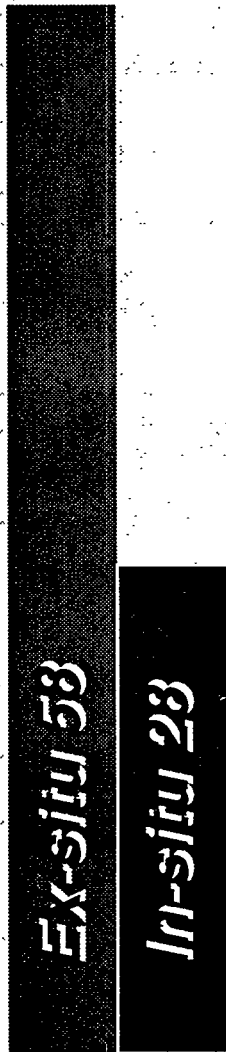
Ex-situ 53

In-situ 28

On-going/Planned 28

Ex-situ 15

In-situ 13

As of January 1997

THE APPLICATION OF CONTAINMENT TECHNOLOGIES ON LANDFILLS AND CONTAMINATED SITES IN EUROPE

Stefan Melchior[1]

1. INTRODUCTION

Remedial action on contaminated sites may include ex-situ or in-situ treatment of contaminants (extraction of solids, liquids and gases or in-situ decontamination) as well as the application of containment technologies. Rumer & Ryan (1995) define containment technology as "the construction of low-permeability barriers around the source zone [of contaminated sites] to contain contaminants combined with manipulation of hydraulic gradients".

The technical focus areas of the 1997 International Containment Technology Conference and Exhibition include vertical, bottom and surface barriers as well as technologies like permeable barriers and stabilization & solidification. Contaminant transport modeling, the test and choice of materials, quality assurance and control, cost and performance criteria, and long-term performance monitoring are integral and essential parts of the technologies and their application. The extent of their use depends on the technology applied as well as on the hazard of the site.

This paper will focus on a description of the systems used to construct walls, floors, and caps on European landfills and contaminated sites. The application of walls, floors, and caps, however, is not only a question of the best available technology but also is strongly governed by the priority of the problem to be solved. Therefore this paper will give a short overview on some environmental, socio-economical and political factors, which influence the application of containment technologies, before short profiles of the currently applied technologies will be presented.

2. BACKGROUND INFORMATION ON CONTAMINATED SITES AND LANDFILLS IN EUROPE

2.1 Precipitation and the Use of Ground Water

The natural conditions vary to a wide extent in the different regions of Europe. The very humid western coasts of Norway, Ireland, Brittain, Northern Portugal and Spain as well as the high mountain ranges (the Alps and some other areas in France, Italy, Croatia, Bosnia and Serbia) receive at least 1,000 mm to > 2,000 mm precipitation per year. Most parts of France, England, Southern Sweden, Denmark, the Netherlands, Belgium and Western Germany get between 600 and 1,000 mm rainfall per year. There are also large semi-arid areas as well in Spain, Eastern Europe and Eastern Scandinavia with only 250 to 600 mm precipitation per year (data from Diercke 1996). While Western Europe has a maritime climate, the winters can get extremely cold in Scandinavia and Eastern Europe. The Mediterranen countries have hot and dry summers.

The average water consumption in Europe is 157 liter per person and day (1988, Flinspach 1992). This is much less than in the U.S.A (397 liter/person/day) or Japan (379 liter/person/day). An average 64 % of the water consumption is covered by ground water and spring water, 36 % by surface water. The Netherlands, France, Austria and Germany rely much more on ground and spring water (63 % to 99 %) than Spain (30 %), the U.K. (27 %) or the U.S.A. (40 %). Ground water protection therefore has a much higher priority in the humid European countries with a high ground water consumption than in those countries, which rely predominantly on the use of surface water.

---

[1] IGB - Ingenieurbüro für Grundbau, Bodenmechanik und Umwelttechnik
Heinrich-Hertz-Straße 116 - D-22083 Hamburg - Germany
Tel.: +49 (40) 22 70 00 - 38, Fax: +49 (40) 22 70 00 - 34, SMelchior@compuserve.com

2.2 Socio-economical Data

The regions with the highest population densities in Europe (> 500 inhabitants per km², see Diercke 1996) are also the traditional industrialized centers: Middle England, Northern France, Belgium, the Netherlands, Western Germany (along the river valleys of Rhine, Ruhr, Saar), Eastern Germany (south of the Elbe river), Northern Italy. Other industrialized centers in Northern Spain, Catalonia, Southern France, Switzerland, Austria, the Czech Republic, Denmark, Sweden, Poland, Hungary, Romania, the Ukraine, Belarus, Latvia and Russia have lower population densities.

Europe has vast economical disparities. Most countries of the former East Block face tremendous problems, while some economies like Hungary and the Czech Republic are growing fast. Even within the European Union (EU) large contrasts still exist. The rich regions around Paris, London, Edinburgh, Stockholm, Bruxelles, Amsterdam, Luxemburg, parts of Western Germany and Denmark have an economic power of more than 125 % of the average gross national product and have a lower unemployment rate than the average. Unemployment is more than 3 % higher and the national product only 75 % of the average in Ireland, Portugal, Greece, most of Spain, Southern Italy, Eastern Germany, parts of England and parts of Finland.

These data show that the densely populated, highly industrialized and ground water consuming countries in Central Europe should have the biggest financial resources to contain waste disposal facilities and contaminated sites while other countries might either not feel as much need to do so (because of lower population densities or less ground water use) or might just not have the economical strength. The paradoxon is that the countries with the biggest environmental pollution problems have the least money to spend on protective or remediation measures.

2.3 Landfills and Contaminated Sites

Boels (1993) presented some data on the waste generation within the EU and other interesting figures. Per year 240 million tons of industrial waste, 104 million tons of municipal waste, and more than 60 million tons sediment sludges are produced. 65 % of the waste is landfilled, 24 % incinerated. The rest is partly recycled. The number of landfill sites is estimated with 60,000 to 120,000, occupying 800 to 1,700 km². Approximately 12.5 billion m³ of landfill gas are annually generated in Europe, 755 million m³ (6 %) are recovered. The estimate of the annual leachate production is 0.1 - 4.0 million m³/a. Efforts to avoid the production of wastes and to increase the rates of incineration and recycling are already reducing the waste generation in some countries.

Table 1 gives an overview of potentially contaminated sites in some European countries. The numbers of potentially contaminated sites include uncontrolled waste dumps, former industrial sites such as steelworks, refineries, the chemical industry, gas works, cokeries, gas stations, mine tailings and heaps as well as warfare-related sites from the World Wars, and contaminated military sites. The figures given in Table 1, however, are inconsistant for several reasons. The definition of potentiallly contaminated sites varies as well as the methods of the surveys. Some countries started the survey earlier than others. No country has yet completed the survey. Therefore the numbers of potentially contaminated sites are supposed to rise. However, only about 10 - 20 % of the potentially contaminated sites are supposed to really need remedial action.

2.4 EU Council Directive on the Landfill of Waste

A very large contrast exists between European regions where only few landfills are operated in a controlled way with up-to-date technology and regions where municipal and industrial waste is still dumped at inappropiate sites (river beds, gravel pits or just any other void or remote area in the

23

	Number of Registered Sites	Rough Estimates of Annual Costs [million US $ /a]
Germany	143,000	530 (large sites in East Germany only)
The Netherlands	110,000	500
United Kingdom	100,000	800
Austria	24,000	90
Spain	46,000	?
Denmark	10,500	57
Finland	10,500	36
Sweden	6,500	34
Greece	5,000	?
Norway	3,000	?
Belgium	2,000	30
France	1,500	94

Table 1   Contaminated Sites in Europe (Data from BMU 1994 and BMBF 1995)

landscape) without any liner or cap. In order to harmonize the technical standard for the landfill of waste in the European Union tried to adopt a Council Directive on the Landfill of Waste (European Union 1995). The proposal for the Directive defined three landfill classes, the general and specific requirements to be fulfilled by these facilities, the types of waste to be accepted (hazardous, non-hazardous and inert waste), waste acceptance and control procedures as well as control procedures for operation, closure and after-care of a landfill. Existing landfill sites should bring their standards up to those required in the Directive. Financial guarantee provisions were proposed to be mandatory to cover the expenses for preventive and remedial action. Annex 1 of the proposal listed general requirements for all classes of landfills including location, water control and leachate management, protection of soil and water (by specific geological barriers, base and surface liners), gas control, nuisances and hazards and stability. Annex 2 regulated the waste acceptance criteria and procedures, Annex 3 the control and monitoring procedures in operation and after-care phases.

However, the Council Directive did not pass the European Parliament because parliament had failed to convince the European Commission to back parliaments amendments on two subjects. First, parliament wanted to remove a derogation within the draft directive for small island, remote mountainous settlements and in rural areas (i.e. 50 % of the EU territory) and second, parliament wanted to impose an end to Britain's co-disposal.

Given this situation the procedures to contain landfills and contaminated sites are still governed only by laws and regulations of the individual countries.

2.5 Major Research and Development Programmes

Research activities of the European Union are implemented in multiannual Framework Programmes. The 4th Framework Programme was approved in 1994 and covers the period 1994 - 1998. It includes

the progamme "Environment and Climate", worth 1 billion US $, which focusses mainly on global change. Subprogramme 2.2.3 coveres "Technologies to Protect and Rehabilitate the Environment"., including research on remediation technologies for "organic waste", "dangerous waste" and the "rehabilitation of contaminated sites".

The "STEP Programme" (1989 - 1992) and the "Environment Programme" (1991-1994) concentrated on risk assessment on contaminated sites and soil and ground water protection through in-situ remediation. Research and development of containment technology did not play a significant role in programmes of the European Community.

Several large national research and development projects on soil contamination and remediation technologies have been set up the Netherlands, Denmark, the United Kingdom and Germany. In 1986 the "Netherlands Integrated Soil Reserch Programme" (NISRP) started. The Danish EPA (Miljøstyrelsen) initiated a programme on the "Evaluation of Remediation Technologies" in 1992. In the U.K. new treatment and containment technologies are funded by the Department of Trade and Industry (DTI) within the programme DEMOS (DTI Environmental Management Options Scheme). DTI and the Department of Environment (DoE) of the Brittish Government fund the joint projects ETIS (Environmental Technology Innovation Scheme) and EBPP (Environmental Best Practice Programme). The Construction Industry Research and Information Association (CIRIA) is also coordinating a research programme on contaminated land. The German Federal Ministry for Education, Science, Research and Technology (BMBF) has funded several large joint R&D projects during the past decade. Four programmes focussed on case-studies and were integrated in the remedial activites at very prominent contaminated sites. Another two large integrated research programmes focussed on the "Development of Advanced Landfill Liner Systems" and on "The Geological Characteristics of Landfill Sites". Of course there are numerous other research activities in Europe, not being integrated in national or multilateral programmes.

3. Vertical Barriers (Walls)

Vertical barriers (cut-off walls, diaphragm walls) are commonly used at contaminated sites in Europe to prevent and control horizontal contaminant transport within the groundwater or in the gaseous phase. There are no regulations demanding the application of walls. Usually the hazard of the site or the presence of an investor to re-use a site control the decision to construct vertical barriers. Vertical barriers are usually combined with hydraulic control measures and sometimes may contain the volume to be treated by in-situ decontamination.

Most often vertical barriers are surrounding the contaminated zone and an inward directed hydraulic gradient is created. Walls, however, are also used only to divert the groundwater inflow or to control the groundwater outflow in combination with extraction wells. Permeable reactive walls and funnel-and-gate solutions are emerging technologies to control and treat contaminated plumes.

The depth of vertical barriers depends on the hydrogeological site conditions (depth of an aquitard) and on the nature of the contaminants (light or dense non-aqueous phase liquids, dissolved contaminants). However, costs and technical constrains limit the depth of walls. 30 m to 60 m are state of the art. Depth of up to 100 m are feasible, but pose severe problems to the use of high-qualitiy-sealing materials.

Cut-off walls shall be low permeable, corrosion-resistant and have a low diffusivity as well as a long service-life. Permeabilities below 1×10^{-10} m/s can be obtained. Slurry walls should be as thin as possible since material costs are a major factor. Because of the complexity of the construction methods, quality controll and quality assurance are very important. Only double-wall-approaches offer a control of the barrier performance. Watertight components like geomembranes, steel or glass may be used. The system-permeability of these walls depend of the quality and integrity of the locks between individual sheets.

The choice for a particular type of cut-off wall strongly influences the quality and costs of the containment. The costs for the disposal of excavated contaminated soil and slurry have to be balanced against the the costs for long-term hydraulic measures and the treatment of pumped liquids.

Vertical barriers are constructed using four principles:

(1) Excavation of soil and placement of sealing material
   (single phase and twin-phase slurry wall, composite wall, interlocking bored-pile wall)

(2) Displacement of soil and installation of sealing material
   (thin wall, street-pile wall, diven cut-off wall)

(3) Reduction of soil permeability in place
   (Injection wall, jet grouting, frozen wall)

(4) Placement of reactive walls
   (permeable reactive wall, funnel-and-gate systems)

Some types of walls (usually thin walls) may also be used in double wall concepts with controllable segments.

Wall types listed under (1) and (2) are predominantly used to contain contaminated sites in Europe. They are briefly described in the following chapters. Injection walls, jet grouting and frozen walls are frequently applied for a variety of construction purposes, however, they are rarely – if ever – used on contaminated sites. Permeable reactive walls and funnel-and-gate systems are emerging technologies, currently being in the state of field demonstrations. There are several guidance manuals for vertical barriers in Europe. Meggyes (in Holzlöhner et al. 1995) gives an overview. Other European contributions to this conference present more detailed information on the design, construction, quality control, and experience with cut-off walls and reactive walls in Europe.

3.1 Slurry Walls

Slurry walls are the most often used vertical barriers. Wall thickness varies from 0.4 m to 1.5 m. The individual panels should overlap laterally at least 2/3 of the wall thickness. They are usually applied if a horizontal, low-permeable layer is located underneath the contaminated zone within reach. The walls are usually inserted and bonded about 1.5 im deep into the horizonal bottom layer.

3.1.1   Single-phase slurry wall

Single-phase walls are standard technology on landfills. Self-hardening slurries (bentonite-cement mixes with or without fillers) are pumped into vertical trenches, which are excavated with grab buckets, clamshells or vertical trench cutters. They are simple to construct. Verticality should be checked using inclinometers. The composition of the slurry has to be defined and tested project-specific (controlling factors are depth of the wall, composition of the ground water, duration of excavation and hardening). Sophisticated slurries (eg. organically modified binders, dense cut-off slurries) can not be used in single-phase walls.

Thus the permeability of single-phase walls usually is higher than the permeability of twin-phase walls. Wall depths typically are limited to 35 m. Advantages of single-phase walls are their robustness, the intimate contact between primary and secondary panels and 20 years of experience on landfills and contaminated sites. The excavated soil and small amounts of slurry have to be disposed of.

3.1.2 Twin-phase Slurry Wall

In twin-phase walls a bentonite suspension is used to stabilize the walls of the trench during the excavation of the soil. In the second phase the bentonite suspension is replaced by the cut-off slurry using tremie pipes (contractor method). The individual panels are either confined by stop-end tubes or constructed overlapping laterally by using a vertical wall cutter, which provides an intimate contact of primary and secondary panels as well as a very low vertical deviation of the axis (appr. 1 %).

While the stabilizing suspension needs to be fluid and of low density, the density of the cut-off slurry has to be at least 0,5 t/m³ higher. Soilcrete, bentonite-cement suspensions and, if long hardening durations are feasible, cement-free suspensions with organically modified binders are used as cut-off suspensions. Incomplete replacement of the stabilizing slurry can be a problem. The excavated soil and the stabilizing slurry have to be disposed of. Walls depths up to 84 m have been reached. Twin-phase walls are applied on landfills and contaminated sites for more than 10 years now.

3.1.3 Composite Cut-off Walls

In composite walls geomembrans or steel sheet-piles are inserted into a single or twin-phase slurry wall to further reduce advective flow. Glass walls are also proposed as additional sealing element. The permeability of composite walls is dominated by the quality of the locks between the individual barrier sheets, which is difficult to control.

Composite walls offer very low permeable systems and are used on landfills and contaminated sites for more than 10 years now. Construction, however, is complex and needs a rigourous quality control. The excavated soil and in case of twin-phase walls also the stabilizing slurry have to be disposed of. At present, wall depth is limited to approximately 30 m.

3.2 Interlocking Bored-pile Walls

Bored-pile walls are constructed of primary and secondary piles, bored with or without casing. The secondary piles cut into the primary ones. The overlapping piles form a low permeable wall. The disadvantage of interlocking bored-pile walls is the large number of joints. On the other hand they allow very flexible geometries and can be constructed underground near structures like pipes or cables.

High pressure should be applied while retracting the casing. The wall thickness should not be below 0,6 m to compensate the possible verticality deviation. Maximum depth is about 20 m.

Jet grouted columns are also used in bored-pile walls. The are constructed using a rotary drilling technique in conjunction with a high-density cutting and filling fluid. While retracting the drilling rod the filling fluid is diverted with high pressures (2 - 100 MPa). The cutted soil is removed and replaced by a cement or clay-cement mix and has to be disposed of. Bored-pile walls are rarely used on landfills and contaminated sites.

3.3 Thin Wall

Broad flanged beams are vibrated into the ground. While retracting the piles a bentonite-cement mix with fillers (> 1.5 t/m³) is injected into the void with high pressure through nozzles at the toe of the beam creating a 0.06 to 0.08 m thin wall. Wall thickness may be doubled due to the penetration of injected fluid into coarse soils. Maximum depth is 20 m.

Thin walls are very cost-effective and can be constructed with high output. No excavated soil or slurry has to be disposed of. There are over 10 years of experience on landfills and contaminated sites. Permeability, however, is higher compared to slurry walls. Cohesive soils with consolidation pressures

may cause problems and a very accurate pile guiding and control is required (permitted misalignment < 0.2 % of thickness at 20 m depth).

3.4 Sheet-pile Wall

Steel sheet-piles (0.01 m to 0.02 m thick) are driven into the ground and connected to each other by locks. Sheet-pile walls are easy and rapidly to construct. They can carry loads and there is no need for the disposal of excavated soil or slurry. Maximum depth is approximately 20 m. After 10 years of experience on contaminated sites, many questions regarding the corrosion and the effect of coatings have been answered. The quality and durability of the locks still is an issue.

3.5 Driven Cut-off Wall

Caissons with detachable and watertight sole plates are driven into the ground and filled with soilcrete. The soilcrete is compacted while retracting the caissons causing the sole plates to detach. Wall thickness is ≥ 0.4 m, maximum depth 20 m. Driven cut-off walls are used on contaminated sites in Europe for over 10 years now. Their permeability is higher compared to slurry walls, but no excavated soil or slurry has to be disposed of.

3.6 Cut-off Chamber Systems

Chambers systems with two thin walls have proven to be effective and economically attractive concepts, especially if a hoizontal, low-pemeable layer lies out of reach at a great depth. At the Rautenweg landfill in Vienna two parallel thin walls (in one sector two parallel single-phase slurry walls) have been constructed 8 m apart. They were connected to each other by cross walls every 50 - 70 m. Into each chamber (400 - 600 m² surface area) a well is installed to pump and maintain the ground water level 0,5 m below the natural level outside the landfill. Below the landfill the ground water is kept additional 0,2 m deeper than within the chambers.

The integrity of each chamber can be controlled. Chamber systems are able to contain LNAPL. A layer with reduced permeability (< 5 x 10^{-6} m/s) at the base of the chambers and underneath the contaminated zone is required to limit the water volume, which has to be pumped. While the installation costs are rather low and no excavated soil or slurry has to be disposed of, the permeability of the walls is rather high causing permanent costs for the operation of pumps and treatment facilities.

3.7 Current Trends - Walls

During recent years there is a trend towards the application of non-complicated walls (single-phase walls) in combination with hydraulic measures and site-specific test and choice of materials. Twin-phase walls are used if very deep walls are required, composite walls are only chosen at sites with very high contamination. Sheet-pile walls are applied at sites where the disposal of excavated materials is expensive. The double thin wall chamber system is a controllable solution with rather low installation costs.

Construction technology, the design of material properties, quality control of walls and locks and the quality and durability of locks have been significantly improved. Reactive walls are a new concept, their application is just beginning.

4. Horizontal Barriers unterneath Landfills and Contaminated Sites (Floors)

The regulations and guidance documents of most European countries require geological and technical barriers underneath new landfills (Meggyes in Holzlöhner et al. 1995 gives an overview on the regulations in several European countries). However, many old landfills are not located at appropriate sites and few have technical barriers at their bases. During the last seven years some

proposals to construct horizontal barriers underneath old landfills and contaminated sites have been published.

4.1 Geological Barriers

New landfills have to be constructed at least 1 m above the highest ground water table. Usually at least a "low permeable" subsoil is required underneath the base liner of a landfill. Some countries (Italy, Germany, Switzerland) require minimum thicknesses of the geological barrier (> 1 m, > 3 m, > 10 m resp.) and regulate permeabilities ($k \leq 1 \times 10^{-7}$ m/s). The issue, if technical barriers may replace geological barriers is currently discussed in several countries.

4.2 Technical Barriers

4.2.1   Base Liners for Landfills

In most European countries base liners for new landfills are mulitlayered systems with a drainage layer above one or two barrier layers (for specific requirements in the individual countries see Meggyes in Holzlöhner et al. 1995).

Areal filters containing perforated pipes are commonly used as drainage systems. The thickness, particle size distribution, permeability and slope of the layer as well as the diameter and distance of the pipes vary. The regulations of some countries allow an individual, site-specific hydraulic design of the drainage system.

The most common barrier is a clay liner (0.5 m to 1.5 m thick, several lifts, compacted wet of optimum, permeability $\leq 1 \times 10^{-9}$ m/s or 1×10^{-10} m/s). In some countries composite barriers with a geomembrane above a clay liner are required on municiple or hazardous waste landfills. Protective layers above the geomembrane as well as a certification for the geomembrane may be mandatory. In Germany and Switzerland asphaltic barriers can be used in composite barriers alternatively to the geomembrane on specified landfills. Specifications for the asphaltic barrier and the supporting layers vary in both countries.

4.2.2   Installation of Floors Underneath Contaminated Sites

In the late 80s and the beginning of the 90s some concepts to construct horizontal barriers underneath existing landfills or contaminated sites have been proposed using long wall technology or tunneling. None of the proposed technologies has been applied for this purpose yet, predominantly due to tremendous costs. Furthermore some systems are only feasible or safe in cohesive soils above the ground water table - conditions, which usually are not given at hazardous sites. Jet grouting to form continuous, low permeable horizontal panels is sometimes considered for small sites, but rarely applied.

4.3 Current Trends - Floors

There is an increasing awareness of the risk of incrustations and clogging of the drainage system. Also several modifications of the design of clay liners or cohesive soil components of composite barriers are currently proposed. There is a trend to use specific clay minerals in order to design the individual lifts of a clay liner either to improve the sorption and the retardation of contaminants or to reduce the risk of shrinkage. Sometimes specific additives (e.g. hydrosilicates, waxes, grouts, minerals) are used to improve the properties of otherwise not suitable barrier materials. Another new concept is the compaction of mineral mixtures (mixed-in-plant) with well defined particle size distribution at low water contents to low porosities in order to avoid shrinkage and to reduce diffusion. In Germany, the risk of desiccation of clay barriers underneath geomembranes due to thermally induced water transport has been a major concern. Research results suggest the use of cohesive

subsoils with high unsaturated conductivities to avoid shrinkage of the barrier. Though geomembranes (HDPE) are widely accepted as effective liners the use of asphaltic concrete is increasing.

5. Horizontal Barriers at the Surface of Landfills and Contaminated Sites (Caps)

Various types of caps are used in Europe. Most traditional landfills are only covered by a layer of soil or rubble. Sometimes a simple soil cover without barrier layer is placed on municiple waste landfills as a temporal cover until the initially high rates of subsidance have declined. Modern landfills, however, contain pretreated wastes and usually have multilayered vegetative caps with a topsoil layer to support the vegetation, a drainage layer to divert water laterally, and one or more barrier layers to limit the infiltration of water (Meggyes in Holzlöhner et al. 1995 gives an overview on the regulations in several European countries). A gas ventilation layer may be added above the subgrade, if the disposed waste produces landfill gas. Geotextiles, protective layers and elements for erosion control may also be part of the design. If the potential subsidance of a contaminated site is low and if someone is interested in re-using the site, the cover might be non-vegetative, i.e. the surface will be sealed by asphaltic layers or pavements.

5.1 Surface Sealing of Contaminated Sites

In the densely populated industrial centers of Europe an increasing number of sites is sealed at their surface to re-use the sites for industrial or other purposes. Standard road construction technology is usually applied. Asphaltic concrete layers, however, might be more bituminous to be more flexible and watertight (< 3 % pores). Pavements without special seals in their gaps are too permeable to form a barrier. Their use has to be accomponied by an additional drainage layer above a liner such as a geomembrane.

5.2 Multilayered Vegetative Covers

Multilayered covers usually have at least a topsoil layer and one or more barrier layers to prevent the transport of water and gases. Drainage layers for water and gases are optional components of multilayered covers and frequently applied.

The thickness of topsoil layers varies to a large extent. Topsoil layers shall support the vegetation and protect the barrier layers against freezing. They are usually not designed in order to maximize evapotranspiration or to protect barrier layers against the penetration of roots or against desiccation.

Some regulations require areal drainage layers with permeabilities $\geq 1 \times 10^{-3}$ m/s. Mineral drainage layers are the standard technology. However, geosynthetic drainage elements are also used if the thickness of a cap has to be minimized or if suitable mineral materials are too expensive.

The following barrier layers are frequently used:
- *Compacted Cohesive Soil Liners* (CSL, natural soils as well as mixed-in-place or mixed-in-plant cohesive soils, compacted wet of optimum in several lifts to low permeabilities),
- *Geomembranes* (usually 1.5 mm to 2.5 mm HDPE),

Rather new concepts include:
- *Geosynthetic Clay Liners* (GCL, needlepunched or stich-bounded products),
- *Capillary barriers* (CB, with a laterally conductive layer (sand) above a coarse capillary block (gravel) with low unsaturated conductivity),
- *Asphaltic Concrete Liners* (ACL, asphaltic sealer with < 3 % pores above a bituminous supporting layer),
- *Modified Cohesive Soil Liners* (MCSL, formed either by adding additives like hydrosilicates, waxes, grouts or minerals to a conventional CSL or by modifiing the construction technology, e.g compaction at low water contents).

These barrier layers are either used alone in *single-barrier-covers* or combined in *composite barriers*. *Controllable composite barriers* can be formed if an additional drainage layer is included between the upper primary and the lower secondary barrier. Most single-barrier systems have a compacted cohesive soil liner. Geomembranes and sometimes geosynthetic clay liners are also used as single barriers. By far the most often applied composite barrier is a geomembrane above a compacted soil liner. There are some examples for the following composite barriers: Geomembrane above GCL, GCL above CSL, CSL above CB, ACL above CSL. Controllable composite liners are rarely applied. Technical leak detection systems using geoelectrical methods or tracer gases are still in the demonstration phase.

5.3 Current Trends - Caps

Caps are the most often used containment technologies. Currently many new designs and components are proposed. Sealed covers are applied to re-use abandoned contaminated industrial sites. Field performance data of vegetative covers have shown that shrinkage due to desiccation and water-uptake by plant roots as well as ion exchange can harm CSL and GCL significantly (Melchior 1997). There is a trend away from wet compacted and active clays towards geomembranes in covers. Alternative barriers are emerging (capillary barriers, asphaltic barriers, modified compacted soil liners). Low leakage rates over decades, however, can only be expected from caps with drainage layers and composite barriers. There are only few examples for systematic approaches for the performance monitoring of caps (lysimeters, inspections during excavations). The same applies for the construction of controllable barriers.

Current issues in research and development are:
- Design of recultivation layers to maximize evapotranspiration and to minimize the desiccation of cohesive clays in barriers
- Thermally induced desiccation of cohesive clays in composite barriers
- Sensitivity of barriers to subsidence
- Development of temporal covers
- Construction technology of capillary barriers
- Performance data and monitoring concepts
- Evaluation of the use of sludges, compost, and ashes in covers.

6. CONCLUSIONS

Remediation of contaminated sites still is a rather young technology. First concerns about ground water pollution lead to "pump and treat" concepts. During the early 80s, contaminated sites were primarily contained using a small number of technical approaches. During the late 80s and the early 90s decontamination and in-situ treatment has been the dominant trend. Today the overoptimistic view on decontamination is replaced by a more realistic approach. Composite strategies using pump-and-treat approaches as well as in-situ treatment and containment technologies are developed taking into account the site-specific conditions.

The challenge is:
o   to find the appropriate containment concept for each individual site,
o   to assess the need and to predict the long term quality of the barriers correctly,
o   to rank the priorities of different sites adequately,
o   to finance the activities through re-use of sites.

A large variety of caps, floors and walls has been applied, ranging from very simple systems to complex controllable multi-component approaches. During the last five years less waste has been generated and less landfills were constructed than expected. Construction technology and quality control have improved in many ways. The "best-available-technology" is defined on the global market. If it is applied on a specific site is more a question of political priorities and economical constraints than

a question of availability. Europe will probably face dramatic changes and challenges in the years to come. It will be very demanding to form the European Union. Today the countries with the biggest need for containment technology in order to prevent further environmental pollution have the least money to be spent on these issues. Responsible parties are often hard to name and to incorporate. The future priority level of environmental issues within the European Union is very hard to predict. At present, containment technology is not a growing market in Europe though the application of containment technology is undoubtedly needed.

REFERENCES

BMU - Bundesministerium für Umwelt, Naturschutz und Reaktorsicherheit & Umweltbundesamt (German Federal Ministery for Environmental Protection, Nature Preservation and Reactor Safety & German Federal Environmental Agency) (1994): International Workshop on Contaminated Sites in the European Union - Policies and Strategies, December 1994, Bonn, Germany. (In English)

BMBF - Bundesministerium für Bildung, Wissenschaft, Forschung und Technologie (German Federal Ministery for Education, Science, Research and Technology) (1995): Internationale Erfahrungen zur Altlastensanierung - Synopse, Bewertung und Prüfung der Übertragbarkeit von Methoden und Konzeption. Berlin, Germany. (International experiences on remedial action, in German)

Boels, D. (1993): The significance of covers and surface isolation of landfills for the protection of the environment. International Symposium "Geology and Confinement of Toxic Wastes", June 1993, Montpellier, France.

Diercke (1996): Diercke Weltatlas. 4. edition, Westermann, Braunschweig, 175 p.

European Union - The Council (1995): Amended proposal for a Council directive on the landfill of waste. Brussels, 36 p.

Flinspach (1992): Grundwasserschutz in Deutschland und Europa. Schriftenreihe der Vereinigung Deutscher Gewässerschutz, 58, p. 7-27. (Ground water protechtion in Germany and Europe, in German)

Holzlöhner, U., H. August, T. Meggyes & M. Brune (1995): Landfill liner systems. A state of the art report. Bundesanstalt für Materialforschung und -prüfung (German Institute for Material Testing). English translation edited by D.M. Anderson & T. Meggyes. Penshaw Press, Sunderland, U.K.

Melchior, S. (1997): In-situ Studies on the Performance of Landfill Caps (Compacted Soil Liners, Geomembranes, Geosynthetic Clay Liners, Capillary Barriers). Proceedings of the International Containment Technology Conference and Exhibition, February 09-12, St. Petersburg, FL, U.S.A.

Rumer, R.R. & M.E. Ryan (1995) (eds.): Barrier Containment Technologies for Environmental Remidiation Applications. John Wiley & Sons, New York, 170 p.

APPLICATIONS OF CONTAINMENT TECHNOLOGIES IN AUSTRALIA FOR CONTAMINATION REMEDIATION/CONTROL: STATUS AND EXPERIENCES

A.Bouazza
Monash University, Department of Civil Engineering, Clayton, Melbourne, Vic. 3150, Australia

R.J. Parker
Golder Associates Pty. Ltd., 25 Burwood Road, Hawthorn, Melbourne, Vic. 3122, Australia

Abstract:

In discussing containment technologies in Australia it is important to understand the factors which influence environmental control of wastes. Although Australia is considered to be an arid country, there is only limited reliance on use of groundwater for domestic purposes and this is mainly in rural areas. In many areas, the groundwater is brackish to saline, thus limiting the use of the water. The limited use of groundwater for domestic purposes and the sparse population of Australia combine to produce an environmental regulatory framework very different to North America and Europe. Up until very recently, the approach to disposal of industrial, mining and domestic waste has been based on the principle of "dilute and disperse". However, this attitude has changed, new regulations have been put forward imposing much greater control over the disposal of all forms of waste. This paper provides an overview of the containment technology in Australia as used in certain states with a discussion on the regulatory aspect. It presents examples of some of the innovative techniques that can be considered in the limited Australian regulatory environment.

INTRODUCTION

In Australia, prior to the mid-1980's, waste disposal sites were generally selected as being suitable because they were sites that no one wanted, ie they were holes in the ground, swamps or derelict land. However, through the late 1980's and early 1990's the approach to site selection changed so that consideration of environmental impact became the fundamental requirement of landfill and waste disposal design. Where environmental impact could not be controlled through natural containment, it became necessary for engineers to develop systems which controlled impact, ie lining and leachate collection systems. Engineers in Australia had been involved in construction of lining systems for waste repositories for many years prior to that time. However, it was not until the late 1980's that the primary focus of lining design changed from compaction specifications typically used for ensuring adequate strength of domestic waste for example, to specifications to ensure adequate seepage performance. At the same time new engineering materials were being introduced to Australia including a class of materials now referred to as geosynthetics. A variety of materials ranging from geotextiles through to flexible membrane liners became available. Geotechnical engineers learnt to use these materials for many purposes ranging from strength enhancement of soil to improving environmental performance of waste retention systems.

At the same time that landfill engineering design began to change focus from management of waste to management of the environment, consideration started to be given to the problem of land contamination. Prior to the mid 1980's there had been little consideration given to the impact of wastes on land and groundwater. Hence there remained a legacy of land degradation that had the potential to impact on the human health and the environment. However, in the late 1980's attention was focussed on a number of high profile former industrial redevelopment sites which were found to be contaminated (eg Bayside in Melbourne, Victoria (Swane, et al 1993), Pulpit Point in Sydney, NSW and Kingston in Brisbane, Queensland (Morphet, et al ., 1992).

The actual scale of the contaminated land problem in Australia is yet to be accurately determined, with some predictions placing the number of contaminated sites in the range of 10,000 (Knight, 1985). As a result of the high costs associated with land remediation considerable attention has been given to the problem of contaminated land and most property transfers in Australia are now accompanied by some form of contamination assessment and in some cases remediation. Significant attention is now given to the problems of soil and groundwater contamination and a consulting and contracting industry has developed in Australia (as in other parts of the world) to service the remediation market.

Since the late 1980's greater attention has also been focussed on derelict land, management of mining wastes and management of other solid waste materials, including land reclamation. Increased environmental regulation has resulted in greater effort being implemented in all of these areas to minimise the impact of mining and civil engineering projects on the environment. This paper discusses several issues in relation to the development of environmental geomechanics in Australia, with emphasis on regulations and containment technology.

ENVIRONMENTAL GEOMECHANICS IN AUSTRALIA

Influence of Regulation

Although environmental geomechanics commenced as a practice sector in Australia with minimal environmental regulation to drive it, there is little doubt that the development of environmental geomechanics has been influenced by legislation and regulation even if it was from overseas experience. During the late 1980's and early 1990's there was very little specific regulation which dictated how landfills should be investigated and designed and contaminated land should be assessed and remediated. Although legislation was in place that effectively required protection of soil and groundwater, there was little guidance on how the legislation should be interpreted or implemented. In the mid-1990's there has been considerably more attention given to the development of policy, regulation and guidance for contaminated land assessment and landfill design throughout Australia. Compared to other jurisdictions, particularly the USA, the regulatory environmental processes in Australia are still poorly defined. However, there is now sufficient legislation, policy and guidance documentation in Australia to claim that there is a regulatory framework that governs the practice of environmental geomechanics.

Environmental legislation in Australia has been mainly the responsibility of the States and therefore environmental practices tend to be State-specific. As a consequence there have been differences in the rate at which environmental geomechanics has developed in each state. Also, the variation in geology and hydrogeology in different parts of Australia has influenced the way in which regulation has developed and the way in which environmental geomechanics is practised. For example, groundwater protection has been the main driver of contaminated land assessment and landfill design in Perth (Western Australia), whereas groundwater protection has not been given the same importance in other parts of Australia where urban populations are less dependant on groundwater as a drinking water source. A regulation review conducted recently (Parker, 1996) highlighted some very interesting aspects. These are discussed briefly in the following section

Landfill Regulations

Brief comments on guidelines and regulation relevant to landfill site selection, design and management in some Australian states are provided in the following:

Victoria - The Victorian Environment Protection Authority controls landfill site selection and management through the State Environment Protection Policy on Siting and Management of Landfills Receiving Municipal Waste (EPAV, 1991). This document provides guidance on site selection, information required for permitting of sites and details of operating requirements for landfills. There is very little guidance provided in this document on design of landfills to protect groundwater and surface water. A draft State Environment Protection Policy (Groundwaters of Victoria) has been published (EPAV, 1994) providing information on groundwater beneficial uses which need to be protected. This document effectively provides performance criteria which have to be met in landfill design (or protection of groundwater in

general). Guidance is provided in an appendix on lining systems required to meet different groundwater protection objectives. An EPAV Bulletin (Publication 448) classifies wastes and dictates disposal options for different waste types.

New South Wales - The Environment Protection Authority of NSW regulates design and management of landfills. Siting considerations are strongly influenced by the Department of Urban Affairs and Planning (DUAP). The EPANSW has formulated issued landfill design document titled "Environmental t Guidelines for Solid Waste Landfills" (1996). This document provide benchmark lining, leachate collection and capping requirements for landfills. The basic lining requirement is for a 0.9 m thick compacted clay lining with hydraulic conductivity $< 1 \times 10^{-9}$ m/s. In "poor hydrological conditions" or areas of significant threat to the environment, geomembrane lining is also required.

Queensland - The responsibility for the development of landfills in Queensland rests with the Department of Environment. Draft policies for landfill management have been in circulation since approximately 1993 and these are currently under further review. It is expected that an Environment Protection Policy Waste will be released soon and the final guidelines for landfills will then be produced. At this time there is a reliance on guidelines from other agencies and bench marking to best practice.

Western Australia - Regulation of landfills in WA is controlled by the Waste Management Division of the Department of Environmental Protection. Guidelines have been developed for five classes of landfill. A document titled Criteria for Landfill Management (Health Dept, WA 1993) sets out requirement for management of landfills. There is a requirement in this document that putrescible (municipal) waste landfills should be lined unless there is a management plan which provides strong technical evidence that lining is not required.

Contaminated Land Assessment and Remediation

The general approach to contaminated land assessment and management throughout Australia is based on use of Australian and New Zealand Environment and Conservation Council (ANZECC) and the National Health and Medical Research Council (NHMRC) document titled "Australian and New Zealand Guidelines for the Assessment and Management of Contaminated Sites" (ANZECC and NHMRC, 1992). This document provides a framework for the conduct of contamination assessment and remediation and allows a staged approach from preliminary site assessment through to remedial treatment of the land. The document provides some guidance on the use of threshold criteria for assessment of severity of contamination although it also permits the use of health and ecological risk assessment. Brief comments on approach to contaminated land assessment and remediation in some Australian states are as follows:

Victoria - Contaminated land is managed in Victoria under the 1970 Environment Protection Act which is intended to provide protection of the beneficial use of all segments of the environment. An important feature of contaminated land assessment in Victoria is the use of Environmental Auditors who are required to review the work of persons assessing and remediating land with the view of the Auditor providing Certification of the suitability of the land for future use. Another important feature of contaminated land management in Victoria is the ability to dispose of contaminated soil to landfill through a system of contaminated soil classification (EPAV, 1995) which dictates which landfills can be used for disposal of contaminated soil.

New South Wales - McFarland (1992) summarised the regulation of contaminated land in NSW under the provisions of the Unhealthy Building Act. With the formation of the EPANSW several initiatives have been implemented to improve the application of the available regulatory controls. In NSW there has been a shortage of landfill space and remedial solutions involving landfill disposal are not favoured by the EPANSW. There has been a greater focus in NSW on the use of remedial technologies and containment than in some other jurisdictions in Australia.

Queensland - The Queensland Contaminated Land Act was passed in late 1991. The stated purpose of the Act is to provide a system to identify and manage land which has been contaminated and to prevent further contamination of land. The system is intended to prevent the inappropriate use of contaminated land and ensure the continued protection of public health and the environment. Under the Act there is a requirement for notification of contaminated land. Notification of contamination or likely contamination will result in automatic listing on the Contaminated Sites Register. Four categories of site listing are used: Probable, Released, Confirmed and Restricted. Guidelines for the assessment of contaminated sites were published in 1992 by the then Chemical Hazards and Emergency Management Unit (CHEM Unit) and reflect the

ANZECC guidelines for the assessment and management of contaminated sites. The Director of Waste Management in the Department of Environment is the final arbiter on the status of a site and the acceptance of a report by a consultant, or other person. The general approach to land remediation in the state is focussed on the landfill disposal of contaminated soil although use of remedial technologies is emerging.

CONTAINMENT TECHNOLOGIES

There is no formally recognised approach to design of landfills in Australia although guidelines are starting to be developed in various states which define how landfills should be constructed to maintain environmental protection. These include EPANSW guidelines for solid waste landfills (EPANSW, 1996) and the EPAV draft groundwater policy (EPAV, 1994).

Parker et al (1993) and Parker (1996) have outlined the approach generally being used for design of landfills in Australia. This involves an iterative process based on selection of lining system, evaluation and comparison with defined environmental objectives. With this process, if the designer cannot meet the defined environmental objectives at any stage in the iterative process then additional leachate control measures are required, eg if clay liner is insufficient to provide adequate protection to environment, then include geomembrane as well and reassess potential impact.

Contaminated Land Remediation

A contaminated site is broadly defined as a site at which hazardous substances occur at concentrations above background levels and where it poses or may pose a hazard to human health or to the environment (ANZECC & NHMRC, 1992). Impacts on human health from contaminated soil can occur as a result of exposure via a number of pathways including; pollution of surface and groundwater, inhalation and ingestion of soil and via uptake and subsequent bioaccumulation by plants and animals. Impact on the environment can occur from a number of routes including; direct uptake of contaminants by plants and animals and migration of contaminants to ground or surface waters. Leakage from both above and below ground storage tanks are obvious examples of facilities where contamination can occur on an industrial site. When considering contamination at an industrial site account must be given to the possibility that contamination may have resulted from past practices rather than current operations. It is also possible that contamination may be brought to the site as filling for leveling or raising of the site. It was not uncommon in the past for industrial wastes to be used as structural filling. Common examples of waste that has been used for general filling in Australia are slags from smelting and refining processes, boiler ash and gas works waste.

Remedial Technologies

Remedial technologies related to containment can generally be categorised under the following broad headings:

- removal and disposal (to a contained landfill)
- containment of contaminants

Removal to Landfill

Doesburg (1992) states that the most common form of remedial treatment for contaminated soil in the USA has been excavation followed by disposal to landfill. Likewise in Australia the most common form of remedial treatment of soil is excavation and disposal at landfill. In Victoria, a well regulated system has been developed for disposal of contaminated soil which can be classified as low level contaminated soil or high level contaminated soil. Other states are generally following similar models. Excavation of contaminated soil and removal to landfill is probably the most common method of site clean-up used to date in Australia. The nature of the contaminated soil will govern the type of landfill approved for disposal. For example, in Victoria contaminated soil can either be classed as "low level contaminated soil" or "Prescribed Waste" (EPAV, 1995). The soil classification dictates which landfill can accept the waste and how it should be transported.

The classification of the waste is based on total concentration and leachability of chemical constituents. Stabilisation of the soil may be required to meet leachability criteria.

In recent years regulatory authorities in a number of states have begun to discourage landfilling as an option for site remediation, because of pressures being placed on existing landfill facilities, difficulties in developing new landfills, community opinion on landfill disposal, and the desire to treat contaminated soils on-site. This is particularly the case in some of the major cities of Australia.

Containment

Containment technologies are used at a contaminated site to isolate areas in the subsurface from the surrounding uncontaminated environment. Containment usually involves installation of a cut-off wall around, or a cap over, the affected area. The barrier may take the form of a slurry wall (eg. soil-bentonite wall or cement-bentonite wall), a grout curtain, a soil-mixed wall, an HDPE liner curtain wall, or a sheet piling cut-off. Containment also may include installation of a cap over the contaminated area to impede infiltration of water into the area and form a separation layer between land users and the residual contamination. In many cases in Australia, buildings and pavements have also been considered as part of a containment or risk control system for management of contaminated land. Containment of contaminated soil is considered as a practical option for management of land but it places restrictions on future use of the land. It has been a common form of remedial treatment in Australia where the regulatory framework to date has permitted a pragmatic attitude to contaminated land. However, careful consideration needs to be given to future management of the land to ensure maintenance of the capping or containment systems.

HOME BUSH BAY OLYMPIC SITE PROJECT (SYDNEY, NSW)

Remediation work at Homebush Bay commenced on site in the latter part of 1992, almost 12 months before Sydney became the host city for the year 2000 Olympic Games. The start of work was preceded by an extensive investigation programme which included sampling and analysis of soils and groundwater over 300 ha of the site. The initial focus of remedial efforts at Homebush Bay has been in regard to waste containment. Geosynthetic materials have played an important role in achieving this objective, by minimising the generation and escape of waste leachate to surface and ground water resources and by controlling human contact with waste materials. Most of the information given herein are based on the paper by Pym & Moss (1996).

Aquatic centre remediation

Construction of the Sydney International Aquatic Centre could not be completed before clean up of an adjacent railway embankment containing gasworks and asbestos wastes and a separate asbestos dump was undertaken. Low permeability geosynthetic liners of special manufacture were selected due to the corrosive nature of the wastes in question. Leachate from the railway embankment recorded pH levels as low as 1.2 and high levels of ammonia were present in the asbestos dump. Neutralisation of the acidic wastes was augmented by the addition of lime during placement. The ammoniacal leachate was treated by air stripping during construction and the landfill was provided with both leak detection and groundwater monitoring system. During construction the main contaminants monitored were asbestos, cyanide gases and ammonia. In total, approximately 255,000 tonnes of waste was contained on site. The decision to position the excavated cells beneath the Aquatic Centre car park, and utilise the bitumen and cement surface as an additional layer of capping was considered to be the incorporation of urban design within the remedial solutions. A secure landfill was constructed adjacent the Aquatic Centre to contain hazardous leachate forming wastes found on the site. Figure 1 presents a schematic section of the as-constructed containment system. The main features of this design are described in the following.

The use of a smooth 2mm thick HDPE as primary liner. For puncture protection the liner was overlain on the side walls of the cells by a non-woven needle punched geotextile. The secondary liner chosen for the project was a geosynthetic clay liner (GCL) comprised of a layer of granulated sodium bentonite sandwiched between two geotextiles. An internal leachate collection system was provided in the cells to enable leachate drainage. Across the base of the cells, and immediately underlying the primary liner, is a

150mm thick layer of sand which serves as the leak detection layer. On the side walls of the cells a ribbed polyethylene geonet was used to provide leak detection, with drainage by gravity to the sand layer described above. The side wall geonet was underlain by a heavy geotextile as a separation layer between the geonet and underlying GCL. The landfill cap was designed to limit infiltration of rainwater and to act as a subgrade for the Aquatic Centre car park.

Haslams Creek

The Haslams Creek South site occupies an area of over 30 ha and was used extensively as an industrial waste dump. The area was selected as the main containment area for pockets of waste from the Olympic Precinct. The site was almost entirely contained by leachate drains, to cut off flows both to Haslams Creek, and towards a brickpit. A geosynthetic membrane was tied vertically into low permeability clays underlying the waste, and below the bed of Haslams Creek. The membrane acts primarily to prevent inflow of seawater to the leachate drain, however it has a dual purpose of acting as dam wall, providing storage for leachate in the case of any pump failure along the extensive drainage system. On both sides of Haslams Creek, a vertical geosynthetic leachate cut-off wall was constructed with an integral leachate drainage system to recover waste leachate prior to escape into the creek. Figure 2 shows a schematic section of the drain and cut off constructed along the banks of Haslams Creek. The HDPE cut-off wall which separates and contains the landfill leachate forms a continuous barrier. HDPE sheets of up to 10 m width were joined in-situ with a proprietary locking device ('Geolock' or 'Interlock'). A water tight seal was formed by the addition of a hydrophilic bead which expands when wetted to fill the void between the locking strips, thereby forming a continuous barrier to leachate flow.
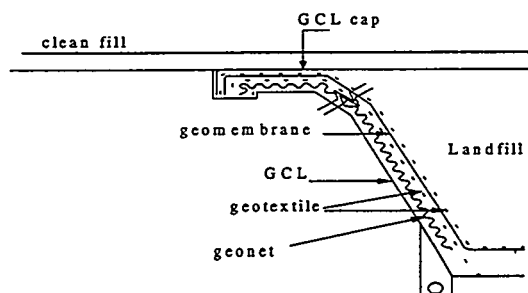
Fig. 1. Secure landfill at the aquatic centre (modified from Pym & Moss, 1996).
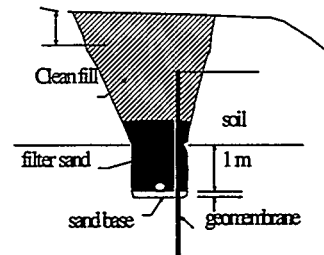
Fig. 2. Leachate cut off wall (modified from Pym & Moss, 1996).

SOUTH EASTERN SAND BELT (MELBOURNE, VICTORIA)

Sand mining has long been practised in the south-east sand-belt region of Melbourne to obtain clean sand for use in construction. Since the late 1960's the abandoned sand mining pits in the region have been used for waste disposal and this trend is increasing with the ever higher demand for new landfill space (although the regulatory pressure for higher standards of waste containment is resulting in most new sites being developed for selective disposal, ie inert waste). During sand mining, the watertable, normally < 5 m below ground level, is lowered up to 40 m. Following cessation of mining and commencement of landfilling, watertable recovery has created a water saturated landfill from which leachate migration occurred soon after landfill closure (Hancock et al, 1994).
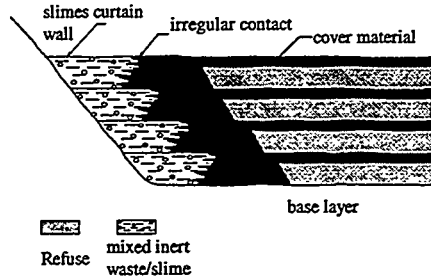
Fig. 3 Slime curtain wall in Clayton 1 landfill
(from Cavey, 1993).
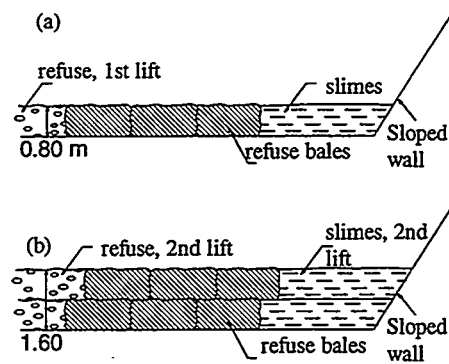
Fig. 4 Slime curtain wall in Clayton 2
landfill (Golder Associates, 1993)

One management technique identified is the use of cut-off walls, formed by hydraulically placing slimes from sand mining (fines washed from the sand), to isolate the landfill from adjoining shallow aquifers. This involves placing wet sand washing slimes mixed with clean fill to achieve a low permeability (in the order of 2×10^{-8} m/s) slurry curtain around the landfill walls (Hancock et al., 1994), as shown in Figure 3. Another alternative successfully used is the use of a sidewall liner in which there is a combination of compacted refuse bales and slimes as shown in Figure 4 (Golder Associates, 1993). This technique was developed specifically to enable greater control on the placement of the slimes and in particular to ensure that the design thickness of the slimes wall could be maintained. At the time of writing this paper, development of the slimes curtain in this manner had commenced. However, quality control data was not available at the time of preparation to this paper to enable comment on performance of the wall.

KINGSTON SITE (BRISBANE, QUEENSLAND)

The Mount Taylor - Kingston Site Recovery Project was one of the first and largest of such projects undertaken in Australia (Morphet et al ., 1992). The Mount Taylor Site was an old gold mine, operated in various modes from 1885 to the 1950's. Mine shafts and pits were later backfilled with domestic and other refuse including, most significantly, acid oil sludge waste (a combination of old engine oil and sulphuric acid). Based on historical information it appeared that the area known as the Main Open Cut was filled with refuse whereas the area referred to as the Northern Pit was filled with the acid oil sludge. The land was later subdivided and houses and a shopping centre constructed. In 1987 a substance that "burns skin and clothing" was reported to be seeping into properties in the area. The rehabilitation was completed in September 1991, resulting in 11 hectares of rehabilitated recreational park land being returned to public use. A range of capping options was decided upon taking account of the needs to: 1) accommodate risks associated with each part of the site; 2) require minimal maintenance; 3) allow public access; and 4) achieve a stable surface over waste material.

Design of Capping

In the Main Open Cut, relatively large future settlement of the refuse needed to be allowed for within the worst part of this area. Much of this area was already covered by an asphalt car park. Of most concern was the differential settlement expected across the fill/intact rock interface along the northern, western and eastern edges of this area. Concrete relieving slabs similar to those used at bridge abutments, or a piled concrete deck could have been used but such solutions would have been costly. It appeared better to tolerate the severe differential settlements, and to take steps to mitigate the resulting damage, and to institute routine monitoring and maintenance to ensure the preservation of an effective seal. This was done by installing a geogrid at the base of a new asphaltic concrete surface course. At least 60mm thickness of asphaltic concrete surface course was installed. Periodic inspections of this area will be made and cracks

that eventually develop will be cleaned with compressed air and sealed with a hot melt filler. In time pavement distortion may become severe and some reshaping and resurfacing will be required. All internal garden beds were recommended to be sealed to reduce their contribution to infiltration into the system.

In the Northern Pit area, where the acid oil sludge had been disposed, two sealing liners were incorporated each capable of confining the sludge alone. The first of these is a compacted clay liner 450mm thick. The second sealing liner is an HDPE geomembrane installed above the clay liner. At the periphery of the sealed area this liner is extended downwards at least 3 m, and at least 1 m into natural ground to act as a short cut off wall and to prevent sludge under pressure finding its way between the existing surface and the capping fill, or through the near surface soils. Protection layers and drainage layers were included above the sealing layers. An important feature of the protection system was the inclusion of a polypropylene reinforced concrete layer. This was intended to act as an intrusion barrier and had to be designed to tolerate possible settlement of the sludge. However, to avoid excessive consolidation settlement of the sludge, the protection barrier and soil layers were kept as thin as possible.

CONTAMINATED SOIL DISPOSAL IN FREEWAY EMBANKMENT (MELBOURNE, VICTORIA)

During 1994 and 1995, two freeway embankments were constructed in the western suburbs of Melbourne using low level contaminated soil. The first of these was located at Ardeer Section of the Western Ring Road and involved the use of about 100,000 m^3 of soil obtained from a former munitions factory which was being remediated. The contaminated soil met Victorian EPA criteria for low level contaminated soil with the principal contaminants being copper (maximum of 1000 mg/kg), lead (maximum of 3000 mg/kg) and zinc (maximum of 5000 mg/kg). The embankment had to be permitted as a landfill given that it was receiving contaminated soil. The concept for the disposal method was to encapsulate the soil in a compacted clay envelope. The soils in the area are a high plasticity clays of basaltic origin. The base sides and cap were specified to be not less than 1 m thick and to have a hydraulic conductivity of not less than $1x10^{-9}$ m/s. The low level contaminated soil was of similar origin to the clay used to encapsulate the contaminated material and therefore also had low permeability when compacted. It was determined that leachate collection would not be necessary for these embankments given that construction would occur over a very short period and the occurrence of leachate generation under the road pavement of the freeway would be negligible.

This novel solution to disposal of a large quantity of contaminated soil, coupled with a need to find a short-fall of construction material of 100s of thousands of cubic meters provided an opportunity for benefits to the owner of the soil (cheaper cost of disposal), the contractor (cheaper cost of fill) and the public who ultimately pay for the road. Control of the fill will remain with the road authority providing institutional control of the soil for a very long time.

FUTURE DEVELOPMENT

Given the rapid development of environmental geomechanics in Australia over a period of less than ten years, it is interesting to speculate how the practice will develop in future. It is clear that with ever increasing concern about the environment and the increasingly stringent regulation that geotechnical engineers and geo-scientists will be called on to solve new problems in the environmental management, many of which are not even contemplated today. It is important to understand the differences in approach that have developed in Australia with respect to landfill design and contaminated land management when compared much overseas practice. In landfill design there has been much reluctance by Australian practitioners to follow the path of prescriptive engineering design. There is much discussion in the industry about the need for broad design guidelines without prescriptive dogmatic regulations on such issues as lining, leachate collection and capping requirements. For example, the Solid Waste Landfills Draft Code of Practice prepared by the Waste Management Association of Australia, clearly attempts to provide broad guidance without dictating any specific requirements for lining or other environmental management measures. The use of such guidelines leaves much to the designer in developing landfill systems that will ensure that unacceptable environmental impact does not occur. With such an approach it will be a challenge for geo-environmental engineers and geo-scientists to be able to provide consistent

assessments and designs which satisfy regulatory authorities who often do not have the same access to engineering expertise as the landfill designers.

Similar trends are evident in the contaminated land remediation industry where there is greater reliance on site management options to limit remedial treatment than there appears to be in some other parts of the world. However, the "internationalisation" of the land remediation industry is more complete and Australia appears to following international trends to a large extent. This is possibly due to the influence of multi-national companies and international financing agencies strongly influencing the remedial industry.

Some of the immediate issues facing geo-environmental engineers are:

Landfill - The rapidly developing use of clay liners for landfills requires better understanding of the nature of Australian soils with respect to leachate seepage characteristics. To date, there is only limited work on the behaviour of Australian soils under differing leachate conditions. There will also be the need to better understand the behaviour of geomembranes and other geosynthetic materials and their interaction with Australian soils, particularly with respect to stability. To date there are only limited facilities for appropriate testing of liners in Australia.

Contaminated Land Assessment and Remediation - Like the landfill design industry there is little information on the nature and fate of chemicals in the Australian environment. Further research is required to tackle some of the major issues involving wide spread use of chemicals such as arsenic in pesticides and lead fall-out in our urban environment. The introduction of health risk assessment will present a challenge to an industry that to a large extent has been focussed on assessment of land using prescriptive guidelines followed by "dig and dump" remediation. The ability to better manage our land and make informed decisions about the real risks posed by contamination is a major challenge.

Mining wastes - The Australian mining industry now has a very strong focus on the management of environmental impact at mining sites. The management of mining wastes is recognised as an important area for research. However, there are many areas for further investigation including, once again, the nature and fate of chemicals in the environment, improved and cost effective design of waste repositories and better methods of storing wastes. Given the importance of mining to Australia, this is one area where significant advances in environmental geomechanics research is being initiated in Australia rather than relying largely on overseas experience.

The development of environmental geomechanics in Australia has led to a some new and interesting opportunities for geotechnical engineers and geologists. It is a sector of geomechanics that is full of challenges and uncertainty. All that the geo-environmental engineer and geo-scientist can be confident of is that there will be new challenges to face as environmental controls and regulation becomes more stringent in Australia.

REFERENCES

Australian and New Zealand Environment and Conservation Council and National Health and Medial Research Council (1992). Australian and New Zealand Guidelines for the Assessment and Management of Contaminated Sites.

Cavey, B.W. (1993). Slimes and clay liners in landfills. Final year project. Monash University, Department of Civil Engineering, Melbourne, Australia.

Doesburg, J. (1992). The Role of Innovative Remediation Technologies. IIR Conferences, Site Remediation, Sydney.

Environment Protection Authority of New South Wales (1996). Environmental Guidelines: Solid Waste Landfills: EPA NSW.

Environment Protection Authority Victoria (1991). State Environment Protection Policy, The Siting and Management of Landfills Receiving Municipal Wastes, Publication Number 265.

Environment Protection Authority Victoria (1994). Draft State Environment Protection Policy, "Groundwaters of Victoria".

Environment Protection Authority of Victoria (1995). Classification of Wastes: EPA Information Bulletin, Publication 448.

Golder Associates (1993). *Engineering review, proposed Fraser Road No2 landfill.* Report for Pioneer Waste Management Pty Ltd.

Hancock, J.S., Phillips, I.R. & Othman, M. (1994). Use of sand washing slimes for leachate containment in landfills. *Proc. 2nd National Hazardous & Solid Waste Convention,* Melbourne, pp. 257-266..

Health Department of Western Australia (1993). *Criteria for Landfill Management*

Knight, M.J. (1985). Scale of the hazardous waste problem in Australia and disposal practice. *Symposium on Environmental Geotechnics and problematic soils and Rocks,* Bangkok (AIT).

Parker, R.J. (1996). Geomechanics-changing with the environment. *Proc. 7th ANZ Conference on Geomechanics,* Adelaide ,Australia, pp. 729-764.

Parker, R.J., Bateman, S. & Williams, D. (1993). Design and management of landfills. *Proc. Geotechnical Management of Waste and Contamination,* Sydney, 209-252.

Pym, J. & Moss, D. (1996). The homebush bay experience: the use of geosynthetics for waste containment and progress through the different facets of the remediation work. *Proc. 3rd National Hazardous & Solid Waste Convention,* Sydney, pp. 299-306.

Swane, I.C., Dunbaven, M. & Riddell, P. (1993). Remediation of contaminated sites in Australia. *Proc. Geotechnical Management of Waste and Contamination,* Sydney, pp. 127-162.

Mc Farland, R. (1992). Contaminated Sites, a regulatory perspective. *IIR Conferences, Site Remediation,,* Sydney.

Morphet R.J., Friday, R.G. & Parker, R.J. (1992). Mt Taylor Kingston gold mine: site recovery project. *Proc. 11th Australian Geological Convention,* Ballarat (Victoria), Geological Society of Australia, pp. 275 &282.

Chapter 2

Slurry Walls: Materials & QA/QC

.

SLURRY WALLS AND SLURRY TRENCHES - CONSTRUCTION QUALITY CONTROL

Raymond J. Poletto[1], P.E. and David R. Good[1], P.E.

ABSTRACT: Slurry (panel) walls and slurry trenches have become conventional methods for construction of deep underground structures, interceptor trenches and hydraulic (cutoff) barriers. More recently polymers mixed with water are used to stabilize the excavation instead of bentonite slurry. Slurry walls are typically excavated in short panel segments, 2 to 7 m (7 to 23 ft) long, and backfilled with structural materials; whereas slurry trenches are fairly continuous excavations with concurrent backfilling of blended soils, or cement-bentonite mixtures. Slurry trench techniques have also been used to construct interceptor trenches. Currently no national standards exist for the design and/or construction of slurry walls/trenches. Government agencies, private consultants, contractors and trade groups have published specifications for construction of slurry walls/trenches. These specifications vary in complexity and quality of standards. Some place excessive emphasis on the preparation and control of bentonite or polymer slurry used for excavation, with insufficient emphasis placed on quality control of bottom cleaning, tremie concrete, backfill placement or requirements for the finished product. This has led to numerous quality problems, particularly with regard to identification of key depths, bottom sediments and proper backfill placement. This paper will discuss the inspection of slurry wall/trench construction process, identifying those areas which require special scrutiny. New approaches to inspection of slurry stabilized excavations are discussed.

QUALITY CONTROL CONSIDERATIONS

The purpose of field quality control is to insure an end product that meets the project goals (structural support, cutoff barrier, etc.). The role of the contractor, engineer and owner will vary depending on their experience, degree of uncertainty of subsurface conditions and project risks. Good quality assurance can identify poor construction practices at an early stage of construction and lead to early corrective measures. Good quality control and record keeping is essential to identify problem areas which may occur as a result of either subsurface or construction problems.

GENERAL COMMENTS ON SLURRY CONSTRUCTION INSPECTION

Slurry is an opaque, viscous fluid which contains suspended solids, and can behave in a complex manner. Since the bottom of the excavation can not be seen, the industry has typically relied on non-standardized, pointed sounding weights to determine elevations and extent of sediment buildup on trench bottoms and backfill slope and surfaces. Well intentioned, but unsubstantiated beliefs promulgated by some in the industry have attempted to explain away quality control concerns as "self-correcting." For example, the proposition that sediment measurement and control is unnecessary because sediments are pushed ahead by the backfill and later excavated. We believe that some current practices are generally inadequate, and have attempted to address these shortcomings by proposing a variety of inspection tools and quality control procedures described herein. The inspection effort described can be an intensive one, requiring an adequate staff, capable of carrying out the demands of inspection. Typically, a project's quality assurance program is staffed with one person to run an on-site laboratory and one performing field inspection. The field inspector will need to call upon the laboratory operator for assistance. The laboratory operator should expect to spend about half the work shift in the field, with the trench inspector outside all that time. Consider training a third inspector when needed for relief, reports and paperwork or in anticipation of the contractor electing to work multiple shifts. As with any

[1]Mueser Rutledge Consulting Engineers, 708 Third Avenue, New York, NY 10017
(212) 490-7110, MueserEng@aol.com

construction, proper construction records are crucial. Records for slurry supported excavations should include: all test results on wall/trench backfill (includes S-B, concrete, etc), excavation progress, materials encountered, top of key elevations, bottom elevations, backfill progress, and wall/trench soundings. The daily record of activities should include information where applicable on project status, unusual events, mixing area status, contractor communications, and all relevant events. It is suggested that the inspector use standard subheadings for each activity on the daily report. Location control is important to inspection. Stationing stakes driven every 3 m (10 ft) are recommended for reference. Elevation control for trench depth determination can then be taken by a string line set between stakes at a known elevation.

SLURRY FOR PANEL AND TRENCH CONSTRUCTION

An ASTM paper published as STP 1129 (1992) and text by Tamaro (1995) describe the necessary properties of hydrated slurry needed for proper stabilization of the excavation. The STP publication contains further discussions on quality control of slurry walls. Test results of slurry may not convey the complete character of the slurry. The inspector should confirm that the mixing operation is producing a consistent slurry and that the tests are made on representative samples of that slurry. Storage ponds that have become bottom laden with thick, gelled bentonite indicate a poor mixing operation. Further, this material may get broken up and pumped into the excavation, which can leave similar clumps and bottom sediments. The inspector should understand the process of the how slurry is made at the site, because it may help solve subsequent concrete or backfill problems. The properties of trench slurry should be viewed with more scrutiny than fresh slurry, because the trench slurry stabilizes the excavation and is displaced by the backfill. Further, trench slurry is subject to modification by contaminated groundwater and suspended solids loosened during the excavation. Water visible at the top of the panel/trench is not uncommon after a heavy rain, or may indicate chemical attack of the slurry. We have observed that a flat sounding weight (described later) is more sensitive to changes in slurry viscosity, and may locate areas of thickened trench slurry which can impair the wall concrete or trench backfill.

The inspector needs to verify that the minimum slurry head is maintained all times. Even short term drops below the minimum slurry level can stress the ground and cause shear plane development, leading to subsequent sidewall failure. It is suggested that a short, lightly weighted tape be used to accurately check and record the slurry level. In the event of unusual loss of slurry accurate and timely measurements of slurry levels are crucial to identify the need for corrective action. The contractor and inspector should be aware at all times where plugging agents are stored, should they be necessary. Even if specifications indicate a low level of slurry will maintain overall stability, slurry levels more than about 1 m (3 ft) below the ground surface tend to promote excavation sidewall sloughing, leading to excessive bottom sediment.

TESTING OF SLURRY PROPERTIES

The required slurry properties differ between panel and trench excavation methods. However, the slurry sampling approach is the same. When sampling for sand content, take the sample near the bottom of the excavation where concentration of sand will be greatest and its presence most harmful. Conversely, if the slurry is to be checked for low viscosity, sample near the top of the slurry column. Identify all slurry samples by location, depth, date and time. Use a clean bailer when sampling. Bailers that are not clean often have faulty valves resulting in a loss of sample or mixing of slurry from different depths.

Testing and control of slurry properties are normally the responsibility of the contractor. However, the inspector should perform quality assurance tests, particularly of the trench slurry to confirm contractor results. Slurry unit weight, sand content, filtration, pH, and viscosity are the minimum tested properties. If chemical attack is a possibility, simple field chemical tests on the clear water

filtrate from trench slurry samples can be used to identify contaminants. When slurry properties are found to be out of specification limits, or are drifting towards noncompliance, prompt corrective action should be taken. Additional observations and samples are needed to understand if there has been a consequence (such as bottom sedimentation) caused by the use of out of compliance slurry.

INSPECTION FOR STABILITY AND KEY

In certain situations, panel/trench stability can be a prime concern due either to soil conditions or the proximity of a structure. The effectiveness of stability monitoring is limited by the time needed to read and interpret results. It is suggested that simple, observable "real time" instrumentation be set up by the inspector. A good stability indicator is stakes driven on a perfectly straight sight line and observation of ground cracking and any changes in structures within the potential influence zone. Simple crack gages should be established at areas of distress in a structure. The inspector should photograph and establish survey control on nearby structures which may be damaged, to document the preconstruction condition. Daily inspection of cracks near the top of the trench and appearance of loose, cracked or overhanging soil should be pointed out to the contractor for removal as the excavation proceeds.

Slurry trenches for groundwater cutoff (hydraulic control) are generally keyed into soil strata of low permeability. The required key depth depends on the key stratum properties, its surface regularity and design goals. Typically keys are from 0.6 to 0.9 m (2 to 3 ft) deep to ensure closure with the key stratum, and to provide a trap for sediment. In a continuous trench, the determination of the depth of the key into the key stratum can be difficult unless there is a distinct material or color change at the top of the key stratum. This problem is made worse where the key material is similar in hardness to overlying strata, or the top of the stratum undulates. With backhoe excavation, as the depth of the excavation increases, there is a greater uncertainty of the location from which bottom samples have been retrieved using the backhoe.

The best remedy to key depth compliance is a complete set of closely spaced borings set on the trench alignment. Excavation can then proceed to a predefined elevation with some confidence. Depth variations can still occur and the inspector must be vigilant. Soundings (measured depths) should be taken at the early excavation of the key material at several locations to determine the deepest cut of the key material. When key materials are first recovered, material from the upper portion of the active excavation slope can flow to the bottom. This will give a sounding that may be falsely high, and therefore the key made too shallow. Additional soundings should be made after a few buckets of excavation to confirm the measurement. If key material is observed, some key has already been excavated; however, typically assume the deepest sounding obtained is the top of key. Bottom of key confirmation for panel walls should be made every 0.3 m (1.0 ft) along the alignment. When a backhoe is used, top of key confirmation may only be possible every 6 to 9 m (20 to 30 ft) depending on excavation limits of the backhoe. After defining the top of key stratum, the volume of recovered key materials should be compared and checked with the theoretical volume of the key. Sounding results should be plotted on a geologic section daily, and compared to expected conditions. Observations of measured quantity of key material which seems to deviate from the expected should be investigated further. When field results indicate a significant deviation from expected conditions, additional borings or a more conservative key depth is needed.

WIDTH DETERMINATION

Panel/trench width determination can be very important if sidewall collapse or sloughing is suspected below the slurry surface. On a recent project a device called the "Hexometer" was constructed to measure trench width with depth. It is a hexagonal shaped caliper hinged at its vertices. A weight kept the device collapsed and allowed it to sink into the slurry. When at

measurement depth, a cable was pulled widening the device until the sidewalls were engaged. A simple measured calibration of cable pull length versus caliper width is then used to determine sidewall width. This device is constructed of square aluminum tubing, and must be kept perpendicular to the trench. Observations of tilt of the lowering rods may indicate on which side of the trench sloughing has occurred. Such a device can not be used within 30 m (100 ft) or more of an active backhoe excavation. It was found that strong currents occur within the slurry for a good distance away from an active backhoe, even when no movement could be detected on the slurry surface.

TREMIE CONCRETE PLACEMENT

In concrete wall construction, reinforcing steel cages are inserted into the panel after the end stop pipes or tubes have been placed within the panel and after cleaning the trench. The panel end stop devices should be securely fastened in position and the cage should be supported properly on guide walls to assure that no cage movement will occur during concrete placement. Concrete should be placed by tremie methods in such a manner that the concrete displaces the slurry progressively from the panel bottom and rises uniformly to the surface and that the concrete and the slurry do not intermix. We recommend that the tremie pipe be fully loaded before discharging concrete (by keeping the pipe hard against the bottom). The pipe should always be embedded within fresh concrete a minimum distance of 2 m (7 ft) and a maximum of 4 m (13 ft). If the tremie pipe is surged during placement, care must be taken to maintain embedment in fresh concrete so that the tremie seal is not lost. The use of a separation plug at the bottom of the tremie, sometimes called a "go devil" is not recommended. The problems resulting from entrapment of the plug within the panel is greater than its perceived benefit. If two or more tremie pipes are used, a sufficient number of ready mixed trucks must be available to charge each tremie hopper uniformly so the concrete is raised essentially level. Normal practice permits the slight lifting but not extraction of end panel pipes during the later stages of the concrete placement. In many cases, concrete is still being placed at the upper level of the panel while end panel stops are being slowly lifted from the bottom. Withdrawal of the panel end stops should be done in a smooth and continuous manner just after the initial set of the last placed concrete occurs. Set times can be estimated by testing small batches of concrete retained from each truck. The tremie hopper should be sufficiently large to receive the occasional surge of concrete and to prevent spillage of concrete from the hopper into the trench. Screen the hopper inlet to prevent the entry of large balls of concrete which are occasionally found in poorly mixed and/or high cement content mixes. Upon removal of end stop pipes the formed panel joint should be scraped prior to placement of concrete.

INSPECTION AND QUALITY CONTROL OF PANEL CONSTRUCTION

When the wall is exposed during excavation, the contractor should check the wall against specified tolerances. After the wall is exposed, clean and remove all protrusions, soil and weak concrete. Keys and inserts should be exposed and prepared for subsequent use. The consequences of poor tremie concrete operation or inadequate slurry desanding may result in occasional leaks at the vertical joint between concrete panels, at horizontal or inclined cold joints or at inserts for tieback anchors. Sealing of leaks at inserts or through a vertical joint must be performed after the wall is exposed. The inspector should check all joints or defects to determine if they are watertight and will not "blow" at a later stage of construction. Defective joints or cracks are chipped out, cleaned and packed with rapid setting cement grout mixes. Occasionally it is also necessary to grout the soil directly behind the wall at the location of the leak.

MEASURING TRENCH SEDIMENT ACCUMULATION

Current field practice requires the determination of sediment thickness by sounding the trench with a pointed weight and slowly "plumbing" the bottom in an attempt to discern resistance due to

48

slurry sediments. We believe this method to be at best highly subjective, probably only useful for revealing gross sedimentation. As an alternative, we have used two weights: a pointed weight to establish the bottom elevation of the trench and a flat bottomed weight to determine "top" of sediments. The flat weight developed is actually somewhat heavier than the pointed weight, but has only about 5 percent or less of the pointed weight's bottom bearing pressure. The edge of the circular flat weight has a rim for collecting a bottom sample. The demarcation between "top" of trench bottom sediments and a heavy sediment suspension at the bottom of the slurry column, is a difficult matter, subject to argument. However, it has been observed numerous times that when the flat weight sounding indicated sediment, the excavator did indeed excavate more sediment. When no additional sediments were recovered, the two measured depths of weights usually agreed, establishing the same bottom depths. Typically, the sampling rim recovered a grit of coarse sand and gravel when sediments were present. The inspector needs to avoid dragging the side of the trench when using the flat weight for sampling. The two weight system is illustrated in Figure 1. A case history by Deming (1997) discusses using the two weight system.
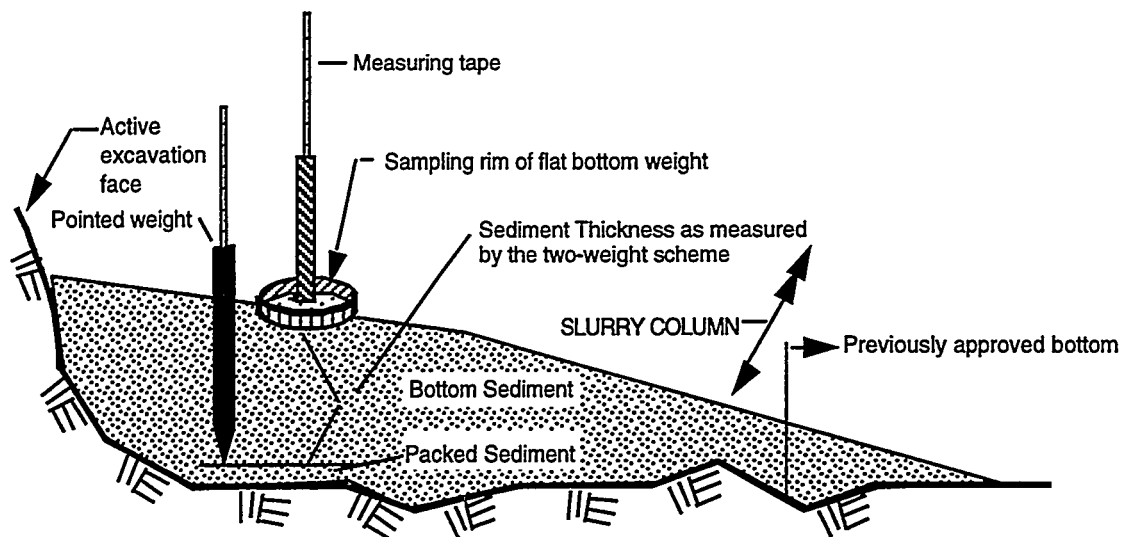
Figure No.1 - Measuring Sediment Thickness at Bottom of Slurry Trench with Two Weight System (Not to Scale)

When taking any soundings, the inspector must keep a tension on the flat weight at all times while lowering. Free falling weights can drift, and the drift can go undetected. Slurry and sediments can hold a weight off vertical for a period of time. Where steep cut slopes occur, the weights can slide down these slopes with little discernable resistance, particularly when weights are allowed to free fall. At the first indication of resistance, the weight should be pulled up sufficient to re-plumb the weight and slowly lowered to determine if a steep slope is present. If a slight impact is felt, plumb the weight up and down to "catch" the slope. This technique is exceptionally useful at turns and corners of trench alignment. Always move the weight up and down to "feel" the bottom, and verify the pointed weight is not lying flat. A clamshell can cause a frontal mud wave when lowered, displacing sediments before the bucket arrives. While this may be less of a problem in a confined panel excavation, sediments in a trench excavation can be pushed away in either direction. This effect can be checked by use of the two weight system and a split spoon sample- which is described later.

49

BACKFILL MIXING INSPECTION

Soil-bentonite backfill testing should be performed prior to backfill placement. At a minimum, we recommend concurrent laboratory testing should include permeability tests at various gradation of fine contents and hydraulic heads. Testing for bentonite content is probably best performed in the field by making sure the proper amount of dry bentonite is added (if used) and that the mix is homogeneous. Proper backfill consistency can be measured by slump immediately before placement. The unit weight of the backfill is checked to verify if it is sufficiently heavier than the slurry. When testing indicates non-compliance, corrective action and re-testing should be performed. An important, but least pleasant inspection function is the "walk through." When thought to be ready, the backfill batch should be spread thin 0.3 to 0.5 m (1 to 1.5 ft) thick for a "walk through" inspection. The inspector is thus able to look for debris, soil clod size, oversize rocks and overall batch homogeneity. After the backfill is ready for final approval, samples may be taken for testing. If dry bentonite is to be added, the approved batch can be squared off and measurements taken to estimate volume for calculating amount of dry bentonite required. It is important to keep unmixed spoils away from completed batches, or batches in progress. This requires a well organized mix area. We recommend that the inspector visit the mixing area periodically during the work day and make a quick sketch of the pad once per day, noting the location and status of backfill.

TRENCH BACKFILL PLACEMENT INSPECTION

Trench backfill placement is generally end dumped by truck when using a central batch and mixing operation, or pushed into the trench by a dozer at the top of the backfill slope when mixing at the trench side. The inspector should check that truck beds are clean of unmixed soil and surface soils are not being plowed into the trench when a dozer is used. The point of backfill placement should be about 3 m (10 feet) in back of the daylighted backfilled slope. We have observed that when backfill is placed right at the visible backfill crest and the crest is pushed along aggressively by constantly moving the backfill placement point, the slurry at the toe of crest tends to pick up part of the backfill making a thick sludge. When the backfill is placed at a single point for an extended period, the backfill slope flattened and the slurry at closeout was free of loose backfill. The backfill slope should be sounded twice per day when placing backfill. If the flat weight is used for sounding, a sample of the backfill surface can be retrieved on the flat weight to check for sedimentation. In addition to the backfill samples recovered by flat weight, it is recommended that a few high quality backfill slope samples also be taken daily or at places where sedimentation from pump discharge or small collapses may contribute sediment. We have found that a 3 inch split spoon soil sampler hung from a cable can provide an excellent sample. The sampler should be rapidly lowered under tension, with only a short bottom free fall, if any. The basket of the sampler should be left in, but bent back to allow soft backfill to penetrate. The distance between the backfill slope and the excavation area is a point of much debate. Clearly it is best to separate the digging and backfill portions of the trench, otherwise sediment and backfill will mix. The "clean" zone between the two portions is difficult to control. We observed that the backfill slope can suddenly slump, racing forward and that sediment from the excavation slope can flow backward. Flat and pointed weight soundings are needed in this area, with sampling to verify that no sediments are entrapped. If this sampling cannot detect the backfill encroaching the bottom sediments, an end stop pipe can be used as a hard boundary between the backfill and excavation sides, as illustrated in Figure No. 2. The end stop when properly designed and used, prevents sediments and bucket spillage from flowing on the previously approved bottom and prevents backfill from surging into the excavation area. The toe of backfill laying against the end stop can be passed through to the excavation side by lifting the end stop for toe cleaning near the end of excavation cycle on the other side. The stop end pipe is lifted forward (by backhoe or crane) to mark the end of approved trench bottom. Fins on opposite sides of the end stop allow it to be moved or fitted tight by rotating its orientation plan. A heavy independent collar with outriggers is used to stabilize the top of the pipe.
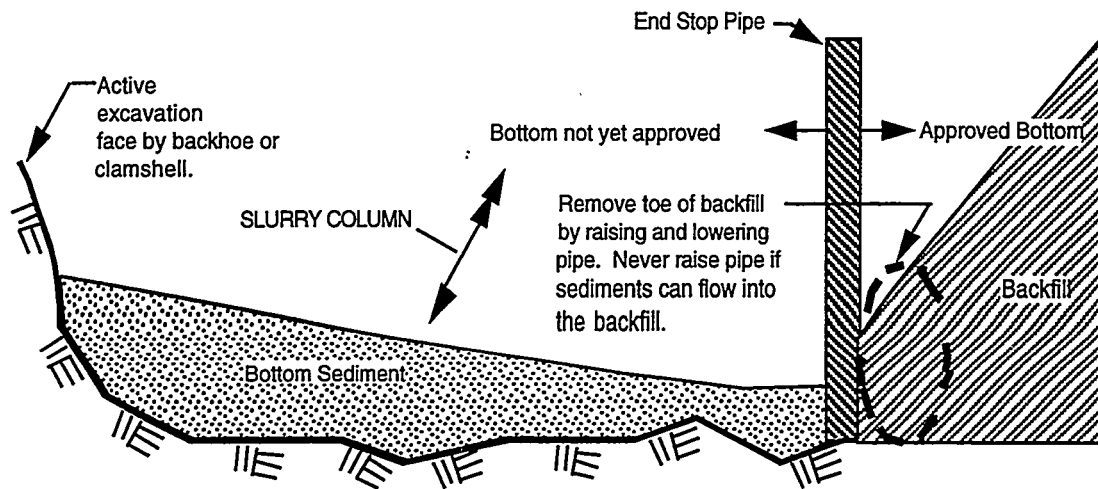
Figure No.2 - Use of an End Stop Pipe to Maintain a Separation Between the Backfill and Excavation (Not to Scale)

As the trench excavation advances, various backfill material is placed into the trench. Typically that backfill is a mixed product of soil and bentonite (S-B) and sometimes replacement with cement and bentonite self hardening slurry (C-B) . Backfill is mixed either along the trench sides or at a central location. Central mixing provides for a more controlled operation and gradation modification when needed. Backfill is placed in the trench, generally starting at a slope excavated at the beginning of the trench, called the lead-in trench. Backfill is placed to allow it to flow down the "lead-in" trench, establishing its own slope until the backfill surfaces or "daylights." Backfill is placed behind the crest of the visible backfill. Cold weather concerns in backfill placement include removal of ice from the trench at backfill placement points and exclusion of frozen backfill.

CONCLUSIONS

Specifications need to be written to reflect the high level of effort necessary to perform quality work, under intensive and meaningful inspection. Many past problems with a slurry wall or trench project can be traced to poor quality control that went undetected. The authors hope that the inspection techniques described herein, and other methods and standards under development will make the construction less of mystery, and nearly similar to foundation subgrade inspections.

REFERENCES

Tamaro, G. J. and Poletto, R. J. (1992) Slurry Walls; Design, Construction and Quality. (ed. D.P. Paul, R.R. Davidson, N.J. Cavalli) ASTM STP 1129, p26-41.

Tamaro, G. J. (1995) Field Inspection Handbook, Slurry Walls, 2nd ed. (D.S. Brock, et al). p9.15-9.33

Deming, P. W. (1997) Design and Construction of a Deep Slurry Trench Barrier, International Containment Technology Conference.

51

THE ORIGINS OF THE SLURRY TRENCH CUT-OFF AND A REVIEW OF CEMENT-BENTONITE CUT-OFF WALLS IN THE UK

Stephan A. Jefferis[1]

Abstract

On the occasion of the first International Containment Technology Conference it is appropriate to look back to the origins of containment walls as well as forward to the new technologies that we may need for the complex chemical and physical environments in which containment may be employed in the future. This paper looks at the development of slurry trench technology from the first concepts in 1938, the first field trials in 1945 and on to the cement-bentonite walls used in the UK today and the issues associated with defining appropriate materials performance.

Introduction

This paper is intended to give an overview of the development of cement-bentonite cut-off walls in the UK and also a perspective on some of the earlier developments of the slurry trench system. The paper is based the author's experience augmented by the published literature. He is aware that individuals and companies may have much more detailed records and he hopes that this paper will prompt a review of such records and publication of a fuller history of cut-off technology and so enhance our understanding of the performance of old containments.

The First Concepts

The concept of excavation under bentonite to form a continuous structural wall was advanced by Christian Veder in 1938 (Xanthakos, 1979) though the use of supporting muds in well drilling is much older and Boyes (1975) notes that a French engineer Fauvelle is credited with the first use of circulating fluid to remove drill cuttings in 1845. Veder (1963) reviews some of the work in the field and the laboratory, and notes that the first applications of early diaphragms were for solution of problems including 'for impermeable cut-offs below earth dams in deposits of sands and gravels with large boulders' (depths about 40 m) and for 'making a reservoir watertight' using a wall of maximum depth 35 m and area 38,000 m². The walls would have been backfilled with concrete and Veder noted that the first experimental diaphragms were carried out in 1950 'using circular concrete elements partly embedded one in another' (though Xanthakos, 1979 notes that concrete test panels were inserted in linear trenches in the 1940s). Hajnal et al. (1984) report that both Veder and Lorenz 'obtained relatively smooth diaphragm walls' in 1950. It seems that the concept of the concrete diaphragm wall was well established by the late 1950s. However, prior to that there had been major developments in cut-off walls backfilled with soil.

The First Trial Cut-Off Wall

The first field trials of a slurry trench cut-off began in September 1945, under the supervision of Major General M. C. Tyler, United States Army (Retired) 'as the originator of the basic idea' (Kramer, 1946). The general's idea was to use a vertical puddle clay cut-off wall to protect levees on the Mississippi river from erosion and sand boils. The initial concept was to excavate the trenches using a trench box for support and then backfill them with puddle clay. However, it was soon found that the trench box concept was impracticable and that 'as an alternative or

[1]Golder Associates (UK) Ltd, 54-70 Moorbridge Road, Maidenhead, Berkshire, SL6 8BN, England, +44-1628-771731, sjefferis@golder.com

auxiliary means of creating the restraining effect of a shield, the possibilities of applying clay slurry, in a manner similar to the utilisation in oil-well drilling operations were given consideration'. Captain J. W. Black, Jr., Corps. of Engineers, US Army, who directed the field experimental work, subsequently developed and demonstrated the practicability of using clay slurry. 'Contemplated also was the less difficult structural and mechanical modification of standard trenching machines, which are factory built for a maximum excavation depth of 24 ft., to obtain depths in the range 35 to 40 ft.'

Field work began in September 1945. Groundwater was at 15 ft below ground level and the excavation had to pass through 'sand with some gravel up to 3/4 in diameter' the paper goes on 'At this juncture it is pertinent to observe that the field work was largely divorced from theoretical considerations; the men assigned to it were chosen primarily on the basis of their experience with practical construction problems, since it was felt that solution of the practical difficulties was of prime importance in the development of the basic idea.' Despite this, those involved with the trials seem to have recognised and exploited all the essential concepts of today's slurry trench walls.

The slurry used in the excavation had a density of 8.5 lb. per gallon (1.02 g/ml) 'as it was essential to maintain sufficient clay content in the slurry to coat and seal the walls of the trench in order to make the hydrostatic pressure effective against them instead of being dissipated through the pervious strata'. 'That this objective was attained successfully was proved by the fact that the loss of water in slurry-filled trench amounted to only a few inches overnight'. A density of 1.02 g/ml corresponds to a clay content of about 3% by weight of water. To achieve such a low water loss with a base slurry containing of the order of 3% clay in a 20 ft deep trench passing through sands and gravels with a slurry level perhaps 15 ft above groundwater level requires a very low filter loss fluid and it seems that it must have been based on sodium bentonite (the mineralogy to the clay is not stated in the paper but the use of bentonite in oil-well drilling was well established by this time, Rogers, 1988).

A major mechanical problem to be solved at the end of the work was identified as 'spill-back' that is spoil spilling from the excavator bucket and contaminating the slurry and eventually settling in the trench, a problem which still occurs today. The trench was backfilled with puddle clay prepared using a box fitted with two rows of paddles to break down clay lumps to puddle consistency.

From the paper it is clear that the essentials of slurry filter cake formation, hydrostatic support and contamination were all identified. It would be interesting to know to what extent the concepts developed in the trials were subsequently used in full-scale works on the levees.

The First Structures

It would seem that the first actual structure formed under slurry, as opposed to trials, was in 1949 at Terminal Island near Long Beach California (Xanthakos, 1979). The wall was some 15 m deep and was excavated under a clay slurry and backfilled with a clay-soil mix. In today's terminology the wall would be described as a soil-bentonite cut-off wall.

By 1968 a substantial number of walls had been constructed. Sherard (1969) gives figures for 'the estimated total area of impervious earth underground wall built by the slurry trench process by United States and Canadian contractors' which show that between 1950 and 1968 some 630,000 m^2 were constructed. The largest job (240,000 m^2) was the construction of cut-off walls for the Dead Sea Dikes Project in Israel, a project to form solar evaporation ponds for the extraction of salts from the waters of the south basin of the Dead Sea. This was a particularly interesting project as water from the Dead Sea containing some 320 g/litre of dissolved salts (density of 1.23 g/ml) had to be used to form the slurry. If it had not been used it would not have been possible to develop a workable slurry of sufficient density to stabilise the trenches against a soil pore water of this density. Because bentonite will not disperse in a water of this salinity the slurry was based on attapulgite clay with additions of local clays. Attapulgite contents in the range 8 to 40 kg/m^3 were used with local clay to build the slurry density to 1350 to 1520 kg/m^3. After excavation under the attapulgite/local clay slurries the trenches were backfilled with local clay soils. The author was fortunate to have the

opportunity to test some of the materials from this project during work for his doctoral thesis. Laboratory prepared mixes were found to have permeabilities generally in the range 10^{-10} to 10^{-9} m/s (Jefferis, 1972).

Cement-Bentonite Walls In Europe

The author has not been able to determine when the first cement-bentonite wall was installed. It seems most likely that the concept was first developed and used in France though it is clear that there was also considerable research activity in Spain. Two important early papers were by Claude Caron of the company Solétanche, Caron (1972) and (1973). The first of these addressed the durability of cement-bentonite materials and the second was a major review of the properties and performance of the cement-bentonite system. Both were substantial works reporting on major programmes of investigation and are a certainly as valid today as when written. Caron notes, in the 1972 paper, that the Solétanche company had already been using what would now be described as single phase cement-bentonite cut-off walls for a few years and, from the author's researches, it seems possible that the first single phase wall may have been installed in 1965. By the time of the 1973 paper Caron was able to record that over 150,000 m^2 of cut-off wall had been constructed. Presumably most of these walls were for the control of nominally clean groundwater, that is they were not for the containment of contaminated sites. It is therefore interesting to note that the records of the Bachy Company in France show that they constructed a slurry trench wall with concrete backfill as early as 1966 to control possible contamination from a refinery (the wall was included as a precaution in case there were spills rather than in response to a spill, Esnault, 1997).

It is clear that there was work in Spain as well as France in the early 1970s and Canizo (1975) published a major review of cement-bentonite research.

In addition to the slurry trench cut-off the vibrated beam method for forming thin cement-bentonite cut-offs should not be forgotten. Maillard and Serota (1963) state that Maillard was the inventor of this 'new method of installing watertight cut-offs', and that a large project in Oberelchingen was completed at the end of 1960 and that by 1963 '129,000 yd^2 had already been constructed'.

Soil-Bentonite Walls In The UK

As in the USA, so it was in the UK that soil-bentonite walls were developed before cement-bentonite walls. It is not clear when the first soil-bentonite wall was installed in the UK. One of the first reported walls was installed in 1963 to keep a gravel workings dry (anon, 1964). This wall was excavated under a bentonite slurry and a soil-pfa-bentonite mix was used for the backfill - the pfa providing extra fines in the mix. Since then soil-bentonite walls have been rather rarely used in the UK and the few applications have generally been at mineral workings (though there have been landfill applications) and have passed largely unreported.

It is not clear why soil-bentonite walls have found so little favour in the UK. It may be in part that they tend to be rather thick, typically of the order of 1.4 to 1.8 m and for economy the excavated soil must be suitable for blending with bentonite to produce the cut-off material. Also soil-bentonite backfill materials may consolidate under the in-situ soil stresses so that there may be some settlement of adjacent ground. In North America soil-bentonite walls are often specified on the basis of the grading of the soil to be used and the quantity of bentonite to be added. Specifications may make no mention of permeability or strength as appropriate values (determined from pre-works trials) will be assumed to be achieved provided the correct mix recipe is followed. Thus specifications are prescriptive, requiring particular mix formulations, bentonite contents, soil gradings etc. though contractors may elect to use their own designs. In the UK it is normal practice to commission cut-off walls (and most other works) on the basis of performance specifications which specify properties such as permeability and strength. Because of the subtleties of the cement-bentonite system it would be unwise to specify them by recipe - though this may be possible if pre-blended 'one-bag' mixes of cement, bentonite and additives are used to prepare the slurries.

54

Development of Cement-Bentonite Walls in the UK

Between 1967 and 1972 the clay cores of three UK embankment dams were repaired using two phase plastic concrete cut-off walls (Little, 1974). The trenches were excavated under a bentonite slurry and backfilled with a plastic concrete. Plastic concrete cut-offs are still used on projects which require deep walls excavated in panels. In the same paper Little notes that a slurry trench cut-off for the Upper Peirce Dam in Singapore had just been completed using a cement-bentonite-fly ash mix without any aggregate (i.e. a single phase wall) and achieved an excellent permeability of 1.2 to 2.1 x 10^{-10} m/s (though the total cement plus fly ash content was relatively high at 378 kg/m^3).

In 1973 Braun published a short paper entitled 'French breakthrough in cut-off wall construction' in the UK journal Ground Engineering. This stated that 'the first ever cut-off wall consisting entirely of solidified bentonite slurry has been completed recently in Paris by Sepicos the French subsidiary company of the worldwide ICOS organisation'. With the benefit only of hindsight it is not clear exactly what made this a first. It is possible that earlier walls in France were composite systems including both structural concrete and cut-off material.

In 1973 the author had recently completed a PhD on excavation slurries and Braun's paper prompted an interest in research on the cement-bentonite system. Of course there had been many earlier papers. However, at that time, the literature on bentonite excavation slurries generally regarded cement as an undesirable and damaging contaminant that could get into bentonite slurries during the concreting of structural diaphragm walls. The idea of deliberately adding cement to a bentonite slurry was slightly difficult to accept. Those working in concrete technology at the time would also have found the cement-bentonite system difficult. Clays, for example, with the aggregate, were regarded as damaging to the strength of concrete and furthermore the use of high water cement ratios (typically 2 to 10) for cement-bentonite materials bordered on the perverse. Thus the concept of a cement-bentonite material did not find ready acceptance in the UK research community. This tended to inhibit research work and also made publication of research findings in the technical literature difficult.

In 1974 Abdurrahman Guner started research on cement-bentonite systems under the supervision of the author. This work was to have a major impact on UK slurry cut-off design. The research soon showed that cement-bentonites when prepared in the proportions implied in the French publications did not set to a reasonable strength. The resulting materials were so weak as to be unusable. However, careful review of the French literature showed that they generally used cements containing ground granulated blastfurnace slag (CLK cements) for the preparation of cement-bentonite mixes. Such cements were not readily available in the UK but slag was available as a separate material. To make the equivalent of a slag cement in the UK it was necessary to blend ordinary Portland cement and slag. In Europe these cements could be purchased as pre-blended systems. The non-availability of slag in the UK was both a disadvantage and an advantage. The disadvantage being that if one wanted to use the materials on site it was necessary to have an additional storage silo and batching system. In the laboratory the great advantage was that the effect of slag could be investigated independently and the system optimised without the limitations to slag/cement ratio imposed by the suppliers. However, it substantially complicated the research as the three component cement-bentonite-water system was extended to a four component system. Guner's investigation of the effects of slag showed that it imparted substantial benefits to the slurry, particularly at high replacement levels, substantially reducing bleed though having more limited effect on fluid loss. High replacement levels also markedly increased the strength of the material and, as found in later research under the author's supervision, much reduced the permeability (Card, 1981).

It is important to note that all this work was done with hydrated bentonite slurries with bentonite concentrations of the order of 2 to 6% by weight of water and total contents of cementitious material (slag plus cement) in the range 95 to about 350 kg/m^3. In some cement-bentonite systems the bentonite is not hydrated and generally rather higher solids contents are used to produce rather stronger materials. Since this time it has been the normal practice, in the UK, to use hydrated bentonite to prepare the cement-bentonite slurry. Systems using non-hydrated bentonite are rare except for small applications such as borehole sealing where hydration would cause delays and require extra plant on site.

During the period of the research the first cement-bentonite 'self-hardening' slurry trench cut-off in the UK was completed (Prentice, 1974). This wall was formed with a mix of bentonite and ordinary Portland cement. Slag was not used and thus to obtain the required strength and permeability (10^{-8} m/s) it was necessary to use higher cement contents than those used in France. The use of a higher cement content clearly has impacts on the economy of the cut-off process but it can be argued that it may be beneficial to the final product. If there is reaction with, or leaching by, the groundwater the higher cement content could, in theory, permit a longer life and thus pure Portland cement mixes should not be forgotten when researching cut-offs for aggressive environments. However, if slag is not used it may be difficult to obtain permeabilities at or below 10^{-9} m/s and the overnight bleed in the trench may be high enough to impact on construction work. For example it may be so severe as to require pumping out before starting work each day.

Guner researched the whole spectrum of cement-bentonite properties from mixing, prolonged agitation (to simulate excavation), bleed and fluid loss, shear, compressive and tensile strengths and much else besides. Figure 1, which gives some of the data presented in his thesis (Guner, 1978, Jefferis, 1981) summarises the effect of slag on strength development.

Figure 1. Effect of Blastfurnace Slag on the Shear Strength of cement-bentonite mixes
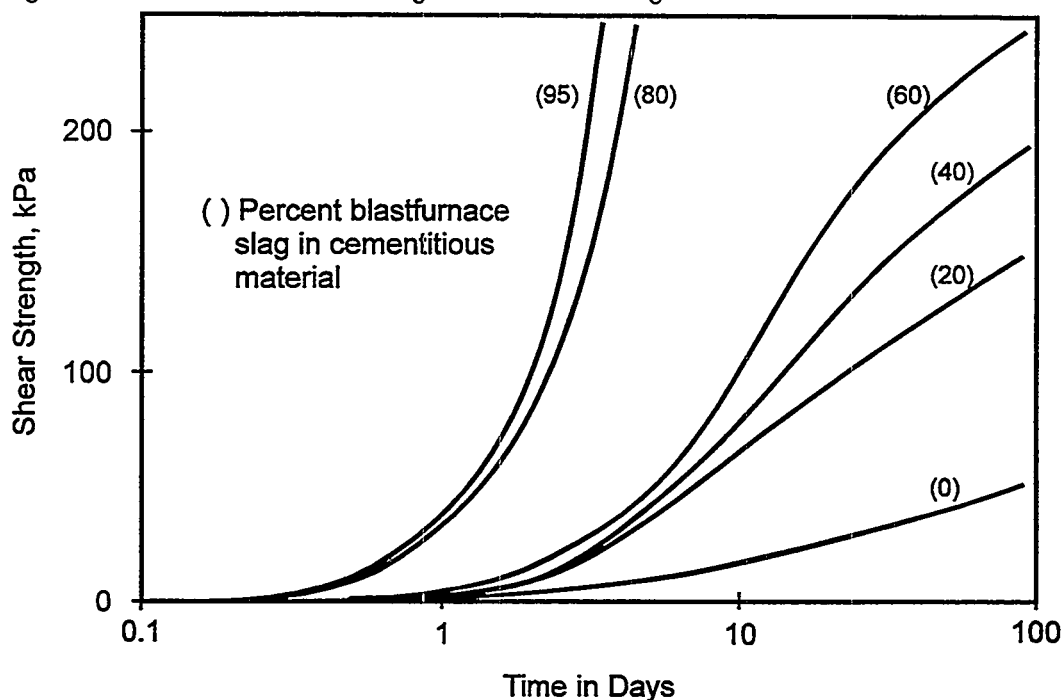
The author is not aware of a fuller presentation of the effects of slag replacement on the strength of cement-bentonite materials (though, even now, papers are published reporting the effects of slag on strength, Krikhaar and de Vries, 1993 and Khera, 1995). Later Card (1981) continued the work and undertook some investigations of the permeability of slag-cement-bentonite mixes and Figure 2 is a typical trend curve derived from his work.

Figure 2. Effect of Blastfurnace Slag on the Permeability of cement-bentonite mixes
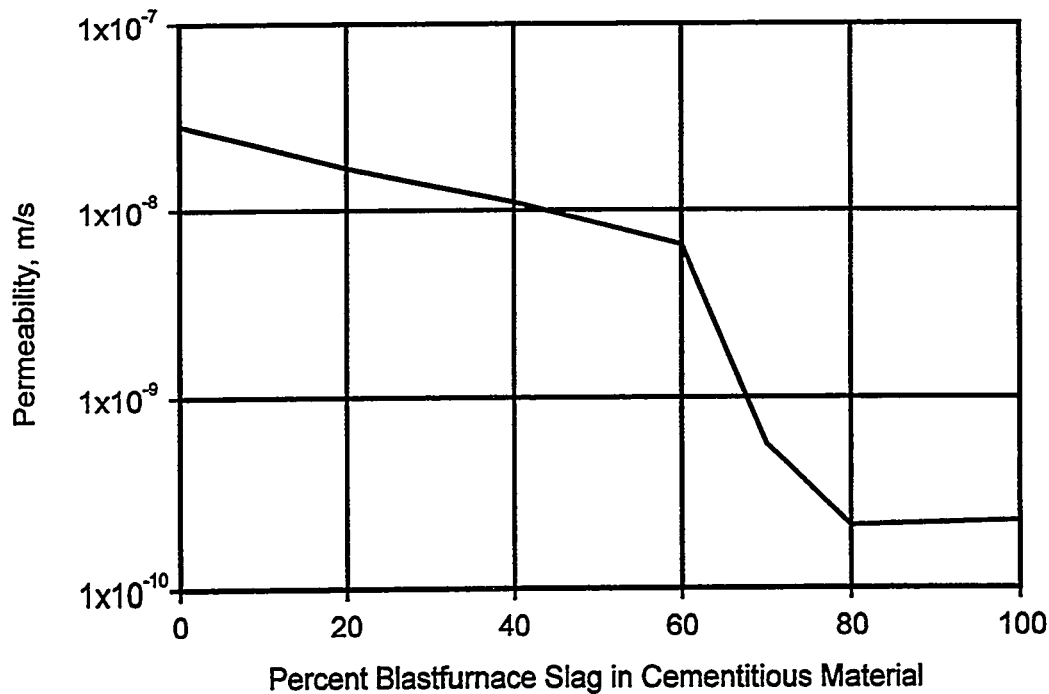
The careful reader, if examining the references, will note that both Guner and Card used the term bentonite-cement and not cement-bentonite in the title of their works. This was the subject of much debate and at the time we felt that bentonite was the dominant constituent in terms of its effect on the material. This may be the case - certainly without it or some other active material the mix would not be stable. However, the author's present view is that the dominant material (excluding water) in terms of proportion in the mix should be stated first and thus cement-bentonites are distinct from bentonite-cements and strictly most of the materials used in the UK should be described as slag-cement-bentonites as the proportion of slag in the mix is typically 65 to 80% of the total cementitious content.

The First UK Slag-Cement-Bentonite Cut-Off Wall

The first slag-cement-bentonite wall in the UK was used to form a cut-off in gravels beneath an earth dam in 1975. The specification required a permeability of less than 10^{-8} m/s after 500 hours permeation under a gradient of 450 and a minimum deformation of 5% under a deviator stress of 125 kPa when tested undrained with a cell pressure of 500 kPa at a sample age of 90 days (Coats and Rocke, 1982). The low specified strength and high strain at failure caused some considerable concern as the requirements did not fit well with the data available from the author's research (and there was little else available in the UK). With hindsight this was a classic example of undertaking research without understanding the demands of the industry. Though it must be allowed that had the UK industry been surveyed prior to starting the research it is doubtful whether it would have been undertaken at all. Slurry walls were hardly the topic of the day! Ultimately a mix was developed with about 100 kg of cementitious material per cubic metre of slurry (70% slag) and 6% bentonite by weight of water. With this type of mix the permeability and strength conditions were not a problem but the strain criterion was, and remains, very difficult to achieve.

Subsequently it was shown that cement-bentonite materials when tested, drained, under effective confining stresses greater than about 50% of their unconfined compressive strength can show a strain at failure of well over 5%. Under undrained conditions failure strains are unlikely to exceed about 1% though mix design and sample size and loading rate will have some effect. It is interesting to note that if samples are not saturated, in the cell, prior to confined undrained testing some drained behaviour may be apparent. The surface of the samples can dry very rapidly during

preparation and mounting in a triaxial cell so ensuring that some effective stress can develop on the sample. Also post failure dilation may cause significant effective stress to develop so that a sample which, if tested unconfined, would fail at <1% strain, when tested undrained, may appear to show a strain without failure of >5%. It follows that in all strain testing saturation of the sample prior to test may be necessary and the sample must be monitored during and after the test to record the first appearance of cracks, failure planes etc.

Saline Soils

No history of cut-off walls would be complete without mention of the 14.5 km of cut-off wall installed on Jordan Arab Potash Project. This project not only involved the first use of an HDPE membrane in a slurry trench but also required the development of one of the most complex and subtle slurry mixes. In the Israeli sector of the Dead Sea a soil-attapulgite wall had been used. In the Jordanian sector it was decided to use a Portland cement-attapulgite-Dead Sea Water mix. The design of the 87,000 m^2 cut-off, completed in 1980, is described in Brice and Woodward (1984) and some of the particular features of the mix are discussed in Jefferis (1985). Subsequent work on saline mixes suggests that the attapulgite clay probably had rather little effect on the fluid properties of the mix. The normal role of the clay, prior to set, is to prevent bleed. After set (and indeed during set) it may react with the cement and in cement-bentonite mixes it seem likely that, over time, all the bentonite reacts with the cement to produce hydration products comparable to those of Portland cement. However, attapulgite develops rather a weak gel unless subjected to prolonged or intense mixing. Hence its effectiveness for bleed control in Portland cement systems can be rather limited. However, the high magnesium ion content of the sea water (of the order of 30 g/litre) was sufficient to produce a strong suspension of magnesium hydroxide via reaction with the cement. This hydroxide, depending on its state of dispersion can have excellent gelling properties and, in the mix, it was this that dominated the bleed control. However, the quantity of magnesium ion was critical. Reducing the concentration led to bleed and increasing it prevented all set as free calcium hydroxide could not exist in the mix. To meet these criteria the water had to be drawn from particular locations around the sea. This example shows that slurries can be produced with chemically active waters and that clays are not the only materials that may be used to control bleed. Special purpose slurries can be designed but the works contract must allow sufficient time.

The HDPE membrane used in the Jordanian sector of the Dead Sea in 1979 was not jointed between panels but was overlapped by 1 m. The first use of a cement-bentonite cut-off in the UK with an HDPE membrane was not until 1990 for gas and leachate control at a landfill site.

The Development of Specifications in the UK

The early specifications for cut-off walls typically required a permeability of $<1x10^{-8}$ m/s and that a strain of >5% should be achieved under a deviator stresses typically in the range 50 to 300 kPa (i.e. the maximum strength should be in this range) when tested under confined triaxial conditions (sometimes specified to be drained and sometimes undrained, though it is now known that 5% strain cannot reliably be achieved, under undrained conditions, for all the material on a cut-off contract). Failure was seldom defined but was generally taken to be the strain at peak deviator stress rather than the strain at which the permeability of the material became unacceptable. This latter strain is the correct criterion for a cut-off but its measurement remains a problem.

Under drained conditions 5% strain (to peak deviator stress) can be achieved provided that an effective confining stress of the order of 50% of the unconfined compressive strength is used. However, the low specified strengths made it very difficult to achieve the required permeability - especially at 28 days. In about 1978 the maximum strength requirement was reversed, in most specifications, to require a minimum unconfined compressive strength of about 100 kPa. It would be reassuring to think that this change was brought about by a better understanding of the material amongst specifiers. Sadly historical accuracy requires it to be noted that it was brought about by a misunderstanding of the then current form of specification. It would be invidious to name the job on

58

which the reversal occurred but it was most welcome as it enabled the greater potential of the materials to be realised for those applications where low strength was not essential - and how many applications actually require a low strength?

The age at test is also an issue for cement-bentonite slurries especially for permeability. In 1983 the first cut-off wall was installed in the UK to control leachate at a landfill. The permeability was specified to be 5×10^{-9} m/s. As this represented some reduction from the then norm of 10^{-8} m/s the enlightened client agreed (after some discussion) that the age at test should not be fixed but that the contractor should be required to test samples at progressively greater ages until the required permeability was demonstrated. Some flexibility over age at test has now become a feature of many specifications. During the late 1980s the permeability requirement was dropped to 10^{-9} m/s. It would seem that this requirement was introduced to match the 10^{-9} m/s that typically was required for landfill liners though the thickness requirement (typically 1 m) was not imported (most cement-bentonite cut-off walls are of order 0.6 to 0.8 m thick).

The Present Situation in the UK

Recently a draft national specification for slurry trench cut-off walls as barriers to pollution migration (Institution of Civil Engineers, 1996) has been published in the UK. This specification includes the following criteria:
Permeability: 'A target permeability of less than 1×10^{-9} m/s is required. However due to inherent variability in mixes and testing, at least 80% of results shall be less than 1×10^{-9} m/s and not more than 5% of results shall exceed 1×10^{-8} m/s'.
Strength: 'The minimum unconfined compressive strength at 28 days age shall be 50 kPa'.
Physical and chemical durability: 'Testing for the indication of attainment of adequate durability characteristics shall be carried out as specified in the Particular Specification (the particular specification is an additional job specific specification that the cut-off designer may require)'.

In relation to durability it should be noted that the design life for a cut-off is seldom explicitly stated and it would seem that specifiers may not always be aware that if specific chemical compatibility testing is required it is likely to take a minimum of 6 months and very possibly much longer depending on the rate of movement of any reaction front through the material (and hence on the permeability of the material). It should be noted that the UK Draft Specification does not include any criteria for deformation behaviour and requires only a minimum and not a maximum strength.

The Future: Issues for Debate

In the UK specifications for cement-bentonite cut-off walls as barriers to pollution migration have been the subject of some debate. Issues are as follows:

Permeability: Current practice is to require a permeability of 10^{-9} m/s and this can be achieved at or after 90 days with cement-bentonite mixes with high levels of slag replacement and with plastic concrete type materials incorporating calcium bentonite, sodium silicates and silanes (Hass and Hitze, 1986) though costs are markedly higher. However, neither of these types of material will show a 5% strain without failure. Membranes may be included in a wall to reduce permeability but is the seal at the toe of the membrane always adequate in aggressive environments? Finally there are still too few field data. Tedd et al (1995) review some of the test procedures which have been tried in the field and report a technique for measuring in-situ permeability in existing walls at discrete locations.

Durability: Water is potentially one of the most aggressive agents for any cement based material as it can leach the more soluble species and particularly free lime and that from the degradation of the calcium silicate hydrates. However, curiously, under confined conditions leaching is not damaging to permeability, indeed it may reduce the permeability by of the order of 100 times. Leaching of cement-bentonite mixes also has the advantage that it reduces the pH of the material and can reduce/eliminate the sensitivity of the material to sulphate attack (ettringite and thaumasite, the principal expansive phases in sulphate attack require alkaline conditions). This may occur naturally

in the ground and thus laboratory immersion tests may be significantly conservative. Interestingly the pH can be re-established should this be required (Jefferis, 1996). The question is: does the material behave in the field in this way? Chemical 'archaeology' of old walls is urgently required to calibrate laboratory models of durability.

Deformation properties: This remains an area for debate in the UK. The fundamental question is: should a strong material be used (perhaps with a strength up to 2 MPa) and hence also a stiff material or should a weak material be used (perhaps with a strength greater than 50 kPa but much less than 2 MPa) and thus of lower stiffness. The theory being that the softer materials should have a higher strain at failure and thus be more tolerant of ground movements. Under unconfined conditions the strain at failure may not be a function of strength but under confined drained conditions plastic type behaviour can be obtained for effective confining pressures greater than about 50% of the unconfined compressive strength. Of course the plastic type behaviour may be limited to the stress-strain curve. It is likely that there will be some increase in permeability at strains less than that at the peak of the curve. Other issues in relation of material strength include:

- Stiffer materials will be better able to resist ground movements but the effects may be marginal as in-situ stresses, if there are ground movements, can be large compared with available wall resistance.
- Chemical damage, either expansive (e.g. sulphate attack) or by leaching may be minimised if the material consolidates under the in-situ stresses to close any cracks or close up voids formed by leaching. Weaker materials will be more easily consolidated by the available in-situ stresses than their stronger counterparts.
- Chemical attack, if controlled by reaction or leaching of a constituent may take longer in mixes of high cement or bentonite content (which generally will be stronger than their low solids counterparts – increasing the bentonite content can markedly increase the strength) as there will be more material to be removed or reacted.

The whole debate on strength and deformation properties is unfortunately poorly informed by field, laboratory or computational investigations. It is an area where research is urgently needed as strength is such a fundamental parameter for a material.

Work is also needed on the field performance of composite systems such as HDPE membranes in slurry trench excavations. How do joints perform in the field and what is the significance of leakage under a membrane at the toe of a wall?

References

Anon, (1964) The formation of dry workings using an impermeable wall, *Cement Lime and Gravel*, November, pp. 3-10.

Boyes, R.G.H. (1975) *Structural and cut-off diaphragm walls*, Applied Science Publishers, pp. 181.

Braun, W.M. (1973) French breakthrough in cut-off wall construction, *Ground Engineering*, Vol. 6, No 3, pp. 16-19.

Brice, G.J. and Woodward, J.C. (1984) Arab potash solar evaporation system: design and development of a novel membrane cut-off wall, *Proceedings of the Institution of Civil Engrs*, Part 1, Vol. 76, pp. 185-250.

Canizo, L. (1975) Las panatallas impermeabilizantes de bentonito cemento. *Boletin de informacion del Laboratorio del Transporte y Mechanica del Suelo*, No 110, Madrid.

Card, G.B. (1981) Properties and performance of bentonite-cement slurries for use in hydraulic cut-offs. *University of London PhD thesis*, pp. 334.

Caron, C. (1972) Pérennité des systèmes argile-ciment ou bentonite-cement dans leurs divers types d'applications, *Construction*, Tome 27, No 10, Paris, pp. 291-296.

Caron, C. (1973) Un nouveau style de perforation: la boue autodurcissable. *Annales de l'Institut Technique du Batiment et des Travaux Publics*, Tome 26, No 311, Paris, pp. 1-40.

Coats, D.J. and Rocke, G. (1982) The Kielder Headworks, Proceedings of the Institution of Civil Engineers, Part 1, 72, pp. 149-176.

Esnault, A. (1997) Private communication.

Esnault, A. and Miralves, J. (1997) Résumé de l'état de l'art des procédés de confinement appliqués aux sols pollués, ADEME, France.

Guner, A. (1978) Properties and behaviour of bentonite-cement slurries. *University of London PhD thesis*, pp. 279.

Hajnal, I., Marton, J. and Regele, Z. (1984) *Construction of Diaphragm Walls, John Wiley.*

Hass, H.J. and Hitze, R. (1986) All-round encapsulation of hazardous wastes by means of injection gels and cut-off materials resistant to aggressive agents, *ESME3 Seminar on Hazardous Waste*, Bergamo, Italy.

Institution of Civil Engineers, (1996) *Draft Specification for cement-bentonite cut-off walls (as barriers to pollution migration),* London.

Jefferis, S.A. (1972) Composition and uses of slurry in civil engineering practice, *University of London PhD thesis*, pp. 169.

Jefferis, S.A. (1981) Bentonite-cement slurries for hydraulic cut-offs, *Tenth International Conference, International Society for Soil Mechanics and Foundation Engineering, Stockholm*, Vol 1, pp. 435-440.

Jefferis, S.A. (1985) Discussion on the Arab potash solar evaporation system, *Proceedings of the Institution of Civil Engrs*, Part 1, pp. 641-6464.

Jefferis, S.A. (1996) Contaminant - barrier interaction: Friend or foe, Mineralogical Society Conference, Chemical Containment of Wastes in the Geosphere, pp. 6.

Khera, R.P. (1995) Calcium bentonite, cement, slag, and fly ash as slurry wall materials, *ASCE Conference, Geoenvironment 2000, Geotechnical Speciality Publication No. 46*, pp. 1237-1249.

Kramer, H. (1946) Deep cut-off trench of puddled clay for earth dam and levee protection, *Engineering News Record*, June 27, pp. 986-990.

Krikhaar, H.M.M. and de Vries (1993) Fundamental behaviour of cement bentonite, *Department of Public Works*, Holland.

Little, A.L. (1974) In-situ diaphragm walls for embankment dams, *Institution of Civil Engineers Conference on Diaphragm walls and Anchorages*, pp. 23-26.

Maillard, R. and Serota, S. (1963) Screen grouting of alluvium by the E.T.F. process, *Institution of Civil Engineers Symposium on Gouts and Drilling Muds in Engineering Practice*, Butterworths.

Prentice, J.E. (1974) Pollution control in alluvial terrain. *Ground Engineering*, Vol. 7, No 5, pp. 26-28.

Rogers, W.F. (1988) *The composition and properties of oil-well drilling fluids*, 5th Edition, Gulf Publishing Company, pp. 818.

Sherard, J.L. (1969) Statistical survey of the diaphragm wall applications, Session 14, *7th International Conference of the International Society of soil Mechanics and Foundation Engineering*, Mexico.

Tedd, P., Quarterman, R.S.T. and Holton, I.R. (1995) Development of an instrument to measure the in-situ permeability of slurry trench cut-off walls, *4th International symposium on Field Measurements in Geotechnics*, Bergamo, Italy, pp. 441-446.

Veder, C. (1963) The excavation of trenches in the presence of bentonite suspensions for the construction of impermeable and load bearing diaphragms, *Institution of Civil Engineers Symposium on Grouts and Drilling Muds in Engineering Practice*, Butterworths, pp. 181-188.

Xanthakos, P.P. (1979) *Slurry Walls*, McGraw Hill Publishers, pp. 622.

.

VERY LOW CONDUCTIVITY SELF-HARDENING SLURRY FOR PERMANENT ENCLOSURES

by Gilbert Tallard, 128 Corlies Ave. Pelham, N.Y. 10803

Abstract:

Attapulgite clay and ground blast furnace slag cement can form a low solids slurry which, after setting and curing, exhibits very low permeability and substantial strength. Compared to better known cement bentonite slurries, the conductivity is 3 orders of magnitude lower and the strength is four times higher at a similar solids content. Coefficients of permeability have been measured in the 10^{-10} cm/sec. range. As a containment barrier, no chemical compound has had detrimental effects on the integrity of the material. Compatibility with leachates at a pH under 2 has been demonstrated. Compared to leachable Ordinary Portland Cement and to bentonite gel shrinkage in the presence of certain organic compounds, the attapulgite clay and the selected slag cement behave as remarkably inert. A number of successful applications as vertical barriers, trenched and by the vibrated beam method, have been installed at remedial sites. Applications by jet grouting have been implemented under utilities to provide continuity. The potential for placement of such materials to form horizontal barriers by jet grouting or frac-grouting/mud jacking techniques, offers the possibility of creating complete enclosures in soils. The purely mineral nature of these slurries ensures long term chemical stability necessary for permanent containment.

Introduction:

Durable ground water vertical barriers are still very much in demand, especially for permanent enclosures. Economics often rules in favor of a controled abandonment rather than treatment and restoration. While soil bentonite have become the panacea for temporary barriers, the need for strict quality assurance for permanent barriers is not well served by this crude construction technique. The self-hardening slurry trenched barrier has always been an attractive proposition in view of the one phase-one way construction technique which limits the number of workers in the hot zone to eventually a single individual, and because of the engineered endproduct which can be controled at every step of the construction process as well as over the long term. Cement bentonite slurries had been used for stable grouts and dam cutoff walls where plastic deformation is a valuable characteristic. Numerous cement bentonite slurry barriers have been installed in ground water contamination cases, inclusive of this country, but with a requirement for hydraulic conductivity limited to 10^{-6} cm/sec. Although we talk about cement bentonite on both sides of the Atlantic, european processed bentonites and blended cements are creating materials quite different from the Wyoming natural bentonites and ordinary Portland cement. When the threshold of hydraulic conductivity has been established systematically by american regulatory agencies at 10^{-7}cm/sec., cement bentonite slurries were out of the waste containment business. Unsatisfied with this exclusion of an appealing technology, this writer has combined some Old and New Worlds experiences to produce a self-hardening slurry, always based on a clay viscosifier and a cement binder principle but using a non bentonite clay and non Portland cement, resulting in much lower permeability , much higher strength and greater chemical resistance to contaminants. With these improvements, self-hardening slurry barriers are back serving the permanent containment industry.

Self-Hardening Slurry:

Self-hardening slurries are always, at a minimum, a clay in a colloidal state that will viscosify water and a finely grained cement. The clay will viscosify water either by pure dispersion as in the case of bentonite or by mechanical crystral stacking as in the case of attapulgite; the clay proportion in water by weight is between 3 and 6% typically. This is enough to generate enough

gel strength to carry in suspension a multiple of its weight of cement. In the United States, cement is always understood as an ordinary Portland type I- II and more rarely type V. elsewhere also a Portland except in countries having a well developed steel industry where blended cements are available and prefered for underground workings. The amount of cement may vary from 10 to 30% by weight of water. The slurry treated eventually with fluidifiers and fluid loss reducing agents, remains fluid under agitation for a number of hours allowing its use as a drilling or trenching fluid. Upon completion of the excavation the slurry is left to rest which allows it to gel due to its thixothropic properties and eventually set in place after a number of hours. The strength gain curve is extremely slow given the very high water cement ratio compounded by the clay cement ratio. Typically, a self-hardening slurry will require at least a year to achieve its ultimate strength. As strength develops, permeability decreases and deformability diminishes. For evaluation these materials are tested at 30 and 90 days. Accelerated curing can simulate a 90 days result in about 10 days. The final strength, between 500kPa and 3MPa permits easy in situ recovery of samples to monitor the barrier over its life cycle.

The construction process which consists in preparing the slurry at a mixing plant that can almost always be set up at a level D protection location, pumping through a slurry line to the barrier installation point and placing the slurry in the cavity created by the excavating or soil displacement tool. Once introduced in the ground, the self-hardening slurry is in place for good and the work is essentially complete at that location. Whether the excavated spoil is disposed alongside the alignment or hauled away is a secondary consideration. Possibly reduced to one man operation in the hot zone, pushed to its limits, with laser grading tools, remote control operation of heavy equipment and excavator's kinetics digital monitoring, a self hardening slurry operation could be entirely remotely controled; the technology is there; the human drive is not.

Cement Bentonite:

As barrier material, cement bentonite barriers achieve, in North America, coefficients of permeability between 10^{-5}cm/sec. and 10^{-7}cm/sec. The choice and amount of bentonite is the prime factor for watertightness at low cement concentrations, whereas at higher cement concentrations, the cement becomes the prime factor. The choice of bentonite as a dispersive clay always ready to exchange ions and loose some water to certain organic compounds found in some waste streams is based on economics and not on sound engineering. Non swelling clays or manufactured "bentonites " may be a better choice especially when the effect of cement is compounded. Portland cement literally destroys bentonite, the flocculation occuring by permutation of sodium by calcium ions from the cement causing the viscosity of the slurry to become excessive and the filtration of the mix becoming many times that of the fresh bentonite mud. Also, driving under the bridges of this country is a constant reminder about the shortcomings of Ordinary Portland cement (OPC) and its propensity to leach uncombined salts (free lime). This is a much smaller problem in cement bentonite than in concretes but it remains an issue when dealing in adverse ground water chemistry at an early age. The sudden demand for water by the dry cement powder at the early stage of the OPC hydration combined with the bentonite flocculation resulting from the lime's calcium exchange with the bentonite's sodium are the reason for the sudden rise in viscosity of the cement bentonite slurry mix during the first few minutes of the mixing process("break over"). A high level of mixing energy and time is required to bring back the viscosity within a practical working range, generally with the addition of fluidifying additives (dispersants, water reducers).

Pore Volume:

Soil laboratories in charge of performing compatibility tests by permeating site leachates through hardened cement bentonite samples, are required to simulate the life cycle of the barrier by passing at an unrealistically high hydraulic gradient a number of sample pore volumes of leachate The pore volume definition derives from the testing of materials with a granular squeleton such as plastic concretes and soil bentonite backfills. It is the percentage of the dry residue weight over the sample weight minus the dry residue, which results in a well graded granular material in the order of 20%. When applying the same definition to a self-hardening slurry where the

moisture content is between 60 and 80 % of the total volume, we obtain for the solidified mass pore volumes of 150 to 400% which is clearly absurd. But nobody in North America has caught up with this issue yet. At similar conductivity, it is clear that it will take much longer to pass 3 pore volume through a self-hardening slurry sample than through a soil bentonite sample; a variable percentage of the total sample volume decreasing with the actual hydraulic conductivity would be reasonable.

The difficulty is to be able to measure the actual porosity of a fresh sample in its working condition and not in its state of ruin. This writer has been eager to find a physical process capable of measuring the actual pore space and its volume in order to explain why so little solids in so much water can create a material of such low conductivity. All porosimetry testing procedures involved some form of dehydration such as caused by vacuum or freeze drying porcesses. A recent observation of cement bentonite through a SEM has provided an imaged view of the pore space environment, but not a quantitative means.

Attapulgite:

Commonly known in the oil drilling industry as salt mud for its mixability with sea water, attapulgite differs in many ways from bentonite. From a crystalline stand point, attapulgite is in needle form with no layer of water and no charged terminals willing to shake hands with ions floating in electrolytic solutions. This makes it very insensitive to its chemical environment. Whereas attapulgite is solely mined in south west Georgia, its close cousin Sepiolite is solely mined in southwest Nevada; other mined areas are in India and in Siberia. The viscosification process is a stacking phenomenon whereby water is adsorbed to an increasingly dispersed complex of needles. This is obtained by high shear mixing, the higher the concentration in solids and the higher the ambient temperature, the quicker the viscosity gained. Without additive, attapulgite mud has a much higher filtrate loss than bentonite.

Fig. 1 Attapulgite microscopic photo
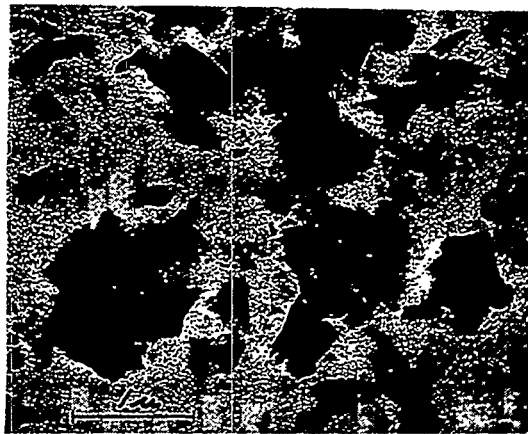
Bentonite microscopic photo (ref.1)

	Attapulgite	Bentonite
% SiO$_2$	55.06	58 - 64
%Al$_2$O$_3$	8.89	18 - 21
%MgO	8.53	2.5 - 3.2
%CaO	3.57	0.1 - 1.0
%Fe$_2$O$_3$	3.39	2.5 - 2.8
%K$_2$O	1.96	.2 - .4
%Na$_2$O	1.75	1.5 - 2.7
%TiO$_2$	.72	0.1 - 0.2
%H$_2$O	16	8.0

Table 1. Chemical compositions of attapulgite and bentonite clays.(ref.2)

Ground Blast Furnace Slag Cement:

In the heydays when making steel was essential to the nation's economy, the NorthEast was awash with blast furnace slag and most cement manufacturers had a slag grinding operation producing an advantageous Portland cement replacement at a rate of 1 to 1. The situation changed with steel manufacturing falling to developing nations with few operating plants active in the US. Atlantic cement was the only firm still grinding blast furnace slag for sometime in Baltimore out of the Bethlehem mills of Sparrows Point, when the environmental movement and the nation's decaying infrastructure awareness came about in the 70's. Since then, the price advantage of ground blast furnace slag coupled with the great chemical advantage to blend cement concretes exposed to harsh environment has renewed interest in the construction industry, particularly for bridge redecking. Low hydration heat is also an advantage for large volume concrete pours such as for the thick mats of the Central Artery Project in Boston. Ground blast furnace slag cement will set by itself when mixed with water, but very slowly. It is best activated by an alkali, be it a clay, Portland cement or caustic soda. Acting as a pozzolan, the hydration product is completely combined and amorphous with no apparent crystallization.

Ingredients	Slag cement	Portland
%SiO2	36.18	19.0 - 25.0
%Al2O3	10.20	3.0 - 8.0
%Fe2O3	.60	.3 - 6.0
%CaO	39.85	60.0 - 67.0
%MgO	11.22	.5 - 5.0
%SO3	.29	1.0 - 3.0
%S	.48	
%Na2O	.21	
%K2O	.37	
Total alkalies	.45	
Loss on ignition	.12	
%residues	.42	

Table 2. Chemical composition of blast furnace slag and Portland cement (ref. 3)

The slow set of slag cement is a distinct advantage when it comes to self hardening slurries. Without any chemical additive, the working time of a slag cement slurry is at least 48 hours without significant loss in rheological properties. This is of significant benefit when working in hot weather, although, a rise in temperature will shorten the set time of an unagitated slurry.
Since self-hardening slurries and stable grout technology originates in Europe, it is over there that the strength properties of blast furnace slag cement at very high water cement ratios was first noticed. The optimum water cement ratio for the best gain in strength by comparison to OPC has not been researched; the range for the W/C bracket commonly used is:

Test performed with the former Universal Atlas Cement slag and type I Portland at 28 days:

W/C	SLAG	OPC type I	gain factor
7.7	.106 MPa	.040 MPa	2.65
3.85	1.590 MPa	.205 MPa	7.75

Table 3. Compared slag and Portland cement type slurries. (ref. 4)

This appears to have remained a well of ignorance on these shores. With the slag cement production being a very small fraction of the total OPC production, the benefits of slag cement is for those few who are well informed. One sure bet is that the infrastructure construction industry (Tiefbau in german) is mostly ignorant about slag cement 's attributes to the detriment of the tax payer that we all are.

The inordinate ability of slag cement to combine water over a long period of time to form a single calcium silicate hydrate (CHS) endproduct instead of a variety of interlocking salts (C_3S, C_2S, C_3A, C_4AF, CSH_2) occuring with OPC in a much shorter hydration period is one explanation for the much lower permeability achieved with slag cement mixes.

CLAY-SLAG CEMENT SLURRIES

Bentonite Slag Cement slurry:

A logical first step is to substitute slag cement for OPC in a cement bentonite slurry. In this substitution, since strength is rarely of interest in containment barriers (if they are not also structural) the immediate benefit is to be able to reduce the cementitious ingredient by half. The rheology of the bentonite slag is excellent since no flash set or relatively quick stiffening of the slurry will occur as it would with OPC. Since the bentonite is much less flocculated, the filtrate loss of the slurry is a small fraction of what it would be with OPC. The problem is that the slurry does not set for a week! which offsets the filtration gains. This can be remedied by adding slag activators to the mix. A small amount of OPC is the most economical but to the detriment of the permeability performance. A low permeability self-hardening slurry (less than 10^{-7}cm/sec.) is created at what can be a saving depending on location, which is an added bonus.

While dispersed hydrated bentonite is still subject to shrinkage within the hardened slurry, the latter will remain succeptible to all inorganic (K_2CO_3, $CaCl_2$) and organic (Xylene, Methanol) chemicals that can steal adsorbed water from within the clay platelet stacks while the permeant is percolating through the sample. Such potential problems do not exist with the attapulgite clay structure and it was logical to prepare the slurry with such a clay so as to create a slurry mix that would maintain its characteristics no matter what contaminant is in the ground.

Attapulgite Slag Cement slurry:

A practical advantage that appeared at the slurry preparation level is due to the lack of electrolytic response, attapulgite can be mixed directly in the batch water at the same time the slag cement is introduced (bentonite must be prehydrated). Furthermore, since the viscosification is mainly due to solids particle friction, the presence of slag accelerates the process by comparison to mixing the attapulgite alone. Such slurries, depending ambient temperature, will start setting between 48 and 72 hours.

Another surprise on the choice of clay came when comparing the strength of two slurries with the same amount of slag cement, one prepared with bentonite and the other prepared with attapulgite:
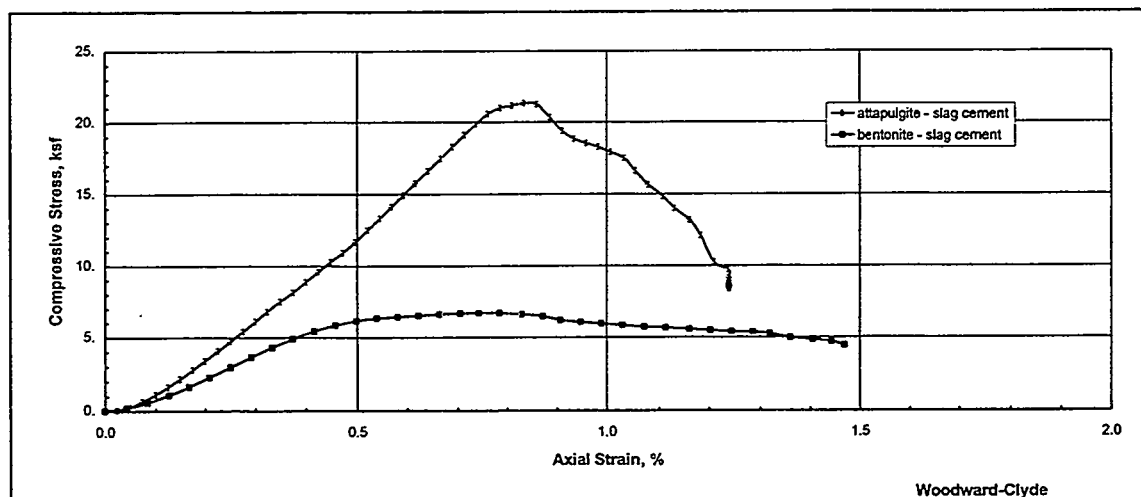
Fig. 2 Effect of clay type on unconfined compressive strength for slag mixes

This is when this writer became convinced of the love affair between attapulgite and slag cement and which the US Patent Office graciously also recognized. And we named it IMPERMIX.

In an attempt to investigate this situation, this writer has obtained SEM photographies of cement bentonite and slag attapulgite hardened slurries. The remarkable differences observed are exagerated due to the SEM preparation method that causes partial dehydration of the samples. Whereas the cement and the bentonite remain identifiable and distinct, the slag attapulgite is one unique body of amorphous appearance. As mentioned above, the pore space of the cement bentonite sample is clearly visible but not such void space appears on the slag attapulgite picture. With the ability to click on one spot of the screen to obtain a spectrograph chemical analysis, it is relatively easy to identify distinct component or judge the degree of sample homogeneity .
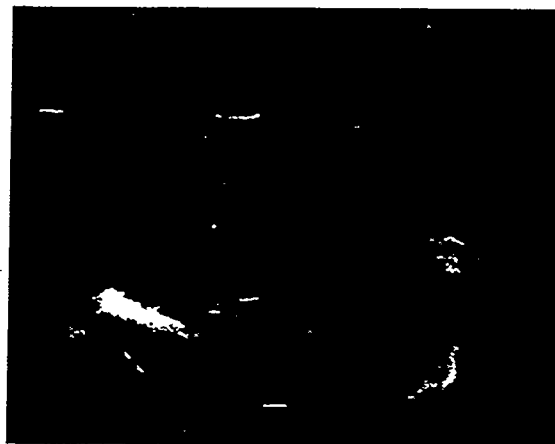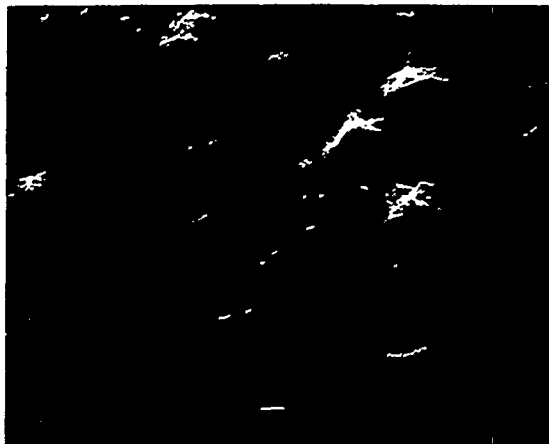
Fully cured cement bentonite.   Fully cured slag attapulgite.

Fig.3   Structure comparison bewteen CB and AS as seen with a S.E.M.(Ref. 5)

Hydraulic conductivity:

The first permeability tests on slag attapulgite slurry go back to 1985 after this writer completed a containment barrier designed as an soil attapulgite backfill slurry trench and with the attapugite slurry prepared with sea water as the only water available on a Texas gulf coast site. A tap water permeability of 10^{-8}cm/sec. was obtained with a mere 12% of slag cement for a total of 15% solids in the slurry, which implies an 85% moisture content. This clearly demonstrated that self-hardening slurries could be back in the business of containmernt barriers and have done so ever since.

Numerous confirmation of this original test, with formulation as low as 10% of slag assures that the sacro-sanct 10^{-7} cm/sec. threshold had been passed with a surprising small amount of materials. In an attempt to optimize the formulation, tests have been conducted with various clay cement ratios and various slag cement contents. After 20% of slag little gain in watertighness is observed and higher contents are limited to structural application. Mineral and organic third constituants have been introduced in an attempt to reduce permeability further and found none that would be cost effective. Certain organic polymers have proven excellent at reducing the filtrate loss which would be of interest when constructing a barrier in very pervious ground with a shallow water table.

As a summary, it is possible to aim at a low 10^{-9}cm/sec. conductivity value for tap water with a (selected) maximum slag content of 20% by weight of water and this appears to be close to the optimum. A K in the 10^{-10}cm/sec. is not out of range. It is two orders of magnitude below the regulatory threshold, and given the barrier continuity inherent to the construction process, it

becomes a strong competitor to HDPE membranes with their great material but potential problems at the bottom seal and the key ways (Hydrotite) seals.

Compatibility testing:

Long term effect by contaminants on barrier material is simulated by percolating the leachate of higher concentration through the sample, and for economic reasons, at very high gradients; for soil bentonite barriers, 3 to 4 pore volumes of leachate through the sample are required . For very low permeability self-hardening slurry, with the inadapted definition of pore volume, as discussed above, only a fraction of the so-called pore volume is passed, even at gradients over 100. The acceptance criterion becomes more the sign of a definite trend towards stability or a clear decrease in conductivity.

Listed organic compounds either in a solute form or as non soluble (NAPL) and denser than water (DNAPL) are the most serious non nuclear contaminants from a barrier standpoint. Most compatibility testing with attapulgite slag cement slurry have been with NAPL and DNAPL, eventually pure methylene chloride. Each time lower permeabilities were observed. Viton membranes have failed but not the samples.
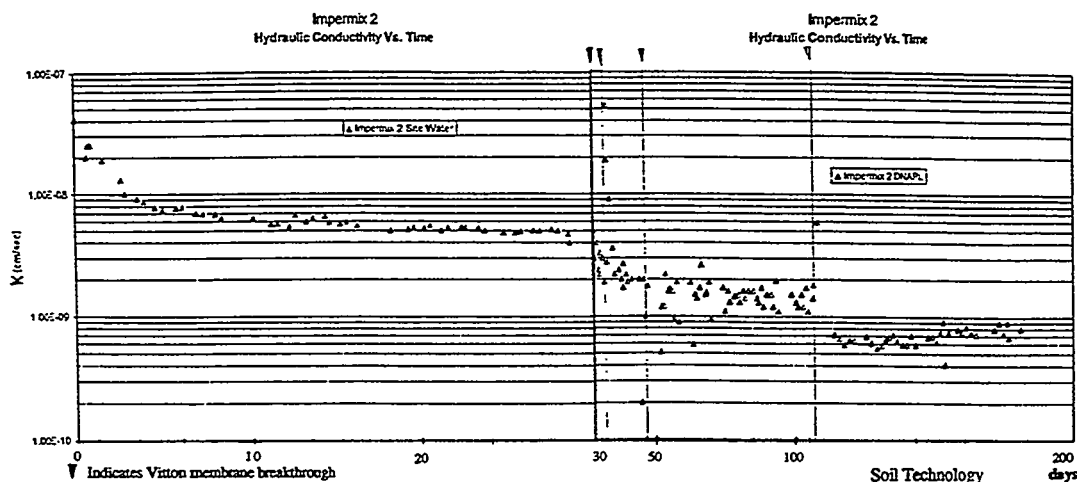
Fig.4 Typical compatibility test performance. (test ref. protected by confidentiality agreement)
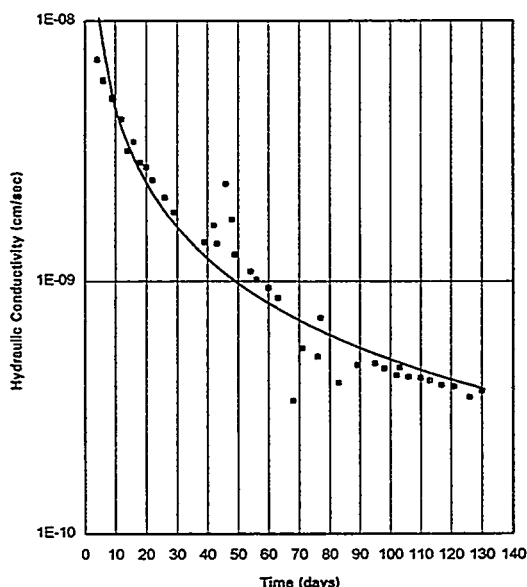
Very low conductivity self-hardening slurry brings unsuspected results. First with regard to very low pH leachates: speed of percolation and the percolate are so small that neutralization occurs very close to the point of entry and no further deterioration occurs. Second, with regard to air or gas. A lab error caused a long term saturated air permeation test simulating methane to turn into a silica gel dried air test. The most surprising after 4 month of testing, dehydration of the sample had occured only in the first 3 mm.at the point of entry. At very low conductivity, the dry air saturated very quickly and stopped dehydrating the sample within a few millimeters.

Fig.5 Permeability test with sulfuric acid solution at pH=2.5 (ETCo R&D)

CONCLUSIONS:

Whereas a lot of attention has been given in the past to the deformability of self-hardening slurries in conjunction with embankment dams construction and repairs, contaminated ground water barriers are seldom subject to significant deformations. In this latter case, low hydraulic conductivity and long term durability in adverse chemical environment are the prevalent parameters. A significant progress in this direction has been achieved by low solids content attapulgite-pure slag cement mixes. The one phase continuous cutoff wall construction method is equal to none when compared to other segmental systems. The potential for engineered controls at all steps of construction and over the long tem is a strong element for good quality assurance. The possibility of incorporating specific additives such as activated carbon or reactive iron sand in the formulation to meet specific requirements is an added advantage.

After achieving very low hydraulic conductivity coefficients such as 10^{-10}cm/sec, the issue of waste containment over the long term turns to diffusion phenomena. Diffusion coefficients vary according to specific chemicals or cocktail of chemicals and their concentration which determines the chemical gradient accross the barrier. The idea that, similarly to a salmon run, chemicals may migrate out through a barrier despite a negative hydraulic gradient due to on site pumping is begining to be a preoccupation for involved parties looking beyond the regulatory horizon. Given the very tight texture of the attapulgite slag cement hard gel, the tortuosity of the material is favorable to a low diffusion coefficient. Lower hydraulic conductivity thresholds, resulting in greater tortuosity will aslo lower diffusion coefficients. This is the new frontier of research where we are currently embarking. Preliminary information may be forthcoming at the time of presenting this paper.

Tables and figures references:

ref.1 Courtesy: Magnolia Petroleum Co. & Attapulgus Minerals and Chemicals Corp. Houston, TX.
ref. 2 Coutesy formely Atlantic Cement now Blue Circle Cement Co. Atlanta , GA
ref. 3 Courtesy of the Milwhite Inc, attapulgite and other minerals manufacturer. Houston, TX.
ref.4 Coutesy Soil Expert International 1975 inter affiliate companies communication, Nanterre, France.
ref.5 IEA lab, N.Bellerica, MA for the account of Liquid Earth Support, Inc.

Bibliography:

ASTM - JOHNSON/FROBEL/CAVALLI Editors, 1984.
Hydraulic barriers in soil and rock; Denver 6/84 ASTM/ASCE ; ASTM STP 874, 1985

D'APPOLONIA D.J., 1880.
Soil bentonite cutoffs, ASCE Journal, geotech. division,106, No.GT4, 1980,pp. 339-417

DUPEUBLE P.,HABIB P., 1978.
Coupures étanches en béton plastique, 13th ICOLD congress, Q. 48, New Dehli 1978.

EVANS J.C., FANG H-Y. and KUGELMAN I.J., Nov.4-6 1985.
Containment of hazardous materials with soil bentonite slurry walls, HMCRI Wash.D.C. 1985.

HAUG M.D.,1980
Optimization of slurry trench cutoff design; PHD thesis, Berkeley, CA, 1980.

JEFFRIES S.A., 1985.
Clay slag cement grouts for pollution control, workshop on blast furnace slag cements,
Kings college, London, 1985.

JEFFRIES S.A.,1992
The design and Performance of CB cutoff walls, a U.K. perspective, CGS,Toronto Sept.24, 1992

KAHL T.W., KAUSCHINGER J.L. and PERRY E.B., 1991
Plastic concrete cutoff walls for earth dams, US Army COE report REMG-GT-15, 1991.

MILLET R.A., PEREZ J.Y. 1981.
Current USA practice, slurry wall specifications, ASCE Journal,107, No. GT8, pp. 1041-1056.

NOGUERA G., 1985
Diaphragm wall for Colbun main dam; 15th. ICOLD congress, Lausanne, Q.58, 1985.

PARE J.J., GLOVER P.J. and DUSSAULT G., 1985.
Construction control of remedial work at LG 3 south dikes; 15th ICOLD congress,Q.58, 1985.

RABIDEAU A.J. 1995
Contaminant Tranport Modeling, sect.10 Assessment of Barrier Containment Technology, Aug.95

RYAN C.R., 1977.
Slurry cutoff walls, interim report, technical course, Resource Management Inc., Feb. 1977.

SCHMEDNECHT F., 1976.
Slurry injection. Construction Digest; January 8th, 1976.

STRUBLE L.,1992
The Performance of Portland Cement, ASTM Standardization News, January 1992

TALLARD G.R., 1984.
Slurry trenches for containing hazardous wastes. ASCE C.E. Magazine, February 1984.

TALLARD G.R., 1990.
New trenching method using synthetic bio-polymers. ASTM STP 1129. June 1990.

TALLARD G.R. ,1992
Hazwaste hydraulic barriers, Update for the 90's 45th CGS conference , Toronto Oct. 92

TAMARO G.,1986
Plastic Concrete Cutoff Walls, Workshop on Remedial Control, W.E.S. October 22, 86

US EPA, 1984.
Slurry trench construction for pollution migration control. EPA.540/2-84-001, US EPA Cincinnati, OH., 1984.

* * * * * * * *

An Improved Method For Interpreting API Filter Press Hydraulic Conductivity Test Results

G. M. Heslin[1], G. M. Filz[2], D. Y. Baxter[1], R. R. Davidson[3]

ABSTRACT: The American Petroleum Institute (API) filter press is frequently used to measure the hydraulic conductivity of soil-bentonite backfill during the mix design process and as part of construction quality control. However, interpretation of the test results is complicated by the fact that the seepage-induced consolidation pressure varies from zero at the top of the specimen to a maximum value at the bottom of the specimen. An analytical solution is available which relates the stress, compressibility, and hydraulic conductivity in soil consolidated by seepage forces. This paper presents the results of a laboratory investigation undertaken to support application of this theory to API hydraulic conductivity tests. When the API test results are interpreted using seepage consolidation theory, they are in good agreement with the results of consolidometer permeameter tests. Limitations of the API test are also discussed.

INTRODUCTION: Determination of the hydraulic conductivity of soil-bentonite backfill is important for backfill mix design, for quality assurance and quality control (QA/QC) during construction, and for assessing the *in situ* performance of soil-bentonite cutoff walls. Laboratory tests can contribute valuable information for all three purposes. In order to perform useful laboratory tests, the following guidelines from the literature should be considered:

- Laboratory testing practices should model field conditions as closely as possible. (Mitchell and Madsen, 1987; Daniel, 1994.)
- Increases in confining pressure can cause significant decreases in hydraulic conductivity. The effect is more pronounced for highly compressible soils. (Barvenik and Ayers, 1987.)
- High gradients can cause reductions in hydraulic conductivity due to seepage induced consolidation and/or migration of fines. (Dunn, 1983; Mitchell and Younger, 1967.)
- The nature of the permeant can influence measured hydraulic conductivity. When evaluating compatibility, samples in the laboratory should be permeated with the same fluid that will permeate the soil in the field. When evaluating compatibility is not the objective, permeation with tap water or 0.01 N CaSO$_4$ is recommended. Permeating with distilled water is not recommended. (Daniel, 1994; Dunn and Mitchell, 1984.)
- Permeameter type is important in compatibility testing. Flexible wall cells can mask hydraulic conductivity increases in cases where the permeant causes the soil to shrink. Conversely, using rigid wall cells without applying overburden pressure can overestimate hydraulic conductivity increases because the soil may shrink away from the cell wall. For many situations, rigid wall cells with an overburden pressure applied, e.g., consolidometer permeameters, provide a good means for compatibility testing. (Mitchell and Madsen, 1987.)
- Lowering pore pressures to apply gradients can cause consolidation of soil specimens and can cause air to come out of solution. (Dunn and Mitchell, 1984.)
- Gradients should be applied by increasing the pore water pressure at the bottom of the specimen. (Dunn and Mitchell, 1984.)
- Saturation of laboratory specimens is enhanced by permeating upwards with small gradients during backpressure saturation. (Dunn and Mitchell, 1984.)
- As long as side wall leakage is prevented and compatibility testing is not the objective, all permeameter types yield about the same results for comparable test conditions. (Daniel et al., 1985.)
- Soil-bentonite samples from the field should be obtained, transported to the laboratory, and tested with a minimum of mixing. (Barvenik and Ayers, 1987.)

---

[1] Graduate Research Assistant, Via Department of Civil Engineering, Virginia Tech, Blacksburg, VA 24061-0105, (540) 231-7406.

[2] Assistant Professor, Via Department of Civil Engineering, Virginia Tech, Blacksburg, VA 24061-0105, (540) 231-7151, filz@vt.edu.

[3] Principal and Vice President, Woodward-Clyde Consultants, 4582 South Ulster St., Denver CO 80237, (303) 694-3946.

In the current state of practice, final acceptance of cutoff walls is generally based on the results of laboratory flexible wall tests and *in situ* tests. For mix design and QA/QC testing, both rigid wall cells and flexible wall cells are used. One type of rigid wall cell that is used fairly often is the API filter press (Barvenik and Ayers, 1987; Daniel and Koerner, 1995). When hydraulic conductivity tests are performed in the API filter press, water is forced down through the soil-bentonite specimen by air pressure applied to water that is placed over the specimen. No overburden pressure is applied to the specimen, so the effective vertical stress at the top of the specimen is zero. The effective vertical stress at the bottom of the specimen is equal to the sum of the applied air pressure, the differential water head across the specimen, and the stress from the buoyant weight of the specimen. Because the slurry is normally consolidated, the void ratio varies significantly from the top of the specimen to the bottom. Consequently, the hydraulic conductivity also varies over the specimen length. Use of the API filter press yields a gross hydraulic conductivity for the entire specimen. Because hydraulic conductivity varies with void ratio, or consolidation pressure, there is a need to determine the appropriate consolidation pressure that corresponds to the measured gross hydraulic conductivity. The seepage consolidation theory of Fox and Baxter (1996) can be used to calculate this pressure.

This paper describes the results of a laboratory investigation that was performed to assess the applicability of the Fox and Baxter theory to hydraulic conductivity tests performed in the API filter press. The API test results are compared to hydraulic conductivities measured in consolidometer permeameters. Some limitations of the API test are discussed, and a modification of the API test procedure is proposed.

MATERIALS: Two base soil gradations, which are shown in Figure 1, were used to prepare the soil-bentonite mixes that were tested in this investigation. The base soils used to fabricate soil-bentonite mixes SB2 and SB3 had Unified Soil Classifications of SC and SM, respectively. SB2 was fabricated by adding 1.5% bentonite by dry weight to the base soil, while SB3 contained 3% added bentonite by dry weight. The bentonite used in this study was a sodium-montmorillonite sold under the trade name Hydrogel 90 by Wyo-Ben, Inc. The bentonite was hydrated in tap water for 24 hours prior to being mixed with the appropriate base soil. After mixing, the water content of each mix was adjusted to achieve a slump between 4 and 6 inches.

TEST EQUIPMENT AND PROCEDURES: Two hydraulic conductivity test methods were used in this investigation. Consolidometer permeameter tests were performed in conventional 1-D consolidation cells that were not equipped to apply backpressure. Samples were 6.35 cm in diameter and initially 2.54 cm tall. Consolidation of the samples was performed in general accordance with ASTM D-2435. Falling head hydraulic conductivity tests were conducted at selected load increments. In these tests, de-aired tap water was permeated upward through the specimen after primary consolidation was complete. Gradients ranged from 7 to 35 and were applied such that a minimum vertical effective stress of 7 kPa was maintained. Inflow volume was measured to the nearest 0.02 ml until the calculated hydraulic conductivity stabilized. Outflow was not measured. The 1-D consolidometer permeameter tests were performed in accordance with the procedures men-

Figure 1. Base Soil Gradations
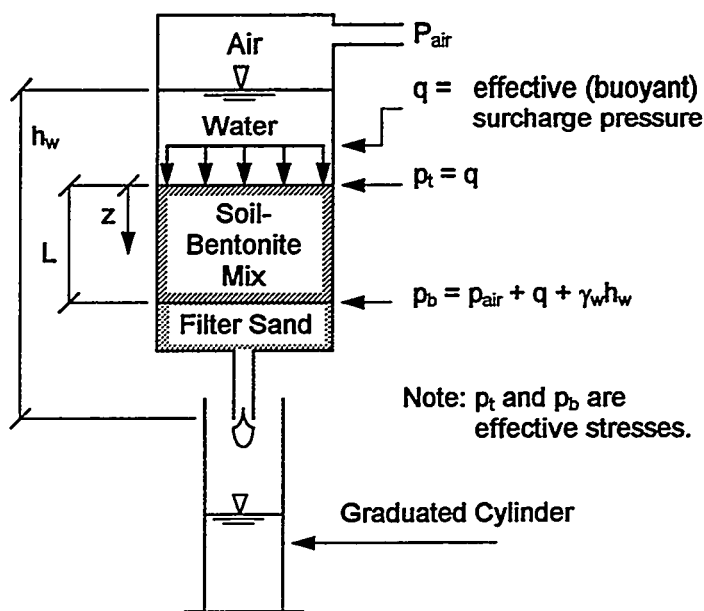
Figure 2. Definition Sketch for Applying the Fox and Baxter (1996) Theory to Hydraulic Conductivity Tests Performed in the API Filter Press

tioned in the Introduction. These tests were used as a baseline to evaluate API test results.

Hydraulic conductivity was also measured in the API filter press using procedures described by Barvenik and Ayers (1987). The API filter press is a rigid wall cell that is normally used to measure the filtrate loss of bentonite-water slurries. As recommended by Barvenik and Ayers, a layer of bentonite paste 0.8 mm thick was placed on the inside wall of the chamber to minimize sidewall leakage. Filter sand, soil-bentonite, and tap water were placed in the chamber as shown in Figure 2. Samples were approximately 7.6 cm in diameter and initially about 5 cm tall. The driving air pressure was regulated to the nearest 1.3 kPa. Sample height was measured to the nearest 0.3 mm with a ruler. Outflow was measured to the nearest 0.1 ml. Inflow was not measured. As described subsequently, hydraulic fractures developed in all API test specimens when this procedure was used. In order to prevent hydraulic fracturing, the procedure was modified to include placing a surcharge weight on the top of the API specimen. A piece of filter paper and a layer of sand approximately 0.7 mm thick were placed on top of the soil-bentonite mix. A 725 g solid steel weight 7.2 cm in diameter was placed inside the chamber on top of the sand. The purpose of the upper sand layer was to ensure that the water pressure would be uniformly applied across the top of the specimen. The buoyant weight of the steel disk provided the surcharge pressure, q, shown in Figure 2.

Barvenik and Ayers (1987) recommend running API tests for 24 hours. It was observed during this study that longer times are often required to reach a condition of steady-state seepage. In many instances the sample was still consolidating after 24 hours. The gross hydraulic conductivity calculated based on the flow rate at 24 hours exceeded the steady-state value by a factor of two or more. The difference between the flow rate at 24 hours and the steady-state flow rate was largest for the initial pressure increment.

THEORY FOR INTERPRETING RESULTS: The schematic of the API filter press in Figure 2 includes definition of terms for applying the Fox and Baxter (1996) seepage consolidation theory. Fox and Baxter assume that the hydraulic conductivity in a normally consolidated soil is related to pressure according to

$$k = k_0 \left(\frac{p_0}{p} \right)^A \tag{1}$$

where k = the hydraulic conductivity; k_0 = a reference hydraulic conductivity; p = the effective major principal stress = the total major principal stress minus the pore water pressure; p_0 = the reference effective major principal stress at which k_0 applies; and A = a material parameter = the slope of the log k versus log p plot where log p is the abscissa.

Note that the slope of the log k versus log p plot is negative, corresponding to decreases in hydraulic conductivity for increases in consolidation stress. However, as written in equation 1, A

is taken as the absolute value of this slope. Also note that for the value of A to be constant, the slope of the log k versus log p plot must be linear. This was shown to be a reasonable approximation over limited stress ranges for the soil-bentonite materials tested in this investigation.

Fox and Baxter assume that Darcy's law applies, side wall leakage is negligible, the stresses induced by self-weight of the soil are negligible compared to the other stresses involved, and the shear stresses between the soil and the container side walls are negligible. Based on these assumptions, Fox and Baxter have shown that the following equations apply at steady-state:

$$p = \left(\frac{z}{L}\left(p_b^{1-A} - p_t^{1-A} \right) + p_t^{1-A} \right)^{\frac{1}{1-A}} \tag{2}$$

and

$$v = \frac{B}{L}\left(p_b^{1-A} - p_t^{1-A} \right) \tag{3}$$

where z = the distance from the top of the specimen; L = the length of the specimen in the direction of flow; p_b = the effective vertical stress at the bottom of the specimen; p_t = the effective vertical stress at the top of the specimen; v = the Darcy (discharge) velocity; B = a material parameter = $k_0 p_0^A / \gamma_w (1-A)$; and γ_w = the unit weight of water.

The effective stress in the sample varies with position, z, according to equation 2. Consequently, the hydraulic conductivity also varies with position according to equation 1. At steady-state, the Darcy velocity is the same for all values of z, and this is reflected in equation 3.

Values of the material parameters A and B can be determined from equation 3 by repeating the API test at two or more applied air pressures, p_{air}. The air pressures should be applied in an increasing sequence so that the sample remains normally consolidated. If two tests are performed, the values of A and B are unique, and can be found by simultaneously solving two instances of equation 3. If three or more tests are performed, the values of A and B that provide the "least squares" best fit to the data can be found using an iterative algorithm.

The gross hydraulic conductivity, $\overline{k}$, of an API test specimen is given by

$$\overline{k} = \frac{v}{\overline{i}} \tag{4}$$

where $\overline{i}$ = the hydraulic gradient applied across the entire specimen

$$= \frac{p_{air} + \gamma_w h_w}{\gamma_w L} = \frac{p_b - p_t}{\gamma_w L}$$

In order to find the mean pressure, $\overline{p}$, that should be associated with the gross hydraulic conductivity, $\overline{k}$, from an API test, equations 1 and 3 can be substituted into equation 4 and solved to obtain the following:

$$\overline{p} = \left(\frac{(1-A)(p_b - p_t)}{p_b^{1-A} - p_t^{1-A}} \right)^{\frac{1}{A}} \tag{5}$$

In summary, the proposed procedure for interpreting hydraulic conductivity tests performed using API filter press test equipment is to repeat the test two or more times using the same specimen with increasing applied air pressures. The best-fit value of the material parameters A and B are obtained from equation 3. For each test, the value of A is used in equation 5 to obtain the value of mean pressure, $\overline{p}$, that corresponds to the gross hydraulic conductivity, $\overline{k}$ (from equation 4).

RESULTS AND DISCUSSION: The results of two consolidometer permeameter tests performed on SB2 are shown in Figure 3. The left plot is the conventional end-of-primary consolidation curve. The right plot is hydraulic conductivity versus specimen void ratio. In the initial unload-reload cycle, no significant change in hydraulic conductivity was measured for a 4-fold reduction in vertical effective stress. In the final rebound, only slight increases in hydraulic conductivity

were measured. Consolidometer permeameter tests conducted on SB3 produced the same type of results. The data in Figure 3 shows that void ratio, rather than current effective stress, controls the hydraulic conductivity of compressible mixes like soil-bentonite. Because void ratio increases are small in unloading, hydraulic conductivity measured in consolidometer permeameters can be related to preconsolidation pressure. This type of comparison is shown in Figure 4 for SB2 and SB3. It can be seen that the data from the consolidometer permeameters fall in narrow bands for each mix.

A total of 7 API specimens were tested using the procedures recommended by Barvenik and Ayers (1987). Based on visual evidence, all of these specimens developed hydraulic fractures that originated at the top of the specimen and propagated to the bottom. Hydraulic fracturing developed at applied air pressures ranging from 7 to 28 kPa and at times from 0 to 9 hours after the application of the air pressure which caused fracturing. Hydraulic fracturing probably occurred because the effective stress at the top of the sample was zero in these tests. To correct this problem, a surcharge of approximately 1.6 kPa was applied, as discussed previously. Although hydraulic fracturing did not occur for any specimens when the surcharge was used, fines were forced out of one specimen when the applied air pressure was 101.7 kPa.

The data from several API tests performed using a surcharge pressure of 1.6 kPa were interpreted using the method described previously. The results are listed in Table 1. It can be seen that the mean pressure, $\bar{p}$, is much less than p_{air}. The mean pressures and the gross hydraulic conductivities from the API tests in Table 1 are plotted with the results from the 1-D consolidometer permeameter tests in Figure 4. The agreement is generally quite good. Exceptions occur for the five API tests indicated in the figure. For test API_7 at an applied air pressure of 101.7 kPa, fines piped out of the specimen. This may have resulted in the relatively high hydraulic conductivity value that was calculated. For tests API_8 and API_15 at applied air pressures of 55 kPa and higher, the measured hydraulic conductivity was lower than the trend of the data for SB3. This response was likely due to migration of fines. The average gradients in these tests were about 140 and 270 at applied air pressures of 55 and 100 kPa, respectively. Because the hydraulic conductivity was lowest at the bottom of the specimen, most of the head loss occurred at the bottom. This variation in head loss produced gradients much higher than the average gradient near the bottom of the specimen. As documented by Dunn (1983) and Mitchell and Younger (1967), gradients of this magnitude can cause migration of fines and reductions in hydraulic conductivity in laboratory specimens. The tendencies for piping and migration of fines at high applied air pressures may place a limitation on the applicability of the API test. At the air pressures which precluded piping and migration of fines, the mean pressures
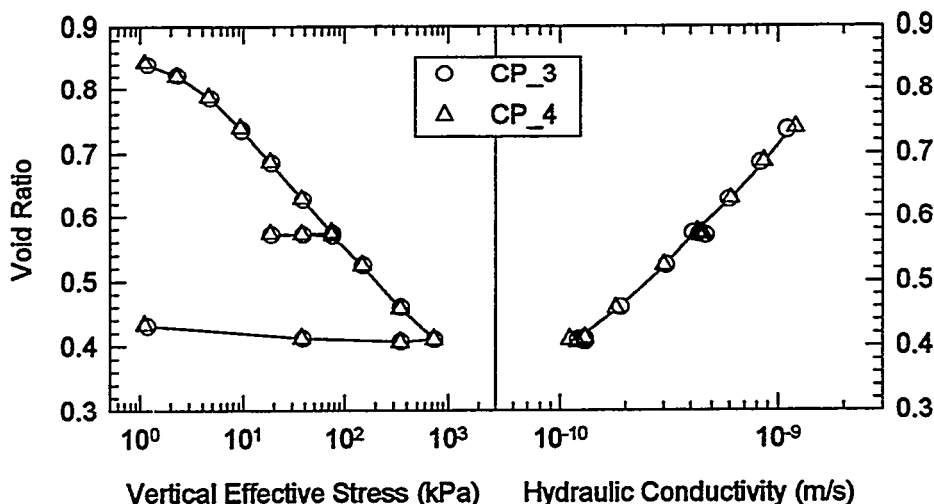
Figure 3. Consolidometer Permeameter Test Results for Mix SB2
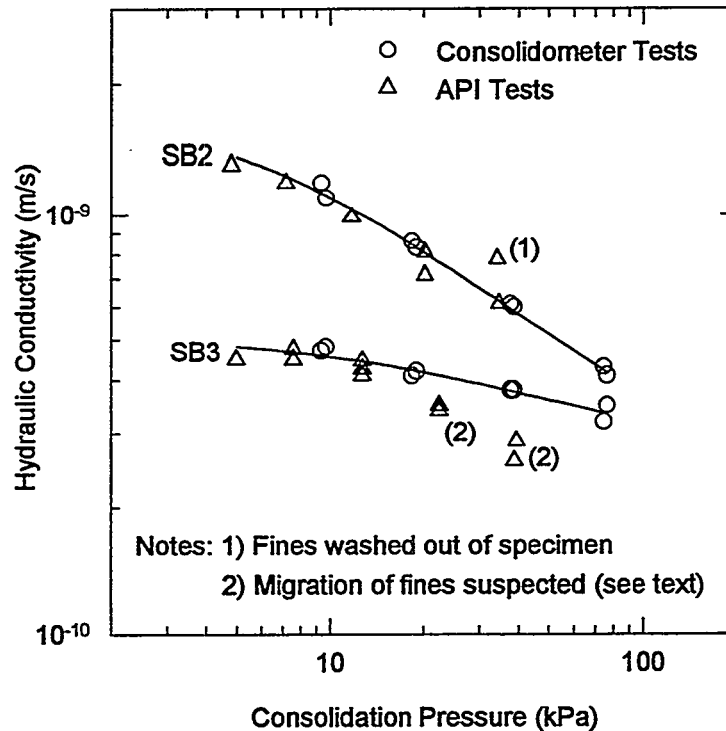
Figure 4. Results of Consolidometer Permeameter and API Tests

Table 1. Summary of API Test Results Shown in Figure 4

Mix	Test	p_{air} (kPa)	p_b (kPa)	$v^{(2)}$ (m/s)	L (m)	$\bar{k}$ (m/s)	A	$B^{(3)}$	$\bar{p}$ (kPa)
SB2	API_7	13.8	15.4	3.79E-08	4.826E-02	1.20E-09	0.427	4.94E-10	7.2
		27.6	29.2	6.22E-08	4.674E-02	9.90E-10			11.7
		55.2	56.8	1.03E-07	4.521E-02	8.10E-10			20.2
		$101.7^{(4)}$	103.3	1.85E-07	4.420E-02	7.80E-10			34.1
	API_10	6.9	8.5	2.28E-08	4.801E-02	1.30E-09			4.8
		13.8	15.4	3.88E-08	4.724E-02	1.20E-09			7.2
		27.6	29.2	6.34E-08	4.572E-02	9.90E-10			11.7
		55.2	56.8	9.18E-08	4.470E-02	7.10E-10			20.2
		103.4	105.0	1.52E-07	4.293E-02	6.10E-10			34.6
SB3	API_8	13.8	15.4	1.74E-08	4.166E-02	4.80E-10	0.145	7.36E-11	7.6
		27.6	29.2	2.89E-08	4.166E-02	4.10E-10			12.6
		$55.2^{(4)}$	56.8	4.81E-08	4.064E-02	3.40E-10			22.5
		$101.7^{(4)}$	103.3	6.83E-08	3.962E-02	2.60E-10			38.7
	API_15	13.8	15.4	1.47E-08	4.674E-02	4.50E-10			7.6
		27.6	29.2	2.87E-08	4.547E-02	4.50E-10			12.6
		$55.2^{(4)}$	56.8	4.53E-08	4.445E-02	3.50E-10			22.5
		$103.4^{(4)}$	105.0	6.99E-08	4.394E-02	2.90E-10			39.3
	API_16	6.9	8.5	8.88E-09	4.191E-02	4.50E-10			5.0
		13.8	15.4	1.65E-08	4.140E-02	4.50E-10			7.6
		27.6	29.2	3.10E-08	4.039E-02	4.30E-10			12.6

Notes: 1) p_t = 1.6 kPa for all tests.
2) Steady-state seepage obtained for measurement of the Darcy velocity, v.
3) Dimensions of B are $kN^{A-1}m^{4-2A}/s$.
4) These data were not used to determine values of A and B. See Figure 4 and discussion in text.

76

ranged from 4.8 to 12.6 kPa. These pressures are generally lower than those expected in soil-bentonite cutoff walls (Evans et al, 1995; Filz, 1996).

CONCLUSIONS: From this investigation, the following conclusions can be made concerning hydraulic conductivity tests performed using the API filter press:

- Using the seepage consolidation theory of Fox and Baxter (1996) to interpret the results of API tests provides good agreement with the results of tests performed in consolidometer permeameters. The gross hydraulic conductivity obtained from the test should be associated with the mean pressure found from the theory.
- API tests should be run with a surcharge. Otherwise, the sample is prone to hydraulic fracture due to the condition of zero effective stress at the top of the specimen.
- Using high driving pressures in the API test can lead to significant overestimates or underestimates of hydraulic conductivity due to piping or migration of fines. For the materials tested in this investigation, apparent errors in the measured hydraulic conductivity occurred at applied air pressures of 55 kPa and above for some samples.
- When used for mix design, API tests should be run to a condition of steady-state seepage. For the materials tested in this investigation, steady-state conditions took up to 48 hours to develop for the first pressure increment applied.

REFERENCES:
Barvenik, M. J. and Ayers, J. E. (1987). "Construction Quality Control and Post-Construction Performance Verification For The Gilson Road Hazardous Waste Site Cutoff Wall," EPA / 600/2-87/065.
Daniel, D. E. and Koerner, R. M. (1995). Waste Containment Facilities: Guidance for Construction, Quality Assurance and Quality Control of Liner and Cover Systems.
Daniel, D. E. (1994). "State-of-the-Art: Laboratory Hydraulic Conductivity Tests for Saturated Soils," Hydraulic Conductivity and Waste Contaminant Transport in Soil, ASTM STP 1142, Edited by D. E. Daniel and S. J. Trautwein, 30-77.
Daniel, D. E., Anderson, D. C., and Boynton, S. S. (1985). "Fixed-Wall Versus Flexible-Wall Permeameters," Hydraulic Barriers in Soil and Rock, ASTM STP 874, Edited by A. I. Johnson, R. K. Frobel, N. J. Cavalli, and C. B. Pettersson, 107-126.
Dunn, R. J. and Mitchell, J. K. (1984). "Fluid Conductivity Testing of Fine-Grained Soils," ASCE Journal of Geotechnical Engineering 110 (11), 1648-1665.
Dunn, R. J. (1983). "Hydraulic Conductivity of Soils in Relation to Subsurface Movement of Hazardous Wastes," Doctoral Dissertation, University of California, Berkeley.
Evans, J. C., Costa, M. J., and Cooley, B. (1995). "The State-of-Stress in Soil-Bentonite Slurry Trench Cutoff Walls," Geoenvironment 2000, ASCE GSP #46, Edited by D. E. Daniel and S. J. Trautwein,
Evans, J. C. (1994). "Hydraulic Conductivity of Vertical Cutoff Walls," Hydraulic Conductivity and Waste Contaminant Transport in Soil, ASTM STP 1142, Edited by Y. B. Acar and D. E. Daniel, 1173-1191.
Filz, G. M. (1996). "Consolidation Stresses in Soil-Bentonite Backfilled Trenches," Proceedings of the Second International Congress on Environmental Geotechnics, Edited by M. Kamon, Osaka, Japan, 497-502.
Fox, P. J. and Baxter, C. D. P. (1996). "Consolidation Properties of Soft Soils from the Hydraulic Consolidation Test," Submitted to the ASCE Journal of Geotechnical Engineering, 1996.
Mitchell, J. K. and Madsen, F. T. (1987). "Chemical Effects On Clay Hydraulic Conductivity," Geotechnical Practice For Waste Disposal '87, ASCE GSP #13, Edited by R. D. Woods, 87-116.
Mitchell, J. K. and Younger, J. S. (1967). "Abnormalities in Hydraulic Flow Through Fine-Grained Soils," Permeability and Capillarity of Soils, ASTM STP 417, 106-141.

EFFECT OF ACIDIC LEACHATE ON MATERIAL DEGRADATION
OF SLURRY TRENCH CUTOFF WALLS

Faouzi Ahtchi-Ali[1],Ph.D. and Michael F. Casper[2]

Abstract

The use of low permeability slurry trench cutoff walls has increased since the early 1980's. This permeability requirement is necessary to minimize the seepage rate of the contaminated groundwater (leachate) through the cutoff wall. The selection of the cutoff wall material (e.g. soil-bentonite, soil-treated bentonite, soil-attapulgite, soil-cement-bentonite, cement-bentonite, etc.) is primarily dependent on the chemical properties of the leachate and construction requirements. To investigate the effect of low pH effluent on wall materials, short and long term compatibility studies were assessed on different wall material mixes. A leachate with a pH of 2.4 was used in this study. In addition, water with a pH of 6.8 was used for comparison of test results.

In order to assess the applicability of wall materials in a cost effective and timely manner, filter press, chemical desiccation, and sedimentation tests were selected to assess the short term effect of the leachate on eighteen slurry samples. These tests were performed on 90 bbl Fed Jel bentonite and 125 bbl Fed Jel treated bentonite (manufactured by M-I Drilling Fluids), and attapulgite slurry samples prepared first with leachate and then with water. The duration of each test varied from 30 minutes to 7 days. Test results obtained from the short term compatibility study indicate that the 90 bbl Fed Jel bentonite slurry degraded under exposure to the leachate, and therefore, the 125 bbl Fed Jel bentonite and attapulgite slurries were selected for the long term compatibility study.

Rigid wall permeability testing was selected to assess the long term effect of the leachate on four soil-125 bbl Fed Jel bentonite and four soil-attapulgite samples. The samples were saturated, consolidated, and subjected to permeation using first water and then leachate. The duration of each test varied from 40 days to 60 days. The test results obtained from the long term compatibility study indicate that the samples were compatible with the leachate.

Finally, flexible wall permeability testing was selected to determine the appropriate mix design with a maximum permeability of 1×10^{-7} cm/sec. The test was performed in accordance with ASTM D-5084 testing method on four soil-125 bbl Fed Jel bentonite samples, and results show that a maximum permeability of 1×10^{-7} cm/sec is achieved at minimum amounts of 2% 125 bbl Fed Jel bentonite and 51% soil fines.

Introduction

Slurry Trench vertical barrier cutoff walls are non structural underground walls that serve as barriers to the horizontal flow of contaminated groundwater. Deep slurry trench cutoff walls have many advantages over other seepage control techniques such as grouting, sheetpiling, vibrating beam, and deep soil mixing. Slurry trenches provide a continuous and uniform seepage barrier. They can extend to greater depths than most methods and require no maintenance or operating costs after installation.

[1] Project Environmental Engineer, August Mack Environmental, Inc., 2624 Lord Baltimore Drive, Suite K, Baltimore, Maryland 21244.
[2] Senior Geologist, August Mack Environmental, Inc., 2624 Lord Baltimore Drive, Suite K, Baltimore, Maryland 21244.

The primary function of the slurry is to maintain trench wall stability. The hydrostatic pressure exerted by the slurry and the filter cake formation on the walls are the two primary factors to be considered for trench wall stability. For a stable trench, the total active pressure exerted by the hydrostatic water pressure and the soil pressure has to be less than the total passive pressure exerted by the slurry. In addition, the weight of the slurry must exert its force not only on the soil pore fluid but also on the soil particles. The filter cake allows the hydrostatic force of the slurry to be more directly transferred to the walls of the trench. Unstable wall conditions are frequently associated with poor cake formation (Jepsen and Place 1985).

This study documents the short and long term effect of the leachate on different wall material mixes. A leachate with a pH of 2.4 was used in this study. Test results obtained from the short and long term compatibility studies indicate that the 90 bbl Fed Jel bentonite slurry degraded under exposure to the leachate.

Short term Compatibility Study on Slurry Samples

Several short term compatibility tests have been proposed to investigate the effect of leachate on slurry trench cutoff wall materials such as filter press, chemical desiccation, and sedimentation tests (Day 1993). These tests were developed by the petroleum, well drilling, and geotechnical disciplines, and they are relatively simple tests which rely on observations and comparative results. There is limited understanding of their application to other disciplines.

The 90 bbl Fed Jel bentonite, the 125 bbl Fed Jel bentonite, and the attapulgite clays were selected for the short term compatibility study. The leachate consists of 20.1 milligrams per liter (mg/L) of Chromium, 6.50 mg/L of Fluoride, 623 mg/L of Nitrate, 522 mg/L of Sulfate, and 8.84 mg/L of Nickel. The leachate (groundwater) was sampled from an on-site existing monitoring well. The slurry properties of these materials are shown in Table 1. Water with a pH of 6.8 was used to prepare these slurry samples.[1]

Table 1. Slurry Properties

Properties	90 bbl Fed Jel bentonite	125 bbl Fed Jel bentonite	Attapulgite
Material by Weight (%)	6.4	5	4.8
Marsh Funnel Viscosity (sec)	42	42	44
Filtrate Loss (ml)	13	14	117
Density (g/cm^3)	1.03	1.02	1.02
pH	7.9	8.8	8.8

For each material, two slurry samples were prepared; first with water and then with leachate. Each slurry sample was subjected to filter press, chemical desiccation, and sedimentation tests which were performed as follows.

Filter Press Test

Slurry samples were prepared in accordance with American Petroleum Institute (API) Standard 12A and tested in accordance with API Standard 13B. Filter press testing was conducted on each slurry sample by pressurizing a chamber filled with slurry to a pressure of 689.5 KPa for 30 minutes to form a filter cake. The volume of water which flows out of the chamber is referred to as filtrate loss. Trench stability is dependent on a low filtrate loss.

For each slurry mix, two identical filter cakes were permeated with leachate and water. A ratio of the flow rate with the leachate to the flow rate with the water exceeding 2 indicates an incompatibility (Day 1993).

[1] 90 bbl and 125 bbl (barrels [42 gallons] of API standard mud per 1 ton of dry bentonite)

The test results are summarized in Figure 1, and indicate that the 90 bbl Fed Jel bentonite resulted in the highest flow rate ratio of 2.

Figure 1. Filter Press Test Results
Flow Ratio (leachate/water)-Pore Volume
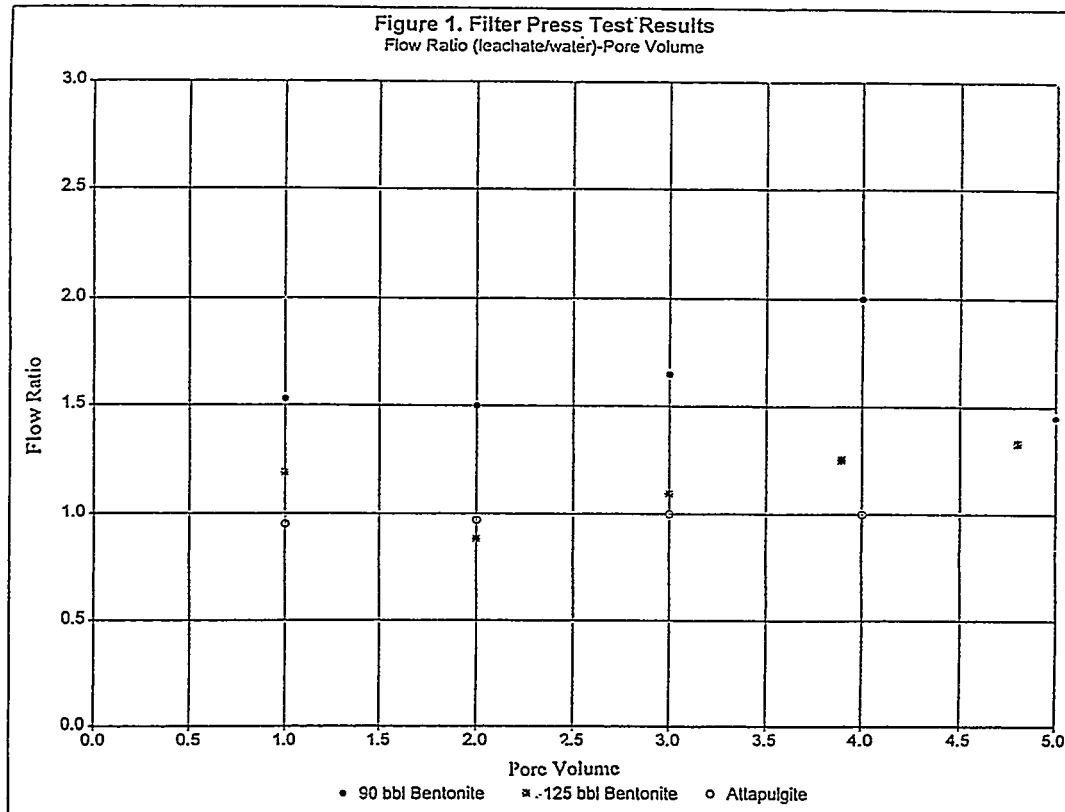
Two mechanisms have been explained (D'Appolonia 1980) that may contribute to the filter cake permeability increase. The first mechanism indicates that soil minerals may be soluble in the leachate, resulting in a mass loss of the bentonite and a corresponding increase in permeability. The second mechanism indicates that the pore fluid substitution may lead to a smaller diffused double layer thickness of the partially bound water surrounding the hydrated bentonite. As a result, the effective size of the bentonite particles is reduced, and the size of the effective flow channels and the permeability are increased. The change in the diffused double layer thickness (t) can be approximated by the following equation (Mitchell 1993).

$$t = (DKT/8\pi\eta\epsilon^2 v^2)^{0.5}$$

where D is the dielectric constant of the medium
      K is the Boltzmann constant = 1.38×10^{-16}
      T is the temperature in degrees centigrade
      η is the electrolyte concentration
      ϵ is the unit electronic charge = 16×10^{-20} coulomb
      v is the cation valence

The diffused double layer thickness (t) will decrease as the dielectric concentration and/or the valence increases. This means that if either the salt concentration of the pore fluid increases or the valence increases when the sodium ion of the bentonite (sodium montmorillonite) is exchanged with the multiple ions (such

as calcium) carried in the leachate, the net effect will be a reduction in the double layer thickness. This will result in increased permeability. Two to four pore volumes of the leachate must be permeated to fully replace the existing pore fluid and complete the cation exchange in order to achieve a steady state condition in which the permeability remains constant (D'Appolonia 1980).

Chemical Desiccation Test

The chemical desiccation test relies on observations of the slurry, and tends to model the most severe exposure. The chemical desiccation test is the process of air drying of the slurry in contact with the leachate on a glass plate. Often severe cracking, chemical reactions, or dissolution of the material particles can be observed (Day 1993).

Slurry samples were prepared in accordance with API Standard 12A. For each slurry mix, two identical slurry samples were prepared; one with leachate and one with water. Each slurry mix was placed on a glass plate. Visual observations were made on each slurry sample during the air drying process which lasted for a few days. These observations revealed that very large cracks formed on the 90 bbl Fed Jel bentonite sample prepared with the leachate and minor cracks formed on the 125 bbl Fed Jel bentonite sample prepared with the leachate. However, no cracks were observed on the attapulgite slurry samples or on the 90 and 125 bbl Fed Jel bentonite prepared with water.

Sedimentation Test

The sedimentation test relies on observations of the slurry, and tends to model the construction process when the slurry is used to support the trench walls. Evidence of flocculation or sedimentation can be observed during the test. Slurry samples were prepared in accordance with API Standard 12A. For each slurry mix, two identical slurry samples were prepared; one with leachate and one with water. Each slurry mix was placed in a glass cylinder. The sedimentation test lasted for a few days. Visual observations made on each slurry sample indicated that no sedimentation or flocculation occurred during the test.

Long Term Compatibility Study on Soil Bentonite and Soil Attapulgite Samples

Soil Sample Selection and Index Properties

Two type of soils, classified as Silty Sand material (SM) with 13% fines and Clayey-Silt material (CL-ML) with 51% fines in accordance with the Unified Soil Classification System (USCS), were selected for the long term compatibility study. Liquid and plastic limit tests were performed on these soil samples using first leachate and then water in order to assess the effect of the leachate on the plasticity index. The test results revealed that the plasticity index remained unchanged. The low pH of the material fines may influence the mix design (Kargbo, et.al. 1993).

Rigid Wall Permeability Test

The 125 bbl Fed Jel bentonite and attapulgite clay were selected for the long term compatibility study since no degradation of these materials was observed during the short term compatibility study. Rigid wall permeability tests, which are more cost effective than flexible wall permeability tests, were performed on eight samples. Each sample was permeated with 1 pore volume of water for a period of 12 days. The permeation continued with 3 pore volumes of leachate for an additional period of 36 days for the samples No. 1 through 4 and 1.5 pore volumes of leachate for an additional period of 13 days for samples No. 4 through 8. The testing parameters for each sample consist of a head pressure of 13.79 KPa and a hydraulic gradient of 19.5. Permeabilities obtained from the rigid wall permeability tests are shown in Figures 2 and 3. The results indicate that the leachate did not affect the permeability of these materials. The sample mixture and permeability test results are shown in Table 2.

81

Table 2. Sample Mixture and Permeability Test Results

Sample #	Sample Mixture Percentage by weight)	Permeability (cm/sec)
1	2% 125 bbl Fed Jel bentonite and 98% SM	2.5×10^{-7}
2	4% 125 bbl Fed Jel bentonite and 96% SM material	1.0×10^{-7}
3	2% 125 bbl Fed Jel bentonite, 40% CL-ML , and 58% SM	1.3×10^{-7}
4	4% of 125 bbl Fed Jel bentonite, 40% CL-ML , and 56% SM	5.2×10^{-8}
5	4% attapulgite and 96% SM	5.3×10^{-7}
6	8% attapulgite and 92% SM	2.3×10^{-7}
7	4% attapulgite, 40% CL-ML, and 56% SM	2.4×10^{-7}
8	8% attapulgite, 40% CL-ML, and 52% SM	1.3×10^{-7}

Figure 2. Rigid Wall Permeability Test
Soil-125 bbl Fed Jel Bentonite

Figure 3. Rigid Wall Permeability Test
Soil-Attapulgite

Time (Days)

• Sample 5   o Sample 6
▪ Sample 7   ✦ Sample 8
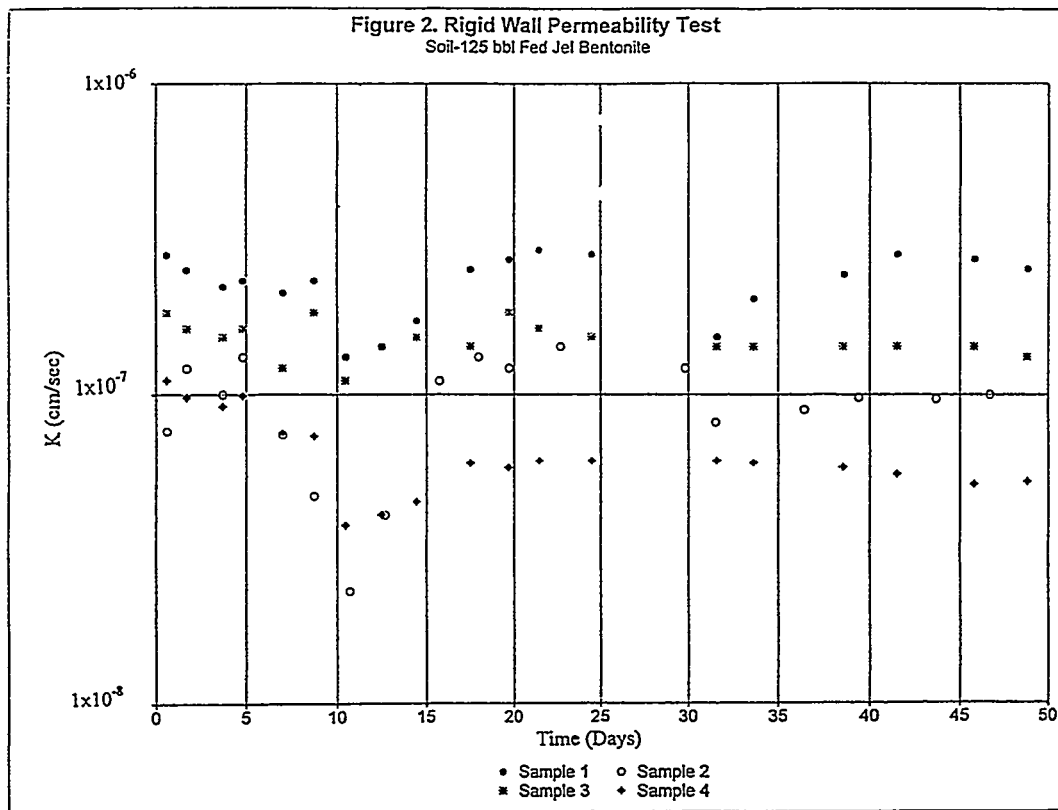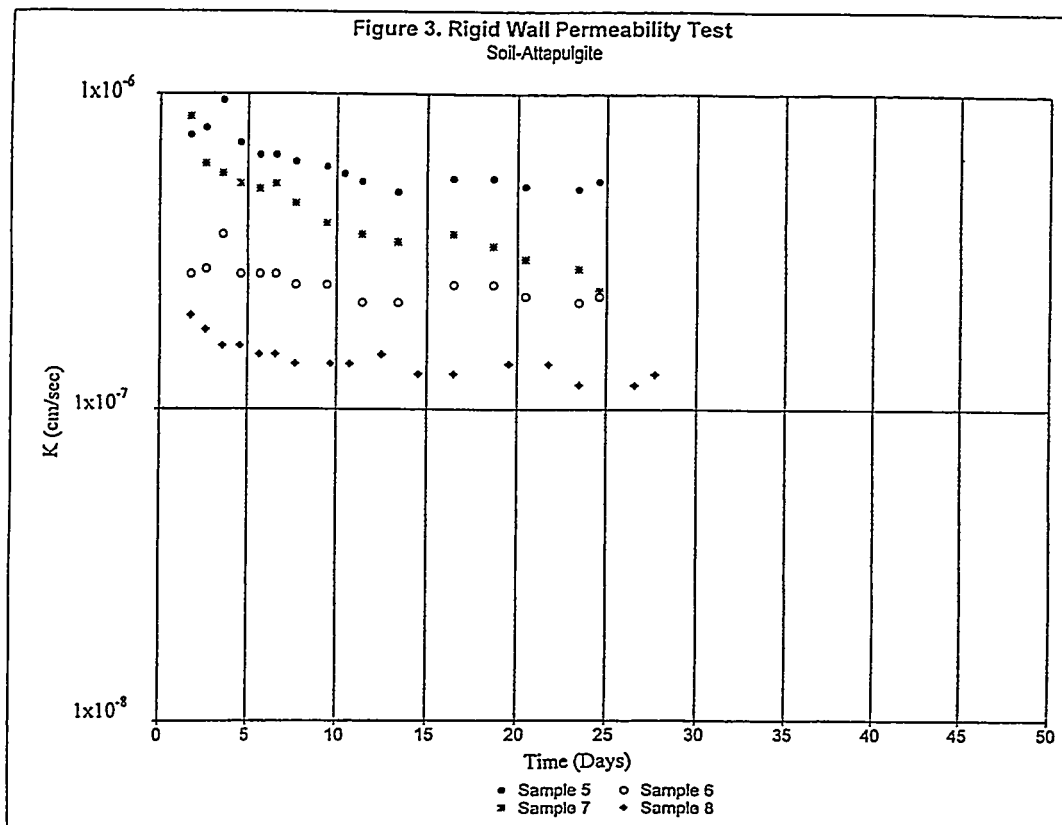
Flexible Wall Permeability Test

The 125 bbl Fed Jel bentonite, which is more cost effective than the attapulgite clay, was selected for the flexible wall permeability testing. The testing was conducted to determine the concentrations of bentonite needed to achieve the maximum permeability of 1×10^{-7} cm/sec. Flexible wall permeability tests were performed in accordance with ASTM D-5084 on four soil-125 bbl Fed Jel bentonite samples with the same mixtures as shown above (samples No. 1 through 4) to determine which mixes would achieve the required permeability. The testing parameters for each sample consist of a confining pressure of 344.75 KPa, a backpressure saturation of 248.22 KPa, and a hydraulic gradient of approximately 30. The permeability test results are 1.35×10^{-7} cm/sec and 1.00×10^{-8} cm/sec for samples No. 1 and 2, and 2.15×10^{-8} cm/sec and 6.10×10^{-9} cm/sec for samples No. 3 and 4 respectively.

Conclusions

The following conclusions are limited to the test results obtained from this study and observations made during the testing.

The material degradation of slurry trench cutoff walls under the exposure of low pH leachate may be assessed in a cost effective and timely manner by conducting short term compatibility studies, which include the filter press, sedimentation and chemical desiccation tests.

The filter press test results have shown that the volume of leachate permeated through the 90 bbl Fed Jel bentonite filter cake was approximately twice the volume of water permeated through the same filter cake. This may be explained by the fact that the degradation of the 90 bbl Fed Jel bentonite under exposure of the leachate has increased the permeability of the filter cake.

Large cracks on the 90 bbl Fed Jel bentonite and minor cracks on the 125 bbl Fed Jel bentonite were observed during the desiccation test for the samples prepared with the leachate.

Rigid and/or flexible wall permeability tests on the soil-90 bbl Fed Jel bentonite were not necessary since the 90 bbl Fed Jel bentonite degraded under exposure of the leachate.

Rigid wall permeability test results revealed that the low pH leachate had no effect on the permeability of samples No. 1 through 8.

Flexible wall permeability test results indicate that only sample No. 1 exhibited a permeability greater than 1×10^{-7} cm/sec due to the low amount of bentonite and low amount of fines in the soil.

Acknowledgments

References

Alther, G., Evans, J.C., Fang, H.Y., and Witner, K. (1985) Influence of Inorganic Permeants upon the permeability of Bentonite: Hydraulic Barriers in Soil and Rock, ASTM-STP 874, pp. 64-73.

D'Appolonia, D.J. (1980) Soil-bentonite Slurry Trench Cutoff Walls: Journal of the Geotechnical Engineering Division, Proceedings of the ASCE, Vol. 106, No. GT4, pp. 339-417.

Day, S.R. (1993) The Compatibility of Slurry Cutoff Wall Materials With Contaminated Groundwater: Geo-Con, Inc., Pittsburgh, PA.

Jepsen, C.P. and Place, M. (1985) Evaluation of Two Methods for Constructing Vertical Cutoff Walls at Waste Containment Sites: Hydraulic Barriers in Soil and Rock, ASTM STP-874, pp. 45-63.

Kargbo, et.al. (1993) Environmental Significance of Acid Sulfate Clays as Waste Covers: Environmental Geology, Vol. 22, No. 3, pp. 218-226.

Mitchell, J.K. (1993) Fundamentals of Soil Behavior: John Wiley & Sons, Inc., New York.

The Effect of Freeze-Thaw Cycles on the Hydraulic Conductivity and Structure of a 10% Sand-Bentonite Mixture

Thomas F. Zimmie[1], Juan D. Quiroz[2] and Christine M. LaPlante[2]

Abstract

Sand-bentonite barriers have often been used for landfill covers and liners at waste containment facilities where clay is not readily accessible. Freeze-thaw effects have been well documented for compacted clay barriers which generally show an increase of hydraulic conductivity from one to three orders of magnitude. However, previous research indicates that sand-bentonite barriers are not affected by three dimensional freeze-thaw cycles. In this paper, a sand-bentonite mixture of 10% bentonite content was subjected to one and three dimensional freezing and thawing in the laboratory. One dimensional freezing simulates in-situ conditions and yields different freezing patterns than three dimensional freezing. Once the specimens reached specified cycles (1, 5, 10, and 15) of freeze-thaw, the hydraulic conductivity was determined. Hydraulic conductivity tests on specimens with an initial value of 4.8×10^{-9} cm/s changed to a value of 4.0×10^{-9} cm/s after fifteen one dimensional freeze-thaw cycles and 3.4×10^{-9} cm/s after ten three dimensional freeze-thaw cycles (i.e., virtually no change in hydraulic conductivity) proving that one dimensional and three dimensional freezing and thawing produce similar results. In addition, frozen thin sections and x-rays were prepared of specimens to evaluate the effects of freeze-thaw on the structure of the soil. A hydraulic conductivity unaffected by freeze-thaw is important in areas where sub-zero degree Celsius temperatures are encountered.

Introduction

The primary goal of a containment barrier is to maintain its hydraulic properties throughout its design life. For landfill design, the typical minimum hydraulic conductivity (k) required by the regulatory agencies is 10^{-7} cm/s (Othman et al. 1994). In areas where clay is not readily available, sand-bentonite mixtures are often used to provide low hydraulic conductivity barriers.

In areas where sub-zero degree Celsius temperatures are encountered the effects of freeze-thaw cycles becomes an important issue. The effects of freeze-thaw on the hydraulic conductivity of containment barriers made of natural materials (i.e., clay) are well documented (Othman et al. 1994). In general, compacted clays show an increase of hydraulic conductivity from one to three orders of magnitude due to freezing and thawing. Such increases in hydraulic conductivity can adversely affect the conditions of the containment facility.

The greatest structural changes in soils can occur when ice lenses are formed. Ice crystals/lenses exert pressure on each other and the surrounding soil, inducing structural changes within the soil. The soil between the ice interlayers is consolidated and crack networks are formed when the ice lenses thaw (Andersland and Anderson 1978, Andersland and Ladanyi 1994).

The main focus of this research was to study the effects of freeze-thaw cycles on the hydraulic conductivity and structure of a 10% (based on total dry weight) sand-bentonite barrier mixture. Previous research indicates that there is no change in hydraulic conductivity for three

---

[1] Professor, Department of Civil Engineering, Rensselaer Polytechnic Institute, Troy, NY 12180, (518) 276-6939, zimmit@rpi.edu
[2] Graduate Research Assistant, Department of Civil Engineering, Rensselaer Polytechnic Institute, Troy, NY 12180, (518) 276-8143, quiroj@rpi.edu

dimensionally (3-D) frozen and thawed sand-bentonite mixtures (Wallace 1987, Wong and Haug 1991, Haug and Wong 1993). In this study, specimens were subjected to one and three dimensional freeze-thaw cycles in the laboratory. One dimensional (1-D) freeze-thaw experiments were performed to simulate in-situ conditions, and 3-D freezing was performed as a control and for comparison to previous research results. Once specified cycles (1, 5, 10 and 15) of freeze-thaw were reached the hydraulic conductivity was determined. In addition thin sections were prepared of frozen specimens and x-rays were taken of thawed specimens to evaluate soil structure.

Freeze-Thaw Effects on Compacted Clays

A number of researchers have shown that freeze-thaw cycling in low hydraulic conductivity compacted clays (typically 10^{-7} to 10^{-9} cm/s) will increase the hydraulic conductivity from one to three orders of magnitude (Chamberlain et al. 1990, Zimmie and LaPlante 1990, Zimmie et al. 1992, Othman and Benson 1992, Wong and Haug 1991). The state-of-the-art paper by Othman et al. (1994) presents the results of a number of research projects dealing with freeze-thaw effects on the hydraulic conductivity of compacted clays and discusses items such as open systems vs. closed systems, dimensionality of freezing (i.e., 1-D vs. 3-D freeze-thaw cycles), number of freeze-thaw cycles, ultimate temperature, rate of freezing and state of stress of soil.

An open system has an external water supply available during freezing while a closed system has no external supply of water during freezing. In most cases properly designed and constructed compacted clay barriers will not have a continuous supply of water available. Chamberlain et al. (1990) and Zimmie et al. (1992) showed that while freezing and thawing in both systems caused increases in hydraulic conductivity, the increases were similar. Since most compacted clay landfill liners and covers are constructed wet of optimum, and thus are almost fully saturated, it is felt that the availability of water in an open system causes little or no additional increase in hydraulic conductivity.

In the field, soil generally freezes one dimensionally as the freezing front descends. However, in the laboratory it is much simpler to apply 3-D freezing to soil specimens, thus saving time and expense. Othman and Benson (1992) examined thin sections from samples that were one and three dimensionally frozen, showing that the structural changes were different depending on the dimensionality of freezing, but that the changes in hydraulic conductivity were similar. Zimmie and LaPlante (1990) and Othman and Benson (1992) evaluated the changes in hydraulic conductivity due to 1-D and 3-D freeze-thaw cycles and concluded that the increases in hydraulic conductivity were similar.

The largest increase in hydraulic conductivity occurs during the first few cycles of freezing and thawing. After three to ten freeze-thaw cycles, increases in hydraulic conductivity are usually not significant (Chamberlain et al. 1990, Zimmie and LaPlante 1990, Othman and Benson 1992, and Wong and Haug 1991).

The amount of hydraulic conductivity increase due to freezing and thawing is a function of effective overburden stress, with the largest increases occurring at low stresses and smaller increases at high stresses. Freezing and thawing generally does some permanent damage, since it takes very high pressures to return the hydraulic conductivity to its unfrozen value (Othman et al. 1994). This could be important in the case of a landfill liner exposed to freezing temperatures prior to waste placement. It is unlikely the stresses produced by waste placement will be sufficient to return the hydraulic conductivity to its original unfrozen value.

Landfill covers are shallow, with low overburden stresses, and hence hydraulic conductivity increases due to freezing and thawing can be expected to be permanent.

86

Freeze-Thaw Effects on Sand/Bentonite Hydraulic Barriers

Previous research indicates that closed system 3-D freezing and thawing performed in the laboratory on sand-bentonite covers does not significantly increase the hydraulic conductivity (Wallace 1987, Wong and Haug 1991 and Haug and Wong 1993). All testing was done at moisture contents wet of optimum since that is common practice for landfill covers and liners. Also, the maximum number of freeze-thaw cycles applied to the specimens in these studies was five and ten.

Wallace (1987) concluded that a 2% sand-bentonite mixture showed no change in hydraulic conductivity for remolded specimens that were subjected to ten freeze-thaw cycles and permeated with a synthetic leachate. Wong and Haug 1991 tested five sand-bentonite mixtures (4.5%, 6%, 8.3%, 13%, and 25%) which were subjected to five freeze-thaw cycles under low confining stresses. A flex-wall triaxial permeameter was used for the 4.5% mixture and a rigid wall set up with a triaxial permeameter was used for the other specimens. In all cases the hydraulic conductivity decreased less than an order of magnitude, which implies no significant change in hydraulic conductivity. Haug and Wong 1993 tested an 8% sand-bentonite mixture subjected to five freeze-thaw cycles and two wet-dry cycles, in rigid molds under no confining stress, using standard Proctor and modified Proctor compactive efforts. An increase in hydraulic conductivity (less than one order of magnitude) was observed but that increase disappeared after the wet-dry cycle for the standard Proctor effort.

In general, these studies indicate that no significant change in hydraulic conductivity occurs for sand-bentonite mixtures subjected to 3-D freeze-thaw cycles in the laboratory. The purpose of this study was to utilize 1-D freezing to better simulate in-situ conditions and to evaluate changes in hydraulic conductivity and soil structure due to 1-D freezing.

Testing Procedure

The testing program consisted of subjecting 10% (bentonite content) sand-bentonite specimens to 1-D and 3-D freeze-thaw cycles. The specimens were molded at about three percent wet of optimum. Once the specimens reached a specified number (1, 5, 10 and 15) of freeze-thaw cycles the hydraulic conductivity was determined. The hydraulic conductivity tests were performed using a flexible wall triaxial device (ASTM D-5084). In addition x-rays and frozen thin sections were used to evaluate the soil structure.

Materials

A poorly graded medium to fine sand was used to provide a uniform medium and to minimize hydraulic conductivity variations between specimens that occur in well graded sands. The grain sizes vary between 0.1-0.8 mm, $C_u = 1.7$, $C_c = 1.2$ and the USCS (Unified Soil Classification System) classification is SP (implying a sand that is poorly graded).

The bentonite selected is a commercial bentonite called Quik-Gel® produced in powder form by Baroid Drilling Fluids. This bentonite is commonly used for seepage barriers. The bentonite consisted of a finely ground sodium montmorillonite which consists of 85% montmorillonite, 5% quartz, 5% feldspar, 2% cristobalite, 2% illite and 1% calcium and gypsum.

Tap water was selected as the mixing fluid in accordance with ASTM D-5084. Preliminary hydraulic conductivity testing in our lab showed that mixing with distilled/deionized water produced piping (soil particles washed out by seepage forces).

Sample Preparation

The following sample preparation procedure was used during this testing program:

1. Dry mixed predetermined sand and bentonite quantities were mixed in a sealed plastic bag (to reduce loss of bentonite) for about 10 to 15 minutes. Note that the bentonite content is based on total dry weight. About 2.5 kg of total dry weight is recommended for thorough mixing.

2. The target amount of water was added to the soil, and mixed thoroughly for 15-20 minutes.

3. The soil was placed in sealed plastic bags and hydrated for a minimum of 12 hours. Moisture equilibrium throughout the sample was verified. If the water contents were within a half percent then the moisture was stabilized throughout the sample.

4. Once the sample was hydrated and the moisture stabilized, the samples were ready for specimen preparation.

Specimen Preparation

After sample preparation a standard Proctor test (ASTM D-698) was performed (Figure 1). Specimens were extruded, then trimmed and placed in a triaxial permeability device to determine the initial hydraulic conductivity vs. water content curve (Figure 2). As expected, the minimum hydraulic conductivity occurs slightly wet of optimum moisture content.

Specimens were prepared at a water content 3% wet of optimum which corresponded to a water content of 22.5% and a γ_{dry} of 15.62 kN/m^3 (99.4 lb/ft^3). The standard Proctor compactive effort was applied to specimens in a 101mm (4 in.) long polyvinyl chloride (PVC) mold with a 76 mm (3 in.) diameter. The specimens were double wrapped with plastic wrap to minimize loss of moisture. The soil specimens prepared in this manner were unconfined in the vertical direction and confined in the lateral direction.

Freezing and Thawing

The specimens were frozen both 1-D and 3-D in the PVC molds in an environmental room at a constant temperature of -15° C. The detailed procedure followed is outlined in LaPlante and Thomas (1989). Several representative specimens were instrumented with thermocouples to show that 1-D freezing was occurring (i.e., the freezing front was descending uniformly across the specimen). When the specimens reached a temperature of -8° C they were allowed to thaw.
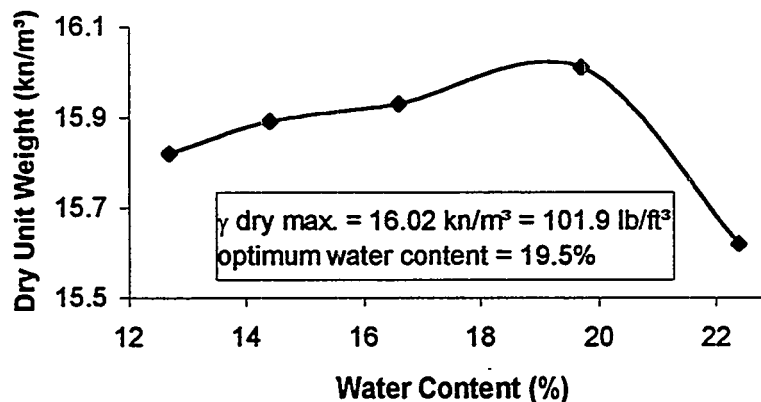
Figure 1. Standard Proctor curve for the 10% sand-bentonite mixture.

The 1-D freezing apparatus consisted of stacked insulation blocks with 101mm (3 in.) holes wherein the specimens were placed. The tops of the specimens are exposed to freezing temperatures while the bottoms are exposed to warmth produced by a heating blanket and air

line, thus establishing a thermal gradient. The freezing of the 1-D specimens typically lasted about 40 hours, starting with an unfrozen temperature about 20° C. Note that the overburden pressure is zero, the most conservative case since overburden pressure would decrease structural and hydraulic conductivity changes produced by freeze-thaw cycles.

Hydraulic Conductivity Testing

At specified numbers of freeze-thaw cycles (1, 5, 10 and 15) the hydraulic conductivity was determined per ASTM D-5084. The specimens were extruded frozen, coated with a thin paste of bentonite, and then they were placed in a triaxial permeability device. The bentonite paste was used to ensure adhesion to the flexible wall membrane and prevent sidewall leakage. The specimens were allowed to thaw and consolidate for one day under an effective stress of 34.4 kPa (5 psi) followed by backpressure saturation to 275.6 kPa (40 psi) for another day. Permeation was initiated and continued until inflow equaled outflow and hydraulic conductivity was constant.
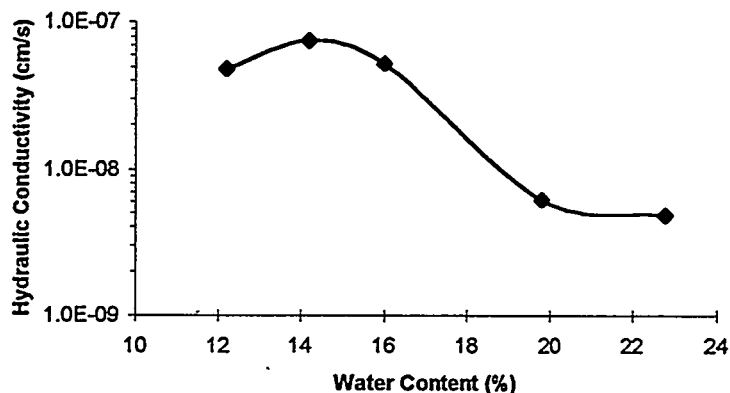
Figure 2. Initial hydraulic conductivity vs. water content curve

Structure Evaluation

Frozen thin sections were prepared to study the macrostructure of the sand-bentonite mixture. The thin sections were milled in a cold room at a temperature of -8° C. The specimens were cut horizontally or vertically and attached to a glass slide with supercooled water droplets. They were then milled to a thickness of about 1 mm and placed on a light board for observation. A more detailed description of the thin section preparation procedure is outlined in Moo-Young (1995).

X-rays were also taken at zero and five 1-D freeze-thaw cycles. The x-rays were performed with the thawed soil in the PVC mold. X-ray results appear more useful than thin section results. The entire specimen can be imaged by x-rays, and cracks caused by freezing and thawing are easily observed. Thin sections only examine a small portion of the specimen, and often major cracks are missed. In addition, the thin section preparation process causes some soil disturbance, whereas specimen disturbance can be avoided by the use of x-rays.

Results and Discussion

The results indicate that there is no effect on the hydraulic conductivity of the sand/bentonite samples due to freezing and thawing. The initial hydraulic conductivity for specimens molded at three percent wet of optimum was 4.8×10^{-9} cm/s. As shown in Figures 3 and 4 the hydraulic conductivity of the sand-bentonite mixture did not change, whether frozen

one dimensionally or three dimensionally. Similar research performed on compacted clays indicate that increases in hydraulic conductivity due to freeze-thaw cycles occur within the first three to ten cycles for 1-D or 3-D freezing (Othman et al. 1994). For comparison Figures 3 and 4 also show the results of freeze-thaw experiments on compacted Niagara Clay specimens molded at three percent wet of optimum. The compacted clay specimens were tested using the same procedures utilized for the sand-bentonite samples (Zimmie and LaPlante 1990).

X-ray and frozen thin section analyses were performed to evaluate the macrostructure of the specimens. The x-rays were taken on the same specimen both before freezing and after five 1-D freeze- thaw cycles. X-rays of the unfrozen specimens indicate a quite homogeneous structure. However, the lift interfaces are quite evident. On x-rays of specimens subjected to five freeze-thaw cycles, the soil structure is still homogeneous and no cracks are evident, however the lift interfaces are much less prominent. This may indicate a healing process.
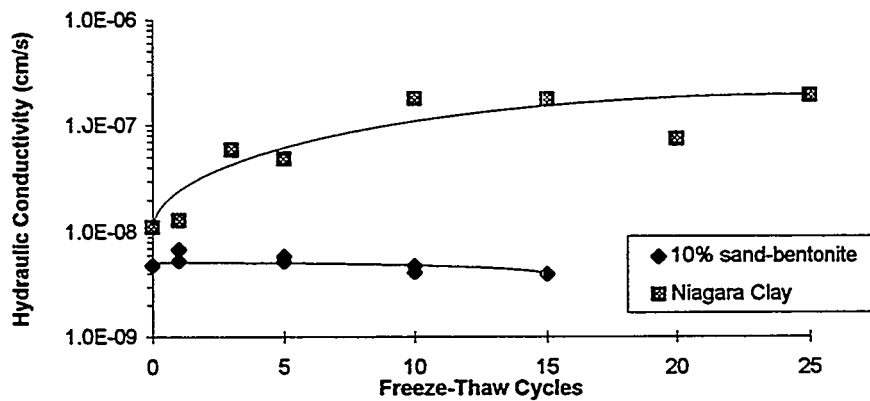
Figure 3. One dimensional freeze-thaw effects on the 10% sand-bentonite mixture and Niagara Clay
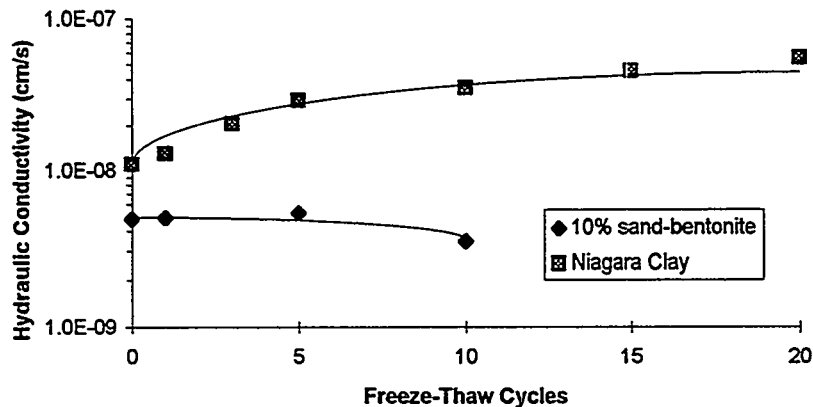
Figure 4. Three dimensional freeze-thaw effects on the 10% sand-bentonite mixture and Niagara Clay.

Both horizontal and vertical thin sections were also prepared to analyze the macrostructure of the sand-bentonite samples. The thin sections did not show any visible structural changes. Thus it appears the freeze-thaw process had little or no effect on the sand-bentonite structure.

The lack of structural changes in the sand-bentonite samples may be due to the nature of the compacted sand skeleton and the montmorillonite clay water interactions. As compared to a compacted clay specimen, the hydrated bentonite restricts flow through the soil matrix lowering the permeability of the sand-bentonite mixtures (Wong and Haug 1991).

The results of this study clearly indicate that sand-bentonite mixtures utilized in containment applications are not susceptible to effects produced by freeze-thaw cycles. Hydraulic conductivity tests performed on 1-D and 3-D frozen specimens showed no significant changes. X-ray techniques and thin section analyses also verified the absence of structural changes in the sand-bentonite samples.

References

Andersland, O.B. and Anderson, D.M. (1978) *Geotechnical Engineering for Cold Regions*, New York, NY.

Andersland, O.B. and Ladanyi, B. (1994) *An Introduction to Frozen Ground Engineering*, New York, NY.

Chamberlain , E.J., Iskander, I. and Hunsiker, S.E. (1990) Effect of Freeze-Thaw on the Permeability and Macrostructure of Soil. In *Proceedings, International Symposium on Frozen Soil Impacts on Agricultural, Range, and Forest Lands*, pp. 145-155. Spokane, WA.

Haug, M.D. and Wong, L.C. (1993) Freeze-Thaw Effects on Hydraulic Conductivity of an Unconfined Soil-Bentonite Cover Material. In *Proceedings, Forty Sixth Canadian Geotechnical Conference*, pp.193-201. Saskatoon, Saskatchewan, Canada.

LaPlante, C.M. and Thomas, M.B. (1989) The Effect of Freeze/Thaw Cycles on the Permeability of Niagara Clay. *Master of Engineering Thesis*, Rensselaer Polytechnic Institute, Troy, NY.

Moo-Young, H.K. (1995) Evaluation of Paper Mill Sludges for Use as Landfill Covers. *PhD Thesis*, Rensselaer Polytechnic Institute, Troy, NY.

Othman, M.A. and Benson, C.H. (1992) Effect of Freeze-Thaw on the Hydraulic Conductivity of Three Compacted Clays from Wisconsin. *Transportation Research Record*, 1369, 118-129.

Othman, M.A., Benson, C.H., Chamberlain, E.J. and Zimmie, T.F. (1994) Laboratory Testing to Evaluate Changes in Hydraulic Conductivity of Compacted Clays Caused by Freeze-Thaw: State of the Art. In *Hydraulic Conductivity and Waste Contaminant Transport in Soils, ASTM STP-1142* (eds. D.E. Daniel and S.J. Trautwein), pp. 227-254. American Society for Testing and Materials, Philadephia, PA.

Wallace, J.F. (1987) Laboratory Testing of Bentonite Amended Soil Mixtures Proposed for a Mine Waste Disposal Facility Liner. In *Geotechnical and Geohydrological Aspects of Waste Management* (eds. D.J.A. Van Zyl et al.), pp. 245-258. Chelsea, MI.

Wong, L.C. and Haug, M.D. (1991) Cyclical Closed-System Freeze-Thaw Permeability Testing of Soil Liner and Cover Materials. *Canadian Geotechnical Journal*, 28, 784-793.

Zimmie, T.F. and LaPlante, C.M. (1990) The Effects of Freeze-Thaw Cycles on the Permeability of a Fine-Grained Soil. In *Proceedings, 22nd Mid-Atlantic Industrial Waste Conference*, pp. 580-593. Philadelphia, PA.

Zimmie, T.F., LaPlante, C.M., and Bronson, D.L. (1992) The Effects of Freezing and Thawing on the Permeability of Compacted Clay Landfill Covers and Liners. In *Proceedings of the Mediterranean Conference on Environmental Geotechnology*, pp. 213-217. Balkema, Rotterdam.

Chapter 3

Slurry Walls: Cementitious & Composite

CONTAINMENT BARRIER AT PRIDE PARK, DERBY, ENGLAND

Peter Barker[1], Annette Esnault[2] and Peter Braithwaite[3]

ABSTRACT

The Pride Park site at Derby occupies 96ha of derelict land close to the city centre. Approximately one third of the site was a closed landfill with a further third being an old gas works site. The remainder comprised former heavy engineering works and gravel pit workings. The River Derwent bounds the site on two sides.

The objectives of the remediation strategy for the site included minimising off-site disposal of contaminated soils and ensuring that contaminants do not migrate into the adjacent river. The eastern part of the site, including the landfill and gasworks sites, was therefore contained by a 600mm wide bentonite cement vertical cut-off wall, with HDPE membrane, sealed by 1m into the underlying mudstone. The cut-off wall is some 3km long and a maximum 10m deep. The works were complicated by the need to construct the wall around 36 existing underground services.

The paper briefly covers the background to the remediation of the site, describes the construction process and discusses design considerations in relation to the durability requirements of the containment barrier in the potentially aggressive environment.

BACKGROUND

Introduction

The Midlands of England was, in the late 18th and early 19th Centuries, the centre of the industrial revolution and the home of the country's iron and steel making industries. By the mid 20th century manufacturing industry had gone into decline leaving vast areas of derelict land often very close to city centres. Over the last few years, efforts have been made to remove this blight and aid regeneration of the region by introducing alternative industries and services.

Derby City, in the East Midlands, is one such area. Derby was the centre for heavy engineering works related to the railway industry. Economic changes have left about 80 hectares of land derelict within approximately 1 mile of the city centre. This area has been stifling the redevelopment of the city. The land was previously used for domestic/industrial landfill, coke and gas production, heavy engineering works and gravel extraction.

In 1992 Derby City Council was successful in bidding for special government funding from the City Challenge Programme. This programme was set up to aid regeneration and promote inward investment and social improvements for decaying industrialised cities. Derby Pride Limited was set up to administer the funding necessary to deliver the city challenge goals, of which the development of Pride Park was the flagship proposal. City Challenge funding provided essential "pump priming" for the project as much of the remediation works had to be implemented before any profit from land sales could be ploughed back into the project.

This paper describes how one of the main elements of the reclamation strategy, the three kilometres long bentonite cut-off wall, was designed and installed to protect a highly sensitive target, the River Derwent, from contamination both during and after reclamation and development works.

---

[1] Bachy, Godalming Business Centre, Catteshall Lane, Godalming, Surrey, GU7 1XW, UK, 01483/427311

[2] Bachy, 4 rue Henri Sainte-Claire Deville, 92563 Rueil Malmaison, Cedex, France, 01/4714 2600

[3] Ove Arup & Partners, 3 Duchess Place, Edgbaston, Birmingham, B16 8NH, UK, 0121/454 8853

Site Description

A number of site investigations had been carried out over parts of the Pride Park site prior to the award of city challenge funds and the retention of Ove Arup & Partners as Reclamation Engineers. These investigations produced some 800 soil samples which were taken for chemical testing, for a total of 22 different determinants. This early work identified major contamination issues to be addressed which included oil, tars, phenols, heavy metals, ammonia, boron and even some low level radioactive materials based below the landfills.

The site is generally level and as shown in Fig. 1 is bounded to the north and east by the River Derwent and to the south and west by the main rail line between Derby and London. Old buildings have been demolished, except two large gas holders which are still in use. The former Derby to London canal, which is completely filled in, runs through the centre of the site as does a trunk combined sewer. In general, the soils follow the sequence of fill (up to 7m thick) overlying alluvium, terrace gravels and Mercia Mudstone. Groundwater was generally about 4m below surface.

Borehole tests had indicated that landfill gas was continuing to be generated within the old closed landfill.

Reclamation Strategy

Figure 1: Site Plan.

Prior to developing the reclamation strategy Arup created a three dimensional contamination model which was used to produce a constraints model identifying particular areas of elevated contamination for both soil and groundwater. For example, the model can be used to identify the constraints imposed by the worst class of very contaminated soils or for particular determinants. The model can also plot contaminants at various depths below surface, which is of prior importance when determining remediation options. The model indicated that the site could generally be split into eastern and western halves. The eastern half, comprising the old landfill and gas works, had the most highly contaminated soils and even more highly contaminated groundwater. The western half which formerly comprised gravel pits and engineering works, had localised and impersistent areas of contamination both in type and level. The groundwater under this part of the site was generally uncontaminated. The two principle objectives considered during the development of the reclamation strategy were to minimise the off site disposal of contaminated soils and to ensure that contaminates do not migrate into the River Derwent.

Below the landfill and gas works, high contamination levels extended to at least 10m below surface which made removal impractical and uncommercial. The strategy for this part of the site was to safely contain the contaminates within the soils and groundwater by enclosing the area with a bentonite cement cut-off wall sealed into the underlying Mercia Mudstone. A gas venting
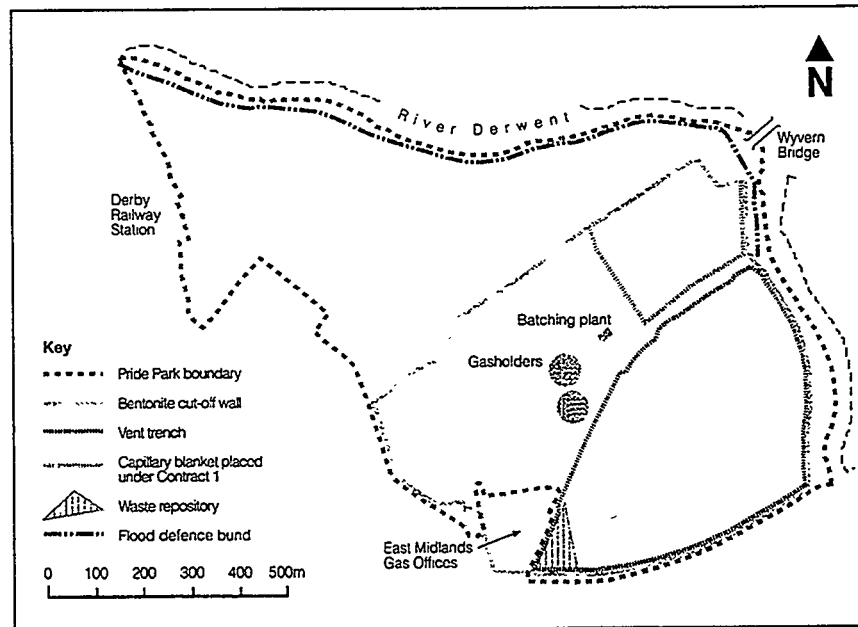
trench would encircle the landfill to prevent landfill gases migrating beyond the limits of the landfill. The surface of the landfill and gas works site within the cut-off wall would be protected by a permeable capillary break blanket. This 650mm thick blanket of graded stone was designed to ensure that in periods of drought the capillary rise of any contaminant would be less than the thickness of the blanket. Precipitation can percolate through and into the landfill but end users are protected by the capillary break blanket. To minimise the amount of material to be removed off site, a fully engineered landfill was designed by Arup and constructed on site. This is located within the bentonite cut-off wall to take 36,000m³ of the most highly contaminated soils arising from the rest of the site.

The western, less contaminated, part of the site would have less intensive treatment, with removal of localised elevated levels of contaminated soils. The basic elements of the reclamation strategy are shown in Fig 1.

Hydrogeological Modelling was used to predict the effect that the bentonite cut-off wall would have on both internal and external groundwater levels. Groundwater levels outside of the wall would rise up gradient by about 0.7m as a result of impedance of groundwater flow created by the wall. This was acceptable to the surrounding structures and ground levels.

Field pumping trials and further hydrogeological analysis were used to predict the rate of groundwater rise within the bentonite cut-off wall. This was complicated by the upward flow of groundwater through the Mercia Mudstone. A system of abstraction and treatment wells would be installed inside of the cut-off wall to control the level of groundwater and ensure that water levels inside the wall would always be at or below those outside. If the wall should fail, or be breached, then clean water would flow into the site rather than contaminated water flowing out. A secondary benefit of the capillary break blanket solution is that by encouraging infiltration through the landfill, over time the soluble contaminates will be washed out of the waste and a gradual clean up of the wastes will occur.

CUT-OFF WALL

Scope

The cut-off wall was to have a minimum thickness of 600mm and to extend from finished reclamation level to penetrate a minimum of 1m into mudstone (Fig 2). The scope of the works is summarised below:

Length	-	3000m
Area	-	22000m²
Max. depth	-	10.2m
Min depth	-	5.1m
Average depth	-	7.4m
Service crossings	-	36 No
Membrane panels	-	560 No
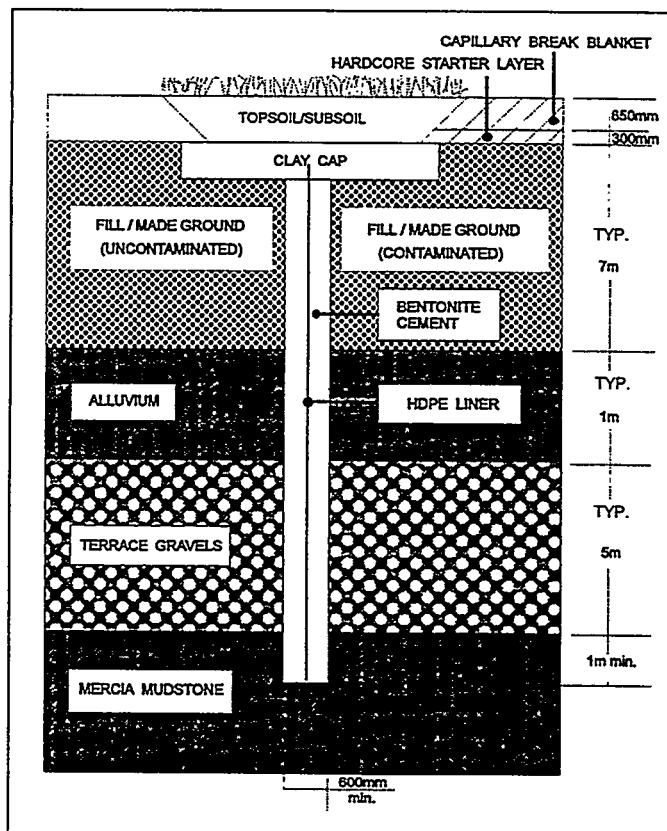
Figure 2: Section through Bentonite Cut-Off Wall.

97

The line of the cut-off wall and also the location of the slurry batching plant is indicated in Fig 1. At the time of writing the cut-off wall is both the longest and has the largest elevational area of any such wall in the UK. At no time previously had service crossings of the frequency and depth of those encountered at Derby been accommodated within a vertical containment barrier.

Specification

The cut-off wall was required to comprise bentonite/cement slurry and HDPE membrane. The slurry was required to achieve a maximum permeability to water of 1×10^{-8} m/sec at an age of 28 days, a minimum undrained shear strength of 25kPa at 14 days, a minimum unconfined compressive strength (UCS) of 150kPa at 90 days, and to have a minimum strain at failure of 3% at an effective confining pressure of >120kPa at 90 days (consolidated drained triaxial compression test). The HDPE membrane was required to have a minimum sheet thickness of 2mm, and no point of the membrane and panel jointing system was to have an overall permeability to water exceeding 1×10^{-9} m/sec. Minimum tensile stress and elongation at yield and break were also specified.

Slurry Mix Design

On the basis of results from previous contracts carried out by Bachy, together with results of laboratory trials utilising materials from sources to be used on site, the following slurry mix design was used:

- Ground granulated blastfurnace slag   120 kg/m³   • Sodium Bentonite   35 kg/m³
- Ordinary Portland Cement   30 kg/m³   • Water   934 litres

Admixtures were used to assist with the mixing process, reduce filter loss in the trench and, when necessary, to retard the initial set of the slurry to enable placing of the HDPE membrane.

Slurry Production

The bentonite/cement slurry was mixed in a batching plant set up on site in the location shown in Fig. 1. An idealised plant layout is shown in Fig 3. Bentonite, cement and ground granulated blastfurnace slag were delivered to site in pressurised tankers in 24 tonne loads. They were stored on site in dry powder silos.

The mixing took place in 3 stages. In the first stage a master mud, comprising approximately 90% of the total mix water and the bentonite powder, was mixed thoroughly (UFB mixer) and stored overnight in tanks to allow hydration. In the second stage

Figure 3: Batch Plant Layout.

the cementitious material (OPC & GGBS) was mixed (FCP mixer) with the remaining 10% of the water. The third stage involved transferring both the hydrated master mud and the freshly mixed

cementitious slurry to a large 10m³ capacity mixer (BRC) where the final slurry was produced. The maximum daily slurry production was 280m³ whilst the average throughout the works was 180m³.

During slurry production, regular checks, up to three times per day, were made on the density of both the master mud and the final slurry (by mud balance) to confirm the correctness of the mixing process. These checks were in addition to weekly calibration of the mixer weigh scales. Checks were also carried out on the viscosity (by Marsh Cone) to confirm suitability for both pumping to the trench and the excavation process. The stability of the mix was checked by placing samples in a 1 litre covered measuring cylinder and measuring any bleed water after a period of 24 hours, with a maximum value of 4%.

Construction - General

On 20 June 1994 Bachy Ltd were appointed by Morrison Construction, the Main Contractor for the works, to construct the vertical containment barrier, designed by Ove Arup and Partners. Construction was programmed to start on 29 June, but due to the late award of the sub-contract, wall construction did not commence until 18 July.

The main constraints to the construction sequence were the requirement for early completion of the road corridor to allow the Wyvern Bridge to be constructed for access to the site over the River Derwent, late access to the East Midlands Gas Depot and Office Area, where the majority of the services were located, and the need to accommodate the 36 service crossings into the overall construction programme (Fig 1).

Excavation of the cut-off wall was carried out by long arm backhoe. As soon as excavation was commenced, the bentonite/cement slurry was pumped (via 100mm diameter steel pipes, maximum distance 1.5km) to the trench. Excavation continued under the slurry until the top of the Mercia Mudstone was identified in the trench arisings. The depth of the trench was then measured using a weighted tape and excavation continued to achieve the required minimum 1m penetration into the mudstone. The depth to the mudstone and final depth of the cut-off wall were recorded at 1m intervals along the whole length of the cut-off wall. The trench arisings were generally placed alongside the trench and removed by Morrison Construction once the slurry on the arisings had set.

Figure 4: Geolock Joint Detail.

When the required depth had been reached, and before the slurry had set, the HDPE membrane was installed. The HDPE membrane was supplied to site in 5.7m wide panels, cut to length in accordance with a schedule of anticipated cut-off wall depths. The Geolock joints (Fig 4) had previously been manufactured and factory fitted by Geotechnics Holland BV.

Expansion profile before installation

Final volume after approximately 40 hours

Each membrane panel was fitted at its base with small sacrificial plates which hook into locating points at the base of a placing frame. The top of the panel was then attached to tensioning devices and the panel tensioned onto the frame. The panel and frame together were then lifted by crane and placed into the fluid slurry to the base of the trench. A further panel and frame together were then lowered into the trench with the joint sections interlocking, the Hydrotite section being located in the female part of the
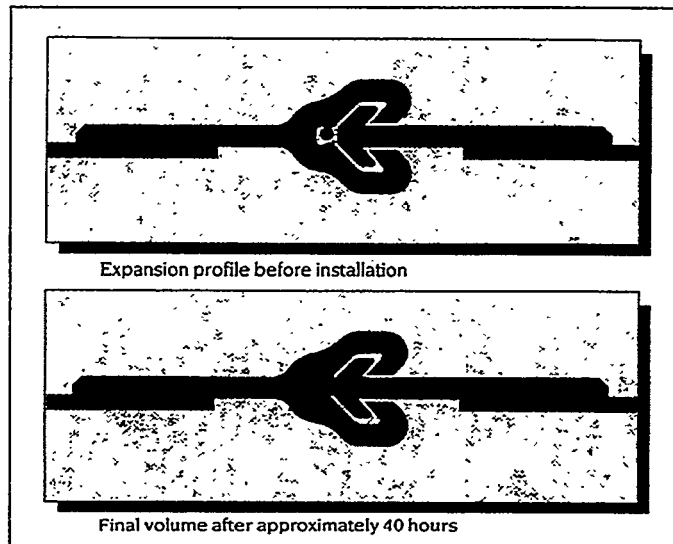
joint as a slack fit. Once the second panel had been installed the first panel was released from the frame (by releasing the tensioning devices) and the frame withdrawn. The locking and sealing of the joint was then completed by the Hydrotite absorbing water from the slurry mix and swelling to potentially ten times its dry volume. The jointing system has been tested in the laboratory in both the USA and UK and found to be effective up to pressures across the joint exceeding 5 bar, which is far in excess of the likely field conditions.

Construction continued with excavation of the trench closely followed by installation of the membrane. Temporary stopends were installed, attached to the Geolock joint, at the end of each working day in order to protect the membrane from damage during excavation for placing of the adjacent panel. The maximum number of membrane panels installed in one day was eight.

Samples of bentonite/cement slurry were obtained from the trench after completion of excavation and before installation of the membrane, at a rate of a sample set every 20m length of wall, or for each day's production. A set comprised 2 samples each from the top, middle and bottom of the wall. Once the samples had been obtained (with a remote sampler operated from the surface) the fluid slurry was placed in 100mm diameter plastic tubes, 450mm long. They were sealed on site and allowed to set for 2 weeks before transfer to a specialist laboratory for testing.
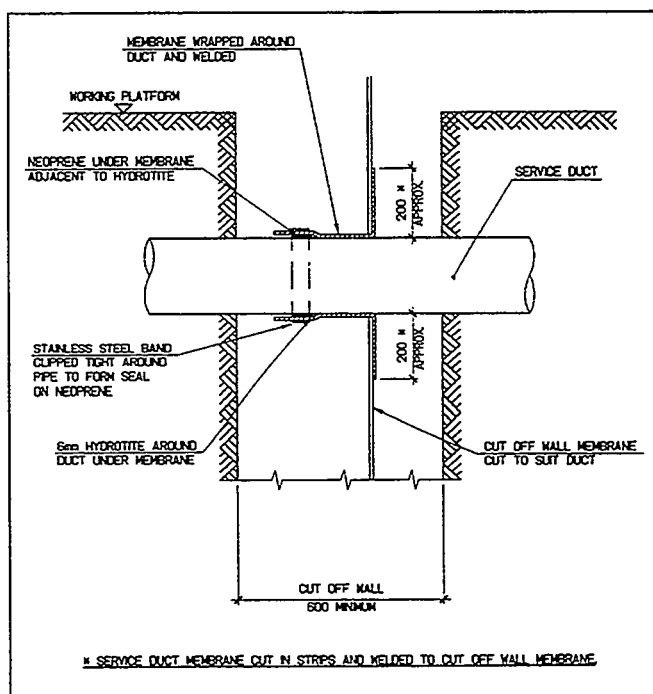
Figure 5: Service Duct Crossing.

Construction - Services

As noted above, the line of the cut-off wall was crossed by 36 services which required to be accommodated. Wherever possible the cut-off wall was completed around the service in advance of the main run, and temporary stop ends installed on the HDPE membrane to allow subsequent connection. The final detail is shown schematically (Fig 5). The method of achieving this detail varied from case to case but can be summarised as follows:

1. Expose service by hand and excavate below the service to the required depth under slurry.
2. Position double male membrane, with cut out for service, on part height frame next to service. With top part of membrane rolled under, move membrane and frame under service. Allow slurry to set.
3. Wrap service with membrane sleeve over neoprene and Hydrotite. Weld membrane and seal with stainless steel band. Unfold membrane panel around service pipe and weld to membrane sleeve.
4. Top up with slurry and install stop ends to await tie-in.

For the deep interceptor service crossings, of which their were two, it was necessary for Morrison Construction to install sheet pile cofferdams to allow access to the sewers and carry out local dewatering. The whole of the cut-off wall was constructed in a period of 26 weeks.

Compliance Testing

A total of 922 samples of slurry were taken for set slurry testing. Tests were carried out on 305 of those, as selected by the Engineer, to determine shear strength (Cu) at 14 days, permeability at 28 days, strain at 90 days and UCS at 90 days. The results are summarised below:

Test type	Requirement	No. of tests	% complying
Cu @ 14 days	> 25 kPa	76	100
Perm. @ 28 days	< 1 x 10^{-8} m/sec	81	90
Strain @ 90 days	> 3% @ > 120 kPa ECP	71	93
UCS @ 28 days	> 150 kPa	77	100

Capping

From an age of 7 days onwards, the top 0.5m of slurry was carefully removed from around the set bentonite/cement slurry by hand and the membrane, which had been left protruding above ground level, was trimmed to the required level with a sharp knife. The ground level was reduced by 0.5m over a width 2.5m either side of the wall centreline, and the whole was backfilled with a clay capping to prevent the slurry from drying and protect it from damage, so as to form the typical detail shown (Fig 2).

CUT OFF WALL DURABILTY

As previously stated, the contamination at the site is mainly represented by heavy metals, polynuclear aromatic hydrocarbons and phenols found in various concentrations in ground and groundwater.

Compounds identified as potentially harmful towards a bentonite/cement slurry are as follows, with a brief description of mechanisms of action:

acids : a destruction of the cementitious compounds occurs upon reaction with the calcium-based components of the hydraulic binder.

sulphates : their reaction with aluminates leads to the formation of expansive salts such as gypsum and ettringite whose crystallisation may provoke cracking.

sulphurs : under certain conditions, their oxidation leads to the formation of sulphates. The oxidation of H_2S generates sulphuric acid which is well known for its aggressivity.

ammonium : a reaction of exchange occurs between Ca++ and NH_4+ leading to a partial dissolution of the cement calcium based components.

phenols : the aggressivity is due to their acid tendency

heavy metals : they may cause expansion and cracking of the cementitious matrix by exchange with calcium ions.

aromatics such as PAHs : when mixed with the slurry, the reaction of hydration may be slowed down due to coating of the particles of cement.

The level of aggressivity depends of course on the concentration of each element. Provided a mixture of Ordinary Portland Cement and Ground Granulated Blast Furnace Slag is used, the following limits are usually taken:

- pH above 4.5
- sulphate : below 6000 mg/l
- ammonium : below 100 mg/l

- sulphides : below 5 mg/l
- phenols : below 10 mg/l
- PAHs : below 10 % in the slurry

The durability of the slurry mix itself was assessed, and whilst the average values calculated in relation to the concentrations of the above contaminants are not considered detrimental to the slurry mix design used on site, the maximum concentrations found on sulphates and ammonium

and the minimum pH values are potentially harmful. However in order for there to be significant deterioration of the slurry there would have to be sufficient quantities, as well as concentrations, of the contaminants in contact with the wall.

Examination revealed that only about 8% of the trial pit samples and 5% of the borehole samples showed contamination of sufficient intensity to have the potential to damage the bentonite/cement slurry. The spacial distribution of these hot spots of contamination showed the majority to be isolated and situated away from the line of the wall. There did appear to be a concentration of hot spots of soil contamination in the area of the north end of the road corridor. However, these were generally from shallow samples, such that the material concerned was to be removed by the bulk earthworks operations.

The cut-off wall as constructed, comprising a 600mm thick bentonite/cement slurry wall and a 2mm HDPE membrane, is therefore sufficient to withstand the contamination revealed.

When needed and within certain limits, the durability of conventional bentonite/cement slurry can be enhanced by the use of specific agents such as pozzolanic materials (fly ash, silica fume, etc.), soluble sodium silicate, special clays, etc. However, it must be pointed out that the use of an HDPE membrane to form a composite cut-off wall is the best available technology with respect to durability and low permeability. As a general rule it is considered that to use an enhanced slurry mix in a composite barrier with HDPE to withstand contamination is unnecessary.

ENVIRONMENTAL MONITORING

An extensive environmental monitoring system was developed prior to any works on site, to monitor air quality, soil and groundwater conditions during and after the reclamation works.

Validating the performance of the cut-off wall is via a series of monitoring holes drilled through the made ground on either side of the wall. As the purpose of the wall is primarily to isolate the heavily contaminated groundwater below the landfill and old gas works from the River Derwent and cleaner groundwater to the east, monitoring is concentrated on analysing the condition of groundwater.

The groundwater extraction system is designed to keep water levels within the cut-off wall at or below that outside, so that monitoring groundwater levels either side of the wall is a good indicator of its continued integrity. Any suspect readings can be backed up by analysing the quality of groundwater. If the analysis indicates that contamination is present outside of the wall, then that section can be remediated by construction an additional length of wall adjacent to the suspect section.

The design life of the wall is anticipated to be about 50 years. As time passes, the groundwater abstraction system will lead to gradual improvements in the water quality within the wall. It is anticipated that by the time the wall reaches the end of its design life, soluble contaminants within the wall will not be significantly greater than those outside and replacement will not be necessary.

CONCLUSIONS

The 3000m long cut-off wall was successfully installed and closed within a period of 26 weeks and testing of slurry samples indicated greater than 90% compliance with the specification. This has resulted in releasing approximately 60ha of land for development, demonstrating the speed of this remediation technique.

The contract value to the Client was £1.57m or £61.6/m^2 which is very competitive with any other form of remediation, including dig and cart away.

Since completion of the cut-off wall, three development plots have been sold off including a major 8.5ha development plot for the construction of a football stadium for Derby County Football Club.

The design and installation of the bentonite/cement slurry wall at Pride Park, Derby has, therefore, demonstrated the cost effectiveness and speed of this form of reclamation solution.

CUT-OFF WALL SYSTEM FOR SUBSURFACE LIQUID CONTAINMENT

R.Carlson, Rollins Environmental Services (TX) Inc., Deer Park, TX, USA
F.Khan, P.E., Rollins Environmental Services (TX) Inc., Deer Park, TX, USA

ABSTRACT
The subject of this paper is the use of a Cut-off Wall System (CWS) in conjunction with conventional soil bentonite slurry walls. The system is a vertical subsurface containment solution for isolating contaminated soils and groundwater in situ, thereby enhancing protection of the environment. The CWS is composed of geomembrane panels and specially designed connectors that form an interlocking subsurface vertical barrier wall. This system provides a cost effective, easily installed, positive cut-off for isolation of mixed and hazardous wastes, and wastes from uncontrolled releases. This application will address manufacturing, fabrication, installation, strength, QA/QC, chemical compatibility, and permeability.

INTRODUCTION
Conventional soil-bentonite (SB), soil-cement (SC), cement-bentonite (CB) and soil-cement-bentonite (SCB) slurry walls have been used for years, primarily in geotechnical applications as subsurface means for cut-off and diversion of lateral flowing liquids, as well as for containment of waste streams resulting from leaking landfills and impoundment basins. Over the last 5 to 6 years, emerging concerns from various regulatory agencies have been voiced questioning the effectiveness of the conventional slurry wall. Some of these concerns addressed the construction techniques and the type of backfill materials used in the mix. In particular, improperly mixed slurry and backfill, collapse of trench during excavation or backfill, long term desiccation of walls due to water table fluctuation, freeze thaw behavior, and chemical compatibility of the wall to the liquids to be contained limit the effectiveness of conventional slurry walls. Some waste constituents would attack and eventually filter through the walls, deeming them useless and ineffective. This has lead to the development of various synthetic panel systems to be used either with or without conventional slurry walls for improved containment and diversion of liquid flows when dealing with chemical waste.

This paper focuses on the development of such a system. In particular, a recently patented subsurface barrier wall system that has received agency approval and is currently in use as part of an ongoing Part "B" corrective work program in Texas, will be explored. This paper will address the design, manufacturing/fabrication, connection clean-out and inspection, grouting, installation methods, chemical compatibility, barrier wall application, and laboratory testing of the system.

DESIGN
The use of High Density Polyethlyene (HDPE) geomembrane to contain lateral flowing liquids from landfills and impoundments has been in existence for a number of years. The geomembrane sheets are available in widths ranging from 4.5 to 9 meters (15 to 30 feet), and are thermally bonded by either an extrusion or fusion process. The basic concept for the synthetic vertical barrier wall is the same as landfill liners, in that it serves as a separator between the two areas. However, the main difference between the two systems is that the HDPE vertical barrier wall panels are the "lock and key" type connection and the use of a grout or hydrophilic gasket as a sealant. The patented barrier wall system uses grout as a sealant which creates a more tortuous path for fluid migration. The installation of the synthetic vertical barrier wall achieved by forming a trench, filling the trench with dense soil to form a primary barrier, inserting the initial panel within the primary barrier to form a secondary barrier, inserting successive panels within the primary barrier system, and finally grouting the interlocks.

The panel design for the connectors and sheets is illustrated by Figures 1 through 4 contained in the Appendix. Figure 1 illustrates a fragmented view of the outer and inner connectors. The outer connector is comprised of a HDPE pipe (typically 7.6 cm) having a slot lengthwise, a flap lengthwise and a bottom

endcap. The inner connector consists of a smaller diameter pipe (typically 5 cm), a flap lengthwise and perforated holes drilled at the bottom of the pipe as shown in Figure 1.

A modular panel consists of a 5 cm diameter inner connector, a 7.6 cm diameter outer connector, and a precut HDPE sheet. Figure 2 shows a schematic cross-section view of a modular panel, wherein a plastic HDPE sheet (typically 100 mil thickness and 2.3 meter wide) has the inner connector (5 cm diameter pipe) attached at one end and the outer connector (7.6 cm diameter pipe) attached to the other end. The inner and the outer connectors are bonded to the HDPE sheet by an extrusion process. A modular panel is connected to the adjacent modular panel by inserting the inner connector of one panel into the outer connector of another connector through the slot as shown in Figure 3. One of the advantages of the connection is its ability to make 90 degree turns, or any other oblique angle by simply changing the location of the slot in the desired direction. Figure 4 illustrates two modular panels connected at a 90 degree alignment.

MANUFACTURING / FABRICATION
Depending upon service requirements, vertical barrier walls can be manufactured from most plastics. The panel wall sheet is typically fabricated from standard 100 mil HDPE, and the HDPE connectors are manufactured through an extrusion die process. The unique design of the pipe connector and flap assembly is very adaptable to panel assembly. The male and female connections are cut to length, end caps secured to the outer tube, and clean-out and grouting holes installed on the bottom of the inner tube. Panel sheets are then aligned and welded to the flap connection. Holes are then placed in the bottom of the panel and brackets placed onto the end of the connection tubes to provide attachments for installation of the panel. Once assembled, the welded seams are tested for leaks in accordance with the project specifications. These panels can either be fabricated under shop or field conditions depending upon project needs.

CONNECTION CLEAN-OUT, INSPECTION & GROUTING, CLEAN-OUT / INSPECTION
The tubular design of the connection allows for thorough clean-out and ongoing inspection of the connection during installation of the system. This is accomplished by inserting an inflatable packer and pipe assembly into the inner pipe creating a water tight seal. As shown in Figure 3, water is pumped through the connection flushing out any materials that may have entered during panel installation. This flush-out process is continued until all the solid material is removed from the connection and washwater appears clear.

GROUTING
Following clean-out of the connection, the preferred grout material is pumped into the connection utilizing the same procedure as described for the clean-out of the connection. Both a cement based non-shrink grout and a three-component epoxy grout were tested, exhibiting excellent strength and permeability properties. The test procedures for permeability were set up to mimic the actual field conditions and are described in detail under the "Laboratory Testing" section of this paper.

INSTALLATION METHODS
A unique aspect of the system is its utilization of a vibratory insertion plate. The insertion plate is fabricated from 1.9 cm carbon steel plate and light weight I-beams and angle iron (see Figure 5) and it can be designed to fit most panel widths and lengths. Its unique pipe bracket design cradles and secures the two connectors and panel membrane, preventing possible damage to the panel during installation. The geomembrane is fixed at its base with 1.9 cm diameter carbon steel pins or dowels protruding from the bottom of the plate. A vibratory driver, (ICE Model 416) supported by a crane, is attached to the top of the insertion plate and used to vibrate the entire assembly into the slurry supported trench. The insertion plate is then removed leaving the geomembrane panel in place. The plate has been prepared to provide a slick surface for easy separation during the removal phase of the operation. In addition, the insertion plate is fitted with high pressure water discharge nozzles to further facilitate its removal following placement of the panel. Subsequent panels are then inserted through the slot of the outer pipe of the preceding panel in place, creating a continuous barrier wall.

CHEMICAL COMPATIBILITY

Prior to specifying panel materials and grouts, compatibility studies, in accordance with the EPA Test Methods 9090, and 9100 should be conducted respectively, using site specific wastes and/or leachates that will come into intimate contact with the panel wall system. Material selection for the modular panels and connections should be based on these waste-to-liner compatibility test results. Both the panel and connection members are made from the same base resin materials. High Density Polyethylene (HDPE) geomembrane materials were chosen for our project located in Deer Park, Texas due to their superior properties against chemical exposure, resistance to water vapor transport, and semi-crystalline plastic make-up which makes it resistant to chemical permeation.

BARRIER WALL APPLICATION

Barrier walls containing geomembranes are an excellent choice in any application where the flow of water or other liquids is to be controlled. There are many different types of applications for vertical barrier walls. The Department of Energy (DOE) and the Environmental Protection Agency (EPA) are presently investigating the feasibility of using barrier walls as part of their final closure of many contaminated sites. The effectiveness of slurry walls in all applications is dependent upon the configurations and depth as well as the associated remedial measures (such as groundwater pumping) applied in conjunction with the barrier wall at a particular site. The site conditions that determine both configuration and associated remedial measures include setting, both geologic and geographic waste characteristics, and the nature of the environmental problems existing at the site. The configurations refer to the positioning of the barrier wall with respect to the source of contamination and groundwater flow characteristics. The three most widely used configurations are: circumferential wall placement, upgradient wall placement, and downgradient wall placement. A circumferential wall is used to completely isolate waste within a site by placing the barrier wall all the way around the waste. A surface barrier layer (cap) is often used in conjunction with the barrier walls in order to greatly reduce the amount of leachate generated within a site. An upgradient wall is placed on the groundwater source side of a waste site. This type of placement can be used where there is a relatively steep gradient across the site, to divert uncontaminated groundwater around the waste. Drainage and diversion structures are likely to be needed to successfully alter the flow of clean groundwater. A downgradient wall is placed at a waste site on the side opposite the groundwater source. The application does nothing to limit the groundwater form entering the site and therefore, is only used in situations such as drainage dividers, where there is limited groundwater flow from upgradient. It should be noted that this positioning does not reduce the amount of leachate being generated, but acts as a barrier to contain the leachate so it can be recovered for treatment. The barrier walls are "keyed" into a low permeability formation below the aquifer in order to contain contaminants that mix or sink to the bottom of the aquifer. In some applications, the barrier wall is used in conjunction with groundwater pumping, surface and subsurface collection, surface sealing, and vapor extraction. The type of remedial measures depends upon site specific conditions.

LABORATORY TESTING

One of the most important properties for barrier walls is low permeability to liquids. There have been hundreds of chemical compatibility tests performed using EPA 9090 test method on HDPE sheets with a variety of municipal and hazardous leachates without a single failure. In fact, it is the author's opinion that the compatibility of HDPE against chemicals is well documented as an efficacious method of containment. Due to the dearth of information, it was imperative to investigate the strength and permeation resistance of the patented interlocks. Laboratory testing of the HDPE interlock connections was performed by a qualified independent testing laboratory to evaluate the tensile property (pull-out) and the hydraulic conductivity of the grouted connection. The test procedures for both the tensile and the permeability (hydraulic conductivity) tests are summarized in the following sections.

Tensile test: The purpose of the tensile test was to determine the force required to pullout the 2 inch inner pipe from the 3 inch outer pipe. The test results obtained were used to make an evaluation of whether the connections could withstand longitudinal forces during the panel insertion and normal operational life of the system. It was monitored and proven during actual panel installation and laboratory testing that the transverse forces experienced by the modular panels during installation will be minimal due to controlled downward movement of the insertion plate, additional spacing provided by the annular space in the connectors, flexibility of the panel connector, and increased sliding motion created by the tubular design of the connectors. The tensile test procedures for assessing the strength of the connections required drilling 1 cm diameter holes at 5 cm centers on both the 5 and 7.6 cm HDPE flap. Two pieces of 3.8 cm angle iron with similar hole pattern was mounted to each side of the HDPE flap to securely clamp the flap. A 15 cm square tube with a longitudinal slit was fabricated as an attachment device to simply mount the angle iron to the upper and the lower platen of the testing apparatus. A calibrated testing machine was used with the loading range set appropriately to achieve one percent accuracy of the indicated load. Load was then applied continuously without shock at a rate of 0.63 cm per minute until failure. A total of six specimens with length ranging from 5 to 32 cm were tested. The test results are summarized in the following table.

TABLE 1. TENSILE TEST RESULTS

SAMPLE NO	SAMPLE LENGTH	MAXIMUM LOAD	MAX. LOAD PER UNIT LENGTH
1	31.75 cm (12.5")	291 kg (640 lb)	916 kg/m (614 lb/ft)
2	4.83 cm (1.90")	36.4 kg (80 lb)	754 kg/m (505 lb/ft)
3	5.38 cm (2.12")	43.6 kg (96 lb)	810 kg/m (543 lb/ft)
4	5.16 cm (2.03")	41.8 kg (92 lb)	810 kg/m (544 lb/ft)
5	29.08 cm (11.45")	277.3 kg (610 lb)	954 kg/m (639 lb/ft)
6	29.01 cm (11.42")	300.0 kg (660 lb)	1034 kg/m (694 lb/ft)

AVERAGE: 880 kg/m (590 lb/ft)

Since the combined weight of the insertion plate and the HDPE panel is lower than the pullout capacity of the interlock (880 kg/m) it is unlikely that the HDPE interlock connection will be separated by the force induced by installation process. The grouting technique requires that the grout be pumped inside the 5 cm pipe then allowed to flow up through the annulus between the 5 and 7.6 cm pipe and overflow at the surface. If the HDPE interlocking connection were to separate during the installation process in an extremely unlikely event, it will obviously be detected during the grouting operation since grout will be lost in the formation and will not fill the 5 cm by 7.6 cm annulus .

Hydraulic Conductivity Test: The hydraulic conductivity tests were performed on the grouted HDPE interlock connections to assess the permeation resistance of the interlock. Special testing procedures and conditions were developed and monitored by qualified independent consultants. A total of five different grout products were tested to evaluate shrinkage and permeability characteristics. The trial mix grout batch proportions are summarized as follows: (a) Bentonite clay grout-Puregold, (b) Cement based nonshrink grout-Euclid, (c) Cement based nonshrink, nonmetallic grout- Five Star Grout, (d) Three-component epoxy grout - Brutem MP, (e) 50% bentonite with 50% Five Star grout and, (f) 75% bentonite with 25% Five Star grout. All grout batches were mixed and placed strictly in accordance with manufacturer recommendations. In order for the grout to fill the 5 cmX7.6 cm annulus, 1.27 cm diameter holes were drilled at the bottom 5 cm of the inner pipe and an end cap was welded to the bottom of the 7.6 cm pipe. Subsequently, a 10 cm diameter half round pipe was welded to the flap of 5 cm and 7.6 cm pipe. The top and the bottom of the 10 cm half round pipe was closed with 250 mil HDPE liner by extrusion process to create a water tight chamber (see Figure 6). A water inlet one-way valve and an air outlet valve were installed on the side of the water pressure chamber. An inflatable donut shaped packer

was inserted at the top of the 5 cm pipe in order to create a seal for pressure grouting. Grout was then pumped into the bottom of the 5 cm pipe until it filled the 5 cm pipe and the annulus between the 5 and 7.6 cm pipes completely and overflowed from the top. The grout was allowed to cure for 7 days at room temperature prior to the hydraulic testing. The sample was allowed to saturate for at least 24 hours at 34.5 kpa pressure. The tests were performed utilizing gradients which consisted of an equivalent hydraulic head of 34.5, 69, and 138 kpa. The tests were started at 34.5 kpa and the permeant volume versus time measurements were recorded and the hydraulic conductivity of the test specimen was determined. Once the steady state flow was established, the hydraulic head was increased to an equivalent of 69 and 138 psi and the volume versus time measurement was repeated. At the conclusion of the permeability tests, the samples were cut for post test inspection.

Based upon inspection and test results, it appears that Five Star nonshrink grout and the three component epoxy grout- Brutem MP exhibited very low permeabilities. In fact, the epoxy grout did not have any flow through the samples after 10 days of tests under 123 kpa of head pressure. The pure bentonite also exhibited low permeability at head pressure less than 34.5 kpa, however, pure bentonite squeezed out of the connection through the slot at a higher pressure. The grout/bentonite mixture exhibited average permeability values of 1.7X10EE-6 cm/sec but did not meet our target values 1X10EE-7 cm/sec. Therefore, a cement based grout or epoxy should be used for head pressure higher than 35 kpa.

CONCLUSION
The potential for conventional slurry wall failures resulting from the incompatibility of clay backfill to certain known chemicals and the lack of construction quality control support the use of secondary wall containment systems. HDPE geomembranes have been used in long term buried applications for years and as bottom liners for landfill applications. Now the technology is available to achieve the same degree of safety, impermeability, and compatibility in a vertical orientation. The geomembrane panel system inserted into the conventional slurry trench and joined side by side by interlocking mechanisms, provides an effective barrier against fluid migration.

There are many known contaminated sites existing throughout the world. Currently the DOE and the EPA are searching for new technologies for the long-term containment of hazardous waste sites. It is the opinion of this author that the geomembrane vertical barrier wall is an innovative technology that provides a viable and superior alternative for waste containment

REFERENCES

Carlson, R.J. (1995); "Cut-off Wall System to Isolate Contaminated Soil", United States Patent Number 5,388,931.

Koerner, R.M. and Guglielmetti, J.L. (1995), "Vertical Barrier", a chapter in International Containment Workshop Final Report, R.E. Rumer, Ed. Baltimore, MD.

Rollins Environmental Services Inc. (1996), Hydraulic Conductivity Test Results of HDPE Interlock Connections, Professional Service Industries, Houston, TX.

Rollins Environmental Services Inc. (1995), Tensile Testing of HDPE Interlock Connections, Professional Service Industries, Houston, TX.

Thomas, R. (1995), "Advances in HDPE Barrier Walls", Proceedings of the 9th GRI Conference - Philadelphia, PA
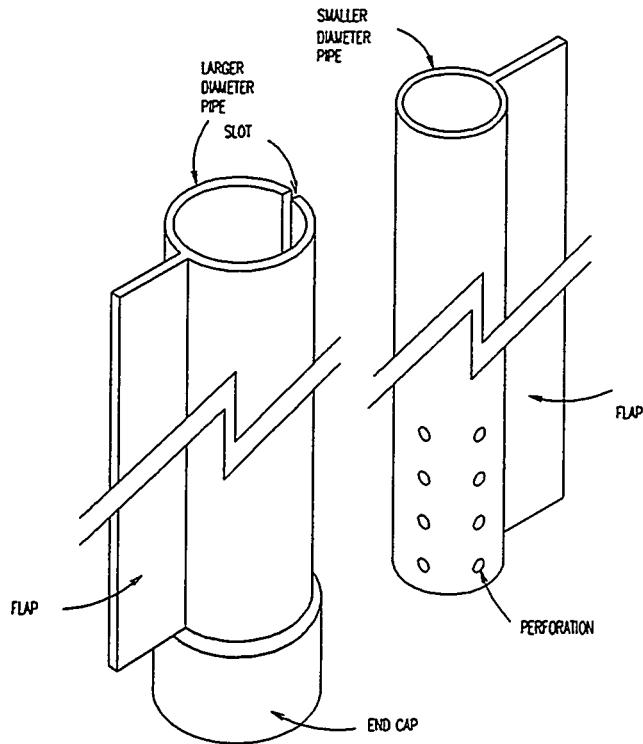
FIG. 1

FRAGMENTED VIEW OF OUTER &
& INNER CONNECTOR
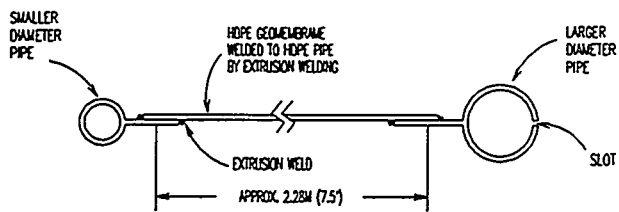
FIG. 2

CROSS SECTION OF A MODULAR PANEL
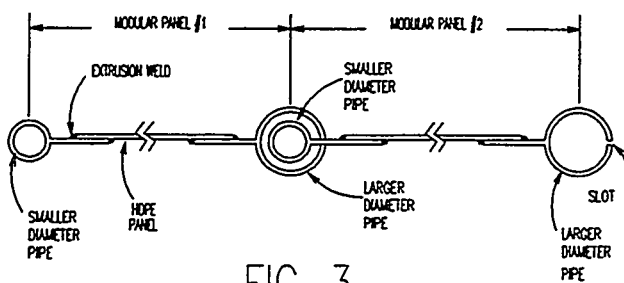
FIG. 3

MODULAR PANELS CONNECTED AT 180 DEG.
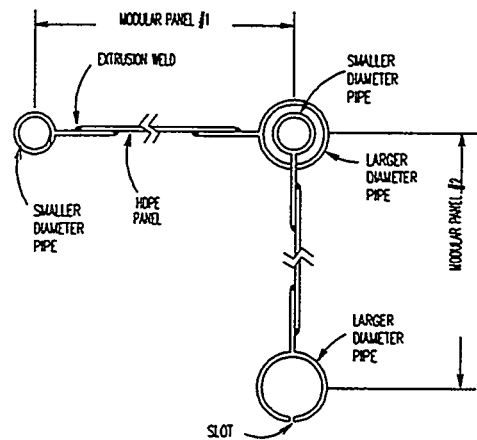
FIG. 4

MODULAR PANELS
CONNECTED AT 90 DEG.
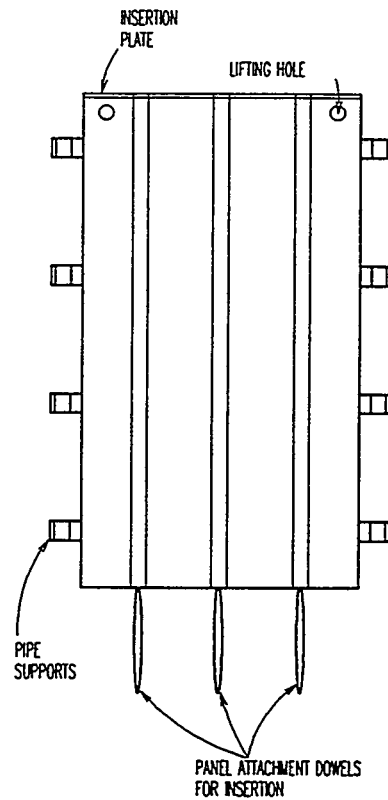
FIG. 5

PANEL INSERTION PLATE

109
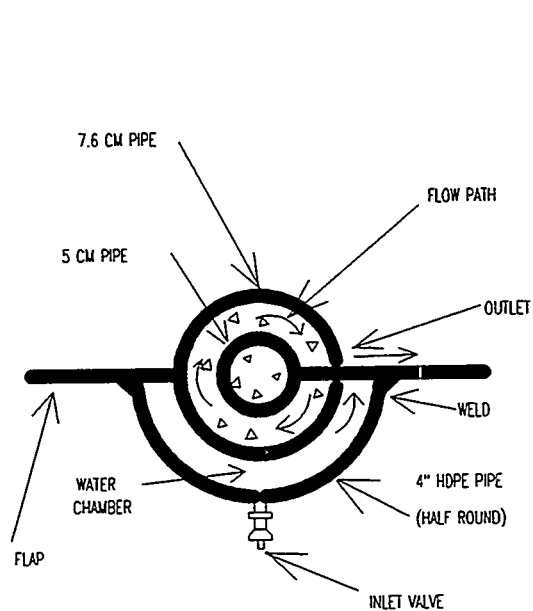
FIGURE 6: PERMEABILITY TEST SET-UP
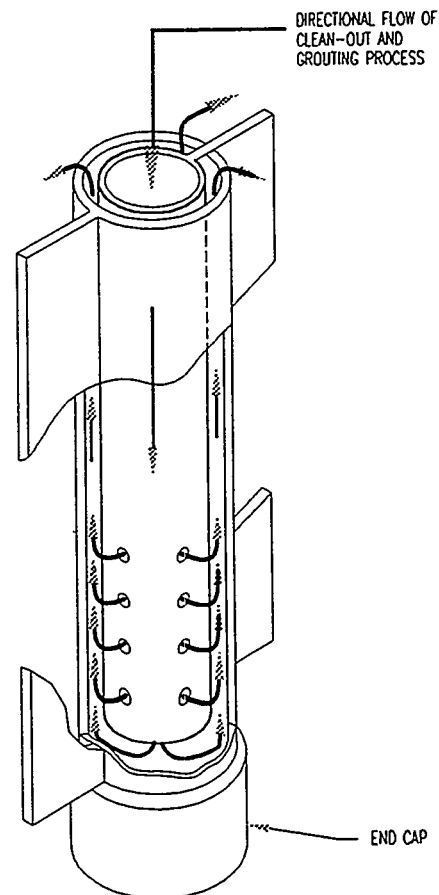
FIGURE 7: CLEAN-OUT AND GROUTING OPERATION
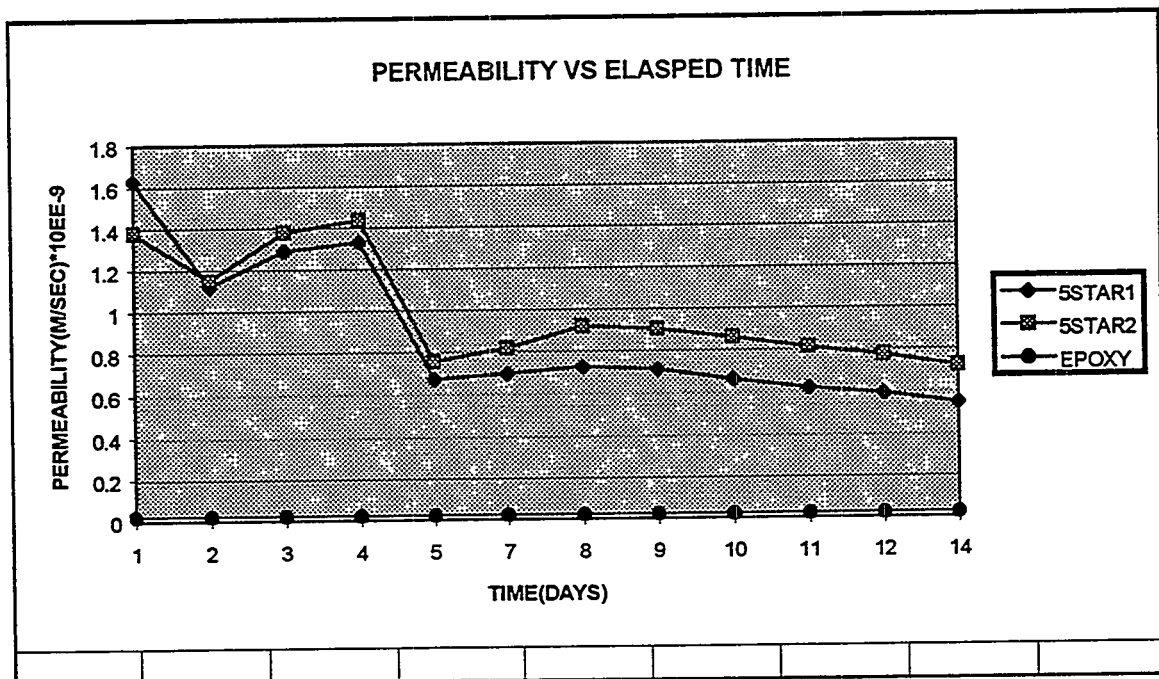
FIGURE 8: PERMEABILITY OF 5 STAR GROUT & BRUTEM MP EPOXY

VERTICAL CUT-OFF WALLS FOR THE CONTAINMENT OF CONTAMINATED GROUND

Hans L. Jessberger[1], Klaus Krubasik[2], R.A. Beine[3]

ABSTRACT

Vertical cut-off walls are widely used for the containment of contaminated sites, where a capping system is not sufficient for the protection of groundwater. Various types of cut-off walls are introduced and new developments are prescribed. Design and testing principles are outlined.

1. INTRODUCTION

Containment techniques are the appropriate measure for old landfills and abandoned industrial sites with contaminated ground and groundwater, too, since the shortage of financial resources in many countries classifies clean-up techniques as too cost intensive in most cases.

The most often used containment techniques are capping systems, which prevent rainwater from penetrating the contaminated portion. These systems may not be sufficient, if:
- there is a groundwater flow through the contaminated portion;
- pollutants above the groundwater level are mobilized in the future,
- volatile contaminants migrate in the unsaturated strata.

In these cases the source of contamination has to be enclosed with a vertical barrier. Furthermore such a barrier may be used in the case of
- seepage water from layered strata,
- when a demarcation for hydraulic measures or in situ clean-up actions is needed.

The vertical barrier (cut-off- wall) cuts off the path between source of emission and the target of impact. In most cases it is imbedded in an impermeable stratum of the soil profile. Inside the enclosure by a cut-off wall, the water table is lowered to remove the contaminated body from the water saturated zone and to create a hydraulic potential towards the enclosure. In combination with a capping system, the lowering of the groundwater level within the enclosure leads to desiccation of the contaminated body and will eventually stop the production of contaminated leachate. Such cut-off walls have been used often recently in geotechnical and water-engineering practice as well as in remediation actions.

2. CUT-OFF WALLS

Cut-off walls can be constructed using various foundation engineering processes. A distinction is made between cut-off walls constructed by excavating the soil and those constructed by soil displacement. Fig. 1 gives a summary of the methods. The designer should bear in mind that with certain methods, excavated contaminated material and/or displaced temporary suspensions (two-phase methods) will need to be disposed off. In the case of sheet pile walls there is no excavated material. In the case of narrow walls, small excess quantities of the sealing material arise. With grout curtain walls there are usually only small quantities of excavated material to be disposed off; in the case of bored pile walls and diaphragm walls the excavated soil and the supporting fluid must be disposed off.

[1] Ruhr-University Bochum, PB 102 148, D - 44801 Bochum, 49 234 700 -6135
[2] Bilfinger + Berger, Bau AG, Carl-Reiß-Platz 1-5, D - 68165 Mannheim, 49 621 459-1
[3] Jessberger + Partner, Consultants, Am Umweltpark 5, D - 44793 Bochum, 49 234 68 775-0

In principle, the cut-off wall material has to be defined separately for each application in preliminary tests, taking account of the soil and groundwater composition and of the leachate. Suitability studies must be undertaken in advance to examine the influence of additives and to evaluate them during the course of construction. The long-term resistance of the cut-off wall depends on the thickness and distribution of the components within the wall as well as on the cut-off wall material selected. Even where similar materials are used (with the same attainable material permeabilities), different cut-off wall systems can achieve different system permeabilities. For example, because of their higher proportion of joints, bored pile walls have a greater system permeability than diaphragm walls.

In most cases cut-off walls will be designed to key into a continuous and sufficiently thick underlying low permeable stratum at such a depth that an adequate seal is guaranteed. The keying depth has to be specified in the design depending on the method and the foundation conditions. The cut-off walls may be used in conjunction with hydraulic head control measures.

Diaphragm walls are generally the most appropriate method for surrounding landfills or contaminated sites. Moreover they allow a more precise identification of the strata encountered. So this paper concentrates on this type of cut-off walls, taking into account thin walls, too.
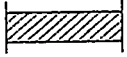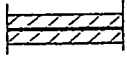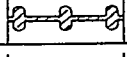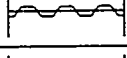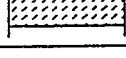
Principle	Cut-off-wall-system	Plan view	Soils	Material
Excavation of soil in place and installation of a sealing material	Diaphragm wall one-phase method		Limited application in the case of peat/-humic acid	Bentonite-cement suspension with/-without filler
	Diaphragm wall two-phase method		Limited application in the case of peat/-humic acid	Bentonite susp., natural concrete
	Composite diaphragm wall		As above, only in the one-phase method	Bentonite-cement suspension, add. sealing elements (e.g. HDPE)
Displacement of soil in place and installation of a sealing material	Thin wall		Suitable for driving or vibrating in	Bentonite-cement susp. with filler
	Sheet pile wall			Steel
Reduction of permeability of soil in place	Grout curtain		Injectable Soils	Cement, clay-cement, susp., silica gels

Fig. 1: Cut-off wall systems (GLR 1993)

3. CUT-OFF DIAPHRAGM WALLS

Diaphragm walls, which can be constructed using the one-phase or the two-phase method, are a succession of primary and secondary panels. Panels can be constructed:
- by a single excavation unit;
- or, more commonly, by three excavation units (two primary and one secondary).

Additives are often mixed with the sealing wall material to improve flow behavior and as retarding agents. Where these substances are used it is necessary to remember that such sealing compounds tend to have higher precipitation values. It is therefore necessary to ensure that the sealing compound is thoroughly mixed to reduce segregation and filtrate water loss. It is necessary to check that the additives used do not affect the stability of the mix.

3.1 One-phase Method

To ensure the continuity of one-phase cut-off walls, panels must be overlapped. The fluid sealing compound is placed in the trench while excavation is still in progress and remains there after

excavation is finished. During excavation the sealing compound has a supporting function and after hardening it performs the sealing function. The suspension consists primarily of bentonite, cement and water plus a filler and any additives. During excavation, some of the existing soil may become incorporated, depending on the soil conditions. Depending on the soil permeability and on the depth of the groundwater level, a filtrate water loss occurs, necessitating topping up with the supporting suspension. The suspension is kept in constant motion, which prevents it from stiffening as a result of the cement content. After excavation of the panel the suspension is left undisturbed thus allowing it to harden.

3.2 Two-phase Method

Two-phase cut-off walls should preferably be constructed using the reciprocating rolling process. The diaphragm is excavated under the protection of a bentonite slurry which serves as the supporting suspension. The actual sealing compound is then introduced by the tremie method, the displaced supporting suspension is pumped out, regenerated and reused. The sealing compound sets in the trench and forms the cut-off wall. Formwork pipes are used on the face to form the boundary of the primary panels. If the hardening behavior of the sealing compound so permits, a pipe need not be used.

3.3 Composite Diaphragm Wall

A composite diaphragm wall is constructed using the one-phase method and incorporating additional components in the sealing compound (fig. 2). This serves to reduce permeability and increase long-term resistance, as well as improving mechanical behavior (e.g. in areas where subsidence occurs). The additional sealing component material must be compatible with the chemistry of the attacking media.

Special care is necessary in the construction of composite diaphragm walls. The objective of including the maximum proportion of solid substance to guarantee adequate strength and low permeability must be balanced against the need to permit subsequent incorporation of the additional sealing components.

Sealing components added to a diaphragm wall may consist of various materials such as HDPE or sheet steel profiles.
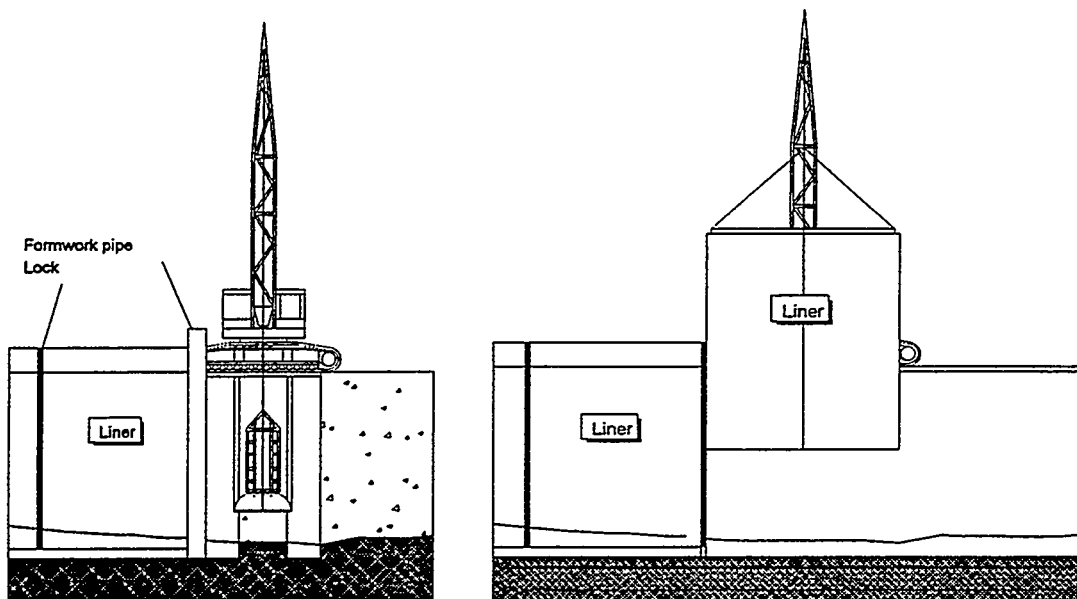
Fig. 2: Construction of a composite diaphragm wall

4. DESIGN

During excavation the trench stability includes two aspects:
— the stability of the soil grains at the walls of the trench,
— the overall stability of the excavation.

The main factors affecting the stability which can be controlled during the execution are:
— the properties of the supporting suspension and its level,
— the length of the panels,
— the time during which the trench is left open with respect to changes in soil and groundwater conditions.

The stability of the trench shall be determined on the basis of stability calculations and trial excavation on site, if there is no comparable experience.

The stability calculations shall take account of
— stabilizing forces,
— groundwater pressures,
— earth pressures out of the three-dimensional geometry,
— shear strength of the soil;
— adjacent loads.

The level of the supporting suspension shall always remain at least 1 m above the highest groundwater level.

Special measures should be adopted in the cases of very soft, especially humus, and highly permeable coarse soils.

The verticality of the panels can usually be held within 0.5 %.
Guide-walls are normally between 0,7 m and 1,5 m deep.

5. CUT-OFF WALL CONSTRUCTION

To excavate the trench for diaphragm walls, grab buckets with different dimensions in thickness and length are used. Having a former width of 2,80 m, nowadays the standard width of an excavation unit is 3,40 m with a thickness of 60, 80 or 120 cm. One-phase walls can be constructed up to a depth of about 30 m and deeper at favorable conditions, limited by the time the supporting suspension may be kept in motion and the output of the grab bucket within this time, which may be between 8 and 36 hours, depending on the mixture of the suspension.
The cement-bentonite slurries used in the one-phase excavation of diaphragm walls must be fluid enough to allow passage of the grab bucket. Contrary to pure bentonite slurries, however, they do not form a very dense filtration cake on the trench walls. In permeable sands and gravels they may lose much of their water content to the surrounding soil and increase their density with time. With regard to mechanical stability and sealing characteristics of the material, this is advantageous. However, at a certain depth and density of the slurry, excavation is halted because the grabs are unable - despite their large weight - to penetrate further into the dense slurry. Cases are known where specified trench depths in excess of 30 m could not be reached or excavation tools were lost in the trench because the slurry became too dense through loss of water to permeable surrounding ground.

Since water loss by the suspension is time-dependent, the trench has to be excavated as quickly as possible. Faster excavation performance than with grabs is achieved with the diaphragm wall cutter, which cuts the ground with two counter-turning wheels studded with roller bits. The cuttings are continuously pumped out of the trench together with the suspension.

In a separation plant all particles larger than fine sand are removed from the suspension, which is then pumped back into the trench. Cement particles are much smaller than fine sand and remain in the suspension.

Due to a greater output of the diaphragm wall cutter, in most soils a depth of about 50 m can be reached using this method. Two-phase walls have been constructed to a depth of more than 100 m.

To construct a composite diaphragm wall sheets of synthetic liner (or sheet piles) are lowered into the trench while the suspension is still sufficiently fluid.

To lower a liner into a trench filled with slurry, shear forces in the slurry, buoyancy of the liner and frictional resistance in the locks have to be overcome. Special lowering devices are therefore necessary. In first applications, sheets of liner were cut to length, fastened onto a heavy steel frame and lowered into the trench. When the final position was reached, the frame was detached from the liner and recuperated. Frame length and therefore wall depth was determined by the boom configuration of the crane and limited to app. 20 m maximum. The frame with its liner offers a large area of wind resistance and makes installment of the liner, even in only slight winds, difficult.

These problems have been solved with a new technique for installing synthetic liners into sealing walls. The custom-tailored sheet, 5,0 m wide and equipped on both sides with interlocks for neighboring sheets, is rolled onto a drum. The drum is mounted on a mobile crawler unit which can be positioned exactly at the point of placement (fig. 3). The diameter of the drum is large enough to avoid permanent deformation of the locks. The interlock is threaded into the lock of the neighboring sheet partition already in place. A crane-held guiding frame is connected to the footing edge of the liner. As the frame is lowered into the slurry-filled excavation it unrolls the liner from the drum and introduces it into its correct position. If necessary, extension sections can be mounted onto the guiding frame during the lowering process. The depth of a sealing wall with synthetic liner is therefore only restricted by the size and power of the crane which has to lift the
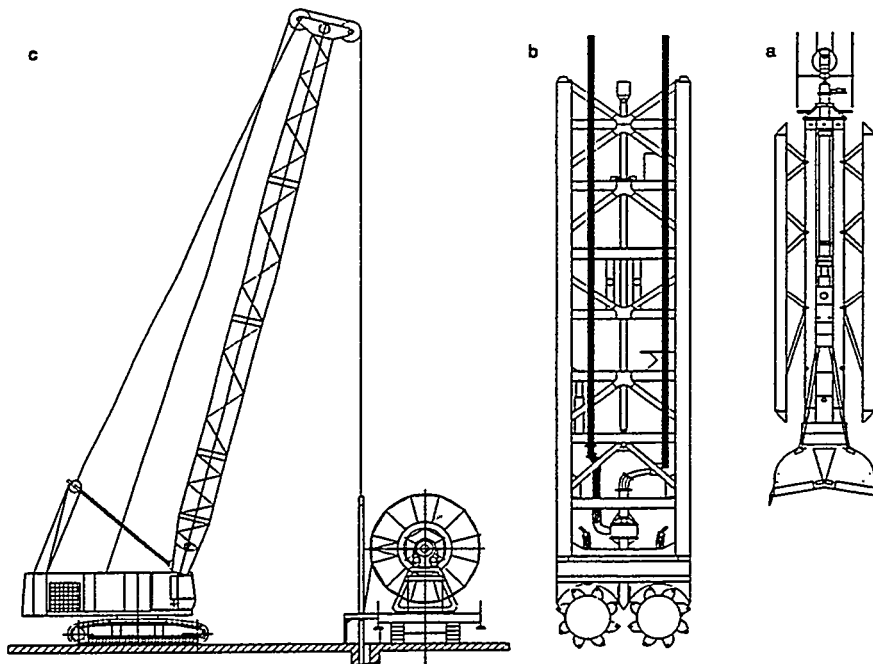
Fig. 3: Schematic illustration of the equipment
a: grab bucket   b: diaphragm wall cutter   c: drum for placing a liner into a diaphragm wall

frame out after placement of the liner. So far synthetic liners have been installed with this technique up to a depth of 35 m. Interlocks between neighboring sections of liners form hollow tubes which can be pumped dry after placement, controlled by camera and welded and/or filled with an appropriate sealing material.

In 1993 the method was applied for the first time in the enclosure of the central waste disposal of Hünxe in Germany, where a composite diaphragm wall was constructed with a length of 950 m and a maximum depth of 35 m. Total wall area was 30.000 m². The cut-off wall was excavated in day and night shifts from both ends simultaneously. One drum unit was able to keep up with excavation by placing up to 6 liner widths per day.

6. TESTING AND QUALITY ASSURANCE

The suitability of mineral sealing compounds must be demonstrated in each individual case by suitability tests. These must be undertaken only by laboratories with the appropriate equipment and expertise. As a general rule, the following should be determined:
- composition and characteristics of the individual components of the mix;
- characteristics of the fresh sealing compound;
- workability and solidification behavior of the sealing compound;
- strength and stress deformation behavior of the hardened sealing compound;
- permeability of the hardened sealing compound;
- unit mass and water content;
- physico-chemical properties related to specific requirements.

Permeability decreases and uniaxial compressive strength increases during hardening of the one-phase or two-phase sealing compound. (Fratalocchi et al. 1996) found that the development of the permeability k of cement-bentonite slurries can be expressed by

$$k(t) = k_o \, (t/t_o)^{-\alpha}$$

k_o: permeability at time t_o (usually 28 days)
α = reduction coefficient

To ensure the quality of the cut-off wall, initial tests and tests during construction must be performed, set out in (GLR 1993).

Examples of mixes for different types of walls are given in fig. 4. For one-phase walls ready mixed construction materials are widely used that obtain very good results, need no time for swelling of bentonite, and spare one mixing unit, too. For two-phase walls sealing compounds were developed with high density and resistance against pollutant attack.

A monitoring program on a one-phase cut-off wall around a hazardous waste disposal site built in the late 70's proved the reliability of the sealing, though it was one of the first cut-off walls in highly aggressive surroundings and had the low standard of that stage of development, in terms of permeability 10^{-7} m/s.

116

	One-Phase Wall	Two-Phase Wall		Thin Wall
		cement-free	with cement and adsorption capacity	
	(%) bentonite (Na) 3.5 (Ca) 14.5 cement 17.5 12.5 water 79 73	(%) silicone reagent* 10 sand and gravel 75 powdered clay 13 fly ash (filler) 2 *incl. water	(%) cement 10 powdered clay 41 coal fly ash 6 additives 0.3 water 42.7	(%) bentonite 1.5 cement 10.5 rock flour 49 water 39
density permeability (i. laborat.)	1,150 kg/m^3 $10^{-9} \div 10^{-10}$ m/s	2,200 kg/m^3 $10^{-10} \div 10^{-11}$ m/s	1,575 kg/m^3 10^{-11} m/s	1,640 kg/m^3 $10^{-8} \div 10^{-9}$ m/s
water/solid-ratio	3.7 2.7	0.11	0.75	0.64
site/year	many	Breitscheid / 1992	Malsch / 1994	many

Fig. 4: Examples of compounds for different types of walls

7. COSTS

The different types of cut-off walls meet different requirements and have different costs. A rough overview is presented in the following, giving a price factor related to a one-phase wall.

Type of cut-off wall	factor
one-phase wall, 60 cm thick	1.0
two-phase wall with plastic concrete	1.4
two-phase wall with cement free sealing	3.3
one-phase wall with HDPE liner	1.6
one-phase wall with sheet piles	2.2
thin wall	0.44
double thin wall as chamber system	0.9

The price for a 15 m deep one-phase wall is about 140 DM/m². Site specific costs relating to worker safety, disposal of excavated soil, loss of slurry, details of top of the wall etc. have to be considered.

8. SUMMARY AND CONCLUSIONS

Cut-off walls for providing containment have been used for 20 years and on many sites in Europe and out of Europe and have developed a high standard. For nearly all requirements a suitable cut-off wall can be designed and constructed. More testing and monitoring, however, should be done to get a better understanding of the interaction between pollutants and cut-off wall materials.

References

Fratalocchi, E., Manassero, M., Pasqualini, E., Spanna, C. (1996) Predicting Hydraulic Conductivity of Cement-Bentonite Slurries. 2nd International Congress on Environmental Geotechnics, Osaka, November 5-8, 1996.

GLR (1993) Geotechnics of Landfill Design and Remedial Works. Technical Recommendations (ed. German Geotechnical Society for the International Society of Soil Mechanics and Foundation Engineering), Ernst & Sohn Berlin.

VALUE ENGINEERING STUDY FOR SELECTION OF VERTICAL BARRIER TECHNOLOGY AT A SUPERFUND SITE

E. E. Bryan[1], J. L. Guglielmetti[2], P. B. Butler[3],and M. P. Brill[4]

Abstract

A value engineering (VE) study was conducted to identify and evaluate vertical barrier technologies and alignments for a Superfund project in New Castle County, Delaware. The objective was to select and recommend the most appropriate vertical barrier(s) for two separate landfills and a portion of the manufacturing plant on the site. A VE team was assembled to identify and evaluate site specific issues related to effectiveness, constructability and cost for numerous vertical barrier technologies. Several cost-effective alternatives were identified that met project objectives. The VE study concluded that a composite vertical barrier system consisting of a soil-bentonite slurry trench and steel sheet piles would provide effective containment of the North Landfill. Additionally, the geologic confining unit specified in the Record of Decision (ROD) was found to be unsuitable as a vertical barrier key and a more suitable, shallow confining unit was discovered. This paper describes the value engineering process and results of the VE study for one of the landfills.

Introduction

The Newport Superfund site encompasses approximately 486,000 square meters (120 acres) in northern New Castle County, Delaware. Figure 1 shows a plan view of the site. The site includes an operations area consisting of portions of two chemical manufacturing plants, two inactive landfills, and adjacent wetlands and upland forested areas. The site is bisected by the Christina River. The North Landfill is bordered by the manufacturing areas on the north and east, by a drainage way and wetlands on the west, and by the Christina River on the south.

Figure 1 Plan View of Site
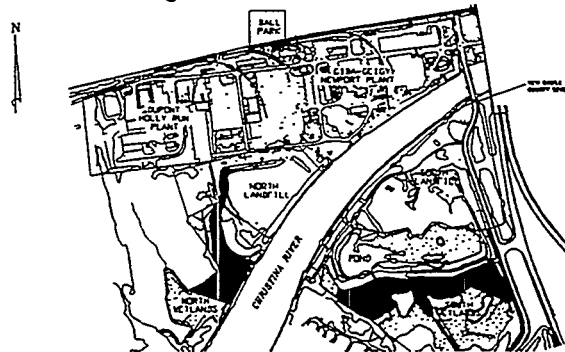
The site has historically been used for the manufacture of organic and inorganic chemicals including pigments, nickel, high-purity silicon, and chromium dioxide. In 1988, the owners entered into an Administrative Consent Order (ACO) with the Environmental Protection Agency (EPA) to complete investigations for the site in accordance with the Comprehensive Environmental Response, Compensation, and Liability Act (CERCLA) and Superfund

[1] DuPont Environmental Remediation Services, Barley Mill Plaza 27, P.O. Box 80027, Wilmington, Delaware 19880-0027, (302) 892-7420, bryanee@csoc.dnet.dupont.com
[2] DuPont Environmental Remediation Services, Barley Mill Plaza 27, P.O. Box 80027, Wilmington, Delaware 19880-0027, (302) 992-6806
[3] DuPont Environmental Remediation Services, Barley Mill Plaza 27, P.O. Box 80027, Wilmington, Delaware 19880-0027, (302) 992-5978
[4] DuPont Environmental Remediation Services, Barley Mill Plaza 27, P.O. Box 80027, Wilmington, Delaware 19880-0027, (302) 892-7576

Amendments and Reauthorization Act (SARA). The site was included on the National Priorities List (NPL) in early 1990. A remedial investigation and feasibility study (RI/FS) was conducted in three phases between August 1988 and August 1992. In August 1993, a Record of Decision (ROD) specifying the remedial actions to take place at the site was issued.

A value engineering (VE) study was conducted for the North Landfill as part of the remedial actions identified in the ROD. The objective of the VE study was to select and recommend the most appropriate vertical barrier(s) and alignment for the North Landfill area of the site.

Value Engineering Overview

Value engineering is a systematic, multidisciplined approach designed to select the most cost-effective implementation of remedies that are also protective of human health and the environment. Value engineering entails evaluating and selecting alternate materials, processes, and construction methods. The VE process is comprised of the following five-phase program:

- Gather information
- Value engineering workshop
- Evaluate VE workshop results
- Field investigations and economic evaluation
- Presentation of conclusions and recommendations

The VE team researched and gathered information on the past operations and regulatory history of the site, site surface and subsurface conditions, and vertical barrier technologies. The VE team also held internal meetings to identify key issues concerning alignment, extent of waste, connections with existing structures, space constraints, and the long-term suitability of in place structures. The VE workshop was then planned.

A two-day VE workshop was held at the site. The workshop was attended by agency representatives, design and construction consultants, owners, health and safety representatives, the project team, and meeting facilitators. The VE workshop provided project background information to all of the participants, generated creative discussion of key issues and vertical barrier technologies identified during the information gathering phase, and organized the ideas generated during the workshop into a usable form for evaluation. A site tour was also conducted as part of the workshop. ,

The ideas developed from the value engineering workshop were evaluated and additional information needed to complete the evaluation process was identified. The selected vertical barrier technologies and alignments were narrowed down based on the criteria of effectiveness, implementability, and cost.

Field investigations were performed to gather the additional information and data needs identified. Soil borings were taken along the southern berm of the North Landfill in order to characterize the berm and underlying geological strata. A radiological survey and thorium migration assessment was conducted to locate and predict the effects of thorium waste on the selected barrier technology. Cross sections of the riverbank area, including the river and its north and south banks, were developed and evaluated to identify areas of extreme grade and possible stability problems. After the additional information was gathered, an economic evaluation was performed and each of the alternatives were evaluated against the requirements of the ROD.

A report presenting the VE team's recommendations for the most cost-effective, vertical barrier technologies and alignment that met the ROD performance standards while protecting human health and the environment was prepared and submitted to the U.S. Environmental Protection Agency (EPA). This report also identified predesign investigations for the recommended technologies and alignment.

Project Issues

Several key issues affecting the selection of vertical barrier technologies were identified prior to and throughout the VE study. One of the primary objectives of the VE study was to select the most appropriate alignment for the vertical barrier. Vertical barrier alignments along the top of the river bank and along the toe of the river bank were evaluated based on the issues identified.

A number of concerns centered around the waste contained within the landfill. The location of radioactive thorium waste reported to be contained along the southern berm of the landfill was of special concern. In addition to health and safety concerns associated with the thorium waste, ensuring that the thorium would be fully contained, would not be released to the environment during construction, and would not decrease the effectiveness of the selected vertical barrier needed to be considered. Other waste issues included constructability of vertical barriers through large debris located within the landfill berms, management of excavated materials, and the need to contain the waste on the berm slope.

The landfill slopes along the river bank and the drainage way on the west side of the landfill also presented several challenges in selecting a technology and alignment. These issues included health and safety concerns during construction, constructability along steep grades, the presence of exposed waste along the slopes, and the destruction of natural habitat on the slopes.

Construction of a vertical barrier along the river would necessitate the implementation of health and safety procedures associated with work on and around water. Increased sediment and erosion controls would be required during construction along the toe of the river bank. Likewise, tidal fluctuations, fast river velocities, flooding and other weather related issues would need to be addressed.

Other issues identified throughout the VE study included evaluating groundwater containment using pump and treat methods versus a deeper vertical barrier, methods of tying the vertical barrier into an existing steel sheet pile barrier on the eastern side of the landfill, and the longevity of technologies.

Value Engineering Workshop

During the VE workshop, each technology was given a relative rating for effectiveness and implementability, and unit cost ranges for installation were given for each technology. The effectiveness criterion was characterized by the ability to be protective of human health and the environment, meet the ROD objectives, reliability and durability, and the amount of waste contained. Construction difficulties, short-term health and safety concerns, short-term environmental impacts, and the ability to monitor the construction and effectiveness of the technology were identified in the implementability criterion. During this evaluation process, the criterion of effectiveness was given the highest weighting.

Each technology was rated as either high, medium, or low for the effectiveness criteria and easy, moderate, or difficult for the implementability criteria. A high effectiveness rating represented a technology that met all, or nearly all, of the ROD performance standards, had proven reliability and durability, and contained all, or nearly all of the waste. Conversely, a low effectiveness rating represented a technology that met few of the ROD performance standards, was not a reliable, durable, or proven technology, and would not effectively contain all of the waste. Similarly, a technology earning an easy rating for implementability would present few or no construction difficulties, short-term health and safety concerns, or short-term environmental impacts and its construction and long-term effectiveness could be easily monitored. On the other hand, a technology with a difficult implementability rating would be extremely difficult or dangerous to construct, would have severe or potentially severe short-term environmental impacts, and could not be easily monitored during construction or for long-term effectiveness.

The following technologies were evaluated during the VE workshop:

- Soil-Bentonite (SB) Slurry Trench
- Cement-Bentonite (CB) Slurry Trench
- Steel Sheet Piling
- Deep Soil Mixing
- Geomembrane - Vibrating Insertion Plate
- Geomembrane - Trench Installation

- Cement-Bentonite - Panel Construction
- Plastic Sheet Pile - Driven
- Cement-Bentonite - Beam Injection
- Jet Grouting
- Permeation Grouting

Of the technologies evaluated, the SB slurry trench, steel sheet piling, and the geomembrane trench installation had high effectiveness ratings. These technologies were also easy or moderately easy to implement. Cement-bentonite panel construction, jet grouting, and permeation grouting were also easily implemented, however, they were less effective than the SB slurry trench, steel sheet piling, and geomembrane trench.

Advantages of the SB slurry trench include the capability of accurately controlling the specification of the backfill and being able to monitor the entire excavation depth. However, installation of a SB slurry trench would require disposal of excavated material and transition down slopes would be difficult. Trench stability problems may also be encountered during installation. Installation of SB slurry trenches ranges between $86 and $129 per square meter ($8 and $12 per square foot).

Advantages of the steel sheet piling include the potential to grout the sheet interlocks to reduce permeability, and the option to coat or treat the steel to increase longevity. Installation of steel sheet piles is non-intrusive, thus reducing health and safety concerns and decreasing environmental impact. Construction difficulties would include relocation of the sheet pile wall around, or excavation and disposal of large obstructions encountered along the wall alignment. Steel sheet pile installation costs range between $215 and $322 per square meter ($20 and $30 per square foot).

Similar to the SB slurry trench, the geomembrane trench could be monitored throughout the entire excavation depth. Likewise, the disposal of excavated material, trench stability, and difficult transition down slopes would apply to geomembrane trench installation. In addition, undetected damage to the geomembrane during trench backfilling would decrease the effectiveness of the vertical barrier. Geomembrane installation in a trench ranges between $129 and $172 per square meter ($12 and $16 per square foot).

The VE team reviewed the ratings for each technology to narrow the number of technologies that warranted further consideration. Separate vertical barrier alignments along the toe of the river bank and on the top of the landfill were discussed.

After evaluating the information generated at the VE workshop, the team concluded that a composite barrier was the most cost-effective approach. A composite barrier system includes two or more vertical barrier technologies. This conclusion allowed the team to narrow the choices for further evaluation to three options.

Option 1 (shown in Figure 2) consisted of a vertical barrier system approximately 671 meters (2,200 ft) long consisting of approximately 610 meters (2,000 ft.) of SB slurry trench and 61 meters (200 ft.) of steel sheet piling. The SB slurry trench would be installed through the landfill berm at the top of the river bank extending from west of the existing sheet pile barrier on the eastern side of the landfill to the drainage way on the west side. Steel sheet piling would connect the existing sheet pile barrier to the SB slurry trench at the east end of the landfill. Steel sheet piling would also be used to traverse the slope from the top of the river bank to the drainage way along the west end of the landfill. The SB slurry trench would then continue north along the drainage way and around the northwest corner of the landfill.

Option 2 consisted of a SB slurry trench installed along the toe of the river bank from the existing sheet pile barrier to the drainage way and continuing north along the drainage way and around

the northwest corner of the landfill as in the previous option. A berm would be constructed at the toe of the riverbank to facilitate construction of the SB slurry trench along this alignment. Short lengths of steel sheet piling would be used to tie the existing sheet pile barrier into the SB slurry trench.

Option 3 consisted of steel sheet pilling along the toe of the riverbank from the existing sheet pile barrier to the drainage way. A SB slurry trench would then be installed northward along the drainage way and around the northwest corner of the landfill similarly to Option 1.

Figure 2 Composite Barrier Option 1
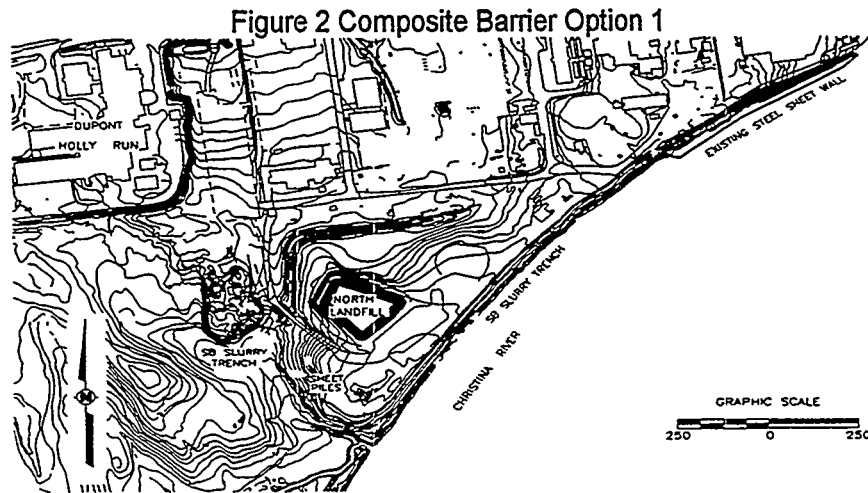
Additional Investigations

The VE workshop and subsequent evaluation of the technologies identified the following additional information and data needs.

- Better characterization of the southern berm of the North Landfill and the subsurface conditions below the berm down to the first Potomac unit.
- Location of the thorium waste and potential effects on effectiveness of selected technologies.
- The grade and stability of the north bank of the Christina River.
- Suitability of stratigraphic unit at the base of the Columbia formation for vertical barrier key.

Field investigations including soil borings, radiological survey and thorium migration assessment, geotechnical testing, and a hydrogeological investigation were performed to gather this additional information. Cross sections of the river bank area including the river were also developed and evaluated to identify areas of extreme grade and possible stability problems.

The Coastal Plain stratigraphic units found beneath the North Landfill (Figure 3) are part of three geologic formations which are found consistently throughout the entire site. The first stratigraphic unit encountered by the VE borings was found to be horizontally continuous under the waste material of the North Landfill and has a sufficient thickness and low permeability to serve as a key for a vertical barrier. This unit is classified as a Holocene or Recent age (less than 1 million years ago) clayey silt. The clayey silt stratum ranges in thickness from 2.1 meters (7 ft.) to 3.8 meters (12.5 ft.). The unit has an average thickness of approximately 3 meters (10 ft.). All of the VE soil borings and previous borings from the RI/FS encountered the clayey silt unit. The base elevation of the upper clayey silt layer is fairly consistent. The clayey silt is a marsh deposit that is believed to have formed in association with the ancient flood plain of the Christina River.

The second stratigraphic unit is the Pleistocene age (1 to 2 million years ago) silts, sands and gravels of the Columbia formation. The VE soil borings showed that the lithology of this unit extends from the bottom (i.e. end) of the clayey silt, at approximately 6.7 meters (22 ft.) below

ground surface (BGS), to approximately the start of the Potomac unit, around 24.5 meters (80 ft.) BGS.

The third stratigraphic unit is part of the Cretaceous age (65 to 135 million years ago) Potomac formation characterized by a mixture of variegated red, gray, purple, yellow and white, frequently lignitic silts and clays containing interbedded white, gray and rust-brown fine to coarse quartz sands and gravels. Because of this interbedding with sands, the permeability of the Potomac "clay" unit found at the base of the Columbia formation is two orders of magnitude higher than the permeability of the upper clayey silt stratum. The average permeability of the first Potomac formation unit is 3.32×10^{-7} m/s and the average permeability of the upper clayey silt confining unit is 3.13×10^{-9} m/s. Additionally, this first Potomac formation is not continuous and does not provide an effective vertical barrier key.

Figure 3 Typical Geologic Cross-Section
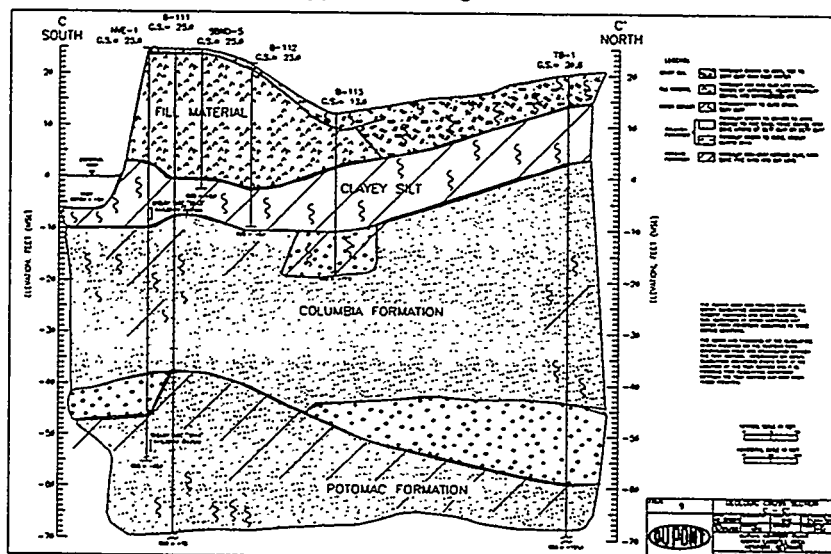
One of the primary concerns for the vertical barrier alignment at the top of the landfill berm was disturbing the buried nickel bearing thorium oxide waste material during barrier construction. The exact location of the thorium waste relative to the landfill berm was unknown. A radiological survey in and around the soil borings was conducted and concluded that there is no thorium within 1.5 meters (5 ft.) horizontally of the VE soil borings. Based on the VE radiological survey, it was concluded that the construction of the vertical barrier through the landfill berm would in no way adversely effect the buried thorium waste material. A thorium migration assessment was conducted to evaluate the effectiveness of a SB slurry trench versus a SB slurry trench embedded with a geomembrane in containing the thorium waste. Modeling showed that because of the extremely low solubility of thorium oxide, as well as the natural sorptive properties of soil and bentonite, thorium would be contained for more than a million years by a SB slurry trench alone. The addition of a geomembrane would increase cost, present additional construction difficulties, and would not provide additional protection nor achieve permanent containment of the thorium.

The ROD stipulated that "A physical barrier wall (an actual wall that limits migration of groundwater to the maximum extent practicable) shall be constructed to extend from the ground surface to the base of the Columbia aquifer keying into the aquitard which separates the Columbia aquifer and the Potomac aquifer". Based on the findings of the VE field investigation, a vertical barrier extended into the upper clayey silt (with fill zone groundwater extraction), will effectively prevent migration of contaminated shallow groundwater into the Christina River. However, for containment of the underlying Columbia formation groundwater, the effectiveness of the Potomac unit as a vertical barrier key is questionable because it is not continuous and

123

exhibits a much higher permeability than the upper clayey silt stratum. Therefore, a deeper vertical barrier to limit Columbia formation groundwater migration to the Christina River may not be effective. Hydraulic containment of this Columbia formation groundwater, using pumping wells, is a more cost-effective method for controlling the movement of this groundwater than a vertical barrier.

Economic Evaluation

An economic evaluation was performed to compare the various technology and alignment options. Based on the VE field investigation findings, shallow and deep barriers keying into the upper clayey silt stratum and first Potomac unit, respectively, were evaluated based on engineering and construction costs. Pumping costs, with or without a vertical barrier to the base of the Columbia Formation, are considered a cost-neutral issue and are not included in this economic evaluation. A summary of estimated costs for each option is presented below.

Estimated Cost

Vertical Barrier Option	Shallow	Deep
#1 - Soil Bentonite Trench - Through Landfill Berm	$700,000	$2,300,000
#2 - Soil Bentonite Trench - Along Toe of Riverbank	$800,000	$2,400,000
#3 - Steel Sheet Piles - Along Toe of Riverbank	$1,700,000	$4,100,000

The above cost estimates include construction, contingency, and engineering costs, but do not include erosion protection, capping, and groundwater pumping.

Recommended Solution

Based on the VE study results, the containment system shown in Figure 4 was recommended to the EPA. This containment system consisted of a SB slurry trench with a minimum width of 1 meter (3 ft.) and a maximum permeability of 1×10^{-9} m/s installed through the landfill berm at the top of the river bank (as close as practical to the edge of the river bank) extending from west of the existing sheet pile barrier to the drainage way. The SB slurry trench would continue up the drainage way and around the northwest corner of the landfill. Steel sheet piling will be used in the transition zones connecting the SB slurry trench to the existing sheet pile barrier and connecting the SB slurry trenches between the landfill berm and the drainage way. The SB slurry trenches and steel sheeting will extend, and be keyed a minimum of 1 meter (3 ft.), into the upper clayey silt confining stratum. A soil cover consisting of 0.3 meters (1 ft.) of low permeability soil having a maximum permeability of 1×10^{-7} m/s, and 0.15 m (6 in.) of topsoil will extend from the vertical barrier along the landfill berm, down the slope to the toe of the riverbank (high tide elevation).

Figure 4 Recommended Containment System

124
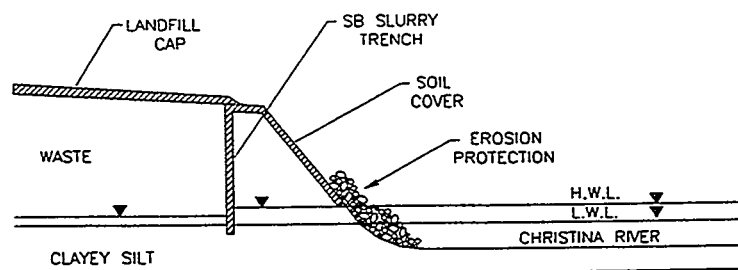
INVESTIGATION OF THE PERFORMANCE OF CEMENT-BENTONITE CUT-OFF WALLS IN AGGRESSIVE GROUND AT A DISUSED GASWORKS SITE

P. Tedd[1]; I.R. Holton[1]; A P Butcher[1]; S. Wallace[2]; P. Daly[3];

Abstract

here has been an increased use of cement-bentonite slurry trench cut-off walls to control the lateral migration of pollution in the UK. Concerns inevitably exist about their performance in chemically aggressive ground particularly in the long term. To address some of the uncertainties a programme of field and laboratory research is being undertaken at a disused gasworks in the UK. Elevated levels of sulphate and other contaminants are present on the site and could potentially change the properties of the cement-bentonite. Two boxes, 10m square in plan, by 5m deep have been constructed, one with and one without an HDPE membrane, to isolate parts of the site. Local hydraulic gradients across the walls have been created by pumping from within the boxes. Isolated lengths of wall have been constructed which are being used to assess and develop in-situ testing techniques such as the piezocone for measuring permeability, strength and overall integrity of the wall.

Introduction

Slurry trench cut-off walls using self-hardening cement-bentonite are currently the most common form of in-ground vertical barrier constructed in the UK to control the lateral migration of pollution (leachate and gas) from contaminated land sites. The single phase method of construction is generally used, in which a continuous trench is excavated under the support of a self-hardening cement-bentonite slurry which sets to form a low permeability barrier. Typically walls are 0.6m wide and less than 12m deep and have been excavated using hydraulic back-actors. Approximately 75% of walls constructed in the UK have had a high density polyethylene (HDPE) membrane, usually 2mm thick, placed in the wall. The slurry mixes generally contain bentonite, cement and blast furnace slag although pulverised fuel ash has been used. Sodium exchange bentonite, described as CE grade (civil engineering) is usually used. Mixing of the slurry is generally a two stage process with bentonite powder and water being pre-mixed in a high shear mixer and the slurry allowed to hydrate for a minimum of eight hours before the cementitious material is added. BRE Digest 395 and Jefferis (1993) provide some background to construction, materials and specifications.

Although this type of cut-off wall to contain contamination has been in use for more than 20 years and there have been few known cases of unsatisfactory performance, there is a lack of in-situ performance data and concerns inevitably exist about their performance in chemically aggressive ground, particularly in the long term. To address some of these concerns, the Building Research Establishment (BRE) in collaboration with British Gas Properties and British Gas Research and Technology, has established a test site to study the in-situ performance of slurry walls in chemically aggressive ground. The objectives of the project are to facilitate production of improved specifications for slurry walls and provide industry with data on their long term in-situ performance in aggressive environments. The test site will also be used to assess and aid the development of improved monitoring methods. This work forms part of a wider research programme currently being undertaken at BRE relating to the redevelopment of contaminated land including site investigation methods, performance of containment systems and building materials, and landfill gas generation. However, this paper is confined to a description of the work undertaken at the test site and the associated laboratory testing. Work on the project is still at an early stage with construction of the cut-off walls being completed in April 1996,

[1]Building Research Establishment, Watford, WD2 7JR, UK
[2]British Gas Properties, Basingstoke, UK
[3]British Gas Research & Technology, Loughborough, UK

Test Site Description

Commercial production of coal gas began in the UK in the first half of the 19th century and continued until the 1970s when it was replaced by natural gas. British Gas owns some 1000 sites many of which may be potentially contaminated from the manufacture and purification of gas. Remediation of many of these gas works has now been undertaken with the object of redevelopment and slurry trench cut-off walls have been used at a number of sites as part of that remediation. British Gas Properties have provided part of a former gasworks for the field study. The gasworks at the site was established prior to 1890 and decommissioned in the mid 1970's. The area allocated for research (the test site) is approximately 50m by 100m and had historically been used as a coal stocking and disposal area. Ground conditions at the test site consist of approximately 3m of made ground, containing spent oxide, coal residues, carbon black and foul lime, overlying stiff Lower Lias clay.

Significant quantities of spent oxide have been found on part of the site. Spent oxide is the residue from iron oxide used in the purification of coal gas to remove hydrogen sulphide and hydrogen cyanide. When the sulphur content reached 50-60% sulphur, the material was termed spent and was either dumped or used for the production of chemicals such as sulphuric acid. The removal of hydrogen cyanides during purification resulted in the formation of complex cyanides with total cyanide contents up to 6%.

Trial pits and boreholes at the site together with chemical analysis were used to assess the ground conditions, and type and level of contamination. Sulphate, total cyanide, sulphur, PAHs, sulphide and arsenic values exceed TTCs (trigger threshold concentrations specified in UK guidance documents) over much of the test site. The water table is approximately 2m below ground level. Values of pH and concentrations of SO_4 in the ground water were very variable. At some locations they were consistently above 10,000 mg/l with a pH value between 2 and 3, which would require a high sulphate resistant concrete. Laboratory tests have shown that such elevated levels of sulphate can cause significant reaction with cement-bentonite (Jefferis, 1992, Tedd et al 1993, and Garvin, 1994).

Construction Of The Test Walls

The cut-off walls were built by Keller Colcrete, a specialist contractor for this type of work. It was specified that the construction method and materials used should be typical of those currently being used in the UK, although it was accepted that different contractors would have slightly different mix designs and suppliers of materials. Construction of the walls by the single phase method inevitably involves some mixing of the surrounding ground and associated contaminants into the slurry. An assessment of the effects of this mixing in of contaminants from the site is an important aspect of the research work. A total of 120m of cut-off wall, 0.6m wide by 5m deep were constructed, comprising two boxes, 10m square in plan, and three independent lengths of wall. The boxes have been built to isolate parts of the site in which the water levels can be raised or lowered to create local hydraulic gradients across the walls of the boxes. A section through one of the boxes indicating the locations of monitoring points and wells is shown in Figure 1. A high density polyethylene (HDPE) membrane was installed in the walls of one of the boxes. The membrane was nominally 2mm thick and was supplied in 5m wide panels which were joined using the SLT 6 channel interlock. A complete box of the panels was made, nominally 5m deep. A nominal 0.5m layer of clay was placed over each box as shown in Fig.1 to prevent rain infiltration. The independent lengths of wall were constructed for the assessment and development of in-situ testing techniques.

During construction of the test walls it was evident that levels of spent oxide contamination varied widely across the site. The two box sections and one 10m length of independent wall were constructed in the more contaminated ground. Where considerable mixing of the surrounding contaminated ground with the slurry occurred in the trench, the slurry did not turn the dark blue colour, characteristic of cement-slag-bentonite slurries, but turned a dark grey and had a strong sulphurous smell. Although the presence of the contamination did not appear to have noticeably affected the setting of the slurry, it will be seen later that the contaminated slurry does have a lower strength and a higher permeability than the uncontaminated slurry.

Figure. 1.   Section through test box
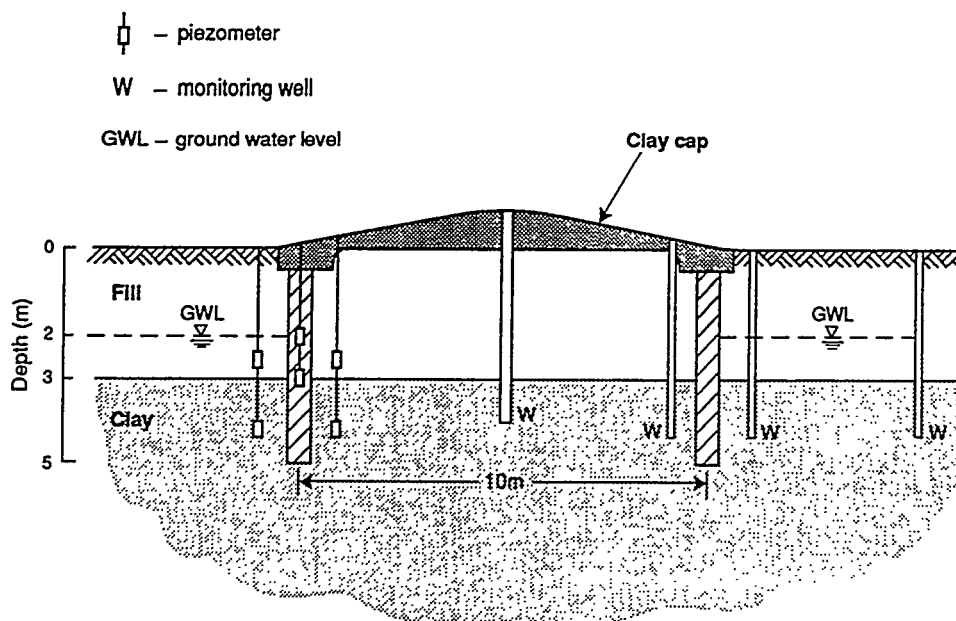
Laboratory Assessment of the Set Slurry

Laboratory assessment of the set material has included the compliance tests to measure permeability, strength and deformation that would normally be carried out on a slurry wall contract, and some long term permeability and various chemical compatibility tests.

Specifications for slurry trench cut-off walls in the UK have usually included requirements for the set slurry to achieve specified values of the permeability, strength and strain at failure at specific ages, usually 28 and or 90 days. Compliance with the specified properties is determined by testing samples of the set material which were cast from the fluid slurry taken from the trench and the mixer. It has been the practice to specify a permeability of less than 1×10^{-9}m/s and a strain at failure of greater than 5% in a consolidated drained triaxial test. However, a draft national standard for cement-bentonite cut-off walls recently published in the UK (ICE, 1996) has removed the 5% strain requirement partly because of the difficulties of achieving it at realistic effective confining pressures together with the 10^{-9}m/s permeability requirement using current materials and mix designs.

The routine compliance tests were performed using 100mm diameter samples cast during construction and cured under water until required for testing. Samples were taken from the bottom and top of the trench, and from the slurry mixer.

Permeability

Permeability testing was carried out in a triaxial cell (flexible wall permeameter) in accordance with ICE (1996). Samples from the mixer and trench were tested. It was anticipated that the properties of samples from the trench, particularly the bottom, could be affected by mixing in of the surrounding ground, and the effect of any chemical reaction between the contamination and cement-bentonite was unknown.

The maximum permeability measured on the samples from the mixer was 5×10^{-10}m/s with a mean value of 8×10^{-11}m/s. However, the measured permeabilities of samples from the trench at approximately 40 days, where significant contamination of the slurry had occurred, were generally at least an order of magnitude larger with a maximum value of 1.5×10^{-8}m/s being measured. By 90 days, the permeability of nearly all samples tested was less than 2×10^{-10} m/s.

127

Figure. 2. Results from laboratory permeability tests
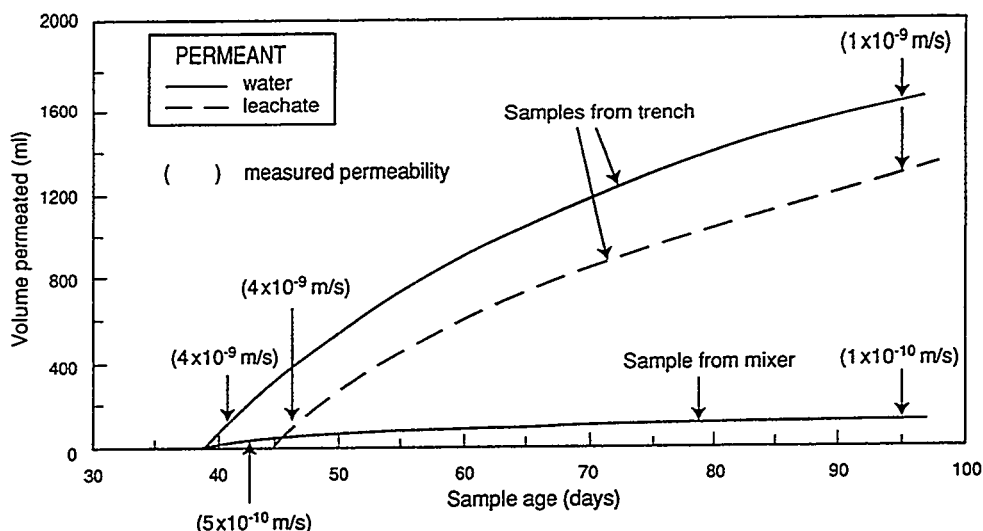
Figure 2 shows the results of permeability tests on three samples, two from the trench and one from the mixer, carried out over a prolonged period in the BRE leachate permeability apparatus. Volume permeated has been plotted against sample age and therefore the permeability is represented by the slope of the line. The sample from the mixer was permeated with tap water. One trench sample was permeated with tap water and the other with site leachate having a sulphate content larger than 10 g/l and a pH of approximately 2.5. Although these tests form part of the chemical compatibility assessment, it is useful to draw the following conclusions from the results presented in Fig 2 in this section on permeability. The initial permeabilities of the trench samples were nearly an order of magnitude larger than that of the sample from the mixer. The measured permeabilities decreased in all the samples with permeation (age of sample) such that the permeabilities of the trench samples had decreased to 1 x 10^{-9}m/s by 90 days. The volume of the sample has decreased at an approximate rate of 0.35ml/day (2.2% of volume permeated). It is not known whether this volume reduction is contributing to the decrease in permeability. There were no significant differences in measured permeability between permeating with tap water and site leachate. Chemical compatibility and the chemistry of the effluent from the samples are discussed later.

Strength
Unconfined compressive strengths (UCS) of samples 100mm diameter by 200mm long were measured at 28 days and 90 days. All the samples failed in a brittle manner by a number of vertical or sub-vertical cracks. The mean UCS of uncontaminated samples from the mixer at 28 days was approximately 360 kPa whereas contaminated trench samples had a mean value of 260kPa. At 90 days, the UCS of the uncontaminated material had increased to 890 kPa and the contaminated material to only 580 kPa.

Deformation characteristics
It has been the practice in the UK to specify that the hardened cement-bentonite should have an axial strain at failure in a consolidated drained triaxial compression test (CDTCT) of greater than 5%. This strain criterion is specified because of a perceived need for a deformable plastic cut-off wall that will not crack when subjected to movement. The deformation properties of cement-bentonite in a CDTCT are complex; they change with age of the material and are particularly sensitive to effective confining pressure. Figure 3 shows the effect of effective confining pressure on 28 day old samples. It is only at the effective confining pressures significantly larger than those in-situ that the 5% strain value can be achieved. At 90 days a significant proportion of the samples tested did not achieve the 5% strain value when using an effective confining pressure of 100kPa.

Figure 3. Effect of effective confining pressure on the strain at failure in a consolidated drained triaxial test.
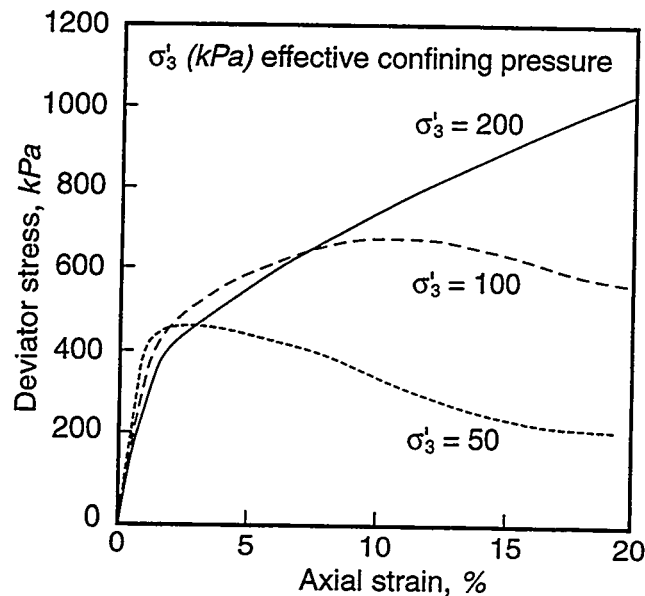
Chemical compatibility

Potential chemical compatibility effects include failure of the slurry to develop the required permeability and strength properties due to mixing in of the contamination (leachates and solids) during construction and change in properties of the set slurry due to the long term permeation of aggressive leachates during operation. Contaminated trench samples and mixer samples have been analysed to determine differences in chemical composition and to investigate any chemical reactions. To assess the chemical compatibility of cement-bentonite with the site leachate, immersion and permeation tests have been undertaken.

Analysis of the contaminated trench samples and a mixer sample approximately 60 days old showed their chemical composition to be significantly different. In particular, sulphur concentrations in the uncontaminated slurry were of the order of 0.8% dried weight compared to values in excess of 10% in the contaminated slurry from the trenches. Iron concentrations of 3% in the contaminated slurry were twice those in the uncontaminated slurry. A 28 day old sample of hardened contaminated slurry was examined using a scanning electron microscope with a cryogenic stage and energy dispersive X-ray analysis (EDS). Only small quantities of ettringite, a mineral resulting from sulphate attack, were detected in the sample. The EDS revealed high concentration of sulphur which could be in the form of thiocynides, sulphides or sulphates.

Immersion tests provide a simple visual indication of any reaction between the leachate and the cement-bentonite. Tests showed that a reaction in the form of surface spalling between cement-bentonite and site leachate initially with a pH of 2.5 does occur, but ceases when the leachate has been neutralised. It has been long recognised that such tests which allow free expansion of the surface material are not representative of conditions in the ground where the cement-bentonite is constrained by the surrounding ground (Jefferis, 1992).

Permeation tests using site leachates or chemical solutions in a triaxial cell where the material is confined provide more realistic conditions for assessing material performance. Permeation of a contaminated trench sample with site leachate is shown in Fig. 2. and it can be seen that there is little difference in permeability compared to the contaminated sample permeated with water. The pH of the inflowing leachate was 2.5 and initially the outflow (effluent) was 14, reducing gradually to 12 after 100 days of permeation. However, the total flow through the sample has been less than three sample volumes (one sample volume is approximately 800ml). It is planned to continue this test.

The effluent from both contaminated trench samples, one permeated with leachate and the other with tap water, was a bright yellow liquid with a strong sulphurous smell. Upon acidification a thick white precipitate appeared which was insoluble in excess acid. Analysis of the effluent samples revealed that all the solutions contained sulphate, dissolved iron cyanide and silica. The presence of the iron cyanide ($3Fe(CN)_6$) in the effluent is explained by considering the pH dependence of spent oxide in solution. Spent oxide (iron ferri cyanide, $Fe_4(Fe(CN)_6)_3$) is essentially insoluble at neutral pH, but its solubility increases rapidly as the solution becomes more alkaline.

$$Fe_4(Fe(CN)_6)_3 \text{ (s)} + 12 H_2O \rightleftharpoons 4Fe(OH)_3 \text{ (s)} + 3Fe(CN)_6^{3-} + 12H^+ + 3e^-$$
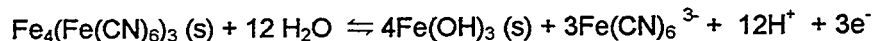
Note: (s) indicates a solid phase

The yellow colour of the samples is characteristic of iron cyanide in solution. Similarly the solubility of aluminium silicates is strongly pH dependent. They are soluble in alkaline conditions but the solubility rapidly falls with increasing H^+ concentration (acidity). Hence, a precipitate would be expected on the addition of acid.

On permeating leachate or water through the contaminated cement-bentonite trench samples, the leachate becomes strongly alkaline and this alkalinity causes the bentonite clay and spent oxide in the sample to dissolve. It would be expected that where this happens in the field, the pH of the effluent would rapidly fall on exiting from the wall and that the dissolved species would rapidly fall out of solution. Thus the conditions in the laboratory permeation test do not represent the field conditions.

The sulphate level in the effluent from the cement-bentonite trench sample which is being permeated with site leachate containing sulphate at levels of between 11,000 and 14,000 mg/l was below 120 mg/l, indicating that most of the sulphate has been absorbed by the cement-bentonite. This has been also found in earlier experiments using sulphate solutions.

Field assessment

Laboratory tests on samples provide an indication of the properties of the hardened cement-bentonite in the trench, but they do not demonstrate that the whole containment system will perform satisfactorily. Few tests have been carried out to measure the in-situ properties of the wall such as permeability and strength let alone system monitoring. Concerns inevitably exist that some intrusive methods could damage the wall. The test walls and boxes provide a unique opportunity to measure the system performance of the boxes and experiment with local in-situ measuring devices. The best measure of the effectiveness of the cut-off wall containment system will come from pumping ground water out of or into the box sections. This will identify whether gross leakage either under the walls or through the walls has developed. However, results from this work are not yet available.

Work to date has concentrated on intrusive in-situ methods of measuring the properties of the wall, especially its permeability. There has often been a need to measure the in-situ permeability of slurry trench cut-off walls, but currently there are no accepted methods. An initial assessment of these various methods and earlier experimental work has been reported by Tedd et al (1995). At the test site the following have been used.

Standpipe Piezometers

Standpipe piezometers with porous tips were installed in the walls at a number of locations when the slurry was two to three days old. Subsequent falling head permeability tests at 28 days in these piezometers gave very low values of permeability, less than 1×10^{-10} m/s. In some piezometers the increased water level established at the start of falling head permeability tests did not alter over a period of many months. It seems likely that the filters of some of these piezometers are blocked.

BRE Packer System

A number of in-situ tests have been undertaken using the BRE packer system (Tedd et al 1995). This involves drilling a 50mm diameter hole in the centre of the wall, isolating part of the hole with a packer and undertaking a falling head permeability test. These tests have given permeability values of the order of 2×10^{-9} m/s for an uncontaminated wall and 5×10^{-9} m/s in the contaminated wall after 90 days.

<u>Piezocone</u>

The piezocone is used for characterising the ground, measuring amongst other properties its strength and consolidation characteristics. Its use in cement-bentonite cut-off walls was first reported by Mannassero (1994), who concluded that it was a promising tool for quality control in terms of evaluating hydraulic conductivity and to some extent in identifying and locating defects. To assess its potential, a 15 cm2 piezocone was used in the independent walls at the test site. The probe was advanced at 2 cm/s. A total of five profiles have been made, two of which were carried out at 28 days in the same wall and gave good repeatability of results in terms of cone resistance, sleeve resistance and pore pressure.

Figure 4. Piezocone profiles of cone resistance, qt, (a) in the same cut-off wall 28 days and 90 days after construction, (b) in a contaminated and an uncontaminated wall at 90 days after construction.

(a)   (b)
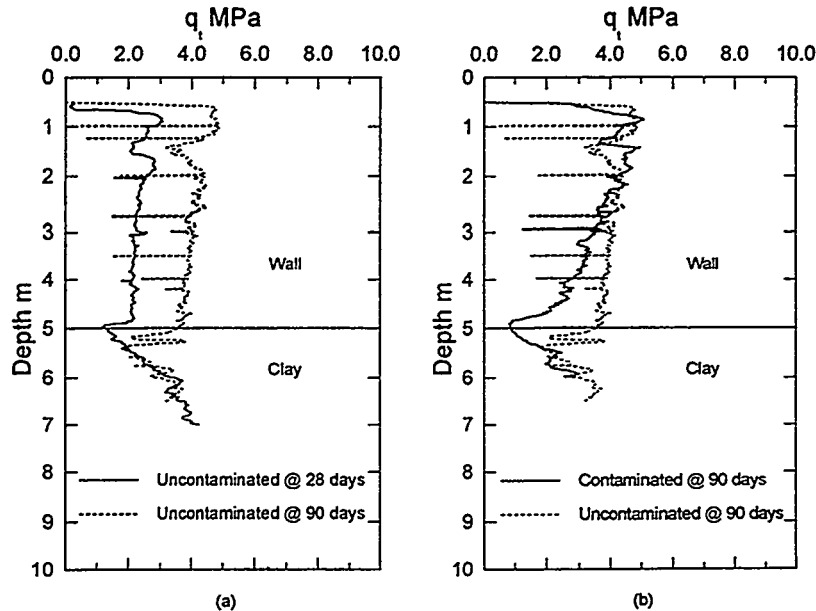
Figure 4a shows profiles of qt (corrected cone resistance) against depth at 28 and 90 days in the same relatively uncontaminated wall. The following observations can be made. For both profiles, qt in the wall decreased very slightly with depth except at about 1.5m depth where there was a fluctuation. There was also a definite decrease in qt at the base of the wall followed by a continuing increase as the cone went into the underlying clay. The profiles show a nearly two fold increase in qt from 28 days to 90 days which compares with a slightly greater than two fold increase in unconfined compressive strength.

Figure 4b shows profiles of qt at 90 days in both the uncontaminated and the contaminated wall. Although qt profiles are similar in the upper 2.5m of the wall, there was a marked decrease in qt in the lower part of the contaminated wall presumably due to the presence of the contamination affecting the strength development. These observations are supported by the UCS laboratory tests.

Results plotted on classification charts (Robertson et al 1986) showed that most of the data classified the cement-bentonite as a clay, however a significant proportion of the data were in or close to the very stiff fine grained cemented sand classification. Similar results were found by Manassero (1994) and reflects the very stiff, strong cemented structure of the cement-bentonite.

The primary objective of using the piezocone was to determine the in-situ permeability. Dissipation tests using the piezocone were undertaken in the walls when they were 90 days old. Permeabilities derived from these tests, using procedures presented by Robertson et al (1992), were of the order of 10-6m/s and several orders of magnitude larger than any other in-situ or laboratory measured values. A possible explanation for the very high permeability values derived from the piezocone dissipation tests is that the cone driving causes localised cracking thus allowing rapid local dissipation of the excess pore pressures generated during driving. This conflicts with the findings of Manassero (1994) and needs further investigation.

Conclusions and future work

The test site is providing a unique facility to study and develop methods to assess the long term performance of cement-bentonite slurry trench walls. This paper provides a brief introduction to the work undertaken. Considerable contamination of the slurry with material possessing high sulphate levels and low pH, has slowed down the rate of development of strength and permeability properties. Despite this retardation, the slurry has set to form a low permeability material at least in the short term. Further development of in-situ permeability measurement is required. Dissipation tests from the piezocone do not appear to give realistic values of permeability in the material used in the cut-off walls at the test site.

Laboratory permeability tests indicate that the set material has a very low permeability even when permeated over a sustained period with the high sulphate low pH site leachate. Pumping from within the two box sections is due to begin in autumn 1996 and this should provide a true assessment of the effectiveness of the containment system; cut-off walls, clay cap and the underlying clay aquiclide.

It is planned to exhume sections of the test walls after a number of years. Non-destrustive methods such a resistivity and self-potential will be assessed for measuring the effectiveness of the walls. Long term laboratory permeability tests and chemical compatibility assessment will continue.

Acknowledgements

References

BRE. 1994. Digest 395. Slurry trench walls to contain contamination.

Garvin,S.L.,Tedd,P. and Paul,V. (1994) Research on the performance of cement-bentonite containment barriers in the United Kingdom. 2nd Int. Symp. on the Environmental Contamination in Central and Eastern Europe. Budapest.pp414-416

ICE (1996) Draft specification for slurry trench cut-off walls construction as barriers to pollution. Institution of Civil Engineers, Great George St, London.

Jefferis,S.A. (1992) Containment-grout interaction, ASCE Speciality Conference. Grouting, Soil improvement and Geosynthetics, New Orleans, pp1393-1402

Jefferis,S.A (1993) In ground barriers. pp111-140. Contaminated Land: Problems and solutions. Ed Cairney,T. Glasgow Backie Academic and Professional.

Manassero,M.(1994) Hydraulic Conductivity Assessment of Slurry Wall Piezocone Tests. Journal of Geotechnical Engineering. ASCE Vol.120,10,pp1725-1746.

Robertson,P.K.,Campanella,R.G.,Gillespie,D and Grieg,J. (1986) Use of the Piezometer cone data. Proc of In-situ 86, ASCE, New York.

Robertson,P.K.,Sully,J.P.,Woeller,D.J.,Lunne,T.,Powell,J.J.M and Gillespie.D.G (1992). Estimating coefficient of consolidation from piezocones tests. Canadian Geotechnical Journal. Vol. 29. 529-550.

Tedd,P., Paul,V. and Lomax,C. (1993) Investigation of an eight year old slurry trench wall. Green'93. Int.Symp. on Waste Disposal by Landfill. Bolton Institute. Balkema 1995.pp581-590.

Tedd,P.,Quarterman,R.S.T. and Holton,I.R. (1995) Development of an instrument to measure in-situ permeability of slurry trench cut-off walls. 4th Int. Symp. on Field Measurements in Geomechanics. Bergamo,Italy. pp441-446.

CONTAINMENT TECHNOLOGY
AT THE "GRIFTPARK" FORMER MGP SITE IN THE NETHERLANDS

Peter W. de Vries[1] and Ben Viveen[2]

Abstract

"Griftpark" is a former highly contaminated gasworks site of approximately 8 hectares situated in Utrecht (The Netherlands). The MGP site is contained by a vertical barrier wall made of a specific mixture of bentonite-concrete and underlying clay layers at depths of 50 to 60 m which are slowly permeable. The barrier wall is 80 cm thick, has an average depth of 64 m, a length of 1260 m and has a total surface area of approximately 70,000 m². The construction of the barrier wall took nearly three years, from 1993 to 1995, to complete and building costs approximated 35 million US$ whereas the total project costs amounted to more than 150 million US$ including water detoxification.

Migration of contaminants in the soil strata is successfully arrested by the construction of the barrier wall which was built conform NEN-ISO 9000/9001 standards. Wall permeability which was tested during a ten months period after construction demonstrates fully warranted reliability. This year a top layer will be installed consisting of an open insolation without foil. After placement of the top the site will be developed into a recreation park. Contaminant migration will permanently be monitored.

1. Introduction

"Griftpark" is one of the most notorious polluted sites in the Netherlands where from 1850 to 1960 a number of gasworks sustained full production. The site of approximately 8 hectares is named after the stream the "Grift" which crosses its borders. It is neighbouring the historic city-centre of Utrecht. For more than a century coal, tar and alike products were transported to and fro by barges which resulted in heavy contamination of the site by aromatics, polycyclic hydrocarbons, phenols, cyanides and hydrocarbons.

Remediation history
After closure in 1960 of the works a number of investigations and feasibility studies were conducted and in 1990 the responsible authorities decided to implement a realistic rehabilitation policy. A strategy of insulating soil contaminants by construction of a barrier wall proved most cost effective. This was followed by control and monitoring of the site. The building activities of the wall started in 1992 and proceeded in stages. A record of interesting aspects such as design and control, quality procedures and contract management are discussed.

---

[1] De Vries Consultancy & Project Management, Bilderdijklaan 6, 3818 WE Amersfoort, The Netherlands tel+ +3133 4611729, fax + +3133 4656867

[2] Heidemij Advies BV, Consulting Engineers, Post Box 264, 6800 AG Arnhem, The Netherlands tel + +3126 3778609 fax + +3126 4457549 , b.viveen@heidf.unisource.nl

Geohydrologic contamination

The first aquifer is located at a depth of 50 m in sandy layers. Between depths of 50 to 65 m series of semi-permeable clay and silt layers are prominent below which sandy layers are extending to great depths containing the second aquifer. The semi-permeable clay layers separate the first aquifer from the second. The first aquifer is severely contaminated by the former gasworks activities whereby mobile contaminants are leaching into the second ground water aquifer and laterally migrating to distances greater than 400m from the source area.

Remediation programme

The following objectives are distinguished for the remediation of the site.

For the source area:

* insulation, control and monitoring of the severely polluted soil and ground water of the source area within approximately 8 ha. This is realized by
  1. ground water abstraction
  2. construction of a vertical barrier wall of 64 m deep joining the slowly permeable clay layers
  3. covering the top of the contaminated soil with an insulation layer which after consolidation is suitable for redevelopment of the site into park grounds.

For the surrounding area by:

* cleaning up of contaminated soil layers and by long term abstraction of the polluted deep ground water.
* ground water detoxification in an off-site water treatment plant.

The total costs of the programme are approximately DFL 300 million (1 DFL = 0,55 c) which are funded by the Ministry of the Environment (90%) and the Municipality of Utrecht (10%).

Assessment and risk analysis

The main objective for the control of mobile contaminants in the soil is to reduce the required ground water abstraction to 50 m3/h or less. The factors which govern leaching and movement of contaminants are dependent on soil properties and the permeability of the barrier wall, underlying clay layers and insulating cover.

* The permeability of the underlying deep clay layer of the site which has an area of approximately 68,000 m2 was investigated. The profile of this layer consists of variable sheets of fine grained sand, loam and clay. The hydraulic permeability is ranging from 25 to 2000 days as a result of the variability of the thickness and composition of the strata. The average hydraulic permeability from the first to the second aquifer is estimated to be 750 days.

* To control horizontal migration of contaminants in the first aquifer a barrier wall of 50 to 64 m deep, 80 cm wide and 1,260 m long (70,000 m2) with a hydraulic resistance of 1000 days was erected. The wall was adapted to the composition, configuration and depth of the semi-permeable clay layer. Various types of building constructions and composition of materials were assessed. The selection criteria used are the permeability and durability of materials under the prevailing chemical conditions and the environmental impact caused by the construction of the wall. Special attention was paid to the inner sealing of the barrier wall with the clay layer and the joints of the wall panels. The wall panels are made of a 50% bentonite and 50% cement mixture which has a hydraulic resistance of 12.5 days/cm.

* The hydraulic permeability of the cover layer of the site is considered to be of minor importance. Therefore, the selection between a closed system of clay layers and/or foil and an open system was based only on economics. The costs of an open system of layers of course metal are lowest i.e. water decontamination and maintenance costs are lower than those of a closed system.

Hydraulic resistance of the barrier wall was assessed by testing of materials and by monitoring the movement of contaminants over a relatively long period of time. The hydraulic insulation of contaminants by the panel joints and panel/clay sealing were examined. Simulation of a worse-case scenario is used to specify guarantees.

2. Design of the barrier wall

The effectiveness of the barrier wall is crucial to the containment of contaminants in the soil strata. Consequently, the design, construction and testing of the wall is completed under strict NEN-ISO 9000/9001 Quality Standards.

2.1 Stepwise construction of the barrier wall

* Two reinforced concrete walls were erected above ground where in between the barrier wall was to be made. This was needed to accurately trace and secure underground pipes and cables and for outlining the contours of the barrier wall.
* A 6 meter deep bentonite-cement wall was constructed to create a zone free of debris in order to prevent downward contamination from the upper layers.
* The construction of the deep wall in connection with the clay layers.

During the building of the barrier wall the development of the wall was regularly evaluated after each phase and quality demands were checked.

* In the first phase two wall elements outside the barrier wall trace were used to test the technique and materials to be used.
* In the second phase a small closed area was used to build part of the barrier wall to the ultimate depth and to test the sealing of the wall with the clay layer. Permeability and seepage were investigated and quality guarantees validated.
* In the third phase the barrier wall was build according to the specifications.
* In the fourth and fifth phases the entire wall construction and its sealing with the clay layers was monitored over a period of ten months and tested for quality validation.

2.2 Contracting

Significant considerations and conditions for contracting works are as follows:

* The prime contractor bears full responsibility for the construction and quality guarantees of the wall and its sealing with the clay layer. This practice resulted in smooth test procedures and legal liability after guarantees are certified .
* Construction techniques and materials such as wall fillings, chemical resistance and permeability were thoroughly tested by independent experts and laboratories before application.

Contractors were carefully selected and a Dutch company who are experts in foundation and remediation were appointed in collaboration with French experts in deep-barrier wall constructions. An affiliation of expertise from external engineering consultants, institutes and government bodies was assigned for supervision, sampling, analyses, testing and environmental impact.

2.3 Detailed design and building preparations

The production procedures for the contract work included the following:

* The removal of all the polluted soil along the course of the barrier wall by dry excavation down to the phreatic level (apr. -1.5m) and replacement by cement-stabilised sand.
* The construction of concrete guide walls 6 m deep into the stabilised sand.
* Making cone penetration tests at regular distances of 7m (the panel width) in between the guide walls to determine the depth and structure of the clay layer.
* Cutting the 6m wall in between the guide walls with a traditional wall cutter and cable crane. For removal of heavy pieces of old foundation rubble hydraulic equipment was used. The excavation was performed using stabilising fluid (bentonite-cement) which hardened out within a few days (1-phase wall technique).
* The construction of the deep barrier wall was performed in two phases:
    - phase 1: excavation of the deep trench with a hydrofraise in panel widths of 7.2m. Each panel was made in three cuttings using excavation stabilizing cutting fluid (bentonite fluid). During construction panel shape and position were checked and registered continuously.
    - phase 2: replacement of the stabilizing cutting fluid by a mixture of 50% bentonite-cement and 50% of the excavated sand.

2.4 Production of quality handbooks, guides and other documents

Contract obligations include publishing of manuals on quality standards, guidelines and procedures. The documents contain both the description of quality standards, definitions, objectives, construction methods, machinery, materials, processes, criteria, certification and relevant aspects of organization, information and time schedules.

Examples are: information of parties, actors and stakeholders, political structures and decision making, contracts, licences and legislation, documentation, sampling and test procedures, terminology and data logging.

Quality standards were established for:
* Overall quality base guidelines with details about planning, sanitation, health and safety, installation testing systems.
* Base guidelines for wall construction with details on cone penetration, drilling and testing, concrete guide walls, 6-meter wall, deep excavation with hydrofraise, bentonite-concrete production and excavation filling, removal of guide walls.
* Basic guidelines for supervision with details on sampling, monitoring, testing and analysis.

Draft documents were prepared before the construction of the wall started. After construction of the wall and evaluation of the test results the draft documents were revised where required. Complementary quality audits were performed to check the quality practice and for additional revisions.

3. Quality assurance during construction

The contract for the project was approved at the end of 1992 although construction activities only started in spring 1993 after installation of quality guidelines and documentation. After consensus about the quality standards and procedures two test panels were manufactured and placed in a test pit to attune the organization and equipment for construction of the barrier wall.

Two major problems arose during the testing procedures in the pit. Firstly the excavated sand was not suitable to be directly mixed with the bentonite-concrete mixture and secondly the last test panel of the wall collapsed during the filling process. Both events caused adjustment of the quality guidelines. The test results of the permeability of the panels in the test pit proved very promising.

The hydraulic resistance ranged from 8000 to 12,000 days which is well above the guaranteed 1000 days. Consequently, the construction of the barrier wall conform the set quality standards was highly successful. Also, provision was made to prevent collapsing of the wall excavation near high pressure gas pipelines and high voltage electricity cables. Higher safety standards at parts of the routing with higher risk were subsequently imposed. At some places of the wall route the underlying clay layer was unusually deep for which the depth of the wall had to be adapted.

The barrier wall was completed and secured in November 1994 and the entire project was finished in April 1995 after making provisions for the river to cross the wall. After completion of the wall ground water abstraction from the insulated site was monitored to calculate the hydraulic permeability from both the barrier wall and the slow permeable clay layer by measuring ground water table, amount of abstracted water, rainfall and evaporation.

4. Results and conclusions

The hydraulic resistance of the bottom stratum was calculated to range between 75 and 175 days with a most probable value of 125 days. The latter is only 1/5th of the expected value of 750 days estimated in the feasibility study but falls within the tolerance range of 25 to 2000 days.
The hydraulic resistance of the barrier wall ranges from 100 to 300 days with a most probable value of 200 days which is also only 1/5th of the required 1000 days. This is thought to be caused by random deficient bonding of the wall and the very deep clay layers. However, the overall hydraulic resistance is within the agreed limits of guaranteed values. Consequently, the insulation of the contaminated site has been successful and can be warranted at a ground water abstraction level of approximately 25 to 30 m3/h which is much lower than the first target of 50 m3/hr.
Although the hydraulic resistance of the bottom stratum is rather low, the resistance of the top 5m layers is much higher than expected. The insulated site comprises a system in which under-pressure can be reached without large fluctuations in the ground water level. This allows for adequate insulation of the site at ground water abstraction levels of 10-15m3/hr and facilitates monitoring of ground water levels outside the contained area.

Chapter 4

Slurry Walls: Soil/Bentonite Case Histories

CASE STUDY
INSTALLATION OF A SOIL-BENTONITE CUTOFF WALL
THROUGH AN ABANDONED COAL MINE

Michael J. Carey[1], Michael J. Fisher[2] and Steven R. Day[3]

Abstract

The site is a 72,846 square meter (18-acre) abandoned strip mine located in Western Pennsylvania used for municipal and industrial waste disposal until the mid-1970's. The waste pit is adjacent and connected to a flooded deep mine which saturated the waste over the past 20 years. The site was placed on the National Priority List in 1984, primarily due to the presence of drums on the surface of the site.

EPA's proposed remedial action for the site included excavation and stockpiling of the waste materials, backfilling the pit with clean materials, constructing a RCRA cell on the clean materials, and disposing of the waste into the cell. The estimated cost of EPA's remedy was approximately $26 million. An alternative action proposed included in-place closure and containment at the site. Many were unsure whether a slurry cutoff wall could be installed through the deep mine adjacent to the waste pit. The proposed alternative of grouting mine voids to facilitate slurry wall installation had never been performed on a Superfund site, and resulted in a cost savings of approximately $15 million. The grout and slurry wall were successfully installed, with complete closure expected by spring of 1997.

Introduction

The project is a Superfund site in Western Pennsylvania. The site shown in Figure 1 is an abandoned strip mine from the Brookville Coal Seam covering an area of approximately 72,846 square meters (18 acres). Adjacent to the northeast side of the strip mine is a deep mine and high wall. The majority of the area immediately surrounding the site is used for agricultural purposes, however, there are several residences 250 meters (820 feet) north of the site.

It is estimated that strip mining at the site began in the early 1900's and concluded in the late 1940's. A 460 meter (1,500-foot) long pit through the center of the site was a remnant of the strip mining operation. The site was operated as a disposal area from the 1950's to 1978. The majority of the material disposed of was dark, coarse foundry sand along with slag, scrap metal, wood, paper, and plastic matter. Drums were placed on the surface of the site, but were removed during a separate project. The disposal operation was halted by the Pennsylvania Department of Environmental Resources in 1978.

The presence of drums at the site attracted regulatory interest. Following preliminary sampling, the site was brought to the attention of EPA for inclusion in the Superfund program and added to the National Priority List in 1984.

[1]Geo-Con, Inc., 4075 Monroeville Blvd., Suite 400, Monroeville, PA 15146, (412) 856-7700, mjcarey0@ccmail.wcc.com

[2]Geo-Con, Inc., 4075 Monroeville Blvd., Suite 400, Monroeville, PA 15146, (412) 856-7700, mjfishe0@ccmail.wcc.com

[3]Geo-Con, Inc., 4582 S. Ulster Street, Stanford Place, Suite 1000, Denver, CO 80237, (303) 740-2600, srdayxx0@ccmail.wcc.com

Site stratigaphy from surface is as follows: 6 to 15 meters (20 to 46 feet) of overburden fill, comprised of mine spoils, landfill materials and fill materials; the Clarion rock formation 6 meters (20 feet) above the abandoned coal mine; the Brookville Coal Seam 1.2 to 2.5 meters (4 to 8 feet) thick; the Brookville Coal Underclay 1 to 2.5 meters (3 to 8 feet) thick; and the Homewood Sandstone formation 10 meters (30 feet) thick.

Contaminants found in the waste were benzo(a)pyrene, dibenzo(a,h)anthracene, chromium, lead and nickel. Because fill material was deposited below the water table into the mine pool, EPA concluded that the site groundwater was contaminated with the same materials found in the waste. Additionally, low levels of vinyl chloride and trichloroethene were detected in the onsite groundwater.

Disposed materials had contaminated onsite shallow groundwater, Clarion Formation groundwater and the Homewood Formation groundwater. Onsite waste materials were considered a current dermal contact risk, and migration of contaminated groundwater considered a potential future risk.

Remedial Actions

Objectives of closure were as follows:

> Prevent migration of contamination through the groundwater;

> Prevent infiltration of surface water into the contaminated area;

> Prevent contact with contaminated materials.

EPA's preferred alternative for remediation of the site included construction of a RCRA compliance landfill at the site. This alternative would have achieved the desired objectives, but had an estimated cost of $26 million. The plan included excavating and stockpiling wastes onsite while the RCRA cell was constructed. The cost of this alternative was high because much of the waste was located below the water table, requiring a dewatering system and treatment of the wastewater before discharge.

The Alternative Remedial Action proposed by the owner and engineer was onsite closure accomplished by installing a soil-bentonite slurry wall around the perimeter of the contaminated area and installation of a low permeability GCL cap. Extraction wells installed inside the slurry cutoff wall would collect contaminated groundwater and send it to onsite water treatment system. Estimated cost of the alternative remedy was approximately $10 million.

The main difficulty at this site was the abandoned deep mine adjacent to the landfill. Landfill closures using soil-bentonite slurry walls and low permeability caps are common. The challenge posed by this closure was the installation of approximately 275 meters (900 linear feet) of slurry wall through the deep mine, because realignment of the slurry wall was not feasible. EPA initially decided the alternative remedy would not be acceptable for this reason, but later agreed to consider the action if a panel comprised of EPA and Army Corps of Engineer experts deemed the installation feasible. The remedial action was approved pending resolution the following:

1. Verification of coal seam underclay presence along the entire alignment of the slurry wall through the deep mine. The underclay acts as the confining or key material for the cutoff wall.

2. Demonstration that the remedial action could control damage to the cutoff wall or cap due to potential mine subsidence.

3.   Demonstration that the remedy would not adversely impact the mine pool and could be feasibly constructed at a reasonable cost.

Slurry Wall and Grouting

The slurry wall technique uses an engineered fluid, water and bentonite (in this case), to support the sidewalls of a deep, vertical trench. The presence of mine voids as high as 2.4 meters (8 feet) made the construction of a slurry wall at this site impossible at this site. Excavating a slurry wall through voids of a deep mine would cause an immediate and catastrophic loss of the slurry.

Mine grouting was selected as the technique to fill the voids. Grouting was performed along the slurry wall alignment for two purposes: to provide containment for slurry wall construction, and to prevent damage to the wall and cap due to potential mine subsidence. Three lines of grout holes were installed along and adjacent to the centerline of the slurry wall. An outer bulkhead was installed 15 meters (50 feet) outside the slurry wall. A second row of grout holes was installed approximately 10.5 meters (35 feet) inside the slurry wall alignment and adjacent to the landfill and highwall. The third row of holes was placed directly along the slurry wall alignment (see Figure 2).

Standard air rotary drilling rigs were used to install the grout holes. 200 millimeter (eight-inch) diameter steel casing was installed through the overburden to the top of the Clarion rock formation. A 100 millimeter (4-inch) diameter hole was drilled through the rock formation. Borings were drilled along all three boring alignments on 3 meter (10-foot) spacings to identify mine voids and highly fractured rock. When voids were encountered, hole spacing was decreased to 1.5 meter (5-foot) on centers.

The contractor performed a mix design to determine the flyash to cement ratio required to meet the strength specification of 100 psi after 7 days for both low and high slump grouts required for the project. The low slump grout, which was required to have a slump in the range of 25 to 75 millimeters (1 to 3 inches), consisted of 9:1 flyash to cement and a water to solids ratio of 0.154. The high slump grout, with a required slump in the range of 200 to 250 millimeter (8 to 10 inches), consisted of 8:1 flyash to cement with a water to solids ratio of 1.3. Both grouts were required to have a minimum compressive strength in 7 days of 100 psi.

Grouting work began with the outer bulkhead borings. To assure detection of all possible voids, the specification required that each outer hole be drilled 0.6 meters (2 feet) into the Brookville Coal Underclay. A low slump grout , prepared at the onsite plant, was injected through a grout pipe inserted to the bottom of the hole. As the pressure built, the pipe was raised creating a column of grout. As the process is repeated in adjacent holes, a bulkhead is constructed. The purpose of the low slump grout is to create a barrier to contain the high slump pressure grouting performed for the inner and slurry wall grout holes.

Once a sufficient number of outer bulkhead holes were completed, work began on the inner and center pressure holes. The inner row of holes were drilled 0.6 meters (2 feet) below the Brookville Coal Underclay and the center pressure was drilled 1.5 meters (5 feet) into the Brookville Coal Underclay. Both sets of holes were pressure grouted with high slump grout, filling voids both in the mine and in the highly fractured rock. Figure 3 is a cross section through the 3 rows of grout holes.

The cutoff wall specified for the project was a 0.6 meters (2 foot) wide soil-bentonite wall installed by the slurry trench technique. The wall was keyed a minimum of 1 meter (3 foot) into the Brookville Coal Underclay, where present, or 1.5 meters (5 feet) into the underlying Homewood Sandstone which also served as a confining zone. In the deep mine area, the cutoff wall is keyed into the Underclay. The wall backfill was specified to have a hydraulic conductivity of 1×10^{-7} cm using a mixture of the excavated soils and 2 % bentonite clay.

The bentonite slurry, used to support the trench, forms a cake on the trench sidewalls, plugging the soils and forming a hydraulic barrier. The permanent wall is formed by replacing the slurry with an engineered low permeability backfill. Trench stability is maintained during construction by controlling slurry properties (density, viscosity, etc.) and by keeping the slurry level in the trench above the groundwater table.

The Contractor performed mix designs to determine that 2% bentonite would need to be added to site soils to assure the wall backfill would meet the performance specification. To achieve the 2% bentonite addition, 1% dry bentonite was added to the spoils removed from the trench. An industry standard, yet a conservative assumption, is that of 1% bentonite is incorporated into the spoils excavated using the slurry trench method.

Slurry for the trench was made by mixing onsite pond water with premium grade sodium/calcium montmorillonite clay, or bentonite. The materials were mixed to a homogeneous, colloidal suspension in a specially designed 12.5 cubic meter (5-cubic yard) colloidal mixer. The slurry was required to have a density of at least 64 pcf and a marsh funnel viscosity of 40 seconds at the plant before introduction to the trench. Typically, 4 to 5 45 kilogram (100-pound) bags of bentonite were added to approximately 3,200 liters (850 gallons) of mix water to ensure trench stability and to meet specifications.

Mine grouting for the project was performed in the fall of 1995. Mine voids along approximately 275 meters (900 linear feet) of slurry wall were grouted. Approximately 250 linear feet of the wall was installed through unmined coal. The grouting program included installation of 660 borings, 9,850 meters (32,500 linear feet) of drilling. A total of 22,300 cubic meters (9,000 cubic yards) of grout was placed.

The slurry wall was installed through the deep mine area in the spring of 1996. Excavation of grout materials did not pose a problem due to the relatively low compressive strength of 100 psi. The wall was completed through the deep mine area without any measurable loss of slurry or backfill cave-ins.

Another anticipated problem was the effect of cement on the bentonite slurry. Bentonite slurry walls constructed through cement stabilized soils have historically had problems with flocculation of the bentonite. Lignosulfanate was approved as an additive to bentonite slurry to counteract this effect. No problems were experienced on this project and lignosulfanate was not required.

Summary and Conclusions

This containment project was started in the summer of 1995, and successful completion is expected in the spring of 1997. Applying engineering and construction ingenuity, project remediation costs were reduced approximately 60% by allowing inplace containment versus excavation and removal to an off-site RCRA hazardous waste landfill.

This project illustrates that cutoff walls can be installed through areas with large voids, such as deep mines. The grouting program was successful in sealing the voids and containing the slurry during construction. The project illustrates the potential for use of grouting and slurry wall installation in combination to provide a cutoff barrier through other types of subsurface voids and fractures.

References

Woodcock, J., Weinzierl, R. and Miller, K. (1996) CERCLA Landfill Closure Utilizing Slurry Wall Construction in Deep Mined Area.

N

POND NO. 1

STOCKPILE
AREA

STOCKPILE
AREA

POND
NO. 2

SLURRY
WALL

POND
NO. 3

INNER PRESSURE GROUT HOLES

CENTER PRESSURE GROUT HOLES

OUTER BULKHEAD GROUT HOLES

MINE VOID AREA

APPROXIMATE
LIMITS OF
FILL AREA

FIGURE 1
SITE PLAN
NO SCALE

145
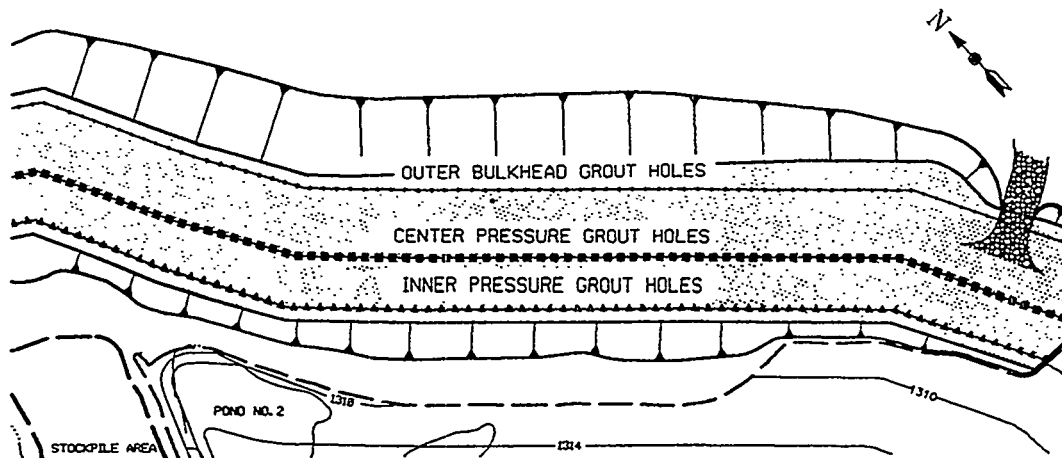
FIGURE 2
ENLARGEMENT OF MINE GROUTING AREA
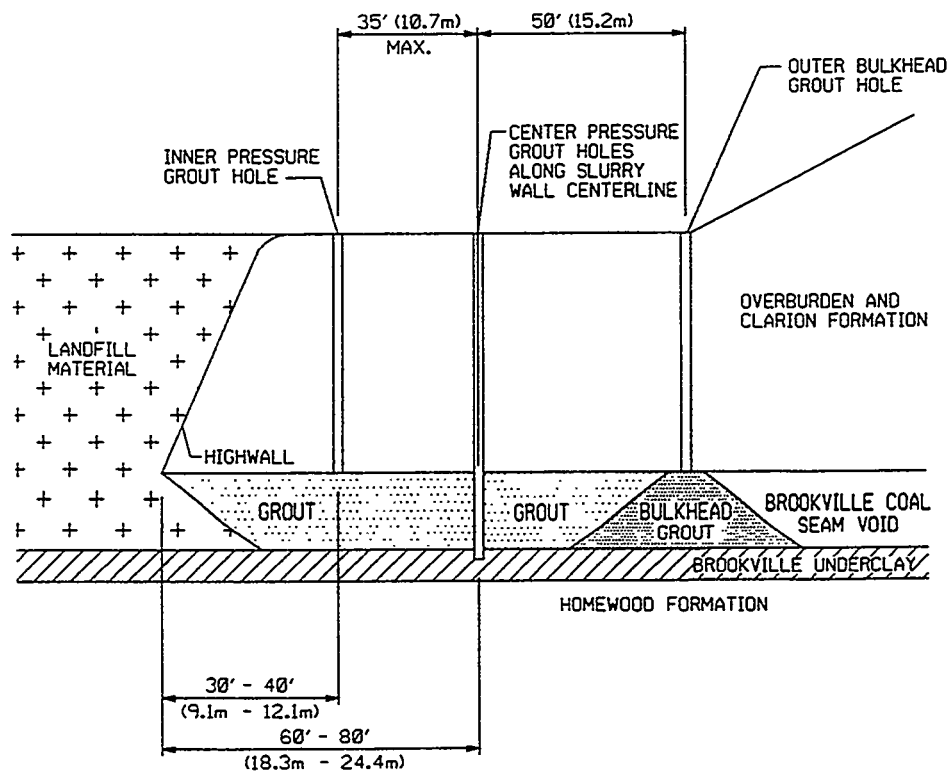
FIGURE 3
CROSS SECTION THROUGH
THE (3) ROWS OF GROUT HOLES

CASE HISTORY: VERTICAL BARRIER WALL SYSTEM FOR SUPERFUND SITE

AUTHORS

M. A. Koelling
C. P. Kovac
Hayward Baker, Inc.

J. E. Norris
Kennedy/Jenks Consultants

ABSTRACT

Design considerations and construction aspects are presented for the installation of a vertical barrier wall system for the Boeing Company at a Superfund Site near Seattle, WA. The construction was performed during 1996. The vertical barrier wall system included: 1) a soil-bentonite (SB) slurry wall, approximately 670 meters (2200 feet) in length, ranging from 12 to 21 meters (40 to 70 feet) in depth; 2) expansion of a cover system over the area enclosed by the SB wall; and 3) surface drainage improvements. Design and construction of the system addressed requirements of a Consent Decree for the site issued in 1993. The paper discusses the development of the design to meet remedial performance goals of preventing migration of contaminants in the soil/groundwater system and aiding aquifer restoration. Secondly, the paper details installation of the SB wall, highlighting the more significant construction issues, which included excavation of the wall through glacially deposited cobbles/boulders/till as well as addressing the severe elevation changes along the wall alignment. Thirdly, the paper presents Quality Assurance (QA) monitoring and testing performed during the construction phase.

INTRODUCTION

The vertical barrier wall system was constructed at the Queen City Farms (QCF) Superfund Site, an area of 1.3 square kilometers (320 acres) located in a rural section of south King County, Washington, approximately 24 km (15 miles) southeast of Seattle. Land use at the site in the 1950's and 1960's included a pig farm, gravel mine, small airport, and hazardous waste disposal ponds. Industrial waste liquids including paint, petroleum products, oils, and organic solvents were disposed in three unlined waste ponds located in the northeastern portion of the site.

Three waste ponds were the focus of an Initial Remedial Measure (IRM) performed in 1986 that included: 1) removal of the ponds' contents and bottoms; 2) surface water diversion; and 3) cover system construction over the ponds. Further remedial investigations and feasibility studies were performed from 1987 through 1992. The Boeing Company agreed to prepare and implement further work measures for site cleanup under a Consent Decree issued in 1993. Boeing conducted this work in cooperation with the U.S. EPA and the State of Washington Department of Ecology.

Further work measures, pertinent to this case history, include the following, as taken in part from the Consent Decree:

- Isolation of contaminated soils by construction of a subsurface vertical barrier wall system around the IRM to minimize intrusion of groundwater from Aquifer 1 and the near-surface water bearing zone;

- Expansion of the existing IRM cover system to include the area bounded by the vertical barrier wall;

The Boeing Company entered into a contract with Hayward Baker Inc. (HBI) in 1995 to provide design/build services for the required items listed above. Kennedy/Jenks Consultants (KJC) provided the engineering design under subcontract to HBI.

SITE CONDITIONS

Prior to completion of project design, the subsurface site conditions were thoroughly characterized by extensive Remedial Investigation (RI) and post-RI field investigations. Figure 1 shows a generalized hydrogeologic cross section of the construction area.

Preconstruction Ground Surface: The site is a sloping meadowland area predominantly vegetated by low grasses and shrubs. Sloping topography present at the outset of construction was a result of grading work performed during the IRM. The upper 1 meter (~3 feet) of soil is predominantly silty sand and gravel. A multilayer PVC geomembrane cover system, installed as part of the IRM, was present over a significant portion of the area to be enclosed by the barrier wall. Ground surface elevations at the site range approximately from 137 to 155 meters (450 to 510 feet) above mean sea level.

Figure 1: Generalized Hydrogeologic Cross Section
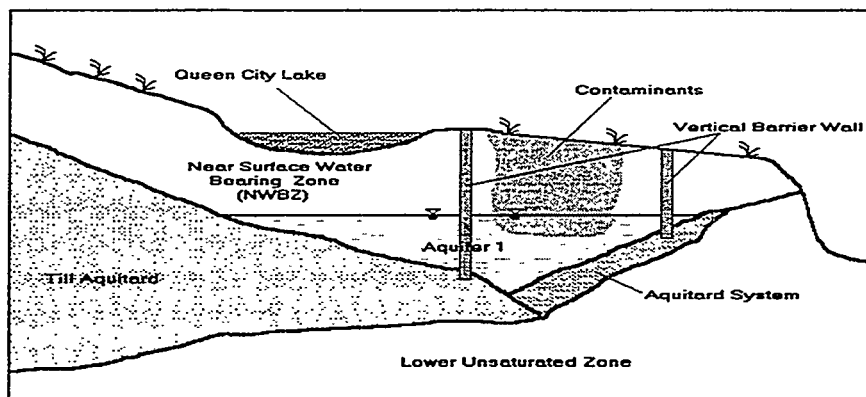
Subsurface: The site is underlain by a complex sequence of glacial deposits, which include open works gravel, dense ablation till, dense lodgement till, and outwash. In general, several strata of hydrogeologic significance include an upper zone of transient groundwater flow [commonly referred to as the Near Surface Water Bearing Zone (NWBZ)], an upper saturated zone referred to as Aquifer 1, a thick Till Aquitard unit, and a thinner layer of silt and sand referred to as the Aquitard System.

Hydrology: The site is bordered on the northwest and south by two seasonal lakes, Queen City Lake and Main Gravel Pit Lake, respectively. Relatively high volumes of runoff enter these lakes in the wet season (November to April). During the rest of the year, runoff is limited, and water levels in the lakes decline dramatically. Water from Queen City Lake discharges through an overflow culvert and also leaks through the lake bottom into Aquifer 1 Surface water from Queen City Lake is discharged to Main Gravel Pit Lake, and some groundwater moving through Aquifer 1 emerges at springs above Main Gravel Pit Lake. Contaminants from the former waste ponds have been detected in Aquifer 1. The primary focus of this project was to substantially reduce the recharge of Aquifer 1 within the barrier wall and prevent groundwater from contacting contaminated aquifer material. Figure 1 depicts the site subsurface and hydrology.

DESIGN CONSIDERATIONS

The remedial performance goal for the vertical barrier wall and cover system extension around and over the IRM area is to prevent contaminants in the subsurface soil from migrating to deeper groundwater and to aid in restoration of Aquifer 1 outside the barrier wall. Foremost among the design considerations for the barrier wall were the proper alignment and depth of the wall, the permeability of the wall backfill (1×10^{-9} m/sec), and the durability of the wall. The wall and cover system were designed to withstand increased hydraulic forces, possible chemical alterations, and potential environmental loading conditions due to seismic events and/or dewatering of the interior

148

formation. The cap system was designed to provide long-term minimization of infiltration through the expanded IRM area, function with minimum maintenance, promote drainage, minimize erosion or abrasion of the cover system material, and accommodate settling and subsidence. In addition to an engineering design review process by Boeing and its site representative, the design also had to be approved by the U. S. Environmental Protection Agency (EPA).

Seepage Cutoff/Barrier Alignment: The design of the wall included establishing its alignment outside known boundaries of contaminated soils and a zone of light non-aqueous phase liquid (LNAPL) present in Aquifer 1. These boundaries, both horizontal and vertical, were determined using data generated from the RI and subsequent site investigations. The wall bottom was designed to be imbedded ("keyed") into the Aquitard System layers to significantly reduce vertical flow beneath the wall. Barrier wall depths were designed conservatively to allow for variability in subsurface conditions.

Hydraulic Modeling: The anticipated hydraulic pressures and gradients acting on the proposed SB wall were evaluated to assure backfill stability against piping/blowout into adjacent formation materials, hydraulic fracture, and erosion of wall backfill at the base of the wall into coarser formational materials due to underseepage. Numerical modeling of the groundwater flow regime in the IRM area was undertaken by KJC to confirm and verify results of pre-design modeling. The purpose of the modeling effort was to quantify the worst-case head increase(s) along the upgradient side of the barrier wall system. The results of the design modeling effort were generally consistent with previous model results. Wall thickness from 0.9 to 1.2 meters (3 to 4 feet) was specified to withstand anticipated hydraulic forces.

Cover System Placement: Initially the cover system was designed to be identical to the cover system installed as a component of the IRM. This approach was pursued to facilitate regulatory agency approval. Alternative designs such as incorporating a geosynthetic clay liner (GCL) were also evaluated prior to construction. The cover system design considered several important factors which included permeability, slope stability (static and dynamic), and drainage.

CONSTRUCTION

The Slurry Wall: Excavation of the slurry wall began on May 7, 1996, and backfilling was completed on September 11, 1996. HBI used a large backhoe with an extended stick to dig the trench length of 670 meters (2200 feet) to depths up to 21.3 meters (70 feet). Along deeper portions of the barrier wall alignment, the construction platform was lowered to facilitate excavation. A crawler crane was equipped with a chisel for boulders and with a clamshell for cleaning the trench bottom. The construction process is shown in Figure 2.

Backfill, comprised of excavation spoils, trench slurry, imported silt, and coarse grain bentonite was first mixed by a dozer in a broad and shallow rectangular mixing area. This enabled homogeneous mixing of ingredients, and facilitated the removal of coarse material from the cuttings. The dozer then pushed the mixed backfill into a deeper and roughly cylindrical mixing pit. In this second stage the backfill was mixed further by a backhoe and loaded into trucks. The backfill was then transported to and placed in the trench.

Backfill placement began at the first portion of open trench as excavation continued at the leading end. Initially the backfill was placed and allowed to flow down a gently sloping portion of the trench, commonly referred to as a "lead in trench." As backfilling continued, the backfill assumed its own angle of repose at the first portion of the trench. Backfill was then placed on the portion of the backfill material progressively exposed above the slurry level in the trench material. This method of placement resulted in the backfill advancing via a continuous slope failure of the backfill material in place, thus ensuring that no pockets of slurry or other sloughed material were incorporated within the wall. Upon completion of backfill placement, a cap of silt, approximately 1 meter (3 feet) thick, was placed over the backfill to prevent desiccation of the top of the wall and to facilitate compaction beneath the cover system tie-in along the top of the wall alignment.

Figure 2: Trench Excavation & Backfilling
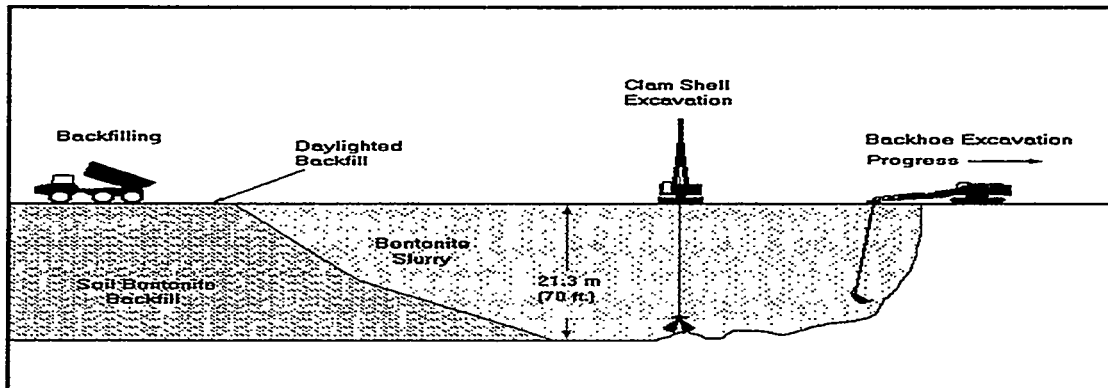
This project site presented several challenges to the typical construction of the soil-bentonite slurry wall. The most formidable was due to the nature of the glacial till in which the wall was constructed. The lodgement till forming a portion of the Aquitard System is well indurated and extremely difficult to excavate. Penetrating the till, a minimum of 0.9 meters (3 feet) required for proper keying-in of the wall, would often completely wear out a set of steel backhoe teeth in less than one 10 hour shift of excavation. Additionally, the barrier wall penetrated through a zone of open works gravel, into which large amounts of slurry were lost. The losses were controlled by either increasing the flow of new slurry to the trench, or by adding other stabilizing agents to the slurry. Due to the relief across the site and variations in the wall bottom elevation dictated by the complicated hydrodynamics of the glacial deposits present, numerous changes in working platform elevation were required along the alignment to complete construction of the barrier wall. The numerous challenges to barrier wall construction resulting from elevation changes were overcome through the strategic use of a combination of sheetpile bulkheads to shore up the backfill at points of change in working platform elevation, and earthen berms for maintaining slurry levels and assuring stability of the trench wall.

The Cover System: The cover system was installed in layers consisting of 0.6 meter (2 feet) of silt or (alternatively) GCL, a 0.762 mm (30 mil) PVC geomembrane, 0.6 meter (2 feet) of sand, 0.6 meter (2 feet) of cobbles, and at least 0.3 meter (1 foot) of cover soil. Each layer was tested to assure compliance with the specifications. The subgrade and the silt were tested for compaction and moisture content using a Standard Proctor test and a nuclear density meter. The gradation of the subgrade, silt, cobbles and sand was measured. Compliant lift thicknesses were attained by placing a grid of stakes marking the elevations each lift needed to reach. The GCL and the PVC geomembrane were tested for material and seam strength, and required the manufacturer's certification of quality.

The principal challenge in construction of the cover system was to attain the specified density of the silt layer under the PVC. Rain during construction frequently rendered the silt too wet for proper compaction. This difficulty was overcome by substituting the GCL for the silt layer over two thirds of the site. The GCL proved to be advantageous because a section of GCL could be placed and covered in one day, whereas the silt had to be placed in several lifts each requiring several days for drying, compaction, and finish rolling.

A significant concern in the cover system design and in use of the GCL was the slope stability of the cap system. To address the issue of slope stability, a slope stability sensitivity analysis was run to determine maximum allowable slopes and slope height. Results of this analysis were incorporated into the design and subsequently added to the new GCL specification to provide maximum slope limits and still allow flexibility in the final grading. An overlapping tie-in of the GCL under the existing cover system was used instead of an anchor trench, after it was determined that the normal loading of the materials overlying the overlap would adequately anchor the GCL.

QUALITY ASSURANCE

A QA/QC testing and monitoring plan was developed and defined in the specifications to provide adequate documentation of project performance. All QA/QC test results and records were reviewed by HBI, KJC, Boeing and their site representative, EPA, and U. S. Army Corps of Engineers (USACOE). Some of the test samples were split, and independent parallel tests were run by both the site representative and HBI. This level of reproducibility provided substantial validation of test results.

The QA/QC testing and monitoring plan was reviewed by all parties. As a part of this plan, the design/build team-and Boeing each provided a qualified individual tasked to observe construction and review QA/QC test results and records. HBI and the site representative each maintained an on-site laboratory, each supported by a more fully equipped, off site and local laboratory. This provided the ability to obtain short-term test results quickly when expediency was required and/or to obtain test results of greater accuracy (e.g. longer run times) for final documentation as required. Results of the QA/QC testing and monitoring plan covered water, bentonite, slurry, trench depth and key, and backfill. The QA/QC testing and monitoring for each of these media is provided in Table 1.

Table 1: QA/QC Testing and Monitoring Plan

Media	Standard	Test	Frequency	Specified Values
Water		pH	Once	As required to hydrate the
		Hardness	Once	bentonite
		Total dissolved solids	Once	
Bentonite	API 13A	Test to show compliance with standard	Per truckload	Certificate of compliance from manufacturer
Pond Slurry	API 13B	Viscosity	Once per shift	Minimum 40 second Marsh Funnel
	API 13B	Unit weight	Once per shift	Minimum 10.06 kN/m³ (64 PCF)
	API 13B	Filtrate Loss	Once every third shift	Less than 25 CC in 30 minutes @ 689.5kPa (100 PSI)
Trench Slurry	API 13B	Viscosity	Once per shift (top & bottom)	Minimum 40 second Marsh Funnel
	API 13B	Unit weight	Once per shift (top & bottom)	Minimum 10.06 kN/m³ (64 PCF)
Backfill	ASTM D-5084	Permeability	Once per 765 m³ (1000 CY)	1×10^{-9} M/SEC (1×10^{-7} CM/SEC) maximum
	ASTM D-1140 (mod)	Fines content	Once per 765 m³ (1000 CY)	Not less than 20 percent passing the #200 sieve
	ASTM D-1140 (mod)	Unit weight[b]	Once per shift	2.36kN/m³ (15 PCF) greater than trench slurry unit weight
	ASTM C-143	Slump	Once per 380 m³ (500 CY)	7.6 - 17.8 cm (3-7 inches)
		Slope Profile[b]	Twice per shift (beginning and end of shift)	No irregularities
Trench		Depth measurement	Once per 3 linear meters (10 linear feet) of trench excavation	Minimum penetration into key
		Key	Continuous	Acceptable key materials

Water: Construction water was tested once at the outset of pumping from the supply well.

Bentonite: Each shipment of bentonite was accompanied by a certification sheet verifying compliance of the lot with American Petroleum Institute standards

Slurry: Pond slurry was tested for viscosity and unit weight once each shift. It was also tested for filtrate loss twice each work week. Two samples of the trench slurry were also tested for viscosity and unit weight once each shift. One sample was taken from the top 3 meters (10 feet) of the slurry, and the second was taken from the bottom of the trench.

Trench: The trench was sounded and a profile developed at least twice a day at 3 linear meter (10 linear foot) intervals. Additionally, the trench was sounded at the completion of each cut to provide the means to locate any areas where materials or construction might later have been found to be non-compliant. HBI maintained tabular and graphical records (updated daily) of the soundings. Classification and verification of the trench key materials (Aquitard System) were performed continuously as the excavation proceeded.

Backfill: Quality control of the backfill was performed primarily before and during the mixing of each 770 m3 (1000 cu. yd.) batch. This involved testing of ingredient materials, design of the mix, and testing of the first batch. This provided HBI with the information necessary to formulate a backfill mix that consistently met specifications. Once the first batch was found to meet all specifications, its mix design was simply repeated in subsequent batches. This early effort expedited the mixing, testing and placing of subsequent backfill batches. As can be seen in Figure 3, the mix design produced a backfill that consistently exceeded permeability specification requirements.

Figure 3:   Permeability Test Results
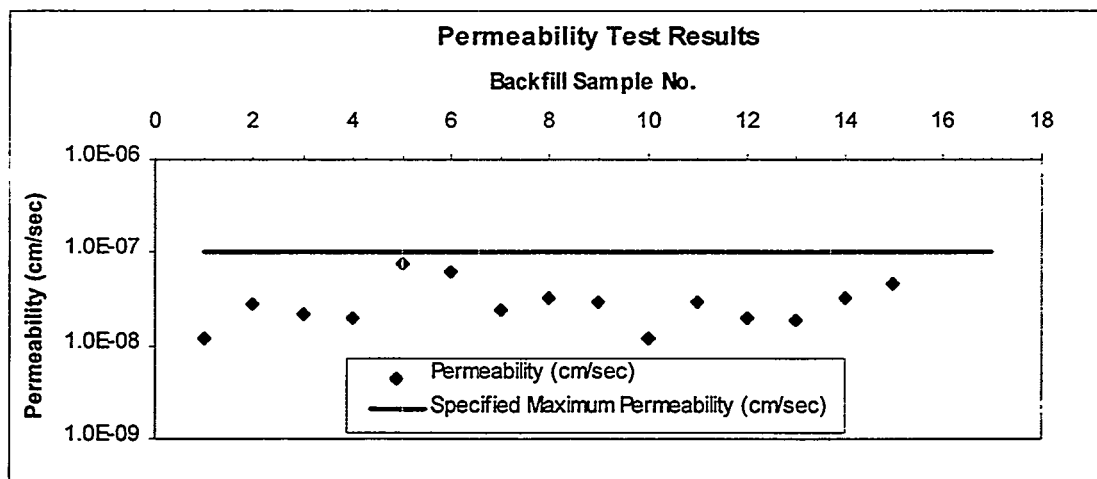
CONCLUSIONS

The barrier wall system for the Queen City Farms site was successfully installed within the scheduled work duration, meeting all requirements of the design/build contract and Consent Decree, and providing Boeing with a quality product. Observations and conclusions are summarized below:

- The selected soil-bentonite slurry wall system proved to be the most economical and constructible barrier wall system for the given site conditions and restrictions;

- Continuous observation of the stratigraphic sequence penetrated by the trenching allowed for timely decisions regarding final keying-in of the barrier wall;

- All permeability testing for the soil-bentonite backfill met or exceeded the required $k=1x10^{-9}$ m/sec ($k=1x10^{-7}$ cm/sec);

- Trench advancement through exceptionally hard till with boulders was anticipated and accomplished with frequent equipment maintenance, bucket teeth replacement, and chiseling effort;

- Slurry loss through open works gravel was controlled by adjusting slurry feed rate, changing slurry viscosity, and/or through use of stabilizing additives, thereby maintaining adequate slurry level and trench stability at all times. However, slurry was detected in various wells

completed in Aquifer 1 across the site, indicating significant transmission of slurry through open works gravel;

- Construction of the barrier wall along an alignment with significant grade changes was successfully performed through efficient use of working platforms, earthen berms, and sheet pile bulkheads;

- Utilization of the GCL liner over a portion of the extended cover system in lieu of the silt layer eliminated difficult soil moisture conditioning requirements during wet weather operations and provided a good technical alternative to be considered for future cap construction.

To conclude, it should be noted that joint cooperation is necessary among various members of the client's project representatives and the design/build team to successfully complete any project, much less one that had the number of design and construction challenges offered by this project. In this regard, the authors acknowledge the efforts of the Boeing Support Services Group, EPA, USACOE and Boeing's site representative, Golder Associates.

M. A. Koelling
C. P. Kovac
Hayward Baker, Inc.
2701 California Avenue SW, Suite 230
Seattle, WA 98116

J. E. Norris
Kenndy/Jenks Consultants
530 South 336th Street
Federal Way, WA 98003

REFERENCES

1. Burke, George K. and Fritz N. Achhorner (1988) Construction and Quality Assessment of the In Situ Containment of Contaminated Groundwater.

2. Golder Associates, Inc. (February 23, 1995) Preliminary Design of Vertical Barrier Wall - Queen City Farms Remediation Project.

3. Golder Associates, Inc. (June 30, 1995) Boeing Queen City Farms Vertical Barrier Wall 1995/1996 Subsurface Investigation Summary for Preliminary Design.

4. Hayward Baker Inc. and Kennedy/Jenks Consultants Inc. (April, 1996) 100% Task Remedial Design Report - Queen City Farms Vertical Barrier Wall System 1995/1996

5. Landau Associates (April 20, 1990) Remedial Investigation Report Queen City Farms King County, Washington

6. U.S. Environmental Protection Agency (November 8, 1993) Consent Decree - Queen City Farms Superfund Site.

KAOLINITIC CLAY-BASED GROUTING DEMONSTRATION

A.Lynn McCloskey[1], Creighton J. Barry[2]; and R. Wilmoth[3]

Abstract

An innovative Kaolinitic Clay-Based Grouting Demonstration was performed under the Mine Waste Technology Program (MWTP), funded by the U.S. Environmental Protection Agency (EPA) and jointly administered by the EPA and the U.S. Department of Energy (DOE). The objective of the technology was to demonstrate the effectiveness of kaolinitic clay-based grouting in reducing/eliminating infiltration of surface and shallow groundwater through fractured bedrock into underground mine workings.

In 1993, the Mike Horse Mine was selected as a demonstration site for the field implementation and evaluation of the grouting technology. The mine portal discharge ranged between 114 to 454 liters per minute (30 to 120 gpm) of water containing iron, zinc, manganese, and cadmium at levels exceeding the National Drinking Water Maximum Contaminant Levels.

The grout formulation was designed by the developer Morrison Knudsen Corporation/Spetstamponazhgeologia (MK/STG), in May 1994. Grout injection was performed by Hayward Baker, Inc. under the directive of MSE Technology Applications, Inc. (MSE-TA) during the fall of 1994. The grout was injected into directionally-drilled grout holes to form a grout curtain at the project site. Post grout observations suggest the grout was successful in reducing the infiltration of the surface and shallow groundwater from entering the underground mine workings. The proceeding paper describes the demonstration and technology used to form the subsurface barrier in the fracture system.

Introduction

A significant environmental hazard to surface waterways nationwide and worldwide is acidic, metal-laden water draining from abandoned mines. The State of Montana has identified more than 20,000 abandoned mine sites, on both public and private lands, resulting in more than 2092 kilometers (1,300 miles) of streams experiencing pollution problems. To address and find technical solutions to the problems created by these sites, the EPA created the MWTP which demonstrates field and pilot-scale technologies to either treat, reduce, or eliminate the existing hazards.

The MWTP Activity III, Project 2, Clay-Based Grouting Demonstration Project was funded by EPA and jointly administered by EPA and the DOE through an Interagency Agreement. EPA contracted MSE-TA through the MWTP to evaluate and develop the subsurface application of a clay-based grouting technology. The Mike Horse Mine site was selected as the demonstration site (MSE, Inc., 1994).

EPA and DOE selected the clay-based grout formulated technology developed by MK/STG. The technology involved injecting clay-based grout into a fractured bedrock system, thereby reducing the amount of ground and surface water infiltrating underground mine workings. Reducing water inflow into underground mine workings was expected to reduce the volume of impacted water discharging from the 300-level adit portal of the Mike

[1] A. Lynn McCloskey, MSE Technology Application, Inc., P.O. Box 4078, Butte, MT 59702, (406) 494-7371, lmcclosk@buttenet.com

[2] Creighton J. Barry, MSE Technology Application, Inc., P.O. Box 4078, Butte, MT 59702, (406) 494-7268, mking@buttenet.com

[3] Roger C. Wilmoth, National Risk Management Research Laboratory, Office of Research and Development, U.S. Environmental Protection Agency (MS 445), 26 W. Martin Luther King Drive, Cincinnati, OH 45268, (513) 569-7509, Roger_Wilmoth@msn.com

Horse Mine and potentially improve water quality downstream from the mine. Because the technology was developed to eliminate the flow of water into the mine workings, it was considered a source-control technology.

The Mike Horse Mine site is owned by American Smelting and Refining Company, Inc. (ASARCO) and is located approximately 24 kilometers (15 miles) northeast of Lincoln, Montana. Presently, slightly acidic waters containing elevated levels of heavy metals discharge from the 300-level portal of the mine directly into Mike Horse Creek. The State of Montana recognized this mine discharge as one of the major contributors of metal loading into the Upper Blackfoot River (Montana Department of State Lands, 1991). Mike Horse Creek is one of three tributaries that make up the headwaters of the Upper Blackfoot River. A portion of the mine workings, where water from Mike Horse Creek was determined to flow into the underground mine workings through the subsurface fractures, was designated as the project area to be used for demonstration of the technology.

Figure 1. Clay-Based Grouting Demonstration site map.
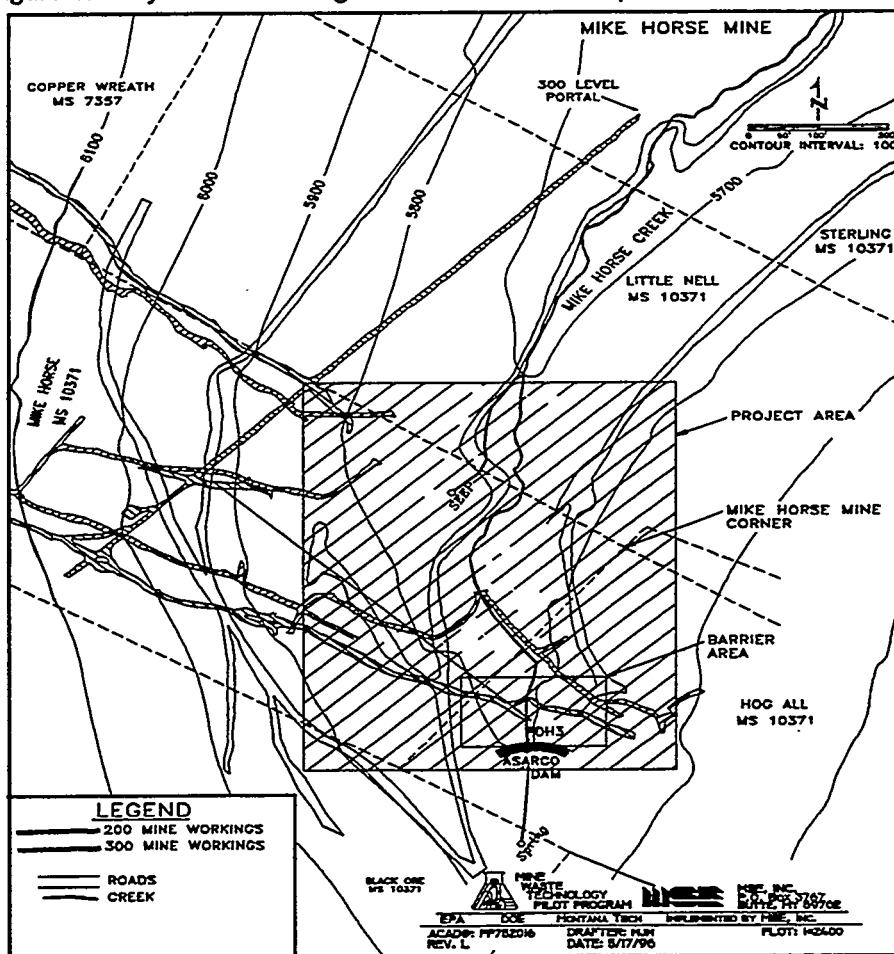
The Clay-Based Grouting Demonstration Project consisted of five major phases: 1) site characterization; 2) grout formulation; 3) Phase I—Grout Injection; 4) Phase II—Grout Injection; and 5) verification monitoring and technology evaluation.

Technology Background

Site Description

The site selected for the demonstration was the Mike Horse Mine, an inactive underground mine in the Heddleston Mining District in Lewis and Clark County, Montana. The Mike Horse Mine was the largest and most productive mine in the Upper Blackfoot Mining Complex. Silver, lead, and zinc-bearing ores of the Heddleston Mining District were discovered in the late 1800's, and development of the district and the Mike Horse Mine began in 1898 (Pardee and Schrader, 1933). ASARCO continued operation of the mine until 1955, when the Mike Horse Mine operation was put out of production due to declining metal prices.

The Mike Horse Mine consisted of 10 underground working levels, which were driven along the veins/faults for distances up to 610 meters (2000 ft). The mine workings extend to approximately 305 meters (1000 ft) below ground surface (bgs). The main haulage drift, at the 300-level, was accessed by a 335 meter (1,100 ft) crosscut tunnel. For this project, the main workings of interest were at the 300-level drift and crosscut tunnel. The elevation at the 300-level portal was the lowest surface expression of the mine. Water entered the mine upgradient of the 300-level through either subsurface fractures or surface flows into the old mine working at other levels. Review of existing mine maps confirmed that mine workings extend beneath the stream bed of Mike Horse Creek; this area corresponded to a losing segment of the creek. This relationship strongly suggested that the water lost from the losing section of the creek was infiltrating the mine workings through fractures and joints in the rock structure underlying the stream and eventually was discharging from the 300-level mine portal back into Mike Horse Creek. MSE-TA proposed applying clay-based grout under the losing portion of Mike Horse Creek to control water infiltrating the mine workings.

Project Objectives and Scope of Work

The primary objective of this project was to demonstrate that the strategic placement of a clay-based grout could control and significantly reduce the inflow of surface water and shallow groundwater to underground mine workings. The primary objective was to control the influx of water into the underground mine workings; thus, eliminating water contact with sulfide ore zones and as a result decreasing the formation of acid mine drainage. The project was not to be viewed as a direct treatment of mine waste, but as a method to control one source of acid mine drainage by managing groundwater flow. The project was designed to test and evaluate the effectiveness of the grouting technology.

Success Criteria Established

Criteria for the success of the grouting technology was established to define and measure the degree of success the technology developers were able to achieve. Field tests were performed prior to grouting to establish baseline conditions at the site. Postgrouting tests were performed, and results were compared to baseline conditions to determine the performance of the grout with regard to hydraulic sealing of the fracture system. Testing methods were modified during progression of the project, as required, to properly characterize the grout effectiveness. The primary objectives used to define the success of the project were as follows (SAIC/SITE, 1995).

1) To show grouting had a probable effect in reducing the *hydraulic connection* between Mike Horse Creek near the project area (drill pad), the groundwater at a monitoring well (monitor well (MW) -4), and the 300-level portal.

2) To verify MK/STG's claim that their clay-based grouting process would reduce *in situ permeability* within known areas of the grout curtain to $<1 \times 10^{-8}$ meters per second (m/sec).

3) To determine MK/STG's claim that exposure of the clay-based grout to acidic materials (pH <5.5) would not increase the hydraulic conductivity of the grout by more that 15% at a confidence level of 95% (*acid resistiveness*).

4) To determine whether the clay-based grouting process reduced the permeability to 10^{-8} m/sec in grout holes, angle drill hole ADH-7 and ADH-8, in which permeability values were greater than 1.27×10^{-6} m/sec based upon pre-grout packer injection tests (*permeability for grout holes ADH-7 and ADH-8*).

Although the main objective was to control point-source influx, the evaluation of the project's success also included the feasibility, cost-effectiveness, and flexibility of the technology to be used in other situations and other applications.

<u>Demonstration History</u>

The clay-based grout technology and the Mike Horse Mine site were selected by EPA for the demonstration in the summer of 1993 under the stipulation that the Mike Horse Mine would be accessible, as per ASARCO's claims, and flow stations would be placed at the drifts in the 300-level to determine the flow produced from each drift. In the spring of 1994, ASARCO decided not to open the Mike Horse Mine; furthermore, ASARCO's future plans for the mine included placing a bulkhead in the 300-level mine workings approximately 150 feet in from the portal entrance. It was decided by EPA in July 1993 to proceed with the demonstration .

In September 1993, ASARCO constructed an earthen dam (referred to as the ASARCO dam throughout this document) upgradient from the Clay-Based Grouting Demonstration Project site to contain and reroute (pipe) water from Mike Horse Creek to an area below the 300-level Mike Horse portal. This system was designed to decrease the amount of surface flow entering the underground workings. This dam was not keyed into the bedrock, allowing for groundwater to move under the dam through the shallow alluvial material on which the dam was constructed.

From spring 1993 to August 1994, pregrout site characterization was performed to provide the baseline parameters necessary to evaluate grout emplacement. During May 1994, the grout formulation was developed in laboratories in the Ukraine by STG using the kaolinitic clay from Troy, Idaho. On September 15, 1994, Phase I of the grout injection was initiated. During Phase I grout injection, approximately 1224 cubic meters (1600 cubic yards (cy)) of clay grout were injected into the fracture system to reduce infiltration of water into the underground mine workings. Due to severe weather conditions at the site, Phase I grout injection was terminated on November 7, 1994. Once Phase I was completed, the technology developers stated that grout injection was only 40 to 50% complete and proposed a second grout injection phase be performed. The Phase II grout injection was scheduled for July and August 1995; however, on May 7, 1995, high water due to spring runoff caused the 300-level portal, which initially was almost totally collapsed, to washout from the mine towards Mike Horse Creek. All flow devices monitoring the 300-level discharge filled with sediment and became inoperative. Since this main critical data source (the 300-level discharge) had been eliminated by the high runoff event, EPA canceled the Phase II—Grout Injection on June 21, 1995.

Pre-Grout Site Characterization

Pre-grout site characterization was performed at the project site to establish baseline information and to determine the locations at which water was infiltrating into the underground mine workings. With respect to the pre-grout site characterization at the Mike Horse Mine site, the following observations and conclusions were established:

- Historic flow and geological data provided surface water flow and fracture information about the Mike Horse Mine drainage system. From this information, the annual averages for the 300-level portal flows were estimated at 3.40 l/s (0.12 cfs), and the annual average stream flow was estimated to range from 0.85 to 85 l/s (0.03 to 3 cfs). A down gradient seep observed flowing every year, was interpreted as a surface expression of the original stream bed of Mike Horse Creek that was changed during historic mining events.

- Stream gauging results illustrated that Mike Horse Creek began to loose water where it flowed directly over the Mike Horse Mine 300-level workings, and the quantity of water lost in this region was less than the quantity of water reentering Mike Horse Creek below the 300-level portal.

- Continuous stream flow measurements included a monitoring plan to provide a water balance for the Mike Horse Mine drainage above the 300-level portal. The data provided baseline stream flow records.

- The 300-level Mike Horse Mine portal discharge data were determined to be critical. Two continuous monitors were placed at the portal. Data from the portal flow monitors supported the conclusion that Mike Horse Creek was hydraulically connected to the Mike Horse Mine in the project area. Direct responses to packer testing performed on August 18 and September 19–20, 1994 were very apparent on the daily flow records provided by MSE-TA's continuous monitoring station. The continuous monitors also provided baseline data used in further interpretations for this project.

- Precipitation data provided useful baseline information for interpretations concerning the 300-level portal discharge and stream flows. The annual precipitation figures show that 1993 was a fairly wet year with respect to long-term averages; however, annual precipitation figures for 1994 and 1995 were below average.

- Groundwater potentiometric elevations contoured for September 9–14, 1994, indicated an anisotropic aquifer system and a significant cone of depression in the vicinity of monitoring well , MW-7. MW-7 was located directly over a large stope that was located less than 7.6 m (25 feet) bgs and is directly connected to the 300-level underground mine workings. Additionally, the alluvial system below the project area was on average between 3.6 and 6.1 m (12 and 20 ft) deep, suggesting a thin (less than 1.5 m (5 ft) thick) bedrock layer between the alluvium and the stope. The bedrock located between the stope and the alluvial layer provided infiltration through the enhanced fractures. The fractures had been enhanced by weathering, subsidence, and historic blasting and mining operations.

- In addition to establishing direct connection between the mine workings and the project area, the packer tests define the variability and magnitude of the hydraulic conductivity of specific intervals of the grout injection holes. These hydraulic conductivity values provide baseline data to calculate and determine the amount of grout that could be injected into the formation.

- A baseline tracer dye study was performed by injecting dye at select points in monitoring wells. The dye was detected in a monitoring well located approximately 9.1 m (30 ft) away from the nearest injection point, in just a few hours. Tracer dye was also determined to be present at the 300-level portal on May 4, 1995.

- Geophysical and geologic logging of the core holes were performed to define the geological units and fractures. A borehole video camera was used to view the borehole walls and water table of grout hole, ADH-7, which was at a drilled depth of 46 m (150 ft). The borehole televiewer measured the borehole and viewed the water table of ADH-7, which was located at 46 m (150 ft) drill depth. The directional survey provided the deviations due to drilling in ADH-7 and ADH-8. Cross sections using this and other surface surveys illustrate that ADH-7 is located 0.9 m (3 ft) from the 300-level mine workings, and the water level in ADH-7 corresponds to the middle of the 300-level mine workings.

- The rock mechanic testing conducted on representative samples from the Mike Horse Mine evaluated the sample density, tensile strength, compressive strength, elastic properties, and hydrofracture pressures required to break the rock. The tensile strength of the rock samples was influenced by the various grades of fracture healing, brecciation, and alteration. Samples with low compressive strengths <3,515,500 kgs/m^2 (<5,000 pounds per square inch (psi)) usually failed along preexisting fractures. High-strength specimens > 17.57 million kgs/m^2 (>25,000 psi) tended to fail violently. It was apparent that the competent rock at the Mike Horse Mine should withstand the forces exerted during grout injection. If maximum grout injection pressures remain below 210,900 kgs/m^2 (300 psi), hydrofracturing should not occur in competent rock; however, if unhealed fractures existed, then grout could initiate reopening of the fractures. At maximum pressures of 421,800 to 464,000 kgs/m^2 (600 to 660 psi), even healed fractures could be reopened.

Grout Injection Procedures

The Phase I field implementation of the grout injection began on September 22, 1994 and was completed on November 7, 1994. A discussion of grout specifications, composition, and procedures is provided in this section.

Grout Hole Specifications

The STG\MK Joint Venture was the technology developer for the Phase I field implementation of the clay-based grouting technology. The concept behind the STG/MK's field implementation plan was to inject grout into the 35° (from horizontal) angle grout holes first. Grout injected into these holes would form a cap over the deeper angled, 45° grout holes that would be grouted second; thus, the cap would force the grout to move deeper rather than shallower in the fracture system. Steeper angled grout injection holes were to be grouted after completing the 35° and 45° grout holes. See Figure 2.

Figure 2. Conceptual cross-sectional view of the subsurface grout barrier design.
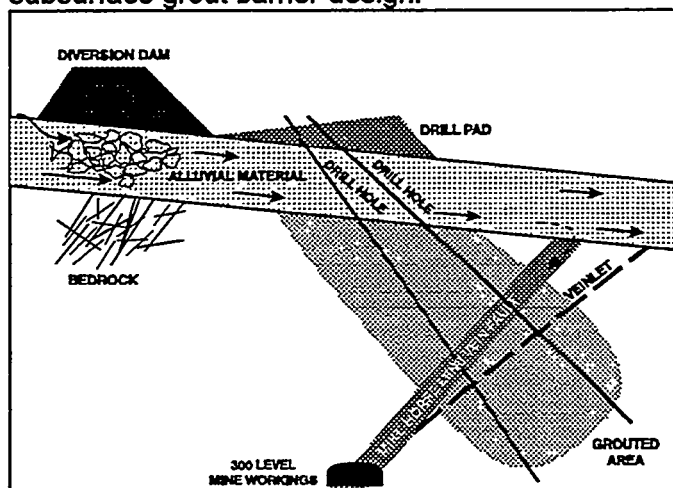
Grout Composition

The grout formulation for the clay-based grout was developed in the Ukraine by STG during May 1994. The overall properties of the clay-based grout depend on the physical and mechanical properties of the clay. The clay used for this demonstration was a kaolinitic clay from near Troy, Idaho. The kaolinitic clay along with water, structure-forming cement, and proprietary chemical additives are formulated into a viscoplastic grout. The grout's properties are such that it retains rheological properties, meaning it retains plasticity and does not crystallize, unlike cement-based grouts. Also, since the pHs of the water at the site range from 5 to 7, the grout composition was adjusted to structurally form and remain stable under lower pH conditions.

The composition of the grout used in the project by weight consisted of 30 to 35% kaolinitic clay, 6 to 7% sulfate resistant cement (Class V), 1 to 1.5% proprietary additive(s), and 56.5 to 63% water; occasionally, sawdust was added as a filler material. The density of the grout was 1350 to 1400 kilogram per cubic meter $(kg/m^3)(6.24 \times 10^{-2} lbs/ft)$, with a dynamic shear strength of 0.64 to 0.68 mm Hg (85 to 90 pascals), a structural viscosity of 37 to 40 centipoise $(37 \text{ to } 40 \times 10^3 \text{ pascals/sec})$, and a compressive strength of 1.0 to 1.5 bars (0.1 to 0.15 megapascals).

The kaolinitic clay was transported by truck to a facility having the ability to crush the clay to minus 8-mesh, as specified by the developers. Sawdust was the filler material designated for grout injection during periods when minimum pressures and large amounts of grout were being injected into large voids.

159

Grout Injection System

Field implementation was performed by Hayward Baker, Inc. (HBI), a ground modification company. They injected the grout into the subsurface at the Mike Horse Mine Project site per the direction of MSE-TA and the developer.

The high-clay grout was mixed in two stages. The first stage consisted of making a clay-water slurry. Four to five tons of clay were added to approximately 5.4 m³ (7 cy) of water over 50 to 60 minutes, increasing the density of the slurry from 1000 to 1350 kg/m³ (62.4 to 84.3 lbs/ft³); the clay-water slurry was then tested for density. The clay-water slurry mixing was performed using a colloidal mixer. After the batch of slurry was mixed thoroughly, it was transferred to a large storage tank.

The second stage of grout mixing consisted of adding a binder material (cement) into a second shear mixer 0.43 m³ (.56 cy). Volumes of binder were metered as they were added into the mixer. Then the clay-slurry mix with the added binder was piped to a hopper containing a screw feeder where the proprietary additive(s) and the fillers were mixed into the grout in proper proportions. In most instances, sawdust was the preferred filler material used in the grout injection. The entire system enabled the continuous injection of grout into the grout holes at the specified pressure until refusal was reached. Testing ports provided samples for grout density, viscosity, injection pressure, and flow rate.

Initially, grout was pumped from the hopper and down the grout injection holes using a Moyno screw pump; however, gravels, approximately ¼ inch in diameter, clogged and ruined the screw pump. The replacement pump specified was a positive displacement pump that had the ability to pump the gravels and other filler material down-hole without binding the pump. The grout was pumped down a 3.8 cm (1½-inch) flexline with a flowmeter/pressure transducer placed at the top of the casing and tremie pipe. The tremie pipe was 3.8 cm (1½-inch), rigid threaded pipe that was connected in 25.4 cm (10-inch) sections.

The grouting was performed in stages with grouted sections 6.1 to 12.2 m (20 to 40 ft) long. The injection rate was anticipated to be 0.94 l/s (15 gpm), but actually varied between 0.06 to 1.26 l/s (1 and 20 gpm). The upstage method of grouting (from the bottom of the hole upward using an inflatable packer) was used for grout injection.

The anticipated allowable pressure for grouting was 703 kg/m² to 1054 kg/m² (1 to 1.5 psi per vertical foot) of drilled borehole. The Aardvark Packer used for Phase I of grout injection was designed to function without slipping up to pressures of 386,650 to 421,800 kg/m² (550 to 600 psi), usually if the grout hole had not been grouted before. However, the nitrogen (piped through 0.64 cm (¼-inch) tygon tubing) used to inflate the packer would start to compress above pressures of 386,650 to 421,800 kg/m² (550 to 600 psi), resulting in the packer slipping in the grout hole. The pressure was measured at the end of the pump and at the well header. Grouting was continued until refusal was reached or the packer slipped. If refusal was reached and the pressure held for longer than 15 minutes, the packer was kept at the staged interval until the back pressure at the header approached (0 psi).

Approximately 1224 m³ (1600 cy) of clay-based grout was injected during the period from September 23 to November 11, 1994. It was determine by the developers at the end of the injection period that only 40% of the grout required had been injected.

Grout Injection Results

During field implementation of grout, the main parameters monitored included continuous monitoring of the discharge at the 300-level portal and continuous monitoring of the water level in the monitoring wells at the project site. Results from the 300-level portal did not show a significant reduction in flow during grout injection; however, this may have been due to the large volume of water blocked within the mine workings. During grout injection, however, the monitoring wells did show significant water level changes during grout emplacement.

Results of the 1223 m³ (1600 cy) of clay-based grout injected, were observed in the monitoring wells continuously monitored. The water level in MW-1 rose approximately .76 m (2.5 ft) due to grout injected in

ADH-14 which closed off a hydraulic connection that had allowed water to infiltrate into the underground mine workings. The elimination of hydraulic connections was also apparent in water level measurements in MW-2. The water level in MW-2 decreased almost 2 feet in response to recharge zones for MW-2 closed by grout injected in ADH-14.

MW-3's initial water level was 33.8 m (111 ft) bgs; however, after grouting at ADH-14, the water level in MW-3 rose and is presently between 5.2 to 4.3 m (17 to 14 ft) bgs. It was concluded that the previous water levels in MW-3 reflected water infiltrating into the mine. This conclusion was made because DDH-3, an open core hole located approximately 3.1 m (10 ft) east of MW-3, had a static water level of 11.6 m (38 ft) bgs. The steep gradient is representative of a dewatering situation. While grouting ADH-14, the fractures hydraulically connecting the mine workings and MW-3 were grouted shut and the water level in MW-3 rose to 5.2 m (17 ft) bgs.

Also, the field implementation plan for the demonstration was modified during grout injection. The modification consisted of drilling near-surface grout holes at steeper angles because cross communication occurred between grout injection holes, and grout surfaced frequently when grout was injected into the shallower 35° grout injection holes. As a result of the modification, the steeper grout holes were drilled closer to the 300-level mine workings. ADH-7 was drilled approximately 0.9 m (3-ft) away from the mine workings. When grout was injected at the 37.2 m (122-ft) packer interval, back pressure did not exist (negative pressures). Sawdust filler was added to the grout formulation to fill the void and try to raise the injection pressure. After 128 m³ (168 cy) of grout were injected into ADH-7, sufficient back pressures were not achieved; therefore, dead plugs were placed at depths of 41 and 39 m (135 and 128 ft). The main quantities of grout (approximately 50%) were placed in two grout injection hole.

A second modification to the field implementation plan was to increase the initial maximum pressures suggested by the developer to a maximum pressure of 421,800 to 456,950 kg/m² (600 to 650 psi). With this modification, the developer was able to hydrofracture healed fractures allowing larger quantities of grout to be injected. Hydrofracturing was performed by decreasing the density of the grout formulation by adding water at a point when high pressures and the grout injection rate had decreased. This allowed grout to penetrate smaller fractures and extend the boundaries of the grout curtain. The higher pressures caused compression of the nitrogen inflated packer, allowing the packer to slip up the grout hole. In some instances, the packer was destroyed when it was shredded by sharp fragments or reached a void that allowed the packer to expand until it burst.

Conclusions and Recommendations

Within the *MWTP, Activity III, Project 2, Clay-Based Grouting Demonstration Project, Interim Report,* (MSE-TA, Inc., 1994) the ability of the clay-based grout, developed by MK/STG, to reduce and/or eliminate flow into subsurface fracture systems was evaluated for its integrity, ability to inhibit water inflow, grouting method, and potential for future implementation.

In summary, the recommendations and conclusions addressing kaolinitic clay-based grout for reducing the permeability of a fractured bedrock system include:

- Kaolinitic clay can provide a substantial reduction in the permeability of a fracture system. From the hydrograph created during this period, portal discharge was shown to have been reduced by up to 29% in March 1995, and up to 42% in May 1995. However, high-flow conditions reflect larger reduction in flow compared to small reductions during the low-flow conditions. Note, the amount of flow reduced is proportional to the high/low-flow conditions of the mine.

- The reduction was also apparent when flow measurements recorded during the first week of April 1996, as measured by ASARCO, read consistently 1.45 l/s (23 gpm). This value was approximately 0.63 l/s (10 gpm) lower than base flow conditions on pregrout years.

- Kaolinitic clay-based grout can provide reduced permeability in fracture systems, and it also maintains its rheological properties in saturated/partially-saturated conditions. It also does maintain its continuity under acidic conditions, this is an advantage when comparing the clay-based grout to other viable grouts.

- However, primary disadvantages of this grout are that it does not provide structural strength for use in civil projects and it should not be used in arid or unsaturated areas, because desiccation and cracking of the grout occurs, allowing water to infiltrate through the grouted area. If the grout is specified for implementation in such conditions, special consideration should be taken. Also, if the soil moisture is significant enough in an unsaturated area, then this grout may be feasible for emplacement of a subsurface barrier.

Acknowledgements

References

1. MSE, Inc. (July 1994), Draft Site Characterization Report—Clay-Based Grouting Demonstration, MWTPP Activity III, Project 2

2. Montana Department of State Lands (February 1991), Abandoned Mine Reclamation Bureau, Environmental Assessment Upper Blackfoot River, Abandoned Mine Reclamation Project, Phase I.

3. Pardee, J. T. and F. C. Schrader, *Metalliferous Deposits of the Greater Helena Mining District*, USGS Bulletin 842, 1933.

4. SAIC/SITE Program *Quality Assurance Project Plan (QAPP) for the Clay-Based Grouting Demonstration Project, Revision 1*, September 28, 1995.

DESIGN AND CONSTRUCTION OF A DEEP SLURRY TRENCH BARRIER

Peter W. Deming, PE[1]

Abstract

A 24 m (80 ft) deep slurry trench surrounding a former chromium manufacturing facility on the Patapsco River in Baltimore, Maryland was constructed in 1995 to contain groundwater and site soils, and to reduce the volume of groundwater extracted to maintain an inward gradient. In 1992, an embankment made of crushed stone was constructed in the Patapsco River to make land for barrier construction outboard of the bulkheads, and to protect the barrier. Stability of the slurry-supported trench excavation in the embankment required construction from an elevated work platform. An extended reach backhoe was used to excavate the deep slurry trench and to clean the trench bottom. Soil-Bentonite backfill was prepared at a central mixing area and transported by truck to the perimeter barrier. A synthetic membrane was inserted partially into the backfill for connection to a multimedia cap, and for redundancy and erosion control in the tidal zone. Hydraulic testing of the aquitard contained by the barrier demonstrated excellent performance of the barrier and bottom closure. Detailed definition of subsurface conditions and the closure stratum was necessary for the design and successful construction of the barrier, and is recommended for comparable slurry trench construction projects.

Project Description

The AlliedSignal Baltimore Works is in the Fells Point area of Baltimore, Maryland, on the Patapsco River waterfront. The 6 hectare (15 acre) site forms the eastern edge of Baltimore's Inner Harbor. In the 1860's the site was constructed by placing fill outboard of the original shoreline, widening a narrow peninsula in the Patapsco River. Fill was placed to a bulkhead structure on the north side of the site and was placed in fingers to create piers along the south side.

A plan view of the site as it appeared in 1988 is shown in Figure 1. Timber and steel bulkhead structures constructed from the 1860's and 1950's, functional but deteriorated, formed the waterfront perimeter in 1988. A typical 1860 era bulkhead is shown in Figure 2. A low level timber deck was constructed in 1948, and circular steel sheetpile cells were constructed in 1967 to create land area for industrial development.

Chromium manufacturing ceased in 1986. Industrial structures were dismantled in 1990 under a consent decree agreement between AlliedSignal (the Owner), the US EPA, and the Maryland Department of the Environment. The consent decree required a layered multimedia cap over the area enclosed by the hydraulic barrier. An inward hydraulic gradient was required in a deep sand and gravel aquifer overlying bedrock and in the shallow groundwater along the land perimeter, and a maximum chromium concentration was specified for the Patapsco River surface waters along the river front perimeter. A subsurface investigation was performed in 1988 to evaluate the feasibility of constructing a deep hydraulic barrier. The barrier alignment was outboard of the bulkhead in order to retain contaminated fill behind the bulkhead structures. An embankment was constructed outboard of the bulkheads to replace these aging waterfront structures, provide land area for barrier construction, and provide long term protection of the hydraulic barrier in the marine environment. The soil-bentonite backfilled slurry trench barrier was selected because of its cost effective long term low permeability performance and the ability of field personnel to verify barrier continuity and positive closure with the underlying bedrock during construction.

---

1   Mueser Rutledge Consulting Engineers, 708 Third Avenue, New York, New York 10017 Tel. (212) 490-7110, MueserEng@AOL.com.

Subsurface Geologic Conditions

Miscellaneous fill along the waterfront perimeter is underlain with 3 to 6 m (10 to 20 ft) of soft organic clay and alluvial sand deposits in the Patapsco River bed. These are underlain by Cretaceous age deposits, consisting of a 5 to 10 m (16 to 33 ft) thick hard clay and compact fine sand aquitard, and a 5 m (16 ft) thick layer of compact coarse sand and gravel aquifer. These materials overly decomposed bedrock. The bedrock surface drops gradually from Elev. -15 m (-50 ft) NGVD at the north side of the site to Elev. -21 m (-70 ft) NGVD at the south perimeter. The upper 1 to 3 m (3 to 10 ft) of bedrock is highly decomposed (locally termed "saprolite") and transitions to crystalline schistose gneiss at depths of 3 to 9 m (10 to 30 ft) below the decomposed rock surface. A typical soil profile is provided in Figure 2. The groundwater level in the Cretaceous gravel and sand aquifer is influenced by the tide, exhibiting ground water fluctuations on the order of 30% to 65% of the measured tide level changes, and bedrock was found to have a slight upward gradient.

Borings for the first deep site characterization and barrier feasibility study were widely spaced around the perimeter of the contaminated site. Borings were drilled using mud rotary methods with wash water and casing to advance and stabilize the boreholes. In situ falling head permeability testing was performed on the deep aquifer and bedrock while advancing these borings. Records of borings made for site development, dating to the 1930's were used to plan this investigation, and were incorporated into the profile depicting subsurface conditions. Split spoon samples were taken to measure compactness of the soil within the excavation profile, and to recover soil for identification and for backfill design mix testing. Laboratory permeability tests were performed on cores of the hard Cretaceous clay and decomposed rock recovered with Geo-Barrel and Pitcher samplers. Tube-a-manchette grout pipes sealed in the completed boreholes were used to test the feasibility of creating the deep barrier with microfine cement grout.

The permeability of the underlying aquifer and bedrock was measured with falling head tests in the boreholes; given the test flows were primarily into the side walls of the boreholes the tests defined the horizontal permeability of each strata. The sand and gravel aquifer overlying bedrock was found to have an average permeability on the order of 10^{-2} cm/sec. The permeability of the decomposed rock ranged from 10^{-5} to 10^{-6} cm/sec. Bedrock permeability decreased to 10^{-7} cm/sec with the transition to crystalline rock. The decomposed rock was chosen as the closure stratum. Because the decomposed rock was relatively consistent, an analysis of seepage below the wall through the decomposed rock found that increasing the depth of the barrier key into bedrock would not substantially decrease inward flows.

The initial feasibility study borings were spaced approximately 122 m (400 ft) on center. A few borings were added to define the soil profile along the final hydraulic barrier alignment when making borings for embankment design, and a final series of design borings was made through the completed embankment, to provide an understanding of that structure and for further definition of the bedrock surface elevation. For design and construction bidding, the elevation of the decomposed rock surface ("closure stratum" or "key stratum") was defined by borings at an average spacing of 34 m (110 ft) along the barrier alignment. Boring spacing ranged from 27 m to 46 m (90 to 150 ft). During construction two borings were added ahead of the trench excavation to determine the surface elevation of the closure stratum.

EMBANKMENT DESIGN AND CONSTRUCTION

The embankment is a 580 m (1900 ft) long zoned structure made of crushed stone grading from rip rap in the wave zone to a sand and gravel "wall zone" inboard adjacent to the bulkhead. Embankment construction was preceded by dredging to remove soft compressible clay sediment to expose a firm sand bearing surface. Temporary pile structures were constructed to support the

bulkheads during dredging. A typical section of the completed embankment is shown in Figure 2. The core of the embankment is 150 to 230 mm (6 to 9 inch) diameter stone. Core stone was placed by bottom dumping below Elev. -3 m (-10 ft) NGVD. Core stone above this elevation and all of the sand and gravel fill inboard was placed with a 6 m^3 (8 yd^3) clamshell bucket. Fill placement was monitored by sonar soundings below Elev. -3 m (-10 ft) NGVD, and by survey rod soundings above. An essential requirement in construction of the embankment was to prepare the wall zone for the future slurry-supported trench excavation by removing all piles and other obstructions and controlling placement of the coarse stone core to prevent intrusion into the barrier alignment.

The embankment was designed to provide a minimum safety factor of 1.3 against static slope failures, and a minimum safety factor of 1.1 under 0.05 g earthquake acceleration. Along the south and west sides of the site, the embankment was 11 m (37 ft) wide from the bulkhead to the crest of the rip rap slope. The outboard slope was 1V:1.75H from the crest to the toe, which rested on medium compact sand. Along the north side the embankment was only 5.2 m (17 ft) wide to provide 2.4 m (8 ft) of draft at the centerline of the former "Back Basin" defining the north property line. The narrower north embankment required a toe berm below Elev. -3 m (–10 ft) for stability.

The gradation of the sand and gravel fill in the embankment wall zone was selected to enhance its performance during underwater placement and to minimize turbidity in the Harbor during embankment construction. Gradation curves are provided in Figure 3. The fill developed an angle of repose of 1V:4H during placement. Mud-rotary borings advanced through the embankment found the sand and gravel fill to be loose and the borehole walls unstable. To enhance stability and reduce future settlement of the embankment surface, the embankment was densified by vibrating a pile probe in the wall zone before the slurry trench was excavated. A testing program was performed to determine the amount of time the vibrating pile probe should be held at final depth (2 minutes), and optimum probe spacing (1.2 m (4 ft)). The coarse gradation and low fines content of the fill made vibratory densification feasible, and resulted in up to 760 mm (2.5 ft) of settlement at the embankment surface (or 7% strain). The sand and gravel fill in the wall zone was coarse enough to raise a design concern that a filter cake strong enough to prevent ravelling of the trench walls would develop during excavation. The contract indicated the excavation rate may have to be controlled for this purpose. However, after densification the trench walls were found to be stable and excavation proceeded with the rate uncontrolled.

A 180 m (600 ft) long and 23 m (75 ft) wide slip along the north side of the site, the former "Back Basin," contained 6 m (20 ft) of very soft organic clay sediment, and was determined to be too narrow for economic dredging. The Back Basin was isolated from the Patapsco River and filled. Fill placement was stabilized with two layers of high strength reinforcing geotextile placed over the soft sediment. Vertical wick drains were installed through a 1.5 m (5 ft) thick sand working platform spaced 1.2 m (4 ft) on center in a triangular pattern to accelerate drainage of pore water from the organic clay. Fill to final grade and 5 m (15 ft) of surcharge was placed in controlled lifts. Settlement occurred almost simultaneous with fill placement, and a total of approximately 1.2 m (4 ft) of settlement was observed.

SLURRY TRENCH DESIGN AND CONSTRUCTION

In the late 1980's when this project design began, slurry trenches deeper than about 18 m (60 ft) were advanced by a combination of backhoe and clamshell equipment. Extended reach backhoes were being developed which could reach to depths of 30 m (100 ft), making backhoe excavation of this 24 m (80 ft) deep trench feasible. The design and contract documents for this project considered the influence of an extended reach backhoe and the deep trench on the performance of the slurry trench construction methods. The contract specified a minimum separation between the excavation and backfill operations, required trench bottom cleaning,

quality control measurement of the trench bottom, and limited the sand content of the slurry.

Key Into Closure Stratum

The slurry trench was designed to be keyed into the underlying decomposed bedrock. Excavation depths ranged from 21 to 24 m (70 to 80 ft) below the surface of an elevated temporary work platform. Closure with bedrock was mandatory for performance of the system because even a small window in the sand and gravel aquifer would allow large inflows to the active head maintenance system. A minimum 1 m (3 ft) key into the decomposed rock was specified. This key depth was intended to permit some allowance for unknown subsurface conditions, and to contain small amounts of trapped bottom sediment and debris while sealing the full thickness of the sand and gravel aquifer with the low permeability soil-bentonite backfill. Trench depths.were measured from a surveyed reference string line at the edge of the trench. Trench depth readings were converted to elevation, and compared to the bedrock elevation defined by borings.

Trench Excavation and Bottom Cleaning

Operated by cranes positioned adjacent to the trench, clamshell equipment can excavate at any location along the trench alignment. However, because the slurry-supported trench walls in the embankment fill could not support the weight of a large backhoe, the backhoe must operate from the solid ground at the leading end of the trench, and can only reach the trench bottom for a distance of 10 to 12 m (35 to 40 ft) from the leading end of the trench. The bucket of a backhoe tips as it is raised through the slurry column, and can spill excavation spoils onto the trench bottom beyond reach of the backhoe for cleaning. If the backfill is pushed too close to the excavation face, excavation debris falling from the backfill and sloughing off of the excavation face will mix with the backfill and cover the bottom undetected. Also, the excavation depth, key material and trench depth cannot be measured and verified. The contract specified a minimum 12 m (40 ft) separation between the toe of the excavation slope and the toe of the backfill slope to obtain and verify closure with bedrock. This separation allowed inspection to verify that the key was excavated into bedrock. The separation permitted measurement of sediment and debris covering the trench bottom. The specifications also required cleaning of the trench bottom, the lower third of the backfill slope, and periodic removal of the backfill toe to remove accumulated sediments and prevent debris entrapment. The contract essentially envisioned clamshell tools would be provided for cleaning the trench bottom beyond the backhoe reach.

The trench bottom was checked for the presence of sediment and debris by measuring trench depth with two weights at the same location (Poletto and Good, 1997). A 16 mm (1 in) diameter steel 4 kg (9 lb) weight was used to define the bottom of the trench. A 127 mm (5 in) diameter flat steel plate weighing 4 to 5 kg (9 to 12 lbs), with a lower bearing pressure was used to define the top of sediment and debris resting on the trench bottom. When these two weights agreed within 150 mm (6 in) the trench bottom was approved for backfill placement. This check was performed immediately before the backfill was advanced. Because both weights were used at the same time, sediment and debris could be "lost" in a hole at the bottom of the trench. The contractor found that a 7 tooth bucket with 200 mm (8 in) long teeth efficiently removed sediment and excavation debris and was able to meet the measurement criteria. A 5 tooth bucket with 460 mm (18 in) long teeth raked through the debris and could not obtain the 150 mm (6 in) sediment criteria.

The contractor requested (and was permitted) a physical separation of the excavation and backfill operations so that the 12 m (40 ft) separation could be reduced, and the trench could be excavated and cleaned with an extended reach backhoe. Excavation was physically separated from the backfill by a 760 mm (30 inch) diameter open steel pipe called an "end stop." The lower half of the end stop pipe had 150 mm (6 inch) angles welded to the diameter; when rotated, the

end stop would contact and disengage the trench side walls. The pipe rested on the trench bottom, and was pinned at the top by steel beams placed across the trench. The end stop prevented the extended stick from passing over the backfill surface and allowed bottom cleaning and measurement before backfill covered the trench bottom. After the excavation reached final depth, the trench bottom was sounded with the flat and pointed weights to check for sediment and debris. With the trench bottom cleaned and approved, the end stop was lifted and moved forward by a crane or backhoe operating at the side of the trench. The toe of the backfill slope advanced with each move. The backfill toe was periodically pushed into the excavation end and isolated there by lowering the end stop. The isolated materials were excavated to prevent accumulation and reduce entrapment of scoured sediment and other debris.

When excavated below the slurry surface, the sand and gravel embankment fill ran to the bottom of the excavation and travelled as much as 10 m (30 ft) from the cut. This occurred because the granular fill had no fines to bind the particles together, and slurry quickly penetrate the clean fill, lubricating particle contacts. Without the required separation or the Contractor's end stop, running sand and gravel would have covered the bottom and the backfill surface, resulting in undetected gravel pockets within the backfill and below the wall. It is likely this would have occurred with each advance of the excavation.

Backfill Placement

In slurry trench construction, backfill is placed behind of the crest of the backfill slope to push the backfill ahead in a mudwave which does not intermix with the trench slurry and is thought to scour debris and sediments from the bottom. The scouring action is probably quite limited, especially for bottom sediment, and can only be lessened as the depth of the trench increases. In a deep slurry trench the large sidewall area may impart a drag force on the backfill, reducing the force pushing the toe of the backfill forward, and increasing the opportunity for entrapment of debris and sediment. Identification and removal of these undesirable materials to prevent entrapment requires aggressive quality assurance and contract provisions supporting removal and monitoring. Backfill was placed at slumps of 80 to 150 mm (3 to 6 inches) and was allowed to build up to 3 m (10 ft) thickness against the end stop. Progress of the advancing backfill was monitored daily. Backfill placed aggressively at the crest of the backfill slope was observed to run down the face of the backfill. The theoretical mudwave performance was observed only when backfill was placed at one location until the trench could not take more backfill. This placement detail resulted in a slight flattening of the backfill slope. Placing backfill at one location is recommended if mudwave performance is desired in the backfill advance.

Slurry Sand Content

Natural fines and sand build up in the trench slurry during excavation, when the backhoe agitates the slurry. More than one quarter of the slurry volume may be composed of sand. After excavation, in a low energy condition, excess sand and silt which cannot be supported by the slurry will fall out of suspension onto the trench bottom until the slurry gel strength acts to hold sand in suspension. If the sand content drops by only 5% in a 24 m (80 ft) deep trench, 1.2 m (4 ft) of sand will be deposited on the backfill surface or bedrock at the bottom of the key. For any given slurry, sedimentation potential increases with time. Construction time increases significantly with increasing depth of a trench excavation. Where a 12 m (40 ft) deep trench   Because excavation and backfill in deep trenches moves forward slowly, and because the large volume of slurry in the trench is not agitated by the backhoe movements, the slurry column has ample opportunity to drop sand. The contract specified active desanding of the slurry to maintain the sand content below 15% for slurry sampled 1.5 m (5 ft) above the trench bottom; the sand content ranged from 6% to 16% in construction, depending on desander use. Split spoon

sampling of the trench bottom and backfill surface showed that sand did not build up on the backfill surface, and the specified backfill slope cleaning was relaxed to a monthly occurrence. When required, bottom cleaning beyond the reach of the backhoe was performed by airlift.

The contractor developed a special desanding plant to control slurry sand content. The desander incorporated a series of vibrating screens and lined cyclones which efficiently removed medium and coarse sands from the slurry in a continuous flow. This desanding plant was able to reduce the slurry sand content from 15% to 7% sand in one cleaning pass. One or two 100 to 150 mm (4 to 6 inch) pumps lifted slurry from depths of 12 to 18 m (40 to 60 ft) providing a continuous supply of slurry to the desanding plant.

Backfill Design

The trench was backfilled with a homogeneous blend of soil and bentonite. Excavation spoils were utilized to prepare a well graded clayey sand and gravel containing from 20% to 35% passing the No. 200 sieve. The specified gradation range is shown in Figure 3. The addition of dry bentonite was required to reduce backfill permeability. Wyo-Ben Inc.'s salt water compatible treated bentonite "SW-101" was specified for the dry addition because brackish Patapsco River water (1,500 ppm chlorides) will leach through the backfill under the inward gradient with time, and the pore water in the excavation spoils contained chlorides. SW-101 bentonite yields 180 barrels per ton (42 gal barrels per 2,000 lb ton) when mixed with fresh water and 90 barrels per ton when mixed with sea water. Permeability testing of design mixes showed the measured permeability of samples prepared with SW-101 to be five times lower than samples prepared with untreated premium bentonite. Testing indicated a 2% addition by dry weight of soil blend was optimal for permeability benefit, but a 3% addition was specified to accommodate field imperfections in bentonite distribution and thoroughness of blending. The average permeability measured in 71 batches was 5×10^{-9} cm/sec, and ranged from 4×10^{-8} to 9×10^{-10} cm/sec. The low permeability was attributed to the use of the SW-101 bentonite, and the contractor's shredding of the natural stiff clay materials and thorough homogenization of the backfill.

For design, gradation tests were performed on natural soils, to define the particle size range of each strata. Particle sizes were numerically combined in proportion within their thickness in the barrier profile to estimate the gradation range of backfill made from excavation spoils, and to verify the desired backfill gradation could be obtained utilizing excavation spoils. This analysis demonstrated materials needed for backfill preparation were present, but both clay and gravel spoils would have to be stockpiled and selectively used during construction. A requirement to stockpile materials and balance the gradation was included in the specifications. The presence of the 8 to 11 m (25 to 35 ft) thick sand and gravel embankment fill along the waterfront perimeter alignment assisted with management of backfill gradation because it provided a dependable source of consistent coarse aggregate. The central mixing operation and truck transport of excavation spoils employed by the contractor supported segregation and selective use of excavation spoils, the gradation of each of the 71 backfill batches was within the specified range.

Backfill was prepared in 230 to 600 m³ (300 to 800 yd³) batches at a central location on a 100 mm (4 inch) thick asphalt surface covering an abandoned concrete building floor slab. The firm mixing surface was an asset to quality control because foreign materials were not picked up into the backfill, but it showed considerable wear after 18,500 m³ (24,000 yd³) of backfill was prepared. The contractor used a travelling hammerhead mill (Caterpillar SS-250 "soil stabilizer") to shred the stiff clay into particles smaller than 6 mm (1/4 inch), blend dry bentonite into the spoils, and homogenize excavation spoils into prepared backfill. The travelling mill operated efficiently within backfill up to 460 mm (18 inches) thick. On the first few passes, the rotating hammerheads pushed a wave of wet spoils ahead and, as the machine walked out of the spoil pile, oversize materials, cobbles, and timber, etc. dropped to the pavement surface for hand collection and

removal. A high-track dozer moved spoils around the mix area to homogenize each batch and mixed bentonite slurry into prepared backfill for final slump adjustment. Backfill was stockpiled at a low slump, and the dry addition was allowed to hydrate while the contractor performed gradation tests and the Owner performed permeability tests for batch approval. Triaxially consolidated specimens were permeated by the constant volume method, and permeability was determined within 24 hours of sampling. Backfill slump was adjusted by adding bentonite slurry, and tested for slump, and approved immediately before loading transport trucks for trench placement. Backfill was placed by direct tailgate dump onto previously placed backfill at the top of the trench backfill.

Trench Stability

Stability of the slurry-supported trench excavation in the embankment fill was analyzed by comparing active earth pressure driving forces with the resisting slurry fluid pressure. The two dimensional analysis determined that a minimum slurry density of 1,160 kg/m³ (72.5 lb/ft³) and a slurry head 1.5 m (5 ft) above high tide would provide a safety factor of 1.29 against a sliding failure of the trench walls in the embankment fill, and 1.15 in the fill and stabilized clay profile of the former Back Basin. The contract required construction of the slurry trench from a raised work platform at Elev. +2.7 m (+9 ft) NGVD, to provide 25 mm (1 ft) of freeboard above the minimum 1.5 m (5 ft) positive slurry head above a monthly high tide of Elev. +910 mm (+3 ft) NGVD. The top of the work platform was 7.6 m (25 ft) wide to support the backhoe excavator and provide allowance for shallow failures of the trench wall. The Contractor chose to use timber mats to support the large excavator on the work platform.

While negotiating an outside corner of the trench alignment, where the embankment was not adjacent to a bulkhead, the slurry trench excavation apparently encountered some of the coarse stone fill at the embankment core and a rapid slurry loss occurred. The loss was stemmed by adding cellophane flakes to the slurry at the excavation face but the large slurry losses continued with two subsequent attempts to continue excavation. To prevent delays, the trench excavation skipped over this segment of the alignment; a slurry overflow trench and lead-in slope were constructed, and barrier construction on the embankment was continued to completion without further incident. The skipped segment was excavated at the end of the project by isolating the slurry loss area with steel sheeting driven across the trench, and moving the alignment inboard.

Approximately 25 m (80 ft) of the trench wall collapsed on the land portion of the alignment. The failure was apparently caused by an unknown soft clay pocket below the fill, and may have been aggravated by low slurry levels. The contract prohibited surcharging the side walls of the slurry trench, therefore straddling the slurry-supported trench with the backhoe was not permitted. However, at this location and at the skipped segment of the embankment, the backhoe was required to straddle the trench alignment because a clamshell was not available to remove spoils and excavate virgin ground. The trench was backfilled with spoils, and then excavated in 10 to 12 m (35 to 40 ft) "panels" isolated by steel sheeting driven across the trench. The sheeting retained soil in place below the backhoe and provided a stable trench wall, but was costly as it was accomplished at time and materials rates within a unit price contract. Slurry trench contracts should include some provision for clearing the excavation of trench wall collapse spoils; overbreak materials, and or other debris. Where stability is questionable, provision of clamshell tools should be mandatory for deep slurry trenches.

Trench Width Measurement

With the elevated slurry head and work platform design, a shallow collapse of the raised work platform could have led to a loss of slurry to the Patapsco River which would have dropped the

slurry head and resulted in a general trench collapse. To confirm that the trench wall was not unravelling and undermining the work platform, the trench width was measured with depth. A hexagonal caliper device was designed and assembled to measure trench width at depths up to 17 m (55 ft). The caliper was expanded to encounter the trench walls by pulling on a central cable. It was lowered into the trench and oriented perpendicular to the trench wall with square aluminum rods. The cable pull was calibrated to the width of the caliper. Readings of trench wall width were taken at 1.5 m (5 ft) depth intervals in several locations, during and after excavation. The caliper device worked well, the readings were repeatable, and this measurement verified the trench sidewalls were stable. The trench was observed to gradually decrease from a typical width of 1500 mm (60 in) at the top to a width of 1000 mm (38 in) at a depth of 8 m (25 ft), and to remain constant thereafter. The sloping side walls were believed to be a result of the long stick backhoe operation, as the trench sidewalls were used by the operator to guide the excavator to the center of the narrow slot with depth.

Excavation Adjacent to Bulkheads

Where the slurry trench excavation was adjacent to the abandoned bulkhead, the bulkhead performed as an interior guide wall. Along the circular steel cells the inboard edge of the trench was tangent to the outboard edge of the cells. The bulkheads remained stable, even with the trench excavation adjacent below the tips of piles supporting the headwall, and the backhoe never engaged the bulkhead framing timbers or support piles. Caliper trench width measurements verified the embankment fill outboard of the circular cell bulkhead was stable and remained in place in the sheet piling arcs. In the Back Basin, the two layers of high-strength woven geotextile at the base of the fill were cut before trench excavation by vibrating steel sheeting pairs along the outboard edge of the alignment. The geotextiles were cut in advance of trench excavation to prevent an undermining of the trench side walls by disturbing the geotextiles; the trench side walls proved to be stable throughout this area.

60 Mil VLDPE Synthetic Membrane Interim Cap

The design included a 60 mil very low density polyethylene (VLDPE) membrane at the top of the barrier to Elev. -1 m (-3 ft) at the outboard edge. VLDPE was specified because its elasticity. The 60 mil thickness was utilized to enhance the endurance of the membrane under installation wear, and to permit welding to the HDPE membrane of the multimedia cap. The membrane provides a redundant barrier and reduces the potential backfill dessication above the water level. It also provides erosion protection of the soft soil-bentonite barrier in the tidal zone within the sand and gravel embankment fill. The synthetic membrane will be welded to the multimedia cap membrane, closing the multimedia cap to inundation in high tide events.

The membrane was inserted into the backfilled barrier using a mandrel. The mandrel panels were overlapped 0.9 m (3 ft) with a maximum separation of 100 mm (4 in) permitted between the membrane panels. The synthetic membrane was inserted up to 4.5 m (15 ft) into the backfilled trench, which appeared to be the maximum depth of the mandrel used. The insertion mandrel and installation procedure were developed by the contractor and worked quite well. Insertion was performed with an open pipe frame mandrel with a 300 mm (1 ft) deep steel plate along the bottom edge. The VLDPE membrane was cut from a roll, laid on the ground outboard of the trench, and aligned with 300 mm (1 ft) placed inboard of the trench wall. The steel plate mandrel edge was pushed into the membrane and the tight radius and friction around the steel plate held the membrane in place. A backhoe pushed the mandrel into the backfill and extracted the mandrel by pulling chains at the top. The mandrel was pulled into the backfill, away from the outer wall, which separated the mandrel from the sheet, leaving the membrane along the outside edge. String tell tales were fastened to the tip of selected sheets to verify the sheet remained at the insertion

depth when the mandrel was extracted. Each sheet was over-pushed 300 mm (12 in) because the membrane typically came up 150 mm (6 in) when the mandrel was extracted. The overlapped joints sometimes engaged an adjacent sheet, especially at depth, but the 100 mm (4 in) clearance generally proved satisfactory if sheets were properly aligned and the mandrel was pushed vertical. A reinforcing geogrid was placed along the top of the barrier to provide stability for working and the membrane was extrusion welded above the backfill surface. The barrier was covered with 150 mm (6 in) of No. 57 stone as an interim cover awaiting construction of the multimedia cap.

Hydraulic Testing And Barrier Performance

Large diameter piezometer pairs installed for long term monitoring of the barrier were used to evaluate barrier performance. The piezometers were installed and tested as the barrier was completed and the interim cover was completed. Interior piezometers located 3 m (10 ft) inboard of the barrier were pumped to lower the groundwater table as much as 7.5 m (25 ft) in the confined aquifer, with no influence on the adjacent piezometer 10 ft outboard of the wall. This testing is described and summarized by others (Ref. 2).

CONCLUSIONS

Successful construction of this deep slurry trench required a careful examination of the slurry trench construction method. The specifications limited the slurry sand content, required trench bottom cleaning, and required separation of the excavation turmoil from the backfill. The contractor's implementation of the end stop, cyclone desander, backfill gradation control, and travelling hammerhead mill supported the construction quality required by the contract documents.

Quality assurance of slurry trenches is difficult because the slurry column prevents visual observation and obscures soundings. Diligent and active field inspection of the trench was especially necessary for this project due to the difficult site conditions, the unknown embankment fill excavation performance, and the environmental sensitivity of the adjacent Patapsco River. Borings on close spacing along the alignment were necessary for quality assurance of the key and bottom closure. The contract drawings included a detailed soil profile along the trench alignment which was used for quality assurance and to track the job progress. Inspection of the excavation and bottom cleaning was difficult in the deep trench with the extended reach backhoe.

Hydraulic testing for performance assessment indicates the barrier performance is excellent. This performance is attributed to consistently obtaining a key into the closure stratum and the cleaning of the trench bottom which enabled the soil-bentonite backfill to positively contact and close with the bedrock.

Acknowledgements

Construction Manager, J.P. Kavney, in the design, contract preparation, and implementation of this remedial construction was fundamental to the success of this project and is appreciated.

References

Poletto, R. and Good, D. (1997) *Slurry Walls and Slurry Trenches - Construction Quality Control,* Proceedings, 1997 International Containment Technology Conference and Exhibition, February, 1997, St. Petersburg, Florida, USA.

Snyder, G. et al (1997) *Performance Assessment Through Hydraulic Testing - Baltimore Works Site with Comparison,* Proceedings, 1997 International Containment Technology Conference and Exhibition, February, 1997, St. Petersburg, Florida, USA.
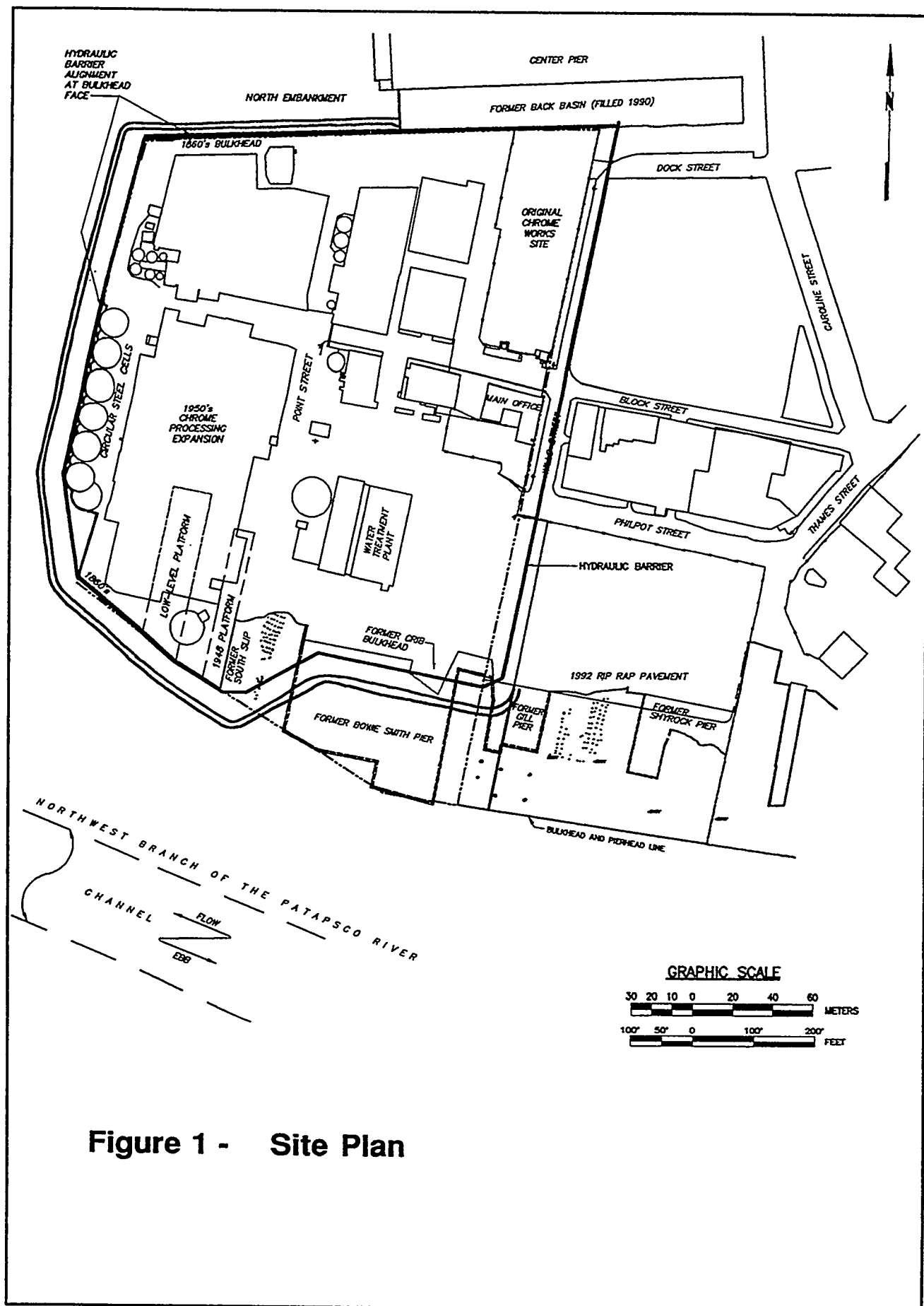
Figure 1 -   Site Plan
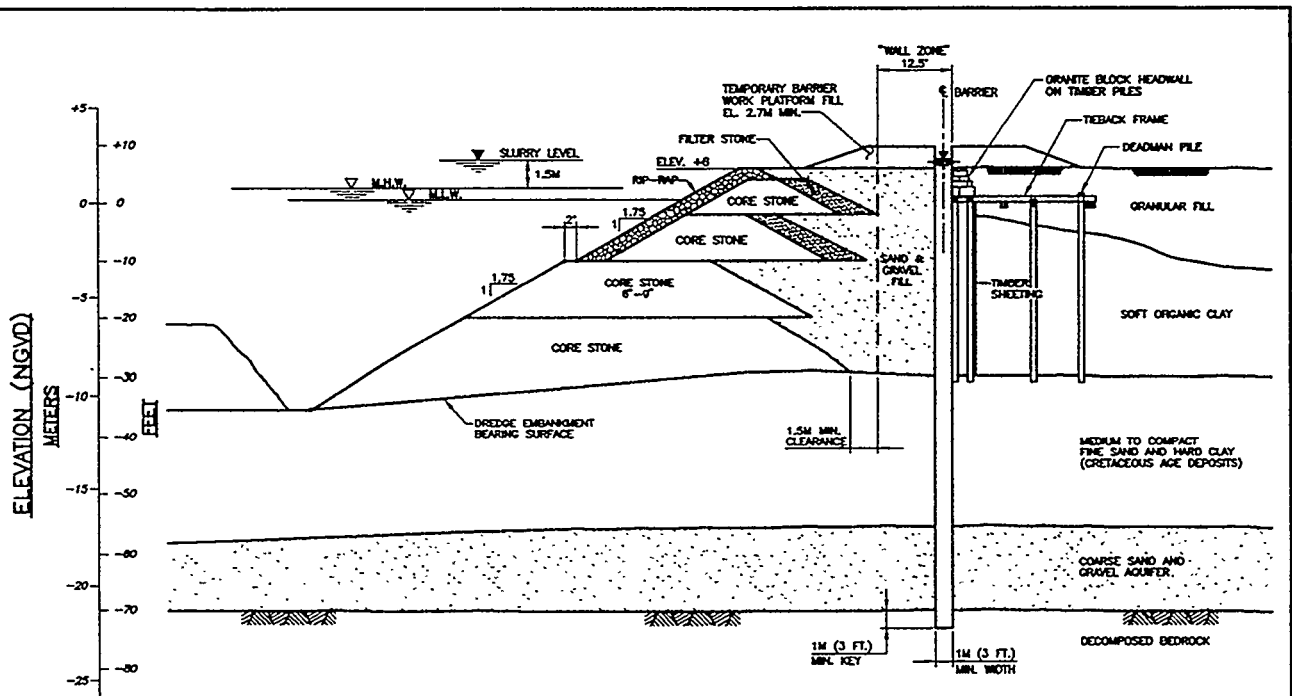
Figure 2 - **Bulkhead Circa 1860 and New Embankment With Active Slurry Trench Excavation**
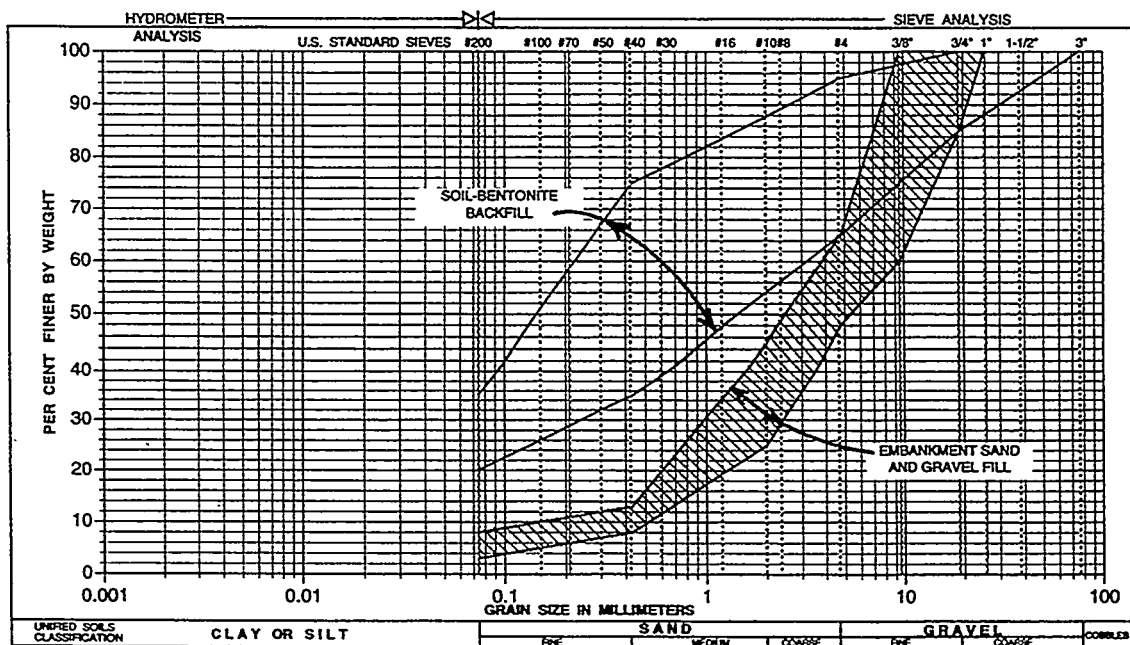
Figure 3 - **Embankment Fill and Backfill Gradation Ranges**

174

MEETING THE CHALLENGE OF CONSTRUCTING
A UNIQUELY DIFFICULT BARRIER WALL

Robert L. Stamnes[1], Howard M. Orlean[2], Neil E. Thompson[3]

Abstract

A soil-bentonite vertical barrier wall with intersecting and round corners was constructed in complex geology and steep terrain to enclose and dewater a 1.4 hectare (3.5 acre) area once used for hazardous waste lagoons and landfills at the Queen City Farms (QCF) Superfund site in Maple Valley, Washington. The barrier system, including cap and barrier wall, was designed to contain light non-aqueous phase liquid (LNAPL), in addition to subsurface soil and ground water contaminated with chromium, polychlorinated biphenyls, polyaromatic hydrocarbons, trichloroethylene, dichloroethylene and vinyl chloride in the dissolved-phase. These contaminants threaten a drinking water aquifer beneath the site. Constructing the vertical barrier was a challenge due to steep slopes of 20 percent along the alignment (19.2 meter elevation change in the top of the wall), a 22.5 meter (75 foot) design wall depth, heavily consolidated clays and silts, open works gravels (gravel without finer soils), and geologic discontinuity. The barrier wall is keyed into either a glacial till or thin clayey-silt aquitard. Extensive earth moving, stepped walls and many construction techniques were used to enable construction of this barrier wall. Commonly accepted constructability criteria would have discouraged the construction of this wall.

Site Conditions

The Queen City Farms Superfund site (the Site) is located about 32 kilometers (20 miles) south-southeast of Seattle, Washington near the town of Maple Valley. The Site is situated in a predominantly rural, wooded and hilly area located between a 360 hectare (900 acre) regional landfill and a large gravel mining operation (Figure 1). The entire Site encompasses approximately 128 hectares (320 acres). Approximately 1.4 hectares (3.5 acres) in the northeast corner of the Site historically contained three (3) unlined lagoons used for disposal of liquid wastes including paint, petroleum products, solvents and oils. To prevent potential exposure to these hazardous substances, the potentially responsible parties (PRPs) conducted an interim remedial measure (IRM). The IRM included draining and clean up the lagoons, and capping the underlying contaminated soils in place.

The Site, including the IRM area, is underlain by consolidated and unconsolidated glacial till, silt, sand and gravel. These soil types pinch out or grade laterally over very short distances across the Site. Four saturated units (aquifers) have been identified beneath the IRM area. These units in order of increasing depth are; Aquifer 1, Aquifer 2, Aquifer 3, and the Deep Confined Water-Bearing Zone (Figure 2). Locally, Aquifer 2 is used as a drinking water source by residences and businesses adjacent to the Site. The hydraulic gradient is vertically downward, from Aquifer 1 to Aquifer 2 and 3. Low concentrations of VOCs (below drinking water standards) have been found in aquifer 3.

[1] United States Environmental Protection Agency, Region 10, 1200 Sixth Avenue, Seattle, Washington 98101, (206)553-1512, stamnes.robert@epamail.epa.gov
[2] United States Environmental Protection Agency, Region 10, 1200 Sixth Avenue, Seattle, Washington 98101, (206)553-6903, orlean.howard@epamail.epa.gov
[3] United States Environmental Protection Agency, Region 10, 1200 Sixth Avenue, Seattle, Washington 98101, (206)553-7177, thompson.neil@epamail.epa.gov

Figure 1
Preliminary Barrier Wall Alignment
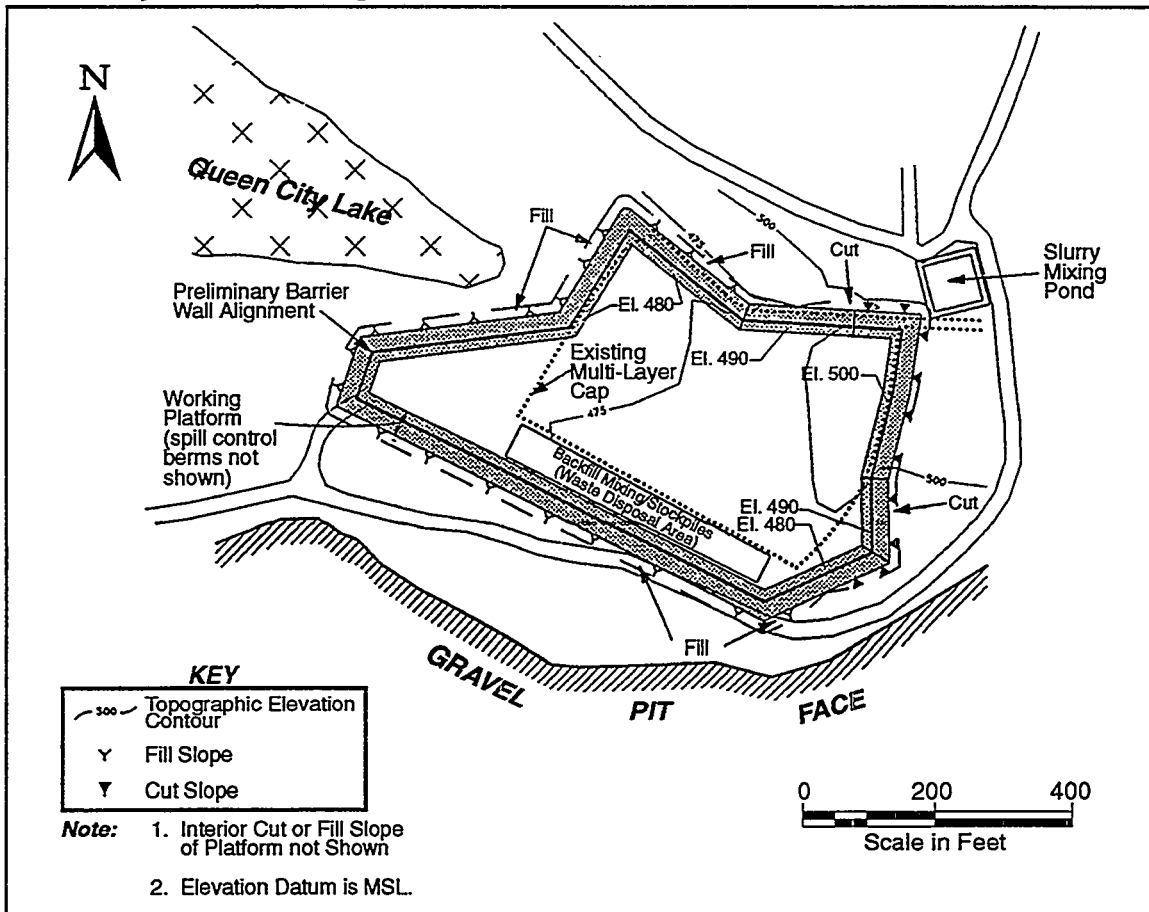
The deep water bearing zone has not been impacted. The deep confined aquifer (deep water bearing zone) maintains a positive hydraulic gradient upward into aquifer 3.

Subsurface soil and Aquifer 1 ground water beneath the IRM area are contaminated with volatile organics, dissolved phase polyaromatic hydrocarbons (PAHs), polychlorinated biphenyls (PCBs) andwater bearing zone has not been impacted. The deep confined aquifer(deep water bearing zone) maintains a positive hydraulic gradient upward into aquifer 3. heavy metals. Free phase dense non-aqueous phase liquid (DNAPL) has not been found. Ground-water monitoring performed during the remedial investigation determined that water level elevations seasonally fluctuate by as much as 6 meters (20 feet) during the year. Contaminants within subsurface soil and Aquifer 1 beneath the IRM are consequently "flushed" down into Aquifer 2.

Thus, the IRM area has continued to serve as a source of contamination to a drinking water aquifer (Aquifer 2). To control the source and prevent further contamination of Aquifer 2, a Record of Decision (ROD) incorporated the provision to place a vertical barrier around the IRM to control inflow of ground water and reduce the transport mechanism for contamination to migrate.

Figure 2
Generalized Cross-Section of Site
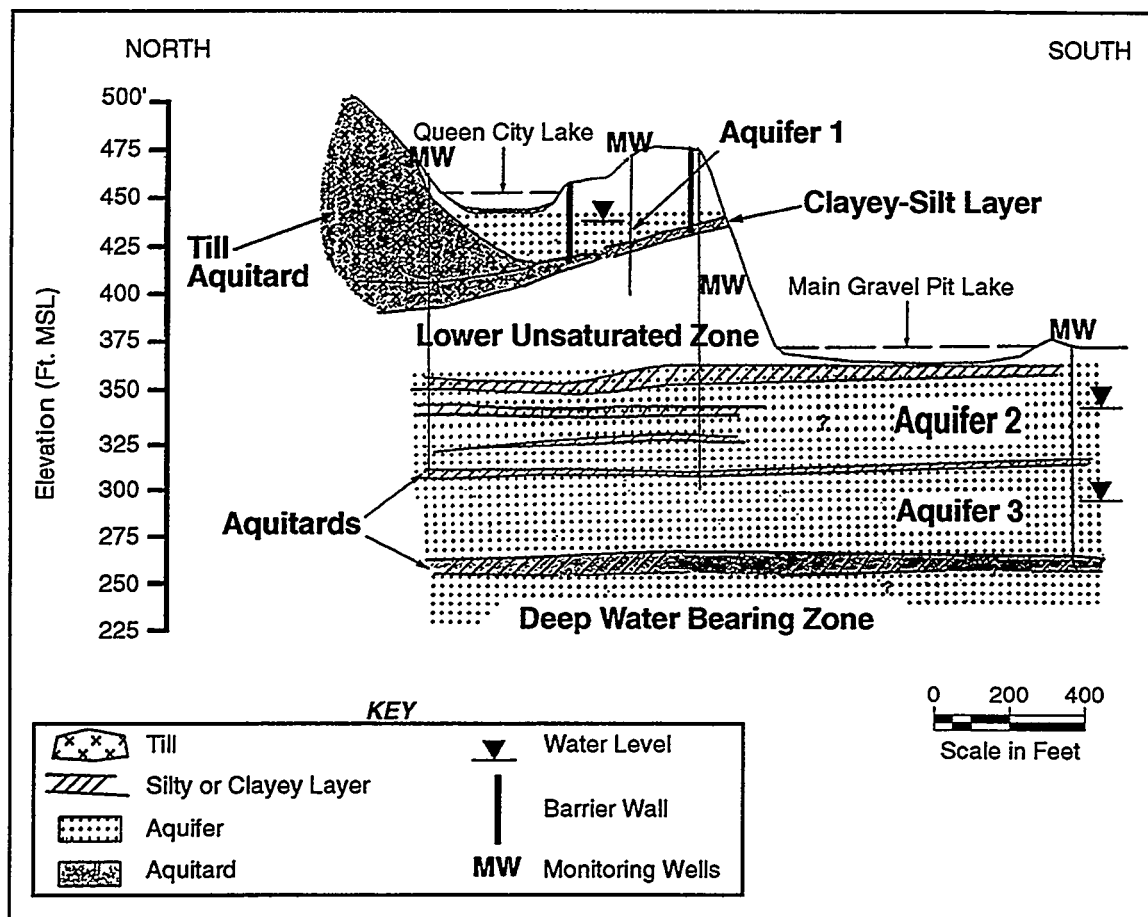
Design Considerations

The Boeing Company (a PRP) selected a design and construction team (Kennedy/Jenks, design; Hayward Baker, construction) to implement the ROD requirements for the vertical barrier wall. Design and construction were intentionally combined to allow selection of the most protective and cost-effective design for this Site. Several issues needed to be considered in design development. They included open works gravel, hard consolidated glacial till, extreme depth of the vertical barrier wall, the variable topography of the site, and the need for special working platforms to construct the barrier wall.

A slurry wall construction technique using a soil-bentonite backfill with a permeability of 10^{-7} centimeters/second was selected. The depth of the vertical barrier from ground surface to interception of the low permeable key layer required trench depths of 23.7 meters (79 feet) below ground surface (bgs). This was deeper than the normal track hoe reach. Therefore special work platforms needed to be constructed at or near the ideal slope of less than 2 percent as measured parallel to the top of the trench (USEPA, 1984).

To meet these requirements, an 18 meter (60 foot) wide working platform (about 9175 cubic meters (12,000 cubic yards) of soil) was cut through the upper portion of the site, lowering the highest elevation from 155 meters to 144 meters (516 feet to 481 feet). This reduced the upper elevation of the wall 10.5 meters (35 feet), with a remaining elevation change along the wall alignment of 7.8 meters (26 feet) for an average slope of 3.0%.

177

This reduced the depth of the slurry trench in this area from 23.7 meters to 15.6 meters (79 feet to 52 feet), within the 21.6 meter (72 foot) depth reach achievable by a modified track hoe (Koehring 1466). Additional excavations were needed at other areas to reach the required depth with this equipment.

To address topographic changes along the wall alignment, steps were created in the working platform. In several locations, to allow the equipment to follow the surface topography better, the platform steps changed as much as 3.9 meters (13 feet). In most locations, the remaining 7.8 meters (26 feet) of elevation drop along the wall was accounted for by the natural 5:1 to 10:1 (horizontal to vertical) slope of the backfill when it was placed from the high end of the trench toward the lower end of the trench. At one location, the 3.9 meter drop was maintained by placing the lower section first and filling over that section with soil to form a work platform for the higher section. The higher section was then excavated through the fill and past the interception with the lower wall section.

The trench bottom was keyed 0.9 meter (3 feet) into an aquitard. The aquitard elevation varied across the Site, requiring many steps in the bottom of the wall. Due to complex stratigraphy, the aquitard elevation was difficult to determine from boreholes spaced about 33 meters (100 feet) apart along the wall alignment. An on-site geologist continuously logged the stratigraphy of the trench to ensure the wall was properly keyed into the aquitard. Large boulders (3.3 meters in diameter) were also encountered within the trench area during wall construction. Boulders were removed by lowering a 12 meter (40 foot) long H-beam from a crane until the rock was chipped away.

Construction Methods

During slurry wall construction, several problems were encountered. These included, the type and quality of soils which varied throughout the site creating trench stability problems, hard consolidated glacial till that posed problems for the equipment and slowed the project down, and open works gravels which caused significant slurry loss during construction.

The lower portion of the trench encountered consolidated glacial till which required a powerful track hoe to cut. Even with this powerful equipment, progress was slow. Glacial till was hard on equipment, resulting in cracks in the boom and replacement of a set of bucket teeth per day.

Where natural glacial till extended to the work platform, trench stability was very good. However, in areas with open works gravels and softer surface soils, a dense slurry in the trench was needed to reduce sloughing. Sloughing and cave-ins were a minor problem.

The following techniques were used to address the 7.8 meter (26 feet) elevation change in topography along the path of the slurry wall. Work platforms were sloped slightly and stepped to account for the remaining 7.8 meters of elevation drop in the wall. Slurry was maintained in each section of uniform platform height until a step in the work platform was reached. Steel sheet pile was placed in the trench to reduce the movement of backfill toward the excavation end of the trench. This allowed placement of as much backfill as possible while the slurry was near the top of the trench. These piles were lifted periodically to allow the backfill to flow under them, metering the amount of released backfill.

Since the steel sheet pile did not hold back the slurry, slurry dropped to the top level of the lower trench and allowed as much as 3.9 meters (13 feet) of upper trench to be unsupported by slurry or backfill. When a drop in the elevation of the platform was reached, the backfill was allowed to seek the height of the lower platform by using its natural angle of repose (5:1 to 10:1, horizontal to vertical). A minimal amount of sloughing did occur in the open, upper trench as a result of lowering the slurry level. However, in glacial till soils, sloughing was not a problem.

On one corner of the project, the lower wall was constructed first and a temporary soil platform built on top of the constructed wall. This allowed the upper wall trench to be constructed through the lower wall (which was already in place) without a loss of slurry. The soil platform was then removed, the surface of the lower wall trimmed, and additional backfill placed on the wall to bring it up to finished grade.

Sloughing of filter cake from trench walls was noted during the operation. This was not unexpected as it has been noted at other installations (Grube, 1992). This was not a concern at this site because the backfill itself was designed to meet the permeability requirements of the barrier, 10^{-7} centimeters/second.

Surface cracks were noted between the natural soils and the wall backfill. These cracks ran parallel to the length of the wall. This type of cracking has been noted by others, especially where fines content in backfill is high (USEPA, 1984). A surface cap placed over the site extended past the outside of the wall reducing the potential for wall failure due to shrinkage.

Excavation in unconsolidated gravels resulted in slurry loss, requiring addition of large volumes of slurry. Excessive loss of slurry was generally controlled by immediate backfilling with side cast materials or soil from previous earthwork. In one area, slurry loss was so significant that a truck load of dry Portland cement, used as a thickening agent, was added to the trench to form a pudding seal in the gravels. This was effective and slurry loss was stopped. Cuttings affected by the cement slurry were side cast and not used in the backfill mix.

Potential loss of slurry to Queen City Lake was a concern. Queen City lake is less than 6 meters (20 feet) from the wall and nearly the entire site drains toward the lake. Special precautions taken to address potential surface runoff problems included silt fencing, hay bales, and construction of dikes between the slurry wall and the lake.

Construction Quality Control/Quality Assurance

Hayward-Baker performed the quality control function. The Boeing Company hired Golder and Associates under a separate contract to perform quality assurance on the project. The quality assurance function controlled the progress on the slurry wall. The Golder and Associates geologist worked very closely with the track hoe operator to acquire and analyze soil samples, and to ensure that design depth was met. As a result, this teaming approach ensured proper keying of the wall into the appropriate aquitard layer. The geologist also kept records of trench sections cleaned prior to backfilling. Testing of slurry and backfill was performed by both Hayward-Baker and Golder and Associates. This confirmation process is similar to that recommended by others (Millet, 1992).

Post Construction Monitoring

In accordance with the ROD, the PRP must keep Aquifer 1 dewatered inside the vertical barrier wall (USEPA, 1992). This is a much more restrictive requirement than that proposed for other sites (Grube, 1992). The integrity of the wall will play a major roll in the cost of maintaining the de-watered condition within the wall. If the wall, cap and underlying aquitard are tight, a single dewatering of the groundwater within the wall may satisfy these conditions for a long time period. If not tight, additional maintenance pumping will be required to ensure Aquifer 1 groundwater evacuation inside the wall.

Water levels in three wells completed in Aquifer 1 and located inside the wall alignment area were continuously monitored during and after construction of the wall. Daily fluctuations in the water levels demonstrate the interrelationship between construction of the wall (the slurry) and Aquifer 1.

These wells continue to be monitored to determine the impact of the wall on the ground water systems. Post remedial groundwater monitoring is in design.

Ground-water monitoring has revealed the presence of bentonite in Aquifer 1. The effects of this on the ability to extract water from Aquifer 1, inside the containment wall, has not been fully evaluated. A full year of monitoring will be completed before the effectiveness of this wall can be evaluated.

Conclusions

Although the Army Corps of Engineers design checklist limits application of soil-bentonite walls to areas with 2 percent or less slope along the alignment, walls can be constructed in areas with much steeper slopes (USACOE,1995). A number of additional problems are encountered, however, and should be recognized and addressed during design and construction. Special precautions should be taken in design and maintenance of such walls, particularly at wall corners, including an extensive depth monitoring program in the area of wall intersections, overlapping intersections to guarantee backfill joints to the bottom of the trench, and cutting back the wall being joined to reduce slumping of backfill. Even with these precautions in place, there is still some increased chance for development of windows at corner joints. Intersecting walls at corners should be avoided if at all possible and continuous walls used.

Potential surface loss of slurry to nearby waterways can be prevented, and requires installation of berms around the project area and aggressive oversight. Silt fences, even if properly installed, can become plugged with bentonite, creating a potential for failure.

Thickening agents, such as the cement used at this site, are available and should be considered, especially where open works gravels are encountered. If thickening agents are used, caution should be exercised in the use of trench cuttings in backfill, as they may adversely impact backfill characteristics. The selected thickening agent should also be readily available on-site for immediate deployment to reduce slurry loss. Thickening agents may affect backfill density. Care should be taken to maintain the suggested difference between the density of the backfill and that of the slurry (USACOE, 1995).

Acknowledgments

John Barich, Marcia Knadle and Grechen Schmidt of USEPA, The Boeing Company, and Golder and Associates.

References

Grube, W.E., Jr. (1992) "Slurry Trench Cut-off Walls For Environmental Pollution Control". In *Slurry Walls: Design, Construction and Quality Control, ASTM STP 1129*, (ed. D.B. Paul, R.R. Davidson and N.J. Cavalli.), American Society for Testing and Materials, pp. 72, 73, Philadelphia, Pennsylvania, U.S.A.

Kennedy/Jenks Consultants. (1996) *Queen City Farms, Vertical Barrier Wall System, Task Remedial Design Report*, Federal Way, Washington, U.S.A.

Millet, R .A., J. Y. Perez, and R. R. Davidson. (1992) "USA Practice Slurry Wall Specifications 10 Years Later. In *Slurry Walls: Design, Construction and Quality Control, ASTM STP 1129*, (ed. D.B. Paul, R.R. Davidson and N.J. Cavalli), American Society for Testing and Materials, p. 64, Philadelphia, Pennsylvania, U.S.A.

Rumer, R. R. and J. K. Mitchell. (1995) *Assessment of Barrier Containment Technologies*, Baltimore, Maryland, U.S.A.

United States Army Corps of Engineers. (1995) *Engineering and Design Checklist for Design of Vertical Barrier Walls for Hazardous Waste Sites, ETL 1110-1-158*, p. B-14, USACOE, Washington, D.C., U.S.A.

United States Army Corps of Engineers. (1994) *Corps of Engineers Guide Specification, 02444 - Soil -Bentonite Slurry Trench for HTWR Projects, Washington, D.C., USA.*

United States Environmental Protection Agency. (1993) *Technical Guidance Document: Quality Assurance and Quality Control for Waste Containment Facilities, EPA/600/R-93/182*, GPO, Washington, D.C., U.S.A.

United States Environmental Protection Agency. (1992) *Record of Decision; Declaration, Decision Summary, and Responsiveness Summary for Final Remedial Action, Queen City Farms Superfund Site, Maple Valley, King County, Washington*, p. 87, Seattle, Washington, U.S.A.

United States Environmental Protection Agency. (1984) *Slurry Trench Construction for Pollution Migration Control, EPA 540/2-84-001*, p. 5-12. GPO, Washington, D.C., U.S.A.

Use of Deep Soil Mixing as an Alternate Vertical Barrier to Slurry Walls

A. David Miller, P.E.[1]

Abstract

Slurry walls have become an accepted subsurface remediation technique to contain contaminated zones. However, situations develop where conventional slurry wall excavation techniques are not suitable. The use of conventional containment wall construction methods may involve removal and disposal of contaminated soils, stability concerns and the risk of open excavations. For these reasons, other installation techniques have received further consideration. Deep Soil Mixing (DSM) has emerged as a viable alternative to conventional slurry wall techniques. In situations dictating limited soil removal for contamination or stability concerns, or where space is a limitation, DSM can be used for installation of the barrier. Proper installation of a DSM wall requires sufficient monitoring and sampling to evaluate the continuity, mixing effectiveness, permeability and key into the confining layer. This paper describes a case study where DSM was used to cross major highways to avoid open excavation, and along slopes to reduce stability concerns. The DSM barrier was tied to an existing conventional slurry wall that had been installed in more stable areas without highway traffic.

INTRODUCTION

Underground vertical barriers are used to prevent lateral migration of contaminants and groundwater. Most often, they consist of a variation of Slurry walls. Slurry wall types typically include: Soil-Bentonite (SB), Cement-Bentonite (CB), Composites, or Bio-Polymer. Other techniques have been used and other variations exist.

Underground barriers date back to the 1940's; most have been installed since the mid 1970's. In recent years, American Society for Testing and Materials (ASTM) has established relevant test standards (US Army (1995), USEPA (1984)).

Vertical barriers generally are used either for new or remedial work. New work would include: new cell construction of a waste facility, dam, or lagoon. Remedial work generally involves mitigating existing conditions. This may include prevention of migration of a contaminant source or plume, protection of existing groundwater, or as an aid in dewatering. Most barriers are installed using hydraulic excavators. This entails excavating a trench while maintaining it full of slurry for hydraulic support of the excavation walls. The trench is then backfilled with an impervious material, typically a blend of soil and bentonite (Figure-1). In some instances, this technique creates an unstable soil condition. Instability may be caused by a high water table or an unusually high surcharge loading near the barrier alignment. Highly contaminated soils, property access or physical constraints may also preclude the use of conventional excavation techniques.

DSM Technology

One method used to install a vertical barrier in situations involving unstable conditions or site constraints is the use of DSM. DSM uses a multiple set of overlapping augers (Figure 2). As these augers penetrate the ground, a fluid (bentonite slurry) is injected through the augers and out the

SCHEMATIC SECTION THROUGH SB SLURRY CUT-OFF
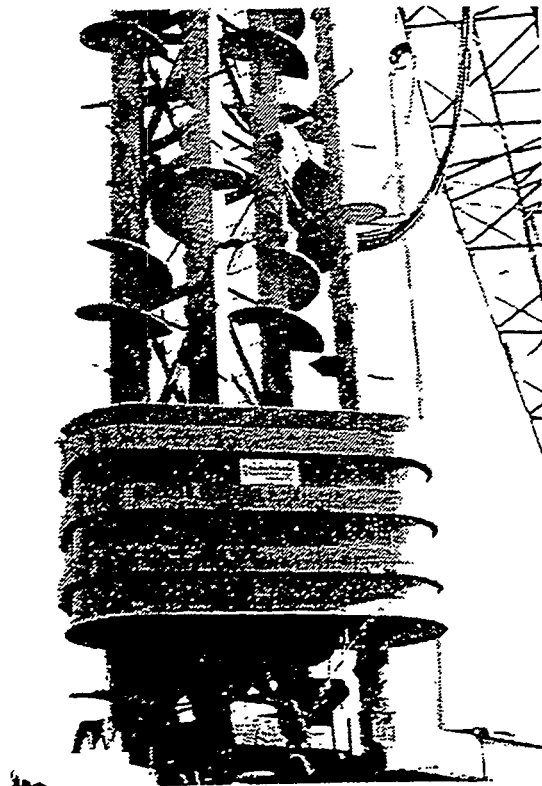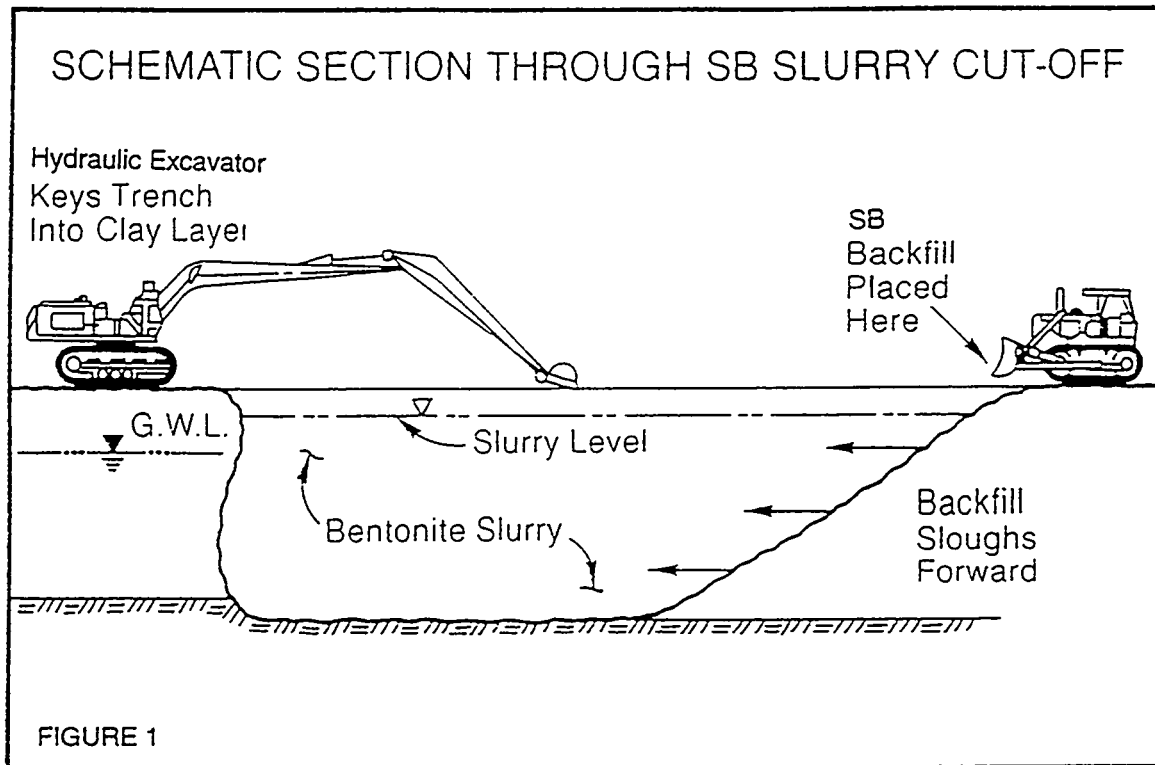
FIGURE 1

FIGURE 2   MULTI-AUGER DSM MIXING MACHINE

cutting face. The augers mix the slurry with the in-situ soils to create a blend of soil - bentonite forming a low permeability barrier. This is accomplished without open excavation, so stability concerns are minimized. Also, a DSM barrier can be installed within inches of existing structures.

DSM creates the barrier in-situ by drilling in a linear arrangement. To assure continuity, the first shaft redrills the print of the last segment (Figure 3). It is a technique that is relatively new to the U.S. The process was developed in Japan primarily for structural retaining walls and excavation support systems. The same equipment has seen more uses for containment walls at contaminated sites in the U.S.

The DSM technique has limitations due to cost. However, some of these costs can be recovered since similar permeabilities can be achieved with DSM compared to more conventional containment walls because DSM does not incur the additional cost of added dry bentonite. Also, due to saturated soil conditions, some waste may be displaced that requires disposal. That is, as the slurry is injected and fewer voids are available to accommodate the slurry, contaminated soils may be displaced. Depending on the level of saturation, there may be spoils generated. These spoils can be disposed of or graded on site.

A comprehensive monitoring plan helps to ensure continuity of the key into the aquiclude. This plan includes monitoring vertical alignment, slurry intake, mixing time, and depth. The slurry properties monitored during installation include viscosity, density, and filtrate loss. Samples of the mix can be sent to a laboratory for permeability and gradation tests. Since immediate lab results are not possible, field QA/QC plays a very important role in the installation process.
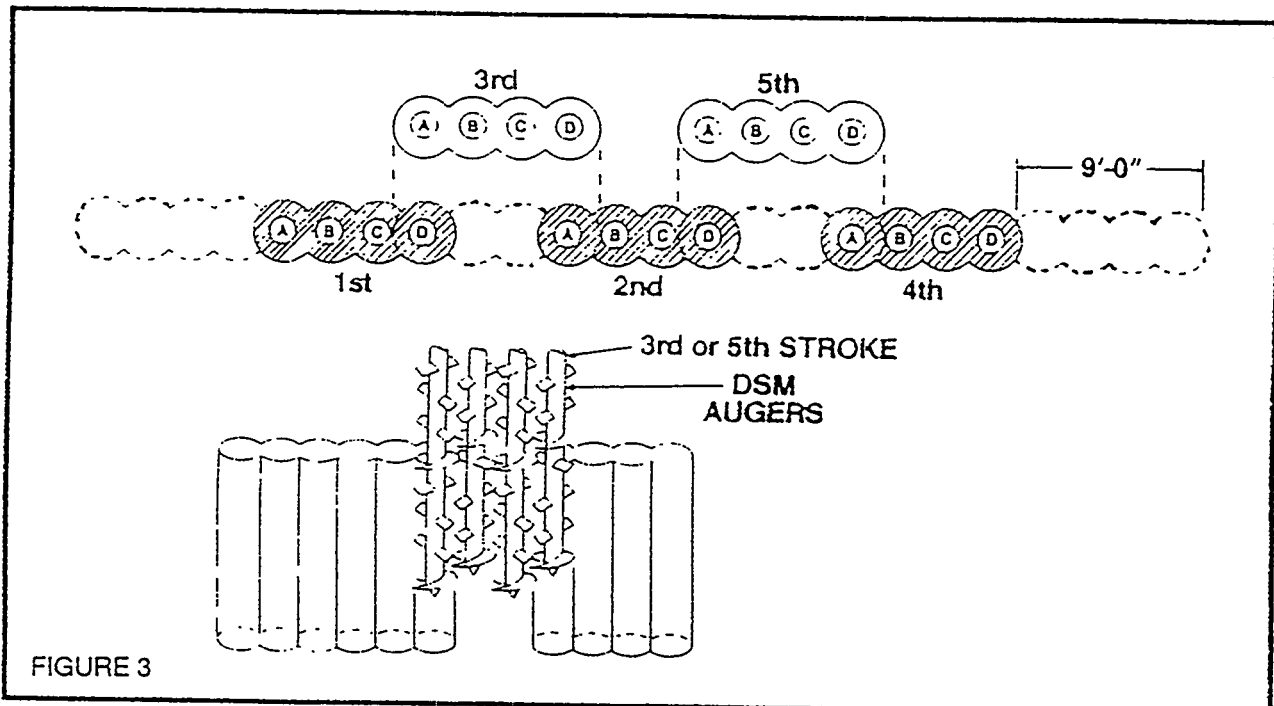
FIGURE 3

APPLICATION OF DSM FOR BARRIER WITH STABILITY CONCERNS

A former chemical facility near Houston, Texas consists of approximately 11.3 acres near the junction of a major Interstate highway and another heavily traveled highway. Historical activities at the site included waste disposal and reclamation. Reclamation of discarded residuals took place from 1958 until 1961, when the site was flooded by a hurricane. In 1964, the Texas Water Pollution

Control Board issued a permit allowing a series of salvage ponds. On-site activities utilized open "pits" as catch basins for spent or waste materials until 1968, when open pit disposal was prohibited within the city limits. From 1968 to 1977, various property owners attempted to reclaim residuals.

In 1983, the remedial Investigation/ Feasibility Study (RI/FS) at the site was divided into two components by the EPA. These are source control and management of migration (MOM). Source control was defined in the ROD as contaminant removal within the site boundaries to remediate surface impoundments and adjacent areas. Previous remedial activities completed included drum disposal, diking and fencing of the site, removal of surface water, demolition and removal of above ground tanks, and underground storage tank removal. Pit sediments will be stabilized and capped. This combined with the containment barrier will completely encapsulate remaining site wastes.

The barrier wall was part of the remedy to prevent off-site migration of DNAPL and impacted groundwater. DNAPL and groundwater recovery systems were also installed. The project's containment barrier was initially designed to be a conventional slurry wall constructed using a hydraulic excavator. However, early in the construction of the slurry wall, it became apparent that groundwater conditions combined with surcharge loads along the barrier alignment would prevent project completion using slurry wall excavation techniques. After the start of construction, it was discovered that the water table was confined and under pressure. In addition, the containment wall crossed major highways and associated feeders in three locations. Concerns over the impact on traffic from work platform and open excavation instigated an evaluation into the advantages of using the DSM technique. DSM process was selected because less excavation would be required to create the work platform, thereby minimizing impact on traffic. Also, the DSM process was able to eliminate the risk of trench collapse from highway ramp surcharge loading.

The lithology along the slurry wall alignment consisted predominately of interbedded sands, clays and silt. The aquiclude used for key material consisted of Upper Chicot clay. This formation was found at depths of approximately 15 - 17 meters. Groundwater pressures effectively raised the groundwater level to within one meter of the ground surface.

The containment barrier was planned as part of a complete encapsulation of the site. The total planned length was approximately 1530 meters. Of this, approximately 400 meters were completed with DSM. The intended key into the Upper Chicot clay was one meter.

Preconstruction laboratory studies were completed to determine the optimum mix ratio to meet the permeability design requirement of 1×10^{-7} cm/sec. As strength was not a factor, the predominant additive considered was bentonite. Due to the soil stratigraphy, which was mostly clay with interbedded sands, mix variations in bentonite content had little effect on barrier permeability.

Construction began using conventional slurry wall techniques. After breaching an intermediate clay layer with the hydraulic excavator, groundwater levels rose. A saturated sand layer was present below the intermediate clay layer. This layer contained a confined aquifer under sufficient hydrostatic head to cause an increase in groundwater elevation after breaching the clay layer. Eventually the confined aquifer created stability problems. This combined with the surcharge effect of an adjacent embankment, contributed to a trench failure at one location.

As a result of this failure, barrier design was reevaluated. The majority of the site was in open areas where minor trench failures could be tolerated. Therefore, on most of the site, stability concerns were alleviated by simply raising the working platform. This created enough elevation difference above the groundwater to allow the bentonite slurry to develop a hydrostatic head that would support the excavation and avoid trench failure. This proved to be very successful and relatively economical. However, greater concerns for stability existed for highway crossings.

The zero tolerance for failure and the additional work platform now required to accommodate the higher work platform within the highway right of way facilitated DSM. It was determined that DSM had specific advantages for this site, including the ability to install a barrier in a relatively discontinuous construction sequence. Traffic could simply be diverted from each side of the highway rather than completely rerouting it. In addition, considerably less effort and room were required to construct a 'work platform (Figure 4). This also accelerated traffic rerouting and highway reconstruction.

FIGURE 4
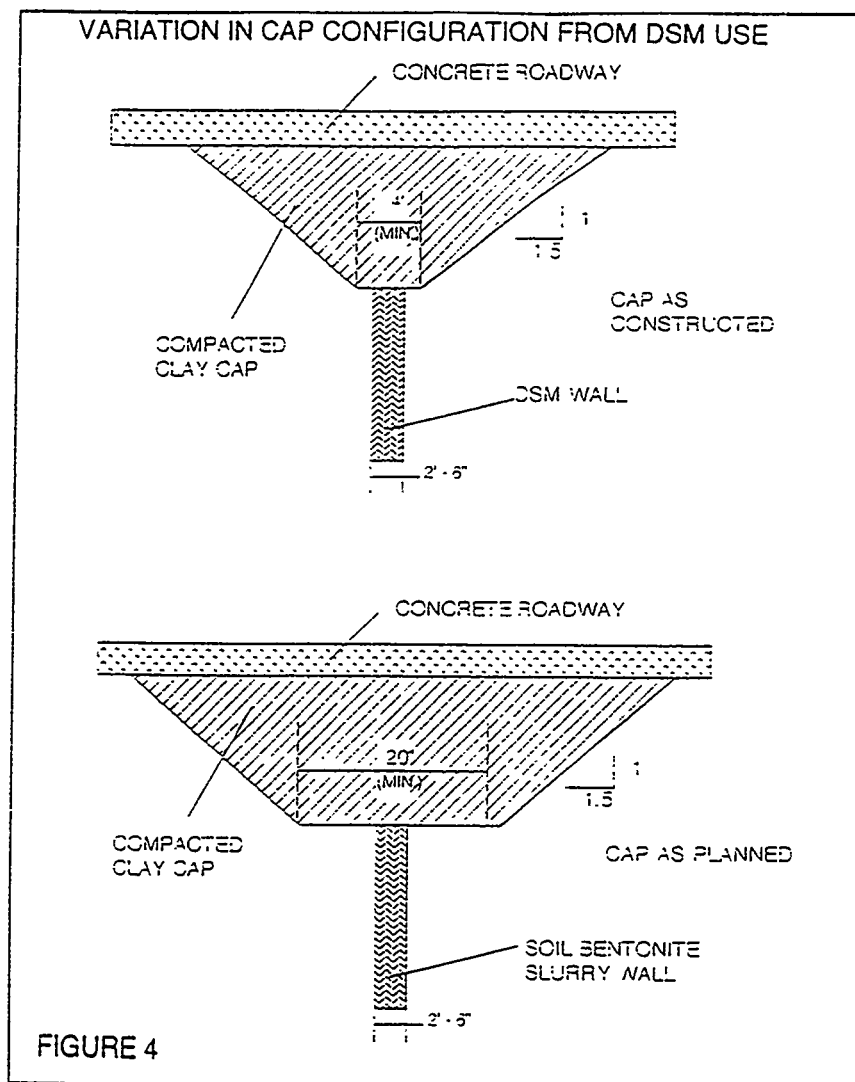
Since the ROD was already approved, it was necessary to obtain EPA's approval of the modification. Plan details, quality control procedures and sequencing were required for formal EPA approval. In addition, EPA had concerns over the minimum thickness of the barrier. The slurry wall had a minimum thickness of about 1 meter, whereas the DSM has an average thickness of approximately 0.8 meters. Initial permeability results alleviated these concerns as they were better

than the 1×10^{-7} cm/sec requirement.

Although DSM was initially only planned to cross the highway in three locations, a small section of barrier wall remained east of the highway (Figure 5). Right of Way concerns with the property owner and the work platform required for a slurry wall in this location made DSM attractive for this zone also.

Sequencing of DSM was such that all crossings involving traffic in the same direction were completed first. Lane crossings involving traffic in the opposite direction were then completed. In order to tie into existing work, the augers were drilled in perpendicular to the alignment of the existing slurry wall. This technique assured a continuous wall between the two distinct installation techniques (Figure 6).

FIGURE 5   SITE PLAN FOR BARRIER WALL

FIGURE 6   TIE IN DETAIL

187
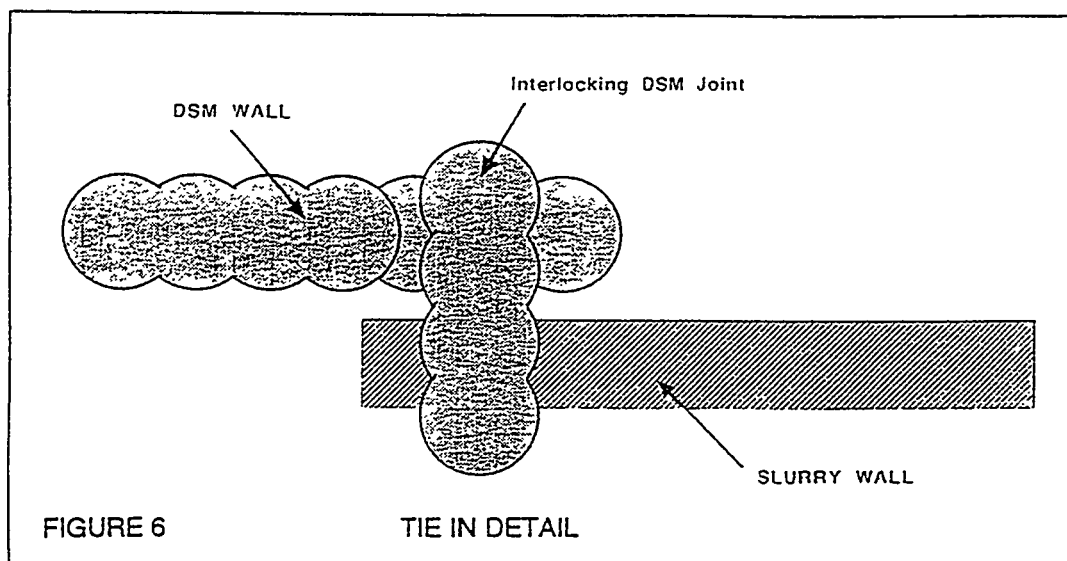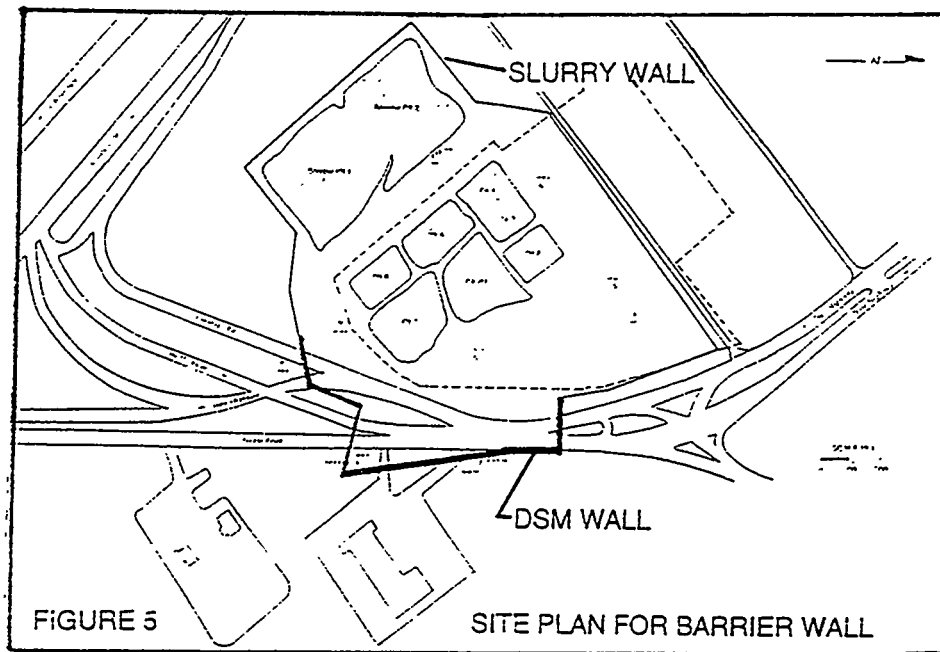
RESULTS ·

A rigorous quality control (QC) program was initiated by the owner. This included monitoring the verticality of DSM strokes, overlapping configuration and depth. These were monitored through a series of ground measurements. The angle of inclination was also monitored in relation to the ground Slurry was monitored on-site for viscosity, unit weight and filtrate loss. Total slurry used was recorded and compared with expected values. In addition, wet samples were taken from the fresh soil-bentonite mixture and tested for permeability. Due to the 5 to 7 day turn around time for lab permeability results, on-site QC was extremely important in the evaluation of the effectiveness of the barrier.

This effort along with careful sequencing by the contractor made for an effective, safe, and timely installation of the DSM barrier wall. Permeability results were all significantly lower than the design target permeability of 1×10^{-7} cm/sec.

This project shows that the amount of bentonite needed for DSM can be limited. The blending action of the augers combined with high clay content soils were able to create an effective containment barrier. During construction of the DSM barrier, no stability problems were noted within the wall alignment. An ongoing monitoring program will determine whether any long term stability problems develop.

CONCLUSIONS

At this site, DSM proved to be an economical, safe and reliable way to address a difficult set of constructibility issues that were also coupled with stringent regulatory requirements and right of way and access concerns. DSM expedited project completion substantially.

Each site has its own set of access concerns, stability problems and soil stratigraphy. A high quality, low permeability containment barrier can be constructed within narrow constraints using DSM.

ACKNOWLEDGMENTS

The author was formerly a Project Manager with Geo-Con, Inc, the contractor for the project. He is now a Project Manager with CDM Engineers and Constructors, Inc. The author would like to thank the owner and Geo-Con, Inc. for assistance in providing the data necessary to complete this paper.

REFERENCES

United States Army Corps of Engineers. (1995) Engineering and Design Checklist for Design of Vertical Barrier Walls for Hazardous Waste Sites, ETL 1110-1-158, pp 8-14. USACOE, Washington. D.C., USA

Yang, David S. (1995), "Vertical Barriers by Deep Mixing", International Containment Technology Workshop. Baltimore, MD, USA August, 1995

Ryan, Christopher R. and Day, Steven R. (1995). "Containment, Stabilization and Treatment of Contaminated Soils using Insitu Soil Mixing", Geoenvironment 2000. ASCE Specialty Conference, New Orleans, LA. USA February. 1995

Schneider. James R. (1994), "Soil / Bentonite Cutoff Walls", ANCOLD Specialty Symposium on Slurry Trench Cut-Offs, Singleton, NSW, Australia, October 1994

Yang, D.S., Kimoto. I.. Luscher, U., Takeshima. S. (1993). "SMW Wall for Seepage Control in Levee Reconstruction", Third International Conference on Case Histories in Geotechnical Engineering, St. Louis, Mo. USA. June 1993.

Grube, W.E. Jr. (1992) Slurry Trench Cut-off Walls For Environmental Pollution Control. In Slurry Wall: Design, Construction and Quality Control, ASTM STP 1129, (eds D.B. Paul, et al.), American Society for Testing and Materials, P.72, Philadelphia, PA, USA

Jasperse, Brian H. and Miller, A. David, (1990), "Installation of Vertical barriers Using Deep Soil Mixing", HazMat Central '90, Rosemont, Il. USA, March, 1990.

United States Environmental Protection Agency. (1984) Slurry Trench Construction for Pollution Migration Control. EPA 540/2-84-001, pp. 5-12 GPO, Washington, D.C., USA

Tallard, G. (1984), "Slurry Trenches for Containing Hazardous Wastes", Civil Engineering, February 1984, pp. 41-45

Chapter 5

Vertical Barriers: Sheet Piling & Geomembranes

INSTALLING A HDPE VERTICAL CONTAINMENT AND COLLECTION SYSTEM IN ONE PASS UTILIZING A DEEP TRENCHER

William M. Bocchino[1], Belinda Burson[2]

Abstract

A unique method has been developed to install high density polyethylene (HDPE) vertical containment panels and a horizontal collection system for the containment and collection of contaminated groundwater. Unlike other means of creating this type of system, this barrier wall and collection system is installed in one step and in one narrow trench, utilizing a one-pass deep trencher.

Originally HDPE vertical barriers were installed using conventional slurry trenching techniques. Use of this method raised questions of trench stability and disposal costs for the trench spoils. In addition, if a collection system was desired, a separate trench or vertical wells were required.

In response to these concerns, a trenchless vibratory installation method was developed. Although this method addressed the concerns of trench stability and disposal costs, it raised a whole new set of concerns dealing with drivable soil conditions, buried debris and obstructions. Again, if a collection system was desired, a separate trench or vertical wells had to be installed.

The latest development, the one-pass, deep trencher, has eliminated or significantly reduced the previously discussed construction concerns. The trencher methods reduce the amount of spoils generated because a trench width of 61 cm (24") is constantly maintained by the machine. Additionally, soil classification and density are not as critical as with a vibratory installation. This is due to the trencher's ability to trench in all but the hardest of materials (blow counts exceeding 35 blows/ft). Finally, the cost to add a collection system adjacent to the cutoff wall is substantially reduced and is limited only to the cost of the additional hydraulic fill and 4" HDPE collection piping. The trench itself is already constructed with the installation of the wall.

Introduction

The following is a review of the evolution of the HDPE Vertical Barrier market and the factors that led to the development of the One-Pass Deep Trenching System.

Since 1980, interlocking high density polyethylene (HDPE) vertical barrier systems have become increasingly utilized especially in areas of limited access, high concentrations of chemicals, and where a containment and collection system is desired in the same trench. Factors which have attributed to the growth of this industry are the regulations and the improved methods of installation.

[1]Groundwater Control Inc., 11511 Phillips Highway, Jacksonville, FL 32256, (904) 886-3700, GCI78@aol.com

[2]Groundwater Control Inc., P.O. Box 73327, Houston, TX 77273-3327, (281) 895-9765, BBurson@compuserv.com

Regulatory Influence

In the past two decades, substantial regulations have been enacted worldwide relating to the management of wastes. In the United States, the Resource Conservation and Recovery Act (RCRA) of 1976 provides for the regulation of waste facilities, and the storage, treatment and disposal of wastes. Under the authorization of RCRA, the US Environmental Protection Agency(EPA) has adopted regulations governing the management and disposal of wastes and the management of contaminated sites.

The Comprehensive Environmental Response, Compensation and Liability Act of 1980 (commonly known as CERCLA or "Superfund") was enacted in response to the dangers of uncontrolled hazardous sites. In an effort to accelerate the Superfund progress and control costs, Congress and the EPA have prescribed "presumptive remedies" to prevent further groundwater and soil contamination which include subsurface barrier walls and geomembrane caps. Under the Hazardous and Solid Waste Amendments of 1984, it was prescribed that hazardous waste landfills, surface impoundments, and ponds used in the containment of hazardous liquids use a double lined system (two or more geomembrane liners with leachate collection and drainage systems above and between each liner). These liner systems are required to be constructed of a geomembrane resistant to the hazardous chemicals stored at the site, thus singling out HDPE as an EPA approved material.

Now, in 1996, twenty years following the initiation of RCRA, HDPE geomembrane is being widely used to contain wastes above and below ground. Just as clay is no longer acceptable to control the vertical migration of leachate and contaminants into the subsurface, it should also not be used to control the horizontal migration of those wastes. Some industry professionals and regulators believe that the same standards enacted for horizontal hazardous containment (liners used in conjunction with a collection system) should be mandated for vertical applications also. Although very few vertical barrier walls consist of a double lined system, the number of HDPE containment and collection systems is steadily increasing.

Products

HDPE has proven to have a low permeability (2.7×10^{-13} cm/sec to water), high chemical resistance and a long service life. "Recent estimates of a 1000-year lifetime for HDPE are not beyond reach. Indeed the time to subsequent half-life of the engineering properties of a properly formulated HDPE geomembrane is many centuries and eminently suited for the containment of waste sites." (Koerner, 1996)

Although many EPA -90 compatibility tests have been performed on HDPE using a variety of chemicals, most of which without failure, some hydrocarbons (aromatic or chlorinated) can reduce the tensile strength of HDPE. Due to the critical nature normally associated with the performance of these containment walls, the manufacturer recommends (and often requires) that a material no less than 2.03 mm (80 mils) be used. This thickness limits the amount of absorption of the chemical and thus the amount of change in tensile strength. In field applications, unlike compatibility tests, the concentrations of contaminants and time of exposure are rarely high enough to cause measurable changes in the physical properties or an increase in permeability.

The most widely used HDPE barrier walls in the world are GSE CurtainWall® and GSE GundWall® as manufactured by GSE Lining Technology, Inc. Over 9 million square feet have been installed to date. These products have been successfully utilized on projects to depths exceeding 30.5 m (100'). The patented interlocks for either system are extruded through a proprietary method to create exceptional quality and consistency with tolerances less than .025 cm (1/100 inch). These interlocks are then joined to panels of 2.03 mm (80 mil) (minimum)

HDPE geomembrane through fusion welding. The dual-wedge welding system used in this process, allows for an air channel to be created which is used to test the integrity of the weld. An added quality control feature is the fabrication of the panels to site specific requirements in a factory-controlled environment.

Sealing of the interlocks is achieved with a chloroprene-based, hydrophilic seal. The seal is an extruded profile which is 8 mm (.3 inches) in diameter. When exposed to water, it can expand up to 8 times its original volume. In the case of the GundWall single channel, sheetpile like interlock (also known as Geolock®), the hydrophilic cord is inserted in a 6 mm (.23 inches) groove in the female profile. This condition creates a positive seal even before expansion takes place.

Unlike grouts or other types of sealants, continuity can be ensured because the seal is an extruded profile and is installed as a continuous piece through-out the entire length of the panel interlock. In fact, if the seal is broken during installation, the panel can be withdrawn and the seal restarted.

The GundWall interlock has been tested by a third party laboratory to document the potential leakage rate. Even at 1.36 bars (20 psi), in an apparatus designed to create a leak, the interlock allows less than 10-7 gallons/min/foot to pass through (GeoSyntec, 1993). Thus, when the geomembrane and interlock permeabilities are combined, the performance of an HDPE system consisting of narrow panels will be less than 10^{-11} cm/s.

In the case of the CurtainWall System, this interlock consists of a multi-channeled profile. The profile allows for multiple seals as well as an electronic method to verify that the panels are interlocked properly to the full depth. This is accomplished by measuring resistance of conductive contact plates. These plates are positioned at the bottom of the interlock. As one plate contacts the other the technician, using a voltage/ohm meter, will note the current flow and insure the continuity of the interlock. This patented system is commonly referred to as E.V.D. (Electronic Verification Device).

Methods of Installation

A containment and collection system, can be accomplished utilizing one of four methods. The first method developed, being to dig and install two separate trenches. The HDPE panels are installed through a bentonite slurry in one trench and then another (usually shallower) trench is excavated adjacent and backfilled with a hydraulic material. Vertical wells are then drilled and used as sumps to extract the leachate collected . Excavating two trenches is obviously redundant and costly.

A second, more recently developed method, utilizes a biopolymer or biodegradable slurry instead of a bentonite slurry. These slurries allow the HDPE panels and collection system to be installed in the same trench. Unlike bentonite, these slurries will either biodegrade or can be reverted. This allows the collection media, placed in the trench with the HDPE panel, to drain clear and free of fines. The largest HDPE cutoff wall in the United States, consisting of over 19 Km (12 miles) of 7.3m (24') wide panels, was installed using a biopolymer slurry.

Factors which control the effectiveness of these biopolymer slurries are groundwater chemistry, depth, and soil classification. Trenches exceeding depths of 60' should be avoided due to the intrusion of fines into the trench and thereby, restricting or clogging of the collection system.

The third method of achieving a containment and collection system in the same trench is in utilizing a trenchless, vibratory method of installing HDPE panels. First, a collection trench is constructed to the required depth. This is followed with the installation of the geomembrane using

modified pile driving techniques. Panels ranging in widths between .91 m and 1.83 m (3' -6') are driven to depths up to 12.20 m (40'). If the design requires that the panels be driven past the bottom of the collection trench, then the properties of the native soils are critical. This construction method is most suited for sites on which the excavation and disposal costs are high, access is limited, or where a collection system is not required.

The fourth and latest method developed for the installation of these systems, is the "one-pass" deep trencher. To date, It has proven to be the fastest and safest method to install this system. Using 1.83 m (6') HDPE interlocking panels this, proprietary, specialty trencher can install a vertical geomembrane wall with a collection system consisting of HDPE pipe and a gravel fill in one trench, in one pass. Production rates exceeding 76 m (250') per day have been documented.

The patented One-Pass trencher is designed and manufactured by the European company, Steenbergen-Hollandrain. This equipment, which is driven by a 450 HP Mercedes engine, can be modified to bring the minimum width of the machine to as little as 4.27 m (14'). Although the working weight of the trencher is 58,974 kg (130,000 lbs), the 6.10 m (20') tracks bring the ground pressure to less than .68 bars (10 psi). These physical attributes help to minimize the amount of preparatory work required on most jobsites, as well as allow this installation method in a wide variety of conditions.
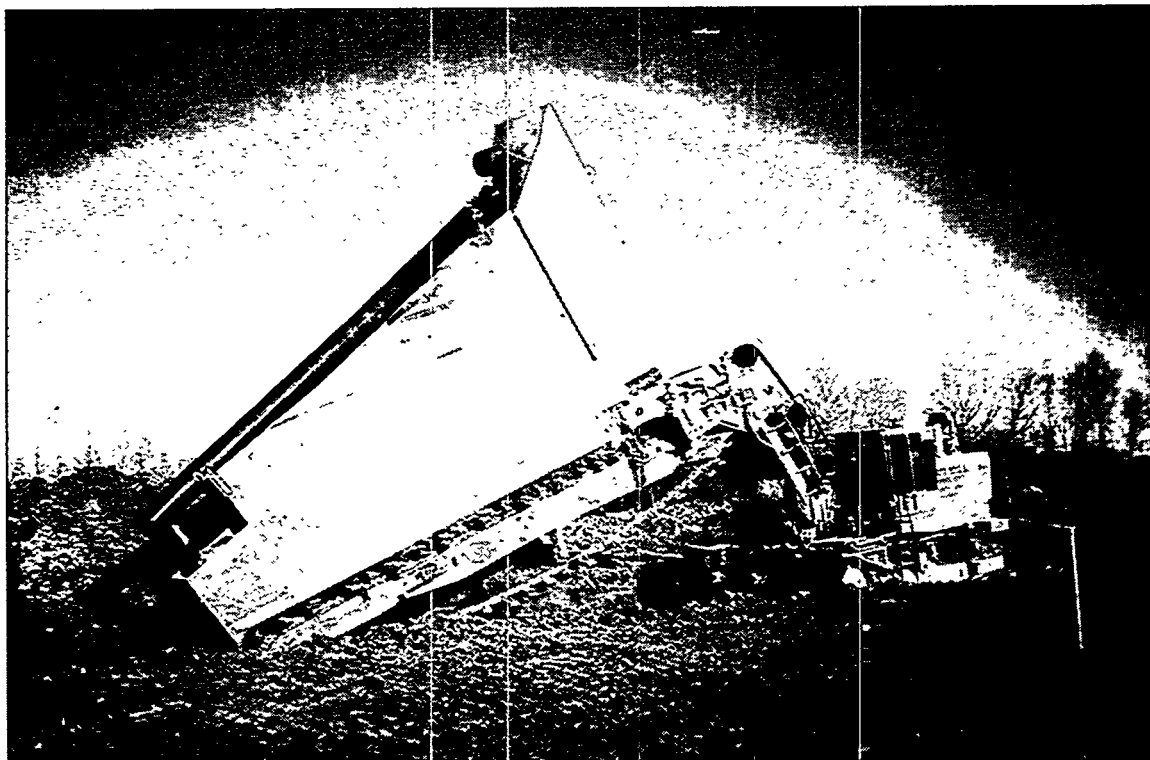
Figure 1. A sump ready for installation using the one-pass deep trencher.

Another attribute that makes this method of installation appealing is the trencher's ability to install an in-line sump (if required) and then trench forward (see Figure1) installing the HDPE barrier wall, collection pipe and gravel pack in one application. The system performance is enhanced by the adjacent location of the barrier to the trench. On a Superfund site in Indiana, the rapid

capture of groundwater was visually evident by the rise in groundwater elevation upgradient of the wall (see Figure 2).

Figure 2. Waste Inc. NPL site in Michigan City, IN. GundWall panels (foreground) seen exiting the rear of the trencher (background). Collection pipe can be seen being fed in above trencher.

In terms of quality control, this method has several advantages. First, the 2.03 mm (80 mil) HDPE panels are lowered into a separate compartment of the steel boot. The boot follows behind the cutting chain of the trencher and acts like a trench box. This boot is sealed from the native soils and allows the installer to visually inspect and place the interlocks in a clean area (see Figure 3). The gravel pack and HDPE collection pipe are placed in an adjacent completely separate compartment of the boot.

Second, the interlock and seal are clearly visible throughout the installation of the panel. Should the seal break, the panel is easily removed and a new seal installed without interference from the surrounding soil.

Finally, the grade of the barrier wall and collection pipe is controlled by a dual laser guidance system mounted on the trencher. The specified grades are programmed into the system and allows for the capability of installing the materials to within hundredths of an inch.

Although this type of system can be installed utilizing a wide panel (exceeding 2.44 m (8')), it is not recommended due to the lack of construction flexibility. Modifications to the work plan during construction of a subsurface barrier are very common. Narrower panels help to make a changed condition proceed more smoothly because they are individual units that can be easily modified. Also, the chances of damaging a wide panel (commonly a roll of geomembrane up to 200' in width with interlocks at either end) are greater due to the tendency of the HDPE to elongate and wrinkle

more so than to deploy. This places undesired stress on the interlock, the weld, and the liner itself. Unlike a narrower panel, if damaged, a wide panel cannot be individually withdrawn from the trench.

Figure 3. Shown here close-up, the HDPE panels leaving the back of the boot at the Hunter Ridge Subdivision, Jacksonville, FL.

Summary

The evolution of the HDPE Vertical Barrier and Collection system has been one which has seen the many different and distinct installation methods be developed. Of these various methods the one-pass method eliminates risks associated with slurry compatibility, feasibility of a vibratory installation, or when constructing two trenches, the possibility of damage to either the containment or collection system.

References

Koerner, R.M. (1996) Remediation vs. Containment of Solid/Liquid Waste Sites. *Geosynthetics World, 6(1),* 6-7.

GeoSyntec Consultants (1993) Final Report Laboratory Test Results GundWall Locking Section with Hydrotite Leakage Potential Testing.

A New Alternative in
Vertical Barrier Wall Construction

Greg F. Rawl, P.G.

Horizontal Technologies Incorporated, 4767 Pine Island Road NW, Matlacha, Florida 33993, USA. Telephone 941-283-5640. Facsimilie 941-283-2222. E-mail: gregrawl@horizontal.com

Abstract

A new proprietary vertical barrier wall system has been developed to revolutionize the construction process by eliminating many of the concerns of conventional installation methods with respect to performance, installation constraints and costs. Vertical barrier walls have been used in the environmental and construction industries for a variety of purposes, usually for cut-off or containment. The typical scenario involves a groundwater contamination problem, in which a vertical barrier wall is utilized to contain or confine the spread of contaminants below the ground surface. Conventional construction techniques have been adequate in many applications, but often fall short of their intended purposes due to physical constraints. In many instances, the economics of these conventional methods have limited the utilization of physical barrier walls. Polywall, the trade name for this new barrier wall technology, was subsequently developed to meet these needs and offer a number of distinct advantages in a variety of scenarios by maximizing confinement and minimizing installation costs. Polywall is constructed from chemically resistant high density polyethylene (HDPE) plastic. It has proven in a half-dozen projects to date to be the most cost-effective and technically sound approach to many containment situations. This paper will cover the development of the technology and will provide a brief synopsis of several installations.

INTRODUCTION

The basic concept of vertical barrier walls is to separate two areas with an impervious vertical boundary. This barrier affects the movement of fluids within or across a hydrogeologic unit so that groundwater flow or other fluid transport is altered. Barrier walls offer a number of benefits, the most attractive of which is the long-term cost-effectiveness of a passive barrier system.

Vertical barrier walls have been used in the environmental and construction industries for a variety of purposes, usually for cut-off or containment purposes. The typical scenario involves a groundwater contamination problem, in which a vertical barrier wall is utilized to contain or confine the spread of contaminants below the ground surface. Conventional construction techniques have been adequate in many applications, but often fall short of their intended purpose due to physical constraints. In many instances the economics of these conventional techniques have limited the utilization of physical barrier walls, so much so that it became obvious that a more cost-effective method was needed. An alternative barrier wall system, Polywall, was subsequently developed by Horizontal Technologies Incorporated (HTI) to meet these needs and offer a number of distinct advantages in a variety of scenarios by maximizing confinement and minimizing installation costs.

DESIGN AND DEVELOPMENT

The initial efforts to develop Polywall were to design a cost-effective cut-off or containment system for water table control and remediation purposes. It became apparent that additional applications could be

developed to meet growing demands due to restrictions on water use and environmental regulations. The barrier wall system evolved from the trencher technology developed for the installation of trenched horizontal wells. For the installation of the trenched horizontal wells, trenchers were developed which trench or cut vertically instead of an angle (typically 65 degrees) as with many other similar trencher applications.

The challenge in developing a new and innovative method to install an impermeable barrier wall was to come up with a cost-effective delivery system that was capable of installing the barrier wall equal to the rate of travel of the trenchers and maximize the amount of continuous impermeable barrier wall with the minimum number of joints. Joints in barrier wall construction not only take time to complete, but are also the most common points of leakage.

The first step was to select the impermeable material for the barrier wall. High Density Polyethylene (HDPE) was chosen as the most suitable geomembrane because of its resistance to a wide range of organic and inorganic chemicals and its durability in the subsurface environment. In addition, HDPE has wide acceptance in the industry, exhibits a degree of flexibility and strength, has excellent material strength, and can be welded easily without compromising strength.

The second step was to develop a method to insert and backfill the geomembrane in the trench. The research and development involved both technical and field staff members using standard and custom-designed material and equipment. The method that was ultimately developed has been utilized successfully in a number of applications.

The installation of the Polywall barrier wall involves trenching a nominal 40 cm (16 inch) wide trench with the cutters in a vertical orientation and delivery of the HDPE geomembrane in a continuous one step operation. The barrier wall is delivered from the installation box that is pulled through the ground behind the cutter assembly and boom. The barrier wall is unrolled in the ground in a vertical orientation from the pre-made rolls that are equipped with a female and male water tight joint system on the beginning and end of the rolls, respectively. A high performance, hydrophilic interlocking waterproof joint system is welded on to the rolls to create runs of virtually any length or configuration. These joints can be visually inspected to insure their integrity. These initially tight fitting HDPE joints, after installation, become essentially impervious when the hydrophilic seals hydrate with either soil moisture or groundwater. There are a number of commercially-available joint profiles, all of which incorporate the hydrophilic seal concept that are suitable for use and have been used successfully in Polywall applications.

Currently the maximum depth capability of the trenching equipment is approximately 10 meters (32 feet) below the base of the installation machine. Installation depths of over 15 meters (50 feet) have been achieved in the installation of trenched horizontal wells with benching. To date, the deepest Polywall installation has been without benching with 8 meter (24 foot) sheets installed to a depth of 7 meters (22 feet) below land surface. Research and development are ongoing to provide greater depths as industry demands.

Polywall is unrolled in a fluid filled environment inside the installation box. A positive hydraulic head above the surrounding strata is maintained on the inside of the box utilizing either water or a fluid additive. The appropriate fluid to maintain a positive head inside the box is selected prior to the start of an installation based upon the hydrogeologic properties of the strata to be encountered. Seals are utilized on the discharge end of the box in order to minimize open areas where the HDPE is being delivered. This limits the loss of fluids from the box and minimizesthe area for which cuttings can enter the box. During the installation, constant pumpage is maintained from the bottom of the box to remove any solids that enter the chamber.

As part of the installation process, the strata's cuttings may be partially fluidized and routed around the installation box at the surface to provide a backfill for the barrier wall. Because the cuttings are fluidized, the backfilling process places very little or no stress on the barrier. When metered slurry deliveries are utilized in conjunction with the trenching process, significant reductions of the hydraulic conductivity of the backfill that comes to rest on both sides of the sheets and joints are achieved. In this manner, an additional degree of impermeability can be achieved. Using a slurry, the barrier wall can also be sealed into underlying impermeable strata, when basal seals are required.

During an installation, when the end of a roll is reached, the forward motion of the trencher is stopped before the end of the roll is pulled out of the box. The empty roll and spool are removed and loaded with a new roll. The full roll and spool are then inserted back into the box while the joint profile connection is simultaneously made.

The HDPE geomembrane may be installed in thicknesses of 1 to 2.5 mm (40 to 100 mil). For most applications either 1mm (40 mil) or 1.5 mm (60 mil) thicknesses are used. Using 1 mm (40 mil) thickness material rolls, lengths of 57 meters (190 feet) have been installed, so that joint profiles are only required at 57-meter (190-foot) spacings. For 1.5 mm (60 mil) thicknesses, HDPE roll lengths of as much as 36 meters (120 feet) in length have been installed successfully. Obviously, as the HDPE geomembrane thickness increases, the length of the sheet that can be rolled to fit into the installation box decreases in proportion to the sheet thickness.

While to date, only HDPE has been used for Polywall installations, other geomembrane materials can be utilized if needed. Examples of other materials that could be utilized are Very Low Density Polyethylene (VLDPE), PVC, or other flexible geomembranes.

APPLICATIONS

The Polywall barrier wall system offers positive control of subsurface environments through isolation, containment or separation. It can be used with in-situ treatment technologies such as physical, chemical and biological reactors. This system can be combined with a variety of in-situ and above grade remediation strategies. Other uses include prevention of leakage through levees, isolation of wetlands and sensitive areas and the control of groundwater flow. A wide variety of civil and hydraulic engineering applications can utilize this technique.

Virtually any length or configuration of the barrier wall can be installed without concern of possible holes or windows inherent in other subsurface cut-off or containment structures. Tight turns, as tight as a 10.5-meter (35-foot) radius, have been accomplished using the delivery system.

This type of barrier wall system offers a number of unique features over other types of cut-off and containment walls. For years, slurry walls have been constructed for this purpose with mixtures of bentonite clay mixed with native soils. This type of "wall" has had varying degrees of success. Polywall can be installed in high hydraulic conductivity material even where piping is a problem, without compromising the integrity of the wall. This innovative subsurface environmental control technology provides a cost-effective alternative to typical barrier systems. The installation costs are often less than conventional techniques such as slurry walls. The installation process is rapid and consequently can be used for emergency conditions where time is critical. The nominal 40-centimeter (16-inch) trench creates a minimum of trenching spoils, most of which are returned into the trench as bedding material for the barrier wall. The system does not require subsurface dewatering and essentially eliminates spoil disposal requirements.

Additional advantages include a lower cost than conventional techniques, rapid installation process, and the accommodation of irregular geometry or topographies. This barrier wall system is compatible with groundwater capture-and-control and contaminant removal strategies. It can also be used with in-situ treatment technologies, such as physical, chemical and biological reactors. Joints can be visually inspected as they are made to insure their integrity.

HYDROGEOLOGIC AND SURFACE CONDITIONS

The barrier wall system can be installed in a variety of subsurface materials with varying hydrologic conditions. To date, applications have been in unconsolidated materials, typically sands, gravels, silts and clays. Occasionally, cobbles, thin limestone or cemented sand and shell layers are encountered and successfully trenched with little or no difficulty. Using a different boom, chain, cutter configurations, and greater power-to-cutter ratios, the ability to trench consolidated strata has been expanded. However, the greatest demand for barrier wall applications appears to be in unconsolidated surficial strata because of its ability to readily transmit groundwater and subsequent contaminant loads.

The hydraulic conductivity of the strata to be trenched is dealt with by selecting the most applicable fluid for the delivery system. In high hydraulic conductivity strata, it is often necessary to adjust the flow rate of the fluid from the box into the formation. In applications where the post-installation hydraulic conductivity around the wall can not be permanently significantly decreased, a bio-polymer additive is utilized. In high hydraulic conductivity strata applications where permanent reductions in hydraulic conductivity are not an issue, a slurry is utilized. High water table conditions are not an issue with the delivery system as long as the load bearing capacity of the working surface is capable of supporting the machinery. All of the machines are track driven so that they are able to traverse poor soil conditions. For example, machines for 7-meter (22-foot) installations currently in use are capable of operating on surface conditions as low as 4900 kilograms per square meter (7 psi). Using equipment mats, this bearing requirement can be reduced by 50 percent.

CASE STUDY ONE: Diesel Fuel Migration

The first commercial installation of this barrier system took place on the banks of the Little River in Star Lake, New York in October 1993. The site was the third largest hydrocarbon plume in the state at the time. In the warmer months, free product was migrating down gradient from an abandoned industrial facility in\to the otherwise remote and pristine river. The Polywall barrier system was successfully employed to cut off the migration of a free product phase diesel fuel plume into a river. The system was continuously installed along the riverbank for a distance of 405 linear meters(1,350 linear feet). This installation consisted of a 1 mm (40 mil) HDPE geomembrane placed vertically from land surface to depths of 3.6 to 4.5 meters (12 to 15 feet) below land surface. The actual installation time was two and one-half days. A trenched horizontal drain was subsequently installed to recover the free product that was trapped on the upgradient side of the barrier wall installation.

CASE STUDY TWO: Fuel Leakage into Bay

Years of refueling naval vessels near Norfolk, Virginia, had left a pier front area contaminated from leaks from a high pressure fuel line. A plume of light non-aqueous phase fuel oil was seeping into the adjacent bay. Its visibility at the surface of the water attracted attention to the need for its remediation. Subsequently, a cleanup system was designed that required a down-gradient barrier wall installed in conjunction with a upgradient Light Non-Aqueous Phase Liquid (LNAPL) recovery trench system. The

purpose of the down-gradient recovery system was to cut off the migration of the LNAPL, while damping the significant tidal fluctuation upon the low groundwater flow rate recovery system. The Polywall system provided the most cost-effective and technically sound installation. The area was a former fill area and the underlying strata were unconsolidated consisting of sand, silt and gravel. The greatest challenge was working adjacent to a bulkhead at the pier front, without having an adverse impact upon the surface water quality of the bay.

The impermeable geomembrane was installed approximately 2 to 2.5 meters (7 to 8 feet) landward of a waterfront bulkhead. The Polywall installation began with the cutting and removal of the concrete pavement for the length of each of the five installation sites for a total width of 1.2 meters (four feet) centered along the proposed location of the barrier wall.

The actual installation involved the removal of pavement and pre-trenching to expose the water table and locate utilities. The minimal disturbance of the area was especially important as underground utility lines were present. The barrier wall was installed in a single pass with 1.5 mm (60 mil) HDPE in five 6.5-meter (22-foot) wide vertical continuous sheets at a depth of 4.5 to 5 meters (fifteen to sixteen feet) below grade. The top of the wall was left two meters (six feet) above the surface and the trench was backfilled with the excavated material. Approximately 150 linear meters (500 linear feet) of Polywall was installed at the site.

As a result of this installation, there has been a significant decrease in seepage into the bay. The light non-aqueous phase liquid collection system has been installed up-gradient of the Polywall to capture fuel oil and is operating successfully. The project was successfully completed in a minimum amount of time without causing a significant disruption of the pier front activities. Polywall was deemed the only acceptable technically feasible alternative that provided assurance of a leak proof non-reactive barrier wall.

CASE STUDY THREE: Asphalt Refinery

An asphalt refinery along the riverfront in Georgia was the site of a complex barrier wall installation, as a variety of obstacles were encountered or had to be worked around. The primary function of the plant is the refinement of crude oil into asphalt products. The site had become suspected of discharging Light Non-Aqueous Phase Liquids (LNAPL's) into the Savannah River and had received the attention of the United States Coast Guard, due to the fact that a visible discharge was observed. In addition, Dense Non-Aqueous Phase Liquids (DNAPL's) were also present and posed an additional problem.

The site was underlain by silty sands down to 4.5 meters (15 feet) below land surface. A clay layer was present at this depth and extended to 12 meters (40 feet) below land surface. Polywall was selected for this project over other technologies because this system provided the most economical answer to this problem. In addition, this option could be installed in a very short time and could be navigated though a maze of above and below ground obstructions. The barrier wall was placed at a depth of six meters (twenty feet) below ground surface and extended approximately 330 meters (1100 feet) parallel to the river front with two sixty-meter (hundred-foot) returns on either end providing 450 meters (1500 feet) of continuous coverage. Interlocking, self-sealing joints were placed at 54 meter (180 foot) intervals using 1mm (40 mil) HDPE Polywall, allowing construction of the continuous wall with only seven joints for the entire wall. Scheduling was critical because of other construction activities taking place that could not be interrupted. The water table fluctuated widely due to the three meter (nine foot) tidal range in the Savannah River without causing a noticeable impact on the installation process. The entire installation was completed in five days.

SUMMARY

The advancement of barrier wall technologies offers an alternative that improves the cost effectiveness and reliability of traditional barrier wall installations, while saving time and streamlining the installation in the process. The unique one-step process has the ability to assist with many challenges in the environmental and construction industries by offering an alternative method of groundwater control.

REFERENCES

Mutch, Robert D. Jr., Ash, Robert E. IV and Caputi, Jeffrey R. (1995) "Advancements in Subsurface Barrier Wall Technology." Proceedings, Superfund XVI, Washington, DC.

Starr, Robert C. and Cherry, John A. (1992) "Applications of Low Permeability Cutoff Walls for Groundwater Pollution Control." Proceedings, 45th Canadian Geotechnical Conference, Toronto, Ontario.

Thomas, Richard W. and Koerner, Robert M. (1995) "Advances in HDPE Barrier Walls"

SEALABLE JOINT STEEL SHEET PILING FOR GROUNDWATER CONTROL AND REMEDIATION: CASE HISTORIES

David Smyth[1], Robin Jowett[2] and Murray Gamble[3]

Abstract

The Waterloo Barrier[TM] steel sheet piling (patents pending) incorporates a cavity at each interlocking joint that is flushed clean and injected with sealant after the piles have been driven into the ground to form a vertical cutoff wall. The installation and sealing procedures allow for a high degree of quality assurance and control. Bulk wall hydraulic conductivities of 10^{-8} to 10^{-10} cm/sec have been demonstrated at field installations.

Recent case histories are presented in which Waterloo Barrier[TM] cutoff walls are used to prevent off-site migration of contaminated groundwater or soil gases to adjacent property and waterways. Full enclosures to isolate DNAPL source zones or portions of contaminated aquifers for pilot-scale remediation testing will also be described. Monitoring data will be used to demonstrate the effectiveness of the Waterloo Barrier[TM] in these applications.

Introduction

Groundwater remediation most commonly involves groundwater extraction by wells or drains, with subsequent treatment of the contaminated water at surface. This pump-and-treat approach can be effective for the control and containment of groundwater but, as indicated by Mackay and Cherry (1989), it generally requires long-term operation and is seldom effective for restoring aquifers in contaminant source zones.

With the recognition of the limitations and inefficiencies of pump-and-treat, there have been strong incentives to develop alternate approaches and new technologies for groundwater remediation. Mackay et al. (1993) and Cherry et al. (1996) describe various methods by which contaminant source zone isolation and plume containment might be achieved. As shown in Figure 1, these methods include source zone isolation using low permeability cutoff walls, long-term hydraulic control of the plume emanating from the source zone using an active pump-and-treat system, or in situ treatment of contaminants emanating from the source zone using permeable reactive walls or Funnel-and-Gate[TM] systems (patented). Hydrogeological conditions and contaminant characteristics will govern the feasibility of these approaches at a given site, but the potential for the use of vertical barriers in source zone isolation and plume containment is apparent.

Renewed interest in recent years in the development and application of barrier wall technologies has been described by Mutch et al. (1994). This has led to advancements such as improved hydraulic performance, enhanced installation methods and extended capabilities at depth or in difficult soil conditions. Given the variety of barrier technologies and the construction techniques available, it is reasonable to assume that there will be technical and cost advantages of using

---

[1] Department of Earth Sciences, University of Waterloo, Waterloo, ON, Canada N2L 3G1

[2] Waterloo Barrier Inc., P.O. Box 385, Rockwood, ON, Canada N0B 2K0

[3] C3 Environmental, P.O. Box 188, Breslau, ON, Canada N0B 1M0

particular barrier walls in different situations. The remainder of this paper describes the development, testing and application of sealable joint steel sheet piling (Waterloo Barrier™) for cutoff wall construction.

Waterloo Barrier

In the late 1980's researchers at the University of Waterloo (UW) required a secure means of isolating portions of an uncontaminated sand aquifer for experimentation involving the controlled release of DNAPL chemicals. Several conventional cutoff wall technologies were investigated and found to be prohibitively expensive for the small scale, closed cell installations or insufficiently watertight. Thus, other construction options for the test cells were explored.

Steel sheet piling has seldom been used in environmental applications due to an unacceptable amount of leakage through the interlocking joints (McMahon et al., 1995). A method of sealing the joints of conventional steel sheet piling to limit the leakage was devised and the construction of a number of test cells using this prototype version of the Waterloo Barrier™ proceeded at Canadian Forces Base Borden in Ontario.

As shown in Figure 2, the Waterloo Barrier™ consists of conventional steel sheet piling with a modified interlock. A sealable cavity is incorporated into the interlock between adjacent sheet piles as the sheet is manufactured. Product specifications are presented in Table 1. The barrier can be installed using conventional pile driving techniques. A foot-plate at the base of the cavity reduces the build-up of compacted soil and the entry of obstructions during driving. After driving, the entire length of each cavity is jetted clean using pressured water or air. The integrity of each cavity can be evaluated for imperfections or blockages using the jetting hose, or using more sophisticated techniques such as downhole fibre optic video equipment. Following the cleaning and inspection of the cavities, the low permeability sealant can be emplaced from bottom to top in each cavity.

Table 1: Waterloo Barrier™ Profile Specifications

Section	Thickness in (mm)	Height in (mm)	Nominal Width in (mm)	Moment of Inertia in^4/wall ft. (cm^4/wall m)	Section Modulus in^3/wall ft. (cm^3/wall m)
WZ 75	.295 (7.50)	8.17 (208)	22.25 (565)	64.8 (8870)	15.9 (860)
WEZ 95*	.375 (9.50)	10.81 (275)	25.0 (635)	134 (18300)	24.9 (1340)

* Available June, 1997

Since 1989, more than 20 test cells have been installed by UW for field research purposes at Borden and another site in southwestern Ontario. These have ranged in dimensions from 1 by 3 to 9 by 9 m, and have extended to depths ranging from approximately 3 to 15 m. Several of these cells have been constructed with concentric double walls, a configuration which facilitates rigorous hydraulic testing. Figure 3, after Starr et al. (1992), shows a schematic diagram of such a double-walled cell in which a hydraulic test was undertaken. The cell extends to a depth of 14.7 m through a surficial sandy aquifer into an underlying aquitard. The sealable cavities were injected with a bentonite slurry. For the test, the water level in the moat bounded by the two walls was maintained at a constant level. At the start of the test, the water level in the internal cell was raised

by approximately 1 m relative to the natural water table in the vicinity of the cell. As the test proceeded, the decline in water level in the internal cell was monitored with time. Corrections were made to these levels to account for losses by evaporation.

In applying an analytical solution to assist in interpretation of the data, it was assumed that the underlying aquitard was impermeable and that all leakage from the internal cell occurred laterally through the barrier wall. In reality, some vertical leakage into the underlying aquitard would have occurred, so this assumption would result in an overestimation of the hydraulic conductivity of the barrier. As shown in Figure 4, the bulk hydraulic conductivity of the cell wall was calculated to be 6 x 10^{-9} cm/sec. Similar tests in other cells, including those sealed with organic polymers, resulted in bulk hydraulic conductivities ranging from 10^{-8} to 10^{-10} cm/sec.

Commercial Applications

The Waterloo Barrier[TM] became available commercially in late 1993 and has been used to provide subsurface containment and control at 18 sites across North America. With application in a wide variety of site conditions, it has been necessary to develop a number of joint sealants to meet project requirements. Issues that may be considered in sealant selection include sealant/contaminant compatibility, the presence of unusual groundwater chemistry such as high salt content, the ability of the sealant to withstand anticipated differences in hydraulic head across the barrier, the effects of wet/dry and freeze/thaw cycles on grout integrity, the removability of the sealant for temporary installations, permeability characteristics, pumpability and thermal expansion characteristics, design life of the system and cost. The types of sealants available include clay-based grouts such as bentonite and attapulgite, cement-based grouts modified with expanding agents, epoxy polymers, urethane polymers, and mechanical inflatable packers.

The ability to document quality assurance and quality control (QA/QC) during the construction process is a desirable attribute of cutoff walls used for environmental applications. With commercialization, QA/QC was another aspect of the Waterloo Barrier[TM] technology that needed to be further developed. As potential leakage through the wall is limited to the sealed joints, QA/QC procedures can be focused on joint integrity prior to sealing and the sealing operation itself. Vertical alignment of piles monitored during driving, and the flushing and probing of the sealable cavities provides documentation regarding the ability to inject sealant the full length of the cavity. Records of grout volume, pumping time and starting depth provide assurance that the entire cavity has been sealed.

Project costs are site specific and are dependant on many factors such as project size, location, profile thickness of the sheet pile, type of sealant used, installed depth, and driving conditions. Overall costs including mobilization, materials, pile installation, joint flushing and sealing, and a QA/QC program and report generally range from $160.00 US to $ 270.00 US per square metre ($15.00 US to $ 25.00 US per square foot) of barrier wall.

Waterloo Barrier[TM] projects undertaken to date have varied considerably with respect to purpose, size, geological conditions and special requirements, but the barrier has proven to be a robust and versatile system for groundwater pollution control. It has been used to control the flow of contaminant plumes to enhance in situ or pump-and-treat remedial measures, to isolate source zones of contamination in the subsurface and adjacent to waterways, to isolate zones of contamination in soils where dewatering and excavation operations were undertaken, and to improve the performance and efficiency of a soil vapor recovery system in the unsaturated zone adjacent to a landfill. In the following section, representative projects are described in more detail.

Source Zone Isolation, Industrial Facility, Washington

At a large industrial facility in Washington, approximately 5,500 sq. m of Waterloo Barrier™ was installed in three enclosures around zones of known subsurface contamination. The barrier was driven to depths ranging from 8 to 15 m in soils that included fill materials, sand, silt and clay with some gravel and organic matter. Installation procedures were disrupted by the occurrence of buried wooden pilings requiring some pre-drilling to facilitate driving of the steel sheeting. A second complication of the installation process, which was overcome by the flexibility of the Waterloo Barrier™ system, was the need to align portions of the cells around existing utilities and beneath parts of operating buildings. The latter entailed barrier installation through the floors of buildings with limited overhead clearance. An attapulgite-cement grout was used to seal the interlock cavities.

Chemical monitoring conducted over the two year period since the barrier was installed has failed to detect the presence of contaminants outside the enclosures. Although the implementation of the ultimate corrective actions at the site has yet to occur, future options include enhanced isolation of the source zone areas within the cells with active pumping, or the removal of a section of barrier and its replacement with a permeable reaction curtain to treat in situ the controlled discharge from the source zone area.

Venus Mine Site, Yukon Territory, Canada

A barrier wall was constructed for the Department of Indian and Northern Affairs to isolate waste rock and tailings at a former mine site from an adjacent surface water system. The waste area was largely bounded by bedrock and natural soils. The barrier was installed to replace a dyke of natural soils along a portion of the perimeter. The barrier was approximately 250 m in length, extending to a depth of about 7.5 m. The dyke and overburden material was primarily a silty clay. A cementitious grout was used for sealing the cavities. Subsurface soil conditions were favorable for sheet pile installation, but unusual aspects of the project were the remote location of the site and associated issues pertaining to mobilization, the influence of the cold climate and temperature variations, the high dissolved solids content of the groundwater, and the sealing of the barrier to the bedrock surface.

The general purpose of the barrier was to reduce groundwater flow and the associated subsurface transport of dissolved contaminants including arsenic and zinc derived from the weathering of the waste rock and tailings from the impoundment towards an adjacent lake. A second function of the barrier was to enhance the stability of the dyke and reduce the surface erosion of the tailings. Additional features of the remedial scheme include a cap to limit infiltration of precipitation and erosion of the impoundment surface, and a decant system for surface water drainage.

The remedial system was installed in September 1995. Preliminary findings of the surface water monitoring program indicate a reduction in the level of contaminants of 80% for arsenic and a 50% for zinc. Monitoring over a longer term will be required to determine the full effect of the barrier wall and capping system on the surface water quality in the lake.

Former Kitchener Landfill, Kitchener, Ontario

In the mid 1970's, methane gas was identified on the residential properties adjacent to a former landfill site. At that time, some gas control systems were installed at the site perimeter. In the late 1980's a decision was made to upgrade the facilities to improve the effectiveness of methane gas containment. Site investigation determined that a perched water table in the landfill would

interfere with conventional vertical extraction wells. A Waterloo Barrier™ cutoff wall was incorporated into the design to provide a barrier to both water and landfill gas, and to direct the gas to horizontal collection lines located above the water level.

In June 1995 approximately 3,125 sq. m of Waterloo Barrier™ was installed in two segments along the boundaries of the landfill that adjoined residential neighbourhoods. The barrier was driven to depths ranging from 4.5 to 9.5 m and extended through the unsaturated zone to beneath the seasonally low water table. Soil conditions consisted of fine sand to silt, but excavation of buried refuse was required at several locations along the wall path. Barrier installation was achieved using a crane-mounted vibratory hammer. The crane was operated from the margins of the landfill mound. Much of the barrier alignment was on the slope created by the landfill mound and engineered cover. Access to the toe of the slope was restricted in the vicinity of the residential neighbourhoods. The sealant used for the interlocks was a cementitious-based grout.

Since installation of the barrier wall, a vacuum has been maintained above the water level, indicating that the gas from this area is being collected and that the Waterloo Barrier™ is functioning as designed.

Lowry Air Force Base, Colorado

In November, 1995 a pilot scale Funnel-and-Gate™ system was installed in the path of a TCE plume at Lowry Air Force Base. Waterloo Barrier™ was utilized to construct the rectangular treatment gate and the low permeability funnel that channels contaminated groundwater into the subsurface treatment zone. The system extended through a fine sand aquifer to the bedrock surface at a depth of about 5.5 m. A cementitious grout modified with silica fume was used to seal the interlocks of the funnel and the two connecting walls of the treatment gate. Up and down gradient sections of the gate were sealed temporarily with a prefabricated mechanical packer system consisting of an injectable grout line and a rubber bladder that was pressurized by air. This temporary seal was maintained while soil in the gate was excavated and the reactive media emplaced.

The gate was excavated to within 10 cm from the base of the piles and remained fully open for a period of at least 12 hours. During this time there was no visible leakage of groundwater water through the sealed joints. A small volume of water up to several cm deep collected on the floor of the excavation, but it appeared that the source of this infiltration was from below. A hydraulic head differential of about 3 m existed between the outside water table and the base of the excavation.

Once the gate was filled with reactive media the temporary mechanical seals were released and the up and down gradient sections of barrier wall were removed thereby opening the gate to allow the flow of contaminated water. The versatility of the Waterloo Barrier™ in constructing irregular layouts on both large and small scale, its ability to form a watertight seal between the funnel and the treatment gate components, and its potential for removability make it particularly useful in Funnel-and-Gate™ construction.

Advantages and Limitations of Waterloo Barrier

Field applications have confirmed several advantages of the Waterloo Barrier™ system. Installation is clean and rapid with minimal waste generation. The system is flexible and can be installed to satisfy customized layouts; for example, the alignment and installation procedures can be modified to accommodate existing infrastructure and natural features. Further, the barrier system, depending on selection of sealant, can be compatible with a wide range of contaminant

conditions. QA/QC documentation of driving, joint flushing and sealing operations may be an advantage in complying with regulatory requirements. The barrier can function as a structural wall facilitating source zone removal by excavation. Hydraulic performance and integrity of the barrier system can be predicted based on the joint inspection and sealing documentation, and the hydraulic test results of numerous enclosures.

There are applications for which the Waterloo Barrier™ may not be appropriate. The vibration and noise associated with pile driving equipment may be a problem in densely populated areas. Hydraulic pile driving equipment, however, can be used to reduce vibration and noise at some sites. Waterloo Barrier™ installation is subject to the same limitations in terms of soils types and attainable depths as conventional steel sheet piling. In bouldery terrain and very dense unconsolidated sediments, the use of sheet piling will not be possible. Steel sheet pile applications are generally restricted to depths of less than 30 m or so. Although installation capabilities for sheet piling at depth can be enhanced by techniques such as the use of water jets at the leading edge of the pile as driving occurs, or by pre-drilling along the wall path, these will add to project costs. At some sites it is necessary to seal the barrier system to bedrock. Although techniques have been developed for sealing the base of Waterloo Barrier™ to underlying rock formations, special precautions will be necessary, and effectiveness of the sealing techniques may be difficult to confirm.

The Waterloo Barrier™ technology has been available for less than three years and although development, field testing and applications to date have demonstrated its effectiveness in the control and containment of subsurface contamination, it is anticipated that the full capabilities including the advantages and limitations of the technology will become more clear as more projects are implemented.

References

Cherry, J.A. , S. Feenstra and D.M. Mackay. (1996) Concepts for the remediation of sites contaminated with dense, non-aqueous phase liquids (DNAPLs), In *Dense Chlorinated Solvents and Other DNAPLs in Groundwater,* (ed. J.F. Pankow and J.A. Cherry), pp. 475-512. Waterloo Press, Portland, Oregon.

Mackay, D.M., and J.A. Cherry. (1989) Groundwater contamination: Limitations of pump-and-treat remediation. *Environmental Science and Technology,* 23 (16), 630-636.

Mackay, D.M., S. Feenstra and J.A. Cherry. (1993) Alternative goals and approaches for groundwater remediation. In *Proceedings of Workshop on Contaminated Soils: Risks and Remedies,* pp. 35-47, Stockholm, Sweden.

McMahon, D.R. et al. (1995) Vertical Barriers: Sheet Piles. In *Assessment of Barrier Containment Technologies,* International Containment Technology Workshop, Baltimore, Maryland (ed. R.R. Rumer and J.K. Mitchell), pp.77-93

Mutch, R.D., R.E. Ash and N.J. Cavalli. (1994) Advancements in subsurface barrier wall technology, in *Superfund XV,* pp. 784-789, Washington.

Starr, R.C., J.A. Cherry and E.S. Vales. (1992) A new type of steel sheet piling with sealed joints for groundwater pollution control, In *Proceedings of the 45th Canadian Geochemical Conference,* pp. 75-1 to 75-9, Toronto.

Acknowledgements

Figure 1: Contaminant source zone isolation using a) low permeability barrier enclosure: b) hydraulic containment by pump-and-treat; and passive contaminant containment and in situ treatment by contaminant containment by: c) permeable reaction curtain and d) Funnel-and-Gate™ system (after Mackay et al., 1993, and Cherry et al., 1996).

WATERLOO BARRIER STANDARD SHEET PILE
PLAN VIEW

WATERLOO BARRIER SEALABLE CAVITY DETAIL
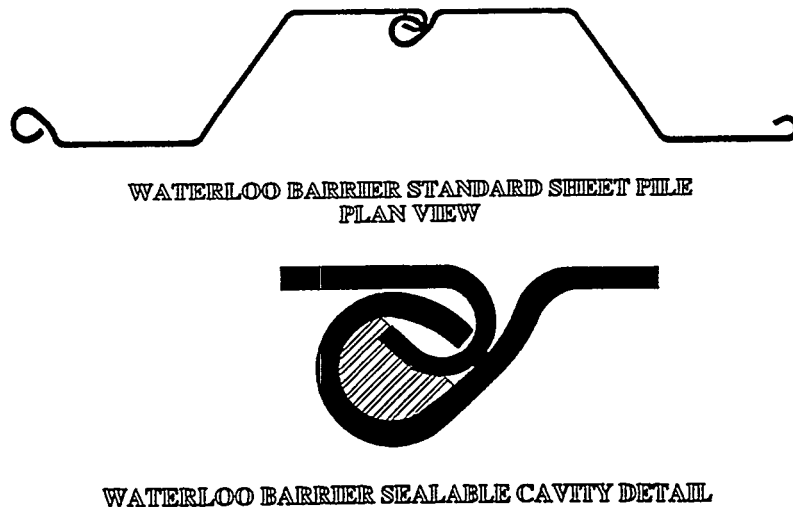
Figure 2: The Waterloo Barrier™ system showing interlocking steel sheet piling and modified joint with the sealable cavity.
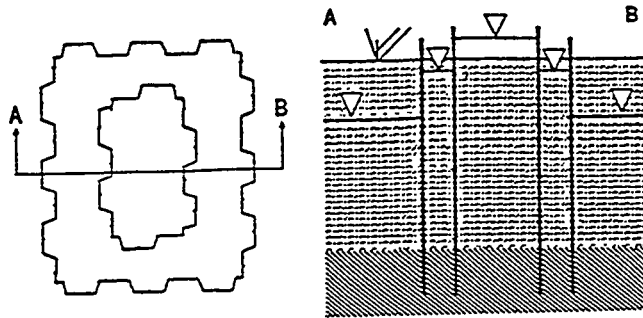
Figure 3: Plan and section view of test cell used to conduct hydraulic testing (after Starr and Cherry, 1992).
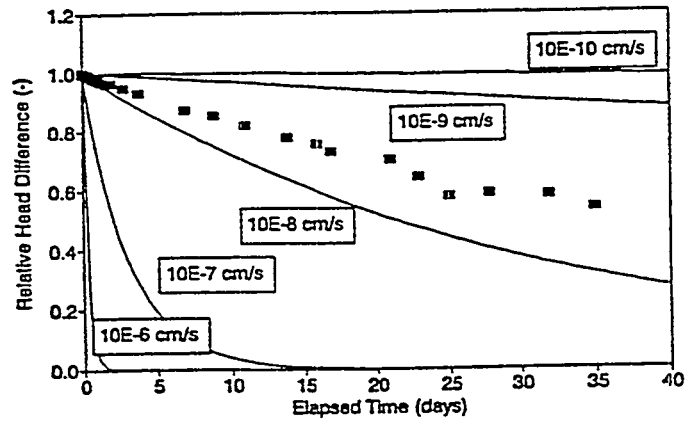
Figure 4: Observed response of representative hydraulic test of test cell showing bulk hydraulic conductivity of barrier wall (after Starr and Cherry, 1992).

USE OF A GEOMEMBRANE STEEL SHEET PILE VERTICAL BARRIER TO CURTAIL ORGANIC SEEPAGE

John L. Guglielmetti and P. Brandt Butler
DuPont Environmental Remediation Services
Barley Mill Plaza 27
P.O. Box 80027
Wilmington, Delaware 19880-0027

ABSTRACT

At a Superfund site in Delaware, contaminated groundwater, seeping out of a riverbank, produced a visible sheen on the river. As part of an emergency response action, a geomembrane steel sheet pile vertical barrier system was installed to contain the sheen and contaminated soil and sediments. The response action presented an engineering challenge due to the close proximity manufacturing facilities, steep riverbank slopes, tidal fluctuations, high velocity river flow, and underground and overhead interferences. A unique vertical containment barrier was developed to stabilize the riverbank slope, curtail sheens on the river, and prevent groundwater mounding behind the vertical barrier. In addition, the cost-effective vertical barrier enables natural chemical and biological processes to contain the organic seepage without requiring a groundwater extraction system.

SITE CONDITIONS

Seeps and sheens were observed along the riverbank immediately adjacent to the Newport Superfund site in Newport, Delaware. The riverbank and the site are composed of fill material placed during the early part of this century. The site was developed by filling in the floodplain. Of particular interest, the fill was placed over a continuous clayey-silt deposit which underlies both the site and river.

The seep area was a 213 meter (700 foot) length of riverbank immediately adjacent to the operating facility as shown in Figure 1. The riverbank ranges from 1.5 to 6.1 meters (5 to 20 feet) above the river's mean high-tide elevation and had steep, tree-brush-rubble covered slopes. The tidal fluctuation of the river is approximately 1.7 meters (5.5 feet).

The seeps were generally located in the intertidal silt and coarse rubble zone. The fine-grained, clayey-silt confining layer outcrops along the riverbank below the fill in this intertidal zone. The seeps are the result of natural expression of groundwater at low-tide. Groundwater flow and discharge in the intertidal zone at low tide produced a sheen on the surface water, necessitating emergency action.

A field investigation determined that the seeps contained organic chemicals derived from heat transfer fluids that were historically used in the site's manufacturing process. These materials have a specific gravity greater than 1, so the source material itself was believed to have flowed through the fill material to the confining layer and followed the top of the confining unit to the riverbank. It was concluded that the visible sheen was a surface tension phenomena created by an interaction between the immiscible organics and the river water.

DESIGN OBJECTIVES

Several design objectives were established by the project team.

- Provide an interim solution which contains the organic contamination entering the river and impacted soils and sediments.
- Avoid premature implementation of the full hydraulic containment and groundwater extraction remedy established by the regulatory agencies.

- Plan for encorporationj of the interim remedy into the final remedy when implemented.
- Minimize intrusion into the river to shorten agency review and approval time and to simplify construction.
- Avoid groundwater mounding which would have impacted building foundations.

SYSTEM COMPONENTS

Figure 2 shows a cross section of the vertical containment barrier system designed to achieve the objectives discussed above. The design included the following four elements:

- **Bulkhead Containment**

  The selected bulkhead was a cantilevered steel sheet pile wall (PZ-35 sheets) driven into the riverbank at the low-tide elevation to the underlying clay unit. This location contained the impacted soils and sediments and the portion of the riverbank where the sheens originated. It also avoided construction in the river beyond the low tide point.

  The sheets were 12.2 meters (40 feet) long and were driven 9.2 meters (30 feet) below grade with 3.1 meters (10 feet) of stickup. The top of the wall was designed for a 100-year flood event. To comply with the anticipated ROD requirement for the vertical barrier, the sheet piles were driven deep below the marsh deposit into the aquitard at the bottom of the Columbia aquifer (the aquifer immediately below the river, see Figure 1). The sheet pile wall can be readily modified at anytime to establish full hydraulic containment.

  A 1.0 millimeter (40 mil) thick high density polyethylene (HDPE) geomembrane was placed against the plant side of the installed steel sheeting from the top of the sheeting to a depth of 0.6 meters (2 feet) below low-tide elevation to prevent sheen seepage through the interlocks above low-tide elevation. A nonwoven, needlepunched geotextile cushion with a mass per unit area of 541 grams per square meter (16 ounces per square yard) was placed against the installed geomembrane for protection from installation damage during placement of the stone backfill.

- **Groundwater Drainage System**

  Since the geomembrane-backed bulkhead would have prevented fill zone groundwater from entering the river, a drainage system was designed to prevent groundwater mounding behind the wall. The groundwater drainage system consisted of excavated trenches along the length and both sides of the bulkhead and drain holes in the bulkhead below the low-tide elevation. This allowed groundwater to drain from behind the barrier and eliminate the buildup of hydrostatic pressure on the plant side of the structure. A nonwoven, needlepunched geotextile filter with a mass per unit area of 271 grams per square meter (8 ounces per square yard) was placed in the trenches, and the trenches were filled with stone. Riprap was placed on the river side at the bulkhead for erosion protection.

- **Contaminant Containment System**

  Contaminant containment consisted of two components. First, the geomembrane, extending to below the low-tide elevation, prevented the sheen from entering the river through the sheetpile joints. Secondly, the geotextile and vent holes served to enhance natural chemical and biological degradation mechanisms. The contaminant readily hydrolyzes in water. In addition, it is biodegradable. Daily tidal fluctuations behind the wall bring a ready source of nutrients and microorganisms to speed natural degradation. The tidal flushing also assured that residual dissolved contaminant levels were reduced to below protective levels before entering the river.

The nonwoven geotextile creates a medium for chemical and biological degradation as it disperses the immiscible contaminants exiting the riverbank. The geotextile chosen was a nonwoven, needlepunched geotextile filter with a mass per unit area of 271 grams per square meter (8 ounces per square yard) and 50-millimeter (2-inch) gravel backfill over the bank.

CONSTRUCTION

The sequence and details of construction included utility relocation, slope preparation, barrier installation, toe-drain installation, dispersion system installation, and backfilling. Actual site work began with slope clearing activities and construction of a temporary road to gain access to the lower riverbank area. Most of the work was conducted from the top of the riverbank, which required access for large equipment. Installation of the drainage trenches was conducted when the river was at or near low-tide elevation.

The initial design step involved the excavation of the drainage trench; however, concerns regarding the potential suspension of impacted sediment by tidal influence resulted in a decision to install the sheet piles first to create a tidal barrier. Sheet pile panels were driven using a vibratory hammer to within a few feet of the design depth. Holes were burned into the sheets (one hole in each sheet), and the sheets were driven to the final design depth. At this depth, the holes were exposed within the gravel drainage trenches to provide hydrostatic relief of groundwater and communication with the river.

The drainage trenches were dug using a long-arm excavator. Access was gained through the temporary road that was routinely regraded, as needed, to accommodate settling and access height needs. Impacted sediment was consolidated on the slope using straw bails and stone for erosion control and drainage. The geomembrane was hung on the plant side of the sheeting, fastened at the top of the sheeting with a nail gun, and fitted flush against the sheet-pile sections as shown on Figure 3. After the geomembrane was installed, the geotextile cushion was hung over the geomembrane and temporarily clamped to the top of the wall.

Before placing the stone backfill, hydrostatic relief was confirmed by observing water level changes within the drainage trench in relation to the tidal cycle as shown on Figure 4. The stone backfill was then placed behind the bulkhead, and the temporary clamps for the geotextile cushion were removed. Figure 5 shows the completed vertical containment barrier system.

PERFORMANCE

Oil sheens have not been observed since the vertical containment barrier system was installed. The river is sampled monthly and, to date, sampling indicates concentrations of organics well below the protective limit established in the order.

SUMMARY

Groundwater seeps in the intertidal zone of a riverbank were causing a release of organic contaminants. A unique, cost-effective passive vertical containment barrier system was designed and constructed to curtail sheens on the river and prevent groundwater mounding behind the vertical barrier without the use of a pump-and-treat system. The barrier system is compatible with the long-term site remedies and will be integrated into future containment designs. The installed systems met all of the design objectives. The project was installed safely, on schedule and under budget.

Figure 1: Riverbank Seep Area

Figure 2: Vertical Containment System Design

Figure 3: Installing Geomembrane Against Steel Piles

Figure 4: Vent Holes in Steel Sheeting
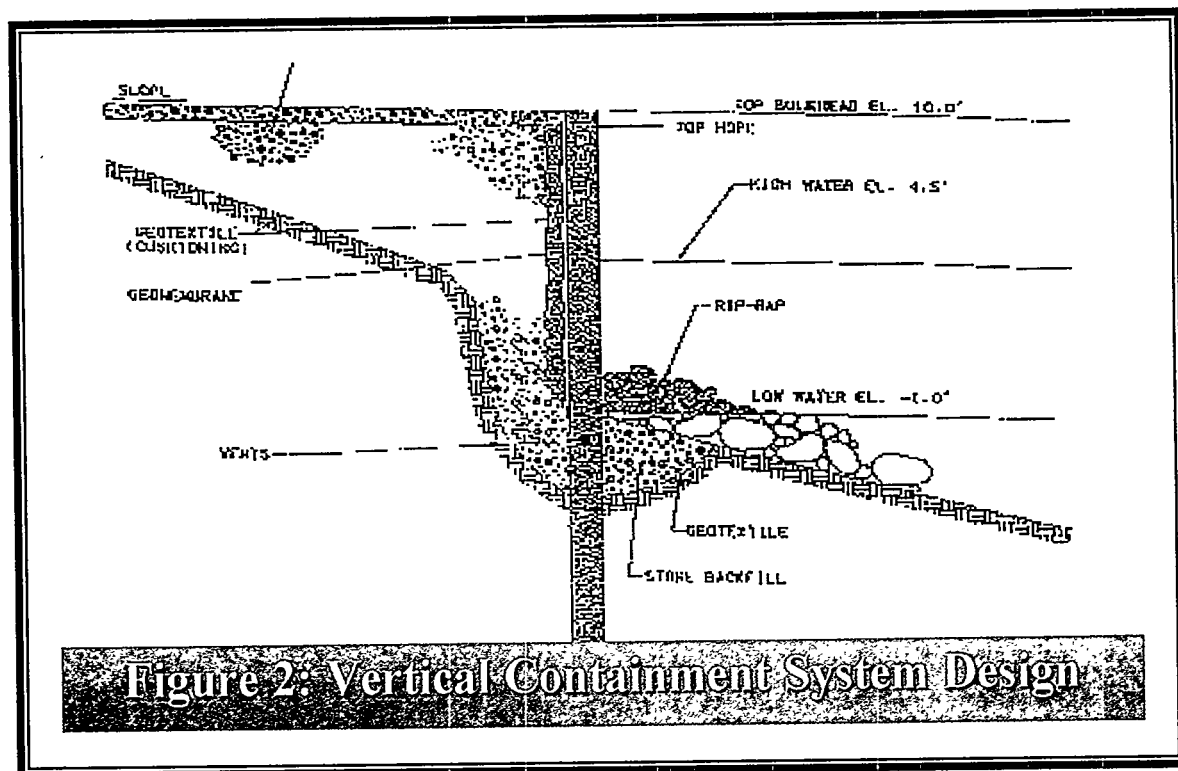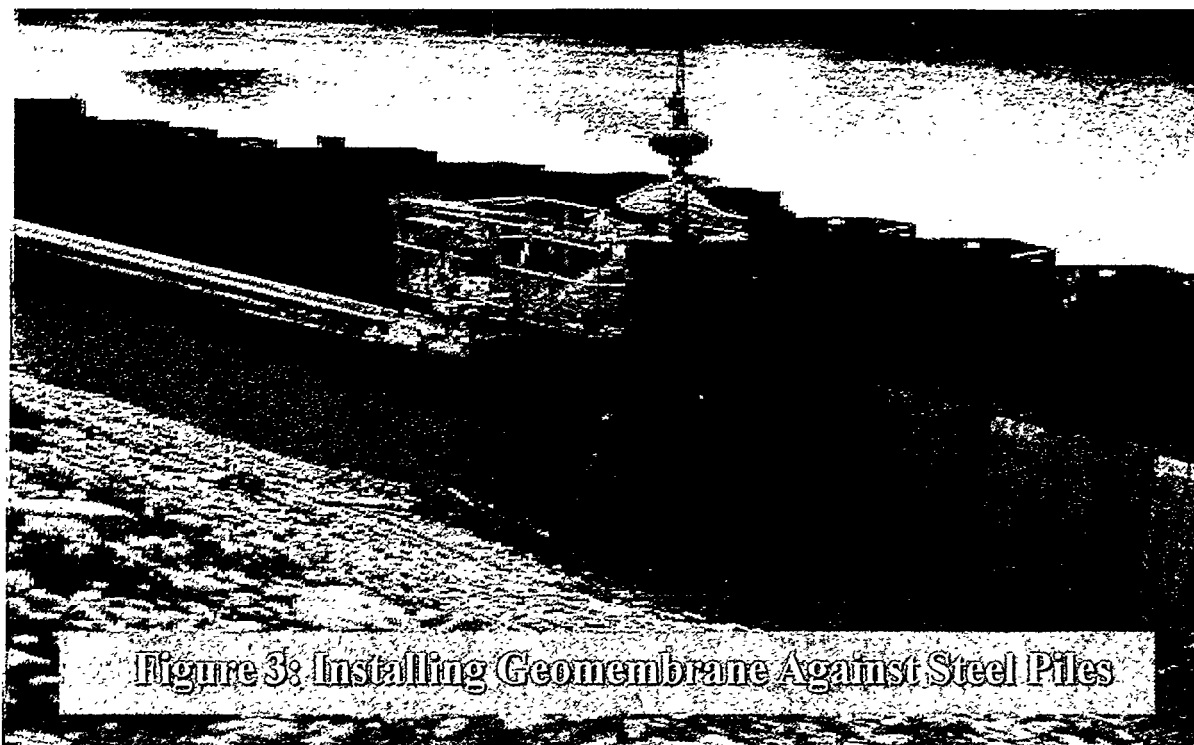
Figure 5: Completed Vertical Barrier System

CASE HISTORIES PORTRAYING DIFFERENT METHODS OF INSTALLING LINERS FOR VERTICAL BARRIERS

G.K. Burke, P.E.[1]
Hayward Baker Inc.
Odenton, Maryland, USA
R.M. Crockford
Keller Colcrete Ltd.
Wetherby, West Yorkshire, U.K.
F.N. Achhorner
Slurry Walls, Inc.
Irving, Texas, USA

ABSTRACT

The installation of liners for vertical barriers is difficult and has been a learning experience for every contractor making the attempt. Soil stratigraphy and hydrogeologic conditions can vary over short distances, creating a variety of problems. This is particularly so when working near landfills and documentation of the as-built condition is poor. Successful installation requires detailed planning and knowledge of what to expect, as well as alternate plans for potential problems. Several successful methods of panel connection will be presented as well as a variety of installation techniques. Project case histories will be reviewed, highlighting the challenges associated with specific construction techniques.

INTRODUCTION

The in-place containment of hazardous materials has long been considered an excellent interim measure to limit migration and assist with many forms of remediation. By constructing vertical barriers around the contaminated area, keying the barriers into an established aquiclude, and capping the area, an environment is provided that can be somewhat controlled. Hydraulic control and/or vapor control systems can be designed for this closed environment to assist with remediation.

For thirty years, soil-bentonite walls have served well to furnish the required degree of hydraulic control. But vapor control required that a moisture control system be added to this system to maintain a degree of impermeability. This increased the attractiveness but also the cost of the system. In the mid 1980's, vertical geomembrane liners began to be considered as an option to remedy the drying condition that soil-bentonite walls experience above the capillary zone. With the increased popularity of geomembrane liners for capping, particularly high density polyethylene (HDPE) materials, vertical geomembrane liners were increasingly considered. Their structural integrity combined with their resistance to a very wide range of contaminants was seen as satisfying the technical requirements for permanent containment as well as being eminently constructable. At about this time, manufacturers focused on developing impermeable interlock systems to aid in the installation of these liner materials. Study and field performance has proven that many of these systems perform satisfactorily if installed properly.

---

[1]George Burke, P.E., Hayward Baker Inc., 1130 Annapolis Road, Suite 202, Odenton, MD 21113

LINER INSTALLATION METHODS

Trench Wall Technique

This method involves digging a slurry trench and unrolling the geomembrane liner in place prior to backfilling, as shown in figure 1. For this system to work, the trench should be stable with relatively smooth sidewalls. The bentonite or biodegradable slurry should not be too heavy so as to minimize the buoyancy problems inevitable with installing liners under fluid (note that nearly all liner materials have a specific gravity less than 1.0).
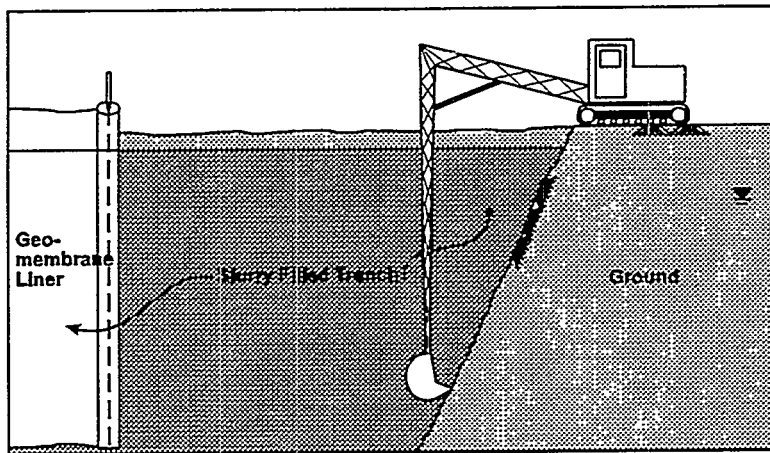
Figure 1. Trench wall technique

The liner roll must be manufactured to be as deep as the trench and be of a diameter so as to fit within the wall's trench width. As the liner is unrolled, it must be held in place. Since buoyancy and displacement by backfill are difficult problems to overcome, methods using trench jacks, bottom weighting, and heavy "key" backfills have all been employed, as well as some specialty systems.

Polywall Technique

Effective to a depth of about 7.5 m, the Polywall method uses custom-built machinery (similar to an oversized utility trencher) to dig the trench, shield a section of wall, vertically install the continuous HDPE liner from a roll, and backfill in one, single-step process (Horizontal Happenings, 1996). Interlocking, self-sealing joints are used to join liner sections. The single-step, continuous pass eliminates the need for trench-stabilizing fluids.

Panel Wall Technique

This installation method is employed where barrier depths exceed easy to handle liner rolls (typically >9 m). In this case, panels are excavated either by crane and digging tools or extended backhoes (figure 2). Panels are typically dug of a size to complete in a shift the amount of liner that can be installed. For instance, if the liner panels are 7 m long by 15 m deep, and two panels are anticipated to be installed in a day, then the first part of the work shift will dig a slot 14 m long by 15 m deep. The liner is next installed and key material placement and backfill is completed (figure 2). Specialty interlock systems are used to join the liners, and stop end tubes protect the interlock for the subsequent panel.
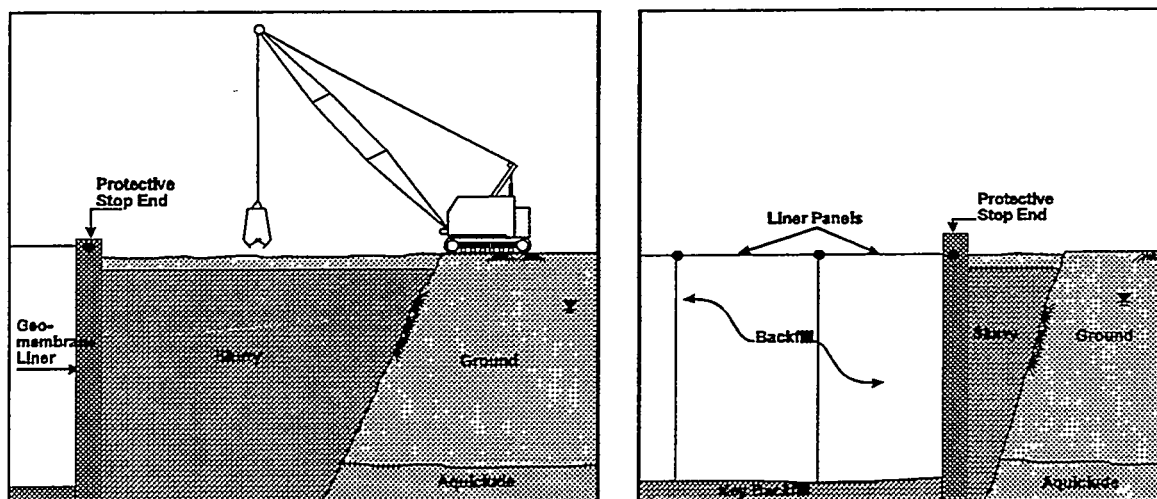
Figure 2. Panel wall technique

Verticality control and trench stability are key factors for this system to work. Structural steel, temporary support systems are used to hold and control the liner, and various "contractor experience" methods are used to facilitate the liner interlock installation. Special care and patience are necessary to assure a continuous barrier is constructed.

Gundwall® Technique

The Gundwall technique uses a vibratory installation method of narrow panels, typically 1.5 - 1.8 m wide. This method has been proven successful in uniform granular soils to depths up to 12 m. The installation equipment consists of a standard vibratory piling hammer, mounted at the top of a special support frame/shield. The support machinery is typically a crane, but recently specialty attachments for hydraulic backhoes are utilized to guide and support the vibratory hammer. The vibratory installation shield can be enhanced with jetting nozzles in order to penetrate and liquefy denser soil formations. For contaminated soils, the Gundwall method is extremely effective since soils need not to be removed during the panel installation. The drawback, however, is the limitation with regard to depth, and unforeseen obstructions which can block the shield penetration. Gundwall panels have been installed from floating barges to stabilize levees.

INTERLOCK/CONNECTION METHODS

The conventional means of connecting liners and maintaining containment integrity are welding and mechanical methods. Specialty interlock systems are also available.

Welding Method

Welding HDPE gives assurance of continuous integrity. The weld can be tested for impermeability and is a strong connection. Unfortunately, it requires a clean environment and a long section of trench so the end can be pulled out and aligned with the next sheet. Neither of these features make it easy to construct in the field.

Mechanical Method

Mechanical connections have proven successful and easy to construct. These utilize a hydrophylic gasket sandwiched between the liner sheets and opposing stainless steel strips, bolted 150 mm on center.

223

Specialty Methods

Specialty interlock systems include those developed by the manufacturer, as shown in figure 3:
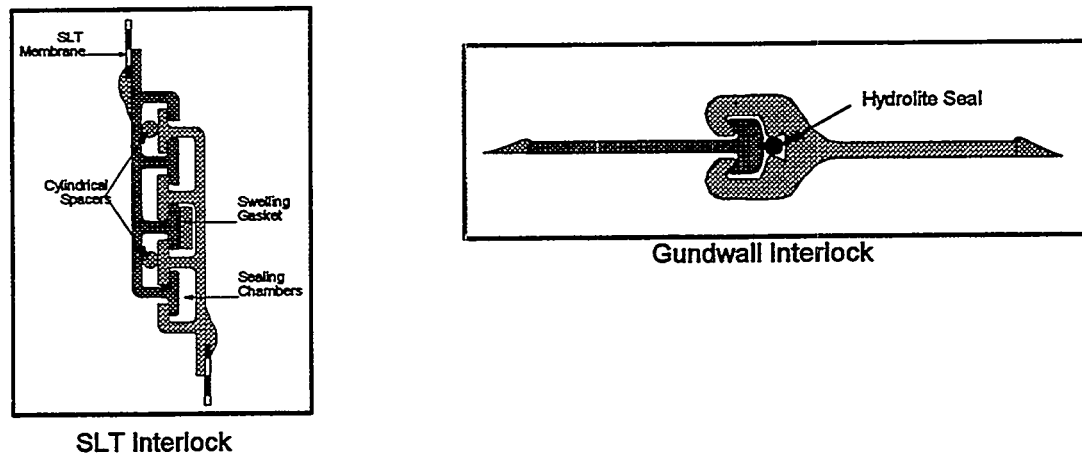
Figure 3. Specialty interlock systems

These also utilize a hydrophylic gasket system as the seal between panels. Specialty systems are typically premanufactured to panel wall requirements to minimize any field welding. Quality of the interlock is good: however, special care is required during installation. Occasionally, problems of unzipping have occurred in the trench, but generally experience has shown excellent end results.

CASE HISTORIES

To illustrate the challenges that can be encountered during installation, several case histories are presented. In nearly every case, the site conditions were different or changed from that expected, and methods were developed to overcome the difficulties.

Municipal Landfill, Oxnard, CA

After closing of the Santa Clara Landfill, an 18-hole golf course was constructed over the site. Adjacent property development created a serious concern over methane gas migration from the landfill. The design remedy included a 7.5 m deep, soil-bentonite slurry wall for hydraulic control and a 4.5 m deep, 1.0 mm HDPE liner (above groundwater level) to control gas migration (Burke, 1992). As the bentonite slurry wall was constructed, the liner was unrolled in the trench prior to backfilling.

Challenge 1   Maintaining the liner in position was difficult. HDPE is buoyant and always subject to float. Backfilling with well mixed soil-bentonite was difficult as this material displaced the liner from the trench. Additionally, a 1.0 mm thick liner did not have enough strength to withstand the rigors of construction handling, occasionally tearing.

Solution 1   Trench jacks installed to the full depth of the liner and set in position every 4.5 lineal meters of wall. These were removed only after the backfill had achieved 1.5 m of cover as measured from the bottom of the liner.

Challenge 2   The wall position was to be located near the property boundary, in existing soil. In several locations along the wall, the alignment required excavation of up to 6 m of municipal waste, an often unstable medium.

| Solution 2 | Municipal waste encountered outside the landfill limits was transported to an active landfill. Wall production was slowed so that the amount of open trench was minimized. |

Petroleum Refinery, Denver, CO

Over the years, leakage from an old existing refinery and tank farm had created a free product (gasoline) plume on the groundwater table. The gradient caused the product to flow into an environmentally sensitive stream at the property boundary.

A combined collection/containment system was designed to be constructed along the stream. This used a biodegradable slurry wall system with a filter backfill and the HDPE liner installed on the down-gradient side. In addition, wing walls and collection sumps were installed at about 15 m intervals to pool the free product.

| Challenge 1 | The ground was marginally stable: the soil was a clean sand with high groundwater. Space was limited, preventing construction of a higher platform. |

| Solution 1 | A liner installation system was designed to unroll the HDPE above ground and wrap it down and across an extended arm in the trench. This allowed for large rolls to be used, involving very few, easily welded seams and minimized the amount of open trench. The greater integrity of an 2.0 mm liner thickness eased handling and installation. |

Ash Landfill, Morgantown, MD

The leachate from an old, above-grade, closed ash landfill was disturbing the ecology down-gradient. Investigation revealed small amounts of heavy metals leaking beyond the landfill. However, very low pH water appeared to be the biggest problem.

A biodegradable slurry wall with filter backfill, collection piping and sumps, and a down-gradient containment liner was designed, along with a series of treatment ponds for the collected leachate. The wall extended along two sides of the landfill, to variable depth of 4.5 - 17.5 m.

| Challenge 1 | The in-place soils were highly unstable. The wall alignment was expected to be beyond the landfill, but intersected it at several locations. This caused a reversal in hydraulic gradient (due to perched water in the landfill) into the trench. |

| Solution 1 | Pre-excavate to a depth of 4.5 m, identify potential seeps, and sump these areas prior to wall construction. |

| Challenge 2 | The leachate, being very acidic (pH of 2.0 as compared to groundwater pH of 4.0-6.0) caused the biodegradable slurry to prematurely lose its viscosity, which reduced the slurry unit weight, made it difficult to establish a cake zone, and the trench became unstable. |

| Solution 2 | The same as solution 1 plus greatly reduced productivity to eliminate any open trench. |

| Challenge 3 | Installing liner panels 17.5 m deep by 6.5 m long is very difficult on even a moderately windy day. |

Solution 3   A very heavy structural frame was built to minimize wind impacts, set and hold the liner in position, and enable key and filter backfill placement, as well as installation of horizontal piping, before frame extraction. Planning and close coordination of activities enabled quality installation.

Municipal Landfill, City of Greenfield, Massachusetts

A biodegradable slurry wall was selected for a collection and cut-off system. The trench was 300 m in length and 12 m deep. A 2.0 mm HDPE liner was installed with a double frame system, meaning that panels are installed in an alternating method, leaving the primary panel mounted on a fixed frame while the secondary panel is lowered. Once the secondary panel is at its final position it becomes the primary panel.

Challenge 1   To develop a composite membrane system that would allow the collection of the methane gas and also cut-off migration from the existing municipal landfill.

Solution 1   A 6 mm thick non-woven Geofabric was attached to the 2.0 mm HDPE liner panels and installed simultaneously into a biodegradable slurry wall.

Challenge 2   Installation of a methane gas collection system within the cut-off system

Solution 2   Once the liner was installed within the open trench, granular backfill was placed to the invert elevation of the collection piping and the collection pipes were installed. During this backfill operation, the Guar-based suspension fluid was collected through the extraction system and biodegraded for final discharge.

Landfill Containment, Cardiff, UK

An impermeable barrier was required around a new shopping and recreation mall, built adjacent to and partially over an old landfill site, to isolate contamination and prevent gas and leachate migration from the landfill.

A combined membrane/cement bentonite slurry wall 1,400 m long to 7 m depth was installed using 2.0 mm thick HDPE and 6, GSE channel interlocks. Individual panels varied in depth from 3.5 to 7 m while panel widths were standardized at 7.5 m between interlocks over most of the walls length.

Challenge 1   The specification called for the membrane to be central within the trench to a tolerance of 150 mm and to achieve verticality better than 1 in 75.

Solution 1   Great care was taken in tensioning each panel on the placement frame, with the top horizontal steelwork support being kept as close as possible to the upper panel edge. Once installed, the membrane panels were suspended in position from poles spanning the trench until the slurry had hardened.

Challenge 2   Ten live services had to be crossed by the slurry trench line. This is believed to be the first time that live service crossings with a continuous membrane had been attempted.

Challenge 3   Electricity, telephone and fibre optic cables were encountered within 1 m of ground surface. These were crossed by passing the free end of the installed panel beneath the cables. The free end was left unsupported on the installation frame and folded back upon itself until the top panel edge was lower than the underside of the cable. The free edge with interlock attached was then pulled beneath the surface using top and bottom ropes such that the interlock maintained verticality.

In one location the cable lay between two right angle bends in the wall and hence the panel was located in isolation beneath the cable. A join-up panel was placed, interlocking onto the panel beneath the cable and the previous wall end panel, at right angles to the installation axis. To marry up two interlocks simultaneously requires considerable skill in the field, the more so when one of the receiving interlocks is on a 90 degree axis.

One 0.6 m cast iron gas main crossing also had to be effected under stringent utility working regulations. The trench was therefore dug dry to as deep as possible prior to introducing a panel beneath the pipe to allow the site welding of a gap-filling membrane panel above the pipe.

Though the wall was installed well within overall program, the service crossings required disproportionate time periods to plan and execute given that the utmost care must be exercised if the services are to remain unaffected by membrane slurry wall construction.

Hydrocarbon Collection and Abstraction, Glasgow, UK

An unusual application of a vertical HDPE barrier was combined with a biodegradable polymer mud trench support medium to fulfil this requirement.

The membrane acted as a barrier to the passage of waterborne hydrocarbons while stone backfill was able to act as a collector drain once the polymer mud, through which it was placed, had degraded. Abstraction was then achieved using wells constructed adjacent to the collector drain.

Challenge 1   Collapsing ground due to poor support characteristics of the polymer mud and previous excavations in the area having loosened the ground.

Solution 1   Initially, mud levels were maintained as high as possible within the trench. When this failed to address the problem, a pre-grouting exercise was undertaken using a cement-bentonite slurry in a 2 m deep trench along the entire slurry wall line. This was then excavated through and was found to support the ground well.

Challenge 2   Several 5 m wide panels were installed prior to the introduction of stone fill such that the angle of repose of the stone maintained with the dug sections rather than causing "flow" into newly excavated lengths. This led to tension cracking of the ground either side of the trench which generated concern for the stability of nearby buildings.

Solution 2   Trench sheets were placed either side of the last panel to be placed at the center point of the panel length. Stone was then backfilled behind the sheets prior to the next panel being introduced. The trench sheets were then pulled and moved to the center point of the new panel, and so on. This eliminated the surface ground movements.

Problem 3   Abstraction wells had to be installed in pockets dug perpendicular to the wall.

Solution 3   To prevent stone slumping and membrane damage two sheet pile sections were placed as a "V" at the point specified for well installation. These protected the membrane and retained the stone while the well pockets were dug and the wells installed and backfilled.

227

SUMMARY

Different containment projects have different containment goals. In addition, ground conditions vary greatly and are not always predictable. Groundwater has a significant impact also, including the chemistry and contaminant concentration(s).

The following aspects should be taken into consideration during the design phase of a vertical geomembrane installation:

Characterization:	· to determine strata and landfill conditions
	· to determine live and abandoned services (utilities)
	· to determine ground contaminants
	· to determine groundwater levels and variations accurately
	· to determine aquiclude depth and suitability
Trench Stability	· ground level relative to water table
	· soils make up and state of compaction/consolidation
	· likely slurry loss/over break into ground
	· safety of installation crew next to trench walls
Liner Installation	· need for liner or not
	· services along route of trench
	· likely obstructions
	· gas or leachate containment
	· complementary collection systems
Key Backfill & Design Backfill	· permeability if used to connect to the aquiclude
	· tremie methods of installation required?
	· filter characteristics for collection systems

In summary, many methods of liner installation have been developed, with proven effectiveness for groundwater and vapor containment. The method selected is dependent on the many aspects identified above, as well as cost and schedule requirements not included with this paper. The best recommendation whenever working below ground is to expect the unexpected.

Acknowledgments

References

"Polywall Does It All", Horizontal Happenings, Volume 2 Issue 1, Fall 1996

Burke, G.K. (1992), "In Situ Containment Barriers And Collection Systems For Environmental Applications," presented at Symposium on Slurry Walls, Canadian Geotechnical Society, Southern Ontario Section, September 1992

CASE STUDY
INSTALLATION OF A HDPE CURTAIN WALL
WITH SHEETPILE TIE-IN ON BOTH ENDS

Robert M. Schindler[1] and Peter C. Maltese[2]

Abstract

The plans for eliminating the off-site migration of non-aqueous phase liquid (NAPL) from a refinery into a nearby river included the installation of a High Density Polyethylene (HDPE) curtain wall and an underdrain system.

A 640 m (2100 lineal feet) HDPE Curtain Wall was installed along the river boundary, tying into an existing sheet pile wall on both ends. The wall varied from approximately 4.5 m (15 feet) deep at the northern end to about 7 m (23 feet) deep at the southern end, running approximately 3 to 3.6 m (10 to 12 feet) inland of an existing wooden bulkhead. The curtain wall was successfully installed through a slurry supported trench.

A 930 m (3050 lineal feet) interception/collection trench was installed parallel to the HDPE Curtain Wall, continuing on beyond the curtain wall on the southern end. The depth of the trench varied from approximately 3 to 4 m (10 to 13 feet) deep. A 20.32 cm (8 inch) diameter perforated HDPE header pipe was placed in the trench to convey groundwater and product to two sumps. The trench is 53.34 cm (21 inches) wide and contained aggregate to approximately 0.9 m (3 feet) below ground. This work was accomplished using the bio-polymer slurry drainage trench (BP Drain) technique.

This paper briefly describes the construction methods utilized during this project, specifically HDPE curtain wall installation thru a bentonite slurry and tie-in to the existing sheet pile wall.

Introduction

At the site of an active refinery, NAPL was entering a river, via groundwater, adjacent to the facility property line. The area of flow was concentrated to a 640 m (2100 lineal feet) stretch. Existing sheet pile walls along the river, upstream and downstream of this open section, directed the NAPL to this area. An HDPE curtain wall was selected to contain the flow because of its excellent resistance to the contaminants found on site.

The challenges presented by this project were the attachment of the curtain wall to the existing sheet pile walls and the selection of an installation method for the curtain wall panels through the soil conditions present, which were known to contain various construction debris and rubble.

---

[1]Geo-Con, Inc., 4075 Monroeville Blvd., Suite 400, Monroeville, PA 15146, (412) 856-7700, rmshind0@ccmail.wcc.com

[2]Geo-Con, Inc., 4075 Monroeville Blvd., Suite 400, Monroeville, PA 15146, (412) 856-7700, pcmalte0@ccmail.wcc.com

Curtain Wall Panel Installation

The curtain wall was installed through a slurry using frames. This method was selected because of the soil conditions along the wall alignment, and the presence of the construction debris and rubble along centerline. By installing the panels through a slurry supported trench, the integrity of the HDPE could be assured.

Although there were no set procedures to install the wall, standard slurry wall techniques and equipment were used. The initial step taken was to excavate a .6 m (2 feet) wide trench, using a bentonite slurry to support the side walls. The slurry was produced at a mix plant which consisted of a 3.82 cubic meter (5 cy) colloidal mixer, and two 15.24 cm (6 in.) trash pumps. A nearby fire hydrant supplied the water used to fill the 3,785.4 L (1000 gallon) mixer. Approximately 181.5 kg (400 lbs.) of bentonite powder was introduced into the water-filled mixer and agitated. Once a fully hydrated slurry was produced (typically after 5 minutes of mixing) it was then transferred to the trench using one of the trash pumps and polyethylene pipe. As the excavator, a CAT 330L, removed the material from the trench, it was replaced with the hydrated slurry from the mix plant.

The excavated spoils were cast to the inside of the trench, away from the river, and spread out. A combination of a trackhoe and a rubber tired loader sorted through the spoils to remove the abundance of construction debris. The debris included items such as brick clusters, wooden lagging, wire, plywood sections and various other construction waste materials. This was a critical step which required thorough removal of all foreign matter which could have possible adverse effects on the integrity of the curtain wall. This debris was transferred to dumpsters in close proximity to the trenching area for proper disposal. Once the debris was separated from the spoils, the remaining material was mixed with a dozer to form a homogeneous mixture of spoils and slurry. To accomplish this, the dozer tracked back and forth through the spoils, using the tracks and blade of the dozer, to blend the materials. At times, additional bentonite slurry was added to the spoils to form a slump which was adequate for proper backfilling of the trench, typically 5.1 to 10.2 cm (2 to 4 inches). Although this is a standard process to construct a low permeability soil-bentonite cutoff wall, the makeup of the contaminants were not completely compatible with bentonite as indicated by the trial mix program which was completed prior to the job startup. Thus, the addition of a curtain wall provided the added impermeability necessary to stop the flow of contaminated groundwater into the river.

Once a lead-in slope was excavated, normal slurry trenching continued. Due to several areas along the centerline of the trench, which contained large pieces of debris, the top of the trench became wider at those sections. Also, at several stations along the trench alignment, abandoned utilities were encountered. All utilities were removed and plugged, prior to panel installation, to avoid interference with the continuity of the curtain wall. This also resulted in portions of the trench becoming wider at the top. In those areas where trench width was increased, portable walkways were utilized to allow for easier access while installing the curtain wall in the trench.

Another item which had to be considered during trenching, was the influence of the nearby tidal river. Tidal influence caused fluctuations in the groundwater elevation, which varied from .6 to 1.8 m (2 to 6 feet) below the working platform. As the groundwater elevation rose, the stability of the trench became a greater concern. Trench stability was controlled by the rheology of the bentonite slurry, level of slurry in the trench, soil conditions, and by limiting the amount of open excavation (portion of trench filled with slurry) prior to the panel installation procedure.

After approximately 21.3 m (70 lineal feet) of trench was excavated to full depth, the initial panel of HDPE curtain wall, which had previously been secured to its frame, was lowered into the slurry filled trench to the proper elevation. The panel was moved into place using a 35 ton, rough terrain crane. Each panel was 12.2 m (40 feet) wide and as deep as required for each section of trench in which it was installed. The geomembrane itself was 80 mil thickness.

Attached to the geomembrane were 160 mil interlocking channels on both edges. These channels were used to connect the series of panels together to form a continuous curtain wall (Figure 1).

Once the panel was lowered to the bottom of the trench, it was positioned with the crane towards the outside wall of the trench, nearest the river. The panel and its frame were stabilized and left in place. Excavation of the trench continued until there was sufficient open trench (trench supported by slurry) to install the next panel. Once this was accomplished, the succeeding panel was attached to a second frame. The panel was elevated, using the crane, and interlocking channels on both panels were aligned to connect the HDPE. A small diameter, hydrophilic, high swelling gasket material was placed between the connections to assure that the joint is watertight. The gasket material was a rubber joint seal which expands up to five times its volume when exposed to liquid. During panel interlocking, the bentonite slurry was used to aid in the lubrication of the HDPE joints and the gasket material to ensure that the gasket would not be broken as the panels slip together.

At several instances during panel installation, wind became a concern. At all times, taglines were utilized to guide the elevated panel into place. Due to the large area of each panel, small amounts of wind would cause interference with typical installation, and create unsafe conditions for employees attempting to restrain the taglines. In several instances, the taglines were tied to equipment to stabilize the panel before lowering it into the trench. On a few occasions, all installations had to cease because the sheets became uncontrollable in higher winds, creating a safety concern.

Once the second panel was successfully installed and stabilized, backfilling of the trench could begin. Previously sorted and mixed backfill was lowered into the trench via the lead-in slope. Due to the low slump of the material, the slope of the backfill was maintained between 2:1 and 4:1. Backfilling continued until the toe of the backfill reached the far end of the first panel, at a minimum. This was determined by regularly sounding the trench with a weighted tape measure. To allow for the backfill volume, slurry trench excavation continued at the opposite end. Once sufficient backfilling was complete, the frame on the initial panel was released and removed from the trench, allowing the HDPE panel to remain in place (Figure 2). Another panel was secured to the frame and prepared for installation. Once adequate trench was excavated, the third panel was connected to the second and submerged under the slurry. This process was repeated until the entire length of trench was complete with the interlocking, nonstructural HDPE wall. At both ends, the curtain wall was tied into an existing metal sheetpile wall.

HDPE Curtain Wall To Sheetpile Tie-In

The most unique feature of this project was the HDPE curtain wall to sheetpile tie-in. It was decided to leave the existing sheetpile in place as a barrier wall. The existing sheetpile effectively cut off groundwater flow from the site to the river, except for a 636 m (2100 lineal foot) section where the sheetpile was not installed in lieu of an existing wooden bulkhead. Over time, the wooden bulkhead deteriorated and came to disrepair. The sheetpile, however, remained in fair condition. The challenge was in coming up with a means of creating a watertight connection between the existing sheetpile and the HDPE curtain wall.

After entertaining numerous ideas and connection variations, a connection using both a mechanical joint and the manufacturers standard curtain wall joint was employed. The manufacturers' HDPE joint (SLT Curtain Wall Interlock ™) as shown in Figure 1 was attached to the sheetpile by means of a mechanical joint (Figure 3). To make the attachment, the ending sheetpile panel was removed using an excavator. A section of interlock was cut to the length of the removed sheetpile section. The edge of the sheetpile where the connection was to be made was thoroughly cleaned, using a wire brush attachment on a hand drill. Once the sheetpile was cleaned, the HDPE interlock was ready to be mechanically attached.

Standard mechanical attachments are most frequently used to attach HDPE liner to an existing concrete structure. The major component of the mechanical attachment is the batten strip. The most commonly used batten strip is made from stainless steel type 301 or 304. Typical dimensions are 5.08 cm (2 inch) wide by 0.64 cm (1/4 inch) thick, coming in lengths of 3 to 3.6 m (10 to 12 feet). They can be cut to the desired length. To facilitate installation, the batten strip is slotted with 0.95 cm (3/8 inch) wide by 1.11 cm (7/16 inch) long slots on 15.24 cm (6 inch) centers. These slots receive the anchor bolts which hold the batten to the concrete structure. The anchor bolts which are most frequently used are 0.95 cm x 9.53 cm (3/8 inch x 3 3/4 inch) anchor length stainless steel bolts. To install, the concrete is drilled and the anchor bolts are set on 15.24 cm (6 inch) centers. A 5.08 cm (2 inch) wide by 0.32 cm (1/8 inch) thick neoprene gasket with an adhesive backing is then applied continuously along the length to be battened. The geomembrane being attached is then pulled into place, cutting undersized holes at the anchor bolt locations, and forcing the membrane down over the anchor bolts. The stainless batten is then positioned with the anchor bolts through the 0.95 cm (3/8 inch) by 1.11 cm (7/16 inch) slots and tightened down to create a watertight seal.

This standard mechanical attachment, with slight alterations, was used to attach the manufacturers' HDPE joint to the sheetpile panels. A standard head 0.95 cm x 5.08 cm (3/8 inch x 2 inch) stainless steel bolt was used in place of the anchor bolts. Then, upon review of the chemical resisitivity properties of the neoprene gasket, it was decided to use a nitrile gasket instead. While neoprene offers moderate resistance to petroleum oils and gasoline, nitrile offers excellent resistance to these products. To attach the interlock, the sheetpile panel and the HDPE interlock were drilled on 15.24 cm (6 inch) centers. The nitrile was then applied continuously along the edge of the sheetpile panel. The bolts were then fed through the sheetpile panel from back to front. The interlock was next placed over the bolts, followed by the stainless steel batten strip. The nuts were then tightened down on the bolts until the nitrile was compressed enough to create a watertight seal.

Now, the section of sheetpile with the HDPE interlock attached to it was complete. The next obstacle which had to be overcome, was driving this sheetpile panel back into the ground without destroying the interlock itself. In order to do this, the next two adjacent sheetpile panels were also removed with the excavator. The sheetpile alignment was then excavated to depth back to the next sheetpile panel section which remained in place. Care was taken not to damage the sheetpile joint with the excavator bucket during excavation. This excavation was done under a slurry to support the trench due to the depth of excavation (approximately 5.45 m (18 feet) deep), groundwater elevation (approximately 0.9 m (3 feet) below ground surface), and soil conditions. The sheetpile panels were then re-installed through the slurry supported trench, using a vibratory hammer. This method allowed the sheetpile panels to be easily installed with no damage to either the sheetpile joints or HDPE interlock. The curtain wall installation then proceeded as previously described.

Summary

The completed curtain wall, which was tied in on both ends to an existing steel sheetpile wall, proved to be a very effective way to control the off-site migration of contaminated groundwater. The addition of a soil-bentonite backfill, in conjunction with the curtain wall, amplified the effectiveness of the cutoff system. After the wall was completed, an interceptor/collection trench was installed approximately 4.6 to 6.1 m (15 to 20 feet) off of the centerline of the curtain wall. This system was used to collect the groundwater which was cut off by the barrier wall. The combination of curtain wall backfilled with soil-bentonite backfill, and the collection trench, was a very successful combination.

Groundwater infiltration into the river has been deferred to the collection trench, therefore, eliminating any future problems for the refinery in this location. The collected groundwater was transferred to a treatment facility where it was conditioned and disposed of properly. This system was installed efficiently and operates as intended.

SLT 80 mil HyperFlex™

HYPERTITE
EXPANSIVE SEAL

DOUBLE TRACK
FUSION WELD

1" APPROX.

SLT CurtainWall
INTERLOCK™ 160 mil
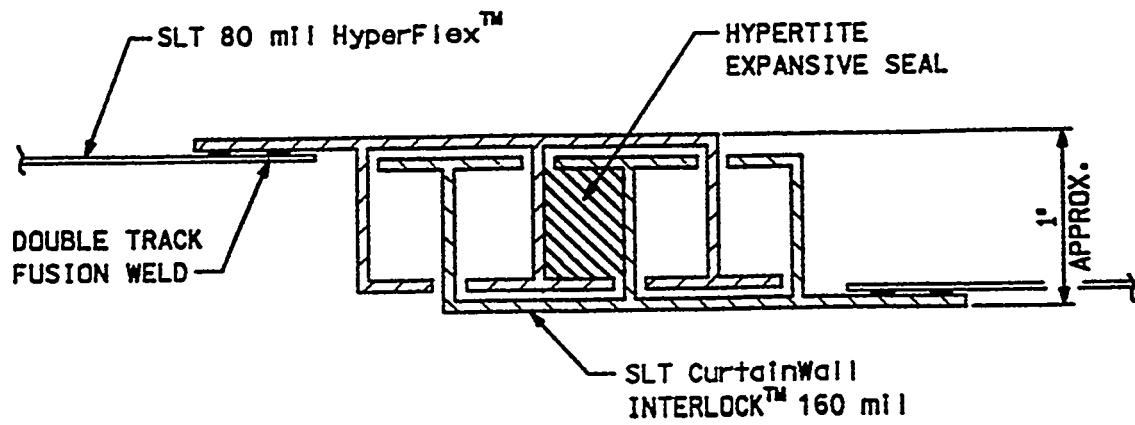
CurtainWall INTERLOCK DETAIL

FIGURE 1

SLURRY
SUPPORTED
TRENCH
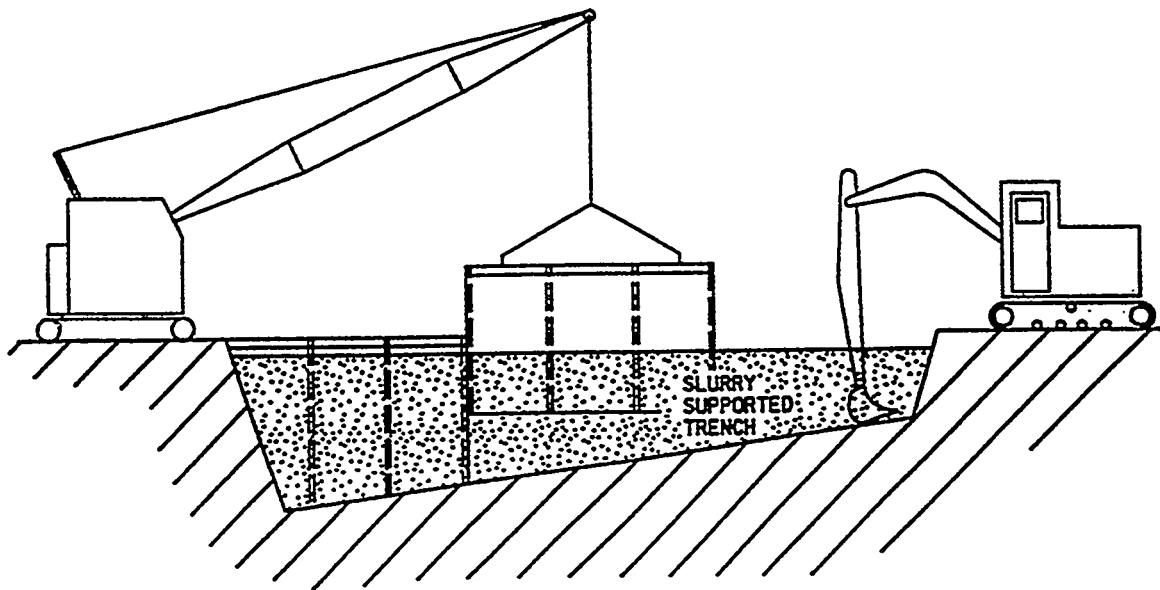
GEOMEMBRANE CurtainWall INSTALLATION

FIGURE 2

STEEL
SHEET
PILES

JOINT

CurtainWall
INTERLOCK

FOR SHEET PILE
CONNECTION SEE
DETAIL THIS SHT.

CurtainWall
INTERLOCK

STEEL BATTEN

SHEET PILE

NEOPRENE GASKET
3" WIDE x $\frac{1}{8}$" THICK
x LENGTH TO SUIT
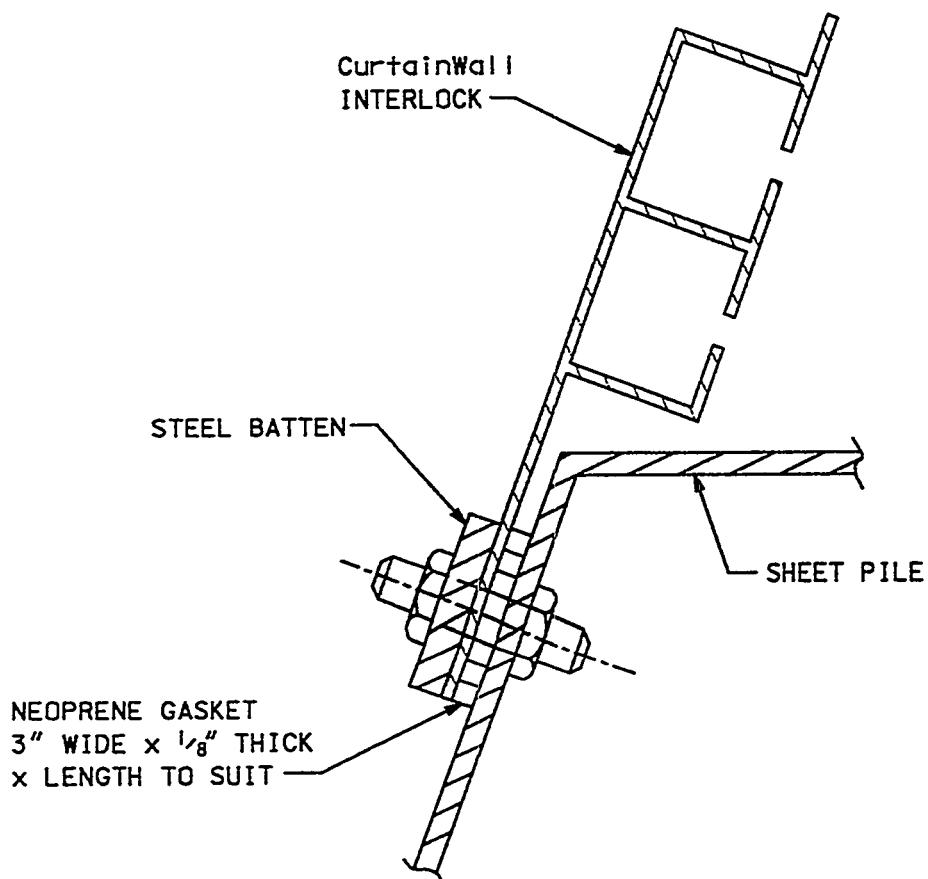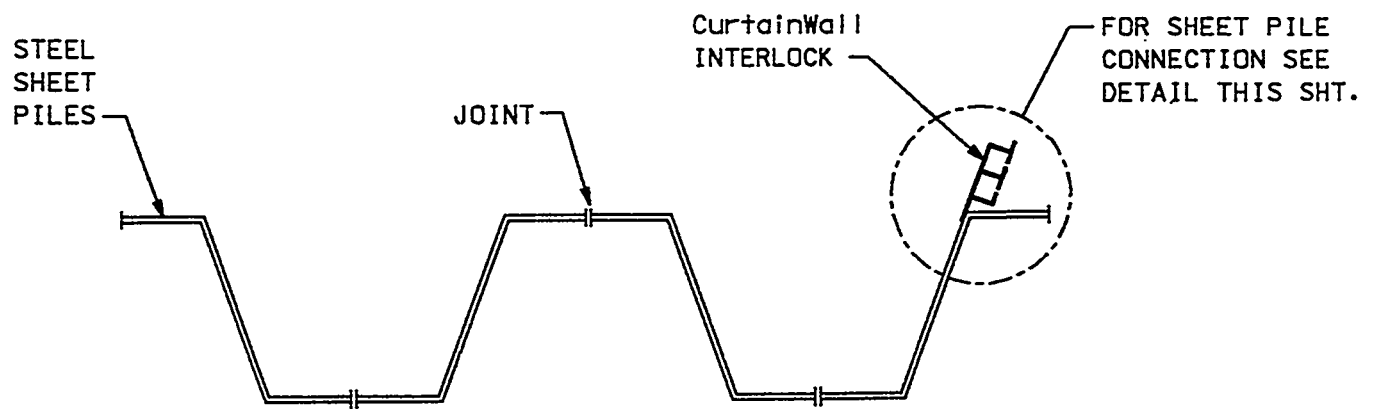
SHEET PILE CONNECTION DETAIL

FIGURE 3

Containment and Recovery of a Light Non-Aqueous Phase Liquid Plume at a Woodtreating Facility

Dan Crouse[1], Greg Powell[2], Steve Hawthorn[3] and Sara Weinstock[4]

Abstract

A woodtreating site in Montana used a formulation (product) of 5 percent pentachlorophenol and 95 percent diesel fuel as a carrier liquid to pressure treat lumber. Through years of operations approximately 378,500 liters of this light non-aqueous phase liquid (LNAPL) product spilled onto the ground and soaked into the groundwater. A plume of this LNAPL product flowed in a northerly direction toward a stream located approximately 410 meters from the pressure treatment building. A 271-meter long high density polyethylene (HDPE) containment cutoff barrier wall was installed 15 meters from the stream to capture, contain, and prevent the product from migrating off site. This barrier was extended to a depth of 3.7 meters below ground surface and allowed the groundwater to flow beneath it.

Ten product recovery wells, each with a dual-phase pumping system, were installed within the plume, and a groundwater model was completed to indicate how the plume would be contained by generating a cone of influence at each recovery well. The model indicated that the recovery wells and cutoff barrier wall would contain the plume and prevent further migration. To date, nearly 3½ years later, approximately 106,000 liters of product have been recovered.

Introduction

This paper presents a case study where a high density polyethylene (HDPE) cutoff barrier wall was installed to contain a light non-aqueous phase liquid (LNAPL) product plume consisting of 5 percent pentachlorophenol (PCP) and 95 percent diesel fuel and prevent it from entering a stream located approximately 15 meters away from the wall. This paper is not intended to be a detailed technical presentation, but only to describe one project where a cutoff barrier wall was installed to successfully contain a plume.

The theory of this cutoff barrier wall installation was to allow groundwater to flow underneath it while containing the floating product. A dual-phase recovery system was also installed to collect the free-phase product and contain the plume by creating a hydraulic gradient towards the recovery wells. Water recovered from the recovery wells was treated and discharged to the receiving stream.

---

[1] Roy F. Weston, Inc./REAC, 2890 Woodbridge Avenue, Edison, NJ 08837-3679, (908) 321-4222

[2] United States Environmental Protection Agency, Environmental Response Branch, 26 West Martin Luther King Drive, Cincinnati, OH 45268, (513) 569-7537

[3] United States Environmental Protection Agency, Region VIII, 999 18th Street, Suite 500, Denver, CO 80202-2405, (303) 312-6061

[4] United States Environmental Protection Agency, 155 West Granite, Butte, MT 59701, (406) 782-7415

Background

Pentachlorophenol is a chlorinated compound used to pressure treat lumber for telephone poles and other materials to prevent damage from termites, wood-boring insects, and rotting. Pentachlorophenol is usually added to diesel fuel as a carrier liquid to allow for easier penetration into the wood grain. This is done by placing the dried lumber into large cylindrical vessels along with the PCP-diesel fuel solution. After treatment, the lumber is transferred to railroad cars and pulled onto a concrete drip pad. From there, the lumber is transferred to drip areas where any excess PCP solution is allowed to drain.

Due to poor handling procedures when transferring the lumber to the railroad cars, coupled with the constant dripping of PCP in the drip area, thousands of liters of PCP have contaminated the groundwater. Estimates of the amount of PCP product that contaminated the groundwater vary from 378,000 to 1,130,000 liters. The contaminated groundwater and product entered a stream located approximately 410 meters north of the facility. The product was visible as an oily sheen that entered the stream at six identifiable seep points.

Prior to installation of the cutoff barrier wall, several seeps of PCP product had been found entering the stream. To prevent this seepage, the contaminated material above the groundwater surface and between the cutoff barrier wall and the stream was excavated, removed, and backfilled with clean fill material. Following excavation, the seeps stopped, and have not returned after 2½ years. In addition, piezometers installed on the down gradient side of the wall did not contain any free-phase product, while those upgradient of the wall did contain product. This indicates that the cutoff barrier is effective in containing the free-phase product.

Recovery Wells

The United States Environmental Protection Agency/Environmental Response Team Center (U.S. EPA/ERTC) tasked the Response Engineering and Analytical Contract (REAC) personnel to complete the following tasks:

- Evaluate the various treatability studies and remedial investigation plans, determine if a pump test is needed to adequately evaluate the effectiveness of a proposed cutoff trench installation, and determine the impact of adjacent site activities on the product recovery system.

- Determine the optimal treatment system for treating the groundwater that would be removed from the cutoff trench, and develop a conceptual design for a total fluid recovery system (including capital costs and operation and maintenance costs) while assisting the Region VIII On-Scene Coordinator (OSC) with oversight activities during development and installation of the product recovery system.

After reviewing previous reports and conducting treatability studies on the contaminated groundwater to determine the optimum method for treatment, it was proposed to install two recovery trenches to intercept the product. The decision for the locations of the two trenches was based on information contained in a Remedial Investigation (RI) Report (Keystone 1992). The first trench installation was stopped during the initial excavation because of poor stability of the trench walls due to its composition of finely grained sands. Unsuccessful attempts were then made to secure the walls with a trench box. It became apparent that the construction of cutoff trenches was inappropriate for this particular condition (WESTON/REAC 1993).

In response, the U.S. EPA Region VIII OSC decided to install a product recovery system consisting of recovery wells. Figure 1 shows the locations of the recovery wells. REAC also

236

installed several piezometers and a recovery well and then conducted a yield test to obtain data to evaluate the aquifer transmissivity data necessary to design the recovery system (WESTON/REAC 1993).

In an attempt to install a recovery system before winter, a preliminary recovery well system was first designed. Pilot borings were proposed for recovery well locations to ensure optimum hydrogeologic conditions, and a preliminary groundwater model was constructed based on the existing data. At that time, surveys, a full-scale pumping test, groundwater elevation data collection, and a full-scale groundwater model were proposed by REAC to evaluate the preliminary design. The baseline groundwater flow model was then developed with the single layer analytical element model (SLAEM) developed by Otto D. L. Stack (WESTON REAC 1993).

Seven piezometers and ten product recovery wells were then installed. Eight of the recovery wells were installed along the axis of the product plume and each of the other two wells were installed along the ends of the cutoff barrier (see Figure 1). The two end wells were installed to prevent the migration of the product around the ends of the cutoff barrier wall. Two pumps were installed in each recovery well. One pump was used to extract contaminated groundwater to create hydraulic containment. The other pump, fitted with a special membrane which only allowed the PCP-diesel carrier fluid to enter, then removed the product. The recovery wells were designed at production rate of 57 L/min each, but actual pumping rates varied from 15 to 170 liters per minute (L/min). The contaminated groundwater was pumped to a 1,135 L/min treatment system built on site with granular activated carbon as the primary treatment method for organics removal. The recovered product was then pumped to horizontal holding tanks for subsequent disposal. After 4 years, the recovery system is recovering an average of approximately 27,000 liters of product per year.

Cutoff Barrier Wall Specifications

To prevent additional migration of the floating product along the groundwater table interface and into the stream, a free-phase product HDPE cutoff barrier wall was also installed (see Figure 1). The average depth to groundwater was 1.5 meters and the thickness of product varied from 5 centimeters to 0.61 meters This 271-meter cutoff barrier was made of 60-millimeter-thick HDPE, and it was installed to 3.7 meters below ground surface (bgs), approximately 2.4 meters into the groundwater, and 15 meters from the stream embankment. Figure 2 contains a detailed sketch of the HDPE cutoff barrier wall. The cutoff barrier wall panels were approximately 3 meter wide.

Cutoff Barrier Wall Installation

A special pneumatic hammer drove a steel plate into the ground to the desired depth to make a slot in which the panels were installed. Each panel had an interlocking edge allowing one panel to slip into another panel forming a solid impermeable barrier. Once the slot was made, the machine would install a panel. Each panel had a slot at the bottom which held a steel plate which was used to force the panel into the ground. Once the panel was installed to the desired depth, the ground bound onto the panel bottom lip, and the steel plate was removed. Successive panels were installed in the same manner as the previous one. The total price of the contract was approximately $ 72,000 for the HDPE panels and its installation. Minor problems were incurred during the installation. The main problem was that the site contained walls of waste slag material approximately 2.75 meters high, 3.6 meters wide, and hundreds of meters long. The ground surface on which the cutoff barrier was installed contained approximately 0.6 meters of slag which hampered the pneumatic hammer somewhat during installation of the panel slots. Overall however, the installation was completed without major delays.

Groundwater Model Calibration

After installation of the recovery wells, additional data were collected and used to calibrate the preliminary groundwater model. The plume (large oblong shaded area) is outlined and the ten recovery wells (EPA-1 through EPA-10) are shown on Figure 1. After entering the new data, the groundwater model was updated and it was very similar to the preliminary model. The groundwater model has been updated at regular intervals with the actual product thickness, recovery pumping rates, and water table elevations input into the model. The results indicated that the existing recovery system is still adequate to contain and remove the product.

Conclusions

The installation of a HDPE vertical cutoff barrier wall to contain an light non-aqueous phase liquid (LNAPL) plume was very successful at this site. For other sites containing an LNAPL plume this type of barrier wall could be appropriate if it was installed in conjunction with some type of system to create a hydraulic gradient.

A unique quality about this project was the entire product recovery system was completed within six months. This included the hydrogeological study, treatability studies, design, construction, and startup.

References

Keystone Environmental Resource, Inc. (Keystone). July 1992. Remedial Investigation Report, Draft Report, prepared for ARCO, Monroeville, PA.

Roy F. Weston, Inc./Response Engineering and Analytical Contract (WESTON/REAC). August 1993. Hydrogeology and Groundwater Modeling Report, prepared for United States Environmental Protection Agency under Contract No. 68-03-3482. Edison, NJ.
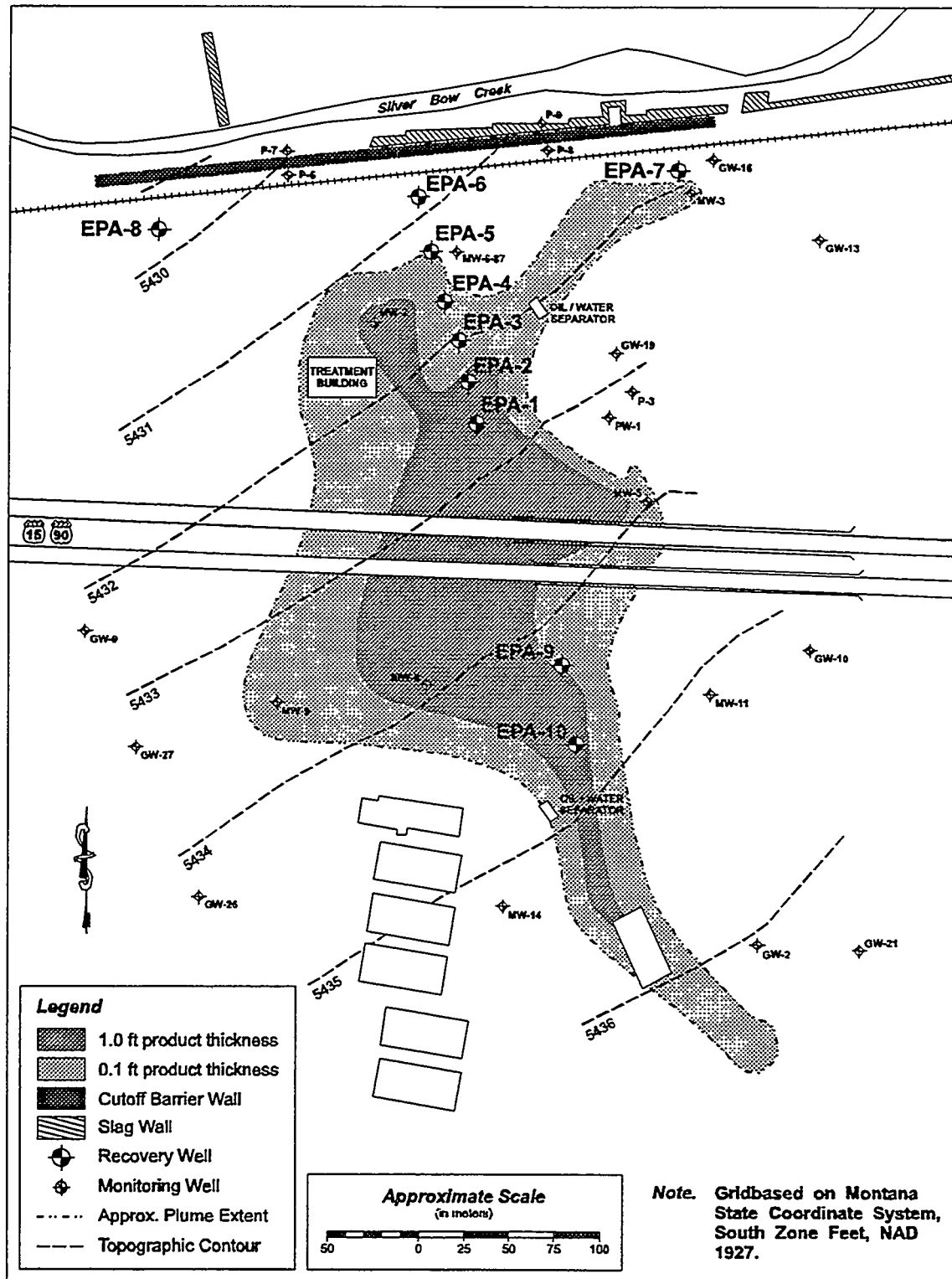
Figure 1. Site map showing the PCP product plume, cutoff barrier wall, and ten recovery wells.
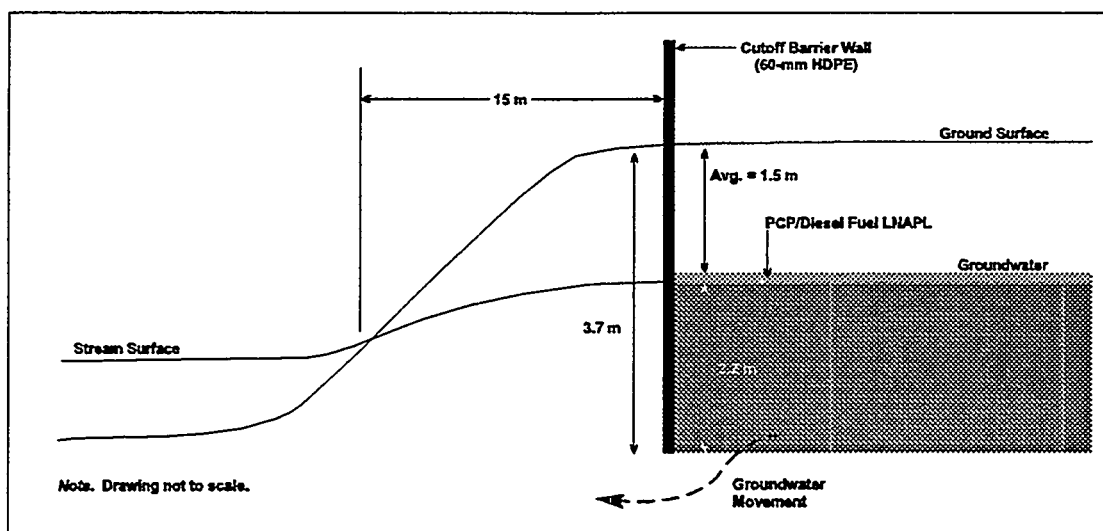
Figure 2. Cross-section sketch of the HDPE cutoff barrier wall.

Chapter 6

Caps: Capillary Barriers

AN ECOLOGICAL ENGINEERING APPROACH FOR KEEPING WATER FROM REACHING INTERRED WASTES IN ARID OR SEMIARID REGIONS

Jay E. Anderson[1]

Abstract

This paper describes application of a soil-plant cover system (SPCS) to preclude water from reaching interred wastes in arid and semiarid regions. Where potential evapotranspiration far exceeds precipitation, water can be kept from reaching buried wastes by 1) providing a sufficiently deep cap of soil to store precipitation that falls while plants are dormant and 2) maintaining plant cover to deplete soil moisture during the growing season, thereby emptying the storage reservoir. Research at the Idaho National Engineering Laboratory (INEL) has shown that 2 m of soil is adequate to store moisture from snowmelt and spring rains. Healthy stands of perennial grasses and shrubs adapted to the INEL climate use all available soil moisture, even during a very wet growing season. However, burrowing by small mammals or ants may affect the performance of a SPCS by increasing infiltration of water. Intrusion barriers of gravel and cobble can be used to restrict burrowing, but emplacement of such barriers affects soil moisture storage and plant rooting depths. A replicated field experiment to investigate the implications of those effects is in progress. Incorporation of an SPCS should be considered in the design of isolation barriers for shallow land burial of hazardous wastes in arid regions.

Introduction

This paper describes an ecological engineering approach for preventing water from reaching buried hazardous wastes in arid or semiarid areas. Ecological engineering is the building of sustainable, self-maintaining ecosystems in which the energy supplied by humans is "small relative to the natural sources, but sufficient to produce large effects in the resulting patterns and processes" (Odum 1962, as cited by Mitsch 1993). Simply stated, this approach uses natural materials and natural ecosystem processes to address environmental problems. Once constructed, the system sustains itself indefinitely with only modest amounts of human intervention; the system runs primarily on solar energy (Mitsch 1993).

Among the most serious problems associated with shallow land burial of hazardous wastes is keeping water received as precipitation from reaching the waste zone. However, in arid and semiarid regions, an elegant ecological engineering solution exists. Under such climates, the potential to evaporate water far exceeds the amount of water received from precipitation. Consequently, what is needed is a way to the store water until it can be evaporated. Many natural aridland ecosystems do just that. The soil serves as a reservoir that temporarily stores any water that is not immediately evaporated, and plants use solar energy to pump that water back into the atmosphere.

We have been studying the potential for applying these concepts in the design of waste burial covers at the Idaho National Engineering Laboratory (INEL) for over a decade (Anderson et al. 1987, 1991, 1993). The INEL is located on the Upper Snake River Plain in southeastern Idaho where average annual precipitation is about 220 mm. At the INEL and similar cold-desert sites, much of the annual precipitation is received during late fall, winter, and early spring while plants

[1] Department of Biological Sciences, Idaho State University, Pocatello, Idaho 83209-8007, (208) 236-3145, andejay@isu.edu

are dormant or just initiating growth. Thus, a cap of soil over hazardous wastes must be sufficiently deep to store water received during that period. The other crucial component of this ecological engineering design is a healthy stand of perennial plants to empty that storage reservoir each growing season (Link et al. 1994). These two components constitute a soil-plant cover system (SPCS). Our research has shown that at the INEL a soil cap 2.0 m thick would more than suffice to store precipitation received while plants are dormant and that drought-tolerant grasses or shrubs will use all of the plant-available soil moisture, even during an exceptionally wet year (Anderson et al. 1991, 1993).

Design Criteria

To determine the depth of soil required in a SPCS, estimates of the water storage capacity of the soil and of the maximum amount of water to be stored are needed. The effective storage capacity of a soil is the difference between the *drained upper limit* and the *lower limit of extraction* (Ritchie 1981). The drained upper limit is the amount of water a soil will hold against the force of gravity. This parameter is estimated by thoroughly wetting the soil and then allowing it to drain. The amount of water remaining in the profile once excess water has drained (but no water has been removed by evapotranspiration) is the drained upper limit (Ratliff et al., 1983). This parameter is analogous to field capacity (e.g. Hanks and Ashcroft, 1980), but is determined *in situ*. The lower limit of extraction is the minimum soil moisture content to which a particular plant species can deplete soil moisture. The lower limit is estimated from the amount of water remaining in the soil when plant growth and activity completely stop (Ritchie, 1981).

Precipitation and evapotranspiration are typically expressed as depths of water, whereas the amount of water in a soil is expressed as a percentage of the total soil volume. Volumetric water content is readily converted to depth. For example, if a soil contains 27% water by volume, a meter depth of that soil will contain 270 mm of water. The INEL soil that is used to cap waste sites has a drained upper limit of 28% (Anderson et al. 1993). The lower limit of extraction varies little among the drought-tolerant perennial species that we have studied, averaging about 11% for that soil (Figure 1). Thus, the effective moisture storage capacity of the soil is 17% by volume, or 170 mm per meter of soil (Anderson et al. 1993).

The second estimate required is the amount of water to be stored. If a good cover of perennial plants is present, rainfall received during the middle and latter parts of the growing season will be quickly evaporated or transpired. For the INEL, most rainfall received during June through September is quickly lost by evapotranspiration (Anderson et al. 1991, 1993). Therefore, the maximum precipitation that might fall from October through May was used to estimate the minimum fill soil requirement. The maximum received during that period for 44 years of record (1950-1994) is 277 mm. If 277 mm water infiltrated the soil, 1.6 m of fill soil would be required to store it, given a storage capacity of 17%. However, the wetting front in a soil will extend below that portion of the profile that is at the drained upper limit. Our data indicate that the wetting front from 277 mm of water might reach 1.8 m (Anderson et al. 1993). Additionally, ponding due to soil subsidence or deep snow accumulation could increase infiltration in local areas. Therefore, we have recommended a minimum fill soil depth of 2 m for the INEL (Anderson et al. 1991, 1993). A substantial portion of precipitation that falls while plants are dormant will be lost by evaporation or sublimation, so a fill soil of 2 m should be quite conservative.

Successful performance of a SPCS requires that water infiltration not exceed the storage capacity of the soil. Therefore, the site should be nearly level so that the potential for water draining onto it from adjacent areas is minimal. Mounding of the cap is not recommended for several reasons. Mounding increases the potential for soil loss by both wind and water erosion. It also increases the potential for deep snow accumulations on leeward exposures, which could result in a large influx of water from melting snow. Finally, mounding will increase runoff from the protective cap,

which could result in insufficient moisture storage in the cap soil to maintain a vigorous stand of perennial plants.

To insure long-term functional integrity of a SPCS with minimal maintenance requirements, it is important to choose plant species that are well adapted to the area and tolerant of periodic drought. The natural vegetation of the INEL typically consists of an overstory of big sagebrush (*Artemisia tridentata*) and an understory of perennial grasses and forbs. We have evaluated water use by four species of drought-tolerant perennial plants that are common at the INEL, big sagebrush and three perennial grasses (crested wheatgrass, *Agropyron desertorum*; Great Basin wildrye, *Leymus cinereus*; streambank wheatgrass, *Elymus lanceolatus*). Crested wheatgrass is an introduced species that has become naturalized in western North America through extensive use for rangeland rehabilitation and reclamation of disturbed sites; the other three species are natives. All four species can remove water from a soil cap to a depth of at least 2.2 m, and a vigorous stand of any of the species would likely use all of the plant-available water that might be stored in the soil, even during an exceptionally wet year (Anderson et al. 1991, 1993). For example, evapotranspiration from the plot of Great Basin wildrye shown in Figure 1 was over 540 mm in 1987, some 2.8 times the average annual precipitation for the INEL. We currently recommend planting crested wheatgrass on soil caps at the INEL because it is easily established and very persistent (Marlette and Anderson 1986), but, as explained below, we are investigating the establishment and functioning of diverse species assemblages of native species.

Other Considerations and Ongoing Research

Researchers at the INEL and elsewhere have demonstrated that burrowing by small mammals (e.g., Laundre 1993) and ants (Blom et al.1994) can increase water infiltration by decreasing the bulk density of soil or creating channels for preferential flow. Burrowing animals also may transport contaminants to the surface (Arthur and Markham 1983, Arthur et al. 1987). A biological intrusion barrier consisting of a layer of rock placed within a protective soil cap will restrict the depth to which mammals can burrow (Hakonson et al. 1983, Hakonson 1986, Reynolds 1990). Tunneling by ants can be obstructed by a layer of gravel placed in the soil (P. Blom, personal communication). Thus, a layer of gravel and cobble placed within a soil cap should restrict animal burrowing, but plant root growth may also be limited to the soil above the intrusion barrier. If roots were restricted to the soil above an intrusion barrier, the effective water storage reservoir of the soil cap would also be limited to the soil above the barrier. In this case, depth of emplacement of the intrusion barrier within a soil profile would be critical. On the other hand, if plant roots penetrated through the intrusion barrier and extracted water from the soil below it, depth of emplacement of the barrier would have little effect on the size of the water storage reservoir.

In 1993, researchers at Idaho State University in Pocatello, and the Environmental Science and Research Foundation in Idaho Falls, Idaho, initiated a large-scale, replicated field experiment to compare the performance of two SPCS designs that include biological intrusion barriers at depths of either 0.5 or 1 m in a 2-m soil profile with that of a soil-only design (Limbach et al. 1994). The major objectives of this study are to examine the effects of placing an intrusion barrier in a soil cap on water percolation, water storage capacity, and plant rooting depths and to determine which species of plants, if any, will grow roots through an intrusion barrier and extract water from the soil below it (which would be necessary if the intrusion barrier were placed at a shallow soil depth). Performance is being monitored under three irrigation treatments: 1) ambient precipitation, 2) "heavy spring," in which sufficient water is added to the soil profile at the beginning of the growing season to bring the total stored water up to approximately 300 mm (which exceeds the highest October - May precipitation recorded at the INEL), and 3) "extended spring/summer," an amount of water equal to that of treatment 2 is applied in 50 mm increments at bi-weekly intervals (depending on natural precipitation events) through the spring and into the summer. These treatments will be modified later in the experiment to determine the amount of water required to cause failure of each of the experimental cap configurations.

The effects of emplacing a biobarrier in a soil profile are shown in Figure 2, which contrasts the moisture profiles during the 1996 growing season in a soil-only cap with those in a cap having a biobarrier 1 m below the soil surface. The wetting front resulting from winter-spring recharge reached 1.2 m in the soil-only cap and 0.8 m in the biobarrier cap. The increase in storage between October 1995 and March 1996 was 130 mm in the soil-only cap and 170 mm in the 1-m biobarrier cap. The capillary break due to the soil-gravel interface at the top of the biobarrier restricted downward movement of water so that all of the recharge water was held above the biobarrier. There was no appreciable change in water content below the biobarrier through the growing season (Figure 2). Under ambient precipitation over three years, we have observed percolation of water below the 1-m biobarrier on only one of 18 plots despite the fact that the 1995 growing season was the wettest on record, when some 250 mm of water were received from March through June. The mean for that period is 100 mm. Percolation below the 0.5-m biobarriers was observed on five of 18 plots in 1995.

The biobarriers clearly are an impediment to root growth. We have evidence for extraction of water below the 0.5-m biobarriers in four of 18 plots and below the 1-m biobarrier in one of 18 plots (Figure 3). We have only seen extraction below the biobarriers when volumetric water content below the barrier was initially at least 25%. There is no evidence of root extraction of water below biobarriers in any of the 24 ambient precipitation plots despite the presence of modest amounts of extractable water below the barriers of most plots. These results indicate that there may be a threshold water content below which plants are unable to detect the presence of extractable water below a biobarrier. On the other hand, the results show that roots can penetrate the biobarriers and extract water from the soil below them if water content is sufficiently high. Future monitoring of our plots should reveal whether this is a predictable outcome and whether water below the barriers will be depleted to the lower limit of extraction.

Regardless of the kind of plants that are initially planted in a SPCS, common native species such as sagebrush and rabbitbrush (*Chrysothamnus* spp.) likely will occupy the site eventually (Link et al. 1994). Furthermore, it may be desirable to establish a diverse plant community initially because a diverse community may be more functionally stable than a monoculture (McNaughton 1977, Tilman and Downing 1994). Such diversity might help to insure the functional integrity of a protective cap under threats from insect or pathogen outbreaks or disturbances such as fire. Thus, developing techniques for establishing a diverse community and evaluating cap performance with diverse species and growth forms present is necessary. Two vegetation types were included in the present experiment. One is a monoculture of crested wheatgrass, and the other consists of a mixture of 12 native species, including five shrubs, five perennial grasses, and two forbs. Native species of shrubs and grasses were transplanted from natural stands within about 2 km of the experimental site in November, 1993, after they became dormant. Forbs and crested wheatgrass were seeded by drilling. Survival and growth of individuals representing all species on all SPCS configurations are monitored. We also are monitoring changes in species composition under the three irrigation treatments. We expect that survival and growth of shrubs may be lower while growth of shallow-rooted grasses may be relatively higher on the plots having an intrusion barrier at 0.5 m than on other plots. Shrubs are expected to have the competitive advantage under the heavy spring irrigation treatment which results in deeper soil recharge, whereas applying a similar amount of water over an extended period during late spring/early summer should benefit perennial grasses. The latter irrigation treatment was based on the prediction that the northern portions of the Great Basin and adjacent Snake River Plain may receive a larger portion of their annual precipitation during the summer months under global climate warming (VEMAP 1995). Results from our studies should provide some basis for predicting what effects climate change may have on vegetation composition of a SPCS. We expect that directional changes in species composition on the native vegetation plots will be apparent within five or six years.

Conclusions

Research at the INEL has shown that a soil-plant cover system consisting of 2 m of soil supporting a healthy stand of perennial plants should suffice to preclude water received as precipitation from reaching interred wastes. Such an ecologically-engineered cover is relatively simple and inexpensive to construct and should provide long-term protection with minimal human intervention, provided that precautions are taken to avoid subsidence, drainage onto the site, or deep accumulations of snow. Questions remain concerning the necessity of placing intrusion barriers in the soil cap to limit burrowing by small mammals or ants and concerning the effects that such barriers will have on SPCS performance. These questions are being addressed in a large-scale, statistically replicated field experiment. Irrespective of the outcome of current studies, however, it is clear that inclusion of a SPCS should be considered in the design of protective caps used to isolate hazardous buried wastes in arid and semiarid regions.

Acknowledgements

References

Anderson, J. E., M. L. Shumar, N. L. Toft, and R. S. Nowak. (1987) Control of the soil water balance by sagebrush and three perennial grasses in a cold-desert environment. *Arid Soil Res Rehab* 1,229-244.

Anderson, J. E., R. S. Nowak, T. D. Ratzlaff, and O. D. Markham. (1991) *Managing Soil Moisture on Waste Burial Sites.* Idaho Field Office, U.S. Department of Energy, Idaho Falls.

Anderson, J. E., R. S. Nowak, T. D. Ratzlaff, and O. D. Markham. (1993) Managing soil moisture on waste burial sites in arid regions. *J. Environ Qual* 22,62-69.

Arthur, W. J. and O. D. Markham. (1983) Small mammal soil burrowing as a radionuclide transport vector at a radioactive waste disposal area in southeastern Idaho. *J. Environ Qual* 12,117-122.

Arthur, W. J., O. D. Markham, C. R. Groves, and B. L. Keller. (1987) Radionuclide export by deer mice at a solid radioactive waste disposal area in southeastern Idaho. *Health Phys* 52,45-53.

Blom, P. E., J. B. Johnson, B. Shafii, and J. Hammel. (1994) Soil water movement related to distance from three *Pogonomyrmex salinus* (Hymenoptera, Formicidae) nests in south-eastern Idaho. *J. Arid Environ* 26,241-255.

Hakonson, T. E. (1986) *Evaluation of Geologic Materials to Limit Biological Intrusion into Low-level Radioactive Waste Disposal Sites.* LA-10286-MS. Los Alamos National Laboratory, Los Alamos, New Mexico.

Hakonson, T. E., J. F. Clime, and W. H. Rickard. (1983) *Biological Intrusion Barriers for Large Volume Waste Disposal Sites.* NUREG/CP-0028, Vol. 3. U.S. Nuclear Regulatory Commission, Silver Spring, Maryland.

Hanks, R. J., and G. L. Ashcroft. (1980) *Applied Soil Physics.* Advanced Series in Agricultural Sciences 8. Springer-Verlag, New York.

Laundre, J. W. (1993) Effect of small mammal burrows on water infiltration in a semi-arid environment. *Oecologia* 94,43-48.

Limbach, W. E., T. D. Ratzlaff, J. E. Anderson, T. D. Reynolds, and J. W. Laundre. (1994) Design and implementation of the Protective Cap/Biobarrier Experiment at the Idaho National Engineering Laboratory. In *In-situ Remediation: Scientific Basis for Current and Future Technologies* (ed G. W. Gee and N. R. Wing), pp. 359-377. Thirty-third Hanford Symposium on Health and the Environment. Batelle Press, Richland, Washington.

Link, S. O., W. J. Waugh, and J. L. Downs. (1994) The role of plants in isolation barrier systems. In *In-situ Remediation: Scientific Basis for Current and Future Technologies* (ed G. W. Gee and N. R. Wing), pp. 561-592. Thirty-third Hanford Symposium on Health and the Environment. Batelle Press, Richland, Washington.

Marlette, G. M., and J. E. Anderson. (1986) Seed banks and propagule dispersal in crested-wheatgrass stands. *J. Appl Ecol* 23,161-175.

McNaughton, S. J. (1977) Diversity and stability of ecological communities: a comment on the role of empiricism in ecology. *Am Nat* 111,515-525.

Mitsch, W. J. (1993) Ecological engineering: a cooperative role with the planetary life-support system. *Environ Sci Technol* 27,438-445.

Ratliff, L. F., J. T. Ritchie, and D. K. Cassel. (1983) Field-measured limits of soil water availability as related to laboratory-measured properties. *Soil Sci Soc Am J.* 47,770-775.

Reynolds, T. D. (1990) Effectiveness of three natural biobarriers in reducing root intrusion by four semi-arid plant species. *Health Phys* 59,849-852.

Ritchie, J. T. (1981) Soil water availability. *Plant Soil* 58,327-338.

Shumar, M. L., and J. E. Anderson. (1987) Transplanting wildings in small revegetation projects. Arid *Soil Res Rehab* 1,253-256.

Tilman, D., and J. A. Downing. (1994) Biodiversity and stability in grasslands. *Nature* 367,363-365.

VEMAP (1995) Vegetation/ecosystem modeling and analysis project: comparing biogeography and biogeochemistry models in a continental-scale study of terrestrial ecosystem responses to climate change and CO_2 doubling. *Global Biogeochemical Cycles* 9,407-437.
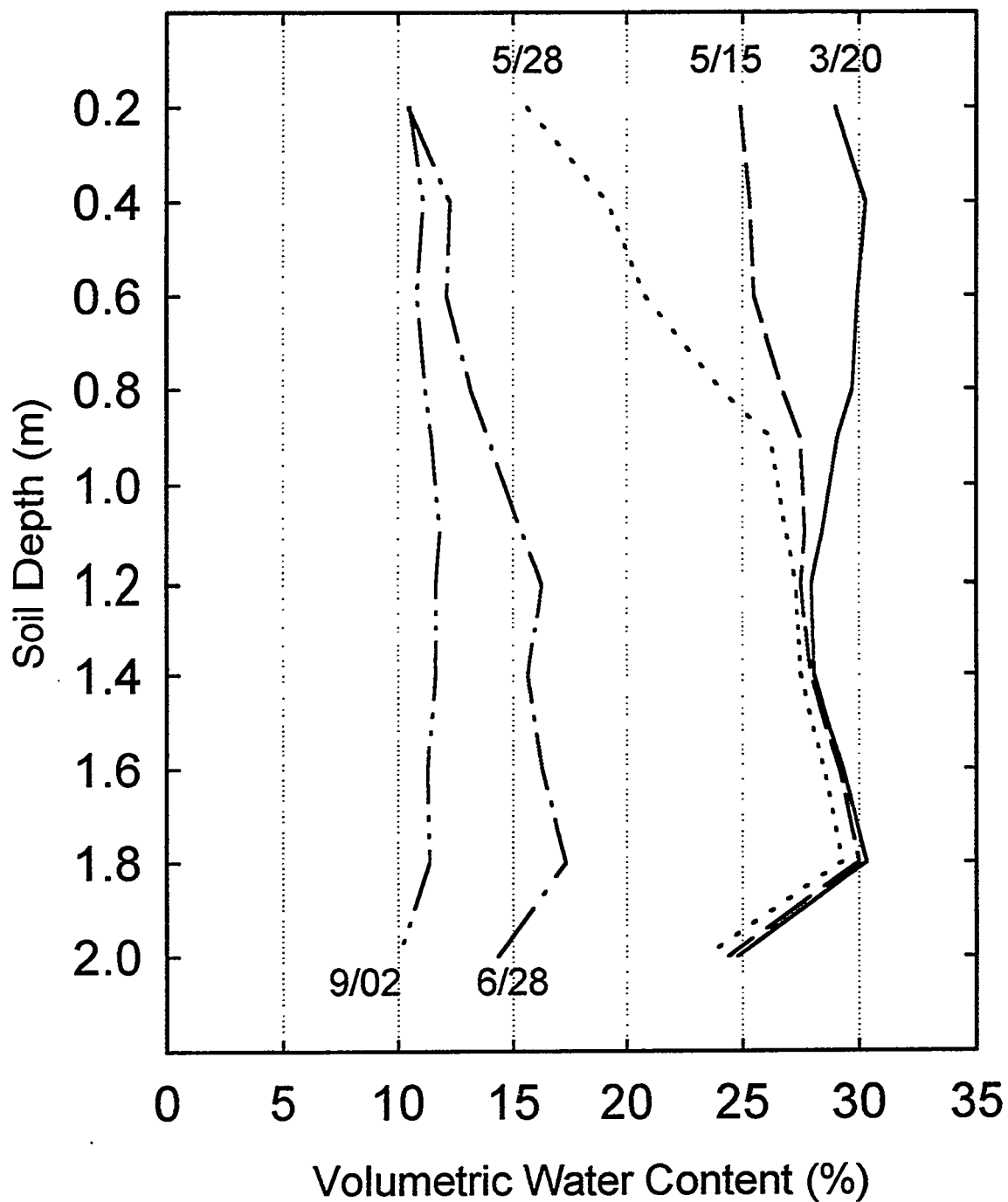
Figure 1. Changes in soil moisture over a growing season for an experimental field plot supporting a stand of Great Basin wildrye (Leymus cinereus). Each line depicts volumetric water content for a particular sampling date. The plot soil was a homogeneous clay loam to a depth of 2.4 m. Supplemental irrigation resulted in volumetric water content being near saturation throughout the profile at the beginning of the growing season. Water content at the lower limit of extraction was estimated from the data for September 2. Redrawn from Anderson et al. (1987).
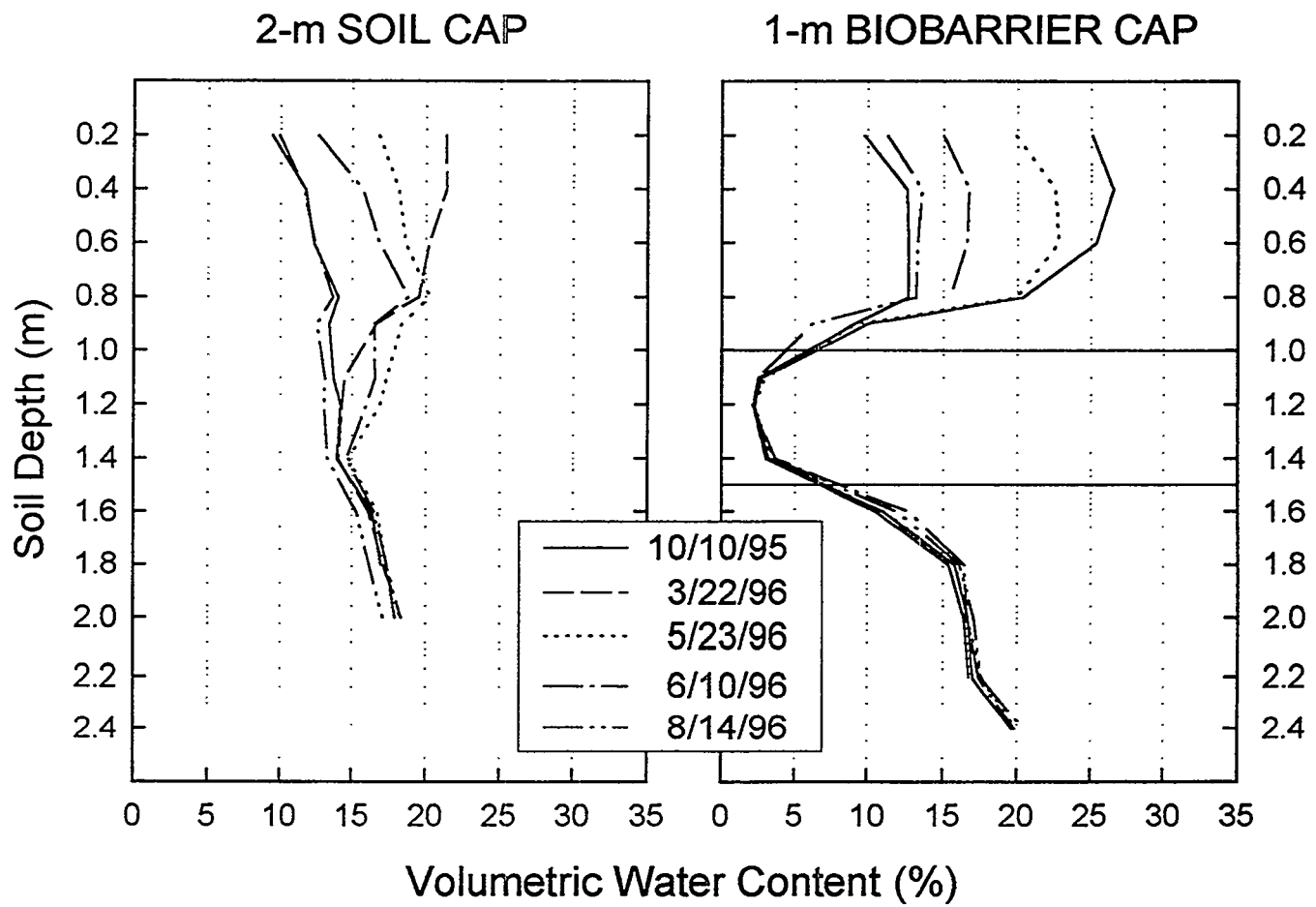
Figure 2. Soil moisture profiles for a soil-only cap and a 1-m biobarrier cap (a 0.5-m layer of gravel and cobble placed 1-m below the soil surface) for the fall of 1995 and the 1996 growing season. Each line depicts volumetric water content for a particular sampling date.
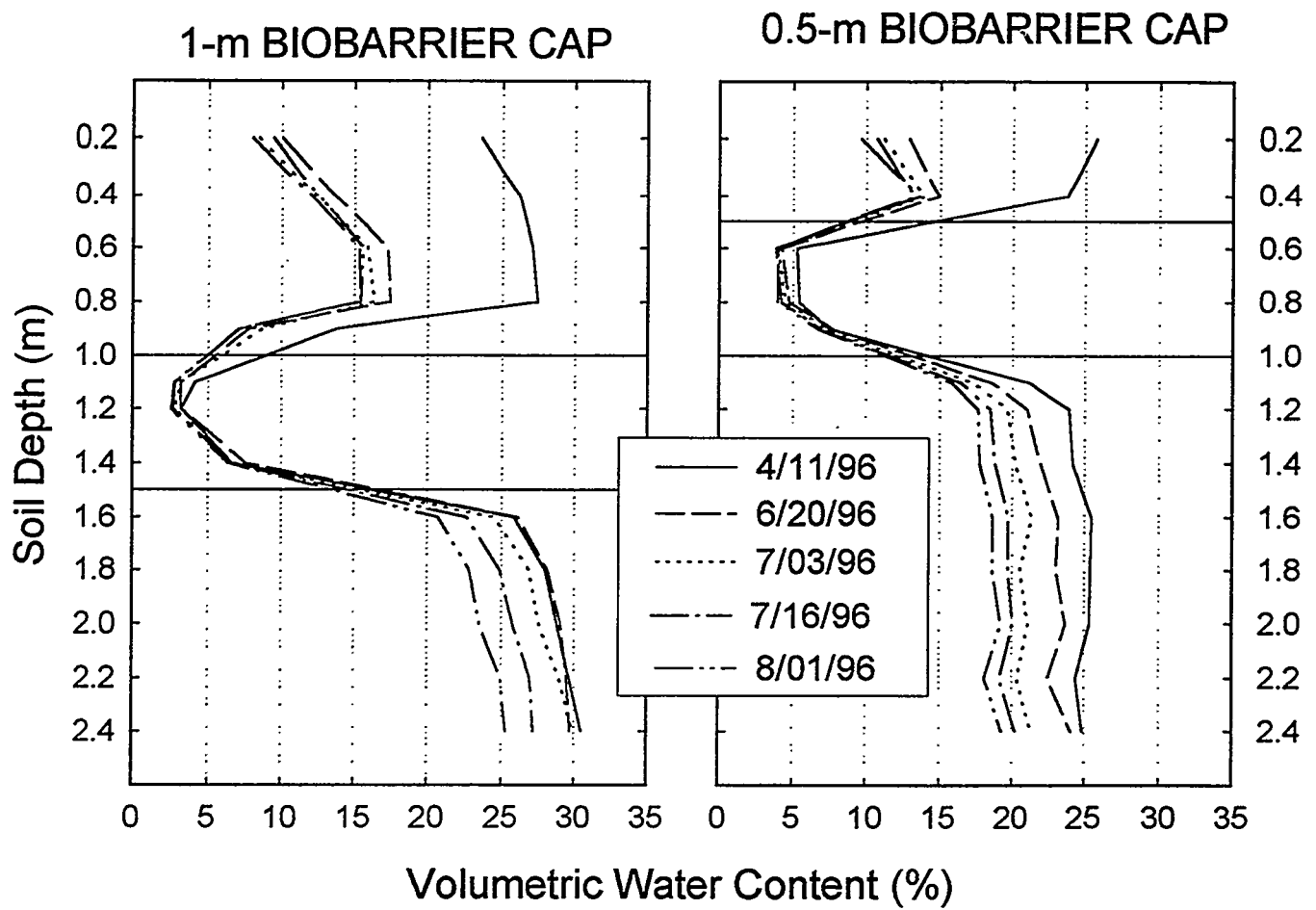
Figure 3. Changes in soil moisture over the 1996 growing season for a 1-m biobarrier cap and a 0.5-m biobarrier cap (a 0.5-m gravel/cobble biobarrier placed either 1 m or 0.5 m below the soil surface). In both cases, the moisture profiles indicate extraction of water by plants from the soil below the biobarrier.

WATER BALANCE OF TWO EARTHEN LANDFILL CAPS IN A SEMI-ARID CLIMATE

by

Milind V. Khire[1], Craig H. Benson[2], and Peter J. Bosscher[2]

ABSTRACT: Water balance data are presented that were obtained from two earthen cap test sections located in a semi-arid region. The test sections were constructed on a municipal solid waste landfill in East Wenatchee, Washington, USA. One test section represents a traditional resistive barrier, and is constructed with a compacted silty clay barrier 60 cm thick and a vegetated silty clay surface layer 15 cm thick. The other test section represents a capillary barrier and has a sand layer 75 cm thick overlain by a 15-cm-thick vegetated surface layer of silt. Extensive hydrological and meteorological data have been collected since November 1992. Unsaturated hydraulic properties of soils, hydrologic parameters, and vegetation have been extensively characterized. Results of the study show that capillary barriers can be effective caps in semi-arid and arid regions. They are also cheaper to construct and can perform better than traditional resistive barriers.

INTRODUCTION

This paper describes a field study of the water balance of two landfill cap test sections. The study is being conducted for three purposes: (i) to study the dynamics of the water balance in a semi-arid climate, (ii) to assess the relative performance of one-dimensional capillary barriers and resistive barriers in a semi-arid region, and (iii) to generate high quality and detailed field data that can be used to evaluate water balance models. This paper describes the test sections, their hydraulic properties, and the water balance data that have been collected. Inferences are also drawn regarding design of capillary barriers in semi-arid regions.

BACKGROUND

Resistive Barriers

Current geoenvironmental practice for minimizing percolation into underlying waste or contaminated soil generally consists of a prescriptive cover consisting of a barrier layer and a vegetated surface layer. The barrier layer may be a layer of compacted clay, a geosynthetic clay liner, a geomembrane, or a combination of these layers (Benson and Khire 1995). In some cases, a drainage layer is included to promote lateral drainage above the barrier layer (Daniel 1994, Melchior et al. 1994).

The prescriptive cover functions by offering hydraulic resistance to flow via low saturated hydraulic conductivity of the barrier layer. Thus, the prescriptive cover is also called a "resistive barrier" (Schulz et al. 1989). Although the premise of the "resistive barrier" design is based on the barrier layer having low saturated hydraulic conductivity, field data have shown that earthen resistive covers in semi-arid and arid climates are generally unsaturated (Khire et al. 1997). Thus, the behavior of a resistive cover is governed primarily by its unsaturated hydraulic properties.

Capillary Barriers

Even though resistive barriers are more commonly used, recent field studies indicate that capillary barriers can be effective at restricting percolation in semi-arid and arid climates (Gee and Kirkham 1984, Gee et al. 1993, Nyhan et al. 1990, Nyhan et al. 1993, Hakonson et al. 1994, Benson and Khire 1995). Capillary barriers are constructed in various forms, ranging from a simple design consisting of two layers to more complex designs that include multiple layers of fine-

---

[1] Asst. Proj. Engineer, GeoSyntec Consultants, Boca Raton, FL 33487 (Miles@GeoSyntec.com)
[2] Assoc. Profs., University of Wisconsin-Madison, Madison, WI 53706 (benson@engr.wisc.edu)

grained and coarse-grained soils (e.g., Stormont 1995). In its basic form, however, a capillary barrier consists of a fine-grained layer overlying a coarse-grained layer (Benson and Khire 1995).

At most water contents, except near saturation, fine-grained soils have higher matric suctions than coarse-grained soils due to their different soil-water characteristic curves. As a result, the apparent hydraulic gradient in a capillary barrier near the fine-grained/coarse-grained interface is normally upward, except when the surface layer becomes nearly saturated. In addition, infiltrated water is stored in the fine-grained surface layer until the matric suction becomes low enough to permit water entry in the coarse-grained layer. Because coarse-grained soils have very low unsaturated hydraulic conductivities at low water contents, the coarse-grained layer impedes flow. These factors constitute the "capillary barrier effect" which restricts percolation. In a system that is approximately one-dimensional, water is stored in the fine-grained layer due to the capillary barrier effect. This stored water is easily removed via evapotranspiration.

Capillary barriers can also be less expensive than resistive barriers because there is no need for moisture-conditioning of the barrier soil. For example, the capillary barrier test section in this study was approximately four times less expensive to construct than the resistive barrier. In addition, capillary barriers are less susceptible to degradation caused by desiccation cracking, because they do not have a wet compacted fine-grained layer. However, capillary barriers do have a unique set of problems, including erosion and biota intrusion of the fine-grained layer and vertical break-through of lateral flows (Khire et al. 1994, Stormont 1995). Nevertheless, the advantages of capillary barriers can be significant for some projects.

TEST SECTIONS

Two test sections were constructed as part of capping activities at the Greater Wenatchee Regional Landfill in East Wenatchee, Washington, USA. East Wenatchee is in central Washington state (236 km east of Seattle). The average annual precipitation is 23 cm, and primarily occurs in late fall and winter as rain or snow. Snowfall typically comprises 30% of annual precipitation.

A schematic of a test section is shown in Fig. 1. One test section is the prescriptive earthen cover for the site. It is a resistive barrier with a 60-cm-thick barrier layer consisting of low plasticity silty clay, covered with a vegetated surface layer consisting of 15 cm of silty soil. The other test section is a capillary barrier. The lower layer of the capillary barrier is a 75-cm-thick medium uniformly graded sand. The surface layer is 15 cm of uncompacted vegetated silt. All soils were obtained on-site. Benson et al. (1994) describe how the test sections were constructed. Both test sections are on a slope of 2.7 horizontal to 1 vertical.
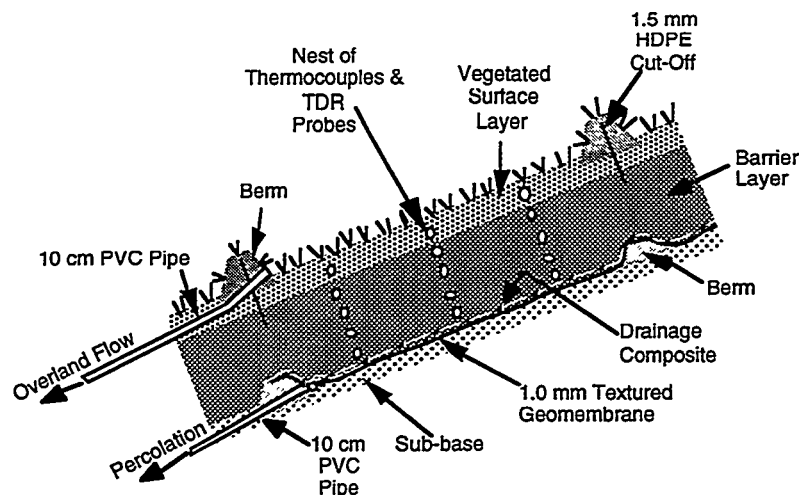
Fig. 1. Schematic of Test Section.

Each test section is 30 m x 30 m, of which a 18.3 m x 12.2 m region is used for monitoring. The test sections are instrumented for continuous monitoring of meteorological data, overland flow, soil water content, and percolation. Percolation is collected using a lysimeter 12.2 m wide x 18.3 m long (Fig. 1) constructed from high density polyethylene geomembrane and a geocomposite drain. Overland flow is collected via diversion berms. Time domain reflectometry (TDR) is used to measure soil water content. A detailed description of the monitoring system is contained in Benson et al. (1994). Soil water storage is computed by integrating soil water contents over the depth of the test sections. Evapotranspiration (E) is computed by subtracting daily overland flow (O), percolation (P_r), and the change in the soil water storage (ΔS) from daily precipitation (P). Lateral flow (L) is assumed zero when computing E. Because the soils have relatively low unsaturated hydraulic conductivities and are saturated only for a small period of time, lateral flow is expected to be less than 0.01% of total precipitation (Khire 1995).

SATURATED AND UNSATURATED HYDRAULIC PROPERTIES OF SOILS

Soil-water Characteristic Curves

Soil-water characteristic curves for the fine-grained cover soils were measured in pressure plate extractors. A hanging column equipped with a Buchner funnel was used for the sand. Only desorption curves were measured. Details of the preparation and testing procedures can be found in Benson et al. (1993). The Haverkamp function (Haverkamp et al. 1977) was fitted through the soil-water characteristic data. The Haverkamp function has the form:

$$\frac{\theta - \theta_r}{\theta_s - \theta_r} = \frac{\alpha}{\alpha + \psi^\beta} \tag{1}$$

where θ is the volumetric water content at matric suction ψ, θ_s is the water content at saturation, θ_r is the residual water content, and α and β are fitting parameters. The fitted functions are shown in Fig. 2, and the fitting parameters are listed in Table 1.
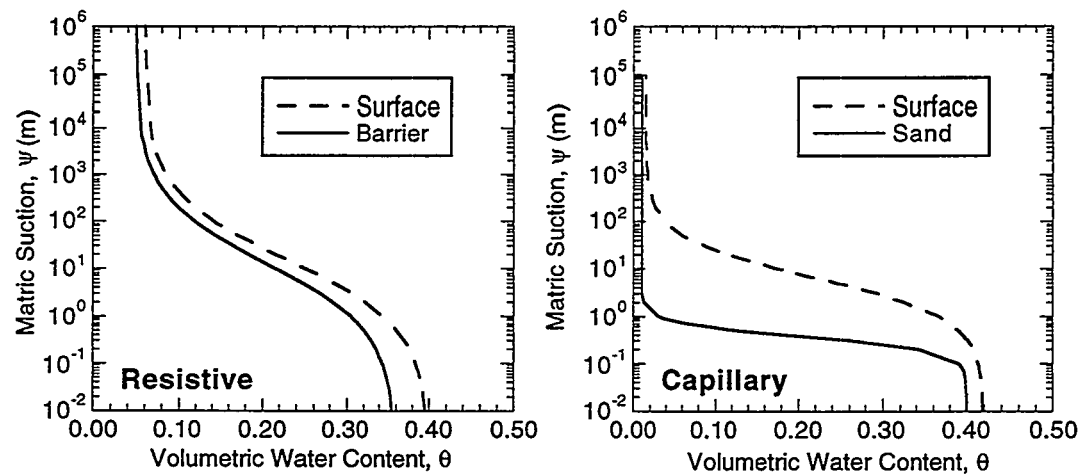
Fig. 2. Soil-Water Characteristic Curves for Resistive and Capillary Barrier Test Sections.

The soil-water characteristic curves for the fine-grained soils from the resistive barrier test section and the surface layer of the capillary barrier test section exhibit a gradual decrease in water content with increasing matric suction, which is expected for fine-grained soils (Hillel 1980). In contrast, water content of the sand from the capillary barrier decreases rapidly for small increases in matric suction due to drainage of large pores (Fig. 2).

Table 1. Haverkamp Fitting Parameters.

| Test Section | Layer | K_s (cm/s) | θ_s | θ_r | Haverkamp Fitting Parameters | | | |
| | | | | | Matric Suction | | Hydraulic Conductivity | |
					α	β (1/cm)	A	B (1/cm)
Resistive	Surface	4.5×10^{-5}	0.40	0.06	80	0.6	300	2.2
Resistive	Barrier	2.2×10^{-7}	0.36	0.05	72	0.6	400	1.3
Capillary	Surface	2.7×10^{-4}	0.42	0.015	650	1.0	90	2.2
Capillary	Sand	2.9×10^{-3}	0.40	0.01	35000	2.9	105	2.9

Hydraulic Conductivities

Saturated hydraulic conductivities (K_s) of the surface layer of both barriers were measured on undisturbed block specimens. Geometric mean hydraulic conductivities for both surface layers are listed in Table 1.

Saturated hydraulic conductivity of the resistive barrier layer was determined both by testing specimens collected in 7.1-cm-diameter thin-wall sampling tubes and by back-calculation from steady percolation during Winter 1993. The hydraulic conductivities obtained using the two methods are essentially the same (Benson et al. 1993). The geometric mean saturated hydraulic conductivity of the specimens is 2.2×10^{-7} cm/s (Table 1). Laboratory tests on re-constituted specimens of the sand yielded a saturated hydraulic conductivity of 2.9×10^{-3} cm/s. Comprehensive details regarding the sampling methods and testing procedures can be found in Benson et al. (1993).

Unsaturated hydraulic conductivity functions (K_ψ) for the surface layers were measured in the laboratory using the instantaneous profile method on block specimens removed from the test sections (Khire et al. 1995). The unsaturated hydraulic conductivity function for the barrier layer of the resistive barrier was measured in the laboratory and field (Meerdink et al. 1996). The unsaturated hydraulic conductivity function for the sand from the capillary barrier was measured in the field using the instantaneous profile method and in the laboratory using a gravity drainage test (Khire 1995). The Haverkamp function was fit through the unsaturated hydraulic conductivity data. The Haverkamp function is:

$$K_\psi = K_s \left(\frac{A}{A + \psi^B} \right) \qquad (2)$$

where A and B are the fitting parameters. Haverkamp fitting parameters for unsaturated hydraulic conductivity are listed in Table 1. The hydraulic conductivity functions are shown in Fig. 3.

The hydraulic conductivity functions for the resistive and capillary barriers exhibit contrasting characteristics. In particular, for matric suctions exceeding approximately 0.5 m, the surface layer of the resistive barrier has lower hydraulic conductivity than the barrier layer. In contrast, for the capillary barrier, the sand layer has lower hydraulic conductivity than the surface layer when the matric suction is greater than 0.5 m. Matric suctions in both test sections are almost always greater than 0.5 m. Consequently, if water infiltrates the surface layer of the resistive barrier, it moves downward into the barrier layer. In the capillary barrier, water that enters the surface layer is impeded at the sand interface due to the low unsaturated hydraulic conductivity of the sand. As a result, water is stored in the surface layer of the capillary barrier, where it can be easily removed via evapotranspiration.

255
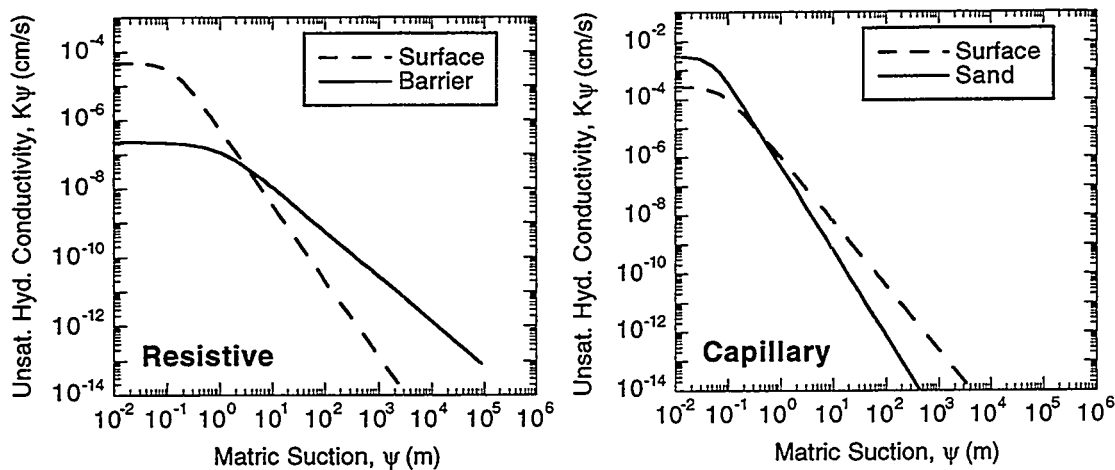
Fig. 3. Unsaturated Hydraulic Conductivity Functions for Resistive and Capillary Barriers.

FIELD WATER BALANCE OBSERVATIONS

Overland Flow

Cumulative overland flow for the resistive and capillary barriers is shown in Fig. 3a. Overland flow is essentially the same for the resistive (12.6% of precipitation) and capillary barriers (11.9% of precipitation). The primary reason for this similarity is believed to be the combined influence of hydraulic conductivity of the surface layer and density of vegetation on both test sections.

The saturated and unsaturated hydraulic conductivities of the surface layer of the capillary barrier are approximately one order of magnitude higher than those for the resistive barrier (Fig. 3). Thus, water should infiltrate more easily in the capillary barrier. However, vegetation on the capillary barrier is less abundant than on the resistive barrier. The percent bare area (area bare of plants/total area) for the capillary barrier is 83%, whereas for the resistive barrier it is 40% (Benson et al. 1993). Dunne and Dietrich (1980) report that the average runoff velocity decreases and the residence time increases as the density of vegetation increases. Consequently, overland flow is lower for slopes having denser vegetation. Apparently the effects of higher hydraulic conductivity and less abundant vegetation for the capillary barrier compensate, and result in essentially the same overland flow as occurs on the resistive barrier. The writers acknowledge, however, that this combined influence is probably coincidental.
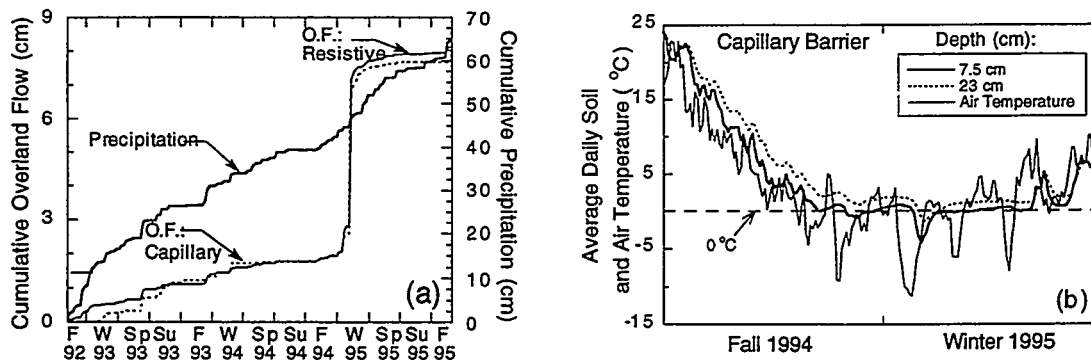
Fig. 3. Overland Flow and Precipitation (a) and Soil and Air Temperature for Capillary Barrier (b).

Overland flow for both test sections was exceptionally high during late Fall 1994 and early Winter 1995. The primary reason for this behavior is that the ground surface was frozen during late Fall 1994 and most of the early part of Winter 1995 (Fig. 3b), which limited infiltration. Thus,

water balance simulations conducted for design of caps should account for freezing of the surface layer, and its effect on overland flow.

Soil Water Content

Volumetric water contents for the resistive and capillary barriers are shown in Fig. 4. For both test sections, the water contents show a periodic behavior. An increase in water content occurs in fall and winter, followed by reductions in spring and summer.

In the resistive barrier, water contents increase gradually at all depths during the winter, and exhibit a time lag with depth corresponding to the slow downward movement of a diffuse wetting front (Fig. 4a). These gradual increases in water content are consistent with the unsaturated hydraulic properties of the soils used to construct the resistive barrier. That is, these soils exhibit gradual changes in water content and hydraulic conductivity as matric suction changes. In addition, because the unsaturated hydraulic conductivity of the barrier layer is greater than that for the surface layer when ψ is greater than 0.6 m, water readily moves from the surface layer into the barrier layer.

Different behavior occurs in the capillary barrier during winter seasons (Fig. 4b). The water content of the surface layer increases gradually as the layer accumulates ("stores") water. The sand, however, remains dry until the surface layer reaches its storage capacity. This behavior is a manifestation of the "capillary barrier effect." After the storage capacity is reached, however, water moves rapidly into the sand, which is reflected by a rapid increase in water content at all depths.
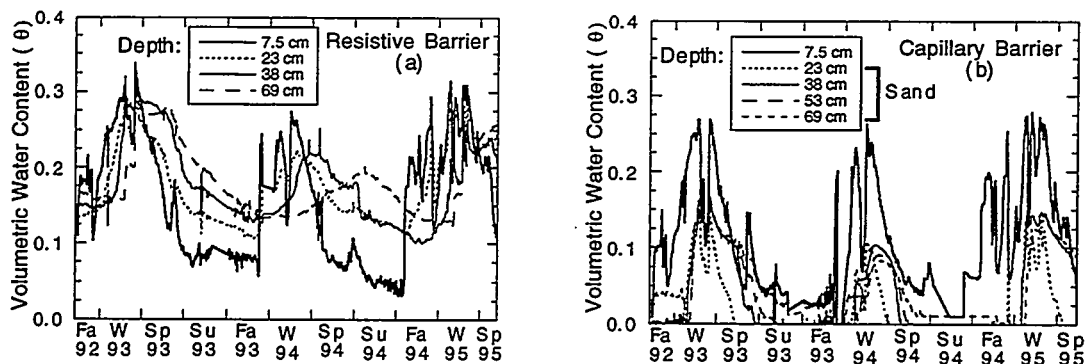
Fig. 4. Soil Water Contents in Resistive (a) and Capillary (b) Barriers.

The data illustrate that the surface layer of a capillary barrier needs to have adequate storage capacity (i.e., a sufficiently thick surface layer) to store water during the severest critical season. Otherwise, breakthrough into the coarse layer will occur, which eventually results in percolation. In Wenatchee, the critical season is winter, when precipitation occurs less intensely, but more frequently and often as snow. Concurrently, evapotranspiration is extremely small. Other seasons may be critical at other sites, but in most cases the critical season corresponds to the period when precipitation is high and evapotranspiration is low. The severest critical season for any site can be determined by evaluating historical meteorological records and performing water balance simulations.

Soil Water Storage and Evapotranspiration

Soil water storage in both test sections shows a periodic behavior that reflects the changes in water content described in the preceding section. An increase in soil water storage occurs in fall and winter, followed by reductions in spring and summer (Fig. 5). At Wenatchee, precipitation is higher in fall and winter, moderate during spring, and fairly low during summer. Conversely, evapotranspiration is low during fall and winter and higher during spring. As a result, soil water storage in the resistive and capillary barriers increases during fall and winter (low

257

evapotranspiration), which is followed by a large decrease in spring and moderate decrease in summer.
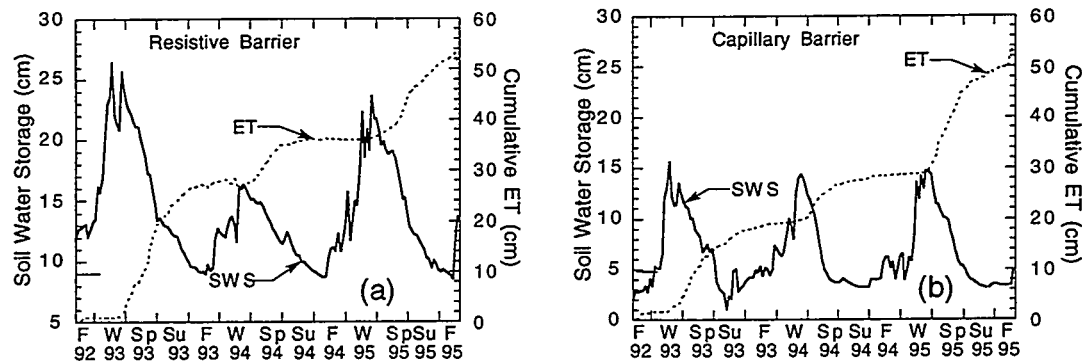
Fig. 5. Soil Water Storage and Evapotranspiration for Resistive (a) and Capillary (b) Barriers.

Soil water storage (S) for the resistive barrier is always higher than that for the capillary barrier, because fine-grained soils retain more water than coarse-grained soils under gravity drainage. In addition, the annual change in soil water storage (ΔS max) is larger for the resistive barrier, primarily because significant changes in water content occur at all depths in the resistive barrier, whereas most storage (and hence any change in storage) in the capillary barrier occurs in the surface layer.

Evapotranspiration is the most significant component of the water balance at this semi-arid site (~80% of precipitation). Evapotranspiration is a function of soil water storage, hydraulic conductivity of the soil, plant transpiration, and energy available to evaporate soil water. Evapotranspiration is low during fall and winter, due to low air temperatures and solar radiation. During spring, as solar radiation and air temperature increase and the growing season begins, evapotranspiration increases rapidly. Evapotranspiration ceases when the water supply in the barrier is exhausted. For example, evapotranspiration persisted into fall in 1993 and 1995 because water was available. In 1994, however, less water was available and evapotranspiration ceased in mid-summer.

A key element of design for either barrier type is ensuring that adequate evapotranspiration will exist to remove water stored during the critical wet period (winter at this site). Adequate evapotranspiration can be achieved by choosing a surface layer having appropriate hydraulic conductivity and thickness. If evapotranspiration is inadequate, water will annually accumulate in the barrier, and percolation will occur (Morris and Stormont 1996). At this site, evapotranspiration was adequate, because soil water storage was reduced to conditions corresponding to residual water content each summer.

Percolation

Percolation for the resistive and capillary barriers is shown in Fig. 6. During the three year monitoring period, the resistive barrier transmitted 3.3 cm of percolation (5.1% of precipitation), whereas the capillary barrier transmitted 0.5 cm of percolation (0.8% of precipitation).

Significant percolation from the capillary barrier occurred only during Winter 1993 when the record snow fall was received. If the surface layer of the capillary barrier had been thicker (i.e., providing additional storage capacity), percolation from the capillary barrier could have been restricted to nearly zero (Khire 1995).

Percolation from the resistive barrier in 1993 and 1994 occurred when the wetting front reached the base of the test section towards the end of winter (Figs. 4, 6). At the end of Winter 1995, however, percolation occurred before the wetting front reached the base (Khire et al.

1997). Percolation also increased dramatically in 1995. The primary reason for this change is new preferential flow through vertical cracks, which apparently formed as the barrier desiccated the previous summer (Benson and Khire 1995, Khire et al. 1997). Animal burrows, found during field reconnaissance in Spring 1995, may also have contributed to the increase in percolation.
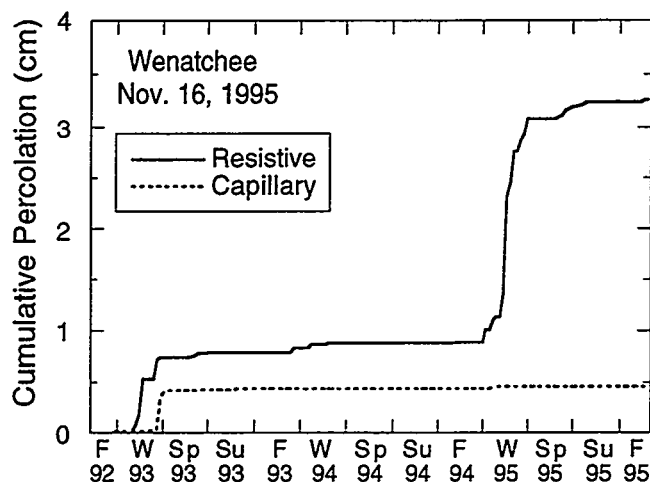
Figure 6. Percolation from the Resistive and Capillary Barriers

SUMMARY AND PRACTICAL IMPLICATIONS

Water balance data have been described in this paper from two test sections representing resistive and capillary barriers. The data show that the capillary barrier effect can be realized at field scale and that capillary barriers can be more effective in restricting percolation in semi-arid and arid climates than prescriptive covers designed as earthen resistive barriers. However, capillary barriers do have a unique set of problems that should be considered during design, including desiccation cracking, biota intrusion, and erosion of the surface layer.

The data also suggest that overland flow is affected by numerous factors, including hydraulic conductivity of the surface layer, density of vegetation, and presence of a frozen surface. Each of these factors should be considered when conducting water balance analyses during design.

Soil water storage capacity of the surface layer also affects the performance of a capillary barrier. A surface layer must be selected such that it has adequate capacity to store infiltrating water during each critical period throughout the design life of the cap. Frequently the critical period occurs when precipitation is more frequent and evapotranspiration is low. However, each site is likely to have a unique critical design period and critical design year. In addition, vegetation must be selected which will yield enough evapotranspiration each year to remove the water stored in the surface layer. Otherwise, water will accumulate and steady percolation will eventually occur. The hydraulic conductivity of the surface layer should be low enough to promote runoff and allow storage of an adequate quantity of water, yet high enough to permit adequate removal of water by evapotranspiration. In addition, vegetation should be selected that is drought-resistant and has a root structure that limits erosion.

ACKNOWLEDGMENT

Pearsall of E. Wenatchee, Washington and Xiaodong Wang of the University of Wisconsin-Madison, who have assisted in construction, instrumentation, and maintenance of the test sections.

REFERENCES

Benson, C., Khire, M., and Bosscher, P. (1993) Final Cover Hydrologic Evaluation, Phase II-Final Report, Environmental Geotechnics Report 93-4, Dept. of Civil and Envr. Eng., Univ. of Wisconsin-Madison.

Benson, C., Bosscher, P., Lane, D., and Pliska, R. (1994) Monitoring System for Hydrologic Evaluation of Landfill Final Covers. *Geotechnical Testing J.*, 17(2), 138-149.

Benson, C. and Khire, M. (1995) Earthen Final Covers for Landfills in Semi-Arid and Arid Climates. *Landfill Closures*, GSP No. 53, ASCE, 201-218.

Daniel, D. (1994) Surface Barriers: Problems, Solutions, and Future Needs. *Proc. 33rd Hanford Symposium on Health and the Environment, In-Situ Remediation: Scientific Basis for Current and Future Technologies*, G. Gee and N. Wing, eds., Pasco, WA, Nov. 7-11, Battelle Press, Columbus, OH, 441-487.

Dunne, T. and Dietrich, W. (1980) Experimental Study of Horton Overland Flow on Tropical Hillslopes II. *Geomorphology Suppl.*, 33, 40-80.

Fayer, M. (1993) Model Assessment of Protective Barriers: Part IV, FY 1992 Work. PNL-8498, UC-902.

Gee, G. and Kirkham, R. (1984) Arid Site Water Balance: Evapotranspiration Modeling and Measurements. Pacific Northwest Laboratory. PNL-5177.

Gee, G., Felmy, D., Ritter, J., Campbell, M., Downs, J., Fayer, M., Kirkham, R., and Link, S. (1993) Field Lysimeter Test Facility Status Report IV: FY 1993. Pacific Northwest Laboratory, PNL-8911, UC-902.

Hakonson, T., Bostick, K., Trulillo, G., Manies, K., Warren, R., Lane, L., Kent, J., and Wilson, W. (1994) Hydrologic Evaluation of Four Landfill Cover Designs at Hill Air Force Base, Utah, Dept. of Energy Mixed Waste Landfill Integrated Demonstration, Sandia National Laboratory, LAUR-93-4469.

Haverkamp, R., Valcin, M., Touma, J., Wierenga, P., and Vauchaud, G. (1977) A Comparison of Numerical Simulation Models for One-Dimensional Infiltration. *Soil Science Society of America J.*, 41, 285-294.

Hillel, D. (1980) *Fundamentals of Soil Physics*, Academic Press.

Khire, M., Benson, C., and Bosscher, P. (1994) Final Cover Hydrologic Evaluation-Phase III. Environmental Geotechnics Report 94-4, Dept. of Civil and Envr. Eng., University of Wisconsin-Madison.

Khire, M. (1995) Field Hydrology and Water Balance Modeling of Final Covers for Waste Containment. Ph.D. Dissertation, University of Wisconsin-Madison.

Khire, M., Meerdink, J., Benson, C., and Bosscher, P. (1995) Unsaturated Hydraulic Conductivity and Water Balance Predictions for Earthen Landfill Final Covers. *Soil Suction Applications in Geotechnical Engineering Practice*, GSP No. 48, ASCE, 38-57.

Khire, M., Benson, C., and Bosscher, P. (1997) Water Balance Modeling of Earthen Final Covers at Humid and Semi-Arid Sites. *J. of Geotechnical Engineering*, in press.

Meerdink, J., Benson, C., and Khire, M. (1996) Unsaturated Hydraulic Conductivity of Two Compacted Barrier Soils. *J. of Geotechnical Engineering*, ASCE, 122(7), 565-576.

Melchior, S., Berger, K., Vielhaber, B., and Miehlich, G. (1994) Multilayered Landfill Covers: Field Data on the Water Balance and Liner Performance. *Proc. 33rd Hanford Symposium on Health and the Environment, In-Situ Remediation: Scientific Basis for Current and Future Technologies*, G. Gee and N. Wing, eds., Pasco, WA, Nov. 7-11, Battelle Press, Columbus, OH, 411-425.

Morris, C. and Stormont, J. (1996) Design of Capillary Barriers for Waste Site Containment, Proc. of the 3rd International Symposium on Environmental Geotechnology, Vol. 1, H-Y Fang and H. Inyang, Eds., 513-522.

Nyhan, J., Hakonson, T., and Drennon, B. (1990) A Water Balance Study of Two Landfill Cover Designs for Semiarid Regions. *J. of Environmental Quality*, 19, 281-288.

Nyhan, J., Langhorst, G., Martin, C., Martinez, J., and Schofield, T. (1993) Hydrologic Studies of Multilayered Landfill Closure of Waste Landfills at Los Alamos. *Proc. of 1993 DOE Environmental Remediation Conference*, Augusta, GA.

Schulz, R., Robert, R., and O'Donnell, E. (1989) Control of Water Infiltration Into Near Surface LLW Disposal Units, Annual Report. US Nuclear Regulatory Commission, NUREG/CR-4918, Vol. 3.

Stormont, J. (1995) The Performance of Two Capillary Barriers During Constant Infiltration. *Landfill Closures*. ASCE GSP No. 53, J. Dunn and U. Singh, Eds., 77-92.

A WATER BALANCE STUDY OF FOUR LANDFILL COVER DESIGNS VARYING IN SLOPE FOR SEMIARID REGIONS

J.W. Nyhan, T.G. Schofield, and J. A. Salazar
Environmental Science Group, Los Alamos National Laboratory, Los Alamos, NM 87544

Abstract
The goal of disposing of radioactive and hazardous waste in shallow landfills is to reduce risk to human health and to the environment by isolating contaminants until they no longer pose a hazard. In order to achieve this, the performance of a landfill cover design without an engineered barrier (Conventional Design) was compared with three designs containing either a hydraulic barrier (EPA Design) or a capillary barrier (Loam and Clay Loam Capillary Barrier Designs). Water balance parameters were measured since 1991 at six-hour intervals for four different landfill cover designs in 1.0- by 10.0-m plots with downhill slopes of 5, 10, 15, and 25%.

Whereas runoff generally accounted for only 2-3% of the precipitation losses on these designs, similar values for evaporation ranged from 86% to 91%, with increased evaporation occurring with increases in slope. Consequently, interflow and seepage usually decreased with increasing slope for each landfill cover design. Seepage consisted of up to 10% of the precipitation on the Conventional Design, whereas the hydraulic barrier in the EPA Design effectively controlled seepage at all slopes, and both of the capillary designs worked effectively to eliminate seepage at the higher slopes.

INTRODUCTION

Institutional control and maintenance of low-level radioactive-waste repositories are expected to cease 100 years after the closure of a waste site. After this time the repository's engineered barriers and geohydrologic conditions need to act passively to isolate the radionuclides for an additional 300 to 500 years (US NRC, 1982). Even though the successful performance of the entire landfill is very much a function of interactive water balance processes (Paige et al., 1996), traditional remedial engineering solutions have ignored these processes, leading to numerous landfill failures (Jacobs et al., 1980; Hakonson et al., 1982). Field water balance data for landfill cover designs do not exist to enable the site operator to adequately define and engineer suitable barriers to prevent the migration of waste materials out of the landfill.

Our approach to developing an effective landfill cover technology is based on the results of ten years of individual shallow land burial studies at Los Alamos and Utah (Abeele, 1986a, 1986b; DePoorter, 1981; Hakonson et al., 1982; Nyhan et al., 1984, 1990a, 1990b). These studies were combined with current European research (Nyhan et al., 1993) to design and emplace the Protective Barrier Landfill Cover Demonstration at the Los Alamos National Laboratory in Los Alamos, New Mexico. The objectives of the present study are: (i) to determine if hydraulic and capillary barriers in three landfill cover designs can change water balance relationships over those observed in landfill covers without engineered barriers; and (ii) to determine how the slope of the landfill cover influences water balance parameters.

MATERIALS AND METHODS
Plot Construction, Design and Rationale
The Protective Barrier Landfill Cover Demonstration was constructed to compare water balance on the conventional landfill cover design, similar to that used in Los Alamos and by the waste management industry for waste disposal (Jacobs et al., 1980), with that on three other designs containing engineered barriers (Fig. 1). The performance of all four designs was evaluated at dominant downhill slopes of 5, 10, 15 and 25% on plots without vegetation. These 16 plots were installed in 1991 in our 8-ha field test facility (DePoorter, 1981) and were instrumented so that a complete accounting of precipitation falling on the plots could be measured. The plots were constructed and instrumented to provide measures of runoff and interflow, as well as seepage and soil water storage as a function of slope length.
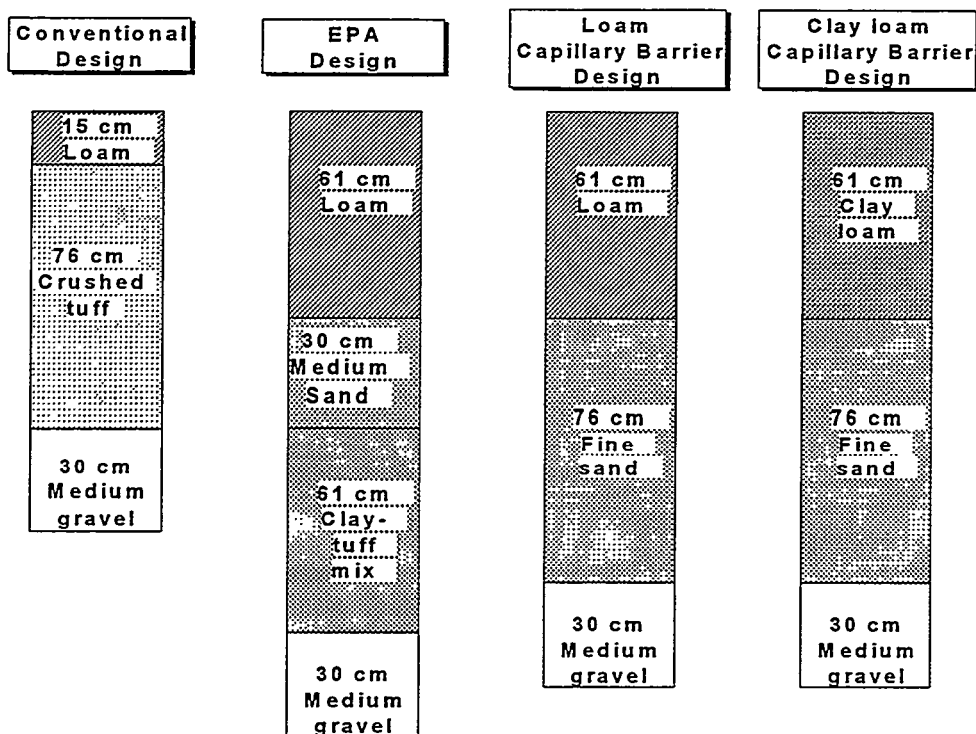
Figure 1. Description of soil layers in the four landfill cover designs at the Protective Barrier Landfill Cover Demonstration. A high conductivity geotextile was installed above the medium gravel layer and the medium sand layer.

The Protective Barrier Landfill Cover Demonstration was emplaced on an east-facing slope similar to the aspect of many of the local landfills where this technology will be applied. The area was surveyed into four pads, each of which received crushed tuff to establish the varying downhill slopes. Four 1.0- by 10.0-m plots were then constructed on each pad (Nyhan et al., 1993). A seepage collection system was installed in the bottom of each of the plots consisting of four metal pans filled with medium gravel (8.0- to 25-mm diam) overlain with a high conductivity MIRAFI geotextile used in previous field studies (Nyhan et al., 1990a); an 11-cm-wide space was left between the sidewalls of the plot and the pan to minimize sidewall effects.

The hydrologic properties of soils used in the field study are presented in Table 1. The soils were analyzed for porosity and for hanging column and thermocouple psychrometric moisture retention characteristics (Klute, 1986). Constant head determinations of saturated hydraulic conductivity were performed as well as pressure plate extractor determinations of moisture retention characteristics (ASTM, 1993). Van Genuchten's RETC code (van Genuchten, 1991) was employed to determine the van Genuchten factors for each soil using analytical procedures described previously (Mualem, 1976; van Genuchten, 1980).

The technology for controlling soil water erosion on all cover designs consisted of applying a 70% ground cover of medium gravel (8.0- to 25-mm diam). The plots with the Conventional Design, similar to that used at Los Alamos waste sites, contained 15 cm of a loam topsoil (Fig. 1) consisting of a 2:1:1 (V:V:V) mixture of an uncharacterized topsoil, sand, and aged sawdust (<9.5-mm diam). This topsoil was not underlain by an engineered barrier, only with 76 cm of crushed tuff (Nyhan et al., 1984, 1990a).

One set of plots contained the EPA-recommended (US EPA, 1989) final cover design (Fig. 1). These plots contained 61 cm of the loam topsoil described previously emplaced on top of 30 cm of a medium sand (0.25 to 0.5-mm diam). The medium sand layer corresponds to the EPA

263

Table 1. Hydrologic properties of soils used in field study as determined with van Genuchten's RETC model (van Genuchten et al., 1991) and laboratory analyses.

| Soil description | van Genuchten factors | | | θ_r | θ_s | Saturated conductivity |
	α	n	m	(cm^3/cm^3)		(cm/s)
Loam topsoil	0.0271	1.539	0.3504	0.0692	0.4209	5.7×10^{-3}
Hackroy clay loam	0.0100	1.548	0.3541	0.0730	0.4839	2.5×10^{-4}
Fine sand (0.05-0.425 mm diam)	.0334	5.472	0.8173	0.0700*	0.4180	1.2×10^{-2}
Medium sand (0.25-0.5 mm diam)	0.0288	3.766	0.7344	0.0376	0.4184	1.3×10^{-1}
Crushed tuff	0.0104	1.707	0.4140	0.0031	0.4079	8.2×10^{-4}
Clay-tuff mix	0.00014	3.992	0.7495	0.0000*	0.4415	6.3×10^{-8}
Medium gravel	-	-	-	-	-	2.0

* Constrained parameter in van Genuchten model.

"drainage layer" and was overlain with the MIRAFI geotextile to provide the EPA-recommended filter layer necessary to prevent fine soil particles from migrating into the drainage layer. The bottom layer in the EPA-recommended final cover, called the "low-permeability layer," usually consists of a 20 mil (0.5 mm) minimum thickness flexible membrane liner (FML) on top of a 60-cm-thick layer of soil with an in-place saturated hydraulic conductivity of $<1 \times 10^{-7}$ cm/s. Since the plastic FML would last less than 35 years (US EPA, 1989), this feature of the EPA design was omitted in our EPA Design. The results of previous research on mixtures of local crushed tuff and sodium-saturated bentonite (Abeele, 1986a, 1986b) indicated that a 1:10 (W:W) dry mixture of finely ground Aquagel (Baroid Drilling Fluids, Farmington, NM) and crushed tuff (called the clay-tuff mixture) should easily provide the low saturated hydraulic conductivity required for this layer (Table 1).

Two designs contained capillary barriers varying only in the type of topsoil (Fig. 1). One of the designs contained 61 cm of the loam topsoil used in the previous designs, whereas the other design contained 61 cm of a Hackroy clay loam classified as a Lithic Aridic Haplustalf (clayey, mixed, mesic family) and used in two previous studies (Nyhan et al., 1984, 1990a). These soils were emplaced on top of 76 cm of a fine sand (0.05-to 0.425-mm diam) made in the sand classifier/blender. The fine sand was specifically chosen to complement the underlying medium-sized gravel in terms of optimizing the relationship between the hydraulic conductivity and the water-holding properties of the capillary barrier (Wohnlich, 1990).

Measurement of Seepage, Interflow, Runoff, and Precipitation
Runoff, precipitation, and seepage were collected year-round from December 1991 through July 1995, as well as interflow (flow occurring along the length of each plot through the medium sand layer in the EPA Design, the fine sand layer in the two designs with capillary barriers, and the crushed tuff layer of the Conventional Design). Water levels in each 100-liter tank used to collect these data were measured with a microprocessor-controlled ultrasonic liquid level sensor (model DCU-7, Lundahl Instruments, Logan, UT) connected to a multiplexed, automated system described previously (Nyhan et al., 1993). The water levels in the tanks were routinely recorded hourly, but much more frequently when the tank was either emptying or when it was nearly full.

Precipitation was measured using a weighing rain gauge and a long-term event recorder.

Measurement of Soil Water Content

Soil water content was routinely monitored once every six hours from December 1991 through July 1995, at each of 212 locations throughout the 16 plots using Time Domain Reflectometry (TDR) techniques with the help of an automated and multiplexed measurement system. Volumetric water content was measured with a pair of stainless steel waveguides (60-cm long, 3-mm diam soil moisture probes; model number 6860, Campbell Scientific, Logan, UT), which are buried parallel and 5 cm apart in the soil and are connected to a 26-m length of RG-8/U coaxial cable. TDR waveguides were emplaced in the Conventional Design at depths of 5-10, 20-80, and 80-86 cm, in the EPA Design at depths of 1-61, 61-91, 96-102, and 92-152 cm, and in the two designs containing capillary barriers at depths of 1-61, 66-126, and 126-132 cm. These TDR waveguides were normally emplaced at downslope locations of 2.63, 4.65, 6.62, and 8.69 m for each soil depth, except at the deepest depths in the Conventional Design and the designs containing the capillary barriers, where they were emplaced at downslope locations of 3.64, 5.66, 7.68 and 9.70 m (to coincide with the bottom end of each of the four seepage pans installed in the bottom of each field plot).

Water Balance Calculations

Daily water balance calculations were performed by determining the daily change in soil water inventory, by summing the daily amounts of precipitation, seepage, interflow, and runoff, and then determining the amount of daily evaporation by difference. As an independent check on these evaporation estimates, evaporation was also estimated from eddy heat flux data collected from a fast-response hygrometer mounted at a height of 12 m on a 92-m meteorological tower at Los Alamos; daily values were estimated from field data collected at 15-minute intervals.

In order to further evaluate the water balance data, daily shortwave radiative energy received by field plots with slopes of 5, 10, 15, and 25% was estimated from pyranometer data collected at a height of 1.2 m from the same meteorological tower described above at the same sampling frequencies. The influences of slope and seasonality of shortwave radiative energy were calculated using the SOLARFLUX model (Rich et al., 1995).

RESULTS AND DISCUSSION

Estimates of Precipitation and Soil Water Inventory

The overall significance of each year's water balance data can best be explained by understanding the spatial and temporal occurrence of precipitation around Los Alamos (Bowen, 1990). Bowen showed that mean annual precipitation is 32.8 cm at White Rock, the only station close to the Protective Barrier Landfill Cover Demonstration with a data base longer than the data collected in this field study. We determined that 2.94-year, 5.56-year, and 20-year events occurred in 1992, 1993, and 1994, respectively.

Soil water inventory data are presented for several layers of the Conventional Design (Fig. 2). The inventory data for the loam topsoil represents the daily average readings of horizontally placed waveguide pairs at a depth of 5 to 10 cm at downslope locations of 2.63, 4.65, 6.62, and 8.69 m. The frequent variations in the TDR measurements at this depth occurred because soil water content usually increased with precipitation events as small as 0.5 cm. Similar data collected at the 15-75 cm depths exhibited less frequent fluctuations because the small precipitation events did not penetrate to the maximum depths over which the measurements were integrated.

Large changes in soil water inventory were observed at both sampling depths in the crushed tuff layer monitored with time in the Conventional Design with the 5% slope (Fig. 2), typical of the changes observed on the three field plots containing this design with larger slopes. The soil water inventories presented for the 15-75 cm depth decrease throughout the summer and fall of

265
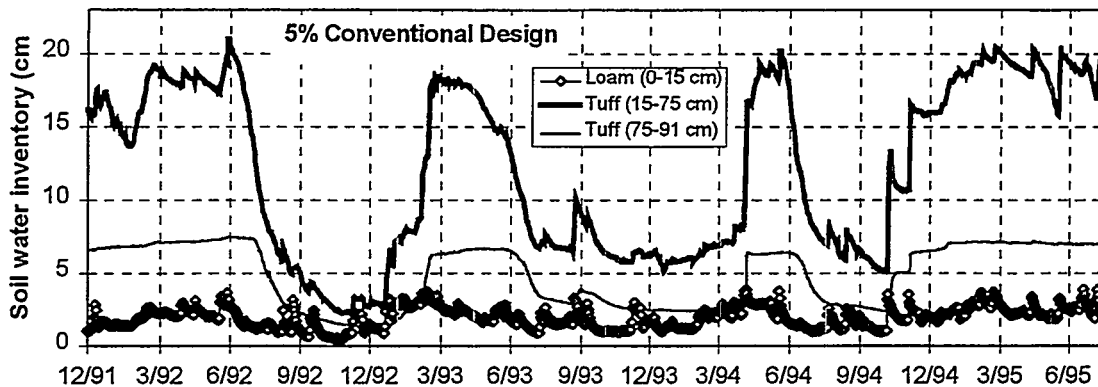
Figure 2. Daily soil water inventory as a function of time for the Conventional Landfill Cover Design with the dominant downhill slope of 5%.

each year and increase during the cooler winter and spring months with snowmelt additions. The data collected at the 75-91 cm depth of the tuff layer (Fig. 2) shows that soil water inventories remained at values greater than 2.9 cm (corresponding to field capacity volumetric water content of 18%) over 69% of the time. Since soil water inventory values greater than 2.9 cm for the tuff correspond to soil water regimes dominated by gravity flow, these time periods represent periods when seepage was observed to occur beneath this lower tuff layer with additions of water from upper layers.

Water Balance Summaries

The most practical comparisons among the four landfill cover designs for a semiarid region, in terms of their usefulness to the burial site operator, should be the overall performance comparison of the water balance parameters for the duration of this field study (Table 2). Using a Two-Factor ANOVA without replication (P <0.05; Steel and Torrie, 1960), there was a significant effect of both landfill cover design and slope on all of the individual water balance parameters listed in Table 2.

As might have been expected in a semiarid environment, 86 to 91% of the precipitation received by all of the landfill cover designs was evaporated from these unvegetated landfill cover designs. Since the soil in the vicinity of the meteorological tower was similar to the Conventional Landfill Cover Design with the 5% slope, we were able to compare the tower hygrometer estimates of water flux with the amounts of evaporation observed in this plot. We discovered that these two estimates agreed quite well: the eddy heat flux data from the meteorological tower (collected from December 1991 through July 1995) amounted to 131.1 cm water, compared with our field plot estimate of 138.9 cm water for the same time period (Table 2). For the years 1992, 1993, and 1994, the meteorological tower estimates were 36.5, 36.2, and 32.7 cm water, respectively, compared with evaporation estimates from the Conventional Landfill Cover Design with the 5% slope of 33.8, 39.6, and 34.7 cm water for the same years.

Evaporation usually increased with increases in slope within each landfill cover design (Table 2) on our east-facing study site, because plots with large slopes intercepted more shortwave radiative energy than plots with smaller slopes (Fig. 3). This effect was dominant during the first and fourth quarters of each year, during times when seepage occurred; i.e., during the fourth quarter of 1993, plots with a 5% slope received 1339 MJ/m^2 shortwave radiative energy compared with the 1561 MJ/m^2 received by the plots with a slope of 25% (Fig. 3). Consequently, the sum of the interflow and seepage usually decreased with increasing slope for each landfill cover design (Table 2).

Evaporation also varied inversely with the ability of each cover design to conduct water into the soil layers in the design (Fig. 1). The smallest amounts of evaporation generally occurred on the

Table 2. Water balance data for all landfill cover designs from December 1, 1991 through July 31, 1995. Total precipitation for this time period was 171 cm.

Landfill cover Design and slope	Water balance parameter (cm)				
	Evaporation	Interflow	Seepage	Runoff	Change in soil water inventory
Conventional Design					
5%	138.9	9.86	17.40	3.04	2.52
10%	143.8	15.12	8.16	3.19	0.45
15%	152.8	10.05	8.60	3.32	-4.57
25%	161.7	6.72	3.09	4.34	-5.69
EPA Design					
5%	154.1	17.07	0.00	1.83	-1.12
10%	154.1	16.02	0.00	1.73	0.00
15%	154.4	15.10	0.00	3.94	-2.23
25%	154.4	12.95	0.00	6.14	-2.27
Loam Capillary Barrier Design					
5%	145.0	14.59	7.62	1.41	2.09
10%	137.9	20.62	3.61	4.75	3.87
15%	150.6	17.85	0.00	3.37	-0.59
25%	155.9	10.69	0.00	5.66	-2.08
Clay loam Capillary Barrier Design					
5%	150.3	10.71	4.84	2.95	2.03
10%	152.5	12.77	0.00	4.44	1.06
15%	156.9	6.83	0.00	6.19	0.21
25%	163.7	1.50	0.00	7.43	-1.39

field plots with the Loam Capillary Barrier Design (Table 2), where water could quickly move through the loam topsoil and the fine sand layers, which had saturated hydraulic conductivities of 0.0057 and 0.012 cm/s, respectively (Table 1). Slightly larger amounts of evaporation occurred on the plots with the Conventional Design than on those with the Loam Capillary Barrier Design, because water had to move through the loam topsoil in the Conventional Design. This water then migrated more slowly through the crushed tuff layer which had a saturated hydraulic conductivity of 0.00082 cm/s (Table 1). The plots with the EPA Design and the Clay Loam Capillary Barrier Design generally had larger amounts of evaporation than the plots with the other designs, because of the low saturated hydraulic conductivities of the clay/tuff mix in the EPA Design and of the clay loam topsoil in the Clay Loam Capillary Barrier Design.

Although runoff did not seem to be related to surface slope on a per event basis. runoff did increase with increasing slope over the 44-month duration of this study for each of the designs. Runoff generally accounted for about 2-3% of the precipitation losses across all of the plots studied (Table 2).

The site operator usually prefers minimal seepage to occur on the landfill. Seepage was definitely decreased with engineered barriers in this study over that observed in the Conventional Design, which did not contain an engineered barrier. Although 9.86 cm of interflow occurred on the Conventional Design with the 5% slope, 17.4 cm of seepage occurred over the life of the field study. The hydraulic barrier in the EPA Design effectively controlled seepage at all slopes, and both of the capillary designs worked effectively to eliminate seepage at the higher slopes
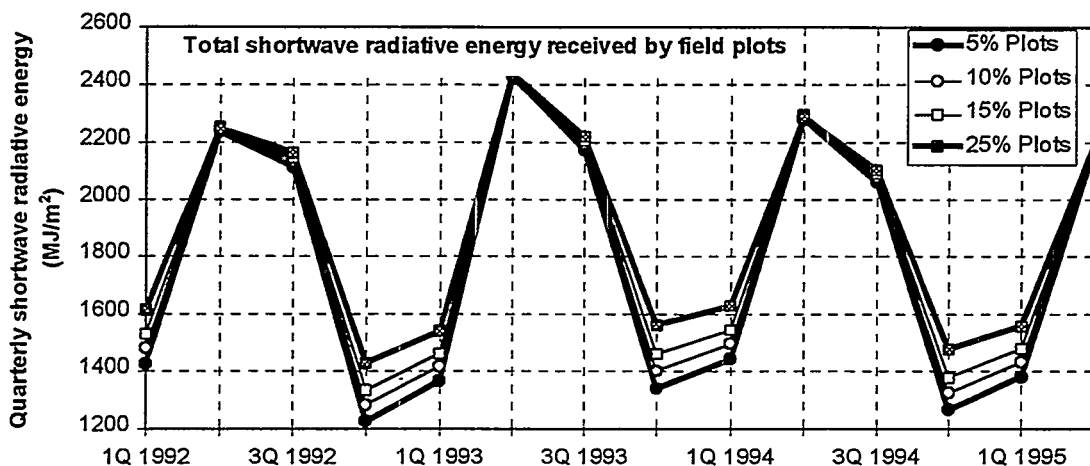
Figure 3. Quarterly total shortwave radiative energy received by field plots with slopes ranging from 5 to 25%. Data were estimated from 15-minute meteorological tower observations that were corrected for slope using the SOLARFLUX model (Rich et al., 1995).

(Table 2), many of which are commonly used on waste sites at Los Alamos and throughout the waste management community.

Current state and federal regulations usually require an engineered barrier to be present in the landfill cover design, a design criterion that is also impacted by risk assessments and cost considerations. Capillary barriers can be used as alternative designs to the EPA Design (US EPA, 1989), with the realization that seepage did occur at 5 and 10% slopes in the Loam Capillary Barrier Design and in the Clay Loam Capillary Barrier Design with a slope of 5% (Table 2). Although the EPA Design does seem to eliminate seepage in field plots with 5 and 10% slopes (Table 2), the EPA design is probably more expensive than alternative designs (Paige et al., 1996). In the case of either engineered barrier, other field data sets similar to that collected in the current study are needed in a variety of climates and with slope lengths longer than 10 m to validate hydrologic models that can be used in design selection.

REFERENCES

Abeele, W. V. (1986a) Consolidation and compaction as a means to prevent settlement of bentonite/sandy silt mixes for use in waste disposal sites. In *Geotechnical and Geohydrological Aspects of Waste Management* (ed A.A. Balkema), pp. 255-264. Rotterdam Press, Boston, MA.

Abeele, W. V. (1986b) The influence of bentonite on the permeability of sandy silts. *Nuclear and Chemical Waste Management*, 6, 81-88.

American Society for Testing and Materials. (1993) Annual book of ASTM standards, Vol. 04.08. ASTM, Philadelphia, PA

Bowen, B.M. (1990) Los Alamos Climatology. Los Alamos Nat. Lab. Rep. LA-11735-MS, Los Alamos, NM.

DePoorter, G. L. (1981) The Los Alamos Experimental Engineered Waste Burial Facility: design considerations and preliminary experimental plan. In *Waste Management '81* (eds. R. G. Post and M. E. Wacks), pp. 667-686, University of Arizona, AR.

Hakonson, T. E., L.J. Lane, J.G. Stegar, and G.L. DePoorter. (1982) Some interactive factors affecting trench cover integrity on low-level waste sites. Technical Report NUREG/CP-0028, Vol. 2, US Nuclear Regulatory Commission, Silver Springs, MD.

Jacobs, D. G., J.S. Epler, and R.R. Rose. (1980) Identification of technical problems encountered in the shallow land burial of low-level radioactive wastes. Oak Ridge Nat. Lab. Rep. ORNL/SUB-80/13619/1, Oak Ridge, TN.

Klute, A. (1986) Methods of soil analysis. Part 1, Second Ed., Am. Soc. of Agronomy, Madison, WI.

Mualem, Y. (1976) A new model for predicting the hydraulic conductivity of unsaturated porous media. *Water Resour. Res.*,12, 513-522.

Nyhan, J. W., G.L. DePoorter, B.J. Drennon, JR. Simanton, and G.R. Foster. (1984) Erosion of earth covers used in shallow land burial at Los Alamos, New Mexico. *J. Environ. Qual.,* 13, 361-366.

Nyhan, J. W., T.E. Hakonson, and B.J. Drennon. (1990a) A water balance study of two landfill cover designs for semiarid regions. *J. Environ. Qual.,*19, 281-288.

Nyhan, J., T. Hakonson, and S. Wohnlich. (1990b) Field experiments to evaluate subsurface water management for landfills in snowmelt-dominated semiarid regions of the USA. In *Contaminated Soil '90* (Eds. F. Arendt, M. Hinsenveld, and W. J. Van der Brink), pp. 1205-1206. Kluwer Academic Publishers, Netherlands.

Nyhan, J. W., G. J. Langhorst, C. E. Martin, J. L. Martinez, and T. G. Schofield. (1993) Field studies of engineered barriers for closure of low level radioactive waste landfills at Los Alamos, New Mexico, USA. Proc. of the 1993 International Conference on Nuclear Waste Management and Environmental Remediation, September 5-11, 1993, Prague, Czechoslovakia, American Society of Mechanical Engineers, Book No. 10354B, 255-266.

Paige, G.B., J.J. Stone, L.J. Lane, D.S. Yakowitz, and T.E. Hakonson. (1996) Evaluation of a prototype decision support system for selecting trench cap designs. J. Environ. Qual., 25, 127-135.

Rich, P.M., W.A. Hetrick, and S.C. Saving. (1995) Modeling topographic influences on solar radiation: a manual for the SOLARFLUX model. Los Alamos Nat. Lab. Rep. LA-12989-M, Los Alamos, NM.

Steel, R.G. and J.H. Torrie. (1960) Principles and procedures of statistics. McGraw-Hill Book Co., Inc., New York, NY.

US Environmental Protection Agency. (1989) Final covers on hazardous waste landfills and surface impoundments. Technical Guidance Document EPA/530-SW-89-047, Washington, DC.

US Nuclear Regulatory Commission. (1982) 10CFR Part 61 licensing requirements for land disposal of radioactive waste. *Federal Register*, 47, 248, 57446-57482.

Van Genuchten, M. Th. (1980) A closed-form equation for predicting the hydraulic conductivity of unsaturated soils. *Soil Sci. Soc. Am. Proc.*, 44, 1072-1081.

Van Genuchten, M. Th., F.J. Leij and S.R. Yates. (1991) The RETC code for quantifying the hydraulic functions of unsaturated soils. US Environ. Protection Agency Rep. EPA/600/2-91/065, Office of Research and Development, Ada, OK.

Wohnlich, S. (1990) CABADIM- a computer model for dimensioning of capillary barriers. In *Contaminated Soil '90* (Eds. F. Arendt, M. Hinsenveld, and W. J. Van der Brink), pp. 429-430. Kluwer Academic Publishers, Netherlands.

THE IMPACT OF A SHALLOW BIOBARRIER ON
WATER RECHARGE PATTERNS IN A SEMI-ARID ENVIRONMENT

John W. Laundré[1]

Abstract

This study attempted to measure the effect of a shallow biobarrier of gravel and cobble on water flow patterns during spring snow melt and recharge. The design consisted of 30 metal culverts 3 m in diameter and 1.6 m long, positioned on end. Test culverts contained 50-cm biobarrier of gravel or cobble and then an additional 50 cm of soil placed above the barrier layer. A neutron probe was used to measure soil moisture above and below the barrier. Measurements were made in the fall and again immediately after snow melt in the spring. During recharge, the biobarriers provided a capillary break which resulted in a pooling of water above the barrier layer. With sufficient snowmelt, the water can penetrate the break and possibly penetrate deeper than in the absence of the barrier layer.

Introduction

Some small mammal species can dig their burrows deep enough to potentially penetrate the protective caps placed on hazardous waste burial areas (Reynolds and Wakkinen 1987, Laundré and Reynolds 1993). The intrusion of burrowing mammals into hazardous waste areas (biointrusion) can lead to subsequent transport of waste off the burial areas (Arthur and Markham 1983) or possible intrusion of water into the waste areas (Laundré 1993). To reduce this biointrusion, attempts have been made to prevent small mammals from burrowing by placing a barrier (biobarrier) within the soil. Typically, this biobarrier consists of a gravel or cobble layer of varying thickness usually placed within less than a meter of the soil surface.

Such a layer establishes a capillary break within the soil that would not exist in the absence of the biobarrier. Capillary breaks can have profound impacts on water movement through the soil profile. These impacts can be especially evident when a pulse of water, typified by heavy rain or spring snowmelt, is added to the soil. In cool semi-arid environments typically there is a large pulse of water added to the soil during spring snowmelt. In these areas, it is unknown whether the presence of a biobarrier would adversely affect the proper function of a protective waste area cap during this time. Consequently, it is important to determine if the attempts to eliminate one compromising factor (small mammal burrows) from a protective cap, inadvertently introduces a second (water intrusion). To this end, a study to investigate the water flow patterns during spring snowmelt above and below a shallow (50 cm) biobarrier layer within a simulated waste cap was initiated.

Methods and Study Area

The experiment was conducted at the Environmental Science and Research Foundation field station on the Idaho National Environmental Laboratory (INEL). The INEL area, located approximately 80 km northwest of Pocatello Idaho, is part of the Great Basin region and is typified by low annual precipitation (20-30 cm) and sagebrush (*Artemisia tridentata*)/grass mixed vegetation. Much of the annual precipitation falls as snow and provides a major recharge pulse of water to the soil during spring snowmelt.

Simulated cap areas consisted of metal culverts 3-m in diameter and 1.6m long positioned on end on local clay loam soil normally used on the burial area of the INEL. The culverts contained a 50-cm biobarrier layer of chipped roofing gravel or 5-10 cm cobble with an additional 50 cm of soil placed above the barrier layer. A cross-section of the design is shown in Fig. 1. Control culverts consisted of 2 m of soil (Fig. 1). All culverts were planted with a sagebrush (*Artemisia tridentata*) and crested wheatgrass (*Agropyron desertorum*) mixture. There were six replicate culverts for the control and 24 replicates for the treatment.

Five neutron probe access tubes were placed in a crossed pattern within the culverts. The tubes extended through the barrier and into the underlying soil. Probe readings were taken every 20 cm in the

---

[1]Department of Biological Sciences, Idaho State University, Pocatello, ID 83209, (208)236-3914, launjohn@fs.isu.edu

tubes. Soil moisture measurements were made in the fall and again immediately after snow melt in the spring. Volumetric moisture content was estimated from neutron probe counts for each 20 cm level of the soil profile. Appropriate 20 cm sample intervals were summed to yield estimates of water amounts in different sections of the soil profile, e.g. above the barrier. Soil water estimates from the fall of one year were subtracted from estimates made the subsequent spring to yield estimates of water added to the various sections of the soil profile.

The amount of water added to the soil profile for the various sample intervals of interest was compared between the control (soil only) and treatment (gravel and cobble) with a t-test design. The null hypothesis tested was no difference in amount water between treatment and control for the desired soil level. The alternate hypothesis was that more water would be present in the treatment levels. Consequently, the $P<0.05$ rejection level used was one-tailed. All statistical tests were conducted with Sigmastat[e] (Jandel Corporation) statistical software.

Results

Water movement patterns above and below the biobarriers were measured during four spring recharge seasons (1992-93 to 1995-96). Winter precipitation (December to February) varied from 4.0 cm to 12.2 cm. In 1995, the INEL received a record 24.7 cm of spring precipitation (March to June).

Soil water content in the upper 50 cm was significantly higher in the culverts with the biobarrier material in 1993 and 1996 (Fig. 2a). There was only sufficient recharge to penetrate beyond 100 cm in the first three seasons (Fig. 2b). Immediately after snow melt (early March) in 1993, moisture levels immediately below the barriers and at the same level in controls were equal. However, deeper in the profile there was more soil water added under the biobarrier layer. Two weeks later water levels in the soil at the level corresponding to 40 cm below the barrier were higher in the control culverts. At the 140- to 180-cm levels, water levels averaged higher below the barriers but the difference was not significant. In 1994, water levels immediately below the barriers were significantly higher than at this level in the controls. For 1995, no water reached the 110-cm level in the controls compared to 0.17 cm at the same depth for biobarrier culverts. In 1996, no water reached depths corresponding to below the biobarrier for treatments or controls. For the post recharge spring precipitation in 1995, there was significantly higher water above the barrier than at the same level in the controls (Fig. 2a). Below the barrier depth, there was significantly more water in the controls (Fig. 2b).

Discussion of Results

Water pooled above the barrier layers, when there was significant amount of winter and spring recharge. This would be predicted based on the impact capillary breaks are known to have on water movement patterns within soils. However, there were two contradicting trends seen at depths below the barrier. Regarding recharge from snow melt, water in culverts containing biobarriers seemed to penetrate more rapidly and deeper into the soil profile than in control culverts. Likely, once water breaches the capillary break, it can move rapidly through the gravel/cobble layer and beyond, as water tension levels are higher in the underlying soil. This pattern is tentative and the opposite is seen when a large amount of water enters the soil in the spring after recharge.

The observed water movement patterns seen have several implications for hazardous waste caps. Regarding spring recharge, the pooling of water above the barrier layer would tend to keep more water in the upper reaches of the soil. This water could be advantageous to enhanced plant growth. There would also be a greater probability of lateral flow of water. The presence of the barrier effectively reduces the water holding capacity of the layer compared to an area without the barrier. Thus, if the capillary layer is breached, water could flow to the waste area more readily than in the absence of the layer.

The volume of water reaching deeper into the soil is variable. For example, in 1994, there was an average of 0.16 cm more water in the soil below the biobarrier than at the same level in control plots. For a square meter area, this equals 1.6 l of water or for a hectare, 16,000 l. In March of 1993, there was 2.9

l/m^2 (29,000 l/h) more water below the barrier. In these cases, the biobarrier may provide a deterrent to burrowing mammals but may increase the risk of water infiltration into a waste area. However, in contrast, for the post recharge season in 1995, there was $29.1/m^2$ (290,000 l/h) more water in the deeper levels in the controls. This reverse pattern in response to the spring precipitation is possibly due to spring plant growth. Once plants start to grow in the spring, they utilize higher amounts of water. It is possible that plants are using the excess water above the barrier rapidly enough to reduce the amount of water reaching the capillary break. In these cases, the capillary break actually can reduce the amount of water reaching deeper into the soil.

Conclusions

The interactions of biobarriers and water flow through the soil is complex. Biobarriers do more than just provide a capillary break to water movement. Factors such as the amount of water recharge and the time of the year it occurs are important. Barriers do retain more water in the upper profile than controls. Consequently, they can have advantages in preventing water from penetrating deeper into the soil, if water levels immediately above the barrier are not high enough to breach it. If biobarriers are used in a waste management situation in semi arid areas, they should be placed deeper into the soil to prevent water from reaching those levels. This deeper placement would provide more water holding capacity above the barrier to contain water above and prevent breaching the capillary break. The recommended depth should contain sufficient soil to hold the maximum precipitation an area may receive. At these levels, the barriers would still function as barriers to mammal burrowing and provide adding protection against water penetration into a waste area. We are currently testing these hypotheses with a design that contains shallow and deeper biobarrier treatments.

Acknowledgments

References

Arthur, W. J. and O.D. Markham. (1983) Small mammal soil burrowing as a radionuclide transport vector at a radioactive waste disposal area in southeastern Idaho. *J. Environ. Qual.*, 12:117-122.

Laundré, J. W. (1993) Effects of small mammal burrows on water infiltration in a cool desert environment. *Oecologia*, 94:43-48.

Laundré. J. W. and T.D. Reynolds. (1993) Effects of soil structure on burrow characteristics of five small mammal species. *Great Basin Nat.*, 53:358-366.

Reynolds, T. D. and W.L. Wakkinen. (1987) Characteristics of the burrows of four species of rodents in undisturbed soils in southeastern Idaho. *Amer. Mid. Nat.*, 118:245-250.

Figure 1. Skematic design (not to scale) of biobarrier test chambers. Each chamber consisted of a metal culvert 3 m diameter and 2.5 m long set on end and filled with test material.

● Native soil
○ Gravel
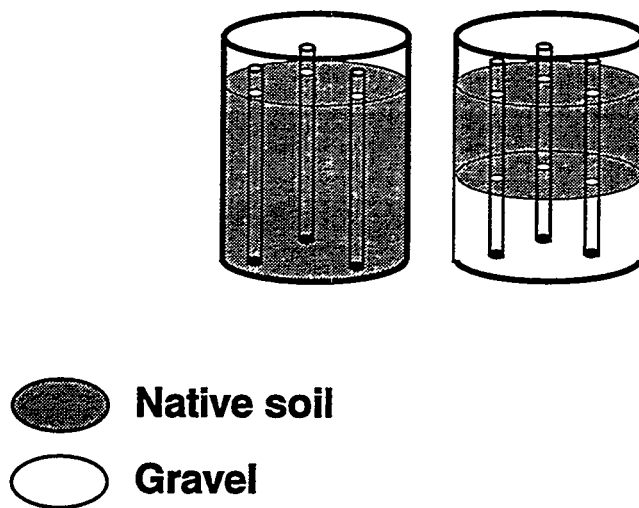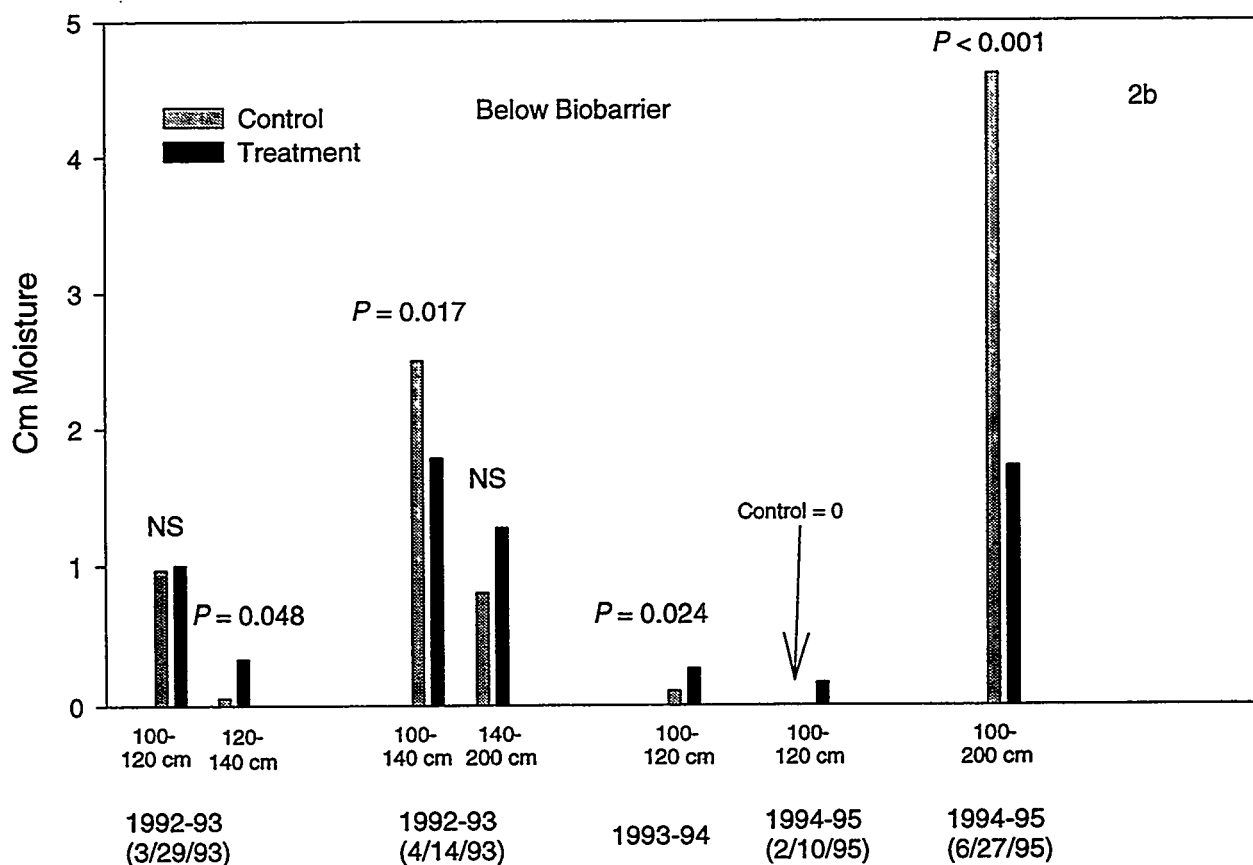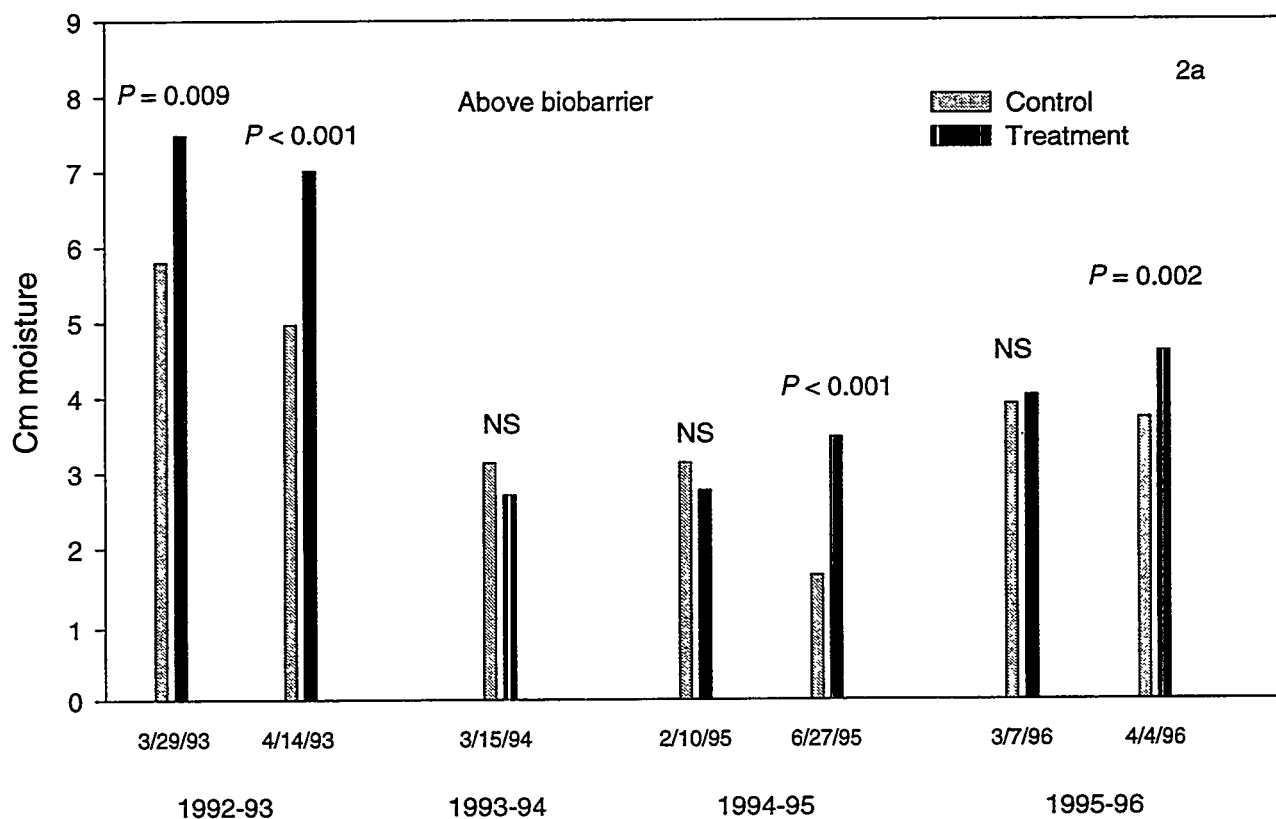
Figure 2. Mean soil moisture measurements for the various sample years and sample intervals.

Numerical Simulations of Capillary Barrier Field Tests

Carl E. Morris[1]
John C. Stormont[2]

Abstract

Numerical simulations of two capillary barrier systems tested in the field were conducted to determine if an unsaturated flow model could accurately represent the observed results. The field data was collected from two 7-m long, 1.2-m thick capillary barriers built on a 10% grade that were being tested to investigate their ability to laterally divert water downslope. One system had a homogeneous fine layer, while the fine soil of the second barrier was layered to increase its ability to laterally divert infiltrating moisture. The barriers were subjected first to constant infiltration while minimizing evaporative losses and then were exposed to ambient conditions. The continuous infiltration period of the field tests for the two barrier systems was modelled to determine the ability of an existing code to accurately represent capillary barrier behavior embodied in these two designs. Differences between the field test and the model data were found, but in general the simulations appeared to adequately reproduce the response of the test systems. Accounting for moisture retention hysteresis in the layered system will potentially lead to more accurate modelling results and is likely to be important when developing reasonable predictions of capillary barrier behavior.

Introduction

Capillary barriers, consisting of fine-over-coarse soil layers, have been suggested as an alternative component for surface cover systems, especially in dry climates (Hakonson et al. 1994; Reed 1989). The contrasting materials of the fine-over-coarse arrangement serve as a barrier to downward flow. Infiltrating water is held in the fine layer by capillary forces and does not move into the coarse layer until the fine soil near the

Figure 1. Schematic of a capillary barrier.

interface approaches saturation. Consequently, a layer of soil underlain by a coarse layer has a greater soil water storage capacity than a simple free-draining system. Soil water is removed from the system by percolation (breakthrough) into the coarse layer or by evaporation and transpiration as shown in Fig. 1. If the fine/coarse interface is sloped, water in the fine layer can also be diverted laterally out of the system under unsaturated conditions, providing another removal mechanism. A capillary barrier acts as a suitable cover system when the transient effects of evapotranspiration, soil water storage and lateral diversion exceed infiltration, thereby keeping the system sufficiently dry so that appreciable breakthrough does not occur.

In order for capillary barriers to be more widely considered as a viable design alternative, engineers need to become more familiar with their performance, and simplified design methodologies need to be developed. An important part of this process is the development and verification of numerical models which can be used to analyze designs. A numerical model

---

[1] Lecturer, Dept. of Civil and Mining Engineering, University of Wollongong, Wollongong, NSW 2522, Australia; rmorris@uow.edu.au

[2] Associate Professor, Department of Civil Engineering, University of New Mexico, Albuquerque, NM 87131, USA; jcstorm@unm.edu

used for design should be capable of reasonably reproducing the response of capillary barriers in field tests.

The focus of this paper is to evaluate the use of a numerical model to simulate the behavior of a pilot scale capillary barrier system. A discussion of several capillary barrier designs is given, along with results of the pilot scale tests. The results of the comparison between the field tests and the numerical modelling results are presented and discussed.

Test Configuration

Two capillary barrier designs were constructed and tested in above grade boxes in 1994-1995 (Stormont, 1996). The boxes were 7.0-m long, 2.0-m wide and 1.2-m high, and were sloped at 10%. Six drains were installed in the bottom of the boxes to collect moisture that percolated into the discrete sections of the test system. Drain 1 collected effluent from the upslope 2 m of the capillary barrier system, drains 2-5 from 1-m segments, and drain 6 collected all water that moved into the last 1 m of the box. The upslope 6 m of the boxes were filled with 250 mm of gravel. The gravel was covered with a local fine-grained soil in one box and with layers of local soil and sand in the second system. An area to collect and drain laterally diverted water was created in the last 1.0 m of the box by completely filling this region with the fine-grained soil. A 170 g/m^2 nonwoven geotextile was placed between the fine and coarse materials to prevent migration of fines into the coarse layer. The geotextile was observed to be hydrophilic, and subsequent tests of similar geotextiles suggests it has a water entry suction of more than 50 mm. The gravel has a water entry suction on the order of 10 mm, and thus it is the gravel, not the geotextile which controls breakthrough.
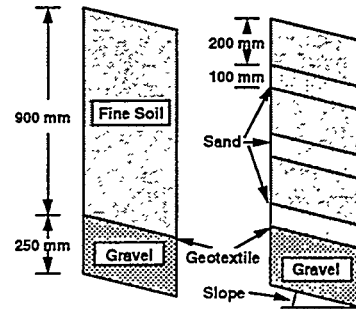
Fig. 2. Profile of system designs.

Profiles of the two designs are shown in Fig. 2. The fine layer of the homogeneous design contained 900 mm of a local, near-surface soil. The second design consisted of alternating layers of 100 mm of a fine-grained sand and 200 mm of the same soil used in the homogeneous system. Initial water content of the soil at the beginning of the tests was between 15 and 18%. The properties of the soils used in the test are given in Table 1. The methods used to derive the data in Table 1 are described in detail in Stormont (1996).

Table 1. van Genuchten (1980) properties for test soils.

	K_{sat} (m/sec)	α (mm^{-1})	n	θ_r	θ_s
soil	1.2x10^{-6}	0.0021	1.87	0.08	0.40
sand	2.1x10^{-4}	0.0039	5.74	0.06	0.39
gravel	0.1	0.493	2.19	0.005	0.42

Lateral Diversion

Capillary barriers can be classified as sloped or non-sloped, depending on the angle of the fine/coarse soil interface. In a non-sloped system, soil water is removed only by evaporation and/or plant transpiration (collectively evapotranspiration, ET) or by percolation (breakthrough) into the underlying coarse layer. If the soil water storage capacity of the fine layer is sufficient to hold the expected infiltration within the ET zone at a particular site, then a non-sloping capillary can provide satisfactory protection against precipitation moving into the underlying waste.

Lateral diversion within a sloped capillary barrier provides an additional means to remove soil moisture from the system. The process is essentially gravity-driven unsaturated drainage within the fine layer. Because the water content of the fine soil increases with depth, lateral diversion is concentrated at the fine/coarse interface where the hydraulic conductivity is the greatest.

276

Laterally diverting water will cause an increase in moisture in the downslope direction, which may result in failure of the barrier. The downslope distance the water can be diverted before breakthrough into the coarse layer occurs is called the diversion length, as shown in Fig. 1.

The simplest capillary barrier design is a homogeneous fine layer of local, near-surface soil over a coarse sand or gravel. In this design, the fine layer of a sloping barrier system serves three main purposes: (1) as a rooting medium for plants; (2) as a soil water storage medium; and (3) as a lateral diversion medium (Stormont, 1996). Field tests and numerical simulations of capillary barriers with homogeneous fine layers indicate that the effective diversion lengths are less than 10 m (Hakonson et al., 1994, Morris and Stormont, 1997). These short diversion lengths are due to the relatively low hydraulic conductivity of the fine soil prior to breakthrough compared to the infiltration rate during stressful periods when the soil is relatively wet (e.g., spring snowmelt). Thus, local soils which are suitable as a rooting and a water storage medium, and are relatively inexpensive, may not be conductive enough to laterally divert substantial amounts of water downslope and out of the system. (I.e., their diversion lengths are expected to be short.)

The diversion capacity can be increased by utilizing unsaturated drainage layers within the fine layer (Stormont, 1995, Morris and Stormont, 1997). Unsaturated drainage layers are one or more relatively conductive layers which drain water laterally within the fine soil while remaining unsaturated. Because soil water tends to accumulate near the fine/coarse interface and unsaturated conductivity increases with water content, a transport layer at the interface will be most effective in removing water from the system through lateral diversion. The two upper unsaturated drainage layers in Fig. 1 provided little lateral diversion since no capillary break was present below them.

This concept of using unsaturated drainage layers was incorporated into one of the pilot scale tests conducted by Stormont (1996) with performance compared to a simple sloping capillary barrier system. Measurements were made of water storage and lateral diversion in the fine soil, and breakthrough into the coarse layer. The systems were initially subjected to a period of constant infiltration and then were exposed to nearly 200 days of ambient climatic conditions.

Pilot-Scale Tests

The covered barriers were subjected to a period of constant infiltration which consisted of adding 130 liters of water to the top of each system over a period of 6 hours daily. The water was evenly distributed over the entire 7-m length, which corresponded to 9.5 mm of precipitation. After 26 days, the response of the layered design approached steady-state and infiltration was halted. Water was added to the homogeneous system for a total of 43 days which was followed by an additional 16 days of monitoring of both tests. The covers were removed from both test plots and the barriers were subjected to ambient conditions for 193 additional days. During the period that the barriers were exposed to ambient conditions, 63 mm of precipitation fell. Though the response to ambient conditions was modelled numerically in this project it is not discussed due to space limitations.

The Model

The numerical simulations of the pilot scale tests were performed using the TRACR3D code developed at Los Alamos National Laboratory. TRACR3D is a finite-differences based code that is capable of simulating transient, 3-dimensional flow in saturated and unsaturated porous media. The model solves Richard's equation using van Genuchten's (1980) constitutive equations for determining the relationships between soil moisture content, matric potential and hydraulic conductivity (Travis and Birdsell, 1991). Upstream weighting of permeability is used in the model to provide robustness under transient conditions, however it may allow more leakage across the interface than actually occurs.

The numerical model used in the study consisted of a grid that was 115 cells in depth, 1 cell wide and 70 cells long. The vertical and horizontal components of the gravity vector were modified to provide the 10 % slope required to simulate the field tests. Water was added to the system over a 6-hour period by designating the top layer of cells as prescribed flow cells. No flow boundaries were set for the top and sides of the model, while the bottom boundary maintained the initial condition of 1% saturation. Flow into the bottom cells of the model was recorded and was considered to be equivalent to the moisture collected from the drains of the field systems. The geotextile layer was not included in the numerical model and no calibration was attempted.

Field Test Results

Homogenous Capillary Barrier

The results of the constant infiltration portion of the test of the homogeneous capillary barrier are given in Fig. 3. The data plotted in the figure is the normalized quantity of water produced from each drain over the test period. The data was normalized by taking the total volume of water produced for each drain and dividing it by the total surface area of the box (7 m by 2 m) (Stormont, 1996). As shown in Fig. 3, all drains produced water, indicating that the capillary barrier failed over its entire 6 m length.

Fig. 3. Water collected from homogeneous capillary barrier field test (from Stormont, 1996).

There was some lateral diversion in the system, but it was less than 2 m, as breakthrough occurred within the first collection cell which was 2 m in length.

Breakthrough first occurred in drain 6 on day 14, and was followed by drain 5 and then the remaining drains. By day 22, all drains were producing water, indicating that failure had occurred along the entire capillary barrier. Drain 6 produced the most water from the system, with the quantity being more than that attributable solely to the infiltration occurring immediately above the collection area (15 mm/day), which suggests that some lateral diversion was taking place. In addition, drain 5 produced more water than drains 1 through 4, further suggesting that some downdip water movement occurred within the fine layer (Stormont, 1996).

When addition of water to the barrier ceased (day 43), water production from drains 1-5 decreased rapidly and approached zero within a few days. However, drain 6 continued to produce water at a decreasing rate, as some lateral diversion of moisture from upslope was probably occurring and no capillary barrier was present to stop the downward flow.

In addition to monitoring the amount of drainage from each system, soil moisture content measurements were made throughout the test period. These data showed that when water was initially added to the barriers, an increase in soil moisture content took place until breakthrough occurred and effluent was being produced. Fig. 4 shows the moisture distribution on day 21 of the test. Even though extensive measurements were made
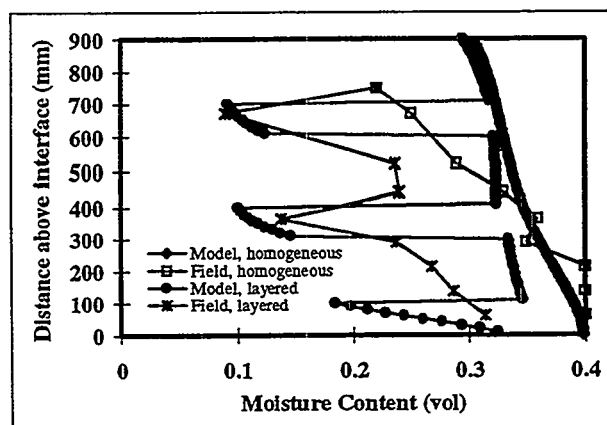
Fig. 4. Soil moisture contents for field and model tests after 21 days (field data from Stormont ,1996).

278

on the system, about 25% of the added water is not reflected in either increased moisture content or effluent production. The source of this error is unknown, but some may be attributable to evaporative losses and problems with the effluent collection system (Stormont, 1996).

Layered Capillary Barrier

The response of the layered capillary barrier system to constant infiltration was markedly different than that of the homogeneous system as shown in Fig. 5. All water was laterally diverted to drain 6 in the system, meaning that the capillary barrier did not fail as no water was collected in drains 1-5. Therefore, the addition of the sand layers into the system increased the lateral diversion distance to at least 6 m. Once infiltration was stopped on day 26, the rate at which water drained from the system decreased rapidly and approached zero by day 50.

Moisture contents were measured to determine the distribution of water in the system for comparison with the homogenous barrier. Fig. 4 shows the moisture distribution within the layered barrier on day 21 of the tests. The upper two sand layers had a lower moisture content than the surrounding fine soil, while the bottom sand layer had a higher average content.

Fig. 5. Water collected from layered capillary barrier for field and model tests (field data from Stormont, 1996).

Fig. 6. Drain outputs from the homogeneous capillary barrier model test.

Numerical Model Results

Homogeneous Barrier

The numerical modelling results for the homogeneous capillary barrier that are comparable to Fig. 3 are presented in Fig. 6. The results shown in Fig. 6 are comparable to the field test data in all but two areas. The shape and the amplitude of the curves are very similar, as are the times at which the effluent begins to flow and diminishes to zero. However, the amount of effluent produced by drain 1 in the model is much greater than that measured in the field, and conversely, the model significantly underpredicts flow from drain 5. The numerical modelling results also tend to be much smoother than the field test data and do not show the sudden decrease in output at day 41 that occurred in all drains. However, the numerical results do show oscillations in drain output that seem to correspond to similar trends in the field test data. The total effluent produced by the homogeneous field barrier was approximately 175 mm versus approximately 300 mm from the numerical model of the same system. However, about 25% of the water added to the field test system was not accounted for and, thus, may explain the difference.

Moisture contents of the homogeneous numerical model and the field test at day 21 are shown in Fig. 4. The field test data is a vertical profile from the middle of the box which was seen to be representative as there was little variation in the profile along the length of the barrier (Stormont, 1996). The numerical data is a vertical profile in the same region, with data from each cell being plotted. There is a definite difference in the soil moisture profile, but there is little difference in the overall average soil moisture content (33 % for the field test, 35 % for the numerical simulation).
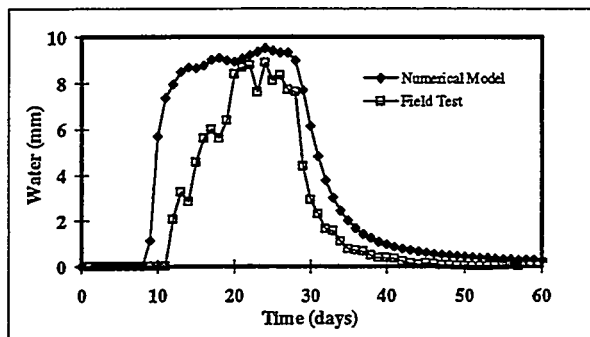
279
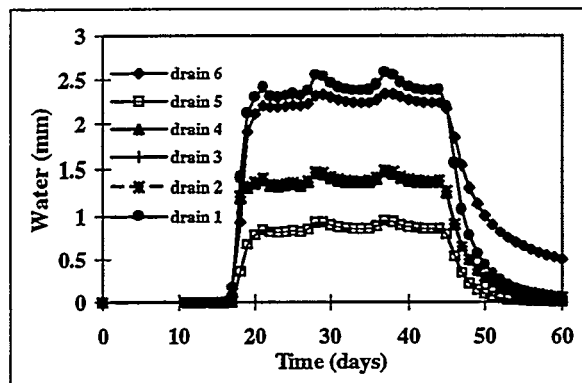
The moisture content measurements were problematic throughout the field tests and, therefore, may not accurately represent the actual soil conditions. This would account for the differences between the observed and simulated values.

<u>Layered Barrier</u>

The numerical model response to the layered capillary barrier also proved to be good as shown in Fig. 5. Like the field test, breakthrough occurred only in drain 6 due to the addition of the lateral diversion layers which increased the diversion length to greater than 6 m. The shape, magnitude and timing of the numerical data was similar to the field data, indicating that the model can effectively represent a layered capillary barrier system.

Soil moisture content distribution for the numerical model and the field test is shown in Fig. 4 for day 21. The soil moisture distribution is considerably different for the two systems, but this is not surprising due to the limits of the field measuring equipment. The major difference between the two data sets is in the fine soil moisture content, with the model giving much higher results. The moisture contents of the sand layers are very similar, providing some confidence in the numerical modelling data. Again, no water balance was conducted on the numerical model since mass balance must be satisfied by the code. However, it should be noted that the numerical model produced approximately 210 mm of effluent versus 150 mm for the layered field test.

Discussion

The difference between the numerical modelling data and the field test data is in most cases likely due to differences between the physical and the TRACR3D models. Soil properties used in the numerical model were based on values measured in the lab that were supposed to mirror conditions found in the field tests. However, it is difficult to obtain uniform, homogeneous placement and compaction of soils in the field. Differences in soil properties and actual thicknesses could affect when breakthrough commences, explaining why the numerical model of the layered system produced effluent 3 days before the field model. This could also be explained by the fact that the numerical model had no losses in the drainage collection system and no water was lost in wetting the coarse layer and drainage system components. In contrast, the numerical model of the homogeneous system takes longer to produce effluent, which could be attributed to higher than lab-measured hydraulic conductivities in the field. In addition, the model does not account for the geosynthetic layer in the field system, the effects of which are unknown.

An additional item that is not addressed that affects the results of the layered tests is the hysteresis of unsaturated flow in the lateral diversion layer (sand). The unsaturated flow characteristics of the sand are based on data from a drying curve which can differ significantly from a wetting curve. Generally, the conductivity for a given moisture content on a drying curve is greater than on a wetting curve. Using the drying curve likely leads to greater effluent production which may be why the model effluent production is greater and starts earlier than the field test. Though not shown in this paper, effluent production is strongly affected by changes in the characteristics of the lateral diversion layer. Work is presently underway to obtain a wetting curve for the sand layer for testing in the numerical model.

One discrepancy between the field test and numerical data that is not readily explained is the low effluent production from drain 5 in the homogeneous model. In the model, there is large lateral flow at the downslope end of drain 5 which causes significant amounts of moisture to flow into drain 6. Water appears to be drawn into the drain 6 area rather than flowing into the underlying coarse layer. This horizontal flow can be reduced by placing a no-flow boundary 200-mm high at the interface at the drain 5-drain 6 boundary. This reduces the flow into drain 6 and increases the flow into drain 5, but does not change the overall effluent production. The reason for this discrepancy requires further investigation.

The drain 1 effluent production for the homogeneous numerical model is much higher than that of the field test data, and produces the most water. Several possible explanations can be suggested for this significant difference, such as the lack of homogeneity in the drain 1 region of the field barrier which causes significant lateral diversion, lateral diversion out of the drain 1 region, and problems with the drain 1 collection system. Some problems with the collection system were encountered, but the difference between the field and model data cannot be directly attributable to drainage difficulties. However, it is reasonable that drain 1 produces more effluent since it services an area twice the size of the other drains.

The soil moisture content profiles determined by the model are significantly different from those measured in the field, but these differences may be attributable to a lack of homogeneity in the field tests, evaporation from the surface, time of measurements, the field measurements, and some problems with the FDR access tubes. The probe used to measure moisture content senses a volume of soil around the probe and reports an average value for that volume. This may have led to inaccurate values, especially for the layered system and near the surface. Additionally, differences could be attributable to evaporation from the surface of the field system, creating a different gradient. Also, the time at which the measurements were made compared to when water was added to the system may influence the near surface soil moisture contents. On the other hand, the numerical solution does not account for hysteresis, which could be significantly affecting the magnitude of the soil water content. The current model does not account for this hysteresis and therefore its affect is unknown.

In summary, it appears that a finite difference code (TRACR3D) can be used to simulate water movement within a capillary barrier system reasonably accurately, including the layered system with increased lateral diversion. However, since the comparisons in this paper are limited, additional modelling of field systems needs to be performed in order to better determine the accuracy and limitations of the model before it can be applied in practice.

Acknowledgment

References

Hakonson, T.E., Bostick, K.V., Trujillo, G., Manies, Warren, Lane, Kent and Wilson (1994) Hydrologic Evaluation of Four Landfill Cover Designs at Hill Air Force Base, Utah. Los Alamos National Laboratory report *LAUR-93-4469*.

Morris, C.E., Stormont, J.C. (1997) Capillary Barriers and Conventional Surface Covers: Estimating Equivalency. *Journal of Environmental Engineering,* 123(1), 3-10.

Reed, J.E. (1989) Some Preliminary Model Studies of Capillary Barriers. *US Geological Circ 1036,* 61-72.

Stormont, J.C., (1996) The effectiveness of two capillary barriers on a 10% slope. *Geotechnical and Geological Engineering,* 14, 243-267.

Stormont, J.C., (1995), The performance of Two Capillary Barriers During Constant Infiltration, *Landfill Closures, Geotechnical Special Publication No. 53,* Dunn and Singh, Eds., 77-92.

Travis, B.J., and Birdsell, K.H. (1991). "TRACR3D: A Model of Flow and Transport in Porous Media." Los Alamos National Laboratories LA-11798-M (UC-814), Los Alamos, NM.

van Genuchten, M. Th. (1980) A closed-form equation for predicting hydraulic conductivity of unsaturated soils. *Soil Sci Soc Am. J.,* 892-898.

The Effects of Heterogeneities on the Performance of Capillary Barriers for Waste Isolation

Clifford K. Ho and Stephen W. Webb[1]

Abstract

The effects of heterogeneities on the performance of capillary barriers is investigated by simulating three systems comprised of a fine soil layer overlying a coarse gravel layer with 1) homogeneous, 2) layered heterogeneous, and 3) random heterogeneous property fields. The amount of lateral diversion above the coarse layer under steady-state infiltration conditions is compared between the simulations. Results indicate that the performance of capillary barriers may be significantly influenced by the spatial variability of the properties. The layered heterogeneous system performed best as a result of horizontal features within the fine layer that acted as additional local capillary barriers that delayed breakthrough into the coarse layer. The random heterogeneous system performed worst because of channeled flow that produced localized regions of water breakthrough into the coarse layer. These results indicate that engineered capillary barriers may be improved through emplacement and packing methods that induce a layered system similar to the layered heterogeneous field simulated in this study.

Introduction

Engineered and natural capillary barriers in the subsurface have been suggested as an effective means of diverting water away from buried waste. These capillary barriers generally consist of two or more interspersed layers of fine and coarse porous materials (such as sand or soil). Because the fine layer consists of larger capillary pressures relative to the coarse layer in unsaturated conditions, downward flowing water can be held in fine layers overlying coarse layers. If the layers are tilted, water can be diverted down-dip along the interface of the two layers. This phenomenon has applications and significant impacts in fields including nuclear waste management (Prindle and Hopkins, 1990; Ross, 1990; Wilson, 1996), landfill cover design (Morris and Stormont, 1996; Webb et al., 1997), and soil remediation (Ho and Udell, 1992).

Unfortunately, nearly all of the predictive models that have been used to assess the performance of capillary barriers have assumed that the regions comprising the fine and coarse layers are homogeneous (Ross, 1990; Prindle and Hopkins, 1990; Oldenburg and Pruess, 1993; Wilson, 1996; Webb, 1996; Webb, 1997). The assumption of homogeneous materials allows uniform, smooth interfaces between the fine and coarse layers, which may over-predict the diversion capacity of actual heterogeneous systems. Homogeneous models also neglect small scale behavior caused by heterogeneities within each layer that may positively or negatively impact the performance of capillary barriers. Therefore, this paper presents a study of the impact of intra-unit heterogeneity on the performance of capillary barriers. Three simulations are presented that include homogeneous, layered heterogeneous, and random heterogeneous representations of a system comprised of a fine soil layer overlying a coarse gravel layer. Comparisons are made between the simulations, and conclusions regarding the effects of heterogeneities are drawn based on the findings.

Numerical Approach

The computational domain is two-dimensional and consists of a fine layer of soil (1 m high x 6 m wide) overlying a coarse layer of gravel (0.3 m high x 6 m wide) as shown in Figure 1. The

[1]Both authors at Sandia National Laboratories, P.O. Box 5800, MS-1324, Albuquerque, NM 87185-1324, (505) 848-0712, ckho@nwer.sandia.gov.
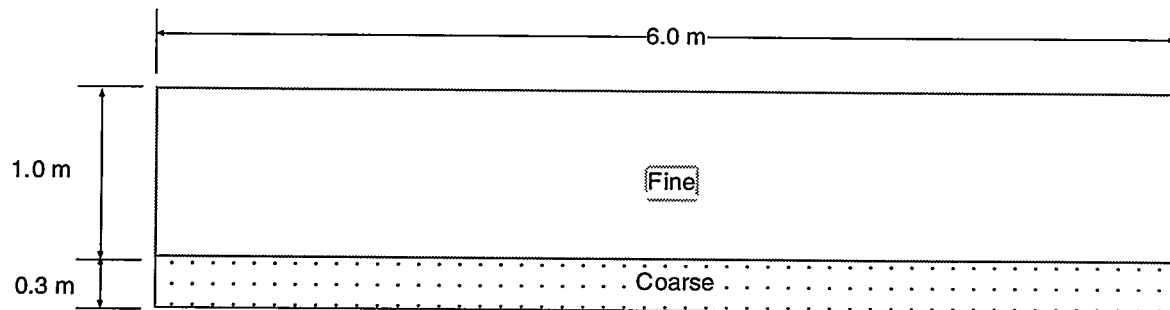
Figure 1. Computational domain used in TOUGH2 (Pruess, 1991) simulations. The domain consists of 150 columns and 65 rows of equally spaced elements (9750 total elements). Each element is 0.04 m wide x 0.02 m high. The bottom coarse layer consists of 15 rows, and the top fine layer consists of 50 rows. The entire domain is tilted 5 degrees clockwise.

domain is discretized into 9750 equally spaced elements that are each 0.02 m high x 0.04 m wide. Boundary conditions include infiltration within each element along the top row at a steady rate of 4.62×10^{-7} kg/sec (1 mm/day), no-flow lateral boundaries, and a saturated boundary that is connected to the ten right-most elements in the bottom row to allow outflow of water. The entire domain is tilted 5 degrees clockwise by rotating the gravity vector in the simulations. The numerical code TOUGH2 (Pruess, 1991) is used to simulate the water movement in the unsaturated domains. TOUGH2 has been validated in numerous studies (Pruess, 1995) and can simulate multiphase transport of air, water, and heat in porous media. In the current studies, the gas phase is passive with a constant temperature and pressure (20°C, 1 bar). Only the transport of liquid water is investigated using the TOUGH2 equation of state module EOS 9.

The properties of the domain are taken from two sources: an internal Sandia report[2] of typical soils and gravel in Albuquerque, NM, and a paper describing capillary barrier experiments performed at Sandia (Stormont, 1995). The means, μ, and standard deviations, σ, of four properties (in natural log space) are listed in Table 1 along with the expected mean value, E, in real space. The four properties that are allowed to vary in the simulations include the saturated conductivity, Ksat (cm/sec), the van Genuchten curve-fitting parameters for capillary pressure and relative permeability, α and β, and the residual liquid saturation, Sr. For the homogeneous simulations, the expected values, E, are used for the fine and coarse layers. For the heterogeneous simulations, unconditioned sequential Gaussian simulations are performed using GSLIB (Deutsch and Journel, 1992) with subsequent standardization to obtain a standard normal distribution of values for all the elements in the domain. Exponential semivariogram models are used with different ranges and anisotropy factors to produce two distinct fields (Figure 2): 1) a layered heterogeneous field and 2) a random heterogeneous field. The layered heterogeneous field displays horizontal features, while the random heterogeneous field contains a "salt and pepper" distribution. The means and standard deviations in Table 1 are then used to map the standardized variables, Z, in Figure 2 to corresponding properties, X, for the fine and coarse layers of the computational domain using the following transformation:

$$X = \sigma Z + \mu \qquad (1)$$

Because the mean, μ, and standard deviation, σ, are in natural log space, the real space property values are found by taking the exponent of the property values, X, given in equation (1).

---

[2]McTigue, D.F., Moisture Retention Properties of Soils from the Chemical Waste Landfill, Sandia National Laboratories, Albuquerque, NM, internal Sandia Letter Report dated 12/9/94.

Table 1. Parameters used in the simulation of homogeneous and heterogeneous property fields. E is the expected value in real space and μ and σ are the mean and standard deviation in natural log space.

	(Fine Layer)			(Coarse Layer)		
	$E^{\dagger}$	μ	σ	$E^{\dagger}$	μ	σ
porosity	0.4	—	—	0.42	—	—
Ksat (cm/sec)	1.43×10^{-4}	-9.10	0.700	10	2.30	6.99×10^{-2}
α (1/cm)	0.021	-4.24	0.864	4.9	1.59	4.52×10^{-3}
β	1.87	0.609	0.184	2.19	0.772	0.157
Sr	0.21	-1.63	0.198	0.012	-5.67	1.58

$^{\dagger}E = \exp(\mu + \sigma^2/2)$

Numerical Results and Discussion

Steady-state liquid saturations and mass flow vectors for each of the three simulations are shown in Figure 3. Recall that the infiltration along the top row of elements is constant and that the domain is tilted 5 degrees clockwise. Also, it is worth noting that the criterion for steady-state conditions is that the mass flow exiting the bottom right corner, which is connected to a saturated boundary, must equal the total mass flow entering the system from infiltration.

The resulting saturation profiles and mass flow vectors are very distinct for the different fields. The homogeneous field (Figure 3(a)) displays a fairly uniform saturation distribution in the fine
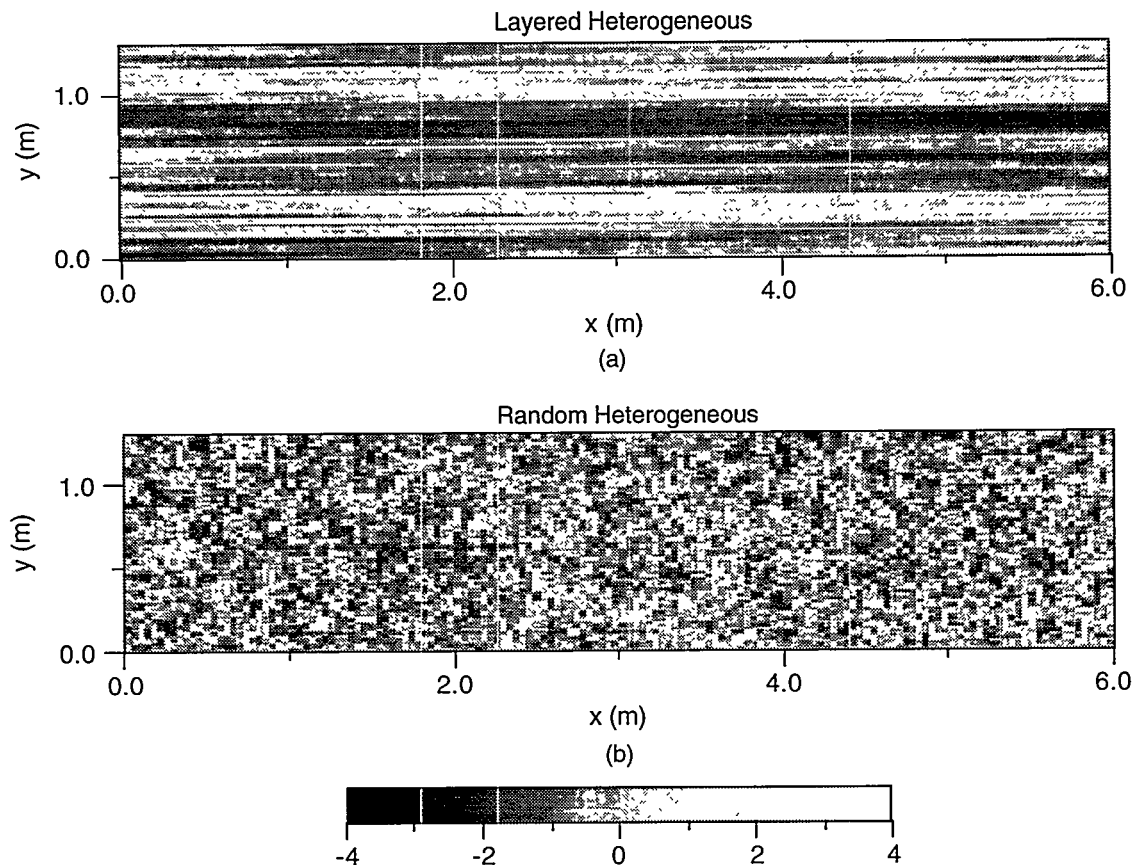
Figure 2. Unconditioned normalized sequential Gaussian simulations using GSLIB (Deutsch and Journel, 1992) with an exponential semivariogram model (seed=1711) and the following range coefficients: a) a=1.0 m and b) a=0.03 m (effective range=3a). The layered heterogeneous simulation was created using an anisotropy factor of 100:1 in the x-direction (anis1=100, anis2=1).
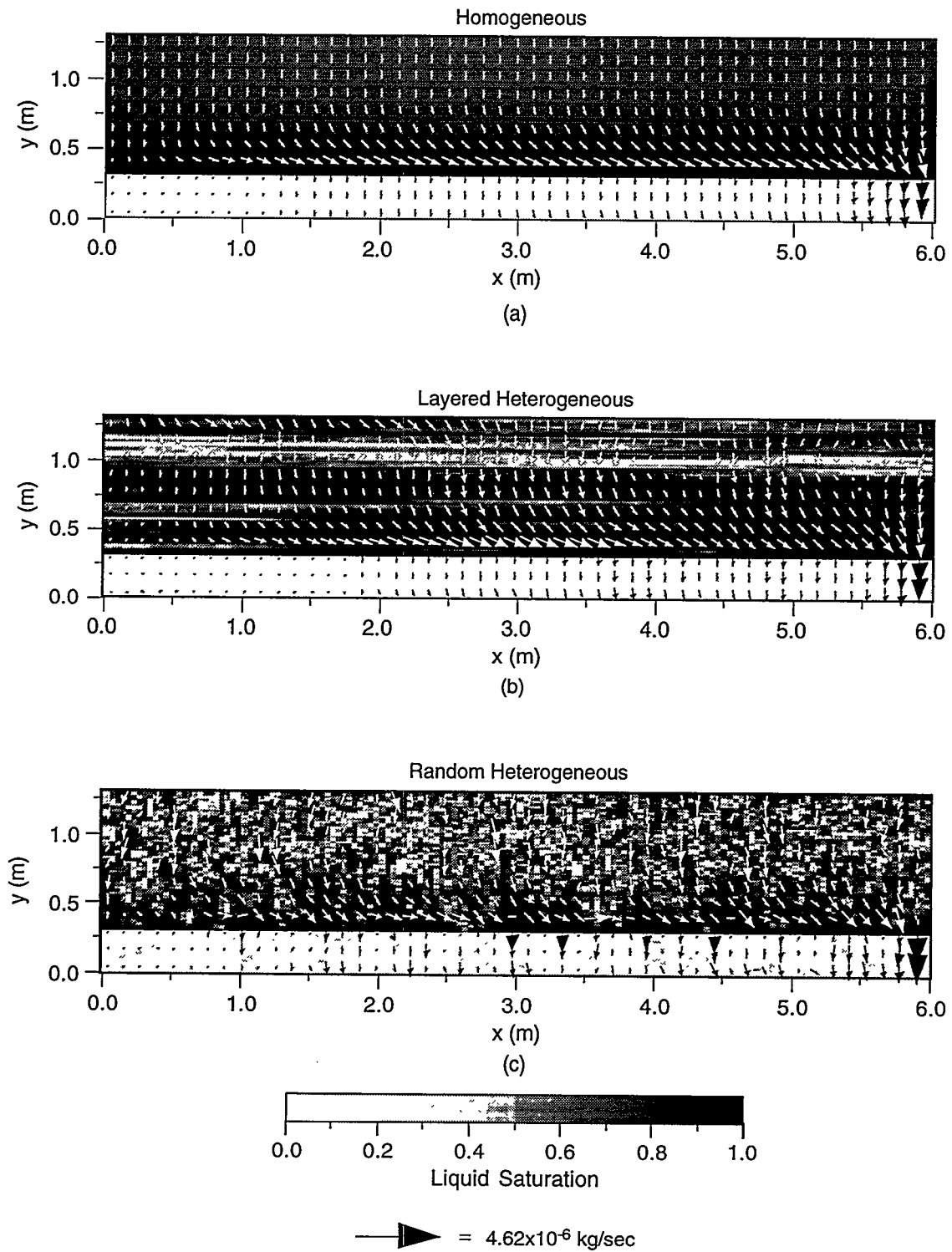
Figure 3. Liquid saturations and mass flow vectors in the a) homogeneous, b) layered heterogeneous, and c) random heterogeneous simulations. The domains are tilted 5 degrees clockwise.

layer, with saturation increasing near the interface of the fine and coarse layers. Water flow is primarily vertically downward except at the interface, where lateral diversion exists. In addition to diversion at the interface, the layered heterogeneous field (Figure 3(b)) also exhibits regions of lateral diversion *within* the fine layer of soil. Local zones of high permeability (and low saturation) within the fine layer at y~1 m act as localized capillary barriers that contribute to additional lateral diversion. The random heterogeneous field (Figure 3(c)) shows localized channeling of downward flow through high permeability zones. The saturation distribution is indicative of the highly variable permeability field that causes the localized flow. The channeled flow results in pulses of water that break through the interface of the fine and coarse layers at frequent intervals.

The diversion capacities of the different fields is quantified in Figure 4, which displays the mass flow rate of water entering the coarse layer divided by the infiltration rate as a function of distance along the interface. Figure 4(a) shows that the layered heterogeneous field has a longer diversion length when compared to the homogeneous field. Initial breakthrough of water into the coarse layer in the layered heterogeneous domain occurs at x~1.5 m, which is greater than twice the diversion distance displayed by the homogeneous model. In contrast, the random heterogeneous field (Figure 4(b)) displays breakthrough even earlier than that of the homogeneous model with intermittent "bursts" of water. The results of a semi-analytical solution using the method of Ross (1990) is also shown, where appropriate van Genuchten functions have been used. Note that the no-flow right boundary causes significantly higher mass flow rates along the right side of the domain, but for distances less than x~5 m, the influence of the right boundary is minimal.

Another useful means of quantifying the performance of capillary barriers is to define a breakthrough ratio, χ, by integrating the mass flow of water entering the coarse layer with respect to distance along the interface and dividing this quantity by the integrated infiltration with respect to distance along the surface:

$$\chi = \frac{\displaystyle\int_0^x \dot{m}(x)\,dx}{\displaystyle\int_0^x q(x)\,dx} = \frac{1}{qx}\int_0^x \dot{m}(x)\,dx \tag{2}$$
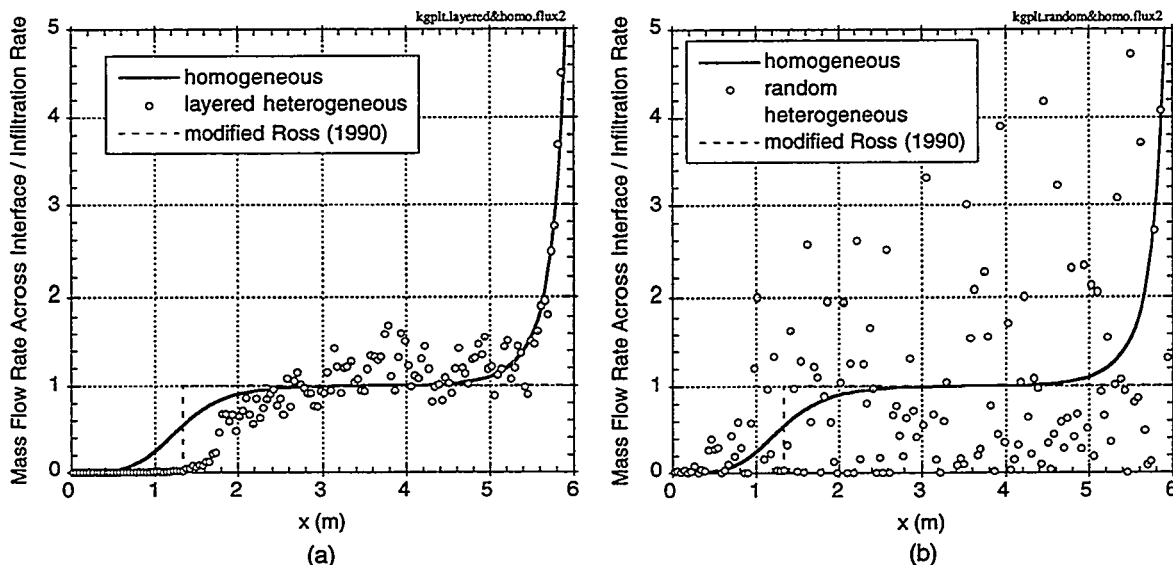
Figure 4. Mass flow rate across the interface of the fine and coarse layers divided by the infiltration (1 mm/day): a) homogeneous and layered heterogeneous b) homogeneous and random heterogeneous. A modified solution of Ross (1990) using homogeneous van Genuchten parameters is also shown.

where $\dot{m}(x)$ is the mass flow rate of water entering the coarse layer at a location x and q is the infiltration rate (assumed constant in this study). Figure 5 shows the breakthrough ratio, χ, for each simulation as a function of distance along the interface of the fine and coarse layers. For any location, x, each curve gives the mass ratio of water entering the coarse layer with respect to the total infiltration entering the system upstream of that location. The results in Figure 5 confirm that the layered heterogeneous system performs best with the greatest amount of diversion above the coarse layer, which results from the sub-unit horizontal features acting as local capillary barriers within the fine layer of soil. The random heterogeneous field performs worst, with breakthrough occurring almost immediately as a result of local channeled flow.
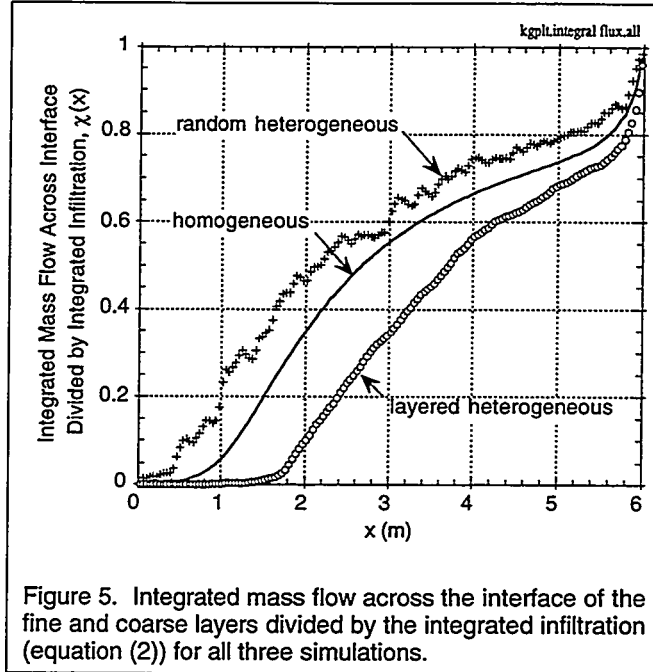
Figure 5. Integrated mass flow across the interface of the fine and coarse layers divided by the integrated infiltration (equation (2)) for all three simulations.

Finally, Table 2 presents average residual and steady-state saturations and water mass in the fine and coarse layers for each simulation. The layered heterogeneous simulation yields the least amount of water in the coarse layer at steady-state, whereas the random heterogeneous simulation yields the most. In contrast, the layered heterogeneous simulation yields the greatest amount of water in the overlying fine layer, which indicates a greater amount of storativity in the fine layer. The features that act as capillary barriers within the fine layer of the layered heterogeneous field increase the storativity, which may provide additional benefits during episodic infiltration events. One final comment should be made regarding the computational performance of each of the simulations. The homogeneous and layered heterogeneous simulations took on the order of several hours to reach steady-state from residually saturated initial conditions. However, the random heterogeneous field had difficulty reaching steady-state from residually saturated initial conditions. A uniform initial saturation greater than residual was imposed to allow the random heterogeneous simulation to reach steady-state. Different initial saturations were imposed, and while the results were identical, the duration and number of time steps required to reach steady-state were highly dependent on the value of the initial saturation.

Table 2. Predicted average saturations and water mass in the fine and coarse layers at residual conditions and steady-state conditions (infiltration = 1 mm/day).

	(Fine Layer)			(Coarse Layer)		
	Homogeneous	Random	Layered	Homogeneous	Random	Layered
Avg. Residual Saturation	0.200	0.201	0.202	1.20×10^{-2}	9.72×10^{-3}	7.17×10^{-3}
Avg. Steady Saturation	0.764	0.785	0.825	4.65×10^{-2}	4.95×10^{-2}	3.92×10^{-2}
Residual Water Mass (kg)	479	482	484	9.06	7.34	5.41
Steady Water Mass (kg)	1830	1880	1976	35.1	37.4	29.6

Conclusions

Simulations have been performed to investigate the effects of heterogeneities on the performance of capillary barriers. Homogeneous, layered heterogeneous, and random heterogeneous representations of a system comprised of a fine soil layer overlying a coarse gravel layer were simulated to determine the amount of lateral diversion above the coarse layer under steady-state infiltration conditions. Results indicate that the performance of capillary barriers may be significantly influenced by the spatial variability of the properties. The layered heterogeneous system delayed breakthrough longest as a result of horizontal features within the fine layer that acted as additional local capillary barriers. Random heterogeneous systems performed worst because of channeled flow that produced localized regions of early breakthrough into the coarse layer. In addition, the storativity in the fine layer of the layered heterogeneous field was greatest, indicating the potential to hold more water from episodic infiltration events. These results indicate that engineered capillary barriers may be improved through emplacement and packing methods that induce a layered system similar to the layered heterogeneous field simulated in this study. On the other hand, the results also indicate that capillary barriers can perform poorly if the fine layer consists of randomly distributed properties. Models of these systems, including conventional homogeneous models, may overestimate the diversion capacity if the intra-unit heterogeneities are not considered.

Acknowledgments

References

Deutsch, C.V. and A.G. Journel (1992) *GSLIB: Geostatistical Software Library and User's Guide*, Oxford University Press, New York.

Ho, C.K. and K.S. Udell (1992) An Experimental Investigation of Air Venting of Volatile Liquid Hydrocarbon Mixtures from Homogeneous and Heterogeneous Porous Media, *J. Contam. Hydrol.*, 11, 291-316.

Morris, C.E. and J.C. Stormont (1996) Capillary Barriers and Subtitle D Covers: Estimating Equivalency, accepted for publication in *Journal of Environmental Engineering*.

Oldenburg, C.M. and K. Pruess (1993) On Numerical Modeling of Capillary Barriers, *Water Resour. Res.*, 29, 1045-1056.

Prindle, R.W. and P.L. Hopkins (1990) On Conditions and Parameters Important to Model Sensitivity for Unsaturated Flow Through Layered, Fractured, Tuff: Results of Analyses for HYDROCOIN Level 3 Case 2, *SAND89-0652*, Sandia National Laboratories, Albuquerque, NM.

Pruess, K. (1991) TOUGH2—A General-Purpose Numerical Simulator for Multiphase Fluid and Heat Flow, *LBL-29400*, Lawrence Berkeley Laboratory, Berkeley, CA.

Pruess, K. (1995) Proceedings of the TOUGH2 Workshop '95, *LBL-37200*, Lawrence Berkeley Laboratory, Berkeley, CA.

Ross, B. (1990) The Diversion Capacity of Capillary Barriers, *Water Resour. Res.*, 26, 2625-2629.

Stormont, J.C. (1995) The Performance of Two Capillary Barriers During Constant Infiltration, in Landfill Closures, *ASCE Geotechnical Special Publication No. 53*, Edited by Bunn and Singh, pp. 77-92.

Webb, S.W. (1997) Comparison of Ross' Capillary Barrier Diversion Formula with Detailed Numerical Simulations, in proceedings of the *1997 International Containment Technology Conference and Exhibition*, St. Petersburg, FL.

Webb, S.W., J.T. McCord, and S.F. Dwyer (1997) The Applicability of the HELP Model in Predicting Tilted Capillary Barrier Performance, in proceedings of the *1997 International Containment Technology Conference and Exhibition*, St. Petersburg, FL.

Webb S.W. (1996), Selection of a Numerical Unsaturated Flow Code for Tilted Capillary Barrier Performance Evaluation, *SAND96-2271*, Sandia National Laboratories, Albuquerque, NM.

Wilson, M.L. (1996) Lateral Diversion in the PTn Unit: Capillary-Barrier Analysis, in proceedings of the *1996 International High Level Radioactive Waste Management Conference*, Las Vegas, NV, 111-113.

Comparison of Ross' Capillary Barrier Diversion Formula
with Detailed Numerical Simulations

Stephen W. Webb[1]

Abstract

Ross (1990) developed an analytical r(ɔn length of a tilted fine-over-
coarse capillary barrier. Oldenburg ar   ation results using upstream
and harmonic weighting to the diver   rmula with mixed results; the
qualitative agreement is reasonable ł   poor, especially for upstream
weighting. The proximity of the wate   at breakthrough is a possible
reason for the poor agreement. In th   Ɪḻd Pruess problem is extended
to address the water table issue. V   / far away from the interface at
breakthrough, good qualitative ana ꞯᵤ....   ed using upstream weighting.

I. Introduction

Capillary barriers, consisting of tilted fine-over-coarse layers under unsaturated conditions, have been suggested as a means to divert water infiltration away from sensitive underground regions. The capillary diversion formula of Ross (1990) (Steenhuis et al.,1991 and Stormont, 1995 present additional variations) is of particular interest because it can be easily used in capillary barrier design and evaluation. Oldenburg and Pruess (1993) compared TOUGH2 (Pruess, 1991) simulation results using upstream and harmonic weighting with Ross' formula; the results were mixed. While the comparison is reasonable qualitatively, the quantitative agreement is generally poor, especially for upstream weighting. A reason that has been proposed for this poor agreement is the proximity of the water table (Pruess, private communication, 1994). In Ross' derivation, the fine-coarse interface is assumed to be infinitely far away from the water table. In Oldenburg and Pruess (1993), the water table is only a few meters below the interface when breakthrough occurs. In order to address the water table proximity question, the Oldenburg and Pruess (1993) model is extended in the present study to allow for different initial water table locations. The applicability of upstream weighting to transient unsaturated flow conditions including capillary barrier behavior is also discussed.

While comparison of Ross' diversion equation with numerical modeling results is of interest, it must be kept in mind that capillary barrier leakage and breakthrough involve complicated unsaturated flow phenomena including fingering (Hill and Parlange, 1972; Glass et al., 1989a,b,c) as discussed by Oldenburg and Pruess (1993). Fingering phenomena are not treated in the analytical solution of Ross or in the TOUGH2 numerical code at present. In addition, heterogeneities and their spatial distribution may have a significant impact on the diversion length of tilted capillary barriers (Ho and Webb, 1997), which are not included in Ross' expression. Therefore, while comparison of Ross' expression with numerical results is of interest, comparison of modeling approaches to actual data is also needed.

II. Ross' Capillary Barrier Diversion Formula

Ross (1990) developed an analytical relationship to calculate the diversion length of a tilted fine-over-coarse capillary barrier with constant infiltration, assuming that the upper boundary (infiltration surface) and the lower boundary (water table) are far away from the fine-coarse interface. The only flow in the system is due to the infiltration. The analysis assumes steady-state conditions and defines breakthrough from the fine to the coarse layer as the occurrence of downward flow through the coarse layer equal to the infiltration rate. This assumption, along with the infiltration surface boundary condition, allows one to calculate the vertical relative permeability in the fine soil at breakthrough and,

---

[1]Sandia National Laboratories, P.O. Box 5800/MS-1324, Albuquerque, NM 87185-1324, (505) 848-0623, swwebb@nwer.sandia.gov.

therefore, the horizontal flow in the fine layer. This horizontal flow is equal to the total amount of water diverted up until breakthrough

$$Q_{max} = K_s \tan \phi \int_0^\infty k_r \, d\psi \qquad (1)$$

where ϕ is the angle of the fine-coarse interface with respect to horizontal. If the relative permeability is given by the quasi-linear function

$$k_r = e^{\alpha \psi} \qquad (2)$$

where α is the sorptive number and ψ is the moisture potential ($\psi = P_c / \rho g$), then the equation reduces to a closed form solution

$$Q_{max} = K_s \frac{\tan \phi}{\alpha} \left[\left(\frac{q}{K_s^*} \right)^{\alpha/\alpha^*} - \frac{q}{K_s} \right] \qquad (3)$$

where the starred value refers to the coarse layer parameter. For constant infiltration, the capillary diversion length is simply the total water diverted by the capillary barrier divided by the infiltration rate

$$L = K_s \frac{\tan \phi}{q \alpha} \left[\left(\frac{q}{K_s^*} \right)^{\alpha/\alpha^*} - \frac{q}{K_s} \right] \qquad (4)$$

where L is the horizontal distance. Equation (1) above is general and can be used with any relative permeability function. Equations (3) and (4) are derived from equation (1) using the quasi-linear relative permeability function. The diversion length can be evaluated numerically for other relative permeability expressions such as van Genuchten (1980) as discussed by Webb (1997).

III. TOUGH2 Numerical Simulations

Oldenburg and Pruess (1993) analyzed a two-dimensional tilted fine-over-coarse capillary barrier with a water table and vertical infiltration using TOUGH2 (Pruess, 1991). For consistency with the Ross derivation, TOUGH2 was modified to include the quasi-linear wetting-phase relative permeability function discussed earlier. A sketch of the capillary barrier problem is given in Figure 1; properties and problem parameters are summarized in Table 1. A fine layer 50 m thick overlies a coarse layer 10 m thick; the layers are tilted at a 5° angle with respect to horizontal. Infiltration occurs at the top of the fine layer at a constant rate of 0.60 m/year, and a water table is specified at 59 m along the left boundary. For the conditions summarized in Table 1 ($\alpha = 0.1$ m^{-1}; $\alpha^* = 4.0$ m^{-1}), the predicted capillary diversion length from Ross (1990) is 39.3 m.

The discretization employed by Oldenburg and Pruess (1993) consisted of thirty rows each 2 m high with varying column widths. The column width was 4 m for the first 80 m downdip which increased thereafter. A higher resolution grid was examined between 32 and 80 m downdip using 2 m wide columns. The results from the original grid and the higher resolution grid are essentially the same.

Figure 1 schematic (axis labels): Z(m) vertical axis with values 0, -20, -40, -60. Y(m) horizontal axis with values 0, 20, 40, 60, 80, 100. Regions labeled "Fine" and "Coarse". Annotations: $\phi=5°$, g (downward arrow).
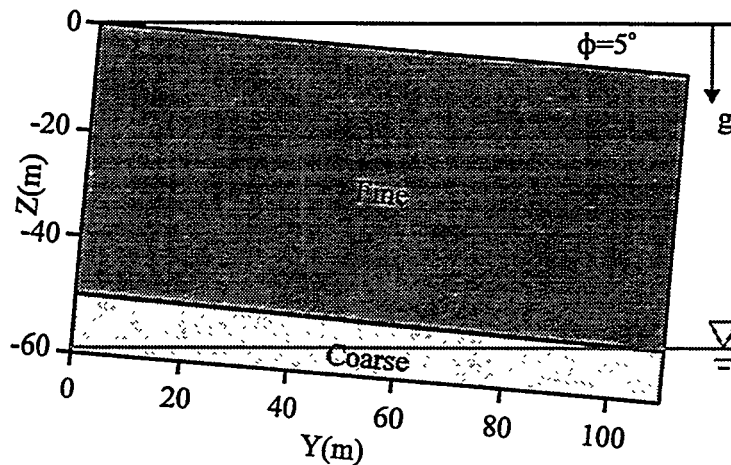
Figure 1
Comparison Problem Schematic
(after Oldenburg and Pruess, 1993)

Table 1
Original Problem Parameters

	Upper Layer (Fine)	Lower Layer (Coarse)
Thickness	50 m	10 m
Length	750 m	750 m
Permeability	$10^{-13}\ m^2$	$2 \times 10^{-13}\ m^2$
Porosity	0.30	0.40
Relative Permeability	$k_r = e^{\alpha\psi}; \alpha = 0.1\ m^{-1}$	$k_r = e^{\alpha^*\psi}; \alpha^* = 4.\ m^{-1}$
Capillary Pressure	$P_c = -10^6\ (1.-S_l)$	$P_c = -10^6\ (1.-S_l)$

Boundary Conditions

Left Side	No flow.
Right Side	No flow.
Top	Constant Infiltration rate (0.60 m/year).
Bottom	Horizontal water table with a depth of 59 m at left boundary.

The results from the capillary barrier simulations are presented as a ratio of the leakage past the fine-coarse boundary divided by the infiltration rate. A value of zero shows complete diversion of the infiltrating water, while a value of 1.0 means no diversion. The ratio should increase with distance downdip until breakthrough occurs, which is defined as a ratio of 1.0. Values higher than 1.0 are expected further downstream when the diverted water flows into the coarse layer.

Oldenburg and Pruess (1993) investigated two different numerical weighting schemes for the permeability-mobility product ($k\ k_r / \mu$). The differences in the two schemes illustrate some of the complexities associated with unsaturated flow modeling. Harmonic weighting, which considers upstream and downstream parameters, is appropriate for steady-state one-dimensional flow without phase change or phase propagation based on flux conservation. However, for transient conditions involving phase propagation, flux conservation is not applicable, and upstream weighting is more appropriate. Upstream weighting, which only uses the upstream parameters, is numerically much more efficient and robust than harmonic weighting.

(a) Harmonic Weighting   (b) Upstream Weighting
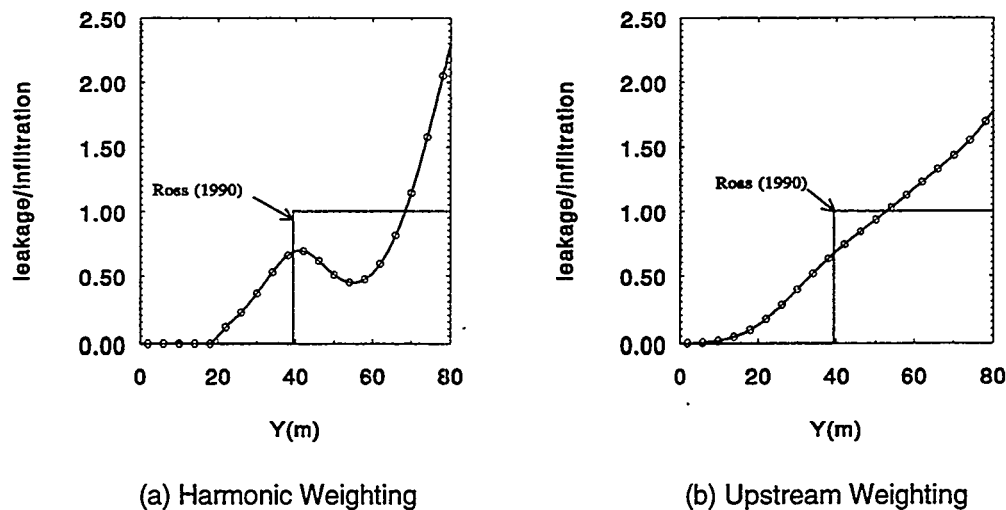
Figure 2
TOUGH2 Leakage/Infiltration Ratio Results

The use of harmonic weighting for transient unsaturated flow can lead to large errors and upstream weighting is preferable (Aziz and Settari, 1979; Tsang and Pruess, 1990). In fact, harmonic weighting can lead to unphysical results in transient analyses of tilted capillary barriers such as the complete saturation of the upper fine layer without any leakage or flow into the lower coarse layer. Upstream weighting results are predominantly shown in the present paper.

The leakage/infiltration ratio as a function of distance downdip is given in Figure 2 for the Oldenburg and Pruess (1993) problem with coarse and fine layer sorptive numbers of 4.0 m^{-1} and 0.1 m^{-1}, respectively. This ratio is shown for harmonic and upstream weighting as calculated by the present author; the results are essentially the same as those in Oldenburg and Pruess (1993) The behavior of the leakage/infiltration ratio is significantly different for the two weighting schemes. The leakage/infiltration ratio using harmonic weighting shows an initial breakthrough at about 40 m. This ratio decreases slightly after this location because some of the water has flowed into the coarse layer. The ratio then increases again. In contrast, for upstream weighting, the ratio increases monotonically with distance. The agreement between the numerical results and Ross' formula is mixed. The comparison is reasonable qualitatively because the breakthrough location is in general agreement. However, the quantitative agreement is poor, especially for upstream weighting, because the leakage/infiltration ratio behavior is considerably different than the Ross (1990) model results for both numerical weighting schemes.

As discussed earlier, one reason that has been proposed for the poor agreement between the numerical simulations and Ross formula is the proximity of the water table. In Ross' derivation, the fine-coarse interface is assumed to be infinitely far away from the water table, while the water table is only a few meters below the interface when breakthrough occurs in the Oldenburg and Pruess (1993) problem. If the water table is near the fine-coarse interface, the moisture content and relative permeability of the coarse material will increase due to the added moisture from the capillary fringe, and the capillary pressure will be reduced. The net effect is to decrease the contrast between the fine and the coarse layers which will reduce the capillary barrier effectiveness. In order to address the water table proximity question, the initial water table location is varied in the present investigation.

In order to perform the modeling with different water table locations, the model domain was expanded. The depth of the coarse layer was increased from 10 meters to 50 meters for a total model depth of 100 meters. The vertical discretization was kept constant at 2 meters similar to Oldenburg and

Pruess (1993), resulting in 50 elements in the z-direction. In addition, since the location of breakthrough is expected to change with water table depth, the y (downdip) discretization was kept at a constant value of 4 meters for a total distance of 800 meters (Oldenburg and Pruess had a total distance of 750 meters) with a total of 200 elements in the y-direction. Therefore, the total grid consisted of 10,000 elements.

The standard version of TOUGH2 (Pruess, 1991) employs a full two-phase treatment of unsaturated flow with conservation equations for both the air and water phases. A Richards' equation treatment, which only considers water movement, is also available (Pruess and Antunez, 1995). As shown by Webb (1996), the full two-phase treatment and the Richards' equation results are essentially the same for the Oldenburg and Pruess capillary barrier problem, and the Richards' equation solution time is only 1/10 of the full two-phase treatment. Therefore, the Richards' equation version has been used in the present study including Figure 2 above. The conjugate gradient solvers of Moridis and Pruess (1995) have also been used.

The water table in Oldenburg and Pruess is at z=-59 meters along the left edge of the domain, or 9 meters (m) below the fine-coarse interface. In the present study, water table locations of 5, 9, 13, 19, 29, 39, and 49 m below the fine-over-coarse interface have been considered with upstream weighting. The problems were run in two parts. Initial conditions were established by running a false transient to steady-state with the water table but without infiltration. The infiltration transient was then performed by using the calculated initial conditions and applying the infiltration uniformly along the top surface. The bottom boundary pressures remained constant during the transient, which provided a sink for the infiltrating water that breaks through. The simulation was run until steady-state conditions were achieved. Leakage across the fine-coarse boundary was then compared to the infiltration rate to determine the leakage/infiltration ratio.

Figure 3 compares the results from TOUGH2 and Ross' (1990) formula for the various initial water table depths. For an initial water table elevation 5 m below the fine-coarse interface, the leakage/infiltration ratio increases monotonically, reaching a maximum value of about 1.7 at 38 m. For an initial water table elevation 9 m below the interface, the leakage/infiltration ratio increases monotonically, and the ratio reaches a maximum value approaching 2.0 at 82 m. These results are similar but not exactly the same as given by Oldenburg and Pruess (1993). Small differences between the two results are expected due to the expanded computational domain employed in the present simulations and the different treatment of unsaturated flow. For an initial water table 13 m below the interface, the leakage/infiltration ratio again increases monotonically, although the ratio shows a tendency to "flatten out" slightly at intermediate distances. The peak ratio is about 2.0 at 126 m downdip.

Results for initial water table depths of 19 m, 29 m, 39 m, and 49 m are also shown in Figure 3. As the initial water table depth increases, three regions are evident. They are 1) initial increase in leakage/infiltration ratio, 2) leakage/infiltration plateau at a value of 1.0, and 3) increase in the ratio above 1.0 as the water table is approached. (The downdip distance corresponding to the intersection of the water table with the fine-coarse interface is simply the initial water table depth divided by tan 5°, or 0.0875.) For example, the leakage/infiltration ratio from 0 to 100 m is essentially the same for water table locations 19 m or more below the fine-coarse interface. The breakthrough location is similar to that predicted by Ross (1990) although considerably more diffuse due to the numerical behavior of upstream weighting (see, for example, Oran and Boris, 1987). The ratio then remains at a value of 1.0 until the water table is approached. The leakage/infiltration ratio then increases to a value of about 2.0 as water flows down to the water table in the capillary fringe region.

In summary, for initial water table depths of 13 m or less, the location of the water table significantly influences the initial behavior of the leakage/infiltration ratio; this range includes the original Oldenburg and Pruess (1993) problem specification of 9 m. For larger initial water table depths of 19 m or more, the initial leakage/infiltration ratio is not affected by the location of the water table.
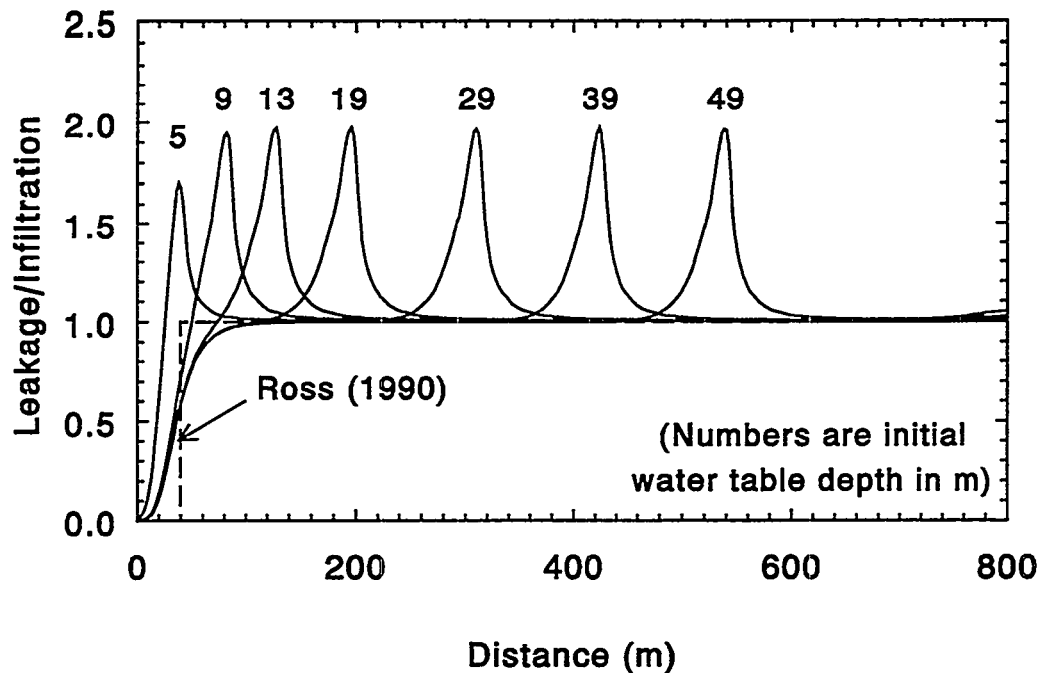
Figure 3
TOUGH2 Leakage/Infiltration Ratio Result
As a Function of Initial Water Table Depth

IV. Discussion and Conclusions

Results from numerical simulations using upstream weighting have been compared to Ross' tilted capillary barrier diversion formula for the Oldenburg and Pruess (1993) capillary barrier problem with variable water table locations. For a sufficiently deep water table, which is consistent with the assumption used by Ross (1990), the simulations are in good qualitative *and* quantitative agreement with Ross' capillary barrier diversion formula. For shallower water tables, including the Oldenburg and Pruess (1993) location, the results are significantly influenced by the water table. These results indicate that upstream weighting can accurately model capillary barrier behavior as evidenced by good agreement between the simulations and Ross' formula for the deeper water table locations.

These results are significantly different than Oldenburg and Pruess (1993). Oldenburg and Pruess concluded that while upstream weighting may describe the general behavior of capillary barriers, it is not able to model the details of capillary barrier flow; harmonic weighting is required to resolve the details of breakthrough. Their conclusion is based on the difference between their upstream weighting results and Ross' (1990) formula as shown in Figure 2. Their conclusion has significant implications in unsaturated flow modeling for capillary barriers. As mentioned earlier, upstream weighting is often required for transient unsaturated flow modeling. Therefore, according to Oldenburg and Pruess (1993), modeling of transient unsaturated flow in capillary barriers involves numerical compromises; while upstream weighting is often required for numerical efficiency and stability, it is not as accurate as harmonic weighting. As mentioned by Oldenburg and Pruess (1993), this compromise not only applies to engineered capillary barriers such as discussed in this paper, but it also has important implications for simulation of natural capillary barrier effects such as encountered in potential nuclear waste repositories.

In contrast, the present study has shown that the disagreement observed by Oldenburg and Pruess (1993) was significantly influenced by the proximity of the water table. If the water table is deep enough, which is consistent with the assumption made by Ross (1990), simulations using upstream

weighting agree well with Ross' capillary barrier diversion formula. Based on the present results, upstream weighting *can* be used to accurately model transient unsaturated flow including capillary barrier behavior.

Acknowledgment

V. Nomenclature

K_s	saturated hydraulic conductivity for fine layer
$K_s^{\bullet}$	saturated hydraulic conductivity for coarse layer
k_r	relative permeability
L	horizontal diversion length
P_c	capillary pressure
q	infiltration rate
Q	total horizontal flux
S_l	liquid saturation
α	sorptive number for fine layer
$\alpha^{\bullet}$	sorptive number for coarse layer
ρ	fluid density
μ	viscosity
ϕ	angle of the fine-coarse interface with respect to horizontal
ψ	moisture potential

VI. References

Aziz, K., and T. Settari (1979) *Petroleum Reservoir Simulation*, Applied Science Publishers, London.

Ho, C.K., and S.W. Webb (1997) "The Effects of Heterogeneities on the Performance of Capillary Barriers for Waste Isolation," 1997 ICTCE Conference, St. Petersburg, FL.

Moridis, G., and K. Pruess (1995) *Flow and Transport Simulations Using T2CG1, A Package of Conjugate Gradient Solvers For the TOUGH2 Family of Codes*, LBL-36235, Lawrence Berkeley Laboratory.

Oldenburg, C.M., and K. Pruess (1993) "On Numerical Modeling of Capillary Barriers," *Water Resour. Res.*, Vol. 29:1045-1056.

Oran, E.S., and J.P. Boris (1987) Numerical Simulation of Reactive Flow, Elsevier, New York.

Pruess, K. (1991) *TOUGH2 - A General-Purpose Numerical Simulator for Multiphase Fluid and Heat Flow*, LBL-29400, Lawrence Berkeley Laboratory, May 1991.

Pruess, K., and E. Antunez (1995) "Applications of TOUGH2 to Infiltration of Liquids in Media with Strong Heterogeneity," in *Proceedings of the TOUGH Workshop '95*, K. Pruess, ed., pp. 69-76, LBL-37200, Lawrence Berkeley Laboratory.

Ross, B. (1990) "The Diversion Capacity of Capillary Barriers," *Water Resour. Res.*, 26:2625-2629.

Ross, B. (1991) "Reply", *Water Resour. Res.*, 27:2157 (see Steenhuis et al., 1991).

Steenhuis, T.S., J.-Y. Parlange, and K.-J.S. Kung (1991) "Comment on 'The Diversion Capacity of Capillary Barriers,' by Benjamin Ross," *Water Resour. Res.*, 27:2155-2156 (see Ross, 1991).

Stormont, J.C. (1995) "The Effect of Constant Anisotropy on Capillary Barrier Performance," *Water Resour. Res.*, 31:783-785.

Tsang, Y., and K. Pruess (1990) *Further Modeling Studies of Gas Movement and Moisture Migration at Yucca Mountain, Nevada*, LBL-29127, Lawrence Berkeley Laboratory.

van Genuchten, M.Th. (1980) "A Closed-form Equation for Predicting the Hydraulic Conductivity of Unsaturated Soils," *Soil Sci. Soc. Am. J.*, 44:892-898.

Webb, S.W. (1996) "Selection of a Numerical Unsaturated Flow Code for Tilted Capillary Barrier Performance Evaluation," SAND96-2271, Sandia National Laboratories.

Webb, S.W. (1997) "Generalization of Ross' Tilted Capillary Barrier Diversion Formula For Different Two-Phase Characteristic Curves," submitted to *Water Resources Research*.

Prediction of Tilted Capillary Barrier Performance

Stephen W. Webb, James T. McCord, and Stephen F. Dwyer[1]

Abstract

Capillary barriers, consisting of tilted fine-over-coarse layers under unsaturated conditions, have been suggested as landfill covers to divert water infiltration away from sensitive underground regions, especially for arid and semi-arid regions. The Hydrological Evaluation of Landfill Performance (HELP) computer code is an evaluation tool for landfill covers used by designers and regulators. HELP is a quasi-two-dimensional model that predicts moisture movement into and through the underground soil and waste layers. Processes modeled within HELP include precipitation, runoff, evapotranspiration, unsaturated vertical drainage, saturated lateral drainage, and leakage through liners. Unfortunately, multidimensional unsaturated flow phenomena that are necessary for evaluating tilted capillary barriers are not included in HELP. Differences between the predictions of the HELP and those from a multidimensional unsaturated flow code are presented to assess the two different approaches. Comparisons are presented for the landfill covers including capillary barrier configurations at the Alternative Landfill Cover Demonstration (ALCD) being conducted at Sandia.

I. Introduction

The Alternate Landfill Cover Demonstration is a series of large-scale landfill test covers that have been constructed at Sandia National Laboratories in Albuquerque, New Mexico (Dwyer, 1995). Each cover is 13 m wide and 100 m long. The 100 m length is crowned in the middle, resulting in two 50 m long sections each with a 5% slope. One side is exposed to ambient conditions, while additional water is added to the other side to stress the barriers to the desired storm events. Two traditional cover designs and four alternatives, including tilted capillary barriers, are being tested and are shown in Figure 1. Plot 1, a RCRA Subtitle "D" cover, is simply topsoil over a compacted soil barrier layer. Plot 2 is a Geosynthetic Clay Liner (GCL) cover with topsoil, sand and a geomembrane on top of the GCL. Plot 3 is a compacted clay cover that simply replaces the GCL in Plot 2 with a compacted clay barrier layer, or a RCRA Subtitle "C" cover. Plot 4 is a tilted capillary barrier consisting of topsoil over sand and gravel layers followed by a barrier layer and another sand layer. Plot 5 is an anisotropic barrier consisting of 2 soil layers over sand and gravel. Finally, Plot 6 is an evapotranspiration cover and is simply topsoil over native soil. Assuming van Genuchten (1980) characteristic curves, properties for the various soils have been estimated and are summarized in Table 1. The wetting phase permeability as a function of capillary pressure, which is particularly useful in determining capillary barrier performance, is shown in Figure 2.

Prediction of the performance of the ALCD landfill covers should consider all unsaturated flow phenomena including precipitation, runoff and evapotranspiration under the arid conditions of Albuquerque, New Mexico. While the HELP model (Schroeder et al, 1994a,b) considers precipitation, runoff, and evapotranspiration, the simplified unsaturated flow modeling in HELP is inappropriate for tilted capillary barriers (Morris and Stormont, 1997). In addition, HELP has demonstrated a trend to overpredict percolation/leakage in semi-arid and arid conditions (Thompson and Tyler, 1984; Nichols, 1991; Fleenor and King, 1995), which are typical of capillary barrier applications. Because some of the covers may experience lateral diversion due to capillary barrier effects, and the ALCD is located in the arid environment of Albuquerque, HELP may not give accurate results. Conversely, many multidimensional unsaturated flow codes suitable for tilted capillary barriers do not have precipitation, runoff, and evapotranspiration models and the flexibility of HELP.

---

[1]All the authors are at Sandia National Laboratories. S.W. Webb's address is P.O. Box 5800/MS-1324, Albuquerque, NM 87185-1324, (505) 848-0623, swwebb@nwer.sandia.gov.
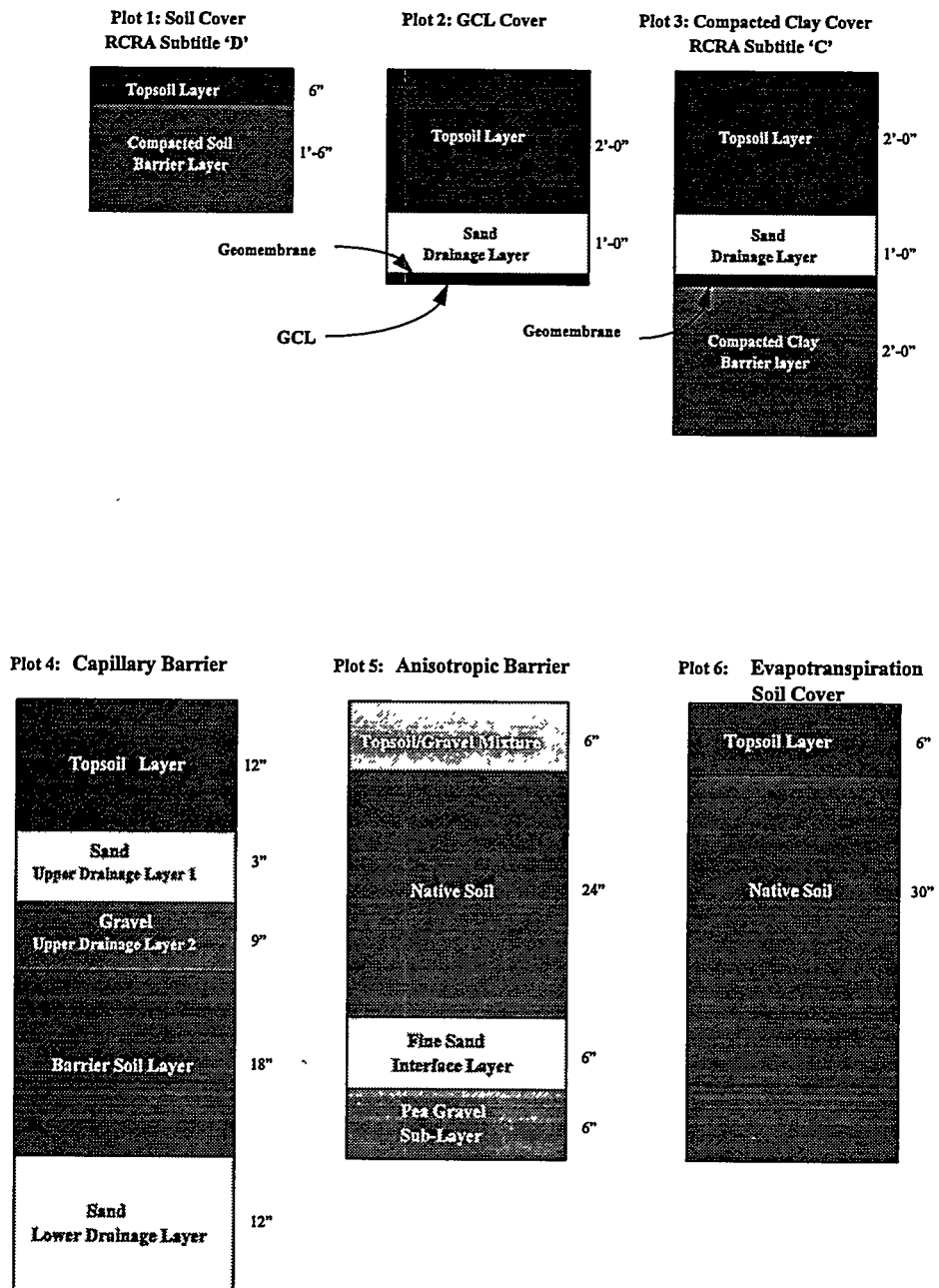
Figure 1
ALCD Landfill Covers

Table 1
Estimated Soil Properties

Soil Type	Saturated hydraulic conductivity (cm/s)[1]	Saturated Moisture Content	Residual Moisture Content	Capillary Pressure Parameter (1/cm)	Shape Parameter
Topsoil	3.0×10^{-4}	0.40	0.06	0.021	2.5
Native Soil	1.0×10^{-4}	0.40	0.08	0.018	2.0
Sand Layers	8.0×10^{-3}	0.39	0.04	0.018	3.3
Gravels	1.3	0.42	0.02	1.0	15.0
Compacted Clay and GCL	1.0×10^{-8}	0.45	0.20	0.005	1.5
Barrier Soil	1.0×10^{-6}	0.42	0.14	0.010	1.73
Geomembrane	4.0×10^{-13}	-	-	0.001	1.2
Topsoil/Gravel	2.0×10^{-2}	0.41	0.04	0.14	6.1

[1] - 1 cm/s ~ 1.03×10^{-9} m^2 for water at 20°C.
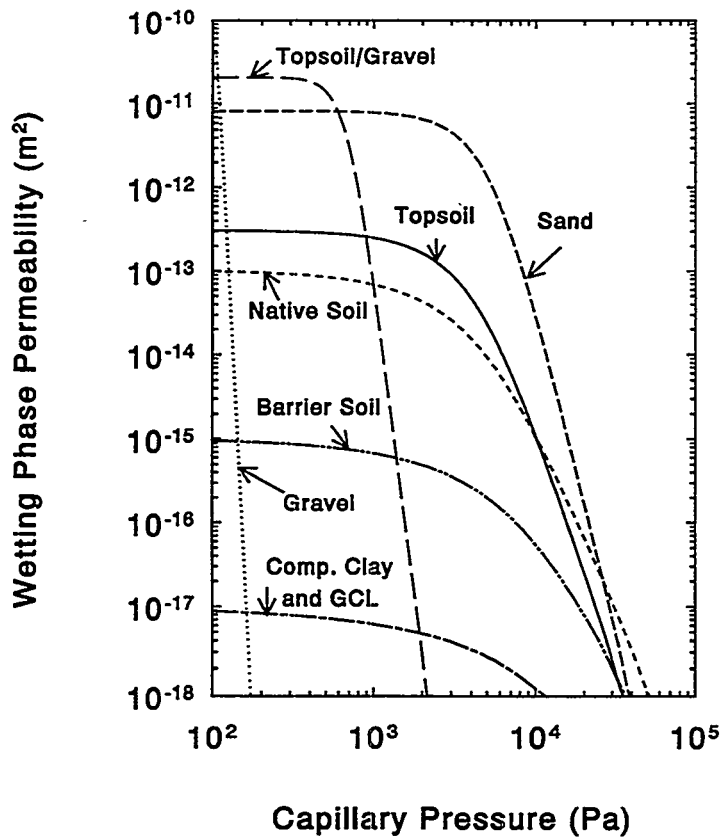
Figure 2
Wetting Phase Permeability vs. Capillary Pressure

In the current study, simulations for the ALCD landfill covers have been performed using HELP Version 3.06. In addition, two methods have been used to evaluate the capillary barrier diversion length of these covers; Ross' capillary barrier diversion formula (Ross, 1990) and detailed TOUGH2 simulations. The results from these approaches are compared for the various landfill covers including capillary barriers.

II. HELP Simulations

For the present study, the HELP simulations have been run for 5 years using Albuquerque precipitation and evapotranspiration assuming a maximum evaporation zone depth of 0.46 m (18 inches) and bare ground (Leaf Area Index = 0). Runoff, which is small for the present simulations, is calculated using a 5 percent slope and a length of about 50 m (150 ft); a soil texture of 5 (SCS Runoff Curve number = 84.5) has been assumed. Similarly, any lateral drainage layer had a 5 percent slope and a length of about 50 m (150 ft).

The layering sequence and appropriate properties for HELP input for each of the plots are summarized in Table 2. The field capacity and wilting point moisture content input parameters, which are used to define moisture storage and unsaturated hydraulic conductivity, are calculated using the van Genuchten two-phase characteristic curves and the parameters in Table 1 for capillary pressures of 0.33 and 15. bars, respectively, consistent with assumptions used in HELP. In all unsaturated layers, the initial moisture content is assumed equal to the wilting point value. In general, the layers are specified as vertical percolation layers. Subject to layering sequence restrictions in HELP, lateral drainage layers are also used. Lateral drainage in HELP is *not* equivalent to tilted capillary barrier behavior because it is based on saturated flow; capillary barrier diversion is an unsaturated phenomena and is much more complex. Nevertheless, lateral drainage layers were specified where possible.

The restrictions imposed by the HELP code for these simulations can be seen by comparing the layering sequences for Plots 4 and 5. In Plot 4, the gravel layer is a lateral drainage layer. In Plot 5, the gravel is specified as a vertical percolation layer even though the layering sequence of Plots 4 and 5 are very similar. The reason for this difference is that HELP does not allow a lateral drainage layer to be the bottom layer in a layering profile. While the layer sequence restrictions may be adequate for a horizontal landfill cap, which is after all the primary use of HELP, the restrictions may not be applicable to tilted capillary barriers, which HELP is *not* designed to model.

The average annual precipitation, runoff, evapotranspiration, lateral drainage, change in moisture content, and percolation/leakage for the simulations are summarized in Table 3 for the various covers. The percolation/leakage values span a wide range. For an average annual precipitation of 24.3 cm, the percolation/leakage for the various covers ranges between 0.002 cm to 15.9 cm. According to HELP, the most effective covers are Plots 2 and 3 due to the geomembrane with a percolation/leakage of 0.002 cm. Plot 5, which is a capillary barrier, is predicted to allow the highest leakage at 15.9 cm. As discussed above, lateral drainage could not be specified for this plot due to HELP restrictions on the layering sequence. Plot 4, which has a similar layering sequence to Plot 5, has a much lower percolation/leakage of 4.8 cm probably due to specification of the gravel as a lateral drainage layer.

III. Capillary Barrier Effect

To estimate the capillary barrier effect of the covers, Ross' formula (Ross, 1990) and the TOUGH2 code (Pruess, 1991) have been used to evaluate the steady-state diversion length of the covers. While Ross' original formula is only directly applicable to the quasi-linear two-phase characteristic curves, Webb (1997a) has recently extended Ross' equation to other two-phase curves including van Genuchten (1980). Comparison of Ross' formula with detailed numerical simulations shows good agreement (Webb, 1997b).

Table 2
Layering Sequences

Plot 1: Soil Cover RCRA Subtitle "D"

Layer	Properties	HELP Layer Type
Topsoil	Topsoil	Vertical Percolation
Compacted Soil Barrier	Barrier Soil	Vertical Percolation

Plot 2: GCL Cover

Layer	Properties	HELP Layer Type
Topsoil	Topsoil	Vertical Percolation
Sand	Sand	Lateral drainage
Geo-membrane	Geo-membrane	Membrane Liner Pinhole Density - 1 hole/acre Install Defects - 10 holes/acre Placement Quality - Good
GCL	GCL	Vertical Percolation

Plot 3: Compacted Clay Cover RCRA Subtitle "C"

Layer	Properties	HELP Layer Type
Topsoil	Topsoil	Vertical Percolation
Sand	Sand	Lateral Drainage
Geo-membrane	Geo-membrane	as above
Compacted clay barrier	Compacted clay	Vertical Percolation

Plot 4: Capillary Barrier

Layer	Properties	HELP Layer Type
Topsoil	Topsoil	Vertical Percolation
Sand	Sand	Vertical Percolation
Gravel	Gravel	Lateral Drainage
Barrier Soil	Barrier Soil	Barrier Soil
Sand	Sand	Vertical Percolation

Plot 5: Anisotropic Barrier

Layer	Properties	HELP Layer Type
Topsoil/Gravel	Topsoil	Vertical Percolation
Native Soil	Native Soil	Vertical Percolation
Sand	Sand	Vertical Percolation
Gravel	Gravel	Vertical Percolation

Plot 6: Evapotranspiration Soil Cover

Layer	Properties	HELP Layer Type
Topsoil	Topsoil	Vertical Percolation
Native Soil	Native Soil	Vertical Percolation

Table 3
Summary of HELP Simulation Results

	Plot 1	Plot 2	Plot 3	Plot 4	Plot 5	Plot 6
Precipitation (cm)	24.3	24.3	24.3	24.3	24.3	24.3
Runoff (cm)	0.15	0.13	0.13	0.02	0.02	0.12
Evapotranspiration (cm)	17.4	6.0	6.0	2.9	8.4	13.1
Lateral Drainage (cm)	0	17.9	17.9	16.6	0.	0.
Change in Moisture Content (cm)	0	0.31	0.31	0.01	0.	0.
Percolation/Leakage (cm)	6.8	0.002	0.002	4.8	15.9	11.1

Table 4
Calculated Capillary Barrier Diversion Lengths

Net Infiltration Rate	Plot 1	Plots 2 and 3	Plots 4 and 5	Plot 6
20 cm/yr	3.4 m	220. m	210. m	0.
2.0 cm/yr	0.25 m	2200. m	2100. m	0.
0.2 cm/yr	0.035 m	17000. m	21000. m	0.

Table 4 presents the calculated capillary barrier diversion length of Plots 1-6 as a function of average net infiltration rate (precipitation minus runoff minus evapotranspiration); note that the average total precipitation from HELP is 24.3 cm/yr. Plot 1 shows a small capillary barrier effect at the topsoil/compacted soil interface which, interestingly, decreases with decreasing infiltration rate. This behavior is contrary to traditional fine-over-coarse tilted capillary barrier behavior which exhibits an increasing diversion length with decreasing infiltration. Plots 2 and 3 show no capillary barrier effect at the topsoil/sand interface. This behavior can be explained by comparing the characteristic curves for the two layers on Figure 2. Since the sand curve is above the topsoil curve, there is no capillary barrier effect for topsoil over sand using the present properties; the curve for the underlying layer must be below the curve for the overlying layer for a capillary barrier effect. Neglecting the geomembrane due to its low hydraulic conductivity and the possibility of local defects, the capillary barrier effect was calculated for the sand/GCL or compacted clay interface. Plots 2 and 3 are identical in this case because the GCL and compacted clay properties are the same. The calculated diversion length for this interface is hundreds of meters or more and is significantly greater than the length of the ALCD covers. Therefore, little, if any, percolation/leakage through the GCL or compacted clay is expected for Plots 2 and 3 due to the capillary barrier effect. While the reality of diversion lengths of 1000 meters or more is questionable, the magnitude of the calculated diversion length indicates a strong capillary barrier effect and minimal percolation/leakage. Similar to Plots 2 and 3, Plots 4 and 5 have no capillary barrier effect at the topsoil(native soil)/sand interface. Plots 4 and 5 *do* have a large capillary barrier effect at the sand/gravel interface; the predicted diversion length for Plots 4 and 5 is similar to Plots 2 and 3 and is significantly greater than the length of the ALCD covers. Finally, Plot 6 has no capillary barrier effect at all.

The results from TOUGH2 simulations show similar results. TOUGH2 is a multidimensional unsaturated flow code that is widely used for simulating flow and transport in fractured and porous media in nuclear waste, environmental, and geothermal applications (Pruess, 1991). Simulations were performed using TOUGH2 based on a net infiltration rate (precipitation minus runoff minus evapotranspiration) of 1, 10, and 100% of normal precipitation of 20 cm/yr for up to 10 years similar to Table 4. For Plots 1 and 6, minimal or no diversion was calculated by TOUGH2, while complete lateral diversion was predicted for Plots 2, 3, 4, and 5 consistent with the results from Ross' formula.

The advantage of using TOUGH2 compared to HELP is the mechanistic calculation of unsaturated conditions in the soil layers. Unfortunately, TOUGH2 does not include precipitation, runoff, or evapotranspiration models or have the flexibility of HELP. Morris and Stormont (1997) attempted to partially address the unsaturated flow issue by extracting the precipitation, runoff, and evapotranspiration data from HELP and using it as input to a mechanistic unsaturated flow code. However, this approach may not be adequate since the unsaturated conditions calculated by the unsaturated flow code were not fed back into HELP. Therefore, we are presenting planning to couple the precipitation, runoff, and evapotranspiration models of HELP with the unsaturated flow modeling of TOUGH2 (Webb, 1996). When this coupling is completed, a more comprehensive evaluation of the performance of the ALCD landfill covers, including capillary barriers, can be performed. Further evaluation is also anticipated when the experimental data from the ALCD become available.

IV. Conclusions

The predicted performance of the ALCD covers from the two approaches can be significantly different. For example, HELP predicts that Plot 5, a tilted anisotropic capillary barrier, allows the most percolation/leakage of any of the ALCD covers. In contrast, the capillary barrier results indicate that Plot 5 is one of the most effective configurations and will allow minimal or no percolation/leakage.

Evaluation of tilted landfill cover performance should consider possible capillary barrier effects. If there is little or no capillary barrier effect, HELP results may be appropriate, although questions about the applicability to semi-arid and arid regions remain. If there is a significant capillary barrier effect, the HELP results are not applicable. For the ALCD project, Plots 2, 3, 4, and 5 are expected to be the most effective designs due to the capillary barrier effect, and little or no percolation/leakage through these covers is expected. Plots 1 and 6 should allow significant percolation/leakage based on the HELP analysis; no significant capillary barrier effect is expected for these two plots.

In the future, HELP and TOUGH2 are planned to be coupled. When this work is completed, the effects of precipitation, runoff, and evapotranspiration based on HELP and the unsaturated flow modeling of TOUGH2 will be combined automatically and should give much more realistic results than either the HELP or TOUGH2 results by themselves.

Acknowledgment

V. References

Dwyer, S.F. (1995) "Alternative Landfill Cover Demonstration," *Landfill Closures - Environmental Protection and Land Recovery,* Geotechnical Special Publication No. 53, Dunn and Singh, eds., ASCE.

Fleenor, W.E., and I.P. King (1995) "Identifying Limitation on Use of the HELP Model," *Landfill Closures - Environmental Protection and Land Resources,* Geotechnical Special Publication No. 53, Dunn and Singh, eds., ASCE.

Morris, C.E., and J.C. Stormont (1997) "Capillary Barriers and Subtitle D Covers: Estimating Equivalency," *Journal of Environmental Engineering,* 123:3-10.

Nichols, W.E. (1991) *Comparative Simulations of a Two-Layer Landfill Barrier Using the HELP Version 2.0 and UNSAT-H Version 2.0 Computer Codes,* PNL-7583, Pacific Northwest Laboratory.

Pruess, K. (1991) *TOUGH2 - A General-Purpose Numerical Simulator for Multiphase Fluid and Heat Flow,* LBL-29400, Lawrence Berkeley Laboratory.

Ross, B. (1990) "The Diversion Capacity of Capillary Barriers," *Water Resour. Res.,* 26:2625-2629.

Schroeder, P.R., C.M. Lloyd, and P.A. Zappi (1994) *The Hydrological Evaluation of Landfill Performance (HELP) Model User's Guide for Version 3,* EPA/600/R-94/168a, U.S. Environmental Protection Agency Risk Reduction Engineering Laboratory, Cincinnati, Ohio.

Schroeder, P.R., T.S. Dozier, P.A. Zappi, B.M. McEnroe, J.W. Sjostrom, and R.L. Peyton (1994) *The Hydrological Evaluation of Landfill Performance (HELP) Model: Engineering Documentation for Version 3,* EPA/600/R-94/168b, U.S. Environmental Protection Agency Risk Reduction Engineering Laboratory, Cincinnati, Ohio.

Thompson, F.L., and S.W. Tyler (1984) *Comparison of Two Groundwater Flow Models - UNSAT1D and HELP,* EPRI CS-3695, Electric Power Research Institute.

van Genuchten, M.Th. (1980) "A Closed-form Equation for Predicting the Hydraulic Conductivity of Unsaturated Soils," *Soil Sci. Soc. Am. J.,* 44:892-898.

Webb, S.W. (1996) *Selection of a Numerical Unsaturated Flow Code for Tilted Capillary Barrier Performance Evaluation,* SAND96-2271, Sandia National Laboratories.

Webb, S.W. (1997a) "Generalization of Ross' Capillary Barrier Diversion Formula For Different Two-Phase Characteristic Curves," paper submitted to *Water Resources Research.*

Webb, S.W. (1997b) "Comparison of Ross' Capillary Barrier Diversion Formula with Detailed Numerical Simulations," 1997 ICTCE Conference, St. Petersburg, FL.

Chapter 7

Caps: Innovative Techniques

Surface Barrier Research at the Hanford Site

Glendon W. Gee, Anderson L. Ward and Michael J. Fayer[1]

Abstract

At the DOE Hanford Site, a field-scale prototype surface barrier was constructed in 1994 over an existing waste site as a part of a CERCLA treatability test. The above-grade barrier consists of a fine-soil layer overlying coarse layers of sands, gravels, basalt rock (riprap), and a low permeability asphalt layer. Two sideslope configurations, clean-fill gravel on a 10:1 slope and basalt riprap on a 2:1 slope, were built and are being tested. Design considerations included: constructability; drainage and water balance monitoring; wind and water erosion control and monitoring; surface revegetation and biotic intrusion; subsidence and sideslope stability, and durability of the asphalt layer. The barrier is currently in the final year of a three-year test designed to answer specific questions related to stability and long-term performance. One half of the barrier is irrigated such that the total water applied, including precipitation, is 480 mm/yr (three times the long-term annual average). Each year for the past two years, an extreme precipitation event (71 mm in 8 hr) representing a 1,000-yr return storm was applied in late March, when soil water storage was at a maximum. While the protective sideslopes have drained significant amounts of water, the soil cover (2-m of silt-loam soil overlying coarse sand and rock) has never drained. During the past year there was no measurable surface runoff or wind erosion. This is attributed to extensive revegetation of the surface. In addition, the barrier elevation has shown a small increase of 2 to 3 cm that is attributed to a combination of root proliferation and freeze/thaw activity. Testing will continue through September 1997. Performance data from the prototype barrier will be used by DOE in site-closure decisions at Hanford.

Introduction

The U. S. Department of Energy (DOE) has been actively pursing surface cover design and construction for the past decade or more (Wing and Gee 1994). A multi-year barrier development program was started at the Hanford Site in 1985 to develop, test, and evaluate the effectiveness of various barrier designs (Wing 1994). A series of reports, now totaling over 120, document the progress of the barrier development work (e.g., Gee et al. 1996). These reports detail field tests, natural analog studies, and modeling of surface barrier performance and provide information on water balance, wind and water erosion, and biotic intrusions studies supporting surface barrier development at the Hanford Site. This paper provides a summary of the surface cover work that has been ongoing at the Hanford Site for more than 10 years. It details a barrier development program specifically designed for 1000-year performance and describes current research activities at a prototype surface barrier, located at the Hanford Site, that could be used at waste sites in arid climates.

Surface Barrier Design

Figure 1 shows the scope of work undertaken during the past 10 years that has been leading toward a final barrier design. As part of the overall development effort, a prototype barrier, incorporating all essential elements of a long-term surface barrier, was constructed at the Hanford Site in 1994. Because of the demand for a barrier that could perform for at least 1,000 yr without maintenance,

---

[1]Pacific Northwest National Laboratory, P. O. Box 999 K9-33, Richland, Washington 99352
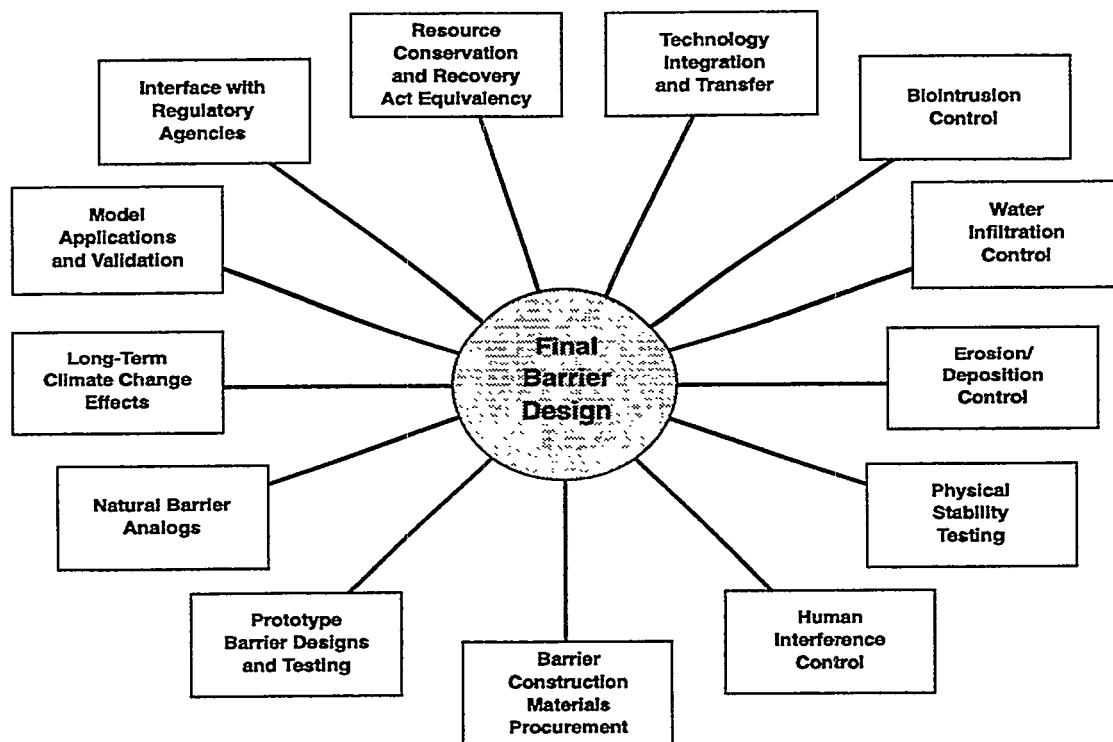
Figure 1. Components of the Barrier Development Program.

natural construction materials (e.g., fine soil, sand, gravel, cobble, basalt riprap, asphalt) were selected to optimize barrier performance and longevity. Most of these natural construction materials are available in large quantities on the Hanford Site and are known to have existed in place for thousands of years (e.g., basalt). The current barrier consists of a fine-soil layer overlying other layers of coarser materials such as sands, gravels, and basalt riprap and is designed to limit recharge to ≤ 0.5 mm yr^{-1} (Figure 2). Each layer serves a distinct purpose. The fine-soil layer acts as a medium in which moisture is stored until the processes of evaporation and transpiration recycle any excess water back to the atmosphere. The fine-soil layer also provides the medium for establishing plants that are necessary for transpiration to take place. The coarser materials placed directly below the fine-soil layer create a capillary break that inhibits the downward percolation of water through the barrier. The placement of fine soils directly over coarser materials also creates a favorable environment that encourages plants and animals to limit their natural biological activities to the upper, fine-soil portion of the barrier, thereby reducing biointrusion into the lower layers. The coarser materials also help to deter inadvertent human intruders from digging deeper into the barrier profile. Low-permeability layers, placed in the barrier profile below the capillary break, alsò are used in the barrier. The purpose of the low-permeability layers is (1) to divert away from the waste zone any percolating water that crosses the capillary break and (2) to limit the upward movement of noxious gases from the waste zone. The coarse materials located above the low-permeability layers also serve as a drainage medium to channel any percolating water to the edges of the barrier. In addition to testing the performance of a capillary barrier design, the prototype is being used to test two different sideslope designs: (1) a relatively flat apron (10:1, horizontal:vertical) of pit-run gravel (commonly called a clean-fill dike) and (2) a relatively steep (2:1) embankment of fractured basalt riprap (Gee et al. 1993b; Ward and Gee, 1997). Figure 2 also shows details of the two sideslope
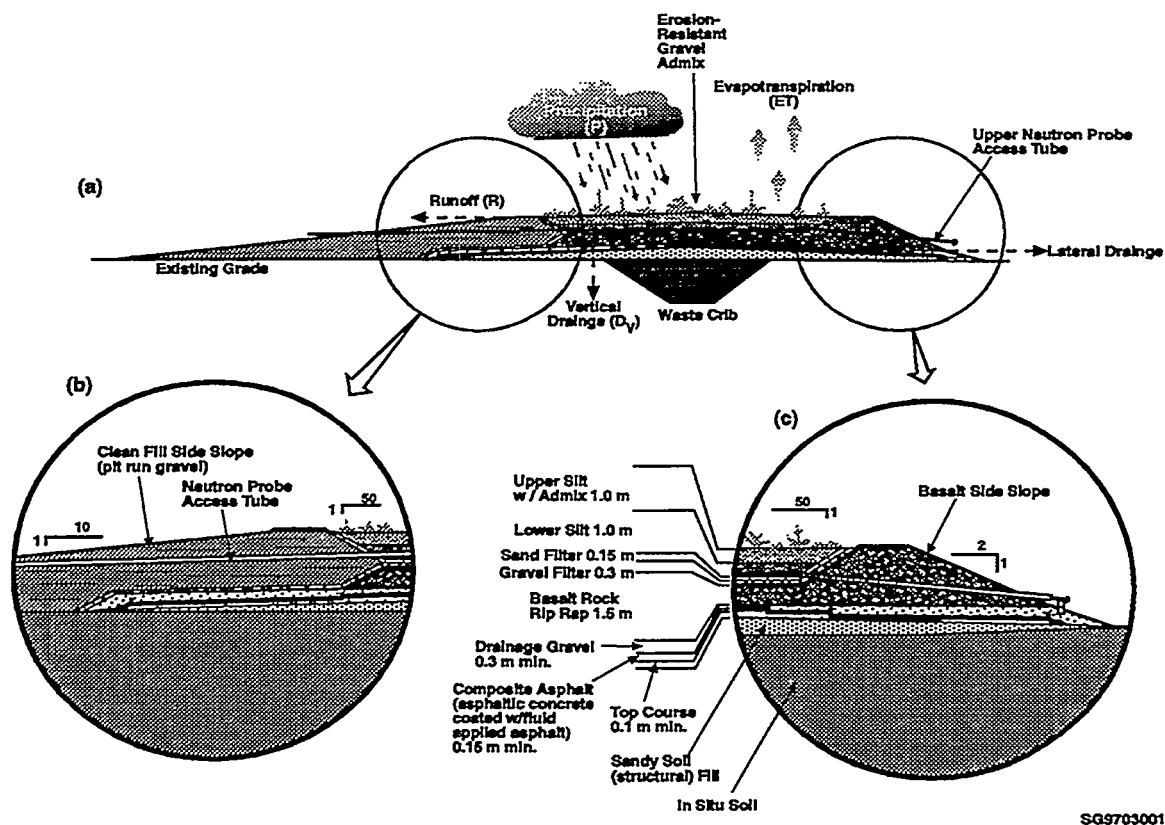
Figure 2. Cross-Section of the Hanford Barrier Showing the Layer Sequence and (a) Interactive Water Balance Processes, (b) Clean-fill Sideslope, and (c) Riprap Sideslope.

configurations used in the prototype barrier. A shrub and grass cover was established on the soil surfaces of the prototype in November 1994. Shrubs were planted at a density of 2 plants/m^2 with four sagebrush (*Artemsia tridentata*) plants to every one rabbitbrush (*Chrysothamnus nauseosus*) plant. Designing a maintenance-free barrier requires an understanding how natural processes affect barrier performance. A series of tests was designed to provide a better understanding of these processes and enable the design of a barrier that passively meets performance objectives.

Results of Field Tests

From November, 1994 through October, 1996, soil (capillary barrier) plots on the northern half of the prototype barrier were subjected to an irrigation regime of three times the long-term average annual precipitation (3X). This treatment included application of sufficient irrigation water on March 24, 1995 and March 25, 1996 to mimic a 1000-yr storm event (70 mm of water) and periodic applications to achieve a precipitation target of 480 mm/yr for the entire water year (November 1- October 31). Survival rate of the transplanted shrubs has been remarkably high; 97% for sagebrush and 57% for rabbitbrush (Gee et al. 1996). A heavy invasion of tumbleweed (*Salsola kali*) occurred in 1995 but was virtually absent in 1996. Grass cover, consisting of a 12 varieties of annuals and perennials (including cheatgrass, several bluegrasses, and bunch grasses), dominated the surfaces, particularly those that were irrigated. Approximately 75% of the surface was covered by vegetation; a cover

value typical of shrub-steppe plant communities. In all respects the vegetated cover appeared to be healthy and normal. There was a surface response to irrigation, with nearly twice as much grass cover on the irrigated surfaces compared to the non-irrigated surfaces (Gee et al. 1996).

Figure 3 shows the temporal changes in water-storage data at the prototype through October 1996. All irrigation and natural precipitation plus all available stored soil water was removed via evapotranspiration (ET) during the first year of surface barrier operation.
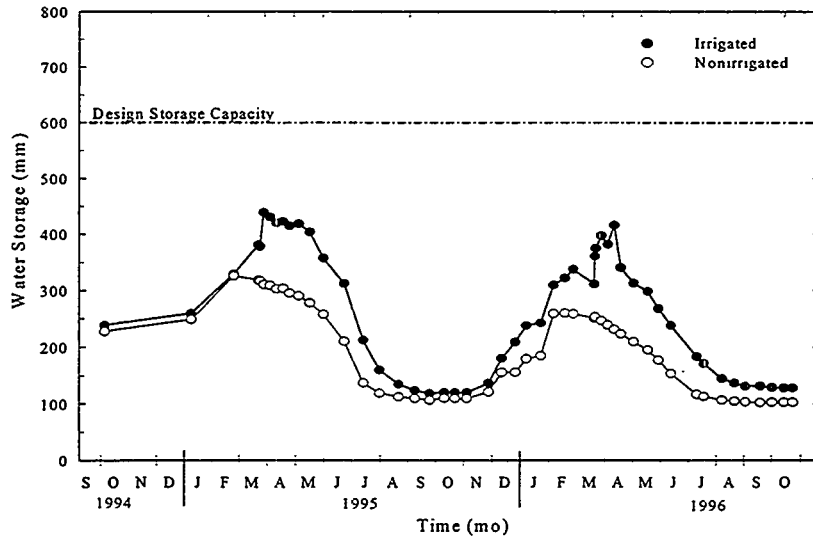
Figure 3. Temporal Change in Soil Water Storage at the Prototype Barrier from 09/30/94 Through 10/31/96.

Water was removed from the entire soil profile so that by late summer (September) of 1995, water content in both irrigated and non-irrigated plots had reached a relatively uniform lower-limit of about 5 vol. % throughout the soil profile. Correspondingly, water storage was reduced to levels near 100 mm (i.e., lower-limit of plant-available water), for both the irrigated and non-irrigated soil surfaces. This is about one-fifth the amount of water required for drainage. Based on these observations and considering the irrigation treatment to represent the extreme in wet climate, the soil cover would not be expected to drain, even under the wettest Hanford climate conditions.

Figure 3 also shows that in 1996, water from the second 1000-yr storm was removed from the soil profile. Since no drainage has occurred the change in storage is attributed to water loss by evapotranspiration, thus demonstrating the continued positive benefits of having vegetation on the barrier surface. Evapotranspiration for the irrigated surfaces was nearly double that for the non-irrigated (ambient) surfaces (Figure 4), suggesting that vegetation is capable of adjusting to water applications. It is apparent that the capacity of vegetation for water consumption has not been exceeded even at the 3X precipitation rates, even after the second year of testing. This further supports the hypothesis that the combination of vegetation and soil storage capacity is more than sufficient to remove all applied water under the imposed test conditions .
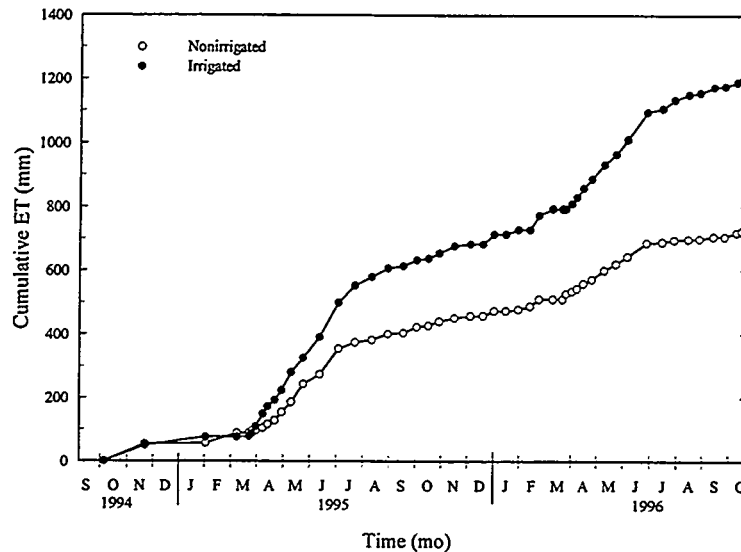
Figure 4. A Comparison of Cumulative ET From the Irrigated and Nonirrigated
Treatments for the Period 09/30/94 Through 10/31/96.

Drainage did not occur from the soil-covered part of the prototype barrier, even under the extreme conditions of 3X precipitation. These observations from the prototype agree with the results of extensive lysimeter testing of capillary barriers designs (Campbell et al. 1990; Gee et al 1993) and suggest that the water storage capacity of the soil is well in excess of the 3X (480 mm) precipitation. In contrast, both sideslope configurations drained although the amount of drainage was less than predictions based on the lysimeter studies. Sideslope drainage was expected since the surfaces are coarse and bare, with no vegetation growing on the basalt riprap and only a sparse (less than 10%) cover growing on the clean-fill gravel (Gee et al. 1993a; Sackshewsky et al. 1995). Figure 5 compares cumulative drainage from the gravel and riprap slopes through 10/31/96. On the nonirrigated treatments, the total amount of drainage from the clean-fill sideslope was greater than that from the basalt riprap sideslopes A similar trend was observed on the irrigated slopes up until November 1995. While irrigation of the soil surfaces started in February 1995, irrigation of the sideslopes did not start until November 1995. A closer look at these results show a seasonally dependence of drainage. While drainage from the clean-fill gravel sideslope was continuous, there was essentially no drainage from the riprap in the summer. In the winter, both sideslope configurations drained at similar rates. It is our hypothesis that advective drying similar to that described by Stormont et al. (1994) and Rose and Guo (1995) may be partly responsible for the lower drainage on the riprap sideslopes and may also have an effect on water storage in the fine-soil cover. Additional testing and numerical modeling will be used to test this hypothesis.

The rapid establishment of vegetation on the soil surface was thought to be responsible for at least three positive benefits to surface barrier performance. First, the vegetation was dominant in the water removal process from the soil surfaces. Second, the surface was stabilized against water erosion

309
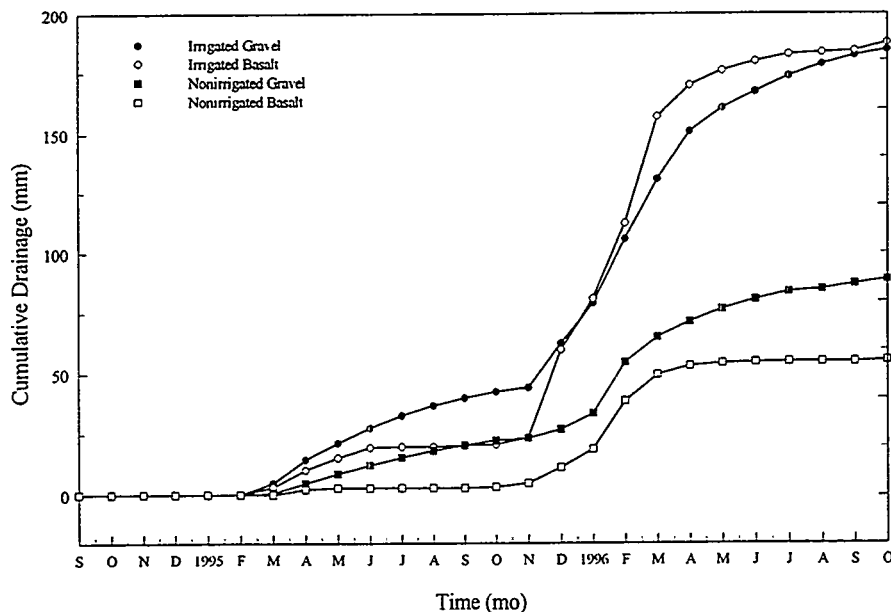
Figure 5. Cumulative Drainage From the Prototype Hanford Barrier for the Period 02/01/95 Through 10/31/96. No Drainage has Occurred From The Soil-Covered Plots.

and runoff. Runoff from the 1000-year storm in 1995 was 1.8 mm (about 2% of the 70 mm applied). There was no runoff in 1996. The improvement was attributed to vegetative growth and plant establishment. Root growth has caused some changes in soil bulk density and likely was presence of vegetation on soil surface Finally, there has been a positive benefit in controlling wind erosion. After plant establishment in November 1994, there have been no measurable losses of soil from the surface of the prototype by wind erosion. This is attributed to the vegetation and lack of surface disturbance during the past two years.

A minimum of 3 years of testing is planned for the prototype barrier. Because only a finite amount of time exists to test a barrier that is intended to function for a minimum of 1,000 yr, the testing program has been designed to "stress" the prototype so that barrier performance can be determined within a reasonable time frame. Continued monitoring of prototype barrier performance for extended periods is desirable because the succession of vegetation types, the full development of root profiles, and the natural colonization of the barrier surface by burrowing animals will occur over a longer time period. Long-term monitoring of the prototype barrier would be a valuable asset for hydrologic model validation studies and in the assessment of the long-term performance of cover systems at the Hanford Site.

Conclusions

The study of surface barriers at the Hanford Site has evolved into an integrated demonstration of key features of barriers designed to minimize water intrusion, erosion, and biointrusion. The results of

field tests, experiments, and lysimeter studies are providing a defensible foundation on which barrier designs can be based. Test results show that for the Hanford Site's arid climate, a well-designed capillary barrier limits drainage to near-zero amounts. A subsurface asphalt layer provides additional redundancy. Data collected under extreme conditions (excess precipitation) provides confidence that the barrier has the ability to meet its performance objectives for the 1,000-yr design life. Data from the prototype surface barrier confirm earlier observations with lysimeters and field plots and show that all available water can be removed from the soil surfaces by evapotranspiration, even under elevated precipitation conditions. Sideslopes, in contrast, drain because they are barren. The sideslope drainage is less than predicted because of advective heating and wind action but is non-zero, thus this drainage must be accommodated in the final design. Asphalt sublayers can be successful in extending areas of surface protection and can divert drainage water away from underlying wastes.

Acknowledgments

References

Campbell, M. D., G. W. Gee, M. J. Kanyid, and M. L. Rockhold. (1990) *Field Lysimeter Test Facility: Second Year (FY 1989) Test Results*, PNL-7209, Pacific Northwest Laboratory, Richland, Washington.

Gee, G. W., D. G. Felmy, J. C. Ritter, M. D. Campbell, J. L. Downs, M. J. Fayer, R. R. Kirkham, and S. O. Link. (1993a), *Field Lysimeter Test Facility Status Report IV: FY 1993*, PNL-8911, Pacific Northwest Laboratory, Richland, Washington.

Gee, G. W., L. L. Cadwell, H. D. Freeman, M. W. Ligotke, S. O. Link, R. A. Romine, and W. H. Walters, Jr. (1993b) *Testing and Monitoring Plan for the Permanent Isolation Surface Barrier Prototype*, PNL-8391, Pacific Northwest Laboratory, Richland, Washington.

Gee, G. W., A. L. Ward, B. G. Gilmore, S. O. Link, G. W. Dennis, and T.K. O'Neil. (1996) *Hanford Protective Barrier Status Report. FY 1996.* PNNL-11367. Pacific Northwest National Laboratory, Richland, Washington.

Link, S. O., N. R. Wing, and G. W. Gee. (1995) The Development of Permanent Isolation Barriers for Buried Wastes in Cool Deserts: Hanford Washington. *J. Arid Land Studies 4:215-224.*

Rose, A. W., and W. Guo. (1995) Thermal Convection of Soil Air on Hillsides. *Environ. Geology* 25:258-262.

Sackschewsky, M. R., C. J. Kemp, S. O. Link, and W. J. Waugh. (1995) Soil Water Balance Changes in Engineered Soil Surfaces, *J. Environ.Qual.* 24: 352-359.

Stormont, J. C., M. D. Ankeny, and M. K. Tansey. (1994) Water Removal from A Dry Barrier Cover System, In *In-Situ Remediation: Scientific Basis for Current and Future Technologies* (ed G. W. Gee and N. R. Wing), pp. 325-346. Parts 1-2. Thirty-Third Hanford Symposium on Health and the Environment. November 7-11, 1994, Pasco, Washington, Battelle Press, Columbus, Ohio.

Ward, A. L. and G. W. Gee. (1997) Performance Evaluation of a Field-Scale Surface Barrier. *J. Environ. Qual.* 26: 694-705 .

Wing, N. R. (1993) *Permanent Isolation Surface Barrier Development Plan*, WHC-EP-0673, Westinghouse Hanford Company, Richland, Washington.

Wing, N. R. and G. W. Gee. (1994) Quest for the Perfect Cap. *Civil Engr.* 64(10):38-41.

PERFORMANCE CHARACTERISTICS OF A SELF-SEALING/SELF-HEALING BARRIER

R.G. McGregor[1] and J.A. Stegemann

Abstract

Environment Canada and the Netherlands Energy Research Foundation are co-developers of a patented Self-Sealing/Self-Healing (SS/SH) Barrier system for containment of wastes which is licensed to Water Technology International Corporation. The SS/SH Barrier is intended for use as either a liner or cover for landfills, contaminated sites, secondary containment areas, etc., in the industrial, chemical, mining and municipal sectors, and also as a barrier to hydraulic flow for the transportation and construction industry. The SS/SH Barrier's most significant feature is its capability for self-repair in the event of a breach. By contrast, conventional barrier systems, such as clay, geomembrane, or geosynthetic clay liners can not be repaired without laborious excavation and reconstruction.

Laboratory investigations have shown that the SS/SH Barrier concept will function with a variety of reactive materials. Self-Sealing/Self-Healing Barriers are cost competitive and consistently exhibit hydraulic conductivities ranging from 10^{-9} to 10^{-13} m/s, which decrease with time. These measurements meet or exceed the recommended hydraulic conductivity required by EPA for clay liners ($<1 \times 10^{-9}$ m/s) used in landfills and hazardous waste sites. Results of mineralogical examination of the seal, diffusion testing, hydraulic conductivity measurement, and durability testing, including wet/dry, freeze/thaw cycling and leachate compatibility are also presented.

Introduction

The properties of an ideal waste containment system include low permeability, resistance to contaminant diffusion and long-term physical and chemical stability. Hydraulic barriers, such as compacted clay and synthetic flexible membrane liners, are most commonly used to obtain low hydraulic conductivities ($<10^{-9}$ m/s). These barriers, especially the compacted clay liners, are also resistant to diffusion, although diffusion of some contaminants can remain significant (Johnson et al. 1989, Mott and Weber 1991). The major concern with clay and synthetic liners is their long-term stability against chemical reactions with leachates (Farquhar and Parker 1988, Schackelford 1994) and resistance to weathering processes such as freeze/thaw and wet/dry cycling (Othman et al. 1994, Bowders and McClelland 1994).

The Self-Sealing/Self-Healing Barrier technology is based on micro-scale properties of diffusion and chemical reactions as shown in Figure 1. The process begins with the reaction of dissolved compounds to form a precipitate at the interface between two materials (i.e. parents). Precipitation reactions at the interface result in a decrease in the aqueous concentrations of the reactive components and thereby create a concentration gradient. This gradient leads to diffusion of additional reagents to the interface, thus resulting in further precipitation until the pores between the two parent materials are completely filled. If the barrier is damaged the remaining parent materials will once again react at the new interface and restart the self-healing process, leading ultimately to a new barrier between the two parent materials (van der Sloot et al. 1995).

---

[1] Water Technology International Corporation, operator of the Wastewater Technology Centre and the Canadian Clean Technology Centre, PO Box 5068, Burlington, Ontario, Canada, L7R 4L7, richard.mcgregor@cciw.ca

The parent materials used in forming the barrier are dependent upon numerous factors such as material availability, transportation costs, mixing facilities, native soil properties and intended barrier application. To reduce costs, waste materials and/or leachates derived from waste materials are incorporated into the barrier design either as a parent material or as matrix material. An example of waste utilization includes using mine tailings to form liner/cover systems for the containment of acidic drainage. Other experimental liners currently being tested use leachates from a variety of waste materials including municpal landfills as one of the parent materials.

Figure 2 shows complete encapsulation of a waste by the Self-Sealing/Self-Healing Barrier. Disruption of the barrier leads to renewed formation of the barrier at the site of the breach. The self-healing ability of the seal is an unique feature of the Self-Sealing/Self-Healing Barrier. By contrast, conventional barrier systems, such as compacted clay/soil, geomembrane or geosynthetic clay liners provide limited self-repair and are extremely costly and difficult to repair if significant damage occurs.
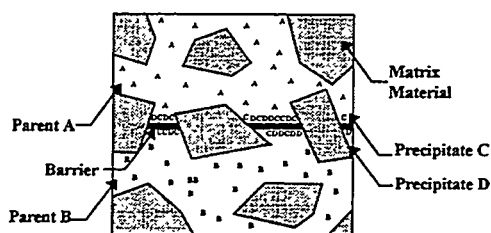
Figure 1 - Microscopic view of self-sealing process showing two parent materials (A and B) reacting to form precipitates C and D.
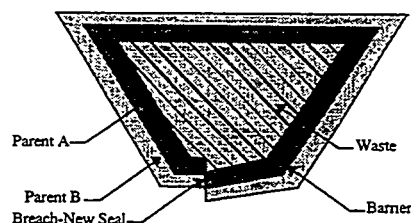
Figure 2 - Schematic showing the application of the barrier as a cover and liner with a self-healed breach.

Experimental Methods

A number of experimental methods were applied in the laboratory for a wide variety of parent combinations. These tests included diffusion testing to measure the resistance of the barrier to contaminant diffusion and hydraulic conductivity testing, to measure the resistance of the barrier to water and leachate flow as well as the effect of wet/dry and freeze/thaw cycling on the barrier's integrity. The results presented in this paper are for a Self-Sealing/Self-Healing barrier system developed for the isolation of mining wastes.

Diffusion tests

Diffusion experiments were conducted to evaluate, both qualitatively and quantitatively the performance of the seal as a diffusive barrier. Experiments used tartrazine dye as an unreactive tracer to indicate the presence of a barrier. These experiments were performed in glass test tubes. Parent materials were placed and allowed to react for a period of 14 days. After a formation period of 14 days, dye was added to the surface of the sample and allowed to diffuse to the interface between the two parent materials. After pre-determined periods of time, the samples were sliced and sampled for chemical and mineralogical analyses. Using colourimetric analysis techniques, the concentration of the indicator was determined for quantitative assessment of the barrier performance.

Leachate compatibility tests

Numerous studies of the interaction of leachate pore water with conventional liner materials have shown that reactions between the two may significantly alter the hydraulic conductivity of the liner (e.g., Shackelford, 1990). To examine its compatibiliy with leachate, the Self-Sealing/Self-Healing Barrier was permeated with various leachates containing a variety of organic and inorganic compounds. The effect of the leachates on the barrier was evaluated by measuring hydraulic conductivity in a 7.62 cm (3") diameter flexible-wall permeameter. This paper will discuss the results of two leachate tests; one acidic leachate containing elevated heavy metals and the other leachate obtained from an active municipal landfill. The method used to measure the hydraulic conductivity of the barriers is outlined in ASTM Method D5084, "Measurement of Hydraulic Conductivity of Saturated Porous Materials Using a Flexible Wall Permeameter". Bladder accumulators were used to isolate the leachate from the panel and a sampling port was installed in the permeameter outlet in order to obtain pore water samples from the barrier sample.

Parameters measured for the leachates included; pH, E_H, alkalinity, temperature, cations (Al, As, Ca, Cd, Co, Cr, Cu, Fe, K, Mg, Mn, Na, Ni, Pb, Si and Zn), anions (Cl, NO_2, NO_3, PO_4 and SO_4) and, in the case of the municipal landfill leachate, ammonia (NH_3) and total organic carbon (TOC). Measurements of pH, E_H, temperature and alkalinity were made immediately after sampling using a flow-through cell to isolate the pore water from atmospheric oxygen. Before each reading the pH electrode was calibrated using pH 4.0 and 7.0 buffers (NBS standard) and E_H measurements were checked using Zobell's solution (Nordstrom 1977). Alkalinity determinations were made using standardized H_2SO_4 and a digital titrator. Table 1 provides partial analyses of the two leachates.

Table 1- Partial analysis of two leachate samples used for compatibility experiments

Leachate	pH	As	Cd	Co	Cr	Cu	Fe	Pb	NO$_3$	TOC
Mun. Landfill	6.55	<0.1	0.001	0.08	0.022	0.003	0.45	<0.04	<1.5	345
Heavy Metals	2.18	28.1	11.1	24.4	25.3	26.3	53.5	10.8	22.5	<1.0

All units mg/L except pH.

Weathering tests

Two sets of experiments were carried out to determine the effect of wet/dry and freeze/thaw cycling on the integrity of the barrier. Freeze/thaw procedures used 3-D freezing methods as discussed by Zimmie and LaPlante (1990). Previous studies of the effects of freeze/thaw on clay have indicated that maximum increases in permeability generally occur within five cycles of freezing and thawing (Othman and Benson 1992, Zimmie and LaPlante 1990). Specimens of the Self-Sealing/Self-Healing Barrier were submitted to one cycle per day of -18°C (±4°C) to 22°C (±5°C). To test for damage due to freeze/thaw, frozen barrier specimens were extruded from the molds, jacketed in thin flexible latex membranes and placed in a 7.62 cm (3") diameter flexible-wall permeameter. Hydraulic conductivity was measured as described in ASTM Method D5084, using distilled water as the permeant. The effective confining stress was kept constant for the tests while the hydraulic gradient was adjusted in order to compensate for decreases in hydraulic conductivity as the samples self-healed.

The effects of wet/dry cycling on the barrier were examined in a second set of experiments. The barrier samples were subjected to one wet/dry cycle per week. During the wet cycle the sample was saturated with distilled water for a period of four days. On the fifth day the sample was placed in an oven and allowed to dry for a period of three days at a temperature of 60°C (±5°C). The specimens were tested in a flexible-wall permeameter as described for the freeze/thaw experiments.

Self-healing tests

To evaluate the self-healing capability of the barrier, two experiments were carried out. The first experiment involved fracturing the barrier using hydraulic pressure by increasing the hydraulic head on a specimen in a flexible-well permeameter until the sample fractured. The second experiment involved mechanical fracturing of the barrier using a blow with a sharp tool. In both cases, the hydraulic conductivity of the barrier was then measured over a period of time to determine if and how fast the barrier would self-heal. Both experiments used ASTM Method D5084 with a distilled water permeant and a varying hydraulic gradient to compensate for the self-healing of the barrier.

Results and Discussion

Diffusion tests

Figure 3 shows the results from diffusion tube experiments using the tartrazine dye. It is clear from the sharp discontinuity near the middle of the profile (i.e. at the interface of the two parent materials) that a barrier had formed. Due to the minor role of advection and the relatively homogeneous nature of the parent materials, the migration of the tartrazine can be predicted by diffusion models based on Fick's second law:

$$\frac{\partial C}{\partial t} = D_e \left(\frac{\partial^2 C}{\partial zz^2} \right)$$

(1)

Calculations of the effective diffusion coefficient (D_e) give values ranging from 0.9-1.5×10^{-6} cm^2/s. These values are lower than those values reported by Johnson et al. (1989) (4×10^{-6} cm^2/s) and Barone et al. (1989)(7.5×10^{-6} cm^2/s) for Cl diffusion through clay-lined disposal sites.
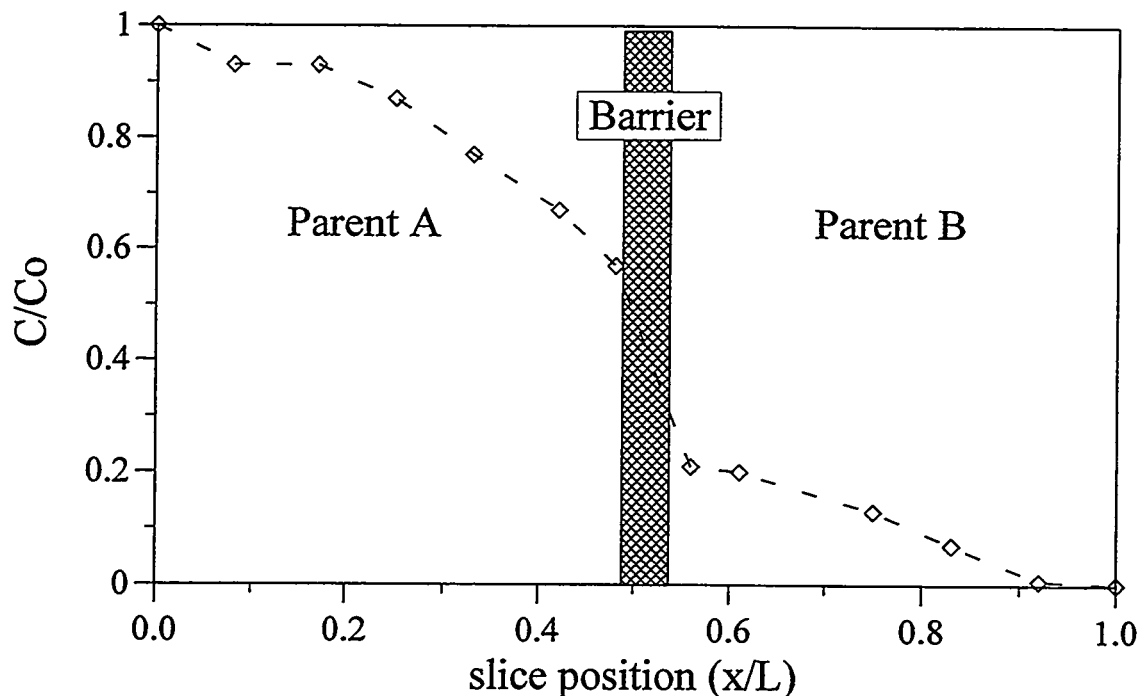
Figure 3 - Diffusion test results showing a tartrazine profile through the barrier. The shaded area represents the interface (cemented) between the two parent materials.

Leachate compatibility tests

Leachate compatibility tests done on samples of the barrier have shown no evidence of negative reactions between the leachate and the barrier. Monitoring of the hydraulic conductivity and outflowing leachate chemistry indicate that neither the acidic, heavy metal leachate or the municipal landfill leachate has an effect on the hydraulic conductivity of the barriers. In addition, the quality of the leachate which is forced through the barrier by the high hydraulic gradient of the hydraulic conductivity test is dramatically improved with many of the potential contaminants being removed from solution through precipitation/adsorption reactions. Results of the first leachate test using an acidic solution containing elevated concentrations of heavy metals showed no breakthrough of the heavy metals ($C/C_o>0.01$), with the exception of Zn which reached a maximum concentration of $C/C_o=0.011$. after eight pore volumes of flow at which point the test was stopped. The second compatibility tested using municipal landfill leachate as the permeate. This test is on-going with the hydraulic conductivity unaffected after two pore volumes of flow and the leachate outflow showing decreased concentrations of heavy metals, nutrients and total organic carbon.

Weathering tests

Figure 4 shows the results of the two weathering tests completed on the barrier. The results for both the freeze/thaw and wet.dry cycling indicate that the barrier's hydraulic conductivity remains well below the United States Environmental Protection Agency's suggested hydraulic conductivity of $1x10^{-9}$ m/s for compacted clay liners (CCL) in Subtitle D landfills after 20 cycles. The weathering tests used are conservative in three respects: 1) the amount of parent provided for rehealing in a laboratory sample is finite, 2) there is no time provided for rehealing between cycles, and 3) even in cover applications, a barrier would not be expected to undergo more than one freeze/thaw cycle annually, and the field conditions for wet/dry cycling would not be as extreme.
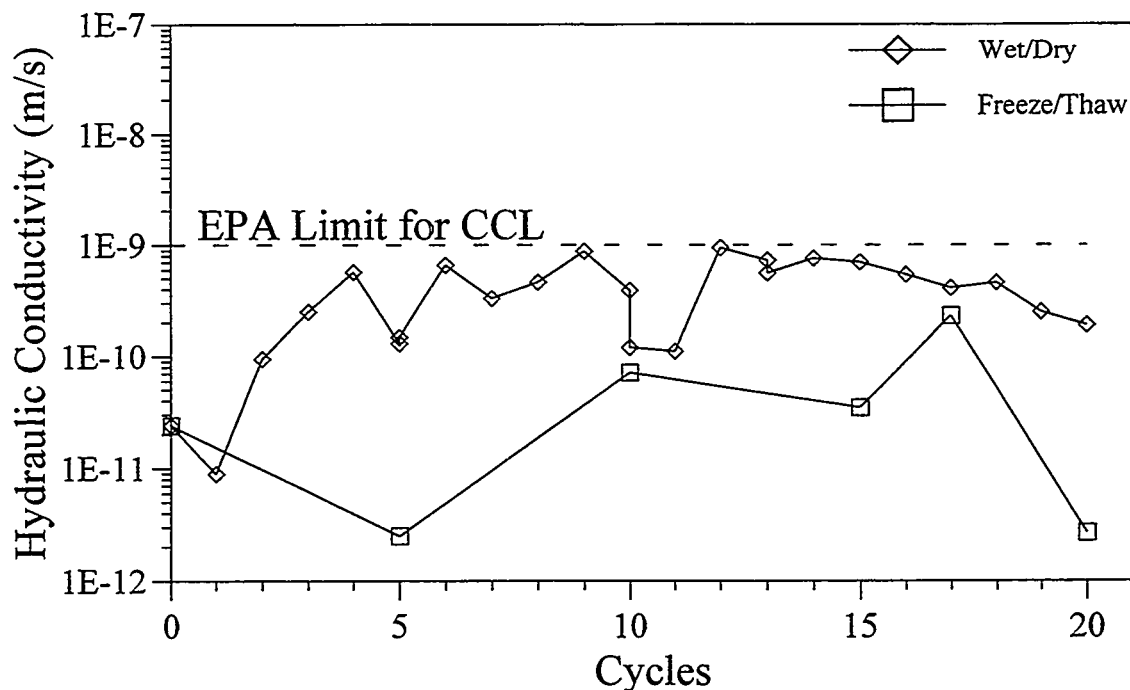
Figure 4 - Plot showing the effect of freeze/thaw and wet/dry cycling on the hydraulic conductivity of the barrier. The suggested EPA limit for compacted clay liners is provided for reference.

Self-healing tests

Figure 5 shows the results of the self-healing test where the barrier was mechanically fractured and then allowed to heal. Prior to and after the fracturing event the hydraulic conductivity of the barrier sample was measuredcontinuously under a constant confining pressure. The results show that the barrier had a hydraulic conductivity of 8.8×10^{-13} m/s prior to fracturing. The initial decrease in hydraulic conductivity is due to healing reactions occurring at the interface between the two parent materials. Immediately after fracturing, the hydraulic conductivity increased to 8.9×10^{-7} m/s, representing the hydraulic conductivity of the parent materials. Within 0.05 pore volumes of flow the hydraulic conductivity of the barrier had decreased to 1.4×10^{-9} m/s indicating that healing was proceeding. After 0.63 pore volumes of flow the hydraulic conductivity had decreased to its original value prior to fracturing.
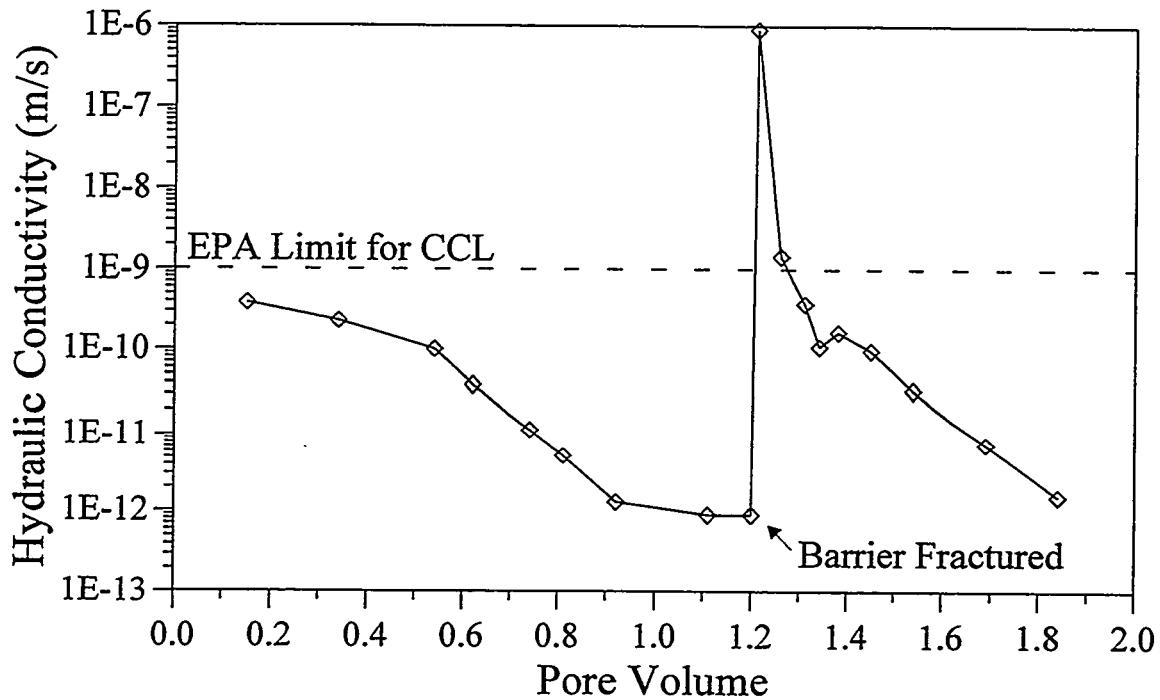
Figure 5 - Plot of hydraulic conductivity versus pore volume showing self-healing of a barrier sample fractured and allowed to self-heal under constant flow.

Conclusions

Diffusion, leachate compatibility and weathering testing on the Self-Sealing/Self-Healing Barrier system suggest that the barrier's performance is equivalent to or exceeds that of compacted clay/soil liners. The Self-Sealing/Self-Healing Barrier system also provides an unique self-healing mechanism which other liner systems such as compacted clay/soil, geomembranes and geosynthetic clay liners can not offer. Cost analysis of installing a Self-Sealing/Self-Healing Barrier system is estimated to be 50% to 80% of that for a compacted clay liner.

Field tests plots of the Self-Sealing/Self-Healing Barrier have been installed and are currently being monitored at a mine site in Northern Ontario and at a municipal landfill site in South Korea.

References

Barone, F.S., E.K. Yanful, R.M. Quigley and R.K. Rowe. (1989) Effect of multiple contaminant migration on diffusion and adsorption of some domestic waste contaminants in a natural clayey soil. *Can. Geotech. J.* 26, 189-198.

Bowders, J.J. and S. McClelland (1994) The effects of freeze/thaw cycles on the permeability of three compacted soils. In *Hydraulic Conductivity and Waste Containment Transport in Soil.* (eds Daniel, D.E. and S.J. Trautwein), pp. 461-481. ASTM STP 1142. Philadelphia.

Farquhar, G.J. and W. Parker. (1988) Interactions of leachates with natural and synthetic liners. *The Landfill-Reactor and Final Storage:Lecture Notes in the Earth Science Volume 20*, (ed P. Baccini), Springer-Verlag, Berlin.

Johnson, R.L., J.A. Cherry and J.F. Pankow. (1989) Diffusive contaminant transport in natural clay: a field example and implications for clay-lined disposal sites. *Environ. Sci. Technol.* 23(3), 340-349.

Mott, H.V. and W.J. Weber. (1991) Factors influencing organic contaminant diffusivities in soil-bentonite cutoff barriers. *Environ. Sci. Technol.* 25(10), 1708-1715.

Nordstrom, D.K. (1977) Thermochemical redox equilibria of Zobell's solution. *Geochimica et Cosmochimica Acta*, 41, 1835-1841.

Othman, M.A. and C.H. Benson. (1992) Effect of freeze/thaw on the hydraulic conductivity of three compacted clays from Wisconsin. *Transportation Research Record*, in press.

Othman, M.A., C.H. Benson, E.J. Chamberlain and T.F. Zimmie (1994) Laboratory testing to evaluate changes in hydraulic conductivity of compacted clays caused by freeze-thaw: state-of-the-art. In *Hydraulic Conductivity and Waste Containment Transport in Soil.* (eds Daniel, D.E. and S.J. Trautwein), pp. 227-254. ASTM STP 1142. Philadelphia.

Shackelford, C.D. (1994) Waste-soil interactions that alter hydraulic conductivity. In *Hydraulic Conductivity and Waste Containment Transport in Soil.* (eds Daniel, D.E. and S.J. Trautwein), pp. 111-168. ASTM STP 1142. Philadelphia.

van der Sloot, H.A., D. Pereboom, R.G. McGregor and J.A. Stegemann (1995) Properties of self-forming and self-repairing seals. In *Proceedings 5th International Landfill Symposium*, in press, Sardinia.

Zimmie, T.F. and C.M. LaPlante. (1990) The effects of freeze/thaw cycles on the permeability of a fine-grained soil. In *Proc. 22nd Mid-Atlantic Industrial Waste Conference*, pp. 580-593. Drexel University, Philadelphia.

LABORATORY TESTING OF CLOSURE CAP REPAIR TECHNIQUES

Peter Persoff[1], George J. Moridis[1], David M. Tuck[2], and Mark A. Phifer[2]

INTRODUCTION

Landfill design requires a low permeability closure cap as well as a low permeability liner. The Savannah River Site, in South Carolina, has approximately 85 acres of mixed waste landfills covered with compacted kaolin clay. Maintaining low permeability of the clay cap requires both that the permeability of the compacted clay itself remain low and that the integrity of the barrier be maintained. Barrier breaches typically result from penetration by roots or animals, and especially cracks caused by uneven settling or desiccation.

In this study, clay layers, 0.81 m in diameter and 7.6 cm thick, were compacted in 7 lysimeters to simulate closure caps. The hydraulic conductivity of each layer was measured, and the compacted clay layers (CCL's) were cracked by drying. Then various repair techniques were applied and the effectiveness of each repair was assessed by remeasuring the hydraulic conductivity. Finally the repaired CCL was again dried and measured to determine how the repair responded to the conditions that caused the original failure. For a full report of this investigation see Persoff et al. (1996).

Six repair techniques have been tested, four of which involve the use of injectable barrier liquids colloidal silica (CS) and polysiloxane (PSX) described below: (i) covering the crack with a bentonite geosynthetic clay liner (GCL), (ii) recompaction of new kaolinite at STD+3 moisture content joined to existing kaolinite that had dried and shrunk, (iii) direct injection of colloidal silica to a crack, (iv) injection of colloidal silica (CS) to wells in an overlying sand layer, (v) direct injection of polysiloxane to a crack, and (vi) , injection of polysiloxane (PSX) to wells in an overlying soil layer .

EXPERIMENTAL
Compacting Kaolin Layers in Lysimeters

The lysimeter design is shown in Figure 1. Each lysimeter consists of two concentric cylinders of 0.6-cm thick gray polyvinyl chloride (PVC), hot-air-welded to a base of 1.2-cm PVC. The inner cylinder divides the flow area beneath the compacted clay layer (CCL) into a 5-cm wide annulus at the outer wall and a 71-cm diameter central region, which are drained separately. During the experiments, however, there was evidence that flow from the edge of the lysimeter can flow to the central drain and vice versa.

The CCL's were constructed from Barden AG-1 kaolin (Kentucky-Tennessee Clay Co., Langley SC). This clay was received powdered at 1% moisture. Its Liquid and plastic limits (ASTM D-4318) were 83 % and 37 % respectively, and its maximum dry density under standard Proctor compaction (ASTM D-698) was 1370 kg/m^3, with an optimum water content of 29.5 %. A sample compacted at 32.5% water (i.e., 3 % wet of optimum, STD+3) had a hydraulic conductivity (ASTM D-5084) of 4.7 x10^{-8} cm/sec.

Kaolin at STD+3 was compacted in each lysimeter in three lifts to form a 7.6-cm-thick (3 inch) CCL. Each lift was compacted with 1047 blows of a Modified Proctor compaction hammer, which was 2.7 times standard compactive effort to compensate for the lack of wall confinement when compacting in the wide lysimeters. Between lifts the surface was scarified to ensure good bonding.

[1]Earth Sciences Division, Lawrence Berkeley National Laboratory, Berkeley, CA 94720 ,
(510) 486-5931, persoff@lbl.gov; (510) 486-4746, gjmoridis@lbl.gov

[2]Westinghouse Savannah River Company, Aiken, SC 29808 (803) 725-2927,
david.tuck@srs.gov; (803) 725-5222, mark.phifer@srs.gov
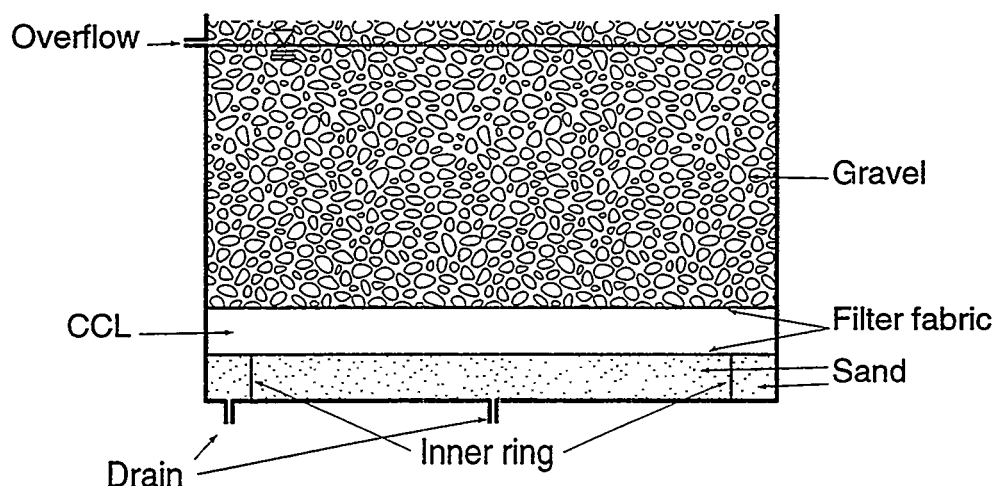
Figure 1. Lysimeter with CCL over sand drainage layer. Flow rates through central and edge drains were measured under constant hydraulic head.

After compaction, the dry density and the moisture content of the compacted clay was checked by taking 1-inch diameter plugs from the compacted clay, weighing, drying, and reweighing. Holes left by removal of plugs were repaired by compaction of additional kaolin into the holes, using a miniature compaction hammer. Similar sampling and recompaction was done several times on each CCL to monitor changes in moisture content and dry density as the kaolin dried.

To measure the hydraulic conductivity, a layer of filter fabric was placed over the CCL, and then 36 cm of gravel was placed over the filter fabric to prevent the CCL from swelling during the test. Water was then maintained at a depth of 36 cm, to give a hydraulic gradient of 4.67. Flow was collected in tared Erlenmeyer flasks. Although the inner ring was supposed to isolate flow from the edge and central areas of the lysimeter, flow usually issued only from either the center or edge drain. This suggested that the filter fabric between the sand and kaolin layers conducted flow across the dividing ring. The hydraulic conductivities of the CCL's in the various lysimeters ranged between 3×10^{-8} and 8×10^{-8} cm/sec, values that compare favorably with the value measured on a sample of the same clay compacted by ASTM D-698 and flow tested by ASTM D-5084.

Drying and Fracture Formation
Following the measurement of as-built hydraulic conductivity of the CCL's, dry air was flowed over their surfaces to dry them. Although in the field drying clay cracks as it shrinks, this behavior was not reproduced in the laboratory. Instead, the CCL's tended to shrink as a unit, gapping away from the walls of the lysimeter rather than cracking. Various techniques were implemented to prevent annular gapping and encourage formation of tension cracks. Tension cracks were successfully produced by aiming a heat gun at a line. These cracks tended to reclose as water diffused from wetter parts of the clay layer, but after sufficient drying they remained open.

After the cracks were established by drying, they were widened to 2 to 4 mm by driving a mason's chisel into each end of the crack and twisting it. During dry back, measurements were made of dry density, moisture content, and areal shrinkage . Data for CCL 6, which are typical for all are shown in Figure 2. Normalized area, which indicates shrinkage, was estimated from gap measurements.

CONDUCTIVITY OF CRACKED CCLs
The hydraulic conductivity of the cracked CCL's was measured to provide a baseline against which to assess the effectiveness of repairs. Measurement of the hydraulic conductivity of the cracked CCL was complicated by two factors: the annular gap between the perimeter of the shrunken CCL and the lysimeter wall, and the tendency of kaolin to swell and reseal itself under ponded water. Before measuring the hydraulic conductivity of a cracked CCL, bentonite paste (1.6 mL water per g of bentonite) was packed into the annular gap. The dry kaolin took water from the bentonite
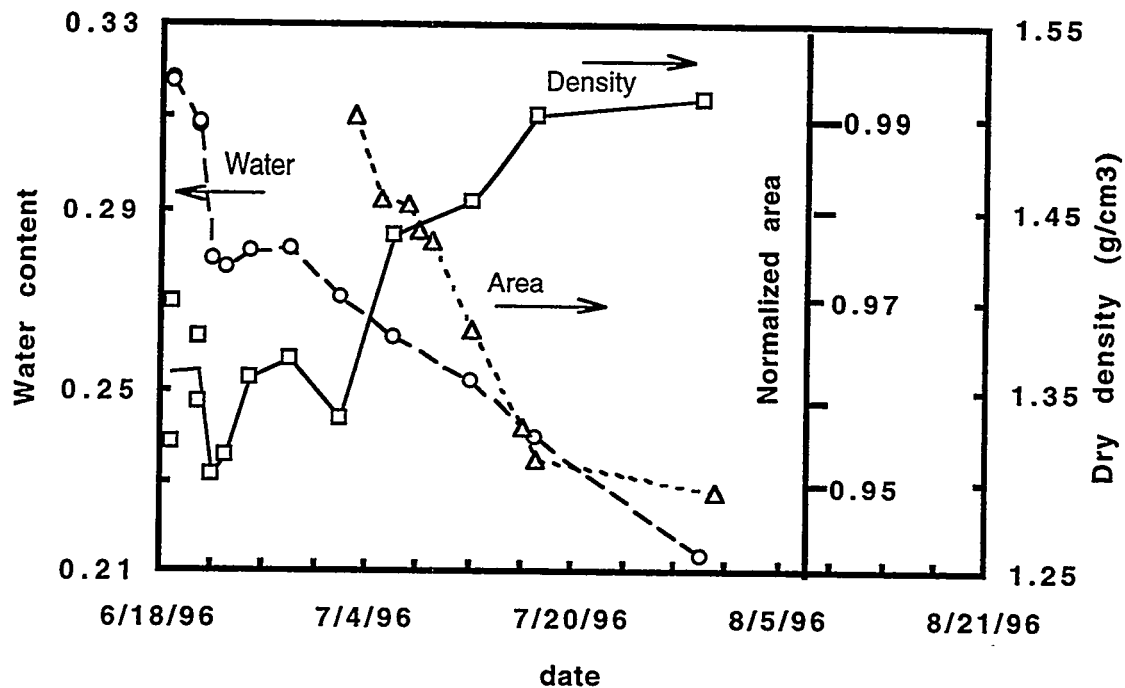
Figure 2 Water content (left axis), dry density and normalized area (right axes)during dry back of CCL 6.

paste, causing it to shrink. The bentonite paste was repacked immediately before starting hydraulic conductivity measurements, but some time was required (generally two days) before it swelled in place sufficiently to stop the flow of water.

Four measurements were made of the hydraulic conductivity of cracked CCL's. Although essentially all the flow in these measurements was through the crack, results are expressed as equivalent conductivity of the entire cracked CCL. Details of these measurements are presented elsewhere (Persoff and Moridis 1996). These measurements showed that the initial hydraulic conductivity of the cracked CCL was greater than 1x10-4 cm/sec but decreased rapidly because of kaolin. If the crack was not propped open it sealed completely (no detectable flow) within 2 days, while if the crack was propped open by filling it with sand (same as used for base layer), the hydraulic conductivity of the cracked CCL decreased to about $1x10^{-5}$ cm/sec.

Testing the repaired clay caps required that they be subjected to a hydraulic head. If the cracks were not sand-propped, this would cause the crack to self-heal and give a false indication of success. Therefore, to ensure that a measurement of low hydraulic conductivity of a repaired clay cap could be attributed to the repair and not to swelling of the kaolin, all cracks were sand-propped before the repair techniques were tested. Although the crack in CCL 2 did self-heal after two days under ponded water, such self healing is not likely to occur In the field. A CCL is generally overlain by a drainage layer of coarse material that prevents the formation of ponded water; also the coarse material enters cracks and prevents them from closing upon rewetting (Caldwell and Reith, 1993).

TESTING THE REPAIR TECHNIQUES

The results of the tests with six repair techniques are summarized in Table 1. All techniques were effective in restoring the hydraulic conductivity of cracked clay caps below the generally accepted standard of 10^{-7} cm/sec except for injection of PSX through soil, which failed because the

Table 1.	Hydraulic conductivity of CCLs as built and after repai					
Lysimeter	2	3	4	5	6	7
K as buit (cm/sec)	3.7E-8	2.7E-8	2.7E-8	5.7E-8	no flow	–
K after crack (cm/sec)	nm b	1.6E-4	7.7E-5	1.9 E-5	nm b	–
repair technique	CS direct to crack	CS through wells in coarse sand	GCL	PSX through wells in JN soil	PSX direct to crack	Recompaction of new kaolin
K after repair (cm/sec)	9.1E-8	no flow , 90 days	2.1E-8	6.0E-6 a	5.4E-8	2.3E-8
results of redrying	crack reopened at surface; K=4.3E-8	b	new crack, increased K to 1E-6 cm/sec		Not tested	b
re-repair			additional patch			
K after repair (cm/sec)			no flow , 20 days			
results of redrying	b		new crack, increased K not measured			
re-repair			additional patch			
K after repair (cm/sec)			8.8E-9			

a incomplete coverage of crack b test still in progress

capillary forces prevented much of the injected PSX from draining down to the clay surface and flowing to cover the crack.

Fracture Covered With GCL (Lysimeter #4)

Lysimeter 4 was repaired by application of Claymax R Bentonite Geosynthetic Clay Liner (GCL) (CETCO, Arlington Heights, IL). A patch of GCL was cut to overlap the entire fracture by 10 cm on both sides and fit closely with the wall. Since the hydraulic conductivity of the cracked CCL had just been measured, the bentonite paste in the annular gap was still watertight, so when hydraulic conductivity was measured, there was no flow from the edge. Flow from the center drain indicated that the repair was successful.

Lysimeter 4 was then redried by flowing a stream of dry air over it. A shallow (1 mm) secondary crack was observed extending out from under the GCL, and presumably connecting with the main crack. Hydraulic conductivity measurement showed that the new crack was carrying flow to the original crack under the GCL, resulting in a permeability (averaged over the entire area) of about 10^{-6} cm/sec, gradually decreasing. The overburden was then removed and a second GCL patch was applied, covering the new crack and overlapping the first patch. Overburden and water head were applied, and the second patch reduced the flow rate to zero. After ten days the test was discontinued with no flow having been observed. A third redrying produced similar results, with new crack formation, and a third repair reduced the hydraulic conductivity to 8.8x10-9 cm/sec.

Excavation of Cracks and Recompaction of New Kaolin (Lysimeter #7)

When cracks are detected, either during construction or in service, the cracked material can be removed and new material recompacted in its place. This is the baseline technology against which the other technologies are to be compared. During the construction of the existing clay caps at SRS, some material dried and cracked and was removed, and new material was joined to it. Thus, this repair technique has actually been implemented in the field. The repair technique consists of compacting new material next to, and joining it to existing compacted material. The desired result

is that the "seam" between the two materials is as tight as the bulk material; and that the seam not constitute a zone of weakness during drying that may occur after construction.

Recompaction of new clay can only succeed if the existing clay is sufficiently plastic to deform when the new clay is joined to it. Observations made in the other lysimeters showed that even 21% water is too dry to accept much compactive effort. It was desired that the clay to be repaired have dried and shrunk sufficiently to develop a significant crack, and yet still be plastic enough to repair. The lysimeter was divided in half by a temporary wall, and new Barden AG-1 kaolin at STD +3 was compacted in half of the lysimeter. This half-CCL was allowed to dry until it was judged by feel to be near the lower limit of water content necessary for successful joining of new clay. The water content was 28.4%. The CCL has also shrunk to 98.2% of its original area; this would constitute a significant crack. The temporary wall was removed, and clay was removed from the vertical surface of the existing clay to leave an oblique surface with a slope of 1 vertical to 2 horizontal. Water was sprayed on the oblique surface and it was scarified, and new material was compacted to fill the lysimeter. No problems with cracking of the existing clay cap were noted. The hydraulic conductivity was measured at 2.3×10^{-8} cm/sec,. indicating a successful repair. Following the flow test, after several weeks under ponded water, the repair was not visible. The laboratory test is continuing with drying of the CCL, to see whether the seam behaves differently from the bulk compacted clay. Presumably when this technique was used in the field, no problem was observed due to inadequate plasticity of the existing clay. Therefore the available evidence confirms that this repair technique was satisfactory.

The Viscous Barrier Liquids

Viscous barrier liquids are low-viscosity grouts that can be injected into soils to gel or solidify in place, blocking water flow. The two types of liquids tested here were selected for low initial viscosity, controllable gel time, effective pore blocking, and non-toxicity. See Moridis et al, (1993, 1995) or Persoff et al. (1994, 1995) for more information about the barrier liquids .

The colloidal silica was NP-5880 (Eka-Nobel, Marietta GA). This is an alumina-modified colloidal silica that typically contains 25% by weight silica, and 0.4% by weight Na_2O; its viscosity is 7 cP, pH 6.5, and density 1.17 g/cm^3. The nominal particle size is 8 nm. This colloid is made to gel by mixing 1 part by volume of CaCl2 brine with 5 parts colloid. The brine concentration controls the gel time. For direct-to-crack injection, 0.32 M $CaCl_2$ brine was used, which gels to a solid in 2 hr, and for through-sand injection 0.28 M $CaCl_2$ which takes twice as long to gel.

The polysiloxane was Dow-Corning 2-7154-PSX-10, with catalyst Syl-Off 4000. (Dow-Corning, Midland MI). This has an initial viscosity of 10 cP. It was used with 3% catalyst by weight, which gives a gel time of 1 hr.

For injection of gelling liquid to succeed as a repair technique, the liquid must (i) flow to the crack through the overburden (clay-sand or drainage layer), (ii) drain into the crack, (iii)gel in the crack before it drains down out of the crack, and (iv) be effective in sealing once it has gelled in the crack. In order to isolate these events, the testing of gelling liquids was conducted in two parts: First, the ability of the gelled liquid to seal the crack was tested by injecting the liquids directly to the crack. Second, the liquids were injected through wells into a layer of overburden, through which they flowed over and into the crack.

Direct PSX Injection Into Fracture (Lysimeter #6)

Bentonite powder was poured into the annular gap at the wall, and followed by packed-in bentonite paste. Sand was poured and packed into the fracture and the barrier liquid was applied to the crack with a pipette. Several 100-g batches of PSX were mixed and applied to the crack, saturating the crack, and allowed to gel. Because this CCL had been dried to a lowest water content of all the CCL's, much of the PSX was imbibed by the kaolin. A total of 700 grams of PSX were applied, until the crack refused to take any more PSX. An additional 200 grams were used to fill large divots formed when the crack was spread by rotating a chisel.

Initially there was a fast flow of water, which was recognized as typical of leakage through the bentonite paste. This flow issued from center drain as well as from the edge drain; however since it was turbid it was interpreted as flow through the bentonite powder. After two days the flow at the center stopped completely and a slow flow continued through the edge drain. In Table 1 this flow rate is interpreted as leakage through the repaired CCL.

Direct CS Injection Into Fractures (Lysimeter #2)
Colloidal silica was applied to CCL 2 in a similar manner as PSX had been to Lysimeter 6. After a total of 470 mL of CS grout had been applied in six injections, the crack would not accept any more. As in Lysimeter 6, there was initially fast flow of turbid water (equivalent to a hydraulic conductivity K of 1×10^{-5} cm/sec) through both drains; after the bentonite swelled a slow flow continued through the center drain, indicating a final hydraulic conductivity of 9.1×10^{-8} cm/sec.

CS Injection Into Sand Overburden (Lysimeter #3)
A practical advantage of injecting gelling grouts through overburden (sand or soil) is that the overburden need not be removed and replaced. In this case the liquid can be injected into a well or trench and must flow downward to the CCL and laterally to the crack, and then drain into the crack. In the field, the crack location may not be known, but generally the CCL is sloped, which will aid the grout in finding the crack.

To test this method of application in the laboratory, the crack was packed with sand to prevent it from self-healing and 15 cm of coarse sand, simulating the actual drainage layer overlying the some of the clay caps at the Savannah River Site was placed over the CCL. Two wells, perforated only in the bottom inch, were located 22 cm from each side of the crack as shown in Figure 3.

The electrical conductivity of CS grout was used to monitor its flow from the well to the crack. Twenty pairs of wires, used as resistivity sensors were arrayed over the surface of the CCL as shown in Figure 3. Sensors 10 through 16 trace out the crack. After this photograph was taken, the coarse sand was placed over the entire CCL, and two 2100 mL grout injections were made from a Mariotte bottle on successive days, first through the north well (between sensors 1 and 2) and then through the south well. The advance of grout through the coarse sand overburden is shown by the decrease in resistance as grout contacted each probe in Figure 4. No outflow was detected during 100 days. Complete flow blockage indicates either that the grout flowed into the crack and sealed it or that a complete layer of grouted sand was formed above the CCL. This lysimeter is now being dried for further testing.

PSX Injection Into Soil Overburden (Lysimeter #5)
This test was done in a similar manner to the preceding test, except a local clay-sand soil was used instead of coarse sand, lightly compacted to a dry density of 1.44 g/cm^3. Following the second injection of PSX, the soil was covered by filter fabric and gravel overburden, and the hydraulic conductivity of the repaired CCL was measured. The flow rate indicated a hydraulic conductivity of 6.0×10^{-6} cm/sec, which is lower by a factor of 3 than the hydraulic conductivity of the sand-packed fracture, but well above the target value for repaired CCL. To diagnose the cause of failure, the soil was mucked out by hand to reveal the grouted plumes, which were in the form of symmetrical mounds. The injected PSX grout spread over the surface of the CCL but did not completely cover the crack, leaving the ends of the crack exposed.

Analysis of numerical simulations of the injection showed that the great majority of grout injected into JN soil was taken up into pore space by capillarity, and did not contribute either to filling the crack or to forming an impermeable zone above the crack. The amount of PSX injected was sufficient to cover the CCL to a depth of 1 cm. If a greater volume of liquid had been injected, greater spreading and saturation of the grout would have resulted, and the design criterion (1×10^{-7} cm/sec) might have been met.
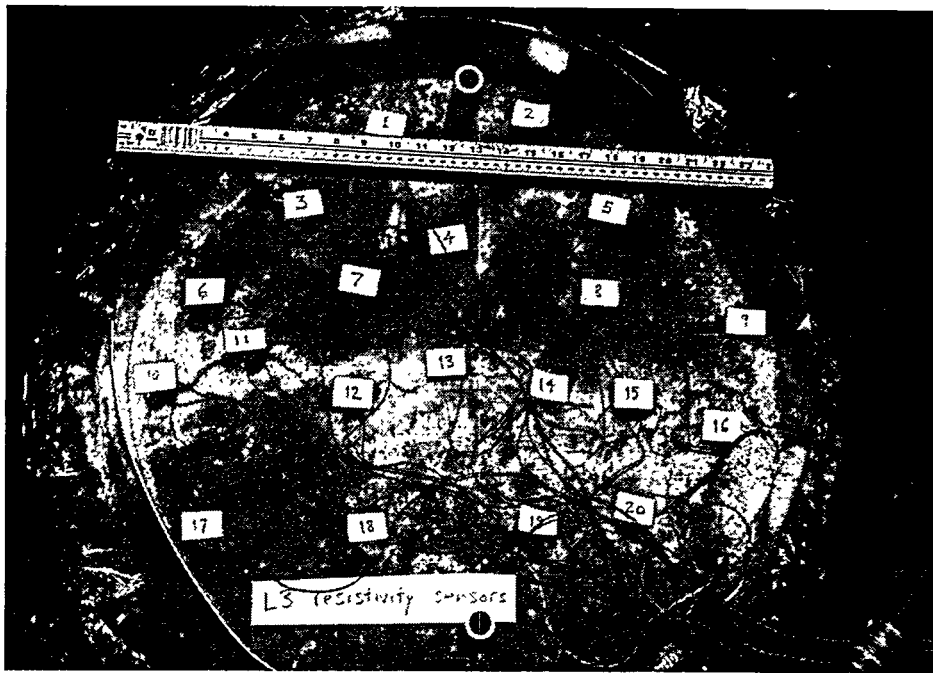
Figure 3. Resistivity sensors and wells arrayed on CCL 3 before covering with coarse sand.
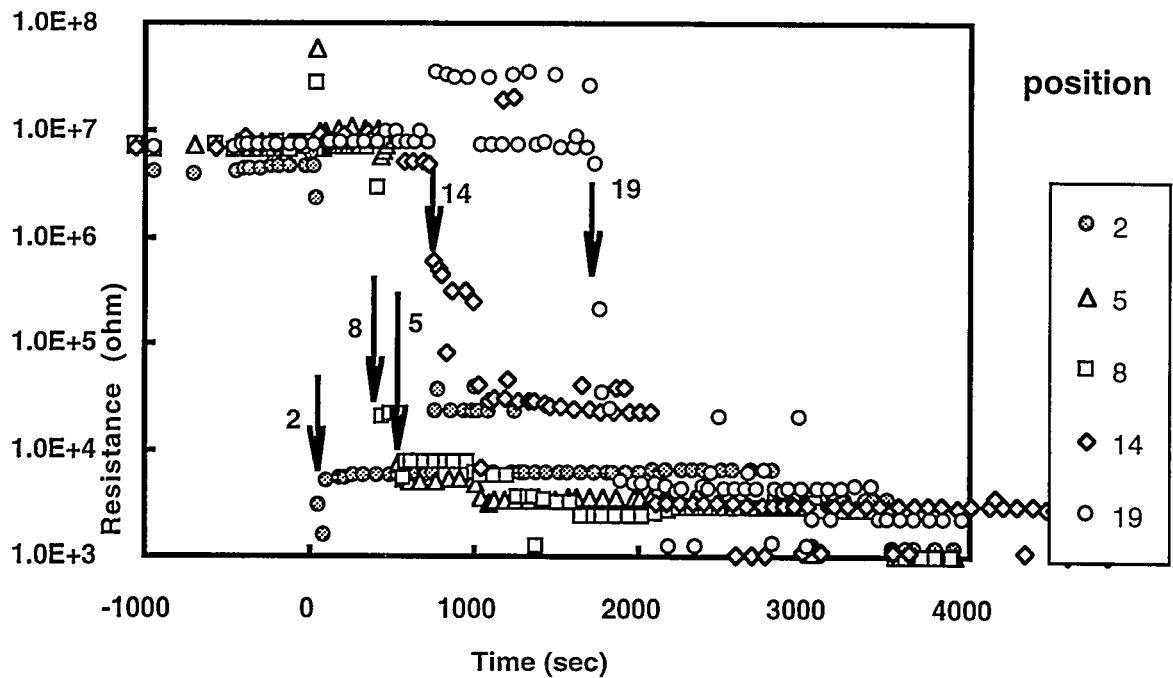
Figure 4. Resistivity measurements showing time of grout arrival at stations 2, 5, 8, 14, and 19.

CONCLUSIONS

The observations support the following conclusions:

.
(1)   Covering a crack with a GCL effectively prevents water from entering the crack, but does not fill the crack. Additional cracks that connect with the repaired crack can therefore bypass the repair.
(2)   Either colloidal silica or polysiloxane, if injected or drained into a crack in compacted clay, seals the crack effectively.
(3)   Colloidal silica can be injected into a sand drainage layer and flow into a crack and seal it.
(4)   Electrical resistivity measurement is an effective technique for tracking the penetration of colloidal silica grout.

ACKNOWLEDGMENTS

REFERENCES

Caldwell, J.A., and Reith, C.C. Principles and Practices of Waste Encapsulation, p. 231Lewis Publishers, Boca Raton, FL, 1993

Moridis, G., Myer, L., Persoff, P., Finsterle, S., Apps, J., Vasco, D., Williams, P., Flexser, S., Muller, S., Yen, P., Freifeld, B., and Pruess, K. (1995) First-Level Field Demonstration of Subsurface Barrier Technology Using Viscous Liquids. Lawrence Berkeley Laboratory Report LBL-37520.

Moridis, G.J., Persoff, P., Holman, H.-Y., Muller, S.J., Pruess, K., and Radke, C.J. New Barrier Fluids for Containment of Contaminants, in Proceedings of ER '93 Environmental Remediation Conference, Augusta GA , Oct. 24-28, 1993, p. 941-948 (Lawrence Berkeley Laboratory Report LBL-34673).

Persoff, P., S. Finsterle, G.J. Moridis, J. Apps, and K. Pruess, "Injectable barriers for waste isolation," AIChE Symposium Series, vol. 91, no. 306, 58-67, 1995. (Lawrence Berkeley Laboratory report LBL-36739).

Persoff, P., Moridis, G.J., Apps, J., Pruess, K., and Muller,S.J. Designing Injectable Colloidal Silica Barriers For Waste Isolation at the Hanford Site, in Proceedings, 33rd Hanford Symposium on Health and the Environment, -- In-Situ Remediation: Scientific Basis for Curent and Future Technologies, Part 1, p. 87-101, Pasco WA Nov 7-11 1994   Lawrence Berkeley Laboratory Report LBL-35447.

Persoff, P., Moridis, G.J., Frangos, W., and James, A. Laboratory Study of Closure Cap Repair Techniques, Final Report, Lawrence Berkeley National Laboratory Report LBNL-39420 , December 1996.

Phifer, M.A., Boles, D., Drumm, E.C., and Wilson, G.V. (1995) "Comparative Response of two barrier soils to post compaction water content variations," in Geoenvironment 2000, vol. 1 Geotechnical Special publication No. 46, American Society of Civil Engineers, New York, NY, p 591-607

CLAY SLURRY AND ENGINEERED SOILS AS CONTAINMENT TECHNOLOGIES FOR REMEDIATION OF CONTAMINATED SITES

Jerald R. Williams[1], Stanislaw Dudka[2], and William P. Miller[2], Donald O. Johnson[3]

Abstract

Clay Slurry and Engineered Soils are containment technologies for remediation of waste disposal sites where leaching, groundwater plumes and surface runoff of contaminants are serious ecological hazards to adjacent environments. This technology is a patent-pending process which involves the use of conditioned clay materials mixed with sand and water to form a readily pourable suspension, a clay slurry, which is either placed into a trench barrier system or allowed to de-water to create Engineered Soils. The Engineered Soil forms a layer impervious to water and air, therefore by inhibiting both water and oxygen from penetrating through the soil the material. This material can be installed in layers and as a vertical barrier to create a surface barrier containment system. The clay percentage in the clay slurry and Engineered Soils varies depending on site characteristics and desired performance standards. For example Engineered Soils with 1-2% of clay (dry wt.) had a hydraulic conductivity (K) of 10^{-8} to 10^{-9} cm/sec.

Tests of tailing materials from a kyanite and pyrite mine showed that the clay slurry was effective not only in reducing the permeability of the treated tailings, but also in decreasing their acidity due to the inherent alkalinity of the clay. The untreated tailings had pH values in the range of 2.4 - 3.1; whereas, the effluent from clay and tailings mixtures had pH values in a slightly alkaline range (7.7-7.9).

Pug-mills and high volume slurry pumps can be readily adapted for use in constructing and placing caps and creating Engineered Soils. Moreover, material on site or from a local sand supply can be used to create clay slurries and engineered soils. Clay materials used in cap construction are likewise readily available commercially. As a result, the clay slurry system is very cost effective compared to other capping systems, including the commonly used High Density Polyethylene (HDPE) liner systems.

---

[1]   Reclamation Technology, Inc., P.O. Box 7574, Athens, GA, 30604-7574, USA; Tel: (706)369-7329; Fax: (706)546-8417; E-Mail: http://rtijw@mindspring.com

[2]   The University of Georgia, 3111 Miller Plant Science Building, Athens, GA, 30602-7272, USA; Tel.: (706)542-0895; Fax: (706)542-0914

[3]   Energy System Division, Argonne National Laboratory, 9700 S. Cass Avenue, ES/362-E340, Argonne, IL 60439-4815, USA.: Tel.: (630)-252-3392, Fax: (630)-252-7288; don_johnson@qmgate.anl.gov

Introduction

Placing toxic and other hazardous waste materials in basins or landfills is a common method of waste disposal. In many such waste disposal sites, leaching of toxic compounds into surface and groundwater is a major environmental hazard. Many waste stockpiles directly threaten human health because nearby residents are exposed to the contaminated soil, dust and surface water (Golden, 1983).

The objective of remediating hazardous waste sites is the protection of human health and the environment by reducing risk. There are three primary approaches which can be used in site remediation to achieve acceptable levels of risk (Cairney, 1993; Cunningham and Berti, 1993);

(1) the hazardous waste can be excavated from the site, treated *ex situ*, and returned to the site;
(2) the hazardous waste can be treated *in situ* to detoxify hazardous constituents;
(3) the hazardous waste can be contained at the site to preclude additional migration of contaminants and exposure to them.

Ex situ and *in situ* remediation technologies are often impractical because of the extremely high costs and limited site access. The excavating and handling of wastes before processing creates the risk of uncontrolled release of contaminants. In addition, secondary contaminants (sludge, contaminated fines) resulting from processing still must be stored in a landfill (Anderson, 1993).

Containment, the third remediation option entails construction of covers and barriers to prevent water and oxygen from moving into the waste. This is the first step in the natural attenuation, bio-remediation process. Containment barriers may consist of plastic liners, concrete/asphaltic mixes, alkaline coal wastes, or compacted clays (Cairney, 1993). The traditional Compacted Clay Covers, used in the Subtitle C landfills, have problems with cracking (EPA, 1988), and are very expensive and difficult to construct. This desiccation cracking causes the barrier to lose its integrity and consequently its ability to block the infiltration of water (Omidi *et al.*, 1996).

The Clay Slurry and Engineered Soils described in this paper are created from a colloidal mixture that, when de-watered, produces capping systems and Engineered Soils with very low permeability (about 10^{-9} cm/sec) that will not lose their integrity with desiccation. Moreover, a dense vegetation cover can easily be established. Laboratory results indicate that the Engineered Soils act as bio-barriers preventing roots from penetrating the cap. This containment system represents a barrier technology which when combined with natural attenuation and bio-remediation can serve as a "walk away" solution for contaminated waste sites.

Scientific background

The available data on the construction of toxic waste disposal site sub-liners suggests that relatively small amounts of swelling clays may be used to construct engineered layers impermeable to both water and gases (e.g. Keren and Singer, 1988). Under the proper chemical conditions, these clays form quite viscous suspensions, which are able to entrain or suspend much coarser particles. In such a state, a suspension of clay and sand might be pumped onto the surfaces and trenches of waste site, or allowed to de-water and placed on a waste area utilizing existing construction equipment. Impermeability is achieved by the clay particles occupying voids between larger grains in the sand/clay slurry matrix, thus inhibiting water flow through those voids (Karen and Singer, 1988). Small amounts of such clays have major effects on the rate of water flow (hydraulic conductivity, K). For example, some clay/sand mixtures containing as little as 2-3% of clay per dry weight, possess a hydraulic conductivity (K) of about 10^{-7} to 10^{-9} cm/sec (Table 1). Hydraulic conductivity was measured by a falling head method (Hillel, 1980). Alternating layers of sand and engineered soils can further decrease the hydraulic conductivity by utilizing a capillary barrier effect (Nicholson et al., 1993).

Table 1.   Saturated hydraulic conductivities (K, cm/s)[a] of sand/clay mixtures

Clay content	K (cm/s)
0% (Sand only)	2.5×10^{-3}
1% (Pumped)	6.1×10^{-7}
1% (Placed mechanically)	4.1×10^{-8}
2% (Pumped)	1.1×10^{-7}
2% (Placed mechanically)	1.4×10^{-9}

[a]   Measured by a falling head method (Hillel, 1980)

The clay/slurry technology may use a local sand supply or may utilize local milled tailings at mineral waste sites to control acid mine drainage (e.g. Gerencher et al., 1991).

Use of mine tailing waste material from a kyanite mine showed that the clay/slurry was effective not only in reducing the permeability of the treated tailings, but also in decreasing their acidity due to inherent alkalinity of clay and the coating of sand mineral particles by the clay (Table 2). The untreated tailings were sandy and highly permeable materials, with pH values in the range of 2.4-3.1 as a result of pyrite oxidation. Adding a small percentage of conditioned clay to the tailings reduced hydraulic conductivities by three orders of magnitude compared to the untreated tailings and brought pH values of the effluent up to a slightly alkaline range (7.7 - 8.5).

Table 2. Saturated hydraulic conductivities (K, cm/s)[a] and pH of leachates from clay and sand tailings[b] mixtures; all mixtures were placed by pumping the slurry.

Treatment	K (cm/sec)	pH
Control	2.5×10^{-3}	2.8
Tailings+0.9% clay	1.6×10^{-5}	6.1
Tailings+1.8% clay	9.2×10^{-7}	7.7
Tailings+3.6% clay	1.3×10^{-7}	8.4
Tailings+5.4% clay	9.4×10^{-8}	8.5

[a] Measured by a falling head method (Hillel, 1980)

[b] Kyanite mine in Georgia.

Process description

The Clay Slurry and Engineered Soils Containment System is a containment process for the bio-remediation and natural attenuation of contaminated sites. The clay slurry technology utilizes a set of established engineering principles and equipment (pug-mills, slurry pumps, etc.) used in oil and gas industries, mineral processing and ore benefaction, and wastewater treatment plants. The first step in the clay slurry process is mixing and conditioning of clays to obtain the low permeability characteristics desired. The conditioned clay, sand and water form a colloidal suspension, which is then pumped on a site or allowed to de-water to create an engineered soil. The engineered soils have very low permeability, and when layered with overlying sand, create a containment system impervious to air and water (Figure 1). This containment system can be effectively utilized at a broad variety of mixed waste sites, including the following: oxidized mine tailings, industrial and municipal waste disposal sites, contaminated soils and sediments, and fly-ash disposal sites.

Various modifications of the clay slurry capping system can be used depending on local conditions at the particular site. If waste material is stored above ground, the cap will form a seal on the surface of the waste to isolate and contain the site. If the waste material is disposed of below ground level (completely or partially), the clay slurry capping system will include vertical walls (barriers) in addition to surface cover to further decrease a risk of the horizontal movement of water and contaminants (Figure 1). At newly constructed waste disposal sites, the waste can be completely encapsulated using Engineered Soils as a liner, and after the landfill has been filled, the site can be capped/closed with the Clay Slurry and Engineered Soils Containment System.

The clay slurry and engineered soil cap usually consists of three layers (Figure 2). The surface layer is a 40-100 cm thick layer with a low clay content and a hydraulic conductivity of about 1×10^{-6} cm/sec. The function of this layer is to support plant growth. The second layer is a highly permeable sand layer (3.5×10^{-3} cm/sec) designed

to shed rainfall and prevent moisture infiltration into the third layer. The third layer of this simple configuration is the low-permeability clay slurry cap or engineered soil with a permeability of about 10^{-9} cm/sec. The six orders of magnitude difference in hydraulic conductivity between the sand layer and the engineered soil layer creates an anisotropic barrier, resulting in a lower hydraulic conductivity for the whole system than that obtained by the sum of its parts. As a result, the Engineered Soil system is, from a practical point of view, impervious to water. About 60-80% of precipitation is removed from the system by surface runoff, and up to 30% escapes into the atmosphere through evapotranspiration. The small percentage of infiltration water that penetrates through the surface layer is either taken up through plant roots or removed by lateral drain flow though the unconsolidated sand layer (Figure 2). No water flows through the Engineered Soil layer; thus none reaches the contained waste. Since water flow into the waste material is eliminated, impaired water outflow and the transport of the contaminants from the site also ceases.

Revegetation and bio-barriers are an integral part of the Engineered Soils and containment systems. The engineered soils act to inhibit from roots from entering the cap thus maintaining integrity of the containment system. Furthermore, establishing a dense vegetative cover is essential for erosion control. Selection of the most appropriate grass seed mix will depend on the desired end use, the site location, and the site conditions. Sowing rates vary according to the location and the requisite end-products. Closely mown sward should be sown at around 300 kg/ha. In the majority of instances, sowing should take place in spring (April-June) or autumn (September). These periods are preferred because soil and climate conditions are optimal at these times.

Conclusions

1. The Clay Slurry and Engineered Containment System is a patent pending process that can be used as a reclamation technology for the remediation of contaminated sites where groundwater contamination, leaching, and surface runoff of contaminants is a concern.

2. The Clay/Slurry proved to be effective in reducing the leaching and runoff of toxic metals from a smelter waste, and in eliminating Acid Mine Drainage in oxidized mine tailings.

3. The clay/slurry and engineered soils are reclamation technologies for the containment of waste sites that are contributing to ecological degradation. The containment system with bio-remediation and natural attenuation can represent a complete site restoration process.

References

Anderson, W.C. (1993) *Innovative Site Remediation Technology: Soil Washing/Soil Flushing*. American Academy of Environmental Engineers, Annapolis.

Cairney, T. (1993) *Contaminated Land: Problems and Solutions*. p.351. Lewis Publishers, Boca Raton.

EPA, Office of Solid Waste. (1988) Criteria for Municipal Solid Waste Landfills (40CFR, Part 258) Subtitle D of Resource Conservation and Recovery Act (RCRA). Draft - Background Document. *Case Studies on Ground-Water and Surface Water Contamination from Municipal Solid Landfills*: EPA/530-SW-88-040. PB88-242466.

Gerencher, E.H., J.Y. Wong, R. van Dyk, and D.E. Konasewich. (1991) The use of mine tailings in concrete surface covers to control acid mine drainage in waste rock dumps. pp. 69-83. **In:** *Proc. 2nd International Conf. on Abatement of Acid Drainage*, Vol. 4. Montreal.

Golden, D.M. (1983) Water pollution arising from solid waste (coal, fly ash, slag) disposal, and measures to prevent water pollution. *Wat. Sci. Tech.* 15, 1-10.

Hillel, D. (1980) *Fundamentals of soil physics*. Academic Press, Inc., San Diego.

Keren, R. and M.J. Singer. (1988) Effect of low electrolyte concentration on hydraulic conductivity of sodium/calcium montmorillonite-sand system. *Soil Sci. Soc. Am. J.* 52, 368-373.

Nicholson, R. V., F.F. Akindunni, R.C. Sydor, and R. W. Gilham. (1991) Saturated tailings covers above the water table: The physics and criteria for design. pp. 443-460. **In:** *Proc. 2nd International Conf. on Abatement of Acid Drainage*, Vol. 1. Montreal.

Omidi, G.H., J.C. Thomas, and K.W. Brown. (1996) Effect of desiccation cracking on the hydraulic conductivity of compacted clay liner. *Water, Air, and Soil Pollut.* 89, 91-103.

Figure 1. Landfill Cap and Trench System (Cross-Sectional Veiw)

Clay Slurry Capping System

Vegetation Cover

Slurry Trench System

Land Surface

Waste

Site Specific Geologic Parent Material
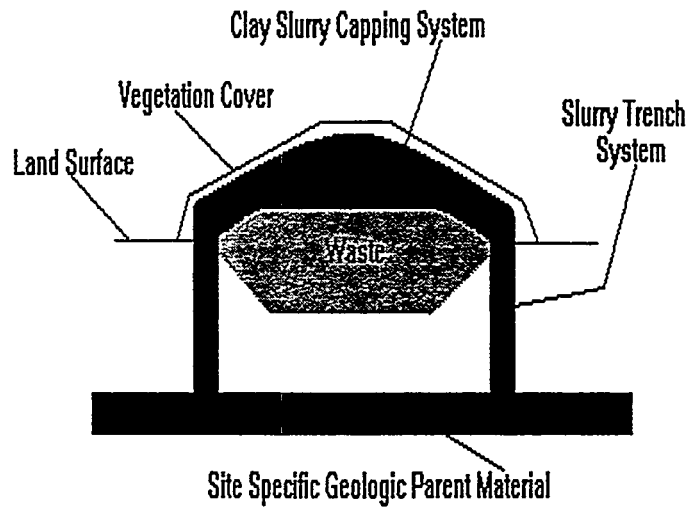
Figure 2. Water Balance of the Clay Slurry Engineered Soils Capping System.

Precipitation (100%)

Evapotranspiration (10-30%)

Surface Runoff (60-80%)

Plant Uptake

Vegetation Zone

Infiltration

Zone of High Permeability (Sand)

Drain Flow

Drain Flow (3-10%)

Engineered Soils - Clay Slurry Containment System
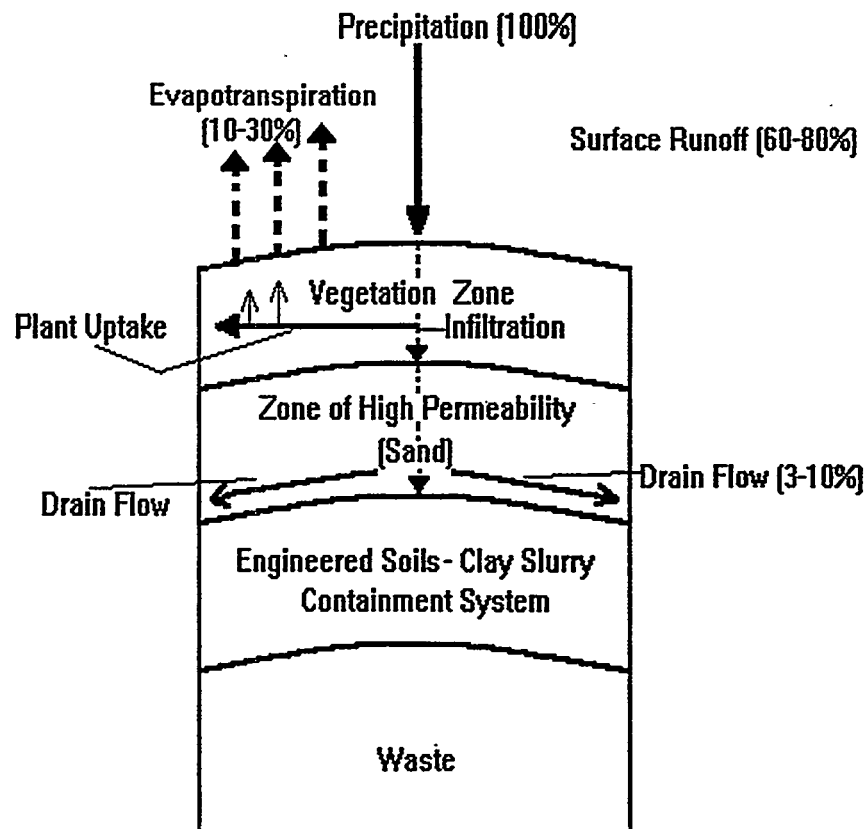
Waste

Poly-Urea Spray Elastomer for Waste Containment Applications

Carol J. Miller, Ph.D., P.E.
Wayne State University
Dept. of Civil and Environmental Engineering
Detroit, MI 48202

S.C.J. Cheng, Ph.D., P.E.
Drexel University
Dept. of Civil and Architectural Engineering
Philadelphia, PA 19104

Rick Tanis
Foamseal
195 Demille Road
Lapeer, MI 48446

INTRODUCTION

Geomembrane usage in environmental applications has increased dramatically following the promulgation of federal regulations resulting from the Resource Conservation and Recovery Act of 1976 (RCRA). Subtitle D rules, formulated under the authority of RCRA, call for minimum performance standards to limit adverse effects of a solid waste disposal facility on human health or the environment (40 CFR 257,258, August 30,1988). These rules set minimum standards requiring new landfill designs to include liner systems and final cover systems. Each state has the responsibility to develop rules that are at least as stringent as the Subtitle D rules.

There are several types of geomembranes currently available for landfill applications, each offering particular advantages and disadvantages. For example, PVC does not show the yield point (point of instability) that HDPE shows, HDPE has a higher puncture resistance than PVC, and PVC will deform much more than HDPE before barrier properties of the geomembrane are lost. Because each geomembrane material exhibits its own particular characteristics the material selected should be chosen based on the individual project requirements. It is preferable to select a design that uses the least expensive material and meets the performance specifications of the project.

Certain problems are common to most of the currently available geomembranes. Most of these relate to potential damage during packaging, transportation, handling and installation of the product. The primary installation defect is inadequate and incomplete seaming of the adjacent (or overlapping) panels. Even minor leaks can lead to considerable environmental damage. Hence, the search for liner materials and methods that are less dependent on construction quality control and field seaming.

A poly-urea elastomeric material developed by FOAMSEAL has recently been evaluated for use in landfill liner applications. The material can be applied in the field to form a continuous, seam-free liner. The polyurea spray elastomer consists of an isocyanate terminated prepolymer reacted with an amine terminated resin. The liquids are pumped by a two component dispense unit at 2000 psi and 155°F and sprayed through a mechanical purge gun in a fan-shaped pattern. They react almost immediately with a gel time of 3 seconds and tack free time of 6 seconds. The elastomer can be walked on in minutes. The application can be by hand or with automated equipment utilizing a transversing spray gun.

The immediate advantages of the spray elastomer for landfill applications include the development of a monolithic, seamless membrane, the direct bonding of the material to soil and almost any underlying support material, the high strength and elongation values to handle settling, the ability to apply the liner directly to surface obstructions such as vent pipes, the high interface friction angle, the composition which is 100% solids with no volatile organic compounds (VOCs), and the ease of repair to damaged areas.

Although there may be a number of potential applications for the FOAMSEAL material, this project was limited to the investigation of the feasibility of the material for landfill liner applications. Standardized laboratory testing of the elastomer was completed at the Geosynthetic Research Institute (GRI) laboratories at Drexel University. The field application was completed at a landfill facility in metropolitan Detroit, with supervision by Wayne State University. The non-standard testing program was completed in the environmental engineering laboratories at Wayne State University. The procedures and results of the standardized testing program were presented in Cheng, et al. (1994). They are summarized in Table 1 and Table 2. The values in Table 1 were compiled for factory sprayed elastomer samples.

TABLE 1 - Mechanical and Hydraulic Properties

Property Tested	Test Standard	Value
Tensile Strength, Maximum Stress	ASTM D 638	20.8 MPa
Tensile, Elongation @ Break	ASTM D 638	450%
Tear Resistance	ASTM D 1004	4.0 N/mm
Strip Tensile, Maximum Stress	ASTM D 1682	17.8 MPa
Strip Tensile, Elongation @ Break	ASTM D 1682	670%
Wide Width Tensile, Maximum Stress	ASTM D 4885	10.3 MPa
Wide Width Tensile, Elongation @ Break	ASTM D 4885	560%
Puncture Resistance	FTMS 101C, Method 2065	16.6 N/mm
Water Vapor Transmission	ASTM E 96	7.1×10^{-10} cm/sec

TABLE 2 - Direct Shear Results (ASTM D 5321)

Sample Details	Friction Angle (°)	Cohesion (psi)
Elastomer Sprayed onto Soil	38.7	2
Elastomer Sprayed onto Geotextile	14.5	0
Elastomer/Geotextile on Soil	37.4	0

FIELD APPLICATION

The field application occured in the summer of 1993 at a site in metropolitan Detroit. The test plot was 100' by 100'. Several spray options were considered and tested. These included direct spray on the prepared clay surface, spray on a non-woven geotextile base, and spray on a woven geotextile base. The application directly on the clay provided excellent bonding (see Table 2). However, there were several problems: excess product loss into cracks, inadequate coverage of cracks, and non-uniform finish. Later applications were tested on moistened clay and appeared to provide better results, primarily due to the quality of the clay surface. Mobilization of clay particles via the high pressure spray did not appear to be a problem. Using the non-woven heat bonded geotextile (2.3 oz/yd^2) as a base appeared to provide the best performance. The majority of the 100' by 100' plot was covered in this manner, with an overlap of 6"between adjacent panels (6' each) of the geotextile base. Coverage of the plot used 11.5' width spray regions (covering two geotextile panels per run) that were overlapped by approximately 4" at the commencement of the next spray. Strength testing at the point of overlap indicated that this joint had greater strength than the parent material, indicating the "seam"would not be a failure point. Half of the sprayed site was covered with a 9"cover soil, while the other half remained exposed. Field samples have been removed at periodic intervals to evaluate the performance over time. Current data suggests negligible degradation or deterioration in the mechanical or hydraulic properties.

NON-STANDARD TESTING

The Foamseal liner material was subjected to a variety of standard tests available for conventional liners to evaluate its suitability for landfill liner applications. Results of these tests were provided in Cheng, et al. (1994). In general, the material properties of the spray elastomer are comparable to both PVC and VLDPE. Mechanical properties, as well as hydraulic properties, were found suitable for landfill liner applications, either exceeding or meeting current regulatory guidelines for liner materials. Additional non-standard testing of the elastomer was completed to examine some of the unique properties and installation considerations specific to the Foamseal material. Many other researchers found it necessary to use non-standard liner testing, among those Estornell and Daniel, 1992; Brown et al., 1987; and Jayawickrama et al., 1988.

Standard permeability testing, using the Water Vapor Transmission (E96) test, shows that the Foamseal liner has a permeability well below the maximum allowable (10^{-7} cm/sec) for landfill liner applications. This test was conducted using a relatively small liner sample which has been sprayed under ideal laboratory conditions. Therefore, it may be claimed that this test does not reflect the actual permeability of a liner sprayed under the non-ideal field conditions.

Non-ideal field conditions may lead to imperfections affecting the integrity of the liner and make it susceptible to leakage. Such imperfections are divided into two types: (1) imperfections which result due to non-ideal conditions during spraying, e.g. weak contact between the elastomer and the fabric due to the presence of dust and soil particles, and (2) imperfections which result after the completion of spraying due to other field activities, e.g. flaws and punctures due to driving heavy machinery over the liner. Therefore, it was found necessary to test the permeability of the liner material using a relatively large sample that accommodates these types of field imperfections.

The Foamseal material provides unique advantages over conventional liners. Among these advantages is the ability of "manufacturing" the liner at the site. The construction of the liner is accomplished by manually spraying the Foamseal material at the surface of a geo-fabric. Current development is underway to automate the entire process using a computer controlled system with non-destructive thickness verification. The manual spray process presents concerns

336

regarding the resulting uniformity of the liner, especially thickness. Therefore, in order to assist the sprayer in achieving the desired thickness, a color coding system was suggested as a first-level monitor that minimum thickness criteria is achieved.

This section provides a discussion of the non-standard experimental tests conducted for the Foamseal material to further investigate its suitability as a landfill liner. The non-standard tests were developed to examine the following issues:

1) large scale leakage
2) leakage lilner defects
3) color coding system for thickness uniformity control

A description of the experimental apparatus, methodology, and results of this investigation is provided.

EXPERIMENTAL METHODOLOGY

1)Large Scale Leakage Investigation:

Figure 1 provides a schematic diagram for the relatively large scale permeability testing apparatus used for this study. This apparatus allows using a larger liner sample (24 inch X 17 inch) which provides a better representation of the liner. This permeameter consisted of two main parts; the lower part is for flow collection and sample support, while the upper part is for maintaining a constant hydraulic head of water. The test sample lies between these two parts. The upper and the lower parts were fastened and sealed to the liner material using silicon caulk to prevent any unwanted sidewall leakage.

The lower part of the apparatus is a clear plastic container with an outflow collection tube fixed at the bottom. This was used to accommodate a 3 inch layer of marble stone which has an observed particle grain size ranging from 0.25 inch to 2 inch. The marble stone was washed thoroughly prior to its use to avoid loss of moisture by absorption. The marble stone was used to support the flawed liner samples. The permeability of the intact liner samples was determined without the marble stone support. The flow passing through the liner sample was collected via the collection tube and measured volumetrically.

The upper part of the apparatus is a plastic container, identical to the lower part, used to maintain up to a 6 inch constant head of water. A red dye was mixed with the water to assist in observing small leakage through the liner.

2) Flaw Formation

The investigation of flow rates through defected liners included both Foamseal and HDPE liners. The Foamseal liner samples used for this investigation were taken from the field spray conducted in an earlier phase of this project. Two methods were used to create a puncture or a flaw in the test samples. In the first method, the liner material was placed on a rigid surface with a marble stone beneath. A one pound steel hammer was used to impact the liner material, forcing the jagged edge of the stone through the liner, creating a puncture. In the second method, flaws were generated by forcing a 1/16" diameter steel nail through the liner. This

23.00" Long X 16.57" Wide

Inflow Pipe
3/16"

Water Surface

6" Constant
Head of Water

Liner w/
Defects

Silicon
Seal

Detail A

Bolt

3.00" Gravel

Geo- Net

Steel
Bars

10 Degrees Base Inclination
Toward The Outflow

Elevation

Outflow Pipe
3/16 " I.D.

Upper Container

Silicon Seal

Silicon Seal

Liner

Lower
Container

Silicon Seal

Bolt

Detail A
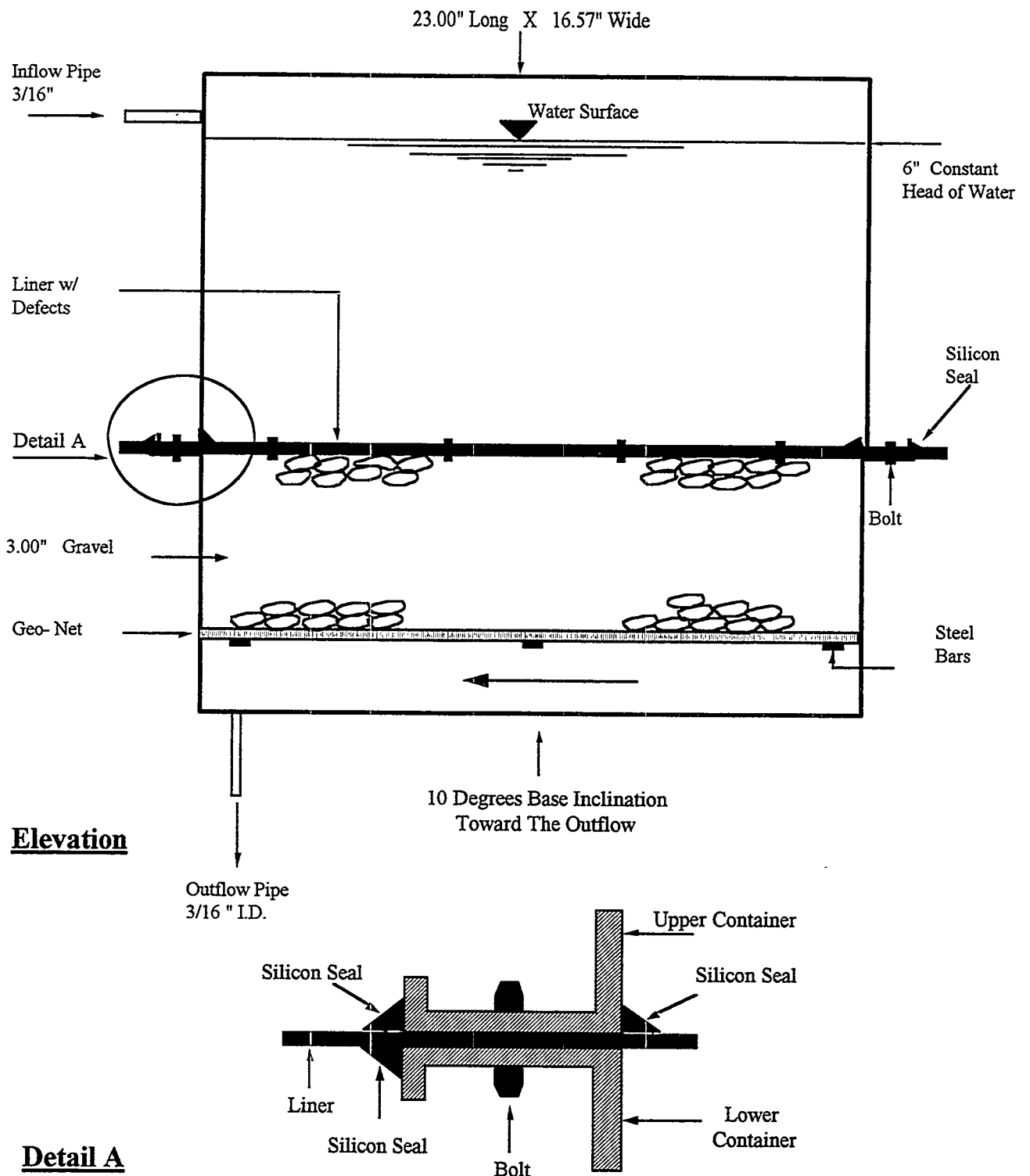
Figure 1 Schematic Diagram For Large-Scale
Permeability Testing Apparatus

method is more easily replicated from sample to sample than the first method. Therefore, it enables direct comparison between the two liners.

3) Color Coding

The color coding system is based on the idea that a unique thickness of Foamseal material is associated with complete coverage of a uniquely colored base material. Complete coverage is defined as the loss of identity of the color of the base material. The required thickness varies among colors depending on their degree of brightness. Therefore, a color coding system can be established by measuring the thickness required to cover each color of a group of colors investigated. The color coding system can then be used to guide the sprayer in achieving the required thickness and controlling the uniformity of the spray.

The color coding idea was tested by using four duplicate white fabric samples (50 inch x 25 inch). Each of the samples was sprayed with a different color. The colors examined were green, black, red, and brown. Each of the colored fabric samples was carefully sprayed with the Foamseal material until complete coverage, as defined above, occurred. The thickness of the liner was measured at different spots within each sample. One purpose of the testing was to determine if, in fact, the thickness associated with color coverage as measured by the human eye was unique. If so, the coding system would be a viable option.

RESULTS AND ANALYSIS

1) Large Scale Leakage

The leakage experiments conducted using the intact Foamseal liner sample were continued for a period of thirty days. As mentioned earlier, these experiments were conducted without the marble stone support under the liner sample. Therefore, due to the weight of the water, tension stress was applied to the sample during the course of the experiment which assisted in magnifying any defects that might exist in the sample. During the course of the experiments, no flow was observed through the liner. In addition, at the end of the experiments the underside of the sample that was not in direct contact with the dyed water was examined, and no staining was observed. This precludes the possibility of even small permeation through the liner sample.

2) Leakage through Defected Liner

Four strikes, using the method explained earlier, were required to make a flaw in a Foamseal liner sample. The sample thickness was approximately 140 mil (slight variation in the thickness, on the order of 10 mil, was noted). The resulting flaw was 3 mm in length. Due to the high elasticity of the material, the flaw closed naturally. This defected sample was used to quantify the rate of leakage through the flaw at a constant hydraulic head of 6 inches of water. Thirteen days were required before any leakage was observed. Afterwards, the flow rate was monitored and found to be 1.3×10^{-4} m^3/year. This experiment was duplicated using a similar liner sample. The experiment is on-going for more than one year without observing any flow.

Similar experiments were conducted using the HDPE liner. The thickness of the liner was 80 mil. The HDPE liner required a greater effort (six strikes) to create the puncture defect. The resulting flaw was 4 mm in length and approximately 0.5 mm in width. It appeared that the HDPE flaw did not heal, remaining open for subsequent leakage. Upon starting the experiment, leakage was observed within several minutes. The flow rate at a constant head of 6 inches of water was 8.7 m^3/year. This experiment was duplicated using a similar liner sample. The resulting flaw was about 2-3 mm in length and 1- 2 mm in width. The flow rate at a hydraulic head of 6 inches of water was measured to be approximately 155 m^3/year. The flow rate was found to vary significantly with the hydraulic head.

Another set of experiments were conducted for both the Foamseal and the HDPE liners. However, in these experiments the flaw was generated using a steel nail. The flow experiments conducted for the Foamseal liner is on-going without observing any flow. However, for the HDPE liner, the flow was observed instantaneously and it was found to vary with the hydraulic head above the liner.

3) Color Coding

Table 3 shows the results of the thickness color coding system evaluated for control of liner thickness. As indicated, a red underlying material would require the thickest liner for coverage. The remaining colors required thickness coverage in order of decreasing thickness as follows: black, brown, and green. The maximum variation in the liner thickness (i.e. the difference between the maximum and the minimum observed thickness), ranged between 0 to 15 mil. The maximum standard deviation was 5.8 mil. This technique could not be used as the ultimate evaluation tool for monitoring liner thickness. However, it is envisioned that it could be used as a continuous, full-coverage check that the process was being completed in a satisfactory manner. Limited destructive sampling at selected points in the liner, or non-destructive ultrasonic thickness evaluation would be used to ensure compliance.

Table 3 Results of the Color Coding System

Color	Average Thickness (mil)	Maximum Thickness (mil)	Minimum Thickness (mil)	Standard Deviation (mil)
Green	105	108	100	4.2
Black	116	117	115	0.6
Black	114	115	112	1.73
Red	157	164	150	4.5
Red	165	175	160	2.9
Brown	105	110	100	5.8
Brown	113	120	110	5.1
Brown	100	100	100	0

REFERENCES

Brown, K. W., J. C. Thomas, R. L. Lytton, P. Jayawickrama, and S. C. Bahrt (1987) Quantification of Leak Rates Through Holes in Landfill Liners. EPA 600/S2-87/062. pp. 1-4.

Cheng, S.C.J., Corcoran, G.T., C.J. Miller, and J.Y. Lee (1994) The Use of a Spray Elastomer for Landfill Cover Liner Applications. *Proceedings of the Fifth International Conference on Geotextiles, Geomembranes and Related Products*, Singapore, 5-9 September, 1994, pp. 1037-1040.

Estornell, P. and D. E. Daniel (1992) Hydraulic Conductivity of Three Geosynthetic Clay Liners. *Journal of Geotechnical Engineering*, 118 (10), 1592-1606.

Jayawickrama, P.W., K. W. Brown, J. C. Thomas, and R. L. Lytton (1988) Leakage Rates Through Flaws in Membrane Liners. *Journal of Environmental Engineering*, 114 (6), 1401-1420.

Koerner, R. (1990) *Designing with Geosythetics*, Prentice-Hall, New Jersey.

PERFORMANCE OF PAPER MILL SLUDGES AS LANDFILL CAPPING MATERIAL

Horace K. Moo-Young Jr.[1] And Thomas F. Zimmie[2]

Abstract: The high cost of waste containment has sparked interest in low cost and effective strategies of containing wastes. Paper mill sludges have been effectively used as the impermeable barrier in landfill covers. Since paper mill sludges are viewed as a waste material, the sludge is given to the landfill owner at little or no cost. Thus, when a clay soil is not locally available to use as the impermeable barrier in a cover system, paper sludge barriers can save $20,000 to $50,000 per acre in construction costs.

This study looks at the utilization and performance of blended and primary paper sludge as landfill capping material. To determine the effectiveness of paper sludge as an impermeable barrier layer, test pads were constructed to simulate a typical landfill cover with paper sludge and clay as the impermeable barrier and were monitored for infiltration rates for five years. Long-term hydraulic conductivity values estimated from the leachate generation rates of the test pads indicate that paper sludge provides an acceptable hydraulic barrier.

Introduction

An integrated approach to waste management typically includes waste treatment, recycling, incineration, and waste disposal. Waste storage and containment is one of the most popular options for waste management. To protect the groundwater from contamination, most modern waste containment systems must have a composite liner and cover that prevent the infiltration of water into the landfill and the escape of leachate from the landfill.

The most important component of the waste containment system is the low hydraulic conductivity barrier layers. Present specifications commonly stipulate that the impermeable barriers of a waste containment facility have a hydraulic conductivity of 1×10^{-7} cm/sec or less (approximately 1 inch/year of leachate infiltrating through the layer). Clay soils are the most popular fine grained soil used as a low hydraulic barrier layer in waste containment systems. When an abundant source of clay is not locally available to the waste containment facility, the cost of construction increases dramatically. To reduce the cost of construction, waste containment facilities in the Northeastern U.S. have utilized paper mill sludges as the hydraulic barrier in landfill covers.

Since 1975, paper mill sludges have been used to cap landfills in the U.S. (Stoffel and Ham 1979; Pepin 1984; Aloisi and Atkinson 1990; Swann, 1991; Zimmie et al., 1995; Zimmie and Moo-Young 1995; Moo-Young and Zimmie 1996). Paper mill sludges are provided to the landfill owner at little or no cost which can reduce the cost of construction by $20,000 to $50,000 per acre. This study looks at the use of paper mill sludges as the impermeable barrier in landfill covers. Test pads were constructed to simulate a typical landfill cover with paper sludge and clay as the impermeable barrier and were monitored for the infiltration rates for five years.

Test Pad Construction

In 1989, Erving Paper mill conducted a study to establish the long-term hydraulic conductivity characteristics of the paper sludge to obtain approval from the Massachusetts Department of Environmental Protection to use sludge as a landfill capping material (Aloisi and Atkinson 1990; Moo-Young 1995). Six test pads simulating typical landfill covers were constructed of primary sludge (test pads 2 and 3), clay (test pad 1), and blended sludge (test pads 4, 5, and 6). (Primary paper sludge is from

[1] Assistant Professor, Department of Civil and Environmental Engineering, Lehigh University, Bethlehem, Pennsylvania, USA.
[2] Professor, Department of Civil Engineering, Rensselaer Polytechnic Institute, Troy, New York, USA.
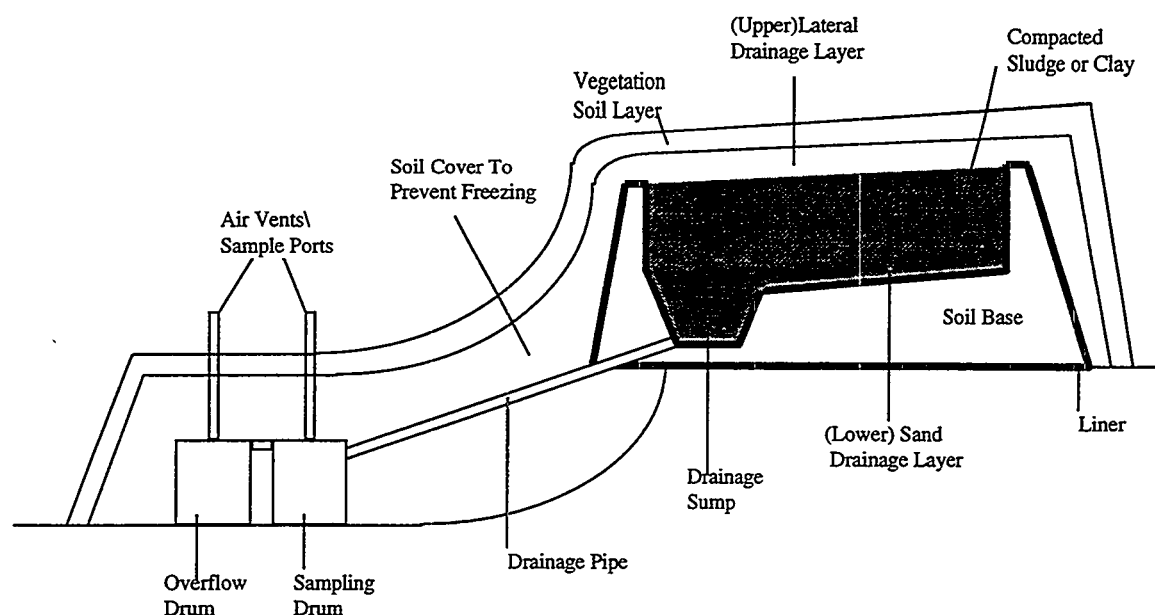
Figure 1 Cross Section of Landfill Test Pad

primary wastewater treatment sludge of the Erving Paper Mill. Blended paper sludge is a combination of primary and secondary wastewater treatment sludge from the Erving Paper Mill.) The geotechnical properties of these sludges used in this study are detailed in the paper by Moo-Young and Zimmie (1996).

The test pads are 7.62 meters in length by 7.62 meters in width (58 m^2 in area). Figure 1 shows the cross section of the test pads. Fine grained sandy soil (lower sand drainage layer) is used to prepare a smooth base with a 6 percent bottom slope and containment berms. A protective geotextile filter fabric covers the base of each test pad. The liner of the test pad consists of a 6 mil agricultural plastic. The leachate collection system consists of PVC piping and two plastic drums in series. The PVC pipe is secured to the liner with gaskets and clamps. A geotextile fabric filtered solids from entering and possibly clogging the leachate collection system.

A (upper) lateral sand drainage layer (15.24 cm in thick) was placed over the test pads liner system for the collection of leachate infiltrating through the overlying cap. A low hydraulic conductivity layer, either clay or paper sludge, was placed above the drainage layer. A 15.24 cm sand layer was placed above the low permeability to facilitate the lateral flow of rain water. A 30.5 cm layer of top soil was placed on top of the sand layer for vegetative support. Table 1 describes the tests pads. Test pad 1 was constructed with a 45.72 cm thick clay barrier,test pad 2 and 3 were constructed with a 45.72

Table 1 Test Pad Description

TEST PAD	BARRIER MATERIAL	THICKNESS (cm)	INITIAL PERMEABILITY (cm/sec)
1	CLAY		3.2×10^{-7}
2	PRIMARY SLUDGE	45.72	5×10^{-6}
3	PRIMARY SLUDGE	91.44	5×10^{-6}
4	BLENDED SLUDGE	45.72	1.4×10^{-6}
5	BLENDED SLUDGE	91.44	1.4×10^{-6}
6	BLENDED SLUDGE	91.44	1.4×10^{-6}

and 91.44 cm thick primary sludge barrier, and test pads 4, 5, and 6 were constructed of 45.72, 91.44, and 91.44 cm thick blended sludge barriers, respectively. Test pad 6 was constructed one year after the construction of test pads 1-5. Test pad 1 was constructed at an initial water content of 20%, and test pads 2-6 were constructed at a high initial water content ranging from 150-200% (Moo-Young and Zimmie 1996). Collection drums were emptied periodically to determine the amount of leachate generated.

During the construction of the test pads, different types of compaction equipment were used to place the sludge cap. Four types of equipment were used: a small ground pressure vibratory drum roller, a vibrating plate compactor, a sheepsfoot roller, and a low ground pressure track dozer. The sheepsfoot roller which was used to compact the clay liner in test pad 1 clogged immediately due to the cohesive nature of the sludge and the high water content. The vibratory methods did not provide homogeneous mixing and did not compact the sludge effectively. The small ground pressure dozer provided the best method for placement and compaction. This equipment successfully eliminated large voids from the sludge material and kneaded the material homogeneously (Moo-Young and Zimmie 1996).

Leachate Generation

Figure 2 illustrates the cumulative leachate production through test pads 1, 2, 3, 4, and 5 over five years (9/13/89-7/25/94) and test pad 6 over 4 years (9/13/90-7/25/94). The breaks in the data represent the winter months when snow covered the test pads and frozen ground conditions occurred. Analysis of the clay test pad (test pad 1) data in Figure 2 reveals that after the installation during the fall of 1989 (0 to 0.25 years) very little moisture percolated through the clay test pad. After the first winter, the clay control pad (test pad 1) generated greater quantities of leachate.
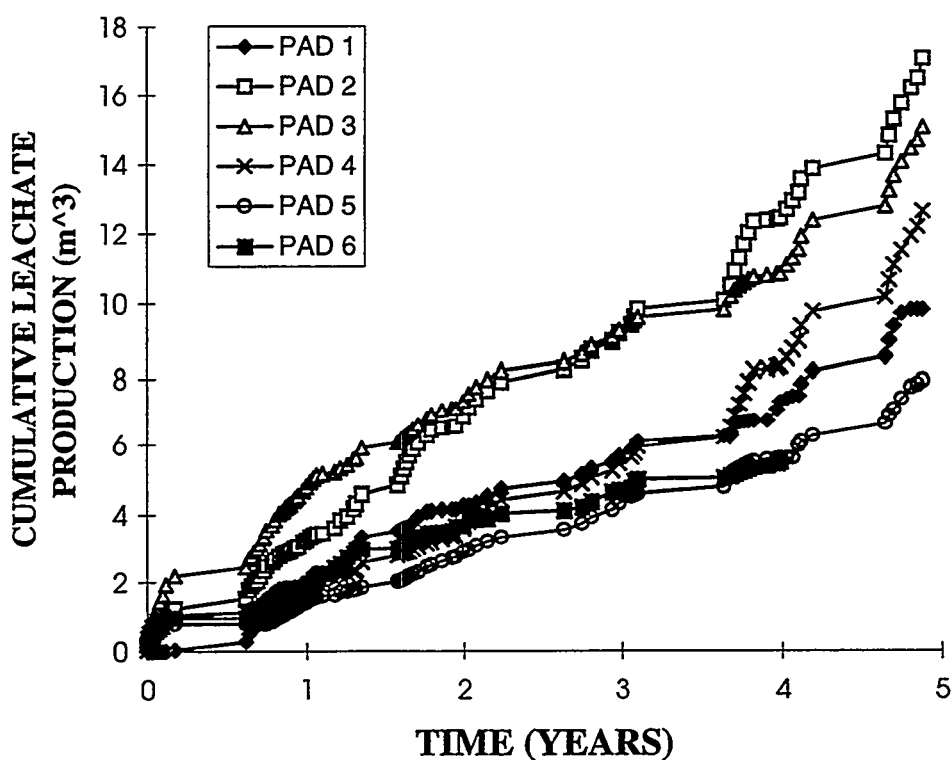
Figure 2 Cumulative Leachate Production

The highest cumulative leachate production over the five years occurred through the 45.72 cm and 91.44 primary paper sludge test plots (test pads 2 and 3). The lowest cumulative leachate production occurs for the two 91.44 cm blended paper sludge test pads (test pads 5 over five years and test pad 6 over four years). After five years, the leachate production for test pads 5 was approximately 20 percent less than the clay control pad, and for test pad 6, the leachate production was approximately 16 percent less than the clay control pad. From this data, it appears that blended paper sludge provided a better hydraulic barrier than primary paper sludge, since the cumulative leachate production through the blended paper sludge barriers was less than the primary paper sludge barrier. Moreover, since blended paper sludge had a lower cumulative leachate production than the clay barrier after four years, it can be inferred that blended paper sludge provides a better hydraulic barrier than clay with time.

Estimated Field Hydraulic Conductivity

Estimations of field hydraulic conductivity or percolation rate is based on the rearrangement of Darcy's law. (k = -Q/iA where k is the field hydraulic conductivity, Q is the flow rate, A is the area of the test pad (58.1 m^2), and i is the hydraulic gradient which equals the barrier thickness divided by the hydraulic head.) Assuming that the low hydraulic conductivity layer was assumed fully saturated, the hydraulic head in the sand drainage layer was assumed to be negligible, and the hydraulic gradient was assumed to be one. An examples of how to compute the hydraulic conductivity is as follows: If the area of the landfill cover is 58.1 m^2, the thickness of the sludge layer 91 cm, the hydraulic gradient is one, and the infiltration rate (flow rate) through the cover is 0.1 m^3/day (1.16 x 10^{-6} m^3/sec), then the hydraulic conductivity through the cover is 2 x 10^{-8} m/sec (2 x 10^{-6} cm/sec). Figure 3 plots the estimated hydraulic conductivity results for test pads 1, 3, and 5, and Table 2 displays the statistical data for each test pad.
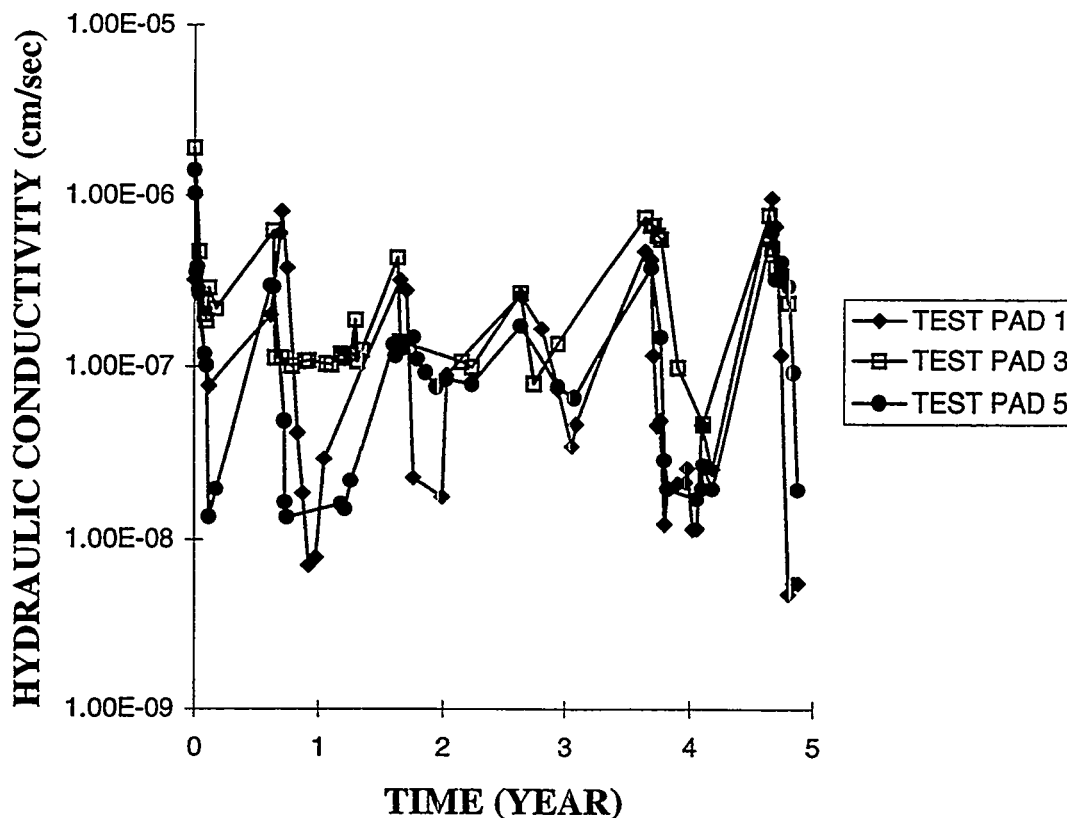
Figure 3 Estimated Hydraulic Conductivity

TABLE 2 Statistical Data From Estimated Hydraulic Conductivity From 9/13/89-7/23/94

	TEST PAD					
	1	**2**	**3**	**4**	**5**	**6**
AVERAGE (cm/sec)	2.3×10^{-7}	3.5×10^{-7}	3.5×10^{-7}	2.7×10^{-7}	1.6×10^{-7}	1.1×10^{-7}
STANDARD DEVIATION (cm/sec)	4.8×10^{-7}	2.8×10^{-7}	3.0×10^{-7}	3.2×10^{-7}	1.8×10^{-7}	1.1×10^{-7}
RANGE (cm/sec)	4.1×10^{-6}	1.5×10^{-6}	1.5×10^{-6}	1.9×10^{-6}	1.0×10^{-6}	5.3×10^{-7}
MINIMUM (cm/sec)	2.3×10^{-9}	1.7×10^{-8}	1.8×10^{-8}	7.9×10^{-9}	8.9×10^{-9}	2.7×10^{-9}
MAXIMUM (cm/sec)	4.1×10^{-6}	1.5×10^{-6}	1.5×10^{-6}	1.9×10^{-6}	1.0×10^{-6}	5.4×10^{-7}

Figure 3 shows the field hydraulic conductivity (percolation rate) for test pads 1 over the five years (9/13/89-7/25/94). Test pad 1 (clay control) had an initial hydraulic conductivity of 3.2×10^{-7} cm/sec. After construction in the fall of 1989 (Fall, winter, spring and summer are represented by 0-0.25, 0.25-0.5, 0.5-0.75, and 0.75-1.0 years, respectively.), there was decrease in hydraulic conductivity. An increase in hydraulic conductivity occurs after the each winter. Hydraulic conductivity changes are determined from the maximum and minimum values during a range of time. (e.g., During the first year, when comparing the maximum and minimum values, test pad 1 shows an increase in hydraulic conductivity of one order of magnitude (Figure 3).) Hydraulic conductivity increases in the clay test pad after the winter months (during the spring) may have been caused by ground freezing conditions. During the summer (e.g., 0.75-1.0 years) and fall (e.g., 0.0-0.25 years), there is an improvement in the test pad's hydraulic conductivity to a value below the regulatory requirement of 1×10^{-7} cm/sec. It can be postulated that the improvements in the field hydraulic conductivity of test pad 1 during the summer and fall may result from the closure of cracks caused by ground freezing.

Blended paper sludges have been used as the landfill cover material by various municipalities (Moo-Young 1995; Moo-Young and Zimmie 1996) and represents a realistic comparison to the clay barrier since it has a lower initial hydraulic conductivity in comparison to primary sludge (Moo-Young 1995). Figures 3 display the estimated field hydraulic conductivity of test pads 5, the 91.44 cm blended sludge test pads, which represents the sludge test pad with the lowest cumulative leachate production. Test pad 5 is characterized by a high initial permeability of 2.1×10^{-6} cm/sec (see Table 1). This value is approximately one order of magnitude higher than the clay test pad.

Test pad 5 varies in a similar manner to the clay test pad. (i.e., there is an increase in hydraulic conductivity during the spring followed by a decrease in hydraulic conductivity during the summer and fall.) In comparison to the clay test pad (test pad 1), during the first year (0.0-1.0 years), test pad 5 (Figure 3) showed an increase in hydraulic conductivity greater than the clay control (Figure 5). During the second, third and fourth years, test pad 5 showed an increase in hydraulic conductivity less than the clay control (as shown in Figure 3) which indicates that the sludge was performing as a better hydraulic barrier than the clay. The variance of test pads 5 (Table 2) is lower than the clay control which indicates that the hydraulic

conductivity for blended paper sludge A does not fluctuate as much as the clay test pad. Similar results were determined for test pad 4 (45.7 cm blended sludge) and test pad 6 (91.4 cm blended sludge).

Figure 3 also plots the estimated hydraulic conductivity results for test pad 3 (91.44 cm primary sludge test pad). Test pad 3 had a high initial hydraulic conductivity of 5×10^{-6} cm/sec (Table 1). Test pad 3 follows the same trend as test pads 1 and 5 with an increase in hydraulic conductivity during the spring of each year (see Figure 3). However, test pad 3 does not provide as effective a hydraulic barrier as test pads 1 and 5. For example, the minimum hydraulic conductivity values during each one year interval for test pad 3 is higher than the minimum hydraulic conductivity for test pads 1 and 5 during the same time (see Figure 3).

Shelby tube specimens were taken from test pads 1 (clay control) and 5 (blended sludge) approximately 3.75 years after construction. After 3.75 years, the clay test pad specimen was dry and stiff with an initial water content of 15% and a hydraulic conductivity of 1×10^{-7} cm/sec. From Figure 3, on June, 1993 (which represents 3.75 years), the hydraulic conductivity value for test pad 1 was approximately 9×10^{-8} cm/sec. Although the laboratory measured hydraulic conductivity was slightly lower, this indicates a good correlation between the determination of the hydraulic conductivity in the field and in the laboratory.

After 3.75 years insitu, a specimen from test pads 5 had a final water content of 125% and laboratory measured hydraulic conductivity of 1.1×10^{-8} cm/sec. From Figure 5, in June, 1993 (which represents 3.75 years), the hydraulic conductivity inferred from the infiltration data for test pad 5 is approximately 2.5×10^{-8} cm/sec, which is slightly higher than the laboratory measured value. This shows

a good correlation between the laboratory and field measured hydraulic conductivity (for this particular time of sampling). After four years, the organic content of test pads 5 decreased from 50 percent to 31 percent. Thus, from the laboratory hydraulic conductivity testing of insitu samples, it can be inferred that the blended paper sludge provides a better hydraulic barrier than the clay control. The clay control was dry and stiff which possibly increased its susceptibility to cracking if differential settlement was to occur. With dewatering, consolidation, and organic decomposition, blended paper sludge provided a better hydraulic barrier than the clay used in this study.

If samples were taken at another time, the laboratory results may have varied relative to the insitu hydraulic conductivity inferred from the infiltration data. Laboratory hydraulic conductivity values obtained for test pads 1 and 5 may represent the lower limits of hydraulic conductivity, since Shelby tubes were used for sampling. (In comparison to the average hydraulic conductivity (Table 2), the hydraulic conductivity values from the Shelby tube samples for the paper sludge and clay are low.) Since no temperature measurements were taken of the test pads, there is no data indicating that freezing and thawing occurred. Since sampling was conducted three months after the winter, there was no definite field evidence which indicated whether freezing and thawing had occurred.

Summary and Conclusions

In this study, six test pads were constructed to compare primary and blended paper mill sludges to compacted clay as a hydraulic barrier. Initially, the leachate production from the blended sludge test pad was greater than the leachate production from the clay test pad. As time increased, the leachate produced from the blended sludge test pad decreased below that of the clay test pad.

After five years, the estimated hydraulic conductivity of the blended paper sludge was similar to the clay control. This indicates that paper sludge can provide an effective hydraulic barrier. With time, the sludge will consolidate and dewater. The blended paper sludge provided a better hydraulic barrier than the primary paper sludge and as good a barrier as the clay. Shelby tube samples taken from the test pads during the third year indicate that the blended paper sludge maintains a lower hydraulic conductivity than the clay test pad.

346

References

Aloisi, W. and Atkinson, D.S. (1990) Evaluation of paper mill sludge for landfill capping material." *Prepared for Town of Erving, MA by Tighe and Bond Consulting Engineering*, Westfield, MA.

Moo-Young, H.K. (1995) *Evaluation of Paper Mill Sludges for Use as Landfill Covers.* Ph.D. Thesis. Rensselaer Polytechnic Institute, Troy, NY.

Moo-Young, H.K. and Zimmie, T.F. (1996) Geotechnical properties of paper mill sludges for use in landfill covers. *Journal of Geotechnical Engineering, ASCE,* 122 (9), 768-775.

Pepin, R.G. (1984) The use of paper mill sludge as a landfill cap. *Proceedings of the 1983 National Council of the Paper Industry for Air and Stream Improvement (NCASI) Northeast Regional Meeting*, NCASI, New York, NY.

Stoffel, C.M., and Ham, R.K. (1979) Testing of high ash paper mill sludge for use in sanitary landfill construction. *Prepared for the City of Eau Claire, WI, by Owen Ayers and Associates, Inc.* Eau Claire, WI.

Swann, C.E. (1991). "Study indicates sludge could be effective landfill cover material. *American PaperMaker,* pp. 34-36.

Zimmie, T.F., and Moo-Young, H.K. (1995). "Hydraulic Conductivity of Paper Sludges Used For Landfill Covers." *GeoEnvironment 2000,* Y.B. Acar and D.E. Daniel (Eds.), ASCE Geotechnical Special Publication No. 46, New Orleans, LA. 2: p. 932-946.

Zimmie T.F., Moo-Young, H.K., and LaPlante, K. (1995), The Use of Waste Paper Sludge for Landfill Cover Material, *Green '93--Waste Disposal by Landfill,* R.W. Sarsby (Ed.), Bolton Institute, Bolton, UK, A.A. Balkema, Rotterdam, Netherlands, p. 487-495.

INNOVATIVE PERMEABLE COVER SYSTEM TO REDUCE RISKS AT A CHEMICAL MUNITIONS BURIAL SITE

Cynthia C. Powels[1], Ingrid Bon[2], Nora M. Okusu[3]

INTRODUCTION/BACKGROUND - An innovative permeable sand cover with various integrated systems has been designed to contain and treat the Old O-Field chemical munitions landfill at Aberdeen Proving Ground, Maryland. The 18,200 m^2 (4.5 acre) landfill was used from the mid 1930s to the mid 1950s for the disposal of chemical, incendiary, and explosive munitions from domestic and foreign origins, together with contaminated wastes associated with the development and production of chemical warfare agents (CWA). The site is suspected to be contaminated with white phosphorous (WP) (which when dry, spontaneously burns when exposed to air), shock sensitive picric acid fuses and has the potential to contain large quantities of CWA-filled munitions. Historically, one to three explosions or fires occurred per ten-year period at the landfill. Such events have the potential to cause a CWA release to the environment, which could potentially affect densely populated areas. Recovery and decontamination projects conducted at the site in the late 1940s and early 1950s used large amounts of decontamination chemicals (containing solvents) and fuels which further contaminated the area. The groundwater downgradient of the landfill is contaminated with volatile organic compounds, metals, explosives and CWA degradation compounds and is currently being contained by a groundwater extraction and treatment system.

A preliminary feasibility study evaluated a variety of potential remedial alternatives for the site including excavation, in-situ treatment, and capping. The capping alternative was selected for its cost effectiveness and potential for in-situ treatment. A focused feasibility study of the capping alternatives yielded an innovative design which aims at not only preventing fires and explosions, but also offering the possibility for in-situ treatment of the wastes in conjunction with the existing groundwater extraction and treatment system. This alternative, the Permeable Infiltration Unit (PIU), was selected in a Record of Decision as the remedial technology for the Old O-Field landfill.

The cover consists primarily of sand which will stabilize the surface of the landfill by filling trenches and erosional holes, minimize the flow of air to the surface of the landfill to prevent white phosphorous-initiated fires, allow for water to percolate to continue the natural degradation of the wastes, and allow for infiltration of chemicals for in-situ treatment. In the event an explosion or fire occurs in the subsurface, the sand will absorb the blast and reduce the migration of CWA vapors due to its self-healing capabilities.

Installed over a minimum of two feet of sand will be a geogrid for stability, a subsurface trickling system for the addition of chemicals and/or water to facilitate in-situ treatment, and a synthetic strip layer for the detection of CWA releases. The subsurface systems will be covered by a minimum of three feet of sand and an erosion control layer comprised of geotextile and six inches of crushed aggregate. A sprinkler system located on top of the cap will work in conjunction with the air monitoring layer: in case an agent release is detected, the sprinklers will be activated to contain and hydrolyze the agent.

The U.S. Army Garrison, APG has tasked the U.S. Army Corps of Engineers (USACE), Baltimore District, with the construction of the PIU. A cost-reimbursable contract was awarded in June 1995 to Roy F. Weston, Incorporated (Weston) for the construction and one year of operation and

---

[1] U.S. Army Garrison, Aberdeen Proving Ground, ATTN: STEAP-SH-ER, APG, MD 21010

[2] U.S. Army Corps of Engineers, P.O. Box 56, Gunpowder Branch, APG, MD 21010

[3] ICF Kaiser Engineers, Inc., 7 East Congress Street, Savannah, GA 31401

maintenance of the PIU. Weston chose to construct the initial sand layer with teleoperated, low ground pressure heavy equipment (developed by Lockheed Martin) in an attempt to remove equipment operators from the most hazardous task of the overall construction. The construction of the PIU is also being coordinated with ICF Kaiser Engineers (ICF-KE) in order to facilitate time-sensitive field investigations which are being conducted by ICF-KE to support evaluation of *in-situ* treatment alternatives. This valuable data, to include information on corrosion rates, microbiological activity within the landfill, chemicals present in the soils, and geotechnical parameters, will be used as the backbone of the integration studies by ICF-KE. These studies will determine the most efficient way for the PIU and the existing groundwater treatment system to work in tandem in order to achieve the goal of the total remediation of the Old O-Field landfill.

HAZARD ASSESSMENT - The Old O-Field landfill poses a challenge to risk-based decision making because of the unconventional hazards at the site. The existence of a large volume and large variety of unexploded ordnance items and potential for CWA in ordnance and bulk containers pose potential risks to human health and the environment that cannot be assessed by standard environmental risk assessment techniques. In comparison to these imminent hazards, standard environmental risks (risks posed to human health and the environment by contaminants at the site) are comparatively small. Risk consists of a combination of the probability of an event occurring and the effects of that event, as follows: Risk = Probability X Effect. In other words, if an event is not likely to occur (small probability) but the effects are very large, then that event may still dominate the total risk. A qualitative risk assessment was performed in which the risk posed by the ordnance and CWA was compared to that posed by the contaminants in the soil, groundwater, and other environmental media. For either human health or ecological endpoints, the magnitude of risks posed by the contaminants in the environmental media is greatly overshadowed by the potential threat of an explosion or fire leading to release of CWA into the atmosphere. Therefore, the risk assessment focused on the probability of the occurrence of an explosion or fire that leads to the release of CWA.

GOALS OF THE REMEDIAL ACTION - The most significant risks posed by the site would result from either the direct volatilization of contaminants to air or dispersal of contaminants due to an explosion or fire at the site. To reduce the risk of the occurrence of these events, specific remedial action objectives/goals were identified as follows:

- Reduce the risk from white phosphorus or incendiary ignition by removing all flammable materials from the site, reducing incidences of animal burrowing or contact, and/or eliminating the supply of oxygen to materials which could spontaneously combust.
- Stabilize surface soils by eliminating and/or filling in trenches and depressions which may erode or collapse, thereby reducing the potential for exposure of WP to air, reducing the potential for shock-induced detonation of a round, and reducing the number of items that could release contents.
- Reduce or eliminate the blast and fragmentation hazards and releases associated with possible ordnance explosions at the site, either through a removal action or by constructing a shrapnel- and vapor-resistant cover.
- Reduce pressure and/or shock that may be transmitted to the buried items during encroachment on the surface by adding fill material above the buried items.
- Reduce the risk of evaporation from potential CWA-filled items located on or near the surface. Release of CWA could be reduced by preventing direct contact with an open atmosphere.

SELECTION OF THE REMEDY - As part of the feasibility study for the site, a large number of potentially applicable remedial technologies were identified and screened. These remedial technologies include:

- Excavation of the contaminated soil and materials and *ex-situ* treatment. The excavation methods considered include robotics, hydraulic, and manual handling.
- *In-situ* treatment technologies, including chemical, biological, and physical treatment options.

- Containment technologies, which includes the construction of blast-resistant covers, multi-media impermeable caps, permeable covers, and lightweight caps.

Due to the high hazards associated with the excavation, handling, and storage of a large volume of contaminated materials and ordnance items, all of the excavation options were eliminated from consideration. The soil at the site and the ordnance items are considered to be highly unstable. Based on historical records, the risk of exposing white phosphorus while disturbing the surface soil is extremely high. This would lead to a fire, which could then result in the explosive release of CWA.

In-situ treatment methods would be extremely hazardous or would not be effective in remediating the containerized materials. The materials within intact containers pose the highest risk due to the potential for an explosive release and the fact that natural degradation of the CWA would not have occurred. However, the leaching of contaminants from soil using water or other solutions appears to be a promising technology when used in combination with a containment technology. Of the containment options, the following technologies were evaluated:

Blast-Resistant Cover - A blast-resistant cover constructed of a composite, lightweight material was eliminated as being prohibitively expensive. Concrete or metal plating placed directly on the site would be extremely heavy and the excess weight of a suitable barrier may increase the risk of an explosion both during and after construction. A supported structure would be difficult to construct at the site due to the poor soil conditions and the danger associated with conducting excavation activities at or near the site.

Lightweight Synthetic Cap - The use of lightweight synthetic materials (such as spray-on foam) offers the advantages of safety to workers during construction because it could be remotely applied and is lightweight. This alternative would stabilize the soil and prevent human and animal contact with munitions and contaminated material buried in the disposal pits. The low density of the foam would result in a relatively small amount of pressure on the trenches and buried items. The foam surface would allow foot traffic and light equipment with minimal pressure applied to the buried materials. In addition, the foam cap would prevent air from reaching the buried materials, thus reducing the fire hazard posed by ignition of incendiary materials, such as white phosphorus. The principal drawback of the foam cap is that it would provide little shrapnel resistance in the event of a detonation; however, the likelihood of an accidental explosion or fire occurring is reduced by this alternative.

Impermeable Multi-Media Cap - An impermeable multi-media cap would consist of several layers of crushed stone, synthetic fabric sheets, a clay liner, a drainage layer, low-permeability soil fill, and topsoil to support vegetation. Construction of this cap would stabilize the soil and trenches; prevent stormwater infiltration through the source area; eliminate human and animal contact with the surface of the field; reduce the possibility of a fire by cutting off oxygen to the current field surface; and reduce the likelihood and potential effects of accidental detonation and evaporative release. To reduce the overall weight of the cap, a combination of natural and synthetic materials may be used in cap construction. Construction methods would also be tailored to minimize the disturbance of the field, although soil compaction would be needed to form the upper topsoil layer. However, the relatively large weight of this cap would pose a safety concern because of the instability of the trenches and the presence of thin-walled munitions and containers within the landfill. In addition, the multi-layer structure would be difficult to repair in the event of an explosion or subsidence.

Permeable Infiltration Unit - A permeable infiltration unit (PIU), would be constructed of sand or other granular materials and would reduce risks from the site similar to those described above for the impermeable cap but, would have the added benefit of being permeable to water. The PIU would be designed to allow infiltration of water or the application of solutions through the wastes, thus allowing natural degradation to continue and further testing of processes to treat the soil and wastes *in-situ.* This alternative would work in conjunction with the downgradient groundwater treatment system to promote leaching of contaminants and produce an ultimate reduction in the volume of the wastes.

Sand also provides the added benefit of being self-healing in the event of an explosion or trench collapse and would be easier to repair than other types of covers. This alternative also includes a subsurface air monitoring system to detect the presence of CWA within the pore spaces of the sand. Also, a sprinkler system will be constructed on top of the PIU. It will be capable of quickly spraying water on the PIU in order to form a vapor barrier within the sand to prevent an air release of CWA and to hasten the hydrolysis of CWA. The PIU would also include a subsurface trickling system to allow subsurface application of water and/or solutions to the site to facilitate *in-situ* treatment.

DESIGN CONSIDERATIONS - In the Record of Decision prepared by ICF-KE, the Army and the regulators selected the PIU as the remedy for the site. ICF-KE then designed the PIU . Some of the design considerations are discussed below.

Rationale for Use of Sand as the Primary Material - Sand will be used as the primary PIU construction material because of its superior blast attenuation properties as compared to soil (Backofen, 1976; Bush et al., 1946). Sand is more capable of dispersing blast effects than other types of soil due to the fact that sand grains are not as cohesive as other soil materials and will absorb blast impulse as the energy passes through the sand bed. In addition, shock waves and blast overpressures are attenuated to a greater extent within the air-filled interstices of a sand bed than in less-porous materials where shock is transmitted through the solid matrix. Also, individual sand particles absorb energy by easily-shattering and forming smaller grain sizes. In soils which are less porous, more cohesive, or shatter less from blast energy, there is less reduction in blast energy (Backofen, 1976; Bush et al., 1946). Therefore, sand is the most appropriate construction material to achieve a large reduction in blast energy.

Soil moisture also affects the attenuation of blast energy and the improved drainage properties of a sand layer again provides better blast resistance compared to more cohesive materials. Blast energy is reduced in multiphase materials in proportion to the differences in density. When a soil is saturated, the voids are filled with water, and the change in density between the void spaces and the soil particles decreases. Therefore, a soil with high moisture content would tend to transmit rather than attenuate the blast energy. In the case of dry sand or moist sand which is well drained, the voids between sand particles are filled with air. The density difference between air and sand will enhance attenuation of the blast energy. For these reasons, dry or moist sand is more appropriate for the attenuation of blast energy (Backofen, 1976; U.S. Army Technical Manual TM5-855-1, 1986; Bush et al., 1946; Cook, 1971). Sand which is moist (but not saturated) will be nearly as effective as dry sand.

Rationale for Sand Layer Thickness - The factors considered in choosing the minimum depth of 1.5 m (5 ft) for the PIU's sand layer included ensuring sufficient amounts of sand to: (1) fill in holes resulting from pit settling and erosion; (2) allow distribution of the weight of equipment/personnel needed to place the sand and allow attenuation of the impulse to the current surface of the site; (3) contain explosive events to the extent practicable.

A 1.5 m (5 ft) thick layer of sand appears to be adequate in the event of subsequent collapse of trenches. A review of available statements, testimony, opinions, and historical data concerning disposal methods at the site indicates that the average depth of the original trenches ranges from 1.5 to 2.4 m (5 to 8 ft). The maximum settling of these trenches is estimated to be 30% of the trench volume. In the extreme case of 30% settlement of a 2.4 m (8 ft) deep trench, the sand layer would need to fill a hole or depression of approximately 0.7 m (2.4 ft). The combination of the initial minimum 0.6 m (2 ft) sand layer and the additional minimum 0.9 m (3 ft) layer would adequately cover the current surface of the site and all disposed material, even in the event of collapse of a large trench.

Working from a layer of sand reduces the pressure exerted by equipment and personnel on the original surface of the site. On a 0.6 m (2 ft) layer of sand, the pressure exerted on the original

surface of the site by a low ground pressure bulldozer is 3,318 kg/m^2 (680 lbs/ft^2), including the pressure exerted by the sand layer. On a 1.5 m (5 ft) layer of sand, the pressure exerted on the original surface of the site by the bulldozer and the sand layer is 3,660 kg/m^2 (750 lbs/ft^2). These pressures are less than the pressure that a person exerts while walking on the original surface of the site.

In addition, increased sand depth increases the explosion containment capability of the PIU. Potential breaching depths (the depth of burial at which no soil or solid materials escape) for various explosive weights beneath dry sand have been evaluated based on the work of Backofen (1976) and Army Technical Manual TM5-855-1 (1986). The explosive weight is the TNT equivalent of the explosive contained within the round and may consist of a single item or a combination of items totaling the given explosive weight. The explosive weight that can be contained by a layer of sand 1.5 m (5 ft) thick is 2.3 kg (5 lb) of explosives. Based on the historical disposal and recovery records, approximately 99.6% of ordnance items believed to be within the site contain a mass of explosive less than this amount. Therefore, a sand layer of a minimum of 1.5 m (5 ft) thick was selected for the PIU.

Erosion Control Layer - Once the final grading has occurred, a permeable erosion control fabric will be placed on top of the sand layer. This layer will be covered with a 15 cm (6 in) thick layer of gravel or crushed aggregate, which will reduce the erosion of the sand from rain and wind effects.

Geogrid Layer - A geogrid layer was designed to provide long-term stability to the overlying air monitoring and subsurface tricking systems, which are explained below. The geogrid will be placed over the initial sand layer. When the original surface of the landfill settles due to corrosion of the existing waste, the geogrid will provide support to the subsurface systems while the sand over the geogrid flows towards the lower layer. Though the subsurface systems are flexible and can tolerate settlement without failures, the geogrid is aimed at preventing problems stemming from large scale settlements. A biaxial geogrid was chosen for this application. High material strength was desired as well as the maximum percent open area and aperture size possible. The material specifications require a minimum of 2,232 kg/m (1,500 lb/ft) long-term allowable design load in the machine and cross machine directions, 2 cm (0.8 in) aperture size and 60% open area. Other considerations were pH resistance in anticipation of the materials that will be added to the PIU to promote the degradation of the wastes. The pH range was specified as 2 to 10 units of pH.

Subsurface Trickling System - Chemicals and/or water will be delivered to the landfill through a network of perforated high density polyethylene (HDPE) piping to promote in-situ degradation of the waste. Treatability studies will be conducted to determine the process by which agents will be mobilized from the munitions and degraded. A combination of chemical and biological treatment is envisioned. Since the characteristics of these chemicals are unknown at the present, HDPE was the material selected for the piping for its wide range of pH resistance. Also, its relative flexibility will provide a more durable network since the system has to be able to withstand settlement.

Air Monitoring System - An air monitoring system currently provides continuous monitoring for CWA vapors in the ambient air around the site. The air monitoring system consists of five Automated Continuous Environmental Monitor (ACEM) systems capable of detecting low levels of CWA in the near-surface ambient air. As configured, the ACEMs will energize a siren and remote alarm when CWA is detected at a preset action level. As part of this project, one sampling port from each ACEM will be dedicated to monitoring the air within the internal air monitoring network (described below).

Internal Air Monitoring Network - Construction of the PIU should reduce the possibility of an explosive release of CWA and should attenuate the flow of vapors from the site to the atmosphere in the event of an evaporative release. However, as a supplement to the ambient air monitoring system described above, a subsurface air monitoring network has been designed as an integral part

of the PIU. A high-permeability conduit, consisting of filter fabric-wrapped synthetic drainage strips, will be installed within the PIU (at an elevation approximately 0.6 m (2 ft) above the original surface of the site) and connected to the ACEM sampling lines. Because the CWA vapors are heavier than air, they will tend to be collected within the sampling network and flow downward toward the perimeter rather than migrating upward through the sand. In addition to this density effect, the large contrast in permeability between the sand layer and the air monitoring network also assists in detection of the CWA vapors by the air monitoring system before the vapors break through the surface of the PIU.

Sprinkler System - Following the completion of the erosion-control layer, a sprinkler system will be installed. The purpose of the system is to subdue any release of CWA and extinguish any fire, should such an event occur. The sprinkler system consists of a series of 14 sprinkler heads, each capable of distributing 3.15 L/s (50 gpm) of water in a 30.5 m (100 ft) radius across the site (and will spray water over the entire 18,200 m^2 (4.5 acre) surface of the PIU) and an activation system which would automatically turn on the sprinkler system in the event that CWA is detected above the preset action levels by the air monitoring system.

IMPLEMENTATION - The PIU is being constructed by Weston under a contract with the Baltimore District, USACE. Contract safety provisions require Weston to operate any equipment over a minimum of 0.6 m (2 ft) of sand. Also, the equipment has to meet a specified ground pressure of less than 3,416 kg/m^2 (700 psf).

Prior to placement of the initial sand layer there were many unknowns concerning the condition of the landfill. An assessment of its conditions had not been possible due to entry restrictions imposed in the mid 80s. Knowledge of the stability of the soils; depth of erosional holes; amount, condition, and type of munitions on the surface of the landfill was limited. The purpose of using teleoperated equipment was to remove the equipment operators from the hazards presented by potentially disturbing ordnance as sand placement, clearing, and debris removal activities were performed.

The teleoperated equipment consisted of a CAT D6H low-ground-pressure (LGP) hydraulic bulldozer and a CAT 320L LGP excavator. The bulldozer was used for the majority of sand placement operations. Concurrent to sand placement, the excavator could perform one of various functions. These were tree clearing, ordnance and debris inspection, sand placement, and debris removal. A saw end effector was used for cutting trees. A high- definition camera was attached to the saw end effector to perform close inspections of items laying on the surface of the landfill. A bucket was used for sand placement applications where the shear forces caused by pushing sand were undesirable. For example, when filling open trenches, the excavator would be used to place sand over munitions or other items of concern followed by sand placement alongside the trench using the bulldozer. A bucket-and-thumb end effector was used to handle non-ordnance items.

While the teleoperated equipment was working on the PIU, LGP trucks delivered sand to the site. The trucks were driven by personnel in EPA level B personnel protective equipment. In order to protect the truck drivers from a potential explosion, safety restrictions required the trucks to operate 15 m (50 ft) away from the leading edge of the sand.

The placement of the initial sand layer was conducted from mid August 1996 to mid November 1996. The work was accomplished safely, without incidents or accidents. The key was the extensive preparation that ensued prior to the accomplishment of the work. At the time of preparation of the safety plans, the APG Safety office required a detailed procedure for addressing above surface ordnance items that presented a probability of explosion or chemical release if disturbed by construction activities. Weston, in conjunction with GeoCenters, the unexploded ordnance subcontractor, developed both manned and unmanned stabilization techniques. An unmanned stabilization entailed the placement of sand with the excavator bucket over the item of concern. Depending on the number and configuration of the munitions, this procedure was combined with the

addition of water to lifts of sand in order to create a cushioning bed. Manned stabilization of munitions consisted of gingerly placing a wooden crate over the item of concern, filling the crate with sand using shovels followed by placement of sand over the box using the excavator bucket. The placement of the wooden crate was to be accomplished by two contractor personnel in EPA level A personnel protective equipment. A team of other two contractor personnel would be standing by at the personnel decontamination station in case of an emergency. They would rescue and decontaminate any injured personnel prior to handing them to the APG emergency responders. Two installation-wide emergency drills were conducted in order to prepare the contractor and the emergency responders in case of an incident during a manned stabilization.

Several ordnance items were found during initial sand layer placement. Their condition ranged from good to badly rusted. Only one ordnance item required manned stabilization. Various containers were also found. Some of these were partially buried, others were located on the surface of the landfill. All containers were filled with sand or a controlled-low-strength-material in an attempt to minimize manned entries for disposal sampling; minimize sampling, analysis, and disposal costs; and prevent the PIU from locally collapsing at the container locations once corrosion occurs.

The central section of the landfill showed erosional holes and soil subsidence. These areas were addressed by placing dry sand onto them with the excavator bucket without disturbing the surface of the landfill. This procedure was repeated during consecutive days until no further sand subsidence was observed. Sand would then be placed over the area with the bulldozer.

STATUS - The construction of the PIU will continue until Fall of 1997 followed by operations and maintenance. Integration studies will be conducted from 1996 to 2002. Full integration of the PIU and the groundwater extraction and treatment system is planned by 2005.

REFERENCES

Backofen, J.E. (1976) Estimation of Depth of Penetration of Impacting Dud Ordnance. Naval Explosive Ordnance Disposal Facility, Report No. DEODF 1-2.

Bush, V., J.B. Conant, and E.B. Wilson, Jr. (1946) Effects of Impact and Explosion. Office of Scientific Research and Development, Washington, D.C.

Cook, M.A. (1971) The Science of High Explosives. Robert E. Krieger Publishing Co., Inc.

Longe, T., J. Choynowski, D. Pope, and G. McKown. (1996) Remediation Support, Old O-Field Preliminary Integration Activities. ICF Kaiser Engineers.

U.S. Army. (1986) Technical Manual TM-955-1, Fundamentals of Protective Design for Conventional Weapons.

ENHANCED SHEAR STRENGTH OF SODIUM BENTONITE
USING FRICTIONAL ADDITIVES

K.E. Schmitt, J.J. Bowders, R.B. Gilbert, and D.E. Daniel

Abstract

One of the most important obstacles to using geosynthetic clay liners (GCLs) in landfill cover systems is the low shear strength provided by the bentonitic portion of the GCL. In this study, the authors propose that granular, frictional materials might be added to the bentonite to form an admixture that would have greater shear strength than the bentonite alone while still maintaining low hydraulic conductivity.

Bentonite was mixed with two separate granular additives, expanded shale and recycled glass, to form mixtures consisting of 20-70% bentonite by weight. In direct shear tests at normal stresses of 34.5-103.5 kPa, effective friction angles were measured as 45° for the expanded shale, 36° for the recycled glass, and 7° for the hydrated granular bentonite.

The strength of the expanded shale mixtures increased nearly linearly as the percentage shale in the mixture increased, to 44° for a bentonite mixture with 80% shale. The addition of recycled glass showed little effect on the shear strength of the mixtures of glass and bentonite. Hydraulic conductivity measurements for both types of mixtures indicated a linear increase with log(k) as the amount of granular additive increased.

For applications involving geosynthetic clay liners for cover systems, a mixture of 40% expanded shale and 60% bentonite is recommended, although further testing must be done. The 40/60 mixture satisfies the hydraulic equivalency requirement, with $k = 5.1 \times 10^{-9}$ cm/sec, while increasing the shear strength parameters of the bentonitic mixture to $\phi' = 17°$ and $c' = 0$.

Introduction

Cover systems are an important component of the overall waste containment scheme for landfills. Cover systems provide drainage to divert rain and surface water away from the waste, and they act as barriers to prevent infiltration into the waste. A typical cover system consists of surface, protective, drainage, barrier, and gas collection layers.

The discussion in this paper is relevant to the barrier component of a cover system. In some cases, the use of a geosynthetic clay liner (GCL) as part of a barrier layer is the most technologically or economically feasible alternative. A GCL typically consists of a thin (<10 mm) layer of dry bentonite sandwiched between two man-made products, such as geomembranes or geotextiles. The geosynthetics are used to facilitate the transportation and deployment of the bentonite. Some geosynthetics may be designed to add strength to the system.

Other ideas for increasing the strength of clay include lime stabilization (National Lime Association, 1975), cement-modified soil (Neal, 1984), and the addition of liquid calcium to soil

[1] Senior Staff Engineer, GeoSyntec Consultants, 2100 Main Street, Suite 150, Huntington Beach CA 92648
[2] Research Civil Engineer, Department of Civil Engineering, ECJ 9.227, University of Texas at Austin, Austin TX 78712
[3] Assistant Professor, Department of Civil Engineering, ECJ 9.227, University of Texas at Austin, Austin TX 78712
[4] Professor and Department Head, Department of Civil Engineering, University of Illinois at Urbana-Champaign, Urbana IL 61801

(Massa, 1990). Such measures have been primarily used in roadway bases and subgrades. They have been successful in reducing the plasticity of soils as well as providing moderate strength increases. The studies did not document the effect on hydraulic conductivity.

Geosynthetic clay liners work well as barriers because bentonite has one of the lowest hydraulic conductivities, k, of any naturally occurring soil (k=1X10^{-10}-1X10^{-9} cm/sec). Initially, flow across the barrier layer causes the dry bentonite to hydrate and swell, thus attaining a low hydraulic conductivity. Bentonite is also highly plastic.

One obstacle to the widespread use of GCLs in cover systems is the low shear strength of bentonite. Typical effective friction angles for bentonite are 7-9° for normal stresses in the range of 25-138 kPa (Grim and Guven, 1978; Daniel, 1993). Such low strength leads to slope instability in cover systems, which is often analyzed as an infinite slope problem. Typical cover systems are designed for 5:1 to 3:1 (horizontal:vertical) slopes. In order to maintain a factor of safety of 1.5 in such cases, it is necessary to have a friction angle of 17° to 27°, well above that of bentonite alone at such normal stresses.

Attempts have been made to internally reinforce GCLs to increase shear strength. Some GCLs are manufactured with needle-punched fibers running through the bentonite to connect the top and bottom geosynthetics. Gilbert et al. (1996a) reported effective friction angles for reinforced GCLs on the order of 23-29° (σ'_n=3.5-69.0 kPa). However, at large displacements there was evidence that the needle-punched fibers separated and pulled-out. The residual friction angle was reduced to that of bentonite alone: ϕ'=9° (σ'_n=3.5-27.6 kPa) at a displacement of 43 mm.

The objective of this research program was to determine the feasibility of increasing the internal shear strength of bentonite by creating admixtures of bentonite and frictional, granular materials. A constraint is that the hydraulic conductivity of the mixture must remain low enough to maintain hydraulic equivalency with a compacted clay liner.

Materials

Two dry, cohesionless, granular additives were mixed with bentonite to form admixtures for shear strength and hydraulic conductivity testing. Expanded shale and recycled glass were used in conjunction with bentonite. Table 1 provides information on the general properties of the three materials.

Table 1. Material Properties.

	Grain Size	Atterberg Limits	Gs	Angularity	Source
Bentonite	Granular 1.18 mm	LL=570 PL=89-97*	2.79	----	Bentonite Corp. South Dakota
Expanded Shale	1.18-2.00 mm	NA	1.50	Subangular	Texas Industries Houston, TX
Recycled Glass	0.43-0.85 mm	NA	2.50	Subangular	Strategic Materials Houston, TX

* NOTE: PL data from Grim and Guven, 1978

Expanded shale was first developed in the early 1900s. Shale or expandable clay is quarried, evaluated for conformance with proprietary specifications and prepared for processing by crushing and screening into various sizes. The raw material is then fired in a rotary kiln at temperatures in excess of 2000°F. After cooling, the expanded shale, also termed lightweight aggregate, is processed to precise gradations for distribution (Valsangkar and Holm, 1990).

356

A scanning electron microscope of the expanded shale magnified 1000 times is shown in Figure 1(a). The porous nature of the material is evident by the "Swiss-cheese" matrix of shale and void space. The result is a lightweight material. By focusing on the edge of one particle, as in Figure 1(b), one can see that the expanded shale is porous at the edge and slightly denser toward the center of the granule. This feature is likely due to the manufacturing process, in which the outside heats faster than the inside. Figure 1(b) also illustrates the angularity of the particle.

Recycled glass is formed by crushing old sheets of plate glass. The recycled product is then prepared for distribution by U.S. sieve size. The glass particles are generally subangular, like expanded shale, and they have sharp, smooth edges, compared to the rough, almost pumice-like edges of the shale (Figure 1(c)).
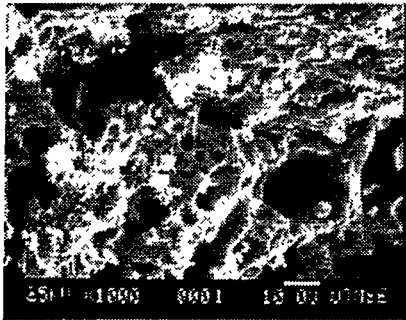
Fig. 1(a).
The Inside of an Expanded Shale Particle
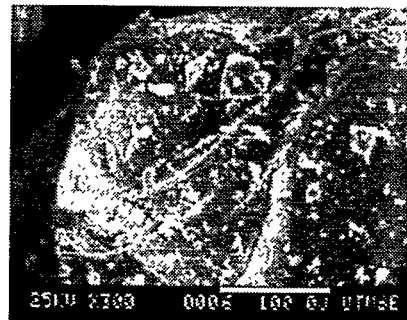
Fig. 1(c).
A Smooth Glass Particle
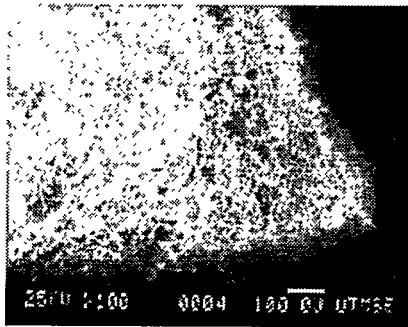
Fig. 1(b).
The Edge of an Expanded Shale Granule
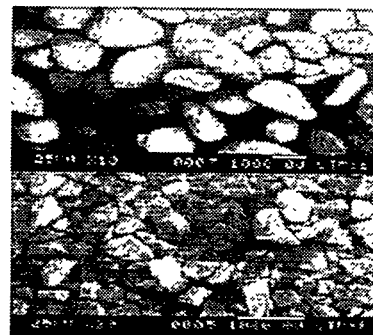
Fig. 1(d). Relative Size and Shape of Shale (top) and Glass (bottom) Particles

Fig. 1. Scanning Electron Micrographs of Glass and Expanded Shale.

Experimental Methods

Strength Testing

Mixtures were formed by combining bentonite at 600% water content, slightly above the liquid limit, with expanded shale or recycled glass on a percentage by dry weight basis. The bentonite content of the mixtures ranged from 20-70%.

Shear strength of the mixtures was evaluated in direct shear testing machines at normal stresses of 34.5-103.5 kPa. ASTM D3080 was followed, with a few exceptions made to accommodate the high compressibility of bentonite. The shear rate in all tests was less than 0.001 mm/min, slow enough to

ensure proper drainage (Gilbert et al., 1996b). Samples were sheared to approximately 10 mm. The complete testing program is outlined in Schmitt (1996).

For tests on mixtures of bentonite and expanded shale, each combination was tested at three normal stresses (34.5, 69.0, and 103.5 kPa), and a linear regression line was fitted through the data to determine effective friction and cohesion values.

For tests involving bentonite and recycled glass, fewer shear tests were performed and mixtures were tested only under an effective normal stress of 103.5 kPa. In such cases, the Mohr-Coloumb envelope for each combination was developed by assuming that $c' = 0$ and $\phi' = \tan^{-1}(\tau/\sigma'_n)$.

Hydraulic Conductivity Testing

The hydraulic conductivity of expanded shale and recycled glass were evaluated individually by constant head tests in accordance with ASTM D2434. All tests on mixtures of bentonite and granular material were performed in flexible-wall permeameters following the general guidance provided in GCL-2 from Geosynthetic Research Institute (GRI) at Drexel University. Samples were prepared in the permeameters with the bentonite and expanded shale or recycled glass in a dry condition, approximately 1.2 cm thick (6-10 times the diameter of the particle), similar to a GCL but without the geotextile and/or geomembrane. Numerous attempts to permeate the samples failed due to sidewall leakage caused by the loss of dry bentonite at the edges of the sample and segregation of the granular additive from the bentonite. A deviation was made from the testing guidelines to prevent leakage problems. A ring of bentonite, 10 mm wide, was placed around the outside of the specimen, with the mixture of bentonite and additive forming an inner ring of 81 mm diameter. The calculation of hydraulic conductivity was modified to account for the added bentonite on the outer edge of the sample by assuming that the total flow (Q_T) through the sample equaled the sum of the flows through the inner (Q_{inner}) and outer (Q_{outer}) rings of soil. In accordance with GRI GCL-2, the samples were backpressure saturated incrementally to a final effective stress of 69.0 kPa at the effluent end of the sample. The samples were saturated at the pressures for a minimum of 48 hours before permeation. The effective stress in the hydraulic conductivity tests falls in the middle of the 34.5-103.5 kPa range of normal stresses used for the strength testing of mixtures.

Results and Discussion

Shear Strength

The drained shear strength of bentonite was represented by an effective friction angle of 7° and an effective cohesion of 7.0 kPa. The expanded shale and recycled glass are dry, cohesionless materials, and the measured friction angles were $\phi'=45°$ for the shale and $\phi'=36°$ for the recycled glass.

For mixtures of bentonite and expanded shale, the measured cohesion was nearly zero in all cases. The friction angels are plotted versus the percentage shale in the mixture in Figure 2(a). Each point on the graph represents the friction angle calculated by a linear regression of the results of 2-4 direct shear tests at varying normal stresses. A steady increase in strength is observed as the percentage expanded shale increases. Tabulated values of shear strength are shown in Table 2.

Figure 2(c) shows the effect of the recycled glass on the effective secant friction angles of mixtures of bentonite and glass. Table 2 provides the shear strength of the mixtures. Recycled glass appears capable of increasing the shear strength of bentonite only slightly with any addition of glass. There is not an increasing trend as the percentage glass in the mixture increases.
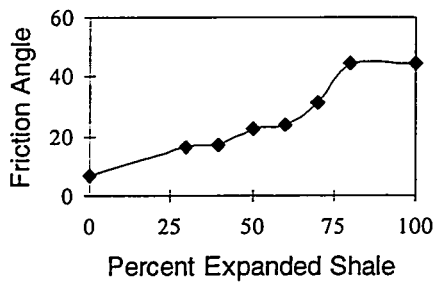
Fig. 2(a)
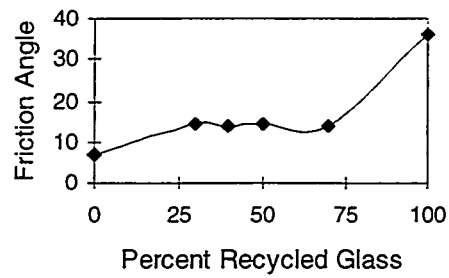
Fig. 2(c)
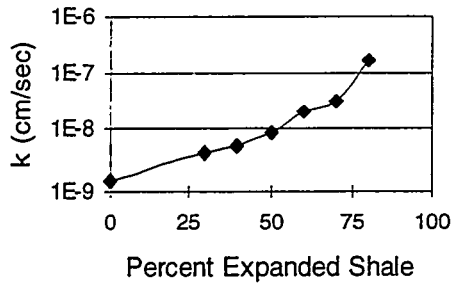
Fig. 2(b)
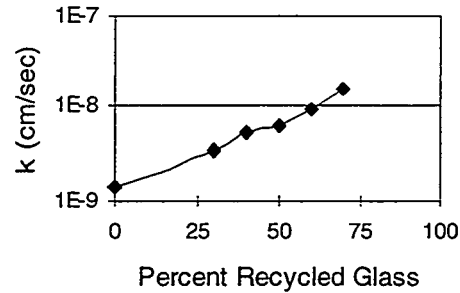
Fig. 2(d)

Figure 2. Effect of Additives on Shear Strength and Hydraulic Conductivity of Mixtures

The difference in the ability of expanded shale and recycled glass to affect a change in the shear strength of bentonite mixtures is likely due to the relative size of the particles used in this study. The largest glass particles used were less than 75% of the size of the smallest expanded shale particles. The larger aggregates likely interlocked better with one another. Larger glass particles may yield better results, but the possibility of rupturing a geomembrane in the cover system increases as the size of the glass particles increases. Furthermore, the expanded shale may work better because its surface is rough and the surfaces of glass are smooth. Rough surfaces provide more sliding resistance than smooth surfaces.

This research study shows clearly that it is possible to increase the shear strength of sodium bentonite in the range of normal stresses of 34.5-103.5 kPa by mixing the bentonite with expanded shale, a granular, frictional material. Application of these results to landfill cover systems requires additional investigation. The normal stresses in many cover systems are well below 34.5 kPa, and designers should not simply extrapolate the data presented here to cover systems. Testing at low normal stresses is a unique challenge, however. Direct shear machines, tilt tables, and triaxial apparatuses present significant obstacles to testing cover systems at low normal stresses. The extension of this research to applications in landfill covers must entail a critical examination of testing options before any data at low normal stresses can be developed.

In the present research, problems were encountered in measuring the cohesion of soil samples in direct shear machines. For reasons that are not completely explained but are consistently reproduced, the direct shear machines used for this testing may tend to produce a cohesion which is an artifact of the machine, not the soil (Schmitt, 1996). Limited triaxial testing of expanded shale confirms that the cohesion measured in direct shear is likely not real. Consequently, the c'=7.0 kPa for bentonite is equally suspect; the cohesion may be machine-induced or the strength envelope may be curved and may intersect the origin. Further work must

359

be undertaken on the subject. Nevertheless, this research shows that the strength of mixtures of bentonite and expanded shale increases as the percentage of expanded shale in the mixture increases. As more frictional particles are available, the degree of interlocking increases and the amount of surface contact between granular particles increases, thus enhancing the sliding resistance within the material. Consequently, the internal shear strength of the mixture increases.

Table 2. Shear Strength of Mixtures.

Percent Bentonite	Percent Additive	Shear Strength of Expanded Shale (all units kPa)			Shear Strength of Recycled Glass (all units kPa)		
		$\sigma_n=34.5$	$\sigma_n=69.0$	$\sigma_n=103.5$	$\sigma_n=34.5$	$\sigma_n=69.0$	$\sigma_n=103.5$
100	0	10.9	15.5	19.4	10.9	15.5	19.4
70	30	10.0	-	31.8	-	-	28.3
60	40	14.0	-	37.0	-	-	28.6
50	50	15.0	28.5	49.3	-	-	28.1
40	60	-	33.7	55.8	-	-	-
30	70	-	-	71.2 73.8	-	-	28.3
20	80	28.0	89.4	136.3 99.5	-	-	-
0	100	56.2 64.2	104.2	128.9 133.5	54.5	84.0	105.0

Notes: σ_n is the nominal effective normal stress at the start of the test.
    See Schmitt (1996) for a discussion of measured cohesion in tests of bentonite and expanded shale separately.

Hydraulic Conductivity

The hydraulic conductivity of the bentonite was measured as 1.5×10^{-9} cm/sec. The granular additives have measured hydraulic conductivities orders of magnitudes higher than bentonite: 1.75 cm/sec for expanded shale and 0.1 cm/sec for recycled glass.

The hydraulic conductivity of bentonite and granular frictional materials increases as the percentage of granular material in the mixture increases. Most regulatory agencies require that the maximum hydraulic conductivity of a liner system not exceed 1×10^{-7} cm/sec. However, regulatory requirements were originally devised for compacted clay liners (CCLs). For GCLs or mixtures of bentonite and shale or glass, the equivalency of a GCL to a compacted clay liner should be evaluated.

The advective flux through a GCL or mixture should be equal to or less than the advective flux through a CCL. A 1.2 cm GCL mixture must have $k=5.1 \times 10^{-9}$ cm/sec to be hydraulically equivalent to a 0.9 m CCL ($k=1 \times 10^{-7}$ cm/sec) under maximum ponding of 0.3 m. Mixtures of 40% expanded shale or recycled glass and 60% bentonite result in low enough conductivity to satisfy the hydraulic equivalency requirement.

Achieving low hydraulic conductivity in mixtures can only be done by ensuring that the bentonite and granular material are mixed thoroughly; segregation of the additive from the bentonite will lead to concentrated zones of high hydraulic conductivity. This practical issue was not addressed as a part of this feasibility study. However, the use of the strength enhancement idea in practice will require extensive research into the manufacturing aspects of the product. Poorly mixed batches will still produce enhanced shear strength but will fail the second and equally important requirement of the project: hydraulic conductivity less than 5×10^{-9} cm/sec.

Conclusions

The objective of this study was to determine whether frictional additives could be combined with bentonite to form admixtures that would have greater shear strength than the bentonite alone while still maintaining low hydraulic conductivity. This would help alleviate the prevailing obstacle to using GCLs in landfill cover systems: the low shear strength provided by the bentonitic portion of the GCL.

In this study, mixtures of bentonite and expanded shale were found to have greater shear strengths than bentonite alone in the range of normal stresses of 34.5-103.5 kPa. A mixture of 40% expanded shale and 60% bentonite is recommended to satisfy the hydraulic equivalency requirement, with k=5.1X10^{-9} cm/sec, and increase the shear strength to ϕ'=17° and c'=0.

Further research should concentrate on evaluating the shear strength of mixtures at low normal stresses (< 35 kPa) typical of landfill cover systems. The large-strain behavior of the mixtures should also be evaluated.

Acknowledgments

References

American Society for Testing and Materials. (1995) *Annual Book of ASTM Standards.* American Society for Testing and Materials, Philadelphia.

Daniel, D. E. (1993) *Geosynthetic Clay Liners in Landfill Covers.* The Solid Waste Association of North America, San Jose.

Geosynthetic Research Institute. (1993) Standard Test Method for Permeability of Geosynthetic Clay Liners (GCLs). Drexel University, Philadelphia.

Gilbert, R. B., F. Fernandez and D. Horsfield. (1996a) Shear Strength of a Reinforced Geosynthetic Clay Liner. *Journal of Geotechnical Engineering* 122(4): 259-266.

Gilbert, R. B., H. B. Scranton and D. E. Daniel. (1996b) Shear Strength Testing for Geosynthetic Clay Liners. *Testing and Acceptance Criteria for Geosynthetic Clay Liners ASTM ATP 1308*, ed. L. W. Well. American Society for Testing and Materials, Philadelphia.

Grim, R. and N. Guven. (1978) *Developments in Sedimentology: Bentonites.* Elsevier Scientific Pub. Co., Amsterdam.

Massa, B. (1990) CaCl Base Stabilization Prolongs Life, Study Shows. *Roads and Bridges* Oct. 1990, p. 58.

National Lime Association. (1975) Quicklime Stabilizes Canal Lining. *Roads and Streets* Jan. 1975.

Neal, D. V. (1985) Cement-Modified Soil(CMS). *Texas Civil Engineer* June/July 1995, pp. 11-14.

Schmitt, K. E. (1996) "Feasibility Study for Enhancing the Shear Strength of Sodium Bentonite Using Additives." *M.S. Thesis*, University of Texas at Austin.

Valsangkar, A. J. and T. A. Holm. (1990) Geotechnical Properties of Expanded Shale Lightweight Aggregate. *Geotechnical Testing Journal* 13(1): 10-15.

Chapter 8

Caps: Performance

IN-SITU STUDIES ON THE PERFORMANCE OF LANDFILL CAPS
(Compacted Soil Liners, Geomembranes,
Geosynthetic Clay Liners, Capillary Barriers)

Stefan Melchior[1]

ABSTRACT

Since 1986 different types of landfill covers have been studied in-situ on the Georgswerder landfill in Hamburg, Germany. Water balance data are available for eight years. The performance of different barriers has been measured by collecting the leakage on areas ranging from 100 m² to 500 m². Composite liners with geomembranes performed best, showing no leakage. An extended capillary barrier also performed well. The performance of compacted soil liners, however, decreased severely within five years due to desiccation, shrinkage and plant root penetration (liner leakage now ranging from 150 mm/a to 200 mm/a). About 50 % of the water that reaches the surface of the liner is leaking through it. The maximum leakage rates have increased from $2 \times 10^{-10} \, m^3 \, m^{-2} \, s^{-1}$ to $4 \times 10^{-8} \, m^3 \, m^{-2} \, s^{-1}$. Two types of geosynthetic clay liners (GCL) have been tested for two years now with disappointing results. The GCL desiccated during the the first dry summer of the study. High percolation rates through the GCL were measured during the following winter (45 mm resp. 63 mm in four months). Wetting of the GCL did not significantly reduce the percolation rates.

INTRODUCTION

Covers for landfills and contaminated sites have a variety of tasks. Usually they shall prevent the direct uptake of contaminants by organisms, control gas fuxes, and reduce the infiltration of rainfall and snowmelt. The design of covers depends on severel factors like the climatic conditions of the site, the geomechanical properties and the environmental risks of the contaminated area, the planned use of the site, and costs. Sites to be used for industrial purposes may be sealed at the surface by layers of asphaltic concrete. In most cases, however, contaminated sites are covered to enable plant growth and recultivation. Such a "green" cover usually should have an erosion-resistant top layer to support the vegetation above several layers which are designed either to laterally drain water or gas or to form barriers against vertical transport of water and gas. The service life of a cover usually is long compared to most other engineered constructions. It varies from several decades to hundreds of years. Though there is a lot of practical experience with the design and construction of covers, little is known of their practical performance. Unlike base liners of landfills covers are exposed to a variety of environmental stresses (e.g. erosion, heat, frost, desiccation, biological turbation, transport and precipitation of colloids, hydroxides, carbonates) in addition to the impact of the waste body (gas and gas condensate, contaminated liquids, subsidence). Therefore it is hard to predict the long-term performance of a cover on the basis of theoretical considerations and laboratory data. For this reason a team of researchers and technicians has set up and operated several in-situ test facilities during the last ten years to study and monitor the performance of multilayered covers with the following barrier layers: compacted soil liners (CSL), geosynthetic clay liners (GCL), capillary barriers (CB), and composite liners (CL) with geomembranes above compacted soil liners. This paper gives a brief overview on the most important results.

THE SITE AND CONCEPT OF THE STUDIES

The Georgswerder landfill is located in Hamburg, Germany. The area of the landfill is 44 ha, its height 40 m. It contains $7 \times 10^6 \, m^3$ of municipal waste of which 3 % is highly toxic liquid industrial waste. The landfill has been closed since 1979. After the detection of high concentrations of 2,3,7,8 TCDD a

[1] **IGB** - Ingenieurbüro für Grundbau, Bodenmechanik und Umwelttechnik
     Heinrich-Hertz-Straße 116 - D-22083 Hamburg - Germany
     Tel.: +49 (40) 22 70 00 - 38, Fax: +49 (40) 22 70 00 - 34, SMelchior@compuserve.com

complex remedial action program was started in 1985 including a multilayered cover (from top to bottom: topsoil / drainage layer / composite liner (geomembrane/compacted soil liner) / gas ventilation layer). Subsidence of the landfill is rather uniform. The average rate is 10 cm/a eight years after capping. Gas collection decreased from 600 m³/h (1986) to 300 m³/h (1995). The temperature within the landfill is 35 °C. The vegetation is formed by grasses and perennial weeds, cut twice a year. In 1995 shrubs, bushes and trees were planted on selected areas of the cover. The climate of Hamburg is humid and temperate, influenced by the close North Sea (there is no comparable climate in the U.S., the closest you can get is Seattle, WA). The average precipitation from 1998 to 1995 was 865 mm/a, distributed almost uniformly over the year. Rainfall intensity usually is low, maximum intensities being around 3 mm/10 min and rarely above 10 mm/h. The long-term average air temperature is 8.7 °C with average values of 0.1 °C in January and 17.5 °C in July. An average of 23 days per year (d/a) show a maximum temperature above 25 °C, 25 d/a have a maximum temperature below 0 °C. The average potential evapotranspiration is 540 mm/a.

In 1987 six test fields with a size of 10 m by 50 m each have been integrated into the northern slopes of the landfill cover to study the water balance and the liner performance of different caps. The layer design is shown in Figure 1. Fields named F are "flat" with an inclination of 4 %, the "steep" fields S have a slope of 20 %. All fields were constructed with the same state-of-the-art technology, materials and quality control as used during the contruction of the cover of the whole landfill. No artificial materials cut through the liners at the boundary of the test fields to avoid the formation of preferential flow paths (details in Melchior & Miehlich 1989 and Melchior 1993). Meteorological data, soil hydrological parameters, surface runoff, lateral discharges within the soil layers as well as the leakage through the liners are measured directly, the latter by collecting the flow in gravel-filled underpans. Topsoil and drainage layers are uniform on all fields, the topsoil (0.75 m) being a sandy loam (25 % < 0.063 mm, 1.1 % organic carbon), the drainage layer (0.25 m) being a sand/gravel mixture (56 % < 2 mm, 38 % from 2 mm to 6.3 mm) with 8.8 % $CaCO_3$. The storage capacity for plant-available water in topsoil and drainage layer is 105 mm (field capacity minus wilting point). Underneath the drainage layer the various test plots contain compacted soil liners, composite liners and an extended capillary barrier. All test fields have been monitored for over eight years now.
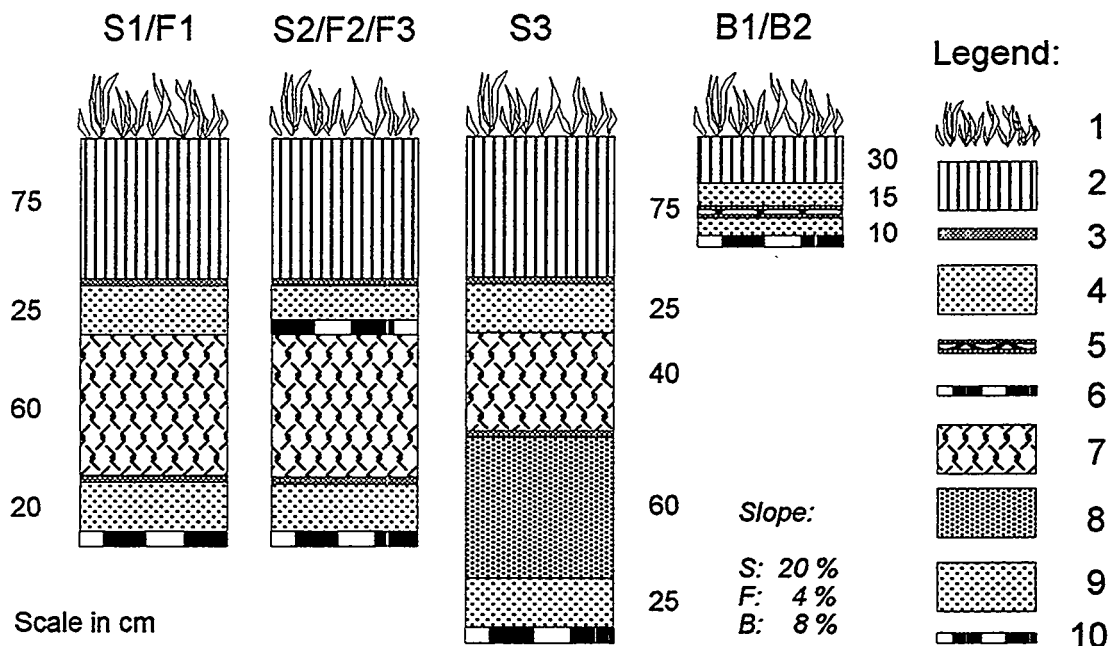
Figure 1   Layer Design of the Test Fields

(1: vegetation; 2: topsoil; 3:geotextile; 4: drainage layer; 5: geosynthetic clay liner; 6: geomembrane (HDPE, 1.5 mm); 7: compacted soil liner; 8: capillary layer; 9: capillary block (only on field S3); 10: geomembrane of underpan)

The test fields B1 and B2 with a size of 100 m² each were constructed in 1994 to monitor the performance of the geosynthetic clay liners Bentofix D 3000 and NaBento under a shallow cover of 0.3 m of topsoil and 0.15 m of drainage layer (Fig. 1). Gundseal, Bentomat, and Claymax SP 500 are installed on three additional small observation plots underneath a similar cover, but without collecting the leakage in underpans.

WATER BALANCE DATA

The water balance data are listed in Table 1. Evapotranspiration and lateral drainage above the liners are the dominant parameters in the water balance. Significant surface runoff only occurred during the first year with scarce vegetation. Later on it is very low and almost independent of inclination. During the 8 years of measurements, however, there have been unusually few thunderstorms with high rainfall intensities and only very few snowmelt events compared to the long-term average. Lateral drainage within the topsoil (interfow) only occurred under steep slope conditions and even then contributed only a few millimeters to the water balance (maximum flow rates around 0.4 mm/d or 0.1 mm/h). There is some variation in the drainage and evapotranspiration data over the years and between the individual fields. In general, the amount of drainage discharge per year is independent of inclination (maxima 40 mm/week and 39 mm/week on fields S and F respectively). The short-term flow rates however are higher on the steep fields (maxima around 23 mm/d or 3.7 mm/h) than on the flat fields (maxima 15 mm/d or 0.9 mm/h). The annual evapotranspiration is higher on the flat fields than on the steep fields due to a higher input of solar radiation in winter, spring and fall. In consequence the annual drainage rates are lower on the flat fields.

LINER PERFORMANCE

Compacted Soil Liner (CSL)
Compacted soil liners have been monitored in three test fields. On fields F1 and S1 three lifts and on S3 two lifts of glacial marl have been compacted to a total thickness of 0.6 m (S1, F1) and 0.4 m (S3) after compaction. They have the following average properties: 17 % clay, 26 % silt, 52 % sand, and 5 % gravel; no organic matter; carbon content, 9.8 % CO_3; 50 % of the clay minerals are illite, 30 % smectite, 20 % chlorite and kaolinite; liquid limit, 20.4 %; plasticity index,8.9; consistency index, 0.8; bulk density, 1.950 g/cm³; water content, 12.1 % dry weight or 23.6 vol.-%; Proctor density, 2.039 g/cm³; optimum water content, 9.6 %; compacted > 95 % Proctor density on wet side of optimum water content; pore volume, 27.0 %; degree of saturation, 0.87; geometric mean of saturated hydraulic conductivity in the laboratory, 2.4 x 10 $^{-10}$ m/s. Due to its graded particle size distribution, its low clay content, and the dominance of relatively inactive clay minerals, the marl shows a low potential for shrinkage compared to other "clay liners".

Figure 2 shows the discharges in the drainage layer above the liner and the liner leakage (the scale of the Y-axes of both discharges differs by the factor 10). The drainage discharge above the liner is high during winter and spring, whereas little happens during the summer. The liner leakage was very low during the first 20 months. In August 1989, however, it rose sharply within a few days after a rather small discharge event above the liner following heavy rainfall. From that time on, both discharges had a similar pattern. This flowpattern and the results of a tracer experiment prove the existence of continuous preferential flowpaths within the liner that allow rapid percolation. In fall 1992, the liner leakage increases again and reaches maximum values. The maximum flow rates have increased from 1 x 10 $^{-10}$ m³ m $^{-2}$ s $^{-1}$ (1988/89) to 2 x 10 $^{-9}$ m³ m $^{-2}$ s $^{-1}$ (1990 and 1991) to 4 x 10 $^{-8}$ m³ m $^{-2}$ s $^{-1}$ (1993 and 1994) on test field S1. On field F1 maximum flow rates increased simultaneously and reached 1 x 10 $^{-7}$ m³ m $^{-2}$ s $^{-1}$ in 1993. The measured soil hydrological data (water content and matric potential) clearly show that upward directed water transport into the dry drainage layer and topsoil has caused a desiccation of the liner and consequently the formation of cracks (details in Melchior 1993 and Melchior et al. 1994). Excavations of the liners in 1993 and 1995 revealed very small fissures between soil aggregates in liners which were not yet penetrated by plant roots (field F1). On field S1 further damage was visible in 1995. Plant roots had massively intruded and completely grown through the soil liner to depths below 1.6 m under the surface of the vegetative cover (e.g. Lotus corniculatus, Cirsium ssp., Rumex ssp., Armoracia rusticana). The marl was brittle, very hard and very dry with cracks several millimeters wide. Figure 3 shows the desiccation of the liner from 1987 to 1995. The

mm/a	1988	1989	1990	1991	1992	1993	1994	1995	Avg.
Precipitation	854.8	713.9	917.3	744.1	853.7	1032.3	1019.9	780.2	864.5
Surface Runoff S1	19.6	1.8	0.9	0.6	0.6	1.0	0.8	0.2	3.2
Surface Runoff F1	5.5	1.2	1.9	1.0	1.7	3.3	1.9	1.0	2.2

Compacted Soil Liners

		1988	1989	1990	1991	1992	1993	1994	1995	Avg.
S1	II	5.8	2.5	4.1	2.3	4.2	5.3	5.2	3.5	4.1
	III	385.8	246.5	317.9	176.9	289.4	343.1	343.8	229.4	291.6
	IV	1.9	3.1	13.3	13.5	48.1	136.2	150.4	149.8	64.5
	ET+dW	441.7	460.0	581.1	550.8	511.4	546.7	519.7	397.3	501.1
F1	III	368.0	182.7	286.4	187.2	226.2	253.4	246.8	155.5	238.3
	IV	7.0	7.8	17.5	8.8	102.7	174.0	165.8	163.5	80.9
	ET+dW	474.3	522.2	611.5	547.1	523.1	601.6	605.6	460.2	543.1
S3	II	12.1	6.2	8.3	5.2	7.6	8.0	7.4	5.9	7.6
	III	395.9	233.8	318.8	200.1	278.6	263.2	248.4	150.6	261.2
	V+VI	8.4	13.9	31.0	32.5	116.8	171.0	184.0	201.4	94.9
	ET+dW	418.8	458.2	558.3	505.7	450.1	589.1	579.3	422.1	497.6

Capillary Barrier

		1988	1989	1990	1991	1992	1993	1994	1995	Avg.
S3	V	8.4	13.9	31.0	32.5	101.7	169.9	172.0	152.7	85.3
	VI	0.0	0.0	0.0	0.0	15.1	1.1	12.0	48.7	9.6

Composite Liners (Geomembrane Above Compacted Soil Liner)

		1988	1989	1990	1991	1992	1993	1994	1995	Avg.
S2	II	13.2	5.9	8.5	5.3	8.3	10.8	9.7	6.8	8.6
	III	354.8	236.6	320.9	191.6	329.8	389.9	388.7	296.6	313.6
	IV	0.6	0.3	0.5	0.7	1.0	1.7	3.0	2.8	1.3
	ET+dW	466.6	469.3	586.5	545.9	514.0	628.9	617.7	473.8	537.8
F2	III	293.2	156.4	262.9	170.9	313.2	412.2	409.0	309.7	290.9
	IV	3.5	0.6	0.4	0.5	0.8	1.3	1.8	1.7	1.3
	ET+dW	552.6	555.7	652.1	571.7	538.0	615.5	607.2	467.8	570.1
F3	III	367.3	155.3	262.1	168.2	325.9	481.1	431.4	328.0	314.9
	IV	4.1	1.4	2.6	2.0	3.5	5.0	5.2	5.2	3.6
	ET+dW	477.9	556.0	650.7	572.9	522.6	542.9	581.4	446.0	543.8

Table 1   Water Balance Data of the Test Fields on the Georgswerder Landfill in mm/a

S1, S2, S3, F1, F2, F3: name of test field (layer design and slope see Fig. 1);
Surface runoff only measured on S1 and F1 (data extrapolated to S2, S3 resp. F2, F3);
II: interflow within topsoil (measured on all fields, no flow on fields F1, F2, F3);
III: lateral drainage within drainage layer above liner;
IV: water collected underneath liner (= V + VI on S3);
V: lateral interflow within capillary layer (only on S3) ;
VI: vertical percolation into capillary block (only on S3);
ET+dW: actual evapotranspiration and change in soil water storage.
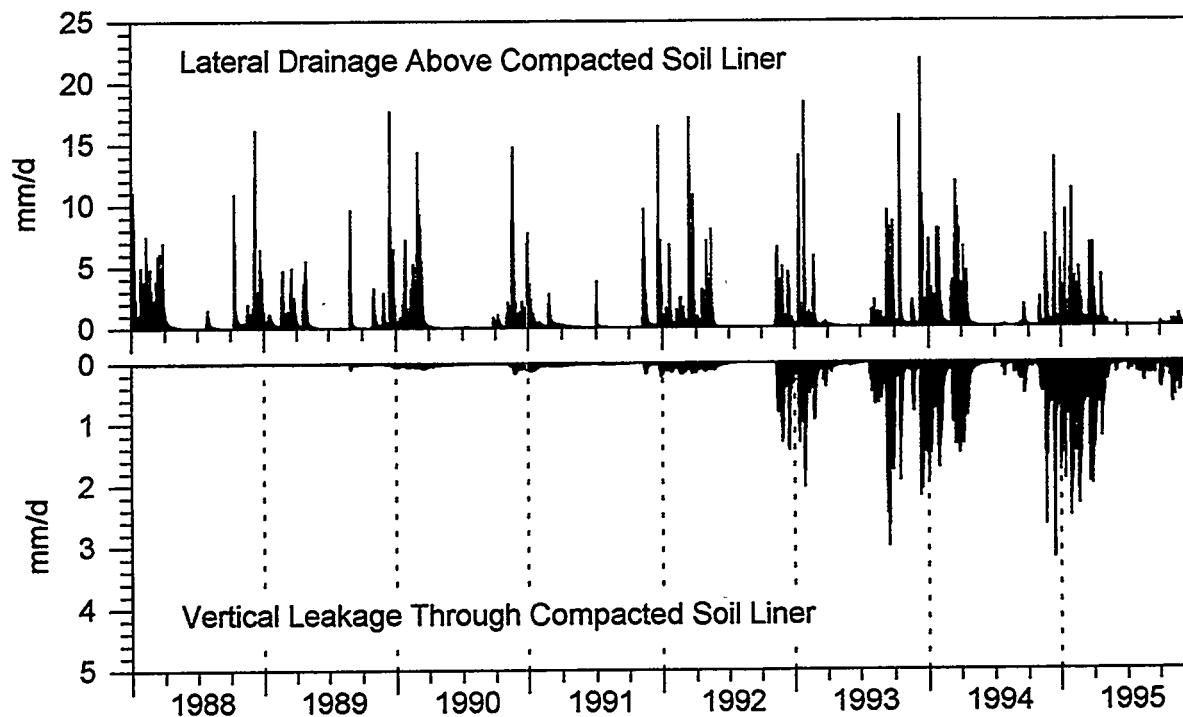
Figure 2   Compacted Soil Liner on Test Field S1: Lateral Drainage and Liner Leakage
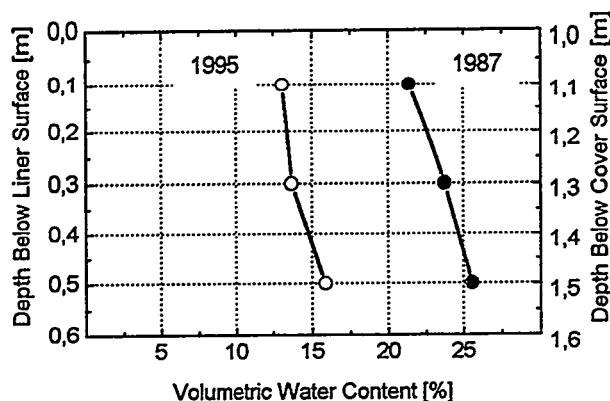
Figure 3   Water Content in the Compacted Soil
                Liner (S1) after Construction and 1995

average water content in 1995 (14.4 vol.-%) is much lower than the water content measured in the laboratory during the determination of the water retention data at soil water tensions of 3,000 hPa (22.6 vol.-%) and 15,000 hPa (17.7 vol.-%). Therefore matric potentials within the liners must have been very low during the dry summer of 1995.

The sequence of increasingly dry summers in 1989, 1992, and 1995 has led to higher percolation rates in the following winters. From 1993 through 1995 136 mm/a to 202 mm/a have leaked through the compacted soil liners (flow "IV" of fields S1 and F1, flow "V+VI" on S3 in Table 1). The sum of the lateral discharge within the drainage layer (flow "III") and the liner leakage represents the potential percolation into the landfill. In 1995 an average of 49 % of the potential leakage actually leaked through the liners.

Geosynthetic Clay Liner (GCL)
GCL appeared on the German market in the early 90s. They are used for a variety of geotechnical purposes including covers for contaminated sites. Laboratory tests have proven a low permittivity of swollen GCL, even after several wet/dry cycles. Being aware of the threat that desiccation poses on compacted soil liners we wondered, if field conditions (root penetration, chemical composition of soil water, variing velocity and intensity of desiccation and moistening) would influence the performance of GCL. Therefore we set up two test fields and three observation plots in April 1994. For two reasons

369

we decided to test the GCL under a rather shallow cover of 0.3 m topsoil (sandy loam, 4 % organic carbon) and 0.15 m drainage layer (gravel, 1 mm to 8 mm): (1) Field tests are time consuming. Therefore we wanted to be sure that plant roots and desiccation would reach the depth of the GCL during the first two years of the study; (2) GCL are used under shallow topsoils in covers for old contaminated sites (on new landfills German regulations require > 1.3 m thickness of topsoil and drainage layer above a liner). We choose a needle-punched GCL (Bentofix D 3000 with natural Na-Bentonite, Naue Fasertechnik) and a stitch-bounded GCL (NaBento with activated Ca-Bentonite, Huesker Synthetic) for the two test fields with underdrains to collect leakage. The American GCL were installed in small plots without underdrains. The concept of the study and the technical set-up were approved by the manufacturers representatives or their distributors in Germany before the construction of the fields. The manufacturers kindly delivered the GCL at no costs. Representatives of the companies were present to supervise the installation of the GCL and to seal the overlaps personally.

The average water content of the GCL during installation had been 10.4 % (April 1994). In November 1994 the GCL were swollen (water content of Bentomat and Claymax 138 % and 152 % resp.). Plant roots had penetrated the GCL. The summer of 1995 was extremely dry in Hamburg (water contents of topsoil and the drainage layer 5 vol.-% and 1 vol.-% resp.). The soil water tension of the GCL exceeded the measurement range of tensiometers. The measured water contents of 29 % (Bentomat) and 37 % (Claymax) also prove the desiccation of the GCL. In fall and winter 1995 the GCL were remoistened again with water contents above 100 %. The depth of freezing did not reach the GCL. Visual inspections of Bentomat and Claymax during the summer of 1995 and also of Bentofix and NaBento in spring 1996 revealed a pronounced soil structure with up to 2 mm wide gaps and cracks between bentonite aggregates of about 1 cm in diameter.
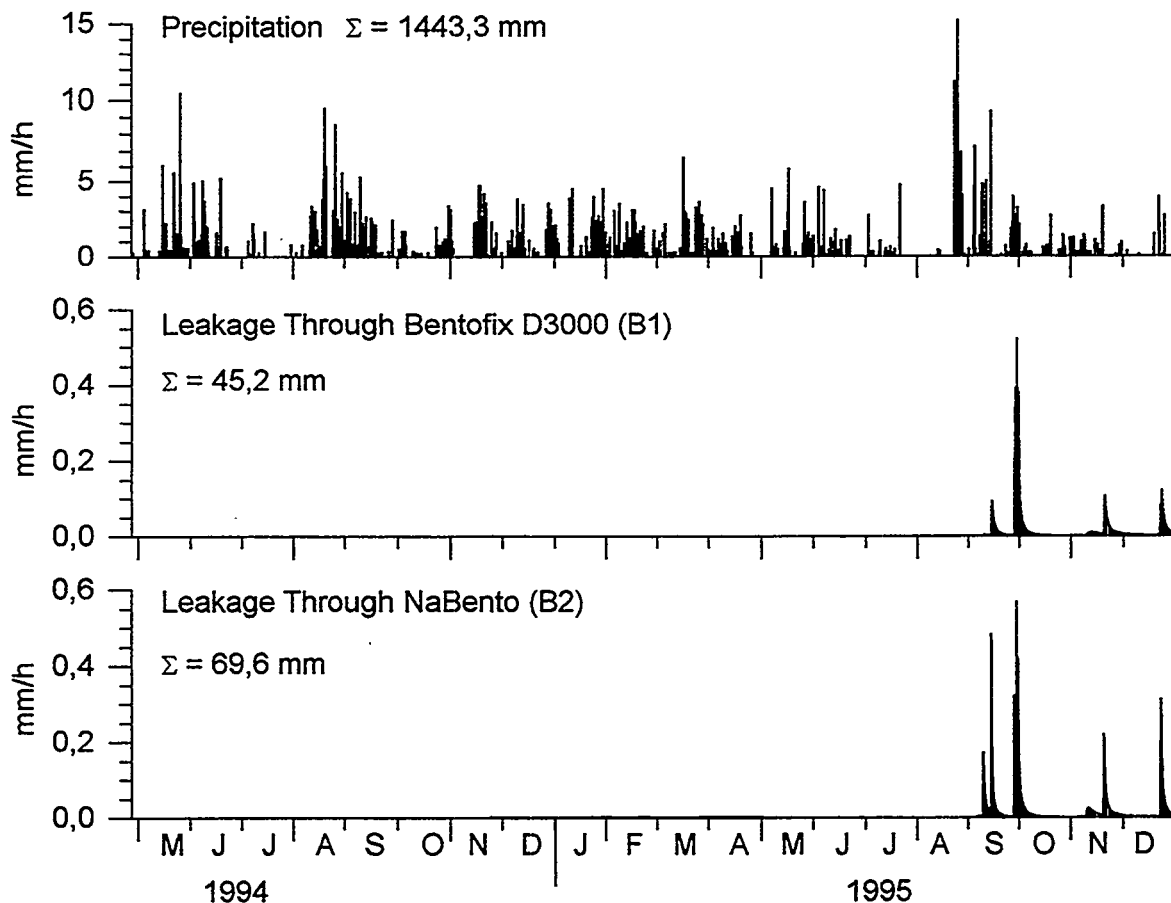
Figure 4   Geosynthetic Clay Liners: Precipitation and Leakage of Bentofix (B1) and NaBento (B2)

The characteristic property of GCL is their ability to rehydrate and swell. Figure 4 shows the precipitation data and the leakage through the GCL until the end of 1995. Both GCL performed excellent during the first winter (0.0 mm and 6.2 mm leakage through Bentofix resp. NaBento). This result demonstrates the proper installation of the GCL including the overlaps. However, after the dry summer of 1995 rainfall first remoistens the topsoil (August) and then produces high leakage rates after every major rainfall event (up to 1×10^{-7} m^3 m^{-2} s^{-1}). Within four months, 45 mm and 63 mm leaked through Bentofix resp. NaBento. During the whole winter of 1995/96 the GCL did not rehydrate and swell enough to seal the preferential flowpaths formed during desiccation. Research to explain the reasons for this very fast decrease of efficiency is ongoing. First results indicate that the mineralogical structure of the bentonite is still intact. However calcium ions have exchanged sodium to a large extent. Consequently the swelling capacity of the bentonite has been reduced to values close to typical values of Ca-Bentonite. Precipitates of humic colloids, carbonates or iron hydroxides have not been found on the surfaces of the bentonite aggregates so far. The leakage through the GCL will be monitored at least until spring 1997.

Capillary Barrier (CB)

The capillary barrier on field S3 consists of 0.6 m of fine sand (78 % of the particles with diameters from 0.1 mm to 0.2 mm) as a laterally conductive capillary layer above 0.25 m of coarse sand and gravel (85 % from 0.63 mm to 6.3 mm), which serves as capillary block. The unsaturated hydraulic conductivity of the capillary layer is 1×10^{-4} m/s at matric potentials above -30 hPa. The capillary barrier is covered by topsoil, drainage layer and two lifts of compacted soil to limit the vertical infiltration into the capillary layer. Figure 5 shows the lateral drainage above the soil liner, the lateral drainage within the capillary layer and the vertical infiltration into the capillary block (the annual water balance data are given in Table 1). The system performed perfectly during the first 4.5 years. In 1992 the compacted soil liner desiccated. Cosequently the leakage through the soil liner along cracks increased dramatically. From November 1992 on several events occurred when the infiltration into the capillary layer exceeded the lateral drainage capacity of the capillary layer and therefore produced vertical leakage into the capillary block (up to 48.7 mm/a in 1995, see Table 1).

In an additional study we tested several material combinations for capillary barriers in a 10 m long tilted trough under various inclinations and infiltration rates (Steinert et al. 1996). Capillary layers with medium or coarse sands had much higher lateral drainage capacities than the material combination used in test field S3. These results show the potential for the use of optimally designed conductive capillary barriers in landfill covers.
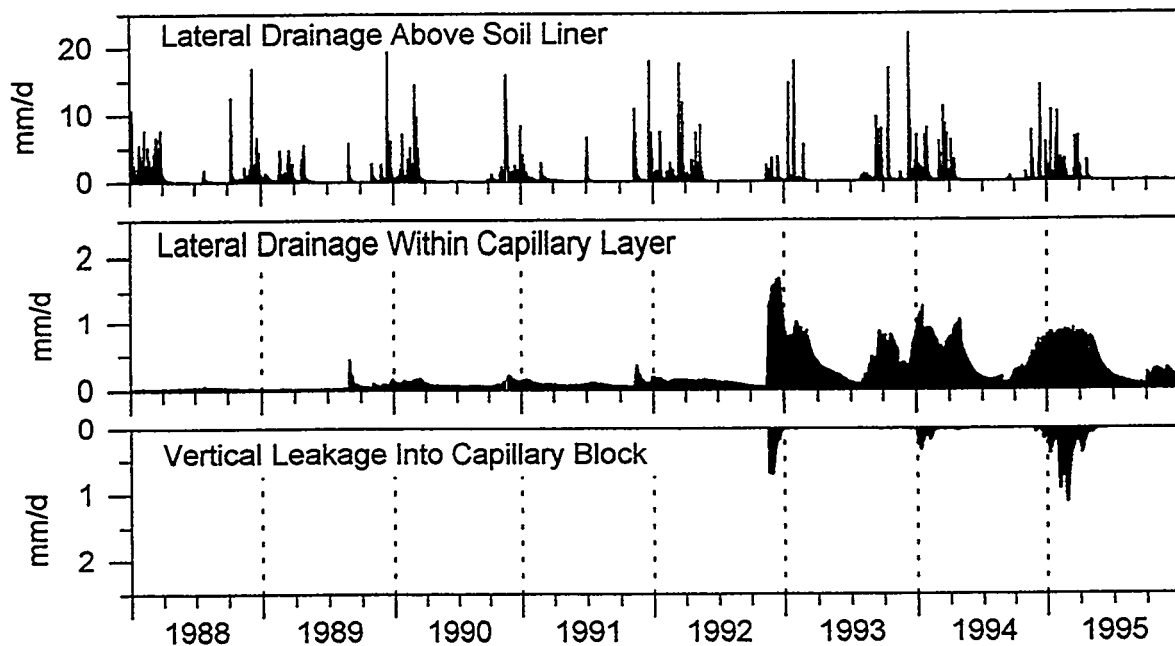
Figure 5   Extended Capillary Barrier on Test Field S3: Lateral Drainage Above the Soil Liner and Within the Capillary Layer and Vertical Leakage into the Capillary Block

Composite Liner (CL, Geomembrane above Compacted Soil Liner)

Composite liners with 1.5 mm thick HDPE-membranes above three lifts of compacted marl (see chapter on compacted soil liners) were tested on three test fields since 1988. On two fields (S2, F2) the geomembranes are welded, on field F3 the geomembranes are installed overlapping in slope direction. The performance of the composite liners is excellent. Table 1 shows that an average of 1.3 mm/a has been collected underneath the liners of fields S2 und F2. On field F3 it has been slightly more (3.6 mm/a). Detailed interpretation of the soil hydrological data and the soil temperature data reveals that the water collected unterneath the composite liner is not the result of leaks within the geomembrane but transported out of the compacted soil liner during hot summer periods when soil temperature is higher at the surface of the soil liner than on its lower boundary. This water transport causes periodical changes of the matric potential within the soil liner. Additional studies on the thermally induced water transport in composite liners (Vielhaber 1995) have shown that the absolute temperature as well as thermal gradients induce a transport of vapor and liquid water from warm to cold regions of the soil. However, in a temperate climate and underneath a thick topsoil the thermally induced downward water transport is very slow, limited to a short period of the year and will not threaten the integrity of the compacted soil liner within several decades.

CONCLUSIONS

Test fields are very useful tools to monitor the performance and water balance of landfill covers. An appropiate technical set-up design is required and time is needed to collect and interpretate valuable data. The most important conclusions after ten years of field studies in Hamburg, Germany are:

- A cover should be designed to maximize evapotranspiration and lateral drainage. However, in humid climates and in semi-arid areas with rare but intensive precipitation, a liner is needed to effectively limit the infiltration into a landfill or contaminated site.
- Compacted soil liners and geosynthetic clay liners are very sensitive to desiccation and shrinkage. Upward water transport into dry topsoil and water uptake of plant roots have caused an irreversible formation of cracks and preferential flowpaths in the tested liners. Plant root penetration and desiccation of CSL and GCL must be prevented by thick topsoils or other protective measures. At present no means are known to control the properties of clays in order to prevent the formation of preferential flowpaths during desiccation or to rapidly re-seal cracks in shrunken cohesive surface liners.
- Capillary barriers are promising components for covers on slopes. However, they must be protected against high infiltration rates into the capillary layer. In humid environments, and most likely also at many semi-arid sites, a lateral drainage component is mandatory. The conductive capillary layer should have a maximum unsaturated conductivity at matric potentials above 30 hPa, achievable with well sorted coarse sands. Well graded materials, silts, loams, and clays are unsuitable for capillary layers. The capillary block should consist of gravel and must provide filterstability to the capillary layer. Within a composite liner (e.g. under a geomembrane) a capillary barrier can provide a secondary liner as well as a system to monitor the performance of the primary liner.
- Composite liners with geomembranes above a compacted soil liner performed best. Geomembranes are very effective and make durable liners if suitable polymers are used and if they are installed properly. The cohesive soil component is able to seal local defects in the geomembrane. Unlike in base liners, however, soil liners are rarely used in covers to retard contaminant transport. Placed under an intact geomembrane, the soil liner is protected against upward directed water losses. In the longterm (after at least many decades) this would no longer be true if the geomembrane would deteriorate completely. Over decades thermally induced water transport may cause desiccation of the soil liner even under an intact geomembrane. In conclusion composite liners with geomembranes are very effective and durable systems. However, there is some potential to make them more cost-effective by reducing the thickness or the quality of the soil component or by replacing the soil liner by a different geomembrane or a capillary barrier.
- Covers should be designed carefully by taking into account the specific boundary conditions of the individual application (e.g. climate, geometry, actual or potential hazard of the site, planned use of the cover, availability of materials, critical influences like differential settlements or aggressive chemicals, and costs). Planners can choose from a variety of options to design a cost-effective and suitable cover.

ACKNOWLEDGMENTS

REFERENCES

Melchior, S. (1993): Wasserhaushalt und Wirksamkeit mehrschichtiger Abdecksysteme für Deponien und Altlasten (Water Balance and Effectiveness of Multilayered Landfill Covers). Ph.D. Thesis, University of Hamburg, Germany. *Hamburger Bodenkundliche Arbeiten,* 22, p. 330.

Melchior, S. & G. Miehlich (1989): Field Studies on the Hydrological Performance of Multilayered Landfill Caps. In: U.S. EPA (ed.): Proceedings of the 3rd International Conference on New Frontiers for Hazardous Waste Management in Pittsburgh, PA. P. 100-108.

Melchior, S, K. Berger, B. Vielhaber & G. Miehlich (1994): Multilayered Landfill Covers: Field Data on the Water Balance and Liner Performance. In: Gee, G. & N.R. Wing (eds.): In-Situ Remediation: Scientific Basis for Current and Future Technologies. Battelle Press, Columbus, Richland, p. 411 - 425.

Steinert, B, S. Melchior, K. Burger, K. Berger, M. Türk & G. Miehlich (1996): Dimensionierung von Kapillarsperren zur Oberflächenabdichtung von Deponien und Altlasten (Dimensioning of Capillary Barriers for Landfill Covers). Research Report no. 1440 569A-39 to the German Federal Institute of Material Testing and the German Ministery for Research and Technology (BMBF), p. 19.

Vielhaber, B. (1995): Temperaturabhängiger Wassertransport in Deponieoberflächenabdichtungen. Feldversuche in bindigen mineralischen Dichtungen unter Kunststoffdichtungsbahn (Thermally induced Water Transport in Landfill Covers). Ph. D. Thesis, University of Hamburg, Germany. *Hamburger Bodenkundliche Arbeiten,* 29, p. 200.

INFERRED PERFORMANCE OF SURFACE HYDRAULIC BARRIERS FROM LANDFILL OPERATIONAL DATA

B.A. Gross[1], R. Bonaparte[2], and M.A. Othman[2]

Abstract

There are few published data on the field performance of surface hydraulic barriers (SHBs) used in waste containment or remediation applications. In contrast, operational data for liner systems used beneath landfills are widely available. These data are frequently collected and reported as a facility permit condition. This paper uses leachate collection system (LCS) and leak detection system (LDS) liquid flow rate and chemical quality data collected from modern landfill double-liner systems to infer the likely hydraulic performance of SHBs. Operational data for over 200 waste management unit liner systems are currently being collected and evaluated by the authors as part of an ongoing research investigation for the United States Environmental Protection Agency (USEPA). The top liner of the double-liner system for the units is either a geomembrane (GMB) alone, geomembrane overlying a geosynthetic clay liner (GMB/GCL), or geomembrane overlying a compacted clay liner (GMB/CCL). In this paper, select data from the USEPA study are used to: (i) infer the likely efficiencies of SHBs incorporating GMBs and overlain by drainage layers; and (ii) evaluate the effectiveness of SHBs in reducing water infiltration into, and drainage from, the underlying waste (i.e., source control). SHB efficiencies are inferred from calculated landfill liner efficiencies and then used to estimate average water percolation rates through SHBs as a function of site average annual rainfall. The effectiveness of SHBs for source control is investigated by comparing LCS liquid flow rates for open and closed landfill cells. The LCS flow rates for closed cells are also compared to the estimated average water percolation rates through SHBs presented in the paper.

Introduction

SHBs, also called "caps" or "infiltration barriers", have been constructed over many contaminated sites as part of the site waste containment or remediation strategy. A primary function of a SHB is to minimize infiltration of water into the underlying wastes. SHBs are almost never used alone; rather, they are one of the up to six basic components used in cover systems. The functions and potential materials for each component of a cover system have been described by Daniel and Gross (1996). The focus of this paper is on "conventional" resistive SHBs incorporating GMBs and overlain by surface and protection layers and drainage layers. The components pertinent to this type of conventional cover system are shown in Figure 1.

Little published information is available on the field behavior of modern multicomponent cover systems (Rumer and Ryan, 1995; Daniel and Gross, 1996). Performance data for SHBs are limited because such data are not normally collected as part of waste containment or remediation projects. A limited number of field studies are currently being conducted to evaluate the performance of cover systems test sections incorporating SHBs (e.g., Melchior et al., 1994; Dwyer, 1995; Khire, 1995; Petersen et al., 1995; Schultz et al, 1995). However, most of the studies have been ongoing for only a few years, or less, and not all of them include a drainage layer over the SHB. Nonetheless, the available data indicate that cover systems with GCL, GMB, GMB/CCL, and GMB/GCL SHBs limit infiltration better than cover systems with CCL barriers that tend to desiccate and crack (Daniel, 1995).

[1]GeoSyntec Consultants, 1004 E. 43rd Street, Austin, TX 78751-4407, (512) 451-4003, BethG@geosyntec.com

[2]GeoSyntec Consultants, 1100 Lake Hearn Drive, Suite 200, Atlanta, GA, 30342-1523, (404) 705-9500, RudyB@geosyntec.com, MajdiO@geosyntec.com
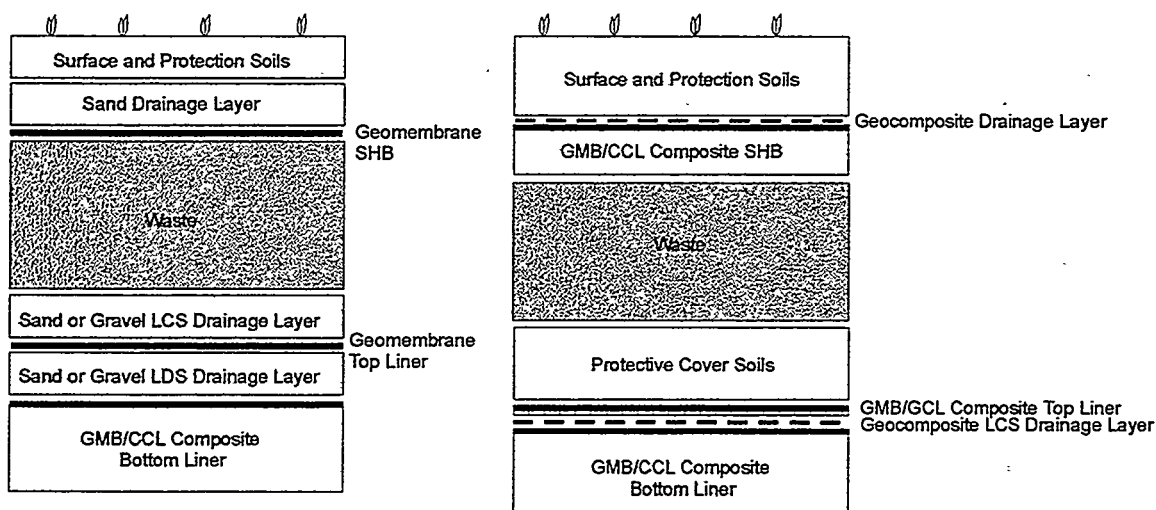
Figure 1. Typical cover systems and double-liner systems for landfills.

The cover system test sections that have been monitored over the longest time period, and that incorporate a drainage layer and CCL or GMB/CCL SHB, appear to be those described by Melchior et al. (1994). In 1987, four cover system test sections were constructed in Hamburg, Germany, a city with an average annual rainfall of about 700 mm. The test sections consisted of, from top to bottom: a 0.75-m thick topsoil layer; a 0.25-m thick gravel drainage layer; and a CCL or GMB/CCL SHB. The geometric mean of the laboratory saturated hydraulic conductivity of the CCL was 2.4×10^{-10} m/s. Precipitation, other meteorological parameters, soil temperature, runoff, lateral drainage, soil moisture content, soil suction, and percolation through the SHB were monitored. For the test section with a CCL SHB, percolation increased each year due to preferential flow through shrinkage cracks which developed in the CCL as it lost moisture by evapotranspiration. In 1992, percolation was 47.9 mm on the steep (i.e., 20%) test slope and 102.5 mm on the shallow (i.e., 4%) test slope. The corresponding CCL SHB efficiencies were 85.7 and 68.7%, respectively, relative to the total amount of water that had percolated to the drainage layer above the SHB. In 1994, percolation through the CCL SHB on the shallow slope was about 200 mm, which corresponded to a barrier efficiency of about 60% (Melchior, 1995). No percolation was observed for the test section with a GMB/CCL SHB, although some water occasionally drained from the CCL component in response to thermal gradients.

Operational data on LCS and LDS liquid flow rates and chemical quality are available for numerous landfill double-liner systems. A landfill double-liner system consists of top and bottom liners, or barrier layers, with a LDS drainage layer between the two liners and a LCS drainage layer above the top liner (Figure 1). These types of LCS and LDS data have been evaluated previously to estimate the rates of leakage though landfill top liners (Bonaparte and Gross, 1990; Gross et al., 1990; Bonaparte and Gross, 1993; Feeney and Maxson, 1993; Maule et al., 1993; Workman, 1994). SHBs are generally subjected to lower average liquid heads, transient liquid heads, lower compressive stresses, and greater differential displacements than landfill top liners. However, the data used to assess the performance of landfill top liners can be used to infer the likely hydraulic performance of SHBs having similar components to the top liners.

The purpose of this paper is to use operational data from modern landfill double-liner systems to assess the likely hydraulic performance of SHBs. The data are a subset of the waste containment facility database being developed by the authors for the USEPA National Risk Management Research Laboratory. The database contains information on facility characteristics (e.g., location and average annual rainfall), types and properties of materials used in the liner and cover systems of the facilities, and quantity and chemical quality of liquid flow into the LCS and LDS sumps of the facilities. Currently, the database includes information on 194 individual cells at 54 double-lined landfill facilities and 17 individual ponds at six double-lined surface impoundment facilities located

throughout the U.S. The top liners for all the cells considered in the USEPA study include GMBs, and are either GMBs, GMB/GCL composites, or GMB/CCL composites. Not all data are available for all facilities (e.g., chemical quality data are not available for some facilities). The current USEPA study is an expansion of the work previously conducted by Bonaparte and Gross (1993) and includes new data for landfill facilities evaluated in their report as well as data for additional landfills. In this paper, the likely efficiencies of SHBs incorporating GMBs and overlain by drainage layers are inferred from efficiencies calculated for landfill top liners. The SHB efficiencies are then used to estimate average water percolation rates though SHBs as a function of site average annual rainfall. In addition, the effectiveness of SHBs for source control is investigated by comparing LCS flow rates for open and closed landfill cells. The LCS flow rates for closed cells are also compared to the average water percolation rates through SHBs presented in the paper.

Liner Efficiency

Bonaparte et al. (1995) defined the "apparent" efficiency of a top liner of a double-liner system using the following equation:

$$\text{Apparent Liner Efficiency (\%)} = (1 - \text{LDS Flow Rate} / \text{LCS Flow Rate}) \times 100 \qquad \text{(Eqn. 1)}$$

The liner efficiency is referred to as "apparent" because liquid flow into the LDS sump may be due to sources other than top liner leakage (Gross et al., 1990). If the only source of liquid flow into the LDS sump is top liner leakage, then Eqn. 1 gives the "true" liner efficiency. The higher the true efficiency of a liner, the more effective it is as a hydraulic barrier. There is no one true efficiency for a hydraulic barrier type; true efficiency is a function of a number of variables, including construction quality, barrier slope, and head of liquid on the barrier.

True liner efficiencies were calculated for 39 individual cells from 15 landfills with GMB or GMB/GCL top liners. The calculated efficiencies are based on LCS and LDS flow rate data covering time periods up to eight years after cell construction. Over two years of data are available for about 81% of the cells, and over five years of data are available for about 33% of the cells. The performance of some of the units with a GMB/GCL top liner was recently evaluated by Bonaparte et al. (1995). The ranges of efficiencies calculated for the two liner types and representative efficiencies to be used in subsequent calculations are presented in Table 1. The values are considered to represent true efficiencies as top liner leakage was the only significant source of LDS liquid flow identified for the cells. The sources of liquid flows from the LDSs of the cells were evaluated using the five-step approach described by Bonaparte and Gross (1990) and Gross et al. (1990). With this approach, the measured LDS flow rates are compared to calculated LDS flow rates from each identified potential source of flow, and LCS and LDS flow chemical quality data are compared to assess whether top liner leakage is occurring. Representative true liner efficiencies of 99% for GMBs alone and 99.9% for GMB/GCL composites were selected for use in further analyses. These representative values are high and reflect the significant liquid containment capabilities of the types of liners in common use today. True liner efficiencies of cells with GMB/CCL top liners can not be calculated directly since LDS flows from these cells include water from consolidation of the CCL component of the top liner. However, based on the detailed evaluation of data in Othman et al. (1996) for liner systems with GMB/CCL top liners, the authors have concluded that the true efficiencies for GMB/CCL composite liners can equal, or exceed, 99.9%.

Table 1. True liner efficiencies.

Liner Types	Number of Cells	Efficiency (%)	
		Range	Rep. Value
GMB	15	97.2 - 99.9	99
GMB/GCL Composite	24	99.3 - 100	99.9
GMB/CCL Composite	------	------	99.9

Inferred SHB Efficiencies and Percolation Rates

The efficiency of a liner is dependent on the liner type, construction quality, head of liquid in the drainage layer over the liner, as well as other factors. For a given rate of infiltration into a drainage layer, the head in the layer will decrease as the inclination of the layer increases and as the hydraulic conductivity of the layer increases. Since increasing liquid head on a liner increases leakage through the liner, the efficiencies of liners should be somewhat higher on steeper side slopes than on shallower base slopes. This conclusion is also applicable to SHBs and is supported by the cover system study by Melchior et al. (1994) described earlier. In that study, the efficiencies of CCL barriers on 4 and 20% slopes were 68.7 and 85.7%, respectively, in 1992. SHBs for municipal solid waste (MSW) landfills are generally constructed with steeper slopes than the average slopes for liner systems (excluding special cases such as landfills in canyons or quarries). The efficiencies of these SHBs may be somewhat higher than the efficiencies given for top liners in Table 1. In addition, SHBs overlain by geonet drainage layers are expected to have higher efficiencies than those overlain by sand drainage layers as a result of the lower heads in geonet drainage layers for a given drainage layer flow rate. Conversely, slopes for hazardous waste landfills and site remediation projects are typically relatively flat (e.g., slope of 2 to 10%), resulting in a potential for lower efficiencies if a suitably permeable drainage material is not placed over the SHB. However, since insufficient data are available to quantify the effects of slope or drainage layer type on the efficiencies of SHBs incorporating GMBs, the efficiencies of SHBs are assumed to be the same as those given in Table 1 for liners.

If the lateral flow rate of water from the drainage layer above a SHB is known, the rate of percolation of water through the SHB can be estimated using Eqn. 1, modified to apply to a SHB rather than a liner, and the efficiencies given in Table 1. The flow rate of water from a cover system drainage layer can be estimated using a water balance model, such as the USEPA Hydrologic Evaluation of Landfill Performance (HELP) computer model developed by Schroeder et al. (1994a,b), a numerical transport model, or field data. For this paper, the HELP model was used to estimate lateral flow rates from a geonet or sand drainage layer overlain by a 0.6-m thick topsoil layer. The HELP analysis was conducted using synthetic weather data generated for a limited number of cities across the U.S. These flow rates were then used to estimate typical average percolation rates through SHBs. The results of this analysis are summarized in Table 2.

Table 2. Estimated percolation rates through SHBs.

Avg. Rainfall (mm/yr)	Avg. Lateral Flow Rate[1] (mm/yr)	Avg. Percolation Rate (mm/yr (liters/hectare/day (lphd)))	
		GMB SHB	GMB/CCL or GMB/GCL SHB
100 - 300	0 - 5	0 - 0.05 (0 - 1)	0 - 0.005 (0 - 0.1)
300 - 600	0.2 - 30	0.002 - 0.3 (0.06 - 9)	0.0002 - 0.03 (0.005 - 0.8)
600 - 800	10 - 100	0.1 - 1 (3 - 30)	0.01 - 0.1 (0.3 - 3)
800 - 1,000	30 - 200	0.3 - 2 (9 - 60)	0.03 - 0.2 (0.8 - 5)
1,000 - 1,600	100 - 500	1 - 5 (30 - 100)	0.1 - 0.5 (3 - 10)

Note: [1] Estimated using HELP model with default data for sandy loam and silty clay loam topsoils, coarse sand and geonet drainage layers, fair grass, 5 and 20% cover system slopes, and 10 years of synthetic weather data generated for select cities in the U.S.

From Table 2, the average rates of percolation through GMB SHBs underlain by high permeability materials (e.g., moist clean sand) are estimated to range from 0 to 5 mm/yr. The estimated average percolation rates through GMB/CCL or GMB/GCL SHBs are one order of magnitude lower and range from 0 to 0.5 mm. For a given SHB type, the higher percolation rates are associated with wetter climates. The values in Table 2 were developed for comparison purposes and are not meant to be applied to a particular site. However, the general methodology given above can be used with project-specific input data and assumptions to evaluate project-specific SHB performance. For the previously discussed cover system study in Germany, Melchior et al.

(1994) reported an average annual precipitation of 830 mm and average annual lateral drainage of 280 mm during the first three years of the study.

Effect of SHB Placement on Source Control

The effectiveness of SHBs for source control can be evaluated by comparing LCS flow rates for open and closed landfill cells. LCS flow rate data are available for 22 closed cells at five hazardous solid waste (HSW) landfills located in the U.S. Data for closed MSW landfills are currently being collected and evaluated by the authors and are not presented herein. The HSW cells were constructed between 1985 and 1989 and closed between 1986 and 1993. Characteristics of the landfill sites and cells and summary LCS flow rate data are presented in Table 3. The cover system of each cell consists of the following components, from top to bottom: (i) topsoil surface and protection layer; (ii) a sand or geonet drainage layer; and (iii) a GMB/CCL SHB. LCS flow rates for the cells are summarized in Table 3 for two periods: (i) the operation period of the cell; and (ii) the post-closure period. After a cell was closed and its cover system installed, LCS flow rates decreased with time, as shown in Figure 2. On average, LCS flow rates during the first year after closure were approximately 22% of the LCS flows during the year prior to closure (i.e., year 0 in Figure 2). The average overall LCS flow rate from the HSW cells for a given year after closure ranged from 1,150 lphd at one year after closure to 0.7 lphd at nine years after closure. In the first eight years after closure, the average overall LCS flow rates were significantly higher than the estimated average percolation rates through GMB/CCL SHBs of 0 to 10 lphd presented in Table 2. The relatively high LCS flow rates are primarily attributed to drainage of preclosure liquid from the waste. At nine years after closure, LCS flow rates are very low. The LCS flows at this time are attributed to drainage of small amounts of preclosure liquid and, potentially, percolation through the SHB.
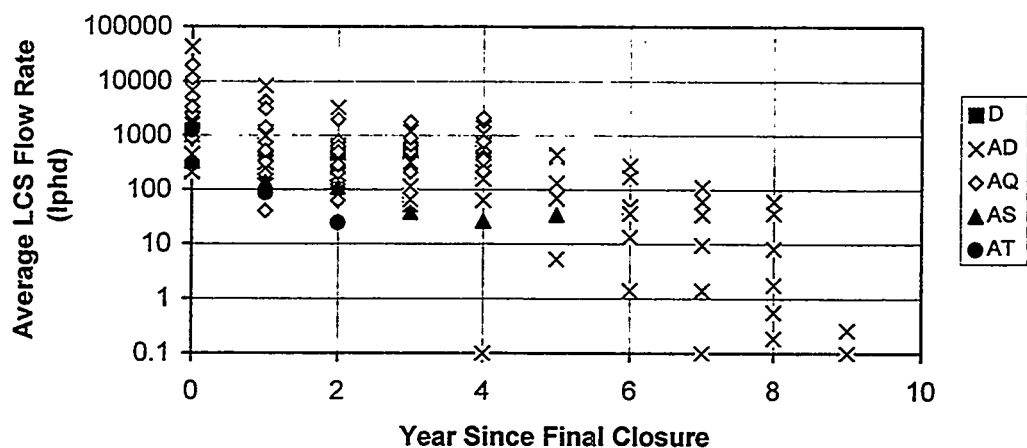
Figure 2. Average LCS flow rates after closure for HSW landfills D, AD, AQ, AS, and AT (flow rates of 0 are shown as 0.1 lphd).

References

Bonaparte, R. and B.A. Gross. (1990) Field Behavior of Double-Liner Systems. In *Waste Containment Systems: Construction, Regulation, and Performance* (ed. R. Bonaparte), pp. 52-83. ASCE Geotechnical Special Pub. No. 26.

Bonaparte, R. and B.A. Gross. (1993) *LDCRS Flow from Double-Lined Landfills and Surface Impoundments*, 65 p. USEPA Risk Reduction Engineering Laboratory, Cincinnati, OH, EPA/600/SR-93/070.

Table 3. Summary of characteristics of landfill cells and LCS flow rates.

Cell No.	U.S. Region[1]	Avg. Annual Rain. (mm)	Cell Area (hec)	Max. Waste Ht. (m)	LCS Mat. Type[2]	Topsoil Layer Thick. (m)	Drainage Layer Type	Drainage Layer Thick. (m)	SHB Mat. Type	Time of Final Close[3] (mon.)	Operation Period Time Period[3] (mon.)[5]	Operation Period Avg. Flow[4] (lphd)	Post-Closure Period Time Period[3] (mon.)	Post-Closure Period Avg. Flow[4] (lphd)
D1	SE	1,630	0.37	7.9	1	0.61	Geonet	0.005	GMB/CCL	8	ND[5]	ND	30-47	486
AD1	SE	1,830	0.57	21	2	0.61	Geonet	0.005	GMB/CCL	38	21-32	374	33-121	28
AD2	SE	1,830	0.57	21	2	0.61	Geonet	0.005	GMB/CCL	36	19-30	1,890	31-119	196
AD3	SE	1,830	0.57	21	2	0.61	Geonet	0.005	GMB/CCL	32	15-26	1,680	27-115	290
AD4	SE	1,830	0.57	21	2	0.61	Geonet	0.005	GMB/CCL	32	15-26	1,080	27-115	140
AD5	SE	1,830	0.53	21	2	0.61	Geonet	0.005	GMB/CCL	24	8-20	34,600	21-108	739
AD6	SE	1,830	0.89	21	2	0.61	Geonet	0.005	GMB/CCL	24	8-19	991	20-108	72
AD7	SE	1,830	1.5	24	2	0.61	Geonet	0.005	GMB/CCL	73	19-77[6]	1,340	78-96	309
AD8	SE	1,830	1.5	24	2	0.61	Geonet	0.005	GMB/CCL	66	13-67[6]	1,910	68-87	253
AD9	SE	1,830	1.3	24	2	0.61	Geonet	0.005	GMB/CCL	58	15-59[6]	1,470	60-79	542
AQ1	NE	970	0.59	21	3	0.61	ND	ND	GMB/CCL	48	50-66	5,070	67-98	1,160
AQ2	NE	970	0.50	21	3	0.61	ND	ND	GMB/CCL	48	50-57	2,620	58-98	383
AQ3	NE	970	0.47	21	3	0.61	ND	ND	GMB/CCL	48	49-58	2,970	59-97	683
AQ4	NE	970	0.64	21	3	0.61	ND	ND	GMB/CCL	57	49-58	2,970	59-97	524
AQ5	NE	970	0.70	21	3	0.61	ND	ND	GMB/CCL	57	51-57	4,480	58-91	748
AQ6	NE	970	0.51	21	3	0.61	ND	ND	GMB/CCL	57	43-63	2,730	64-91	496
AQ7	NE	970	0.77	21	3	0.61	ND	ND	GMB/CCL	57	43-54	1,250	55-91	131
AQ8	NE	970	0.76	21	3	0.61	ND	ND	GMB/CCL	57	47-58	4,290	59-91	533
AQ9	NE	970	0.54	21	3	0.61	ND	ND	GMB/CCL	57	51-58	720	59-91	599
AQ10	NE	970	0.86	21	3	0.61	ND	ND	GMB/CCL	57	53-58	954	59-91	664
AS1	SE	1,420	1.0	9.8	4	0.46	Geonet	0.005	GMB/CCL	31	18-35	318	36-78	60
AT1	W	740	2.6	11	2	0.30	Sand	0.23	GMB/CCL	11	10-12	1,250	13-37	55

Notes: (1) NE = northeast, SE = southeast, and W = west.
(2) LCS drainage layer material types are: 1= sand; 2 = sand on base and geonet on side slopes; 3 = gravel over geonet; and 4 = geonet.
(3) All times given are since end of cell construction.

(4) lphd = liters/hectare/day = 0.0365 mm/yr.
(5) ND = no data available.
(6) Intermediate cover soil has been placed over the cell.

379

Bonaparte, R., M.A. Othman, N.S. Rad, R.H. Swan, and D.L. Vander Linde. (1997, in press) Evaluation of Various Aspects of GCL Performance. Appendix F in *Report of 1995 Workshop on Geosynthetic Clay Liners* (eds. D.E. Daniel and H.B. Scranton). USEPA National Risk Management Resource Laboratory, Cincinnati, OH, EPA Report No. ___.

Daniel, D.E. (1995) Soil Barrier Layers Versus Geosynthetic Barriers in Landfill Cover Systems. In *Landfill Closures ... Environmental Protection and Land Recovery* (eds. R.J. Dunn and U.P. Singh), pp. 1-18. ASCE Geotechnical Special Pub. No. 53.

Daniel, D.E. and B.A. Gross. (1996) Caps. In *Assessment of Barrier Containment Technologies: A Comprehensive Treatment for Environmental Remediation Applications* (eds. R.R. Rumer and J.K. Mitchell), pp. 119-140. NTIS Pub. No. PB96-180583.

Dwyer, S.F. (1995) Alternative Landfill Cover Demonstration. In *Landfill Closures ... Environmental Protection and Land Recovery* (eds. R.J. Dunn and U.P. Singh), pp. 19-34. ASCE Geotechnical Special Pub. No. 53.

Feeney, M.T. and A.E. Maxson. (1993) Field Performance of Double-Liner Systems. In *Proceedings, Geosynthetics '93 Conference*, Vol. 3, pp. 1373-1387.

Gross, B.A., R. Bonaparte, and J.P. Giroud. (1990) Evaluation of Flow from Landfill Leakage Detection Layers. In *Proceedings, Fourth International Conference on Geotextiles*, Vol. 2, pp. 481-486.

Khire, M.V. (1995) *Field Hydrology and Water Balance Modeling of Earthen Final Covers for Waste Containment*, 166 p. University of WI - Madison, Environ. Geotechnics Rep. No. 95-5.

Maule, J., J. McCullogh, and R. Lowe. (1993) Performance Evaluation of Synthetically Lined Landfills. *TAPPI Journal*, 76:12, 80-90. Technical Association of the Pulp annd Paper Industry.

Melchior, S. (1995) speaker at International Containment Technology Workshop, Baltimore, MD.

Melchior, S., K. Berger, B. Vielhaber, and G. Miehlich. (1994) Multilayered Landfill Covers: Field Data on the Water Balance and Liner Performance. In *In-Situ Remediation: Scientific Basis for Current and Future Technologies* (eds. G.W. Gee and N.R. Wing), pp. 411-425. Battelle Press.

Othman, M.A., R. Bonaparte, and B.A. Gross. (1996) Preliminary Results of Study of Composite Liner Field Performance. In *Proceeding of the 10th Geosynthetic Research Institute (GRI) Conference*, pp. 110-137. Drexel University, Philadepphia.

Petersen, K.L., S.O. Link, and G.W. Gee. (1995) *Hanford Site Long-Term Surface Barrier Development Program: Fiscal Year 1994 Highlights*. Pacific Northwest Laboratory, Richland, Washington, PNL-10605.

Rumer, R.R. and M.E. Ryan. (1995) Conclusions. In *Barrier Containment Technologies for Environmental Remediation Applications Technologies* (eds. R.R. Rumer and M.E. Ryan), pp. 139-155. John Wiley & Sons, Inc., New York.

Schultz, R.K., R.W. Ridky, and E. O'Donnell. (1995) *Control of Water Infiltration into Near Surface LLW Disposal Units Progress Report of Field Experiments at a Humid Region Site, Beltsville, Maryland*, 20 p. U.S. Nuclear Regulatory Commission, NUREG/CR4918, Vol. 8.

Schroeder, P.R., C.M. Lloyd, and P.A. Zappi. (1994a) *The Hydrologic Evaluation of Landfill Performance (HELP) Model User's Guide for Version 3*, 84 p. USEPA Office of Research and Development, Washington, D.C., EPA/600/R-94/168a.

Schroeder, P.R., T.S. Dozier, P.A. Zappi, B.M. McEnroe, J.W. Sjostrom, and R.L. Peyton. (1994b) *The Hydrologic Evaluation of Landfill Performance (HELP) Model Engineering Documentation for Version 3*, 116 p. USEPA Office of Research and Development, Washington, D.C., EPA/600/R-94/168b.

Workman, J.P. (1993) Interpretation of Leakage Rates in Double-Lined Systems. In *Proceedings, 7th Geosynthetic Research Institute Seminar*, pp. 91-108. Drexel University, Philadelphia, PA,.

Geosynthetic Clay Liners - Slope Stability Field Study

David A. Carson[1], David E. Daniel[2], Robert M. Koerner[3], Rudolph Bonaparte[4]

Abstract

A field research project was developed to examine the internal shear performance of geosynthetic clay liners (GCLs). Several combinations of cross sections were assembled using GCL materials that were available at the time of project initiation. The cross sections utilized were intended to simulate landfill cover applications. Thirteen (13) resulting test plots were constructed on two different slope angles, and each plot is instrumented for physical displacement and soil moisture characteristics. Test plots were constructed in a manner that dictated the shear plane in the clay portion of the GCL product. The project purpose is to assess field performance and to verify design parameters associated with the application of GCLs in waste containment applications. Interim research data shows that test slopes on 2H:1V show global deformation, but little internal shear evidence, and the 3H:1V slopes show little derformation at approximately 650 days. The research is ongoing, and this paper presents the most recent information available from the project.

Introduction

Geosynthetic Clay Liners (GCLs) are increasingly offered as an alternative to a compacted clay liner (CCL) providing low hydraulic conductivity in waste containment designs. US EPA and others have facilitated workshops and symposia in recent years to foster a better understanding of the qualities of GCLs (Daniel and Estornell, 1991, Daniel and Boardman, 1993, Daniel and Scranton, 1996, Koerner, Gartung and Zanzinger, editors, 1995). GCL applications continue to expand, and technical comparisons have been made between GCLs and the traditional CCLs. Technical properties of CCLs and GCLs are presented in detail in Daniel and Boardman (1993), and GCLs have many desirable properties. One property that remains unproven in the long term is internal shear strength which relates directly to geotechnical slope stability. The curiosity about this property emerges from our understanding of the technical properties of bentonitic clay, commonly used in GCLs. Bentonitic clay has undesirable engineering properties when hydrated, such as low shear properties under low overburden pressures. Relatively low overburden pressures are present in most landfill cover applications.

Modern landfill covers contain many natural and geosynthetic components, presenting the designer with a long-term performance and stability design challenge. Landfill covers are a common application for GCLs. Some GCLs are specifically designed to serve in slope applications. All interfaces between natural and/or geosynthetic layers must be analyzed for interface friction and resulting effects on slope stability. Interfaces result from site-specific design, varying for each project. This project focuses on only one property, the internal shear characteristics of GCLs. Other interfaces and shear properties were selected to be satisfactory for the purposes of this experiment. This research effort was initiated

---

[1] US Environmental Protection Agency, Office of Research and Development, 26 W. Martin Luther King Drive (ML-CHL), Cincinnati, OH 45268-3001

[2] University of Illinois at Urbana-Champaign, 1114a Newmark Civil Engineering Laboratory, 205 N. Mathews Avenue, Urbana, IL 61801-2352

[3] Geosynthetic Research Institute, 33rd Ave. and Lancaster Walk, Rush Bldg. (#10) - West Wing, Philadelphia, PA 19104

[4] GeoSyntec Consultants, 5775 Peachtree Dunwoody Road, Suite 200F, Atlanta, GA 30342

with the assistance of GCL manufacturers to gain greater understanding of the shear and slope stability characteristics of GCLs.

Materials and Methods

The project required the participation and convergence of researchers, GCL manufacturers, available land, a geosynthetics installation construction team, and monitoring personnel. The project began via experimental design, followed by construction of the individual slopes involved in the testing matrix. With all GCLs represented, the project was constructed at full scale beginning in November, 1994. Thirteen (13) test plots were constructed and instrumented for physical displacement, and for soil and GCL clay moisture conditions, the primary indicators of slope stability and long-term performance.

Experimental Design

The research team evaluated the available resources, and decided that the land would support two slope angles. Slopes of 3H:1V (18.4 degrees) and 2H:1V (26.6 degrees) were selected. These slopes were to represent typical landfill cover applications, and a more aggressive slope nearer the minimum factor of design safety (for this particular experiment), respectively. It was also determined that all GCLs would be tested side-by-side for symmetry. Each plot consists of two roll widths, to include a field constructed seam running vertically along the length of the slope. Slope lengths were to accommodate a 9.2m (30 ft) vertical elevation change. This resulted in GCL panel lengths of 29m (95 ft) for the 3H:1V slopes, and of 20m (67 ft) for the 2H:1V slopes. Each plot was to be isolated from the other, and separated by unused ground in approximately 3m (10 ft) widths to accommodate monitoring, plot isolation and drainage.

GCLs Involved in Study

Five products from all four GCL manufacturers (at the time of project initiation) were included in the study. The GCLs included in this study are described in Table 1.

Table 1. GCLs Involved in Study

Product	Substrate as Field Placed	Superstrate as Field Placed	Structure	Roll Width	
				m	ft
Bentofix NS	NP-NW GT	NP-NW GT	needle punched and burnished	4.7	15.5
Bentofix NW	W-SF GT	NP-NW GT	needle punched and burnished	4.7	15.5
Bentomat ST	NP-NW GT	W-SF GT	needle punched	4.6	15.0
Claymax SP500	W-SF GT	W-SF GT	stitch bonded, 100mm spacing	4.2	13.8
Gundseal	HDPE-T GM or none	none or HDPE-T GM	adhesive bonded	5.3	17.5

Key: NP-NW GT   = needle punched nonwoven geotextile
      W-SF GT   = woven slit film geotextile
      HDPE-T GM   = high density polyethylene, textured both sides, (GM orientation varied per plot)

Table 2 describes the configuration of the test plots and the identifying letter, represented graphically in Figure 1 (for 2H:1V slopes). Recall that all plots have geosynthetic erosion control products applied to rapidly establish vegetation, except plot M, which is an experimental control. Broad categories for the project plots covered these primary component studies:

1)   Some cross sections contained composite barriers consisting of a GCL overlain by a geomembrane, and some had only a GCL used without a geomembrane, and

2)   Some cross sections contained geosynthetic drainage composites, and others had GCL overlain by sand and a geotextile to form a drainage layer.

Table 2. Configuration and Description of Test Plots

Plot	GCL	Target Slope*	Actual Slope*	Cross Sections (described from top to bottom)
A	Gundseal	18.4	16.9	cover/GC/GM/GCL (bentonite up)/subgrade
B	Bentomat ST	18.4	17.8	cover/GC/GM/GCL/subgrade
C	Claymax SP500	18.4	17.6	cover/GC/GM/GCL/subgrade
D	Bentofix NS	18.4	17.4	cover/GC/GM/GCL (NW GT side up)/subgrade
E	Gundseal	18.4	17.8	cover/GC/GM/GCL (bentonite down)/subgrade
F	Gundseal	26.7	23.6	cover/GC/GM/GCL (bentonite up)/subgrade
I	Bentofix NW	26.7	24.8	cover/GC/GM/GCL/subgrade
J	Bentomat ST	26.7	24.8	cover/GT/granular drain/GCL/subgrade
K	Claymax SP500	26.7	25.5	cover/GT/granular drain/GCL/subgrade
L	Bentofix NW	26.7	24.9	cover/GT/granular drain/GCL/subgrade
M	None (Control)	26.7	23.5	cover/subgrade
N	Bentofix NS	26.7	23.0	cover/GC/GM/GCL (NW GT side up)/subgrade
P †	Gundseal	26.7	23.5	cover/GC/GM/GCL (bentonite up)/subgrade

Key: GC   = geotextile/geonet/geotextile drainage composite, thermally bonded
       GM   = geomembrane
       GCL   = geosynthetic clay liner
       GT   = geotextile
       NW GT= nonwoven geotextile
       †   = replaced plots G and H, lost prior to testing
       *   = units: degrees

Instrumentation

Instrumentation was devised to suit this type of long-term field testing. Parameters that would indicate the performance of the plots are moisture properties, to determine hydration of subgrade and GCL, and movement of the GCL panels down slope. To monitor this behavior, three instruments were utilized.

Moisture sensor in soil subgrade is monitored by the use of electrical resistance moisture probes calibrated to the subgrade soils found under each plot. To monitor relative subgrade moisture , gypsum blocks were employed. The sensors were placed at evenly spaced intervals in a 5 row by 2 column grid along the vertical centerline of each GCL panel. Each probe has electrical leads that extend beyond the boundary of each panel to accommodate measurement. The location of the

383
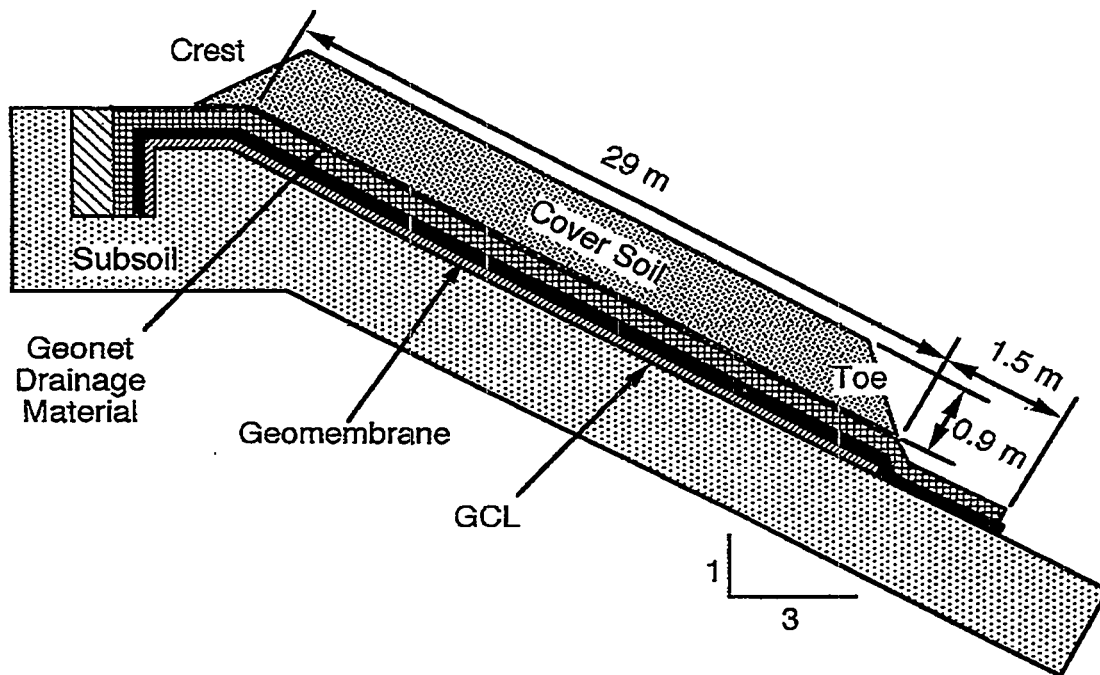
Figure 1. Cross section of 3H:1V test plot. (Scranton, 1996)

sensors is shown in Figure 2.

Moisture sensor in or near bentonitic clay within GCL was similar in function to the gypsum blocks used for soil subgrade, but were fiberglass wafers. These probes were inserted into the clay portion of each GCL blanket. Calibration of these sensors for use in granulated bentonite confirmed known inaccuracies at high moisture levels, as this was not their intended design use. The GCL bentonite probes were placed in a similar grid as the soil subgrade sensors, with electrical leads that also extended beyond the boundary of each panel.

GCL deformation - translational movement was monitored by a series of steel wires encased in polymer sleeves. The flexible, stranded stainless steel wire was encased in plastic sleeve tubing to allow movement of the wire inside the sleeve. The wires were connected to the GCL in a similar grid as the moisture sensors, and were attached to both the top and bottom textile of each GCL panel. This kind of monitoring would allow the detection of translation movement of both top and bottom textiles used to create each GCL. The design was modified for Gundseal, a GCL which is comprised of granulated bentonite adhered to a geomembrane overlain by an extremely lightweight geotextile web (or in most cases, no geotextile at all). Monitoring displacement data for Gundseal products is difficult in this experiment due to our inability to monitor both surfaces effectively. The lightweight geotextile may be incompatible with our displacement monitoring system. The steel wires are brought to the surface monitoring area at the crest of each slope (in two locations, one for each panel) and placed in tables constructed to indicate any movement. Deadweights are attached to the free end of the wires to provide tension.

Construction Sequence

Construction of each plot followed the following sequence, weather during construction was generally rainy and cool, leading to subgrades that were relatively wet:
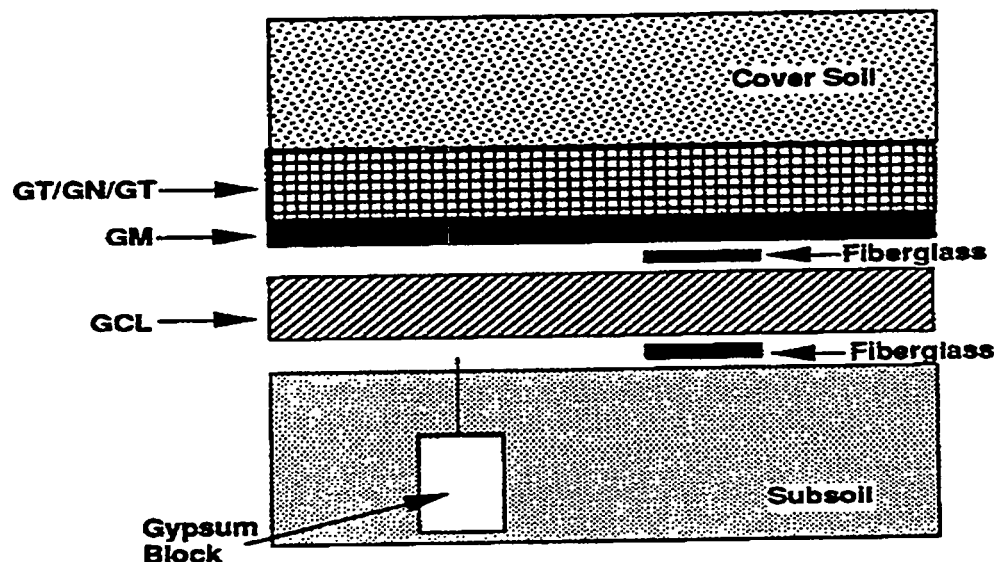
Figure 2. Location of Moisture Sensors, typical. (Scranton, 1996)

- Subgrade preparation
- GCL deployment
- Geomembrane deployment and seaming (where required)
- Drainage layer installation (either geocomposite or GCL/sand/geotextile)
- Cover soil emplacement
- Removal of bottom buttress
- Installation of erosion control geosynthetics
- Hydro seeding of slope surface

At the completion of the construction sequence, the experiment had not yet begun. This is due to the fact that all materials that overlay the GCL might be contributing to the stability of the slope. Near the end of construction, the largest supportive force, the soil toe buttress (necessary for construction) was removed, and the overlying geosynthetics were then severed to begin the experiment.

Results and Discussion

Results are being collected as the project progresses. This paper provides a brief overview and discussion of data collected up to the point of writing. Below is a discussion of events that have occurred.

Field Performance - Post-Construction

The slopes were monitored after construction while finishing touches were placed on formal monitoring gauge stations. During this period, two slopes (former plots G and H) were lost in translational slides. Each slide was caused by low interface friction between the overlying textured geomembrane sliding on top of the underlying GCL (in these cases, a woven slit-film material interfaced with textured geomembrane), which remained intact. The slides mimicked a large-scale direct shear test, with the cover materials sliding off of the underlying GCL. The two plots were later replaced with another plot P as shown in Table 1. Although the slides are under investigation, it is clear that interface friction properties between GCL and overlying geomembrane were inadequate for this experiment. Both slides occured in relatively short time frames, 20 and 50 days after construction, respectively.

The slides are not indicative of the internal shear characteristics of GCLs, since the project was not

385

designed to study interface friction, and inferences regarding long-term performance should not be drawn from this pre-experimental event. This phenomenon does point up the importance of understanding all interface friction (and internal friction) properties of all materials (natural and synthetic) for application on slopes. Further information will be available in upcoming technical outputs from this project.

All other plots remained stable throughout the construction process, showing minimal motion. The plots appeared to have survived construction well with no unusual occurrences.

Field Performance - Experimental Commencement

The slopes were monitored for approximately 5 months before severing of the geotextiles at the crest of each slope. In order to sever all overlying geosynthetics, access to the crest of the slope was cleared of soil and a sacrificial protective geomembrane slip sheet was opened to sequentially expose all layers overlying the GCL. Textiles and/or geomembranes were carefully severed at each layer. For GCLs other than Gundseal, only the bottom geotextile remained intact. For Gundseal, only the geomembrane remained intact (for bentonite up applications). The severing was uneventful, and no unusual events were observed. It is at severing that the experiment began. After severing, it is primarily the clay that resides within any individual GCL that resists movement on each plot.

Slide of Plot F

Plot F experienced a slide at approximately 10 months into the experiment. Plot F did not yield logical experimental results and remains under investigation. As with the post-construction slides discussed erlier, the GCL remained on the slope, while overlying materials slid in a block down slope. Panel F was constructed such that the clay of the GCL was positioned between two geomembranes, one as part of the GCL, and the other provided as an overlying geomembrane. This arrangement should prevent any hydration of bentonitic clay within this cross section, yet this is not what was observed. Wetting of the GCL progressed quickly, beyond expectations. Samples were removed to check moisture monitoring probes, which were verified. Analysis continues as the cause of this slide, but includes these possible explanations:

a)   excessive moisture entered during construction
b)   the GCL or overlying geomembrane was flawed
c)   surface water was fed into the GCL by displacement gauges
d)   surface water was fed into the GCL and conducted by space between the geomembrane and GCL

Of these possible explanations, most were prevented as a result of installation care, except a combination of explanations "c" and "d." A definitive explanation remains elusive, but one possible explanation is that some aspect of experimental design funneled water to the interface, causing rapid hydration of the GCL in a system where this is otherwise unlikely.

Data Summary

Data is voluminous for this research, and has been summarized in Table 3. The table shows indications of deformation and hydration status at the time of writing. As can be seen from this data, some motion is detected on 2H:1V plots at the time of writing. No other slides have been experienced on any other test plots.

Future Research

This effort will continue as long as facilities and human resources permit. Monitoring continues on a monthly basis. Final technical project reports will be forthcoming from the authors and US EPA in 1997and upon project conclusion. Details of this project are included in Daniel and Scranton, (1996).

Table 3. Project data summary.*

Plot	GCL	Maximum Total Deformation (mm)	Maximum Differential Deformation (mm)	Hydration Status		Comment
				GCL/ Subgrade	Subgrade	
A	Gundseal	<10	<10	low	moderate	
B	Bentomat ST	<25	<25	low	moderate	
C	Claymax 500SP	<25	<10	wet	wet	
D	Bentofix NS	<35	<15	wet	wet	
E	Gundseal	<25	<10	moderate	wet	
F	Gundseal			wet	wet	Slid
I	Bentofix NW	<170	<10	wet	wet	
J	Bentomat ST	<450	<30	moderate	wet	
K	Claymax SP500	<750	<75	moderate	moderate	
L	Bentofix NW	<280	<125	moderate	moderate	
M	None (Control)			unknown	unknown	No GCL
N	Bentofix NS	<30	<10	wet	wet	
P	Gundseal			low	low	No deform. gauges

* = approximated since construction (approx. 650 days), data through November, 1996

References

Daniel, D.E., and Boardman, B.T. (1993) *Report of Workshop on Geosynthetic Clay Liners*, EPA/600/R-93/171, US EPA Office of Research and Development, Cincinnati, Ohio.

Daniel, D.E. and Estornell, P.M. (1991) *Compilation of Information on Alternative Barriers for Liner and Cover Systems*, EPA/600/2-91/002, US EPA, Office of Research and Development, Risk Reduction Engineering Laboratory, Cincinnati, Ohio.

Daniel, D.E. and Scranton, H.B. (1996) *Proceedings of 1995 Workshop on Geosynthetic Clay Liners*, EPA/600/R-96/149, US EPA, Office of Research and Development, National Risk Management Research Laboratory, Cincinnati, Ohio.

Koerner, R.M. Gartung, E., and Zanzinger, H., editors. (1995) *Proceedings of an International Symposium on Geosynthetic Clay Liners*, A.A. Balkema Publishers, Rotterdam, Netherlands.

Scranton, H.B. (1996) *Field Performance of Sloping Test Plots Containing Geosynthetic Clay Liners*, thesis presented to the Graduate School of the University of Texas at Austin in partial fulfillment of the requirements for the degree of Master of Science in Engineering.

Prediction of Long-Term Erosion From Landfill Covers in the Southwest

Clifford E. Anderson[1] and John C. Stormont[2]

Abstract

Erosion is a primary stressor of landfill covers, especially for climates with high intensity storms and low native plant density. Rills and gullies formed by discrete events can damage barrier layers and induce failure. Geomorphologic, empirical and physical modeling procedures are available to provide estimates of surface erosion, but numerical modeling requires accurate representation of the severe rainfall events that generate erosion. The National Weather Service precipitation frequency data and estimates of 5, 10, 15, 30 and 60-minute intensity can be statistically combined in a numerical model to obtain long-term erosion estimates. Physically based numerical models using the KINEROS and AHYMO programs have been utilized to predict the erosion from a southwestern landfill or waste containment site with 0.03, 0.05 and 0.08 meter per meter surface slopes. Results of AHYMO modeling were within 15 percent of average annual values computed with the empirical Universal Soil Loss Equation. However, the estimation of rill and gully formation that primarily degrades cover systems requires quantifying single events. For southwestern conditions, a single 10-year storm can produce erosion quantities equal to three times the average annual erosion and a 100-year storm can produce five times the average annual erosion.

Introduction

As a result of implementing new solid waste regulations for existing facilities, many communities now find it advantageous to close their existing landfills and use regional facilities. Consequently, many existing facilities are being closed and a smaller number of new landfills are being constructed. The regulations for closure of municipal waste landfills in New Mexico follow the Federal regulations established by the Resource Conservation and Recovery Act (RCRA, 1976, Subtitle D program, 40 CFR 258) and require that the top soil layer have a surface slope of not less than 0.02 meter per meter, and not greater than 0.05 meter per meter. This minimum slope is required because the surfaces of a landfill are subject to substantial local settlement due to the normal process of decomposition of solid waste. Covers for hazardous waste remediation will generally have similar slopes. The application of minimum slope criteria provides for a surface that is relatively free of local depressions and pond areas where excess precipitation can accumulate. Because surfaces of waste containment sites can have differential settlement depths of one meter or more, the use of slopes steeper than 0.02 meter per meter will further minimize the future occurrence of ponding. It is common for designers and regulators to try to approach the 0.05 meter per meter limit. There has even been some discussion about changing the regulations to allow slopes of 0.08 or 0.10 meter per meter.

In many areas of the United States, the vegetative cover will form a protective blanket that effectively inhibits erosional processes on the cover system. But for many areas of the southwest United States, natural vegetation on covers is sparse, with vegetation covering only 10 to 20 percent of the surface. The native plants that have evolved for this environment commonly establish root systems that collect moisture from the surrounding areas and store moisture during drought periods. While it is possible to provide revegetation with nonnative species to provide a higher plant density, such attempts to modify the native plant community are frequently unsuccessful. In order to sustain the nonnative species, supplemental watering may be required, but introduction of water is not

---

[1] University of New Mexico, Dept. of Civil Engineering, Albuquerque, NM 87131,
(505) 277-4809, ceanders@unm.edu

[2] University of New Mexico, Dept. Of Civil Engineering, Albuquerque, NM 87131,
(505) 277-6063, jcstorm@unm.edu

normally advisable for long-term post-closure operations. The most likely long-term success with reseeding will be found by restoring the native plant community and density. Furthermore, some native plant species depend upon the naturally occurring depressions as a source of moisture. When conditions are created that minimize local depressions, some native plant species cannot be sustained.

If the native plant community is to be utilized for southwestern cover systems, there will likely be no opportunity to establish a continuous erosion blanket. Much of the land surface will be exposed to the impacts of rainfall and surface runoff, with the resulting transport of soil through erosion. Erosion has been shown to be greatly affected by the intensity of rainfall and the steepness of the terrain. The impact from raindrops initiates local soil movement, but it is the conveyance across slopes that causes the local soil movement to become erosion. A decision to create greater surface slopes can have consequences for cover erosion that will become obvious only after severe rainfall events. Erosion does not usually occur as a uniform lowering of the surface, but by the formation of rills or small gullies. Rills can be defined as the smallest channel, formed by runoff, that can be destroyed by minor surface disturbance, such as plowing. Gullies are the somewhat deeper channels, formed where no defined channel recently existed. The distinction between the two is not precise, and the terms are frequently used interchangeably. Rills and gullies have the potential to cut through the top soil (erosion) layer of a cover system and damage the underlying barrier soil layer or liner. Such damage could compromise the protection that the cover system was designed to provide.

This paper will assess the potential for erosion on a typical southwestern waste containment site and quantify the relative impact of slopes on erosion, and on rill or gully formation. For this project a typical cover environment near Artesia, New Mexico was selected. This example does not reflect the exact conditions of any existing or proposed solid waste facility, but was selected to provide a measurable example of physical phenomena. The estimation of erosion can be accomplished using three basic procedures described as (1) a geomorphologic evaluation, (2) an empirical equation or procedure and (3) mathematical modeling of the physical processes. These three procedures will be applied to the Artesia example case.

A Geomorphologic Procedure

A geomorphologic evaluation involves the consideration of the geology, hydrology and specific land forms of a site, and comparing the results with similar conditions so that the analysis can be used to predict what will happen over time. It is the simplest in terms of mathematical procedure, but perhaps the most complex in terms of factors that must be considered and the level of expertise required to implement an evaluation. An example of a geomorphologic approach is provided by the US Bureau of Land Management publication *Gully Erosion* (Harvey, et al, 1985). This document may be applied to cover erosion to evaluate "(1) Threshold conditions for gully initiation (2) The stages of gully evolution (3) Current stability of a gully system (4) Long-term gully erosion rates and subsequent yields."(Harvey, et al, 1985, p.3)

The *Gully Erosion* report also describes the physical processes that are present in gully or rill formation. Of particular note for a cover system is the erosion initiated at points where there is an abrupt increase or convex change in the longitudinal profile, called a nickpoint. Erosion is initiated at nickpoints, and the nickpoints migrate upstream. The upstream migration can continue until intercepted by a physical barrier or until the drainage basin is so small that runoff can no longer initiate erosion of the steepened section. At waste containment sites, the interface between the top surface and the steeper side slopes is a likely location for the initiation of nickpoint erosion.

Among the geomorphologic thresholds that may be used to identify the potential for erosional processes, of particular note for this study is the shear stress threshold indicator that defines a line below which gully incision does not occur. The equation for the gully shear stress indicator is:

$S = 0.008 \, A^{-0.26}$ (Harvey, et al, 1985, p.73)   Where: A = area in square miles
(1 square mile= 259 hectare)
and   S = slope in meter per meter

This equation is based on work by J.C. Brice in the Medicine Creek Drainage Basin, Nebraska, 1966. Only six watersheds from this study were below 250 ha (the smallest with 40 ha) and application to small waste containment sites may not be directly transferrable. Nevertheless, Table 1 shows the results when the gully indicator equation is applied to very small drainage basins.

Table 1. Application of the gully indicator equation

Basin Area (ha or hm²)	Threshold slope (meter/meter)
0.5 (1.24 acre)	0.041
2.0 (4.94 acre)	0.028

A figure showing a similar relationship between basin area and slope for gully erosion is included in *Engineering Analysis of Fluvial Systems* (Simons, Li and Associates, 1982, p. 5.38). This figure was based on 1975 data from the Piceance Creek area in western Colorado. The data indicates that for drainage basins smaller than 1300 ha, the zone between gullied and ungullied is not precisely defined and both gullied and ungullied conditions are found for slopes between 0.025 and 0.065 meter per meter. Thus, a geomorphologic evaluation of conditions similar to those found at waste containment surfaces raises concerns about gully erosion potential, and the formation of definitive conclusions requires a site specific geomorphologic investigation.

An Empirical Procedure: the Universal Soil Loss Equation

An example of an empirical procedure applicable to cover system erosion evaluation is the Universal Soil Loss Equation (USLE). This equation is described in detail in *Predicting Rainfall Erosion Losses* (Wischmeier and Smith, 1978). The USLE has been used throughout the United States and is particularly directed to the prediction of erosion from agricultural lands, but the procedure does include methodology for use in pasture, range and idle land, and for areas disturbed by construction. The USLE equation is:

$$A = R \; K \; L \; S \; C \; P$$

where A is the computed soil loss per unit area, R is a rainfall runoff factor, K is a soil erodibility factor, L is a slope length factor (a ratio of field length to a 22.1 m test plot), S is a slope steepness factor (a ratio of field slope to a 0.09 meter per meter slope), C is a vegetative or mulch cover and management factor, and P is a conservation practice factor. The USLE is limited to the determination of average annual erosion rates and cannot establish erosion from specific events and peak erosional years. The aerial extent and surfacing of many waste containment sites provide similar conditions to those described in the procedures for USLE. However, there is no direct method within the USLE procedure to determine the depth or magnitude of the gully or rill erosion that may be an integral part of the erosion process.

Mathematical Modeling with AHYMO and KINEROS

There is no known procedure that presents an accurate measure of the physical processes concerning erosion on a cover. However, there are several procedures that combine modeling of some physical processes along with application of empirical equations. One applicable methodology includes the determination of storm water runoff hydrographs using hydrologic modeling, the estimation of sediment wash loads (fine silts and clays that can be suspended in runoff) using the storm based Modified Universal Soil Loss Equation (Williams, 1975), and estimation of channelized sediment transport rates using regression equations developed from more complex sediment transport procedures. This computational methodology has been included in the *AHYMO Computer Program* (Anderson, 1994). The sediment volume for any storm event can

be computed from the above procedure. All of the runoff events for a period can be accumulated to obtain an average annual volume. An average annual sediment yield can also be computed by using a statistically weighted function of the 2, 5, 10, 25, 50 and 100-year sediment yields.

As an alternative, the *KINEROS, Kinematic Runoff and Erosion Model* (Woolhiser, et al, 1990) provides a computerized procedure to compute rainfall hydrographs and erosion quantities. "KINEROS is a distributed, event-oriented, physically based model describing the processes of surface runoff and erosion from small agricultural and urban watersheds." (Woolhiser, et al, 1990, p.3) The KINEROS model derives its name from the kinematic wave equations that are used to solve for overland flow and flow through channels, and from the capability to compute the quantity of erosion. Successful use of the model to simulate runoff and erosion at the Walnut Gulch Experimental Watershed in southern Arizona is described in the KINEROS documentation. Of the six sediment transport relations available with KINEROS, the tractive force relation (Meyer and Wischmeier, 1969) and the Bagnold/Kilinc relation (Kilinc and Richardson, 1973) were selected for this case study.

Estimates of Gully and Rill Erosion

None of the procedures described above provide a method to compute the extent of rill or gully erosion, but the study by Kilinc and Richardson (1973) presents the results of erosion simulation tests made on a 1.52 m by 4.88 m watershed test bed. Artificially simulated rainfall using a sprinkler system was run using rainfall intensities that varied from 3.175 to 11.68 cm per hour, using uniform bed slopes from 5.7 to 40 meter per meter, with 24 one-hour test runs. Of special interest for cover systems are the regression equations that quantify rill area, rill volume and rill depth as functions of slope and rate of runoff. Because the regression equations were established based on a constant rainfall and runoff rate for a one-hour simulation, it is not possible to directly apply the equations to a hydrograph computation. However, incremental hydrograph quantities can be combined with the regression equations in a spreadsheet to estimate the volume of rill erosion for the peak one hour of runoff. Because the regression equations are based on a single 7.4 m^2 test bed, there is no mechanism to accommodate dimensional scale effects with the computations.

Rainfall

Rainfall is the driving condition for most moisture and erosion that can impact a cover system. While snow melt may also produce moisture, it is of lesser consequence for erosion throughout much of the southwest US. For the Artesia site, rainfall conditions for a one-hundred (100) year period were simulated with the US Army Corps of Engineers, *Hydrologic Evaluation of Landfill Performance (HELP) Model* (HELP3) (Schroeder, et al., 1994). This model uses probabilistic methods to identify the daily rainfall, or lack thereof, for every day in the 100-year period. The HELP3 simulation for the Artesia area used synthetic precipitation data for the nearby city of Roswell, New Mexico. For the 100-year simulation, a total of 156 days had precipitation greater than 2.2 cm; this is the precipitation threshold expected to produce measurable runoff. The values computed by HELP3 were compared with the 24-hour precipitation amounts in the *Precipitation Frequency Atlas of the Western United States, Volume IV-New Mexico (NOAA Atlas)* (National Weather Service, 1973). It was found that the values computed by HELP3 were substantially less than the NOAA Atlas values as shown on Table 2.

Table 2. Precipitation frequency values for 24-hour storm

Return period	From NOAA Atlas maps	Computed by HELP3
2-year	4.95 cm	3.35 cm
10-year	8.13 cm	4.85 cm
100-year	12.70 cm	6.96 cm

For erosion event computation, extreme rainfall events must be accurately represented. Therefore, revised synthetic precipitation data was created using the Extreme Value Type I distribution and procedures described in *Applied Hydrology* (Chow, et al, 1988). This resulted in 137 daily events greater than 2.2 cm for a 100-year simulation, and extreme event values in agreement with the NOAA Atlas.

The simulation of runoff and erosion required that the depth of cumulative precipitation be simulated throughout a 24-hour period, with special concern about the rainfall intensity during the peak hour. Review of the NOAA Atlas showed that the six-hour precipitation was approximately 80 percent of the 24-hour precipitation for the Artesia, NM site. Similarly, the peak 1-hour precipitation was 60 percent of the 24-hour precipitation. The NOAA Atlas contains a table of adjustment factors to obtain 5, 10, 15 and 30-minute precipitation estimates as a ratio of the peak hourly precipitation. All of these factors can be combined to obtain a distribution of a typical rainfall event based on the 24-hour value. Table 3 shows the ratios that were developed. The data from Table 3 was applied to each of the 137 daily rainfall quantities to form 137 rainfall distribution tables.

Table 3. Rainfall distribution factors

Time	24-hr	6-hr	1-hr	30-min	15-min	10-min	5-min
Percent of 24-hour	100.0	80.0	60.0	47.4	34.2	27.0	17.4
Percent of 1-hour	166.67	125.0	100.0	79.0	57.0	45.0	29.0

Establishing Input Parameters for Erosion Simulations

In order to simulate runoff from a typical cover system using numerical methods, it was necessary to establish some physical parameters that would be used in the models. For this study the following values were selected: cover system area at 2.02 ha (5.0 acres), surface dimensions at 142.2 m by 142.2 m, a coarse sandy loam or loamy fine sand surface soil, median bed material gradation (D_{50}) of 0.50 mm, and a ground cover with 10-percent native grass cover. Surface slopes of 0.02, 0.05 and 0.08 meter per meter were used to simulate three potential surface configurations.

Results from the Universal Soil Loss Equation Analysis

The average annual sediment yield from the USLE is tabulated in Table 4. These values are based on a rainfall-runoff factor (R) of 80; a length-slope factor (LS) of 0.318 at a 0.02 meter per meter slope, 1.15 at a 0.05 meter per meter slope, and 2.14 at an 0.08 meter per meter slope; a soil erodibility factor (K) for coarse sandy loam or loamy fine sand of 0.20; a cover factor for 10-percent native grass of 0.35; and a conservation practice factor of 1.0. Table 4 summarizes the results from the USLE.

Table 4. Average annual sediment yields based on the USLE

Slope = 0.02 m/m	Slope = 0.05 m/m	Slope = 0.08 m/m
4017 kg/ha/year	14437 kg/ha/year	26864 kg/ha/year
8128 kg/year for 2.02 ha	29211 kg/year for 2.02 ha	54359 kg/year for 2.02 ha

Results from the AHYMO and KINEROS Modeling

When the 137 largest rainfall events of the 100-year period were evaluated with the AHYMO computer program, only 115 events showed measurable runoff. A summary of the AHYMO sediment yields is contained in Table 5. The average annual sediment yields computed by the AHYMO program are within 15 percent of the values computed with the USLE.

The KINEROS model was also used to compute storm water runoff and sediment yields for the 137 largest rainfall events in the 100-year period. Because the KINEROS model uses more physically based parameters to compute runoff, different runoff rates are computed for the 0.02, 0.05 and 0.08

meter per meter slopes. Table 6 presents the sediment yields from the KINEROS model for the tractive force (Meyer and Wischmeier, 1969) and the Bagnold/Kilinc (Kilinc and Richardson, 1973) transport equations. The sediment yields computed by the KINEROS program are substantially larger than the values computed with the USLE.

Table 5. Sediment yield using AHYMO

Event frequency	24-hr rainfall (cm)	Sediment (kg) at 0.02 m/m slope	Sediment (kg) at 0.05 m/m slope	Sediment (kg) at 0.08 m/m slope
100-year	12.70	54848	184349	326523
10-year	8.13	23387	79415	141648
2-year	4.95	6214	21509	38818
Average annual	-----	9320	31841	57018

Table 6. Sediment yield using KINEROS

Event frequency	24-hr rainfall (cm)	Sediment (kg) at 0.02 m/m slope	Sediment (kg) at 0.05 m/m slope	Sediment (kg) at 0.08 m/m slope
Tractive force equation:				
100-year	12.70	69691	293695	439358
10-year	8.13	15961	76335	155589
2-year	4.95	1371	8131	19220
Average annual	-----	5515	26310	52429
Bagnold/Kilinc equation:				
100-year	12.70	49735	247084	456987
10-year	8.13	14293	77420	171734
2-year	4.95	1711	11673	29271
Average annual	-----	4939	27568	61564

Results of Rill Erosion Evaluation

The regression equations computed by Kilinc and Richardson (1973) were combined in a spreadsheet to estimate rill erosion. Two rainfall events were used for this analysis: (1) a 100-year storm, and (2) a 10-year storm. The rainfall was simulated on the 1.52 m by 4.88 m area used with the original test setup. Table 7 is a summary of the spreadsheet computations. These values for rill depth, area and volume demonstrate the variability with changes in surface slopes. They can not be directly scaled to predict rill erosion for a specific site.

Table 7. Estimates of Rill Erosion for a 1.52 m by 4.88 m test area.

Surface slope	Ave. rill depth	Ratio: rill area to surface area	Ratio: volume rills to total sediment volume	Volume rills
100-year storm (24-hour precipitation=12.70 cm)				
0.02 m/m	0.033 cm	0.093	0.088	230 cm^3
0.05 m/m	0.182 cm	0.108	0.122	1459 cm^3
0.08 m/m	0.433 cm	0.117	0.144	3764 cm^3
10-year storm (24-hour precipitation=8.13 cm)				
0.02 m/m	0.011 cm	0.072	0.049	59 cm^3
0.05 m/m	0.060 cm	0.084	0.068	376 cm^3
0.08 m/m	0.144 cm	0.091	0.080	970 cm^3

Conclusions

The function of any specific top slope can be greatly impacted by construction measures designed to control erosion. While mitigative measures such as revegetation, application of mulches, construction of terraces, placement of gravely soils, construction of nickpoint barriers, and use of convex slopes may reduce erosion, it is the combination of slope, runoff and transportable soil that generates surface erosion. Some of the techniques presented in this study may serve as an outline for further erosion investigations at existing or proposed landfill and waste remediation sites.

The case study presented herein demonstrates that the slope of a final cover can have a profound impact on the amount of erosion and on the size of rills or gullies. Geomorphologic considerations indicate that gully formation may be initiated when slopes reach maximum regulatory levels. The average annual estimates of erosion using the USLE change substantially when slopes are increased above 0.02 meter per meter. In arid climates, a significant percentage of erosion and formation of rills may come from single events that are represented by 10-year to 100-year storms. A single 10-year storm can to produce erosion quantities equal to three times the average annual erosion and a 100-year storm can produce five times the average annual erosion. A cover not experiencing problems for many years, may suddenly be compromised by a single catastrophic event. In order to predict the long-term performance of a cover, it is necessary to consider the major precipitation events that are likely to occur over the design life of the cover system.

References

Anderson, C.E. (1994) *AHYMO Computer Program User's Manual.* Albuquerque, NM.

Chow, V.T., D.R. Maidment and L.W. Mays. (1988) *Applied Hydrology.* Mc-Graw-Hill, New York, N.Y.

Harvey, M.D., C.C. Watson and S.A. Schumm. (1985) *Gully Erosion.* U.S. Department of Interior, Bureau of Land Management, Denver, CO.

Kilinc, M. and E.V. Richardson. (1973) *Mechanics of Soil Erosion from Overland Flow Generated by Simulated Rainfall.* Colorado State University, Hydrology Papers No. 63, Fort Collins, CO.

Meyer, L.D. and W.H. Wischmeier. (1969) Mathematical simulation of the process of soil erosion by water. In *Transactions of the American Society of Agricultural Engineers,* 12(6), 754-762.

National Weather Service. (1973) *NOAA Atlas 2, Precipitation-Frequency Atlas of the Western United States, Volume IV-New Mexico.* U.S. Department of Commerce, National Oceanic and Atmospheric Administration, Silver Spring, MD.

Schroeder, P.R., T.S. Dozier, P.A. Zappi, B.M. McEnroe, J.W. Sjostrom, and R.L. Peyton. (1994) *The Hydrologic Evaluation of Landfill Performance (HELP) Model: Engineering Documentation for Version 3 and User's Guide for Version 3.* EPA/600/9-94/168a and b, U.S. Environmental Protection Agency, Risk Reduction Engineering Laboratory, Cincinnati, OH.

Simons, Li and Associates. (1982) *Engineering Analysis of Fluvial Systems.* Fort Collins, CO.

Williams, J.R. (1975) Sediment-yield prediction with universal equation using runoff energy factor. In *Present and Prospective Technology for Predicting Sediment Yields and Sources, Proceedings of the Sediment-Yield Workshop, USDA Sedimentation Laboratory, Oxford, Mississippi, November 28-30,1972.* ARS-S-40, U.S. Department of Agriculture, Agricultural Research Service.

Wischmeier, W.H. and D.D. Smith. (1978) *Predicting Rainfall Erosion Losses - a Guide to Conservation Planning.* Agriculture Handbook Number 537, U.S. Department of Agriculture, Science and Education Administration, Washington, DC.

Woolhiser, D.A., R.E. Smith, and D.C. Goodrich. (1990) *KINEROS, A Kinematic Runoff and Erosion Model: Documentation and User Manual.* U.S. Department of Agriculture, Agricultural Research Service, ARS-77, Springfield, VA.

A SENSITIVITY ANALYSIS OF HAZARDOUS WASTE DISPOSAL SITE CLIMATIC AND SOIL DESIGN PARAMETERS USING HELP3

D.D. Adelman[1] And J. Stansbury[2]

ABSTRACT: The Resource Conservation and Recovery Act (RCRA) Subtitle C, Comprehensive Environmental Response, Compensation, And Liability Act (CERCLA), and subsequent amendments have formed a comprehensive framework to deal with hazardous wastes on the national level. Key to this waste management is guidance on design (e.g., cover and bottom leachate control systems) of hazardous waste landfills. The objective of this research was to investigate the sensitivity of leachate volume at hazardous waste disposal sites to climatic, soil cover, and vegetative cover (Leaf Area Index) conditions. The computer model HELP3 which has the capability to simulate double bottom liner systems as called for in hazardous waste disposal sites was used in the analysis.

HELP3 was used to model 54 combinations of climatic conditions, disposal site soil surface curve numbers, and leaf area index values to investigate how sensitive disposal site leachate volume was to these three variables. Results showed that leachate volume from the bottom double liner system was not sensitive to these parameters. However, the cover liner system leachate volume was quite sensitive to climatic conditions and less sensitive to Leaf Area Index and curve number values. Since humid locations had considerably more cover liner system leachate volume than arid locations, different design standards may be appropriate for humid conditions than for arid conditions.

I. Background.

The federal Resource Conservation and Recovery Act (RCRA) is the primary legislation that deals with hazardous wastes and solid wastes (Cohen, 1989). Subtitle C of RCRA deals specifically with hazardous wastes. There are several components to Subtitle C. These included: (1) identification and listing of hazardous wastes; (2) standards applicable to generators of hazardous wastes including record keeping, labeling, use of suitable containers, information on storage and transport, development of a manifest system for tracking purposes; (3) standards for transportation of hazardous wastes; (4) a permit system for treatment, storage and disposal of hazardous wastes; (5) authorization of state hazardous waste regulation; (6) inspection of hazardous wastes; (7) enforcement provisions of hazardous waste regulations; and (8) assistance to states in terms of financial and other resources to implement hazardous waste regulations. Amendments including guidance on designing a hazardous waste landfill found in Title 40 Code of Federal Regulations Parts 264, 265, 267, and 270 were made to RCRA in 1984 to correct deficiencies in the 1976 legislation.

To limit leachate production and subsequent migration from the bottom of hazardous waste landfills, RCRA guidance was developed for the design of top cover and bottom liner (leachate control) systems. The HELP3 computer model (EPA, 1994), developed for design of solid waste landfills, can also be used to help design hazardous waste disposal sites. The objective of this research was to investigate the sensitivity of hazardous waste disposal leachate volume to climatic conditions, soil cover conditions, and vegetative cover conditions using

---

[1]Water Resources Engineer, Adelman And Associates, 4535 Y Street, Lincoln, NE 68503-2344.

[2]Assistant Professor, 129 Engineering Building, University of Nebraska-Lincoln, Omaha, NE 68182-0178.

HELP3. Double bottom liner systems, called for in hazardous waste disposal sites, were simulated in this analysis.

HELP3 documentation is divided into two parts: soil, waste, and synthetic liner design parameters; and climatic variables including air temperature, precipitation, evapotranspiration, and solar radiation (EPA, 1994).

HELP3 simulates moisture movement through the landfill assuming unsaturated conditions. The landfill soil, waste and synthetic liner design parameters include: layer thickness, layer texture, total porosity, field capacity, wilting point, saturated hydraulic conductivity, drainage length, and drainage slope. The soil curve number value selected for the landfill is specific to the surface soils used in the cover system. The synthetic liner has specific design variables including pinhole and defect density per unit area, and placement quality which is described as perfect, excellent, good, poor, and worst case (EPA, 1994). HELP3 operates as an unsaturated zone advective flow model and has been used in some research to simulate unsaturated conditions at sites other than landfills (Lokke, 1992).

For this study, air temperature, evapotranspiration and solar radiation were synthesized by the model. Rainfall data used in this study were actual data from the model database (EPA, 1994).

The leachate volume or production from a solid or hazardous waste landfill is the final output from the model. Although the model does not have a contaminant transport component, knowledge of the quantity of leachate from a landfill gives the designer information on the quantities of hazardous materials that could be escaping from the landfill. This information would indicate the danger the landfill poses to underlying groundwater. In addition, the model can be used to predict contaminant transport via groundwater to surface water resources.

II. Methods And Procedures.

A hypothetical hazardous waste disposal site consisting of twelve different layers was simulated for this research. The layers correspond to RCRA guidance (Cohen, 1989) for design of hazardous waste landfills. The uppermost layer was a 15.3 cm layer of loamy sand to support a grass cover. The next three layers composed the upper liner system consisting of a 30.5 cm layer of gravel followed by a 0.3175 cm High Density Polyethylene (HDPE) synthetic liner that was underlain by a 30.5 cm layer of material referred to in the HELP3 User's Manual as a barrier soil (i.e., compacted clay). Below the cover liner system was a 914.4 cm depth of hazardous waste with a density of 312 kg/m^3. This was underlain by a 15.2 cm layer of loamy sand. A double constructed bottom liner system was beneath the hazardous material layer. The two liner systems each consisted of the same makeup as the cover liner system (i.e., a 30.5 cm gravel layer separated from a 30.5 cm barrier soil layer by the 0.3175 cm thick HDPE layer). The geomembrane liners were assumed to each have defect and pinhole densities of 2.0 per 0.40 hectares (one acre) and to each have poor placement quality.

HELP3 includes an extensive data base on precipitation for several locations in each state (EPA, 1994). HELP3 runs were made for six locations in the United States. The following locations and climates were simulated: Olympia, Washington (very humid climate with annual precipitation at 129.4 cm); Miami, Florida (humid climate with annual precipitation at 146.2 cm); Topeka, Kansas (subhumid climate with annual precipitation at 86.1 cm); North Platte, Nebraska (semiarid climate with annual precipitation at 49.4 cm); Bakersfield, California (arid climate with annual precipitation at 14.5 cm); and Phoenix, Arizona (very arid climate with annual precipitation at 18.1 cm). These six climates were chosen to evaluate how varying climate affects leachate volume production and migration through a hazardous waste disposal site.

HELP3 runs were also made for three different soil cover conditions. The United States Department of Agriculture (USDA) Natural Resources Conservation Service Curve Number Method (USDA, 1972) is used in HELP3 to represent different surface cover soil conditions. These soil conditions (i.e., curve numbers) are related to the amount of precipitation that will infiltrate the cover soil and that could ultimately percolate through the cover liner system. Curve number values can range from 40 to 100. For example, a dry, highly permeable, flat soil surface would have a curve number of 40, while a saturated, highly compacted, steeply sloping soil surface would have a curve number of 100. For these simulations, curve number values of 70, 80 and 90 were used because these values represent the range of values that might be expected for surface soils at hazardous waste sites. The higher curve number values result in the greatest runoff from the disposal site surface and least percolation to the cover liner system (USDA, 1972).

HELP3 runs were also made for three different vegetative cover conditions. Leaf Area Index (LAI) (ASAE, 1981) was used to represent the vegetative condition of the cover. LAI ranges from a theoretical minimum value of zero for no vegetation to 5 for "excellent grass" (EPA, 1994). HELP3 uses LAI to represent how much transpiration by the cover vegetation occurs at the surface of a disposal site and, therefore, learns how much moisture is left for percolation to the cover liner system. LAI values of 1.0, 1.5, and 2.0 were used in this analysis to evaluate the effect of varying vegetative cover conditions that might typically be found at hazardous waste landfills on leachate production.

Fifty-four combinations of climatic conditions, curve number values, and LAI values were simulated using HELP3. The 30-year sum of leachate volume through the cover HDPE synthetic liner and the 30-year sum of leachate through the uppermost HDPE synthetic liner of the bottom double liner system were recorded for each run.   The area of the site was assigned a value of one acre to estimate leachate production on a unit area basis.

III. Results And Discussion.

The 30-year leachate volume through the uppermost HDPE liner of the lower double liner system ranged from 0.00765 m^3 at Olympia, Washington to 0.00090 m^3 for Phoenix, Arizona. These are very low values. It was noted during these runs that most of this leachate was drained off through the 30.5 cm gravel collection layer of the very bottom liner system of the bottom double liner system, and the amount of leachate getting through the very bottom HDPE liner was usually negligible.

Leachate volumes passing through the upper liner system (cover) for each of the above 54 runs are tabulated in Table 1. Table 1 reveals that climate has a major influence on the leachate volume getting through the cover liner system. Olympia, Washington with a very humid location is shown to have significantly more leachate volume than the other five less humid locations regardless of the other parameter values. Table 1 reveals that the curve number value of the cover soil has some influence on leachate volume. However, the influence is less than that of climatic conditions. The higher the curve number value, the more runoff and, therefore, the less deep percolation into the surface or cover of the hypothetical disposal site. Table 1 reveals that the LAI value of the cover vegetation has little influence on leachate volume compared to climatic conditions and curve number value.

IV. Conclusion.

Leachate volume through the cover liner system was much higher in areas with high precipitation. This is not an unexpected result. However, the low volumes of leachate passing through the cover liner system and the negligible leachate passing through the bottom of the landfill may indicate that the landfill design requirements are overly conservative, especially in

Table 1. 30-Year Sum of Leachate Passing Through the Cover Liner System (m³)

Location	Curve Number	Leaf Area Index		
		1	1.5	2
Bakersfield, CA	70	0.132	0.111	0.115
	80	0.132	0.110	0.109
	90	0.121	0.109	0.098
Miami, FL	70	4.747	4.377	4.206
	80	4.395	4.057	3.902
	90	2.856	2.643	2.548
North Platte, NE	70	0.663	0.592	0.544
	80	0.613	0.539	0.448
	90	0.408	0.372	0.329
Olympia, WA	70	10.538	10.533	10.540
	80	10.330	10.331	10.347
	90	9.321	9.357	9.390
Phoenix, AZ	70	0.105	0.092	0.091
	80	0.102	0.093	0.092
	90	0.079	0.072	0.070
Topeka, KS	70	2.736	2.678	2.620
	80	2.544	2.496	2.429
	90	1.769	1.740	1.687

areas with arid climates. Therefore, cover liner system design could be allowed to vary depending on the climate where a hazardous waste disposal site is located.

V. References.

ASAE. (1981) Design and Operation of Farm Irrigation Systems, p. 829. American Society of Agricultural Engineers, St. Joseph, MI.

Cohen, C. (1989) Index to the Code of Federal Regulations, 1989, p. 3509. Congressional Information Service, Bethesda, MD.

EPA. (1994) The Hydrologic Evaluation of Landfill Performance (HELP) Model: User's Guide for Version 3, p. 184. U.S. Government Printing Office, Washington, D.C.

Lokke, D.M. (1992) Vadose Zone Travel Time Modeling With Application to Nitrates, 174 p. University of Nebraska-Lincoln.

U.S.D.A. (1972) NRCS-National Engineering Handbook, Section 4: Hydrology, p. 9-2. U.S. Government Printing Office, Washington, D.C.

Cost Comparisons of Alternative Landfill Final Covers

Stephen F. Dwyer[1]

Abstract

A large-scale field demonstration comparing and contrasting final landfill cover designs has been constructed and is currently being monitored. Four alternative cover designs and two conventional designs (a RCRA Subtitle 'D' Soil Cover and a RCRA Subtitle 'C' Compacted Clay Cover) were constructed of uniform size, side-by-side. The demonstration is intended to evaluate the various cover designs based on their respective water balance performance, ease and reliability of construction, and cost. This paper provides an overview of the construction costs of each cover design.

Engineering Background

The US Department of Energy (DOE) is in the midst of a major clean-up effort of their facilities that is expected to cost billions of dollars. These cost estimates; however, are based on "state-of-the-art" technologies, of which many are inadequate. Consequently, work has begun on the development or improvement of environmental restoration and management technologies. One particular area being researched is landfill covers. As part of their ongoing environmental restoration activities, the DOE has many radioactive, hazardous, mixed waste, and sanitary landfills to be closed in the near future (Hakonson et al., 1994). These sites, as well as mine and mill tailings piles and surface impoundments, all require either remediation to a 'clean site' status or capping with an engineered cover upon closure. Additionally, engineered covers are being considered as an interim measure to be placed on contaminated sites until they can be remediated. The Alternative Landfill Cover Demonstration (ALCD) is a large-scale field test at Sandia National Laboratories, located on Kirtland Air Force Base in Albuquerque, New Mexico. Its intent is to compare and document the performance of alternative landfill cover technologies of various costs and complexities for interim stabilization and/or final closure of landfills in arid and semi-arid environments. The test covers are constructed side-by-side for comparison based on their performance, cost, and ease of construction. The ALCD is not intended to showcase any one particular cover system. The focus of this project is to provide the necessary tools; i.e., cost, construction and performance data, to the public and regulatory agencies so that design engineers will have less expensive, regulatory acceptable alternatives to the conventional cover designs.

The covers are each 13 m wide by 100 m long. The 100 m dimension was chosen because it is representative of hazardous and mixed waste landfills found throughout the DOE complex (approximately 2 acres in surface area). All covers were constructed with a 5% slope in all layers. The slope lengths are 50 m each (100 m length crowned at the middle with half of the length - 50 m - sloping to the east and the other half toward the west). The western slope is monitored under ambient conditions (passive monitoring). A sprinkler system was installed in the eastern slope of each cover to facilitate stress testing of the covers (active monitoring).

Continuous water balance and meteorological data is currently being obtained. It will be actively collected for a minimum five-year post construction period. In addition, periodic measurements of vegetation cover, biomass, leaf area index, and species composition are being taken.

---

[1] Principal Investigator, Sandia National Laboratories, MS 0719, P.O. Box 5800, Albuquerque, NM, USA 87185.

General Costs of Construction

The covers were independently designed. The designs were packaged into a set of construction bid documents that included drawings and specifications for each test cover. The covers were divided into two separate bid packages. Phase I was bid in FY95 while Phase II, due to funding constraints, was bid in FY96. The phase I covers built in FY95 include a conventional RCRA Subtitle 'D' Soil Cover, a conventional RCRA Subtitle 'C' Compacted Clay Cover, and the Geosynthetic Clay Liner (GCL) Cover. The phase II covers built in FY96 include the Capillary Barrier, Anisotropic Barrier, and Evapotranspiration (ET) Cover.

Each phase of construction was competitively bid with the low bidder receiving a firm fixed price contract. The costs to construct each cover design were broken out of the overall contract with the help of the general contractor and applicable subcontractors. The entire process including the bid package preparation, bid process, contract award, and construction activities were performed similar to that on an actual landfill cover project.

Costs for each cover design were developed as follows: (1) common costs such as mobilizing, demobilizing, and seeding were evenly assessed to each cover; (2) all other costs such as materials and labor were carefully allocated to each cover design. A summary of the cost per meter for each cover is presented in figure 7.

Conventional EPA Landfill Covers

Two conventional cover designs were installed to provide a baseline for comparison of the alternative cover designs. Traditional Test Cover 1 (Figure 1) is a basic Soil Cover that is generally installed over typical municipal landfills. This cover design meets minimum requirements set forth for RCRA Subtitle 'D' governed landfills (US Dept. of Energy, 1993). This cover is 60 cm thick. It is constructed of essentially two layers. The bottom layer is a 45 cm thick compacted soil barrier layer. Only native soil was used in this layer. The soil was compacted 'wet of optimum' to 95% of maximum dry density. The soil was placed as specified to meet the maximum 1×10^{-5} cm/sec saturated hydraulic conductivity requirement of Subtitle 'D' regulated facilities. The top vegetation layer is 15 cm of topsoil loosely laid. This layer provides for vegetation growth and erosion protection.

Subtitle 'D' RCRA-Cover
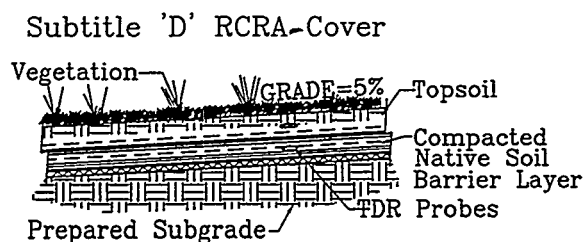
Figure 1 - Conventional Test Cover 1

The Soil Cover was the simplest and least expensive of all of the covers installed. Costs include obtaining and placing the 60 cm thick fill soil and seeding. The bottom 45 cm barrier soil layer required compaction. This barrier layer was installed in three 15 cm compacted lift depths. Compaction was relatively easily achieved using a vibratory compactor. The cost of construction for this cover design was $52.42 per square meter.

This cover, however, is generally considered inadequate at controlling infiltration into the underlying waste it is designed to isolate from the surrounding environment. An EPA sponsored

study revealed that a large percentage of landfills utilizing this cover design have failed (US Environmental Protection Agency, 1988).

Traditional Test Cover 2 (Figure 2) is a Compacted Clay Cover that is generally installed over hazardous waste landfills. This cover was designed and installed to meet minimum requirements set forth for RCRA Subtitle 'C' regulated landfills (Landreth et al, 1991). It is 1.5 m thick. The typical profile for this cover consists of three layers. The bottom layer is a 60 cm thick barrier layer. The barrier layer's primary purpose is to prevent the downward movement of water into underlying waste. Laboratory tests revealed that the native soil required amendment to meet the saturated hydraulic conductivity requirement (maximum of 1×10^{-7} cm/sec). It was constructed of native soil mixed with 6% bentonite by weight. The lifts were compacted to a minimum of 98% of maximum dry density (ASTM D698). During fill and compaction, the soil was kept at a water content 'wet of optimum' so as to remold the soil. The combination of the compaction requirements, soil amendment, and placement ('wet of optimum') was necessary to yield a maximum hydraulic conductivity of 1×10^{-7} cm/sec. Constructing the barrier layer was very difficult. The most economical means of obtaining the bentonite was having it trucked in from Wyoming. It arrived in two-ton bags. The bentonite then required to be evenly mixed with the soil prior to its installation in the cover. After mixing, it was wetted, placed on the cover and compacted. The moist amended soil proved to be much more difficult to work with than the plain native soil. It was sticky to spread and slippery to drive on. The compaction was extremely difficult to achieve. It was compacted in four approximately 15 cm compacted depth lifts. Substantial quality control was required to ensure the material and placement was as specified.
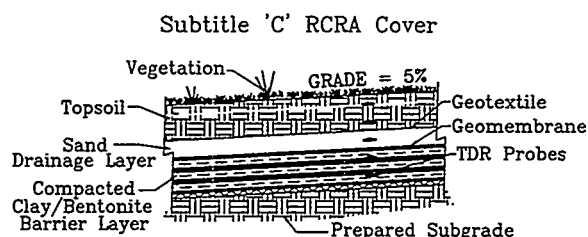
Figure 2 - Conventional Test Cover 2

A 40 mil linear low density polyethylene geomembrane was placed directly on top of the clay barrier layer. The surface of the clay barrier layer was smooth-roll compacted and prepared to allow for intimate contact between it and the under-surface of the geomembrane to essentially obtain a composite barrier layer. The geomembrane was purchased and trucked to the site. The cost of the geomembrane includes not only the material cost but shipping costs. It can get very expensive if a partial load is shipped rather than a full load because the full cost of that truck's time and mileage will be billed to that shipment. This is true for all geosynthetics used. On this project, we were able to have full loads shipped. The installation of the geomembrane required spreading it in place and heat welding the seams. All seams were tested for adequacy. Any and all defects found in the geomembrane were patched and tested for adequacy.

The middle layer is a 30 cm thick drainage layer. The primary purpose of the drainage layer is to quickly route any water that has passed through the vegetation layer laterally to collection drains normally located at the perimeter of the landfill. This layer was constructed of sand placed directly on the geomembrane. The average hydraulic conductivity of the sand installed was 1×10^{-1} cm/sec which is an order of magnitude better than the minimum 1×10^{-2} cm/sec called for in Subtitle 'C'. It was trucked to the site and spread in place in a single lift.

A nonwoven polyester needlepunched geotextile was placed directly on top of the sand drainage layer. This served as a filter between the drainage layer material and top layer. The rolls of

geotextile were placed on the sand and rolled into place. Joints were simply overlapped; no physical seaming was performed.

The top layer is a 60 cm thick vegetation layer comprised of loosely laid soil. This layer's primary purpose is to provide for vegetation growth, erosion protection, and protect the underlying layers from such events as harmful freeze/thaw cycles. It allows for storage of infiltrated water that can later be evaporated. It is 45 cm of native soil covered by 15 cm of topsoil.

The Compacted Clay Cover was by far the most difficult and expensive cover design to install. The construction cost of this cover design amounted to $157.58 per square meter.

Alternative Designs

Any and all compaction of soil in the alternative designs was compacted 'dry of optimum' rather than 'wet of optimum' as currently recommended with the conventional covers (Daniel, 1993). This was done in an effort to mitigate the potential for desiccation cracking.

Alternative Test Cover 1 (Figure 3) is a Geosynthetic Clay Cover identical to the traditional compacted clay cover with the exception that the problematic clay barrier layer was replaced with a manufactured sheet, a geosynthetic clay liner (GCL), installed in its place.

Geosynthetic Clay Liner (GCL) Cover

Figure 3 - Alternative Test Cover 1
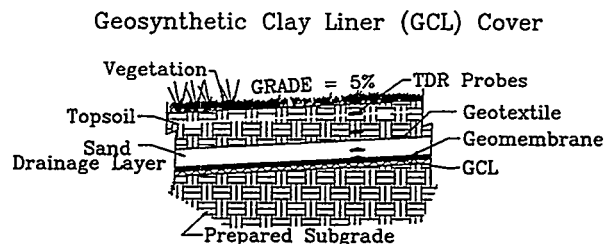
The GCL is the bottom barrier layer covered with a geomembrane, drainage layer and vegetation layer, respectively. The GCL sheet installed is a composite of two nonwoven fabrics sandwiching a layer of bentonite. The hydraulic conductivity of the GCL is 5×10^{-9} cm/sec.

Replacing the 60 cm thick clay (amended soil) barrier layer with a GCL drastically reduced the cost and difficulty of construction. The topsoil, sand drainage layer, geotextile, and geomembrane were installed similarly to that in the Compacted Clay Cover. The GCL was purchased and trucked to the site. The rolls were simply rolled into place. Joints were overlapped with no physical seaming. The construction cost of this cover design was $92.89 per square meter.

Alternative Test Cover 2 (Figure 4) is a Capillary Barrier. The Capillary Barrier comprised of a fine-grained layer of soil placed over a coarse-grained layer emphasizes a sufficient contrast between the hydraulic conductivity's of the fine-grained layer versus the coarse-grained layer. This contrast lends to the effect that flow through the cover is greatly slowed under unsaturated conditions.

This cover system consists of 4 primary layers: (1) a surface or topsoil layer; (2) an upper drainage layer; (3) a barrier soil layer; and (4) a lower drainage layer. The topsoil layer is 30 cm thick. This surface layer is placed to enhance evapotranspiration, protect against desiccation of the barrier soil layer, and provide a medium for growth of vegetation. This vegetation increases evapotranspiration and protects against surface erosion. The upper lateral drainage layer is 22 cm of gravel overlain by 8 cm of sand. The sand serves as a graded filter to prevent topsoil from

clogging the drainage layer. The gravel allows for lateral drainage of any water that has percolated through the topsoil. The barrier soil layer and lower drainage layer comprise the capillary barrier. The barrier soil layer is compacted soil 45 cm thick. The lower drainage layer is 30 cm of sand.
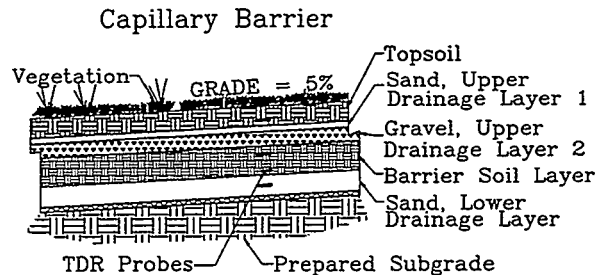
Capillary Barrier

Figure 4 - Alternative Test Cover 2

The Capillary Barrier was installed without any geosynthetic materials. The lower sand drainage layer is washed concrete sand. It was placed in one lift. The barrier soil layer was then placed on the sand. The first lift of the soil had to be carefully placed so as to keep a smooth uniform transition between the soil and sand. In order to minimize weight and thus not disturb the interface between the soil and sand, a small dozer with steel tracks was used to spread the soil. This took longer than using larger equipment with rubber tires and was slightly more expensive. The soil was placed in three 15 cm deep lifts. Compaction was relatively easily achieved. It was compacted to a minimum of 95% of maximum dry density. The gravel upper drainage layer was then placed in one lift. It was clean pea gravel, a readily available material. A sand upper drainage layer was then placed in one lift on the gravel. Again, special care was required to keep a smooth interface between the sand and gravel. The small dozer was again used to spread the sand into place. The 8 cm deep layer of sand called for in the design proved impractical. Fifteen cm of sand seemed to be the thinnest practical depth. No allowance was given to the contractor for the additional sand used because he bid the job based on the assumption he would be able to evenly spread an 8 cm thick lift of sand. The construction cost of this cover design was $96.45 per square meter.

Alternative Test Cover 3 (Figure 5) is referred to as the Anisotropic Barrier. The design of the Anisotropic Barrier attempts to limit downward movement of water while encouraging lateral movement of water. This cover is composed of a layering of capillary barriers. The various layers are enhanced by varying soil properties and compaction techniques that lead to the anisotropic properties of the cover.

Anisotropic Barrier
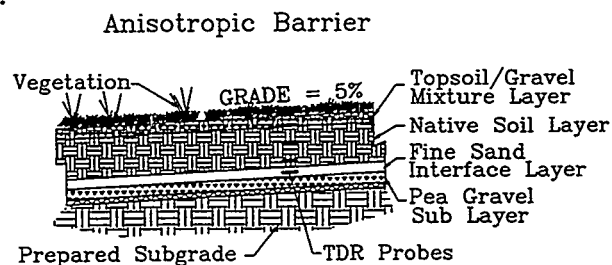
Figure 5 - Alternative Test Cover 3

This cover system consists of 4 layers: (1) a top vegetation layer; (2) a cover soil layer; (3) an interface layer; and (4) a sublayer. The vegetation layer is 15 cm thick. It is comprised of a mixture of local topsoil and pea gravel. The gravel to soil mixture by weight was 25%. This layer encourages evapotranspiration, allows for vegetation growth, and reduces surface erosion. The

cover soil layer is 60 cm of native soil. Its function is to allow for water storage and eventual evapotranspiration, as well as, serve as a rooting medium. The interface layer is 15 cm of fine sand. This layer serves as a filter between the overlying soil and the underlying gravel. It also serves as a drainage layer to laterally divert water that has percolated through the cover soil. The sublayer is 15 cm of pea gravel. It serves as a capillary break. The interface layer and sublayer combined also serve a dual purpose as bio-barriers.

The Anisotropic Barrier was installed without any geosynthetic materials. The pea gravel sublayer was installed in one lift. The same clean pea gravel as that used on the Capillary Barrier was used on this cover. The sand interface layer was installed in one lift by the small steel tracked dozer to maintain the clean interface between the sand and gravel. The sand was also washed concrete sand. The native soil layer was then installed in one lift on the sand . It was also spread with the small dozer. The only compaction on this soil layer was due to equipment traffic on it during construction. The topsoil/gravel layer was mixed adjacent to the cover then trucked on and spread in one lift. The gravel used was clean pea gravel. The construction cost of this cover design was $74.92 per square meter.

Alternative Test Cover 4 (Figure 6) is referred to as an Evapotranspiration (ET) Cover. The ET Cover is a soil cover with an engineered vegetative covering. This cover encourages water storage and enhances ET. It is 90 cm thick. The bottom 75 cm was compacted while the top 15 cm of topsoil was loosely placed. The soil allows for water storage, which when combined with the vegetation will increase, evapotranspiration.

Evapotranspiration Soil Cover
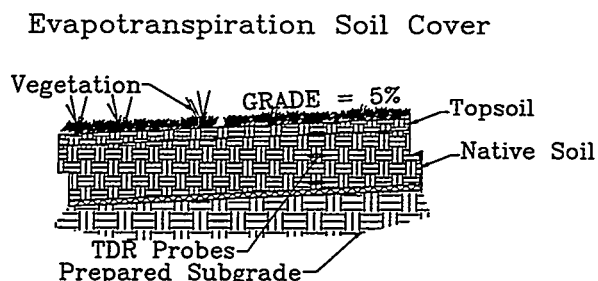
Figure 6 - Alternative Cover 4

The ET Cover was constructed similarly to the RCRA Subtitle 'D' Soil Cover. The RCRA Subtitle 'D' Soil Cover's shallow depth is one of the primary reasons for its inadequacy. Computer modeling revealed that if the depth were increased to 90 cm in the Albuquerque climate, this would essentially eliminate water infiltration into underlying waste. The ET Cover was easily constructed placing five 15 cm thick compacted depth lifts overlain by one lift of topsoil. The construction cost of this cover was $72.66 per square meter.

Alternative Acceptance

A study (Wentz, 1989) performed by the University of North Dakota concluded that the deciding factors affecting which hazardous waste management technology is to be used are from most important to least important: 1) government regulations, 2) economics, 3) public relations, and 4) process / technology. Great effort has gone into obtaining regulatory involvement and eventual acceptance of the technologies involved in this project. Each of the alternative designs is less expensive and easier to construct than the conventional Compacted Clay Cover and much more effective than the plain Soil Cover.

405

Expected Benefits

The probable outcome of this demonstration is the acceptance of alternative cover designs that are significantly less costly than conventional designs. Given the thousands of acres of buried waste sites to be covered, the payoff from this demonstration may be on the order of many millions of dollars in savings.

Acknowledgments

The work was funded by the United States Department of Energy Office of Science and Technology through the Subsurface Contaminants Focus Area.

Summary

The construction costs for each of the six landfill cover designs is shown below in figure 7. These costs may vary depending on the size and location of the site, but the ratios should remain about the same.
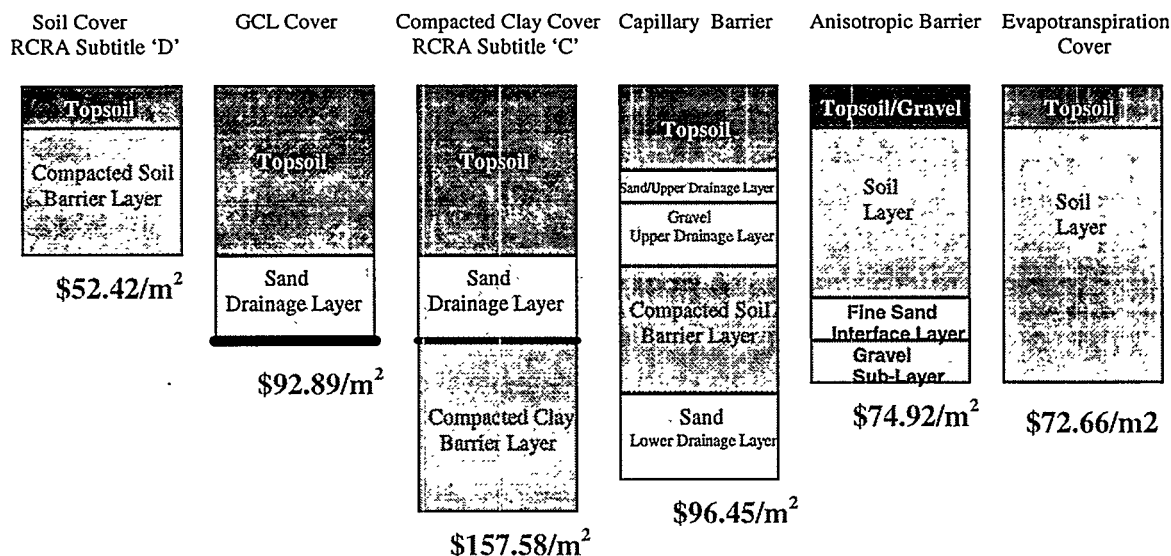
Figure 7 - Summary of Construction Costs

References

1. Daniel, DE, RM Koerner (1993) Quality Assurance and Quality Control for Waste Containment Facilities. *Technical Guidance Document. EPA/600/R-93/182;* chapters 1 -5.

2. Hakonson et al (1994) Hydrologic Evaluation of Four Landfill Cover Designs at Hill Air Force Base, Utah. Los Alamos National Laboratories Document *LA-UR-93-4469.*

3. Landreth, RE, DE Daniel, RM Koerner, PR Schroeder, GN Richardson (1991) Design and Construction of RCRA / CERCLA Final Covers. *Seminar Publication: EPA/625/4-91/025;* chapters 1- 7.

4. US Department of Energy - Office of Environmental Guidance, RCRA Information Brief "Closure of Municipal Solid Waste Landfills (MSWLFs)" (1993)., *EH-231-036/0793.*

5. US Environmental Protection Agency, Office of Solid Waste (1988) Case Studies on Ground Water and Surface Water Contamination from Municipal Solid Waste Landfills. *EPA/530-SW-88-040.*

6. Wentz, Charles A,. (1989) *Hazardous Waste Management,* p.374.

ALTERNATIVE LANDFILL COVER TECHNOLOGY DEMONSTRATION AT KANEOHE MARINE CORPS BASE HAWAII

L.A. Karr and B. Harre
Naval Facilities Engineering Service Center
Port Hueneme, CA 93043

T.E. Hakonson
Colorado State University
Fort Collins, CO 80523

Abstract

Surface covers to control water infiltration to waste buried in landfills will be the remediation alternative of choice for most hazardous and sanitary landfills operated by the Department of Defense. Although surface covers are the least expensive method of remediation for landfills, they can still be expensive solutions. Conventional wisdom suggests that landfill capping technology is well developed as evidenced by the availability of EPA guidance for designing and constructing what has become known as the "RCRA Cap". In practice, however, very little testing of the RCRA cap, or any other design, has been done to evaluate how effective these designs are in limiting infiltration of water into waste.

This paper describes a low cost alternative to the "RCRA Cap" that is being evaluated at Marine Corps Base Hawaii (MCBH) Kaneohe Bay. This study uses an innovative, simple and inexpensive concept to manipulate the fate of water falling on a landfill. The infiltration of water through the cap will be controlled by combining the evaporative forces of vegetation to remove soil water, with engineered structures that limit infiltration of precipitation into the soil. This approach relies on diverting enough of the annual precipitation to runoff, so that the water that does infiltrate into the soil can easily be removed by evapotranspiration.

Introduction

Landfill covers (caps) are the least expensive method to effectively manage the human and ecological risks associated with hazardous waste landfills. Landfill covers will be the remediation technology chosen for many of these landfills. Unfortunately, very little testing of the EPA's RCRA Cap, or any other cap has been performed. The Kaneohe study demonstrates the effectiveness of two designs, one involving a 20% enhancement of runoff, and the other a 40% enhancement of runoff, along with a conventional soil cap to serve as a basis of comparison. The equivalency of the three designs to the EPA RCRA design will be evaluated by comparing the field monitoring data with the predicted performance of the RCRA design using the HELP model. The goal of this study is to demonstrate the effectiveness of alternative landfill cap designs that manipulate the fate of meteoric water in a high precipitation area.

The fate of meteoric water falling on the landfill is often referred to as the water balance of the site. A simplified representation of water balance describes surface runoff and one dimensional movement of water in the soil profile to the plant rooting depth. For net rates and amounts, the water balance equation is:

$$dS/dt = (P - R - ET - L)/dt \qquad \text{Equation (1)}$$

where:
- dS/dt = Time rate of change in soil moisture per unit of time
- P = Precipitation per unit area, cm H_2O/m^2
- R = Runoff per unit area, cm H_2O/m^2
- ET = Evapotranspiration per unit area, cm H_2O/m^2
- L = Percolation below the root zone per unit area, cm H_2O/m^2
- dt = Unit of time used to solve equation

The concept of mass balance, relative to the design of landfill covers, accounts for the strong interactions between the various terms of Equation 1. For example, a reduction or elimination of the runoff term (R), increases infiltration of water into the soil, resulting in increased soil moisture storage followed by an increase in ET and/or percolation. Likewise, a reduction of ET must be followed by increased percolation in order to maintain hydrologic mass balance. In this study, the runoff term is enhanced, thus decreasing soil moisture storage and the amount of water available for ET and/or percolation.

The concept of water balance, and especially methods to manipulate its various components, has served as the basis for several studies to design, test, and evaluate a variety of capping alternatives for radioactive and hazardous waste landfills (Nyhan et al. 1990; Hakonson et al. 1992; Hakonson et al. 1993; Lane 1984; Lane and Nyhan 1984). For example, past studies have emphasized the role of vegetation in removing soil moisture via evapotranspiration, the use of subsurface barriers to intercept and laterally divert percolating water, and surface management practices to control runoff and erosion.

Nearly all of the past work has been conducted in arid or semi-arid environments with annual precipitation of less than 20 inches per year (Nyhan et al. 1990; Hakonson et al. 1992; Hakonson et al. 1993; Lane 1984; Lane and Nyhan 1984). The annual average precipitation at MCBH Kaneohe is 38 inches, an amount greater than can be removed from the soil by evapotranspiration.

The study at MCBH Kaneohe focuses on enhancing surface runoff, thereby reducing the amount of soil water that must be partitioned between the ET and percolation terms in Equation 1. The theory behind these designs is to limit percolation of water through the cap by enhancing runoff to limit infiltration of precipitation into the soil (Figure 1) and using the very powerful evaporative forces of vegetation to remove that moisture which does infiltrate into the soil. The approach relies on diverting enough of the annual precipitation to runoff, using water harvesting structures (WHS), so that the water that does infiltrate into the soil can easily be removed by evapotranspiration. In addition to soil moisture removal, vegetation also serves to control erosion of the landfill cap.

The objectives of the MCBH study are to compare the hydrologic performance of two infiltration control designs, one involving a 20% enhancement of runoff and the other a 40% enhancement, with a conventional soil cover design. Preliminary calculations, based on MCBH climate, suggested that water harvesting structures installed on about 20% and 40 % of the cover surface would be effective in reducing infiltration by those amounts leading to very low levels of percolation. The equivalency of the three designs to the EPA RCRA design are being evaluated by NFESC and CSU by comparing the predicted performance of the WHS designs with RCRA using EPA's HELP3 model (EPA/600/R-94/168a&b). Figure 1 shows the experimental plots. Note that there is a replicate of each design, resulting in six plots.

Each plot is 6.10 m x 9.14 m long, The cap designs to limit infiltration consisted of a non-layered soil profile with two levels of water harvesting structures installed on the cover surface (Figure 1). The water harvesting structures are essentially rain gutters which feed into the runoff collector. The collector then leads to a sediment trap and a collection tank (Figure 2). Leachate through the soil cap is collected in a gravel layer that is lined with permalon. Each of the plots has a 0.6m soil layer over a 0.3m gravel layer. The plots all have a plywood cutoff wall on the upslope side of the plot to inhibit lateral movement into the plot area. Cutoff walls are not used between the plots to avoid the edge effects experienced in other experiments (TOM reference). The leachate collection area is less than the plot surface area because the plot borders are not isolated.

Instrumentation

The Kaneohe study uses instruments to measure the fate of meteoric water. An onsite meteorological station is used to collect meteorological data. Precipitation is measured with tipping buckets. Soil moisture is measured with a time domain reflectometry (tdr) system at four locations within each plot. Runoff is measured using a 5 psi pressure transducer, which measures the collection tank level, and with a flowmeter, which measures the volume pumped out of the collection tank (Figure 2). The drain pipe leads to a collection tank with a pressure transducer, which measures collection tank level. A tipping bucket, which measures low volume flowrates into the leachate collection tank, is also used to measure percolation through the cap. A flowmeter, which measures the volume pumped out of the leachate collection tank is also used. Sediment yields are collected in a sediment trap and weighed to determine the mass. The only parameter not measured is evapotranspiration. Evapotranspiration is estimated by solving the water balance equation . All of the data is collected by dataloggers and downloaded through a modem each night.

Canopy and Ground Cover

Cover is characterized on all of the plots using a modified point frame technique (Levy and Madden 1933). The point frame is positioned at 10 equidistant locations (Pieper 1973) perpendicular to the 9.14 m axis of each plot resulting in 61 measurements per point frame position and 61 0 measurements per plot. Canopy cover is determined by recording the type of vegetation first contacted by the point frame pin. The canopy cover categories included grass, shrub, forb, and standing dead. Ground cover is estimated by recording the first type of material contacted by the pin as it touches the ground surface. Categories of ground cover include litter, basal root crown, bare soil, and gutter.

Biomass and Species Composition

Biomass estimates are made by dividing each plot into 3 sections, the upslope 3 meters, a midslope 3 meters, and a lower 3 meters. A quadrat of 0.0804 m^2 is randomly thrown into each section. The quadrat is positioned on the ground surface and all the plant material within the boundary of a vertical projection of the quadrat, including plant material hanging into the quadrat, is clipped and bagged for drying and weighing. Biomass estimates are made on standing live plants, standing dead plants, and litter. Material is classified as live if the plant was predominately green and extending above the ground surface. Some dead plants are partly lying on the ground surface and partly off the ground surface. Dead plant material that is predominately on the ground surface is classified as litter while that predominately off the ground surface is classified as standing dead. Plant material is segregated into either shrub, forb, grass, standing dead, or litter. Samples are air dried for several days and then weighed.

Taxonomic identification of species present on the plots was performed during May 1996. Point frame data is analyzed with ANOVA using each transact (10/plot) as a replicate sample (Snedecor and Cochran 1989).

Preliminary Results

Measured, CLIGEN generated precipitation, and 30 year average precipitation is shown in Figure 3. The weather input to the model was with Kahuku (a site just up the coast on Oahu) parameters entered into the weather generator CLIGEN, which are almost identical to MCBH Kaneohe Bay. The monthly values are the long term average precipitation values for the 30 year simulation. The 30 year average values are from historical records of precipitation at MCBH Kaneohe Bay. The measured values are from the meteorological equipment at the MCBH site.

The relative performance of the various cover types in generating runoff and percolation is summarized in Figure 4. These preliminary, short term results support the concept of using runoff enhancement to manage landfill site water balance. The designs statistically increased runoff over the soil cover design and reduced percolation to about one quarter to one third of that measured from the soil cover.

The results also demonstrate that the hydrologic response of the MCBH Kaneohe cover designs is highly dependent on season and a related variable, the amount of precipitation falling during a particular month. Most of the runoff and percolation was associated with a few months in winter when most of the precipitation occurs. Additionally, months with threshold precipitation above about 10 cm, generated most of the runoff or percolation. Summer months generally received less than 10 cm and produced little of the runoff and percolation measured on the plots.

References

Hakonson, T. E., L. J. Lane, and E. P. Springer (1992). "Biotic and Abiotic Processes," Reith, C. C. and Thomson, B. M. (eds.) in Deserts as Dumps, The Disposal of Hazardous Materials in Arid Ecosystems University of New Mexico Press, ISBN 0-82631297-7.

Hakonson, T. E. and L.J. Lane (1992). "The Role of Physical Process in the Transport of Man-made Radionuclides in Arid Ecosystems," R. M. Harrison (ed.) in Biogeochemical Pathways of Artificial Radionuclides, John Wiley & Sons.

Hakonson, T.E., K.L. Manies, R.W. Warren, K.V. Bostick, G. Truijillo, J.S. Kent, and L.J. Lane (1993). Migration barrier covers for radioactive and mixed waste landfills. IN Procs. Second Environmental Restoration Technology Transfer Symposium, San Antonio, TX, January 26 - 28, 1993.

Hakonson, T. E., L. J. Lane, J. W. Nyhan, F. J. Barnes, and G. L. DePoorter (1990). Trench cover systems for manipulating water balance on low-level radioactive waste sites. M. S. Bedinger and P. R. Stevens, (eds.), PP. 73-80, IN: Safe Disposal of Radionuclides in Low-Level Radioactive Waste Repository Sites: Low Level Radioactive Waste Disposal Workshop, USGS Circ.- 1036.

Lane, L.J. (1984). "Surface Water Management: A User's Guide to Calculate a Water Balance Using the CREAMS Model," Los Alamos National Laboratory Report, LA10177-M.

Lane, L.J., and J.W. Nyhan (1984). 'Water and Contaminant Movement: Migration Barriers," Los Alamos National Laboratory Report, LA-1 0242-MS.

Nyhan, J. W., T. E. Hakonson, and B. J. Drennon (1990). "A Water Balance Study of Two Landfill Cover Designs for Semiarid Regions," Journal of Environmental Quality, Vol. 19, No. 2, pp. 281-288.

Nyhan, J., T. Hakonson, and S. Wohnlich (1990). "Field Experiments To Evaluate Subsurface Water Management fro Landfills in Snowmelt-Dominated Semiarid Regions of the USA," F. Arendt, M. Hinsenveld, and W.J. van den Brink (eds.) IN: Contaminated Soil'90, pp. 1205-1206.

Levy, E.B. and E.A. Madden. 1933. The point method of pasture analysis. New Zealand J Agr. 46: 267-279.

Pieper, Rex D. 1973. Measurement techniques for herbaceous and shruby vegetation. Department of Animal, Range and Wildlife Science. New Mexico State University, Las Cruces, N.M.

Snedecor, George W. and W.G. Cochran. 1989. Statistical Methods (8th Ed). Iowa State University Press, Ames, Iowa.
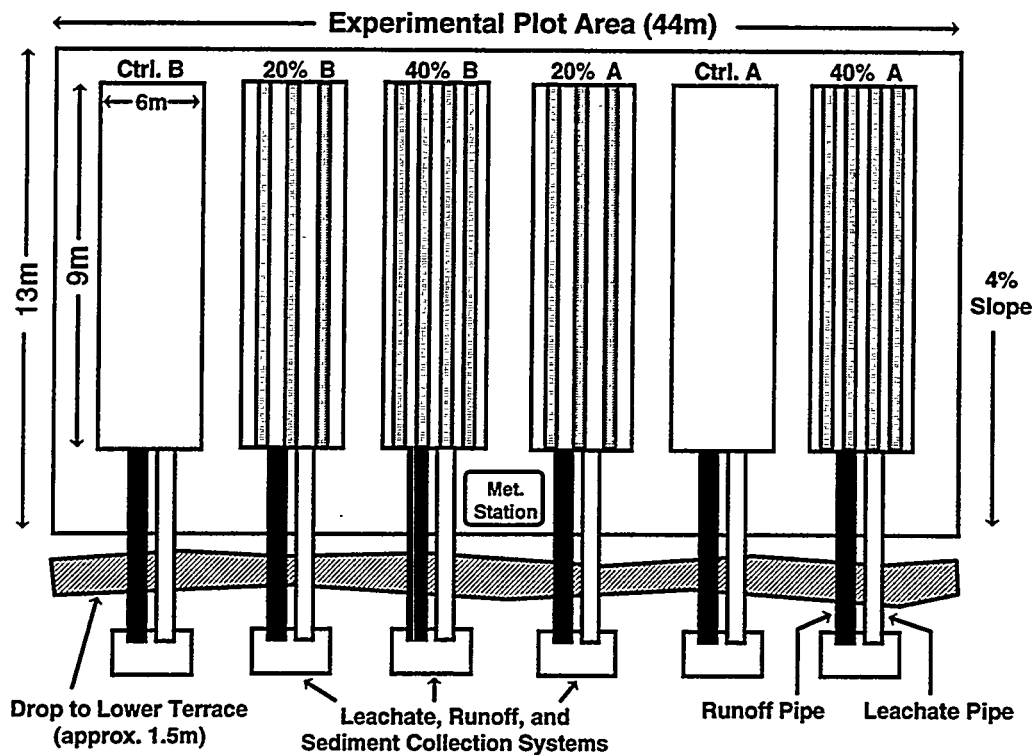
Figure 1. Experimental Plots

Labels in figure:
Experimental Plot Area (44m)
Ctrl. B 20% B 40% B 20% A Ctrl. A 40% A
6m
13m
9m
4% Slope
Met. Station
Drop to Lower Terrace (approx. 1.5m)
Leachate, Runoff, and Sediment Collection Systems
Runoff Pipe Leachate Pipe
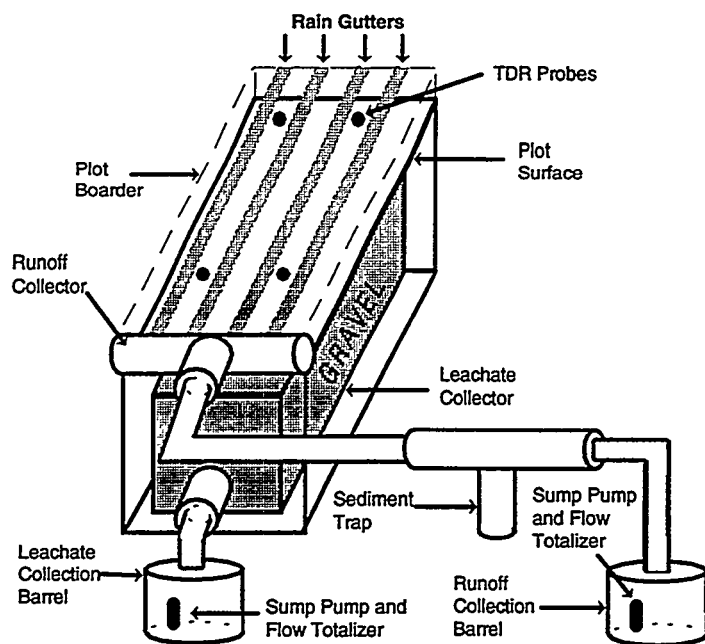
Figure 2. Detail of Experimental Plot

Labels in figure:
Rain Gutters
TDR Probes
Plot Boarder
Plot Surface
Runoff Collector
GRAVEL
Leachate Collector
Sediment Trap
Sump Pump and Flow Totalizer
Leachate Collection Barrel
Sump Pump and Flow Totalizer
Runoff Collection Barrel

Figure 3 Measured, 30 YR Average, and HELP3 Predicted Monthly Precipitation at MCBH
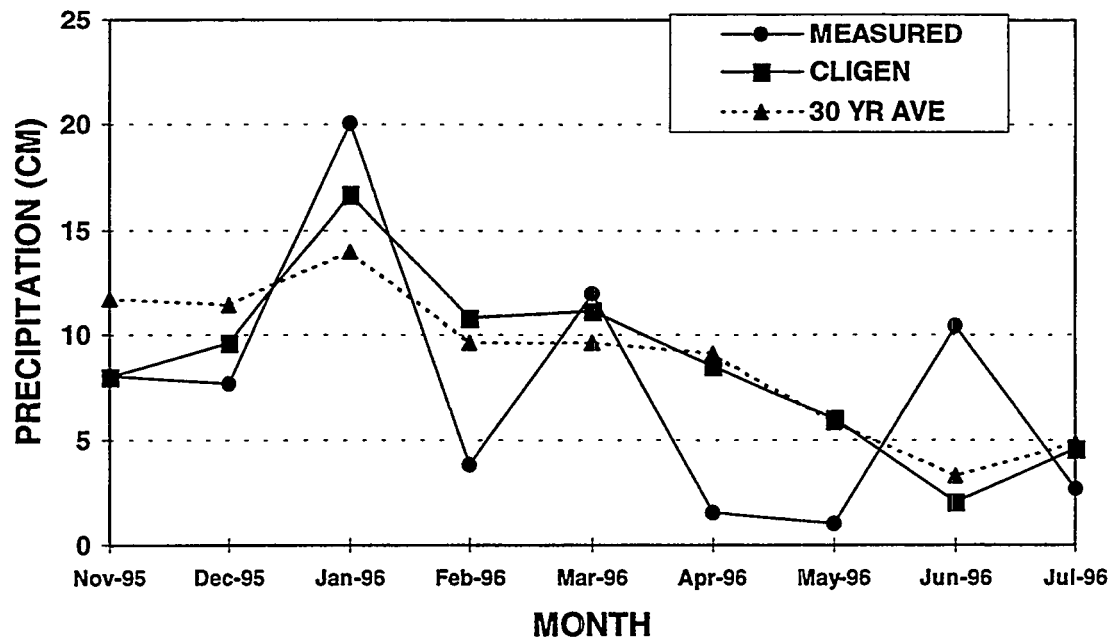
Figure 4. Relative Amount of Runoff and Percolation Produced
From Runoff Enhancement, Soil, and HELP3 Simulated RCRA
Cover Designs at MCBH for Period 11/95 - 7/96
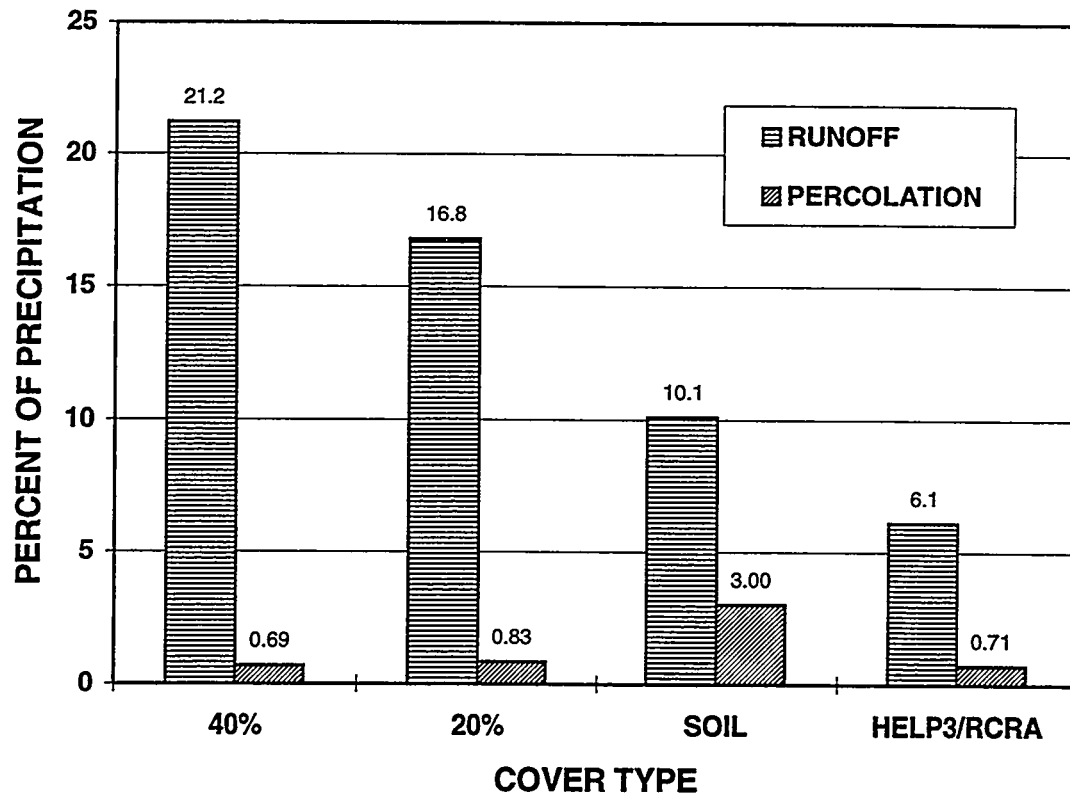
ENVIRO-GEOTECHNICAL CONSIDERATIONS IN WASTE CONTAINMENT SYSTEM DESIGN AND ANALYSIS

H. Y. Fang[1], John L. Daniels[2], and Hilary I. Inyang[3]

ABSTRACT

The effectiveness of waste control facilities hinges on careful evaluation of the overall planning, analysis and design of the entire system prior to construction. At present, most work is focused on the waste controlling system itself, with little attention given to the local environmental factors surrounding the facility sites. Containment materials including geomembranes, geotextiles and clay amended soils have received intense scrutiny. This paper, however, focuses on three relatively important issues relating to the characterization of the surrounding geomedia. Leakage through naturally occurring low-permeability soil layers, shrinkage, swelling, cracking and effects of dynamic loads on system components are often responsible for a waste containment breach. In this paper, these mechanisms and their synergistic effects are explained in terms of the particle energy field theory. It is hoped that this additional information may assist the designer to be aware or take precaution to design safer future waste control facilities.

INTRODUCTION

The performance of waste containment systems hinges on effective planning, analysis, and design of the entire system prior construction. Several investigators exemplified by Inyang and Tumay (1995), have analyzed various containment system configurations. At present, most work focuses on the configuration of systems such as vertical barrier (wall), bottom seal (liner) and top seal (cap) barriers. Little attention is given to probable changes in the characteristics of the media in which containment systems are embedded. In this paper, three relatively important areas are discussed: (1) leakage through "impervious" low-permeability soil layers; (2) shrinkage, swelling and cracking of site soils, and (3) dynamic behavior of contaminated site soils. Fang (1995) has explained interactions between contaminants and fine-grained soils in terms of particle-energy field theory. Limited laboratory test results presented herein, may not be conclusive enough to establish the compliance of every physico-chemical phenomenon in soils with the theory but they may provide some insight into the factors that need to be considered in the design of waste containment systems and monitoring of the geomedia around such systems. Some investigators (Andersland and Al-Moussani, 1987; Wright, 1993; and Miller and Mishra, 1989) have devised approaches to assess the influence of flaws on the effectiveness of barrier systems and soil characteristics. This conceptual assessment may be an adequate explanation for the generation of flaws described in these references.

LEAKAGE THROUGH LOW-PERMEABILITY SOIL LAYER

Figure 1 is a schematic diagram illustrating a typical layout of some waste controlling systems. As seen in the figure, the contact border area between wall (points a-b) and low-permeability soil layer (points b-c) are contaminated. Soils are three-dimensional systems; they have a two dimensional areal extent and a depth dimension. Soils show areal limitations and changes with depth. Horizontal as well as vertical transitions into another soil type may be gradual or abrupt, depending on geologic and pedogenetic factors.

[1]Distinguished Research Professor and [2]DuPont Graduate Fellow and [3]Director, DuPont Young Professor, Center for Environmental Engineering and Science Technologies (CEEST), and Dept. of Civil and Environmental Engineering, University of Massachusetts, Lowell, MA 01854

The top layer which starts from the surface deposit of decaying plant litter to a depth at which the organic matter is completely humified, is called the A-horizon. The horizon containing the parent material is commonly called the C-horizon. Between the A- and C- horizons lies the B-horizon which is usually a locus of accumulation of material in suspension or colloidal solution eluviated from the A-horizon by percolating precipitation water. The interaction of waste controlling facilities and the A- and B-horizons are generally of greater concern as the geologic formations that comprise the C-horizon are more stable. Exceptions to this are realized in gypsum, karst and similar formations.

Soil is the cumulative result of geological ages under changing environments, combined with the physical effects of weathering and biological processes. Soils are creations of climatic forces and influenced by local environmental factors. As a result of these factors, soil's in-situ (undisturbed) condition shares many essential properties with living systems. Furthermore, microfauna that are dispersed in soils render soils actual living systems. No soil is truly impervious. Boring logs often show fungi, tree roots and bacteria distributions in all the soil profiles and horizons. In geotechnical engineering practice, it is customary to consider in-situ soils as being "undisturbed." The disturbance threshold for significant effects on moisture and contaminant migration is plausibly lower than that for strength changes. Thus, for all practical purposes, waste disposal site soils may be considered as being disturbed.

In general, voids exist in geomedia as indicated in Fig. 2. Leakage mechanisms through these soil layers have several stages: (a) leakage through soil cracks and tree roots, (b) Leakage due to change of state of matter of the pore fluid existing between soil particles (e.g. solid, liquid and gas), and (c) leakage through horizontal capillarity action. Some leakage mechanisms have been discussed previously (Fang, 1996), however, additional experimental data are presented herein to support earlier discussions. Table 1 presents the comparison of characteristics between man-made hydraulic barriers and natural "impervious" low-permeability soil layers.

Figure 3 shows the laboratory model experiment on a barrier wall made with a sand-bentonite mixture. Arrows indicate that leakage follows the horizontal capillary routes between layers of material where the density of material are different. The variables y_1 and y_2 represent sands of similar composition, but with differing void ratios. It is clearly indicated that horizontal capillary action is an important factor that causes leachate seepage through low-permeability soil layers.

SHRINKAGE, SWELLING AND CRACKING

Shrinkage, swelling and cracking in soil are natural processes that occur frequently in earthen structures due to internal energy imbalance in the soil mass. The two common causes of energy imbalance in surficial soils are nonuniform moisture and temperature distribution. This phenomenon is significant around many hazardous/toxic waste sites. Fluid movement around waste sites may be unsaturated, of low velocity, unsteady and nonuniform. Gases and/or solids may be dispersed in the permeating liquids. Significant volume changes and cracking may be associated with fluid transport in such a complex system. An illustration of probable configurations of cracks that may result from desiccation (Inyang, 1994) is presented in Figure 4.

When water is removed from soil, the soil will shrink and water added will increase the soil volume. Several important points from this relationship indicate that (a) swelling and shrinkage is not a reversible process. This means that swell is not equal to the shrinkage, (b) shrinkage process is in the thermal energy field, and the swelling is in the multi-media energy field, (c) swelling-shrinkages will lead to cracking and fracture of the soil. Cracking represents the pre-failure phenomena of a soil and fracture is the behavior of a soil at failure condition. There are four types of cracking, namely shrinkage cracking, thermal cracking, tensile cracking and fracture cracking. The mechanisms of each

415

type have been discussed by Fang (1994). Figure 5 shows the volume change hysteresis between drying and wetting of soils. The cracking patterns of fine-grained soils due to interactions with landfill leachate are discussed as follows:

(1) Cracking-Fracture Behavior when Soil is Drying: As wet or moist fine-grained soil loses water, the soil particles move closer and closer together. If the drying process is from the soil surface downward, the dehydrated surface layer shrinks while the water resistance between the upper and lower layers and in the layers themselves prevent an adjustment to the volume decrease of the surface layer. Under the drying process, the cracking pattern is controlled by thermal energy.

(2) Cracking-Fracture Behavior when Soil is Saturated: The entrance of water into a porous dry soil system can also cause cracking/fracture of soil mass. In this case, these causes and phenomena are more complicated than in drying condition, because they are controlled by multi-media energy fields which include thermo-electro-magnetic energies as discussed by Fang (1994, 1995).

(3) Cracking Patterns: Cracking pattern and mechanisms of contaminated soil differ with those of non-contaminated soil. Because the adsorption characteristics, dielectric constants and surface tension are different for different contaminant/soil combinations, cracking patterns are also different from soil to soil. Based on laboratory results, the contaminated pore fluid (pH = 2 or pH = 11) produces larger volume changes. Some acids such as aniline ($C_6H_5NH_2$), acetic acid ($C_2H_4O_2$), and carbon tetrachloride (CCl_4), show greater volume changes than other acids. Soil structural changes such as flocculation or dispersion will affect cracking pattern. Flocculation produces larger areas of cracking than dispersive structures.

Therefore, an assessment of cracking potential and macroporosity as it relates to leachate migration through natural soil depends upon the prevailing conditions.

DYNAMIC BEHAVIOR OF CONTAMINATED SOIL

The characteristics of soil under either static or dynamic loads at the pre-failure stage are controlled by multi-media energies (environmental factors) and not by mechanical energy (loading) alone. Under the static load, soil particles are close together and there is less room for particle interaction with the environment. However, for the dynamic load, the space between particles are larger, and there is more room for soil to interact with the environment. Laboratory experiments indicated (Du, et al. 1986; Naik, 1986) that when dynamic loads are imposed on contaminated soils, they cause the acceleration of failure in comparison with static load. In general, if pH value decreases (acid), it will increase soil strength as indicated by conventional static load such as unconfined, direct and triaxial shear tests. However, during dynamic load test, indications are that strength decreases as the pH value decreases. It is a controversial finding as reported. In field conditions, these dynamic loadings frequently occur as earthquake loading, blasting, machine vibration, pile driving, moving vehicles, etc.

SUMMARY AND CONCLUSIONS

(1) Leakage through low-permeability soil layers is more critical than conventionally used vertical barriers. Mechanisms of how leachate can seep through natural soil layers are explained. The barrier wall laboratory model constructed of a sand-bentonite mixture and surrounded by sands of varying density underscores horizontal capillarity.

(2) Soil cracking is a natural phenomena due to internal energy imbalance in the soil mass

and changes in local environments, but especially sensitive to conditions caused by hazardous waste sites.

(3) Dynamic loading can cause more damage in the hazardous waste site than static loading, because the bonding energy created by acidity is destroyed by excitation under dynamic loads.

(4) These three relatively important aspects must be considered for analysis and design of waste controlling facilities. All explanations of how and why are based on the recently developed particle-energy-field theory. Limited laboratory test results presented herein may not be comprehensive enough to draw general conclusions, but will give some sign of warning to the designer who considers these aspects.

REFERENCES:

Andersland, O.B. (1987) Crack formation in soil landfill covers due to thermal contraction. *Waste Management & Research*, 5, 445-452

Du, B. L., Mikroudis, G. K. and Fang, H. Y. (1986) Effect of pore fluid pH on the dynamic shear modulure of clay, *ASTM STP 933*, 226-239.

Fang, H. Y. (1994) *Cracking and fracture behavior of soil, Fracture Mechanics Applied to Geotechnical Engineering*, ASCE. NY, 102-117.

Fang, H. Y. (1995) *Environmental geotechnology, Encyclopedia of Environmental Control Technology*, v. 9, chapter 2, Gulf Publ. 13-117.

Fang, H. Y. (1996) *Leaking mechanism of impervious soil layer, Proc. 2nd International Congress on Environmental Geotechnology*, Japan, Nov.

Inyang, H.I. (1994) Waste containment technology, long term performance aspects. A presentation to U.S. E.P.A. office of solid waste and emergency response, GDR Inc.

Inyang, H.I. and Tumay, M.T. (1995) Containment systems for contaminants in the subsurface. A chapter in the *Encyclopedia of Environmental Control Technology*, Gulf Publishing Company, 175-215.

Miller, C.J. and Mishra, M. (1989) Modeling of leakage through cracked clay liners-II : A New Perspective. *Water Resources Bulletin* 25 (3) 557-563.

Naik, D. (1986) Effect of temperature and pore fluid on shear characteristic of clay. *Proc. 1st International Symposium on Environmental Geotechnology*, v. 1, 382-390.

Wright, S.J. (1993) Non-Intrusive Crack detection in clay landfill cover liners. *Engineering Hydrology, Proc. of the Symposium* 491-496.
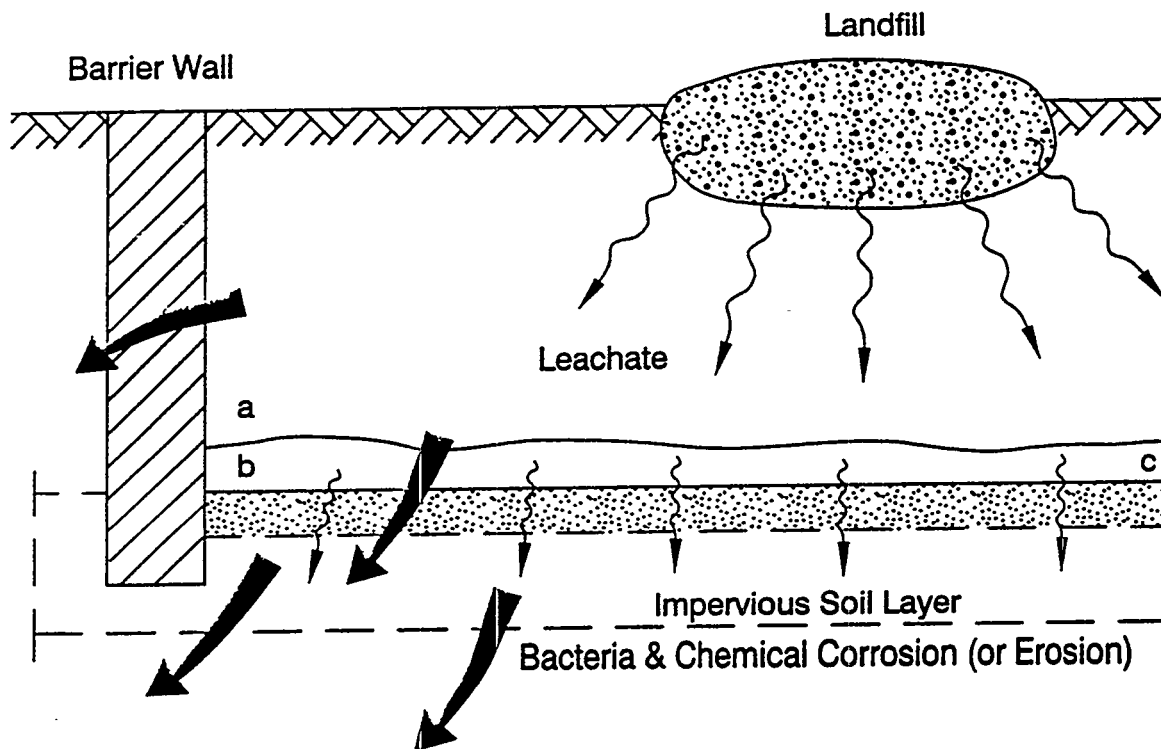
Figure 1. Schematic diagram illustrates landfill site, hydraulic barrier and natural impervious soil layer.

Table 1. Comparisons of characteristics between barrier wall and impervious soil layer.

Characteristics	Barrier Wall	Impervious Soil Layer
(1) Construction Procedure	Man-made	Natural
(2) Material Source	Selected	Natural
(3) Material Type	Uniform fine-grained soil	Natural A- & B- horizons & profiles
(4) Cracking Potential	Low (small cracks)	High (larger cracks)
(5) Contact Area with Pollution	Limited area (Fig. 1: a-b)	Larger area (Fig. 1: b-c)
(6) Risk Potential	Low	High
(7) Scientific Knowledge	Sufficient	Very Little
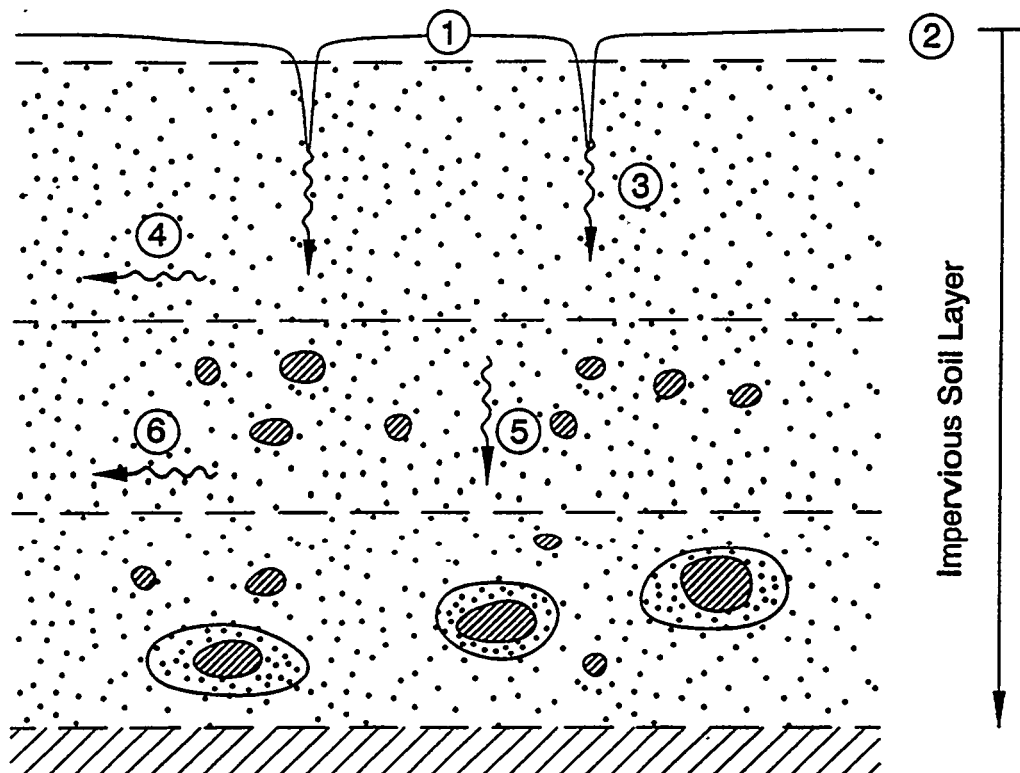
Figure 2. Leaking routes: horizontal direction through voids (1,3,5) and horizontal capillary action (4,6).
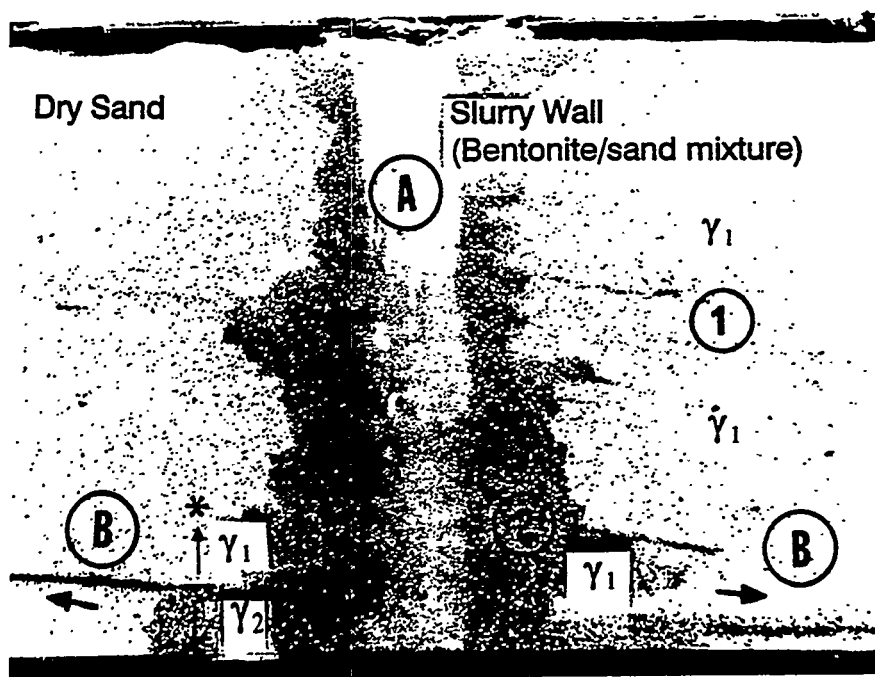
Figure 3. Laboratory model study indicates that the possibility of contaminated water seeping through slurry wall due to horizontal capillary action.
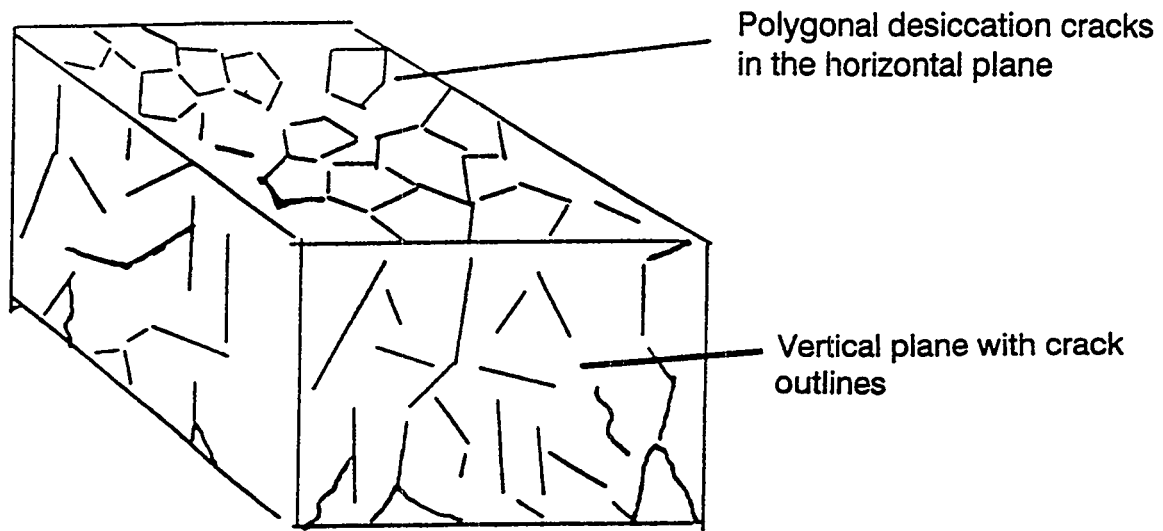
Figure 4.   Illustration of crack network in a dessicating clay soil (Inyang, 1994)
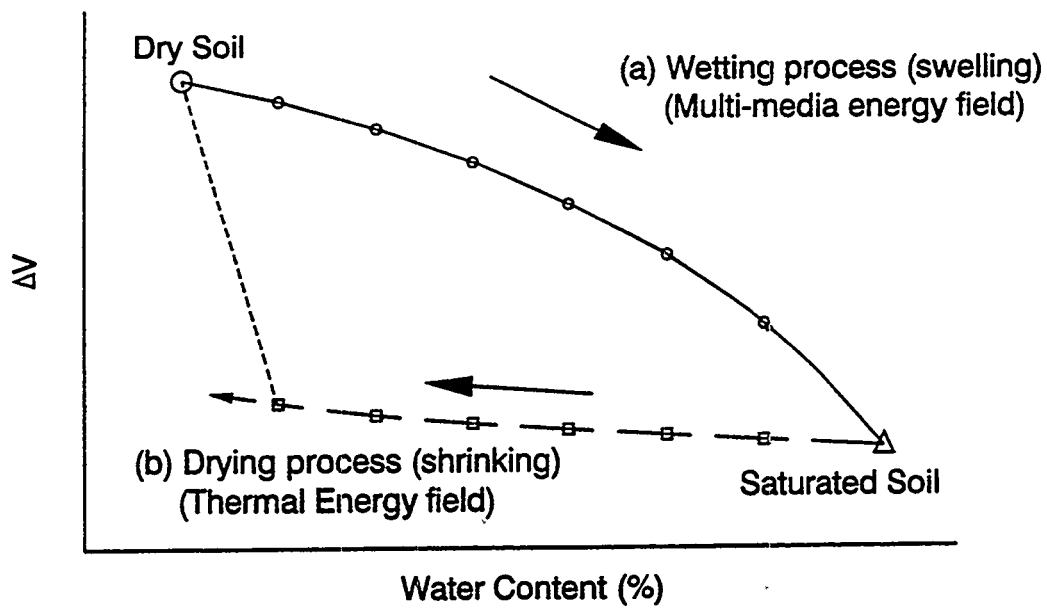
Figure 5. Effect of wetting or drying processes on soil behavior.

MODELING OF GEOSYNTHETIC REINFORCED CAPPING SYSTEMS

B. V. S. Viswanadham[1], D. König[2] and H.L. Jessberger[3]

Abstract

The investigation deals with the influence of a geosynthetic reinforcement on the deformation behavior and sealing efficiency of the reinforced mineral sealing layer at the onset of non-uniform settlements. The research program is mainly concentrated in studying the influence of reinforcement inclusion in restraining cracks and crack propagation due to soil-geosynthetic bond efficiency. Centrifuge model tests are conducted in the 500 gt capacity balanced beam Bochum geotechnical Centrifuge (Z1) simulating a differential deformation of a mineral sealing layer of a landfill with the help of trap-door arrangement. By comparing the performance of the deformed mineral sealing layer with and without geogrid, the reinforcement ability of the geogrid in controlling the crack propagation and permeability of the mineral sealing layer is evaluated.

1. Introduction

In the life span of a landfill, the capping systems encompassing the waste are more or less subjected to non-uniform settlements due to the compressible nature of the waste. Excessive non-uniform settlements could damage the mineral sealing system, which reflects in the form of cracks in the tension zone and loss of hydraulic barrier efficiency of the mineral sealing layer (Fig. 1a, 1b). The mineral sealing layer is defined as one of the components of capping system, which is generally made-up of compacted clay of low permeability characteristics. The occurrence of cracks in the mineral sealing layer could take place depending on the plastic behavior of sealing material and the presence of overburden stresses will suppress this tendency. The sealing material characteristics like, consistency, compactive effort, plasticity, clay content, etc. can significantly influence the tensile strength characteristics of the cohesive soil. The integrity of the liner is mainly achieved by maintaining the good deformable characteristics of the mineral sealing layer throughout the different stages of construction. Due to the non - availability of the suitable sealing material, low overburden stresses and anticipated large non-uniform settlements in the case of surface capping systems, the adoption of geosynthetic reinforced capping systems could be an efficient solution to enhance the deformation behavior of the mineral sealing layer system (Fig. 1c).

In such situations, geosynthetic materials such as geogrids can be used as a reinforcing elements within the mineral sealing layer, which can withstand relatively high in-plane tensile strains and stresses induced by non - uniform settlements. The idea behind this technique is to make use of the tensile strength of the reinforcement to limit/prevent the clay liner from cracking. The clay liner deformations impose lateral tensile stresses along the soil - reinforcement interface in the tension zone which are resisted by the tension mobilized in the reinforcement in the form of interface bond stresses, as shown in Fig. 1c. In this paper, the behavior of reinforced mineral sealing layers is explored using centrifuge modeling technique. In particular, the effectiveness of a geogrid reinforcement placed within the top portion of the model mineral sealing layer (with and without reinforcement) is examined by assuming that the critical zone of deformation is positioned on the convex side of the deformed mineral sealing layer. In this study, it is mainly concentrated to evaluate the deformation behavior of the mineral sealing layer with and without geogrid. The creep effects of the geosynthetic material are not covered in the scope of the present work.

---

[1]Institute for Soil Mechanics and Foundation Engineering IA 4/126, Faculty of Civil Engineering, Ruhr - University of Bochum, 44801 Bochum Germany, Tel: +49 (234) 700-6135, Fax: +49 (234) 7094-150 (formerly)

[2]Institute for Soil Mechanics and Foundation Engineering IA 4/126, Faculty of Civil Engineering, Ruhr - University of Bochum, 44801 Bochum Germany, Tel: +49 (234) 700-6135, Fax: +49 (234) 7094-150)

[3]Institute for Soil Mechanics and Foundation Engineering IA 4/126, Faculty of Civil Engineering, Ruhr - University of Bochum, 44801 Bochum Germany, Tel: +49 (234) 700-6135, Fax: +49 (234) 7094-150

2. Review of earlier works

The geotechnical problems concerning the deformability of mineral sealing systems were highlighted by Daniel (1983). The centrifuge tests carried out by Jessberger and Stone (1991) and Scherbeck and Jessberger (1993) have revealed that the loss of sealing efficiency of a liner system subjected to non-uniform settlements is influenced by: (i) normal stress resulting from overburden, (ii) shear strength of the sealing material, (iii) stiffness of the sealing material in tension and compression, (iv) tensile characteristics of the sealing material and (v) thickness of the mineral sealing layer. Bredariol et al. (1995) have studied the effect of differential settlement on the permeability of the lining system and they have reported that the soil alone in the un-reinforced compacted liners cannot restrain or mobilize such high tensile strength in order to retain it's integrity function.
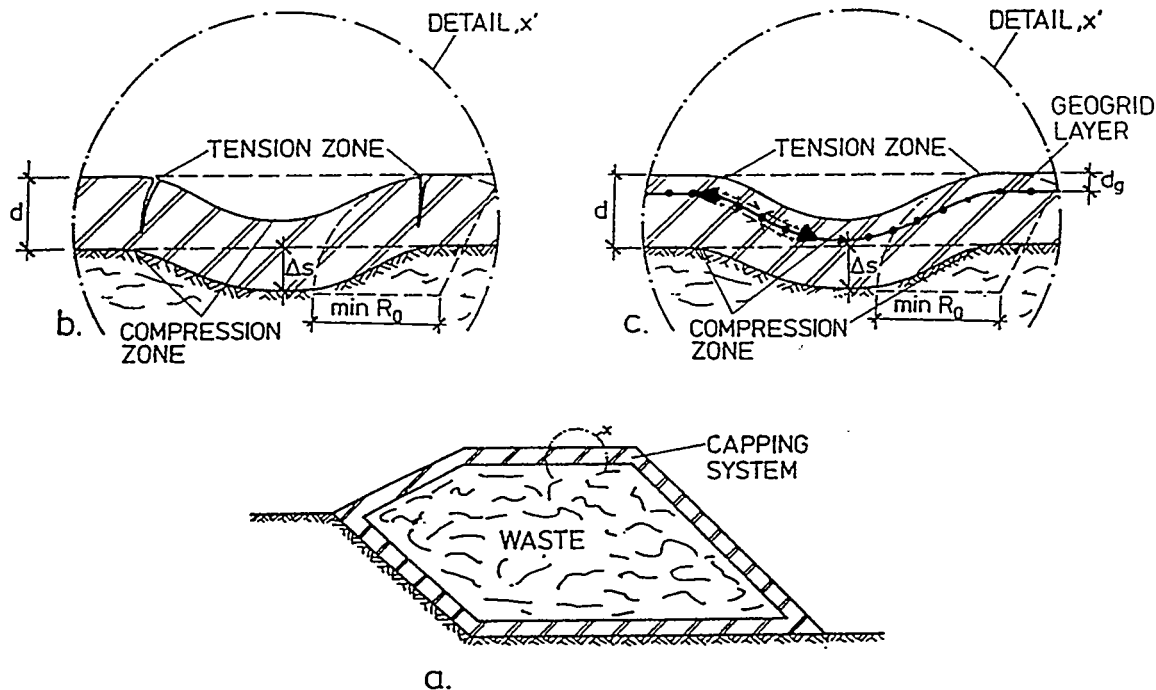
Fig. 1 Landfill capping system subjected to non-uniform settlements

It is evident from the literature review (Christie and El Hadi 1977, Chaudhari and Char 1985, and Smoltczyk and Henne 1991) that by introducing a geosynthetic material as a reinforcement within the soil system has positive influence, but the exact investigations dealing with the evaluation of the geosynthetic reinforcement and it's influence on the deformation behavior were not carried out. Many investigators (for e.g., Bourdeau et al.1982 and Espinoza 1994) have considered the influence of deformed geosynthetic layer as a tension membrane effect and the geosynthetic material is assumed to provide anchorage resistance by frictional forces away from the settled region. The mechanism by which tensile forces and strains are transmitted from soil to the reinforcement largely depends on the roughness characteristics of the embedded geosynthetic material, such as, geometry, opening size, stiffness, soil-reinforcement interaction and interlock. However, there is a lack of information about the crack propagation and soil-geosyntehtic bond efficiency in restraining the cracks.

3. Modeling and model test package

3.1 Centrifuge modeling

Centrifuge modeling, because of it's ability to reproduce identical stress levels in a small - scale model at those present in a full scale prototype, is a useful tool for the investigation of geotechnical problems (Schofield 1980). Since cracking is a condition heavily influenced by the presence of prototype stress levels, the application of centrifuge modeling is very significant. Centrifuge modeling also provides

excellent opportunities to change and vary boundary conditions during model investigations. Centrifuge scaling relationships have been extensively described elsewhere (Jessberger and Güttler 1988).

The geometry of the prototype, e.g. liner thickness, geogrid location from the top surface, curvature, etc., is scaled down in the model by a scale factor n = 50. Consequently, the tests were performed in an enhanced acceleration field of 50 gravity's. The selection of model geogrids has been carried out by considering the bandwidth characteristics of the prototype geogrids. The process of scaling down the prototype reinforcement to obtain model reinforcement has been discussed in detail by Bhamidipati (1996).

3.2 Equipment for centrifuge model testing

The centrifuge model tests were performed in a rectangular steel box of internal dimensions 848 mm long x 398 mm wide X 500 mm high. The front side is formed by a Perspex window through which deformations of the model can be photographically observed while the model is 'in flight' on the Centrifuge. In this strong box, a mineral sealing layer of a thickness 1.25 m and of a capping system area of approx. 850 m^2 of a landfill is modeled (Fig. 2). In order to generate a displacement profile at the base of the model mineral sealing layer a trap-door mechanism is fitted in the floor of strong box. Between the trap-door unit and the mineral sealing layer, thin layers of fine gravel and fine sand are placed in order to maintain the continuos displacement profile. The symmetrical trough shaped deformation profile is formed with a 1.25 m settlement at the center and the influencing length of 20 m in prototype dimensions respectively.
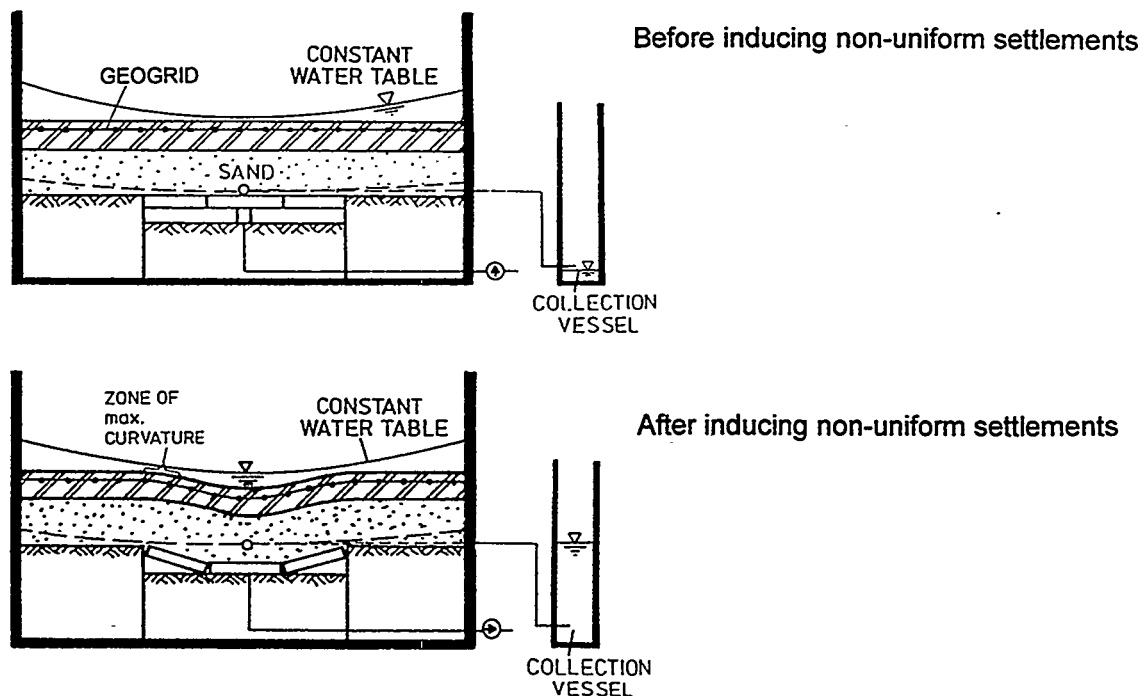
Fig. 2 Schematic diagram showing centrifuge model test package

The deformation behavior of the model mineral sealing layer was monitored during the centrifuge test by (i) Linear Variable Differential Transducers (LVDTs) located on the surface, (ii) two photo cameras observing the cross-section of the mineral sealing layer, and (iii) two video cameras mounted along with the model observe the surface and cross-section of the mineral sealing layer. The information recorded is used to arrive at the settlement contours and the corresponding strains in the cross-section. The permeability behavior of the mineral sealing layer is observed by (i) monitoring the water table on the surface and (ii) recording the amount of water passing through the mineral sealing layer, which is measured in the collecting vessel (Fig. 2).

3.3 Model preparation and procedure for centrifuge model testing

After all the internal components have been fitted into the strong box including trap-door unit a 37.5 mm thick layer of fine gravel overlain by a 37.5 mm thick fine sand is rained into the strong box. The speswhite kaolin clay was used a model material (Liquid Limit W_L= 45.85%; Plasticity Index I_P= 16.5%; Permeability k = 1x10^{-9} m/s) for the mineral sealing layer. Kaolin slurry (80 % by weight) was placed by hand to a predetermined depth over the sand layer. A consolidation unit was then attached to the strong box and the slurry was one-dimensionally consolidated with sequential load increments up to maximum consolidation pressure of 1270 kPa. In the case of centrifuge test with a reinforcement inclusion, two stage consolidation procedure was adopted. The procedure involves consolidating the slurry in the first stage, laying the model geogrid, and finally consolidating the slurry in the second stage. Finally, a mineral sealing layer of 25 mm thickness (model dimensions) is maintained.

After completing the consolidation phase a shallow trench was excavated in the consolidated liner. The provision of shallow trench on the top surface of the model sealing layer helps in preventing any sort of leakage's along the sides of the wall during the centrifuge test. A grid of discrete markers were fixed in the cross-section of the model sealing layer for subsequent digitization from 'in flight' photographs. A row of discrete markers were also fixed on to the geogrid by using an adhesive.

The centrifuge testing is carried out in two phases. In the phase I - (i) the soil is allowed to consolidate, which is recorded with the help of LVDT's installed on the surface of the mineral sealing layer and (ii) allowed the upper and lower water tables to stabilize (Fig. 2). The periodical settlement and observation stages have been maintained in the second phase. Once after attaining the steady state in the system, the step-wise lowering of trap-door unit and observation stage was carried out in phase II. The observation period, which was maintained represents a period of approx. 50 days in prototype dimensions. The lowering of trap-door starts at a predetermined rate of 1 mm/min. (model dimensions) until the full trap-door settlement is achieved.

3.4 Testing program

In the present study, three centrifuge model tests were reported. Table I gives brief specifications of each of three tests. The tests reported were without any overburden stress. Two types of model reinforcements - MGG1 and MGG3, were used in the present study. The model geogrid materials MGG1 and MGG3 representing prototype geogrids are with a secant stiffness of 3000 kN/m and 460 kN/m at 7 % strain respectively.

TABLE I Details of centrifuge model tests				
Test Code	Thickness of Clay liner d [mm]	Consistency Index I_c [-]	Geogrid location from the top surface d_g [mm]	Reinforcement type
BDS3	25	0.63	--	Un-reinforced
BDS4	25	0.64	5	MGG1
BDS7	25	0.73	5	MGG3

4. Results and discussion

Fig. 3 presents the observed cracking patterns for the mineral sealing layers without and with reinforcement inclusions after centrifuge tests. After reaching a settlement ordinate level a = 0.5m, the un-reinforced mineral sealing layer has started developing cracks in the tension zone (Fig. 3a). The occurrence of cracks take place in the present model along the convex side of maximum curvature zone, due to mobilization of maximum strain along the extreme outer fiber of the mineral sealing layer. The cracking is observed to be very distinct with one or two wide cracks. The observation of cracks were not noticed in the bottom portion of the sealing layer in the central region. This could be attributed due to (i) the interaction between the model sealing layer and the bottom sand layer and (ii) the self-weight of the mineral sealing layer. In the case of mineral sealing layer reinforced with a geogrid MGG3 (J_G = 460 kN/m at 7 % Strain), after attaining a = 0.5m, the sealing system was observed to crack in the maximum

curvature region (Fig. 3b). The cracking pattern and their distribution in the maximum curvature zone was found with small crack widths and at regular intervals of crack spacings. As shown in Fig. 3c, the mineral sealing layer reinforced with a geogrid MGG1 (J_G = 3000 kN/m at 7 % Strain), it is noted that the reinforcement has not allowed the soil to crack even after attaining the maximum settlement of a = 1.25m. Only a very tiny hair cracks of small width were observed at very closed spacings in the tension zones of the deformed reinforced mineral sealing layer (Fig. 3c). The reason for not able to observe formation of cracks in the mineral sealing layer reinforced with model geogrid MGG1 is due to good compatibility between soil and geogrid tensile strength characteristics.
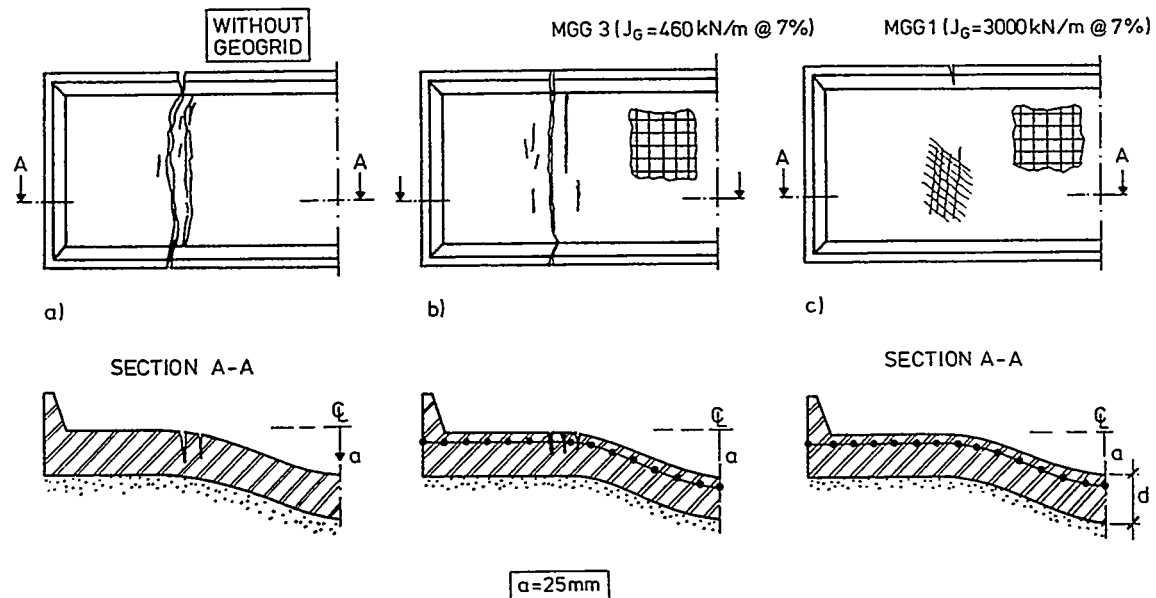
Fig. 3 Surface and Cross-section of the model mineral sealing layers after centrifuge tests

Fig. 4 shows the schematic representation of the dependence of the permeability of the clay liner on the settlement level and the curvature of the liner. The data is obtained by measuring the variations in and outflows with time during centrifuge test. As can be seen from Fig. 4, in the case of un-reinforced mineral sealing layer a un-controllable flow through liner is registered after reaching a = 0.5 m. Where as in the case of mineral sealing layer reinforced with MGG3, a marked flow through the liner is recorded and in the case mineral sealing layer reinforced with MGG1, a very negligible amount of change in the permeability of the liner is noted. The model reinforcement materials adopted in the present investigations have shown a significant influence on the deformation behavior of reinforced mineral sealing layers. By adopting a suitable reinforcement inclusion a continuous deformation behavior of reinforced mineral sealing layer is observed against the discontinuous behavior of the un-reinforced mineral sealing layer after reaching deformation limit.

The influence of induced deformations on the un-reinforced and reinforced mineral sealing layer can be assessed through the strain level across the cross-section of the mineral sealing layer. The outer fiber strain can be specified by the geometrical values of elongation and the curvature based on beam theory. By comparing the deformation behavior of the un-reinforced and reinforced mineral sealing layers and the experimental observations, it evident that in the case of mineral sealing layer reinforced with geogrid, a strain distribution has taken place in the tension zone due to soil - geogrid interaction. This has been further analyzed by comparing the strain levels in the geogrid and the soil at the soil - geogrid interface. As can be seen from Fig. 5, the response of reinforcement to all settlement levels is indicated that for a magnitude of strain in the soil, the geogrid tries to mobilize an almost equal amount of strain. The correlation between the soil strain and the geogird strain at the soil-geogrid interface suggests that in order to prevent the occurrence of cracks on the surface of the mineral sealing layer due to non-uniform settlements, the geogrid strain shall be 1 to 1.2 times the strain in the soil at the soil-geogrid interface. The observations made in the experimental investigations suggests that the role of reinforcement is to

provide adhesion due to soil - geogrid interaction, such that less strains are induced and tension is avoided. Based on the test results, it can be concluded that the extent of withstanding large tensile deformations depends mainly on the stiffness, geometry of the reinforcement and the stiffness of the soil.
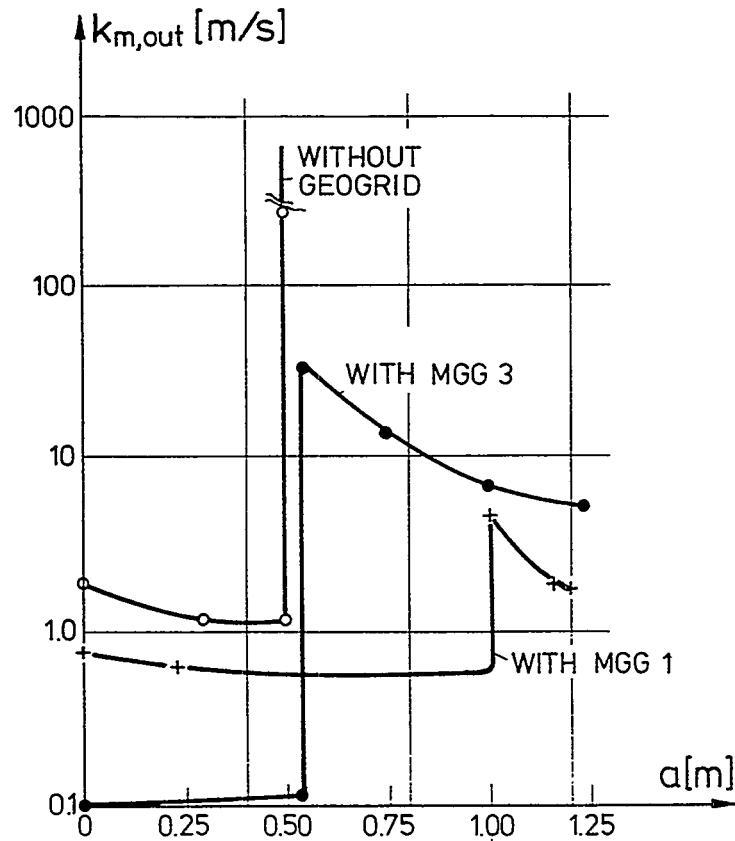
Fig. 4 Permeability behavior of the mineral sealing layers with and without geogrid
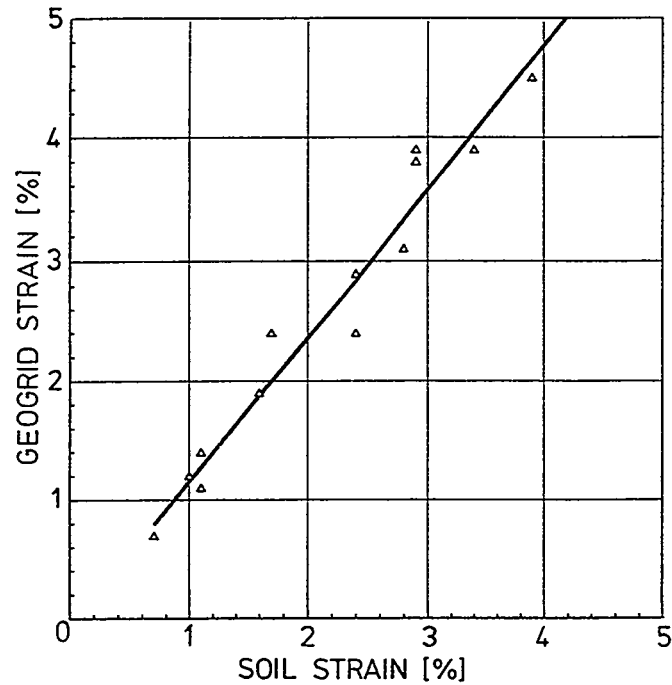
Fig.5 Strain in the soil and geogrid in the maximum curvature zone

5. Conclusions

From the model tests presented in this paper, the following conclusions can be drawn:

(i) The geosynthetic reinforced mineral sealing layers can withstand much greater tensile deformations without loosing it's sealing efficiency than the comparable mineral sealing layer without any reinforcement inclusion.

(ii) The extent of withstanding large tensile deformations depends mainly on the stiffness, geometry of the reinforcement and the stiffness of the soil.

(iii) The role of the reinforcement is to provide adhesion due to soil - geogrid interaction, such that less strains are induced and tension is avoided.

(iv) Further studies have to be focused on the theoretical considerations involving soil - geogrid interaction. However, in the case of non-availability of suitable sealing material, low overburden stresses, and large non-uniform settlements the reinforcement of mineral sealing layer seems to be an alternative solution to improve the deformation capacity.

References

Bhamidipati, V. V. S. (1996) Geosynthetic Reinforced Mineral sealing layers of Landfills. Sr. Nr. 28, Dissertation of the Institute for Soil Mechanics and Foundation Engineering, Ruhr University Bochum, Germany.

Bourdeau, P. L., Harr, M. E., and Holtz, R.D. (1982) Soil-Fabric Interaction- An analytical model. Proc. of 2nd Int. Conf. on Geotextiles, Vol. II, Las Vegas, pp.387-391.

Breardiol, A.W., Martin, J.P., Cheng, S.C., and Tull, C.F. (1995) Flexural cracking of compacted clay in Landfill Covers. Geoenvironment 2000, vol.2, ASCE, Geotechnical special Publication Nr. 46, Proc of the Specialty Conference sponsored by Geotechnical Engineering and Environmental agency, New Orleans, Louisiana, Feb. 24-26, 1995, pp 914-931.

Chaudhari, A.P., and Char, A.N.R. (1985) Flexural behavior of Reinforced Soil Beams. Journal of Geotechnical Engineering, ASCE, Vol. 111, No.11, pp. 1328-1333.

Christie, I.F., and El Hadi, K.M. (1977) Some aspects of the design of earth dams reinforced with fabric. Proc. of C.R. Coll. Int. Soils. Textiles, Paris.

Daniel, D.E.(1983) Shallow Land Burial of Low-Level Radioactive waste. Journal of Geotechnical Engineering, ASCE, Vol.109, No.1, pp.40-55.

Espinoza, R. David. (1994) Soil - Geotextile interaction: Evaluation of Membrane support, Journal of Geotextiles & Geomembranes, 13, pp. 281-293.

Jessberger, H.L., and Güttler, U.(1988) Bochum Geotechnical Centrifuge, Proc. of Centrifuge 88, Paris, 25-27 April, France, pp. 37-44.
8
Jessberger, H.L., Stone, K.J.L. (1991) Subsidence effects on Clay barriers. Geotechnique, Vol.41, No.2, pp.185-194.

Scherbeck, R., and Jessberger, H.L. (1993) Assessment of deformed mineral sealing layers, Proc. Waste Disposal by Landfill-Green'93, eds. Sarsby, pp. 477-486.

Schofield, A.N. (1980) Cambridge Geotechnical Centrifuge Operations, Geotechnique, Vol. 30, No. 3, pp. 227-268.

Smoltczyk, U., and Henne, J. (1991) Criteria for evaluating geotextile reinforced clay liners supporting wastes on compressible foundations- Summary of an ongoing study. Proc. of the 10th Eur. Conf. on Soil Mechanics and Foundation Engineering, 26-30 May, Florence, Balkema, pp. 563-567.

Chapter 9

Grouting

Progress in Forming Bottom Barriers Under Waste Sites

By: Ernest E. Carter,P.E. CARTER TECHNOLOGIES
9702 Garden Row
Sugar Land, Texas
Fax 281-495-0540
voice 281-495-2603

ABSTRACT

The paper describes an new method for the construction, verification, and maintenance of underground vaults to isolate and contain radioactive burial sites without excavation or drilling in contaminated areas. The paper begins with a discussion of previous full-scale field tests of horizontal barrier tools which utilized high pressure jetting technology. This is followed by a discussion of the TECT process, which cuts with an abrasive cable instead of high pressure jets. The new method is potentially applicable to more soil types than previous methods and can form very thick barriers. Both processes are performed from the perimeter of a site and require no penetration or disturbance of the active waste area. The paper also describes long-term verification methods to monitor barrier integrity passively.

INTRODUCTION

There are many sites with buried radioactive waste or underground tanks which are now considered to pose a hazard to groundwater but which are dangerous or enormously expensive to remove. A better alternative may be to develop a means of constructing a verifiable containment barrier around and under these sites. Jet grouting has been used to successfully construct arched horizontal water barriers 15 meters below ground level. This was done by Halliburton Services in preparation for tunneling portions of the Washington Subway in 1989. This type of barrier is 99 percent effective but this may not good enough because it is hard to verify. To be accepted, a method must be 100 percent effective and also verifiable.

Several tests were performed between 1992 and 1995 in an attempt to demonstrate the feasibility of constructing a horizontal barrier by means of a SoilSaw™ type process in which jet grouting hardware physically moves through the entire volume of the barrier. This concept is preferred because it does not depend on the unverified penetration of fluid jets between adjacent holes. The TECT™ Process[1] now under development, builds upon the experience gained in the prior work and also increases the scope of the work beyond horizontal barriers to that of in situ construction of full vault structures around a buried waste with passive leak detection.

---

[1] TECT is a trademark of Carter Technologies

EARLY WORK

In late 1992 a preliminary test of the concept of horizontal barrier construction was funded by Halliburton NUS Corporation. The concept was based on the SoilSaw™ Barrier System[2] technology which is essentially a special type of linear Jet Grouting. The method uses high pressure jets of grout slurry to cut the soil and blend it into a homogenous slurry which must flow around the apparatus as the device advances through the ground. In the vertical SoilSaw™ System, a heavy steel pipe with multiple jet nozzles on its underside, is reciprocated to liquify the soil with a high energy blast of cementitious slurry. The beam sinks in on its free end to a 45-degree angle. As the machine advances through the soil, it leaves a mixed-in-place barrier wall behind it. Early tests showed production rates in excess of 10 square meters per minute (100 square feet per minute), and the ability to hold a very uniform vertical wall thickness in soft wet soil.

The basic horizontal panel construction concept tested, was performed by placing multiple directionally drilled parallel pipes under the waste site, describing the path of a barrier to be constructed. In the early tests the directional drilling was simulated by placing the pipe in an excavated and surveyed trench and backfilling the trench. The pipes, which pass in a long arc under the waste site, describe the edges of the horizontal grout panel to be constructed. A jetting tool with multiple soil cutting nozzles was attached to the end of two adjacent pipes. By mechanically pulling on the pipes at the other end, the cutting tool was advanced into the soil, cutting and mixing the soils in its path with the grout slurry. The cutting tool pulls another pipe behind it which stays within the liquid panel and becomes the "pulling" pipe for the next panel. This helps assure that the next pipe is always joined to the previous one.

These early tests were based on two simple "tools." The first was a "rigid bar" tool which had 64 forward facing jet nozzles across its 2.74 meter (9-foot) width. The tool was about 7.5 cm (3 inches) thick and extended 15 cm (6 inches) to either side of the pulling pipes. The second tool was a "rotating bar" tool with jet nozzles at a 15-degree angle from the axis of the tool, which were rotated around the axis of the tool by a hydraulic motor. This tool was about 22.5 cm (9 inches) thick and cut a path about 3 meters (10 foot) wide. These tools were designed, built, and tested with a small budget and a very short 90-day timetable for design, construction and testing. Neither one of these tools had the same type of cutting action and efficiency as the vertical SoilSaw™, but they could be constructed quickly. The grout used in making these panels was a cement kiln dust mixed to a specific gravity of 1.7 (about 13.9 pounds per gallon). This grout was cheap and useful for testing but was not expected to offer good properties for a real barrier.

1992 FIELD RESULTS

The soils at the Duncan, Oklahoma test site were composed of compacted grey sands which were far too hard to read on a pocket penitrometer, which can only register about 4,900 kg/ sq meter (5 tons per square foot.) It was estimated that the actual hardness was about 9,800 kg /sq meter (10 tons per square foot.) The soil also contained many lumps of harder sandstone rock and red clay.

The rotating bar tool was tested first and appeared to cut very slowly, with an advance rate of one to two feet per minute. The tool returned about 3 volumes of waste grout for every volume of panel formed. Pulling force on the tool was about 9,100 kg (10 tons) of force. It did form a cut approximately 35 cm (14 inches) thick with a surface roughness of plus or minus 2.5 cm (1 inch) on both top and bottom. The swivel on the tool was prone to mechanical failure and had to be repaired about every 3 meters (10 feet) of travel. On its last run the tool suffered a catastrophic failure deep underground after having traveled less than 12 meters (40 feet). A cross section cut across the path of this tool shows a very substantial and impressive panel. A section of this panel about 3

---

[2]SoilSawTM Barrier System is a trademark of Halliburton NUS Corp.

432

meters (10 foot) square was excavated and brought to the surface.

The rigid bar tool proved quite durable and succeeded in making two sets of joined panels approximately 30 meters (100 feet) long and three panels wide. The 2.74 meter (9-foot) wide tool could be pulled through the ground at about 4 meters (13 linear feet) per minute. On the third panel, the progress of the tool would frequently be stopped and could only be restarted by pulling harder or in some cases by backing up the tool by pulling on the other end. The pulling unit was a 18,000 kg (40,000 pound) class trackhoe. Maximum pulling force was measured at about 20,000 pounds. The stoppage was believed to be caused by pulling the bar too fast for it to make a complete thickness cut. Excavation showed excessive rock in the path of this panel. The tool had 64 jets of 2 mm (.078 inch) diameter operating at about 246 kg/sq meter (3,500 psi).

Large 10 meter (30 foot) square areas of both sets of panels were excavated and washed with a high-pressure water hose. The panels were very rough and had inclusions of rock. They also had clay stuck to the surface of the panel which was not removed by the high pressure water. The joint between adjacent panels appeared to be continuous and as sound as the body of the panels. The thickness of the panels varied from 3 cm to 32 cm (one inch to six inches) thick. It was not possible to conclusively determine that there were no actual holes through the barrier because of the tightly adhering clay and rocks. No permeation testing was performed. The visual quality of the panels was poor since they were very rough and fractured easily when excavated. About 60 meters (200 linear feet) of cross section cut was made without any convincing evidence of a hole in the panels. A hole due to subsidence is a strong possibility because the grout used in the test was too low a density to support the overburden weight. The cutting action of this tool was far from optimal and resulted in pressure increases within the area around the tool. This caused several eruptions in which liquid grout fractured to the surface. In general these two tests verified that horizontal barrier construction was possible but they also demonstrated the necessity of grout density control and longitudinal jet movement to obtain uniform barrier thickness.

SECOND GENERATION TOOLS

In mid 1994 a second series of tests funded by DOE, was performed using a new rigid bar tool and two new "second generation" tools. Both of these new tools attempted to provide jet movement longitudinal to the cut in the manner of the vertical SoilSaw™.

The "mechanical reciprocating" tool consisted of a box-like steel frame with a moving "jetting head" which reciprocated laterally across the face of the cut. The reciprocation of the jetting head was powered by reciprocation of a steel rod inside one of the pulling pipes. Movement of the rod operated a cable and pulley system which reciprocated the jetting head across the face of the tool on a brass "V" block. The other pulling pipe provided the high pressure grout slurry to the tool. This tool provided a cutting action very similar to the vertical SoilSaw™ and was designed to cut a 30 cm (12-inch) thick path between pulling pipes spaced 3 meters (10 feet) apart and also to cut an additional 15 cm (6 inches) outboard of each pulling pipe. The tool was designed to work in both sand and clay soils and to swallow and pass rocks up to football size with ease.

The "flex tool" was a catenary design in which the tool consists of a flexible member forming a "U" shape between the two pulling pipes. Opposed reciprocation of the pulling pipes causes the jetting elements of the tool to move laterally around the face of the cut. The flex tool concept appears mechanically simple since it has no moving parts. Operation of the flex tool is complex and depends in frictional conditions, soil bearing conditions, and properly sequenced mechanical pull on the pulling pipes. The flex tool concept is intended for large full scale barriers cutting panels a minimum of 50 meters wide. The flex tool concept allows a very large spacing between adjacent directional drilled holes as well as much greater tolerance in positioning of these holes. The test program, however, specifically called for a tool to operate between pulling pipes spaced 3 meters (10 feet) apart. The miniature flex tool was designed to meet this goal by using high pressure hoses to carry the fluid and spring steel as the tensile body of the tool.

A new rigid bar tool was also constructed which was essentially a 7.5 cm (3 inch) diameter pipe with jets every 5 cm (2 inches) across its 3 meter (10 foot) width.

1994 FIELD TEST RESULTS

The test area selected for this work was only a few hundred yards away from the previous one but it contained a hard, red clay soil. This soil was significantly tougher than the soils in the previous tests and was intended to qualify the tools for additional testing at a DOE (FERNALD) site known to have clay soil. (The FERNALD soil was actually classified as glacial till but it had the physical properties of hard, impermeable, sticky clay.) All of the tools failed to perform for different reasons. The rigid bar tool was unable to cut a complete path between adjacent jets and thus could not advance reliably. The tool was destroyed during this test. The old rigid bar tool was then pressed into service, and while it proved indestructible it also failed to advance through the hard clay soil even though it was pulled by a large D-6 dozer.

The other two tools appeared to cut well enough but suffered unrelated mechanical breakage. The Flex tool was set up but failed to reciprocate as planned. Apparently, after the first few strokes the curvature geometry of the cut became distorted and resulted in breakage of the tool. Insufficient data was recorded to determine the exact cause of the failure, but it was believed that the 1.5 meter (5 foot) radius of the catenary was simply too small for this type of tool.

The mechanical reciprocating tool was then set up and tested briefly. The internal cable pulley tensioner on the unit was insufficient to allow the device to make a full stroke under pulling load. The jet pattern on both of this and the Flex tool appeared to cut a sufficient path for passage of the tool but it was apparent that repairs or adjustments on the tools would be required for them to work properly.

1995 FIELD TESTS

With renewed DOE funding, the flex tool was modified to operate on a 9 meter (30 foot) wide cut and was taken to the field again in 1995. A redesigned version of the rotating tool was also commissioned and built. The new rotating tool was powered by a mechanical drive shaft and had mechanical teeth as well as high pressure jets. Instead of a full-scale field test these tools were tested by jetting with plain water while puling the tools through a pile of loose dirt. This was done to reduce the expense of a full scale test and allow more time for modification of the tools in the field. During initial testing the rotating tool developed problems due to the large amount of power transmitted through the long drive shaft and was abandoned in favor of the more promising flex tool concept. The 9 meter (30 foot) wide flex tool suffered some initial breakage problems but was later modified by increasing the flexibility of the areas prone to breakage. This tool showed promise in the testing to date, operating as designed and making several 30 meter (100 foot) long runs through shallow undisturbed native ground using only water through the jets. This tool cut at a rate of about 50 square feet per minute. Since water was used as the cutting media, no barrier was constructed. No additional funding has become available for testing this tool with grout. At this writing no additional work is scheduled.

ANALYSIS

The jetted barrier techniques described have thus far seen insufficient testing to demonstrate their promise. Of the systems tested, the flex tool appears to hold the most promise. Development should focus on the full scale 30 to 50 meter wide version. Large rocks, significantly bigger than the thickness of the barrier may be a problem. Plugging of the jet nozzles due to debris in the system is also an issue requiring constant preventive measures. Design improvements in the

hardware are needed to provide the ability to recover from breakage or plugging of the tool under ground. One barrier to development of the past approaches is the expense of field testing. This technology is difficult to simulate at small field scale. The optimum width of a panel is about 100 times its thickness. A new full scale jetting tool is currently proposed for DOE funding which will try to solve these problems as well as synergistically incorporating many of the concepts described below.

BUOYANT BARRIER CONCEPTS

Another type of advanced barrier construction method under development is the buoyant lift concept. Plate Tectonics describes the continents of the earth as plates floating on dense molten fluid. Buoyant lift barriers utilize a special ultra-high-density grout injected into a thin basin-shaped cut to float the entire waste site upward on a thick layer of the grout. When this grout hardens, a continuous barrier basin layer is created under the waste site. In the TECT™ Process[3], a buoyant lift barrier is formed by a mechanical cutting cable which operates between guide pipes in directionally drilled holes. Each guide pipe has several parallel steel cables banded to it before it is drawn into the hole. One cable from each pipe is joined together into a continuous loop. This cable is placed under tension and circulated like a band saw, to cut a path between the guide pipes.

Instead of cutting and mixing a thick layer of the native soil, this process makes only a thin horizontal cut. As the cut is made, a very low viscosity, but very dense grout is pumped into this cut from portals in the guide pipes. The guide pipe's portals are repositioned as the cut proceeds. This dense grout flows back to the surface through the annular space between the pipe and the hole as it carries cuttings and heat back to the surface. It also supports the weight of the soil and rock above the cut and causes the soil block to rise buoyantly on the free end. Additional grout flows into the cut from a trench around the perimeter. The grout is more dense than the soil overburden and causes large unsupported areas to rise upward. Mechanical anchors keep the floating block centered in the cut and help keep the lift even and level. This process can produce 1 meter thick barriers which are made from essentially pure grout with no soil content to limit their physical properties. Since grout is not wasted as in high pressure cutting, the new process is expected to produce little if any waste.

FRACTURING

Hydraulic Fracturing has been suggested as a means for creating a horizontal cut and even heaving a block upward. Fractures propagate along the planes of least principle stress and thus depend on existing soil conditions more than the skill of the contractor to determine the direction and orientation of final position the fractures. The trouble with fracturing is that there is no way to prevent a fracture from following an existing plane of weakness in the soil which may cause it to enter a contaminated soil and then erupt to the surface. It is also difficult to confirm that a continuous plane has been created. It is also difficult to be sure that the fracture will not close again after it is opened. Use of a dense grout instead of pressure is a subtle but important distinction. A grout with specific gravity of 3.0 is dense enough to float a typical soil block. The basalt rock in Idaho has a 2.5 average bulk density.

Forming barriers with dense grout is unlikely to increase the size of any fractures in rock above the cut. If the grout should enter an existing fracture or fissure in the floating block, it will fill up the fracture without enlarging it.

When working in rock layers such as columnar basalt which contains large vertical fractures it is

---

[3] TECT is a trademark of Carter Technologies

possible for these fractures to consume an virtually unlimited volume of a low viscosity grout. To address this condition, a specially configured guide pipe with a floating piston valve, is used to inject an alternating flow of cementitious grout and a super set accelerator. These two materials react to cause an "instant set" in portions of the grout, which is then capable of plugging desk-sized chasms. Another means is the use of thixotropic grouts which are fluid when moving or shaken but quickly gel when their flow velocity decreases as they enter a fracture network.

GROUTS

The TECT grout is a cementitious grout which is extensively modified with additives to increase its ductility and decrease its permeability. Specific density is about 3.0 but can be adjusted for the application. The grout remains fluid for several weeks but eventually hardens to a ceramic-like product. After approximable 12 months of curing, the grout approaches its final matrix condition which is thermodynamically stable and resistant to chemical attack. This grout was developed for arid climates. The grout is significancy less permeable than cement or cement/bentonite materials. Permeability is approximately 1×10^{-8} cm/sec. A similar grout is under development which will be designed to remain soft and plastic. These grouts are much more costly than plain concrete, but at a typical cost of three to five dollars a gallon are still economical compared to chemical grouts.

HDPE SYNTHETIC LINER

Once the block of soil containing the waste site is severed from the earth, and floating free on a half meter (20 inch) thick layer of grout, a series of chains may be attached to the guide pipes and pulled under the floating block to verify continuity of the barrier. New sections of guide pipe are pulled in as old sections are pulled out. Large one-piece sheets of HDPE liner are then attached to the guide cables by flexible strips and pulled under the floating block. Single sections of HDPE liner joined by a sliding mechanical interlock joint, may also be pulled under the block to form a complete bottom liner. The HDPE sheet would be folded over the berm surrounding the block. After the grout hardens, which takes about 3 months, an airtight cap structure is constructed by conventional methods. This bottom liner may be joined to a top HDPE liner by heat fusion welding to form an air-tight seal. The multi-layer cap above this would consist of layers of clay and soil doped with bitter tasting chemicals and covered with a structural concrete cover, buried below the frost line.

PROCESS VERIFICATION AND LONG TERM MONITORING

Because a continuous cutting member has passed through the entire barrier surface, the continuity of the barrier is initially verified by its passage. After a barrier panel has been formed and lifted to its full thickness, it is possible to drag a chain or other mechanical proving bar through the liquid panel to verify that it is continuous and has no "holes". Also the visible heave at the ground level provides compelling evidence that the barrier has reached full thickness.

Once a barrier basin has been constructed it is important to be able to continue to demonstrate the integrity of the barrier on a regular basis. This can be done by constructing an airtight vault and monitoring changes inside the vault versus changes outside the vault. If a basin barrier is formed with TECT™, (or some other process which forms an airtight basin), an airtight cap can be added by conventional methods. A structural and airtight cap is instrumented with atmospheric pressure sensors, humidity sensors, sound sensors, and fluorocarbon tracer gas sensors. By monitoring records of the differences in fluctuations of these variables inside and outside the barrier, the continued integrity of the barrier can be passively assessed.

Various sensors would be installed below the cap to monitor soil gas pressure, humidity, chemical concentrations, and sound. External buried sensors and cap mounted sensors will measure atmospheric pressure, and other corresponding values such as ground temperature. A data logger

436

will record these values over many years along with rainfall and other data. Analysis of this data stream over many years will serve to verify continued integrity of the barrier vault. Build up of decomposition gas from the waste, if any, may be withdrawn through a vent pipe on a regular basis. Tracer gas or odor chemicals may be introduced into the vault to allow maintenance surveys to locate leakage.

CABLE SAW EQUIPMENT

One method for making the initial cut for a buoyant lift barrier is the Diamond Wire Cable Saw. Diamond wire saws have been used in rock quarry work for over 25 years. A power driven pulley pulls a continuous diamond studded cable through a drilled channel with coolant circulation to remove rock chips and heat. In solid rock, the maximum area of a cut is a function of wear rates and the length of the wire available. In soil, the wear on the cable is significantly reduced and it should be possible to make cuts as large as 15 meter (50-foot) wide by 150 meter (500-foot) long with ordinary aircraft cable roll lengths. The cable is spooled on a surface mounted unit. Replacement of broken cables is performed by pulling an additional cable into the cut and re-weaving the ends into a continuous loop. Failure of any mechanical system during the work can be overcome by pulling a new unit into place with the extra cable on the guide pipes.

FIELD EXPERIENCE

A full-scale buoyant barrier using wire saw cutting has not yet been demonstrated in field scale. Football-sized basalt rocks have been floated in buckets full of the TECT grout. In the previously described horizontal barrier tests, it has been observed that when a low density liquid grout panel is formed, that the overburden pressure will squeeze out the grout and allow the overburden soil to subside. It was also observed that allowing pressure to develop in the freshly formed horizontal panel will cause the ground to heave as the thickness of the panel increases. In these tests, this additional pressure also caused fractures to break through to the surface in soil having planes of weakness. If similar subsurface pressure was generated by the hydrostatic head of dense fluid at grade level, fracturing would not occur within the floating block, because the forces would be balanced. Existing voids and passages would do no more than fill with grout to the level of the grout in the perimeter trench.

PROCESS COMPARISONS

Problems in construction of horizontal barriers by the SoilSaw™ method include the problem of rocks and unexpected soil conditions. Geological data from borings is frequently incomplete or misleading because "toughness" of a soil is difficult to quantify. Toughness is the amount of jetting energy a material can absorb. Current SoilSaw™ based systems which cut with high pressure jets are very sensitive to soil toughness. Another significant problem in development of these jetting technologies is the scale at which they must be tested. These systems are difficult to test without using full scale equipment. This testing requires a large amount of equipment to be mobilized and large volumes of highly perishable liquid grout materials to be blended.

The TECT buoyant lift process may avoid both these problems. Since it cuts soil mechanically with a cable saw, it is expected to be less sensitive to soil toughness. It is expected to be more tolerant of rocks. The TECT™ process was originally proposed to form barriers in solid rock. The concept can be inexpensively tested in small scale and then scaled up with fewer uncertainties. One significant advantage of the concept is that it does not require high pressure grout pumping systems and should therefore cost less to construct. Also there are no small jet orifices to plug. The most important feature of TECT is the HDPE enhanced, airtight liner and cap system which not only assures current integrity but allows continual passive monitoring of the vault.

MATHEMATICAL MODELING OF PERMEATION GROUTING AND SUBSURFACE BARRIER PERFORMANCE

S. Finsterle, C.M. Oldenburg, A.L. James, K. Pruess, and G.J. Moridis

ABSTRACT

The injection of solution grouts into the subsurface can be used to form underground barriers for the containment of contaminants. The technology requires identifying suitable grout materials, specifically fluids which exhibit a large increase in viscosity after injection and eventually solidify after a controllable period, thus sealing permeable zones. We have developed a new fluid property module for the reservoir simulator TOUGH2 to model grout injection, taking into account the increase of liquid viscosity as a function of time and gel concentration. We have also incorporated into the simulator a model which calculates soil hydraulic properties after solidification of the gel within the pore space. The new fluid property module has been used to design and analyze laboratory experiments and field pilot tests in saturated and unsaturated formations under a variety of subsurface conditions. These applications include modeling barrier emplacement in highly heterogeneous soils in the vadose zone, grout injection into the saturated zone in combination with extraction wells for flow control, the design of verification strategies, and the analysis of barrier performance. In this paper we discuss the modeling approach and present simulation results of multiple grout injections into a heterogeneous, unsaturated formation.

1. INTRODUCTION

The injection of solution grouts into the subsurface is a technique used to encapsulate pollutants, to emplace underground barriers for containment of contaminant, and to prevent the spread of existing plumes. Furthermore, on-site containment and control of ground-water flow patterns can prevent off-site migration during active cleanup operations, and may increase the efficiency of traditional remediation techniques. A number of barrier fluids have been identified as suitable for permeation grouting of soils in both the saturated and unsaturated zone. These fluids exhibit a low initial viscosity which increases at a controllable rate after injection. The grout eventually solidifies, sealing the permeable zones of an aquifer. Work on the identification of appropriate barrier fluids and the generation of basic knowledge on their rheological properties is reported in Moridis et al. (1994). We will focus here on an aqueous silicon-based chemical grout, the gelation of which is induced and controlled by increasing the ionic strength of the gelling agent.

Numerical models are tools for the design of subsurface barrier systems, the optimization of the emplacement strategy, and the assessment of the barrier's integrity. Computer programs designed to simulate in-situ gelation for the application of enhanced oil recovery have been previously presented (Scott et al., 1985; Hortes, 1986; Todd, 1990). The main emphasis in these works is on the kinetics of the gelation process. We are interested in the performance of shallow barriers emplaced in both the saturated and the vadose zone. Each application poses its specific problems. In the saturated zone, the dilution of the solution grout by native water has to be considered. Emplacement issues such as the absence of strong gravity effects and the question of how to achieve complete volumetric coverage between injection ports and near plume boundaries require special attention (Moridis et al., 1996). Due to space limitation, we focus here on vadose zone applications. When grout is injected into unsaturated soils, the grout plume slumps under gravity and spreads due to capillary forces, leaving the soil only partially saturated. The reduction of porosity and permeability is thus a function of final gel saturation, and multiple injections may be required to achieve complete filling of the pore space. Modeling these processes includes the simulation of multiphase flow effects, the concentration and time-dependent increase of viscosity of the grout-water mixture, and a model description of the hydraulic properties of the partially grouted soil.

Lawrence Berkeley National Laboratory, Earth Sciences Division, University of California, One Cyclotron Road, Mail Stop 90-1116, Berkeley, CA 94720, (510) 486-520, SAFinsterle@lbl.gov

For the purpose of this work, we have extended the capabilities of the TOUGH2 code (Pruess, 1987; 1991), a numerical simulator for non-isothermal flows of multicomponent, multiphase fluids in porous and fractured media. In this paper we describe the physical processes considered and the modeling approach used for the development of the numerical simulator, and discuss its application for the design of a subsurface barrier system.

2. MODELING APPROACH

2.1 Process Description

Injection of a water-based grout into an unsaturated porous medium leads to a system which consists of three separate phases, namely the solid grains, a non-condensable gas, and an aqueous phase containing chemical grout in dissolved or colloidal form. After the initiation of the gelling process, the viscosity increases, turning the gel-water mixture into a non-Newtonian, visco-elastic fluid that eventually solidifies. The appearance of a new phase, i.e. the solidified gel, leads to changes in the physical and chemical properties. Contact angles and interfacial tensions vary with the chemical properties of the gel-water mixture, and adsorption and filtration of gel clusters may occur. By the time the grout is completely gelled, the resulting "new" porous medium has a lower porosity, a new pore structure, reduced permeability, and different wettability characteristics.

Controlled barrier emplacement becomes very difficult if the gelation kinetics are significantly affected by the soil mineralogy or pore water chemistry. Detailed knowledge about chemical and hydraulic heterogeneity over a range of scales would then be required to predict the behavior of the gel. A robust technology therefore relies on a solution grout material that is minimally affected by pH, salinity, and activity of the soil and pore water. In this case, no need for chemical interaction modeling arises. We use surface-modified colloidal silica grouts especially manufactured for this type of application. In our modeling approach, the following major assumptions are made:

(i) The chemical process of gelation is not explicitly modeled. Instead, we calculate the viscosity of the liquid phase as a function of grout concentration and time. The viscosity of pure grout as a function of time is measured in the laboratory and represented by a *gel time curve*. Mixture viscosity varies with the concentration of gel in the aqueous phase, and is described by a *mixing rule*.

(ii) The grout is treated as a miscible, aqueous solution, i.e. it does not form a separate phase. After completion of the gelling process, we assume that the gel, which is a fluid of very high viscosity, solidifies. By doing so, the porosity of the grouted soil is reduced. The new porous medium thus has a lower permeability and different characteristic curves in the region affected by the grout. The transition of the grout from a highly viscous fluid to a solid part of the matrix is described by the *solidification model*.

(iii) Injection and redistribution of grout in the unsaturated zone is modeled using TOUGH2 (Pruess 1987; 1991). We consider multiphase flow of the three components water, air, and chemical grout. Flow processes account for relative permeability and capillary pressure effects, and allowance is made for appearance and disappearance of phases and components. The empirical gel time curve and mixing rule are used to describe liquid phase viscosity. The solidification model describes the transformation of viscous gel into a "new" porous medium.

The conceptual approach as well as the specific quantitative correlations described in the following sections are in need of detailed testing through laboratory and field experimentation.

2.2 Gel Time Curve and Mixing Rule

Within the unsaturated zone, the pore space is occupied by two fluids: the gaseous phase, consisting of air and water vapor, and the liquid phase which is composed of water, grout, and dissolved air. The viscosity of the liquid phase depends on grout concentration and time. The increase of pure grout viscosity as a function of time is described by the gel time curve, a

parameterized function which can be fitted to laboratory data. Based on the measurements of Moridis et al. (1994) we suggest the use of an exponential function of the form

Gel Time Curve: $\qquad \mu_{gel} = a_1 + a_2 \cdot \exp(a_3 \cdot t)$ (1)

where t is time, and a_1, a_2, and a_3 are fitting parameters. After injection, the grout suspension will be diluted due to mixing with pore water. The mixing rule calculates the viscosity of the liquid phase, μ_l, as a function of gel concentration, X_l^{gel}, and time. One of the following mixing rules can be used:

Linear Mixing Rule: $\qquad \mu_l = X_l^{gel} \cdot \mu_{gel} + \left(1 - X_l^{gel}\right) \cdot \mu_w$ (2)

Power-Law Mixing Rule: $\qquad \mu_l = \left(\dfrac{X_l^{gel}}{\mu_{gel}^{\,b}} + \dfrac{1 - X_l^{gel}}{\mu_w^{\,b}} \right)^{-1/b}$ (3)

Figure 1 shows the viscosity of the liquid phase as a function of time and gel concentration. The upper part of Figure 1 shows the viscosity measurements for a colloidal silica gel (symbols). The solid line is the fitted gel time curve (Eq. 1) which provides the viscosity as a function of time for pure gel (X_l^{gel}=1). A linear mixing rule (Eq. 2) has been applied and is visualized in the lower part of the figure where viscosity (in centipoise) of the liquid phase is contoured as a function of gel concentration and time. Strictly speaking, the concepts of a gel time curve and mixing rule are only meaningful as long as the grout is completely miscible with water, and as long as the grout-water mixture is Newtonian. For practical purposes, however, this model is reasonable since grout plume movements are very slow once a high viscosity has been reached.
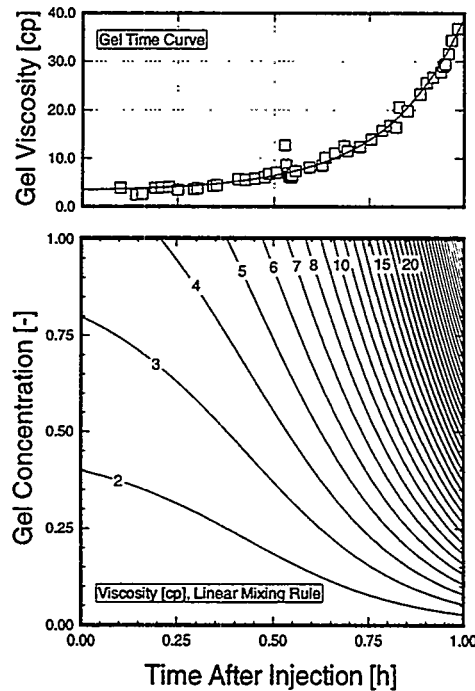
Figure 1. Viscosity in centipoise of pure gel as a function of time (gel time curve) and gel concentration (mixing rule).

2.3 Solidification Model

As discussed above, the gel is modeled as a liquid, the viscosity of which increases with time as gelation proceeds, until solidification occurs. After complete solidification, the soil exhibits new

440

properties that must be derived based on assumptions about the pore structure of the partially grouted soil. The parameters to be recalculated are porosity, permeability, relative permeability and capillary pressure functions, and initial liquid saturation. All these properties are a function of the final grout content prior to solidification.

The Solidification Model is based on the assumption that all of the liquid in the pore space eventually solidifies if the grout in the liquid phase exceeds a certain minimum concentration, X_{min}^{gel}. We introduce a parameter A as follows:

$$A = 1 \qquad \text{for} \qquad X_l^{gel} \geq X_{min}^{gel} \qquad (4a)$$

$$A = \frac{X_l^{gel}}{X_{min}^{gel}} \qquad \text{for} \qquad X_l^{gel} < X_{min}^{gel} \qquad (4b)$$

Setting X_{min}^{gel} to 0.2, for example, means that all the liquid with a gel concentration greater than 0.2 eventually solidifies. The fluid with lower gel concentrations solidifies incompletely.

The liquid saturation at the time solidification occurs is denoted by S_l^{sol}. All soil characteristics and initial conditions referring to the new porous medium are denoted by a star (*). The porosity of the grouted medium is reduced by the amount of gel that solidifies:

$$\phi^* = \phi(1 - A \cdot S_l^{sol}) \qquad (5)$$

The porosity reduction leads to a decrease of absolute permeability. The partial clogging of the pore space by grout is conceptually similar to the permeability reduction due to phase interferences in a multiphase flow system. The Permeability Reduction Model (PRM) describes the permeability reduction as a function of the solidified grout saturation:

$$k^* = k \cdot PRM \qquad (6)$$

Because the grout-water mixture is the wetting fluid, the permeability reduction factor (PRM) is described by the relative permeability function of the non-wetting phase, $k_{r,nw}(S_{nw})$, evaluated at $S_{nw} = (1 - A \cdot S_l^{sol})$. The permeability reduction might in fact be stronger because not only are the small pores sealed by the wetting grout, but continuous gel adsorption at the pore walls reduces the diameter of the remaining larger pores. Other permeability reduction models can be found in Verma and Pruess (1988), Todd (1990), and Oldenburg and Spera (1992).

Due to the reduced pore sizes, the capillary pressure p_c^* of the grouted soil is expected to be more negative for a given water content. We apply Leverett's scaling rule to calculate the capillary pressure of the new medium based on the capillary pressure function of the original soil:

$$p_c^*(S_l^*) = p_c(S_l^{ori}) \sqrt{\frac{k}{k^*} \cdot \frac{\phi^*}{\phi}} \qquad (7)$$

Note that the original p_c -function is evaluated at a saturation related to the original porosity value:

$$S_l^{ori} = A \cdot S_l^{sol} + S_l^* \cdot \left(\frac{\phi^*}{\phi}\right) \qquad (8)$$

Given a certain liquid saturation S_l^* of the grouted soil, Eq. (8) provides the original liquid saturation S_l^{ori} corresponding to the same water content. The capillary pressure p_c is then obtained and rescaled by applying Leverett's model (Eq. 7). Finally, the liquid saturation after solidification is calculated as the volume of the ungelled pore fluid divided by the porosity of the new medium.

Note that the solidification model has to be applied to each grid block of the discretized flow region to provide initial conditions and soil properties of the grouted medium for subsequent simulations.

441

3. APPLICATION

Numerical simulations were performed to design a horizontal grout barrier beneath a potentially leaking underground storage tank. A two-dimensional vertical model was developed, and a heterogeneous, anisotropic permeability field was generated with a geometric mean permeability of 1.55×10^{-12} m^2 and a standard deviation of one order of magnitude. We modeled multiple grout injections from two layers of horizontally drilled boreholes; the spacing between the wells is 1.0 m. The layout of the wells is shown in Figure 2. The first grout injection is made through the lower array of boreholes at a rate of 12 kg per minute and per meter borehole for an injection period of 1 hour. A gel time curve has been selected such that gel viscosity is doubled after 2 hours, and that it solidifies after 6 hours.

Figure 2 shows contours of grout content , i.e., the product of liquid saturation, grout concentration, and porosity, at the end of the first injection. Highest grout contents are in the immediate vicinity of the boreholes, where the initial soil gas and pore water are completely displaced due to the injection overpressure. After redistribution of the plume due to gravity and capillary forces, however, maximum grout contents are encountered beneath the injection ports due to gravitational slumping of the plume. The relatively fast gelation prevents the plume from slumping down even further. Note that the spreading of the plume leads to an incomplete occupation of the pore space by grout, i.e., partial plugging and insufficient permeability reduction will occur if only one injection is performed.

After solidification of the gel, the porosity of the grouted region is reduced, leading to the permeability field shown in Figure 3. Subsequently, a secondary injection is performed from the upper set of boreholes for 30 minutes. The grout from the secondary injection ponds on the low permeability layer produced by the primary injection (Figure 3), assuring high final grout saturations and thus enhancing the continuity of the subsurface barrier. The permeability field after solidification of the second plume is shown in Figure 4, along with the concentration contours of a potential spill from the underground storage tank. The model plume is effectively contained.

4. CONCLUDING REMARKS

Emplacing a subsurface barrier for temporary or permanent containment of contaminants requires identification of suitable barrier liquids, the development of an emplacement technology, as well as a numerical model for performing design calculations. In this paper we have presented a numerical simulator for modeling multiple injections of chemical grouts into the saturated and unsaturated zones of a heterogeneous aquifer. Assuming that the gelation process is not affected by soil and pore water chemistry, the code calculates the increase of viscosity as a function of time and gel concentration. A solidification model has been developed which assigns new properties to the zone partially occupied by grout. Application of the solidification model enables the repeated simulation of multiple grout injections, and performance studies of the barrier system can be conducted. Modeling capabilities are also essential for the verification studies including hydraulic, pneumatic, and tracer testing to assess permeability reduction and the continuity of the barrier. Furthermore, the design of a monitoring system can be supported by modeling.

Model calculations have been performed to design a horizontal barrier system in the unsaturated zone of a highly heterogeneous formation. Two layers of grout have been injected from a series of horizontally drilled wells. The simulations demonstrate that the combined action of gravity and capillarity leads to a substantial spreading of the gel plume, resulting in incomplete filling of the pore space. The second injection, however, assures high final grout contents due to ponding of the gel plume on the first layer of solidified grout.

We believe that uncertainties in formation characteristics and gel behavior should be addressed by appropriate grout specification and a robust design of the containment system. Nevertheless, modeling of multiphase flow effects is useful for the simulation of barrier emplacement in the unsaturated zone. The extended TOUGH2 code is considered to be a useful tool for modeling the behavior of grout plumes and for the design of subsurface barrier systems.
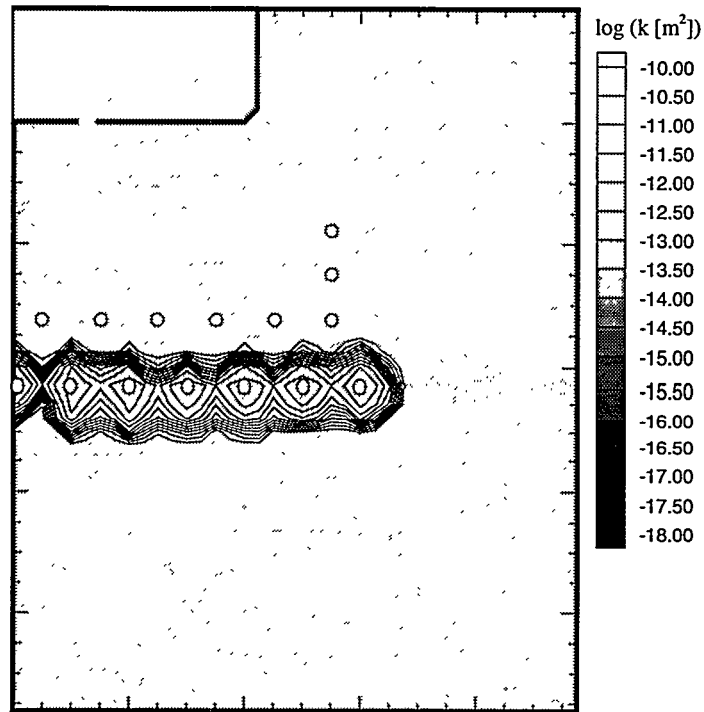
Figure 2. Initial permeability field (shaded) and gel content (contour interval is 0.04) after 30 minutes of grout injection.
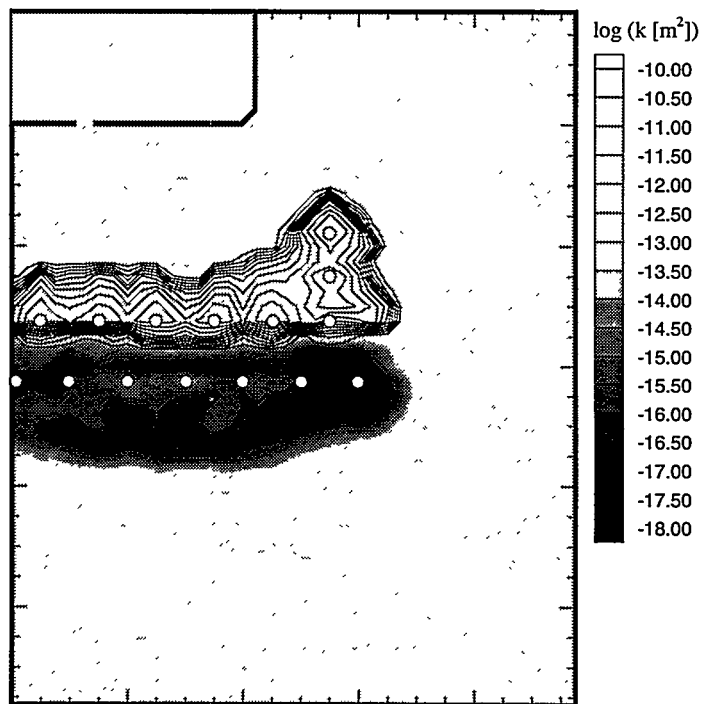
Figure 3. Permeability field (shaded) and gel content (contour interval is 0.04) prior to solidification of secondary grout plume.
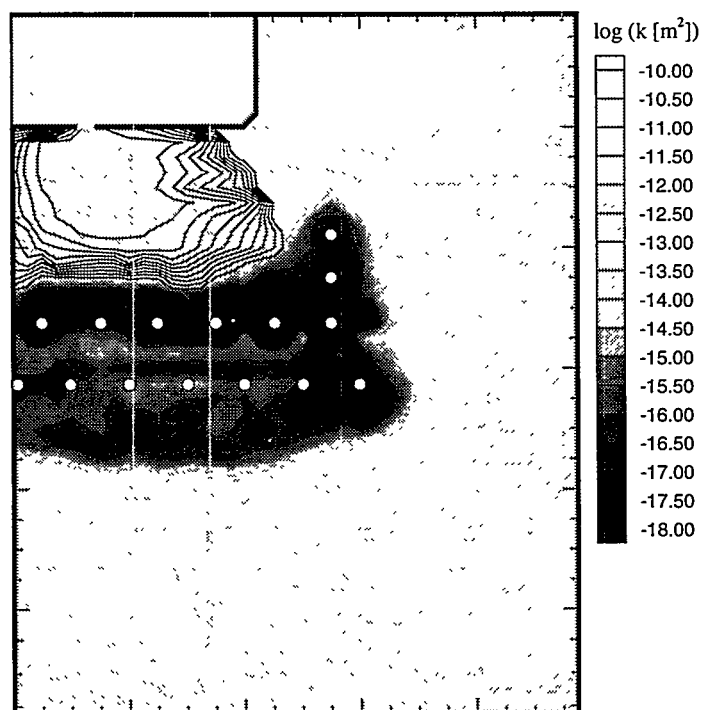
Figure 4. Final permeability field and containment of contaminant by subsurface barrier.

REFERENCES

Finsterle, S., G.J. Moridis and K. Pruess. (1994) A TOUGH2 equation-of-state module for the simulation of two-phase flow of air, water, and a miscible gelling liquid. Report LBL-36086, Lawrence Berkeley National Laboratory , Berkeley, Calif.

Hortes, E. (1986) Development of a reservoir model for polymer/gel treatments. Report 87-3, University of Texas at Austin, Texas.

Moridis, G.J., P. Persoff, H.-Y. Holman, S. J. Muller, K. Pruess, P. Witherspoon and C.J. Radke. (1994) Containment of contaminants through physical barriers formed from viscous liquids emplaced under controlled viscosity conditions. FY 1993 Annual Report LBL-29400, Lawrence Berkeley National Laboratory, Berkeley, Calif.

Moridis, G.J., P. Persoff, J. Apps, A. James, C. Oldenburg, A. McGrath, B. Freifeld, L. Myer, L. Pellerin and K. Pruess (1996) A design study for the isolation of the 281-3H retention basin at the Savannah River Site using the viscous barrier technology. LBL-38920, Lawrence Berkeley National Laboratory, Berkeley, Calif.

Oldenburg, C. M. and F. J. Spera. (1992) Hybrid model for solidification and convection. *Numerical Heat Transfer*, Part B, (21), 217-229.

Pruess, K. (1987) TOUGH user's guide. Report LBL-20700, Lawrence Berkeley National Laboratory, Berkeley, Calif.

Pruess, K. (1991) TOUGH2 - A general-purpose numerical simulator for multiphase fluid and heat flow. Report LBL-29400, Lawrence Berkeley National Laboratory, Berkeley, Calif.

Scott, T., L. J. Roberts and S. R. Short. (1985) In situ gel calculations in complex reservoir systems using a new chemical flood simulator, SPE #14234, presented at the Annual Technical Conference at Las Vegas, Nevada, September 22-25.

Todd, B. J. (1990) Numerical modeling of in situ gelation in porous media, Ph.D. dissertation, Dept. of Chem. and Petr. Eng., Univ. of Kansas.

Verma, A., and K. Pruess (1988) Thermohydrological conditions and Silica redistribution near high-level nuclear wastes emplaced in saturated geological formations. *J. Geophys. Res.*, *93*, 1159-1173.

Advanced Hydraulic Fracturing Methods to Create In Situ Reactive Barriers

Larry Murdoch[1,2], Bill Slack [1,4], Bob Siegrist[3], Steve Vesper [4], Ted Meiggs [5],

[1] FRx Inc
PO Box 37945
Cincinnati, Ohio 45222
513- 469-6040

[2] Department Geological Sciences
Clemson University, Clemson, SC 29634

[3] Environmental Sciences Division,
Oak Ridge National Laboratory; and
Environmental Science & Engineering Division,
Colorado School of Mines,
Golden, CO, 80401-1887

[4] CGEST, University of Cincinnati
1275 Section Rd., Cincinnati, OH 45234

[5] Foremost Solutions, 14250 Braun Rd., Golden, CO, 80401

Many contaminated areas consist of a source area and a plume. In the source area, the contaminant moves vertically downward from a release point through the vadose zone to an underlying saturated region. Where contaminants are organic liquids, NAPL may accumulate on the water table, or it may continue to migrate downward through the saturated region. In either case, NAPLs or other compounds in this area may dissolve and potentially contaminate large volumes of groundwater. The contaminant plume itself typically consists of dissolved compounds that move horizontally away from the source by ambient groundwater flow, potentially impacting supplies of drinking water or other receptors. Early developments of permeable barrier technology have focused on intercepting horizontally moving plumes with vertical structures, such as trenches, filled with reactive material capable of immobilizing or degrading dissolved contaminants (e.g. Gillam, 1996). This focus resulted in part from a need to economically treat the potentially large volumes of contaminated water in a plume, and in part from the availability of construction technology to create the vertical structures that could house reactive compounds.

Contaminant source areas, however, have thus far remained largely excluded from the application of permeable barrier technology. One reason for this is the lack of conventional construction methods for creating suitable horizontal structures that would place reactive materials in the path of downward-moving contaminants. Methods of hydraulic fracturing have been widely used to create flat-lying to gently dipping layers of granular material in unconsolidated sediments. Most applications thus far have involved filling fractures with coarse-grained sand to create permeable layers that will increase the discharge of wells recovering contaminated water or vapor (Murdoch et al., 1994). However, it is possible to fill fractures with other compounds that alter the chemical composition of the subsurface. One early application involved development and field testing micro-encapsulated sodium percarbonate (Vesper etal., 1993), a solid compound that releases oxygen and can create aerobic conditions suitable for biodegradation in the subsurface for several months.

METHODS OF HYDRAULIC FRACTURING

Hydraulic fracturing begins by injecting fluid into a borehole until the pressure exceeds a critical value and a fracture is nucleated. Coarse-grained sand, or some other granular material, is injected as a slurry while the fracture grows away from the borehole. Guar gum gel, a viscous fluid, is commonly used to facilitate transport of the granular material into the fracture. After pumping, the guar gum gel is decomposed by an enzyme added during injection and the fracture resembles a thin layer or bed in the subsurface (Murdoch et al, 1994).

The injection pressure required to create hydraulic fractures is remarkably modest. For example, at the beginning of injection during a test at 2 m depth, the pressure increased abruptly to 490 kPa (70 psi), but then decreased sharply when the fracture began to propagate. Injection pressure decreased from 200 to 100 (30 to 15 psi) throughout most of the duration of propagation (Murdoch et al, 1994). Slightly greater pressures are required to create fractures at greater depth.

Fracture Form

Conventional methods of hydraulic fracturing generally produce a single parting (multiple fractures require repeated operations) and the form of the fracture depends on the state of stress, the degree of stratigraphic layering or fabric in the enveloping formation, and perhaps other factors. In overconsolidated or bedded sediments, hydraulic fractures typically are equant to elongate in plan and dip gently towards their parent borehole (Fig. 1).
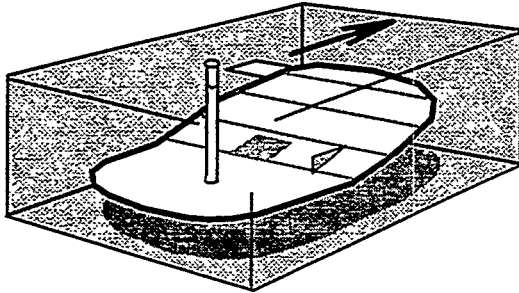
Figure 1. Idealized hydraulic fracture. Arrow points to the preferred propagation direction. White square overlies thickest area at center of fracture. Triangle shows dip angle.

In most cases, the fractures have a preferred direction of propagation so that they are asymmetric with respect to the borehole. The area of the fracture containing the thickest material, however, nearly always occurs in the vicinity of the center of the fracture, so that the propagation direction affects the distribution of injected material (Murdoch et al., 1991). Fractures typically climb in the preferred direction of propagation and will reach the ground surface along that direction if sufficient fluid is injected. The propagation direction can be related to distribution of vertical load at the ground surface, with the fractures propagating toward regions of diminished vertical load. At some locations, the vertical load has been manipulated (say, by positioning a drill rig near the injection point) to influence the propagation direction, whereas at other locations this approach has been impractical or ineffective.

Hydraulic fractures have been created between 1.2 and 16m below the ground surface during recent projects. Nearly all of them have been in silty clay, and most have been in glacial drift that probably was overconsolidated so that the form outlined above is typical. Maximum dimensions increase with depth, but are in the range of 7 to 10 m. Bulk volumes of granular material filling the fractures also increases with depth, ranging from 0.15 m^3 (5 ft^3) for shallow fractures to 1.25 m^3 (44 ft^3) for deeper ones. The average thickness of material filling a fracture ranges from 5 to 10 mm, but can be as much as 25 mm.

The sizes of the features that can be created using conventional hydraulic fracturing methods is remarkable considering the modest injection pressures and power required. However, conventional methods offer scant opportunity to influence the geometry of the fractures. Where surface loading is impractical, the direction of propagation can be difficult to anticipate, and the degree of asymmetry about the injection point cannot be influenced at all. This drawback can be of minor consequence where fractures are used for recovery because subsurface flow occurs beyond the lateral extent of the fractures so the natural variations in geometry have a only secondary effect. The drawback is more serious, however, where fractures are filled with reactive materials and used to degrade contaminants in place. In this application, the ability to influence the location of a fracture will help ensure that reactive material uniformly cuts across potential contaminant migration pathways.

Monitoring

The fracturing procedure is monitored by recording both pressure and deformation of the ground surface as functions of time. The ground surface over a shallow hydraulic fracture will lift to form a broad, gentle dome. The amount of uplift is similar to the fracture aperture (Murdoch et al., 1991), so the pattern of uplift can be used to infer the location and thickness of material filling the fracture at depth. Accordingly, the dome typically will be slightly asymmetric and the point of maximum uplift (the apex of the dome) will be displaced away from the injection point in the preferred direction of propagation.

Net ground displacements accompanying fracturing can be measured using optical leveling methods, or the inclination of the ground surface can be measured in real time using an array of tiltmeters. The tilt signal can be inverted to estimate uplift and, in particular, to sense the position of the apex of the dome. The tiltmeter data show that in most cases, fractures develop a preferred direction early and then continue to grow in this direction throughout propagation.

Directional Fracturing

Conventional methods of hydraulic fracturing have been modified to provide a mechanism for influencing the preferred direction of propagation of gently dipping fractures. The purpose here has been to develop a capability either to make fractures that are highly asymmetric in a particular direction, or to make fractures that are symmetric where they might otherwise be asymmetric. The first capability will allow reactive material to be placed beneath waste pits, buildings, tanks or other potential sources that cannot be penetrated by a vertical boring, whereas the second one will ensure that reactive material can be uniformly distributed in contaminated ground.

Methods of directional fracturing use an energetic water jet concurrent with slurry injection. The jet is supplied by a narrow tube that passes through a seal at the wellhead and extends to the depth of the fracture. The jet is oriented perpendicular to the tube so that its direction can be controlled by rotating the supply tube. Slurry flows down the annulus between an outer casing and the supply tube and is entrained by the jet when it reaches the depth of the fracture. The preferred direction of propagation follows the direction of the jet. During operation, tiltmeters are used to detect the propagation direction and the jet is rotated to either oppose or enhance that direction.

Field applications of the method have demonstrated the ability to induce propagation in a particular direction by directing the jet in that direction. The uplift is roughly symmetric about the injection point over most fractures created using conventional methods at a test site in the vicinity of Cincinnati, OH (Fig. 2a). Uplift that is highly asymmetric is created by operating the jet concurrent with slurry injection (Fig. 2b). Thickness of injected material is roughly proportional to the uplift, so that the injected material is concentrated to the NW of the borehole in Figure 2b. Several borings confirmed this inference.

Other field tests have involved using the directional system to improve the symmetry of the fractures. The success of this application appears to hinge on the time required to detect the direction of propagation; when propagation direction is detected early (within the first minutes of injection) it can be arrested or changed, when it is detected later the directional methods (in the current embodiment) have limited effect and the fracture continues to propagate in its preferred direction.

The directional methods developed thus far will diversify the applications of hydraulic fractures during the emplacement of reactive compounds. The system may be improved by increasing the power of the controlling jet, and experiments with this aspect of the technology are in progress.
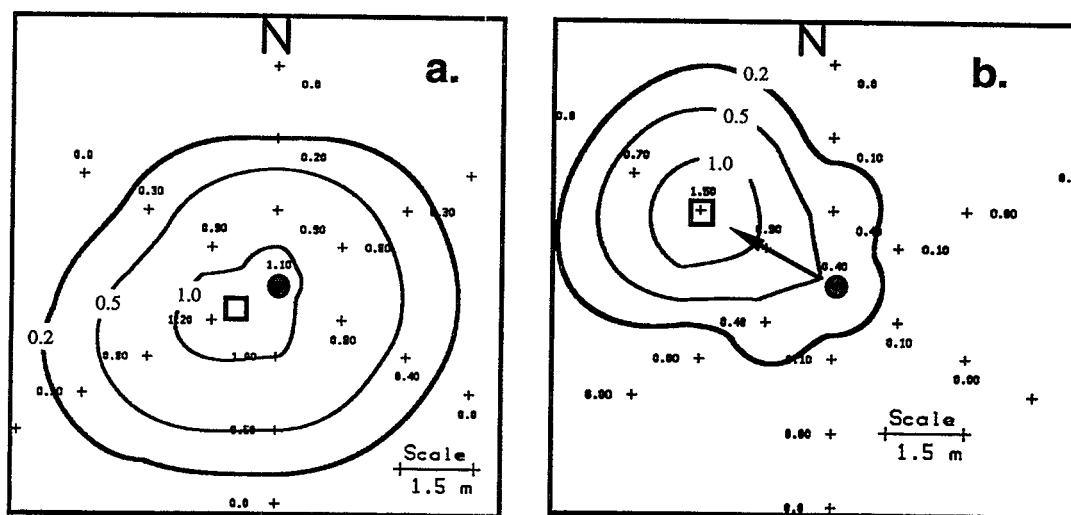
Figure 2a. Relatively symmetric uplift (cm) over conventional fracture; b.) Asymmetric uplift over fracture created with directional method. Jet pointing in direction of arrow during slurry injection. Square: maximum uplift

APPLICATIONS

Hydraulic fractures have been used to create sheet-like layers filled with a wide range of reactive compounds, from materials that alter redox conditions, to ones that adsorb contaminants or slowly leach beneficial materials. Early tests used a solid percarbonate, which slowly releases oxygen, to create fractures that developed aerobic conditions to enhance biodegradation in the subsurface. The early work demonstrated the viability of this approach but used material created using microencapsulation methods, which was too expensive for widespread application. However, recent formulations of similar oxygen releasing compounds (e.g. Marlow, 1996) are less expensive so this application may receive renewed interest.

Applications that are currently under investigation include filling fractures with porous ceramic granules to stimulate biodegradation, with adsorptive materials that can be treated using in situ with biodegradation, or with redox-altering materials to either oxidize or reduce contaminants.

Biodegradation Using Porous Ceramics

Biodegradation at some sites can be augmented by injecting populations of organisms capable of degrading contaminants along with the nutrients they require to thrive. This approach can be facilitated by colonizing granules of a highly porous ceramic made from diatomaceous earth (trade name, Isolite) with the selected microbial population. The granules also form a permeable bed through which nutrients can be injected.

Hydraulic fractures were filled with inoculated Isolite to augment bioremediation at a site where long-chain hydrocarbons used for cutting oil resulted in TPH values in excess of 2000 mg/kg. Samples from the site indicated that the population of heterotrophic and autotrophic organisms was too sparse to accomplish degradation, according to Stavnes et al. (1996), who describe the details of this study. Moreover, the site is underlain by weathered, fine-grained sediments of low permeability so that closely spaced conventional wells would be required to effectively deliver liquid nutrients.

Laboratory studies identified and refined a consortium of cutting-oil-metabolizing bacteria culled from samples taken from the site. Bench-scale tests indicated that this consortium effectively

reduced TPH values in site soils. A solution containing the bacteria consortium and nutrients was circulated through packed columns filled with Isolite, causing bacterial growth on the porous ceramic granules and effectively inoculating the Isolite for subsurface injection (Stavnes et al., 1996).

Sets of hydraulic fractures stacked one above the other were created with the innoculated Isolite at two locations. Location 1 contained four fractures at depths of 2.4, 3.4, 4 and 4.6 m, whereas Location 2 contained only two fractures at slightly greater depths, 4.6 and 5.2 m. The fractures were filled with between 0.25 and 0.5 m^3 of Isolite (grain size: 1 to 2 mm), which created layers as thick as 2.5 cm and 6 to 8 m in maximum dimension.
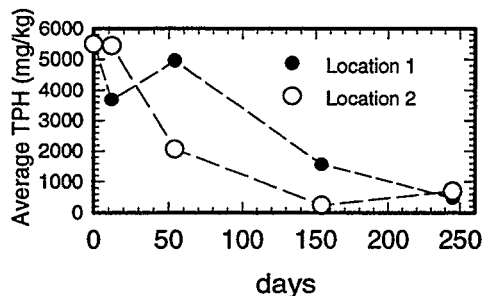
Figure 3. Average TPH concentrations from soil samples as a function of time.

The intention was to utilize the Isolite-filled fractures as in situ bioreactors that would degrade contaminants in their vicinity, although the optimal operation of the fractures was unclear. Accordingly, fractures at Location 1 were augmented by injections of nutrients, additional microbes, and a surfactant was added to increase bioavailability. Later, air was injected at Location 1 to enhance aerobic conditions. In contrast, Location 2 was left idle, although several wells were screened in the fractures and may have provided some passive aeration (Stavnes et al., 1996).

Soil samples were obtained 12, 54, 154 and 245 days after fracturing and analyzed for TPH. Samples were taken from the 11 locations in vicinity of the Location 1, and 4 locations in the vicinity of Location 2, as well as from more distant areas to act as control. The average concentrations from those sampling events indicate that the TPH concentrations remained roughly constant during the first 54 days at Location 1 and then decreased after that time (Fig. 3). Concentrations apparently decreased slightly earlier at Location 2. By day 154, average concentrations at both locations decreased to 20 percent of initial values and by day 254, the average concentrations were roughly 10 percent of initial values. Student t-tests performed on the data indicate that the reduction in concentration compared to initial measurements at both locations is statistically significant by day 154, assuming $\alpha=0.1$, and the confidence increases with time so by day 254 the reductions in concentration are significant assuming $\alpha=0.05$. Samples taken in the contaminated zone beyond the region that was unaffected by the reactive fractures yielded TPH values between 1700 and 3140 mg/kg throughout the study period and showed no systematic change in concentration with time.

Adsorption and biodegradation

It can be important in some circumstances to arrest contaminant; for example, where vertical flow is rapid enough to outpace degradation kinetics, or where contaminants (e.g. metals) cannot be degraded at all. One approach to this scenario uses fractures filled with granular activated carbon (GAC) to adsorb chlorinated solvents, coupled with techniques to periodically degrade the adsorbed solvents using biodegradation. A proof-of-concept field test has been conducted at an uncontaminated site, and a field test at a contaminated site is on going.

The proof-of-concept field test involved creating a fracture filled with GAC and inoculating the material with a consortium of TCE-degrading methanotrophic organisms. It was assumed that the GAC could adsorb TCE, and we sought to evaluate the ability of the organisms to degrade solvent without actually having any solvent in the ground. This was accomplished by injecting a mixture of air and 3 percent methane into the GAC-filled fracture for 3 months in an effort to stimulate the growth of the introduced organisms. Samples were obtained weekly and tested in small batch reactors in the laboratory for their ability to degrade TCE. The samples were also used to evaluate the activity of methane monooxygenase using the conversion of naphthalene to napthol

in batch reactors, and to measure the number of TCE-degrading organisms using cell counts and SEM analyses.

The results show that samples from the GAC-filled fracture will degrade TCE in batch reactors throughout the 3-month-long test, whereas TCE concentrations in control reactors were unchanged. Moreover, the lab tests consistently showed a conversion of naphthalene to naphthol, which indicates that methane monooxygenase was produced. These results parallel an increase in the microbial population from 10^6 to 10^7 CFU per gm GAC.

These results indicate that it is possible to maintain conditions that will favor in situ degradation of TCE using methanotrophic organisms in GAC-filled hydraulic fractures. On going field tests will evaluate the extension of these results to field conditions where TCE is present.

Redox compounds

The use of redox agents for in situ treatment of organics and inorganics is evolving as an effective means of in situ treatment (Siegrist et al., 1995; 1996, Gates et al., 1996), and implementation of in situ redox zones using hydraulic fracturing is also being explored. As of this writing, laboratory and field experiments are ongoing involving hydraulic fractures filled with redox agents for interception and destruction of DNAPL compounds, such as TCE, in low permeability media, such as silts and clays (Siegrist et al., 1995; 1996). A major part of this work involves a comparative field test that is ongoing at the DOE Portsmouth Site in Ohio where multiple test cells have been emplaced in clean and contaminated sites. These cells are being used to evaluate in situ remediation of DNAPL compounds in silty clay media by both enhanced air flushing and in situ destruction. All of the test cells involve hydraulically emplaced fractures at four to five depths in the range of 1 to 6 m with diameters of ~10 m. Two of the test cells involve fractures that form permeable barriers of either zero-valent iron particles or a special potassium permanganate grout. The work is being completed by a multi-institutional, interdisciplinary team comprised of scientists and engineers from ORNL, Lockheed Martin at Portsmouth, FRx Inc., University of Cincinnati, and the Colorado School of Mines.

The test cells at Portsmouth were installed in September, 1996, and process operation and performance monitoring occurred during fall 1996 with further experimentation planned for spring 1997. Pre- and post-operational monitoring has involved onsite/offsite analyses of more than 600 samples, coupled with 3-dimensional in situ instrumentation emplacement using direct-push and sidewall sampler devices to measure subsurface biogeochemical properties and contaminant treatment efficiency.

In the test cells containing redox reactive fractures, continuous cores were collected across the emplaced fracture zones nearly 3 months after fracture emplacement. Each core was carefully examined and dissected with analyses made for Eh, pH, TOC and WC. DNAPL compound degradation tests were also completed to define destruction efficiency and potential as a function of distance from the reactive fracture. Initial results indicate highly reactive zones were present in these two permeable barrier cells with very high DNAPL degradation efficiencies (e.g., >99%) in fracture treatment zones of varying thickness (e.g., 1 to 10 cm). Further information on this work will be available in forthcoming publications during 1997.

CONCLUSIONS

Hydraulic fracturing methods offer a mechanism for gently dipping layers of reactive compounds. Specialized methods using real-time monitoring and a high-energy jet during fracturing allow the form of the fracture to be influenced. This technique allows asymmetric fractures to be created beneath potential sources (e.g. tanks, pits, buildings) that should not be penetrated by boring.

The technique appears to be particularly versatile. Field applications thus far have created fractures filled with zero-valent iron to reductively dechlorinate halogenated hydrocarbons, or

granular activated carbon to adsorb compounds. Porous ceramic granules innoculated with organisms have been used to biologically degrade cutting oil, and slowly dissolving solid peroxides have been used to create aerobic conditions in the subsurface. The most challenging application has been to fill fractures with granules of potassium permanganate, a strong oxidant that degrades a wide range of organic chemicals. It appears that hydraulic fracturing methods will allow reactive barriers to be created with nearly any solid compound for which subsurface injection is permissible.

The flat-lying treatment zones created using these methods can be operated passively or actively to intercept vertically migrating contaminants. Both organics and inorganics can be intercepted, removed, and either immobilized or degraded. This is an exciting compliment to vertical permeable barriers and provides a means to strategically contain, and even treat in situ, contaminant source areas.

ACKNOWLEDGMENTS

REFERENCES

Gates, D.D., R.L. Siegrist, and S.R. Cline. (1995) Chemical oxidation of volatile and semi-volatile organic compounds in soil. *Proc. Air and Waste Management Assoc. Conference*, June.

Gillam, R. W. (1996) Metal enhanced degradation of halocarbons: Technology development and implementation. in *Groundwater and Subsurface Remediation*, H. Kobus, B. Barczewski, and H-P Koschitzky, ed. Springer, Berlin, 159-169.

Marlow, H. (1996). The use of oxygen release compound (ORC) for groundwater bioremediation, Session 12, *American Chemical Society Symposium on Emerging Technologies in Hazardous Waste Management*, Birmingham, AL, Sept. 9-11.

Murdoch, L. et al. (1994) Alternative Methods for Fluid Delivery and Recovery. EPA/625/R-94/003.

Murdoch, L.C., et al. (1991). The feasibility of hydraulic fracturing of soil to improve remedial actions. Final Report USEPA 600/2-91-012. NTIS Report PB91-181818.

Siegrist, R.L. and K.S. Lowe (eds.) (1996) *In Situ Remediation of DNAPL Compounds in Low Permeability Media: Fate/Transport, In Situ Control Technologies, and Risk Reduction.* A series of focus papers by an ad hoc consortium sponsored by the U.S. DOE Office of Science & Technology. Oak Ridge National Laboratory report, ORNL/TM-13305. 200 pp.

Siegrist, R.L., et al. (1995) Field evaluation of subsurface manipulation by fracturing, permeation dispersal, and horizontal well recirculation using unconfined test cells. *National Ground Water Association Annual Educational Conference*, Indianapolis, IN,October.

Stavnes, S., C. A. Yorke, and L. Thompson. (1996) In situ bioremediation of petroleum in tight soils using hydraulic fracturing. *HazWaste World/Superfund XVII Conference*, Washington, D.C. Oct. 16.

Vesper, S. J., L.C. Murdoch, S. Hayes, and W.J. Davis-Hoover. (1994) Solid oxygen source for bioremediation in subsurface soils. *Journal of Hazardous Materials* 36:265-274.

DEVELOPMENT OF A DESIGN PACKAGE FOR A VISCOUS BARRIER AT THE SAVANNAH RIVER SITE

G.J. Moridis, A. James and C. Oldenburg
Earth Sciences Division, Lawrence Berkeley National Laboratory
1 Cyclotron Rd., MS 90-1116
Berkeley, CA 94720

1. INTRODUCTION

This paper describes elements of a design for a pilot-scale field demonstration of a new subsurface containment technology for waste isolation developed at the Lawrence Berkeley National Laboratory (LBNL), which uses a new generation of barrier liquids for permeation grouting. The demonstration site was Retention Basin 281-3H, a shallow catchment basin at the Savannah River Site (SRS), originally built to control contaminated runoff for the H Reactor, and which has been contaminated mainly by radionuclides.

The LBNL viscous barrier technology employs barrier liquids which, when injected into the subsurface, produce chemically benign nearly impermeable barriers through a very large increase in viscosity. The initially low-viscosity liquids are emplaced through multiple injection points in the subsurface and the intersecting plumes merge and completely surround the contaminant source and/or plume. Once in place, they gel or cure to form a nearly impermeable barrier. The technology can also be applied to encapsulate wastes in the subsurface. In applying this technology it is important to match the barrier liquid to the waste and to the soil conditions, and to control the gel time and the barrier emplacement (Moridis et al., 1994; Persoff et al., 1994, Moridis et al., 1995).

The barrier liquid to be used in this application is Colloidal Silica (CS), an aqueous suspension of silica microspheres in a stabilizing electrolyte. It has excellent durability characteristics, poses no health hazard, is practically unaffected by filtration, and is chemically and biologically benign. The increase in viscosity of the CS following injection is due to a controlled gelation process induced by a strong electrolyte added immediately prior to injection at ambient temperatures. The CS has a tendency to interact with the geologic matrix, and therefore, a surface-modified formulation is used. This CS variant is significantly less susceptible to soil (Moridis et al., 1995), and is stabilized at a near-neutral pH by a permanent particle charge produced by partial isomorphic replacement of surficial Si by Al. Detailed information on the CS properties and behavior, as well as on the interaction with the SRS soils and on the selection procedure can be found in Moridis et al. (1996).

2. PROBLEM DESCRIPTION AND ISOLATION APPROACH

Basin 281-3H is a shallow retention/seepage basin at the Savannah River complex, which contains standing water and is contaminated mainly by radionuclides. Of particular concern are ^{137}Cs, ^{90}Sr, and ^{238}Pu. The groundwater table is thought to be shallow (possibly a perched water table) and to vary seasonally between 1.2 and 3.6 m from the surface. Most of the contamination is believed to be in the top 0.3-0.6 m from the surface and from the basin bottom. In addition to the contamination in and around the basin, a pile of contaminated excavated soil is located on the west side of the basin. Radionuclide-laden water migrates towards the water table through infiltration of rainfall or when a rising watertable intercepts the contaminated zone, and creates a plume carried by the regional groundwater flow. Waste containment and isolation are a prerequisite for placement of the soil pile in the basin.

Current plans for Retention Basin 281-3H call for removal of the contaminated water from the basin, moving the contaminated soils into the basin, and isolating the basin from the surrounding environment. Waste isolation includes (a) establishing a hydraulic barrier beneath the contaminated material in the basin to prevent infiltration of contaminated water, and (b) placement of a low permeability cap on top of the contaminated material. The humid conditions at the site dictate the use of CS: CS is water based, and as such it can easily seal the water-filled pores. Compared to the other baseline technologies (such as slurry walls and removal and disposal) the LBNL subsurface

barrier technology offers several advantages. It entirely isolates the affected area from the regional groundwater flow by providing barriers to both horizontal and vertical flow. It makes possible the isolation of waste through the least intrusive approach. Because it relies on permeation, no soil is excavated during injection and the risk of human exposure is substantially reduced.

3. DESIGN OBJECTIVES AND CRITERIA

The design criteria include: (a) spatially averaged hydraulic conductivity between the isolated soil volume and the surroundings of 10^{-9} m/sec or less, (b) minimum cumulative thickness of the grouted soil horizons in the direction of potential flow of 0.9 m (3 ft) or more, and (c) demonstrated lack of hydraulic communication between the isolated volume and the surrounding soils. In this paper, however, we do not discuss verification-related design issues.

4. BARRIER SPECIFICATIONS AND CONCEPTUAL MODEL

Figure 1 is a plan view of the retention basin 281-3H. The basin dimensions are 61 m (200 ft) by 36.6 m (120 ft) by 1.83-2.44 m (6-8 ft). Figure 2 is a cross-section of the basin prior to barrier emplacement. The soil pile (i.e. the most contaminated soils) is first placed at the bottom of the basin and is distributed as uniformly as possible. The top 0.6 m (2 ft) of the soil of the area within the basin fence are then stripped and placed in the basin. The contaminated soils are then be covered with 0.6 m (2 ft) of clean soil to provide the necessary physical and radiation protection for the barrier emplacement operations.

The barrier conceptual model and geometry are shown in Figure 3, and involve the creation of a compound barrier system which seals all the permeable zones to a depth of 6.1 m (20 ft) and incorporates(a) a minimum of 0.9 m (3 ft) and a maximum of 1.2 m (4 ft) cumulative thickness of grouted horizons, coupled with and complementing (b) the naturally low permeability of soils at the basin site. This design provides a needed additional level of safety, and protection and isolation of all potential primary and secondary sources of contamination to a depth of 6.1 m (20 ft) from current grade. The primary sources are the contaminated soils inside the sealed basin, and the secondary sources are created by contaminants outside the basin. Preliminary permeability data (Moridis et al., 1996) indicate that acceptable permeable zones to a depth of 6.1 m are rather few and quite thin. Emplacement of this barrier in essence involves injections at multiple target zones, but the total thickness of CS-grouted horizons is not expected to exceed 0.9-1.2 m. The total volume of CS is estimated between a minimum of 910,000 kg and a maximum of 2,135,000 kg.

The main reason for adopting this conceptual design is the fact that the bulk of radioactivity is estimated to be at least 200 Ci, and is expected to be concentrated mainly in the soil pile. These soils will be placed at the bottom of the basin. A significant amount of water, the primary migratory vehicle of the contamination, will remain in the basin after drainage and will be in contact with highly contaminated materials. The additional level of safety required by the radioactivity necessitates the sealing of any conductive pathways between the bottom of the basin and the groundwater. Such conductive pathways are suggested by the fact that the water level fluctuations in the basin cannot be fully accounted for by rainfall and evapotranspiration. The barrier conceptual model in Figure 3 is based on the assumption that low permeability sediments are present underneath the basin, with discontinuous zones of locally high permeability. Such a soil profile is suggested by preliminary permeability analyses (Moridis et al., 1996). Should the natural sediments underneath the basin involve zones with hydraulic conductivities of 10^{-6} m/sec or higher in a matrix with a predominant hydraulic conductivities of 10^{-8} m/sec, the creation of the barrier in essence complements the naturally low permeability. In this sense the barrier emplacement in the lower horizons (beneath the basin) involves identification and sealing of the permeable layers, while the CS at the bottom of the basin will prevent contaminant migration from the basin toward the groundwater.

5. THE BARRIER EMPLACEMENT METHOD

After evaluating several barrier emplacement alternatives, lance injection was selected as the barrier emplacement method. Lance injection offers several attractive features. The injections are closely spaced, and accurate emplacement is easy to achieve. It requires no drilling fluids, and no cuttings or slurry are expelled during penetration. Three lances can be simultaneously forced into the soil

using a hydraulic mechanism, thus increasing the rate of barrier emplacement while eliminating the risk of contaminant dispersion in the air, which could pose a problem when using pneumatic techniques such as ODEX for well drilling. It has a significant cost advantage compared to traditional well drilling techniques because it doesn't require well completion. Injection begins from the top of the intended injection zone, and proceeds downward (downstage method). It eliminates the downward spread of contaminants, a common problem of drilling methods. Lance injection results in a barrier consisting of overlapping grout bulbs (see Figure 3), and allows repeated injections and/or re-treatment of the grouted zones. It allows visual monitoring of work at all times, and is compatible with many methods of emplacement and post-injection barrier verification.

6. BARRIER EMPLACEMENT DESIGN CALCULATIONS

6.1. Injection Grids and Strategy

The injection pattern involves two grids (Figure 1) : the primary grid (i.e. the first pass) and the secondary grid (second pass), which is offset from the primary and injects into the centers of the primary grid. The grid spacing is expected to range between 0.6 and 1.5 m, and will be more accurately estimated after additional permeability tests. The injection strategy is dictated by the saturation conditions of the subsurface, and differs for saturated and unsaturated conditions. Unsaturated conditions allow somewhat higher pressures, simultaneous injection from all three lances (in 3-pronged systems), and shorter gel times. Saturated conditions could preclude simultaneous use of more than two lances (to avoid less than satisfactory coverage), and require lower injection pressures and longer gel times (several hours long).

Simulations of constant pressure gel injection into a fully saturated two-dimensional Cartesian mesh have been performed in order to continue the exploration of gel content between multiple side by side injection ports. For all simulations, a gel of 4.5 cP viscosity is injected into a horizontal, 2-D water saturated domain with a uniform permeability of 5×10^{-13} m^2 (0.5 darcy).

The simulations involve port spacings and pressures expected in field application, and model two different injection scenarios in order to maximize gel content between ports. Figure 4 is a plan view illustrating gel placement after 1800s (0.5 hrs.) of simultaneous 2 port injection and 1.5 hrs. natural evolution. Observations are made at t = 2 hrs. Port locations are labeled and the 2-D grid is halved along the line of symmetry at port 2. Grid blocks between injection ports 1 and 2 are 1 mm in length (x axis). Initial pressure conditions throughout the domain were set at roughly 2.22091×10^5 Pa (2 atm or 32 psi) based on a subsurface depth of 4.57 m (15 ft). The constant pressure injection was set at 6.89×10^5 Pa (100 psi). Contour lines of gel mass fraction in Figure 4 indicate that there is a zone between the two injection ports with less than 10 % gel due to this injection scheme. If injection were continued, this area would eventually be filled with gel and a low gel zone would not exist. The relevancy of this series of simulations is to show that given an injection period beyond which we cannot extend, there may exist a zone between injection ports of low gel content. If this is the case, a manner in which to maximize gel coverage in the area between the injection ports is the selection of optimal injection schemes.

Figure 5 shows grout placement at t = 2 hrs. for the second injection scheme, a staggered gel injection. Gel injection occurs via port 1 for 0.5 hrs. at 6.89×10^5 Pa (100 psi), followed by injection from port 2 at the same constant pressure for the next 0.5 hrs. The system is then allowed to evolve naturally. Comparison of these two simulations shows that the staggered scheme increases gel content in the zone between ports for the same time allowed for injection from all ports and essentially the same amount of injected gel. The obvious conclusion is that a staggered injection scheme favors a more effective and uniform filling of the pore space with CS.

6.2. Injection Under Variably Saturated Conditions

The TOUGH2 simulator (Pruess, 1991) using the EOS11 (Finsterle at al., 1994) gelation module was used to perform preliminary simulations of water injection under saturated and unsaturated conditions. For these preliminary calculations, we inject water only with no CS present. From a series of simulations, we constructed injection curves. The injection curves are plots of water injection rate vs. lance tip pressure for injection at constant pressure conditions for various values of

permeability. The approximately linear relations between pressure (P), permeability (k), injection rate (q), and viscosity (m) in the system allow relatively easy interpolation between curves, and straightforward approximation of injection rates and pressures.

The conceptual model of the system considers a single lance injection in a two-dimensional radial (r-z) system with homogeneous isotropic permeability. Parameters for the problem are presented in Table 1. In Figures Figure 6 and 7 we show the injection curves for unsaturated and saturated injection scenarios, respectively. The injection rate plotted is the time averaged mass injection rate over the first 10 minutes of injection.

The injection curves for unsaturated conditions (Figure 6) show that injection rates are relatively small for the low k formations expected at the site. We see further that there is a k below which we effectively cannot inject water over any reasonable time period due to the low injection rate. Note that injection curves for all lower k's will plot between the x-axis and the $k = 5 \times 10^{-14}$ m^2 curve. Thus the surface defined by the constant k curves has a very sharp drop-off at about $k = 5 \times 10^{-13}$ m^2. As k increases above 10^{-13} m^2, injection rates increase significantly. The corresponding hydraulic conductivity K values (in m/sec) are obtained by multiplying k by the factor 9.81×10^6. In Figure 7 we show the injection curves for saturated conditions. Under saturated conditions, injection rates are slightly smaller than in unsaturated conditions due to the need to displace existing water in the formation under saturated conditions. We observe the same steep edge to the surface defined by the permeability curves as observed in the unsaturated case. However, as k increases, we do not see as rapid an increase in injection rates as we see for the unsaturated conditions.

These simulations show that it may be difficult to inject significant quantities of water or gel over any practical time frame into the low-permeability formations expected at the H-Area site. The simulations do not account for permeability heterogeneity or anisotropic permeability which may allow higher injection rates. To account for the effects of the CS viscosity (expected to be in the 5-6 cP range), the pressures or injection rates illustrated in Figures 6 and 7 have to be scaled accordingly by dividing rates or multiplying pressures by the CS viscosity.

7. REFERENCES

Finsterle, S., G.J. Moridis, and K. Pruess (1994) *A TOUGH2 Equation-Of-State Module for the Simulation of Two-Phase Flow of Air, Water, and a Miscible Gelling Liquid.* Lawrence Berkeley Laboratory Report LBL-36086, Berkeley, CA.

Moridis, G.J., P. Persoff, H.-Y. Holman, S.J. Muller, K. Pruess, P.A. Witherspoon, and C.J. Radke (1994) *Containment of Contaminants through Physical Barriers Formed from Viscous Liquids Emplaced Under Controlled Viscosity Conditions, FY 1993 Annual Report.* Lawrence Berkeley Laboratory Report LBL-29400, Berkeley, CA.

Moridis, G.J., L. Myer, P. Persoff, S. Finsterle, J.A. Apps, D. Vasco, S. Muller, P. Yen, P. Williams, B. Freifeld, and K. Pruess (1995) *First-Level Field Demonstration of Subsurface Barrier Technology Using Viscous Liquids.* Lawrence Berkeley Laboratory Report LBL- 37520, Berkeley, CA.

Moridis, G.J., P. Persoff, J. Apps, A. James, C. Oldenburg, A. McGrath, B. Freifeld, L. Myer, L. Pellerin and K. Pruess (1996) *A Design study for the Isolation of the 281-3H Retention Basin at the Savannah River Site Using the Viscous Barrier Technology.* Lawrence Berkeley Laboratory Report LBL- 38920, Berkeley, CA.

Persoff, P., G.J. Moridis, J.A. Apps, K. Pruess and S.J. Muller (1994) Designing injectable colloidal silica barriers for waste isolation at the Hanford site. In *Proceedings, 33rd Hanford Symposium on Health and the Environment, In-Situ Remediation: Scientific Basis for Current and Future Technologies,* (eds. G.W. Gee and N.R. Wing), pp.87-100. Battelle Press, Richland, WA.

Pruess, K (1991) *TOUGH2 - A General-Purpose Numerical Simulator for Multiphase Fluid and Heat Flow.* Lawrence Berkeley Laboratory Report LBL-29400, Berkeley, CA.

ACKNOWLEDGMENTS

Table 1. Parameters for the Injection Curve Simulations

Parameter	Symbol	Value
porosity	ϕ	0.3
compressibility	COM	4.4×10^{-8} Pa^{-1}
permeability	k	$10^{-11} - 5 \times 10^{-14}$ m^2
temperature	T	15 °C
viscosity of injected water	μ	1.136×10^{-3} Pa s
lance injection interval	L_i	0.16 m
lance injection depth	d_i	6.49 m
max. capillary pressure	$P_{cap\ max}$	10^5 Pa
residual liquid saturation	S_{lr}	0.20
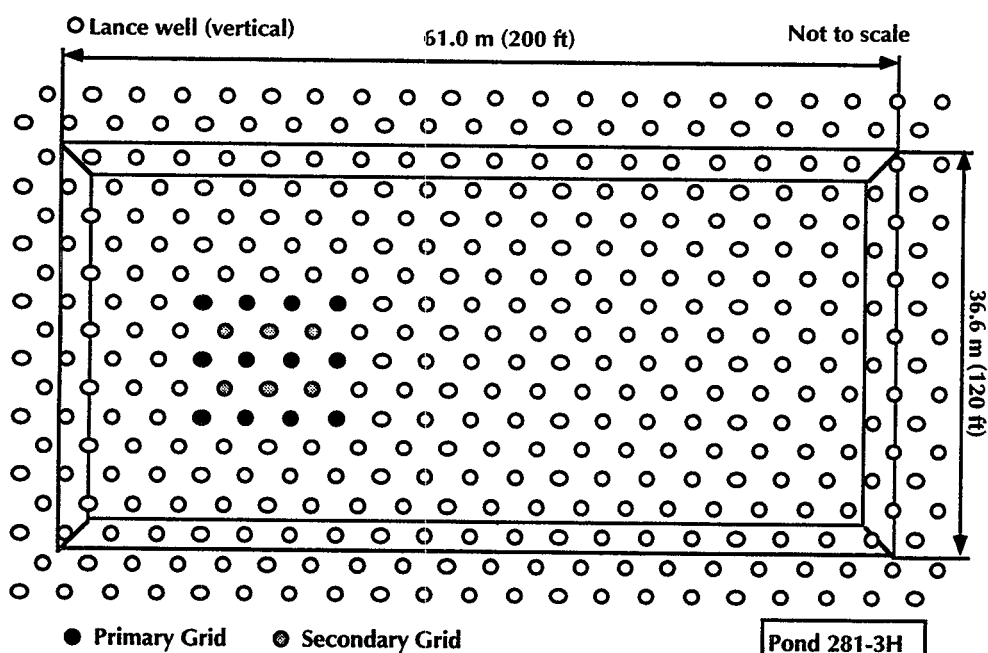
Figure 1. Plan view of the basin and of the subsurface barrier emplaced using lance injection.
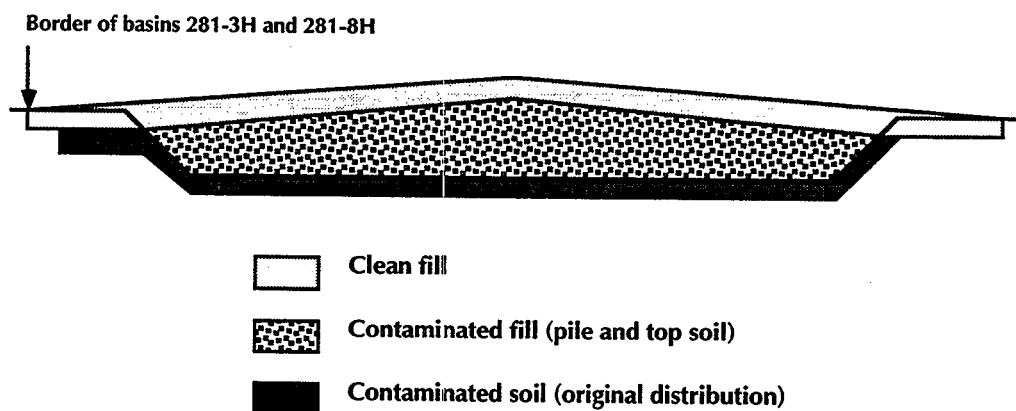
Figure 2. A schematic of the barrier immediately before the barrier emplacement.
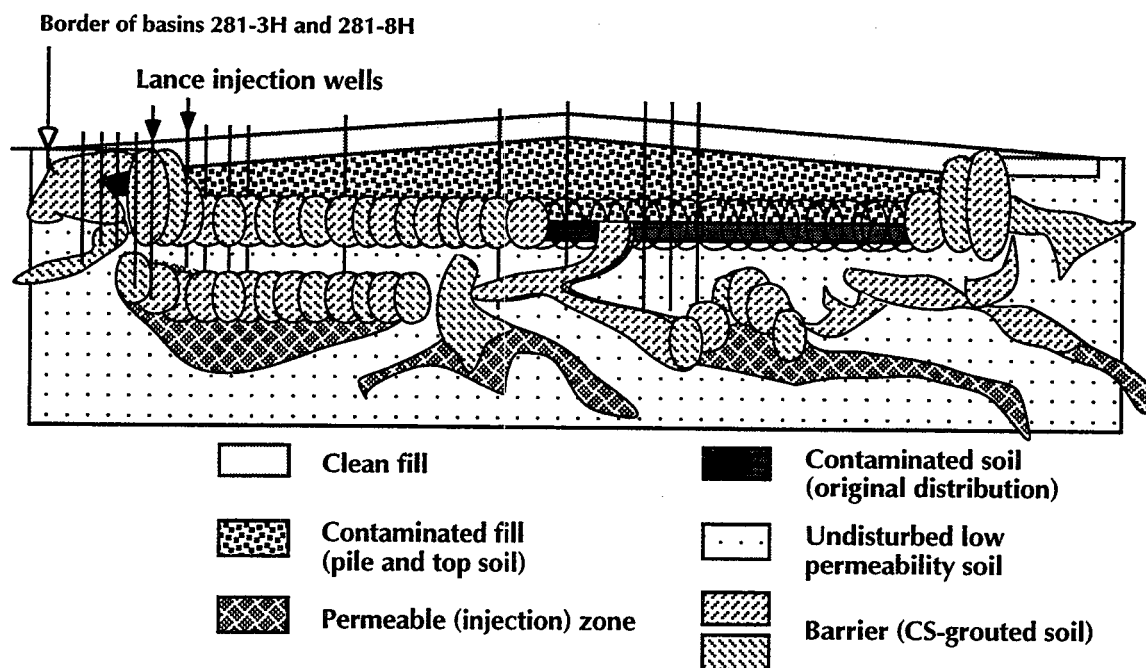
Figure 3. Conceptual model of the barrier.

Border of basins 281-3H and 281-8H

Lance injection wells

Clean fill

Contaminated fill
(pile and top soil)

Permeable (injection) zone

Contaminated soil
(original distribution)

Undisturbed low
permeability soil

Barrier (CS-grouted soil)
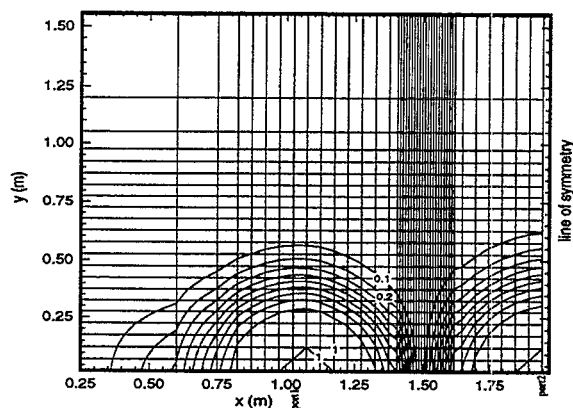
Figure 4. Simultaneous 2 port grout injection.
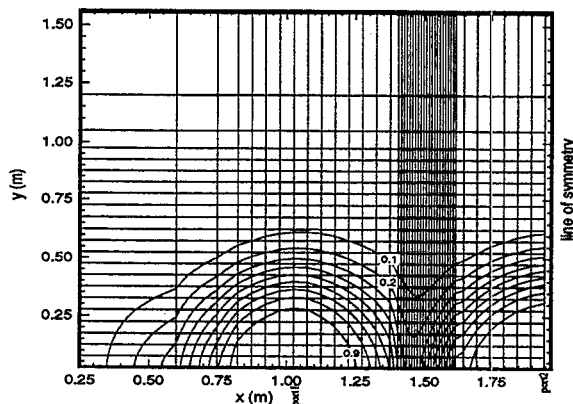
Figure 5. Staggered middle port injection.
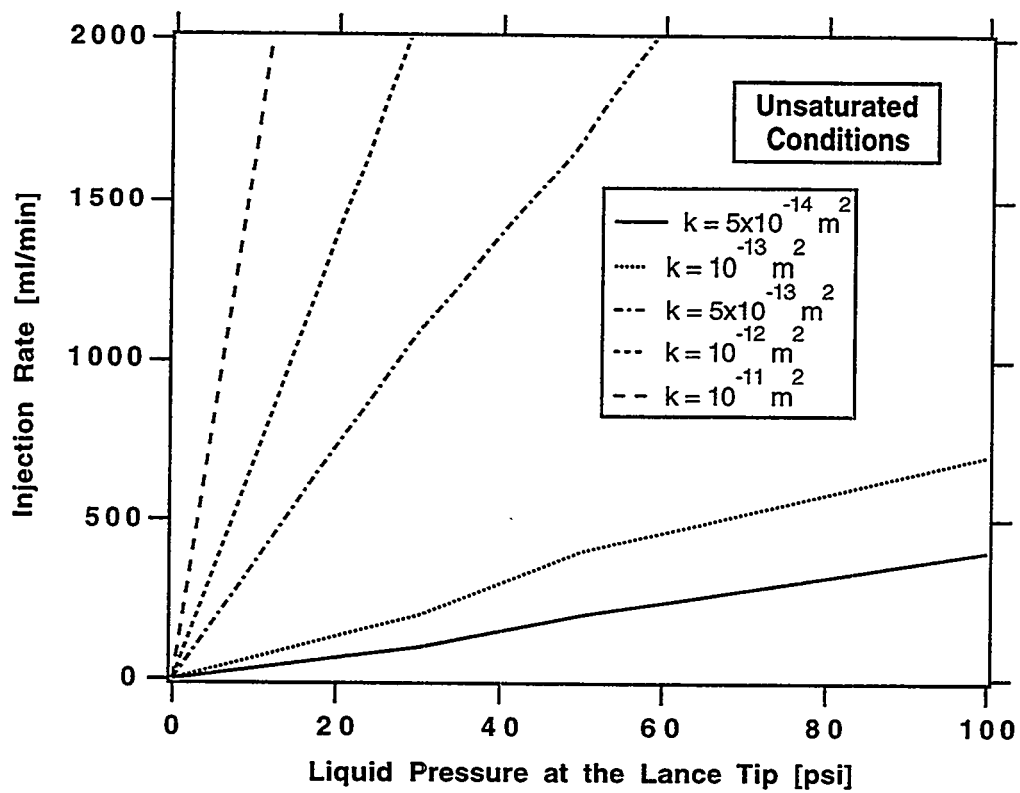
Figure 6. Injection curves for unsaturated conditions (water injection).
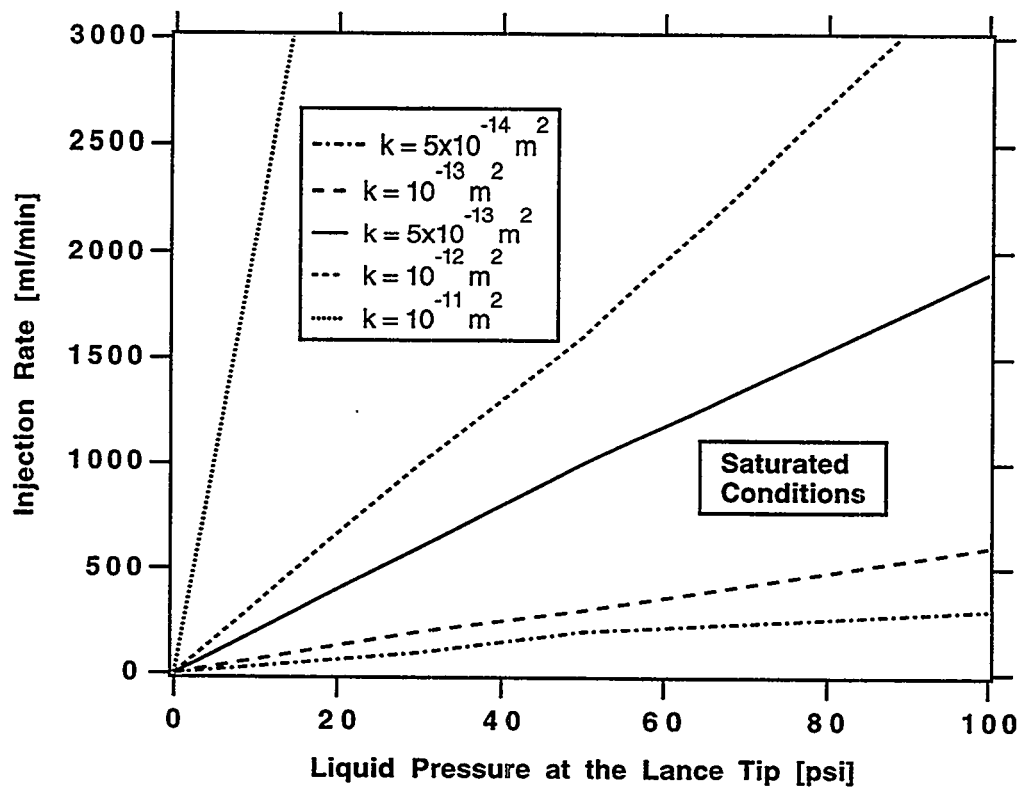
Figure 7. Injection curves for saturated conditions (water injection).

Bedrock Refractive-flow Cells: A Passive Treatment Analog to Funnel-and-Gate

Vincent Dick[1] and David Edwards[2]

Abstract: *Funnel-and-gate technology provides a mechanism to passively treat groundwater contaminant plumes, but depends on placement of a sufficient barrier ("funnel") in the plume flow path to channel the plume to a pass-through treatment zone ("gate"). Conventional barrier technologies limit funnel-and-gate deployment to unconsolidated overburden applications. A method has been developed which allows similar passive treatment to be applied to bedrock plumes. Rather than use barriers as the funnel, the method uses engineered bedrock zones, installed via precision blasting or other means, to refract groundwater flow along a preferred path to treatment (gate). The method requires orienting the refractive cell based on the Tangent Law and extending refractive cell limbs down gradient of the gate to disperse head and control flow. A typical Refractive-Flow cell may be "X" shaped, with each limb 3-10 ft [1-3 m] wide and several tens to a few hundred feet [10 - 100 m] in length. Treatment takes place at the center of the X. MODFLOW modeling has been used to successfully simulate desired flow. Engineered blasting has been used at full scale application to create bedrock rubble zones for active collection/flow control for several years. The method provides a previously unavailable method to passively treat contaminated groundwater in bedrock at low cost.*

Introduction: In-situ remediation technologies are becoming increasingly attractive to industry, remediators and regulators. These technologies minimize the management of waste above ground, avoid potential exposures and associated health concerns at the surface, and avoid the "problem relocation" issues that result from removing contaminated soil and water from a site to a separate, off-site-treatment or disposal location.

In particular, the funnel-and-gate groundwater treatment approach (McMurty and Elton, 1985; Burris & Cherry, 1992) has drawn significant attention due to the apparent simplicity of design, installation, allowance for variable in-situ treatment techniques, and the associated cost savings that derive from these factors. The funnel-and-gate approach, in concept, relies upon the installation of barriers to groundwater flow (the "funnels") that divert flow to centralized permeable pass-through areas (the "gates"), where in-situ treatment takes place. A growing number of pilot and field-scale projects of funnel-and-gate technology, combined with a variety of treatment techniques at the gate, are showing promise for reasonable-cost, low-maintenance techniques to passively treat contaminant plumes in-situ (Suthersan, 1997). Applications of funnel-and-gate and background discussion can be found in Starr & Cherry (1990) and Starr et al. (1992).

However, effective deployment of funnel-and-gate applications depends on the ability to install sufficiently low-hydraulic-conductivity or impermeable barriers to divert groundwater flow through single or multiple gates (see Starr and Cherry, 1990; Sutherson, 1997). The primary available barriers for the funnel-and-gate approach are sealable, locking-flange sheet-pile walls (Starr et al., 1992) or conventional low-hydraulic-conductivity slurry walls. Other innovative barrier-placement techniques are also being developed. Deployment of sealable sheet piles requires subsurface geotechnical conditions amenable to conventional sheet-pile driving, i.e., low- to moderate-density unconsolidated sand or granular materials of finer grain size. Highly heterogeneous materials and, in particular, materials such as glacial tills where cobble- or boulder-size obstructions exist, may prevent effective emplacement or limit the installation of such sheet-pile barriers as funnels. Installation of slurry walls as an alternative typically requires excavation and above-ground management of large volumes of potentially contaminated soil. Lastly, use of commercially available techniques to create a funnel barrier is either impractical or prohibitively expensive in bedrock.

[1]Haley & Aldrich, Inc., 189 N. Water St., Rochester, New York, 14604 USA, (716)327-5507, vbd@HaleyAldrich.com

[2]Haley & Aldrich, Inc., 189 N. Water St., Rochester, New York, 14604 USA, (716)327-5519, dae@HaleyAldrich.com

The development of refractive flow and treatment (RFT) systems was intended to provide an alternative analogous to the funnel-and-gate barrier approach and to provide a mechanism for the type of in-situ treatment that funnel-and-gate can provide, but in geologic settings where barrier emplacement may be impractical. Conceptually, refractive-flow cells in an RFT system are oriented zones of engineered high-hydraulic-conductivity materials in otherwise low-hydraulic-conductivity settings that are used to refract groundwater flow along a preferred path to an in-situ, high-hydraulic-conductivity treatment cell. Similar high-hydraulic-conductivity downgradient cells are used to disperse the treated groundwater back into the host formation. The engineered high-hydraulic-conductivity zones refract groundwater flow, rather than rely on a barrier to divert flow, as is done in conventional funnel-and-gate technology. This paper provides an overview of the RFT concept, the fundamentals of the physical basis for the concept, and a description of some potential applications. Analysis of the physics and modeling of the concept are provided in Edwards et al. (1996a). A detailed description of treatment cells in an RFT system and potential methods for treating contaminated groundwater are described in Edwards et al. (1996b).

Refractive-Flow Concept

Groundwater streamlines in the subsurface are refracted when passing from one porous material to another with a different hydraulic conductivity, similar to the manner in which light is refracted as it passes a contact between two materials having different refractive indices. However, unlike the refraction of light, which behaves according to Snell's Law, a sine function, the refraction of groundwater streamlines behaves according to a tangent function (see, for example Freeze and Cherry, 1979; Fetter, 1988). As indicated in Figure 1, a groundwater flow impinging upon a boundary between a geologic material of hydraulic conductivity K_1 and a second geologic material of greater hydraulic conductivity K_2 is refracted to a new flow direction, which is based on a tangent function of its angle of incidence, θ_1, and the ratio of K_1 to K_2. The tangent law is expressed as:

$$K_1 / K_2 = \tan(\theta_1) / \tan(\theta_2) \qquad (1)$$

In broad terms, if the first geologic medium has a hydraulic conductivity K_1 that is two or more orders of magnitude smaller than the hydraulic conductivity K_2 of the second geologic material, then angles of refraction approaching 90° are possible. Accordingly, it should be feasible in concept to engineer a high-hydraulic-conductivity in-situ cell that refracts streamlines of contaminated groundwater and conveys them along preferred paths.
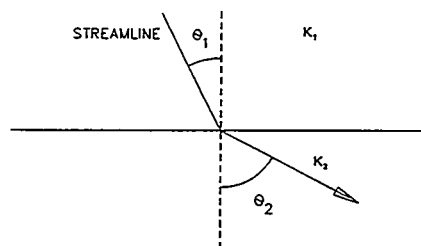
Figure 1   Refracted Streamline Across Boundary Between Low-K (K₁) and High-K (K₂) Materials.

Containing streamlines in the engineered high-hydraulic-conductivity material over long distances means only localized treatment cells are necessary to treat the contaminated groundwater before streamlines pass back out of the cell. In concept, the distinction between a refractive-flow cell and a conventional funnel-and-gate barrier is shown in Figure 2.
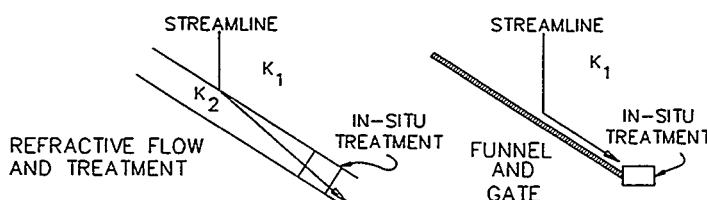
Figure 2   Difference Between RFT Flow Refraction and Funnel-and-Gate Flow Diversion.

Figure 3 depicts an idealized single, infinitely long refractive-flow cell, oriented obliquely to a groundwater-flow streamline. Hydraulic conductivity of the native material on either side of the refractive-flow cell is designated as K_1, and hydraulic conductivity of the refractive-flow cell is designated as K_2. Thickness of the cell is designated by T, and projected length of the streamline in the cell, measured parallel to the cell wall, is designated by S. The incident angle θ_1 and refracted angle θ_2 are measured with respect to a line oriented normal to the planar boundary between the native material and the refractive-flow cell. Points "A," "B" and "C" are designated to allow trigonometric relationships of the streamline refraction along the path of length L to be determined in terms of W, a capture-zone width, and T.
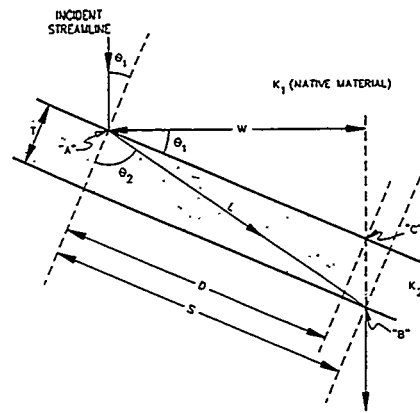
Figure 3 Geometry of a Theoretical RFT Cell (High Conductivity = K_2) in a Low-Conductivity (K_1) Matrix.

As can be deduced from Figure 3, the relationship between capture-zone width, refractive-flow-cell thickness and hydraulic-conductivity ratio for the idealized system is given by (Edwards et al., 1996a):

$$\log (W/T) = \log [\sin (\theta_1)] + \log [(K_2/K_1)-1] \qquad (2)$$

This equation can be used to qualitatively investigate impacts of different streamline angles of incidence and refractive-flow-cell thicknesses on capture widths for RFT systems.

Figure 4 depicts a log-log plot of W/T versus K_2/K_1, based on Equation 2, for several illustrative angles of incidence, i.e., 30 and 50 degrees. For large differences between hydraulic conductivity between the native material and the refractive-flow cell, the log of (W/T) is nearly a linear function of the log of (K_2/K_1). Some nonlinearity is apparent for very small values of K_2/K_1. As shown in Figure 4, a refractive-flow-cell width of approximately 6 feet [2 m], where the refractive-flow cell has a hydraulic conductivity two orders of magnitude greater than that of the native material, would yield a theoretical spacing of approximately 600 feet [185 m] (two orders of magnitude difference between W and T) in an idealized refractive-flow system. In an actual system, the spacing would, for various reasons, be smaller.
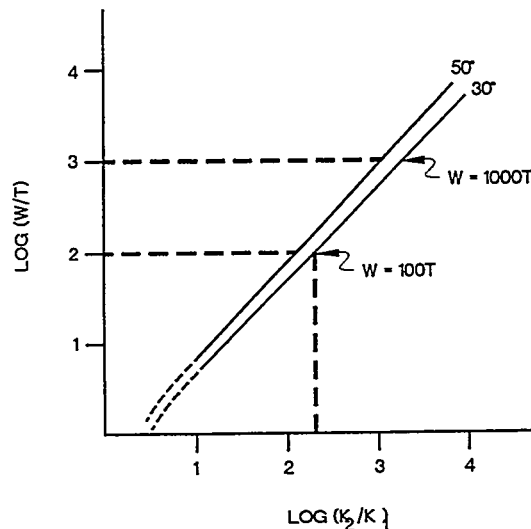
Figure 4 Variability of Refractive Cell Dimensions W and T, Relative to Ratio of Cell Conductivity (K_2) and Native Conductivity (K_1).

It is emphasized that the system described so far is idealized and, for actual design purposes, changes in system-scale flow patterns and variability of several other parameters would need to be characterized using numerical modeling in order to plan for groundwater capture and treatment with

461

an appropriate factor of safety. However it is notable by viewing Equation 2 and Figure 4 that the predominant variable affecting idealized refractive flow is the hydraulic-conductivity contrast between the installed refractive-flow cell and the adjacent native rock or soil. Therefore, despite native system heterogeneities and variability of some of the parameters, if the hydraulic conductivity contrast between the installed refractive-flow-cell materials and the adjoining native rock or soil materials is sufficiently high, then flow refraction to successfully contain and treat a contaminant plume is attainable.

Preliminary Modeling

MODFLOW, an USGS finite-difference model for groundwater flow, was used to simulate groundwater flow patterns for a number of RFT configurations. Figure 5 depicts a contoured MODFLOW output for isopotential lines of groundwater entering into and exiting an illustrative RFT system configured as an "X". This particular RFT system is configured so as to allow upgradient refractive-flow cells to capture a plume and direct it to a treatment zone located at the cross point of the "X", and to allow hydraulic head to be dispersed downgradient from the treatment zone so treated water flows refractively back into the native formation downgradient from the treatment zone.
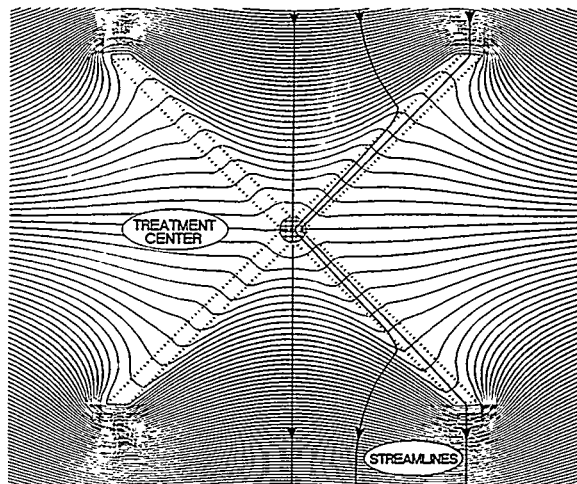
Figure 5 Results of MODFLOW Simulation Depicting Streamline Refraction and Capture with an "X-Shaped" RFT System.

The modeling for which results are shown above assumes isotropic, heterogeneous conditions. Accordingly, hydraulic gradients are assumed to be coincident with streamline directions. More detailed analysis of RFT systems and discussion of model-output variability, based on such influences as anisotropy and heterogeneity, is discussed in Edwards et al. (1996a).

Applications Specific to Bedrock Settings

Engineered blasted-bedrock systems for enhanced pump-and-treat remediation in low-hydraulic-conductivity fractured-bedrock settings have been operated successfully for several years (see Begor et al., 1990; Smith and Heeks, 1992; Gehl, 1994; McKown et al., 1995; Loney et al., 1996). In these systems, a zone of highly-fractured bedrock is created by detonating explosives in timed sequence in a series of closely-spaced shotholes. Typical blasted-bedrock zones are created in either linear or radial configurations, depending on site requirements. Linear configurations are utilized for downgradient hydraulic control of contaminant plumes, whereas radial configurations are used in the interior of contaminant plumes to accelerate contaminant-mass removal (see Loney et al., 1996). Blasting to create such systems requires careful design and engineering to determine the type, volume, and distribution of explosive charges needed to obtain sufficient subsurface fracturing, yet limit vibrations to sensitive structures, utilities, etc. Shotholes are drilled 3 to 6 feet [1 to 2 m] apart, using overburden casing to maintain the hole open for explosives loading. Typical loads range from 0.5 to 1.5 lbs. of charge per-unit-foot of depth [0.6 to 2.2 kg/m], with crushed stone being used as stemming to maintain blast debris in shot holes. Loadings of lesser value, closer shothole spacing, or different linear arrangements are used where blast zones are close to sensitive structures.

When actively pumped, blasted-bedrock trenches typically yield orders-of-magnitude more groundwater per recovery well than conventional systems would and at much lower cost (see Loney et al., 1996). This is due to increased fracture connectivity as well as order-of-magnitude increases in hydraulic conductivity. Post-construction investigations of some blasted-bedrock systems 200 to 1,200 feet [e.g., 60 to 370 m] in length, and 30-60 ft. [9 to 19m] in total depth have shown that the high-hydraulic-conductivity rubble zones created using only linear (not staggered) arrangements of shot holes have generally had thicknesses of 3 to 6 feet [1 to 2 m]. Larger blasted-bedrock-zone widths than those created historically can be achieved using "staggered" or "diamond" patterns of shotholes, similar to those employed in the construction of bedrock utility trenches. Therefore, if linear or, preferably, staggered arrangements of shotholes are used to create refractive-flow cells in bedrock, then contrasts in hydraulic conductivity between native material (K_1) and blasted bedrock forming the refractive-flow cell (K_2) can be sufficient to achieve a degree of refraction needed for capture and treatment. Numerical modeling is typically necessary to determine suitable orientations of refractive-flow cells in bedrock, considering existing site hydrogeology, possible refractive-flow-cell widths, dimensions of the contaminant plume, and surface structures affecting placement and orientation of the RFT system.

Typical cost for installing an engineered blasted-bedrock zone in the northeastern U.S. ranges from approximately $150 to $250 per linear foot [$500 to $800 per linear meter] of trench in terms of lateral dimensions. Typical depth of penetration into bedrock, exclusive of overburden depth, is approximately 25 to 40 feet [8 to 12 m] (Loney et al., 1996).

Treatment Cells - Treatment cells in RFT systems can be installed in bedrock using several different methods (e.g., conventional caisson-installation techniques). A variety of in-situ treatment technologies can effectively be employed to reduce, oxidize, biodegrade, volatilize, sorb or precipitate out dissolved contaminants in groundwater. These technologies include zero-valent-iron for chemical reduction, electron-acceptor and nutrient delivery systems for biodegradation, sparging systems for volatilization, carbon or resins for sorption, and chemical or electrochemical systems for in-situ reduction, oxidation or precipitation (see Starr and Cherry, 1990; Edwards et al., 1996b).

Design of treatment cells in RFT systems must account for residence time of contaminated groundwater within the treatment cell or cells. The desired residence time can be manipulated by varying such factors as treatment-cell dimensions, grain size or fracture apertures and density of media used in treatment- or refractive-flow cells, imposed gradient across a cell, etc.

Other RFT Applications and Design Concerns

Overburden Applications - Although an example is given here of an RFT application in bedrock, RFT systems do not need to be limited to bedrock settings. Applications in bedrock allow for totally in-situ installations, since the bedrock can be explosively fractured and left in place to create a refractive-flow cell. Refractive-flow cells, however, can also be created in native soils or fill materials of low hydraulic conductivity using conventional trenching or other techniques to remove pre-existing materials and replace them with clean porous media of high hydraulic conductivity, such as sand. Application of an RFT system in an overburden setting does potentially create the issue of having to manage large quantities of overburden materials removed from the trench, and so it would be desirable to locate the upgradient refractive-flow cells of an overburden RFT system sufficiently downgradient from the contaminant plume so that excavated materials do not need to be specially managed.

Use of Refractive Cells For Flow Diversion - Use of refractive-flow cells need not be limited to downgradient collection and treatment. Refractive-flow cells can be placed upgradient from a source area and used to divert the bulk of groundwater flow around it in a manner similar to which run-on is controlled around sanitary landfills. This may reduce the rate of growth and development of a plume and/or allow for greater residence time in a downgradient in-situ reactor. An understanding the variability of hydrogeologic parameters of the effected system is important in determining the proper

placement, orientation, and dimensions of refractive-flow cells to accomplish the desired diversion. Examples of diversion configurations that have been preliminarily modeled for proof of concept appear in Figure 6. Again, it is noted that these are example configurations only, and that site-specific configurations that accommodate sensitive structures, utilities, etc. can be developed to meet design objectives.

Idealized vs. Real World Conditions - As with any subsurface system, it is important that variabilities in parameters that could affect an RFT system be considered both individually and in terms of their synergistic effects. This can best be accomplished through sensitivity analysis during numerical modeling. Variability of native-material hydraulic conductivity, engineered-cell hydraulic conductivity, heterogeneities in both systems and desired residence times should all be considered relative to overall system design.
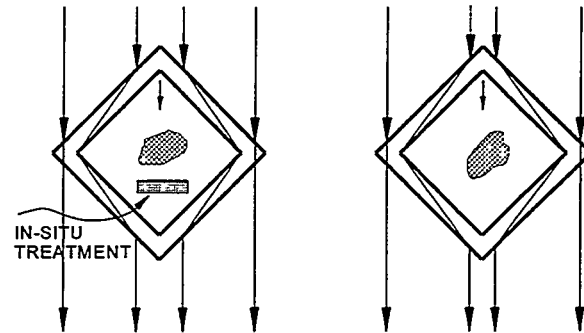
Figure 6   *Example of Refractive Cells Used to Refract Flow Around Contaminant-Source Area.*

Other factors such as contaminant-concentration variability, potential changes in groundwater flow direction, specific forms of the contaminant (dissolved phase or NAPL) and diffusion may also be important. Once the potential variability of these parameters is determined, an appropriate factor of safety for system design can be estimated. It is anticipated for most systems that the primary factors controlling application and design will be hydraulic conductivity contrasts between refractive-flow cells and native materials, hydraulic gradients across the system and required residence times to effectively treat contaminated groundwater in-situ.

Adequate numerical modeling to account for variability of these parameters and to determine a final deployed configuration and a factor of safety will be necessary for most RFT systems. However, it is anticipated that the capital costs of characterization, modeling, design, and deployment should still be comparable to those of many, if not most, of active remediation systems that could be employed at a contaminated site. As with other in-situ, and especially in-situ/passive-treatment, technologies, it is anticipated that while capital costs for RFT and active systems will be comparable, overall design-life cost in constant dollars will be lower for RFT systems due to significantly lower operation and maintenance costs.

Summary and Conclusion

In-situ remediation of contaminated groundwater has numerous advantages over traditional remedial methods involving groundwater extraction, treatment, and discharge. Once constructed, in-situ methods appear relatively unobtrusive, occupy less land space, and require fewer restrictions on surface activities. In addition, many such systems avoid potential problems of exposure and waste management associated with many ex-situ or active-treatment systems. Further, overall design-life costs may be much lower than those for conventional remedial approaches.

This paper presents a new technology, called Refractive Flow and Treatment (RFT), for in-situ capture and treatment of contaminated groundwater found in bedrock or overburden materials of low to moderate hydraulic conductivity. Refractive-flow cells in RFT systems are engineered to have higher hydraulic conductivities than those of adjacent native or fill materials, typically by several orders of magnitude. The refractive-flow cells are oriented in the subsurface so as to passively

capture, refract and/or channel contaminated groundwater in a predetermined manner. The contaminated groundwater captured by a refractive-flow cell is channeled, without pumping, to one or more downgradient in-situ treatment cells, associated also with an RFT system. The groundwater, once treated, is refracted back into the adjacent native or fill materials. During RFT operation, no groundwater is extracted at the surface, and no added energy is required for in-situ capture or dispersal. Energy may or may not be required for treatment, depending on the treatment method employed.

As conceived, RFT technology offers an analog to emerging funnel-and-gate technologies but, unlike funnel-and-gate systems, can be deployed in settings where sheet piling or other barriers used for funnel-and-gate cannot be emplaced. These settings, for instance, include sites where contaminated groundwater exists in bedrock or glacial till with boulders.

RFT technology is a new technology that is currently being extended to a number of different applications. One is to place refractive-flow cells upgradient to a contaminant-source area for the purpose of diverting the bulk of clean, flowing groundwater around the source area, thereby reducing the rate of contaminant dissolution and migration. This approach can increase residence time in downgradient in-situ reactors.

References

Begor, K.F., Miller, M.A. and Sutch, R.W. (1989) Creation of an artificially produce fracture zone to prevent contaminated ground-water migration. Groundwater, v.27, 57-65.

Burris, D.R. and J.A. Cherry. (1992) Emerging plume management technologies. In situ treatment zones. Eighth Annual Air and Waste Management Meeting, Kansas City, MO, June 21-26.

Edwards, D.A., Dick, V.B. and J.W. Little (1996a) Refractive-flow-and-treatment systems: Part 1, Refractive flow. (in preparation)

Edwards, D.A., Dick, V.B. and J.W. Little (1996b) Refractive-flow-and-treatment systems: Part 2, Treatment zones. (in preparation)

Fetter, C.W. (1988) *Applied Hydrogeology,* p 140. Merrill Publishing Co., Columbus, Ohio.

Freeze, R.A. and Cherry, J.A. (1979) *Groundwater,* p. 172-173. Prentice-Hall, Inc., Englewood Cliffs, New Jersey.

Gehl, R.W. (1990) Hydraulic enhancement and control strategies for remediation of a contaminated fractured bedrock aquifer, *in Proceedings of the Focus Conference of Eastern Regional Groundwater Issues,* National Water Well Association, p. 265-273.

Loney, J.E., Edwards, D.A. and Little, J.W. (1996) Groundwater capture and remediation with engineered blasted-bedrock zones. Northeastern Geology and Environmental Sciences, v. 18, no.3, 195-200.

McKown, A.F., Smith, L.P., and J.E. Loney (1995) Blast trenches for groundwater remediation, *in Proceedings of 21st Annual Conference on Explosives and Blasting Techniques,* p. 305-322. International Society of Explosives Engineers.

McMurty, D.C. and R.O. Elton (1985) New approach to in-situ treatment of contaminated groundwaters. Environmental Progress, v. 4, no. 3, 168-170.

Smith, L.P. and Heeks, R.E. (1992) Innovative remedial technologoy applied to chlorinated solvents in fractured rock, *in Proceedings of the 5th annual hazardous materials and environmental management conference,* p.102-

117, Central, Chicago.

Starr, R.C. and J.C. Cherry (1990). In situ barriers for groundwater pollution control. Prevention and treatment of soil and groundwater contamination in the petroleum refining and distribution industry, Montreal, Quebec, October, 16-17.

Starr, R.C. and J.C. Cherry, and E.S. Vales. (1992). A new type of steel sheet piling with sealed joints for groundwater pollution control, 45th Canadian Geotechnical Conference, Toronto, Ontario, October 26-28.

Suthersan, S.S. (1997) Remediation Engineering: Design Concepts, p. 187-214. CRC Press, Inc., Boca Raton, Florida.

LONG-TERM DEGRADATION (OR IMPROVEMENT?) OF CEMENTITIOUS GROUT/CONCRETE FOR WASTE DISPOSAL AT HANFORD

Mel G. Piepho[1]

ABSTRACT

If grout and/or concrete barriers and containments are considered for long-term (500 yrs to 100,000 yrs) waste disposal, then long-term degradation of grout/cement materials (and others) need to be studied. Long-term degradations of a cementitious grout monolith (15.4mW x 10.4mH x 37.6mL) and its containment concrete shell and asphalt shell (each 1-m thick) were analyzed. The main degradation process of the concrete shell was believed to be fractures due to construction joints, shrinkage, thermal stress, settlement, and seismic events. A scenario with fractures was modeled (flow and transport model) for long-term risk performance (out to a million yrs). Even though the concrete/grout is expected to fracture, the concrete/grout chemistry, which has high Ph value, is very beneficial in causing calcite deposits from calcium in the water precipitating in the fractures. These calcite deposits will tend to plug the fracture and keep water from entering. The effectiveness of such plugging needs to be studied more. It's possible that the plugged fractures are more impermeable than the original concrete/grout. The long-term performance of concrete/grout barriers will be determined by its chemistry, not its mechanical properties.

1.0 INTRODUCTION

Most groundwater flow/transport codes assume constant hydraulic/transport properties. However, for simulations of waste-disposal performance, long time periods (greater than 500 years) are required. Long time periods are needed because the release of contaminant particles can be very slow and take a long time to reach a peak release and take an even longer time to reach a peak concentration in the groundwater. Over long time periods, degradation of man-made barriers can be expected. These degradations (for example, cracking of concrete) will change the flow and transport properties of the barriers and waste form. Degradation of the engineered barriers was assumed in the Grout Waste (grout monoliths with concrete and asphalt shells) Performance Assessment performed at Hanford, Washington (Piepho 1994; Kincaid et al. 1995). Saturated conductivities, porosities, and moisture-retention curves were changed in discrete steps over time. The effects of the time-degradation of the barriers (or shells) and the grout monolith on groundwater are shown. Also, recommendations are made on the effectiveness of concrete shells (barriers) and grout waste forms, and how more accurate modeling of their long-term performance can be accomplished.

2.0 CONCEPTUAL MODEL

The goal of the grout monolith with its concrete and asphalt shells (barriers) in the vadose zone is to slow down the contaminants (radionuclides), that are placed in the grout monolith, in reaching the water table to an acceptable rate. Slowing releases of contaminants will reduce the amount of contaminants that is potentially consumed from drinking-well water as shown in Figure 1.

Figure 1 shows the 2D flow-and-transport model domain which consists of the vadose zone, and the water table (top of groundwater) is the lower boundary. The upper boundary consists of a small constant water infiltration rate of 0.1 cm/yr. The side boundaries are no-flow boundaries. Flow and transport in the aquifer and drinking-water doses from the well are calculated with simpler models,

---

[1] Daniel B. Stephens & Associates, Inc.; 1845 Terminal Dr., Suite 200; Richland, Washington 99352; Phone (509) 946-6627; Fax (509) 946-6712; e.mail: stephens@oneworld.owt.com

but are included in the analysis. In effect, waste contaminants slowly flow out of the grout vault (primarily due to cracks in the outer shells), flow vertically through the vadose zone to the groundwater, enters the groundwater and flow horizontally to a drinking well located about 100 m horizontally from the waste grout monolith, and is consumed by a human drinking water from the well. The performance measure (bottom line) of the disposal system is the magnitude and timing of the peak drinking-water dose to man.

The focus of this report is the degradation of the grout disposal vault (especially the concrete shell) which is shown in Figure 2 (the central compliance case is described in Section 4.0). The purpose of the high-density polyethylene (HDPE) liner between the grout and concrete shell is to provide a flow path for excess grout water from the monolith to the catch basis below the vault. The catch basin is filled with gravel and has an outlet for the excess water to be pumped (pump is not shown) out of the catch basin for the short-term.

The degradation processes for concrete with rebar and grout monoliths include 1) seismic loading, 2) rebar corrosion, 3) construction joints/cracks, 4) drying shrinkage, 5) thermal stress, 6) chemical degradation, 7) settlement, 8) externally applied loads, and 9) weathering. The main long-term degradation of the asphalt shell, which is not the focus here, is bio-degradation (bacteria) and cracking promoted by the slow hardening of the asphalt.

3.0 MATHEMATICAL MODELS FOR CRACKS IN POROUS MEDIA

Two different models were used to model the moisture retention and relative permeability of cracks that are smaller than the cell size. These models are referred to 1) backfill soil model, and 2) composite model.

One model which was not used, but is worthy to mention, is the "dual-porosity" model. The dual-porosity model was not used primarily because data, especially for the crack-matrix interface coupling, did not exist. The total contaminant flux through the barriers is calculated accurately by the two chosen crack models described in next section.

3.1 BACKFILL-SOIL CRACK MODEL

The backfill-soil model for cracks assumes that the cracked porous media (like cracked concrete) has backfill-soil unsaturated properties. In other words, backfill-soil moisture-retention and relative-permeability properties and transport properties are assumed not only for the crack, but for the entire computational cell. An equivalent saturated conductivity and diffusion coefficient is calculated for the entire computational cell. For example, the saturated conductivity and diffusion coefficient for the cracked concrete are estimated by the following equations (Harr 1962, Piepho 1994):

$$^{eq}K_{sat} = ECF * 3 \times 10^{-2} + (1 - ECF) * 3.75 \times 10^{-10} \qquad \text{(cm/s)} \qquad (1)$$

where ECF is the Effective Crack Fraction in concrete, which is the volume fraction of the through cracks (no dead ends) divided by the volume of the bulk concrete and varies with time; 3×10^{-2} cm/s is the saturated conductivity value of backfill soil, 3.75×10^{-10} cm/s is the saturated conductivity value of the initial concrete. The effective diffusion coefficient for the cracked concrete is given by the following equation (Crank 1975, Piepho 1994)

$$D_{eq} = ECF * D_m + (1 - ECF) * 5 \times 10^{-8} \qquad \text{(cm}^2\text{/s)} \qquad (2)$$

where D_m is the diffusivity of solute (2.5×10^{-5} cm²/s) in pure water, 5×10^{-8} cm²/s is the diffusivity value of solute in non-cracked concrete.

These properties were used as input to the Grout/Glass Performance Assessment Code System-GPACS (Piepho 1994a) for flow, transport, and dose calculations. The same total water flux

through the equivalent cell should be the same as a cell with matrix properties and crack properties. The break-through time through the equivalent cell will not be accurate, but this information is not needed as the early fluxes will be buffered by the large vadose zone and will not affect the peak dose from the drinking well. The cracks dominate the hydraulics in both the asphalt barrier and concrete vault when the cracked cells are conservatively assumed to have backfill soil properties.

The open-gravel properties for cracks could also be used in lieu of backfill-soil properties. The gravel properties are not as conservative as the backfill-soil properties since gravel does not have high moisture-retention capability nor high relative permeability. The gravel properties represent cracks that are air filled, and air-filled (dry) cracks are barriers to water flow instead of conduits. Hence, gravel properties were not assumed in this analysis. Backfill soil properties were assumed so that the analysis would be more conservative.

3.2 COMPOSITE MODEL

The composite model (Klavetter and Peters, 1986) combines the crack properties and the barrier matrix properties to form the composite material (both cracks and matrix) properties. The composite model was chosen so that the pressure head could be kept continuous and still preserve mass when cracks occur in the concrete barrier. The model consists of the following equations and assumptions. For a given pressure head, the saturation for the fractures (S_f) and for the matrix (S_m) are calculated using the van Genuchten (1978) moisture retention curves with backfill soil parameters for S_f and with concrete parameters for S_m. The composite material saturation (S_c) is calculated by the following equation:

$$S_c = (S_f * ECF + S_m * (1 - ECF) * e_m)/e_c \qquad (3)$$

where ECF = effective crack fraction (sum of crack apertures over given length), and varies over time; e_m = porosity of matrix; e_c = effective porosity of composite material = $ECF + (1 - ECF) * e_m$. The relative permeability ($k_{r,c}$) of the composite material is given by the following equation:

$$k_{r,c}(S_c) = [K_f * ECF * k_{r,f}(S_f) + K_m * (1-ECF) * k_{r,m}(S_m)]/^{eq}K_{sat} \qquad (4)$$

where ECF = Effective Crack Fraction (sum of crack apertures over given length or crack volumes over cell volume), and varies over time; K_f = fracture saturated conductivity = 3×10^{-2} cm/s; $k_{r,f}$ = relative permeability of crack which is a function of S_f (Mualem-1976 model is assumed); K_m = matrix saturated conductivity = 3.75×10^{-10} cm/s; $k_{r,m}$ = relative permeability of matrix (concrete) as a function of S_m; $^{eq}K_{sat}$ = composite material saturated conductivity, where the backfill-soil Ksat is used for the cracks and concrete properties are used for the matrix.

This model assumes that the pressure heads in the both the cracks and matrix are all equal for a given computational cell.

4.0 SIMULATION CASES AND RESULTS

The following cases describe the release scenarios of the grout-vault system with time-dependent degradation of the asphalt barrier, concrete vault and grout. Because of the time dependence of property parameters, these cases are more complex than cases with fixed parameters. To gain a better understanding of the time-dependent degradation cases, more details are provided in Piepho (1994). The cases are briefly described here.

Case 1.0 (Central Compliance): The asphalt and concrete shells are assumed to crack at 5000 and 5150 years, respectively, after disposal (1 mm crack every meter). The concrete moisture-retention curves are changed to those of backfill soil (see Section 3.1) and the grout's conductivity increases by a factor of 10 due to micro cracking. At 20,000 years after disposal, increased cracking in the

469

concrete doubles its conductivity and biodegradation of the asphalt increases the conductivity by a factor of 10. At 40,000 years after disposal, the asphalt shell is assumed to be all gone (conductivity increases by a factor of 100) due to bio-degradation, the grout's conductivity increases by a factor of 10, and the concrete shell's conductivity increases by a factor of 10. The diffusion coefficient of the contaminant in each of the materials also increases over time. Also, since some salts (primarily sodium nitrate) are stored in the grout, there is expected to be an osmotic potential which will attract water vapor from the surrounding unsaturated soils to the high salt concentrations near the grout. This water vapor will then condense and form a liquid water source that will effectively increase the advection to and from the grout. See Figure 2 for details of this case.

Case 1.1 (Delayed Cracking): Same as central compliance case (Case 1.0) except that the asphalt and concrete shells crack at 10,000 years instead 5,000 years and 5,150 years, respectively.

Case 1.2 (No HDPE Flow Path): Same as central compliance case (Case 1.0) except that there is no high-density polyethylene liner included in the model as well as no gravel in the catch basis. The purpose of this case was to quantify the performance of the liner/catch basis design.

Case 1.3 (Composite Model): Same as central compliance case (Case 1.0) except that a composite flow and transport model (see Section 3.2) was used to model the cracked concrete and asphalt shells.

The drinking-water doses are shown in Figure 3 for each of the four cases. The effects of the cracks in the concrete and asphalt shells on the dose is rather apparent as the dose increases dramatically after cracks occur as cracks greatly enhance the advection of water into and out of the grout monolith. If the major cracking sequence is delayed to 10,000 years, the doses are much lower for the first 10,000 years (Case 1.1). However, if the cracking sequence is delayed, then more contaminant mass is available later in time to reach the groundwater, causing a higher dose later in time than the other cases. The high-density polyethylene liner appears to be beneficial in reducing doses because it routes some of the contaminated grout water to the catch basin beneath the vault where advection is smaller (Case 1.2). The composite model, which should be more realistic, shows a reduction in dose for the first 40,000 years, but higher doses after 40,000 years. This indicates that the composite model is not as conservative as the backfill-soil model for the first 40,000 years, but is more conservative after 40,000 years.

However, the chemistry of the concrete shell, grout, and Hanford water were not included in this analysis, and this chemistry can be very important in regards to water flow in concrete cracks. At Hanford, and other sites, the water, infiltrating through the soils, contains carbon dioxide (CO_2) which combines with calcium hydroxide (CaOH) in the high Ph concrete to form calcium carbonate (CaO_3) as precipitate in the pores and cracks that have the infiltrating water. In other words, the flow paths in the concrete (cracks or pores) will be plugged with calcium carbonate, which will inhibit or stop the flow of infiltrating water. This chemical process was not included in this analysis partly because hydraulic properties for calcium carbonate (calcite) were not known and the time for plugging was not known. It is possible that the calcite is more impermeable than the concrete (or grout) itself, which would mean that the cracked concrete would be a better infiltration barrier than the initial uncracked concrete (same for the grout monolith). This principle would apply to any cementitious media that has calcium hydroxide and high Ph as long as carbon dioxide is present in the infiltrating water.

5.0 CONCLUSIONS AND RECOMMENDATIONS

The the most important hydraulic parameters were found to be the hydraulic parameters (moisture-retention, relative permeability, and saturated conductivity values) for cracks. If no cracks are present, then the Ksat (or permeability) of the asphalt barrier and concrete vault are the most important parameters.

Since it may be impossible to defend a no-cracking scenario for low-permeability barriers in the long term (> 500 years), the hydraulics and chemistry of cracks need to be known. One recommendation for future studies of long-term performance of cementitious barriers is to measure the hydraulic properties of the cracked composite material together as a function of time for various sizes (apertures) of cracks. As the calcite forms and plugs the cracks, the saturated conductivity should greatly decrease. A cracked cementitious barrier may actually be a better barrier than the uncracked one. In summary, the long-term performance of cementitious barriers will depend on the chemistry of the material and the soil water, not the mechanical features of the material. The chemistry will be present much longer than the initial mechanical features.

6.0 REFERENCES

Crank, J. (1975) *The Mathematics of Diffusion*, p. 273, Oxford University Press.

Harr, M. E. (1962) *Groundwater and Seepage*, p. 27, McGraw-Hill Book Company, New York.

Kincaid, C. T., J. W. Shade, G. A. Whyatt, M. G. Piepho, K. Rhoads, J. A. Voogd, J. H. Westsik, Jr., M. D. Freshley, K. A. Blanchard, and B. G. Lauzon. (1993) *Performance Assessment of Grouted Double Shell Tank Wastes Disposal at Hanford.* WHC-SD-WM-EE-004, Rev. 1, Westinghouse Hanford Company, Richland, Washington.

Klavetter, E. A. and R. R. Peters. (1986) *Fluid Flow in a Fractured Rock Mass.* SAND-85-0855, Sandia National Laboratories, Albuquerque, New Mexico.

Mualam, Y. (1976) "A New Model for Predicting the Hydraulic Conductivity of Unsaturated Porous Media". In *Water Resources Research*, Vol 12 (3), 513-522.

Piepho, M. G. (1994) *Grout Performance Assessment Results of Benchmark, Base, Sensitivity and Degradation Cases.* WHC-SD-WM-TI-561, Rev. 0, Westinghouse Hanford Company, Richland, Washington.

Piepho, M. G., W. H. Sutherland, and P. D. Rittmann. (1994a) *The Grout Performance Assessment Code System (GPACS) with Verification and Benchmarking.* WHC-SD-WM-UM-019, Westinghouse Hanford Company, Richland, Washington.

van Genuchten, M. Th. (1978) *Calculating the Unsaturated Hydraulic Conductivity with a New Closed-Form Analytic Model.* Report 78-WR-08, Water Resources Program, Dept. of Civil Engineering, Princeton University, Princeton, New Jersey.

Figure 1. Conceptual Model
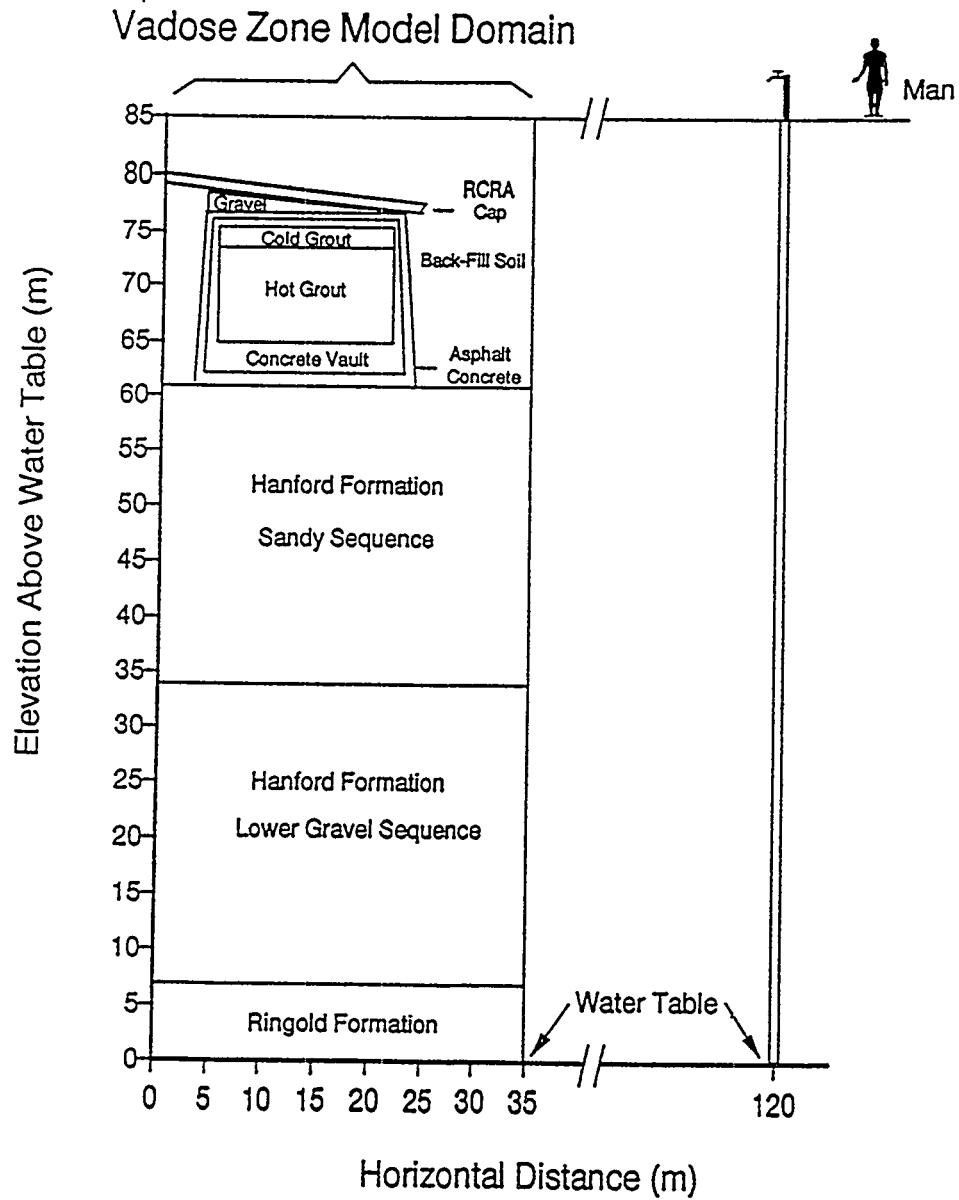
Figure 2. Features within the Model of the Central Compliance Case (Case 1.0) Not to scale
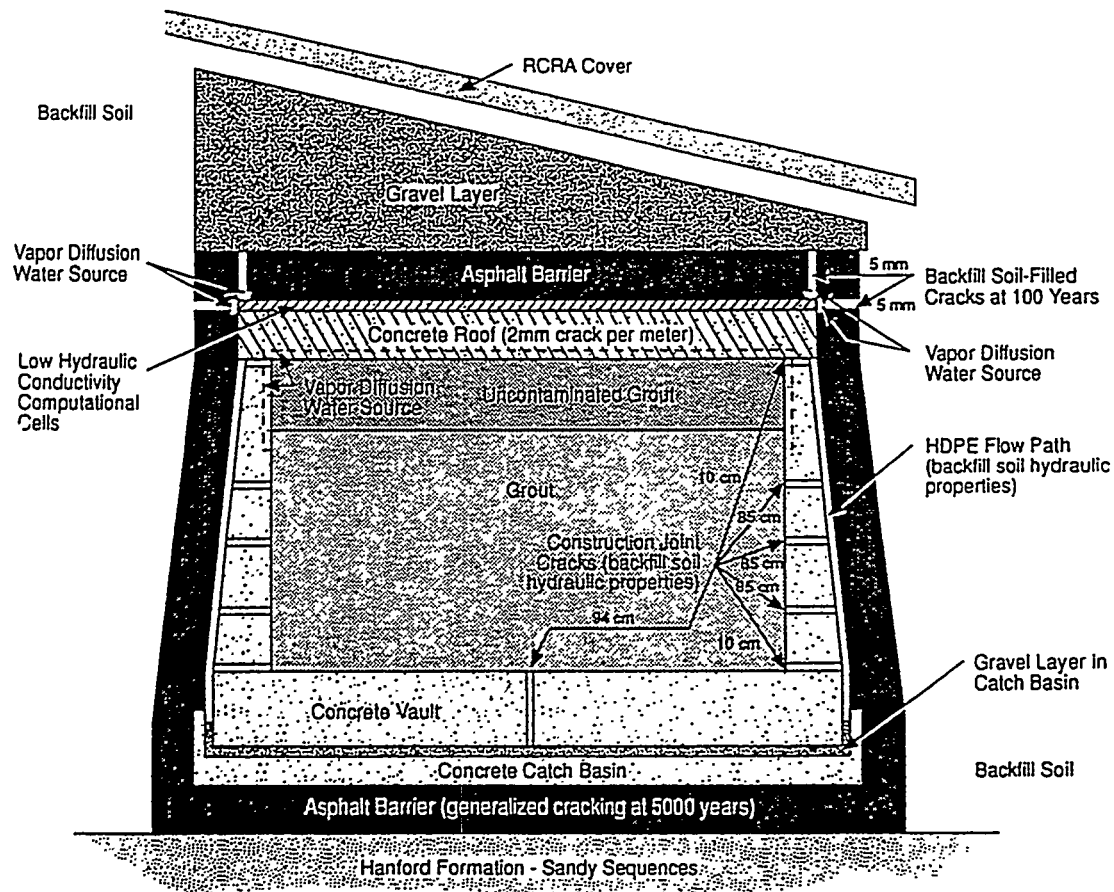
Figure 3. Drinking-Water Doses for Compliance Cases
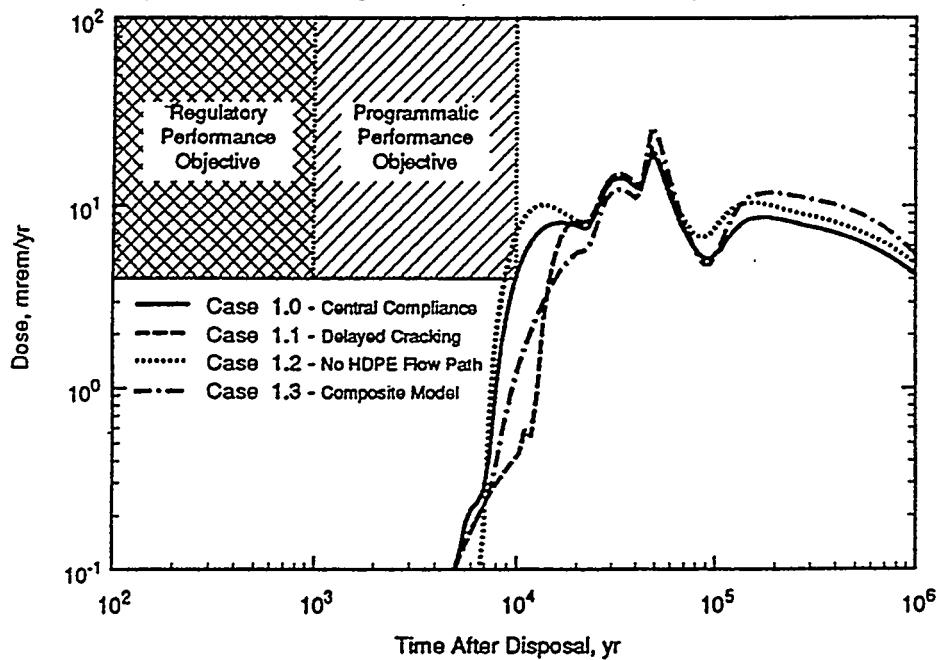
IN-SITU CONTAINMENT OF BURIED WASTE
AT BROOKHAVEN NATIONAL LABORATORY

Brian P. Dwyer
Sandia National Laboratories
MS-0719
P.O. Box 5800
Albuquerque, NM 87185-0719
(505) 845-9894

John Heiser
Environmental & Waste
Technology Center
Brookhaven National Laboratory
P.O. Box 5000
Upton, NY 11973-5000
(516) 344-4405

Willis Stewart & Steve Phillips
Applied Geotechnical Engineering
and Construction, Inc.
P.O. Box 1280
Richland, WA 99352
(509) 372-0459

ABSTRACT

The primary objective of this project was to further develop close-coupled barrier technology for the containment of subsurface waste or contaminant migration. A close-coupled barrier is produced by first installing a conventional cement grout curtain followed by a thin inner lining of a polymer grout. The resultant barrier is a cement polymer composite that has economic benefits derived from the cement and performance benefits from the durable and chemically resistant polymer layer. The technology has matured from a regulatory investigation of issues concerning barriers and barrier materials to a pilot-scale, multiple individual column injections at Sandia National Labs (SNL) to full scale demonstration. The feasibility of this barrier concept was successfully proven in a full scale "cold test" demonstration at Hanford, WA. Consequently, a full scale deployment of the technology was conducted at an actual environmental restoration site at Brookhaven National Lab (BNL), Long Island, NY. This paper discusses the installation and performance of a technology deployment implemented at OU-1 an Environmental Restoration Site located at BNL.

INTRODUCTION

The US Department of Energy (DOE) Complex sites have experienced numerous loss of confinement failures from underground storage tanks, piping systems, vaults, landfills, and other structures containing hazardous and mixed wastes. Consequently, efforts are being made to devise technologies that provide containment of waste sites either as a safety net to "catch" future contaminant leakage/migration or as an interim step while final remediation alternatives are developed. A subterranean barrier fixes the volume of waste and reduces the possibility of contaminant migration into local geologic media or groundwater. Failure to treat contamination in situ will also result in exorbitant restoration costs at a later date. In addition, the legal ramifications for not treating many of these waste sites could be detrimental to the responsible parties.

The primary objective of this project was to develop and demonstrate at a field scale an economical subsurface barrier technology capable of containing virtually any waste form(s) within the existing subsurface media, disposal, or storage structures. The barrier was designed to cost substantially less than any known alternative remedial action such as: cryogenic, soil-saw, or circulating air barriers; excavation and treatment; vapor extraction, etc. In addition, the barrier design provides interim, or permanent containment or can enhance other remedial options such as stabilization and removal. A secondary objective of the project was providing a demonstration barrier for integrity verification. The technology of choice was perfluorocarbon gas tracers. BNL provided the expertise in this area.

Conceptually a close-coupled barrier is built by first installing a conventional cement grout curtain followed by a thin lining of polymer grout. The resultant barrier is a cement polymer composite that has economic benefits derived from the cement and performance benefits from the durable and chemically resistant polymer layer. It is essential that materials (grouts) and emplacement techniques are compatible; therefore, they were developed and demonstrated simultaneously. This is not a trivial issue. Barrier materials must simultaneously be emplaceable, i.e., compatible with emplacement equipment and site geology, withstand a wide variety of chemical, thermal, physical and radiological conditions, and meet acceptable longevity requirements.

BACKGROUND

SNL has been investigating placement methods and cementitious grouts for subsurface barriers. During the summer of FY'94 SNL placed several pilot scale individual jet-grouted cement columns, conical and v-trough shaped configurations, and a 7 X 7 matrix of columns at a clean site near the Chemical Waste Landfill at Sandia. At the same time BNL was invited to demonstrate a polymer grout using the same placement equipment. FY'94 barrier evaluation testing consisted of infiltration testing and lab analysis of core samples. In FY'95, a team composed of Brian Dwyer of SNL, John Heiser of BNL, and Applied Geotechnical Engineering Construction, Inc. (grouting contractor) was assembled to complete the design, installation, and integrity validation of a full scale subsurface barrier. The test was conducted at a benign (cold) site in Hanford, WA. A cone shaped cementitious "bath tub" was constructed and the inside lined with a polymer binder that BNL has been developing for applications where impermeability and long-term durability are required (Siskind and Heiser, 1993) (Heiser and Columbo, 1994). The final containment product is a composite barrier having the cost savings associated with using relatively inexpensive neat cement grout to form the structural backdrop; thereby, minimizing the volume of the more expensive polymer grout required to attain the desired containment objectives. FY'95 testing (barrier integrity validation) was expanded to include more rigorous infiltration testing (falling head test with TDR and soil moisture block probes strategically located), gas tracer evaluation and also stress/strain monitoring of the waste form during grouting. Figure 1 is a conceptual profile of the close-coupled cement/polymer barrier installation at BNL.
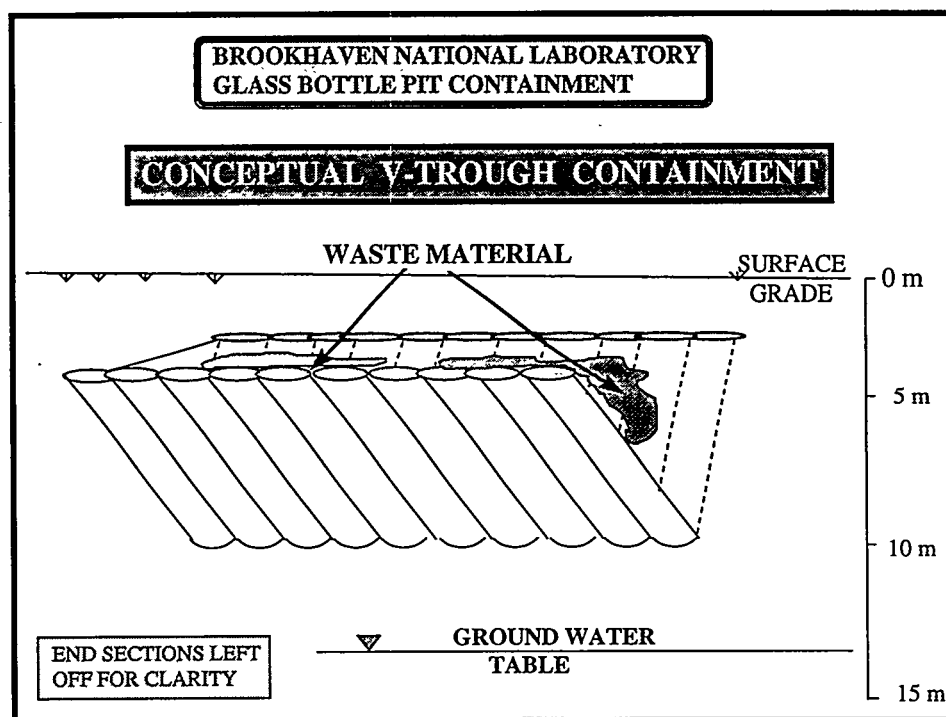
Figure 1. Schematic of Close-Coupled Barrier Demonstration.

TEST SITE

The deployment test site selected for the field-scale demonstration is noted as the AOC 2C Glass Holes location. The Glass Holes area is located inside OU-IV, BNL, and the Glass Hole pit chosen was G-11 (1 of 17 Glass Hole pits in OU-IV). BNL is located in central Long Island, New York state. The geologic media consists of unconsolidated glacial deposited sediments primarily composed of fine to coarse grained quartzose sand with lessor amounts of gravel. Groundwater beneath Pit G-11 is approximately 13 meters below grade. Groundwater sampling in the OU-IV area has shown the presence of volatile organic, heavy metals, and fission products. Historical records indicate that the Glass Hole pits were typically excavated with a clam-shell to depths of 6 to 7 meters. Waste materials and backfill were placed into the individual unlined pits in lifts with final backfill to grade. Most of the constituents in Pit G-11 are unknown.

TECHNOLOGY DESCRIPTION

Jet grouting is a technique first developed in Japan in the 1970s. This technique injects grout at high pressure (~400 bars) and velocity; thereby, completely destroying the soil's structure. The grout and soil are intimately mixed, forming a homogeneous columnar mass. Jet grouting is feasible in virtually all soil conditions ranging from clays to gravels (Kaushinger, Perry and Hankour, 1992). However, the soil type affects the effective diameter of the grout column, i.e., the efficiency of the process. For example, the diameter of a grouted column in clay soil is less than in sandy soil due the energy absorbing characteristics of the clay vs. The sand. This effect will be minimal and in the worst case will require slightly reduced spacing of the installation bore holes (columns), increased jetting pressures, and decreasing withdrawal rates.

BARRIER INSTALLATION

This project demonstrated a Systems Approach to construction of a subsurface barrier. This includes the integrity of barrier materials, emplacement equipment, verification techniques, and post monitoring instrumentation to produce a close-coupled engineering barrier. More specifically, during this project the first step was construction of a tertiary barrier consisting of two rows (honeycombed) of interconnected vertical and inclined portland based grout columns installed adjacent to and below Pit G-11 forming a v-shaped trough with the waste pit contents undisturbed on the inside. Figure 1 exhibits a conceptual view and Figures 2 and 3 are plan and cross sectional views. Next, the inside of the cement v-trough was lined with a low viscosity, chemically resistant polymer (AC-400) to form a secondary barrier to contaminant movement. The composite cement-polymer barrier provides isolation of the pit contents from the underlying groundwater. Next, the primary barrier was formed by injecting cementitious grout material at relatively low pressure into the waste form; thereby, stabilizing/solidifying the entire waste form. Prior to hardening of the grouted waste form, concrete demolition tubes (dywidags), and steel retrieval picking eyes were strategically placed to enable controlled fracturing of the monolithic waste form into smaller retrievable monoliths (~ 1.2 m X 1.2 m X 2.7 m deep) once the large monolith was fully cured. After complete curing of the concrete monolith, an expansive demolition grout placed in the dywidag tubes facilitated cracking the large monolith into the smaller more manageable stabilized cells or monoliths. Each cell can now be containerized, transported and stored, disposed to other facilities, or other actions taken in accordance with BNL closure plans.
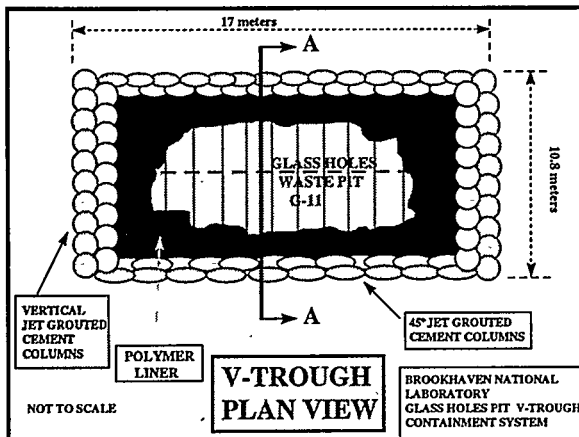
Figure 2. Plan view of glass holes pit G-11.
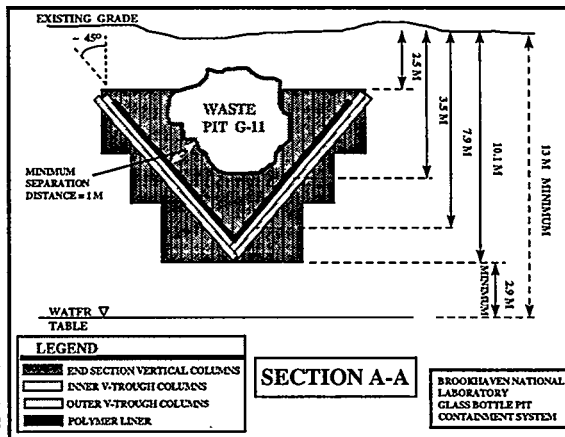
Figure 3. Cross Section A-A of glass hole pit G-11.

EQUIPMENT AND MATERIALS

The barrier was emplaced using a Casa Grande C6S, track mounted drill/grouting rig. The unit is depicted in Figure 4. The grouting assembly includes the following components: 1) a track mounted drill rig capable of conventional rotary/percussion drilling any direction conceivable; 2) a sub-assemble that connects up to three pressure lines to the drill string; 3) pump systems capable of delivering a single or multiple grouts to the drill string at pressures ranging from 10 to 600 bars complete with volume and pressure measurement.
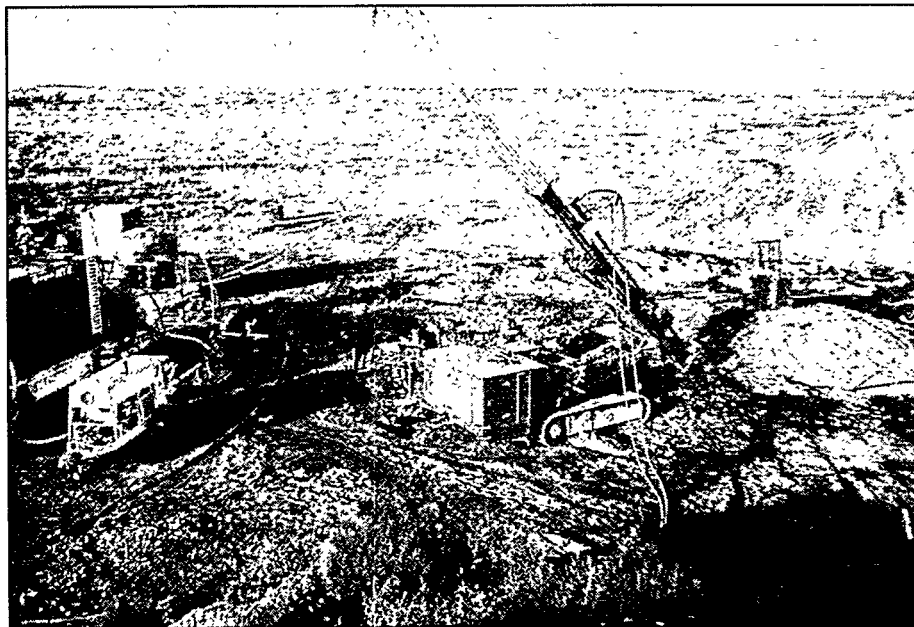
Figure 4. Casa Grande C6S Jet Grouting Rig.

The polymer used as the secondary barrier is a conventional acrylic polymer manufactured by Geochemical Corp. known as AC-400. The resin is polymerized using a catalyst in combination with a promoter. The promoter is mixed in with half the monomer resins (Part A) and the catalyst is mixed into the other half (Part B). The polymerization reaction begins when parts A and B mix together downhole external to the drill string. The mixing occurs as part of the soil mastication/mixing that occurs from the high pressure jetting. The tertiary barrier and the primary stabilizing barrier materials was neat cement, a 0.9: 1 mixture of water to portland cement.

477

INTEGRITY VERIFICATION

Currently there is no suitable methodology for validating the containment integrity of an emplaced barrier (Heiser, 1994). Because of the large size and deep placement of subsurface barriers detection of leaks is challenging. Nonintrusive geophysical techniques appear inherently inept for this task. These techniques identify/image anomalies in the subsurface but cannot distinguish small variations, such as cracks or gaps because the resolution in insufficient. Consequently, detection of discontinuities (small cracks or gaps) on the order of inches at relatively shallow depths (< 30 m) has not been possible using existing geophysical techniques. In addition to problems with nonintrusive viewing of the subsurface, the emplacement techniques such as jet, compaction, or permeation grouting have potential flaws. Permeation and compaction grouting for instance, results in very unpredictable grout placement in the majority of soil types, i.e., most soils are heterogeneous in nature. Consequently preferential grout flowpaths result in no guarantees of barrier location. Conversely, during a jet grouting emplacement soil heterogeneity has a much less negative impact. Although problems can occur when a borehole becomes misaligned or a jet nozzle is partially obstructed by cobble or varying soil types/densities, leaving a gap in the final barrier. Panel or thin diaphragm wall jet grouting may leave gaps between panels and/or at the junctions or horizontal and vertical barrier walls and may be thinner, and thus more prone to cracking. Additionally at the time of gel formation separations or "tears" may occur if localized settling takes place. In the demonstrations at BNL and Hanford, two overlapping rows of jet grouted columns were placed (honeycomb configuration); thereby, substantially decreasing the likelihood of barrier flaws.

Validating the integrity of the barrier at BNL was achieved in two ways: (1) adherence to Test Plan QA/QC barrier construction procedures; and (2) use of a novel approach developed at BNL. QA/QC procedures included rigid specifications for grout mixtures, injection pressures, and drilling geometries to ensure barrier continuity by emplacement of multiple or redundant barrier walls. The second verification technique utilizes perfluorocarbon tracers (PFTs) to locate breaches in the barrier. The feasibility of the PFT technology was established during the demonstration at Hanford, WA.

The equipment and materials required for PFT technology includes: the tracer gases, injection equipment, samplers and analyzers. Negligible background concentrations of PFTs occur naturally in our environment, consequently, very small quantities of PFTs are needed to conduct a verification test. PFTs are nontoxic, nonreactive, nonflammable, environmentally safe (contain no chlorine), and are commercially available. PFT technology is the most sensitive of all non-radioactive tracer technologies and concentrations in the range of 10 parts per quadrillion of air (ppq) can be routinely measured. The PFT technology is a multi-tracer technology permitting up to six PFTs to be simultaneously deployed, sampled, and analyzed with the same instrumentation. This increases flexibility and lowers the cost of experimental design and data interpretation. All six PFTs can be analyzed in 15 minutes on a laboratory based gas chromatograph.

Low detection limits allows detection of very small breaches in a barrier. Breaches are located by injecting a series of PFTs on one side of a barrier wall and monitoring for those tracers on the other side. The injection and monitoring of the PFTs was accomplished through geoprobe wells strategically placed inside and around the subsurface barrier. The location, quantity and type of tracer detected on the monitoring side of the barrier indicates the size and location of the breach. Obviously, the larger the opening in a barrier the greater the amount of tracer transport across the barrier. Precise location of breach requires more sophistication in the tracer methodology. Multiple tracer types can be injected at different points along the barrier (both vertical and horizontal). Investigation of the spectra of tracers coming through a breach then gives a location relative to the various tracer injections points.

The concentration of PFTs in the gas innoculation mixture was determined using computer codes to make first approximations of expected dilutions during subsurface transport. Because the required gas detection concentration outside the barrier is known, a back calculation determines

the required source concentration (assuming certain gas permeability constants for the soil and barrier layers). These assumptions and model predictions determines the initial sampling numbers and duration.

PFTs will potentially assist in locating and sizing breaches in a subsurface containment system. The technology has regulatory acceptance and is used commercially for non-waste management practices (e.g. detecting leaks in underground power cables, radon intrusion into basements). This technology has been used in a variety of soils and locals and will be applicable to the entire DOE complex as well as commercial waste sites.

MONITORING

Gas tracers may be used to validate barrier continuity after emplacement, to re-check corrective actions that may be used to seal or repair a breach, and may also be useful to periodically check a barrier to determine the long term integrity.

CONCLUSIONS

The successful deployment of a multiple material close-coupled barrier at BNL indicates the technology can be used for remediation of subsurface waste sites with: (1) current loss of containment; (2) high probability of near term loss of containment; and/or (3) loss of containment caused by retrieval or in situ remedial actions. Furthermore, this technology is applicable to any surface waste form that has the potential to release mobile contaminants. Unlike many other subsurface barrier technologies, close-coupled barriers are applicable to a wide range of waste materials and geohydrologic conditions. This is extremely advantageous because nearly every subsurface barrier has site specific conditions that require the flexibility offered by this technology; more specifically, this technology offers an ability to place barrier materials that are compatible with virtually any waste form in almost any geologic setting.

Demonstration of this technology in a very difficult geologic setting is the next step toward final development of: (1) the subsurface barrier equipment and materials, and (2) the cost data to allow potential end users a method to estimate the cost of implementation of this technology at their site.

In the area of barrier verification, it appears that QA/QC procedures during barrier construction in conjunction with tracer gas validation and post emplacement monitoring are the most effective candidates available at this time.

ACKNOWLEDGMENTS

REFERENCES

J. Heiser, "Subsurface Barrier Verification Technologies", Brookhaven National Laboratory, Upton, NY, June 1994, BNL-61127.

J. H. Heiser and P. Colombo, "Polymer Containment Barriers for Underground Storage Tanks", Waste Management '94, February 28 - March 3, 1994, Tucson, AZ.

J. H. Heiser and L.W. Xfilian, "Laboratory Evaluation of Performance and Durability of Polymer Grouts for Subsurface Hydraulic/Diffusion Barriers", Brookhaven National Laboratory, Upton, NY, 1994, BNL-61292.

Kaushinger, J.L., Perry, E.B., and Hankour, R., 1992, "Jet Grouting: State-of-the-Practice", in Grouting/Soil Improvement and Geosynthetics, ASCE.

B. Siskind and J. Heiser, "Regulatory Issues and Assumptions Associated with Barriers in the Vadose Zone Surrounding Buried Waste", Environmental and Waste Technology Center, Brookhaven National Laboratory, Upton, NY, February 1993, BNL-48749.

Chapter 10

Jet Grouting

Constructing Bottom Barriers with Jet Grouting

M. Shibazaki, Chemical Grouting Company, Tokyo, Japan
H. Yoshida, Chemical Grouting Company, Tokyo, Japan

Abstract

Installing a bottom barrier using conventional high pressure jetting technology and ensuring barrier continuity is challenging. This paper describes technology that has been developed and demonstrated for the emplacement of bottom barriers using pressures and flow rates above the conventional high pressure jetting parameters.

The innovation capable of creating an improved body exceeding 5 meters in diameter has resulted in the satisfying connection and adherence between the treated columns.

Besides, the interfaces among the improved bodies obtain the same strength and permeability lower than 1×10^7 cm/sec as body itself.

A wide variety of the thickness and the diameter of the improved mass optimizes the application, and the method is nearing completion. The paper explains an aspect and briefs case histories.

1. Introduction

Containing subsurface pollutants in the ground requires both horizontal and vertical barriers. In Japan, there are numerous methods of constructing vertical barriers for containing pollutants, but few are available for horizontal or bottom barriers.

In cut and cover work, the soil at the bottom of the excavated section must be improved to be watertight for dry work. A soil improvement method depends on the degree of water cutoff required, however, one of the best method in terms of water cutoff efficiency combines a high-pressure water jet with grouting. This can be utilized to construct bottom barriers for containing pollutants.

A major feature of the method known as Jet Grouting is that it can be used to selectively improve only the desired region of soil. Another feature is that it requires a small drilled hole from the ground surface to the bottom barrier than that of other methods. For example, a bottom barrier with a diameter of 5 m can be constructed by this method through a borehole diameter of around 15 cm (6 inches). This feature is well suited to the purpose of emplacement of a containment barrier. Moreover, the method provides high quality. When a special cement slurry is used, the hydraulic conductivity is on the order of 10^7 cm/sec. Another feature of the method is that it facilitates a good connection among horizontal barriers because of the thorough filling of the gaps with grout.

2. The basic concept of bottom barrier construction

Figure 1 explains the basic concept to form a horizontal barrier by first inserting a pipe in the ground, then rotating it at a given depth to cut the soil with liquid jet, and finally withdrawing the pipe while emitting a jet of grout (usually cement slurry) which mixes with the cut soil to form a solidified body.

The barrier continuity of the solidified bodies can be seen perfect, in Figure 2. Figure 3 also shows an accurate continuity in vertical barriers. This is because the jet washes mud off the rough surfaces of walls and fills them with grout to create perfect cohesion.

3. Technological aspects

Conventional jet grouting usually produces a cylindrical body about 2 m in diameter. In applying this method for a bottom barrier, it is important to make a body as large as possible. Construction of a barrier exceeding 5 meters in diameter needs new specifications for the water jet used to cut soil and manufacture a jetting equipment satisfying these specifications. The solutions of these tasks are outlined below.
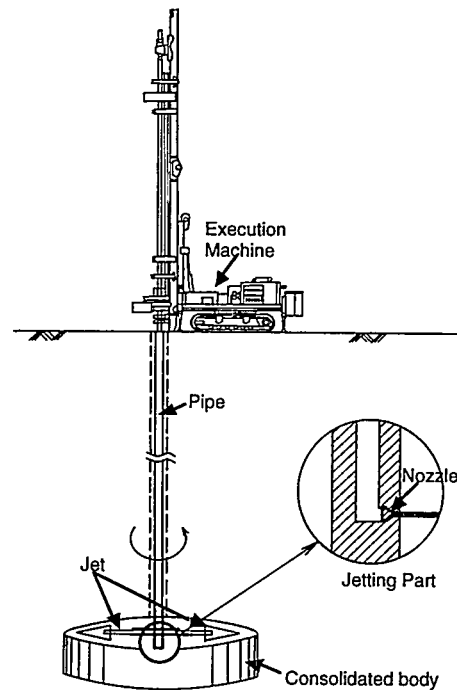
Fig. 1 Conceptual View of Jet Grouting

Fig.2 Overlapping of New Jet Grouting Column
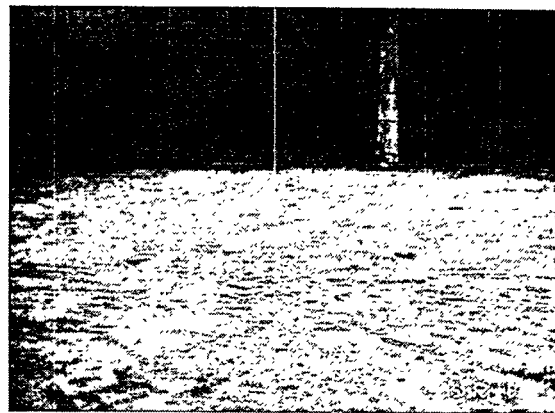
Fig.3 Perfect Continuity between Vertical and Bottom Barrier

3.1 High-pressure water jet

In conventional jet grouting (triple fluid system), water energy of 49 kW (discharge pressure: 40 MPa; flow rate: 75 l/min) is usually applied. In order to construct a barrier with a diameter of 5 m, however, the cutting distance and the improved area have to be extended by 2.5 times and more than 6 times, respectively. The major factors of water jet cutting ability are discharge pressure, flow rate, cutting speed and number of passes made by the water jet. A basic cutting experiment conducted in

simulated ground (sand layer) has led to an empirical cutting distance formula as the following.

$$L_m = \left(4.95KP^{-1.4}Q^{1.6}N^{-0.2}V_n^{-0.3}\right)^{-0.7}$$ Valid for sandy soil of SPT between 5 and 50

where L_m : Radius of barrier (m)
         K : Constant by Jetting liquid (Cement Slurry 2.5 Water 1.0)
         P : Discharge pressure (kgf/cm^2) (200~500 kgf/cm^2)
         Q : Flow rate (ltr/min) (70~300ltr/min)
         N : Number of passes (1~20)
         V_n : Tangential velocity at a nozzle outlet (m/sec) (0.1~0.2 m/sec)

Based the above formula, and taking safety, economy and depreciation of existing equipment into consideration, the discharge pressure of 30 MPa and the flow rate for each of two nozzles of 300 ltr/min have been set, equivalent of energy of 594 kW for a double fluid system. Selection of the cement slurry of double fluid system minimizes the quantity of secondary waste disposal.

3.2 The jetting devices

A smaller borehole demands a smaller drill string pipe. Consequently, a new jetting pipe with a diameter of 5 inches was developed after technical examination. Of vital importance are creating a hydrodynamically efficient way of jetting through a slender pipe, and preventing the pipe from abrasion by means of cement particles.

3.3 Efficient jetting condition

Fluid is emitted perpendicular from a pipe as shown in Figure 1. The soil cutting efficiency of the water jet depends on the focusability on both the shape of the nozzle and the condition of the upper stream toward the nozzle. Turbulence caused in bends and changes in sections must be reduced and then a laminar flow must be arranged in the straight part of the pipe before the nozzle. A relation between jet diffusion and the length of the straight part of a pipe is empirically determined below. This formula indicates that the length of the straight part of a jet pipe must be more than 50 times the internal diameter of the pipe.

$$A = 4C^2 L\left\{1 - \sqrt{2}P_i L / C_1 r_0 U_0^2\right\}^{4/3}$$

Where   A : Spread of jet/ Area of a nozzle outlet
         C, C1 : Empirical constants
         L : Distance from nozzle outlet
         P_i : Colliding pressure of the jet
         ρ_0 : Density of liquid
         U_0 : Velocity of jet at nozzle outlet

As previously mentioned, however, it is impossible to use a pipe having a such a straight section with this method. Therefore a bent pipe is applied and a configuration of a 5-inch-diameter pipe that minimizes jet diffusion is empirically obtained as a result of effecting radius of curvature and pipe diameter on jet diffusion.

Also, research into pipe materials has led to the development of a special alloy that is sufficiently resistant to cement particle abrasion and alkaline corrosion caused by cement slurry. These efforts made it possible to create a jet of cement slurry that is well focused, using jetting parts that can withstand more than 500 hours of successive operation.

4. Case histories

4.1 Bottom slab for preventing deformation of retaining wall

A basement of a new building required soil improvement so as to prevent deformation of walls on construction. The work was constrained from environmental aspects as listed below.

(1) Mostly soft soil condition
(2) As the site is adjacent to houses and highways, minimization of subsidence is a primary concern.
(3) Shoring struts are not available due to constructing a theater and an automated parking lot in the basement.
(4) A tight schedule.

Figure 4 illustrates the sequence of excavation in view of these constraints. Figure 5 also explains the lay-out considering soil condition and economy into consideration. The lay-out of an improved body, compressive strength, shear strength and buckling were considered in terms of the horizontal axial forces that would act on them. The unconfined compressive strength of an improved body must exceed 10 kgf/cm². The results proved entirely satisfactory with respect to time, cost and safety. The achievements are listed below.
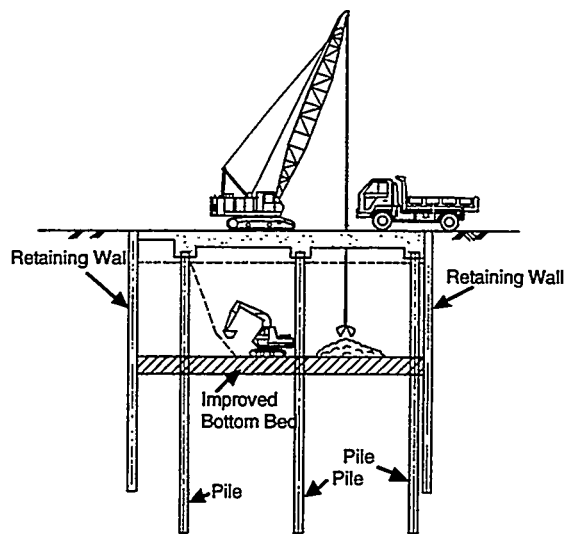
Fig. 4 Excavation Concept
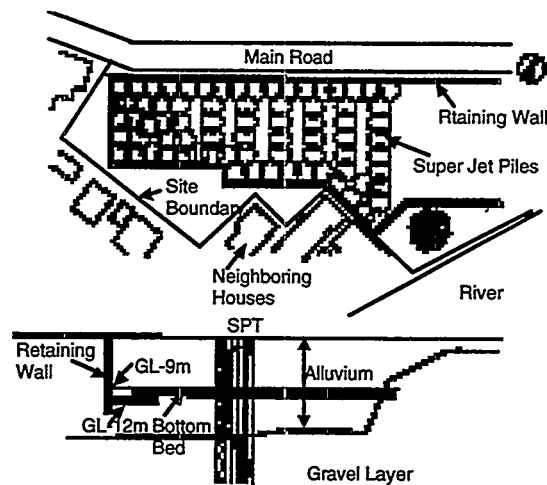
Fig. 5 Plan and Profile of the Site

486

(1) The exposures in Figure 6, have gained diameters exceeding 4 meters and satisfying continuity both between the bodies of improved soil and between the bodies as well as the retaining wall.

(2) The strength of the bodies averaged 14 kgf/cm² as ascertained by core tests clearing the design value and the coefficient of variation proved 25%, respectively.

(3) Figure 7 plots the maximum deformation of 2 mm at the top of the retaining wall and also indicates a maximum retaining wall deformation of 10 mm, keeping the displacement within the simulation before the work.

(4) No settlement of the adjacency.

4.2 Withstanding uplift and water cutoff

This case history briefs a ground modification at the bottom of a launching shaft 50 meters in depth for tunneling as a kicker slab for withstanding the uplift pressure of ground water and for cutting-off the groundwater leveling to 18 meters below the surface.

Figure 8 profiles at the bottom of the section to be excavated was a permeable sand layer with a coefficient of permeability of 10^{-3} cm/sec. An improved bottom bed that was demanded with quality which can resist water penetration, groundwater uplift pressure, the weight of the retaining wall and lateral soil pressure, respectively.

The thickness of the improved soil bed could be determined from the balance between groundwater uplift pressure and the dead weight of the soil bed, and the failure due to bending and shearing. These considerations led to the design goal of a body of improved soil 5.7 m thick and an unconfined compressive strength of 50 kgf/cm², as illustrated in Figure 8.

Another device and expertise were utilized for achieving drilling accuracy which is of vital importance at the depth of 50 meters. In this case, the targeted borehole accuracy cleared 1/250 with the aid of sensors (special clinometer) confirming perpendicular.

Excavation within the walls took place after the following.
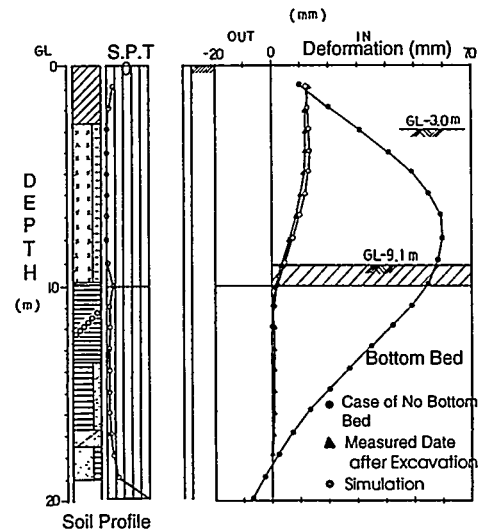
Fig. 7 Deformation of Retaining Wall

Fig.6 Underground Open Space Surrounded by Vertical Walls and Wrapping SUPERJET Piles
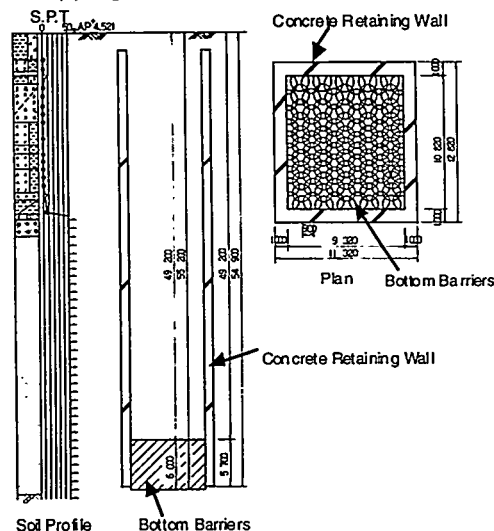
Fig. 8 Plan and Profile of the Site

487

(a) The perpendicular accuracy of the boreholes was verified.
(b) A pumping test confirmed the cutoff performance of the bottom bed.
(c) Tests of core samples obtained by boring indicates that the average unconfined compressive strength of the bottom bed reaches 83 kgf/cm^2, much better than the design goal.

Figure 9 shows, the surface of the bottom bed which allow no groundwater coming in and that withstands the uplift pressure of groundwater without displacement of the bed.

5. Conclusion

Jet Grouting technology in construction field has proved potential even in the requirements of pollution containment and constructing bottom barriers for the purpose with the modified technology is expected to become more common.
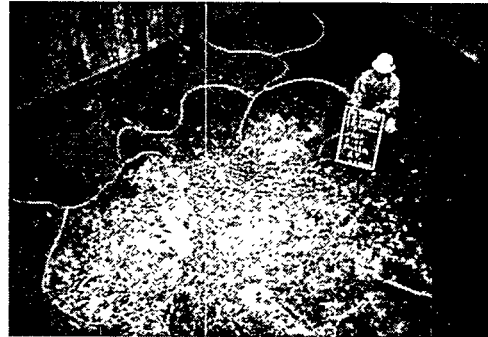
Fig.9 The Surface of the Bottom Bed after Excavation

References

1. K. Banno and H. Yoshida, "Immobilization of Contaminated Soil using Jet Grouting Method", Waste Management '92, Tucson, Arizona.
2. H. Yoshida, R. Asano, and H. Kubo, "Development of SuperJet Method", International Symposium on Soil Improvement and Pile Foundation, Nanjing, China.
3. M. Shibazaki and H. Yoshida, "Historical View of the Soft Ground Improvement Method Utilizing Water Jet", Proceedings of the 8th American Water Jet Conference, Houston, Texas.
4. H. Yoshida, S. Jimbo and S. Uesawa, "Development and Practical Applications of Large Diameter Soil Improvement Method", The Second International Conference on Ground Improvement Geosystems, Tokyo, Japan.
5. M. Shibazaki, "State of the Art Grouting in Japan", The Second International Conference on Ground Improvement Geosystems, Tokyo Japan.

The application of Flowmonta for environmental problems

Dr. Ingo Sass, Dr. Ortwin Caldonazzi, Thomas de Beyer

FlowTex GUT

FlowTex GUT GmbH
Gesellschaft für Großbohr- und Umwelttechnik
Chausseestraße 1
06317 Amsdorf
Germany

Tel: +49 34601 40168
Fax: +49 34601 40159
e-mail: gut@romonta.de

Abstract

The combination of Horizontal Directional Drilling techniques with High Pressure Injection techniques led to the development of Horizontal Directional Injected Barriers under ground. Specially developed injection fluid mixture of Montan wax, cement and bentonite is the basis for the Flowmonta process.

The first field test was made in a mining's landfill in 1993. It confirmed the basic procedure. In a two-stepped, large-scale test in 1995, different injection techniques and injection fluids were tested. Intensive investigations in the field and in the laboratory were made. The Flowmonta-barrier then was excavated to enabled the direct observation and evaluation of the extent of the injections. During the first phase of the test several mixtures and injection techniques were tested, In the second phase a complete three dimensional sealing basin was created. The permeability of this sealing basin was tested in-situ. After excavation, hydraulic and mechanical surveys were made in the laboratory. By using the one-phase jet grouting technique, a penetrative depth of 1,2 meters on each side of the drilling was reached. A test using the Duplex technique resulted in a penetration of up to 2 meters and more on each side of the center bore. The permeability of the injection area was lowered By two exponential orders compared to the surrounding soil. SEM-images showed the structure of the injected material, as well as Montan wax spheres to have of 0,2 μm to 2 μm in diameter. X-ray diffraction, annealing and toluene-extraction gave a semiquantitative proportion analysis. Montan wax disproportion effects were observed in the barrier. Recently geophysical investigation methods still give no satisfying data.

Introduction

The innovative application of Horizontal Directional Drilling (HDD) to solve environmental problems led to the development of horizontal wells and horizontal directional injected barriers. Horizontal wells have been in use for several years, the barriers are recent development. For the establishment of the horizontal barriers an injection fluid of Montan wax, cement and bentonite was used. The name Flowmonta evolved because Montan wax was used. The word Flowmonta is used for the procedure as well as for the installed apron. This technology is based on the high pressure injection of Montan wax bearing fluids out of horizontal directed drillings. Because of the lateral extension of the injection fluid an elongated impermeable apron is created. Several aprons, overlapping each other can build a continuos basin. This makes the shaped and continuos encapsulation of contaminated areas possible.
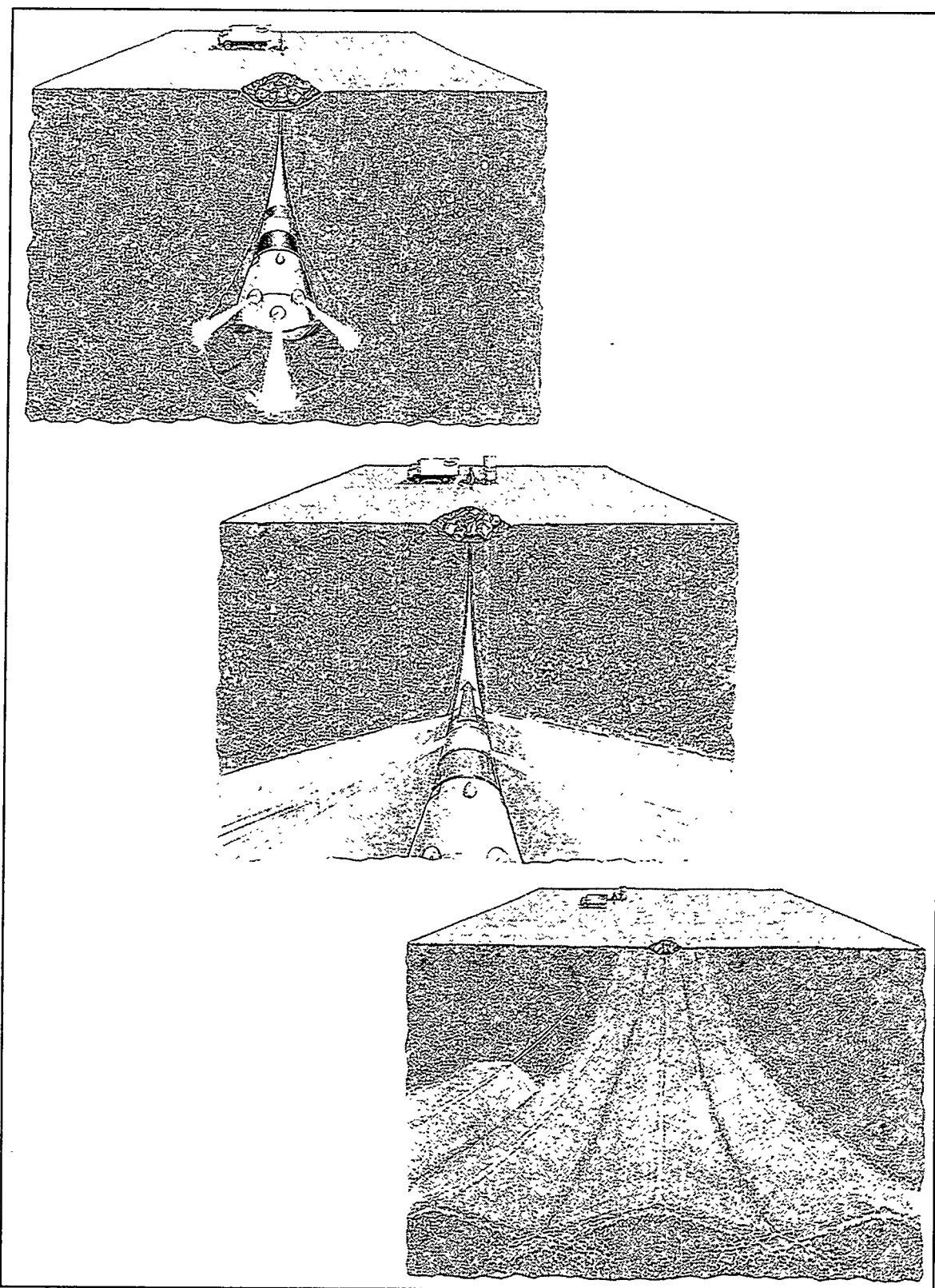
Fig 1:   The Flowmonta procedure

This new and inexpensive containment technology, the Flowmonta technology, was tested in 1993 and 1995 in two large field tests. The results were scientifically analyzed. The first test, in

1993, was carried out in a mining landfill (Goitsche, Sachsen-Anhalt, Germany). This test confirmed the basic working procedure. In a two-stepped, large scale test in 1995, different injection techniques and injection fluid mixtures were tested. Intensive investigations in the field and in the laboratory were made. This paper deals predominantly with the field test of 1995.

The Flowmonta procedure

First, a pilot tunnel is made using a normal horizontal directional drilling under a dangerous waste area or some other type of contamination. During the following pull back procedure, the injection fluid is injected out of two or more nearly opposite jets (in a special jetting head) under high pressure. On both sides of the pilot tunnel an apron is created. Several aprons installed parallel create a continuous layer. Sufficient overlap of the aprons has to be guaranteed.

The injection fluid is a mixture of Montan wax, cement and bentonite. Alternative mixtures are possible as long as they satisfy the standards for processing, injecting and behavior in the ground. The addition of Montan wax reduces the viscosity of the mixture while processing and injecting and also reduces the permeability of the installed layer.

Montan wax

Montan wax is extracted from lignite. The robust leaf wax and resin of plants is preserved in some lignite reservoirs. The Amsdorf mining produces 80% of the world's Montan wax. Its origin and the influences of the coaling process give Montan wax a complex structure. The substance of Montan wax is divided into three groups. The wax itself is about 80% of its entire matter and is made of esters from long chained alcohol and acids. The remaining parts are resins and asphalt. The medium chain length is C 28. Montan wax dispersions are produced for environmental technology applications.

Field Test

In 1995 a test area was set up in Amsdorf, (near Halle a.S.) Germany. There the technology, the injection procedure and the injection mixture was tested by ten drillings in the first phase. With five additional drillings a sealing-basin was created. Although the ground conditions were unfavorable for jet grouting (highly consolidated glacial debris and clay/silt), the applicability of the Flowmonta procedure was proved.
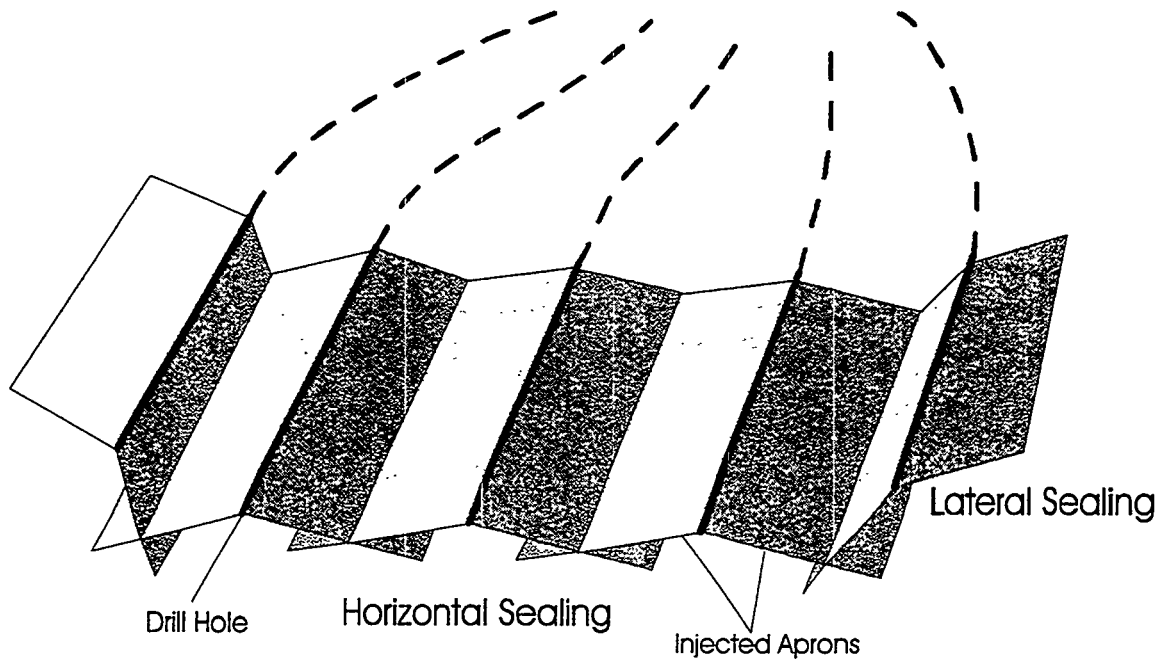
Fig. 2: Sealing-basin

Drilling process

The HDD is used to create the pilot tunnel where the jetting head will run. HDD is conventionally used for the trenchless installation of pipes and cables under roads, railway crossings and environmentally valuable areas. The basic principle of this technique is to hydromechanical cut through the soil with fluid pressures up to 600 bar. The nozzles are located at the tip of the rotating drilling head in an angle to the drill string. A jet of drill fluid (mud) cuts a microtunnel in the soil. The dislodged soil is carried backwards by the drill fluid. The bore navigation is controlled by the rotation of the drilling head. Navigation is also supported by the angled portion of the drilling head, located on the opposite side of the nozzles. When the rotation is stopped, while thrust is still being applied, the nozzles cut only on one side and the wedge shaped drilling head is forced to change its direction.
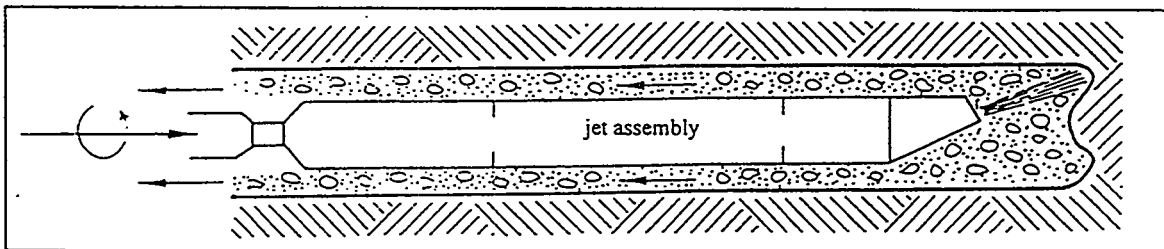
Fig. 3: Jet assembly

The position of the drilling head is determined by using a magnetic locating system. A probe right behind the drilling head measures its position relative to a geomagnetic field and an artificial magnetic field generated by an electric loop on the surface. With these measurements and the length of the drill string the exact position of the drill head is calculated by a computer. The accuracy of the locating system is about 2 % of the depth of the bore tunnel under earth's surface.

Injection technique

After the pilot tunnel is finished the drill jet assembly is replaced by an injection head. The installation of the impermeable layer of a Montan wax-cement-bentonite mixture is accomplished by jet grouting while pulling the injection head back through the pilot tunnel. The high pressure injection jet cuts the soil. The injection mixture comes out of two or more nozzles positioned opposite or in an angle to the drill string and penetrates the soil using the hydromechanical cutting principle. The drill string can be rotated or held in an exact position. If the string is pulled back without rotation, an apron is cut into the soil. If rotation is applied, then a horizontal column is produced.
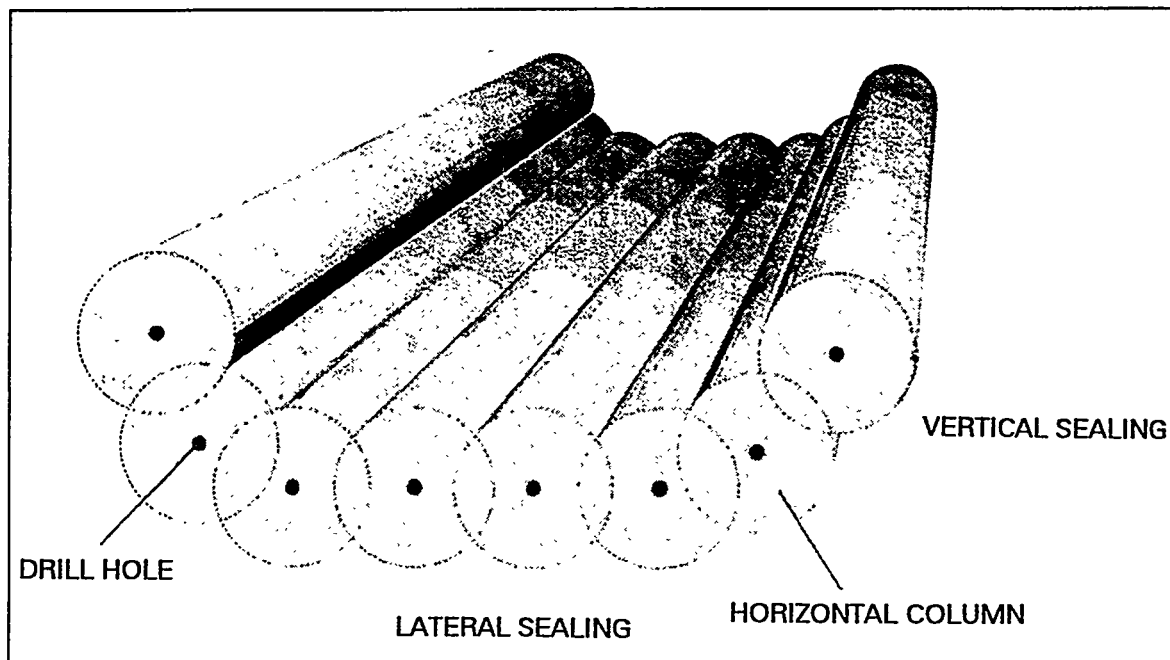
Fig. 4: Flowmonta columns

To build a perfect sealing layer several parallel and continuously injected stripes have to be made. Aprons produce a layer of a few centimeters to decimeters thickness. Horizontal columns result in a layer thickness of about 1 meter. So, for stronger sealing, horizontal columns are more effective.

There are three basic variations of injection technique:

-One   phase   technique   (Jet   grouting)
The injection fluid is also the fluid for the jet that cuts the soil and mixes with it. Standard drill rods with one central channel are used.

-Two   phase   technique   (Duplex   technique)
The injection fluid is also the fluid for the cutting jet but is supported by compressed air. The scope of the injection increases. Duplex drill rods must be used.

-Three   phase   technique   (Triplex   technique)
The cutting jet and the injection jet are split. A water coated air jet cuts the soil and immediately afterwards the injection fluid is injected. A triplex rod with separate channels for each medium is necessary. The scope of this technique is the highest.

The economy of high pressure injections depends on their reach under different soil conditions. With increasing cohesion the scope decreases. In coarse soils the bulk density is the limiting factor. The dimension of the single grain is important because even the biggest grain must be covered completely by the injection fluid. If not, so called „injection shades" occur and may cause

493

highly permeable spots in the barrier. The best results are obtained in medium sand, but the complete range between 2 µm and 600 µm is suitable for high pressure injection.

Two different types of drilling are possible:
-       dead end drilling
-       standard horizontal drilling, that arrives at the resurfaces

Injection procedure

The injection procedure is dependent on the type of drilling and injection tools in use. Standard horizontal drilling is performed using standard tools. After exiting at the surface, the drillhead is replaced by a special injection tool. It is equipped with lateral injection jets only. There are no jets on the top.

Injections using dead end drilling are done with a drillhead that is equipped with nozzles for drilling and nozzles for injecting. While drilling all nozzles are in operation, but because of the smaller diameter of the injection nozzles only the drill nozzles work efficiently. Having reached the end of the microtunnel (the dead end) the drill nozzles are blocked and only the injection nozzles remain in operation.

In both cases the injection occurs during drill string pull back. While injecting the cut soil mixes with the injection fluid and is carried out of the pilot tunnel. A chemical reaction causes the mixture that remains in the soil to solidify into a mass of plastic consistency.

Injection mixture

The injection mixture maintain certain qualities for the original mixing process and after solidification:
-       processability (viscosity, bulk density)
-       stability, rigidity and permeability
Fluids used for vertical jet grouting walls usually consists of water bentonite and/or cement. Cement adds the required rigidity to the injection and guarantees a minimal time for processing.

The mixtures being used for sealing contain a certain amount of bentonite, or other clay, to guarantee permeability. The addition of Montan wax to a mixture of bentonite and cement reduces the viscosity during preparation and injection and increases the scope of the jetting. Further, Montan wax's hydrophobic properties makes the sealing resistant to aggressive liquids. For the test injections the following ingredients were chosen:
-       Montan wax in dispersion (20 % solid particles)
-       Tixoton (active bentonite with a high percentage of montmorillonite)
-       Portland cement
-       water, pH $\approx$ 4
There are certain limits to the variation of the ingredients. A mixture with high viscosity is hard to prepared and limits jet penetration because of high flow resistance.

The Montan wax used for the injection is a wax dispersed in water and consisting of 12 - 25 % Montan wax. This dispersion has the following properties:
-       pH $\approx$ 7
-       density (25°C) = 0,99 - 1 g/cm^3
-       dynamic viscosity (25°C) = 2 - 10 mPas

Spreading of the injections

In a cross-section the injected aprons are club shaped. At the ends of the actual injected apron, several 4 cm thick and up to 5 m long fissures spread out and flow towards the surface.

The microtunnels have diameters of 10 - 15 cm. The width of the injected apron is about 0,3 m to more than 2 m. Directly at the microtunnel, they are 3 cm to 6 cm thick. The maximum apron thickness is about 8 - 12 cm a approx. 0,25 m to 1,1 m distance to the microtunnel.

The spreading of the injection fluid is characterized by two shapes:

- injected aprons formed by actual jet grouting (club shaped)
- thin, long fissures opened and filled by the high (frac-)pressure injection process

The actual injected apron was made by the hydromechanical cutting of soil particles up to 15 cm in diameter. They are typically club shaped. The spreading of the thin layers usually starts from the outer extents of the „clubs". These fissures were produced by the high pressure called the frac-pressure of the injection procedure. The way of the fissures usually follows some preexisting microfissures. No influence of the ground water level has been observed.

Assessment of the injections in the field test

The length of each drilling was 90 m. The lateral distance between the central drillings produced a horizontal plane of 1,2 m. The distance of the outer two lateral drillings was about 0,85 m. They were positioned 0,6 m above the central drillings.

From a geological point of view, the sealing barrier was injected in a 3,7 m thick silt layer. This layer was embedded by two layers of clay. The maximum depth of the drillholes was 7,5 m below the surface. The injections were in the central 55 m of the drillings. The injection nozzles were placed nearly opposite to each other on the drill string with an angle of 150° in a downward direction.

The chosen distance between each drilling was too large to guarantee a complete crossing of two neighbored injected aprons. The one phase technique was not able to have a scope larger than 0,6 m. However the extent of the opened and filled fissures made a continuous sealing layer. To calculate the permeability only the 4 cm thin layers were used

In the first phase of the field test 8 injections using the Duplex technique were carried out. These injections reached a scope of more than 2 m on each side of the drilling hole. They were also shaped more regular. The support of the jetting from pressured air was very efficient, especially in the very cohesive soil conditions.

495
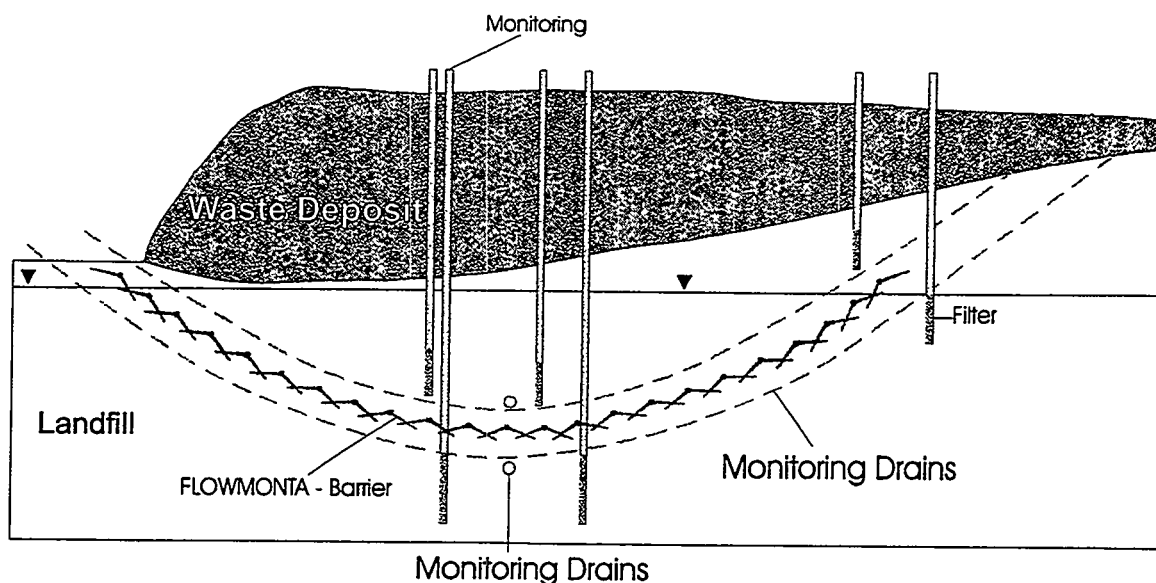
Fig. 5   Sketch of the location of monitoring wells at pumping test

Résumé of the scientific analysis

To find the best mixture of cement, bentonite and Montan wax laboratory tests were made before and during the first field test was started:

Geoelectric:
The geoelectrical resistance in the field test area were measured before and after the injections. No characteristic changes were observed. The resolution of this investigation method was not able to show a change in resistance caused by a thin layer about 7,5 m below the surface.
Measurements after the first excavations showed a slight decrease above and an increase of the electrical resistance below the injected layer. The decrease is explained by a small amount of water on top of the injected layer. The increase is caused by the injected material itself. Montan wax has a very high electrical resistance.

Permeability:
The permeability of the injected layer and the surrounding soil was tested with pumping tests. For these pumping tests eight observation wells were installed above and below the injected layer. The determination of injected layer permeability was produced with a long term pumping test using the concept of a semi-confined aquifer. In a period of five weeks a rate of 3 liters/hour was pumped out of the well below the injected layer, all other wells were observed. The permeability of the soil was defined in a range between $2,6*10^{-7}$ and $9,5*10^{-8}$ m/s, the permeability of the injected layer was in the range of $6,9*10^{-9}$ to $7,5*10^{-10}$ m/s. Permeability of samples of the soil and of the injected material was tested in permeameters. The laboratory tests showed permeability data for the injected layer in a range of $2,8*10^{-9}$ to $1*10^{-10}$ m/s. Tests on gas permeability were not successful.

The permeability of the injected layer was about two orders of magnitude below the already low soil permeability. The sealing effect of the injected layer is very good when the observing the hydrographs of the observation wells during the pumping test of well below the injected layer. The water level below the injected layer dropped depending on the distance observation to pumping well up to 1 m. The water level inside the injected basin hardly changed.

Annealing and toluene extraction:
To determine the distribution of the ingredients inside the injected barrier it was analyzed to quantify the amount of Montan wax, minerals and soil. The annealing test and the toluene extraction lead to the results with a fault range of ± 1 %. These analyses showed the increase of Montan wax content from the drillhole (8%) to outer fissures (14% in 2 m distance).

X-ray diffraction:

The mineral content was analyzed using X-ray diffraction. Montan wax could not been detected with this method. Also, the quantity of soil in the injected barrier could not been analyzed, because there was no prominent soil-mineral absent in the pure injection mixture. The estimated amount of soil inside the injected barrier was 20% to 80%.

Texture analysis

On thin sections and SEM-photographs the structure of the injected barrier was analyzed. The thin sections showed a very dense texture, but no porosity or directional structures. The SEM-photographs showed some spherical particles with sizes from 0,2 µm to 2µm which were identified as Montan wax. The cement forms a net around the spherical Montan wax and thin clay minerals. The pore radius achieved by the duplex technique was 40 nm whereas pore radius achieved by the one phase technique was 23 nm. The pore radius of injections without Montan wax was 230 nm. The porosity of all samples was 50% -60%. The advantage of Montan wax bearing mixtures is the small diameter of the pores below the flow effective pore size.

Shear strength

The addition of Montan wax reduced the cohesion from 240 kN/m² to 150 kN/m² but had no influence on the 43° angle of shear. These properties are adjustable by changing the percentage of the ingredients. The properties are to be conformed to the properties of the soil.

Chances of further applications for Flowmonta

For the application of Flowmonta at a waste deposit site, monitoring wells should be installed inside and outside and drainages inside of the Flowmonta barrier. Also, the waste deposit should be covered to protect against precipitation and to trap gases.

Incapsulation of a Waste Deposit
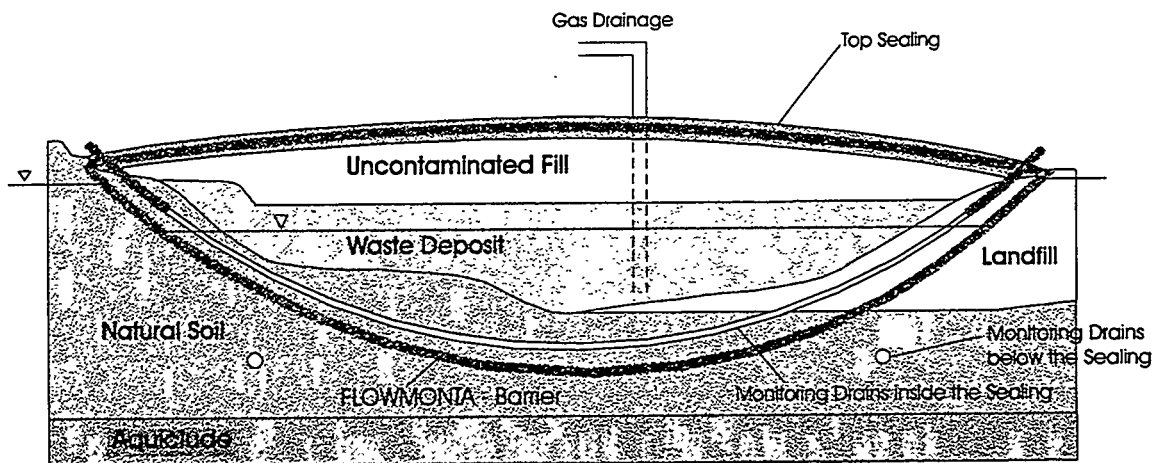
Fig. 6: Encapsulation of a waste deposit

Flowmonta also works the other way round. On a smaller scale the Flowmonta technique was recently tested to seal foundations. Jet grouting is performed very close to moist walls and under the floor of cellars. The advantage of this procedure is the ability to fit the sealing three dimensionally to the shape of the foundations. Smaller drill pipes can be used and therefore narrow curves are possible. Even confined space is no longer a problem. Machinery can be placed away from the working area. A short period after the injections are done the walls are and stay dry.

Flowmonta can also be used to keep excavations below the ground water level dry. The procedure is the same as described above. In these examples, the goal is to keep the water out, as opposed to keeping the contamination in. Construction work can be done without lowering the ground water table in the surrounding area.

The latest Flowmonta technique application idea is the immobilization of contaminated spots. Experience shows that most contaminants are not spread over a large deposit area, but are limited to hot spots. A geophysical survey can locate the contaminant's position. The horizontal directional drilling technique makes it possible to encapsulate a certain contaminated hot spot. Inside this hot spot in-situ remediation can be realized more effectively than in a hole waste deposit.

Investigations are in progress to immobilize contamination by the in-situ blending with hydrophobic, Montan wax bearing mixtures to wrap up each toxic particle. This is achieved by a combination of jet grouting and heating the injected area. The melting Montan wax creeps over the grains and covers each contaminant particle.

Use of Jet Grouting to Create a Low Permeability Horizontal Barrier Below an Incinerator Ash Landfill

A.J. Furth[1] ; G.K Burke, P.E.
Hayward Baker Inc.
Odenton, Maryland, USA
W.L. Deutsch, Jr., Ph.D. P.E.
Roy F. Weston, Inc.
West Chester, Pennsylvania, USA

ABSTRACT

The City of Philadelphia's Division of Aviation (DOA) has begun construction of a new commuter runway, designated as Runway 8-26, at the Philadelphia International Airport. A portion of this runway will be constructed over a former Superfund site known as the Enterprise Avenue Landfill, which for many years was used to dispose of solid waste incinerator ash and other hazardous materials. The site was clay capped in the 1980's, but in order for the DOA to use the site, additional remediation was needed to meet US EPA final closure requirements. One component of the closure plan included installation of a low permeability horizontal barrier above a very thin (approximately 0.61 to 0.91 meters) natural clay stratum which underlies an approximately 1020 m^2 area of the landfill footprint so as to insure that a minimum 1.52 meter thick low permeability barrier exists beneath the entire 150,000 m^2 landfill. The new barrier was constructed using jet grouting techniques to achieve remote excavation and replacement of the bottom 0.91 meters of the waste mass with a low permeability grout. The grout was formulated to meet the low permeability, low elastic modulus and compressive strength requirements of the project design. This paper will discuss the advantages of using jet grouting for the work and details the development of the grout mixture, modeling of the grout zone under load, field construction techniques, performance monitoring and verification testing.

INTRODUCTION

Runway 8-26 will consist of an approximately 1,525-meter-long bituminous runway/taxiway pavement system that will be located east of the existing airport, and will handle only commuter airline traffic. A portion of the eastern end of the runway system, measuring approximately 300 meters in length, will cross the footprint of the existing, 150,000m^2 Enterprise Avenue Landfill.

In order to meet Federal Aviation Administration (FAA) airspace clearance requirements, it is necessary to elevate the runway significantly above existing landfill site grades. This will be accomplished using an earthen embankment. The flat top of the embankment will accommodate a 45.8 meter-wide runway and turnaround area as well as adjacent, grassed 'outfield' areas. The proposed top of embankment grades correspond to embankment fill thicknesses that range from approximately 2.1 to 7.3 meters above the surface of the landfill. The landfill itself extends some 3 to 4 meters higher than adjacent natural grades. The landfill mass consists of 6 meters of predominately incinerator ash and bulk miscellaneous debris such as concrete, asphalt, rock and metal. Hazardous materials were also deposited at the site. A leachate head of approximately 1.2 to 1.8 meters has developed at the base of the landfill. The site is presently clay-capped.

The geologic environment beneath the landfill includes a surficial, low permeability silty clay stratum which directly underlies the waste mass and which varies in thickness across the landfill footprint. In particular, the thickness of this stratum is less than 3 meters over approximately 75% of the footprint, including a 1020 m^2 area in which the thickness is between 0.61 and 0.91 meters. The remaining landfill footprint is underlain by 7.3 to 9.1 meters of the silty clay material. The silty clay stratum is underlain by a sand and gravel stratum which is further underlain by alternating deeper clayey and granular soil strata. The various granular soil layers constitute regional aquifers, the

[1]1875 Mayfield Road, Odenton, Maryland 21113

499

deeper of which supply drinking water to a large population. Because of the environmental concern that these deeper aquifers may become contaminated from the downward migration of landfill leachate over time, several environmental safeguards were designed into a secure closure of the landfill prior to construction of the overlying earthen embankment and runway pavement. These include:

1. Capping of the landfill using a geosynthetic-based final cover system that includes a low-permeability, flexible membrane liner, drainage net, and filtration and cushioning geotextiles,

2. Dewatering of the leachate within the waste mass to the extent possible so as to minimize the vertical driving head of residual leachate which remains within the landfill. This, in turn, will minimize the potential for downward migration of leachate through the surficial silty clay stratum which underlies the waste mass.

3. A system of groundwater monitoring wells, screened within the deeper granular strata, which allows the groundwater quality within these strata to be determined by analytical testing over time.

4. Thickening of the low-permeability barrier layer in the 1020 m^2 area of the landfill footprint where the natural silty clay stratum layer thins to 0.61 to 0.91 meters, by constructing a minimum 0.91 meter thick, low-permeability grout zone within the waste mass directly above the top of the silty clay stratum. This would be accomplished using jet grouting techniques.

The intent of the jet grouting approach was to decrease the permeability of the predominately granular ash waste mass within the 0.91 meter grout zone directly above the thin, natural, silty clay stratum. The thickness of the jet grouted mass, combined with the thickness of the existing thin, silty clay barrier, would be at least 1.52 meters, which was determined to be an acceptable, environmentally secure thickness that would preclude downward vertical migration of residual landfill leachate.

JET GROUTING TECHNOLOGY

Jet grouting was originally developed in Japan during the late 1960's and early 1970's and has found increased acceptance in Europe and worldwide (Bell, et al., 1991). Within the past few years, there has been a significant increase in the technology's acceptance in North America. As jet grouting continues to evolve, it is proving itself in the emerging market of infrastructure improvement (Drooff, et al., 1995) as well as in groundwater control and the more familiar application of structural support (Pellegrino and Bruce, 1996). The jet grouting technique is continuing to be developed as an effective tool for hazardous site remediation.

Jet grouting is often described as a high velocity erosion process (Kauschinger, et al., 1992) that uses ultra-high pressures (300 to 600 bars) to impart energy to a fluid which is used as the soil cutting medium. This energy causes erosion of the ground and the simultaneous placement and mixing of grout in the soil. As shown in Figure 1, jet grouting has developed into three main systems, referred to as Single-Rod, Double-Rod, and Triple-Rod. Depending upon the system being utilized, jet grouting can manufacture a product of cement slurry mixed with in situ soil, or nearly complete replacement of soil with an engineered cement slurry. The resulting final product is referred to as Soilcrete.

The Single-Rod system uses a high pressure grout jet(s) to erode the soil and mix it with the grout. This process is also referred to as chemical churning pile (CCP) or jet pile (Kauschinger, 1992)

In the Double-Rod System the addition of a second component of compressed air, shrouded around a high pressure grout jet(s), enhances the erosion and replacement effect of the high pressure grout

jet(s). The compressed air helps to prevent the soil cuttings from falling back on the jet stream and helps to remove the soil debris by lifting it to the surface (Burke, Heller, and Johnson, 1989).

In the Triple-Rod System, three components (water, compressed air, and grout) are injected simultaneously into the soil. The combined high pressure water jet, compressed air, and grout volumes enables a higher percentage of soil to be removed from the ground and can be used for a nearly full replacement of the in situ soil with a cement grout product (Kauschinger, 1992).

Typically, the Single- and Double-rod systems are best suited to cohesionless sandy soils, while the Triple-rod system can create superior Soilcrete quality across a wider range of soil types and offers more control over injection rates. This is particularly important when the work is beneath or adjacent to sensitive structures (Drooff, et al., 1995).
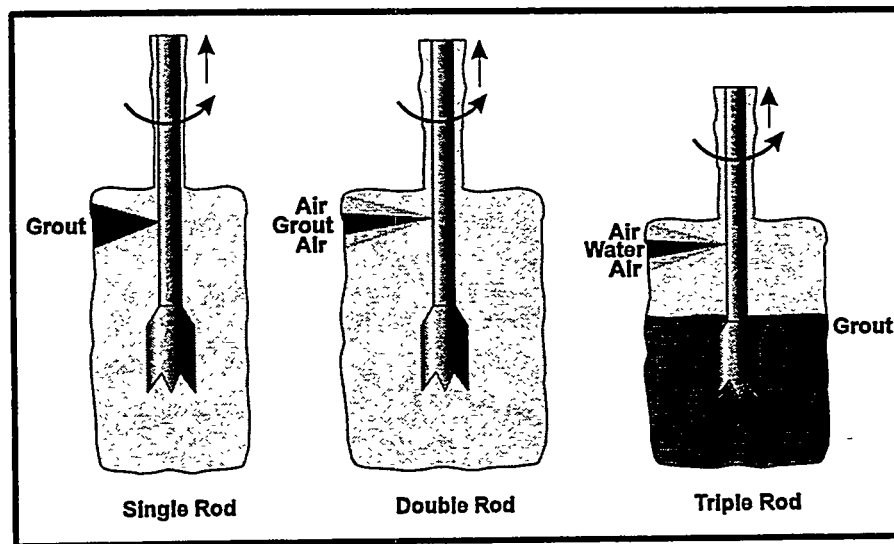
Figure 1: Jet Grouting Systems

DESIGN ISSUES

The design of the grout zone was developed consistent with three main performance criteria:

1. The permeability of the cured grouted landfill mass must not exceed 1×10^{-9} m/sec (using landfill leachate as the permeant) so as to be sufficiently impermeable to act as a low permeability horizontal barrier.

2. The compressive strength of the cured grouted landfill mass must be sufficiently high (900 kPa) so as to be capable of safely supporting the overlying landfill waste ash and earthen embankment loadings.

3. The elastic modulus of the cured grouted landfill mass must be sufficiently low (124,100 kPa specified) to allow the material to respond in a flexible, pliable manner without cracking during consolidation of the underlying silty clay stratum induced by the earthen embankment loadings.

As part of the design process, an analysis of the cracking potential of the cured grout zone was also completed using a finite element based computer program. This program permits computations, at selected locations within the grout zone, of the normal (compression and tension) and shear stresses which will be induced by the applied embankment loadings. This data can be used to predict whether cracking of the grout zone will occur by assuming that the potential for cracking is directly related to

501

development of tensile stresses in this zone. Should tensile stresses develop, it is reasonable to conclude that cracking will only occur if the tensile stresses exceed the tensile strength of the cured grout. In this manner, a Factor of Safety (FS) against cracking can be calculated as the ratio of the minimum measured tensile strength of the cured grout to the calculated maximum tensile stress in the grout zone determined from the finite element analysis. A Factor of Safety value greater than 1.0 is indicative of a theoretical no cracking scenario.

The maximum calculated tensile stress in the grout zone based on the Finite Element analysis was 123 kPa. The minimum tensile strength of cured grout specimens was measured in the laboratory to be 225 kPa based on a total of 4 direct tension tests. The calculated Factor of Safety against potential cracking of the grout zone from the applied earthen embankment loadings was calculated to be an acceptable 1.85.

Grout Mixture Development

The modeling indicated that a grout mixture be developed to meet the low permeability and low elastic modulus parameters. The difficulty was in developing a cementitious grout mixture which could be pumped at a pressure of 400 bars and at a volume that would ensure effective replacement of the in situ soils.

Due to the runway construction schedule, only two months were available to identify the optimum grout mixture for this work. Therefore, preparation of grout mixtures was begun immediately following notification of the contract award. An initial grout mixture was selected that had been previously used in field construction and that met the permeability requirements but had an elastic modulus in excess of the model analysis requirements. This base mixture (referred to here as HB1) included 11% by weight cementitious materials (Portland cement and NewCem) and 89% by weight of a hydrated bentonite mixture. NewCem is a blast furnace slag consisting of calcium, aluminum, and magnesium silicates that is ground to a fineness exceeding that of Portland cement (Blue Circle Cement: Specification Data Sheet, 1992).

In an effort to lower the elastic modulus of the grout mixture, slight modifications to the HB1 mixture were made in the laboratory to identify the most effective neat grout mixtures. These modifications involved adding higher percentages of bentonite. Once the most effective mixtures had been identified, additional test samples were prepared by mixing the neat grouts with various percentages of incinerator ash material taken from the site, to simulate in situ Soilcrete product expectations. Figure 2 illustrates the achieved strengths and permeabilities as a function of percentages of ash materials.

Neat Grout Sample No.	Incenerator Ash Added (%)	Unconfined Compressive Strength (kPa)	Permeability (m/sec)	Elastic Modulus (kPa)	Projected Permeability (m/sec @ 28 days)
1	30	26.9 @14 days	1.4×10^{-8} @ 23 days	2482.2 @ 14 days	1.0×10^{-8}
2	15	55.2 @ 14 days	5.3×10^{-8} @ 14 days	not tested	3.0×10^{-9}
3	5	103.4 @ 14 days	3.0×10^{-8} @ 14 days	not tested	1.0×10^{-9}
HB1	0	910.1 @ 28 days	8.1×10^{-11} @ 28 days	118,180.3 @ 23 days	8.1×10^{-11}

Figure 2: Strength and Permeability versus Ash Percentage

Within several days following mixing of the grout and ash materials, it was noted that set of the samples only occurred in those samples with the higher cement/ash ratios. It was further evident from the observations and testing that slight expansion of samples had occurred and therefore it is believed that the ash material had caused an unforseen chemical reaction that affected the strength and, more significantly, the permeability of the grout/ash mixtures.

Although the initially proposed approach was to inject a neat grout mixture which would mix with the ash to achieve the desired strength, permeability and elastic modulus parameters, the developed test data indicated that in order to meet the targeted parameters for the grouted mass, a near full replacement of the ash material (in excess of 95%) in the targeted grout zone would be necessary to minimize grout/ash chemical reaction. Therefore, to ensure that the design objectives were met during production grouting, a double-cut drilling and grouting program was developed that would excavate the greatest amount of waste ash and thus allow the maximum volume of replacement of ash with a neat grout mix in the target grout zone.

QUALITY CONTROL

Adjacent to the area to be grouted, six, pre-production tests were conducted on groups of three, interconnected Soilcrete columns in order to determine the maximum grout injection point spacing consistent with creating a continuous, low permeability, grouted waste mass. Varying parameters of center-to-center column spacing were employed as shown in figure 3. Lift and rotation speeds, and nozzle size were also varied, as shown in figure 4. Air and grout jet pressure remained constant for all six tests.
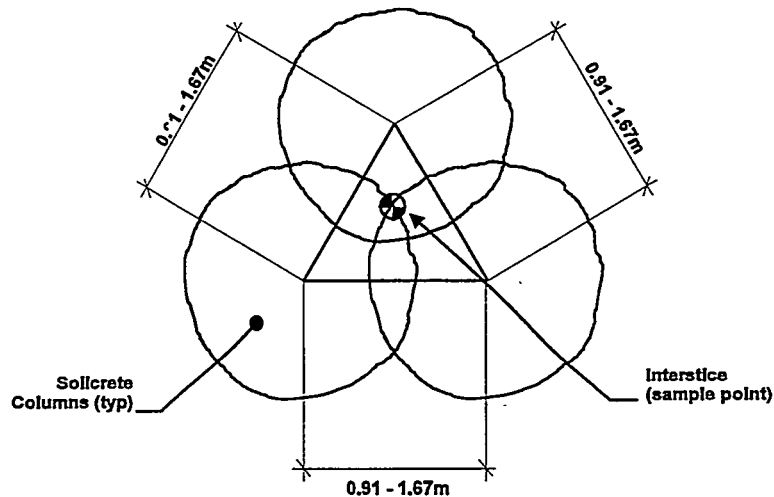
Figure 3: Test Column Layouts

Test Group	C/C Spacing (meters)	Nozzle Size (mm)	Lift Rate (mm/min)	Rotation (rpm)	Grout Pressure (Bars)	Air Pressure (Bars)
1	0.91	4.0	450	18	400	8
2	1.06	5.5	400	16	400	8
3	1.22	5.5	400	16	400	8
4	1.22	5.5	300	12	400	8
5	1.37	5.5	300	12	400	8
6	1.67	5.5	215	8	400	8

Figure 4: Test Column Parameters

503

Based upon the retrieval results of Soilcrete samples cored at the interstice of each test group, the final layout plan for production work was developed to allow the most acceptable results for providing a continuous, fully grouted zone. The test program illustrated that a 1.67 meter, center to center spacing of jet grouted columns could be used for the production work.

CONSTRUCTION

The site characteristics, which involved working in an open area with no sensitive structures nearby, made this project an ideal application for double-rod system jet grouting, and, as previously noted, in order to excavate and replace the greatest amount of waste ash, a double-cut drilling and grouting program was developed. The grout was volumetrically batched on site. Initially, the bentonite was hydrated overnight and then mixed with the pre-weighed and bagged NewCem/Portland cement materials using a colloidal shear mixer. Due to the volumes of grout required, the grout mixture was stored temporarily in a 4 cu yd agitator tank immediately following batching.

Prior to production grouting, every injection location was pre-drilled to provide an accurate, top of clay elevation. Jet grouting was performed by rotary hydraulic drilling and grouting of alternate locations in a single shift in order to allow the fresh Soilcrete to initially cure prior to grouting adjacent columns. Given that the site investigation had confirmed the thickness of the existing natural clay stratum in the target grout zone to be a minimum 0.61 meters, a 0.91 meter thickness of jet grouting was required to meet the project requirement of a 1.52 meter minimum thickness beneath the entire landfill. At each column location, the double system drill rod was advanced to full depth and grouting initiated to cut and grout a 0.91 meter lift. The drill rod was then advanced through the initial lift and a secondary cut made to ensure near complete replacement of the waste material. Spoil material created by the process was ejected from the drill annulus, and temporarily contained in preparation for subsequent permanent, on-site disposal.
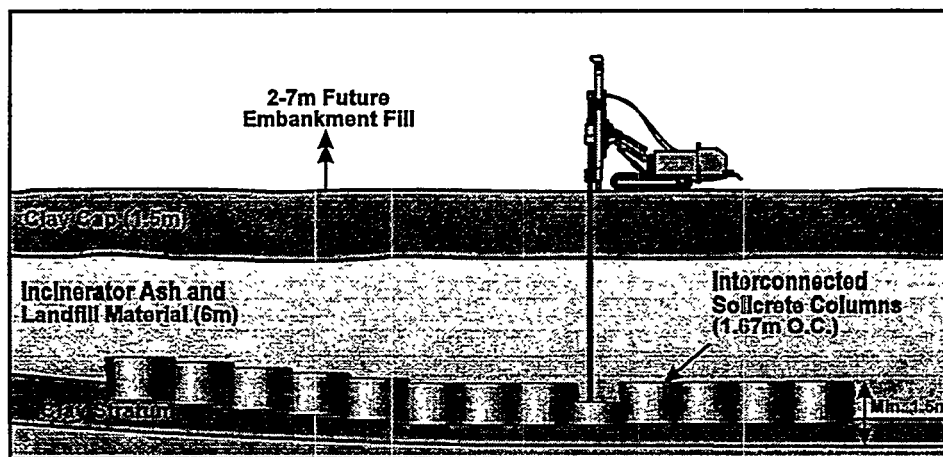
Figure 5: Jet Grouting Construction Profile

QUALITY ASSURANCE

In order to verify the consistency of the fully grouted zone, Cone Penetrometer Testing (CPT) was performed at interstitial points throughout the grouted area. Evaluation of CPT results confirmed that the grouting program had achieved a high percentage of replacement and that a minimum 0.91 meter, low permeability grout zone had been achieved at the bottom of the landfill, directly atop the thin, underlying natural clay stratum. As shown in figure 6, the CPT was able to clearly identify the three, in situ materials - waste ash, Soilcrete and clay.
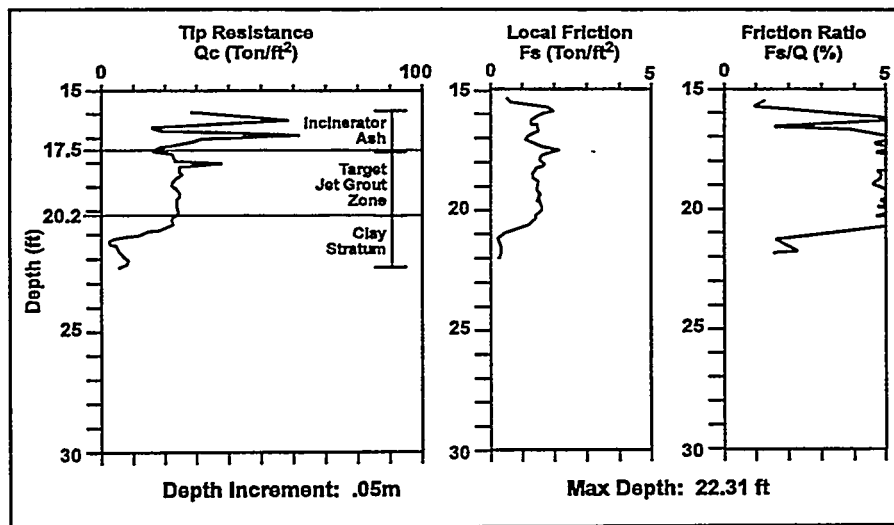
Figure 6: Typical Cone Penetrometer Test Result

SUMMARY

The use of jet grouting to remediate the landfill achieved:

- Minimal exposure of hazardous material during the removal and replacement of the waste ash.

- The timely completion of remediation needed to meet runway construction scheduling requirements.

- The low permeability barrier needed to meet EPA final closure requirements.

- The ability to resolve unforeseen conditions, without project delay, by the modification of typical construction techniques to meet site-specific conditions.

ACKNOWLEDGMENTS

REFERENCES

Bell, A. L., Crockford, R.M. and G. D. Mandley (1991) Soilcrete Jet Grouting in Tunnel Construction in Cohesive Soils at Burnham-on-Sea, Somerset, England. *Proceedings of the 6th International Symposium on Tunneling.* London, U.K. pp 249-261

Burke, G.K., Heller, R.A., and L.F Johnsen (1989) Jet Grouting for Underpinning: The Cutting Edge. *Geotechnical News.* Volume 7, No 1

Drooff, E.R., Furth, A.J., and J.A. Scarborough (1995) Jet Grouting to Support Historic Buildings. *Proceedings of ASCE National Convention on Foundation Upgrading and Repair for Infrastructure Improvement*, San Diego, CA. pp 42-55

Kauschinger, J.L., Perry, E.B., and R.Hankour (1992) Jet Grouting: State of the Practice. *Proceedings of Grouting, Soil Improvement and Geosynthetics.* New Orleans, LA. pp 169-181

Pellegrino, G and D.A. Bruce (1996) *Jet Grouting for the Solution of Tunneling Problems in Soft Clay. In Grouting and Deep Mixing* (ed. Yonekura, Terashi and Shibazaki). pp 347-352. Balkema, Rotterdam

Multi-Point Injection: A General Purpose Delivery System for Treatment and Containment of Hazardous and Radiological Waste

J. L. Kauschinger[1], J. Kubarewicz[2], and S.D. Van Hoesen[3]

Abstract

The multi-point injection (MPI) technology is a proprietary jetting process for the in situ delivery of various agents to treat radiological and/or chemical wastes (Kauschinger 1996). A wide variety of waste forms can be treated, varying from heterogeneous solid waste dumped into shallow burial trenches, bottom sludge (heel material) inside of underground tanks, and contaminated soils with widely varying soil composition (gravel, silts/clays, soft rock). The robustness of the MPI system is linked to the use of high speed mono-directional jets to deliver various types of agents for a variety of applications, such as: pretreatment of waste prior to insitu vitrification, solidification of waste for creating low conductivity monoliths, oxidants for insitu destruction of organic waste, and grouts for creating barriers (vertical, inclined, and bottom seals). The only strict limitation placed upon the MPI process is that the material can be pumped under high pressure.

The subsequent sections of this paper present the construction procedures implemented to inject ordinary cement grout to form solidified monoliths of miscellaneous solid waste. The solid waste was used as a physical surrogate for the actual trench waste buried within Department of Energy disposal sites. The results from solidifying solid waste deposited into B-25 type steel boxes (4.3 m^3), several shallow pits (2.4 m. X 3 m. X 1.2 m. deep) and a deep concrete box (4.3 m X 4.3 m X 4.9 m. deep) are presented in this paper. Very detailed hydraulic conductivity tests were performed on the waste solidified in the B-25 box. The spatial variation of the hydraulic conductivity (K_{fs}) and matrix flux potential (ϕ_m) were measured within the B-25 box over 150 mm intervals within three different bore holes. All conductivity tests were performed under a constant head using a field measuring device termed a Guelph Permeameter (Reynolds, et. al. 1985). The well flow theory developed by Elrick and Reynolds (1989) was used as the basis for extracting the material properties from the data measured on the solidified monoliths. Once the conductivity tests were performed the B-25 box monolith was cut into half for visual examination of the inner core of the monolith. Photographs of the inner core of the monolith are shown so that the reader can relate the visual aspects of the treatment to the measured conductivity.

General Features of the MPI Process

The construction activities required for implementing the MPI process involve three basic steps: installation of plastic ("cuttable") pipe usually by percussion drilling; assembly of a lifting frame and loading of jetting tools into the plastic pipe, then lastly high speed injection. The exact sequence of injection, layout of injection holes, type of lifting frame and material injected into the ground would be dictated by the actual remediation activity. The following sections cover the application of creating a monolith from solid waste deposited into shallow pits. However, the essential feature of installing cuttable plastic pipe and using mono-directional high speed jets for injection are the basic elements of the MPI system would be the same no matter the application.

The utilization of percussion driven plastic pipe prevents waste cuttings from being ejected to the surface when the injection is performed with at least 1.5 meters of soil cover. With less soil cover the jets have greater potential for breaking through to the surface. However, measured ground

---

1). Technical Director, Ground Environmental Services, 200 Berry Glen Court, Alpharetta, Georgia. 30202, (770) 993 - 3538 U.S.A.
2). Technology Coordinator, Jacobs Engineering, 125 Broadway, Oak Ridge, Tennessee
3). Program Manager, Lockheed Martin Energy Systems, Oak Ridge, Tennessee 37830

flows are dense (unit weight = 1.76 g/cc), and is easily contained within a sand bag moat which supports the lifting frame. Furthermore, since all injection is done remotely there is no chance of worker exposure or contamination of capital equipment even if ground flows do occur. Ultimately, the ground flow hardens as a solidified mass, which acts as a concrete cap over the buried waste.

A significant operational feature of the MPI system is related to the ability to re-use the same bore hole liners (plastic pipe) to perform additional injection or repair defects in the treatment. This would allow a simple repair to a cutoff wall if "windows: were detected from anomalies in piezeometric head data. Furthermore, the re-injection feature of the MPI system allows repeated treatments to be done when remediating soil. Clean-up of chlorinated solvents could be done with oxidants (permanganate, peroxide) which tend to react quickly over several days to weeks. The oxidants could be re-injection over time so that there would be a stimulation of the reaction after the initial treatment has lost its effectiveness.

Construction Procedures for Installing the MPI System

The details to deploy the MPI system is discussed in relation to forming a homogeneous monolith. The results from three different jobs are presented to illustrate the various construction steps. These projects include: the solidification of waste inside of a B-25 box (Duncan, Oklahoma project); shallow pits formed in the lake bed near Salt Lake City; and the injection performed in a concrete vault in Oak Ridge, Tennessee.

A wide variety of plastic pipe were tested for application as a casing which is cuttable by a high speed jet. The exact material type is dependent on the application. The installation of the plastic casing is accomplished via a specially designed percussion drive system. This drilling technique does not generate spoil material, and the percussion equipment can be easily adapted for remote control. Plastic casing was driven through non-hazardous, miscellaneous solid waste, with depths that varied from 1.5 to 4.9 meters. The other major difference between any of the three tests sites was the degree of waste containerization. At Duncan, Oklahoma and in Salt Lake City all solid waste was encapsulated within some sort of container (plastic bag, cardboard drum or box sealed with shrink wrap, or within steel drums). Encapsulation of the waste creates a barrier to grout infiltrating the waste. Low pressure grout only penetrates water accessible void space. The photograph in Figure 1 is illustrative of the encapsulated waste form used in Duncan and Salt Lake City sites.

Figure 1 General View of Miscellaneous Solid Waste Used in Salt Lake City Test Beds for Demonstrating the MPI Process

507

The waste deposited into the concrete box at Oak Ridge was not containerized due to the large volume (75 m^3) required to fill the concrete box. This waste was highly compressible and the final stratigraphy of the soil and waste treated at Oak Ridge was as follows:

surface – 2.4 m.   medium dense sapprolite (fill soil)
2.4 – 4.0 m.   heterogeneously placed bags, cardboard, wooden pallets, steel drums, and miscellaneous metal,
4.0 - 4.9 m.   sand bottom layer

Of the eight plastic casings installed through the above-referenced soil/waste form, four were driven totally through the waste to a depth of 4.0 meters.. The other four plastic casings were driven to about 3.5 meters. All plastic pipe were driven with a 64 kilogram (140-pound) standard penetration hammer, which was dropped 76.2 cm. (30 in.) under gravity. Typically, all casing required around 3,300 blows per meter to penetrate through the waste material. After 500 blows, if the casing had not advanced more than 10 mm, the driving was terminated. Even after such a severe pounding (over 5000 blows per 1.5 meters of waste), all the plastic casings were intact and could withstand additional pounding. Since the Oak Ridge field demonstration was scheduled for only a few days, there was no opportunity to change over to a heavier drive hammer for pounding all casing to the 4.0 meter depth.

As part of the demonstration in Oak Ridge a few plastic pipe were driven through the natural soil down to a depth of 8 meters. The plastic pipe only required about 65 blows per meter for penetrating the soil stratigraphy. Furthermore, it only required about 10 minutes to drive the plastic pipe the 8 meters. The soil stratigraphy in this area of Oak Ridge is typically residual soil (sapprolite), which is underlain by weathered to decomposed shale.

The second step in deploying the MPI technology is assembling the disposable lifting frame over the area to be injected. The lifting frame serves the purpose of allowing the jetting tools to be lifted from a remote location. The lifting frame also provides local containment over the area injected. The photograph in Figure 2 shows two workers removing the jetting tools from the lifting frame assembly used during the Salt Lake City demonstration. The plastic wrap covering the frame is clean (no airborne releases) even though 800 bar jetting pressures were used within 300 mm of the surface. The slight amount of ground flow was contained within the sand bag moat.
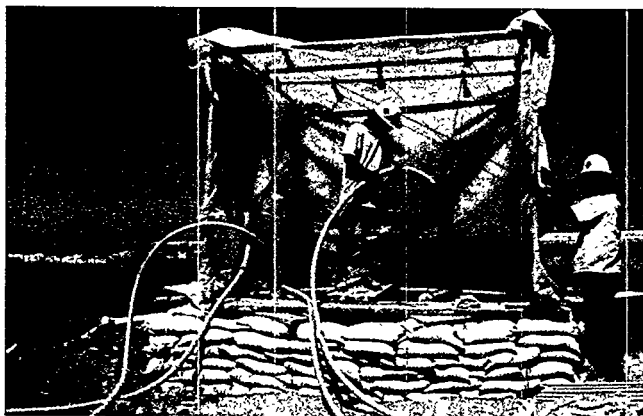
Figure 2   Photograph Illustrating the Lifting Frame Used to Perform the MPI Process on Miscellaneous Solid Waste Deposited in Pit 3 at Salt Lake City Test Site

The final stage of the MPI process is injection of the chemical agents. All demonstration work used a water cement grout (proportioned 1:1 by weight). The MPI injection sequence is similar to an upstage grouting process. Each hole is sequentially injected for about 20 to 200 seconds. Thereafter, the hose/jet monitor assembly is lifted remotely. The sequence of injecting a discrete layer of waste at a time allows precise control over the type of treatment a particular zone of waste receives, i.e. treatment is injected in a plate-like fashion. Different types of injection can be performed at different elevations.

Duncan, Oklahoma Test Site: Solidification of Miscellaneous Waste In Steel B-25 Boxes

An initial concern with using the MPI system to form homogeneous monoliths was related to the possibility of robust containers (ex. steel drums) causing the jets to deflect. Under extreme conditions of jetting inside a steel drum no treatment may penetrate outside the drum. This action would prevent waste from being mixed by the turbulent action of the various jets hitting the waste with high speed grout. If there are a large number of robust containers then there may be large areas of untreated waste. Therefore, field tests were undertaken to understand the ability of a high speed mono-directional jet to cut through steel drums. Jetting pressures between 500 to 800 bars developed sufficient jet velocity to cut holes into steel drums. However, the higher jetting pressures produced a more efficient process. The photograph in Figure 3 is illustrative of a hose suspended jetting tool cutting a steel drum. When conventional jet grouting (rotating jets) was used with 800 bar pressure, no holes could be cut into the drums, (even after several minutes of jetting). This would require closely spaced holes during conventional jetting to assure that no untreated waste was left behind.

Figure 3   Close-up Photograph Illustrating Mono-Directional Jets Cutting a Fifty - Five Gallon
Steel Drum; Pump Pressure = 800 Bars

Formation of a homogeneous monolith is predicated upon the dispersion and turbulent action of the jetstreams to create a "jet-washing machine" effect. This mechanism is the key to homogeneously mixing and cutting the waste for intimate contact with the solidification agents. Quantification of the homogeneity of the treatment was evaluated by performing a series of constant head Guelph Permeameter tests. The test procedure involved core drilling 100 mm diameter holes into the monolith at about 100 to 200 mm depths. At each increment two constant head conductivity tests were performed, (10 cm. and 20 cm. water head). The measured time-flow data was used to calculate the hydraulic conductivity (K_{fs}) and matrix flux potential (ϕ_m) of

the solidified waste. Typically, it required from 48 to 72 hours to obtain a steady state flow. Three conductivity tests, with three levels each, were performed inside each borehole drilled into the monoliths formed in Duncan. The depths at which each of the nine conductivity tests were conducted are listed in Table 1 along with the corresponding values of conductivity. The first tests were typically done at a depth of about 400 - 500 mm. This location was near the original contact between the soil cover and waste placed into the steel B-25 box. The data in the table indicate that at two locations (32a, 33a) the conductivity was around 1.0 x E-06 cm/sec. The conductivity measured at bore hole location 31a was greater (more pervious). The reason for this higher measurement is related to stopping the MPI injection below level "31a". It was of interest to examine the influence which stopping the injection "short" of completion had upon the conductivity. The other conductivity data listed in Table 1 indicate that the monolith was of relatively low conductivity with eight of the nine conductivity values being between 1.0 to 10.0 x E-07 cm/sec. It should be re-emphasized that ordinary cement grout was used during the injection. It was of interest to only examine how homogeneously grout was introduced into the solid waste. Afterward, the monolith was cut into two pieces along the transverse direction. The photograph of the solidified waste, shown in Figure 4, reveals two well-cemented blocks. The section shown on the left side of the photograph represents the internal core of the waste, while the other side was the outer skin caste against the walls of the B-25 box.

Table 1. Hydraulic Conductivity Values Measured Using Guelph Permeameter in Waste Solidified Using Cement Grout Delivered by the Multi-Point Injection Process, Duncan, Oklahoma Site, B-25 Box No.3

Hole ID	Test Depth (mm)	Hydraulic Conductivity (cm/sec)
31a	475	1.9 X E-04
31b	660	1.0 X E-06
31c	813	4.2 X E-07
32a	475	1.7 X E-06
32b	685	1.3 X E-06
32c	787	6.2 X E-07
33a	406	1.4 X E-06
33b	584	1.2 X E-07
33c	762	2.7 X E-06

Figure 4   Photograph Depicting Monolith of Waste Sawed into Two Pieces;
Left Half Is Internal Core of Solidified Waste;
Right Half is Outer Skin Caste Against Steel Shell of B-25 Box

Salt Lake City Demonstration: Shallow Pits

There were three shallow pits used during the MPI demonstration conducted at the Salt Lake City test site. The first pit was used to examine the influence which different types of waste has upon the cutting ability of a high speed jet. The second and third pits were used to examine the influence which the number of injection points and duration of jetting has upon the formation of a monolith. The remaining discussion will focus upon the test data collected on Pit 2 and Pit 3.

The injection performed in Pit 2 utilized seven injection holes which were arranged according to the layout shown in Figure 5. The hole spacing varies from 130 cm to 160 cm (51 to 62.5 inches), with most holes being about 142 cm. (56 inches) apart. MPI monitors were placed within each bore hole and the injection was performed using the procedure specified previously. A total of six levels of injection were performed to solidify the one meter of waste. The total volume injected was equal to about 15,000 liters of grout. The volume of injection represents about twice the total volume of the waste deposited in Pit 2. The over-injection resulted in ground flow of material breaking through to the surface. This ground flow was contained within a sand bag moat constructed beneath the lifting frame (see previous Figure 2). There was never any airborne releases of grout observed during any phase of the injection work.

The purpose of the injection performed in Pit 3 was to demonstrate the formation of a low-conductivity monolith using a smaller amount of grout. The total volume injected was about 1/3 the total volume injected in Pit 2. There were five injection holes used in Pit 3, which were arranged with an injection hole in each of the four corners and one at the center of the 2.4 m. X 3.0 m plan area of the pit. The holes spacing varied from 150 cm to 285 cm. (58.5 to 112.5 inches), with most holes being about 183 cm (72 inches) apart. A total of six levels of injection were performed to solidify the one meter of waste. The total volume injected was equal to about 5000 liters of grout. The volume of injection represents about 75% of the total volume of waste deposited in the pit. The injection resulted in minor ground flow of material breaking through at the surface when the jets were within 45cm (18 inches) of the ground surface. There was about 22 cm thickness (9 inches) of ground flow, which was contained within a sandbag moat constructed beneath the lifting frame. The ground flow represents about 25 percent of the total volume of waste deposited in the pit. The ground flow density was measured as 1.76 g/ml, which is so heavy, to prevent any airborne releases of grout.

Four core holes (CH-1, CH-2, CH-3, and CH-4) were drilled into each of the two pits, see location map in Figure 5. The core hole layout for Pit 3 was nearly the same as Pit 2. One hydraulic head was used in the Guelph permeameter tests to calculate the conductivity of the solidified waste. The conductivity test results from the eight Guelph Permeameter tests conducted for both pits is summarized in Table 2. Typically, the hydraulic conductivity measured on the Pit 2 monolith were about 4.0 to 7.0 X E-07 cm/sec. There was one inconclusive test (CH-3) in Pit 2. Although the majority of the interior of CH-3 resembled a concrete pipe (from bore hole camera survey), a segment of the core hole cut across a portion of a steel drum. The drum had not been penetrated by the jet and the saw dust inside of the drum was left untreated. In general, the hydraulic conductivity measured in Pit 2, along with the overall appearance of the exhumed waste (see photograph in Figure 6) produced a low conductivity, uniform monolith.

The results from the conductivity testing on Pit 3 were more complicated to interpret due to a mishap during the injection. The two injectors located in the Southern corners of Pit 3 had rotated slightly inside the plastic pipe when the jetting pressure was initially applied to the hose, i.e. hose unwrapping during initial pressurization. This hose rotation caused several of the jetstreams to be pointed into the soil adjacent to the trench. Therefore, less jets were directed into the waste. The work plan for the Salt Lake City demonstration required use of packers at each injection hole. This appliance would provide the torsional restraint needed to assure that the hoses never rotate.

However, the contractor claimed that they did not have the budget to include this item as part of the demonstration. The five nozzle jet configuration had previously been tested for stability during injection under 800 bars. This jetting tool had always cut small, uniformly round holes into the plastic casing. This is an indicator that the jetting tool remains stationary during injection. Therefore, with a few operational changes (which were known prior to the demonstration) the MPI monitors can be aimed in the correct direction for performing the solidification. Even though the two injectors along the Southern perimeter of test Pit 3 had rotated, the measured hydraulic conductivity were around 1 X E-05 cm/sec, which is comparable to the conductivity of the natural soils at Oak Ridge. The Northern half of the monolith had much lower conductivity measured at around 7.0 X E-07 cm/sec. Therefore, it would appear that about half of the waste in Pit 3 was solidified as a monolithic structure, using an average injection hole spacing of about 183 cm (72 inches). These jetting parameters produce surface cuttings which are about equal to 25% of the total waste volume, which formed a solid cap over the buried waste.
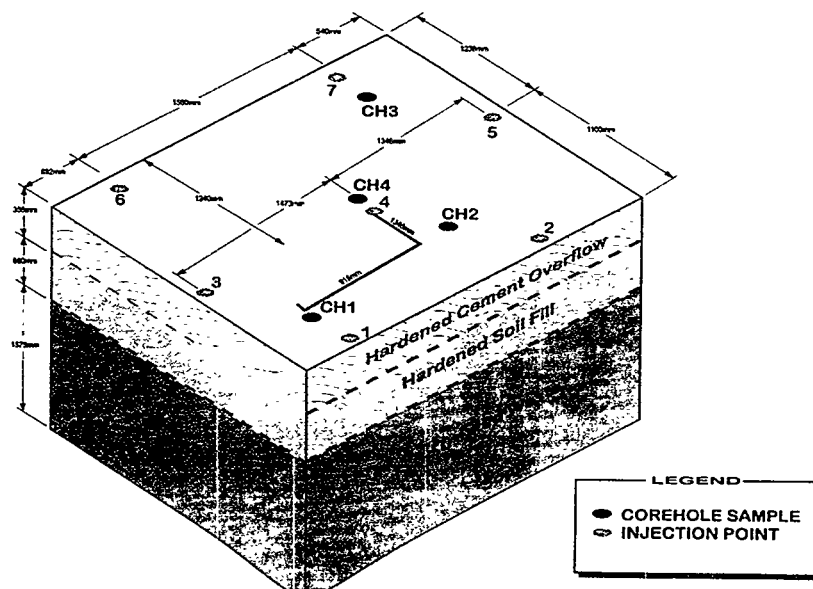
Figure 5 Sketch Illustrating the Overall Dimensions of Pit 2 , with Plan Location of MPI Injection Hole Pattern and Core Hole (CH) Layout Used for Guelph Permeameter Testing

Table 2 Summary of Guelph Permeameter Tests Conducted on Monoliths Formed in Pit 2 and Pit 3

Pit No.	Corehole ID	Permeation Test (cm) From	(cm) To	Waste Thickness Permeated (cm)	Percent Cored Waste Recovery	Hydraulic Conductivity	
Pit 2	CH-1	69.5	116.8	47.3	47%	3.7 X E-07	
	CH-2	57.8	129.5	71.7	72%	7.3 X E-07	
	CH-3	34.3	105.4	71.1	71%	Inconclusive	Core hole intersects steel drum
	CH-4	55.9	83.8	27.9	28%	6.2 X E-07	
Pit 3	CH-1	81.5	128.3	46.8	47%	1.2 X E-05	
	CH-2	75.4	119.4	44.0	44%	1.9 X E-05	
	CH-3	57.7	129.5	71.8	72%	7.2 X E-07	
	CH-4	71.6	116.8	45.2	45%	6.0 X E-07	
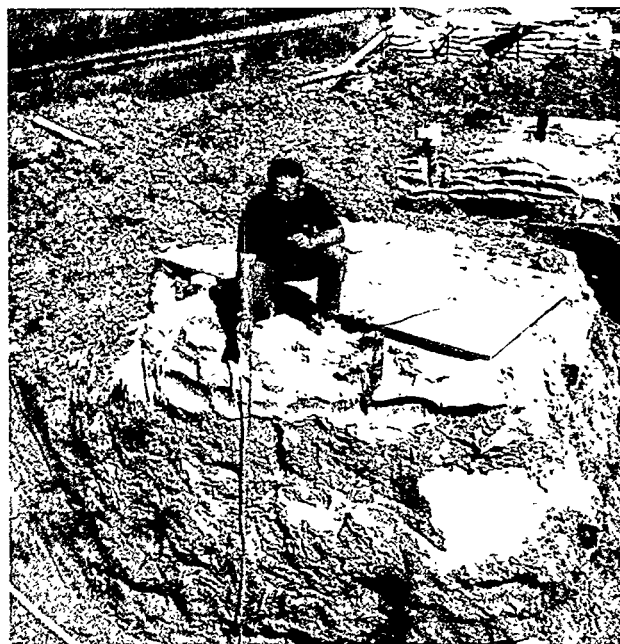
Figure 6   Close-up Photograph of Exhumed Monolith of Solidified Miscellaneous Waste Formed
in Pit 2 During the MPI Demonstration in Salt Lake City

Conclusions

The MPI process has been demonstrated at three sites. The work conducted in Duncan, Oklahoma, and Salt Lake City indicate that low conductivity monoliths (1.0 to 10.0 X E-07 cm/sec) of miscellaneous solid waste can be formed using mono-directional jets spaced apart at about 1.5 to 1.8 meters. The cuttings which are generated represent about 25% of the total volume of waste. The work conducted in Oak Ridge showed that it is practical to drive plastic pipe through 4.0 meters of solid waste and 7.6 meters of natural soil at Oak Ridge. The injection conducted in Oak Ridge indicated the need for field QC/QA over the selection of the jetting time. A bore hole camera and clear plastic pipe can be easily incorporated into the MPI process. The field QC/QA would allow a more rational basis for selecting the jetting times, which would also lead to better control over generated waste. The injection done in Oak Ridge also indicated that the MPI process can form a continuous wall of cement grout in dense sandy clay soils. This was accomplished without generating any cuttings to the surface. This observation will have significant impact on reducing the waste management associated with using the MPI Process to form a continuous cutoff wall.

References:

Elrick, D..E.,   Reynolds, W. D., and Tan, K.A., (1989), Hydraulic conductivity measurements in the unsaturated zone using improved well analysis, Ground Water Monitoring Review, Summer, 184 - 193.

Kauschinger, J.L." U.S. Bureau of Copyright and Patent Application Covering Multi Point Injection", U.S. Patent Pending, All Rights Reserved.

Reynolds, W.D., and Elrick, D. E., (1985), In situ measurement of field-saturated α-parameter using the Guelph Permeameter, Soil Science, 140(4), 292-302.

JET GROUTING FOR A GROUNDWATER CUTOFF WALL
IN DIFFICULT GLACIAL SOIL DEPOSITS

Richard F. Flanagan[1] and Frank Pepe, Jr.[2]

ABSTRACT

Jet grouting is being used as part of a groundwater cutoff wall system in a major New York City subway construction project to limit drawdowns in an adjacent PCB contamination plume. A circular test shaft of jet grout columns was conducted during the design phase to obtain wall installation parameters. The test program also included shaft wall mapping, and measurements of; inflows, piezometric levels, ground heave and temperature, and jet grout hydraulic conductivity. An axisymmetric finite element method groundwater model was established to back calculate the in-situ hydraulic conductivities of both the surrounding glacial soils and the jet grout walls by matching observed inflows and piezometric levels. The model also verified the use of packer permeability test as a tool in the field to evaluate the hydraulic conductivities of jet grout columns. Both the test program and analytic studies indicated that adjustments to the construction procedures would be required to obtain lower hydraulic conductivities of the jet grout walls for construction. A comparison is made with the conductivities estimated from the test program/analytic studies with those from the present construction.

INTRODUCTION

The construction of a new subway connection between two existing subway lines in New York City requires the use of jet grouting to construct a series of cutoff walls. The new connection will be made by passing under the existing subway box near 40th Road and Northern Boulevard and then gradually rising to meet the existing subway invert elevation near 39th Avenue as shown on Figure 1. The cutoff walls will form a watertight enclosure to permit dewatering inside the enclosure while preventing the migration of an adjacent PCB contamination plume, just outside the cutoff walls. The cutoff walls generally extend into rock with a grout curtain in the upper portion of the rock. During construction, differential hydraulic heads across the cutoff walls will range from 6 m to about 14 m. The jet grouting is being used in areas where conventional diaphragm (i.e. slurry) cutoff walls could not be constructed due to the presence of existing surface and subsurface structures and utilities. The total length of the jet grout cutoffs are about 230 m.

A jet grouting test program which included various instrumentation was developed and conducted during the design phase to provide data on the performance of jet grouting in the variable glacial deposits. The principle purpose of the test program was to evaluate the applicability of jet grouting as cutoff walls and to demonstrate whether jet grouting could successfully grout the soil deposits and encapsulate boulders which occur in the glacial till deposits at the site.

A computer model was developed to simulate the test program. Hydraulic conductivities of the jet grout columns and adjacent soils were "back-analyzed" from this computer model by matching the observed drawdowns and inflows of the test shaft. The computed jet grout column hydraulic conductivities gave similar results to those measured from a series of packer permeability field tests in the jet grout columns. Analytic studies for the final cutoff wall utilizing these computed jet

---

[1] Senior Professional Associate, Parsons Brinckerhoff Quade & Douglas, One Penn Plaza, New York, New York 10119, (212) 465-5209, FlanaganR@PBWorld.com

[2] Professional Associate, Parsons Brinckerhoff Quade & Douglas, New York One Penn Plaza, New York, New York 10119, (212) 465-5215, Pepe@PBWorld.com

grout column hydraulic conductivities indicated that in the glacial till with boulders, there would be enough drawdown with undesirable contamination plume transport towards the excavation and that design changes would be needed.

Construction is underway, and to date, quality control, testing, consisting of 68 packer permeability tests, indicate that the design changes made for construction have lowered the hydraulic conductivities. Pump testing inside the cutoff walls in underway and early results indicate that most of the jet grout wall sections are performing as planned.

SITE AND SUBSURFACE CONDITIONS

The project site is located in northwestern Queens County, New York. The site is covered with roadways and buildings and below is the existing New York City Transit (NYCT) Queens Boulevard subway, line as shown on Figure 1.
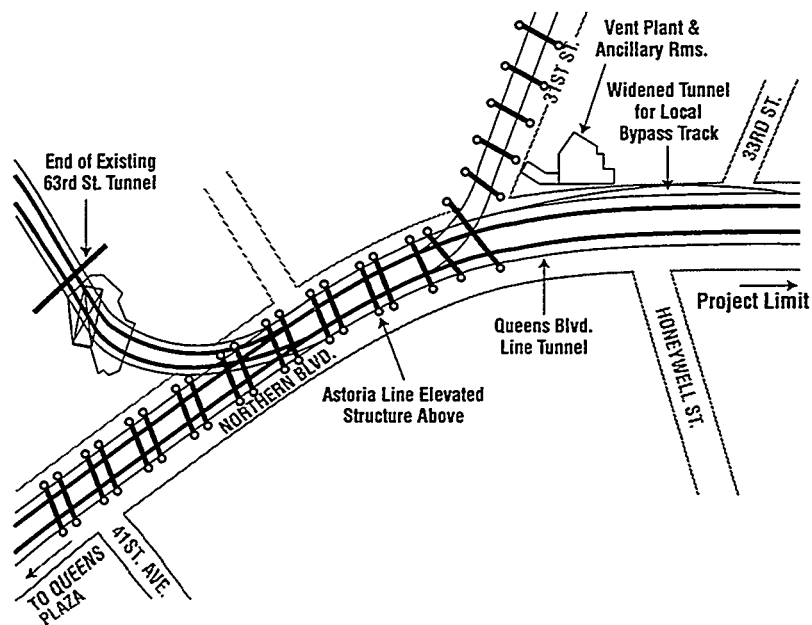
Figure 1: 63rd Street Connection Project Alignment

The site is underlain by metamorphic bedrock which is covered by glacial and interglacial deposits as well as post-glacial materials. The terminal moraine of the last Wisconsin ice advance is located approximately three miles southeast of the site and has major influence on the site's soil conditions. The glacial deposits can generally be divided into three main groups: mixed glacial deposits, glacial till, and outwash/reworked till deposits. The stratification is complex and significant variations in the thickness and distribution of the individual units is common. This heterogeneity is typical of glacial depositional environments found at the rear of terminal moraines.

The generalized subsurface profile at the test site is presented in Figure 2, and in descending order consist of:

- Miscellaneous fill consisting of a heterogeneous mixture of coarse to fine sand, silt, gravel, brick fragments, wood metal and other building rubble.

515

- Mixed glacial deposits which vary from loose to medium dense coarse- to fine-sand with less than 10 percent silt size particles, to soft to stiff varved silt and clay and very fine sand.

- Reworked glacial till/outwash deposits consisting of dense to very dense, well to poorly graded coarse to fine sands with less than 10 percent particles finer than the number 200 U.S. Standard Sieve. Boulders and cobble size particles are also commonly encountered in these deposits. Pump tests indicate that hydraulic conductivity in the outwash sands are high as 2×10^{-2} cm/sec.

- Glacial till deposits which are generally interlayered with the reworked till and outwash deposits and consist of heterogeneous mixture of sand silt and gravel with and without a cohesive binder. The till materials are generally dense to very dense, contain boulders and cobbles and between 15 and 40 percent particles passing the number 200 sieve.

- Bedrock consisting of slightly fractured to sound granite gneiss and schistose gneiss.
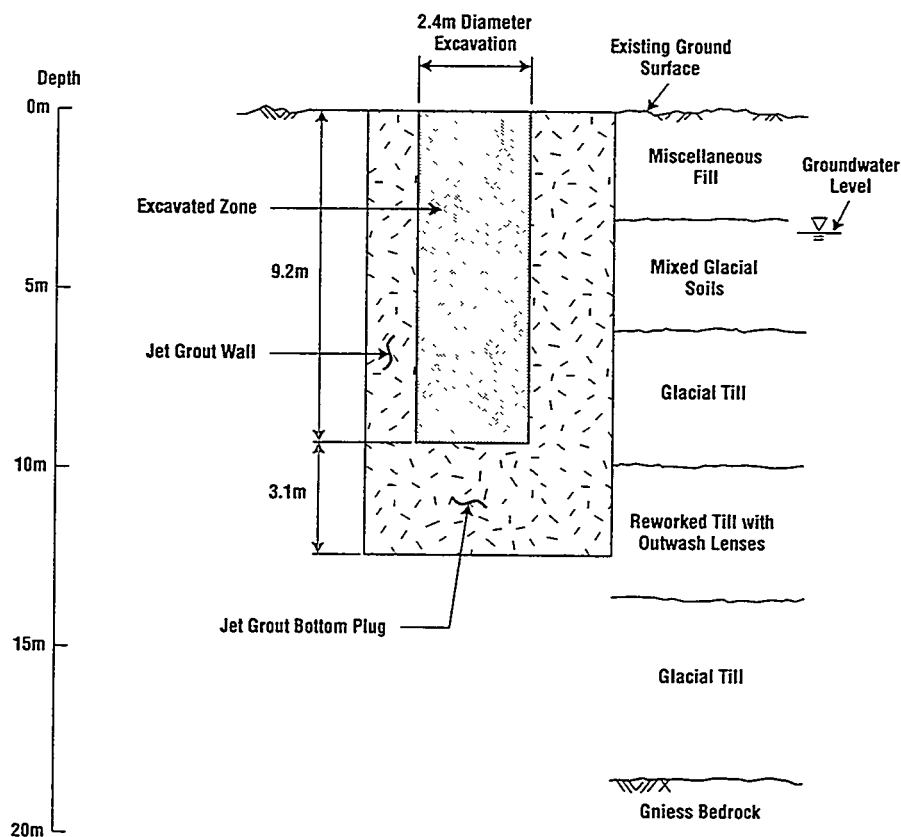
Figure 2: Soil Profile and Section at the Jet Grout Test Cell

JET GROUTING TEST PROGRAM

The jet grouting test program was developed to evaluate the use of jet grouting to form continuous low permeability cutoff walls in the extremely variable soil conditions existing at the site. The key issues for the cutoff walls which were addressed in the test program included:

- Jet grout wall continuity and encapsulation of boulders
- Jet grout wall hydraulic conductivity
- Jet grout column diameter

The plan and location of the jet grout test section is presented in Figure 3. Also shown on Figure 3 are the locations and types of instrumentation installed in the vicinity of the test cell. The test cell consisted of a circular ring of interconnected jet grout columns which form the walls of an 2.4 m diameter shaft. As indicated in the figure, two different configurations of jet grout columns were used to form the cell walls: one half formed by a single row of columns installed at 840 mm centers, and the other half by a double row with the outermost columns installed at 890 mm centers. The overall length of the wall columns was 12.3 m of which the lower 3.1 m form the outer portion of the jet grouted invert cutoff. The inner portion of the invert cutoff was formed by a group of 3.1 m long closure columns which were formed by grouting the soil zone from 9.2 to 12.3 m below grade.
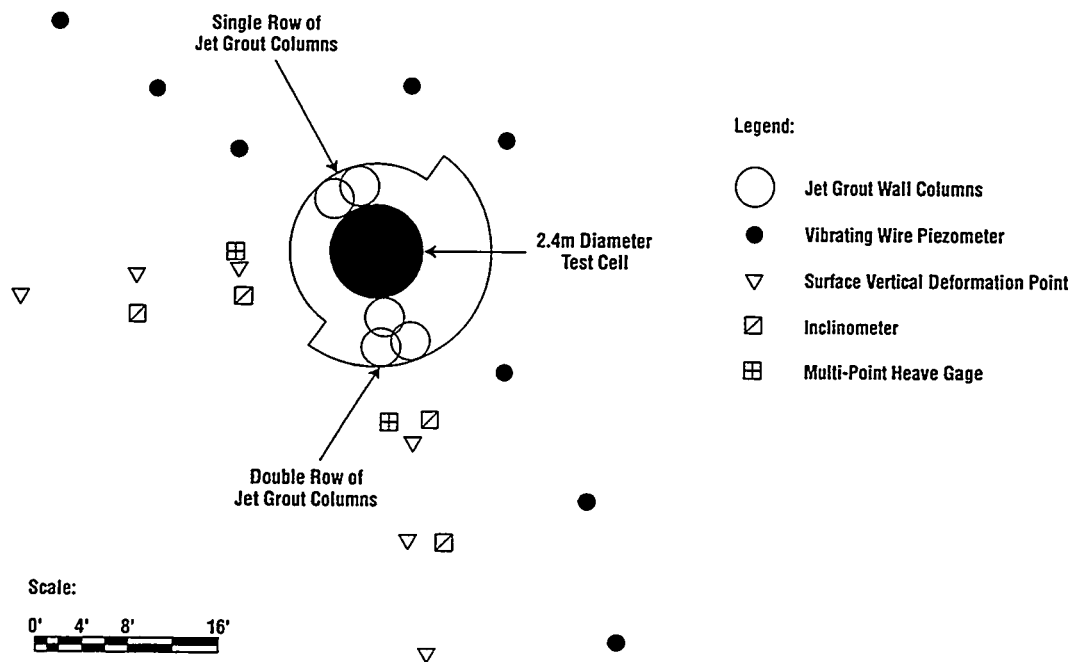
Figure 3: Jet Grout Test Cell and Instrumentation Layout Plan

The test shaft was instrumented with inclinometers (to measure horizontal displacements), piezometers (to measure groundwater drawdowns), thermocouples (to measure ground temperatures) and vertical displacement markers (to measure vertical ground movements). Also mapping of the shaft walls and seepage inflow measurements were done during and after the shaft excavation.

The jet grouting contractor Hayward Baker Inc. of Odenton, Maryland elected to use the triple fluid jet grouting method which uses a combination of air, water and grout injected into the soil to form the jet grouted columns. The triple fluid system used a high pressure water jet encapsulated in a cone of air to cut and erode the soil while injecting the cement grout which mixes with the remaining soil to form the jet grouted soil column. The Hayward Baker jet grouting system utilized a single air/water cutting nozzle positioned approximately 250 mm above the grout injection ports.

The jet grouting installation parameters were varied to evaluate the effects on the constructed columns. The triple fluid system utilized a water jet at 40.7 mPa, air at 620 to 900 kPa and grout at 520 to 900 kPa. During grouting, the withdrawal rate varied between 150 to 350 mm/min but most typically 300 to 350 mm/min. The corresponding rotation rate ranged from 5 to 20 rpm with most

517

around 10 to 12 rpm. The grout flow was monitored at 120 to 175 l/min with the most typical at 145 l/min.

Ejected grout waste was monitored. The ratio of waste to soil treated volume was estimated to be between 75% to more than 100%. Verticality checks were made routinely for each column using a level. These checks were done during both pre-drilling and jet grouting by holding the level on the exposed drilling rods. This check only provided a verticality check at the ground surface and not the deviation at the column bottom. Thus, more rigorous verticality monitoring was done on selected columns. This was accomplished by placing inclinometer casing inside the drill rods and measuring deviations with an inclinometer probe. Once the borehole was drilled to its final depth, the drill head was lifted off the casing and the inclinometer casing with centralizers was inserted into the drill rods and placed to the bottom. Subsequently, the inclination was measured with the inclinometer probe lowered inside the inclinometer casing. The deviation from the vertical, varied from 0.6% to 5.5%. The upper value occurred in one column with an inexperienced rig operator. However, the average deviation with an experienced operator was 1.8%. Seven of ten data sets showed a near linear deviation displacement increasing with depth.

Post jet grout coring was done at 18 locations with a triple tube diamond core barrel. The cores were taken at both the center and edge of selected columns. The average core recovery of samples taken in the center of columns was 61%, after excluding boulders. During excavation mapping, ungrouted or soft grout/soil zones and to a lessor extent, voids were observed. The former was prevalent in soil zones with a predominant fines content.

A series of 16 packer permeability (hydraulic conductivity) tests were done vertically along the jet grout column from the ground surface prior to shaft excavation. These tests, done in cored holes, utilized a single inflatable packer. The tests were run on both the single and double row columns at locations corresponding to the center and overlapping sections. The packer test results are presented in Figure 4 (log scale). Tests with no or negligible "takes" are indicated with a hydraulic conductivity of 10^{-7} cm/sec. Four tests are not included because water return to the ground surface was observed. This may be due to a poor seal between the packer and core hole or water escaping around boulders and back into the borehole above the top packer. Two other packer tests were excluded because it was believed that the test zone extended out the bottom of the columns. Figure 4 also includes data from the construction phase.

The majority of the packer permeability tests, from the test program, were done below a 6m depth, generally in the boulder till. Figure 4 illustrates that hydraulic conductivities ranged from 10^{-7} cm/sec to 3.5×10^{-4} cm/sec. Tests done at the center of columns gave similar results regardless of whether the test was located in the single or double row columns. However, based on limited data, it appears that tests done in column overlapping zones yielded lower hydraulic conductivities. The overall average horizontal hydraulic conductivity is about 7×10^{-5} cm/sec.

Higher hydraulic conductivity was obtained in zones with higher boulder density. The correlation between a zone of higher hydraulic conductivity and boulder density was confirmed by the shaft mapping whereby boulders could be observed directly. The influence of boulders on the higher hydraulic conductivity is probably due to lack of continuity of the soil-cement grout mass around boulders, i.e., incomplete encapsulation of boulders with grout. The result of this phenomena is leakage paths.

The piezometers indicated groundwater drawdowns during shaft excavation and reached a maximum of about 0.3 m. The drawdowns indicated a steady state during the few weeks the shaft was completely open. The pattern of drawdown was uniform on both the double and single side of the shaft. The drawdown pattern also indicated a radius of influence of about 150 m.
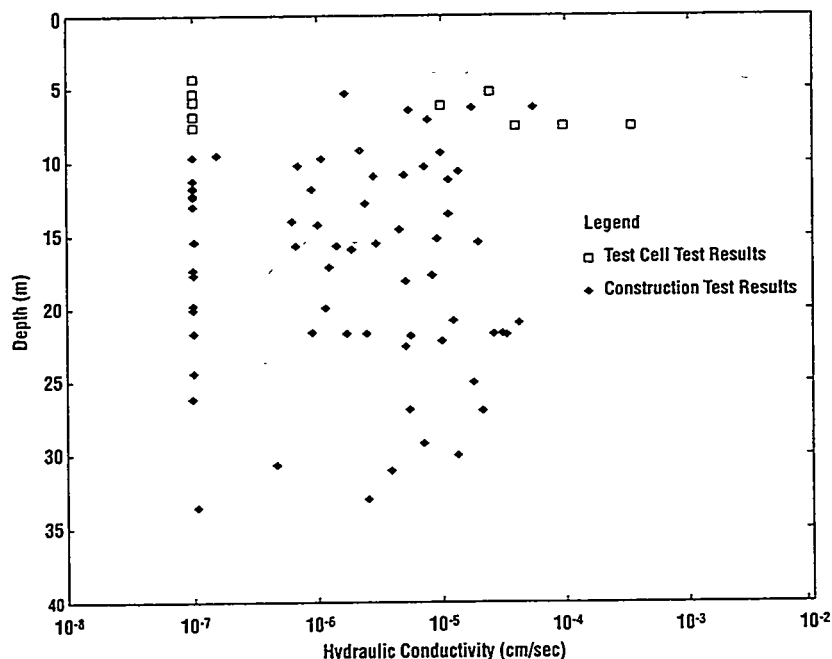
Figure 4: Packer Permeability Test Results

Observed seepage into the shaft was noted in the invert and in shaft walls approximately 5.2m below the ground surface. Active seeps were too small to measure individually. Much of the seepage appeared as surface "sweating" or dripping. The total inflow rate, however, was possible to measure and is approximately 0.3 to 0.4 l/min. This rate of seepage was generally constant with time while the shaft was completely open.

GEOHYDROLOGICAL ANALYSIS AT THE TEST SECTION

Geohydrological analyses of the field test program data were done. The primary purpose of these analyses was to "back-compute" the hydraulic conductivity of the jet grout walls and provide a check on the packer permeability tests. A secondary purpose was to estimate the hydraulic conductivities of the soils and provide an insight into the jet grout treatment behavior.

A two-dimensional axisymmetric profile groundwater model was developed to simulate a jet grout lined shaft. Partial penetration was included in the model geometry since the test cell did not fully penetrate the underlying glacial till strata. The geomechanics software, FLAC, a Lagrangian finite difference method produced by the Itasca Consulting Group, Minneapolis, MN was used for these analyses. The model was designed to include the known soil stratification and contained elements to simulate the jet grouted walls and invert cutoff. The thickness of the jet grouted mass was based on the known geometry of the single overlapping columns. A horizontal bottom boundary was fixed at the known rock surface as a no-flow boundary. The outer radial boundary was fixed at 155 meters as a constant head boundary (i.e."radius of influence"). This distance was estimated from the pattern of drawdowns of nearby adjacent piezometers. This radius of influence compares very favorably with an estimated 135 meters radius of influence for equilibrium conditions based on pump tests done later for this project. The test site has a shallow perched groundwater condition. This condition was simulated by applying at the outer radial boundary, two fixed heads. One head corresponded to the shallow or perched groundwater, the other to the deeper groundwater levels.

Soil and jet grout hydraulic conductivities were systematically varied and values of Root Mean Square Error (RMSE) based on differences between the computed and observed groundwater levels were generated. Analyses with apparent minimum RMSEs and computed inflows that that approximately matched the estimated observed inflows indicated the following hydraulic conductivities:

- Upper glacial till and mixed glacial soils - 7.5×10^{-6} cm/sec
- Lower glacial till and reworked till deposits - 1×10^{-4} cm/sec to 4×10^{-4} cm/sec
- Upper Jet Grout Wall (located in mixed glacial deposits and upper glacial till) - 1×10^{-7} cm/sec
- Lower Jet Grout Wall (located in lower glacial till with boulders) - 2.5×10^{-5} cm/sec

There is good agreement, between the hydraulic conductivity from the model (2.5×10^{-5} cm/sec) and the average horizontal hydraulic conductivity of the field packer permeability tests (7×10^{-5} cm/sec) for the jet grout wall located in till with boulders. It was concluded that packer permeability testing is a reasonable tool to find the upper bounds of hydraulic conductivity of jet grout columns.

FINAL REQUIREMENTS FOR JET GROUT CUTOFF WALL CONSTRUCTION

It was determined that jet grout columns, as constructed in the test shaft, would be inadequate for groundwater drawdown control in the final cutoff wall due to the too high hydraulic conductivity in the till with boulders. Inadequate drawdown control would result in undesirable contamination plume transport. Cutoff wall analyses indicated that hydraulic conductivities would need to be lower than the mid 10^{-5} cm/sec range computed above. Analyses indicated that lower hydraulic conductivity could be achieved by tight multiple rows of overlapping columns. Hence, project specifications were written to have three overlapping jet grout column rows, to achieve a 2100 to 2700 mm total wall width. Columns were also specified to have a maximum hydraulic conductivity of 1×10^{-6} cm/sec. Furthermore, during the wall construction an intensive packer permeability test program would be conducted on the jet grout columns. Any columns that grossly exceeded the maximum allowable hydraulic conductivity would require remediation, such as additional jet grouting. After column installation, a second and final phase of testing is required. This final testing would consist of completing the entire enclosed cutoff system and then conducting a pump test inside the enclosure. The wall would be considered adequate if the groundwater drawdowns outside the cutoff are less than 610 mm. Should the external drawdowns exceed this latter number, remediation would be required. The jet grout walls, in some locations extend from the bottom of the invert of the existing subway to top of rock. The contact between the jet grout columns and the subway invert or the top of rock represent critical points for leakage. Requirements were established that these interfaces are to be tested with packer permeability tests by straddling the interface. Any zones with "takes" are to be grouted. The rock beneath cutoff walls are also to be packer tested with followup cement grouting if the results indicated a permeability in excess of 1 Lugeon (1.3×10^{-5} cm/sec)

CONSTRUCTION OF THE FINAL JET GROUT CUTOFF WALL

Construction of the jet grout cutoff walls on one contract is complete on two out of three wall sections. Pacchiosi Drill USA constructed the cutoffs with a triple fluid system. The water nozzle is about 1220 mm above the grout ports. Verticality of columns were measured during installation through the drill rods with an in-place inclinometer. Vertical deviations were typically less than 1%. Some general jet grouting parameters are:

- water jet pressure- 45 mPa
- water injection rate - 95 l/min
- air pressure - 1.2 mPa
- grout pressure - 5 mPa to 20 mPa but typically about 16 mPa

- grout injection rate – 130 to 150 l/min
- withdrawal rates – 80 to 160 mm/min, typically 115 mm/min
- rotation rates – 7 to 9 rpm

Packer permeability tests have been conducted on the columns to evaluate hydraulic conductivity. Figure 4 illustrates the computed hydraulic conductivity as a function of depth. Locations of tests with "no takes" are plotted with a hydraulic conductivity of 1×10^{-7} cm/sec.

The construction phase data in Figure 4 does not include remediation efforts for zones of hydraulic conductivities that exceed design requirements. Some remediation has been done, consisting of either additional jet grouting or chemical grouting, and the results are still being evaluated. A comparison, between the test program and construction phase, of the frequency distribution of hydraulic conductivities (from packer permeability tests) without consideration of depth, is as follows:

Hydraulic Conductivity (cm/sec)	Test Program	Construction
> 5×10^{-6}	50%	60%
5×10^{-6} - 5×10^{-5}	30%	38%
> 5×10^{-5}	20%	2%

It should be noted that the table above has limited data for the test program in comparison to the sample size of the construction phase data.

CONCLUSIONS

A test program of an enclosed jet grout cutoff shaft resulted in inflows and groundwater drawdowns when excavated. Packer permeability tests in the jet grout columns, where located in glacial till/boulders, indicate a horizontal permeability of about 7×10^{-5} cm/sec. This compares favorably with a 2.5×10^{-5} cm/sec hydraulic conductivity back computed from geohydological analyses. It was concluded that packer permeability testing is a reasonable tool to evaluate the upper bound of hydraulic conductivity. Hydraulic conductivity of the values above would not be acceptable for the final cutoff wall. Construction of the final cutoff wall was specified to be closely spaced overlapping three rows of jet grout columns. Quality of the final wall would be subject to a rigorous testing program that include packer permeability testing and a pump test.

Construction is proceeding with several jet grout cutoff wall sections already constructed. Packer permeability testing of these walls indicate that the changes made to the original requirements of the jet grout test shaft have significantly reduced hydraulic conductivities but some remediation is necessary to address local areas of higher hydraulic conductivities. Recently commenced pump testing inside the cutoff walls indicate, to date, that most of the jet grout wall sections have satisfactory performance.

Chapter 11

Stabilization/Solidification

DEEP SOIL MIXING FOR REAGENT DELIVERY AND CONTAMINANT TREATMENT

N. Korte[1], O.R. West[2], F.G. Gardner[1], S.R. Cline[2], J. Strong-Gunderson[2], and R.L. Siegrist[2]

J. Baker, AlliedSignal, Inc., P.O. Box 419159, Kansas City, Missouri 64141-6159

[1]Oak Ridge National Laboratory, 2597 B 3/4 Road, Grand Junction, Colorado 81503

[2]Oak Ridge National Laboratory, P.O. Box 2008, Oak Ridge, Tennessee 37831

ABSTRACT

Deep soil mixing was evaluated for treating clay soils contaminated with TCE and its byproducts at the Department of Energy's Kansas City Plant. The objective of the project was to evaluate the extent of limitations posed by the stiff, silty-clay soil. Three treatment approaches were tested. The first was vapor stripping. In contrast to previous work, however, laboratory treatability studies indicated that mixing saturated, clay soil was not efficient unless powdered lime was added. Thus, powder injection of lime was attempted in conjunction with the mixing/stripping operation. In separate treatment cells, potassium permanganate solution was mixed with the soil as a means of destroying contaminants in situ. Finally, microbial treatment was studied in a third treatment zone. The clay soil caused operational problems such as breakage of the shroud seal and frequent reagent blowouts. Nevertheless, treatment efficiencies of more than 70% were achieved in the saturated zone with chemical oxidation. Although expensive ($128/yd^3), there are few alternatives for soils of this type.

INTRODUCTION

Many treatment processes can be applied successfully in coarse-grained media. Treatment of contaminated clay soils, however, is a much more difficult problem (Siegrist et al. 1996). In general, it appears that invasive techniques such as mixing or fracturing are required. For example, Deep Soil Mixing (DSM) had been successfully used for full-scale treatment of a contaminated clay soil at the Portsmouth Gaseous Diffusion Plant near Piketon, Ohio (Siegrist et al. 1995). That project demonstrated that volatile organic compounds (VOCs) could be successfully removed from soils above the water table. The most cost-effective approach was the use of air stripping in conjunction with the soil mixing. Treatment efficiency was determined by the amount of mixing both in terms of the drilling rate and the number of times each cell was mixed. The success of the Portsmouth project led to the consideration of potential applications in the saturated zone and at greater depths. Thus, a program was designed to determine whether DSM could be used to deliver treatment reagents that would either destroy the contaminants or alter the subsurface conditions such that air stripping could be performed.

The field work was conducted at the Department of Energy's Kansas City Plant (KCP) located in Kansas City, Missouri. The objective was to evaluate three treatment approaches in a highly-contaminated, silty-clay zone at the KCP. Typical soil characteristics for the KCP site are shown in Table 1.

Besides working in wet, silty clay, another difference for the Kansas City project was the need to drill deeper. The Portsmouth project had only required drilling to approximately 5 m (15 ft). At the KCP, much of the contamination resides on a bedrock surface found at a depth of approximately 15 m (45 ft). Thus, both reagent delivery and drilling depth were to be evaluated. Three treatment approaches were to be studied. These were the injection of (1) a biotreatment solution consisting of a TCE-degrading microorganism and nutrient solution, (2) potassium permanganate, and (3) calcium oxide (lime). The lime injection technique was developed from laboratory studies that showed that the wet clay soils did not mix readily. The laboratory data in Fig. 1 shows that the addition of powdered lime caused the soil to become friable, easily mixed, and amenable to air stripping (West et al. 1995).

Table 1. Characteristics of soil underlying the study site

Property	Range
Unified Soil Classification (soil classification system for foundation and hydraulic structures)	CL to CH (clay in which plastic limit ranges from low to high)
Moisture content	19% (above the water table) - 33% (below the water table)
Plastic limit (moisture content at which the soil can be molded)	18 to 20%
Liquid limit (moisture content at which a soil-water mixture will flow)	33 to 50%
Dry bulk density	1.33 to 1.48 g/cc
Total organic content	0.4 to 0.7%
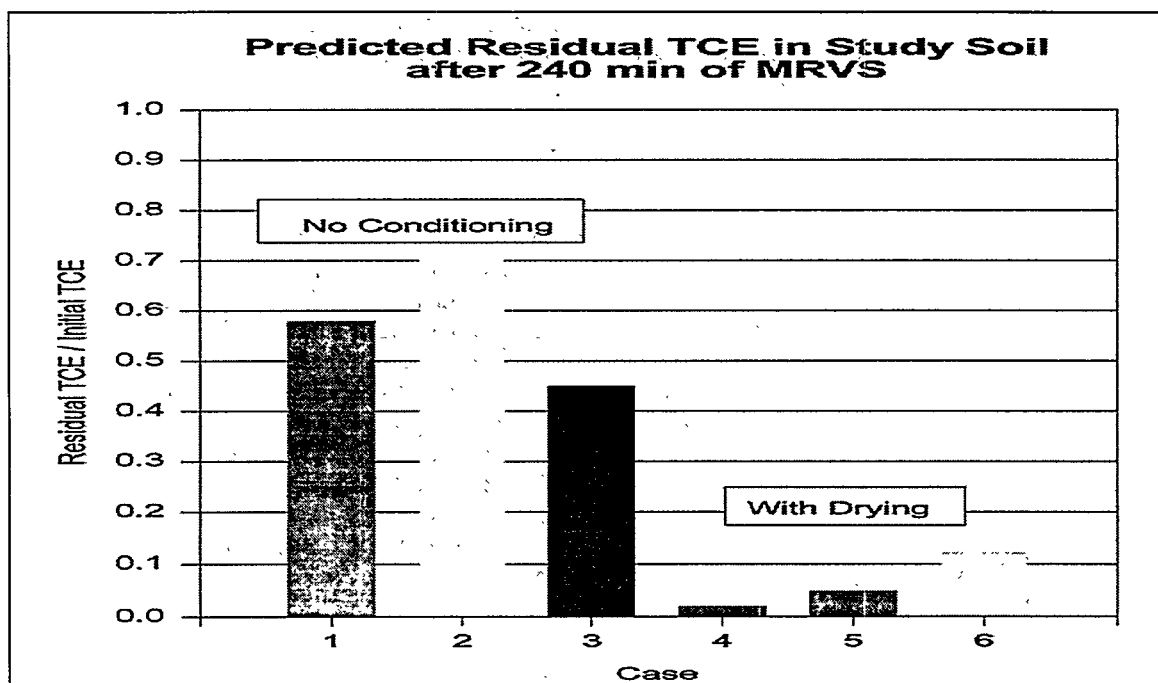
Fig. 1. Predicted residual TCE in study soil after 240 min of MRVS.

EXPERIMENTAL

Initially, the amount of contamination present was evaluated. This was accomplished by drilling, sampling and performing on-site VOC analyses. Calculations of the amount of trichloroethene (TCE) present were made using two methods. First, a commercial software package was used to fit a three-dimensional spatial function to the measured soil TCE concentrations (Dynamic Graphics 1993). The algorithm used in this package selects an interpolating function with "minimum curvature" that agrees with the observed concentration values (Briggs 1974). The interpolating TCE function is then evaluated at points on a rectangular grid that encompasses the soil volume of interest. In the second approach, the mean TCE concentration was calculated from the estimated mean of the pretreatment soil TCE data. The mass of TCE was then calculated as follows:

$$M_{TCE} = \overline{C}_{TCE, \text{ measured}} \, V_{demo} \, \sigma_{soil}$$

where $\overline{C}_{TCE}$, measured is the average TCE concentration in the pretreatment samples collected from the demonstration site. The results of these mass estimates are shown in Table 2.

Table 2. Summary of TCE mass estimates

Method	Estimate of mean TCE concentration in the region, $\mu g/kg$	Estimated TCE mass, kg
1. Average grid TCE concentration	60,990	637
2. Average measured TCE concentration	113,308	1,183

Geo-Con (Pittsburgh, PA) was hired to perform the soil mixing. The work was performed with a Manitowac 4000 Crawler crane coupled with a CH200 drilling platform and an 80 cm^2 (12.75 square inch) kelly bar. Drilling with a 3.1-m (10-ft) diameter blade was performed initially. Unfortunately, the 3.1 m (10 ft) blade required so much water for drilling that the work area was quickly flooded. Thus, a 2.45-m (8-ft) diameter blade was used for the remaining work. With the 2.45 m (8-ft) blade, it was possible to drill to 15 m (45 ft) with air instead of water.

The microbial treatment solution was added at 50 to 65 L/0.33 m (13 to 17 gal/ ft) in the top 7 m (23 ft). The potassium permanganate solution (5 wt % KMnO$_4$) was added such that the loading was approximately 5-7g KMnO$_4$/kg of soil. Such a high loading is needed because KMnO$_4$ reacts with natural soil organic matter, and naturally-occurring minerals, as well as the contaminants. Unfortunately, when the lime injection was attempted, the pressure available from the vendor's equipment could not overcome the back-pressure resulting from the stiff clay soil.

Auger depth, temperature, and certain other parameters were measured in a nearby trailer by means of transducers or sampling ports attached to the auger shroud. Real-time VOC measurements, of the off-gas, measured with a flame-ionization detector (FID) correlated to auger depth, were automatically logged and plotted during the mixing step. A Hewlett-Packard 5890 Gas Chromatograph was also used for on-site soil and water VOC analyses.

DRILLING AND REAGENT DELIVERY OBSERVATIONS

The drilling rate with the 2.45-m (8-ft) diameter blade was nominally 0.33 m- (1- ft) per-minute. Although drilling was successful, on occasion the air would find a preferential pathway and release pressure to the surface. For reagent addition, the procedure was to drill to depth in order to pre-mix the soil. The treatment agents were added as the auger was raised.

As noted above, the reagent delivery rate was approximately 50 to 65 L/0.33 m (13 to 17 gal/ft) for the biotreatment solution. Because only the vadose zone and upper portion of the clay aquifer were to be treated with this method, reagent delivery was performed to approximately 7 m (23 ft). Reagent delivery was straightforward but it was observed that this amount of fluid was not adequate to facilitate thorough mixing of the soil. Subsequent drilling into the biotreatment cells resulted in visual observations that some of the soil showed little evidence of having been mixed. A larger volume of solution should be used for future tests of this type to ensure that the mixing is adequate. Another operational issue with the biotreatment solution is that the microbes are grown on site and need to be injected at their peak activity. Thus, equipment problems, occurring at an inopportune time, can severely affect the treatment. Such a problem occurred in this instance because the seal on the auger shroud broke several times and had to be repaired while the biotreatment cells were being mixed. Because of the onset of darkness this problem limited the amount of mixing that could be performed. With a nonperishable reagent, delivery might have waited until the following morning.

The injection rate with the potassium permanganate ranged from 115 to 230 L/0.33 m (30 to 60 gal/ft). The larger amount of fluid permitted the cells to be well-mixed. However, as adjacent cells were drilled with air, there were a number of blowouts in which a stream of previously applied treatment reagent was forced into a preferential pathway and blown to the surface. Some of these blowouts occurred three or more meters from the auger and sprayed an equal amount vertically. Such blowouts constitute a safety problem because their location and timing were unpredictable. Because blowouts during reagent delivery had been recognized as a potential problem, field personnel minimized time spent in the immediate vicinity of the auger and shroud. However, this problem may limit the use of this method in locations difficult to shield. In addition, blowouts prevented maintaining as much control over the reagent delivery and dispersal as was desirable. Although the amount of reagent added was controlled, that which flowed out over the surface could not be measured. For example, blowouts combined with an injection rate that was too high, resulted in an estimated 30% loss of the $KMnO_4$ reagent in one test cell. The work area was bermed so no reagent was discharged from the work zone. However, the $KMnO_4$ flowed over the ground making it impossible to know how much was mixed in the subsurface. Adjacent work areas also required addition of gravel before drilling or moving the crane because the soil was
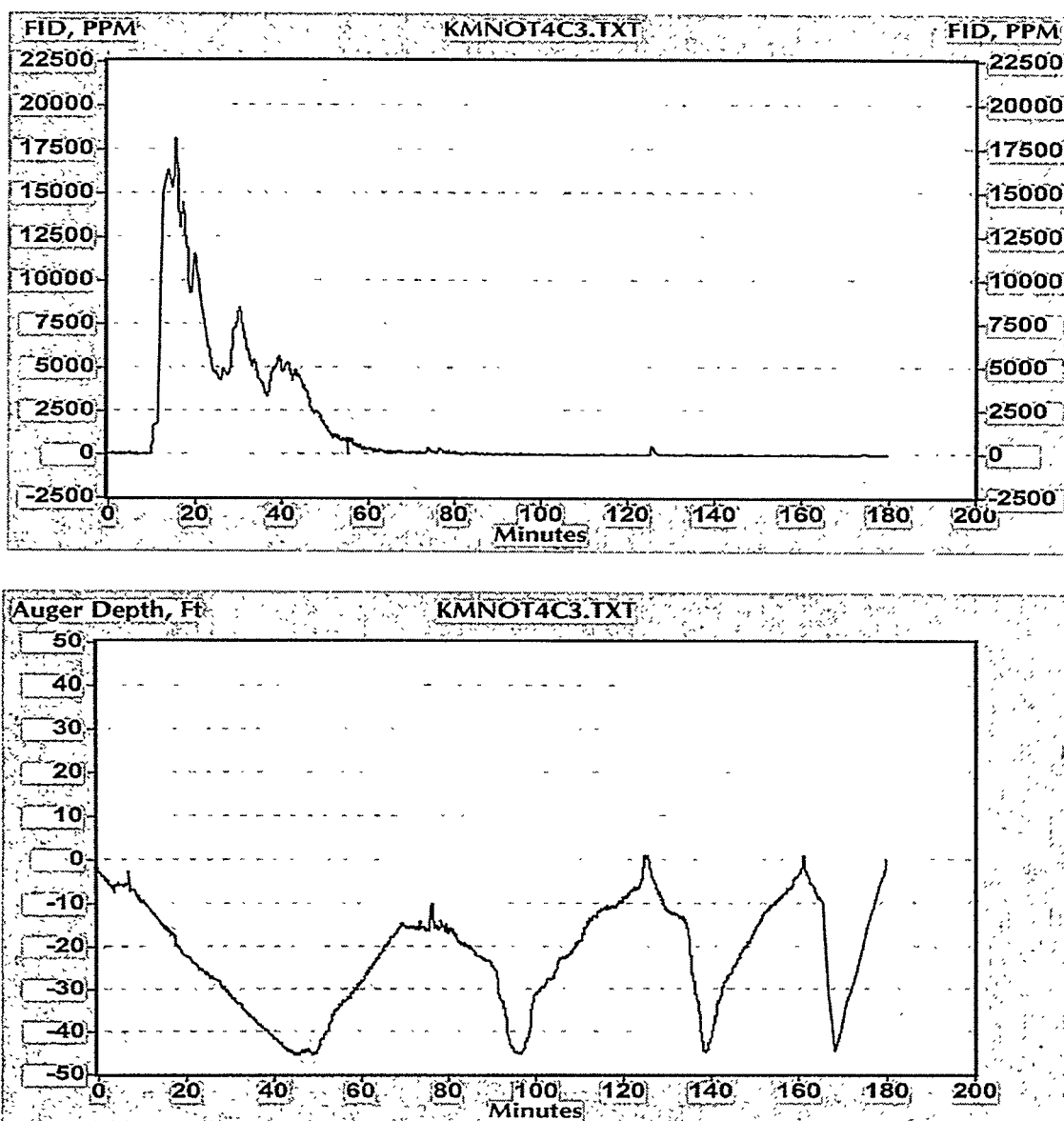
Fig. 2. Predicted residual TCE in study soil after 240 min of MRVS.

saturated by the lost reagent. To ensure adequate mixing, each $KmnO_4$ cell was mixed three times, from top to bottom, following reagent addition. The visual appearance of the soil in the mixed cells did indicate that it was well-mixed with reagent. Figure 2 shows the total VOCs as measured with an FID as related both to time and auger depth for one of the $KMnO_4$ cells. These data demonstrate that there was some removal of volatile contaminants during the air drilling step and that the more easily volatilized contaminants were located near the water table surface (approximately 5 m or 15 ft).

Delivery of the dry, powdered lime was attempted next but was unsuccessful. It was determined that the vendor-supplied equipment could deliver 517 cm Hg (100 psi), while calculations indicated that 930 cm Hg (180 psi) were required. Other factors causing the unsatisfactory powdered lime delivery were the limited experience available with the method which led to a flawed design in the delivery system, which created the unexpectedly high back-pressure. Thus, the lime injection was abandoned. Because blades and delivery systems compatible with dry powder injection are available, this technique should be attempted in the future.

DISCUSSION AND RECOMMENDATIONS

The average TCE mass reduction for the bioaugmentation cells was expected to be low because TCE concentrations were high enough to be toxic to the organisms. The average reduction for the bio cell was 38%. For the $KMnO_4$ injection, an average TCE removal of 67% was observed. Total VOC removal was probably higher because cis-1,2-dichloroethene (DCE) was also present and is more easily oxidized than TCE. However, the tight clay soils prevented the achievement of oxidant loading as high as was possible in the laboratory (5 to 7 g/kg vs 16 g/kg). Thus, 90% removal was achievable in the laboratory system as compared to an average of 67% in the field. In one cell, mixed to approximately 8 m (25 ft), removal was 81% (Fig. 3).

Post-treatment soil properties were not adversely affected by the treatment. $KMnO_4$ was not detected in the post-treatment soil samples and some soil organic matter also remained. The exchangeable Mn data suggested relatively homogenous distribution of the oxidant within the subsurface and also provided evidence of some $KMnO_4$ migration outside of the treatment zone.

The results demonstrate that soil mixing has applicability for tight clay soils and for work in the saturated zone. On the other hand, practitioners should expect operational problems with regard to reagent delivery rates and blowouts. These will probably be sufficiently site specific that both treatability studies and careful on-site monitoring will be required.

ACKNOWLEDGEMENTS
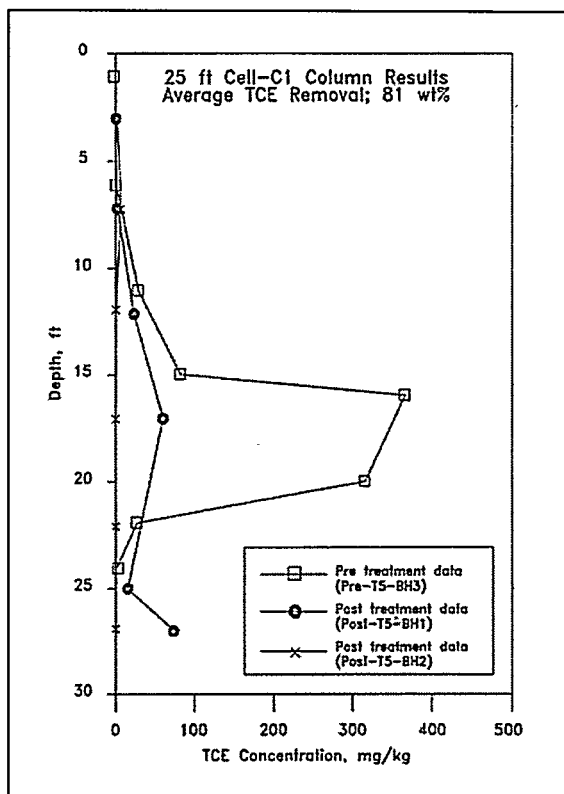
Fig. 3. TCE results (T5C1 Column).

REFERENCES

Briggs, I.C. (1974) Machine contouring using minimum curvature. *Geophysics,* 39, 39-48.

Dynamic Graphics. (1993) *Earth Vision: Three-Dimensional Visualization Software.* Dynamic Graphics, Inc., Bethesda, Maryland.

Siegrist et al. (1995) In situ mixed region vapor stripping in low permeability media: 2. Full-scale field experiments. *Environmental Science and Technology,* 29 (9), 2198-2207.

Siegrist, R.L. and K.S. Lowe, eds. (1996) "In Situ Remediation of DNAPL Compounds in Low Permeability Media: Fate/transport, In Situ Control Technologies, and Risk Reduction". A series of focus papers prepared by an Ad Hoc Consortium sponsored by the U.S. Department of Energy and the American Petroleum Institute. ORNL/TM-13305. Oak Ridge National Laboratory, Oak Ridge, TN 37831.

West, O.R., P.A. Cameron, D.R. Smuin, N.E. Korte, and A. J. Lucero. (1995)
Innovative treatment for TCE-contaminated saturated clay soils. Paper presented at the Industrial and Engineering Chemistry Special Symposium, American Chemical Society, Atlanta, Georgia, September 17 - 20, 1995.

FIELD APPLICATION OF INNOVATIVE GROUTING AGENTS FOR IN SITU STABILIZATION OF BURIED WASTE SITES

Guy G.Loomis[1] and Richard K. Farnsworth[2]

Abstract

This paper presents field applications for two innovative grouting agents that were used to in situ stabilize buried waste sites, via jet grouting. The two grouting agents include paraffin and a proprietary iron oxide based cement grout called TECT. These materials were tested in specially designed cold test pits that simulate buried transuranic waste at the Idaho National Engineering Laboratory (INEL). The field demonstrations were performed at the INEL in an area referred to as the Cold Test Pit, which is adjacent to the INEL Radioactive Waste Management Complex (RWMC). At the RWMC, 56,000 m^3 of transuranic (TRU) waste is co-mingled with over 170,000 m^3 of soil in shallow land burial. Improving the confinement of this waste is one of the options for final disposition of this waste. Using jet-grouting technology to inject these materials into the pore spaces of buried waste sites results in the creation of buried monolithic waste forms that simultaneously protect the waste from subsidence, while eliminating the migratory potential of hazardous and radioactive contaminants in the waste.

Introduction

At the INEL, over 56,000 m^3 of TRU waste is buried and co-mingled with 170,000-225,000 m^3 of soil. In 1994 and 1995, use of high-pressure jet-grouting technology was shown to be potentially cost-effective in stabilizing simulated buried waste pits at the INEL in situ, without increasing its volume (Loomis and Thompson 1995; Loomis et al. 1995). The process involved injecting both single and two phase materials into the waste to fill the void spaces. This simultaneously eliminated the possibility of subsidence and reduced the general hydraulic conductivity of the buried waste site. Proof-of-concept tests were performed using Portland cement and a high-priced acrylic, two-phase polymer material. Based on the results, the Department of Energy's (DOE's) Subsurface Contaminants Focus Area authorized creation of an In Situ Stabilization project, aimed at demonstrating in situ stabilization on an actual radioactive waste site at the INEL. As part of this project, funding was authorized to evaluate different innovative stabilization materials that would be both less costly than the acrylic polymer, and more effective than Portland cement. The grout materials that were selected include molten paraffin, and a proprietary iron oxide based cement grout called TECT. The purpose of this report is to summarize the results of their field evaluations.

Field Demonstration Procedures

Field demonstration procedures include constructing and grouting the pits, and coring and destructive examination of the stabilized monoliths. Procedural aspects are summarized below.

---

1 Lockheed Martin Idaho Technologies Co., Idaho National Engineering Laboratory, P. O. Box 1625, Idaho Falls, Idaho, 83415-3710, (208) 526-9208, guy@inel.gov

2 Lockheed Martin Idaho Technologies Co., Idaho National Engineering Laboratory, P. O. Box 1625, Idaho Falls, Idaho, 83415-3710, (208) 526-6986, frn@inel.gov

Pit Construction

Two full-scale test pits, 1.8 m x 1.8 m x 1.8 m (6-ft x 6-ft x 6-ft) , were constructed for the demonstrations. Each pit used cardboard boxes and metal and cardboard drums of waste, to simulate the type of waste packaging that was used in waste disposal actions at the INEL (Arranholz and Knight 1991). The simulated waste contents included paper, cloth, metal, asphalt, organic sludge, salts, and wood. For environmental purposes, sulfate salts were used to simulate any nitrate salt wastes, and canola oil was used to simulate the regal oil and halogenated hydrocarbons in the organic sludge wastes. The waste packages were backfilled in a typical landfill technique and covered with a 0.9-m (3-ft) overburden of compacted soil.

Grouting the Pits

Once buried, each pit was grouted with either molten paraffin or TECT. Injection was performed using the Casagrande™ drill and high pressure injection pump system. This is the same system used on prior jet grouting experiments at the INEL (Loomis and Thompson 1995; Loomis et al. 1995). To prepare for injection, the drill stem is driven through to the bottom of the waste seam. Once inserted, the drill stem is withdrawn in precise increments while rotating the drill stem and injecting the grout. The single component fluids are injected in situ at pressures up to 41.4 MPa (6000 psi).   In prior studies using tracers in the waste (Loomis and Thompson 1995), it was found that the use of high pressure injection equipment does not result in any contamination spread during injection. Figure 1 shows a diagram of the grout hole orientation for each pit. Grouting is performed sequentially, in pre-arranged 51-cm (20-in) triangular spacings. Use of this spacing guarantees that all of the packages in the waste will be punctured and filled. Because of their single component nature, both paraffin and TECT were grouted as single phase materials.
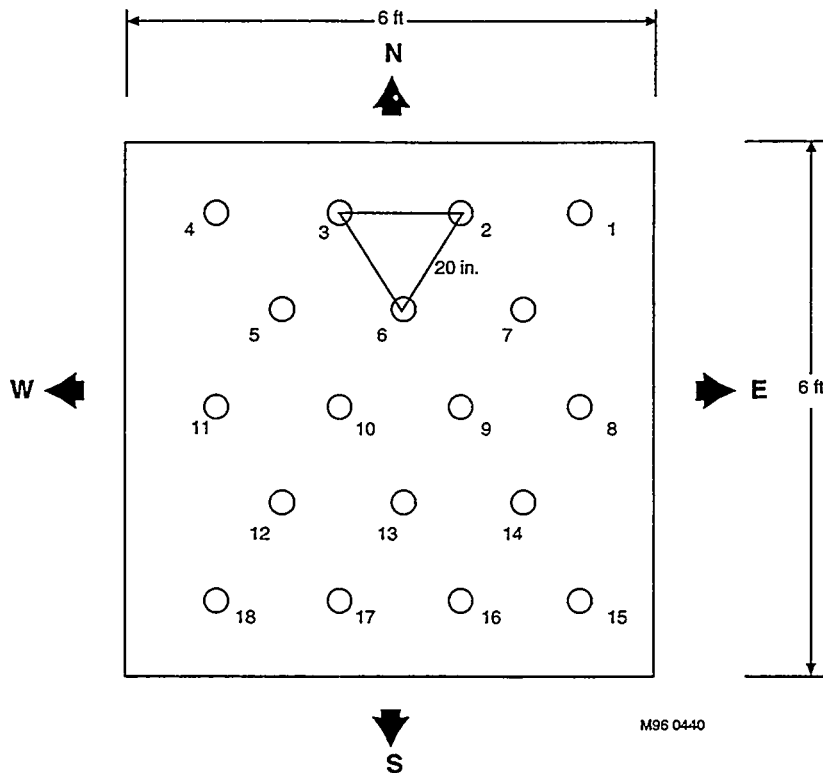
Figure 1. Orientation of Grout Holes for Each Simulated Waste Pit

Operational variables associated with jet-grouting include pump pressure, drill stem rate of rotation, amount of time per step (dwell time) and vertical step size. The variables are set based on preliminary field trials in the INEL soil. Grout effectiveness is then measured by observing the amount of grout returns, and the ease of operations for grouting each pit.

The two innovative grouts selected for this study (TECT and paraffin) had previously met a set of preliminary lab acceptance criteria outlined in Shaw and Weidner (1996). This criteria included information on particle size (<3 mm), set time (>120 min.), viscosity (<30 cP, no phase separation), cure temperature (<100°C), materials compatibility (with waste) and safety (non-hazardous component materials). Selected materials were then prioritized based on both product availability, cost and readiness. A description of TECT and paraffin materials is shown below.

TECT is a high performance cementatious grout designed for block encapsulation of buried waste by the jet grouting process. The low viscosity grout has been formulated to allow mixing and delivery in ordinary concrete mixer trucks. TECT grout remains liquid longer than portland cement slurries but eventually hardens into a very dense, very low permeability solid, resembling kiln-fired ceramics. The grout has a low heat of hydration and is formulated to tolerate and stabilize small amounts (10% by volume) of organic contamination. Heavy metals contacted by the grout are stabilized by changes in grout pH during curing, initially rising to 12 and then falling below 9. After approximately 12 months of curing, the grout approaches its final matrix condition, which is both thermodynamically stable and highly resistant to chemical attack.

Paraffin grout is a low-temperature, wax-based grout originally developed for stabilizing hydrofluoric acid leaks in surface impoundments. Additives in the grout allow the molten wax to blend with and permeate soils, regardless of their moisture content; they also cause the grout to bond to water, and wet the surfaces of buried debris. The paraffin is designed to fully encapsulate buried waste and isolate it from environmental groundwater. The grouted area will self heal any fractures and greatly minimize potential airborne dust if the material is excavated at a later date.

Coring Phase

Coring was not performed on the paraffin and TECT pits until two weeks after grouting, to allow sufficient time to cure/solidify. Curing/solidification was monitored by tracking the internal temperature of the monolith, using a thermocouple that was inserted into the pit during grouting along with a data logger. Coring was accomplished using standard rotational drilling equipment.

Destructive Examination Phase

Prior to destructive examination, the resultant monolith was excavated, to evaluate whether the resultant monolith was free-standing. The monoliths were then destructively examined, using a backhoe to slice 15-cm (6-in) sections off the monolith. Observations and photographs were recorded/taken after each sectioning interval. Destructive examinations were not performed until three weeks after grouting.

Test Results

This section includes discussions on field trials, grouting the simulated waste pits, temperature measurements during curing, and coring and destructive examination of the resultant monoliths.

Grouting of Pits

TECT PIT - Jet-grout injection of the TECT material was performed in one day, using the same Casagrande™ equipment used in previous jet-grout injections of Portland cement (Loomis and Thompson 1995; Loomis et al. 1995). The only change was that the injection nozzle size was increased to 3 mm (rather than 2.3 mm), to accommodate the higher viscosity TECT material. The proprietary TECT grout was premixed in a local ready mix plant and delivered to the site of testing in the truck. Two field trials in INEL soil were used to determine initial jet grouting parameters of 41.4 MPa (6000 psi) pump pressure, a 5-cm (2-in) step size, two drill stem revolutions per step, and a 6-sec. dwell time. A total of 11 holes (instead of the planned 18 holes),1.8-m (6-ft) deep, were then jet grouted in the TECT pit over 80 minutes. Additional holes could not be grouted because the planned supply of TECT grout was exhausted (apparently due to using more grout per hole than anticipated). Total injected volume for TECT grout was 4417 liters (1167 gal), an average of 401 liters (106 gal) per 1.8-m (6-ft) hole. Total estimated grout returns were 188 liter s (50 gal), resulting in 4199 liters (1117 gal) of grout left in the pit. This amount represents 138% of the total estimated void volume of the pit even though only 61% of the pit was grouted. Therefore, it appears that grout injection was successful at filling all voids in the grouted portion of the pit, as well as most of the ungrouted portion, and even some voids in the INEL soil surrounding the simulated pit. Clean-up of the system was easily accomplished, via a simple water flush.

Paraffin Pit - To prepare to grout paraffin, considerable modifications had to be made to the feed system. This was due to the potential plugging of the supply system, caused by heat losses in the lines and pumps that could cool and solidify the pre-heated paraffin. The system modifications required heat taping and insulation of all high pressure hoses, as well as the high pressure pump. In addition, the paraffin material had to be delivered to the testing area in a large (12,000 liter), heated tanker truck at 60°C. The tanker truck contained 5300 liters (1400 gal) of molten paraffin and 5300 liters (1400 gal) of 80° C water, to keep the paraffin hot during transport. Gravity feeding was employed to transport the molten paraffin to the high pressure pump, via heated and insulated lines. Cleanup was performed by switching the supply line in the tanker truck to the hot water supply, and pumping hot water through the Casagrande™ equipment.

Grouting was performed as planned, with 15 holes (rather than the planned for 18, due to more grout per hole than anticipated) grouted in 90 minutes. Dwell time for each step was set at 3 seconds (down from 4 seconds, during field trials), while maintaining other operational parameters at 2 rotations per step, 5 seconds per step, and 41.4 MPa (6000 psi) pump pressure. After the second hole, jet-grouting was accompanied with considerable grout returns of what appeared to be pure paraffin (ie., not mixed with soil) emanating from previously grouted holes in the pit. The amount of these returns were copious, with pure paraffin emanating from adjacent and distant holes in the pit. Management of the grout returns was performed by digging shallow canals form the top surface of the pit to a spoils collection pit, 0.76-m (2.5-ft) wide, 0.6-m (2-ft) deep, and 1.5-m (5-ft) long. Following jet-grouting, cleanup of the apparatus was found to be easier than anticipated.

Total grout injection was 4613 liters (1227 gal), or an average of 304 liters (82 gal) per hole. Total returns were estimated at 1474 liters (392 gal), meaning that 3139 liters (835 gal) remained in the pit. This represents 104% of the estimated void volume, even though only 83% of the pit holes had been completed. Therefore, it appears that paraffin was also able to fill the entire void volume of the grouted pit, plus some. The lower fill volume of paraffin(relative to TECT), is probably due to the reduced dwell time of paraffin's injection, which resulted in less void volume filled in the soils surrounding the simulated pit. Paraffin also appeared to be more permeable than the cementitious TECT grout, prior to hardening. The permeable nature of paraffin was evidenced by

the standing head of liquid paraffin, 7.5-10 cm (3-4 in) thick, left over the top surface of the pit. The standing head of paraffin filled any residual void spaces in the monolith, by gravity feeding and permeating paraffin into the waste up to 8 hours following grouting.

Grout Field Trials

Field trials were performed on INEL soil using a thrust block of concrete designed to contain any spoils returns. Use of the thrust block was also evaluated as a rudimentary design for controlling contamination spread (due to spoils returns) on the surface of actual radioactive burial sites. On both material injections, it appeared that the thrust block concept worked as planned, with minimal grout material outside of the thrust block, even with minimal (i.e, 15-cm) soil overburden.

Temperature Time History of the TECT and Paraffin Pits

During grouting, a 1.3-cm (0.5-in) diameter, 2.9-m (9.5-ft) copper tube (with a sealed end cap) was placed in the middle grouted portion of both the TECT and paraffin pits. The copper tubes were inserted into center holes in each pit immediately after it was grouted (Hole 9 for the TECT pit and Hole 5 for the paraffin pit). Type T thermocouples were then inserted into the copper tubes. The thermocouples were collected to a data logger programmed to record the interior temperatures of each monolith in 10 minute intervals. Use of this interior thermocouple served as an effective monitor of the time required for curing/solidifying each monolith. The TECT pit reached a peak temperature of almost 55°C approximately 15 hrs after grout injection, then proceeded to cool to 45°C over approximately 105 hrs. This is consistent with the Portland type 2 cement data obtained in Loomis and Thompson (1995). In contrast, the paraffin material stayed molten for over 75 hours before solidifying at 49°C, and then took another 115 hours to reach 45°C. The relatively long time period to solidify is due to the higher temperature (over 64°C) of the paraffin material, upon injection, and the thermally insulative nature of both the soil and paraffin.

Evaluation of cores

Cores and video logs of the TECT and paraffin pits were obtained to determine the extent of grout pervasiveness and structural integrity of the monoliths. Three cores were obtained in the TECT pit, and two cores in the paraffin pit. Grout pervasiveness was evaluated by examining the percent recovery of each core. Any gasps in the cores were most likely due to erosion by the lubricating water stream, which occasionally washed out any loose ungrouted soil debris or poorly cured grout, and lower core recoveries would be observed. The cores extended through 0.9 m (3 ft) of overburden and 1.8 m (6 ft) of monolith.

TECT Pit - Examination of the cores in the TECT pit showed excellent recovery of the solid monolith. Recoveries for core holes 1, 2 and 3 were 82%, 93%, and 100%, respectively. The lower recovery in core holes 1 and 2 is probably due to the presence of soil inclusions in the cores that were washed out by the lubricating core drill water.

Paraffin Pit - The paraffin pit had even better recoveries than TECT. Recoveries were 100% on both cores and the cores were complete and solid. A possible reason for the complete recoveries is the permeable nature of the paraffin, which allowed all absorbent waste materials (i.e., cardboard, paper, wood surfaces and clay soil inclusions) to become permeated with the paraffin.

Destructive examination of the pits

The destructive examination of the TECT and Paraffin pits was performed using a standard backhoe. The examination was accomplished by first isolating the pit from the surrounding overburden material and then removing 15-cm (6-in) increments of the pit. Field notes, samples, and photographs were recorded/taken throughout the destructive examination.

TECT PIT - Destructive examination of the TECT pit revealed that the TECT grout had cured, creating a solid monolith out of the original soil/waste matrix. The cured monolith was extremely hard and difficult to dismantle, due to its cohesive and solid nature. Retrieval of the pit required a standard backhoe to be extended 0.9-1.2 m (3-4 ft) above the pit, then dropped to create enough force to break off a 15-cm (6-in) slice. Once the destructive examination had uncovered 45 cm (18 in) of the pit, it became apparent that the pit was a hard, cohesive monolith with no void spaces. As the face was further exposed, it became obvious that all of the waste containers that had been punctured and exposed to grout injection, and that jet-grouting had filled all the voids and mixed with interstitial soils to form a solid soilcrete mix. Included in the soilcrete mix were numerous inclusions of ungrouted clay soil (estimated at 15% of the volume). However, the inclusions are completely encapsulated in the general soilcrete matrix. The only concern with was that the interface between TECT soilcrete and waste was sufficient to encapsulate the waste, but not sufficient to incorporate any contamination present on the surface of the waste. This result, coupled with its extreme hardness, suggests that TECT grout should only be used for long-term stabilization purposes-- not for interim stabilization purposes, prior to retrieval.

At the 76-cm (36-in) layer, a drum of completely encapsulated well mixed organic sludge and TECT was uncovered. The texture of this material was a solid mass. In prior grouting experiments with Portland cement and methacrylic polymer (Loomis and Thompson 1995; Loomis et al. 1995), the canola oil based sludge stimulant and the grout never hardened; upon performing a destructive examination, the resultant mixture remained a relatively non-viscous, flowable sludge.

Paraffin Pit - Destructive examination of the paraffin pit was performed 21 days following the paraffin injection. By this time, the paraffin pit had solidified to form a complete monolith out of the soil/waste matrix, with no ungrouted voids.

Prior to the destructive examination, it was observed that the top surface of the pit had a residual layer of paraffin 7.5-cm (3-in) thick from the spoils rejection. Upon removing this layer, it was found that the paraffin in this layer had permeated into the soil to a depth of 9 cm (3.5 in). In addition, destructive examination of the pit found that the inclusions of clay soil in the general soilcrete mixture had soaked through with paraffin, leaving no positions in the face of the pit with dry soil (as was the case with TECT). The paper, wood, and metal that was retrieved from the dig face were also soaked in paraffin, such that any contaminant on these materials would have been encapsulated and not readily aerosolizable. Apparently, the molten paraffin had low enough viscosity to literally soak all waste forms prior to curing. Therefore, paraffin appears to be more acceptable for using as an interim stabilization material, prior to retrieval, than the TECT grout.

During excavation, it was observed that the paraffin-stabilized organic sludge had a soft, viscous consistency, much like lard. This is less desirable than the solid organic material observed for TECT, indicating that paraffin may be less desirable for long-term stabilization purposes. The resultant lard-like mixture is much less fluid (i.e. more durable) than the previously evaluated cement and methacrylic materials, however (Loomis and Thompson 1995; Loomis et al. 1995).

Conclusions/Recommendations

Both paraffin and TECT grout have been field-demonstrated as potential innovative stabilization materials for in situ stabilization of buried waste sites. It appears that both of these materials are implementable in the field, with properties superior to Portland cement (with regards to encapsulation of both organic sludges and salts), and costs (along with some properties) significantly less expensive than methacrylic polymer. Due to its relative hardness, and better

ability in stabilizing organic sludges, TECT appears to be the preferred material for long-term stabilization purposes. In contrast, paraffin is recommended for interim stabilization activities, due to its ability to better permeate the surfaces of potentially contaminated debris.

Specific conclusions are as follows:

1. The TECT material can efficiently be jet-grouted into buried waste with minimum grout returns, and no indication of void space in the stabilized monolith. In contrast, paraffin results in copious grout returns. However, the long-term, multi-day cooling of the paraffin pit results in considerable permeation of ungrouted soils, leaving the contents of the pit (both soil and waste) more thoroughly soaked than the TECT pit (therefore improving micro-encapsulation of any loose surface contamination on the waste).

2. The resultant TECT monolith is more difficult to retrieve than the paraffin pit, because of the high compressive strength [greater than 6.9 MPa (1000 psi)] of the resultant soilcrete. In addition, the inability to permeate the surface of certain potentially contaminated debris wastes may cause a contamination control concern with TECT grout, if it were to be retrieved. In contrast, the paraffin monolith, while freestanding, can be easily retrieved with a standard backhoe, along with an anticipated reduction in contamination spread.

3. The thrust block concept for secondary waste management works well for controlling grout returns for the TECT grout. Application of this idea will require some modification or expansion of the volume for paraffin, however. In either case, the concept appears workable for field application, and needs to be developed further.

Both of these materials can be recommended for jet grouting field application to buried transuranic waste sites, or even radioactively contaminated soil zones (based on the results of the field trials in INEL soil). Based on cost estimates that were separately prepared for these materials, it appears that the cost of remediating a 1-acre site with these materials is $4.8 M for paraffin, and $12 M for TECT. In contrast, the costs for standard Portland cement and methacrylic polymer are $1.2 M and $60 M, respectively. In the future, it is recommended that a spoils return management strategy be refined for application of the molten paraffin grout. It is also recommended that modifications to the drilling system need to be engineered for radioactive applications (to improve issues associated with contamination control of the drill stem, upon withdrawal).

References

Arranholz, D. A. and J. L. Knight (1991) *A Brief Analysis and Description of Transuranic Wastes in the Subsurface Disposal Area of the Radioactive Waste Management Complex at INEL*, EGG-WTD-9438, Idaho National Engineering Laboratory, EG&G, Inc., Idaho Falls, Idaho 83415.

Loomis, G. G. and D. N. Thompson. (1995) *Innovative Grout/Retrieval Demonstration*, INEL-94/001, Idaho National Engineering Laboratory, Lockheed Idaho Technologies Company, Idaho Falls, Idaho 83415.

Loomis, G. G., D. N. Thompson, and J.H. Heiser (1995) *Innovative Subsurface Stabilization of Transuranic Pits and Trenches*, INEL-95/0632, Idaho National Engineering Laboratory, Lockheed Idaho Technologies Company, Idaho Falls, Idaho 83415.

Shaw, P. G. and J. R. Weidner (1996) *Laboratory-Performance Criteria for In Situ Waste-Stabilization Materials*, INEL-96/0069, Idaho National Engineering Laboratory, Lockheed Martin Idaho Technologies Company, Idaho Falls, Idaho 83415.

REMEDIATION BY IN-SITU SOLIDIFICATION / STABILISATION OF ARDEER LANDFILL, SCOTLAND

M. WYLLIE - ICI Explosives - Ardeer Operating Services - Ardeer Site - Stevenston Ayrshire KA20 3LN, Scotland

A. ESNAULT - Bachy - 4, rue Henri Sainte-Claire Deville - 92563 Rueil-Malmaison, France

P. BARKER - Bachy - Foundation Court - Godalming Business Centre - Catteshall Lane - Godalming Surrey GU7 1XW, England

ABSTRACT : The Ardeer Landfill site at ICI Explosives factory on the west coast of Scotland had been a repository for waste from the site for 40 years. In order to safeguard the local environment ICI Explosives, with approval of Local Authorities and the Clyde River Purification Board put into action a programme of investigation and planning which culminated in the in-situ treatment of 10,000 m3 of waste within the landfill by a deep mixing method using the "Colmix" system. The paper describes in varying degrees of detail the remediation from investigation to the execution of the in-situ stabilisation and presents the post construction monitoring results.

I. INTRODUCTION

The landfill site is located on the west coast of Scotland approximately 30 miles south-west of Glasgow. It is situated on a peninsula with the First of Clyde to the west and the Garnock Estuary to the south and east. The town of Irvine lies on the opposite shore of the estuary. ICI Explosives is the operator and owner of the site.
The unlined landfill is on the south-eastern tip of the peninsula and has been a repository for waste from the manufacturing operations on the site for approximately 40 years. The Garnock Estuary is recorded as being a Site of Special Scientific Interest (SSSI).

II. ASSESSMENT

The assessment of the landfill site to determine the degree and extent of contamination and the need or otherwise for remediation was carried-out in accordance with ICI's Safety, Health and Environment policies and guidelines (1).

III. HISTORICAL REVIEW

Prior to the start of disposal operations in the mid 1950's, the area had been a natural salt-marsh. The landfill was in use until 1993. From examination of available disposal records and with a knowledge of the manufacturing operations on the Site, it became clear that there was the potential for the generation of acidic groundwater and, from this, leachate.
An assessment was made of analytical results obtained over a number of years, by both ICI Explosives and the Clyde River Purification Board, on samples of run-off in the salt-marsh area. The assessment indicated that, although there was no immediate, major problem with polluted leachate, there was a trend to increasing acidity and metal levels in the leachate. Further investigative, sampling and analytical work was therefore undertaken, in line with ICI company procedures.

IV. SITE INVESTIGATION

4.1. Monitoring Wells and Trial Pits

Monitoring of groundwater within and adjacent to the landfill was undertaken between 1983 and 1992 using ten monitoring wells. The continued deposition of waste, however, resulted in some of these wells being destroyed. In 1992 additional investigation were undertaken which involved

sampling the surviving wells, installation and sampling of eight new wells and excavation and sampling of shallow trial pits in the intertidal zone. This work (2) was carried-out by what was then ICI's Brixham Environmental Laboratory (now Zeneca BEL). The hydrogeology of the site is divided into two aquifers, which are separated by a relatively impermeable boulder clay. The lower aquifer in the Carboniferous, is not of concern. The upper aquifer, within the alluvial and aeolian sands and above the boulder clay, exists across the whole of the Ardeer site and is in hydraulic continuity with both the Garnock Estuary and the sea.

Both inside and outside the landfill, groundwater was found at a depth of about 3 to 4 metres. Permeability tests were carried out in 11 monitoring wells and values of between 4×10^{-6} and 1×10^{-5} m/s were recorded, with an average of 2×10^{-5} m/s. Analysis of the samples revealed that the groundwater beneath the landfill was acidic with elevated metal concentrations and that there appeared to be an attenuated plume of contamination in the direction of the estuary. The groundwater quality 'upstream' of the landfill was found to be good.

4.2. Geoprobe Survey (3)

The monitoring wells in the landfill had identified areas of groundwater with low pH. The geographical extent of these areas, however, was not known. A series of investigations was therefore undertaken using a hydraulically powered drive point probe (Geoprobe) mounted on the back of an Iveco four-wheeled drive van. The system works on the principle that a single 'grab' of groundwater is taken, rather than having to install and develop a monitoring well. The advantage is that a large number of samples can be undertaken quickly at different locations, and at considerably less cost than the installation of a well. Once the boreholes were drilled, the probe was pulled back up to the surface. A new slotted probe base was added and the probe re-inserted into the borehole. The groundwater was extracted from the hollow probe using a Waterra inertial pump and had its pH, temperature and electrical conductivity measured in the field. Samples of the groundwater were taken for chemical analysis. The results of the analysis were made available to the field team by noon the following day, allowing further probeholes to be drilled in the areas of highest contaminant concentration to give better definition of plume boundaries.

4.3. Conclusions

Resultats of the analysis of the groundwater throughout the landfill showed high concentrations of metals in the areas where low pH dominates. In order to assess the significance of the occurrence of the most abundant metals comparisons were made with the Environmental Quality Standard (EQS) levels proposed by the Scottish Office (highest concentrations of particular materials acceptable in a saltwater estuary).

5. RISK ASSESSMENT

A Risk Assessment was carried-out by ICI Explosives to consider the potential impact of the closed landfill on man and the environment. The likely effects were assessed in four areas viz : airborne contaminants ; landfill surface ; groundwater beneath the landfill ; groundwater discharge to the Garnock Estuary.

Investigation into the first three areas indicated no significant risk.

The groundwater beneath the landfill, however, was recognised as being contaminated, and there was evidence that it was moving towards the mud flats adjacent to the estuary. This area, consequently, was studied more closely to ascertain if there was any detectable effect on the flora and fauna.

This was difficult due to the effects of past discharges of effluent to the estuary. Chemical analysis, however, indicated an effect on the pH and metal content of the interstitial water within the mud flats. The contaminant levels found were compared with available standards, (eg EQS's), and against the toxicity of the metals to species likely on or in the mud flats.

Consideration of the data obtained suggested that there was a long term, low level risk to the flora and fauna likely to be in or on the mud flats. This led to the conclusion that it would be appropriate to neutralise the low pH waste within the landfill in order to reduce the dissolution and mobilisation of metals in the groundwater.

6. REMEDIATION STRATEGY

As data became available from the site investigations, all the known remediation techniques were considered and assessed in turn as to suitability for application to the landfill. ICI invited several specialist contractors to discuss, in detail, the various options. The techniques fell into three broad categories.

The first of these categories, 'Removal of Contamination' included soil washing, vapour extraction, thermal desorption and excavation/removal to an external landfill. The first three were not considered feasible due to the variety of contaminants, hydrogeological conditions and quantity of material. The fourth was discounted due to the high safety, health and environmental risks associated with excavation, handling and transportation of such large quantities as well as the difficulties likely to be encountered in finding a landfill licenced to accept the contaminated material.

The second category, "Immobilise or Contain' included hydrodynamic containment, vitrification and chemical dispersion which were considered not feasible due to the nature and variety of the contaminants, the hydrogeological conditions, and the quantity of material involved. Capping, either alone or in combination with sub-surface barriers, was seen as an option worth consideration. Hydrogeological model simulation with various areas of capping and lengths of vertical barrier were computed and showed that there could be a high degree of control of the groundwater flow into the River Garnock and the mudflats between landfill and river. The disadvantages were that it would not treat or remove the contamination and even the highest specification of installation and materials would have a potentially limited life. Solidification was deemed to be a viable option. As the data from the site surveys confirmed the localisation of the low pH contamination within the landfill, so the potential for stabilisation as a realistic option became firmer.

Of the third category 'Treat to Render Harmless' only pump and treat was seen to be a viable technique for the landfill, but there were reservations due to the very large volumes involved and the inevitably excessive timescale such a scheme would consequently be required to operate.

From the above considerations, an overall strategy for the Ardeer Site Landfill remediation was developed (Fig. 1). The key starting point was determined to be a site trial to attempt in-situ stabilisation of an area of very low pH. If successful, the stabilisation would be extended to treat the area of lowest pH within the landfill as defined by the Geoprobe surveys and hydrogeological modelling. A period of monitoring post-stabilisation would be required to prove the effectiveness of the treatment but, if successful, the extent of final remediation works could be significantly reduced.

It was also decided that ICI would continue the work in conjunction with Bachy, the specialist ground/environmental contractor.

7. WASTE SAMPLING AND CHARACTERISATION

Following the decision that the treatment of the 'hot-spot' area was to be undertaken, it was necessary to characterise the material to be treated. Physically, the fill material was mostly a white/brown to grey/black granular solid interspersed with a small proportion of rubbery material. On analysis the samples were shown to be a mixture of siloxane materials with normal sand at the base of the fill.
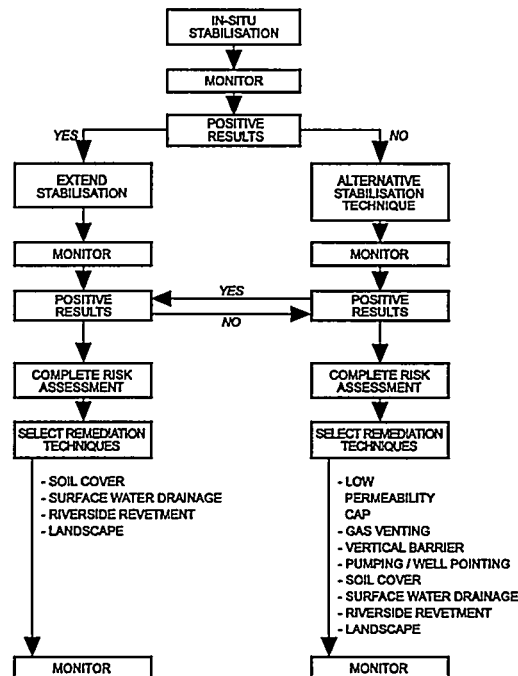
Fig. 1 - Ardeer landfill remediation :
Preferred engineering solution
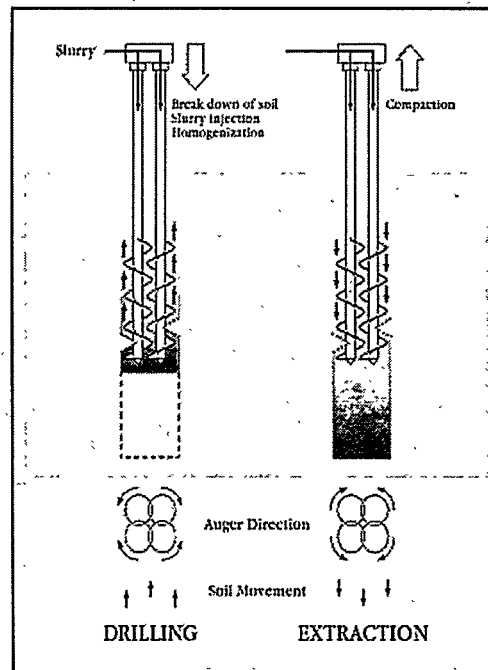
Fig. 2 - Construction of Colmix columns

8. LABORATORY TRIALS

A study was performed at Bachy's Laboratory in France to evaluate the feasibility of treating specific areas of Ardeer Landfill by in-situ stabilisation using the patented Colmix process. The aim of the treatment was to neutralise the acidic wastes and to increase the pH to a level where heavy metals would not be mobilised. In addition a hardened mass would be obtained and,

subsequently the permeability and leachability of the treated area would be reduced. The stabilisation agents were utilised in the form of an aqueous suspension of several powders, the mix being referred to as a 'slurry'. The liquid slurry was required to exhibit characteristics compatible with the Colmix process, i.e., low viscosity and good stability. The selected materials to perform the treatment were as follows : calcium hydroxide (slaked lime) as a neutralisation agent, Portland cement (OPC) as a binder, Flyash (PFA) as a filling agent.

The performance of the stabilisation process was evaluated using two different types of leaching tests : Acid Neutralisation Capacity (ANC) and the French Leaching Test. The ANC was used to determine the buffering capacity of the stabilised waste. The test reflects the ability of the mix to withstand the agressivity of acids by maintaining alkaline conditions. The ANC is obtained by measuring the magnitude of shifts in pH due to the addition of increasing amounts of acid. The 'French Leaching Test' is currently used, in France, to evaluate the efficiency of stabilisation/solidification processes on wastes.

After a preliminary evaluation of several cement based slurry compositions and the examination of the physical and chemical characteristics of the waste, two potential mixes (Mix N° 47 & 48) were selected to stabilise the low pH waste by the Colmix process. Their performance was evaluated with respect to their rheological, mechanical and leaching properties.

The ANC is directly linked to the composition of the slurry. Tests showed that the use of both flyash and lime in sufficient quantities is necessary to obtain a good performance.

The leaching tests performed with two extraction fluids, water and acetic acid, did not show any significant difference between the mixes tested.

Results of permeability tests on the mixes, at 3 and 6 x 10-8 m/s respectively, are of the same order of magnitude and significantly less than the overall permeability of the waste which averaged 2 x 10-5 m/s.

The recommendation was therefore that Mix N° 48 at a dosage of 310 l/m3 of waste should be used initially for the site trials. The final composition and the ratio slurry to waste would be optimised during the trials on site.

9. SITE TRIAL

9.1. Colmix Process and Plant Operation / Equipment

The Colmix process was developed in the late 1980's and creates columns of stabilised soil in the ground. The soil mass is broken down during the drilling process using multiple overlapping counter-rotating augers. At the same time slurry is introduced into the ground at the required dosage. Once the required depth has been reached the augers are rotated in the opposite direction and slowly withdrawn so as to further mix and compact the soil/slurry mixture (Fig. 2).

The Colmix equipment used at the Ardeer site was selected in order to provide the most economic means of treating a mass block of ground. The base machine, a Banut 500 fitted with quadruple auger equipment, was chosen to give the necessary stability and torque to penetrate the waste to the required depth of 5 metres. Support equipment included two dry powder storage silos (OPC and PFA), screw feeds, an A6R slurry mixer, an AR 1500 agitator and two PH15 pumps with one in reserve. For the trial bagged lime was used, introduced into the A6R mixer manually.

The slurry was pumped from the agitator to the rig by the pumps via four 38 mm diameter pipes, each line dedicated to one of the four augers. The correct dosage of slurry was achieved by a Lutz system using a flowmeter on the outflow of the agitator linked by cable via the controls to a Tarracord computer in the rig. Relevant information is displayed on a screen in the cab, and printouts are subsequently obtained for each column. The printouts include volume injected, torque, time and drilling speed.

9.2. Work on Site

Site trials commenced in September 1994 and were scheduled for completion by the end of the year. A technical specification was agreed jointly by ICI and Bachy and covered raw materials (cement, lime, flyash and water), the slurry mix (density, viscosity, stability, pH and ANC) and the stabilised waste (ANC, permeability, leachability and strength). Tests on the slurry mix and the stabilised waste were carried-out at regular intervals.

The scope of work included 261 columns constructed tangentially to treat an area 25 metres by 8 metres in plan to a depth of 5 metres. This approximated to 10 % of the total area to be treated (Fig. 3). The slurry mix was altered to Mix N° 47 during the course of the trial to enable comparisons of the two alternatives to be made.

SITE TRIAL COLUMN LAYOUT

LEGEND
COLUMN CLEAR AND 5m DEEP
OBSTRUCTION FOUND , CLEARED AWAY , DEPTH 5m
OBSTRUCTION FOUND , COLUMN LESS THAN 5m DEEP.
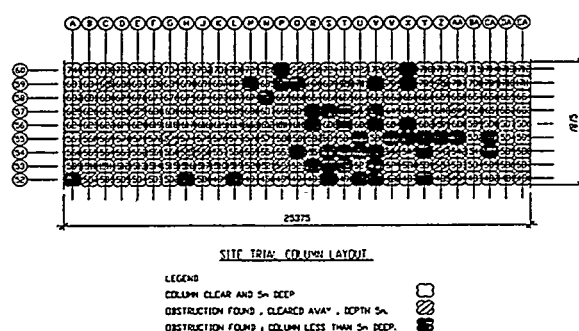
Fig. 3 - Plan of trial area : Column layout with obstructed columns

10. SITE TRIAL ASSESSMENT

The trial was evaluated in relation to the provisional specification agreed prior to the start of the works. Samples were taken during the construction of the columns.

To determine the ANC tests were performed on both the slurry and the treated waste. The fresh slurry samples were taken directly from the mixing plant and were tested at 14 days. The treated waste samples were obtained both from the augers by redrilling (to be tested at 14 days) and in-situ after at least 28 days by 'push in tube'. Almost all the results fell within the specific limits i.e. ANC > 5 meqH/g at pH 9 (Fig. 4) for slurry and ANC > 2 meqH/g for treated waste. The results using Mix n° 47 were slightly better than those obtained with Mix n° 48.

Preliminary attempts to measure the unconfined compressive strength on samples taken both from the augers by redrilling and in-situ from 'push in tubes', showed results which were not considered a fair reflection of the treatment. This was due to difficulties in obtaining and making representative samples from the augers after redrilling, and damage caused to the material when obtaining 'push in tube' samples. It was therefore decided to carry out in-situ mechanical tests using an ultra light dynamic penetrometer. A total of 18 columns were tested plus an additional 3 outside the treated area. The effectiveness of the treatment was then proven with over 99 % of the results above the specified value i.e. > 200 kPa at 28 days. A comparison with the results obtained in the untreated area demonstrated the increase due to the stabilisation/solidification (Fig. 5).

For permeability four tests were carried out at 28 days on samples taken from the augers during construction of the columns. Another set of four samples was also collected in-situ by 'push in tube'. The permeability values were slightly higher than that specified i.e. < 1 x 10-7 m/s. Nevertheless, it was considered that the sampling procedures again did not reflect the true nature of the treated waste, resulting in an overestimation of the permeability. No difference was apparent between the two slurries.

Seven samples were tested for leachability for information only. The results obtained show the reduced leachable amount of heavy metals and the increase in pH compared with the waste. No distinction was apparent between the two slurries.

In conclusion, the results of the trial were judged satisfactory as almost all of the specified values were reached. It was decided to carry-out the main works using Mix N° 47 at a dosage of 230 litres per metre of column, which it was agreed would give the necessary assurance of meeting the specified requirements.

543

Sample Ref.	Slurry Ref.	AGE days	ANC @pH9 meq H+/g
F1	48	7	7,77
F5	48	18	8,67
F6	48	18	8,64
BS1	48	14	6,25
BS5	48	14	6,25
F16	48	14	9,60
F19	48	14	9,00
F22	48	14	9,50
MIX 48		mini	6,25
		max	9,60
		average	8,21
F8	47	14	9,25
F11	47	14	10,00
BS4	47	14	6,50
F13	47	14	12,00
MIX 47		mini	6,50
		max	12,00
		average	9,44

Column Location	Slurry Type	Age at test (d)	Length tested (m)	Cumulation (cm) where qd < 1MP	% where qd > 1 MPa
1618	48	75	3,25	0	100 %
1619	47	86	5	19	96,5 %
1630	48	78	4,25	0	100 %
1631	48	91	3	0	100 %
1635	48	91	3,5	0	100 %
1636	48	90	3,5	20	94,5 %
1671	48	74	2,5	0	100 %
1672	47	84	3,25	0	100 %
1602	48	76	3	0	100 %
1604	48	76	5	2	99,6 %
1645	48	91	5	4,5	99,1 %
1647	48	91	3	0	100 %
1686	X	WASTE	5	84	
1628	X	WASTE	5	4,5	
1870	X	WASTE	5	114	
1985	47	7	3	0	100 %
1927	47	7	3	0	100 %
1869	47	7	5	18,5	96,3 %
2399	47	28	5	0	100 %
2300	47	28	3,25	0	100 %
2242	47	28	3,5	0	100 %

Fig. 4 - ANC tests on slurry tests

11. MAIN WORKS

After succcessful completion of the trial area the instruction was given to continue with the main works, to complete the treatment of a plan area of 80 metres by 25 metres to a depth of 5 metres. The total number of columns to be constructed was 2668, leaving a balance of 2407 to be completed within the time period January to June 1995. Minor alterations were made to the equipment and to the method of working in order to optimise production.

Sampling and testing for the main works initially followed the same regime that was used for the site trials. Midway through the programme, however, the frequency was decreased. Samples from 39 columns were tested for ANC and there was 100 % compliance with the specification i.e. > 2 meqH+/g at pH9.

Samples from 19 columns were tested for permeability and the results ranged from 1.1 x 10-7 to 4.8 x 10-7 m/s. Although outwith the original specification the rate was considered to be at a sufficiently low level.

The ultra light dynamic penetrometer was again used for testing the mechanical strength. A total of 49 columns were tested. 99 % were above the specification i.e. > 200 kPa at 28 days.

12. POST-CONSTRUCTION MONITORING

The Main Works were completed in June 1995 and in November 1995 fourteen additional groundwater monitoring wells were established in and around the treatment area. These additional wells supplemented the existing wells, some of which were lost during the construction period.

It was decided to monitor the groundwater at 3 monthly intervals with the first samples being taken in January/February (Q1) 1996. It is anticipated that a period of 18-24 months will be required to establish the success, or otherwise, of the project. At the time of writing only two sets of results were available (i.e. Q1 and Q2 1996) therefore it is too early to detect any trends. General observations, however, indicate that the very low pH's (i.e. 1,5 to 2) are not present in the groundwater (pH3 being the lowest). Metal concentrations, on the whole, appear to be down, although there are several exceptions. Temperatures in the wells immediately adjacent to the treatment area are higher than average suggesting heat of neutralisation.

In addition to the groundwater monitoring, a separate ecological study is taking place in the Garnock Estuary. The study involves annual surveys of meiofauna communities in the intertidal zone adjacent to the landfill. The first survey was carried-out in summer 1994 (i.e. before remediation work started) and subsequently in summer 1995 (at the end of the construction period) and summer 1996. At the time of writing the 1996 report was not available so no conclusions can be drawn at this stage.

13. REFERENCES

1. ICI SHE Document N° E-001 : 'Assessing Soil and Groundwater Contamination'
2. Grinell A.J. & Rumford S.P. (1993) - Ardeer Landfill, Groundwater pH Survey
3. Grinell A.J., Rumford S.P. & Murray-Smith R.J. (1994) - Ardeer Landfill, Probing Survey.
4. Barker P., Wyllie M., Esnault A. (1996) - Investigation, planning and execution of the remediation of Ardeer Landfill, Scotland

PILOT DEMONSTRATION FOR CONTAINMENT USING *IN SITU* SOIL MIXING TECHNIQUES AT A CHEMICAL DISPOSAL SUPERFUND SITE

S.J. Zarlinski, P.E.
N.W. Kingham
R. Semenak

Kiber Environmental Services, Inc.
3786 Dekalb Technology Parkway, N.E.
Atlanta, Georgia USA 30340

ABSTRACT

Kiber Environmental Services, Inc. (Kiber), under contract to McLaren-Hart Corporation and the site PRP group, performed technical oversight and on-site sampling and analyses at the confidential site located in Texas. The site consists of 15,000 cubic meters (20,000 cubic yards) of contaminated materials that were to be solidified on-site. The contaminants included heavy metals, PAHs, oil and grease, and volatile organics. Groundwater is less than 1 meter from the surface. Kiber was retained after several unsuccessful efforts to find on-site containment methods that effectively solidified the waste pits while achieving the performance goals. The PRP group then contracted with Kiber to perform the treatability and pilot oversight studies. The full-scale pilot demonstration was performed by Geo-Con.

Pilot-scale treatment was performed to evaluate the effectiveness of *in situ* solidification treatment at achieving the site specific performance criteria, including an unconfined compressive strength of greater than 170 kPa (25 psi) and a permeability of less than 1×10^{-6} cm/sec. Technical oversight and on-site sampling and analysis were provided to evaluate pilot-scale application of the selected technology and verify treatment effectiveness. The project was divided into several subtasks. First, laboratory treatability testing was conducted to verify that performance specifications were achievable using the proposed reagent formulations. Next, a pilot demonstration was performed by Geo-Con using a Manotowoc 4000 crane equipped with a 1.5-meter diameter auger to evaluate shallow soil mixing. The final task included a comparative study between the performance of test specimens collected using wet sampling techniques versus *in situ* post-treatment coring.

Detailed sampling and analyses were performed on site to evaluate basic material characteristics of the treated uncured material, including pH, moisture content and cement content. These evaluations were then used in conjunction with geotechnical evaluations, including unconfined compressive strength and permeability. UCS and permeability testing was performed after sample curing to determine the potential applicability of the tests for screening of treatment effectiveness during full-scale treatment.

Review of the data from permeability and strength evaluations of the treated mixtures, based on wet sampling, indicated that the treatment was effective at achieving the site-specific treatment criteria, including an unconfined compressive strength of greater than 170 kPa (25 psi) and a permeability of less than 1×10^{-6} cm/sec. Review of data from post-treatment core samples indicated that they were unable to achieve the criteria for strength and permeability. Investigations of the treatment, sampling and analyses were performed to fully assess possible sources for the failure of the testing to meet site criteria. Based on these investigations, wet sampling was identified as a more accurate measurement of the UCS and permeability than core sampling.

PILOT DEMONSTRATION

Representatives of Kiber were on site throughout the pilot demonstration to assist in remediation and technical oversight activities and perform on-site laboratory testing. The contractor selected to perform the pilot demonstration was Geo-Con. The primary objective of the pilot demonstration was to confirm that existing technical specifications for the project could be achieved. Specifically, testing was performed to ensure that the waste material could be stabilized to the required depths and areal extent, using *in situ* technology and non-proprietary admixtures. Treatment criteria included a minimum UCS of 170 kPa and a maximum permeability of 1×10^{-6} cm/s. The pilot study included two test areas. Test Area A was treated using an admixture formulation with 20% by-weight addition of Type I Portland cement. Treatment of Test Area B was performed with a 20% by-weight addition of cement and a 3% bentonite addition.

Pilot treatment was initiated by Geo-Con using a 1.5-meter diameter auger fitted with reagent-slurry injection ports. The auger was attached to a Manotowoc 4000 crane utilized to advance and withdraw the auger during treatment. A separate engine, suspended from the boom, was used to rotate the auger during advancement into the sludge. Treatment was performed by injecting the reagent slurry through the auger, while simultaneously advancing the auger into the untreated sludge. The auger was continuously rotated throughout the process in order to blend the grout with the sludge. The reagent grout was added to the untreated material on a batch basis for each column treated. Prior to initiating treatment, a slurry of the requisite amount of reagent and water was determined for each column based on the depth to be treated, the diameter of the column and the density of the sludge. In this manner, the weight of the sludge to be treated was estimated, and therefore, the weights of the reagent and water to be added for each column determined.

For Test Area B, involving two reagent admixtures, the treatment process was initiated by pumping the bentonite slurry until all slurry had been injected. Generally, injection of the bentonite slurry occurred over the first complete penetration and withdrawal of the auger. At this point, pumping was initiated for the cement slurry. Injection of the cement slurry generally occurred during the second complete penetration and withdrawal of the auger. Blending continued until 6 to 8 complete penetrations and withdrawals were performed for each column. Treatment of Test Area A was completed using similar protocols except there was no initial bentonite slurry addition. The following summarizes operating parameters for each test area:

TEST PIT	REAGENT (%)		WATER:REAGENT		PENETRATIONS		COMMENTS
	Cement	Bentonite	Cement	Bentonite	#	Total Time	
1A	20	0	1.4	-	1	3:05	Oversaturated/Under Mixed
3A	20	0	1.4	-	7	7:35	Oversaturated
6A	20	0	0.8	-	12	20:00	Over Mixed
10A	20	0	0.8	-	6	10:00	Dye Additive
14A	20	0	0.8	-	8	10:30	Change in Ratio
24A	20	0	0.8	-	6	10:00	Adjusted Ratio
28A	20	0	0.7	-	6	9:24	Initial Ratio
7B	20	3	0.7	11.76	5	8:46	-
8B	20	3	0.7	10	6	12:14	-
9B	20	3	0.7	11.76	6	10:32	-
15B	20	3	0.7	10	6	12:06	-
17B	20	3	0.7	11.76	5	8:50	-
19B	20	3	0.7	11.76	5	8:35	-

SAMPLING AND ANALYSES OF WET SAMPLES

Based on experience from similar types of projects, and current industry practice, the preparation of wet samples was chosen as the primary method to obtain samples for subsequent performance evaluation testing. The wet sampling method is similar to the method utilized in the concrete industry whereby samples of the uncured material are placed into cylindrical molds, cured under controlled conditions, and then tested. This method is commonly specified for both *ex situ* and *in situ* stabilization and solidification projects, and is accepted by many regulatory agencies.

Sampling activity at the site was performed during treatment of both Test Area A and B. A total of 13 sample locations were identified: 7 within Test Area A, and 6 within Test Area B. Sampling at each location was performed immediately after treatment at depths of 1 and 2 meters below mean sea level (MSL). Sampling was performed by advancing a hollow steel tube into the center of each specified column. The tube was suspended from the bucket of a track hoe and advanced into the column by lowering the bucket of the track hoe. The hollow tube was equipped with a hydraulically activated cap covering the bottom. To sample, the tube was lowered to the requisite depth for sampling. Once at the necessary depth, the cap was hydraulically opened and the treated sludge was allowed to seep into the tube. After retrieving the sample, the cap was hydraulically sealed over the bottom of the tube, and the entire sampling apparatus was removed from the treated column. Once removed, the cap was again opened and the treated sludge allowed to drain into a prepared 20-liter bucket.

Visual observations of the treated material were performed immediately to ensure that the samples represented treated sludge and did not include untreated product from neighboring columns. Additional observations were also noted regarding the homogeneity of the treated sludge. After verification of the treated sample matrix, the bucket was removed from the exclusion zone, decontaminated and transported to the on-site laboratory.

Upon receipt of the treated materials at the on-site laboratory, screening analyses were performed for physical and chemical properties, and samples were remolded for curing and later testing. Screening analyses included material pH, moisture content, bulk density and cement content testing. The screening analyses were performed to provide information relative to treatment effectiveness and the potential variability of the *in situ* mixing process. Review of the results provides data for comparison of the various columns. Replicate analyses allowed for estimations of the treatment effectiveness, including reproducibility and uniformity of treatment.

Based on the moisture content results, a good correlation was observed between the water:reagent ratio and the moisture content of the treated materials. Lower moisture content values were obtained for columns developed with the lowest water:reagent ratios while higher water:reagent ratios resulted in treated materials with the highest moisture contents. For columns developed with similar water:reagent ratios, moisture content values varied by less than 20%. This good reproducibility indicates consistent application of the treatment process.

Material pH was performed to evaluate reagent addition. While pH of treated materials is known to vary with cure time, a review of the pH immediately after reagent addition can be used to verify treatment. The treated pH ranged from 11.45 to 12.16. This indicates that the pH of the material was increased significantly from untreated values of approximately 6.5. This increase is attributed to the alkalinity of the cement. Due to the buffering capacity of the sludge and the cement, it is not possible to directly correlate reagent addition to pH. However, the values do indicate that consistent quantities of reagent were added to each column.

The cement content testing is intended as a relatively quick and inexpensive test to be used at construction sites to determine compliance with specifications. Review of the cement content results revealed values from 5% to 33% by weight. Cement content was only performed as a qualitative evaluation of reagent addition. As such, quantitative interpretations of the results are

inappropriate. The cement content results are useful for verifying that cement was added to each column but should not be used for estimations of actual addition rates.

In addition to the screening analyses, individual test specimens were compacted for curing and later geotechnical testing. Each specimen was compacted by filling the mold in thirds and tamping the entire mold to minimize void spaces. This process was continued until the mold was full of compacted material. Due to the wet nature of the treated materials, compactive effort was not a concern. Also, no rodding of the materials was performed during this process. Specimen sizes were 7.6 cm in diameter and 15.2 cm in height for strength testing, and 7.6 cm in diameter and 7.6 cm in height for permeability testing.

All specimen compaction was performed immediately upon receipt in the laboratory trailer. Visual observations revealed that no setting of the treated material had occurred by this time (approximately 2 hours after treatment). That is, the treated sludge was still wet, pliable, and had not begun to solidify into a monolithic structure. Compaction of the test specimens did not disturb the material, and did not hinder the setting process. Any oversized particles which would bias the strength and permeability testing were removed. Every effort was made not to perform additional blending of the treated sludge during compaction beyond that required to assure that representative material was compacted into each mold. Each compacted specimen was placed in a ziplock bag with a moist paper towel to promote curing in a humid environment. All samples were cured at room temperature which was between 15 and 20 (°C).

A testing program was implemented that included geotechnical testing and visual observations of wet sampled specimens (discussed above), core drilling of the cured pilot test areas, and excavation of the cured pilot demonstration areas with a hydraulic excavator. Wet sampled treated materials were tested for UCS in accordance with ASTM D 2166 at cure times of 1, 2, 3, 4, 5, 6 and 7 days. Permeability testing was performed to estimate the quantity and flow rates of water through a material under saturated conditions. Permeability testing was performed after a minimum cure time of 7 days in general accordance with EPA SW-846 Method 9100 and incorporated several guidance parameters outlined in ASTM D 5084. The following table summarizes the UCS and hydraulic conductivity test results:

TEST	UNCONFINED COMPRESSIVE STRENGTH (kPa)							PERMEABILITY
PIT	1 Day	2 Day	3 Day	4 Day	5 Day	6 Day	7 Day	>7 Days (cm/sec)
1A	34	-	62	97	97	90	83	8×10^{-7}
3A	55	97	117	131	117	110	138	6×10^{-7}
6A	62	131	159	165	172	186	186	3×10^{-7}
10A	131	331	352	359	400	427	372	1×10^{-7}
14A	90	138	200	200	193	221	248	2×10^{-7}
24A	103	248	290	248	283	338	338	1×10^{-7}
28A	117	193	228	283	331	338	262	2×10^{-7}
7B	62	76	97	117	124	152	124	3×10^{-7}
8B	90	97	110	131	152	138	186	7×10^{-7}
9B	83	97	124	145	152	179	193	4×10^{-7}
15B	55	-	131	-	103	-	117	3×10^{-7}
17B	62	90	103	103	103	172	152	3×10^{-7}
19B	69	97	110	117	117	193	124	3×10^{-7}

CORE SAMPLING AND TESTING

Core sampling of each demonstration area was performed after a minimum 7 day cure time to 1) inspect the cured monoliths for uniformity of mixing and/or homogeneity, and 2) determine the overall effectiveness of treatment. Cored samples were collected for UCS and permeability testing. A total of 12 sampling locations were identified: 7 in Test Area A, and 5 in Test Area B. All core sampling was performed using a Shelby tube sampler. Sampling was initiated by advancing a 8.9 cm diameter seamless steel tube into the center of a treated column. The tube and sample was then withdrawn from the hole. The driller then extracted the sample from the steel tube and transferred the material to a clear acrylic tube. Sampling was continued, in the same manner, in increments of approximately 1 meter to the bottom of the treated material. Visual observations during sampling indicated steam being released from each core location indicating increased temperatures due to heat of hydration, even after cure times greater than 7 days.

The samples were delivered to the laboratory for visual descriptions, extrusion and further geotechnical testing. The treated samples were extruded from the tubes using only hand pressure. The extruded cored specimens appeared disturbed and difficult to handle. Most specimens had numerous cracks and microfractures throughout the entire specimen. Comparison of the core specimens and the wet samples revealed several differences. The wet samples exhibited good integrity and material handling, while the core samples had little integrity. Each core was fragile and brittle in nature. Close examination of the core specimens revealed microfractures throughout the entire sample. These fractures were generally small and were only readily apparent upon close inspection of the materials. Each core also had numerous large fractures apparently caused by the sampling process.

Each of the core samples was then subjected to UCS and hydraulic conductivity testing. The results of treated analyses performed on the core samples collected from Test Pit A reveal UCS values ranging from a low of 69 kPa to a high of 476 kPa, with an average value of 338 kPa. Test Pit B results revealed values ranging from 55 kPa to as high as 310 kPa, with an average strength of 152 kPa. Permeability analyses performed on the Test Pit A core samples revealed values ranging from 6×10^{-5} cm/sec to 4×10^{-6} cm/sec with an average of 2×10^{-5} cm/sec. Permeability results for Test Pit B core samples revealed values ranging from 5×10^{-5} cm/sec to 2×10^{-6} cm/sec, with an average value of 1×10^{-5} cm/sec.

Sampling of an additional 6 coring locations (3 in each test area) was performed after cure times in excess of 60 days. As with the 7 day coring samples, the additional core samples indicated that the waste and reagent admixtures were well mixed; however, the samples were extremely fragile and brittle. Additional UCS and permeability evaluations were also performed on these core samples. The data indicates that, for Test Pit A, core samples achieved an average UCS value of 207 kPa and an average permeability value of 4×10^{-4} cm/sec. For Test Pit B, average values included a strength of 62 kPa and a permeability of 2×10^{-4} cm/sec.

Several theories were developed for potential causes of the differences between the wet samples and the *in situ* core samples. Generally, the potential causes include differences in curing, and sampling procedures and protocols. The potential differences in curing primarily focus on the heat of hydration which is sustained within the treated monolith for weeks after treatment. This heat of hydration is much greater in the *in situ* monolith due to the mass effect of a large volume of treated material. Wet samples, curing in the laboratory trailer, do not experience such a mass effect and achieve relatively low heat of hydration temperatures for a fairly short period of time. These increased, sustained temperatures are observed during full-scale *in situ* treatment using similar reagents. Experience indicates that the heat of hydration does not negatively impact the effectiveness of solidification treatment. The investigators do not attribute the poor core sample data to the heat of hydration.

Groundwater can often cause a decrease in treatment effectiveness through repeated cycles of wetting and drying, or through contaminants which may inhibit the curing process. Visual observations performed during sampling indicate that the individual core samples were not saturated with groundwater. These observations confirm moisture content data, which indicated that the core samples produced moisture contents similar to the wet samples. Therefore, the investigators do not attribute the poor core samples to potential groundwater effects.

Other potential causes of poor curing for the *in situ* materials include chemical contaminants within the treated matrix which may inhibit effective curing. As outlined above, groundwater was not observed to be a problem; therefore, the introduction of chemical contaminants through the groundwater is not likely. Similarly, any contaminants within the sludge matrix which may have interfered with effective curing would have affected the wet samples as well.

The geotechnical characterization data indicates that the 7-day core samples are similar to the wet samples. Although the core samples are fractured throughout, the actual material matrix appears similar to the wet samples. The investigators believe that the main cause of the increased permeability values is due to the sampling method. Core sampling requires invasive techniques which imparts a considerable amount of disturbance to the material. It is theorized that this sampling technique is responsible for the microfractures visible throughout the core samples. The wet samples and core samples are physically similar, in terms of appearance, moisture content and density values. However, the visual observations confirm the presence of numerous cracks and fissures which can cause channeling during permeability testing. The increased permeability values may be a result of this channeling.

LONG TERM CURES

Additional UCS and permeability testing was performed to evaluate the various treated materials at extended cure times. These analyses were performed on specimens collected using both wet sampling and coring techniques. Testing was only performed on samples from Test Pit A.

| SAMPLE NUMBER | CURE TIME (Days) | DENSITY | | MOISTURE CONTENT | | UCS (kPa) |
		BULK (g/cm^3)	DRY (g/cm^3)	EPA (%)	ASTM (%)	
WET SAMPLES						
6A-5.5	90	1.46	0.85	42	72	496
10A-3	103	1.44	0.85	41	70	1000
14A-5.5	104	1.43	0.83	41	70	469
24A-3	90	1.52	0.90	41	70	786
28A-5.5	105	1.47	0.88	40	67	862
CORING SAMPLES - 7 DAY CORE						
10A (4-6)	103	1.41	0.95	33	49	621
24A (4-6)	103	1.28	0.78	40	65	241
CORING SAMPLES - 60 DAY CORE						
8A (2.5-5)	104	1.36	0.77	44	77	131
20A (5-7.5)	104	1.36	0.82	40	68	214

Permeability testing was performed on two Test Pit A wet cured samples. The hydraulic conductivity of the two samples were 6x10^{-8} cm/sec for 6A-5.5 and 5x10^8 cm/sec for 24A-3. These permeability tests achieved the lowest hydraulic conductivity values obtained for any testing performed on the site materials. The extended wet cured samples achieved a hydraulic

conductivity approximately one order of magnitude less than the wet cured samples analyzed after only 7 days of curing. The values are also three to four orders of magnitude less than the core samples analyzed.

DATA SUMMARY

Samples from Test Pit A were analyzed to evaluate their ability to achieve the project specific goal of an unconfined compressive strength of greater than 170 kPa and a hydraulic conductivity of less than 1×10^{-6} cm/sec:

- Wet samples collected during treatment of Test Pit A achieved an average UCS of 228 kPa after 7 days of curing
- Core samples collected from Test Pit A after approximately 7 days of curing achieved an average UCS of 338 kPa.
- Core samples collected after approximately 60 days of curing achieved an average UCS of 207 kPa.
- Wet samples analyzed after extended cures of up to 104 days achieved an average UCS of 724 kPa.
- No significant difference was noted between UCS testing performed immediately after coring, and after extended cure times of greater than 100 days.
- Wet samples collected during treatment of Test Pit A achieved an average hydraulic conductivity of 4×10^{-7} cm/sec after 7 days of curing.
- Core samples collected from Test Pit A after approximately 7 days of curing achieved an average hydraulic conductivity of 2×10^{-5} cm/sec.
- Core samples collected from Test Pit A after approximately 60 days of curing achieved an average hydraulic conductivity of 4×10^{-4} cm/sec.
- Wet samples analyzed after extended cures of up to 104 days achieved an average hydraulic conductivity of 6×10^{-8} cm/sec.

Samples from Test Pit B were also tested to evaluate their ability to achieve the project specific goal of an unconfined compressive strength of greater than 170 kPa and a hydraulic conductivity of less than 1×10^{-6} cm/sec:

- Wet samples collected during treatment of Test Pit B achieved an average UCS of 172 kPa after 7 days of curing.
- Core samples collected after approximately 7 days of curing achieved an average UCS of 152 kPa.
- Core samples collected from Test Pit B after 60 days of curing achieved an average UCS of 62 kPa.
- Wet samples collected during treatment of Test Pit B achieved an average hydraulic conductivity of 5×10^{-7} cm/sec after 7 days of curing.
- Core samples collected from Test Pit B after approximately 7 days of curing achieved an average hydraulic conductivity of 1×10^{-5} cm/sec.
- Core samples collected from Test Pit B after approximately 60 days of curing achieved an average hydraulic conductivity of 2×10^{-4} cm/sec.

CONCLUSIONS

The investigators concluded that waste material at the site can be stabilized to the required depths and areal extent, using *in situ* mixing technologies and non-proprietary admixtures. Also, the waste material can be stabilized such that the stabilized material has a minimum unconfined compressive strength of 170 kPa and a maximum permeability of 1×10^{-6} cm/sec, consistent with the overall intent of the original project specifications. Due to the problems associated with obtaining core samples which become significantly disturbed during sampling, wet sampling methods were recommended at the site as more appropriate for obtaining samples for unconfined compressive strength and permeability testing.

IMPLEMENTATION OF AN EX SITU STABILIZATION TECHNIQUE AT THE SAND SPRINGS SUPERFUND SITE TO SOLIDIFY AND STABILIZE ACID TAR SLUDGES INVOLVING A QUICK-LIME BASED STABILIZATION PROCESS AND INNOVATIVE EQUIPMENT DESIGN

R.W. McManus, P.E., SOUND Environmental Services, Inc., Dallas, Texas
P. Grajczak, P.E., ARCO, Corporate Environmental Remediation, Los Angeles, California
J.C. Wilcoxson, ARCO, Exploration and Production Technology, Plano, Texas
S.D. Webster, U.S. Environmental Protection Agency, Region 6, Dallas, Texas

ABSTRACT

An old refinery site was safely remediated a year before schedule and for 25% less than final engineering estimates for the stabilization remedy thanks to energetic project management and innovative design involving ex situ stabilization/solidification of acid tar sludges. A quicklime based process, Dispersion by Chemical Reaction (DCR™), was employed to solidify and stabilize (SS) over 103,000 cubic meters (135,000 cubic yards) of petroleum waste, mostly acidic tarry sludge. The SS process was selected over competing methods because it afforded minimal volume increase, could readily achieve Record of Decision (ROD) specified physical and chemical treatment goals, could be implemented with treatment equipment that minimized emissions, and could be performed with low reagent usage and at low cost. To ensure treatment goals were achieved and an accelerated schedule met, a custom designed and fabricated transportable treatment unit (TTU) was employed to implement the process. The treated material was visually soil-like in character, it was left in stockpiles for periods of time, and it was placed and compacted in the on site landfill using standard earth-moving equipment.

PROJECT BACKGROUND AND HISTORY

The Sand Springs project was the remediation of a former Sinclair refinery that operated in the first half of the century. The operation left behind 103,000 cubic meters (135,000 cubic yards) of petroleum waste, mostly acidic sludge, concentrated in several earthen pits. The site was placed on the National Priority List in 1986 and ARCO, Sinclair's successor in business, volunteered to cleanup the site. Subsequently, ARCO, EPA Region VI, and the Oklahoma State Department of Health entered into a consent decree under which ARCO agreed to remediate the site (*Consent Decree* 1989).

Most of the site's waste originated from an old fuel stabilization process that was in use between 1870 and the late 1940's. The process involved mixing raw crude oil with concentrated sulfuric acid in a batch mode. The acid catalyzed polymerization of unstable hydrocarbons found in the crude. The sludge resulting from the process was treated as waste and discarded. Typical acid sludge waste contains a high percentage of heavy molecular weight hydrocarbons, high acidity, and is often saturated with sulfur dioxide. The waste consistency varied from coal-like to thick, slow-flowing tar. The Sand Springs acid tar had an average total organic carbon content of 33%, total petroleum hydrocarbon content of 196,000 mg/kg, and pH of 0.3. In several areas, total petroleum hydrocarbon content exceeded 40% (*ARCO Final Independent Task Report* 1992).

The Record of Decision (ROD) issued for the site required solidification/stabilization of all petroleum sludges and containment of the resulting matrix in a hazardous waste cell to be constructed on site. All waste plus one foot of underlying soils was to be removed, processed and placed in an on site landfill. The selected solidification/stabilization technology was to provide for the protection of public health and the environment comparable to incineration, a treatment originally contemplated by the EPA.

The project site was located in an industrial area of Sand Springs, Oklahoma and had limited acreage available for landfill construction. Control of airborne emissions and limiting the final volume of the landfill were the major technical considerations for remedial design.

TECHNOLOGY SELECTION

According to the Consent Decree, selecting the treatment technology was to be done in two stages. In the first stage, ARCO had to prove that the waste could be treated by solidification in a manner consistent with the ROD. Specifically, the waste had to be solidified to 1. remove all free liquid, 2. provide structural strength consistent with RCRA cell design, 3. reduce waste toxicity or mobility, and 4. meet RCRA land disposal restrictions. To accomplish this a selected group of vendors was invited to try their respective processes in bench tests. Only three vendors were successful in meeting the objectives specified in the ROD. These vendors were then invited to a full scale demonstration at the site.

Each of the three vendors proposed a unique process and used a different type of solidification agent. The first process used cement/lime mixture and relied on in situ mixing of waste using shallow tilling technique. The second process used quicklime and involved pre-mixing of sludges with water. The third process required neutralization followed by in situ mixing with organophillic clays. Each technology produced a matrix that met the requirement of the ROD.

Following successful field demonstration of solidification, ARCO solicited bids for the technical oversight and know-how for the process. Upon careful evaluation of the bids, which included evaluation of the total cost of the project, the contract was awarded to SOUND Environmental Services, Inc., of Coppell, Texas. The process offered by SOUND was a lime-based method for converting oily and tarry waste into a soil-like product compactable to high compressive strength and low permeability material and referred to as Dispersion by Chemical Reaction (DCR).

QUICKLIME STABILIZATION

Research performed in the late 1960's and early 1970's by Professor Friedrich Bölsing at the University of Hanover, in then West Germany described the dynamics involved in the hydration of alkali earth metal oxides, such as quicklime, in organic waste matrices; that is, mixes of oily waste, water, and inert materials. Dr. Bölsing discovered means of managing the alkali earth metal oxide hydration reaction in such a manner as to most efficiently take advantage of reactions and interactions in the stabilization of organic wastes. These processes have been described in several patents and are referred to as Dispersion by Chemical Reaction or DCR.

DCR PROCESS

The DCR Process is a lime-based process applicable to the stabilization of organic wastes. The process has been used in Europe for over 15 years to convert oily wastes into a solid, free flowing soil like material used for on site closure, fill and road subgrade material. Oil and oil-like compounds can be dispersed homogeneously to form a dry pulverulent solid by means of the process. This holds true for any mix of organics as a separate phase, or with mixtures of oils and inorganic materials. Any oil containing system, (i.e., tank bottoms, oil contaminated soil, as well as organic sludges in unlimited concentrations) can be transformed into dry powdered solids.

DCR technology takes advantage of certain chemical compounds that, upon reacting with water, form highly pulverulent solids with high specific surface areas. These chemical reactions are termed 'dispersing reactions'. Alkali earth metal oxides, such as common quick lime, have this characteristic. An alkali earth metal oxide, upon hydration with a stoichiometric amount of water, will form the corresponding hydroxide as shown in Equation 1.

1. $CaO + H_2O > Ca(OH)_2$
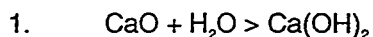
In this reaction, the specific surface area of the material dramatically increases as the particle size decreases and the porous nature of the material increases. In the case of a powdered or ground calcium oxide, the specific surface area increases from approximately 1 m^2/g to over 30 m^2/g in the exothermic reaction that forms the hydroxide.

Oils and oily substances can be converted from mobile, liquid materials into pulverulent dry solids by taking advantage of dispersing reactions as described above. This is possible by pre-distributing the oily material in the alkali earth metal oxide prior to affecting the hydration reaction. The oil is carried through the exothermic hydration reaction and is adsorbed homogeneously throughout the hydroxide. The oil is eliminated from the oily phase by virtue of being adsorbed onto the hydroxide in molecular thickness across dramatically increased surface area. Due to the nature of the reaction and elimination of the oil as a liquid phase the conversion is virtually irreversible short of dissolving the calcium hydroxide substrate. In addition, the elimination of the liquid oil and formation of calcium hydroxide in most waste matrices results in an end product with desirable engineering characteristics. Specifically, these characteristics are low permeability and high compressive strengths when compacted. The process -- pre-distribution of an oily waste to be immobilized into a material subject to dispersing reactions, then effecting the dispersing chemical reaction, converting the liquid into a dry pulverulent solid -- is referred to as DCR (Bölsing 1988). The process is protected by several patents.

Quick lime, or calcium oxide, is generally applied to the stabilization of sludges without knowledge of the underlying system dynamics. The simple mixing of calcium oxide into an organic sludge, consisting of oily waste, water and inert material, can have dramatically varying results, including fires (ARCO Sand Springs Superfund Site Tier 2 pilot scale tests describe such an incident). Experience managing the exothermic hydration reaction is necessary for safe and efficient field implementation.

There are five means of carrying out the DCR process so as to accomplish the pre-distribution of the oil component in the required amount of calcium oxide prior to the hydration reaction. These five means involve sequential addition (blending reagent and waste prior to water addition), creating emulsion to inhibit lime-water interaction, adding reaction retarding reagent to slow hydration, hydrophobizing the calcium oxide to retard hydration, or rapid mixing to pre-distribute the oil prior to the hydration reaction. Each of these methods allows pre-distribution to take place prior to hydration. The first four methods also serve to attenuate the hydration reaction. Attenuation of the hydration reaction is beneficial in controlling maximum reaction temperatures.

There is an important distinction between this approach to organics solidification and those approaches involving cement based reagents. When cement or related reagents are generally applied to heavy organic sludge, the goal is to produce a solid matrix which will hold the oil over time (Connor 1990). The success of the solidification is dependent upon the long-term integrity of the matrix, thus leaving the product vulnerable to potential re-coalescing of oils if the matrix is destroyed mechanically, chemically, or by age.

The DCR process, in contrast, is not dependent upon the matrix to hold the liquid phase organic. The liquid phase is actually eliminated in the dispersing reaction. The organic is surface adsorbed on the hydroxide particles and not present as a free liquid. DCR-treated material has the appearance of a brown, silty soil and can be handled as ordinary soil. Successful treatment is not dependent upon the integrity of the matrix. This allows for the stockpiling of treated material before placement and compaction without degrading its qualities.

This soil-like character of the DCR treated material was particularly important at the Sand Springs project. It allowed the excavation, treatment, and placement work activities to proceed

independent of each other. In order to provide process flexibility, a provision was made for stockpiling material at the load and discharge end of the treatment unit.

EMISSIONS

One of the main problems of lime-based stabilization is emissions generated as a result of the exothermic hydration reaction. Heat generated during the reaction can quickly raise the temperature of the treated material to above 100°C speeding up release of volatile organics. Because of the project location, the site was surrounded by operating businesses, ability to control emissions was one of the main factors in selection and development of treatment technology. Therefore, following award of the solidification contract, ARCO commissioned an extensive study aimed at defining and developing means of emission controls.

The study included elaborate bench tests that used commercial agents and raw waste from the site. The goal was to determine rate of emissions versus time and its dependence on temperature of reaction. Early in the study it was determined that only benzene could potentially cause concern, other components in the emitted stream were well below action levels.

The test runs involved the main steps of the DCR process as intended for the full scale operation. Concentrations of benzene in the vapor stream and temperature of the reaction environment were measured over time. The results showed that temperature inside the freshly mixed material increased rapidly reaching 105°C at which point steam was visible rising from the surface. The temperature would plateau for few minutes and start a slow decrease indicating that the reaction is complete and the mixture entered a cooling stage. Concentration of benzene increased rapidly following closely the temperature rally, however, it rapidly declined after reaching a sharp peak shortly after peak temperature. Benzene emissions decreased to near the limits of detection (<5 ppm) within 30 minutes of lime addition and mixing (*Additional Bench Scale Study Report* 1993).

FIELD APPLICATION

An economic analysis was performed to determine the desired treatment operation throughput to meet schedule requirements and minimize costs. The main challenge was combining neutralization and excavation rates (all waste had to be neutralized prior to excavation to control sulfur dioxide emissions) with treatment and waste placement rates that would match the rate of landfill construction on a cramped site. The analysis indicated that a plant capable of treating 135 tonnes (150 tons) per hour would provide optimum operating environment and lowest cost. However, construction of a unit this large represented a challenge. Construction of permanent structures on site was not desirable and building a transportable plant required extensive engineering. Moreover there was no experience available for this technology -- the European designs were generally capable of processing 9 to 14 tonnes (10 to 15 tons) per hour; the Sand Springs plant was to handle over 10 times this rate. Additionally, the project schedule demanded that the plant be ready for operation in less than a year.

TREATMENT UNIT DESIGN

To achieve the desired throughput capacity and provide for operational flexibility the TTU was to include a dual processor, sequencing batch system. The system involved two parallel batch mixing units that were fed by a single rate modulated feeder. The batching was computer controlled using a programmable logic controller (PLC) so overlapping batch operations could be efficiently conducted. The sequencing of batch feed-mix-discharge in two trains produced in effect a continuous operation from feed to product. Moreover, the design provided for a flexibility to operate at half the rate using only one train.

The PLC based batching controls provided for flexible implementation of the DCR process. The batch mixing sequence of waste load, water addition, lime addition, hydrophobizing on-off, and mix duration enabled process implementation be carried out in the manner determined to be the most cost effective and produce the best results. Several batching sequences based on DCR theory and bench scale results were tried during project start-up. For instance, one sequence tested was mixing unmodified lime with waste for 30 seconds, then adding the water required for lime hydration, and mixing for an additional 30 seconds. This followed the sequential addition model of application. The method found most effective in dispersing the tar with the least reagent usage was selected for application to most of the sludges.

The PLC-based system for the TTU was designed with an operator friendly man-machine interface. A PC interface provided for real-time point-and-click control of treatment parameters through graphical displays of actual equipment operations. Plant operating parameters, such as batch cycle time, batch weight, reagent addition, and water addition, were automatically recorded for each batch, and output was available in a variety of reporting formats. The control system was also designed to monitor all rolling equipment for various operating faults. Automatic shutdown occurred to protect personnel and equipment when out of specification conditions were detected. In addition, should one treatment train experience a mechanical problem, the system would automatically revert to single train operation, disable the problem treatment unit, and signal the mechanical fault. This feature proved invaluable in maintaining continuous treatment efforts and high operational efficiency.

The following paragraphs describe the major TTU components. The discussion begins with the plant's headworks and ending with the discharge and stacking of the treated material. The following discussion corresponds to the general equipment layout shown in Figure 1.

Figure 1. Equipment Layout
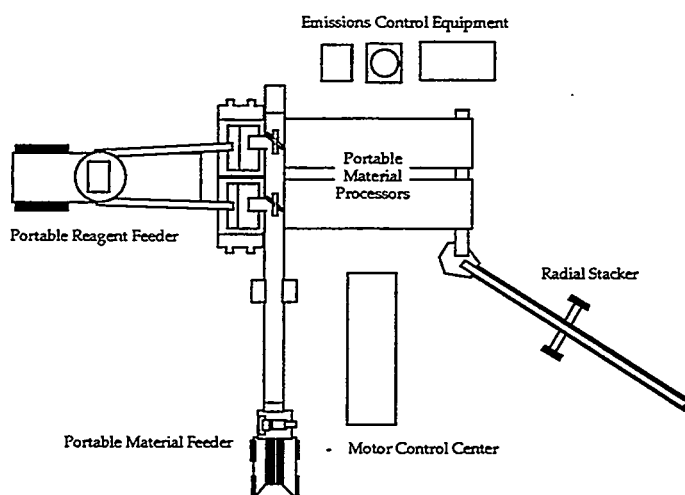
Portable Material Feeder   At the headworks of the TTU was a portable material feeder equipped with a grizzly screen. This unit consisted of a feeder-breaker, commonly used for crushing rocks, and a material conveyer system. The headworks, common to both material processor units, fed two parallel weigh batch hoppers. The feeder-breaker reduced the neutralized waste to nominal 6.3 cm (2.5") minus material. Design feed rate was 138 cubic meters per hour (150 cubic yards per hour). The feeder-breaker was capable of delivering over 190 cubic meters per hour (250 cubic yards per hour).

Portable Reagent Feeder   The portable reagent feeder system consisted of a small (20 cubic meter) lime day tank, a hydrophobizing spray system, and dual (2) lime feeder systems. Each lime feeder system consisted of a horizontal auger on a load cell, and an inclined, aero-mechanical conveyer. Lime storage silos fed the day tank on demand, when called for by a low level indicator in the tank. The tank provided 30 to 60 minutes of surge capacity to the lime system, and provided a point to apply hydrophobizing reagent. As the lime is blown into the day tank, it is sprayed with a hydrophobizing agent. From the day tanks the lime was gravity fed into the horizontal augers, metered and transferred to the weigh batch hoppers via high volume aero-mechanical conveyors.

Dual Portable Material Processor Unit   Both of the TTU portable material processor units were identical and consisted of a weigh batch hopper, a high intensity shear mixer, and an adjustable speed, slow moving walking floor conveyer. Their purpose was three-fold: to precisely control the amount of lime and water added to the waste, to blend lime and water into the waste and create a homogeneous mixture; and finally, to provide for controlling emissions during and immediately after the reaction. Either unit could be locked-out for maintenance or repairs, while the other unit remained in operation.

Each weigh batch hopper had a separate bin for waste and lime. Bins were constructed with steep walls lined with plastic sheets to prevent sticking. Lime and waste were fed to the mixer below through two independently operating clam shell gates. The mixers blended neutralized raw waste, water, and lime into a homogeneous mixture. The amount of lime and water added to each batch, as well as cycle time, was adjusted to waste composition. After blending, the reacting mixture was dropped onto the walking floor conveyor. The conveyor would allow for up to 45 minutes of retention time for tarry waste to be stabilized by the DCR process. The final product was a soil-like, moist and warm to touch material. In order to control emissions slight vacuum was maintained inside all segments of the material processing units. The product was collected from the walking floors and stockpiled using a radial stacker.

Processor unit treatment parameters were managed from a control room above the motor control center. From this location the treatment unit operator could visually observe raw waste loading and treated material discharge. Treatment parameters, including batch size, reagent addition, water addition, mixer shaft speed, batching sequence and timing, and walking floor speed, could be altered in real time to adjust to changes in material feed or changes in treated material character.

Emissions Control   The TTU was designed with three emissions control systems to reduce particulate and organic vapors to acceptable levels. The TTU itself contained five main sources of emissions: the lime day tank, both weigh batch hopper and mixer assemblies, and both walking floor conveyers. Each stream was treated separately.

Dust generated in lime transfer operations was controlled by baghouse equipment, both on the lime day tank and the storage silos.

Gas streams from the weigh batch hoppers and mixers contained mostly lime dust and were processed through a hydrostatic precipitator where water was mixed into the gas stream using impellers. The process produced dust free stream of gas and diluted lime slurry. Waste lime slurry generated by the precipitator was mixed with raw waste and passed through the treatment process.

Gas stream from walking floors was vented first to a spray tower. The spray tower knocked down steam and dust and cooled the air stream causing condensation of large fraction of organics. The air stream was then polished on vapor-phase activated carbon before being released to the atmosphere. A flow equalization basin on site served as a source of water and a repository for condensate.

TREATMENT OPERATIONS

The design and fabrication of this unique piece of treatment equipment were carried out under extremely tight time constraints. Only nine months was allowed in the project schedule to design, fabricate and mobilize the unit. The equipment was delivered on nine standard trailers, set up at the site, and operational within one day of the target date. Following startup and shake out, the equipment averaged single-shift production of over 1000 tonnes of throughput per eight hour operating day (125 tonnes per hour).

A total of 103,000 cubic meters (137,000 cubic yards) of waste was processed at the site through the unit within 13 months of operation. Use of the DCR process in concert with the custom-designed transportable treatment unit proved most successful in treatment of the Sand Springs acid tar waste. The resulting material was homogenous, soil-like, easy to transport and readily compacted in the landfill. The agent to waste ratio varied from 6 to 15%, however, stayed on average in the 7-8% range. Water addition ranged from 3 to 6% by weight. Expansion factor averaged 7%.

Material properties of the treated waste resembled a natural soil of fine particle size, such as a silt. The soil was non-cohesive in nature and was easily placed and compacted to the specified 90% of maximum dry density (ASTM 1557). Typical physical properties of the material are presented in Table 1. All samples of the treated material passed the TCLP as required by the project specifications.

Table 1. Treated Material Physical Properties

Item	Test Method	Treatment Standard	DCR Treated (typical)
Unconfined Compressive Strength	ASTM 1633	>1.76 Kg/cm^2 (25 psi)	9.8 Kg/cm^2 (140 psi)
California Bearing Ratio		>5	33
Liquid Release	EPA 9096	<5% wt. loss @ 1.76 Kg/cm^2 (25 psi)	0.25%
Permeability	EPA 9100	(not specified as a treatment standard)	5 x 10^{-5} cm/sec
pH Stability	EPA 600	>3.89x10^{-3} mg/g	12.0 mg/g

REFERENCES

ARCO Final Independent Task Report - Additional Site Characterization (1990), Morrison Knudsen Engineers, Inc., Remedial Design/Remedial Action Source Control Operable Unit, Sand Springs Petrochemical Complex.

Additional Bench Scale Study Report (1993), Remedial Design/Remedial Action Source Control Operable Unit, Sand Springs Petrochemical Complex, Consolidated Final Design Report, Volume II, Waste Excavation Treatment and Handling Design, Part 2, Section 7, Atlantic Richfield Company.

Bölsing , Dr. F. (1988), *DCR Technology in the field of Hazardous Compounds*, Ministry of Economics, Technology and Traffic, Federal Republic of Germany.

Conner, Jesse R. (1990), *Chemical Fixation and Solidification of Hazardous Wastes,* p. 183. Van Nostrand Reinhold, New York.

Consent Decree (1989), United States of America and the State of Oklahoma, ex rel. Oklahoma State Department of Health as the plaintiffs versus the Atlantic Richfield Company as the Defendants, Civil Action No. 89-C-447B, Filed May 30, 1989.

Stabilization/Solidification
of Battery Debris & Lead Impacted Material at
Schuylkill Metals, Plant City, Florida
by
Tina Anguiano & David Floyd
ENTACT, Inc.
Irving, Texas

ABSTRACT

The Schuylkill Metals facility in Plant City Florida (SMPCI) operated as a battery recycling facility for approximately 13 years. During its operation, the facility disposed of battery components in surrounding wetland areas. In March of 1991 the U.S. EPA and SMPCI entered into a Consent Decree for the remediation of the SMPCI site using stabilization/solidification and on-site disposal. In November of 1994, ENTACT began remediation at the facility and to date has successfully stabilized/solidified over 228,000 tons of lead impacted battery components and lead impacted material. The ENTACT process reduces the size of the material to be treated to ensure that complete mixing of the phosphate/cement additive is achieved thereby promoting the chemical reactions of stabilization and solidification. ENTACT has met the following performance criteria for treated material at the SMPCI site:

- Hydraulic Conductivity less than 1×10^{-6} cm/s
- Unconfined Compressive Strength greater than 50 psi
- Lead, Cadmium, Arsenic, Chromium TCLP Leachability below hazardous levels

The ENTACT technology has exceeded the standard performance criteria commonly used to evaluate the effectiveness of remedial solutions. During the course of this project, several studies were conducted to further evaluate the performance of the stabilized/solidified material in its final disposal condition. The effectiveness of the physical containment was tested by performing the first of its kind in-situ permeability testing of the stabilized/solidified material. This paper describes the ENTACT technology, the results of performance testing and the results of other studies performed on the stabilized/solidified material.

PROJECT BACKGROUND & HISTORY

Schuylkill Metals of Plant City, Inc. (SMPCI) was a battery recycling facility from 1972 to 1986. The 17.4 acre site consisted of a 2.3 acre processing area, a 2.2 acre wastewater holding pond, and approximately 10 acres of associated marshes. During operation, the process area was filled with pieces of rubber and plastic battery casings and sulfuric acid solution. Acid washdown wastewater was stored in the 2.2 acre holding pond and initially neutralized with lime and later ammonia. In 1982, the facility was placed on the National Priorities List. In June 1986, SMPCI discontinued operations as a battery recycling facility. Stabilization/Solidification of lead impacted soil, battery components, debris and on-site disposal was designated as the selected remedy in the Record of Decision in 1990. A Consent Decree was entered into between the United States Environmental Protection Agency (US EPA) and SMPCI in 1991. As part of the selected remedy, the following performance criteria were chosen for the treated material:

- Toxicity Characteristic Leaching Procedure (TCLP) Lead, Cadmium, Chromium, and Arsenic less than 5 mg/L, 1 mg/L, 5 mg/L, and 5 mg/L, respectively

Tina Anguiano/David Floyd
ENTACT, Inc.
1616 Corporate Court Suite 150
Irving, Texas 75038

- Unconfined Compressive Strength greater than 3.51 kg/cm^2 (50 psi)
- Hydraulic Conductivity less than 1 x 10^{-6} cm/sec

THE TREATABILITY STUDY

In July 1994, under the direction of the Potentially Responsible Party (PRP), ENTACT began a treatability study. It was designed to meet the performance criteria using Stabilization/Solidification (S/S) technologies for on-site disposal of stabilized/solidified material within a portion of the upper aquifer and surrounding wetlands. The Treatability Study was structured to imitate in-situ field conditions. Process equipment was designed to provide for efficient and reliable performance through the duration of the project.

The treated material requiring stabilization/ solidification was approximately 64% soil, 30% battery casing debris, and 6% peat, by volume. The hydrophilic nature of peat inhibits the solidification action of cement. Previous studies of the SMPCI material had noted difficulty in achieving hydraulic conductivity due to the peat component. The goal for the first phase of the Treatability Study was to reduce the hydraulic conductivity of the waste material to meet the performance criteria specification. ENTACT performed numerous rounds of hydraulic conductivity tests with varying additives and processing methods. Hydraulic conductivity performed during the first stage of testing on 14 different samples yielded values ranging from 3.7x10^{-3} cm/s to 3.4x10^{-7} cm/s. Through several iterations of the first phase of testing, it was determined that particle size reduction, moisture content and additive content were the critical components in achieving the hydraulic conductivity specification. During the ENTACT Treatability Study, the percentage of peat material used in each sample did not noticeably affect the hydraulic conductivity of the treated material.

Samples prepared for hydraulic conductivity testing were sized, blended with additive in stainless steel containers, compacted into cylinders using standard compaction in accordance with ASTM 690, and allowed to cure for seven days prior to testing. The mix ratio of contaminated soils reflected the actual distribution percentage at the site. Particle size reduction was performed only to the extent that was feasible for large scale treatment equipment for ebonite and plastic battery cases components. The reduction of particle sizes to less than 1.27 cm (½ in.) was deemed essential for obtaining the hydraulic conductivity performance criterion of the lead impacted soil.

With completion of the first phase testing, additive blends, moisture content and particle sizing was optimized and a design mix was determined. Bench scale testing for hydraulic conductivity was conducted on six samples using the design mix, (See TABLE I). Two of the samples were molded into 10.2 cm (4 in.) diameter cylinders and submitted for rigid cell falling head hydraulic conductivity tests in accordance with EPA SW 846 Method 9100, the remaining four samples were molded into 7.1 cm (2.8 in.) diameter samples and submitted for triaxial cell falling head hydraulic conductivity also in accordance with EPA SW 846 Method 9100.

It was determined during the bench scale testing that the falling head procedure using a rigid mold proved to be less consistent due to problems with sealing the rigid sample and the inability to provide for saturation of the sample. Throughout the project hydraulic conductivity testing a triaxial flexible wall falling head device was utilized.

The unconfined compressive strength of all of the bench scale blends was well above the performance criteria of 3.51 kg/cm^2 (50 psi) with a range from 22.22 kg/cm^2 to 26.85 kg/cm^2.

TABLE I
Treatability Study - Bench Scale Hydraulic Conductivity Test Results

Sample No.	Type of Test	Specimen Diameter (cm)	Initial Moisture Content, % of dry weight	Initial Dry Density (g/cm^3)	Hydraulic Conductivity (cm/sec)
1	Falling Head - Rigid	10.2	21.6	1.43 (89.2 pcf)	3.0×10^{-4}
2	Falling Head - Rigid	10.2	21.6	1.44 (89.9 pcf)	4.8×10^{-8}
5	Triaxial	7	21.6	1.49 (93.1 pcf)	8.0×10^{-7}
6	Triaxial	7	21.6	1.47 (91.9 pcf)	3.0×10^{-8}
7	Triaxial	7	21.6	1.43 (89.3 pcf)	1.5×10^{-7}
8	Triaxial	7	20.0	Not Measured	1.7×10^{-6}

The final phase of the Treatability Study consisted of numerous types of leaching tests to evaluate the effectiveness of the containment technology in restricting the mobility of metals within the waste material. Stabilized/Solidified samples were subjected to Toxicity Characteristic Leaching Procedure (TCLP) analysis, modified TCLP using synthetic site ground-water, modified TCLP using site ground-water, Synthetic Precipitate Leaching Procedure (SPLP), and modified ANS 16.1 test.

TCLP analysis was performed in accordance with SW 846 Method 1311 except where modifications were noted, (i.e., ground-water used as leachate). Untreated samples were analyzed for TCLP arsenic, cadmium, chromium, lead, calcium, and phosphorus. Lead was found to be the only contaminant exhibiting a toxicity characteristic. The SPLP analysis is similar to the TCLP analysis with the exception that the extraction fluid used is specific to the project location. The SMPCI site is located in the East US region; thus, extraction fluid #1 with a pH of 4.2 was used. Since a relatively impermeable monolith was to be created on-site, the modified ANS 16.1, (MANS) test procedure more closely simulated the actual disposal scenario than the other leachate procedures. The MANS procedure consists of hanging a cylindrical Stabilized/Solidified sample within a known volume of site ground-water and analyzing the leachate at time intervals of up to 90 days. This procedure more closely simulates the monolith siting in ground-water and surrounded by marshes. Table II presents a portion of the analytical results from the final phase of the Treatability Study using the design mix formulation.

The Treatability Study determined that ENTACT's Stabilization/Solidification treatment technology exceeded the performance criteria for hydraulic conductivity, unconfined compressive strength and reduced the leachability of lead to acceptable levels as measured by both the TCLP test and the MANS test. ENTACT found that particle size reduction, addition content and moisture content were critical elements in the success of the stabilization/solidification process. ENTACT holds a patent for the four phosphate/cement blends for the stabilization/solidification of lead impacted material and for the stabilization/solidification equipment used to achieve successful treatment of this material.

TABLE II
TREATABILITY STUDY - LEACHING TEST RESULTS

Sample	TCLP Lead (mg/L)	TCLP Lead Synthetic Site Ground-water (mg/L)	TCLP Lead Site Ground-water (mg/L)	SPLP (mg/L)	AN 16.1 Site Ground-water 7 hours (mg/L)	AN 16.1 Site Ground-water 2 days (mg/L)	AN 16.1 Site Ground-water 4 days (mg/L)	AN 16.1 Site Ground-water 19 days (mg/L)	AN 16.1 Site Ground-water 90 days (mg/L)
Untreated	10.2	0.28	0.16	0.12					
Treated A	2.19	2.06	1.07	1.55	0.013	0.023	<0.005	0.03	0.007
Treated B	2.29	1.44	0.73	0.92	0.017	0.018	<0.005	0.041	0.03
Treated C	1.19	0.80	0.68	0.95	0.008	<0.005	<0.005	0.012	0.02
Treated D	0.10		0.12						
Treated E	0.36		0.15						
Treated F	0.16		0.08						

SITE PERFORMANCE

To date, more than 228,000 tons of material from the SMPCI site have been stabilized/solidified and placed back in the excavation area. With more than 450 treatment quality assurance samples analyzed, hydraulic conductivity has averaged approximately 3.95×10^{-8} cm/sec, Unconfined Compressive Strength (UCS) has averaged more than 45.7 kg/cm^2 (650 psi), and TCLP Lead has averaged less than 0.24 mg/L.

ADDITIONAL STUDIES

SPLP Analysis

In addition to standard performance tests, several additional studies have been conducted to further evaluate the containment properties of this Stabilized/Solidified material. The US EPA National Risk Management Research Laboratory collected and analyzed twenty two treated samples for SPLP lead leachability. Six samples were collected in June 1995, six in July 1995, and two each month from August through December 1995, (See Table III).

SPLP Lead test results were below the TCLP action level of 5 mg/L, with the exception of Sample #175. As the study progressed, the SPLP results trended downward while the pH remained consistent. The downward slope of the SPLP data is due in part to a reduction in the amount of cement used in the Stabilization/Solidification process. The analysis revealed SPLP results as low as 0.13 and 0.15 mg/L lead respectively for the two batches, #289 and #294, collected in December 1995.

TABLE III
STABILIZED/SOLIDIFIED MATERIAL SPLP RESULTS
(Meagher-Harzell, 1996)

Sample Batch #	US EPA SPLP Lead (mg/L)	US EPA pH	Sample Batch #	US EPA SPLP Lead (mg/L)	US EPA pH
99	1.32	12.37	144	3.31	11.93
100	1.29	12.39	163	1.6	12.29
103	1.38	12.41	175	14.9	12.04
105	1.6	12.38	200	0.77	12.39
107	0.94	12.3	201	0.42	12.51
112	1.75	12.43	215	0.57	12.46
139	1.13	12.16	220	0.34	12.44
140	1.38	12.13	240	0.44	12.37
141	2.14	12.23	249	0.71	12.45
142	3.16	12.22	289	0.13	12.15
143	3.08	12.14	294	0.15	12.12

Boutwell Test

An in-situ hydraulic conductivity test for Stabilized/Solidified environmental material was performed at the SMPCI site. The test used to evaluate the hydraulic conductivity of the Stabilized/Solidified material as compacted in the field was the state of the art Boutwell Two-Stage Borehole Field Permeability Test (Boutwell Test). The Boutwell Test was designed to measure the hydraulic conductivity of soils in the field rather than with laboratory procedures. The first stage of the Boutwell Test measures the hydraulic conductivity in the vertical direction and the second stage measures the hydraulic conductivity in the horizontal direction. The test is performed by boring a hole into the treated, placed, and compacted material. The Boutwell Test apparatus is inserted into the bore hole and filled with water to saturate the underlying soil. The apparatus sits flush with the bottom of the bore hole and seals the vertical wall of the hole to prevent the horizontal movement of water during the first stage. After saturation, the rate of water infiltration is measured for 24 hours. With time the rate of water infiltration approaches a limit which is calculated to provide the hydraulic conductivity of the material. The second stage of the test involves drilling a smaller diameter hole through the original boring. The vertical wall of the inner boring remains exposed to allow the horizontal movement of water. The measured water level drop during the second stage is the result of infiltration in both the horizontal and vertical directions. The water level drop is adjusted to compensate for infiltration in the vertical direction based on the vertical hydraulic conductivity developed during the first stage.

BOUTWELL TWO-STAGE BOREHOLE
FIELD PERMEABILITY TEST
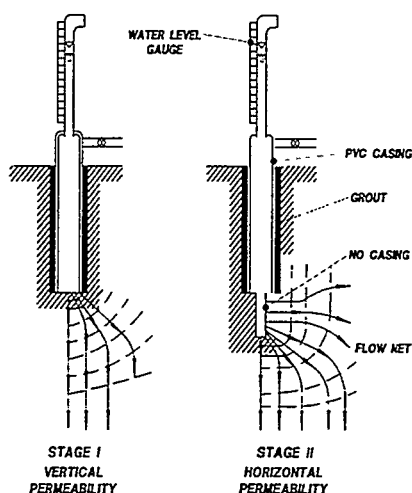
Of the nine locations tested at the SMPCI site, the apparent permeabilities from the first stage of the Boutwell Test were all less than 1×10^{-6} cm/sec except for one location at which a leak was detected. Because the infiltration of water had not reached the steady state condition at the end of the tests, i.e., the hydraulic conductivity was still falling, it is evident that the actual hydraulic conductivity of the material is less than the reported hydraulic conductivity. Due to the time-dependent nature of the physical properties of the stabilized/solidified material, it is very difficult to determine the actual vertical and horizontal permeabilities, since they decrease with the curing time of the treated material. However, the results indicated that the vertical hydraulic conductivity should be lower than 5.1×10^{-7} cm/sec, the mean value of the apparent hydraulic conductivity for the eight locations. An attempt was made to determine a conservative value for the actual hydraulic conductivity using the "Stage One Only" method, and a conservative value of two for the horizontal to vertical hydraulic conductivity ratio. Based on this method, the average vertical hydraulic conductivity for the treated in place material at the SMPCI site is 3.6×10^{-7} cm/sec. (Boutwell, 1995) The hydraulic conductivity results are presented in Table IV.

TABLE IV
BOUTWELL IN-SITU HYDRAULIC CONDUCTIVITY TEST RESULTS
(Boutwell, 1995)

Test	Hydraulic Conductivity (cm/sec)	
	Vertical	Horizontal
FP - 2	3.7×10^{-7}	7.5×10^{-7}
FP - 3	5.1×10^{-7}	1.0×10^{-7}
FP - 4	4.4×10^{-8}	8.8×10^{-7}
FP - 5	1.1×10^{-7}	2.1×10^{-7}
TSB - 1	2.8×10^{-7}	5.7×10^{-7}
TSB - 2	6.2×10^{-7}	1.2×10^{-6}
TSB - 3	3.3×10^{-6}	6.5×10^{-6}
TSB - 4	5.4×10^{-7}	1.1×10^{-6}
OVERALL		
Log Mean	3.6×10^{-7}	7.2×10^{-7}
Std. Dev.	0.519	0.519

CONCLUSION

The Stabilized/Solidified material at the SMPCI Site exceeded all of the performance criteria. The TCLP and SPLP tests were used to evaluate the stabilization process by measuring the leachability of lead in the treated material because TCLP on the untreated sample exceeded the performance criteria. The unconfined compressive strength and hydraulic conductivity tests were used to evaluate the solidification process by measuring physical properties of the treated material.

The Stabilization/Solidification treatment technology that has been used at the SMPCI Site has proven to be a very effective method for containing lead contaminated soils. Stabilized/Solidified material serves the same function as a low hydraulic conductivity layer in a landfill system. The hydraulic conductivity of the Stabilized/Solidified material is comparable to that of a compacted clay liner. The treated material is much thicker than a two-foot thick clay liner. Added thickness to the low hydraulic conductivity material causes an increase in the amount of time water takes to travel from the surface of the containment system to the underlying soil and ground-water. Also, the concern of damage occurring to the low hydraulic conductivity layer during and following installation is alleviated due to added durability resulting from the greater thickness. This Stabilization/Solidification treatment system is an option that may be considered for sites requiring environmental containment and may out perform other technologies.

REFERENCES
Boutwell, Gordon, Two-Stage Field Permeability Tests, October 1995.

Meagher-Hartzell, Evelyn and Jim Rawe, Science Applications International Corporation, *Schuylkill Metals Site Summary Analytical Report*, April 1996.

Chapter 12

Barrier Materials

A CASE STUDY - USING A MULTI-GROUT BARRIER
TO CONTROL ^{90}Sr RELEASE AT ORNL

J. D. Long[1], D. D. Huff[2] and A. A. Naudts[3]

Abstract

During summer 1996, low-pressure permeation grouting was performed inside portions of four unlined, shallow waste disposal trenches at a radioactive waste burial ground that was opened in 1951 at the Oak Ridge National Laboratory (ORNL). The objective was to selectively control sources that release about 25 percent of all strontium 90 (^{90}Sr) discharged from the ORNL complex. A unique grouting methodology was adapted to control interaction of wastes with natural runoff at this humid site. Driven sleeve pipes were injected 4 to 5 times with multiple formulae of type III portland cement-based grouts, ultra fine cement-based grouts, and acrylamide grouts. Multiple-hole grout injection was monitored continuously using real time monitoring equipment. Apparent Lugeon values were calculated during grouting operations and grout formulae were continually adjusted during injection to maximize permeation, durability, and economy. Over 500 m^3 of combined grout types were emplaced. At the completion of production grouting, the effectiveness of grout spread and in situ hydraulic conductivity of the grouted mass were assessed. The average residual hydraulic conductivity measured in more than 20 check pipes was less than 1 x 10^{-6} cm/sec. Hydrologic monitoring has been established to determine the overall effectiveness of the project for ^{90}Sr control.

Introduction

After decades of living with a seemingly insurmountable environmental remediation task, an innovative site investigation provided the basis for cost-effective remediation of a radioactive waste burial ground at ORNL (ORNL 1995). Contamination sources in portions of four existing waste disposal trenches were determined to be responsible for more than 70 percent of the ^{90}Sr leaving the burial ground and about 25 percent of all ^{90}Sr discharged from the ORNL complex. By controlling the contamination sources in these four trench sections (which comprised less than 1 percent of the total site area), about $4 million and 3 years of effort were saved, as compared to other remedial strategies. A unique low-pressure permeation grouting methodology developed by one of the authors (Naudts 1996) was used to control the contamination sources.

The technical objective was to reduce the in situ hydraulic conductivity of the waste disposal trench sections identified as containing ^{90}Sr sources such that groundwater would tend to flow around these sections rather than through them, effectively isolating contamination sources from groundwater flow and reducing the off-site transport of ^{90}Sr. A target average residual (after grouting) in situ hydraulic conductivity of equal to or less than 1 x 10^{-6} cm/sec was established for the waste materials based on the average in situ hydraulic conductivity of the surrounding natural ground being about 1 x 10^{-4} cm/sec (ORNL 1995). It is important to note that the action memorandum (regulatory decision document) did not require a commitment to "encapsulate the wastes."

---

[1]Lockheed Martin Energy Systems, Inc., P.O. Box 2008, Building 1053, MS 6338, Oak Ridge, TN, USA 37831-6338, (423) 574-8656, L5g@ornl.gov

[2]Earth and Engineering Science Division, Lockheed Martin Energy Research, Inc., P.O. Box 2008, Building 1509, MS 6400, Oak Ridge, TN, USA 37831-6400, (423) 574-7859, ddh@ornl.gov

[3]ECO Grouting Specialists, Ltd., 73 Credit Road, Cheltenham, Ontario, Canada LOP 1CO, (905) 838-0150, Alex<ecogrout@passport.ca>

Groundwater and weather conditions dictated that the work be fast-tracked to take advantage of the dry season. Design was initiated in early January 1996 and grouting was completed October 21, 1996. Drilling into the waste materials was prohibited for safety and security reasons. The following paper provides brief background information and an overview of the technical aspects of the project.

Site Conditions

The project site is a 23-acre burial ground for radioactive and industrial wastes at Waste Area Grouping (WAG) 4, southwest of the ORNL main complex in Oak Ridge, Tennessee. The site layout is shown in Figure 1. The burial ground was operated from 1951 until about 1974 and received wastes from DOE sites and DOE contractors from throughout the Southeast. The preponderance of the waste disposal records were destroyed by fire in 1957; consequently, little information was known about the types of wastes, contaminant concentrations, and the boundaries of the waste disposal trenches. Available information suggested that, primarily, solid wastes were disposed at the site. The waste form was highly variable consisting of materials such as absorbent paper, clothing, glassware, scrap metal, dirt, filters, lumber, irradiated piston rings, powders, wire, depleted uranium, carcasses of animals used in biological experiments, transuranic (TRU) wastes, oils, solvents, a few large pieces of equipment, and a small metal building. Some waste materials were buried in metal, wooden, plastic, fiber, or concrete containers; others were dumped into the trenches without containers. Potentially explosive metallic sodium, packaged in metal drums or glass containers, may have been present. The contaminants of concern were ^{90}Sr, ^{137}Cs, ^{60}Co, ^{3}H, U, Th, and TRU isotopes; however, ^{90}Sr was the principal contaminant of concern based on concentration, mobility, and radiotoxicity (Jacobs ER Team 1995).

Figure 1. WAG 4 grouting site layout. (Note: only grouted portions of trenches are shown.)
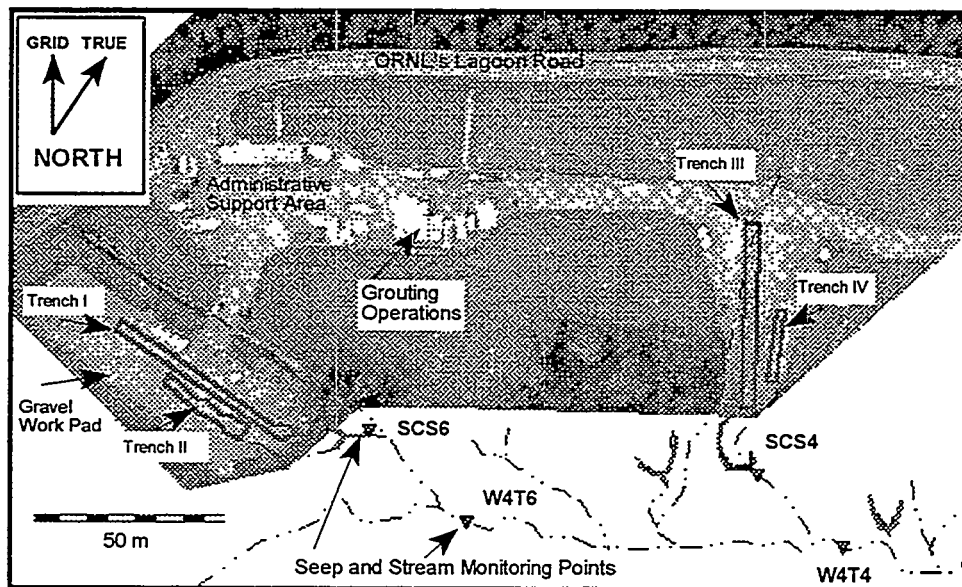
The sections of waste disposal trenches targeted for grouting were about 30 to 53 m long, 2 to 4 m wide, and 4 to 6 m deep. The trenches had been excavated down through residual soils to weathered shale and limestone in an uphill-to-downhill direction and covered with about 1.2 to 1.5 m of loose soil and porous construction debris. No geotechnical information was available; groundwater information was available from the site investigation previously cited (ORNL 1995) and from ongoing groundwater monitoring efforts.

The waste disposal trenches were seasonally inundated by percolating surface water and upwelling groundwater. This water flowed down through the waste materials, collecting contaminants and discharging down hill in the form of contaminated seeps and contaminated groundwater. Numerous seeps were present at the site; however, only a small fraction of the seeps were highly contaminated. At the start of grouting, groundwater levels varied from 0 to about 2.4 m below the existing ground surface (existing means prior to placement of the crushed stone working surface described later).

Grout Materials

Since the waste materials in any particular trench were unknown and potentially highly variable, it was anticipated that the void size amenable to grouting could be highly variable, as well. Also, prior experience has demonstrated that repeated injections of multiple grout formulae are necessary to achieve low in situ hydraulic conductivity (Naudts 1996, SEG in publication). Thus, it was deemed necessary to be able to inject a wide range of different grout types to maximize grout permeation, durability, and economy.

The technical specifications required the grouting subcontractor to be able to batch up to 20 different formulae of type III portland cement-based grouts, up to 5 different formulae of ultra fine cement-based grouts, and 10 to 20 percent solutions of acrylamide grouts. The cement-based suspension grouts contained up to 8 different ingredients: water, cement, bentonite, fly ash, silica fume, natural pozzolan (pumice), dispersing agent/retarder, and viscosity modifier. The grout mixes were specially formulated to repel water, generate low heats of hydration, have zero bleed, have high resistance against pressure filtration, remain mobile (i.e. cohesion less than 100 pa) for 24 hours, and not reach initial set for 72 hours. The low cohesion and delayed set were keys to enabling multiple injections of grout into the same zones of the trenches. A grout formulation/compatibility study was conducted as part of design to establish the desired rheological characteristics of the cement-based suspension grouts and to attempt to simulate accelerated aging of the grouts in the trench fluids. No testing was performed with the acrylamide solution grouts since engineering properties and durability are well documented elsewhere (Karol 1990, Spalding et al. 1986).

Although not investigated during this project, portland cement-based grouts offer an added treatment benefit for certain radionuclides, since the increased pH from grouting yields increased precipitation and sorption of ^{90}Sr. During grouting, reductions in radiation levels within the sleeve pipes and concentrations of radiostrontium in groundwater samples taken from the trenches were observed after just one stage of grouting with portland cement-based grouts.

Method of Grout Injection

Sleeve pipes (or *tube-a-manchettes)* were used to enable the injection of a multitude of grouts in various stages and phases without installing secondary holes. Also, the use of sleeve pipes enabled performance of in situ hydraulic conductivity tests for investigative and verification purposes. Properly installed sleeve pipes offer many advantages over the use of open-ended grout pipes for environmental remediation applications (Huff et al. 1996). Figure 2 shows a schematic of the sleeve pipe specified for this project. Important attributes are the heavy gauge construction and massive steel drive point to allow installation by driving, the injection ports, the rubber sleeves which act as one-way check valves, and the sleeve protector(s) which protect the rubber sleeves during driving.

Preparation for Grouting

As discussed elsewhere (Huff et al. 1996), the most important element of site preparation was covering the trenches with multiple layers of geotextile and crushed stone to create a "clean" working platform and to direct surfacing grout away from the work area.

Figure 2. Sleeve pipe detail. (Note: sleeve pipes were driven to refusal below trench bottom.)
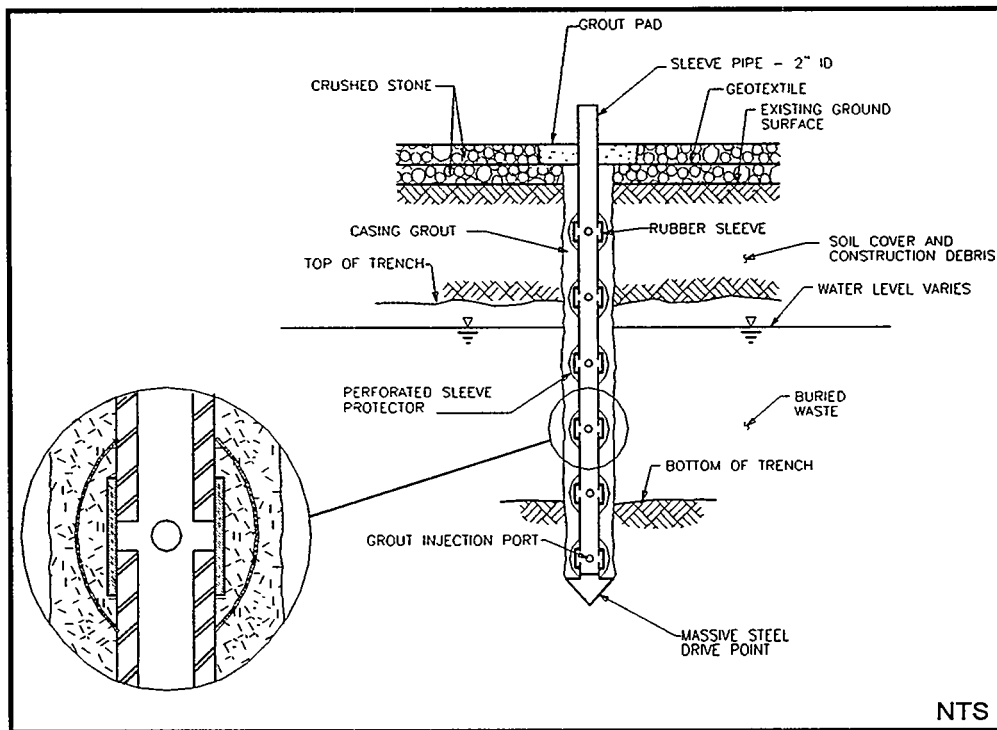
Sleeve pipes and groundwater monitoring wells were installed semi-remotely by driving with a portable, track-mounted, diesel-powered pile driver, using remote controls for operation to avert potential explosive hazards. Figure 3 shows driving of a sleeve pipe in progress. A total of 250 sleeve pipes and over 30 groundwater monitoring wells were installed. Of this total, only 7 additional pipes were installed due to the original pipes encountering obstacles and not reaching full depth.

Figure 3. Sleeve pipe driving in progress.
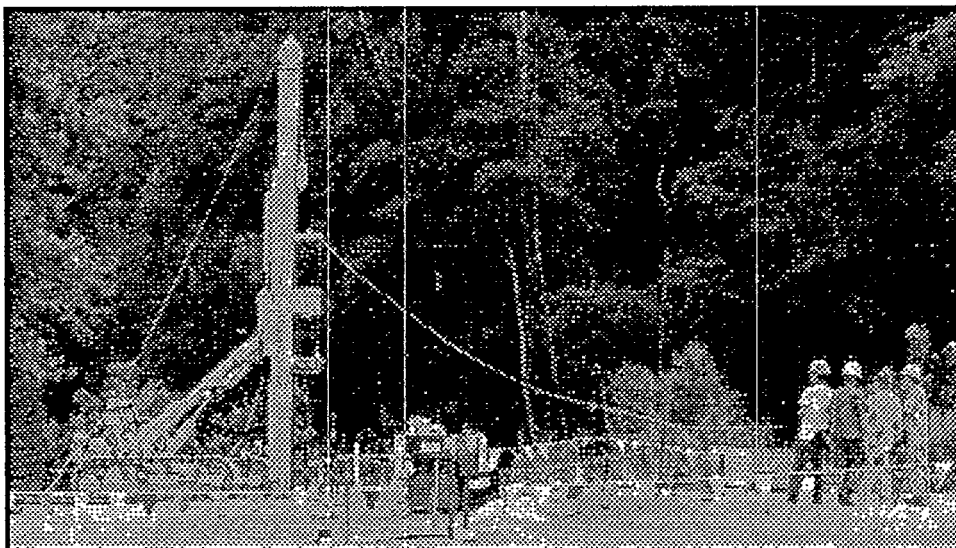
Groundwater samples were collected from the trenches after driving pipes to assess any chemical or radiological changes from breaching containers; no significant changes were noted.

After installation of sleeve pipes and groundwater monitoring wells, grout pads were cast around each pipe to seal the opening made in the ground surface. Using a double packer arrangement, pre-determined quantities of weak, brittle casing grout were injected through each sleeve into the annulus between the sleeve pipe and the subsurface to prevent grout from flowing immediately upward to the ground surface. Upon curing, the casing grout at selected sleeves was cracked by applying water pressure to provide access out of the sleeve pipe to the subsurface. Subsequently, initial in situ hydraulic conductivity tests (or water tests) were performed to measure permeability and further test for large voids prior to grouting. Since the hydraulic conductivity (permeability) is related to void sizes in the subsurface target volume, this information was used to determine the starting grout mixes and the amenability of the subsurface to the grout formulations. [For a detailed discussion on amenability theory and water testing refer to Naudts (1996)]. This step was critical, since no other geotechnical information was available for the waste materials. For the most part, the test results indicated that the initial in situ hydraulic conductivity was very high (1×10^{-1} cm/sec or higher) and that the waste materials were amenable to starting mixes using portland cement-based grouts. Installation of casing grout and initial water testing were also performed semi-remotely.

Grouting

Following completion of initial in situ hydraulic conductivity testing for a given trench section, production grouting activities began at the downhill end of each targeted trench section and progressed up hill pushing groundwater ahead of the grout front. Figure 4 shows grouting operations in progress. By starting grouting at the downhill end of the targeted trench section, it was possible to contain grout spread (it did not run uncontrolled down hill in the trench). But most importantly, this grouting sequence greatly reduced dewatering requirements and the potential for pushing groundwater up into the work zone. Only groundwater which was displaced upward and out of the groundwater monitoring wells and sleeve pipes with failed sleeves (less than 15 percent of sleeve pipes had leaking sleeves after driving), was pumped out of the trench during grouting. We were required to collect and treat surfacing groundwater. A total of about 76 m³ of combined flush water and groundwater were collected and treated during the course of the project. At Trenches I, III, and IV, the grouting program was started at mid-trench locations. Bulkheads were built with thixotropic, low-sag grout to keep subsequent grout injections from flowing down hill by gravity.

Figure 4a and 4b. Grouting plant operations and delivery to target area via sleeve pipes.

(a)   (b)

Grout injection pressures and flow rates were monitored using real time data collection/display

575

equipment. Apparent Lugeon values (ALVs) (Naudts 1996) were calculated throughout the grouting program by treating the entire grouting operation as an extended hydraulic conductivity test using grout as the test fluid. By comparing the initial in situ hydraulic conductivities of the formation with the ALVs, grout formulae were continually adjusted, specifically rheology, solids content, and particle size, to place the most competent grout with the highest possible solids content in the subsurface target volume. Calculation of ALVs enabled quick response to the subsurface for a specific grout formulation. If the ALV remained constant, the grout's solids content was increased while adjusting its rheology. Depending on the formation's response to the adjustments, a change to ultra fine cement-based suspension grouts was made, when the decrease in ALV could not be reached with regular cement-based grouts.

Grout injection quantities were continuously compared to estimated theoretical quantities of grout take. As stated earlier, during injection of the cement-based suspension grouts, changes were made to the grout formulations based on the ALV trend. This increased the likelihood that the quantity of grout required to fill the "theoretical grout cylinders" around the grout pipes was injected. If the reduction in ALV was too fast to allow construction of the "theoretical grout cylinder," a reduction in viscosity, thixotropy, and/or solids content was made. A combination of hydro-fracturing and permeation grouting was utilized during acrylamide grouting to maximize treatment of the waste materials.

Grouting was conducted in multiple holes simultaneously, with multiple injections made into the same zone of waste. Each sleeve was injected at least twice with type III portland cement-based grout, subsequently with ultra fine cement-based grout, and finally with acrylamide grout. At each successive stage, the ALVs decreased and the grout volumes accepted by the media became smaller, as the overall permeability of the treated zone gradually decreased.

The total theoretical trench volume grouted was about 1000 m^3. A total of 34 m^3 of casing grout, 370 m^3 of type III portland cement-based grouts, 65 m^3 of ultra fine cement-based grouts, and 51 m^3 of acrylamide grouts (10 percent solution) were injected, corresponding to about 50 percent of the estimated total trench volume. Remarkably, the total injected quantity of grouts was within 10 percent of the total estimated quantity. The total void volume was estimated to be about 40 percent.

Verification

Upon completion of grouting operations for each trench, the residual in situ hydraulic conductivity of the grouted waste materials was measured through check pipes (sleeve pipes that were installed prior to grouting, but not used for production grouting), using a permeameter attached to the grout packers. Testing theory was based on earlier work by Cambefort and Naudts (Naudts 1996). Equipment and testing procedures were specially developed for this project. Average (calculated statistically as a geometric mean) residual in situ hydraulic conductivity measured in 23 check pipes was 0.90×10^{-6} cm/sec. Measured values ranged from 1.0×10^{-7} cm/sec to 1.5×10^{-5} cm/sec. Twenty-two of the twenty-three measured values were on the order of 10^{-6} cm/sec or less.

Hydrologic monitoring (of flow and ^{90}Sr concentration) is being performed to assess the effectiveness of grouting in reducing ^{90}Sr transport. Pre- and post-treatment relationships of flow vs. concentration are being compared. Grouting is expected to reduce ^{90}Sr release at White Oak Dam, the final discharge point for the ORNL complex, 20 percent from pre-treatment conditions, although, it may take 10 years to reach that level.

Conclusions

Professionally executed, low-pressure permeation grouting is a powerful method of source control for solid low-level radioactive wastes in burial trenches. Hydrologic monitoring is being performed to evaluate the overall effectiveness of grouting in reducing the off-site transport of ^{90}Sr.

The multi-phase, multi-stage, low-pressure sleeve pipe grouting process, utilizing a multitude of portland and ultra fine cement-based suspension grouts, in conjunction with acrylamide solution grouts, was successful in dramatically reducing the in situ hydraulic conductivity of trenches filled with a myriad of radioactive and other wastes of an unknown nature. With proper engineering controls, the work can be performed safely without environmental insult and with generation of only small volumes of wastes.

In spite of the fact that no secondary grout pipes were placed, the average residual in situ hydraulic conductivity of the materials in the trenches, as measured through more than 20 check pipes, was reduced to less than 1×10^{-6} cm/sec. The ability to achieve this low target value is believed to be primarily due to the application of repeated injections of multiple grout formulae into the same zones of the trenches, application of advanced engineering principles such as the apparent Lugeon theory, tight monitoring/direction of the grouting program, and proper quality control. Also key to the success of the grouting program were the use of cement-based suspension grouts with delayed set times which made it possible to inject the same zones of the waste disposal trenches multiple times before the grout reached initial cure. Finally, the use of sleeve pipes reduced potential exposure of workers to contaminants, provided the vehicle for multiple injections of grouts, and enabled hydraulic verification of the end product without drilling into the waste materials. Having been left in place, the sleeve pipes can be re-accessed in the future for hydrologic evaluation and remedial grouting, if needed.

The total project cost, including engineering, construction management, site preparation, waste management, etc. is projected to be about $4 million.

References

Huff, D., J. Long, and A. Naudts. (1996) Radwaste source control by surgical strike - a cost-effective strategy. *Radwaste Magazine*, 3 (6), 20-26.

Jacobs ER (Environmental Restoration) Team. (1995) *Engineering Evaluation/Cost Analysis for Waste Area Grouping 4 Seeps*, DOE/OR/02-1490&D2, Oak Ridge, Tennessee.

Karol, R. (1990) *Chemical Grouting Second Edition, Revised and Expanded*, Marcel Decker, Inc., New York.

Naudts, A. (1996) Grouting to improve foundation soil. In *Practical Foundation Engineering Handbook (ed. R. W. Brown)*, pp. 5.277-5.400. McGraw-Hill Book Co., New York.

ORNL. (1995) *Site Investigation Report for Waste Area Grouping 4 at Oak Ridge National Laboratory, Oak Ridge, Tennessee*, ORNL/ER-329, Oak Ridge, Tennessee.

ORNL. (1995) *Supplement to a Hydrologic Framework for the Oak Ridge Reservation, Summary of Groundwater Modeling*, ORNL/TM-12191, Oak Ridge, Tennessee.

SEG (Scientific Ecology Group). (in publication) *Grouting of Simulated Radioactive Waste Trench at SEG Site in Kingston*, TN, ORNL/ER-387, Oak Ridge, Tennessee.

Spalding, B., S. Lee, C. Farmer, and L. Hyder. (1986) *Demonstration of In Situ Immobilization of Buried Transuranic Waste Using Acrylamide Grout*, RAP86-69, Oak Ridge, Tennessee.

EFFECT OF DILUTION AND CONTAMINANTS ON STRENGTH AND HYDRAULIC CONDUCTIVITY OF SAND GROUTED WITH COLLOIDAL SILICA GEL

Peter Persoff[1], John Apps[1], George Moridis[1], and Joyce M. Whang[2]

INTRODUCTION

Colloidal silica (CS) is a low-viscosity liquid that can be made to gel by addition of brine. This property allows it to be injected into, or mixed with, soil, so that after gelling the colloidal silica blocks the pore space in the soil and forms a barrier to the flow of contaminated groundwater or non-aqueous liquids (NAPLs). Gelled-in-place CS was first studied for the petroleum industry (Jurinak et al., 1991, Seright 1993) and later for protecting groundwater quality (Yonekura et al 1992, 1993, Noll et al. 1992, Persoff et al. 1994, 1995, Moridis et al. 1996). Noll (1992) investigated the use of colloidal silica diluted so that its solids content was reduced from 30% (a typical nominal value for material as delivered) to values as low as 5%. The more dilute colloids could still be made to gel, although more slowly, and the resulting gel was weaker. Because the proposed application of colloidal silica grout involves emplacing it in the subsurface by permeation, jet grouting, or soil mixing where its role as a barrier will be to resist flow of contaminants, the effects of these contaminants on the properties of the grouted soil is also of interest.

This work comprised four tasks. In Task 1, samples of grouted sand were prepared with a range of CS dilutions, for measurement of hydraulic conductivity and unconfined compressive strength. In Task 2, these properties were measured on samples of grouted sand that incorporated 5% volumetric saturation of NAPLs. In Task 3, samples, prepared without any contaminants, were immersed in contaminant liquids and tested after 30 and 90 days.

Task 4 was added because NAPL contamination in the samples of Tasks 2 and 3 impelled modifications in the test methods, and comparison of the results of Task 2 and Task 1 suggested that these modifications had introduced errors. In Task 4, samples were tested both ways, to confirm that in Tasks 2 and 3 strength was underestimated and hydraulic conductivity was overestimated. Despite the existence of these known systematic errors, the inclusion of control samples in Tasks 2 and 3 permits conclusions to be drawn from these data.

MATERIALS
The CS used in this work was DuPont Ludox SM, with 29.5 weight percent silica. The sand was Monterey #0-30 sand, a silica sand. Brines were made from distilled water and reagent NaCl, and distilled water was used for dilutions. pH adjustment was done by titration with concentrated HCl.

METHODS

SAMPLE PREPARATION
Task 1: Uncontaminated Monterey sand grouted with five dilutions of CS.
First the grout was prepared and then it was combined with the soil or sand in a mold to make each sample. The CS was first diluted from its as-received silica concentration of 34.3 wt % with distilled water. For grouts that required pH adjustment, the pH was then lowered to approximately 8.5 by titration with concentrated HCl. Next, NaCl brine was added with constant swirling of the diluted colloid, and final pH adjustment was done. pH adjustment was done in two stages to minimize the time needed to adjust pH after the brine was added.

[1]Earth Sciences Division, Lawrence Berkeley National Laboratory, Berkeley, CA 94720, (510) 486-5931, persoff@lbl.gov; (510) 486-5193, jaapps@lbl.gov; (510) 486-4746, gjmoridis@lbl.gov.

[2] Du Pont Central Research and Development, Jackson Laboratory, J-24 Chambers Works, Deepwater, NJ 08023, (609) 540-4275, whangjm@a1.jlc.umc.dupont.com

Three hundred forty g of sand and 78 mL of grout were mixed to fill each 5 cm diameter x 10 cm long (2 x 4 inch) cylinder mold. The bottoms of the plastic cylinder molds were removed and replaced by caulked-on lids; this allowed the samples to be slid out of the molds for testing. To prepare each sample, the liquid grout was poured into the mold, and the pre-weighed sand was poured slowly into the liquid while gently shaking the mold to settle the sand. These amounts of sand and grout were found to fill the mold without excess liquid or solid.

Table 1. Formulae for Task 1 samples.

Volume liquid per sample (mL)	Volume colloid per sample (mL)	Silica concentration after dilution (wt %)	Added brine [NaCl], Molarity	volume brine per sample (mL)	final [NaCl], Molarity	volume distilled H$_2$O	mass sand per sample (g)	final pH
78	13	4.9	1.8	13	0.3	52	340	6.95
78	20	7.4 [a]	1.2	13	0.2	46	340	6.95
78	26	9.8	1.2	13	0.2	39	340	6.48
78	52	19.7[a]	0.6	26	0.2	0	340	10 (not adjusted)
78	71.5	27.0	1.2	6.5	0.1	0	340	10 (not adjusted)

[a] these formulae also tested in Tasks 2 and 3

Task 2: Monterey sand, contaminated with NAPL, grouted with two dilutions of CS.

The data of Wilkins *et al.* (1995) suggest that in the NAPL-contaminated unsaturated zone of sandy soil, volumetric saturation of water and NAPL are typically 10 and 5 % of pore space. Samples for Task 2 were made as for Task 1a, except that the sand was prepared by addition of first water, and then NAPL, to produce these saturations in the sand before the sand was poured into the mold. The dilution water in the grout was reduced to compensate for the water pre-added to the sand. Three NAPLs were used in this task: C$_2$Cl$_4$ (perchloroethylene, PCE), CCl$_4$, C$_6$H$_5$NH$_2$ (aniline). Samples were also prepared with 10% water saturation and no NAPL.

Task 3: Uncontaminated Monterey sand grouted with two dilutions of CS, immersed in contaminants.

Samples were prepared as for Task 1, and then immersed in one of nine liquids: the three NAPLs, water saturated with each of the three NAPLs, water saturated with an equimolar mixture of the three NAPLs, HCl diluted to pH 3, and distilled water.

TEST METHODS
Measurement Of Unconfined Compressive Strength.
Unconfined compressive strength was measured by ASTM C-39-86, using a loading rate of 50 lb./min. In this test, flat and parallel sample ends are assured by capping the ends. For Task 1, the samples were capped with Cylcap sulfur mortar, according to ASTM C-617-72 To avoid exposing personnel to NAPLs during the capping and testing, different capping and testing procedures were used for Tasks 2 and 3. Hydrostone, a gypsum plaster, was used so that the capping could be done in a hood without exposing the samples to heat. Also, after capping, the samples were enclosed in zip-lock plastic bags and tested in the bags.

Measurement Of Hydraulic Conductivity.
Hydraulic conductivity was measured in a flexible wall permeameter by ASTM D-5084, at a net confining pressure of 207 kPa (30 psi). As with the strength measurements, safety considerations required that the technique be modified for Tasks 2 and 3. Sample preparation was designed to prevent the latex membrane from contacting the solvent and also to prevent any evaporation of the solvent. To prevent the latex membrane from contacting the solvent, 0.076-

mm (0.003-inch-) -thick Teflon sheet, (Boart Longyear, Salt Lake City) was wrapped around the sample with a 1-cm overlap, held in place with vacuum grease. More details are presented elsewhere (Persoff *et al.* 1997).

RESULTS

Task 1: Effect of dilution on strength and hydraulic conductivity
The compressive strength and hydraulic conductivity of Monterey sand grouted with CS are shown in **Figure 1.** The sample consolidates to some degree during measurement of hydraulic conductivity under 207 kPa (30 psi) confining pressure. The volume of each sample was measured both before and after measurement of hydraulic conductivity, and finally the total solids were determined by drying the sample. From these data the dry density and (assuming a density value for the solids) the porosity before and after consolidation was calculated. These porosity data are shown in **Figure 2.** The difference between the initial and final porosity is a measure of sample consolidation that occurs when the sample is subjected to the confining pressure; the confining pressure caused minimal consolidation of the grouted Monterey sand.
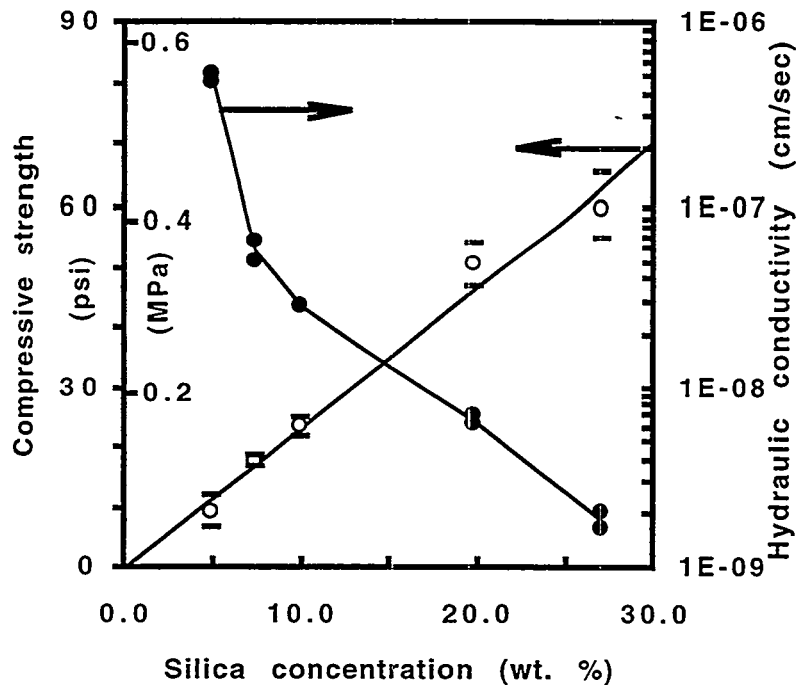
Figure 1. Compressive strength and hydraulic conductivity of samples of Monterey sand grouted with various dilutions of Ludox SM. Error bars are standard deviation of five strength measurements; duplicate hydraulic conductivity measurements are shown. The strength line is a least-squares fit, not forced through the origin.

Tasks 2 and 3: Effect of inclusion of NAPLs on strength and hydraulic conductivity.

The results of measurements on Task 2 and 3 samples are shown in **Tables 2 and 3.**

DISCUSSION

Strength of Task 1 samples.
Figure 1 shows that as the silica content of the grout is reduced by dilution, the strength of the sample decreases and the hydraulic conductivity increases. The Monterey sand itself is not cohesive, and any strength results from the cementing effect of the grout, which increases

linearly with the amount of silica in the grout. This suggests that the colloidal particles bond not only to each other but also to the silica surface of the sand.

The strength of sand grouted with colloidal silica and sodium silicate-glyoxal grouts was investigated by Yonekura and Miwa (1993). They found that the strength of sand grouted with colloidal silica was independent of gel time in the range 10 sec - 1 hr, and continued to increase during 1000 days of aging. Tested at 100 days, the strength was 95 psi, and the ultimate strength was more than twice that.
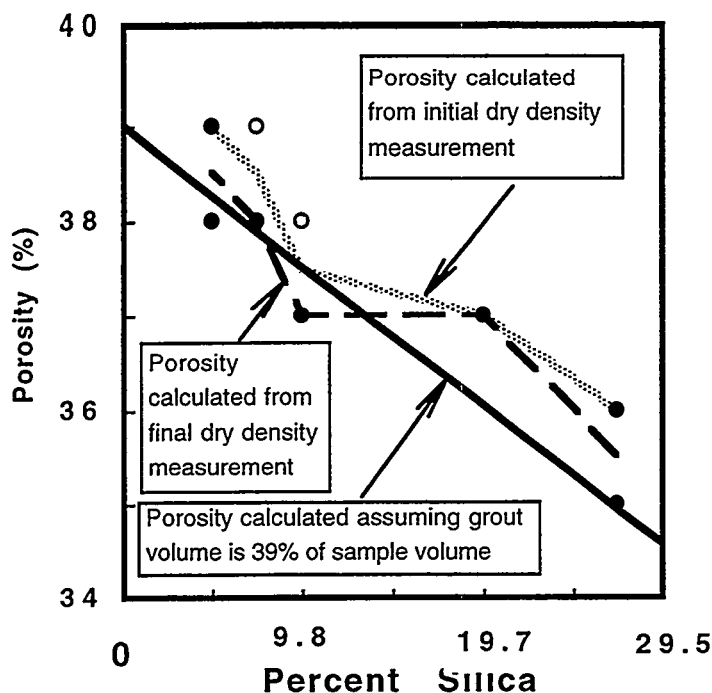
Figure 2. Porosity of Task 1 samples before and after consolidation.

Table 2. Compressive strength and hydraulic conductivity of samples of Monterey sand, contaminated with NAPLs and grouted with two dilutions of CS (Task 2).

percent silica	contaminant	unconfined compressive strength (kPa)		hydraulic conductivity (cm/sec)	
		mean of 5	std. dev	mean of 2	difference between 2
7.4	PCE	149.9	8.14	3.30E-07	1.00E-07
	CCl$_4$	129.3	8.96	7.95E-07	3.10E-07
	aniline	129.7	10.7	2.80E-07	1.00E-07
	water	128.0	9.03	2.55E-07	1.50E-07
19.7	PCE	273.9	15.4	1.35E-08	1.00E-09
	CCl$_4$	296.3	21.7	4.25E-08	2.10E-08
	aniline	236.3	20.8	1.33E-08	7.50E-09
	water	295.9	36.0	2.40E-08	1.60E-08

Table 3. Unconfined compressive strength (kPa) of samples immersed in various liquids (Task 3).

percent silica	not immersed (Task 1)		immersion liquid	30 day immersion		90 day immersion	
	mean of 5	std dev		mean of 3	std dev	mean of 3	std dev
7.4	123.9	7.24	water	181.8	17.6	165.7	4.76
			PCE	186.9	13.9	168.2	8.55
			CCl$_4$	170.9	17.5	169.0	2.90
			aniline	93.29	18.1	116.3	3.10
			water s/w PCE[b]	189.3	10.5	179.6	12.6
			water s/w CCl$_4$	201.5	12.1	169.8	10.8
			water s/w aniline	161.3	1.10	138.2	23.2
			water s/w mix of 3	174.5	14.0	170.1	6.55
			pH 3	166.1	11.1	155.8	6.55
19.7	349.6	26.4	water	492.0	21.2	533.8	55.4
			PCE	493.8	6.55	567.3	6.14
			CCl$_4$	499.7	3.38	535.1	11.1
			aniline	327.0	41.7	355.6	27.5
			water s/w PCE	456.9	38.2	533.3	29.6
			water s/w CCl$_4$	463.8	19.8	553.0	33.8
			water s/w aniline	497.5	41.5	413.4	22.1
			water s/w mix of 3	501.5	38.1	587.1[a]	0.00[a]
			pH 3	531.9	24.3	601.4[a]	2.21[a]

[a] mean and difference between two samples.

[b] s/w = saturated with

Hydraulic conductivity of Task 1 samples.

The hydraulic conductivity of the grouted sand or soil is the principal property of interest. Generally a value of 10^{-7} cm/sec is taken as the criterion for acceptable barrier material. The data in Figures 3 and 4 show that this criterion is met by all the samples made with at least 7.4 % silica. This number represents therefore the lower limit for dilution of Ludox SM for use as a barrier material.

Figure 1 shows a strong effect of the silica concentration on the permeability of the Monterey sand samples. The hydraulic conductivity of the grout in these samples was unaffected by consolidation. The sand grains themselves are effectively impermeable and the measured hydraulic conductivity can be understood to represent the hydraulic conductivity of the gelled Ludox SM itself, multiplied by a factor of approximately 0.38, representing the volume fraction of the sample occupied by gelled grout.

The relationship between silica concentration and hydraulic conductivity can be explained, at least qualitatively, by considering the structure of the gelled grout. By volume, the gelled grout is mostly water, and the space between the gelled chains of silica particles constitutes a network of pores through which water can flow. The low value of hydraulic conductivity results from a highly divided flow path with many small pores. At 27.0 % silica the grout is (100 - 27.0/2.65) = 90% water by volume, and at 7.4 % it is about 97% water. This 8 % increase in flow area is too small to

account for a 30-fold increase in the hydraulic conductivity. Flow resistance results from viscous drag on water as it flows through a tangle of chains of gelled particles. Increasing the silica concentration by a factor of (27.0/7.4)=3.67 reduces the space between chains. This space between chains may be considered as a measure of the effective radius of pores. Approximate the pores as Hagen-Poiseuille flow in parallel tubes: for fixed pressure gradient and viscosity, the flow through each tube is proportional to the fourth power of the radius. Flux, or Darcy velocity, is thus proportional to the square of the radius. While the geometry of the system is not defined well enough to permit actual calculation of the change in permeability, the effect of reduced friction drag by chains of silica particles can account for the increase in permeability.

Effects of test-method modifications for Tasks 2 and 3

Three groups of samples included in Tasks 1, 2, and 4 were tested by both unmodified and modified methods. Matched data in Table 4 show that the samples of Tasks 1 and 2, identical in composition but differing in the test method, gave different results. This suggested that the modifications (introduced because of NAPL contamination) had the effect of increasing the measured hydraulic conductivity and decreasing the measured strength. To confirm this, in Task 4, additional samples were prepared without contamination, and tested by both methods. The results of these tests are summarized in Table 4.

Table 4 shows that the modified test method for strength causes an underestimate of strength, but only for the stronger samples (19.7 and 27.0 % silica). This is reasonable because the requirement for the capping compound is that it not fail before the sample. Similarly, (although here the small number of samples makes the conclusion less certain) the use of Teflon sheet caused an overestimate of the hydraulic conductivity. In the light of these results, we caution that the results of Tasks 2 and 3 can be interpreted only to determine the effects of inclusion or immersion in contaminants *relative to the water control.*

The use of Teflon sheet or tape (with some variation as to materials and method of wrapping) to protect latex membranes appears to be the standard method for preparing contaminated samples for ASTM D-5084 (Daniel and Trautwein, 1994). In Task 4 (Table 4), we treat the overestimate in hydraulic conductivity as an additive factor representing a parallel flow path. For a 5-cm diameter sample (and at 200 kPa confining pressure) this wall effect is equivalent to 3.4E-8 or 3.0E-8 cm/sec hydraulic conductivity. This degree of error becomes significant when measuring samples as tight as these.

Table 3 shows that samples gained strength during the immersion, except for samples immersed in aniline and water saturated with aniline. In that sense, immersion in aniline weakened the samples.

Table 4. Comparison of values measured with modified and unmodified test methods.

Property	% silica	ASTM	Task 1 not modified			Task 2 modified			Task 4 not modified			Task 4 modified		
			n	mean	s**	n	mean	s**	n	mean	s**	n	mean	s**
Unconfined compressive strength(kPa)	7.4	C-39	5	123.9	7.24	5	128.0	9.0						
	19.7	C-39	5	349.6	26.4	5	295.9	36.0						
	27.0	C-39	5	416.4	35.1				4	416.1	18.6	3	367.5	9.7
Hydraulic conductivity (cm/sec)	7.4	D-5084	2	4.95E-08	1.7E-08	2	2.55E-07	1.5E-07						
	19.7	D-5084	2	6.65E-09	7.0E-10	2	2.40E-08	1.6E-08						
	27.0	D-5084	2	1.9E-9	0.4E-9				1	5.0E-9		1	3.9E-8[a]	

a after this measurement, the sample was remeasured using the unmodified method, and hydraulic conductivity was 9E-9 cm/sec.
**standard deviation, or difference between 2 measurements

CONCLUSIONS

1. The unconfined compressive strength of sand grouted with Ludox SM is proportional to the concentration of colloidal silica particles, up to a maximum of approximately 400 kPa (60 psi).

2. The hydraulic conductivity of sand grouted with Ludox SM decreases with increasing concentration of colloidal silica particles. For silica particle concentration greater than 7.4 % by weight , the hydraulic conductivity is less than 1.0×10^{-7} cm/sec; that is, it meets the generally accepted criterion for a barrier material. In this range, the log of hydraulic conductivity decreases approximately linearly with increasing concentration of colloidal silica particles.

3. Monterey sand provided a skeleton to prevent consolidation of grout under confining pressure. Under these conditions measured k is therefore a function of the grout, and variation of k with Si content can be explained on the basis of flow through a network of Si chains.

4. Samples immersed in water continued to gain strength for 95 days. Immersion of samples for up to 95 days in aniline, or in water saturated with aniline, weakened the samples. Immersion for up to 95 days in the other test liquids (PCE, CCl_4, water saturated with these NAPLs, water saturated with the mixture of 3 NAPLs, and HCl diluted to pH 3) had no statistically significant effect, i.e., they gained strength during 95 days of immersion the same as those immersed in water.

ACKNOWLEDGMENT

REFERENCES

Daniel, D.E. and Trautwein, S.J., Eds., Hydraulic Conductivity and Waste Contaminant Transport in Soils, ASTM STP 1142, American Society for Testing and Materials, Philadelphia. 1994

Jurinak, J.J. and Summers, L.E. "Oilfield Applications of Colloidal Silica Gel", Society of Petroleum Engineers Reservoir Engineering, Nov. 1991, 406-412.

Noll, M.R. Bartlett, C. ,and Dochat, T.M. "In Situ Permeability Reduction and Chemical Fixation Using Colloidal Silica," Proceedings of the Sixth National Outdoor Action Conference on Aquifer Restoration, May-11-13 1992, Las Vegas, NV, sponsored by National Ground Water Assn.

Persoff, P. Moridis, G.J. Apps, J.A., and Whang, J.M. Effect of dilution and contaminants on strength and hydraulic conductivity of sand and soil grouted with colloidal silica gel, manuscript in preparation, 1997

Persoff, P. Moridis, G.J. Apps, J.A., Pruess, K. and Muller. S.J. Designing Injectable Colloidal Silica Barriers For Waste Isolation at the Hanford Site, in Proceedings, 33rd Hanford Symposium on Health and the Environment, -- In-Situ Remediation: Scientific Basis for Current and Future Technologies, Part 1, p. 87-101, Pasco WA Nov 7-11 1994 (Lawrence Berkeley Laboratory report LBL-35447)

Persoff, P., S. Finsterle, G.J. Moridis, J. Apps, and K. Pruess, "Injectable barriers for waste isolation," AIChE Symposium Series, vol. 91, no. 306,58-67, 1995. (Lawrence Berkeley Laboratory report LBL-36739).

Seright. R.S. Reduction of Gas and Water Permeabilities Using Gels. Presented at Society of Petroleun Engineers Rocky Mountain Regions Low Permeability Reservoirs Symposium , Denver CO April 12-14, 1993 (SPE 25855).

Sydansk, R.D. "A Newly Developed Chromium (III) Technology," Society of Petroleum Engineers Reservoir Engineering, Aug 1990, 346-352.

Wilkins, M.D., Abriola, L.M., and Pennell, K.D. "An experimental investigation of rate-limited nonaqueous phase liquid volatilization in unsaturated porous media: Steady state mass transfer," Water Resources Research 31(9) 2159-2172, (1995).

Yonekura R. and Kaga,M. "Current Chemical Grout Engineering in Japan" Grouting, Soil Improvement, and Geosynthetics, Geotechnical Special Publication No. 30, American Society of Civil Engineers, 1992, 725-736.

Yonekura R. and Miwa, M. Fundamental properties of Sodium Silicate Based Grout. Eleventh South East Asian Geotechnical Conference , Singapore, May 4-8, 1993.

Application of Soil Barriers for Encapsulation of Contaminants Using Special Blocking Materials and Sealing Technologies

by Hans-Jürgen Kretzschmar, DBI Gas- und Umwelttechnik GmbH Freiberg, Germany;
Istvan Lakatos, Hungarian Academy of Sciences, Miskolc - Egyetemvaros, Hungary

1   Remediation Task

Soil contaminations are ground water contaminations in most cases in Germany. Therefore, environmental pollution will be mobilized and increased. Soil contaminations are existin below nonthighted old waste disposals, below industrial plants of the chemical, energetical and metallurgical industry, and below fuel stations.

The exploration of environmental damages in Germany has proven thousands of such soil pollutions endangering surrounding soil and water. If an immediate remediation of soil by lifting out is not possible, because pollution is layering too deep (f.e. 50 m) or the area is built on, encapsulation of the contamination area and its isolation from ground water flow is necessary.

Soil and water compatible blocking materials and reliable technologies for penetration of impermeable substances are preconditions of successful encapsulation. Scientific-technical research in both methods has developed practical useable methods following these principles:

- Treated soil zone has to be made impermeable by blocking material that prevents convective or diffusive transport of contaminants
- Blocking materials are resistant over a long time against chemical, microbiological, hydraulic, mechanical and radioactive attacks, and are water neutral
- Encapsulation technologies are characterized by simple and economical handling under field conditions.

Montanwax-dispersion, in most cases, and Polymersilicate-solution, in a few cases, are used as blocking materials in developed and short characterized technologies.

2   Blocking Material Montanwax

Montanwax is comparable in a chemical sense with recent plant waxes. It is recovered from a special location of Middle Germany brown coal mining, extracted from the coal, and produced to a pumping dispersion. A brown coal seam including bright Montanwax layers is shown in fig. 1.

Montanwax is a natural stable material existing for about 30 million years under aerobic and inaerobic conditions in soil.

This water neutral natural product has to adapt for the specific application cases by special recipes. Its base properties have been proven satisfactory by the results in table 1, characterizing it as a suitable blocking material.

Montanwax-dispersions are used pure as blocking material, but they can also adapt to mixture with inorganic substances (mineral solids) as an application.

3   Encapsulation Technologies

The following methods for tightening are in practical application:

- Injections through wells to create vertical and/or horizontal impermeable barriers, using normal or high pressure
- Slit walls with mud cake on walls and tight fill in soil
- Surface sealing as sealing and covering layer by casting or spraying
- Well filled with coiled tubing.

3.1 Well Injections

The simplest technology is pore volume filling injection by overhydrostatic but underpetrostatic displacement pressure to penetrate the soil pores by Montanwax.

However universal technology is jet grouting at high pressures to 50 MPa in maximum, 10 - 20 MPa in average. The scheme of boreholes and injecting is shown in fig. 2. After drilling of each injection well in predesigned tracks, drill-pipes are returned and jets cut the soil in two sections of 2 to 3 m length. Soil and Montanwax injection mud are mixed in the left and right sections, forming the impermeable layer.

High pressure injection is suitable for most soil types, especially in fine and middle sands with small pores. Wells can reach a length of 1000 m and a depth of 300 m. At present, jet grouting in deviated wells is the only applicable method for the post tightening of old waste disposals and for encapsulation of soil pollutions in built on areas.

Tightness of the sealing zone can be controlled by geoelectrical and geohydraulical measurements or by special control wells below, or behind, the sealing zone.

3.2 Slit Walls

A mud filled soil slit is produced by the method of continous slit cutting (fig. 3). Segments of serial slit sections form the slit of desired length. On each slit wall, mud cakes are growing up to 6 cm thick forming vertical sealing layers against ground water flow.

Montanwax in the cake acts as an impermeabilizer and chemical stabilizer. The slit itself is filled up by removed soil mixed with Montanwax on the surface with special mixing equipment. By this method, a stable slit wall is constructed with a maximum thickness of 1 m. The continuity of the wall is controlled during the slitting process.

The maximum depth of the slit wall is about 100 m.

Special field equipment was developed for continuous cutting if vertical barriers are only constructed. In high populated areas, this technology is not applicable.

3.3 Surface sealing

Rain flushes out contaminants from soil and transports them by ground water. The same process occurs on mining slopes, including dangerous substances. The wind is able to blow out and to transport dry contaminated soil particles from mud and waste disposals. In these cases, the contamination areas or the slopes, are covered watertight and windtight as shown in fig. 4.

Montanwax-dispersion is adapted to the special soil type achieving the highest sealing effect. Montanwax-dispersion or mixture is sprayed on the surface area by pumps and flexible tubes, or by heliocopters in repeated fly overs. The sealing layer is relatively thin using this equipment. A sealing and covering layer with the thickness to 0,5 m is producible by means of conventional building site equipment, similar to the construction of cement layer. In this case, mixing equipment for Montanwax and on site soil is used.

4 Application Cases

Typical field examples of these technologies are demonstrated.

4.1 Base Sealing below Tar Basin

Residuals of German brown coal industry (tars, muds) were disposed previously in open soil basins without presealing the basin. At present the contaminants penetrate the soil to the ground water layer.

Below this basin, an impermeable barrier was injected through horizontal wells at high pressure by the FLOWMONTA process. Fig. 5 shows the used FLOWMONTA drilling injection equipment in the upper part. The lower part illustrates the white coloured wing of a dug out injection beam. This wing is in average 10 cm thick and 2 m long. It acts like a thick plastic foil.

This barrier prevents a deeper penetration of contaminants from the tar basin in the ground water layer.

4.2 Slit Wall around Chemical Waste Disposal

Residuals of the chemical industry were disposed in a large open pit of Middle German brown coal mining from 1918. Especially after 1945, deposing of CCH distillation residuals, waste tars, mangan muds and HCH waste isomers (Hexachlorcyclohexan) was increased. In a period of 20 years, about 70 000 t HCH were disposed.
The 50 m deep hole is now included in the ground water flow because the water level has increased after finishing of mining activities in this region. In water wells along the ground water flow lines, a high water pollution was measured.
To prevent the water flow through the disposal, a 50 - 60 m deep slit wall is necessary. The wall is based in a clay layer as a natural horizontal seal. By this combination of natural and artifical seals, the chemical danger can be controlled. Fig. 6 shows a view of the bright coloured slit wall.

4.3 Surface Sealing

Mercury contamination to a depth of 12 m was explored below a removed chemical plant in Middle Germany. At present a suitable remediation process does not exist. The area should be used for the new construction of a factory. The surface has to be covered to protect it from rain. As in the Fig. 7 illustrated Montanwax-dispersion was penetrated in the soil by several spraying and rolling. By this repeated method, a „sandwich" package of Montanwax layers was formed. The soil below this package remains dry and the mercury immobile.

5 Conclusion

Montanwax sealing technologies have developed to field application for soil and ground water protection by several drilling and construction methods.
Montanwax, as a seldomly located natural product, has surprisingly suitable tightness properties for remediation of waste disposal and soil contaminations. All field experiences and research work show a permanent impermeabilization of soil.

Table 1. **Properties of Montanwax**

Impermeability	$k = 10^{-10} \dots 10^{-11}$ m/s extremely impermeable $= 10^{-2} \dots 10^{-3}$ mD	DIN 18 130
Chemical Stability	Lab tests over several years with acids, bases and waste disposal fluids; No change of impermeability	DIN 18 130 5491
Microbiological Resistance	No degradation of wax substance in lab tests, bacterial growing possible without damage	DIN 53 739 38 412
Toxicity	fish tests were successful, water neutrality proven	EC 84/449C.1
Fire-Explosion-Safety	nonburning in soil, nonexplosive	DIN 51 794
Radon Stability	no degradation in Radon environment, stable impermeability	DIN 5491
Flow properties as dispersion	viscosity at different recipes $\eta = 5 \dots 100$ mPas	

DIN = Deutsche Industrie Norm (German Industry Standard)
EC = European Committee Rule
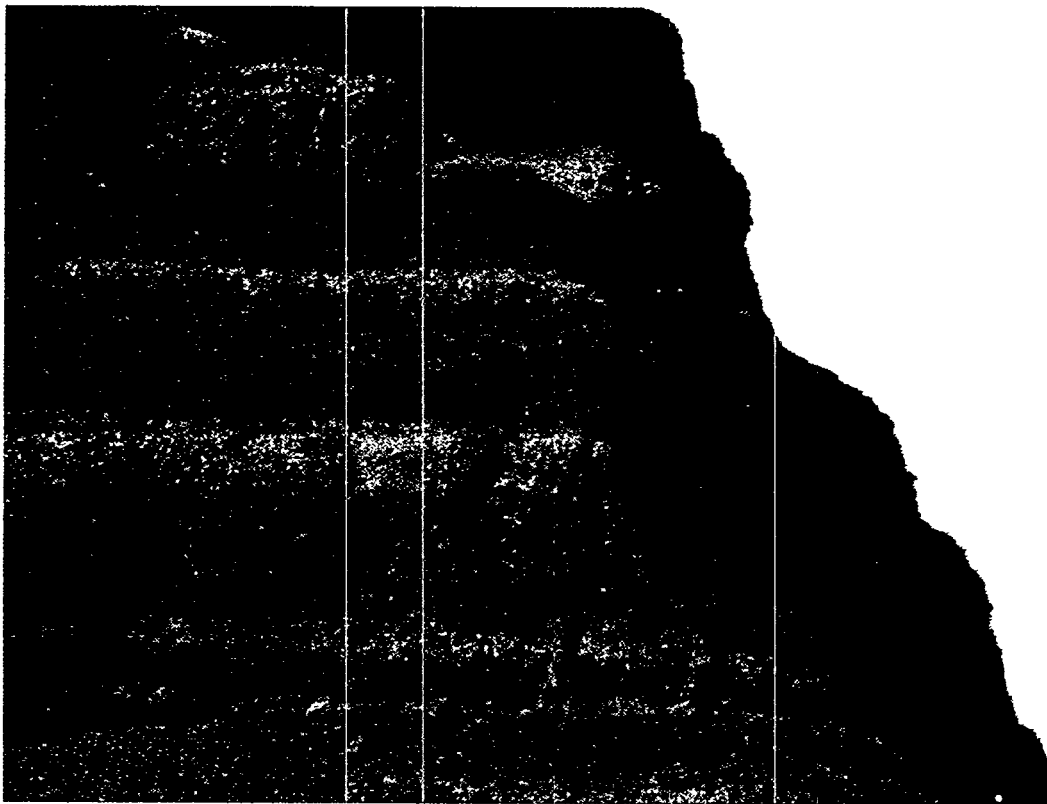
Fig. 1   Brown coal seam with bright Montanwax layer
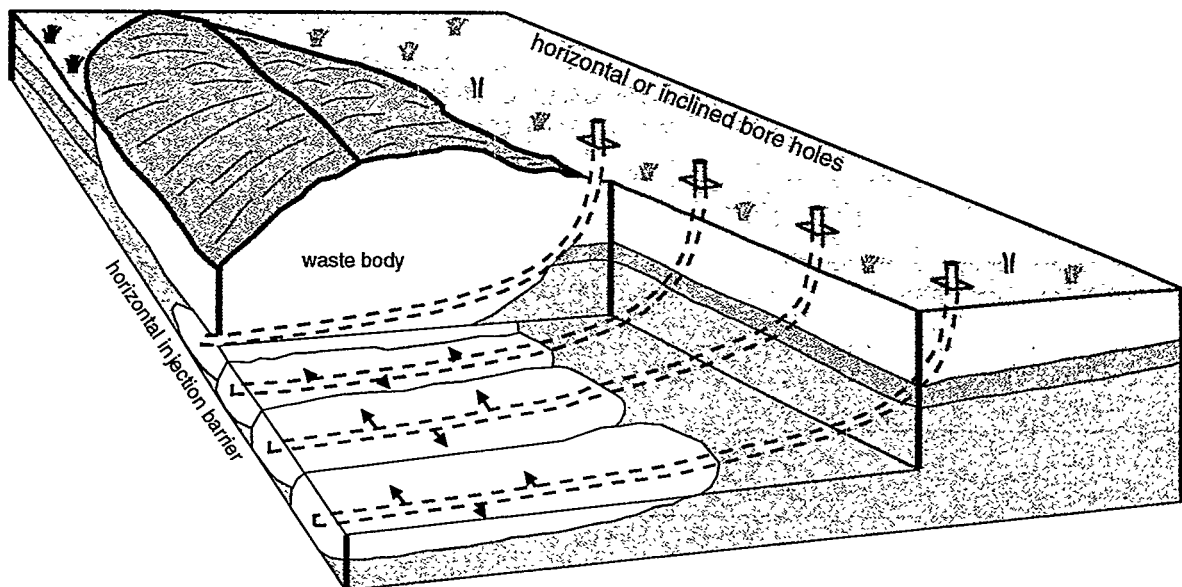
Fig. 2   Base barrier below waste disposal by horizontal wells
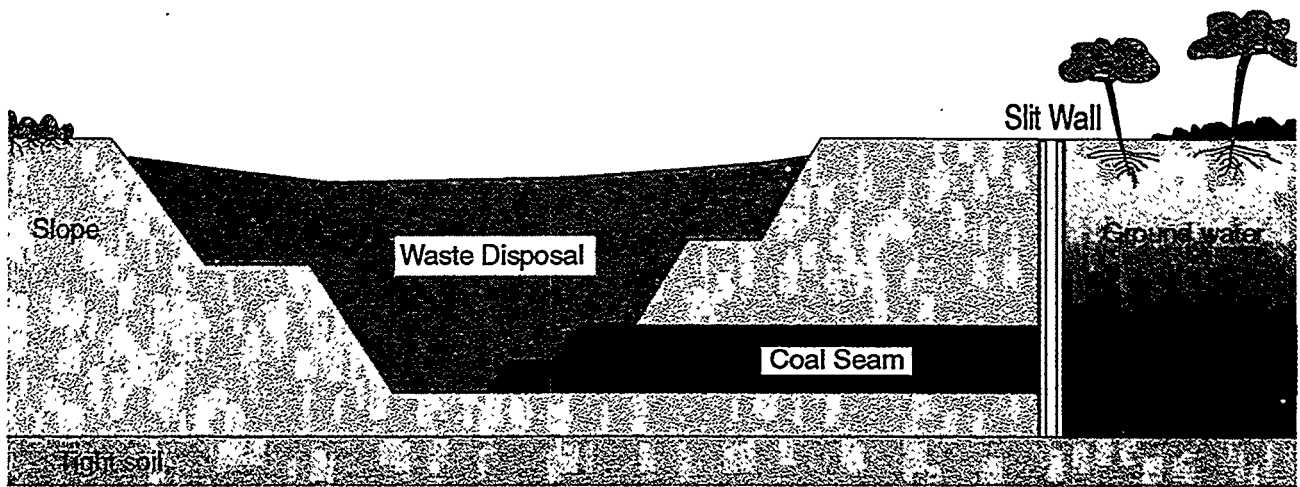
Fig. 3   Slit wall as vertical barrier at a waste disposal
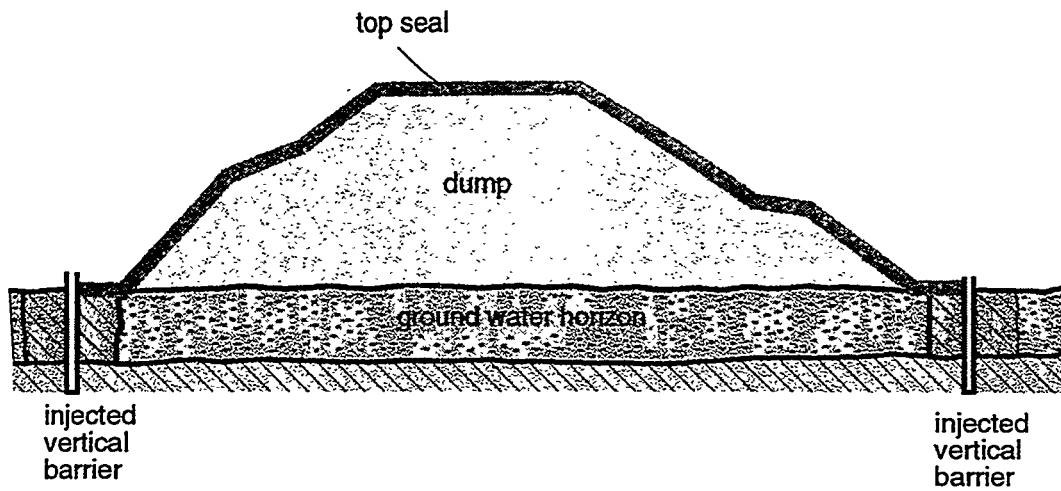
Fig. 4   Surface sealing scheme of a dump
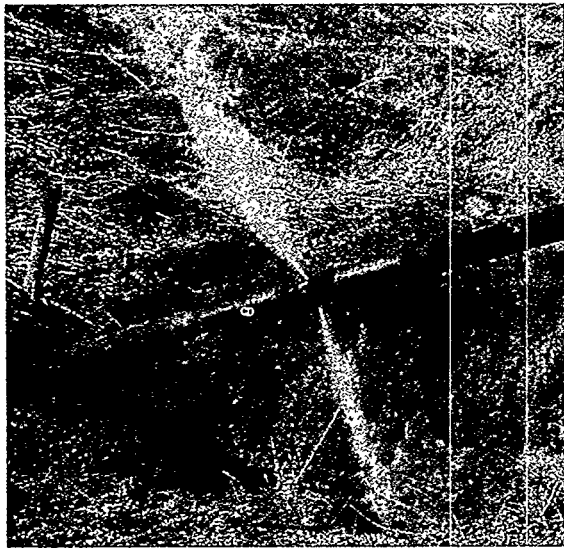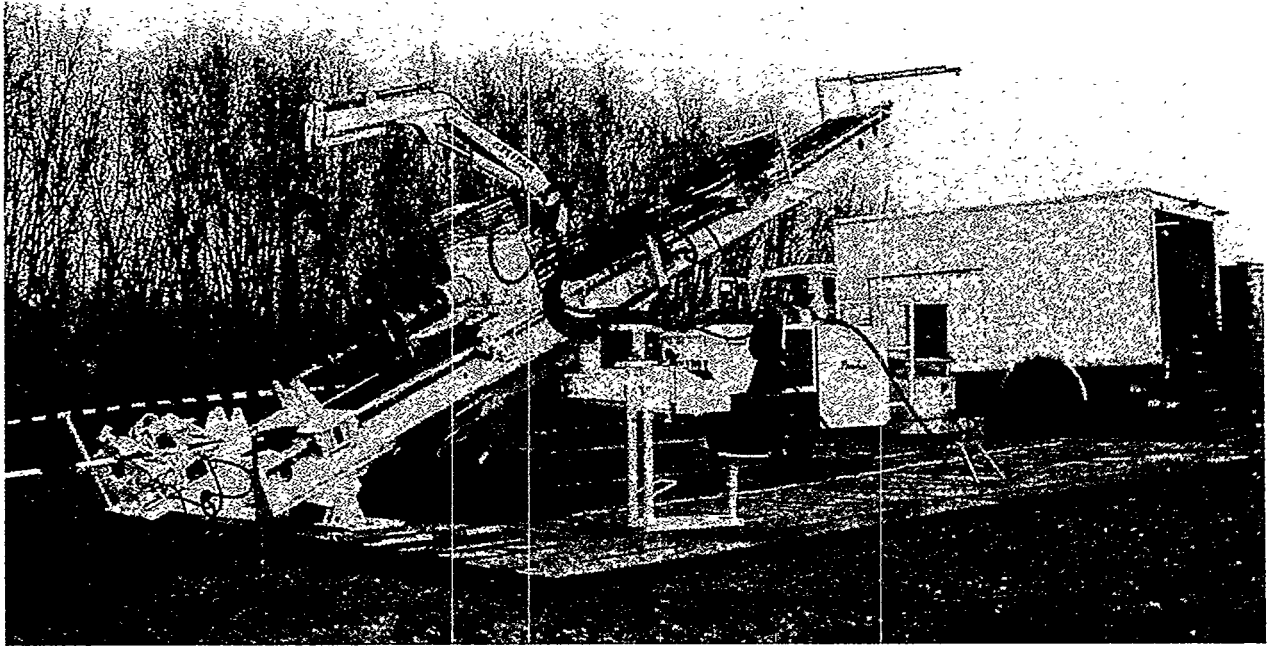
Fig. 5   FLOWMONTA equipment for horizontal base sealing by jet grouting and sealing wing

Fig. 6   Montanwax bright coloured slit wall around an open cast mining hole

591
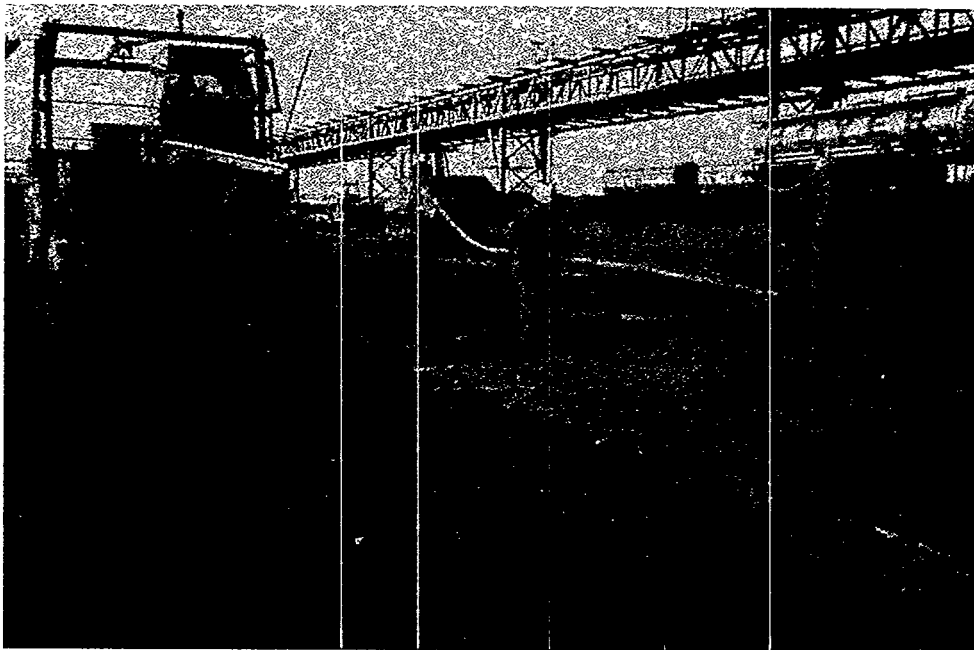
Fig. 7   Construction of surface sealing above a mercury contamination

LAB SCALE TESTING OF NOVEL NATURAL ANALOG
IN SITU STABILIZATION AGENTS

Peter Shaw

Idaho National Engineering Laboratory

Lockheed Martin Idaho Technology Co.

2525 N Fremont

Idaho Falls, Idaho 83415-3710

ABSTRACT

This report summarizes the laboratory-scale test results on several novel in situ treatment and stabilization agents for buried hazardous and radioactive waste. Paraffin, hematite and phosphate materials were examined when combined with soil and other wastes representative of what might be present at buried waste DOE sites. Hematite was made from the reaction of agricultural iron and lime slurries to form gypsum and iron oxide/hydroxide. Common household paraffin was melted, both with and without a zeolitic additive, waste added and then cooled. Magnesium phosphate was made from the reaction of magnesium oxide and phosphoric acid or potassium biphosphate to form, magnesium phosphate. All were tested with soil and some with additional waste sumulants such as ash, machine oil and nitrate salts. The following laboratory-generated data indicate that all waste encapsulation materials tested are appropriate materials, for field in situ testing. Compressive strengths of treated Idaho National Engineering and Environment Laboratory (INEEL) soil and the waste encapsulation material were sufficient to prevent collapse of the void space in waste, i.e., greater than the NRC 60 psi minimum. The mineralogy and microstructure of hematite was amorphous but should progress to an interlocking crystalline solid. Phosphate was crystalline with characteristics of higher temperature ceramics. Paraffin is non crystalline but encapsulates even very fine grained INEEL soils. Each agent appears to be chemically and physically inert to possible waste materials such as, nitrates and machine cutting oil. Two of the agents hematite and phosphate react favorably with ash increasing the metals retention at higher waste loadings than Portland cement. Hematite, phosphate and zeolite decrease leaching of most hazardous metals from waste when compared to untreated waste and soil. Solution pH, time for reaction initiation, and viscosity values are conducive to jet-grouting application.

Introduction

This report summarizes the laboratory-scale test results for paraffin, hematite and phosphate binders as potential in situ stabilization agents for buried hazardous and radioactive waste. In insitu waste encapsulation is less-expensive alternative than "remove and treat" solutions contemplated at the at the Idaho National Engineering and Environment Laboratory (INEEL) and other government and industrial facilities.[1] A specific waste application is long-term stabilization of Transuranic-contaminated waste pits and trenches INEEL. Laboratory tests were used to determine long term durability, leach resistance of each binder with soil and selected wastes and the implementability of such agents for jet grouting application.

Phosphate and hematite are synthetic analogs of natural encapsulating materials (cements). These materials have long term durability by being in equilibrium with the environment in which they occur. Materials in equilibrium will remain intact as long as the natural environment remains unchanged.[2] Paraffin is an unreactive long chain aliphatic that penetrates well into soil when melted, seals dissimilar materials and is relatively impervious to physical and biological decay.

Hematite natural analog is formed from the reaction of agricultural iron sulfate and lime to form gypsum and iron oxide/ hydroxide; $FeSO_4 \cdot 7H_2O + Ca(OH)_2 = Fe(OH)_2 \cdot 5H_2O + CaSO_4 \cdot 2H_2O$. Over time, the iron hydroxide oxidizes to hematite (Fe_2O_3), goethite ($FeO[OH]$), ferri-ferrous iron oxides, and oxyhydroxides.[2] Iron Sulfate and fly ash were also used with the ash providing the active ingredient calcium oxide. Calcium sulfate and iron oxides are proposed as primary waste encapsulation materials, because they have formed and are forming by natural processes in the desert INEEL soils.

Phosphate natural analog material were made from the reaction of dolomite and potassium biphosphate or (phosphoric acid,) to give Monazite; KH_2PO_4 (H_3PO_4)+ MgO +$5H_2O$ = $MgKPO_4 \bullet 6H_2O$ $MgKPO_4$ $(MgHPO_4 \bullet 6H_2O)$.[3] Magnesium phosphate is proposed as a primary waste encapsulation material since the structure is able to incorporate significant amounts of uranium (U) and thorium (Th) in its crystal structure which immobilizes them. These are naturally stable leach resistant materials as illustrated by deposits of U and Th in phosphate minerals.

Paraffin was examined when melted alone or with zeolite to increase metal absorption. Common American paraffin with a density of 0.92 g/cc and a melting temperature $60^{\circ}C$ was used in lab testing with a lower temperature type paraffin (melting temperature $45^{\circ}C$) used in the in situ application. A standard natural calcium zeolite, gismodine, with a nominal formula of $CaO\text{-}Al_2O_3\text{-}SiO_2\text{-}H_2O$ was also tested to increase metal retention. It was premixed with the paraffin and soil before any spiked metals were added in the standard EPA toxicity characterization leaching procedure (TCLP) leach test.

The successful in situ application of any of these agents would provide encapsulation and isolation of buried waste materials from the environment. Preventing water intrusion into the waste, which dissolves and transports waste components, is achieved by (a) filling the void space in the waste with rock-like material to eliminate subsidence, (b) providing a physical barrier to prevent water from reaching the waste, and (c) chemically adsorbing contaminant ions in solution to prevent their further movement.

Several properties of the natural analog agent and resulting wasteforms were obtained in lab test to access the agent's effectiveness and implementability: Compressive strength and density indicate strength and compatibility of treated INEEL soil, and other waste materials such as debris, ash, nitrates, machine cutting oil, and metallic iron;[1] with the waste encapsulation material. The leachability of hazardous metals using TCLP gives an idea of short term leachability of hazardous constituents encapsulated by the waste isolation material. Field application parameters such as viscosity, reaction temperature and set time test suitability for in situ jet grouting application.

Sample Preparation

Preparation of Compressive Strength Wasteforms

Compressive strength testing was performed on samples with varying soil contents, waste types, and initial reagents. TCLP testing was done only on soil or ash waste containing waste forms. Test specimens containing soil and/or other waste and the waste isolation material were prepared by mixing the dry ingredients in the case for hematite and phosphate and adding water (or microwave melting paraffin) in beakers while stirring. The contents are poured or scooped into cylinders. The cylinders had been coated with a thin film of vacuum grease so the sample could be easily removed. They are made from plastic pipe or cut from 1.27 cm (0.5 inch) I.D plastic or glass tubing to make cylinders that are twice as high as wide. The minimum diameter for most compressive strength testing is 5 cm. Small samples were chosen for waste minimization purposes to allow comparison when these agents will be used on actual mixed waste samples.

The samples are allowed to set then removed from the tubes air dried and weighed. Dimensions of the samples both wet and dry and the corresponding weights were taken to calculate bulk densities for each waste form. Compressive strengths were measured in accordance with the ASTM procedure C39-86. Replicate soil and isolate material combinations with various soil ratios and waste types gave reproducibility and data quality information with an overall measurement precision of 20-50%. Sample compositions and results are summarized in Table 1.

Table 1. Compressive Strength of Soil, Waste and Isolation Material.

Paraffin	Zeolite	INEEL Soil	Waste	Density	Compressive Strength
weight percent				g/cc	psi
27	0	73	0	1.4	316±123
19	0	81	0	1.5	323±180
32	12	56	0	1.3	416±158
22	8	69	0	1.4	349±187
			Nitrate		
20	0	55	24	1.3	352±64
24	9	43	24	1.3	439±223
			Machine Oil		
23	0	62	14	1.3	152±35
28	11	49	12	1.3	382±272
FeSO$_4$	Ca(OH)$_2$	Soil	Ash		
4	0	0	76	1.5	335±130
8	4	15	19	1.5	65±5
9	8	0	33	1.3	60±15
12	15	0	15	1.3	101±30
31	15	0	0	1.5	154±48
20	11	21	0	1.6	176±92
16	8	45	0	1.6	126±25
8	4	67	0	1.5	164±34
			Iron		
14	7	35	5.3	1.2	119±27
14	7	29	11	1.4	86±33
14	7	18	21	1.4	106±22
14	7	0	39	1.5	97±17
			Nitrate		
14	7	34	5.4	1.2	62±15
14	7	28	11	1.2	61±14
14	7	18	21	1.1	54±7
14	7	0	39	1.1	60±16
			Oil		
15	7	10	4.6	1.4	232±26
26	13	0	16	1.5	262±56
27	13	0	11	1.5	206±37
KH2PO4	MgO	Soil	Ash		
38	11	0	35 ash+ debris	1.8	1300±100
12	4	0	70	1.9	4008±1350
18	6	0	60	2	6708±350
21	7	48	0	1.8	4000
18	6	58	0	1.7	3000

Paraffin samples were melted and mixed with soil. Zeolite was added to the soil and wax before the additional TCLP metal soil was introduced. Paraffin sample compositions were 43-82 wt% soil, 19-31 wt%

paraffin, and 0-12 wt% zeolite mixed with no other ingredients, or 24 wt% reagent grade potassium nitrate, or 12-14 wt% Texaco Regal Oil (same type used in much of incoming waste to the INEEL from machining),[3]

Hematite samples were prepared by mixing the required amount of waste dry into 1-to-1 mole ratio of lime and iron sulfate waste isolate material and adding water to initiate the reaction and liquefy. Waste concentrations were 0-67 wt% soil, 0-76 wt% fly ash, 0-39 wt% reagent grade potassium nitrate, 0-16 wt% Texas Regal Oil and/or 0-39 wt% reagent grade, 325 mesh, metallic iron powder. Waters of hydration from the Iron sulfate heptahydrate contribute to the high water loadings of these samples.

Phosphate samples were prepared by mixing the required amount of waste dry into 1-to-1 mole ratio of magnesium oxide and potassium biphosphate waste isolate material. About 10 to 12 wt% water was added to make a moldable paste and stay within stoichiometric constraints of the hydrate product. The phosphate samples were mixed with soil, ash or ash and ground up debris simulating buried waste. Waste concentrations were 50-75 dry wt% soil as the waste, 35 wt% ash/debris or 60-70 wt% fly ash.

TCLP Spiked Soil, Ash and Sample Preparation

Leachability of hazardous metal constituents encapsulated by the waste isolation material is determined using TCLP. Hematite and paraffin waste isolation binder material were combined with a toxic metal-spiked INEEL soil. Hematite and phosphate samples were also combined with toxic metal spiked ash. An ASTM class F coal fly ash from Jim Bridger plant and dried and ground INEEL soil were used as base material. The soil had been prepared to contain about 1 wt% each of the 8 EPA metals in the oxide by mixing with reagent grade oxides of silver (Ag_2O), arsenic (As_2O_3), barium (BaO), cadmium (CdO), chromium (Cr_2O_3), mercury (HgO), lead (PbO), and selenium (SeO_2). The final soil concentration for all TCLP metals was 7.5% (75,000 ppm). The ash had been prepared to contain about 0.1 wt% total of 8 EPA metals in the oxide by mixing with reagent grade oxides of silver (Ag2O), arsenic (As2O3), barium (BaO), cadmium (CdO), chromium (K2CrO4), mercury (HgO), lead (PbO), and selenium (SeO2). The final ash concentration for all TCLP metals was 7640 ppm, about 900 ppm of each metal.

Three INEEL spiked soil and two ash samples with no added binder agent were leached as controls to account for the natural attenuation of the soil or ash one INEEL unspiked soil sample was run as a blank. All controls were made into monoliths then crushed or sized for the test. The controls were dampened sufficiently to form into cylinders. Phosphate/ash and paraffin /soil samples were leached for 24 hours in 0.01 N Acetic Acid (EPA #2 test solution). The hematite/ash and hematite soil sample was leached with the buffered salt (EPA #1 test solution). The approximate compositions are given in Table 2 as determined by inductively coupled plasma (ICP).

Results

Compressive Strength

Table one lists sample composition and unconfined compressive strength (UCS) results. All sample soil/waste types were stronger than the Nuclear Regulatory Commission (NRC) minimum requirement for containment of radioactive waste of 60 psi, even after the short curing time of 10 days. A formulation of 67 wt% waste simulated the composition which when injected would sufficiently fill all available voids assuming 35-40% porosity. This indicates that any of the waste isolation material s would prevent open-space collapse if injected into buried waste at the INEEL, even in the presence of common wastes such as ash, nitrates, or machine oil. Data suggest that oil under 20 wt% may actually increase the strength for some mixtures of materials. Most samples were air dried and lost up to 10 wt% of their water during the average curing time of 10 days.

Table 2. TCLP Leaching for Soil, Waste, and Isolation Material Mixtures.

Binder	Soil	Metal	Ag	As	Ba	Cd	Cr	Hg	Pb	Se
weight percent			Concentration in leachate (ppm)							
0[a]	0	92	7.5	40.8	389	368	368	<0.3	20.7	92.6	62.8
0[b]	0	98	1.6	13±3	46±8	76±14	88±20	<0.01	7±4	22±5	84±28
0[b]	0	98	1.5	13±3	54±10	79±14	63±15	<0.01	20±7	31±7	67±22
0[b]	0	100	0	<0.3	<0.7	0.14	<0.05	<0.3	<2.5	<0.4	<1.4
KH2PO4	MgO	Ash	Metal								
0[a]	0	99	0.68	2	0.93	0.72	28.4	12.1	3.3	0.074	7.3
0[b]	0	99	0.76	0.31	18.6	1.33	38.2	25.4	17.1	0.26	6.77
18[b]	6	60	0.46	<0.05	2.39	0.03	<0.01	0.03	0.0013	<0.10	9
FeSO4		Ash	Metal								
1[a]		81	0.6	2.1	1.1	.33	31.6	.182	2.2	2.1	.72
4[a]		75	0.55	0.75	0.32	0.21	20.7	0.34	0.42	0.53	2.9
13[a]		55	0.41	<.005	0.2	0.14	16.3	0.55	0.006	0.41	0.1
FeSO4	Ca(OH)2	Soil	Metal								
14[a]	7	63	0.54	<0.3	<0.7	<0.07	147	<0.3	<2.5	11.4	<1.4
28[a]	14	38	0.33	<0.3	<0.7	<0.07	418	<0.3	<2.5	13.8	<1.4
paraffin	zeolite	Soil	Metal								
23[b]	0	76	1.1	6±0.2	7±2	17±1	10±1	<0.01	1±0.1	9±1	76±19
26[b]	0	74	0.15	3±0.1	2±0.8	5±0.6	3±0.6	<0.01	6±2	5±1	3±0.5
27[b]	10.2	61	1.2	7±0.2	13±3	9±1	11±2	<0.01	13±4	9±2	20±5
30[b]	11.4	58	0.15	3±0.1	2±0.8	2±0.3	3±0.6	<0.01	2±0.7	2±0.5	10±3
TCLP Regulatory limit[c]			5.0	5.0	100	5.0	1.0	0.2	5.0	1.0
UTS(d)			0.3	5	7.6	0.19	0.86	0.025	0.37	0.16

< indicates detection limit for that element, three times the standard deviation
a. Sample leached in 0.1 N Sodium Acetate
b. Sample leached in 0.1 N Acetic Acid
c. 45FR 33119, May 19, 1980, as amended at 55 FR 22684, June 1, 1990.
d. Universal Treatment Standards, Proposed EPA 40 CFR Part 261, Vol. 59 No 180, September 19, 1994

Paraffin samples ranged from 119 to 685 psi UCS, hematite range from 54-262 psi and phosphate from 1300-6700 psi. The average UCS for all paraffin samples is fairly consistent 341±168 psi with only oil seriously weakening the matrix. Potassium nitrate did not weaken the paraffin but had a very negative effect on hematite strength. The average compressive strengths for room temperature paraffin samples were higher than the hematite. The Texaco Regal Motor oil weakened the paraffin alone but in the less than 20 wt% range it did not weaken the paraffin/zeolite or the hematite samples. Compressive strengths of hematite samples with oil averaged 233±28 psi and without oil 155±25 psi, and those of paraffin and oil samples with the zeolite averaged 381±271 psi and without 152±15 psi. The binding of oil by the zeolite

may have made it less likely to tie up metals in the following TCLP Test. Phosphate samples are now being tested on oil and nitrate salt wastes but for soil and ash have compressive strengths in the Portland cement range at very high waste loadings

TCLP

Generally the samples with the binder had lower metal concentrations in the leachate than the control samples containing only spiked INEEL soil or ash. As expected the organic material that depends on encapsulation for containment does not show nearly the decrease as does the inorganic natural analog materials which have both chemical and encapsulate properties. Paraffin treated samples were 3 ± 2 times lower in TCLP metals concentration than the untreated ones with arsenic, cadmium and barium concentrations consistently below the controls. Zeolite added to paraffin was only partially effective at reducing concentrations of metal leached below those of the paraffin alone. The factor decrease in concentration from additive and binder over the binder alone for these metals averaged 2.5 ± 0.5. No significant reduction in leachate concentration due to the additive was observed for cadmium, arsenic, mercury and selenium. The metal concentration decrease over the control (soil with no binder) averaged 3 ± 1.9 .

Hematite samples had reductions in leach rates from spiked soil and ash up to a factor of 400 over ash or soil with no additive. The decrease in concentration of heavy metals in solution in the case of hematite is primarily due to the chemical adsorption of the toxic metal ions onto the iron compounds XRD data in the case of both ash and soil indicate that, the iron material has not had time to crystalline. In all leach testing the hematite product turns into a mud like material when immersed. Thus in terms of containment the hematite waste form would render the waste nonhazardous as the resulting leachate is below TCLP limits even if water penetrated though the barrier. The Iron based materials appear to have no effect on the aqueous concentration of cadmium, enhancing its release in some cases.

Phosphate material had metal removal factors from the ash in the thousands for mercury and cadmium but did not remove selenium. The difference in an acid and salt leach from ash is apparent in this control sample. This material had the best waste form properties over all in terms of density, compressive strength and TCLP metal leaching. The leach data was obtained from 4 different labs and had overall uncertainty estimated to be 30%, for sample preparation, leaching and analysis of the eight metals.

Field Application Parameters

Field parameters such as reagent ratios, viscosity of injection solutions/slurries, soil solubility, heat generation upon mixing and solidification rate (curing time) , were qualitatively determined for each agent as applicable. The viscosity of paraffin appeared to be similar to that of water upon melting (above 60°C, 140 °F). Similar materials have been jet-grouted. The potential of premature hardening upon release from the nozzle for in situ injection in 7°C (45°F) soil was mitigated in the field trial with a special low melting point material (45°C) being used. There is little viscosity change beyond this point up to the boiling point of 200°C (400°F) according to the vendor giving a sufficient range for safe operation. Soil immediately settles to the bottom of the container with paraffin alone with little or no miscibility with INEEL soil or inorganic waste. Zeolite seems to increase miscibility with soil. In field trials a surfactant was added which greatly enhanced soil miscibility. The final paraffin product appears to be an excellent material for retrieval. It is waxy with complete retention of dust noted upon fracturing. Machine oil softens the paraffin upon set however the metal leach retardant additive restored hardness to that of other samples.

Field parameters for the hematite included the heat and pH changes of the ferrous sulfate hydrate and slaked lime reaction itself. Six titrations showed (a) a stoichiometric reagent ratio is acceptable, (b) no distinct endpoint as the iron hydroxide decomposes, buffering the solution, and (c) a final pH of 6.5-7.5. The ferrous sulfate hydrate slaked lime reaction initiation time · and heat of reaction at both room temperature and zero C was examined by simple calorimetry measurements. The reaction initiates immediately upon mixing and generates maximum heat within 1 minute at room temperature and 2

minutes, at zero C. The XRD results indicate that reaction continues slowly toward a crystal phase. The 5-8°C temperature rise for beaker size quantities depends primarily on the amount of waste isolate material. An estimate from these experiments is 10 calories per gram of waste isolate material. The viscosity of slaked lime rises exponentially (1-5000 centipoise) throughout the range tested (0-65 wt%) and can be adjusted for purposes of jet-grouting application by dilution. The viscosity for soluble iron sulfate shows little viscosity change (1-4 centipoise) up to saturation (48% in hot water). Going beyond that, i.e. maintaining a slurry, is difficult as the solid ferrous sulfate recyrstallizes, immediately settling to the bottom of the container. Air oxidizes the solution forming insoluble and less reactive iron oxide.

Field parameters for the phosphate magnesium oxide reaction have not been specifically or fully addressed. Observations from the reactions using ash and soil show that (a) a sub stoichiometric reagent ratio (phosphate rich) is acceptable as basic oxides in the soil and ash react with the phosphate, (b) no distinct endpoint is visible as the phosphate buffers the solution, and (c) a final pH is near neutral. The reaction initiation time and heat of reaction at room temperature was examined by simple calorimetry and thermocouple measurements. The reaction unless retarded with boric acid initiates within 5 minutes of mixing and generates maximum heat within 15 or 20 minutes, at room temperature rising to 70 °C. The XRD results[3] indicate that reaction is usually incomplete with unreacted MgO but a monazite type structure is formed. The reaction continues after initial set and can be enhanced by soaking in phosphate solution. The 50°C rise depends on the amount of waste isolate material and reaction retardants including the waste material itself. This reaction is approximately 10 times "hotter" that the hematite reaction with an estimated reaction heat of 100 calories per gram of waste isolate material. The viscosity of the reagents for purposes of jet-grouting applications has not been measured. It is thought that a two component mixture could be injected with a saturated KH_2PO_4 solution (83.5% in hot water) or 85 wt% phosphoric acid and a 60 wt% MgO slurry. The viscosity characteristics for insoluble MgO slurries seem similar to the lime ($Ca(OH)_2$) ones measured.

Conclusions

Data indicate that phosphate and hematite materials tested are effective in reducing leaching for buried waste containment. All the materials are effective in enhancing the durability and filling in voids over soil alone. The phosphate material has some implementability issues that need resolution before jet grouting can be attempted whereas the paraffin and hematite have been field tested. Wasteforms with soil and wastes have compressive strength greater than the NRC 60 psi minimum. This is sufficient to prevent collapse of the void space in waste in shallow land burial. Iron oxide/gypsum and paraffin are cheaper than phosphate and have been used in field trials following this testing. All agents are cheap enough for massive application in containing buried wastes Phosphate and gypsum/iron oxide remove hazardous metals from solution by adsorption and would pass TCLP limits for most EPA toxic metals in typical DOE buried wastes. Paraffin alone is a macroencapsulate and has no chemical interaction to prevent leaching. The addition of zeolite needs some development to enhance leach resistance in a TCLP type test. All appear to be chemically and physically inert with respect to the bulk of the waste materials likely to be found at the INEEL.

References
1. Vigil, M. J., (1989), "Subsurface Disposal Area (SDA) Waste Identification (1952-1970) Emphasis," EGG-WM-8727, EG&G Idaho, Inc.
2. Stumm W., Morgan J., (1981), "Aquatic Chemistry," 780 pp., John Wiley and Sons., New York.
3. Singh D., Waugh A.S., Cunnane J. C, (1994), "Chemically Bonded Phosphate Ceramics for Low Level Mixed Waste Stabilization," Proceeding ACS Symposium on Emerging Technologies in Hazardous Waste Management VI, September 19-21, Vol. 1, , pp. 562-564.

ECONOMIC ALTERNATIVES FOR CONTAINMENT BARRIERS

Peter J. Nicholson, Brian H. Jasperse, and Michael J. Fisher[1]

Abstract

Fixation, barriers, and containment of existing landfills and other disposal areas are often performed by insitu auger type soil mixing and jet grouting. Cement or other chemical reagents are mixed with soil to form both vertical and horizontal barriers. Immobilization of contaminants can be economically achieved by mixing soil and the contaminants with reagents that solidify or stabilize the contaminated area. Developed in Japan, and relatively new to the United States, the first large scale application was for a vertical barrier at the Jackson Lake Dam project in 1986. This technology has grown in both the civil and environmental field since. The paper describes current United States practice for Deep Soil Mixing (over 12 meters in depth), and Shallow Soil Mixing for vertical barriers and stabilization/solidification, and Jet Grouting for horizontal and vertical barriers. Creating very low permeability barriers at depth with minimal surface return often makes these techniques economical when compared to slurry trenches. The paper will discuss equipment, materials, soil and strength parameters, and quality control.

Introduction and Origin Of Insitu Soil Mixing

Soil mixing, both deep and shallow, and jet grouting are now accepted technologies in both the civil construction and environmental remediation markets in the United States. However, this recently accepted technology had an unorthodox path to acceptance.

In 1962 Norman Liver, working for Intrusion-Prepakt Co. in Cleveland, patented an auger-based soil mixing technique that has become the basis for the world's current technology. Originally there was little acceptance in the United States and development was stagnant; but in the early 1970s and into the 1980s, the Japanese took the technology and made rapid advances. By the late 1980s, approximately 2,000,000 cubic meters of soil mixing and jet grouting were being performed annually in Japan, much of it in their coastal cities, ports and harbors (1995 DSM). Current Japanese practice utilizes soil mixing to transform soft clays into hardened, cemented barriers, water and contaminant cutoff walls and mass foundations for piers, wharves and buildings. Over 200 rigs work continuously in this $1.0 billion-plus per year industry in Japan. In comparison, the United States, with twice the population, has six rigs.

Acceptance in the United States

Insitu soil mixing re-emerged in the United States in 1986 when a Japanese specialist company, Seiko-Kogyo, performed a demonstration in California. Seiko was assisted by Geo-Con, a domestic specialty foundation contractor. The next year, Geo-Con and SMW Seiko redesigned and won a $16 million contract for Morrison-Knudsen Co. to use the process on a Bureau of Reclamation project, Jackson Lake Dam in Wyoming. The soil mixing was used to provide a vertical cutoff and also improve the capability of the dam's foundation to resist liquefaction. After the commencement of this work, a project in Michigan for a contaminant containment barrier was performed in 1987 to 1988; and since then, many other various soil mixed wall and cutoff barriers have been constructed.

Presently over 50 projects have been completed in the United States. In the soft clays of Boston, deep and shallow soil mixing have been used for over 56,000 square meters (600,000 square feet) of structural and cutoff walls. Presently, the largest project to date in the United States is

[1]President, Executive Vice-President and Assistant Project Manager, Geo-Con, Inc., 4075 Monroeville Blvd., Suite 400, Monroeville, PA 15146, (412) 856-7700, pjnicho0@cmail.wcc.com, bhjaspe0@ccmail.wcc.com, mjfishe0@ccmail.wcc.com.

underway in Boston as part of the enormous Central Artery/Tunnel construction program. In this project deep soil mixing, shallow soil mixing and jet grouting will be used to solidify 600,000 cubic meters (780,000 cubic yards) of organic silts and soft clay. The design for this Fort Point Channel section is to provide mass solidification of unstable soils improving the compressive strength from 36kPa (0.75 kips per square foot) to an average of 2400kPa (50 kips per square foot), equivalent to the strength of a soft rock. This ground treatment and solidification will allow deep excavation, 18 meters (60 feet) plus below the water table, for cut and cover tunnel sections to provide a link between I-93 and the Massachusetts Turnpike.

The Insitu Soil Mixing Process

Deep Soil Mixing

Insitu soil mixing in the United States is divided into two general categories: Deep Soil Mixing (DSM) which is generally considered treatment depths greater than 12 meters (40 feet) and Shallow Soil Mixing (SSM) which is generally considered treatment depths less than 12 meters (40 feet) deep.

For DSM the typical equipment used consists of a set of two to four mixing tools, top driven by either hydraulically or electrically powered motors. These motors and the shafts they power ride up and down a set of specially designed leads, which in turn are supported by a crane or may be structurally integrated into the crane body itself. The mixing tools consist of thick-walled rods, usually 250 to 300 mm (10-12 inch) diameter, with 50 to 75 mm (2-3 inch) diameter center holes, for slurry conveyance. Attached along each rod are mixing paddles which are designed to overlap with the paddles on the adjacent, counter rotating rod to create a pugmill-like mixing environment for the soils and injected slurry. At the bottom of each rod is a cutting head, also with a hollow center, that is designed to lift the soil to the mixing paddle area where it is blended with the previously injected slurry (Figure 1). As the rods and paddles penetrate the soil, they continuously rotate and mix the slurry and soil together. When the bottom of the stroke is reached, further slurry is injected while the shafts maintain that depth and mix for a short period to ensure blending of the bottom of the column. The rods are then slowly pulled from the ground with continued rotation and slurry injection at a reduced rate.
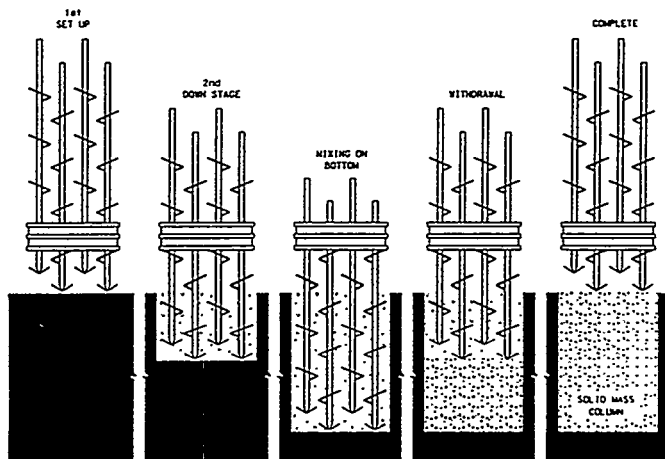
Figure 1: Multiple Shaft Auger Mixing System

The multiple-shaft design provides several benefits. For installing barrier or cutoff walls, a pattern of overlapping of adjacent panels is adopted. Primary strokes are spaced at appropriate intervals, and secondary strokes later re-penetrate the outer shafts of the primary strokes to ensure continuity of the wall. Other drilling and mixing patterns can be created that will allow block treatment and perimeter enclosures (Figure 2). In this way contaminants can be enclosed or treated and solidified into a cemented (or other reagent) mass.
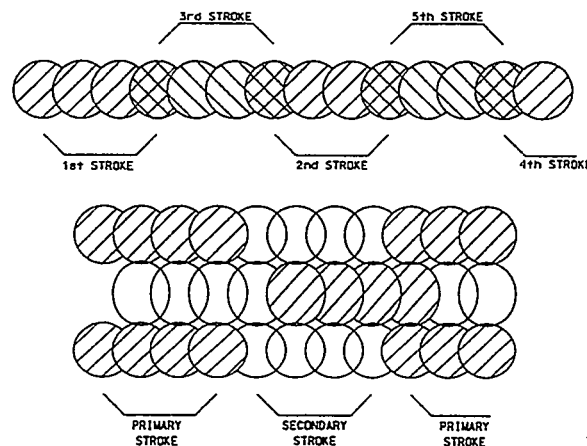
Figure 2: Multiple Shaft Auger Mixing Patterns

Shallow Soil Mixing (SSM)

Many applications of insitu soil mixing, particularly in the environmental remediation area, are located near the ground surface (less than 12 meters [40 feet] deep). In these cases it is often possible to use a single, large-diameter tool to perform the mixing process. This method, SSM, is usually faster and far less expensive, largely because the equipment is simpler and the larger diameters employed mean much more soil can be treated in each meter of penetration. For example a typical DSM system will treat 1.5 to 2.25 m3 per meter of stroke (0.6-0.9 cy/foot), whereas an SSM system will treat 5 to 9 m3 per meter of stroke (2-3.5 cy/foot)

SSM equipment consists of a single-auger mixing tool generally 2-4 meters (6-12 feet) in diameter. This process was developed in the United States and utilizes standard domestic cranes to support a caisson turntable and a Kelly bar driven mixing tool. The Kelly bar is hollow-stemmed to allow for slurry injection. The mixing tool has carbide cutting teeth, combined with a short auger flight that contains jet ports to inject the slurry into the soil.

SSM can be used to treat a number of contaminants through stabilization, solidification, fixation, neutralization and permeability reduction. It is very effective on heavy metals and can treat low levels of organics. With the use of lime as a reagent, acidic soils and sludges can be neutralized. The following shows reagents and the contaminants on which they are generally effective:

Contaminant	Solution	Reagent
Heavy Metals	Stabilization	Cement, flyash, kiln dust
PCBs	Stabilization, fixation	Cement, flyash, bentonite proprietary reagents
Organics	Stabilization, solidification	Cement, flyash, bentonite proprietary reagents
Creosotes	Stabilization	Cement, flyash
Acidic Soils and Sludges Dust	Stabilization, neutralization	Lime, cement flyash, kiln dust
Asbestos	Stabilization	Cement, flyash, lime

Technical and Economic Considerations

Insitu mixing offers many technical and economic advantages over conventional slurry wall trench installation for barriers.

Less spoil disposal -- Since the soils and slurry are mixed insitu, the amount of spoil removed is limited to approximately the volume of slurry added, usually from 10-30% of the treated volume. In trench excavation, all of the soils must be removed. In cases where the soils are contaminated, it is obvious that the savings in disposal costs can be significant.

Capable of greater treatment depths -- Standard depths of 25 meters (82 feet) are available in one stroke. By adding sections of mixing tool, depth is limited only by time and soil type. Depths of treatment of up to 40 meters (131 feet) have been completed in the United States and 60 meter (200 feet) depths have been achieved in Japan.

No open trench -- When the mixing tools are withdrawn, that section of the wall is complete. This eliminates open trenches that pose potential safety and quality control problems due to possible trench collapse. Exposure to volatilization of VOCs is minimized.

Less working area is required -- Since the mixing is performed insitu, space for above-ground mixing is not required. The batching of the cement is containerized and the slurry may be pumped great distances if required. Distances of 600-1200 meters (2000-4000 feet) are not uncommon.

Superior mixing of slurry with soil -- The pugmill mixing environment that is created by overlapping mixing paddles produces a very homogeneous product. Conventional methods mix the soil backfill above ground with tracked excavating equipment resulting in uneven blending. By mixing insitu, the amount of slurry or reagent required also is minimized.

Better quality control is achieved -- During this mixing process, there are a number of quality control measures that are used to control mix quality and ensure thorough blending. Specific gravity of the slurry is controlled at the mixing plant to ensure the proper proportions of agents are blended. In-line flow meters are used with digital readouts to instantaneously monitor flow rates and record total flows. When integrated with penetration rate controls, the flow rate per foot can be optimized and controlled. Electronic monitoring of penetration of the shaft will record instantaneous penetration rates as well as record total distance traveled (depth). Testing of the final mixed-in-place soil and slurry is accomplished by grab samples at various depths after withdrawal of the tools from the hole. Subsequent core or test drilling will confirm that the proper amount of slurry injection and mixing have been performed.

Barrier and Stabilization Materials

Generally, the purpose of the soil mixing treatment is to increase the strength and/or lower the permeabilities of insitu soils in order to construct a barrier or stabilize contaminants. Cement is by far the best reagent for strength increase, but it can be cost prohibitive if massive amounts are needed to achieve the required strengths. Other reagents, some of which are process by-products and economically purchased, can be mixed with cement to reduce cement usage or can be used alone. Types of strength increasing reagents follow:

    Cement
    Lime Kiln Dust (alone or with cement)
    Flyash (with cement)
    Lime (alone)
    Gypsum (with cement)

Use of these reagents also lowers the permeability of the final soil mixed product.

Sands and coarse grained soils are the easiest to mix, but even very stiff clays can be treated, albeit with slower penetration rates and increased slurry usage. The following table shows a range of typical values for strength and permeability of treated soils. This data is based on over twenty-five projects performed in the United States using DSM, SSM, and jet grouting.

Soil Type	Cement Usage	UCS	Permeability
Sludge	240 to 400 kg/m³ (400 to 700 lbs/cy)	70-350 kPa (10-50 psi)	1×10^{-6} cm/sec
Organic silts and clays	150 to 260 kg/m³ (260 to 450 lbs/cy)	350-1400 kPa (50-200 psi)	5×10^{-7} cm/sec
Cohesive silts and clays	120 to 240 kg/m³ (200 to 400 lbs/cy)	700-2100 kPa (100-300 psi)	5×10^{-7} cm/sec
Silty sands and sands	120 to 240 kg/m³ (200 to 400 lbs/cy)	1400-3500 kPa (200-500 psi)	5×10^{-6} cm/sec
Sands and gravels	120 to 240 kg/m³ (200 to 400 lbs/cy)	3000-7000 kPa (400-1000 psi)	1×10^{-5} cm/sec

Note: Strengths can generally be increased with additional cement.   Permeability can be lowered with the use of bentonite or proprietary reagents.

Although adding cement does decrease the permeability of soils, it generally is not to the order of magnitude required for effective insitu barriers. Bentonite is by far the superior material to mix into the soil for this purpose. Generally, cement is also added to create a soil-cement bentonite product, which is impermeable, flexible, and has some strength. The following table shows results compiled from several projects.

Soil-Cement-Bentonite Soil Mixing Project Results

Soil Types	Job Type	Water/ Cement Ratio	Bentonite/ Water Ratio	Additional Reagent Ratios*	Grout/ Soil Ratio	UCS 28 day (kPa)	Hydraulic Conductivity (cm/sec)
Fine sandy silt, silty sand, trace gravel	Jet Grouting	2	0.05	None	0.36	120 - 140 (14 day)	3.3 x 10(-7)
Medium dense sand to sandy gravel, loose silty sand to soft sandy silt	Deep Soil Mixing (DSM)	1	0.04	None	0.32	420	9 x 10(-8)
Sand, sand with clay	DSM	1.2	0.064	FA/W=.21	0.3	1,400 to 8,400	6x10(-7) to 2x10(-8)
CL-ML	DSM/Jet Grout	1.5	0.02	FA/W=.4 Gyp/W=.2	0.38	1729	1 x 10(-7)

* Additional reagents include fly ash and gypsum

Costs

As previously stated, the largest DSM project in the U.S. is currently underway in Boston involving 600,000 m3 (800,000 cy) of treatment. Additional sections of both shallow and deep mixing, as well as jet grouting, have since been bid. Some of the work will be carried out to depths of 40 meters (130 feet) below existing ground and 37 meters (120 feet) below the mean sea level on land reclaimed from the harbor. Costs for the work in a busy industrial area even to these depths are surprisingly economical.   Prices for shallow soil cement mixing at approximately $65 per m3 ($50 per cy) have been bid. For deeper work, both DSM and jet grouting, the prices have varied from as low as $120 per m3 ($90 per cy) for DSM to a range of $190-$220 per m3 ($150-$170 per cy) for jet grouting (1994-1996 Various Bid Documents).

A typical DSM cutoff or barrier wall can be installed in place, with cement or a combination cement-bentonite, for as little as $150/m2 ($15/sf). Production rates are on the order of 100-150 m2/shift (1000-1500 sf/shift).

Applications of DSM

Jackson Lake Dam

The Bureau of Reclamation's Jackson Lake Dam project was the first major application of DSM in America-1986. This dam, located near Jackson Hole, Wyoming, was built in the early 1900s and required major safety upgrades. DSM was used on the project to construct a deep cutoff wall to minimize seepage through the foundation. In addition, because of seismic considerations, liquefaction of the underlying sands was a major concern. A honeycomb pattern of DSM was used here to contain the soils in the event of liquefaction.

Cutoff construction -- Reduction of seepage under the dam foundation was to be obtained by a cutoff wall on the upstream face. Conventional methods of constructing the wall were rejected as too costly and problematic because of the nearness of the lake itself and also the depth required, 34 meters (112 feet).

To construct the cutoff wall, a three-auger shaft machine, of Japanese design with leads integral to the crane, was employed. The cutting heads and mixing paddles were 86 cm (34 inches) in diameter and the shafts were 46 cm (18 inches) on center. This configuration created a wall with a minimum width of 60 cm (24 inches). The permeability required in the silty sand foundation material was 1×10^{-5} cm/sec and the strength required to resist seismic forces was 4500 kPa (660 psi).

DSM for Liquefaction Control -- In order to improve the soils underlying the dam to resist liquefaction, a different pattern of DSM was adopted. Here, honeycomb-shaped cells were installed using a Seiko-designed two-auger mixing tool. With a UCS of 4500 kPa (660psi) and a corresponding shear strength of 1400 kPa (200 psi) for the soil-mixed columns making up the cells, the sandy soils would be contained during an earthquake.

The Jackson Lake project was completed in 1988 with all permeability and strength criteria being achieved. A total of 100,000 cubic meters (130,000 cubic yards) of soil were treated for containment and barrier purposes to the satisfaction of the Bureau of Reclamation.

Bay City, Michigan

Shortly after the Jackson Lake project commenced, the first DSM project using American-made equipment began. This application was a vertical cutoff wall to control the migration of PCBs from an industrial site in Bay City, Michigan. Approximately 2 km (1.5 miles) of wall was required to be constructed around two different contaminated sites and was extended into the underlying glacial till to provide an aquaclude. Because impermeability was a key requirement, a bentonite-cement slurry was employed as the injection and mixing medium to achieve a permeability of less than 1×10^{-6} cm/sec.

The American designed and made equipment employed a four-auger mixing shaft arrangement with 0.9 m (3 feet) diameter cutting heads. The leads were free-standing and supported by a standard Manitowoc crawler crane. Rather than electric motors, as used on the Japanese equipment to drive the auger and mixing paddle shafts, this design employed hydraulic motors powered by a Caterpillar diesel engine.

On this project certain obstacles and structures prevented the use of DSM to install the wall in some areas. Where this occurred, jet grouting was employed to complete the wall and containment. Jet grouting employs a single rod with a small diameter bit, typically 100mm (4"), bit to advance it into the ground. In this process, high pressure pumps are used to deliver slurry at 40 MPa (6000 psi) through 2 to 3 mm diameter nozzles. In some cases compressed air is used to increase the efficiency of the jets in mixing the soil. This use of both DSM and jet grouting represented the first U.S. combined application of these techniques on a single project.

Since these early projects in 1986-1989, over 50 DSM projects have been completed in the United States. Because of the flexibility of the patterns that can be employed, the depths that can be achieved, the technical and quality superiority, and economics, it is likely that this technology will be employed on more and more projects in the future.

New Technology

During the last several years, at least two new soil-cement mixing methodologies have been developed. Two of these, Jacsman and Geo-Jet, promise further refinement in the speed and quality with which soil and cement can be mixed.

Each of these methods employs mechanical mixing as in conventional soil-cement mixing, but combine it with the hydraulic action of high pressure jets, as used in jet grouting, to achieve rapid advancement of the tools and add energy to mixing.

In the Jacsman system, two mixing shafts are mounted on a rotary head. The shafts counter-rotate at speeds of 20-40 rpm while jet nozzles, mounted along the mixing heads, spray a mixture of cement and water into the ground . The jets intersect and mix the area between the mixing paddles. Since there is 360 degree rotation of both shafts, the jets also engage soil throughout the treated soil area. This process is similar to that of a milkshake machine with the added benefit of jets of milk to break the ice cream down. As of 1996, the Jacsman has been successfully employed on approximately 20 projects in Japan to depths up to 20 meters (65 feet).

Geo-jet is a process invented by a Californian, Lonnie Schellhorne, a few years ago. In this process a single-axis rotary head drives a single flight, auger shaped tool. At or near the advancing blade of the tool, high pressure jets are assembled to break the soil immediately after it has been shaved by the advancing auger. As with Jacsman, the speed of advance is helped by the combination of the auger cutting action with the mixing action of the high pressure hydraulic jets of cement milk.

Both new technologies, Jacsman and Geo-jet, may provide a superior product to the current "mechanical only" mixing methods being used in both shallow and deep mixing. Sampling that has been done on soils mixed with the Geo-jet technique have shown good mixing.

Summary and Conclusions

Soil mixing has come full circle, from its invention in the United States in the 1960s, through its development in Japan during the 1970s and 1980s, to its acceptance as a significant technique for ground treatment and soil remediation in both the civil and environmental fields.

Soil mixing is an ideal solution for barriers and containment in most soils:
* Its high strength and homogeneity ensure a permanent barrier;
* Low permeabilities make it ideal for water and contaminant barriers;
* Spoil production is reduced compared to trenching methods;
* A high degree of confidence in quality can be assured;
* Jet Grouting and SSM can be used to supplement or solidify; and
* New techniques combining jet and mechanical mixing will bring costs down.

The use of the techniques described provide the engineer and the owner with a sophisticated, sure method of controlling the migration of wastes.

References

(1995) DSM Association Brochure.
(1994-1996) Various Bid Documents for Central Artery/Tunnel, C09, A8, C3A1.

Frozen soil barriers for hazardous waste confinement

J.G.Dash[a] H.Y. Fu[b] and R.Leger[a]

ABSTRACT

Laboratory and full field measurements have demonstrated the effectiveness of artificial ground freezing for the containment of subsurface hazardous and radioactive wastes. Bench tests and a field demonstration have shown that cryogenic barriers are impenetrable to aqueous and non aqueous liquids. As a result of the successful tests the US Department of Energy has designated frozen ground barriers as one of its top ten remediation technologies.

INTRODUCTION

Artificial ground freezing has been employed for many years in large scale engineering projects to bond soils for load-bearing strength during construction and excavation, and to seal tunnels and mine shafts against flooding from groundwater [Frémond 1994, Andersland 1995]. A newer application of artificial ground freezing is in hazardous waste management, to prevent the escape of liquid contaminants from waste sites. Studies have shown that the hydraulic conductivity of moist soils is reduced considerably at subzero temperatures [Horiguchi 1983, Nakano 1991]. Here we report on freezing techniques that can achieve low conductivities of various liquids in normally highly permeable ground. Bench tests of the technique showed that coarse and arid soils can be made impermeable to non aqueous liquids and to concentrated brines. Following the laboratory tests a field demonstration of a cryogenic barrier was carried out successfully for the US Department of Energy. On the basis of these tests the DOE designates ground freezing among the top ten waste management technologies.

LABORATORY MEASUREMENTS

The laboratory study was carried out in small test cells (see Fig.1) which permit a variety of soil measurements over a range of temperatures and temperature gradients [Dash 1994]. Temperatures down to -30°C can be imposed on selected zones of the soil column by individually controlled thermoelectric cooling elements. The cells contain provisions for monitoring liquid movement *in-situ*, injecting and removing liquids, testing the porosity by pressurized gases, profiling temperature and electrical conductivity along the soil column, and measuring the permeability of the frozen zone to various fluids under moderate hydrostatic pressure.

Soils and chemicals

The soils were uncontaminated samples from U.S. Department of Energy nuclear reservations: a coarse sand from Hanford, Washington, and a clay soil from Oak Ridge, Tennessee. The test fluids were dilute aqueous solutions of potassium chromate (K_2CrO_4), trichloroethylene (TCE) and radioactive cesium ($^{137}CeCl_2$), concentrated $CaCl_2$ brine, and pure decane. The choice of soils and chemicals provided an appreciable range of the characteristics of liquid contaminants at many of the DOE's leaking nuclear waste sites.

Temperature profile and thermomolecular pressure

In operation, a central region of the soil column was cooled to subzero temperatures, while the portions above and below were maintained above freezing. The temperature gradients were important for achieving low permeabilities at moderate temperatures, particularly essential in the

---

[a] Physics Department., University of Washington, Seattle, Washington 98195-1560, Fax (206)543-9523; email dash@phys.washington.edu

[b] Quantum Institute, University of California, Santa Barbara, California

coarse sandy soil. The gradients produce a thermomolecular ('frost heave') pressure inward, tending to cause migration toward the central lowest temperature (Dash 1989a). which produces a non porous frozen region. Such barrier regions can withstand great hydrostatic pressure gradients: Barrier core temperatures of only a few degrees below freezing can oppose hydrostatic pressures of many atmospheres. An additional important characteristic is that non porous frozen barriers are impenetrable to non aqueous liquids. A technique for creating thick non porous barriers quickly is described below.

Construction of thick non porous cryogenic barriers

A method was developed for remote injection of water into a selected zone and freezing the water in place, to produce non porous cryogenic barriers. The technique can limit the injected water to a closely delimited region. The method allows construction of a barrier of arbitrary thickness, regardless of the initial soil moisture level. The technique is illustrated in Fig.2. Using this method we prepared non porous zones 2-5 cm thick for permeability measurements with various liquids, as described below.

Tests with chromate and TCE solutions

Tests of non porous barriers with potassium chromate and trichloroethylene solutions were performed over a period of several months, in test cells of the design shown in Fig.1. The test parameters (soil type, initial moisture content, test liquid, hydrostatic head, and test duration) and calculated hydraulic conductivity are summarized in Table 1. Hydraulic conductivities were calculated according to Darcy's law. Since no leakage was detected in any of the tests, the tabulated conductivity K is the maximum possible value consistent with the limited duration of the observations. There were no technical difficulties preventing longer tests, but the overall duration of the project was constrained by a project completion deadline. Nevertheless, the test times were sufficiently long to show that the barriers were 'impermeable' according to standard classifications (Baer 1972).

Table 1. Results of chromate and TCE tests against non porous barriers

Soil	Moist[1]	Solution[2]	T°C[3]	Head[4]	Time[5]	K[6]
Hanford	0	Cr	-26	34	72	7.6
"	"	"	-17.5	"	67	8.2
"	15	"	-28	25	90	8.3
"	0	TCE	-15	30	48	12.9
"	"	"	-10	"	64	9.7
Oak Ridge	"	Cr	-26	"	"	"
"	"	"	-17.5	"	26	23.9
"	"	"	-15	"	60	10.4
"	7.5	TCE	-10	"	16	38.8
"	"	"	-15	"	50	12.4
"	20	"	-16	"	48	12.9
"	"	"	-10	"	68	9.1

---

[1] Initial soil moisture level, as volume fraction of water relative to saturation. 0% is produced by air drying. During testing the soil was fully saturated in the barrier zone, but remained at its initial unsaturated level below the barrier.

[2] Cr = K_2CrO_4 solution; TCE = trichloroethylene solution.

[3] Temperature of central 1 cm of barrier.

[4] Hydrostatic head of contaminant solution, in cms.

[5] Duration of test, in hours.

[6] Hydraulic conductivity of barrier in units of 10^{-11}cm/sec.

Barriers without injected water

Four experiments with chromate solution were conducted to test the effectiveness of cryogenic barriers with only the original moisture level and no water injection into the barrier zone. No leakage was detected in any of these tests, which can be attributed to the efficiency of the thermomolecular pressure in opposing the transport.

Radioactive cesium

A special cell was designed for gamma ray logging measurements with ^{137}Ce. This isotope is a fission product in the manufacture of plutonium, and is one of the principal radioactive components in underground storage tanks at Hanford. The characteristic radiation is a highly penetrating gamma ray (662 keV). The radiation can be transmitted through the walls of the test cell with only slight attenuation, thus permitting continuous profiling of the isotope's distribution without removing the soil. The cell was similar to the others, except for a radiation enclosure of thick walled lead shields to protect personnel and reduce background activity. The cell and shields were mounted on a motor-driven frame, which enabled vertical scanning of the radioactivity along the soil column. Detection was obtained by a scintillation detector fitted with a narrow angle collimator, which provided a spatial resolution of a few millimeters along the soil column. The results are summarized below. As in the tests with chromate and TCE solutions, no leakage was detected in any of the cesium measurements. The conductivities in Table 2 are the maximum K's consistent with the duration of the tests.

Table 2. ^{137}CsCl$_2$ tests of non porous barriers

Soil Type	Time(hrs)	Temp.	Head(cm)	K(cm/sec)
Hanford	99.5	-13°C	2.5	2.5 x 10^{-9}
"	124.8	-16°C	2.5	2.0 x 10^{-9}
Oak Ridge	123.8	-25°C	0.5	10.1 x 10^{-9}
"	122.5	-10°C	0.5	10.2 x 10^{-9}

Decane

Decane is useful for measurements of hydraulic conductivity in frozen and partially saturated soils [Andersland 1994], because decane remains liquid at low temperature (m.p. -31°C), and has a viscosity comparable to that of water. We carried out leakage measurements with decane on a 6 cm thick non porous region having a core temperature of -25.5°C., well within the range of decane's liquid phase. Pure decane was injected on top of the soil column, sufficient to produce a hydrostatic head of 28 cm. The liquid column height was monitored during the next two days. The results, if ascribed to leakage through the barrier, indicate an average conductivity K=5.3 x 10^{-8} cm/sec. However, all or part of the change may have been due to mixing of the decane with the unfrozen water above the freezing zone, rather than to actual penetration or transport through the barrier. Nevertheless, the measured rate, if ascribed to leakage, still designates the barrier as "impervious".

Calcium chloride brine

The most stringent test of a cryogenic barrier is the containment of brines and other 'antifreeze' liquids, where the temperature of the barrier is higher than the freezing point of the mixture. Nevertheless, it is possible to contain such fluids for extended periods. When liquid contacts the barrier it induces melting whenever the freezing point of the brine is lower than the temperature of the ice. As melting proceeds the brine is diluted by the meltwater, raising the local freezing point. Melting will continue as long as the supply of solute maintains a local freezing point below the temperature of the ice. The melt rate is limited by thermal conduction to supply the latent heat of fusion and by molecular diffusion of solute toward the interface. Since thermal conduction is typically much faster than molecular diffusion, the erosion rate will be governed primarily by the latter, and the rate will fall steeply as the diffusion path length increases. Thus, the lifetime of the barrier depends on its initial thickness, its temperature profile, the solidus curve of the liquid, and

the diffusion rate of the solute through the soil. A quantitative analysis and extensive testing would be required before reliable quantitative estimates could be obtained for the useful lifetime of barriers against brines and other antifreeze fluids. However, the qualitative trends, as described above, lead one to believe that the parameters of thickness, temperature, and soil permeability may be combined so that a barrier could remain intact for virtually any finite period.

A test with concentrated $CaCl_2$ brine was carried out in coarse Hanford soil, with a non porous barrier approximately 5.5 cm thick. The barrier's temperature increased monotonically in both directions from the center, from a minimum of -25.5°C. at its core. Since the freezing point of the saturated solution was -46°C, contact with the liquid caused immediate melting. The progress of melting was monitored by the height of the liquid column, changes of height being due to the volume change between ice and water (or solution). During the six day test the erosion was initially rapid, then fell non exponentially with increasing time, as expected. The rate at the end of five days implied an *effective* hydraulic conductivity no greater than 2.8×10^{-7} cm/sec. However, it is to be emphasized that the monotonically decreasing rate implies that the brine was still contained within the frozen zone.

FIELD DEMONSTRATION

A full-scale cryogenic barrier was demonstrated for five months at a clean site in Oak Ridge, Tennessee [Scientific Ecology Group 1995]. The design of the frozen region, shown in Fig.3, provided a full surround of the subsurface region. Freeze pipes were installed in a double row, inclined at a 45° angle to establish an inverted vee-shaped subsurface barrier. The pipes were set on 2.5 m centers in each row, with rows 1.2 m apart.

After the installation of piping, refrigeration was supplied by two large mobile units delivering $CaCl_2$ heat exchange fluid circulating at -20°C. A complete subsurface enclosure of frozen ground was obtained in about two weeks. By the end of the demonstration period the barrier wall thickness averaged more than two meters.

Barrier integrity was tested by measuring the ionic conductivity across the frozen zone, which showed negligible ionic transport through the frozen walls. Ground penetrating radar examination of the barrier wall after excavation of the interior unfrozen region showed a continuous frozen zone throughout the wall section.

Diffusion transport was determined by chemical tracer tests before and after freezing. Because the barrier was installed in low permeability clay soil, it was necessary to prepare the area in order to obtain a critical test of the barrier's effectiveness, Before freezing a sand trench was dug transecting the barrier region, to provide a route for rapid transport of fluid, and therefore a stringent measurement of the effectiveness of freezing to block transport. Before freezedown, substantial hydraulic conductivity through the sand trench was obtained by chemical tracers. Four hours after the injection of fluorescein in the center of the site it was detected in a monitoring well outside of the sand trench. After freezedown the site was injected with rhodamine solution: extended observation detected essentially no tracer outside of the barrier for the duration of the demonstration.

The demonstration provided a practical example on which to base the cost of frozen ground barriers. After subtracting the special expenses for extra sensors and test support, the first year's cost per cubic meter for installation and maintenance is estimated as $200, and the average maintenance cost over a 15-year period is estimated as $2.20 per cubic meter per year. The estimate of long term cost is based on calculated thermal losses in a typical soil, equipment amortization expense, power and maintenance costs (Dash 1989b). By comparison, costs of grout and other barrier materials range from $20 to more than $750 per cubic meter (DOE 1995).

A unique advantage of the cryogenic technology as compared to other techniques is its ability to achieve complete subsurface enclosure down to depths of several hundred meters (Jones 1982).

This feasibility, together with the competitive overall cost for long term maintenance, makes it possible to protect aquifers and surface waters from leaking waste sites for durations as long as required.

The bench tests and demonstration were deemed completely successful by the Office of Technical Development of the US Department of Energy [DOE 1995]. In 1996 the DOE designated frozen soil barriers as one of its top ten remediation technologies [Weapons 1996]. The DOE has recently awarded a contract for the installation of a cryogenic barrier around a radioactive site at the Oak Ridge National Laboratory.

CONCLUSIONS

Laboratory measurements have tested the hydraulic permeability of frozen soil to several liquids. The soils were samples of a coarse sandy soil from Hanford, Washington, and a clay soil from Oak Ridge, Tennessee. A method was developed to create barriers of nonporous frozen soil, and such barriers were created in both types of test soils. The liquids were dilute aqueous solutions of potassium chromate, trichloroethylene, and radioactive cesium; a concentrated calcium chloride brine, and pure decane. No leakage through the barriers was detected in any of the tests. Due to time constraint, the tests were of relatively short duration. Nevertheless, the permeabilities were no greater than 4×10^{-10} cm/sec, placing the barriers in the category 'impermeable'.

A field test of frozen ground containment was performed in a clean site at Oak Ridge, Tennessee. The site was prepared to insure that an adequate test could be completed in a few months. Since the native soil is a low permeability clay, a sand-filled trench was constructed to transect the barrier region. Before freezing, the trench provided a rapid flow path for liquids from the site. After the frozen barrier was in place, no transport of tracer chemicals from within the containment region was detected in test wells outside of the region. The barrier was also examined by ground penetrating radar and electrical conductivity.

On the basis of the laboratory tests and field demonstrations, the Department of Energy has included cryogenic barrier technology as one of its top ten remediation technologies.

REFERENCES

Andersland OB and Ladanyi B 1994 *Intro. to Frozen Ground Engineering*, Chapman and Hall
Andersland OB Davies SH and Wiggert DC 1994. *Performance and formation of cryogenic containment barriers in dry soils: Barrier performance.* Michigan State U. Rept to RUST Geotech, Inc., private comm.
Baer J 1972. *Dynamics of Fluids in Porous Media.* Elsevier Press NY; also Dover Publ. 1988.
Dash, JG 1989a. *Thermomolecular pressure in surface melting: motivation for frost heave.* Science **246**, 1591.
Dash, JG 1989b. *Ice technology for hazardous waste management.* Waste Man. 11, 183.
Dash, JG, Fu H and Leger R, 1994. *Bench scale testing of Hanford and Oak Ridge Soils: Formation and diffusion testing of cryogenic barriers,* U. Washington , Rept to Martin Marietta Systems Inc. Hazardous Waste Remedial Actions Program.
Frémond M 1994 ed. *Ground Freezing 94.* Balkema publ.
Horiguchi K and Miller RD 1983, *Permafrost: 4th Intl. Conf. Proc.* Nat. Acad. Press Wash DC pp 504-508.
Jones MB 1982. *Ground freezing technology advances with speed.* Tunnels and tunneling 14, 31.
Nakano Y 1991. *Ground Freezing 91,* ed Y Xiang & W Changsheng, Balkema Rotterdam pp 65-70.
US DOE, 1995. *Frozen Soil Barrier Technology.* Office of Innovative Technology Summary Report.
Scientific Ecology Group, 1995. *Demonstration of Ground Freezing Technology at SEG Facilities in Oak Ridge, TN,* Report to Martin Marietta Systems Inc. Hazardous Waste Remedial Actions Program.
Weapons Complex Monitor: Waste Management and Cleanup 1996, *Top Ten Technologies Listed by DOE-Environmental Management* Exchange/Monitor Publ Feb.13 p.6.

FIGURE LEGENDS

Fig.1. Schematic drawing of a test cell.
Fig.2. Sequence of steps in creating a non porous cryogenic barrier.
Fig.3. Sketch of the barrier installation in the full field demonstration.

Fig. 1

Fig. 2

612

outer freezing grid

○ ○ ○ ○ ○ ○ ○ ○ ○ ○ ○ ○ ○

○ ○ ○ ○ ○ ○ ○ ○ ○ ○ ○ ○ ○

○ ○   inner freezing grid   ○ ○

○ ○   ○ ○

○ ○   ○ ○   13.4 m

○ ○   ○ ○

○ ○   ○ ○

○ ○   ○ ○

○ ○   ○ ○

○ ○ ○ ○ ○ ○ ○ ○ ○ ○ ○ ○ ○

○ ○ ○ ○ ○ ○ ○ ○ ○ ○ ○ ○ ○

17.1 m

ground level

7.8 m
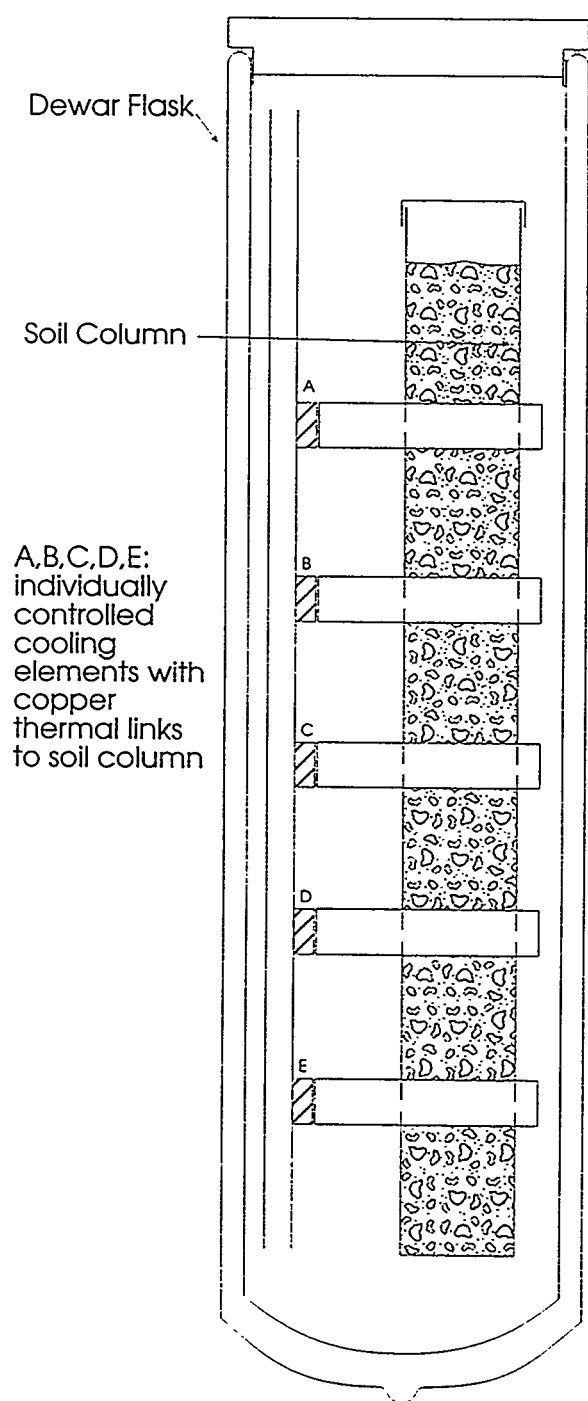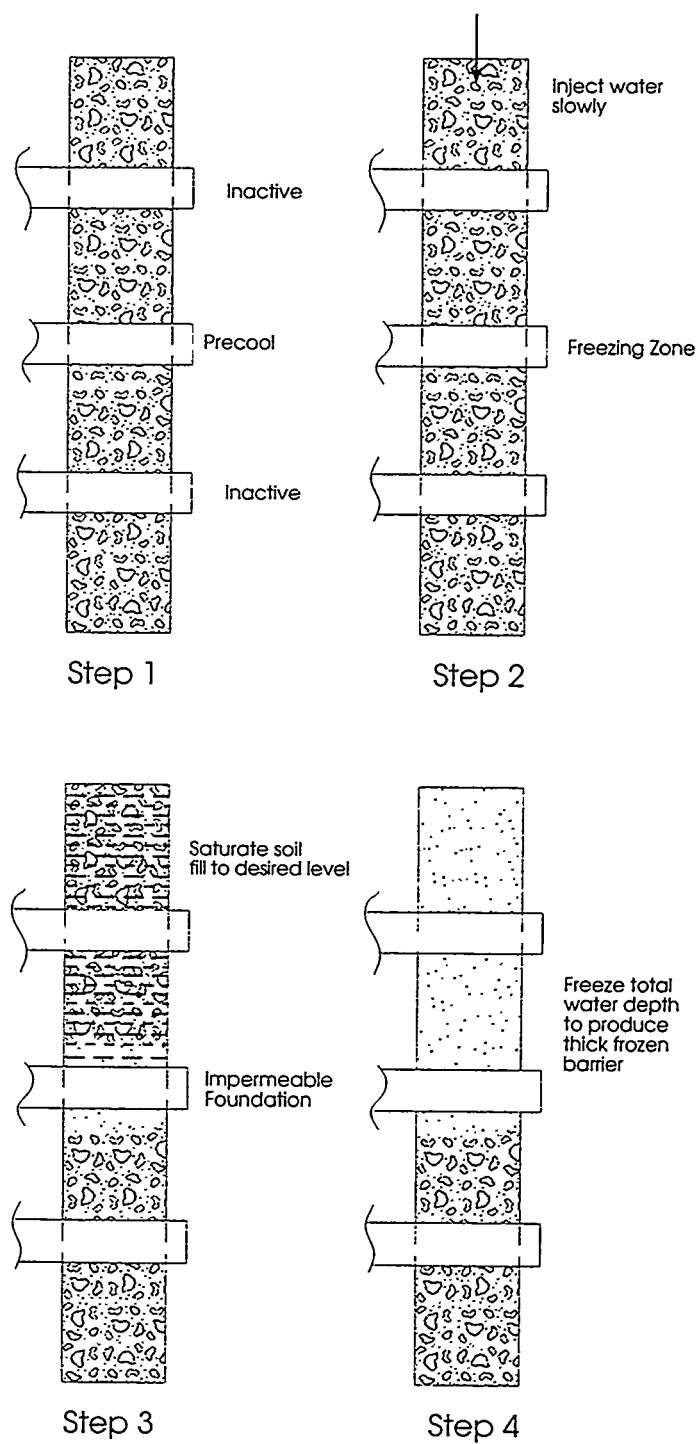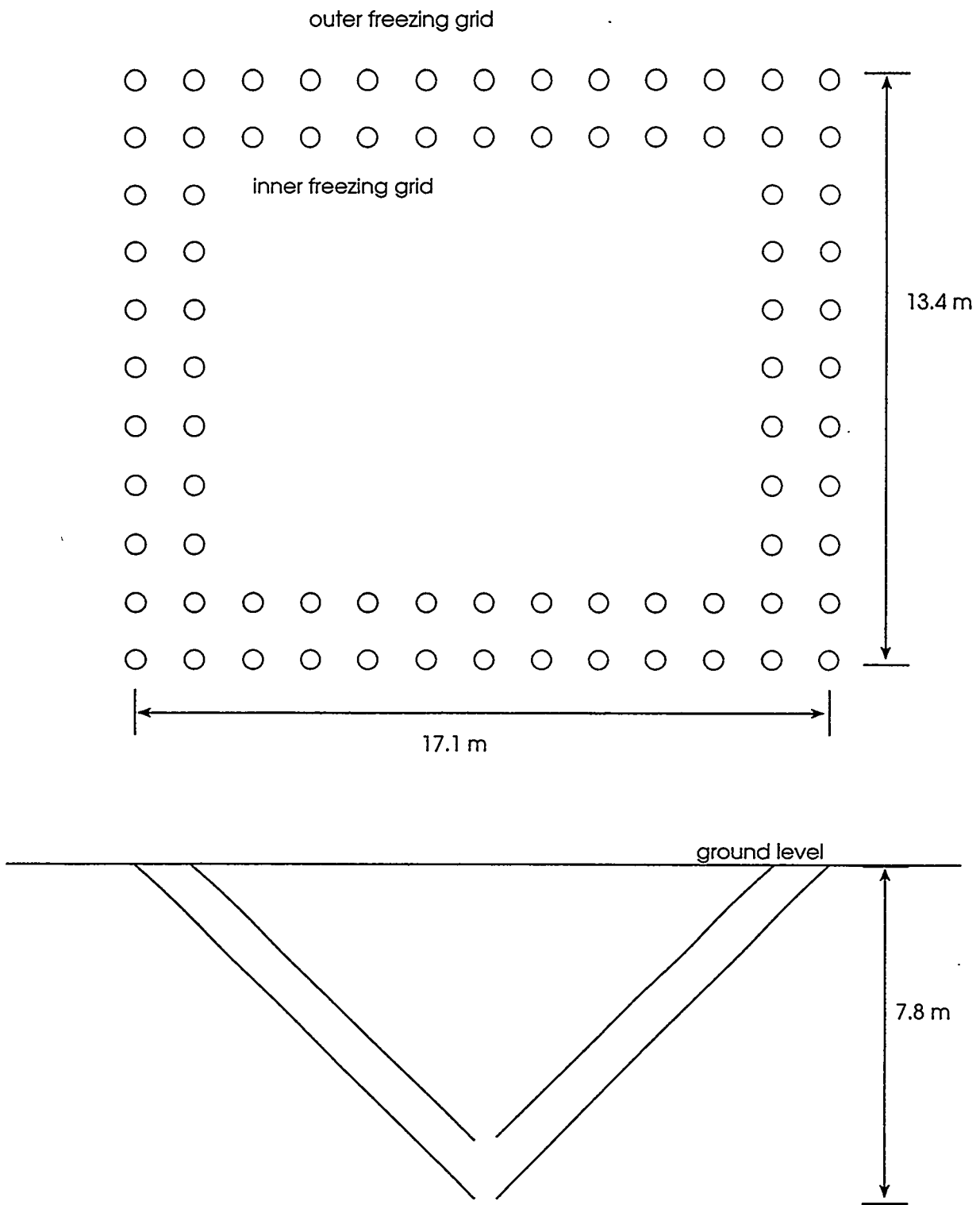
Fig. 3

SILICATE GROUT CURTAINS BEHAVIOUR FOR THE PROTECTION OF COASTAL AQUIFERS

M. Elektorowicz[1], R. Chifrina[2], R. Hesnawi[3]

Abstract

Tests were performed to evaluate the behaviour of silicate grout with different reagents (ethylacetate - formamide SA and calcium chloride SC) in pure silica sand and natural soils from coastal areas containing organic matter, clayey soil and silica sand. The grouted specimens were tested with simulated fresh and salt water. The setting process during chemical grouting in the soil and sand was studied. The grouting of soil and sand with SA caused a transfer to the environment of some compounds: sodium formate, sodium acetate, ammonia and part of the initial ethylacetate and formamide. This process had a tendency to decrease for approximately 4 months. The stability of specimens was low. The grouting of soil and sand with SC caused no significant contamination of the environment. The increase of pH of environmental water was even less than with SA grouting. Also, the stability of specimens is higher in comparison with SA grouting. Salt water protected the specimens grouted with SA and SC from destruction and prevented contamination.

Introduction

Human activities and environmental conditions such as leaching, contaminant spills and saltwater intrusion affect groundwater quality. Grout curtains (eg. silica gel) may be used for the protection of aquifers. Generally, grouting leads to the consolidation of dispersed matter such as sand and soil. Grouting with silicate gel attracts attention because the silicate gel transformation products are similar to the natural silicates of sand and soil. The properties, the transformations and the preparation methods of silica and silicate gel were investigated for many years (Gmelins 1959).

In principle, silica gel consists of molecules of silicic acids which tend to condensate in linear or branched chains. This process is known as condensation polymerisation (Myshlaeva et al. 1974). As a result, the formation of $(-Si-O-Si-)_n$ bonds and the elimination of water occur.

These silicon-oxygen bonds have a tetrahedral configuration because silicon is tetravalent. The polymer chains consist of associated tetrahedra. However, due to existence of 3d-orbitals, silicon is able to coordinate 6 atoms or groups having small sizes, eg. OH^-, F^-. Therefore, the formation of a 3-dimensional network as a result of condensation polymerization is beneficial.

Condensation polymerization depends on the pH and temperature of the medium. An increase in temperature leads to the acceleration of the process. When pH increases, silicate ions appear. The complexity of these ions depends on pH (Gmelins 1959). In the range of pH 13.5-10.9, a dimeric form of silicate ions exist. A pH decrease leads to the formation of more complex polymeric silicate ions which are stable in alkaline solution and have a negative charge. Alkali-ion (sodium in the case of sodium silicate) is a counter-ion. Further pH decrease to neutral conditions and the elimination of sodium cations cause the rapid aggregation of colloid particles and their setting as a powder-like substance. So, silicates, especially sodium silicate, are useful for the grouting of soils and sand.

For a rapid and convenient preparation method of sodium silicate gel with appropriate mechanical and physical properties, some agents were used (Karol 1990). Historically, calcium chloride was used as the first agent. Sodium silicate and calcium chloride were injected in the ground producing a strong gel. The cation exchange reaction follows:

$$SiO_2 \cdot Na_2O + CaCl_2 + H_2O \rightarrow Ca(OH)_2 + SiO_2 \cdot NaCl$$

---
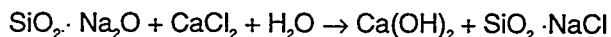
[1]Assistant Professor, [2]Research Associate, [3]Graduate Student, Department of Civil Engineering, Concordia University, 1455 boul. de Maisonneuve W, Montreal, Quebec, H3G 1M8

Having a high solubility in water, sodium chloride is eliminated from the silica. Consequently, the polymerization of the introduced liquid and the aggregation of colloid particles occur rapidly. The polymerization rate and the setting time depends on the SiO_2/Na_2O ratio and the $CaCl_2$ content.

It was later found that the elimination of Na^+ and H_2O occurred with the addition of some organic compounds instead of $CaCl_2$ to sodium silicate (Karol 1990). Practically all these compounds contain a carbonyl group: aldehydes, ketones, amides, esters. In the fifties, the first patents proposed the use of ethylacetate and formamide in France (Caron 1957) and the USA (Peeler 1959) to catalyze the polymerisation process. These patents formed the basis of many formulations and were used in Europe and the USA till now.

The ease of introduction, the control of grout distribution in the ground containment and the good mechanical and physical properties of grouted ground determine the success of these methods. However, for practical reasons, all organic compounds should be verified for their potential impact on soil and groundwater quality. It is necessary to investigate the chemical processes occurring in the grouted ground and control their end and by products as well as the influence on the environmental groundwater and saltwater. After two years, it was found that the quality of groundwater changes as a result of the effluent from the constructions grouted with sodium silicate and ethylacetate (Muller-Kirchenbauer 1985).

Tests were performed to evaluate the behaviour of silicate grout with different reagents (ethylacetate - formamide and calcium chloride) in pure silica sand and natural soil from coastal areas containing organic matter, clayey minerals and silica sand. The grouted specimens were tested in an environment which simulated fresh and salt water. The setting process occurring during chemical grouting in the soil and sand was studied.

Methodology of experimental work

Pure silica sand with particle size diameters between 0.30 mm to 0.42 mm was used. The particle size distribution of the natural soil consisted of 60% fine sand, 25% coarse sand and 15% silt and clay. Among the primary minerals, quartz and feldspars were dominant in the natural soil. Organic matter was estimated to be less than 1% as organic carbon. The calcium carbonate content was estimated to be 1.2%. The permeability of silica sand was 7.2×10^{-2} cm/s and of natural soil was 1.86×10^{-4} cm/s.

Sodium silicate was supplied by Fisher Ltd. and consists of 28.9% SiO_2 and 9.8% Na_2O by weight (ratio SiO_2/Na_2O is 3.22). The solution was 62.4% water by weight. This sodium silicate was used to prepare two types of grout: 1) grout SC, where sodium silicate was mixed with calcium chloride, and 2) grout SA where sodium silicate was mixed with ethylacetate and formamide. The pH of the initial sodium silicate was 11.3 (20°C).

To obtain SC grout, 50% sodium silicate was mixed with 50% calcium chloride using a magnetic stirrer until the solution was homogenized. To obtain SA grout, 5% ethylacetate and 5% of formamide was diluted with 40% of tap water. The mixture was mixed thoroughly, combined with 50% sodium silicate and remixed with a magnetic stirrer. The setting processes of SA samples, cured for 4 months in open air, were investigated using IR spectra.

Both SA and SC grouts were used for preparing laboratory grout specimens. Following preliminary test results, 40 ml of grout mixture was used to stabilize 100 grams of dry natural soil or silica sand in experiments. This mixture was mixed in a container using a hand stirrer. Then, the grout-soil mixture was poured and pressed into aluminum cylinder molds with 7.20 cm length and 3.22 diameter. Both ends of the mold were covered with plastic wrap and an O ring to prevent leakage as well as to prevent any change in moisture content during the settlement period.

After curing for 1, 3 and 7 days, the specimens were subjected to a constant head permeability

test without removing them from the mold. A laboratory standard apparatus for the permeability test was adapted to measure the permeability (gradient approximately 18) of grouted specimens. The effluent from these tests was examined with a UV-VIS spectrophotometer Perkin Elmer 2S and IR spectrophotometer Perkin Elmer 599B.

To evaluate the effect of water chemistry on the specimens permanence and to determine the possible impact on the environment media by grouted with SA and SC specimens, the following experiment was executed. Both sand and natural soil grouted specimens, cured for one day in open air, were removed from the mold and placed in two plastic containers filled with freshwater (groundwater) and saltwater (seawater) up to 60 days.

Both containers were subjected to a constant pressure of 69 kN/m^2 (10 psi). The initial pH of salt and fresh water was 7.7 and 8.0 respectively. The pH of water samples was measured with a pH meter (Accumet 1003). The silicate concentration in water was estimated by the Voinovitch method using UV-VIS spectrophotometer (Voinovitch 1966). Salt water contained much more magnesium as Mg (408 mg/l) and calcium as Ca (384 mg/l) than freshwater (21 and 43 mg/l respectively). For measurements of liquid samples (ethylacetate, formamide, their mixture, upper layers from the effluent etc.), a 10 mm quartz cuvette was used. The reproducibility of the measurements was ± 0.02%.

For IR spectra measurements, air dried grout samples and their mixtures with soil and sand as well effluent lower solid layers were grinded, mixed with dry potassium bromide, and pressed into pellets. For liquid samples, the IR spectra were measured using barium fluoride plates. The reproducibility of the band maxima was found to be ±10 cm^{-1} in the region of 4000-2000 cm^{-1} and ± 3.5 cm^{-1} in the region of 2000-200 cm^{-1}.

Results and Discussion

1. Chemical processes in grout

To clarify the interaction between sodium silicate and ethylacetate/formamide additive, white precipitate samples released from silicate gel were examined by IR spectra immediately after setting and during the 4 months. The IR spectra are shown in Fig. 1.

This comparison leads to the conclusion of rapid transformations of the initial components ethylacetate and formamide. The bands at 1739 cm^{-1} in ethylacetate spectrum and at 1680 cm^{-1} in formamide spectrum, both attributed to C=O stretching vibrations, disappeared in the spectrum of SA grout. Instead, the very intensive band at 1600 cm^{-1} and a small shoulder at 1680 cm^{-1} were observed.

Considering the other observed bands at 1360 and 770 cm^{-1}, it can be concluded that the spectrum of fresh grout included the spectrum of sodium formate besides some discrepancy in C=O stretching band (Table 1). Further observations during the 4 month curing period showed that the band at 1680 cm^{-1} disappeared completely and the band at 1600 cm^{-1} shifted to 1580 cm^{-1}.

The ratio of bands at 1360 cm^{-1} and 1600 (1580) cm^{-1} was measured. A decrease of this ratio during the curing period was observed (Fig. 2). This indicates that both bands do not belong to the same compound. While the 1360 cm^{-1} band certainly belongs to sodium formamide (Table 1), the band at 1600 cm^{-1} is a mixture of two bands associated with two compounds. Contrastingly, the ratio would be constant during all the curing period. The IR spectrum of sodium acetate also does not coincide completely with the observed IR spectrum of SA grout (Table 1). It was assumed that an intermediate complex between the sodium ion of sodium silicate and the carbonyl group of ethylacetate formed.

The spectrum of freshly prepared SA grout contains bands attributed to Si-O stretching and deformation vibrations and to bands connected with organic components. The assignment of these bands can be clarified by comparing the IR spectra of initial compounds to those that might appear

during this process: sodium formate and sodium acetate, formic and acetic acids, etc. (Table 1).

Table 1 The bands (cm^{-1}) and assignment of the initial and proposed end products of SA grouting

Name	vO-H[a]	vC-H	vC=O or as vC...O	vC=O or s vC...O		
Ethylacetate $CH_3COOC_2H_5$		2980s2940w[c] 2905w[b]	1739vs	1450w1370s 1242vs	1040s	
		2940w[d]	1735vs	1450w1370s 1240vs	1040s	
Acetic acid CH_3COOH	3042sb[e]	2631w	1714vs	1413m1294s	1015m	
Sodium acetate[e] (trihydrate) CH_3COONa	3427m	2981 2935	1557s	1414m1344 m	1020m	
Formamide[e] $HCONH_2$	3319vsb	2881s2767w	1682vs		1050m	
Formic acid[e] HCOOH	3118vsb		1722vs	1391s1308s	1181s 1062w	812m
Sodium formate[e] HCOONa	3412m	2715w	1605s	1340mb		774s 722w
Silica[e]			1630w[f]	1360m	1099sb[g] 960w	810m
Sodium silicate[d] Na_2O SiO_2	3400sb				1000sb[g]	
Grout SA: Na_2O SiO_2[d], Ethyl acetate, Formamide		2940w2840m 2760w2705w	1600-1580s	1360m	1050sb[g]	770s
Effluent after[d] permeability test	3400w	2940w2840m 2760w2705w	1680w 1600-1580s		1050sb[g] 950w	790w[h] 770s
Soil initial[d]	3400w		1630w[f]	1420w1360 m	1090sb[g]	790s[h]

Notes: [a]-type of vibrations: v-stretching, s-symmetric, as-asymmetric; [b]-relative intensity and form of bands: s-strong, vs-very strong, m-medium, w-weak, b-broad;[c]-(Aldrich 1981), [d] data from present work, [e] (Sigma 1986), [f,h]- attributed to deformation vibrations of OH and Si-O bonds respectively, [g]-attributed to stretching vibrations of Si-O bond.
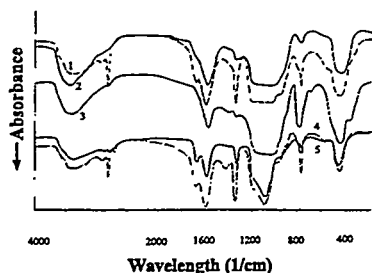
Figure 1 IR spectra of freshly prepared grout SA (1), after 4 months of curing in open air (2), modelled mixture of SA grout with soil (3), effluent after permeability test of sand grouted with SA, upper layer (4), lower layer (5)
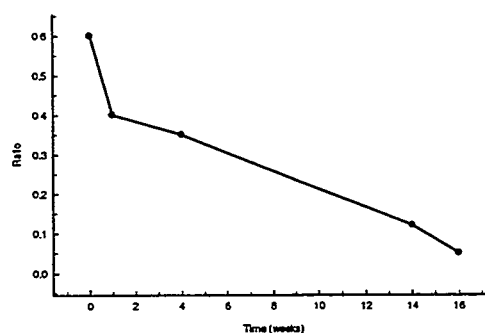
Figure 2 Ratio of absorbance of bands 1360 and 1600 cm^{-1} in IR spectra of SA grout cured in open air

In this situation, the sodium ion remained attached to the oxygen of silicon-oxygen bond. The sharing of the positively charged sodium ion between two oxygens with negative charge resulted in lesser polarization of both bonds. Therefore the position of asymmetric stretching carbonyl vibration can not be equal to that in a completely ionic bond, like in sodium acetate (Nakamoto 1986).

Generally, it can be assumed that transformations in SA grout with initial pH 11.3 occurs according to the following equations:

I $[Si_2O_5]^{-2}$ $2Na^+$ + $2H_2O$ + $2O=COC_2H_5CH_3$ ⇒ $[Si_2O_5]^{-2}....2Na^+....2O=COC_2H_5CH_3$ + H_2O ⇒
                                                         (intermediate complex)

$[Si_2O_5]^{-2}$ $2H^+$ + $2Na-OCOCH_3$ + $2C_2H_5OH$
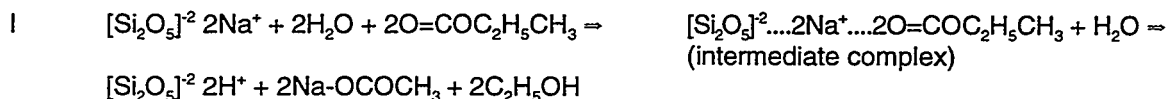
The intermediate complex was stable. The band at 1580 cm^{-1} was found after 4 months of curing a grout sample in open air (Fig.1). For high pH, formamide readily undergoes hydrolysis (Coffey 1965):

$$\text{NaOH}$$
II $HCONH_2$ + H_2O ⇒ $HCONH_4$ ⇒ $HCOONa$ + NH_3 + H_2O

Therefore, in the ^1R spectrum of freshly prepared SA grout, intensive bands related to sodium formate were observed, and the grout odor was similar to ammonia. From the foregoing, the end products of grouting with SA process are: NH_3 (or NH_4OH in water), C_2H_5OH, formate and sodium acetate. All these products are highly water soluble.

2. Chemical processes in soil and sand grouted with SA

In soil and sand specimens grouted with SA, the content of organic compounds introduced was small (approximately 4%). From the spectrum of the modelled mixture of soil and solid SA grout (Fig. 1), only the absorbance of two bands at 1580 cm^{-1} and 1360 cm^{-1} can be measured. Due to losses of organic components during grouting and curing, carbonyl organic compound content became smaller. Therefore, observations and measurements of bands related to carbonyl were difficult.

A curing time of 1, 3, and 7 days at room temperature was provided for the specimens to study the durability of the grouting process with SA and the stability of specimens afterwards. Permeability tests performed with these specimens showed a decrease three (soil) and four (sand) orders of magnitude less than ungrouted specimens after curing for 1 and 3 days. Curing for 7 days exhibited a permeability increase of up to initial value in case of soil specimens and to a value of 2 orders of magnitude less compared to ungrouted specimens in case of sand specimens.

Effluent from permeability tests were untransparent mixtures, colourless for sand specimens and brown for soil specimens. With time, precipitation was observed and mixtures were dividing in two layers: lower solid precipitate and upper liquid layer that became transparent. The IR spectra of samples from the two effluent layers from sand specimens before dividing the layers was completed and are shown in Fig. 1. These spectra are similar to the SA grout spectra discussed above.

This indicates that the grouting process mechanism remained unchanged when the grout was mixed with natural soil or pure sand. However, part of the sodium silicate was eliminated from specimens during permeability tests, probably in the form of intermediate complex with ethylacetate. Also, the band at 1680 cm^{-1} which connected with formamide was more intensive than in spectra of fresh SA grout. The ratio between band absorbencies related to organic compounds and silica was higher for the upper layer. So, the grouting process of sand and soil with SA is slower than the grouting of only SA. Therefore, it should be expected that the presence of initial organic components could also be a source of environment contamination during grouting of sand and soil.

After dividing effluent layers from soil specimens and the upper brown layer became transparent, it was subjected to UV-VIS spectra measurements. These spectra are shown in Fig. 3.

618

The absorbance in the UV-VIS region was high for the specimens after 1 day of curing and decreased with curing time. It is known (Kononova 1961) that humic compounds as a part of soil organic matter when extracted at high pH are brown. During the curing process the extraction of organic matter from soil took place till the pH was high.
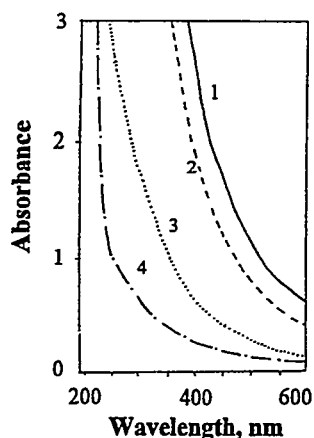
Figure 3 UV-VIS spectra of effluent (upper layer) from soil specimens grouted with SA after 1 (1), 3 (2), 7 (3) days of curing and UV spectrum of tap water (4)

3. The influence of groundwater quality on specimens with SA and SC

The experiments for which the soil specimens were allowed to cure in fresh and salt water were conducted for 60 days. Measurements were executed on the 1st, 7th, 14th and 28th day. The water samples were examined by UV spectra and the silicate content was determined (Fig. 4a). The pH of these samples was measured and is shown in Fig. 4b. It was found that the pH of salt water samples was less than the pH of fresh water samples. The pH of water in which specimens grouted with SA were cured was higher than the pH of specimens cured with SC. Practically the same behaviour was exhibited by dependence of silicate content measured using UV spectra.

When soil and sand specimens grouted with SA were allowed to cure in fresh water, they were destroyed after 13 and 4 days respectively. After curing in salt water, no changes in structure were observed for 60 days. The stability of soil and sand specimens grouted with SC in fresh water was higher in comparison with SA: 60 and 30 days. Curing in salt water did not lead to any visible changes.

Generally, both SA and SC grouted specimens were not affected by saltwater. The thin white layer on the specimens surface was examined by IR spectra. It was found that this thin layer contained carbonates. Hence, the precipitation of calcium and magnesium carbonates occurred. The resulting core from these carbonates on the specimens surface prevented the transfer of sodium silicate (and sodium salts in case of SA grout) in environmental water as well as an increase of its pH. Due to this core, the mechanical stability of specimens also increased.
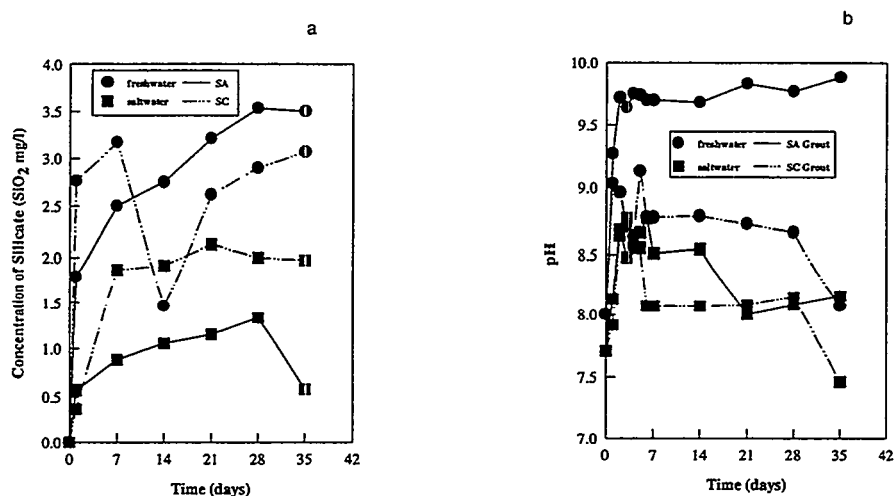
Figure 4 Concentration of silicate (a) and pH of water
(b)

Conclusions

1. SA grouting of soil and sand caused a transfer to the environment of some compounds: sodium formate, sodium acetate, ammonia and part of the initial ethylacetate and formamide. This process had a tendency to decrease for approximately 4 months. The stability of specimens was low.

2. SC grouting of soil and sand caused no significant contamination of the environment. The increase of pH of environmental water was even less than with SA grouting. Also, the stability of specimens is higher in comparison with SA grouting.

3. Salt water protected the specimens grouted with SA and SC from destruction and prevented contamination.

References

Caron C. (1957) French Patent 1,154,835, Soletanche
Gmelins Handbuch der Anorganichen Chemie (1959) 15b, Verlag Chemie, GMBH
Karol, R.H. (1990) Chemical Grouting, Marcel Dekker Inc., N-Y-Basel.
Kononòva, M., Nowakowski, T., Newman A. (1961), Soil Organic Matter: Its Nature..., Pergamon
Muller-Kirchenbauer, H., Barchert K.M., Friedrich, W. (1985) Bautechnik, 4, pp. 130-142
Myshlaeva L.V., Krasnoshekov V.V. (1974) Analytical Chemistry of Silicon, JWS
Nakamoto K. (1986), Infrared and Raman Spectra of Inorganic and Coordination Compounds, JWS
Peeler P. (1959) US Patent 2,209,415, Diamond Alkali
Rodd's Chemistry of Carbon Compounds, Ed. by S.Coffey, 1965, V.1, part C, Elsevier
The Aldrich Library of IR Spectra (1981), Ed. by C.J. Pouchert
The Sygma Lybrary of FT-IR Spectra (1986) v. 1., Ed. by R. J. Keller
Voinovitch, T., Debras-Guedon, J., Louvrier, J. (1966), The analysis of Silicates, Israel

ENGINEERED CLAY-SHREDDED TYRE MIXTURES AS BARRIER MATERIALS

Abir Al-Tabbaa and Thirugnanasam Aravinthan

Abstract

An engineered clay consisting of kaolin and bentonite was mixed with shredded tyre in various weight percentages and examined for use as a constituent in a landfill liner. The clay-tyre mixtures properties in terms of compaction, unconfined compressive strength, permeability to water and paraffin, leachability, stress-strain behaviour, free swell behaviour and swelling pressure were investigated. The results show that the dry density and strength reduced with the addition of tyre and also with increased tyre content but that good interaction was developed between the clay and tyre. The strain at failure increased showing reinforcing effect of the tyre. The permeability to paraffin was considerably reduced compared to that to water due to the presence of the tyre which caused high swelling pressures to develop. The leachability results indicate initial high concentrations leaching out of the soil-tyre mixtures which will be subjected to dilution in the environment. This work adds evidence to the potential advantages of using soil-tyre mixtures as a landfill liner material.

Introduction

In the UK 25 million car tyres and 3 million truck tyres are discarded each year. Of this total amount 18% is used for retreading, 6% for regeneration (e.g. granulation, carbon/oil extraction and steel recovery) and 9% for incineration proposals. This leaves 67% which is stockpiled, landfilled or illegally dumped. The best way to reduce the environmental and health hazards associated with scrap tyres is to minimise, and ultimately eliminate, stockpiling.

Waste tyre material has been utilised successfully on playgrounds and football fields and in paving materials. A potential use of scrap tyre, which has received little attention, can be in soil stabilisation. Shredded tyre can be mixed with different soils to improve their engineering properties for specific applications. The main concern in all these applications is the possible leaching of heavy metals from the tyre into the soil and groundwater. To date, only very few studies have been conducted to evaluate the potential engineering applications of shredded tyre in soil-tyre mixtures (e.g. Baykal et al, 1992, 1995, Black and Shakoor, 1994, Baykal and Alpatli, 1995 and Lyons et al, 1995).

The work reported by Black and Shakoor (1994) showed that some heavy metals such as iron, zinc and chromium could leach out of the tyre in concentrations which would not be acceptable depending on the maximum concentration levels imposed. This conclusion was however reached using severe leaching tests. Because of the potential serious problem of contaminants leaching out of the tyre, this paper investigates the mixing of shredded tyre with soil in such a way as to reduce the general leaching of heavy metals from the tyre to acceptable levels. The paper therefore only considers the mixing of shredded tyre with clayey soils because clays have some ability to adsorb heavy metals.

School of Civil Engineering, The University of Birmingham, Birmingham B15 2TT, UK, (0044) 121 414 5051/5049, A.Al-Tabbaa@bham.ac.uk

One application which could be of considerable value is the use of clay-tyre mixtures in landfill liner and cover materials. Baykal et al (1992, 1995) and Baykal and Alpatli (1995) observed that shredded tyre has a capacity to absorb petroleum based hydrocarbons and by doing so swells to sometimes three times its original size. This applies swelling pressure on the material causing the permeability of the soil-tyre mixture to decrease. This is an interesting finding because organic chemicals particularly hydrocarbons when permeated through soils cause an increase in permeability sometimes by three orders of magnitude because they cause the diffuse double layer to contract. Hence the presence of tyre in the landfill liner material could counterbalance this effect. Obviously, on the one hand, the swelling pressure should be high enough to be effective and on the other, it should not exceed the overburden pressure on the liner so as not to jeopardise the integrity of the liner. Also, tyre has the ability to absorb hydrocarbons without releasing them hence to reduce their leaching out of the landfill liner into the soil and groundwater environment.

The effect of tyre on the strength of soil-tyre mixtures is found to be dependent on the shape of the tyre particles. Lath-shaped particles are reported to increase the strength acting as reinforcement (Baykal & Alpatli, 1995) while circular and angular particles reduce it (Black & Shakoor, 1994, Lyon et al., 1995 and Blackwell, 1995).

The work presented in this paper assesses the behaviour of typical tyre material used in the UK and extends the work already published by others. It examines the behaviour of a specific engineered clay, mixed kaolin and bentonite clay, in clay-tyre mixtures for applications in landfill liner materials. A specific hydrocarbon, paraffin, is used as the permeant and the behaviour is compared to that due to water. The behaviour is investigated in terms of a number of properties of the soil-tyre mixtures such as compaction, strength, stress-strain behaviour, permeability, free swelling behaviour, cracking and leachability.

Materials

An engineered clay consisting of 80% kaolin and 20% bentonite was used. The bentonite was included for its high cation exchange capacity and hence ability to adsorb heavy metals. The shredded tyre used was obtained commercially (Leigh Environmental) in 1 to 8mm angular mixed size free of any scrap metal. The tyre was sieved into two size groups of 1-4mm, 4-8mm and mixed with the soil in percentages ranging from 6% to 20% by weight.

It was not possible to carry out bulk chemical analysis of the shredded tyre to identify the percentages of heavy metals present in it. Hence, the results of the chemical analysis work presented by Black & Shakeer, 1994 on American tyre was used as an initial guideline. They found large amounts of iron, zinc and chromium present and leaching in much higher concentrations than the maximum allowable concentration levels set up the U. S. Environmental Protection Agency (Federal Register, 1992), the worst being chromium. Based on those results, optimum percentages by weight of tyre to be added to the soil were selected such that the percentage added would be expected to produce acceptable concentrations of the heavy metals in leaching tests. The smallest size tyre produced the highest leached concentrations of heavy metals as would be expected because of the large surface area associated with it. Therefore the percentages, by weight, of shredded tyre which were added to the soil were 6% of the 1-4mm, and 15% of both the 4-8mm tyre grading.

Paraffin (molecular structure: $C_{12}H_{26}$ and weight: 170) was used as the petroleum based hydrocarbon in all the tests. Shredded tyre pieces were immersed in paraffin for one hour to assess their susceptibility to swelling by paraffin and found to increase in volume by up to 190% while immersion in water caused 110% increase in volume. Gasoline, used by others increased in volume by 120% after 30 minutes and 250% after one week (Baykal et al., 1995).

Experimental procedure

Standard compaction of the clay and clay-tyre mixtures was carried out using the Dietert compactor with ten blows on either side of the sample. The samples were 38mm in diameter and were trimmed to 76mm high and then tested for their unconfined compressive strength (UCS). Up to three samples were tested for repeatability and gave dry density variation of up to ±5% and UCS variation of up to ±17%.

For the permeability measurements rigid wall permeameters were used and the permeability was measured using the flow pump method (Head, 1992). The confining pressure was not measured. The use of the flow pump speeded up the initial saturation process, produced permeability values within a few days and allowed sufficient permeant to be collected for leachability analyses. A pore pressure transducer at the inflow position measured the pore water pressure there. The vertical permeability was the measured using Darcy's law: $k = (Q \gamma L)/(A \Delta u)$ where Q is the quantity of water discharged per unit time, γ is the unit weight of water, L is the height of sample, A is the cross-sectional area of the sample and Δu is the pore water pressure at the inflow position. The samples were compacted at a moisture content 3% above optimum to give low permeability. Permeability was measured using water, acidic water (sodium acetate solution, pH=4.9 to simulate leaching conditions in the ground) and paraffin as permeants. Up to three samples were tested and gave a variation of up to ±32%.

The leachate analysis was carried out on the distilled and acidic water effluents from the permeability flow pump tests. The heavy metals investigated were zinc, nickel and copper. For comparison purposes, the leachate concentrations were measured once a reasonable quantity of leachate solution of around four pore volumes was obtained.

To correlate the concentrations with those obtained from the Toxicity Characteristic Leaching Procedure (Federal Register, 1986), which is considered a worst case scenario, the TCLP test was carried out on separate samples. In this test a 25g sample of each of the soil, tyre and soil-tyre mixtures was placed in 500mL of each of the two water permeants mentioned above as extraction fluids. The mixture was agitated at 30rpm for 17 hours. The contents were then centrifuged and subsequently filtered to separate the liquid (leachate solution) from the solids. The leachate solutions were then passed through an atomic absorption spectrometer to quantify the concentrations of certain heavy metals in them.

The free swell and swelling pressure tests were carried out in standard oedometers, 75mm in diameter and 19mm high (BS1377, 1991). For comparison purposes, three moisture contents were used for each mix, the optimum and 5% above and below. The samples were compacted in a standard Procter mould and extruded using a cutting ring. The samples were all water compacted. When tested, both water and paraffin were used as the permeant. In most cases swelling was complete within 24 hours.

Results and discussion

Compaction

The compaction behaviour of the clay alone and with the 6% and 15% of 1-4 and 4-8 mm size tyre respectively was investigated in terms of dry density vs. moisture content. The results are shown in Figure 1. The figure shows that the maximum dry density slightly decreased and optimum moisture content stayed the same as the amount of tyre increased. A decrease in the dry density is expected due to the lighter weight of tyre compared to the soil. However the decrease in the dry density was mainly due to that effect which shows that good compaction was achieved. These results are consistent with other published work although in other instances a slight increase in the optimum moisture content was observed as the tyre content increased (Blackwell, 1995; Black & Shakoor, 1994). On physical examination of the compacted samples,

good interaction was observed between the tyre and the clay which improved as the moisture content increased. Cracking was observed with the lower moisture content mixtures and it was minimised when compacting the samples at least 2% above the optimum moisture content.

Unconfined compressive strength (UCS)

The compacted samples were then tested for their unconfined compressive strength and the results are shown in Figure 2. The figure shows that the introduction of the tyre causes a decrease in the UCS with the optimum mixtures producing the highest strengths. These results agree with those observed using angular and round-shaped tyre (Black & Shakoor, 1995 and Lyons et al 1995). Considering the compaction and UCS results together, it seems that although the mixes on the wet side of optimum compacted better than those on the dry side, they produced lower strengths.

Figure 1. Compaction behaviour of clay and clay-tyre mixtures.
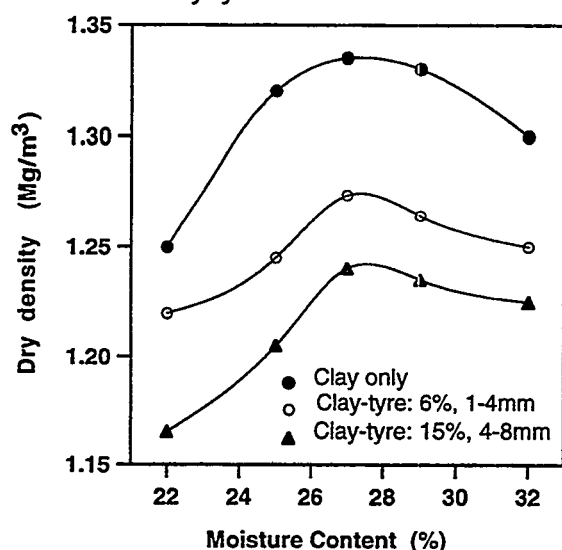
Figure 2. Unconfined compressive strength of clay and clay-tyre mixtures.
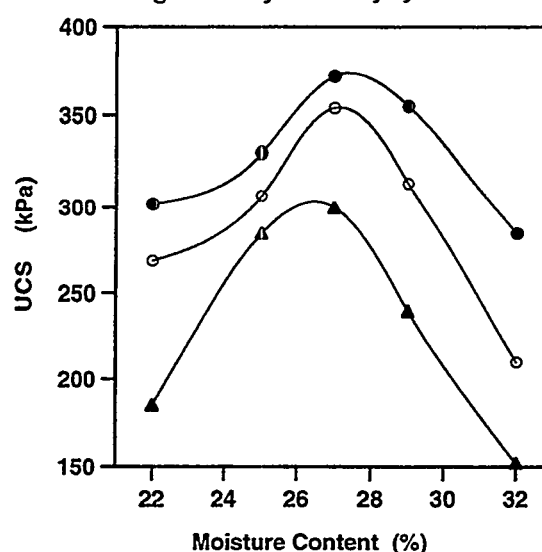
Stress-strain behaviour

The stress-strain behaviour was investigated during the UCS tests and the results are given in Figure 3. The results show that the very initial stiffness of all the mixes remains the same. Following that and leading to the point of failure the stiffness decreased as the tyre content increased. The strain at failure increased as the tyre content increased. The decreased stiffness up to failure indicates a more ductile behaviour and the increased strain at failure indicates that the presence of the tyre has a reinforcing effect on the soil. This behaviour agrees with that observed by Lyon et al (1995) on lath-shaped tyre particles.

Permeability

The permeability was measured using three permeants: distilled water, acidic water and paraffin. The three permeants were used in succession so the permeability was measured using the same sample and hence facilitated direct comparison. The results are shown in Table 1 and show that by using distilled water as the permeant, the permeability of the clay-tyre mixtures increased compared to the clay alone. This agrees with the results reported by Black & Shakoor, 1994. However the increase is not significant indicating good interaction between the clay and tyre and that the development of large pores and cracks was minimal. When acidic water was used as the permeant, the permeability slightly increased for both the clay and clay-tyre mixtures. This is due to the acidic environment which facilitates flocculation and hence a higher permeability. When paraffin was the permeant, the permeability of the clay increased over ten times. This is the

expected effect of hydrocarbons with lower dielectric constants caused the diffuse double layer to shrink and the permeability to increase. When paraffin was permeated through the clay-tyre samples the permeability decreased below the permeability of the clay alone. The permeability to paraffin compared to water reduced by over fifty times when using 15% of 4-8mm tyre grading. The observed trend in the permeability behaviour agrees well with that observed for gasoline by Baykal et al (1992) and Baykal & Alpatli (1995) who report a decrease in permeability of clays of seven times to gasoline compared to water.

Figure 3. Stress-strain behaviour of clay and clay-tyre mixtures.
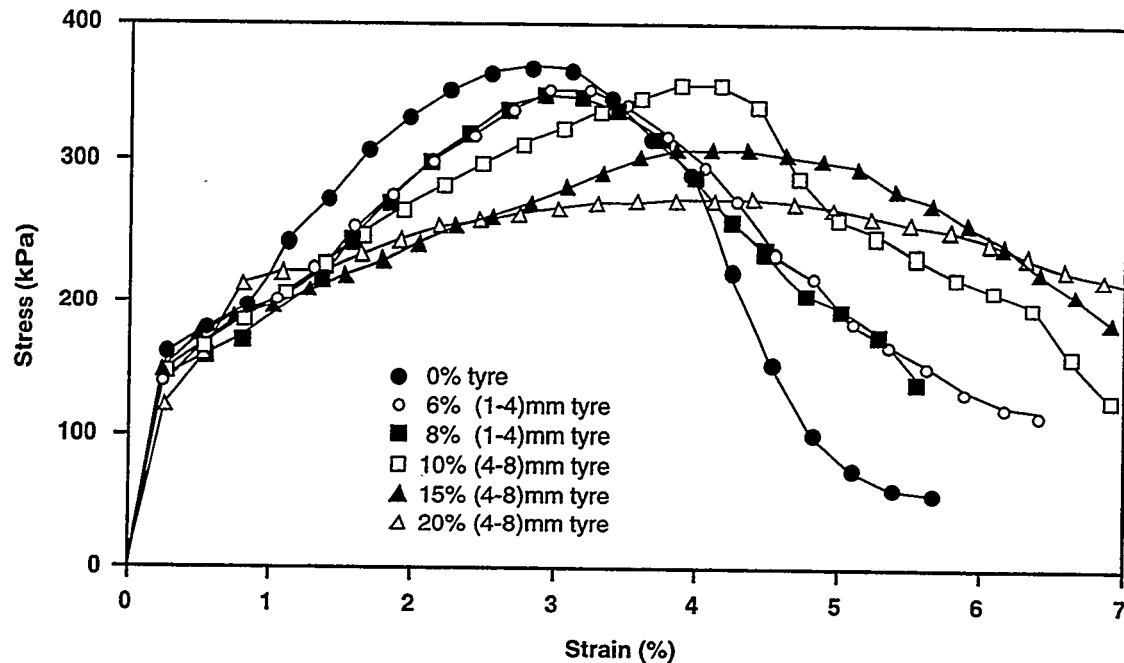
Table 1. Permeability of clay and clay-tyre mixtures to different permeants.

material	Permeability ($\times 10^{-9}$ m/s)		
	distilled water	acidic water	paraffin
clay	2.0	2.8	26
clay-tyre: 6%, 1-4mm	4.2	5.7	0.93
clay-tyre: 15%, 4-8mm	6.3	8.2	0.12

Leaching

The leachability results in terms of concentrations of zinc, nickel and copper are reported in Table 2. Also reported are the zinc concentrations from the TCLP test from a related study (Blackwell, 1995) for comparison purposes. The concentrations shown are those for the acidic water permeant as no detectable concentrations were measured when water was the permeant. As can be seen the leached concentrations of Zn are similar to those produced in the TCLP test. The TCLP test is considered a worst case scenario because the agitation ensures full exposure of the tyre to the leaching solution. Less exposure would be expected when a leachate is permeated through a clay-tyre mixture. However, the TCLP uses a ratio of solid (soil-tyre material) to fluid (extraction fluid) of 20:1 to allow for dilution into the environment. This dilution is not facilitated as the leachate solution permeates through the clay-tyre material. Hence the quantity of leachate which needs to be collected is 20 times that actually collected. A detailed investigation of how the leachate concentrations of heavy metals change with time would give a better understanding of the leaching behaviour. A correlation will need to be established between the two leaching tests to enable a meaningful comparison between the results.

Table 2. Leaching results of tyre and clay-tyre mixtures using acidic water.

	tyre grading mm	% tyre	concentration (mg/L)			
			Zn	Ni	Cu	TCLP Zn**
tyre	1-4	100	9.65	1.72	0.05	10.37
	4-8	100	8.43	0.73	n/d	8.57
clay-tyre	1-4	6	1.42	0.03	n/d	1.64
clay-tyre	4-8	15	1.24	n/d	0.24	1.56
maximum*			5.00	0.05	3.00	5.00

* Drinking water standards from Severn Trent Laboratories, UK. **From Blackwell (1995).

Free swell and swelling pressure tests

Figures 4 (a) and (b) show the maximum free swelling of the clay and clay-tyre mixtures at different moisture contents using water and paraffin as the permeant respectively. Figure 4 (a) shows the swelling which takes place without tyre compared to the reduced amount of swelling which takes place following the introduction of the tyre particularly at moisture contents away from optimum. This could be due to the presence of cracks which accommodated the water. Figure 4(b) shows the limited amount of swelling which takes place when paraffin is the permeant compared to water for the clay alone. This is probably related to the fact that bentonite becomes non-plastic in the presence of hydrocarbons and hence does not swell and also due to shrinking of the diffuse double layer of both kaolin and bentonite in the presence of paraffin (Baykal et al, 1995). It also shows the considerable increase in swelling which takes place on the introduction of the tyre. These observations show the same trend as those reported by Baykal & Alpatli (1995) for gasoline permeated pure kaolin and bentonite clays.

Figure 4. Maximum free swell of clay and clay-tyre mixtures with (a) water and (b) paraffin as the permeant.

(a)   (b)
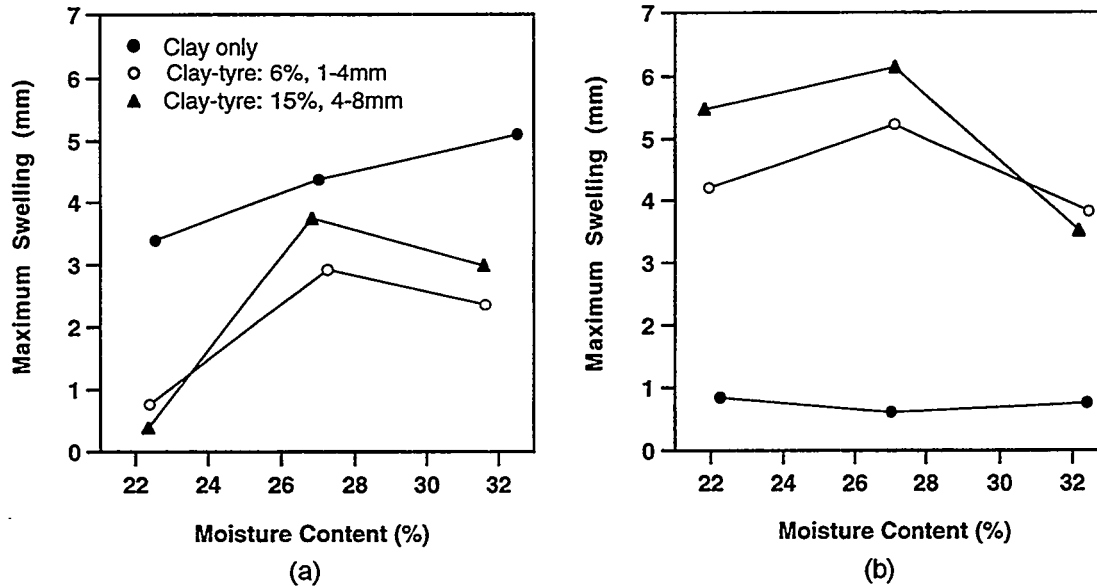
Figures 5(a) and (b) show the corresponding swelling pressures developed with similar trend to that of swelling. Again this shows how the swelling pressure of the water permeated samples reduced as the tyre is introduced while it increased considerably for paraffin permeated samples. It also shows how in the absence of the tyre the swelling pressure of paraffin permeated samples is low and hence the swelling pressure is due to the large expansion of the tyre particles. These swelling pressures will need to be assessed in relation to the overburden pressure and hence the required swelling pressure could be achieved by adding the appropriate percentage of tyre.

Conclusions

The addition of tyre to soil produces a mixture with desirable properties for use as part of a landfill liner. The permeability of soil-tyre mixtures to paraffin was considerably reduced compared to that to water due to the presence of the tyre which caused reasonable swelling pressures to develop. The developed pressures should be assessed in relation to the overburden pressure and the required pressure could be achieved by using the appropriate tyre content. The strain at failure increased showing reinforcing effect of the tyre. The dry density and strength reduced with the addition of tyre and also with increased tyre content but good interaction was developed between the clay and tyre particles. Such detrimental effects will need to be taken into account. The leachability results indicate initial high concentrations leaching out of the soil-tyre mixtures which will be subject to dilution in the environment. Leachability analyses will need to be assessed in relation to real in situ situations.

Figure 5. Swelling pressure for clay and clay-tyre mixtures with (a) water and (b) paraffin as the permeant

(a) (b)
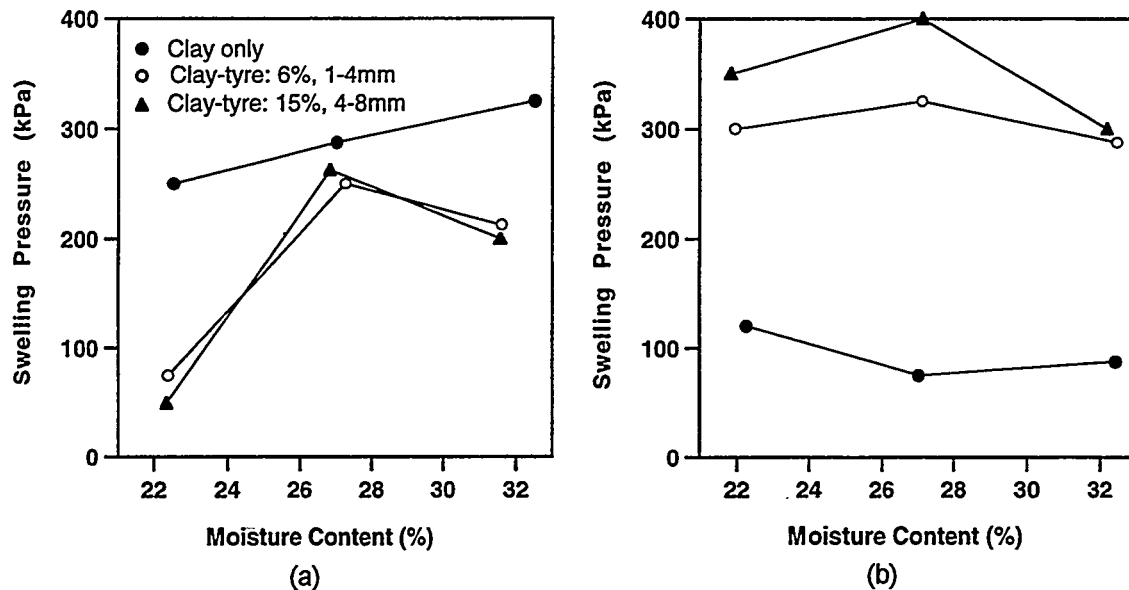
References

Aravinthan T (1996)   Soil-tyre mixtures: swelling and stress-strain behaviour, MSc thesis, University of Birmingham.

Baykal, G, Yessiler, N and Koprulu, K (1992) Rubber clay liners against petroleum based contaminants, Proceedings , Environmental Geotechnology (M Usmen & Y Acar (eds)), Balkema, pp 477-481.

Baykal, G, Kaval, A and Alpatli, H M (1995) Rubber-kaolinite and rubber-bentonite liners, Waste disposal by landfill, Green'93, Sarsby (ed.) Balkema, pp 399-404.

Baykal, G and Alpatli, H M (1995) Permeability of rubber-soil liners under confinement, ASCE Geotechnical Special Publication No. 46, Eds Y B Acar and D E Daniel, ASCE, pp 718-731.

Black, B A and Shakoor, A (1994) "A geotechnical investigation of soil-tire mixtures for engineering applications", Proc. of 1st Int. Conf. on Environmental Geotechnics, Bitech Publications, pp 617-623.

Blackwell, O (1995)   Soil-tyre mixtures for geotechnical applications, MSc thesis, University of Birmingham, UK.

BS1377 (1991) Methods of testing soils for civil engineering purposes, British Standards Institutions, London.

Federal Register (1986) "Toxicity Characteristics Leaching Procedure", Vol. 51, No. 216, pp40643-40652.

Federal Register (1992). CFR 57, Washington, D.C. p. 60848.

Head, H K (1986) Manual for laboratory testing, Pentech Press, London.

Leigh Environmental Limited (Rubber Processing Division), Wolverhampton WV10 7DQ, UK.

Lyons J C, Hitchens, D G and Monticello, D A (1995) Recovery of scrap rubber tires from landfill for construction uses, Waste disposal by Landfill, Green'93, Sarsby (ed.), Balkema, pp 327-334.

DESIGN OF DRY BARRIERS
FOR CONTAINMENT OF CONTAMINANTS IN UNSATURATED SOILS

Carl E. Morris[1]
Bruce M. Thomson[2]
John C. Stormont[2]

ABSTRACT

A dry barrier is a region of very dry conditions in unsaturated soil that prevents vertical migration of water created by circulating dry air through the formation. Dry soil creates a barrier to vertical water movement by decreasing the soil's hydraulic conductivity, a concept also used in capillary barriers. A dry barrier may be a viable method for providing containment of a contaminant plume in a setting with a thick unsaturated zone and dry climate. The principal factors which determine the feasibility of a dry barrier include: 1) an arid environment, 2) thick vadose zone, and 3) the ability to circulate air through the vadose zone. This study investigated the technical and economic considerations associated with creating a dry barrier to provide containment of a hypothetical 1 ha aqueous contaminant plume. The concept appears to be competitive with other interim containment methods such as ground freezing.

INTRODUCTION

Remediation activities that take place following release of a contaminant to the soil environment may be categorized as: containment of pollutants, removal of contaminated soils, removal of mobile constituents, or in-situ stabilization or degradation of the contaminants. Recent developments associated with containment and remediation technologies have provided increasingly effective waste management options in soil formations with shallow depths to groundwater. However, there remains a need for containment and remediation alternatives at sites where a thick unsaturated zone is present beneath the pollutant source. One possible method that could be applied at sites where a thick unsaturated zone exists is the use of a dry barrier. A dry barrier is a layer of geologic material in which the soil moisture content is reduced to very low values by circulating dry air through it. Drying the soil layer creates a barrier to water movement by reducing the hydraulic conductivity to extremely low values. For example, the hydraulic conductivity of a typical sand may decrease by three orders of magnitude as its moisture content is decreased from 20 to 10 percent (Morris and Thomson, 1995). The coarser the material, the greater the reduction in its hydraulic conductivity as it dries. Figure 1 illustrates the concept of a dry barrier in a sub-surface application. Dry barriers may also be effective for landfill covers (Stormont et al., 1995).

This paper briefly introduces the theoretical concepts associated with creation of a dry barrier, and then summarizes the components of the design process. The results of a feasibility study for creating a dry barrier at a hypothetical site in Albuquerque, NM are presented. This paper considers both the technical and economic aspects of installing and operating a subsurface dry barrier system to provide containment of a 1 ha contaminant plume for a period of 10 years.

THEORETICAL CONSIDERATIONS

The design of a dry barrier is necessarily site specific and depends on many variables. Table 1 is a summary of the principal variables that must be considered. The most important information required is the areal extent and location of the contaminant plume so that the depth and size of the barrier can be determined. The second most important information is knowledge of the

---

[1] Dept. of Civil and Mining Engineering, University of Wollongong, Wollongong, NSW, 2522, Australia

[2] Dept. of Civil Engineering, University of New Mexico, Albuquerque, NM, 87131

seasonal meteorological conditions, principally precipitation, temperature and humidity. The size of the barrier, combined with the meteorological conditions at the site will determine the air flow required to maintain the system, while the hydraulic characteristics of the soils in which the air injection and extraction wells are to be installed determine well locations and designs. Lastly, the electric power rate structure must be known so that the system can be designed and operated under the most cost-effective conditions.
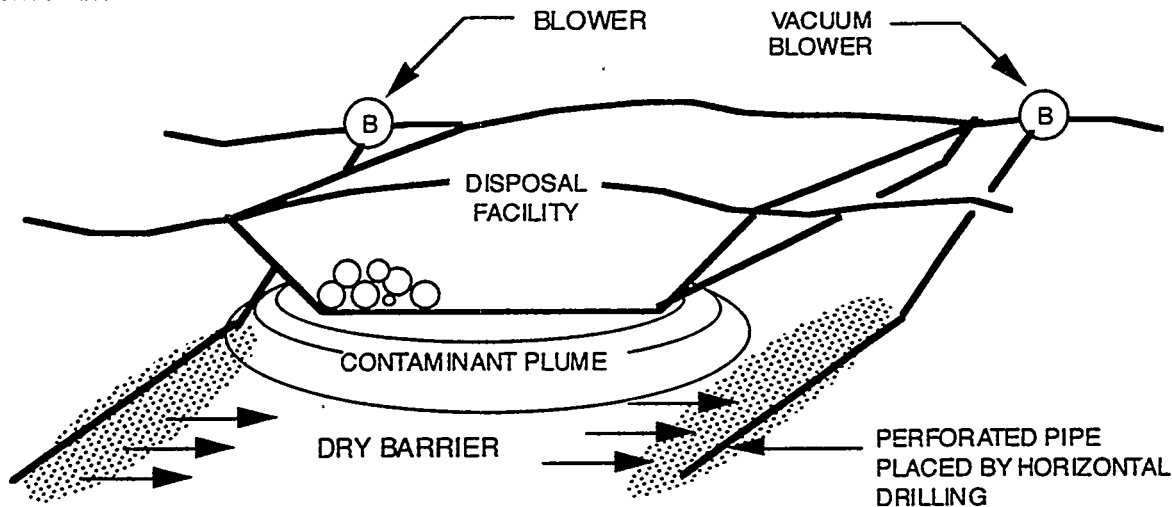
Figure 1. Schematic diagram of the dry barrier concept.

The variables presented in Table 1 are all related and interdependent. A change in any one variable will propagate through the design and affect the well spacing, size of the blowers, motors and piping. Because of this interdependence, the design process may require several iterations to produce an optimum system.

Moisture Removal in Subsurface Environments. Air movement is a convenient method for removal and transport of water and other volatile constituents from subsurface soils. When designing a dry barrier two factors must be considered regarding moisture removal: the mass of moisture to be removed per unit time and the ability of air to evaporate and transport this moisture. Under steady-state conditions, the mass of moisture that must be removed to maintain a dry barrier is simply the vertical water flux that infiltrates through the soil column due to atmospheric precipitation. Infiltration rates depend on factors such as climatic conditions, soil type, slope, vegetative cover and exposure. The mass of moisture to be removed from a dry barrier per unit time is simply the mass infiltration rate times the area of the barrier.

The ability of air to remove moisture depends on its temperature as well as its relative humidity. In a subsurface barrier the soil will have a large thermal mass and will be at a different temperature than that of atmospheric air. As a first approximation, the subsurface soil temperature is equal to the annual average air temperature and can be assumed to be constant. The ability of air to remove water by evaporation is termed its drying potential (W_{DP}), which is the difference between the saturated

Site Variable	Importance
Three dimensional extent of contaminant plume	Determines areal extent and minimum depth of barrier
Soil characteristics	Determines well spacing and blower sizes.
Annual precipitation	Calculate moisture removal requirements
Daily temperature and humidity of air	Calculate ability of air to remove moisture
Power rate structure	Determine tradeoffs between operating and capital costs

Table 1. Dry barrier site and design variables

humidity ratio (W_s) and the actual humidity ratio (W). Therefore, if the air has a high humidity ratio, its drying potential is low and vice versa. The drying potential can be calculated as: $W_{DP} = W_s - W$ (ASHRAE, 1993). The saturated humidity ratio (W_s) is a function of temperature and atmospheric pressure. The humidity ratio of a gas (W) depends on these variables as well as relative humidity. Values for these parameters can be calculated (ASHRAE, 1993) or found in a psychrometric chart or table. If the air is warmer than the soil (i.e. summer), the relative humidity of the air decreases as it cools to the soil temperature in the dry barrier resulting in little drying capacity of the air. In the winter months the opposite will happen; the soil will warm the air, thereby increasing its drying potential.

The monthly variations in humidity ratio (W) throughout the year for Albuquerque are illustrated in Figure 2. The maximum humidity ratio (W_s) and the drying potential (W_{DP}) are also plotted using the air temperature to define W_s. Figure 2 shows that the maximum drying potential occurs in the summer months. If the air is injected into a subsurface barrier, compensation must be made to account for the change in air temperature from ambient to that of the soil. Figure 3 shows the same data corrected to the Albuquerque subsurface soil temperature of 13 °C. The humidity ratio shows the same trend as in the previous figure, low in the winter and high in the summer, but a major change is seen in the drying potential of the air. Because the soil temperature is assumed to be constant throughout the year, the drying potential reaches a maximum during the winter and drops to near zero during the summer months. This is opposite to the trend shown in Figure 2.

Figure 2. Humidity ratio of air for Albuquerque, NM, showing drying potential of air.

Daily drying capacity of Albuquerque air varies from a high of approximately 0.01 kg H_2O/kg air to a low of -0.002 kg H_2O/kg air. Negative values during the summer months could result in condensation of moisture in the relatively cool soil matrix. From the daily data one can calculate an annual average drying potential for a subsurface barrier of 0.0059 kg H_2O/kg air.

For a given drying potential (W_{DP}) and water infiltration rate (G_r), the volume of air (Vol_a) required to remove the annual infiltrating water mass is:

$$Vol_a = \frac{G_r}{W_{DP} \, r_a} \quad (1)$$

Figure 3. Humidity ratio and drying potential of air for Albuquerque, NM, corrected to average soil temperature.

Vol_a represents the total volume of air needed to remove the annual mass of water infiltration. If the drying occurs over a portion of the year, this volume of air must be delivered in this period by using a correspondingly larger daily flow rate than that assuming flow for the entire (365 day) year. If the system is to be run

only during night hours, the calculation must also include this factor. Depending on the operations schedule, one or more air flow rates for the barrier can be calculated. The next step is to determine the pressure drop through the system so that the air circulation system can be sized.

Air Flow Hydraulics. The pressure drop through the soil is important in sizing blowers and is a function of the site variables identified in Table 1. These parameters are the air velocity; the intrinsic soil permeability; the screened length of the injection and extraction wells; the distance over which the pressure drop will occur; and the viscosity of air . Air flow through the soil can then be calculated using Darcy's law. This is valid provided the pressure differential is less than about 0.2 atmospheres; larger pressure differentials require consideration of compressibility.

Pipe sizes and materials for the air handling system must be selected to provide acceptable head losses. Head losses are a function of air flow rate, pipe size, geometry, roughness, and length. The pressure drop for the piping system must then be added to the pressure drop for the air flow through the soil matrix to find the total pressure drop through the system. The pressure drop can then be used to select appropriate air blowers.

SUBSURFACE DRY BARRIER DESIGN PROCESS

The dry barrier design process begins by identifying the site characteristics identified in Table 1. The second step is to determine the annual average infiltration rate at the site. This is a difficult parameter to measure, and most often must be estimated from meteorological data and soil conditions. Surface vegetation is especially effective at collecting and transpiring soil moisture to the atmosphere and will significantly decrease the infiltration rate to the point of virtually eliminating it in some instances (Hakonson et al., 1992). Water balance models such as the HELP model (Schroeder et al., 1984) may be used to estimate infiltration rates in the absence of field measurements. The next step in the design process is to calculate the seasonal values of the drying potential of the air (W_{DP}). The drying potential and the annual infiltration are then used to calculate the required annual volume of air to remove the water infiltration flux using equation (1).

To this point the dry barrier design process is relatively straightforward as there has not been consideration of economic factors. The next step in the design process is to lay out the subsurface air circulation system using a combination of air injection and extraction wells. Due to the very slow downward migration of water through unsaturated soil, it is possible to base the air flow calculations on annual average conditions at the site. Since the objective is to create a horizontal barrier beneath a contaminant plume, the use of horizontal well technology is especially appropriate, however, a system of vertical air circulation wells may be equally effective (Birdsell et al., 1994). The air handling system (piping, blowers, and vacuum blowers) can be designed once the wells are located. The size of the blowers will be determined by the air flow hydraulics through the unsaturated soil and through the piping system. The initial step in the design process is based on 12 months of operation of the air handling system.

Once a preliminary system design has been completed, an economic analysis must be performed. This will consist of determining both the capital costs and the operations and maintenance (O&M) costs. The capital costs consist of the costs of constructing the wells and the air handling system. Operations and maintenance costs principally consist of power costs for running the blowers.

There are tradeoffs between capital and O&M costs in the design process. A system operating continuously, 365 days per year will have the lowest capital costs because the air volume required to create the dry barrier (equation 2) is pumped over a period of an entire year. Therefore, the smallest blowers and pipes, and largest well spacing can be used, however, this system will also have the highest O&M costs. There are two situations that may be taken advantage of to reduce O&M costs: 1) seasonal periods in which the drying potential of the air is low or even negative, and 2) a time-of-day rate structure which offers cheaper electric rates during off-peak hours. An

example of the first situation is illustrated in Figure 3; the drying potential of Albuquerque air during the summer months is so low that negligible soil moisture removal will occur. Therefore, a more cost effective method of maintaining a dry barrier may be to increase the size of the air handling equipment so that the same mass of moisture can be removed in 265 days rather than 365. The second situation is also realized in Albuquerque where the local utility offers off-peak electric rates that are less than half of the peak load rates. Again, the designed system must be larger to account for its discontinuous operation.

EXAMPLE DESIGN OF A DRY BARRIER

The design process is illustrated for a subsurface dry barrier beneath a hypothetical one hectare site in Albuquerque, NM. The parameters used in the analysis, which are based on actual data and conditions for Albuquerque, are listed in Table 2. The first step in the design process is the determination of the amount of moisture to be removed from the system on a yearly basis. Using values from Table 2 determine that 1×10^5 kg/year of water must be removed from the soil to create a barrier. Note that an engineered cover such as might be constructed over a landfill may significantly reduce the annual infiltration rate. Once this value is known, air flow rates can be calculated for various operating options.

Parameter	Value
Annual precipitation	20.6 cm
Annual infiltration to depth	1 cm
Length of barrier	100 m
Width of barrier	100 m
Soil permeability	10^{-10} m^2
Annual average temperature	13° C
Viscosity of air	1.8×10^{-5} kg/m-s
Density of air	1.2 kg/m^3

Table 2. Design parameters for a subsurface dry barrier located in Albuquerque, NM.

Air flow required to remove moisture from the barrier depends on the drying potential, (Figure 3). The drying potential shows a marked decrease for the 100 days of summer. Because drying during this period is limited, one operating alternative option is to operate the system for 265 days each year. The average drying potentials (W_{DP}) are 6 g H_2O/kg air and 7 g H_2O/kg air for 365 day and 265 day operation respectively. Also, due to the electric rate structure in Albuquerque, a second option to explore would be the possibility of operating the system only during off-peak hours. The local electric utility offers off-peak rates that are significantly lower and apply for 108 out of 168 weekly hours. The combination of operating options leads to 4 scenarios to be examined. Four air flow rates were calculated for these four scenarios. These are summarized in Table 3.

	365-day operation	265-day operation
Continuous	0.45 m^3/s	0.53 m^3/s
Off-peak	0.70 m^3/s	0.82 m^3/s

Table 3. Required air flow rates to maintain a dry barrier in Albuquerque, NM

The piping system was designed next and blowers selected. The use of horizontal air injection and extraction wells was assumed in this design. 100 m spacing between the two wells was used to calculate the pressure drop in the subsurface formation for each of the flow rates listed in Table 3. The final step in the design process is selection of blowers for each of the operating options. Four blowers were identified from a manufacturer for each of the four air flows and pressure drops determined in the designs. Table 4 lists the power requirements under each option condition.

	365-day operation	265-day operation
Continuous	3 kW 4 hp	3.75 kW 5 hp
Off-peak	7.5 kW 10 hp	9 kW 12 hp

Table 4. Power requirements for air injection or extraction wells for four operating scenarios for a dry barrier in Albuquerque, NM.

The cost of installing a subsurface dry barrier is difficult to project due to the large variation in costs of well drilling, and this is especially true of drilling horizontal wells. Wilson and Kaback (1993) compiled data on horizontal wells drilled in the U.S. and found that unit costs per meter of length varied from $103/m to $3,000/m. The analysis presented here used costs of $354/m and $715m based on similarities to projects described by Wilson and Kaback (1993). These costs should be considered as lower and upper bounds in this analysis.

Information needed to determine the overall cost of drilling horizontal wells includes the depth of the screen, the entry angle of the borehole, the radius of curvature of the hole, and the screened length of the well. Based on the unit drilling costs of $354/m and $715/m, the total horizontal well installation costs range from $129,600 to $261,600, for the two wells required to create a dry barrier system.

Comparison of Alternative Operating Scenarios. If the dry barrier system is expected to operate for many years , the best option will likely be a configuration that yields the lowest annual power costs. Table 6 lists the yearly power requirements and costs for the four operating options. The table shows that operating 24 hours a day during the non-summer months (265 days/year) gives the lowest annual power costs. Though there are differences in operating costs between the four operating scenarios, the difference is not large and a more complete economic analysis than that given here may be required to identify the best design.

	365-day operation	265-day operation
Continuous	$5,160 52,560 kW-hr	$4,455 47,700 kW-hr
Off-peak	$6,587 84,471 kW-hr	$5,543 73,172 kW-hr

Table 5. Operating costs and power requirements for a dry barrier system in Albuquerque, NM

System Costs. An economic analysis of this design was performed, based on system lives of 2, 5 and 10 years. The cost that would be incurred when installing and operating the subsurface dry barrier were broken into three categories: construction, capital, and operation and maintenance. The construction and capital equipment costs will be similar for the three proposed project lifetimes; only the operating costs will vary. The construction and capital costs are estimated to range from $155,600 to $287,600, depending on which unit drilling cost is used. Operating costs are approximately $9,500 per year based on the continuous 265-day operation scenario. The annualized costs for the three project lifetimes for the two drilling costs are summarized in Table 6.

Drilling cost	Total Annualized Costs		
	2 year life	5 year life	10 year life
$354/m	$87,300	$40,620	$25,060
$715/m	$153,300	$67,020	$38,260

Table 6. Annualized costs for a subsurface dry barrier system in Albuquerque, NM.

CONCLUSIONS

This study considered the technical and economic feasibility associated with use of a dry barrier to achieve containment of mobile constituents in unsaturated soils. This is a new technology that has not yet been demonstrated at a full scale. Successful application of a dry barrier system principally depends on three factors: 1) the presence of fluid-borne contaminants, 2) climatic conditions conducive to evaporation of water from soil, and 3) site characteristics which are compatible with construction and maintenance of a dry barrier system. These considerations are discussed below.

It is important that the climatic conditions at the site must be compatible with removal of water by evaporation. The annual infiltration rate must be small to minimize the mass of water to be removed. This may be met in arid and semi-arid environments with low annual precipitation, or an engineered process may be designed to reduce infiltration rates through the use of impervious or

vegetative covers. It is likely that dry barriers will see their principal application in arid climates characterized by an annual evaporation-to-rainfall ratio greater than about four.

Site characteristics must be considered in determining the feasibility of a dry barrier. Of particular importance is the presence of a thick, high permeability unsaturated zone to allow circulation of large volumes of dry air. A thick unsaturated zone is needed to circulate air between injection and extraction wells without undo influence from the surface. High permeability is needed to keep pressure drops, and therefore pumping costs, low.

The analysis presented in this report suggests that drilling costs are by far the most expensive part of a subsurface dry barrier application. Improvements in horizontal drilling technologies will reduce the costs substantially, however, it is clear that alternative methods of developing a subsurface dry barrier are also needed.

For non-volatile and non-degradable constituents it must be recognized that dry barriers represent only a containment mechanism and one that is effective only as long as air is actively circulated through the formation. The barrier would function until remediation activities either removed the contaminants from the soil matrix or rendered them permanently immobile. In this regard the technology is similar to cryogenic methods which provide containment by freezing the soil (Dash, 1991). Under these circumstances the dry barrier concept appears to be technically and economically viable as a temporary containment strategy. If volatile constituents are present, a dry barrier, in addition to providing containment, would be an effective remediation process that would remove contaminants from the subsurface environment.

REFERENCES

American Society of Heating, Refrigerating and Air-Conditioning Engineers, (1993) *ASHRAE Handbook 1993 Fundamentals*, Washington, D.C.

Birdsell, K.H., Rosenberg, N.D., Edlund, K.M. (1994) *Performance of Horizontal versus Vertical Vapor Extraction Wells*. Los Alamos National Laboratory, LA-12783-MS.

Dash, J.G. (1991) Ice Technology for Hazardous Waste Management, *Waste Mgt.*, 11, pp. 183-191.

Hakonson, T.E., Lane, L.J., Springer, E.P. (1992) Biotic and Abiotic Process, Ch. 4 in *Deserts As Dumps?*, Reith, C.R. and Thomson, B.M. (editors), Univ. of New Mexico Press, Albuquerque, NM pp. 101-146.

Morris, C.E., Thomson, B.M., and Stormont, J.C. (1994). *Assessment of Dry Barriers for Containment of Mobile Constituents in the Unsaturated Zone*. Sandia National Laboratories Report, SAND94-2094, Albuquerque, NM.

Morris, C.E, and Thomson, B.M. (1996) Water and Vapor Transport in a Two-Layer Soil System, Proc. *3rd Intl. Symposium on Environmental Geotechnology*, San Diego, CA, pgs 282-291.

Schroeder, P.R., Morgan, J.M., Walski, T.M, Gibson, A.C. (1984) The Hydrologic Evaluation of Landfill Performance (HELP) Model, Vols. I and II, EPA/530-SW-84-010, U.S. Environmental Protection Agency, Washington, D.C.

Stormont, J.C. (1995) Alternative Barrier Layers for Surface Covers in Dry Climates. in *GeoEnvironmental Issues Facing the Americas, Special Geotechnical Publication No. 47*, American Society of Civil Engineers.

Wilson, D.D. and Kaback, D.S. (1993) *Industry Survey for Horizontal Wells*. Final Report, Westinghouse Savannah River Company, WSRC-TR-93-511.

EFFECT OF pH ON THE HEAVY METAL-CLAY MINERAL INTERACTION

Orhan Altýn, H.Önder Özbelge, Timur Doğu, Tülay A. Özbelge
Middle East Technical University, Department of Chemical Engineering, 06531,Ankara, Turkey.
oaltin@rorqual.cc.metu.edu.tr

ABSTRACT

Adsorption and ion exchange of Pb and Cd on the surface of kaolinite and montmorillonite were studied with a strong emphasis on the pH values of solutions containing heavy metal ions. The pH range studied was 2.5 - 9. For kaolinite at a clay/solution ratio of 1/10 (w/w), Pb removal changes from 20 to 30% for an initial Pb concentration of 1640 ppm, and Cd removal changes from 10 to 20% for an initial Cd concentration of 1809 ppm. Due to its high exchange capacity, montmorillonite can remove more heavy metal than kaolinite. Removal rates for montmorillonite can reach up to 90% for both Pb and Cd. In the pH range of 3-6, there is a plateau for the removal rates. At pH values higher than 6, removal seems to increase artificially due to the precipitation of heavy metals. Under similar conditions for both clays, the rate of removal of Pb is always higher than that of Cd. As the pH value decreases for montmorillonite, there is a strong tendency for decreased surface area and swelling, as indicated by BET surface area measurements, adsorbed layer thickness and pore size distribution data. In the range of pH values studied, X-ray diffraction analysis showed the appearance of a characteristic (001) peak for montmorillonite, indicating that the crystalline structure of the clay was intact during the experiments.

INTRODUCTION

One of the many factors affecting the ion exchange and sorption properties of minerals is the pH of soil-solution. The amount of Pb and Cd sorbed in montmorillonite and kaolinite depends on the kind of exchangeable cation(Garcia-Miragaya et al. 1976, Ziper, 1988) and pH (Harter, 1983, Schulthess and Huang, 1990). The medium pH determines electrostatic behaviour between the layers of montmorillonite and edges of both montmorillonite and kaolinite. Yong et al.(1992) indicated that the solution pH and electrolyte concentration influence the development of both positive and negative surface charges. In addition to surface charges, the organic content of clay minerals is affected by the medium pH. Organic matter is present in mineral surface soils in proportions as small as 0.5% to 5 % by weight. Cabbar et al. (1996) investigated the effect of different concentrations of humic substances on the physical characteristics of montmorillonite, including porosity and surface area. The pH of a clay soil-solution affects the interlayer distance of montmorillonite and the surface area available for ion exchange. The ratio of Si and Al sites is therefore a function of pH.

The objective of this study is to identify the effect of pH on the removal of Pb and Cd using unmodified montmorillonite and Ca and Na saturated kaolinite and montmorillonite. The effects of pH on important physico-chemical parameters were also determined, including: i. Surface area, ii. organic content, iii. pore size distribution, iv. porosity, and v. X-ray diffraction.

EXPERIMENTAL

In this work the following sets of experiments were performed to characterize the clay minerals studied: 1. Chemical analysis, 2. X-ray diffraction analysis, 3. Particle size analysis, 4. Surface area analysis and porosity determination and 5. Ion exchange equilibrium experiments.

1. Chemical analyses of montmorillonite(M) and kaolinite(K) were performed by inductively coupled plasma (ICP) and X-ray fluorescence (Table 1.)

Table 1. Chemical compositions obtained by XRF and ICP for montmorillonite(M) and kaolinite(K).

| | | | | | | | | | percent | | | ppm | | | |
	SIO_2	Al_2O_3	Fe_2O_3	CaO	K_2O	FeO	Na_2O	MgO	LOI	Cu	Cr	Pb	Ni	Cd	Zn
M	63.0	16.5	6.00	1.80	1.00	0.01	3.20	2.35	6.17	50	120	ND	91	ND	75
K	68.0	20.0	1.80	0.50	0.80	0.07	0.19	0.41	6.96	20	56	ND	27	ND	55

M: montmorillonite, K: kaolinite
ND: not detected, LOI : Loss of ignition.

2. X-ray diffraction measurements of both montmorillonite and kaolinite were carried out according to the method outlined by Mehra and Jackson (1960). Using this method, the removal of organics was achieved by treating the soil with hydrogen peroxide and iron oxides, and cementing agents were removed by sodium dithionite. In order to asses the effect of nitric acid on the crystal structure of montmorillonite, X-ray diffraction patterns were obtained for different pH-adjusted clay minerals. In the range of pH values studied, the X-ray diffraction analyses showed the appearance of the characteristic (001) peak for montmorillonite, indicating that crystalline structure of the clay did not change.

3. For the particle size analysis, the clay minerals received were sieved to 200 mesh size and, using an image analyzer, the average particle size was found to be 20 μ.

4. The external surface area determinations of clays were based on the BET(Brunauer-Emmett-Teller) equation using a Micromeritics ASAP 2000, N_2-adsorption surface area analyzer. Unmodified montmorillonite and kaolinite samples were degassed overnight at 80 °C. In addition, completely Na-saturated and pH-adjusted montmorillonite samples were analyzed. These pH-adjusted clays were freeze-dried and then degassed at 40 °C under vacuum before analysis. By the freeze drying technique, it was possible to measure the surface area of the clay at any swelled condition. The BET surface areas of unmodified montmorillonite and kaolinite were 14.7 and 13.6 m^2/g, respectively. However, if the montmorillonite was swelled by adding demineralised water in a 10/1(w/w) water to clay ratio, it was found that the BET area was 110 m^2/g. After swelling, the porosity of montmorillonite increased to 0.93 from 0.61 for the unmodified montmorillonite.

5. Experiments to evaluate the heavy metal removal by ion exchange, adsorption and precipitation were conducted for montmorillonite and kaolinite clay minerals as follows. Two kinds of ion exchange equilibrium experiments were carried out : i. Unmodified montmorillonite and kaolinite containing mainly Ca, Mg, Na, K cations, and ii. Completely Ca and Na saturated montmorillonite and kaolinite. The heavy metal stock solutions were prepared by dissolving $Pb(NO_3)_2$ and $Cd(NO_3)_2.4H_2O$ (Merck grade) in demineralised water. The experiments were performed in 50 cc polyethylene centrifuge tubes. In the first kind of experiments, 2 gr. of air-dried clay minerals were washed using demineralised water , and the pH of the slurry was adjusted. The solution containing Pb and Cd ions were added to this pretreated sample. The solution to clay ratio was kept at 10:1. The slurry was shaken for 24 hours at a rate of 180 strokes per minute. After shaking, the samples were centrifuged and the pH of the clear supernatants were measured. In the second kind of equilibrium experiments, both montmorillonite and kaolinite were saturated with Ca and Na ions by applying the procedure given by Harter(1992). In this procedure, soils were saturated with 0.5 M $CaCl_2$ and 0.5 M NaCl and then washed with 0.5 mmole/L $CaCl_2$ and 0.5 mmole/L NaCl , respectively. In both types of experiments, the pH range was between 2.5 and 9. The pH of each sample was adjusted with dilute HNO_3 and NaOH solutions.

Determinations of Pb, Cd, Mg and Ca were performed using atomic absorption spectroscopy (Philips PU9300X) and Na and K ions were analyzed with a flame photometer (Jenway).

RESULTS AND DISCUSSION

Adsorption Experiments With Montmorillonite

A. With unmodified clay

Ion exchange and adsorption curves for both Pb and Cd show the same pH dependence, although the amounts removed by montmorillonite and kaolinite are different. Figure 1 shows the removal of Cd and Pb by ion exchange and adsorption on montmorillonite, at pH values 2.5 - 3.0 , the percent removal of Cd is less, compared to those in the pH range 3.5 - 5, where the existence of a plateau is noticed. Adsorption of Cd and Pb or other cations is believed to be controlled by competitive ion-exchange reactions (Schulthess and Sparks,1988); that is, at low pH, the H^+ cation completely exchanges with the metal cation. The removal of Cd is around 40 percent at pH 2.54 but increases to 50% at pH values between 3 and 5.3. It is clear that after pH 5.7, the removal of Cd increases rapidly with pH. This could be attributed to increased surface area of the small pores, as implied by Table 2 and Figure 6; however, precipitation at high pH values seems to be more important. Because, precipitation causes blockage of the entrance of small pores,
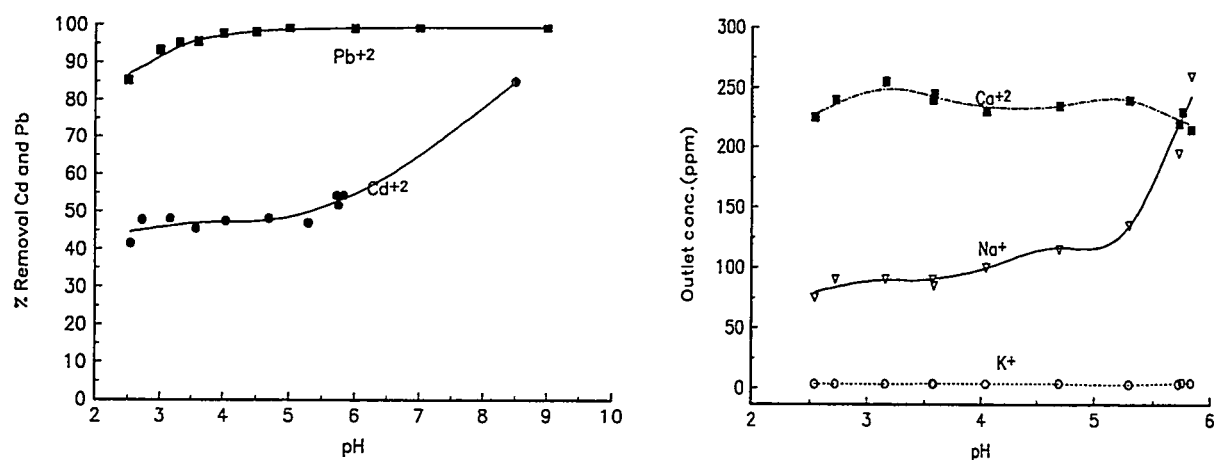
Figure 1. Removal of Cd and Pb by original montmorillonite. (Initial concentrations of Cd and Pb: 1760 and 1781 ppm, respectively)

Figure 2. Extracted Ca, Na, K from original montmorillonite by using Cd.
(the same experiment in fig.1)

and consequently, the diffusion of ions to the interlayers of clay becomes impossible, it is likely that the ion-exchange and adsorption mechanism takes place on the surface of the soil.

In Figure 2, it is seen that the amount of Ca and K replaced by Cd remains almost constant in the pH range 2.5 - 6. The amount of Na replaced seems to be less than Ca. This is contrary to the natural behaviour of Na. This behaviour results from the fact that, during the washing and pH adjustment, most of the Na present originally in the clay is extracted.

B. With saturated clay

The existence of many cations in the clay minerals affects the pH adjustment. Therefore, in the second set of experiments, the soil is saturated by only Ca and Na. The pH was adjusted in three days to reach the desired value. In Fig. 3 and 4 , Ca and Na saturated montmorillonite was exposed to Cd or Pb ions. In both cases, ion exchange plateaus of cations have been observed. When the percentages of Cd adsorbed by the Na saturated and Ca saturated montmorillonite are compared in Fig.3, it is seen that the percentage of Cd adsorbed is larger in the case of Na saturation. This result is mainly due to the replacing power of ions with respect to their charges and ionic sizes. Hellfrich (1962) stated that the ion exchanger tends to prefer counter ions of higher valence and smaller equivalent volume. The valence of Cd is 2, while the valences of Na is 1 and that of Ca is 2. The hydrated radii of Na, Cd and Ca are 0.358, 0.426 and 0.412 nm (Nightingale, 1959), respectively. These lead to the conclusion that Cd replaces Na easily due to the valence effect, while the size effect is not appreciable or is overcome by the valence effect. The same behaviour is observed in Fig. 4 for the case of Pb.
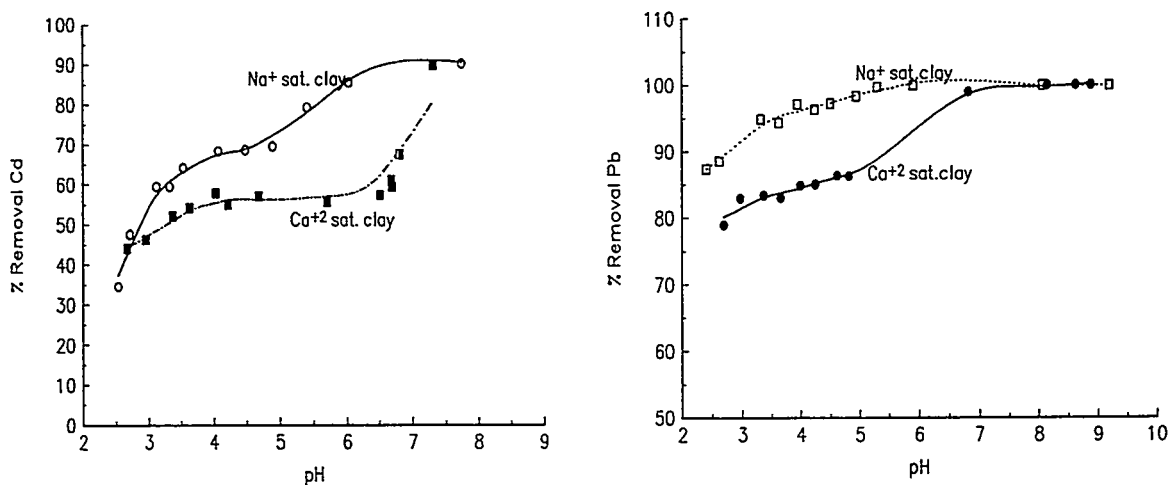
Figure 3. Cd removal by Ca and Na saturated montmorillonite.(Initial concentration of Cd:1770 ppm)

Figure 4. Pb removal by Ca and Na saturated montmorillonite.(Initial concentration of Pb:2060 ppm)

When the percentage of adsorbed Cd and Pb are compared in Fig. 3 and Fig. 4 in the pH range 2.5 - 5, it is observed that the amount of Pb adsorbed is higher. This is due to the fact that the hydrated radius of Pb is 0.401 nm while that of Cd is 0.426 nm; consequently, the ionic volume effect becomes important.

Adsorption Experiments With Kaolinite

Montmorillonite has a larger specific surface area than kaolinite due to its interlayer structure. The interlayers have an ability to expand depending on the concentration and the type of cations. Therefore, the surface area can be controlled by the cation used as the saturating agent. Norrish (1954) found that low concentrations of Na-solutions could swell the montmorillonite layers almost 20 times, but this is not the case for calcium. Since the kaolinite has a different kind of interlayered structure, ion exchange and

adsorption occurs on the surface of the clay particles, especially on the broken bonds. In Figure 5, the results of the adsorption experiments performed with kaolinite are given. The percentages of adsorbed Pb and Cd are almost identical to the results obtained with montmorillonite, except that the corresponding percentages are lower in the case of kaolinite due to the lower exchange area per unit mass of kaolinite.
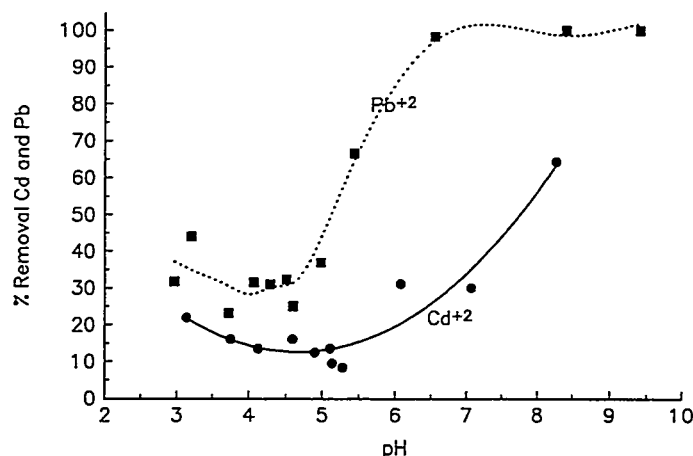
Figure 5. Cd and Pb removal by Na saturated kaolinite.(Inlet concentrations Cd: 1809 and
Pb : 1641 ppm.)

Surface Area Measurements

The dependence of the surface area of montmorillonite on the type and the concentration of ion used for saturation and pH was studied experimentally. The ions used for saturation were Ca and Na at 0.5 mmole/L and the pH range was 2.5 - 9. At the end of each saturation experiment, the clay was freeze-dried and the surface area was determined by the BET method. N_2 - adsorption surface area values are given in Table 2.

Table 2. Surface area and cumulative adsorption properties of montmorillonite at different pH values.

pH	BET-N_2 Surface Area (m²/gr)	Cumulative Adsorption (cm³/gr)
2.5	23.17	0.075
4.0	46.89	0.085
5.5	61.36	0.097
9.0	72.21	0.098
no pH adjust.	72.90	0.087

Organic Matter Content

Soil organic matter (SOM) content of the clay minerals is the another important physico-chemical parameter. In particular, the clay organic matter affects the amount of ions adsorbed per unit mass of clay since SOM influences the cation complexation mechanism and the organic matter (humic and fulvic matter) have active groups which adsorb cations (Yong et al., 1992). The affinity of organic matter towards

cations is effected by acidity (Grimshaw, 1971). The experimental values of carbon content measured by an LECO-CHN elemental analysis instrument are seen in Table 3 for both montmorillonite and kaolinite. As seen in the table, for both clays the change in carbon content is very small in the pH range of 2.5 - 5.5.

Table 3. Carbon contents on montmorillonite and kaolinite at different pH values.

pH	Original clay	2.5	4.0	5.5
% C in Mont.	0.16	0.13	0.13	0.12
% C in Kaol.	0.42	0.39	0.43	0.40

Pore Size Distribution

In figure 6, the pore size distributions of montmorillonite are given in the pH range 2.5 - 9. If the clay particle size of $2x10^{-6}$ m is considered, the size range covered in the figure can be divided into two groups: extraparticular pore size range (pore diameter larger than $2x10^{-6}$ m) and intraparticle pore size range (pore diameter less than $2x10^{-6}$ m). The pH dependence of pore volume as a function of pore size is interesting. In the intraparticular range the pH dependence is high, whereas in the extraparticular range there is almost no pH effect. In the micropore region (diameters less than $0.4x10^{-6}$ m) as pH is decreased, a decrease of pore volume is observed, which is attributed to the collapse of micropores in the low pH range.
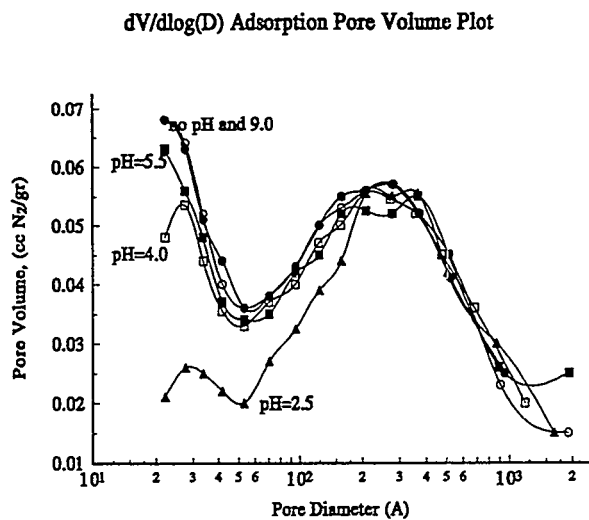
Figure 6. Pore size distribution of montmorillonite at different pH values.(The clay is saturated with Na ion)
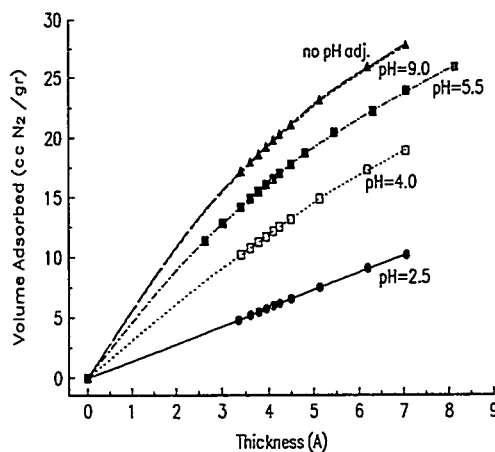
Figure 7. N_2-adsorbed layer thickness of montmorillonite at different pH values.

Adsorbed Layer Thickness In The Pores

With the classical BET method, the surface area and pore size distribution information obtained spans the pore size down to 20 Å. In the micropore region, information in the quantitative sense can be obtained by the method suggested by Boer et al. (1966). The thickness of the N_2- adsorbed in the micropores can be found by using Harkins and Jura's equation (Harkins and Jura, 1943). In figure 7, the volume of N_2 - adsorbed is plotted as a function of thickness at various pH values. It can be seen that at low pH values. the volume adsorbed decreases, indicating that the micropores close at low pH values as indicated in fig. 7.

CONCLUSIONS

The adsorption and ion - exchange of Cd and Pb is higher in montmorillonite in comparison to kaolinite due to the larger cation exchange capacity and surface area of montmorillonite. At low pH values (2.5 - 3) the hydrogen ion competes with metal cations (Fig.1 and 2) and the percent removal of metals becomes less. At intermediate pH values, there is a plateau observed for both montmorillonite and kaolinite. Above pH 6, precipitation becomes dominant. Consequently, the affinity of metal ions towards these clay minerals depends on the pH of the soil solution. The adsorption of Pb is always higher than that of Cd in both clay minerals because the hydrated radius of Pb is smaller than that of Cd. Therefore, the ionic volume is an important factor which determines the amount of ion adsorbed in the interlayers of clay minerals.

The experiments conducted (the N_2-layer layer thickness values calculated and pore size distribution results) to evaluate the effect of pH on the surface area of montmorillonite show that the clay layers collapse at low pH values (Table 2 and Fig.7). The organic content value of clay minerals doesn't show any appreciable change with pH, and there is no nitric acid effect observed on the crystalline structure of montmorillonite in the pH range studied.

REFERENCES

Boer, J.H. et al., (1966) The t-curve of multimolecular N_2-adsorption, J.of Colloid and Interface Science, 21,405-414.

Cabbar, C., Doğu, G., Doğu, T. and McCoy, B. J. (1996) Single-pellet dynamics for the soil organic matter effect on the dichloromethane sorption, AIChE J., 42(7), 2090-2093.

Garciya-Miragaya, J. and Page, L.A. (1976) Influence of ionic strength and inorganic complex formation on the sorption of trace amounts of Cd by montmorillonite, Soil Sci. Soc. Am. J., 40,658-663.

Grimshaw, W. Rex (1971) The Chemistry and Physics of Clays and Allied Ceramic materials, Wiley - Interscience, New York.

Harkins, W. D. and Jura, G. (1943) An adsorption method for the determination of the area of a solid without the assumption of a molecular area and the area occupied by N_2-molecules on the surface of solids, J. Chem. Phys., 11, 431-432.

Harter, R. D. (1983) Effect of soil pH on adsorption of lead, copper, zinc and nickel, Soil.Sci. Soc. Am. J., 47, 47-51.

Harter, R. D. (1992) Competitive sorption of cobalt, copper and nickel ions by a calcium saturated soil, Soil Sci. Soc. Am. J., 56, 444-449.

Hellfrich, H. (1962) Ion Exchange, Mc Graw Hill, New York.

Mehra, O.D. and Jackson, M.L. (1960) Clays and Clay Minerology, 7, 317.

Nightingale, E.R. Jr. (1959) Phenomenological theory of ion solution. Effective radii of hydrated ions, J.Phys. Chem., 63, 1381-1387.

Norrish, K. (1954) Manner of swelling of montmorillonite, Nature, 6, 256-257.

Schulthess, C. P. and Sparks, L. D. (1988) A critical assessment of surface adsorption models. Soil Sci. Soc. Am. J., 52, 92-97.

Schulthess, C. P. and Huang, C. P. (1990) Adsorption of heavy metals by silicon and aluminum oxide surfaces on clay minerals. Soil Sci. Soc. Am. J., 54, 679-688.

Yong, R. N., Mohammed, O. M. and Warkentin, P. B. (1992) Principles of Contaminant transport in Soils, Elsevier, Amsterdam.

Ziper, C., Komarneni, S. and Baker, E. D. (1988) Specific cadmium sorption in relation to the crystal chemistry of clay minerals. Soil Sci. Soc. Am. J., 52, 49-53.

Chapter 13

Reactive, Low Permeability Materials

VERTICAL BARRIERS WITH INCREASED SORPTION CAPACITIES

Heike B. Bradl[1]

Abstract

Vertical barriers are commonly used for the containment of contaminated areas. Due to the very small permeability of the barrier material which is usually in the order of magnitude of 10^{-10} m/s or less the advective contaminant transport can be more or less neglected. Nevertheless, there will always be a diffusive contaminant transport through the barrier which is caused by the concentration gradient. Investigations have been made to increase the sorption capacity of the barrier material by adding substances such as organoclays, zeolites, inorganic oxides and fly ashes. The contaminants taken into account where heavy metals (Pb) and for organic contaminants Toluole and Phenantrene. The paper presents results of model calculations and experiments. As a result, barrier materials can be designed „tailor-made" depending on the individual contaminant range of each site (e.g. landfills, gasworks etc.). The parameters relevant for construction such as rheological properties, compressive strength and permeability are not affected by the addition of the sorbents.

Introduction

The remediation of contaminated areas can be carried out basically by three methods:
- treating the contamination on site (in situ)
- treating the contamination off site (ex situ)
- encapsulating the contamination by vertical and horizontal barriers.

State of the art for encapsulating measures are vertical barriers which can be executed as diaphragm walls (either by the one-phase method or by the two-phase method), composite walls, bored pile walls and jet grouting walls (Arz et al. 1991). Diaphragm walls can be executed by either the one-phase or the two-phase method.

When using the two-phase method, the supporting liquid, which consists of a bentonite-water suspension, is replaced by the remaining barrier material once the trench has been excavated. When using this method, special attention has to be paid to the joints between primary and secondary cut. Also the replacement of the supporting suspension by the secondary mass (which can be a concrete or another bentonite-cement slurry) must be executed carefully. Therefore the work expense and the costs for executing vertical barriers in the two-phase methods are high. When using the one-phase method, the supporting liquid is used as the final barrier material and remains in the trench. This method has several advantages as for costs, simplicity of execution and work expense. Also there are no joints between adjacent cuts as the cuts overlap. The barrier material consist of a cement-bentonite-water slurry, which is prepared on site using large mixing plants. It is very convenient to use prefabricated mixtures. On site only water is added and the slurry can be used.

The slurry has to meet several requirements concerning rheological properties, permeability, compressive strength and chemical stability against contaminants. The permeability of the barrier material is usually in the order of magnitude of 10^{-10} m/s or less. Therefore the advective transport of contaminants can be neglected. Nevertheless, there will always be a diffusive contaminant transport through the barrier which is caused by the concentration gradient. This transport has to be taken into account especially when considering the long-term aspects of contaminated site encapsulation.

---

[1] Bilfinger + Berger Bauaktiengesellschaft, Research and Development, Carl-Reiss-Platz 1-5, D-68165 Mannheim, Germany, (621) 459-2613, fue.bilberg@t-online.de

A research project has been started to investigate the effect of adding substances with high sorption capacities such as organoclays, zeolites, inorganic oxides, and fly ashes to the prefabricated slurry. Different slurries with various additives have been investigated. The parameter relevant for construction are Marsh funnel time, yield point and permeability. The additives have been characterized by X-ray investigations, cation exchange capacity (CEC), determination of specific surface, pore distribution and micropore volume. For the fly ashes time-dependent investigations with the help of X-ray and scanning electron microscope have been made. Also model calculations have been made for the contaminant transport in slurry walls. The paper presents some preliminary results which are very promising. It is possible to design barrier materials with increased sorption capacities without affecting the relevant construction parameters.

Experimental

Prefabricated Mixtures

The follwing prefabricated mixtures have been used in the investigations: (1) DiWa-Mix K mod 2-200 by Anneliese BUT, Ennigerloh, Germany, (2) Solidur 274 F and (3) Solidur 274 MS by Dyckerhoff, Wiesbaden, Germany. DiWa-Mix K mod 2-200 consists of Na-bentonite and special hydraulic binder which is characterized by long workability. Therefore it is often used for composite cut-off walls. Solidur 274 F is also characterized by long workability and low amount of filtrate water and is mostly used for the encapsulation of contaminated areas. Solidur 274 MS has been especially modified for extremely agressive leachate waters. From each sample a blank was prepared as follows: 1 kg dry powder were mixed with 4,65 kg of water for 5 minutes using an Utraturrax mixing apparatus. Then rheological properties (Marsh funnel time, yield point, filtration water volume, density) have been determined. For the methods used see Kreisel (1996). Permeability and uniaxial strength were determined after 21 days of storing the samples under water. All tests were conducted at room temperature (21°C).

Additives

To increase the sorption capacity of the slurry different substances have been added to the blanks. Samples were investigated containing 1% and 5% additive. The dry additive is added to the suspension receipe, which means that the volume of water and prefabricated mixture is not changed. The following additives have been investigated: (1) Organophilic bentonite IBECO Organosorb from the IBECO Company, Mannheim, (2) two zeolites, IKO-SORB Z from IBECO company and Zeolite „Brunner" from Romania, (3) fly ash SAFA-GKM from SAFA Company, Baden-Baden, Germany and (4) water treatment sludge from water treatment plant Hamburg, Germany.

Inorganic Oxides

Oxides and hydroxides of Aluminum, iron and manganese are also able to adsorb contaminants, especially heavy metals. For example, goethite (α-FeOOH) and hematite (α-Fe$_2$O$_3$) form very small crystals (10-100 nm) and have a very large specific surface of 300 - 500 m²/g. As oxides and hydroxides possess variable surface charges only, they contribute to the cation exchange by proton dissociation of M-OH and M-OH$_2$ groups. Here water treatment sludge was used, which consists of amorphous ferrihydrite 5 Fe$_2$O$_3$ $\cdot$ 9H$_2$O and to a very small extent of Goethite (FeOOH).

Fly Ash

Fly ash is produced as a by-product at coal incineration. The accompanying rock of the coal melts at temperatures of 1300°C and forms microfine glassy particles. Fly ashes are pozzolanes which form solid crystals if water is added. Here hard coal fly ash SAFA-GKM from SAFA Company, Baden-Baden, Germany was used.

Organophilic Bentonites

Organophilic bentonites are bentonites where the inorganic interlayer cations have been substituted by organic cations like DMDO (dimethyl-dioctadecyl-ammonium) or OBDM (octadecyl-benzyl-dimethyl-ammonium). The distance between the layers increases by this substitution and the surfaces properties of the clay mineral change. The originally hydrophilic surface becomes hydrophobic and is able to adsorb organic contaminants. The mechanism is described by Schall and Simmler-Hübenthal (1994).

Figure 1: Adsorption mechanism of organic contaminants on the surface of an organophilic bentonite (redrawn after Schall and Simmler-Hübenthal 1994).
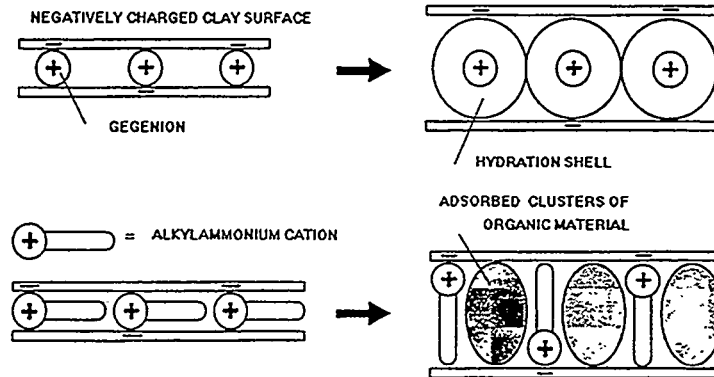
Zeolites

Zeolites are alumosilicates of the general formula $M_{2/z} \cdot Al_2O_3 \cdot x\ SiO_2 \cdot y\ H_2O$, where M is a metal ion of valence z. The mineralogical structure is shown in figure 2.

Figure 2: Molecular structure of a zeolite (Klinoptiolithe) after Czurda (1994)
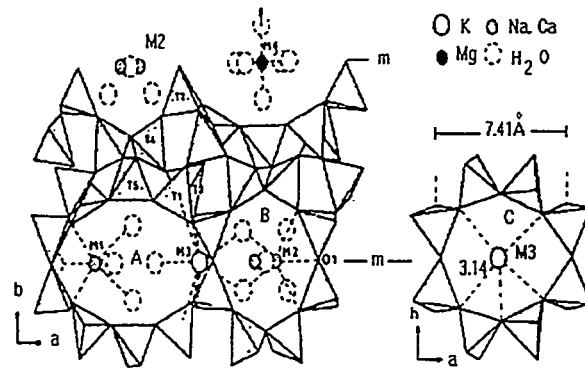
The characteristic molecular feature of a zeolite is a three-dimensional channel system. The sieving effect is caused by the different pore size.

Discussion of Results

<u>Mixing Experiments</u>

Table 1 presents some results of mixing tests with 5% additive. As for permeability, values increased from order of magnitude $1x10^{-13}$ m/s for the blank to 10^{-10} for a slurry upgraded with fly ash. Yet this value is still acceptable for construction purposes. Also the other parameters investigated have not shown any deleterious effects caused by the mixing of additives. One exeption was the water treatment slurry; most samples did not harden within 28 days so permeability and compressive strength could not be determined.

Table 1: Suspension properties of Dyckerhoff 274 F with various additives; blank: 1kg Dyckerhoff 274 F and 4,5 kg water, mixtures with 5% additive

Parameter	Blank	Fly ash	Org. Bentonite	Sludge	Zeolite Ikosorb-Z
Permeability [m/s]	$1x10^{-13}$	$4,5x10^{-10}$	$2,5x10^{-12}$	$2,4x10^{-11}$	$3,7x10^{-12}$
Compressive Strength [N/mm²]	0,52	0,50	0,58	n.b.	0,67
Marsh funnel time [sec]	46	37	35	49	37,5
Density [kg/m³]	1160	n.b.	1150	1115	1116
Yield point [N/m²]	19,9	12,3	9,2	12,0	12,3
filtrate water [ml]	31,5	41,5	51,5	40	39,5

Table 2 presents an overview of results for all additives and prefabricated mixtures investigated. With the exeption of water treatment sludge all additives could be used. Organophilic bentonites can make some problems during the mixing process because of their hydrophobic surface which results in the formation of lumbs.

Table 2: Results of mixing experiments for prefabricated mixtures with various additives

Additive	DiWaMix K	Solidur 247 F	274 MS	273
Organophilic Bentonite	X	--	X	X
Zeolite	X	X	X	X
Fly ash	X	X	X	X
Water treatment sludge	--			
	X = Well suited; addition possible without changing rheological properties -- = Addition not possible without changing rheological properties			

<u>Sorption Experiments</u>

Sorption experiments have been carried out for Lead for additives zeolite, organophilic bentonite and water treatment sludge and for Toluole for additives zeolite, fly ash, organophilic bentonite, diatomite and water treatment sludge. Figure 3 shows the adsorption isotherms for Lead. For this heavy metal, the water treatment sludge showed the highest sorption followed by the zeolites

(Brunner from Rumania and IKOSORB Z from IBECO). Also the organoclay showed a consider-able sorption for Lead.

Figure 3: Adsorption isotherms for Lead for additives Zeolite, organophilic bentonite and water treatment sludge.

Adsorption Isotherms Lead
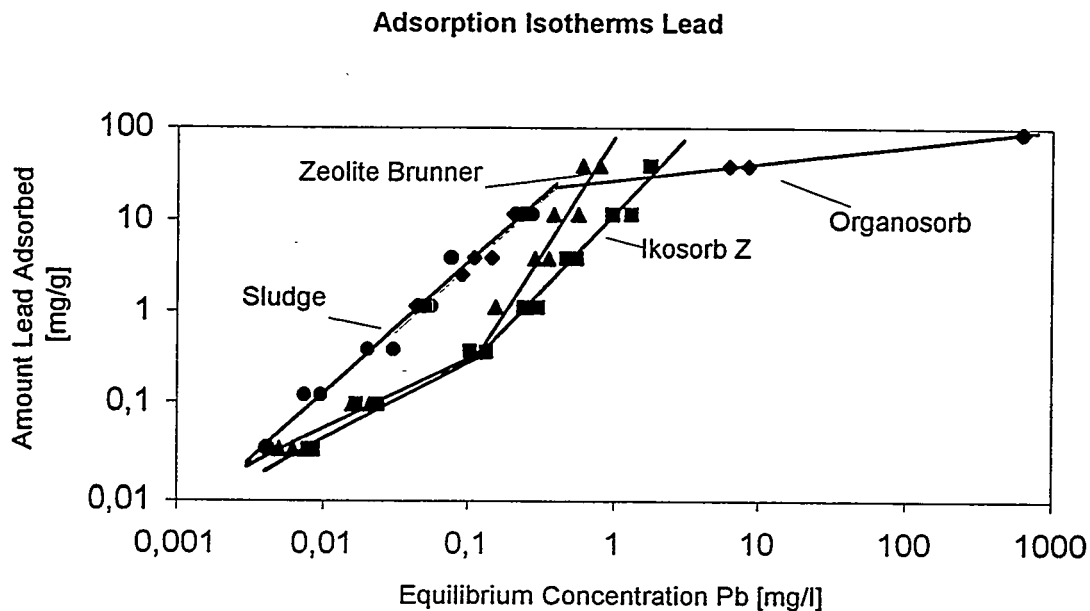
Figure 4: Adsorption isotherms for Toluole for additives zeolite, fly ash, organophilic bentonite, diatomite and water treatment sludge

Adsorption Isotherms Toluole
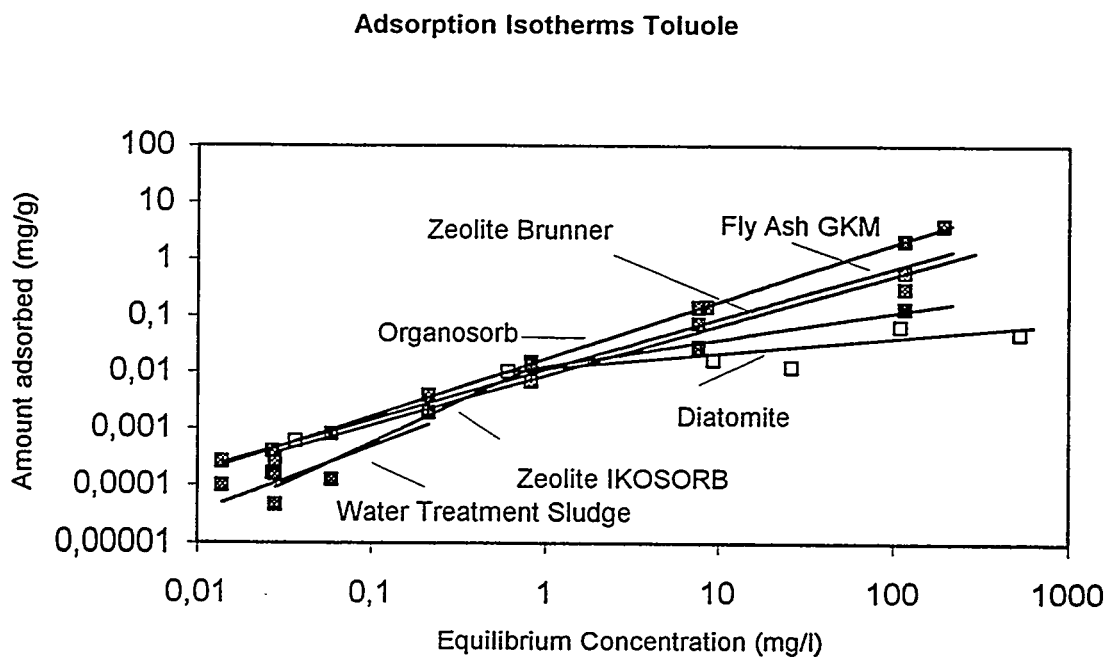
Figure 4 shows the adsorption isotherms for additives zeolite, fly ash, organophilic bentonite, diatomite and water treatment sludge.

As expected the organophilic bentonite shows the best sorption potential for Toluole but also fly ash and the zeolites are well suited as a sorbent for this contaminant.

Model Calculations

For a slurry upgraded with fly ash, model calculations for Phenantrene have been made (Grathwohl 1995). The relative concentration C/Co in the slurry wall as a function of place and time can be determined with the help of the analytical solution of the advective-dispersive equation according to Ogata and Banks (1961):

$$\frac{C}{C_o} = 0.5 \left[erfc\left(\frac{x - tv_r}{2\sqrt{tD_a}}\right) + \exp\left(\frac{xv_r}{D_a}\right) erfc\left(\frac{x + tv_r}{2\sqrt{tD_a}}\right) \right]$$

Mechanical dispersion is neglected. Figure 5 shows a direct comparison between Phenantrene transport in a conventional slurry and a slurry upgraded with fly ash. Contaminant transport is heavily retarded by sorption so that the contaminant penetrates only a few centimeters into the slurry wall material.

Figure 5: Comparison of Phenantrene transport in a conventional one-phase slurry wall (dotted line; De = 3.9 · 10^-7 cm²/s; α = 13.2) and in a slurry upgraded with fly ash (straight line; De = 1.6 · 10^-7 cm²/s; α = 1890) after 10, 30 and 300 years (i = 0.1; k_f = 2.6 · 10^-10 m/s) redrawn after Grathwohl 1995.
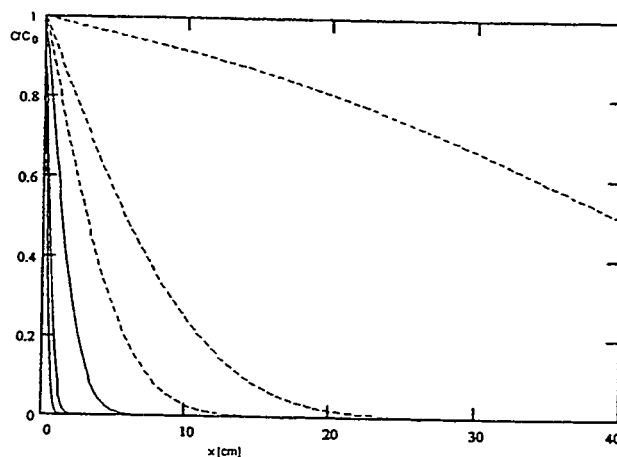
Conclusions

The results of mixing and sorption experiments show that it is possible to mix slurry material with substances of high sorption capacity without changing rheological properties and permeability of the barrier mass. Results for a slurries upgraded with fly ash, zeolite, organophilic bentonite, and water treatment sludge are presented. Sorption experiments have been carried out for Lead and Toluole. For Phenantrene model calculations show a considerable increase in long-term safety for vertical barriers. After 300 years Phenantrene has penetrated only the first few centimeters of a slurry wall. Thus the long-term safety of vertical barriers can be increased considerably.

References

Arz, P., Schmidt, H.G., Seitz, J.M. and S. Semprich. (1991) Grundbau. *Sonderdruck aus dem Beton-Kalender*, p. 132, Ernst & Sohn, Berlin.

Czurda, K.A. (1994) Multimineralische Abdichtung. *Schr. Angew. Geologie Karlsruhe* 30, 4 - 21.

Grathwohl, P. (1995) Quantifizierung des diffusiven und advektiven Transports ausgewählter organischer Schadstoffe in mineralischen Dichtwänden. *Unpublished report*, 44 pp. Tübingen.

Kreisel, T. (1996) Untersuchungen von Dichtwandmassen mit erhöhtem Sorptionsvermögen. *Unpublished Diploma Thesis* FH Kaiserslautern, 179 pp. Kaiserslautern.

Ogata, A. and R.B. Banks. (1961) A solution of the differential equation of longitudinal dispersion in porous media. *U.S. Geol. Surv. Prof. Paper* 411-A, Washington D.C.

Schall, N. & Simmler-Hübenthal, H. (1994) Organophile Bentonite zur Sicherung von Altlasten. In 10. Bochumer Altlastenseminar: *Sicherung von Altlasten* (ed H.L. Jessberger) pp. 203 - 212. Balkema, Rotterdam.

Sorption of Cesium and Strontium on Savannah River Soils impregnated with Colloidal Silica

N. Hakem[1]; I. Al Mahamid[1]; J. Apps[1], G. Moridis[1].

Abstract

The sorption behavior of cesium and strontium on Savannah River Site Soils impregnated with Colloidal Silica, was studied using a batch experimental method. The samples were prepared by addition of CS and an aqueous solution of $CaCl_2$ to the soil materials. Sorption studies were conducted after the gelation of the CS samples had occurred. The variation of the sorption ratio, R, as a function of cesium or strontium concentration was examined. The Freundlich isotherm was used to fit the data and very good results were obtained.

Introduction

Colloidal silica (CS) is being considered as an injectable low viscosity fluid for creation of impermeable barrier containment of low level radioactive waste at the Savannah River Site (SRS), South Carolina.

To determine the effectiveness of the barrier, it is desirable to predict the transport behavior of radionuclides through the barrier. This transport can be modified by several mechanisms such: co-precipitation, adsorption or diffusion (Adeleye et al. 1994). If precipitation or strong adsorption occurs, radio-contaminants will be immobilized and the CS barrier will retard radionuclide migration. If the radionuclides diffuse through the CS barrier, the barrier will be less effective in preventing groundwater contamination (Persoff et al. 1994).

The purpose of this work is to study the sorption of cesium and strontium on the colloidal silica and soil from SRS. ^{137}Cs and ^{90}Sr ions, respectively, are present in the radioactive waste and potentially mobile as dissolved species under the conditions prevailing at the SRS.

The sorption experiments were performed using a batch method, at different concentrations of radionuclides and at constant pH. The sorption is measured by gamma counting for cesium, by Inductively Couple Plasma (ICP), and by liquid scintillation counting (LSC) for strontium.

Experimental

Reagents

Reagents used in the experiments were: CsCl, ultra pure reagent, $CaCl_2$. 2 H_2O 99 % pure and $SrCl_2$. 6H_2O 99.8 % pure (J.T. Baker Inc., Phillipsburg, NJ). The isotopes ^{137}Cs and ^{90}Sr (Isotopes Products Laboratories, Burbank, CA) were received respectively as CsCl and $SrCl_2$ in 0.1 M HCl. An Ecolite cocktail liquid (ICN Biomedicals, Inc Irvine, CA) was used as a scintillation solution for the radioactive counting. We used Nyacol DP5110 Colloidal Silica (PQ Corporation, Ashland, MA) with the characteristics described in Table 1.

---

[1] Earth Sciences Division, MS 70A-1150, Lawrence Berkeley National Laboratory, University of California, Berkeley, CA, 94720, USA

Table 1. Characteristics of Colloidal Silica Used in our Experiments

Density (g/mL)	1.20
SiO_2	30 %
Na_2O	< 0.1 %
Al_2O_3	< 0.25 %
pH	6.5
Surface specific area (m^2/g)	220
Sites SiO_2/nm^2	8
Sites Al_2O_3/nm^2	< 0.5
Particle Diameter (nm)	14

All solutions were prepared with freshly deionized distilled CO_2-free water and were stored under argon atmosphere.

Apparatus and methods

The concentration of ^{137}Cs was measured using the 661.7 KeV gamma-ray of ^{137}Ba and the concentration of ^{90}Sr was measured by liquid scintillation counting. We used a high purity germanium (HPGe) detector designed at LBNL and a liquid scintillation counter, RackBeta, from Pharmacia Inc, Finland.

The pH measurements were performed using a semimicro Ross combination pH electrode calibrated with NIST-traceable standard buffers solutions. The reference solution was 3 M KCl. All experiments were performed at ambient temperature (23 ± 1° C). The experiments using radiotracers were conducted in an argon atmosphere glove box. Polyethylene vials were used to contain the samples and were kept on a low speed shaking table during the experiment.

Samples were collected from each vessel and filtered through 4.1 nm Centricon-30 filters (Amicon Corporation, Beverly, MA). Filters were pre-saturated with the same solutions.

Sample preparation

We carried out three series of experiments using cesium with ^{137}Cs as radiotracer, three series with strontium and three series using strontium with ^{90}Sr as radiotracer. For the cesium sorption study, the initial concentration of CsCl was varied from 10^{-3} to 10^{-8} M. We added 3.0×10^{-9} M of the radioactive isotope ^{137}Cs to each solution in order to use a γ analysis technique that provides a lower detection limit than chemical methods. For the strontium study, the initial concentration of $SrCl_2 \cdot 6H_2O$ was varied from 10^{-2} to 10^{-7} M, ICP being used to determine the concentration of strontium in the solution. For the system with ^{90}Sr, the concentration of strontium as $SrCl_2 \cdot 6H_2O$ was varied from 10^{-4} to 10^{-8} M ; we also added 10^{-9} M of ^{90}Sr to each solution to obtain a better detection limit using the liquid scintillation counter. A fourth series with vials containing only Cs or Sr solutions with the different concentrations mentioned above have used as blank samples to correct for any sorption on the walls of the vials. The sorption study of cesium was carried out over a period of 97 days. Table 2 describes the material present in each experimental vial.

Table 2. Description of materials present in experimental vials

Series #	Material	weight of soil (g)	Volume of Colloids (ml)	Volume of 0.3 M $CaCl_2$ (ml)
1	Soil, 5-10 ft depth	15	4.5	0.9
2	Soil , 10-20 ft depth	15	4.5	0.9
3	DP5110	0	4.5	0.9
4	Blank	0	0	0

For each vial of each series we added 30 mL of the corresponding cesium or strontium solution. The mixtures of series 1, 2, and 3 were prepared two days before the addition of any solutions to allow for the colloidal silica gelling process to occur.

The soil consists mainly of quartz(60%) and clay (28%), with minor presence of geothite (6%) and hematite (6%). The clay mineral in the <2 mm size fraction is primarily kaolinite (99%) with a very minor amount of vermiculite (1%). The soils were dried in an oven for 16 h at 100° C before addition of colloidal silica and calcium chloride.

Results and Discussion

To evaluate the sorption of each element, we used the sorption ratio coefficient which is defined

as: $R = \dfrac{C_0 - C_f}{C_0}$ where :

C_0 = initial concentration of the element of concern (Sr or Cs) (M)

C_f = final concentration of the element of concern (Sr or Cs) (M)

a) Cesium Sorption

For cesium, the sorption is significant for all systems as R is generally higher than 0.9 and occasionally reached a value of 1. As can be seen in figure 1, the curve is almost flat in the range from 10^{-6} to 10^{-8} M. This part of the curve represents the maximum uptake and is considered as the fixation capacity of the materials studied. At higher concentrations of cesium (10^{-5} to 10^{-3} M) the sorption decreases due to incomplete saturation of the free sites on the substrate by cesium ions (Hakem *et al.* 1995).

Figure 2 shows clearly that the sorption is very fast and occured within the first few days. A complete sorption equilibrium was established in 8 days for all series.

b) Strontium Sorption

The sorption data obtained by ICP showed that the presence of calcium, silica, and alumina in the samples interfered with the strontium measurement leading to higher values of Sr concentrations. In addition, the detection limit of the ICP is about 1.25×10^{-6} M, which is higher than some of our experimental concentrations. Figure 3 shows a general tendency of decrease in sorption as a function of Sr concentration; however, the errors in the measurements are high. We are repeating this study with ^{90}Sr. The presence of ^{90}Sr allows us to achieve a detection limit less than 10^{-9} M with the liquid scintillation counter. This work still in progress.

Data Analysis

We used the Freundlich isotherm to interpret the experimental results. This isotherm is described by the equation : $Q_{ads} = k \; C_{eq}^{n}$ (Sposito 1989)

Q_{ads} and C_{eq} are the concentrations of the nuclide in the solid and liquid phases respectively after the sorption.

n and k are positive values determined by plotting log Q_{ads} against log C_{eq}. Logk and n are the y intercept and the slope, respectively, of the resulting straight line.

The curves obtained for cesium and strontium are plotted in figures 4 and 5, respectively. We obtained straight lines for all experimental systems indicating that the Freundlich isotherm fits our data very well. In table 3, we report the values of n and k for each element. We obtained values

of n between 0 and 1 which suggest that the structure of the adsorbant surface is heterogenous with an exponential energy distribution of the adsorption sites (Sposito 1989).

Table 3. Values of n and k for cesium and strontium

System	Cesium		Strontium	
	n ± 0.05	logK ± 0.1	n ± 0.05	logK ± 0.1
Soil, 5-10 ft depth	0.700	-2.90	0.970	-2.99
Soil10-20 ft depth	0.810	-2.60	0.930	-3.21
CS	0.820	-2.40	1.190	-2.39

Conclusion

The high sorption ratio, R, for both cesium and strontium suggests that they can be immobilized in the soil at SRS.

Generally cesium sorption is higher than that of strontium because cesium ions have a lower hydration energy which enables the cations to shed their hydration shell upon entering the clay interlayers (28% of soil composition) (Cornell, R.M. 1992).

The sorption behavior on geological material is highly specific and each measured sorption is valid only for specific conditions including pH, concentration of the element considered, presence and concentration of competing ions, temperature, time for equilibrium and method of separation of solid and liquid phases. Therefore, all realistic conditions prevailing at the site of interest must be taken into account.

For a better understanding of the role of CS as a gel liquid barrier, both desorption and diffusion studies must be done on such material.

Acknowledgement

References

Adeleye, S.A, P.G. Clay and M. O. A. Oladipo. (1994) Sorption of caesium, strontium and europium ions on clay mineral. *J. of Materials Science .*, 29, 954-958.

Cornell, R.M. (199 Adsorption of cesium on mineral: a reveiw. *j.of Radioanalytical and Nuclear Chemistry,* 2) *Articles.,* 171(2), 483-500.

Hakem, N, B. Fourest, and R. Guillaumont. (1995) Sorption of radionuclides at tracer level on mineral colloids. *Sixth Annual International Conference on High level Radioactive Waste Management.,* 237-239.

Persoff, P, G.J. Moridis, J. Apps, K. Pruess, and S.J. Muller. (1994) Designing injectable colloidal silica barriers for waste isolation at the Hanford Site, *Thirty-third Hanford Symposium on Health and the Environmant.,* 87-100.

Sposito, G. (1989) *The chemistry of soils,* pp.153-154. Oxford University Press.
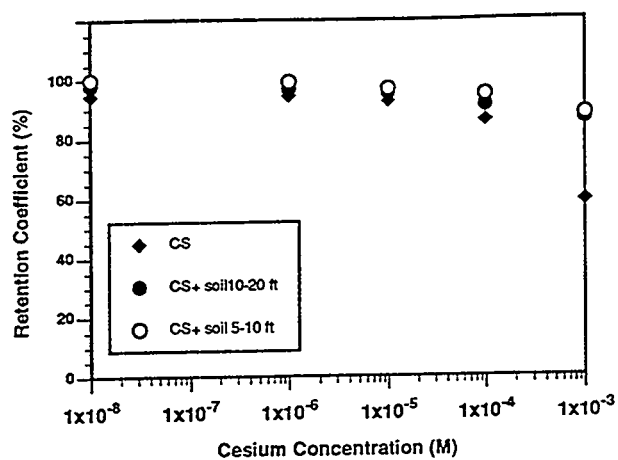
Figure 1. Sorption of Cesium as a Function of its Concentration
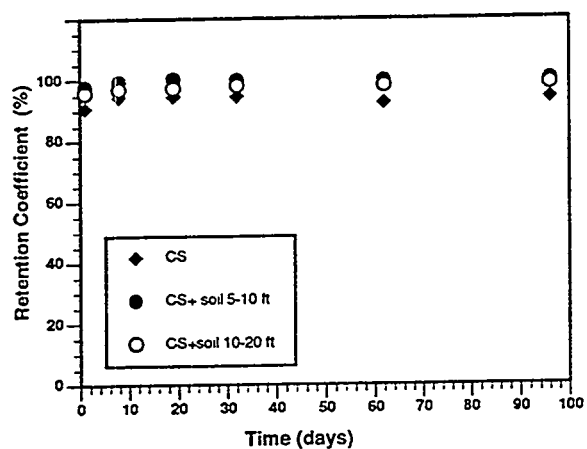
Figure 2. Sorption of Cesium at 1 E-6 M as a Function of Time
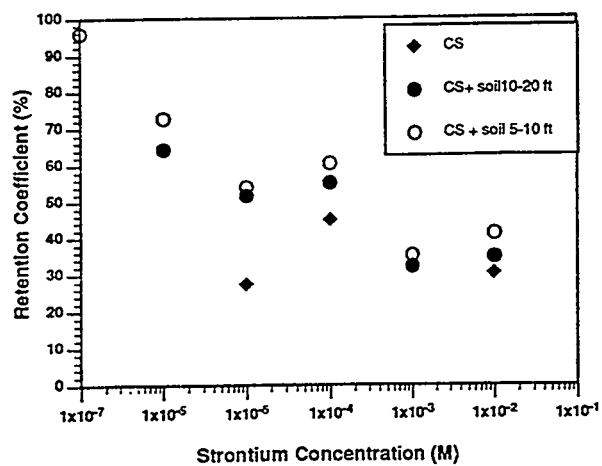
Figure 3. Sorption of Strontium as a Function of its Concentration

656
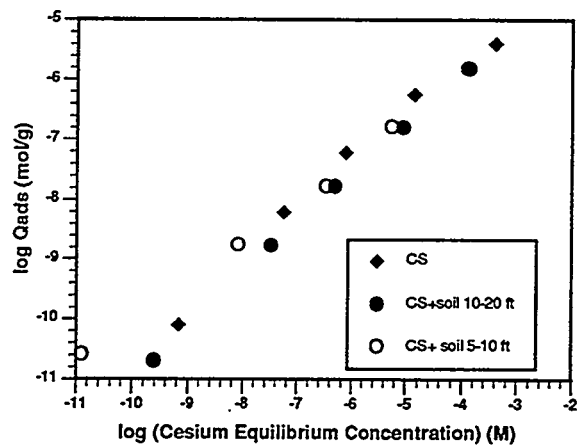
Figure 4. Variation of the Amount Adsorbed as a Function of Cesium's Equilibrium Concentration
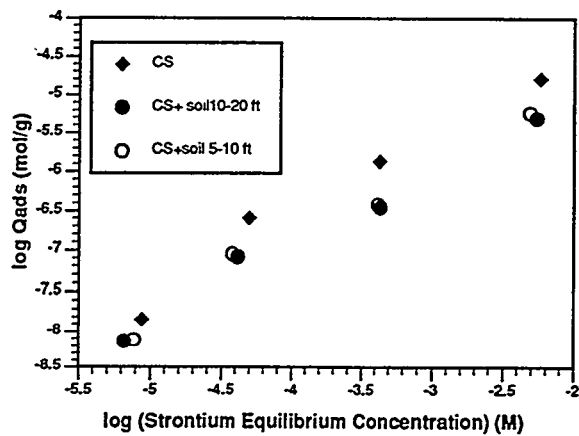
Figure 5. Variation of the Amount Adsorbed as a Function of Strontium Equilibrium Concentration

MASS TRANSPORT OF HEAVY METAL IONS AND RADON IN GELS USED AS SEALING AGENTS IN CONTAINMENT TECHNOLOGIES

I. Lakatos[1], K. Bauer[1], J. Lakatos-Szabó[1] and H.-J. Kretzschmar[2]

Abstract

The diffusion and hydrodynamic mass transport of multivalent cations, mostly Cr(III) and Cr(VI) ions and radon in polymer/silicate gels and Montanwax emulsions were studied. It was concluded that the self-conforming gels may decrease the hydrodynamic mass transport in porous and fractured media by 4-6 orders of magnitude. In water saturated systems, however, the diffusion transport can be restricted by hydrogels only to a moderate extent. On the other hand, the high and selective retention capacity of gels towards different diffusing species may open new vistas in the sealing technologies. Similar results were obtained for transport phenomena of radon. The almost perfect quenching process of radon and its nuclides in gels and emulsions further enhances the positive effects of the encapsulation methods. The laboratory experiments provided valuable new information to design the different containment technologies.

Introduction

The basic idea of subsurface blocking is that by placing a gel or clay barrier around a heavily contaminated area the transport of hazardous materials can be reduced to extremely low levels. Since the hydrodynamic mass transport and the permeability in porous media might be decreased drastically, optimistic expectations were revealed about the application of gels and clay barriers. These could be established in the facts that extensive studies on determination of transport phenomena in clays, cements, concrete, polymers and other covering materials have been carried out though the contributions of the hydrodynamic and diffusion factors were often not determined separately. Thus, the earlier approach completely ignores that even though the contaminants might be effectively localised by these methods, the chemical mass transport remains mostly unchanged. Thus, as it was definitely proved in the past years, the chemical mass transport is not only commensurable with the convective one, but sometimes it becomes the major migration factor of species. Therefore, a detailed research program was initiated with the aim at determining the transport of heavy metal ions and radon through polymer/silicate gels and Montanwax clay suspensions. The experimental results obtained by the laboratory studies are evaluated in respect to practical application of these materials in containment technologies.

Mass Transport of Heavy Metal Ions in Gels

Application of hydrated gels for containment of hazardous materials opened up new vistas in environmental protection. The diffusion and hydrodynamic mass transport of different chemical species in self-conforming phases may be of crucial importance because these processes may influence significantly the *in-situ* formation of artificial barriers in subsurface regions and the ef-

---

[1] Research Laboratory for Mining Chemistry, Hungarian Academy of Sciences
3515 Miskolc-Egyetemváros, PO Box 2. Hungary, Fax.: 36-46-367-211

[2] DBI Gas- und Umwelttechnik GmbH,
Halsbrücker Str. 34., 09599 Feiberg, Germany, Fax.: 49-3731-365-432

ficiency of technologies to be applied in relevant areas. Since multivalent cations used frequently as cross-linkers are also in the focus of the environmental pollution, the investigations were concentrated mainly on determination of the diffusion transport of different chromium ions in gels containing a water soluble polymer and an alkali silicate.

Experimental Conditions

The diffusion measurements were carried out in a conventional dual cell apparatus. The gel phase, having 30 mm diameter and 20 mm thickness, was fixed into the connecting glass tube. The gel contained a hydrolized polyacrylamide in concentration of 0 - 2.5 g/l and an alkali silicate (SiO_2) in concentration of 12.5 - 62.5 g/l. The cross-linker solutions always contained sufficient amounts of HCl to control the gelation time and to maintain the pH in range of 8.0-8.5. The model tests were performed by chromium ions added as chromium(III) chloride and chromium(VI) dichromate. The ion concentrations in the cells were determined by flame AAS method. The total mass balance in cells were followed by a special computer program. The diffusion coefficient and the break-through time were obtained by the slope and the intersection point of the linear section of the curves shown in Fig. 1. The specific ion retention capacity of gels was calculated by the difference in the break-through times (t_0 and t_1) obtained for non-adsorbing and adsorbing species and the actual diffusion flux.

The hydrodynamic mass transport through gels was studied in a horizontal model having 100 cm length and 4 cm diameter. Original soil and sand materials were used as carrier solid materials. The permeability of such porous systems against water was greater than 10 D. After the permeability measurements an appropriate gel phase was placed into the model. The composition of gel was the same as mentioned above. In the final stage of tests repeated permeability measurements were performed at different pressure gradients until hydrodynamic equilibrium was set. The results were calculated by Darcy's law.
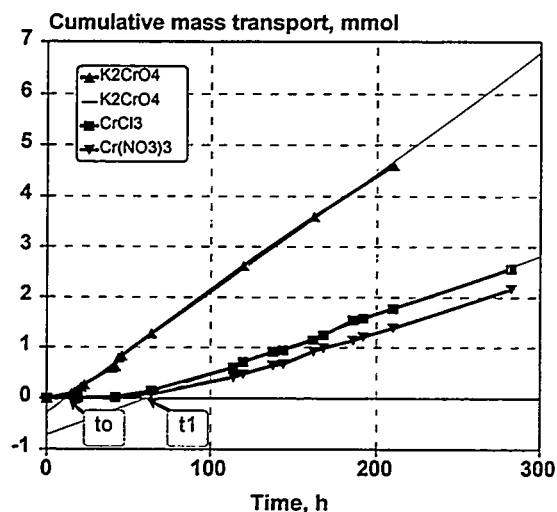
Fig. 1. Cumulative mass transport of different chromium ions in polymer/silicate gels
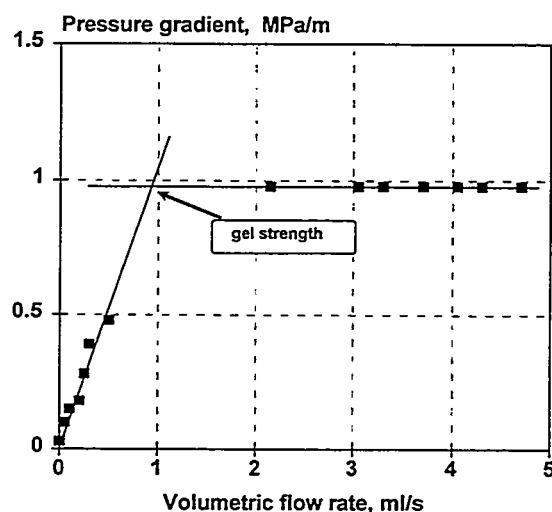
Fig. 2. Hydrodynamic mass transport of water in gel at different pressure gradients

Hydrodynamic Mass Transport in Gels

The laboratory studies focused on application of self-conforming gels in containment technologies can be summarized as follows:

1) The hydrodynamic liquid transport in gels can be described by the Darcy's relationship up to a certain pressure limit (Fig. 2.). By statistical measurements this limit (gel strength) is about 10 bar/m for polymer/silicate gels in the temperature range of 0-30 °C.

659

2) Presence of gel in porous media may significantly influence the permeability. Although the volumetric flow rate remained pressure-dependent until the gel is stable, the residual permeability was usually less than 0.1 mD in non-consolidated models. Consequently, the permeability was reduced by 5 orders of magnitude by gel treatment.

Taking the viscosity of fluids also into account, it is clear that application of hydrogels leads to drastic restriction of flow flux in subsurface regions: the predictable reduction of the hydrodynamic mass transport may exceed 6-7 orders of magnitude for gases and 4-5 orders of magnitude for liquids depending on surface characteristics (wettability) of the solid/liquid systems.

General Feature of Diffusion Mass Transport in Gels

On the basis of the preliminary studies the diffusion flux of the different chromium ions in a well defined polymer/silicate gel can be characterized as follows:

1) After break-through the cumulative transport of all ions increases linearly in time if the absolute change of the original concentration gradient is negligible (Fig. 1.). That fact suggests indirectly that the transport phenomena can be described by the Fick's I. law.

2) The effective diffusion coefficient of chromium ions in gel is only 10% less than in an aqueous phase. The difference in the diffusion coefficients is proportional to the effective hydrodynamic radii of the ions.

3) The break-through times found for Cr(III) and Cr(VI) ions differ significantly. This fact can not be explained by the effective diffusion coefficients. The relatively long break-through time obtained for Cr(III) ions might be traced back to ion adsorption, hydrolysis and precipitation of the corresponding compounds in the slightly alkaline media of the gel.

4) The diffusion coefficient and the specific ion retention capacity are independent of the gel geometry, but the break-through time increases linearly with the thickness of gel (Figs 3. and 4.).

5) The temperature has a significant effect on transport phenomena: the diffusion coefficient increases with temperature and that change can be described by the Arrhenius equation. Similarly, the break-through time and the ion retention capacity are proportionally lower at elevated temperature.

In addition, the existence of competitive processes allow us to predict that the one-dimensional random-walk equations may not be used for calculation of the mean diffusion distance of adsorbing ions in gels. On the other hand, the experimental findings imply that the diffusion transport is only slightly hindered in gels despite the fact that the retention capacity increases and the diffusion flux decreases proportionally with the thickness and volume of gel.

Effect of Gel Composition on Diffusion Transport

The main components of any barriers may have a pronounced impact on migration of species. Therefore, it was important to determine the effect of gel composition on the transport phenomena . In this respect the experimental results can be summarized as follows:

1) The effective diffusion coefficient of Cr(III) ions decreases linearly with the silicate and the polymer content (Figs 5. and 6.).

2) Under identical gel geometry and experimental conditions the break-through time increases considerably on both the silicate and the polymer content.

3) The specific retention of Cr(III) ions show behavior similar to the break-through time. Namely, the amount of diffusing species retained by the blocking phase gradually increases with the quantity of the structure forming components of the gel.

Deff, 10E-10 m3/s

8

6

4

2

1 2 3 4

I, cm
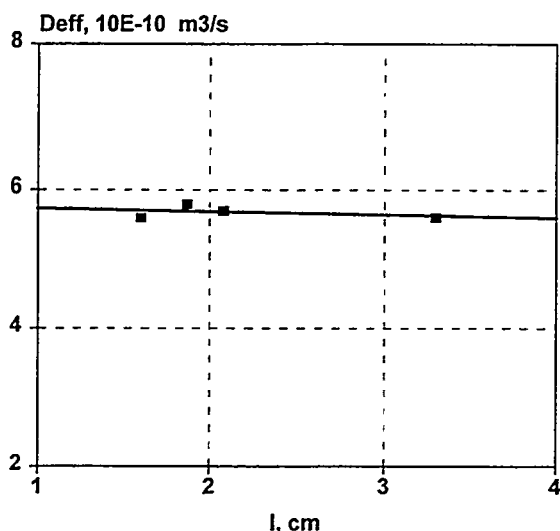
Fig. 3. Dependence of the effective diffusion
coefficient of Cr(III) ions on gel thickness

Break-through time, h

200

150

100

50

0

1 2 3 4

I, cm
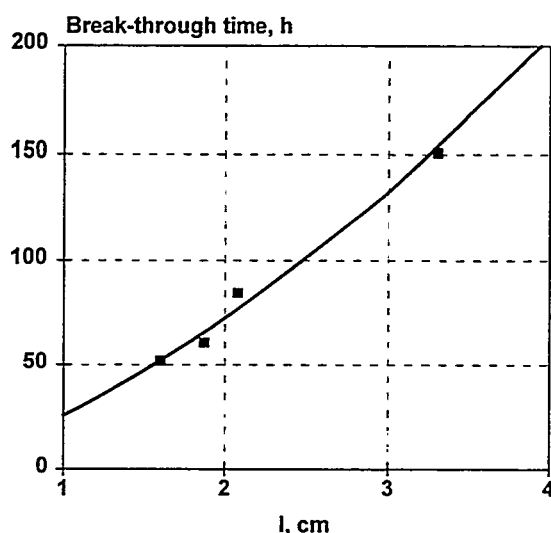
Fig. 4. Dependence of break-through time of
Cr(III) ions on gel thickness

4) However, the relative effects of the major components differ significantly. The sensitivity of transport properties towards the silicate content is roughly one order of magnitude less than the effect of polymer concentration.

Further, it is worth mentioning that other components of the gel may also have a substantial impact on the transport and retention properties. For example, the original pH of the barrier phase may modify the shares of processes leading to net retention of diffusing species. Since the diffusion coefficients in gels hardly differ from values characteristically found in the aqueous phase, the effect of gel composition on migration of heavy metal ions puts the gel type barriers in a different light and it turns our attention to the importance of those methods which selectively improve the retention capacity.

Description and Interpretation of Diffusion Transport in Gels

The migration of ions in gels can be interpreted similarly as the diffusion of charged species in porous media saturated with water. The basis of this hypothesis is that the dual network of cross-linked polymers and the polymerized silicate forms a flexible structure of gel and its "pore space" is filled with the solvent. Below it will be shown that this assumption is consistent with the ex-perimental findings. Using this approach the following conclusions could be drawn:

1) The effect of gel components can be interpreted through the *formation factor* (F). Thus, the experimental data might be correlated with the structure of gel (Figs 7. and 8.). On the basis of this theoretical treatment the Fick's I. law can be modified to the following form:

$$\frac{dn}{dt} = -D_{eff}A\frac{dc}{dx} = -D\frac{A}{F}\frac{dc}{dx} = -D\frac{A\Phi}{\tau^2}\frac{dc}{dx} = -D\frac{A_{eff}}{\tau^2}\frac{dc}{dx}$$

and that new relationship also proves the linear relationship between the transport parameters and the gel composition.

2) According to the experimental results the dual networks of gels induce high capillary forces to imbibe spontaneously and steadily retard the water, but this chain network hinders the migration of ions only to a negligible extent, e.g. the migration path of different metal ions in gels is merely 20% longer than in straight capillaries (Figs 7. and 8.).

As far as the practical application of the polymer/silicate gel is concerned it was concluded that the diffusion flux can be controlled effectively by the gel composition. It is obvious, however, that in placing gels around a contaminated area, the migration of heavy metal ions will be efficiently restricted only in those cases where the original porous or fractured media is only partially saturated with water or it is completely free of any liquids (e.g. gas saturated).
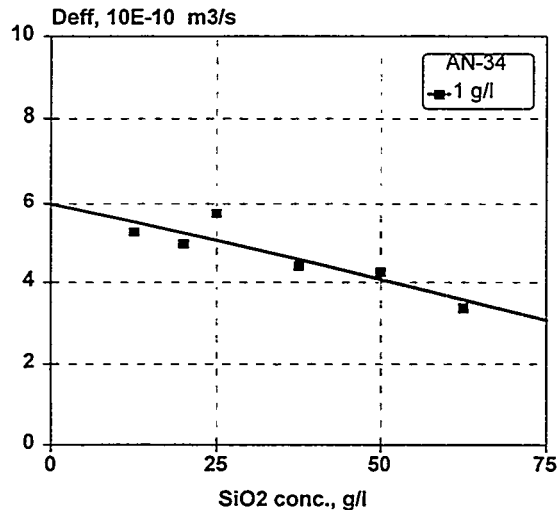
Fig. 5. Effect of silicate content on the effective diffusion coefficient of Cr(III) ion
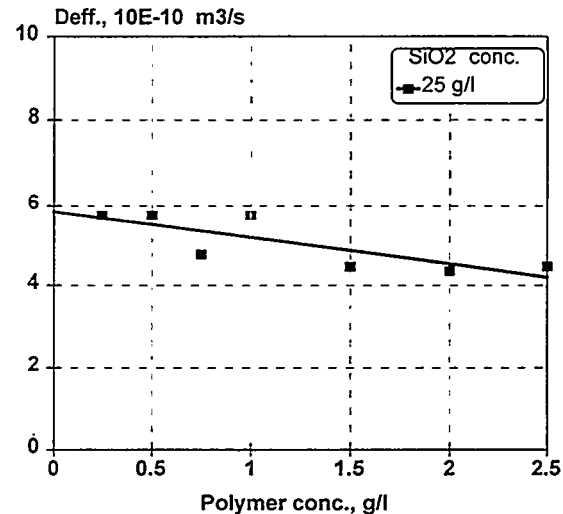
Fig. 6. Effect of polymer content on the effective diffusion coefficient of Cr(III) ion
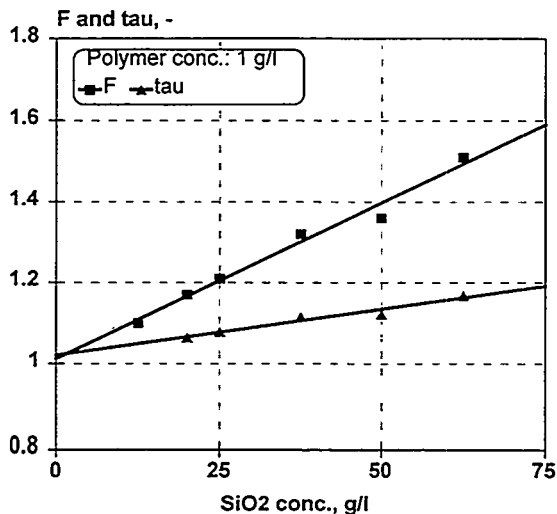
Fig. 7. Effect of silicate content on formation factor and tortuosity of gel
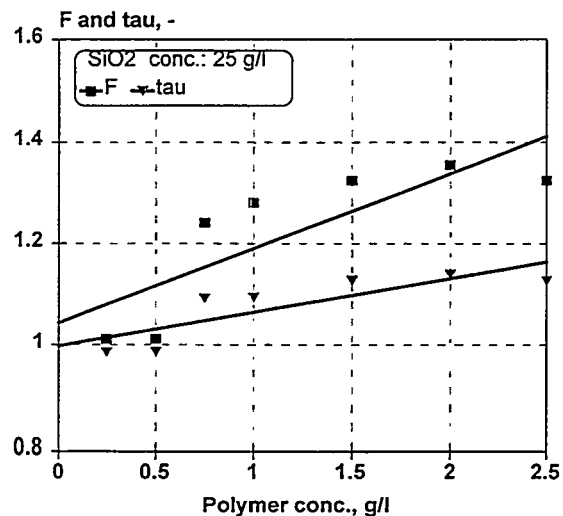
Fig. 8. Effect of polymer content on formation factor and tortuosity of gel

Diffusion of Radon in Gels and Montanwax Emulsions

The geochemical radon sources and nuclear waste depositories emanating high intensity radon flux represent continuous and serious hazard for humans. The radon gas (^{222}Rn) originating from ^{238}U isotope is omnipresent in the natural environment. Radon's high mobility can be attributed to gas and liquid phase transport and the leaching process of precursor nuclides. Consequently, an efficient restriction of radon migration in subsurface regions must form a central issue in environmental protection. Recently, self-conforming gels are proposed to decrease the flow of radon gas in porous media. This later technical solution may raise hopes because they can easily

be adapted to a great variety of local circumstances and tailored to any integrated environmental technologies without extensive destruction of surface facilities.

Experimental Conditions

The gel and the clay barrier significantly differ from each other regarding their chemical nature and placement technology. These facts must be considered when constructing the experimental arrangements and the samples to be analyzed. In the present case a cationic polymer (Polyquat 20) is cross-linked by anionic ortho-silicates. Under natural conditions the blocking effect is accomplished by injecting the self-conforming mixture into the target subsurface region. The samples to be exposed to radon must be prepared accordingly. For the serial analysis artificially consolidated porous media having 50% porosity and > 10 D permeability were used. Other aspects of the experimental technique and the calculation method were detailed earlier by CSIGE at al (1995). The fundamental difference between the gel and clay barriers is that no solid carrier is required in the later case. The sealing material is usually prepared at the surface from liquid (e.g. Montanwax emulsion) and solid components and then it is filled into a ditch sited around the contaminated area. The experimental arrangements of these tests were modified accordingly. More information on these laboratory studies was published recently by LAKATOS et al. (1996).

Diffusion Coefficient of Radon in Different Media

The absolute and effective diffusion coefficients of radon in different media are listed in Table 1. Comparing these data the following conclusions may be drawn:

1) The diffusion mass transport of radon in porous and fractured systems might be reduced by 5-6 orders of magnitude using self-conforming hydrogels and Montanwax clay suspensions if the pore space is originally filled by gaseous substances.

2) The diffusion coefficient of radon is 30% less in polymer/silicate gels than in pure water. The difference can be explained by the solid content and the structure of gel.

3) In porous media saturated with polymer/silicate gels the effective diffusion coefficient of radon is 60-70% less than in the aqueous phase. Thus, the diffusion radon transport can be reduced only slightly by gels in those systems where the original saturating media is water.

4) In Montanwax emulsions used for preparation of clay suspensions the calculated effective diffusion coefficient is 30% greater than the characteristic value in water. The phenomena can probably be traced back to the higher diffusion rate of radon in organic phases.

5) The diffusion transport of radon in concentrated clay suspensions is similar to that in porous media filled with gels. The effective diffusion coefficient of radon in such media is dependent on solid content, particle size distribution, porosity, tortuosity and the composition of the liquid phase used for preparation of suspensions. The experimental results clearly show that the hydrophobic sealing material is practically impermeable against water; however, the presence of the organic phase in suspension may increase slightly the diffusion mass transport of radon.

Table 1. **Diffusion coefficient of radon in different media**

Media	Diffusion coefficient, cm^2/s^1
Air	$\approx 1.0 \cdot 10^{-1}$
Water	$\approx 1.0 \cdot 10^{-5}$
Polymer/silicate gel	$\approx 7.0 \cdot 10^{-6}$
Porous media saturated by polymer/silicate gel	$\approx 3.3 \cdot 10^{-6}$
Montanwax emulsion	$\approx 1.3 \cdot 10^{-5}$
Clay suspension	$\approx 6.0 \cdot 10^{-6}$

The study of radon diffusion revealed that the gas phase migration of radon in natural porous media can be drastically reduced by the injection of gel-forming materials and placement of clay suspensions into the target area. Particularly, the Montanwax dispersion might be effective under natural conditions because of its hydrophobic capability and potential for mechanical entrapment of oil droplets by small size pores. Hence, their applications in different environmental technologies might be very effective. In natural water-saturated surface and subsurface systems, however, the positive effect derives mostly from restriction of the hydrodynamic mass transport, while the reduction of the diffusion mass transport remains within moderate limits. Despite that unfavorable fact, one beneficial property of both the polymer/silicate gels and clay system is that the quenching process is almost perfect in the sealing phase: on average less than 1% of the inlet radon concentration could be detected at the outlet surface of the sample having merely 3-4 cm thickness. It should be underlined that in this respect the daughter nuclides of radon may concentrate in the sealing materials until they completely decay.

Conclusions

The diffusion and hydrodynamic mass transport of chromium ions and radon in polymer/silicate gels and Montanwax emulsions were studied. On the basis of the experimental results the following conclusions were drawn:

1) The self-conforming gels may decrease the hydrodynamic mass transport in porous and fractured media by 4-6 orders of magnitude. In water saturated systems however, the diffusion mass transport can be restricted by hydrogels only in a moderate extent.

2) The high and selective retention capacity of gels towards hazardous species, which might be built artificially into the sealing phase, may extend the weaponry of containment technologies.

3) Similar results were obtained for transport phenomena of radon in porous media saturated by gels and Montanwax emulsions as mentioned above. The almost perfect quenching process of radon and its nuclides in gels and emulsions enhances significantly the positive effects of the encapsulation methods.

The laboratory experiments provided valuable new information and data to design the different containment technologies and formulate the barrier-forming materials and solutions.

Symbols

c	concentration, mol/l
n	number of moles, mol
t	time, s
x	thickness of sample, m
D	diffusion coefficient , m^2/s
F	formation factor, -
τ	tortuosity, -
Φ	porosity or volume fraction of water in gel, -

References

Csige, I., Hakl, J., Lakatos I. (1995) Measurement of Effective Diffusion Coefficient of Radon in Porous Media with Etched Track Radon Monitors. *Radiation Measurements*, 25 (1-4), 659-660.

Lakatos, I., Bauer, K., Lakatos-Szabó, J., Csige, I., Hack, J., Kretzschmar, H.-J. (1996) Diffusion of Radon in Polymer/Silicate Gels and Clay Barriers Applied in Environmental Protection. *In Environmental Pollution* (ed. Nath, B., Láng, I., Mészáros, E., Robinson, J. P., Hens, J.), pp. 522-529. European Centre for Pollution Research, London

MODIFICATION OF CLAY-BASED WASTE CONTAINMENT MATERIALS

Kofi Adu-Wusu[1], Joyce M. Whang[2] and Michael F. McDevitt[3]

Abstract

Bentonite clays are used extensively for waste containment barriers to help impede the flow of water in the subsurface because of their low permeability characteristics. However, they do little to prevent diffusion of contaminants, which is the major transport mechanism at low water flows. A more effective way of minimizing contaminant migration in the subsurface is to modify the bentonite clay with highly sorptive materials.

Batch sorption studies were conducted to evaluate the sorptive capabilities of organo-clays and humic- and iron-based materials. These materials proved to be effective sorbents for the organic contaminants 1,2,4-trichlorobenzene, nitrobenzene, and aniline in water, humic acid, and methanol solution media. The sorption capacities were several orders of magnitude greater than that of unmodified bentonite clay. Modeling results indicate that with small amounts of these materials used as additives in clay barriers, contaminant flux through walls could be kept very small for 100 years or more. The cost of such levels of additives can be small compared to overall construction costs.

Introduction

The goal of subsurface physical containment systems or waste containment barriers is to prevent migration of contaminant plumes. Advection and diffusion are the major mechanisms of contaminant movement through containment barriers. To minimize advection through barriers, materials with low permeability are used. Diffusion can be reduced by sorption. However, common waste containment materials such as bentonite clays have low sorption characteristics.

Previous investigators have measured the effects of additives that can be used to increase the sorption of contaminants (Brixie & Boyd, 1994; Evans, et al., 1994; Mott & Weber, 1992). The enhancement of barrier sorption characteristics must be achieved without creating any deleterious effects on the other properties of the materials, especially the hydraulic conductivity. In this study, the sorption of organics was measured for the following possible high sorptivity additives: organo-clays, natural humus, iron oxyhydroxide, iron carbonate, and activated carbon. Modeling was used to estimate the long term performance of barrier walls having these additives.

Experimental Method

Sorbents

The sorbents evaluated in this study were: (1) unmodified sodium bentonite clay (Hydrogel 125) from Wyo-Ben, Inc. (Billings, MT); (2) trimethylphenylammonium (TMPA) clay - modified sodium bentonite clay (organo-clay) prepared in our laboratory; (3) hexadecyltrimethylammonium (HDTMA) clay - modified sodium bentonite clay (organo-clay) prepared in our laboratory; (4) iron oxyhydroxide from an industrial byproduct; (5) iron carbonate from an industrial byproduct; (6) natural humus; and (7) powdered activated carbon.

---

[1] DuPont Central Research and Development, Glasgow 300, P. O. Box 6101, Newark, DE 19714-6101, (302) 451-9835, aduwusk@a1.esvax.umc.dupont.com

[2] DuPont Specialty Chemicals, Jackson Laboratory J-24, Chambers Works, Deepwater, NJ 08023, (609)540-4275, whangjm@a1.jlcl01.umc.dupont.com

[3] DuPont Central Research and Development, Experimental Station, P. O. Box 80304, Wilmington, DE 19880-0304, (302) 695-4882, mcdevimf@esvax.dnet.dupont.com

Chemicals

Chemicals used were reagent grade from Aldrich Chemical Company (Milwaukee, WI). The contaminant chemicals used were 1,2,4-trichlorobenzene, nitrobenzene, and aniline. They were selected because of their varying hydrophobic characteristics. 1,2,4-trichlorobenzene was applied in solutions of 20 ppm, which is close to its solubility limit. The more water soluble chemicals nitrobenzene and aniline were tested at 500 and 450 ppm, respectively.

Known concentrations of solutions of the contaminant chemicals were prepared with distilled water using glass containers at room temperature ($23 \pm 1°C$). Dissolution of the chemicals was speeded up by agitating in a shaker bath overnight.

Humic acid (technical grade) and methanol were used to mimic different subsurface solution media. TMPA bromide and HDTMA bromide, which are quaternary ammonium compounds, were used to prepare the organo-clays.

Organo-Clay Preparation

The organo-clays were prepared by adding an amount of quaternary ammonium compound of interest (HDTMA bromide or TMPA bromide) equal to the cation-exchange capacity (CEC) of the sodium bentonite clay. CEC of sodium bentonite clay (Hydrogel 125) ~ 90 cmol/kg.

A solution of quaternary ammonium bromide was added to a clay suspension (1:25 (w/w) clay/water) and tumbled for 5/6 hours. The organo-clay suspension was then centrifuged and washed four times with distilled water. It was followed by air-drying and storage at room temperature ($23 \pm 1°C$).

Sorption Tests

A batch sorption run was conducted by adding 20 mL of a solution of the contaminant of interest to known mass of sorbent in a 30 mL Corex glass centrifuge tube equipped with a Teflon® lined screw-cap. Several soil-solution ratios were employed for each sorbent. The tubes were rotated end-over-end in a tumbler for 24 hours at 8 rpm.

At the end of the 24-hour equilibration period, the soil-solution mixtures were centrifuged for 10 minutes at 9500 rpm to settle the solids. DuPont Sorvall SS-3 centrifuge with SS-34 rotor was used for centrifugation. About 13-mL aliquots of the supernatants were removed and placed in glass tubes with Teflon®-lined caps for analysis. The amount of contaminant sorbed was determined from the initial and final concentrations of contaminant in solution.

Control and blank runs were conducted simultaneously with the main sorption runs. A control is a solution of the contaminant without sorbent. A blank, on the other hand, is a suspension of sorbent and contaminant-free solution. Control and blanks permit correction for analytical interference due to sorbent extracts as well as correction for interaction between chemical and container or handling losses. All sorption runs were conducted at room temperature ($23 \pm 1°C$).

Chemical Analysis

The concentrations of contaminants in the supernatants were determined using a gas chromatograph equipped with flame ionization, mass spectrometer, or electron capture detectors. TMPA and HDTMA were analyzed using the titration method outlined in Furlong and Elliker (1953) and Zhang et al. (1993).

Experimental Results and Discussion

Tables 1, 2 and 3 are summaries of partition coefficient data for the sorption of 1,2,4-trichlorobenzene, nitrobenzene, and aniline, respectively. These data are for sorption experiments conducted in water solution medium. The partition coefficients were obtained from linear regression analysis of sorption isotherm data. Correlation coefficients (r^2) for all the isotherm data were greater than 0.88, with 95% of them greater than 0.97. Measurements of sorption of nitrobenzene to iron oxyhydroxide and iron carbonate were inconclusive. The partition coefficient is the ratio of contaminant in the sorbed and solution phases. Higher values indicate more sorption.

Tables 1, 2 and 3 all indicate that sorption of each contaminant by each of the various sorbents in water medium was increased by several orders of magnitude compared to unmodified clay. The most effective sorbents for 1,2,4-trichlorobenzene (Table 1) were activated carbon, TMPA-clay, HDTMA-clay, and natural humus. For nitrobenzene (Table 2), the sorbents that were most effective were activated carbon, TMPA-clay and natural humus/HDTMA-clay. Activated carbon, natural humus and TMPA-clay proved to be the best sorbents for aniline (Table 3).

Iron oxyhydroxide exhibited average sorptivity. Iron carbonate and unmodified clay exhibited minimal sorption in most cases. Natural humus had selective sorption characteristics. Natural humus was effective for aniline but not as effective for 1,2,4-trichlorobenzene and nitrobenzene.

Table 1. Sorption data for 1,2,4 trichlorobenzene in water. Initial concentration = 20 mg/L.

Sorbent	Partition Coefficient, L/kg	R^2
Activated Carbon	630,000	0.96
TMPA-Clay	3,100	1.00
HDTMA-Clay	470	0.98
Natural Humus	150	0.94
Iron Oxyhydroxide	65	0.98
Iron Carbonate	2	0.97
Unmodified Clay	2	0.88

Table 2. Sorption data for nitrobenzene in water. Initial concentration = 500 mg/L.

Sorbent	Partition Coefficient, L/kg	R^2
Activated Carbon	7000	1.00
TMPA-Clay	230	0.97
Natural Humus	87	0.99
HDTMA-Clay	72	0.92
Unmodified Clay	<1	

Table 3. Sorption data for aniline in water. Initial concentration = 450 mg/L.

Sorbent	Partition Coefficient, L/kg	R^2
Activated Carbon	900	0.96
Natural Humus	440	0.99
TMPA-Clay	140	0.96
HDTMA-Clay	89	0.99
Iron Oxyhydroxide	74	0.95
Unmodified Clay	47	1.00
Iron Carbonate	2	0.89

667

The affinity of a contaminant for a given sorbent was related to its hydrophobicity. 1,2,4-trichlorobenzene demonstrated the greatest sorptivity for a sorbent, followed in decreasing order by nitrobenzene and aniline.

The effect of solution medium on sorption is shown in Tables 4 and 5. The trends in Tables 4 and 5 indicate humic acid and methanol solution media decrease sorption. The decrease in sorption was more marked in the methanol solutions than humic acid solution. However, the relatively high sorptivity exhibited by even the 3:7 methanol/water (v/v) solution indicates both TMPA- and HDTMA- clays are promising sorbents for applications involving water-miscible organic constituents. The above observations were based on experiments with 1,2,4-trichlorobenzene and TMPA-clay and HDTMA-clay. The same deductions are expected for the other contaminants and sorbents tested in this study.

Modeling Predictions

To determine the likely impact of adding such sorptive materials to a barrier wall, the one-dimensional advection-dispersion equation was used to describe transport through a barrier (Rabideau, 1996).

$$R_f \frac{\partial C}{\partial t} = -v \frac{\partial C}{\partial x} + D \frac{\partial^2 C}{\partial x^2}$$

C is the volume-averaged aqueous phase contaminant concentration, t is time, x is the distance from the entrance side of the barrier, v is the interstitial fluid velocity, D is the dispersion coefficient, and R_f is the retardation factor, defined by

$$R_f = 1 + \frac{\rho_b K_d}{n}$$

where ρ_b is the bulk density, K_d is the partition coefficient, and n is the porosity. An analytical solution has been derived by Rabideau (1996) for flux at the exit side of the barrier for the following boundary conditions

$C(x,0) = 0$
$C(0,t) = C_o$
$C(L,t) = 0$

where C_o is the concentration at the entrance side of the barrier, and L is the wall thickness.

Table 4. Effect of solution medium on the sorption of 1,2,4 trichlorobenzene on TMPA-Clay. Initial concentration = 20 mg/L.

Solution Medium	Partition Coefficient, L/kg	R^2
Water	3100	1.00
Humic Acid (15 ppm)	1100	0.99
1:9 Methanol/Water (v/v)	330	0.95
3:7 Methanol/Water (v/v)	250	0.95

Table 5. Effect of solution medium on the sorption of 1,2,4 trichlorobenzene on HDTMA-Clay. Initial concentration = 20 mg/L.

Solution Medium	Partition Coefficient, L/kg	R^2
Water	470	0.98
Humic Acid (15 ppm)	410	0.97
1:9 Methanol/Water (v/v)	220	0.94
3:7 Methanol/Water (v/v)	91	1.00

Figure 1 shows the predicted flux at the exit side of a barrier (plotted on a semilog scale) for the following conditions.
- wall thickness 1 m
- hydraulic conductivity of the wall 10^{-7} cm/s
- concentration at the entrance side of the barrier 100 ppm
- hydraulic gradient 0.01
- dispersivity 10^{-6} cm^2/s
- bulk density 1.7 g/mL
- porosity 40%
- partition coefficients 0, 1, 3 l/kg

Under these conditions, the steady state flux would be 300 ng/m^2/year. The broken line in Figure 1 marks a hypothetical target flux of 0.3 ng/m^2/year, or 0.1% of the steady state flux. As seen in Figure 1, the model predicts that flux will remain this low after 100 years if the material in the barrier wall has a partition coefficient between 1 and 3 L/kg or greater.

The data in Tables 1-5 indicate that for the materials tested, partition coefficients of 100's or 1000's L/kg can be attained. When mixed with inert materials, partition coefficient scales with the amount of the sorbent; hence, mixes containing 0.1% to 1% sorbent materials would give net partition coefficients on the order of 1 to 3 L/kg or more. Some barrier materials, such as cement-based materials, may affect the sorbents; hence confirmation tests should be conducted with proposed mixes. For mixtures of modified and unmodified clays, sorptivity of the mixture should equal the weighted sum of the sorptivity of the clays.

In many situations, pump-and-treat is used in conjunction with a barrier wall to prevent migration of contaminants through the wall. With the addition of sorptive materials, it may be possible to avoid using pump-and-treat. Without pump-and-treat, there could be an increase in the hydraulic gradient across a barrier. Figure 2 shows the fluxes predicted at the exit side of a 1 m barrier after 100 years for various hydraulic gradients and partition coefficients. Other conditions are the same as in Figure 1. At low hydraulic gradient, changes of hydraulic gradient

Figure 1. Model predictions of flux through a 1 m wall, hydraulic gradient 0.01.
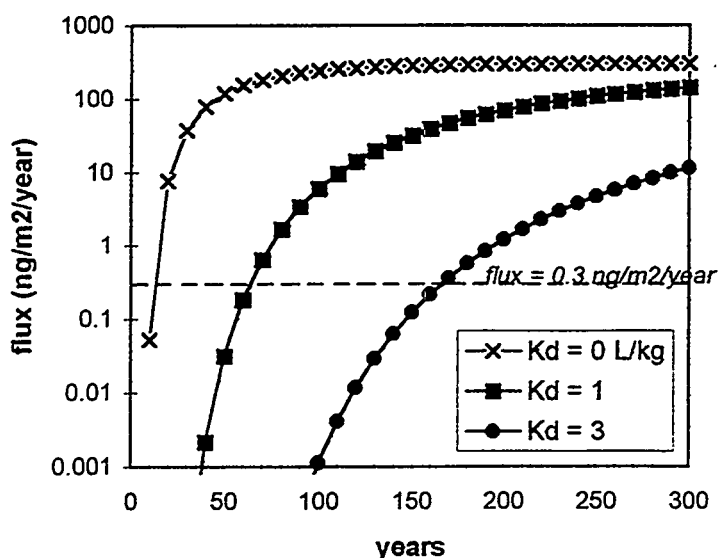
have little effect on flux. Under these conditions, advection contributes little to net flux; flux is primarily the result of diffusion. At high hydraulic gradients, partition coefficient of 10 L/kg or more may be needed for flux to be lower than the hypothetical target of 0.3 ng/m^2/year.

Cost

Table 6 lists approximate costs for the sorbents tested, sample application rates, and material costs for adding these sorbents to a barrier wall at these rates. Costs are given per square-meter of a 1 m-thick wall. Actual application rates and costs will be site-specific. Construction of conventional slurry walls typically costs $20-80/m^2 (Filz & Mitchell, 1996). The incremental cost of using additives is essentially the cost of materials.

Conclusions

In laboratory results, activated carbon, trimethylphenylammonium (TMPA)-clay, hexadecyl-trimethylammonium (HDTMA)-clay and natural humus were very effective sorbents for removing organic contaminants (1,2,4-trichlorobenzene, nitrobenzene and aniline) from water and water-miscible solution media. Hence, their use as components of waste containment barrier materials will greatly enhance the sorptive properties of waste containment barriers. This in turn will lead to long barrier breakthrough times.

Figure 2. Model predictions of flux through a 1 m wall after 100 years.
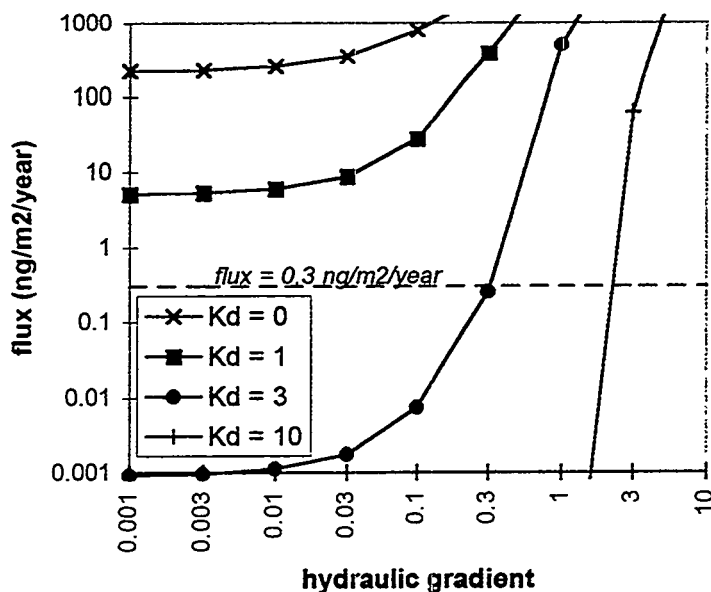
Table 6. Costs of sorbents

Sorbent	$/kg	application rate	$/m^2
Activated Carbon	$2.	0.01%	$0.4
TMPA-Clay	$0.50	0.1%	$0.9
HDTMA-Clay	$0.50	1.%	$9
Natural Humus	<$0.10	1.%	<$2.
Iron Oxyhydroxide	<$0.10	1.%	<$2.

The sorptivity of iron oxyhydroxide material was average but it is relatively effective for highly hydrophobic organic contaminants (e.g. 1,2,4-trichlorobenzene).

Natural humus was selective in its sorptive behavior. As a result, it may be useful for certain contaminant-specific applications (e.g. aniline) because it is the most inexpensive among the effective sorbents mentioned earlier.

Humic acid and methanol solution media reduced the sorption capacity of the sorbents. However, the sorption achieved was relatively high. This implies the use of the sorbents found effective as additives to waste containment barriers would represent a significant improvement in containment technology for situations having water-miscible solution media.

For a given sorbent, 1,2,4-trichlorobenzene showed the greatest sorption followed in decreasing order by nitrobenzene and aniline. This order is inversely related to the solubility of the contaminants.

Model predictions show the effect of partition coefficient on flux through a barrier wall. For sample run conditions, adding the tested sorbents in concentrations of 0.1% to 1% may be sufficient for maintaining low contaminant flux for 100 years. The cost of such sorbents is likely to be small.

For specific field applications, tests should be run for the proposed barrier wall mixtures using site groundwater. In addition to batch tests and modeling, column studies may also help predict long term performance of barrier walls.

References

Brixie, J.M., S.A. Boyd. (1994) Treatment of contaminated soils with organoclays to reduce leachable pentachlorophenol. *J. Environ. Qual, 23*: 1283-1290.

Evans, J.C., T.L. Adams, K.A. Dudiak (1994) Enhanced slurry walls as treatment zones for inorganic contaminants. In *Hazardous and Industrial Wastes, Preceedings of the Twenty-Seventh Mid-Atlantic Industrial Waste Conference* (ed. A.K. Sengupta), pp. 712-721.

Filz, G.M., J.K. Mitchell. (1996) Design, construction, and performance of soil- and cement-based vertical barriers. In *Assessment of Barrier Containment Technologies: A Comprehensive Treatment for Environmental Remediation Applications* (ed. R.R. Rumer, J.K. Mitchell), pp. 296-298. NTIS publication #PB96-180583

Furlong, T.E. and P. R. Elliker. (1953) An improved method of determining concentration of quaternary ammonium compounds in water solutions and in milk. *J. Dairy Sci., 36*: 225-234.

Mott, H.V. and W.J. Weber, Jr. (1992) Sorption of low molecular weight organic contaminants by fly ash: considerations for the enhancement of cutoff barrier performance. *Env. Sci. Tech., 26*: 1234-1242.

Rabideau, A.J. (1996) Contaminant transport modeling. In *Assessment of Barrier Containment Technologies: A Comprehensive Treatment for Environmental Remediation Applications* (ed. R.R. Rumer, J.K. Mitchell), pp. 296-298. NTIS publication #PB96-180583.

Zhang, Z. Z., D. L. Sparks, and N. C. Scrivner. (1993) Sorption and desorption of quaternary amine cations on clays. *Environ. Sci. Technol., 27*: 1625-1631.

Biofilm Treatment of Soil for Waste Containment and Remediation

J.P. Turner[1], M.L. Dennis[1], Y.A. Osman[2], J. Chase[2], L.A. Bulla[2]

[1]Department of Civil and Architectural Engineering
University of Wyoming
P.O. Box 3295 University Station
Laramie, WY 82071-3295

[2]Department of Molecular Biology
University of Wyoming
P.O. Box 3354 University Station
Laramie, WY 82071-3354

ABSTRACT

This paper examines the potential for creating low-permeability reactive barriers for waste treatment and containment by treating soils with Beijerinckia indica, a bacterium which produces an exopolysaccharide film. The biofilm adheres to soil particles and causes a decrease in soil hydraulic conductivity. In addition, B. indica biodegrades a variety of polycyclic aromatic hydrocarbons and chemical carcinogens. The combination of low soil hydraulic conductivity and biodegradation capabilities creates the potential for constructing reactive biofilm barriers from soil and bacteria.

A laboratory study was conducted to evaluate the effects of B. indica on the hydraulic conductivity of a silty sand. Soil specimens were molded with a bacterial and nutrient solution, compacted at optimum moisture content, permeated with a nutrient solution, and tested for k_{sat} using a flexible-wall permeameter. Saturated hydraulic conductivity (k_{sat}) was reduced from 1×10^{-5} cm/sec to 2×10^{-8} cm/sec by biofilm treatment. Permeation with saline, acidic, and basic solutions following formation of a biofilm was found to have negligible effect on the reduced k_{sat}, for up to three pore volumes of flow.

Applications of biofilm treatment for creating low-permeability reactive barriers are discussed, including compacted liners for bottom barriers and caps and creation of vertical barriers by in situ treatment.

BACKGROUND

The phenomenon of bacterial-induced decreases in permeability of porous media (often termed "plugging" or "clogging" in the literature) is well-known in several fields of science and engineering. In most cases, bacterial plugging is considered to be a problem. For example, injection of water into petroleum reservoirs is a common form of enhanced oil recovery. Bacteria and nutrients present in the injected water have been observed to cause severe plugging and loss of water injectivity, reducing the recovery effectiveness (e.g., Cerini et al. 1946; Hart et al. 1960; Kalish et al. 1964; numerous others). In-situ bioremediation involving the injection of nutrients into the ground to stimulate the growth of indigenous bacteria capable of degrading contaminants has led to biofilm plugging, reducing the effectiveness of bioremediation (Taylor and Jaffe 1991). Sewage infiltration ponds may become severely plugged by biofilm, creating a maintenance problem (e.g., Allison 1947; McCalla 1950; Calaway 1957; Mitchell and Nevo, 1964).

Mechanisms of Bacterial Plugging

Aquatic bacteria show a strong tendency to adhere to surfaces of porous media (Mitchell and Nevo 1964; Jones et al. 1969; Marshall et al. 1971). Following initial colonization, bacteria adhere irreversibly to solid surfaces by means of their exopolysaccharide surface structures and begin to form a confluent biofilm within which the bacterial cells are enmeshed in a matrix of acid mucopolysaccharide (Fletcher and Floodgate 1973; Costerton et al. 1987). This adherent plugging biofilm is responsible for decreasing the permeability of porous media. Previous investigations have not reported bacterial plugging of soils sufficiently to meet the generally accepted criteria of hydraulic conductivity (k) less than 10^{-7} cm/sec required for waste containment barriers (see summary by Dennis 1996). However, previous studies strongly suggest that the potential exists for achieving lower values of k by manipulating variables such as bacterial species, nutrient composition, soil type, and preparation technique.

Application to Containment Technology

The performance of contaminant barriers depends upon many factors, including the type of wastes being contained, the materials used to construct the barrier and their compatibility with the waste materials, quality of construction, and long-term durability under adverse environmental conditions. Materials used for barriers should be inexpensive, have low hydraulic conductivity, low molecular diffusivity, and must be durable enough to last for tens and possibly hundreds of years (Mitchell and Jaber 1990). This study is based on the hypothesis that when certain types of bacteria are introduced into soil and stimulated with the appropriate nutrients, the resulting biofilm develops a strong surface adhesion to the soil particles and results in clogging of the soil pore spaces. If this process can be controlled to meet engineering and construction specifications, it offers the potential for materials with low hydraulic conductivity capable of acting as barriers to contaminant transport. The objective of the study described herein is to investigate the feasibility of developing new, low-cost barrier materials bioengineered for waste containment.

LABORATORY STUDY OF BIOFILM FORMATION AND PERFORMANCE

Soil

Laboratory tests were conducted to evaluate the effects of biofilm on soil hydraulic conductivity. The soil used in this study is classified as SM, silty sand, in the Unified Soil Classification System and consists of a naturally occurring, poorly-graded, fine to medium-grained sand mixed with 17 percent (by weight) kaolinite. Selection of the sand-clay mix was based primarily on initial hydraulic conductivity. When compacted at a water content slightly wet of optimum, this soil exhibits a saturated hydraulic conductivity of $k \approx 1 \times 10^{-5}$ cm/sec. This value of k would make the soil unacceptable for use as a compacted soil liner by approximately two orders of magnitude (Landreth 1990; Daniel 1993). Further information on the soil characteristics is given by Dennis (1996).

Bacteria and Growth Medium

The Beijerinckia indica species used in this study is a laboratory isolate (strain CO-1) derived from cultures obtained from the American Type Culture Collection of B. indica ATCC# 9038. B. indica is an aerobic, free-living, non-pathogenic soil bacterium. All bacteria were cultured on a solid medium containing per liter: 20 g glucose, 1.0 g yeast extract, 1.0 g NaCl, 0.8 g K_2HPO_4, 0.2 g KH_2PO_4, 0.5 g $MgSO_4 \cdot 7H_2O$, 75 µg $FeCl_3$, and 15 g agar. The pH of the medium was adjusted to 5.5 before autoclaving. The nutrient solution has the same composition, without agar. B. indica inoculum was prepared by growing the bacterial cultures on 150 mm x 15 mm plates of the solid nutrient medium, scraping and rinsing the bacterial colonies from the plates, and suspending them in liquid medium. The resulting inoculum contained 10^{13} to 10^{14} bacterial cells per mL.

Specimen Preparation and Testing

Approximately 3000 g of air-dried soil was used to make three specimens from a single batch of soil. A volume of water (control specimens) or bacterial inoculum corresponding to the desired moisture content was mixed thoroughly into the soil. Specimens were compacted using a standard Proctor hammer (weight = 24.5 N; 30.5 cm drop height) in a cylindrical mold 7.1 cm in diameter and 8.6 cm high. Because the mold is smaller than a standard Proctor mold, three lifts and ten blows per lift (rather than 25) were used for a compactive energy of 619 kN-m/m³, approximately the same as the standard Proctor method of 593 kN-m/m³. Following compaction, the soil specimen was weighed, extruded from the mold, sheathed in a rubber membrane, and placed in the flexible-wall permeameter.

Fig. 1 is a schematic diagram of the permeameter system. Specimen confining stress was controlled by regulating the pressure on the cell reservoir. Hydraulic gradient was controlled through the pressures applied to the inflow and outflow reservoirs. Bladder accumulators were used on the inflow and outflow lines to keep bacterial and nutrient solutions (permeant) from coming into contact with the
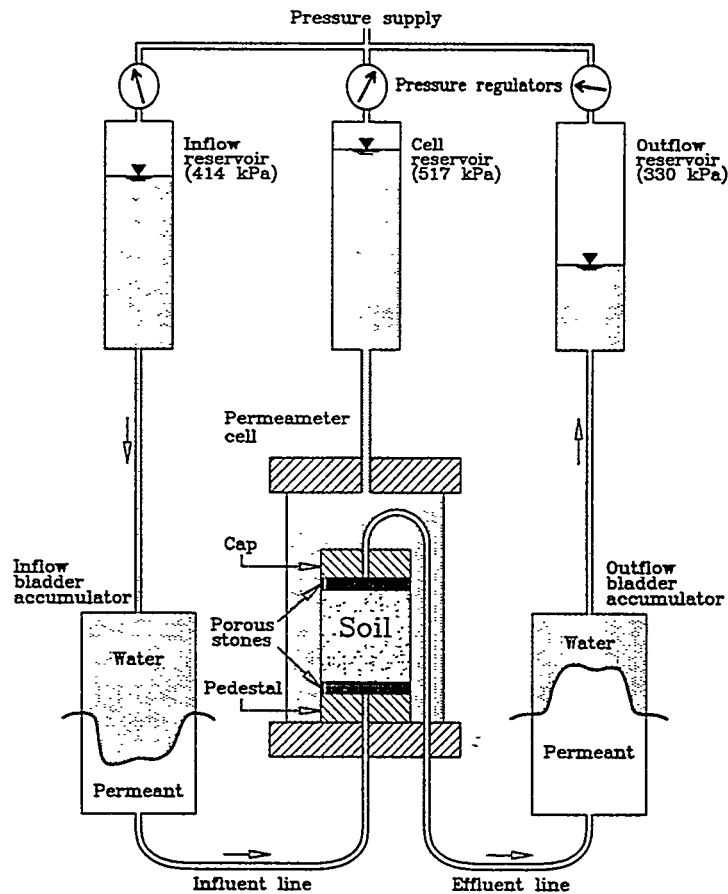
Figure 1. Flexible-wall permeameter

plumbing of the pressure control panel. After a compacted specimen was placed in the permeameter cell, the cell was filled with water and a confining stress of 34 kN/m² was applied. Nutrient solution (or water for control specimens) was allowed to pass slowly into the bottom of the specimen under atmospheric pressure. For control specimens, the outflow end of the specimen was subjected to a vacuum of 42 cm Hg to assist in the displacement of air. Specimens molded with bacteria were not subjected to vacuum, to avoid anything that might inhibit bacterial growth. Full saturation was achieved by applying back pressure to the pore fluid to dissolve air bubbles trapped in the soil. Cell pressure was increased to 517 kN/m² and pore pressure was increased to 414 kN/m². Pressure increases were applied gradually in increments of 35 kN/m² such that the effective stress never exceeded 103 kN/m².

Specimen saturation was verified by conducting checks of Skempton's B pore pressure coefficient. B-checks were conducted by increasing the cell pressure by a known amount with the specimen drain lines closed and recording the resulting change in pore water pressure by means of a pressure transducer connected to a no-flow drain line. In theory $B = 1.0$ for soil which is fully saturated ($S = 100$ percent) because water is essentially incompressible relative to the soil matrix and all of the increase in cell pressure is carried by the pore fluid. If gas is present in the pore fluid, B will be less than 1.0 owing to its high compressibility. During permeation of the soil specimens with nutrient solution, the aerobic B. indica bacteria produce gas, mostly CO_2, which decreases the degree of saturation. Once the nutrient is replaced by some other permeant, such as water, gas production ceases and S increases. For purposes of comparing hydraulic conductivities of various specimens with and without bacterial treatment it is important to report results for the same degree of saturation, since hydraulic conductivity varies with S. Degree of saturation was monitored as often as possible by conducting B-

checks for all specimens, beginning with initial saturation and continuing through permeation with nutrient solution, water, and/or chemical solutions. It was observed that treatment of specimens with bacteria generally reduced the measured value of B compared to control specimens. Following steady-state flow for relatively long periods without nutrients, B would increase to above 0.80 for biofilm-treated specimens. The degree of saturation can conservatively be assumed to be at least 95 percent for $B \geq 0.80$. All values of hydraulic conductivity reported herein for biofilm-treated specimens correspond to values of $B \geq 0.80$.

Measurements of hydraulic conductivity were performed using the constant head test. Pressure in the outflow reservoir was lowered while the pressure in the inflow reservoir was held constant at 414 kPa. Most tests were conducted with a pressure difference across the specimen of 84 kPa, which corresponds to a hydraulic gradient of 100. This gradient was not exceeded in any test.

Test results for thirteen specimens are reported in this paper. This includes five control specimens (i.e., no biofilm treatment and permeated with water only) and eight specimens treated with B. indica. The bacteria-treated specimens were permeated with nutrient solution to establish a plugging biofilm for periods ranging from 7 to 22 days, followed by permeation with either water or chemical solutions intended to challenge the biofilm. Chemical permeants included a saline solution of $0.5N$ NaCl, an acidic solution of HCl ((pH = 3), and a basic solution of NaOH (pH = 11). Hydraulic conductivity and values of B were monitored as often as possible during permeation with the various pore fluids.

RESULTS

Table 1 summarizes the hydraulic conductivity test results. In general, final hydraulic conductivities of biofilm-treated specimens were approximately three orders of magnitude lower than that of the control specimens without biofilm treatment. Fig. 2 illustrates the typical observed behavior, in this case for a specimen permeated with hydrochloric acid solution (pH = 3). For the first 24 hours of the test, nutrient solution was permitted to reside with no flow. Then nutrient solution was passed through the specimen for 16 days, corresponding to 2.0 pore volumes of flow. During most of the nutrient stimulation period k was in the range of 2 to 3×10^{-8} cm/sec, then decreased to approximately 1×10^{-8} cm/sec. This sudden decrease in k was observed in all specimens permeated with nutrient for more than two weeks and is believed to be caused by a buildup of CO_2 which decreases the degree of saturation, as reflected in measured values of $B \approx 0.2$. Upon permeation with acidic solution, B gradually increased to greater than 0.8 and hydraulic conductivity leveled off in the range of 2 to 3×10^{-8} cm/sec. For the three specimens permeated with hydrochloric acid, the number of pore volumes of acidic solution passed through the specimens ranged from 2.4 to 3.1. Specimens permeated with saline and basic solutions exhibited behavior similar to that of the specimen shown in Fig. 2. Individual results of all tests are too extensive to report herein, but the interested reader is referred to Dennis (1996) for full details.

TABLE 1. Summary of Hydraulic Conductivity Test Results

Bacterial Treatment	Final Permeant or Test Condition	Number of Tests	Final Hydraulic Conductivity (cm/s) (average)
none	water	5	1.2×10^{-5}
B. indica	saline (0.5 N NaCl)	2	1.3×10^{-8}
B. indica	acidic (pH = 3)	3	2.7×10^{-8}
B. indica	basic (pH = 11)	3	1.7×10^{-8}
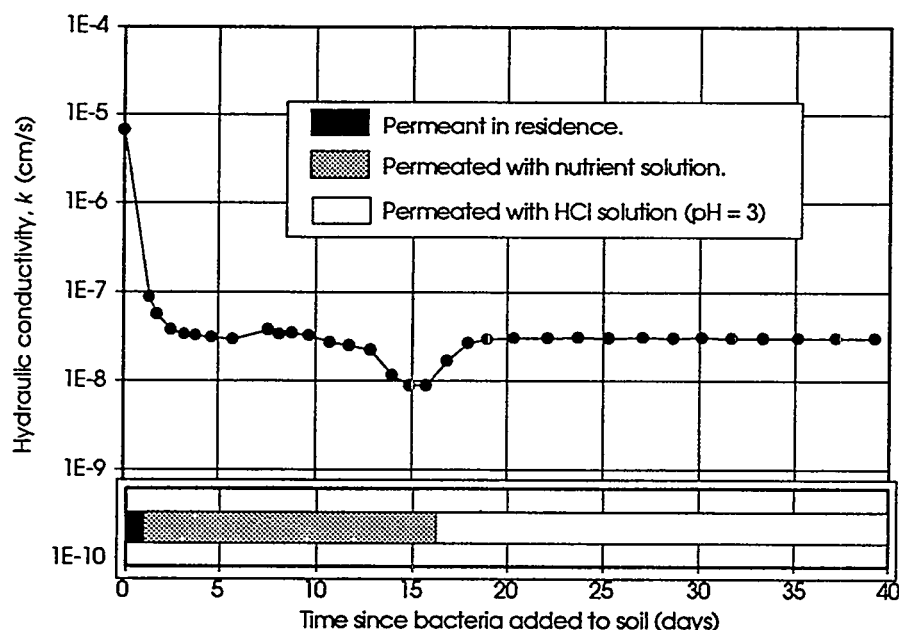
Figure 2. Hydraulic conductivity versus time, specimen permeated with acidic solution

BIODEGRADATIVE CAPABILITIES OF BEIJERINCKIA SPECIES

The biodegradative capabilities of the Beijerinckia species are well documented in the literature. This bacterium has been reported to have high degradative capabilities for different xenobiotic compounds. Various species of Beijerinckia were able to grow on biphenyl or m-xylene as a sole carbon source and were capable of cooxidizing many aromatic hydrocarbons as well (Kim and Zylstra 1995). Gibson et al. (1975) reported a mutant strain of Beijerinckia capable of oxidizing the carcinogens: benzo [a] pyrene and benzo [a] anthracene. Other Beijerinckia species have been reported to degrade the polycyclic hydrocarbons acenaphthene and acenaphthylene (Mahaffey et al. 1988; Schoken and Gibson 1984; Kryohara et al. 1983).

DISCUSSION

The test results described above suggest that biofilm treatment of soils may offer a means of constructing waste containment barriers using locally available soil and low-cost bacterial and nutrient solutions. This technology, although requiring much further research, might be applied in several ways. For example, soil could be mixed on a large scale with a bacterial/nutrient solution, placed in lifts, and compacted to form liners or caps for landfills or surface impoundments. The tests described above were intended to simulate as closely as possible the mixing and compaction process. In addition to hydraulic conductivity, other required engineering properties such as adequate shear strength and ductility would need to be evaluated. Further research at a prototype scale is needed to develop this technology for field applications. Use of biofilm-treated soil for this purpose would be an attractive alternative at sites where suitable low-permeability soils are not available for constructing compacted clay liners. For many such facilities the soil is modified by the addition of bentonite (Daniel 1993) or by transporting suitable low-permeability soils from distances which increase costs substantially. Biofilm treatment may offer a cost-effective alternative, although the technology is not yet developed sufficiently to allow cost comparisons.

A second potential application is where bacterial and nutrient solutions are injected into closely-spaced wells to create in situ vertical barriers, or cutoff walls. Establishment of such a barrier would depend upon many factors, such as initial soil hydraulic conductivity, thickness of the resulting biofilm barrier, nutrient requirements, hydraulic gradients, and many others. Construction of in situ vertical barriers would have the advantage of avoiding excavation, which is necessary when constructing a slurry trench cutoff wall. This technology, however, does require full-scale testing to evaluate its feasibility.

A final potential application of biofilm barriers is the use of biofilm for waste containment combined with in situ treatment. It may be possible to develop a soil-plugging biofilm from bacteria which also biodegrade soil and groundwater contaminants to less harmful substances. B. indica was chosen for this study, in part, because it offers the biodegradation capabilities described earlier.

SUMMARY AND CONCLUSIONS

Significant reductions in hydraulic conductivity can be achieved through bacterial treatment of soil. A feasibility study was conducted to determine if the hydraulic conductivity of a silty sand could be reduced sufficiently to make it suitable for waste containment. Reductions of several orders of magnitude were observed when the soil was mixed with a solution containing the biofilm-producing bacterium Beijerinckia indica, compacted close to optimum moisture content, and permeated with nutrient solution. Final values of hydraulic conductivity were in the range of 1 to 3 x 10^{-8} cm/sec. The biofilm produced by B. indica exhibited resistance to various inorganic chemical solutions. Soil specimens with well-established biofilm showed essentially no changes in k when permeated with a 0.5 normal saline solution and acidic and basic solutions. The biofilm apparently persists and maintains a low hydraulic conductivity in the absence of nutrient solution. One specimen of this study was permeated for 51 days with non-nutrient solutions and there was no increase in k.

Results of this study and previous research showing the ability of B. indica to degrade various contaminants demonstrate a potential for using this bacterium to construct reactive biofilm barriers. Substantial research is required to develop this technology for practical applications. Issues requiring further study include: long-term durability of biofilm; resistance to a wider variety of chemicals; effects of biofilm on engineering properties of soil such as strength and compressibility; and the effects of biofilm on other contaminant transport properties of soil such as diffusion, adsorption, etc. In addition, the range of soil types for which biofilm barriers can be established must be determined. This study represents an initial investigation which suggests that biofilm barriers could eventually form the basis of an effective, economical, and innovative waste containment and treatment technology.

ACKNOWLEDGMENTS

REFERENCES

Allison, L.E. (1947) Effect of microorganisms on permeability of soil under prolonged submergence. *Soil Sci.*, 63, 439-450.

Calaway, W.T. (1957) Intermittent sand filters and their biology. *Sewage and Ind. Wastes*, 29, 1-5.

Cerini, W.F., W.R. Battles, and P.H. Jones. (1946) Some factors influencing the plugging characteristics of an oil-well injection water. In *Petroleum Techn. Pub. No. 28*, AIME, 52-63.

Costerton, J.W. *et al.* (1987) Bacterial biofilms in nature and disease. *Ann. Review of Microbiol*, 42, 435-464.

Daniel, D.E. (1993) Clay liners. Ch. 7 in *Geotechnical Practice for Waste Disposal*, Ed. by D.E. Daniel, Chapman & Hall, London, 137-163.

Dennis, M.L. (1996) Hydraulic conductivity of compacted soil treated with biofilm. M.S. Thesis, Univ. of Wyoming, Dept. of Civil & Arch. Engrg., Laramie, WY.

Fletcher, M. and G.D. Floodgate. (1973) An electron microscopic demonstration of an acid polysaccharide involved in the adhesion of a marine bacterium to solid surfaces. *J. Gen. Microbiol*, 74, 325-334.

Gibson, D.T., V. Mahadevan, D.M. Jerina, H. Yogi, and H.J. Yeh. (1975) Oxidation of the carcinogens benzo [a] pyrene and benzo [a] anthracene to dihydrodiols by a bacterium. *Science*, 189, 295-297.

Gupta, R.P. and D. Swartzendruber. (1962) Flow-associated reduction in hydraulic conductivity of quartz sand. *Soil Sci. Soc. of America Proc.*, 26, 6-10.

Hart, R.T., T. Fekete, and D.L. Flock. (1960) The plugging effect of bacteria in a sandstone system. *Can. Min. Metall. Bulletin*, 53, 495-501.

Holm, L.A. (1993) Strategies for remediation. Ch. 13 in *Geotechnical Practice for Waste Disposal*, Ed. by D.E. Daniel, Chapman & Hall, London, 289-310.

Jones, H.C., I.L. Roth, and W.M. Sanders III. (1969) Electron microscopic study of a slime layer. *J. Bacteriol*, 99, 316-325.

Kalish, P.J., J.E. Steward, W.F. Rogers, and E. O. Bennett. (1964) The effect of bacteria on sandstone permeability. *J. Petroleum Techn.*, 16, 805-814.

Kim, E. and G.J. Zylstra. (1995) Molecular and biochemcial characterization of two meta-cleavage dioxygenases involved in biphenyl and m-xylene degradation by Beijerinckia sp. strain B1. *J Bacteriol*, 177, 3095-103.

Kiyohara, H., M. Sugiyama, F.J. Mondello, D.T. Gibson, and K. Yano. (1983) Plasmid involvement in the degradation of polycyclic aromatic hydrocarbons by a Beijerinckia species. *Biochem Biophys Res Commun*, 11, 939-945.

Landreth, R.E. (1990) Landfill containment system regulations. In *Waste containment systems: construction, regulation, and performance*, GSP No. 26, ed. by R. Bonaparte, ASCE, New York, 1-13.

Mahaffey, W.R., D.T. Gibson, and C.E. Cerniglia. (1988) Bacterial oxidation of chemical carcinogens: formation of polycyclic aromatic acids from benz[a]anthracene. *Appl. Environ. Microbiol*, 54, 2415-2423.

McCalla, T.M. (1951) Studies on the effect of microorganisms on rate of percolation of water through soils. *Soil Sci. Soc. of America Proc.*, 15, 182-186.

Marshall, K.C., R. Stout, and R. Mitchell (1971) Mechanisms of the initial events in the sorption of marine bacteria to surfaces. *J. Gen. Microbiol*, 68, 337-348.

Mitchell, J.K. and M. Jaber. (1990) Factors controlling the long-term properties of clay liners. In *Waste containment systems: construction, regulation, and performance*, GSP No. 26, ed. By R. Bonaparte, ASCE, New York, 84-105.

Mitchell, R. and Z. Nevo. (1964) Effect of bacterial polysaccharide accumulation on infiltration of water through sand. *Appl. Microbiol*, 12(3), 219-223.

Schocken, M.J. and D.T. Gibson. (1984) Bacterial oxidation of the polycyclic aromatic hydrocarbons acenaphthene and acenaphthylene. *Appl. Environ. Microbiol.*, 48, 10-16.

Taylor, S.W. and P.R. Jaffe. (1991) Enhanced in-situ biodegradation and aquifer permeability reduction. *J. Envir. Engrg.*, 117(1), ASCE, 25-46.

METALS ATTENUATION IN MINERALLY-ENHANCED SLURRY WALLS

Jeffrey C. Evans
Bucknell University
Lewisburg, PA 17837

Troy L. Adams
Woodward-Clyde Consultants
Blue Bell, PA 19422

Michael J. Prince
Bucknell University
Lewisburg, PA 17837

ABSTRACT

In current practice, a soil-bentonite slurry trench cutoff wall is a mixture of water, soil, and bentonite that is designed to serve as a passive barrier to ground water and contaminant transport. This study evaluated the transformation of a passive slurry trench cutoff wall barrier to an active barrier system. Conventional soil-bentonite vertical barriers presently serve as passive barriers to contaminated ground water. An active barrier will not only fulfill the functions of the present passive barrier system, but also retard contaminant transport by adsorptive processes.

Attapulgite, Na-chabazite, and Ca-chabazite were added to "activate" the conventional soil-bentonite backfill. Batch extraction tests were performed to determine the partitioning coefficients of cadmium and zinc between the liquid and solid phase when in contact with the backfill mixes. Batch extraction and mathematical modeling results demonstrate the ability of an active barrier to retard the transport of cadmium and zinc. The reactivity of the soil-bentonite vertical barrier depends heavily on the inorganic being adsorbed. The reactivity of the barrier also depends on the adsorptive capabilities of the clay minerals added to the conventional soil-bentonite vertical barrier. The results of laboratory studies suggest that passive barrier systems can be transformed to active systems. Further, the data suggests that although conventional soil-bentonite vertical barriers are presently designed as passive barriers, they already have adsorptive capacity associated with active barriers.

INTRODUCTION

The most commonly employed method for implementing a vertical barrier for site remediation is through the use of a soil-bentonite slurry trench cutoff wall (a mixture of bentonite-water slurry, soil, and, as needed, additional bentonite). Their design, construction and use to control ground water flow is well documented (Xanthakos, 1979, Millet and Perez, 1981, Evans et. al., 1985, Spooner et. al, 1985, LaGrega et. al., 1994). The most common role of this vertical barrier is to serve as a vertical passive barrier to horizontal ground water flow. Constructed around the site, the wall controls the flow of ground water, inhibiting clean water from entering the site and minimizing the rate at which contaminated water flows from the site. This study evaluated the transformation of a passive slurry trench cutoff wall to an active, low permeability barrier system. Conventional soil-bentonite slurry walls presently serve as passive barriers to contaminated ground water. An active, low permeability barrier not only fulfills the functions of the present passive barrier systems, but also further reduces contaminant transport by adding an active enhanced retardation ability to the vertical barrier.

The geochemical attenuation studies described in this paper demonstrate that the bentonite used in conventional vertical barriers already offers some degree of active treatment through its natural affinity for heavy metal ions. The ions adhere to the surface of the clay mineral by adsorption. Further this paper describes the addition of other natural clays such as chabazite (a zeolite) and attapulgite to enhance the barrier's ability to retard contaminant transport through increased adsorption of heavy metal contaminants.

Specifically, geochemical attenuation studies were conducted on conventional soil-bentonite and minerally-enhanced vertical cutoff walls. Batch extraction tests were performed to determine the partitioning coefficients of cadmium and zinc between the liquid and solid phase when in contact

with the adsorbent. Mathematical modeling of breakthrough of the contaminants under study was conducted to compare conventional soil-bentonite barriers with enhanced barriers.

BASIS OF SLURRY WALL BARRIER ENHANCEMENT

For this work, studies of the enhancement of the soil-bentonite barriers focused on adsorption by clay minerals. The adsorption of ions at the solid surface occurs as the solute comes in contact with the mineral. The distribution or partitioning coefficient, K_d, represents the partitioning of ions between the liquid and solid phase. Adsorption equilibrium is quantified by the amount of solute adsorbed per mass of adsorbent versus the concentration of solute in solution at equilibrium. Concentration of adsorbed species versus concentration in free solution at constant temperature is an adsorption isotherm.

Adsorption capacity is quantified by adsorption isotherms to illustrate how the contaminant is partitioned between the liquid and solid phase when in contact with the clay minerals. The Freundlich isotherm is often used to illustrate adsorption capacity. The Freundlich equation is expressed as:

$$x/m = K_d C_e^{1/n} \qquad (1)$$

where
x = the mass of the solute
m = the mass of the adsorbent
C_e = the equilibrium concentration of the solute
K_d = partitioning or distribution coefficient
$1/n$ = the slope of the isotherm.

At sufficiently low concentrations, the isotherm is linear and the Freundlich equation simplifies to:

$$(x/m) = K_d C_e \qquad (2)$$

Thus, K_d is the slope of the straight line describing the relationship between the equilibrium concentration of the contaminant sorbed to the adsorbent (on the solid phase) and the concentration of the contaminant in the liquid phase.

Materials used in this study include bentonite, attapulgite, Na-chabazite and Ca-chabazite. Bentonite is a smectitic clay soil containing the clay mineral montmorillonite. The structure of montmorillonite is widely known and the cation exchange capacity is typically between 70-130 meq/100g (Grim, 1968, Weaver and Pollard, 1973). Attapulgite has a 2:1 layer structure with five octahedral positions and four Si tetrahedra on either side of the octahedral sheet (Weaver and Pollard, 1973). It is associated with montmorillonitic clays and can be changed to montmorillonite under certain hydrothermal conditions. It has a cation exchange capacity of 20 to 30 meq/g (Grim, 1968). Na-chabazite and Ca-chabazite are zeolitic clays. "Zeolite is an aluminosilicate with a skeletal structure containing voids occupied by ions and molecules of water having a considerable freedom of movement that leads to ion-exchange and reversible hydration" (Tsitsishvili et. al., 1992). Zeolite is referred to as a molecular sieve because it allows water to pass through its framework and retain molecules within its intracrystalline pores. Zeolites have the capability to allow water and other cations to move through its crystalline structure. The ions can exchange with others while the water can be removed or replaced continuously (Tsitsishvili et. al., 1992). The cation exchange capacity is 100 to 300meq/100g (Grim, 1968).

No effort was made to optimize the mix at this stage of concept development. Based on construction and cost considerations, each mix was enhanced with 5% of adsorbing mineral for this study.

ADSORPTION STUDIES: LABORATORY TESTING PROCEDURES

The bentonite-water slurry in these studies was prepared using 95% water and 5% bentonite by mass. The mixture was blended in a high speed colloidal shear mixer for 10 minutes. The Marsh viscosity of the slurry was measured and was typically 45 seconds.

All the soil backfill mixed in this research was made from Ottawa sand, bentonite-water slurry, and 5% (by mass) of each mineral that was desired. Four mixtures were developed and tested. There mixtures included a baseline mix of sand-bentonite and mixtures which included calcium chabazite, sodium chabazite and attapulgite added to the baseline mixture. Slurry was added to each mixture until the backfill was visually judged to have a consistency of backfill having a 3-6 inch slump (consistent with field practice). The mixtures were as follows:
- Sand-bentonite: sand, slurry, 5% bentonite
- Sand-bentonite with attapulgite: sand, slurry, 5% bentonite, and 5% attapulgite
- Sand-bentonite with Na-chabazite: sand, slurry, 5% bentonite, and 5% Na-chabazite
- Sand-bentonite with Ca-chabazite: sand, slurry, 5% bentonite, and 5% Ca-chabazite

A 1000 mg/l stock solution of the contaminant (cadmium or zinc) was made. The desired test concentrations of the contaminant were made by dilution. A 20:1 liquid: soil ratio was used for all batch extraction tests. A volume of 125 ml of contaminant was added to 6.25g (dry mass) of soil in an 125 ml Erlenmeyer flask. The soil used in the batch extraction tests was hydrated. The water content was determined before the test in order to calculate the mass of hydrated soil that was equivalent to a dry mass of 6.25g.

Three replicates of each concentration of zinc and cadmium solutions were tested for reproducibility and to obtain an average equilibrium concentration for each isotherm. The test specimens were mixed on a rotary mixer table for 24 hours. After mixing, approximately 12 ml of the sample was then centrifuged to remove all solids that were in suspension. The concentration of the contaminant in the supernatant was then determined using atomic absorption spectrophotometry. Knowing the original concentration of the metal and the equilibrium concentration in the supernatant, the concentration on the soil was calculated by difference.

Isotherm data were calculated and plotted using spreadsheets. The spreadsheet was also used to generate the best fit straight line through the data and going through the origin. The spreadsheet was used to determine the slope of the line and thus the partitioning or distribution coefficient K_d.

ADSORPTION STUDIES: PRESENTATION AND DISCUSSION OF RESULTS

The results for each of the backfill mixtures with cadmium are presented on Figures 1 and 2. The K_d values are presented in Table 1. Based on these data, the distribution coefficient for sand-bentonite with attapulgite is about 5 times greater than that of sand-bentonite alone. The chabazite mixtures resulted in distribution coefficients about 2 times that of sand-bentonite alone.

Table 1. Isotherm Results for Cadmium

Backfill Mixture	K_d (L/kg)
Sand-bentonite	27
Sand-bentonite with attapulgite	149
Sand-bentonite with Na-chabazite	49
Sand-bentonite with Ca-chabazite	49
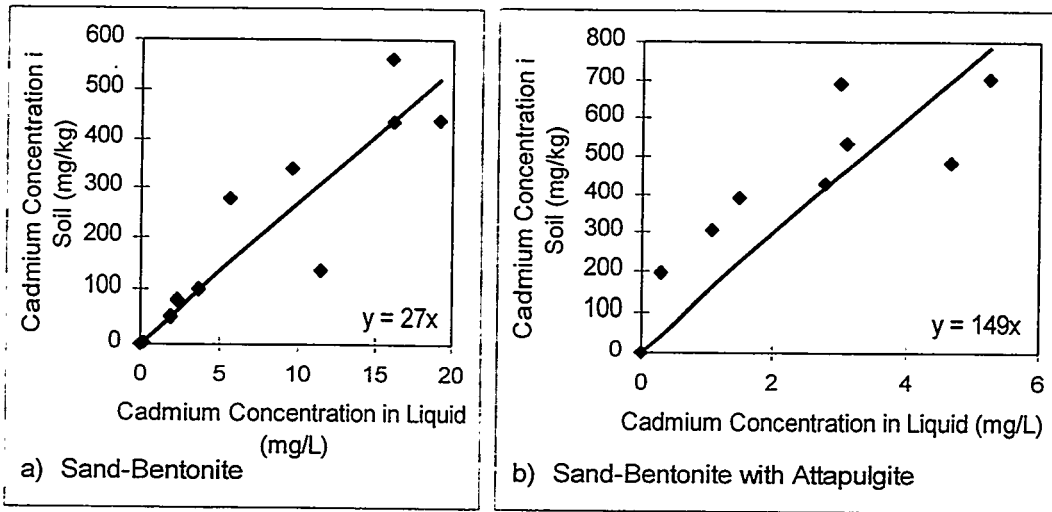
Figure 1. Cadmium Isotherms for a) Sand-Bentonite and
b) Sand-Bentonite with Attapulgite
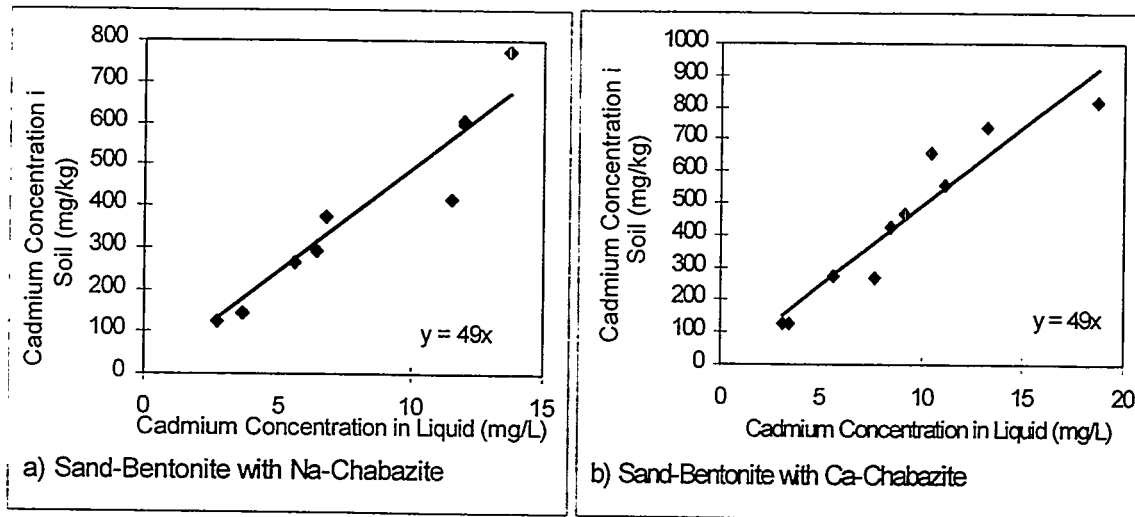
Figure 2. Cadmium Isotherms for Sand-Bentonite with a) Na-chabazite and
b) Ca-chabazite

The results for each of the backfill mixture with zinc are presented on Figures 3 and 4 and in Table 2. For zinc, the sand-bentonite with Na-chabazite mixture has the best adsorptive capability

Table 2. Results of Freundlich Isotherm for Zinc

Backfill	K_d (L/kg)
Sand-bentonite	28
Sand-bentonite with attapulgite	38
Sand-bentonite with Ca-chabazite	48
Sand-bentonite with Na-chabazite	72
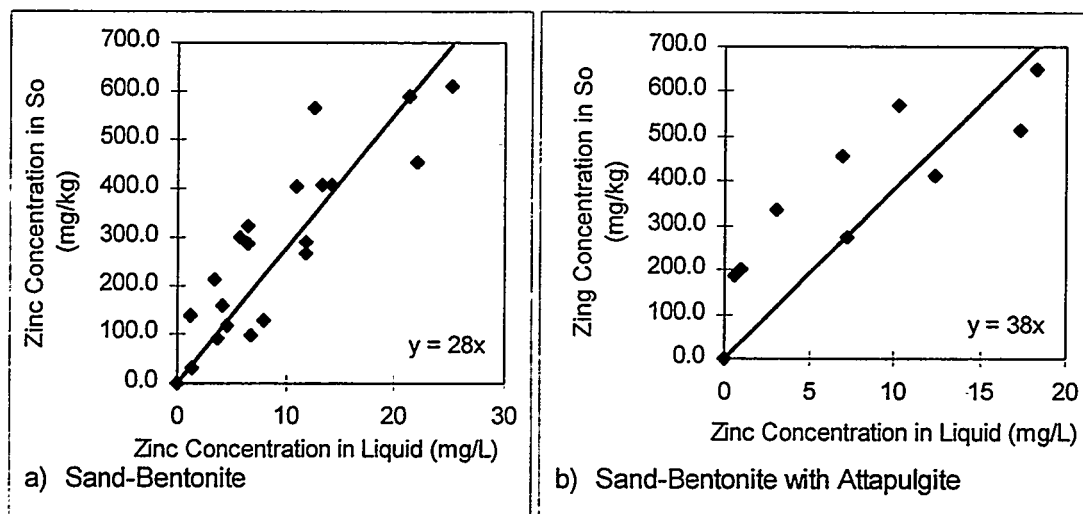
Figure 3. Zinc Isotherms for a) Sand-Bentonite and b) Sand-Bentonite with Attapulgite
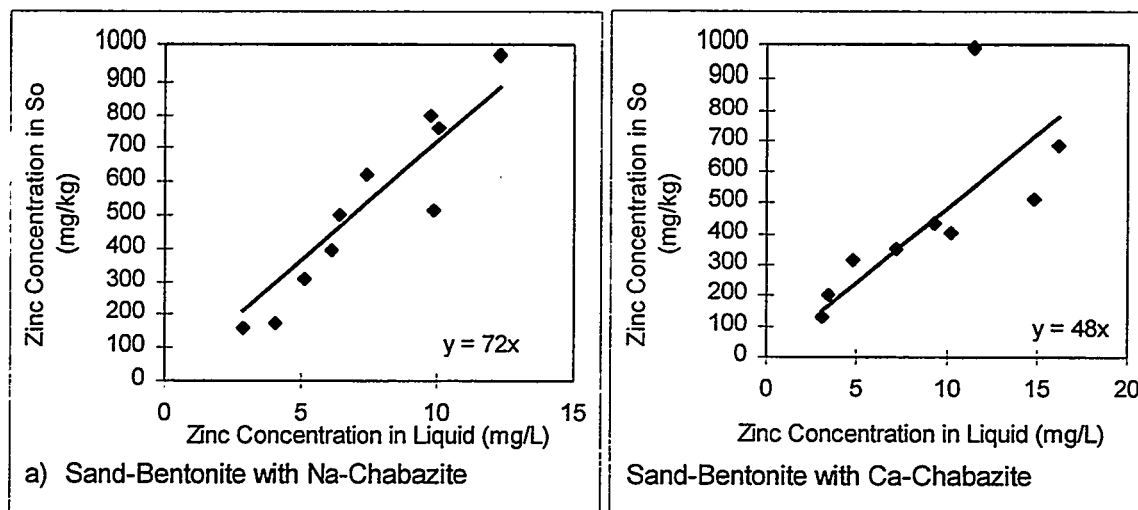
Figure 4. Zinc Isotherms for Sand-Bentonite with a) Na-chabazite and b) Ca-chabazite

HYDRAULIC CONDUCTIVITY STUDIES: LABORATORY TESTING PROCEDURES AND RESULTS

Hydraulic conductivity tests were performed on sand-bentonite and sand-bentonite with chabazite backfill mixtures. Each sample contained 5% bentonite and the sand-bentonite with chabazite backfill mixture also contained 5% Na-chabazite.

Samples of sand-bentonite backfill and sand-bentonite with Na-chabazite backfill were placed in fixed wall permeameters (2.5 cm high by 10 cm in diameter) by tamping to remove any air that may have been trapped in the specimen. Samples were permeated with distilled water until steady flow was achieved. Hydraulic conductivity tests were performed on sand-bentonite and sand-bentonite with chabazite backfill and the results are shown in Table 3. The average hydraulic conductivity of the backfill mixture tested is 1×10^{-8} cm/s. Thus, the addition of 5% chabazite did not affect the hydraulic conductivity of the vertical barrier, enabling this active barrier to continue to function as a passive barrier. Note that under some contaminant conditions, hydraulic conductivity increases may occur (Alther, et. al. 1985).

Table 3. Hydraulic Conductivity of Sand-Bentonite and Sand-Bentonite with Na-chabazite

Hydraulic Conductivity (k), cm/s	
Type of Backfill	Fixed Wall
Sand-Bentonite	1×10^{-8}
Sand-Bentonite-Chabazite	1×10^{-8} and 1.5×10^{-8}

MATHEMATICAL MODELING OF AN ACTIVE BARRIER

Contaminant transport was modeled using the advection-dispersion-adsorption equation (Rowe et al., 1995). The solution to the equation is dependent on the form of the adsorption isotherm and the choice of boundary conditions. The recommended boundary conditions of van Genuchten and Parker (van Genuchten and Parker, 1984) were used. The predicted effluent concentrations for these conditions is given by:

$$Ce*(T) = 0.5 erfc[(\frac{P}{4RT})^{0.5}(R-T)] + 0.5 \exp(P) erfc[(\frac{P}{4RT})^{0.5}(R+T)] \quad (3)$$

where C_{e*} is the dimensionless effluent concentration (Ce/Co), Co is the inlet concentration, T is the number of pore volumes of liquid through the bed (vt/L), P is the Peclet number (vL/D), v is the average interstitial liquid velocity, t is time, L is the bed length and D is the dispersivity which accounts for both molecular diffusion and mechanical dispersion. R is the retardation factor, which for a linear isotherm is given by :

$$R = 1 + \frac{\rho Kd}{\epsilon} \quad (4)$$

where ρ is the average bed density, Kd is the linear partition coefficient of the contaminant between the pore liquid and the soil and ϵ is the porosity. Note the use of this equation limits model predictions to concentration ranges where the adsorption isotherm is linear.

Equation (3) was used to model contaminant transport through environmental barriers in the field. The following parameters were used to simulate field conditions; L=75 cm, hydraulic gradient (i) = 1 and porosity (ϵ) =0.4. Additional parameters were calculated as described below. The interstitial velocity was calculated from Darcy's law (Freeze and Cherry, 1979):

$$v = k*i/\epsilon \quad (5)$$

The bed density was calculated using the fundamental relationship:

$$\rho = (1-\epsilon)\rho_s \quad (6)$$

where ρ_s=2.65 g/cm^3, (density of solids), and

and the dispersivity was calculated from the empirical correlation (Rowe et al., 1995):

$$D = De + 1.75 \, d*v \, (m/a) \quad (7)$$

where:
d=50 microns (grain size)
D_e=5e-6 cm^2/sec (molecular diffusivity)

This information, coupled with experimentally derived partition coefficients and hydraulic conductivity values, was used to predict contaminant break-through times (defined to be Ce*= 0.05) for each barrier material.

RESULTS AND DISCUSSION OF MATHEMATICAL MODELING

The advection-dispersion model for cadmium, with k=1x10^{-7} cm/s, is presented on Figure 5. The breakthrough time for an unmodified soil-bentonite cutoff wall was computed to be 51 years and with the attapulgite enhancement to be 270 years. Since the sodium and calcium chabazite had similar distribution coefficients, the breakthrough time of 89 years was the same for both.
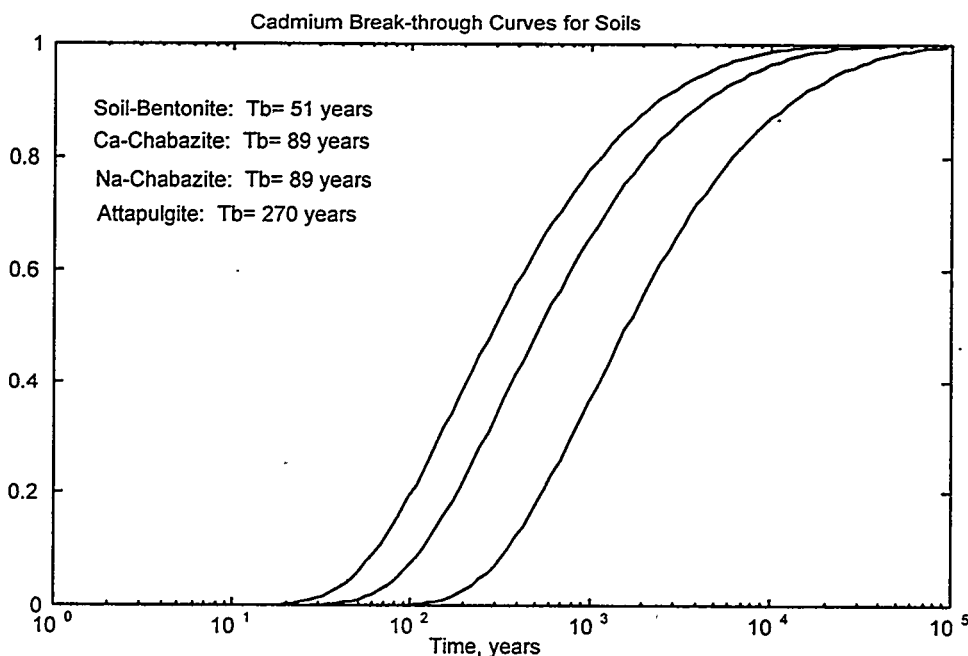
Figure 5. Cadmium Breakthrough Curves

The advection-dispersion model for zinc, with k=1x10^{-7} cm/s, is presented on Figure 6. The unmodified sand-bentonite breakthrough time is 49 years compared with the 130 years for the enhanced wall Na-chabazite. Breakthrough times of 68 and 87 years were computed for sand-bentonite with attapulgite and sand-bentonite with Ca-chabazite, respectively.
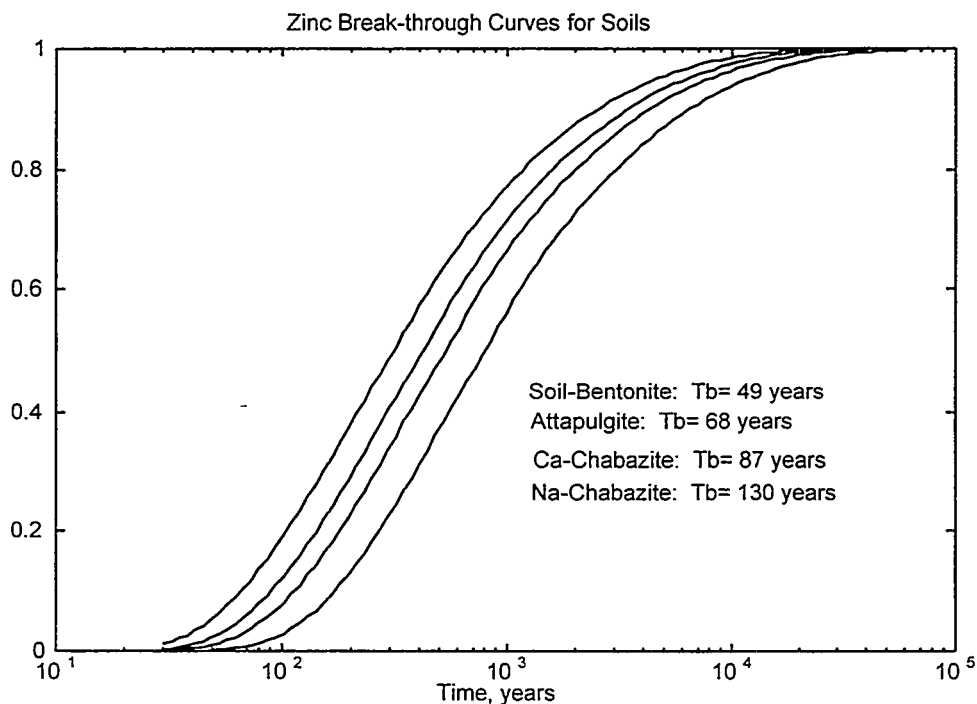
Figure 6. Zinc Breakthrough Curves

As expected, hydraulic conductivity has an effect on the time it takes for cadmium and zinc to breakthrough a 0.75m wide vertical barrier. However, the transport process becomes increasingly diffusion controlled as the hydraulic conductivity decreases. Thus, as the hydraulic conductivity decreased from 10^{-6} to 10^{-7} cm/s, the breakthrough time of cadmium and zinc increased about 60% (see the Table 4). However, a further decrease in hydraulic conductivity from 10^{-7} to 10^{-8} cm/s, resulted in less than 5% improvement in breakthrough time.

Table 4. Effect of Hydraulic Conductivity on Breakthrough

Backfill Type	Cadmium Time, years			Zinc Time, years		
	k (cm/s)			k (cm/s)		
	10^{-6}	10^{-7}	10^{-8}	10^{-6}	10^{-7}	10^{-8}
Sand-bentonite	30	51	54	32	49	54
Sand-bentonite with attapulgite	162	270	277	41	68	72
Sand-bentonite with Ca-chabazite	52	89	97	52	87	95
Sand-bentonite with Na-chabazite	52	89	97	78	130	145

SUMMARY, CONCLUSIONS AND RECOMMENDATIONS

This study has demonstrated that conventional soil-bentonite vertical barriers can be transformed from being passive to active barriers for metal (zinc and cadmium) contamination. Further, the data suggests that although conventional soil-bentonite vertical barriers are presently designed as passive barriers, they already have adsorptive capacity associated with active barriers. The reactivity of the soil-bentonite vertical barrier depends heavily on the inorganics being adsorbed. The reactivity of the barrier also depends on the adsorptive capabilities of the clay minerals added

to the conventional soil-bentonite vertical barrier. In order for an active barrier to perform efficiently, the inorganic being removed must be adsorbable and the clay constituents of the vertical barrier must have affinity for the particular inorganic. More studies are planned using other inorganics (in particular, those which are not readily adsorbed) to validate the transformation of passive barrier systems to active systems. Extension of the concept to organics is also in progress. The cost-benefit analysis should be performed to determine if this technology is worthwhile. The approach used in this paper is limited to the range of concentrations over which the isotherm is linear (at higher contaminant concentrations the isotherm may become non-linear). However, this range of contaminant concentrations is certainly realistic for many sites.

Specific conclusions are:
1) isotherm data coupled with math modeling indicate that reactive barriers have the potential to significantly improve barrier effectiveness.
2) as presently constructed, soil-bentonite vertical barriers function as both passive barriers and active treatment zones; designers can incorporate this behavior into the barrier design.
3) addition of attapulgite significantly increased the adsorptive capacity of the traditional soil-bentonite backfill.

REFERENCES

Evans, J. C., Fang, H.-Y., and Kugelman, I. J. (1985) Containment of Hazardous Materials With Soil-Bentonite Slurry Walls. *Proc. of the Sixth National Conference on Management of Uncontrolled Hazardous Waste Sites,* Washington, DC, pp. 369-373.

Alther, G. R., Evans, J. C., Witmer, K. A., and Fang, H.-Y. (1985) Inorganic Permeant Effects Upon Bentonite. *Hydraulic Barriers in Soil and Rock*, ASTM STP 874, pp. 64-74.

Freeze, R. A. and Cherry, J. A. (1979) Groundwater. Prentice-Hall, Inc., Englewood Cliffs, New Jersey.

Grim, R. E. (1968) Clay Mineralogy. McGraw-Hill, Inc.,. New York, New York.

LaGrega, M. D., Buckingham, P. L., and Evans, J. C., (1994) Hazardous Waste Management. McGraw-Hill, Inc., New York, New York.

Millet, R. A., and Perez, J. Y. (1981) "Current USA Practice: Slurry Wall Specifications." *J. Geotech Engrg.* ASCE, 107(8): 1041-1056.

Rowe, R. K., Quigley, R.M., and Booker, J. R. (1995) Clayey Barrier Systems for Waste Disposal Facilities. E & Fn Spon, London, U. K.

Spooner, Philip., et al. (1984) Slurry Trench Construction for Pollution Migration Control. EPA-540/2-84-001, U. S. Environmental Protection Agency, Cincinnati, OH.

Tsitsishvili, G. V., Andronsikashvili, T. G. and Kirov, G. N., and Filizova, L. D. (1992) Natural Zeolites. Ellis Horwood Limited, New York, New York.

van Genuchten, M. and Parker, J., (1984) "Boundary Conditions for Displacement Experiments through Short Laboratory Soil columns", Soil Sci. Soc. of Am. Jl, 48(4), 703-708.

Weaver C. E. and Pollard, L. D. (1973) The Chemistry of Clay Minerals. Elsevier Scientific Publishing Company, New York, New York.

Xanthakos, P. P. (1979) *Slurry Walls* McGraw-Hill, Inc.,. New York, New York.

Chapter 14

Permeable Reactive Walls:
Materials Development/Characterization

LONG TERM PERFORMANCE OF THE WATERLOO DENITRIFICATION BARRIER

W.D. Robertson and J.A. Cherry
Department of Earth Sciences
Waterloo Centre for Groundwater Research,
University of Waterloo,
Waterloo, Ontario, Canada N2L 3G1
Tel: (519)888-4567, Fax: (519)746-7484

Abstract

Beginning in 1991 a series of laboratory tests and small scale field trials were initiated to test the performance of an innovative permeable reactive barrier for treatment of nitrate from septic systems. The barrier promotes denitrification by providing an energy source in the form of solid organic carbon mixed into the porous media material. Advantages of the system for nitrate treatment are that the reaction is passive and in situ and it is possible to incorporate sufficient carbon mass in conveniently sized barriers to potentially provide treatment for long periods (decades) without the necessity for maintenance. However, longevity can only be demonstrated by careful long term monitoring of field installations. This paper documents four years of operating history at three small scale field trials; two where the denitrification barrier is installed as a horizontal layer positioned in the unsaturated zone below conventional septic system infiltration beds and one where the barrier is installed as a vertical wall intercepting a septic system plume at a downgradient location. The barriers have successfully attenuated 50-100% of NO_3^--N levels of up to 170 mg/L and treatment has remained consistent over the four year period in each case, thus considerable longevity is indicated.

Other field trials have demonstrated this technology to be equally effective in treating nitrogen contamination from other sources such as landfill leachate and farm field runoff.

INTRODUCTION

The observation that septic systems can generate nitrate concentrations several times higher than the drinking water limit of 10 mg/L as N, has lead to attempts to introduce alternative septic system designs that provide improved attenuation of nitrogen. Several such systems have been developed including the "RUUK" system (Laak, 1981) which uses dedicated plumbing to separate household greywater and blackwater so that the greywater can be utilized as a carbon source for denitrification; the "peat" system (Brooks et al., 1984) which uses a layer of spaghnum peat moss to attenuate nitrogen by incorporation into fungal biomass; and recirculating sand filters (e.g. Piluk and Hao, 1989) which return a portion of the nitrified effluent back into the septic tank where carbon availability and anaerobic conditions allowed denitrification to occur. A necessary condition for these alternative systems to be practical for use in household wastewater treatment is that they be mechanically simple are low cost and have minimal maintenance requirements.

A new alternative septic system design that has been under development at the University of Waterloo for the past six years utilizes nitrate-reactive porous media barriers to promote denitrification. In these the nitrate reactive capability is derived from solid carbon material mixed into the porous media. This system referred to as the Waterloo Denitrification Barrier can be constructed as a horizontal layer installed below an otherwise conventional septic system infiltration bed or it can be installed as a vertical wall intercepting a nitrate plume at some downgradient location (Robertson and Cherry, 1991). A variety of solid carbon materials have been shown to be effective for use in such barriers including straw, cellulose, wood chips, compost and sawdust (Vogan, 1993; Carmichael, 1994). The performance, over a one year period, of three pilot scale field trials; two where the denitrification barriers were installed as horizontal layers and one where it was installed as a vertical wall, have been described previously (Robertson and Cherry, 1995). In these it was shown that the barriers achieved 60 - 100% attenuation of nitrate levels of up to 125 mg/L as N during their first year of operation. It was recognized however, that such barriers would have to operate for much longer periods (many years to decades) without significant maintenance or necessity for carbon replenishment in order to be practical for widespread use. Thus the longevity of the carbon material used in the barriers is considered to be crucial to the success of this technology. Although simple mass balance calculations show that is possible to incorporate sufficient solid carbon

material in conveniently sized barriers to potentially achieve denitrification for decades or longer (Robertson and Cherry, 1995), it is difficult to estimate the fraction of the carbon mass that will be ultimately available for denitrification. Thus, long term performance monitoring must be undertaken. This paper documents the longer term (three to four years) operating performance of the three pilot scale field trials described previously (Killarney and Borden layers and Long Point wall).

SYSTEM DESCRIPTIONS

At the Killarney site a denitrification layer was installed in 1992 as a 2 m^2 test plot below a conventional septic system infiltration bed servicing a seasonal-use cottage. The denitrification barrier consisted of three sublayers including, at 0.4 - 0.75 m depth, a mixture of silty fine sand and sawdust; at 0.75 - 0.90 m depth, silty fine sand and leaf compost; and at 0.90 - 1.0 m depth, silty fine sand and rye seed (Fig. 1). Silty fine sand was used so that the layer would have the capacity to remain tension-saturated and thus anaerobic even when positioned above the water table. During initial operation in 1992 and 1993 the test plot was periodically dosed by pumping from an adjacent septic tank, then beginning in 1994 loading was derived primarily from blackwater from a single low flush toilet. The initial loading rate in 1992-93 lead to a porewater residence time within the upper silt-sawdust layer of about one month. When the effluent source was switched in 1994 loading increased, however the amount was not measured directly.

At the Borden site a denitrification layer was installed in 1992 below a conventional 18 m^2 septic system infiltration bed serving a seasonal-use wash trailer and adjacent utility building with a small washroom used year round. The barrier consists of a mixture of silty fine sand and sawdust placed at 0.7 - 1.2 m depth (Fig. 1). Chloride breakthrough during initial loading suggested that effluent residency in the denitrification layer was about 2 weeks.

At the Long Point site the barrier was constructed as a 0.6 m thick wall emplaced to 1.5 m depth in the path of a horizontally migrating septic system plume (Fig. 1). The barrier, in this case, was designed to be of similar permeability to the surrounding formation sand and consists of mixture of a medium sand and sawdust. Porewater residency within the barrier was estimated to be about 10 days based on calculations using the Darcy equation.

At the Killarney and Borden sites where the barriers were positioned above the watertable, porewater samples were retrieved by applying suction to porous cup lysimeters. At the Long Point site where the barrier was positioned below the watertable, short tipped piezometers were used.

More detailed information regarding the construction and operation of these field trials is presented in Robertson and Cherry (1995).

LONG TERM PERFORMANCE

Figure 1 shows nitrogen behavior in the barriers during recent monitoring while Table 1 compares porewater chemistry entering and leaving the barriers. At the Long Point site loading to the septic system was temporarily discontinued in 1996, thus monitoring results from the Fall of 1995 are shown. At all three sites there continues to be substantial attenuation of nitrogen in the barriers. At the Long Point site upgradient nitrate - N levels of 68 mg/L are attenuated to 11 mg/L, while at Killarney input nitrate - N levels of 59 mg/L are depleted to 1 mg/L. At Borden the input nitrate - N level of 31 mg/L is depleted to less than 1 mg/L. Comparison of chloride levels (Table 1) suggests that the observed nitrate attenuation can not be attributed to source variability or to dilution thus it is likely that attenuation results from a biodegradation reaction, presumably denitrification. Figure 2 indicates that similar degrees of nitrogen attenuation have occurred consistently over the periods of operation. Most complete nitrate attenuation occurs at the Killarney site (up to 170 mg/L as N) where residence time is longest (several weeks to one month) whereas somewhat less complete nitrate removal occurs at the Long Point site (about two thirds removal) where residence time is shortest (about 10 days). At the Borden site total inorganic nitrogen (nitrate + ammonium) is shown on Figure 2 instead of nitrate only, because relatively low total nitrogen levels (both nitrate and ammonium) were often observed in the shallowest monitoring point within the barrier (0.7 m depth) presumably as a result of denitrification already being active at this depth position. Consideration of total inorganic nitrogen then allows comparisons to be made with the effluent itself.

DISCUSSION

The degree of nitrogen attenuation observed during recent monitoring appears equally as good as that observed during the first year of operation. Breakthrough curves indicate that treatment has been reasonably consistent throughout the periods of operation. These trials have demonstrated that the sawdust carbon source used in these barriers is sufficiently labile to provide an adequate carbon supply for denitrification yet is sufficiently resistant to biodegradation in anaerobic environments to be relatively long lived. Sawdust thus appears to be a good carbon source for use in denitrification barriers such as these, where porewater residence times are on the order of several days or longer.

It is of interest to estimate the amount of carbon mass that has been consumed by denitrification during the periods of operation. The stoichiometry of the denitrification reaction:

$$5\ CH_2O + 4\ NO_3^- \ 6\ 5\ CO_2 + 2N_2 + 3H_2O + 4\ OH^- \hspace{4cm} 1$$
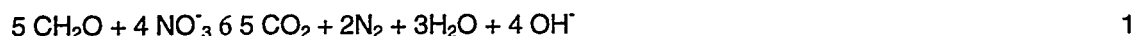
indicates that about one gram of carbon is consumed for each gram of nitrate nitrogen attenuated. Considering the previous estimates of residence time, and assuming porosity of 0.3, flow rates through the barriers are estimated to average 100 L/day, Borden; 6 L/day, Killarney; and 20 L/day, Long Point. Considering the chemistry given in Table 1 as representative of average conditions, the amount of nitrate - N attenuated is 31 mg/L, Borden; 58 mg/L Killarney and 67 mg/L, Long Point. Carbon consumption would thus be 3 g/day, Borden; 0.3 g/day, Killarney; and 1.3 g/day, Long Point. The total amount of carbon originally contained in the barriers was estimated to be 300 kg, Borden; 22 kg. Killarney and 26 kg Long Point. Thus during four years of operation at Borden and Killarney, denitrification should have consumed only about 1.5 % and 2% respectively of the carbon available while after 3 years of operation at Long Point only about 5% of the organic carbon should have been consumed. While carbon consumption may also result from other reactions such as dissolved oxygen and sulfate reduction in some cases and leaching of excess DOC, previous calculations (Robertson and Cherry, 1995) have suggested that carbon loss from these reactions will be less than that from denitrification. Thus, simple mass balance calculations suggest that these installations potentially still retain substantial additional capacity to attenuate nitrate. However, only through continued monitoring will it ultimately be established how much of the carbon mass is available for denitrification.

Although these field trials deal only with treatment of nitrate from sewage, Waterloo Denitrification Barriers have also be used successfully in the treatment of nitrate in farm field runoff (Robertson et al., 1991; Blowes et al., 1994) and nitrate derived from landfill leachate (Byerley and Robertson, 1995).

CONCLUSIONS

These field trials have demonstrated that Waterloo Denitrification Barriers can operate successfully for long periods (years) without maintenance. Because of this characteristic and its simple mode of construction, this technology may offer a practical alternative to conventional septic systems at locations where nitrate control is desirable.

REFERENCES CITED

Blowes, D.W., W.D. Robertson, C.J. Ptacek and C. Merkley, 1994. Removal of agricultural nitrate from tile-drainage effluent water using in-line biorectors. J. Contaminat Hydrol. V. 15, pp. 207-221.

Brooks, J.L., C.A. Rock and R.A. Struchtemeyer, 1984. Use of peat for on-site wastewater treatment: II. Field studies. J. Environ. Qual. V. 13, pp. 524-529.

Byerley, B.T. and W.D. Robertson, 1995. Remediation of landfill leachate using infiltration and reactive barrier technology: A field study. In: M. Moo-Young et al. (eds.), Environmental Biotechnology: Principles and Applications, Kluwer Academic Publishers, The Netherlands, pp. 417-430.

Carmichael, P.A., 1994. Using wood chips as a source of organic carbon in denitrification: a column experiment and field study implementing the funnel and gate design. M.Sc. Thesis, Univ. of Waterloo, Waterloo, ON., 155 p.

Laak, R., 1981. Denitrification of blackwater with graywater. ASCE, J. Environ. Eng. Div. V. 107, pp. 581-590.

Piluk, R.J. and O.J. Hao, 1989. Evaluation of on-site waste disposal system for nitrogen reduction. ASCE, J. Environ. Eng. Div. V. 115, pp. 725-740.

Robertson, W.D. and J.A. Cherry, 1995. In situ denitrification of septic system NO_3^- using reactive porous media barriers; field trials. Ground Water. V. 33, pp. 99-111.

Robertson, W.D. and J.A. Cherry, 1991. Denitrification of septic tank effluent. U.S. patent number 5, 318, 699, issued June 7, 1994.

Robertson, W.D., D.W. Blowes and C. Ptacek, 1991. Agricultural redox reactor. U.S. patent number 5, 330, 651, issued July 19, 1994.

Vogan, J., 1993. The use of emplaced denitrifying layers to promote nitrate removal from septic effluent. M.Sc. thesis, University of Waterloo, Waterloo, ON 232 pp.

	YEAR 3		YEAR 4		YEAR 4	
	Long Point Wall		Killarney Layer		Borden Layer	
	In (2-3)	Out (3-3)	In (0.3)	Out (0.6)	In (0.7)	Out (1.1)
Date	10/95	10/95	7/96	7/96	7/96	7/96
Cl mg/L	52	55	68	54	47	60
NO_3-N mg/L	68	10.8	59	1.2	31	0.4
NH_4-N mg/L	0.9	0.5	23	40	0.2	4.3
DOC mg/L	4.9^5	4.0^5	36^1	17^2	38^3	17^2
Fe mg/L	0.03	3.4	<0.2	7.8	0.24	3.2
AlK (as $CaCO_3$ mg/L	280	500				
pH	7.0	6.7	6.3	6.6	7.0^4	6.6
EC (ΦS)	1302^5	1093^5	801	773	764	718

1) WD 1-0.4 (9/96)
2) 9/96
3) 8/96
4) 10/94
5) 9/95

Table 1   Comparison of water quality entering and leaving the denitrification barriers after three to four years of operation.
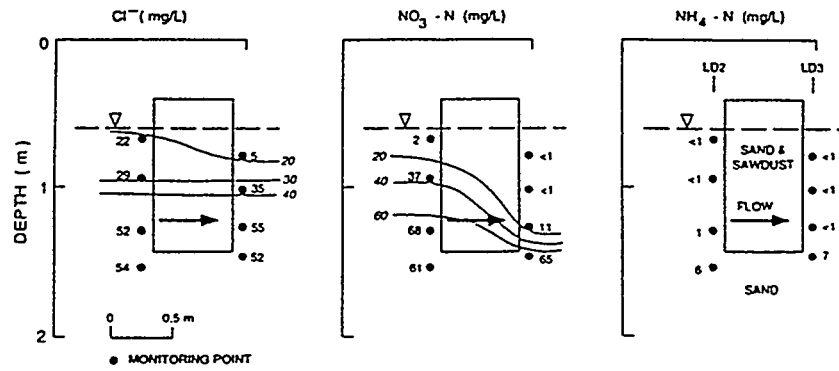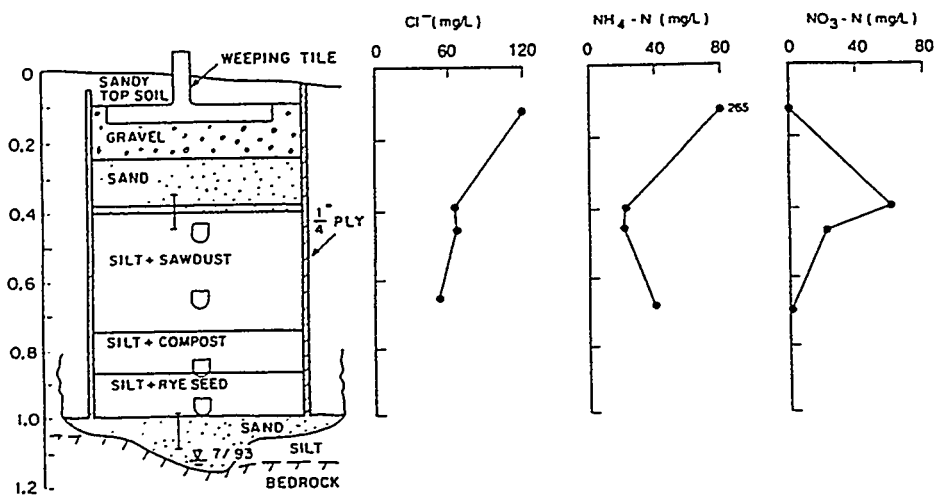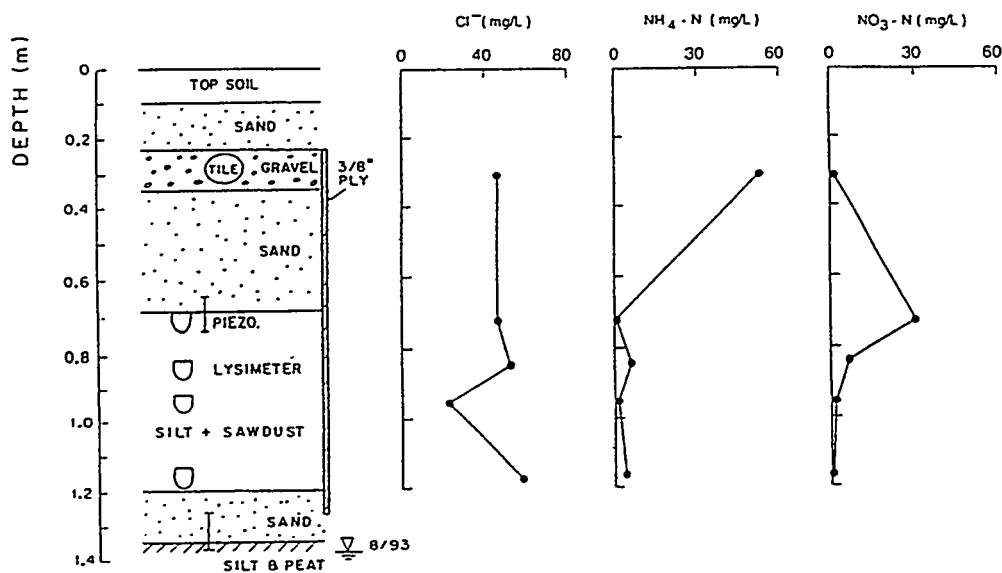
Figure 1.   Behavior of inorganic nitrogen during migration through the Long Point Wall and Killarney and Borden denitrification layers after three to four years of operation.
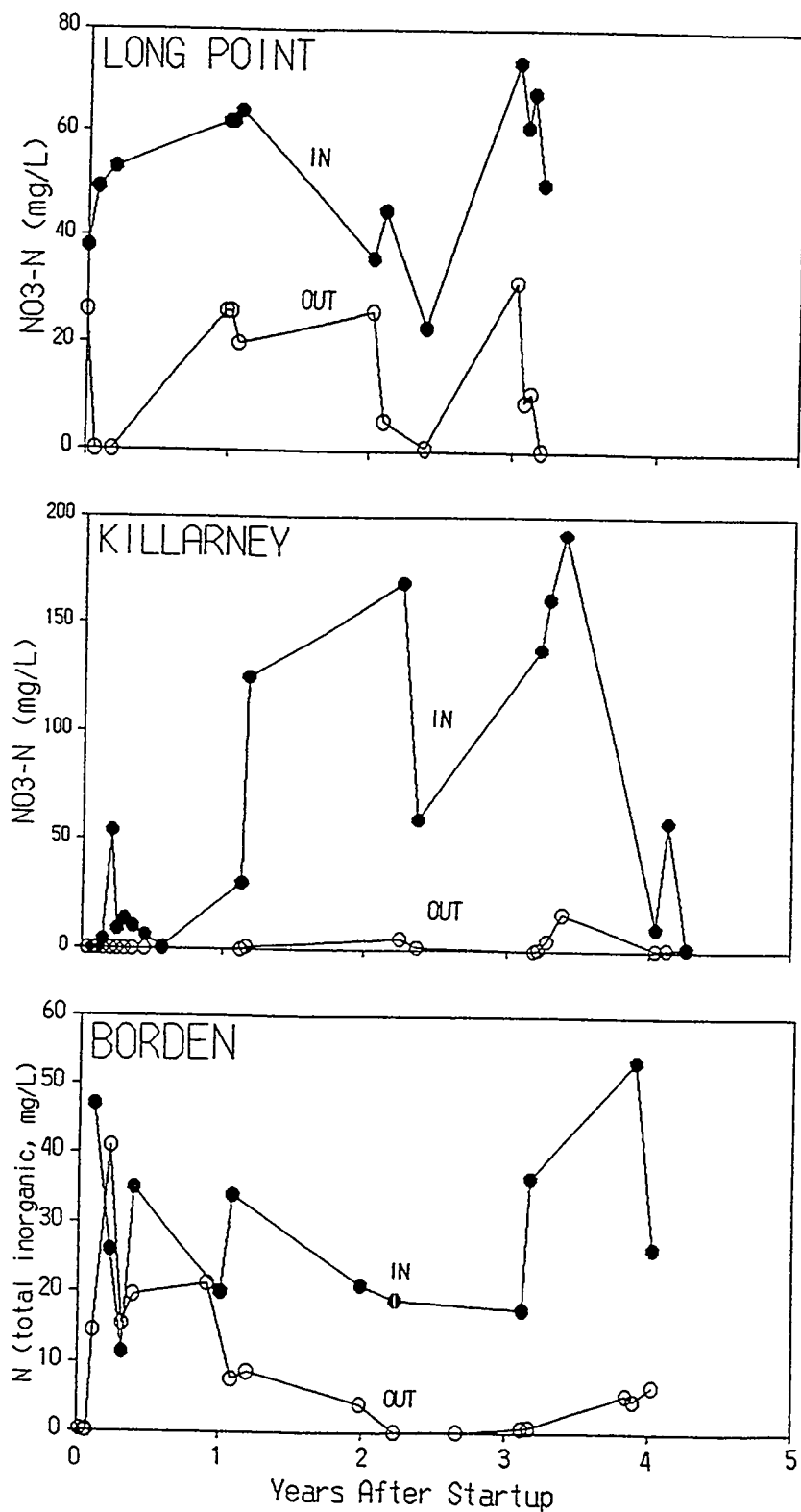
Figure 2. Trend of nitrate (Long Point and Killarney) and total inorganic nitrogen levels (Borden) entering and leaving the denitrification barriers. (In is piezometer LD2-3, Long Point; 0.35 or 0.4 m depth, Killarney; septic tank effluent, Borden. Out is piezometer LD3-3, Long Point; 0.6 m depth, Killarney; 1.1 m depth, Borden.)

Phosphorous Adsorption and Precipitation in a Permeable Reactive Wall : Applications for Wastewater Disposal Systems

Michael J. Baker[1] , David W. Blowes[1,2] , Carol J. Ptacek[3,1]

1. *Department of Earth Sciences, University of Waterloo, Waterloo Ont N2L-3G1*
2. *Waterloo Centre for Groundwater Research, Waterloo Ont. N2L-3G1*
3. *National Water Research Institute, Environment Canada, Burlington Ont L7R 4A6*

Abstract

A permeable reactive mixture has been developed using low cost, readily available materials that is capable of providing effective, long-term phosphorous treatment in areas impacted by on-land wastewater disposal. The reactive mixture creates a geochemical environment suitable for P-attenuation by both adsorption and precipitation reactions. Potential benefits include significant reductions in phosphorous loading to receiving groundwater and surface water systems, and the accumulation of P-mass in a finite and accessible volume of material. The mixture may be applied as a component within surface treatment systems or in subsurface applications such as horizontal or vertical permeable reactive walls. The mixture averaged > 90% treatment efficiency over 3.6 years of continuous-flow laboratory column experiments. The mixture was further evaluated at the pilot-scale to treat municipal wastewater, and the field-scale to treat a well-characterized septic system plume using an *in situ* funnel and gate system. Average PO_4-P concentrations in effluent exiting the reactive mixture range between 0 - 0.3 mg/L. Mineralogical analyses have isolated the phases responsible for phosphorous uptake, and discrete phosphate precipitates have been identified.

Correspondence Address :

Mike Baker
Department of Earth Sciences, University of Waterloo
Waterloo, Ontario N2L-3G1
Telephone : 519-888-4878 (ext. 5643)
e-mail : mbaker@cgrpc.watstar.uwaterloo.ca

Introduction

Reactive materials which remove contaminants passively, under porous flow conditions are a promising new approach for the prevention and remediation of contaminated groundwaters. These materials may be utilized in surface applications under controlled conditions, or alternatively in subsurface applications, such as *in situ* permeable reactive walls.

Reactive materials focused on treating a wide range of groundwater contaminants are currently under development (Blowes et al., 1995). These materials may be classified into two distinct groups. The first type of material promotes chemical reactions that destroy the contaminant or transform it to a more benign species (e.g. reductive dehalogenation, denitrification, biodegradation); the second class attempts to provide sufficient levels of treatment by transferring contaminant mass from the aqueous phase to the solid phase using geochemical reactions (e.g. adsorption, ion exchange, precipitation).

Phosphorous contamination of soils, groundwater, and surface water from wastewater disposal practices is presently an important environmental concern in heavily developed riparian areas. Phosphorous is the limiting nutrient in most inland surface waters and excess inputs can adversely effect the natural trophic state of those waterbodies (Schindler, 1977). Field studies have documented elevated phosphorous concentrations in groundwaters that receive wastewater effluent (Harman, 1992; Robertson, 1994; Walter et al., 1995). A reactive mixture has been developed (Blowes, Ptacek, and Baker, 1995) to provide long-term phosphorous treatment by coupling adsorption and precipitation reactions (Ptacek et al., 1994; Baker et al., 1996). The benefits of the system are twofold. First, the effluent phosphorous concentrations reaching receiving soil and water systems are significantly reduced, and secondly, a significant mass of phosphorous is accumulated in a finite and accessible volume of material which allows for retrieval and future disposal, or alternatively, acceptable rates of release.

A permeable reactive mixture can be applied to areas of wastewater treatment in several ways. The mixture can be incorporated as a horizontal barrier to intercept and treat infiltrating wastewater (Figure 1A). Alternatively, a module-based system can provide phosphorous treatment prior to soil disposal (Figure 1B). In areas where a groundwater phosphorous plume has already developed, a vertical treatment wall can be placed perpendicular to the groundwater flow path upgradient of surface water discharge (Figure 1C).

Methods of Investigation

Various materials were acquired and evaluated in the laboratory to assess the treatment efficiencies of adsorption and precipitation reactions. The most promising materials appear to be a specific group of alkaline metal oxides manufactured as by-products of steel manufacturing. A mixture containing 50 wt% silica sand, 45 wt% crushed limestone, and 5 wt% metal oxide was incorporated into a long-term laboratory column experiment under conditions of dynamic flow and cumulative phosphate loading. The column was constructed from acrylic plastic (20 cm long ; 6.35 cm diameter) and a phosphate solution (3.30 mg/L PO_4-P) was administered through Teflon tubing connected to a multi-channel variable speed peristaltic pump (Figure 2A). The column received continuous inputs of the feed solution at representative groundwater velocities over a period of 3.6 years (1250 pore volumes) under saturated conditions. Flow rates and effluent chemistry were monitored over time. The column solids were sampled periodically and mineralogical analyses were performed to assess the distribution of solid-bound phosphorous within the column, and to provide direct evidence of the geochemical reactions responsible for P-uptake.

The reactive mixture was further evaluated at the pilot-scale to test the reactive mixture under more realistic wastewater conditions. A porous flow treatment module was constructed to remove phosphorous from pre-treated municipal wastewater at the Waterloo sewage treatment plant. Primary clarifier effluent was first directed through a Waterloo biofilter[tm] for primary wastewater treatment and to provide an effluent suitable for porous flow. A portion of the biofilter effluent was then directed through a cylinder (0.5 m diameter ; 0.5 m height), containing the reactive mixture. Wastewater was applied at an average flow rate of 26 L/day over a period of 133 days, or approximately 101 pore volumes of treatment (Figure 2B).

A funnel and gate in situ treatment system was installed to test the reactive mixture capabilities in removing phosphate from a well-characterized septic system plume, and aslo to evaluate the funnel and gate in situ design. The installation consisted of 1.67 m long inter-connected impermeable metal sheet piling (funnel) which directed groundwater flow through a permeable treatment gate (1.8 m length ; 2.0 m width ; 1.0 m depth) containing the phosphorous reactive mixture (Figure 2C). Chemical profiles of the groundwater at the site were monitored over a 779 day period.

Results

Column Experiments

Phosphate concentrations in the effluent solution remained below detection (< 0.01 mg/L PO_4-P) for approximately the first 50 pore volumes and then increased to low and steady concentrations over the remainder of the 3.6 year study period (Figure 3A). The average concentration in the effluent was 0.27 mg/L PO_4-P or > 90% phosphate removal efficiency over the course of the experiment. The shape of the breakthrough curve suggests that both adsorption and precipitation reactions are responsible for the observed reduction in phosphate. Geochemical speciation modelling performed using MINTEQA2 (Allison et al., 1990) indicate that the column effluent is supersaturated with respect to hydroxyapatite ($Ca_5(PO_4)_3OH$, and at saturation with respect to tricalciumphosphate (β-$Ca_3(PO_4)_2$). Mineralogical analyses performed on the column solids reveal that the bulk of the phosphorous mass is preferentially concentrated at the base of the column and that phosphate is being accumulated on the surfaces of oxide phases as well as precipitated as microcrystalline hydroxyapatite, possibly by replacement of existing calcite.

Pilot-scale treatment cell

Breakthough curves for the treatment module at the sewage treatment plant are shown in Figure 3B. The average influent concentrations into the unit were 3.93 mg/L (Total P) and 2.50 mg/L (Ortho-P). Average concentrations in the effluent were 0.14 mg/L (Total-P) and 0.05 mg/L (Ortho-P). Treatment efficency of > 95% was achieved over the 133 day study period.

Funnel and gate system

Breakthrough curves generated from the funnel and gate system are shown in Figure 3C, for monitoring wells 4 m and 0.4 m upgradient of the treatment gate, as well as directly inside the treatment gate. Concentrations within the plume core, 4 m upgradient of the treatment system remained high (2-3 mg/L). Concentrations 0.4 m upgradient of the treatment gate decreased over time from 1.5 mg/L to 0.40 mg/L. Similar reductions were observed for the more conservative solutes such as Cl, Na, and NO_3^-. The dilution effect may be the result of complex groundwater flow paths that have developed due to the installation. For the first 221 days of operation, concentrations in the treatment gate were below detection (< 0.01 mg/L). For the duration of the 779 day monitoring period, average phosphate concentration in the wall remained steady and low (≈ 0.19 mg P/L).

Conclusions

Long-term laboratory, pilot, and field-scale experiments have demonstrated the potential for a permeable reactive mixture to remove phosphorous from wastewater effluent. Results from the field trials were consistent with results obtained from controlled laboratory experiments. Treatment efficiencies range between 85-100%. The reactive mixture, incorporating an alkaline iron oxide, removes phosphate from solution by accumulation on oxide surfaces and precipitation of microcrystalline hydroxyapatite ($Ca_5(PO_4)_3OH$). This technology has the potential to provide significant environmental benefits by preventing excess loading of phosphorous into soil, groundwater, and surface water systems. Current demonstration projects include incorporation of the reactive mixture into high efficiency domestic onsite wastwater disposal systems.

References

Allison, J.D., Brown, D.S., Novo-Gradac, K.J., 1990. MINTEQA2/PRODEFA2, A geochemical assessment model for environmental systems: Version 3.0 user's manual. U.S. Environ. Prot. Agency, Athens, GA, 106 pp.

Baker, M.J., Blowes, D.W., Ptacek, C.J., 1996. Development of a reactive mixture to remove phosphorous from on-site wastewater disposal systems. In Proceedings of Disposal Trenches, Pre-treatment, and Re-use of Wastewater. Waterloo Centre for Groundwater Research Annual Septic System Conference, May 13, 1996 Waterloo, Ontario, pp. 51- 56.

Blowes, D.W., Ptacek, C.J., Baker, M.J. 1995. U.K. patent application # 9523113.0, November 10, 1995.

Blowes, D.W., Ptacek, C.J., Cherry, J.A., Gillham, R.W., Robertson, W.D., 1995. Passive remediation of groundwater using in situ treatment curtains. In: Acar, Y.B. and Daniel, D.E. (Eds.), Geoenvironment 2000, Characterization, Containment, Remediation, and Performance in Environmental Geotechnics, Geoctechnical Special Publication No. 46, Vol 2, American Society of Civil Engineers, New York, pp. 1588-1607.

Harman, J. 1992 Impacts on a Sand Aquifer from a Septic System at a School : Nitrate, Phosphate and Organic Carbon. M.Sc. Thesis. University of Waterloo, Waterloo Ont, 250 pp.

Ptacek, C.J., Blowes, D.W., Robertson, W.D., Baker, M.J. 1994. Adsorption and mineralization of phosphate from septic system effluent in aquifer materials. Proceedings of Wastewater Nutrient Removal Technologies and Onsite Management Districts. Waterloo Centre for Groundwater Research Annual Septic System Conference, June 6, 1994. Waterloo, Ontario. pp. 26-44.

Robertson, W.D. 1995. Development of steady-state phosphate concentrations in septic system plumes. Journal of Contaminant Hydrology, 19, 289-305.

Schindler, D.W. 1977. Evolution of phosphorous limitation in lakes. Science, 195, 260-262.

Walter, D.A., Rea, B.A., Stollenwerk, K.G., Savoie, J. 1995. Geochemical and hydrologic control on phosphorus transport in a sewage-contaminated sand and gravel aquifer near Ashumet pond, Cape Cod, Massachusetts. U.S. Geological Survey. Open-File Report 95-381.
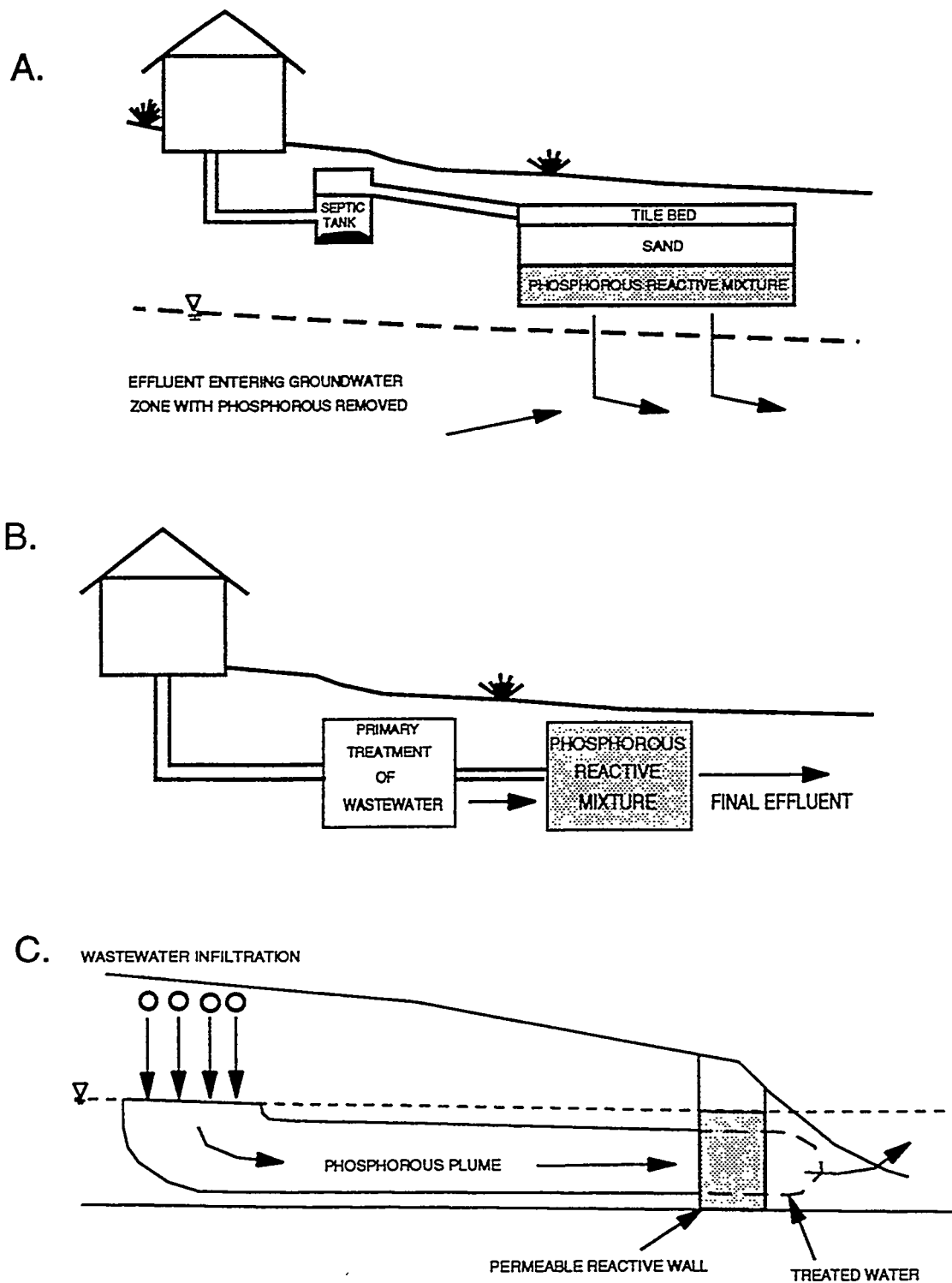
Figure 1. Potential applications of a permeable reactive mixture to remove phosphorous from wastewater discharges. A. Horizontal barrier underlying zone of infiltration in a conventional septic system. B. Modular unit which removes phosphorous from pre-treated effluent. C. Vertical *in situ* reactive wall installed downgradient of existing zone of contamination.
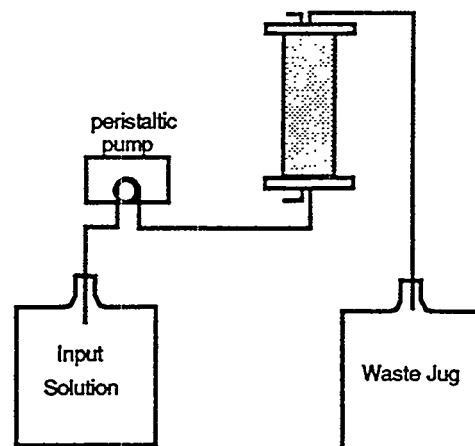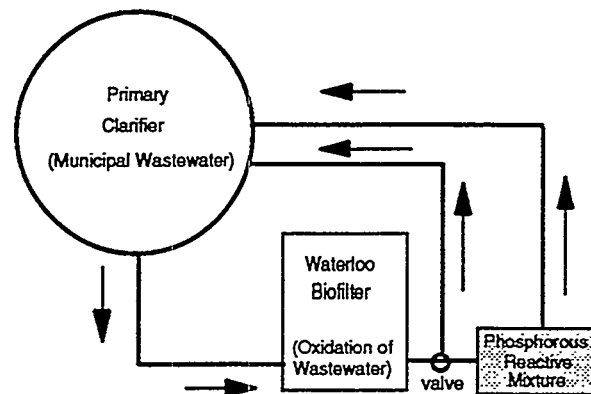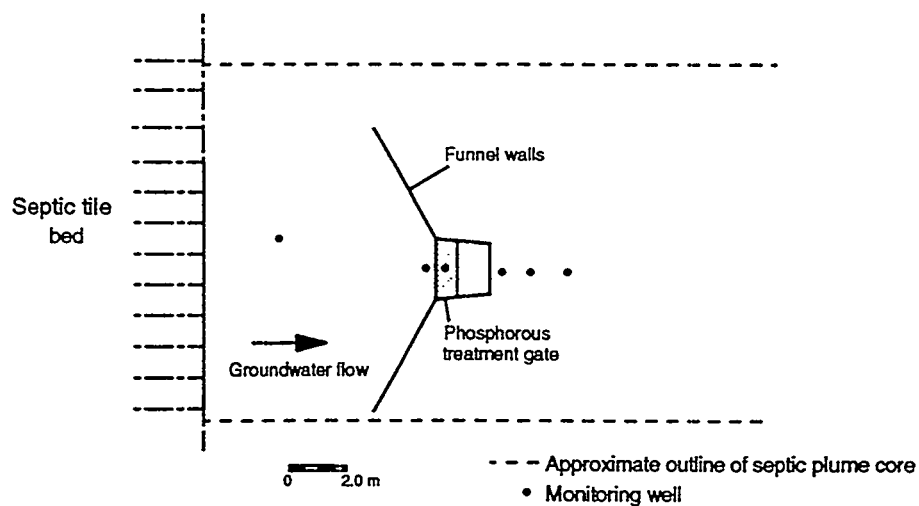
Figure 2. Methods of investigation during development of reactive mixture. A. Laboratory column experiment ; B. Pilot-scale treatment of municipal wastewater ; C. Field-scale funnel and gate *in situ* treatment system
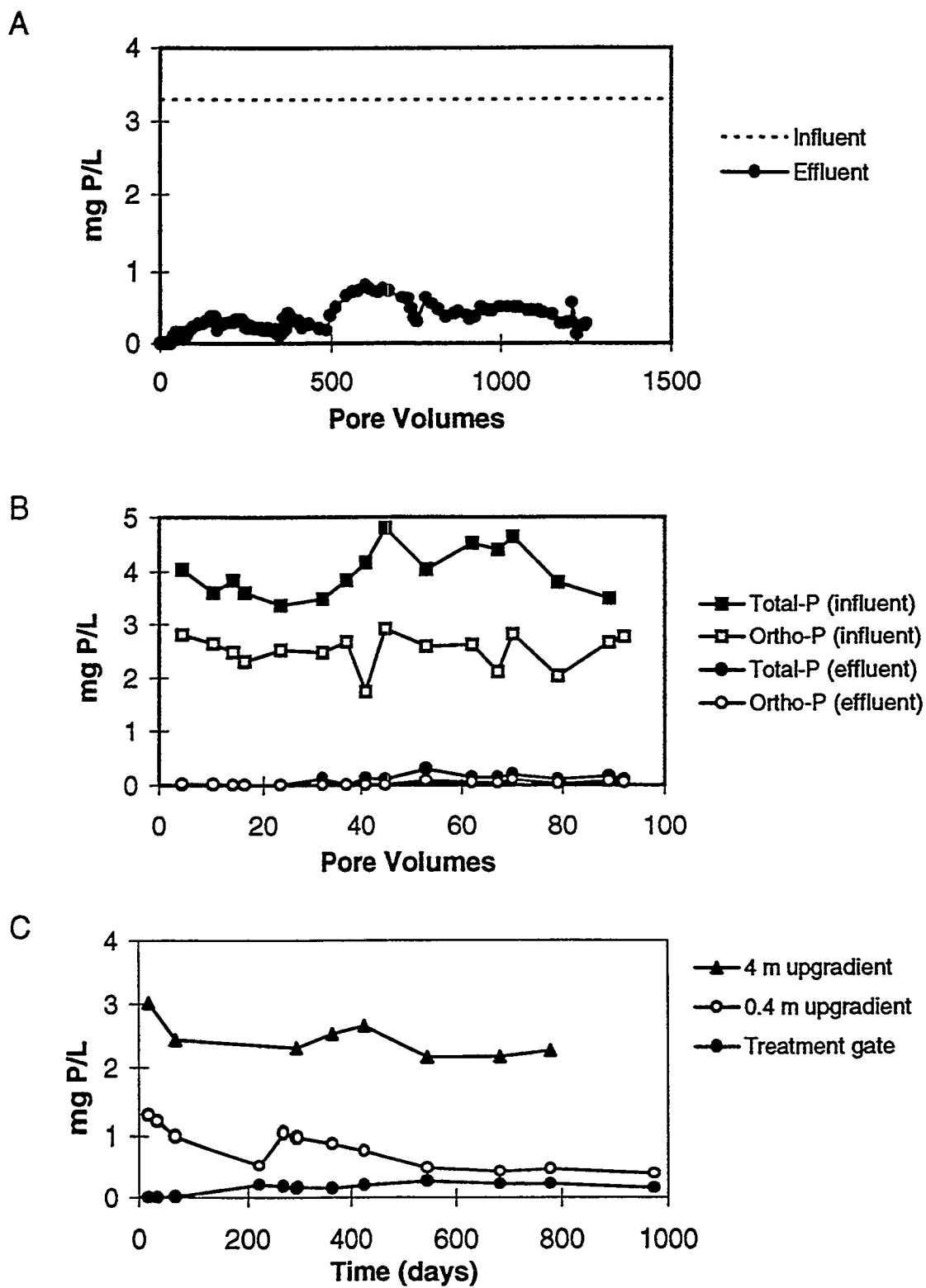
Figure 3. Breakthrough curves for laboratory and field tests. A. Laboratory column ; B. Municipal wastewater treatment system ; C. Funnel and gate system.

CREATION OF A SUBSURFACE PERMEABLE TREATMENT BARRIER USING IN SITU REDOX MANIPULATION

J.S. Fruchter, C.R. Cole, M.D. Williams, V.R. Vermeul, S.S. Teel,
J.E. Amonette, J.E. Szecsody, S.B. Yabusaki

Abstract

The goal of in situ redox manipulation is to create a permeable treatment zone in the subsurface for remediating redox-sensitive contaminants in groundwater. The permeable treatment zone is created just downstream of the contaminant plume or contaminant source through the injection of reagents and/or microbial nutrients to alter the redox potential of the aquifer fluids and sediments. Contaminant plumes migrating through this manipulated zone can then be destroyed or immobilized.

In a field test at the Hanford Site, ~77,000 L of buffered sodium dithionite solution were successfully injected into the unconfined aquifer at the 100-H Area in September 1995. The target contaminant was chromate. No significant plugging of the well screen or the formation was detected during any phase of the test. Dithionite was detected in monitoring wells at least 7.5 m from the injection point. Data were obtained from all three phases of the test (i.e., injection, reaction, withdrawal). Preliminary core data show that from 60% to 100% of the available reactive iron in the targeted aquifer sediments was reduced by the injected dithionite. One year after the injection, groundwater in the treatment zone remains anoxic. Total and hexavalent chromium levels in groundwater have been reduced from a preexperiment concentration of ~60 μg/L to below the detection limit of the analytical methods.

Introduction

Subsurface contaminants at U.S. Department of Energy sites occur in both the vadose and groundwater-saturated zones. Many groundwater plumes are already dispersed over large areas (km^2) and are located tens to hundreds of meters below the ground. This type of dispersed, inaccessible contamination, which is more difficult than other types of contamination to treat using excavation or pump-and-treat methods, can be treated successfully by the in situ manipulation of natural processes to change the mobility or form of the contaminants.

An unconfined aquifer is usually an oxidizing environment; therefore, most of the contaminants that are mobile in the aquifer are those that are mobile under oxidizing conditions. If the redox potential of the aquifer is made reducing, then a variety of contaminants can be treated (Fruchter et al. 1994). The goal of in-situ redox manipulation (ISRM) is to create a permeable treatment zone in the subsurface for remediation of redox- sensitive contaminants in the groundwater (Figure 1). The permeable treatment zone is created by reducing the ferric iron to ferrous iron within the clay minerals of the aquifer sediments. This reduction can be accomplished with chemical reducing agents such as sodium dithionite or through the stimulation of naturally occurring iron-reducing bacteria with nutrients (e.g., lactate). After the aquifer sediments are reduced, any reagent or reaction products introduced into the subsurface are removed. Redox-sensitive contaminants that can be treated by this technology include chromate, uranium, technetium and some chlorinated solvents (e.g., carbon tetrachloride). Chromate is immobilized by reduction to highly insoluble chromium hydroxide or iron chromium hydroxide solid solution. This is particularly favorable because chromium is not easily

reoxidized under ambient environmental conditions. Uranium and technetium are also reduced to less soluble forms, and chlorinated solvents are destroyed by reductive dechlorination. In the study reported in this paper, the target contaminant is chromate.

* Potential Candidate for Redox Treatment
** Favorable Candidate for Redox Treatment
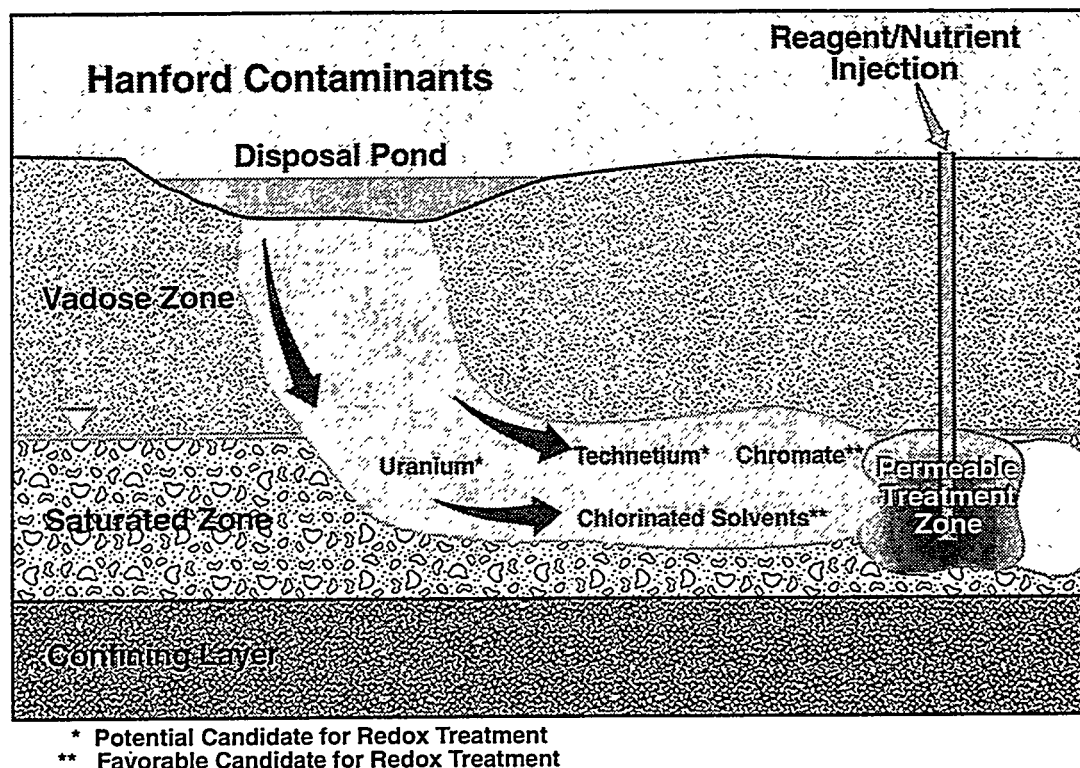
Figure 1. In situ permeable treatment zone concept.

Bench- and Intermediate-Scale Experiments

Work to date has focussed on the chemical reduction method. Sodium dithionite was found to reduce the structural ferric iron found in the clays of the Hanford Site soils (Amonette et al. 1994). Batch laboratory experiments indicate that the half-life of the dithionite ion is ~18 h when in contact with onsite sediments. This half-life allows adequate time for reduction of solids in the aquifer while ensuring that dithionite does not remain as a contaminant in the groundwater for extended periods of time.

Following the completion of bench-scale experiments, an intermediate-scale dithionite injection was completed in a 7-m-long, 0.20-m-thick, 11-degree, wedge-shaped flow cell. The cell was constructed at Oregon State University and packed with sands similar to Hanford sediments. The wedge shape of the flow cell approximated the radial flow field around an injection/withdrawal well. These experiments are described in Fruchter et al. (1996).

In addition to the bench- and intermediate-scale experiments, mathematical models were used in conjunction with reagent and site-characterization information to define nominal specifications for the field experiments (Williams et al. 1994). Important design factors include: site hydrogeology, well and corehole placement, reagent concentration, injection and withdrawal rates, and duration for each stage (injection, reaction, and withdrawal) of the ISRM field experiment.

Field-Scale Experiments

The Hanford Site's 100-H Area (Figure 2) was chosen for the ISRM field test. The site is located southwest of the old 100-H Reactor and is located ~730 m from the Columbia River. The site is relatively uncontaminated, with only low levels (<100 μg/L) of hexavalent chromium in the groundwater. Sixteen wells were drilled and completed, including an injection/withdrawal well, upper and lower zone monitoring wells, and up- and downgradient monitoring wells (Figure 2). Prior to the full-scale injection, a series of site-characterization activities, including hydraulic tests and a bromide tracer injection/withdrawal test, were completed. A "mini" dithionite test injection was also completed and are described in Vermeul et al. (1995) and Fruchter et al. (1996).
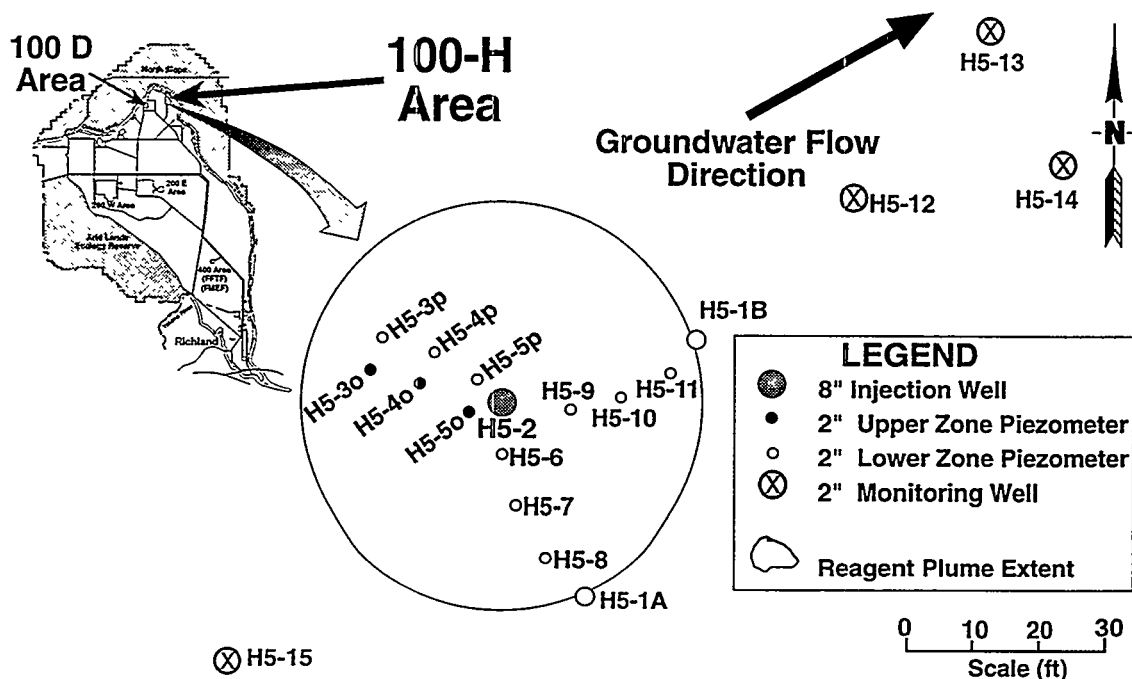
Figure 2. Location of the 100-H Area and wells used in the ISRM field test.

The full-scale dithionite injection experiment was initiated on September 7, 1995, and was designed to produce a 15-m-dia. reduced zone. Approximately 77,000 L of buffered sodium dithionite solution were injected into the aquifer during a 17.1-h injection phase. The injection design incorporated three different concentrations of reagent, decreasing over time, to minimize cost and amount of derived waste; tracer concentration was constant. After a reaction time of 18.5 h, which provided time for the reagent to react with the iron within the sediments, the spent reagent was withdrawn from the aquifer during an 83-h withdrawal phase (4.8 injection volumes) through the injection/withdrawal well. The withdrawal phase was designed to remove any unreacted reagent and buffer, reaction products (e.g., sulfate/sulfite), mobilized metals, and bromide tracer.

Samples collected from the extraction stream during the withdrawal phase of the experiment were analyzed for sulfate, sulfite, and bromide using ion chromatography. Based on integration of the extraction stream concentration data, it was estimated that 87% of the injected sulfur mass (as dithionite) and 90% of the injected bromide were recovered during the withdrawal phase. Measurements also showed that mobilization of naturally occurring trace

metals in the sediments was minimal. The withdrawal water from this experiment was stored in a 380,000-L modular storage tank installed at the site. Following regulatory approval, stored purgewater was discharged to the ground.

Effectiveness of Treatment

Two months after the injection, core samples were collected from the treated zone to determine the extent of reduction. Preliminary core data show that, in general, from 60% to 100% of the available reactive iron within the targeted zone was reduced by the injected dithionite (Figure 3). Data also indicated 1) a general trend of increasing percent reduced with depth; this is consistent with the experiment design, which targeted the bottom 1.3 m of the aquifer and 2) a general trend of decreasing percent reduction with increasing distance from the injection/withdrawal well.
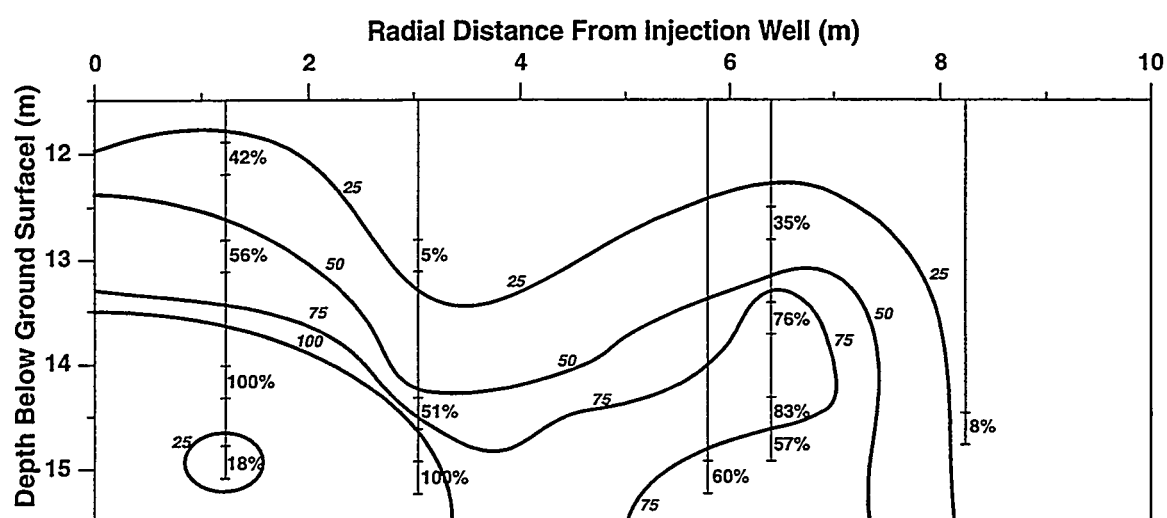
Figure 3. Percentage of available reactive iron reduced by the dithionite injection at the ISRM test site.

It should be noted that a comparison of samples collected from the interior portion of a core sample were significantly more reduced than the outer portion of the core, indicating that some of the cores may have been partially reoxidized during core sampling and/or during handling/storage of the core samples. Subsequent core samples will be collected to assess the decrease in reductive capacity of the treatment zone over time. These core samples will be collected using more rigorous procedures to reduce the potential for atmospheric oxygen contamination during collection.

Comparison of Pre- and Postexperiment Hydraulic Tests

Pre- and postexperiment slug interference test responses were compared for selected ISRM observation well sites to assess the impact of the applied field experiment on existing in situ hydraulic properties. As indicated in Spane (1996), slug interference response transmission (i.e., from the stress well to the point of observation) is highly dependent on the aquifer-interwell transmissivity. The shape and amplitude of the slug interference response are primarily controlled by the elastic storage (S) and vertical anisotropy (K_v/K_h) of the aquifer materials. A comparison of the pre- and postexperiment slug interference responses (for

707

identical test conditions), therefore, should provide a direct means of evaluating any changes in in situ hydraulic properties induced by the experiment application.

Preliminary postexperiment analyses indicate the presence of a small zone (e.g., 2.5 to 10 cm of reduced permeability immediately outside the wellbore. The cause of this zone of reduced permeability is unknown but may be attributed to entrapment of suspended or colloidal material in the sandpack zone immediately outside the well screen during the withdrawal phase of the experiment. This near-well reduction in permeability caused no adverse effects during the injection or withdrawal phases of the field experiment and is not expected to result in any significant degradation in the overall hydraulic performance of the treatment zone.

It should be noted that a direct comparison of slug interference responses was not possible because the aquifer thickness increased from 2.4 to 3.2 m for the pre- and postexperiment tests, respectively; the increase in aquifer thickness (i.e., rise in the water table) was due to historically high Columbia River stage. To eliminate the uncertainties associated with this change in aquifer thickness, additional slug interference tests will be conducted once water levels have returned to their preexperiment conditions. This second phase of hydraulic testing will provide a direct, and more definitive, comparison.

Long-Term (Postexperiment) Monitoring of Wells

Monitoring of the groundwater at the ISRM site has been ongoing since the injection/ withdrawal experiment, initially on a biweekly frequency and then, after ~6 mo, on a monthly frequency. Water samples were collected from the wells at the site and measured for geo-chemical field parameters (pH, conductivity, dissolved oxygen [DO], and hexavalent chromium). Archive samples were also collected, with one set preserved in nitric acid for trace metal analysis (if needed). Three rounds of groundwater samples for all the wells at the site were analyzed for trace metals using ICP/MS. In addition to the wells within the treatment zone, up- and downgradient monitoring wells were sampled and analyzed.

Postexperiment monitoring data are presented for wells along a transect in a generally up-to downgradient direction (Figure 4). DO concentrations in the wells before the injection/ withdrawal experiment ranged between 1.9 to 6.1 μg/L. Following the experiment, DO concentrations in most of the wells within the reduced zone were ~0 μg/L (i.e., <0.05 μg/L) (see Figure 3).

Total chromium concentrations before the experiment ranged from 46 to 71 μg/L within the treatment zone. Following the injection/withdrawal experiment, total chromium concentrations within the treatment zone declined to below the detection limit of the analytical method (ICP/MS; 2 ppb). Hexavalent chromium concentrations have also been reduced to below the detection limit of the analytical method (diphenylcarbazide; 8 μg/L) (Figure 5). The general trends seen in DO concentrations are also seen in the chromium measurements at the site (compare Figures 4 and 5).

Although no negative impacts on the aquifer have been observed downgradient of the reduced zone, a larger and longer reduced zone is needed to adequately monitor and address downgradient effects. The small scale of the ISRM treatment zone makes quantification of downgradient effects difficult because of edge effects and uncertainty in gradient direction.
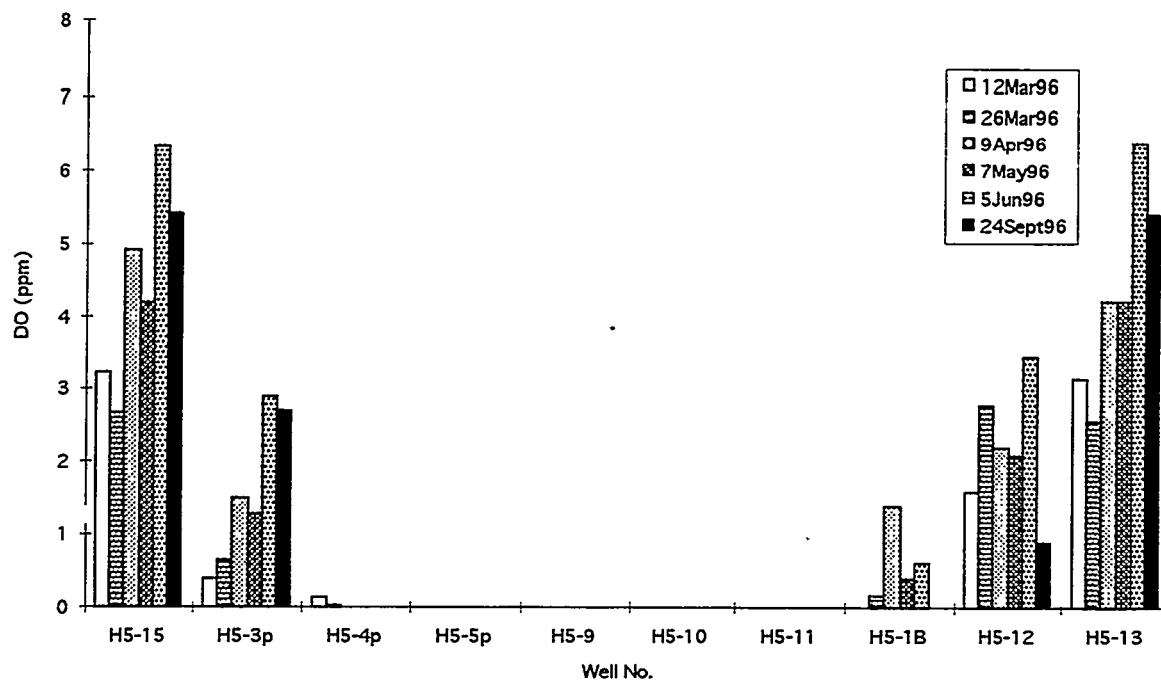
Figure 4. Dissolved oxygen measurements along an up- to downgradient transect during postexperiment monitoring.

Note: Detection limit = 8ppb.
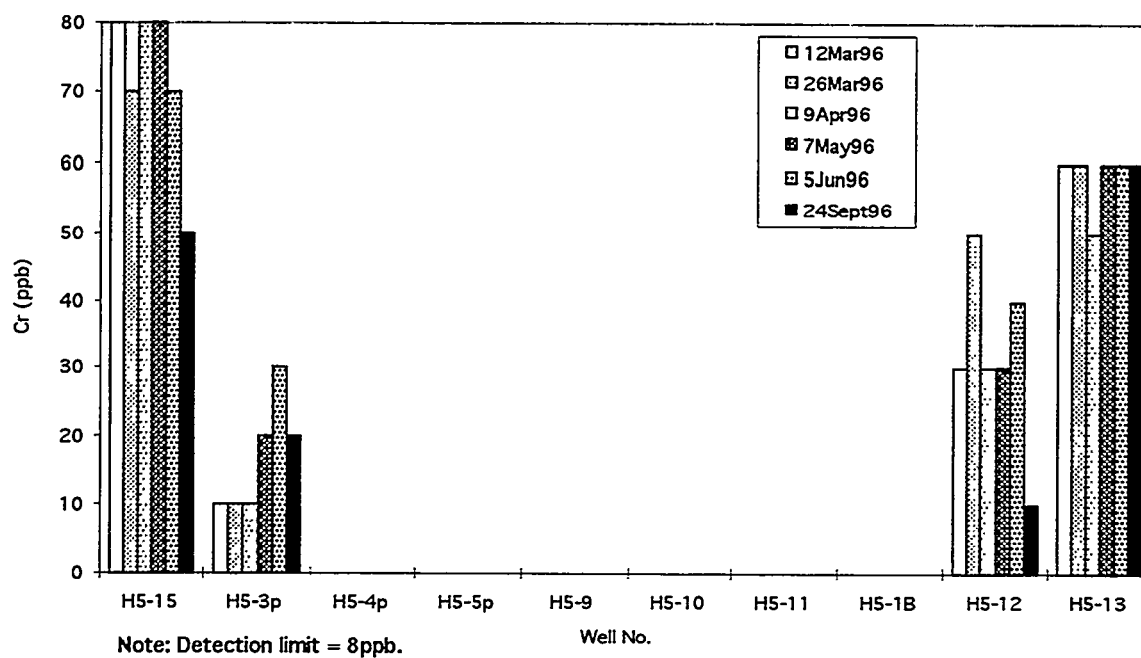
Figure 5. Hexavalent chromium measurements along an up- to downgradient transect during postexperiment monitoring.

Proposed Treatability Test

In response to a request from the Environmental Restoration Contractor for the Hanford Site, a proposal was developed for the emplacement of a pilot-scale permeable treatment zone using ISRM for the treatment of chromium-contaminated groundwater in the 100-D Area (see Figure 2). The dimensions in the nominal design of the pilot-scale treatment zone are 46 m long by 15 m wide. The approach taken for the barrier emplacement is similar to the field experiment conducted at the 100-H Area.

Summary

A buffered sodium dithionite solution (~77,000 L) was successfully injected into the unconfined aquifer at the Hanford Site's 100-H Area in September 1995. No significant plugging of the well screen or the formation was detected during any phase of the test. Dithionite was detected in monitoring wells at least 7.5 m from the injection point. Injection, reaction, and withdrawal data were obtained from all three test phases. One year after the injection, groundwater in the treatment zone remains anoxic. Total and hexavalent chromium levels have been reduced from a preexperiment concentration of ~60 μg/L to below detection limits.

Acknowledgments

References

Amonette, J.E., et al. (1994) Abiotic Reduction of Aquifer Materials by Dithionite: A Promising In-Situ Remediation Technology. *Proceedings of the Thirty-Third Hanford Symposium on Health and the Environment - In Situ Remediation: Scientific Basis for Current and Future Technologies.* (ed. GW Gee and NR Wing), Battelle Press, Richland, WA. pp. 851-882.

Fruchter, J.S., et al. (1994) *Interim Report: Manipulation of Natural Subsurface Processes: Field Research and Validation.* Pacific Northwest Laboratory, Richland, WA. PNL-10123.

Fruchter, J.S., et al. (1996) *In Situ Redox Manipulation Field Injection Test Report - Hanford 100-H Area.* Pacific Northwest National Laboratory, Richland, WA. PNNL-11372.

Spane, F.A. (1996) Applicability of slug interference tests for hydraulic characterization of unconfined aquifers: (1) analytical assessment. *Ground Water,* 34(1), 66-74.

Vermeul, V.R., et al. (1995) *Geologic, Geochemical, Microbiologic, and Hydrologic Characterization at the In Situ Redox Manipulation Test Site.* Pacific Northwest Laboratory, Richland, WA. PNL-10633.

Williams, M.D., et al. (1994) In-Situ Redox Manipulation Field Experiment: Design Analysis. *Proceedings of the Thirty-Third Hanford Symposium on Health and the Environment - In Situ Remediation: Scientific Basis for Current and Future Technologies.* (ed. GW Gee and NR Wing), Battelle Press, Richland, WA. pp. 1131-1153.

PERMEABLE SORPTIVE WALLS FOR TREATMENT OF HYDROPHOBIC ORGANIC CONTAMINANT PLUMES IN GROUNDWATER

Peter Grathwohl, Gerald Peschik[1]

Abstract

Highly hydrophobic contaminants are easily adsorbed from aqueous solutions. Since for many of these compounds sorption increases with increasing organic carbon content natural materials such as bituminous shales and coals may be used in permeable sorptive walls. This, however, only applies if sorption is at equilibrium, which may not always be the case in groundwater treatment using a funnel-and-gate system. In contrast to the natural solids, granular activated carbons (GACs) have very high sorption capacities and reasonably fast sorption kinetics. The laboratory results show that application of GACs (e.g. F100) is economically feasible for *in situ* removal of polycyclic aromatic hydrocarbons (PAH) from groundwater at a former manufactured gas plant site (MGP). For less sorbing compounds (such as benzene, toluene, xylenes) a combination of adsorption and biodegradation is necessary (i.e. sorptive + reactive treatment).

Introduction

The adsorption of hydrophobic organic contaminants from the aqueous phase generally increases with decreasing solubility of the compound (or increasing octanol/water partition coefficient, K_{OW}) and increasing organic carbon content of the aquifer solids. Natural materials with high organic carbon content such as coals or bituminous shales cause significant retardation of organic contaminants from groundwater. Such materials with high sorption capacities may be used in permeable walls for *in situ* removal of strongly hydrophobic contaminants in groundwater (e.g. for polycyclic aromatic hydrocarbons (PAHs) which are a common problem at former manufactured gas plant sites, MGPs). Much more efficient is adsorption onto activated carbon, which is already a well-established technology for *ex situ* treatment of drinking water, polluted groundwater or waste water. In large scale horizontal filters granular activated carbon (GAC) combined with slow sand filtration (Bauer et al., 1994) was used successfully for long term removal of pesticides from River Thames water. For successful use in a permeable wall or in a funnel-and-gate system permeability and sorptive properties of the adsorptive wall material (adsorbent) must be optimized. Both the permeability and the sorption rates depend on the grain size of the adsorbent, the permeability increasing with increasing grain size, and the sorption rates decreasing with increasing grain size squared.

In general, an economically efficient *in situ* groundwater treatment system which relies an adsorption of the contaminants must fulfill the following requirements:

1. Long regeneration cycles (3 - 10 years). Thus high sorption capacities or adsorption combined with biological or abiotic degradation of less sorbing compounds are required.

2. Relatively high permeability in comparison to that of the aquifer in order to prevent steep hydraulic gradients.

3. Fast sorption kinetics in order to achieve high retardation factors even at high groundwater flow velocities (short contact times in funnel-and-gate applications).

4. No decrease in permeability or "chemo-/biofouling" of the adsorbent due to competitive adsorption of dissolved organic matter or the growth of a biofilm which may plug adsorbent

[1] Applied Geology, University of Tübingen, Sigwartstr. 10, 72076 Tübingen, Germany
phone: +49 7071 297 5429, Fax: +49 7071 5059, grathwohl@uni-tuebingen.de

pores (although biodegradation of contaminants would be highly desirable for a sorptive + reactive wall).

This paper presents the basics of adsorption and results of a laboratory study for *in situ* removal of hydrophobic contaminants (PAHs) from the groundwater at a former MGP site where a funnel-and-gate system (slurry wall funnel and a permeable sorptive gate) will be used for *in situ* treatment of the PAHs in the groundwater. Different granular activated carbons (GAC) were used in batch experiments to determine the adsorption isotherms and the sorption kinetics of selected PAHs. Long term column tests with contaminated groundwater from the site were performed in order to investigate the PAH transport in GACs and additionally in a natural bituminous shale sample.

Background

Sorption/Retardation

The retardation of contaminants, e.g. in a sorptive permeable wall, can be calculated based on the sorption coefficient K_d:

$$R_d = 1 + K_d \frac{\rho}{n}$$

where ρ denotes the bulk density and n the porosity of the filter (in packed beds both values lie within a narrow range). R_d may be interpreted as the number of pore volumes which can be displaced before breakthrough of the contaminant occurs. K_d denotes the ratio between the sorbed and aqueous concentrations of the contaminant. If sorption is nonlinear (which is often the case for strongly hydrophobic contaminants and strong adsorbents such as GAC), K_d can be calculated in a first approximation from the commonly-used Freundlich type adsorption isotherm:

$$K_d = \frac{C_s}{C_w} = K_{Fr} C_w^{1/n-1}$$

where C_s, C_w and K_{Fr} denote the equilibrium solid and aqueous concentrations of the solute and the Freundlich sorption coefficient, respectively. The Freundlich exponent *1/n* is usually smaller than 1, resulting in decreasing K_d values with increasing concentration of the contaminant.

Natural Adsorbents

For most hydrophobic compounds and natural adsorbents K_d can be estimated based on the organic carbon content (f_{oc}) of the solids (Fig. 1) and the organic carbon normalized sorption coefficient K_{oc} of the specific organic compound ($K_d = K_{oc} f_{oc}$). Mineral surfaces do not contribute significantly to the sorption of organics in natural and organic carbon-containing materials. K_{oc} depends on the octanol/water partition coefficient (K_{ow}), which for soil organic matter may be calculated based on empirical correlations (e.g. Karickhoff et al., 1979):

$$K_d = K_{oc} f_{oc} = 0.62 f_{oc} K_{OW}$$

Such empirical K_{oc} - K_{ow} relationships are representative for organic matter in soils (e.g. humins). As shown in Fig. 1 for mature (aged or fossil) organic matter such as coals and kerogen, the K_{oc} values can be up to a factor 30 higher than those for soil organic matter (Grathwohl, 1990). Therefore even relatively small amounts (10%) of sorptive additives with high K_{oc} would result in significant equilibrium sorption of hydrophobic contaminants.
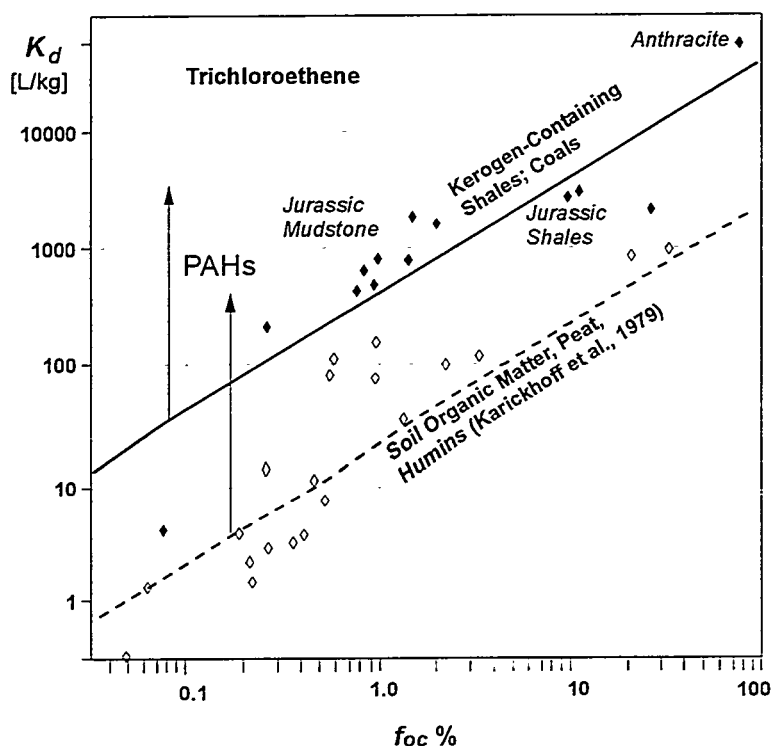
Fig. 1: Sorption coefficients measured for trichloroethene (TCE) versus the organic carbon content (f_{oc}) of natural soils, sediments and coal samples. Open symbols: geologically young organic matter in top soils; filled symbols: fossil organic matter in sedimentary rocks, shales and coals (Grathwohl, 1990). For PAHs the K_d values are expected to be much higher (by a factor 100 - 1000).

Activated Carbon Adsorption

Adsorption capacities for organic compounds using activated carbons are much higher than in naturally occurring organic sorbents. Fig. 2 shows literature data on adsorption of a variety of organic compounds onto activated carbon (F300). Distribution coefficients (K_d) were calculated based on the Freundlich sorption isotherms (K_{Fr}, $1/n$) for an aqueous concentration of 10% of the pure compound's water solubility. For compounds with high water solubilities ($S > 1$ mg/l) an almost linear inverse relationship between K_d and S is observed (solid line in Fig. 2). Since bulk density and porosity in a packed bed of granular activated carbon are both close to 0.5, K_d in a GAC permeable wall is approximately equal to the retardation factor R_d.

Sorption Kinetics and Permeability

The data shown in Figs. 1 and 2 are valid for equilibrium sorption, which is not always applicable since the mean residence times (contact times) in a permeable sorptive wall may be too short for complete equilibration. Sorptive uptake of solutes by a porous adsorbent particle is diffusion limited. This results in K_d values which increase with the square root of time for short-term sorptive uptake (less than 50% of sorption equilibrium reached). Fast equilibration would be achieved for small particles with high surface to volume ratios. Small particles, however, result in low permeabilities. In a funnel-and-gate system the permeability of the gate has to be as least as high as in the aquifer. In a first approximation the permeability (K) increases with the grain radius of the adsorbent particle squared and the intergranular porosity. Since the porosity in loose packed beds will generally lie within a relatively narrow range, between 0.4 and 0.6, the main factor influencing the permeability is the size of the adsorbent particles. For typical groundwater flow velocities and a thickness of the sorptive wall of about 1 m -2 m, the mean residence time of contaminated groundwater will range from less than a day to a few days. If the mean residence time is too short for equilibration, the K_d values will be much smaller than expected for equilibrium conditions, which would in turn result in an early breakthrough of the contaminant through the sorptive wall.
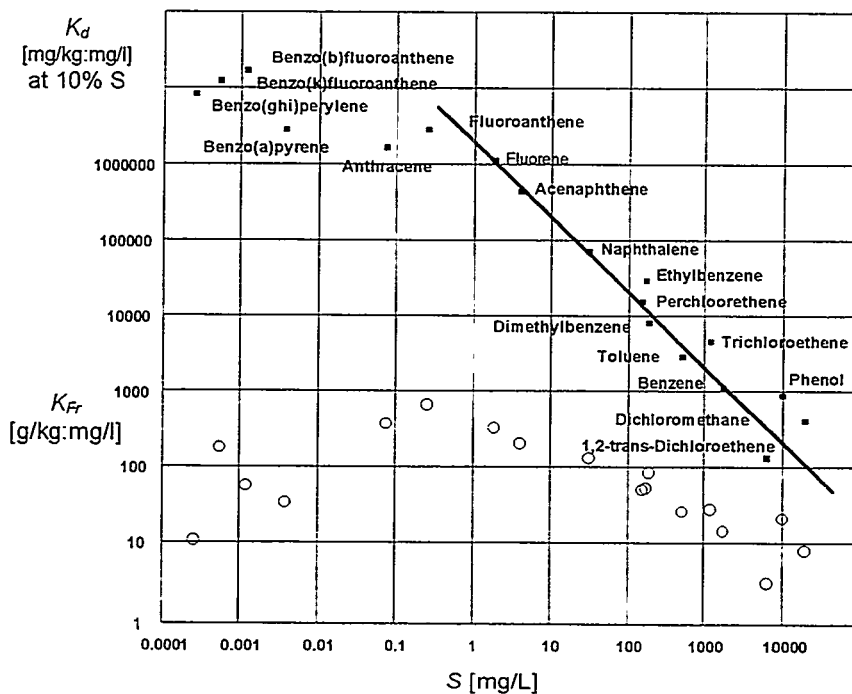
Fig. 2: Freundlich sorption coefficients K_{Fr} (open symbols) as reported in the literature (American Water Works Association, 1990; Sontheimer et al., 1985) for GAC (F300) and distribution coefficients (K_d : filled, labeled squares) were calculated for a concentration of 10% of the water solubility S [mg/L] of the respective compounds.

The chart y-axes are labeled K_d [mg/kg:mg/l] at 10% S and K_{Fr} [g/kg:mg/l]; the x-axis is labeled S [mg/L]. Plotted labels include Benzo(b)fluoroanthene, Benzo(k)fluoroanthene, Benzo(ghi)perylene, Benzo(a)pyrene, Anthracene, Fluoroanthene, Fluorene, Acenaphthene, Naphthalene, Ethylbenzene, Perchloorethene, Dimethylbenzene, Toluene, Trichloroethene, Benzene, Phenol, Dichloromethane, 1,2-trans-Dichloroethene.

Experimental

Column Tests with Contaminated Groundwater (MGP Site)

A natural bituminous shale sample and 3 different GACs were used in laboratory column tests in order to investigate the transport of PAHs in a permeable sorptive wall planned at a former MGP site in Southern Germany. PAH concentrations in the column effluent (16 EPA PAHs) were determined by GC/MS after liquid-liquid extraction (cyclohexane). Breakthrough of PAHs in the bituminous shale column was already observed after approximately 10 displaced pore volumes, indicating that the equilibrium sorption capacity was not reached (by far). In the GAC columns no breakthrough was observed and PAHs were concentrated in the first few centimeters of the packed bed (Tab. 1), as determined by methanol extraction of thin GAC layers after the column test.

The results obtained for the GAC indicate that sorption at these relatively slow flow velocities is reasonably close to equilibrium (typical flow velocities in drinking water treatment are much higher) and the retardation factors to be expected are higher than 3000.

Tab. 1: Column tests for removal of PAHs (16 EPA PAHs) from contaminated groundwater (PAH concentration approx. 2500 µg/L, predominantly naphthalene and acenaphthene)

Adsorbent (GAC)	F100	D15/1	C40/4 (pellets)	Bit. Shale
Origin	Chemviron	Lurgi	Carbo Tech	Lias ε (Aalen)
Grain Size [mm]	0.5 - 3	1.25	4.2	2 - 4
BET-Surface Area m^2 /g	770	1102	1281	16
Column Length [cm]	14	13	13	21
Porosity (intergranular)	0.52	0.68	0.61	0.48
Run Time [days]	23	23	23	112
Pore Volumes Displaced	885	731	814	1097
Flow Velocity [m/day]	5.3	4.0	4.6	2.1
Mean Residence Time [h]	0.6	0.76	0.68	2.6
PAH penetration depth	< 1.5 cm	< 1.5 cm	< 4 cm	breakthrough

714
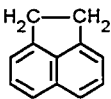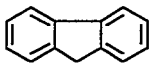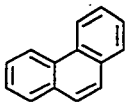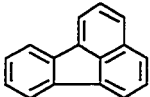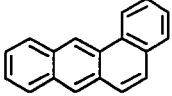
Batch Experiments on Sorption of PAHs onto GAC

Batch experiments were performed in order determine the equilibrium adsorption isotherms and the sorption kinetics of selected PAHs (Acenaphthene, Fluorene, Phenanthrene, Fluoranthene and Benz(a)anthracene) for three different GACs and a C_{18}-modified silica gel used as reference sorbent (Tab. 2). Chemico-physical properties of the PAHs selected for this study are shown in Tab. 3.

Tab. 2: Properties of GACs used in batch experiments.

Property / GAC	F 100	C 40/4 (Pellets)	TE 143	C_{18}-
Origin	Bituminous Coal	Bituminous Coal	Coconut	Silica Gel
Manufacturer	Chemviron	Carbo Tech	Pica	IST
BET Surface Area [m^2/g]	770	1280	993	$f_{OC} = 0.19$
Total Pore Volume [cm^3/g]	0.422	0.630	0.483	-
Average Pore Radius [Å]	10.95	9.87	9.71	-
Radius [mm]	0.8-1.0	1.0-2.0	0.4-0.5	20 - 35 μm

Tab. 3: Properties of PAHs selected for this study

Compound	Structure	Mol.-Mass [g/mol]	S^* [mg/l]	log K_{OW}[#]	Melting-Point [°C]
Acenaphthene (Ace) $C_{12}H_{10}$		154	3.47	4.33	96
Fluorene (Fln) $C_{13}H_{10}$		166	1.98	4.18	116
Phenanthrene (Phe) $C_{14}H_{10}$		178	1.29	4.46	101
Fluoranthene (Fla) $C_{16}H_{10}$		202	0.26	5.33	111
Benz(a)anthracene (BaA) $C_{18}H_{12}$		228	0.014	5.61	158

* Sims and Overcash (1983); [#] Mackay and Shiu (1977)

For the determination of the adsorption isotherms 0.05 g samples of pulverized GAC were equilibrated for 4 days with 100 ml deionized water which was spiked with the selected PAHs at an initial concentration of 10%, 25%, 50%, 75% and 90% of the respective water solubilities. Sorptive uptake was monitored for a time period of 7 days using 0.15 g GAC (not pulverized) at an initial PAH concentration of 20% of their water solubility. All experiments were performed in

crimp top vials with teflon coated butyl rubber septa. Analysis of PAHs in the aqueous phase was performed by GC/MS (SI-Mode) after filtration (using glass fiber filters) and liquid-liquid extraction (by cyclohexane). The mass sorbed was calculated from the measured aqueous concentration based on mass balance considerations. The aqueous concentrations of Benz(a)anthracene and in part Fluoranthene dropped below the detection limit (therefore no data are shown for these compounds). Performance of the laboratory method was checked by extraction of the C_{18} solids with supercritical CO_2 (SFE at 120 °C and 296 bar for 40 min, using 4% methanol as modifier). Equilibration of the C_{18} silica gel was finished after 24 h and no significant loss of the PAHs was observed after 7 days. The recovery rate after supercritical extraction of the C_{18} solids was > 80% whereas recovery rates for the GACs (pulverized before extraction) were less than 5% using SFE.

K_d and K_{Fr} determined in the equilibrium sorption experiments (Fig. 3, Tab. 3) agree reasonably well with literature data shown in Fig. 2. The PAHs investigated, however, showed no increase of K_d or K_{Fr} with decreasing water solubility (as was observed for the C_{18} silica gel). The K_d values measured in the sorption kinetic experiments were much lower than expected from the equilibrium values (Tab. 4). The sorption kinetic data agreed very well with the numerical solution of Fick's second law for intraparticle diffusion in a finite bath (Fig. 4). The apparent diffusion coefficients were between 1×10^{-12} and 1×10^{-13} m^2 s^{-1}.
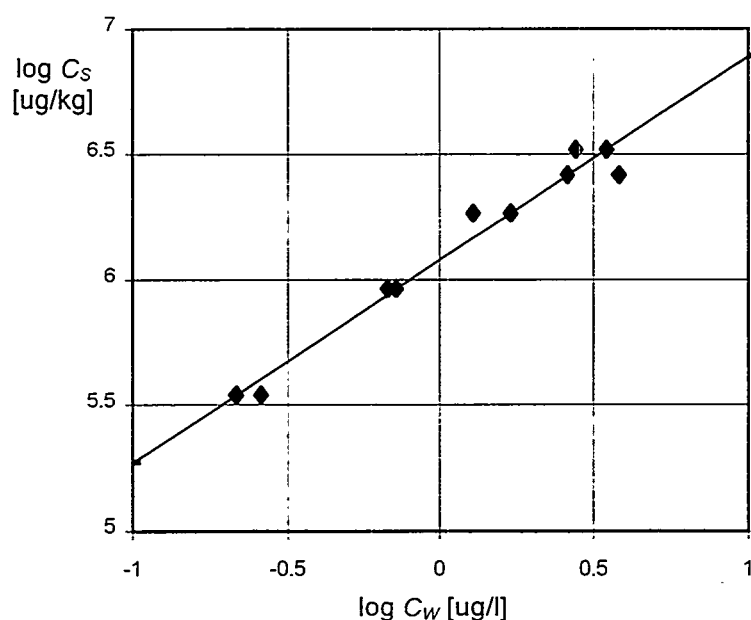
Fig. 3: Freundlich adsorption isotherm of Fluorene on GAC (F100; GAC pulverized for fast equilibration)

Tab. 4: Freundlich coefficients $(K_{FR}, 1/n)$, equilibrium K_d and K_d values measured in the batch kinetic experiments after 24 h, 3 days and 7 days $(K_d *)$.

	F 100			C 40/4			TE 143			C_{18} Silica		
	Ace	Fln	Phe	Ace	Fln	Phe	Ace	Fln	Phe	Ace	Fln	Phe
log K_{Fr}	6.2	6.1	5.9	6.0	5.9	5.7	5.2	5.6	5.7	4.8	5.0	5.2
1/n	0.59	0.81	0.56	0.87	0.99	0.70	0.92	0.67	0.56	0.81	0.82	0.79
log K_d at 10 % S	5.2	5.6	5.0	5.6	5.8	5.1	5.0	4.9	4.7	4.3	4.6	4.8
log K_d * 24 h	3.4	3.7	4.1	3.2	3.2	3.3	3.3	3.3	3.4	4.6	4.9	5.1
log K_d * 3 days	4.0	4.3	4.4	3.6	3.7	3.7	4.5	4.4	4.2	4.6	4.9	5.1
log K_d * 7 days	4.0	4.5	4.7	3.9	3.9	3.9	4.8	4.8	4.6	4.7	5.0	5.3
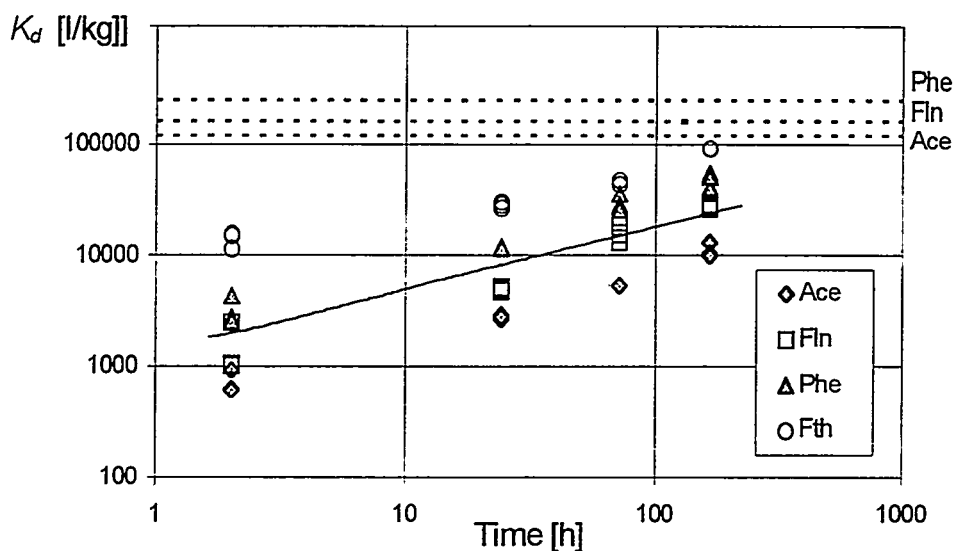
Fig. 4: Sorption kinetics of Acenaphthene (Ace), Fluorene (Fln), Phenanthrene (Phe) and Fluoranthene (Fth) onto GAC (F100). The solid line was calculated using a numerical model (Crank-Nicolson implicit/explicit scheme) for sorptive uptake of Fln in a bath of limited volume. Dashed, horizontal lines denote the equilibrium K_d (Ace, Fln, Phe).

Conclusions

Permeable sorptive walls containing granular activated carbon are applicable for removal of highly hydrophobic organic contaminants such as the polycyclic aromatic hydrocarbons commonly occurring at former manufactured gas plant sites. For natural adsorbents such as kerogen containing bituminous shales, the mean residence time in a sorptive wall probably in many cases is too short for equilibration. For GAC the retardation factors and thus the regeneration times may also be much shorter than expected on the basis of the equilibrium sorption capacity (which is extremely high). For compounds with higher water solubilities than the PAHs a combination of adsorption onto activated carbon and biodegradation (e.g. for phenols and BTEX) may be required to eliminate these less sorbing (but bioavailable) contaminants in a sorptive + reactive wall. This issue will be addressed in further investigations on site and in situ at the MGP site in southern Germany.

References

American Water Works Association (1990): Water Quality and Treatment, 4th ed.

Bauer, M., Buchanan, B., Colbourne, J., Forster, D., Goodman, N., Kay, A., Rachwal, A., Sanders, T., (1994): The GAC/slow sand filter sandwich - from concept to commissioning.- Water Supply, 14, 159-175

Grathwohl, P. (1990): Influence of organic matter from soils and sediments from various origins on the sorption of some chlorinated aliphatic hydrocarbons: Implications on K_{oc}-correlations.- Environ. Sci. Technol., 24 (11): 1687-1693

Grathwohl, P., Reinhard, M. (1993): Desorption of trichloroethylene in aquifer material: Rate limitation at the grain scale.- Environ. Sci. Technol., 27 (12): 2360-2366

Karickhoff, S.W., Brown, D.S., Scott, T.A. (1979): Sorption of hydrophobic pollutants on natural sediments.- Water Research, 13 (3): 241-248

Sontheimer, H., Frick, B.R., Fettig, J., Hörner, G., Hubele, C., Zimmer, G. (1985): Adsorptionsverfahren zur Wasserreinigung.- DVGW-Forschungstelle am Engler Bunte Institut der Universität Karlsruhe (TH)

Sims, R.C., Overcash M. R. (1983): Fate of polycyclic aromatic compounds in soil plant-systems. Residue Review, 88, 1-68

Mackay, D., Shiu, W.J. (1977): Aqueous solubility of polynuclear hydrocarbons.- J. Cem. Eng. Data, 22, (4), 399-402

ACTIVE CONTAINMENT SYSTEMS INCORPORATING MODIFIED PILLARED CLAYS

Peter Lundie[1] and Neil McLeod [2]

Abstract

The application of treatment technologies in active containment systems provides a more advanced and effective method for .the remediation of contaminated sites. These treatment technologies can be applied in permeable reactive walls and/or funnel and gate systems. The application of modified pillared clays in active containment systems provides a mechanism for producing permeable reactive walls with versatile properties. These pillared clays are suitably modified to incorporate reactive intercalatants capable of reacting with both a broad range of organic pollutants of varying molecular size, polarity and reactivity. Heavy metals can be removed from contaminated water by conventional ion-exchange and other reactive processes within the clay structure. Complex contamination problems can be addressed by the application of more than one modified clay on a site specific basis. This paper briefly describes the active containment system and the structure/chemistry of the modified pillared clay technology, illustrating potential applications of the in-situ treatment process for contaminated site remediation.

Introduction

The application of Active Containment utilising permeable treatment walls provides a means for treating mobile pollutants without the need to physically contain groundwater emanating from a contaminated site. The In-situ treatment technology described in this paper incorporates the use of modified pillared clays designed for application in permeable reactive walls and/or funnel and gate systems. Pillared clays are expanded smectite clays with a fixed interlamellar spacing. The clay layers are held apart by reactive polymer compounds which act as molecular props or pillars. The pillared clay structure and chemistry is described in the following Technical Overview section and the Active Containment approach is illustrated in the Application section.

Technology Overview

The treatment technology is essentially an advanced immobilisation (chemical fixation) process targeted at soils contaminated with both organic and inorganic/heavy metal waste materials. The process is based on the use of modified pillared smectite clays which incorporate reactive species. Once intercalated, the reactive properties of the clay and the presence of reactive species will ensure that the waste contaminant is effectively immobilised within the substrate material. The pillaring effect facilitates the passage of contaminated water through the clay bringing the pollutants into direct contact with intercalated reactive species and enables the reactive clays to be used in permeable reactive walls.

---

[1] Director, Envirotech (Scotland) Ltd, The Mill of Brotherfield, Brotherfield, Skene, Aberdeen, Scotland AB32 6SQ Tel/Fax: 0044-1224-740406.

Director, Environmental Resource Industries Disposal Pty Ltd, Unit 2, No 7 Pitt Way, Myaree 6154, Perth, Western Australia. Tel: 0061-9-330-8282; Fax: 0061-9-330-8283.

[2] Technical Director, Envirotreat Ltd, LCP House, Kingswinford, United Kingdom DY6 7NA. Tel/Fax: 0044-1384-288876.

The prime objectives of intercalation are:-

1.   To create adequate interlamellar spacing to accommodate larger molecules (e.g. PCB's and PAH's) and to increase the effective surface pillaring agents.

2.   To create an organophilic environment of varying polarity to attract organics into the interlamellar spaces by absorption/adsorption.

3.   To provide a reactive environment in which the organic substrates can be permanently bonded to the clay surface and pillaring agents.

4.   To provide an active medium for effective treatment of heavy metals both cationic and anionic (eg CrO_4) by interaction with the intercalated species and/or by cation exchange processes .

By selective use of available smectite clays and intercalation of appropriate quaternary ammonium ions in conjunction with other relatively low cost pillaring agents and reactants (principally Fe/Al compounds), it is possible to produce highly efficient and multifunctional treatment media which can be applied on a cost effective basis.

Envirotreat, in collaboration with the University of Birmingham, England, have developed a range of modified organoclays and inorgano-organoclays which address the stated objectives of intercalation. A diagrammatic representation of the generic modified clay is as shown in Figure 1.

Figure 1.

Modified Pillared Clay
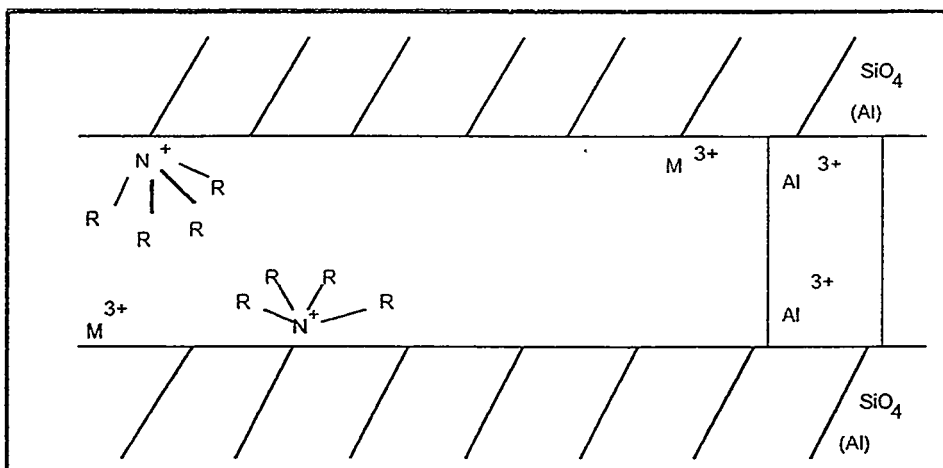
Clay pillared by Hydroxy Aluminium species - typical spacing 18-20A°
M^{3+} represents transition metals; $N(R_4)^+$ represents quaternary ammonium ions.

The potential reactivity of modified clays with organic compounds can be classified as a combination of hydrophobic association, Lewis acid/base bonding (e.g. Al - Cl), transition metal ligand bonding and hydrogen bonding.etc. Once intercalated and bonded to the modified clay, the organic molecules have the potential for further reactivity with other organics/inorganics forming polymeric structures. This reactivity is enhanced by the confined environment within the pillared clay structure which brings the molecules in close proximity to each other in similar fashion to catalysis techniques using zeolites etc.

A range of modified clays of varying hydrophobicity and chemical composition have been developed which are designed to address the issues of hazardous waste treatment and contaminated land remediation (which can require the treatment of a complex range of organic pollutants in addition to heavy metals etc). Batch absorption tests have been carried out with representative organic chemicals viz. 50ml samples of the target organic pollutant were added to a 50mg sample of clay in each case; the samples were then sealed and placed on a motor driven carousel for 48 hours; the clay was then removed by centrifugation and the residual organic concentration was determined by UV/Visible Spectrophotometry. The results obtained with Benzene (a neutral planar molecule with no substituted reactive groups) are as shown in Table 1.

Table 1 - Absorption of Benzene with Modified Clays

Clay Used	Equilibrium concentration (ppm)	Amount absorbed (ppm)	Equilibrium concentration (mmols/mL)	Amount absorbed (mmols/g)
1	250	1410	3.21×10^{-3}	18.1
2	290	1370	3.72×10^{-3}	17.6
3	580	1080	7.44×10^{-3}	13.8
4	200	1460	2.56×10^{-3}	18.7
5	290	1370	3.72×10^{-3}	17.6
6	650	1010	8.33×10^{-3}	12.9
7	250	1410	3.21×10^{-3}	18.1

Initial Benzene concentration 1660 ppm

Whilst all clay variants showed a level of reactivity, certain clays were found to be more reactive due to their inherent composition and structure (the most reactive clay was found to be a transition metal aluminium pillared organoclay). This pattern has been demonstrated with other representative organic species. Where there are complex organic contamination problems, the objective would be to use more than one clay formulation as deemed appropriate.

Conventional smectite clays exhibit cation exchange properties in similar fashion to zeolites which can be utilised in the treatment of cationic species/toxic heavy metals under controlled conditions. They are not however suitable for the treatment of problematic anionic and anionic complexed species, in particular Chromates/Dichromates, Arsenates and Ferri/Ferrocyanides etc.

Modified pillared clays have been shown to be effective in absorbing anionic species. Laboratory demonstration trials have been carried out at Bachy, France on Hexavalent Chromium solutions. Straight-line absorption graphs were obtained using a modified aluminium pillared clay. This clay formulation provided a reactive media for both cationic Cr^{3+} and anionic $CrO_4^{2-}/Cr_2O_7^{2-}$.

Demonstration of In-Situ Treatment Process using Cementitious Materials / Modified Clays

The prime objective of the development programme was to demonstrate that the treatment process could be carried out in-situ using auger mixing and injection techniques. It was decided to carry out in-situ stabilisation/solidification treatment trials using cementitious materials incorporating modified clays. For application in permeable reactive walls, the pillared clays would be used alone or in conjunction with small amounts of cementitious materials as necessary.

The development programme comprised of laboratory treatment trials followed by a full scale site trial demonstration of the in-situ treatment process at a Ministry of Defence site in West Drayton, London, UK. The site trial was carried out using a modified continuous flight auger injection and mixing system developed by May Gurney Limited, a leading UK civil engineering contractor.

Laboratory Treatment Trials

A series of treatment grouts were prepared in the laboratory based on mixes of Ordinary Portland Cement, Pulverised Fly Ash and modified clays. Soil-grout mixes were prepared using samples of contaminated soil obtained from the Ministry of Defence site. This site has been contaminated with both organics (predominantly PAH's) and heavy metals. Testing procedures were carried out to determine the leachability and physical properties of the treated material. Leachability was evaluated using the Toxic Characteristic Leaching Procedure (TCLP). Physical properties tested included Unconfined Compressive Strength, Durability and Permeability. Target objectives were agreed for Leachability (<50x drinking water standards for the UK) and Unconfined Compressive Strength (>50 psi/350 kPa). Target criteria were achieved in all cases and optimum grouts were developed for use in the site trial. It was decided to use a transition metal aluminium pillared organoclay in the site trial focusing on the 6 WHO PAH's commonly specified by regulatory bodies in drinking water standards [Benzo (a) Pyrene, Benzo (b) Fluoranthene, Benzo (ghi) Perylene, Benzo (k) Fluoranthene, Fluoranthene, Indeno (1,2,3 cd) Pyrene] and toxic heavy metals. Target leachate levels <10µg/l for PAH's ; <2.5mg/l for Cr / Pb ; <150mg/l for Cu ; <250mg/l for Zn. The modified clay was produced in slurry form (20g clay per litre); the slurry was then utilised as a source of water for OPC/PFA mixing and hydration purposes.

Site Trial

Following discussions with the Ministry of Defence, it was agreed to treat an area of $6m^2$ with average depth 2.5m giving a total volume of $15m^3$. A grid treatment plan was prepared based on producing overlapping columns (maximum 50% overlap) using a 600mm∅ modified auger. Soil-grout columns were constructed in-situ by advancing the auger into the soil down to the depth of the column, mixing the soil in-place throughout the auger descent and then injecting the grout slurry into the soil with simultaneous mixing on the auger withdrawal. A number of grout variables were tested as shown in Table 2. Each treatment column was designated a specific grout mix.

Table 2 - West Drayton Site Trial - Mix Options

OPTIONS		A	B	C	D	E	F
Weight of PFA (kg)		80	80	80	80	80	-
Weight of Cement (kg)		30	30	25	25	20	80
Weight of Lime (kg)		-	1	4	4	-	-
Weight of Bentonite (kg)		-	-	-	-	-	8
Volume	Clean Water	26	26	26	30	23	110
(litres)	Clay Solution	20	20	20	16	17	30
	Total	46	46	46	46	40	140
Soil:Grout Ratio (by weight)		5:1	5:1	5:1	3.5:1	5:1	5:1
Weight of Soil Column (kg)		1200	1200	1200	1200	1200	1200
Weight of Grout/Column (kg)		240	240	240	340	240	240
Grout:Soil Ratio (solids only)		14%	14%	13.5%	20%	14%	8%

Initial concentrations of the 6 WHO PAH's and selected toxic heavy metals (ie Chromium, Copper, Lead and Zinc) were determined from untreated soil samples as shown in Table 3.

Table 3 - Untreated Soil Samples - Average Concentration

CONTAMINANT	6 WHO PAH(ug/l)	Cr (mg/l)	Cu (mg/l)	Pb (mg/l)	Zn (mg/l)
SOIL CONCENTRATION	9900	53	473	2820	693

Following the site trial, the treated area was left to cure in-situ. Core samples were taken after nominally 28 and 56 days respectively. A series of tests were carried out on the core samples to assess the effectiveness of in-situ treatment; these tests included leachability, unconfined compressive strength, pH, durability and permeability. The results for pH and leachability are as shown in Table 4. Toxic heavy metals were analysed from three random samples (options A, C and D respectively). Unconfined compressive strength values greatly exceeded target parameters (average value 1337 kPa); durability tests satisfied ASTM criteria for wet-dry and freeze-thaw testing parameters and permeability values were typically in the order of 1×10^{-9} m/s.

The overall volume increase at the end of the site trial was measured to be $1 m^3$ i.e. 6.6%. This was considered to be a satisfactory result taking into account the significant overlap.

Table 4 - TCLP Leach Test Results and pH Values

MIX OPTIONS	pH VALUE	6 WHO PAH $Conc^n$ (ug/l)	Cr (mg/l)	Cu (mg/l)	Pb (mg/l)	Zn (mg/l)	TTM (mg/l)	ERF* PAH's	ERF* TTM
A	10.3	<0.5	0.01	0.24	0.03	0.23	0.51	2×10^4	0.8×10^4
B	8.7	<0.5	-	-	-	-	-	2×10^4	-
C	10.9	<1.0	ND	0.13	0.04	ND	0.17	1×10^4	2.4×10^4
D	10.2	<0.9	ND	0.31	0.02	0.01	0.34	1.1×10^4	1.2×10^4
E	9.9	<1.2	-	-	-	-	-	0.8×10^4	-
F	10.7	<0.5	-	-	-	-	-	2×10^4	-

* ERF:- Empirical Remediation Factor (Soil Concentration÷Leachate Value)

Target leachate criteria as specified on page 3 were satisfactorily achieved in all cases. Empirical remediation factors ranged from $0.8 - 2.4 \times 10^4$.

Potential Applications of the In-Situ Remediation Process

The in-situ remediation process can be used (i) to treat areas of contaminated land by forming blocks of overlapping columns in conjunction with cementitious materials and/or (ii) to treat contaminated sites by the formation of reactive treatment walls using primarily modified pillared clays.

Application of Modified Pillared Clays in Active Containment Systems (Treatment Walls)

Modified pillared clays can be applied in active containment technologies. The pillaring effect facilitates passage of polluted groundwater through the clay structure wherein the pollutants can be removed by interaction with the intercalated reactive species. The modified clays have the capability to treat both organic and inorganic pollutants.

Permeable Treatment Walls can be constructed in-situ using auger drilling techniques. Other in-situ application methods are available or under development; WCI Umwelttechnik GmbH have developed a patented Permeable Treatment Bed where the treatment materials are contained within a prefabricated double wall [1].

The treatment wall can either completely surround the contaminated site or form part of a combined physical and active containment system (depending on specific site remediation requirements and hydrogeology etc). This in-situ treatment process provides a cost effective and practical solution to remediation of sites with complex contamination problems.

The Active Containment System can be applied as described below:

1.   As a permeable treatment wall surrounding the periphery of the site (figure 2).

2.   As a treatment wall combined with a conventional physical containment approach. This approach provides a safeguard should the external containment wall fail (figure 3).

3.   In a funnel and gate approach using pillared clays in bulk form (figure 4).

4.   In combination with "hot-spot" treatment utilising the in-situ process described in the paper (figure 5 illustrates treatment wall with "hot-spot" treatment).

The approach adopted will depend to a large extent on the site hydrogeology and logistical considerations and will vary from site to site.

T : Columns constructed using treatment materials.
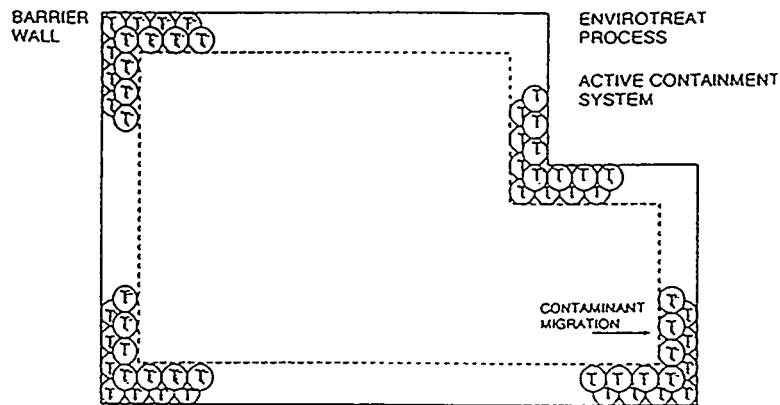
Figure 2. Permeable treatment wall.
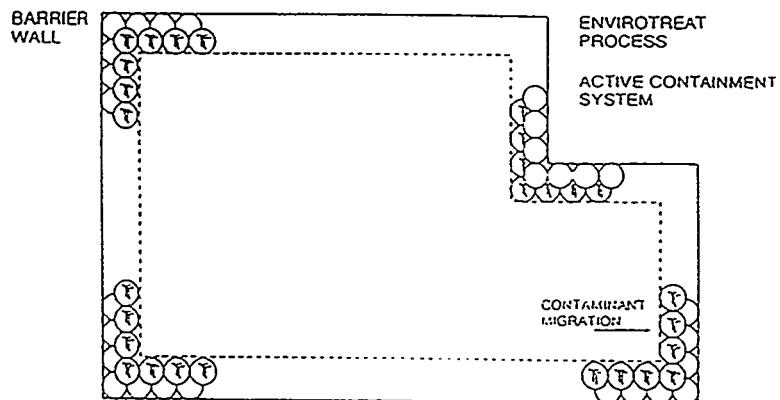
Figure 3. Treatment wall combined with containment
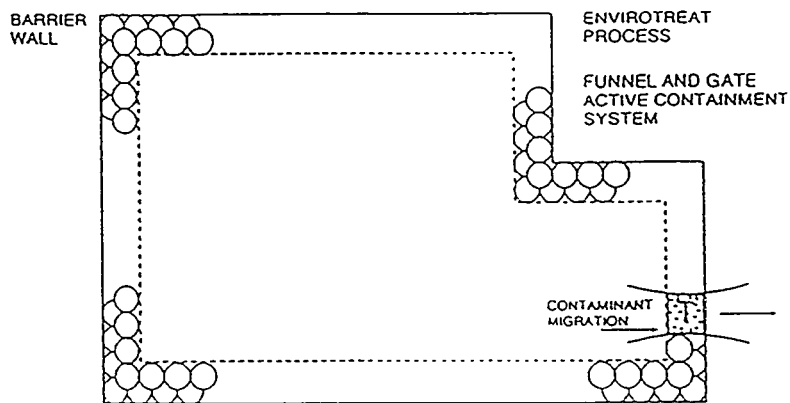
Figure 4. Funnel and gate
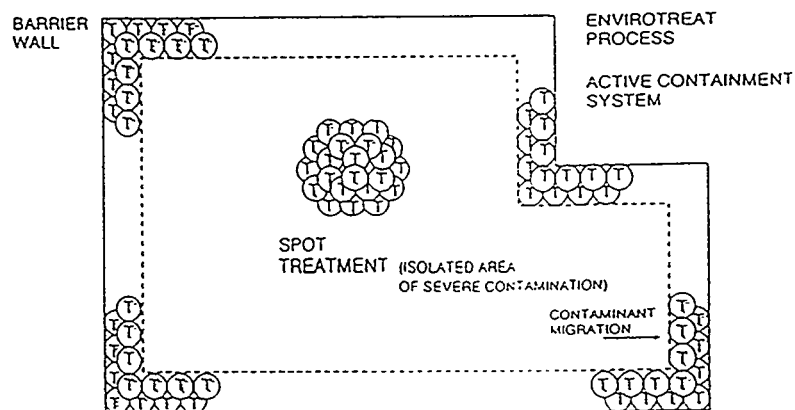
Figure 5. Treatment wall with hot-spot treatment.

Conclusions

The Active Containment System incorporating modified pillared clays is an advanced immobilisation technology which can be applied for use in permeable treatment walls. The treatment technology can address a broad range of contamination problems and can be applied using conventional civil engineering plant and equipment.

References:

[1]   Burmeier H : "Permeable Treatment Beds", Paper presented at NATO/CCMS Pilot Study Meeting on Evaluation of Demonstrated and Emerging Technologies for the Treatment and Clean-up of Contaminated Land and Groundwater (Phase II) held in Adelaide, South Australia, February 1996.

HYDROLOGIC CHARACTERIZATION OF THE FRY CANYON, UTAH SITE PRIOR TO FIELD DEMONSTRATION OF REACTIVE CHEMICAL BARRIERS TO CONTROL RADIONUCLIDE AND TRACE-ELEMENT CONTAMINATION IN GROUND WATER

D.L. Naftz[1], G.W. Freethey[1], J.A. Davis[2], E. Feltcorn[3], R. Wilhelm[3], R. Breeden[4], R.R. Spangler[5], S.J. Morrison[6]

The Fry Canyon site in southeastern Utah (fig. 1) has been selected as a long-term demonstration site to assess the performance of selected reaction-barrier technologies for the removal of uranium and other trace elements from ground water. Project partners at the Fry Canyon site include the U.S. Environmental Protection Agency (USEPA), Bureau of Land Management (BLM), Department of Energy (DOE), Utah Department of Environmental Quality (UDEQ), and U.S. Geological Survey (USGS). Objectives of the field demonstration project include (1) hydrologic and geochemical characterization of the site prior to emplacement of barriers; (2) design, installation, and operation of selected reaction-barrier technologies; and (3) evaluation of barrier(s) performance and commercialization potential.

The Fry Canyon site has many advantages for the field demonstration of reactive chemical barriers: (1) the site is managed by BLM; (2) the site has not been reclaimed; (3) the site is in a remote area and does not present a hazard to domestic water supplies or known biological resources; (4) sufficient volumes and areas of shallow contaminated ground water are present and will support cost effective installation and monitoring of multiple in-situ chemical barriers; and (5) the USEPA gave the site a No Further Action Planned (NFRAP) rating in 1990, thus preventing conflicting activities at the site during long-term field demonstrations.

The Fry Canyon site consists of unreclaimed tailings, leach pads, and leach ponds remaining from uranium upgrading and copper heap-leaching operations and is located on property managed by the BLM. Ground water is present at the site in a 0.61- to 1.5-meter-thick colluvial aquifer underlain by Cedar Mesa Sandstone (fig. 2). Monitoring wells were completed in the colluvial aquifer during September 1996. Initial hydrologic and geochemical data were collected to ensure that a consistently high concentration of uranium in the ground water and an adequate volume of ground water was present to support field demonstration projects.

---

[1]U.S. Geological Survey, 1745 W 1700 S, Salt Lake City, UT 84104, (801) 975-3389
[2]U.S. Geological Survey, 345 Middlefield Road, MS 465, Menlo Park, CA 94025, (415) 329-4484
[3]U.S. Environmental Protection Agency 6602J, Radiation and Indoor Air, 401 M Street S.W., Washington, DC 20460, (202) 233-9422
[4]U.S. Environmental Protection Agency (P2-HW), Region 8, 999 18th Street, Suite 500 Denver, CO 80202-2466, (303) 312-6522
[5]Consultant, 1460-C North Ave., Grand Junction, CO 81501, (970) 241-2544
[6]Weston, Inc., P.O. Box 14000, Grand Junction, CO 81502, (970) 248-6373
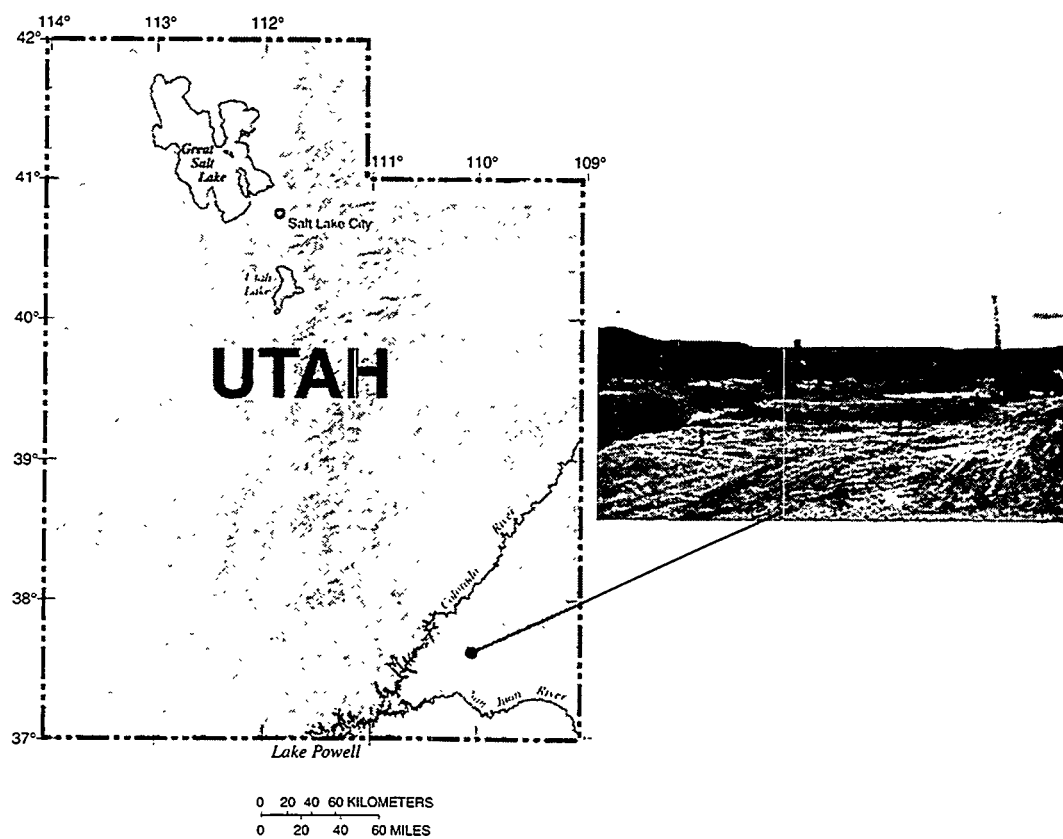
Figure 1. Location of the Fry Canyon study site in Utah.
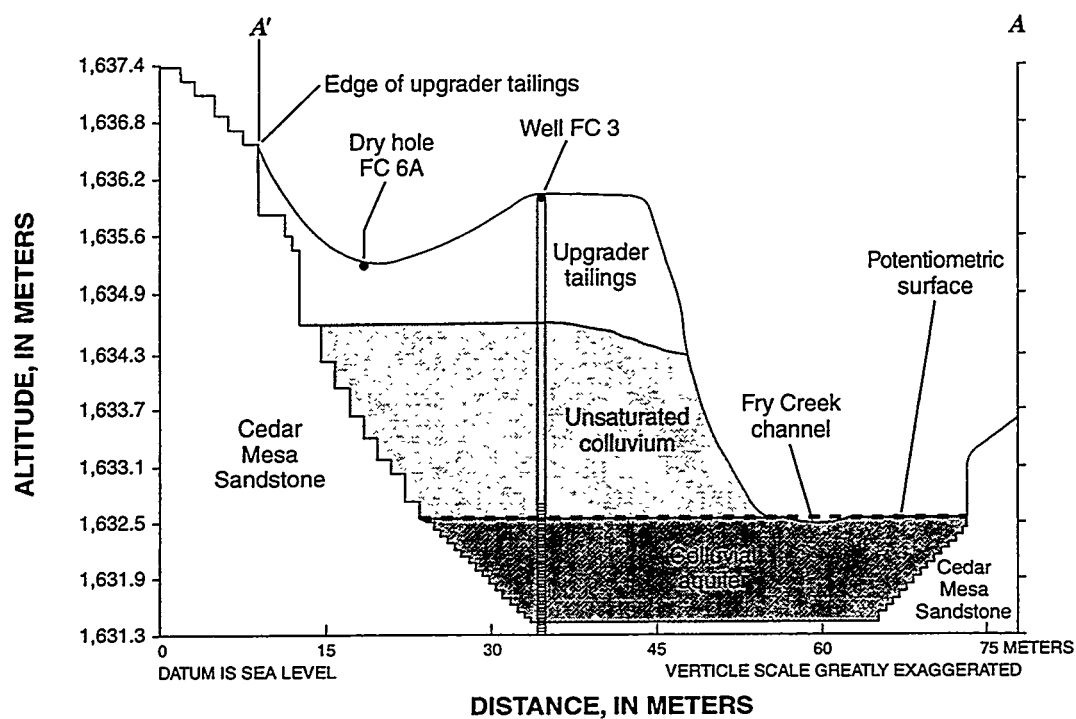
Figure 2. Hydrologic cross section of Fry Canyon, Utah. (See fig. 3 for location of section.)

Dissolved (0.45-micrometer filter) uranium concentration measured in water from seven wells ranged from 0.078 parts per million (ppm) at the upgradient background well to 3.8 ppm at a well located on the upgrader tailings. Monitoring of uranium concentration during a 1-hour pumping cycle of the well containing water with the highest uranium concentration indicated no substantial decrease in uranium concentration with time. Total uranium in subsurface sediment samples collected from the saturated zone of the colluvial aquifer ranged from 2.95 ppm to 21.2 ppm. Total uranium concentration was higher in the unsaturated colluvium, indicating that rainwater has infiltrated through the tailings on the surface and concentrated substantial quantities of uranium within the unsaturated colluvium.

Water levels in the colluvial aquifer measured during mid-October indicate ground-water flow to the northwest, almost parallel to Fry Creek (fig. 3), a perennial stream. Discharge measured in Fry Creek above the tailings on December 18, 1996, was 1.02 liters per second. A representative hydrologic cross section (A-A') was constructed (fig. 2) at right angles to the ground-water flow direction to calculate the volume of water flowing through the colluvial aquifer and the mass of exported uranium. The hydraulic gradient calculated for cross section A-A' is 0.009 meter per meter, and the saturated area is about 46.4 square meters. Hydraulic conductivity (K) value for the lithology of the colluvial aquifer (mostly clean sand with some silt and gravel) is approximately 27 meters per day (Freeze and Cherry, 1979). Using this K value, about 11,300 liters per day is flowing through the colluvial aquifer at section A-A'. Uranium mass export through cross section A-A' is calculated to be about 43 grams per day.

Selected barrier materials, including amorphous ferric oxyhydroxide (AFO), phosphate, and iron filings, are currently undergoing laboratory evaluations for possible field demonstration at the Fry Canyon site. Initial experiments using 6.7 grams per liter of hydroxyapatite were able to completely remove 14.3 ppm of dissolved uranium (VI) from solution. Extrapolation of these results indicate that hydroxyapatite can remove uranium (VI) from at least 3,600 pore volumes of ground water at the Fry Canyon demonstration site. Commercial sources of phosphate (bone meal and phosphate rock) are currently being tested for use in the initial chemical barrier field demonstrations.

Additional site characterization activities are currently (1997) underway to address preliminary barrier-design questions and to obtain the necessary permits for barrier emplacement and operation. Initial installation and field demonstration of the reactive barriers is scheduled to begin during May 1997.

Emplacement of the reactive barriers at the Fry Canyon site will be achieved using simple, inexpensive, and well established construction methods. A bulldozer will be used to move approximately 3.5-m of overburden from above the colluvial aquifer. A backhoe will be used to construct a 1.5-m trench into the colluvial aquifer for placement of the reactive barrier material for both barriers. The barrier material will be keyed into the underlying confining unit and oriented perpendicular to ground-water flow. The barriers will be separated by bentonite. Approximate barrier dimensions (thickness x length x height) will be 0.9 m x 3.0 m x 1.5 m. Many small active and abandoned mine and mill sites throughout the Western United States should be suitable for using these emplacement methods.

References
Freeze, R.A., and Cherry, J.A. (1979) Groundwater, p. 29. Prentice-Hall, Inc. Englewood Cliffs, New Jersey.
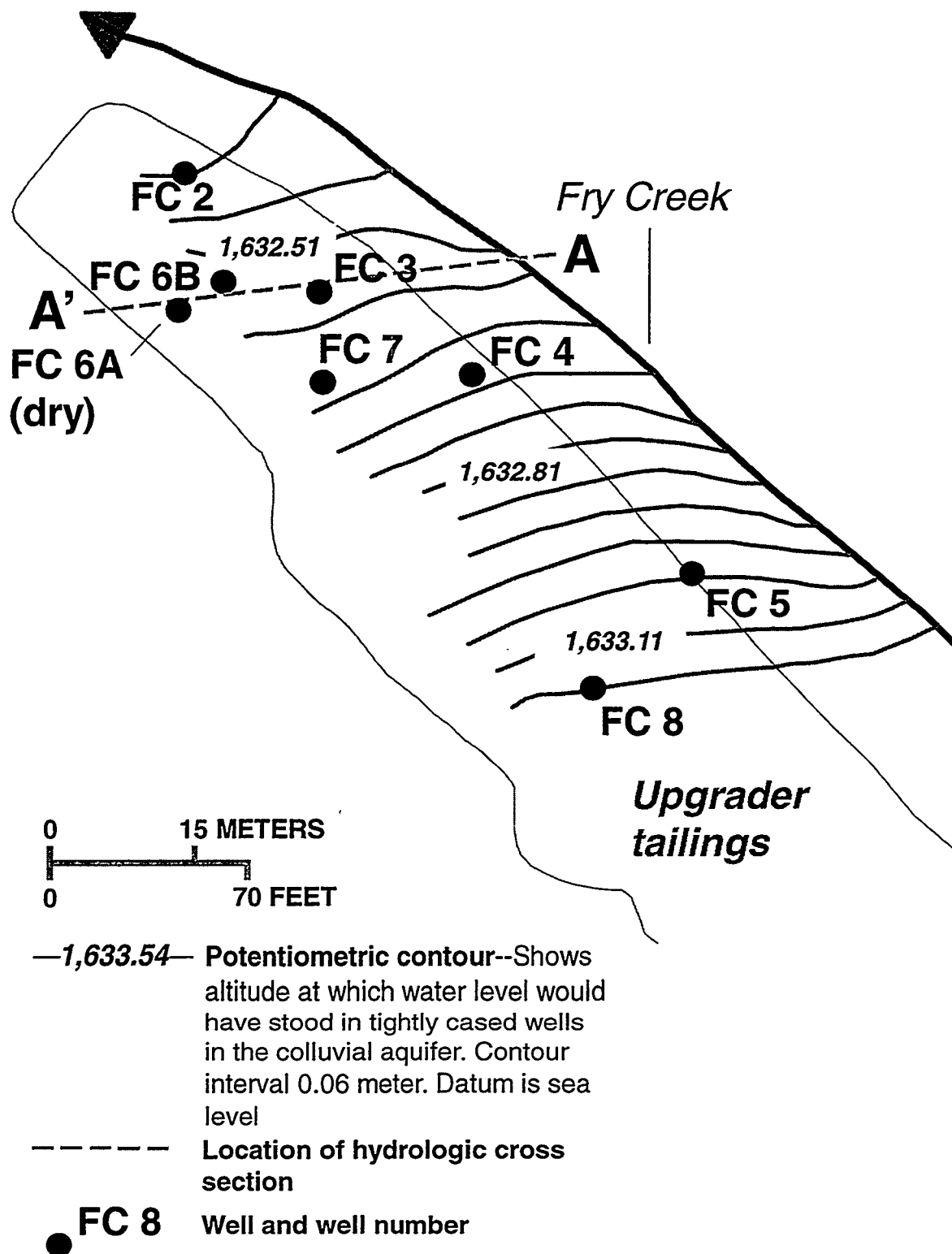
Figure 3. Potentiometric surface of the colluvial aquifer during mid-October 1996 and the location of hydrologic cross section A-A', Fry Canyon, Utah.

BEAR CREEK VALLEY CHARACTERIZATION AREA
MIXED WASTES PASSIVE IN SITU TREATMENT
TECHNOLOGY DEMONSTRATION PROJECT - STATUS REPORT

David Watson[1], Maureen Leavitt[2], Chris Smith[3], Thomas Klasson[4],
Bill Bostick[3], Liyuan Liang[4], and Duncan Moss[2]

Abstract

Historical waste disposal activities within the Bear Creek Valley (BCV) Characterization Area (CA), at the U.S. Department of Energy (DOE) Oak Ridge Y-12 plant, have contaminated groundwater and surface water above human health risk levels and impacted the ecology of Bear Creek (Figure 1 and 2). Contaminates include nitrate, radioisotopes, metals, volatile organic chemicals (VOCs), and common ions. This paper provides a status report on a technology demonstration project that is investigating the feasibility of using passive in situ treatment systems to remove these contaminants (e.g. Figure 3). Although this technology may be applicable to many locations at the Oak Ridge Y-12 Plant, the project focuses on collecting the information needed to take CERCLA removal actions in 1998 at the S-3 Disposal Ponds site (Phase 3).

Phase 1 has been completed and included site characterization, laboratory screening of treatment media (sorbents and iron), and limited field testing of biological treatment systems. Batch tests using different Y-12 Plant waters were conducted to evaluate the removal efficiencies of most of the media. Phase 1 results suggest that the most promising treatment media are Dowex 21k resin, peat moss, zero-valent iron, and iron oxides. Phase 2 (scheduled for completion in 1997) will include in-field column testing of these media to assess loading rates, and concerns with clogging, by-products, and long-term treatment efficiency and media stability. Continued testing of wetlands and algal mats (MATs) will be conducted to determine if they can be used for in-stream polishing of surface water. Hydraulic testing of a shallow trench and horizontal well will also be completed during Phase 2.

Introduction

This project is being conducted to determine if passive in situ treatment systems can be used to meet treatment goals in BCV tributaries and/or groundwater downstream of the tributaries. Given the localized nature of known contaminant pathways and the fractured bedrock geology, the treatment system (e.g. Figure 3) will likely include a trench or horizontal well to capture and treat groundwater by means of a train of individual treatment media to remove the contaminants of concern (i.e., radionuclides, metals, organics). In accordance with treatment needs, the trench may be supplemented by any of three bioremediation technologies: constructed wetlands, MATS, or phytoremediation systems. The level of sophistication required to address the difficult subsurface matrix and the complex array of contaminants requires prudent evaluation of treatment efficiencies and operational issues to determine the optimal remedy for each pathway. The technology demonstration project consists of three phases as follow.

Phase 1: Site characterization and preliminary screening of treatment technologies. The objectives of Phase 1 are to characterize possible demonstration sites near the S-3 Ponds; to screen treatment media; and to conduct preliminary testing of wetlands, MATs, and phytoremediation.

---

[1]Oak Ridge National Laboratory, MS-6400, Oak Ridge, TN, 37831-6400, (423)241-4749, watsondb@ornl.gov

[2]SAIC, Oak Ridge, Tennessee

[3]Lockheed Martin Energy Systems Inc., Oak Ridge Tennessee

[4]Oak Ridge National Laboratory, Oak Ridge, Tennessee

Phase 2: Field evaluations of treatment technologies and hydraulics study. The objective of Phase 2 is to obtain the data needed to design treatment systems for the three pathways identified during phase 1. This will be accomplished by conducting long-term, in-field column tests and by installing two shallow trenchs or horizontal wells and conducting 30-day pumping tests.

Phase 3: Implementation of CERCLA removal action. The objective of Phase 3 is to design and install treatment systems at the three contaminant pathways. The systems will include a groundwater capture trench coupled with in situ or ex situ treatment(s) and, if appropriate, will operate in conjunction with constructed wetlands, MATs, or phytoremediation.

Purpose

This paper provides an update on the status of the project and an overview of the results of Phase 1 media screening and site characterization activities. Additional discussion of the Phase 1 results is provided in the Phase 1 Report (SAIC 1997a). The overall project scope is described in the BCV Technology Demonstration Action Plan (SAIC 1996) and the Phase 2 Workplan (SAIC 1997b). Detailed descriptions of the hydrogeology and contamination of the site is provided in the BCV CA remedial investigation report (LMES 1996). Bostick et al. (In these proceedings) also describe results of some of the iron testing conducted during Phase 1.

Site Setting

The S-3 Ponds (Figure 1) consisted of four unlined ponds constructed in 1951 on the west end of the Y-12 Plant. The ponds had a storage capacity of 40 million liters. Liquid wastes, primarily nitric acid plating wastes containing various metals and radionuclides (e.g., uranium and technetium), were disposed of in the ponds until 1983. Tetrachloroethylene (PCE) was also disposed in the ponds. Pond wastes that remained were neutralized and denitrified in 1984, and the site was capped.

Waste disposal activities at the site have created a mixed waste plume of contamination in the underlying regolith and competent shale bedrock. The ponds are located on a hydrogeologic divide. The plume is over 400 feet deep directly beneath the ponds and extends 4000 feet along geologic strike both east and west of the ponds. Contamination from the plume discharges to three tributaries of Bear Creek (i.e., NT-1, NT-2, and the upper stem of Bear Creek). The total dissolved solids (TDS) content of the groundwater plume is >40,000 mg/L near the ponds. The S-3 plume also contains elevated levels of nitrate and other ions, metals, uranium, technetium, and PCE. The plume is stratified, and the distribution of contaminants is dependent on geochemical characteristics of the contaminants and groundwater. For example, nitrate and technetium, which are not highly particle reactive, have the most extensive distribution in groundwater. Uranium and metals that are more reactive are not as deep and have not migrated as extensively away from the ponds.

Summary of Phase 1 Activities

The scope of phase 1 included the following activities:

- collecting hydraulic and geochemical information on potential S-3 trench installation locations (i.e. adjacent to tributaries NT-1, NT-2, and upper Bear Creek);
- test the ability of sorbents (e.g., zeolites, peat moss, activated carbon, Dowex 21k resin, iron oxides) to remove uranium and other metals from two Y-12 groundwater types;
- test the ability of zero-valent iron (ZVI) to reduce the concentration of uranium and other metals, technetium, nitrate, and VOCs in three Y-12 groundwater types;
- assess the effectiveness of wetlands, MATs, and phytoremediation technology in removing nitrate, uranium, and other metals from contaminated surface water; and
- select trench installation locations and the media to use in Phases 2 and 3.

Field Characterization Activities

The field characterization focused on identifying the major flowpaths for groundwater contaminants to discharge to the tributaries around the S-3 Pond area and select the target sites for trench installation. The following activities were part of the field characterization:

- conducting creek walk-overs to collect field data from surface water and identify seeps;
- on the basis of creek walk-over data, installing 30 temporary 2.54-cm-diameter (1 inch) pushprobes by means of geoprobe technology and conduct chemical analyses; and
- installing four 10-cm-diameter (4 inch) piezometers in primary seepage pathways to collect more complete chemical analyses, conducting pumping tests, and using as a source of water for long-term column tests in Phase 2.

Media Tested

The advice of nationally recognized experts was sought with regard to treatment technologies and media to test as well as potential site-specific issues. On the basis of their ideas, the screening protocols were established and treatment media agents were selected.

The technologies/media in Table 1 were tested with one or more Y-12 water types during Phase 1.

Table 1. Media Tested During Phase 1

Media category	Advantages	Products Tested
Sorbents	Predictable performance, potential low cost and low maintenance	Peat moss, activated carbon, Dowex 21k resin, iron oxides, amberlite IRC-718, zeolites, TRW coal-based sorbent, biobeads, phosphate rock, Ionac SR-4
Zero-valent iron	Extended treatment periods possible; passive; potential low cost	Masterbuilder, Fisher, palladium-coated, cercona iron foam
Biological means	Passive; affects both metals and nitrate	Wetlands, algal mats, phytoremediation

Water Types Tested

Four types of Y-12 site water were collected and used for Phase 1 testing. The water types, characteristics, and primary media tested are listed in Table 2.

Table 2. Y-12 Water Types Tested During Phase 1

Water source	Media tested	Characteristics
East End (VOCs only)	ZVI, and activated carbon	Carbon tetrachloride dominated (1 mg/L)
Boneyard/Burnyard (BYBY) water	Sorbents, Zero-valent iron	Uranium (1 mg/L), VOCs (1 mg/L PCE, 1,1,1-trichloroethane and), low TDS (<1000 mg/L)
S-3 Ponds (NT-1 piezometer)	Sorbents, ZVI, algal MATs, and phytoremediation	high TDS (up to 40,000 mg/L), nitrate (up to 20,000 mg/L), metals, technetium (>10,000 pCi/L), low pH (4-6) and PCE (<1 mg/l)
Spring SS-4	Wetlands and algal mats	Low TDS, uranium (0.2 mg/L), and nitrate (70 mg/L)

Other inorganics and their maximum concentrations at the S-3 Ponds NT-1 site are barium (380 mg/L), cadmium (4 mg/L), calcium (>10,000 mg/L), strontium (340 mg/L), zinc and nickel (20 mg/L), and copper (3.1 mg/L).

In some instances, the natural waters were spiked with higher levels of VOCs and uranium to represent possible worst-case conditions.

Phase 1 Results

Specific findings are noted in the following subsections.

Field Characterization

Field characterization efforts have delineated three primary pathways for contaminated groundwater to discharge to surface water (Figure 1) at the S-3 site.

- Two shallow pathways (pathways 1 and 2; Figure 1) conduct uranium-contaminated groundwater to the main stem of Bear Creek adjacent to the former S-3 Ponds. Groundwater in pathway 1 is also contaminated with high TDS, nitrate, technetium, and elevated levels of some metals. Groundwater in pathway 2 is primarily contaminated with uranium and has lower TDS content.
- One deeper along strike pathway (pathway 3; Figure 1) conducts nitrate, PCE, technetium, metals, and high TDS-contaminated groundwater to NT-1. This deeper along strike flow path extends to NT-2 although, at NT-2, some of the metals and VOCs are not present.

The use of trenches or horizontal wells to intercept contaminated groundwater prior to discharging to the tributaries appears feasible at all three pathways.

Treatment Technologies

Uranium removal - Most of the technologies/media from all categories showed positive results for uranium removal in low TDS water (i.e., BYBY) (Figure 4). For this water type the best sorbent performers were Dowex 21K resin (>18mg/g), peat moss (4 mg/g), and iron oxides (powdered form only). In some cases (Dowex 21K resin), the agent's loading capacity under equilibrium conditions could not be determined because the media achieved maximum uranium removal at all concentrations tested. ZVI also efficiently removed uranium through reduction and precipitation and/or through corrosion, precipitation, and sorption mechanisms. MATs (70-100% removal) and the constructed wetlands (30-46% removal) were able to remove uranium from surface water containing lower concentrations of uranium (<0.2 mg/L).

Very few media were able to provide uranium removal under the high TDS conditions in NT-1 piezometer water (Figure 4). The principle interference in NT-1 appears to be nitrate, although high calcium and aluminum concentrations also contributed to low removal by several sorbents. Peat moss had lower removal efficiencies in this water, but still provided 0.9 mg uranium removed per gram of peat moss used. Zero valent iron is also a candidate for treating of S-3 water. The long-term potential for uranium mobilization will be assessed during Phase 2 column testing.

Metals Removal - Sorbents were relatively ineffective in removing other metals from NT-1 test water. Amberlite IRC-718 and MATs removed some metals from the NT-1 water but not enough to continue as a primary treatment mechanism for the more concentrated groundwater. MATs showed promising results for removing aluminum, barium, calcium, cadmium, magnesium, manganese, nickel and strontium from more dilute surface water (e.g., SS-4 water). ZVI removed metals during batch experiments, but not during preliminary column experiments. This discrepency is attributed to pH changes and more rapid corrosion of ZVI in batch tests and the longer residence time for metals to be exposed to the iron (in comparison with residence times in column tests).

Nitrate Removal - Nitrate removal is an important consideration, as demonstrated by nitrates interference on removal of other contaminants in NT-1 water. Some nitrate reduction in the lower concentration surface water was observed in the wetlands and MATs systems, but more testing is required to establish the maximum rate of removal. In addition, the effect of biomass grown in a peat moss/ZVI environment is also being evaluated as a potential medium for nitrate removal. This combination of components appears to provide a reducing environment, a support matrix, and some degradable carbon to support nitrate removal. Further investigation of these options will be continued in Phase 2.

VOC Destruction - Both Fisher and Masterbuilder iron removed VOCs from test water but Masterbuilder iron produced a shorter half-life than Fisher iron. The half-lives of Masterbuilder and Fisher iron were <1.0 hours and >11 hours, respectively, for batch studies conducted on BYBY water containing PCE and trichloroethylene (TCE). For 1,1,1-TCA, the half-lives were 1.21 hours and 4.18 hours, respectively. Palladium coating enhanced the effectiveness of both iron forms, but the gain may be too small to compensate for the added cost of palladium treatment. The calculated half-life for palladium-coated Masterbuilder iron was 0.21 hours while the uncoated was 0.25 hour. The rate of degradation for daughter products of carbon tetrachloride (chloroform and dichloromethane) were too slow for Fisher iron to be a viable candidate for treatment of carbon tetrachloride. Further investigation of the fate of daughter products will be performed in Phase 2.

Phase 1 Conclusions

Contaminants reach Bear Creek through at least 3 discrete pathways in fractured bedrock. Conceptual treatment systems (e.g. Figure 3) for each of the contaminant pathways were developed by considering chemical, hydraulic, and waste management/discharge issues.

The following table describes the treatment media, target contaminants, and the issues to be resolved in Phase 2.

Table 3. Concerns to be resolved in Phase 2.

Media	Targets	Issues
Dowex 21K resin	Uranium	Reduced performance with elevated TDS, effective only for uranium
Peat Moss	Uranium, metals, VOCs, nitrate	Unsure of long-term performance
Zero-valent iron	Uranium, metals, VOCs	Colloid release of Uranium; VOC byproducts
Iron oxides	Uranium, VOCs	Colloid release of uranium
Algal Mats	Uranium, metals, nitrate	Requires sunlight, nitrate reduction capacity unclear, full-scale engineering needed
Wetlands	Uranium, nitrate	Fate of accumulated uranium, winter effects
TRW	Uranium	Not commercially available, effective only for uranium

References

Energy Systems (Lockheed Martin Energy Systems, Inc.). 1996. *Report on the Remedial Investigation of Bear Creek Valley at the Oak Ridge Y-12 Plant*, Oak Ridge, Tennessee, DOE/OR/01-1455/D1/V1-V6.

SAIC. 1996. *Bear Creek Valley Characterization Area Technology Demonstration Action Plan.* Y/EN-5479.

SAIC. 1997a. *Bear Creek Valley Technology Demonstration Phase 1 Report.* 96-128PS/013097.

SAIC. 1997b. *Treatability Study on the Bear Creek Valley Characterization Area at the Oak Ridge Y-12 Plant, Oak Ridge, Tennessee, Phase II Work Plan.* Y/ER-278

Figure 1. Contaminant migration pathways.

NT-2
| NITRATE - BOTH >50 mg/L |
| URANIUM - <0.003-0.037 ppm |
| GROSS ALPHA - 97-1581 pCi/L |
| GROSS BETA - 78-824 pCi/L |

GW-835
| NITRATE - 29 mg/L |
| URANIUM - 1.7 mg/L |
| GROSS ALPHA - 370 pCi/L |
| GROSS BETA - 280 pCi/L |
| TECHNETIUM - 150 pCi/L |

GW-834
| NITRATE - 2300 mg/L |
| URANIUM - 0.0037 mg/L |
| GROSS ALPHA - 9000 pCi/L |
| GROSS BETA - 78-824 pCi/L |
| TECHNETIUM - 22,000 pCi/L |

GW-837
| NITRATE - 1400 mg/L |
| URANIUM - 2.6 mg/L |
| GROSS ALPHA - 790 pCi/L |
| GROSS BETA - 4300 pCi/L |
| TECHNETIUM - 10,000 pCi/L |
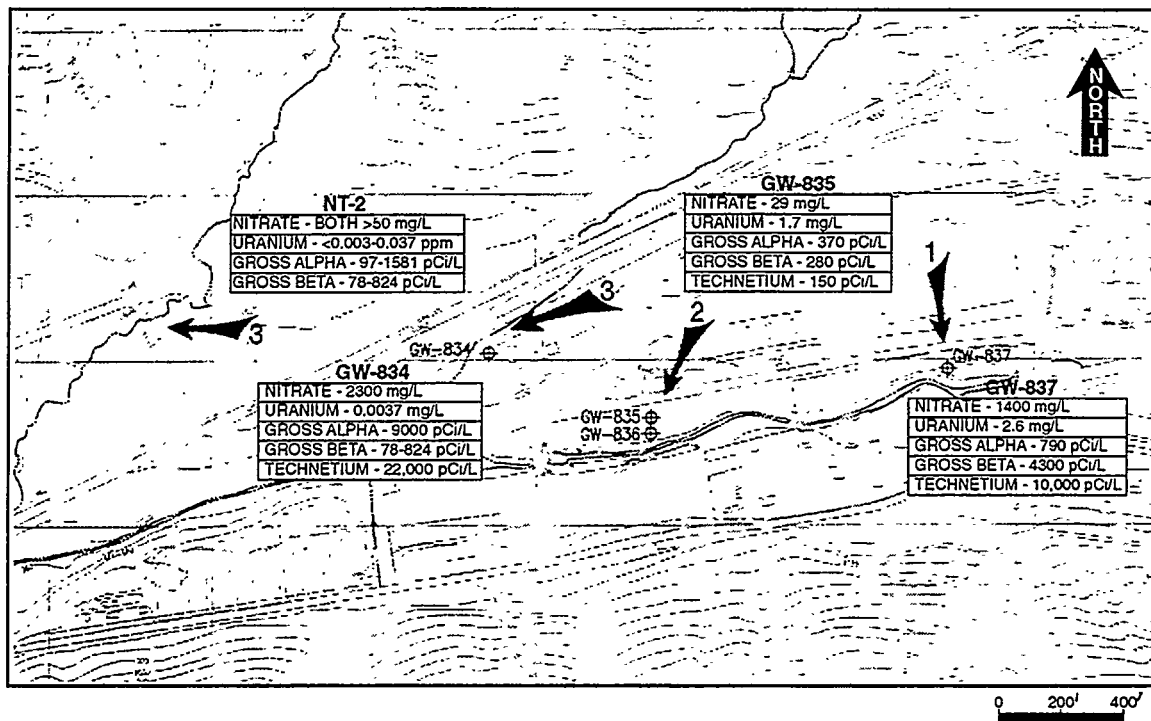
Figure 2. Conceptual model of groundwater transport.

Density driven

Updip migration of plume

Along strike flow of plume >100 ft deep

■ > 10,000 mg/L nitrate
▨ 1,000 - 10,000 mg/L nitrate
☐ 100 - 1,000 mg/L nitrate

BC-140

735
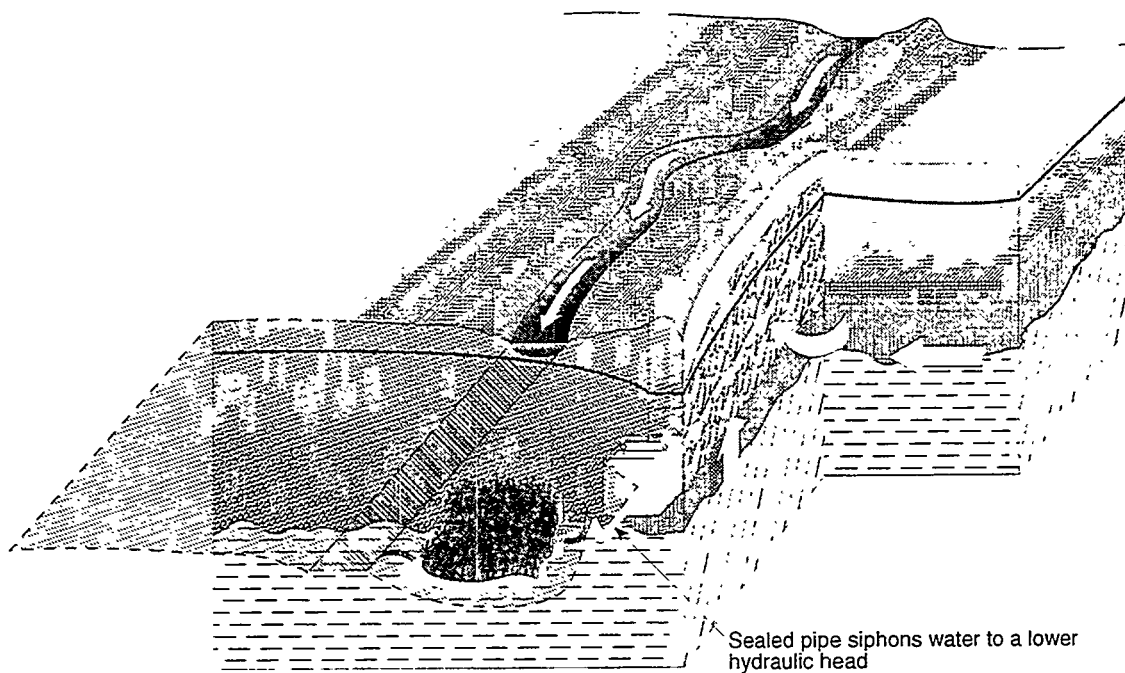
Figure 3. Conceptual treatment system design.

(a) BYBY Water

(b) NT-1 Water
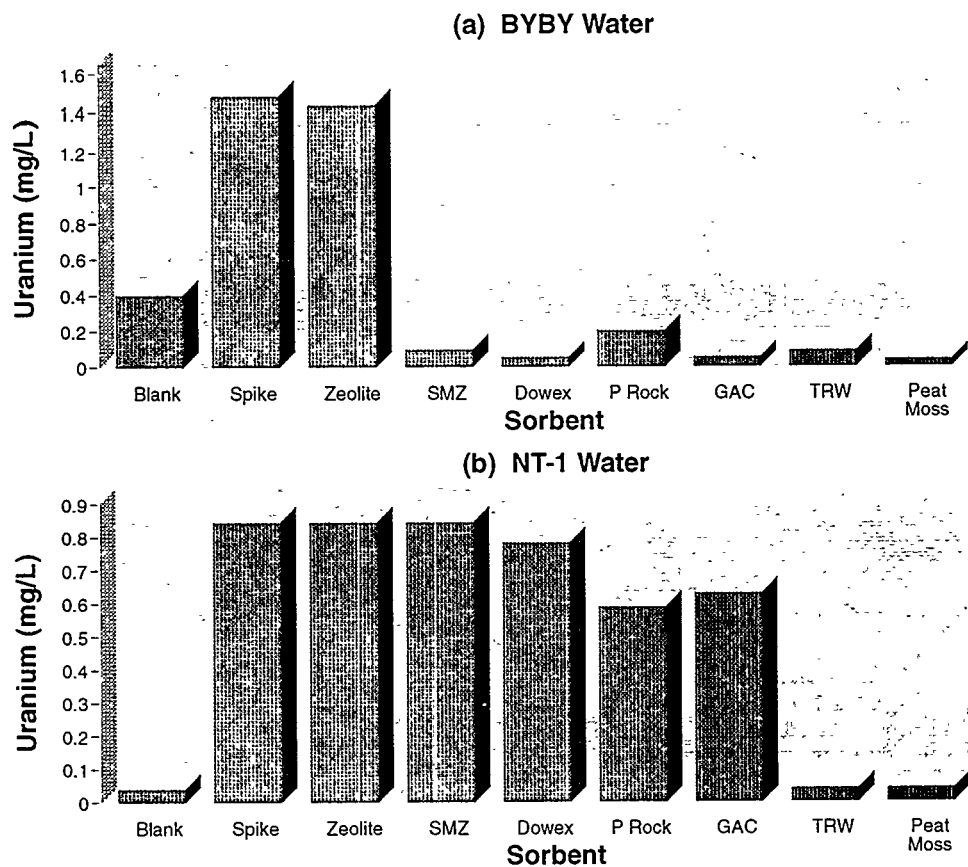
Figure 4. Batch study results from (a) low ionic strength BYBY water,
(b) high ionic strength NT-1 piezometer water.

In Situ Precipitation and Sorption of Arsenic from Groundwater: Laboratory and Ex Situ Field Tests

Joyce M. Whang, [1] Kofi Adu-Wusu, [2] William H. Frampton, [3] J.Gray Staib[3]

Abstract

Permeable, reactive walls may provide long term, low-maintenance prevention of off-site migration of contaminated groundwater. Laboratory and ex situ field tests conducted on several arsenic-contaminated groundwaters indicate that both precipitation and sorption can remove arsenic to levels of less than 10 ppb. Precipitation has been induced by adjusting pH, adding selected cations, and/or reducing the oxidation-reduction potential. Adjusting pH or adding cations was most effective when there were high levels of other ionic species with which arsenic could coprecipitate. Reducing the oxidation-reduction potential was effective on a variety of groundwaters. Humate was an effective sorbent at low pH; aluminum and iron materials were effective over a large range of conditions. Long term performance of precipitation systems can be limited by formation of precipitate on reactive surfaces. Long term sorption can be reduced by competing ions, such as phosphate. Laboratory and ex situ field tests indicate that reactive walls may have lifetimes of decades or more.

Introduction

Laboratory and ex situ field tests have been conducted to determine the likely efficacy of various materials that could be used in permeable, reactive walls to treat arsenic-contaminated groundwater. Previous investigators have measured high rates of sorption of arsenate to iron (Fuller, et al., 1993) and aluminum (Anderson and Malotky, 1979) materials. Other investigators have also shown that zero-valent iron removes heavy metals from groundwater, apparently by reductive precipitation (Cantrell, et al., 1995). Data on inorganic chemistry (Weast, 1980) further indicate conditions under which chemicals can be precipitated from groundwater. Identification of optimal materials for field applications is likely to be groundwater-specific. Laboratory and ex situ field tests were conducted with several arsenic-contaminated site groundwaters. The materials tested were selected based on expected (1) effectiveness at removing arsenic, (2) availability in large quantities at low cost, (3) high permeability, and (4) low toxicity.

Materials

Laboratory jar tests for were conducted with reagent grade forms of the following: $Ca(OH)_2$, $Mg(OH)_2$, $CaCO_3$, $MgCO_3$, $CaCl_2$, $CaSO_4$. Technical grades of bauxite, activated bauxite, and activated alumina were also tested. The humate tested was a highly weathered soil organic matter that was produced from the mining of titanium ore in Stark, Florida. Iron-based industrial mixes were co-products from the processing of titanium ore. "Industrial FeOOH mix" contained primarily FeOOH, $Fe(OH)_2$, and $Fe(OH)_3$. "Industrial $FeCO_3$ mix" was primarily $FeCO_3$. These mixes also contained other metal hydroxides and metal carbonates, respectively.

Laboratory column tests were conducted with 4- and 8-mesh Drierite-brand $CaSO_4$. The median diameters of these materials were 7 and 4 mm, respectively. Ex situ field column tests were conducted with zero-valent iron filings; crushed, sieved bauxite; and site sand. The iron was Peerless brand, 8-16 mesh. Two sizes of bauxite were used: 4-mesh - 10 mm and 8-10 mesh.

[1] DuPont Specialty Chemicals, Jackson Laboratory J-24, Chambers Works, Deepwater, NJ 08023, (609)540-4275, whangjm@a1.jlcl01.umc.dupont.com
[2] DuPont Central Research and Development, G300, P. O. Box 6101, Newark, DE 19714
[3] DuPont Central Research and Development, Experimental Station, Wilmington, DE 19880

Groundwater was tested from 5 wells from 3 sites. Table 1 gives some of the key constituents of the groundwaters tested.

Methods

Precipitation Tests

Jar tests were conducted by adding 100 mL of contaminated groundwater to powdered precipitant. In most cases, 1 to 6 g precipitant was used. For some tests, as little as 0.3 g or as much as 250 g was used. The mixtures were shaken vigorously for 1 minute, and then less rapidly for 16 to 24 hours. pH was measured, and filtered samples were analyzed using graphite furnace atomic absorption spectroscopy.

Sorption Tests

Batch sorption tests were conducted by adding 20 mL of contaminated groundwater to known masses of sorbent material in glass centrifuge tubes. Several soil-solution ratios were used. The bottles were rotated end-over-end in a tumbler for 24 hours at 8 rpm. At the end of the 24-hour equilibration period, the soil-solution mixtures were centrifuged for 10 minutes at 9500 rpm to separate the solids. After centrifugation, supernatant was removed and analyzed for arsenic using graphite furnace atomic absorption spectroscopy.

Freundlich isotherm plots were used to evaluate results from several soil-solution ratios. Using these isotherms, sorbent usage rates were estimated based on the initial arsenic concentration in the groundwater. The potential lifetimes over which sorbing walls would be effective were then calculated for 1 m walls and 7.5 cm/day groundwater velocity according to the following formula: lifetime = (wall thickness)*(bulk density)/(porosity)/(velocity)/(usage rate).

Laboratory Column Tests

Laboratory column studies were conducted using an Ismatec variable speed peristaltic pump to drive groundwater through flexible wall columns containing $CaSO_4$ particles. The columns, of diameter 4.1 to 4.7 cm, had 6.4 to 8.6 cm of $CaSO_4$ followed by 1.3 to 3.0 cm of sand. Porous stones on the two ends of the column helped distribute the flow of groundwater across the cross section. The column materials were held in heat shrink tubing under confining pressure. Groundwater was pumped at velocities equivalent to groundwater flow of 1.8 m/day through an aquifer of 30% porosity. This elevated flow rate was used to expedite the experiment. Water samples were collected during the tests and analyzed for phosphorus, arsenic, calcium, sulfur, and/or pH.

Ex Situ Field Column Tests

In ex situ field column tests, water was pumped directly from a well to columns of reactant materials. 7 columns were run in parallel. A gear pump or a peristaltic pump was used to pump groundwater from the well to a manifold system with an overflow. An 8-cartridge Ismatec variable speed peristaltic pump was used to deliver groundwater from the manifold to the columns. Table 2 gives the specifications for the columns. Column 1 was made with the 4-mesh - 10 mm bauxite. Columns 3, 4, and 5 were made with the 8-10 mesh bauxite. Column 6 was made with an 80/20 mixture of sand and 8-10 mesh bauxite.

Table 1. Key constituents of groundwaters tested

	As, ppb	Fe, ppm	P, ppm	SO$_4$, ppm	pH
Site 1	1000	<0.5	1400	300	8
Site 2, Well 1	10000	800	40	9500	2
Site 2, Well 2	1000	8	<1	800	7
Site 2, Well 3	150	30		1700	6
Site 3	250	30	1700		6.5

Results

Batch sorption tests and precipitation jar tests were conducted for removing arsenic from the various groundwaters. Tables 3 through 7 give the results of these tests.

Table 2. *Ex situ field column tests*

Column	material	diameter cm	length cm	flow rate mL/min	residence time hr	average linear velocity cm/day
1	bauxite	11	91	1.4	56	39
2	iron	11	91	1.5	61	36
3	bauxite	4.6	5	0.20	4	29
4	bauxite	4.6	10	0.18	9	26
5	bauxite	1.4	48	5.1	0.1	9200
6	sand/bauxite	1.4	51	5.1	0.1	12000
7	iron	1.4	42	5.9	0.1	8300

Table 3. Site 1: 1000 ppb As, 1400 ppm P, pH 8

Precipitation Tests

Precipitant	g/(100mL)	final As, ppb	final P, ppm	final Ca, ppm	final pH
$CaCO_3$*	3.5	900	1000	2.3	9.1*
$Mg(OH)_2$*	3.4	800	330		10.9*
$Ca(OH)_2$	3.4	<10	<1		12.5
$CaCl_2$	2.6	10	1.2	12000	5.2
$CaSO_4$	5.7	700	12	720	7.2
$CaSO_4$ and $Mg(OH)_2$	1.4 1.0	<10	2.7	120	9.5

* these tests were conducted 8 months later; initial pH was 9.6

Sorption Tests

Sorbent	final As, ppb	final P, ppm	life, years
industrial FeOOH mix	<10	<1	3
activated alumina	<10	7	1
industrial $FeCO_3$ mix	<10	9	2

Table 4. Site 2, Well 1: 10000 ppb As, 800 ppm Fe, 9,500 ppm SO_4, pH 2

Precipitation Tests

Precipitant	g/(100mL)	final As, ppb	final pH
$Ca(OH)_2$	0.3	8	2.8
$CaCO_3$	0.4	6	2.9
$Mg(OH)_2$	0.4	<5	4.9
$MgCO_3$	0.5	<5	4.4

Sorption Tests

Sorbent	final As, ppb	final pH	life, years
humate	<5	3.5	30
activated alumina	<5		10
activated bauxite	9	6.2	3

Table 5. *Site 2, Well 2: 1000 ppm As, 8 ppm Fe, 800 ppm SO$_4$, pH 7*

Precipitation Tests

Precipitant	g/(100mL)	final As, ppb	final pH
Ca(OH)$_2$	2.8	300	12.5
CaCO$_3$	3.8	1300	7.6
Mg(OH)$_2$	3.6	300	9.8
MgCO$_3$	5.2	1000	9.3
Fe^0	10	660	9.0
Fe^0	30	150	9.2
Fe^0	100	<5	9.7

Sorption Tests

Sorbent	final As, ppb	life, years
activated bauxite	<5	400
activated alumina	15	300
industrial FeCO$_3$ mix	<5	
bauxite	24	

Table 6. *Site 2, Well 3: 150 ppb As, 30 ppm Fe, 1700 ppm SO$_4$, pH 6*

Precipitation Tests

Precipitant	g/(100mL)	final As, ppb	final pH
Ca(OH)$_2$	2.8	<5	11.9
CaCO$_3$	3.8	130	6.0
Mg(OH)$_2$	3.6	<5	9.3
MgCO$_3$	5.2	60	8.1
Fe^0	250	<5	7.2

Sorption Tests

Sorbent	final As, ppb	final pH
activated alumina	<20	10.6
industrial FeCO$_3$ mix	<20	6.4
bauxite	<20	5.8
industrial FeOOH mix	<20	7.1

Table 7. *Site 3: 250 ppb As, pH 6.5*

Sorption Tests

Sorbent	final As, ppb	final pH	life, years
activated bauxite	16	6.9	4000
bauxite	40	6.4	800
industrial FeCO$_3$ mix	50	6.5	700
activated alumina	30	7.6	100

Laboratory column tests were conducted in which groundwater from Site 1 was pumped through columns of CaSO$_4$ particles. Arsenic removal was poor. Phosphorus was initially removed to <50 ppm. After 1.5 to 2 days, phosphorus in the water treated with 4-mesh CaSO$_4$ rose. Calcium in the treated water dropped at this time. Phosphorus remained low in the 8-mesh-treated water until 4.7 days, when calcium dropped. The 8-mesh CaSO$_4$ treated three times as much water as the 4-mesh CaSO$_4$ before phosphorus levels rose to greater than 100 ppm.

Ex situ field column tests were conducted at Site 3. In Columns 1 and 2, which were designed to simulate expected residence time in a reactive wall, arsenic was consistently removed to <10 ppb by bauxite and by zero-valent iron. Zinc was also removed by the zero-valent iron column from 10 ppm to <10 ppb. In Columns 2 and 3, which were designed to simulate expected ground water velocities in a reactive wall, arsenic was again removed to <10 ppb by bauxite. Figure 1 shows the cumulative removal of arsenic in Columns 5 to 7.

Discussion

Lime, dolomite

Increasing pH was effective for removing some or all of the arsenic in all of the groundwaters tested. It was most effective in the low pH groundwater of Site 2, Well 1 (Table 4). In this case, slight increases in pH resulted in reduction of arsenic to <10 ppb. In the high phosphorus groundwater from Site 1 (Table 3), arsenic was removed to <10 ppb only when pH was raised to 12.5. In the neutral groundwaters of Site 2, Wells 2 and 3 (Tables 5 and 6), arsenic removal increased with increasing pH. However, arsenic level remained high even at pH 12.5 in the 1000 ppb arsenic groundwater of Site 2, Well 2.

It is theorized that the removal of arsenic in these cases is primarily by coprecipitation. The low pH groundwater of Site 2, Well 1 has high levels of iron and other metals that precipitate quickly with slight increases of pH. Arsenic in wastewater is commonly treated by coprecipitation with iron. The equilibrium of phosphorus, which is present at high levels in Site 1 groundwater, shifts from the monoprotonated state (HPO_4^{2-}) to the unprotonated state (PO_4^{3-}) at pH 12.3. Unprotonated phosphate salts (e.g. $Ca_3(PO_4)_2$) are usually less soluble than monoprotonated phosphate salts (e.g. $CaHPO_4$) (Weast, 1980).

Calcium salts

Arsenic was removed from the groundwater of Site 1 when calcium concentration was increased using calcium salts (Table 3). With the addition of the highly soluble salt calcium chloride, arsenic was removed to 10 ppb. The less soluble salt calcium sulfate had less impact on arsenic concentration.

Again, it is theorized that arsenic is being removed primarily by coprecipitation. As seen in Table 3 addition of calcium salts also reduced the concentrations of phosphorus in this groundwater. At neutral pH, the monoprotonated and diprotonated forms of phosphate dominate, and the calcium salts of these anions (i.e. $CaHPO_4$ and $Ca(H_2PO_4)_2$) have high enough solubility that very high levels of calcium are needed to precipitate most of the phosphorus.

Figure 1. Cumulative arsenic removal in ex situ field column tests.
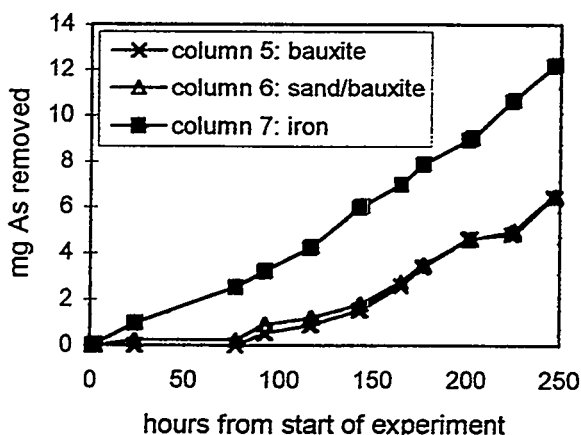
Calcium chloride is so soluble that it would be difficult to build a long-lasting wall of it. It might be possible to treat arsenic at Site 1 by injecting calcium chloride solution. A wall could be built using calcium sulfate, or its widely available, less pure form gypsum, to remove much most of the phosphorus and some of the arsenic.

Zero-valent iron
Zero-valent iron was often effective in removing arsenic from the neutral pH groundwaters of Site 2, Wells 2 and 3 (Tables 5 and 6) and Site 3 (Figure 1).

Zero-valent iron creates reducing conditions. Under reducing conditions, arsenic shifts from the +5 valence of arsenate (AsO_4^{3-}) to the +3 valence of arsenite (AsO_3^{3-}) to the unoxygenated +3 valence (As^{3+}) (Ferguson, 1972). Sulfate (SO_4^{2-}) is reduced to sulfide (S^{2-}). Hence, arsenic may precipitate as the highly insoluble arsenic sulfide (As_2S_3), or it may coprecipitate with ferrous sulfide (FeS).

Sorbents
Arsenic was readily sorbed by many aluminum-, iron-, and humus-based materials. As indicated in Tables 5 and 7, batch tests indicate that a 1 m wall of these sorbing materials can often be expected to be effective for removing arsenic for theoretical lifetimes of hundreds of years or more. Lifetime is reduced when there are high concentrations of competing ions, such as the phosphorus of Site 1 (Table 3), or when pH is very low, as at Site 2, Well 1 (Table 4).

Combination technologies
For Site 1 (Table 3), tests indicated that arsenic can be reduced to less than 10 ppb by using calcium sulfate and magnesium hydroxide to attain modest increases of pH and calcium concentration. Such a combination technology may be implemented more easily than calcium hydroxide or calcium chloride alone, because (1) there is less concern about excessively high pH resulting from using calcium hydroxide alone, and (2) less salt is need to reach these intermediate calcium levels than to reach the calcium levels associated with calcium chloride. The increase of pH causes a shift of phosphate from the diprotonated state ($H_2PO_4^-$) to the monoprotonated state (HPO_4^{2-}). The monoprotonated calcium phosphate salt ($CaHPO_4$) is about two orders of magnitude less soluble than the diprotonated calcium phosphate salt ($Ca(H_2PO_4)_2$) (Weast, 1980).

Table 3 shows that a sorbing wall is expected to be effective for a lifetime of only a few years for the groundwater of Site 1. As discussed above, this is probably because of the high levels of phosphorus in this groundwater. However, Table 1 also shows that calcium sulfate is effective for removing phosphorus from the groundwater of Site 1. Hence, it may be most feasible to remove arsenic from the groundwater of Site 1 using a wall having two layers. Groundwater would first pass through a calcium sulfate layer, where most of the phosphorus and some of the arsenic would be precipitated. Groundwater would then pass through a finishing layer of sorbent, where arsenic would be removed. By using this approach, it may be possible to design a wall with a longer effective lifetime.

Long-term removal based on laboratory column tests
In laboratory column tests using calcium sulfate as a precipitant, arsenic removal was minimal, but phosphorus was initially removed to very low levels. These results were expected based on jar tests (Table 3). This test was conducted (a) because calcium sulfate could be used in conjunction with an a sorbing material, and (b) to determine the long term effectiveness of precipitation removal. As indicated above, 8-mesh calcium sulfate treated three times as much water as the 4-mesh calcium sulfate. This ratio is consistent with the ratio of surface areas expected for these particles based on median diameters of 7 and 4 mm. These results suggest that phosphorus removal is limited by surface area of the precipitant. The highest concentrations of calcium in solution are near the precipitant surfaces, so precipitation is expected to occur near these surfaces. Precipitation on the surface reduces the solubility of the calcium sulfate, resulting in less calcium in solution and less phosphorus removal.

If removal of phosphorus is directly proportional to surface area and inversely proportional to the square of the average particle diameter, then the results from this experiment can be extrapolated to estimate that a 1 m thick wall of 1.0-1.3 mm particles of calcium sulfate would remove phosphorus from a 1400 ppm phosphorus, 15 cm/day groundwater for a lifetime of 20 years.

Long-term removal based on ex situ field tests

The results in Figure 1 show that arsenic was still being removed at a high rate at the end of this experiment. However, based on the total removals measured, lower bound estimates can be calculated for the lifetimes of 1 m thick walls intercepting a 400 ppb arsenic, 7.5 cm/day groundwater. These calculations indicate an iron wall would remove arsenic for at least 50 years. A wall of bauxite or a sand/bauxite mixture would remove arsenic for at least 20 years. Note that because the sand/bauxite mixture is 20% bauxite, a pure bauxite wall could actually be expected to remove arsenic for at least 100 years.

Conclusions

Laboratory tests indicate conditions under which the following materials may be effective for removing arsenic from groundwater.

- lime, dolomite, to increase pH
- $CaCl_2$, $CaSO_4$ to increase calcium concentration
- zero-valent iron to create reducing conditions
- aluminum-, iron-, and humus-based materials to sorb the arsenic

Lime, dolomite, $CaCl_2$, and $CaSO_4$ were most effective when there were high levels of other ionic species with which arsenic could coprecipitate. Reducing the oxidation-reduction potential was effective on a variety of groundwaters. Humate was an effective sorbent at low pH; aluminum and iron materials were effective over a large range of conditions. Certain ions, such as phosphate, compete with arsenic for sorption sites and reduce the long term effectiveness of sorbents. In some cases, combinations of materials may lead to less extreme conditions or longer expected wall lifetimes. Selection of materials is very site-specific.

Batch sorption tests have indicated that some sorbing materials may be expected to treat groundwater for theoretical lifetimes of hundreds or thousands of years. Laboratory studies indicate that in cases of high levels of precipitation, long term performance can be limited by formation of precipitate on reactive surfaces. Limited ex situ field column tests have indicated lifetimes of decades or more. Further testing is needed to better determine expected lifetimes.

References

Anderson, M.A., D.T. Malotky. (1979) The adsorption of protolyzable anions on hydrous oxides at the isoelectric pH. *J. Colloid Interface Science, 72(3)*, 413-427.

Cantrell, K.J., D.I. Kaplan, T.W. Wietsma. (1995) Zero-valent iron for the in situ remediation of selected metals in groudnwater. *J. Haz. Mat., 42*, 201-212.

Ferguson, J.F., J. Gavis. (1972) A review of the arsenic cycle in natrual waters, *Water Research, 6:* 1259-1274.

Fuller, C.C., J.A. Davis, G.A. Waychunas. (1993) Surface chemistry of ferrihydrite: part 2: kinetics of arsenate adsorption and coprecipitation. *Geochimica et Cosmochimica Acata, 57*, 2271-2282.

Weast, R.C. (1980) *CRC Handbook of Chemistry and Physics*, CRC Press, Inc, Boca Raton, Florida.

USE OF A PERMEABLE BIOLOGICAL REACTION BARRIER FOR GROUNDWATER REMEDIATION AT A URANIUM MILL TAILINGS REMEDIAL ACTION (UMTRA) SITE

Milind S. Thombre, Bruce M. Thomson[*], Larry L. Barton[**]

Department of Civil Engineering, University of New Mexico, Albuquerque, NM 87131, Phone: (505) 277-2722, Fax: (505) 277-1988

ABSTRACT

Previous work at the University of New Mexico and elsewhere has shown that sulfate reducing bacteria are capable of reducing uranium from the soluble +6 oxidation state to the insoluble +4 oxidation state. This chemistry forms the basis of a proposed groundwater remediation strategy in which microbial reduction would be used to immobilize soluble uranium. One such system would consist of a subsurface permeable barrier which would stimulate microbial growth resulting in the reduction of sulfate and nitrate and immobilization of metals while permitting the unhindered flow of ground water through it.

This research investigated some of the engineering considerations associated with a microbial reducing barrier such as identifying an appropriate biological substrate, estimating the rate of substrate utilization, and identifying the final fate of the contaminants concentrated in the barrier matrix.

The performance of batch reactors and column systems that treated simulated plume water was evaluated using cellulose, wheat straw, alfalfa hay, sawdust, and soluble starch as substrates. The concentrations of sulfate, nitrate, and U(VI) were monitored over time. Precipitates from each system were collected and the precipitated U(IV) was determined to be crystalline $UO_{2(s)}$ by X-ray Diffraction.

The results of this study support the proposed use of cellulosic substrates as candidate barrier materials.

INTRODUCTION

Uranium contaminated ground and surface waters near abandoned mill tailings piles is a matter of concern in many western United States. Inexpensive and effective remediation techniques are needed which separate uranium and other contaminants from aqueous waste plumes. In nature, uranium generally exists in either the U(VI) or the U(IV) oxidation state. Under oxidizing conditions U(VI) is present as the uranyl ion UO_2^{2+} which is soluble in water and, therefore, mobile in the aqueous environment. Under reducing conditions insoluble U(IV) is stable and presents a smaller threat to water resources. In recent years, several researchers have discovered that anaerobic bacteria can mediate the reduction of U(VI) to U(IV). Sulfate reducing bacteria have been found to be capable of reducing U(VI) with subsequent precipitation of U(IV) species (Lovley and Phillips, 1992, Barton et al, 1995). This knowledge forms the basis of a proposed remediation strategy for containment and remediation of groundwater associated with a Uranium Mill Tailings Remedial Action (UMTRA) site near Shiprock, NM. The proposed system involves the use of a permeable biological reaction barrier.

A permeable barrier is defined as an in-situ wall that intercepts a contaminated groundwater plume and treats through various physical, chemical, or biological reactions. Remediated groundwater passes through the barrier with minimal impact on the ground water hydrology (Thomson et al., 1991, Thombre et al., 1996). A conceptual representation of the proposed permeable reaction barrier is presented in Figure 1.

The principal contaminants at the Shiprock site include high concentrations of U, SO_4^{-2}, NO_3^-, and selenium (Se). The mechanisms for removal of the contaminants are microbial reduction of NO_3^- and SO_4^{-2} and subsequent precipitation of U. Under strongly reducing conditions provided by sulfate reduction, U(VI) has been found to be removed as insoluble U(IV) phase $UO_{2(s)}$. However, most U(VI) reduction work to date has focused on pure cultures of sulfate reducing bacteria using low molecular weight organic acids as substrates. These substrates are not practical for an actual application due to their high cost and the fact that they

---

[*] To whom all correspondence should be addressed, e-mail bthomson@unm.edu
[**] Department of Biology, University of New Mexico, Albuquerque, NM 87131, Phone: (505) 277-2537

would be quickly degraded, thus providing a short usable life for a remediation process. The ideal barrier material should satisfy the following criteria

1) support bacterial growth over the design period of the permeable barrier;
2) be relatively inexpensive and readily available;
3) comprise a manageable volume for use in such a barrier.

It is postulated that plant residues can meet these criteria.

The purpose of the this study was to examine the suitability of using low cost cellulosic materials as substrates for mixed culture anaerobic bacterial growth. Potential carbon sources chosen in this study were wheat straw, alfalfa hay, sawdust, commercially available cellulose and soluble starch.

The focus of this paper is to address some fundamental aspects of using a permeable barrier such as:

1) identification of an appropriate substrate for growth of bacteria ;
2) estimating substrate utilization rates; and,
3) identifying the final form of the contaminants concentrated in the barrier matrix.

EXPERIMENTAL SECTION

The suitability of cellulosic substrates for mixed culture sulfate reduction was investigated using batch reactors and laboratory soil columns.

Batch Experiments-Materials and Methods

Batch experiments were carried out in 250 ml glass bottles acting as batch reactors. Organic substrates and nutrients were added to each bottle. The bacterial medium had a chemical composition similar to that of groundwater at the Shiprock site and consisted of per L: Na_2SO_4, 22 g; $NaNO_3$, 5.5 g; $NaHCO_3$, 2.5; Na_3-Citrate, 14.705 g; K_2HPO_4, 0.005 g; $FeSO_4.7H_2O$, 0.1 g; KCl, 0.5 g; $MgSO_4.7H_2O$, 0.5 g; $UO_2(NO_3)_2.6H_2O$; trace metals solution, 20 ml; the pH was adjusted to 7.0 with 50% NaOH. The bottles and caps were autoclaved at 250°F for 30 minutes and were then sealed with rubber butyl stoppers and aluminum caps in an aseptic environment. The reactors were then inoculated with a mixed bacterial culture collected from ground water at the Shiprock UMTRA project site. The head space in each reactor was purged with nitrogen gas for 15 minutes to provide an anaerobic environment.

Sampling and analyses were carried out at 0, 1, 3, 5, 10, 20, 38, 60 and 90 days. Uranium concentration in the samples was measured by a colorimetric method using a hexanol extraction technique (Meloan et al., 1960). The Lowry method for protein measurement was used to determine the biomass concentration (Lowry et al., 1951). Sulfate and Nitrate concentrations in the samples were analyzed by ion chromatography using a Dionex Model 2110i. Samples were filtered using Gelman Acrodiscs, pore size 0.2 μm. Cellulose was analyzed using the Sulfuric Acid digestion method (Updegraff, 1969). Transmission Electron Microscopy and X-ray Diffraction were used to identify the phase of the reduced uranium.

Laboratory Column Experiments-Materials and Methods

Two inch diameter Plexiglass columns, 2 feet long were used to conduct column tests (Figure 2). Influent and effluent ports were separated from the packing material by 2 stainless steel screens. Sample ports were machined into the column walls at 2 inch intervals consisted of teflon fittings (Swagelok # 7/16-20) to allow sampling using a hypodermic needle attached to a syringe. Each carbon source was dispersed in the sand in the column. Wheat straw and alfalfa hay were ground to less than 2 mm. Sawdust passing through a #10 sieve was used. The different carbon sources were mixed with treated silica sand in 100g portions to obtain a fraction of organic carbon by weight of 2.5%.

The simulated plume water was pumped upflow through the columns at a flow rate of 15 ml/hr. Flow rates were adjusted to obtain a hydraulic residence time of one day. About two pore volumes of influent solution were then passed through the column to prepare the column for the introduction of the bacterial inoculum. Each column was inoculated with one pore volume of the

mixed bacterial culture from the Shiprock site. Effluent samples were collected on a daily basis. Initial samples were analyzed for SO_4^{-2}, NO_3^- and U. Samples were also collected, at weekly intervals, from the various sampling ports along the length of the columns to generate vertical concentration profiles. Substrate utilization was estimated by measuring the chemical oxygen demand (COD) of representative soil samples, at the beginning and conclusion of the column experiments. The closed-reflux colorimetric method (Standard Method 5220D) was used for the determination of COD (APHA, 1992).

RESULTS AND DISCUSSION
Batch Experiments
<u>Concurrent reduction of Uranium U(VI) and Sulfate</u>

The reduction of sulfate and soluble uranium in the batch reactors was plotted for all the five substrates and is shown in Figures 3 and 4. As seen from the figures, the batch reactor containing soluble starch as the sole carbon source did not show any appreciable reduction of either sulfate or soluble uranium. Soluble starch is more rapidly degraded than the other solid organic carbon sources tested. Under anaerobic conditions, a fermentation occurs with the formation of appreciable amounts of lactic, acetic, and butyric acids (Alexander, 1961). Acidic conditions are unfavorable for the existence of sulfate reducers which explains the limited reduction of sulfate and uranium.

<u>Transmission Electron Microscopy and Energy Dispersive X-ray Spectroscopy</u>

The black precipitate resulting from the batch reactors was mounted on a copper grid and air dried overnight. The precipitate was then examined by transmission electron microscopy at the Department of Earth and Planetary Sciences, University of New Mexico, using a JEOL 2010 electron microscope operating at 200 kV. The elemental composition of the precipitate was determined by energy-dispersive X-ray analysis. The precipitate was entirely extracellular, as confirmed by viewing different locations on the sample. Also, the precipitate appeared to be comprised of microcrystals of Uraninite (UO_2), which was later confirmed by X-ray diffraction. An energy-dispersive X-ray analysis was carried out to identify the elemental composition of this precipitate (Figure 5), using a Link EDS system (spot size, 5 nm) attached to a Link light element detector. The copper signal (Cu) was from the sample grid, and the titanium signal (Ti) was from the sample holder.

<u>X-ray Diffraction</u>

X-ray Diffraction Analysis was performed to confirm the phase of the uranium precipitate. The analysis was carried out in the X-ray Diffraction laboratory at the 'Department of Earth and Planetary Sciences', University of New Mexico. The precipitate resulting from the microcosm containing cellulose as the substrate, was collected in a glass vial and freeze-dried. The powder was mounted on a glass slide with acetone. The X-ray Diffractometer was equipped with a graphite monochromater and a nickel filter and used $CuK\alpha$ radiation with a wavelength of 1.54060 A^o. The X-ray diffraction pattern is shown in Figure 6. Table 1 compares the measured X-ray diffraction pattern with the Lattice spacing values for uraninite ($UO_{2(s)}$) obtained from the Joint Committee on Powder Diffraction Studies (JCPDS) data card 5-550.

Table 1: Comparison of Measured X-ray diffraction pattern with JCPDS data file card for Uraninite (5-550).

l k h	2-theta	Relative Intensity	Measured d-spacings	JCPDS d-spacings	Error (%)
1 1 1	28.245	100	3.154	3.16	0.18
0 0 2	32.717	48	2.693	2.73	1.35
0 2 2	46.943	49	1.930	1.925	0.25
1 1 3	55.696	47	1.637	1.648	0.66

The pattern closely matches with the JCPDS pattern to within 1.5% error confirming that the uranium phase is 'Uraninite' (UO_2).

Column Experiments

Nitrate and nitrite concentrations measured in the sawdust column effluent during the course of the experiment are shown in Figure 7. The initial persistence of nitrate in the effluent indicated that a time lag of about 4 days occurred before conditions necessary for denitrification of influent nitrate were established. The observed nitrate removal was slow and incomplete. As seen from Figure 7, significant nitrite concentrations were observed in the effluent indicating incomplete denitrification. Therefore, on day 41, the hydraulic residence time was increased to 3 days as it was apparent that slow microbial kinetics limited reduction of these contaminants in the columns. The effluent nitrate and nitrite concentrations rapidly decreased and by day 55, complete denitrification was observed. Sulfate reducing conditions were subsequently established, which was manifested as a grayish-black region in the sand column resulting from $FeS_{(s)}$ precipitation. It is important to recognize that little or no sulfate reduction occurred in the columns until all the nitrate was reduced. This provides confirmation of sequential reduction of dissolved oxygen, nitrate, and, sulfate. This preferential reduction occurs due to the decreasing amounts of energy released by microbial reduction of each electron acceptor (Stumm and Morgan, 1996).

Effluent U(VI) concentrations were monitored weekly. Complete U(VI) removal (99.94%) was observed on day 60 when the effluent soluble U(VI) concentration was measured as 5.04 ppb. No U(VI) reduction was seen prior to day 60, which is consistent with the concept of sequential reduction.

Chemical results obtained during the wheat straw and alfalfa hay column experiments were similar to those of the sawdust column. However, contaminant removal rates in the sawdust column were slower compared to the wheat straw and alfalfa hay columns due to the presence of significantly higher percentage of lignin in sawdust.

The precipitates formed in the column were collected and subjected to an elemental composition using a Transmission Electron Microscope. The precipitate was found to be extracellular and comprised of micro-crystals of $UO_{2(s)}$ which is consistent with the findings from the batch experiments.

The rate of substrate utilization is an important variable which will influence the design of the permeable barrier. Knowing the rate of substrate utilization, it is possible to estimate the mass of substrate required. Table 2 lists substrate consumption over a period of 70 days for the different columns:

Table 2: Comparison of substrate utilization in column experiments.

Column Type	% substrate utilization in 70 days
Sawdust	6.8
Wheat Straw	11.3
Alfalfa Hay	11.9

Since lignin compounds are known to be relatively resistant to microbial attack, it can be concluded that substrate consumption values from Table 2 represent the utilization of cellulose for each of the substrates. As expected, wheat straw and alfalfa hay were degraded more than sawdust which has much higher lignin content.

CONCLUSIONS

Based on the results of this study, the following conclusions were reached:

1)   A mixed culture of bacteria were able to utilize cellulose as a substrate and to achieve reduction of NO_3^- and SO_4^{-2}.

2)   More than 95% removal of soluble U(VI) was observed in batch and column experiments. X-ray diffraction studies indicate that U(VI) reduction results in the formation of an insoluble Uraninite ($UO_{2(s)}$).

3)   Approximately 16% utilization of cellulose was reported over a period of 90 days in the batch experiments. The reaction was first order with a rate constant, $k = 2.0 \times 10^{-3}$/day.

4)   Removal efficiency for U(VI) in the soil columns was dependent on the hydraulic residence time. Longer residence times provided greater removal efficiency.

5)   Substrate utilization for the sawdust column was slower as compared to the wheat straw and alfalfa hay columns. This may be related to the relative percentages of cellulose in the three materials.

6)   The results obtained during this research support the concept of a permeable biological reaction barrier for removal of groundwater contaminants such as nitrate, sulfate and U(VI).

ACKNOWLEDGMENTS

REFERENCES

Alexander, M. (1961) Introduction to Soil Microbiology, John Wiley & Sons, Inc., New York, NY.

APHA, AWWA, WEF. (1992) Standard Methods for the examination of water and wastewater, 18th edition.

Barton, L.L., B. M. Thomson, K. Choudhary, M. S. Thombre, K. Steenhoudt. (1995) Removal of Uranyl Ion by Anaerobic Bacteria, International Journal of Environmentally Conscious Design & Manufacturing, Vol.4, Number 3-4, pp 65-70.

Lovley, D.R., E. J. P. Phillips. (1992) Reduction of Uranium by Desulfovibrio desulfuricans, Applied and Environmental Microbiology, 58:850-856.

Lowry, O.H., N. J. Rosebrough, A. L. Farr, R. J. Randall. (1951) Protein Measurement with Folin Phenol Reagent, Journal of Biological Chemistry, Vol. 193, pp. 265-275.

Meloan, C.E., P. Holkeboer, W. W. Brandt. (1960) Spectrophotometric Determination of Uranium with Benzohydoxyamic Acid in 1-Hexanol, Analytical Chemistry, Vol.32, No.7, June.

Stumm, W., J. Morgan. (1996) Aquatic Chemistry, John Wiley & sons, Inc., 3rd Edition, pp. 475-476.

Thombre, M.S., B. M. Thomson, L. L Barton. (1996) Microbial reduction of Uranium using Cellulosic Substrates, Proc. HSRC-WERC Joint Conference on the Environment, Albuquerque, NM, 1996.

Thomson, B.M., S. P. Shelton, E. Smith. (1991) Permeable Barriers: A New Alternative for Treatment of Contaminated Groundwater, 45th Purdue Industrial Waste Conference Proceedings, Lewis Publishers, Inc., Chelsea, MI pp. 73-80.

Updegraff, D.M. (1969) Semimicro Determination of Cellulose in Biological Materials, Analytical Biochemistry, 32:420-424.
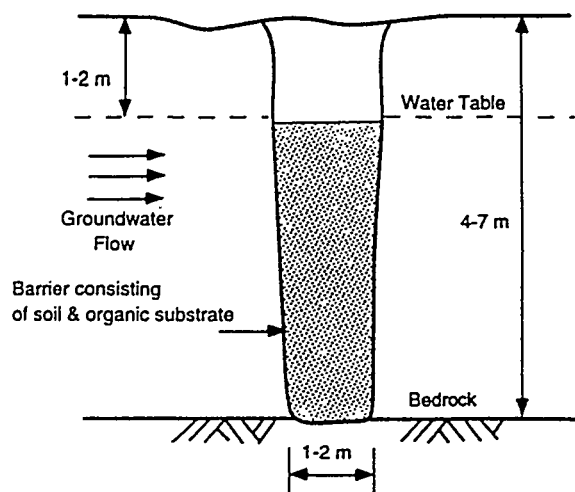
Figure 1: Conceptual representation of the proposed permeable barrier.

Figure 2: Schematic diagram of the column system.

Figure 3: Reduction of sulfate with time in batch reactors.
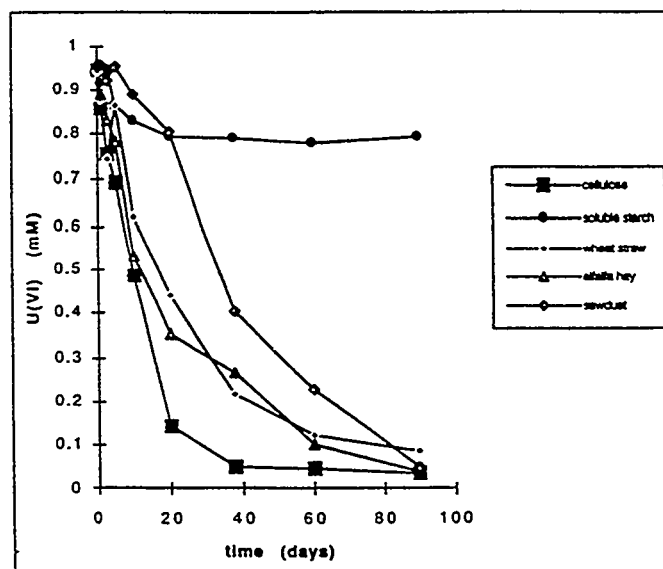
Figure 4: Reduction of soluble U(VI) with time in batch reactors.

749
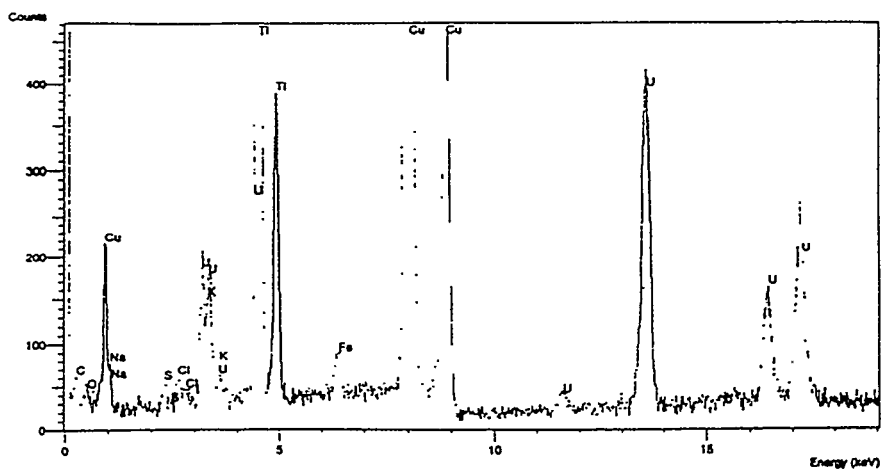
Figure 5: Results of the energy dispersive X-ray analysis.
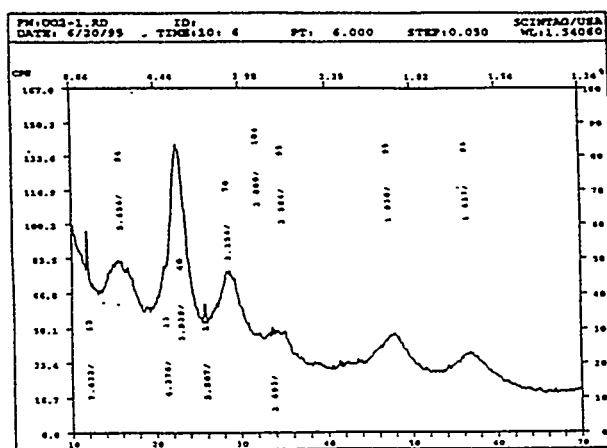
Figure 6: Results of the X-ray Diffraction analysis.
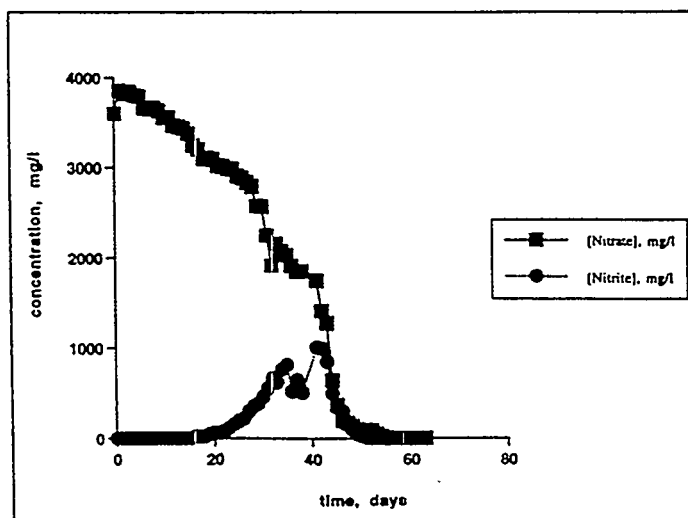
Figure 7: Effluent Nitrate and Nitrite, sawdust column.

Chapter 15

Permeable Reactive Walls: Zero-Valent Metals

.

Redox-Active Media for Permeable Reactive Barriers

T.M. Sivavec*, P.D. Mackenzie, D.P. Horney and S. S. Baghel

Abstract

In this paper, three classes of redox-active media are described and evaluated in terms of their long-term effectiveness in treating TCE-contaminated groundwater in permeable reactive zones. Zero-valent iron, in the form of recycled cast iron filings, the first class, has received considerable attention as a reactive media and has been used in about a dozen pilot- and full-scale subsurface wall installations. Criteria used in selecting commercial sources of granular iron, will be discussed. Two other classes of redox-active media that have not yet seen wide use in pilot- or full-scale installations will also be described: Fe(II) minerals and bimetallic systems. Fe(II) minerals, including magnetite (Fe_3O_4), and ferrous sulfide (troilite, FeS), are redox-active and afford TCE reduction rates and product distributions that suggest that they react via a reductive mechanism similar to that which operates in the Fe^0 system. Fe(II) species within the passive oxide layer coating the iron metal may act as electron transfer mediators, with Fe^0 serving as the bulk reductant.

Bimetallic systems, the third class of redox-active media, are commonly prepared by plating a second metal onto zero-valent iron (e.g., Ni/Fe and Pd/Fe) and have been shown to accelerate solvent degradation rates relative to untreated iron metal. The long-term effectiveness of this approach, however, has not yet been determined in groundwater treatability tests. The results of a Ni-plated iron column study using site groundwater indicate that a change in reduction mechanism (to catalytic dehydrohalogenation/hydrogenation) accounts for the observed rate enhancement. A significant loss in media reactivity was observed over time, attributable to Ni catalyst deactivation or poisoning. Zero-valent iron systems have not shown similar losses in reactivity in long-term laboratory, pilot or field investigations.

Introduction

Permeable treatment walls have emerged as an important low-cost alternative to pump-and-treat systems for treating groundwater contaminated with chlorinated solvents. For an *in-situ* reactive wall to offer substantial reductions in operation and maintenance costs relative to a conventional pump-and-treat system, it should be truly passive and should not require post-construction operation at the site. To meet this requirement, a robust, reactive media that will continue to reduce contaminants at a constant and predetermined rate over an economically viable period is necessary. The formation and escape of reaction by-products that are less desirable (e.g., more toxic) than the starting contaminant or that affect the hydraulic permeability of the reactive medium or surrounding aquifer are to be avoided. Transport, geochemical, and microbiological factors may also affect the reactivity, hydraulic performance and lifetime of the medium over time and these effects must be accounted for in barrier design.

The reductive dechlorination of chlorinated solvents such as TCE, PCE, 1,1,1-TCA and carbon tetrachloride has been studied in a number of aqueous-heterogeneous systems including zero-valent metals, bimetallic systems, minerals and reduced mineral systems. Zero-valent iron, in particular, has received considerable attention as a reactive media in laboratory, pilot and field studies (Gillham and O'Hannesin 1994). Research at GE Corporate Research and Development has focused on the development of a mechanistic understanding of chlorinated solvent/iron interactions including the factors that affect reductive dechlorination rate and hydraulic performance in field application. Long-term column treatability studies have been used to quantify the effects of significant operating parameters such as groundwater characteristics, velocity, inorganic precipitates, and potential biofouling (Mackenzie *et al.* 1995).

---

* General Electric Corporate Research and Development Center, Bldg. K1, Room 5A45, P.O. Box 8, Schenectady, NY 12301-0008, (518) 387-7677, sivavec@crd.ge.com

This paper addresses three classes of redox-active media, zero-valent iron, Fe(II) minerals, and bimetallics, and evaluates each with respect to long-term performance. Particular attention is paid to solvent reduction rates measured in column studies, reduction mechanisms, and reduction pathways that TCE, a very common groundwater contaminant, follow in each system.

Zero-Valent Iron and Selection Criteria

In this laboratory, dechlorination rates of chloroethenes (e.g., PCE, TCE, DCE isomers and VC) have been determined for approximately thirty commercial iron materials in various physical forms. The specific surface area of these metals, measured by BET Kr adsorption, was found to vary by as much as four orders of magnitude (from 0.0004 to 5 m^2/g). A linear correlation between dechlorination rate constant and iron surface area has been determined (Sivavec et $al.$ 1995). Although many different forms of zero-valent iron, including filings, turnings, chips, and powders are commercially available, today only low-cost, granular cast iron, a recycled product from the automotive industry, is considered practical in in-$situ$ groundwater treatment applications.

Recycled cast iron filings generally outperform all other iron metal candidates in that they have very high specific surface areas (generally >1 m^2/g, measured by Kr adsorption, BET) and hence afford high iron surface area concentrations (i.e., iron surface area/volume aqueous phase >5000m^2/L) in 100% iron zones. Requirements that we have used in selecting commercial, granular iron for application in 100% iron treatment zones include: (1) large particle sizing that affords a hydraulic permeability greater than the aquifer material (one order of magnitude is considered acceptable), (2) a high specific surface area (~1 m^2/g), (3) a high proportion of Fe^0 relative to iron oxide determined by XPS depth profile analysis, (4) first-order dechlorination rates determined in long-term column studies (>100 pore volumes site groundwater), (5) product mass balances and daughter products that also degrade, and (6) low cost and high volume availability. Several commercial suppliers of cast iron have been shown to meet these criteria.

When observed pseudo-first-order degradation rate constants, k_{obs}, are normalized for iron surface area, rate constants measured in batch and column systems can be compared (Johnson et $al.$ 1996). Surface area-normalized rate constants k_{SA} for a series of batch and column experiments in which TCE was reacted with one source of low-cost, granular iron are compared in Table 1. Specific reaction rate constants k_{SA} ($Lh^{-1}m^{-2}$) are remarkably uniform, differing by less than a factor of four, even though the rate comparisons in Table 1 do not take into account the effects of different groundwater characteristics, iron surface modification due to precipitates or groundwater velocity.

Recent work has focused on the use of emplacement methods other than standard excavation that may allow deeper reactive walls to be constructed at potentially lower cost. In jet grouting

Table 1. Comparison of surface area-normalized first-order dechlorination rate constants k_{SA} measured for TCE reduction in batch and column systems. All experiments were performed under anaerobic conditions using untreated Peerless cast iron with specified particle size- distributions and initial TCE concentrations of 0.5-18 mg/L.

system	water	granular iron source	m^2/L	k_{SA} $Lh^{-1}m^{-2}$
batch	DI	Peerless -50 mesh to dust	180	1.9×10^{-4}
batch	DI	Peerless -20 mesh to dust	126	1.7×10^{-4}
batch	DI	Peerless -8 + 50 mesh	25-250	1.3×10^{-4}
batch	site gw #1	Peerless -8 + 50 mesh	25-250	2.5×10^{-4}
column	site gw #1	Peerless -8 + 50 mesh	3810	1.2×10^{-4}
column	site gw #1	guar gum / Peerless -8 +50	4850	9.5×10^{-5}
column	site gw #2	Peerless -8 + 50 mesh	4210	8.0×10^{-5}
column	site gw #2	Peerless -8 + 50 mesh	4760	5.7×10^{-5}

and soil fracturing, the use of a viscosity-building agent such as guar gum is necessary to produce an iron slurry suitable for pumping high density granular iron to great depths. As shown in Table 1 (entry 6), the addition of guar gum and an enzymatic breaker to a granular iron column did not affect the reactivity or reaction pathway. Guar gum degradation products are highly water soluble and were flushed from the iron column at normal groundwater velocities.

Zero-Valent Iron: The Role of the Oxide Surface

Iron corrosion processes in aqueous systems have been studied extensively. Until recently, corrosion processes in which dilute aqueous concentrations of chlorinated solvents act as the oxidizing agent have not been investigated with respect to fate of the chlorinated solvent. The net reductive dechlorination reaction promoted by zero-valent iron (eq. 3) may be viewed as the sum of an anodic and cathodic reaction occurring at the iron metal surface (eqs. 1 and 2, respectively). Under aerobic conditions, dissolved oxygen can compete with the chlorinated

$$Fe^0 \rightarrow Fe^{2+} + 2e^- \tag{1}$$

$$\underline{RCl + 2e^- + H+ \rightarrow RH + Cl^-} \tag{2}$$

$$Fe^0 + RCl + H^+ \rightarrow Fe^{2+} + RH + Cl^- \tag{3}$$
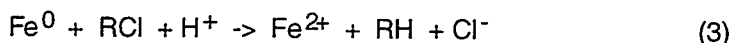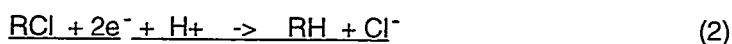
solvent as the favored oxidant (eq. 4). This effect is seen in the rapid consumption of dissolved oxygen at the entrance to the iron system (column or barrier), resulting in iron oxide and iron hydroxide precipitates that have been shown to foul a system's hydraulic performance (Mackenzie *et al.* 1995). Water, itself, may also serve as the oxidant as in eq. 5. Both reactions 4 and 5 can result in an increased pH in weakly buffered systems. Under anaerobic conditions, the corrosion of iron induced by water (eq. 5) also leads to the formation of iron hydroxide precipitates that may passivate the iron surface and affect its redox properties.

$$2Fe^0 + O_2 + 2H_2O \Longleftrightarrow 2Fe^{2+} + 4OH^- \tag{4}$$

$$Fe^0 + 2H_2O \Longleftrightarrow Fe^{2+} + H_2 + 2OH^- \tag{5}$$
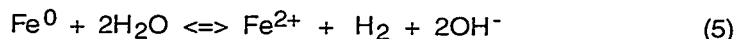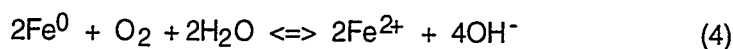
Early work on the nature of the passive film on iron (Nagayama *et al.* 1962) has suggested that the composition of the passive film consists of an inner layer of magnetite (Fe_3O_4), a mixed Fe(II,III) oxide, and an outer layer of maghemite (γ-Fe_2O_3), an Fe(III) oxide. More recent electron diffraction studies have confirmed the γ-Fe_2O_3/Fe_3O_4 structure. (Kuroda *et al.* 1982).

Recently, we have postulated that the reduction of chlorinated hydrocarbons by iron metal may occur by a reaction of surface-bound Fe(II) at the iron metal-water interface (Sivavec and Horney 1995b). The surface-bound Fe(II) species at the passive oxide-water interface may serve as mediator for the transfer of electrons from Fe^0 to adsorbed chlorinated hydrocarbon (Figure 1).

Scanning electron microscopy (SEM) of cross-sections of commercial iron filings (thermally treated by the vendor), such as those used in permeable barriers, indicate film thicknesses of between 0.75 and 7.5 µm (Sivavec *et al.* 1995b). The oxide films on these low-cost cast iron filings also appear quite porous relative to films coating electrolytically-deposited iron metals Depth profile analysis of these iron metal surfaces using an argon ion sputtering/x-ray photoelectron spectroscopy (XPS) technique has been used to measure passive oxide film thicknesses (Sivavec *et al.* 1995).

In general, oxide film on iron may be removed or modified as protective layers by reductive dissolution processes. The corrosiveness of a particular aqueous species can be measured by effects on anodic polarization curves. In the presence of chloride ion, for example, stainless steel and cast iron show large current density increases with breakdown of the passive film and consequent pitting attack. Organic acids, mineral acids, chloride, sulfate, ferrous ion, and complexing agents at appropriate aqueous concentrations can increase corrosion rates.
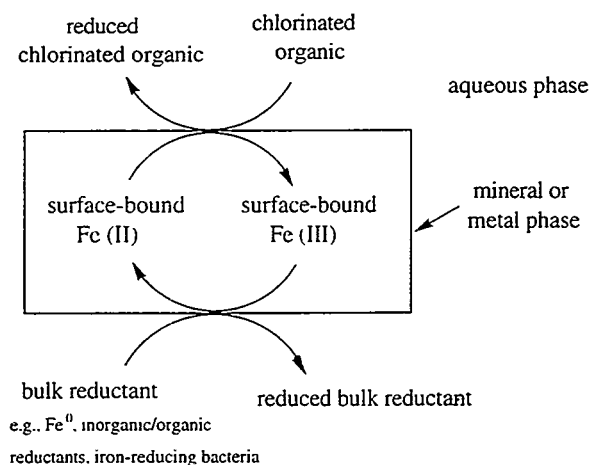
Figure 1. General reaction scheme for chlorinated solvent reduction at surface-bound Fe(II) sites.

Related Fe(II) Mineral Systems

Reduced forms of iron and sulfur are abundant natural reductants in anaerobic soils and sediments. Redox reactions between these reductants and organic pollutants are often greatly accelerated in natural systems because of microbial mediation or because the electron transfer is mediated by Fe(II)/Fe(III) cycling (Stumm 1992). For example, recent studies have shown that surface-bound, reduced iron species play the important role of electron transfer mediator in reductions promoted by iron-reducing bacteria (Heijman *et al*.1995). The high specific surface areas of iron-bearing minerals and the reduced redox potential of a surface-bound Fe(II) species relative to aqueous Fe(II) appear to facilitate transformations of reducible organic substances in natural systems (Figure 1).

In our investigations of chloroethene reduction promoted by ferrous sulfide (specifically, troilite FeS) and magnetite (Fe_3O_4), insight into the mechanism of Fe^0-promoted reduction and potential reactive media for new *in-situ* barrier application were sought. Reductive dechlorination of TCE, DCE and VC by FeS (troilite, as analyzed by XRD and XPS) was studied in batch and column systems. TCE reduction rate constants, normalized to metal or mineral surface areas, are given in Table 2. Product distributions and intermediates were determined to be very similar in the FeS and iron metal system, suggesting a common reduction mechanism The major hydrocarbon product in both the FeS and iron metal systems was acetylene. In the presence of iron metal, however, acetylene was further reduced to ethene and ethane (Figure 2). The TCE degradation product distribution in the magnetite system was identical to that seen in the Fe^0 system. Significantly smaller concentrations of C_3-C_6 hydrocarbon products were observed in all systems, consistent with coupling of intermediate carbon-centered radicals at Fe^0 and mineral surfaces.

Table 2. Comparison of surface area-normalized first-order dechlorination rate constants k_{SA} measured for TCE in granular iron, iron sulfide and magnetite systems.

system	water	redox mediium	m^2/L	k_{obsd} h^{-1}	half-life h	k_{SA} $Lh^{-1}m^{-2}$
column	site gw #2	granular iron (Peerless)	4210	0.337	2.06	8.0×10^{-5}
column	site gw #2	granular iron (Peerless)	4760	0.271	2.55	5.7×10^{-5}
column	site gw #2	ferrous sulfide (troilite, FeS)	1050	0.792	0.9	7.5×10^{-4}
batch	deionized	magnetite, Fe_3O_4	81	0.00152	454	1.9×10^{-5}

Both Fe^0 and Fe(II)-containing mineral systems reduce chlorinated ethenes, for example, via two connected degradation pathways: (a) reductive β-elimination and (b) sequential hydrogenolysis (Figure 2) (Sivavec and Horney, 1997; Roberts et al., 1996). The two pathways result in different intermediates. Of particular concern is the formation of DCE and VC from TCE or PCE through the sequential hydrogenolysis route, as these are toxic and slower to degrade. Even low concentrations of DCE and VC daughter products (typically <5% relative to TCE or PCE in 100% iron systems) may determine the size of an iron barrier depending on site characteristics. The chloroacetylene intermediate in the β-elimination pathway, by contrast, is a very short-lived intermediate and is rapidly reduced to ethene.

A

TCE $\xrightarrow[-Cl^-]{2e^- + H^+}$ cis-DCE $\xrightarrow[-Cl^-]{2e^- + H^+}$ VC $\xrightarrow[-Cl^-]{2e^- + H^+}$ ethene $\xrightarrow{2e^- + 2H^+}$ ethane

$\Big\downarrow {}^{2e^-}_{-2Cl^-}$ **B**

chloroacetylene $\xrightarrow[-Cl^-]{2e^- + H^+}$ acetylene $\xrightarrow{2e^- + 2H^+}$ (to ethene)
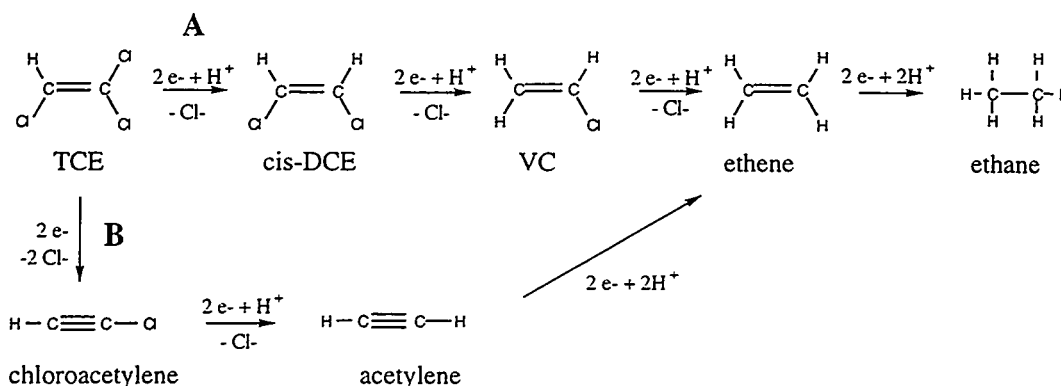
Figure 2. Proposed pathways for reduction of trichloroethylene (TCE) promoted by Fe(II) minerals and zero-valent iron. Pathway (A) represents sequential hydrogenolysis (the minor pathway) and pathway (B) represents reductive β-elimination (the major pathway).

Experiments employing $^{13}C_2$-labeled TCE and granular iron verified that all C_2-C_6 hydrocarbon products originated from TCE and that CS_2 and CO_2 were not produced from TCE. XPS analysis of the native FeS surface indicated only oxidized forms of sulfur and no sulfide. This and other data suggests a mechanism of chloroethene reduction promoted by surface-bound Fe(II) or possibly protonated iron sulfide surface groups and not by surface-bound sulfur species as proposed in the pyrite/carbon tetrachloride system (Kriegman-King and Reinhard 1994).

Although the observed reduction for TCE and its daughter products in the FeS column system suggest that this material may outperform granular iron (Table 2), the difference in cost between the two materials rules out use of FeS, at least in large installations. Interestingly, other forms of ferrous sulfide do not afford similar, fast solvent degradation rates, suggesting that the reactivity of Fe(II) minerals may be influenced by the electrochemical properties of the mineral and not just Fe(II) content.

Reactive Fe(II) sites may also be generated downgradient from an iron wall, where Fe(II) may be adsorbed onto native mineral oxide surfaces. Solvent degradation rates that may be attributed to reaction at Fe(II)-modified mineral sites downgradient of the wall may be significant in iron wall installations where pH is well-buffered and where Fe(II) may more readily escape precipitation within the Fe^0 zone.

Bimetallic Systems, Ni/Fe

The reductive dechlorination of chlorinated solvents by bimetallic systems has also been actively researched. Some of these metallic couples, including Ni/Fe, and Pd/Fe, demonstrate significant acceleration in degradation rate (Shoemaker et al., 1995; Muftikian et al. 1995) . The rate enhancement observed in some bimetallic systems may be attributed to corrosion-inducing effects promoted by the second, higher reduction potential metal. Bimetallic systems that include common hydrogenation catalysts such as Ni and Pd and a metal capable of generating hydrogen

(e.g., zero-valent iron, eq. 5), provide a second reduction pathway by which solvents are dechlorinated: catalytic dehydrohalogenation (replacement of halide with hydrogen) followed by hydrogenation (addition of hydrogen).

Evidence obtained in this study which supports a catalytic dehydrohalogenation/hydrogenation mechanism operating in the Ni/Fe system includes: (1) a dependence of rate on hydrogen concentration, (2) similar rates and product distributions measured in supported Pd/H_2 and supported Ni/H_2 systems, and (3) catalyst deactivation by site groundwater leading to significant loss in media reactivity.

Unlike zero-valent iron systems, bimetallic systems based on zero-valent iron have not been subjected to long-term column treatability studies. Such studies have been shown to be useful in determining the effects of a number of significant parameters such as groundwater characteristics, velocity, mineral precipitates and the potential for biofouling. The importance of mineral precipitates and other issues particular to a catalytic dehydrohalogenation system, including catalyst deactivation, is illustrated by the results of a column study in which Ni-treated granular iron was treated with TCE-contaminated site groundwater. Nickel (0.5 mol% plated onto -8+50 mesh granular iron filings) was selected over other hydrogenation catalysts based on cost and reactivity considerations.

First-order TCE degradation rates and products were measured routinely over a period of time in which 250 pore volumes of site groundwater (containing 2.1-3.3 mg/L TCE) were introduced into the Ni/Fe-packed column at a velocity of 1.6 m/d. The initial TCE reduction rate, k_{obsd}, measured over the first 76 pore volumes was greatly accelerated relative to an untreated iron column. However, very significant decreases in TCE reduction rate were measured over time until a dechlorination rate was obtained that was similar to that measured for the same untreated iron (Figure 3). TCE degradation rates remained first-order, indicating a uniform loss of media reactivity throughout the column That the Ni remained on the surface on the iron was determined by measuring the total Ni concentration in the column effluent as a function of time. After introducing 10 pore volumes of groundwater to the column system, a steady-state effluent concentration of 1-2 µg/L total Ni was measured.
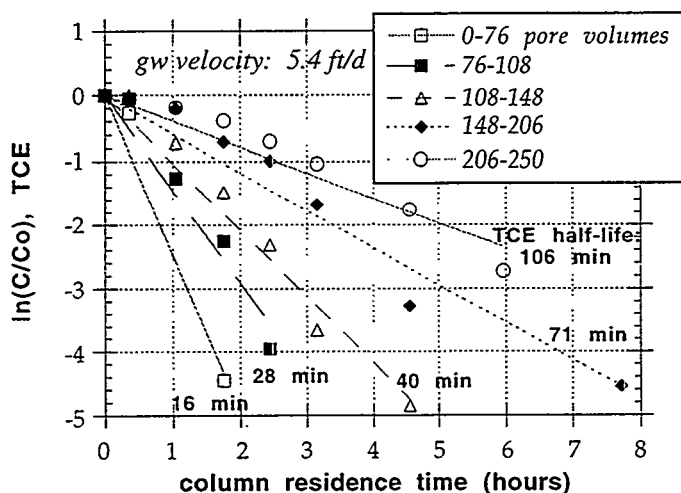
Figure 3. First-order kinetic model fit for TCE dechlorination data measured in a Ni-plated iron/site groundwater column study. A significant loss in media reactivity was observed over time, attributable to Ni catalyst deactivation .

One indicator that a catalytic dehydrohalogenation/hydrogenation mechanism was operating early in the column study was the complete absence of chlorinated degradation products (e.g., cis-DCE and VC produced from TCE) before the effects of catalyst deactivation were seen. Ethane was the major product determined in mass balance studies just as in supported Ni/H_2 and supported

758

Pd/H$_2$ systems. Low concentrations of cis-DCE and VC (less than 10% relative to [TCE]$_0$) begin to appear after 108 pore volumes, as catalyst deactivation occurs.

Conclusions

The high sensitivity of the Ni/Fe media to site groundwater treatment is made clear in this study. Caution should be exercised in the use of iron-supported catalysts in subsurface groundwater treatment applications as hydrogenation catalysts, in general, are well-known to be prone to deactivation. It is important to note that noncatalytic, granular Fe^0 systems have not shown similar losses in reactivity in long-term laboratory, pilot or field investigations. More recent work has focused on new emplacement methods for subsurface reactive zones (Shoemaker *et al.*, 1995). Advancement of the technology in this direction may further broaden the choice of reactive media

References

Gillham, R.W. and S.F. O'Hannesin (1994) Enhanced Degradation of Halogenated Aliphatics by Zero-Valent Iron. *Ground Water, 32,* 958-967.

Heijman, C.G., E. Grieder, C. Hollinger, C. and R.P. Schwarzenbach (1995) Reduction of Nitroaromatic Compounds Coupled to Microbial Iron Reduction in Laboratory Aquifer Columns. *Environ. Sci. Technol., 29,* 775-783.

Johnson, T.L., M.M. Scherer and P.G. Tratnyek (1996) Kinetics of Halogenated Organic Compound Degradation by Iron Metal. *Environ. Sci. Technol., 30,* 2634-2640.

Kriegman-King, M. and M. Reinhard (1994) Transformation of Carbon Tetrachloride by Pyrite in Aqueous Solution. *Environ. Sci. Technol., 28,* 692-700.

Kuroda, K., B.D. Cahan, G. Nazri, E. Yeager and T.E. Mitchell (1982) *J. Electrochem. Soc., 129,* 2163.

Mackenzie, P.D., S.S, Baghel, G.R. Eykholt, D.P. Horney, J.J. Salvo and T.M. Sivavec (1995) Pilot-Scale Demonstration of Chlorinated Ethene Reduction by Iron Metal: Factors Affecting Iron Lifetime. In *Emerging Technologies in Hazardous Waste Management VII*, pp 59-62. Atlanta, GA; American Chemical Society.

Muftikian, R., Q. Fernando and N. Korte (1995) A Method for the Rapid Dechlorination of Low Molecular Weight Chlorinated Hydrocarbons in Water. *Water Res., 29,* 2434.

Nagayama, M. and M. Cohen (1962) *J. Electrochem. Soc., 109,* 781.

Roberts, A.L., L.A. Totten, W.A. Arnold, D.R. Burris and T.J. Campbell (1996) Reductive Elimination of Chlorinated Ethylenes by Zero-Valent Metals. *Environ. Sci. Technol., 30,* 2654-2659.

Shoemaker, S.H *et. al.* (1996) Permeable Reactive Barriers. In *Assessment of Barrier Containment Technologies* (eds. R.R. Rumer and J.K. Mitchell), pp. 301-353. NTIS, Springfield, VA.

Schreier, C.G. and M. Reinhard (1995) Catalytic Dehydrohalogenation and Hydogenation using H$_2$ and Supported Palladium as a Method for the Removal of Tetrachloroethylene from Water. Prepr. Pap. ACS Natl. Meet., Am. Chem. Soc., Div. Environ. Chem., 35(1), 749-751.

Sivavec, T.M. and D.P. Horney (1997) Reduction of Chlorinated Solvents by Fe(II) Minerals. Prepr. Pap. ACS Natl. Meet., Am. Chem. Soc., Div. Environ. Chem., 37(1).

Sivavec, T.M. and D.P. Horney (1995a) Reductive Dechlorination of Chlorinated Ethenes by Iron Metal. Prepr. Pap. ACS Natl. Meet., Am. Chem. Soc., Div. Environ. Chem., 35(1), 695-698.

Sivavec, T.M. and D.P. Horney (1995b) Reductive Dechlorination of Chlorinated Ethenes by Iron Metal and Iron Sulfide Minerals. In *Emerging Technologies in Hazardous Waste Management VII*, pp 42-45, Atlanta, GA; American Chemical Society: Washington, DC.

Stumm, W. (1992) *Chemistry of the Solid-Water Interface: Processes at the Mineral-Water and Particle-Water Interface of Natural Systems*. Wiley, New York.

Degradation of Trichloroethylene (TCE) and Polychlorinated Biphenyl (PCB) by Fe and Fe-Pd Bimetals in the Presence of a Surfactant and a Cosolvent

Baohua Gu[*], Liyuan Liang, Paula Cameron, Olivia R. West, and Nic Korte

ABSTRACT

Surfactants and cosolvents are being used to enhance the removal of dense non-aqueous phase liquids (DNAPL) such as trichloroethylene (TCE) and polychlorinated biphenyls (PCBs) from contaminated soils. However, the waste surfactant solution containing TCE and PCBs must be treated before it can be disposed. This study evaluated the use of zero-valent iron and palladized iron filings to dechlorinate TCE and a PCB congener (2,3,2',5'-tetrachlorobiphenyl) in a dihexyl sulfosuccinate surfactant solution. Batch experimental results indicated that TCE can be rapidly degraded by palladized iron filings with a half-life of ~27.4 min. PCB was degraded at a slower rate than TCE with a half-life ranging from ~100 min to ~500 min as the concentration of surfactant increased. In column flow-through experiments, both TCE and PCBs degrade at an enhanced rate with a half-life about 1.5 and 6 min because of an increased solid to solution ratio in the column than in the batch experiments. Results of this work suggest that Fe-Pd filings may be potentially applicable for ex-situ treatment of TCE and PCBs in the surfactant solutions that are generated during surfactant flushing of the contaminated soils.

INTRODUCTION

Enhanced soil washing with surfactants has been proposed as an alternative method for remediating soils that are contaminated with polychlorinated biphenyls (PCBs) and nonaqueous-phase liquids (NAPLs) such as trichloroethylene (TCE). Surfactants can dramatically increase the solubility of organic compounds in groundwater and lower their interfacial tensions; both effects can significantly increase the extraction efficiency of pump-and-treat systems (Pennell et al., 1993; Fountain et al., 1991; Abdul and Ang, 1994). Previous studies (Pennell et al., 1993; Fountain et al., 1991) have successfully applied this technique to remove various hydrocarbons, PCBs, and polycyclic aromatic hydrocarbons (PAHs) from soil. For example, surfactants have been used extensively in enhance oil recovery to increase the mobility of crude oil (Gogarty, 1983; Nelson, 1989). In this process, surfactants and cosolvents are blended to reduce interfacial tension between oil and water to less than 0.01 dynes/cm (10^{-6} N/m), a reduction of over four orders of magnitude. In both laboratory and field experiments, Abdul and Ang (1994) reported that PCBs can be effectively removed from soils by the surfactant washings. They observed more than 85% of PCB removal from a laboratory soil column after 105 pore volume washings.

However, a significant problem associated with the surfactant washing is the generation of large quantities of secondary wastes that must be properly treated or disposed of. Although many treatment techniques are available and known to be effective to degrade TCE and PCB contaminants in the absence of surfactants, few studies have evaluated the treatment techniques to degrade these contaminants in the presence of surfactants and cosolvents. Among various treatment techniques, the use of zero-valence iron metal for reduction of chlorinated organic compounds such as TCE has been an area of significant recent research (Gillham and O'Hannesin, 1994; Matheson and Tratnyek, 1994; Liang et al., 1996). Field demonstration of this treatment technology at the Borden site in Ontario (O'Hannesin, 1993) and other commercial sites, and subsequent detailed laboratory studies have been reported (Gillham and O'Hannesin, 1994; Matheson and Tratnyek, 1994; Campbell and Burris, 1995; Liang et al., 1995; Sivavec and Horney, 1995; Mackenzie et al., 1995). Several investigators also discovered that a bimetallic preparation of Fe with a small amount of Pd (0.05% by weight) can substantially enhance the

[*]Corresponding author. Environmental Sciences Division, Oak Ridge National Laboratory, P.O. Box 2008, MS-6036, Oak Ridge, TN 37831-6036.

dechlorination rate of the chlorinated volatile organic compounds (Mallat et al., 1991; Muftikian et al., 1995; Korte et al., 1995; Liang et al., 1995; Schreier and Reinhard, 1995). Similarly, Sivavec (1996), Gillham (1996), and Appleton (1996) have reported that nickel-coated iron bimetal can also greatly enhance the dechlorination kinetics of many chlorinated volatile organic compounds. The bimetallic system provides faster (about 1-2 orders of magnitude) dechlorination kinetics and more complete dechlorination than reduction by iron alone. As an example, the reported half-life for 1,2-*cis*-dichloroethylene (*cis*-DCE), when exposed to zero valence iron is over 30 hours. In contrast, the half-life is only several minutes when the iron is properly treated with palladium (Liang et al., 1995; Korte et al., 1995). In addition, dichloromethane (DCM) and PCB compounds that do not react with zero valence iron are also dechlorinated by palladized iron (Muftikian et al., 1995; Korte et al., 1995; Liang et al., 1995; West et al., 1996).

The present study was undertaken to evaluate if zero-valence Fe and Fe-Pd bimetals can degrade TCE and PCBs in the presence of surfactants and cosolvents. It is hoped that zero-valence Fe and Fe-Pd bimetals can be potentially applied for in-situ and/or ex-situ treatment of surfactant wastes that are generated during the surfactant washing of soils contaminated with TCE and/or PCBs.

MATERIALS AND METHODS

TCE and PCB [2,3,2',5'-tetrachlorobiphenyl (PCB)] were the two target contaminants used for the present study. The surfactant (dihexyl sulfosuccinate or Aerosol MA-1) was obtained from Cytec Industries Inc. (West Paterson, NJ) and was used without further purification. Both ethanol and isopropanol were used as cosolvents for the study. Additionally, the surfactant itself contains ~5% isopropanol and methyl isobutylcarbinol. All chemicals used were analytical reagents except the surfactant solution.

Dechlorination of TCE was first studied in batch experiments using zero-headspace extractors (or ZHEs) to prevent TCE volatilization losses (Associate Design & Manufacturer Co., Alexandria, VA). The essential components of the ZHE are composed of a stainless steel cylinder and a piston (Gu and Siegrist, 1996). The upward movement of the piston is controlled by applying a positive pressure at the bottom of the piston. At a given time of reaction, a sample can be taken or displaced by slowly raising the piston so that no headspace is left in the ZHE as a result of sample withdrawal. Two reactive or reductive materials were studied to determine their effect in degrading TCE in the presence of surfactants and cosolvents. They were 40-mesh iron filings obtained from Fisher Scientific (Pittsburgh, PA) and 40-mesh Pd-coated iron filings (0.05% Pd) obtained from Johnson Matthey Inc. (West Deptford, NJ). Experimentally, 20 g of Fe or Fe-Pd filings were added to ZHEs, to which 100 mL of aqueous solution containing TCE, surfactant (2% or 4%), and cosolvent (2%) was added. The initial TCE concentration was ~2 mg/L. A ZHE without the addition of Fe or Fe-Pd filings was prepared similarly as a control. All ZHEs were then mounted on a rotary shaker and rotated at 30 rpm. At various time intervals of reaction, 4 mL of aqueous sample was taken through the sampling valve from the same ZHEs and immediately injected into 4 mL of hexane for the extraction of TCE. The extraction of TCE was accomplished by shaking the samples in hexane for 24 h; the samples were then allowed to settle for at least 1 h so that a clear hexane layer formed and could be observed and sampled for analysis. It should be noted, however, that since all samples were taken from the same ZHE, there was a slight increase in solid to solution ratio with sampling time that may slightly overestimate the reaction kinetics.

Degradation of PCBs was studied in 5-mL glass vials with 2 g 100~200-mesh Fe-Pd filings (with 0.1% Pd) because our preliminary studies showed that PCBs degrade very slowly with Fe-filings alone or when coated with a relatively small amount of Pd. The experimental procedures were similar to those described for TCE degradation studies except that 5-mL glass vials were used because PCBs are semi-volatile organic compounds, and the extraction of PCBs was accomplished with a mixture of methanol-hexane (1:2).

The concentration of TCE or PCB was analyzed by means of gas chromatography (GC) (Hewlett-Packard, 5890 Series II) equipped with a HP-5 fused-silica column (0.32 mm × 50 m) and an electron capture detector (ECD). TCE in hexane or PCB in methanol-hexane (1–2 µL) was directly injected into the GC column, and its concentration was determined in reference to TCE or PCB standards prepared in hexane or obtained from Ultra Scientific Inc. (North Kingston, RI). For biphenyl analysis, a flame ionization detector (FID) was used on the same GC.

Column experiments were performed to evaluate the reaction kinetics between TCE or PCB and Fe or Fe-Pd filings under the flow-through conditions. Two columns of 1x5 cm were used for TCE degradation studies whereas two columns of 2.5x5 cm were used for the PCB degradation studies because of a relatively slow reaction kinetics of PCBs in comparison with that of TCE. The two columns were wet-packed with Fe or Fe-Pd filings and connected in series through a three-way valve so that a sample can be withdrawn between the two columns. After flushing the packed columns with several pore volumes (>10) of the reactant solution, samples were taken at the inlet, outlet, and between the two columns for the analyses of TCE, PCB, or their byproducts, as described earlier. This sampling process was repeated at different time intervals and at three different flow rates which determined the residence time of TCE or PCB in the column.

RESULTS AND DISCUSSION

Degradation of TCE in the presence of 2% Aerosol surfactant and 2% ethanol is shown in Fig. 1. TCE degraded much faster (~2 orders of magnitude) by Fe-Pd filings than by Fe-filings. The degradation of TCE appeared to follow the pseudo-first-order rate law with an estimated half-life of 27.4 min in Fe-Pd system and ~1200 min in Fe-filing system. Results of TCE degradation in Fe-Pd is comparable with TCE degradation in the same system without the presence of surfactants and cosolvents (Liang et al., 1995) and suggest that the presence of surfactants (2%) and cosolvents (2%) did not significantly influence the dechlorination kinetics of TCE.
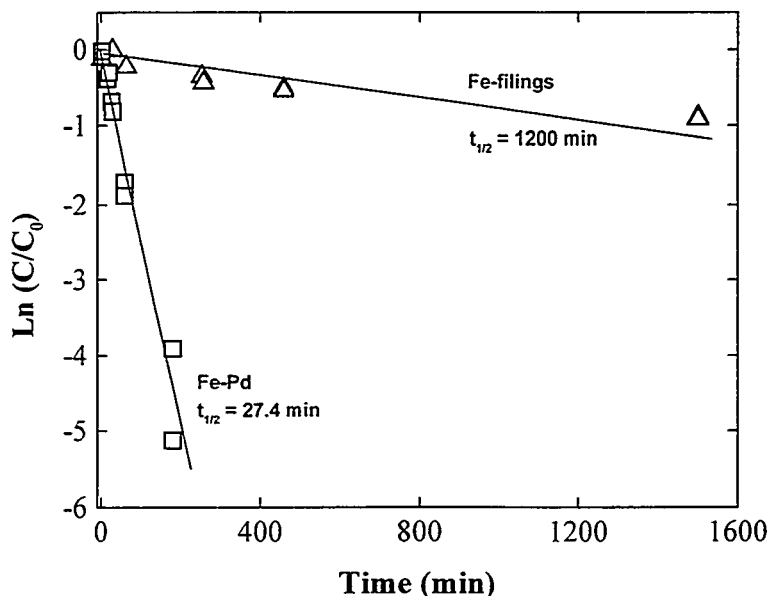
Fig. 1. Reactions between trichloroethylene (TCE) and iron and palladized iron filings in the presence of 2% Aerosol surfactant and 2% ethanol. Initial TCE concentration was ~2 mg/L.

The formation of byproducts during TCE degradation in Fe or Fe-Pd filings was not observed by direct analysis of TCE in hexane by the GC-ECD. Attempts were made to analyze byproducts by the purge-and-trap system but were unsuccessful because of the foaming of surfactants during the purging process. In the absence of surfactant, however, Liang et al. (1995) have reported the formation of byproducts such as cis-DCE and vinyl chloride. In particular, these byproducts persisted at a relatively high concentration in the system with Fe-filings only. On the other hand, no DCE isomers were observed and about an order of magnitude less amount of vinyl chloride was observed in the Fe-Pd system. Similar observations have been reported (in the absence of surfactants or cosolvents) by using the Ni/Fe bimetallic system although Fe-Pd appears to be more effective than Ni/Fe in enhancing the dechlorination kinetics of TCE and its byproducts (Appleton, 1996; Sivavec, 1996; Gillham, 1996).

Degradation of PCBs was studied in 100~200-mesh Fe-Pd filings (with 0.1% Pd) because our preliminary studies have shown that PCBs do not degrade appreciably with Fe-filings alone or with a low amount of Pd coated on Fe filings (West et al., 1996). Results (Fig. 2) indicated that PCB degraded slowly in comparison with TCE, particularly in the presence of a relatively high concentration of surfactant. The degradation half-lives were about 100 and 306 min in the presence of 2% and 4% Aerosol surfactant. These observations suggest that surfactant reduced the degradation rates of PCB by Fe-Pd filings. In the absence of surfactant, West et al. (1996) reported that PCBs degraded rapidly under similar conditions with a half-life on the order of ~10 min.
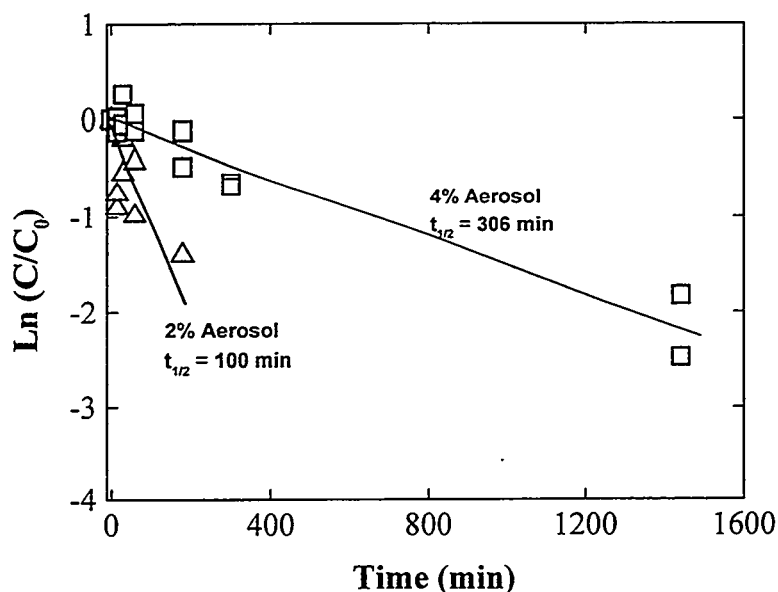
Fig. 2. Reactions between 2,3,2',5'-tetrachlorobiphenyl (PCB) and palladized iron filings in the presence of 2% and 4% Aerosol surfactant. Initial PCB concentration was ~1.2 mg/L.

Major reaction byproducts during PCB degradation were identified as 2,2'-dichlorobiphenyl (DCB), 2,3,2'- and 2,5,2'-trichlorobiphenyl (TCB) (Fig. 3). Small amounts of biphenyl were also identified for PCB degradation in the 2% Aerosol surfactant but were not in the 4% surfactant solution. These results again indicate that the presence of high concentrations of surfactant could have influenced the degradation rate of PCBs. On the basis of these reaction byproducts, the degradation of 2,3,2',5'-PCB by Fe-Pd filings appears to follow a step-wise dechlorination process as evidenced by the appearance of less chlorinated byproducts, which are 2,3,2'-TCB followed by 2,5,2'-TCB and 2,2'-DCB.

It should be indicated, however, that a mass-balance analysis indicated a relatively low recovery of PCBs (<60%), suggesting that other processes such as adsorption may also play a role in removing PCBs from the solution phase. It is known that PCBs can be strongly adsorbed or partitioned by various media such as minerals and the walls of many containers (Nkedi-Kizza et al., 1985; Baker et al., 1986). Additionally, the corrosion products of iron, iron hydroxides, may also adsorb significant amounts of PCBs. In this case, the Fe-Pd filings may act as adsorbents followed by the dechlorination of PCB on the Fe-Pd surfaces. Adsorption of PCBs on Fe-Pd filings can be evidenced when only Fe-filings were used as a reactive media. A substantial amount of PCB can be removed or adsorbed by the Fe-filings alone but no detectable amounts of byproducts can be identified in the system (data not shown). This observation indicates that Fe-filings do not actually degrade PCBs.
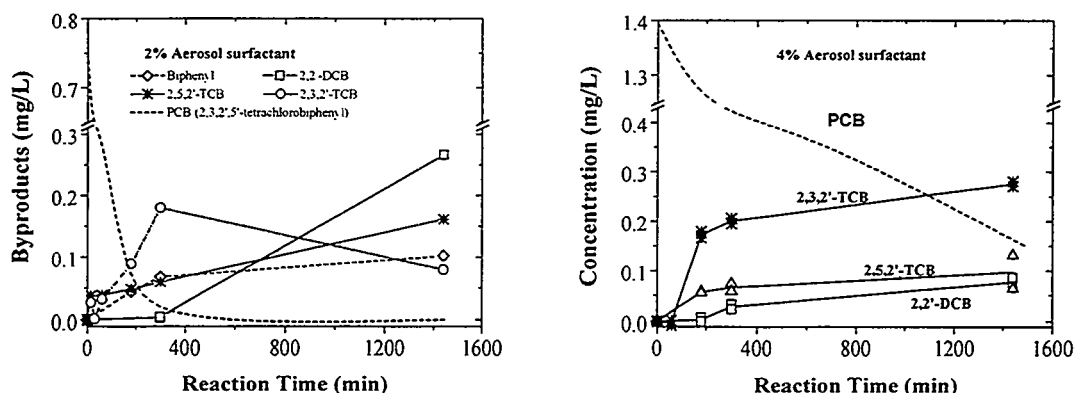
Fig. 3. PCB degradation byproducts with 100-200-mesh Fe-Pd filings in 2% and 4% Aerosol surfactant.

In laboratory column studies (Fig. 4), both TCE and PCB appear to degrade much faster than that were observed in the batch experiments. The degradation half-life for TCE was only about 1.5 min and was ~6 min for the degradation of PCB in the presence of 2% Aerosol surfactant and cosolvent. These observations are explained by the fact that a much higher solid to solution ratio is used in the column experiments than in the batch experiments. This increased solid to solution ratio greatly increased the available surface area of Fe-Pd filings to react with TCE or PCB. As has been indicated by other investigators (Matheson and Tratnyek, 1994; Muftikian et al., 1995), the dechlorination of these chlorinated organic compounds is a surface-controlled reaction process. The higher is the specific surface area, the faster is the reaction kinetics. Similar observations were also reported by Liang et al. (1995). An additional contributing factor to an increased reaction rate in the column experiments may be attributed to an initial adsorption process, particularly in the case of PCBs, as discussed earlier. The column experiments for the PCB was run for ~9 h. We observed a consistently increased C/C_0 with the reaction time in the effluent of the first column (Fig. 4, PCB). These results may well illustrate that surfaces of Fe-Pd filings became relatively saturated with PCB or surfactant as the PCB-surfactant solution was continuously displaced into the column. PCB removal as a result of the partitioning into and degradation on the Fe-Pd surfaces decreased with time. On the other hand, this reaction-rate dependence on the reaction time was not observed for the degradation of TCE within the experimental error and within the limited reaction time period (Fig. 4). These results are consistent with the batch experiments that the degradation of PCBs appears to be more strongly influenced by the presence of surfactant and by the adsorption process than that of TCE (Liang et al., 1995). It is important to note that a decreased reactivity between Fe-Pd and PCBs with time may also be partially attributed to a Pd-catalyst-poisoning effect. Sivavec (1996) reported the similar poisoning effect using Ni-Fe system. Therefore, further studies are certainly needed to

evaluate the long-term performance of Fe-Pd bimetal system in degrading TCE and PCBs in the presence or absence of surfactants or cosolvents.
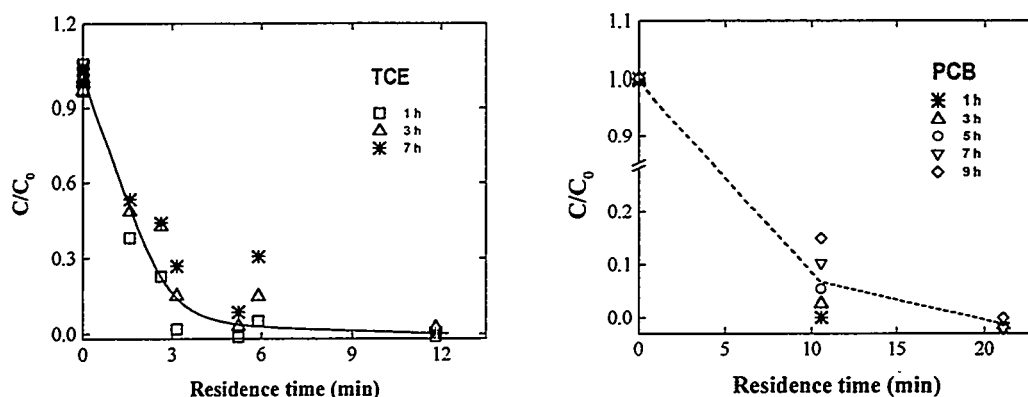
Fig. 4. Degradation of TCE and PCB in two packed columns (connected in series) with Fe-Pd filings in 2% Aerosol surfactant and 2% isopropanol. Samples were taken at the inlet, outlet, and between the two columns at various time intervals.

In summary, both laboratory batch and column experiments showed that TCE can be rapidly dechlorinated by Fe-Pd filings despite the presence of surfactants and cosolvents. PCBs can also be degraded by Fe-Pd filings but are at a reduced rate. A high concentration of surfactant may further reduce the rate of PCB degradation. The degradation of PCBs appears to follow a step-wise dechlorination process to less chlorinated byproducts such as 2,3,2'-TCB, 2,2'-DCB, and biphenyl. Results of this work suggest that Fe-Pd bimetal may be potentially applicable for ex-situ treatment of surfactant washing solutions containing chlorinated organic compounds such as TCE and PCBs, as long as a sufficient residence time is provided for their reactions with Fe-Pd filings. Fe-filings alone may be used to degrade TCE in the surfactant solution. However, a much longer residence time is required by using Fe-filings than by using Fe-Pd filings.

ACKNOWLEDGMENT

REFERENCES

Abdul, A. S. and C. C. Ang. (1994) In situ surfactant washing of polychlorinated biphenyls and oils from a contaminated field site: Phase II pilot study. Ground Water 32, 727-734.

Appleton, E. L. (1996) A nickel-iron wall against contaminated groundwater. Environ. Sci. Technol. 30, 536A-539A.

Baker, J., P. D. Capel, and S. J. Eisenreich. (1986) Influence of colloids on sediment-water partition coefficients of polychlorobiphenyl congeners in natural waters. Environ. Sci. Technol. 20, 1136-1143.

Campbell, T. J. and D. R. Burris. (1995) Sorption of PCE in a reactive zero-valent iron system. 209th National Meeting, American Chemical Society (ACS) 35, 775.

Fountain, J. C., A. Klimek, M. G. Beikirch, and T. M. Middleton. (1991) The use of surfactants for *in situ* extraction of organic pollutants from a contaminated aquifer. *J. Haz. Mat.* 28, 295-311.

Gillham, R. W. (1996) Ni/Fe as reactive barriers. *Remediation Technologies Development Forum (RTDF) Permeable Barriers Action Team Meeting, December 11-12, Denver, CO.*

Gillham, R. W. and S. F. O'Hannesin. (1994) Enhanced degradation of halogenated alliphatics by zero-valence iron. *Ground Water* 32, 958-967.

Gogarty, W. B. (1983) Enhanced oil recovery by the use of chemicals, Part I. *J. Pet. Technol.* 35, 1581.

Gu, B. and R. L. Siegrist. Alkaline Dechlorination of Chlorinated Volatile Organic Compounds. (1996). Oak Ridge National Laboratory, ORNL/TM-13263. Oak Ridge, TN 37831.

Korte, N. E., R. Muftikian, C. Grittini, Q. Fernando, J. L. Clausen, and L. Liang. (1995) ORNL-MMES research into remedial applications of zero-valence metals. 2. Bimetallic enhancements. *209th ACS National Meeting, ACS* 35, 752.

Liang, L., J. D. Goodlaxson, N. Korte, J. L. Clausen, and D. T. Davenport. (1995) ORNL/MMES research into remedial applications of zero-valence metals. 1. Laboratory analysis of reductive dechlorination of trichloroethylene. *209th ACS National Meetings, ACS* 35, 728-731.

Liang, L., N. Korte, J. D. Goodlaxson, J. Clausen, Q. Fernando, and R. Muftikian. (1996) Byproduct formation during the reduction of TCE by zero-valence iron and palladized iron. *Environ. Sci. Technol.* (in review).

Mackenzie, P. D., S. S. Baghel, G. R. Eykholt, D. P. Horney, J. J. Salvo, and T. M. Sivavec. (1995) Pilot scale demonstration of reductive dechlorination of chlorinated ethenes by iron metal. *209th ACS National Meeting, ACS* 35, 796.

Mallat, T., Z. Bodnar, and J. Petro. (1991) Reduction by dissolving bimetals. *Tetrahedron* 47, 441-446.

Matheson, L. J. and P. G. Tratnyek. (1994) Reductive dehalogenation of chlorinated methanes by iron metal. *Environ. Sci. Technol.* 28, 2045-2053.

Muftikian, R., Q. Fernando, and N. Korte. (1995) A method for the rapid dechlorination of low molecular weight chlorinated hydrocarbons in water. *Water Res.* 29, 2434.

Nelson, R. C. (1989) Chemically enhanced oil recovery: the state of the art. *Chem. Eng. Prog.* 85, 50-57.

Nkedi-Kizza, P., P. S. C. Rao, and A. G. Hornsby. (1985) Influence of organic cosolvents on sorption of hydrophobic organic chemicals by soils. *Environ. Sci. Technol.* 19, 975-979.

Pennell, K. D., L. M. Abriola, and Jr. W. J. Weber. (1993) Surfactant-enhanced solubilization of residual dodecane in soil columns. 1. Experimental investigation. *Environ. Sci. Technol.* 27, 2332-2340.

Schreier, C. G. and M. Reinhard. (1995) Catalytic hydrodehalogenation of chlorinated ethylenes using palladium and hydrogen for the treatment of contaminated water. *Chemosphere* 31, 3475-3487.

Sivavec, T. M. (1996) Ni/Fe as reactive materials. *Remediation Technologies Development Forum (RTDF) Permeable Barriers Action Team Meeting, December 11-12, Denver, CO.*

Sivavec, T. M. and D. P. Horney. (1995) Reductive dechlorination of chlorinated ethenes by iron metal. *209th ACS National Meeting, ACS* 35, 695.

West, O. R., L. Liang, W. L. Holden, N. E. Korte, Q. Fernando, and J. L. Clausen. (1996) Degradation of polychlorinated biphenyls (PCBs) using palladized iron. *ORNL/TM-13217* , Oak Ridge National Laboratory, Oak Ridge, TN 37831.

Zero-Valent Iron for the Removal of Soluble Uranium in Simulated DOE Site Groundwater[1]

W. D. Bostick, R. J. Jarabek, and J. N. Fiedor
Lockheed Martin Energy Systems, Inc.[2]
Oak Ridge, Tennessee, USA

J. Farrell
University of Arizona
Tucson, Arizona, USA

R. Helferich
Cercona, Inc.[3]
Dayton, Ohio, USA

ABSTRACT

Groundwater at the Bear Creek Valley Characterization Area, located at the Oak Ridge Y-12 Plant, is contaminated with regulated metals and volatile organic compounds (VOCs) due to former site activities and disposal practices. The contaminant of principle concern, from the perspective of protecting human health, is soluble uranium, which is present in some waters at concentrations up to a few parts-per-million. We present product speciation and relative reaction kinetics for removal of soluble uranium under oxic and anoxic conditions with use of zero-valent iron. Under oxic conditions, U(VI) is rapidly and strongly sorbed to hydrous ferric oxide particulate ("rust"), whereas uranium is slowly and incompletely reduced to U(IV) under anoxic conditions.

1. INTRODUCTION

Groundwater at the Bear Creek Valley Characterization Area, located at the Department of Energy's Oak Ridge Y-12 Plant, is contaminated with regulated metals and volatile organic compounds (VOCs) due to former site activities and disposal practices. A technology demonstration is being planned to investigate the feasibility of using passive, in-situ treatment systems at the site (Watson, et al., 1997). Zero-valent iron (ZVI) is identified as a leading technology for use in this remediation effort.

We report on the efficacy of zero-valent iron (ZVI) and select sorbents (primarily iron oxide media) for the removal of some of the contaminants of potential concern in the Bear Creek Valley water systems. Soluble uranium is considered to be the primary contaminant of interest, and its treatment is the primary focus of our investigation.

Recently, Cantrell et al. (1995) demonstrated that zero-valent iron was able to effectively remove soluble uranyl ion (i.e., U^{+6}) from solution. They suggest that this removal could occur by any of three different mechanisms: (1) reduction of U^{+6} by either Fe^0 or Fe^{+2} to form insoluble U^{+4} (i.e., $UO_2 \cdot nH_2O$); (2) sorption of U^{+6} to insoluble iron oxide corrosion product (hydrolyzed Fe^{+3}); or (3) some combination of reduction and sorption. Thermodynamically, reduction of U^{+6} to U^{+4} by zero-valent iron is slightly

favored, especially in acidic solution, as indicated by the modest positive value for the standard cell potential, E^0 in Eq. 1:

$$Fe^0 + 1.5UO_2^{+2} + 6H^+ = Fe^{+3} + 1.5U^{+4} + 3H_2O, \quad E^0 = +0.17V. \tag{1}$$
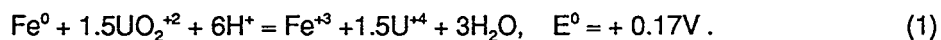
However, reduction of U^{+6} to the less soluble U^{+4} species (e.g., $UO_2 \cdot xH_2O$) is reported to be controlled primarily by kinetic, not thermodynamic factors (Wersin et al. 1994, and references cited therein). Similarly, reduction of U^{+6} by ferrous ion (Fe^{+2}) has been reported to be kinetically slow except in the presence of strong acid (Baes 1953).

Some of the more important reactions that may occur during treatment of inorganic contaminants with ZVI (Fe^0) include the following four processes:

Anaerobic corrosion:	$2H_2O + Fe^0 = Fe^{+2} + H_2 + 2OH^-$.	(1)
Aerobic corrosion:	$O_2 + 2Fe^0 + 2H_2O = 2Fe^{+2} + 4OH^-$.	(2)
Cementation:	$M^{+n} + Fe^0 = M^{+n-2} + Fe^{+2}$.	(3)
Sorption/Ion Exchange:	$>OH + M^{+n} = >OM^{+n-1} + H^+$.	(4)
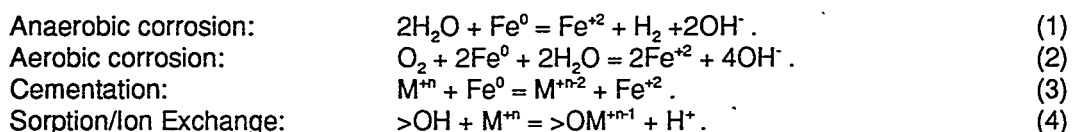
In the Eqs. 1–4, M^{+n} represents a cationic metal contaminant, and $>OH$ represents an exchangeable site on the hydrous metal oxide at the iron substrate or on its detached corrosion product. Note in the simplified Eq. 4 that, depending upon the solution pH, the surface site may have a net positive ($>OH_2^+$) or negative ($>O^-$) charge. The exchange of protons to and from the oxide surface creates specific site types available for adsorption. For most iron-containing minerals, the solution pH value that results in no net charge on the mineral (i.e., the point of zero charge, or pzc) is typically in the range of ~6–8 (Sylva and Nitsche 1995). As the solution pH value falls below the pzc of the substrate, the net surface charge becomes more positive, favoring the sorption of anionic species; conversely, as the pH is increased above the pzc, the substrate becomes more negatively charged, favoring the sorption of cationic species.

In addition, the ferrous iron (Fe^{+2}) reaction product in Eqs. 1–3 can be oxidized by air to form ferric ion (Fe^{+3}), which can subsequently hydrolyze and precipitate from solution at near-neutral and alkaline pH values, as illustrated in the simplified Eq. 5:

$$Fe^{+2} + 1/4O_2 + 5/2H_2O = Fe(OH)_3(s) + 2H^+. \tag{5}$$
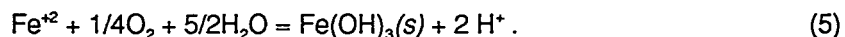
Hydrolyzed ferric iron [$Fe(OH)_3(s)$, and its polymer, ferrihydrate] and other iron oxide minerals are effective reagents for removing many toxic and radioactive trace element contaminants from solution by sorption (as depicted in Eq. 4) or a combination of coprecipitation and sorption. Sorption of uranyl ion to these and other mineral phases is well documented (Langmuir 1978, Hsi and Langmuir 1985, Ho and Miller 1986, Koss 1988, Hakanen and Lindberg 1992). Excellent reviews of the chemistry of radionuclides in the geosphere have been prepared by Leiser (1995) and by Silva and Nitsche (1995).

The "cementation" (or reductive precipitation) reaction described by Eq. 3 refers to the process by which a metal deposits by reaction of its ion with a more readily oxidized metal. Iron is most commonly used as the sacrificial anode for the galvanic couple.

In this report, we present data on the predominant reaction mechanism (viz., reductive precipitation, Eq. 3, vs sorption, Eq. 4) and the relative kinetics for removal of soluble uranium (U^{+6}) with use of mild steel coupons under the two limiting conditions of oxic (aerobic) and anoxic gas purge. The main purge gas mixture is nitrogen with carbon dioxide (20%), which maintains the partial pressure of CO_2 approximately constant.

We use x-ray photoelectron spectroscopy (XPS) to monitor the uranium oxidation state at the Fe^0 surface. This is a surface-sensitive technique (i.e., beam interaction depth ≤ 100 Å) that provides

information on the various chemical states of elements on a substrate. For example, Muftikian et al. (1996) recently used XPS to probe the nature of a palladium-iron bimetallic surface, used to increase the reductive dehalogenation of organic contaminants in water, and Wersin (1994) used this technique to establish that some sulfide minerals can partially reduce U^{+6} under anaerobic conditions. We complimented the XPS data with information from scanning electron microiscopy with energy-dispersive x-ray analysis to gain further information on the spatial distribution of elemental components.

2. MATERIALS

Water samples. Contaminated groundwater at the site can be categorized into distinct groundwater plumes with characteristic composition features. Water Type 1 is represented by water from North Tributary 1 (NT-1), flowing near a former waste burial site; this water system contains relatively high levels of dissolved metal ion contaminants and total dissolved solids (TDS). Nitrate ion is present at levels >7000 mg/L, and ^{99}Tc (present as soluble pertechnetate ion, TcO_4^-) dominates the total radio-activity in the NT-1 water. Water Type 2 is represented by water from Groundwater Sampling Well 087 (GW-087), near the so-called boneyard/burnyard (BYBY) region of the site. The BYBY water system contains relatively low levels of TDS, and the principal contaminants of concern are trace VOCs and soluble uranium. Representative data for these water systems are summarized in Bostick et al. (1996). For purposes of testing using a reproducible source of material, a synthetic surrogate was formulated to reproduce the essential composition of the authentic BYBY water (see Table 1).

Uranium spike and tracer. Soluble uranium was added to test solutions in the form of uranyl nitrate $[UO_2(NO_3)_2 \cdot 6H_2O]$, either as natural isotopic abundant material or material enriched with the gamma-emitting isotope ^{233}U.

3. METHODS

Iron coupon testing. Small coupons (~1.4 cm dia. by 0.16 cm thick) are punched from mild steel plate, and a small string hole is drilled. The steel used contains small traces of Al and Si in the bulk phase. An inert kevlar™ fiber string is attached, and the surface of the coupon is cleaned by dipping it into warm ~6 molar HCl for ~10 min. The coupon is rinsed with distilled water and suspended in a 1-L three-neck flask with moist gas purges and instrumented with calibrated sensors for solution pH, redox potential (Eh), and dissolved oxygen. Redox potential measurements were made with an Orion Pt-calomel electrode, and results are corrected to give equivalency to the Standard Hydrogen Electrode (SHE). For anoxic conditions, the test solution (~300 mL of BYBY surrogate) is prepurged with a mixture of 80% nitrogen and 20% carbon dioxide to displace any dissolved oxygen. The test vessel is placed in a radiological glove box, also equilibrated with purge gas. When the coupon is removed from the test vessel, it is rinsed with deaerated distilled water and placed in a gas-tight transfer vessel to prevent exposure to air before the coupon is analyzed. For aerobic conditions, pure oxygen is added to the purge gas blend to yield equivalent dissolved oxygen to solution purged with laboratory air. The CO_2 in the gas purge mixture helps to maintain some important kinetic and sorptive parameters at near-constant values. For example, the solution pH remains within a relatively narrow range (near pH 6.0), and the predominant speciation for soluble uranium under these conditions is expected to be a near-equal mixture of $UO_2(CO_3)^0$ and $UO_2(CO_3)_2^{-2}$; see, for example, Payne and Waite (1991) and Miyahara (1992).

Table 1. Formulation of Synthetic BYBY Surrogate Water

Compound	Amount compound added per liter solution		Concentration (mg/L) (as-formulated)	Value reported in Authentic BYBY, mg/L[a]
	mmol	mg		
$MgSO_4 \cdot 7H_2O$ [FW = 246.5]	0.25	61.1	Mg = 6.02; SO_4 = 23.8	Mg = 5.1–8.5 SO_4 = 8–21
$CaCl_2 \cdot 2H_2O$ [FW = 147.0]	0.28	41.1	Ca (total) = 50; Cl = 19.8	Ca = 38–76 Cl = 20–33
$Ca(OH)_2$ [FW = 74.1]	0.97	71.8		
$NaHCO_3$ [FW = 84.0]	0.53	44.8	Na = 12.3	Na = 13–18
$K_2CO_3 \cdot 1.5H_2O$ [FW =165.2]	0.92	15.2	K = 7.2	K = 3.9–6.1
NO_3^-	NA	NA	NA	NO_3^- = 0.06
Total Alkalinity (As $CaCO_3$, mg/L)			132	81–238
pH			[~6.0][b]	~6.2–7.2 [b]

[a] Range of values, as summarized in Bostick et al., Report K/TSO-35P.

[b] Note: simulant was prepared by adding the stated chemicals to de-ionized water; calcium ion was solubilized, and the final pH was adjusted, by bubbling a gas mixture (80% N_2/20% CO_2) into slurry overnight. After the solution is stored for several days, excess CO_2 is lost, gradually raising the solution pH value to ~7.2 (authentic BYBY samples behave similarly).

Gamma counting. Solutions traced with gamma-emitting radionuclide (^{233}U) were counted on a Packard Auto-Gamma 500C instrument. For determination of soluble uranium activity, solutions are filtered with use of 0.2-μm pore Millipore™ membrane media.

X-ray photoelectron spectroscopy (XPS). XPS spectra were obtained using a PHI (Perkin Elmer) 5000 series spectrometer, using an Al anode at a power of 400W (15 kV). The analysis pressure was kept < 10^{-7} torr. All data reduction for the XPS data was performed with the aid of GOOGLY software written by Dr. Andrew Proctor. Spectra were obtained for several stable U species (e.g., U^{+6} as uranyl nitrate and as UO_3, and U^{+4} as UO_2. Binding energy is referenced to the C 1s band (284.5 eV). Curve fitting of the U 4f band envelopes was accomplished using the Levenberg-Marquardt damping method.

4. RESULTS

Figure 1 illustrates the relative kinetics for removal of soluble uranium under the limits of aerobic and anaerobic conditions. For the aerobic test, the final solution pH was ~5.8, and the Eh (SHE) was +510 mV. Assuming that uranium species are in equilibration with the dominant iron redox couple, thermodynamic considerations predict that U^{+6} would be the predominant form in both solid and aqueous phases (Pourbaix, 1974); the XPS peak position for U (381.5 eV) indicates that U^{+6} is the form of U on both the coupon surface and the detached corrosion product. However, mass balance indicates that the preponderance (~80–90%) of insoluble U activity was avidly sorbed onto the detached hydrated ferric oxide corrosion product, rather than being associated with the iron surface. The pseudo-first-order uranium removal kinetics gave a half-life of ~9.2 h.
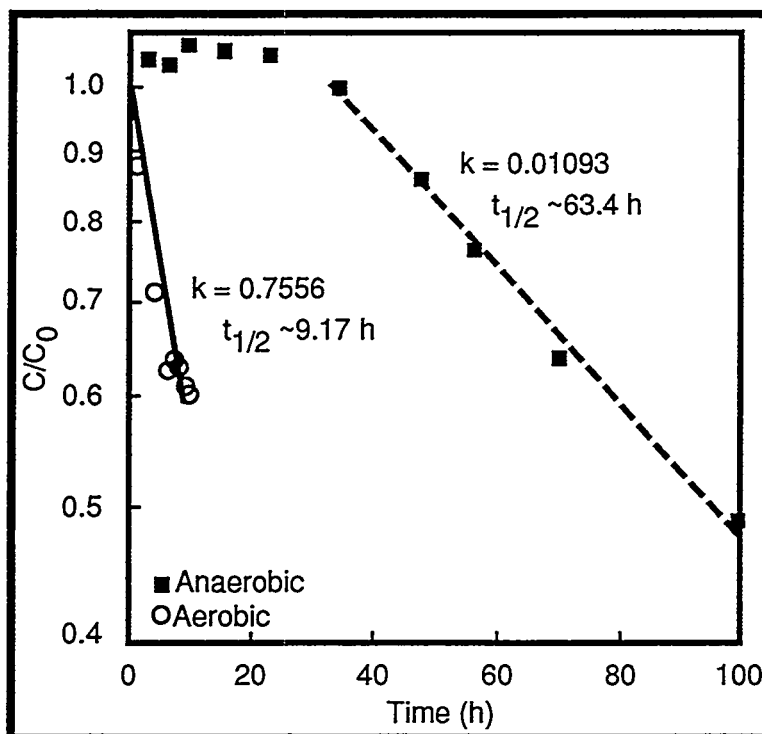
Fig. 1. Relative kinetics of aerobic and anaerobic experiments. (See text for experimental detail.)

Anaerobic testing (Fig. 1) had notably slower relative kinetics for the removal of soluble uranium, with an apparent "induction" phase of > 30 h, before yielding pseudo-first-order uranium removal kinetics with half-life of ~63 h. Unlike the aerobic test, under the anoxic conditions almost all of the uranium activity removed from solution remained bound to the iron/iron oxide surface. The final recorded solution pH value was ~6.0, and the Eh (SHE) value was -35 mV (i.e., strongly reducing). Again, referenced to the thermodynamic predictions presented in Pourbaix, the predominant stable solid-phase uranium species should be U^{+4} (i.e., UO_2 or its hydrate). Examination of the coupon surface by XPS indicated that uranium was partially reduced; by curve-fitting, it is estimated that the relative proportions of U^{+4} to U^{+6} was ~3:1. Briefly exposing the coupon to dry laboratory air caused partial reoxidation of U (i.e., U^{+4} to U^{+6} became ~1:1). Amorphous UO_2 hydrates are reported to be readily oxidized in air to U_3O_8, whereas crystalline UO_2 (uranite) is relatively stable (Katz and Rabinovitch, 1951).

5. CONCLUSIONS

Batch-testing using ZVI under aerobic conditions, analogous to conditions that may prevail near the inlet of a cannister or trench for treatment of an aerated surface water, indicate that soluble uranium is effectively and rapidly removed. Testing with use of iron coupons under controlled conditions indicate that, under fully oxic conditions, sorption of U^{+6} to hydrated Fe^{+3} corrosion product(s) is the predominant removal mechanism. The strong affinity for uranium by iron-containing minerals is well-documented [e.g., see Hakanen and Lindberg (1992), Ho and Miller (1986), Hsi and Langmuir (1985), Koss (1988), and Leiser (1978)]. A potential concern is the possible redispersion and/or desorption of U^{+6} on detached fine particulate corrosion product; in-situ treatment by ZVI of subsurface water, with low levels of dissolved oxygen, should minimize this effect.

Our data show that under similar reaction conditions (pH, U speciation), but with the exclusion of dissolved oxygen, soluble uranium is slowly removed at the surface of the iron by partial reduction of U^{+6} to sparringly soluble U^{+4} species. These results are similar to those recently reported by Grambow et al. (1996), who suggest that U^{+6} in anaerobic brine solution is sorbed to magnetite (Fe_3O_4), and then slowly and incompletely reduced at the iron surface. Analogously, Wesin et al. (1994) report on the kinetically slow partial reduction of U^{+6} to U^{+4} at the surface of sulfide minerals under strongly-reducing anoxic conditions. Reduction of uranium may be beneficial, in terms of limiting its solubility and mobility, but the relatively slow reaction kinetics may mandate a long residence time in the reductive medium.

REFERENCES

Baes, C. F., Jr. (1953), *The Reduction of Uranium(VI) by Ferrous Iron in Phosphoric Acid Solution: The Formal Electrode Potential of the U(IV)/U(VI) Couple*, Report ORNL-1581, Oak Ridge National Laboratory, Oak Ridge, Tennessee.

Bostick, W. D., R. J. Jarabek, W. A. Slover, J. N. Fiedor, J. Farrell, and R. Helferich (1996), *Zero-Valent Iron and Metal Oxides for the Removal of Soluble Regulated Metals in Contaminated Groundwater at a DOE Site*, K/TSO-35P, Lockheed Martin Energy Systems, Inc., Oak Ridge, Tennessee.

Cantrell, K. T., D. I. Kaplan, and T. W. Wietsma (1995), Zero-Valent Iron for the In-Situ Remediation of Selected Metals in Groundwater, *J. Haz. Mater.*, **42**, 201.

Grambow, B., E. Smailos, H. Geckeis, R. Mueller, and H. Hentschel (1996), Sorption and Reduction of Uranium (VI) on Iron Corrosion Products under Reducing Saline Conditions, *Radiochim. Acta*, **74**, 149.

Hakanen, M., and A. Lindberg (1992), *Sorption of Uranium on Rocks in Anaerobic Groundwater*, Report JYT-92-25, Nuclear Waste Commission of Finnish Power Companies, Helsinki, Finland.

Ho, C. H., and N. H. Miller (1986), Adsorption of Uranyl species from Bicarbonate Solution onto Hematite Particles, *J. Colloid Interface Sci.*, **110**(1), 165.

Hsi, C.-K. D., and D. Langmuir (1985), Adsorption of Uranyl onto Ferric Oxyhydroxides: Application of the Surface Complexation Site-Binding Model, *Geochim. Cosmochim. Acta*, **49**, 1931.

Katz, J. J., and E. Rabinowitz (1951), *The Chemistry of Uranium*, Part I. McGraw-Hill Publishers.

Koss, V. (1988), Modeling of Uranium (VI) Sorption and Speciation in a Natural Sediment-Groundwater System, *Radiochim. Acta*, **44/5**, 403.

Langmuir, D. (1978), Uranium Solution-Mineral Equilibria at Low Temperatures with Applications to Sedimentary Ore Deposits, *Geochim. Cosmochim. Acta*, **42**, 547.

Leiser, K. H. (1995), Radionuclides in the Geoshere: Sources, Mobility, Reactions in Natural Waters and Interactions with Solids, *Radiochim. Acta*, **70/71**, 355.

Miyahara, K. (1992), Sensitivity of Uranium Solubility to Variation of Ligand Concentrations in Groundwater. *J. Nucl. Sci. & Technol.*, **30**(4), 314.

Muftikian, R., K. Nebesny, Q. Fernando, and N. Korte (1996), X-Ray Photoelectron Spectra of the Palladium-Iron Bimetallic Surface used for the Rapid Dechlorination of Chlorinated Environmental Contaminants, *Environ. Sci. & Technol.*, **30**, 3593.

Payne, T .E., and T. D. Waite (1991), Surface Complexation Modelling of Uranium Sorption Data by Isotope Exchange Kinetics, *Radiochim. Acta* **52/53**, 487.

Pourbaix, M. (1974), *Atlas of Electrochemical Equilibria in Aqueous Solutions*, 2nd English ed., National Assoc. of Corrosion Engineers, Houston, Texas.

Silva, R. J., and H. Nitsche (1995), Actinide Environmental Chemisrty, *Radiochim. Acta*, **70/71**, 377 .

Watson, D., C. Smith, T. Klasson, and M. Leavitt (1997), Bear Creek Valley Characterization Area Mixed Wastes passive In-Situ Treatment Technology Demonstration Project, *Proc. 1997 Internat. Containment Technol. Conf. & Exhibit.*, St. Petersburg, Florida, February 9–12.

Wersin, P., M. F. Hochella, Jr., P. Persson, G. Redden, J. O. Leckie, and D. W. Harris, (1994), Interaction between Aqueous Uranium (VI) and Sulfide Minerals: Spectroscopic Evidence for Sorption and Reduction. *Geochimica et Cosmochemica Acta*, **58**(13), 2829.

Injection of Colloidal Size Particles of Fe^0 in Porous Media with Shearthinning Fluids as a Method to Emplace a Permeable Reactive Zone

By K. J. Cantrell[*], D. I. Kaplan and T.J. Gilmore

Abstract

Previous work has demonstrated the feasibility of injecting suspensions of micron-size zero-valent (Fe^0) particles into porous media as a method to emplace a permeable reactive zone. Further studies were conducted to evaluate the effects of several shearthinning fluids on enhancing the injectability of micron-size Fe^0 particles into porous media. In contrast to Newtonian fluids, whose viscosities are constant with shear rate, certain non-Newtonian fluids are shearthinning, that is, the viscosity of these fluids decreases with increasing shear rate. The primary benefit of using these fluids for this application is that they increase the viscosity of the aqueous phase without adversely decreasing the hydraulic conductivity. A suspension formulated with a shearthinning fluid will maintain a relatively high viscosity in solution near the Fe^0 particles (where the shear stress is low) relative to locations near the surfaces of the porous media, where the shear stress is high. The increased viscosity decreases the rate of gravitational settling of the dense Fe^0 colloids (7.6 g/cm3) while maintaining a relatively high hydraulic conductivity that permits pumping the colloid suspensions into porous media at greater flowrates and distances. Aqueous solutions of three polymers at different concentrations were investigated. It was determined that, the use of shear thinning fluids greatly increases the injectability of the colloidal Fe^0 suspensions in porous media.

Introduction

A significant amount of effort has been directed to laboratory and field research studies on the use of zero-valent iron (Fe^0) as a material to remediate certain groundwater contamination problems (Tratnyek 1996; Fairweather 1996; Wilson 1995). Fe^0 is a very strong chemical reductant and has the capability to dehalogenate several halogenated-hydrocarbon compounds which are common groundwater contaminants [e.g., trichloroethylene (TCE), trichloroethane (TCA), carbon tetrachloride] (Gillham and O'Hannesin 1994; Matheson and Tratnyek 1994; Orth and Gillham 1996; Roberts et al. 1996). Fe^0 can also chemically reduce many highly mobile oxidized metal contaminants (e.g., CrO_4^{2-}, UO_2^{2+}, MoO_4^{2-}, and TcO_4^-) into their less mobile forms (Gould 1982; Cantrell et al. 1995).

In situ chemically reactive barriers or in situ treatment zones are permeable zones emplaced within the aquifer which react with contaminants as contaminated groundwater flows through the zone. Fe^0 shows great promise as an in situ reactive barrier material because of its applicability to a broad range of contaminants, rapid reaction kinetics, and the low cost and wide availability of the material (Wilson 1995). Several in situ reactive barriers composed of Fe^0 have been constructed to date using trench-and-fill techniques, i.e., digging a trench in the flow path of a contaminant plume and backfilling the trench with reactant material (Gillham et al. 1994; Yamane et al. 1995) or auger techniques (Puls et al. 1995). Although the trench-and-fill approach is effective, it is limited to sites where the aquifer material is porous, as opposed to fractured, depths that are shallower than about 20 m, and aquifers which are relatively thin (because excavations must be dewatered during construction). Although many sites have these characteristics, many important sites do not.

[*]Senior Research Scientist, Battelle, Pacific Northwest National Laboratory, P.O. Box 999, Mailstop K6-81, Richland, WA 99352. kj_cantrell@pnl.gov

Because of these factors and the fact that trench construction tends to be the single greatest expense for this remediation technique, innovative methods for installation of reactive barriers in the subsurface are needed, especially in geologic settings where current barrier installation technologies are of limited practical value (fractured media and/or at depths of greater than 20 m).

Or previous work has demonstrated the viability of an innovative approach for emplacement of an in situ treatment zone composed of Fe^0 (Kaplan et al. 1994; Kaplan et al. 1996; Cantrell and Kaplan 1997). In this approach, colloidal size (1-3 micron diameter) Fe^0 particles are injected as a suspension into the subsurface. As the suspension of particles moves through the aquifer material, the particles are filtered out on the surfaces of the aquifer matrix. As a result of the high density of the Fe^0 particles (7.6 g/cm^3), it appears that the primary removal mechanism of Fe^0 colloids in aqueous solution passing through sand columns is gravitational settling (Kaplan et al. 1996; Cantrell and Kaplan, 1997).

In this article, the use of shearthinning or pseudoplastic viscosity amendments for improving the emplacement of the colloidal Fe^0 suspensions in porous media is studied. In contrast to a Newtonian fluid, whose viscosity is independent of shear rate, certain non-Newtonian fluids are shearthinning, a phenomena in which the viscosity of the fluid decreases with increasing shear rate (Chhabra 1993). By increasing the viscosity of the colloidal Fe^0 suspension through the addition of a shearthinning polymer, the rate of gravitational settling of the Fe^0 particles will decrease, however, an increase in viscosity of the injection suspension will also have the adverse effect of decreasing the effective hydraulic conductivity of the porous media. The use of shearthinning fluids in the formulation of a Fe^0 colloid suspension will result in a high viscosity near the suspended Fe^0 particles (due to low shear stress of the fluid near the particles) and a lower viscosity near the porous media surface, where the fluid is experiencing a high shear stress. These properties allow the development of a Fe^0 colloid suspension solution which both is viscous enough to keep the Fe^0 particles in suspension for extended time periods to enhance colloid mobilization into the aquifer and yet will not cause an adverse decrease in hydraulic conductivity. The objective of this study was to evaluate the effect that three shearthinning fluids had on Fe^0 colloid emplacement in sand columns containing coarse-grained sand. Three non-toxic polymers were investigated. A synthetic high molecular weight polymer (vinyl polymer, VP), a biopolymer (gum xanthan, GX), and a cellulose type polymer (carboxymethyl cellulose, CMC).

Experimental Methods and Materials

Three polymer compounds were selected for testing the efficacy of shearthinning fluids to enhance the emplacement of Fe^0 colloid suspensions: a synthetic high molecular weight polymer (vinyl polymer, VP), a biopolymer (gum xanthan, GX), and a cellulose type polymer (carboxymethyl cellulose sodium salt, CMC). The VP (product name Slurry Pro CDP) was obtained from K. B. Technology, Chattanooga, Tenn. GX and CMC were obtained from Sigma Chemical Co. Commercially available Fe^0 colloids (Product Number S3700; International Specialty Products, Wayne, NJ) were used in these experiments. The colloids had a diameter of 2 ± 1 μm, bulk density of 2.25 g cm^{-3}, particle density of 7.6 g cm^{-3}, Fe concentration of 98.1%, C and N concentrations of <1%, and O concentration of 0.7%.

Colloid suspensions were made by first adding an anionic surfactant to water, 0.001% Aerosol, (Sigma Chemical Co., St. Louis, MO). The Fe^0 colloids were then dispersed in the surfactant solution and finally the polymer was added to the Fe^0-surfactant suspension. If the surfactant was not added before the polymer, the Fe^0 colloids would form into clumps and not disperse. The viscosity of the polymer solutions at various concentrations were measured with Ubbelohde type viscometers immersed in a constant temperature water bath at $25.0 \pm 0.1°C$. The measurements were conducted according to manufacturer's (Cannon Instrument Co., State College, PA) instructions.

Slurry injection experiments were conducted using 1.0-m long sand columns (with the exception of one 3.05-m long column) constructed with PVC pipe with a 4.4-cm inner diameter. The ends of the columns were fit with PVC tapered reducers to provide an even distribution across the cross-sectional area of the sand column. The tapered reducers were connected to 12.7-mm outer diameter, 7.9-mm inner diameter tygon tubing. A piece of 390-mesh (36-μm openings) nylon screening located between the ends of the PVC column and the tapered reducer was used to act as a bed support. Most columns were filled with washed 20-30 mesh (0.84 mm - 0.60 mm) quartz sand (Accusand, Unimin Corporation, Le Sueur, MN). Two columns were filled with 30 - 40 mesh (0.60 mm - 0.42 mm) and 40 - 50 mesh (0.42 mm - 0.30 mm) sand. The columns were packed to an average porosity of 32 ± 2 %. The pressure within the columns was measured using a pressure gauge to observe any affects that the shearthinning fluids had on the hydraulic conductivity of the columns and to determine if emplacement of the iron colloids would affect hydraulic conductivity.

Colloid suspensions (1.0 % w/w) were pumped into the columns using a Fluid Metering Inc. LAB Pump (Oyster Bay, NY), Model QD-1,. Darcy flow velocities used in these experiments were 0.154 cm/sec (436 ft/day), 0.051 cm/sec (144 ft/day), and 0.010 cm/sec (28 ft/day). Each column received 3, 10 or 30 pore volumes of Fe^0 colloid suspension. After injection of the colloid suspension into the column, an influent solution of 0.01 M $CaCl_2$ was pumped overnight at a rate of 0.2 cm/min (9.4 ft/day, ~2 pore volumes). The $CaCl_2$ flush was meant to simulate the influx of groundwater that could potentially carry away Fe^0 colloids that remained in suspension. Following the $CaCl_2$ flush, the columns were cut into 10-cm increments. The colloid concentrations in the sand collected from each 10-cm column increment were determined in two 0.5 to 3-g samples (dry). The Fe^0 in the column sand samples were dissolved in 3.6 M H_2SO_4 and then the concentration of dissolved Fe was determined by the o-phenanthroline colorimetric method (Olsen and Ellis 1982). A negative control, sand without Fe^0 colloids, and a positive control, 0.001, 0.005 or 0.01 (w/w) Fe^0 colloid in sand, were carried through all analyses. The analytical precision for the Fe^0 colloid analyses was ± 0.5%.

Results and Discussion

Studies were conducted to evaluate the effects of several shearthinning fluids on the emplacement of suspensions containing micron-size Fe^0 particles into sand columns. Three polymers were evaluated: three concentrations (0.005%, 0.01% and 0.02%) of VP, and two concentrations (0.04% and 0.08%) of GX and CMC. Figure 1 shows the iron concentrations measured in the sand columns as a function of column length for the VP slurry at an injection rate of 0.154 cm/sec, and a throughput of 3 pore volumes. Results obtained for an experiment containing no polymer were also included for comparison. It is apparent that when no VP is added, the distribution of iron within the column is greatest at the inlet and rapidly decreases with distance from the inlet. At the lowest VP concentration (0.005%), increased filtration of the Fe^0 colloids near the inlet is also evident; however, the decrease in Fe^0 concentration with distance from the inlet is much less than for the case with no polymer added. For the higher concentrations of VP (0.01% and 0.02%) the distributions of Fe^0 throughout the columns are essentially uniform. This is a desirable attribute for a chemically reactive barrier because this would result in the most efficient utilization of the Fe^0 reactant. Injection experiments conducted with GX and CMC at both concentrations tested also produced very flat distribution profiles of Fe^0 within the column that were very similar to the VP results (not shown). These results suggest that each of the polymers tested are very effective at reducing gravitational settling of the Fe^0 colloids within the sand columns. This is especially encouraging because it suggests that the use of shearthinning fluids as a carrier solution for Fe^0 colloids will be an effective means of emplacing iron into the subsurface.

The results of the viscosity measurements of the polymeric solutions, pressure measurements in the column experiments and the hydraulic conductivity values calculated from the final pressure measurements and Darcy's Law are listed in Table 1. Interestingly, the slowest settling rates of the Fe^0 colloids (not shown) do not correspond to highest measured viscosities reported in Table 1. For example, the 0.01% and 0.02% VP solutions have similar viscosities to the GX solutions but lower viscosities than the CMC solutions; however, the settling rates observed for the VP solutions were much slower than any of the GX or CMC solutions. In addition, the back pressures developed with VP tended to be very low, nearly the same as pure water. The back pressures observed for GX solutions with similar viscosities to the VP solutions were significantly higher. The implication of these results is that although each of the polymers is able to prevent gravitational settling of Fe^0 colloids during injection into porous media, VP is superior with respect to maintaining the highest hydraulic conductivity within the sand columns. In fact, the VP solutions produced hydraulic conductivities which are nearly the same as that observed for water. In other words, VP exhibited much better shearthinning properties than did GX and CMC. This is a desirable attribute for a Fe^0 suspension used to form a chemically reactive barrier because the primary limitation on how far Fe^0 can be emplaced from an injection point will depend on the pore velocity, which is directly dependent upon the hydraulic conductivity.

Further experimental testing of the effects of shearthinning solutions on the injection of Fe^0 colloids was limited to VP. Results of three column experiments conducted with 0.01% VP, an injection rate of 0.154 cm sec^{-1}, and variable throughput (3, 10, and 30 pore volumes) are illustrated in Figure 2. In each case the iron concentration profile along the column remains nearly uniform. The average Fe^0 concentration throughout the column is proportional to the throughput (i.e., 3 PV $\approx$ 0.1%, 10 PV $\approx$ 0.3%, and 30 PV $\approx$ 1.0%).

Another set of experiments was conducted to determine the effects of lowering the injection flow rate (Figure 3). Darcy velocities used in these experiments were 0.154 cm sec^{-1}, 0.051 cm sec^{-1}, and 0.010 cm sec^{-1}. Three pore volumes of 0.01% VP solution was used for the 0.154 cm sec^{-1} and 0.051 cm sec^{-1} experiments. Only 2 pore volumes was used in the 0.010 cm sec^{-1} experiment. The concentration of iron along the column of the 0.051 cm sec^{-1} experiment are nearly 2.5 times the concentration of iron in the 0.154 cm sec^{-1} experiment. This is likely the result of greater gravitational settling at the lower flow rate. Despite the higher concentrations of iron in the 0.051 cm sec^{-1} experiment, the concentration profile remain fairly constant along the length of the column. The concentrations of iron along the 0.010 cm sec^{-1} column experiment are nearly the same as for the 0.051 cm sec^{-1} column experiment; however, it is likely that higher concentrations would have been observed if three instead of two pore volumes of solution were injected into this column.

The effect of particle size of the porous media was evaluated by conducting three column injection experiments with three different particle size ranges of sand (0.30 mm - 0.42 mm, 0.42 mm - 0.60 mm, and 0.60 mm - 0.84 mm). These experiments were conducted at 0.01% VP, 0.154 cm sec^{-1} darcy velocity, and a three pore volume throughput (Figure 4). The two experiments conducted with the two smaller particle size ranges (0.30 mm - 0.42 mm and 0.42 mm - 0.60 mm) removed more iron colloids from solution than did the largest particle size range (0.60 mm - 0.84 mm). Results from each of these experiments produced fairly flat iron concentration profiles; however, there was more variability in the results from the 0.42 mm - 0.60 mm and 0.30 mm - 0.42 mm experiments than for the 0.60 mm - 0.84 mm mesh experiment. In addition, the 0.42 mm - 0.60 mm and 0.30 mm - 0.42 mm results were nearly the same. Fe^0 concentrations in the 0.60 mm - 0.84 mm column were consistently less than the two smaller particle size ranges. This is likely the result of larger pores in the 0.60 mm - 0.84 mm particle size column, which permitted the Fe^0 colloids to pass through the column more freely.

Conclusions

The use of shearthinning fluids greatly improves the emplacement profile of suspensions of micron-size Fe^0 particles in porous media relative to suspensions without shearthinning fluids. These fluids will also permit the use of much lower flow rates than would be possible without them. Lower flow rates are desirable because it will increase the distance from the well that the slurry can be effectively injected,decreasing the number of injection wells required to emplace the barrier, thereby decreasing the installation cost of the barrier. This will greatly increase the range of subsurface environments that this emplacement technology can be used. It was also found that VP was superior to GX and CMC because the VP suspensions created the lowest backpressure, resulting in the highest hydraulic conductivity. The results of this work also indicate that additional data collected from column experiments at various suspension concentrations would allow the development of a simple empirical model for predicting the emplacement of the Fe^0 colloids as a function of suspension flow rate, concentration and total throughput.

Table 1. Viscosity of polymeric solutions, initial backpressure (with deionized water) in 1.0-meter column experiments conducted at 0.154 cm/sec (5.5 m/hr), final back pressure after 3 pore volumes throughput of polymeric solution containing 1.0% Fe^0 colloids, and the hydraulic conductivity determined from the final backpressure measured in the column.

Polymeric Solution	Viscosity m^2/s	Initial Pressure N/m^2	Final Pressure N/m^2	Hydraulic Conductivity m/s
0.000%	1.0×10^{-6}	1.4×10^4	1.4×10^4	1.04×10^{-3}
0.005% VP[a]	1.7×10^{-6}	1.4×10^4	1.7×10^4	9.1×10^{-4}
0.01% VP	2.6×10^{-6}	1.4×10^4	1.4×10^4	1.04×10^{-3}
0.02% VP	4.1×10^{-6}	1.4×10^4	1.4×10^4	1.04×10^{-3}
0.04% GX[b]	2.6×10^{-6}	1.5×10^4	2.8×10^4	5.4×10^{-4}
0.08% GX	5.0×10^{-6}	1.4×10^4	4.8×10^4	3.1×10^{-4}
0.04% CMC[c]	7.7×10^{-6}	1.4×10^4	2.0×10^4	7.3×10^{-4}
0.08% CMC	15.6×10^{-6}	1.6×10^4	5.1×10^4	3.0×10^{-4}

[a] VP = vinyl polymer
[b] GX-gum xanthan
[c] CMC = carboxymethylcellulose

Acknowledgements

References

Cantrell, K.J., D.I. Kaplan, and T.W. Wietsma. (1995) Zero-valent iron for the in-situ remediation of selected metals in groundwater. *Haz Waste Techno,* 42, 201-212.

Cantrell, K.J., and D.I. Kaplan. (1997) Retention of zero-valent iron colloids by sand columns: Application to chemical barrier formation. *J. Environ Eng,* (in press).

Chhabra, R.P. (1993) *Bubbles, Drops and Particles in Non-Newtonian Fluids.* CRC Press, Boca Raton, Florida.

EPA (1983) *Methods for Chemical Analysis of Water and Wastes, EPA/600/4-79/020.* Environmental Monitoring and Support Laboratory, U. S. Environmental Protection Agency, Cincinnati, Ohio.

Fairweather, V. (1996) When Toxics Meet Metal. *Civil Eng*, May, 44-48.

Gillham, R.W., and S.F., O'Hannesin. (1994) Enhanced degradation of halogenated aliphatics by zero-valent iron. *Ground Water*, 32, 958-967.

Gillham, R.W., D.W. Blowes, C.J., Ptacek and S.F., O'Hannesin (1994) Use of zero-valent metals in in-situ remediation of contaminated ground water. In *In-situ remediation: Scientific Basis for Current and Future Technologies* (eds. G.W. Gee and N.R. Wing), , pp. 913-930. Battelle Press, Columbus, Ohio.

Gould, J.P. (1982) The kinetics of hexavalent chromium reduction by metallic iron. *Water Resour*, 16, 871-877.

Kaplan, D.I., K.J. Cantrell, T.W. Wietsma and M.A. Potter (1996) Formation of a chemical barrier with zero-valent iron colloids for groundwater remediation. *J. Environ Qual*, 25, 1086-1094.

Kaplan, D.I., K.J. Cantrell, and T.W. Wietsma (1994) Formation of a barrier to groundwater contaminants by the injection of zero-valent iron colloids: Suspension properties. In *In-situ remediation: Scientific basis for current and future technologies* (eds. G. W. Gee and N. R. Wing), pp. 820-838. Battelle Press, Columbus, Ohio.

Matheson, L.J., and P.G. Tratnyek (1994) Reductive dehalgenation of chlorinated methanes by iron metal. *Environ Sci Technol*, 28, 2045-2053.

Olson, R.V., and R. Ellis Jr. (1982) Iron. In *Methods of soil analysis, Part 2. 2nd ed.*, Agron. Monogr. 9. (Eds A. L. Page et al.), pp. 301-312. ASA and SSSA, Madison, Wis.

Orth, W.C., and R.W. Gillham. (1996) Dechlorination of trichloroethene in aqueous solution using Fe^0. *Environ Sci Technol*, 30, 66-71.

Puls, R.W., R.M. Powell, and C.J. Paul. (1995) In situ remediation of ground water contaminated with chromate and chlorinated solvents using zero-valent iron: A field study. Preprint of Extended Abstracts from the 209th ACS National Meeting, Anaheim, Cal, 35, 788-791. Anaheim, CA. Div Of Environ Chem, Am. Chem Soc, Washington, D.C.

Roberts, A.L., L.A. Totten, W.A. Arnold, D.R. Burris, and T.J. Campbell. (1996) Reductive elimination of chlorinated ethylenes by zero-valent metals. *Environ.Sci Technol*, 30, 2654-2659.

Tratnyek, P.G. (1996) Putting corrosion to use: remediating contaminated groundwater with zero-valent metals. *Chem & Ind*, July 1, 499-503.

Wilson, E.K. (1995) Zero-valent metals provide possible solution to groundwater problems. *Chem Eng News*, 73, 19-22.

Yamane, C.L., S.D. Warner, J.D. Gallinatti, F.S. Szerdy, T.A. Delfino, D.A. Hankins, and J.L. Vogan. (1995) Installation of a subsurface groundwater treatment wall composed of granular zero-valent iron. Preprint of Extended Abstracts from the 209th ACS National Meeting, Anaheim, Cal, 35, 792-795. Anaheim, CA. Div Of Environ Chem, Am Chem Soc, Washington, D.C.
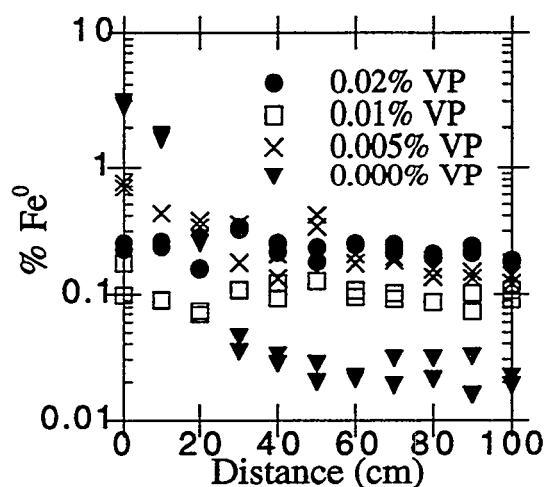
Figure 1. Fe[0] concentrations retained in 1.0-m long sand columns obtained with VP injection solutions at three concentrations.

Figure 2. Fe[0] concentrations retained in 1.0-m long sand columns obtained with 0.01% VP injection solution at three throughput volumes (one pore volume is approximately 0.35 L).

Figure 3. Fe[0] concentrations retained in 1.0-m long sand columns obtained with 0.01% VP injection solution injected at three flow rates.
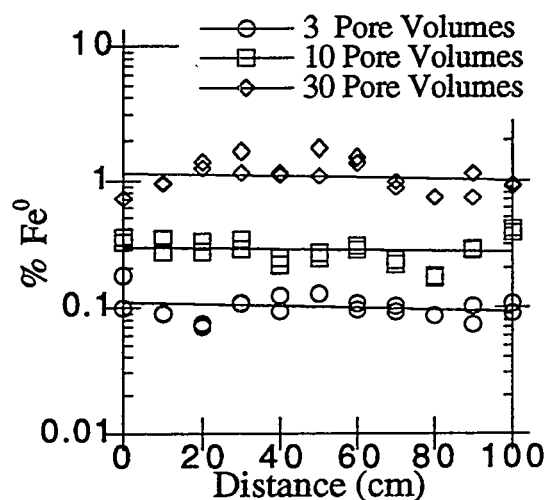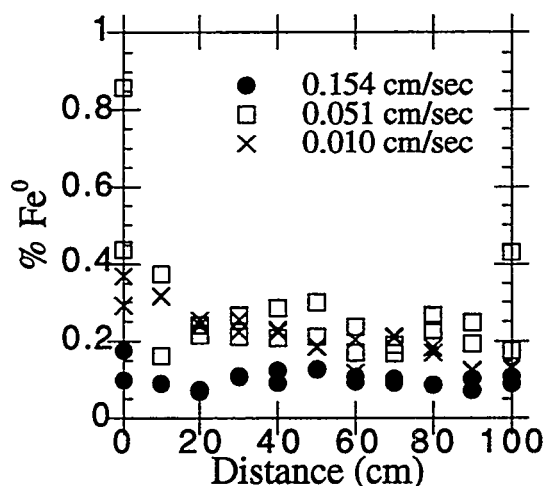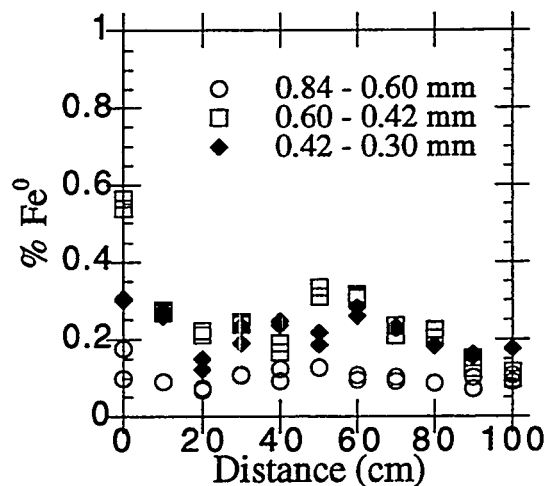
Figure 4. Fe[0] concentrations retained in 1.0-m long sand columns obtained with 0.01% VP injection solution for three particle size ranges of porous media.

Extending Hydraulic Lifetime of Iron Walls

P.D. Mackenzie[*], T.M. Sivavec, and D.P. Horney

Abstract

Iron walls for control of groundwaters contaminated with chlorinated solvents and reducible metals are becoming much more widely used and field studies of this technology have proven successful to date. However, there is still much uncertainty in predicting long-term performance. This work focuses on two factors affecting the lifetime of the iron media: plugging at the treatment zone entrance and precipitation in the bulk iron media.

Plugging at the system entrance is due principally to dissolved oxygen in the incoming water and is an issue in aerobic aquifers or in ex-situ canister tests. In an in-situ treatment system, plugging would result in a dramatic reduction in flow through the iron zone. Designs to minimize plugging in field applications include use of larger iron particles and admixing sand of comparable size with the iron particles.

Mineral precipitation in the bulk iron media can lead to porosity losses in the media, again reducing flow through the treatment zone. Decreases in reactivity of the iron media may also occur. The nature of the mineral precipitation and the factors that affect extent of mineral precipitation are examined by a variety of tools, including tracer tests, aqueous inorganic profiles, and surface analysis techniques. At short treatment times, measured porosity losses are due mainly to entrapment of a film of H_2 gas on the iron surfaces and also to $Fe(OH)_2$ precipitation. Over longer treatment times precipitation of $Fe(OH)_2$ and $FeCO_3$ in low carbonate waters and of $Fe(OH)_2$, $FeCO_3$ and $CaCO_3$ in higher carbonate waters will begin to dominate porosity losses. Preliminary results of an on-going study to control pH in an iron zone by admixing iron sulfide with iron show no difference in extent of carbonate precipitation versus a 100% iron system, suggesting that these systems are supersaturated with respect to carbonate precipitation. Hence, the benefit of pH control for minimizing carbonate precipitation in these systems has not been established.

Plugging at Entrance to Iron Zones

In laboratory columns and in ex-situ canister tests, researchers have consistently observed a plugging of the pore spaces at the entrance to the iron system as manifest by the formation of a "solidified" zone of iron. Such hardening of the iron particles results in the near 100% occlusion of the pores across a given cross section. In laboratory systems fed with a positive displacement pump, this results in a rapid rise in pressure at the system entrance. In passively-fed systems the result would be a dramatic reduction in flow through the iron zone.

Previous work suggested that this plugging is due to high dissolved oxygen in the incoming water (Mackenzie et al. 1995b). Dissolved oxygen profiles show that the oxygen is consumed rapidly at the system entrance and does not reach the bulk of the iron media. It reacts with the iron at the system entrance to form ferric (oxy)hydroxides. These amorphous, gelatinous materials can bridge or cement individual particles together, effectively blocking a significant fraction of the pore spaces for water flow. When the iron mass at the entrance to plugged columns is examined, it is found to be hardened into a solid mass and so the low hydraulic permeability of this material is not unexpected. By contrast, the iron at the exit of the column remains free-flowing individual grains.

To establish definitively that dissolved oxygen in the incoming water is the source of the plugging at the entrance to iron systems, a column experiment was conducted in which a single iron source (0.42 - 1 mm VWR) was treated with the following waters: site groundwater (300 mg/L carbonate as $CaCO_3$) which had been stripped with nitrogen to remove dissolved oxygen, as-received site groundwater with high dissolved oxygen, and deionized water that had been aerated to a high dissolved oxygen level. Figure 1 summarizes these results. When the groundwater was stripped

General Electric Corporate Research and Development Center, Bldg. K1, Room 5A47,
P.O. Box 8, Schenectady, NY 12301-0008, (518) 387-6831, mackenzie@crd.ge.com

of dissolved oxygen the column showed no signs of pressure build up/ plugging. When the feed was switched to the as-received groundwater, pressure rose very quickly. In a separate column experiment using aerated deionized water, the pressure rose very quickly from the start. Thus, plugging occurred with water with no carbonate but high dissolved oxygen and did not occur with water with high carbonate and low dissolved oxygen. This confirms that dissolved oxygen is the principal source of plugging at column entrances.

Wavelength dispersive spectroscopy analysis of a plug taken from the entrance to a plugged iron column showed no calcium, minimal carbon and high levels of iron, confirming that the plugging is due to iron oxides and not carbonate precipitates.

Several approaches for scavenging oxygen without leading to system plugging have been identified. Figure 2 compares two approaches. The rapid pressure rise seen with the smaller iron particles (0.42 - 1 mm) was dramatically reduced by using larger iron particles (1 - 4.8 mm), leading to longer system lifetime. The large particles afford larger pore spaces and less particle-to-particle contact, hence they are harder to bridge together. A further lifetime extension is achieved by admixing sand particles of the same size with large iron particles. In all of these cases, the iron retained its ability to remove dissolved oxygen. Cercona pellets (93% ion, balance aluminosilicate, 2.4 - 3.4 mm) also performed very well - showing no plugging tendencies until they lost their ability to remove dissolved oxygen from the water.

The best system identified to date for scavenging dissolved oxygen from water is admixing large iron particles with sand of a similar size. Smaller sand particles may become lodged in the pore spaces between iron particles and not serve the role of separating the iron particles and minimizing the particle-to-particle contact that can lead to bridging and plugging. The uniform shape of the Cercona pellets has the same effect.

The best systems have treated > 2600 pore volumes of highly aerated water without plugging. For a groundwater flow of 0.3 m/day (1 foot/day), this translates to a zone 0.5 m (1.5 feet) thick of oxygen-scavenging material to yield an operational life of 10 years. A less oxygenated water will require a smaller oxygen-scavenging zone. In these designs, it is envisioned that after the oxygen-scavenging zone the bulk media would consist of the more typical iron media - 100% iron and perhaps smaller particle size - to maximize zone reactivity and minimize zone thickness.

Since it is associated with high dissolved oxygen levels, plugging is anticipated to be an issue only for walls emplaced in aerobic aquifers and for *ex-situ* canister tests where significant dissolved oxygen is introduced by the pumping of water above ground. It should not be an issue in an anoxic aquifer.

Porosity Changes in Bulk Iron Media

A second factor that will affect the lifetime of iron walls is loss of system porosity. From a variety of techniques, including tracer tests, aqueous inorganic profiles, and surface analysis of iron, it is well established that porosity losses and mineral precipitation occur in iron systems. In order to control precipitation and hence porosity losses, it is important to understand some of the factors that affect mineral precipitation and to understand which precipitates form under given conditions. Factors that affect the type and extent of precipitation include: pH, carbonate level, iron corrosion rate, and residence time in the system. Observation from various treatability studies will be used to illustrate the impact of these variables (General Electric and ETI 1996, Horney *et al.* 1995, Mackenzie *et al.* 1995a).

To measure how porosity changes over time, a tracer test technique suitable for use in iron columns was developed. Eykholt et al. (1995) discuss the details of the technique, which consists of monitoring the breakthrough curve of a non sorbing tracer (D_2O, deuterium oxide) at various sample ports in a column system. Comparison of measured tracer curves with theoretical predictions, based on the van Genuchten model (van Genuchten 1981), and with curves measured at the start of the experiment allows estimation of the changes in porosity over time.

Porosity losses in iron systems can be attributed both to precipitation of minerals and evolution of H_2 gas. Under the anaerobic conditions that exist in the bulk of the media, iron is reduced by water:

$$Fe^0 + 2H_2O <-> Fe^{2+} + H_2 + 2OH^- \tag{1}$$
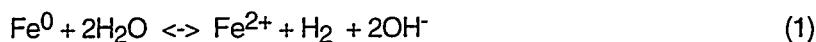
The resultant rise in pH can lead to the precipitation of ferrous hydroxide:

$$Fe^{2+} + 2OH^- <-> Fe(OH)_{2(s)} \tag{2}$$

In carbonate-containing waters, the rise in pH from the anaerobic corrosion of iron will shift the carbonate-bicarbonate equilibrium and lead to the precipitation of calcium carbonate and ferrous carbonate (siderite):

$$HCO_3^- + OH^- <-> CO_3^{2-} + H_2O \tag{3}$$

$$Fe^{2+} + CO_3^{2-} <-> Fe(CO_3)_{(s)} \tag{4}$$

$$Ca^{2+} + CO_3^{2-} <-> Ca(CO_3)_{(s)} \tag{5}$$

The equilibrium constants controlling these relationships are summarized below.

Equilibrium Expression	Equilibrium Constant
$(H^+)(CO_3^{2-})/(HCO_3^-) = K_2$	$K_2 = 4.7 \times 10^{-11}$
$(Fe^{2+})(OH^-)^2 = K_{Fe(OH)2}$	$K_{Fe(OH)2} = 8 \times 10^{-16}$
$(Fe^{2+})(CO_3^{2-}) = K_{FeCO3}$	$K_{FeCO3} = 3.2 \times 10^{-11}$
$(Ca^{2+})(CO_3^{2-}) = K_{CaCO3}$	$K_{CaCO3} = 2.8 \times 10^{-9}$

Thus, three main precipitates may form due to the chemistry in the iron zone: $Fe(OH)_2$, $FeCO_3$, and $CaCO_3$. All of these precipitates will reduce the pore volume in an iron system. H_2 evolution and retention will also lead to porosity losses. Although no distinct gas bubbles were observed during tracer tests, the formation of a thin film of H_2 gas on the surface of the iron particles could be significant in reducing measured porosity.

In typical iron column experiments, the pH value rises quickly and then levels off, suggesting a balance between anaerobic corrosion of iron and precipitation of basic species.

Figure 3 shows a set of tracer curves measured at the start and during an iron column experiment (Mackenzie 1995a). The tracer curves are for the second and the third column in an experimental set up consisting of four columns in series. A simulated groundwater was used for this part of the experiment, consisting of 40 mg/L $CaCO_3$ with pH adjusted to about 8 with CO_2. The second tracer test was measured after about 1750 hours of operation, when 210 pore volumes (2900 L) had been treated. The measured breakthrough curves correspond to porosity losses of 5 - 10% throughout the system.

Typical inorganic profiles measured in column systems show most of the loss of inorganics (calcium and carbonate) occurs early in these systems. This appears inconsistent with the uniform nature of the porosity losses measured here and in other column studies (see below) and suggests that the porosity losses are due either to $Fe(OH)_2$ precipitation or to the formation of a film of H_2 on the iron particles, processes that would occur throughout the iron zone.

Iron samples removed from the column and analyzed by x-ray photoelectron spectroscopy (XPS) and wavelength dispersive spectroscopy (WDS) showed the presence of oxidized iron and

carbonate and non-detectable amounts of calcium, pointing to iron-based precipitates as the dominant species.

The relative impact of carbonate precipitates can be discerned by considering the total amount of carbonate introduced into the system. Up to the time of the tracer test, approximately 1.2 mol carbonate were introduced. Using a molar volume of 35 ml/mol, representative of $CaCO_3$, this corresponds to about 42 ml of precipitate formed, or about 0.3% of the total system pore volume of 13.6 L. Hence, only a small portion of the porosity losses measured here can be attributed to carbonate precipitates, either calcium or ferrous. Given the porous nature of the precipitate film as observed by scanning electron microscopy, there is the possibility that the precipitates effectively occupy a greater volume than their molar volume, trapping stagnant water that is "lost" to the system. However, the magnitude of this effect is probably not large enough to account for the porosity losses measured here.

Some estimate of the magnitude of the amount of Fe^{2+} formation, and hence the amount available to precipitate, can be made based on measured anaerobic corrosion rates (Reardon 1995). Using 1 mmol Fe^{2+} /kg iron/day as a typical rate, about 5 mol Fe^{2+} would have been formed in this experiment up to the time of the tracer test. At the pH levels measured in these columns (8.5-10), all of this would be expected to precipitate. Using a molar volume of 26.4 ml/mol for $Fe(OH)_2$, this corresponds to about 1% of the system pore volume. (This approximation is not rigorous in that it does not consider the volume previously occupied by the Fe^0). In addition, at this anaerobic corrosion rate, the amount of H_2 produced in one day would result in a 10% porosity loss if it were all retained in the system.

Overall, for the system described here, a low alkalinity, simulated groundwater, the measured porosity losses appear due to H_2 entrapment and also to $Fe(OH)_2$ precipitation. The formation of this precipitate is very pH sensitive (equation 2). Reducing the pH in the system from 9 to 7.5 results in a three order of magnitude increase in equilibrium Fe^{2+} concentration and should dramatically limit the extent of $Fe(OH)_2$ precipitation. For a low carbonate groundwater, this could minimize porosity losses over long times.

When the feed to this system was switched to a high carbonate groundwater (approximately 400 mg/L alkalinity and hardness as $CaCO_3$) only a small additional increase in porosity losses was observed after treating 110 pore volumes of this water. There was no change in porosity in the second column and the third column increased from a 5% to about a 10% loss. Such a small change is somewhat surprising given the much higher amount of carbonate in this water. The inorganic profiles showed gradual loss of calcium and carbonate throughout the system, rather than the more typical pattern of fairly rapid initial loss. The total carbonate actually lost in this part of the experiment would account for about a 2% loss in porosity throughout the whole system and may explain the small porosity loss increase observed with this water. More extensive carbonate losses had been expected. XPS and WDS analysis of iron after this part of the experiment confirmed the presence of calcium as well as carbonate and oxidized iron, showing all three precipitates to be present. The relatively unchanging porosity losses measured throughout this experiment may be indicative of a steady state balance between precipitation and sloughing off of precipitates and their subsequent migration out of the system. However, they are more likely controlled by a thin film of entrapped H_2 gas on the surface of the iron particles, which reaches a stable film thickness. Over longer treatment times, mineral precipitation may dominate porosity losses.

At the measured pH values, the calculated equilibrium carbonate levels are lower than those measured. Hence, the column effluents are supersaturated with respect to $CaCO_3$ and probably also with respect to $FeCO_3$. $CaCO_3$ precipitation from supersaturated waters can be inhibited by the presence of magnesium and naturally occurring organics (Greenberg et al. 1992). In addition, the precipitate layer formed early in the experiment may be inhibiting the formation of more precipitate by limiting access to the metal surface. In either case, in this and in other systems (see below) carbonate precipitation is not entirely controlled by pH and the effect of pH control on minimizing carbonate precipitation and porosity losses is not well understood.

In another experimental study using a groundwater with moderate alkalinity (110 mg/L as $CaCO_3$), a tracer test after 1770 hours of operation, when 560 pore volumes (215 L) had been treated showed 5-15% porosity loss throughout the system (Horney 1995). Inorganic profiles from this point in the experiment were not measured, but assuming complete loss of carbonate, only a 2.5% porosity loss is expected. A tracer test measured later in the experiment showed no additional loss of porosity. These observations again point to the importance of H_2 entrapment and $Fe(OH)_2$ precipitation in controlling porosity losses early in a treatment process.

Inorganic profiles obtained in a third study show the impact of residence time on extent of carbonate precipitation (General Electric and ETI 1996). Figure 4 shows the carbonate profile across a column system at two different flow rates. The calcium profile behaved similarly. The lower residence time (150 min versus 1400 min) at the higher velocity results in less precipitation, showing that carbonate precipitation is a rate controlled process. At the lower velocity, an "equilibrium" value is reached, although again, the solution is supersaturated with respect to carbonate. At the higher velocity, the residence time is not sufficient for this level to be reached. This effect has impact for "aging" studies run at accelerated velocities. The lower carbonate loss at higher velocities means the iron is not "aged" as extensively as may be anticipated. Indeed, inorganic profiles obtained at even higher velocities resulted in a situation in which the carbonate loss per unit time was actually less despite the higher throughput.

In these last two studies, carbonate loss always exceeded calcium loss, indicating the formation of both $FeCO_3$ and $CaCO_3$ precipitates, as well as $Fe(OH)_2$.

These studies show that, for short treatment times, measured porosity losses are most likely due to entrapment of a film of H_2 gas on the surface of iron particles and also to precipitation of $Fe(OH)_2$. In low carbonate waters, $Fe(OH)_2$ and $FeCO_3$ are the dominant precipitates and, in higher carbonate waters, $Fe(OH)_2$, $FeCO_3$ and $CaCO_3$ all precipitate. These precipitates will control porosity losses over longer treatment times. Solutions often appear to be supersaturated with respect to $CaCO_3$ precipitation and so the benefit of pH control for minimizing carbonate precipitation in these systems is not well established.

Controlling Precipitation and Porosity Losses

A study currently underway is designed to examine how pH control affects mineral precipitation and porosity losses in iron systems. Several researchers have found good control of pH in iron systems through the addition of sulfur-based minerals. For instance Sivavec et al. (1995) have shown that admixing iron sulfide with granular iron results in controlled pH while still maintaining good reactivity (Sivavec 1995). Modeling results of Holser et al. (1995) suggest that controlled pH will lead to less precipitation. Despite these observations, previous studies have not measured the extent of mineral precipitation and porosity losses in these systems. In the current program, inorganic profiles and tracer tests for columns containing 100% granular iron and 15 wt% FeS and 85 wt% granular iron are being compared. Columns are being run at a velocity of 1.2 m/day, with about a 12 hour residence time.

The FeS/Fe system has shown good pH control, with the effluent pH about 7.8 versus 8.8 for the Fe-only column. Figure 5 shows the carbonate profiles are identical after 20 pore volumes. The calcium profiles are also identical. This suggests that pH alone does not control the extent of carbonate precipitation and that some other factor(s) must be important. Indeed, as above, both effluent streams are supersaturated with respect to calcium carbonate precipitation. This does not appear to be a rate effect as both profiles show a fairly rapid decrease to the final value with no further change throughout the rest of the system.

Tracer tests have not been conducted at this point. Based on input carbonate levels, porosity changes attributable to carbonate precipitation should only account for about a 1% loss up to the first sample port - below what can be detected by this method. Any measurable change in porosity will presumably be due to H_2 film entrapment or $Fe(OH)_2$ precipitation. The extent of

precipitation of Fe(OH)$_2$ could be greatly affected by pH control in this range, and hence a significant difference in porosity changes between these two systems over long times is possible. The inorganic profiles will continue to be monitored to look for changes over time.

References

Eykholt, G.R., S.S. Baghel, T.M. Sivavec, P.D. Mackenzie, D.H. Haitko, and D.P. Horney. (1995) Conservative flow tracers for iron column studies. In *ACS Division of Environmental Chemistry Proceedings, 35(1)*, Anaheim, CA, pp. 818-821.

General Electric Corporate Research and Development Center and EnviroMetal Technologies, Inc. (1996)*Treatability Studies: GE Appliances Hazardous Waste UST Closure EPA ID#WID006121347*. Final report submitted to Wisconsin Department of Natural Resources, March 1996.

Greenberg, A.E., L.S. Clesceri, and A.D. Eaton. (1992) Calcium carbonate saturation. In *Standard Methods for the Examination of Water and Wastewater*, p 2-29. American Public Health Association, Washington, DC.

Holser, R.A., S.C. McCutcheon, and N.L. Wolfe. (1995) Mass transfer effects on the dehalogenation of trichloroethene by iron/pyrite mixtures. In *ACS Division of Environmental Chemistry Proceedings, 35(1)*, Anaheim, CA, pp. 778-779.

Horney, D.P., P.D. Mackenzie, J.J. Salvo, and T.M. Sivavec. (1995) *Zero-Valent Iron Treatability Study for Groundwater Contaminated with Chlorinated Organic Solvents at the Paducah, KY GDP Site*, Final Report submitted to Lockheed Martin Energy Systems, Inc, US DOE Contract No. DE-AC05-840R21400, Subcontract No. 1CP-GEC43C, Dec 1995.

Mackenzie, P.D., S.S. Baghel, G.R. Eykholt, D.P. Horney, J.J. Salvo, and T.M. Sivavec. (1995a) Pilot-scale demonstration of reductive dechlorination of chlorinated ethenes by iron metal. In *ACS Division of Environmental Chemistry Proceedings, 35(1)*, Anaheim, CA, pp. 796-799.

Mackenzie, P.D., S.S. Baghel, G.R. Eykholt, D.P. Horney, J.J. Salvo, and T.M. Sivavec. (1995b) Pilot-scale demonstration of chlorinated ethene reduction by iron metal: factors affecting iron lifetime. In *Emerging Technologies in Hazardous Waste Management VII*. ACS Industrial & Engineering Chemistry Division, Sep 17-20, 1995. pp. 59-62.

Reardon, E.J. (1995) Anaerobic corrosion of granular iron: measurement and interpretation of hydrogen evolution rates. *Environ. Sci. Technol., 29(12)*, 2936-2945.

Sivavec, T.M. (1995) US Patent 5,447,639. Method for Destruction of Chlorinated Hydrocarbons in Aqueous Environments.

Sivavec, T.M., D.P. Horney, and S.S. Baghel. (1995) Reductive dechlorination of chlorinated ethenes by iron metal and iron sulfide minerals. In *Emerging Technologies in Hazardous Waste Management VII*. ACS Industrial & Engineering Chemistry Division, Sep 17-20, 1995. pp. 42-45.

van Genuchten, M.T. (1981) Analytical solutions for chemical transport with simultaneous adsorption, zero-order production and first-order decay. *J. Hydrology, 49*, 213-233.
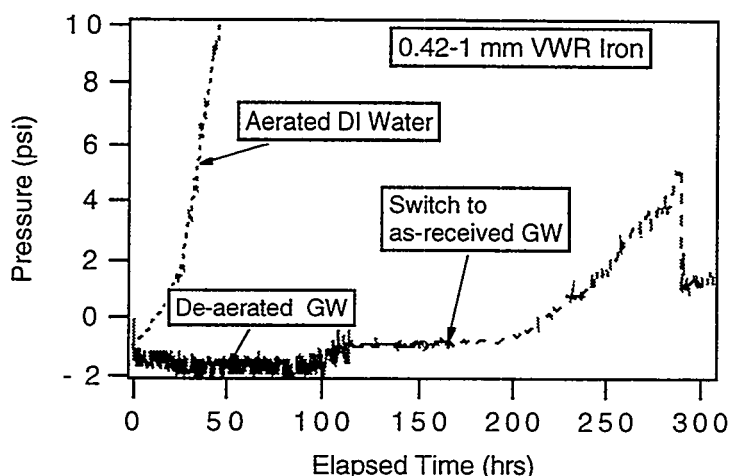
Figure 1. Plugging Tendencies of Different Waters. Aerated deionized water rapidly plugged an iron column, as evidenced by the rapid pressure rise. De-aerated site groundwater showed no plugging tendencies, whereas switching to the as-received, highly aerated site groundwater resulted in rapid plugging. (Note that the negative pressure values are due to a shift in the pressure transducer calibration and do not indicate sub atmospheric pressures.)
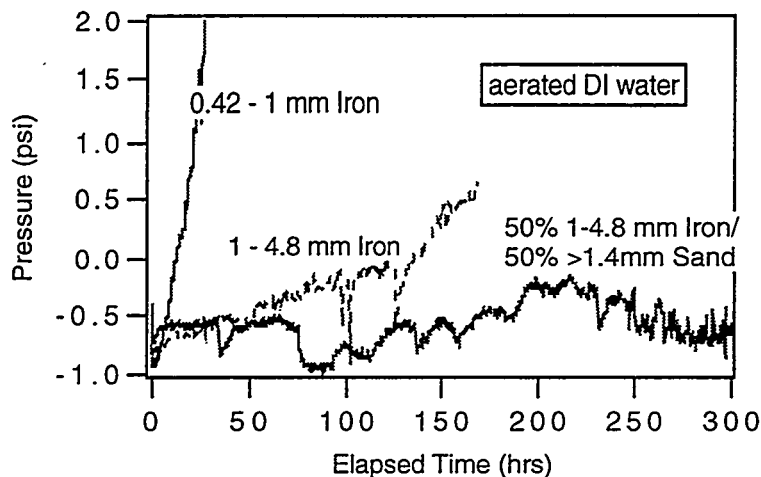
Figure 2. Approaches for Controlling Plugging Due to Dissolved Oxygen. The rapid pressure rise, indicative of system plugging, seen with the smaller iron particles is dramatically reduced by using larger iron particles and iron/sand mixes, leading to longer system lifetime.
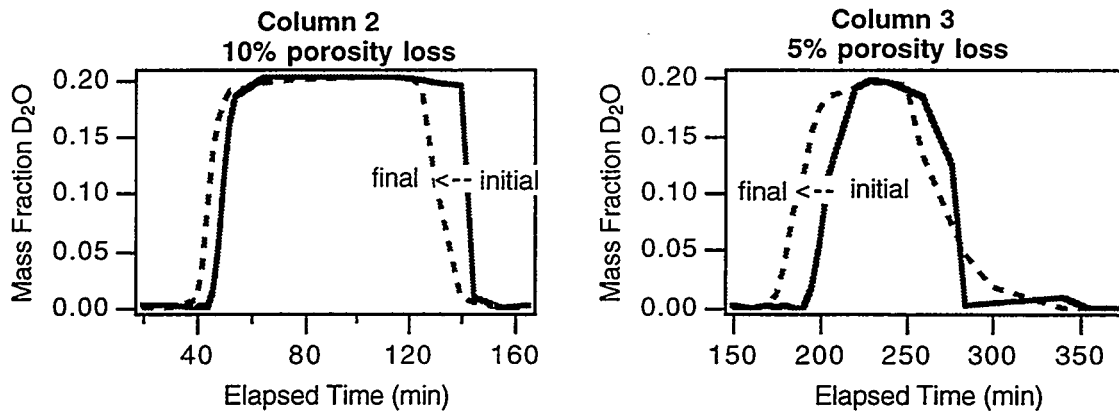
Figure 3. Porosity Losses in Iron Columns After Treating Low Alkalinity, Simulated Groundwater. In this mullet-column system, porosity losses occurred throughout the bulk of the iron media, as indicated by the shift in non-sorbing tracer curves to the left in all of the columns. This suggests the importance of $Fe(OH)_2$ as a precipitate.
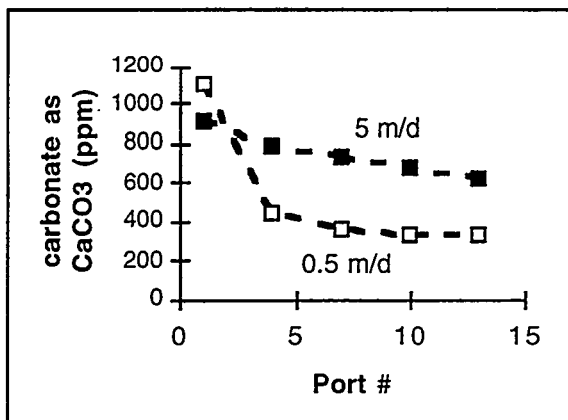
Figure 4. Effect of Residence Time on Carbonate Precipitation. Carbonate loss is less at the higher velocity due to the reduced residence time. Carbonate precipitation is a rate-dependent process.
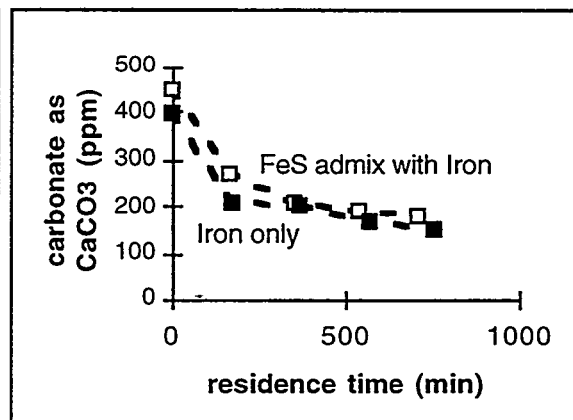
Figure 5. Effect of pH Control on Carbonate Precipitation. The effluent pH of the FeS/Fe column was 8.4 versus 9 for the Fe only column, yet there is no difference in the extent of carbonate precipitation.

787

PERMEABLE TREATMENT WALL DESIGN AND COST ANALYSIS

Chris Manz[1] and Kenneth Quinn[2]

ABSTRACT

A permeable treatment wall utilizing the funnel and gate technology has been chosen as the final remedial solution for one industrial site, and is being considered at other contaminated sites, such as a closed municipal landfill. Reactive iron gates will be utilized for treatment of chlorinated VOCs identified in the groundwater. Alternatives for the final remedial solution at each site were evaluated to achieve site closure in the most cost effective manner. This paper presents the remedial alternatives and cost analyses for each site. Several options are available at most sites for the design of a permeable treatment wall. Our analysis demonstrates that the major cost factors for this technology are the design concept, length, thickness, location and construction methods for the reactive wall. Minimizing the amount of iron by placement in the most effective area and construction by the lowest cost method is critical to achieving a low cost alternative. These costs dictate the design of a permeable treatment wall, including selection of a variety of alternatives (e.g., a continuous wall versus a funnel and gate system, fully penetrating gates versus partially penetrating gates, etc.). Selection of the appropriate construction methods and materials for the site can reduce the overall cost of the wall.

INTRODUCTION

Permeable treatment wall technologies have been evaluated as a groundwater remedial alternative at many sites throughout the world. A permeable treatment wall is, in general, a wall of reactive material that will treat the contaminants of concern. Two general approaches are, either a continuous wall of permeable treatment material (iron, carbon, etc.), or a treatment wall which utilizes the funnel and gate technology. The funnel and gate technology utilizes a barrier wall (i.e. sheet piling, slurry walls, etc.) to funnel groundwater to a permeable portion of the wall (gate) for treatment. In particular, iron wall systems have been considered as technically viable alternatives for treatment of chlorinated volatile organic compounds (VOCs), and some other contaminants as well (Matheson and Tratnyek, 1994; Starr and Cherry, 1994; Powell, Puls, and Paul, 1994). Chlorinated VOCs passing through the gate are destroyed by the metal enhanced reductive dehalogenation (MERD) process as illustrated in Figure 1.

As with any emerging technology, the cost of the technology decreases as more cost effective methods are found to implement the technology. The intent of this paper is to compare traditional remedial measures with some alternative design concepts and construction methods for this technology.

---

[1] Montgomery Watson - Wisconsin Program, 11925 West Lake Park Drive - Suite 200, Milwaukee, WI 53224, (414) 359-1144, Fax: (414) 359-1145, chris.manz@us.mw.com

[2] Montgomery Watson - Wisconsin Program, One Science Court, Madison, WI 53711, (608) 231-4747, Fax: (608) 231-4777, kenneth.quinn@us.mw.com

SITE DESCRIPTIONS

Industrial Site

A permeable treatment wall utilizing the funnel and gate technology has been chosen as the final remedial solution for an industrial site in Milwaukee, Wisconsin. The site has a shallow water table (approximately 2-3m (7-10ft) below grade) within clay and silty soils with relatively low permeability (1 x10^{-4} to 1x10^{-5} cm/sec). A groundwater and soil vapor extraction system was installed at the site in 1995 as an initial source control measure to reduce source area concentrations. Chlorinated VOCs (primarily TCE and its degradation products, with up to 50 ug/L of vinyl chloride) are present at the site, downgradient of the existing remediation system. A funnel and gate treatment wall will be installed with reactive iron gates for treatment of chlorinated VOCs identified in the groundwater (Figure 2).

After the initial source control measure was implemented, alternatives for the final remedial solution were evaluated to address the entire site and achieve site closure in the most cost effective manner. The two biggest factors in achieving site closure were to remediate local soil and groundwater to below state regulatory standards and to ensure no contamination migrates off-site. Soil excavation with a perimeter groundwater extraction and treatment (GWT) system was considered, but soil disposal costs made that option economically undesirable. Operation of the existing GWT system, in conjunction with a perimeter GWT system at the property boundary, was also considered. As shown in Table 1, the most cost effective alternative was implementation of the permeable treatment wall at the site. This allows the existing source control system to continue operation for only two more years; thus eliminating long term operation and maintenance (O&M) costs; and ensures no contamination will migrate off-site, as all groundwater will be treated by the permeable treatment wall.

Table 1 - Industrial Site Remedial Alternatives Cost Analysis

Remedial Alternative	Capital Cost	Annual O&M Cost	10 Year Net Present Worth (10%)	20 Year Net Present Worth (10%)	30 Year Net Present Worth (10%)
Excavation & Disposal w/ GWT System	$1,139,300	$55,000	$1,477,253	$1,607,548	$1,657,780
Existing and Perimeter GWT w/ SVE	$269,250	$75,220	$731,447	$909,643	$978,341
Permeable Treatment Wall	$440,206	$27,120	$606,847	$671,094	$695,920

Landfill Site

Remedial action options are being considered at a closed, unlined landfill site in Wisconsin. Groundwater beneath (and within) the site has up to 5,000 ug/L of chlorinated VOCs. A major component of the VOCs at the site is vinyl chloride. The landfill has only minor methane gas levels, but the site does not have a final, low permeability cover, which is now required by state regulations.

The subsurface conditions consist of up to 13.7m (45ft) thick sequence of unconsolidated deposits overlying a thick dense lean clay till. The clay till is >30.5m (>100ft) thick with a permeability of <1x10^{-6} cm/sec and forms a base to the shallow aquifer. The upper 13.7m (45ft) is typically heterogeneous. The upper 10.7m (35ft), consists mostly of organic clay with minor silt and sand layers. The lower ten feet is typically an outwash sand and gravel. Migration of the vinyl chloride primarily occurs within the sand and gravel deposit at depth. Migration in the shallow organic clay appears to be limited (probably due to its high retardation factor for chlorinated VOCs) and is present only in the thin silt and sand stringers. The organic clay/silt and sand zone has a bulk permeability of less than 1x10^{-4} cm/sec and the sand and gravel has a permeability of greater than 1x10^{-3} cm/sec.

The remedial action system currently required under the state's solid waste rules would consist of a landfill cover and gas extraction system. In addition, a groundwater extraction and treatment system would be installed to protect off-site groundwater quality. The landfill cover and gas extraction system is a requirement of the state regulatory agency to limit the rate of leachate generation and migration of contaminants away from the landfill. If a low permeability cover is installed, a landfill gas system would be required to extract potentially explosive gas that would accumulate beneath the low permeability landfill cover. If accumulated gas is not extracted, it could pose an explosive hazard to surrounding structures.

The rationale for a landfill cover is to semi-permanently limit the rate of leachate generation, thereby protecting groundwater in the long term. This is appropriate at sites where the contaminant is continuing to leach from the landfill. However, the groundwater is within the waste at this site, and the highest VOC concentrations are below the waste. Therefore, the only benefit of a cover is to limit direct exposure to the waste. An upgraded, low permeability cover would not provide significant groundwater protection at this site. Therefore, the two options to be considered are the landfill cover/gas extraction/GWT system and a permeable treatment wall. The costs for these alternatives are outlined in Table 2.

Table 2 - Landfill Site Remedial Alternatives Cost Analysis

Remedial Alternative	Capital Cost	Annual O&M Cost	10 Year Net Present Worth (10%)	20 Year Net Present Worth (10%)	30 Year Net Present Worth (10%)
Landfill Cover, Gas Extraction System, and GWT System	$3,550,000	$100,000	$4,164,457	$4,401,356	$4,492,691
Permeable Treatment Wall	$1,975,000	$20,000	$2,107,891	$2,155,271	$2,173538

BARRIER WALL DESIGN AND ANALYSIS

Industrial Site

In the design of the permeable treatment wall for each specific site, costs are a major driving factor that affects the design. One factor to consider is the location of the wall. The treatment wall must be placed where it will capture and treat all of the contaminated groundwater to the limits established by the regulatory agency. The farther downgradient from the source area the wall is located, the longer the overall length may be. As the treatment wall is moved closer to the source area, the larger the capital costs savings for wall construction will likely be. Another factor affecting costs is the expense of the iron for gate construction. The treatment gates are constructed utilizing zero valent iron (Vogan et al, 1994), which costs approximately $413/metric ton. Efficient use of iron for treatment is essential to keeping the cost of the treatment wall to a minimum.

At the Milwaukee industrial site, both a continuous permeable treatment wall and a funnel and gate system were evaluated. A confining clay layer exists at approximately 5.5m (18ft) below grade. Based on the geology, the treatment wall will be installed to approximately 6.1m (20ft) to anchor into the confining layer. At the eastern property boundary, the confining clay layer dips down to approximately 6.7m (22ft) and a more permeable sand seam is present with a higher groundwater velocity. In the design of the treatment gate, the gate thickness is calculated and is directly proportional to the groundwater velocity. As a cost saving measure, it was decided to move the location of the wall upgradient of this more permeable zone. Otherwise, in the more permeable zone, the barrier wall would need to be deeper and the treatment gates would have to be thicker. At $413/metric ton for iron, the thinner, shallower gates will significantly reduce the cost of the treatment wall.

A continuous permeable treatment wall involves installing a continuous wall of zero valent iron for treatment of all site groundwater as it passes through the wall. The continuous wall at the Milwaukee site would have to be approximately 335m (1,100ft) long. In evaluating the costs for this option, it was determined that the amount of zero valent iron required in the treatment wall to meet the discharge standards (0.2 ug/L vinyl chloride) would cost approximately $1.5 million alone. Based on this analysis, a funnel and gate approach for the site was adopted.

Technologies for barrier walls were evaluated based on effectiveness and costs. The barrier wall for the Milwaukee site has a length of 335m (1,100ft) and a depth of approximately 6.1m (20ft.) The following technologies were found to be technically feasible and were evaluated based on costs: 1) Steel sheet piling with interlocking seal ($200k - $250k), 2) Soil-bentonite slurry wall ($175k -$225k), and 3) Geomembrane panels with interlocking seals ($175k - $225k). The final decision on the barrier wall will be determined based on contractor's bids and recommendations for construction.

Landfill Site

The downgradient perimeter of the landfill site is approximately 305m (1,000ft) long. The depth of the base of the aquifer is approximately 13.7m (45ft). A continuous permeable treatment wall at this site is not practical because the volume of iron that would be needed is very large $(1,912m^3 (67,500ft^3))$, which makes that option not economically feasible. Therefore, the funnel and gate approach is currently considered to be the only economically feasible approach. The funnel's low permeability wall would probably be constructed of a typical slurry wall because of the depth and length of the wall. However, as mentioned for the Milwaukee site, the geomembrane panels may be similar in cost and could be considered at this site.

PERMEABLE GATE DESIGN AND ANALYSIS

Industrial Site

As illustrated in Figure 2, the Milwaukee industrial site will have three treatment gates located in the barrier wall. Extensive groundwater modeling was completed to ensure all contaminated site groundwater would pass through the treatment gates and that no contaminated groundwater would travel around the barrier wall. The groundwater modeling and the contaminant concentrations determined how wide and thick the treatment gates must be. As derived from the first order decay rate equation, the formula for the thickness of the treatment gate is:

$$T=\ln(C_{final}/C_{initial})((GW_{gate\ velocity})/\text{decay constant})(FS)$$

where: T = thickness of the gate
C = groundwater contaminant concentration
$GW_{gate\ velocity}$ = groundwater velocity through the gate
FS = factor of safety

For the Milwaukee site, the groundwater velocity is approximately 0.15m/day (0.5ft/day) in the gate, the limiting contaminant is vinyl chloride, which has a concentration of 50 ug/L ($C_{initial}$) and a very low regulatory standard of 0.2 ug/L (C_{final}), and a factor of safety of two (2) is being utilized. The decay rate (1.87 d^{-1}) was measured in a bench scale treatability study that was conducted by Envirometals, Inc. using site groundwater. Based on these requirements, the treatment gate will be approximately 4m (13ft) high, 1.5m (5ft) wide, and 1m (3ft) thick. The iron costs for each gate will be approximately $7,000.

Construction of the treatment gates at the Milwaukee site will likely be completed utilizing a trench box. Other treatment gate installation techniques were considered, but due to the shallow depth of the wall, the trench box is the most cost effective option. Either a prefabricated box or driven steel sheet pilings will be placed in the trench and filled with the zero valent iron filings. After the box is full, the trench box or sheet piling will be removed, and the gate construction will

be complete. Total installation costs for each treatment gate is estimated to be approximately $10,000. Some other treatment gate installation techniques will be discussed in the next section.

A method to reduce fouling of the treatment gate will be utilized at the site. Some potential methods include: mixing a small percentage of native soils with the iron in the treatment gate; a removable cassette filled with iron or another oxygen sink; or the use of large iron chips as an oxygen sink followed by a transition zone to the smaller, more reactive iron filings (Mackenzie et al, 1995). Installation of one of these methods will reduce long term O&M costs of the treatment gate.

Landfill Site

The treatment gates are a significant portion of the cost for the funnel and gate system at the landfill site discussed here. This is due to two factors, the relatively large depth to the base of the aquifer (13.7m (45ft)) and the relatively high VOC concentrations, primarily vinyl chloride. The design for the gate considered two design concepts and two construction techniques.

The two design concepts are a fully penetrating gate verses a partially penetrating gate. The fully penetrating gate would place iron filings throughout the entire saturated zone, allowing essentially horizontal flow of groundwater through the gate. A partially penetrating gate would place iron filings only within the high permeability sand and gravel zone, at the base of the unconsolidated zone. The portion of the gate above this zone would be backfilled with a low permeability seal, to prevent migration through this area. Flow in the shallow, lower permeability portions of the aquifer would have to travel down to the high permeability zone. An alternate approach to this design would be to have a thick gate at depth, in the higher permeability sand and gravel zone and a thinner gate in the lower permeability organic clay zone. However, the potential for short circuiting through this type of gate is too great and the partially penetrating gate is preferred. Given the large ratio of permeability between the organic clay and the underlying sand and gravel (greater than 10 times), the rate of additional flow from the organic clay zone into the sand and gravel would be less than 10%. Given the safety factors built into the wall, this additional flow in the lower zone would be insignificant.

The typical gate construction used to date is a cofferdam or trench box construction. This may be because the first pilot and full scale systems were very shallow, so that a cofferdam was the lowest cost approach. The other approach to be considered for this site is the use of tangential caissons. This type of construction would include installing a slurry wall, drilling caissons into the slurry wall for the gate, and backfilling with the appropriate material (iron filings, bentonite seal or stone filter). Table 3 shows the cost for a typical gate (7.5m (25ft) wide, 3.1m (10ft) thick by 13.7m (45ft) deep) using both of these construction methods for both a partially penetrating and a fully penetrating gate.

Table 3

Alternative Gate Capital Costs	Trench box Construction	Tangential Caissons
Fully Penetrating (40 ft of iron)	$562,000	$425,000
Partially Penetrating (15 ft of iron)	$435,000	$300,000

As illustrated in Table 3, the use of tangential caissons is more cost effective at this depth and size of gate. The partially penetrating gate is very effective at reducing the cost of the gate by placing iron only within the zone of preferential groundwater flow and still effectively treating the contaminated groundwater.

CONCLUSIONS

Permeable treatment walls are a cost effective remedial alternative to achieve closure at contaminated sites. Long term O&M costs are significantly less than conventional remediation systems. Varying design and construction techniques allows for the technology to be utilized at sites with different geological and hydrogeological characteristics. Fitting the proper design concepts and construction techniques with the hydrogeologic setting is critical in achieving a low cost and effective system.

Industrial Site
The permeable treatment wall appears to be the most cost effective remedial alternative to achieve closure at the site. Design of the permeable treatment wall at this industrial site considered the location of the wall with respect to the hydrogeology and the type of wall to be placed. A continuous wall would require a large volume of iron, which controls the cost of this system. The location of the wall within the lower permeability material near the source area, reduces the overall length of the barrier wall, limits the thickness of the gates, while still collecting all the VOC contaminated groundwater at the site.

Landfill Site
The permeable treatment wall appears to be the most cost effective remedial alternative to achieve closure at the site. The lowest cost option for construction of a funnel and gate system at this landfill utilizes a partially penetrating gate constructed by tangential caissons. This design concept and construction method is controlled by the depth to the confining layer, approximately 13.7 m (45ft), and the presence of a deep, high conductivity sand and gravel zone. Placement of the iron in this zone, limits the volume of iron needed, and the cost to treat the contaminated groundwater at the site.

REFERENCES

Matheson, L.J., and P.G. Tratnyek. 1994. Reductive dehalogenation of chlorinated methanes by iron metal. Environmental Science and Technology 28, pp. 2045-2053.

Starr, R.C., and J.A. Cherry. 1994. In Situ Remediation of Contaminated Groundwater: The Funnel and Gate System. Groundwater, Volume 32, No. 3 pp. 465-476.

Powell, R.M., R.W. Puls, and C.J. Paul. 1994. Chromate reduction and remediation utilizing the thermodynamic instability of zero-valence iron. Innovative Solutions for Contaminated Site Management. Miami, FL.

Vogan, J.L., J.K. Seaberg, B. Gnabasik, and S. O'Hannesin. 1994. Evaluation of in-situ groundwater remediation by metal enhanced reductive dehalogenation - Laboratory column studies and groundwater flow modeling. 87th Annual Meeting of the Air & Waste Management Association, Cincinnati, OH, June 19-24, 1994.

Mackenzie, P.D., Baghel, S.S., Eykholt, G.R., Horney, D.P., Salvo, J.J., Sivavec, T.M. 1995. Pilot-Scale Demonstrations of Chlorinated Ethene Reduction by Iron Metal: Factors Affecting Iron Lifetime. I&EC Special Symposium of the American Chemical Society, Atlanta, GA, September 17-20, 1995.
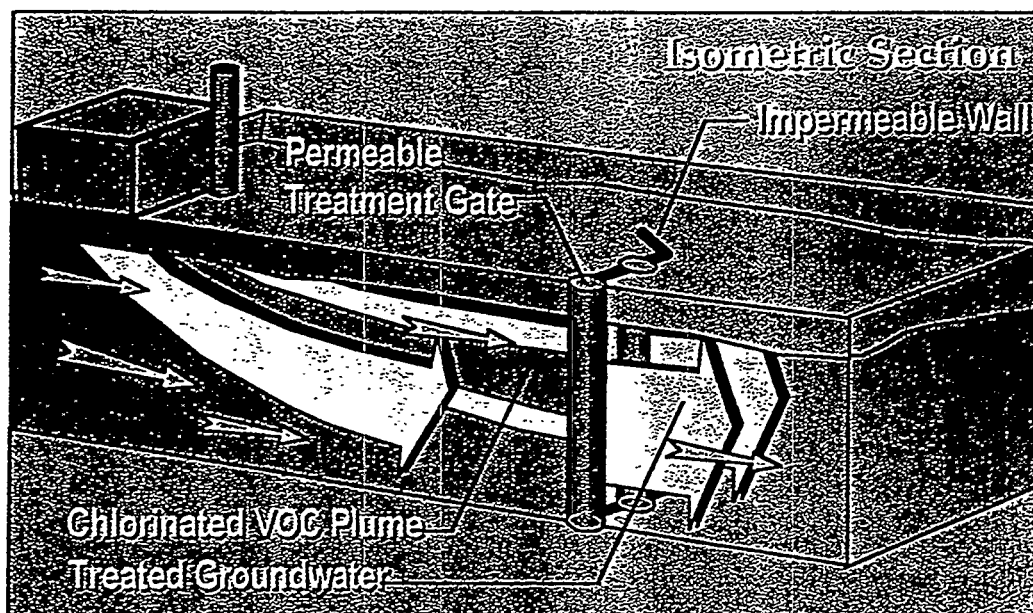
FIGURE 1
TYPICAL FUNNEL AND GATE CONFIGURATION
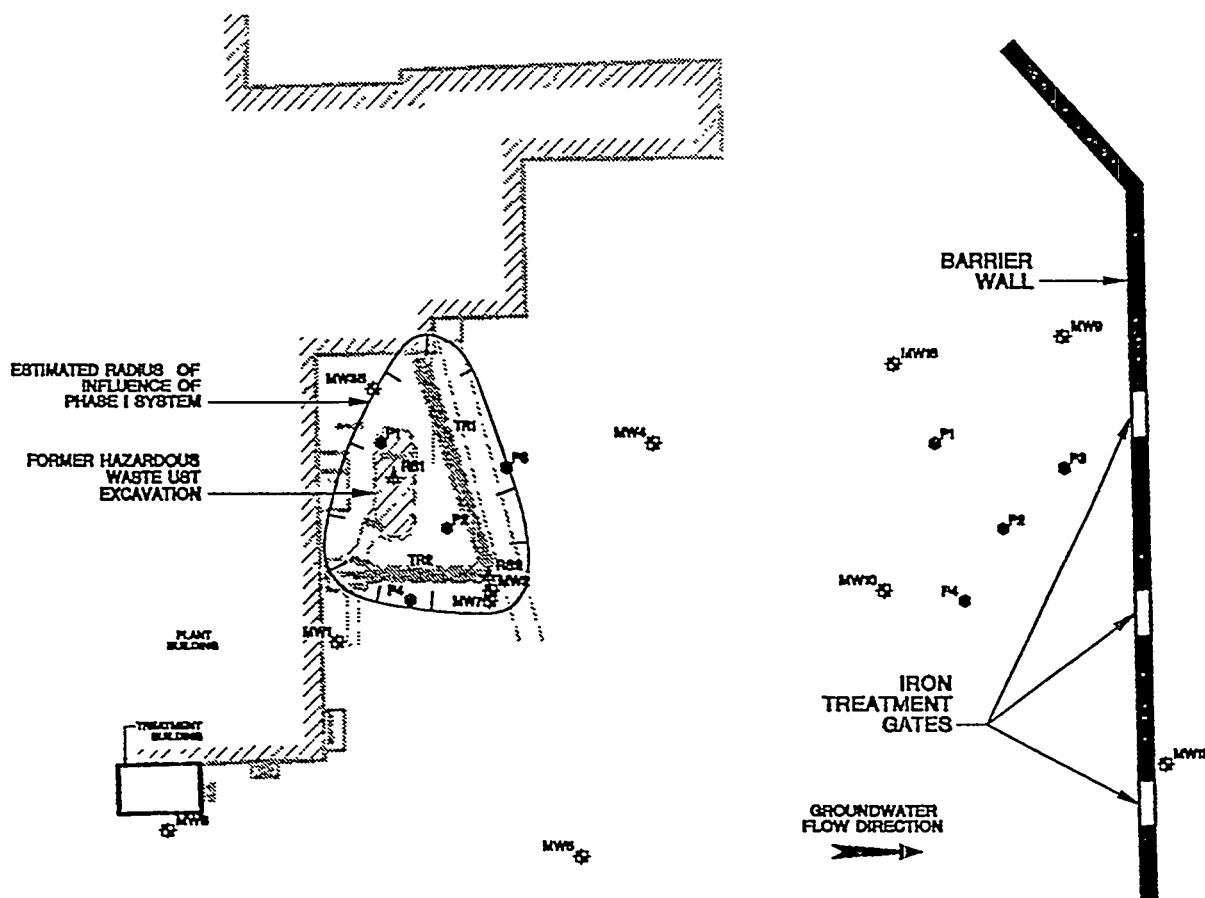
FIGURE 2
INDUSTRIAL SITE FUNNEL AND GATE

RCRA Corrective Measures Using A Permeable Reactive Iron Wall
U.S. Coast Guard Support Center, Elizabeth City, North Carolina

William L. Schmithorst[1] and James A. Vardy[2]

Abstract

A chromic acid release was discovered at a former electroplating shop at the U.S. Coast Guard Support Center in Elizabeth City, North Carolina. Initial investigative activities indicated that chromic acid had migrated into the subsurface soils and groundwater. In addition, trichloroethylene (TCE) was also discovered in groundwater during subsequent investigations of the hexavalent chromium (Cr VI) plume. Corrective measures were required under the Resource Conservation and Recovery Act (RCRA).

The in-situ remediation method, proposed under RCRA Interim Measures to passively treat the groundwater contaminants, uses reactive zero-valent iron to reductively dechlorinate the chlorinated compounds and to mineralize the hexavalent chromium. A 47 meter by 0.6 meter subsurface permeable iron wall was installed downgradient of the source area to a depth of 7 meters using a direct trenching machine. The iron filings were placed in the ground as the soils were excavated from the subsurface. This is the first time that direct trenching was used to install reactive zero-valent iron filings. Over 250 metric tons of iron filings were used as the reactive material in the barrier wall. Installation of the iron filings took one full day.

Extensive negotiations with regulatory agencies were required to use this technology under the current facility Hazardous Waste Management Permit. All waste soils generated during the excavation activities were contained and treated on site. Once contaminant concentrations were reduced the waste soils were used as fill material.

Introduction

The U.S. Coast Guard Support Center is located near Elizabeth City in northeastern North Carolina. The facility occupies approximately 800 acres, and is situated along the southern bank of the Pasquotank River, approximately eight miles upstream of its confluence with Albemarle Sound. The primary functions of the SCEC are the support, training, operation and maintenance associated with USCG aircraft.

The TCE/Cr (VI) site is located on the northeast part of the SCEC facility. The site is located immediately north of Building 79 which formerly housed an electroplating shop. The former electroplating shop was in use for approximately 30 years until 1984. The site is currently designated as a RCRA Solid Waste Management Unit (SWMU). The site plan is shown in Figure 1.

The first indication that a release of waste(s) from the facility had occurred was discovered during demolition of the former plating shop in December 1988. The demolition contractor discovered a hole approximately 0.5 meters in diameter in the concrete floor slab of the former plating shop below a tank which had contained chromic acid. The hole had penetrated a 122 meter (m) long, 0.3 m by 0.6 m concrete air-return duct connected to the central hangar heating distribution system. A water main break in the hangar approximately 5 years prior to the

[1] Parsons Engineering Science, Inc., 401 Harrison Oaks Blvd., Suite 210, Cary, NC 27513, (919) 677-0080, bill_schmithorst@parsons.com

[2] U.S. Coast Guard Civil Engineering Unit, SCEC, Bldg. 19, Elizabeth City, NC 27909, (919) 335-6847, javardy@ecsu.campus.mci.net

demolition of the former plating shop had flooded the air return duct, possibly spreading contaminants from the plating shop. The quantity of waste lost from the release(s) is unknown. Soil excavated beneath the floor of the former plating shop was found to contain chromium at concentrations up to 14,500 mg/kg. The majority of the contaminated soil at the site was believed to have been excavated at that time. However, subsequent investigations indicated that the groundwater had been impacted by Cr (VI). Additional environmental investigative activities indicated the presence of chlorinated compounds in groundwater.

Site Setting

The USCG facility is situated within the North Carolina Coastal Plain Physiographic Province. Topographically, SCEC and the surrounding area is essentially flat, and for the most part between 2.1 m and 3 m above mean sea level. Approximately 75 meters to the north, the site is bordered by the Pasquotank River.

The area of concern is underlain by surficial Pleistocene to Recent aged sediments. These sediments are comprised mainly of sandy clays and fine grained sands with varying amounts of silt and clay. The subsurface hydrogeologic environment is very heterogeneous with the primary groundwater flow direction towards the Pasquotank River. A continuous layer consisting of clayey fine sand to silty clay is present at a depth of approximately 7 m below land surface. Depth to groundwater at the site is approximately 2 m below ground surface.

Groundwater Contamination

Cr (VI) and TCE are primarily found in a silty fine sand to fine sand zone approximately 5 m to 6 m below land surface. Shallow contaminant migration in groundwater is restricted by lower permeability silty to clayey fine sand. Contaminants migrating in the groundwater are eventually discharged to the adjacent river. Concentrations of TCE detected in groundwater exceed 10 mg/L. In addition, Cr (VI) concentrations in groundwater exceed 5 mg/L. The regulatory limit for TCE is 0.005 mg/L and for Cr is 0.1 mg/L.

Corrective Measures

An in-situ permeable iron treatment wall was utilized as the corrective measure to remediate the Cr (VI) and TCE plume. A 46 m long by 0.6 m wide permeable treatment wall consisting of more than 250 metric tons of zero-valent iron was constructed to a depth of approximately 7 m below land surface using a continuous trenching machine. This was the first time that a continuous trencher has been used to install such a system. The continuous trencher is comprised of a cutting chain mounted on a tracked vehicle. A trench box is mounted directly behind the cutting chain and a hopper used for feeding granular material is mounted directly on top of the trench box. As the native material was excavated by the trencher, granular zero-valent iron was placed in the trench. The granular iron was continuously fed to a hopper permitting uninterrupted installation of the iron filings. The application rate of iron was measured by the feed rate of iron placed into the hopper. Installation of the iron filings was completed in one day. Costs for the iron were reduced by installing the iron from a depth of 2 m to 7 m below land surface. A schematic of the iron filings wall is shown in Figure 2.

The treatment wall was constructed downgradient of the source area to utilize the natural groundwater hydraulic gradient to transport the contaminants to the treatment zone. Contaminants are reduced prior to passing through the entire thickness of iron filings. The hydraulic conductivity of the treatment wall is greater than the hydraulic conductivity of the surrounding native material, thus not diverting the contaminant plume away from the treatment area. Treatability and groundwater flow modeling studies were conducted by the University of Waterloo and the USEPA National Risk Management Research Laboratory. The purpose for the treatability studies were to determine the effectiveness of the zero-valent iron as a treatment material and to determine the residence time needed to completely reduce the contaminants. Determination of the residence time provided the data needed to calculate the thickness of the wall.

Reaction Chemistry

TCE and Cr (VI) have been shown to be reduced by elemental iron. The net reaction of water, elemental iron and a chlorinated organic compound is suggested in the following equation, where X-Cl represents a chlorinated organic compound (Gillham and O'Hannesin, 1994):

$$2Fe^{o} + 3H_2O + X\text{-}Cl \rightarrow 2Fe^{2+} + 3OH^- + H_2 + X\text{-}H + Cl^-$$
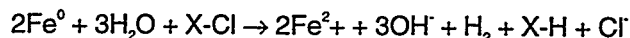
Cr (VI) has also been shown to reduce in the presence of iron metal (Powell et al., 1995). The net reaction in the presence of elemental iron is shown as:

$$Fe^{o} + CrO_4^{2-} + 4H_2O \rightarrow Fe(OH)_3 + Cr(OH)_3 + 2OH^-$$
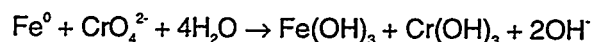
The reduction of chromate in the presence of elemental iron occurs rapidly.

Regulatory Considerations

The USCG facility is operating under a Hazardous Waste Management Permit. Therefore, all investigative and corrective measures activities are governed by regulations under RCRA. Investigative procedures and corrective measures are controlled by procedural functions as referenced in the permit and applicable regulations. Due to the regulations associated with a RCRA site, it can be challenging to propose a new innovative technology that has not yet been proven to work on a field scale level. The primary concern of the regulatory community besides the protection of human health and the environment is the consideration that if a responsible party obligates a substantial amount of funds to an innovative technology, sufficient funds may not remain to proceed with alternative measures if the technology fails. These concerns and others had to be addressed before proceeding with construction of the treatment wall.

A considerable amount of time was required to meet the regulatory requirements and answer all regulatory concerns. To meet the requirements of the Hazardous Waste Management Permit the project was approached as a RCRA Interim Corrective Measure. Under the permit, the waste soils generated during trenching activities were classified as remediation wastes. In order to meet regulatory requirements for handling of remediation wastes, a Corrective Action Management Unit (CAMU) was constructed to contain the waste soils. The CAMU completely contained the waste soils to prevent any release to the environment.

Engineering Considerations

Prior to installing the treatment wall, the main concern was the potential for liquids or a mud slurry to flow away from the work area and contaminate the surrounding environment. Therefore, berms consisting of plastic and hay bales were placed around the trenching area to prevent the contaminated soil and groundwater from flowing over land surface and impacting the surrounding environment. High capacity pumps and a large tanker were kept on standby at the site in case the volume of fluids and excavated soil exceeded the capacity of the bermed area. As a precaution, the top 1 m of soil was excavated to provide an area to hold fluids.

In addition, a storm sewer line that crossed the trenching area had to be cut to permit the trenching operation in the area. The upstream and downstream ends of the storm sewer were plugged to prevent potential runoff from entering the trench. The downstream end of the storm sewer had to be plugged because the discharge end of the line is in the river and the river is influenced by wind tides that also could flood the excavation.

Approximately 280 cubic meters of contaminated soils were generated during trenching activities. Results from the analysis of samples collected from the stockpiled soils indicated that chromium levels were at background levels. This was probably due to mixing and dilution effects from the trenching process. However, TCE remained at elevated concentrations making the soils a listed waste. The contaminated soil was transported to the CAMU and worked with earth moving equipment. TCE concentrations were reduced to below detectable concentrations within a few weeks. The USCG was then permitted to use the soil as backfill at the base.

In addition, health and safety conditions were monitored during construction. Respiratory protection equipment was available in case an upgrade in protection was required.

Problems Encountered During Construction

The major problem encountered during construction activities was caused by undermining of the soils beneath the concrete pavement. The undermining and weight of the trenching equipment caused large sections of the concrete to fracture and even collapse near the trench.

In addition, the trenching process created a loose slurry of fine sand, silt and clay that retained much of the groundwater as it was excavated. The soil slurry did not accumulate in piles as anticipated and tended to flow. Overland flow was controlled by the plastic and berms set up around the site. However, soil did flow back into the top of the trench as the trenching equipment was advanced. Subsequently, the first 1 m of contaminated soil had to be excavated from the trench after the trenching was complete.

A more accurate method of measurement should be applied to the rate of application of iron. This could possibly involve measuring the flow rate directly in the hopper on the trencher. In addition, due to the fluid-like nature of the soil cause by the mixing action of the cutting chain, subsurface soil mixed with the iron as it was applied resulting in a final treatment wall containing a mixture of native material and iron. However, treatability studies conducted by the University of Waterloo indicate that a mixture of iron with native material will create an effective treatment wall. One way to reduce costs is to limit the volume of iron used by mixing the iron with sand. This was not attempted for this project because the density differences between sand and iron would make it difficult to obtain a homogeneous mixture.

Conclusions

The effectiveness of the iron filings wall will be determined through long term monitoring using groundwater monitoring wells and multi-level samplers. One of the principal concerns with the long term viability of the treatment wall is the potential for changes in the hydraulics of groundwater flow along the wall. Due to the nature of the in-situ chemical reactions with iron, the pH of the groundwater in the immediate vicinity of zero-valent iron treatment wall can increase substantially. The increase in pH may cause precipitation of naturally occurring metals and carbonates along the interface of the treatment wall and the native subsurface material resulting in a loss of permeability of the treatment wall material. Decreasing permeability of the iron filings may cause the contaminant plume to flow around the treatment wall.

This project demonstrates the ability to translate an innovative technology and basic research into a viable field scale application, thanks to the efforts of the USEPA, the University of Waterloo, and the U.S. Coast Guard Civil Engineering Unit.

References

Gillham, R.W. and O'Hannesin, S.F. (1994) Enhanced degradation of halogenated aliphatics by zero-valent iron. *Ground Water*, 32: 958-967.

Powell, R.M., Puls, R.W., Hightower, S.K. and Sabatini, D.A. (1995) Coupled iron corrosion and chromate reduction: mechanisms for subsurface remediation. *Env. Sci. Technol.* 29:1913-1922.

FIGURE 1

SITE PLAN

CONCRETE PATCH 0.2m

UNDISTURBED EARTH

MINIMUM 0.6m
COURSE AGGREGATE

EXCAVATED NATURAL SOILS

0.6-1.2m

0.6m

8.5m

7m

EXISTING CONCRETE

IRON FILINGS WALL CROSS SECTION
N.T.S

MINIMUM 0.6m
COURSE AGGREGATE
0.6-1.2m EXCAVATED NATURAL SOILS

CONCRETE PATCH 0.2m

48m
IRON FILINGS

UNDISTURBED EARTH

8.5m

EXISTING CONCRETE

IRON FILINGS WALL LONGITUDINAL SECTION
N.T.S

1.2m

CONCRETE PATCH

0.6m

0.6m

0.6m

70m

EXISTING CONCRETE

IRON FILINGS

48m

EXISTING CONCRETE

9m

IRON FILINGS WALL PLAN VIEW
N.T.S

PLASTIC SHEETING

EXISTING CONCRETE

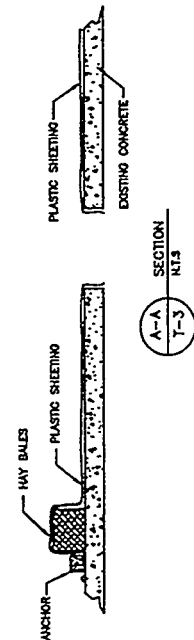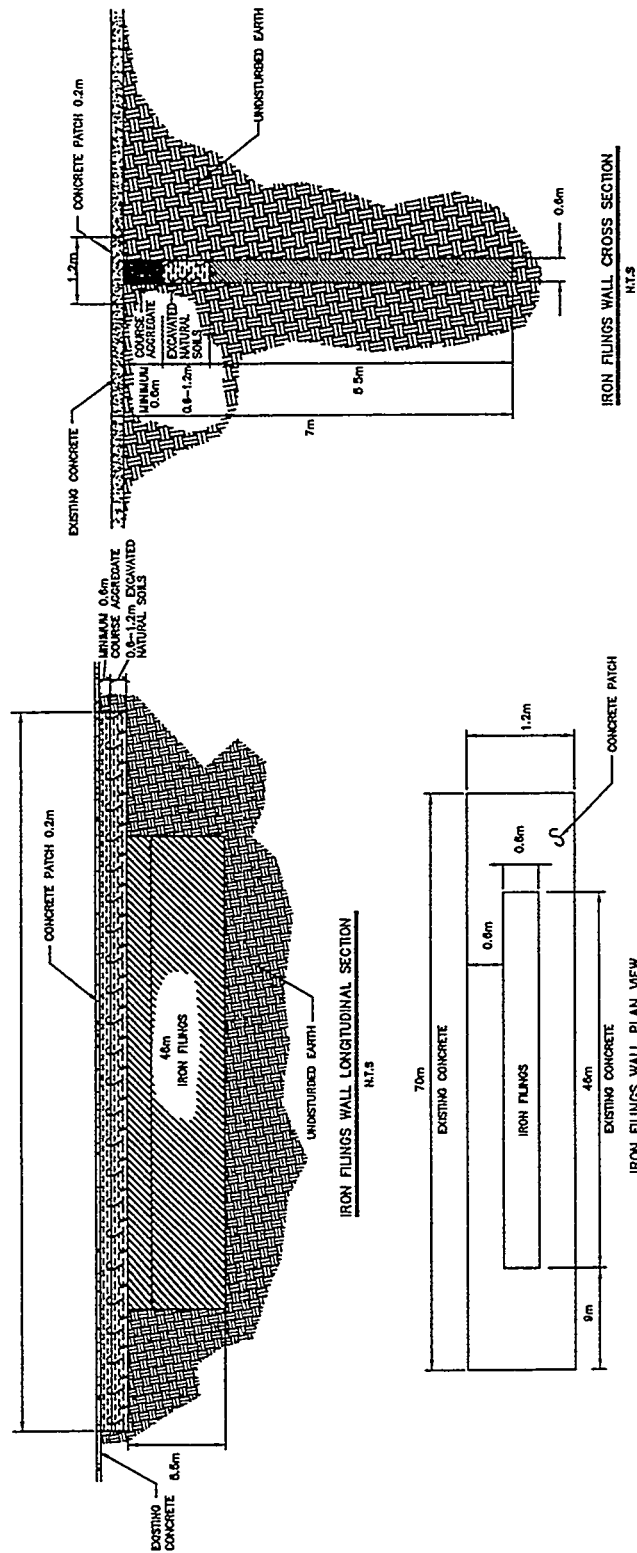HAY BALES

PLASTIC SHEETING

ANCHOR

A-A
T-3
SECTION
N.T.S

FIGURE 2

IRON WALL DETAILS
TREATMENT

800

# IDENTIFICATION OF PRECIPITATES FORMED ON ZERO-VALENT IRON IN ANAEROBIC AQUEOUS SOLUTIONS

Thea Schuhmacher[1]
Levine·Fricke·Recon
1920 Main Street
Suite 750
Irvine, CA
92614-7211
Tel. (714) 442-7296
Fax (714) 955-0683

M.S. Odziemkowski
University of Waterloo
Earth Science Dept.
Waterloo, ON
N2L 3G1
Tel. (519) 885 1211
Fax (519) 746-0183

E.J. Reardon
University of Waterloo
Earth Science Dept.
Waterloo, ON
N2L 3G1
Tel. (519) 885 1211
Fax (519) 746-0183

R.W. Gillham
University of Waterloo
Earth Science Dept.
Waterloo, ON
N2L 3G1
Tel. (519) 885 1211
Fax (519) 746-7484

Abstract

The formation of precipitates has been identified as a possible limitation in the use of granular iron for *in situ* remediation of groundwater. This study was undertaken to identify the precipitates that form on the iron surfaces under conditions of differing water chemistry. Two laboratory column tests were performed using 100 mesh, 99% pure electrolytic iron. A 120 mg/L calcium carbonate ($CaCO_3$) solution passed through one column and a 40 mg/L potassium bromide (KBr) solution through the other. The $CaCO_3$ treated iron formed a whitish gray coating on the first centimeter of the column but the KBr treated iron did not display any visible precipitates. X-ray diffraction, Raman spectroscopy, and scanning electron microscopy were used to identify the precipitates. Calcium carbonate and ferrous carbonate ($FeCO_3$) phases were only present on the surface of the iron removed from the influent end of the column treated with a $CaCO_3$ solution. Iron surfaces analyzed from both the influent and the effluent end of the KBr treated iron and the effluent end of the $CaCO_3$ treated iron indicated the presence of magnetite (Fe_3O_4) precipitates.

Introduction

Laboratory tests have shown significant degradation of several chlorinated organic compounds in the presence of iron (Gillham and O'Hannesin, 1994) and over the past few years zero-valent iron has been successful in passive *in situ* remediation of contaminated groundwater. According to the direct electron transfer mechanism (Matheson and Tratnyek, 1994), iron corrodes anaerobically through oxidation by water and serves as a source of electrons to reductively dechlorinate organic compounds present in aqueous solution. The corrosion of iron produces an alkaline environment and can be represented by the following equation:

$$Fe^0 + 2\,H_2O \rightarrow Fe^{2+} + 2\,OH^- + H_{2(g)} \qquad (1)$$
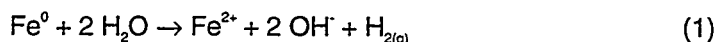
As the iron corrodes, Fe^{2+} and OH^- are produced which may lead to the formation of inorganic precipitates on the iron surfaces. Precipitation of other mineral phases can also occur depending on the ions available in solution. For example, if carbonate ions (CO_3^{2-}) are present in solution, they might react with cations such as Ca^{2+} and Fe^{2+} to form calcium carbonate ($CaCO_3$) and iron carbonate ($FeCO_3$) phases (Equations 2 and 3)

$$Ca^{2+} + CO_3^{2-} \rightarrow CaCO_{3(s)} \qquad (2)$$

$$Fe^{2+} + CO_3^{2-} \rightarrow FeCO_{3(s)} \qquad (3)$$

Precipitates may reduce the performance of both reactive *in situ* barriers and above-ground reactors by blocking reaction sites causing a decrease in the rate at which organics degrade or by reducing the permeability of the iron material. To investigate the manner in which precipitates affect the performance of iron metal, it is of particular importance to first identify the inorganic precipitates formed on the iron surfaces. The precipitates that form on zero-valent iron in anaerobic aqueous solutions were identified using various analytical techniques including x-ray diffractometry (XRD), scanning electron microscopy (SEM), and electron-dispersive x-ray

spectroscopy (EDS). Iron samples were removed from columns after several pore volumes of simulated groundwater passed through them. In these methods the iron samples were exposed to atmospheric oxygen during the transfer process and thus the character of the surface film could have been modified. Therefore, Raman spectroscopy was also used to identify surface film(s) formed on the iron without exposure of the iron sample to the atmosphere. This vibrational spectroscopy technique, in addition to EDS, provides information about functional groups and molecular species on the metal surface.

Methods

Simulated groundwater was pumped through laboratory columns packed with 100 mesh electrolytic iron powder (99% pure) to form inorganic precipitates on the iron surfaces. A 40 mg/L potassium bromide (KBr) solution was deaerated with zero-oxygen nitrogen and passed through one column and a 120 mg/L calcium carbonate ($CaCO_3$) solution that had been deaerated and equilibrated with a 5% CO_2/95% N_2 gas mixture was passed through a second column. The source water was pumped to the columns using a multi-channel peristaltic pump at a flow rate of approximately 0.23 ml/min. The residence time of solution in the column was approximately 13.3 hours. Silicone tubing (1.65 mm I.D.) passed through the pump assembly with all other tubing made of Teflon® and each solution was maintained under their specific atmospheres for the duration of the experiment.

The laboratory set up for the columns was similar to that described in Gillham and O'Hannesin (1994) except that a 19 L glass carboy was used to contain the influent solution. Each 16 cm long Plexiglas™ column had an internal diameter of 5.08 cm and had sampling ports located at 4, 8, and 12 cm from the influent end. The ports were constructed of nylon Swagelok® fittings (0.16 cm O.D.) tapped into the column, into which a syringe needle (16G1½) was inserted. Teflon® tubing (0.159 cm I.D.) was used for the influent and effluent lines.

After 158 and 166 pore volumes had passed through the $CaCO_3$ and the KBr columns respectively, the columns were disassembled in an anaerobic controlled environment chamber and freeze-dried. These samples were analyzed using a x-ray diffractometer equipped with a diffracted beam monochromator. The samples were also analyzed by using a scanning electron microscope equipped with an analytical energy dispersive x-ray analyzer under various magnifications. Energy dispersive x-ray analysis was used for qualitative elemental analysis on different areas of each specimen.

Raman spectra were obtained with a Dilor OMARS-89 spectrometer equipped with a diode-array optical multichannel analyzer and a microscope. Potassium bromide and calcium carbonate treated iron samples were taken for *ex situ* analyses from both influent and effluent locations of the columns. All samples were prepared and maintained under an anaerobic atmosphere.

Results and Discussion

Several freeze-dried samples removed from the influent, middle, and effluent portions of both the $CaCO_3$ and KBr treated columns were analyzed by x-ray diffraction. All spectra obtained were identified as Fe_3O_4 (magnetite) or α-Fe_2O_3 (hematite) according to their peak intensities and locations. Though visibly coated with a whitish/gray precipitate, iron samples removed from the influent portion of the $CaCO_3$ treated column showed only Fe_3O_4 to be present. This indicates that if carbonates were present there was an insufficient amount in the bulk samples to be detected by x-ray diffraction.

Several crystalline features were observed by scanning electron microscopy. Most of the carbonate precipitates were present within the first 4 centimeters of the column treated with the $CaCO_3$ solution, and the greatest abundance was found within the first centimeter. Inorganic profiles of Ca^{2+} and CO_3^{2-} indicate significant decreases in concentrations by the first port which confirms that precipitation occurs at the influent end of the column. Scanning electron photographs from iron samples removed from the influent end of the $CaCO_3$ treated column appeared similar to aragonite ($CaCO_3$) crystalline morphology (Bishop, 1967 and Schneidermann and Harris, 1985) and siderite ($FeCO_3$) crystalline morphology. The crystalline features resembling siderite were analyzed by energy dispersive x-ray spectroscopy and were found to contain Fe, C, and O. SEM photographs of iron samples removed from the effluent end of the $CaCO_3$ treated iron column and the influent and effluent end of the KBr treated iron column did not show defined crystalline structures, therefore, Raman spectroscopy data was used to supplement the XRD and SEM findings.

A sample of the $CaCO_3$ treated iron was removed from the influent end of the column after 158 pore volumes of solution had passed through the column. The iron surface revealed a strong Raman signal at 1083-1084 cm^{-1}. This band is assigned to the symmetric stretching vibration of a carbonate anion (Herman, *et al*, 1987). Pronounced shifts in the 100-500 cm^{-1} region were observed in the region representative of external lattice vibrational modes for the $CaCO_3$ treated iron samples (Figure 1). The $CaCO_3$ treated iron samples produced bands at 148 and 197-199 cm^{-1}. Given that the spectra are accurate to ± 1 cm^{-1}, the bands found for the influent sample removed from the $CaCO_3$ treated column gave the closest match to the vibration bands of aragonite (Herman *et al.*, 1987), a polymorph of calcite. The bands do not match calcite as shown in Figure 1. The presence of other calcium carbonate phases and ferrous carbonates (i.e. carbonate green rust (GR1) ($Fe^{III}_2Fe^{II}_4(OH)_{12}CO_3 \cdot 2\ H_2O$), ankerite ($CaFe(CO_3)_2$)) could be excluded because the Raman spectrum for such phases were not detected on the iron surface.
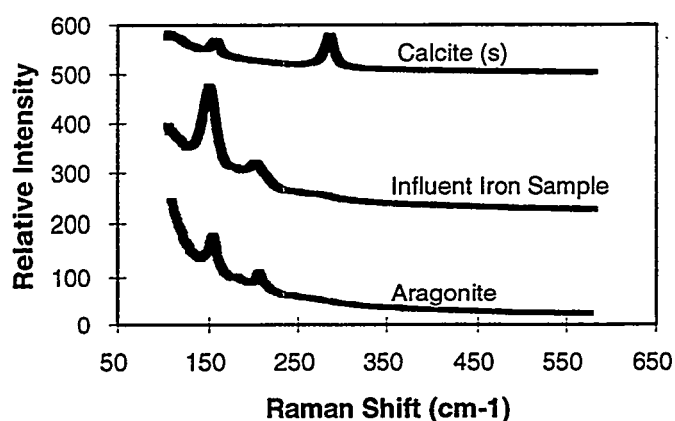
Figure 1: Raman spectra in the 100-600 cm^{-1} region for carbonate treated iron samples

Samples removed from the influent and effluent ends of the KBr treated iron and the effluent sample taken from the $CaCO_3$ treated iron produced similar spectra. For these samples, the primary precipitate identified was magnetite (Fe_3O_4). For the influent and effluent samples of the KBr treated iron only magnetite bands were identified. Stretching bands for magnetite were located at 542 and 666 cm^{-1} for the influent sample and at 546 and 665 cm^{-1} for the effluent sample. In the same region, spectra for the effluent iron sample treated with a 120 mg/L $CaCO_3$ solution showed bands at 545 and 666 cm^{-1} (Figure 2). These bands are all representative of magnetite, as reported by Balkanski et al. (1975) and from spectra obtained from a standard magnetite sample.
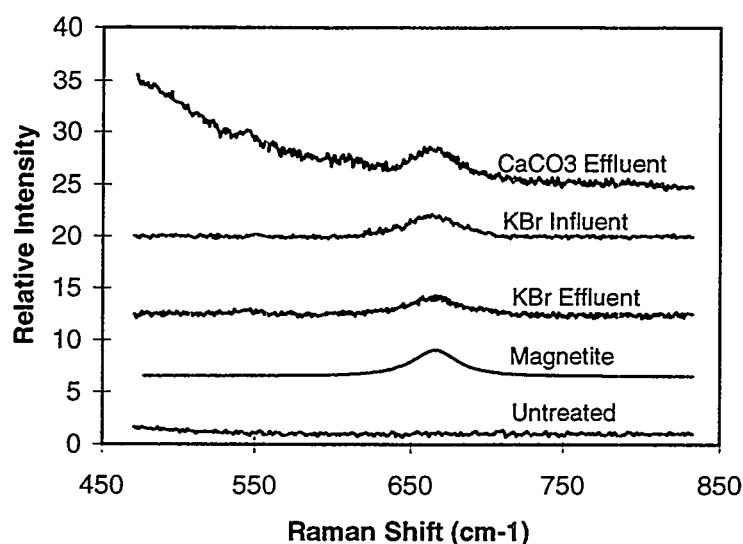
Figure 2: Raman spectra for iron samples in the 500-900 cm^{-1} region.

Conclusions

The production of Fe^{2+} and OH^-, through the oxidation of iron by water, leads to the formation of several precipitates depending on the available ions in solution. Raman spectroscopy was successful in identifying the precipitates that form on iron surfaces as this technique does not expose the iron sample to atmospheric oxygen which can alter the composition of the surface film. If the contacting solution contains calcium carbonate, precipitates such as aragonite and possibly siderite form in addition to magnetite. The carbonate phases precipitate from solution to form solids near the influent end of the column leaving the iron in the remainder of the column covered by a magnetite film.

References

Balkanski, M. *et al.* (1975) *Light Scattering in Solids.* Proceedings of the Third International Conference on Light Scattering in Solids, Flammarion Sciences, Brazil.

Bishop, A.C. (1967) *An outline of crystal morphology.* Hutchinson Scientific and Technical, London.

Gillham, R.W. and O'Hannesin, S.F. (1994) Enhanced degradation of halogenated aliphatics by zero-valent iron. *Groundwater,* 32(6), 958-967.

Herman, R.B. *et al.* (1987) Discrimination among carbonate minerals by Raman spectroscopy using the laser microprobe. *Applied Spectroscopy,* 41(3), 437-440.

Matheson, L.J. and Tratnyek, P.G. (1994) Reductive dehalogenation of chlorinated methanes by iron metal. *Nature,* 259, 200-201.

Schneidermann, N. and Harris, P.M. (1985) *Carbonate Cements,* p. 138. Society of Economic Paleontologists and Mineralogists, Oklahoma.

Enhanced Zero-Valent Metal Permeable Wall Treatment of Contaminated Groundwater

by
Debra R. Reinhart,[1] Jacqueline W. Quinn,[2] Chris A. Clausen,
Cherie Geiger, Nancy Ruiz, Ghassan F. Afiouni

Abstract

On-going research at the University of Central Florida, supported by NASA, is investigating the use of sonicated zero-valent metal permeable treatment walls to remediate chlorinated solvent contaminated groundwater. Use of ultrasound within the treatment wall is proposed to enhance and/or restore the activity of the zero-valent metal. Batch studies designed to evaluate the destruction of chlorinated hydrocarbons using enhanced zero-valent metal reduction found a nearly three-fold increase in reaction rates after ultrasound treatment. Column studies substantiated these results. It is hypothesized that ultrasound serves to remove corrosion products from the iron surface and will prolong the reactive life and efficiency of the permeable treatment wall, thus decreasing long-term costs of wall construction and maintenance.

Introduction

Chlorinated solvents are used by a wide range of industries including dry cleaners, electronic equipment manufacturers, metal parts fabricators, insecticide and herbicide producers, military equipment manufacturers, etc. These solvents replaced petroleum derived mineral spirits and have distinct advantages because of their nonflammability. The persistence and mobility of these hydrocarbons in the subsurface was largely unanticipated, therefore historical disposal practices have lead to widespread groundwater contamination. For example, trichloroethene (TCE) has been found at more than 791 of 1300 National Priority List sites (Clement International Corporation, 1993), primarily as a groundwater contaminant.

Treatment of chlorinated hydrocarbon contaminated groundwater is usually accomplished by pumping the groundwater to the surface and removing the contaminant through oxidation or air stripping. More recently, efforts have focused on the physical, biological, or chemical treatment of these contaminants in place. An innovative technique which has been the topic of numerous laboratory studies, and more recently several pilot and full-scale efforts, uses zero-valent metals to promote the reductive dehalogenation of chlorinated hydrocarbons (Gillham and O'Hannesin, 1994).

Zero-valent zinc and iron significantly enhanced the reductive dehalogenation of aliphatic compounds with iron being particularly attractive due to its low cost and availability (Gillham et al., 1993). Batch tests in which aqueous solutions of a wide range of chlorinated methanes, ethanes, and ethenes were added to 100-mesh iron filings resulted in degradation rates that were three to seven orders of magnitude greater than natural abiotic rates reported in the literature (Gillham and O'Hannesin, 1994). Generally, the rates increased with the degree of chlorination and with increasing iron surface area to solution ratio. The chlorinated products of degradation subsequently degraded to non-chlorinated compounds. Similar results have been obtained by Vogan et al. (1994) who propose that the corrosion of iron, while occurring independently of volatile organic compound degradation, likely provides the electron source needed for the reduction.

Although the reaction mechanism for zero-valent metal catalyzed chlorinated solvent destruction is not precisely known, it appears to involve simultaneous oxidation of iron and reductive

---

[1] Associate Dean, College of Engineering, University of Central Florida, P.O. Box 162993, Orlando, FL 32816-2293

[2] NASA Kennedy Space Center, Environmental Program Office, JJ-D, Kennedy Space Center, FL 32899

806

dechlorination, as shown below for trichlorethene (TCE) (adapted from Matheson and Tratnyek, 1994):

$$Fe^{\circ} \longrightarrow Fe^{2+} + 2e^{-}$$

$$C_2HCl_3 + 3H^{+} + 6e^{-} \longrightarrow C_2H_4 + 3Cl^{-}$$
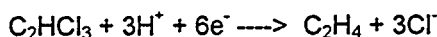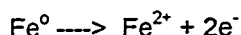
Thus, the destruction of one mole of TCE yields three moles of chloride and results in a pH increase due to the consumption of protons. Degradation rates, however, have been found to decline with increasing pH (Gillham et al., 1993) presumably because of surface deposition of iron precipitates. Laboratory studies generally account for most of the chloride mass generated (98 to 100 percent), however, carbon mass balances are usually much lower, probably due to the volatility of the carbon endproducts (Orth and Gillham, 1996).

Zero-valent metals have application to groundwater treatment in both in situ and-ex situ situations, however, they are most frequently used as the reactive component of a permeable treatment wall. A permeable treatment wall is conceptually very similar to a concrete slurry wall, only their functions are completely opposite. When-used at a remediation site, slurry walls attempt to confine a contaminant plume to a restricted volume thereby preventing its spread to uncontaminated regions. Slurry walls are virtually impermeable by design, whereas permeable treatment walls, as their name implies, are designed to permit larger volumes of water to pass through them than through surrounding soils. As the contaminated groundwater flows through the treatment wall, chlorinated solvents are chemically altered to acceptable alternative species. Emerging on the downstream side of the treatment wall is contaminant-free groundwater. No pumps or other above-ground treatment are required, as the natural groundwater gradient carries the contaminant through the treatment wall.

Corrosion of iron is inherent to the electron transfer process driving dechlorination of the solvents. It has been documented that this corrosion process leads to precipitation or fouling of the zero-valent metal surface (Gillham and O'Hannesin, 1994). Corrosion leads to a decrease in the degradation rate of this surface mediated process and may also reduce the permeability of the treatment wall.

The dechlorination of chlorinated compounds has also been shown to be effectively accomplished using ultrasound (Bhatnagar and Cheung, 1994; Kotronarou et al., 1992; Orzechowska et al., 1995), suggesting that ultrasound could be a potent remedial technique for contaminated groundwater. In addition, since the most common use of ultrasound is to clean surfaces, ultrasound may enhance the permeable treatment wall efficiency through surface maintenance. Suslick and Casadonle (1987) observed that nickel particles were several hundred-fold more active in hydrogenation reactions after being sonicated.

The term ultrasound is applied to periodic stress waves, often loosely referred to as either sound or acoustical waves, that occur at frequencies above the limit of human hearing, or in excess of 20,000 Hertz. Stress waves are aptly named because they create a deformation stress of the medium through which they are passing. At their upper extreme, ultrasonic frequencies are so high that their extremely short wavelengths are comparable to the agitation of molecules caused by heat (Heuter and Bolt, 1955).

Sonication has been applied to the destruction of compounds such as parathion (Kotronarou et al., 1992), pentachlorophenate (Petrier et al., 1992), and chlorinated hydrocarbons (Cheung et al., 1991). The mechanism for destruction has been hypothesized to involve the thermal dissociation of water during bubble collapse to produce hydroxyl radicals which react with target compounds (Bhatnagar and Cheung, 1994). In addition, thermal destruction (or pyrolysis) has been reported to occur within the cavitation bubble at the extremely high temperatures induced by sonication (Kotronarou et al., 1992). The destruction of chlorinated hydrocarbons by

sonication usually results in a decline in pH due to the production of hydrochloric acid. As is observed during zero-valent metal reactions, the rate of reaction increases with decreasing pH.

The purpose of the study described herein was to evaluate the effects of sonication on zero-valent metal destruction of chlorinated hydrocarbons. If degradation rates can be enhanced, reaction times will be reduced for equivalent final contaminant concentrations. Consequently, reactor or permeable wall size can be reduced in the application of this technology to field-scale projects, significantly decreasing treatment cost. The effects of ultrasound were examined using batch and column tests and will be evaluated at field scale in the near future.

Methods and Materials

Batch Studies. Aqueous samples of TCE were exposed to 20-kHz ultrasound in a 0.5-L Tedlar™ bag. The bag reactors were filled with 0.5 L deionized water and 0 to 2.5 g of iron, then purged with nitrogen. TCE was added in a 5000 ppm methanol solution to achieve final concentrations of 5 to 20 mg/L. Iron was washed with a ten-percent sulfuric acid solution prior to use to remove surface contamination. Bags were placed on a shaker table (160 shakes/min) to maintain well mixed conditions. Samples were removed periodically from the bags and analyzed for TCE. Zero-headspace conditions were maintained at all times.

Ultrasound was introduced using a 450-W Branson Ultrasonic water bath with an ultrasonic intensity of approximately 0.16 W/cm^2. Ultrasound treatment of bags containing iron consisted of one of the following catagories: no sonication, sonication prior to introduction of TCE, or sonication after 14 days of contact with TCE. Length of sonciation varied from 30 mintutes to three hours. To minimize temperature impacts during sonication, water was either allowed to flow continuously through the ultrasound bath or the tank was emptied and refilled every 30 minutes. Reagents were obtained from Fisher Scientific, all at least 99 percent purity and used as received. One hundred-mesh iron, obtained from Mallinckrodt Chemicals (Paris, KY 40361) was used for all tests reported herein. Control bags were constructed to evaluate possible sorption and ultrasound effects exclusive of iron treatment.

Column Studies. Column studies are ongoing and are being conducted in an up-flow mode using four different combinations of iron and native aquifer material: 50-mesh iron particles, from Science Kit and Boreal Laboratories, acid-washed heated cast-iron chips from the Peerless Corp., unwashed Peerless iron, and acid-washed heated cast-iron chips from Master Builder's Supply (Streetsboro, Ohio). The Peerless and Master Builder's Supply iron chip mesh sizes were distributed as follows: 43 percent of the iron was retained on mesh size 20 and 40 percent on mesh size 40. The remaining fraction of the iron particles included iron dust. Four of the ten-cm diameter, one-meter long Plexiglass columns contain 20-percent by weight iron and 80-percent by weight construction-grade sand. A fifth column serves as the experimental control and contains 100-percent sand. Unbuffered solutions of 15 mg/L TCE in deionized water flow through the columns at a rate of 4.7 mL/min. Samples are collected at multiple depths along the columns to monitor TCE destruction. Ultrasound was introduced to the 50-mesh iron column at 50 percent maximum power using a 15.9 mm-diameter stainless-steel long-ship auger drill bit inserted 15 cm through the bottom of the column and threaded for connection to a Fisher Sonic Dismembrator Model 300 (Watt) ultrasonicator.

Analysis. TCE was analyzed following EPA Method 624. Each sample was injected with 5.0 µL of internal standard, bromochloromethane. A five-ml portion of the sample was transferred to a purge vial. Helium was bubbled through the sample for a period of eleven minutes to transfer the TCE onto a Vocarb 3000 trap. The desorb time from the trap was four minutes at 250°C and the trap bake time was seven minutes at 260°C. A Hewlett-Packard gas chromatograph (Model 5890) equipped with a 0.25-mm id, 60-m long Vocol capillary column was programmed for a three-minute hold at 60°C, and a 15°C/min rise to 180°C held for three minutes.

Iron surface area was measured using a Porous Material, Inc BET Sorptometer. The 100-mesh iron surface area was found to be 1.76 m^2/g.

Results

Batch Studies. Ultrasound effects on the dechlorination of TCE were monitored during a series of experiments involving intermittent introduction of ultrasound. The first control, with no iron and no ultrasound exposure, was shaken for two weeks. The second control, contained no iron but was exposed to ultrasound for 30 minutes. TCE data were collected before ultrasound, immediately after exposure and then one hour later. For the control with no ultrasound exposure and no iron, less than two percent of TCE was lost over 14 days. TCE destruction during 30 min of sonication alone (no iron) also resulted in less than two percent loss. Fifty-five percent of the experiments were performed in duplicate.

To quantify the results, data were analyzed assuming first-order kinetics. Bags which received ultrasound treatment were monitored, for the purpose of developing rate constants, beginning 24 hours after sonication ended to prevent inclusion of TCE destruction which may have occurred during treatment. Concentrations were transformed to natural logarithms and results of linear regression between transformed concentrations and time were examined. TCE breakdown products, primarily cis-dichloroethene and ethene were found to increase over time, indicating destruction and not simply sorption of TCE onto the iron surface. Iron concentrations, length of sonication, half-lives for TCE disappearance, first order rate constants normalized per m^2 iron and length of monitoring period are provided in Table 1. Sonicated bags which indicate no monitoring before ultrasound received ultrasound treatment prior to exposure to TCE.

Table 1. Results of Batch Tests Using Iron and Ultrasound (US)

Iron, g/L	US Exposure, hrs	Half-Life, days	1st Order Rate Constant, min^{-1} $(x10^6)$*	Days Monitored Before/After US
0	0	---	No Loss[+]	14/0
0	0.5	---	No Loss[+]	0/14
1	0	36.2	7.56	28/0
1	0.5	31.2	8.61	0/28
3	0	24.6	3.71[+]	28/0
3	0.5	21.9	4.17	0/28
5	0	16.2	3.69[+]	28/0
5	0.5	13.5	4.06	14/14
5	1	5.3	10.3[+]	0/28
5	2	5.2	10.5	14/14
5	3	5.2	10.6[+]	14/14

*normalized per m^2 iron
[+]represents an average of duplicates

Comparison of first order rate constants normalized per m^2 of iron suggest that the addition of ultrasound to reactors containing iron increases reaction rates significantly. Sonication for one-half hour appears to increase reaction rates an average of about 12 percent compared to similar iron concentrations which received no treatment, regardless of when the ultrasound treatment occured relative to TCE exposure. However, rate constants nearly tripled (average increase of 184 percent) after a minimum of one hour of ultrasound treatment. While rate constants continued to increase with increasing length of treatment, the difference in rate increases between one hour and three hours of treatment was less than four percent.

Ultrasound has been shown to effectively degrade organic compounds in other studies. Many of these studies use a horn or probe configuration for the energy delivery system, similar to that used in the current column study (Cheung et al., 1991; Bhatnagar and Cheung, 1994; Orzechowska et al., 1995). Other studies use small volumes of samples (25 to 100 mL) irradiated for periods up to 3 hours by ultrasonicators operating at a high frequency, such as 530 kHz (Petrier et al., 1992) or high ultrasonic intensity, approximately 75 W/cm^2 (Kotronarou et al., 1992). In light of these findings, sonication of a large volume (500 mL) of liquid in an ultrasonic bath operating at 20 kHz with relatively low ultrasonic intensity (0.16 W/cm^2) under the circumstances of our research may not provide sufficient energy to degrade significant amounts of TCE. In addition, evaluation of reaction rate constants is delayed sufficiently to exclude these effects. The improvement in TCE destruction is therefore assumed to be due to removal of corrosion products which have accumulated on the iron surface. Scanning electron microscopy (SEM) has also shown that iron "aged" in 200 ppm TCE for 30 days exhibited significant calcification on the surface as compared to "unaged" iron. Following ultrasound application, the SEM showed that the surface was visibly cleaner.

Column Studies. Results from columns have provided important information regarding long-term performance of reactive iron, as seen in Table 2. The increase in half-lives over time suggests that gradual but significant iron aging has occurred. Comparison of TCE removal by washed and unwashed Peerless iron showed that washed iron is ten times more reactive than unwashed. Surprisingly, little difference was initially observed among the three types of iron used.

Table 2. Results of Column Studies

Column	TCE Half-Life, min	No. of Pore Volumes Passing through Column
50-Mesh Iron	240	1-20
	289	200-225
	618	300 - 315
Peerless Iron	246	50-60
	720 - 805	80 - 140
Master Builder Iron	225	50-60
	800	80 - 140
Unwashed Peerless	2567	50-60

The effects of ultrasound on the 50-mesh iron column were explored once deterioration in column performance (increased half life) was observed over an extended period of time (300 plus pore volumes). Ultrasound was introduced at over a one-hour period. An immediate reduction in half life was observed over the next 30 pore volumes. Unfortunately, air was drawn into the feed bag shortly thereafter, introducing oxygen to the column. The half life immediately returned to the pre-ultrasound level, presumably due to the build-up of oxidized iron products on the iron surface. Ultrasound was again introduced, and, as can be seen in Figure 1, half-lives fell dramatically and have remained at low levels to date (for around 60 pore volumes).

Half lives calculated for TCE disappearance over the lower section of the column, which contains the probe, and the upper section of the column before and after sonication indicate that impacts of sonication extend beyond the end of the probe. Prior to sonication, the lower half of the column, which receives the highest concentrations of TCE, exhibited a half-life approximately 1.5 times that of the upper section. After sonication, both half lives dropped significantly. The lower section exhibited a half-life decrease of approximately 70 percent, while the half life for the upper section of the column dropped 22 percent. Although certainly not to the degree of the lower section, the iron in the upper section of the column appears to have benefited from sonication.
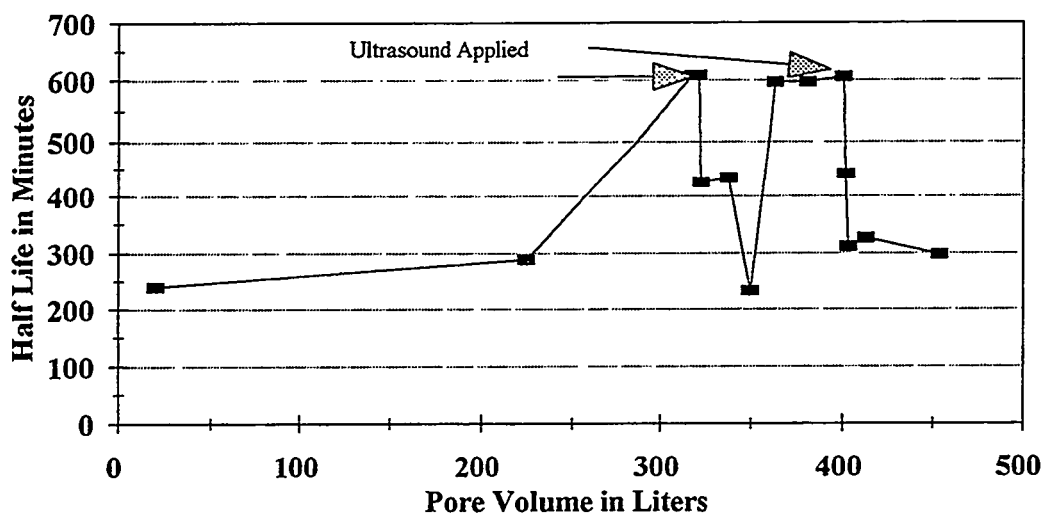
Figure 1. Performance of 50-mesh Iron Column Following the Introduction of Ultrasound

During the ultrasound application, dispersion of brown colloidal material was observed (iron precipitates). This material tended to be removed further up the column with the advective flow. No increase in pressure drop along the column was experienced after ultrasound treatment which would suggest plugging of the column. Some short-circuiting of TCE down the column was measured during ultrasound introduction. Short-circuiting was not observed for a lithium tracer added to the TCE solution. Therefore it is assumed that TCE volatilization occurred as a result of local high temperatures induced by ultrasound. Once ultrasound was discontinued, the TCE movement through the column returned to normal.

Future Studies

Zero-valent iron studies are continuing in four areas: batch studies, column studies, sandbox studies, and design for full-scale wall installation. Batch studies are intended to further evaluate the effects of ultrasound as well as the impact of carbonate buffering on iron kinetics. In addition, batch experiments have been designed to evaluate the effect of exposure of iron to the atmosphere after acid washing but before subsurface installation. Laboratory columns will continue to be used to evaluate the long-term performance of iron and ultrasound impacts. A bench-scale sandbox is currently operating to evaluate, in three-dimensions, zero-valent metal treatment of TCE and ultrasound delivery systems.

Laboratory studies are underway to estimate the radius of influence of an ultrasonic probe in aquifer solids. From this information, a prototype system will be developed for field-scale testing. Manufacturing implications, such as power requirements and probe design, must be determined to assess costs for field scale application. Conversations with ultrasound manufacturers indicate this is a practical technology.

Using data collected in the laboratory, a field-scale permeable wall installation is in planning stages. After discussion with NASA personnel, Launch Complex 34 (LC 34) has been selected as a suitable site for installation of the reactive wall. LC 34 has been used by NASA and its

contractors since the early 1960s. TCE was routinely used to flush Saturn rockets prior to launch, frequently resulting in the loss of TCE. Spills of other materials have occurred as well. The site has been the subject of a contamination assessment and remedial investigation and is fairly well characterized. Analysis of groundwater has identified four volatile organic compounds (VOCs) including TCE and daughter products cis- and trans-1,2 dichloroethene, and vinyl chloride. TCE concentrations range from non-detectable to 310 mg/l. Field-scale construction is anticipated in late 1997.

The wall will be constructed using deep-soil mixing, a relatively new construction technique to the environmental engineering field. Similar to trenching, deep-soil mixing can be used to increase soil strength and reduce permeability. However, soil excavation is not required. Deep-soil mixing uses a crane-supported set of leads which guide a series of hollow augers into the subsurface. A cement-based grout is injected through the augers as the mixing shafts penetrate the soil. Once the design depth is reached, the mixing shaft rotation is reversed and the mixing process is repeated as the auger shafts are brought to the surface, leaving behind a soilcrete column (Geo-Con, 1989).

Deep-soil mixing has possible applications to permeable treatment walls where sandy soils dominate the lithology of the contamination site. Instead of excavating soil down to design depths, only a portion of the excavation occurs, specifically in the upper few feet of the subsurface where there is little chance of finding chlorinated solvents. The mixing augers blend the existing sandy soils with iron shavings which are injected through hollow augers. The upper subsurface is removed to allow volume increases as the mixing action redistributes the soil within the column. Deep-soil mixing rigs have never been used for this application, and there is no field testing to support this possible form of permeable treatment wall construction, although several companies supplying this technology have been contacted and have expressed great interest.

Conclusions

The attractiveness of reductive dechlorination using zero-valent metal lies primarily in its passive nature. The addition of chemicals or ultrasound increases cost and complexity and therefore must be well justified in terms of reduced reactor volume, increased treatment efficiency, or prolonged reactive wall life. Preliminary results from batch and column tests reported herein suggest that the use of ultrasound increases TCE dechlorination reaction rates significantly. This enhancement presumably occurs as a result of displacement of corrosion products covering the surface of the zero-valent iron. This effect was supported by Scanning Electron Microscopy. Future tests must explore the mechanisms behind this enhancement. In addition, the practical use of ultrasound for in situ groundwater treatment is being investigated using sand-box models and cost implications are being evaluated. Finally, field-scale testing will evaluate construction techniques and the effectiveness of full-scale implementation of ultrasound techniques.

References

Bhatnagar, A. and H. M. Cheung (1994), "Sonochemical Destruction of Chlorinated C1 and C2 Volatile Organic Compounds in Dilute Aqueous Solution," *Environmental Science and Technology,* Vol 28 (8): 1481-1486.

Cheung, H. M., A. Bhatnagar, and G. Jansen (1991), "Sonochemical Destruction of Chlorinated Hydrocarbons in Dilute Aqueous Solution," *Environmental Science and Technology,* Vol 25 (7): 1510-1512.

Clement International Corporation (1993), *Toxicological Profile for Trichloroethylene,* Prepared for the US Department of Health and Human Services, Atlanta, Ga.

Fairweather, V. (1996) "When Toxics Meet Metal," *Civil Engineering,* May: 44-48.

Gillham, R.W. and S.F. O'Hannesin, (1994), "Enhanced Degradation of Halogenated Aliphatics by Zero-Valent Metal," *Groundwater*, 32: 958-965.

Gillham, R.W., S.F. O'Hannesin, and W.S. Orth (1993), "Metal Enhanced Abiotic Degradation of Halogenated Aliphatics: Laboratory Tests and Field Trials," presented at the Haz Mat Central Conference, Chicago, IL, March 9-11.

Geo-Con (1989) *DSM Geotechnical Improvement Process Technical Brief*, T-DSM-01-89.

Heuter, T. F. and R. H. Bolt (1955) *Sonics*. New York: Wiley Science.

Kotronarou, A., G. Mills, and M. R. Hoffmann (1992), "Decomposition of Parathion in Aqueous Solution by Ultrasonic Irradiation," *Environmental Science and Technology*, Vol 26 (7): 1460 - 1462.

Matheson, L.J. and P.G. Tratnyek (1994), "Reductive Dehalogenation of Chlorinated Methanes by Iron Metal," *Environmental Science and Technology*, Vol 28 (12): 2046 - 2053.

O'Hannesin, S. F.(1993) "A Field Demonstration of a Permeable Reaction Wall for the In Situ Abiotic Degradation of Halogenated Aliphatic Organic Compounds," University of Waterloo Thesis, Waterloo, Ontario, Canada.

Orth, S. W. and R.W. Gillham, (1996), "Dechlorination of Trichloroethene in Aqueous Solution Using Fe," *Environmental Science and Technology*, Vol 30 (1): 66.

Orzechowska, G. E., E. Poziomek, V. F. Hodge, W. H. Engelmann (1995), "Use of Sonochemistry in Monitoring Chlorinated Hydrocarbons in Water," *Environmental Science and Technology*, Vol 29 (5): 1373-1379.

Petrier, C., M. Micolle, G. Merlin, J. Luche, and G. Reverdy (1992), "Characteristics of Pentachlorophenate Degradation in Aqueous Solution by Means of Ultrasound," *Environmental Science and Technology*, Vol 26 (8): 1639-1642.

Spooner, Philip et al. (1985) *Slurry Trench Construction for Pollution Migration Control*, Noyes Publications, Park Ridge, New Jersey.

Suslick, K.S. and D. J. Casadonle (1987), " Heterogeneous Sonocatalysis with Nickel Powder,"*J. Am. Chemical Society*, 109: 3459.

Vogan, J. L., J.K. Ealberg, B. Gnabasik, and S. O'Hannesin (1994), "Evaluation of In Situ Groundwater Remediation by Metal Enhanced Reductive-Dehalogenation - Laboratory Column Studies and Groundwater Flow Modeling," presented at the 87th Annual Meeting and Exhibition of the Air and Waste Management Association, Cincinnati, OH, June 19-24.

Chapter 16

Permeable Reactive Walls: Field Studies

DEVELOPMENTS IN PERMEABLE AND LOW PERMEABILITY BARRIERS

Stephan A. Jefferis[1], Graham H. Norris[2] and Alan O. Thomas[3]

Abstract

The concept of the reactive treatment zone whereby pollutants are attenuated as they move along a pathway in the ground has enabled a re-thinking of many of the concepts of containment. In particular it offers the potential for the control of the flux from a contaminated area by controlling the contaminant concentration in the pathway(s) as well as or instead of using a low permeability barrier. The paper outlines the basic concepts of the reactive treatment zone and the use of permeable and low permeability reactive systems. The paper then gives a case history of the installation of a permeable barrier using an in-situ reaction chamber.

Introduction

The use of containment systems is now widely accepted for municipal and toxic waste landfill sites, but up to now it has been more reluctantly accepted for the remediation of contaminated land. This reluctance perhaps stems from a desire to use process orientated treatment technologies as a permanent means of dealing with contaminated land problems. However, as the effectiveness of some in-situ treatment technologies remains in doubt and the costs of treatment in general remain relatively high, interest in containment continues to develop and particularly in combining treatment with containment and the prospects for using intrinsic processes as low cost longer term remedial options (Bardos and van Veen 1996).

Terminology

In the UK it is common practice to refer to barrier systems which impede groundwater flow as passive containment systems and the term active containment has been coined for those which reduce pollutant flux by treating the contaminant(s) in a flow path between a source and a receptor. However, these terms are not universally accepted. For example, in Canada and the USA, active containment is often used to describe processes where there is an energy input such as pump and treat systems and the term permeable barrier is used for the UK active containment. In this paper the more general term reactive treatment zone will be used for in-ground systems involving reactions which tend to reduce contaminant concentrations in a pathway and passive containment for barriers which solely impede flow.

Reactive Treatment Zones

The reactive treatment zone concept provides a new framework for the analysis of barrier behaviour. The essential feature of the treatment zone is that chemicals can be prevented from escaping from a source zone without necessarily containing the carrier fluid (almost always water,

[1]Golder Associates (UK) Ltd, 54-70 Moorbridge Road, Maidenhead, Berkshire, SL6 8BN, England, +44-1628-771731, sjefferis@golder.com
[2]Nortel Ltd, Oakleigh Road South, New Southgate, London N11 1HB, England +44-181-945-3556, graham.norris@nt.com
[3]Golder Associates Geoanalysis s.r.l., Turin , Italy +39-11-5683800, athomas@golder.com

but gases are also amenable to such treatment). This highlights the fact that chemical and physical phenomena are interlinked in barriers and that they should not be regarded as independent. The interlinking may be regarded as a continuum with two extreme situations:

- Permeable reactive treatment zones. The best known example is the use of zero valent iron to dechlorinate solvents in groundwater (Gilham and O'Hannesin, 1992).
- Low permeability active containments, e.g. exploiting the chemistry of, or adding species to, low permeability barriers such as a soil-bentonite (Evans, 1991) or cement-bentonite (Jefferis, 1996).

Reactive treatment zones can be distinguished from passive (low permeability) containments by considering the controls on the flux, J for any contaminant which may be written as:

$$J = k\,i\,A\,C$$

For a traditional passive barrier, the flux is controlled by ensuring that the permeability of the system, k is low and hence that the flow through the barrier is low. However, as a result the area of flow, A will be high as the barrier must surround the source and the concentration, C of the contaminant species and the gradient, i (unless modified by pumping) also will be high.

An alternative way to reduce the flux is to reduce the concentration of the contaminant(s). If this can be achieved then the flux can be reduced and the permeability ceases to be the controlling parameter and it may be high or low as appropriate to the application. With a high permeability system the gradient, i will be low as the carrier fluid is allowed to escape and the area for flow may be less than that of a containment as it may be deliberately focused with an engineered system or naturally higher permeability regions may be exploited. This may simplify monitoring and where necessary in-situ control. If space is available the input concentration may be varied by selecting the position of the reactive zone in relation to the contaminant source and/or intrinsic remediation, in the ground, may be exploited upstream or downstream of the reactive treatment zone. It should be noted that reactive treatment zones often will be used as pathway control mechanisms to prevent contaminants from a source reaching a receptor rather than as source clean-up technologies (at least in the short term).

Reactive Zone Configurations

In principle a reactive treatment zone or zones should enclose the all pathways from the pollutant source to the receptors. In practice this may require that the zone(s) are very extended and as the flow through any element may be uncertain, large volumes of reactive material may be necessary to ensure sufficient residence time under all hydrological conditions. Optimisation of the deployment of the reactant is therefore an important consideration for any reactive treatment. Possible configurations include:

- The use of injection wells to introduce chemicals into the natural groundwater flow
- The use of passive wells containing replaceable canisters etc. of treatment materials that may dissolve into the natural groundwater flow
- Treatment zones close to the source which reduce pollutant concentrations to levels at which natural intrinsic remediation can operate in zones down gradient of the source.
- Funnel and Gate^{TM} systems.

It is also important that it should be possible to monitor and, if appropriate, control the processes within the treatment zone. The requirements for monitoring and control can present problems for in-situ treatments or intrinsic remediation in an undefined area, given the heterogeneity typically associated with ground conditions and the large volumes of soil that may require treatment. Martin and Bardos (1996) describe examples of in-situ treatment zones where treatment remains in the ground but under conditions of better definition. The gate of a Funnel and Gate^{TM} system is an example of such a system where monitoring and control can be particularly straightforward.

The Permeability of Reactive Treatment Zones

A reactive treatment zone must include some process which removes, destroys precipitates or otherwise attenuates the contaminants migrating from the source(s) towards the receptor(s). Processes which may be employed alone or in combination include: chemical reaction, physical separation, biological degradation and sorption.

Many of these processes will rely on an interaction between the flowing groundwater and a solid phase in the treatment zone and although the permeability of the zone is not the controlling parameter it may be necessary to consider it. For example, a moderate to high permeability may be necessary if problems such as ponding within a containment are to be avoided. Designing and maintaining such a permeability may pose some problems as the reaction rate in the zone may be dependent on the surface area of a solid phase within it. As a result it may be necessary to use finely divided (and hence low permeability) materials to limit the required residence time of the contaminants in the zone. Also precipitates or biological slimes may form within the zone. Thus careful consideration must be given to the initial permeability of the treatment zone and to processes which may lead to its reduction over time.

Low Permeability Reactive Zones

Reactive treatment zones may be designed to be of low permeability so that the physical effect of a barrier is enhanced by chemical reaction(s). For example, heavy metals may be precipitated by the high pH of cement-bentonite walls though credit is seldom given for this in the design of containments (except for the containment of radionuclides in purpose designed repositories).

A significant amount of work has been reported on the effect of contained chemicals on the physical properties of barrier materials such as clay liners and cement or soil-bentonite walls. The prime focus of much of this work has been the assessment of the damage to the impermeability of a barrier that may be caused by contained chemicals. Much less work has been reported on the beneficial effects of chemicals, though an examination of the literature shows that some work focused on the damage has actually demonstrated beneficial effects.

Interactions in low permeability systems are potentially much more complex than in high permeability systems as it is necessary explicitly to consider the effects of chemical and mineralogical changes on the permeability and not just design to minimise their impacts. At the laboratory scale it has been demonstrated that the chemical history of a containment material and its permeability can be strongly interlinked. For example, leaching a cement-bentonite material by sustained permeation with water, so reducing its pH, will usefully reduce its permeability and also inhibit expansive cracking and damage if it is exposed to sulphates. High pH, if required, can be re-established by permeation with lime and this can further reduce the permeability but it will re-establish sensitivity to sulphates (Jefferis 1996).

That such interaction can occur is not surprising but it does raise questions about the interpretation of laboratory investigations of chemical damage to barriers using samples that have not been exposed to the chemical history that occurs in-situ (including, and very importantly, periods of leaching by water). Also it has been demonstrated that some chemical damage can be reversed by re-introduction of appropriate chemical species. It follows that there is considerable potential to modify the behaviour of barriers once in the ground. This could be to repair them, extend their life, protect them from damaging species or modify or re-charge their chemical activity. It is therefore quite simplistic to consider cement-bentonites and indeed most mineral barrier systems as having a unique permeability. They are physically and chemically active and if we can learn to exploit this activity new barriers concepts may be forthcoming.

A Case History of a Permeable Reactive Zone

In addition to the problems of design of reactive treatment zones with appropriate chemical reactions there can be significant practical problems in fitting such systems to the circumstances of a site and this is illustrated by the following case history.

At an industrial site in Belfast, Northern Ireland, currently being used for the manufacture of electronic components, historic spillages of chlorinated solvents had led to an intense though localised contaminant source and plume. A site investigation identified the following contamination in the groundwater:

- Trichloroethene (TCE) at concentrations up to 390 mg/L
- Trichloroethane (TCA) at concentrations between 100 and 600 µg/L
- Tetrachloroethene (PCE) at concentrations of the order of 100 µg/L.

A particular problem with chlorinated solvents is that they tend to be of low solubility (typically less than about 1000 mg/L) and thus can remain as a free phase product in the ground for substantial times but the regulatory control levels are typically of the order of tens of µg/L i.e. of the order of one hundred thousand times less than their solubility. Also they are generally recalcitrant and not easily biodegraded. Thus even quite a modest chlorinated solvent spill may persist in the groundwater and continue to pollute it for a substantial length of time.

The soil profile at the site was complex, with glacial till interbedded with lenses of silts, sands and gravel. In-situ pumping tests showed that the till acted as an effective barrier to the vertical and lateral migration of the contaminants but the silt, sand and gravel lenses were sufficiently permeable to allow off site migration of dissolved solvents from the source which included free phase solvents present as a dense non-aqueous phase liquid (DNAPL). There were also smaller discrete lenses of clay or clayey silt which complicated the flow regime.

In-situ permeability tests and pumping tests conducted to evaluate potential remedial strategies showed that conventional pump and treat remediation would require numerous extraction wells to address the thin saturated zone and this, together with the presence of a free product DNAPL source, meant that such a system would have to be maintained for many years. Similarly there would be major problems with a soil vapour extraction system.

Reductive Dechlorination

One of the best known and researched reactive treatments is the use of iron filings to reductively dechlorinate chlorinated solvents (Gilham and O'Hannesin, 1994). The process essentially leads to the development of an extremely reducing environment, allowing reactions occurring on the surface of the iron to strip halogens from the dissolved organic compounds as they flow through the zone. The reaction is abiotic and chlorinated solvents are converted to chloride ions and various hydrocarbons.

The process does not degrade the resulting hydrocarbons but as non-chlorinated species they have much higher permissible regulatory control concentrations. Also they are much more readily bio-degraded by intrinsic remediation processes occurring in the ground. The iron filings reactive containment is thus a conversion process which reduces toxicity. This demonstrates a general principle that a reactive treatment zone need not degrade contaminants to basic species such as carbon dioxide and water but need only convert them to species which are acceptable toxicologically and environmentally in the local setting.

The iron filings technology seemed to have potential for the Belfast site and samples of the site groundwater obtained from sampling wells were shipped to EnviroMetal Technologies Inc., Guelph, Ontario for treatability studies. The results of these studies are reported in Thomas et al. (1995). Briefly, a series of laboratory column studies were undertaken to determine the degradation kinetics of the species of interest, and to identify whether there were any constraints imposed by the natural geochemistry of the site groundwater. The results showed that TCE, PCE and TCA were completely degraded from initial starting concentrations in the test groundwater

samples of 300,000, 170 and 200 µg/L respectively. The half life of TCE in the site water was estimated to be 1.2 hours in the presence of iron filings. In contrast small concentrations of cis dichloroethene (DCE) and vinyl chloride (VC) built up in the water as a result of the dechlorination of the TCE etc. with VC reaching a peak, at the end of the column, of 700 µg/L in the initial studies.

The reason for this is that although the dechlorination does not appear to be a stepwise process (i.e. tetrachloroethene to tri and then di chloroethene, vinyl chloride and ultimately chlorine free hydrocarbons) and it would seem that the majority of the solvent is dechlorinated in a single step, a small amount may be released from the surface of the iron prior to full degradation. This leads to a temporary increase in species such as DCE and VC as these species are more slowly dechlorinated by iron filings. Considerable care was necessary in the design to ensure that they would be satisfactorily degraded. Otherwise the net effect of the treatment zone could be to increase the concentrations of these species which would be most unsatisfactory particularly as vinyl chloride has markedly lower regulatory control limits than many other chlorinated solvents.

Further column studies were then undertaken at lower flow rates, the increased residence time resulting in much earlier degradation of the parent compounds thus enabling estimation of the degradation rate of vinyl chloride. From these laboratory trials it was concluded that a residence time in contact with the iron filings of about 12 hours was required for the site water to achieve removal of all chlorinated species to below regulatory limits. This result together with the results of a groundwater modelling exercise enabled the calculation of the required reactive zone thickness from the estimated groundwater flow rate and the required residence time of the contaminated groundwater in contact with the iron filings.

Design of the Reactive System

A preliminary review of the site situation concluded that the optimum strategy for deployment of the iron filings was in the gate of a Funnel and Gate™ system. However, the site geology and site circumstances placed a number of constraints on the design:

- The contaminant source extended to within a few metres of the site boundary, outside which there was a public road. The reactive treatment zone therefore needed to be very compact.
- The solvent source was underlain by a thin layer of clay which had inhibited its migration to greater depths. If this layer were penetrated by the gate the free product solvents would sink and pollute a lower aquifer stratum.
- The groundwater perched on the thin clay layer was shallow and showed seasonal variations in depth. It would be difficult to maintain any significant depth of horizontal flow in a gate seated on this layer.
- A perched water table also existed in the fill covering the surface of the site. In wet seasons this water, if allowed to enter the gate, could dominate flow through it and unacceptably reduce the residence time. It therefore had to be excluded.
- Because of the proximity of buildings and the risk of damage by vibration and also the cost, sheetpiles could not be used to form either the funnel of the gate of the system.
- If a slurry trench procedure were used to form the system then it was imperative that the iron filings were not inundated and thus blocked by slurry from the wall construction. It would therefore be necessary to contain the iron or to construct the slurry wall before placing the iron filings. Prior excavation could allow local collapses during placement of the iron and thus a poor seal between the wall and the iron filings.

- The residence time of groundwater within the reactive treatment zone is critical. A zone that is too thin may lead to the escape of lower chlorinated species such as vinyl chloride which can pose a greater toxicological or environmental threat. Extensive groundwater modelling studies were undertaken to ensure that the design residence time could be achieved.
- The clean-up was being undertaken voluntarily by the site owner.

After consideration and rejection of many reactive treatment zone designs the in-situ reactor configuration shown in Figure 1 was finally developed as best fitting the site constraints. In place of the previously used horizontal flow reactive treatment zones the flow was arranged to be vertical in a 12 m tall by 1.2 m diameter steel reactor shell which was filled with iron filings as shown in the figure. This design enabled the reactor to be placed between the contamination and the site boundary. This could not have been achieved with a horizontal flow regime as the design calculations had shown that the flow path length needed to be at least 5 m plus entry and exist zones to collect and disperse the flow. The vertical flow direction within the reactor also ensures that the full depth of the iron filings will be saturated whatever the seasonal variation in groundwater level.

Figure 1. Reactor configuration, elevation and plan view

822
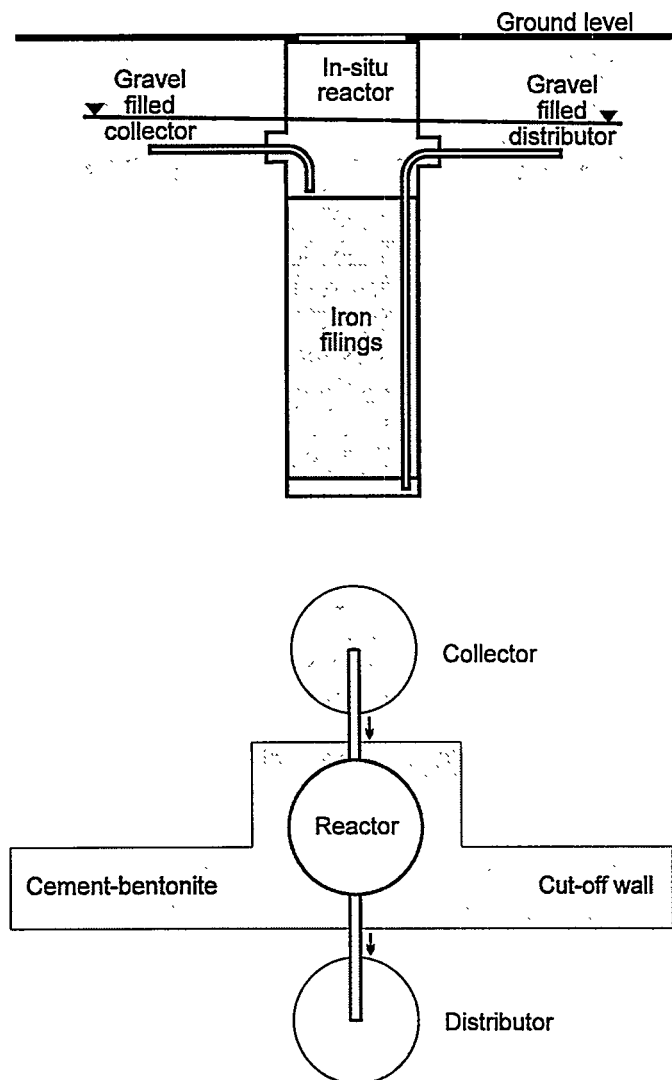
The reactor was placed in an enlargement in a cement-bentonite cut-off wall (see Figure 1, plan view) which was used to funnel the flow to the reactor. This wall was toed into a deep aquiclude layer at 10 m and the enlargement was taken to a depth of slightly over 12 m to accommodate the reactor shell. The cut-off and enlargement penetrated through the clay layer on which the chlorinated solvents were retained. However, as the cut-off material was designed to have a permeability of $<10^{-9}$ m/s minimal downward migration of solvents will occur.

Because of the relatively low permeability and heterogeneity of the adjacent soil it was decided that the flow to the reactor should be collected via an upstream high permeability collector and that downstream of the reactor there should be a similar distributor. The collector and distributor were formed from gravel filled piles taken down to the top surface of the thin clay layer. A gravel backfilled trench, excavated under a degradable polymer slurry, could have been used to form the collector and distributor but there were concerns about the effect of any remaining polymer on the iron filings and so augered pile holes were used.

Finally the internal geometry of the reactor was arranged so that the pipework connections to the gravel filled collector and distributor piles could be made from within the clean environment of the reactor shell without the need for any hand excavation or for anyone to enter the excavations all of which were undertaken either with a backhoe under cement-bentonite slurry or with a piling auger. During the works airborne solvent concentrations were monitored and found to be undetectable.


Results

To date, results from the reactor must be regarded as provisional and only indicative rather than definitive. There are two issues:
- The flow rate through the reactor was very low during the first months of operation (this was expected from the hydrological investigation). However, this has meant that uniform flow conditions have not been established in the reactor and that the internal pore water chemistry is very sensitive to disturbance of the flow regime
- Sampling from within the relatively modest volume of the reactor has proved to be a problem if traditional procedures are used. Only small volumes of water can be withdrawn if the local chemistry within the reactor is not to be disturbed. Particular techniques are being developed to obtain small but representative samples from the reactor whilst avoiding the need to purge the sampling tubes.

The results of two campaigns of sampling within the reactor and in the upstream collector are shown in Figure 2. The results relate to times of 4 and 7 months after installation of the reactor. The figure shows separate plots for the inorganic species sodium and chloride and for the chlorinated solvent species. Sodium is unaffected by the reactions within the reactor and it can be seen that its concentration is effectively constant throughout the reactor. In contrast chloride increases markedly due to the contribution from the dechlorination of the solvents. At 4 months chloride peaks at about 3 m into the reactor but by 7 months high values are seen throughout the central length of the reactor as would be expected once a steady flow has been achieved.

Figure 2 shows that all the chlorinated solvents are rapidly degraded on entry to the reactor. At 7 months TCE is reduced to of order 5 µg/L within the reactor but is slightly higher at exit due to some backflow from the distributor during sampling. DCE is formed in the early part of the reactor but is at non-detectable levels at the sampling point 3 m into the iron filings bed. Unfortunately some TCE has been drawn back into the reactor, from the downstream area, by the sampling process, leading to the production of DCE in the later stages of the reactor and this accounts for its presence at the sampling points at 4.5 and 6m (the end of the reactor) into the bed.

Figure 2. Chemical Concentrations upstream of, and in the reactor
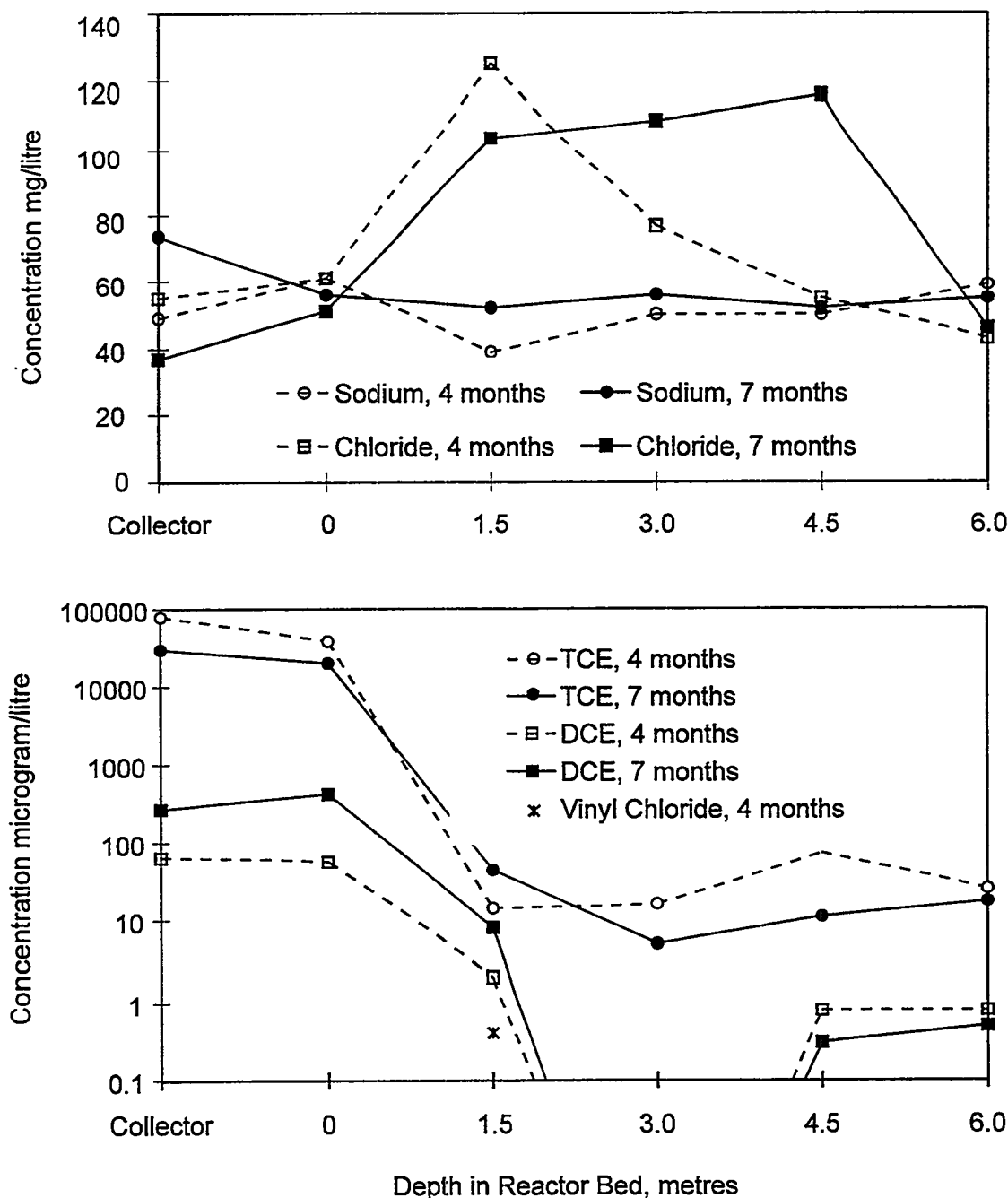
On each sampling occasion TCA was at undetectable levels. Vinyl chloride was found at a single sampling point within the reactor at 4 months (at a level of 0.4 μg/L) but not in the collector or distributor and it was not detected at all at 7 months.

TCE was found at the end of the reactor at both 4 and 7 months. This is because of contamination that was present downstream prior to the installation of the reactor and as the flow rate through the reactor was very low during the initial months this contamination has not been swept out. Also there was some reverse flow through the reactor induced by pumping during the commissioning and sampling processes.

With regard to the remaining downstream contamination it is interesting to note, that at times of low seasonal flow, there is potential for the recycling groundwater from wells downstream of the reactor to the upstream·collector (by pumping) to treat the downstream area should treatment of this contamination be required. Also the reactor will work with the flow in either direction. Thus, if, for some reason, the flow should be reversed naturally then the site would be protected from the inflow of any contaminants spilled or remaining outside the reactor system.

Monitoring of the reactor is continuing and very recent sampling has, as expected, shown further reductions in solvent concentrations within the reactor and at 6 m into the bed TCE is now at 2 µg/L and DCE is undetectable despite the continuing high input concentrations of TCE etc.

Conclusions

The reactive treatment zone concept offers not only a new tool for the control of contamination but also forces a re-thinking of low permeability barrier systems. Prior to the development of the concept, contaminant/barrier interaction had generally been considered only as a possibly damaging process which could increase the permeability of a barrier. Now barrier interactions should be seen differently. They may be deliberately engineered to be beneficial.

Reactive treatment zones may be most economically employed as pathway control procedures but will contribute to the slow clean-up of a source. The pathway control they offer is their essential feature and it may be argued that they should not be designed to achieve more than slow source clean-up as this minimises the rate at which any treatment chemicals, energy or other process inputs are required i.e. it minimises the process demands and operating costs whilst maximising the opportunity for natural, intrinsic, remediation.

At the present time a significant limitation to the use of reactive treatment zones is the rather narrow range of contaminants that can be treated and the complications introduced by mixed contaminants etc. However, work is in progress and the technology has strong parallels with intrinsic remediation (e.g. intrinsic bioremediation) and it is likely that the reactive treatment zone concept will find much application in stimulating intrinsic degradation or attenuation.

The Funnel and Gate™ concept is a powerful adjunct to the technology as it can allow the treatment zone to be at some distance from the source, if this is required by surface or buried structures, geological conditions or process optimisation (e.g. exploiting natural dilution or attenuation in the soil) etc. · Sites need not be capped to prevent rainwater ingress, indeed it can be an advantage in driving groundwater flow to a treatment zone.

The concept of an in-situ reactor adds further flexibility to the design of reactive treatment zones, allowing more precise control of the reactive zone and also recharging or recovery and replacement of the active material should this be required. Furthermore several reactors may be linked in series to treat mixed contaminants.

Although most reactive treatment systems which have been advanced to date have been for the control of groundwater pollution there is no reason why other systems such as reactive caps should not be developed to control, for example, the escape of semi-volatile or volatile organics from petroleum impacted sites or gas or odour from landfills. Bio-oxidation zones to control methane migration through unsaturated soils offer some exciting prospects but there could be difficulties with excessive local heating.

Low permeability reactive treatment zones are a more specialist application and may require site capping or groundwater pumping (and treatment) to avoid ponding. Reactive treatment zone concepts will be useful where long term secure containment is necessary as chemical interactions can provide additional security and lifetime to a physical containment. Furthermore the concepts may be useful in developing in-situ repair strategies for barriers which have suffered damage and in analysing the effects of reaction on the permeability of these systems.

References

Bardos, R.P. and J. van Veen. (1996) Longer term or extensive treatment technologies. *Land Contamination & Reclamation*, 4(1), pp. 19-36.

Evans, J.C., Y. Sambasivam and Z.R. Zarlinski. (1991) Attenuating materials in composite liners, Waste Containment Systems: Construction, Regulation and Performance, *ASCE Geotechnical Special Publication*, No 26.

Gilham, R.W. and S.F. O'Hannesin. (1994) Enhanced degradation of halogenated aliphatics by zero-valent iron, *Groundwater*, 32(6), pp. 958-987.

Gilham, R.W. and S.F. O'Hannesin. (1992) Metal catalysed abiotic degradation of halogenated organic compounds, *IAH Conference "Modern trends in Hydrogeology"*. Hamilton Ontario, Canada, pp. 94-103.

Jefferis, S.A. (1996) Contaminant - barrier interaction: friend or foe? *Mineralogical Society Conference, Chemical Containment of Wastes in the Geosphere*.

Martin, I. and R.P. Bardos. (1996) A review of full scale treatment technologies for the remediation of contaminated soil. *(Final report for the Royal Commission on Environmental Pollution, October 1995). EPP Publications, 52 Kings Road, Richmond Surrey*.

Starr, R.C. and J.A. Cherry. (1994) In situ remediation of contaminated groundwater: The funnel-and-gate system, *Groundwater*, 32, pp. 465-476.

Thomas, A.O., D.M. Drury, G. Norris, S.F. O'Hannesin, and J.L. Vogan. (1995) The in-situ treatment of trichloroethene contaminated groundwater using a reactive barrier - results of laboratory feasibility studies and preliminary design considerations. *Contaminated Soil '95, W.J. van den Brink, R. Bosman & F. Arendt (eds)*.

TWO PASSIVE GROUNDWATER TREATMENT INSTALLATIONS AT DOE FACILITIES

W.D. Barton[1], P.M. Craig[2], W.C. Stone[3]

ABSTRACT

Groundwater is being successfully treated by reactive media at two DOE sites. Passive treatment utilizing containerized treatment media has been installed on a radioactive groundwater seep at Oak Ridge National Lab, Oak Ridge, Tennessee, and on a TCE plume at the Portsmouth Gaseous Diffusion Plant in Piketon, Ohio. In both applications, flow is conducted by gravity through canisters of reactive treatment media. The canister-based treatment installation at ORNL utilizes a natural sodium-chabazite zeolite to remove radiological cations (Sr, Cs) from contaminated groundwater at greater than 99.9% efficiency. Portsmouth is currently conducting tests on three different types of treatment media for reductive dehalogenation of TCE.

The advantages of canister-based treatment over uncontained media reactive walls are:
- Flow characteristics through the media are improved to minimize "short-circuits";
- Flow rate and treatment performance can be easily monitored;
- Treatment media can be prepared off site, hauled to the site, and easily installed;
- Treatment media is easily changed out when depleted;
- Workers are not in direct contact with contaminated treatment media; and,
- Depleted media may be disposed of in the treatment canisters.

This paper describes the development and performance of these systems, including the contaminants, groundwater modeling, geochemistry, treatment media, installation methods and performance.

INTRODUCTION

Groundwater is being successfully treated by reactive media at two DOE sites. Passive treatment utilizing containerized treatment media has been used to remediate a radioactive groundwater seep at Oak Ridge National Lab (ORNL), Oak Ridge, Tennessee, and a TCE plume at the Portsmouth Gaseous Diffusion Plant (PORTS) in Piketon, Ohio. At both sites, contaminated groundwater is intercepted and conducted through canisters of treatment media by gravity flow, providing containment by passive groundwater collection and treatment.

Effective plume containment can be achieved with conventional pump and treat systems or by passive capture. Where hydrogeologic and topographic conditions are appropriate, passive capture is more efficient and may reduce capital as well as M&O costs. At some sites, pump-and-treat systems are anticipated to operate for years to remove a diminishing but never ending quantity of contaminant. The development of these passive treatment systems is an attempt to provide long term containment of contaminants without the expense of pumping large amounts of groundwater.

In both of these treatment applications, flow is conducted by gravity through canisters of reactive treatment media. The canister-based treatment installation at ORNL utilizes a natural sodium-chabazite zeolite (an inorganic ion-exchange resin) to remove radiological cations (Sr, Cs) from contaminated groundwater at greater than 99.9% efficiency. The PORTS treatment facility is designed with multiple treatment bays to simultaneously conduct tests of different treatment media. Initial treatment media experiments have focused on reductive dehalogenation by zero-valence iron.

[1]P-Squared Technologies, Inc., 10938 Hardin Valley Road, Knoxville, TN 37932, (423) 691-3668, bbarton@p2t.com
[2]P-Squared Technologies, Inc., 10938 Hardin Valley Road, Knoxville, TN 37932, (423) 691-3668, pmcraig@p2t.com
[3]Lockheed Martin Energy Systems, Inc., P O Box 2008, MS-7358, Oak Ridge, TN 37831, (423) 574-0333one@ornl.gov

PASSIVE FLOW-THROUGH REACTOR FOR ^{90}SR REMOVAL

Waste Area Group 5, Seep C Location

Waste Area Group 5 (WAG 5) is a low-level radioactive waste burial ground located in Melton Valley, south of the ORNL main plant. WAG 5 consists of two principal sections, the northern section used for retrievable storage of transuranic waste and the southern section for trench burial of low-level radioactive wastes. The 20-hectare (50-acre) site began receiving waste in 1958 and ceased receiving waste in the 1970s. Waste materials were placed in unlined trenches which were filled with mostly uncompacted waste and subsequently covered with less than one meter of soil. The trenches were constructed in relatively parallel sets numbering 5 to 25 trenches and were excavated roughly perpendicular to geologic strike with their long axis parallel to topographic slope. Direct rainfall and shallow storm-flow enters the unlined and uncapped trenches and migrates through the waste materials from trench to trench and eventually to seeps at the toe of the slope. These seeps have been found to be contaminated with dissolved radioactive materials which vary in their constituents depending on the contents of the trenches through which the water passes. WAG 5 Seep C was one of the most contaminated seeps, accounting for approximately 15% of all radioactive contamination entering the White Oak Creek Embayment from the ORNL complex. The location of WAG 5 and
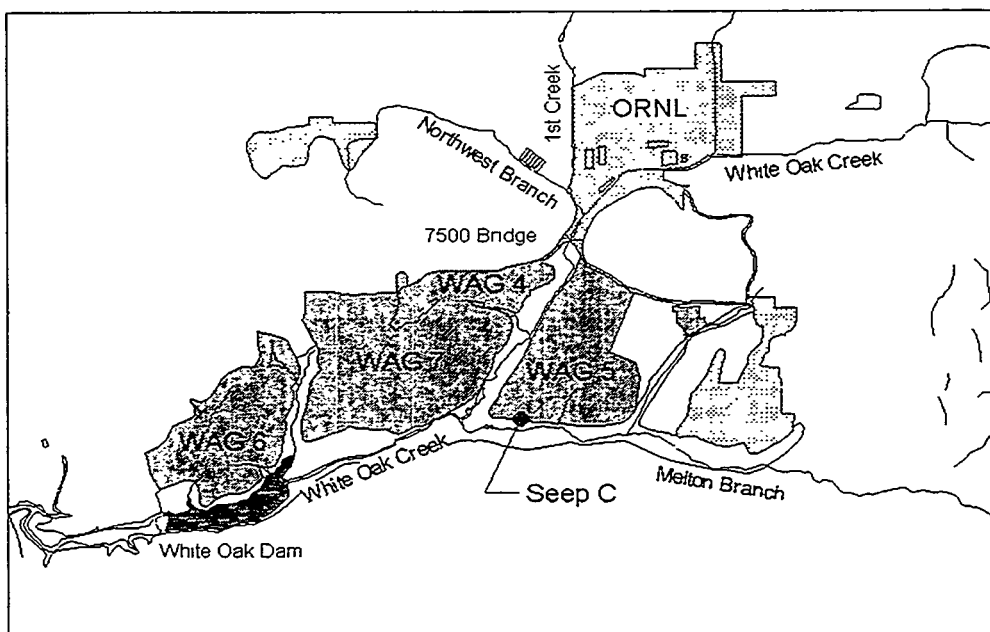
Figure 1. Map of ORNL Showing Location of WAG 5 Seep C.

Contaminants

The primary contaminant of concern at WAG 5 Seep C is Strontium 90 (^{90}Sr). In 1995, the average influent concentration of ^{90}Sr was approximately 386nCi/L. The total flux of contaminants and contaminant concentration varies with the amount of water flow through the trenches. As flow increases, the total flux of contaminants increases but contaminant concentration decreases due to dilution.

Geologic Setting

WAG 5 is located over aquitard units of the Conasauga Shale formation. The trenches which waste was placed were excavated to the top of shaly bedrock, a depth of approximately 5 m (15 ft). The floor of the waste trenches is located at the interface between soil and bedrock. In this geologic unit, the top of bedrock is the most weathered and fractured, and therefore the most hydraulically conductive zone. Groundwater flows only through networks of pervious, connected fractures and tends to flow in a lateral rather than vertical direction. Seep C is located near Melton Branch where the fractured soil/bedrock interface surfaces, just above the stream channel.

Seep Geochemistry

Seep C waters are of the calcium-magnesium-bicarbonate type, typical of near surface groundwater at ORNL. The pH has been measured to be neutral to slightly acidic (7.0-6.8). Alkalinity is moderate at 260 mg/l as $CaCO_3$. The seep water chemistry is dominated by the controls of CO_2 - calcium carbonate equilibria and as such is a highly buffered system (resistant to perturbations in pH). Sampling data analyzed by a thermodynamic model indicates that the seep water as it flows from the ground is undersaturated with respect to calcium carbonate and saturated with respect to several iron-bearing minerals.

Seep C Project Development

The Seep C intercept project began with the assembly of a team of ORNL scientists and engineers who had submitted proposals for Department of Energy development funding to investigate a variety of passive groundwater treatment approaches. The approaches included such diverse activities as bench scale testing of various types of treatment media, artificial wetlands research, and research into techniques for installing treatment media into the ground in the path of the groundwater.

Shortly after the establishment of the passive groundwater treatment team, the Seep C site was identified as a priority site for remediation and a CERCLA removal action was initiated. Rather than continue pursuing research on contaminated groundwater in general, several members of the passive treatment development team began to focus on Seep C as a potential passive treatment site. Ion-exchange, the exchange of cations between an aqueous solution and an insoluble solid in contact with it, has been effectively used in pumped columns to remove radionuclides and other metals. Bench scale testing confirmed that a natural zeolite (sodium chabazite) ion-exchange resin in use at the ORNL radioactive water treatment plant would be suitable for low flow rate treatment of radioactively contaminated seepage.

Field tests of Seep C flow through zeolite treatment media were conducted, and the results indicated that as long as the groundwater had direct contact with the zeolite for approximately 20 seconds the radionuclides would be adsorbed onto the zeolite, effectively removing ^{90}Sr from groundwater. Subsequently, DOE, Martin Marietta Energy Systems, Inc. Environmental Restoration Division, and the Tennessee Department of Environment and Conservation (TDEC) agreed to a full scale installation of a passive treatment system at Seep C. The concept at this point was to intercept the laterally flowing groundwater with a French drain upgradient from Seep C, conduct the water from the drain to a concrete vault where the water would pass through a horizontal trough filled with treatment media. Flow would be completely by gravity. The contaminants would be removed by the treatment media and the clean water would discharge to the adjacent stream. A discharge criteria was negotiated with TDEC which allowed discharge to Melton Branch if a minimum of 90% of the ^{90}Sr was removed from the water.

Physical Modeling

A mock-up of a treatment unit was constructed and tested for hydraulic properties of flow through the system. Dye tracer tests performed on the plexiglass mock-up treatment unit demonstrated that a horizontal flow treatment unit would have problems with short-circuits along preferential flow paths, especially along the edges. This testing eventually led to the use of steel drum canisters and downward vertical flow as the preferred treatment approach.

Numerical Modeling

A numerical groundwater model was developed to determine the amount of water anticipated to be captured and routed through the treatment canisters. The accuracy of the groundwater model was one of the critical factors in the design of the facility, because the model was used to determine the upper and lower limits of flow through the treatment system.

Seep C Interception and Treatment System Configuration

The final design and installation of the treatment system consisted of a 23 m (75 ft) long French drain, a 3 X 3.5 m (10 X 12 ft) concrete vault, connecting piping, canisters of treatment media, and monitoring instrumentation. Figure 2 shows a schematic diagram of the interception and treatment facility. The contaminated groundwater is intercepted by the French drain and routed to the low point of the drain to a pipe which connects the drain to the treatment vault. Within the treatment vault, the groundwater flows into a manifold which conducts the flow to any one or all of four primary treatment drums in parallel, then through any one or all of four secondary treatment canisters. The flow is then sampled and discharged to Melton Branch.
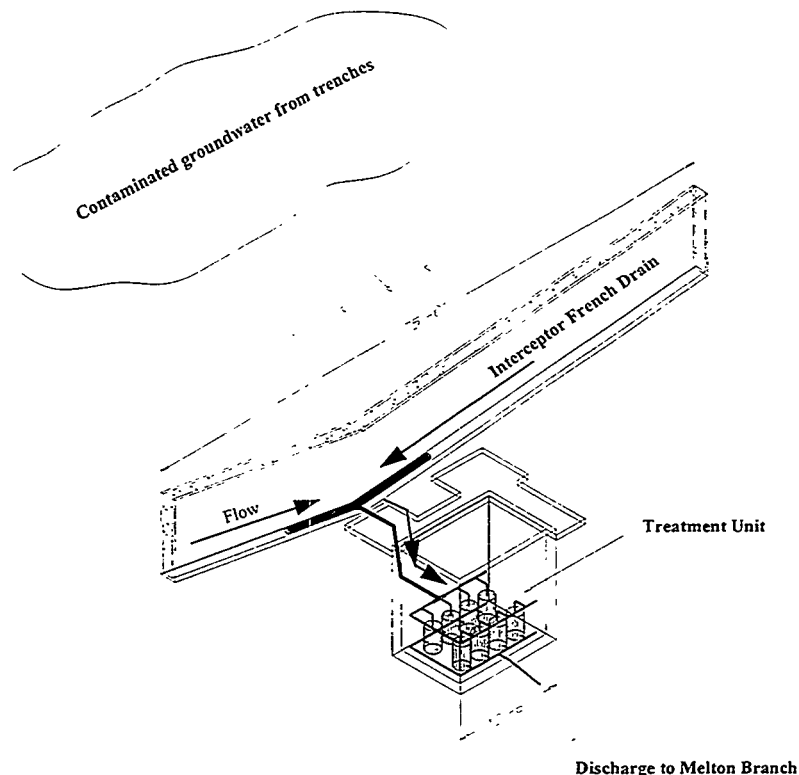
Figure 2. Seep C Interception and Treatment System.

Residence time of groundwater in the treatment canisters is a function of the flow rate, but even at high flow residence time is substantially longer that the minimum required for effective groundwater treatment. Design flow rates for the system ranged from a minimum of 6,250 to a maximum of 24,500 liters per day (1650 to 6500 gpd). Based on this range of flow rates, the residence time of the groundwater in contact with the ion-exchange media ranged from approximately 10 minutes for low flows to 3 minutes for high flows.

Seep C Treatment System Performance

The Seep C treatment system was completed in November 1994, and has been in continuous operation since that time. During 1995, samples have been collected of the influent and effluent as part of the system performance monitoring. The system has consistently removed >99% of the ^{90}Sr from the intercepted groundwater. The system has also experienced clogging problems due to iron precipitation, and efforts are ongoing to reduce the effects of iron oxidation on the system. These efforts have included the introduction of nitrogen into the French drain to limit oxygen transfer (which produced mixed results) and experimentation with the addition of a dispersing agent to the groundwater upstream of the canisters to keep iron from flocculating. The useful life of the zeolite was estimated to be approximately 3000 bed volumes or one year. Due to clogging problems the zeolite canisters have been changed more frequently than that.

The interception and containment of Seep C contaminants has reduced the total radionuclides into the White Oak Creek Embayment by approximately 15%. Figure 3 shows the total ^{90}Sr discharges at the ORNL compliance boundary for the years 1993, 1994, and 1995. It is clear that the installation of the WAG 5 Seep C treatment system has resulted in a substantial reduction in off-site discharges for 1995 compared to the discharges for 1993, a year with similar average runoff.

Figure 3. Contaminant Discharges at White Oak Dam.

PASSIVE FLOW-THROUGH REACTOR FOR TCE REMOVAL

Introduction

A facility for treating TCE contaminated ground water and testing in-situ treatment media for TCE removal was developed for the Portsmouth Gaseous Dif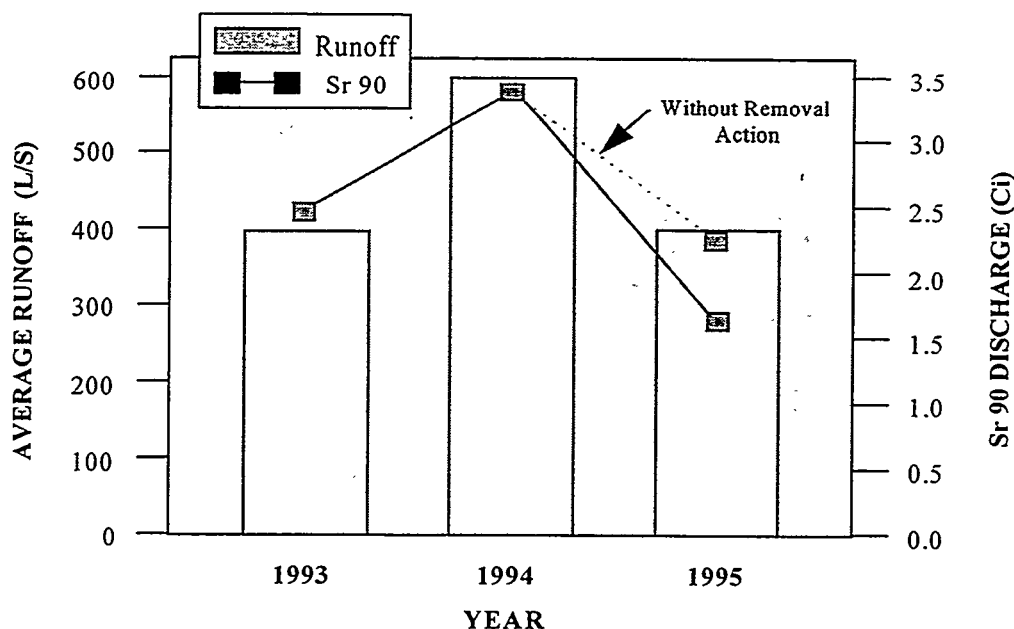fusion Plant (PORTS) Piketon, Ohio. The goals of the project were to intercept and decontaminate the groundwater and test different types of experimental treatment media on the groundwater under full scale field conditions. To intercept contaminated groundwater a horizontal well approximately 425 m (1400 ft) in length was installed from the TCE plume to the site of the treatment facility. The treatment facility was designed and constructed such that the flow from the horizontal well can be split between treatment bays where experimental treatment media is placed in 55-gallon drum cartridges.

X-120 TCE Plume Location

The TCE plume, known as the X-120 plume, is located in the southwest corner of the PORTS site. The plume is the result of TCE spills which began nearly 40 years ago at a training facility building on the PORTS site. The training building has since been demolished, and the site is a relatively flat grass covered field. The off-site migration of the plume has been relatively slow, as the natural groundwater migration is limited by the placement of a large volume of low-permeability fill soil for expansion of industrial facilities. Figure 4 shows the southwest corner of the of the PORTS site, the location of the X-120 Plume, and the X-120 Treatment Facility.

X-120 System Configuration

Ground water is collected in a horizontal well and is conducted to the treatment facility. The treatment facility is located in the bottom of a large existing ravine such that ground water flows by gravity from the plume to the facility. The treatment system consists of three treatment bays located within the small metal building. The treatment bays allow side-by-side tests of reactive media under realistic groundwater conditions. The facility was designed to accept experimental treatment media in 55-gallon drum canisters for testing. After flowing through the treatment media, the groundwater is conducted through activated carbon canisters to assure removal of solvent prior to discharge to the environment.

Geologic Setting

The PORTS site geology consists of a shale aquiclude overlain by successive layers of stream and lake deposits. The Sunbury Shale is a thin, but highly impermeable layer, located at a depth of approximately ten meters below ground surface. Immediately above the shale is the Gallia unit, which is a shallow aquifer. The Gallia is a heterogeneous mix of gravel, sand, and silt, deposited as braided

831
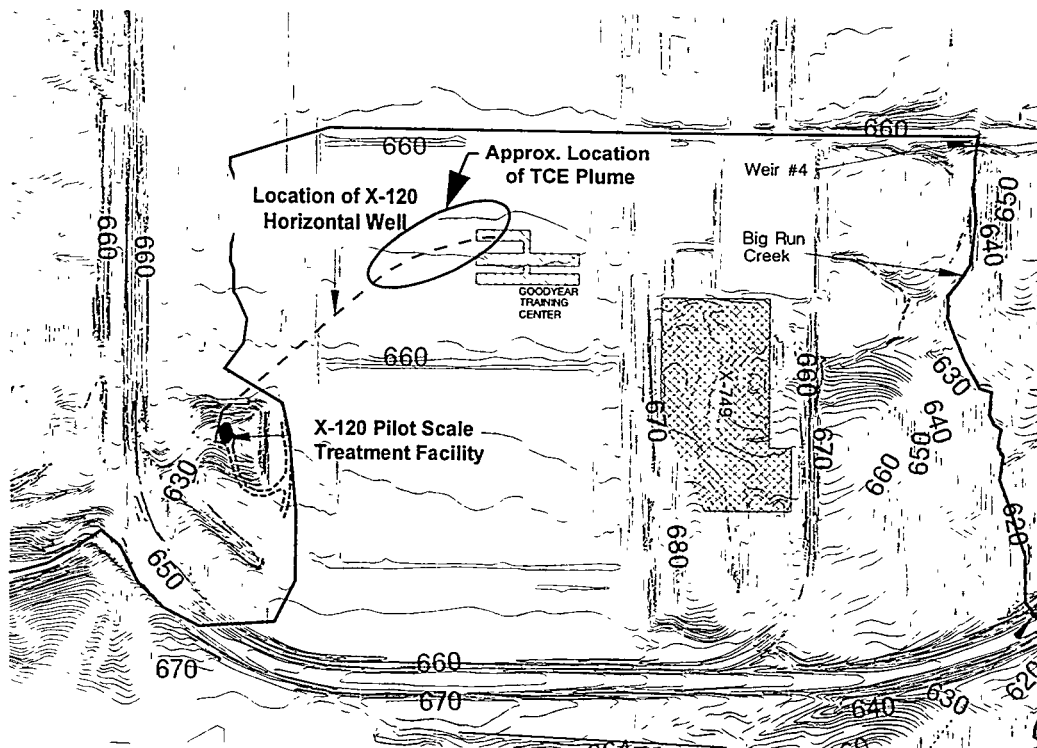
Figure 4. Southwest Corner of the PORTS Site Showing X-120 Area

stream bed sediments, containing localized zones of relatively high hydraulic conductivity. Higher conductivity zones tend to be at the bottom of the Gallia with lower conductivity zones above. Conductivities in the Gallia range from .4 to 8 m/day (1.4 to 26 ft/day). Above the Gallia unit is the Minford clay, consisting of fine silts, lacustrine clays, stream alluvium and compacted fill. Virtually all groundwater migration occurs in discontinuous high conductivity zones located at the bottom of the Gallia immediately above the Sunbury.

Groundwater Modeling and Plume Capture
An extensive program of groundwater modeling was performed to develop anticipated capture zones and flow rates with which to design the interception and treatment facility. By modeling and analysis of the geology, it was determined that no barriers were needed to direct and contain the groundwater; containment would be achieved by the placement of a horizontal well beneath the plume in the high conductivity zone of the Gallia. In spite of the presence of high conductivity zones, the groundwater flow rate is controlled by low conductivity soils and is quite low, in the range of .003 to 3 cm/day (.0001 to 0.1 ft/day).

The model predicted that the horizontal well would deliver a steady-state flow of approximately 6.8 L/min (1.8 gpm), with an initial TCE concentration between 140 and 200 ppb. The orientation of the horizontal well was chosen to get the maximum screen length within the 100 ppb contour of the TCE plume. Based on the modeling, the horizontal well was designed to be 5 cm (2 in) in diameter and 410 m (1344 ft) in length with a screen length of 150 m (500 ft). The head difference between the well screen and the treatment facility was approximately 3 m (10 ft).

Design and Installation
The X-120 Treatment Facility and horizontal well were designed in 1995 and constructed between June 1995 and February 1996. The system was designed to contain the X-120 plume, conduct the groundwater through the treatment facility by gravity flow, provide a facility for experimental media testing, and ensure that the groundwater was cleaned prior to discharge. It was designed to be operated as an unmanned facility, with automatic sampling, analysis, data recording, and alarm systems.

Treatment Process Operations

The facility began processing groundwater with experimental treatment media in March, 1996. The actual flow rate of water delivered by the horizontal well ranges from 3 L/min to 4.5 L/min (0.8 to 1.2 gpm) and the TCE concentration ranges from 100 to 200 ppb. The inlet pressure measured at the point where groundwater enters the building fluctuates between 275 and 317 millibars (4 and 4.6 psi). The only major change in the system as designed has been to install a prefilter for removing suspended materials and to scavenge the dissolved oxygen from the groundwater. Once inside the treatment facility the water flows into a manifold where it is routed through three parallel treatment bays.

The initial treatment media experiments involve the dehalogenation of TCE by three types of zero-valence iron. The media are: (1) fine-grade iron filings (equivalent to 40-mesh), (2) stock iron filings (8 to 50-mesh), and (3) palladized iron filings obtained by chemically plating palladium (at 0.05% of iron) on 40-mesh iron filings. Each of the treatment bays containing iron filings consists of three 55-gallon drums of treatment media with a sand layer at the bottom and top of the drum and a layer of iron between. Only one drum was used in the palladized iron treatment train, with only a 6-in layer of reactive material, due to the substantially faster reaction rate of palladized iron. Figure 5 shows a schematic diagram of the experimental treatment system. The chemical processes of reductive dehalogenation are beyond the scope of this paper, however, a substantial amount of the research on this topic is referenced in the *Reprints of Papers Presented at the 209th American Chemical Society National Meeting,* Anaheim, California, April 2-7, 1995, Vol. 35 No. 1.
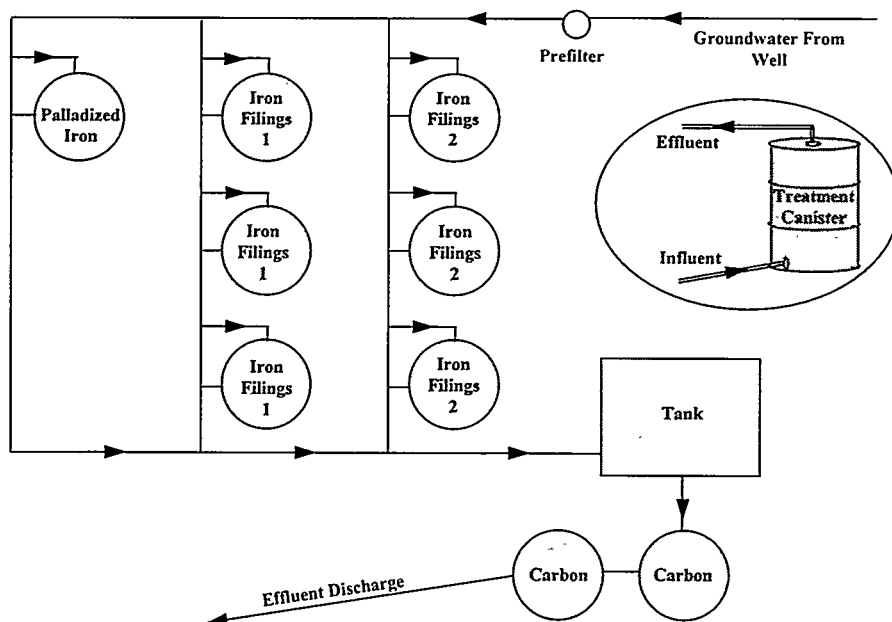
Figure 5. Schematic of Treatment System

Experimental Treatment Results

Performance of the experimental treatment media for the months of March and April, 1996, was described in the report, "*Interim Report on the X-749 /X-120 Groundwater Treatment Facility a Field-Scale Test of Trichloroethylene Dechlorination using Iron Filings, Liang, et.al., May 1996*", and the following conclusions are presented. TCE was effectively removed in all three treatment trains. For the first week, initial concentrations of 170 ppb TCE were reduced in all three treatment trains to below the detection limit of 2 ppb. After 51 days of operation, effluent concentrations were <2 ppb for iron filings 1, 3 ppb for iron filings 2, and 12 ppb for the palladized iron.

Degradation of treatment media was observed in each of the media types. Initial half-lives were: 14 minutes for iron filings 1, 19 minutes for iron filings 2, and 1.4 minutes for the palladized iron. After 51 days, the half-lives of the media were 16 minutes for iron filings 1, 35 minutes for iron filings 2, and 4.1 minutes for the palladized iron. Increases in the half-lives were anticipated because previous lab experiments at ORNL indicated that for prolonged periods of reaction, the reagent deteriorated and the reaction rate constants were reduced.

CONCLUSIONS

Contaminated groundwater is being effectively treated by cartridges of reactive media. The ion-exchange resin at WAG 5 Seep C has consistently removed >99.9% of the strontium and cesium present in the groundwater, and has resulted in a 25% reduction in the discharge of total radioactivity from ORNL. The experimental treatment operations at the PORTS X-120 site have demonstrated successful treatment of TCE contaminated groundwater by reductive dehalogenation for the limited time the system has been operational. Groundwater modeling at these two sites provided accurate predictions of groundwater interception and flow rates to support facilities design. In both systems the use of 55-gallon drum cartridges of treatment media has provided predictable flow with minimal short-circuiting, easy replacement of depleted media, and the ability to effectively monitor influent and effluent streams.

REFERENCES:

Environmental Consulting Engineers, 1994. *"Design Support of WAG 5 - Seep C Removal Action,"* Prepared for Martin Marietta Energy Systems, Inc. under Contract No. 17B-99987V K23. Oak Ridge, Tennessee.

Borders, D.M., D.S. Hicks, R.S. Clapp, T.M. Scanlon, 1995. *"Effectiveness of ^{90}Sr Removal Actions in the White Oak Creek Watershed,"* ER Surface Water Project at ORNL - Technical Bulletin No.2, FY96BUL2.V2, Oak Ridge National Laboratory, Oak Ridge, Tennessee.

Science Applications International Corporation, 1994. *"Remedial Investigation Work Plan for the Groundwater Operable Unit at Oak Ridge National Laboratory, Oak Ridge, Tennessee,"* ORNL/ER-221&D0, Oak Ridge National Laboratory, Oak Ridge, Tennessee.

Liang, L., O.R. West, N.E.Korte, J.D. Goodlaxson, F.D. Anderson, C.A. Welch, and M. Pelfry, 1996. *"Interim Report on the X-749/X-120 Groundwater Treatment Facility, a Field-Scale Test of Trichloroethylene Dechlorination using Iron Filings,"* Portsmouth Gaseous Diffusion Plant, Piketon, Ohio.

Environmental Consulting Engineers, 1995. *"Technical Specification, Horizontal Groundwater Collection Well for the X-120 Pilot Scale Treatment Project,"* Prepared for Lockheed Martin Energy Systems, Inc. under Contract No. 90B-99229C. Portsmouth Gaseous Diffusion Plant, Piketon, Ohio.

Environmental Consulting Engineers, 1995. *"Develpoment of Calibrated Groundwater Flow and Transport Models for Evaluating Remediation Alternatives at Portsmouth Gaseous Diffusion Plant and their Application to the Design of the X-120 Horizontal Well,"* Prepared for Lockheed Martin Energy Systems, Inc. Portsmouth Gaseous Diffusion Plant, Piketon, Ohio.

Environmental Consulting Engineers, 1995. *"X-120 Conceptual Design Description/Criteria,"* Prepared for Martin Marietta Energy Systems, Inc. under Contract No. 90B-99229C. Portsmouth Gaseous Diffusion Plant, Piketon, Ohio.

Porous Reactive Wall For Prevention of Acid Mine Drainage: Results of a Full-scale Field Demonstration

S. G. Benner, D. W. Blowes and C. J. Ptacek
Department of Earth Sciences
University of Waterloo
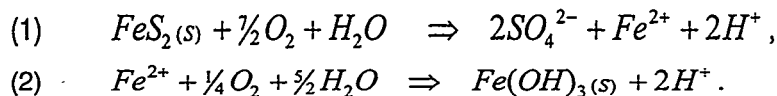Waterloo, Ontario, Canada

Abstract

A porous reactive wall was installed in August, 1995, to treat mine drainage flowing within an aquifer at the Nickel Rim mine site, near Sudbury, Ontario. The reactive mixture was designed to maximize removal of metals and acid generating capacity from the groundwater by enhancing sulfate reduction and metal sulfide precipitation. The installed structure, composed of a mixed organic substrate, is 15 meters long, 3.6 meters deep and the flow path length (wall width) is 4 meters. Results of sampling nine months after installation, indicate that sulfate reduction and metal sulfide precipitation is occurring. Comparing the chemistry of water entering the wall to treated water exiting the wall nine months after installation: SO_4 concentrations decrease by >50% (from 2400-4800 mg/L to 60-3600 mg/L), Fe concentrations decrease by >95% (from 260-1300 mg/L to 1.0-40 mg/L), pH increased from 5.8 to 7.0 and alkalinity increased from 0-60 mg/L to 700-3200 mg/L as $CaCO_3$. After passing through the reactive wall, the net acid generating potential of the aquifer water was converted from acid producing to acid consuming.

Introduction

Acidic metal-rich drainage from mines and mine wastes is the largest environmental problem facing the North American mining industry (Feasby, 1991; USDA, 1993). Conventional treatment strategies for acid mine drainage (*e.g.,* lime neutralization) involve high capital and operating costs and produce large volumes of metal-rich sludge. Permeable reactive walls are a passive, *in situ* treatment technology that may provide an effective and less expensive remedial alternative. This paper describes the installation of the first full-scale permeable reactive wall for the prevention of acid mine drainage and presents results of that installation.

Acid mine drainage

The oxidation of sulfide minerals in mine-wastes, and the subsequent oxidation of dissolved Fe(II), produces acidic drainage through the reactions (Nordstrom, 1979; Dubrovsky et al, 1984):

$$(1) \qquad FeS_{2\,(S)} + \tfrac{7}{2}O_2 + H_2O \quad \Rightarrow \quad 2SO_4^{2-} + Fe^{2+} + 2H^+,$$

$$(2) \qquad Fe^{2+} + \tfrac{1}{4}O_2 + \tfrac{5}{2}H_2O \quad \Rightarrow \quad Fe(OH)_{3\,(S)} + 2H^+.$$

This reaction sequence results in the production of H^+, Fe^{2+} and SO_4^{2-} to the water. Similar reactions, involving other sulfide minerals can release dissolved As, Cd, Cu, Ni, Pb, and Zn.

In mine tailings impoundments, the oxidation of sulfide minerals and the oxidation of Fe^{2+} are often de-coupled (Morin and Cherry, 1988; Blowes et al, 1990). Sulfide oxidation (Reaction #1) occurs in the unsaturated zone of the tailings and the reaction products (SO_4^{2-}, Fe^{2+}, H^+) are carried downward by infiltrating precipitation water into the underlying aquifer. At most sites, the H^+ released by sulfide oxidation is attenuated by reaction with minerals contained in the tailings, and underlying aquifer material. Dissolved Fe^{2+}, and SO_4^{2-}, however, remain in solution and are

displaced downward through the tailings and into underlying aquifers, resulting in the development of a plume of tailings-derived water. When the resulting groundwater plume, containing high concentrations of SO_4^{2-}, Fe^{2+} and other metals discharges to oxygenated surface-water bodies, Fe^{2+} is oxidized releasing two moles of H^+ per mole of Fe^{2+} (Reaction #2). The resulting low pH conditions are harmful to biota, and increase the mobility of dissolved metals such as Cd, Cu, Ni, and Pb, greatly enhancing their bioavailability. In many cases the flux of low quality water from tailings impoundments will continue for many decades, even centuries (Morin and Cherry, 1988; Blowes et al, 1990).

Current methods for the prevention and treatment of acid mine drainage include preventing the infiltration of meteoric water, preventing the oxidation of sulfides, and treatment of the acidic water discharge (Blowes et al, 1994). Conventional treatment of discharge waters involves oxidation and precipitation of Fe-oxyhydroxides by addition of lime. This approach can be effective but often involves high operating costs and produces large volumes of metal-rich sludge.

Sulfate reduction as a treatment strategy

Wakao (1979) suggested that mine waters could be treated through the precipitation of metal sulfides by using sulfate-reducing bacteria to reduce dissolved SO_4^{2-} contained in the drainage water. Bacterially mediated reduction of sulfate can be expressed as:

$$(3) \quad SO_4^{2-} + 2CH_2O + 2H^+ \Rightarrow H_2S + 2CO_2 + H_2O,$$
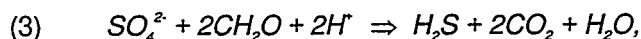
where CH_2O represents organic carbon. In the presence of soluble metals, hydrogen sulfide can react to form metal sulfides;

$$(4) \quad Fe^{2+} + H_2S \Rightarrow FeS_{(s)} + 2H^+.$$

Elements such as As, Cd, Cu, Ni, Pb and Zn can also react with H_2S to form other sulfide minerals.

This reaction sequence results in decreased concentrations of dissolved SO_4^{2-}, Fe, and other metals, an increase in alkalinity and increase in pH. All of these changes are desirable. Recently, interest in sulfate reduction has focused on its utility during remediation of acid mine drainage using constructed wetlands. The primary method of exploiting sulfate reduction in wetlands has been to direct acidic, metal and sulfate-rich surface water into the subsurface by an induced hydraulic gradient (Machemer and Wildeman, 1992). A variety of laboratory and field-scale projects have demonstrated the potential effectiveness of this process (Dvorak et al., 1992; Machemer and Wildeman, 1992; Eger and Wagner, 1995).

The success of these wetland projects has been mixed. In many cases sulfate reduction and metal sulfide-precipitation has resulted in improved water quality. However, three factors have hampered this approach. First, high acidity can quickly consume the buffering capacity of the reactive organic material, resulting in a decrease in pH. Because sulfate reduction is optimized at moderate pH (Brock and Madigan, 1991), these acidic conditions limit treatment capacity. Second, where neutral pH conditions have been maintained, the residence times within the reactive mixture are often not sufficient to remove the mass of sulfate and metals entering the system (Eger and Wagner, 1995). Third, in northern latitudes, and high elevations, cold temperatures decrease both biological and chemical reaction rates.

Blowes et al, (1990) proposed *in-situ* treatment of water contaminated with mine-related wastes by sulfate reduction within the saturated zone of the tailings or within permeable reaction

zones installed into the aquifer down-gradient of tailings impoundments. By treating the water prior to the oxidation of the Fe^{2+}, the generation of additional acidity is prevented. Additionally, because contaminated groundwater is treated without pumping, the volume of water that is necessary to treat is smaller. Subsurface treatment is also advantageous because temperatures are generally higher during winter months and it is easier to maintain the reduced geochemical conditions necessary for sulfate reduction below the water table.

Reactive wall technology

We have attempted to exploit advantages of treatment within the aquifer using the emerging remediation technology of a permeable reactive wall. This method consists of installing an appropriate reactive material into the aquifer, so that contaminated water flows through the material. The reactive material induces chemical reactions that remove the contaminants from the water or otherwise cause a change that decreases the toxicity of the contaminated water (Blowes and Ptacek, 1992; Gillham and O'Hannesin, 1992, 1994; Robertson and Cherry, 1995; Baker, 1993; Ptacek et al., 1994). For the treatment of groundwater affected by leachate derived from mine wastes, organic carbon is used in the treatment wall to enhance sulfate reduction and metal sulfide precipitation (Blowes and Ptacek, 1994, Blowes et al., 1995).

A two year laboratory study was undertaken to assess the viability of using sulfate reduction in a porous reactive wall to treat groundwater similar to leachate water from inactive mine-tailings impoundments (Waybrant, 1995; Waybrant et al., 1995). Batch studies were conducted to select the optimal organic substrate for inducing sulfate reduction. This work indicated that a variety of organic materials are effective at inducing sulfate reduction (Waybrant, 1995; Waybrant et al., 1995).

Column experiments were conducted using the results of the batch experiments to simulate the dynamic flow and geochemical conditions that exist within a contaminated aquifer (Waybrant, 1995; Waybrant et al., in prep.). The influent water contained high concentrations of SO_4, Fe, Zn, and Ni and was maintained under anoxic conditions. Sulfate, Fe and Ni concentrations were significantly decreased and alkalinity increased after passing through the columns, indicating that, under dynamic flow conditions, rates of sulfate reduction are sufficient to treat fluxes typically found in contaminated aquifers on a sustained basis.

In Autumn 1993 and 1994, pilot-scale test cells were installed into the aquifer at the Nickel Rim mine site near Sudbury, Ontario, Canada (Blowes et al., 1995). The permeable cells of reactive material were designed to allow groundwater to flow through them to evaluate the potential of inducing sulfate-reduction and metal-sulfide precipitation reaction under field conditions. The test cells continue to induce sulfate reduction 12 and 24 months after installation, indicating that the reactive wall technology for the treatment of mine-contaminated waters was transferable to a field setting.

Methods

In August of 1995 a full-scale porous reactive wall was installed into the aquifer at the Nickel Rim mine site (Benner et al., in submittal). Based on previous laboratory and field studies, a mixture of 40% leaf compost, 40% municipal compost, and 20% wood chips was selected for the organic source material. The organic material was mixed with 50% (by volume) washed pea gravel to obtain a hydraulic conductivity capable of accommodating the flux rates in the Nickel Rim aquifer. To obtain a uniform mixture of gravel and organic material, a 40 meter. inclined conveyer belt was used. The organic materials and the pea gravel were simultaneously added to the conveyor and allowed to cascade into a conical pile. The materials were mixed as the pile formed at the end of the conveyer. This process was repeated until a uniform mixture was obtained.

The reactive wall was installed by cut and fill excavation; as the aquifer material was removed to underlying bedrock, the trench was back-filled with the organic carbon and gravel mixture (Figure 1). Sand fill was added at the up and down-gradient sides of the wall to square off the organic mixture with the sloping sides of the trench. The installed wall is approximately 15 meters long, 3.6 meters deep, and 4 meters wide. Nested piezometers were installed and sampled along a line parallel to flow, providing a cross-sectional sampling profile. Sampling and analysis were conducted as described in Waybrant (1995) and Bain (1996).

Initial Results and Discussion

The aquifer down-gradient of the reactive wall receives surface water recharge. Therefore, the water flowing through the reactive wall occupies only the lower portion of the down-gradient aquifer while the upper portion of the aquifer contains untreated water. Sampling nine months after installation indicates that the reactive wall is greatly improving groundwater quality. Comparing water entering the wall to treated water exiting the wall; sulfate concentrations decrease >50% (from 2400-4800 mg/L to 60-3600 mg/L), Fe concentrations decrease >95% (from 260-1300 mg/L to 1.0-40 mg/L), pH increases from 5.8 to 7.0 and alkalinity (as $CaCO_3$) increases from 0-60 mg/L to 700-3200 mg/L (Figure 2). The water entering the wall has an average net acid producing potential of 6-46 meq/L and the water exiting the wall has a average net acid consuming potential of 16-45 meq/L (Benner et al., in submittal).

Maintaining permeability

It is anticipated that the permeability of the porous reactive wall will not decrease with time. The gravel-compost mixture was chosen so that the material is gravel supported which should prevent a significant decrease in permeability by compaction. The precipitation of sulfide minerals is not expected to decrease permeability because sulfate reduction and metal sulfide precipitation result in the exchange of a less dense material (organic material) for a more dense material (metal sulfide). Organic carbon (density $\cong 1$ gm/cm^3) is being converted to CO_2, much of which is lost from the reactive wall as alkalinity. This mass lost from the wall is being replaced by the precipitation of Fe-sulfides (density $\cong 4$ - 5). The laboratory column studies using a similar material show no decrease in permeability after 30 months and 75 pore volumes (Waybrant, 1995).

Estimating the potential longevity of a reactive barrier

The ultimate success of the permeable reactive wall will be determined by the longevity over which sulfate reduction and subsequent metal-sulfide precipitation is maintained. The ability of the wall to transform the groundwater from acid producing to acid consuming is dependent on the removal of Fe. Therefore, change in Fe concentrations as water passes through the wall is a useful measure of the reactive wall effectiveness. It is assumed that the limiting factor will be the ability of the organic carbon to induce sulfate reduction.

Previous research suggests that not all of the carbon is "available" for sulfate reduction (Eger and Wagner, 1995). If the total carbon that can be used for sulfate reduction is limited, the thickness of the permeable reactive wall will be proportional to its longevity. In addition, the amount of available organic carbon may also be a function of the amount of time that the sulfate and organic carbon are in contact. The longer the contact time, the larger fraction of the organic carbon will be available for inducing sulfate reduction.

The flow path length and residence time in the reactive wall at Nickel Rim can be compared with the results of column experiments conducted by Waybrant et al. (1995). In the

laboratory 300-1000 mg/L Fe was removed in the column with a residence time of 15 days and a travel path length of 0.3 m. Assuming a groundwater velocity in the Nickel Rim aquifer of approximately 16 meters/year and a wall thickness of 4 meters, the residence time is about 90 days (Benner et al., in submittal). Therefore the wall residence times are six times longer, and path length is 12 times longer than the laboratory columns. Concentrations of Fe range between 200 and 1000 mg/L at Nickel Rim, similar to concentrations used in the laboratory columns. An estimate of reactive wall longevity by comparison with column longevity is appropriate.

In the laboratory column (Waybrant et al, 1995), a minimum of 10% of the carbon has been consumed by sulfate reduction and metal sulfide precipitation. Assuming that 10% of the carbon in the porous reactive wall at Nickel Rim is available, an approximate calculation of longevity can be made. The wall contains approximately 1,500,000 moles of carbon. Assuming that a minimum of 10% of that carbon (~150,000 moles) is available, the minimum amount of Fe that can be precipitated as sulfides by that carbon is 75,000 moles (based on stoichiometry of Reactions #3 and #4). Given a porosity of 0.4, groundwater velocity of 16 m/a, and a cross-sectional area of 45 m^2, the flux of water through the wall is 288 m^3/a. Assuming an Fe concentration of 1000 mg/L, the annual flux will be about 5,100 moles/yr. This suggests that the reactive wall will be effective for a minimum of 15 years (Benner et al., in submittal).

Cost of installation

Materials and installation costs for the porous reactive wall were approximately $30,000.00 (U.S. funds). Approximately half of that cost was materials and half was installation. This value does not include costs of monitoring and assessment. Estimates of capital and operating expenses for a pump and treat facility at the Nickel Rim site are greater than one million dollars. Costs will vary from site to site depending on the physical and chemical characteristics of the contaminated groundwater plume.

Conclusions

The potential use of permeable reaction walls for remediation and prevention of acid mine drainage has been evaluated through a full-scale field installation. The results of this installation indicate that sulfate-reduction and metal-sulfide-precipitation reactions can be initiated and sustained, at rates that are suitable for treatment of plumes of tailings-derived water, under field conditions.

These studies indicate that permeable reactive walls, using bacterially mediated sulfate reduction, are a potentially effective treatment strategy for remediation of groundwater plumes impacted by drainage from mining activities. The discharge from the full-scale wall will continued to be monitored for a minimum of three years. Research is ongoing to more fully describe the biogeochemical transformations within the reactive wall.

References

Bain, J.G. *The Physical and Chemical Hydrogeology of Sand Aquifer Affected By Drainage From the Nickel Rim Tailings Impoundment.* M.Sc.Thesis, University of Waterloo, Waterloo, Ontario;1995.

Baker, M.J. *Laboratory investigations into the potential for solid mixtures containing industrial products to remove phosphate from solution.* M. Sc.Thesis, University of Waterloo, Waterloo, Ontario;1993.

Baker, M.J., Blowes, D.W., and Ptacek, C.J. 1996. Development of a reactive mixture to remove phosphorous from on-site wastewater disposal systems. *In: Waterloo Centre for Groundwater Research Conference Proceedings for Disposal Trenches, Pre-Treatment, and Re-Use of Wastewater,* University of Waterloo, Waterloo, Ontario, May 13, 1996. pp. 51-56.

Blowes, D.W. and Jambor, J.L. 1990. The pore-water geochemistry and the mineralogy of the vadose zone of sulfide tailings, Waite Amulet, Quebec, Canada. *Appl. Geochem.* 5, 327-346.

Blowes, D.W. and Ptacek, C.J. University of Waterloo, W., Canada, assignee. System for Treating Contaminated Groundwater. U.S. 5514279.1994. 329,826. C07F 1/58. 210/617; 210/719; 210/720; 210/721; 210/747.

Blowes, D.W. and Ptacek, C.J. 1994. Acid neutralization mechanisms in inactive tailings impoundments. **In:** Anonymousp. 271-292.

Blowes, D.W., Ptacek, C.J., Bain, J.G., Waybrant, K.R., and Robertson, W.D. 1995. Treatment of mine drainage water using in situ permeable reactive walls. *In: Proceedings of Sudbury '95 - Mining and the Environment.,* Sudbury, Ontario, May 28 - June 1, 1995. Hynés, T.P. and Blanchette, M.C. Eds.Vol. 3., pp. 979-987.

Blowes, D.W., Ptacek, C.J., and Jambor, J.L. 1994. Remediation and prevention of low-quality drainage from tailings impoundments. **In:** ; Blowes, D.W., Jambor, J.L. Eds. 22th ed. Nepeon, ON: Mineralogical Association of Canada, p. 365-379.

Brock, T.D. and Madigan, M.T. *Biology of Microorganisms.* 6th ed. Englewood Cliffs, New Jersey: Prentice Hall;1995.

Cohen, Y. 1986. Organic pollutant transport. *Environ. Sci. Tech.* 20, 538-544.

Dubrovsky, N.M., Morin, K.A., Cherry, J.A., and Smyth, D.J.A. 1984. Uranium tailings acidification and subsurface contaminant migration in a sand aquifer. *Water Poll. Res. J. Canada,* 19, 55-89.

Dvorak, D.H., Hedin, R.S., Edenborn, H.M., and McIntire, P.E. 1992. Treatment of metal-contaminated water using bacterial sulphate reduction: Results from pilot-scale reactors. *Biotech. Bioeng.* 40, 609-616.

Eger, P. and Wagner, J. 1995. Sulfate reduction for the treatment of acid mine drainage: Long term solution or short term fix? *In: Proceedings of Sudbury '95- Mining and the Environment.,* Sudbury, Ontario, May 28 - June 1, 1995. Hynes, T.P. and Blanchette, M.C. Eds.Vol. 2., pp. 515-524.

Gillham, R.W. and O'Hannesin, S.F. 1992. Metal-catalysed abiotic degradation of halogenated organic compounds. *In: IAH Conference "Modern Trends in Hydrogeology".,* Hamilton, Ontario, May 10-13, 1992. pp. 94-103.

Gillham, R.W. and O'Hannesin, S.F. 1994. Enhanced degradation of halogenated aliphatics by zero-valent iron. *Ground Water,* 32, 958-967.

Machemer, S.D. and Wildeman, T.R. 1992. Adsorption compared with sulphide precipitation as metal removal processes from acid mine drainage in a constructed wetland. *J. Contam. Hydro.* 9, 115-131.

Morin, K.A., Cherry, J.A., Dave, N.K., Lim, T.P., and Vivyurka, A.J. 1988. Migration of acidic groundwater seepage from uranium-tailings impoundments, 1. Field study and conceptual hydrogeochemical model. *J. Contam. Hydro.* 2, 271-303.

Nordstrom, D.K., Jenne, E.A., and Ball, J.W. 1979. Redox equilibria of iron in acid mine waters. **In:** *Chemical modeling of natural systems.* ; Everett, A.J., Ball, J.W. Eds.

Ptacek, C.J., Blowes, D.W., Robertson, W.D., and Baker, M.J. 1994. Adsorption and mineralization of phosphate from septic system effluent on aquifer materials. *In: Proceedings of the Waterloo Centre for Groundwater Research Annual Septic System Conference: Wastewater Nutrient Removal Technologies and Onsite Management Districts.,* Waterloo, Ontario, June 6. pp. 26-44.

Robertson, W.D. and Cherry, J.A. 1995. In situ denitrification of septic system nitrate using reactive porous media barriers: Field trials. **In Press** *Groundwater.*

Wakao, N., Takahashi, T., Sakurai, Y., and Shita, H. 1979. The treatment of acid mine water using sulphate-reducing bacteria. *J. Ferment. Technol.* 57, 445-452.

Waybrant, K.R., Blowes, D.W., and Ptacek, C.J. 1995. Selection of reactive mixtures for the prevention of acid mine drainage using porous reactive walls. *In: Proceedings of Sudbury '95 - Mining and the Environment.,* Sudbury, Ontario, May 28 - June 1, 1995. Hynes, T.P. and Blanchette, M.C. Eds.Vol. 3., pp. 945-953.

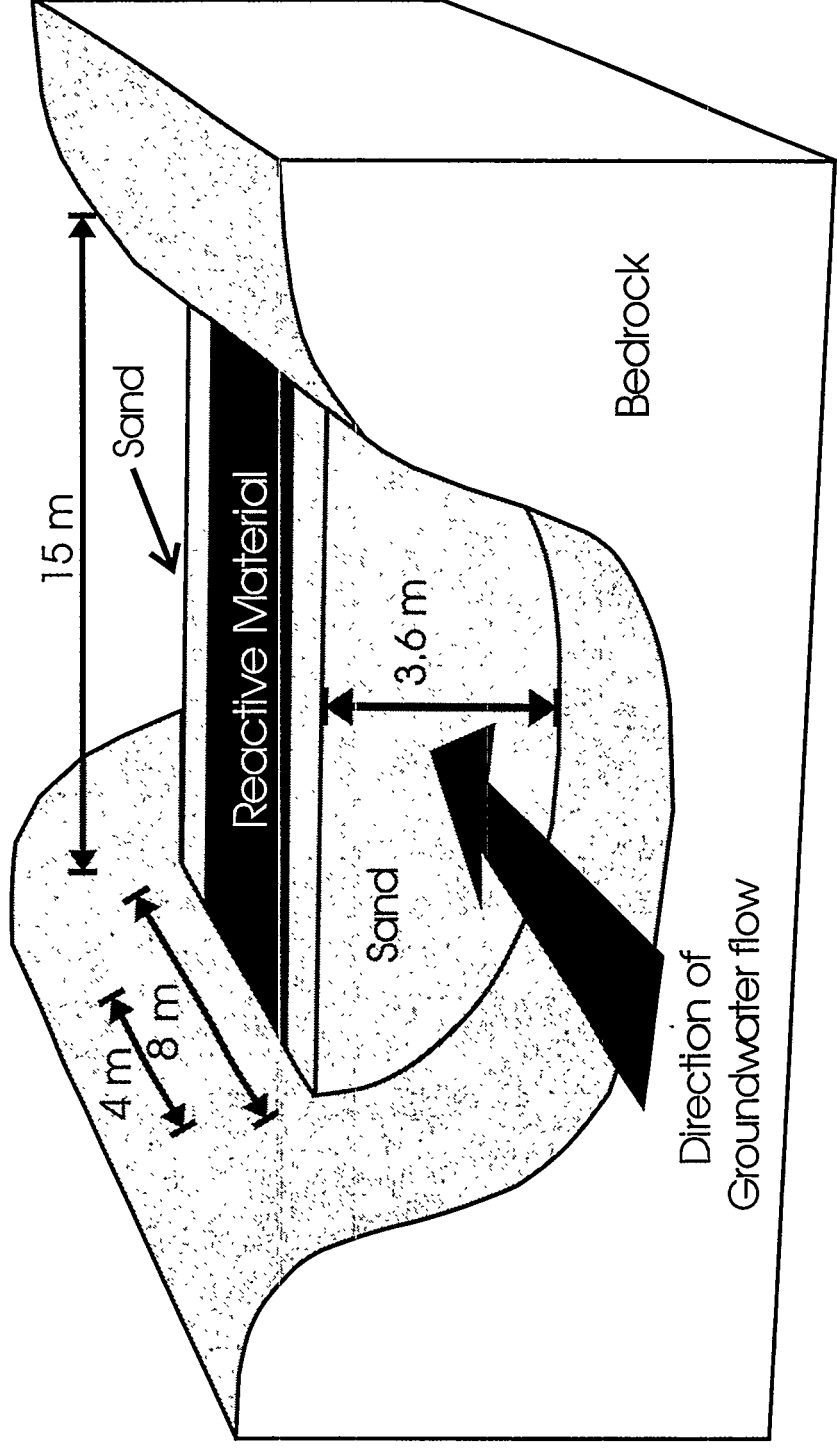# Porous Reactive Wall Installation

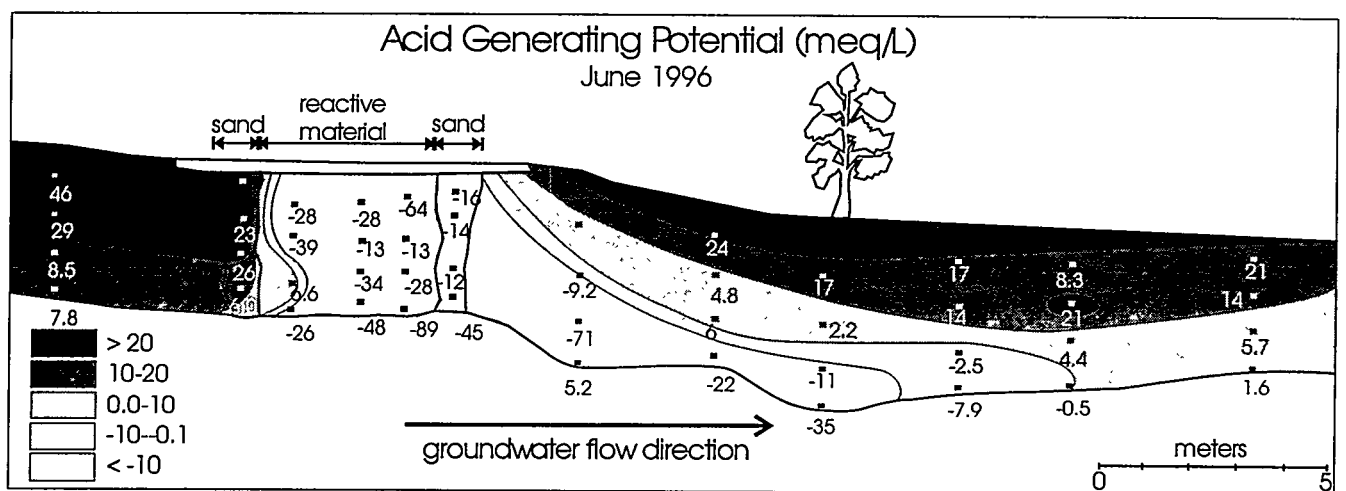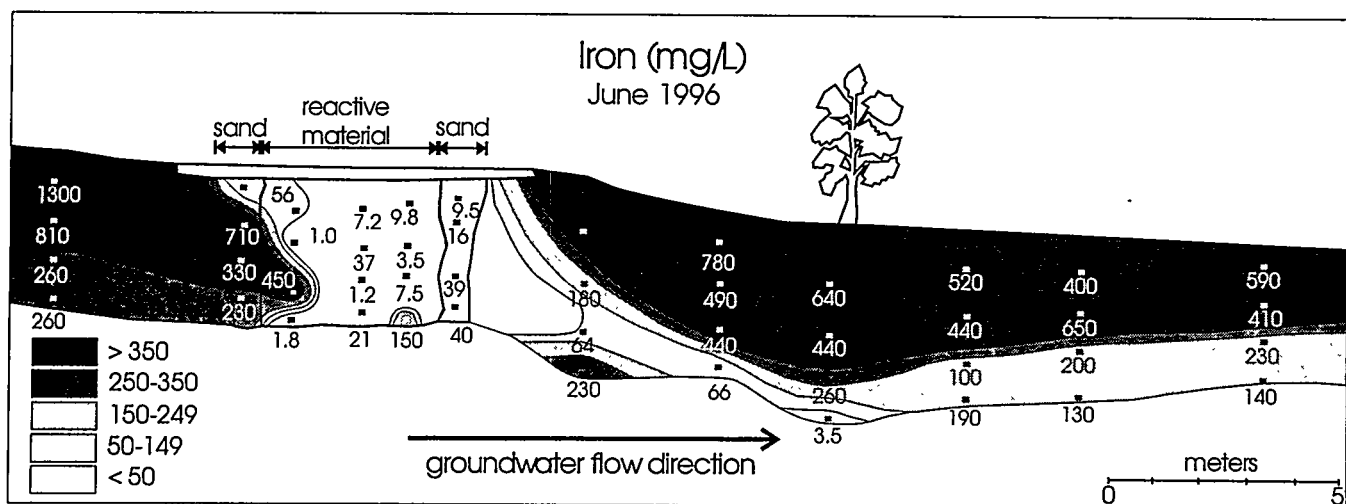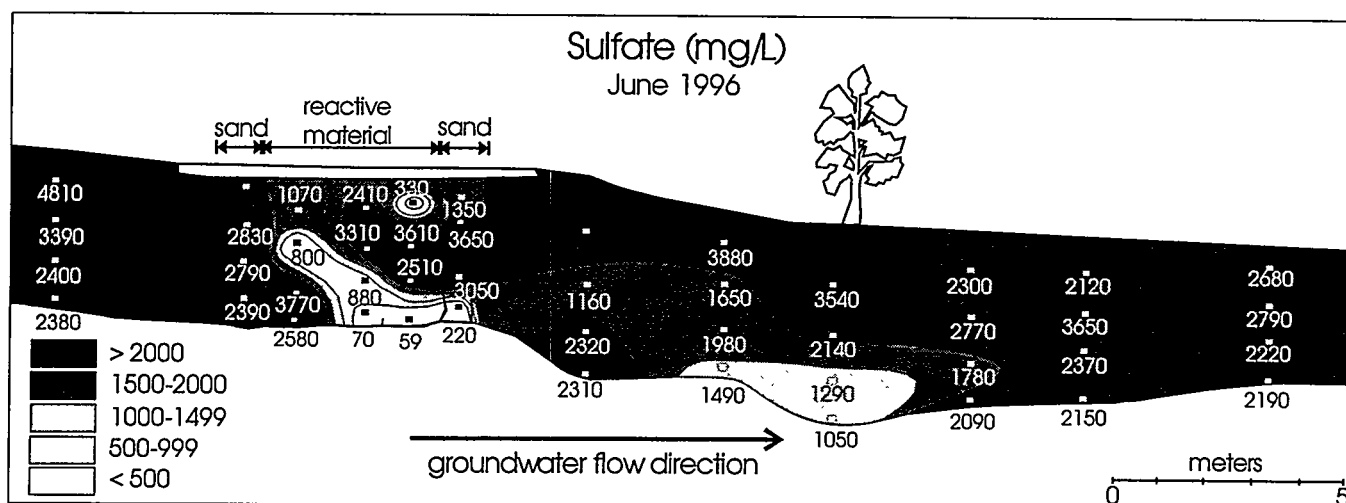Figure 1. Schematic diagram of porous reactive wall installation

Figure 2. Cross-sectional view of reactive wall and adjoining aquifer. Small squares indicate sample locations. Profiles of sulfate, iron and "Acid Generating Potential" 9 months after installation are shown.

IN SITU REMEDIATION OF URANIUM CONTAMINATED GROUNDWATER

Brian P. Dwyer[1] and Dianne C. Marozas[2]

ABSTRACT

In an effort to develop cost-efficient techniques for remediating uranium contaminated groundwater at DOE Uranium Mill Tailing Remedial Action (UMTRA) sites nationwide, Sandia National Laboratories (SNL) deployed a pilot scale research project at an UMTRA site in Durango, CO. Implementation included design, construction, and subsequent monitoring of an in situ passive reactive barrier to remove Uranium from the tailings pile effluent. A reactive subsurface barrier is produced by emplacing a reactant material (in this experiment - various forms of metallic iron) in the flow path of the contaminated groundwater. Conceptually the iron media reduces and/or adsorbs uranium in situ to acceptable regulatory levels. In addition, other metals such as Se, Mo, and As have been removed by the reductive/adsorptive process. The primary objective of the experiment was to eliminate the need for surface treatment of tailing pile effluent. Experimental design, and laboratory and field preliminary results are discussed with regard to other potential contaminated groundwater treatment applications.

INTRODUCTION

Until recently, remediation of contaminated groundwater utilized pump and treat or a related variation. Experience gained in this area has shown that pump and treat schemes are not cost effective in treating the majority of groundwater contamination problems. As an alternative to active pump and treat treatment systems efforts are being made to devise passive in situ treatment techniques. More specifically related to this project is the more than 230 million tons of uranium mill tailings at mill sites throughout the United States (U.S. Environmental Protection Agency, 1987). Uranium and other metals in the mill tailings piles have contaminated subsurface soils and groundwater beneath many of these sites. Plumes migrating from mill tailings sites have been found to contain uranium concentrations on the order of several hundred parts per billion (ppb), which is in excess of the proposed drinking water maximum contaminant level of 20 ppb. Remediation costs of the existing contaminated groundwater associated with the 24 Uranium Mill Tailings Remedial Action (UMTRA) sites have been estimated at about $ 1 billion. Consequently, innovative improvements are necessary to lower the cost of cleaning up the remaining UMTRA sites.

This project demonstrated field scale installation of a reactive barriers at the Durango, Colorado, UMTRA site. Conceptually a reactive barrier treatment system diverts contaminated groundwater with relatively impermeable vertical subsurface walls into a narrow higher permeability treatment zone. The treatment zone contains reactant materials or biota which selectively remove contaminants. Contaminant removal is achieved by one or a combination of the following mechanisms: (1) chemical, (2) physical, and (3) biological. Although the initial costs of a passive system will likely be more than an active system, the payback will be in the form of far less maintenance and operation costs over time.

TEST SITE: BODO CANYON DISPOSAL CELL, DURANGO, COLORADO - UMTRA SITE

Surface remedial action has been completed at the Uranium Mill Tailings Remedial Action Project site in Durango, Colorado. Contaminated soil and debris was moved to the Bodo Canyon

---

[1]Sandia National Laboratories, P.O. Box 5800, Albuquerque, NM 87185-0719, (505) 845-9894, bpdwyer@sandia.gov
[2]Sandia National Laboratories, P.O. Box 5800, Albuquerque, NM 87185-0719, (505) 844-5504, dcmaroz@sandia.gov

Disposal site is in La Plata County, Colorado, approximately 2.5 km from the town of Durango. The land within 1.5 km surrounding the site is uninhabited. Movement of the mill/tailings to the Bodo Canyon disposal site was completed in the fall of 1990. A total of 2.5 million cubic yards (yd^3) of contaminated materials were relocated to the disposal cell. (Jacobs Engineering Group, 1994)

The disposal cell at Bodo Canyon was designed to limit the amount of new infiltrating precipitation. However, fluids disposed of with the contaminated tailings are currently draining from the disposal cell and UMTRA groundwater prediction models estimate three more years of drainage. The draining fluids (leachate), have been collected in a subsurface engineered collection gallery and drained via gravity to a lined retention basin for treatment. Previous treatment included conventional chemical flocculation/settling in a lined retention basin. Once confirmed clean, treated water is released into a nearby arroyo.

LABORATORY TESTING

For a reactive material to be effective in a passive barrier treatment system, the reactant must be capable of simultaneously removing metals from contaminated groundwater and maintaining sufficient hydraulic conductivity to facilitate the passage of fluid through the barrier for long periods of time. Table 1 shows the concentration of detectable metal constituents in Bodo Canyon tailings pile pore fluids and levels of metals acceptable to the Colorado Department of Public Health and Environment (CDPHE). Based on this information, uranium was chosen as the main target for chemical removal by the passive barrier design.

Table 1. Metal Concentrations in Bodo Canyon Tailings Pile Pore Fluids.

Element	Concentration (mg/L)	CDPHE Requirements
As	0.16	0.5
Se	0.17	monitor
Zn	0.49	0.5
U	2.6	2.0
Ra-226	1.1 pCi/L	3.0 pCi/L
Mo	0.89	-
Mn	3.3	-

Many inorganic reactive materials have been proposed for use in removing uranium and other contaminant metals from solutions similar to uranium mill tailings fluids. Some of these include: metallic iron (Cantrell, K.J., et. al., 1995), ferric oxyhydroxide, clinoptilolite, coal, fly ash, peat, hydroxyapatite, sawdust, and titanium oxides (Morrison, S. J. and Spangler, R.R., 1992), (Morrison, S.J., et. al., 1995); taconite and scoria (Jacobs Engineering Group, 1991), and sodium dithionite (Amonette, J.E., et. al., 1994). In these studies, uranium and other metals were removed from solution primarily by sorption, reduction, and precipitation mechanisms.

Metallic iron, metallic iron in contact with a copper catalyst (copper screen), and a patented iron foam were selected for the Bodo Canyon passive barrier demonstration based on numerous laboratory successes in removing uranium and other metals from solutions similar to those at Bodo Canyon and from the actual tailing pond leachate. All of these reagents are environmentally benign in nature and should continue to react with metal contaminants for long periods of time without the need for outside intervention. Availability and cost were also primary considerations in the selection process, because substantial quantities will be required in many future field treatments. By testing multiple materials in the Bodo Canyon demonstration, information on

longevity, cost, and effectiveness will be obtained for use in designing passive barriers for other sites.

Results from laboratory studies conducted by other researchers, on uranium and molybdenum removal by metallic iron are shown in Table 2. Metallic iron immobilizes uranium by chemical reduction and subsequent precipitation. Amorphous Ferric Oxyhydroxide (AFO) adsorbs uranium and other contaminants from groundwater without affecting the redox condition of the system. When metallic iron is in contact with a minor amount of catalytic metal such as copper, the rate of reduction is markedly increased (Sweeny, K.H., and Fischer, J.R., 1973). A bimetallic copper-iron reagent is being tested in order to see if metals such as Mo, V, and Se present in Bodo Canyon fluids (Table 1) can be removed more rapidly by reductive treatment than iron alone (Table 2).

Table 2. U and Mo Removal with Metallic Iron - Bodo Canyon Tailings Fluid
(Data from: Cantrell et al., 1995 and Morrison et al., 1995)

	Reactant	Starting Concentration (mg/L)	Ending Concentration (mg/L)	Contact Time (hours)	CDPHE Requirements
U	Metallic Iron	8.7	.040	2	2.0
	Metallic Iron	2.5	.002	2	2.0
	AFO	2.38	.001	4	2.0
Mo	Metallic Iron	26.0	2.5	88	-
	Metallic Iron	4.5	.09	88	-

Although both reductive and adsorptive chemical treatment systems have been shown to remove uranium from solution in laboratory tests, it is also known that the removal efficiency can vary depending on site specific hydrogeochemical conditions such as pH, major element concentration, and mineralogy. In order to obtain engineering information on how site specific conditions at Bodo Canyon will affect reactivity of the permeable barrier a series of laboratory tests on chemical reactivity and hydraulic conductivity were conducted. Laboratory work determined the following characteristics of various potential treatment materials: (1) the capacity of the reactive material to remove target contaminants; (2) the capability of the reactive material to maintain sufficient hydraulic conductivity and to minimize flow losses because of plugging during the desired treatment interval; and (3) the compatibility of the treatment material with site specific geochemical conditions such as pH, redox, ionic strength, and major element concentrations. The laboratory experiments also aided in formulating the following engineering design parameters: (1) develop volume requirements and subsequent cost data for treatment material; (2) estimate treatment material capacity; and (3)estimate treatment material longevity.

PROJECT SCOPE

Demonstrate at a field scale that an in situ, passive geochemical barrier can be used to selectively remove contaminants from a plume. The entire experiment was conducted inside a 11m X 18.3m X 1.83m deep pre-fabricated leak proof retention basin. In effect this treatment system simulates the flow and subsequent treatment of contaminated ground water in a controlled environment. Consequently, the risk of contaminant release during the experiment is eliminated. Figure 1 is a schematic of the general layout of the tailings pile, the old treatment retention pond, and the new treatment system.
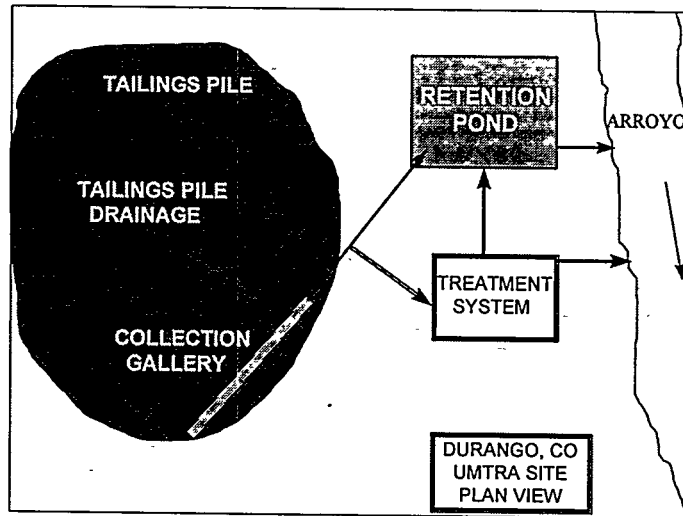
Figure 1. General location schematic.

OBJECTIVES

1. passive diversion of tailings pile effluent into treatment zone;
2. passive removal of selected contaminants from tailings effluent;
3. effective treatment of a simulated contaminated groundwater having representative (geochemistry and geohydrology) conditions of other UMTRA sites;
4. evaluate treatment efficiencies and associated costs for different treatment materials; and
5. extrapolate the longevity of each material.

Laboratory data was used to design treatment configurations 1 and 2 shown in Figures 3 and 4, respectively. More specifically: material saturated hydraulic conductivity and required residence time for contaminant removal were the primary parameters used to determine material volumes, thickness, and densities.

TREATMENT SYSTEM OPERATION

The new treatment system selectively transforms the unwanted contaminant (uranium) into a less toxic and mobile state, i.e., this is essentially a chemical filtration process. Treatment system chemistry is shown in Figure 2. The purified water is collected in the underdrain and diverted to the existing retention pond until treatment effectiveness is verified.
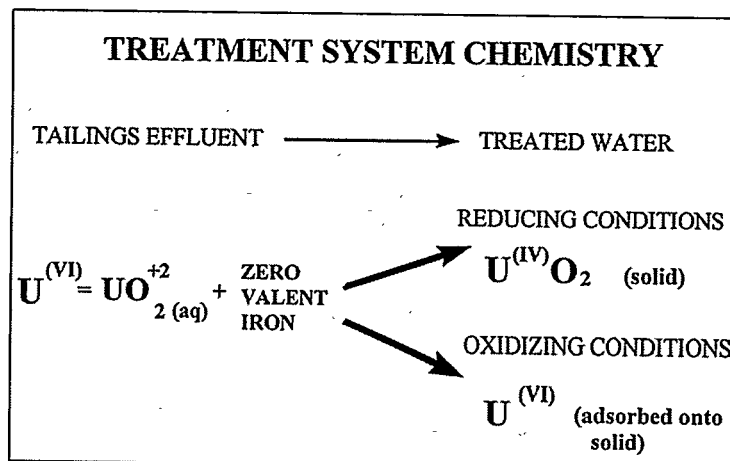
Figure 2. Treatment system chemistry.

Treatment Configuration 1 is an engineered ground water treatment system consisting of a subsurface drainfield similar to a residential septic leach field (Figure 3), that evenly distributes contaminated groundwater above a treatment zone was constructed inside of the retention basin. Contaminated groundwater percolates via gravity through the treatment zone where target contaminants (uranium, selenium, and molybdenum) are transformed and/or removed. The experiment tests three different materials (zero valent iron, iron foam, and a bimetallic iron/copper) using two different configurations in an effort to identify the optimum treatment media. In addition, field stability and form of the immobilized contaminants shall be evaluated for the duration of the project - 4 years. A second treatment configuration (Figure 4) utilizing a plug flow reactor design was used to evaluate an iron foam produced by Cercona, Inc. of Dayton, Ohio; and the zero-valent iron (provided by International Steel Wool).
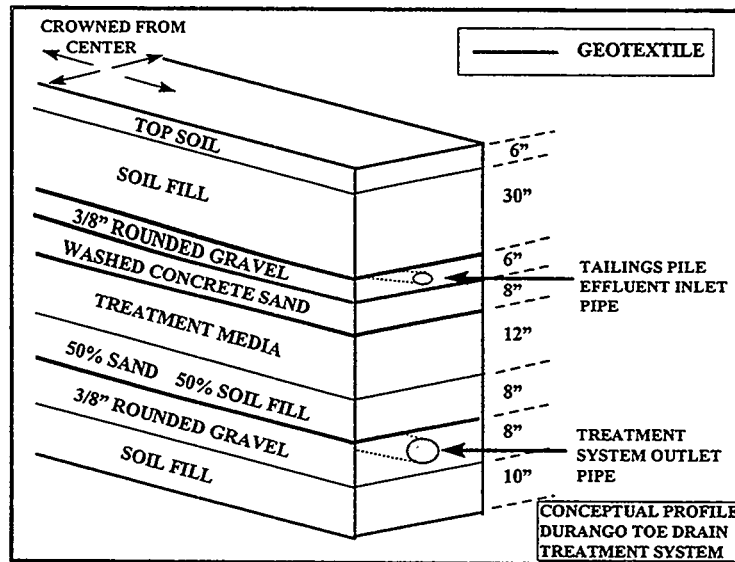
Figure 3. Configuration 1 - leach field cross section.
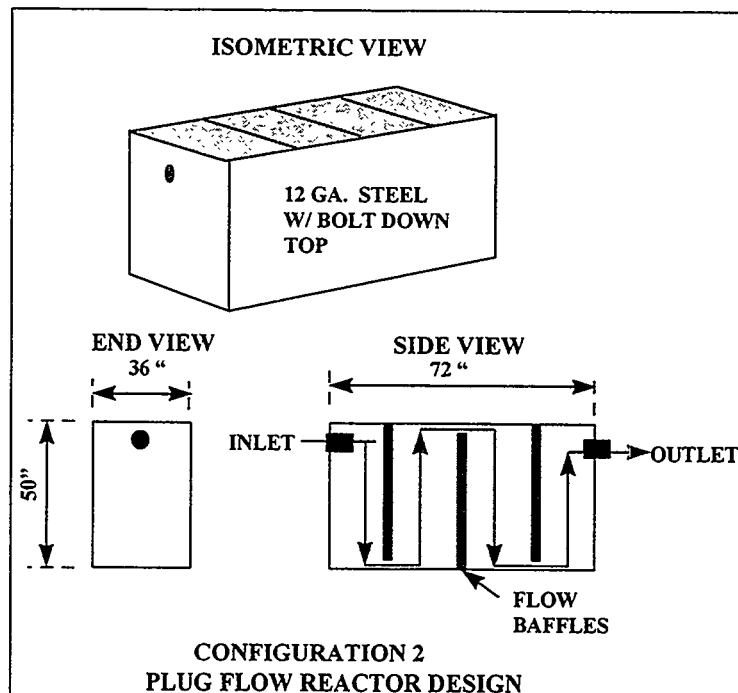
Figure 4. Configuration 2.

848

RESULTS

Operation of the field pilot test began in May, 1996 and is scheduled to continue through 1999. The results to date are very promising. Figures 5, 6, and 7 exhibit pilot test removal efficiencies of the iron foam treatment media. The field results essentially coincide with previous laboratory data. Previous research has shown that the rate of contaminant removal by metallic iron can be directly related to surface area of the reactant. Metallic iron foam could be the alternative reactive media that provides increased surface area for reaction as well as improved hydraulic conductivity. Metallic iron foam products have between .1 and 5 m^2/g of surface area. In comparison, steel wool has a surface area of about 5.6E-3 m^2/g. Batch experiments on the foam with Bodo Canyon water showed that uranium was removed to less than detectable levels within 10 hours of contact. A second parameter which will determine the feasibility of using zero valent iron as a long term solution is treatment effectiveness over time. Laboratory testing indicated that the metallic iron treatment media will maintain sufficient hydraulic conductivity during the desired treatment interval (4 years). Initial saturated hydraulic conductivity of the zero-valent iron (steel wool) was 6.4 x 10^3 cm/s; and the iron foam was 0.53 cm/s. Oxygenated water simulating a worst case plugging scenario was used to simulate changes that occur due to oxidation of the iron. After more than 700 pore volumes of water passed through the reactive zone the column still maintained its capacity.

Figure 5. Uranium Removal.

Figure 6. Nitrate Removal.

Figure 7. Molybdenum Removal.

CONCLUSIONS

Before reactive barriers can be accepted as a reliable and efficient method of addressing uranium mill tailing groundwater problems, field studies such as this Durango, CO pilot are needed to provide efficiency, longevity, and control information to interested parties. The nature of uranium mill sites, i.e., multiple contaminants, requires a technology capable of handling problematic contaminants using an in situ barrier.

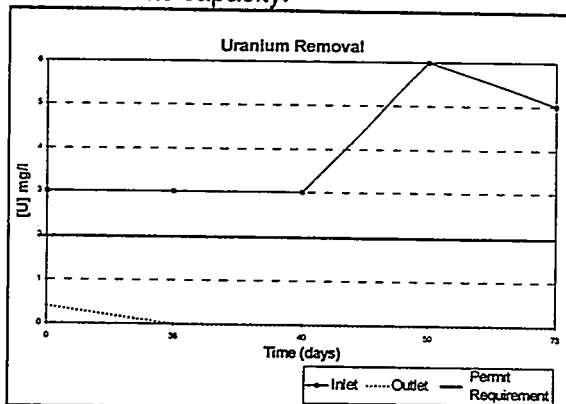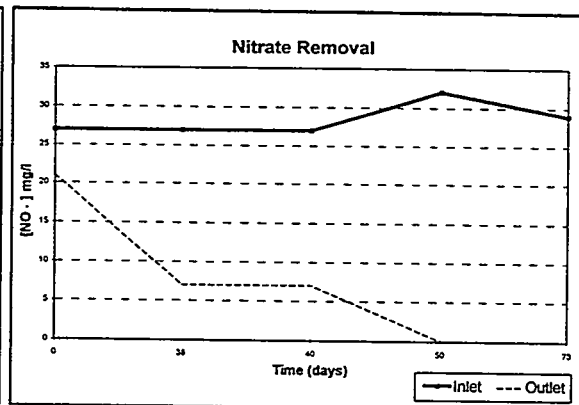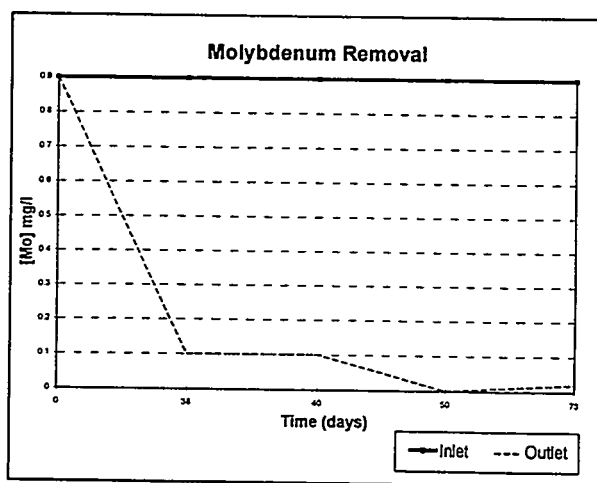Results from the Durango experiment have and will continue to be incorporated into reactive barrier designs for other uranium mill tailings remediation efforts. Information is being collected regarding removal efficiencies of uranium, selenium, molybdenum and other elements in an effort to broaden the technology application. During the expected project duration (3 more years), reactive zones will be examined to identify the long-term stability of the reaction products. This information will assist designers of future in situ reactive barrier installations. Finally, the costs and associated benefits of using this treatment approach will be determined.

REFERENCES

1. Amonette, J.E., Szecsody, J.E., Schaer, H.T., Templeton, J.C., Gorby, Y.A., and Fruchter, J.S., 1994, Abiotic reduction of aquifer materials by dithionite: A promising in-situ remediation technology, in: In-Situ Remediation: Scientific Basis for Current and Future Technologies, edited by G.W. Gee and N.R. Wing, pp. 851-882.

2. Cantrell, K.J., Kaplan, D.I., and Wietsma, T.W., in press, Zero-valent iron for the in situ remediation of selected metals in groundwater, Journal of Hazardous Materials, 1995.

3. Jacobs Engineering Group, 1991, Alternative geochemical barrier materials, U.S. DOE Contract Report No. DE-AC04-82AI14086.

4. Jacobs Engineering Group, 1994, UMTRA Project Water Sampling And Analysis Plan, Durango, Colorado, U.S. DOE Contract Report No. DOE/AL/62350-87D.

5. Morrison, S. J. and Spangler, R.R., 1992, Extraction of uranium and molybdenum from aqueous solutions: A survey of industrial materials for use in chemical barriers for uranium mill tailings remediation, Environmental Science and Technology, Vol. 26, No. 10, pp. 1922-1931.

6. Morrison, S.J. and Spangler, R.R., and Tripathi, V.S., 1995, Adsorption of uranium (VI) on amorphous ferric oxyhydroxide at high concentrations of dissolved carbon (IV) and sulfur (VI), Journal of Contaminant Hydrology, Vol. 17, pp. 333-346.

7. Puls, R. W.; Powell, R.M., and Paul, C.J. In situ remediation of ground water contaminated with chromate and chlorinated solvents using zero-valent iron: a field study, in: ACS Division of Environmental Chemistry Proceedings, Anaheim, CA, 1995, Vol. 35, No. 1, pp. 695-698.

8. Sweeny, K.H., and Fischer, J.R., 1973, Decomposition of halogenated organic compounds using metallic couples, U.S. Patent 3,737,384, 6 pp.

9. U.S. Environmental Protection Agency, 1987. Standards for remedial actions at inactive uranium processing sites; proposed rule. Federal Register, V. 53, Vol. 14, 40 CFR Part 192, Part III, pp. 36000-36008.

In-situ POROUS REACTIVE WALL FOR TREATMENT OF Cr(VI) AND TRICHLOROETHYLENE IN GROUNDWATER

D.W. Blowes[1], R.W. Puls[2], T.A. Bennett[1], R.W. Gillham[1], C.J. Hanton-Fong[1] and C.J. Ptacek[1]

[1]Department of Earth Sciences, University of Waterloo, Waterloo, Ontario, Canada
[2]R.S. Kerr Environmental Research Laboratory, U.S. Environmental Protection Agency, Ada, OK

A permeable reactive wall for treating groundwater contaminated with hexavalent chromium (Cr(VI)) and trichloroethylene (TCE) was installed at the U.S. Coast Guard Support Center in Elizabeth City, NC in June, 1996. The porous reactive wall is 46 m long, 0.6 m wide, and 7.3 m deep. The reactive wall was installed in less then six hours using a continuous trenching technique which simultaneously removed the aquifer material and replaced it with reactive material. The wall is composed of 100% elemental iron in the form of iron filings. Preliminary laboratory experiments, with site groundwater and reactive materials similar to the full-scale wall components, were successful in decreasing 11 mg/L Cr(VI) to < 0.01 mg/L and 1700 µg/L TCE to < 1 µg/L. Detailed field monitoring commenced in November, 1996. The monitoring program includes groundwater sampling upgradient, downgradient and within the reactive wall, and collection of core samples for mineralogical and microbiological study. Preliminary results from the monitoring program indicate that the wall successfully removes Cr(VI) from influent concentrations of 6 mg/L to < 0.01 mg/L, and TCE from 5600 µg/L to 5.3 µg/L within the wall.

INTRODUCTION

Treatment of contaminated groundwater using permeable reactive barriers may provide an approach to groundwater remediation that is effective and less expensive than conventional treatment approaches. Conventional pump-and-treat systems require pumping contaminated groundwater to the ground surface, where the contaminants are removed, and the water is subsequently discharged. Because of slow dissolution processes, and other mass transfer limitations, pump-and-treat remediation techniques may require operation for long time periods, resulting in high treatment costs (Mackay and Cherry, 1989). *In situ* treatment, using permeable reactive walls circumvents these higher operational costs because treatment occurs within the aquifer, without the need for groundwater extraction.

Permeable reaction walls are installed into aquifers by excavating aquifer material in the path of the plume of contaminated groundwater, and replacing this material with a reactive mixture (Figure 1). The reactive mixture is designed to promote the removal of the contaminant as the groundwater flows through the permeable barrier. Permeable reactive barriers have been designed for the treatment of many contaminants including dissolved metals (Blowes and Ptacek, 1992, 1994), chlorinated hydrocarbons (Gillham and O'Hannesin, 1992, 1994), dissolved nutrients (Robertson and Cherry, 1995; Baker et al., 1996), gasoline derivatives (Bianchi-Mosquera et al., 1994), and acid mine drainage (Blowes et al., 1994, 1995a; Waybrant et al., 1995; Benner et al., 1996). This paper describes the design, installation and preliminary field results from a reactive barrier designed for the combined treatment of hexavalent chromium (Cr(VI)), and halogenated hydrocarbons, trichloroethylene (TCE), dichloroethylene (DCE) and vinyl chloride (VC). The reactive barrier was installed at the United States Coast Guard Support Center, near Elizabeth City, North Carolina, in June, 1996.

## SITE DESCRIPTION

The field site is located at the United States Coast Guard Support Center near Elizabeth City, NC, on the south bank of the Pasquotank River (Figure 2). The river at this location is approximately 3 km wide. Surficial sediments on the base consist of typical Atlantic coastal plain sediments. At the site, upper imported fill material is underlain by silty clays, which overlie a thin

sandy clay layer which occurs at about 1.5 m below the ground surface. Fine to medium grained sands dominate from 4 m to 20 m below the ground surface. At the site of Cr(VI) contamination, a fine grained layer occurs approximately 8 m below the ground surface (Puls et al., 1994). A dense gray clay unit, the Yorktown confining unit, persists at a depth of 20 m. Groundwater flow is directed toward the Pasquotank River. Hydraulic conductivity measurements made at the site show significant variability ranging from 0.1 to 26 m/day in the shallow portion of the aquifer. The average hydraulic conductivity in the vicinity of the contamination site is estimated to be 17 m/day. Groundwater velocities, calculated using the field measured hydraulic conductivity, a representative hydraulic gradient of 0.003, and an estimated porosity of 0.38, vary from 8.7×10^{-4} to 0.23 m/day.

The source of dissolved chromium at the site was identified as a former plating shop located in Hangar 79 (Puls et al., 1995). The plating shop operated for more than 30 years. During this period, acidic chromium plating solutions were released through a hole in the concrete floor into the underlying geological materials. The release of chromium has resulted in the development of a plume of groundwater containing dissolved Cr(VI) at concentrations in excess of 0.05 mg/L, with maximum concentrations of 8 mg/L. The plume extends 65 m from the plating shop, terminating at the Pasquotank River. In addition to chromium, an extensive plume of chlorinated solvents is present at the site, and overlaps with the Cr(VI) plume (Puls et al., 1995). The two plumes are narrow in the vertical dimension, with most of the contamination occurring between 4 and 7 m below the ground surface.

Selection of Reactive Materials

Material selected for use in the reactive barrier is required to result in the attenuation of dissolved chromium and the destruction of the chlorinated hydrocarbons. Numerous reduced phases have been identified to have the potential to reduce dissolved Cr(VI). After testing a range of solid phases, Blowes and Ptacek (1992) concluded that elemental iron (Fe^0) has the potential to induce the rapid reduction and removal of Cr(VI) from synthetic groundwater. Subsequent batch tests conducted by Powell et al. (1995) confirmed the potential for Cr(VI) removal using Fe^0. Flow-through column experiments indicate the potential for continued removal of Cr(VI) at concentrations of up to 20 mg/L for periods in excess of 100 pore volumes (Blowes and Ptacek, 1992; Blowes et al., 1995b, submitted). Mineralogical study of the reacted solids obtained from the batch and column experiments indicates that the principal mechanisms limiting Cr(VI) mobility is the reduction of Cr(VI) to Cr(III) and the formation of Fe(III)-Cr(III) oxyhydroxide phases. The most abundant of these phases is goethite. The mechanism of Cr(VI) removal by Fe^0 can be written as:

$$Fe^{\,o} + HCrO_4^- + 2H_2O + H^+ \hookleftarrow Fe(OH)_3 + Cr(OH)_3$$
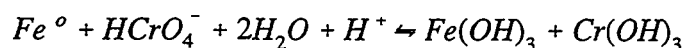
The reaction product occurs as a mixed Cr(III) - Fe(III) oxyhydroxide phase with Cr(III) contents that attain up to 23% of the total cation mass (Blowes et al., 1995b, submitted).

Elemental iron also is used as a means of enhancing abiotic reductive dechlorination of organic compounds (Gillham and O'Hannesin, 1992, 1994). Elemental iron has been shown to result in the degradation of a wide range of chlorinated methanes, ethanes and ethenes with half-lives that are three to eight orders of magnitude less than those observed to result under natural abiotic conditions (Gillham and O'Hannesin, 1994). Degradation of the compounds present at the Elizabeth City site has been observed to occur in the presence of Fe^0 in laboratory and field scale experiments.

Elemental iron was selected as a reactive component of potential mixtures for use in a full-scale reactive wall at the Elizabeth City site. Laboratory batch and column experiments were conducted to assess the potential for combined treatment of Cr(VI) and halogenated hydrocarbons. Batch experiments were conducted using three sources of Fe^0, mixed with either silica sand or local aquifer material. The results of the batch tests indicated removal of Cr(VI) and halogenated hydrocarbons at rates that were sufficient for treatment of these contaminants.

Column tests were conducted to assess the potential for groundwater treatment under dynamic flow conditions. In these tests groundwater collected from the Elizabeth City site was used. The concentrations of Cr(VI) and halogenated hydrocarbons in this water were increased to 11 mg/L Cr(VI) and 1700 µg/L TCE to be similar to the maximum concentrations observed at the field site.

Six column tests were conducted using differing mixtures of elemental iron, silica sand and site aquifer material. The columns used were 50 cm long and 3.8 cm internal diameter. Sampling ports were positioned along the length of the column at distances of 2.5, 5, 10, 15, 20, 30, 40 and 50 cm from the inlet end. A peristaltic pump was used to feed solution from a collapsible teflon bag to the bottom influent end of the columns. The initial flow velocity was 0.6 m/day (2 ft/day). A second set of three column experiments was conducted at a lower flow velocity of 0.3 m/day (1 ft/day).

All column experiments indicated removal of Cr(VI) and halogenated hydrocarbons at rates that are suitable for groundwater treatment using a reactive barrier. At the column effluent concentrations of Cr(VI) were consistently < 0.01 mg/L and concentrations of TCE were consistently < 1 µg/L. Based on these results a reactive material composed of 100% elemental iron was selected for use in the field scale installation. Laboratory results illustrating the degree of treatment using this material are presented in Figure 3. This selection was made to avoid the necessity for mixing reactive materials at the site and to avoid the possibility of zonation within the reactive barrier due to incomplete mixing. The source of elemental iron was selected based on cost and logistical considerations.

Configuration of Reactive Barrier

Two principal configurations for the reactive barrier were considered, a funnel-and-gate system consisting of an impermeable funnel attached to a permeable gate containing the reactive material, and a continuous reaction barrier. Numerical simulations were conducted using two and three dimensional groundwater flow and transport models. The boundary conditions used in the simulations were based on conditions observed at the field site. The simulations were conducted using extreme low and high hydraulic conductivity values observed at the site and hydraulic conductivity values estimated for the reactive material through laboratory experiments. The results of the simulations indicated that groundwater flow velocities through the funnel-and-gate configuration were greater than through the continuous barrier configuration. In the absence of an underlying confining layer, the potential for diversion of flow below or around the barrier edges was greater in the funnel-and-gate configuration. The simulation results indicated that the anticipated residence time within the reactive material was greater in the continuous barrier than in the funnel-and-gate system. The simulation results suggested that for a similar volume of iron, the same capture zone and residence time could be attained using both the continuous wall and funnel-and-gate configurations. Based on these considerations, and the comparative costs of installation, a continuous barrier configuration was selected. The barrier installed was 46 m (150 ft) long, 7.3 m (24 ft) deep and 0.6 m (2 ft) wide (Figures 1,2).

Reactive Barrier Installation

The reactive barrier was installed in under 6 hours using a continuous trenching technique on June 22, 1996. The continuous trenching machine excavated aquifer material while simultaneously depositing reactive material into the aquifer. The trenching technique provided an efficient and effective means of installing the reactive material into the aquifer. Rehabilitation of the site following installation of the reactive barrier was provided by the U.S. Coast Guard and their site contractors.

Post-installation Monitoring

In November 1996, a monitoring network of bundle type piezometers was installed in the aquifer upgradient, within, and downgradient of the reactive barrier by researchers from the University of Waterloo and U.S. Environmental Protection Agency. This monitoring network included three cross-sections of five bundle piezometers each across the barrier (Figure 4). Each of the bundle piezometers contained seven to eleven sampling ports. Water samples were collected from these ports for immediate measurement of field parameters, including pH, Eh, electrical conductivity, turbidity, alkalinity, and concentrations of dissolved oxygen, dissolved Cr(VI), and dissolved Fe(II). Occasional measurements were made to determine the concentrations of dissolved H_2S. Filtered (0.45 µm) samples were collected for determination of dissolved inorganic constituents, and unfiltered samples were collected for determination of total concentrations. Separate samples were

collected for determination of the concentrations of halogenated hydrocarbons.

The preliminary results indicate that the groundwater pH rises sharply within the reactive barrier, from upgradient values of 6 to 7, to barrier values of 9 to 10.5. The pH returns to near neutral values within 1 m downgradient of the barrier. The groundwater Eh exhibits a corresponding sharp decrease, from upgradient values of 100 to 500 mV, to very low values of -400 to -600 mV within the barrier. Within 1 m downgradient of the barrier, the Eh returns to relatively oxidized conditions. Concentrations of Cr(VI) decrease from 2 to 8 mg/L in the upgradient plume to consistently < 0.01 mg/L in the barrier and in the downgradient sampling points (Figure 4).

Concentrations of TCE upgradient of the wall reach a maximum of 5600 µg/L, then decrease sharply proceeding through the wall. The extent of treatment varies depending on location along the length of the wall. The maximum concentration of TCE detected at the downstream margin of the wall is 5.3 µg/L. In the treated water plume downgradient of the wall, TCE concentrations increase to a maximum of 50 µg/L. The increase in TCE concentration downgradient of the wall probably reflects slow desorption of organic compounds bound to the aquifer sediment. With increasing time the downgradient concentrations are expected to decline to below the MCL (maximum contaminant level; 5 µg/L).

CONCLUSIONS

A full-scale reactive barrier was installed at the U.S. Coast Guard Base, near Elizabeth City, NC. The design of the barrier was based on bench-scale treatability studies, and the results of numerical groundwater flow and transport model simulations. The configuration of the treatment system is a continuous reactive barrier, 46 m (150 ft) long, 7.3 m (24 ft) deep and 0.6 m (2 ft) wide, containing 100% elemental iron as iron filings. The reactive barrier was installed in less than 6 hours using a continuous trenching technique. The trenching technique provided an efficient and effective means of rapidly installing the treatment barrier. Preliminary results from the field site indicate effective treatment of Cr(VI) is attained near the upgradient side of the reactive barrier. Concentrations of TCE approach or attain the MCL within the barrier.

ACKNOWLEDGEMENTS

DISCLAIMER

Although the research described in this article has been funded wholly or in part by the United States Environmental Protection Agency, it has not been subjected to the Agency's peer and administrative review and therefore may not necessarily reflect the views of the Agency and no official endorsement may be inferred.

REFERENCES

Baker, M.J., D.W. Blowes and C.J. Ptacek (1996) Phosphorous adsorption and precipitation in a permeable reactive wall: Applications for wastewater disposal systems. Submitted to the *1997 International Containment Technology Conference and Exhibition*, St. Petersburg, Florida, Feb. 9-12, 1997.

Benner, S.G., D.W. Blowes and C.J. Ptacek (1996) Porous reactive wall for prevention of acid mine drainage:

Results of a full-scale field demonstration. Submitted to the *1997 International Containment Technology Conference and Exhibition*, St. Petersburg, Florida, Feb. 9-12, 1997.

Bianchi-Mosquera, G.C., R.M. Allen-King and D.M. Mackay (1994) Enhanced degradation of dissolved benzene and toluene using a solid oxygen-releasing compound. *Ground Water Monitoring and Remediation*, 120-128.

Blowes, D.W. and C.J. Ptacek (1992) Geochemical remediation of groundwater by permeable reactive walls: Removal of chromate by reduction with iron-bearing solids. In *Proceedings of the Subsurface Restoration Conference, Third International Conference on Groundwater Quality Research*, June 21-24, 1992, Dallas, Texas, pp. 214-216.

Blowes, D.W. and C.J. Ptacek (1994) System for treating contaminated groundwater. United States Patent 5,362,394.

Blowes, D.W., C.J. Ptacek, J.G. Bain, K.R. Waybrant and W.D. Robertson (1995a) Treatment of mine drainage water using *in situ* permeable reactive walls. In *Proceedings of Sudbury '95 - Mining and the Environment*, (Eds. T.P. Hynes and M.C. Blanchette), May 28 - June 1, Sudbury, Ontario, Vol. 3, pp. 979-987, CANMET.

Blowes, D.W., C.J. Ptacek, C.J. Hanton-Fong and J.L. Jambor (1995b) *In-situ* remediation of chromium contaminated groundwater using zero-valent iron. In *Proceedings of the 209th American Chemical Society National Meeting, Environmental Chemistry Division*, Anaheim, CA, April 2-7, Vol. 35, pp. 780-783.

Blowes, D.W., C.J. Ptacek and J.L. Jambor (1994) Remediation and prevention of low-quality drainage from mine wastes. In *Environmental Geochemistry of Sulphide Mine Wastes*, (Eds. J.L. Jambor and D.W. Blowes), Geological Association of Canada-Mineralogical Association of Canada Short Course, Waterloo, Ontario, May, 1994, Vol. 22, pp. 365-380.

Blowes D.B., C.J. Ptacek and J.L. Jambor (1996) In-situ remediation of chromate contaminated groundwater using permeable reactive walls. Submitted to *Environ. Sci. Technol.*

Gillham, R.W. and O'Hannesin, S.F. (1992) Metal-catalysed abiotic degradation of halogenated organic compounds. In *Modern Trends in Hydrogeology*, IAH, Hamilton, Ontario, May 10-13, pp. 94-103.

Gillham, R.W. and O'Hannesin, S.F. (1994) Enhanced degradation of halogenated aliphatics by zero-valent iron. *Ground Water*, 32:958-967.

Mackay, D.M. and J.A. Cherry (1989) Groundwater contamination: pump-and-treat remediation. *Environ. Sci. Technol.*, 23:630-636.

Powell, R.M., R.W. Puls, S.K. Hightower and D.A. Sabatini (1995) Coupled iron corrosion and chromate reduction: Mechanisms for subsurface remediation. *Environ. Sci. Technol.* 29:1913-1922.

Puls, R.W., R.M. Powell and C.J. Paul (1995) *In situ* remediation of ground water contaminated with chromate and chlorinated solvents using zero-valent iron: A field study. In *Proceedings of the 209th American Chemical Society National Meeting, Environmental Chemistry Division*, Anaheim, CA, April 2-7, Vol. 35, pp. 788-791.

Puls, R.W., D.A. Clark, C.J. Paul and J. Vardy (1994) Transport and transformation of hexavalent chromium through soils and into groundwater. *J. Soil Contam.* 3:203-224.

Robertson, W.D. and J.A. Cherry (1995) In situ denitrification of septic-system nitrate using reactive porous media barriers: Field trials. *Ground Water*, 33:99-111.

Waybrant, K.R., D.W. Blowes and C.J. Ptacek (1995) Selection of reactive materials for the prevention of acid mine drainage using porous reactive walls. In *Proceedings of Sudbury '95 - Mining and the Environment*, (Eds. T.P. Hynes and M.C. Blanchette), May 28 - June 1, Sudbury, Ontario, Vol. 3, pp. 945-953, CANMET.
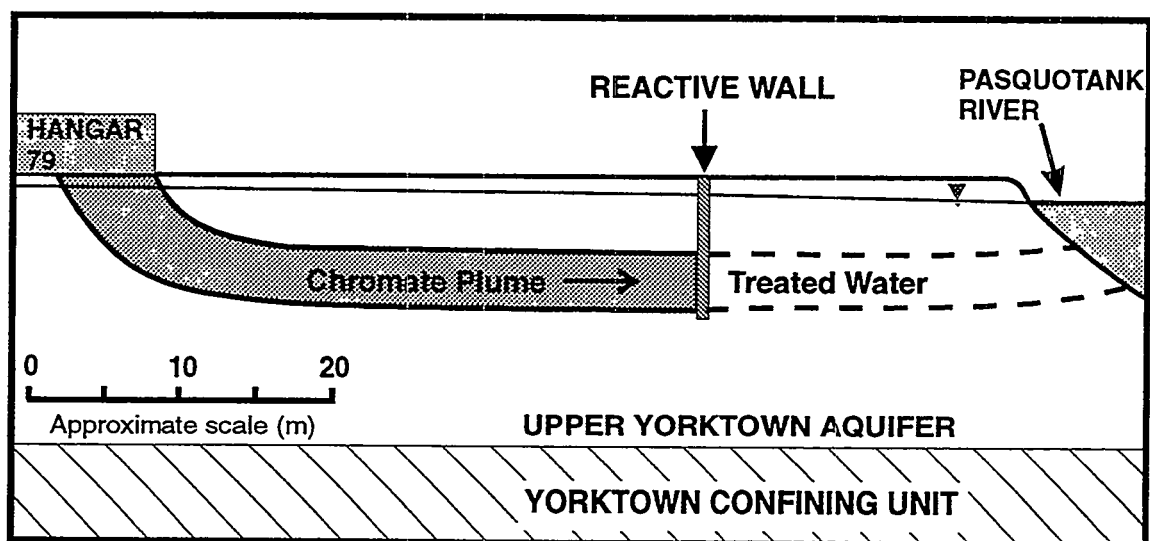
Figure 1. Schematic cross-section of the field site illustrating the extent of Cr(VI) contamination in the aquifer, the position of the reactive barrier and the hydrogeology of the field site.
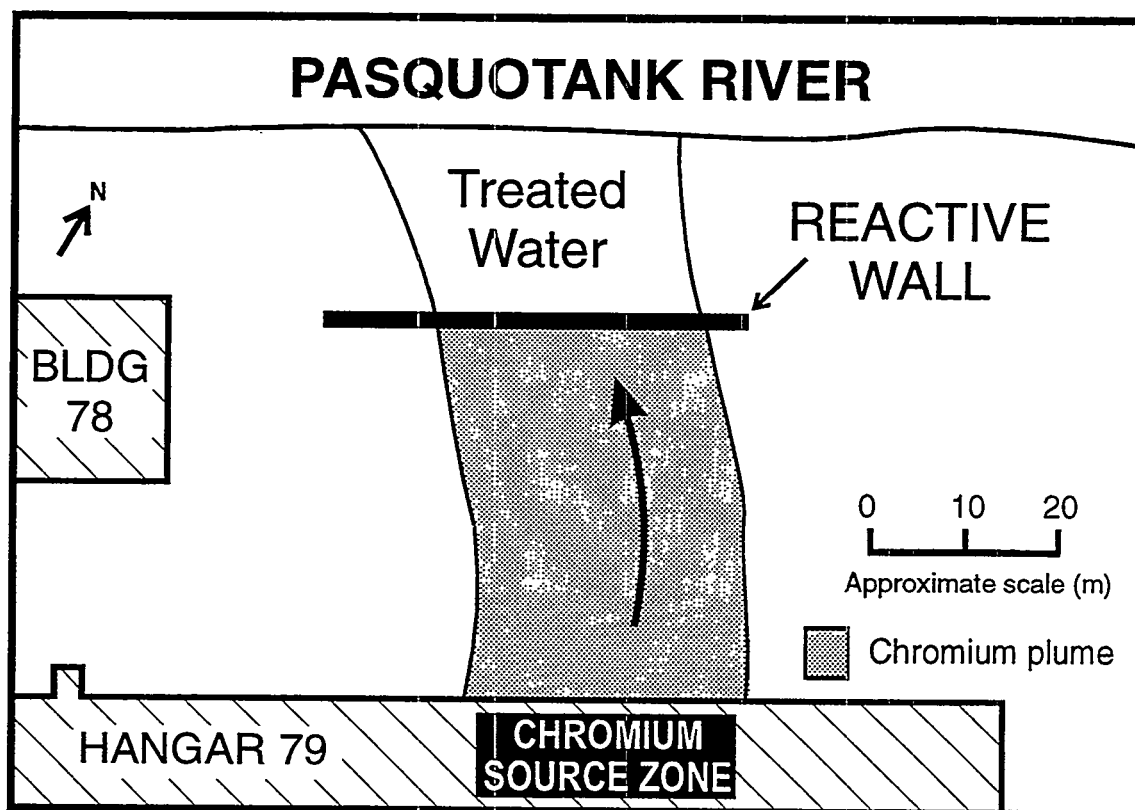
Figure 2. Areal view of the study area showing the extent of Cr(VI) contamination in the aquifer and the position of the reactive barrier.
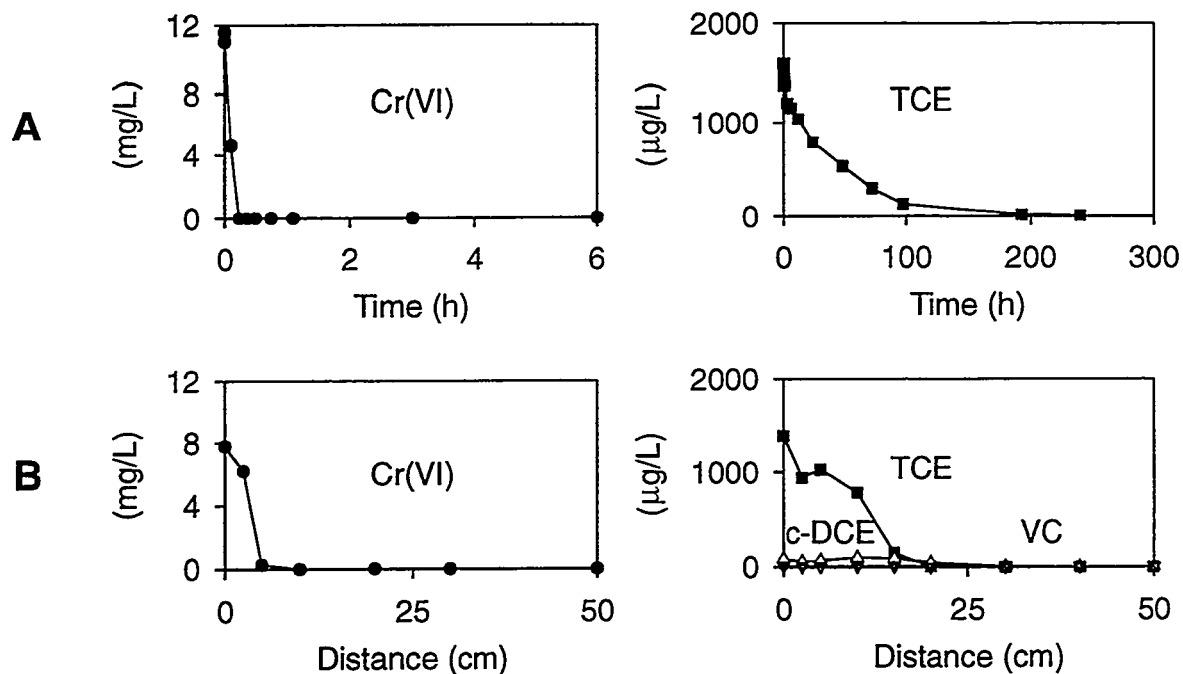
Figure 3. Laboratory results for (A) batch tests and (B) column tests after >100 pore volumes, conducted with the elemental iron used in the full scale reactive barrier.
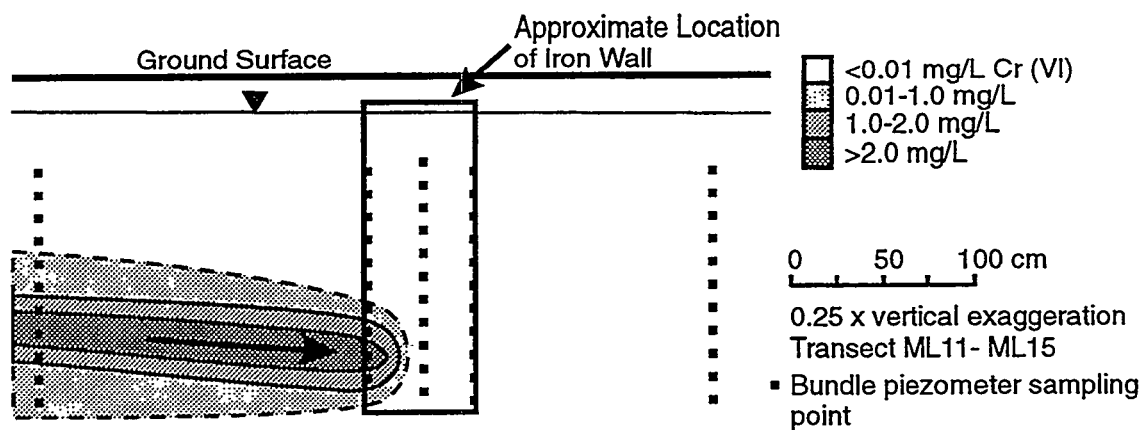

Figure 4. Cross-section of the reactive barrier showing Cr(VI) concentrations entering the wall (November 1996 data).

Enhanced Degradation of VOCs: Laboratory and Pilot-Scale Field Demonstration

R.W. Gillham[1], S.F. O'Hannesin[1], M.S. Odziemkowski[1], R.A. Garcia-Delgado[2], R.M. Focht[3], W.H. Matulewicz[4] and J.E. Rhodes[4]

Abstract

The potential for using zero-valent metals to remediate contaminated groundwater has been recognized since the early 1990s. This paper reports on possible enhancements achieved by plating small amounts of nickel onto the iron surfaces. The half-life for trichloroethene, for example, was shown to decrease from about 30 min in the presence of granular iron to about 3 min with the enhanced iron. Based on the results of the laboratory tests, an above-ground pilot-scale field test using the enhanced iron was initiated in New Jersey in July 1996. Groundwater at the site contains dissolved tetrachloroethene, cis 1,2-dichloroethene and trichloroethene at concentrations of up to 15, 1 and 0.5 mg/L, respectively. A granular iron treatment canister has been in operation at the site since November 1994. Performance of a canister containing the enhanced iron represented a substantial improvement over the canister containing only iron, but the performance was substantially below expectations based on the results of the laboratory tests. Investigations are continuing in an attempt to determine the cause of the difference in laboratory and field performance.

Introduction

The concept of using granular iron for the in situ remediation of groundwater contaminated by chlorinated organic compounds was introduced by Gillham and O'Hannesin (1992). The concept has since stimulated considerable research concerning the degradation process (Gillham and O'Hannesin, 1994; Matheson and Tratnyek, 1994; Sivavec and Horney, 1995; Orth and Gillham, 1995; Roberts et al., 1996 for example), and further studies concerning implementation of the technology (Yamane et al., 1995; Focht et al., 1996). Indeed, the technology currently shows considerable promise as a cost-effective method of groundwater remediation.

Though granular iron appears to be an effective and robust agent in the degradation of chlorinated organic contaminants, there is evidence that plating a small amount of a second metal on the iron surfaces can result in a substantial increase in degradation rates. This was first demonstrated by Sweeny (1973), using copper as the second metal. More recently, various researchers have shown that small amounts of palladium, when plated onto granular iron, could result in degradation rates that are a factor of ten or more greater than iron in the absence of palladium (Muftikian et al., 1995; Grittini et al., 1995). The apparent increase in activity could have important benefits in reducing the amount of material required for in situ applications and could also broaden the scope of application to include above-ground treatment.

Tests conducted at the University of Waterloo have focused on nickel as the second metal. In these tests, various amounts of nickel, ranging from about 0.08 to 0.5% by weight have been plated onto granular iron by electroless methods using nickel chloride as the source of nickel and sodium hypophosphite as the reductant. Using column procedures, the nickel-iron (Ni-Fe) material gave half lives of about 3 min for trichloroethene (TCE), compared to about 30 min using iron alone. Furthermore, the production of dichloroethene (DCE) isomers and vinyl chloride (VC) was

---

[1] Dept. of Earth Sciences, University of Waterloo, Waterloo, Ontario N2L 3G1
[2] University of Malaga, Malaga, Spain
[3] EnviroMetal Technologies Inc., 42 Arrow Road, Guelph, Ontario N1K 1S6
[4] Rodes Engineering, P.C., P.O. Box 258, Haddonfield, N.J. 08033-0403

much less using the Ni-Fe material than iron alone. Tests using simulated groundwater (40 mg/L calcium carbonate) ran for over 2400 pore volumes, with no apparent loss in reactivity.

Encouraged by the results of the early laboratory tests, an above-ground field trial was initiated to evaluate performance at an industrial site. This paper presents the results of laboratory tests conducted to evaluate the potential for application at the site and to develop parameters for design of the field installation. Results of the initial field test are also presented.

Laboratory

The site selected for the test was in Wayne, New Jersey, where an above-ground reactor using granular iron had been in operation since October 1994 (Vogan et al., 1995). Water used in the column tests was shipped from the site to the University of Waterloo.

The column procedures were similar to those described in Gillham and O'Hannesin (1994). A 20 cm long acrylic column with an internal diameter of 3.81 cm was packed with laboratory-prepared nickel plated iron. The iron used in the test was obtained from MasterBuilders Inc. of Cleveland, Ohio. Seven sampling ports were located along the column at distances of 2.5, 5, 7.5, 10, 12.5 and 17.5 cm from the influent end, and samples could also be collected from the influent and effluent solutions. Each port was constructed using a nylon fitting which held in place a syringe needle 3.8 cm long. The needle tips were located along the central axis of the column. The pore volume was determined by weight, giving a value of 116 mL with a porosity of 0.51. The column was initially flushed with carbon dioxide to avoid air entrapment during wetting and the test was conducted at room temperature $\approx 23°C$. A peristaltic pump was used to feed the site water to the bottom of the column. The ports along the column were sampled periodically until steady state concentration profiles were achieved. Samples were analysed using pentane extraction and a gas chromatograph equipped with an ECD detector, and also by headspace analysis using a PID detector.

The column test was conducted with a flow velocity of 1133 cm/day (37.2 ft/day), giving a residence time of 0.42 hr. The main organic compounds detected in the water obtained from the site were tetrachloroethene (PCE, 10,000 µg/L) and cis 1,2-dichloroethene (cDCE, 1,000 µg/L). Lower levels of trichloroethene (TCE, 400 µgL) and vinyl chloride (VC, 120 µg/L) were also detected. A total of 152 pore volumes of water was passed through the column. Figure 1 shows the steady state concentration profiles. The PCE concentration declined rapidly along the column, reaching a value of 350 µg/L in the effluent. Fitting the first-order decay model to the data gave a half life of 5.6 min with an r^2 value of >0.9. The cDCE concentration declined rapidly with non-detectable values after a travel distance of 7.5 cm, while the TCE was non-detectable after a travel distance of 20 cm. Half lives of 0.84 and 3.8 min were obtained for cDCE and TCE, respectively. No VC was detected in the column over all sampling times. Assuming the VC had just disappeared by the first sampling point gave a half life of <0.53 min. The column showed reducing conditions throughout with redox potentials (Eh) of -350 mV, and relatively constant pH values ranging from 6.8 to 7.0. Nickel concentrations of 0.07 mg/L were measured in the column effluent.

In order to degrade all the contaminants at the field site to the Federal MCLs (PCE, 5 µg/L; cDCE, 70 µg/L; TCE, 5 µg/L; VC, 2 µg/L), the residence time within the enhanced iron required for PCE, cDCE, TCE and VC would be 1.0, 0.05, 0.40, 0.05 hrs, respectively. Because the compounds degrade simultaneously, and because there was no evidence of the formation of chlorinated degradation products, the laboratory data suggested that a residence time of 1.0 hr would be adequate. Allowing for a degree of uncertainty and possible variations in the influent concentration, the reactor was designed to give a residence time of 1.5 hr.

Results of previous laboratory tests using groundwater from the site and the same iron material but without the nickel plating gave a required residence time of about 24 hr. Clearly the sixteen-

fold improvement obtained with the Ni-Fe material could have major implications with respect to the design and economics of treatment systems.

Field Application

In July of 1996, a reactor containing the enhanced iron was installed at the facility in Wayne, New Jersey. Printed circuit boards had been manufactured at the facility until 1984 and the site is currently involved in remedial investigation activities and cleanup. The remedial action to date involves the use of an above-ground reactor containing granular iron. The reactor was installed, and has been operating successfully, since November 1994. The volume of iron in the reactor is 7.8 m^3, the flow rate is about 2.0 L/min (0.5 gpm) and the residence time is about 24 hr (Vogan et al., 1995; US EPA, 1997).

Groundwater is extracted from the overburden and shallow bedrock at the site by passive recovery techniques, using stone-filled collection trenches. Water from two deep wells and two artesian wells also discharges to the collection trench. The groundwater then flows to a sump, where it is pumped to the top of the treatment reactor. The water flows downward through the reactive material and exits the bottom of the reactor through a collection pipe submerged in coarse sand. In this test, the enhanced iron and the iron reactor were operated in series, with the effluent from the enhanced iron passing to the top of the existing iron reactor. Should the enhanced iron not perform to expectations, the iron reactor would act as a contingency. Effluent from the iron reactor is returned to the aquifer through six injection wells.

The enhanced-iron reactor was 0.9 m in diameter and 1.8 m in height (Figure 2), and was fitted with seven sampling ports along its length, located at distances of 7.5, 15, 23, 38, 53, 69 and 84 cm, from the influent surface of the reactive material. Ports were also installed such that samples of influent and effluent water could be collected. The granular iron used in the test was obtained from MasterBuilders Inc. of Cleveland, Ohio, and was plated with nickel at a commercial facility in Ontario. A total weight of 1633 kg of the enhanced iron was placed in the reactor to a depth of 1.0 m (0.65 m^3). The grain size of the enhanced iron was 0.25 to 2.0 mm and the specific surface area was 3.1 m^2/g. The specific surface area of the iron before plating was considerably lower at 1.1 m^2/g. A pore volume of 260 L was calculated using an estimated porosity of 0.4.

At an average flow velocity of 1674 cm/day (pumping rate of 3.0 L/min and residence time of 1.4 hr), 1200 pore volumes of water passed through the reactor over the three month test period. The influent water had concentrations similar to those measured in the site water used in the bench scale tests, with concentrations of 10000, 1200, 500 and 260 µg/L for PCE, cDCE, TCE and VC, respectively. Figure 3, obtained at 1171 pore volumes, is an example of the results showing the concentration for each compound versus distance along the reactor (cm). A steady decline in PCE concentration was observed with an effluent concentration of 500 µg/L. In this case the half life was calculated to be 19 min ($r^2 = 0.84$); however, over the seven sampling events, the half life for PCE varied from 13 to 67 min with an average value of 31 min. With an initial TCE value of 500 µg/L, an increase in concentration was observed at the first sampling port (7.5 cm) to a maximum of 3870 µg/L, followed by a steady decline with an effluent value of 477 µg/L. The substantial increase in TCE was attributed to the dechlorination of PCE. A half life of 20 min ($r^2 = 0.89$) was calculated from the peak concentration, while over the entire test period, values ranged from 11 to 59 min with an average value of 33 min. Only a slight decline in cDCE concentration was observed along the length of the canister from an influent value of 1286 µg/L to an effluent value of 1100 µg/L. The VC concentration showed considerable variation, with no consistent evidence of degradation. The slow decline of cDCE and variable VC concentrations were attributed to the production of these compounds due to the dechlorination of PCE and TCE. Half lives could not be calculated for these compounds. Low concentrations, <0.01 mg/L of dissolved nickel were found in effluent samples from the enhanced iron reactor.

The variations in the half lives of PCE and TCE were not consistent with time and therefore do not appear to reflect a loss of reactivity over time. Rather the variation is believed to be the result of considerable variation in flow rate. Because flow rate was not recorded continuously, the average was used in all half life calculations. In spite of the high degree of variability, it is evident that the behaviour of the Ni-Fe material in the field reactor differs significantly from the results of the laboratory tests. In an attempt to identify the cause of the difference in behaviour, a second laboratory column test was conducted using a sample of the commercially plated iron installed at the site. Table 1 compares the half lives obtained in the laboratory and field using enhanced iron, and those typical of the iron reactor installed in 1994.

Table 1: Laboratory and field half lives (minutes) generated from both enhanced iron (NiFe) and iron (Fe) systems.

	Laboratory			Field	
	Fe Only	Lab NiFe	Comm NiFe	Comm NiFe	Fe Only
	Half Lives (minutes)				
PCE	36	5.6	40	31	120
TCE	42	3.8	10	33*	120
cDCE	222	0.84	5.0	NA	342
VC	54	<0.53	9.0	NA	NA

* Half life calculated from the peak concentration.
NA = not applicable

The field average half lives of 31 and 33 min obtained for PCE and TCE, respectively, in the enhanced iron reactor were about four times greater than values obtained in the initial column test using laboratory-plated iron. However, the values are about four times lower than those obtained from the iron reactor. The substantial increase in TCE concentration observed in the field, is not consistent with the laboratory tests, nor with the results obtained from the iron reactor. Typical increases observed for TCE from PCE are usually about 5% in some iron systems. The short half lives observed in the laboratory for cDCE and VC were not observed in the field.

Half lives of 40 and 10 min were calculated for PCE and TCE, respectively, in the laboratory test using the commercially-plated iron. Though these values are reasonably consistent with the field values, particularly for PCE, the increase in TCE concentration observed in the field was not observed in the laboratory test, and the reasonably low half lives for cDCE and VC obtained in the laboratory test were also not observed in the field.

It is clear that the commercially plated iron was significantly different from the material plated in the laboratory and this, at least in part, could explain the underperformance of the field installation. Scaling up of the laboratory method of preparation to a commercial process is presently under investigation. Insufficient mixing to provide uniform plating and drying in an oxygen-rich environment are particular factors that may have adversely affected the performance of the commercial material.

Conclusions

The results obtained in the initial column test using water from the industrial site and laboratory-prepared nickel-iron were highly encouraging. Half lives were about a factor of ten lower than normally obtained using iron alone and were comparable to values obtained using the nickel-iron material and laboratory-prepared water. The ten-fold enhancement could substantially reduce the amount of reactive material required and could therefore broaden the scope of problems for which the technology is applicable.

The field demonstration reactor performed substantially better (by a factor of about 4) than the reactor that contained only iron. Though providing further reason for encouragement, the performance did not meet expectations based on the results of the initial laboratory tests. The supplemental laboratory tests suggested the underperformance of the commercially produced nickel-iron material to be a result of inadequacies in the commercial plating process.

A further issue that was not explored in detail in this study concerns catalyst poisoning. In previous tests using laboratory-prepared water, there was no apparent loss of reactivity with the passage of several hundred pore volumes of solution through the columns. In the present tests using groundwater from the industrial site, there was no clear evidence of loss of reactivity over time; however, because of the variability in the flow rate in the field test and the relatively short duration of the tests, it can not be concluded that catalyst poisoning would not be an issue. Further, it would not be reasonable to generalize from the results obtained for this particular site to other sites having different groundwater chemical characteristics.

Results of both the laboratory tests and field trial support the ultimate utility of the nickel-iron reactant in the degradation of chlorinated organic compounds. However, further development of commercial plating methods and further evaluation of the potential for catalyst poisoning are required in order to advance the technology to the stage of commercial implementation.

References

Focht, R.M., J.L. Vogan and S.F. O'Hannesin. (1996) Field Application of reactive iron walls for in-situ degradation of volatile organic compounds in groundwater. Remediation, 6(3), 81-94.

Gillham, R.W. and S.F. O'Hannesin. (1994) Enhanced degradation of halogenated aliphatics by zero-valent iron. Groundwater, 32(6), 958-967.

Gillham, R.W. and S.F. O'Hannesin. (1992) Metal-catalysed abiotic degradation of halogenated organic compounds. IAH Conference "Modern Trends in Hydrogeology". Hamilton, Ontario, Canada, 94-103.

Grittini, C., M. Malcomson, Q. Fernando and N. Korte. (1995) Rapid dechlorination of polychlorinated biphenyls on the surface of a Pd/Fe bimetallic system. Environ. Sci. Technol., 29(11) 2898-2900.

Matheson, L.J. and P.G. Tratnyek. (1994) Reductive dehalogenation of chlorinated methanes by iron metal. Environ. Sci. Technol., 28(12), 2045-2053.

Muftikian, R., Q. Frenando, N. Korte. (1995) A method for the rapid dechlorination of low molecular weight chlorinated hydrocarbons in water. Water Res., 29(10), 2434-2439.

Orth, W.S. and R.W. Gillham. (1996) Dechlorination of trichloroethene in aqueous solution using Fe^0. Environ. Sci. Technol., 30(1), 66-71.

Roberts, A.L., L.A. Totten, W.A. Arnold, D.R. Burris and T.J. Campbell. (1996) Reductive elimination of chlorinated ethylenes by zero-valent metals. Environ. Sci. Technol., 30(8), 2654-2659.

Sivavec, T.M. and D.P. Horney. (1995) Reductive dechlorination of chlorinated ethenes by iron metal. Presented at the 209th ACS National Meeting, Anaheim, California, 35(1), 695-698.

Sweeny, K.H. and J.R. Fischer. (1973) Decomposition of halogenated organic compounds using metallic couples. U.S. Patent # 3,737,384.

Vogan, J.L., R.W. Gillham, S.F. O'Hannesin, W.H. Matulewicz. (1995) Site specific degradation of VOCs in groundwater using zero-valent iron. Presented at the 209th ACS National Meeting, Anaheim, California, 35(1), 800-804.

United States Environmental Protection Agency. (1997) EnviroMetal Technologies Inc., Metal-enhanced dechlorination of volatile organic compounds using an above-ground reactor: Innovative technology evaluation report, Cincinnati, Ohio.

Yamane, C.L., S.D. Warner, J.D. Gallinatti, F.S. Szerdy, T.A. Delfino, D.A. Hankins, J.L. Vogan. (1995) Installation of a subsurface groundwater treatment wall composed of granular zero-valent iron. Presented at the 209th ACS National Meeting, Anaheim, California, 35(1), 792-795.

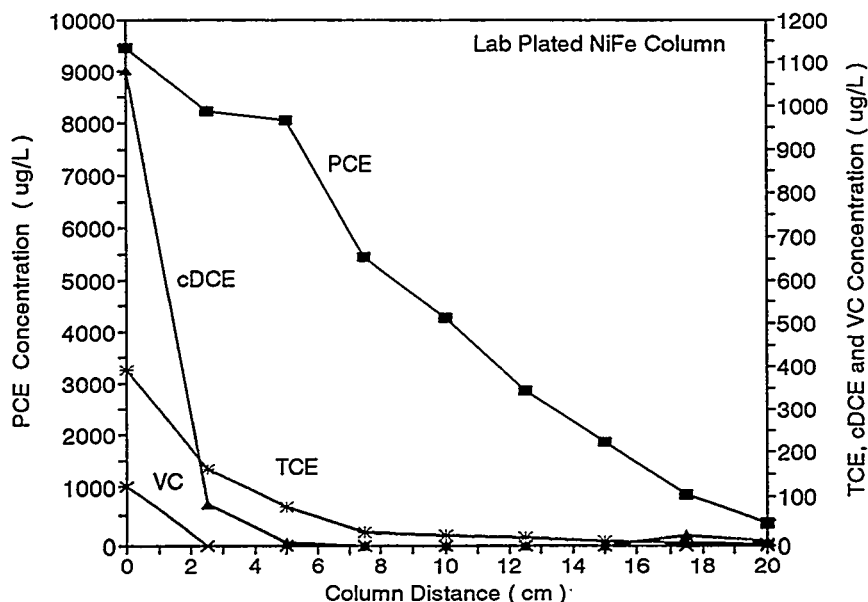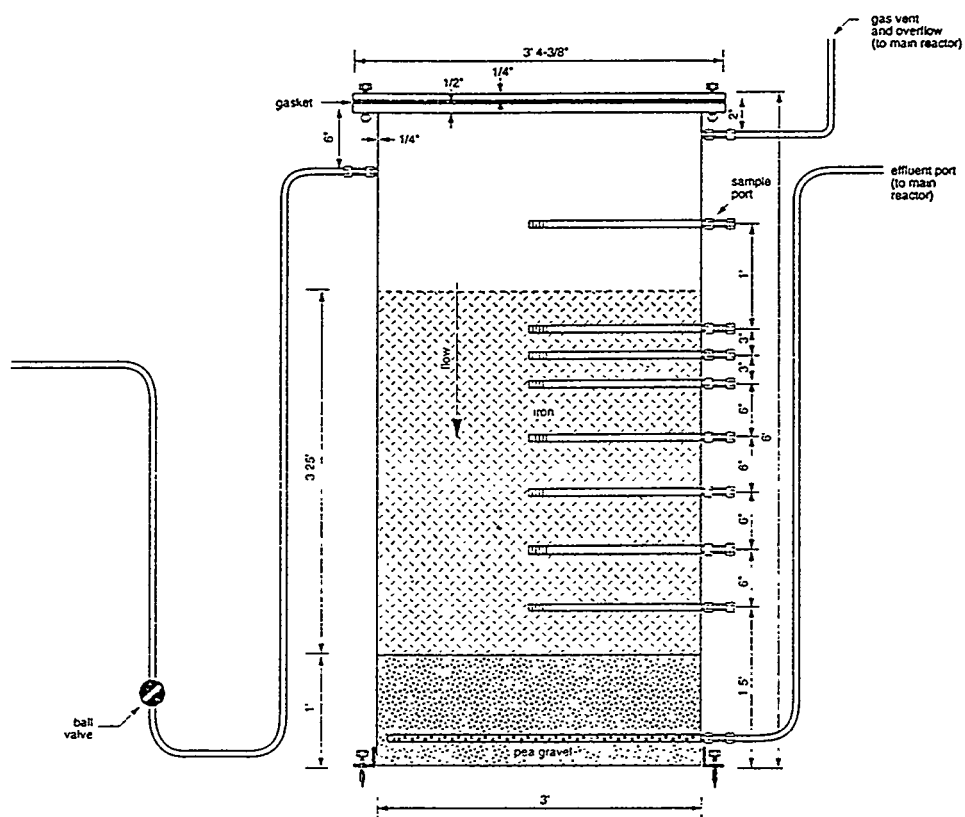**Figure 1:** PCE concentration and other organic concentrations (µg/L) versus column distance (cm).

Figure 2: Schematic of Ni-Fe reactor.

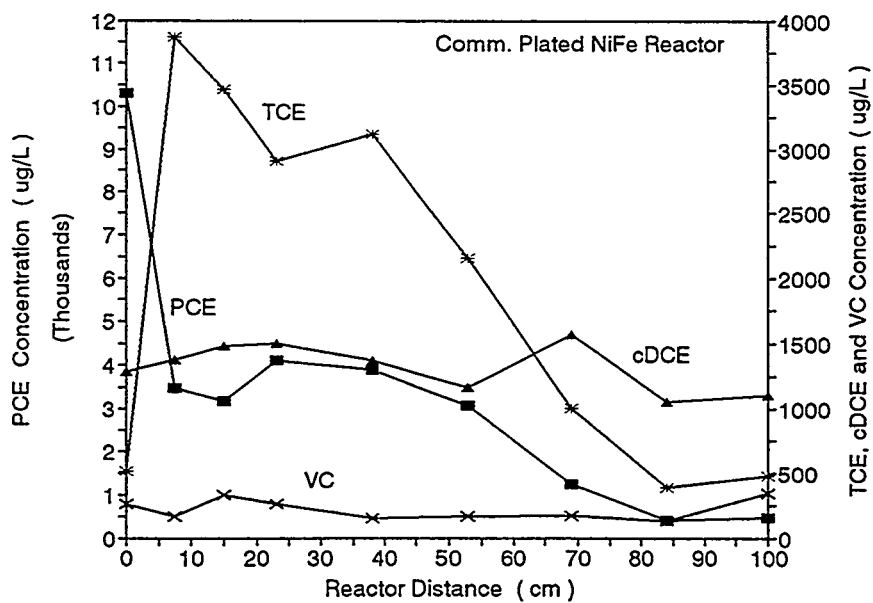**Figure 3:** PCE concentration and other organic concentrations (μg/L) versus reactor distance (cm).

INTEGRATED FUNNEL-AND-GATE/GZB PRODUCT RECOVERY TECHNOLOGIES FOR IN *SITU* MANAGEMENT OF CREOSOTE NAPL-IMPACTED AQUIFERS

J.G. Mueller[1], S.M. Borchert[1], E.J. Klingel[2], D.J.A. Smyth[3], S.G. Shikaze[3],
M. Tischuk[4], and M.D. Brourman[4].

Introduction

An *in situ* source management system was modeled and designed for the containment and recovery of creosote non-aqueous phase liquid (NAPL) at a former wood treating facility in Nashua, New Hampshire. The conceptual system was based on the integration of patented technologies for physical source containment and management (*i.e.,* funnel-and-gate technology) with patented *in situ* product recovery (*i.e.,* GZB technology - described below). A funnel-and-gate physical barrier was proposed to mitigate the continued flow of NAPL into the Merrimack River. The purpose of the funnel was to divert groundwater (and potential NAPL) flow through two gate areas. Where required, an *in situ* system for product recovery was integrated. Mathematical modeling of the combined technologies led to the selection of a metal sheet pile barrier wall along 650 feet of the river's shoreline with the wall anchored into an underlying zone of lesser permeability. Multiple GZB wells were placed strategically within the system. This combination of technologies promised to offer a more effective, cost-efficient approach for long-term management of environmental concerns at Nashua, and related sites.

Objectives

The relative inefficiency and high operating expense of an existing pump-and-treat approach to contain NAPL at the Nashua site highlighted the need for more cost efficient approaches for *in situ* source management. Considering challenges by similar problems at other sites, the objective of these efforts was to define an *in situ* system to prevent the continued seepage of NAPL to the Merrimack River in a scientifically valid, more cost-effective manner thereby reducing the life-cycle cost of managing the site remediation.

Site Description

• Wood treating operations at the Nashua, NH site were conducted between the years of 1923 until 1983. The site is approximately 97 acres, and is bounded by Greeley Park on the southern side, the Merrimack River on the eastern and northern sides, and the Boston & Maine Railroad to the west.
• In 1981, NAPL seepage into the Merrimack River was reported. A series of site investigations concluded that the former Lagoon Area (where two creosote wastewater impoundments were formerly located) was a source of these materials.
• NAPL is more viscous than water (33 centistokes at 15°C), and has a density of 1.05 g/cc at 25°C.

---

[1]SBP Technologies, Inc., 105 Gregory Square, Pensacola, FL 32501, (904)470-0055, 75357.1357@compuserve.com.

[2]IEG Technologies Corporation, 5015-D West W.T. Harris Blvd, Charlotte, NC 28269, (704)599-4818, 102022.2042@compuserve.com

[3]University of Waterloo Centre for Groundwater Research, Waterloo, Ontario, CANADA N2L 3G1, (519)888-4567 ext. 2899, dsmyth@sciborg.uwaterloo.ca

[4]Hanson Environmental & Legal Group, 436 Seventh Ave, Pittsburgh, PA 15219, (412)227-2177 brourman@fyi.com

• NAPL is present as thin layers within a layer of fine-grained sand and silt overlying a discontinuous till layer, or directly over bedrock.

• two main zones of high product saturation were delineated at depths of 9.3 to 10.7 m below land surface (bls) and 12.3 to 13.3 m bls, dependent upon topography.

• NAPL is migrating from west to east (into the Merrimack River) preferentially through these higher-permeable sand and silt lenses (ca. $K_h = 1 \times 10^{-3}$ cm/sec).

• depth to groundwater	=	7.3 m bls
• Darcian velocity	=	2.68×10^{-7} m/sec
• K_h (horizontal hydraulic conductivity)	=	ca. 1.0×10^{-3} cm/sec
• K_v (vertical hydraulic conductivity) estimated	=	ca. 1.0×10^{-4} cm/sec
• Horizontal hydraulic gradient (i) toward river	=	0.029
• Thickness of treatment zone (H)	=	5.5 to 7.6 m

Technical Approach

The technical design consisted of a funnel-and-gate system to manage and contain NAPL in conjunction with vertical groundwater circulation wells (German: Grundwasser Zurkulations Brunnen = GZB) to enhance product recovery. The funnel-and-gate system consisted of low conductivity cutoff walls (funnels) with one or more openings (gates). The system was designed such that the cutoff wall barriers physically impede the transport of NAPL and diverts the flow of groundwater to the gate areas. A series of GZB recovery wells are installed at strategic locations on the upgradient side of the barrier to enhance NAPL recovery.

Funnel-and-Gate Barrier Wall

The funnel-and-gate system (3,5) is an *in situ*, passive technology that can be used to manage and physically contain myriad constituents of interest in ground water, including free phase product. The system consists of low conductivity cutoff walls (funnels) with one or more openings (gates). Hence, the purpose of the funnel is to divert groundwater and, potentially, free-phase product (NAPL) flow through the gate area which contains a system for recovery and/or treatment.

GZB Groundwater Circulation Technology

The basic principle of GZB operation (Figure 1) focuses on the creation of vertical ground water circulation cells in the aquifer (1,4). This is accomplished by moving water from the lower portion of the aquifer into the GZB well through a lower screen section of the well. The water is then pumped vertically upward through the GZB well casing, allowing it to exit through an upper screen section of the same well. Exiting water mounds in the area surrounding the upper screen section of the GZB well thus producing a positive hydraulic head. Natural equilibration of hydraulic potential (negative at the GZB well bottom, positive at the well top) results in circular ground water flow through the aquifer, with both a horizontal and vertical component. As such, the GZB well facilitates *in situ* soil flushing using circulating ground water as a carrier and encourages NAPL movement in the direction of the GZB well wherein it is collected and recovered for reuse.

System Design and Modeling

During the initial design and modeling phase, various configurations of the barrier installation were examined. The purposes of these examinations were to: 1) establish a mathematical modeling system to predict efficacy of various system configurations; 2) utilize site-specific data to calculate hydraulic and NAPL flow regimes as they are influenced by barrier installation and ground water circulation cells; and 3) identify the most efficacious funnel-and-gate/GZB configuration for the Nashua site.

Funnel-and-Gate Modeling

The effective application of a funnel-and-gate system at the Nashua site required an accurate understanding of the aquifer hydraulics. Accordingly, 3-dimensional numerical modeling of ground water

866

flow analysis was performed. The model used was Frac3DVS (6), an efficient simulator of saturated-unsaturated groundwater flow and solute transport in porous and fractured porous media (2). A 3-dimensional, rectangular computational domain of 383.3 m in the x-direction (approximately parallel to the Merrimack River), 133.3 m in the y-direction (approximately parallel to the direction of ground water flow), and 30 m in the vertical z-direction was established. Site specific factors pertaining to hydraulic control, NAPL distribution, and geology were integrated into the modeling initiatives.

GZB System Modeling

Site specific modeling was conducted to define the effective radius of influence for GZB systems either in the gate areas or those positioned behind the barrier wall. The model assumed both natural ground water flow, and accelerated ground water flow through the gate areas (as induced by the barrier wall). The resulting flow fields of single or multiple GZB installations differs from natural groundwater flow field (0.10 m/d using i=0.029, Kh=1.0x10^{-3} cm/sec and 25% porosity) or accelerated ground water flow (0.13 m/d due to the barrier wall) only in a limited area around the GZB. The 3-dimensional flow field in a defined, limited aquifer region was obtained by superposition of a horizontal uniform flow field, computed in a vertical cross section and representing either the natural ground water flow or accelerated flow, and of radially symmetric, vertical flow fields for each GZB. Superposition of the different flow fields with their own discretization was achieved by interpolating and adding the different flow vectors at the various nodes of a simple rectangular grid with variable grid distances independently chosen for each Cartesian coordinate. The rectangular grid allowed for some refinements near the wells and their screen sections. More details of the numerical computations are given in Herrling et al. (1).

NAPL Modeling

In an effort to define the radius of influence that the GZB well will have on NAPL recovery, the vertical and horizontal pressure gradients needed to enhance NAPL flow were modeled by KEY Environmental, Carnegie, PA. For vertical movement of NAPL through the groundwater saturated zone, the entrance pressures were calculated using eight different hydraulic conductivities (determined from 8 grain size distributions on soil cores at 2-foot intervals), a wetting angle of 35 degrees, and an interfacial tension of 16.1 dynes/cm. NAPL saturation curves were established in the lab and capillary pressure was also taken into account. Horizontal migration was calculated using the concept of natural ground water flow slowly displacing the NAPL due to the "water-flooding" occurring, or pressure build-up behind each NAPL droplet as induced by circular ground water flow.

Integrated System Modeling

To ensure capture of ground water and NAPL, the physical location of the funnel walls considered alignment of the barrier system relative to the principal direction of ground water flow, accounting for seasonal/tidal variations. To ensure NAPL containment and recovery, multiple construction scenarios were considered which included simulations of various gate locations, gate widths, sheet pile lengths (e.g. depth of penetration).

RESULTS AND DISCUSSION

Funnel-and-Gate Modeling

A total of 11 application options were modeled. The initial models considered various combinations of total wall length (160, 210, or 283 m), number of wall segments (1, 3 or 4 wall segments), number of gate areas (2 or 3 gates), and depth of wall penetration into the formation (15 or 16.7 m). The width of the gate areas was modeled at 10 m. Rationale for considering these various barrier configurations focused on the analysis of performance and economics of the installation. For example, in the domain used, wall penetration to a depth of 16.7 m simulated complete connection with lower permeability bedrock which, in theory, would minimize underflow. Conversely, barrier penetration to a depth of 15 m simulated a potential underflow component which is perhaps more representative of actual field conditions since complete connection to bedrock in situ is unlikely. Moreover, permeability differences between the aquifer and the bedrock confining layer appears to be of gradual transition occurring over a distance of 1.7

to 3.3 m. Thus, in the event that complete connection into bedrock was determined to be unlikely, or unnecessary, to reduce underflow, then the installation of the barrier to a depth of 15 m would represent a more cost efficient design.

In the final analysis, the most effective means of physical containment was a steel sheet pile wall approximately 216.7 m in length installed along the river's edge to a depth of 16.7 m (no gates). This wall length was determined efficient to contain completely all areas of potential NAPL migration. At the north and south ends of the wall "wing walls" were placed each 43.3 m total length (Figure 2). Each wing wall was designed with a 10 m gate area in the middle of the wing section. In this configuration, the majority of the modeled streamlines approaching the barrier wall were diverted towards either the north or south gate areas. Complete anchoring of the sheet pile barrier into a lower permeability material helped prevent modeled underflow.

GZB Modeling

The GZB was modeled with an internal flow of 4 m^3/h and a saturated thickness of 7.6 m (flow rates of 1 and 2 m^3/h were also modeled). To ensure sufficient ground water flow and NAPL capture, with particular attention given to units positioned in the gate areas, the calculated practical radius of influence was based on 30% of the stagnation point (see Stamm [4] and Herrling et al [1]). This yielded a radius of 8.3 m. Based on these calculations, one pore volume sweep of the aquifer circulation cell areas occurs once every 8 days. This flow was determined sufficient to capture NAPL directed toward the areas via the barrier wall.

NAPL Modeling

Results showed entrance pressures from 0.18 to greater than 0.34 m of water column. Horizontal pressures were lower, confirming field observations, that NAPL seemed to be migrating more readily horizontally in relatively more permeable zones. Thus, to induce vertical migration of NAPL flow, the greatest hydraulic head that the GZB would need to be overcome is 0.34 m.

Integrated Systems Modeling

Integrated modeling solved issues associated with the number, dimensions, and placement of gates, location and number of GZB wells, and diversion of flow either around or beneath the system. For example, the residence time of impacted ground water and NAPL within the gate areas must be sufficient for the necessary capture of the diverted NAPL (i.e., GZB well recovery).

Figure 2 presents the preferred system design which integrates 5 GZB wells into the funnel-and-gate barrier. Multiple (four) GZB enhanced product recovery systems were placed strategically upgradient of the barrier wall to manage and remove contained product. These four GZB systems were placed in areas of known or suspected NAPL accumulation (e.g., natural bedrock depressions), and considered transitional flow regimes affected by the installation of the funnel-and-gate system. Additional GZB product recovery systems may be integrated at a later date to further enhance NAPL recovery.

Effective management of the flow in the gate areas was critical to control any diverted NAPL. Accordingly, in addition to the 4 source management GZB wells, a single GZB unit was placed at the southern gate to recover migrating NAPL. Modeling considering hydraulics and NAPL movement demonstrated no need for a similar unit in the northern gate area. Induced hydraulics through the gates (as a function of funnel construction) was considered in the integrated design. Given the GZB practical radius of 8.3 m (30% of the stagnation point) and a gate width of 10 m, the positioning of a single GZB system would be sufficient to recover any diverted NAPL.

Technical Limitations/Uncertainties

In the Spring of 1997, field testing of two initial GZB systems will address several uncertainties that were identified during the modeling efforts described above. These include:
- Further assessing the need for anchoring of the barrier wall into a layer of lower permeability.

- Evaluating alternatives means of reducing the potential for NAPL underflow beneath the barrier wall (*e.g.*, grouting, placement of additional GZB NAPL recovery wells).
- Validating the estimated rate of NAPL recovery from the GZB wells to ensure efficiency of operations.
- Validating mathematical calculations that modeled the affect of the GZB wells to overcome the density flow of the NAPL to an acceptable degree, yielding a practical zone of influence.

Potential Advantages

Despite the uncertainties mentioned above, the integrated technologies hold promise for several advantages:

- Use of Waterloo Barrier™ technology for the integrated system allows for barrier installation immediately along the river's edge thus providing complete and immediate *in situ* containment of NAPL entering the Merrimack River.
- GZB systems will collect NAPL from the entire saturated zone, thus avoiding problems with fluctuation in groundwater levels.
- GZB/funnel-and-gate design requires no groundwater removal which:
  i) greatly reduces long-term economic liability associated with the operation and maintenance of groundwater pre-treatment systems,
  ii) negates the need for groundwater discharge permits, and
  iii) is not influenced by water infiltration and groundwater or river flow that will impede the performance of simple upgradient hydraulic barriers.
- GZB/funnel-and-gate systems represent an innovative *in situ* source management and containment technologies with potential applicability to other sites (especially those without existing groundwater treatment plants).

References

1. Herrling, B., Buermann, W. and Stamm, J. 1991. Hydraulic circulation systems for *in situ* bioremediation and/or *in situ* remediation of strippable contamination. *In*. R.E. Hinchee (ed), *In Situ* Bioreclamation, Applications and Investigations for Hydrocarbon and Contaminated Site Remediation. Butterworth-Heinemann, Boston, MA. Pages 173-195.

2. Shikaze, S.G., C.D. Austrins, D.J.A. Smyth, J.A. Cherry, J.F. Barker and E.A. Sudicky. 1995. The Hydraulics of a Funnel-and-Gate System: A Three-Dimensional Numerical Analysis. IAH Congress XXVI: Solutions '95, Edmonton, Alberta, Canada.

3. Smyth, D., J. Cherry and R. Jowett. 1995. Treat Groundwater in Place: *In situ* funnel- and-gate system corrals water for treatment. Soil & Groundwater Cleanup. December Issue:36-43.

4. Stamm, J. 1995. Vertical circulation flows for vadose and groundwater zone *in situ* (bio)-remediation. *In*. R.E. Hinchee (ed), *In Situ* Aeration: Air Sparging, Bioventing, and Related Remediation Processes. Bioremediation 3(2): 483-492

5. Starr, R.C. and J.A. Cherry. 1994. *In situ* remediation of contaminated groundwater: the funnel-and-gate system. Groundwater 32:465-476.

6. Therrien, R. and E.A. Sudicky. 1993. User's Guide for FRAC3DVS - an efficient simulator for 3-dimensional, saturated-unsaturated groundwater flow and chain-decay transport in porous or discretely-fractured porous formations. Waterloo Centre for Groundwater Research, University of Waterloo, Canada.

GZB *IN SITU* Technology for Removal of Creosote - Nashua, NH

SBP Technologies, Inc.
Environmental Engineers and Bioremediation Specialists

Site Lithology
Fine Sand
F-C Sand & Gravel
Fine Sand
Fine Sand Some Silt
Till
BEDROCK

Feet Below Grade
0 ft
10 ft
20 ft
30 ft
40 ft
50 ft
55 ft

GW Table

Groundwater Circulation

NAPL LAYER

Bentonite
Sandpack
Bentonite
Sandpack
Bentonite

NAPL Collection Unit

24" Borehole dia.
16" O.D. Irrigator Screen
Standard Pump
Variable Speed Pump
Packer
17.9" O.D. Double Cased IEG Screen (oleophilic)
2.8" O.D. Double Cased IEG Screen (oleophilic)

SBP Technologies, Inc.
Environmental Engineers and Bioremediation Specialists

NAPL Thickness and Remediated Areas
Nashua, NH

Merrimac River

SBP 102
SBP 101
SBP 104
SBP 106

1.0
5.0
10.0

LEGEND
— Property Line
— Sheet Pile Wall
Proposed GZB Location
Extent of NAPL Remediation
NAPL Thickness Isopleth
5.0

GRAPHIC SCALE
APPROXIMATE SCALE IN FEET
0   30   60   90   120

Emplacement of Zero-valent Metal for Remediation of Deep Contaminant Plumes

David W. Hubble, Robert W. Gillham and John A. Cherry[1]

Abstract

Some groundwater plumes containing chlorinated solvent contaminants are found to be so deep that current *in situ* remediation technologies cannot be economically applied. Also, source zones are often found to be too deep for removal or inaccessible due to surface features. Plumes emanating from these sources require containment or treatment. Containment technologies are available for shallow sites (<15 m) and are being developed for greater depths. However, it is important to advance the science of reactive treatment - both for cut off of plumes and to contain and treat source zones. Zero-valent metal technology has been used for remediation of solvent plumes at sites in Canada, the UK and at several industrial and military sites in the USA. To date, all of the plumes treated with zero-valent metal (granular iron) have been at depths less than 15 m. This paper gives preliminary results of research into methods to emplace granular iron at depths in the range of 15 to 60 m. The study included review of available and emerging methods of installing barrier or reactive material and the selection, preliminary design and costing of several methods. The design of a treatment system for a 122 m wide PCE plume that, immediately down gradient from its source, extends from a depth of 24 to 37 m below the ground surface is used as a demonstration site. Both Permeable Reactive Wall and Funnel-and-Gate™ systems were considered. The emplacement methods selected for preliminary design and costing were slurry wall, driven/vibrated beam, deep soil mixing and hydrofracturing and injection. For each of these methods, the iron must be slurried for ease of pumping and placement using biodegradable polymer viscosifiers that leave the iron reactive. A methodology was developed for cost estimation and selection of the most economical emplacement method based on site specific variables: 1) depths to top and base of plume, 2) contaminant concentration(s), 3) flow velocity and 4) the degradation rate(s) of the contaminants in the site groundwater in contact with the reactive medium chosen. For the demonstration site, a permeable reactive wall system was chosen and the emplacement method selected was hydrofracturing and injection of iron in two 76 mm thick walls.

Introduction

Many contaminant plumes that threaten surface and groundwater resources are comparatively deep (ie > 15 m or 50 ft depth below ground surface). Similarly, contaminant source zones, especially those from dense non-aqueous phase liquid (DNAPL) chemicals, are often found to be too deep or inaccessible for remediation due to surface and subsurface structures or other site features. These source zones cannot be easily removed by excavation for *ex situ* treatment or landfilling. Therefore, the plumes emanating from such sources require some form of *in situ* isolation (containment) or treatment. Containment technologies are available for comparatively shallow sites and are under development for greater depths. The pump-and-treat remediation method, which can be applied to great depths, is suitable for plume capture or control if the source is removed or contained, but is futile or uneconomical on a project life cycle cost basis for restoration of plumes from active DNAPL source zones (Pankow and Cherry, 1996).

For contaminants that are persistent, toxic and relatively mobile (ie they can diffuse through or flow out via imperfections in "impermeable" barriers) it is considered important to achieve treatment of plumes and to contain and treat source zones. One such class of contaminants is chlorinated aliphatic hydrocarbon compounds, which includes many chlorinated solvents. These contaminants have been shown to be degraded, using zero-valent metal, by reductive dehalogenation (Gillham and O'Hannesin, 1994). However, while several sites have been treated with this process, no sites have been remediated where the installation depth was greater than 15 m (50 ft).

---

[1] Department of Earth Sciences, University of Waterloo, Waterloo, Ontario, Canada, N2L 3G1, (519) 888-4567, fax (519) 746-0183, dwhubble@UWaterloo.ca.

The purpose of this study was to investigate methods for installing granular iron to treat chlorinated solvents in a deep groundwater plume. The application could be in a Permeable Reactive Wall (PRW) or Funnel-and-Gate™ (F&G) system. The model case for the study is the CS-10 Source Area plume at the Massachusetts Military Reservation (MMR) in Cape Cod, MA (Hubble and Gillham, 1997a). The plume extends from the water table (about 24 m or 80 ft depth) to about 37 m (120 ft) depth and is about 122 m (400 ft) wide. The soils are glacial outwash deposits (typically compact sand and gravel) with an underlying silty sand aquitard at about 60 m (200 ft) depth. The maximum concentration of tetrachloroethene (PCE) is 200 μg/L and the groundwater flow velocity is about 300 mm/day (1 ft/day).

The study included an assessment of the methods currently available for installing low permeability containment materials at depths greater than 15 m, and selecting those methods that were considered to be adaptable to the properties of granular iron. The adaptability of these emplacement methods to the two primary types of remediation system (PRW and F&G) was then considered and a choice of system for the CS-10 source area plume case was based on site conditions and cost. For the selected methods and treatment system type, the study included assessment of:
- emplacement method
- equipment availability (contractors)
- experience - including constructability, quality control, performance
- cost for 15 m (50 ft) demonstration (pilot) and 122 m (400 ft) full treatment lengths

The primary concern is that the reactive material is installed so that it functions as intended and treats the groundwater (see discussion of treatment integrity below). The methods that have been used for the construction of low permeability barriers or containment walls have been reported in Rumer and Mitchell (1996). Adapting these methods to the installation of granular iron requires considering the problem of bulk materials handling. Specific issues concern particle density, abrasiveness and friction.

Selection of Type of Reactive Barrier System

In a continuous PRW system, the whole width of the contaminant plume flows through the emplaced wall under natural gradient conditions. The contaminant is treated by reactive material as it flows through the wall. In the F&G system, low permeability barrier walls (funnels) channel the plume through reactive material in a gate or in multiple gates. Gates must be proportionately thicker (longer flow path) than a comparable permeable wall, due to the amount of flow diverted by the adjacent funnels. The features of PRW and F&G systems of importance for deep installations and possible emplacement methods used for installing them are summarized in Tables 1 and 2. The cost factors listed in Table 1 indicate that the selection of a system type must be based on site specific criteria and be accompanied by a representative conceptual model of the plume flow system and 2D or 3D numerical modelling of the impact of the F&G on the flow system.

For a continuous PRW that is placed perpendicular to the flow direction (and if the hydraulic conductivity of the reactive material remains above that of the contaminated zone) it can be shown that the flow system is only slightly affected by the PRW. Thus, the treatment wall area can be about the same as the plume cross-section. This is not the case for the F&G system, since the funnels dramatically change the flow system (Shikaze et al., 1995). A limited number of runs using a 3D finite element flow model (FRAC3DVS, Ibid) were performed for the CS-10 source area plume. Since anisotropy of hydraulic conductivity in the outwash materials of the site could not be relied upon to decrease the downward deflection of flowlines, an isotropic flow condition was assumed (K = 0.08 cm/s). The results indicated that for isotropic conditions and with the aquitard layer at great depth (60 m) with respect to the plume base (37 m) the hanging F&G system required significantly more depth of installation to capture the plume. For example, assuming 17 m (55 ft) wide funnels and 15 m (50 ft) wide gates, it was estimated that to capture the plume, the funnel walls would have to extend at least 12 m (40 ft) deeper than the plume (and about 12 m (40 ft) wider on each side). A large cost difference between the PRW and F&G systems was estimated based on the extra depth required for this site and a PRW configuration was selected for further design and cost estimation.

Table 1 - Features of PRW and Funnel-and-Gate Systems Affecting Deep Emplacement

Feature	PRW System	Funnel-and-Gate (F&G) System
Construction Methods	Available barrier emplacement methods must be adapted for iron rather than bentonite & cement.	Vertical "impermeable" barrier walls and seepage cut off walls (funnels) use well established construction methods. Economical emplacement of reactive material in deep gates requires innovation
Areal Dimensions	Area of PRW need only be slightly greater than the vertical and lateral extent of the plume. Suited to plumes which only extend over a portion of the aquifer depth.	*Fully penetrating systems* require more width (depending on flow parameters, funnel:gate ratio, number of multiple gates, etc.) Require greater installation depth than a PRW, unless the plume extends to an aquitard. *Partially penetrating systems* need more area to capture the plume due to underflow and require 3D modelling.
Cost Factors	A single methodology and materials handling system can be used for construction, lowering mobilization and operational costs.	Funnel walls expected to be cheaper per sq. ft than reactive walls of comparable thickness. Gate zones may cost less on a per unit volume basis, but the volume of reactive material required will be about the same. Use of two methods materials on a site will add to costs.

Table 2 - Emplacement Methods for Deep PRW and Funnel-and-Gate Systems

Continuous Permeable Reactive Walls (PRW)	Funnel-and-Gate (F&G) Systems

Slurry Wall
Driven, Vibrated or Jetted Mandrel
    driven/vibrated Beam
    wick drain
    other hollow section driving technologies
Soil Mixing
    Deep Soil Mixing/Soil Mixed Wall
    placement/mixing with hollow stem augers
    placement using drill pipe/mixing by jetting
Hydraulic Soil Fracturing and Iron Injection
Jet Grouting
Overlapping or Staggered Holes
Soil Saw or other Trenchers
	Slurry Wall Funnels
	    slurry wall emplaced gate
	    caisson gate
	    gate formed by soil freezing
	Mandrel Installed Sheet Pile Funnel
	    sheet pile box gate
	    caisson gate
	Deep Soil Mixing/Soil Mixed Wall
	    iron mixed into native soil for "gates"
	    soil-bentonite mixed in for "funnels"
	Hydraulic Soil Fracturing and Injection
	    iron slurry in gates
	    soil-bentonite slurry for funnels
	other methods as listed for PRW

Reactive Material Selection and Reaction Rates

The granular iron used in the application of the zero-valent metal technology has come from several commercial sources (suppliers of construction material additives). Commercial iron has been reported to degrade PCE in a first order reaction, with a half life of 0.6 hr (reaction rate, k, of 1.2 hr^{-1}) in laboratory column tests (Focht *et al.*, 1996). A treatability test using commercial iron and groundwater sampled from the CS-10 source area plume gave a similar result: a half life 0.8 hr (first order reaction rate, k, of 0.8 hr^{-1}) for a column containing 75 percent iron and 25 percent sand on a weight basis (Hubble and Gillham, 1997b). Work is underway at the University of Waterloo on the development of an enhanced iron material that gives a half life on the order of 3 min for PCE, or at least 10 times lower than commercial iron. The granular iron is enhanced by deposition of an alloy containing nickel metal. It was recognised that this enhanced iron had potential uses in above ground canisters for pump-and-treat applications, but it also would have significant implications for deep *in situ* remediation - in that the more highly reactive material could be mixed into the ground at lower iron:soil ratios, or could be emplaced in walls at a fraction of the thickness of commercial granular iron.

Emplacement Methods Selected for Design and Costing

The site-specific information required for selection of an emplacement method includes:
- geology and geotechnical properties of soils
- depth to water table
- equipment capability, availability and depth limitations
- cost for mobilization (and demobilization), materials and equipment operation ($/m^2
  of wall) and disposal of excess soil, if any

Based on the site conditions at MMR and the equipment available in North America, the methods listed in Table 2 that meet the geological and equipment criteria are:
- slurry wall
- driven/vibrated beam (D/VB, also know as vibrating beam)
- deep soil mixing/soil mixed wall (DSM/SMW)
- vertical soil hydraulic fracturing and injection (or fracwall)

The first three methods are described in Rumer and Mitchell (1996) and vertical soil hydraulic fracturing and injection (or hydrofracturing) is reported in Hocking (1996). Each method was considered to be suitable for use in the soils and to the depths required. However, none have been used to emplace granular metal or metal/sand mixtures. Discussions with equipment owners and consideration of the bulk materials handling problems led to the conclusion that all of these methods would require that the metal or metal/sand mixture be conveyed as a slurry (Hubble,1996).

The two primary types of viscosifier available are natural biodegradable polymers derived from plant polysaccharides (cellulose or starch) and synthetic polymers of long chained organic molecules (Ege, 1984). For permeable zone emplacement, the advantage of the natural polysaccharides (such as those derived from zanthum or guar bean) is that they can be biodegraded by premixed enzymes, whereas the synthetic polymers require post-emplacement flushing with chemicals appropriate to the bonds to be broken. To suspend iron particles in a viscous but pumpable gel, it is necessary to "cross-link" the polysaccharide chains, forming covalent bonds between adjacent chains. Enzyme products are also available to break these bonds. Thus, a blend of enzymes appropriate to the polymer and cross-linker used can first "de-link" the cross-linked gel, then break down the polysaccharide chains to glucose and/or mannose (sugar) molecules. Since these sugars are water soluble, it might be expected that the iron would be left unaffected with respect to reaction rate with chlorinated solvents. However, fully coating the metal particle surfaces, on which the dechlorination reactions take place (Odziemkowski and Gillham, 1997), gives rise to concern about the impact of organic polysaccharide molecules and their breakdown products on the charge transfer mechanisms at the reaction sites on the iron and enhanced iron surface. To date, column tests with commercial and enhanced iron show both beneficial and detrimental effects of the polymer at early time. At steady state in the column, the PCE half-life was found to increase by a factor of about 2 (Hubble and Gillham, 1997b). To accommodate the polymer's effect on reaction rate and factors such as lower temperature in the field, precipitate formation and the treatment of degradation by-products, the design half life values used for method selection were 2.75 hr for commercial iron and 12 min for enhanced iron.

Treatment Integrity and Quality Assurance

Performance of a containment wall (*containment integrity*) should be evaluated in terms of the rate of contaminant mass transport through the barrier, plus the effect of mass leakage through defects. Reactive wall performance or *treatment integrity* can be measured in terms of the contaminant mass flux after exit from the most down gradient wall and the effect of mass flux from localized zones in the wall(s) where little or no reaction has taken place. Imperfections in a treatment wall do not necessarily result in "failure" since enough degradation may take place that remediation criteria are satisfied.

Based on a review of reports on containment barrier technologies and discussions with engineers and contractors working with the four selected methods, the methods were ranked in decreasing order of

confidence with respect to treatment integrity in the order listed above. Slurry walls can be constructed to a high degree of integrity and, if specified, the excavated wall space can be probed and verified for shape and orientation before the slurried reactive material is tremied in. The D/VB mandrel causes soil displacement and provides a minimum width of wall. The DSM/SMW methods rely on adding a measured volume of reactive slurry and uniformly mixing it with the *in situ* soil. Treatment integrity will be affected by mix variations and windows in the wall if there are deviations in vertical alignment. Hydrofracturing is the newest of the 4 methods relative to barrier construction and, due to lack of field experience, is initially considered to have the least quality control. More variability is expected in the wall thickness achieved and there is a possibility of small windows, if the advancing fracture front flows around obstructions such as boulder or cobble zones. Experience with granular iron slurry in the laboratory and a field mix trial indicates that the iron/polymer mix remains homogenous during handling and pumping. For hydrofracturing of reactive slurry, the thickness variability can be accounted for in design (i.e. inject a quantity of slurry for an average wall thickness that is some factor (TVF) higher than the minimum thickness that can be relied upon for treatment). To improve treatment integrity to an acceptable level, at least two parallel fracture walls are recommended (Hubble, 1996).

Quality assurance concerns evaluation of factors that affect treatment integrity during or after construction. A continuous PRW constructed using any of the selected methods can be investigated for uniformity of thickness, homogeneity of iron content and continuity at joints, or the possibility of windows by some combination of vertical and angled boreholes, tracer tests, geophysical testing (downhole, crosshole and surface techniques), geotechnical measurements and detailed monitoring of up gradient and down gradient contaminant concentrations and inorganic geochemistry.

Quantity Estimation and Cost Analysis

Estimates of the quantity of iron or enhanced iron needed for remediation of the CS-10 source area plume were based on the groundwater velocity and contaminant concentration of the plume and the design half life of the contaminant with the iron selected. A required treatment thickness of 190 mm (7.3 in) of 100 percent commercial iron or 14 mm (0.53 in) of enhanced iron was calculated and this results in the number of walls and quantities listed in Table 3 for each method of PRW construction.

Table 3 - PRW Design Quantity Comparison for CS-10 Source Area Plume

Method & Iron[1]	No.Walls	Wall Thickness (mm)			Total Thickness (mm)		Iron Weight	
		Design	TVF[2]	Average	Design	Average	%[3]	tonnes
Slurry Wall: C. I.	1	610	1.2	730	610	730	53	182
E. I.	1	610	1.2	730	610	730	6	14.4
FracWall C. I.	3	61	1.5	92	183	277	100	178
E. I.	2	51	1.5	76	102	152	28	17.5
SMW/DSM: C. I.	2	610	1.29	785	1220	1570	32	205
E. I.	1	700	1.29	900	700	900	5	15.5
D/VB: C. I.	2	102	1.25	127	204	254	97	154
E. I.	1	102	1.25	127	102	127	28	14.8

[1] Material Types: Commercial Iron (C. I.) and Enhanced Iron (E. I.).
[2] Design (minimum) thickness calculated for treatment required. Average thickness used for quantity and cost estimation. Thickness Variability Factor (TVF) * design thickness = average thickness. TVF accounts for equipment differences.
[3] Iron weight as a percent of dry weight of iron/sand mix.
Design variables: velocity = 300 mm/day, PCE concentration = 200 µg/L, t1/2 = 150 and 12 min for C.I. and E.I., respectively.

The estimation of iron quantities in Table 3 allows for porosity changes due to the iron/sand mixing and the variation in construction methods, together with the treatment thickness required. For example, in slurry wall construction, a minimum practical width of wall is 0.6 m and the iron must be mixed with sand. Using the design quantities in Table 3 and mobilization and unit costs estimated by specialized contractors, the costs illustrated in Figures 1 to 5 were determined. The total cost for each method is influenced by the mobilization charge, so that the relative cost of the various methods will differ for other sites depending on mobilization charges. For very large projects, the difference in mobilization charge may become less important than the $/m² charges for wall construction. Since the hydrofracturing method uses smaller (and less) equipment, the mobilization cost for it is lowest. Also, the fracturing method involves drilling boreholes spaced down to near the top of the plume and initiating the fracture from that elevation, while the other methods require operation over the width and length of wall from the ground surface down to the top of the plume. For a depth of 24 m to the plume and a 12 m deep treatment zone at the CS-10 site, the operational cost for the hydrofracturing method is less than for the other three methods. For other site conditions, the cost ranking may change.

Based on the costs shown in Figures 1 and 2, a decision was made to proceed with a 15 m demonstration width using iron emplaced with the hydrofracturing method in two parallel 76 mm fractures. The quality control program for the demonstration will include active resistivity geophysical mapping during injection consistent with Hocking (1996). Before and after monitoring of inclinometer casing, pressure transducers and borehole (crosshole) radar tomography will provide complementary information to the organic and inorganic sampling in discrete interval groundwater sampling points.

Conclusions

For the Otis CS-10 Source Area plume, hydrofracturing is estimated to be the most economical method of emplacing an iron slurry into a PRW. Depending on site-specific conditions (particularly the plume depth interval) the slurry wall, DSM/SMW and D/VB methods may be more suited to other sites. Plume-specific treatability study are also required to show that after the chosen polymer breaks and bio-chemical degradation and flushing takes place, the iron will react with the influent contaminant plume and that degradation by-products will also be degraded before leaving the treatment wall.

References

Ege, S.N. (1984) *Organic Chemistry.* p.740-795, 1120-1122, D.C. Heath & Co., Toronto.

Focht, R., J. Vogan and S.F. O'Hannesin (1996) Field Applications of Reactive Iron Walls for In-situ Degradation of Volatile Organic Compounds in Groundwater. *Remediation 6(3), 81-94.*

Gillham, R.W. and S.F. O'Hannesin. (1994). Enhanced Degradation of Halogenated Aliphatics by Zero-valent Iron. *Ground Water, Vol. 32, 958-967.*

Hocking, G. (1996) Azimuth Control of Hydraulic Fractures in Weakly Cemented Sediments. Presented at *2nd North American Rock Mechanics Symposium,* Montreal.

Hubble, D.W. (1996) Emplacement Methods for Permeable Reactive Walls and Funnel-and-Gate Systems for Remediation of Deep Plumes, Presentation to the *Massachusetts Military Reservation Innovative Technology Public-Private Partnership meeting, June 7, 1996.* Otis ANGB, MA.

Hubble, D.W. and R.W. Gillham. (1997a) Emplacement Methods for Remediation of the CS-10 Source Area Contaminant Plume using Zero-valent Metal. Institute for Groundwater Research report to Massachusetts Military Reservation, Cape Cod, MA.

Hubble, D.W. and R.W. Gillham. (1997b) Treatability Study for the CS-10 Source Area Plume. Institute for Groundwater Research report to Massachusetts Military Reservation, Cape Cod, MA.

Odziemkowski, M.S. and R.W. Gillham. (1997) Surface Redox Reactions on Commercial Grade Granular Iron (Steel) and their Influence on the Reductive Dechlorination of Solvent. Micro Raman Spectroscopic Studies. *In submittal.*

Pankow, J.F. and J.A. Cherry. (1996) *Dense Chlorinated Solvents and other DNAPLs in Groundwater,* p. 85, 489-496. Waterloo Press, Portland, OR.

Rumer, R.R. and J.K. Mitchell (ed.) (1996) *Assessment of Barrier Containment Technologies - A Comprehensive Treatment for Environmental Remediation Applications.* NTIS, Springfield, VA.

Shikaze, S.G., C.D. Austrins, D.J.A. Smyth, J.A. Cherry, J.F. Barker and E.A. Sudicky. (1995) Hydraulics of a Funnel and Gate System: Three-Dimensional Numerical Analysis. Presented at I.A.H. Conf., Edmonton, AB.

Figure 1 - *Continuous PRW Costs: 50 ft Wall with Commercial Iron*
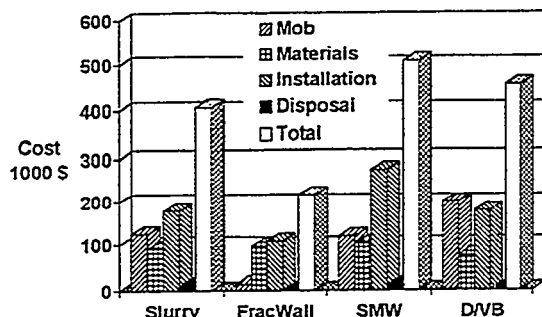

Figure 2 - *Continuous PRW Costs: 50 ft Wall with Enhanced Iron*
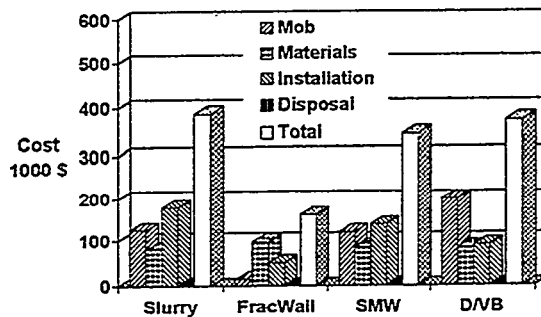

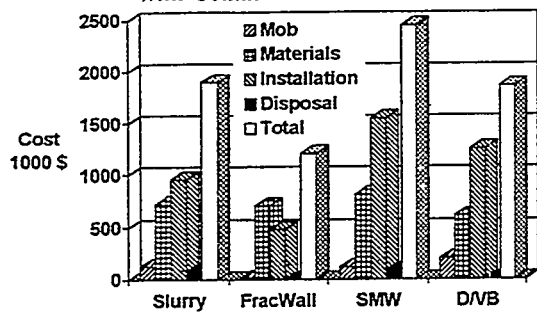Figure 3 - *Continuous PRW Costs: 400 ft Wall with Commercial Iron*

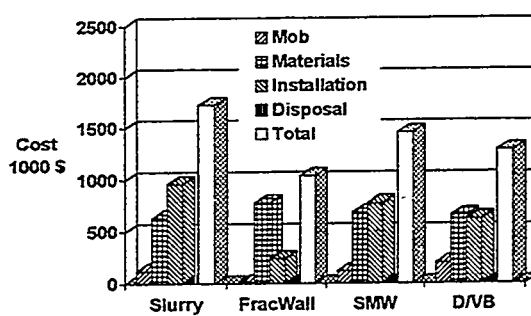Figure 4 - *Continuous PRW Costs: 400 ft Wall with Enhanced Iron*

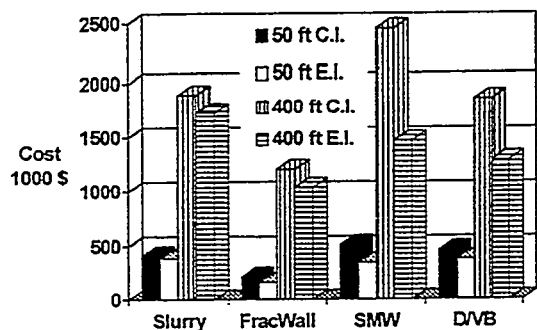Figure 5 - *Continuous PRW Costs: Summary*

Note: costs exclude engineering design and monitoring

Acknowledgements

878

Chapter 17

Modeling: Groundwater Flow

HYDRAULIC PERFORMANCE OF PERMEABLE BARRIERS FOR IN SITU TREATMENT OF CONTAMINATED GROUNDWATER

David J.A. Smyth; Steven G. Shikaze; John A. Cherry
Department of Earth Sciences
University of Waterloo
Waterloo, Ontario, Canada

Abstract

The passive interception and in situ treatment of dissolved contaminants in groundwater by permeable reactive barriers has recently gained favor at an increasing number of sites as an alternative to conventional approaches to groundwater remediation such as the pump-and-treat method. Permeable reactive barriers have two essential functions. The first is that the barriers must be installed in a position such that all of the plume passes through the reactive system. The second function is to achieve acceptable treatment of the contamination by physical, chemical or biological means within or downgradient of the barrier.

In this paper, issues associated with the hydraulic performance of permeable reaction barriers are evaluated using a three-dimensional groundwater flow model. The efficiency of plume capture by permeable wall and funnel-and-gate systems is examined for some generic and for site-specific hydrogeologic systems. The results have important implications to decisions pertaining to the selection, design and installation of permeable reactive barrier systems.

Introduction

Full restoration of the subsurface at contaminated sites to original natural conditions is proving to be an elusive goal. Full restoration requires removal or remediation of sources of contamination, options that are not always feasible or affordable. The most expedient risk-based remedial solutions may involve the implementation of management and control systems to reduce the migration of contaminants from the site to acceptable levels. In a groundwater context, this will involve control or remediation of plumes of dissolved contaminants, possibly in combination with source zone control or isolation.

Until recently, remediation of contaminant plumes has been attempted using conventional pump-and-treat systems. While plume control and management may be successfully attained using pump-and-treat systems, the approach has been shown to have several technical and practical limitations (Mackay and Cherry, 1989). The poor efficiency of contaminant recovery in heterogeneous hydrogeological settings and in the presence of longterm sources of contaminants in the subsurface necessitates the operation of pump-and-treat systems for periods of years to decades to maintain control or achieve remediation on contaminant plumes in many situations. In addition to the efficacy of contaminant recovery, other limitations of pump-and-treat systems include the cost burden of longterm operating and maintenance measures, and problems associated with the collection, treatment and disposal of recovered groundwater.

An alternative to pump-and-treat remediation which is increasingly being considered for many sites involves the passive interception and in situ treatment of the contaminant plume by a permeable engineered barrier (Shoemaker, et al., 1996). Treatment is achieved within or downgradient of the barrier

by one or a combination of physical, chemical or biological mechanisms. Permeable reactive barriers have two essential functions. The first is that the barrier must be installed in a manner to facilitate interception or capture of the contaminant plume at some distance downgradient of its source. The second function is the treatment or removal of contaminants to acceptable levels. In situ treatment of contaminants has recently been the focus of extensive research and development efforts. As Shoemaker et al., (1996) indicate, potential treatment technologies have been identified for a barrier of typical groundwater contaminants such as dissolved organic compounds, including chlorinated solvents, petroleum hydrocarbons and selected pesticides, electroactive metals, nitrate, phosphate and sulfate-rich mine drainage. Although further development and demonstration are required, considerable attention has also been directed towards issues pertaining to the design and construction of permeable barriers and the emplacement of the treatment medium.

Permeable Reactive Barriers

Excluding treatment zones created through the injection of chemicals and subsequent modification of reactivity of aquifer materials, the most simple conceptual form of a permeable barrier can consist of a permeable engineered wall. The wall, which contains the appropriate medium for treatment with a hydraulic conductivity in excess of that of the surrounding aquifer/aquitard system, is constructed across the path of the plume such that complete plume capture is achieved. As groundwater flows through the wall, contaminants are removed or degraded, allowing water of acceptable quality to emerge downgradient of the wall. In 1991, O'Hannesin, and Gillham (1992) installed a metallic iron/coarse sand wall at Canadian Forces Base Borden to remove chlorinated solvents by reductive dechlorination in an experimental plume. Blowes et al. (1995) provide another example of a permeable reactive wall; in their case, a permeable organic barrier was emplaced across a bedrock valley to promote sulfate reduction and the precipitation of metals from groundwater seepage derived from a mine tailings near Sudbury, Ontario.

A second version of a permeable reactive barrier is the funnel-and-gate ™ system. Vertical cutoff walls or barriers of low hydraulic conductivity are installed in a manner to direct or funnel groundwater through permeable gates or chambers, in which contaminant treatment occurs. Conceptually, a funnel-and-gate ™ system offers the advantage over permeable walls of restricting treatment to focused zones, thereby requiring smaller initial volumes of treatment media and facilitating subsequent rejuvenation or replacement of treatment media, if necessary, at appropriate times after initial installation. Focht et al., 1996) describe the use of funnel-and-gate system employing two barrier walls constructed with sealable-joint steel sheet piling (Waterloo Barrier ™) to direct the flow of a portion of a contaminant plume through a central treatment gate. Metallic iron is being used to remove several chlorinated solvents within the treatment gate.

A third form of a permeable reactive barrier involves the use of passive interceptor wells (Wilson and Mackay, 1995). Single or multiple rows of wells are installed across the plume. Interception of the plume is achieved by the cumulative effects of convergence of groundwater flow to open wells from the upgradient direction, and subsequent divergence of groundwater flow downgradient from the wells. Reactants or nutrients, which induce or enhance degradation reactions, are introduced to the groundwater such that contaminant concentrations decrease downgradient of the interceptor wells. Using a solid metal peroxide powder (ORC ™ - Oxygen Releasing Compound) in removable sock harnesses within unpumped wells, Chapman et al. (1996) describe the addition of oxygen to groundwater beneath a former gasoline service station to promote the aerobic biodegradation of petroleum hydrocarbons. Well installation technology has a demonstrated record of success. Its adaptation to permeable reactive barriers, particularly those at depth, may provide advantages in comparison to other barrier design and installation practices, but it will only be appropriate for some treatment technologies which rely on the release of chemicals or nutrients to the contaminant plume.

Hydraulics of Permeable Barrier Systems

Shoemaker et al., (1996) indicate there has been relatively little experience with the actual construction and monitoring of permeable reactive barriers to date. Thus, there has been little opportunity to evaluate the performance of permeable reactive barriers relative to their intended design objectives. The hydraulic characteristics are one of several factors important to the design and performance of permeable reactive barriers.

Starr and Cherry (1994) examined funnel-and-gate systems in a homogeneous, isotropic aquifer using a two-dimensional flow model. They evaluated issues pertaining to hydraulic conductivity contrasts between the treatment gate and the surrounding medium, funnel configuration and length, gate width, and orientation of the system relative to principal directions of horizontal groundwater flow. A primary result of their analysis was that the hydraulic efficiency of a funnel-and-gate did not improve appreciably as the hydraulic conductivity of the gate was increased in excess of an order of magnitude greater than the surrounding aquifer. Because Starr and Cherry (1994) applied a two-dimensional model, their results essentially simulated a funnel-and-gate system fully penetrating a surficial aquifer underlain by a low permeability aquitard.

Shikaze et al. (1995) extended the analysis of funnel-and-gate systems to three dimensions using a numerical, FRAC3DVS, for variably saturated groundwater flow and contaminant transport. The model was developed by Therrien and Sudicky (1996). The analysis focused primarily on systems which penetrate partially or are hanging in a surficial aquifer.

Incorporating particle tracking along streamlines, the model provided graphical output showing the fate of particles as groundwater flows towards a funnel-and-gate system. As particles approach the system, some within the capture zone are diverted through the gate, while others are diverted either laterally around or vertically beneath the barrier walls of the funnel. The funnel-and-gate system included two funnel barriers 10 m in length, and a gate opening of 2 m in width. The three-dimensional analysis, consistent with that of Starr and Cherry (1994), confirmed that the size of the capture zone and the flux of water through the gate increased as the contrast of hydraulic conductivity between the gate treatment medium and the surrounding aquifer was increased to a factor of 10, but further increases in hydraulic conductivity of the gate above this value did not yield appreciable increases in the size of capture zone or flux through the gate. The analysis performed by Shikaze et al. (1995) showed a decrease in submergence of flow beneath a funnel and gate system, and an increase in flux through the gate, as the ratio of vertical to horizontal hydraulic conductivity was decreased.

In this paper, the three-dimensional analysis initiated by Shikaze et al. (1995) has been extended to examine several issues pertaining to the hydraulics of permeable barrier systems, including walls and funnel-and-gate systems. The computational domain has been set-up in a manner consistent with Shikaze et al. (1995). It is 100 m, 50 m and 10 m in the x, y and z directions, respectively. The aquifer, with the exception of one simulation, is homogeneous; it has a hydraulic conductivity of 1×10^{-2} cm/sec, and a porosity of 0.33. All simulations described in this paper involve steady-state, fully saturated groundwater flow conditions. Constant-head boundary conditions have been established in the XZ-plane at y=50 m and y = 0 m, with a hydraulic gradient of 0.005 parallel to the y axis. All other boundaries of the domain have been specified as zero flux.

A portion of the domain for a sample simulation is shown in Figure 1. It shows a perspective view of a hanging funnel-and-gate system approximately in the middle of the flow domain. The funnel barrier walls are assumed to be impermeable, and the permeable treatment gate has been assigned a thickness of 1 m in the direction of groundwater flow. Particles of groundwater approaching the funnel-and-gate system are either captured by the treatment gate or are diverted around or beneath the barrier. The capture zone can be determined graphically by including all streamlines passing through the gate. This approach was applied to simulations of several configurations of permeable reactive barriers.

Figures 2 and 3 represent the hydraulic capture of permeable reactive walls positioned near the middle of the domain. Its hydraulic conductivity is a factor of 10 greater than that of the surrounding aquifer. For the partially penetrating or hanging system (Figure 2), slight convergence of groundwater flow to the permeable wall occurs along its lateral and bottom boundaries has occured. For the fully penetrating system, similar convergence of groundwater flow occurs along its lateral boundaries. Simulations by Wilson and Mackay (1995) identify similar hydraulic capture characteristics for rows of unpumped wells. The hydraulic capture provided by such permeable barriers exceeds slightly the cross-sectional area of the barrier perpendicular to groundwater flow. These simulations further suggest that the flux of groundwater and contaminants entering the permeable barrier will be similar to those present in the aquifer.

Figure 4 represents the hydraulic capture of a partially penetrating or hanging funnel-and-gate system near the middle of the domain. The results of three simulations are shown. In all cases, the thickness of the treatment gate was 1 m, and the ratio of length of impermeable barrier funnels to the width of the gate was 5:1. In case a, the hydraulic conductivity of the treatment gate was a factor of 10 greater than that of the surrounding aquifer; in case b, the contrast was a factor of 5. In case c, anisotropy was incorporated in the aquifer, such that the horizontal component of hydraulic conductivity of the aquifer ($K_{H-AQUIFER}$) was twice that of the vertical component ($K_{V-AQUIFER}$); the hydraulic conductivity of the treatment gate was a factor of 10 greater than ($K_{H-AQUIFER}$). The results of the simulations are remarkably similar, suggesting modest sensitivity between zone of capture and contrast in hydraulic conductivity values between the aquifer and the gate. Further, the zone of capture does not increase appreciably if anisotropy involving a contrast of a factor of 2 between the horizontal and vertical components of hydraulic conductivity is present.

Figure 5 represents the hydraulic capture of a fully penetrating or keyed funnel-and-gate system. Similar to the parameters used for Figure 4 (case a), this simulation incorporated a ratio of funnel length to gate opening of 5:1, and a contrast in the hydraulic conductivity between the gate and the aquifer of 10. The hydraulic capture encompasses an area approximately three times greater than the cross-sectional area of the gate, and hence the flux of groundwater and contaminants through the gate is a similar factor greater than through an equivalent zone of aquifer.

To accommodate treatment of typical plumes, it is likely that wide funnel-and-gate systems with multiple gates would be required. Using the same factor of 10 for the contrast in hydraulic conductivity between the gate and aquifer as most of the previous examples, Figures 6 and 7 represent the hydraulic capture of hanging multiple gate systems. The capture-zone areas for the systems are defined by the overlap of zones associated with all gates. To achieve plume capture, the simulations suggest that low ratios of funnel length to gate width are required. Further, the funnel-and-gate system may need to extend to depths significantly below the base of the plume.

Hydraulics of Field Demonstrations

To date, field demonstrations of prototype permeable reactive barriers have been applied in relatively simple physical hydrogeological settings, although contaminant and groundwater geochemistry may have been quite complex. Representative examples include:

- the hanging permeable wall at CFB Borden (O'Hannesin and Gillham, 1992), which was installed several metres downgradient from the source of a small experimental solvent plume. One issue of concern was fluctuation in groundwater flow directions, which caused less than ideal plume capture.
- a keyed permeable wall across a small bedrock valley to treat mine tailings-derived groundwater seepage in the Sudbury, Ontario area (Blowes et al., 1995). Shallow groundwater flow was largely restricted to the unconsolidated deposits within the valley, so plume capture appears to be assured.

- a keyed a permeable wall along part of an industrial property boundary in California (Warner et al., described by Shoemaker et al., 1996). Lateral low permeability walls, which isolate the shallow subsurface from that on adjoining properties, essentially direct the flow of groundwater through the treatment walls. The surficial aquifer is underlain by an aquitard at a depth of approximately 6 m.
- a keyed funnel-and-gate system extending through a surficial aquifer to an underlying aquitard at a depth of approximately 4.5 m in New York State (Focht et al., 1996). Based on predictive modelling and some preliminary post-installation analysis, a portion of plume approximately 6.25 m in width was captured by the system, which includes two funnel barriers 4.5 m in length on either side of a central gate with an opening of 3.6 m.

To our knowledge, no hanging funnel-and-gate systems have yet been installed for demonstration purposes; thus, assessment of hydraulic performance of hanging systems is not possible. A hanging system adjacent to a river has been proposed as a possible remediation action at a former industrial facility in the north eastern United States. The system would be large, involving a total length of as much as 250 m. Using the numerical model used for our current study, conceptual analysis of possible designs for the system has been conducted using site specific data. Consistent with the simulations of simple hypothetical settings, results demonstrate the need to balance the length of funnel to width-of- gate ratio. If the ratio is too high, there is evidence to suggest that submergence of groundwater flow beneath the system will occur, resulting in contaminants bypassing treatment and entering the river.

Implications and Summary Conclusions

On the basis of numerical simulations in the simple hydrogeological domains considered for this study, the hydraulic efficiency of permeable walls, and by inference passive well systems (Wilson and Mackay, 1995), appear to be more favourable than those for funnel-and-gate systems for intercepting flow of contaminated groundwater. While funnel-and-gate systems may provide hydraulic capture effectively when installed through an aquifer to an underlying aquitard, their potential hydraulic performance needs to be considered carefully for applications where only partial penetration of an aquifer can be achieved. The analysis conducted for relatively simple hydrogeological settings provides a general indication of the hydraulic performance of permeable reactive barriers. It is clearly recognized, however, that additional complexities associated with geological conditions, contaminant distribution in the subsurface, site structures and on-going operations must be considered for applications of permeable barrier technologies at actual sites. For example, the presence of layers of high hydraulic conductivity may exert major control over contaminant migration, and it may be a technical challenge to design a permeable barrier to accommodate treatment of non-homogeneous contaminant loadings. Also, at many sites, it may not always be feasible to construct a barrier perpendicular to principal groundwater flow directions as a consequence of restricted access to the subsurface or fluctuations in the groundwater flow system. Further, it is clear that decisions pertaining to selection of permeable barrier designs will not be made based on hydraulic performance alone. Issues pertaining to the choice of treatment media, sequential treatment of multi-contaminant mixtures, hydraulic characteristics of the media, longevity and performance of the media in the subsurface, the need for periodic replacement of the media, and costs and availability of the treatment media may influence the selection of a particular barrier design. It is also apparent that barrier selection could be influenced by the overall objectives of the remedial projects. For example, some barrier designs may offer distinct advantages if the barrier is to be used for control of contaminant migration from subsurface sources, or permeable barriers could be optimally placed to treat core source areas of plumes and enhance intrinsic remediation schemes for overall plume management..

David J.A. Smyth; Steven G. Shikaze; John A. Cherry
Department of Earth Sciences, University of Waterloo, Waterloo, ON, Canada N2L 3G1
Phone: (519) 888-4567 x2899; Fax: (519) 746-5644; e-mail: dsmyth@sciborg.uwaterloo.ca

References

Blowes, D.W., Ptacek, C.J., Bain, J.B., Waybrant, K.R. and W.D. Robertson, 1995. "Treatment of mine drainage water using in situ permeable reactive walls," Sudbury '95 Conference on Mining and the Environment, May 28th - June 1st, Sudbury, Ontario, Vol. III, pp. 979-987.

Chapman, S.W., Byerley, B.F., Smyth, D.J.A. and D.M. Mackay, 1996. "A pilot test of passive oxygen release for enhancement of in situ bioremediation of BTEX-contaminated groundwater," Ground Water Monitoring and Remediation (submitted).

Focht, R., Vogan, J. and S. O'Hannesin, 1996. "Field application of reactive iron walls for in-situ degradation of volatile organic compounds in groundwater," Remediation, Summer 1996, pp. 81-94.

Mackay, D.M. and J.A. Cherry 1989. "Groundwater contamination: Limits of pump-and-treat remediation," Environmental Science and Technology, V. 23, pp. 630-636.

O'Hannesin, S.F. and R.W. Gillham, 1992. "A permeable wall for in situ degradation of halogenated organics," 45th Canadian Geotechnical Society Conference, October 25-28, Toronto, Ontario.

Shikaze, S., Austrins, C.D., Smyth, D.J.A., Cherry, J.A., Barker, J.F. and E.A. Sudicky, 1995. "The hydraulics of a funnel-and-gate system: A three-dimensional analysis," Solutions '95: International Association of Hydrogeologists Congress, June 5 to 7, Edmonton, Alberta.

Shoemaker, S.H., Greiner, J.F. and R.W. Gillham, 1996. "Permeable reactive barriers," in Rumer, R..R. and J.K. Mitchell, eds., "Assessment of Barrier Containment Technologies: A Comprehensive Treatment for Environmental Remediation Applications," U.S. Department of Energy/U.S. Environmental Protection Agency/DuPont Company, pp. 301-354.

Starr, R.C. and J.A. Cherry, 1994. "In situ remediation of contaminated ground water: the funnel-and-gate system," Ground Water, V. 32, pp. 465-476.

Therrien, R. and Sudicky, E.

Wilson, R.D. and D.M. Mackay, 1995. "A method for passive release of solutes from an unpumped well," Ground Water, V. 33, pp. 936-945.

Figures

Figure 1: Three-dimensional view of streamlines and particles in a sample model domain. Particles are shown at the beginning and end of each streamline. Hydraulic capture is determined by transmission of streamline through the permeable barrier (gate).
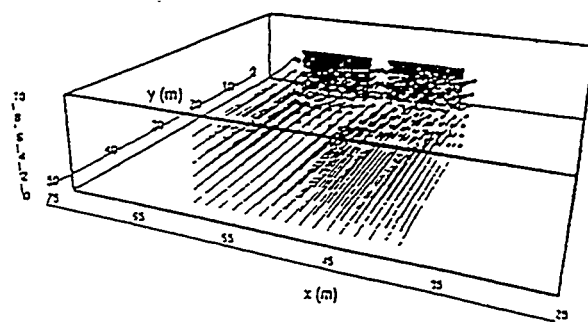

Figure 2: Hydraulic capture of a partially penetrating or hanging permeable reaction wall in an isotropic aquifer; $K_{wall} = 10K_{AQUIFER}$. The permeable barrier is perpendicular to the direction of groundwater flow.
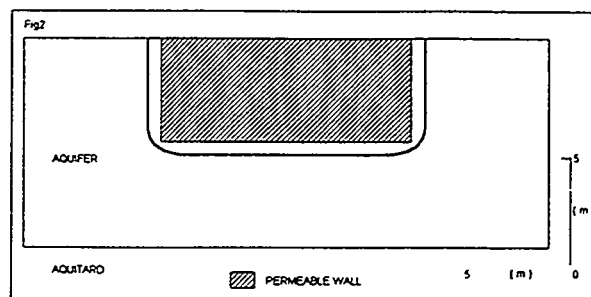
Figure 3: Hydraulic capture of a fully penetrating or keyed reaction wall in an isotropic aquifer overlying an aquitard; $K_{wall} = 10K_{AQUIFER}$.
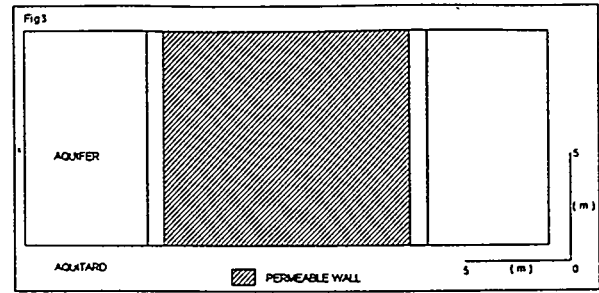
Figure 4: Hydraulic capture of a partially penetrating or hanging funnel-and-gate system in an isotropic aquifer; in a; $K_{wall} = 10K_{AQUIFER}$ and in b, $K_{GATE} = 5K_{AQUIFER}$. In c, the aquifer is anisotropic; $K_{wall} = 10K_{AQUIFER}$; $K_H = 2K_v$.
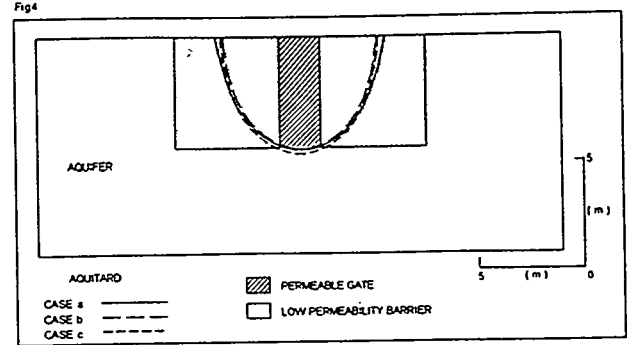
Figure 5: Hydraulic capture of a fully penetrating or keyed funnel-and-gate system in an isotropic aquifer overlying an aquitard; $K_{wall} = 10K_{AQUIFER}$.
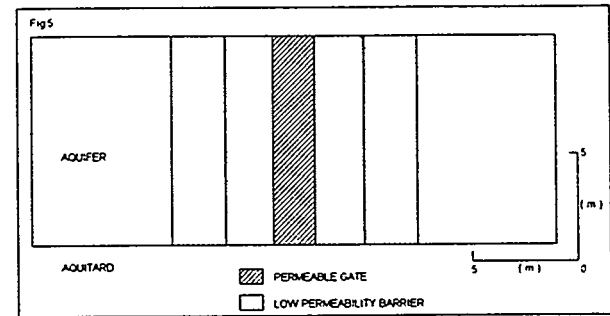
Figure 6: Hydraulic capture of a partially penetrating or hanging multiple gate system; $K_{wall} = 10K_{AQUIFER}$.
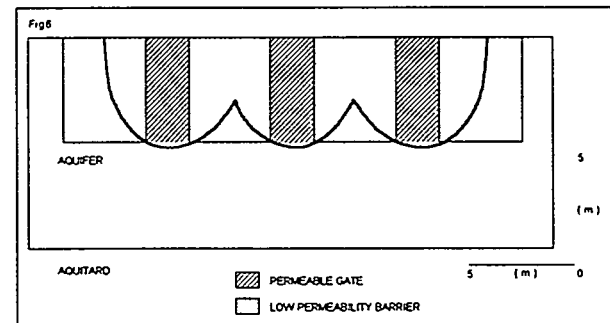
Figure 7: Hydraulic capture of a particular penetrating or hanging multiple gate systems; $K_{wall} = 10K_{AQUIFER}$ Capture to depths of approximately 5 m is achieved by the system which extends to 7.5 m.
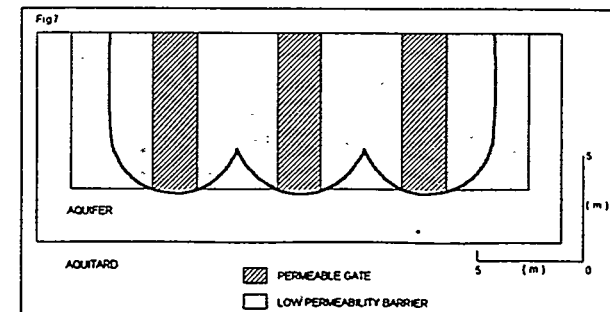
ARRAYS OF UNPUMPED WELLS: AN ALTERNATIVE TO PERMEABLE WALLS FOR IN SITU TREATMENT

Ryan D. Wilson* and Douglas M. Mackay

Abstract

At sites where the installation of permeable walls may be impractical for technical or financial reasons, treatment zones may be created with arrays of unpumped wells. Convergence and divergence of naturally flowing ground water through the wells provides hydraulic control and downgradient mixing. An array of wells, installed either within the gate of a funnel-and-gate or alone, can serve either as a set of in situ reactors or as a means to release amendments that promote biodegradation or other reactions downgradient.

In this paper, the application of arrays of unpumped wells will be demonstrated using two-dimensional flow and transport modeling and pilot scale field data. Various configurations of reactive media or amendment-releasing devices are considered in the simulations, illustrating the impacts on hydraulic performance of the wells and thus the required spacing of wells to achieve various remedial goals.

Introduction

Recently, it has been observed that *active* remediation techniques (pump-and-treat, oxygen/nutrient injection, etc.) have not been effective in reaching and/or maintaining aquifer cleanup goals (Mackay and Cherry, 1989; Cherry et al., 1996). Thus, much effort has been directed at *semi-passive* approaches that offer effective treatment while providing significant cost savings through reduced equipment and maintenance requirements.

The installation of a continuous permeable wall in the path of a contaminant plume is one semi-passive approach that has received some recent attention. These walls can either be constructed of reactive material (McMurty and Elton, 1985; Gillham and Burris, 1992; Robertson and Cherry, 1995), or can be instrumented to allow the introduction of amendments that promote degradation downgradient of the wall (Devlin and Barker, 1994). Two methods of continuous permeable wall installation are 1) excavation and backfilling (with or without installation of a temporary structure such as sheet pile), which involves mobilization of expensive heavy equipment and is limited to installations of perhaps 10 to 15 m, and 2) incorporation of reactive material into the aquifer during auger drilling. It may be possible to construct deeper walls by this second method (50 to 60 m), but ensuring continuous coverage will require a large number of overlapping auger holes. In either case, once installed, the material in the wall cannot easily be
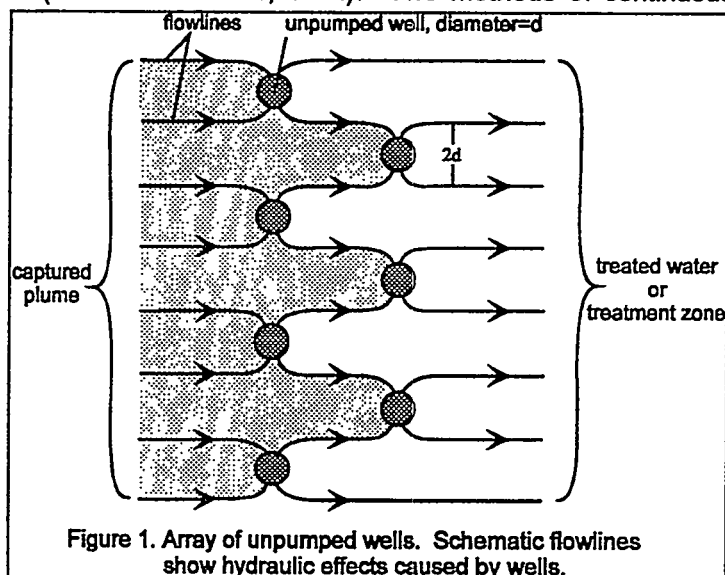

Figure 1. Array of unpumped wells. Schematic flowlines show hydraulic effects caused by wells.

* corresponding author

removed or replaced when the treatment mechanism degrades or fails.

A promising alternative is to install an array of closely spaced unpumped wells to create what can be thought of as a discontinuous permeable wall (Figure 1). Ground water converges under natural flow conditions to the well in response to the hydraulic conductivity contrast between well and aquifer (Halevy et al., 1967). The wells provide a contactor space for installation (and removal if desired) of treatment materials or devices. This approach offers some potentially significant financial and practical advantages: 1) well materials and installation contractors are readily available, 2) well installation in most subsurface conditions is straightforward, 3) deep installations are possible (>50 m deep wells in unconsolidated material is common), and 4) only a fraction of treatment materials are needed to cover the same width as a continuous wall.
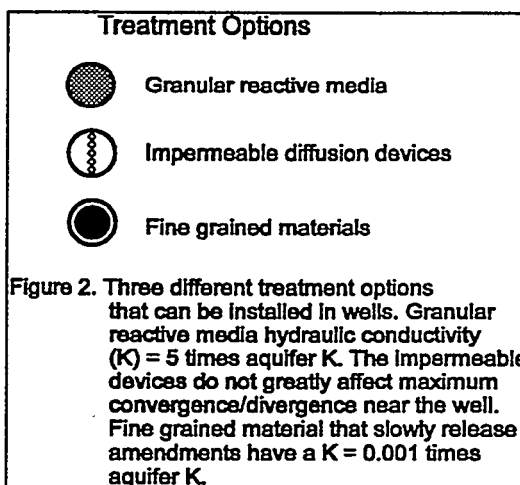
In the context of well arrays, we will consider two contaminant removal approaches. In the first, contaminants are destroyed in the wells as a result of contact with reactive material. The two basic criteria that must be satisfied for complete treatment with reactive media are 1) the contaminant must contact the reactive media, and 2) contact must be long enough for the degradation reaction to go to completion. The first criterion means that the contaminant plume must be completely captured by the well array (i.e., no plume may move through the array without flowing through a well). Thus an essential design parameter is the spacing of wells in an array. If wells are too far apart, some of the plume could migrate through the array untreated, resulting in a pinstripe effect of treated and untreated plume. The second criterion refers to residence time within the zone containing reactive media, and is a requirement common to discontinuous and continuous walls. For treatment in well arrays, longer residence time requirements will mean that the plume will have to flow through more than one well, i.e. require installation of multiple row arrays.

In the second approach, amendments (electron acceptors and/or donors, microbial nutrients, abiotic oxidizers or reducers) are released in the well to promote or sustain degradation reactions in and/or downgradient of the wells. Two constraints that control this approach are 1) amendment supply must at least equal plume demand, and 2) amendments must be spread out sufficiently downgradient of the array by divergent and laterally dispersive flow. Well spacing criterion can be relaxed slightly in the case of passive amendment release because even weak lateral dispersion can be relied on to enhance spreading of amendment downgradient of the arrays. The general utility of arrays of wells for plume treatment by this approach is developed in greater detail by Wilson and Mackay (1996). That work examines the role of appropriate well spacing on the above constraints in the design of effective treatment well arrays.

Treatment Options

Three general physical configurations of treatment options can be installed in wells (Figure 2). Each configuration results in different well hydraulic behavior, which impacts on well spacing. Granular material can be placed in removable baskets in wells. Once installed, these materials would likely result in the wells being at most 2 to 5 times more hydraulically conductive than the host aquifer. Zero valent iron is one example of reactive granular material that has enjoyed recent success installed in permeable walls.

Impermeable devices that slowly release amendments by diffusion can be installed in wells such that the large hydraulic conductivity contrast

Treatment Options

Granular reactive media

Impermeable diffusion devices

Fine grained materials

Figure 2. Three different treatment options that can be installed in wells. Granular reactive media hydraulic conductivity (K) = 5 times aquifer K. The impermeable devices do not greatly affect maximum convergence/divergence near the well. Fine grained material that slowly release amendments have a K = 0.001 times aquifer K.

between well and aquifer is maintained. For example, thin-walled tubing can be installed in a well in some fashion to maximize vertical coverage but not impede water flow through the well. Highly concentrated amendment solution (or gas) is introduced into the tubing, and amendment diffuses at a fixed rate through the tubing wall in response to the imposed concentration gradient (Wilson and Mackay, 1995).

Fine grained materials are available that slowly release amendments to ground water flowing through wells. One example is an oxygen-releasing compound (Chapman et al., 1996) which, in its current formulation (Regenesis, Inc., San Juan Capistrano, CA) is placed in a tube-like filter sock and suspended in wells such that an annular space exists between the sock and the well screen. Upon contact with water, the material reacts with water to slowly release oxygen. The sock itself is of very low hydraulic conductivity, thus oxygen release to flowing ground water occurs primary at the surface of the sock. Flow through the well, then, is constrained to the annular space, the dimensions of which affect the downgradient spreading of oxygen, as examined later in detail.

Lateral Impact of Treatment Options

The steady-state hydraulic behavior of unpumped wells instrumented with the three above treatment configurations was compared in a series of two-dimensional steady-state flow simulations using a finite element model (Pinder and Frind, 1972). A two-dimensional finite element model that employs the Laplace Transform Galerkin (LTG) method (Sudicky, 1989) to derive time-continuous solutions was used to model the release and transport of amendment. While mathematically de-coupled, the models are capable of using the same nodal coordinates generated by a grid-building program that allows for irregular grid discretization and the areal definition of circular wells within the grid.

The modeled aquifer was assigned properties similar to the well-studied aquifer at C.F.B. Borden, Ontario (Sudicky, 1986). The assigned longitudinal and lateral dispersivities are typical of the Borden aquifer (Sudicky, 1986), and correspond roughly to a scale of observation on the order of meters to 10's of meters (Gelhar, 1986). The transport parameters for the treatment wells and the aquifer for each simulation are compiled in Table 1. All the simulations assumed a uniform hydraulic conductivity (K) field as the simplest and visually clearest case. Simulations in random K fields (not shown) do not change the conclusions drawn herein. The simulations were run to 60 days, by which time concentrations near the well had essentially reached a steady state. Therefore, no further significant downgradient spreading within the domain shown will occur after that time. For the granular reactive media, hydraulic influence of the well was inferred by making

Table 1. Parameters used in 2-D modeling

Flow	hydraulic gradient (Dh)	0.0043
	porosity (h_e)	
	aquifer	0.35
	granular reactive media	0.35
	well with impermeable diffusive devices	1.0 [1]
	fine grained material	0.50
	hydraulic conductivity (K_{xy})	
	aquifer	8.42 m/d
	granular reactive media	42.1 m/d [1]
	well with impermeable diffusive devices	8420 m/d [1]
	fine grained material	0.00842 m/d [1]
Transport	longitudinal dispersivity (a_l)	0.05 m
	transverse dispersivity (a_t)	0.005 [1] m
	retardation	1.0 [1]
	solute free solution diffusion coefficient (D^*)	1.7×10^{-4} m^2/d [1]

All parameters from Sudicky (1986) except those which were assumed herein[1] and from Lyman et al., (1982)[1]. D^* is that of oxygen.

the well a source of contaminant-free (i.e. treated) water and examining that distribution downgradient. This assumes that the residence time in the well was adequate for complete treatment. In the case of amendment release, the effect of the well on the flow field can be inferred from the distribution of amendment downgradient. It was assumed that amendment was released from the wells at constant levels from time zero on. In all cases, concentrations were normalized to 1 for direct comparison.

Figure 3 illustrates the difference in hydraulic behavior of an unpumped well instrumented with the three treatment options. Using the 0.1 relative contour of treated water to define the area affected, the lateral impact of the well containing the granular media (3a) is limited to a

Figure 3. 60 day simulation results showing distribution of (a) treated water from a well containing granular reactive media, distribution of amendment from a well containing (b) impermeable diffusion devices, and (c) a cylinder of fine grained material with a 2 cm annular space between the cylinder and the well. Hydraulic influence of the well in in each case can be inferred from the distribution of treated or amended water. The wells are 20 cm in diameter.
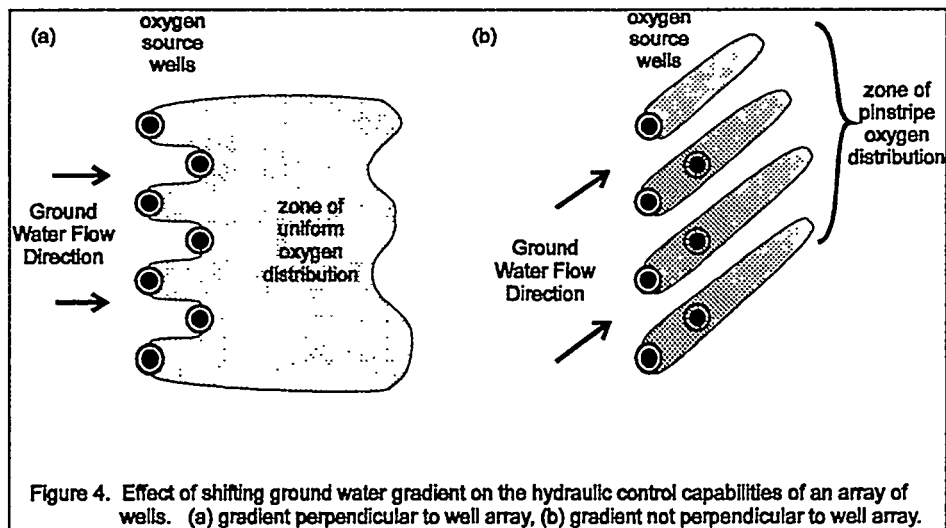
cross-sectional width roughly twice the well diameter. According to the borehole dilution literature (Halevy et al., 1967), this is the maximum impact that can be expected. This means that for complete plume treatment, maximum well spacing will be about twice the well diameter. For treatment by amendment release using the tubing devices (3b), the impacted area downgradient is slightly wider due to the enhancing influence of lateral dispersion. In this case well spacing wider than twice the diameter can be allowed if the relative concentration contour at which the released amendments coalesce is sufficient to support complete treatment (for more detail on this see Wilson and Mackay, 1996). The lateral impact in the case of amendment release from wells containing cylinders of low permeability material with an open annular space around them is significantly smaller (3c), and thus the required well spacing for complete treatment could conceivably be very small, necessitating the installation of multiple rows of wells

Concerns about Spatial and Temporal Variability

Once installed, a continuous wall may not be able to adjust to temporal or spatial changes in plume concentration. If the rate of reaction does not increase with increasing plume concentrations and is not sufficiently rapid to completely degrade periodic and/or localized high contaminant loadings, breakthrough of plume could occur in those places. To prevent breakthrough of contaminants where high plume concentration zones exist, the wall may need to be overdesigned with respect to the average concentration of contaminants it can treat. This means that at some points along the wall, a great deal more treatment material will be used than is necessary. This may also be true for arrays of wells when stationary or low permeability media are used. However, the release of amendment from diffusive release devices can accomodate spatial and temporal plume concentration variations after installation by changing the concentration gradient driving the amendment release.

The remedial performance of arrays of wells (and walls to a lesser extent) can be affected by shifting ground water gradient vectors. Arrays of wells and continuous walls are generally installed perpendicular to the mean plume flow direction. If the gradient shifts, the width of treatment area exposed to the plume is reduced. In the case of multi-row arrays of wells, shifting gradients can result in part of the plume flowing through the array without contacting a well. An example of this is shown in Figure 4, which is from a recently completed pilot scale field test (Chapman et al., 1996), simplified for clarity. In that study it was found that oxygen distribution was more uniformly distributed when the ground water flow gradient was

Figure 4. Effect of shifting ground water gradient on the hydraulic control capabilities of an array of wells. (a) gradient perpendicular to well array, (b) gradient not perpendicular to well array.

perpendicular to the well array (Figure 4a). When the gradient vector shifted during the test, the oxygen distribution was affected as shown in Figure 4b. It is therefore important that seasonal or other predictable shifts in ground water gradient be accounted for in system design.

Conclusions

The installation of arrays of closely spaced unpumped wells to form a discontinuous wall is a viable alternative to continuous permeable walls, especially where installation of the latter is not practical. Unpumped wells provide a hydraulic conductivity contrast that forces ground water to converge and diverge from the well. The wells also provide a contactor space for either granular reactive media or devices or materials that release amendments to promote in situ degradation reactions downgradient of the array.

To achieve complete hydraulic control of a plume (required for treatment with granular reactive media), wells are spaced roughly twice their diameter apart to a total width approximately equal to the plume width. Thus the fraction of plume width occupied by a well array (assuming adequate residence time is provided) is about one half that required for a continuous wall. In the case where amendments are released, wider well spacing (smaller fraction of total plume width) can be permitted because enhanced spreading due to lateral dispersion means that complete plume control is not strictly required.

Unlike continuous walls, arrays of wells can be readily adapted to temporal and spatial variations in plume concentration, especially where they are equipped with amendment release devices. The flexibility provided by well arrays should allow fine tuning of the degradation reactions as remediation proceeds, allowing a maximization of resources without the need for feeder pumps and other expensive equipment prone to failure.

Since there are engineered gaps in arrays of wells, care need be taken to allow for variations in ground water flow direction in well array design. If the gradient shift is dramatic

enough, there is a possibility that flowpaths could evolve that do not travel through the treatment zone.

Corresponding Author:
Ryan Wilson
Department of Earth Sciences, University of Waterloo,
Waterloo, Ontario, Canada, N2L 3G1
Tel: (519) 888-4567 ext 5372, Fax: (519) 746-5644
e-mail: rdwilson@sciborg.uwaterloo.ca

References

Bianchi-Mosquera, G.C., R.M. Allen-King, and D.M. Mackay (1994) Enhanced degradation of dissolved benzene and toluene using a solid oxygen-releasing compound. Ground Water Monitoring and Remediation. v. IX, no. 1, pp 120-128.

Chapman, S.W., B.T. Byerley, D.J. Smyth, R.D. Wilson, and D.M. Mackay (1996) A detailed pilot test of passive oxygen release for enhancement of in situ bioremediation of BTEX contaminated groundwater. Proceedings of Petroleum Hydrocarbons and Organic Chemicals in Ground Water: Prevention, Detection, and Remediation, Houston, Texas, Nov. 13-15, Published by National Ground Water Association, In Press.

Cherry, J.A., S. Feenstra, and D.M. Mackay (1996) Concepts for the remediation of sites contaminated with dense non-aqueous phase liquids (DNAPLS). *In* Dense Chlorinated Solvents and other DNAPLs in Groundwater, J.F. Pankow and J.A. Cherry, Eds. Waterloo Press, Portland, Oregon, pp. 475-506.

Devlin, J.F. and J.F. Barker (1994) A semipassive nutrient injection scheme for enhanced in situ bioremediation. Ground Water. v. 32, no. 3, pp. 374-380.

Gelhar, L.W. (1986) Stochastic Subsurface Hydrology From Theory to Applications. Water Resour. Res., v. 22, no. 9, pp 135S-145S.

Gillham, R.W. and D.R. Burris (1992) In situ treatment walls - Chemical dehalogenation, denitrification, and bioaugmentation. *Proceedings* of Subsurface Restoration Conference, Third International Conference on Ground Water Quality Research, Dallas, Texas, June 21-24, pp. 66-68. Published by National Center for Ground Water Research, Rice University.

Halevy, E., H. Moser, O. Zellhofer, and A. Zuber. 1967. Borehole dilution techniques: A critical review. Isotopes in Hydrology. International Atomic Energy Agency, Vienna, pp 531-564.

Lyman, W.J., W.F. Rheel, and D.H. Rosenblatt (1982) *Handbook of Chemical Properties Estimation Methods*, Chapter 4. McGraw Hill, Inc., N.Y..

Mackay, D.M. and J.A. Cherry (1989) Groundwater contamination: Pump-and treat remediaton. Environ. Sci. Tech., v. 23, no. 6, pp. 630-636.

McMurty, D.C. and R.O. Elton (1985) New approach to in-situ treatment of contaminated groundwaters. Environ. Progress, v. 4, no. 3, pp. 654-663.

Pinder, G.F. and E.O. Frind (1972) Application of Galerkin's procedure to aquifer analysis. Water Resour. Res., v. 8, no. 1, pp. 108-120.

Robertson, W.D. and J.A. Cherry (1995) In situ denitrification of septic-system nitrate using reactive porous media barriers: Field trials. Ground Water. v. 33, no. 1, pp. 99-111.

Sudicky, E.A. (1989) The Laplace transform Galerkin technique for efficient time-continuous solution of solute transport in double-porosity media. Geoderma, v. 26, pp. 209-232.

Sudicky, E.A. (1986) A natural gradient experiment on solute transport in a sand aquifer, 5. Spatial variability of hydraulic conductivity and its role in the dispersion process. Water Resour. Res., v. 22, no. 13, pp. 2069-2082.

Wilson, R.D. and D.M. Mackay (1995) A method for passive release of solutes from an unpumped well. Ground Water. vol. 33, no. 6, pp. 936-945.

Wilson, R.D. and D.M. Mackay (1996) Passive release wells for in situ remediation of contaminant plumes. Proceedings of Petroleum Hydrocarbons and Organic Chemicals in Ground Water: Prevention, Detection, and Remediation, Houston, Texas, Nov. 13-15, Published by National Ground Water Association, In Press.

Implementation of
a Funnel-and-Gate Remediation System

Kent O'Brien and Gary Keyes, P.E.

Geraghty & Miller, Inc. (Richmond, California)

Neil Sherman

Louisiana-Pacific Corporation (Samoa, California)

Abstract

A funnel-and-gate™ system incorporating activated carbon was deemed the most attractive remediation method for an active lumber mill in the western United States. Petroleum hydrocarbons, chlorinated solvents, pentachlorophenol, and tetrachlorophenol were detected in on-site groundwater samples. The shallow aquifer consists of a heterogeneous mixture of marine deposits and artificial fill, underlain by low-permeability siltstones and mudstone.

In the funnel-and-gate™ system, a low-permeability cutoff wall was installed to funnel groundwater flow to a smaller area (a "gate") where a passive below-grade treatment system treats the plume as it flows through the gate. Groundwater flow modeling focused on the inhomogeneities of the aquifer and the spatial relationship between gate(s) and barrier walls.

The gate design incorporates several factors, including contaminant concentration, flow rate, and time between carbon changeouts. To minimize back pressure and maximize residence time, each gate was designed using 1.25-meter (4-foot) diameter corrugated metal pipe filled with a 1.25-meter (4-foot) thick bed of activated carbon. The configuration will allow water to flow through the treatment gates without pumps. The installed system is 190 meters (625 feet) long and treats approximately 76 L/min (20 gpm) during the winter months.

* * *

Introduction

Funnel-and-gate™ systems are gaining attention because they minimize the lifetime costs of implementing remedial actions in situation where containment of contaminated groundwater is required. The term "funnel-and-gate" refers to the installation of low-permeability barriers downgradient of impacted groundwater which are arranged so as to direct the flow of groundwater through treatment gates (Starr and Cherry, 1994). The flow through treatment gates is driven by natural groundwater gradients, eliminating costly extraction pumps and above-ground treatment systems. The treatment gates are designed specifically to treat the groundwater contamination flowing through the gates. In addition, groundwater monitoring and system compliance issues can generally be streamlined for even greater cost savings. It is a developing technology which is currently operating successfully at a site in Mendocino County, California.

Background

Louisiana-Pacific Corporation owns and operates a studmill south of Fort Bragg in Mendocino County, California. The studmill occupies approximately 16 hectares (40 acres) of land. The mill building is located adjacent to a creek, segments of which have been filled to increase log deck capacity. The creek has also been dammed to provide the mill with fire-suppression water.

The area surrounding the mill has been developed as a residential area. Domestic water for the residences is primarily provided through shallow groundwater wells. Groundwater in the area occurs at a depth of approximately 3 meters (10 feet) below ground surface (bgs) from an aquifer consisting of sands and silty sands which extends to a total depth of approximately 4 to 6 meters (12 to 18 feet) bgs. Below this aquifer, a low-permeability weathered bedrock is encountered consisting of clayey siltstones. The underlying bedrock consists of very low-permeability siltstone and sandstone.

Since the early 1980s, soil and groundwater investigations have identified petroleum hydrocarbons, chlorinated solvents (wood-treating compounds), and pentachlorophenol (PCP) (a wood-treating compound) beneath the site.

Development of Final Remediation Strategy

A strategy for final remediation at the site was developed consisting of a combination of source removal by excavation, isolation of the residual impacted soils, in-situ natural degradation of these residuals, and institutional controls for on-site groundwater usage. While institutional controls effectively prevent on-site exposure, preventing off-site migration required the installation of engineered controls. Although the ultimate success of the on-site groundwater remediation program will be determined by natural attenuation processes, protection of the off-site groundwater resource is being achieved using the emerging technology of the funnel-and-gate™ groundwater treatment system.

The funnel-and-gate™ approach consists of the combined application of two proven technologies: slurry-wall hydraulic barriers and activated carbon adsorption. The treatment technologies considered for the gates included native iron reactive zones for dechlorination and treatment of such chlorinated hydrocarbons as trichloroethene (TCE), air sparging for removal of dissolved volatile or aerobically biodegradable compounds, and activated carbon for adsorption of both chlorinated and nonchlorinated hydrocarbons. Granular activated carbon was selected as the most appropriate for this application because the native iron reactive zones would not be effective on the diesel and BTEX, and air sparging would not be reliable at either stripping or biodegrading the TCE and PCP.

Application of the funnel-and-gate™ technology to the site involved installing multiple permeable treatment gates along a downgradient slurry wall. The gates were spaced along the hydraulic barrier at intervals designed to minimize impacts to the natural groundwater flow regime. The effectiveness of the system is monitored using monitoring wells placed up- and downgradient of the treatment gates to provide verification that water leaving the gates meets water-quality objectives.

Groundwater Flow Patterns

A key site condition which made the funnel-and-gate™ approach feasible was the high contrast between permeabilities in the water-bearing shallow aquifer and in the bedrock. In order to minimize the disruption of the natural groundwater flow patterns, there were three key concerns that needed to be addressed.

The first was the effect on water levels both up- and downgradient of the wall. Modeling showed that pressure required to move water through the gate was slightly greater than the natural gradient and was a function of the gate configuration and permeability of the gate.

The "analytic element method" groundwater modeling technique was used to optimize the total number of gates and their locations. This method was developed at the University of

Minnesota Department of Civil and Mineral Engineering by Dr. Otto D. L. Strack. The analytic element approach and its application to groundwater flow is described in the book *Groundwater Mechanics* (Strack, 1989a) and in various conference proceedings (Strack et al., 1987 and 1989, and Strack, 1987 and 1989b).

The computer code selected for the modeling study at the Louisiana-Pacific Corporation site is the two-dimensional groundwater flow code SLAEM (the Single-Layer Analytic Element Model). This code implements the analytic element method for simulation of single-layer, steady-state groundwater flow systems. Streamlines are calculated from the velocity vector using a standard numerical integration technique (second-order Runga-Kutta algorithm).

Transmissivities were determined by aquifer testing and model calibration. The model was calibrated by matching the groundwater contour maps for the site with contour maps generated by the model. The global transmissivity value assigned to the model, 19.5 m^2/day (210 ft^2/day), was based on aquifer testing. Embedded in this background transmissivity were two permeability inhomogeneities. These are identified in Figure 1. The first was assigned a transmissivity of 2.6 m^2/day (28 ft^2/day), and forms a lower transmissivity band curving south to northeast. The second inhomogeneity has a transmissivity of 0.33 m^2/day (3.5 ft^2/day) and runs along the position of the creek and pond downcut through the full thickness of the shallow, saturated sediments. Head-specified line sinks were used to represent the pond and that portion of the creek upstream from the pond. The gradient across the site was assumed to be 0.046 m/m (0.046 ft/ft).

Groundwater streamlines were generated for several combinations of gate lengths and spacings. Successful designs were obtained for a broad range of combinations. One example of a workable system is shown in Figure 1, incorporating four gates and an L-shaped barrier arrangement. The calculated streamlines shown on the top drawing of Figure 1 demonstrated that all groundwater flowing beneath the studmill will pass through the treatment gates.

The second concern was ensuring that groundwater could readily access a treatment gate. Because of the nonuniform distribution of hydraulic transmissivities across the site, water could be impeded in its lateral movement toward and away from the gates, which could have resulted in undesirable hydraulic mounding behind the portion of the wall midway between gates. To minimize this effect, gravel-filled collection and distribution galleries are installed at each gate to collect water from the upgradient side of the gate, ·guide it through the gate, and then redistribute it uniformly after treatment (bottom drawing of Figure 1).

The third concern was that of inadvertently inducing untreated groundwater to flow around the ends of the barrier. This potential effect was evaluated using computer modeling. Use of the model resulted in designing a curved hydraulic barrier that routed the water from underneath the mill through the gates and avoided flow of contaminated water around the ends of the barrier (Figure 1).

Underflow of Barrier

A comparison of the transmissivity of the shallow drinking-water aquifer with that of the underlying bedrock indicated that the hydraulic conductivity of the bedrock is approximately one-thousandth of that of the overlying shallow aquifer. This resulted in a conservatively calculated underflow equal to less than 1% of the total flow through the combined aquifers.

Number and Location of Gates

Due to the complex geology and the influence of the funnel-and-gate™ arrangement on the flow lines across the site, the total flux of water at the barrier cannot be easily calculated. However, the flow can be approximated by taking the cross-sectional flow of a region where the particle traces generated by the computer model are relatively straight. In the area under the mill, the flow lines are relatively unaffected by the presence of the funnel-and-gate™ system. This length is approximately 122 meters (400 feet) of potentially impacted aquifer.

The combined flow rate through all four treatment gates is the product of the transmissivity, the length of the cross-sectional area, and the hydraulic gradient. This results in a total flow of approximately 76 liters per minute (L/min) (20 gallons per minute [gpm]). The flow through each gate is therefore estimated as one-fourth of the total flow, or 19 L/min (5 gpm) per gate.

Gradient Control

Figure 2 shows the plan and cross-section views of the treatment gate with collection and distribution galleries installed to guide water through the gates. Because the aquifer will tend to have higher horizontal than vertical permeability, the collection and distribution galleries are downcut into the aquifer to expose a large cross-sectional area to groundwater flow. This design minimizes the pressure required to move water from the aquifer into the gallery and then to the carbon treatment gate. This is also important on the downgradient side of the wall, where infiltration of water will be limited by the infiltration rate of the aquifer. The installation of these collection and distribution galleries further ensures that the pressure drops across the wall will minimally affect the natural groundwater gradients and flow patterns.

Gate Design

For the purpose of designing the carbon gates, a very large margin of safety was factored into the mass of carbon installed in each gate. The estimated gate flow rate is 19 L/min (5 gpm). The time between changeouts has been selected to be 4 years, although more frequent changeouts could easily be accommodated. In the vicinity where the gates are installed, concentrations of compounds of concern have ranged from nondetect to the low parts per billion. A concentration of 200 micrograms per liter (μg/L) was used in this design to account for the loading due to natural occurring wood-degradation compounds. Using the average carbon loading efficiency of 1% and the constraint of a relatively thin aquifer results in a carbon bed 1.25 meters (4 feet) tall placed within a cylinder 1.25 meters (4 feet) in diameter.

The selection of a moderate carbon grain size and the design of the treatment gates shown in Figure 2 minimizes the pressure loss across the treatment gate by presenting a large cross-sectional flow area through the carbon. This prevents water from backing up behind the gate and increasing the hydraulic head on the upgradient side of the barrier. The pressure required to move the water through the gates corresponds to an increase in water differential of approximately 5 centimeters (2 inches). The treatment gates themselves therefore have a negligible effect on groundwater elevation.

Monitoring points are located upgradient, within the carbon bed, and downgradient of the treatment gate (Figure 2). Samples are collected from the monitoring points to verify that the treatment gate is being effective in removing contaminants. Upon detection of a compound of concern at a concentration above water-quality objectives at the midgate measuring point, the carbon will be removed and replaced.

Carbon replenishment is a relatively easy procedure. Wet spent carbon will be vacuumed out as a slurry, using above-ground slurry pumps. Fresh carbon will be emplaced after dewatering the gate using the upgradient monitoring well which is completed in the gravel packing adjacent to the gate. While water is being evacuated and the gate is dry, fresh carbon will be poured into the gate to the desired thickness.

Conclusion

Funnel-and-gate™ systems will become increasingly popular as alternatives to long-term conventional pump-and-treat systems. Funnel-and-gate™ systems provide a reliable means of controlling groundwater flow to prevent contaminant migration and facilitate cost-effective, in-situ treatment of a limited number of gates.

Creative design and implementation can result in very reasonable capital costs. The design, permitting, and installation of the complete system at the Mendocino County site cost less than $500,000 US. System startup occurred in September 1995. Subsequent monitoring of groundwater elevations and groundwater quality indicates that the system is working effectively.

AUTHORS

Kent O'Brien and Gary Keyes
Geraghty & Miller, Inc.
1050 Marina Way South
Richmond, CA 94804
Telephone: (510) 233-3200

Neil Sherman
Project Manager
Louisiana-Pacific Corporation
One L-P Drive, P.O. Box 158
Samoa, CA 95564
Telephone: (707) 443-7511

REFERENCES

Starr, Robert C., and John A. Cherry. "In Situ Remediation of Contaminated Ground Water: The Funnel-and-Gate System." Ground Water, May-June 1994, 32:3, 465-476.

Strack, O. D. L. 1987. The Analytic Element Method for Regional Groundwater Modeling. Proceedings of "Solving Groundwater Problems with Models," Denver, Colorado.

———. 1989a. Groundwater Mechanics. Prentice Hall, Englewood Cliffs, NJ.

———. 1989b. Multi-Layer Aquifer Modeling Using the Analytic Element Method. Proceedings of "Solving Groundwater Problems with Models," Indianapolis, Indiana.

Strack, O. D. L., K. D. Barr, S. Robertson, and J. K. Seaburg. 1989. Single and Multi-Layer Applications of Analytic Element Modeling. Proceedings of "Solving Groundwater Problems with Models," Indianapolis, Indiana.

Strack, O. D. L., C. R. Fitts, and W. J. Zaadnoordijk. 1987. Application and Demonstration of Analytic Elements Models. Proceedings of "Solving Groundwater Problems with Models," Denver, Colorado.
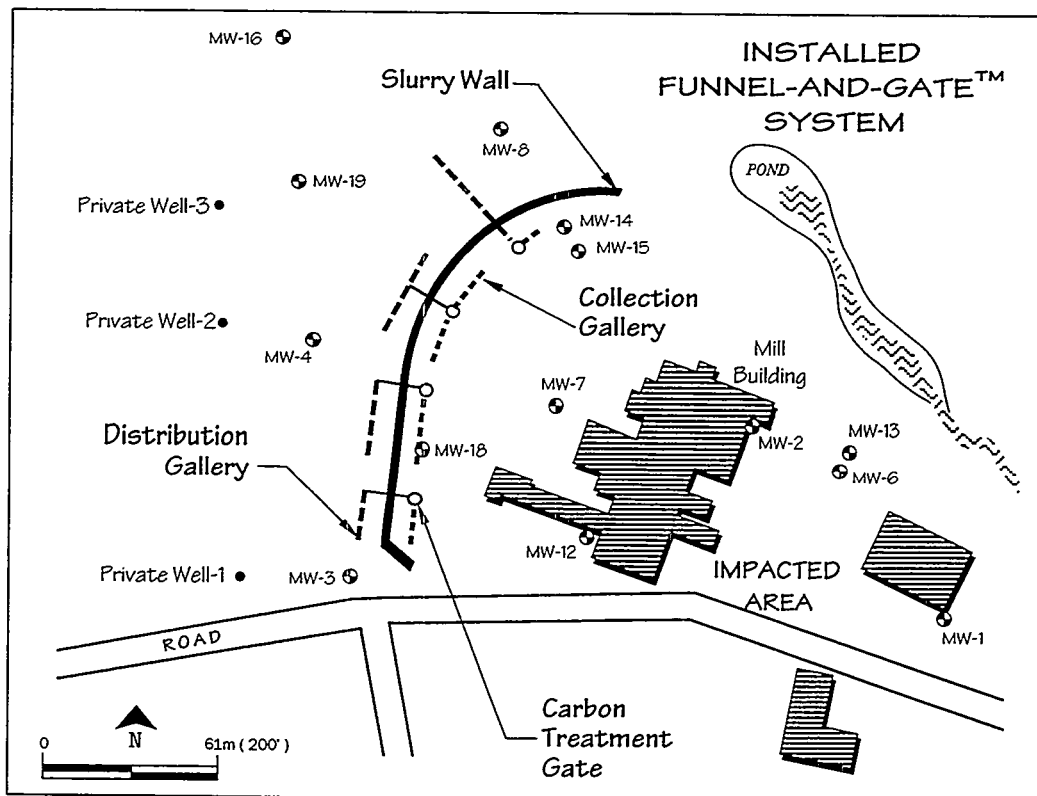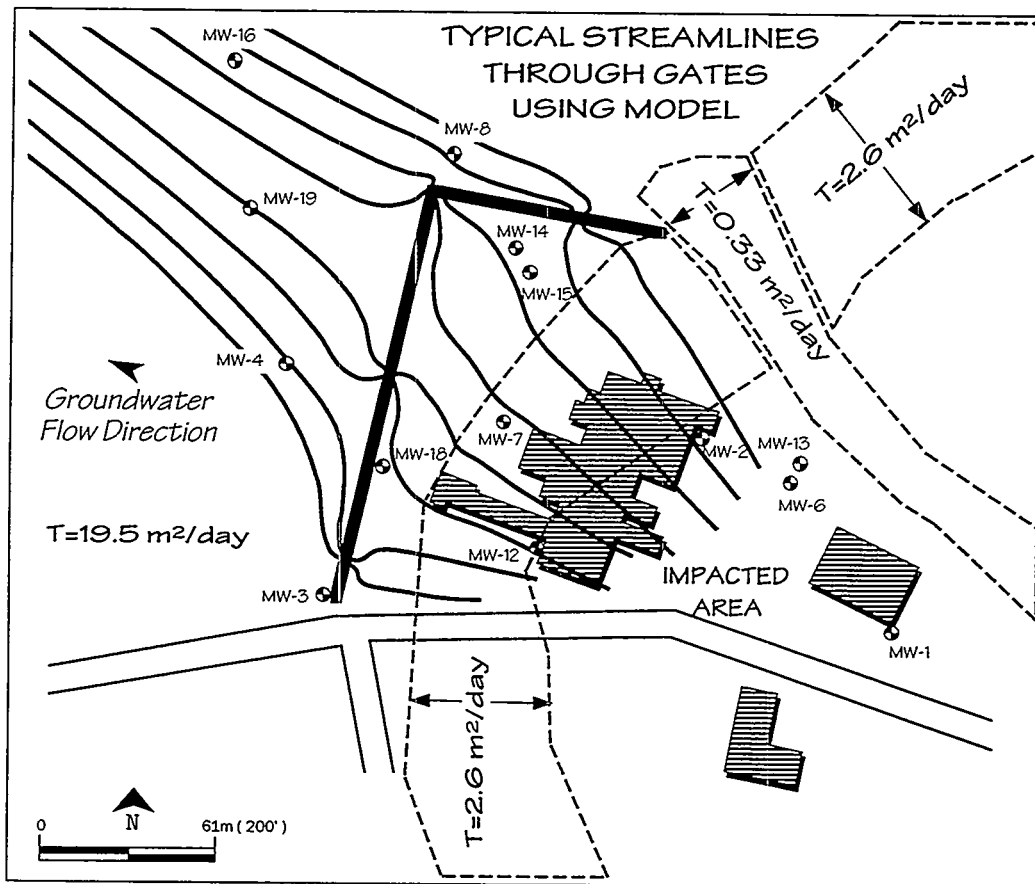
Figure 1 - Streamlines through gates (top drawing) with configuration of funnel-and-gate™ system (bottom drawing).
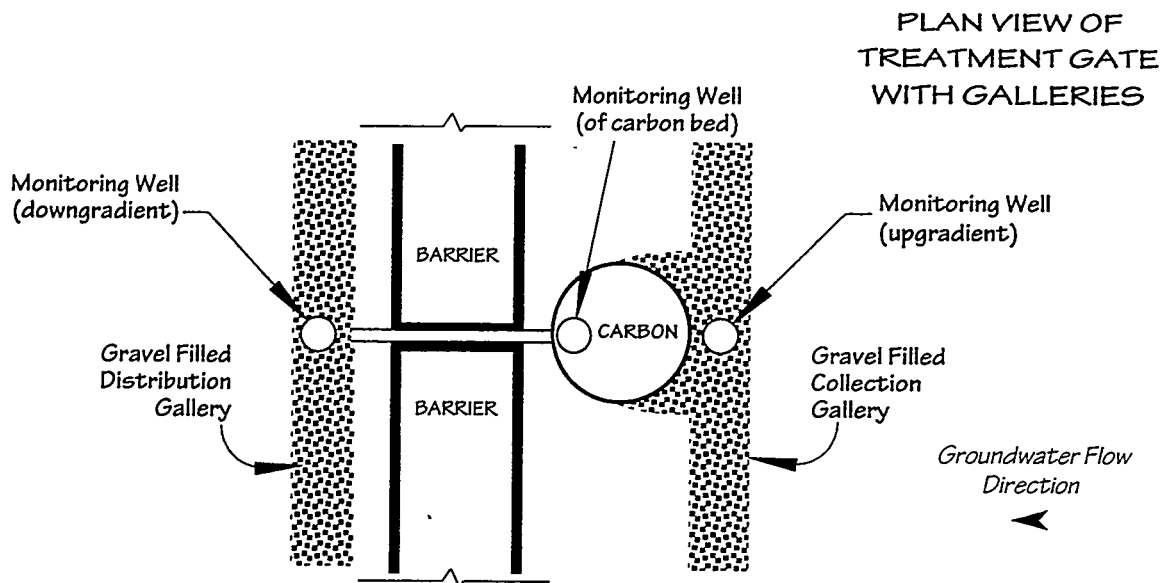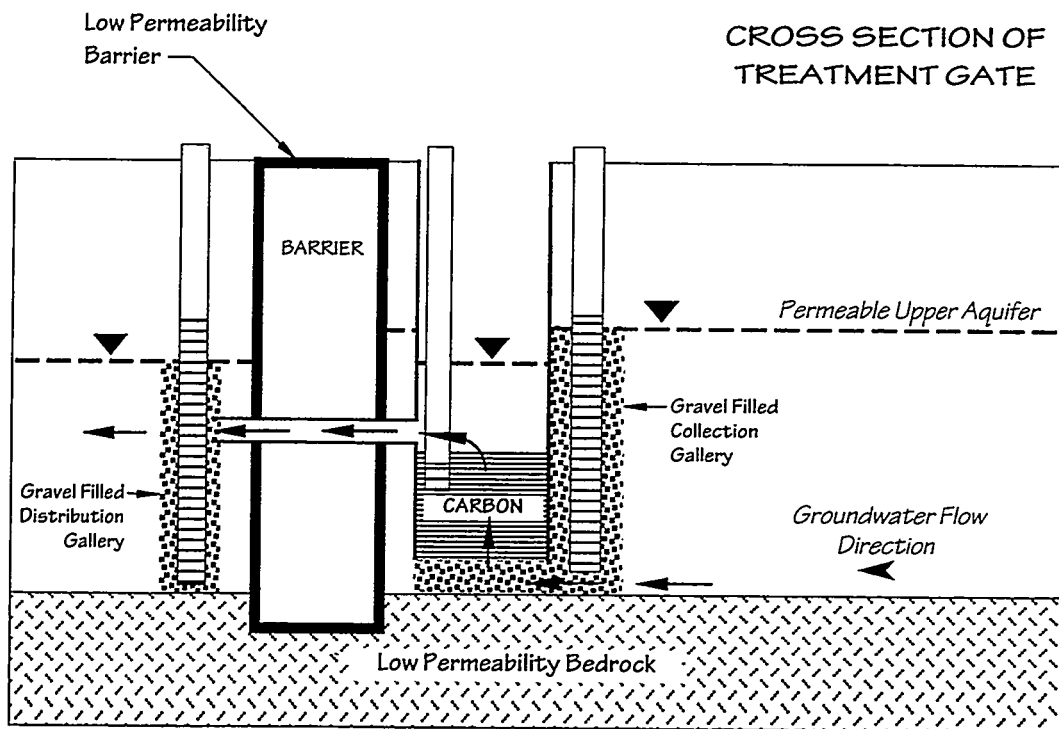
Figure 2 - Cross Section (top drawing) and Plan View (bottom drawing) of Treatment Gate

Impact of Vertical Barriers on Performance of Pump-and-Treat Systems

Kevin Russell* and Alan Rabideau
Department of Civil Engineering
State University of New York at Buffalo
Buffalo, NY 14260
* Now at HydroQual, Inc., Syracuse, NY

Abstract

Although aquifer remediation by pump-and-treat (PAT) is widely practiced, it is generally implemented as an effective means of plume containment, rather than as an efficient means of contaminant mass removal. The use of slurry cutoff walls has been recognized as a means of improving the performance of PAT with respect to hydraulic control. As part of a study on the use of decision analysis in the design of aquifer remediation systems, the economic tradeoffs between capital costs and risk reduction were compared for several alternative PAT strategies. This work included an evaluation of the use of vertical barriers as components of PAT systems, using numerical experiments to examine the impacts of vertical barriers on PAT reliability. The results indicated that the use of vertical barriers in conjunction with PAT can significantly improve the simulated system performance, but that the magnitude of the predicted enhancement and cost-effectiveness of the barrier system are dependent on site characteristics, barrier placement, and modeling assumptions.

Decision analysis for design of pump-and-treat systems

The decision analysis (DA) framework was established from a risk-based philosophy of engineering design. The work of Freeze et al. (1990) pioneered the applicability of DA in a hydrogeologic setting by relating risks to the uncertainties associated with the subsurface. In applying DA to subsurface remediation, alternative designs are compared on the basis of a net present worth objective function

$$\Phi_j = -\sum_{t=0}^{T} \frac{1}{(1+i)^t} \left[B_j(t) - C_j(t) - P_F(t) C_F(t) \right] \tag{1}$$

where Φ_j is the DA objective function value for the jth remedial alternative, t corresponds to a time increment (e.g., year), the total planning horizon is T, B_j are economic benefits, C_j are deterministic costs, P_F is the probability of system failure, C_F is the cost of failure, and i is the market interest rate.

With Eq. 1, costs, risks (probabilistic costs), and benefits are summed over the total planning horizon to obtain the expected net present worth (NPW) of an alternative. In general, benefits are disregarded when considering site remediation, and the negative sign preceding the summation implies that the NPW is expressed in terms of expected overall costs. The alternative with the lowest NPW is therefore chosen as the "best" decision. The deterministic cost term in Eq. 1 represents both capital and operation/maintenance (O&M) costs. If restoration of the site is accomplished during the decision horizon, the time-dependent O&M costs become zero at the point that system operation ceases.

The probability of failure relates to the performance of an alternative under hydrogeological uncertainty. Two definitions of failure have been applied in published studies of PAT: (1) *hydraulic containment failure* occurs when groundwater within the designated boundary of the contaminated region escapes the extraction network, and (2) *concentration compliance failure* occurs when contaminant concentrations exceed regulatory limits at specified compliance points. While these definitions are related, they may lead to different results, as discussed below.

Failure probabilities are predicted by using stochastic simulation models to assess the ability of a remedial alternative to satisfy the design constraints. For remediation design, Monte Carlo methods have been recommended for failure analyses (Freeze et al., 1990), and heterogeneity of the hydraulic conductivity field is usually considered the main source of uncertainty (e.g., Massmann et al., 1992; Houyoux, 1995). Failure analysis for PAT remediation is typically accomplished by generating realizations of heterogeneous hydraulic conductivity fields and simulating the performance of the PAT system for each realization. Simulation model results are then compared with the design constraints and classified as failures or successes.

The most problematic aspect of incorporating failure into the objective function is the treatment of failure costs, which may include fines, taxes, litigation, costs of future remedial activities, loss of public goodwill, and any loss of revenues from the site that result when the remediation system does not meet the design constraints (Freeze et al., 1990). Due to the difficulty in rigorously quantifying these factors, sensitivity analysis is often used to bracket a range of failure costs.

Estimation of cleanup times may be accomplished through a variety of methods. A common approach is to construct a site-specific numerical model of contaminant transport using the measured plume as initial conditions. Although researchers have identified many chemical factors that may limit contaminant removal, such as kinetic desorption and dissolution, these processes are difficult to incorporate into commonly used advective-dispersive simulation models. For the purpose of preliminary design and/or feasibility assessment, consideration of reactions is generally limited to equilibrium sorption and/or first-order decay.

Methodology

As part of the decision analysis study, a series of simulations was performed in an effort to quantify the influence of engineered vertical barriers on the cost, reliability, and effectiveness of PAT systems. The approach is summarized as follows:

- An inactive waste site located near Buffalo, NY, was selected as a case study. The focus of ongoing remedial efforts is a dissolved VOC plume, which, prior to the onset of remediation, had been migrating through the unconfined aquifer under natural gradient conditions toward an adjacent stream. Details regarding the site history are provided elsewhere (Buechi, 1995; Russell, 1996).

- Site-specific two-dimensional models of groundwater flow and contaminant transport were constructed using MODFLOW (McDonald and Harbaugh, 1988), and MT3D (Zheng, 1993).

- Several alternative PAT designs were developed, including various configurations of vertical barriers, based on the initial assumption of homogeneity with respect to hydraulic conductivity. The optimization package MODMAN (Greenwald, 1993) was used to identify cost-effective well configurations. Slurry walls were simulated using the MODFLOW Horizontal Flow Barrier (HFB) package (Hsieh and Freckleton, 1993).

- The potential influence of hydraulic conductivity heterogeneity was considered by generating multiple realizations of heterogeneous hydraulic conductivity (K) distributions using the sequential Gaussian approach (Deutsch and Journal, 1990). The simulated K-fields were used as inputs to MODFLOW and MT3D simulations for each of the proposed designs.

- For the capture zone (CZ) definition of failure, reverse particle-tracking was performed using MODPATH (Pollock, 1989), and the CZ associated with each proposed design was delineated using SURFER® (Golden Software, 1994). Based on a visual comparison of the capture zone with the identified plume boundaries, the designs were designated as a "success" or "failure" for each realization. Failure probabilities were estimated based on a relative frequency of occurrence.

- Failure probabilities based on the concentration compliance definition were generated by performing MT3D simulations of contaminant transport and tracking the predicted concentrations at hypothetical monitoring wells located adjacent to a downgradient stream bordering the site.

- Probability distributions for cleanup time were generated from the MT3D results.

- Capital and operating costs were estimated using the RACER software (Delta, 1996).

- The alternative designs were compared on the basis of expected net present worth (Eq. 1).

Slurry Wall Design

Candidate slurry wall designs were generated using a structured trial-and-error approach. Initially, several PAT configurations were identified by specifying various numbers of wells and applying MODMAN to determine the well placement that minimized the total pumping rate while maintaining inward hydraulic gradients along the plume. After identifying an "optimal" PAT design, promising slurry wall configurations were then added to the base case based on a "performance function" developed to reflect the impact of the wall on plume capture characteristics. Configurations were developed for slurry walls located both upgradient and downgradient of the plume boundary.

A number of requirements were imposed on the candidate slurry wall designs, including a typical value (10^{-7} cm/sec) for the wall hydraulic conductivity and constraints on the east-west locations of the slurry walls due to the proximity of site boundaries. The wall depth was set equal to the estimated aquifer thickness (30 meters), and a typical construction value of one meter was specified for the wall thickness. The design variables for slurry walls were therefore limited to the up/downgradient placement and the horizontal geometry, including the north-south (NS) position, the length of the main NS wall section, the length of angled wall sections extending from the main section, subsequently referred to as wingwalls, and the angle between the wingwall and the main wall section. A site schematic with slurry wall design variables is depicted in Figure 1.

Since the purpose of slurry walls in this project was to improve the performance of PAT systems, the design performance function was based on the extent to which a wall configuration increased reliability. For preliminary design, the width of a PAT system capture zone was modeled under homogeneous conditions, and an average capture zone width was used as a surrogate estimator for reliability. The slurry wall design performance function (φ_S) was defined by:

$$\varphi_S = \frac{\Delta_A + \Delta_B}{2(L+2d)} \tag{2}$$

where Δ_A and Δ_B are the modeled changes in capture zone width versus the base case (i.e., no wall) at representative locations along the plume axis, L is the length of the main wall segment, and d is the length of each wingwall segment, as shown in Figure 1.

Eq. (2) was developed to represent a ratio of "benefits" to "costs", i.e., the increase in CZ width per unit increase in volume of installed wall. Configurations associated with the largest values of the performance function were considered the most "efficient" and were selected for further analysis.

Based on the above approach, approximately 20 slurry wall configurations were selected for further evaluation; detailed results are presented elsewhere (Russell, 1996). In general, slurry walls without wingwalls performed poorly, and in some cases decreased the capture zone width. Although no clear trends in the performance function value with varying downgradient wall configuration were observed, long slurry walls with short wingwalls generally performed better than short walls with long wingwalls. The opposite effect was observed for upgradient wall configurations. Attempts were also made to reoptimize the PAT system with the barriers initially in place, but similar results were obtained.

To illustrate the methodology and key results, a subset of the alternative designs is presented here. A three-well PAT system (28 gpm total) was chosen as the "base case", and the upgradient and downgradient slurry walls with the highest values of the performance function were selected for comparison. Plan views and simulated capture zones for the three designs are shown in Figures 2a-2c. The capture zones shown in these figures represent steady-state conditions under the assumption of homogeneity in hydraulic conductivity.

Stochastic analysis

After the preliminary designs were generated for a homogeneous aquifer, stochastic simulations were performed by considering K as a lognormal correlated random field. Estimates of cost, cleanup time, and failure probability were generated for each design and used to compute the net present worth. Although a range of K statistics was considered in the DA study, the illustrative results presented here are based on a "moderately heterogeneous" aquifer with a log variance of 1.5. A typical K realization is shown in Fig. 3, and a typical "failure", based on the capture zone definition, is shown in Fig. 4.

The estimated costs associated with each design included both capital and operating costs, calculated using current information implemented in the RACER software (Delta Research, 1996), based on the assumption that extracted water would be treated by air stripping prior to off-site disposal. Results from the stochastic simulations were used to construct discretized probability density functions for the predicted cleanup times. In general, the mean cleanup times were on the order of 50 years, with small increases noted for the slurry wall designs due to the increased capture zone and consequent dilution of the extracted water with clean water from outside the plume. Uncertainty in the cost of failure was addressed by considering a range from $1M to $10M.

Results

The results from the NPW calculations were used to assess the influence of various modeling assumptions on the decision-making process (Russell, 1996). Excerpts from these results are shown in Table 1 for the three-well system considered here. Of particular interest to this work is the definition of PAT failure, and the influence of this modeling assumption is broken out in the table. Based on estimated net present worth, the slurry wall designs would be chosen only when the assumed cost of failure was high, approaching $10 M as shown in Table 1. The orientation of the selected wall depends upon which definition of failure is adopted.

Minor variations were noted among the other alternative PAT designs considered, although the fundamental trends were consistent and reflected in the three-well results presented here: *addition of slurry walls to PAT systems improved system reliability (i.e., resulted in lower estimates of failure probability), but at considerable capital expense compared to the operation costs for this relatively low flow-rate system.*

905

Design	Compliance Failure			Capture Zone Failure		
	P_F	Net Present Worth ($M)		P_F	Net Present Worth ($M)	
		$C_F = $1M$	$C_F = $10M$		$C_F = $1M$	$C_F = $10M$
3-well PAT	0.60	1.2*	6.6	0.46	1.2*	5.3
3-well PAT with downgradient wall	0.22	2.0	4.0*	0.35	2.0	5.2
3-well PAT with upgradient wall	0.56	2.8	7.8	0.16	2.6	4.0*

Table 1. Summary of NPW calculations for three-well PAT designs.

Discussion

By definition, optimization strategies for PAT yield capture zones that approximate the plume boundaries as closely as possible. Hence, it is not surprising that simulated failure probabilities are large when heterogeneity is superimposed on a design that was optimized for a homogeneous aquifer. A number of strategies are available for improving the reliability of a PAT design, including overdesign of the pumping system, use of injection wells, and as considered here, vertical barriers. Slurry walls represent a relatively large capital cost and were economical for the site under consideration only when the assumed cost of failure was relatively large. While this result may not be generally applicable, it highlights the value of the decision analysis approach in comparing site-specific alternative design strategies.

An interesting result of this research concerned the sensitivity of the generated failure probabilities to the definition of failure. For the case study, the use of a concentration-based compliance definition favored the installation of a downgradient barrier, as this design most directly protected the downgradient compliance points. Upgradient barriers were favored when the capture zone concept was used to identify failure, as the barrier effectively reduced the influence of the natural hydraulic gradient and produced a wider capture zone. If the methods presented here are to be widely applied, development of a consensus regarding the definition of failure for PAT systems will be required.

References

Buechi, S.P. (1995) Groundwater Modeling at a Contaminated Site. M.E. Project Report, Department of Civil Engineering, State University of New York at Buffalo, Buffalo, NY.

Delta Research Corporation. (1996) Remedial Action Cost Engineering and Requirements System: RACER User Manual. Niceville, FL.

Deutsch, C.V. and Journel, A.G. (1992) GSLIB Geostatistical Software Library and User's Guide. Oxford University Press, Inc., New York, NY.

Freeze, R.A., Massmann, J., Smith, L., Sperling, T., and James, B. (1990) Hydrogeological Decision Analysis: 1. A Framework. Ground Water, 28(5), 739-766.

Golden Software, Inc. (1995) SURFER® for Windows: Version 6 User's Guide. Golden, CO.

Greenwald, R.M. (1993) Documentation and User's Guide: MODMAN An Optimization Module for MODFLOW Version 3.0. GeoTrans Inc., Sterling, VA.

Hsieh, P.A. and Freckleton, J.R. (1993) Documentation of a Computer Program to Simulate Horizontal-Flow Barriers Using the U.S. Geological Survey's Modular Three-Dimensional Finite-Difference Ground-Water Flow Model. *USGS Open File Report 92-477*, Sacramento, CA.

Houyoux, M.R. (1995) An Evaluation of Decision Making for Aquifer Restoration. M.S. Thesis, University of North Carolina Department of Environmental Sciences and Engineering, School of Public Health, Chapel Hill, NC.

Massmann, J., Freeze, R.A., Smith, L., Sperling, T. and James, B. (1991) Hydrogeological Decision Analysis: 2. Applications to Ground-Water Contamination. *Ground Water, 29*(4), 536-548.

McDonald, M.G. and Harbaugh, A.W. (1988) A Modular Three Dimensional Finite-Difference Ground-Water Flow Model. *U.S. Geological Survey Techniques of Water Resources Investigations, Book 6*, Chapter A1.

Pollock, D.W. (1989) Documentation of Computer Programs to Compute and Display Pathlines Using Results from the U.S. Geological Survey Modular Three-Dimensional Finite-Difference Ground-Water Flow Model. *USGS Open File Report 89-381*, Reston, VA.

Rumer, R.R. and Ryan, M.E., (eds.). (1995) Barrier Containment Technologies for Environmental Remediation Applications. J. Wiley & Sons, Inc.

Russell, K.T. (1996) "The Use of Decision Analysis for Groundwater Remediation Design," M.S. Thesis, Department of Civil Engineering, State University of New York at Buffalo, Buffalo, NY.

Zheng, C. (1990) MT3D. A Modular Three-Dimensional Transport Model for Simulation of Advection, Dispersion, and Chemical Reactions of Contaminants in Groundwater Systems. S.S. Papadopulos & Associated, Rockville, MD.
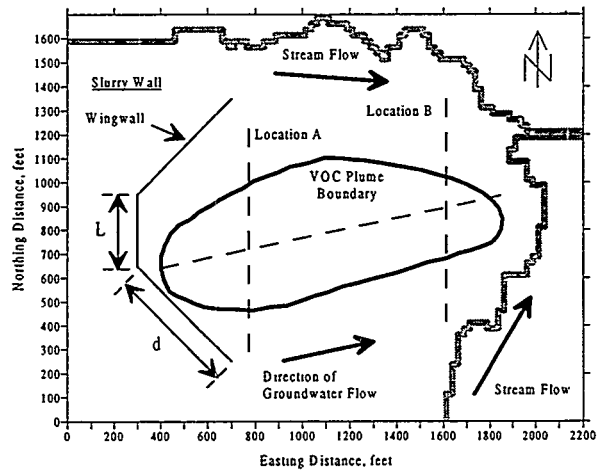
Figure 1. Slurry wall design variables and site schematic.

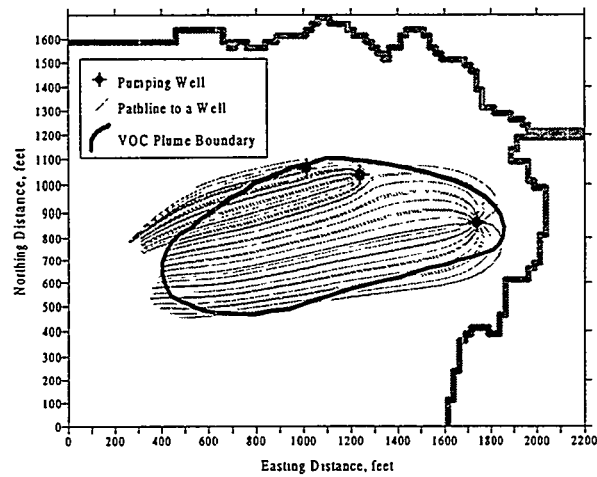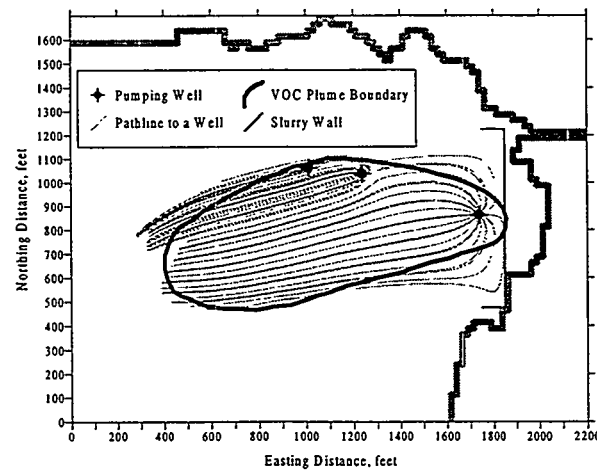**Figure 2a. Capture zone for 3-well PAT with no slurry wall.**

Figure 2b. Capture zone for 3-well PAT with a downgradient slurry wall.

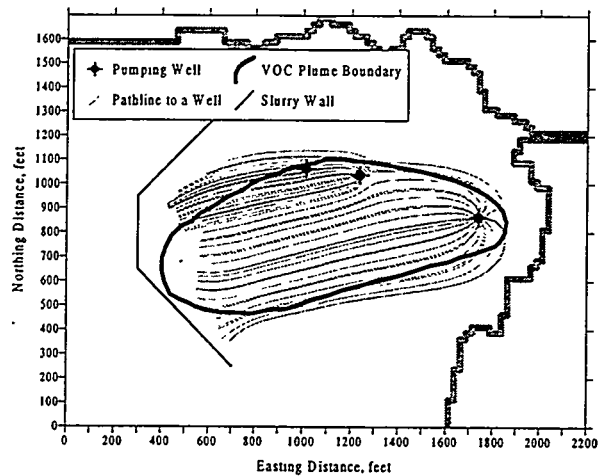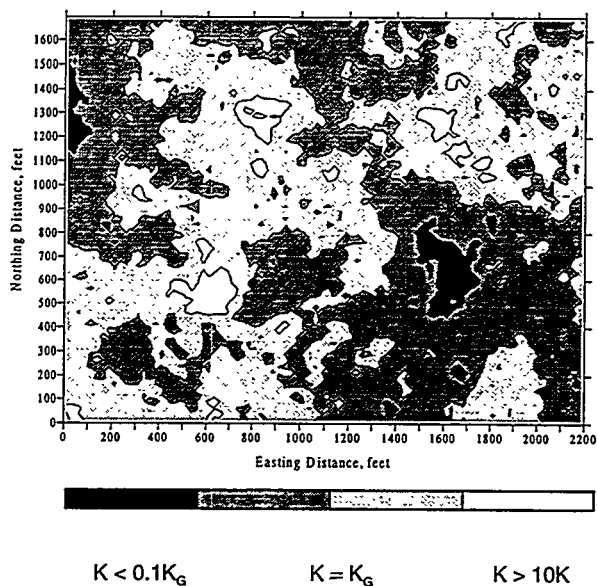**Figure 2c. Capture zone for 3-well PAT with an upgradient slurry wall.**

$K < 0.1K_G$ $K = K_G$ $K > 10K$

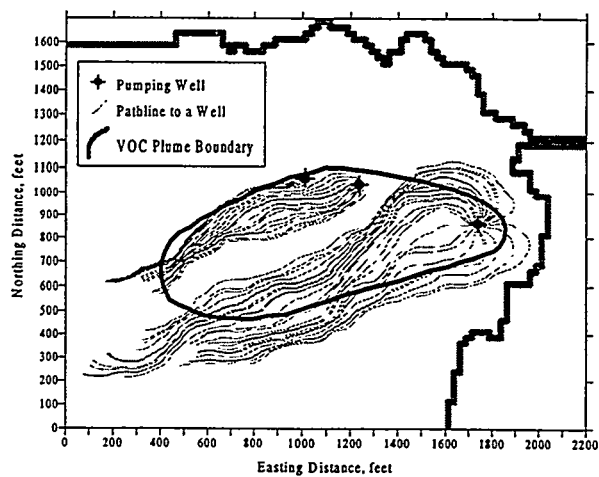**Figure 3. Typical hydraulic conductivity realization (K_G = geometric mean).**

Figure 4. Typical capture zone failure.

USE OF COMPUTER MODELING TO AID IN HYDRAULIC BARRIER DESIGN

Warren T. Dean, Jeffrey A. Johnson, William J. Seaton[1],
Brandon J. Fagan, James M. Fenstermacher[2]

ABSTRACT

Releases of No. 6 and No. 4 fuel oil were discovered at a private boarding school. The releases impact a nearby pond with non-aqueous phase liquid hydrocarbon (NAPL), and threaten to impact an adjacent wetland. Prior to implementation of a permanent remedial solution, such as surfactant treatment and bioremediation, immediate containment of the NAPL was proposed via a barrier-gate containment system. The proposed barrier-gate containment system consisted of a high-density polyethylene barrier, horizontal wells, three flow-through gates, and downgradient infiltration galleries.

Computer modeling of groundwater and NAPL flow was conducted utilizing a finite element multiphase model to evaluate the impacts to local hydrogeology associated with the barrier. These impacts included upgradient groundwater mounding and restriction of groundwater flux to the wetland. Model simulations aided in the identification of improvements to the initial barrier design and guided subsequent design modifications. Results of the simulations indicate the usefulness of computer modeling in containment system design.

INTRODUCTION

A release of No. 6 fuel oil was discovered in 1972 at a private boarding school, followed by a release of No. 4 fuel oil detected in 1984. The releases originated from two underground storage tanks (USTs) at the same location, and resulted in the seepage of non-aqueous phase liquid hydrocarbon (NAPL) from the bank of a small pond located on the school property. The NAPL plume also threatens to impact a wetland adjacent to the pond. The pond and wetland are recognized for their uniqueness and aesthetic quality in an urban/suburban environment. The pond and wetland are approximately 85 meters from the original UST source area, with approximately 6 meters of vertical topographic relief between the source area and the pond. Approximately 1.5 to 2 meters of groundwater head difference occurs over the same distance.

A trench was constructed in 1985 to intercept NAPL. Past reports indicated that up to a meter of NAPL existed in some on-site wells, and by 1990 the school responded with the installation of two groundwater depression and hydrocarbon recovery wells. Several operational difficulties limited the success of this remedial effort. Specifically, the rate of migration and recovery of the heavy fuel oil was very low, and the viscous nature of the product fouled air-operated recovery pumps. Additionally, the capture zone of the existing recovery system was limited by aquifer yield and practical drawdown limits required to minimize vertical NAPL smearing.

To overcome these difficulties, the school's environmental remediation contractor redesigned the existing treatment system and implemented containment of NAPL impacting the surface waters (CHES, Inc., 1994). Based on investigative efforts conducted to supplement understanding of the site, the contractor recommended the implementation of a barrier-gate containment system to provide long-term control of NAPL migration and to support a subsequent permanent remedial

---

[1] Environmental Systems and Technologies, Inc., 2608 Sheffield Drive, Blacksburg, VA 24060, (540) 552-0685, admin@www.esnt.com

[2] Clean Harbors Environmental Services, Inc., 1501 Washington Avenue, Braintree, MA 02184, (617) 849-1800

solution to the release (CHES, Inc., 1996). An appropriate containment technology was required to maintain existing hydraulic flow patterns while controlling migration of NAPL potentially mobilized by surfactant effects of biological degradation and seasonal hydraulic loading along the barrier.

A barrier-gate containment system was subsequently designed consisting of a high-density polyethylene barrier for NAPL containment, horizontal well sections upgradient of the barrier for groundwater and hydrocarbon collection, and three gate relief points for hydraulic control (Figure 1). Water collected in the horizontal well sections would pass through the barrier-gates and recharge the aquifer through high conductivity infiltration galleries (Figure 2).

GROUNDWATER AND NAPL MODELING

Initially, the approximate size and location of the proposed barrier were evaluated with a steady-state groundwater flow model using site characterization and field monitoring data. The preliminary modeling results revealed the need for greater understanding of site groundwater hydrology prior to implementation of the barrier-gate containment system.

Of consideration in the barrier design was the containment of NAPL and the prevention of significant alteration to existing groundwater flow patterns that could potentially introduce hydrocarbon into areas not previously impacted. Also of concern was minimizing disruption of groundwater flux to the wetland. An additional consideration was the potential for groundwater mounding to force NAPL to the ground surface. To address these concerns, additional groundwater and NAPL flow modeling were undertaken. The objectives of the modeling were to 1) understand and minimize the potential impacts of the containment system on the natural groundwater flow regime and 2) evaluate the containment and migration of the NAPL with the barrier in place.

Groundwater Flow Model Calibration

The modeling effort utilized the computer code ARMOS (AReal Multiphase Organic Simulator) (ES&T, 1996). ARMOS is a finite element numerical model capable of simulating groundwater and NAPL flow and recovery in an unconfined aquifer. Unlike other vertical equilibrium models that assume a sharp oil-water interface in the soil, ARMOS describes soil capillary phenomena that give full consideration to the retention of residual hydrocarbon in the unsaturated and saturated zones.

Based on field data, the site was conceptualized as an unconfined sand and gravel aquifer with a constant bottom elevation at vertical datum. The model consisted of 3,800 nodes with variable grid spacing ranging from approximately 10 meters in the upgradient portion of the site to 0.6 meters in the vicinity of the proposed barrier.

Prior to simulating the potential effects of the barrier-gate containment system, the groundwater flow model was calibrated to observed data. Because of the sensitivity to potential groundwater mounding, the groundwater flow model was calibrated to the spring seasonal high water table. The model calibration criterion was defined as 10 percent of the observed groundwater head difference over the site. In the spring, the groundwater elevations range from approximately 9.2 meters above vertical datum in the eastern portion of the site to approximately 7.4 meters near the pond, for a head difference of 1.8 meters. Consequently, the calibration criterion was defined as a maximum of 0.18 meters of difference between the observed and predicted heads.
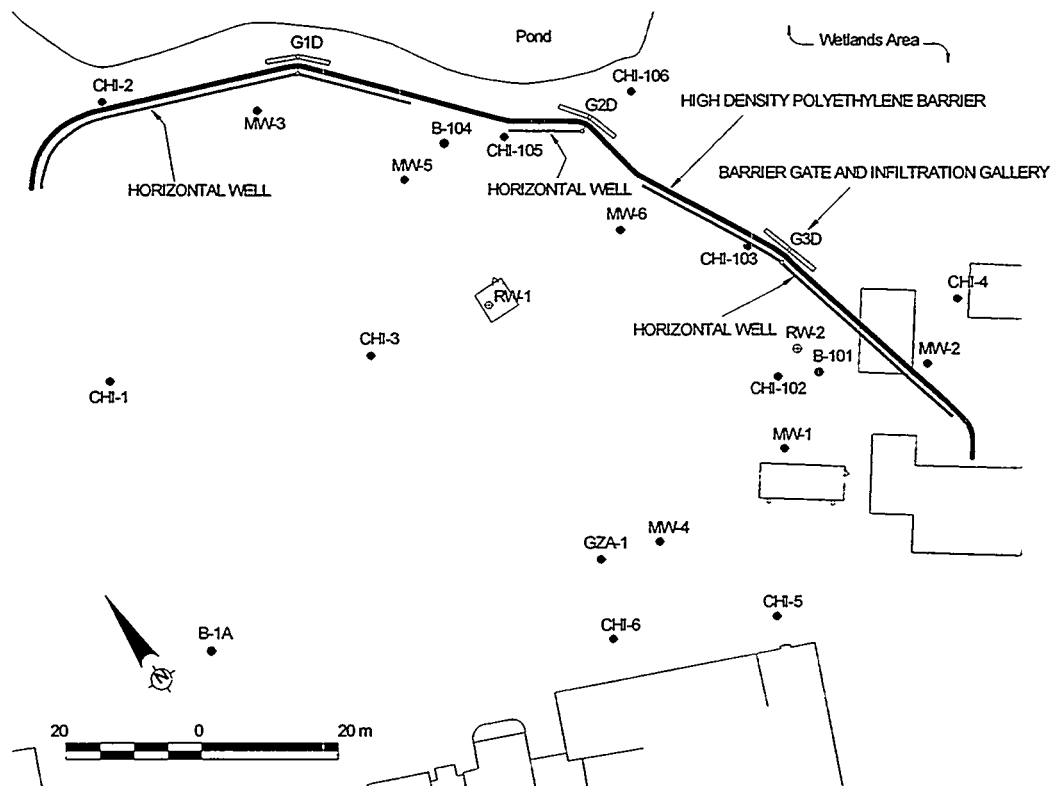
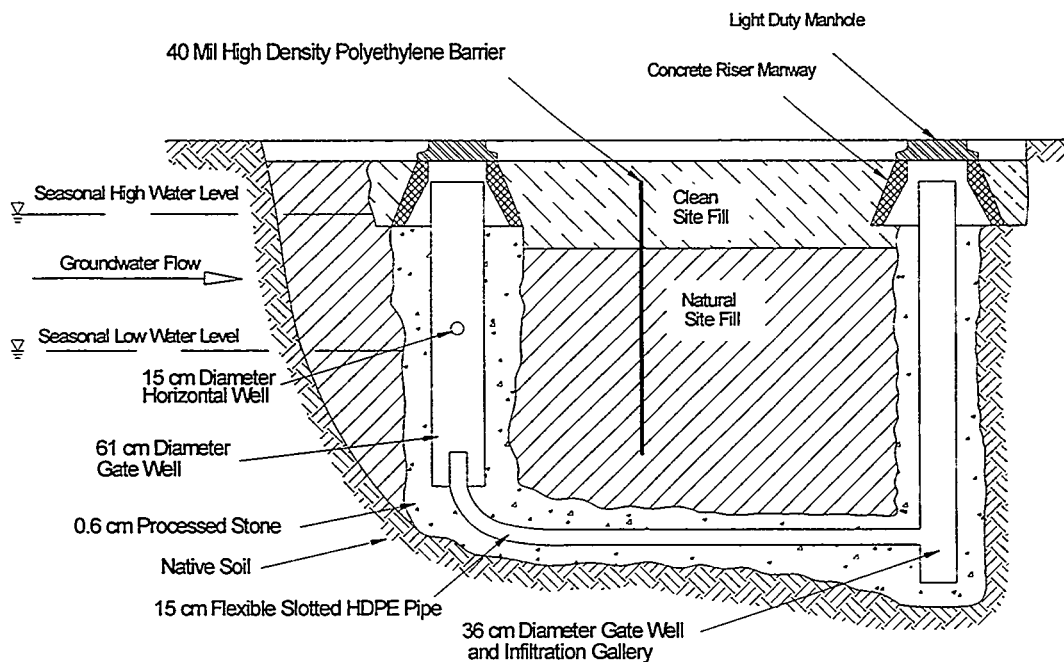Figure 1. Proposed barrier-gate containment system.

Figure 2. Schematic cross-section of flow-through barrier-gates.

The initial conditions were defined as the Spring 1994 water table elevations at the monitoring wells. The pond and boundary conditions were defined as constant heads. The model was calibrated by adjusting aquifer soil property zones (Figure 3) until the difference between the predicted heads and the Spring 1994 observed water table did not exceed the calibration criterion (Figure 4). The base hydraulic conductivity value of 1.5 m/day was based on aquifer withdrawal test data.

Figure 3. Aquifer property zones used in the model.

Hydraulic conductivity values ranged from 1.5 m/day to 42.7 m/day (Table 1), and were within the range of published values for a sand and gravel aquifer (Domenico and Schwartz, 1990). Zone 4 corresponds to a subsurface gravel drain.
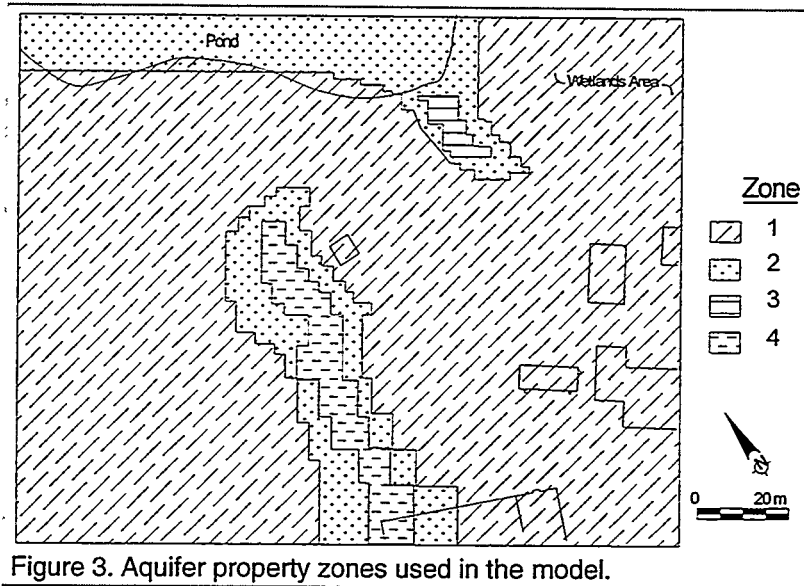
Table 1. Aquifer parameters utilized in the model.

Parameter	Zone			
	1	2	3	4
Hydraulic Conductivity	1.5 m/day	15.2 m/day	19.8 m/day	42.7 m/day
Porosity	0.30	0.35	0.35	0.40
Field Capacity	0.20	0.20	0.15	0.15
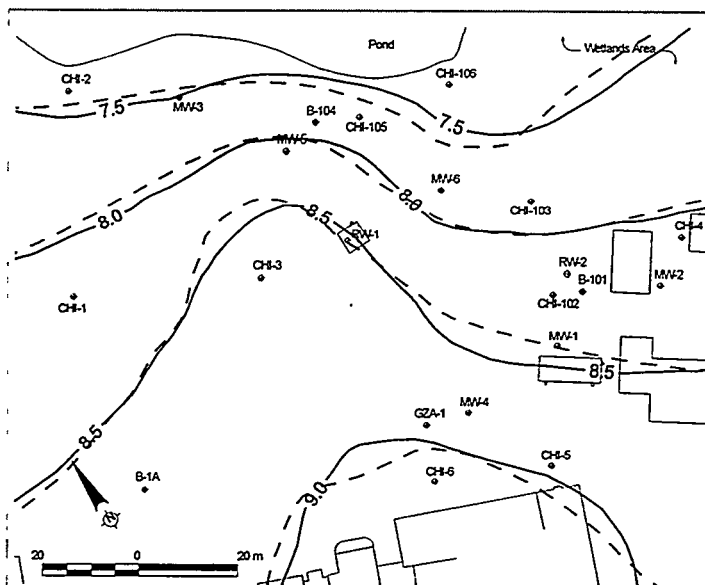
Figure 4. Comparison of observed (solid contours) to predicted (dashed contours) water table elevations. Elevations are in meters above vertical datum.

Model Verification

The model was verified utilizing aquifer withdrawal test data. The aquifer withdrawal test consisted of pumping 10.0 L/min from RW-2 for 7 hours and observing changes in head at monitoring wells CHI-102, MW-1, CHI-103, and MW-2. Observed drawdowns ranged from 0.10 m in CHI-2 and MW-1 to 0.04 m in MW-2. Because all of the drawdowns were smaller than the calibration criterion, the model was not verified against the observed drawdowns. Instead, the model was verified by specifying the observed drawdown in the recovery well and duration of the withdrawal, and predicting the corresponding pumping rate and cumulative volume of water recovered. The model verification yielded reasonable results considering the short

duration of the aquifer withdrawal test (Table 2).

Table 2. Results of Model Verification.

	Pumping Rate	Cumulative Recovery
Observed	10.0 (L/min)	4,353 (l)
Predicted	11.9 (L/min)	5,151 (l)
Deviation	19%	18%

Simulations with Barrier in Place

After model calibration, simulations were conducted to evaluate the effect of the proposed containment barrier on the natural groundwater hydraulics without flow through the horizontal well and barrier-gate relief points. The barrier was simulated as a narrow zone of extremely low hydraulic conductivity. Model results indicated that without the gate relief points, groundwater mounding of 0.6 meters above the calibrated water table was likely to occur, with potential loss of NAPL around the northern end of the barrier.

Additional simulations were conducted to evaluate the flux of water that would be required to pass through the horizontal well and gate system to prevent significant changes in the water table. The criterion for deviation from the calibrated water table elevation was defined as ten percent of the regional water table gradient, 0.18 meters. To simulate the action of water passing through the horizontal well and gate system, pumping nodes were placed along the horizontal well with the simultaneous injection of equal volumes of water along the infiltration galleries. As seen in Figure 1, the northernmost horizontal well section supplied gate G1D, a short section in the central portion of the barrier supplied gate G2D, and the southernmost section supplied gate G3D.

Initial simulations indicated that a flux of 388 liters per day (L/day) through the southernmost well section to gate G3D was sufficient to prevent a head difference greater than 0.09 meters in the vicinity of the southern end of the barrier. However, while simulating the flow of 494 L/day and 353 L/day of water through the northern and central barrier-gates, respectively, a maximum difference of greater than 0.54 meters still occurred near gate G1D (Figure 5). Increasing the flux by an order of magnitude along the northern well section resulted in a slightly smaller areal extent of mounding, but the height of the mound remained unacceptable at 0.54 meters.
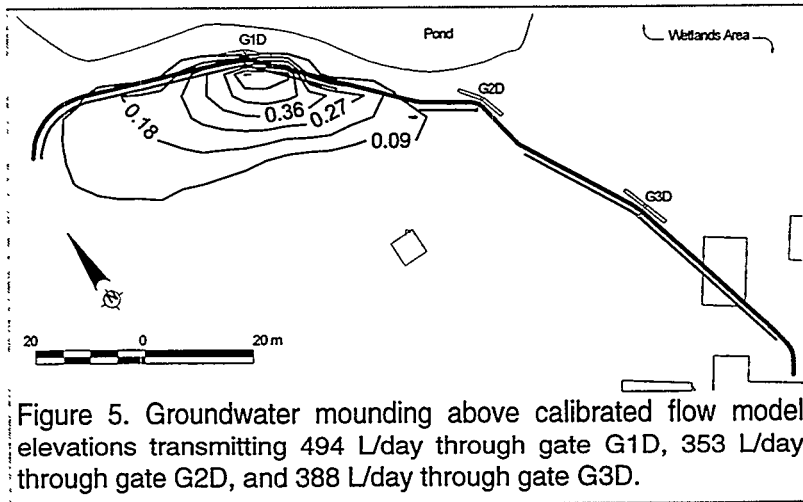
Figure 5. Groundwater mounding above calibrated flow model elevations transmitting 494 L/day through gate G1D, 353 L/day through gate G2D, and 388 L/day through gate G3D.

MODIFICATIONS TO CONTAINMENT SYSTEM DESIGN

The results of additional flow simulations raised concerns about the practicality of accommodating a sufficient flux of water through the northern and central barrier gates to prevent significant mounding. Furthermore, the flow modeling indicated that the infiltration gallery at G1D was inadequate for the required flux. The model results suggested that the volume of water would need to be collected over a greater length of horizontal well section, and hence would require greater infiltration area downgradient of the barrier. In addition, the horizontal well section immediately north of G3D transmitted water away from the gate.

Consequently, the alignment and length of the barrier were slightly modified, a barrier-gate was added between G1D and G2D, the infiltration galleries were lengthened, and the horizontal well was made continuous from the northern end of the barrier to approximately 15 meters south of MW-6 (Figure 6). Mounding smaller than the deviation criterion was achieved with a simulation that transferred 26,000 L/day through G1D and G2D, 8,500 L/day through G3D, and 350 L/day through G4D. The modified design allowed the collection of water over a greater length of horizontal well, and infiltration through an additional gate relief point and longer infiltration galleries.
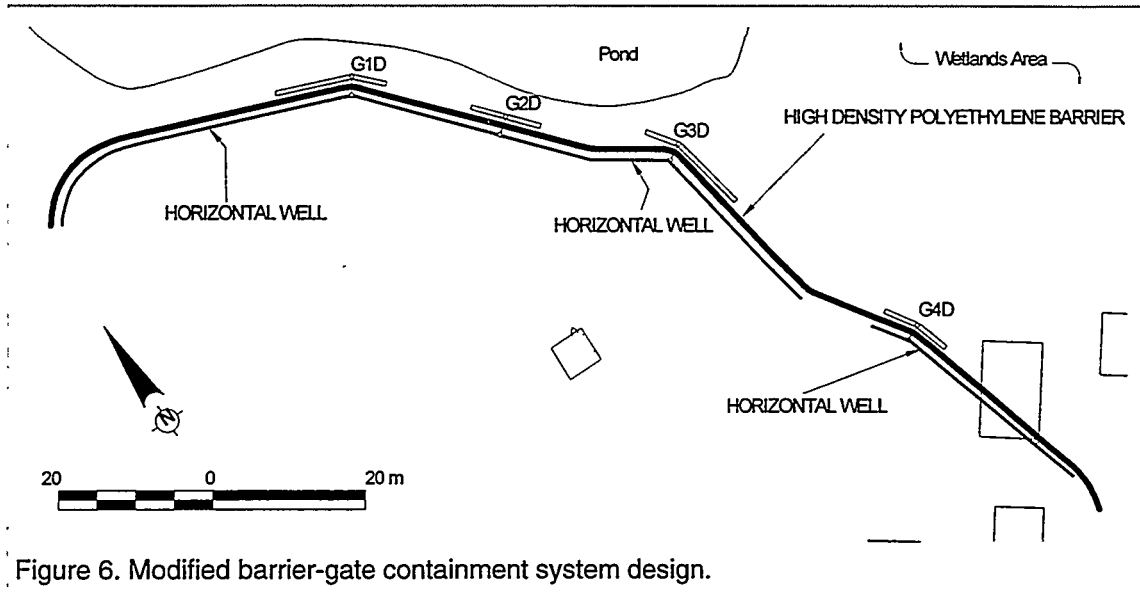

Figure 6. Modified barrier-gate containment system design.

NAPL FLOW MODELING

To evaluate the potential effectiveness of the barrier design to contain the existing NAPL plume, simulations of NAPL flow were conducted using the barrier-gate containment system model. A shallow, high conductivity French drain was simulated trending north-south from the leading edge of the hydrocarbon plume to the horizontal well near gate G1D. The French drain was modeled to evaluate its effectiveness in enhancing the flow of NAPL to the containment system.

The composition of the hydrocarbon was initially modeled as one-third No. 6 fuel oil and two-thirds No. 4 fuel oil based on the release history. The hydrocarbon fluid parameters required for the model were assumed as a weighted average of literature values for fresh No. 6 and No. 4 fuel oils (ES&T, 1996). Specifically, the density was assumed as 0.92 g/cm³ and the oil-water viscosity ratio as 2,148:1. The initial NAPL distribution was defined from representative values of monitoring well gauging events (Figure 7). Under these conditions, the volume of oil was calculated to be 70 m³.

After a simulation time of 10 years, the model results indicated that the area of greatest hydrocarbon thickness migrated eastward toward the barrier, and the French drain enhanced the migration of the leading edge of the plume toward the barrier (Figure 8).
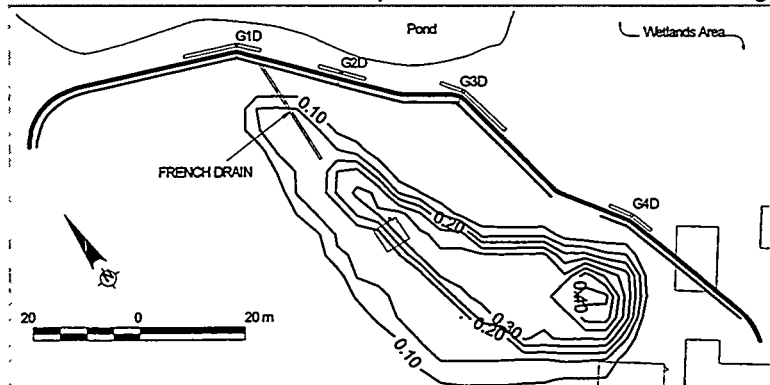

Figure 7. Initial NAPL distribution. Thicknesses are in meters.

The predicted mobile fraction of NAPL decreased in thickness as hydrocarbon mass was transferred to the residual phase by transport through the soil. The model results predicted that the NAPL plume will be adequately contained by the barrier-gate system.
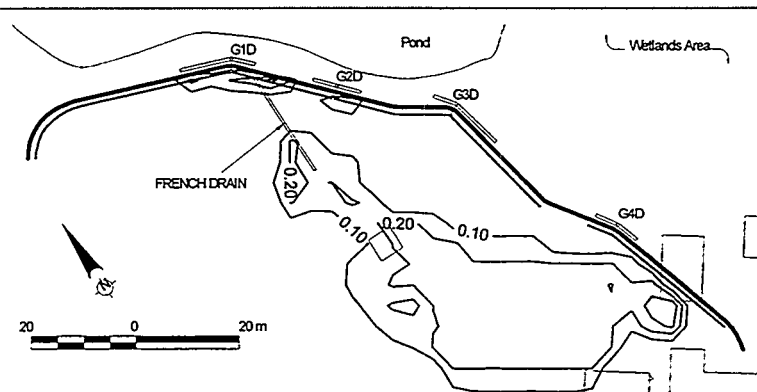

Figure 8. NAPL distribution after a simulation time of 10 years. Thicknesses are in meters.

Additional hydrocarbon flow simulations were conducted by varying the hydrocarbon composition from pure No. 4 fuel oil to pure No. 6 fuel oil to evaluate the potential mobility differences that could impact the long-term treatment of the site. This assessment was utilized to evaluate the effects of changes in viscosity and variations in residual fractions that may remain in the soil during a potential biotreatment program. The results indicated that regardless of hydrocarbon composition the model predicted that the NAPL plume will be contained by the barrier-gate system.

BARRIER IMPLEMENTATION

The modified barrier-gate containment system was successfully field implemented in November 1996. Groundwater gauging has been conducted monthly since that time and will continue at that frequency until November 1997. The available groundwater gauging data indicate no discernible disruption in groundwater hydrology as a result of the barrier.

CONCLUSION

Groundwater flow modeling was used in an iterative fashion to evaluate a conceptual design, provide a basis for modifications, and assist in developing the containment system design. The result is a potential increase in the effectiveness of the proposed system. In addition, the effectiveness of the design for the containment of the existing hydrocarbon plume was evaluated through the model. Future gauging data will be used to evaluate the model results and effectiveness of the barrier design. The utility of computer modeling as a tool to aid in containment system design is illustrated through this study.

REFERENCES

CHES, Inc. (1994) Subsurface Site Evaluation Summary Report, CHES File No. EN-1157, Clean Harbors Environmental Services, Inc., Braintree, MA.

CHES, Inc. (1996) Supplemental Report to the Phase III-Remedial Action Plan, CHES File No. EN-1157, Clean Harbors Environmental Services, Inc., Braintree, MA.

Domenico, P.A. and Schwartz, F.W. (1990) Physical and Chemical Hydrogeology, p. 65, John Wiley and Sons, New York, NY.

ES&T, Inc. (1996) ARMOS, Areal Multiphase Organic Simulator for Free Phase Hydrocarbon Migration and Recovery, Technical and User Guide, Environmental Systems & Technologies, Inc., Blacksburg, VA.

The Design Of In-Situ Reactive Wall Systems - A Combined Hydraulical-Geochemical-Economical Simulation Study

G. Teutsch; J. Tolksdorff
Applied Geology, University of Tübingen, Germany

H. Schad
I.M.E.S. GmbH, Wangen, Germany

Abstract

The paper presents a coupled hydraulical-geochemical-economical simulation model for the design of in-situ reactive wall systems. More specific, the model is used for cost-optimization and sensitivity analysis of a funnel-and-gate system with an in-situ sorption reactor. The groundwater flow and advective transport are simulated under steady-state conditions using a finite-difference numerical model. This model is coupled to an analytical solution describing the sorption kinetics of hydrophobic organic compounds within the reactor (gate). The third part of the model system is an economical model which calculates (a) the investment costs for the funnel-and-gate construction and (b) the operation cost based on the number of reactor refills, which depends on the breakthrough time for a given contaminant and the anticipated total operation time. For practical applications a simplified approximation of the cost-function is derived and tested.

Introduction

In-situ reactive walls either in the form of continuous permeable walls or funnel-and-gate systems are discussed as an alternative technology for the clean-up of soil and groundwater contaminations. The technology seems most favorable where the source of contamination cannot be (entirely) removed due to logistical, technical or economical reasons and the pump-and-treat approach is inefficient, due to the heterogeneity of the aquifer and the chemical properties of the contaminant.

In order to cost-optimize the design of an in-situ reactive wall system, the hydrogeological conditions at a specific site, the hydrogeochemical processes occurring within the permeable wall or the gate-reactor and the construction design have to be considered all together. A general analysis of the sensitivity of the different processes/factors involved requires the use of mathematical simulation tools. Due to the non-linearity of the nonuniform flow and reactive transport parts of the system, a modular numerical/analytical model was developed to adequately simulate the entire system behavior and to calculate the respective investment and operation costs.

The Model Concept

· The hydraulical-hydrochemical-economical model system was partly aggregated out of generally available public-domain software modules and partly programmed for the specific purposes of this study.

The Hydraulical Model

In this study the block-centered finite-difference public-domain code MODFLOW (McDonald & Harbaugh, 1984) was used to simulate the *groundwater flow* in two (horizontal) dimensions, assuming isotropic and homogeneous aquifer conditions. More complex flow conditions, including three-dimensional flow, heterogeneous parameter distributions etc., could equally be represented if required. The *advective transport* was simulated using the public-domain code MODPATH (Pollock, 1989), which calculates the advective paths based on a (linearised) particle tracking approach.

Figure 1 shows the model setup with the funnel-and-gate system and the respective discretisation in the center of the model domain. The flow is controlled through the constant head boundaries at the top and bottom of the model domain. The domain size was chosen large enough not to affect the flow field in the vicinity of the funnel-and-gate system. A special routine was developed and implemented to automatically calculate the width of the funnel-and-gate capture zone, given a set of hydraulic parameters and the angle between the mean groundwater flow direction and the funnel orientation (see Fig. 1).
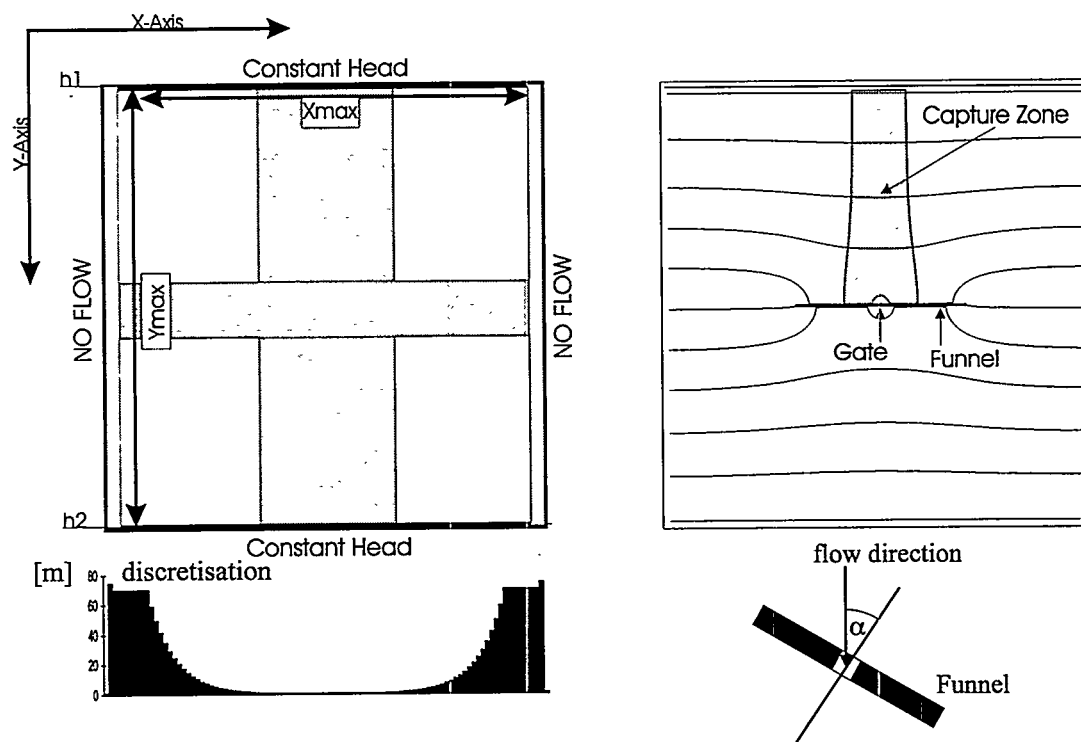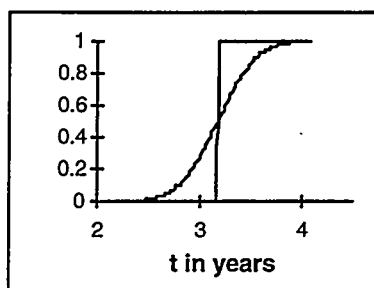
Fig. 1: Model setup and resulting flow field

The Hydrochemical Model

In this study, the groundwater contamination is assumed to be caused by hydrophobic organic compounds which may be removed within an in-situ sorption reactor/filter. Hydrophobic contaminants like the group of polycyclic organic hydrocarbons (PAHs) are most commonly found at former gasworks sites and wood impragnation plants. Individual PAH-compounds are characterized by (a) their octanol-water partitioning coefficient K_{ow}, which describes the hydrophobicity and (b) the distribution coefficient K_d between the mobile (solute) and the immobile (solid) phase, which describes the sorptivity. It should be noted that the K_{ow}- and K_d-values may range over several orders of magnitudes within the PAH-group. In practice, the maximum allowable concentration C_m for one component out of the entire cocktail controls the design of the sorption reactor/filter.

Based on the work published by Grathwohl (1997 - this volume) and others the sorption kinetics of hydrophobic organic compounds is described as an unsteady-state intra-particle diffusion process, which can be parametrized using the apparent diffusion coefficient D_a . D_a can be measured in laboratory experiments for individual component-sorbent combinations. An analytical solution which describes the intra-particle process was derived by Rosen (1952).To obtain the analytical solution, the follo ving assumptions had to be made: (a) the flow is one-dimensional, (b) the sorption isotherm is linear, (c) the sorbent is formed of ideal spheres with a constant radius and (d) the surface and pore diffusion processes can be treated together with one apparent diffusion parameter D_a. Numerous sorption experiments have demonstrated the applicability of this approach for a large number of natural geological materials (sorbents) as well as for activated carbon (Grathwohl, 1997 - this volume).

Figure 2 shows the concentration breakthrough profile resulting from equilibrium and also for non-equilibrium sorption together with the analytical solution developed by Rosen (1952). It is seen that in the case of non-equilibrium sorption (S-shaped curve) the earlier breakthrough of the contaminant may require a more frequent exchange of the sorbent material.

918

Fig. 2: Equilibrium and non-equilibrium (S-shaped) sorption breakthrough curves based on the analytical solution by Rosen (1952)

$$C_w(x,t) = \frac{C_0}{2} \cdot erfc\left\{\left[1 + \frac{n}{(1-n)\cdot \rho_s \cdot K_d} \cdot \left(1 - \frac{v_a \cdot t}{x}\right)\right]\right.$$
$$\left. \cdot \left[2 \cdot \left(\frac{R^2 \cdot n \cdot v_a}{15 \cdot D_a \cdot \rho_s \cdot K_d \cdot (1-n)\cdot x}\right)^{1/2}\right]^{-1}\right\}$$

The Economical Model

The economical model comprises the investment and the operational costs for the funnel-and-gate system. Functional relationships were developed for various construction techniques. These were normalized per unit area or volume in order to provide a flexible calculation basis. Within these relationships the technical limitations (e.g. max. depth) of the individual construction techniques were considered.

A summary of the *investment cost* data is presented in Table 1. The total investment costs are calculated by simply multiplying the per-unit values with the dimensional data of the funnel-and-gate system and adding the one-time cost for site installation. In Table 2 the cost per unit volume for the sorbent material (e.g. activated carbon F-100) is presented together with the technical specifications of the sorbent. The data in Table 2 is used for the calculation of the *operational costs*, which depend on the number of sorbent refills required during the anticipated operation time of the funnel-and-gate system. The operational costs are discounted for the net interest rates (without inflation) and the net price increase rates (without inflation) during the operation time of the system (LAWA, 1994).

Construction technique	maximum excavation depth [m]	subsurface material	site installation [DM]	unit cost
I. Funnel				
clamshell	50 m	unconsolidated rock	150000 DM	170 DM/m²
hydraulic trench cutter	100 m	hard rock	150000 DM	200 DM/m²
vibration beam	20 m	unconsolidated rock	100000 DM	100 DM/m²
vibration beam with high pressure erosion	30 m	unconsolidated rock	100000 DM	110 DM/m²
backhoe with extended boom	10 m	unconsolidated rock and weathered hard rock	20000 DM	100 DM/m²
bored pile wall	30 m	unconsolidated rock and weathered hard rock	30000 DM	200 DM/m²
II. Gate				
gate construction (reinforced concrete)	50 m	unconsolidated rock and weathered hard rock	--	2000 DM/m³

Tab. 1: Funnel-and-gate per-unit construction costs

activated carbon F-100	1000 [DM/m³]
flow effective porosity n	0,5 [-]
particle density in water ρ_s	1,2 [g/cm³]
diameter of carbon particles (=2 R)	$1,6 \cdot 10^{-3}$ [m]

Tab. 2: Sorbent (F-100) per-unit costs and material properties

Simulation Results

The results of the *numerical flow* and the *advective transport simulation* are summarized in Figure 3. It shows the width of the capture zone (treatment zone), which has to be chosen according to the width of the contaminant source zone, as a function of the funnel-length as well as the gate-length. As expected, various funnel- to gate-length ratios can be chosen to obtain the same width of the capture zone. The diagram shows the results for two sets of hydraulic conductivity ratios. The continuos line shows the results for a hydraulic conductivity ratio $K_{Gate}/K_{Aquifer} = 1$, and the dashed line shows the results for a conductivity ratio $K_{Gate}/K_{Aquifer} = 10$. It should be noted that the results for both conductivity ratios are almost identical. This result seems to contradict the simulation results presented by Starr and Cherry (1994), who came to the conclusion that the gate hydraulic conductivity should be in general about 10 times higher than the aquifer hydraulic conductivity. However, we can show that the factor 10 ratio is obtained only if the model domain size is chosen too small and therefore the calculated width of the capture zone becomes affected by the model boundary conditions. In general, the width of the capture zone of a funnel-and-gate system is controlled by the effective hydraulic conductivity of the aquifer-gate combination, which can be approximated by the harmonic mean of $K_{Aquifer}$ and K_{Gate}. Therefore, $K_{Gate} = 10$ $K_{Aquifer}$ has not a significant effect on the width of the capture zone.
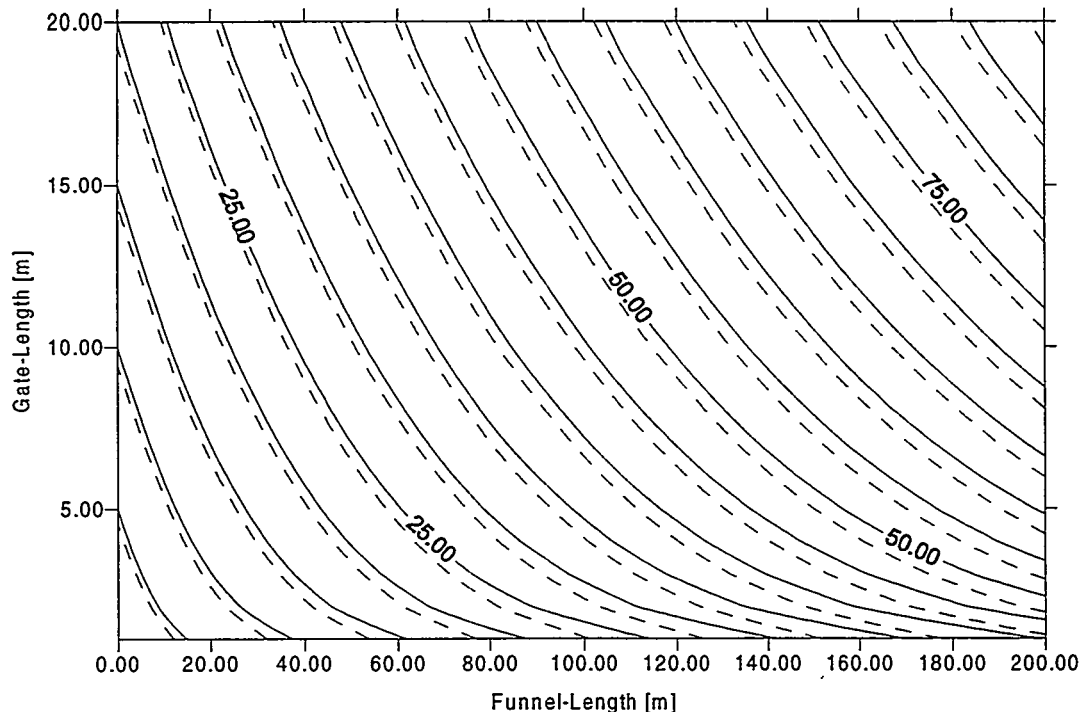

Fig. 3: Width of capture zone for different funnel-lengths and gate-lengths

Based on the *hydrochemical and economical model* described above, the investment and operation costs for a given operation period of the funnel-and-gate system can be calculated. In Figure 4, the diagram on the left side shows the linear functions of the investment costs (continous lines) superimposed on the non-linear functions of the capture zone widths for different funnel-lengths and gate-lengths. The diagram can be used to identify the investment cost-optimum for the required width of the capture zone. It is also useful for cost comparisons between alternative construction techniques. The diagram on the right shows the total cost of the system for a given operation time, including the investment and the operation costs. The complex shape of the total cost functions is caused by the (non-continous) operational cost function, which reflects the regular exchange of the sorbent within the gate/reactor system. The length of the "steps" in the cost function depend on the gate-length, i.e. on the volume of sorbent exchanged at one time. It should be noted, that for a better clarity the isolines of the *width of capture zone* were omitted in the right diagram.

It is interesting to note that for the data-set presented in this paper, the isolines of the *total costs* have a similar shape and orientation as the isolines of the *width of the capture zone*. This means that, given a certain width of the capture zone, the total costs of the system are not very sensitive to the absolute length of the funnel L_{ga} or the gate L_F but they are sensitive to the product of the two lengths. This result could be very important for sites where due to limited space only a certain size of the gate or the funnel might be acceptable. Of course, a smaller gate, which is cheaper to construct, would require a more frequent exchange of the sorbent and this is considered in the cost calculation.
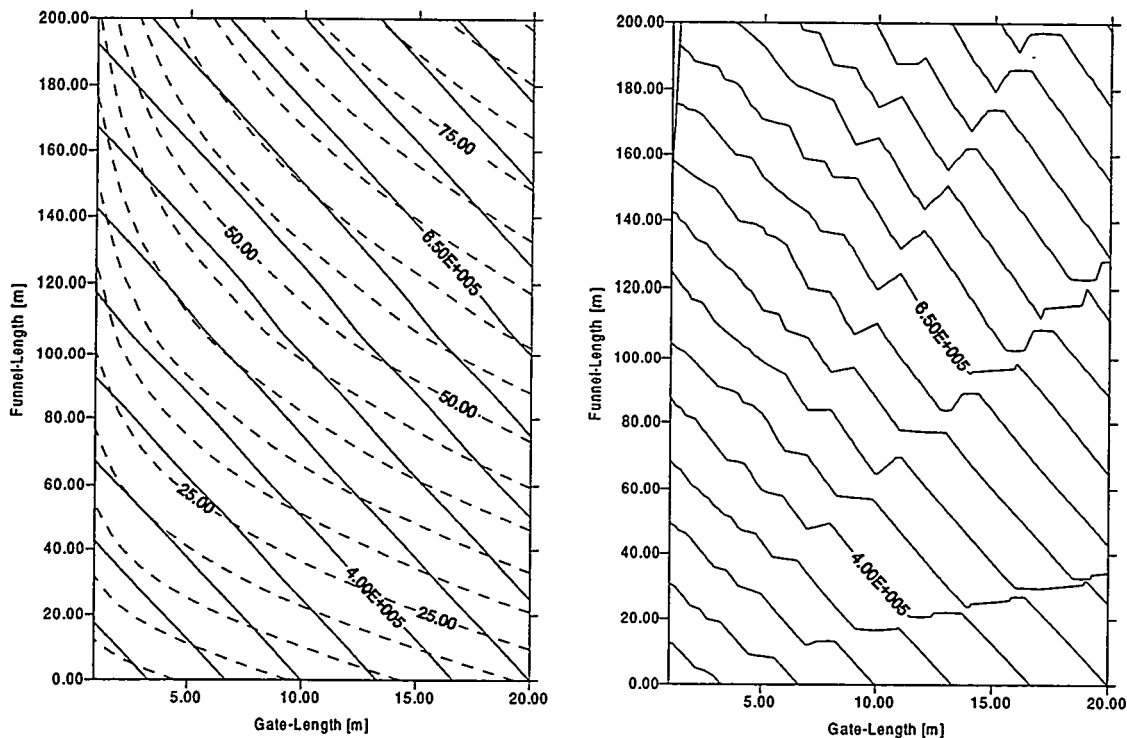
Fig. 4: Funnel-and-gate investment and total cost (construction technique: hydraulic trench cutter, $t_{op} = 50$ y, $C_0/C_m = 10^3$, $T_{Ga} = 0.5$ m, $K_{Aq} = 10^{-3}$m/s, grad h $= 10^{-3}$, $K_d = 10^4$ cm^3/g, $D_a = 10^{-13}$ m^2/s, m = 10 m)

Simplified Cost-Function

The analysis of the results shows that for a considerably wide parameter range the non-linearities of the model system are not too severe. Therefore, to make the model more easily applicable in practice, the attempt was made to linearize and simplify the equations in order to develop an explicit cost formula which includes a reduced set of physical parameters together with the per-unit costs.

For this purpose, the hydraulic model results (comp. Fig. 3) were approximated using a linear regression model of the form: $z = a + b_1 * x + b_2 * y$. The hydrochemical model was simplified assuming equilibrium sorption (comp. Fig. 2), where the contaminant breakthrough is approximated using a simple retardation

factor. The already simple economical model was not modified. Figure 5 shows the comparison between the output of the full numerical/analytical model, the model with the simplified hydraulical component and the model with the simplified hydraulical and the simplified hydrochemical component. Given a limited range of validity, both approximation models perform surprisingly well. The more complex approximation which takes into account the sorption kinetics produces results extremly close to the full numerical solution. The error is generally smaller than 5% in total cost, i.e. certainly better than the anticipated overall precision of the entire simulation.

The COST FORMULA provided represents the simplified hydraulical model but includes the non-equilibrium sorption solution. It should be noted, that the isolines indicating the *width of capture zone* were omitted in this plot for better clarity

Summary and Conclusions

A coupled hydraulical-hydrochemical-economical numerical model was developed for the design-optimization of funnel-and-gate systems with sorption reactors. To facilitate the practical implementation of the model, a simplified version was derived, which proved to be extremely accurate for a wide range of input parameter values. The derived COST FORMULA is a useful tool not only for the purpose of cost-optimization but also to study parameter sensitivities within the coupled system.

In the next phase of the study, the model system will be extended to include some other reactor types/reactions and also more complex flow conditions.
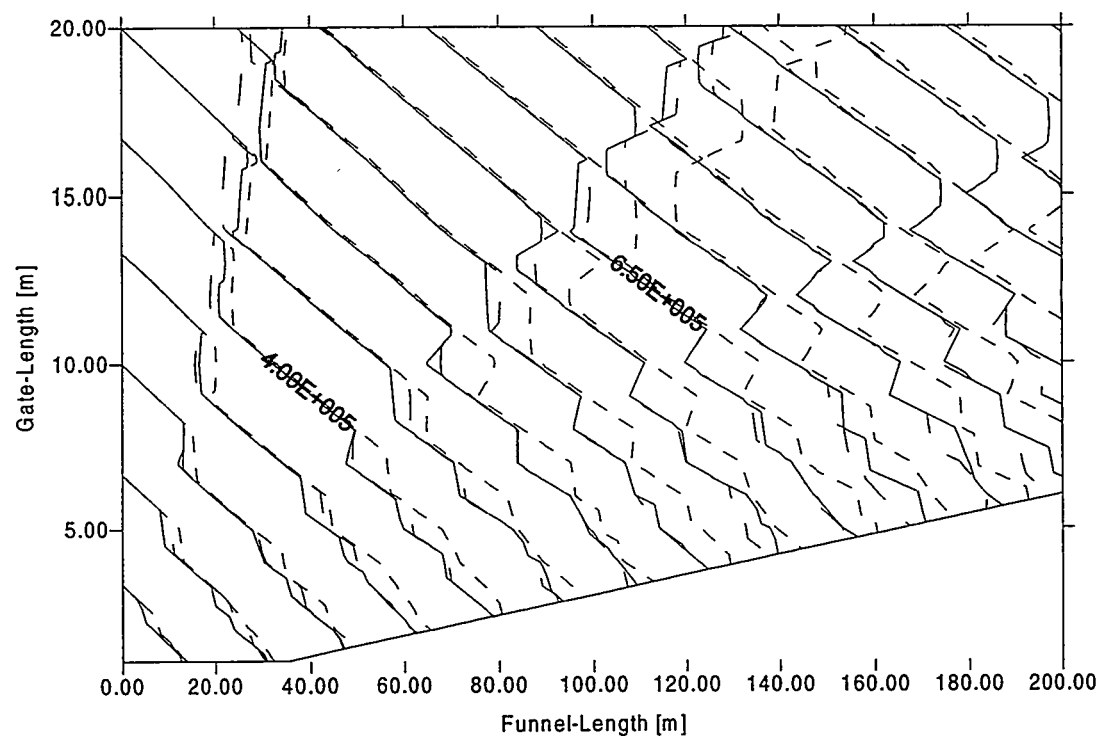

Fig. 5: Comparison between the full numerical [__], the simplified hydraulical [_ _] and the simplified hydraulical-hydrochemical model [---] (parameters as in Fig. 4)

COST FORMULA

$$ToC = SiC + m \cdot \left\{ FuC \cdot L_F + T_{GA} \cdot L_G \cdot \left[(AcC + GcC) + AcC \cdot DF \right] \right\}$$

with

$$DF = (1+P) \cdot \frac{(1+I)^N - (1+P)^N}{(1+I)^N \cdot (1-P)}$$

$$N = int\left(\frac{t_{op}}{t_{Br}} \right), \quad P = (1+0.02)^{int(t_{Br})} - 1, \quad I = (1+0.03)^{int(t_{Br})} - 1$$

$$t_{Br} = \left\{ 1 - \left[arc\ erfc\left(\frac{2 \cdot C_m}{C_0} \right) \cdot 2 \cdot \sqrt{\frac{R^2 \cdot n \cdot v_a}{15 \cdot D_a \cdot K_d \cdot \rho_s \cdot (1-n) \cdot T_{GA}}} - 1 \right] \cdot \frac{(1-n) \cdot \rho_s \cdot K_d}{n} \right\} \cdot \frac{T_{GA}}{v_a}$$

$$v_a = \frac{(1.401 \cdot L_G + 0.319 \cdot L_F - 1.375) \cdot K_{Aq} \cdot grad\ h \cdot \cos\alpha}{L_G \cdot n}$$

Legend

α	angle of groundwater-flow [deg]		L_F	length of funnel [m]
ρ_s	density of sorbent particles [g/cm³]		L_G	length of gate [m]
AcC	activated carbon specific-cost [DM/m³]		m	aquifer thickness [m]
C_0	inflow concentration of contaminant [mg/l]		N	number of reactor refills [-]
C_m	maximal allowable concentration [mg/l]		n	porosity [-]
D_a	apparent diffusion coefficient [m²/s]		P	net price increase (without inflation) [-]
DF	discount factor [-]		R	radius of sorbent particles [m]
FuC	funnel construction specific-cost [DM/m²]		SiC	site installation cost [DM]
GcC	gate construction specific-cost (reinforced concrete) [DM/m³]		t_{Br}	breakthrough time [s]
grad h	hydraulic gradient [-]		T_{GA}	gate thickness [m]
I	net interest rate (without inflation) [-]		ToC	total cost [DM]
K_{Aq}	aquifer hydraulic conductivity [m/s]		t_{op}	total operation time [s]
K_d	distribution coefficient [cm³/g]		v_a	average groundwater flow velocity [m/s]

Acknowledgments

References

Grathwohl, P. (1997) Permeable Sorptive (+ Reactive) Walls for Treatment of Hydrophobic Organic Contaminant Plumes in Groundwater *1997 International Containment Technology Conference*, Feb. 9-12, St. Petersburg, Florida, USA

LAWA (1994) Leitlinien zur Durchführung von Kostenvergleichsrechnungen, Länderarbeitsgemeinschaft Wasser, München

McDonald, M.G. and Harbaugh, A.W. (1984) A modular three-dimesnional finite-difference groundwater flow model. U.S. Geological Survey, Open-File Report 83-875, 528 pp, National Center Reston, Virginia, USA

Pollock , D.W. (1989) Documentation of computer programs to compute and display the pathlines using results from the U.S. Geological survey modular three-dimensional finite-difference groundwater flow model, Dept. of the Interior, U.S. Geological Survey, Open File Report 89-381, Reston, Virginia

Rosen, J.B. (1952) Kinetics of a fixed bed system for solid diffussion into spherical particles *Journal of Chemical Physics*, 20 (3), 387-394

Starr, R.C.and Cherry, J.A (1994) In situ remediation of contaminated Ground Water: The Funnel-and-Gate System *Ground Water* 32(3) : 465-476

Authors addresses
Dr. Georg Teutsch, Joachim Tolksdorff
Univ. of Tübingen, Applied Geology, Sigwartstr. 10, 72076 Tübingen, Germany, Tel.: +49 7071 297-6468 or -4690, Fax: +49 7071 5059, e-mail: georg.teutsch@uni-tuebingen.de

Dr. Hermann Schad
I.M.E.S. GmbH, Kocherhof 4, 88239 Wangen, Germany, Tel.: +49 7528 97130, Fax: +49 7528 97131, e-mail: hermann.schad.imes@t-online.de

Evaluation of Remedial Alternatives of a LNAPL Plume Utilizing Groundwater Modeling.

Terrence Johnson[1], Steven Way[2] and Greg Powell[3]

Abstract

The TIMES model was utilized to evaluate remedial options for a large LNAPL spill that was impacting the North Platte River in Glenrock, Wyoming. LNAPL was found discharging into the river from the adjoining alluvial aquifer. Subsequent investigations discovered an 18 hectare plume extended across the alluvium and into a sandstone bedrock outcrop to the south of the river. The TIMES model was used to estimate the LNAPL volume and to evaluate options for optimizing LNAPL recovery. Data collected from recovery and monitoring wells were used for model calibration. A LNAPL volume of 5.5 million L was estimated, over 3.0 million L of which is in the sandstone bedrock. An existing product recovery system was evaluated for its effectiveness. Three alternative recovery scenarios were also evaluated to aid in selecting the most cost-effective and efficient recovery system for the site. An active wellfield hydraulically upgradient of the existing recovery system was selected as most appropriate to augment the existing system in recovering LNAPL efficiently.

Introduction

In March 1994, oil was discovered to be seeping from a 100-meter (m) stretch along the banks of the North Platte River in Glenrock Wyoming. Initial investigations revealed a light nonaqueous phase liquid (from here on referred to as 'LNAPL', hydrocarbon, or 'product') plume on the water table within the alluvium. The thickness of the plume in the vicinity of the river was approximately 0.3 m. The plume was subsequently traced upgradient through the alluvium over 600 m to the south of the river. The alluvium terminates against the weathered Foxhills Sandstone Formation. Ongoing site investigations have shown that the LNAPL plume extends over 750 m from the river into the sandstone bedrock. The LNAPL plume covers an area of over 18 hectares with product thickness ranging from a sheen to over 3 m.

LNAPL was originally released in the unconsolidated overburden overlying the sandstone to the south where the plume is the thickest. Over time, the LNAPL drained from the sandstone northward to the alluvium following the natural hydraulic gradient. Potential sources of the spill include three now-abandoned oil refineries that operated at various times between 1920 and 1980 refining diesel and gasoline products. Also, three crude-oil-transporting pipelines pass through the plume in hydraulically upgradient areas. Oil fingerprint and boiling point analyses have identified the product to be a mixture of gasoline and diesel compounds with a flash point of approximately 100 °F.

The contaminated zone is shallow and unconfined, consisting of alluvial deposits and sandstone bedrock outcrop. From the North Platte River, the alluvium extends 450 m to the south making an abrupt contact with the bedrock outcrop (Figure 1). The alluvium is very permeable and is comprised mainly of poorly sorted sands and gravels. Paleochannels of higher permeability have been identified within the alluvium by electromagnetic geophysical methods (Rogers et al., 1995). The bedrock has

[1]Groundwater Modeler, Roy F. Weston, Inc./REAC, 2890 Woodbridge Ave., Edison, New Jersey 08837-3679, (908)321-4241, johnson.terrance@epamail.epa.gov.

[2]Onsite Coordinator, U.S. Environmental Protection Agency, Region VIII, 999 18th St., Suite 500, Denver, Colorado, (303)312-6808.

[3]Work Assignment Manager/Hydrogeologist, U.S. Environmental Protection Agency, Environmental Response Team Center, 26 W. Martin Luther King Blvd, Cincinnati, Ohio 45268.

a low permeability and its competence increases with depth and is highly fractured in some areas. Bedrock channels of higher permeability due to differential weathering have also been identified (Rogers et al., 1995).

The site is located in an arid temperate climate with less than 25 cm of annual rainfall. Depth to groundwater ranges from 2.4 to 3.6 m below ground surface. Groundwater moves from the bedrock to the alluvium and flows north towards the river. Groundwater flow is controlled primarily by regional flow between the river and the aquifer with negligible recharge from rainfall. Groundwater table elevations at the site are quite transient, fluctuating annually by more than 1 m near the river. These fluctuations are due to snow melt in the spring and controlled releases from an upstream dam during the summer. Fluctuations in the groundwater table induces fluctuations in LNAPL thickness. Due to fluid entrapment and release, hydrocarbon thicknesses are greater when the water table elevation is low in the fall and winter. Thus, LNAPL recoveries are lower when the water-table elevation is high in the spring and summer.

Remedial Actions

Initial remedial measures focused on preventing seepage to the river and recovering LNAPL. A dual-phase recovery system was installed consisting of five recovery wells and a 200-m long hydraulic barrier slightly downgradient of the recovery wells and perpendicular to the groundwater flow direction (Figure 1). The hydraulic barrier consists of 4.25-m long sections of high-density polyethylene panels installed to a depth of 5 m below ground surface creating an underflow weir for groundwater flow. The 60-cm diameter recovery wells were fitted with separate LNAPL and water recovery pumps. The lower pump recovers groundwater continuously, depressing the water table creating a cone of depression for LNAPL flow. The upper pump, a floating LNAPL-skimmer pump equipped with hydrophobic filters, intermittently recovers accumulated LNAPL. Active recovery of LNAPL and groundwater began in November 1994. To date, LNAPL flow to the river has been contained, and as of June 1996, over 100,000 L of product and over 50 million L of groundwater have been pumped and treated to meet discharge permit limits.

As stated, product recovery is variable due to fluctuation in the river water levels. During the spring and summer of 1996 (not included in the modeling analyses), product recovery was very inefficient (i.e., high water and very low product recovery). This was due to unusually high river levels and a reduced free LNAPL volume in the vicinity of the recovery wells as a result of fluid entrapment and product depletion due to recovery. Additionally, the existing system does not address the bulk of the LNAPL volume which is 500 m to the south in the bedrock and southern-most alluvium (see Figure 2). A recovery system upgradient would be subject to reduced water-table fluctuation and address LNAPL recovery in the bulk of the plume. Product can be more efficiently recovered to the south where plume thickness is greater and the aquifer saturated thickness is smaller. In addition, such a system would intercept product flowing towards the river and ultimately eliminate the need for the existing system.

Numerical modeling can be used to cost-effectively integrate site characterization data and to optimize remedial options. Groundwater and separate-phase hydrocarbon modeling has been used to assess and design remedial options at spill sites (Parker, et al., 1991; Parker, et al., 1994; and Lui and McNulty, 1996). A great deal of site data is currently available: fluid level data is routinely collected from the over 80 monitoring wells at the site; pumping- and slug-test data; geologic and geophysical survey data; and LNAPL and groundwater analytical data are also available. The objectives of this modeling analysis are to (1) estimate the volume of floating product in the shallow aquifer; (2) evaluate the effectiveness of the existing system for long-term LNAPL recovery; and (3) evaluate alternative options for optimizing long-term LNAPL recovery.

LNAPL Recovery and Groundwater Flow Modeling

The site conceptual model assumes that groundwater and LNAPL flow is two-dimensional, horizontal, and transient. Recovery wells, trenches and hydraulic barriers are fully penetrating and the aquifer is heterogenous and isotropic. Groundwater flow is controlled primarily by regional inflow/outflow with no recharge from precipitation, and there are no current sources of LNAPL to the aquifer. It was assumed that the flow of LNAPL is dependent on the groundwater gradient but that groundwater flow is independent of the presence of LNAPL. This allows independent calibration of groundwater flow using corrected water-table elevations. In this modeling approach, the groundwater flow model is first calibrated as if LNAPL were not present, followed by calibration of the hydrocarbon recovery model using the calibrated groundwater model; i.e., groundwater flow calibration was single-phase-flow simulations and LNAPL-recovery calibration was dual-phase (water and LNAPL) simulations.

The TIMES model (TriHydro Integrated Model for Environmental Solutions) by TriHydro (1995) was used for this analysis. TIMES is a newly developed finite-element model that simulates the two-dimensional horizontal or vertical flow of water, air and LNAPL, and dissolved-phase transport in porous media. The model generically simulates heterogeneous and anisotropic hydraulic properties. Sources and sinks simulated by TIMES include pumping and injection, areal recharge, and boundary inflow and outflow. TIMES solves the governing equations subject to the appropriate initial and boundary conditions to determine areal LNAPL and groundwater flow. The governing equations are given in previous work by Kaluarachchi and Elliot (1995) and Parker et al. (1994). TIMES uses the van Genuchten capillary model (van Genuchten, 1980) to determine the distribution of LNAPL and water in the formation above the LNAPL/water interface and requires estimating soil capillary parameters α and N. TIMES computes free LNAPL specific volume at each monitoring point from product thickness data. Areal integration of LNAPL specific volumes provide an estimate of free product volume over the site. TIMES is visually interactive and displays model variables in the spatial and temporal domains during execution. It also allows easy manipulation of data input and output.

Figure 1 shows the model domain; the modeled area covers approximately 54 hectares. The North Platte River forms the northern domain boundary. Model domain was chosen to be within the area where reliable fluid level data is available. A finite-element mesh consisting of 4200 triangular elements was constructed for this exercise. Nodal spacings range from 35 m on the periphery of the domain to 2.4 m in the vicinity of the recovery systems, where greater model resolution is desired.

Table 1 is a summary of model calibrated hydraulic parameters. To the extent possible, hydraulic parameters were initially estimated from site data, i.e., pump test, slug test and geologic logs, and were adjusted during model calibration to better match observed data. Four soil zones were simulated (see Figure 1): alluvium, upper alluvium, alluvial overbank, and sandstone bedrock. The soil zones were delineated based on geophysical terrain conductivity analysis (Rogers et al., 1995) and geological logs. Aquifer bottom elevation (not included in Table 1) was treated as a spatial variable that was estimated from geologic logs. Table 2 shows the fluid parameters used in hydrocarbon flow simulation. Fluid properties were obtained from laboratory analysis of product samples and from the literature.

Corrected April 1994 water-table elevations, augmented by minimum water table elevation at monitor wells where April 1994 data were unavailable, were used to initialize the groundwater-flow model. This represents low river stage, low groundwater elevations, and maximum oil thicknesses at the site. To provide a conservative estimate of hydrocarbon volume, maximum monitor well LNAPL thicknesses were used as initial conditions in the product recovery model. Figure 2 is a contour map of the 18-hectare plume simulated. At the time of modeling, the plume was not fully defined towards the southern end, but contours had to be closed for modeling purposes. Zero LNAPL thicknesses were inserted beyond the area where product thicknesses are available in order to close contours. Additional site assessment will fully delineate the plume extent.

To simulate observed fluctuation in piezometric surface at the site, the piezometric heads at boundary nodes were allowed to fluctuate in accordance with observed data. To the north, in the vicinity of the river, the historical river stage fluctuation was applied. Further south, a smaller fluctuation was

Table 1. Calibrated Hydraulic Parameters.

Aquifer hydraulic Parameters	Alluvium	Upper Alluvium	Alluvial overbank	Bedrock
Hydraulic Conductivity (m/day)	61	12	12	6
Specific Yield (-)	0.21	0.21	0.09	0.09
Porosity (-)	0.34	0.34	0.35	0.35
Soil Capillary Parameters				
α (m^{-1})	18	18	18	6
N (-)	3.0	3.0	3.0	2.0
S_{or} (-)	0.1	0.1	0.1	0.15
S_{og} (-)	0.05	0.05	0.05	0.09

α and N are pore size distribution parameters; and S_{og} and S_{or} are maximum saturated and unsaturated zone hydrocarbon residual, respectively.

Table 2. Fluid Properties

ρ_{ro}	η_{ro}	β_{ao}	β_{ow}
0.84	2.1	3.2	1.4

ρ_{ro} is the hydrocarbon specific gravity, η_{ro} is the hydrocarbon to water dynamic viscosity ratio, β_{ao} the water to hydrocarbon surface tension ratio, and β_{ow} the ratio of water surface tension to hydrocarbon-water interfacial tension.

simulated to reflect a dampening of the river fluctuation over distance. In the product recovery model, perimeter boundary nodes were specified as zero hydrocarbon flow. Recovery wells and trenches were simulated as point sinks and a series of closely spaced wells, respectively. From wells and trenches, water recovery was simulated by specifying the maximum drawdown as the water control elevation and allowing the model to calculate the flux. Product recovery was simulated by specifying zero hydrocarbon thickness at the well.

Model calibration was performed to determine the soil hydraulic and capillary parameters that simulated observed monitor well hydrographs and recovery of LNAPL and water over time. The groundwater table was not allowed to fluctuate during hydrocarbon model calibration. TIMES has a faster execution with smaller hydrocarbon mass balance errors when boundary fluctuation is neglected from LNAPL-recovery simulations. During calibration, the groundwater and hydrocarbon flow was simulated from April 1994 to December 1995. Groundwater and product recovery began in November 1994.

Figure 3 shows observed and simulated hydrographs at three monitor wells (MW-3, PZ-5, and PZ-17). Non-zero starting points reflect data gaps. The model simulated observed groundwater fluctuations with reasonable accuracy. Figure 4a shows the observed and simulated cumulative water recovery from the five recovery wells currently operated at the site. Simulated water recovery (34 million L) is within 13 percent of observed water recovery (30 million L) over the calibration period.

Figure 4b shows observed and simulated cumulative hydrocarbon recovery over the 560 day calibration period. Simulated cumulative LNAPL recovery (66,000 L) is within 3 percent of observed (68,000 L).

Model Simulations

The first critical piece of information evaluated by the model was the free product volume. This is important in determining the extent of the pollution problem and the LNAPL distribution between the bedrock and alluvium. A product volume of 5.5 million L has been preliminarily estimated, over 3.0 million L of which is in the bedrock.

The calibrated hydrocarbon and groundwater flow model was used to evaluate the effectiveness of the existing barrier-wall/recovery-well system against three alternative recovery options: (1) a funnel and gate system 300 m south of the barrier wall consisting of hydraulic barriers funneling LNAPL towards a centrally located passive downgradient well; (2) an active wellfield 450 m south of the barrier wall in the upper alluvium where aquifer saturated thickness is small and groundwater fluctuation is less; and (3) a 200-m long passive bedrock trench 550 m south of the barrier wall. Figure 1 shows the location of the existing and alternative systems. The wellfield in the upper alluvium consisted of four wells spaced 30 m apart and operated at 1 m of drawdown at the wells. Simulations were executed for 10 years, and each scenario assumed continued operation of the existing system. The new systems were assumed to be operational in spring 1996, i.e., two years into the simulation.

Table 3 summarizes the simulation results. The predicted 10-year recovery at the barrier wall is only 238,000 L or less than 5 percent of the estimated product volume. By contrast, predicted recovery by the wellfield, bedrock trench, and funnel and gate systems are 33, 18 and 12 percent of product volume, respectively. Note that the neglect of water table fluctuation and the use of maximum LNAPL thicknesses introduces conservatism to the predicted LNAPL recovery and drainage rates. For the wellfield, the only active system evaluated, the predicted additional water recovery is 0.8 L/sec. The active wellfield scenario meets the objective of increased recovery in a timely manner. The additional water treatment for this scenario is justified based on the predicted doubling of the LNAPL recovery over the other options and guaranteed hydraulic plume control halting LNAPL migration towards the river. This hydraulic plume control resulted in a lower predicted LNAPL recovery for the active wellfield over the passive options (Table 3).

Conclusions and Recommendations

The groundwater flow and hydrocarbon recovery model TIMES was used to estimate spill volume and to evaluate options for optimizing product recovery at a hydrocarbon spill site. Model parameters were estimated from site data, and the groundwater flow and hydrocarbon recovery models were calibrated from site data. The recovery options evaluated include an existing active barrier-wall/recovery-well

Table 3. Predicted LNAPL and water recovery for three scenarios after 10 years

Alternative Systems	LNAPL Recovery (L)	LNAPL Recovery at Barrier Wall (L)	Water Recovery Rate (L/sec)
existing recovery system	-	238,000	0.8
funnel and gate system	401,000	238,000	0.8
well field in upper alluvium	1,591,000	216,000	1.6
bedrock trench	746,000	238,000	0.8

system, an active wellfield in the upper alluvium, a passive funnel and gate system, and a passive bedrock trench. A product volume of 5.5 million L was estimated, over 3.0 million L of which is in the bedrock. The active wellfield in the upper alluvium appears to be the best option for efficient and timely recovery of bulk product. The increased LNAPL recovery by the active wellfield justifies the additional groundwater pumpage and guarantees hydraulic plume control over passive systems. In addition, this system will intercept product flowing north towards the river and may ultimately result in the existing barrier-wall/recovery-well system being decommissioned.

The TIMES model was instrumental in the decision-making process by allowing an objective evaluation of the long-term performance of the various recovery options. The basis for evaluating the options were LNAPL recovery efficiency and time. The availability of adequate site data allowed the estimation of model parameters and effective model calibration. This in turn increased our confidence in the model results. The effective use of a model requires that the adequacy and quality of the input data be evaluated prior to modeling. This is especially true in complex hydrogeologic systems like the one dealt with in this exercise.

References

Kaluarachchi, J. J. and R. T. Elliot (1996) Design Factors for Improving the Efficiency of Free-Product Recovery Systems in unconfined Aquifers. *Groundwater, volume 33, 909-916.*

Lui, K. and G. McNulty (1996) Modeling Ground-Water Remediation at an Oil Refinery. In Proceedings *1996 Annual Convention and Exposition, Civil Engineers Influencing Public Policy,* (not yet published).

Parker, J. C., J. J. Katyal, J. L. Zhu, V. J. Kremesec and E. L. Hockman (1991) Free Product Recovery at Hydrocarbon Spill Sites with Fluctuating Water Tables. In proceeding *5th National Outdoor Action Conference, NWWA.*

Parker, J. L. Zhu, T. G. Johnson, V. J. Kremesec and E. L. Hockman (1994) Modeling Free Product Migration and Recovery at Hydrocarbon Spill Sites. *Groundwater, volume 32, 119-128.*

Rogers, N. T., S. K. Sandberg, and G. Powell (1996) The Effective use of Electromagnetic Methods to Delineate a Fluvial Paleochannel System controlling Oil Migration Near Glenrock, Wyoming. In Proceedings *Symposium on the Application of Geophysics to Engineering and Environmental Problems* (eds R. S. Bell and M. H. Cramer), pp 917-926.

TriHydro Corporation (1996) TriHydro Integrated Modeling for Environmental Solutions; TIMES Version 1.0 User's Guide. TriHydro, Laramie, WY.

van Genuchten, M. Th. (1980) A closed-form equation for predicting the hydraulic conductivity of unsaturated soils. *Soil Sci. Soc. Amer. J., 44, 892-898.*

Figure 1. Site Location, Soil Zones and Recovery Systems Evaluated.

LEGEND

——— SOIL ZONE BOUNDARY

⬧ RECOVERY WELL

▭▭▭ HYDRAULIC BARRIER

▭▭▭ TRENCH

Scale 1:18000

204/FIG1.DWG   10/4/96
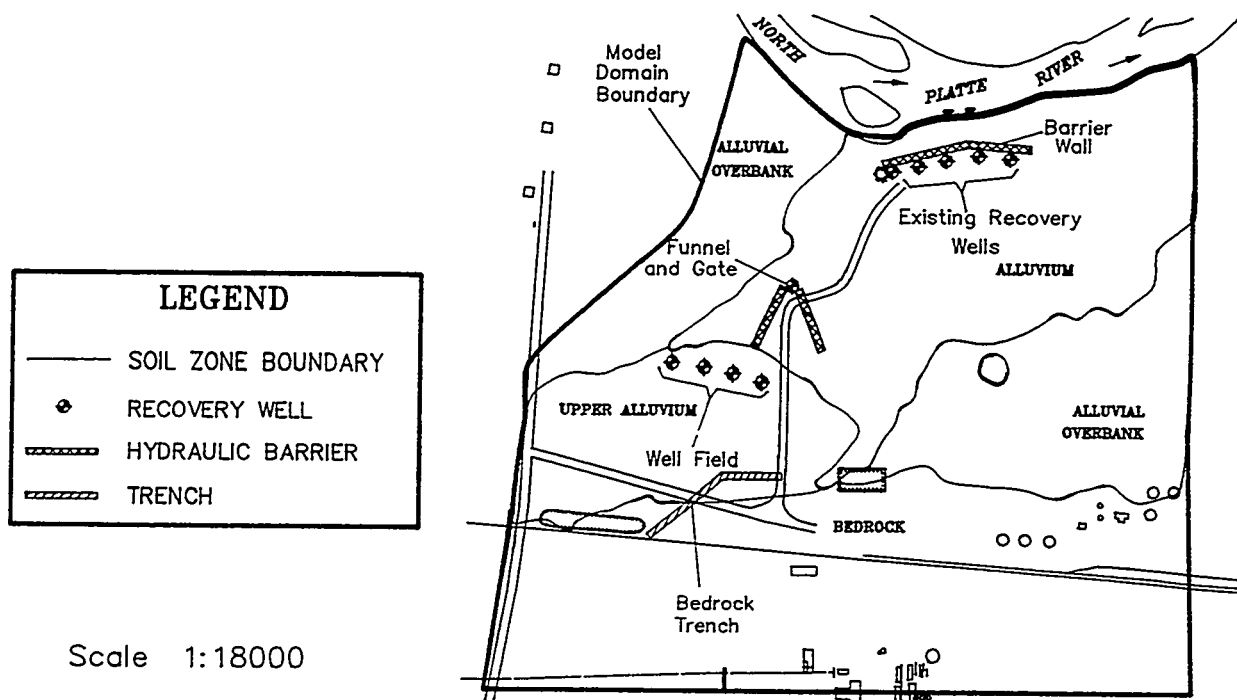
Figure 2. Initial LNAPL Thickness Contours

LEGEND

—— LNAPL CONTOUR (m)

—— WATER TABLE
CONTOUR (m AMSL)

SCALE 1:18000

FIGURE 3. Simulated and Observed Hydrographs

FIGURE 3. Simulated and Observed Hydrographs

FIGURE 4a.
Simulated and Observed Water Recovery

FIGURE 4b.
Simulated and Observed LNAPL Recovery

Chapter 18

Modeling: Transport Through Barriers

MODELING BIODEGRADATION OF ORGANIC POLLUTANTS DURING TRANSPORT THROUGH PERMEABLE REACTIVE BIO-WALLS

by

Michael A. Malusis[1] and Charles D. Shackelford[2]

ABSTRACT

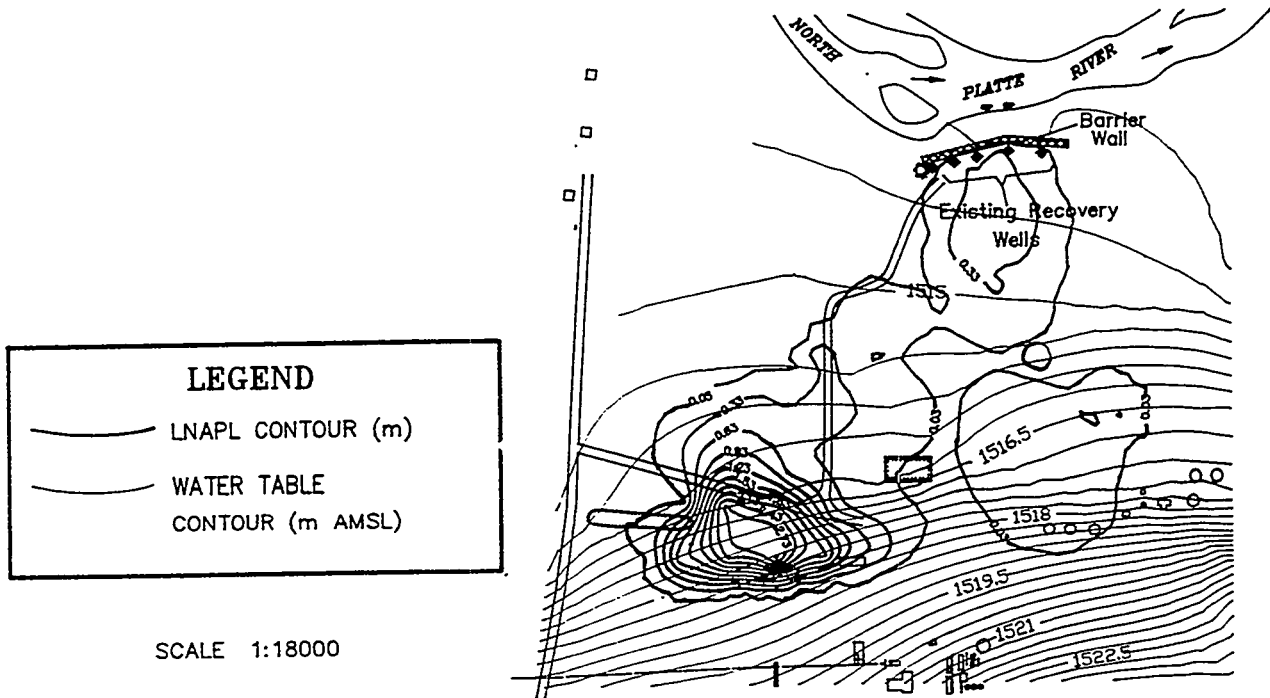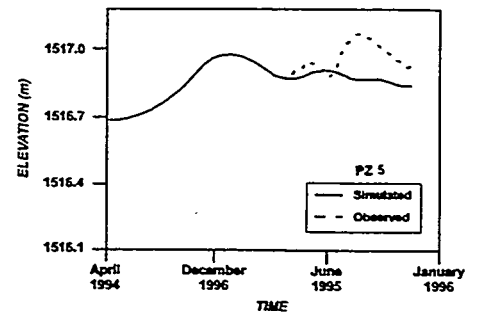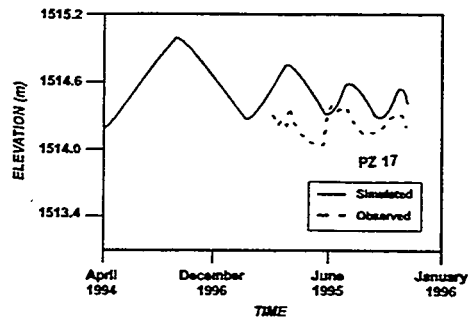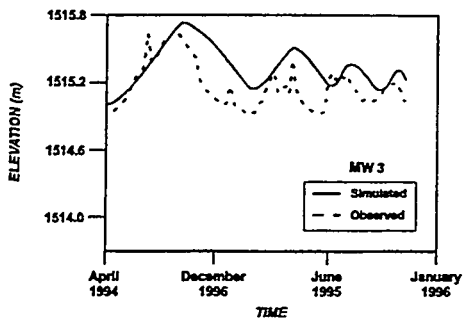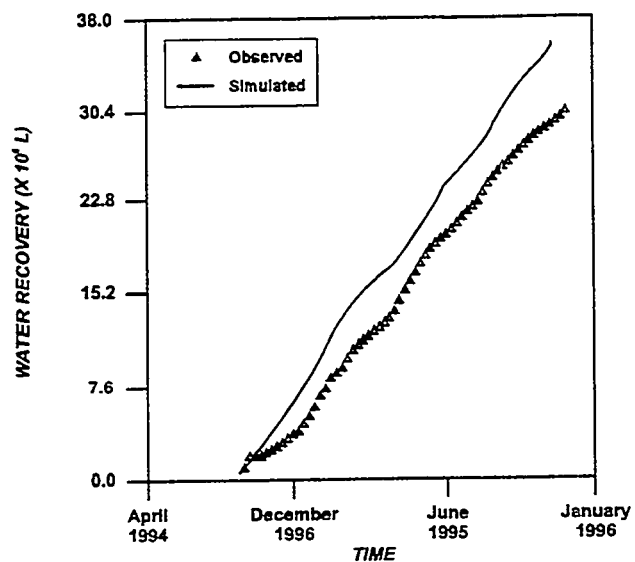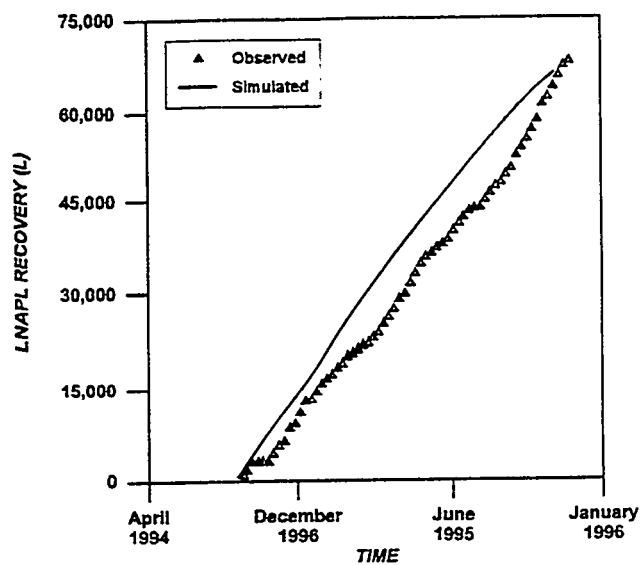One-dimensional solute transport through a permeable reactive bio-wall (PRB) (i.e., a permeable reactive wall with microbial reagents) is simulated in this study using the advection-dispersion equation with a biodegradation sink term. The biodegradation process is modeled using either linear, first-order kinetics or the Monod non-linear kinetics expression. Solute breakthrough curves for first-order and Monod kinetics are compared for a range of influent pollutant concentrations (c_0) and for different values of microbial mass (M_t) using typical PRB design values and Monod growth parameters (μ_{max}, K_c). The results indicate that values of pollutant concentration downgradient of a PRW predicted using first-order and Monod kinetics are similar when c_0 is small relative to K_c (ie., when $K_c/c_0 \geq 10.0$) and/or when M_t is large such that $\beta = \mu_{max}M_t/K_c \geq 5.0$. However, first-order kinetics provides unconservative estimates of the downgradient concentration for smaller K_c/c_0 or β and, therefore, should be used with caution.

INTRODUCTION

A relatively recent development for passive, *in situ* remediation of polluted groundwater is the use of permeable reactive walls (PRWs). Target pollutants are degraded or otherwise removed during passage through a PRW by means of chemical and/or biochemical reactions with reagents incorporated within the wall. The concept of passive remediation using PRW systems was proposed first in 1985 (McMurtry and Elton 1985) and is receiving increased attention at both the laboratory and field scale for removal of a variety of organic and inorganic pollutants (e.g., Gillham and Burris 1992; Morrison and Spangler 1993; Faulkner and Skousen 1994; Blowes et al. 1995; Eykholt and Sivavec 1995). The primary motivation for this increased attention is that the operating costs associated with PRW technology are thought to be lower for long-term groundwater treatment than more active remediation approaches such as pump-and-treat (Burris and Cherry 1992).

A simple conceptual model of a PRW, shown in Fig. 1, is a trench excavated downgradient of the contaminant plume and backfilled with a coarse material (e.g., sand, gravel) containing the required chemical and/or biological reagents. The pollutants move through the PRW with the natural groundwater flow and undergo the necessary chemical and/or biochemical reactions to reduce the downgradient concentrations to acceptable levels.

In recent years, research has been devoted to PRWs that utilize microorganisms to degrade groundwater pollutants. For example, field testing has been proposed to evaluate the potential for passive bioremediation of BTEX (i.e., benzene, toluene, ethylbenzene, and xylene) (Gillham and Burris 1992; Barker et al. 1994) and TCE (Smyth et al. 1994). While much of the effort has been directed toward the use of oxygen and/or nutrient sources as reagents in the PRW to stimulate the activity of indigenous microorganisms (e.g., see Gillham and Burris 1992; Bianchi-Mosquera et al. 1994), the concept of adding a selected, non-indigenous bacterial population to a PRW has been reported in some studies (e.g., Burris and Cherry 1992; Kuyucak and St. Germain 1994; Smyth et al. 1994; Thomas and Ward 1995). These systems, referred to as permeable reactive bio-walls (PRBs) or in-line microbial filters (Burris and Cherry 1992), are attractive in situations where (1) the activity of indigenous microorganisms is not sufficient to achieve the required pollutant removal, or (2) the metabolic pathway for the pollutant may be undesirable with the indigenous population. The latter situation is illustrated by the generation of vinyl chloride

[1] Grad. Res. Asst. and Ph.D. Candidate, Dept. of Civil Engineering, Colorado State University, Ft. Collins, CO 80523. (970)491-2559(phone); mm788363@engr.colostate.edu (e-mail)

[2] Assoc. Prof., Dept. of Civil Engineering, Colorado State University, Ft. Collins, CO 80523. (970)491-5051 (phone); (970)491-3584 (fax); shackel@lance.colostate.edu (e-mail)
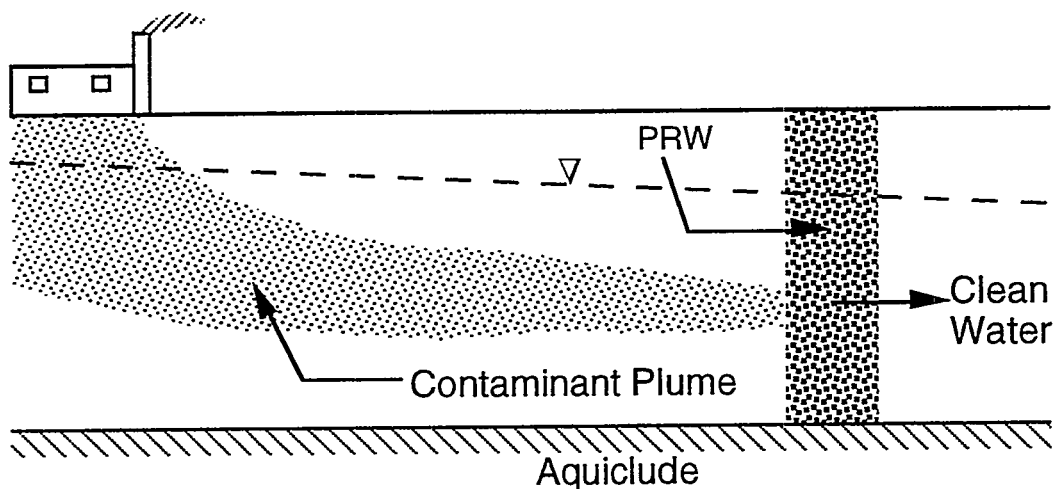
Fig.1 - Conceptual model of a permeable reactive wall (PRW) application

during anaerobic, reductive dechlorination of TCE by methanogenic cultures (e.g., see Freedman and Gossett 1989). However, biodegradation of TCE by *Pseudomonas cepacia* PR1 (referred to as PR1) under aerobic conditions without generation of vinyl chloride (Gillham and Burris 1992; Krumme et al. 1993). The potential use of PR1 in a PRB system for aerobic biodegradation of TCE currently is being investigated (Malusis et al. 1997).

Simulation of the biodegradation process is important for predicting the pollutant removal that occurs during transport through a PRB and involves selection of a biodegradation kinetics expression. For example, the *in situ* biodegradation process has been modeled using linear, first-order kinetics (e.g., see Bedient et al. 1994). Although biodegradation processes generally follow mixed-order reaction rates, the incorporation of a first-order decay reaction in the solute transport equation is convenient because the equation can be solved analytically.

A non-linear kinetics expression given by Monod (1942) has been used *in lieu* of the first-order expression to describe *in situ* biodegradation. The Monod kinetics expression generally is considered more appropriate than first-order kinetics for describing microbial utilization of organic substrates and has been modified to account for oxygen- and/or nutrient-limited biodegradation, inhibition at low substrate concentration, and cell death (e.g., see Borden and Bedient 1986). However, the solute transport equation with Monod kinetics must be solved numerically. The purpose of this paper is to evaluate the implications of using linear versus Monod kinetics expressions to model biodegradation during one-dimensional transport through a PRB by comparing theoretical solute breakthrough curves developed using typical PRB design parameters.

SOLUTE TRANSPORT BACKGROUND

One-dimensional transport of an organic solute through a PRB can be described using the advection-dispersion equation with equilibrium sorption and a biologically active source/sink term, or

$$R_d \frac{\partial c}{\partial t} = D \frac{\partial^2 c}{\partial x^2} - v \frac{\partial c}{\partial x} + \left[\frac{\partial c}{\partial t} \right]_b \tag{1}$$

where R_d is the retardation factor [dimensionless], c is the solute concentration [ML^{-3}], t is the transport time [T], D is the hydrodynamic dispersion coefficient [L^2T^{-1}], x is the distance in the direction of transport [L], v is the seepage velocity [LT^{-1}], and the subscript b denotes the biologically active term. Equation 1 assumes that (1) flow and transport are one-dimensional, (2) the porous medium is homogeneous and incompressible, (3) the dispersion process is Fickian,

(4) sorption is instantaneous, linear, and reversible, and (5) biotransformation occurs in the aqueous phase only.

The value of R_d for organic solutes traveling through a PRB can be considered equal to unity (i.e., $R_d = 1$) unless the PRB contains a source of organic carbon as a sorptive reagent (e.g., activated carbon). For the purposes of this paper, we will assume that the PRB contains only a biological reagent (i.e., microorganisms). Therefore, Eq. 1 can be simplified to

$$\frac{\partial c}{\partial t} = D\frac{\partial^2 c}{\partial x^2} - v\frac{\partial c}{\partial x} + \left[\frac{\partial c}{\partial t}\right]_b \tag{2}$$

Solute breakthrough curves for a PRB can be developed by solving Eq. 2 for x=L, where L is the wall thickness. The results generally are presented as a plot of effluent (downgradient) concentration relative to the initial (upgradient) concentration (c_e/c_0) versus time, t, or pore volumes of flow, T (= vt/L) (e.g., see Shackelford 1991).

First-Order Kinetics

First-order biodegradation kinetics can be incorporated into Eq. 2 by expressing the source/sink term as follows:

$$\left[\frac{\partial c}{\partial t}\right]_b = -\lambda c \tag{3}$$

where λ is the solute decay constant [T^{-1}]. Therefore, the applicable equation for transport through a PRB with first-order biodegradation is

$$\frac{\partial c}{\partial t} = D\frac{\partial^2 c}{\partial x^2} - v\frac{\partial c}{\partial x} - \lambda c \tag{4}$$

Closed-form analytical solutions of Eq. 4 are published for various initial and boundary conditions (e.g., see Van Genuchten and Alves 1982). The following initial and boundary conditions were applied in this study:

$$c(x,0) = 0 ; \qquad c(0,t) = c_0 ; \qquad \frac{\partial c}{\partial x}(\infty,t) = 0 \tag{5}$$

where c_0 is the source concentration of the pollutant [ML^{-3}]. The resulting solution to Eqs. 4 and 5 is given as follows (van Genuchten and Alves 1982):

$$\frac{c(x,t)}{c_0} = \frac{1}{2}\left\{\exp\left[\frac{(v-u)x}{2D}\right]\text{erfc}\left[\frac{x-ut}{2(Dt)^{1/2}}\right]+\exp\left[\frac{(v+u)x}{2D}\right]\text{erfc}\left[\frac{x+ut}{2(Dt)^{1/2}}\right]\right\} \tag{6}$$

where $u = v[1 + (4\lambda D/v^2)]^{1/2}$.

Breakthrough curves for a PRB are developed by setting x=L in Eq. 6, where L is the thickness of the PRB. The limiting case of steady-state transport for a PRB of thickness L is described using a simplified form of Eq. 6 (Eykholt and Sivavec 1995), or

$$\frac{c(L,\infty)}{c_0}=\exp\left[\frac{(v-u)L}{2D}\right] \tag{7}$$

Monod Kinetics

The Monod kinetics expression relates the substrate (pollutant) concentration to the specific growth rate, μ, of the microorganisms, or

$$\mu = \mu_{max} \frac{c}{K_c + c}$$ (8)

where the maximum specific growth rate, μ_{max} [T^{-1}], and the half-saturation coefficient, K_c [ML^{-3}], are growth parameters that typically are measured in laboratory tests. Published values of μ_{max} and K_c for some common pollutants are shown in Table 1.

Table 1 - Monod kinetics growth parameters for selected pollutants (after Cookson 1995)

Chemical Compound	Microbial System[1]	μ_{max} (hr^{-1})	K_c (mg/L)
Benzene	UAC	0.28	6.57
4-Chlorophenol	UAC	0.02-0.025	16.0-17.0
1,2 Dichlorobenzene	UAC	0.066	3.74
Ethylbenzene	UAC	0.216	10.07
Phenol	SR	0.004	2.00
Toluene	UAC	0.523	7.75
p-Xylene	UAC	0.140	2.47

[1] UAC = unidentified, acclimated culture; SR = sulfate-reducing

The change in substrate (pollutant) concentration based on Monod kinetics is written as follows (Bedient et al. 1994):

$$\left[\frac{\partial c}{\partial t}\right]_b = -\frac{\mu_{max} M_t c}{\left(K_c + c\right)}$$ (9)

where M_t is the total microbial concentration [ML^{-3}]. Substitution of Eq. 9 into Eq. 2 yields the following expression:

$$\frac{\partial c}{\partial t} = D\frac{\partial^2 c}{\partial x^2} - v\frac{\partial c}{\partial x} - \mu_{max} M_t \frac{c}{K_c + c}$$ (10)

Equation 10 is valid for describing transport through an PRB provided that cell death is negligible and that microbial growth is not being limited by a substance other than the substrate, such as an essential nutrient (e.g., NO_3^-) or electron acceptor (e.g., O_2). For the purposes of this study, it is assumed that an excess of these substances are provided and maintained in the PRB.

In this study, Eq. 10 was solved by discretizing the transport domain into intervals of time (Δt) and space (Δx) and applying an implicit-in-time, centered-in-space finite difference formulation. The resulting approximate solution for the solute concentration, c, at a given time t in discretized cells of thickness Δx along the path of transport is as follows:

$$\left[1 + \frac{2D\Delta t}{(\Delta x)^2} + \frac{\mu_{max} M_t \Delta t}{\left(K_c + c_i^t\right)}\right]c_i^t = c_i^{t-\Delta t} + \left[\frac{D\Delta t}{(\Delta x)^2} - \frac{v\Delta t}{2\Delta x}\right]c_{i+1}^t + \left[\frac{D\Delta t}{(\Delta x)^2} + \frac{v\Delta t}{2\Delta x}\right]c_{i-1}^t$$ (11)

where c_i^t is the solute concentration in cell i at time t, $c_i^{t-\Delta t}$ is the solution concentration in cell i at the previous time, c_{i+1}^t is the solute concentration in cell i+1 at time t, and c_{i-1}^t is the solute

concentration in cell i-1 at time t. A distribution of solute concentration can be determined for a given time t over the transport domain of interest by solving Eq. 12 for each cell using an iterative procedure. This procedure was implemented using the software EXCEL (Microsoft Inc., Redmond, WA, 1992-93, Version 4.0)

Based on Eqs. 3 and 9, the first-order kinetics expression represents a limiting case of Monod kinetics when $K_c/c \gg 1$ such that

$$\left[\frac{\partial c}{\partial t}\right]_b = -\frac{\mu_{max}M_t}{K_c}c = -\beta c \tag{12}$$

where β is a constant provided that the total microbial mass, M_t, is constant, i.e., cell death, growth, and transport from PRB are negligible. While these processes probably are not negligible, the assumption of M_t = constant is reasonable if (1) the PRB is equipped with an injection system to periodically replenish the treatment zone with new cells, or (2) the PRB contains replaceable "cassettes" of reactive material with the microbes fixed to the coarse particles, as described by Gillham and Burris (1992) for a funnel-and-gate wall. Therefore, M_t is assumed constant in this study. Differences in simulated transport through a PRB using first-order versus Monod kinetics were evaluated by comparing breakthrough curves developed using Eqs. 6 and 11 for different values of K_c/c_0 under the condition that $\lambda = \beta = \mu_{max}M_t/K_c$.

RESULTS AND DISCUSSION

A comparison of breakthrough curves for transport with first-order versus Monod kinetics was made using four cases. Values of L, v, D, μ_{max}, and K_c were 1.83 m (6 ft), 1.06×10^{-5} m/s (3.0 ft/day), 1.94×10^{-6} m^2/s (1.8 ft^2/day), 6.05×10^5 s^{-1} (7.0 day^{-1}), and 7.0 mg/L, respectively, in each case. Values of μ_{max} and K_c represent average values for a BTEX compound based on the published values in Table 1. A different microbial mass, M_t, was used in each case (0.2, 1.0, 2.0, 5.0 mg/L), resulting in β = 0.2, 1.0, 2.0, and 5.0 day^{-1}, respectively. Values of M_t are based on cell concentrations of 2×10^8, 1×10^9, 2×10^9, and 5×10^9 cells/mL, respectively, where the mass of an individual cell is 10^{-12} mg (Bouwer and McCarty 1984). Breakthrough curves were developed using c_0 = 70, 35, 7, 3.5, 1.4, 0.7, 0.35, and 0.14 mg/L. The corresponding values of K_c/c_0 are 0.1, 0.5, 1.0, 2.0, 5.0, 10.0, 20.0, and 50.0, respectively.

Solute breakthrough curves with Monod decay (β = 1.0 day^{-1}) are shown for selected K_c/c_0 values in Fig. 2(a) along with the trends developed using first-order kinetics (λ = 1.0 day^{-1}) to illustrate the convergence of Monod kinetics toward first-order kinetics as K_c/c_0 increases. The results indicate that the use of first-order kinetics rather than Monod kinetics results in smaller, less conservative relative concentration values when K_c/c_0 is small (e.g., K_c/c_0 = 0.1). However, the breakthrough curves for Monod and first-order kinetics become more similar as K_c/c_0 increases.

Comparison of the steady-state, relative concentration values for each case in Fig. 2(b) indicates that the difference between Monod and first-order kinetics can be minimal for large values of K_c/c_0, regardless of the value of β. For example, the steady-state concentrations for $K_c/c_0 \geq 10.0$ are only slightly different than the values obtained using first-order kinetics in all cases. The significance of this result is that first-order kinetics is reasonable for modeling biodegradation in a PRB when the influent pollutant concentration is smaller than K_c by an order of magnitude or more, provided that the microbial mass is held constant and an excess of nutrients and oxygen is supplied. In addition, the results in Fig. 2(b) show that first-order kinetics may be acceptable for smaller values of K_c/c_0 (i.e, larger source concentrations) as the microbial mass in the PRB is increased (i.e., as β is increased).

The total microbial mass in the PRB has a distinct impact on the difference in steady state, relative concentration values obtained using Monod kinetics versus first-order kinetics, as shown in Fig. 3. For example, there appears to be little consequence associated with the use of first-order biodegradation kinetics versus Monod kinetics when β = 5.0/day for $K_c/c_0 \geq 0.5$. As
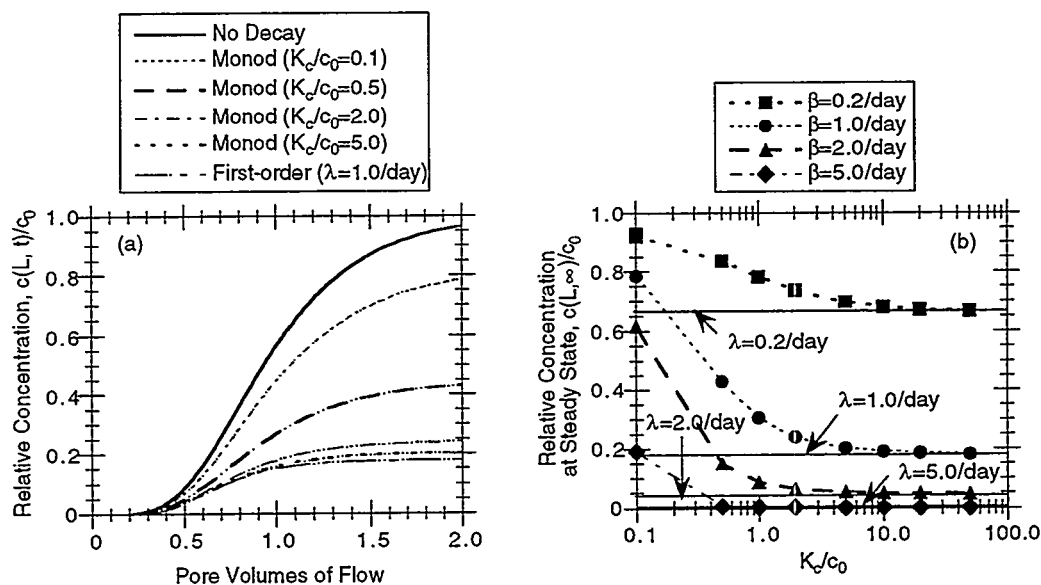
Fig. 2 - The influence of K_c/c_0 on pollutant biodegradation in a PRB based on Monod versus first-order kinetics expressions: (a) breakthrough curves (β=1.0/day); (b) relative concentration at steady-state, $c(L,\infty)/c_0$.
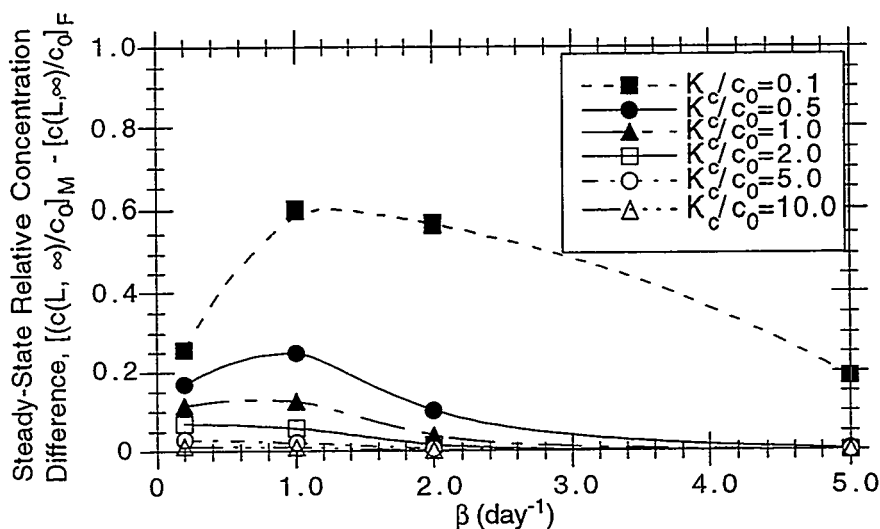
Fig. 3 - Influence of β on the difference in steady-state, relative concentration values obtained using Monod kinetics, $[c(L, \infty)/c_0]_M$, and first-order kinetics, $[c(L, \infty)/c_0]_F$

indicated earlier, β = 5.0/day corresponds to a cell concentration in the PRB of 5×10^9 cells/mL for the conditions considered in this study. A cell concentration this large is possible, although costly, to maintain in a PRB equipped to replenish the treatment zone with new cells. Of course, the required cell concentration and, therefore, β depends on the source concentration as well as the desired level of pollutant removal. The use of first-order kinetics for smaller values of β (e.g., β=0.2/day) can be unconservative, especially for small K_c/c_0.

CONCLUSIONS AND RECOMMENDATIONS

Accurate modeling of the transport process through a PRB requires careful selection of a biodegradation kinetics expression. First-order kinetics is more convenient to use than Monod kinetics since the resulting transport equation can be solved analytically. However, first-order kinetics can provide unconservative estimates of steady-state pollutant concentrations downgradient of a PRB depending on the magnitude of the influent pollutant concentration, the Monod degradation constants, and/or the microbial mass in the treatment zone. Monod kinetics rather than first-order kinetics is recommended unless it can be shown that first-order kinetics can be applied appropriately for the conditions of interest. For example, first-order kinetics may be appropriate for anaerobic systems. A modified Monod kinetics expression is recommended for modeling biodegradation limitations associated with (1) a lack of required nutrients or electron acceptor (e.g., O_2), (2) inhibition at low pollutant concentration, (4) cell death, growth, and transport, and/or (5) interaction between mixtures of pollutants.

ACKNOWLEDGMENTS

REFERENCES

Malusis, M.A., D.J. Adams, K.F. Reardon, C.D. Shackelford, D.C. Mosteller, and A.W. Bourquin. (1997) Microbial Transport in a Pilot-Scale Biological Treatment Zone. *In Situ and On-Site Bioremediation: The 4th Annual Symposium*, New Orleans, LA, April 28-May 1 (in preparation).

Barker, J.F., D. Smyth, and J.A. Cherry. (1994) Controlled In-Situ Groundwater Treatment. *NATO/CCMS Pilot Study Meeting on the Evaluation of Demonstrated and Emerging Technologies for the Treatment and Cleanup of Contaminated Land and Groundwater*, Oxford, UK, Sept. 19-22.

Bedient, P.B., H.S. Rifai, and C.J. Newell. (1994) Biodegradation Reactions and Kinetics. In *Ground Water Contamination:Transport and Remediation*, Chapter 8, pp. 207-249, PTR Prentice Hall, Englewood Cliffs, NJ.

Bianchi-Mosquera, G.C., R.M. Allen-King, and D.M. Mackay. (1994) Enhanced Degradation of Dissolved Benzene and Toluene Using a Solid Oxygen-Releasing Compound. *Ground Water Monitoring and Remediation*, 9(1), 120-128.

Blowes, D.W., C.J. Ptacek, J.A. Cherry, R.W. Gillham, and W.D. Robertson. (1995) Passive Remediation of Groundwater Using *In Situ* Treatment Curtains.*Geoenvironment 2000*, ASCE Geotechnical Specialty Publication No. 46, 1588-1607.

Borden, R.C. and P.B. Bedient. (1986) Transport of Dissolved Hydrocarbons Influenced by Oxygen-Limited Biodegradation: 1. Theoretical Development. *Water Resources Research*, 22(13), 1973-1982.

Bouwer, E.J. and P.L. McCarty. (1984) Modeling of Trace Organics Biotransformation in the Subsurface. *Groundwater*, 22(4), 433-440.

Burris, D.R. and J.A. Cherry. (1992) Emerging Plume Management Technologies: In Situ Treatment Zones. *Proceedings, 8th Annual Meeting of the Air and Waste Management Association*, Kansas City, MO, June 21-26.

Cookson, J.T. (1995) *Bioremediation Engineering: Design and Application.* 524 pp., McGraw-Hill, New York.

Eykholt, G.R. and T.M. Sivavec. (1995) Contaminant Transport Issues for Reactive-Permeable Barriers. *Geoenvironment 2000*, ASCE Geotechnical Specialty Publication No. 46, 1608-1621.

Faulkner, B.B. and J.G. Skousen. (1994) Treatment of Acid Mine Drainage by Passive Treatment Systems. *Proceedings, International Land Reclamation and Mine Drainage Conference*, Pittsburgh, PA, April 24-29, 250-255.

Freedman, D.L. and J.M. Gossett. (1989) Biological Reductive Dechlorination of Tetrachloroethylene and Trichloroethylene to Ethylene under Methanogenic Conditions. *Applied and Environmental Microbiology*, 55(9), 2144-2151.

Gillham, R.W. and D.R. Burris. (1992) Recent Developments in Permeable In Situ Treatment Walls for Remediation of Contaminated Groundwater. *Proceedings from Subsurface Restoration Conference, 3rd International Conference on Ground Water Quality Research*, Dallas, TX, June 21-24.

Kuyucak, N. and P. St-Germain. (1994) Possible Options for In Situ Treatment of Acid Mine Drainage Seepages.*Proceedings, International Land Reclamation and Mine Drainage Conference*, Pittsburgh, PA, April 24-29, 311-318.

Krumme, M.L., K.N. Timmis, and D.F. Dwyer. (1993) Degradation of Trichloroethylene by *Pseudomonas cepacia* G4 and the Constitutive Mutant Strain G4 5223 PR1 in Aquifer Microcosms. *Applied and Environmental Microbiology*, 59(8), 2746-2749.

McMurtry, D.C. and R.O. Elton. (1985) New Approach to *In-Situ* Treatment of Contaminated Groundwaters. *Environmental Progress*, 4(3) 168-170.

Monod, J. (1942) Recherches sur la Croissance des Cultures Bacteriènnes. Herman &Cie, Paris.

Morrison, S.J. and R.R. Spangler. (1993) Chemical Barriers for Controlling Groundwater Contamination. *Environmental Progress*, 12(3), 175-181.

Shackelford, C.D. (1991) Laboratory Diffusion Testing for Waste Disposal-A Review. *Journal of Contaminant Hydrology*, 7, 177-217.

Smyth, D.J.A., J.A. Cherry, and R.J. Jowett. (1994) Funnel-and-Gate for In Situ Groundwater Plume Containment. *Proceedings, Superfund XV*, Washington D.C., November 28-December 1, 1994.

Thomas, J.M. and C.H. Ward. (1995) Ground Water Bioremediation. *Geoenvironment 2000*, ASCE Geotechnical Specialty Publication No. 46, 1456-1466.

van Genuchten, M.Th. and W.J. Alves. (1982) Analytical Solutions of the One-Dimensional Convective-Dispersive Solute Transport Equation. *U.S. Dept. of Agriculture*, Technical Bulletin No. 1661, 151 pp.

FLOW RATES THROUGH EARTHEN, GEOMEMBRANE, & COMPOSITE CUT-OFF WALLS

by Choosak Tachavises[1] and Craig H. Benson[2]

Abstract: Flow rates through soil-bentonite (SB), geomembrane (GM), and composite geomembrane-soil (CGS) cut-off walls were determined using a numerical model of ground water flow. Various geological and wall conditions were simulated. Results of the simulations show that flow rates past all wall types are affected by hydraulic conductivities of the aquifer and underlying confining layer. Flow rates past GM walls with perfect joints are very low, provided the confining layer has low hydraulic conductivity. However, if a small fraction of the joints are defective, GM walls can be ineffective in blocking flow. CGS walls with a low hydraulic conductivity shell are less sensitive to joint defects. CGS walls with good shells typically have lower flow rates than SB and GM walls, even if the CGS wall contains defective joints.

INTRODUCTION

Cut-off walls are frequently used for in situ containment of wastes, contaminated soils, and groundwater. One of the key factors affecting the performance of a cut-off wall is flow rate. Different flow rates can be achieved by using walls of different types, such as earthen soil-bentonite (SB) walls, geomembrane (GM) walls, and composite geomembrane-soil bentonite (CGS) walls. Flow rates through earthen walls are readily estimated using hand calculations, but more sophisticated methods are needed for GM and CGS walls. In this study, numerical models were used to determine flow rates through different walls. The flow rates obtained from the models were then used to compare flow rates for the different wall types.

BACKGROUND

Wall Types and Hydraulic Conductivity

Schematics of SB, GM, and CGS walls are shown in Fig. 1a. A SB wall is formed by placing a mixture of soil and bentonite into a trench filled with bentonite slurry. The soil-bentonite mixture displaces the slurry when it is placed into the trench. The hydraulic conductivity of most soil-bentonite backfill samples from field mixtures varies from 10^{-6} to 10^{-8} cm/s (Ryan 1987, Evans 1994). A hydraulic conductivity of 10^{-7} cm/s is typically specified for a vertical cut-off wall because, with careful design and construction, it is the lowest hydraulic conductivity that can be readily and economically achieved (LaGrega et al. 1994). However, for some projects, calculations of site specific flow rates through the wall show that a hydraulic conductivity of 10^{-6} or 10^{-5} cm/s is suitable (LaGrega et al 1994). In this study, SB walls were simulated having backfill hydraulic conductivities, K_{sb}, of 10^{-6} cm/s and 10^{-7} cm/s.

A GM wall is formed by inserting thin (1 to 2 mm thick) panels of geomembrane (typically high density polyethylene, HDPE) directly into the soil in which flow is to be blocked. The panels are joined by an interlocking joint that typically contains a synthetic sealant that swells in water. In cohesionless soils, which comprise most cutoff wall applications, a GM wall may be installed using vibratory methods (Dunn 1993, Koerner and Guglielmetti 1995). In more difficult soils, installation can be performed via driving a mandrel attached to the bottom of the panel.

Different methods may be used to form joints between panels (Daniel and Koerner 1995). Two common joints are shown in Fig. 1b. Limited data exist regarding the hydraulic conductivity of

---

[1] Ph.D. Candidate, Dept. of Civil & Environ. Eng., Univ. of Wisconsin-Madison, Madison, WI 53706

[2] Assoc. Prof., Dept. of Civil & Environ. Eng., Univ. of Wisconsin-Madison, Madison, WI 53706

GM joints (K_j). Results of recent flow box tests at the University of Wisconsin-Madison (Rochford 1996) suggest that K_j varies from 10^{-12} cm/s (approximate "hydraulic conductivity" of geomembranes, Giroud and Bonaparte [1989]) when the joint is perfect, to 10^{-4} cm/s when the joint is poor. In this study, joint were defined as perfect ($K_j = 10^{-12}$ cm/s), fair ($K_j = 10^{-8}$ cm/s), or poor ($K_j = 10^{-4}$ cm/s). Geomembrane panels were assigned a hydraulic conductivity of 10^{-12} cm/s.

A CGS wall is a combination of SB and GM walls, and is analogous to the "composite liner" used in waste containment systems (Giroud and Bonaparte 1989). CGS walls are formed by installing interlocked geomembrane panels into a trench filled with soil-bentonite, or other backfill materials such as cement-bentonite (Manassero and Viola 1992, Cavalli 1992). In this study, the soil-bentonite was assumed to be the backfill in a CGS wall, and is called the "shell." The hydraulic conductivity of the shell (K_s) should vary within the same range as the hydraulic conductivity of SB walls, whereas the hydraulic conductivity of GM panel (K_{gm}) and GM joint (K_j) should vary within the same ranges as for GM walls. Nevertheless, to broaden the study of shell quality effects on the performance of CGS walls, shell hydraulic conductivities (K_s) defined as good ($K_s = 10^{-7}$ cm/s), fair ($K_s = 10^{-5}$ cm/s), and poor shell ($K_s = 10^{-3}$ cm/s) were used. The hydraulic conductivity of GM panels (K_{gm}) and joints (K_j) were the same as those used in modeling GM walls.
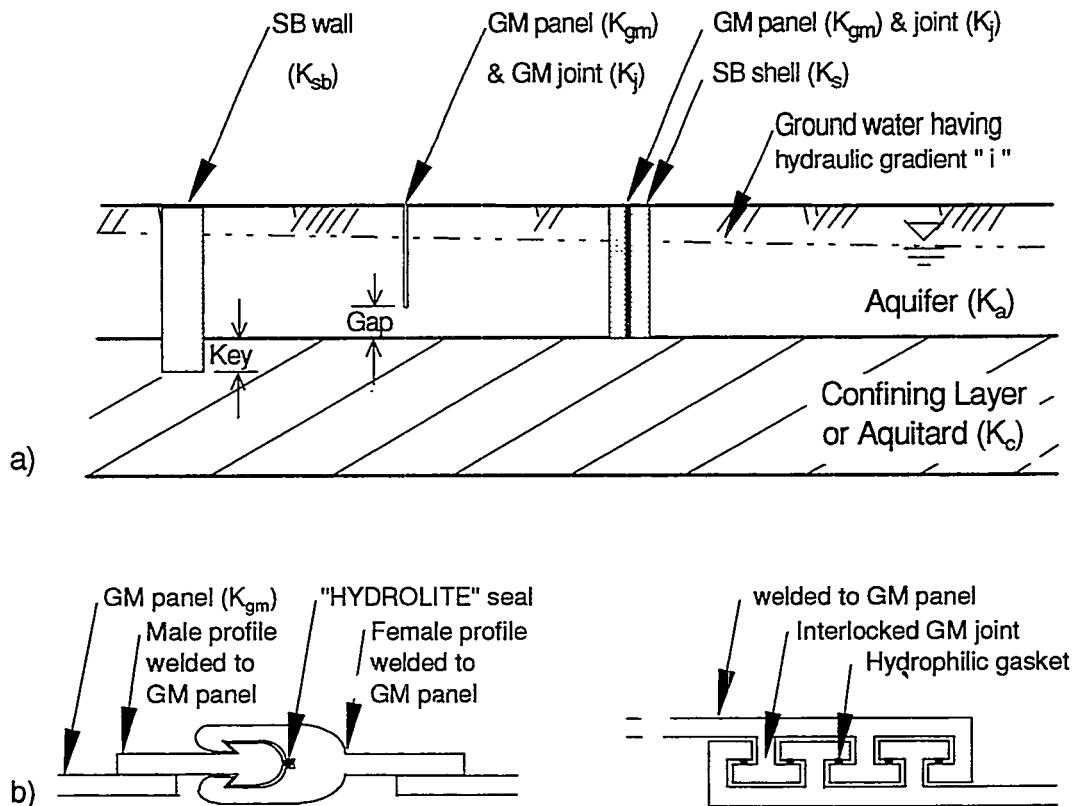
Fig. 1   Schematics of SB, GM, and CGS cut-off walls (a) and examples of GM wall joints (b) (after Koerner and Guglielmetti 1995).

Wall Depth & Width

The depth of cut-off walls may be selected so that the wall is fully penetrating (e.g., the wall is "keyed" into an underlying confining layer, Fig. 1a) or is hanging (gap exists between aquifer and confining layer, Fig. 1a). Generally, the selection of depth and the use of a keyed or hanging wall

is determined by contaminant and geological conditions (Evans 1991). The effects of key depth and key quality are described in Tachavises and Benson (1997). For a given wall type, Tachavises and Benson (1997) show that key depth has little effect on flow rate provided the wall is in intimate contact with the underlying confining layer having hydraulic conductivity about the same as that of the key. In this study, all modeled walls were fully penetrating, but were placed directly on top of the confining layer (no key existed). Keys were eliminated to prevent the effect of key on flow rates pass beneath the walls and then to permit a better assessment of the relative performance of different cut-off walls.

Considerations in selection of cutoff wall thickness include wall type, contaminant flux, wall continuity, construction method, and cost. The practical range of wall thicknesses is often defined by the construction equipment and methods. For example, cutoff walls excavated using a backhoe or clamshell are usually 0.6 to 0.9 m thick, with occasional walls as narrow as 0.4 m and as thick as 1.5 m (Filz and Mitchell 1995). In this study, SB and CGS walls were assumed to be 0.9 m thick, which is a common width of cut-off wall trenches (Evans 1993). The thickness of GM wall was assumed to be 1.5 mm, the thickness of typical geomembranes. GM panels are commonly 1 to 3 m wide (Koerner and Guglielmetti 1995). Thus GM walls were assumed to have panels 1.6 m wide. All GM joints were modeled as equivalent continuous porous media having a thickness of 1.5 mm and width of 0.1 m. CGS walls were assumed to have panels 1.6 m wide and 1.5 mm thick. For most simulations, only one joint with two adjacent panels was modeled.

Defects

All cut-off walls contain defects, such as poor seams, punctures, zones of higher hydraulic conductivity (e.g., "windows"), or inadequate keys. In this study, however, the only defects considered were poor joints (GM walls, CGS walls) or pervious backfill (SB and CGS walls). Defects that were not considered may have a significant negative impact on flow rate through a cutoff wall. The reader is encouraged to keep this limitation in mind when interpreting the results presented subsequently.

NUMERICAL MODEL

The groundwater flow model MODFLOW (McDonald and Harbaugh 1989) was used to simulate flow through SB, GM, and CGS walls. MODFLOW is a three-dimensional finite difference computer program that solves the groundwater flow equation for a variety of geological conditions. The finite difference grids were selected by conducting parametric studies assessing mass balance errors and computational efficiency. Grids were selected that had small mass balance errors, but permitted completion of a simulation within a reasonable time frame (< 4 hr). Grid spacings for all simulations met recommendations described in Anderson and Woessner (1992). A typical finite-difference grid is shown in Fig. 2.

More than 200 different cases were modeled. Walls were installed to block flow in a 30-m-thick aquifer underlain by a 30-m-thick confining layer. The 30 m depth corresponds to the limiting depth for typical trench excavations completed using a backhoe with a modified boom (LaGrega et al 1994). The confining layer was made 30 m thick to eliminate boundary effects that might be caused by a deeper, underlying layer. A horizontal hydraulic gradient of 0.001 was applied using constant head conditions at the upstream and downstream faces of the modeled region. No flow boundaries were used at the base of the confining layer and on the vertical sides parallel to the regional hydraulic gradient.

Hydraulic conductivities of the aquifer (K_a) and confining layer (K_c) were varied between 10^{-2} to 10^{-6} cm/s and 10^{-5} to 10^{-8} cm/s, respectively. These ranges represent the hydraulic conductivities of

materials that comprise aquifers and aquitards (Freeze and Cherry 1979). The porosity of most earthen materials varies in a very much smaller range, and has significantly less effect on groundwater flow compared to hydraulic conductivity. Thus, a porosity of 0.4 was used for all materials. All materials were assumed to be homogeneous and isotropic.
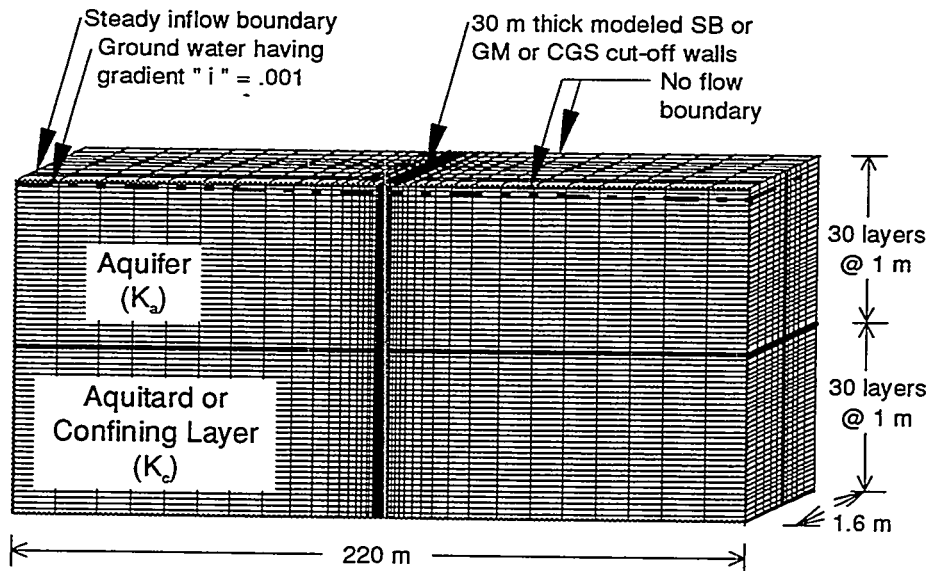

Fig. 2. Schematic of Finite Difference Grid.

RESULTS AND DISCUSSION

Soil-Bentonite (SB) Walls

Results for the SB walls are shown in Fig. 3. Flow rates through the SB walls vary up to 347 times, from 2.5×10^{-5} to 8.8×10^{-3} m³/day/m-wall, depending on the hydraulic conductivity of the backfill (K_{sb}), confining layer (K_c), and aquifer (K_a).

Backfills having lower hydraulic conductivity result in lower flow rate "past the wall," which includes flow through the wall and flow driven through the confining layer beneath the wall. Lower flow rates are expected when less pervious backfills are used because less water can pass through the wall.

The significance of backfill hydraulic conductivity (K_{sb}) also depends on the hydraulic conductivity of the confining layer, K_c. When K_c is reduced form 10^{-5} to 10^{-8} cm/s, the flow rate past the wall with less pervious backfill ($K_{sb} = 10^{-7}$ cm/s) decreases nearly an order of magnitude. In contrast, the flow rate past the wall with more pervious backfill ($K_{sb} = 10^{-5}$ cm/s) decreases by only a factor of 2. Flow rate past the wall is sensitive to K_c and K_{sb} because these hydraulic conductivities affect the relative fractions of flow rate driven through the confining layer and passing through the wall. When K_c decreases, less flow goes through the confining layer, and more flow goes through the wall. Consequently, when K_c is lower, K_{sb} has greater impact on total flow past the wall.

Effectiveness of the SB wall (i.e., flow rate past the wall relative to flow rate when no wall exists) is also affected by aquifer hydraulic conductivity (K_a). Fig. 3 shows that the effectiveness of a wall increases as the ratio of the aquifer and backfill hydraulic conductivities (K_a/K_{sb}) increases.

When this ratio is less than about two orders of magnitude, the SB wall is nearly ineffective. In addition, K_a/K_{sb} is more significant when the hydraulic conductivity of the confining layer, K_c, decreases.
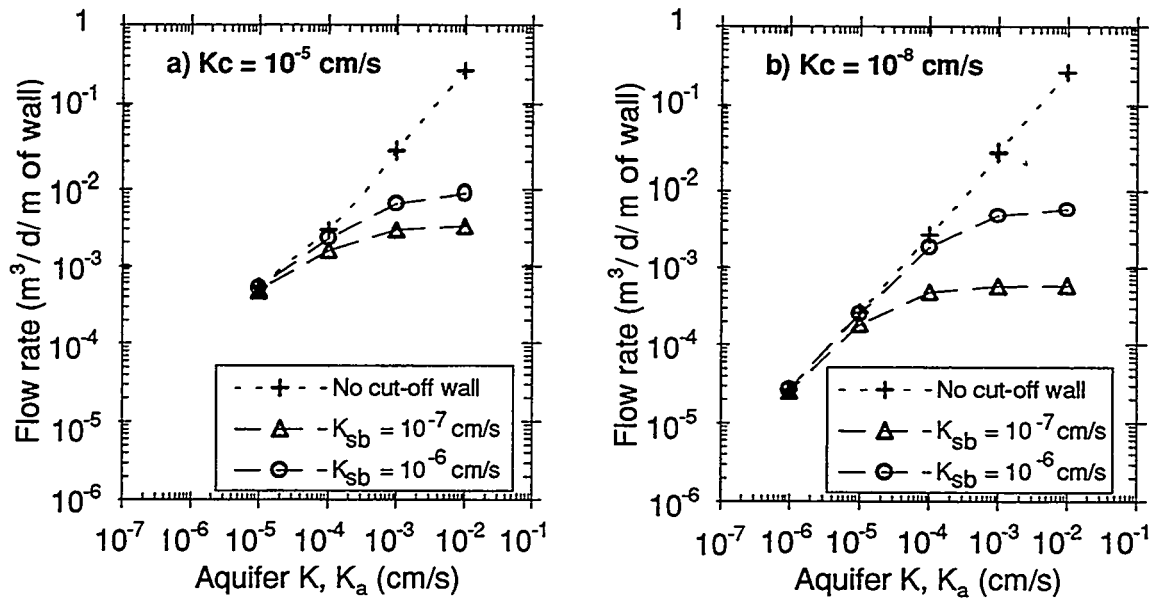

Fig. 3. Flow rate past a SB wall as a function of K_a for $K_c = 10^{-5}$ cm/s (a) and $K_c = 10^{-8}$ cm/s (b).

Geomembrane (GM) Walls

Flow rates past GM walls vary up to 40,200 times, from 6.5×10^{-6} to 2.6×10^{-1} m³/day/m-of-wall, depending on K_j, K_c, and K_a. Flow rates past GM walls having perfect joints are as much as 300 to 40,000 times lower than flow rates through GM walls having fair or poor joints, depending on the values of K_c and K_a, used in the simulation.

Selected results of simulations of GM walls are shown in Fig. 4. The hydraulic conductivity of the confining layer affects flow past GM walls in the same way as for SB walls. When the confining unit is less pervious, flow rates past GM walls decrease, because less water can be driven beneath the wall. In fact, if the joints are perfect and the confining layer has low K_c, flow rates past GM walls can be very low (as much as 100 times lower than for similar SB walls). If the joints are not perfect, however, lower K_c results in a much smaller decrease in flow rate.

The effect of aquifer hydraulic conductivity (K_a) on flow rate past GM walls is also similar to that for SB walls, i.e., the flow rate increases as Ka increases. However, as the quality of the joints is improved (i.e., K_j is lowered), flow rate past the wall becomes less sensitive to K_a. Furthermore, when the joints are perfect and the confining layer has low hydraulic conductivity, flow rate past the wall is very low and practically unaffected by K_a.

Joint quality has a significant effect on flow rates past GM walls. For example, GM walls having poor joints are ineffective in blocking groundwater flow for all K_c and K_a (Fig. 4). Significantly lower flow rates are obtained if the joints are of fair quality. If the joints are perfect, flow rates are very low provided the confining layer has low hydraulic conductivity. These findings suggest that care must be exercised during construction to ensure that joints in GM walls are effective. Otherwise, flow rates may be much higher than anticipated.
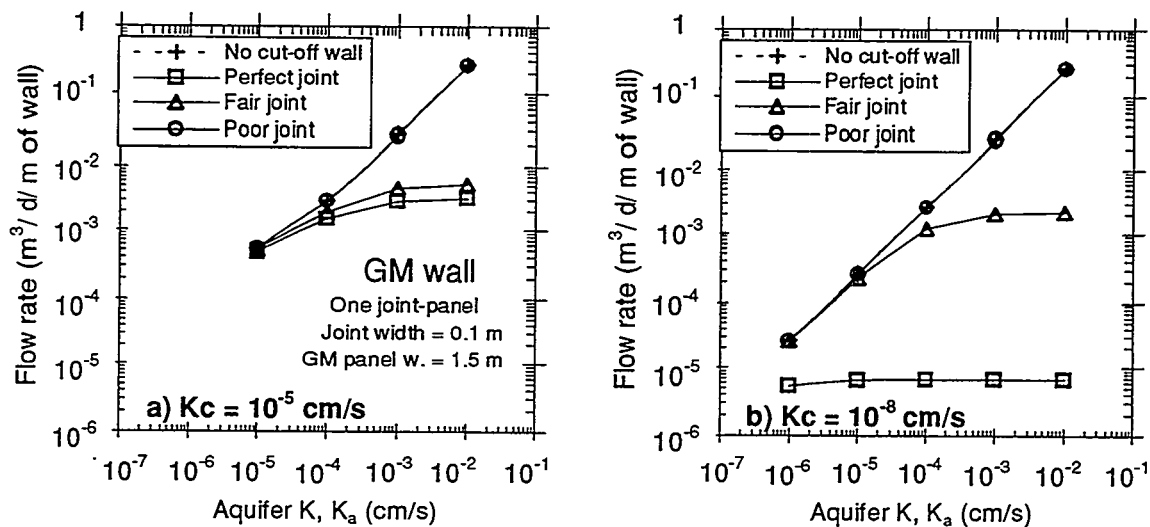
Fig. 4. Flow rates Past GM walls for $K_c = 10^{-5}$ cm/s (a) and $K_c = 10^{-8}$ cm/s (b).

Composite Geomembrane-Soil (CGS) Walls

Flow rates past CGS walls vary up to 41,700 times (5.31×10^{-6} to 2.2×10^{-1} m³/day/m-of-wall), for different joint, shell, aquifer, and confining layer hydraulic conductivities (K_j, K_s, K_c, and K_a). Furthermore, flow rates past CGS walls having perfect joints and a good shell are as much as 320 times lower than flow rates past CGS walls with fair joints and a fair shell, and up to 32,600 times lower than flow rates through CGS walls having a poor shell and poor joints. In addition, CGS walls having poor joints and a poor shell have no influence on ground water flow, for all K_c and K_a.

Flow rates are shown in Fig. 5 for CGS walls with poor and good shells underlain by a confining layer with $K_c = 10^{-8}$ cm/s. Flow rates through CGS walls are affected by the aquifer hydraulic conductivity (K_a) in the same way that SB and GM walls are affected; i.e., flow rates past the wall decrease as K_a decreases. In addition, flow rate is more sensitive to K_a when K_c is lower, because more water is forced to flow through the wall (not shown).

Flow rates past CGS walls are less sensitive to joint hydraulic conductivity (K_j) than GM walls. The shell limits the amount of flow that can pass through the wall in the same manner that a clay layer limits flow through geomembrane defects in a composite liner (Giroud and Bonaparte 1989). In particular, flow rates past CGS walls having a good shell and fair joints (Fig. 5a) are an order of magnitude lower than flow rates past comparable GM walls (Fig. 4b). For poor joints, flow rates past CGS walls are two-orders of magnitude lower than comparable GM walls (Figs. 5a, 4b). In contrast, if the shell is of poor quality, flow rates past CGS walls and GM walls are nearly identical, because the shell has no impact on flow through the joints. In addition, when the joints are perfect, flow rates past CGS and GM walls are also identical regardless of the shell quality, which is expected.

Flow rates past CGS walls having poor or fair joints are lower than flow rates past SB walls having hydraulic conductivity of 10^{-6} or 10^{-7} cm/s if a good quality shell exists. The flow rates are lower because the area of flow is smaller (primarily through the joints instead of the entire wall) and the flow is restricted by the low hydraulic conductivity of the shell. In fact, if a good shell exists, similar flow rates are obtained for CGS walls with fair or poor joints. However, if the shell is poor, flow rates past CGS walls having fair or poor joints are larger than flow rates for SB walls having $K_{sb} = 10^{-7}$ cm/s.
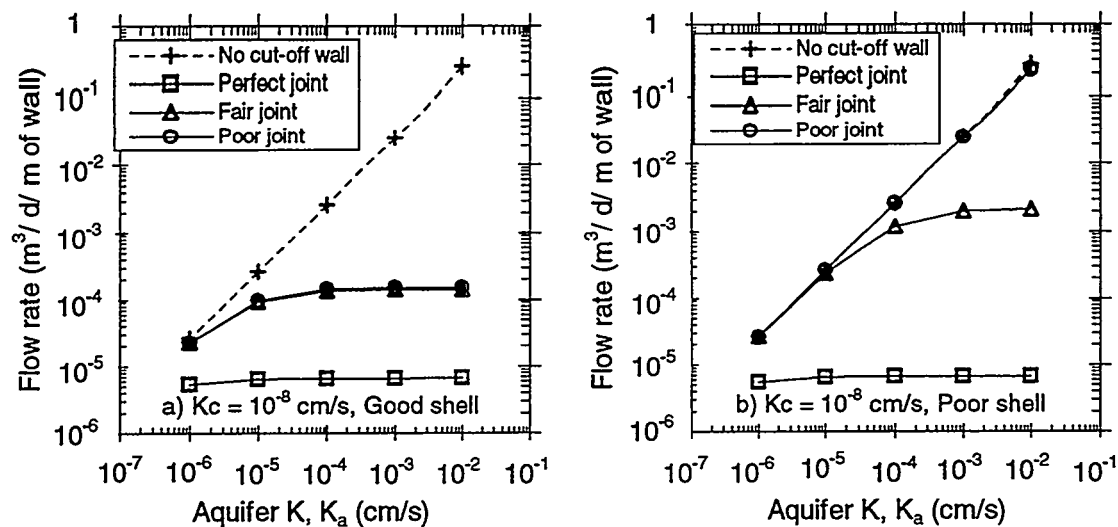
950

a) Kc = 10^{-8} cm/s, Good shell

b) Kc = 10^{-8} cm/s, Poor shell

Legend (both plots):
- No cut-off wall
- Perfect joint
- Fair joint
- Poor joint

Y-axis: Flow rate (m^3/ d/ m of wall), values 1, 10^{-1}, 10^{-2}, 10^{-3}, 10^{-4}, 10^{-5}, 10^{-6}

X-axis: Aquifer K, K$_a$ (cm/s), values 10^{-7}, 10^{-6}, 10^{-5}, 10^{-4}, 10^{-3}, 10^{-2}, 10^{-1}

Fig. 5. Flow Rates Past CGS Walls: K$_c$ = 10^{-8} cm/s (good shell) (a) and K$_c$ = 10^{-8} cm/s (poor shell) (b).

Frequency of Defective Joints

Most of the simulations of GM and CGS walls were conducted with a single joint. However, a limited number of simulations were conducted with multiple joints, where only a fraction of the joints were defective. Typical results of these simulations are shown in Fig. 6. The flow rate can be much higher than anticipated even if a small fraction of the joints are defective; that is, the fraction of defective joints has little effect on flow rate past a GM wall compared to the presence of defective joint. The flow focuses on the defects, which act as permeable preferential pathways through the wall. Furthermore, as the confining layer becomes less pervious (K$_c$ is lower), the effect of defects becomes more dramatic, even if the fraction of defects is small (not shown). This occurs because more water is forced through the wall, and effectively the defects, when K$_c$ is lower.

SUMMARY

Numerical modeling of three-dimensional ground water flow under various geological and cut-off wall conditions was performed to determine flow rates through SB, GM, and CGS walls. Flow rates were then compared to study the relative performance of the walls. SB walls were modeled having backfill hydraulic conductivities (K$_{sb}$) of 10^{-6} and 10^{-7} cm/s. GM walls were modeled having various quality joints, which were represented by joint hydraulic conductivities, K$_j$ = 10^{-12} cm/s (perfect joints), K$_j$ = 10^{-8} cm/s (fair joints), or K$_j$ = 10^{-4} cm/s (poor joints). CGS walls were modeled with similar joint hydraulic conductivities, and shells having hydraulic conductivity, K$_s$ = 10^{-7} cm/s (good shell), 10^{-5} cm/s (fair shell), or 10^{-3} cm/s (poor shell).

Results of the simulations show that flow rates past all wall types are sensitive to the hydraulic conductivities of the aquifer (K$_a$) and the confining layer (K$_c$). Lower flow rates are obtained when either K$_a$ or K$_c$ is decreased. Flow rate past the wall also becomes more sensitive to changes in wall properties (backfill hydraulic conductivity, quality of joints) as K$_c$ decreases, because more flow is forced through the wall.
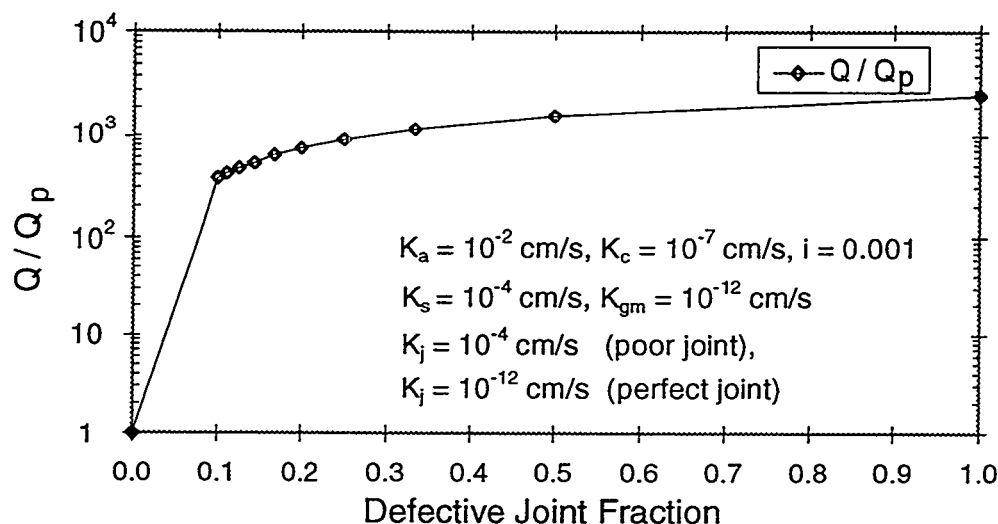
951

Fig. 6. Relative Flow Rate Past Wall vs. Fraction of Defective Joints.

Very low flow rates are obtained for GM walls having perfect joints, particularly when K_c is low. However, much higher flow rates occur when the joints are defective, even if only a small fraction of the joints are defective. In fact, when the joints are poor, GM walls are ineffective in blocking flow. GM walls with fair joints have flow rates falling midway between the flow rates for SB walls having hydraulic conductivities of 10^{-6} and 10^{-7} cm/s. It is important to note, however, that the SB walls were assumed to be free of defects. If windows exist in SB walls, it is likely that similar flow rates would be obtained for SB walls and GM walls with fair joints. Work on this aspect is underway. Nevertheless, the findings of this study show that care must be exercised to ensure that GM walls are free of defects. Otherwise, the flow rate past the wall may be much higher than intended.

Flow rates for CGS walls are less sensitive to joint quality if the shell has low hydraulic conductivity, primarily because the area of flow is essentially limited to the area of joints, which is very small. This small area is also relatively impervious, because it is surrounded by shell material having low hydraulic conductivity. As a result, CGS walls with good shells have lower flow rates than SB walls with comparable backfill hydraulic conductivity. This behavior is directly analogous to that of composite liners consisting of a clay layer overlain by a geomembrane.

The findings in this study indicate that CGS walls with good shells are the most reliable passive vertical flow barriers. The shell and geomembrane complement each other, because defects in either material are unlikely to be hydraulically connected. Unfortunately, CGS walls are costly, and it is unclear whether the additional redundancy afforded by the CGS wall outweighs the additional cost. The authors are currently investigating this topic.

ACKNOWLEDGMENT

REFERENCES

Anderson, M. and Woessner, W.(1992) *Applied Groundwater Modeling: Simulation of Flow and Advective Transport*, p 381. Academic Press Inc., San Diego, C.A.

Cavalli, N. (1992) Composite barrier slurry wall. *Slurry Walls: Design, Construction, and Quality Control*, ASTM STP 1129 (eds. D. Pual, R. Davidson, and N. Cavalli), pp. 78-85, ASTM, Philadelphia, PA.

Daniel, D. and Koerner, R. (1995) *Waste Containment Facilities: Guidance for Construction, Quality Assurance and Quality Control of Liner and Cover Systems*. ASCE Press, New York, NY

Dunn, K. (1993) HDPE vertical barriers. *GundWALL Product Catalog*, enclosure 3. Gundle Lining Systems, Inc., Houston, TX

Evans, J. (1991) Geotechnics of hazardous waste control systems. *Foundation Engineering Handbook 2nd edition* (ed. H-Y Fang), pp. 750-777. Van Nostrand Reinhold, New York, NY

Evans, J. (1993) Vertical cutoff walls. *Geotechnical Practice for Waste Disposal* (ed. D. Daniel), pp. 430-454. Chapman & Hall Inc., London.

Evans, J.(1994) Hydraulic conductivity of vertical cutoff walls. *Hydraulic Conductivity and Waste Contaminant Transport in Soil*, ASTM STP 1142 (eds. D. Daniel and S. Trautwein), pp. 79-94, ASTM, Philadelphia, PA.

Freeze, R. and Cherry, J. (1979) *Groundwater*. Prentice-Hall, Inc., Englewood Cliffs, NJ

Giroud, J. and Bonaparte, R. (1989) Leakage Through Liners Constructed with Geomembranes-Parts I and II. *J. of Geotextiles and Geomembranes, 8*, 27-107.

Koerner, R. and Guglielmetti, J.(1995) Design, construction, and performance of soil- and cement-based vertical barriers. *Assessment of Barrier Containment Technologies: A Comprehensive Treatment for Environmental Remediation Applications* (eds. R. Rumer and J. Mitchell), pp. 45-75, Springfield, VA

LaGrega M., Buckingham P., and Evans, J. (1994) *Hazardous Waste Management*. McGraw-Hill Inc., New York.

Manassero, M. and Viola, C. (1992) Innovative aspects of leachate containment with composite slurry: a case history. *Slurry Walls: Design, Construction, and Quality Control*, ASTM STP 1129 (eds. D. Pual, R. Davidson, and N. Cavalli), pp. 181-193, ASTM, Philadelphia, PA.

McDonald, M. and Harbaugh, A. (1988) *A Modular Three-dimensional Finite-difference Ground-water Flow Model*, US Geological Survey, Reston, VA.

Rochford, W. (1996) Relative Performance of Various Cut-Off Wall Designs for the Indiana Harbor Project, MS Thesis, Dept. of Civil & Environ. Eng., Univ. of Wisconsin-Madison, In preparation.

Mitchell J. and Filz G. (1995) Design, construction, and performance of soil- and cement-based vertical barriers. *Assessment of Barrier Containment Technologies: A Comprehensive Treatment for Environmental Remediation Applications* (eds. R. Rumer and J. Mitchell), pp. 45-75, Springfield, VA

Ryan C. (1987) Vertical barriers in soil for pollution containment. *Geotechnical Practice for Waste Disposal '87*, ASCE GSP 13 (ed. R. D. Woods), pp. 182-204, ASCE, New York.

Tachavises, C. and Benson, C. (1997) Significance of Defects in Vertical Cut-off walls. To be submitted to ASCE *In Situ Remediation '97*. In preparation.

SELECTION OF DISTRIBUTION COEFFICIENTS FOR CONTAMINANT FATE AND TRANSPORT CALCULATIONS: STRONTIUM AS A CASE STUDY[1]

D. I. Kaplan[2], K. M. Krupka, R. J. Serne, S. V. Mattigod, and G. Whelan

Abstract

As part of an ongoing project funded by a cooperative effort involving the Office of Radiation and Indoor Air (ORIA) of the U.S. Environmental Protection Agency (EPA), the Office of Environmental Restoration (EM-40) of the Department of Energy (DOE), and the Nuclear Regulatory Agency (NRC), distribution coefficient (K_d) values are being compiled from the literature to develop provisional tables for cadmium, cesium, chromium, lead, plutonium, strontium, thorium, and uranium. The tables are organized according to important aqueous- and solid-phase parameters affecting the sorption of these contaminants. These parameters, which vary with contaminant, include pH and redox conditions; cation exchange capacity (CEC); presence of iron-oxide, aluminum-oxide, clay, and mica minerals; organic matter content; and solution concentrations of contaminants, competing ions, and complexing ligands. Sorption information compiled for strontium is used to illustrate our approach. The strontium data show how selected geochemical parameters (i.e., CEC, pH, and clay content) affect strontium K_d values and the selection of "default" K_d values needed for modeling contaminant transport and risks at sites for which site specific data are lacking. Results of our evaluation may be used by site management and technical staff to assess contaminant fate, migration, and risk calculations in support of site remediation and waste management decisions.

Background

The sorption of most contaminants is affected by geochemical factors such as pH and redox conditions; CEC; presence of iron-oxide, aluminum-oxide, clay, and mica minerals; organic matter content; and solution concentrations of contaminants, competing ions, and complexing ligands. The term "sorption" will be used throughout this paper as an inclusive term for adsorption, precipitation, and coprecipitation. For example, a great deal of research has been directed at understanding and measuring the extent to which strontium sorbs to sediments (Ames and Rai 1978, Strenge and Peterson 1989). The primary motivation for these studies is the need to understand the environmental fate and mobility of ^{90}Sr, particularly as it relates to site remediation and risk assessment. ^{90}Sr contamination has been identified at 11 of the 45 Superfund National Priorities List (NPL) sites contaminated with radioactive substances considered in EPA/DOE/NRC (1993). Important geochemical parameters affecting K_d values for strontium are CEC; pH; concentrations of calcium and stable strontium in the aqueous and solid phases; mineralogy; and solution ionic strength (Kokotov and Popova 1962, Ames and Rai 1978, Rhodes 1957, and Prout 1958).

Among the most important questions to be addressed in developing a database or table of K_d values is the relationship between the concentrations of a dissolved adsorbate, such as strontium, and the

---

2 All authors: Pacific Northwest National Laboratory (PNNL), P.O. Box 999, Richland, WA 99352.
D. I. Kaplan: (509)372-3004, di_kaplan@pnl.gov
K. M. Krupka: (509)376-4412, km_krupka@pnl.gov
R. J. Serne: (509)376-8429, rj_serne@pnl.gov
S. V. Mattigod: (509)376-4311, sv_mattigod@pnl.gov
G. Whelan: (509)372-6098, g_whelan@pnl.gov

extent to which the adsorbate partitions to the solid phase, i.e., what is the shape of the adsorption isotherm. When the adsorption changes in a linear manner with dissolved absorbate concentration, the K_d model is appropriate. When the ratio of the adsorbed concentration to the dissolved concentration of an adsorbate varies as its total concentration increases, then a nonlinear sorption model, such as the Freundlich or Langmuir models, is more appropriate. However, it is important to realize that the actual model used to describe an adsorption isotherm is not only dependent on the type of contaminant and adsorbent, but also on the range of contaminant concentrations used in the experiment.

Strontium Geochemistry

Sorption information compiled for strontium is used to illustrate our approach for evaluating K_d values for use in a provisional table. The mobility and fate of strontium in geologic systems are affected by several important geochemical processes, including aqueous speciation, precipitation/coprecipitation, and adsorption.

Aqueous Speciation

Dissolved strontium is expected to be predominantly present as the uncomplexed Sr^{2+} ion. There is little tendency for strontium to form complexes with inorganic ligands (Faure and Powell 1972). The solubility of strontium is not greatly affected by the presence of most inorganic anions because it forms only weak aqueous complexes with dissolved carbonate, sulfate, chloride, and nitrate. Stevenson and Fitch (1986) concluded that strontium should not form strong complexes with fulvic or humic acids based on the assumptions that strontium would exhibit similar stability with organic ligands as calcium. Thus, organic and inorganic complexation is not likely to greatly affect strontium speciation in natural groundwaters.

Precipitation

Because strontium generally exists in nature at much lower concentrations than calcium, it commonly does not precipitate as a pure strontium phase (Faure and Powell 1972). Instead it forms coprecipitates (solid solutions), via atomic substitution for calcium, with calcite ($CaCO_3$) (or aragonite, $CaCO_3$), and anhydrite ($CaSO_4$). Calcite can allow the substitution of several hundred parts per million strontium at ambient temperature before there is any tendency for strontianite to form (Faure and Powell 1972).

Adsorption

The extent to which strontium partitions from the aqueous phase to the solid phase at pH values less than 9 is expected to be controlled primarily by cation exchange for a wide range of sediment types and pure mineral phases (McHenry 1958, Ames and Rai 1978, Strenge and Peterson 1989, Lefevre et al. 1993, Serne and LeGore 1996). Evidence to support the cation exchange mechanism includes the observations that strontium adsorption is rapid and reversible. Serne and LeGore (1996), for example, determined that ^{90}Sr adsorption was reversible; that is, strontium could be easily desorbed (exchanged) from the surfaces of sediments. Natural sediments that had been in contact with ^{90}Sr for approximately 27 yr could be leached of adsorbed ^{90}Sr as readily as similar sediments containing recently adsorbed strontium, indicating that ^{90}Sr does not become more recalcitrant to leaching with time. Furthermore, the presence of other cations known to adsorb onto surfaces via cation exchange, e.g., calcium, magnesium, and potassium, influences the extent to which strontium sorption occurs (Jackson and Inch 1989). Correlations have also been reported between strontium sorption and parameters that influence cation exchange, such as CEC (Akiba and Hashimoto 1990), surface area (Jackson and Inch 1980, Inch and Killey 1987), pH (Rhodes 1957, Prost 1958), and sediment texture (Peterson et al. 1996, Serne and LeGore 1996).

Numerous studies have been conducted to elucidate the effects of competing cations on strontium adsorption (Ames and Rai 1978, Kokotov and Popova 1962). These experiments consistently show

that, on an equivalence basis, strontium will out compete most Group 1A and 1B elements (alkaline and alkaline earth elements) for exchange sites. A ranking of the most common groundwater cations by their ability to replace strontium from an exchange site is stable $Sr > Ca > Mg > K \geq NH_4 > Na$ (Kokotov and Popova 1962). Calcium exists in groundwaters at concentrations typically two orders of magnitude greater than stable strontium and typically more than twelve orders of magnitude greater than ^{90}Sr. Consequently, mass action would improve the likelihood of calcium out competing ^{90}Sr for exchange sites.

Approach

Two underlying assumptions were made to assist in the selection of strontium K_d values for the provisional table. It was assumed that the adsorption of strontium (1) occurs by cation exchange, and (2) follows a linear isotherm within the strontium concentrations considered in this study. A data set was compiled from the literature consisting of strontium K_d values and several important ancillary parameters (i.e., CEC, pH, clay content, surface area, and concentration of dissolved calcium). The K_d values included in the data set were measured in systems consisting of natural sediments (as opposed to pure mineral phases), low ionic strength (<0.1 M), pH values between 4 and 10, strontium concentrations less than 10^{-4} M, low humic material concentrations (<5 mg/L), and no organic chelates (e.g., EDTA). These environmental conditions were selected to approximate those existing in far-field environments. The compiled K_d values were analyzed by statistical methods to evaluate the variability of the data and to determine if simplified equations could be developed for predicting best, minimum, and maximum estimates of K_d values as a function of important geochemical parameters.

The range of concentrations over which strontium adsorbs linearly has been reported to be quite wide. Akiba and Hashimoto (1990), Adeley et al. (1994), and Rhodes and Nelson (1957) reported these linear ranges to be 10^{-10}-10^{-3}, 10^{-12}-10^{-4}, and 10^{-10}-10^{-5} M strontium, respectively. Using the average strontium concentration reported for rivers, 0.11 mg/L (1×10^{-6} M) (Hem 1985), as an indication of the strontium concentrations likely to be encountered in groundwaters, it suggests that, as a first approximation, strontium concentrations in a contaminated aquifer will likely fall within the linear adsorption range. An important implication of this conclusion is that a table of K_d values for strontium does not have to provide values for multiple concentrations of dissolved strontium in the system to be modeled.

Results - Strontium K_d Values

Sixty-three K_d values for strontium were chosen from the literature. The descriptive statistics for the variability of these K_d values (in mL/g) are shown in Table 1. The correlation coefficients (r) between strontium K_d values and CEC, pH, clay content (wt.% of size fraction less than 2 µm), surface area, and dissolved calcium concentration are 0.84, 0.28, 0.82, 0.00, and 0.17, respectively. These analyses were used as guidance for selecting appropriate K_d values for a provisional table for strontium.

Table 1. Descriptive Statistics for the Variability of Strontium K_d Values.

Number of Values (n) = 63	Standard Error = 183 mL/g
Range = 10,198.4 mL/g	Median = 15 mL/g
Minimum = 1.6 mL/g	Mode = 21 mL/g
Maximum = 10,200 mL/g	Standard Deviation = 1,458 mL/g
Mean = 355 mL/g	Confidence Level (95%) = 367.2 mL/g

Figure 1 shows the great variability of compiled K_d values for strontium as a function of pH, CEC, and clay content. The experimental conditions used in the studies selected from the literature also varied with respect to test duration, analytical procedures (e.g., filtration and mixing conditions), and ionic strength. These factors also contribute to the scatter of the K_d values. The variability in strontium K_d can be as much as three orders of magnitude for different geochemical conditions. For example, between the narrow CEC range of 5.5 to 6.0 meq/100 g, nine K_d values for strontium are reported (McHenry 1958, Keren and O'Connor 1983, Serne et al. 1993). The K_d values for strontium range from 3 mL/g for a surface noncalcareous sandy loam collected from New Mexico (Keren and O'Connor 1983) to 70 mL/g for a carbonate surface soil collected from Washington (McHenry 1958). Thus, more than an order-of-magnitude variability in strontium K_d values may be expected at a given CEC level. Another important issue is that 83% of the observations exist at CEC values less than 15 meq/100 g (Figure 1B). Therefore, the few K_d values associated with CEC values greater than 15 meq/100 g may have had a disproportionally large influence (Neter and Wasserman 1974) on the regression calculation [K_d=-272+126(CEC), n=63, r=0.84, P≤0.001]. Consequently, estimates of strontium K_d values using these data may be especially inaccurate for low CEC sediments, such as sandy aquifers. We attempted to improve the prediction of strontium K_d values at low CEC by limiting the data included in the regression analysis to those with CEC values less than 15 meq/100 g. The strontium K_d values calculated from the resulting regression equation [K_d=10+4.05(CEC), n=57, r=0.52, P≤0.05] are more similar to those of this reduced (<15 meq/100 g) data set, and, perhaps more important, do not yield negative K_d values at CEC values less than 2.15 meq/100 g. Including both CEC and pH as independent variables further improved the predictive capability of the equation [K_d=-42+14(CEC)+2.33(pH), n=27, r=0.88, P≤0.001] for the full data set as well as the reduced (<15 meq/100 g) set of strontium K_d values.

Because CEC data are not always available to contaminant transport and risk assessment modelers, clay content, the more commonly available parameter, was also used in the regression analysis. Multiple regression analysis was conducted using clay content and pH as independent variables to predict CEC and strontium K_d values. The pH values and clay contents were highly correlated to sediment CEC for the entire data set (n=30, r=0.93, P≤0.001) and for those data limited to CEC values less than 15 meq/100 g (n=27, r=0.75, P≤0.01). Thus, it is not surprising that clay content and pH were correlated to strontium K_d values.

A provisional, full factorial table (Table 2) of strontium K_d values was created in part by using the results of the regression analysis. The table requires knowledge of the CEC or clay content and the pH of the system in order to select the appropriate minimum and maximum estimate of the strontium K_d value. The table includes three pH categories for each of three CEC or clay content categories. A two-step process was used in selecting the appropriate K_d values for each cell. For the first step, the appropriate regression equations were used to calculate K_d values. Additionally, the 95% confidence limits of the regression coefficients were used to calculate minimum and maximum K_d

Table 2. Provisional Table for Strontium K_d Values Based on Cation Exchange Capacity (CEC) (meg/100 g), Clay Content (%), and pH. [For dilute ionic strength waters, <0.1 M.]

CEC	< 3 meq/100 g			3 - 10 meq/100 g			10 - 50 meq/100 g		
Clay	< 4%			4 - 20%			20 - 60%		
pH	< 5	5 - 8	8 - 10	< 5	5 - 8	8 - 10	< 5	5 - 8	8 - 10
Minimum Estimate	1	2	3	.10	15	20	100	200	300
Maximum Estimate	40	60	120	150	200	300	1,500	1,600	1,700

Figure 1. Strontium K_d Values as a Function of Sediment pH (A), CEC (B), and Clay Content (C).
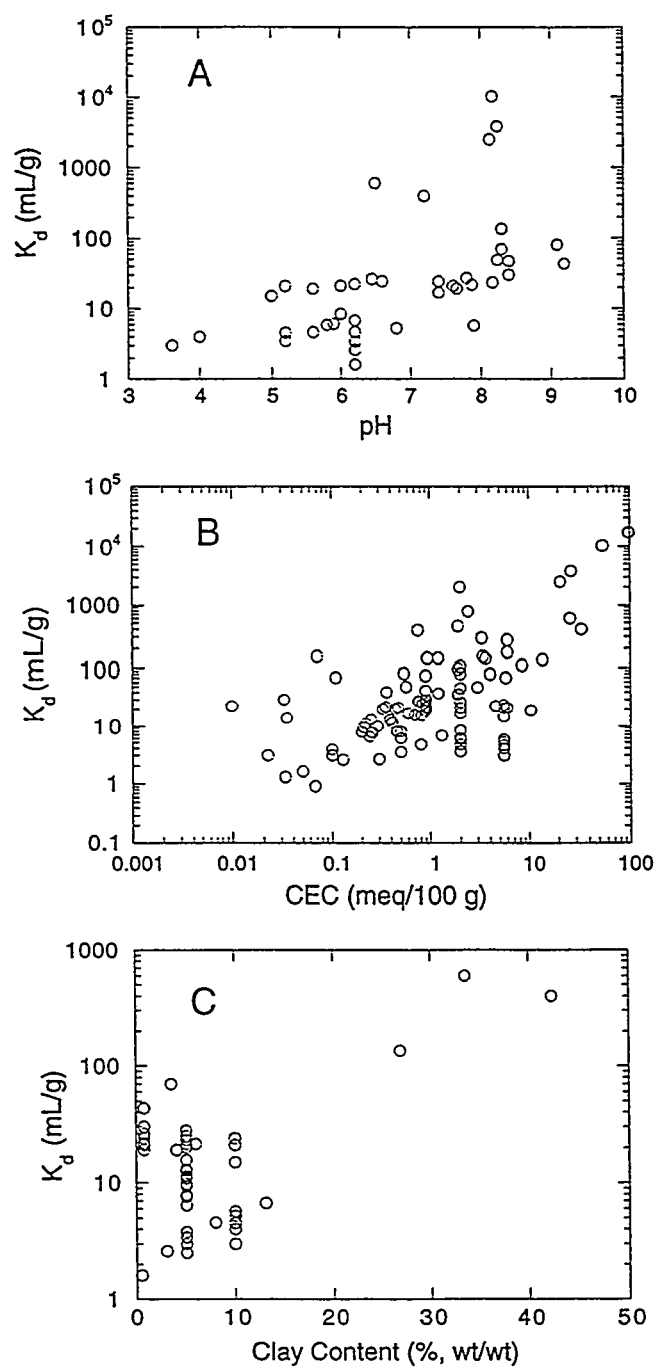
values for each category in the table. These calculated values were then slightly adjusted by "eyeing the data" to keep all K_d regression sets consistent with respect to the original Kd data sets. The clay contents associated with the CEC values in Table 2 were calculated using regression equations derived from the compiled set of K_d-CEC-clay data.

Conclusions

The sorption of contaminants in soil-water environments is affected by several aqueous- and solid-phase geochemical parameters. These include pH and redox conditions; cation exchange capacity; presence of iron-oxide, aluminum-oxide, clay, and mica minerals; organic matter content; and concentrations of contaminants, competing ions, and complexing ligands. The sorption of strontium at low concentrations is controlled primarily by cation exchange. This conclusion is supported by the K_d values reported for strontium as a function of pH, CEC, and clay content. Strontium K_d values compiled from the literature exhibit as much as three orders-of-magnitude variability for certain geochemical conditions.

Strontium K_d values were compiled from the literature. Only those K_d values that were measured under conditions relevant to typical far-field environments were included in the compilation. Statistical analyses of the compiled data set were used to provide guidance to select and identify meaningful trends between the strontium K_d values and the sediment parameters, such as pH, CEC, and clay content. Selection of the most appropriate K_d values for strontium require a combination of objective and subjective decisions. The objective decisions were based on regression analysis of soil properties and strontium K_d values. The subjective decisions were based on expert opinion and were used primarily to maintain consistency between data sets.

Modelers involved with site remediation and risk assessment predictions can use these minimum and maximum K_d values [which incorporate important geochemical functionality unique to each contaminant and site] as conservative bounding values. For a conservative calculation relative to off-site migration of a contaminant, the user would select the minimum K_d value at site-relevant geochemical conditions. For assessing the risks and costs associated with site remediation, however, the maximum value at the relevant conditions should be considered the more conservative value for clean-up techniques such as soil washing and pump and treat. The availability of bounding K_d values, moreover, allows modelers to conduct sensitivity analyses to determine if and how the selected K_d values affect their conclusions. Work is continuing on compiling provisional tables of K_d values for cadmium, cesium, chromium, lead, plutonium, thorium, and uranium.

References

Adeleye, S.A., P.G. Clay, and M.O.A. Oladipo. (1994) Sorption of caesium, strontium and europium ions on clay minerals. *J. Mater Sci*, 29, 954-958.

Akiba, D. and H. Hashimoto. (1990) Distribution coefficient of strontium on variety of minerals and rocks. *J. Nucl Sci Tech*, 27, 275-279.

Ames, L. and D. Rai. (1978) *Radionuclide Interactions with Soil and Rock Media. Volume 1: Processes Influencing Radionuclide Mobility and Retention, Element Chemistry and Geochemistry, Conclusions and Evaluation.* EPA 520/6-78-007A (PB-292 460), p. 428. U.S. Environmental Protection Agency, Las Vegas, Nevada.

EPA/DOE/NRC (Cooperative Effort by the U.S. Environmental Protection Agency, U.S. Department of Energy, and U.S. Nuclear Regulatory Commission). (1993) *Environmental Characteristics of EPA, NRC, and DOE Sites Contaminated with Radioactive Substances.* EPA 402-R-93-011, p. 84. U.S. Environmental Protection Agency, Washington, D.C.

Faure, G. and J.L. Powell. (1972) *Strontium Isotope Geology.* Springer-Verlag, p. 188. Berlin, Germany.

Hem, J.D. (1985) *Study and Interpretation of the Chemical Characteristics of Natural Water.* Water Supply Paper 2254, p.263. U.S. Geological Survey, Alexandria, Virginia.

Inch, K.J. and R.W.D. Killey. (1987) Surface area and radionuclide sorption in contaminated aquifers. *Water Pollution Res J. Canada,* 22, 85-98.

Jackson, R.E., and K J. Inch. (1989) The in-situ adsorption of ^{90}Sr in a sand aquifer at the Chalk River Nuclear Laboratories. *J. Contam Hydrology,* 4, 27-50.

Keren, R. and G.A. O'Connor. (1983) Strontium adsorption by noncalcareous soils - exchangeable ions and solution composition effects. *Soil Sci,* 135, 308-315.

Kokotov, Y.A. and R.F. Popova. (1962) Sorption of long-lived fission products by soils and argillaceous minerals III: Selectivity of soils and clays toward ^{90}Sr under various conditions. *Soviet Radiochem,* 4, 292-297.

Lefevre, R., M. Sardin, and D. Schweich. (1993) Migration of strontium in clayey and calcareous sandy soil: Precipitation and ion exchange. *J. Contam Hydrology,* 13, 215-229.

McHenry, J.R. (1958) Ion exchange properties of strontium in a calcareous soil." *Soil Sci Soc Amer Proc,* 22, 514-518.

Neter, J. and W. Wasserman. (1974) *Applied Linear Statistical Models.* Richard D. Irwin, Inc., p. 842. Homewood, Illinois.

Petersen, L.W., P. Moldrup, O.H. Jacobsen, and D.E. Rolston. (1996) Relations between specific surface area and soils physical and chemical properties. *Soil Sci,* 161, 9-21.

Prout, W.E. (1958) Adsorption of radioactive wastes by Savannah River Plant soil. *Soil Sci,* 84, 13-17.

Rhodes, D.W. (1957) The effect of pH on the uptake of radioactive isotopes from solution by a soil. *Soil Sci Soc Amer Proc,* 21, 389-392.

Rhodes, D.W. and J.L. Nelson. (1957) *Disposal of Radioactive Liquid Wastes From the Uranium Recovery Plant.* HW-54721, p. 33. Westinghouse Hanford Company, Richland, Washington.

Serne, R.J., J.L. Conca, V.L. LeGore, K.J. Cantrell, C.W. Lindenmeier, J.A. Campbell, J.E. Amonette, and M.I. Wood. (1993) *Solid-Waste Leach Characteristics and Contaminant-Sediment Interactions. Volume 1: Batch Leach and Adsorption Tests and Sediment Characterization.* PNL-8889 Vol. 1, p. 112. Pacific Northwest National Laboratory, Richland, Washington.

Serne, R.J. and V.L. LeGore. (1996) *Strontium-90 Adsorption-Desorption Properties and Sediment Characterization at the 100 N-Area.* PNL-10899, p. 70. Pacific Northwest National Laboratory, Richland, Washington.

Strenge, D.L. and S.R. Peterson. (1989) *Chemical Data Bases for the Multimedia Environmental Pollutant Assessment System (MEPAS): Version 1.* PNL-7145, p. 533. Pacific Northwest National Laboratory, Richland, Washington.

One-dimensional Contaminant Transport Model for the Design of Soil-Bentonite Slurry Walls

Ashutosh Khandelwal*, Alan Rabideau*, and Jennifer Su**
*Department of Civil Engineering, 207 Jarvis Hall
State University of New York at Buffalo
Buffalo, NY 14260-4300
**DuPont Inc.

ABSTRACT: A user oriented computer model (TRANS1D) was developed for application to the analysis and design of vertical soil-bentonite barriers. TRANS1D is a collection of analytical and numerical solutions to the one dimensional advective-dispersive-reactive (ADR) equation. The primary objective in developing TRANS1D was to enable the designer of a barrier system to evaluate the potential system performance with respect to contaminant transport, without performing difficult and time consuming field or laboratory experiments.

Several issues related to model application are discussed, including identification of governing transport processes, specification of boundary conditions, and parameter estimation. Model predictions are compared with the results of laboratory column experiments conducted with soil bentonite barrier material under diffusion-dominated conditions. Good agreement between model calibrations and experimental results was noted, with calibrated diffusion coefficients for organic contaminants consistent with literature values.

INTRODUCTION

The migration of contaminants through soil-bentonite (SB) slurry walls is influenced by advective-dispersive transport, sorption, and reaction processes. Molecular diffusion is expected to be the dominant transport mechanism due to the low hydraulic conductivity of SB barrier walls (Gray and Weber, 1984). Although there has been a considerable amount of research on contaminant transport through clay barriers having similar hydraulic conductivities as those of SB slurry walls (Rowe et al., 1995; Shackelford and Redmond, 1995; Johnson et al., 1989), few studies have focused on the applicability of mathematical models in predicting the transport of contaminants through SB barrier walls; an exception is the work of Mott and Weber (1991).

The purpose of this paper is to address issues related to the applicability of simulation models for predicting the transport of contaminants in a barrier wall under conditions usually encountered in the field. A contaminant transport code (TRANS1D) has been developed for application to the analysis and design of subsurface barriers. In TRANS1D, concentration and flux-based solutions to the one-dimensional ADR have been implemented for various assumptions regarding sorption, decay, and boundary conditions. Issues related to the model application are discussed below, including identification of governing transport processes, implementation of boundary conditions, and calibration of model parameters. Model predictions are compared with the results of laboratory-scale SB column experiments.

MODELING APPROACH

The one-dimensional ADR equation describing transport of a single solute through a homogeneous porous media subject to sorption onto the solid phase can be written as:

$$\frac{\partial C}{\partial t} + \frac{\rho_b}{n}\frac{\partial S}{\partial t} = -v\frac{\partial C}{\partial x} + D\frac{\partial^2 C}{\partial x^2} - \lambda_a C - \lambda_s \frac{\rho_b}{n}S \tag{1}$$

where C is the volume-averaged aqueous phase contaminant concentration, t is time, S is the sorbed phase mass fraction, ρ_b is the bulk density, n is the porosity, x is distance from the contaminated side of the barrier, v is the fluid velocity, D is the dispersion coefficient, λ_a is the decay coefficient for the aqueous phase, and λ_s is the decay coefficient for the solid phase.

The dispersion coefficient is typically represented as consisting of two components:

$$D = a_l v + \frac{D_m}{\tau} \tag{2}$$

where a_l is the media dispersivity, D_m is the free aqueous diffusion coefficient of the solute, and τ is the media tortuosity.

Sorption processes are commonly modeled using a first order mass transfer approach:

$$\frac{\partial S}{\partial t} = \alpha(S_e - S) \tag{3}$$

where a is the sorption rate coefficient, and S_e is sorbed phase concentration in equilibrium with the aqueous phase, as determined by the equilibrium model considered. Two commonly used equilibrium models are the linear and Freundlich isotherms:

$$S_e = K_d C \tag{4}$$

$$S_e = K_f C^{n_f} \tag{5}$$

where K_d is the sorption coefficient, and K_f and n_f are Freundlich parameters.

When the sorption process is rapid and linear, the commonly applied retardation factor approach is used and Eq. (3) is eliminated. In TRANS1D, both the equilibrium and mass transfer approaches have been considered.

In modeling contaminant transport in low-permeability barriers, the dependent variable of interest is frequently the contaminant flux f, defined as:

$$f = nvC - nD\frac{\partial C}{\partial x} \tag{6}$$

Boundary Conditions

The various boundary conditions implemented in TRANS1D are summarized in Table 1. The first- and third-type entrance conditions have been commonly used in modeling contaminant transport under advection-dominated conditions. The decaying source condition is applicable when the contaminant source undergoes first order decay and is not replenished by an active source. This condition takes the form of the first type entrance condition when there is no source decay. The finite mass boundary, as proposed by Rowe and Booker (1985), is based on the assumption of a finite quantity of contaminant in the contained area. This scenario results in a declining contaminant concentration at the barrier entrance as the contaminant is transmitted through the barrier. The mixing zone boundary condition, as proposed by Rabideau et al. (submitted manuscript), considers the presence of a uniform concentration zone at the entrance of the barrier. Contaminant transport into the uniform concentration zone is assumed to be advection-dominated. Once the contaminant is inside the mixing zone, contaminant transport into the barrier wall is influenced by both advection and dispersion. This condition is applicable for laboratory columns that incorporate a mixing zone to evenly distribute contaminant at the entrance.

The semi-infinite and second-type exit boundary conditions have been referenced extensively in the groundwater literature. The semi-infinite exit boundary condition is based on the assumption that the exit boundary has negligible impact on transport. The second-type exit boundary condition is based on the assumption of no dispersive flux at the exit boundary. Khandelwal and Rabideau (1996) suggested the inapplicability of this condition under diffusion-dominated

transport, such as would be expected in a slurry wall. The flushing exit boundary condition implies that the contaminant is rapidly transported away from the exit as it emerges. The mixing zone exit boundary condition assumes the presence of a uniform concentration zone at the exit boundary. As in the case of mixing zone entrance boundary, the transport into the uniform concentration zone is assumed to be influenced by both advection and dispersion, while the transport out of the mixing zone is assumed to be primarily advection-dominated.

Table 1: Boundary Conditions Implemented in TRANS1D

	Name	Mathematical Representation
Entrance Boundary Conditions	Ist-Type	$C(t,0) = C_0$
	Third-Type	$vC(t,0) - D\dfrac{\partial\ C(t,0)}{\partial\ x} = vC_0$
	Decaying	$C(t,0) = C_0 e^{-\lambda t}$
	Finite Mass	$C(t,0) = C_0 - \dfrac{1}{H_f}\int_0^t f_0(c,\tau)d\tau$
	Mixing Zone	$C(t,0) = \dfrac{Q_i}{V_{mi}}\int_0^t C_{in}(\tau,0)d\tau - \dfrac{A}{V_{mi}}\int_0^t f_0(C,\tau)d\tau$
Exit Boundary Conditions	Semi-infinite	$C(t,\infty) = 0$
	Second-type	$\dfrac{\partial\ C}{\partial\ t}(t,L) = 0$
	Flushing	$C(t,L) = 0$
	Mixing zone	$C(t,L) = \dfrac{A}{V_{me}}\int_0^t f_L(C,\tau)d\tau - \dfrac{Q_e}{V_{me}}\int_0^t C(\tau,L)d\tau$

where C_0 is an intial concentration at the inlet boundary of the barrier, H_f is the width of contaminant source zone, $f_0(C,\tau)$ is the flux at the inlet boundary as defined by Eq. (6), Q_i is the column flow rate, Q_e is the flow rate of fluid flushing the barrier exit, V_{mi} and V_{me} are the volumes of uniform concentration zones at the inlet and outlet of the barrier, respectively, L is the barrier thickness, A is the barrier cross sectional area, C_{in} is a time-varying influent concentration at the column entrance, and $f_L(C,\tau)$ is the flux at the exit boundary of the barrier as defined by Eq. (6).

Solution Technique

TRANS1D implements solutions for concentration and flux using three computational approaches: 1) *analytical*, based on closed-form solutions, 2) *finite layer*, based on numerical inversion of Laplace-transformed solutions (e.g., Rowe and Booker, 1985), and 3) *numerical*, based on split-operator finite element solutions (Miller and Rabideau, 1993).

Comparison with Laboratory Experiments

To assess the performance of the ADR in predicting contaminant transport through slurry walls, laboratory column experiments were performed using SB. For the results presented here, the columns were prepared using local backfill soil and 6% (by weight) sodium bentonite. The experiments were performed using flexible-wall permeameters under saturated conditions. A summary of experimental conditions is shown in Table 2. Back pressure saturation was first achieved by consolidating the test column under 4 psi confining pressure and then increasing the back pressure in increments of 5 psi. After full saturation was achieved, an aqueous solution of a mixture of trichloroethylene (TCE) and aniline was permeated through 1/8" Teflon tubing into the column. The measured influent concentrations of TCE and aniline were described by second-order polynomials, and the constants (P_0, P_1, P_2) are summarized in Table 2. The columns were equipped with glass wool diffusers (approximately 0.5 cm thick) at the entrance and exit

boundaries to evenly spread the contaminants. The flow rates and hydraulic gradients were measured periodically and did not change appreciably during the course of the experiments. At the end of each experimental run, subsamples from the columns were sectioned at an approximate interval of 0.5 cm and the total mass of contaminants (both aqueous and sorbed) was measured. As shown in Table 2, total mass recoveries of 82-86% for TCE and 92-95% for aniline were obtained. The total mass recovery of less than 100% is attributed to volatilization losses during sectioning of the column. For modeling, the observed data were adjusted proportional to the noted mass recovery for both TCE and aniline.

The resulting spatial mass profiles were compared to ADR predictions generated by calibrating the sorption and dispersion coefficients (assuming equilibrium sorption), using nonlinear regression. The model incorporated the mixing zone boundary condition at the entrance and exit boundaries. The relative contributions of sorbed and aqueous phases to the total extracted mass were calculated by assuming linear equilibrium between phases (Eq. 4). For the hydraulic gradients listed in Table 2, a media dispersivity of 5% of the column length (e.g., Gelhar $et\ al.$, 1992) results in negligible hydrodynamic mixing. Therefore, the estimated dispersion coefficients were considered approximately equal to the effective diffusion coefficients (D_m/τ). Measured spatial contaminant profiles and model fits are shown in Figures 1-3. The estimated values of sorption and diffusion coefficients are shown in Table 3.

As can be seen from Figures 1-3, the measured concentration profiles are generally consistent with the hypothesis that diffusion-dominated transport conditions exist within the barrier wall. Higher contaminant concentration profiles were obtained for aniline than for TCE, as the columns were permeated with higher concentration of aniline. The mass concentration profiles generated by fitting the ADR equation assuming equilibrium sorption resulted in reasonably good fits. The parameter estimation results in values of the diffusion coefficient varying from 1.06×10^{-6} to 3.25×10^{-6} cm^2/sec for TCE and 0.87×10^{-6} to 4.37×10^{-6} cm^2/sec for aniline, with average diffusion coefficients of 2.2×10^{-6} cm^2/sec for TCE and 2.3×10^{-6} cm^2/sec for aniline. Similar ranges of diffusion coefficients have been observed by other researchers for compacted clays (Barone $et\ al.$, 1992; Johnson $et\ al.$, 1989). The parameter estimation results in calibrated values of the sorption coefficient from 0.001 to 0.226 cm^3/gm for TCE and 0.002 to 0.09 cm^3/gm for aniline, with average sorption coefficients of 0.15 cm^3/gm for TCE and 0.03 cm^3/gm for aniline.

Variations in the calibrated values of diffusion and sorption coefficients are observed for the same contaminant under similar experimental conditions. One plausible explanation is the correlation between sorption and diffusion coefficients in the automated parameter estimation process. As shown in Table 3, relatively higher values of the diffusion coefficient are estimated with higher values of the sorption coefficient. It is noted that the transport model predictions are insensitive to small values of the sorption coefficient, and a sorption coefficient below 0.01 cm^3/gm can be considered negligible. A complete discussion of sensitivity and correlation between model parameters is available elsewhere (Khandelwal $et\ al.$, submitted manuscript). Batch isotherm experiments with the SB matrix resulted in estimated sorption coefficients of 0.41 cm^3/gm for TCE and 0.25 cm^3/gm for aniline, which are higher than observed in the column experiments. This apparent difference between batch and column results is also suggested by the fact that fixing the sorption coefficient to batch experimental values yielded unreasonable values for diffusion coefficients calibrated from the columns (estimated diffusion coefficient higher than D_m).

The model calibration was also performed with nonequilibrium sorption incorporated into the ADR equation. In this case, the values of dispersion coefficient, sorption coefficient, and sorption rate coefficients were simultaneously estimated. The model fits resulted in similar predictions and the estimated dispersion and sorption coefficients were essentially equal ($\pm$ 5%) to the values estimated by assuming equilibrium sorption. Also, the estimated mass transfer rates were large (> 10^{-3} 1/sec), suggesting the absence of nonequilibrium sorption in the columns.

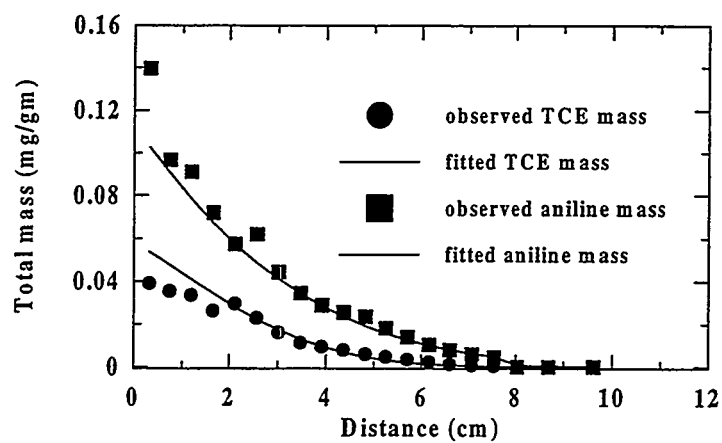**Figure 1: Observed and fitted mass of contaminants in SB column experiment 1**

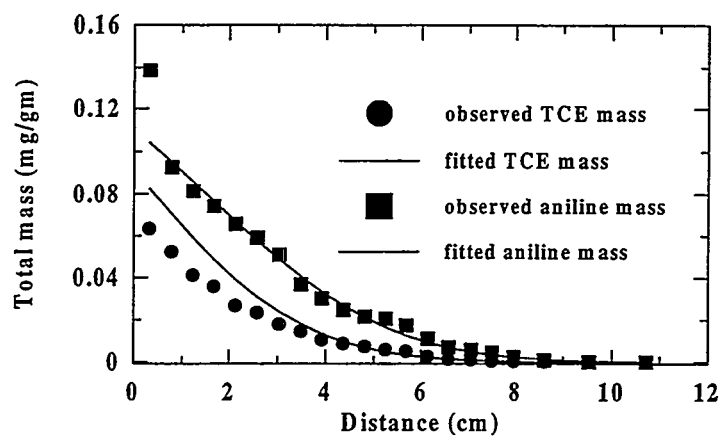**Figure 2: Observed and fitted mass of contaminants in SB column experiment 2**

Figure 3: Observed and fitted mass of contaminants in SB column experiment 3
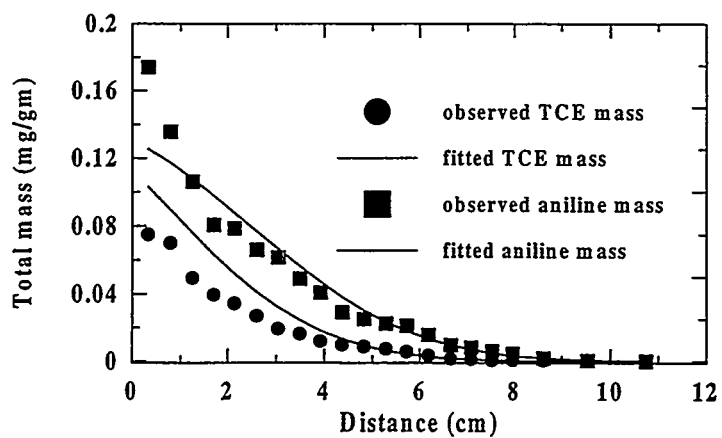
<p style="text-align:center">Table 2: Summary of experimental conditions.</p>

Parameter	Experiment 1	Experiment 2	Experiment 3
Duration (days)	21	18	29
Hyd. Conductivity (cm/s x 10^8)	2.67	3.76	2.93
SB column length (cm)	11.3	12.6	11.2
Porosity	0.339	0.337	0.342
Hydraulic gradient	6.4	6.0	6.1
% Mass recovery (TCE)	86.6	82.5	86.6
% Mass recovery (aniline)	95.0	92.1	94.9
P_o^{TCE} (mg/l)	491.8	481.8	488.1
P_1^{TCE} (mg/L-d)	0.298	-3.29	-6.16
P_2^{TCE} (mg/L-d^2)	-0.0557	-0.0185	-0.019
$P_o^{aniline}$ (mg/l)	879.1	871.0	871.1
$P_1^{aniline}$ (mg/L-d)	-6.11	3.72	-0.16
$P_2^{aniline}$ (mg/L-d^2)	0.016	-0.29	-0.07

<p style="text-align:center">Table 3: Parameter estimates assuming equilibrium sorption.</p>

#	TCE	TCE	Aniline	Aniline
	D_m/t (cm^2/sec*10^6)	K_d (cm^3/gm)	D_m/t (cm^2/sec*10^6)	K_d (cm^3/gm)
1	1.06	0.001	4.37	0.09
2	3.25	0.224	1.48	0.002
3	2.05	0.226	0.87	0.01

SUMMARY AND CONCLUSIONS

A contaminant transport model (TRANS1D) has been developed to predict the transport of contaminants for the design and analysis of subsurface barriers. In TRANS1D, concentration and flux-based solutions to the one-dimensional ADR equation are implemented for numerous boundary conditions. Various reaction scenarios including nonlinear and nonequilibrium sorption, and decay have also been included in the model. The solutions of the ADR equation under various conditions were obtained using *analytical*, *finite layer*, and *numerical* techniques. Applications of TRANS1D for the analysis and design of SB slurry walls are discussed elsewhere (Guglielmetti and Chien, 1996; Adu-Wusu *et al.*, 1997).

As part of a program of model testing, the model was calibrated to data obtained from laboratory scale SB column experiments. The column experiments were designed to mimic, to the extent possible, conditions similar to those likely to be encountered in the field. Based on the results of model calibrations, it was concluded that the ADR model (assuming linear equilibrium sorption) was able to   describe spatial concentration profiles of contaminants. The calibration process resulted in reasonable values for diffusion coefficients. Also, nonequilibrium sorption did not significantly influence transport of TCE and aniline under the conditions present in the column experiments discussed in this paper.

The limitations of the model include representations of a barrier as a homogeneous material, with no variation in properties in space or time. Given the basic heterogeneity of soil and difficulty associated with maintaining highly controlled construction environments, slurry walls are likely to be better represented by incorporating spatial and temporal variability. Also, complex chemical reactions occurring in a barrier may not be well represented by the various reactions considered in this model at the current stage of development. However, the modeling framework presented in this paper should provide reasonable and conservative estimates for contaminant transport and is therefore recommended as a starting point for design.

REFERENCES

Adu-Wusu, K., J. M. Whang, and M. F. McDevitt (1997) Modification of clay-based waste containment materials. Proceedings of *1997 International Containment Technology Conference and Exhibition*.

Barone, F. S., R. K. Rowe, and R. M. Quigley (1992) A laboratory estimation of diffusion and adsorption coefficients for volatile organics in a natural clayey soil. *Journal of Contaminant Hydrology*, 10, 225-250.

Gelhar, L. W., C. Welty, and K. R. Rehfeldt (1992) A critical review of data on field-scale dispersion in aquifers. *Water Resources Research*, 28(7), 1955-1974.

Gray, D. H. and W. J. Weber (1984) Diffusional transport of hazardous waste leachate across clay barriers. *Proceedings of the 7th Annual Madison Waste Conference*, Sept 11-12, Univ. of Wisconsin, 373.-380.

Guglielmetti, J. L. and C.C. Chien (1996) Containment technology and industry's approach. *Proceedings of the Twenty Eighth Mid-Atlantic Industrial and Hazardous Waste Conference*, Buffalo, NY, 127-133.

Johnson, R. L., J. A. Cherry, and J. F. Pankow (1989) Diffusive contaminant transport in clay: a field example and implications for clay-lined waste disposal sites. *Environmental Science & Technology*, 23, 340-349.

Khandelwal, A. and A. J. Rabideau (1996) Modeling of diffusion dominated transport in soil/bentonite slurry walls," Proceedings of the *Twenty Eighth Mid-Atlantic Industrial and Hazardous Waste Conference*, Buffalo, NY, 134-141.

Khandelwal, A., A. J. Rabideau, and P. Shen. Analysis of diffusion and sorption of organic solutes in soil-bentonite slurry walls. Submitted to *Environmental Science & Technology*.

Miller, C. T. and A. J. Rabideau (1993). Development of split-operator Petrov-Galerkin methods to simulate transport and diffusion problems. *Water Resources Research*, 29(7), 2227-2240.

Mott, H. V. and W. J. Weber, Jr. (1991) Factors influencing organic contaminant diffusivities in soil bentonite cutoff barriers. *Environmental Science & Technology*, 25(10), 1708-1715.

Rabideau, A. J., A. Khandelwal, and D. Millar. Application of simplified contaminant transport models to the design of vertical barriers. Submitted to *Journal of Environmental Engineering*.

Rabideau, A. J. and A. Khandelwal. Analysis of the impact of nonequilibrium sorption on contaminant transport in slurry walls. Accepted for publication in *Journal of Environmental Engineering*.

Rowe, R. K., and J. R. Booker (1985) 1-D pollutant migration in soils of finite depth. *Journal of Geotechnical Engineering*, 111(4), 479-499.

Rowe, R. K., R. M. Quigley, and J. R. Booker (1995) *Clayey barrier systems for waste disposal facilities*, E & FN Spoon, London.

Rumer, R. R. and J. K. Mitchell (1995) *Assessment of barrier containment technologies*. NTIS Publication # PB96-180583.

Shackelford, C. D. and P. L. Redmond (1995) Solute breakthrough curves for processed kaolin at low flow rates," *Journal of Geotechnical Engineering*, 121(1), 17-32.

INCORPORATION OF SEDIMENTOLOGICAL DATA INTO A
CALIBRATED GROUNDWATER FLOW AND TRANSPORT MODEL

Nicolas J. Williams[1], Steven C. Young[2], David H Barton[3], Brian T. Hurst[4]

Abstract
Analysis suggests that a high hydraulic conductivity (K) zone is associated with a former river channel at the Portsmouth Gaseous Diffusion Plant (PORTS). A two-dimensinoal (2-D) and three-dimensional (3-D) groundwater flow model was developed based on a sedimentological model to demonstrate the performance of a horizontal well for plume capture. The model produced a flow field with magnitudes and directions consistent with flow paths inferred from historical trichloroethylene (TCE) plume data. The most dominant feature affecting the well's performance was preferential high- and low-K zones. Based on results from the calibrated flow and transport model, a passive groundwater collection system was designed and built. Initial flow rates and concentrations measured from a gravity-drained horizontal well agree closely to predicted values.

Introduction

A prerequisite for accurate groundwater transport simulation is proper delineation of high hydraulic conductivity (K) and low-K deposits that exert primary control on groundwater flow paths. A common problem associated with modeling heterogeneous aquifer systems is that the available K data is too sparse and/or uncertain to map a three-dimensional (3-D) K field for direct input into a groundwater model. In order to construct plausible K fields, hydrogeologists often use geostatistical and/or inverse techniques. These techniques have robust algorithms for generating and evaluating K fields, but they can be misapplied if not used jointly with geological data.

This paper demonstrates how the incorporation of geologic data was critical to a groundwater flow and transport model at Portsmouth Gaseous Diffusion Plant (PORTS). For comparative purposes, a previous model result used at the site is presented whose K field was determined primarily by an automatic inverse calibration technique. Although the previous model provides excellent calibration to measured hydraulic heads, the model's K field and velocity field are inconsistent with geological and plume migration data.

The development of a calibrated two-dimensional (2-D) and 3-D groundwater flow and solute transport model was needed to evaluate different remedial alternatives for the capture of a trichloroethylene (TCE) plume. The 2-D model was used to demonstrate that horizontal wells would be more effective for plume capture than a funnel-and-gate option. The funnel-and-gate model consists of using two subsurface impermeable barriers to funnel groundwater to a vertical extraction well. The 3-D model focused on optimizing the location of the horizontal well and quantifying its performance under several scenarios. The groundwater flow models were based mainly on the sedimentological model of the site with adjustments for recent construction-related impacts on the aquifer.

Site Stratigraphy
PORTS lies within the abandoned Portsmouth River Valley in southern Ohio. An analysis of approximately 300 subsurface boring logs from the southern portion of the site suggests that contiguous deposits of relatively clean silts and sands are associated with a former river channel. Piezometric contours of quarterly water table measurements from 70 wells show large-scale diverging and converging flow patterns consistent with the location of silts and sands inferred from the boring logs.

[1]P-SQUARED Technologies, Inc., P.O. Box 22668, Knoxville, TN, 37933, (423) 691-3668, nicolas@p2t.com

[2]P-SQUARED Technologies, Inc., P.O. Box 22668, Knoxville, TN, 37933, (423) 691-3668, syoung@p2t.com

[3]P-SQUARED Technologies, Inc., P.O. Box 22668, Knoxville, TN, 37933, (423) 691-3668, dbarton@p2t.com

[4]P-SQUARED Technologies, Inc., P.O. Box 22668, Knoxville, TN, 37933, (423) 691-3668, bhurst@p2t.com

Figure 1 shows a simplified stratigraphy at PORTS with approximate thicknesses and estimated K values. The Sunbury Formation was heavily eroded in certain areas by the ancient Portsmouth River. The unconsolidated deposits are divided into two major units: Gallia Sand Member and Minford Clay Member. The Gallia has the most transmissive and heterogeneous deposits at PORTS. It consists of the floodplain, point-bar, and channel lag deposits of the ancient Portsmouth River. The Gallia is considered the main aquifer at the site. For this reason considerable emphasis was placed on dividing the Gallia deposits into textural facies that could help define large-scale patterns in the K field. The facies classification scheme was limited to sand, gravelly sand, and clayey mixture. The snad unit consists of mostly sand and/or sandy silt and has the highest K. The gravelly sand unit consists of mostly sandy gravels or gravels and was limited to less than 15% clay. When the sandy gravels or gravels had more than 15% clay, they were classified as clayey mixture. The Minford Clay Member deposits are primarily associated with lacustrine deposits and have been reworked during cut-and-fill activities.

Ground Elevation

| Minford Clay Member |
| 0.0-12.2 m Thick |
| 0.19 m/day |
| Gallia Sand Member |
| 0.0-4.3 m Thick |
| 6.1 m/day |
| Sunbury Shale |
| 0.6-6.1 m Thick |
| 0.00003 m/day |
| Berea Sandstone |
| 7.6-9.1 m Thick |
| 0.05 m/day |

Figure 1. Stratigraphy.

There are many construction-related impacts on the aquifer. Several manmade trenches and subsurface barriers, shown in Figure 2, affect groundwater flow at PORTS. Along the northern and eastern boundaries of the X-749 Landfill and in the southern portion of the site are bentonite slurry walls used as subsurface barriers. The estimated K value of these barriers is 10,000 times lower than the K value associated with the Gallia deposits, so the barriers can be approximated as impermeable barriers in the numerical model. Along the southeastern and western boundaries of the X-749 Landfill, permeable trenches have been installed with an estimated K value of 85.3 m/day (280 ft/day) (HAZWRAP 1994). The permeable trenches were installed to improve drainage towards
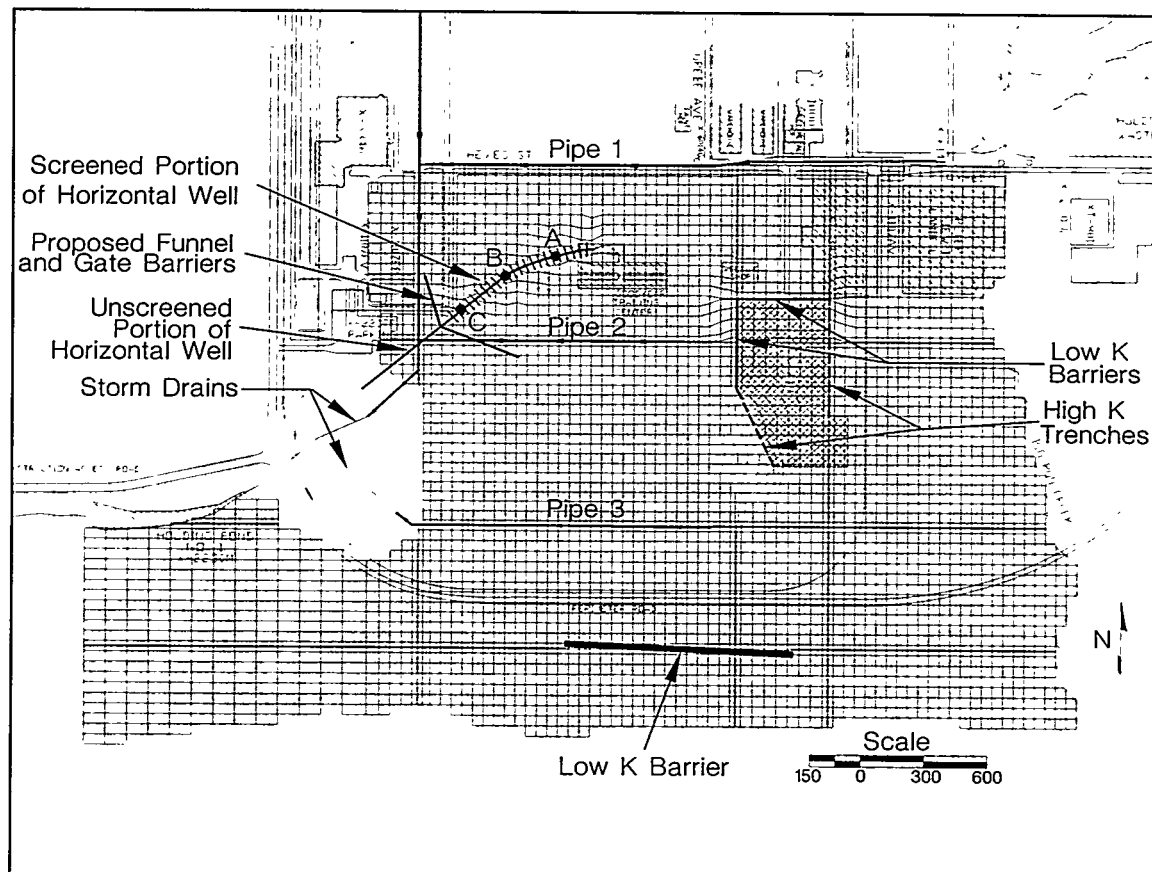

Figure 2. Site Map and Model Grid.

969

two extraction wells. Construction and grading have change the topography across much of the site. More fill than cut has occurred in the X-749/X-120 area. A stream and its tributaries on the western side of the model were filled with compacted clay.

Groundwater Flow Model

The groundwater flow model consisted of a finite-element, saturated-unsaturated flow model using FRAC3DVS (Therrien et al 1994). An accurate delineation of the site stratigraphy is a keystone to an accurate model at PORTS, because highly variable K values are assigned to the stratigraphic units. The model grid is shown in Figure 2 and consists of five element layers with 21,500 elements and 26,400 nodes.

The K and dispersivity values (α) assigned to the different model layers are summarized in Table 1. In regions where local streams have eroded the Sunbury Shale, a weathered shale material type was used. A K value was assigned to each Gallia unit by performing a multiple linear regression analysis on pump test results and the thickness of the Gallia textural units at each well location. The assignment of a K value for each Gallia textural unit permits the calculation of a continuous transmissivity field for the entire Gallia layer. For each unit, a transmissivity is calculated as the product of the unit thickness in each element and the unit-specific K value. The Gallia transmissivity for each element is determined by summing the transmissivities for the three units. To calculate the Gallia K value for each element, the Gallia transmissivity is divided by the Gallia's total thickness at that element.

Table 1. Hydraulic Values Assigned to the Stratigraphic Layers.

Unit	$K_x=K_y$ (m/day)	$\alpha_x=\alpha_y$ (m)
Minford Clay	0.43	0.9
Alluvium	0.21	0.9
Low-K Channel	0.03	0.9
Gallia Clayey Mixture	0.43	1.8
Gallia Gravelly Sand	1.00	1.8
Gallia Silty Sand	7.80	1.8
Weathered Shale	0.003	1.8
Sunbury Shale	0.00003	0.3
Berea Sandstone	0.03	0.9

An alluvium material type was included around Big Run Creek, Holding Pond No. 1, and a small stream on the southern boundary (see Figure 1) to account for floodplain and stream alluvial deposits. In the northwest, the Gallia K field was modified by including a low-K zone. This K zone represents a former drainage channel that was partially filled with compacted clay during the construction of the plant. The effect of the low-K channel can be seen in water table plots for the site, dry wells in the vicinity, and very low-K values from pump test results in this area (Young et al 1995). The low-K channel was delineated by superimposing the topography maps of the pre- and post-construction period. The Minford Clay Member includes layers of fine silts, lacustrine clays, and compacted fill. For the steady-state flow model, the most important impact of the Minford on the groundwater flow system is its spatial distribution of the recharge.

Groundwater Solute Transport Model

To efficiently simulate solute transport and particle tracking in complex stratigraphy, P-SQUARED Technologies, Inc. (P2T), developed the particle-tracking code PTRAX (Benton et al 1995). Particle tracking is a powerful and versatile tool that offers several advantages over finite-difference and finite-element modeling for solute transport. These advantages include the mapping of flow paths, reverse tracking to delineate capture zones, and less grid refinement in regions where dispersion length values are small.

Hydrodynamic dispersion is the parameter that describes the mixing of solute in groundwater and incorporates the effects of both molecular diffusion and mechanical dispersion. The most reliable estimates for dispersivity are normally based on analysis of well controlled tracer experiments and/or detailed measurements of hydraulic conductivity. Neither of these results are available for any of the five stratigraphic layers. The most reliable data presented by Domenico and Schwartz (1990) suggest that the maximum longitudinal dispersivity is on the order of one meter for plumes in materials like the Gallia. For a steady-flow field, lateral dispersivity values are typically about 1/10 of the longitudinal dispersivity, and vertical transverse dispersivity values are about 1/100 the longitudinal dispersivity.

The main advantage of using PTRAX to simulate solute transport is reduced grid discretization. The Peclet constraint limits dispersivity to values greater than one-half the discretization distance for finite-difference and finite-element solute transport methods (Anderson et al 1992). At PORTS, the general discretization in the z-direction is 0.6-9.1 m (2-30 ft). By the Peclet constraint, the effective minimum dispersivity in the z-direction is 0.3-4.6 m (1-15 ft) due to numerical dispersion as a result of discretization. Since PTRAX uses a random walk algorithm to simulate dispersion, it is not limited by the Peclet constraint, and the effective dispersivity in the z-

Figure 3. Model Head for Layer 4, Gallia.

direction is 0.003 m (0.01 ft). The other big advantage is that PTRAX uses distance as the variable of integration. This allows for shorter run times and it always satisfies the Courant constraint. The Courant constraint states that a contaminant cannot travel more than one element length in a time step. Adequate discretization is necessary to delineate the velocity field properly.
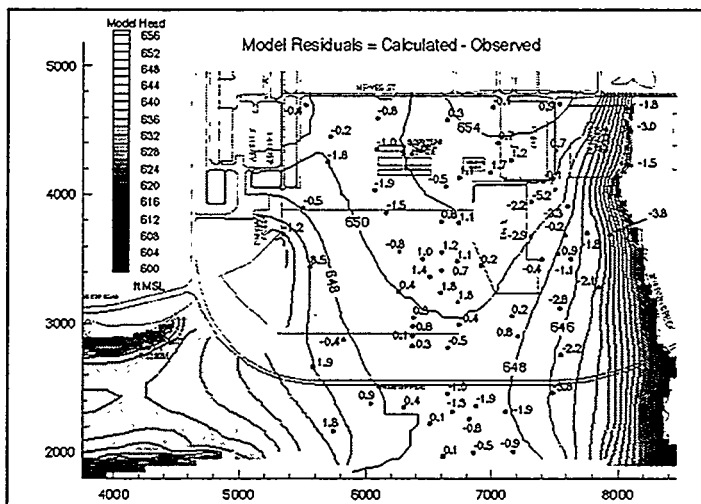
To simulate solute transport with particle tracking, the plume concentrations need to be mapped to individual particles, which are then tracked and mapped to a concentration. Since no detectable concentrations were found in the Minford or Sunbury units, all of the TCE plume was assumed to be located in the Gallia deposits. Each element in the Gallia was assigned a concentration based on its centroid location with respect to the TCE map. The volume of the element and its associated concentration was used to calculate the amount of mass in the element. The mass was then divided into discrete particles of smaller mass. Each particle was tracked through the velocity field to each specified time step. Then the mass of the particles in an element were summed to calculate the mass in that element. This mass was then converted to a concentration based on the volume of each element containing particles. Seeding of the particles was accomplished by randomly distributing the particles through the element using a Latin-Hypercube method. Each element was subdivided into roughly equal volume cubes, enough for one particle per cube. Each particle was then randomly placed in the subcube.

Flow Model Calibration

Conventional groundwater flow model calibration involves adjusting model parameters to improve the match between measured and simulated water table elevations. Without adequate consideration to flow constraints, a groundwater model can appear to be calibrated, but it may not accurately predict groundwater flowpaths. Thus, proper model calibration must include data beyond hydraulic head values. The flow model calibration and validation were based on hydraulic heads and base flow to Big Run Creek. The hydraulic head data set used for calibration represents the average water table values measured during April 1995. The hydraulic heads calculated by FRAC3DVS for the Gallia layer are contoured in Figure 3 with the model residuals. The root-mean-square (RMS) error was 0.42 m (1.39 ft) and the arithmetic mean was -0.13 m (-0.41 ft). From weir measurements, the estimated base flow contribution to Big Run Creek is 27.3 liters per minute (lpm) (7.2 gallons per minute [gpm]) (Young et al 1995). The flux to Big Run Creek from the flow model is 19.3 lpm (5.1 gpm). Given that 0.42 m is less than the seasonal variations observed at the majority of the wells and is small compared to the nearly 15.2 m (50 ft) head differential across the model domain, the favorable agreement between the predicted and measured base flows suggests that the groundwater flow model is adequately calibrated. The fluid mass balance for the model domain is excellent since the model error between total inflows and outflows is less than 0.01%.

Transport Model Calibration

To ensure a calibrated solute transport model that could accurately predict the migration of the TCE plume, it was necessary to perform historical plume development (history matching). Because of the limitations of the site characterization data and the TCE data base, history matching focused on the general trends associated with the bulk movement of the TCE plumes during the last 39 years and on the TCE breakthrough curves from 1988 to 1995 for selected wells. Because the distribution and the amount of released TCE is unknown and plume sampling did not begin until 1988, there is insufficient data to realistically evaluate a numerical simulation of the full evolution of the TCE plumes. Although the TCE data are insufficient to accurately characterize the 3-D structure of the X-120 and X-749 plumes, the data is sufficient to characterize the general configuration of the plumes. To evaluate the solute transport model, the assumption is made that the current plume configurations were caused by a TCE release that began 39 years ago at the Goodyear Training Center (X-120 Area) and at the X-749 Landfill.

To produce the 39-year path lines for TCE transport, modifications to the calibrated flow model are required. From 1955 to 1991, it is assumed that all the model inputs are valid except that there are no low-K barriers nor a low-K cap at the X-749 Landfill. To simulate a flow field from 1955 to 1991, all low-K barriers were removed from the numerical model and the infiltration rate used at the landfill was increased. In 1991, a low-K cap and low-K barriers were installed at the X-749 Landfill. To produce the flow field for 1991 to 1995, only the low-K barrier installed south of the X-749 Landfill was removed from the numerical model. The 39-year path lines and 1995 TCE plume are shown in Figure 4.

One of the groundwater models used to assess remediation alternatives before the P2T model was a MODFLOW model (G&M 1989) which was calibrated to a flow field similar to the one in Figure 3. A major difference between the models was the method used for calibration and development of the Gallia K field. In the G&M model, the K field was determined primarily from an inverse technique of automatic calibration. This produced an impressive RMS of 0.03 m (0.11 ft). However, this low RMS is misleading because it was obtained by producing an unreasonable K field for the Gallia. The highest K value assigned to the Gallia is at the location where the Gallia boreholes have extremely slow recovery times and whose logs indicate high clay contents. Similarly, some of the lowest K values assigned correspond to locations where pump test data and subsurface logs suggest that the K value should be the highest. In explaining the spatial K pattern, G&M (1992) does not discuss any geological data, but suggests that the high K zone represents point bar deposits.

Figure 5 shows the 39-year TCE flow paths produced by coupling flow results from the G&M (1992) model to MODPATH (Pollock 1989). For these simulations the G&M input parameters to MODFLOW (McDonald and Harbaugh 1988) were adjusted to omit the slurry walls and low-K cap at the X-749 Landfill, and MODPATH was modified to incorporate the retardation. The TCE flow paths in Figure 5 are not consistent with the current TCE plume location. Areas of major concern include significant downward movement into the Berea Sandstone and the absence of TCE plume migration south of the X-749 Landfill. As a result of the significant inconsistency between predicted TCE
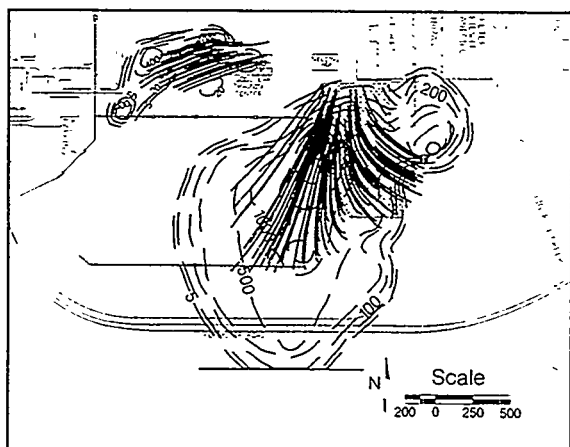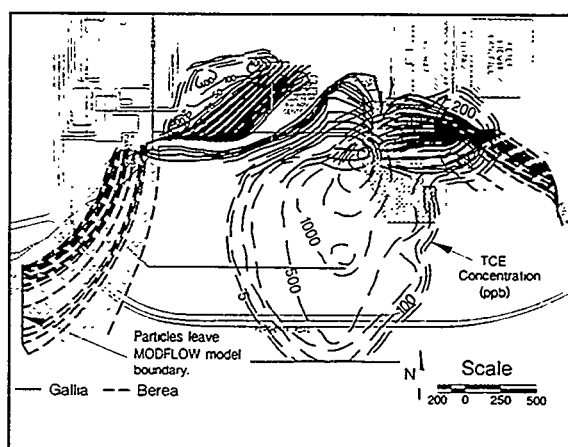

Figure 4. 39-Year Pathlines, P2T Model.

Figure 5. 39-Year Path Lines, G&M Model.

migration and current TCE plume location, the approach to develop a groundwater flow model based primarily on inverse techniques to adjust the K field and optimize the head calibration appears to be inadequate at PORTS.

Appropriate FRAC3DVS and PTRAX runs were performed to simulate the evolution of the X-120 and X-749 plumes from January 1988 until September 1994 for breakthrough curves. The simulations included two flow fields in order to account for the installation of the low K barriers and cap at the X-749 landfill in September 1991. As shown in Fig. 6, the simulated and measured breakthrough curves for the well X-749-13G have consistent trends and have similar concentrations. Overall, the results suggest that the solute transport model provides a credible simulation of the transport processes at PORTS.

Model Application

The primary focus of the 2-D model was to demonstrate that horizontal wells would be more effective for plume capture than a funnel-and-gate system. The evaluation of alternative collection systems was primarily based on the ability to passively collect groundwater. The 214.9 m (705 ft) barriers were implemented as no-flow boundaries by selectively decoupling nodal connections. Table 2 provides the predicted groundwater flow rates for 12 different groundwater collection scenarios with the water table elevation set to 196.6 m (645 ft). The model results indicate that the horizontal well is most effective for collecting groundwater. The simulations suggest that barriers are not a cost-effective option for collecting groundwater in the X-120 region if a horizontal well is to be part of the groundwater collection system (Young et al 1994).

Table 2. Modeled Groundwater Collection Systems.

Type of Collection Facility	Presence/ Absence of Barrier	Groundwater Collected (lpd)
F&G with Vertical Well at A	Present	2884
	Absent	2786
F&G with Vertical Well at B	Present	3153
	Absent	3025
F&G with Vertical Well at C	Present	791
	Absent	685
58.5 m of screened HW	Present	5898
	Absent	5780
117.2 m of screened HW	Present	7226
	Absent	7105
190.2 m of screened HW	Present	7435
	Absent	7355

F&G = funnel and gate system
HW = horizontal well
VW = vertical well

The 3-D model focused on optimizing the location of the horizontal well and quantifying its performance under several transport scenarios. As might be expected in a fluvial aquifer, the most dominant features affecting the performance of the well were preferential high- and low-K zones. For maximum flow withdrawal, the well performance was simulated with a hydraulic head of 196.6 m (645 ft) mean sea level (MSL). The 196.6-m elevation represents the lowest head that could be maintained without desaturating the Gallia deposits. The mean flow rate of 11.0 lpm (2.9 gpm) and 7.0 lpm (1.86 gpm) is predicted for well heads of 196.6 m (645 ft) MSL and 197.2 m (647 ft) MSL, respectively (Young et al 1995).
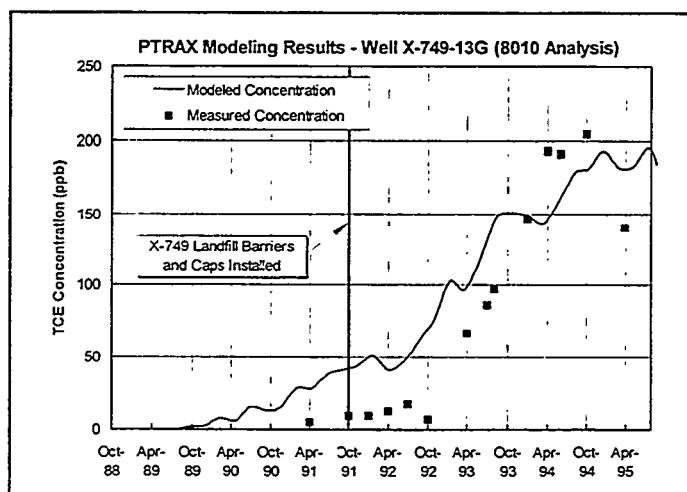

Figure 6. TCE Breakthrough Curve.

TCE Plume and Remediation

A passive ground water collection system using a horizontal well was recommended for collecting the TCE plume. It is passive because the groundwater flows into the well only due to the hydraulic gradients produced in the surrounding groundwater system. Key design criteria for the horizontal well

are its location, length, and head losses. The collected contaminated groundwater will be passed through a reactive media that will facilitate the breakdown of the TCE by reductive dehalogenation; it is driven solely by hydraulic head.

Among the two most important variables required to properly design the well is the delineation of the X-120 TCE plume and the K field of the Gallia deposits near the TCE plume. Before the evaluation of the horizontal well's performance, the selection of the X-120 area looked promising based on the high-K values presented in the G&M report (1989) and the plume configuration. G&M reported K values from 13.7 m/day (45 ft/day) to 18.9 m/day (62 ft/day). The TCE plume configuration was developed based on a review of all TCE monitoring data (Young et al 1995), a consideration for the low-K channel in the Gallia, and numerous TCE measurements from mini-piezometers installed via cone-penetrometers in April 1995. No DNAPL source terms were associated with any of the plumes.

The predicted performance of the horizontal well for the case of 196.6 m (645 ft) hydraulic head shows a TCE removal percentage and concentration entering the X-120 treatment facility of 40% and 60 parts per billion (ppb) at 5 years and 70% and 9 ppb at 30 years. Model results predict the majority of the residual TCE after 30 years resides in the low-K channel. The X-120 treatment facility was completed in 1996. The predicted flow to the treatment facility was 6.8 lpm (1.8 gpm) to 8.3 lpm (2.2 gpm). The average measured flow during the first two months of operation was 3.4 lpm (0.9 gpm) to 4.5 lpm (1.2 gpm). The predicted initial TCE concentration was 100-200 ppb and the average measured concentration was 75-100 ppb (Liang et al 1996).

REFERENCES

Anderson, MP and WW Woessner (1992). *Applied Groundwater Modeling*, Academic Press, Inc., San Diego, CA.

Benton, DJ, SC Young, and NJ Williams (1995). *Description and Verification of PTRAX: A Random Walk Model for Predicting Groundwater Solute Transport*, Environmental Consulting Engineers, Inc., Knoxville, TN.

Domenico, P and F Schwartz (1990). *Physical and Chemical Hydrogeology*, John Wiley & Sons, New York, NY.

Geraghty and Miller, Inc. (1990). *Site-Wide Ground-Water Flow Model of the Portsmouth Gaseous Diffusion Plant, Piketon, Ohio*, Geraghty and Miller, Inc., Reston, VA.

Geraghty and Miller, Inc. (1992). *Quadrant I: Description of Current Conditions at the Portsmouth Gaseous Diffusion Plant, Piketon, Ohio*, Geraghty and Miller, Inc., Reston, VA.

HAZWRAP (1994). *Draft Interim Measures Report for the X-749 Landfill and X-120 Area, Portsmouth Gaseous Diffusion Plant, Piketon, Ohio*, Hazardous Waste Remedial Action Program (HAZWRAP).

Liang, L, et. al. (1996). *Interim Report on the X-749/X-120 Groundwater Treatment Facility: A Field-Scale Test of Trichloroethylene Dechlorination using Iron Fillings*, Department of Energy.

McDonald, M and A Harbaugh (1988). *Chapter A1: A Modular Three-Dimensional Finite-Difference Ground-Water Flow Model*. U.S. Geological Survey Book 6 Modeling Techniques. Scientific Software Group, Washington, D.C.

Pollock, D (1989). *Documentation of Computer Programs to Compute and Display Pathlines Using Results from the U.S. Geological Survey Modular Three-Dimensional Finite-Difference Ground-Water Flow Model*. U.S. Geological Survey, Reston, VA, Open File Report 89-38.

Therrien, R, EA Sudicky, and RG McLaren (1994). *User's Guide for FRAC3DVS: An Efficient Simulator for Three-Dimensional, Saturated-Unsaturated Groundwater Flow and Chain-Decay Solute Transport in Porous or Discretely-fractured Porous Formations*, Software Edition 2.02, Waterloo University, Canada: Waterloo Groundwater Centre for Research.

Young, SC, NJ Williams, and DH Barton (1994). *X-120 Groundwater Modeling Study: Evaluation of Alternative Groundwater Collection Systems*, Environmental Consulting Engineers, Inc., Knoxville, TN.

Young, SC, NJ Williams, BT Hurst, and DH Barton (1995). *Development of Calibrated Groundwater Flow and Transport model for Evaluating Remediation Alternatives at Portsmouth Gaseous Diffusion Plant and Their Application to the Design of the X-120 Horizontal Well*, Environmental Consulting Engineers, Inc., Knoxville, TN.

Hydraulic Studies of In-Situ Permeable Reactive Barriers

R.M. Focht; J.L. Vogan, EnviroMetal Technologies Inc., 42 Arrow Road, Guelph, Ontario, Canada N1K 1S6, Tel.: (519) 824-0432, Fax: (519) 763-2378, E-mail: eti@beak.com

S.F. O'Hannesin, Institute for Groundwater Research, University of Waterloo, Waterloo, Ontario, Canada, N2L 3G1, Tel.: (519) 888-4567 Ext. 3159, Fax: (519) 746-1829, E-mail: sfohanne@sciborg.uwaterloo.ca

Abstract

Groundwater flow velocity is a critical parameter in evaluating the field performance of in-situ permeable reactive barriers. Laboratory column tests indicate that bromide is a suitable conservative tracer for use in field tracer studies involving granular iron. Conservative tracer tests have been conducted to determine groundwater velocity and flow patterns through pilot-scale funnel-and-gate trials involving the EnviroMetal Process. Other methods of measuring in-situ velocities have also been evaluated. Once accurate groundwater flow velocities are known and concentrations of VOCs are measured, field degradation rates can be calculated. Both parameters are necessary for the design and costing of full-scale treatment systems.

Introduction

In-situ permeable treatment zones containing granular iron are currently being used at several private and government facilities in the United States to remediate groundwater contaminated with dissolved chlorinated solvents. This method of treatment involves placing granular iron in permeable zones, across the path of groundwater containing VOCs. As the contaminated groundwater flows through the permeable zones, the chlorinated solvents are degraded in the granular iron (Gillham, 1996). This passive treatment system offers many advantages over conventional pump-and-treat systems. In particular, the contaminants degrade to nontoxic chemicals, and with proper placement, only contaminated water is treated. Because the technology, once installed, is fully passive, substantial reductions in operation and maintenance costs are anticipated. Full-scale in-situ treatment zones have been installed at five government and industrial facilities in the U.S. and one in Belfast, Northern Ireland. Five smaller, pilot-scale units are in place at other sites in the U.S.

The primary factors affecting the installation cost of a reactive iron system are plume dimensions, upgradient VOC concentrations, and groundwater velocity. These parameters affect the treatment zone dimensions, particularly the "flow-through" thickness of the reactive zone required to give the necessary residence time in order for the VOCs to degrade to their MCLs. The residence time in these systems is highly sensitive to groundwater velocity, and therefore accurate determination of this parameter is necessary for the development of a full-scale design. Furthermore, precise knowledge of the actual velocity through a treatment zone is necessary in order to determine if a treatment zone is performing to expectations. This paper presents the results of attempts to measure the velocity through two pilot-scale in-situ treatment zones, and discusses the implications of these results for future application(s) of the technology.

Groundwater models are often used to predict velocity through these treatment systems. In many cases, seldom is there sufficient site data to define detailed hydrologic conditions (model parameters) in the small area surrounding a pilot-scale system. If such data does exist, then the model results are only as accurate as the data itself. For example, the predicted groundwater flow velocities and ultimately treatment zone dimensions, which are proportional to flow velocity, will have the same level of uncertainty as the hydraulic conductivity data used in the model. Clearly, a direct measurement of flow velocity would prove beneficial and would not carry the same

975

uncertainty as sparsely collected and/or estimated aquifer properties, allowing smaller safety factors to be applied during design.

Conservative Tracer Selection

Of the several tracers available, based on the results of laboratory tests and regulatory considerations, bromide was considered the most appropriate. A bench-scale bromide tracer test was conducted using a column of 100% Master Builders iron. The column was in operation for about two weeks prior to the tracer injection. Using weights determined when the column was dry, fully saturated and at the time of the test, the water-filled pore volume was determined to be 250 mL. A 563 mg/L bromide solution (as sodium bromide) was pumped into the column at a rate of 0.32 mL/min for about one pore volume and then replaced with background water. The effluent from the column was connected to a fraction collector which advanced every 20 minutes. By measuring the weight of the collection vials before and after receiving the effluent, the volume of solution in each vial was determined. By measuring the bromide concentration in each of these samples, the two breakthrough curves in Figures 1 and 2 were determined.

The center of mass of both the influent and effluent curves (relative concentration of 0.5) corresponds very closely with one pore volume. Though a relative retardation factor of 1.06 was calculated, within the certainty of the measurements, it is reasonable to conclude that bromide behaved as a conservative tracer. This conclusion is supported by similar results obtained by Bennett, 1996). As the two field sites considered in this paper both contained 100% Master Builders iron, bromide was selected as the tracer for the field tests.

Field Test - Colorado Site

A pilot-scale in-situ treatment system was installed in November 1995 at a government facility in Colorado. This system consisted of a 3 m long by 3 m wide x 5.5 m deep (10 ft x 10 ft x 18 ft deep) permeable treatment section, flanked by 4.6 m (15 ft) of sheet piling on either side (Figure 3). Results of a groundwater modeling exercise conducted prior to installation indicated that the velocity through the reactive zone would be approximately 60 cm/day (2 ft/day).

Three independent methods of velocity measurements were examined:

(i) calculation using water level elevation data and Darcy's equation
(ii) use of a conservative tracer
(iii) an in-well heat pulse flow meter.

The rate of horizontal groundwater flow in the vicinity of the reactive wall was calculated using Darcy's Law as follows:

$$V = Ki/n$$

where:

V = average linear groundwater velocity (L/T);
K = hydraulic conductivity (L/T);
i = hydraulic gradient (L/L); and
n = porosity of aquifer or iron materials (dimensionless).

L and T are dimensions of length and time, respectively.

A value for the hydraulic gradient, i, of 0.02 was determined from hydraulic head measurements taken in June 1996 in the vicinity of the wall. Because of the relatively low gradient and the small

dimensions of the site, differences in water levels were on the order of 1.5 cm or less. A value of 760 cm/day (25 ft/day) was used for the aquifer hydraulic conductivity; and a value of 0.35 was estimated for the aquifer porosity. Given these values, a groundwater velocity of 45 cm/day (1.4 ft/day) was calculated. The hydraulic conductivity value of 760 cm/day was used because it gave the best calibration to measured water levels in the modeling studies; however, a review of data from previous investigations suggests that the hydraulic conductivity of the aquifer in the vicinity of the installation may be higher than 760 cm/day. Should this be the case, the velocity in this area could be higher than 45 cm/day.

Velocities were also measured using a down-hole heat-pulse flow meter manufactured by KV Associates of Falmouth Massachusetts (Kerfoot, 1988). These measurements were made in October 1996 in 5 cm (2 in) diameter wells in the vicinity of the installation. The heat-pulse meter provides both magnitude and direction readings over a small vertical interval. All readings were taken at a depth of approximately 90 cm above the base of the well screen. Water level measurements in October 1996 showed similar elevation patterns to those measured previously.

Results of the flow meter measurements are shown in Table 1. Remarkably similar magnitudes of velocity, of about 11 cm/day (0.4 ft/day), were measured in most wells, and the directions appeared to be reasonably consistent with the direction of flow indicated by water level measurements. That is, northerly flow (out of the treatment zone) was indicated in wells N4, N5, and N6 and a strong westerly flow direction was indicated in well N2. Flow directions in wells N7 and N9 were northwesterly, away from the creek to the east of the installation. A west to southwesterly component in well N1 is not consistent with the interpreted flow directions based on water elevations. Note that both the flow meter and water table maps indicate that flow was not occurring through the system in a north-south direction (i.e., directly perpendicular to the orientation of the treatment zone). This will reduce the size of the upgradient capture zone from that predicted by the model of the system.

In conducting the bromide tracer test, only a small volume of tracer, 9.5L (2.5 gal) of water containing 1,000 mg/L bromide, could be introduced into the relatively small gate area without disrupting the flow field. Downgradient monitoring wells were then monitored every two hours using an ion-specific electrode. Over the course of the test period, bromide concentrations in wells in the iron downgradient of the injection wells could not be differentiated from background values even though concentrations decreased substantially in injection wells. The small injection volumes spread over the screened interval of the wells likely resulted in long, thin, cylindrical slugs only a few centimeters in diameter. It is suggested that the thin slugs would not disperse significantly over the time or distance of the tracer test. This being the case, the downgradient monitoring wells would need to be directly aligned, to within a few centimeters, with the injection well along a groundwater flow line. As described above, the in-well flow meter measurements, performed after the tracer test, indicated that the flow direction was not aligned with the well placement. Thus the tracer test was unsuccessful, providing no useful information.

In summary, estimates of groundwater flow velocity ranged from about 11 cm/day using the in-situ flow meter to 45 cm/day (or higher) using the observed water table and estimated hydraulic conductivity. Both estimates are significantly lower than the 60 cm/day value predicted by the mathematical model. It is quite likely that the velocity varies at the site in response to both seasonal variations in the water table elevation and the water level in the adjacent creek.

Pilot-Scale System, New York

A pilot-scale system of similar size (Figure 4) was installed at an industrial facility in New York in May 1995. In August-September 1996, tracer tests and in-situ velocity meter measurements were performed at the site to ascertain velocity through the system. A groundwater model of the treatment system indicated a flow rate of about 30 cm/day through the reactive iron section.

Groundwater velocities determined from monthly water level measurements varied from a low of 6 cm/day (0.2 ft/day) to a maximum of 40 cm/day (1.3 ft/day) over an initial six-month monitoring period. Because of surveying inaccuracies in the early data, the latter value is considered the most reliable. Using water level measurements from August 1996, a velocity of 23 cm/day (0.75 ft/day) was calculated.

Groundwater velocity was also measured using a down-hole heat-pulse flow meter. A single measurement made in one well installed in the iron gave a velocity of 20 cm/day (0.7 ft/day). Unfortunately, subsequent measurements were influenced by excavation activities upgradient of the installation and were therefore unreliable.

A tracer test similar to that conducted at the Colorado site provided to be equally unsuccessful. That is, bromide concentrations in wells in the iron downgradient of injection wells could not be differentiated from background. As in the Colorado test, we suggest that the thin slugs of bromide created by injecting solution into the upgradient wells bypassed the downgradient wells, due to a non-perpendicular component of flow through the wall.

Estimates of groundwater flow velocity at this site ranged from about 20 cm/day using an in-situ flow meter to 40 cm/day using measured water levels. It is quite likely that the velocity varies at the site in response to seasonal water table gradient variations. Given these values (and pending additional velocity estimates from recent water level measurements), velocities of about 20 to 40 cm/day were used in calculations of VOC degradation rates.

Summary

The tracer tests, using bromide as a conservative tracer, proved to be unsuccessful in determining in-situ groundwater velocities at both sites. Accepting that bromide is conservative in granular iron, as indicated by the laboratory test, then the problem would appear to be intercepting a small target by the downgradient monitoring wells. This could be solved by introducing a larger target, but it is unclear how this could be achieved without disrupting the natural flow system. In addition, though the equipment requirements for a tracer test are modest, they are time consuming and thus costly. Calculations using water table elevations are limited by the accuracy of measurement (small gradients over short distances) and the uncertainty in hydraulic parameters (porosity and hydraulic conductivity). The heat-pulse velocity meter gave magnitudes that were in the range anticipated, but the directional vectors were, in some cases, suspect. Because of the ease of use, velocity probes such as the K-V meter used in this study, or other in-situ probes (Ballard, 1996 for example) appear to offer the greatest promise for velocity determinations in permeable reactive barriers. Though the results obtained in this study using the K-V meter appeared to be consistent with other measurements, a more comprehensive evaluation of their accuracy is warranted.

References

Ballard, S. (1996) The In Situ Flow Sensor: A Ground-Water Flow Velocity Meter. Ground Water 34(2) 231-240.

Bennett, T.A. (1996) (University of Waterloo) personal communication.

Gillham, R.W. (1996) In Situ Treatment of Groundwater: Metal-Enhanced Degradation of Chlorinated Organic Contaminants. " Advances in groundwater Pollution Control and Remediation" 294-274.

Kerfoot, W.B. (1988) Monitoring Well Construction and Recommended Procedures for Direct Groundwater Flow Measurements Using a Heat-Pulsing Flowmeter. "Groundwater Contamination: Field Methods, ASTM STP 963" American Society for Testing and Materials, Philadelphia, 146-161.
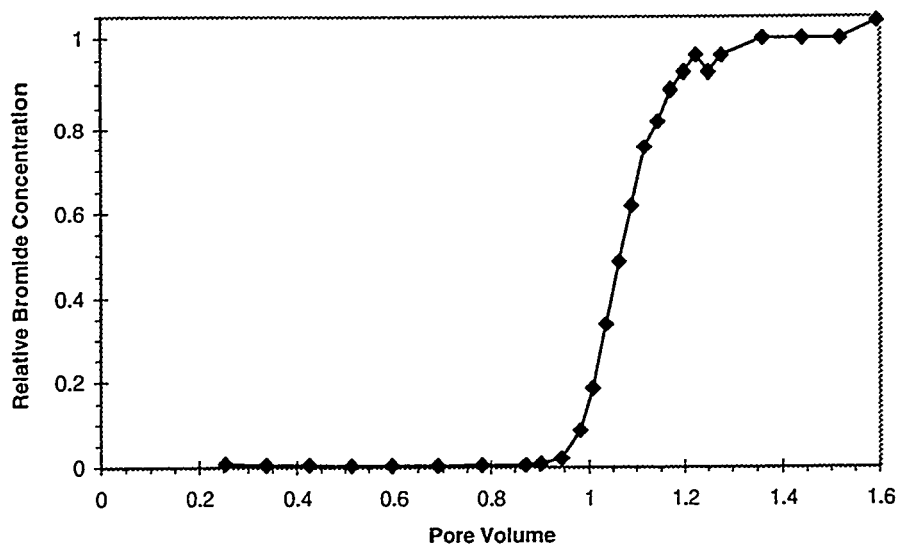
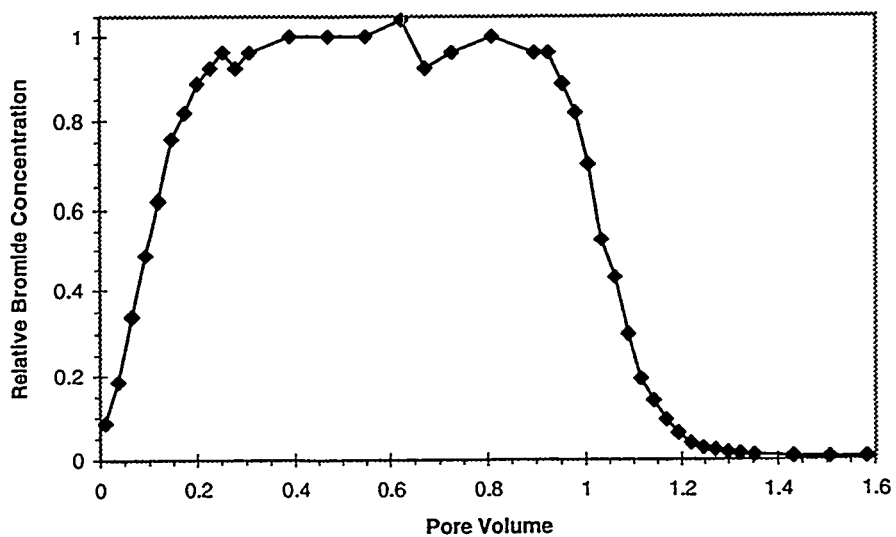Figure 1: Bromide breakthrough curve measured in the laboratory.

Figure 2: Background water breakthrough curve measured in the laboratory.
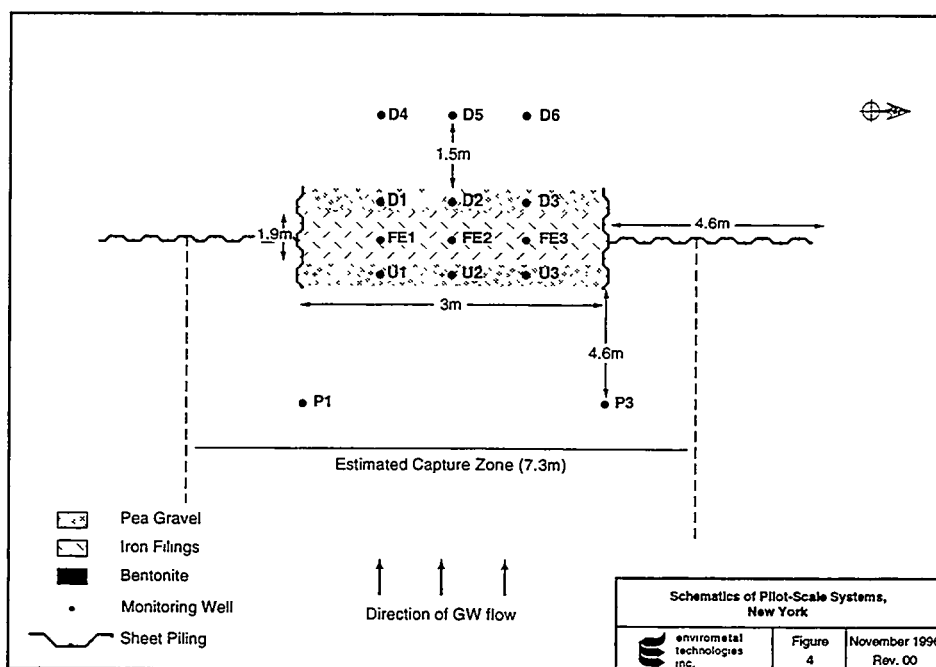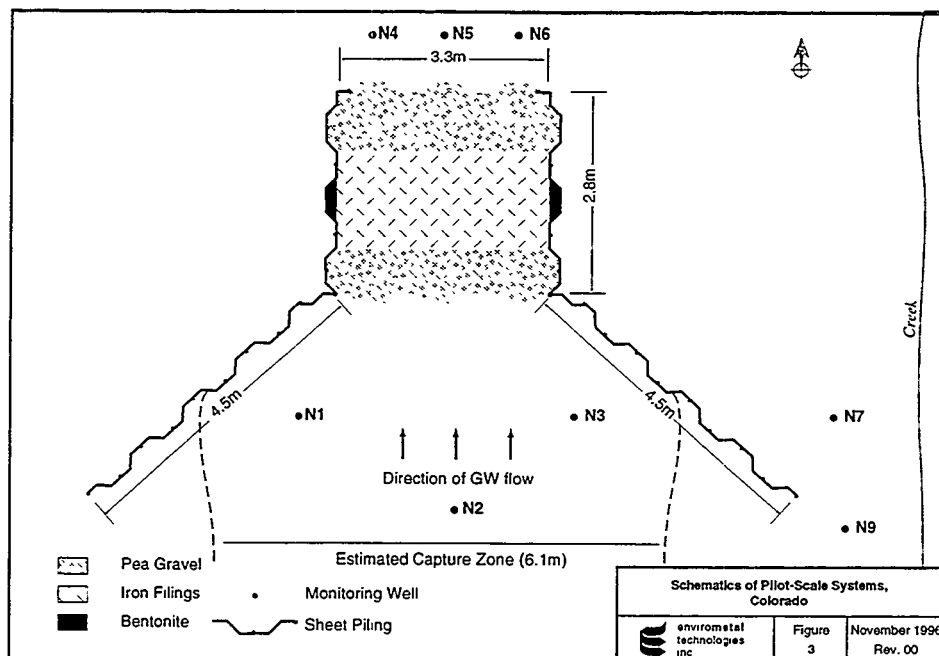
Pea Gravel
Iron Filings   Monitoring Well
Bentonite   Sheet Piling

Schematics of Pilot-Scale Systems, Colorado

envirometal technologies inc   Figure 3   November 1996 Rev. 00

Pea Gravel
Iron Filings
Bentonite
Monitoring Well
Sheet Piling

Direction of GW flow

Schematics of Pilot-Scale Systems, New York

envirometal technologies inc.   Figure 4   November 1996 Rev. 00

Table 1: In-Situ Velocity Meter Results, Colorado Site

Well Location	Groundwater Velocity (cm/day)	Groundwater Direction
N1	11	west-southwest
N2	10	west
N3	-	
N4	14	north-northwest
N5	6	north-northwest
N6	13	north-northwest
N7	11	northwest
\N9	10	west-northwest

Chapter 19

Performance Criteria

EUROPEAN QUALITY ASSURANCE AND QUALITY CONTROL FOR CUT-OFF WALLS AND CAPS

Stephan A. Jefferis[1]

Abstract

Cut-off walls and caps both may be seriously compromised by small areas of substandard materials or work. Quality assurance/quality control is therefore of crucial importance and the paper sets out the issues that need to be addressed when designing a quality plan for a containment. Consideration is given to the purpose of the containment, the parameters to be controlled, specifications and standards and tests on raw and manufactured materials and on the in-situ containment. It is not the purpose of the paper to give detailed test procedures but rather to identify the questions that must be answered to develop a quality plan.

Introduction

Cut-off walls and caps are fundamental components used in the management of many contaminated sites. However, a particular problem with these systems is that a small area of damage or poor quality material can seriously compromise the performance of the whole system. It follows that good quality assurance and quality control procedures are essential to the creation of properly functional systems and to give confidence to owners and regulators that a containment will perform satisfactorily over its design life.

The need for appropriate QA/QC during construction and for the records to be retained during the life of the containment may be focused by considering the possible plight of the owner of a containment 20 years from now. The containment has an area of several hundred thousand square metres and there appears to be leak and contaminants may be escaping (the inverse situation may be equally unacceptable, external groundwater is leaking into the containment and must be pumped out, treated and disposed at possibly very high costs). Has the cap failed? Is there flow through the base and/or through the walls? No construction records are available and an expensive programme of investigation must be undertaken to find the leak or leaks under intense pressure from the regulatory authorities and in an adversarial legal environment. In this position an owner may wish that better QA/QC had been employed and/or that the records had been kept. Furthermore it should be remembered that there need not be an actual leak to trigger an investigation. If there are no construction records to document the containment an investigation may be necessary to prove compliance.

What should be Controlled?

A fundamental question that must be asked when selecting procedures for inclusion in any QA/QC plan is what should be controlled? There can be a tendency to select parameters for measurement because testing is easy or procedures have been codified in some standard though very likely one borrowed from another industry sector. It is also necessary to ask questions of the type: Will the results be useful? Are the proposed parameters good indicators of the potential failure mechanisms? Will they identify unsuitable materials

---

[1]Golder Associates (UK) Ltd, 54-70 Moorbridge Road, Maidenhead, Berkshire, SL6 8BN, England, +44-1628-771731, sjefferis@golder.com

or practices? If testing is intrusive will it impact on the performance of the final structure? Then the procedures themselves must be examined. Are they suitable for use in the harsh environment of a construction site or are they more appropriate to the research and development laboratory? Can they be performed reasonably quickly by staff available to the works? Are the results reproducible? Is the repeatability between duplicate tests such that unacceptable work can be quickly detected?

Finally the nature of the specification itself needs to be considered. Two generic types may be identified: performance specifications which require the completed structure to achieve certain performance standards e.g. a cut-off wall might be specified to have a permeability of less than 1×10^{-9} m/s and that this should be maintained for 25 years. A prescriptive specification for the same cut-off could require that it had a bentonite content of 50 kg/m^3 and a cement content of 175 kg/m^3 and that the slurry should be mixed for 3 minutes in a high shear mixer prior to pumping to the trench. Generally in Europe, performance specifications are preferred though most specifications actually include elements of prescription for example to prohibit the use of inappropriate materials.

Specifications and Standards

Cut-off walls have been used in Europe for the containment of contamination for many years but, as yet there are only a few national specifications or guidance documents for cut-off walls and the associated raw materials and many of the latter have been borrowed from other industries. Documents of note include:

France: ADEME (1997) Résumé de l'état de l'art des procédés de confinement appliqués aux sols pollués, France, Esnault, A. and Miralves, J. This is a very recent overview publication and at present only the summary is available.

UK: Draft national specification for cement-bentonite cut-off walls (as barriers to pollution migration). This was published by the Institution of Civil Engineers in April 1996. It was prepared by Jefferis S.A. and Doe, G. with the guidance of an expert working group. The final version should be completed by mid 1977.

Europe: Before the above French and UK documents were published a European guidance document was produced by Technical Committee ETC 8 (1993) of the International Society of Soil Mechanics and Foundation Engineering under the chairmanship of Professor Jessberger. The committee had representatives from: France, Germany, Holland, Italy, Spain, Switzerland and the UK and thus it collected a range of European experience. Fundamentally the document is concerned with landfills but much of the guidance on caps and cut-off walls is equally appropriate to contaminated land problems.

A European standard on Execution of special geotechnical work, diaphragm walls (prEN1538, 1996) is also currently nearing completion. This is mainly a standard for structural walls but it does include some specification items for cut-off walls.

For geomembranes to be incorporated in cement-bentonite cut-off walls the draft UK specification listed above recommends that the National Sanitation Foundation (NSF) Standard 54-1993 (or later) is used pending production of a European specification.

For caps the ETC 8 publication lists some European specifications that may be used for materials/products to be incorporated in capping systems.

How should it be Controlled?

A quality plan for a containment must involve consideration of all aspects of the system and not just the site work. The following sections detail some of the points that may need to be considered:

Pre-construction Research and Development

Prior to the construction of a cap or a cut-off wall with new materials or in soils with complex physical or chemical features it may be necessary to undertake some research and development work. The level of research will depend on the current state of knowledge of the performance of the proposed cut-off or cap system. The research and development work required may include:

- Assessment of the performance of the containment materials under the credible range of site conditions e.g. aggressive chemical and physical environments (freezing, rainfall, drought etc.).
- Development of site control procedures, in particular identifying the important parameters for the raw materials, manufactured components or on-site processes and codifying them into specifications (including specification of test instruments and test frequency).
- For cut-offs, selection of appropriate batching and mixing plant and mix sequence (order of addition of materials, especially admixtures such as dispersing agents, accelerators and retarders). Because of the sensitivity of both clays and cements to chemical admixtures the timing of their introduction to the mix may have significant impact on the properties - especially the flow properties.
- For natural clay cap materials, clay selection, control and placement procedures including lift height and compaction plant will be important.

Performance data, under a range of operating conditions, are slowly becoming available on containment materials such as native clays, geocomposite liners, cement-bentonite materials and geomembranes but for many systems data are still limited. Testing for compatibility with unusual chemical or physical conditions is not a rapid processes. For example it may take several years for a reaction front to penetrate through a sample of a low permeability inorganic material and for the effects of the reaction(s) to be fully manifest. Also for caps and shallow cut-offs walls the in-situ confining stress may be low and data obtained under high stresses (so as to enable high gradients and thus rapid chemical flux may be quite inappropriate). Jefferis (1992) gives a brief overview of the movement of a reaction front with permeability change for cement-bentonite materials.

In the UK these materials issues can be rather poorly addressed. Specifications for materials and processes are seldom job specific and contracts normally put the burden on the contractor to undertake compatibility testing and select or develop suitable materials. This is in line with the UK practice to favour performance specifications over prescriptive specifications but the time required for material development is not always recognised.

Purpose of the Containment

It is important that those who are involved with the construction QA/QC should know the purpose of the containment and the fundamentals of the design. For example, a containment which includes PCBs or similar materials may require a quite different focus from a landfill for inert waste. It may seem self-evident that those on site should have this information. However, the author has observed sites where the personnel were not properly aware of the significance of the design issues and the consequences of failure. Particular issues that may need to be reviewed include:

- The local circumstances and especially the hydrogeology,

- The design and constructability of the vertical barriers, cap and other elements of the containment,
- The failure mechanisms and their consequences. The consequences of failure of containments or elements of a containment may be very different depending on the contained chemicals, geology, hydrogeolgy etc. Sensitive situations should be addressed at the design stage and the site staff should be aware of them.
- The integration of caps and cut-offs to form a containment introduces problems of the interconnection of the two systems. These connections require particularly careful detailing and site QA/QC as they may vary substantially from site to site and there may be no background level of experience.

Tests on Raw Materials and Products at the Manufacturer's Works

It is common practice to require quality control data from the manufacturer for materials to be incorporated in the works. For materials such as geomembranes and geocomposites the manufacturer's data is likely to have been tailored, so far as is practicable, to the particular needs of the cap and cut-off industries. However, for the manufacturer's of cement, blastfurnace slag, pulverised fuel ash and bentonite, barrier walls may represent only a minor use of their materials and their standard control tests will have been developed for other industries such as structural concrete or oil-well drilling. As a result there can be problems in selecting materials for systems such as cement-bentonite slurries or bentonite-sand liners when only the results of generic tests devised for some other industry are available. Furthermore there may be no general agreement in the industry as to the appropriate properties of such materials to ensure their satisfactory performance in containment applications i.e. there may not be agreement on the best tests and the best properties.

An outline on materials testing is given in ETC 8 (1993) and this may be regarded as a compilation of European practice for cut-off walls for landfills. It identifies a number of classes of materials including:

Water: Two types of water are considered:
Drinking water: ETC 8 notes that this may be accepted as supplied. No additional testing is specified.

Industrial water: for this pH, electrical conductivity and total hardness tests are required to be measured. The total hardness result will give and indication of the combined calcium plus magnesium ion concentration but will not identify the individual concentrations. In the UK where the majority of bentonites that are used for the preparation of cement-bentonite materials are natural calcium bentonites converted to the sodium form with an excess of sodium carbonate the sensitivity of the clays to calcium and magnesium ions is quite distinct. This may be as a result of the different interactions of these ions with sodium carbonate. With calcium ions highly insoluble calcium carbonate will be precipitated. However, magnesium carbonate is markedly more soluble and thus the ions will not be precipitated and may damage the swelling the bentonite at levels as low as 50 mg/litre whereas calcium may not be damaging until about five times this level. The author would therefore suggest that tests on water should separately identify the calcium and magnesium ion concentrations and not just the total hardness. Of course if dissolved salts in the mix water may be an issue the simplest test of all is to mix bentonite with the water and compare the properties of the resulting slurry with those of a slurry prepared with distilled water.

Hydraulic Binder: For the hydraulic binding agent (a generic term for cementitious materials) ETC 8 (1993) requires only the Blaine value (fineness by air permeability) and the proportion of slag noted on the delivery ticket. For most UK cements, unless specially blended, the proportion of slag will be nil. Slags are almost always used in cement-bentonite slurries in the UK but the

slag cements are usually prepared by blending Portland cement and slag on site. Clearly, and not unreasonably, cements are now regarded as sufficiently well understood and controlled that site testing is not required and figures quoted on a delivery ticket are acceptable. (Despite the fact that, as already noted, the manufacturer's tests on a cement are most unlikely to include any assessment of the behaviour of the material in a cement-bentonite system.) An alternative way of viewing this is to say that cement is produced on such a major scale that specially prepared cements for slurries (other than slag addition) are likely to be unavailable. The cut-off wall contractor must accept what he is given and design his product to be tolerant of any variations in the properties of his chosen cement over time (though he may select his cement from a particular works always provided the haulage costs are not thereby made excessive).

Bentonite: The bentonites available locally in Europe almost always occur naturally as calcium bentonites. In cut-off walls they may be used directly in the calcium form or, more usually, (at least in the UK) they are used in the sodium form. The conversion having been done by the suppliers by adding sodium carbonate generally in excess of the theoretical requirement for conversion so the bentonites have a pH in the range of about 9 to 10.5 and pH may be included as a control parameter on the fresh material. Calcium bentonite is less easily dispersed to fine particles in water than sodium bentonite and therefore calcium bentonite suspensions show more bleeding and less marked gel and viscosity than sodium bentonites at the same concentrations. This can be both an advantage and a disadvantage. As an advantage more of the clay can be incorporated into a slurry without it becoming unworkably thick. Thus if chemical interactions are expected in the ground and the clay is intended to be a sacrificial material (or indeed an inert material) more of it can be incorporated thus perhaps increasing the life of the barrier. However, high concentrations lead to higher costs for the cut-off. In contrast, sodium bentonites are much more rheologically active and can impart good bleed control to a cement-bentonite slurry. However, the slurry may be too thick at concentrations over about 6% by weight of water (though this figure will be very sensitive to the source and treatment of the bentonite). Of course in a cement-bentonite slurry a sodium bentonite will undergo exchange with calcium from the cement. The important feature of sodium bentonite is that a higher degree of dispersion can be achieved prior to cement addition than with calcium bentonite and that it is the author's opinion that some of this dispersion remains after interaction with the cement. Presently unpublished work by the author also suggests that, over time, the bentonite in a cement-bentonite mix reacts to form hydrates similarly to those from the hydration of cement itself. The author is now very hesitant to adopt interpretations of the behaviour of hardened cement-bentonite systems which consider the clay and cement fractions as having independent existence and thus which may seek to hypothesise that particular chemicals may damage the clay or the cement fraction. The author recommends that specifications for the future recognise that cement-bentonite is a composite hydrate system and not a mixture of independent cement and bentonite phases.

Materials Standards: European countries will have national specifications for hydraulic binders and European norms are being developed. For bentonite there are fewer standards and more diversity. Typical standards include:
a) Engineering Equipment and Materials Users Association (EEMUA), Publication No. 163, Drilling fluid materials (1988).
b) Oil Companies Materials Association, Specification No. DFCP-4 Drilling fluid materials, Bentonite (1973).
c) American Petroleum Institute, Specification 13A, Specification for drilling fluid materials (1993).
d) Deutsche Norm DIN 4127, Diaphragm wall clays for supporting liquids, Requirements, testing, supply, inspection (1986).

Specifications (a) and (b) are effectively identical. Specification (c) is more rarely used. Specification (d) is not generally used in the UK but will be followed in Germany for excavation slurries.

None of the above specifications a, b and c which are used in the UK are for bentonite for containment systems and recently the UK Federation of Piling Specialists has set up a working party to develop a specification for bentonite for use as excavation slurry, that is to develop a specification similar to (d), the German standard for bentonite for excavation slurries. The fact that it is not yet available is causing some problems as specifications may be borrowed and for example the EEMUA specification is often cited though suppliers may offer a 'civil engineering grade bentonite' which may be better optimised than the EEMUA grade for construction work including cut-offs. To develop a specification for bentonite for use in cement-bentonite materials would be much more complex but it may be achieved.

ETC 8 (1993) specifies that, for the bentonite, the yield value, filtrate loss, water intake value (using the Enslin method) and proportion of grains over 0.125 mm diameter (if appropriate) should be determined but does not provide any control values.

Admixtures: Few specifications in the UK provide any detailed controls on the chemistry of admixtures though phrases of the type: 'admixtures if used must not have any deleterious effect on the performance or durability of the wall' may be included. These are very difficult criteria to meet and tended to suppress the use of admixtures. However, in the UK the demand for a slower setting slurry when geomembranes are being installed in trenches led to their more general use (and in situations where it could be argued that the barrier effect was largely achieved by the membrane and thus a slightly more lenient view could be taken of the cement-bentonite performance). Typically, today admixtures will be used to improve the fluid properties of the slurry, modify its set time and improve the permeability of the hardened material. In the UK admixtures are the province of the contractor and formulations are likely to be commercially confidential.

For the bentonite in geocomposites some type of clay modification is very likely to be employed. This optimisation of the properties will be by the supplier and again generally will be confidential. This can complicate investigations of the use of the materials in special chemical environments where a fuller knowledge of the clay chemistry can be helpful.

On-site Acceptance Tests for Materials and Products Prior to Use

Raw materials such as cement and bentonite may be delivered in bulk tankers and the powders transferred directly to on-site silos so it is important to have rapid procedures to confirm acceptance or rejection of the materials before they are transferred to a silo. For cement the manufacturers certificate may be acceptable (though as noted above, generally it will be concerned with concrete rather than cut-offs). For clays, in the UK there is rather more variation and no agreed acceptance criteria.

The problem is particularly evident for cement-bentonite systems as many are prepared on site with raw materials which may show subtle variations between sources and deliveries. Specific testing is necessary to identify the properties that are required of the bentonite (and cement) to produce an acceptable cement-bentonite. Even if the variations between sources and deliveries have no significant effect on the properties of the slurry and the hardened product it may be difficult to demonstrate this and variation in raw materials adds an expensive extra cost to control of site prepared systems. Research on acceptance procedures has not been done generically and specifications may cover a range of properties including liquid limit, filtrate loss, water absorption, particle size (e.g. amount retained on a 100 mesh sieve when dry and a 200 mesh sieve after dispersion in water), a variety of rheological properties (e.g. Marsh funnel

time, apparent and plastic viscosities and ten second and ten minute gel strengths), bleeding, pH etc.

Fundamentally we need to develop more appropriate tests for identification of 'good' bentonites for cement-bentonite walls and bentonite-sand liner systems etc. and also rapid tests that can be used on site to confirm that a bentonite delivery conforms.

ETC 8 (1993) offers tests for the factory prepared 'one-bag' mixes that are available in Germany and these include: rheology, density, filter loss and water intake capacity. These mixes are optimised by the supplier and, on-site, all that is necessary is to use a suitable mixer to disperse the material in water, at the correct concentration, separate hydration of the bentonite is not required. The strength of one-bag mixes may be quite high at 1 MPa or greater. In the UK it is normal practice to use hydrated bentonite and strengths of the hardened slurries are usually less than 1 MPa, indeed the draft national specification (Institution of Civil Engineers, 1996) requires only that the strength is above 50 kPa - the UK thinking being that weaker mixes will show more plastic behaviour under the effective confining stresses typical of the conditions in most slurry trenches (it will be rare that confining stresses approach 1 MPa). The use of 'one-bag' mixes greatly simplifies the necessary on-site QA/QC and transfers much of the risk associated with the performance of the material to the supplier. These mixes may gain much wider acceptance in the UK if their potentially higher strength can be accepted though cost also will be an issue. They can have permeabilities significantly below 10^{-9} m/s.

For fabricated materials such as geocomposites and geomembranes the on-site acceptance tests may be subsumed into the manufacturer's tests. However, for all geomembranes there is the issue of the joints. For example, for geomembranes used in slurry trenches a jointing strip generally has to be welded onto the geomembrane sheet. This welding may be done locally to the project and not under factory conditions as the panel lengths may not be known in advance of the start of trenching operations and may need to be tailored to the actual depth of the trench. For these geomembranes there are therefore two issues: the weld for the joint strip and the joint which will be formed in the trench. Separate QA/QC procedures will be needed for these two joints and the geomembrane itself.

On-Site Control Tests for Materials Prepared on-Site

In the early days of cement-bentonite slurry trench cut-off walls, in the UK, the following parameters were often included in the on-site testing plan: apparent viscosity, plastic viscosity, gel strength at 10 seconds and 10 minutes, Marsh funnel flow time, sand content, density, filtrate loss, pH and bleeding at 3 hours and 24 hours (details of the procedures for most of these tests are given in Rogers, 1988).

All these parameters were measured for the hydrated bentonite slurry prior to the addition of the cement and also on the freshly prepared cement-bentonite slurry. Tests were also undertaken on samples taken from three depths in the trench excavation (top 1 m, middle and bottom 1 m). On a modest sized site this array of tests could keep two full-time slurry test technicians busy and cause enormous debate between the various parties involved in the work as the results were almost always markedly variable and inevitably some results would be outside the pre-set limits. Surprisingly slowly, it became apparent that the tests were poor indicators of the performance of the hardened slurry. Many of the fluid properties were strongly dependent on the age of the sample and the intensity of the last mixing. Others such as fluid loss and pH scarcely varied and were of more use in a research laboratory developing new materials. Density is a useful indicator of the total solids content of the mix and hence a check on the overall batch proportions. However, the equipment generally used (the mud balance) with a resolution and repeatability of about 0.05 g/ml cannot resolve the solids content to better than about 40 kg/m^3 which is quite inadequate to test a mix which may contain only 200 kg/m^3 total solids. Bleeding

is probably the most useful parameter as it can identify an unstable mix - though only some hours after mixing and thus it is an inappropriate parameter for the immediate control of slurries.

The conclusion is therefore that although all the tests gave some information about the slurry and were part of the learning/confidence building process for slurry systems it is now recognised that they can detect only gross errors in the slurry production process - errors which can be identified with much better precision by targeting tests on critical parameters. However, it is important to note that the array of tests can be abandoned for a much smaller range of tests because we have a better understanding of the system. If the system is changed, for example, by the use of different clays, special admixtures etc. or equally importantly, changes in site practice relating to mixing or excavation plant etc. then it may be necessary to re-introduce these or new tests until confidence has been re-established in the new system and more specific control parameters identified.

The sampling device used to remove samples from a slurry trench also deserves a brief comment. For a deep wall the hydrostatic pressure on the sampler will be substantial and the seals must be reliable and the equipment must be capable of operating under pressure. If there is uncertainty about the tightness of the sampler (and if it is of the type that is operated after lowering to depth - in the UK the usual form of sampler is an open tube which is dropped down a wire to mate against a plug set at the end of the wire, a capping plug is dropped following the tube and the whole assembly then raised as a unit) it should be dropped to the full depth of the trench and then removed again without operating the slurry sampling mechanism. If slurry is found to have invaded the sampler then it must be serviced, replaced or its design changed.

Laboratory Tests on the Products

Because of the difficulty of testing containment systems at full scale it is normal practice for specifications to include laboratory tests on elements of the containment such as permeability tests on hardened cement-bentonites or site batched bentonite-sand liner materials. Tests may be carried out on specimens cut from geomembrane sheets and also on welded joints. A particular problem with all such testing is to identify an acceptable failure rate. For example in the UK draft national specification for cut-off walls the permeability requirement is as follows: 'a target permeability of less than 1×10^{-9} m/s is required. However due to inherent variability in mixes and testing, at least 80% of results shall be less than 1×10^{-9} m/s and not more than 5% of results shall exceed 1×10^{-8} m/s'

In-situ Testing of Elements of the Containment System

Many problems relating to containment specifications could be resolved if there were satisfactory test procedures for the measurement of in-situ performance. To date, for cut-off walls, attempts based on core sampling or the insertion probes have had little success. Test boxes have been constructed contiguous with walls and have proven permeabilities to the $<10^{-8}$ m/s level and to the $<10^{-9}$ m/s level though this is much slower (time-scales of several months of monitoring per test) and more elaborate. Alternative procedures currently being evaluated include:
- The insertion of a piezometer sealed with a packer into the wall (Tedd, 1995),
- Precise analysis of pressure responses in boreholes adjacent to a wall following the injection of water, at a controlled flow rate for a defined period, into a borehole on the remote side of the wall (Eiben and Jefferis, 1994),
- Penetration of a piezocone into the wall (Manassero, 1992 but note Tedd, 1995 queries the results of the test),
- 'Archaeological' investigation of the adjacent water levels, chemistry and materials quality of old walls.

The European state of the art for in-situ performance assessment is developing for cut-off materials and caps. The ideal of a rapid, reliable non-damaging procedure still remains elusive.

Verification

Verification of the performance of a containment is fundamental to regulatory and stakeholder acceptance. Instrumentation therefore may need to be put in place, during containment construction, to monitor the normal performance of the barrier and so indicate abnormal behaviour. It will also be necessary to ensure that someone or some organisation 'holds and owns' the information and that action is taken if the performance deviates from a specified standard.

Conclusions

Containments are large complex systems that may be compromised by small imperfections. Quality plans must be developed specifically for them. This short paper offers few answers but it is hoped that it will serve to highlight some of the problems and force questions such as 'why' and 'how' to be addressed in relation to testing regimes.

One final question remains 'who guards the guards'. QA/QC plans are not merely another cost item to be minimised. Those involved in the quality plan must have independence and authority.

References

Esnault, A. and J. Miralves. (1997) Résumé de l'état de l'art des procédés de confinement appliqués aux sols pollués, *ADEME*, France

American Petroleum Institute. (1993) *API Specification 13A, Specification for drilling fluid materials.*

Deutsche Norm DIN 4127. (1986) *Diaphragm wall clays for supporting liquids, Requirements, testing, supply, inspection.*

Eiben, Th. and S.A. Jefferis. (1994) Implementation of interactive numerical modelling and hydraulic testing in the design and quality control of low permeability barrier systems, *Meeting on measurement of low permeability in soil and rocks*, University of Surrey, Guilford, England.

Engineering Equipment and Users Association. (1988) *Publication No. 163, Drilling fluid materials.*

Institution of Civil Engineers. (1996) *Draft Specification for cement-bentonite cut-off walls (as barriers to pollution migration)*, London.

Jefferis, S.A. (1992) Contaminant - grout interaction, *ASCE Specialty conference*, Grouting, Soil improvement and Geosynthetics, New Orleans pp. 1393-1402.

Manasero, M. (1994) Hydraulic conductivity assessment of slurry wall piezocone tests, *Journal of Geotechnical Engineering*, ASCE Vol. 120, 10, pp. 1725-1746.

Oil Companies Materials Association. (1973) *Specification No. DFCP-4 Drilling fluid materials, bentonite.*

prEN1538. (1996) Execution of special geotechnical work, diaphragm walls, *Draft European Standard*, British Standards Institution, London.

Rogers, W.F. (1988) *The composition and properties of oil-well drilling fluids*, 5th Edition, Gulf Publishing Company, pp. 818.

Technical Committee ETC 8. (1993) *Geotechnics of landfill design and remedial works Technical recommendations - GLR*, Second Edition, Edited by the German Geotechnical Society for the International Society of Soil Mechanics and Foundation Engineering, Ernst & Sohn, pp. 158.

Tedd, P., R.S.T. Quarterman, and I.R. Holton. (1995) Development of an instrument to measure the in-situ permeability of slurry trench cut-off walls, *4th International symposium on Field Measurements in Geotechnics*, Bergamo, Italy, pp. 441-446.

Strategies to Facilitate Stakeholder and Regulator Support for Technology Deployment

Thomas D. Burford[1]

Abstract

Implementation and deployment of new and innovative environmental technologies is impossible without regulator, enduser and stakeholder support. Technologies being developed for different needs require different strategies to facilitate this endorsement. Areas addressed will include technologies developed to meet site specific cleanup needs and those developed for multiple site applications. A third area deals with using site specific technologies at previously unidentified locations. In order to expand the application of these technologies to other sites a plan to include potential site regulators and stakeholders early in the development process should be considered.

The Subsurface Contaminant Focus Area has developed a Stakeholder Communication Plan. This plan, in addition to lessons learned from current technology development projects that have successfully obtained this type of support, will provide the basis for the information provided in this paper. The object of this paper is to suggest strategies that could facilitate the implementation and deployment of technologies at environmental sites by involving regulators and stakeholders at the proper·time for various applications.

Introduction

Implementation and deployment of new and innovative environmental technologies for containment of contaminated sites is impossible without stakeholder support. Stakeholders are those individuals or organizations who have an interest in or are potentially impacted by U.S. Department of Energy's (DOE) efforts to accomplish its mission (Ref. 1). Technologies are being developed for different needs across the DOE Complex that require different strategies to facilitate this endorsement. The areas that will be addressed in this paper will include those technologies developed for multiple site applications and technologies being developed to meet site specific cleanup needs.

The Subsurface Contaminant Focus Area has developed a Stakeholder Communication Plan which identifies the process the Focus Area is implementing. This pre-decisional draft document is available through the Lead Organization at Savannah River DOE. This paper will discuss the key elements of this Plan and lessons learned from current technology development projects that have successfully obtained stakeholder support and discuss their strategies. These strategies could facilitate the implementation and deployment of technologies at environmental sites by involving regulators and stakeholders at the proper time for the various applications identified above.

There are numerous public groups or organizations who have an interest in or are affected by DOE actions. These groups include the National Governors Association, the Western Governors Association (WGA), the Southern States Energy Board, the Community Leaders Network, Site Specific Advisory Boards, Indian Tribes, local governments, nearby property owners, national and local public interest groups, and some agricultural business groups (Ref. 2).

Technology Deployment for Multiple Sites Implementations

These groups can play a special role for technologies like the Alternative Landfill Cover Demonstration (ALCD) that has the potential to be deployed at any arid site where a cover is required as part of its

---

[1] Thomas D. Burford, Sandia National Laboratory, 1515 Eubank Avenue SE, MS-0719, P.O. Box 5800, Albuquerque, NM 87185-0719, (505) 845-9893, tdburfo@sandia.gov

closure actions. This technology is being developed to provide an alternative to a baseline technology which is driven by design guidance from the U.S. Environmental Protection Agency (EPA) and not based on site specific or contaminant specific performance criteria. Therefore a strategy to involve stakeholders and regulators early in the development process is the best way to facilitate the acceptance of this technology following its successful development.

The ALCD is providing a side-by-side comparison of EPA cover designs against four alternative covers in the areas of cost, constructability and performance. A key issue with facilitating this site-wide deployment is including a mix of stakeholders who have a wide influence over any or all potential deployment sites. To meet this goal the ALCD has received endorsement by a committee from a western states' and federal government initiative to accelerate and improve clean up of federal lands.

The ALCD initiative originated in 1992, when the Western Governors Association, the Secretaries of Defense, Energy, Interior, and the Administration of the Environmental Protection Agency formed a federal advisory committee to cooperate on the cleanup of federal waste management sites in the region. This committee, known as the Committee to Develop On-Site Innovative Technologies (DOIT), has sought the guidance of key players to help identify, test and evaluate more cooperative approaches to deploying promising innovative waste remediation and management technologies in order to clean up federal waste sites in an expeditious and cost-effective manner (Ref. 3).

After granting its endorsement the WGA began monthly meetings with key ALCD technology developers and a diverse set of stakeholder personnel. During these meetings the WGA became familiar with the goals and objectives of the technical project. Although direct funding was not realized from this endorsement the WGA provided approximately $130K of in kind services in the form of site tours, monthly meetings, multiple stakeholder meetings and document reviews. This leveraging of funding provided resources that could not have been used with existing funding for the technical project.

Test cover designs were sent out for review to a group of technical peers that were independent of the project and deemed industry experts. This review ensured the technical validity of the designs to be constructed. The revised test plans were then sent to regulatory representatives from Environmental Departments from fifteen western states and three EPA Regional Offices. Comments from all reviews were incorporated into the design guidance.

Another review process included sending a general overview of the demonstration to members of the DOIT Committee and special interest groups identified by the DOIT Committee. These interest groups included representatives from such entities as environmental groups like the Sierra Club, Indian Tribes, government agencies, neighborhood associations, local businesses, engineering firms, and politicians. Over 1000 groups participated in this phase. Comments were forwarded through the WGA for consideration. Regularly scheduled meetings were held with some these special interest groups, the WGA, the New Mexico State Legislature and Sandia National Laboratories. These meetings kept interested parties informed of advancements, progress, and answered questions and concerns.

Products of this stakeholder involvement are many, including letters of support from regulators, private industry and end-user sites. There is significant interest from industry to participate in this test. They are willing to fund the construction of other covers using their own designs or materials allowing the Principal Investigator (PI) to collect data for comparison against the EPA and other alternative covers. (This emphasizes the visibility this project has received from its involvement with the WGA DOIT Committee, and the significance that involving regulators will have on future deployment opportunities.) Tours of the test cell facility have been conducted for DOE Headquarters, a variety of regulators and end-users, and environmental restoration groups from Oakland, CA., LMITCO, ID., Rocky Flats, CO., and the Nevada Test Site (NTS)to name a few.

Technology Deployment for Site-Specific Needs

Another technology development area addresses the deployment of a technology that meets a site specific need. This involves a different strategy, initiated by identifying these site-specific needs through participation in overviews of contaminated sites at a DOE facilities. Following the identification of these needs an overview of potential technologies that could meet these needs was presented to technology transfer, environmental site managers and Site Technical Coordination Group (STCG) personnel. This overview included technologies that had been developed and were now commercially available and technologies that were currently being developed at different stages of development.

Following the overview the site technology transfer personnel arranged for a meeting of technology developers, of potentially deployable technologies, with a team of environmental site task leaders, state regulators and the local EPA region. These meetings proved to be the key in gaining support which was evidenced by the receipt of letters from the STCG Chairman and the EPA Region liaison in support of deployment of this technology to meet the site need. A project time line with roles and responsibilities of project personnel, which included National Labs, two EPA offices, state regulators, and operating contractors for the site, was prepared and reviewed.

The success of the previous meetings resulted in leveraged funding from site contractors and the EPA that was instrumental in obtaining a quick start prior to funding receipt for the proposed technology. Bi-monthly conference calls with team representatives and key Focus Area personnel were used to develop the remediation strategy and identified pre-deployment characterization needs. These calls were also used to inform the site of lab and bench-scale technical activities, and discuss the results of sample analyses conducted on site groundwater samples.

This effort that has resulted in the support for this in-situ treatment technology has also produced additional opportunities for deployment of other technologies at this site location. By bringing key stakeholders and regulators together in a timely fashion and addressing concerns on technology performance and schedules technologies can be deployed for site cleanup in keeping with the Ten Year Strategic Goals of the sites.

Recommended Strategies to Facilitate Stakeholder and Regulator Support

Technologies that have the potential to be deployed at multiple sites will generate the biggest return on investment; therefore, special attention should be given to ensure stakeholder and regulator participation. For these technologies that are being developed to meet global needs, similar to the cover demonstration test case, a strategy to facilitate stakeholder and regulatory support should include the following items.

1) A stakeholder group (SG) should be identified, early in the technology development process, whose endorsement would facilitate the global acceptance of the technology being developed.

2) Use the expertise of the SG to develop a network of regulators and special interest groups to participate in meetings and project reviews.

3) Work with the stakeholder group to develop a time line for document reviews, project reviews and other key issues in sync with the specific technology development project plan.

4) Provide an overview of planned activities with the team and provide regular feedback on status and progress during development efforts.

5) Through the SG provide site tours, when appropriate, for other regulatory and special interest groups from specific sites where the technology may be used.

6) Solicit letters of support, document all review comments and responses, and maintain a file of all interactions with the SG.

7) It is recommended that these strategies be developed with the assistance of the Focus Areas using the expertise and networks that have already been established with many of the stakeholder groups.

Site-specific technologies usually require adherence to more stringent regulations, resulting in the regulator and stakeholder involvement being more focused. Technologies must show they have proven the ability to perform within these regulatory boundaries. For technologies that are being developed to meet site specific needs, similar to the in-situ treatment technology discussed, the key elements leading toward deployment and regulatory and stakeholder support would include the following:

1) Identify technology needs for the specified sites. Data should include risks, schedules, extent of contamination and how this activity fits into the site 10 year plan.

2) Validate and prioritize the site needs. This would be done by the Focus Area Lead Office and is a key element in obtaining funding for future development.

3) Identify commercially available solutions (proved and unproved) and emerging technologies currently under development. This would identify areas for future development needs should an appropriate technology be unavailable in either of these categories.

4) Demonstrate technology at a similar "cold" site as a proof of concept in a like environment. This element would provide the opportunity for working with site regulators and stakeholders. Their involvement would begin with review of the test plan, development of the data quality objectives and assessment, generation of the criteria for acceptance, and overview of the actual demonstration.

5) The evaluation of the technology performance will summarized with cost data, which will lead to its acceptance, or result in minor modifications, or will not be deployed at all.

6) Develop a deployment plan for the accepted technology or in the case of a modified or rejected technology a lessons learned will be recorded (Ref. 4).

7) These strategies could be developed by the Focus Areas using their expertise and networks that have already been established with many of the stakeholder groups.

In order to expand the application of site specific technologies to other sites with similar needs these potential sites need to be identified early in the development process. When these sites are identified the technology developers need to include these sites by developing an alternative site listing using the needs documents and 10 year plans to identify sites with similar needs, and identify key personnel at the alternative sites. These key individuals should be aware of the technology development efforts and invited to participate in correspondence, conference calls, technical reviews and be aware of the activities occurring in the previous section in regards to site specific deployment. By providing these individuals the opportunity to become familiar with the technology being developed. This would also allow the other sites the opportunity to their regulators and stakeholders of these development activities. When the technology becomes available for deployment decisions could be made quickly, regarding their ability to meet the site need.

The effort put forth to follow these three steps could prove invaluable in facilitating the deployment of a technology at a secondary site. As technologies are being developed and deployment opportunities are missed due to funding or technical problems and the ability to quickly turn a technology around for use at another site will result in significant cost savings for both developers and end-users.

The strategies identified here can help facilitate the acceptance of technologies by regulators and stakeholders if they are implemented in a timely fashion. The Subsurface Contaminant Focus Areas (SCFA) has worked to successfully deploy technologies and gain regulatory and stakeholder acceptance for the past two years. They have a Stakeholder Communication Plan and a Program Plan that are available for distribution.

References

1. "Subsurface Contaminants Focus Area (SCFA) Stakeholder Communication Plan", December 6, 1996, Page 2.

2. "Subsurface Contaminants Focus Area (SCFA) Stakeholder Communication Plan", December 6, 1996, Page 7.

3. Dwyer, Stephen., "Landfill Covers for Dry Environments" Spectrum 96, Seattle WA.

4. Subsurface Contaminant Focus Area, Program Plan October 1, 1996, Pages 5-10.

IDENTIFICATION OF LONG-TERM CONTAINMENT/STABILIZATION TECHNOLOGY PERFORMANCE ISSUES

Gretchen E. Matthern[1] and Dave F. Nickelson[2]

Abstract

U.S. Department of Energy (DOE) faces a somewhat unique challenge when addressing in situ remedial alternatives that leave long-lived radionuclides and hazardous contaminants onsite. These contaminants will remain a potential hazard for thousands of years. However, the risks, costs, and uncertainties associated with removal and offsite disposal are leading many sites to select in situ disposal alternatives. Improvements in containment, stabilization, and monitoring technologies will enhance the viability of such alternatives for implementation.

DOE's Office of Science and Technology sponsored a two day workshop designed to investigate issues associated with the long-term in situ stabilization and containment of buried, long-lived hazardous and radioactive contaminants. The workshop facilitated communication among end users representing most sites within the DOE, regulators, and technologists to define long-term performance issues for in situ stabilization and containment alternatives. Participants were divided into groups to identify issues and a strategy to address priority issues. This paper presents the results of the working groups and summarizes the conclusions. A common issue identified by the work groups is communication. Effective communication between technologists, risk assessors, end users, regulators, and other stakeholders would contribute greatly to resolution of both technical and programmatic issues.

Introduction

DOE's Office of Science and Technology sponsored a two day workshop designed to investigate issues associated with the long-term in situ stabilization and containment of buried, long-lived hazardous and radioactive contaminants. DOE faces a somewhat unique challenge when addressing in situ remedial alternatives that leave long-lived radionuclides and hazardous contaminants onsite. These contaminants will remain a potential hazard for thousands of years. However, the risks, costs, and uncertainties associated with removal and offsite disposal is leading many sites to select in situ disposal alternatives. Improvements in containment, stabilization, and monitoring technologies will enhance the viability of such alternatives for implementation.

Containment and stabilization are best achieved through use of an integrated set of in situ technologies which treat, confine, or minimize the waste source term. Accurately characterizing the waste and the site as well as verifying the performance of these technologies is an important component of containment and stabilization. A broad range of technologies contribute to the system including placement techniques and materials for subsurface walls and floors, covers, and instrumentation for characterization, verification, and monitoring. The primary difference between containment and stabilization techniques is the location of their application relative to the waste. Containment structures are placed to surround or enclose the waste in a defined volume, reducing communication with the outside environment. Stabilization techniques work within the waste to minimize contaminant transport and provide structural stability. In either case, the reduction in mobility can be accomplished through

---

[1] Gretchen E. Matthern, Lockheed Martin Idaho Technologies Co., Idaho National Engineering Laboratory, P.O. Box 1625, Idaho Falls, Idaho 83415-3710, (208) 526-8747, gtn@inel.gov

[2] Dave F. Nickelson Lockheed Martin Idaho Technologies Co., Idaho National Engineering Laboratory, P.O. Box 1625, Idaho Falls, Idaho 83415-3710, (208) 526-9061, dfn@inel.gov

the physical properties of the structure, such as reduced permeability, or by chemical interaction with the structure, such as adsorption of specific contaminants.

Barriers and covers are the two major classes of containment technologies. A barrier is an engineered sub-surface structure which surrounds the waste but is not in the waste. It prevents movement of contaminants from the enclosed region by containment or redirection of subsurface water flow and provides a chemical treatment or hydraulic barrier. A cover is an engineered surface structure which controls surface infiltration and transport of water, minimizes animal, plant, and human intrusion, and resists wind and water erosion. It is designed to maintain integrity with minimal maintenance regardless of shifts in climate or waste settling. Both barriers and covers are designed to remain functional in the waste and site environment for at least as long as required by the end user (regulators, site owners, and stakeholders).

Stabilization techniques are engineered sub-surface structures which encapsulate and mix with the waste and provide a stable interface between the waste and the surrounding environment. They provide structural stability to the waste and the waste site and minimize contaminant movement through chemical interaction, physical barriers, or encapsulation. Stabilization minimizes the infiltration of water into the waste from all directions. Stabilization materials are selected with a design goal to perform without significant deterioration at least as long as required by the end users.

Monitoring techniques include instrumentation, data interpretation, and prediction of contaminant movement for characterization of the site and verification of the remediation. Characterization concerns include identifying the chemical and physical properties of the waste and the waste site. This data is used to ensure the proper design of containment/stabilization structures and material specifications. Monitoring is used during construction to verify proper installation; after construction, monitoring is used to verify the proper functioning of the structure, identify failures in the structure and determine the overall effectiveness of the engineered containment/stabilization technology system.

Importance of Long-Term Issues

The definition of long-term is site specific because it is based on the contaminants of concern, the applicable regulations for the site, the future use of the site and public sentiment towards the site. As presented at the workshop, the definition of long-term ranges from 30 to 10,000 years, across the DOE complex. For the purposes of discussion, at the workshop, long-term was defined as greater than 500 years. This time span is beyond that of general commercial construction performance data. This time period requires durability to be based on more than experience or direct time measured data. Measures for this time span must be scaled and modeled to predict future performance.

The remediation options available to address long-term threats contributes to the importance of resolving technical issues for containment/stabilization technology systems. There are three major options: 1) do nothing, 2) retrieve/treat/store/dispose, and 3) treat/contain/immobilize in situ. None of these options releases DOE from its long term responsibilities for these wastes.

The first option is not appropriate for many sites due to the long-term risk posed by the wastes. The second option is commonly used at hazardous waste sites to remove the primary source term. However, a few key differences exist between hazardous and mixed waste sites. Retrieval of mixed wastes presents radiological as well as chemical exposure potentials for remediation workers. While these hazards can be adequately addressed, the costs associated with the monitoring and personal protection equipment are significant. Treatment of the retrieved waste is the next step. The waste is not homogeneous in nature so treatment will require some form of separation/sizing process before the waste is treated. The treatment system has to be designed, tested, and permitted before waste processing can begin. While the technologies for the treatment required of the waste are available, adapting these technologies to function in a radiological environment is not simple and the cost of such a facility is very high. After the waste is treated, it must have an appropriate facility for storage or disposal. Currently there are no approved facilities with sufficient volume and content capacity to

handle the waste. Building the appropriate facilities is technically feasible, but costly. In addition, siting of theses facilities is difficult because no one wants the waste near them. Storage facilities are more easily built, but they represent only an interim solution and are not necessarily less costly to build and operate than a disposal site.

The third option of in situ management of the waste can offers several advantages when addressing long-term threats, if suitable technology is available. Leaving the waste in place eliminates the costs and risks associated with retrieval and does not require siting of a new disposal site. In situ treatment of wastes does not trigger Land Disposal Restrictions. For some wastes, carefully designed in situ treatments can convert mixed waste into low level waste by immobilizing or destroying the characteristic components of the wastes.

As evidenced by discussions during the workshop, the public is frequently sensitive to the cost vs risk reduction ratio offered by a technology. The high cost of retrieval approaches along with the risks and difficulties in storing the retrieved waste have made the public consider other alternatives. In most cases, even if the waste is retrieved, it will remain on the original site indefinitely. Even if the final product is a transuranic waste (TRU) mixed waste suitable for Waste Isolation Pilot Plant (WIPP), the public is keenly aware of the uncertainties surrounding the opening date of the WIPP repository. Faced with the likelihood of the waste remaining on site, the public is interested in the most cost effective way to safely manage the waste.

Long-Term Performance Issues

The workshop facilitated communication among end users representing most sites within the DOE, regulators, and technologists to define long-term performance issues for in situ stabilization and containment alternatives. Participants were divided into groups to identify issues and a strategy to address priority issues. The technical issues fell into three major categories: performance modeling, performance criteria, and prevention and mitigation of failure. A common issue identified at the workshop that impact many aspects of long-term issue resolution is the importance of effective communications. Improved communications between technologists, risk assessors, end users, and regulators, and other stakeholders would contribute greatly to resolution of these issues.

Performance Modeling

The requirement for long-term performance causes direct experimentation on materials and mock-up systems to be imperative, but insufficient to answer the issues associated with performance. When designing a remediation alternative for a site, risk reduction, long-term performance, and cost must be carefully balanced. Risk reduction and long-term performance are based on a set of assumptions about the current conditions of the waste and the site, the future conditions of the waste and site, and the ability of the stabilization/containment structure to accommodate those changes while maintaining its functional integrity. Modeling based on intuitive, analytic, numerical and expert-judgement must be used to predict performance. The first step is to develop conceptual models of the system design and the geological and ecological environment that encompasses the system. The predictive tools developed must reflect the uncertainties and adequacy of the data that describes the performance, both initial and with time, of the designed stabilization and containment system.

Using such predictive tools early in the remediation process can guide data collection by identifying the parameters to which the model is most sensitive and allows the model to be improved based on its prediction of measurable quantities. The major issues identified include: 1. definition of boundary conditions, 2. definition of performance standards and time periods, 3. understanding how data can be applied to different spatial and temporal scales, 4. accounting for future reasonable changes in the environment, and 5. developing appropriate analog studies.

Performance Criteria

There is no commonly developed or commonly defined baseline of performance criteria for containment/stabilization technologies. The need for a "universal" set of performance criteria has been recognized but the criteria are difficult to develop because the CERCLA system is organized to develop site specific criteria only and is not really required to look at similar sites when developing criteria. Success, as defined by the regulatory community could be substantially improved if an approved and widely accepted performance criteria were used for all technology applications. Stabilization/containment requires the following criteria to be considered: integrity, continuity, durability, permeability of barrier, repairability/maintenance, and system approach. An integral part of developing "universal" criteria is improving design interfaces. The more informed end users are early in the CERCLA process, the better the initial criteria will be. Technology developers need to clearly identify the technical site criteria needed for their technology to function effectively. End users need to distinguish between technical and non-technical components of performance requirements and to distinguish between requirements and preferences. Technology developers need to actively seek input from multiple sites while they are developing or refining a technology and to address non-technical concerns with the same rigor as technical concerns.

Prevention and Mitigation of Failures

There are three primary issues to be addressed in improving the prevention and mitigation of deterioration of stabilized/contained structures: the definition of failure and success, the logistics of design and measurement, and the challenge of life-cycle funding. The following discussion emphasizes the principle elements of each of these issues as identified by the workshop participants.

Definition of Failure and Success - A stabilization structure can be considered to have failed if a physical defect in the structure develops or if the release of contaminants is detected. One of the tough questions is how much of a defect or what level of contamination is a problem. Most action limits are risk based and therefore site specific. Stabilization structures need to be designed based on the characteristics of the specific site and on the risks posed by the site. How large of a defect or release constitutes failure must be determined prior to the design of the stabilization structure and the monitoring system. Standards or guidelines, similar to those developed by EPA for design of covers, need to be developed at an upper level for other stabilization techniques. Each site then needs to define the specific requirements and preferred properties for stabilization systems.

High quality site characterization is very important. This data drives the risk analysis for the contaminants and the modeling and design of the stabilization system. Site characterization should include detailed exploration of the nature and extent of the contaminants and the physical, chemical, hydrogeological properties of the subsurface. The workshop participants opinion was site characterization should consider potential future uses of the surrounding area since future land use changes can affect the subsurface properties of the remediation site. When the stabilization system is required to perform for hundreds to thousands of years, historical data on climatic cycling may be used to predict future cycles.

Logistics of Design and Measurement - Verification can be divided into two areas: verification of "as built" and verification of "as functions". The "as built" portion focuses on the construction phase of the project and is tied to quality assurance (QA) field inspections and verification of construction and materials as the stabilization structure is built. It asks "Is the structure built as designed and how can that be shown?" The "as functions" portion focuses on the performance of the stabilized structure after construction. It asks "Does the structure perform as designed and how can that be shown?"

The "as built" portion of verification is more readily accomplished than the "as functions" portion because design drawing with specific dimension and material specifications are available and much of the structure may be exposed during construction. Mass balances can be made for injected materials and the materials under observation are well defined in location and composition. In addition,

the construction phase has a well defined time span. The verification of "as functions" for a stabilization structure is much more complex. For a stabilization structure to perform as designed, the structure must not develop defects and the proper structure for that particular site must have been as it was initially designed. The time frame within which problems can occur and be identified is very poorly defined and may span hundreds of years. In addition, the root cause, of failures is difficult to identify but critical to improving the design of stabilization structures. For example, a crack may be due to settling, changes in the contaminants' interaction with the material, or changes in the water table; the crack is a symptom of a more fundamental change in thesystem. Repair of the crack would not necessarily address the real problem, resulting in numerous small repairs with no ultimate success.

Challenge of Life-Cycle Funding - The design of stabilization structures to require minimal monitoring and maintenance is key to keeping the life cycle costs of containment/stabilization reasonable. The key words for this approach are self-repair, self-heal and equilibrium with the environment. Self-repair applies primarily to structures and includes designing to compensate passively for defects such as cracking and subsidence. Self-healing refers primarily to materials used in construction of the stabilization structure. These materials may deform under stress, possess several stable hydration states, or compensate for physical and chemical changes in the environment through another mechanism. Equilibrium implies a lack of driving force which leads to a stable system. Equilibrium may not be desired in the short term if the stabilization structure is a reactive barrier, but it is always desirable in the long-term. Equilibrium systems are especially important for very long-lived radionuclides and for metals, which have an effectively infinite half-life. One of the challenges is to find material and structures which are at equilibrium with the waste and the site over the long-term, recognizing that the conditions of the waste and the environment can shift over time.

Effective Communication

The workshop participants emphasized that the resolution of long-term performance issues that must be overcome to successfully implement containment/stabilization technology systems relies not only on technology innovations, but also the utilization of effective communications. Improved communication can enhance any technology development process but is crucial when one begins to implement containment/stabilization technology systems for the purpose of long-term in situ disposal.

Containment/stabilization technology systems that can address long-term threats pose some unique communication challenges for technology developers and end user(s). First and foremost, in order to develop a technology system that can be implemented, remedial action objectives must be defined and understood by both the developers and end user. An effective technology system also requires multiple technical disciplines working together to achieve these objectives. As the technology system approaches deployment, it will be critical for all stakeholders to agree on the success criteria. A successful deployment will be determined as much by technology performance as by the expectations and perceptions of all stakeholders.

Determine Requirements and Objectives - Effective communications can have the most impact to successful deployment if it can be achieved early in the technology development stage. Although the long-term problems being addressed by DOE have been around for decades, remedial action has proceeded slowly. A major cause of this inaction is our inability to establish the requirements for remediation. This is also a major obstacle to the development of improved containment/stabilization technology systems.

The requirements for remediation are derived from regulations, federal site cleanup agreements, remediation objectives, risk-based decisions, and the capabilities of the remedial technologies. To complicate matters, sites with long-term threats inherently have multiple stakeholders with differing agendas. Development of a clear, concise and verifiable set of agreed upon requirements is a difficult task. But without such requirements, development of a "deployable" containment/stabilization technology system is difficult.

The technology developer must have a clear understanding of the remedial action objectives. Unfortunately many of these crucial requirements will not be firmly established until a cleanup decision has been made. These objectives are established by the end users and their regulators to ensure that a remedial action is protection of human health and the environment. Unlike other requirements that may not be fully understood until the cleanup decision has been made, remedial action objectives are established early in the decision process to guide the evaluation of remediation alternatives. In turn, these objectives provide the basis for the performance criteria of any successfully implemented technology system.

The technology developer must be cognizant of the remediation schedule. Technologies that are not demonstrated as effective or implementable within the time constraints driven by the site cleanup agreements have no hope of being deployed. The end user will be restricted to selection of perhaps less implementable or more costly technologies to achieve his objectives within his time constraints.

A key to the success in establishing sufficient requirements is to involve the potential end user(s), site regulators, and other stakeholders early in the technology development process. Their expectations ultimately establish the performance objectives that the technology provider must address in order to successfully deploy a containment/stabilization technology system.

Important concepts for the technology developer to consider during this phase include:

- work toward a consensus on the performance objectives: these ultimately establish the technology system's success criteria.

- involve end user(s) and regulators on a routine basis to gain their confidence and trust: the technology developer has a natural barrier to overcome. The end user will be hesitant to expend his energy and time on innovative solutions if he has little confidence in its success.

- obtain a commitment by the end user at the appropriate level of authority: this level of authority will increase as the technology approaches deployment.

- jointly sponsored projects can enhance the likelihood of success. If the end user has committed his resources, the quality of his participation will likely be improved.

Define Technology Interfaces – A deployable containment/stabilization technology system will be comprised of multiple technologies that must operate in an integrated fashion to provide the confidence that remedial action objectives can be achieved. These technologies may include surface covers, subsurface barriers, in situ stabilization, and monitoring for quality control, verification, and long-term performance assessment. The interfaces between these technologies must be defined to ensure success of the overall technology system. Each of the technologies within a containment/stabilization technology system contribute to ensuring that the remedial action objectives can be achieved. However, it is unlikely that a single technology component can ever provide adequate confidence that the objectives can be met. For example, placement of a surface cover without verification of its integrity and long-term monitoring for potential contaminant migration will likely not satisfy anyone's remediation objectives. A successfully deployed containment/stabilization technology system needs to ensure that the interface between the multiple technology components are well-defined, and that each component contributes to ensuring that the remediation objectives are achieved.

The key to defining these interfaces is to involve the various technical disciplines during the early phases of the project when objective and requirements are being defined. It is important that the capabilities and limitations of the various technologies that comprise a containment/stabilization technology system be understood not only by the technology developers but also by the end user(s) and regulators. As the performance objectives for the overall technology system are defined, the specific technology functions required to achieve these objectives are also defined. The "handoff" between these technologies are determined by establishing the interface requirements. These requirements form the basis for performance specifications of each of the technology components.

Deployment of Technology Systems - Deployment of a containment/stabilization technology system at a demonstration site is crucial in establishing confidence in the technologies. The lack of field performance data is a major barrier in the deployment of innovative technology. However, meaningful deployment demonstrations can not occur without the involvement and concurrence of site owners and their regulators. Deployment demonstrations require the technology developer to step into a new world of rules and processes controlled by the site owners and their regulators. The technology developer cannot succeed on his own. The working relationships developed with the end user and other stakeholders through the activities discussed previously will be a primary contributor to the successful deployment demonstration.

Involving potential end users from multiple sites can also enhance deployment. Common objectives can be incorporated into the containment/stabilization technology system. Demonstration at one site can then assist in establishing a precedence and can enhance regulatory reciprocity among states and EPA regions. Involving multiple sites also allows lessons learned and data to be more readily transferred between sites. And finally, involvement of multiple end users will enhance the commercial viability of a technology system. Industry interest and participation in the development of innovative containment/stabilization technology systems is increased if the potential market can be defined during the development stage.

CONSIDERATIONS IN THE DEVELOPMENT OF SUBSURFACE CONTAINMENT BARRIER PERFORMANCE STANDARDS

Steve Dunstan[1], David Lodman[2], and Andrew P. Zdinak[3]

Abstract

The U.S. Department of Energy (DOE) is supporting subsurface barriers as an alternative remedial option for management of contamination problems at their facilities. Past cleanup initiatives have sometimes proven ineffective or extremely expensive. Economic considerations coupled with changing public and regulatory philosophies regarding remediation techniques makes subsurface barriers a promising technology for future cleanup efforts.

As part of the initiative to develop subsurface containment barriers as an alternative remedial option, DOE funded MSE Technology Applications, Inc. (MSE) to conduct a comprehensive review to identify performance considerations for the acceptability of subsurface barrier technologies as a containment method. Findings from this evaluation were intended to provide a basis for selection and application of containment technologies to address waste problems at DOE sites. Based on this study, the development of performance standards should consider: 1) sustainable low hydraulic conductivity; 2) capability to meet applicable regulations; 3) compatibility with subsurface environmental conditions; 4) durability and long-term stability; 5) repairability; and 6) verification and monitoring. This paper describes the approach for determining considerations for performance standards.

Introduction

Subsurface containment barriers represent one of the more promising remedial options available for management of subsurface contamination problems. For over a century, subsurface barriers have been used on construction sites as engineered structures to reduce problems caused by groundwater intrusion. Barrier technologies as applied to waste remediation is a relatively new application and specific performance standards have not been established.

For purposes of this study, a subsurface barrier is defined as an installed structure that sufficiently alters the flow and transport processes in the subsurface such that the existence of any contaminants within the barrier do not pose a threat to human health and the environment. Barrier containment systems are used for remedial applications such as: 1) accomplish source term containment; 2) control contaminant migration; 3) control contaminated groundwater; 4) divert contaminated groundwater from drinking water intake; and 5) divert uncontaminated groundwater flow. There are other classes of barriers, such as permeable reactive barriers, which were not addressed by this study. These barriers have similar components, but would require a different set of design criteria and performance considerations.

The use of barriers as a site cleanup option is not necessary to completely inhibit contaminant or contaminant effluent migration. Rather, the purpose is to engineer a cost-effective solution that will allow specific long-term control of the contaminants of concern at the site. The purpose of developing achievable performance standards for containment barrier technologies is to ensure acceptable contaminant concentrations outside the confines of a barrier that do not exceed established regulatory guidelines (i.e., such as maximum contaminant levels).

---

[1]Steve Dunstan, MSE Technology Applications, Inc., P.O. Box 4078, Butte, MT 59702, (406) 494-7427, dfawcett@buttenet.com

[2]David Lodman, MSE, Inc., Suite 281, 381 Shoup Avenue, Idaho Falls, Idaho 83402, (208) 523-1171

[3]Andrew P. Zdinak, MSE Technology Applications, Inc., P.O. Box 4078, Butte, MT 59702, (406) 494-7223, dfawcett@buttenet.com

To be used successfully for waste remediation, a subsurface barrier will need to: 1) provide long-term compatibility with environmental conditions indigenous to the site; 2) provide long-term compatibility with contaminants specific to the site; 3) have low effective hydraulic conductivity and diffusivity to minimize migration contaminants; 4) minimize risk outside the containment area to acceptable levels per Federal or State guidelines established to protect human health and the environment; 5) be verifiable; and 6) be economically feasible. From this basis, performance considerations for subsurface containment barriers can be developed. However, it must be emphasized that site- and application-specific criteria will need to be determined based on the proposed remedial strategy for the contaminated site.

Basis For Remediation

The U.S. Environmental Protection Agency (EPA) and other Federal agencies have developed a number of approaches for remediating hazardous waste sites. The EPA has pursued three strategies for the minimization of acceptable risks associated with subsurface hazardous waste sources. They are: 1) destruction or degradation of contaminants by implementing some form of remediation technology (in situ and/or ex situ); 2) in situ contaminant stabilization; and containment of contaminants; or 3) isolation by the installation of a low-hydraulic conductivity barrier around the source zone, possibly combined with manipulation of the hydraulic gradient within the zone or either ex situ or in situ treatment systems. Of particular interest to this investigation are containment technologies to control subsurface contaminant migration.

Containment technologies are attractive because they can provide a cost effective remedial alternative when compared to treatment methods for site remediation. Subsurface barriers prevent contamination from becoming more widespread, and also allow for application of certain in situ treatment technologies that could otherwise not be implemented due to hazardous nature of the treatment process. Perhaps of added significance, is the use of containment options as an interim action until promising, cost-effective, and innovative technologies can be more fully developed for field application.

For the above stated reasons, there is increasing interest in the use of subsurface barriers for in situ containment of subsurface contamination problems at facilities and properties under management by DOE. DOE has initiated an active program to evaluate and further develop containment technologies.

Subsurface Barrier Performance Standards Development

As part of this development process, DOE tasked MSE to conduct a comprehensive investigation of relevant issues associated with containment technologies to identify performance considerations for accepting these technologies as an alternative remedial option.

Using a subsurface barrier to contain waste is a simple concept, however, developing a basis for performance standards for using subsurface barrier technology involved an extensive review to develop an understanding of the application of subsurface containment barriers for site remediation. This study involved evaluating a number of interactive components associated with containment barriers. These evaluation categories included: 1) regulatory issues, 2) site characterization aspects, 3) engineering aspects (i.e., emplacement and barrier material), and 4) economic aspects. The following is a brief discussion of these evaluation categories and their importance to development of performance considerations.

Regulatory Issues

In 1980, Congress enacted the Comprehensive Environmental Response, Compensation, and Liability Act (CERCLA), better known as the Superfund Program. The primary purpose for CERCLA was to provide funding and enforcement authority for cleaning hazardous waste sites from past industrial processes, and for responding to uncontrolled hazardous substance releases. Under CERCLA,

remediation efforts do not require a permit, but require a Record of Decision (ROD) declaration that state the preferred remedy for the site.

Most waste sites under evaluation for remediation within the DOE complex are being addressed as a result of responsibilities and requirements placed on DOE by CERCLA (MSE, Inc.) As such, regulatory aspects for determining performance standards for a subsurface containment barrier for application at DOE facilities were reviewed under CERCLA. Within these regulations, a basis for the development of performance standards for subsurface barriers is specified, but this process is typically highly interpretative and requires application-specific requirements to be determined during the remedy selection process. Numerous regulations were closely reviewed to ensure the use of a particular subsurface barrier is appropriate and identify relevant regulatory requirements.

Under CERCLA, performance requirements for a specific site are defined during the remedy selection process. The remedy selection process for short-term removal actions and long-term remedial actions, is defined in the National Oil and Hazardous Substances Pollution Contingency Plan (NCP) and implemented by EPA. Subsurface barriers may be considered as an interim measure under the removal process, a long-term solution, or a component of a long-term solution under the remedial process. A barrier designed under a final remedial action for use with an alternate treatment process, such as pump-and-treat, would most likely fall under the CERCLA regulations and all subsequent applicable and/or relevant and appropriate requirements (ARARs). A barrier used in conjunction with a removal process may or may not need to meet all the specified ARARs under CERCLA, and the performance standards needed to meet the goals of a cleanup action would be negotiated by the Potentially Responsible Parties (PRPs) and State, Tribal, and/or Federal agencies. For this study, evaluation of regulatory issues focused on subsurface containment barriers for long-term site remediation.

CERCLA encompasses most other Federal and State environmental regulations as ARARs. Identification of ARARs must be done on a site-specific basis and involves a two-part analysis: a determination whether a given requirement is applicable; if not, then a determination whether it is both relevant and appropriate. No applicable regulatory standards have been established for subsurface containment barriers; therefore, the ARAR analysis as part of the remedy selection process will stipulate which relevant and appropriate requirements will need be addressed. As previously stated, this analysis is highly interpretive and inconsistently applied between EPA regions and State regulatory agencies.

The process used to select remedies for contaminated sites, and the required performance of any selected remedy may change substantially in the coming months. The reauthorization of CERCLA is currently being debated in Congress, with an important area of debate focusing on the remedy selection process. Reforms proposed to Congress would eliminate the requirement that alternatives meet ARARs. The preference for permanent remedies and treatment over containment would be eliminated, which would favor, in some cases, the use of subsurface barriers as the preferred remedial alternative. Additionally, changes in the current risk assessment process are being considered (Environmental Reporter). Legislative and administrative reforms are discussed in more detail in the conclusion section.

Site Characterization Aspects

There is always a need for information and certain factors must be carefully examined to the extent necessary to assess the overall suitability of applying subsurface barriers for site remediation. The physical relationships regarding geological, hydrogeological, and geochemical characteristics and their interaction with a barrier, in association with the contaminant physical and chemical characteristics, are crucial to containment design and implementation. To understand these properties and environmental interrelationships typically involves a multi-disciplinary site investigation. Investigation findings are used to define the contamination problem and provide the fundamental information for developing a remedial strategy for the site. Key assessment areas and effects on barrier application are discussed in the following sections.

The stratigraphy and hydrogeology of subsurface formations and any heterogeneities in and around a hazardous waste site must be well characterized prior to designing a containment system. Lateral and vertical stratigraphic and structural discontinuities (i.e., faults, fractures, etc.) can significantly impact a barrier wall and floor material configuration, wall emplacement and material installation methods, barrier integrity, and costs. The existence of a naturally occurring confining layer of suitable thickness and hydraulic conductivity underneath a waste site may be effective as a containment floor. Project economics could be positively impacted if a vertical barrier could be keyed to such a naturally occurring barrier. If no naturally occurring low hydraulic conductivity layer is within a reachable depth, then a very expensive bottom impervious layer must be constructed which would complicate containment design and significantly increase cost.

One of the issues of greatest concern in the affective long-term containment of wastes is whether prolonged contact between the barrier materials, waste materials, and leachate will adversely affect the properties and performance of the barrier. The major concern is whether interaction of the leachate and the barrier will cause an increase in the hydraulic conductivity of the barrier over time. Although considerable research has been conducted and there is extensive information about specific interaction of certain barrier materials and contaminants, many issues still remain that require site-specific testing (compatibility tests) to ensure the selected barrier type will meet the performance requirements needed to meet the required design functions (Mitchell).

Geophysical investigation methods can be used to greatly enhance the understanding of the geologic and hydrogeologic conditions at the site. Proper planning for and use of geophysical methods can result in a significant savings during site characterization in terms of both time and money (Telford and EPA). Geophysical methods, like any other means of measurement, have advantages and limitations. There is no single, universally applicable surface or borehole geophysical method to meet all site characterization needs. Furthermore, some methods are quite site-specific in their performance. Therefore, the user must be able to select the method or methods carefully and understand how they should be applied to specific site conditions and to meet project requirements.

Engineering Aspects

For purposes of this study, review of engineering considerations focused on barrier emplacement methods and types of barrier materials. Case studies and technical literature were extensively reviewed to identify common design components, and performance and acceptance considerations. Barrier technologies (emplacement methods and material types) that were evaluated include slurry walls, composite cut-off walls with geomembrane, grouted barriers, mixed in-place cut-off walls, in situ vitrified cut-off walls, and cryogenic cut-off walls. This study also included placing a solicitation in the Commence Business Daily to request information directly from technology developers concerning design specifications and performance requirements.

From this investigation, factors that will limit and ultimately decide the type of method used include: 1) depth of emplacement; 2) required permeability; 3) site topography; 4) site access and work space; 5) geotechnical constraints; 6) soil characteristics; 7) characteristics of confining layer; 8) compatibility issues; and 9) costs. Depth to confining layer is the primary parameter that governs the emplacement method selected. If the confining layer is not acceptable, then a bottom barrier may need to be designed and constructed to achieve total waste containment.

From an engineering perspective, containment technologies fall into proven and experimental methods for barrier emplacement and material types. Selection of the most appropriate technology is directly related to the evaluation of site conditions. Experimental barrier technologies will typically require additional testing to determine successful implementation, and may require greater uncertainty acceptance due to the more experimental nature of applying unproven developmental technologies to site-specific needs.

Economic Aspects

Hazardous waste site management is obligated to consider regulatory requirements, public opinion, engineering, design, monitoring, and other factors, as well as, costs. Even though costs have no bearing on the development of performance standards, they have a significant role in the remedy selection process. We reviewed data on containment technologies, primarily focusing on the key factors that control costs. The cost of implementing, maintaining, monitoring, and possibly removing a subsurface barrier at the end of its life cycle can influence the selection of this type of remedial alternative.

Conclusions

Design criteria and performance standards are distinct, significant entities. Design criteria specify the material and procedures by which the barrier will be constructed, whereas performance standards specify the necessary chemical and physical characteristics required of a barrier material (Barvenik) Ideally, an optimal combination of performance standards and design criteria can be achieved when developing performance specifications for a barrier application at a contaminated site. Based on this study, the following considerations were identified and should be addressed for determining performance requirements for applying subsurface containment barriers for successful application at a DOE waste site.

Sustainable Low Hydraulic Conductivity - The primary performance criteria for containment is the maintenance of low hydraulic conductivity. Hydraulic conductivities is a function of the barrier material and its thickness. Design planning for the containment system will need to focus on the barrier emplacement technique and type of barrier material that will meet the specified hydraulic conductivity for containment. Data from the literature indicates that hydraulic conductivities in the range of 10^{-7} cm/sec, or less, are achievable with proven, natural materials. Clay materials have the capability of achieving 10^{-7} to 10^{-8} cm/sec hydraulic conductivity, and synthetic materials can achieve conductivities several orders of magnitude lower. Experimental materials for subsurface barriers presently under development should be required to perform at similar or lower levels of hydraulic conductivity to eliminate pathways and risk factors posed by the contamination problem.

Capability to Meet Applicable Regulatory Standards - Consideration has been given to the ability of the barrier to control releases such that applicable State and Federal Regulations are met. At a minimum, a barrier will require a combination of low permeability and sufficient barrier thickness to ensure acceptable control with respect to leakage over the desired time period. Under the Superfund Program, remedy selection involves meeting two threshold criteria: 1) protectiveness of human health and the environment and 2) compliance with ARARs. The degree of protectiveness is determined by the risk assessment performed during the Remedial Investigation/Feasibility Study (RI/FS) for the site. Typically, containment technologies can be designed to reduce contaminant exposure to acceptable risk levels. Compliance with ARARs is a highly interpretive process and specific requirements can be inconsistently applied between EPA regions and State regulatory agencies.

Compatibility with Subsurface Environmental Conditions - Before choosing the type of subsurface barrier to control hazardous constituents at a waste site, a number of different compatibility issues must be considered to make defensible decisions regarding the type and kind of barrier to use at a site. Once again, these issues are all site-specific and compatibility tests must be conducted to determine if a barrier option will provide the required performance and longevity needed to meet the design function of the barrier. The barrier material must be able to retain its hydraulic conductivity over time and this is governed by different compatibility issues such as: 1) compatibility of the barrier and the contaminant(s) present at the site; 2) compatibility between the barrier and soil or geologic conditions at the site; 3) compatibility of the barrier with the groundwater (if present) at the site; and 4) compatibility between the barrier materials and the emplacement method.

Durability and Long-Term Stability - The containment barrier must be able to withstand certain environmental and natural forces such as seasonal fluctuations (i.e., extremes in wet and dry periods),

subsidence, and other natural phenomena. A subsurface containment system will be required to be sustainable with regard to hydraulic conductivity and durable with regard to the natural and artificial degradation factors. Additives can be added to barrier materials to minimize the effect of degradation by contaminants and synthetic materials can be engineered to be minimally effected by caustic environments. The effectiveness and long-term performance of containment barriers depend on the level of construction quality control (CQC) that is implemented. CQC plays a fundamental role in confirming the design objectives and ensuring performance requirements can be achieved.

Repairability – Barrier repairabiltiy has been given little attention but is very important consideration for long-term performance. Using a subsurface barrier as a remedial option at a DOE hazardous waste site (radioactive and mixed waste problems) may include short- and long-term applications. Either case will require the following: 1) capability to identify damage; 2) capability to detect degradation; 3) capability to competently repair a subsurface barrier breach or discontinuity that has been caused by some catastrophic event or some type of emplacement problem; and 4) compatibility of the repairing method with the installed subsurface barrier. A well-planned subsurface barrier project ideally takes these factors into account during barrier design, material selection, and emplacement method.

Verification and Monitoring – From a regulatory perspective, once the barrier is emplaced the question remains on how to ensure performance. A performance monitoring program will have to be initiated to evaluate how closely the design is performing to specifications, as well as, to look for signs of any potential increase of contaminant levels from the contaminant area. Performance monitoring may be conducted to satisfy any of the following objectives: 1) evaluate the integrity of the containment barrier; 2) estimate the containment efficiency in relation to design; 3) evaluate changes in water quality by control of contaminant migration; and 4) evaluate the ability of the contaminant barrier to retain its performance over time. These issues can be addressed by developing a monitoring and verification program. Geophysical techniques can be used to verify and check the structural integrity of the containment barrier. A performance monitoring program will provide an early indictor of potential loss of contaminants or releases of contaminants through the barrier.

Other Considerations

Regulatory reforms and economic factors are emerging issues that may influence the acceptance of containment technologies as an alternative remedial option. Senate Superfund Bill 8 proposes a major reauthorization of the Superfund Program. A number of key reforms proposed under this bill would effect the remedy selection process to favor selection of containment strategies (API Memorandum.) Major reforms under this proposed bill are: 1) must select a cost-effective remedy that protects human health and the environment, including groundwater; 2) replace the rigid statutory preference for permanence and treatment with flexibility to allow considerations of all cleanup options, including containment; 3) replace the ARAR process and requires applicable laws to be developed which are administrated consistently; and 4) Reopen record of decision (ROD) to evaluate more cost-effective remedies.

In response to recent and past legislative efforts to reauthorize Superfund, EPA announced 20 new administrative reform initiatives designed to "fundamentally redirect Superfund to make it faster, fairer, and more efficient" (EPA.) Two reform initiatives that directly favor the acceptance of containment strategies for site remediation were the creation of a National Remedy Review Broad and updating remedy decisions. The National Remedy Review Broad reviews those Superfund sites where the estimated cost of the regions preferred alternative either exceeds $30 million or exceeds $10 million and is 50% or greater than the cost of the least costly, protective, ARAR-compliant alternative. This broad has ruled in favor of more cost-effective remedies and in some instances selected containment-type alternatives. However, at federal facility sites where the primary contaminant is radioactive waste, EPA has raised the cost trigger to $60 million and has eliminated the "50% greater than least cost alternative criterion." Discussions with the Departments of Defense and Energy on thresholds for such sites are ongoing at EPA Headquarters level.

EPA has reopened ROD to consider proven or innovative technologies with "well understood capabilities." This reform is also cost-driven, particularly if the existing remedy is not technically achievable or out-of-date with current remediation science and technology. Groundwater cleanup decisions were the most obvious candidates for this initiative. For example, for aquifers contaminated with dense non-aqueous phase liquids ("DNAPLs"), EPA states that groundwater pump-and-treat remedies will be superseded by isolation and containment of the DNAPL source, with EPA seeking to remove that source only to the degree practicable. As stated, these reforms favor the acceptance of containment technologies as stand-alone remediation strategy to address contamination problems at DOE sites.

Not a performance issue, but economics is becoming increasing importance in the remedy selection process. The cost of a barrier solution is an important consideration needing careful analysis, and there are many factors involved. One important trend is that regulators are increasingly open to discussion of cleanup costs. There is a growing willingness in the regulatory community to consider cost an important factor in remedy selection process, specifically when comparing costs to future land use benefits.

References

Arbuckle, et al. Environmental Law Handbook, 11th. Edition, Government Institutes, Inc., p. 488, 1991.

Barvenik, M. J., GZA GeoEnviromnental, Inc. Design Options Using Vertical Barrier Systems, ASCE 1992 International Convention & Symposium, Environmental Geotech Symposium, New York, NY, September 14-17, 1992.

Environmental Reporter, "Current Development", Vol. 26, No. IQ, The Bureau of National Adias, Inc., Washington, D. C., p. 522, July 7, 1995.

Grube, W.E. Jr., "Slurry Trench Cut-off Walls for Environmental Pollution Control," SLURRY WALLS: Design. Construction and Quality Control ASIXf SIP 1129, David S. Paul, Richard R. Davidson, and Nicholas L. Cavalli Ets. American Society for Testing Materials, Philadelphia, 1992.

Mitchell J.R., "Hazardous Waste Containment," Groundwater in Engineering Geology, London, 1986.

MSE, Inc., Subsurface Barriers Performance Standards: Interim Report, Butte, Montana, 1996.

MSE, Inc., Subsurface Barriers Performance Standards, Butte, Montana, 1996.

Rumer, R. and K. E. Ryan (Editors), Barrier Containment Technologies for Environmental Remediation Applications, p 4-5. John Wilq Jb Sons, New York, NY, 1995.

Telford, W. M., L. P. Geldart, and R E. Sheriff, Applied Geophysics, 2nd Ed., Cambridge University Press, New York, 1990.

U.S. Army Corps of Engineers, Soil-Bentonite Slurry Trench for HTRW Projects Guide Specification for Military Construction, CEGS 02444, September 1994.

U.S. EPA, Use of Airborne, Surface, and Ironhole Geophysical Techniques at Contaminated Sites, EPA/C2S/R921007, 1990.

Senate Staff, "Summary of Key Provisions of S.8, The Superfund Cleanup Acceleration Act of 1997, Introduced on January 21, 1997."

U.S. EPA, et. al., "EPA's Superfund Reforms: A Report on the First Year of Implementation," Morgan, Lewis & Bockius LLP, Washington, D.C. 20036, December 1996.

Performance of Engineered Barriers

V. Rajaram[1], Paul V. Dean[2], Sharon A. McLellan[3], Amy Mills[4],
Pierce L. Chandler[5], Gary W. Snyder[6], and Dominique L. Namy[7]

Abstract

Engineered barriers, both vertical and horizontal, have been used to isolate hazardous wastes from contact, precipitation, surface water and groundwater. The primary objective of this study was to determine the performance of subsurface barriers installed throughout the U.S. over the past 20 years to contain hazardous wastes. Evaluation of Resource Conservation and Recovery Act (RCRA) Subtitle C or equivalent caps was a secondary objective. A nationwide search was launched to select hazardous waste sites at which vertical barrier walls and/or caps had been used as the containment method. None of the sites selected had an engineered floor. From an initial list of 130 sites, 34 sites were selected on the basis of availability of monitoring data for detailed analysis of actual field performance. This paper will briefly discuss preliminary findings regarding the design, construction quality assurance/construction quality control (CQA/CQC), and monitoring at the 34 sites. In addition, the short-term performance of these sites (less than 5 years) is presented since very little long-term performance data was available.

Introduction

The field performance of engineered barriers is important to meeting the containment goals at hazardous waste sites. Soil-bentonite slurry walls and caps have been installed at several sites in the U.S. to contain hazardous wastes. Data on design, CQA/CQC, performance monitoring, operation and maintenance (O&M), and cost were obtained for 34 sites by contacting regulatory agencies, contractors, and site owners. Large quantities of performance related data were obtained at some sites that were constructed in the 1980s, and limited performance data were obtained for sites constructed in the 1990s. However, quality of performance data at the sites

---

[1]   Tetra Tech EM Inc., 1921 Rohlwing Rd., Suite D, Rolling Meadows, IL 60008,
(847) 255-4166, rajarar@ttemi.com

[2]   Tetra Tech EM Inc., 1593 Spring Hill Rd., Suite 300, Vienna, VA 22182, (703) 287-8806,
deanp@ttemi.com

[3]   Tetra Tech EM Inc., 200 EastRandolph Dr., Suite 4700, Chicago, IL 60601, (312) 856-8747,
mclells@ttemi.com

[4]   U.S. Environmental Protection Agency, Office of Research and Development,
401 M St., SW (H-8501), Washington, DC 20460, (202) 260-0569,
mills.amy@epamail.epa.gov

[5]   Black & Veatch, 5729 LBJ Freeway, Suite 300, Dallas, TX 75240, (214) 770-1500

[6]   Black & Veatch, The Curtis Center, Suite 850W, Philadelphia, PA 19106, (215) 928-2233,
snydergw@bv.com

[7]   Inquip Associates, Inc., P.O. Box 6277,McLean, VA 22106, (703) 442-0143,
103244.2012@compuserve.com

varied considerably from site to site. This paper will detail the current industry practice for vertical barrier design, CQA/CQC, and monitoring, and present preliminary findings regarding the short-term performance of the containment system (vertical barrier, cap, and any active pumping from within barrier) observed at the 34 sites. A draft report documenting the study will be available in the spring of 1997.

Selection of Study Sites

The scope of the study was to select between 30 and 40 sites for detailed evaluation from 130 sites known to have installed engineered barriers. The sites were screened to identify those sites with sufficient performance-related data available to permit evaluation of performance. The principal screening criteria were design, CQA/CQC during installation, and monitoring. Other relevant criteria included the type of barrier, geologic setting and geographic distribution, and whether the vertical barrier is integrated with a cap or active pumping from within the barrier. Availability of adequate monitoring data was considered crucial to a meaningful evaluation of the performance of engineered barriers. Therefore, the sites selected for detailed evaluation tend to represent well-monitored and documented sites. As such, these sites are not necessarily representative of the universe of vertical barrier sites. To select the 30 to 40 sites, the project team used weighting criteria. The weights assigned to these criteria were 15 percent each for design and CQA/CQC data, 35 percent for monitoring data, 10 percent for barrier type and 25 percent for other criteria (such as cost of barrier, geologic setting and distribution, integration with a cap or active pumping, and innovative technologies). The weights reflect the importance of the criteria in determining the performance of engineered barriers. Of the 34 selected sites, 26 have soil-bentonite barriers, two have cement-bentonite barriers, two have soil-cement-bentonite barriers, one has a concrete barrier, one has sheet piles, one has a plastic-concrete barrier, and one has a clay barrier. Figure 1 illustrates a typical soibentonite slurry trench cross section.

Data Analysis

Site summaries were prepared for the 34 sites, and included site description and history, geologic and geohydrologic setting, nature and extent of contamination, containment remedy, and performance evaluation. The sites then were rated as exceeding, meeting or not meeting acceptable practice for design, CQA/CQC, and monitoring. Acceptable practice was defined by the project team's experience and assessment of established industry practice, supplemented by discussion with engineers and contractors, and review of recent literature (US Army Corps of Engineers 1995; Evans 1994; Barvenik 1992; McCandless and Bodocsi 1987).

Acceptable industry practices for design, CQA/CQC, and monitoring of vertical barriers are presented in Tables 1, 2, and 3, respectively. The tables contain the factors and their respective weightings (as defined by the project team) that were used to determine whether acceptable industry practices were met. (Meaningful weights could not be assigned for monitoring practices.)

Evaluation of the critical design elements at vertical barrier sites studied included:

- Spacing of geotechnical borings
- Geohydrologic investigations of subsurface strata
- Backfill mix testing
- Long-term backfill compatibility testing
- Key depth in aquitard
- Barrier wall thickness
- Surface cap to provide physical protection of the top of the wall
- Control of trench bottom cleanliness prior to backfilling

Consideration of these design parameters increases the likelihood that the vertical barrier will perform as designed.

The vertical barrier CQA/CQC elements that were followed at most sites included the following:

- Continuous inspection of construction
- Confirmation of the key
- Slurry and backfill testing
- Backfill slope sounding and sampling
- Post-construction testing of the barrier wall, by drilling and permeability testing of samples

Adherence to CQA/CQC elements is important for a vertical barrier to perform as designed. For example, when the confirmation of the key was not performed by sampling at the key depth or the inspection of construction sediment and erosion control was inadequate, site review revealed that problems with leakage were more likely to occur.

The most successful way to ensure adequate performance in the long-term is to conduct thorough design studies and provide competent field quality control during construction (Evans 1993). Performance monitoring is a surrogate measure of actual performance of the vertical barrier, and may indicate problems. The monitoring program at most sites consisted of the following:

- Paired piezometers at several locations across the wall to monitor the gradient
- Periodic comparison of baseline and post-construction groundwater quality at key downgradient locations
- Pumping rate from inside the wall

Six sites had data from pumping tests that measured the average as-built hydraulic conductivity of the barrier. Four of the 34 sites used geophysical techniques to measure the post-construction integrity of the vertical barrier.

Performance of Vertical Barriers

Using the criteria detailed in Table 1, 2 and 3, the sites were evaluated for design, CQA/CQC, and monitoring as compared with acceptable practice. For design, 14 sites were rated "exceeds acceptable practice," 15 sites were rated "meets acceptable practice," 2 sites were rated "does not meet acceptable practice," and 3 sites were not rated. For CQA/CQC, 22 sites were rated "exceeds acceptable practice," 8 sites were rated "meets acceptable practice," 1 site was rated "does not meet acceptable practice," and 3 sites were not rated. For monitoring, 11 sites were rated "exceeds acceptable practice," 10 sites were rated "meets acceptable practice," 11 sites were rated, "does not meet acceptable practice" and 2 sites were not rated. Of the 34 sites evaluated, 5 were rated "exceeds acceptable practice" in all three categories, and 1 site was rated "meets acceptable practice" in all three categories. No sites were rated below acceptable practice in all three categories.

At four of the 34 sites in the study leaks were detected at the key and subsequently repaired. Interestingly enough, three of these sites were rated "exceeds acceptable practice" as compared with currently established practices for design, CQA/CQC, and monitoring. The fourth site at which a leak was detected had design which was below acceptable practice and monitoring which met acceptable practice (CQA/CQC was not rated). This indicates that other factors may be affecting performance, although the sample size is too small for drawing definitive conclusions. However, the importance of defining the variability of the geology and geohydrology at the site, and in particular, the key horizon cannot be overemphasized. The CQA/CQC program only ensures that the methods and materials used in constructing the barrier meet the design specifications.

1016

Seven sites had design and CQA/CQC which met or exceeded acceptable practice, but monitoring which did not meet acceptable practice. It is therefore unclear whether the barriers at these sites are performing as intended or leaks have gone undetected. Furthermore, it is unclear whether current industry practice for monitoring is sufficient to detect leaks from vertical barriers where a reverse hydraulic gradient is not present. (In this regard, currently accepted industry practice may not be *acceptable* or satisfactory for adequately demonstrating barrier performance. Further work needs to be done to address this issue.)

The performance of most of these barriers over the typical 30-year design life is yet to be determined since a majority of these sites are less than 10 years old (although thus far most of the barriers are performing as designed). The performance evaluation at the 34 sites studied confirm that one of the most likely places for leakage is at the bottom of the barrier when it is keyed incorrectly into the aquitard. In this regard, special consideration should be given to the following:

- The quality of the aquitard should be investigated thoroughly -- in particular for bedrock formations where additional measures such as grouting below the bottom of the wall may be required
- The thickness of the wall and the depth of key into the aquitard should be determined by parameters such as geological conditions, hydraulic gradient, and depth of the wall
- The key confirmation is very critical during CQA/CQC
- The monitoring program (paired piezometers and groundwater quality) should be designed to detect leakage at the key horizon, and the integrity of the barrier should be determined by stressing the barrier utilizing pumping tests
- The cap should be integrated with the top surface of the barrier to maximize containment system effectiveness

References

Barvenik, M. O. J. 1992. "Design Options Using Vertical Barrier Systems." Presented at the American Society of Civil Engineers 1992 International Convention & Symposium, Environmental Geotech Symposium. New York. September 14-17.

Evans, J. C. 1994. "Vertical Cutoff Walls." American Society of Civil Engineers, New Jersey Section. June 15.

McCandless, R. M., and Bodocsi, A. 1987. Investigation of Slurry Cutoff Wall Design and Construction Methods for Containing Hazardous Wastes. U.S. Environmental Protection Agency. EPA/600/S2-87/063. November.

U.S. Army Corps of Engineers. 1995. Checklist for Design of Vertical Barrier Walls for Hazardous Waste Sites. ETL. 1110-1-158. Department of the Army. Washington, D.C.
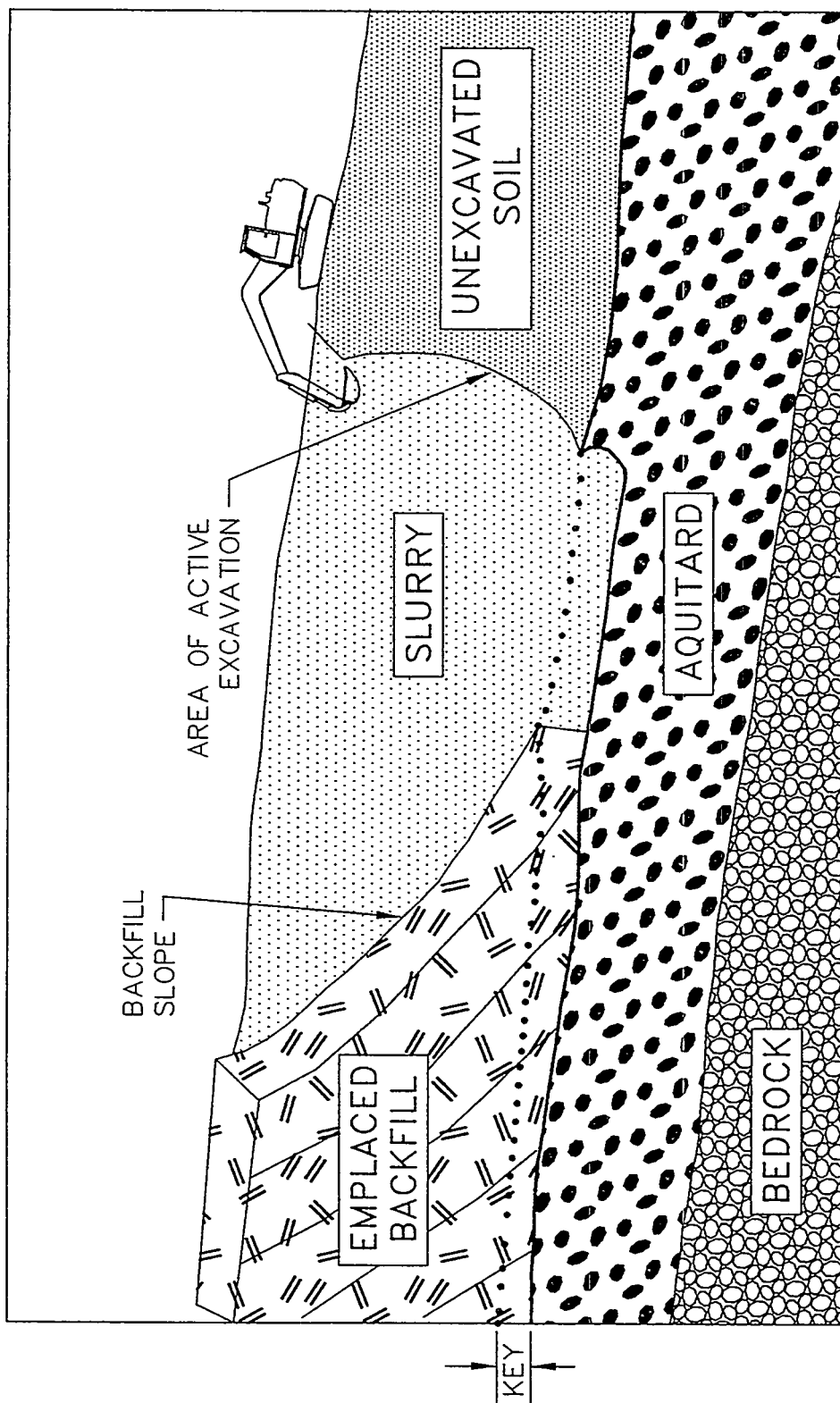
FIGURE 1. SOIL-BENTONITE SLURRY TRENCH CROSS-SECTION

TABLE 1
CONTAINMENT BARRIER DESIGN PERFORMANCE MATRIX

Category	Weight	Does Not Meet Acceptable Practice	Meets Acceptable Practice	Exceeds Acceptable Practice
Hydrogeologic Investigation	10	None	Yes	>
Feasibility Determination	5	None	Yes	>
Geotechnical Design Investigation				
Borings along alignment	10	1 boring/>60 m	1 boring/30-60 m	1 boring/<30 m
Geotech. physical testing	5	None	Yes*	>
Barrier Design				
Groundwater modeling	5	No Modeling	Feasibility Modeling	Design Performance Modeling
Alignment & key depth+	10	<0.6 m	0.6-1.2 m Key	>1.2 m
Wall thickness/hydrofracture	10	<0.6 m	0.6-1.2 m	>1.2 m
Trench stability & analysis	5	None	Analytical	Numerical
Backfill Permeability testing/optimization	2	<3	3 Tests	>3
Trench slurry compatibility	2	<3	3 Tests	>3
Long term backfill compatibility	5	<3	3 Tests	>3
Barrier penetration details	2	None	Contractor Designed	Designer Designed
Barrier cap details	3	None	Physical Protection	>
Cap/barrier interface	2	None	Component Overlay	Physical Connection
Protection from dessication	2	<0.3 m	0.3-0.6 m Clay Cap	>0.6 m
Protection from surface loading	2	None	Spanning Elements	>
Protection from subsurface breach	2	None	Physical Protection	>
Construc. sediment & erosion control	2	None	Contractor Designed	Designer Designed

* Representative gradation, limits, unit weight and key permeability.
+ Soil key shown. Rock key rated 1 (to fracture bedrock-no grouting), 2 (0.15-0.3 m into sound rock), 3 (>0.3 m).

TABLE 2
CONTAINMENT BARRIER CQA/CQC PERFORMANCE MATRIX

Category	Weight	Does Not Meet Acceptable Practice	Meets Acceptable Practice	Exceeds Acceptable Practice
Specialty Contractor Experience	10	<4	4 - 6 Comparable Projects	>6
Trench Excavation Methods	5	No Inspection	Periodic Inspections	Constant Inspection
Trench Width, Verticality & Continuity	10	No Inspection	Periodic Inspection	Measured
Trench Sounding (slope & bottom)	10	>6 m	3 - 6 m	<3 m
Trench Bottom Cleaning	5	None	Yes *	>
Trench Key Confirmation (sampling & sounding)	15	<	Occasional Sampling (~6 m)	Sample all bottom excavation
Slurry Mixing	2	<	Agitation >12 hrs. Hydration	>
Slurry Viscosity Testing	2	<2	2 per shift	>2
Slurry Viscosity	2	<40	40+seconds (marsh funnel)	40++seconds (marsh funnel)
Slurry Sand Content Tests	2	<2	2 per shift	>2
Slurry Sand Content	2	>15%	<15 %	<<15%
Backfill Slump Testing	2	<	1 per 300 - 500 cubic m	>
Backfill Slump	2	<7.5 cm or >15 cm	Most tests 7.5 - 15 cm	All tests 7.5 - 15 cm
Backfill Gradation Testing	3	<	1 per 3 - 5 m	>
Backfill Permeability Testing	3	<	1 per 3 - 5 m	>
Backfill Target Permeability	3	>	5x10-7 - 1x10-7 cm/sec	<
Backfill Mixing/Placement	2	Loosely Controlled	Controlled Mix/Place	Central Mix/Guided Placement
Capping Confirmation	5	None	QC Tested	>
Barrier Continuity	2	Interrupted	Continuous	Continuous & Confirmed
Post Construction Barrier Sampling/Testing	5	None	Some	Regular & Documented
As-Built Records	5	None	Const. Completion Report	Report, Drawings, Test Results
Groundwater Head Monitoring	2	None	Monitored Fluctuation	Periodic & Across Barrier
Final Barrier Alignment Survey	1	None	Surveyed	Surveyed & Monumented
Barrier Construction Specification	10	None	Barrier	Barrier & CQA & Others
CQA/CQC Program & Testing Specified	5	None	Designer Specified	Independent Duplicate QA Test
Groundwater Chemistry Monitoring	1	None	Some	Periodic & Across Barrier

* Observation of trench width and equipment verticality.

TABLE 3
CONTAINMENT BARRIER MONITORING PERFORMANCE MATRIX

Category	Does Not Meet Acceptable Practice	Meets Acceptable Practice	Exceeds Acceptable Practice
Groundwater Quality	Inadequate number or location of wells and/or inadequate analytical program	Adequate number and location of wells to assess nature and extent of groundwater plume	Hydrogeologic studies may have included fate and transport modeling. Analytical trends are monitored
Hydraulic Head	None	Piezometer pairs across barrier	Equally spaced pairs across barrier
Hydraulic Stress Tests	None	Post construction at barrier	At post construct, after 5 years, and when barrier integrity is questioned
Settlement Monitoring	None	Near structures	Near structures and regularly (e.g., quarterly, annually)
Physical Samples & Permeability	None	At select locations	At regular intervals (e.g., quarterly, annually)
Inclinometer & Barrier Movement	None	At slopes which exhibit failure or potential for failure	Regularly (e.g., quarterly, annually) at slopes which exhibit failure or potential for failure
Geophysical Testing	Not applicable	None	Limited testing
Desiccation	Not applicable	None	Limited testing
Earth Stress	Not applicable	None	Limited testing

PREDICTIVE TOOLS AND DATA NEEDS FOR LONG TERM PERFORMANCE OF IN-SITU STABILIZATION AND CONTAINMENT SYSTEMS: DOE/OST STABILIZATION WORKSHOP, JUNE 26-27, PARK CITY, UTAH*

By

David J. Borns
Geophysics Department
Org. 6116/MS-0750
Sandia National Laboratories
Albuquerque, New Mexico 87185-0750

ABSTRACT

This paper summarizes the discussion within the Predictive Tools and Data Needs for Long Term Performance Assessment Subgroup. This subgroup formed at the DOE Office of Science and Technology workshop to address long-term performance of in situ stabilization and containment systems. The workshop was held in Park City, Utah, 26 and 27 June, 1996.

All projects, engineering and environmental, have built-in decision processes that involve varying risk/reward scenarios. Such decision-processes maybe awkward to describe but are utilized every day following approaches that range from intuitive to advanced mathematical and numerical. Examples are the selection of components of home sound system, the members of a sports team, investments in a portfolio, and the members of a committee. Inherent in the decision method are an understanding of the function or process of the system requiring a decision or prediction, an understanding of the criteria on which decisions are made such as cost, performance, durability and verifiability. Finally, this process requires a means to judge or predict how the objects, activities, people and processes being analyzed will perform relative to the operations and functions of the system and relative to the decision criteria posed for the problem. These risk and decision analyses are proactive and iterative throughout the life of a remediation project. Prediction inherent to the analyses are based on intuition, experience, trial and error, and system analysis often using numerical approaches.

This subgroup recommends the following steps for the combined landfill and plumes focus area: (1) that the focus area encourage an interaction between technology developers, possible customers, performance/risk assessment programs, regulators and stakeholders to define reasonable boundary conditions; (2) that the focus area develop methods to quantitatively relate changes in observable properties of the containment system (e.g., evaporation, permeabilities of system components or solubilities of waste forms) to capability of the total system to meet performance or regulatory performance criteria (e.g.: cumulative release to water table); and (3) that the focus area encourage and support a trial application of an integrated process of performance predictions through several stages of the design cycle at specific focus area or EM-40 site(s).

1. Introduction:

The DOE Office of Science and Technology facilitated a workshop to address long-term performance of in-situ stabilization and containment. This workshop was held in Park City, Utah, 26 and 27 June 1996. The objectives of this workshop included the (1) development of a framework or logic tree to support long term risk analysis of in-situ disposal alternatives and (2) to recommend paths or investments by the focus area to address issues regarding long term performance. This paper summarizes the discussions of a subgroup covering the **predictive tools** and **data needs** for long term performance assessment. As with any summary of a group discussion, it is difficult to capture equally all of the view points expressed.

2. The methodology and needs of long-term performance assessment

Performance assessment is a methodology for gauging the relative risk incurred by a series, or sequence of actions. Current approaches are largely based on rules-of-thumb (e.g., it is best to remove the contaminant, or, cap the landfill with clay to reduce water influx). However, rules-of-thumb often depend on site-specific factors and, therefore, may not actually reduce risk. In some cases they might increase risk (e.g., clay caps dry up and form cracks in arid environments).

The National Research Council (1994) and the Congressional General Accounting Office (1996) have concluded that the present risk-based approaches for prioritizing hazardous waste sites are inadequate. Basically, these current approaches do not completely and consistently prioritize sites that present the greatest risk nor prioritize remediation strategies that result in the greatest reduction of risk. Such conclusions stem from the following: (1) There is inadequate data (e.g. waste inventories) to support site assessment; *(2)* some parameters are site-specific; (3) The assessment process doesn't reflect significant types of contaminants and pathways; and (4) legal requirements often do not reflect a significant reduction of the greatest risks. Different approaches to assess risk and to prioritize risk reduction are needed. These new approaches need to couple risk or performance assessment of a total system *(total system performance assessment models)* with data needs and uncertainties that are site-specific *(probabilistic decision analysis;* Miller and others, 1993). Such approaches are coupled and iterative. They will also address the site-specific predicted risk reduction, guide specific site characterization, and identify the uncertainties related to available data and understanding of the processes (e.g.: contaminant fate and transport). The *risk and cost reduction* results from the: (1) selection of remediation strategies that reduce risks; (2) elimination of cost from discontinuing of remediation strategies that do not reduce risk; and (3 the cost of remediation design and collection of the supporting data being optimized.

The technical process of *performance assessment* may appear obtuse and unfathomable. However, we use such processes in our everyday lives, for example, buying a car, selecting an area where to live, or choosing a career. The approach here is to build upon the familiar everyday aspects to develop a process that can be applied to environmental remediation (Figure 1 and 2). The evaluation of the familiar process of buying a car (Figure 2) results in these possible paths: (1) collect more data or gain a better understanding (e.g.: look at additional models or makes of cars); (2) eliminate some the alternative strategies (e.g., evaluate fewer makes and models; (3) relax a decision criteria (e.g., accept a smaller engine); or (4) chose "no action" (e.g.: decide to delay buying a new car).

Remediation activities are based on regulations that vary with country, state, responsible party, and type of waste, or specific site agreement. However, they all include a similar assessment process which predicts (considering the effects of the engineered system and natural systems) the cumulative release of a contaminant at a given boundary (Figure 2). The terminology (as defined in Sec. 2.2) is added to figures to show the regulatory framework.

2.1. Risk versus Performance

For the DOE restoration activities, risk has largely covered life-cycle cost and schedule issues. However, the goal of stabilization and containment is the protection of health and the accessible environment. Therefore, the primary risk addressed in long term performance is the risk-to-health or environment. As a consequence, any analysis of cost or schedule risk are only secondary to the risk-to-health standard being predicted to be achieved. Risk-to-health is a concept that is not easily quantified and standardized. In practice, it is difficult to measure a group value of what is "acceptable" risk (e.g., safe maximum driving speed). When the public intuition contradict analytic evaluations for specific risks, Starr and Whipple (1980) observe that the necessary consensus may not develop, and a political resolution will be required. Congress

has not defined "acceptable" risk ; except where a zero risk approach is mandated. Generally, Congress delegates responsibility to regulatory agencies, such as EPA, the state or tribal equivalents, to set standards that address acceptable risk. Any predictive tool for long term performance can only address the compliance with the regulatory or performance standard and cannot address "what is safe" or "what is acceptable risk" as developed by public consensus or political action.
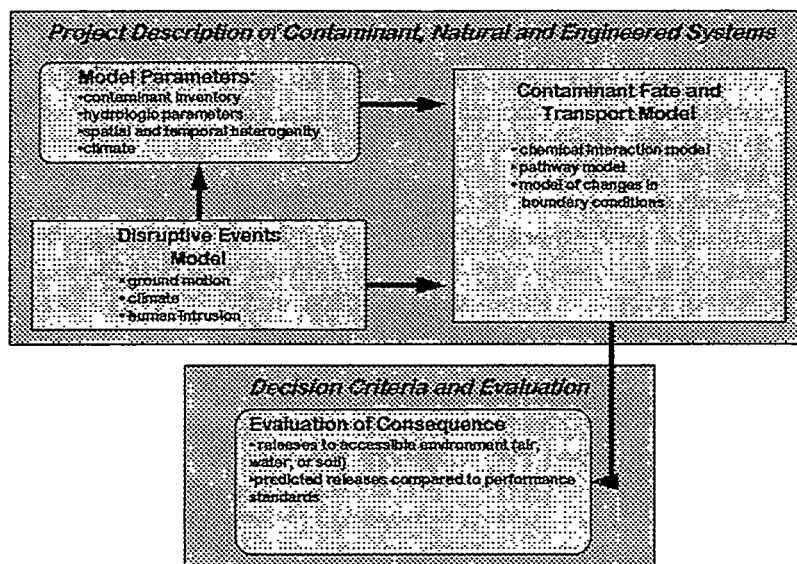
Figure 1: Performance assessment model structure (modified from Miller and others, 1993)

2.2. New terms: disposal system, barrier, passive institutional control, active institutional controls, controlled area, accessible environment, and undisturbed performance definitions (modified from 40CFR190 series, 40CFR260 series):

2.2.1. *"Disposal system"* means any combination of engineered and natural barriers that isolate contaminants after disposal

2.2.2. *"Barrier"* means any material or structure that prevents or substantially delays movement of water or the migration of contaminants to the accessible environment

2.2.3. *"Passive Institutional Control"* means: (1) permanent markers placed at a disposal site, (2) public records and archives; (3) government ownership and regulations regarding land or resource use; and (4) other methods of preserving knowledge about the location, design, and contents of a disposal system

2.2.4. *"Active Institutional Control"* means: (1) controlling access to a disposal site by any means other than passive institutional controls; (2) performing maintenance operations or remedial actions at a site, (3) controlling or cleaning up releases from the site; or monitoring parameters related to monitoring disposal system performance *note; the period of active controls may be limited to a maximum of 100 years for 40CFR190+ wastes and 30 years for RCRA type wastes*

2.2.5. *"Controlled Area"* means: (1) A surface location, to be identified by passive institutional controls, that encompasses no more than 100 square kilometers and extends horizontally no more than five kilometers in any direction from the outer boundary of the originate contaminants in the disposal system; and (2) the subsurface underlying such a surface location

2.2.6. *"Accessible Environment"* means (1) the atmosphere; (2) land surface; (3) surface waters; (4) oceans; and (5) all of the lithosphere that is beyond the controlled area

2.2.7. *"Undisturbed performance"* means the predicted behavior of the disposal system, including consideration of the uncertainties in the predicted behavior, if the disposal systems are not disrupted by human intrusion or the occurrence of unlikely events.
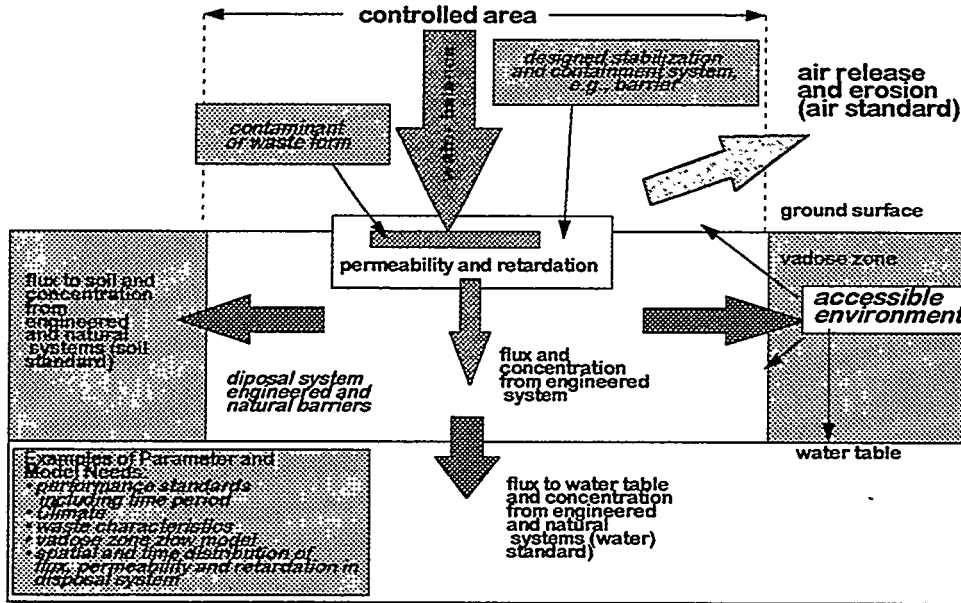
Figure 2. Conceptual Processes and Parameters of an Engineered and Natural Stabilization System

3. Performance/Risk Assessment

All projects, engineering and environmental, have built-in decision processes that involve varying risk/reward scenarios (Lockhart and Roberds, 1996). Developers, endusers and stakeholders evaluating in-situ stabilization and containment systems are faced with a similar problem of selection. Inherent in this decision process and the prediction of long term performance are interlinked and iterative steps such as: *(1) Decision Criteria; (2) Project Description and Model; and (3) Evaluation.*
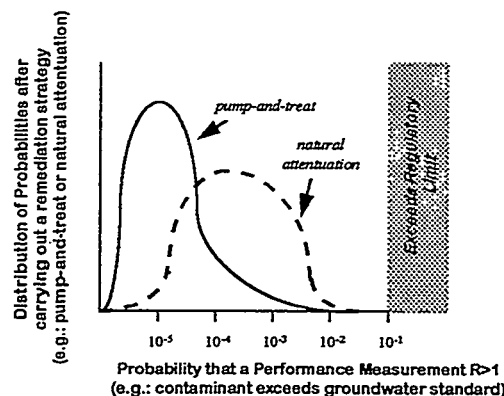
Figure 3: Hypothetical Example of Prediction for Two Remediation Strategies (Miller et al., 1993)

1025

This decision analysis process evaluates alternative strategies and can also guide data collection and decision criteria selection. In Figures 3 and 4, we present hypothetical examples .Figure 3 represents a descriptive probabilities model comparing performance of two remediation strategies (pump-and-treat versus natural attenuation). In this hypothetical model, both strategies meet the performance criteria. Therefore, the least expensive strategy, natural attenuation, will be chosen. Investments can be prioritized by *probabilistic decision analysis.* Figure 4 shows that an investment may reduce the uncertainty for parameter (e.g., fluid flow pathways) and may result in a prediction of compliance for a remediation strategy, which did not comply originally.
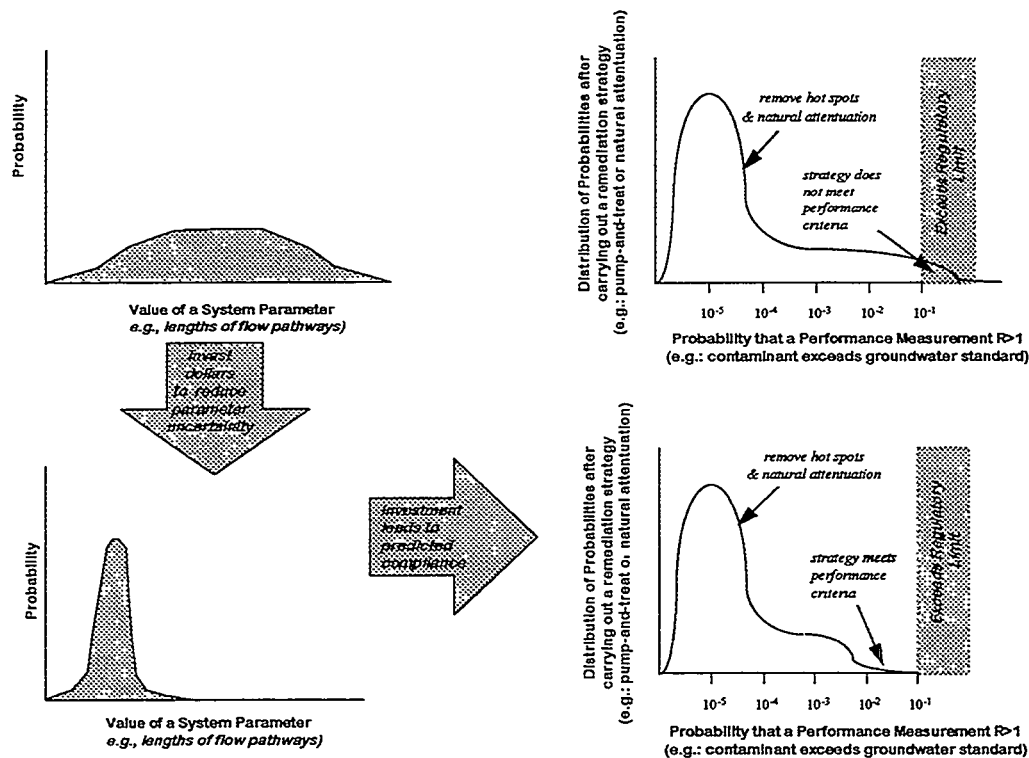
Figure 4: Hypothetical Example of Cost and Performance Effect due to investment in uncertainty reduction (e.g., lengths of fluid flow pathways); modified from Miller and others (1993)

4. Specific Predictive Tool and Data Needs Relative to Stages of Integrated Engineering Decision and Uncertainty Analysis

Tables 1 and 2 describe respectively the needs for predictive tools and data to support long term performance predictive. The evaluation of arid DOE sites demonstrates the difficulties in obtaining important parameters. Evaporation (or evapotranspiration) cannot be reliably calculated in either humid or arid environments. Even for the best estimates, judgement is required, and the uncertainties are large. The recharge estimates are in error by as much as 100% or more.

Table 1: Predictive Tools for in-situ containment and stabilization of DOE sites

Predictive Tool	Use	Possible Sources

Regional/Local Hydrologic Modeling	• water balance
	• process model for vadose zone flow, contaminant retardation and transport
	• changes in water table
		1. analog studies
		2. analytic and numerical models (Kramer and Cullen 1995; Fayer et al. 1992; White et al. 1995):
		  • driving forces and controls
		  • flow transport processes

Design Modeling	• process model for fluid flux, contaminant retardation and transport through the design/ engineered system
	• calculation of flux and concentration to natural disposal system
		3. analog studies
		4. analytic and numerical models
		  • driving forces and controls
		  • flow and transport processes

Groundwater/Air Transport Modeling	• components of natural attenuation
	• calculation of possible releases to accessible environment
	• process model for fluid flux, contaminant retardation and transport through the design/ engineered system
		5. analog studies
		6. analytic and numerical models
		  • driving forces and controls
		  • flow transport processes

Table 2: Data Needs for in-situ containment and stabilization of DOE sites

Data Needs	Required Parameters

1. Process Model/Understanding
2. Boundary Conditions
3. Design
  • Waste Characteristics
4. Performance Standards
5. Regulatory/Interagency Agreement Standards
  • Performance Standards
  • Time Period
6. Uncertainties/sensitivity of process model parameters
  • Understanding of how data can be applied to different scales
  • Spatial and temporal heterogeneity
    – geology
    – flow/transport system
    – waste
    – engineered design
7. Environmental Changes
  • Climatic
  • Pedogenetic
  • Tectonic
  • Igneous
  • Human generated including human intrusion
  • Analog Studies
	1. Boundary Conditions
	  • performance standards
	    – air, ground, soil, and water
	    – period of performance (30, 10000 yrs)
	2. Material properties
	  • bulk density
	  • particle density
	  • specific soil surface area
	3. Hydrogeologic parameters
	  • effective porosity
	  • mass water content
	  • volumetric water content
	  • infiltration capacity
	  • saturated hydraulic conductivity
	  • soil/water characteristic curves
	  • conductivity/pressure head relationship
	4. Parameters related to Climate (e.g.:)
	  • rainfall
	  • evapotranspiration
	  • temperature, etc.)
	5. Chemical parameters of Waste, Engineered and Natural Systems
	  • solubilities
	  • cation exchange capacity
	  • partition coefficients
	  • diffusion coefficients
	  • biodegradation rates
	  • chemical degradation rates
	  • radioactive decay rates
	  • organic matter content

5. Recommendations:

This subgroup suggests that :

(1) *The subsurface contaminant focus area encourage an interaction between technology developers, possible customers, performance/risk assessment programs, regulators and stakeholders to define reasonable boundary conditions,*

(2) *The focus area develop methods to quantitatively relate changes in observable properties of the containment system (e.g., permeabilities of system components or solubilities of waste forms) to capability of the total system to meet performance or regulatory performance criteria; and*

(3) *The focus area encourage and support a trial application of an integrated process of performance prediction at specific focus area or EM-40 site(s).*

6. References

General Accounting Office (GAO) (1996) Federal facilities: Consistent relative risk evaluations needed for prioritizing cleanups, *GAO letter report*, 06/07/96, GAO/RCED-96-150

Fayer, M. J., M. L. Rockhold, and M. D. Campbell (1992) Hydrologic modeling of protective barriers: comparison of field data and simulation results. *Soil Sci. Soc. Am. J.* 56:690-700.

Kramer, J.H. , and S.J. Cullen (1995) Review of vadose zone flow and transport models. In *Handbook of vadose zone characterization and monitoring.* LG Wilson, LG Everett, and SJ Cullen, eds., 730 p., Lewis Publishers, Boca Raton, Florida.

Lockhart, C. W., and W. J. Roberds (1996) Worth the risk?, *Civil Engineering*, April, 62-64

Miller, I., R. Kossisk, and M. Cunnane (1993) A new methodology for repository site suitabilitiy evaluation, in *Waste Managment*, 494-501

National Reseacrh Council (1990) Rethinking high-level radioactive waste disposal - *a position paper of the Board of Radioactive Waste*, National Academy Press, Washington, DC·

Starr, C., and C. Whipple (1980) Risks of risk decisions, *Science*, 208, 1114-1119

White, M.D., M Oostrom, and RJ Lenhard (1995) Modeling fluid flow and transport invariably saturated porous media with the STOMP simulator. 1. Nonvolatile three-phase model description. *Adv. Water Resour.* 18:353-364.

Wilson, L. G., L. G. Everett, and S. J. Cullen, editors (1994) *Handbook of Vadose Zone Characterization and Monitoring*, 730p., Lewis Publishers, Boca Raton.

REACTIVE BARRIER TECHNOLOGIES FOR TREATMENT OF CONTAMINATED GROUNDWATER AT ROCKY FLATS

D.C. Marozas[1], G.E. Bujewski[1], and N. Castaneda[2]
[1]Sandia National Laboratories
P.O. Box 5800, MS 0719
Albuquerque, NM 87185-0719

[2]US Department of Energy, Rocky Flats Field Office
P.O. Box 464
Golden, CO 80402-0464

ABSTRACT

The U.S. Department of Energy (DOE) Office of Science and Technology Subsurface Contaminants Focus Area is supporting the investigation of reactive barrier technologies to mitigate the risks associated with mixed organic/radioactive waste at several DOE sites. Groundwater from a small contaminated plume at the Rocky Flats Environmental Technology Site (RFETS) is being used to evaluate passive reactive material treatment. Permeable reactive barriers which intercept contaminants and destroy the VOC component while containing radionuclides are attractive for a number of reasons relating to public and regulatory acceptance. *In situ* treatment keeps contaminants away from the earth's surface, there is no above-ground treatment equipment that could expose workers and the pubic and operational costs are expected to be lower than currently used technologies. This paper will present results from preliminary site characterization and in-field small-scale column testing of reactive materials at RFETS. Successful demonstration is expected to lead to full-scale implementation of the technology at several DOE sites, including Rocky Flats.

INTRODUCTION

Reactive barriers are an emerging, alternative *in situ* approach for remediating groundwater contamination that combines subsurface fluid flow management with a passive chemical treatment zone (Figure 1).
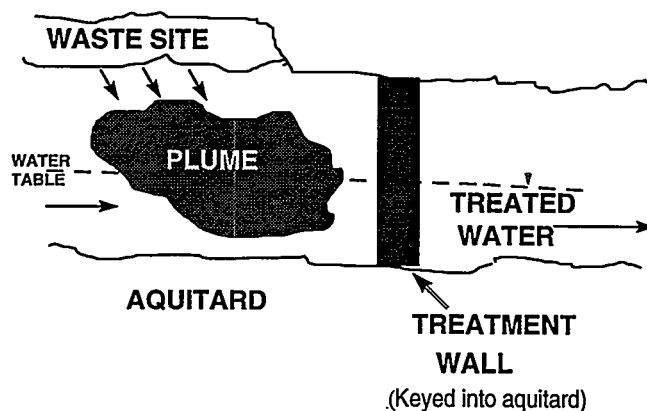
Figure 1. Conceptual Model of a Reactive Barrier System

Because the reactive barrier approach is a passive treatment, a large plume can be treated in a cost-effective manner relative to traditional pump and treat systems (Mackay and Cherry, 1989) while more effectively reducing risk to human and environmental health. In the last several years

several reactive barriers have been piloted in the field both as Environmental Protection Agency (EPA) research projects (Puls et al., 1996) and as commercial installations (Wilson, 1995). A review of the state of the art of permeable reactive barrier systems was prepared by Shoemaker et al. from information presented at the 1995 Containment Conference. These pilot and commercial installations have proven that passive reactive barriers can be a cost-effective and efficient approach for remediation of many groundwater contamination problems. However, thus far, only simple, single reagent reactive systems have been used to remediate groundwater plumes.

It is clear, however, that many of the DOE's waste streams are not simple problems but are oftentimes mixed waste streams that can contain complex mixtures of metals, radionuclides, and organic contaminants which cannot be fully treated by simplistic chemical approaches. Several research programs are in progress to address removal of contaminants using reactive barrier approaches for problems throughout the DOE complex (Bostick et al., 1995; Cantrell et al., 1994; Cantrell et al., 1995; Dwyer et al., 1996; Horney et al., 1995; Korte et al., 1995; Morrison and Spangler, 1993; Thomson, 1995). Treatment of complex waste streams by reactive barrier technologies will require development of robust chemical treatment zones that can passively treat a wide range of contaminants within as small a treatment zone volume as possible, that can meet long-term performance criteria in a cost-effective manner, and that can be practically applied in the field. To address the need for reactive systems that will target multiple contaminants, reactive materials used in common reactive barriers are being demonstrated at a contaminated groundwater site at DOE's Rocky Flats Environmental Technology Site.

REACTIVE BARRIER DEMONSTRATION

The groundwater used in this demonstration site is taken from a small seep, Seep SW059 at the RFETS. This groundwater is contaminated with chlorinated organic compounds, toxic metals, and radionuclides, all at concentrations slightly above the Action Level Framework identified in the Rocky Flats Cleanup Agreement. Site management has identified reactive barriers as an option for addressing contamination from this Seep.

Treatment of this particular groundwater plume at Rocky Flats by a reactive barrier will require development of a treatment system that can passively remove a wide range of contaminants within as small a treatment zone volume as possible. Laboratory and on-site column tests will be used to test reagents suitable for use in the reactive zone. The final design may require a treatment train approach or mixed reagent (i.e., reductive/adsorptive) systems capable of treating both organic and metal/radioactive waste. The purpose of the program is not to develop new treatment agents but to combine currently available treatment approaches to solve specific problems of contaminant mixtures. Promising reagents such as zero-valent iron (Gillham, 1995), bi-metallic enhanced zero-valent iron (Korte et al., 1995), surfactant-enhanced zeolite (Haggerty and Bowman, 1994), foamed iron materials (Bostick, in prep) and commercially available sorbents including Humasorb™ (Sanjay et al., in prep) and Ensorb™ (Connor et al., 1996) are treatment media candidates for laboratory screening during the testing program. The behavior of alpha-emitting contaminants as they move through the treatment columns will also be assessed during the study.

Key issues for the demonstration include: 1) identification of reactive materials to be used to destroy organics in the plume, and identification of reactive materials to capture toxic metals and radioactive contaminants; and 2) establishment of the destruction/reaction rates for design of a remediation system. The benefits of this demonstration to DOE will be an assessment of the technical and engineering issues surrounding the use of permeable reactive barriers for metals/radioactive waste treatment.

PRELIMINARY FIELD CHARACTERIZATION STUDY

Table 1 shows the concentrations of contaminants of concern at Seep SW059 to RFETS. The source of the contamination at SW059 appears to be the Mound source area which lies about 152 m south of the Seep (Figure 2). Because the groundwater collection system for a passive treatment system would most likely be sited between the Mound source area and the Seep and only a few monitoring wells are currently in place in this area, a characterization program was undertaken to survey the contaminant components and their concentrations in the area between the Mound source and the Seep.

Table 1.   Concentrations of Contaminants of Concern at Seep SW059

Chemical Name	Average Detect	Tier I Action Level	Tier II Action Level
Antimony (µg/L)	13.6	600	6
Manganese (µg/L)	269.8	18,300	183
Thallium (µg/L)	4.6	200	2
Antimony (µg/L)	11.3	600	6
Americium-241 (PCi/L)	0.25	14.5	0.145
Cesium-134	.40	151	0.151
Plutonium-239/240	0.05	151	0.151
Uranium - 233, -234	3.40	298	2.98
Uranium - 238	3.02	76.8	0.768
Carbon Tetrachloride (µg/L)	33.9	500	5
Tetrachloroethene (µg/L)	11.6	500	5
Trichloroethene (µg/L)	16	500	5
Vinyl Chloride (µg/L)	1.7	200	2

A GeoProbe® was used to sample water in the vicinity of the Mound and SW059 at RFETS (Puls et al., 1996). Eighteen individual holes were pushed with the GeoProbe® but sufficient water yields to conduct chemical analyses were found in only nine of those wells (Figure 2). An HNU 311 portable GC with a photoionization detector was used to quantify target analytes on site and duplicate samples were taken for off-site analyses of major anion and cations, organic components, metals, and radionuclides. Concentrations of selected contaminants are shown in Figure 2. Knowledge of the site geology and results from the GeoProbe® survey indicate that the concentration and nature of the organic contamination can vary throughout the area and transport of the contaminants may be in large part controlled by sand channels that preferentially direct flow. Additional GeoProbe® characterization will be conducted by RFETS to better characterize contaminant flow and transport in the area to aid in the design of an effective collection system for the passive barrier treatment test.

SEEP SW059

| U-238 - 12 |
| CCl4 - < .5 |
| TCE - .98 |

| U-238 - 12 |
| CCl4 - 1.4 |
| TCE - <.5 |

| U-238 - 12 |
| CCl4 - < .5 |
| TCE - .5 |

| U-238 - 1.2 |
| CCl4 - < .5 |
| TCE - 16 |

| CCl4 - 1.3 |
| TCE - .95 |

| CCl4 - < .5 |
| TCE - 74 |

| U-238 - 8.3 |
| CCl4 - 110 |
| TCE - 60 |

| U-238 - 11 |
| CCl4 - 3 |
| TCE - 4.4 |

| U-238 - 6.1 |
| CCl4 - 3.7 |
| TCE - 210 |

| U-238 - 1.4 |
| CCl4 - 8.6 |
| TCE - 860 |

⊚ GeoProbe Hole Location
▦ Seep SW059
◈ Surface Water

| CCl4 - <.5 |
| TCE - 22 |

| U-238 - 5.9 |
| CCl4 - 48 |
| TCE - 2000 |

MOUND AREA
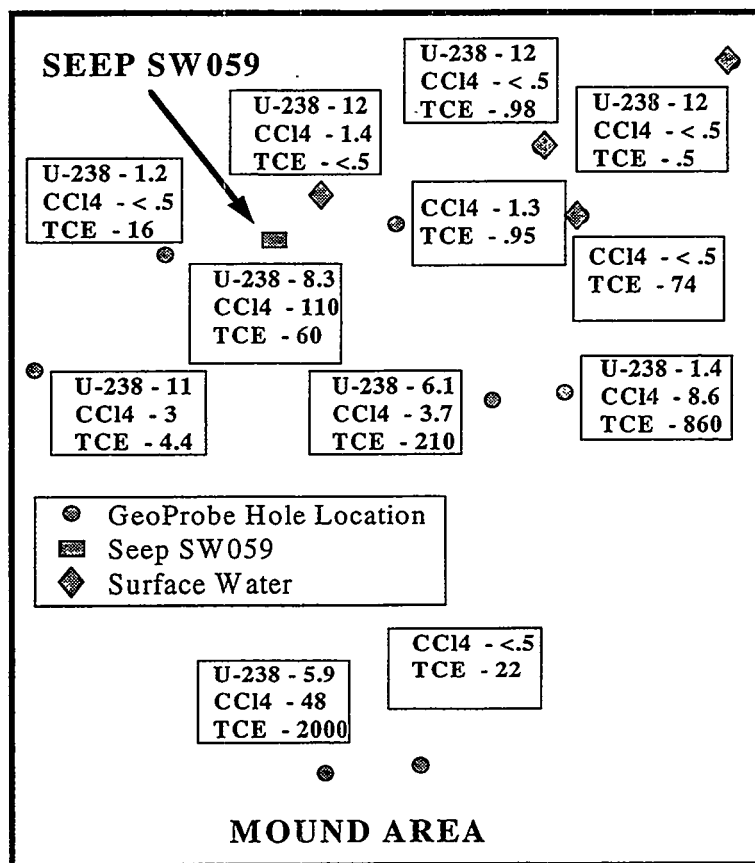
Figure 2. Analytical results of selected contaminants in the Mound-SW059 Area

ZERO-VALENCE IRON PRELIMINARY TESTING

A zero-valence iron treatment approach will be used to treat organic contaminants at SW059. EnviroMetal Technologies Inc. is in the process of developing the treatment media design for the organic contaminant load at the site. Zero-valence iron has been shown in laboratory testing (Bostick et al. (in prep), Cantrell et al. 1995) and field testing (Dwyer et al., 1996) to be an effective media for stopping the migration of uranium contaminants in groundwater. To test the applicability of zero-valence iron for uranium removal for the site specific conditions at SW059, a series of column tests were conducted at the seep. Water was pumped directly from the seep through 2.54 cm wide glass columns containing 25.4 cm lengths (approximately 30 g) of commercially available steel wool as the zero-valence material. A 25 µ polypropylene bag filter was used at the inlet from the seep to minimize pumping fine particles into the columns. Influent and effluent water samples were taken for analyses of uranium, organic components, major and trace metals at Sandia National Laboratories.

The flow rate to the columns was kept at 5 ml/min for one day, then increased to 10 ml/min for one day, then increased to 30 ml/min for four days. Results showed that the uranium component of the water was quickly removed by minimal contact in the steel wool columns (Table 2). The rate of flushing was increased to determine if this might affect uranium removal and to speed the rate of rusting in the columns. It should be emphasized that the purpose of the column tests was to characterize uranium behavior in the iron beds, and that the residence time was not sufficient to strongly affect the organic content (Table 2). Measurements of dissolved oxygen, pH and temperature were taken in the field with a Corning® Checkmate® field portable measuring

system. Concentration of dissolved oxygen in the seep typically ranged between 5 to 6 mg/L. The pH was 8 and the temperature ranged from 13 to 21 °C. Interest in the severity of rusting caused by the dissolved oxygen content of the water was of particular concern because the water source was close to the ground surface and was therefore expected to carry high concentrations of oxygen. However, the GeoProbe® screening also revealed that some of the wells in the area between the Seep and the Mound carried measurable ferrous iron content which indicates reducing conditions.

Table 2. Results of SW059 Field Column Tests Of Zero-Valence Iron

	Influent	Effluent 5 ml/min	Effluent 10 ml/min	Effluent 30 ml/min	Analytical Method
U - 238 (µg/L)	4.5	< 0.95	< 0.95	< 0.95	EPA6020
Carbon tetrachloride (µg/L)	40	< 0.5	< 0.5	< 1.5	EPA8260
Chloroform (µg/L)	12	28	15	15	EPA8260
Trichloroethene (µg/L)	26	21	14	16	EPA8260
cis-1,2 dichloroethene (µg/L)	14	12	9	7.7	EPA8260
1,1,1-Trichloroethane (µg/L)	4.1	3.8	2.5	2.6	EPA8260

CONCLUSION

Results of the preliminary characterization have been used to develop a more detailed characterization plan for the site. This characterization effort will provide design information on the mixture of contaminants and the redox condition of the water that will be treated by the passive barrier system. The column tests indicated that uranium content of the water was quickly removed by zero-valence iron. It is therefore anticipated that the removal of the chlorinated organic component by the zero-valence iron will be the key factor in determining the residence time required in a reactive barrier design. Laboratory testing of additional reactive media will be used to test the concept of removal of the radioactive component ahead of the organic treatment zone to facilitate the eventual disposal of the media materials. Additional laboratory and field testing will be done to determine the effect of the various treatment media on the behavior of plutonium and americium at the site and to identify suitable methods for removing excess iron from the stream that passes through the reactive barrier. EnviroMetal Technologies Inc. will conduct laboratory testing for design of residence time for the reactive barrier.

Reactive barriers are an emerging, alternative, in situ approach for remediating groundwater contamination that combines subsurface fluid flow management with a passive chemical treatment zone. The reactive barrier technology demonstration planned for Rocky Flats will treat both metal and radioactive waste streams by intercepting contaminants and destroying the VOC component while containing radionuclides. This demonstration will assess the technical and public acceptance issues surrounding the use of permeable reactive barriers for metals/rad waste treatment.

REFERENCES

Bostick, W.D., P.E. Osborne, G.D. Del Cul, and D.W. Simmons. (1995) Treatment of aqueous solutions contaminated with Technetium-99 originating from uranium enrichment activities: Final Report, Oak Ridge National Laboratory, K/TCD-1120, April, 1995.

Bostick, W.D., R.J. Jarabek, W.A. Slover, J.N. Fiedor, J. Farrell, R. Helferich. (in prep) Zero-valent iron for the removal of soluble uranium and other regulated metals in contaminated groundwater at a DOE site, 1997 International Containment Technology Conference and Exhibition.

Cantrell, K.J., P.F. Martin, J.E. Szecsody. (1994) Clinoptilolite as in-situ permeable barrier to strontium migration in ground water, in In-Situ Remediation: Scientific Basis for Current and Future Technologies, 33rd Hanford Symposium, ed. by G.W. Gee and N.R. Wing, pp.839-850.

Cantrell, K.R., D.I. Kaplan, and T.W. Wietsma. (1995) Zero-valent iron for the in-situ remediation of selected metals in groundwater, J. Haz. Mater., 42, pp. 201.

Connor J.A., and Clifford, D.A., (1996) Benefits of Ensorb™ in-situ immobilization technology for remediation of DOE sites, Groundwater Services, Inc. , Houston, TX. 11 pp.

Dwyer, B.P., D.C. Marozas, K. Cantrell, W. Stewart, (1996) Laboratory and field scale demonstration of reactive barrier systems, Sandia National Laboratories Report SAND96-2500, 10 pp.

Gilham, R.W. (1995) Resurgence in research concerning organic transformations enhanced by zero-valent metals and potential application in remediation of contaminated groundwater, Division of Environmental Chemistry, American Chemical Society, 209th ACS National Meeting, April 2-7, 1995, Anaheim, CA, Vol. 35, No. 1, pp. 691-694.

Haggerty, G.M. and R.S. Bowman, Sorption of chromate and other inorganic anions by organo-zeolite, Environ. Sci. Technol., Vol. 28, No.3, pp. 452-458.

Horney, D.P., P.D. Mackenzie, J.J. Salvo, and T.M. Sivavec. (1995) Zero-valent iron treatability study for groundwater contaminated with chlorinated organic solvents at the Paducah, KY, GDP site, US DOE Contract No. DE-AC05-840R21400, 181 pp.

Korte, N.R., R. Muftekian, C. Gritteni, Q. Fernando, J.L. Clausen, and L. Liang. (1995) ORNL/MMES research into remedial applications of zero-valent metals; bimetallic enhancements, Division of Environmental Chemistry, American Chemical Society, 209th ACS National Meeting, April 2-7, 1995, Anaheim, CA, Vol. 35, No. 1., pp. 752-754.

Mackay, D.M., and J.A. Cherry. (1989) Groundwater contamination: pump-and-treat remediation, Env. Sci. and Tech., Vol. 23, pp. 630-636.

Morrison, S.J., and R.R. Spangler. (1993) Chemical barriers for controlling groundwater contamination, Environmental Progress, Vol. 12, 175-181.

Puls, R.W., C.J. Paul, F. Beck. (1996) Rocky Flats GeoProbe investigations in Mound and Seep 059 Areas, internal report.

Puls, R.W., C.J. Paul and R.M. Powell. (1996) Field Test of In-Situ Reactive Barrier Using Zero-Valent Iron for Remediation of Chromate-Contaminated Ground Water, In Great Lakes Geotechnical and Geoenvironmental Conference, In Situ Remediation of Contaminated Sites, University of Illinois at Chicago, May 16-17, 1996.

Sanjay, H.G., M. Tiedge, J.J. Stashick, K.C. Srivastave, H.R. Johnson, D.S. Walia. (in preparation) Development of HUMASORB™, A lignite-derived humic acid for removal of metals and organic contaminants from groundwater, ARCTECH Inc., Chantilly, VA.

Shoemaker, S.H., J.F. Greiner, and R.W. Gilham. (1995), Permeable Reactive Barrier, Section 11, in Assessment of Barrier Containment Technologies, ed. by R.R. Rumer and J.K. Mitchell, pp. 301-353.

Thomson, B.M. (1995) Permeable barriers for groundwater remediation at a uranium mill tailings remedial action project (UMTRA) site. Written communication to the International Containment Technology Workshop.

Wilson, E.K. (1995) Zero-valent metals provide possible solution to groundwater problems, Chemical and Engineering New, July 3, 1995, pp.19-22.

.

.

Chapter 20

Performance Monitoring

.

TRACER VERIFICATION AND MONITORING
OF CONTAINMENT SYSTEMS (II)

C. V. Williams[1], S. Dalvit Dunn[2] and W. E. Lowry[3]

Abstract

A tracer verification and monitoring system, SEAtrace™, has been designed and field tested which uses gas tracers to evaluate, verify, and monitor the integrity of subsurface barriers. This is accomplished using an automatic, rugged, autonomous monitoring system combined with an inverse optimization code. A gaseous tracer is injected inside the barrier and an array of wells outside the barrier are monitored. When the tracer gas is detected, a global optimization code is used to calculate the leak parameters, including leak size, location, and when the leak began.

The multipoint monitoring system operates in real-time, can be used to measure both the tracer gas and soil vapor contaminants, and is capable of unattended operation for long periods of time (months). The global optimization code searches multi-dimensional "space" to find the best fit for all of the input parameters. These parameters include tracer gas concentration histories from multiple monitoring points, medium properties, barrier location, and the source concentration. SEAtrace™ does not attempt to model all of the nuances associated with multi-phase, multi-component flow, but rather, the inverse code uses a simplistic forward model which can provide results which are reasonably accurate. The system has calculated leak locations to within 0.5 meters and leak radii to within 0.12 meters.

Introduction

In-situ barrier emplacement techniques and materials for the containment of high-risk contaminants in soils are currently being developed. Because of their relatively high cost, the barriers are intended to be used in cases where the risk is too great to remove the contaminants, the contaminants are too difficult to remove with current technologies, or the potential movement of the contaminants to the water table is so high that immediate action needs to be taken to reduce health risks. Consequently, barriers are primarily intended for use at the high-risk sites where few viable alternatives exist to stop the movement of contaminants in the near term. Assessing the integrity of the barrier once it is emplaced and during its anticipated life is a very difficult but necessary requirement.

The goal of any verification/monitoring technology development should be to develop a system which automatically assesses barrier integrity in real time while avoiding expensive and time consuming data analysis. Surface-based and borehole geophysical techniques do not provide the degree of resolution required to assure the formation of an integral in-situ barrier. Tracer measurements have been suggested as a viable assessment technique for subsurface barriers (References 1 and 2).

Sandia National Laboratories (SNL) and Science and Engineering Associates, Inc. (SEA), through the Subsurface Contaminant Focus Area and the Federal Energy Technology

[1] Sandia National Laboratories, Dept. 6621 MS 0719, P. O. Box 5800, Albuquerque, NM 87185-0719, (505) 844-5722, cvwilli@sandia.gov

[2] Science & Engineering Associates, Inc., 1570 Pacheco Suite D-1, Santa Fe, NM 87501, (505) 983-6698, sddunn@seabase.com

[3] Science & Engineering Associates, Inc., 1570 Pacheco Suite D-1, Santa Fe, NM 87501, (505) 983-6698, blowry@seabase.com

Center, are jointly developing a quantitative subsurface barrier assessment system that uses gaseous tracers. This system, called SEAtrace™, is able to locate and size leaks in subsurface barriers in unsaturated medium with a high degree of accuracy. It uses gaseous tracer injection, in-field real-time monitoring, and real time data analysis to evaluate barrier integrity. The approach is:

- conservative as it measure vapor leaks in a containment system whose greatest risk is posed by liquid leaks;
- applicable to any impermeable type of barrier in the unsaturated zone;
- inexpensive as it uses readily available, non-toxic, non-hazardous gaseous tracers does not require an inordinately large number of sampling points and injection/
- sampling points and injection/sampling points can be emplaced by direct push techniques; and
- capable of assessing not only a barrier's initial integrity, but can also provide long term monitoring.

Approach

SEAtrace™ is based on the simple and predicable transport process of binary gaseous diffusion in porous media. Diffusion is an attractive process to utilize for leak detection because the tracer concentration histories measured at locations distant from the source are highly sensitive to both the size of the breach and the distance from the leak source. This sensitivity allows a global optimization modeling methodology to iterate to a leak geometry and location by minimizing errors in the transport calculations. Thus, SEAtrace™ is made up of two distinct functional components: a monitoring system and an optimization code.

A schematic of the SEAtrace™ system is shown in the Figure 1. Multiple sample points are located outside the barrier, as well as one or more injection/sample ports inside the barrier. These ports are connected to a stand-alone data acquisition and analysis system. A tracer gas (typically sulfur hexafluoride or carbon dioxide, but other gases can be used) is injected into the barrier, creating a large source volume of the tracer. If the barrier has a breach, the tracer will diffuse from within the barrier into the surrounding medium where the exterior monitoring ports will measure the amount of tracer in the soil gas with time. These concentration histories then can be input into the global optimization code. The code iterates to find a best fit solution given the input parameters.
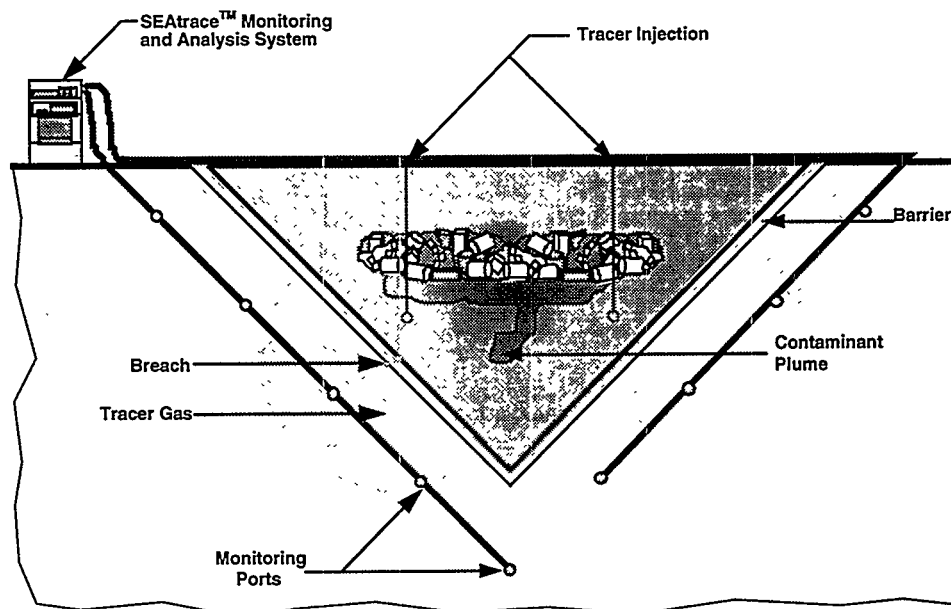
Figure 1. A typical SEAtrace™ verification/monitoring system installation.

Sample ports can be emplaced using a direct push tool. The spacing and configuration of the sampling points are critical to the effectiveness and cost of the monitoring system. Site specific parameters (geology, anticipated source concentration, barrier construction and geometry, properties of the tracer gas, etc.) will determine the optimum port locations. However, numerical simulations have shown that for typical vadose zone conditions, ports spaced on a 5- to 10-m grid between 1 to 2 m from the barrier would adequately detect a breach anywhere on the barrier.

The data acquisition and analysis system is a stand-alone field unit based on the SEA MultiScan™ autonomous soil gas analysis system. The system reliably monitors up to 64 soil gas vapor ports in real-time. It is capable of unattended operation for long periods of time (months). MultiScan™ records all pertinent data and performs many self diagnostic tests to assure the accuracy of the measured concentrations.

If any tracer gas is detected outside the barrier, the concentration history data is analyzed. To overcome the difficulties of standard analysis, SEAtrace™ uses a global optimization model to effectively search multi-dimensional "space" to simultaneously find the best fit solution based on all of the input parameters. The general methodology of this approach rigorously searches for a set of parameters that will best characterize the leak. It uses a forward diffusion model which calculates concentration histories from the multi- parameter "space". These calculated concentrations are compared to the measured concentrations using an objective function. For this project, the objective function was defined as the sum of the squares of the differences between the predicted and measured tracer concentrations. A stochastic method is then employed to minimize the objective function, thus finding a best

fit to the data given a range of defined parameters. The stochastic method chosen is called Simulated Annealing (reference 3). The technique selects points from the given input ranges for each parameter at random. Using these values, the objective function is evaluated.

The process is repeated, the two values for the objective functions are compared, and the code chooses which is more accurate. This point is remembered and the process repeated with a new set of parameter values. The parameter values are chosen using a probability distribution that relies on the objective function of previous points in a complex way. Because the parameter space which is being searched is multidimensional, there may be multiple local minima (minima within the dimensional space to which the inversion code may converge but which in fact are not the correct answer). The nature of the simulated annealing algorithm allows it to sample many of these local minima without being trapped by any of them (reference 3).

The analysis code was designed such that different forward models can be incorporated as they are developed. Presently, the code incorporates a one-dimensional spherical diffusion model:

$$C(r,t) = \frac{r_o}{r} C_o \, erfc\left(\sqrt{\frac{(r-r_o)^2}{4D(t-t_o)}}\right), r > r_o, \, t > t_o$$

where:

r = distance from the leak center,
C = concentration for a given r and t
D = effective diffusivity of the tracer through the soil pores
t_o = the time that the leak began,
r_o = the constant radius of the leak after time t_o, and
C_o = the constant source concentration

The model assumes a constant source concentration is maintained inside the barrier, the flux exiting the leak is not restricted by diffusion through the leak (a function of the barrier

thickness, source concentration, and leak dimensions and flow properties), and that the medium outside the barrier has a constant diffusivity. Further, it neglects gravity, advective flow of the tracer, and adsorption/desorption of the tracer. While this diffusion model is simplistic, determining the location of the leak has been found to be insensitive to the majority of the assumptions. As long as the concentration isopleths are spherical (e.g. gravity is not a significant factor in the tracer movement and the medium diffusivity is homogenous), and the location of the monitoring ports are well known, SEAtrace™ can accurately predict the location of a leak with the forward model. Predicting the size of the leak is more difficult. To accurately calculate the leak size, not only must the isopleths be spherical, but all of the other assumptions used in deriving the forward model must be valid.

In the present version of the code, the size and location of the leak and the time the leak began are treated as unknowns; the source concentration and diffusivity can be treated as either variables or constants; the plane of the barrier is considered to be unknown; and the location of the sampling points are assumed to be known. A range of values must be input for each variable.

A series of benchmark studies were performed on the inverse code to examine the ability of the code to accurately determine model parameters for various settings of parameters and locations of leaks. The code was able to return accurate estimates (within 0.5 m) of the leak location throughout the testing. The leak radius and the source concentration were found to be strongly coupled and exerted significant influence over one another. The code was less able to accurately predict these values if both were treated as unknowns. However, if the source concentration was input as a constant value within a factor of two of the actual value, the code was able to predict the leak radius to within 0.2 m.

Proof-Of-Concept Field Test

A small-scale field demonstration was conducted to test the basic assumptions and components of the SEAtrace™ system. The demonstration was conducted in Technical Area 3 at SNL. The site was chosen as it had been well characterized in previous studies of vapor movement in the vadose zone and monitoring ports were already installed, making it cost effective.

A schematic of the small-scale field demonstration set-up is shown in Figure 2. The barrier was simulated by a non-permeable geomembrane on the surface of the ground and a thin film bag provided the "barrier" volume. A valve assembly was used to connect the source volume to the soil via a baseplate having a defined diameter opening (the leak).
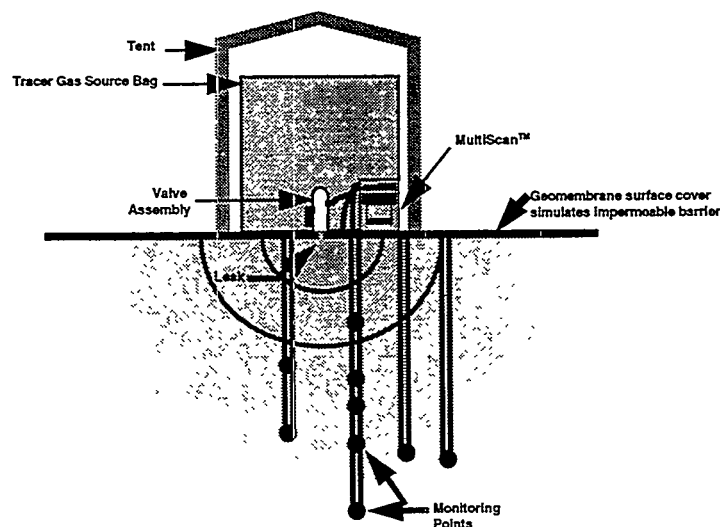
Figure 2: Field test installation.

This configuration was expeditious but far from ideal. Measurements from subsurface sampling ports very near the soil surface were effected by atmospheric changes, as was the source concentration; wind and temperature fluctuations caused some advective movement of the tracer gas into the medium; and the monitoring ports were in a plane perpendicular to the "barrier", making it very difficult for the code to calculate the leak position. Nevertheless, the site was adequate for a proof-of-concept test.

A total of five tracer tests were performed. For the first test, a combination of the source bag being buffeted by wind gusts combined with an inadequate seal between the geomembrane and the soil surface allowed the tracer to be pumped through the leak in between the membrane/soil surface interface. This resulted in an unknown effective leak radius which was much larger than the defined leak in the baseplate. These problems were minimized for the remaining tests. During the second test, heavy rains caused surface moisture infiltration near the defined leak. The localized saturated region restricted diffusion of the tracer gas into the medium. Concentrations measured at the majority of the monitoring ports were not significantly above background levels. An electrical storm damaged the photoacoustic analyzer during the third test, causing data collection to be terminated after only 36 hours. Only four ports recorded increased concentrations of the tracer during this time frame. The fourth test proceeded smoothly, but within days of the start of the fifth test the source volume began to leak, causing a steady and significant decrease in the source concentration. Even with all of the difficulties, SEAtrace™ was able to consistently predict the location of the leak to within 0.5 m , and the leak radius to within 0.15 m (Table 1). Additionally, the measured concentration histories at points equidistant from the leak were very similar, confirming that the diffusion was roughly spherical and the field monitoring system continuously collected data for long periods of time (several months), under very harsh conditions.

Table 1. Summary of field results. All data collected was processed; input concentration was held constant at average measured value for the test duration.

	Test #1	Test #2	Test #3	Test #4	Test #5
x(m); calculated	3.5 +/- 0.4	3.5 +/- 0.4	3.7 +/- 0.6	2.9 +/- 0.2	2.5 +/- 0.4
x(m); actual	3.0	3.0	3.0	3.0	3.0
z(m); calculated	3.1 +/- 0.4	3.0 +/- 0.3	3.0 +/- 1.0	2.9 +/- 0.7	2.5 +/- 2.6
z(m); actual	3.0	3.0	3.0	3.0	3.0
r(m); calculated	0.34 +/- 0.08	3.E-02 +/ 3.E-03	0.16 +/- 0.09	0.19 +/- 0.02	0.27 +/- 0.06
r(in); actual	unknown	unknown	0.05	0.10	0.10

State Of The Art

The SEAtrace™ has been modified to integrate monitoring system and the data analysis system into a single unit. This unit is capable of performing sample collection and automatic data analysis in real-time, as soon as a leak is detected. The system is capable of handling multiple leaks in a barrier, whether they are on the same or different planes of the barrier. While the system is presently using the simplistic one-dimensional spherical model, the code has been written modularly so that different forward models can easily be added as they are

developed. Assumptions used with this model are being evaluated with a numerical multi dimensional, multi component flow code, T2VOC a version of the LBNL TOUGH code. SEAtrace™'s sensitivity to gravity, heterogeneous diffusive transport properties, and a non-constant source concentration are being modeled. The sensitivity of the code to barrier thickness has been evaluated and a more realistic forward model for thick barriers has been developed.

The integrated SEAtrace™ system will be tested on a sub-scale, subsurface barrier installation with known breaches of various sizes and shapes. These test objectives include:

- determine effect of barrier thickness and the leak radius on the exit flux;
- determine effect of the leak geometry the isopleths;
- testing how well SEAtrace™ can define multiple leaks on the barrier and how the location of the leaks affects the systems results;
- determine if SEAtrace™ can accurately locate a leak given an existing background concentration of the tracer in the medium; and
- testing how different tracer gases affect the systems results;

The test volume will be a small scale barrier with both internal and external monitoring points. The configuration of the barrier were chosen to be realistic, easily constructed, and capable of allowing multiple leaks to be tested during the same test sequence. The barrier will be v-shaped trench, 5 meters deep by 15 meters long (Figure 3). The side walls and ends will be sloped 45° from horizontal - a slope shallow enough to minimize construction hazards but steep enough to be economically viable to use at a real site. A vertical wall will be formed at one end of the trench after the trench has been excavated. This will allow the SEAtrace™ system to be tested in one of the most typical barrier configurations (a vertical cut-off wall). The backfill material between the constructed vertical wall and the excavated sloped wall will be well graded and compacted. This will allow the system to be field tested in a medium of known homogeneity.
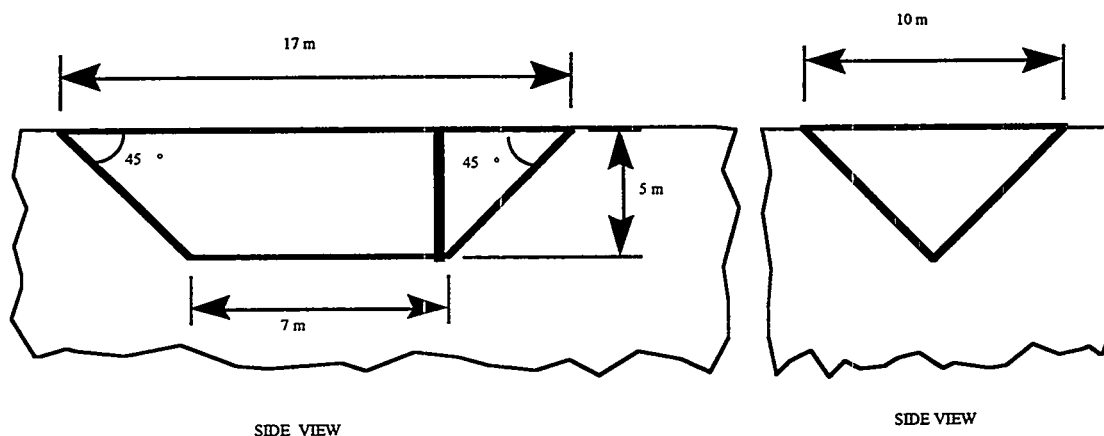
Figure 3. Sub-scale barrier test geometry.

The trench will be lined with an impermeable geomembrane. Well-defined leaks will be engineered into the barrier wall. The trench will be backfilled with native soil and a cover will be placed over the barrier to form a closed volume. Leaks were chosen to cover a wide variety of geometries, with the baseline leak defined as a 5.1 cm (2 in.) radius leak 0.6 m (2 feet) thick. The effect of barrier thickness will be evaluated by comparing the baseline leak with leaks of the same diameter but different lengths (0 and 1.2 meters, 0 and 4 feet, respectively). The effect of leak radius will be tested by comparing the baseline leak (81 sq. cm.) with leaks larger (180 and 1100 sq. cm.) and smaller (5 and 45 sq. cm.). The effect on leak location will be tested by comparing results from baseline leaks located in the center of a

barrier wall and on a joint of the barrier. The effect of leak geometry will be determined by comparing results from leaks of the same area but different geometries (one spherical and one rectangular).

It is anticipated that four different test sequences will be performed. Each sequence will use different combinations of leaks, and will last from one to two weeks. In addition to determining the effects of the leak and barrier geometries on the systems' results, the test sequences have been designed to determine 1) the effect of an existing background concentration of the tracer in the medium (background concentrations can be caused by planer diffusion through a barrier or by a contaminant which is in the soil gas prior to construction of the barrier which the gas analyzer mistakenly identifies as the tracer); 2) how well the system can differentiate between multiple leaks of close proximity; and 3) how results differ with different tracer gases.

Summary

The SEAtrace™ system is an integrated verification and monitoring system for subsurface barrier installations. The global optimization methodology, coupled with real-time autonomous soil gas sampling and analysis, provides a capable and sophisticated barrier assessment system. This system will provide a quantitative, real-time indication of the location and size of breaches in the barriers, either immediately after installation or during the course of their lifetime. Initial proof-of-concept field tests and calculational work indicate that the system is capable of locating a leak within 0.5 meters and sizing the leak within 0.2 meters.

SEAtrace™ is applicable to impermeable barrier installations above the water table. The system requires multiple vapor sampling points be installed around the perimeter of the barrier and one or several tracer injection ports be emplaced inside the contained volume. Vapor point installation can be accomplished in virtually any geologic media, using a variety of techniques. Any barrier type, including grout wall, cryogenic, viscous, and sheet barriers are viable applications fore the SEAtrace™ system.

References

1. Heiser, J. H., "Subsurface Barrier Verification Technologies", BNL-61127, Brookhaven National Laboratory, June 1994.

2. Betsill, J. D. and Gruebel, R. D., "VAMOS, The Verification and Monitoring Options Study, Current Research Options for In-Situ Monitoring and Verification of Contaminant Remediation and containment within the Vadose Zone", TTP#AL2-2-11-07, May 1995.

3. Ahmed Oenes, "Application of Simulated Annealing to Reservoir Characterization and Petrophysics Inverse Problems," Ph.D. Thesis, New Mexico Institute of Mining and Technology, 1992.

CONTAINMENT PERFORMANCE ASSESSMENT THROUGH HYDRAULIC TESTING - BALTIMORE WORKS SITE WITH COMPARISON

G. Snyder[1], G. Mergia[2] & S. Cook[3]

Abstract

The Baltimore Works site containment consists of a circumferential vertical barrier, multimedia cap, and active intragradient conditions predicated upon low leakage and minimal groundwater extraction through time. The soil-bentonite barrier, keyed into decomposed bedrock, measures 3300 linear feet (1006 m) by 3 feet (0.91 m) thick with a depth ranging from 65-80 feet (19.8-24.4 m). Interior groundwater extraction wells equipped with pumps and controls are dynamically actuated by continuously monitored water levels from paired piezometers spaced every 280 linear feet (85.4 m) around the barrier perimeter. To confirm barrier performance and adequate distance-drawdown response, the containment was rigorously tested and monitored. Detailed pre-design investigations and construction quality assurance (CQA) provided a confidently constructed barrier. Further monitoring and testing to prove the containment's performance prior to construction included tidal monitoring, slug and pump testing, site-wide drawdown testing, and groundwater/surface water quality monitoring. This paper discusses the barrier specifics and details of the performance testing. The test data is presented to support the performance assessment. Testing methods are discussed and compared to other industry examples where hydraulic testing was used in performance assessment. Finally, some recommendations for further industry testing are discussed.

SITE OVERVIEW

The Baltimore Works site is located in Baltimore, Maryland, on a peninsula of the Patapsco River adjacent to the active Inner Harbor area. The site is approximately 20 acres (8.1 hectares) and is bounded on three sides by water. The site topography is relatively flat with elevations ranging form +5 feet (1.52 m) mean sea level (MSL) to +11 feet (3.35 m) MSL, draining to the adjacent waterway. Harbor tide varies approximately 2.5 feet (0.76 m) with historical mean low and high levels at -0.4 foot (-0.12 m) and +4 feet (1.22 m), respectively.

The site is underlain by 65-80 feet (19.8-24.4 m) of unconsolidated soils overlying the Baltimore Gneiss. The unconsolidated soils are composed of typical Coastal Plain sequences (Snyder et al. 1993). The shallow unconfined interval is composed of fill, silts, and Pleistocene sands. An underlying 10-15 foot (3-4.5 m) thick confining clay exists across the majority of the site. The underlying Cretaceous sands are coarse, dense and permeable. The basal gneiss grades from clayey decomposed rock to more competent bedrock over a transition zone of 10-25 feet (3-7.6 m). Prior to barrier installation, shallow groundwater above the confining clay moved radially offsite; whereas, deep groundwater below the confining clay moved in a regional northwest to southeast direction.

The site soils and groundwater are contaminated with chromium from more than 140 years of chrome ore processing. This waste intensive process involved roasting chrome ore, leaching with acids, and adding limes and soda ash to form various specialty chemicals. Consequently, the site groundwater significantly varies in constituent concentrations and pH.

[1] Black & Veatch, The Curtis Center, Suite 850W, Philadelphia, Pennsylvania 19106, (215) 928-2233, snydergw@bv.com

[2] Black & Veatch, The Curtis Center, Suite 850W, Philadelphia, Pennsylvania 19106, (215) 928-2227, mergiag@bv.com

[3] Black & Veatch, The Curtis Center, Suite 850W, Philadelphia, Pennsylvania 19106, (215) 928-2236, cooksm@bv.com

CONTAINMENT REMEDY

The site remediation is a RCRA corrective action consisting of active containment. Dredging and construction of a rock embankment provided a stable zone for construction of an encompassing soil-bentonite (SB) hydraulic barrier (Snyder et al. 1994). A multimedia cap of geosynthetic clay liner (GCL) and 60 mil geomembrane covers the 15 acres (6.1 hectares) within the SB barrier. The active containment required an intragradient condition whereby regularly spaced cross-barrier piezometer pairs (12 deep aquifer pairs and 4 shallow aquifer pairs) are to always show a head differential of at least 0.01 foot (0.003 m) less inside than outside. The water level for an inboard piezometer will be compared with the outboard piezometer of the pair at hourly intervals to determine compliance. Groundwater and adjacent surface water quality are also used to monitor performance of the containment.

DESIGN PRINCIPLE AND MODEL

The regulatory performance standards necessitated an aggressive approach to limit inflow and groundwater withdrawal. The design objective of the containment was to construct continuous horizontal and vertical low permeability barriers and minimize the groundwater extraction. Initial design groundwater modeling, utilizing MODFLOW-3D, indicated that a well constructed low permeability vertical barrier adequately keyed into the low permeability floor material would allow for groundwater extraction by wells and result in a tolerable flow requiring treatment. Frequently spaced extraction wells, intermediate to the regularly spaced piezometer pairs, were the chosen withdrawal alternative. Pumping was designed and tested with controls and logic to slowly extract groundwater at varying rates to account for tidal effects, all in an effort to minimize groundwater withdrawal and corresponding long-term operation costs. Figure 1 illustrates the plan arrangement of the barrier, extraction wells, and monitoring piezometers.

Figure 1 - Site Plan
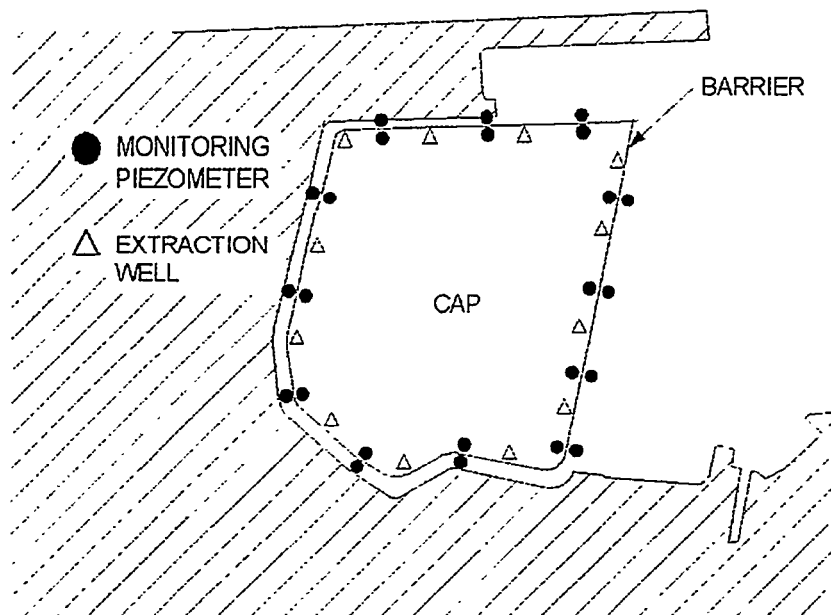
Groundwater modeling estimated that future groundwater extraction must exceed 2000 gallons per day (7.57 m³/day) in order to meet performance standards. No further design modeling was performed. Rather, the client opted to build a quality constructed containment, test the pumping system prior to final construction, and accommodate any unanticipated changes during construction.

SB VERTICAL HYDRAULIC BARRIER

The SB barrier measured 3300 feet (1006 m) long, 65-80 feet (19.8-24.4 m) deep, and approximately 3 feet (0.91 m) thick. Geotechnical design investigations confirmed the alignment and decomposed rock key material. Slurry and backfill compatibility testing was performed. Backhoes were used to excavate the trench in two passes. Backfill consisted of recycled excavated spoils, minimal imported fines, hydrated slurry, and a dry addition of treated saltwater compatible bentonite. Full-time CQA ensured a quality constructed product and included such elements as frequent trench sounding, bottom sounding and physical inspection, and parallel CQA testing for slurry and backfill parameters. CQA testing descriptions are presented by others (Deming 1997).

CQA permeability testing, 1 per batch (300-800 cubic yards (229-612 m^3)), provided an average permeability of 4 x10^9 cm/sec. Physical inspection of the key samples indicated a consistent material and adequate key penetration (4-6 feet (1.2-1.8 m)). The constructed result was a continuous low permeability barrier as determined by physical CQA testing. Additional post-construction hydraulic testing was performed to assess the barrier performance and to evaluate the ability of the planned pumping system to meet the groundwater extraction requirements.

HYDRAULIC MONITORING

Hydraulic monitoring was used to assess the post-construction performance of the barrier and validate assumptions relating to the designed pumping system. This was accomplished using five series of hydraulic tests or monitoring including: long-term groundwater monitoring, slug testing, pumping tests, cross-barrier testing, and site-wide drawdown testing.

Inboard and outboard piezometer pairs (Figure 1) were designed to the same specification as the final groundwater extraction wells. In this way, inboard piezometers could be tested to assess future extraction prior to final extraction well construction.

The procedures, results, and conclusions of these hydraulic tests are discussed below.

Water Level Monitoring

Existing wells and installed cross-barrier piezometer pairs, inside and outside the barrier, were monitored periodically before, during, and after construction to assess the impact of the barrier on groundwater flow and monitor fluctuations throughout hydraulic testing. Site monitoring proved very useful in tracking the change of the site water levels. Water levels in the shallow-most fill layer rose at an average rate of 0.35 foot (0.107 m) per month during and immediately after barrier completion. This rise was attributed to infiltration on the uncapped site, and high periods of water level rise correlated to rainfall, which was also tracked. The deep groundwater response to infiltration was delayed relative to the fill. The water level information at several locations proved useful in maintaining a site-wide water budget.

Slug Testing

Slug tests were run on many of the newly installed cross-barrier paired piezometer locations as a standard installation procedure. The objective was to look for unexpected variability in the hydraulic conductivity of the monitored layers. Data revealed the harmonic mean of hydraulic conductivity was effectively equal to hydraulic conductivities as determined in the calibrated site groundwater model.

Pumping Tests

Pumping tests were performed for two purposes: first, to refine the assumed aquifer parameters and examine distance-drawdown impacts, and second, to evaluate the barrier integrity. High stress adjacent to the barrier provides the greatest likelihood of revealing any imperfections in the barrier in the vicinity of pumping. Such stress has been used at several containment sites to evaluate barrier integrity (Leonards et al. 1985). Individual pumping tests were performed in the deep aquifer at four locations inside the site perimeter. Some limited testing was done prior to barrier construction.

Pumping was conventionally performed and revealed hydraulic conductivity values as shown in Table 1. Data was reduced with the Hantush-Jacob and Theis methods utilizing image well theory to compensate for the barrier boundary condition. Hydraulic conductivity values agreed with aquifer averages. Tests further revealed rapid distance-drawdown, attributed to the low storage of the confined deep sand aquifer. All interior tests showed pumping was able to impact the next adjacent inboard monitoring piezometer, approximately 280 feet (85.4 m), at moderate flow rates and in less than one hour. Pumping in the deep aquifer had little to no impact on the shallow zone indicating little downward leakance where the confining layer was present. Design distance-drawdown assumptions were supported. Pumping tests confirmed the low storage coefficient of the deep aquifer. During pumping tests the outboard piezometers were also monitored automatically for head changes. In the four test locations, even with up to 25 feet (7.6 m) of drawdown, the outside piezometers did not indicate influence from the pumping well. Thus, barrier integrity in the vicinity of pumping and monitoring was confirmed. Figure 2 shows a typical monitoring arrangement and result.

Table 1 - Pumping Test Hydraulic Results

Piezometer No.	IP10[1]	IP5	IP11	IP8
K (avg.) feet/day (m/day)	24.5 (7.47)	23.1 (7.04)	36.0 (10.97)	42.2 (12.86)
S (avg.) feet/day (m/day)	2.5E-4	6.0E-5	1.2E-6	8.0E-12
1 - Test performed prior to barrier construction				

Figure 2 - Pumping Test Cross-barrier Water Levels
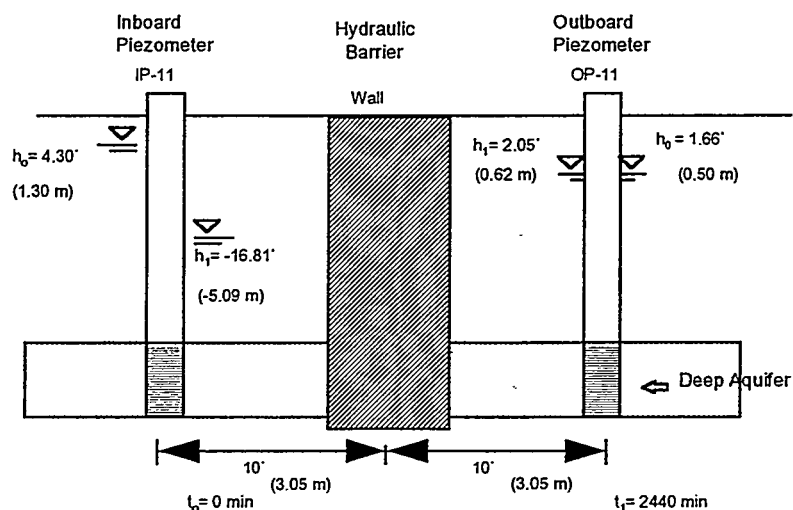
Cross-Barrier Tests & Tide Monitoring

Tidal fluctuations outside the barrier provided an opportunity to examine the interior influence caused by a stress, albeit minor, outside the barrier. All piezometer pairs were monitored at various times. Tide information was also gathered. Data analysis computed lags and tidal efficiency, water level change relative to tidal change, by comparing the outboard and inboard pairs to the tidal data. Figure 3 shows a typical response. Efficiencies were calculated by peak matching. More robust least squares methods (Erskine 1991) were evaluated, but because of the multitude of tidal cycles recorded, the peak matching method was used. Tidal effects were significantly dampened by the barrier's presence, but were still present. This was attributed to pressure propagation through the wall or through the underlying rock.

Figure 3 - Cross-Barrier Test
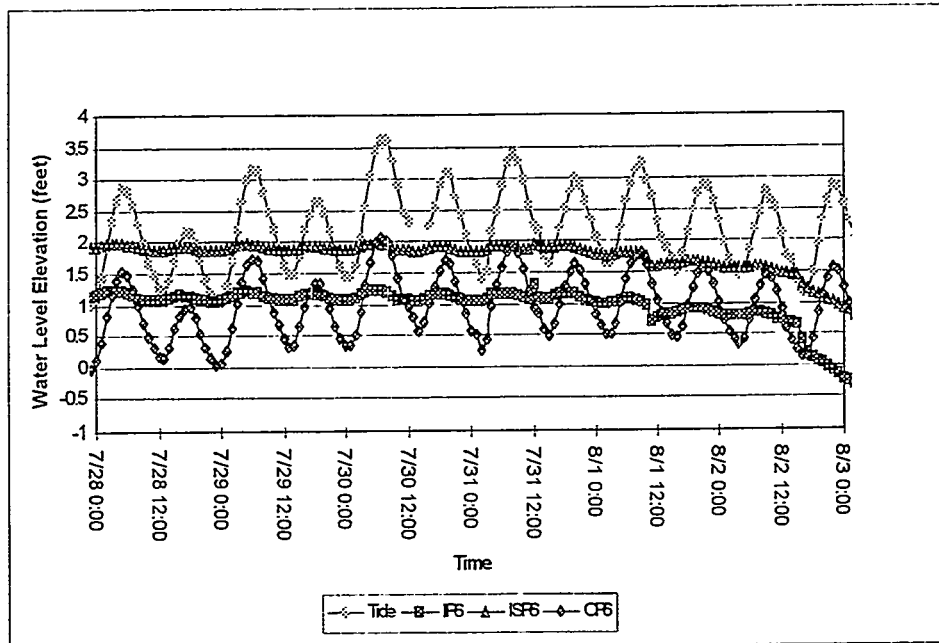
Efficiencies were calculated at tested locations around the site. Table 2 lists calculated efficiencies. Inboard efficiencies were stable and effectively equal considering efficiency calculation methods. Stable values indicate continuous wall integrity around the monitored perimeter and an effective cutoff of adjacent surface water influence. This is especially evident when comparing inside efficiencies to corresponding outside efficiencies.

Table 2 - Cross-Barrier Test Tidal Efficiency

	Piezometer Location	2	3	4	5	6	7	8	9	10	11
Deep	Efficiency Inside Barrier %	9	9	11	10	8 ·	8	9	10	6	9
Aquifer	Efficiency Outside Barrier %	48	ND	56	76	85	82	81	65	49	49

Site-Wide Drawdown Testing

In accordance with the observational method of testing to confirm the groundwater extraction design assumptions, several interior piezometers were pumped simultaneously to simulate the groundwater withdrawal during post-construction extraction well pumping. The test objectives were to confirm that distance-drawdown could be achieved as calculated and to determine if pumping quantities were comparable to modeled flow rates and within design criteria.

Temporary pumps, piping, and water level monitoring equipment were installed in five deep inboard piezometers around the site perimeter. These withdrawal points were spaced around the site approximating the future extraction wells. Transducers were placed in most of the piezometer pairs and supplemented by hand water level measurements before, during, and after pumping. Pumping continued for approximately 6 weeks at varying flow rates.

Tests confirmed earlier pumping test results by showing rapid drawdown propagation in the confined aquifer. Figure 4 shows the impact of pumping on site-wide average water levels. Pumping continued until an inward gradient was established at all piezometer pairs. Observed flows were significantly higher than the design flow, approximately ten times. However, it must be noted that pumping did not represent the long-term steady state condition because significant inflow was occurring from storage in the shallow unconfined interval as well as from infiltration into the uncapped site.

Figure 4 - Water Level Averages vs. Rainfall and Pumping
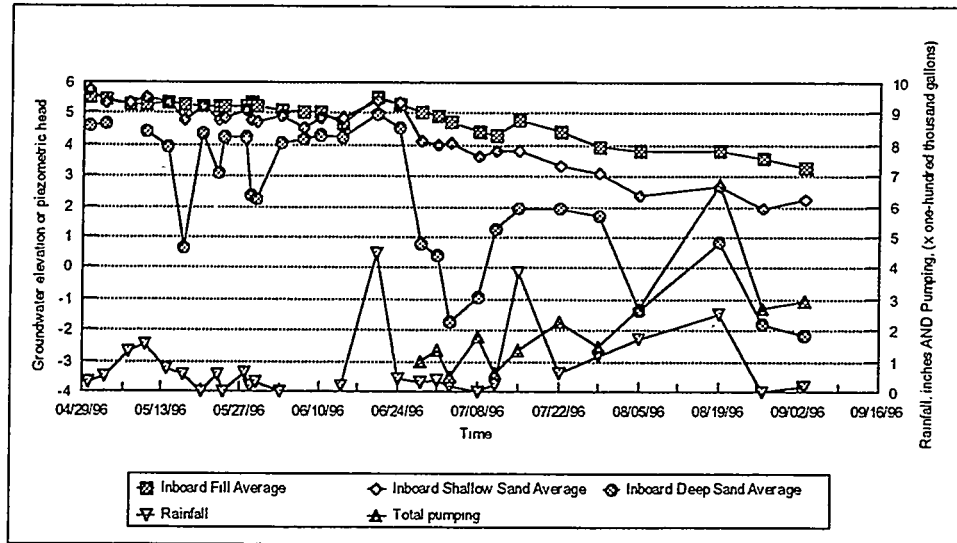
To better understand the balance of water flow during pumping, a water budget for the site was compiled. The water budget approach estimated total inflows into the system and outflows out of the system within the hydraulic barrier above the bedrock. Inflow includes precipitation recharge through rainfall infiltration. Outflow includes pumping. The total change in aquifer storage estimated from the average water levels in the fill layer is compared with the difference between inflow and outflow. Unaccounted inflow into the system is estimated to be in the range of 15,000 to 20,000 gallons per day (56.8 to 75.7 m^3/day). The present estimate indicates that this amount of water may initially need to be pumped from the aquifers to meet the site perimeter head gradient criteria.

The test concluded that the site-wide pumping could achieve regulatory compliance. The worst case with no site cap and water draining from storage still enabled extraction to obtain desired water levels. The pumping rate was much greater than modeled, but tolerable considering the design capacity of the system. The pumping rate is expected to decrease as steady state is reached and storage is depleted.

COMPARISON TO SIMILAR SITES

Hydraulic testing at containment sites provides a means to stress the barrier, accentuating barrier/key imperfections, and measuring integrity after construction. However, such testing is apparently not widely used. Literature research only revealed a limited number of sites where tests were documented. Most instances where stress induced testing was performed, groundwater quality or other monitoring indicated that possible leakage was occurring and the tests were performed for verification. At the Gilson Road site in Nashua, New Hampshire, pumping tests were performed shortly after barrier construction and again after years of operation to evaluate reaches of the barrier where performance was suspect (Barvenik and Ayres 1987). Testing results were conclusive (Haley & Aldrich 1994). At the Edgeboro Landfill in New Jersey, groundwater quality monitoring identified a suspect breach of the barrier and leakage was confirmed by pumping tests and head monitoring (Sadat Associates Inc. 1995). At the Kane & Lombard site in Maryland, pumping tests were used successfully to define barrier performance and bulk hydraulic conductivity prior to full-scale pumping implementation (Ecology and Environment, Inc. 1994). Also, pumping tests were used at the Braidwood Nuclear Power Plant barrier test sections to confirm bulk hydraulic conductivity prior to final barrier construction (Perez 1974). However, these sites represent only a few documented cases were stress testing and monitoring were used to evaluate performance out of a total of perhaps 300 containment barriers constructed in the United States.

SUMMARY AND CONCLUSIONS

Containment performance assessment was conducted at the Baltimore Works site and evaluated prior to final remedial construction using a series of hydraulic tests and monitoring. Long-term water level monitoring and budgeting revealed minimal containment leakage. Slug testing and pumping stress testing confirmed site conductivities and demonstrated necessary distance-drawdown response. Pumping tests were also conclusive in measuring wall integrity near the pumping locations. Cross-barrier tests used tidal influence as a stress condition to further examine site-wide barrier performance, identifying a continuous and effective barrier. Site-wide drawdown testing provided an observational approach rather than a simulated approach to analyzing site-wide drawdown response prior to build-out of the final groundwater withdrawal system and containment cap.

Hydraulic testing and monitoring is a useful method to evaluate barrier performance and a necessary step to confirm groundwater extraction assumptions prior to withdrawal system build-out. Stressing the barrier may accentuate imperfections enabling corrective action prior to completion of remedial construction. Such testing has not been widely used or documented among containment sites in the United States. However, such testing and documentation could provide substantive proof of the integrity of the containment as an effective remedial alternative.

REFERENCES

Barvenik, M.J. and Ayres, J.E. (1987), *Construction Control and Post-Construction Performance Verification for the Gilson Road Hazardous Waste Site Cutoff Wall.* EPA/600/2-87/065.

Deming, P.W. (1997), Design and Construction of a Deep Slurry Trench Barrier. Contribution to the 1997 International Containment Technology Conference and Exhibit, February 9-12, 1997.

Ecology and Environment, Inc. (1994), *Five Year Review Report - Kane and Lombard Site Operable Unit One.*

Erskine, A.D. (1991), The Effect of Tidal Fluctuations on a Coastal Aquifer in the UK. *GROUNDWATER,* 29(4), 556-562.

Haley & Aldrich Inc. (1994), *Remedial Action Evaluation Study, Gilson Road Superfund Site.*

Leonards, G.A., Schmednecht, F., Chameau, J.L., and Diamond, S. (1985), Thin Slurry Cutoff Walls Installed by the Vibrated Beam Method. *Hydraulic Barriers in Soil and Rock, ASTM STP 874,* A.I. Johnson, R.K. Frobel, N.J. Cavalli, and C.B. Pettersson, Eds., American Society for Testing and Materials, Philadelphia, 1985, 34-44.

Perez, J.Y. (1974), *Pumping Test in Slurry Trench Test Section, Braidwood Nuclear Station, Braidwood, Illinois,* Woodward-Clyde Consultants, Chicago, IL.

Sadat Associates, Inc. (1995), *Evaluation of Cutoff Wall Efficiency Area O, Edgeboro Landfill, East Brunswick, New Jersey.*

Snyder, G.W., Murphy, V.P., and Deming, P.W. (1993), Remediation of a Coastal Ore Processing Facility. *Proceedings from AEG/ASCE Geoenvironmental Site Characterization Symposium.*

Snyder, G.W., Ponton J.R., and Deming, P.W. (1994), Dredging with Environmental Controls Baltimore, Maryland Inner Harbor. *Proceedings of Dredging '94.*

A New Geophysical Method for
Monitoring Emplacement of Subsurface Barriers

W. Daily and A. Ramirez
Lawrence Livermore National Laboratory
Livermore, California 94550

February 1997

Abstract

Visualizing subsurface structures is an old and venerable problem. Many geophysical methods have been developed to meet the challenge and some of these have already been applied to visualizing placement of subsurface barriers. Unfortunately, none of these methods have yet demonstrated the ability to yield detailed structure or to reliably evaluate their performance.

Electrical resistance tomography (ERT) is a relatively new geophysical technology which has already proven useful for imaging many underground process. In this paper we discuss how this method may be useful for imaging barriers.

This paper describes the state of ERT technology, summarizing its capabilities as well as its limitations. Then we will demonstrate how the method might be used by showing relevant case histories of high resolution images of subsurface processes. Three dimensional images can be generated which might map barrier boundaries or delineate missed zones. The high speed data acquisition and image reconstruction may even make possible near real time information to guide barrier construction or augmentation.

Introduction

The goal of this paper is not to document our experience using electrical resistance tomography (ERT) to monitor the emplacement or to verify the integrity of a subsurface barrier, for the technique has not yet been used for either purpose. Rather, our goal is to document the capabilities of ERT with particular emphasis on how these capabilities could be used for such purposes. To accomplish this, we will summarize the results of two recent experiments in which fluids have been introduced into the subsurface and their movement and eventual distribution mapped in some detail using ERT. We will also show an example of the use of ERT to image bentonite layers in the subsurface, a reasonable electrical analog to many permeability barriers. Using these examples we will point out the lessons which might be applicable for using ERT to map subsurface barriers and for verifying their performance.

We will describe two applications of ERT to mapping subsurface fluid movement which has relevance to monitoring barrier emplacement as most barriers are introduced as fluids which are designed to change permeability once they are in place. The first example will be the imaging of a dense non aqueous phase liquid (DNAPL) as it is added to a sandy aquifer and particularly as it moves along a clay barrier. The second example will be the imaging of a light non aqueous phase liquid (LNAPL) as it moves through unsaturated sands.

Electrical resistance tomography (ERT) is a technique for reconstruction of subsurface electrical resistivity distribution. The result of such a reconstruction is a 2 or 3 dimensional map of the electrical resistance distribution underground made from a series of voltage and current measurements from buried electrodes (see LaBrecque *et al.*, 1996).

To do ERT surveys we place a number of electrodes in boreholes and/or at the ground surface to sample the subsurface impedance distribution using an automatic data collection and switching system. A few hundred 4 electrode electrical impedance measurements are collected using of

these electrodes. These data are processed to produce electrical tomographs using state of the art data inversion algorithms.

The inversion algorithm solves both the forward and inverse problems. The forward problem is solved using a finite element technique. The objective of the inverse routine is to minimize the misfit between the forward modeling data and the field data, and a stabilizing functional of the parameters. The stabilizing functional is the solution's roughness. This means that the inverse procedure tries to find the smoothest resistivity model which fits the field data to a prescribed tolerance. For additional details, the reader is referred to LaBrecque *et al.* (1996).

DNAPL release experiment

The experiment was conducted in a double wall steel tank 10 meters square and 5 m deep at the Oregon Graduate Institute of Science and Technology in Beaverton, Oregon. This tank allowed for a safe release of perchloroethylene (PCE) into a soil section constructed of sand and clay. Two layers of powdered bentonite were included as barriers. The tank was saturated with 4 ohm m pore water to within about 25 cm of the surface. Four coplaner electrode arrays were used to generate two dimensional (2D) images in three planes; L1, L2, L3 and L4. Each array contained 10 lead electrodes spaced evenly between 50 cm and 275 cm depth. One hundred eighty nine liters (50 gallons) of PCE was released at a single point on the surface approximately midway between arrays L2 and L3. The release rate averaged about 2.0 liters/hr.

Both bentonite layers, the lower extending all the way across the tank and the upper extending only half way across the tank, are clearly imaged (see lower right panel in Figure 1). They are also clearly not uniform; the non uniform thickness reflects the difficulties installing these structures in the tank as well as imperfections in the inverse process (artifacts), although determining the relative importance of the two in the image is not possible as the tank was not dismantled after the experiment. However, as far as we can determine ERT gives a reasonable sectional view of variability in these confining layers which is impossible to achieve with conventional logging or even surface radar methods. This result is an example of the capabilities of ERT to delineate in cross section the shape, extent and continuity of a hydraulic barrier. We note here that had imaging of this hydraulic barrier been the goal, the shape and extent of the barrier could be discerned from this image without the need to compare before and after data as is necessary for lower contrast targets.

Imaging the PCE release requires such a comparison of before and after data which is shown in the other panels in Figure 1. A pixel by pixel subtraction of the background image leaves only the relatively small changes in resistivity distribution induced by the PCE and removes the larger natural heterogeneity of the soil. At 3.5 hours the changes were quite small but the most significant feature is located below the release point--a resistive anomaly arching around the end of the upper clay. This anomaly probably forms as the resistive PCE displaces the more conductive pore water. Other small anomalies in this image are probably from unrelated but natural changes in the pore water conductivity and from data noise.

About 21 hours and 42 liters into the release the anomaly has grown large enough to extend from the release point, arch around the upper clay and reach down to just touch the lower confining layer. Apparently, most of the PCE continues to spill over the edge of the upper layer with little residing on top. Reflecting the dynamic nature of the system, the same small unrelated anomalies are still present (evidence that they are not from random data errors) and now a few others are forming. The weak disconnected features forming along the top of the lower clay may be small accumulations of PCE even at this early stage.

By August 18, at 45 hours, the anomaly begins to spread horizontally along the top of the lower clay as might be expected of the plume as more PCE reaches that layer. The appendage pointing up to the right in plane L2-L3 is not expected and we cannot explain its presence.

The release ended Sunday at noon, August, 20 after 189 liters (50 gallons) was released. On Monday, August 21 the tomographs show a different picture from that 3 days earlier. Only a small remnant is left of the arching anomaly from the surface and around the upper clay. This is understandable if it represented the downward moving PCE which by this time has mostly drained and been replaced by water. However, now a resistive anomaly almost 2 m long sits at the top of the lower clay layer, centered directly below the edge of the upper layer. From this tomograph we conclude that the bulk of the PCE has drained from the sands and is pooled on the lower layer. A 2 m diameter pool of 6 cm uniform thickness would accommodate the volume released and so the anomalies are consistent with a PCE pool at this location. Imaging the PCE movement and eventual fate is an example of how ERT might be used to verify the integrity of a hydraulic barrier, the PCE acting as a fluid tracer added to the system to see if it can breech the barrier. The PCE was also mapped by video images of the dyed DNAPL, taken from inside several glass wells and the distribution so determined agreed well with that inferred from the ERT images.

Difference images were constructed for 4, 16 and 25 days after the release ended. In these images there are two clear trends. First, the anomaly associated with the free product plume breaks apart into separate pieces and each part becomes weaker with time. One explanation is that the free product is moving into topographically lower regions of the clay surface which are out of the image plane. The second trend is that anomalies unrelated to the PCE release are becoming more important. Especially prominent are those at the top right in the image planes. These may be due to the addition of fresh pore water to the tank as a result of heavy rains during the experiment.

From the results showing PCE drainage through the sand and residence on the clay barrier we conclude that similar application of ERT may also be useful for validating the integrity of other barriers. For example, before and after comparison images might delineate the difference between tracer water that is stopped by the barrier and water that may find a path through the barrier. As shown in the above example, ERT image differences are very sensitive to small changes in subsurface resistivity (5% changes can be reliably imaged) and therefore should be sensitive to small volume tracer leakage.

LNAPL release experiment

This experiment was conducted in another double wall steel tank, similar to that described for the DNAPL experiment, at the Oregon Graduate Institute. In this case one hundred gallons of unleaded gasoline was released at a single point on the surface approximately midway between ERT arrays named L2 and L3. The release rate was 80 ml/m. The phreatic surface was held at 90 cm depth during the entire experiment.

ERT data was collected each day between planes L1-L2, L2-L3, L3-L4 (these planes are coplaner) and between L5-L3, L3-L6 (these planes are approximately orthogonal to the first set of planes at L3) during the release, and three times after the release ended. The baseline images at 1 Hz are shown in the top panel in Figure 2. The other panels shows those reconstructions after pixel by pixel subtraction of the background images from subsequent images. (Plane L3-L4 did not always converge so that they are missing in the figure.) These difference images show only changes in resistivity distribution.

On September 12 about 18 hours and 86.4 liters into the release, the image clearly shows a 10 to 40 ohm m resistive anomaly forming directly above the water table in L2-L3 and L5-L3-L6. Notice, however, that it is not uniform or even continuous. In fact, the largest resistivity changes are not directly beneath the release point but rather in plane L3-L5. We believe these anomalies are an indirect indicator of the LNAPL (Daily *et al.,* 1995) moving into a soil of heterogeneous permeability. There are several mechanisms which might be responsible for the resistivity changes associated with the LNAPL. First, is a spatial redistribution of the pore water in the capillary fringe as a result of changes in the pore water suction potential when the water-air boundary is replaced by a water-gasoline boundary. Second, is a displacement of capillary water by increased hydrostatic pressure as the gasoline enters the pore space. What ever the

mechanism, we see a similar effect as was observed in the 1992 gasoline release at OGI (Daily *et al.,* 1995) and believe that the anomalies in Figure 2 are caused by the same mechanism as seen in the earlier data.

On the morning of September 13 about 189 liters had been released, half the total planned release volume. Now the LNAPL anomaly is much stronger, especially in L5-L3-L6 where the resistivity has changed more than 50 ohm m. However, there is little change in the distribution which implies that the preferred paths initially established by the plume are not substantially altered with continued flow. This pattern continues on September 14th (not shown) as the release continues.

Then, after 378 liters (100 gallons), the release ended at 1400 hours on September 15th. The images of that date in Figure 2 were taken between 1700 and 2000 hours on that date and the LNAPL anomaly is noticeably smaller in magnitude implying a relaxation of the plume--perhaps draining of LNAPL out of the image planes. On the 16th of September (not shown), the LNAPL anomaly continues to weaken. In part of L2-L3 it has all but disappeared although in plane L3-L6 changes are imperceptibly small. This heterogeneous behavior suggests complex movement of the plume even in this relatively simple geologic setting.

Although the largest magnitude resistivity changes result from the LNAPL plume near the water table, smaller changes occur well below these. We believe that at least some of these are real and result from an air sparging experiment which was concluded in the tank only about 14 days before the LNAPL release began. Thermal, ionic concentration, and dissolved air concentration gradients are just some of the mechanisms which may have driven these weak changes in the ERT planes in the saturated sands.

Summary and Conclusions

These results are intended to demonstrate the capabilities and limitations of ERT to provide detailed images of subsurface fluid movement, especially where it is possible to compare baseline data with that taken later. Because barriers are generally emplaced as fluids, changes that these fluids produce in subsurface resistivity distribution can be used to map the shape and extent of the barrier material during injection. We have found that such difference imaging is very powerful for high resolution and high sensitivity imaging (see also, Ramirez *et al.,* 1996; Ramirez *et al.,* 1993; Daily and Ramirez, 1995). Both examples discussed here were of electrically insulating fluids. Barrier materials may be either electrically insulating or conducting, but the insulating cases described here are the more difficult to image and so we have shown the worst case.

The DNAPL experiment also demonstrates the capabilities of ERT to provide images of subsurface barriers, in this case bentonite layers in a sandy soil, without the benefit of having data before it is placed. Our experience (see Daily and Ramirez, 1995; Ramirez *et al.,* 1993) is that if a layer has sufficient electrical contrast with the surrounding soil, it can be imaged directly (without comparing before and after images). The results of both case studies pertain to the verification of barrier performance if a fluid tracer is used to validate the barriers hydraulic integrity.

References

Daily, W. and A Ramirez, (1995) Electrical Resistance Tomography During In Situ Trichloroethylene Remediation at the Savannah River Site, *J. Applied Geophysics,* 33, 239-249.

Daily, W., A. Ramirez, D. LaBrecque and W. Barber, (1995) Electrical Resistance Tomography at the Oregon Graduate Institute Experiment, *J. of Applied Geophysics,* 33, 227-237.

Ramirez, A., W. Daily, D. LaBrecque, E. Owen and D. Chestnut, (1993) Monitoring an Underground Steam Injection Process Using Electrical Resistance Tomography, *Water Resources Research,* 29, no. 1, pp 73-88.

Ramirez, A., W. Daily, A. Binley, D. LaBrecque and D. Roelant, (1996) Detection of Leaks in Underground Storage Tanks Using Electrical Resistance Methods, UCRL-JC-122180, October, *J. Engineering and Environmental Geophysics*, in press.

LaBrecque, D. J., M. Miletto, W.Daily, A. Ramirez and E. Owen, (1996) The Effect of Noise on OCCAM's Inversion of Resistivity Tomography Data, Geophysics, *61*, 538-548, March-April.

DNAPL Release

3.5 hrs 7.0 liters
allplane_0816late_1indabs_ncs

21 hrs 42.0 l
allplane_0817_1indabs_ncs

45 hrs 94 l approx.
allplane_0818_1indabs_ncs

1 day after spill ended
190 l approx
allplane_0821_1indabs_ncs

4 days after spill ended
allplane_0824_1indabs_ncs

16 days after spill ended
allplane_0905_1indabs_ncs

Bentonite barriers

25 days after spill ended
allplane_0914_1indabs_ncs

Figure 1. ERT of 1 Hz data from three collinear planes before and during release of perchloroethylene (PCE) into a saturated soil. The right most image in the third row was taken before the release with the right gray bar showing the range of reconstructed resistivities. The other images show changes fro this background during and after the release with the left gray bar representing the resistivities. The arrow shows the DNAPL release point in plane L2-L3.

0　　　　　resistivity difference, m ohm-m　　1.0e+05

3.0　　　4.0　　　5.0　　　6.0
log10 (resistivity, m ohm-m)
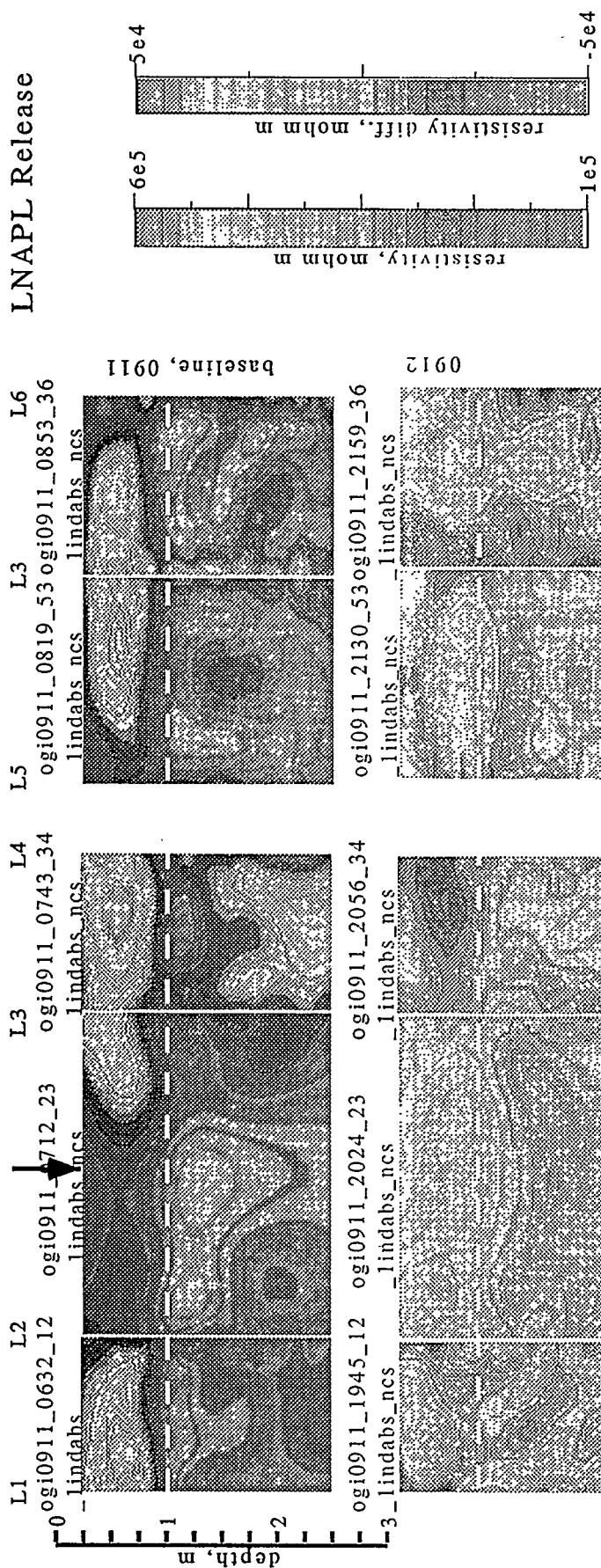
LNAPL Release

Figure 2. ERT results for LNAPL data acquired at 1 Hz. The first row are baseline images taken on 09/11. before the release started. The arrow shows the LNAPL release point in plane L2-L3 and the dashed line is the location of the water table. Below the baseline data are difference images taken during the gasoline release.

Large-area, Long-term Monitoring of Mineral Barrier Materials

A. Brandelik and C. Huebner, Karlsruhe Research Center, Karlsruhe, Germany

Forschungszentrum Karlsruhe
IMK
Postfach 3640
D-76021 Karlsruhe, Germany

1. Abstract

Clay-type mineral layers are used for bottom and surface barriers in environmental containment, such as landfill designs. Their performance in terms of isolation depends on the water content and its variation with the time. Sensitive long-term areal mapping of the moisture content can detect in time drying or shearing failures that will have a negative impact on the performance of the barrier. Based on the measurement of the dielectric coefficient (not of the unpredictable electric conductivity as proposed by others), we use the combination of two sensors; the cryo-moisture sensor and the cable network sensor in the clay-type mineral layer. The cryo-moisture sensor measures the depth profile of the absolute water content and the change of density on a small area (diameter approx. 0.2 m). It is selfcalibrating and very accurate. The cable network sensor is a net of moisture sensitive radiofrequency cables. It is buried in the barrier layer and determines variations of the water content of approximately 3% (by volume) with a spatial accuracy of approx. 4 meters. We have used the cryo-sensor since 1992 and already started installing the cable network on an area of approx. 2000 m² within a waste disposal surface barrier at Karlsruhe. This system is non-destructive and allows long-term monitoring. It is predicted to operate for longer than 20 years. The calculated costs of acquisition, installation and operation are $ 4.-/m² in the first year.

2. Introduction

The disposal of toxic wastes threatens aquifers worldwide. Governments require closure-cost guarantees on new landfill containments and propose or prescribe monitoring of old sites as well. Groundwater monitoring as a preventive measure avoiding groundwater pollution is illogical. At the time when the protection system gives an alert, it is too late (Cullen 1992). The long-term advantages to the public of an early warning are obvious. The monitoring system should give a warning based on small changes which can predict dangerous changes. Also, monitoring should have a good local resolution to enable a minor repair to be made of the barrier system in case of spot failures. Usually, the waste containment sites have a bottom barrier and a surface barrier, but old sites often do not have the bottom barrier. This also applies to our test site, the Waste Disposal West of the city Karlsruhe. The bottom barrier is missing. In addition, this disposal site is situated in the industrial dockyard of the river Rhine. In such cases, the surface barrier has to be reconstructed more carefully. The surface barrier at the Karlsruhe site is a combination of root soil, filter layer of sand and gravel, high density and highly saturated clay mineral, a capillary layer of sand and a capillary barrier layer of gravel. Considering the high slope, no plastic liner has been included. Three years ago we installed some of our cryo-sensors (patents granted in 1992) on this sensitive site (Fig. 1).

Next spring (1997), we will install our new (patent granted in 1996) cable sensor system for large-areas above, in and under the clay layer of 2000 m². In this paper, we report on our experience with the first sensor type and give preliminary results of the second, based on other test fields. Finally, we will extrapolate these results to installation at the Karlsruhe dumping site expected to begin in spring 1997.

According to regulations, the surface barrier has to include a clay-mineral layer because of its

a. stability; old material, it will not change with time,

b. plasticity; it can follow deformation, and

c. low water conductivity.
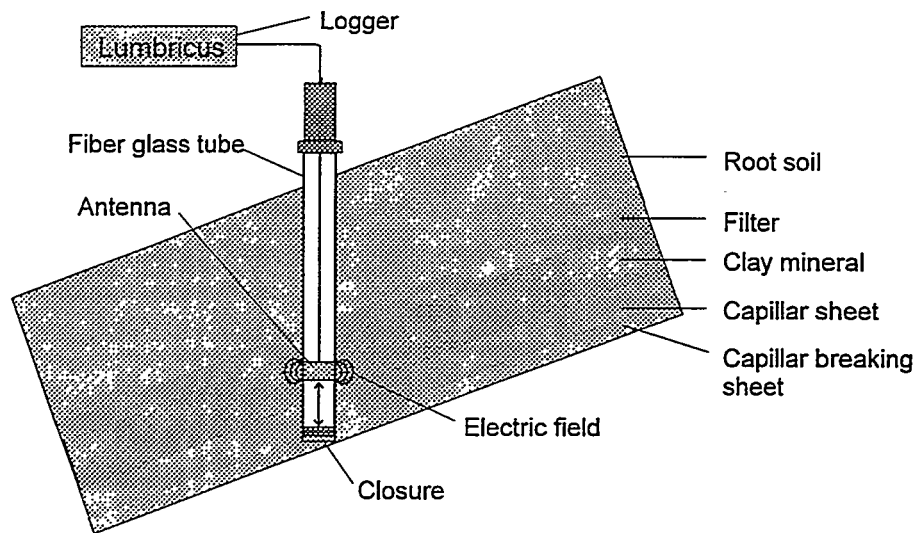
Fig.1 Surface barrier with cryo-sensor

The primary task of a monitor system is the measurement of the hydraulic conductivity of this clay-mineral layer. Direct measurement of this parameter is possible with lysimeters only. They are very expensive, so that their use is limited to small areas. Other common monitoring methods are indirect methods. The most commonly used indirect parameters are the water content and the density of the clay-mineral. Soil-physical and soil-mechanical models relate these parameters to the hydraulic conductivity. A unique property of clay is shrinking and swelling as a result of changing water contents. A commonly used rule-of-thumb says that some water loss in the clay barrier has already induced a higher hydraulic conductivity and, consequently, facilitates leaching of the waste disposed beneath the layer. Based on this rule-of-thumb, several authors and promoters recommend to monitor the water content (Kramer 1996) as a reliable sufficient indirect alert parameter to warn against possible leaching. This is what we are doing. Our first soil moisture sensor (the cryo-moisture sensor) can measure the absolute water content (volume) with an accuracy of ±1.5%. The same device measures the relative dry density of the soil mixture within the same volume and at the same time. Using these two features we wished to measure the leaching behavior of the surface barrier.

Generally, this report deals with monitoring of the surface barrier alone. Nevertheless, the second sensor, the flat-band cable sensor, is suitable for installation in the bottom barrier as well.

We have learned that the water content and density, or the change of density, are necessary but not sufficient to predict leaching. This conclusion is based on our laboratory test involving a measuring volume of 1.6 m³ and from the studies of (Holzloener 1993), (Savadis and Mallwitz 1993) as well. They investigated the role of other parameters, like gravimetric pressure, soil suction characteristic, particle size distribution, etc. These parameters are constant and can be measured before construction. The changes of the water content and density remain as the variable parameters. So, their monitoring can furnish reliable criteria of prediction. The clay-mineral in this surface barrier has a dry density of 1.85 g/cm³ and a volumetric water content of more than 35%. It is compressed to a Proctor density of 0.97. We measured the shrinking behavior of this material and found that within the range of water contents from 35% to 30% the shrinkage exceeds 10% (Fig. 2). This is the critical range that we have to detect and in which the loss of water content is correlated with shrinkage (enhancement of the dry density).
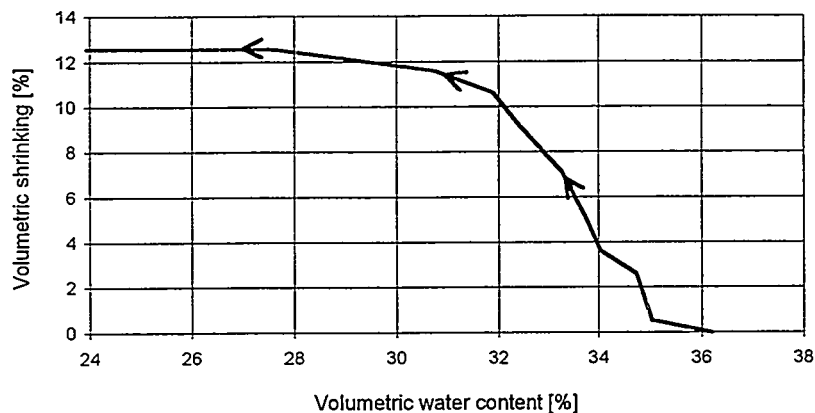
Fig.2 Drying induced shrinkage

There are a lot of devices recommended for water content measurements (Wilson 1995). Some of them, e.g. the neutron-sensor, are also combined with the density measuring feature. The common drawback of the water content measuring devices is their calibration. They need a soil specific calibration. This is always done in the laboratory and not in-situ as would be necessary. Brandelik et al. (1996) also reviewed the advantages and disadvantages of these common techniques. The range of water contents at shrinking is narrow, approx. 5%   (Fig. 2). The accuracy of a device has to be significantly less than this 5 % value. We have found that an ex-situ calibrated sensor cannot fulfill this requirement. By contrast, our cryo-sensor, introduced in the next paragraph, fulfills this requirement.

3. Measurements with the Cryo-sensor

Every soil moisture measuring device has to be calibrated with respect to the specific soil, but the water content and density are very sensitive to laboratory preparation. The soil matrix of an extracted sample can change its sorption and water penetration capabilities as a result of sampling. The laboratory measurements of water mobility often differ from experiences gathered on the site, especially on waste disposal mounds. In order to get realistic results, every soil parameter has to be evaluated in the field, in the natural state and not in a laboratory. To do this, we developed a cryo-soil moisture sensor "LUMBRICUS" which consists of a measuring tube and a data logger (Fig.1). In autumn 1993 six measuring tubes were installed in the test lysimeter field of the waste disposal mound in Karlsruhe. The measurement was focused on the water content and change of density, to obtain numerical parameters for the function which relates the density and water content to the hydraulic conductivity. The cryo-sensor "LUMBRICUS" calibrates itself in-situ without disturbing the measurement volume and without any laboratory preparation. The sensor can be used in long-term monitoring too. (Our first cryo-sensor has operated in a test field since 1990.)

The dielectric coefficient of the soil mixture is measured outside a fiber glass tube, 0.13 m in diameter and 2.5 m in length, which is pushed into the soil, in this case through the surface barrier. Then the same measuring volume is frozen by filling liquid nitrogen into the tube. Then, the dielectric coefficient of the frozen soil is measured again (after the whole amount of water changed its phase into ice). The great difference of the dielectric coefficients between water (approx. 80) and ice (approx. 3.2) and their volumetric portions in the soil mixture gives a very accurate (±1.5 %) absolute measure of the volumetric water content, because the changes of solid and air due to change of temperature are negligible. This patent protected measuring method (licensee METEOLABOR AG) is the central part of the sensor function. From two measurements (unfrozen and frozen) one can determine two unknown quantities. So, the sensor measures not only the volumetric water content, but also the relative dry density. The advantage

of this unique feature is that these important parameters can be obtained in an inherent on-site and long-term measurement. Figures 3 and 4 show these two quantities measured at the dumping site.
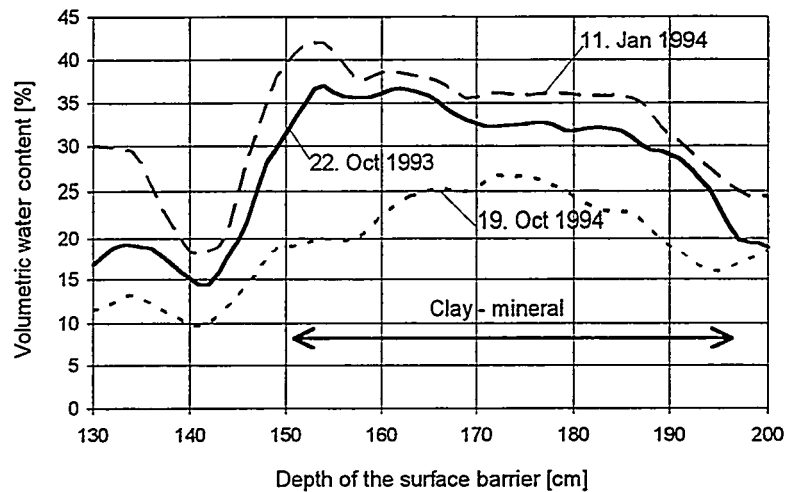
Fig.3 Moisture profile
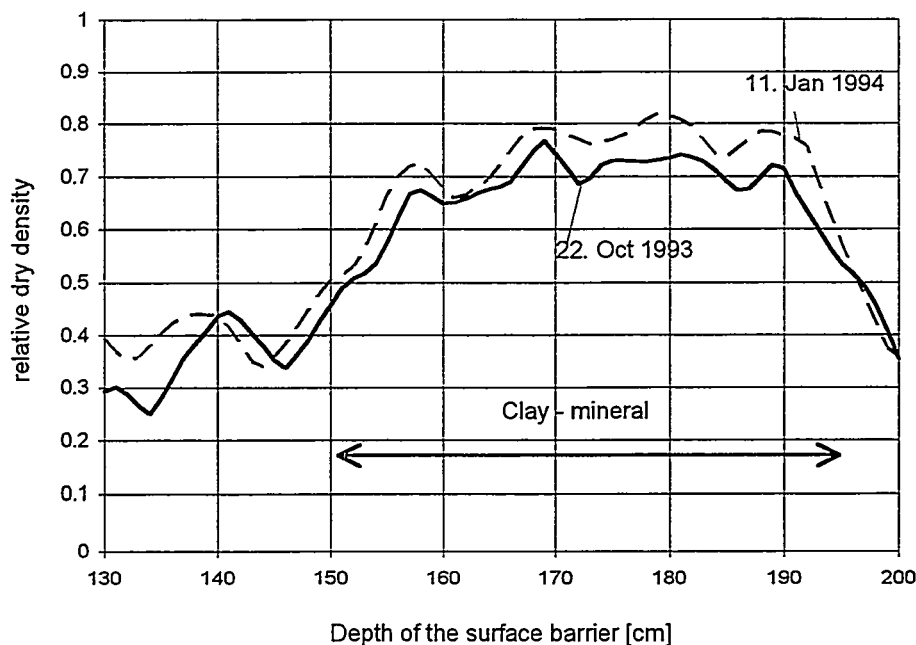
Fig.4 Density profile

Figure 3 shows the moisture increase after the wet winter. Figure 4 shows some compaction during that period. Please note that

(a) the measurement accuracy of the relative density is only ±4 %,and

(b) the depth resolutions of both quantities are very fine (approx. 3 cm).

The cryo-method and the sensor have been described in detail by (Brandelik and Krafft, 1996) and (Brandelik and Huebner, 1994).

We were not satisfied with the poor accuracy of the density measurement. To compensate for this deficiency, we designed the LUMBRICUS antenna so that it would be able to qualitatively detect a very small compaction (Fig. 5). The antenna is the actual sensor part, which moves up

and down in the tube. This antenna yields a measurement pair. If the barrier material, clay, shrinks, it opens an air gap between the tube and the material. In this case, the measurement pair shows a difference. This difference can alert the disposal operator to make a more complete inspection. Figure 5 shows a measurement on our 1.6 m³ laboratory container with exaggerated drying by an electrical heater. The third profile in Figure 3, measured on 19 October 1994 (after a very hot summer), shows the virtual water content profile on the same tube. The corresponding real profile is not displayed.

Depth in an experimental vessel [cm]
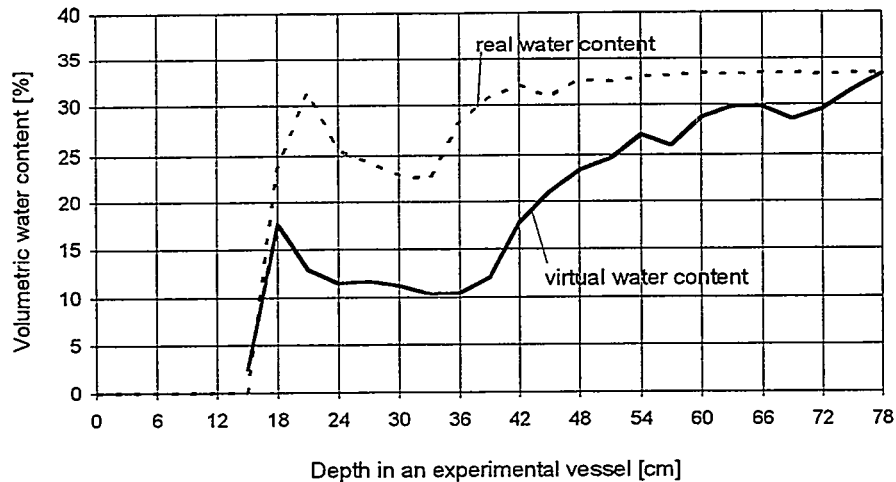
Fig.5 Detection of shrinkage

Conclusion: The waste disposal site operator gets an alert from the very accurate measurement of the water content when drying proceeds, a small air gap will be detected. This is the second stage of alert. To get a numerical result about shrinking of the clay mineral barrier, the measurement of the relative density has to be repeated. For this measurement a new (second) freezing cycle has to be done. Between the two cold measurements the water content is measured and the air gap detected in the warm condition. If the loss of water content is correlated with an enhancement of density, the critical situation is reached. Calculations including the other parameters (like gravimetric pressure, suction potential, etc.) will allow the question to be answered whether the barrier isolates, fails temporarily, or fails irreversibly. This sensor measures only in the close vicinity of the tube. A cost analysis indicates that every 4000 m² has to be equipped with a tube if an extended area is to be monitored. It may be to use the sensor only for the absolute calibration of the cable net sensor system, which will be introduced in the next paragraph.

4.The Cable Net Sensor System

The electric properties of an unshielded flat-band cable also depend on the surrounding materials. The electric loss, signal velocity, phase shift, ability of signal transmission and reflection will be modified by the surrounding material, in our case by the clay-mineral. If we measure these quantities, we can calculate the complex dielectric coefficient of the material. So, we can design a relative measuring device which can be calibrated relative to water content. Time Domain Reflectometry (TDR) has been extensively introduced as a moisture measuring method. These devices only measure the signal velocity. Sometimes the electric loss is included.The devices made with this technique are usually shorter than 0.5 m and are not suitable for application in large areas. By contrast, we use several redundant measurements and the effect of cross-talk between cables (Brandelik et al. 1995). With this approach, we are able to design a cable sensor of some ten meters length. In order to demonstrate this method, we first measured the integral pulse propagation time along a buried cable of 30 m length. Figure 6 shows the change of pulse propagation time correlated with rain events during this test.
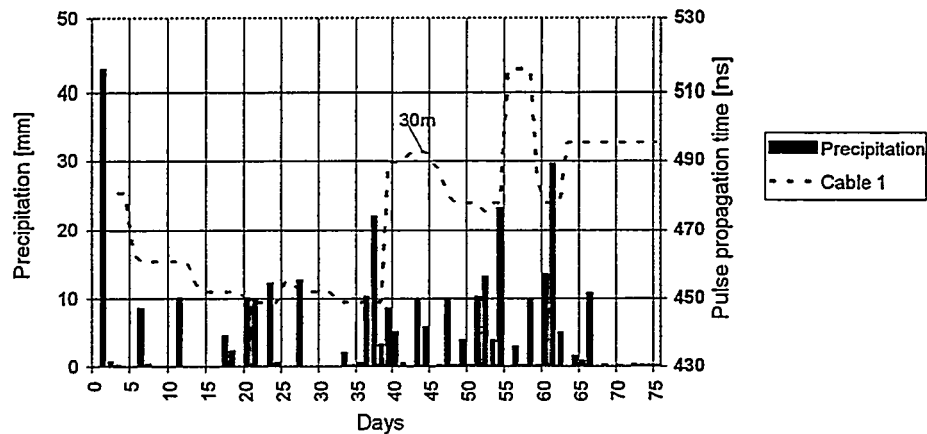
Fig.6 Soil moisture measurement with cable sensor

We can calibrate these time changes relative to integral water content changes. Moreover, if we use the inverse analysis (Lundstedt and Stroem 1986), we can get the differential water content distribution as well.

Measurements with this cable in barrier material (high density, highly saturated clay-mineral) used in practical application yield that a cable may 20 m long. Figure 7 shows the design of the cable net that we are going to instal in spring 1997. With this net pattern we will be able to detect a volumetric moisture change of 3 % with a spatial resolution of approx. 4 meter.
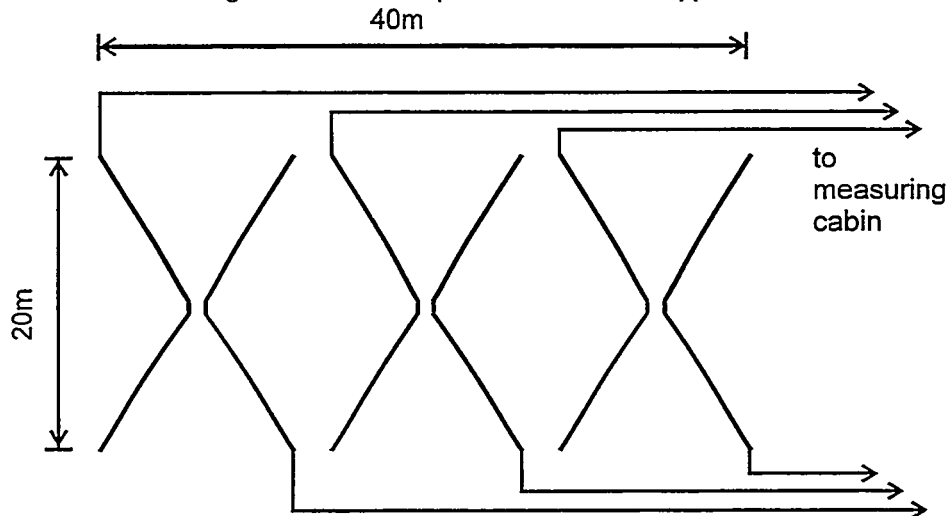
Fig.7 Cable net pattern

Of course, such a cable sensor can be buried vertically. We installed this arrangement during the reconstruction of a petrol station as well.

We note that this cable net sensor is a relative measuring device (in contrast to the absolute measuring cryo-sensor). It needs calibration from other absolute data. To make use of the advantages of both sensors we will instal the cable net sensor together with our cryo-sensors. We had already fabricated the optimized cable. It is 6 cm wide and 1.3 mm thick.

For further hydraulic research on the test site, the cable net sensor will be installed not only in the clay mineral, but above and under that layer as well.

The calculated costs of acquisition, installation and operation in the first year are $ 4 / m².

5. Acknowledgments

6. References

Brandelik, A. et al. (1996) Zerstoerungsfreie In-situ-Messung der Feuchte und Dichteaenderung von mineralischen Deponieabdichtungen. *Muell und Abfall*, 28 (4), 263-268.

Brandelik, A. and C. Huebner. (1994) Calibration of remotely sensed soil moisture. *Proceedings of the European Remote Sensing Conference*, September 26-30, Rome.

Brandelik, A., C. Huebner and R. Schuhmann. (1995) Feuchtesensor fuer ausgedehnte Schichten. German Patent No.19501196.

Brandelik, A. and G. Krafft. (1996) Measurement of Bound and Free Water in Mixtures. In *Microwave Aquametry (ed.* A. Kraszewski), IEEE Press, New York.

Cullen, S.J., J.H. Kramer, L.G. Everett, and L.A. Eccles. (1992) Is Our Ground Water Monitoring Strategy Illogical? *Ground Water Monitoring Review,* 12 (3), 103-107.

Holzloehner, U. (1993) Transportvorgaenge und Bodendeformation unter Einwirkung von Austrocknung und aeußeren Spannungen. *2. Arbeitstagung 17-19 March 1993, BMFT Verbundvorhaben Deponieabdichtungssysteme.* Bundesanstalt fuer Materialforschung und -pruefung, Berlin.

Kramer, J.H. (1996) Landfill Vadose Zone Monitoring Strategies. *International Ground Water Technology,* 2 (1).

Savadis, S. and K. Mallwitz. (1993) Selbsheilungsvermoegen mineralischer Dichtmassen hinsichtlich Durchlaessigkeit in gestoerten Dichtschichten/Dichtungssystemen an Deponien. *2. Arbeitstagung 17-19 March 1993, BMFT Verbundvohaben Deponieabdichtungssysteme.* Bundesanstalt fuer Materialforschung und -pruefung, Berlin.

Wilson, L.G., L.G. Everett, and S. J. Cullen. (1995) *Handbook of Vadose Zone Characterisation and Monitoring.* Lewis Publishers, Chelsea, Michigan.

7. Correspondence

Dr. Alexander Brandelik

Forschungszentrum Karlsruhe
IMK
Postfach 3640
D-76021 Karlsruhe, Germany
Tel.:   +49 (0) 7247-823913
Fax: +49 (0) 7247-824742
Email: chris@imkhp5.fzk.de

GEOMEMBRANES WITH INCORPORATED OPTICAL FIBER SENSORS FOR GEOTECHNICAL AND ENVIRONMENTAL APPLICATIONS*

David J. Borns
Geophysics Department
Org. 6116/MS-0750
Sandia National Laboratories
Albuquerque, NM 87185-0750

ABSTRACT

This research covers the development of optical-fiber sensors and the methods to incorporate the sensors within geomembranes during manufacture. Such systems are being developed to monitor the effects of strain on geomembranes including the location of tears. Other possible measurements utilize moisture and fluid-level sensors. Since the use of geomembranes in geotechnical and environmental applications is widespread and monitoring systems are generally lacking, the potential for this technology is significant. For example, a geomembrane-and-sensor system addresses the need to monitor landfill stabilization in general and specifically the behavior of geomembranes used in liner and cover designs.

We have demonstrated that glass and plastic fibers can be attached to a geomembrane (1) during extrusion and lamination and (2) by hot shoe welding, glued tape runners, and welded runners. Using these methods, we have manufactured 30 m lengths of geomembrane with continuous optical fiber across the length. Our preliminary focus has been on strain sensors to monitor landfill subsidence. We have utilized existing and newly developed strain sensors, e.g., microbend, Bragg grating, and adsorption band sensors. These sensors have been installed as arrays into several test membranes at a manufacturing scale (e.g., 3 to 4 m wide). The prototype monitoring systems were installed in laboratory test frames, and the sensors measured the strains across the membranes as they were loaded. We plan to scale these experiments up to the size of landfill cover system using a test cell under construction.

1. Introduction

The technology of smart structures and smart materials has been developed for defense and space applications. These smart structures have been utilized in monitoring weapons tests, aircraft, naval ships, and the space shuttle. The term, "smart," refers to the incorporation of multiple sensors within the structures or materials during construction (Udd, 1995). Such sensors and monitoring systems are often optical fiber based for reasons of cost, environment (e.g., high temperature, limited space, radio or other electromagnetic interference).

Sandia National Laboratories are now applying the smart structure approach to the design of engineered structures used in environmental restoration. For DOE complex restoration projects, we are designing "smart" landfill covers and linings by incorporating sensors developed in the smart structures applications of the defense programs. Such sensors include optical fiber-based strain and moisture sensors. For the landfill applications, we have developed methods to incorporate optical fiber sensor systems with the plastic sheets (geomembranes or geosynthetic membranes) used as engineered components in, for example, landfill liners and covers. A significant need exists to monitor the geomembranes and the surrounding cover or liner materials for the effects of water accumulation, subsidence and age.

This development of optical-fiber sensors incorporated within geomembranes addresses needs to monitor the effects of strain on geomembranes including the location of tears. Other possible measurements, as mentioned, utilize moisture and fluid-level sensors. Since the use of

geomembranes in geotechnical and environmental applications is widespread (Koerner, 1994) and monitoring systems are generally lacking, the potential for this technology is significant. For example, a geomembrane-and-sensor system monitors the behavior of geomembranes used in liner and cover designs.

2. Project Status

This research covers the development of optical-fiber sensors and the methods to incorporate the sensors within geomembranes. Such systems are being developed to monitor the effects of strain on geomembranes including the location of tears. Other possible measurements utilize moisture and fluid-level sensors. We have demonstrated that glass and plastic fibers can be attached to a geomembrane: (1) during extrusion and lamination and (2) by hot shoe welding, glued tape runners, and welded runners. Using these methods, we have manufactured 30 m lengths of geomembrane with continuous optical fiber along the length. Our preliminary focus has been on strain sensors to monitor landfill subsidence. We have utilized existing and newly developed strain sensors, e.g., microbend, Bragg grating, and adsorption band sensors. These sensors have been installed as arrays into several test membranes at a manufacturing scale (e.g., 3 to 4 m wide). The prototype monitoring systems were installed in laboratory test frames, and the sensors measured the strains across the membranes as they were loaded. These sensors represent both distributed and point measurement devices. Also, constitutive and numerical models for several cover designs have been developed to describe the strain behavior of geomembranes. These models have guided the selection of sensors and bounding conditions for testing. We plan to scale these experiments up to the size of landfill cover system using a test cell under construction.

3. Development of Sensors and Manufacturing Methods

This report summarizes efforts supported by *the Subsurface Contamination Focus Area of the DOE Office of Science and Technology* to design materials, sensors, and manufacturing methods for an integrated geosynthetic membrane monitoring system (GMMS). The design matrix (Table 1) summarizes the geomembrane monitoring system design based on the manufacturing and laboratory testing program during the period 11/1/95 to 7/20/96 during the initial year of the project. This prototype design will be the basis of the field scale tests planned for FY97 and the initial implementation designs in FY97 and FY98. We have demonstrated that glass and plastic fibers can be attached to a geomembrane (1) during extrusion and lamination and (2) by hot shoe welding, glued tape runners, and welded runners. Using these methods, we have manufactured 30 m lengths of geomembrane with continuous optical fiber across the length. The design matrix (Table 1) spans several manufacturing methods (1: Extrusion; 2: Lamination; 3: Hot Shoe Welded Runners; and 4: Hot melt or Glue Gun Strips and Runners) and sensor types (A: absorption-type; B: Bragg grating; C: microbend; and D: other). The various combinations of manufacturing and incorporation methods with a variety of sensors will provide flexibility to address the site specific needs within the DOE complex: such as (1) the area of implementation; (2) existing, under construction or planned implementations; and (3) the types of parameters that need to be monitored.

Significant portions of this work cover manufacturing materials and methods were accomplished through a cooperative agreement with National Seal Corporation, a subsidiary of Waste Management Inc. (WMX). National Seal has provided access to and use of their experimental production facility, their production line, research and development personnel, technical support and materials.

Table 1: Membrane Design Matrix

Membrane Design Matrix	Fiber type		Sensor Type			
Methods of Incorporation	*plastic*	*glass*	*absorption-type*	*bragg grating*	*microbend*	*other*
Extrusion	• there may be high degradation of fiber • plastic survives relative higher strains • relatively lower cost • less imbrittle- • ment with age	• Al-clad glass works well • fiber exhibits good bounding with membrane • successfully extruded 30 ft. lengths of geomembrane with Al-clad fiber	• distributed sensor • fails in same strain range as geomembrane (□5%) • promising, undergoing performance testing currently • uses inherent properties of fiber without modification • therefore, can be used any-where basic fiber can be incorporated	• distributed sensor • failure @ 1.5% strain • currently relatively high cost ($500/sensor) • in some configuration permits three dimensional strain to be determined	• point sensor • low cost of manufacture	• use of commercially available sensors, such as Measurand Inc.'s BEAM fiber optic curvature sensor • does not survive high temperatures • relative low cost
Lamination	• less degradation of plastic	•	• same as above	• same as above	• same as above	• same as above
Hot Shoe Welded Runners	• very promising	• very promising	• same as above	• same as above	• same as above	• survives lower temperatures of application
Hot melt or Glue Gun Strips and Runners	• promising • some degradation with higher temperature melts	• promising	• same as above	• same as above	• same as above	• survives lower temperatures of application

4. Laboratory Proof-of-Concept Tests

• We have constructed and used a large laboratory scale load frame that permits testing of fibers 10's of meters in length.

• Initial bench scale tests were performed with fiber optic sensors imbedded in laminated polyethylene. Laminated membrane and sensors were placed in a load frame. The deformation of the laminated membrane was successfully monitored by the fiber optic strain sensor. Figures 1 and 2 show that the change in optical transmission through the fiber (vertical axis) is related to deflection or displacement of laminate membrane (horizontal axis, Fig. 1), and to strain at different locations on the membrane relative to position where load is applied (horizontal axis, Fig. 2)

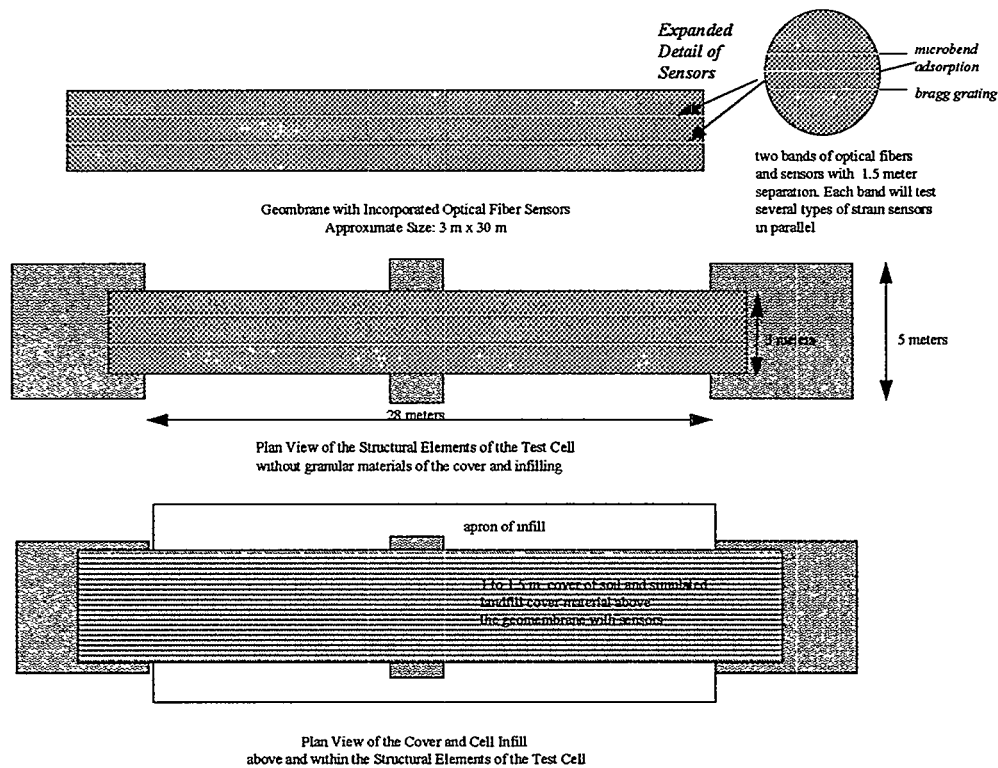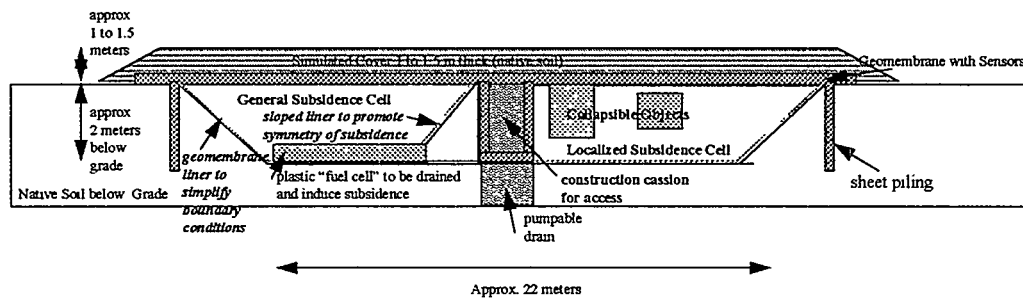## 5. Numerical Modeling of Membrane and Cover interactions During Subsidence

We successfully installed the structural computer model, ABAQUS. With this code, we were able to duplicate test problems originating from Savannah River's work on cover design. Once we completed this benchmark exercise, we began modeling the proposed field scale test of the geomembrane monitoring system (see Section 6). This numerical modeling serves several purposes: (1) the numerical models determine the effects of the scale up from laboratory to field scale; (2) the modeling provides design parameters for the field scale test, such as the amount of subsidence required to achieve critical strains on the membranes; (3) the modeling defines significant parameters, such as the friction coefficient between the geomembrane and the

surrounding soils, that affect deformation of the geomembrane and the landfill cover systems; and (4) the modeling is the initial step in developing a design and performance assessment system for landfill cover systems in general.

6. Field Scale Test

The goal of the Geosynthetic Membrane Monitoring System Project is to initiate and complete a field scale test of the optical fiber based strain monitoring system during FY97. This field scale test will utilize a geomembrane/sensor system fabricated on the scale of a production run geomembrane, which meets ASTM performance standards. The geomembrane will be placed within a cover and fill system similar to landfill designs proposed within the DOE complex. The proposed schedule depending on funding is: (1) to begin construction of the test facility in October 1996 and complete construction before January 1997, (2) to install and begin testing the prototype geomembrane and sensors in January 1997, (3) to complete testing in July 1997, and (4) to complete data analysis and design recommendation by the end of September 1997.

6.1. Objectives of Field Scale Test Cell

The **primary** objectives of the field scale test are to **(1)** demonstrate the capabilities of a sensor system to measure strain of a geomembrane due to *general* subsidence of the landfill components; and **(2)** demonstrate a sensor system to measure strain of a geomembrane due to *local* subsidence in response to collapse of containers within the landfill

6.2. General Description of Test Facility

For this initial stage of field scale testing, the testing will be basically a two dimensional approximation of the subsidence effects. We start with this two dimensional approximation to simplify assumptions (e.g., the effects of membrane welds) and to conserve resources (e.g.: integrated membranes and sensors, space, and funding). Based on progress in FY96, we conclude that a prototype membrane with incorporated sensors (approximately 3 m wide by 30 m long) can be provided for the field test (Figure 3 and 4). Figure 3 shows the basic elements of the field scale test and how these elements will be used to simulate a landfill cover design. The prototype geomembrane will incorporate two parallel lines of optical fibers with sensors. The separation of the lines will be approximately 1.5 m (or 5 ft.). This distance is based on the recommendations of our industrial partner, National Seal Corporation, as representing a characteristic need for spatial resolution in actual landfill applications.

As stated in the objectives, general subsidence and localized subsidence are our first consideration (Figure 4). The conceptual design reflects these priorities and provides two cells over which subsidence can be simulated (Figures 3 and 4). Figures 3 and 4 show the detailed design elements of the test cell in cross section and map view. In one cell (General Subsidence Cell), subsidence will be simulated either by controlled removal or addition of liquid from a buried fuel bladder or by vacuum removal of sand layer within the fill. In the other cell (Localized Subsidence Cell), subsidence will be simulated by collapsing foam objects, vacuum removal of sand fill within objects or trap doors that will mimic the collapse of waste containers.

SENSOR RESPONSE RELATIVE TO APPLIED LOAD LOCATION
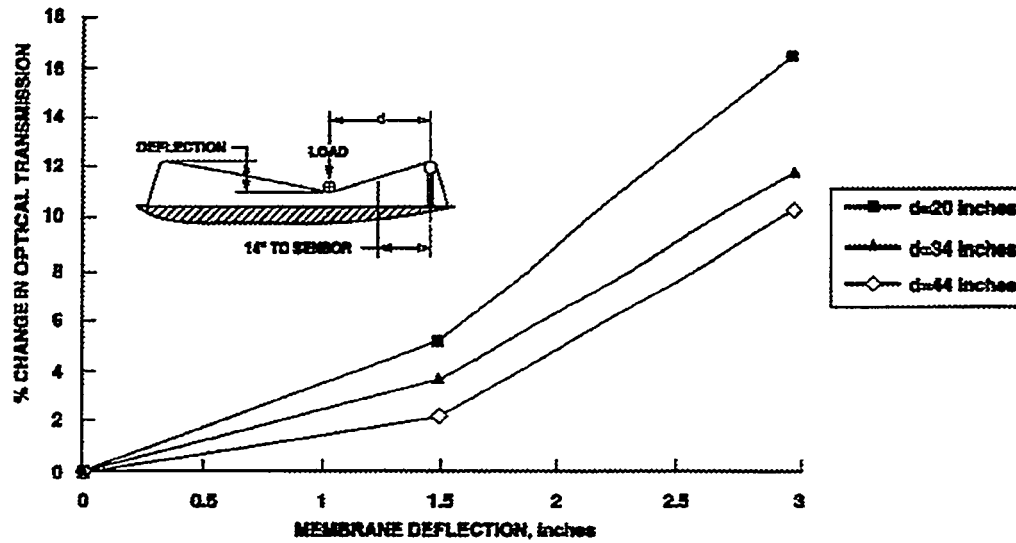
Figure 1: Change in optical transmission (vertical axis) relative to deflection or displacement of laminate membrane (horizontal axis)

STRAIN RESPONSE OF EMBEDDED FIBER-OPTIC SENSORS
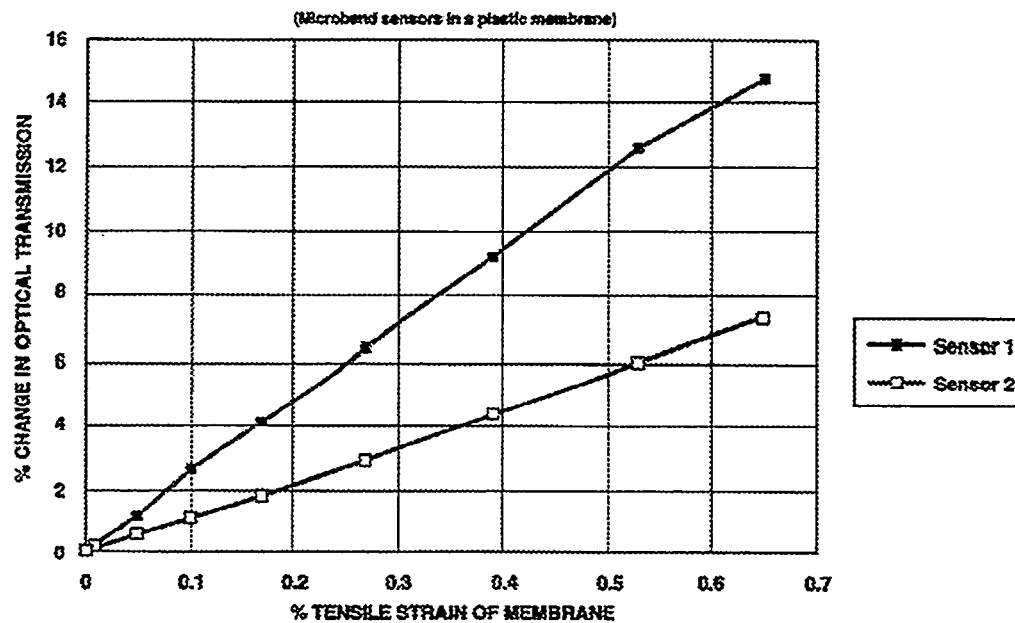
Figure 2: Change in optical transmission (vertical axis) relative to strain at different locations on the membrane relative to position where load is applied (horizontal axis)

Geombrane with Incorporated Optical Fiber Sensors
Approximate Size: 3 m x 30 m

two bands of optical fibers
and sensors with 1.5 meter
separation. Each band will test
several types of strain sensors
in parallel

Plan View of the Structural Elements of tthe Test Cell
without granular materials of the cover and infilling

apron of infill

1 to 1.5 m cover of soil and simulated
landfill cover material above
the geomembrane with sensors

Plan View of the Cover and Cell Infill
above and within the Structural Elements of the Test Cell

Figure 3: Elements of the Conceptual Design for the SMART Geomembrane Test Cell

Figure 4: Cross-Section of the Field Test Facility Showing Two Cells to Test General and Local Subsidence

General Subsidence Cell

•Subsidence will be simulated either by
controlled removal of liquid from a buried fuel
bladder or vacuum removal of a sand layer within
the fill. Use of fuel bladder would permit several
cycles of subsidence to be studied
•Constitutive modeling suggests that at 5%
axial strain shear banding develops in the
geomembrane indicating onset of failure.
Al-coated glass fibers fail at approximately 5%
axial strain
•Numerical models(ABAQUS) suggest that
approximately 15 cm of displacement of the
geomembrane during subsidence in this test
cell will result in 5% axial strain.

Localized Subsidence Cell

•Subsidence will be simulated by collasping foam
forms, vacuum removal of sand fill within objects
or opening trap doors to mimic collapse of waste
containers
•Criteria is similar to general subsidence cell.
Constitutive modeling suggests that at 5% axial
strain shear banding develops in the geomembrane
indicating onset of failure. Al-coated glass fibers
fail at approximately 5% axial strain.

7. Future Implementations

The initial implementations of the SMART geomembrane approach is to measure strains associated with subsidence. In some landfills, subsidence can be localized over collapsing waste drums and boxes. Our preliminary analysis of landfills in general suggests that significant subsidence occurs across the excavation slope of the landfill. This localization of subsidence is in response to the difficulty in compacting the fill and cover material over the excavation slope. For the initial implementation, we propose to demonstrate our SMART Geomembrane System to monitor subsidence and landfill cover deformation over the excavation slope. To accomplished this objective, we propose to place orthogonally two 4 by 50 m geomembrane strips top of the geomembrane included in the cover design at the top of the existing geomembrane components of a cover design (Figure 5). The optical fibers will exit the monitoring membrane where the designed cover membrane terminates under the apron of the cover or erosion barrier. To this system, we can add other optical fiber sensors to monitor fluid level, pore pressure and moisture content. For example, an array of fluid level sensors within the geomembranes of the liner can monitor leachate accumulation.
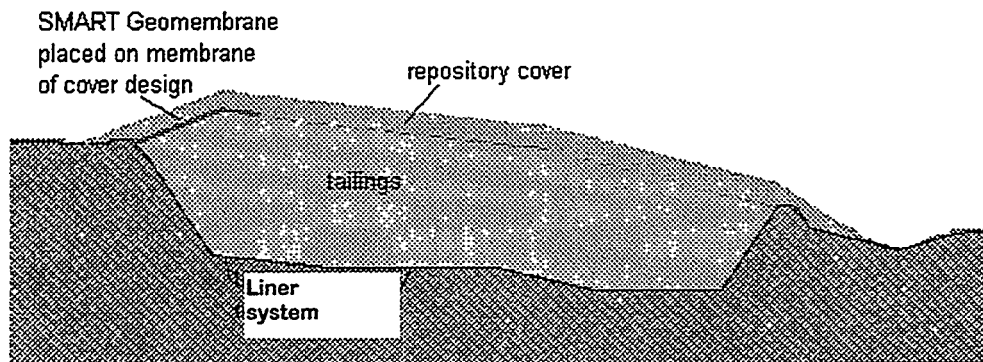
Figure 5: Cross-Section view of initial concept of implementing a SMART geomembrane monitoring system with an existing cover and liner design

8. References

Koerner, R. M. (1994) Designing with Geosynthetics, Prentice Hall, 783 p., Englewood Cliffs, New Jersey
Udd, E. editor, (1995) Fiber Optic Smart Structures, John Wiley and Sons, 671p., New York

GROUND PENETRATING RADAR INVESTIGATION
OF A FROZEN EARTH BARRIER

David Lesmes[1], David Cist[2], and Dale Morgan[2]

Introduction

In March of 1994, the U.S. Department of Energy Office of Science and Technology performed a subsurface ground freezing demonstration at the Scientific Ecology Group (SEG) test site in Oak Ridge, Tennessee. The objective of this demonstration was to evaluate the effectiveness of frozen soil barriers to isolate point sources of contamination by surrounding the contaminant by an impermeable wall of frozen soil. The engineering results of this study can be found in SEG's final report (SEG, Inc. 1995), and in the 1995 Proceedings of the International Containment Technology Workshop (Rumer and Mitchell 1995). The ground freezing demonstration at SEG extended from March to October of 1994. At the end of the demonstration, MIT's Earth Resources Laboratory was invited to test the utility of ground penetrating radar (GPR) to help characterize the structure and integrity of the frozen soil barrier. This paper reports the results of these investigations which were performed on November 5 and 6 of 1994.

Background

Geophysical imaging methods sense discontinuities in subsurface physical properties. The effectiveness of a geophysical investigation is determined by the contrast in the physical properties between the object of investigation and the surrounding material and the inherent resolution of the imaging method. Since the electrical properties of frozen soils are very different from the electrical properties of unfrozen soils, electrical methods of exploration, such as resistivity and ground penetrating radar, are effective methods for imaging frozen soil structures (Annan and Davis, 1976). In a separate study, ISOTRON, Inc., was contracted by DOE to conduct a non-intrusive characterization of the frozen soil barrier using an electrical resistivity technique (SEG, Inc. 1995). To augment these electrical resistivity studies, we were asked to perform a GPR investigation of the frozen soil barrier. In these investigations we used a high-frequency GPR system (225 MHz- 900 MHz) to map the thickness and continuity of the frozen soil barrier.

The velocity of radar wave propagation is dependent upon the dielectric constant of the medium (ε):

$$V = \frac{c}{\sqrt{\varepsilon}} ,$$

where c is the electromagnetic velocity in free space. The attenuation of radar waves is a function of the electrical conductivity of the medium (σ), the frequency of the propagating signal, and to a lesser extent, the dielectric constant of the medium. Radar wave attenuation is highest in media with high conductivity and the attenuation increases with increasing frequency. Practical estimates for the depth of penetration for GPR include not only the medium attenuation but also the frequency response and characteristics of the acquisition system (Davis and Annan, 1989).

The electrical properties of water saturated and frozen soils can be estimated using effective media theories. The Hanai-Bruggeman (H-B) equation is an effective media model that has been widely used to predict the electrical properties of porous media (e.g., Sen, et al 1981; Samstag 1992; Greaves, et al 1996).The H-B equation gives the following result for the complex dielectric constant (ε^*) of a water saturated soil:

----

[1]Boston College, Department of Geology and Geophysics, Chestnut Hill, MA 02167-3835, (617) 552-0839, lesmes@bc.edu.

[2]Earth Resources Laboratory, Department of Earth, Atmospheric, and Planetary Science, Massachusetts Institute of Technology, 42 Carleton Street, Cambridge, MA 02142, (617) 253-8027, cist@erl.mit.edu, morgan@erl.mit.edu

$$\varepsilon^* = \varepsilon_w^* \phi^m \left(\frac{1 - \varepsilon_g^*/\varepsilon_w^*}{1 - \varepsilon_g^*/\varepsilon^*} \right)^m$$

where

$$\varepsilon^* = \varepsilon + i\frac{\sigma}{\omega} \ .$$

ϕ is the volume fraction of the pore solution, m is the cementation index, and subscripts g and w refer to the soil grain and the pore solution, respectively. The same mixing formula can be used to compute the electrical properties of frozen soil, in which case the complex dielectric constant of ice is substituted for the complex dielectric constant of water (ε_w^*).

Table 1 lists the electrical properties of groundwater, ice, soil, and frozen soil. Also listed in this table are the electromagnetic velocities for these materials. The soil properties are computed using the H-B equation, assuming a soil porosity of 30 percent, a quartz grain dielectric constant of 4.5, and a cementation index of 2 (typical for rocks and soils). Ground water conductivities can range from 10^{-3} S/m to 5 S/m. We have chosen an average ground water conductivity of 0.1 S/m for this example.

Table 1. Electrical properties of ground water, ice, soil and frozen soil.

Material	$\varepsilon/\varepsilon_0$	σ (S/m)	v (m/ns)
Ground Water	78	0.1	0.03
Ice	3.1	10^{-7}	0.17
Soil	14	0.009	0.08
Frozen Soil	4.0	1.7×10^{-8}	0.15

The object of this experiment was to exploit the contrast in the electrical properties of ice and water by using ground penetrating radar to map the structure and continuity of the frozen soil barrier. Electromagnetic waves in frozen soil should be faster and attenuate less than in water saturated soil. Furthermore, the interface between the frozen soil (small ε) and the unfrozen soil (large ε) should be marked by a strong reflection and rapid signal attenuation. Variations in the amplitude and continuity of the reflectors should provide information as to the uniformity of the frozen soil barrier.

GPR is similar to seismic reflection in that a series of reflections are recorded as a function of time. A velocity must be assumed to transform these two-way travel times into depths. In the following analysis we have used the velocity of ice to make this transformation. This is an upper limit for the true velocity of the frozen soil and therefore the depth estimates in Figures 4 and 5 are maximum depths. Slower formations (i.e. unfrozen soil) will have true depths (or thicknesses) that are less than the estimated depths.

Data Collection and Processing

Figure 1 is a schematic diagram of the ground freezing system used in this demonstration. A plan view of the frozen soil barrier is shown in Figure 2. The interior of the barrier was heated and thus unfrozen. This unfrozen soil was removed prior to our arrival, leaving the walls of the frozen soil barrier exposed. The excavated interior of the frozen pit was approximately 9 m long, 6 m wide, and 4.5 m deep. The orientation of the walls of the pit reflected the orientation of the cooling pipes which were used to freeze the soil, such that the NW and SE walls were nearly vertical and the NE and SW walls were inclined at an angle of approximately 45 degrees.

The native soil into which the freeze pipes were placed consisted of fine red clay with chert fragments, typical of the Oak Ridge area. Therefore, except for the SE wall, the barrier consisted of frozen native clay. An artificial sand channel was constructed on the SE side of the barrier. The position of the sand channel in the SE wall is shown in Figure 3. The sand channel extended from the face of the SE wall to a distance of approximately 4.5 m to 6 m away from the wall.

Radar profiles were measured on all four of the exposed walls and along the floor of the frozen pit. These profiles were collected using a constant off-set between the transmitter and receiver and using both the 900 MHz and the 450 MHz antennas. Horizontal scans of the walls

were made by moving the antennas along a profile that was approximately 1.5 m from the surface of the pit. This corresponds to line A A' for the SE wall illustrated in Figure 3. Vertical profiles were also collected at the midpoints of the SE and the NW walls. This corresponds to line B B' for the SE wall in Figure 3.

A variety of data processing procedures can be applied to the raw radar data. In the following display of results the data have been high-passed filtered to remove a low-frequency electromagnetic transient component from the recorded signals and a constant gain of 200 has been applied to the data. This minimum amount of processing was chosen to preserve the amplitude information both from trace to trace and with time. In this format, it is easy to recognize the fall off in signal amplitude which we associate with the back of the frozen barrier (Figures 4a and 4b).

The constant gain processing is useful for imaging the structure of the back of the barrier (late time arrivals), however, early time arrivals of high amplitude are over amplified and therefore clipped at a constant (maximum) amplitude. To better resolve the internal structure of the barriers, we have also processed the data using an exponential gain function which corrects for spreading losses and intrinsic attenuation(Figures 5a and 5b). The exponential gain function increases with increasing travel time (or depth) but it is constant from trace to trace.

Results

Figure 4a is the horizontal radar profile measured across the SE wall using the 900 MHz antennas. This profile was collected across the sand channel, along line A to A' in Figure 3. The sand channel is very distinctive in this profile as it is marked by late arriving signals with strong amplitude. The clay sections of the SE wall are very similar to the clay sections measured on the other clay walls. Assuming a constant ice velocity for both the sand and the clay, the sand has an apparent thickness of approximately 4.5 m, whereas the clay has an apparent thickness of approximately 1.7 m. The actual thickness of these zones depends upon the true velocity of the clay and sand.

In addition to the horizontal profiles, we also collected vertical profiles on the SE and the NW walls. The vertical profiles extended from the surface of the pit to the floor of the pit, as illustrated in Figure 3 for the SE wall (B to B'). Figures 4a and 4b are the horizontal and vertical profiles, respectively, measured on the SE wall. The sand channel, marked by late arrivals of high amplitude, is evident in both the horizontal and the vertical sections. Figure 5a and 5b show these same sections plotted using an exponential gain function. The internal structure of the sand channel is better resolved in the exponential gain section. A large diffractor is located at an apparent depth of 3 m in the sand channel. Also, reflections from the bottom of the channel cause the characteristic triangle which extends to a depth of approximately 1 m into the section. The observed heterogeneity in the clay sections may indicate heterogeneous zones within the frozen clay or they may be artifacts caused by the metallic cooling pipes.

By measuring reflections as a function of the transmitter and the receiver separation about a common mid-point, it is possible to determine the true velocity of the medium and therefore the true depth to the reflector (e.g., Yilmaz 1987). We collected common mid-point (CMP) data on both the sand section of the SE wall and on the NW clay wall. Several reflectors were evident in the CMP data collected on the SE "frozen sand" wall. The computed velocities for these reflectors were all in the range of 0.15 m/ns, which is in good agreement with the estimated velocity for frozen soil (Table 1). One major reflector at a shallow depth was resolved in the CMP data measured on the NW wall. The velocity of this layer was computed to be 0.09 m/ns which is much less than the velocity of ice or frozen soil. It may be that just the near surface of the clay is unfrozen and therefore has a slow velocity. However, if this was indeed the case then a higher velocity head wave should have been detected. One possible interpretation is that the clay may not have been completely frozen. It was evident in the field, that the water in the clay wall froze in heterogeneous clumps, which is in contrast to the sand wall where the freezing was homogeneous. Another possibility is that the two-phase mixing formula may be inappropriate for clay which has a very large specific surface area. Even a small amount of bound water (one monolayer) on the surface of the clay particles can cause significant enhancements in the dielectric response. In which case, three phase mixing models are required to properly predict the dielectric response of the material (e.g., Samstag, 1992).

Conclusions

The radar measurements of the sand channel in the SE wall indicate that it has a radar velocity of 0.15 m/ns, which is the predicted velocity of frozen soil, and that the sand channel is frozen to a distance of approximately 4.5 m from the face of the SE wall. A relatively large object, which causes a characteristic diffraction, is off-set a distance of approximately 3 m from the face of the sand channel.

The NW clay wall had a measured radar velocity of 0.09 m/ns which is much slower than the velocity of ice and frozen soil. The freezing in the clay may be more heterogeneous than the freezing in the sand, which would reduce the radar velocity in the clay, and perhaps cause the clay to be more permeable to non-aqueous phase solvents. Alternatively, bound water on the surface of the clay particles may lead to an enhancement in the dielectric response which would result in an over estimate of the unfrozen bulk water in the clay. More studies on the electrical and transport properties of frozen clays are required to better understand these problems. Based on the amplitudes of the radar signals it appeared that the "frozen clay" walls were between 1.5 m and 2.7 m thick. Most of the energy was concentrated in the first 20 ns of signal (1.5 m), however, strong reflections were detected up to times of approximately 35 ns (2.7 m).

In the application of any geophysical technique it is important to understand the limitations of the data, particularly in terms of the resolution and uniqueness of the method. GPR provides relatively high resolution, however, it is inherently non-unique because there is an ambiguity between the medium velocity and the depth to a reflector. If absolute constraints are available at fixed points, then the interpretation can be considerably improved. For example, if we knew the actual thickness of the ice wall at a fixed point, or the true velocity structure, then we could more accurately map variations in the ice wall thickness away from that point.

GPR can also be used for monitoring changes in the subsurface properties. For example in this application, GPR could be used to monitor the distribution of ice, as the ice wall is forming. In any non-destructive testing of barriers, it is best to design and implement the testing apparatus as an integral part of the barrier. In this experiment, for example, monitoring wells could have been installed so that cross-borehole radar measurements could be made both within the frozen barrier and across the barrier, and used in conjunction with continuously recording TDR sensors.

References

Annan, A. P., and J. L. Davis, Impulse radar soundings in permafrost, *Radio Science*, 11, 383-394.

Davis, J. L., and A. P. Annan (1989), Ground-penetrating radar for high-resolution mapping of soil and rock stratigraphy, *Geophysical Prospecting*, 37, 531-551.

Greaves, R. J., D. P. Lesmes, J. M. Lee, and M. N. Toksöz (1996), Velocity variations and water content estimated from multi-offset, ground-penetrating radar, *Geophysics*, 61(3), 683-695.

Rumer, R. R., and J. K. Mitchell (1995) Assessment of Barrier Containment Technologies: A Comprehensive Treatment for Environmental Remediation Applications, Proceedings of the 1995 International Technology Workshop, Baltimore, MD.

Samstag, F. J., 1992, An effective-medium model for complex conductivity of shaly sands in the salinity, frequency, and saturation domains: PhD thesis, Texas A&M University.

Scientific Ecology Group, Inc. (1995) Final Report: Demonstration of Ground Freezing Technology at SEG Facilities in Oak Ridge, TN.

Sen, P. N., C. Scala, M. H. Cohen, 1981, A self-similar model for sedimentary rocks with application to the dielectric constant of fused glass beads, *Geophysics*, 46, 781-795.

Yilmaz, O. (1987), *Seismic Data Processing*, Society of Exploration Geophysicists, Tulsa, OK.

Acknowledgments
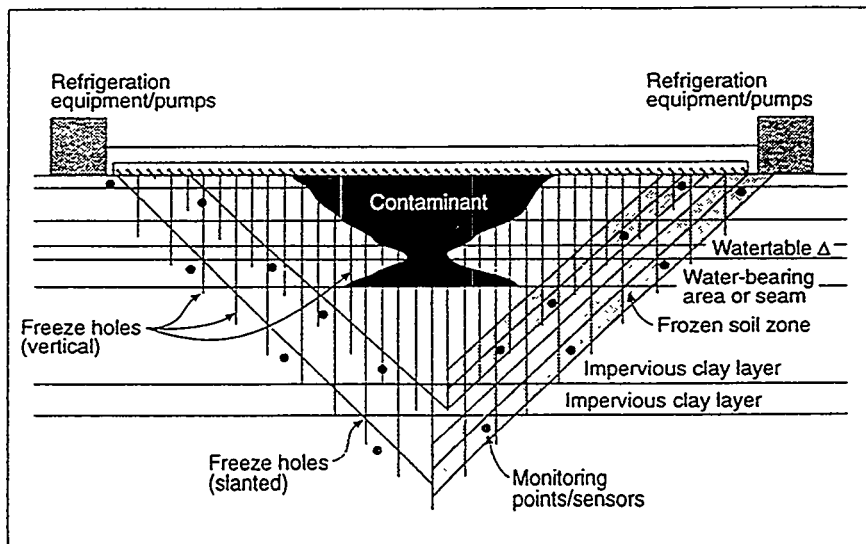
Figure1. Configuration of demonstration of ground freezing system at Oak Ridge, TN. (from Rumer and Mitchell 1995).
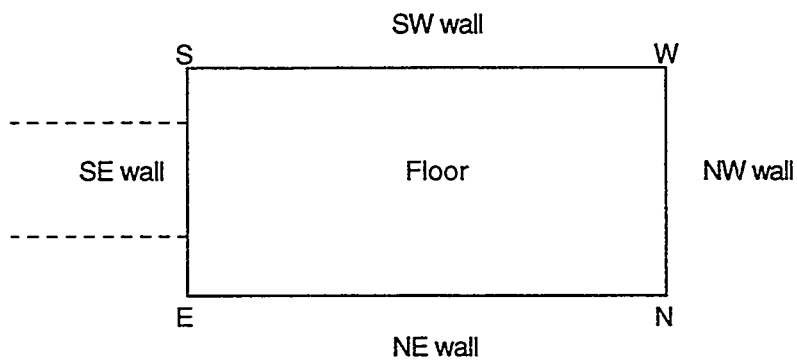
Figure 2. Plan view of frozen pit. Sand channel in SE wall is indicated by dashed lines.
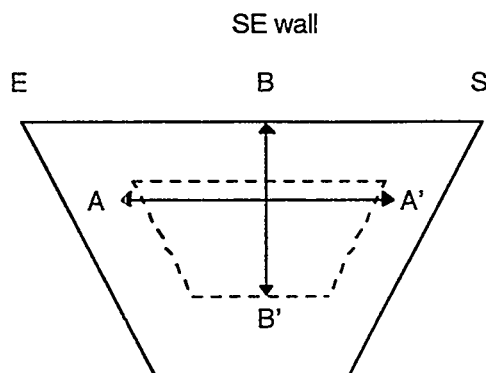
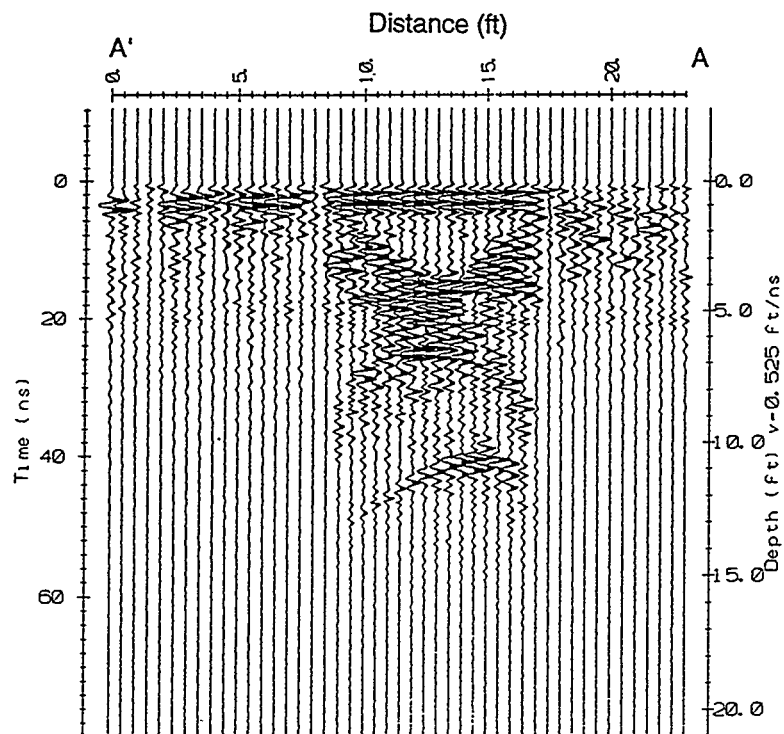Figure 3. Cross-sectional view of SE wall. Position of sand channel is indicated by dashed lines.
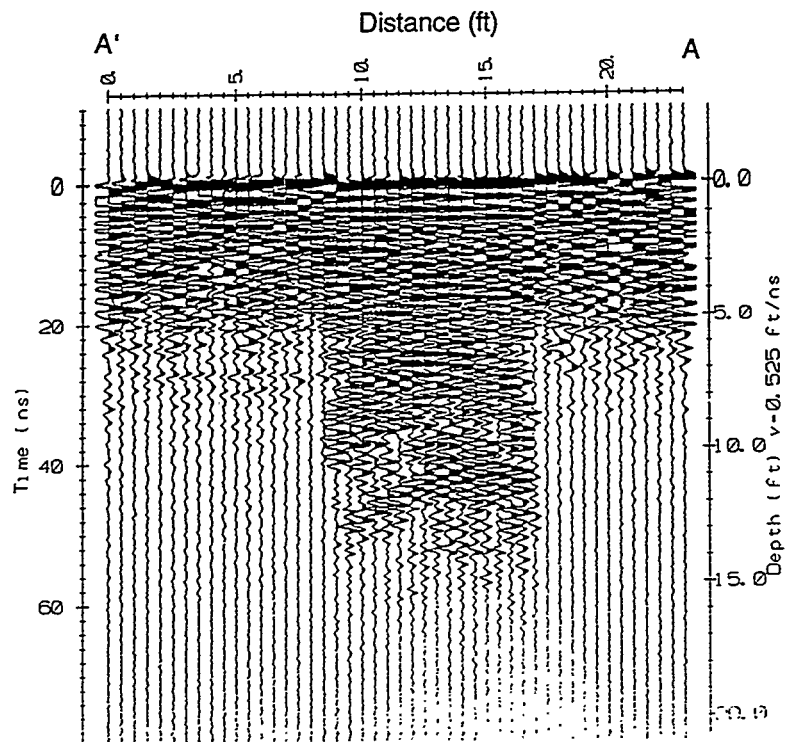
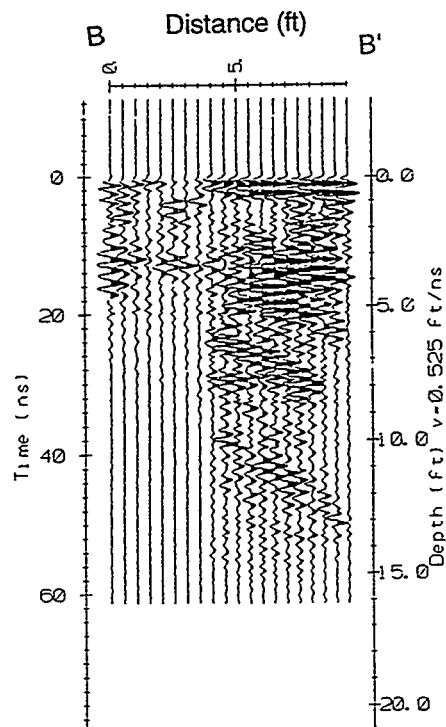Figure 4a. Radar profile (900 MHz) of the SE wall measured horizontal to the surface at a depth of 1.5 m. Constant gain of 200.
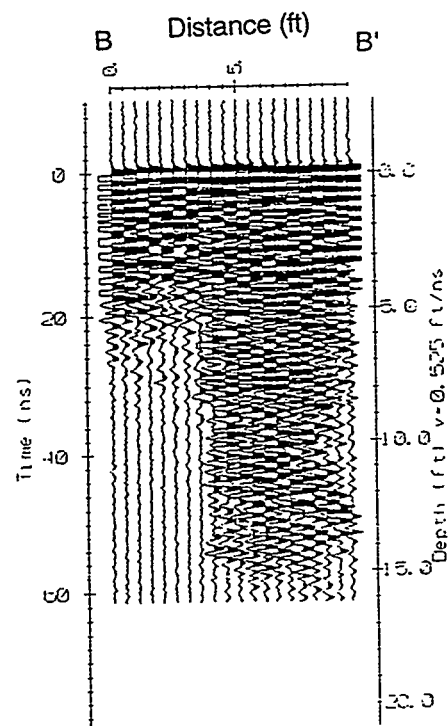
Figure 4b. Radar profile (900 MHz) of the SE wall measured vertical to the surface. Constant gain of 200.

Figure 5a. Radar profile (900 MHz) of the SE wall measured horizontal to the surface at a depth of 1.5 m. Exponential gain.

Figure 5b. Radar profile (900 MHz) of the SE wall measured vertical to the surface. Exponential gain.

PRINCIPLES AND OBJECTIVES OF CONTAINMENT VERIFICATION AND PERFORMANCE MONITORING AND TECHNOLOGY SELECTION

David K. Reichhardt[1], Andrea T. Hart[2], J. David Betsill[3]

Abstract

While a number of technologies or methods of subsurface imaging and monitoring exist, most require some adaptation to meet the site-specific objectives of a particular in situ waste containment/stabilization verification and monitoring program. The selection of methods and their site-specific adaptation must be appropriate for the remediation and be based on sound, scientific principles. Given this, specific information about the site and the objectives of the containment or remediation are required to design and implement an appropriate and effective verification and monitoring program, which must be considered in the initial stages of the project.

Site and technology information that must be considered and how it affects the selection and adaptation of monitoring technologies is presented. In general, this information includes the objectives of the containment or remediation, the verification and monitoring systems, and the physical properties of the site and the waste containment/stabilization system. The objectives of the containment or remediation and the verification and monitoring system must be defined to provide a goal for the technology developer's design. Knowledge of the physical properties of the site and the waste containment/stabilization system are required to ensure the proper technology is selected. A conceptual framework and examples are given to demonstrate the impacts of these aspects on technology selection.

Introduction

Several general site needs or objectives are presented as possible drivers for verification and monitoring systems. These include short-term containment of a waste form, long-term containment of a waste form, and in situ remediation or treatment. Each of these in situ remedial alternatives require different verification and monitoring approaches. These approaches range from imaging the subsurface, monitoring potential[4] distributions, and direct sampling of the subsurface materials. The primary techniques for subsurface barrier verification and monitoring include imaging, mapping potential distributions, and direct sampling.

Objectives of Site Containment and/or Remediation

The ultimate drivers for determining the verification and monitoring strategy used at a site where some form of in situ containment option is to be applied are the final objectives of the in situ containment. These may range from short-term isolation of a waste form during a removal activity to long-term

---

[1]David K. Reichhardt, MSE Technology Applications, Inc., P.O. Box 4078, Butte, MT 59702, (406) 494-7195, dfawcett@buttenet.com

[2] Andrea T. Hart, MSE Technology Applications, Inc., P.O. Box 4078, Butte, MT 59702, (406) 494-7410, ahart@buttenet.com

[3] J. David Betsill, Sandia National Laboratories, Mail Stop 0719, P.O. Box 5800, Albuquerque, New Mexico 87185

[4] In this text, *potential* is used to describe pressure differential of a selected media, for example, groundwater or soil gas.

isolation of waste from the surrounding environment. Other objectives may include an in situ remediation such as with the use of reactive or permeable barriers. The verification and monitoring must be designed such that the objectives of the in situ containment can be shown to be initially met (i.e., verification) and is maintained over time (i.e., monitoring). For example, a containment system designed for short-term use may not require long-term monitoring, yet some form of as-built information demonstrating containment continuity and proper placement as specified in the design would be useful; whereas a system designed for long term isolation of a contaminant would require emphasize measuring on changes in containment performance addressed through monitoring.

With respect to containment/remediation objectives the above, subsurface barriers can be defined by either a specified set of dimensions, or by a change in the transport and fate of the contaminants in the subsurface. If the objective of the subsurface barrier emplacement is to install a feature with some specified set of dimensions and continuity, then ideally, the verification process will produce some form of image of the structure. (The concept of imaging is discussed in Section 3.1) If the objective is to alter the fate and transport of the contaminants, initial verification may be difficult, however, monitoring over time will indicate if the fate and transport processes that control the movement of contaminants has been altered as planned. Imaging may aid in the assessment of the changes in fate and transport processes by defining the changes in the physical system for modeling purposes.

To adequately verify the emplacement of and monitor the performance of a containment or remediation system, some measurable characteristics of the system must be defined to assess its effectiveness. For the different general objectives given in this paper, some possible measurable characteristics will be discussed.

Short-Term Containment of a Waste Form

Short-term containment types of subsurface barriers may be employed during retrieval and/or for treatment of waste in the subsurface. The purpose for such structures is often to limit contamination of additional soils by the accidental spillage of waste during removal. For example, if drums of waste are being excavated, a barrier system may prevent contamination of additional soil in the event a drum is accidentally ruptured. Other short-term containment systems may be designed to provide excavation shoring, without which over excavation may be required for slope stability.

For these types of short-term applications, verification of the continuity and dimensions of a barrier may be adequate. Additionally, some data demonstrating the effectiveness of the barrier system upon completion of the removal activity may be required.

Long-Term Containment of a Waste Form

Long-term containment systems are often proposed for sites where no removal action is planned for the foreseeable future either because the risk involved with exposure to workers is much greater than the risk of leaving the waste in the ground or the cost of removing the waste is greater than the potential cost of the risk of leaving it in place. The purpose of these types of structures is often to prevent further release of contaminants from a source term into the subsurface. Long-term containment of a waste form may require initial verification that the containment system has been installed as planned; however, demonstration that it is performing as planned will require monitoring changes in the system over time.

In Situ Treatment of Contamination

Barriers in which the planned purpose is in situ treatment typically require a flux of contaminated media through the barrier. Ideally, the contaminated media will not flow around the barrier, nor will the barrier significantly impede the flow of contaminated material. To evaluate the performance of such a system,

an understanding of the flow regime prior to the installation of the treatment system is required as well as an analysis of the impacts to the flow regime after installation of the treatment system. Such a system will require verification that the system has been emplaced as designed and that it is functioning properly.

A properly functioning treatment system may be characterized by up- and down-gradient contaminant concentrations and the rate at which these concentrations change over time. In addition to contaminant concentrations, the changes in the hydraulic head over time can give an indication of the performance of such a system.

Verification and Monitoring Systems

As described to in Section 2, verification and monitoring are primarily defined by the time at which they are conducted although, verification tends to be weighted more toward imaging types of technologies and monitoring tends more toward detecting changes in the system performance. Some of the technologies used for verification and monitoring are briefly discussed in the following sections. These discussions are focused on the principles and not necessarily on specific methods. The principles on which verification and monitoring can be based include analysis of subsurface property distributions, potential distributions, and material distributions. The changes in these distributions can be used to assess the existence and performance of the subsurface containment and/or remediation system.

Property Distributions

The transport of contaminants through the subsurface is governed by a number of material properties which include, but are not limited to, intrinsic permeability, soil chemistry, soil structure, and fluid properties (chemistry, density, viscosity, etc.). The distribution of these properties in the subsurface will control the fate and transport of contaminants in the subsurface. Images of subsurface structures can be considered maps of the property distributions. Property distribution maps are valuable tools, yet they require a definition of the relationship of the barrier to the property. For example, a subsurface barrier may be defined as the portions of the soil with 60% grout and 40% soil matrix. A map of the subsurface this composition would result in an image of the barrier. The barrier may also be defined in terms of other soil properties such as permeability. A map of the permeability distribution (given some defined permeability for a barrier) would also constitute an image of the barrier.

To define the extent of a barrier based on a change in the distribution of the transport and flow parameters of the soil requires insight into how the soils change when a barrier is emplaced (Borns, 1995). When a grout material such as cement bentonite is injected into the subsurface, the boundary between grouted and ungrouted soil cannot be assumed to occur entirely within some small discrete zone. This is due to several factors. The effective radius of the grout injection is not constant over the length of the injection due to changes in soil properties, the injection pressure and grout velocity change with respect to the distance from the injection port (the change will result in a net decrease in both pressure and velocity), and residual fluids from the grout will permeate the formation (the permeation distance is also variable depending on the soil type). These factors lead to permeability changes in the form of filling of pore space by the grout and the destruction of the soil matrix by the grouting action. Other changes include the introduction of additional fluids into the formation and changes in the pore water chemistry from the introduction of new fluids. The conceptual grout panel and permeability distributions shown in Figure 1 illustrate how the boundary between grouted and ungrouted soil might actually exist.
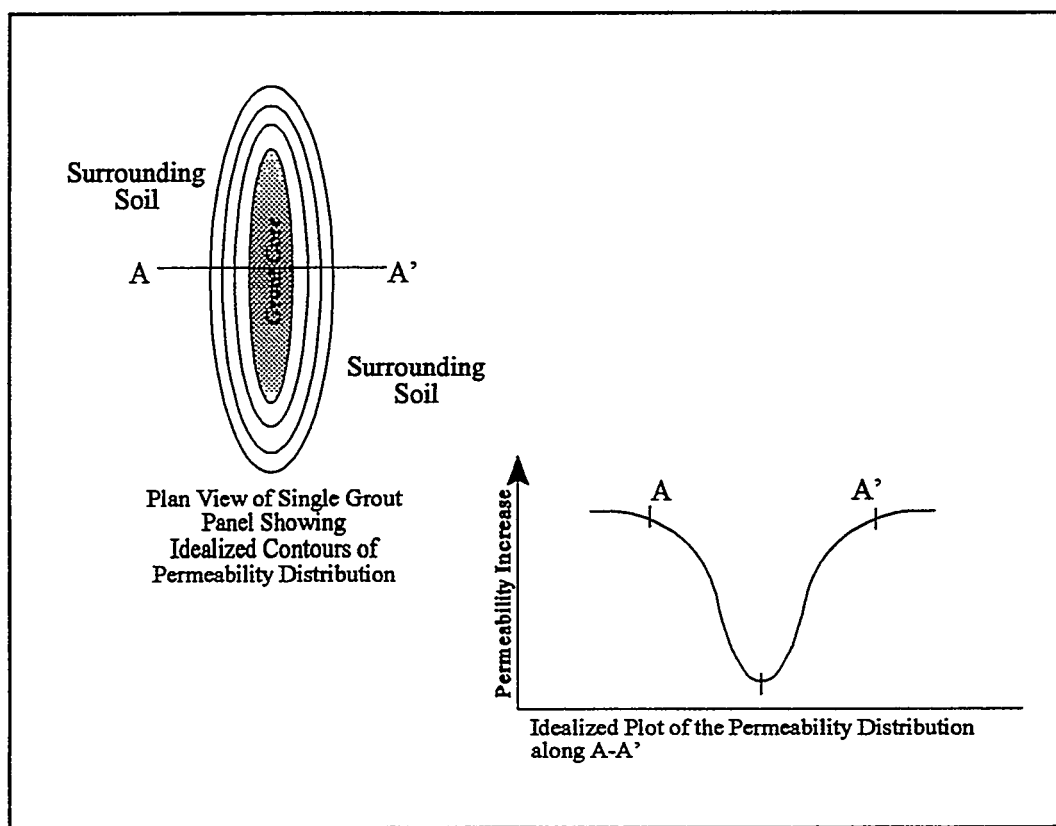
Figure 1. Plan view and plot of conceptual permeability distribution for grout panel.

Property distribution maps or images have been suggested for in the verification stages of a subsurface barrier project. Often the property distribution map is made by geophysical measurements of the subsurface. A variety of geophysical methods exist which can map changes in physical properties such as electrical resistivity, dielectric properties, and seismic velocities. While these properties do not directly relate to properties affecting the flow fields, changes in these properties are a result of changes in the properties affecting the flow fields.

A considerable amount of research has focused on understanding these relationships. Poley, *et al* (1978) presented data on very high frequency dielectric measurements for borehole formation analysis. Sen, *et al* (1981) presented a model for the dielectric constant of sedimentary rocks based on studies of fused glass beads. Feng and Sen (1985) presented a model of conductive and dielectric properties of partially saturated rocks. Olhoeft (1987) studied the electrical properties of soils for a frequency range from 10^{-3} to 10^{+9} Hz. Knight and others (1987, 1991) and Endres and Knight (1991) have studied the relationship between dielectric properties, resistivity, and seismic velocity for a series of sandstones in an attempt to develop relationships between these properties and the porosity and percent of pore fluid in the rocks.

These studies have focused primarily on naturally occurring sedimentary rocks. Many of the grout types proposed for use are hydraulic cements (i.e., Portland Cement based) or innovative new chemical grouts (polymers, colloidal silica, paraffin, etc.). Very little data exists for developing relationships between the electrical properties and seismic properties of the grouts and the fate and transport properties. However, the properties of the grouts in relation to the host soils should be determined in order to properly select the geophysical methods used to map the barrier. Without a significant contrast in the physical properties between the grout and host soil, geophysical methods cannot be used to develop an image of the subsurface.

The highest resolution property distribution maps are attained when the residual or difference between the property distribution before grouting and after grouting are calculated. This effectively highlights only the change, and all other aspects of the distribution which remains constant are removed from the image. Therefore, it is desirable to collect data before and after injection using the same methods from the same locations. Other factors which affect resolution include control of measurement locations, and the ability of the method to resolve small changes in a property.

Potential Distributions

The distribution of soil gas and groundwater potential in the subsurface can be used to determine contaminant transport paths within and around a subsurface barrier. Additionally, this information can be used to determine material permeability and/or detect zones of low permeability in the barrier, which could be considered as a leak.

Because a subsurface barrier is a three dimensional (3D) object in a 3D potential field that changes with time, the data must be collected in three dimensions as a function of time. As soils and grouts go through wetting and drying cycles, the intrinsic permeability of each will change (Wilson, 1995). Wetting and drying cycles may be caused by water driven from the grout during curing and by seasonal changes in the water table and soil moisture levels. Nested, or multi level monitoring systems coupled with automatic data loggers can be used to acquire sufficient data in three dimensions and as a function of time for a proper evaluation of the potential distribution in and around the subsurface barrier.

Potential distribution monitoring systems are particularly well suited for long-term monitoring systems. They can be passive systems which do not require energy to be put into the system, or as active systems which require some form of energy put into the system as with the geophysical methods. This may be important when long-term monitoring costs and logistics are considered.

To effectively design a passive system which monitors changes in potential field, predictive models should be developed to ensure adequate sampling points exist and at the same time ensure that the system is not over sampled. It should be remembered that every sampling point may require a borehole, which will provide a potential transport path for contaminants. This is true for many of the geophysical methods if used from boreholes as opposed to the ground surface.

Material Distributions

Material distributions can be obtained from soil samples, groundwater samples, and soil gas samples. Soil sample data may be used to map the presence of grout material in the soil, which will define the extent of the barrier. Groundwater chemistry data can be used to monitor for contaminant concentrations or liquid tracers, this data may be an indicator of how well the barrier is functioning. Soil gas samples can be used to monitor for vapor phase contaminants or for gaseous tracers, as with the groundwater chemistry data, this data may also be an indicator of barrier performance.

The soil composition data is perhaps the most straight forward data set to use. This data can be used to directly determine the penetration or mixing of the grout with the soil. Some destructive sampling may be necessary to provide "ground truth" data for correlation to other verification and monitoring methods. However, this may require destructive sampling of the barrier, which may not be desirable.

Groundwater chemistry can be collected without compromising the barrier system by planing the placement of sampling points outside of the barrier. Groundwater chemistry can be used to develop fate and transport models. The chemical analysis may include analysis for specific tracers injected into the subsurface to determine if the barrier is leaking, or for contaminant concentrations to monitor for leaks or treatment of groundwater by a permeable or reactive barrier system.

Soil gas monitoring systems can also be used in similar fashions as groundwater monitoring systems. Leaks in a barrier can be detected and located by the presence of gas phase tracers or contaminants.

A limitation of direct sampling as a means of verification and monitoring is in the number of samples required to properly characterize an area. Both the indirect physical property measurements (geophysical methods) and the potential field measurements tend to average the data over an area determined by the sample spacing. The data obtained from direct measurements can be averaged over an area defined by the sampling frequency, but this requires statistical considerations to the representativeness of the data. The development of variograms and the use of krigging are often employed for this purpose.

Discussion

Several general site containment/remediation needs were presented as possible drivers for different verification and monitoring systems. These include short-term containment of a waste form, long-term containment of a waste form, and in situ remediation or treatment. Each of these in situ remedial alternatives will require different verification and monitoring approaches. These approaches range from imaging the subsurface, monitoring potential distributions, and direct sampling of the subsurface materials.

Additionally, some of the basic principles of subsurface barrier verification and monitoring were also presented. These addressed issues of imaging, mapping potential distributions, and sampling. Imaging is best achieved using geophysical principles coupled with the results of direct sampling. Passive potential field monitoring was presented primarily as a means of long-term monitoring of a system; however, it can be used in an active mode (i.e., pump test, etc.,) to verify the initial integrity of a barrier system. Direct sampling was presented as a means of verifying barrier performance.

While a number of technologies exist to addresses each of these issues, a fundamental understanding of when to apply a basic principle to meet the needs of a specific site must be addressed. Each of the verification and monitoring principles presented can be adapted to meet the site specific verification and monitoring needs given an understanding of the needs and principles of the technology. Such an understanding will also aid in the selection of the appropriate technologies for the site.

Conclusion

Verification and monitoring are integrally tied to the objectives of the subsurface containment and/or remediation. A clear statement of the objectives is the basis for planning the verification and monitoring. Additionally, the physical system in which the verification and monitoring system is to be deployed must be understood to properly select and adapt the verification and monitoring methods. Therefore, in order to develop a verification and monitoring plan which meet the objectives of the remediation system and functions in the physical system present at the site, the verification and monitoring must be considered in the initial stages of the project development. Subsequently, a site-specific verification and monitoring system can be designed for optimum effectiveness and performance.

References

Borns, D.J., 1995, Geophysical characterization of subsurface barriers, Sandia National Laboratories, New Mexico, Sandia Report SAND95-1461.

Endres, A. L., and R. J. Knight (1991) The effects of pore-scale fluid distribution on the physical properties of partially saturated tight sandstones. J. Appl. Phys. 69(2), 1091-1098.

Feng, S., and P. N. Sen (1985) Geometrical model of conductive and dielectric properties of partially saturated rocks. J. Appl. Phys. 58(8), 3236-3243.

Knight, R. J. and A. Nur (1987) The dielectric constant of sandstones, 60 kHz to 4 MHZ. Geophysics, 52, 644-654.

Knight, R. J. (1991) Hysteresis in the electrical resistivity of partially saturated sandstones. Geophysics, 56(12) p. 2139-2147.

Olhoeft, G. R. (1987) Electrical properties from 10^{-3} to 10^{+9} Hz — Physics and Chemistry: in *Proc. of the 2nd Int'l. Symp. on the Physics and Chemistry of Porous Media*, Schlumberger-Doll Research, Ridgefield, CT, October, 1986, Am. Inst. Phys. Conf. Proc. 154, J.R. Banavar, J. Koplik and K. W. Winkler, eds., NY, AIP, p. 281-298.

Poley, J. Ph., J. J. Nooteboom, and P. J. de Waal (1978) Use of VHF dielectric measurement for borehole formations analysis. Log Anal., p. 8 -30

Sen, P.N., C. Scala, and M.H. Cohen (1981) A self similar model for sedimentary rocks with application to the dielectric constant of fused glass beads. Geophysics, 46, 781-795.

Wilson, L.G.; Lorne G. Everett; S.J. Cullen (1995) *Handbook of Vadose Zone Characterization and Monitoring*, p. 730. Lewis Publishers, Boca Raton.

ACOUSTIC TOMOGRAPHY AND 3-D RESISTIVITY IMAGING
OF GROUT FILLED WASTE CELLS

Frank Dale Morgan[1], David Lesmes[2], Chantal Chauvelier[1], Weiqun Shi[1]

Introduction

The Scientific Ecology Group, Inc., (SEG) was contracted by Martin Marietta Energy Systems, Inc., to demonstrate and evaluate four grout compounds for use in stabilizing radioactive waste trenches at the Oak Ridge National Laboratory (ORNL). The demonstration site was constructed at SEG's Gallaher Road test facility in Kingston, Tennessee. SEG's objectives in this project were to compare the effectiveness of the candidate grouts and grouting procedures to hydrologically isolate the waste contained within the trenches and to stabilize the trenches against subsequent subsidence. In a separate agreement with Martin Marietta Energy Systems, MIT was contracted to demonstrate the feasibility of using high-frequency acoustic tomographic imaging to evaluate the performance of the various grouts and grouting procedures, and to monitor the stability of the grouted test cells over time.

The test trench consisted of four contiguous cells, each 14' long x 12' wide x 12' deep. The native soil in which the test cells were constructed consisted of fine red clay which is typical of the Oak Ridge area. A plan view of the test cells is shown in Figure 1, and a cross-sectional view of one of the cells within the trench is shown in Figure 2. Each cell within the trench was filled with approximately 75 cubic yards of simulated waste. The simulated waste, which included 55 gallon drums and HEPA filters, consisted of approximately 35% metal, 15% wood, and 50% paper/plastic. After the cells were loaded with the simulated waste, the trench was covered by three feet of soil to grade, to duplicate the trench configuration commonly found at ORNL.

Each cell was filled with a different type of grout. Table 1 lists the grout type for each cell, as well as the seismic velocity (Vp) and electrical resistivity (ρ) of the dry and water saturated grouts. Cells 1, 2, and 3 were grouted using a low-pressure slotted pipe permeation grouting procedure with a maximum pressure of 75 psi. Cell 4 was grouted using high pressure multi-port grout injection but was not accessible for this study.

The initial permeation grouting of Cells 1, 2, and 3 turned out to be ineffective. The cells were therefore regrouted all with a microfine cement. Because of these technical problems the infiltration tests, which were initially designed to test the hydraulic conductivity of the cells, were never performed.

Table 1. Seismic velocity (Vp) and electrical resistivity (ρ) of the dry and water saturated grouts used for each cell. Cells 1, 2, and 3 were re-grouted using microfine cement.

Cell	Grout Type	Vp (m/s) dry	Vp (m/s) wet	ρ (Ω-m) dry	ρ (Ω-m) wet
1	Portland 1 cement with fly ash and bentonite	2030	2350	519	40
2	Microfine cement	2370	2470	912	6
3	Portland 3 cement	2390	2570	2550	26

[1]Earth Resources Laboratory, Department of Earth, Atmospheric, and Planetary Science, Massachusetts Institute of Technology, 42 Carleton Street, Cambridge, MA 02142, (617) 253-8027, morgan@erl.mit.edu, chantal@erl.mit.edu, shi@erl.mit.edu

[2]Boston College, Department of Geology and Geophysics, Chestnut Hill, MA 02167-3835, (617) 552-0839, lesmes@bc.edu

Geophysical Experiments

Recently, researchers at the Sandia National Laboratory have used cross-well seismic tomography to verify and monitor the emplacement of injected-grout subsurface barriers into native soils (Harding, 1994; Elbring, et al, 1995; Dwyer, 1995). The scale of these investigations was on the order of meters to tens of meters, which is much smaller than the cross-well surveys that are typically made in petroleum exploration. In these investigations velocity anomalies on the order of twenty percent were observed after grout injection.

A similar approach was used in the current study to (1) assess the effectiveness of the grout injection into the waste-filled cells, (2) attempt to monitor the invasion of fluid into the cells during the hydraulic tests, and (3) assess the structural stability of the cells over the duration of the experiment. In addition to the cross-well acoustic experiments, we also tested the feasibility of using electrical resistivity tomography, induced polarization, ground penetrating radar, and seismoelectric measurements to jointly image the waste cells. The results of the acoustic tomography and electrical resistivity imaging experiments are presented in this paper.

In addition to the frequency content of the transmitted waves, the following three factors affect the resolution of the tomographic images derived from the cross-well acoustic experiments: (1) the angular coverage of the area to be imaged, (2) the velocity structure of the subsurface, and (3) the algorithm used to invert the cross-well acoustic data. Elohi Geophysics, Inc., was subcontracted by MIT to collect the cross-borehole acoustic data. A DHT-1 high frequency (10 kHz) piezoelectric transducer was used as the down hole source, and high frequency hydrophones (15 kHz) were used as receivers. In these experiments the angular coverage was limited, because the depth of the boreholes was only 12 feet. Given the composition of waste in the cells, we were expecting to see velocity contrasts that could be as large as 200 to 300 percent. Most inversion codes cannot handle velocity contrasts greater than 20 percent. Therefore, new approaches of regularizing and optimizing the tomographic inversion code, to handle very large velocity contrasts, had to be developed and tested.

Results

Because of engineering changes instituted by SEG, we were unable to execute the monitoring experiment as originally planned. Rather, we have collected data after the original grouting of the cells, and then again after the re-grouting of the cells. It was clear from the seismic data, that the re-grouting of the cells had a significant impact on the structure and integrity of the cells. The initial grouting procedure was so ineffective that it was nearly impossible to propagate seismic energy across the cells. After re-grouting, the average velocity is higher than before re-grouting, indicating also a more consolidated grout. The seismic experiments proved to be an extremely useful method for evaluating the overall average effectiveness of the grouting. In general, an effective grout job will result in high average velocities and low signal attenuation. An ineffective grout job will result in low average velocities and high signal attenuation.

Overall, the seismic data had a very small signal-to-noise ratio. This was worse for the earlier data-set because of the high attenuation caused by the unconsolidated behavior of the first grouting. Figure 3 shows a common source gather in cell#1 before and after re-grouting. Both sets of traces were lowpass filtered at 5kHz., and show very different signal-to-noise ratio. Because of the poor signal-to-noise ratio the error in estimating the traveltimes is significant. This necessitates a high level of regularization or smoothing in the inversion.

3-D inversion was performed on the electrical resistivity data acquired at the site (Shi et al., 1996). Figure 4 shows the vertical slides of the 3-D inversion in cell#3. Note that the decrease in resolution with depth is a consequence of the geometry in the data acquisition and can, therefore be improved.

Conclusions and Limitations

The cross-well acoustic experiments showed that there was a significant increase in the seismic velocities of the cells from the initial grouting to the later re-grouting of the cells. Therefore, despite the limitations encountered in the acoustic imaging experiments, it can be reasonably concluded that the second re-grouting was generally successful. A more powerful seismic source and increased stacking of the signals would improve the signal to noise and thus improve the effective resolution of the tomographic images. However, when dealing with very heterogeneous media it may only be possible to obtain a crude statistical characterization of the media. The utility of such a characterization is dependent upon the specific application; e.g., this methodology would be useful in assessing the overall structural integrity of the cell, but it would probably not be capable of identifying individual fractures within the cell.

The seismic inversion turned out to be quite difficult not only because of the high level of noise but also because of the high velocity contrasts and the poor angular coverage of the raypaths. When the velocity contrasts are high, the raypaths do not sample similarly the entire velocity field. Regularization is therefore required to compensate the lack of ray coverage in some parts of the model, but it simultaneously smears out the solution reducing the resolution (Scales et al., 1990). For near surface environmental and engineering geophysical problems, *high resolution* is by definition *essential*. A challenging problem for the inversion community is to obtain *robust* methods that increase resolution and reduce the smoothing caused by regularization. The angular coverage problem can be vastly improved by adding some receiver geophones to the surface. This would improve the resolution of the central near surface zone. To obtain a similar improvement in resolution at depth, boreholes deeper than the body of interest are required. These techniques were not implemented for the current experiment because of the physical layout.

The resistivity inversion was more effective than the acoustic in resolving spatial changes within the cells. Moreover, the 3-D characteristics of the resistivity gives a global view of the cell, while the cross-well acoustic is only restricted to a 2-D section. Figure 5 shows the acoustic and the resistivity results for the same section (Cell#3: 12 - 5). Some similar features appear on this specific section. However, a direct correspondence between the two images is not expected in general, because velocity and resistivity depend on different properties of the material .

References

Dwyer, B. F., 1995, Feasibility of permeation grouting for constructing subsurface barriers, Environmental Restoration Technologies Group, Sandia National Laboratories, Albuquerque, New Mexico.

Elbring, G., Allen, G., and Levine, R., 1995, Crosshole compressional and shear wave seismic tomography, DOE Landfill Stabilization Report.

Harding, R. S., 1994, Crosswell seismic monitoring of a permeation grouting experiment, Geotechnical Test Range- Sandia National Laboratories. Sandia National Laboratories, Albuquerque, N. M..

Scales, J.A., Docherty, P., and Gersztenkorn, A., 1990, Regularization of non-linear inverse problems: Imaging the near-surface weathering layer: Inverse Problems, vol. 6, 115-131.

Shi, W., W., Rodi, W., Mackie, R.L., and Zhang, J., 1996, 3-D dc electrical resistivity inversion with application to a contamination site in the Aberjona Watershed, Proc. SAGEEP, Keystone, Colorado, Environmental and Engineering Geophysical Society, 1257-1267.

Acknowledgments
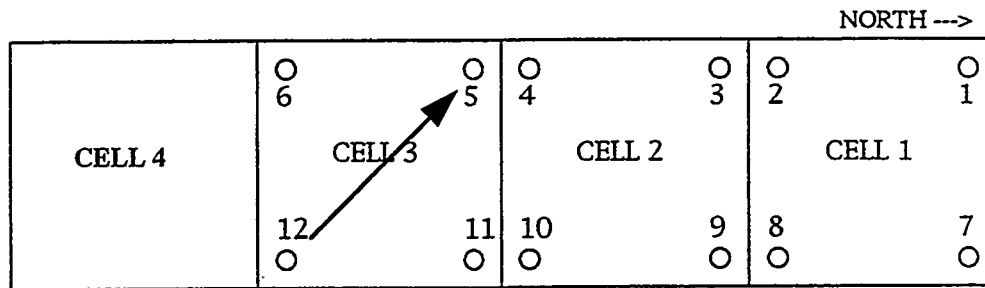
Figure 1. Plan view of simulation waste trench, showing geophysical observation holes in cells 1, 2, and 3.
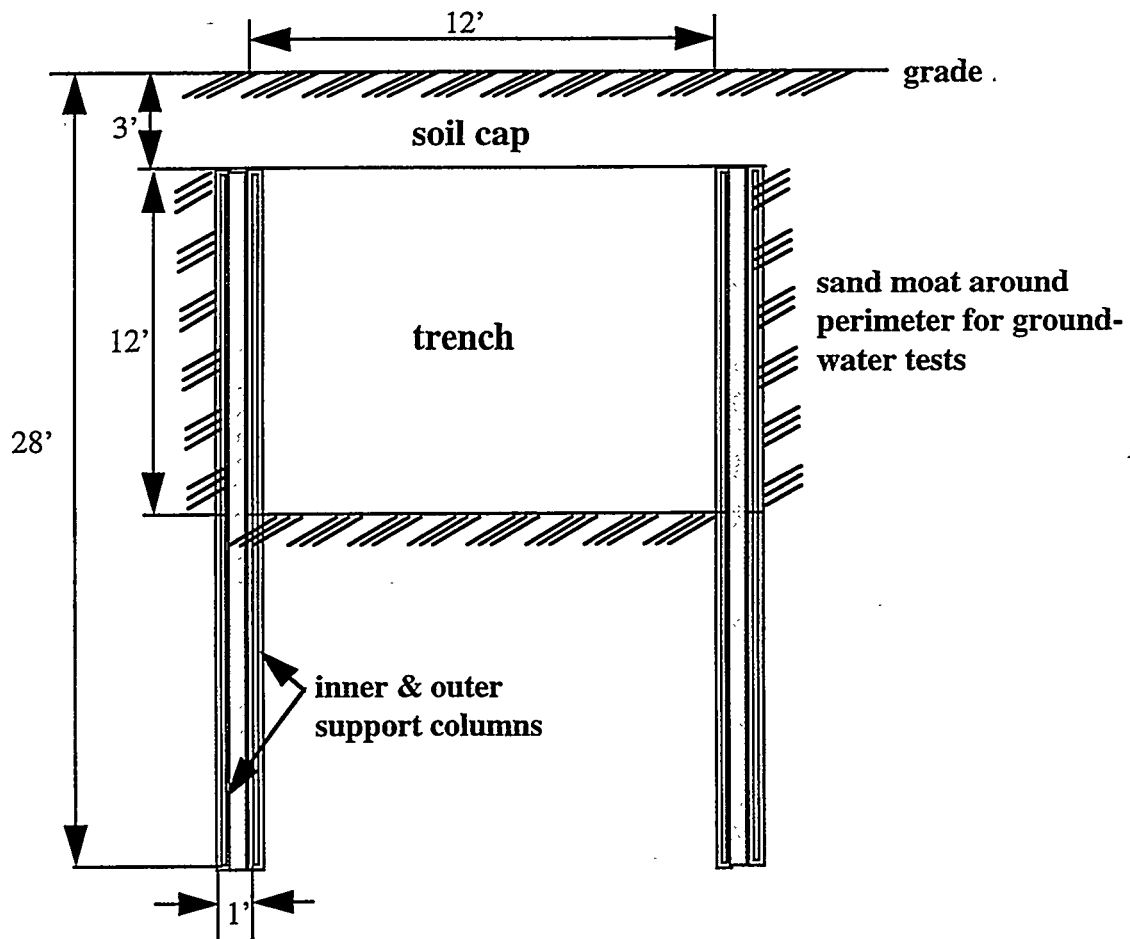
Figure 2. Cross-section of a cell within the simulated waste trench.

Source gather at depth 6.71ft. (2.045m.): Cell#1 (1 --> 8).
Data acquired **before** regrouting and lowpass filtered at 5kHz.
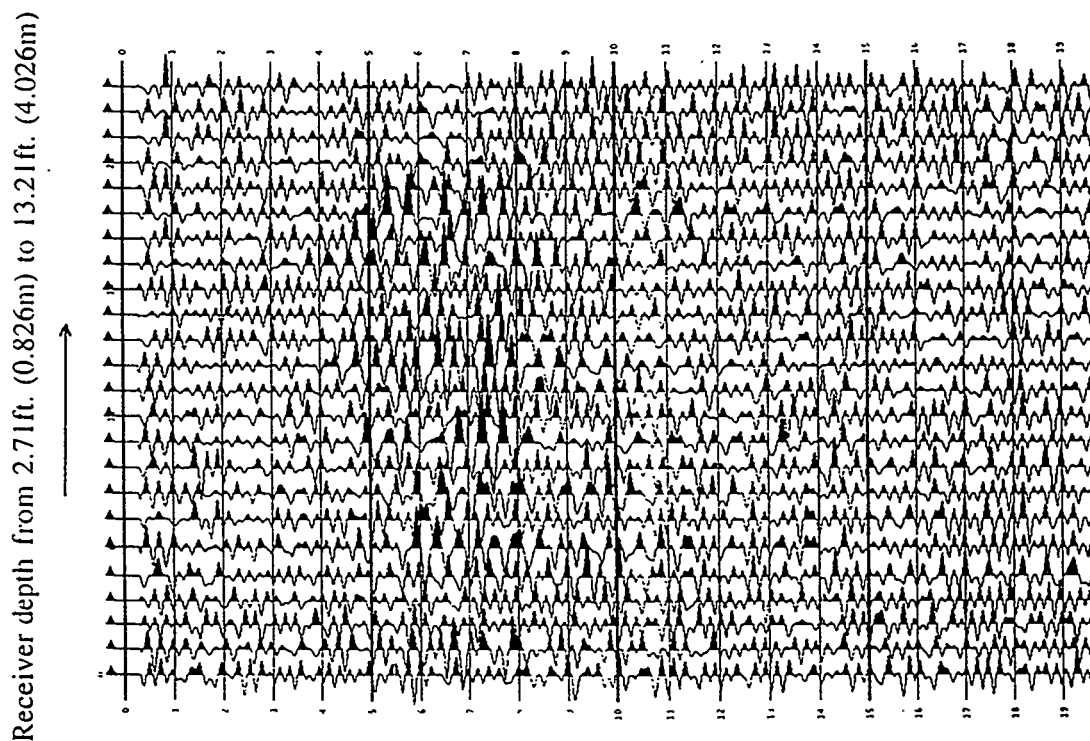
Source gather at depth 6.54ft. (2.0m.): Cell#1 (8 --> 1).
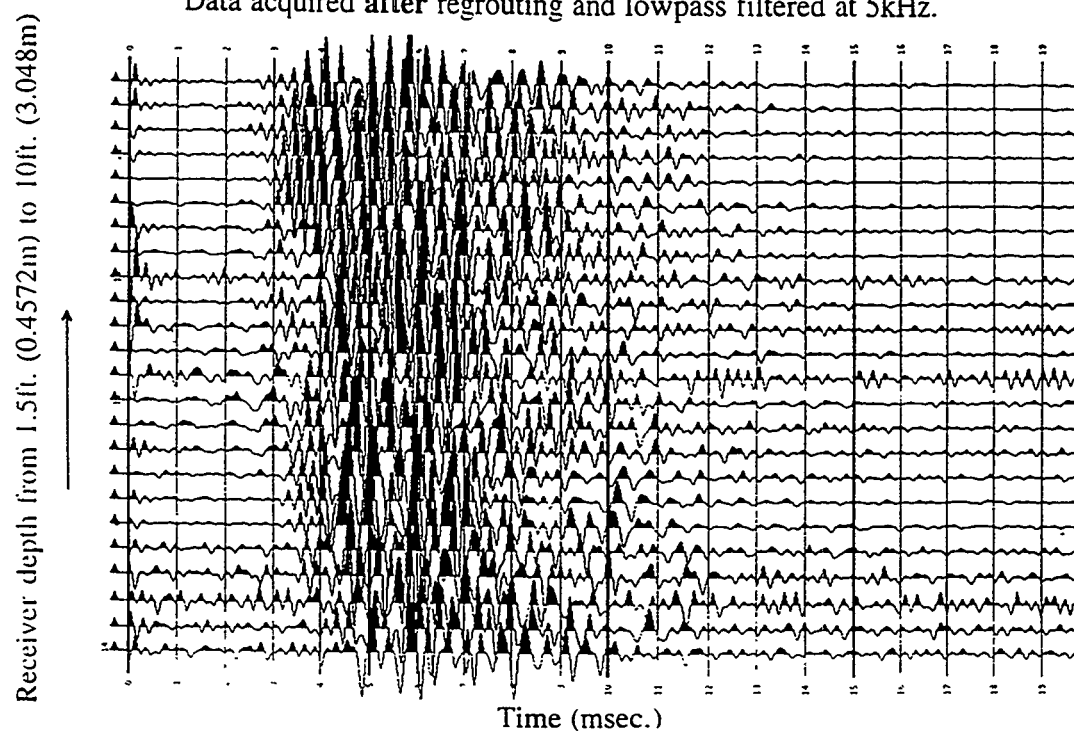Data acquired **after** regrouting and lowpass filtered at 5kHz.

Time (msec.)

Figure 3: Common source gather before (top) and after re-grouting (bottom). The data were lowpass filtered at 5kHz in both cases.
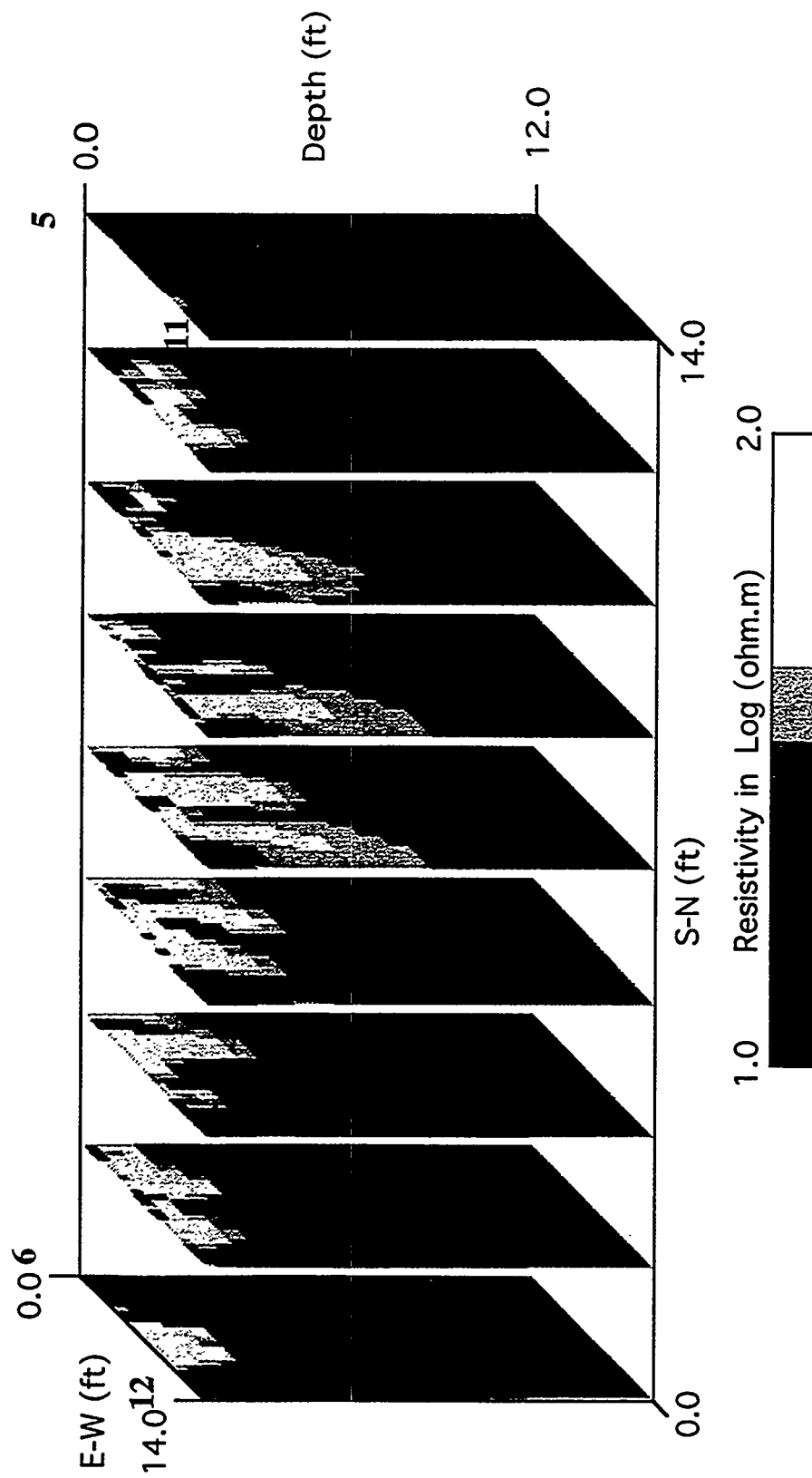
Figure 4 . 3-D electrical resistivity inversion results (vertical cross-sections) on cell 3.
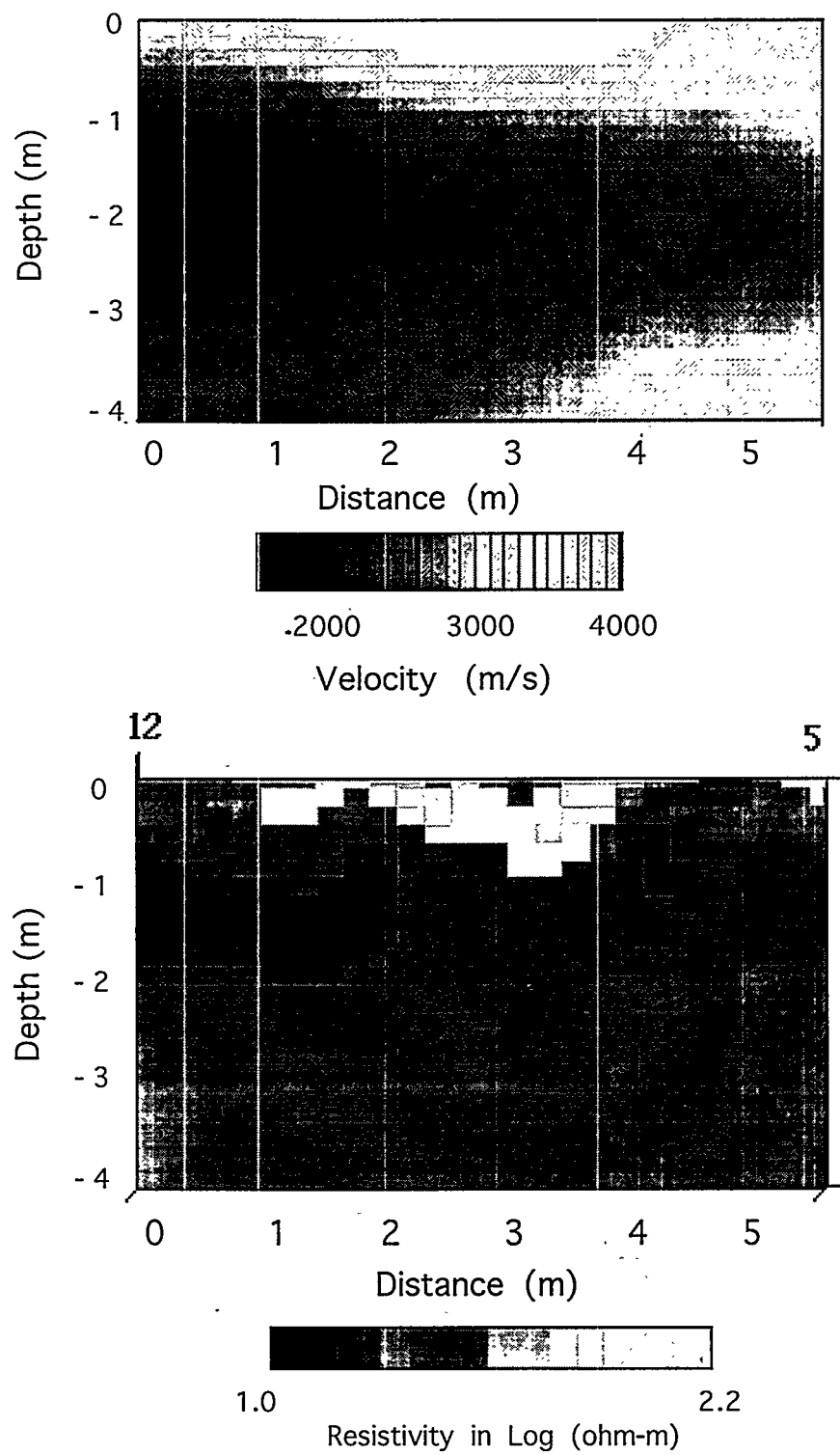
Figure 5: Cell#3 (12 -> 5) Velocity reconstruction (top) and Resistivity results (bottom).

DIELECTRIC CONSTANT AND ELECTRICAL CONDUCTIVITY OF CONTAMINATED FINE-GRAINED SOILS AND BARRIER MATERIALS

Abidin Kaya[1], H. Y. Fang[2] and Hilary I. Inyang[3]

ABSTRACT

Characterization of contaminated fine-grained soils and tracking of contaminant migration within barriers have been challenging because current methods and/or procedures are labor and time-intensive, and destructive. To demonstrate the effective use of both dielectric constant and electrical conductivity in the characterization of contaminated fine-grained soils, pore fluids were prepared at different ionic strengths, and were used as permeates for kaolinite, bentonite and a local soil. Then, both dielectric constant and electrical conductivity of the soils were measured by means of a capacitor over a wide range of frequencies and moisture content. It was observed that although each soil has its unique dielectric constant and electrical conductivity at a given moisture content, increases in ionic strength cause a decrease in the dielectric constant of the system at very high frequencies (MHz), whereas the dielectric constant increases at low frequencies (kHz). Electrical conductivity of a soil-water system is independent of frequency. However, it is a function of ionic strength of the pore fluid. It is clearly demonstrated that dielectric constant and electrical conductivity of soils are functions of both moisture content and ionic strength, and can be used to characterize the spatial and temporal levels of contamination. This method/procedure can be used in estimating the level of contamination as well as the direction of contaminant movement in the subsurface without the use of extensive laboratory testing. Based on obtained results, it was concluded that the proposed method/procedure is promising because it is non-destructive and provides a quick means of assessing the spatial distribution of contaminants in fine-grained soils and barriers.

INTRODUCTION

Identification and/or characterization of contaminated fine-grained soils constitute necessary steps in the development of effective remediation systems. However, existing methods and/or procedures are far from satisfactory because they require extensive soil-pore fluid sampling in the laboratory and field. Pore-fluid sampling has inherent difficulties. For example, contamination may occur during the sampling and testing. For a method to be satisfactory, it should be non-destructive, reproducible, cost-effective and very precise. Furthermore, the arrival times of contaminants within specific locations in soil-based barriers need to be assessed through monitoring for risk assessment. Thus, there is the need to develop a satisfactory method to identify and characterize contaminated fine-grained soils. It was the objective of this paper to determine the effectiveness of dielectric constant and electrical conductivity to identify and characterize presence of contaminants in subsurfaces. In this study, dielectric constant and electrical conductivity of kaolinite, bentonite, and a local soil were determined as functions of ionic strength, moisture content, and frequency in order to analyze water-soil mineral interaction, as well as polarization of the diffuse double layer.

The dielectric constant and electrical conductivity of soils vary with physicochemical states of the soil-pore water. Particularly, ionic charge is an important parameter. It should be pointed out that, dielectric constant and electrical conductivity of soils have been studied extensively, not only in the field of civil engineering, but also the in the field of agronomy, where there has been the need to develop method(s)/ procedures to determine both temporal and spatial moisture content of soils. It has been reported by Topp et al., (1980) that use of such procedures have been very successful and satisfactory in determining moisture content both in the field and laboratory. Also, Knigt and Nur (1987) used the concept of dielectric constant and electrical conductivity to determine the saturation level of petroleum reservoirs.

Dielectric Constant of Materials

---

[1] Post Doctoral Fellow, [2] Distinguished Research Professor, [3] Du Pont Young Professor, Center for Environmental Engineering and Science Technologies, (CEEST), and Dept. of Civil and Environmental Engineering, University of Massachusetts Lowell, Lowell, MA 01854

Dielectric constant of a system of a material is a measure of its polarizability upon application of an electrical field: the higher the polarization, the higher the dielectric constant. Dielectric constant consists of real and imaginary parts. The real part reflects the polarizability of the material, whereas the imaginary part reflects ohmic and polarization losses. Thus:

$$\varepsilon = \varepsilon' + i\varepsilon'' \tag{1}$$

where ε' is the real part of dielectric constant, ε'' is the imaginary part, and $i = (-1)^{0.5}$. However, application of Eq. 1 to soil-water systems has not been precise because of the complications in measurement of the imaginary part of the dielectric constant and surface electrical conductivity of soil particles.

Many empirical and semi-theoretical mixing formulations (Fricke, 1952; Okanski, 1959; Sachs and Spiegler; 1964; and Thevenayagam, 1995) are available to estimate dielectric behavior of soil-fluid systems. All of the formulations are mainly modifications of Maxwell's original derivation which is stated as:

$$\varepsilon = \frac{v_1 \varepsilon_1 (\frac{2}{3} + \frac{\varepsilon_2}{3\varepsilon_1}) + v_2 \varepsilon_2}{v_1 (\frac{2}{3} + \frac{\varepsilon_2}{3\varepsilon_1}) + v_2} \tag{2}$$

where v_1 and v_2 are volumes of liquid and solid, respectively; and ε_1 and ε_2 are the dielectric constants of solid and liquid.

Unfortunately, these formulations fail to predict both electrical conductivity and the dielectric constant of soils because of the complex interaction between soil minerals, water molecules and ions. For example, the complex formulation presented by Thevenayagam (1995) involved the use of dielectric constant values of 10 for kaolinite and 40 for montmorillonite for matching the predicted and measured dielectric constant, although both soil minerals have a dielectric constant of about 4.5.

Electrical Properties of Soil-Pore Fluid Systems

The electrical conductivity of a material is the inverse of the electrical resistance, as shown in Equation 3.

$$\sigma = \frac{1}{R}\frac{L}{A} \tag{3}$$

were R is resistance, L is length, and A is cross-sectional area.

The values of electrical conductivity of saturated soils are usually in the range of about 0.01 to 1.0 S/m. Generally, the variables that affect the electrical properties of soils are texture, structure, soluble salts, moisture content, temperature, density, and frequency at which measurements are conducted. The soluble salt content is the most important since ions increase the electrical conductivity of the system. Although there are several semi-theoretical and empirical formulations to determine the electrical conductivity of soil-pore fluid systems, none of them is satisfactory (Kaya, 1996, and Kalinski, 1992). It should be mentioned that all the presented are derivations of:

$$\sigma^n = \sum v_i \sigma_1 \tag{4}$$

where σ is conductivity of the surface and v is the volume fraction of substance and n is a constant (+1 or -1).

The main limitation of formulations to predict the electrical conductivity of soil-pore fluid systems is the surface conductivity due to polarization of diffused double layer under applied electrical field. Polarization of diffuse

double layer varies with the type of soil mineral and type of ions present in the system. Although this issue deserves lengthy discussion, it will not be discussed further due to space limitations.

MATERIALS AND METHODS

The soils used in this study and their physico-chemical properties are presented in Table 1. Although the procedure for measuring the dielectric constant and electrical conductivity of soils is discussed in detail in Kaya (1996) as well as Kaya and Fang (1997), it is briefly stated herein. The soils were saturated with pore fluids at different ionic concentrations, then the samples were placed in a U-shaped plexiglass cell. The cell (2 cm x 4 cm) was covered by silver plates to eliminate impurities. The separation distance between conducting areas was 2 cm. All the measurements were conducted within a minute or so to eliminate the impurities resulting from overheating by the applied current.

Table 1. Physicochemical properties of tested soils.

	Kaolinite	Bentonite	Local Soil
Specific Gravity	2.55	2.6	2.62
Liquid Limit	42	440	27
Plastic Index	13	370	4
Main Cation [a]	Na	Na	na
CEC (meq/100g)	24	87	na
pH	6.3±1 (10% solid)	8.5±1 (5% solid)	4.6±1 (10% solid)
Surface Area[b] (m^2)	13	27.7	na

na: Not available, na: Na- Method, b: BET method

RESULTS

Figures 1, 2 and 3 present the dielectric constant and electrical conductivity of soils at various ionic concentrations as a function of porosity at 13 MHz. In the figures, values of the dielectric constant of soils are plotted with solid lines, whereas electrical conductivities are plotted with dashed lines. It can be seen that as ionic concentrations in the pore fluid increases, the dielectric constant of soils decreases at a given porosity. On the other hand, electrical conductivity of the soils increases as the ionic concentration in the pore fluid increases, as expected. It should be noted that when ionic concentration is low, i.e. the pore fluid DDI H$_2$O (Distilled-Deionized water) and 0.001 M NaCl in DDI, the electrical conductivity of the soil-water system increases. This is due to contributions from the surface conductivity of the clay particles influenced by the polarization of the diffused double layer. Rhodes et al. (1976), reported a similar phenomenon.

Inspection of Figures 1, 2 and 3 shows that each soil has unique dielectric constant and electrical conductivity. The variations in the amount of dielectric constant are noticeable when kaolinite and the local soil are compared. For example, at a porosity of 0.7, the dielectric constant is about 72 for kaolinite whereas it is about 55 for the local soil when the pore fluid is DDI H$_2$O. However, such a direct comparison was not possible for bentonite because of the nature of this soil. It should be noted that, overall, the dielectric constant of soils can be used to identify the soil type in a given soil-water system. However, comparisons across various soil types may not always be accurate. The same conclusions are also valid for electrical conductivity of the soil-pore fluid system.

Figure 4 shows dielectric constant and electrical conductivity of kaolinite with NaCl and CaCl$_2$. It is seen that for the same molar concentration, the dielectric constant of CaCl$_2$ is lower than that of NaCl, whereas the electrical conductivity is higher. This can be explained with ionic strength, which can be determined by Equation 5:

$$I = \frac{1}{2}\sum_{1}^{n} m_i z_i^2$$

(5)

where m is the total concentration of ion, z is the valence of ion and i = 1,2,3,....n. When the ionic strength of 0.01 M NaCl is 0.01 M and that of 0.005 M CaCl$_2$ is 0.015 M (it is assumed in the calculations that molal = molar). For all

practical purposes, the ionic strengths are very close, thus it is reasonable to expect similar dielectric constants and electrical conductivities. However, it should be pointed out that there are some other factors that can influence both dielectric constant and electrical conductivity such as ionic mobility, etc. Further discussion can be found in Kaya (1996) and Kaya and Fang (1997).

Figures 5 and 6 show dielectric constants and electrical conductivities of kaolinite and bentonite, at 100% moisture content (n=0.72) and 300% moisture content (n=0.89) respectively, as a function of frequency. From the figures, electrical conductivity of soils remains almost constant over a wide frequency range, although there is a considerable increase in electrical conductivity of soil-pore fluid with increase in ionic concentration.

As ionic concentration in the pore fluid increases the dielectric constant of soil-pore fluid system decreases at very high frequencies (MHz frequency range) whereas it increases at low frequency ranges (kHz range). This can be explained by hydration of water molecules and relaxation time. As ions attracted to water molecules, they can not orient themselves in the direction of externally applied electrical field at high frequencies whereas they will move toward anode and cathode at low frequencies according to the Debye theory. The Debye theory predicts the relaxation time,

$$\tau = \frac{4\pi\eta\alpha^3}{kT} \tag{6}$$

where α is the radius of molar structure, η is the coefficient of internal friction, k is Boltzman's constant and T is the absolute temperature (K).

As seen from Eq. 6, the relaxation time ($2\pi f \tau = 1$) is inversely proportional to frequency. At high frequencies, hydrated ions will not contribute to dielectric constant of the system since they cannot orient themselves in the direction of externally applied electrical field due to lack of time. However at low frequencies, not only all ions orient themselves in the direction of externally applied electrical field but also move toward anode and cathode which makes the medium conductive, ultimately give rise to the dielectric constant of the system. Additional information on the interaction of water and ions, and their effects on dielectric constant of water is provided by Kaya (1996).

As mentioned above, there are no available formulations that accurately predict the dielectric constant of a soil-water system because the formulations assume that the system comprises only two phases, namely soil and water using mixture rules. The dielectric constants of soil and water are treated as real, not complex, because these components are assumed to be insulating (i.e., $\varepsilon''= 0$). An obvious limitation of these methods is that they do not take into account electrochemical interactions among the components. The effect of charge accumulation on dielectric constant of soil water system is established in this study. Furthermore, to model the dielectric constant of a soil-water mixture, the basic components are redefined. Instead of mixing the dielectric constant of dry soil and water to predict the dielectric constant of water saturated soils, as was always done, mixing the dielectric constants of wetted soil and water is proposed. It is beyond the scope of this paper to discuss such formulations herein. Nonetheless, the dielectric constant and electrical conductivity of a soil-water system can be successfully used to predict contamination in the subsurface.

PRACTICAL APPLICATIONS OF RESULTS

The presented methodology and results can be used in the identification and characterization of contaminated fine-grained soils. The advantage of this methodology, once the system is installed, is that spatial and temporal variations in the physico-chemical state of fine-grained soils can be determined readily in a non-destructive manner. Consequently, this reduces the cost of data collection and the potential for contamination during sampling and testing. For example, such a system can be easily adapted to check for contamination from a landfill. Both the dielectric constant and electrical conductivity of pore fluids up stream and down stream can be measured, and the contamination source can be identified without performing elaborate testing procedures. Another potential

application of this technique is in the assessment of growth of contaminant concentrations in the aqueous phase within specific locations in relatively intact barriers.

CONCLUSIONS

The following conclusions can be drawn from this work :

(1)   Dielectric constant and electrical conductivity of contaminated fine-grained soils are considerably different from those of non-contaminated soils.

(2)   As ionic concentration in the pore fluid increases the dielectric constant of the soil-pore fluid decreases at MHz frequency range, whereas it increases at kHz frequency range.

(3)   As ionic concentration in pore fluid increases the electrical conductivity of soil-pore fluid increases, however, it remains constant with frequency for all practical purposes.

(4)   Both dielectric constant and electrical conductivity of a soil-pore fluid system can be used to determine spatial and temporal variations in physico-chemical state of pore fluid in a non-destructive and rapid manner.

REFERENCES

Arulanandan, K., 1991. "Dielectric Method for Prediction of Porosity of Saturated Soil." J. of Geotech. Engg., ASCE, 117: 319-330.

Endres, A.L., and Knight, R.J., 1993. "A Model for Incorporating Surface Phenomena into the Dielectric Response of a Heterogeneous Medium." J. Colloid and Interface Sci., 157: 418-425.

Fricke, H., 1942. "A Mathematical Treatment of Electric Conductivity and Capacitance of Disperse Systems." Experientia, 10: 376-377.

Kalinski, R.J., 1992. "Surface Geoelectrics for Characterizing Ground Water Protective Layers and Compacted Soil Liners." A Ph.D. Thesis Submitted to the University of Nebraska, Lincoln.

Kaya, A., and Fang, H.Y., 1997. "The Effect of Pore Fluid Contamination on Dielectric and Electrical Conductivity of Soil-Fluid Systems." ASCE Enviro. Engg., J., vol. 123(2) pp. 169-177.

Knight, R. J. and nur, A., 1987, The Dielectric constant of sandstones, 60 kHz to 4 Mhz," Geophysics, Vol. 52, pp. 644-654.

Kaya, A., 1996. "The Effect of Pore Fluid Contamination on Selected Physico-Chemical Properties of Fine-Grained Soils." A Ph.D. Thesis Submitted to Lehigh University.

Okanski, C.T., 1959. "Effect of Interfacial Conductivity on Dielectric Properties." J. Chem. Phys. 23: 1559-1566.

Okoye, C.N., Cotton, T.R. and O'Meara, D., 1995. "Application of Resistivity Cone Penetration Testing for Qualitative Delineation of Creosote Contamination in Saturated Soils." Geoenvironmental 2000, ASCE: 151-160.

Rohades, J.D.; Ratts, P.A.C., and R.J. Prather, 1976. "Effects of Liquid-Phase Electrical Conductivity, Water Content, and Surface Conductivity on Bulk Soil Electrical Conductivity." Soil Sci. Soc. of Amer., 40: 651-655.

Sachs, S.B., and Spiegler, K.S. "Radiofrequency Measurements of Porous Conductive Plugs, Ion Exchange Resin-Solution Systems." J. Phys. Chem., 68: 1214-1222.

Sen, P.N., 1981. "Dielectric Anomaly in Homogeneous Materials with Application to Sedimentary Rocks." App. Phys. Lett., 39: 667-668.

Smyth, C.P., 1955. "Dielectric Behavior and Structure; Dielectric Loss, Dipole Moment and Molecular Structure, McGraw Hill: 441.

Thevenayagam, S., 1995b. "Frequency-Domain Analysis of Electrical Dispersion of Soils." Geotech Engg., J., ASCE, 121: 618-628.

Thevenayagam, S., 1993. "Electrical Response of Two-Phase Soils: Theory and Applications." J. Geotech. Engg., 119: 1250-1275.

Topp, G.C.; Davis, J.L., and Annan, A.P., 1980. "Electromagnetic Determination of Electrical Conductivity Using Time Domain Reflectometry: Soil and Water Experiments in Coaxial Lines." Water Resour. Res., 24: 945-952.
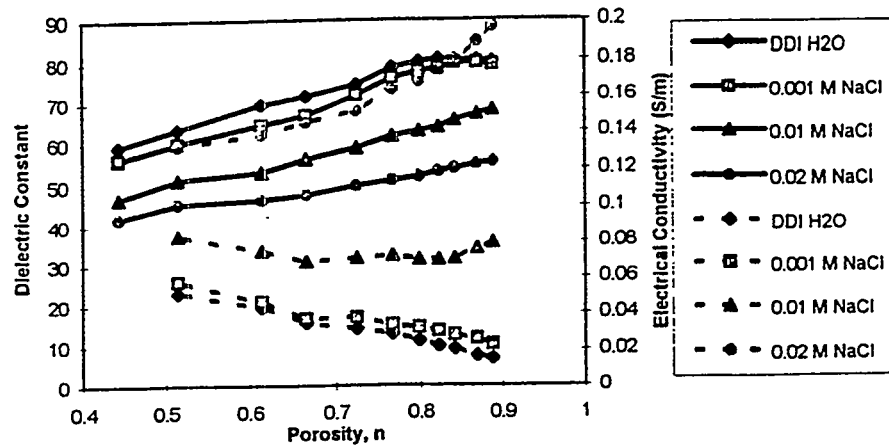
Figure 1. Dielectric constant (sold lines) and electrical conductivity (dashed lines) of kaolinite at various porosity at 13 MHz.
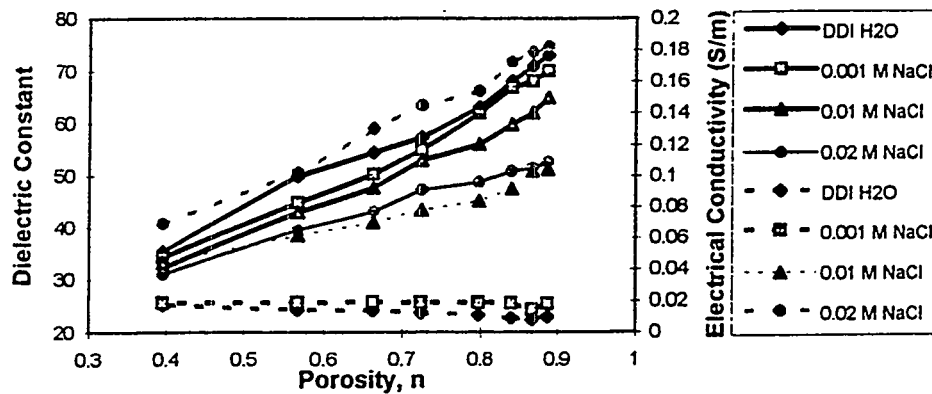
Figure 2. Dielectric constant (sold lines) and electrical conductivity (dashed lines) of a local soil at various porosity at 13 MHz.
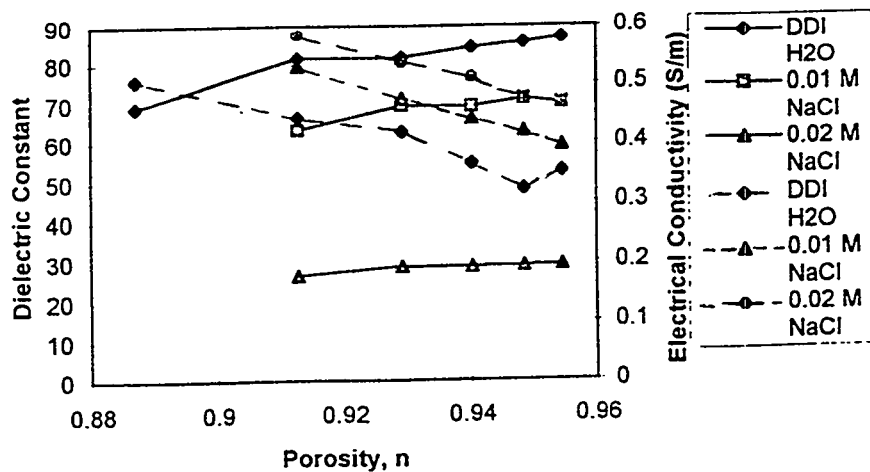
Figure 3. Dielectric constant (sold lines) and electrical conductivity (dashed lines) of bentonite at various porosity at 13 MHz.
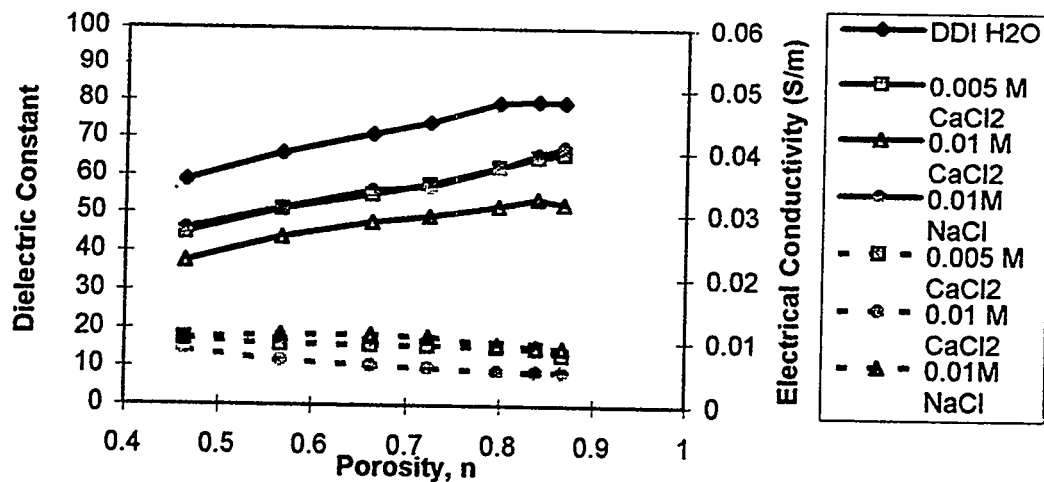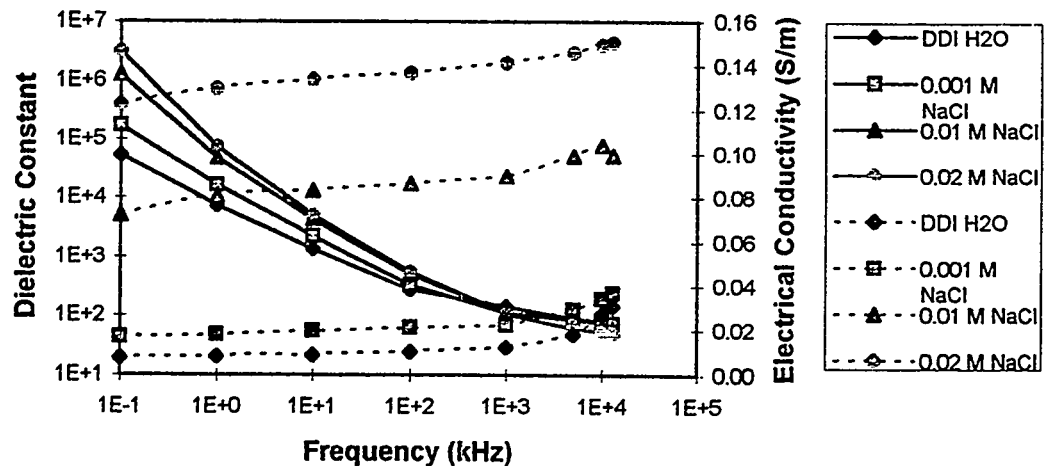
Figure 4. Dielectric constant (solid lines) and electrical conductivity (dashed lines) of kaolinite with NaCl and CaCl$_2$ as a function of porosity at 13 MHz.

Figure 5. Dielectric constant (solid lines) and electrical conductivity (dashed lines) of kaolinite at 100% moisture content as a function of frequency.
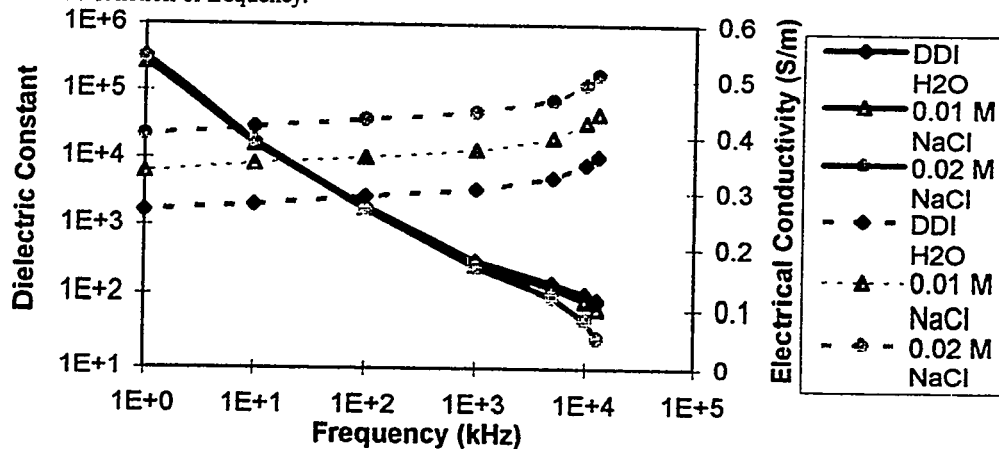
Figure 6. Dielectric constant (solid lines) and electrical conductivity (dashed lines) of bentonite at 300% moisture content as a function of frequency.

Conference Participants

Conference Participants

Mr. Thomas Aalto
U.S. Environmental Protection Agency
Region 8
999 18th ST, STE 500
Denver CO 80202
USA
phone: 303/312/6949
fax: 303/312/6064
e-mail: aalto.tom@epamail.epa.gov

Ms. Allison Abernathy
U.S. Environmental Protection Agency
MC 5701, 401 M ST SW
Washington DC 20460
USA
phone: 202/260/9925
fax: 202/260/5646
e-mail:
abernathy.allison@epamail.epa.gov

Ms. Mary Ann E. Abrahamson
U.S. Environmental Protection Agency
1445 Ross Avenue
Dallas TX 75019
USA
phone: 214/665/6754
fax: 214/665/6660
e-mail:

Mr. Fritz N. Achhorner
Slurry Walls, Inc.
111 Fox Glen Circle
Irving TX 75062
USA
phone: 972/717/6505
fax: 972/717/6232
e-mail:

Mr. Wayne S. Adaska
Portland Cement Association
5420 Old Orchard RD
Skokie IL 60077
USA
phone: 847/966-6200
fax: 847/966-8389
e-mail: wayne_adaska@portcement.org

Mr. Donald D. Adelman
Adelman & Associates
4535 Y ST
Lincoln NE 68503-2344
USA
phone: 402/471-3960(W) or 464-0035(H)
fax: 402/471-3132
e-mail:
Adelman@NRCDEC.NRC.STATE.NE.US

Dr. Faouzi Ahtchi-Ali
August Mack Environmental, Inc.
2624 Lord Baltimore DR, STE K
Baltimore MD 21244
USA
phone: 410/597-9889
fax: 410/597-9849
e-mail: ahtchif@erols.com

Dr. Abir Al-Tabbaa
Department of Engineering
University of Cambridge
Trumpington Street
Cambridge CB2 1PZ
UK
phone: 44-1223/332600 dept phone
fax: 44-1223/332662 dept fax
e-mail: altabbaa@civ-fs1.bham.ac.uk

Dr. Sam R. Allen
TRI/Environmental, Inc.
9063 Bee Cave RD
Austin TX 78733
USA
phone: 512/263-2101/1-800-880-8378
fax: 512/263-2558
e-mail:

Dr. George C. Allen
Sandia National Laboratories
MS-0719, P.O. Box 5800
Albuquerque NM 87185-0719
USA
phone: 505/844/9769
fax: 505/844/0543
e-mail: gcallen@sandia.gov

Mr. Orhan Altin
Department of Chemical Engineering
Middle East Technical University
06531 Ankara TURKEY
phone: 090/312/2104363
fax: 090/312/2101264
e-mail: oaltin@rorgual.cc.metu.edu.tr

Mr. Clifford E. Anderson
Department of Civil Engineering
University of New Mexico
Tapy Hall
Albuquerque NM 87131
USA
phone: 505/277-4809
fax: 505/277-1988
e-mail: ceanders@unm.edu or
jcstorm@unm.edu

Dr. Jay E. Anderson
Department of Biological Sciences
Idaho State University
Box 8007
Pocatello ID 83209-8007
USA
phone: 208/236-3145
fax: 208/236-4570
e-mail: andejay@isu.edu

Mr. Brian D. Anderson
Boeing
22715 SE 168th Way
Maple Valley WA 98038
USA
phone: 206/391/3753
fax: 206/391/7605
e-mail: briand.anderson2@boeing.comm

Ms. Tina M. Anguiano
ENTACT, Inc.
1616 Corporate Court, STE 150
Irving TX 75038
USA
phone: 972/580-1323
fax: 972/550-7464
e-mail:

Dr. John A. Apps
Earth Sciences Division
Lawrence Berkeley National Laboratory
University of California
MS 90-1116
1 Cyclotron Road
Berkeley CA 94720
USA
phone: 510/486-5193
fax: 510/486-5686
e-mail:

Mr. Aran T. Armstrong
U.S. Department of Energy
850 Energy Drive
Idaho Falls ID 83401
USA
phone: 208/526/5199
fax: 208/526/6249
e-mail: armsat@inel.gov

Mr. John E. Auger
DuPont
Barley Mill Plaza, Bldg 27-1106
Lancaster Pike & Rt. 141
Wilmington DE 19805
USA
phone: 302/892/1450
fax: 302/892/1583
e-mail:

Conference Participants

Ms. Martha E. Bailey
Office of Environmental Restoration
U.S. Department of Energy
19901 Germantown Rd
EM-43 Cloverleaf
Germantown MD 20874-1290
USA
phone: 301/903/8098
fax: 301/903/3675
e-mail: martha.bailey@em.doe.gov

Mr. Arthur C. Baker
Earth Tech, Inc.
P.O. Box 274128
Tampa FL 33688
USA
phone: 813/931-1707
fax: 813/948-3409
e-mail:

Mr. Michael J. Baker
Department of Earth Sciences
University of Waterloo
Waterloo Ontario N2L-3G1
CANADA
phone: 519/888-4567 ext. 5643
fax: 519/746-3882
e-mail:
mbaker@cgrpc.watstar.uwaterloo.ca

Ms. Claudia L. Baldwin
Sherwood Geotechnical Services
16 Erinvale ST
Corinda Qld 4075 AUSTRALIA
phone: 13-7/3379-2806 or 3278 1060
fax: 13-7/3278 1004
e-mail:

Mr. Shane Banks
ENTACT
3233 N. Clifton
Chicago IL 60657
USA
phone: 773/281/2455
fax: 773/281/2526
e-mail:

Mr. Peter J. Barker
Bachy Ltd
Foundation Court, Godalming Business
Centre
Catteshall LN
Godalming, Surrey England GU7 1XW
UK
phone: 44-1483/427-311
fax: 44-1483/417-021
e-mail: pjl@bachy-s.demon.co.uk

Ms. Felicia F. Barnett
Office of Technical Services
Waste Management Division
U.S. Environmental Protection Agency
Region 4
100 Alabama Street
Atlanta GA 30365
USA
phone: 404/562/8659
fax: 404/562/8628
e-mail:

Mr. Michel Barraque
Institut Francais du Pétrole
1 & 4, avenue de Bois Préau
92852 Rueil-Malmaison FRANCE
phone: 33-01/47526613
fax: 33-01/47527014
e-mail:

Mr. Edwin F. Barth
Office of Research & Development
U.S. Environmental Protection Agency
26 W Martin Luther King DR
MS489
Cincinnati OH 45268
USA
phone: 513/569-7669
fax: 513/569-7676
e-mail: barth.ed@epamail.gov

Mr. William (Bill) D. Barton
P-Squared Technologies, Inc.
10938 Hardin Valley RD
Knoxville TN 37932
USA
phone: 423/691-3668
fax: 423/691-0611
e-mail: bbarton@P2T.com

Mr. Edward R. Bates
Office of Research & Development
U.S. Environmental Protection Agency
26 W Martin Luther King DR
MS489
Cincinnati OH 45268
USA
phone: 513/569-7774
fax: 513/569-7676
e-mail:

Mr. Paul M. Beam
U.S. Department of Energy
1000 Independence Ave. SW
19901 Germantown RD
Washington DC 20585
USA
phone: 301/903/8133
fax: 301/903/3877
e-mail: paul.beam@em.doe.gov

Ms. Mary Beck
U.S. Environmental Protection Agency
Region 3
841 Chestnut BLDG (3HW90)
Philadelphia PA 19107
USA
phone: 215/566/3429
fax: 215/566/3113
e-mail: beck.mary@epamail.epa.gov

Dr. Reinhard A. Beine
Jessberger + Partner
Am Umweltpark 5
44793 Bochum GERMANY
phone: 49-234/68 775-0
fax: 49-234/68775-10
e-mail:

Ms. Anita Bekesi
Florida State University
2035 E Paul Dirac DR
226 Morgan BLDG
Tallahassee FL 32310-3700
USA
phone: 904/644-5524
fax: 904/574-6704
e-mail:

Mr. Douglas A. Bell
Headquarters
U.S. Environmental Protection Agency
401 M Street, SW
Washington DC 20460
USA
phone: 202/260/8716
fax: 202/260/5646
e-mail:

Mr. David J. Bennett
Dow Corning Corp.
1133 Connecticut Ave NW #600
Washington DC 20036
USA
phone: 202/785/0585
fax: 202/785/0421
e-mail: usdccb23@ibmmail.com

Dr. Craig H. Benson
Dept. of Civil & Environmental
Engineering
University of Wisconsin-Madison
2214 Engineering BLDG
1415 Engineering DR
Madison WI 53706
USA
phone: 608/262-7242
fax: 608/263/2453
e-mail:

Conference Participants

Dr. Kozimierz Beran
Partia Kupiecka RP
ul. Grunwaldska 17
35-959 Rzeszow POLAND
phone: 48-17/52-48-74
fax: 48-17/52-13-46
e-mail:

Ms. Marianne Bessellieu
W.E.S., Inc.
'A Full Service Company'
1802 N Lakemont AVE
Winterpark FL 32792
USA
phone: 407/599-2124
fax: 407/599-2125
e-mail:

Dr. J. David Betsill
Sandia National Laboratories
Environmental Restoration Tech.Dept.
6621
P.O. Box 5800 Mail Stop 0719
Albuquerque NM 87185-0719
USA
phone: 505/844-9578
fax: 505/844-0543
e-mail: jdbetsi@sandia.gov

Mr. Charles Biedermann
Lockheed Martin
P.O. Box 2908
Largo FL 34649
USA
phone: 813/545-6793

Mr. Steven R. Birdwell
Remedial Construction Services
9720 Derrington
Houston TX 77064
USA
phone: 713/955-2442
fax: 713/890-5172
e-mail:

Mr. Joseph L. Birkmier
Zeneca, Inc.
1800 Concord Pike
P.O. Box 15438
Wilmington DE 19850-5438
USA
phone: 302/886-4252
fax: 302/886-5933
e-mail:

Mr. Paul Biscuti
Atlantic Environmental Services Inc.
P.O. Box 188
188 Norwich AVE
Colchester CT 06415
USA
phone: 860/537-0751
fax: 860/537-6347
e-mail: atlantic@worldnet.att.net

Mr. Curt W. Black
Office of Environmental Assessment
U.S. Environmental Protection Agency
1200 Sixth AVE - OEA-095
Seattle WA 98101
USA
phone: 206/553/1262
fax: 206/553/0119
e-mail: black.curt@epamail.epa.gov

Dr. David W. Blowes
Department of Earth Sciences
University of Waterloo
200 University AVE W
Waterloo Ontario N2L 3G1
CANADA
phone: 519/888-4878
fax: 519/746-3882
e-mail: Blowes@sciborg.uwaterloo.ca

Mr. Steve Blume
GSE Lining Technology
19103 Gundle RD
Houston TX 77073
USA
phone: 800-435-2008 or 713/443-8564
fax: 713/875-6010
e-mail:

Mr. William Bocchino
Groundwater Control, Inc.
P.O. Box 60218
Jacksonville FL 32220
USA
phone: 904/783-0477
fax: 904/695-0881
e-mail: GCI78@aol.com

Mr. Peter Bock
National Seal Company
7943 Pecue LN
Baton Rouge LA 70809
USA
phone: 504/751-2700
fax: 504/751-2789
e-mail:

Ms. Ingrid Bon
U.S. Army Corps of Engineers
P.O. Box 56 Gunpowder Branch
Aberdeen Proving Ground MD 21010
USA
phone: 410/612-0489
fax: 410/612-0490
e-mail:
ingrid_bon_@zzerro@ccmail.nab.usace.
army.mil

Dr. Rudolph Bonaparte
GeoSyntec Consultants
1100 Lake Hearn Dr. NE Suite 200
STE 200F
Atlanta GA 30247
USA
phone: 404/705/9500
fax: 404/705/9400
e-mail:

Ms. Marge Bonura
W.E.S., Inc.
6389 Tower Lane
Sarasota FL USA
phone: 941/371-7617
fax: 941/378-5218
e-mail:

Ms. Susanne Borchert
SBP Technologies, Inc.
105 Gregory Square
Pensacola FL 32501
USA
phone: fax: 904/470-0058
e-mail:

Dr. David J. Borns
Geophysics Department
Sandia National Laboratories
Org. 6116/MS-0750
Albuquerque NM 87185-0750
USA
phone: 505/844-7333
fax: 505/844-7354
e-mail: djborns@sandia.gov

Dr. William D. Bostick
Environmental and Chemical Technology
Department
Lockheed Martin Energy Systems, Inc.
K-25 Site
Post Office Box 2003, HWY 58
Oak Ridge TN 37831-7274
USA
phone: 423/574-6827 or 576-4138 (sec)
fax: 423/576-8558
e-mail:

Conference Participants

Dr. Abdel Malek Bouazza
Dept. of Civil Engineering
Monash University
Wellington Road, Clayton
Melbourne, VIC 3168 AUSTRALIA
phone: 61-3/9905 4956
fax: 61-3/9905 4944
e-mail: Bouazza@Eng.monash.edu.au

Mr. Andrew Bouie
BDM
Quince Diamond Executive Center
555 Quince Orchard RD, STE 400
Gaithersburg MD 20878-1437
USA
phone: 301/212-6205

Dr. Heike B. Bradl
Research and Development
Bilfinger + Berger Bauaktiengesellschaft
Carl-Reiß-Platz 1-5
D-68 165 Mannheim GERMANY
phone: 49-621/459-2613
fax: 49-621/459-2350
e-mail: fue.bilberg@t-online.de

Mr. Peter A. Braithwaite
Ove Arup & Partners
Edgbaston House
3 Duchess Place
Edgbaston, Birmingham England B16 8NH
UK
phone: 44-121/454-6261
fax: 44-121/454-8853
e-mail:

Dr. Alex Brandelik
Institute for Meteorology and Climate Research
Research Center Karlsruhe
Postbox 3640
D-76021 Karlsruhe GERMANY
phone: 49-7247/823913
fax: 49-7247/824742
e-mail:

Mr. William C. Brandon
U.S. Environmental Protection Agency
JFK Federal Building, HBT
Boston MA 02203-2211
USA
phone: 617/573/9629
fax: 617/573/9662
e-mail:

Mr. Louis (Buddy) B. Breaux
EnviroWall - Barrier Member
Containment Corp.
9433 Highway 23
Belle Chasse LA 70337-1738
USA
phone: 504/398-0501
fax: 504/398-0503
e-mail:

Mr. Ulrich Brinkmann
Krupp Hoesch Steel Products, Inc.
180 Interstate North PKWY
Atlanta GA 30339-2194
USA
phone: 770/661-3401
fax: 770/661-8625
e-mail:

Mr. Ron Broadrick
Earth Tech, Inc.
P.O. Box 274128
Tampa FL 33688
USA
phone: 813/931-1707
fax: 813/948-3409
e-mail:

Mr. Richard K. Brown
Wyo-Ben, Inc.
P.O. Box 1979
Billings MT 59103
USA
phone: 406/652-6351
fax: 406/656-0748
e-mail:

Mr. Eric E. Bryan
DuPont Environmental Remediation Services
Barley Mill Plaza 27 Rts. 141 &48
P.O. Box 80027
Wilmington DE 19880-0027
USA
phone: 302/892-7420
fax: 302/892-1514
e-mail: bryanee@csoc.dnet.dupont.com

Ms. Grace E. Bujewski
Sandia National Laboratories
Dept. 6621, MS-0719
P.O. Box 5800
Albuquerque NM 87185-0719
USA
phone: 505/844-3330
fax: 505/844-0543
e-mail: gebujewski@sandia.gov

Mr. Thomas D. Burford
Environmental Restorations
Technologies Dept.
Sandia National Laboratories
P.O. Box 5800, MS 0719
Albuquerque NM 87185-0719
USA
phone: 505/845-9893
fax: 505/844-0543
e-mail: tdburfo@sandia.gov

Mr. George K. Burke
Hayward Baker Inc.
1130 Annapolis RD
Odenton MD 21113
USA
phone: 410/551-8200 or 1980
fax: 410/551-1900
e-mail:

Mr. John M. Burns
Olin Corporation
550 Forest Lane NE
Cleveland TN 37312
USA
phone: 423/336/4057
fax: 423/336/4280
e-mail: jburns@corp.olin.com

Dr. David R. Burris
Armstrong Laboratory, AL/EQL
139 Barnes DR, STE 2
Tyndall AFB FL 32403
USA
phone: 904/283-6035
fax: 904/283-6090
e-mail: david_burris@ccmail.aleq.tyndall.af.mil

Ms. Belinda Burson
Groundwater Control Inc.
P.O. Box 73327
Houston TX 77273-3327
USA
phone: 281/895-9765
fax: 281/895-9768
e-mail:

Mr. Brent N. Burton
Lockheed Martin Idaho Technologies Co.
P.O. Box 1625
Idaho Falls ID 83415-3920
USA
phone: 208/526/8695
fax: 208/526/6852
e-mail:

Conference Participants

Dr. P. Brandt Butler
DuPont Environmental Remediation
Services
Barley Mill Plaza, BLDG 27
P.O. Box 80027
Wilmington DE 19880-0027
USA
phone: 302/992-5978
fax: 302/892-7637
e-mail:
butlerpb@m.csoc.umc.dupont.com

Mr. James R. Butner
Parsons Engineering Science
2901 W Busch BLVD
STE 901
Tampa FL 32618
USA
phone: 813/933-4650
fax: 813/932-7416
e-mail:

Ms. Joaquin Caballero
ENTACT, Inc.
802 S Woodrow Wilson
Plant City FL 33567
USA
phone: 813/754-7004
fax: 813/754-7708
e-mail:

Ms. Darcy J. Campbell
U.S. Environmental Protection Agency
999 18th ST, STE 500
Denver CO 80202
USA
phone: 303/312/6560
fax: 303/312/6065
e-mail:

Dr. Hugh J. Campbell, Jr.
E.I. DuPont De Nemours & Co., Inc.
1007 Market ST
B12218
Wilmington DE 19898
USA
phone: 302/892-1268
fax: 302/892-7641
e-mail:
campbehj@a1.csoc.umc.dupont.com

Dr. Kirk J. Cantrell
Applied Geology and Geochemistry
Group
Battelle, Pacific Northwest National
Laboratory
P.O. Box 999
Mail Stop K6-81
Richland WA 99352
USA
phone: 509/376-2136
fax: 509/376-5368
e-mail:

Mr. Michael J. Carey
Geo-Con, a Woodward-Clyde Company
4075 Monroeville BLVD
Corp. One, BLDG. II, STE 400
Monroeville PA 15146
USA
phone: 412/856-7700
fax: 412/373-3357
e-mail:

Mr. Kenneth W. Cargill
GeoSyntec Consultants
1100 Lake Hearn Dr. NE Ste. 200
Atlanta GA 30342
USA
phone: 404/705/9500
fax: 404/705/2000
e-mail:

Mr. Robert J. Carlson
Remedial Construction Department
Rollins Environmental Services Inc.
15 Chestnut Hill Court
Woodlands TX 77380
USA
phone: 281/478-2103
fax: 281/478-2102
e-mail:

Mr. David A. Carson
NRMRL
U.S. Environmental Protection Agency
5995 Center Hill AVE
Cincinnati OH 45224
USA
phone: 513/569-7527
fax: 513/569-7879
e-mail: carson.david@epamail.epa.gov

Mr. Ernest E. Carter
Carter Technologies
9702 Garden Row
Sugar Land TX 77478
USA
phone: 281/495-2603 or 0540
fax: 281/495-2603 or 0540
e-mail: ernie_carter@prodigy.com

Ms. Meghan F. Cassidy
U.S. Environmental Protection Agency
Region 1
JFK Federal Building
Mailcode HBI
Boston MA 02203
USA
phone: 617/573/5785
fax: 617/223/5580
e-mail:

Mr. Skip Chamberlain
Office of Technology Systems (EM-53)
U.S. Department of Energy
Cloverleaf 1182
19901 Germantown RD
Germantown MD 20874-1290
USA
phone: 301/903-7248
fax: 301/903-7234
e-mail: grover.chamberlain@em.doe.gov

Mr. Matthew J. Charsky
U.S. Environmental Protection Agency
401 M ST SW (5202 G)
Washington DC 20460
USA
phone: 703/603-8777
fax: 703/603-9133
e-mail:

Dr. Calvin C. Chien
Core Resources Section
DuPont Specialty Chemicals
Barley Mill Plaza 27/2228
Routes 141 & 48
Wilmington DE 19805
USA
phone: 302/892-7439
fax: 302/892-7641
e-mail:

Dr. Dennis Don Chilcote
Ecolight
3248 16th AVE S
Minneapolis MN 55407-2348
USA
phone: 612/729-0878
fax: 612/729-0878
e-mail:

Dr. Chung-Tien Chin
Moh and Associates, Inc.
11/Fl., No. 35, Lane 11, Kwangfu North
Road
Taipei 105 Taiwan REPUBLIC OF
CHINA
phone: 886-2/7535399
fax: 886-2/7662343
e-mail: maatpcc.1@tpts1.seed.net.tw

Conference Participants

Mr. Yoon-Jean Choi
U.S. Environmental Protection Agency
JFK Federal BLDG
MC HBS
Boston MA 02203
USA
phone: 617/223-5505
fax: 617/573-9662
e-mail:

Mr. Marcelo Chuaqui
ECO Grouting Specialists Ltd.
73 Credit RD
Cheltenham Ontario LOP 1C0
CANADA
phone: 905/838-0150
fax: 905/838-3825
e-mail:

Ms. Jo Ann Cola
U.S. Environmental Protection Agency
75 Hawthorne ST (H-6-4)
San Francisco CA 94105
USA
phone: 415/744/2238
fax: 415/744/2180
e-mail: cola.joann@epamail@epa.gov

Mr. Scott J. Colburn
Lockheed Martin Energy Systems
P.O. Box 2003
831 Tri-County Bld.
Oliver Springs TN 37840
USA
phone: 423/435-3470
fax: 423/435/3290
e-mail: colburnsj@ornl.gov

Mr. Brewster Conant
Dept. of Earth Sciences
University of Waterloo
Waterloo Ontario N2L 3G1
CANADA
phone: 519/885-1211
fax: 519/746-7484
e-mail: bconatj@sciborg.uwaterloo.ca

Mr. Joseph P. Congdon
Montell Polyolefins
2801 Centerville RD
Wilmington DE 19808
USA
phone: 302/996-6198
fax: 302/996-6138
e-mail:

Ms. Donna Conley
SBP Technologies, Inc.
105 Gregory Square
Pensacola FL 32501
USA
phone: 904/470-0055
fax: 904/470-0058
e-mail:

Mr. John A. Connor
Groundwater Services, Inc.
5252 Westchester, STE 270
Houston TX 77005
USA
phone: 713/663-6600
fax: 713/663-6546
e-mail: jacannor@gsi-net.com

Mr. Harry Craig
Oregon Operations Office
U.S. Environmental Protection Agency
Region 10
811 SW 6th AVE
Portland OR 97204
USA
phone: 503/326/3689
fax: 503/326/3399
e-mail: craig.harry@epamail.epa.gov

Mr. Michael E. Crain
U.S. Army Corps of Engineers
(CEMRO-ED-GH)
215 N 17th Street
Omaha NE 68102-4978
USA
phone: 402/221-7787
fax: 402/221-7769
e-mail:

Mr. James M. Cramer
Nilex Corporation
Corporate Headquarters
6810 S Jordan RD
Englewood CO 80112
USA
phone: 303/766-2000
fax: 303/766-1110
e-mail: jcramer@nilex.com

Dr. Daniel G. Crouse
Roy F. Weston, Inc./REAC
2890 Woodbridge AVE
Edison NJ 08837-3679
USA
phone: 908/321-4222
fax: 908/494-4021
e-mail: crouse.dan@epamail.epa.gov

Mr. Kim Dahlstrom
Ringstedvej 20
DK-4000 Roskilde DENMARK
phone: 45/463003101
fax: 45/46300311
e-mail: kda@mst.dk

Dr. William D. Daily
Lawrence Livermore National Laboratory
P.O. Box 808, L-156
BLDG 131, RM 2660
Livermore CA 94550
USA
phone: 510/422-8623
fax: 510/422-3013
e-mail: daily1@llnl.gov

Mr. James M. Damon
Sevenson Environmental Services, Inc.
2749 Lockport RD
Niagra Falls NY 14302
USA
phone: 716/284-0431
fax: 716/284-1796
e-mail:

Dr. David E. Daniel
Dept. of Civil Engineering
University of Illinois at
Urbana-Champaign
1114a Newmark Civil Engineering
Laboratory
205 N Mathews AVE, MC-250
Urbana IL 61801
USA
phone: 217/333-1497
fax: 217/265-0318
e-mail:

Mr. John L. Daniels
Cntr. for Environ. Eng. & Science
Technologies
University of Massachusetts - Lowell
One University AVE
Lowell MA 01854
USA
phone: 508/934/2291
fax: 508/934/3092
e-mail: danielsjcwoods.uml.edu

Mr. Winn J. Darden
WVCO
P.O. Box 2280
Eugene OR 97402
USA
phone: 541/484-9621 x298
fax: 541/343-4207
e-mail:

Conference Participants

Ms. Kathryn L. Davies
U.S. Environmental Protection Agency
Region 3
841 Chestnut BLDG (3HW41)
Philadelphia PA 19107
USA
phone: 215/566-3315
fax: 215/566-3001
e-mail: davies.kathy@epamail.epa.gov

Ms. Katherine L. Davis
DuPont Environmental Remediation
Services
Barley Mill Plaza, BLDG 27/1210
P.O. Box 80027
Wilmington DE 19880-0027
USA
phone: 302/892-7596
fax: 302/892-7643
e-mail:
DavisKL@A1.CSOC.UMC.dupont.com

Mr. Steven R. Day
Geo-Con, a Woodward-Clyde Company
Standford Place 3, STE 600
4582 S Ulster ST
Denver CO 80237
USA
phone: 303/740-2600 or 740-2714 (DL)
fax: 303/740-2650
e-mail:

Mr. Philip R. DeLuca
Sevenson Environmental Services, Inc.
2749 Lockport RD
Niagra Falls NY 14302
USA
phone: 716/284-0431
fax: 716/284-1796
e-mail:

Mr. Michael DeRosa
ENTACT
3233 N Clifton
Chicago IL 60657
USA
phone: 773/281/2455
fax: 773/281/2526
e-mail:

Mr. Warren T. Dean
Environmental Systems and
Technologies, Inc.
2608 Sheffield DR
Blacksburg VA 24073
USA
phone: 540/552-0685
fax: 540/951-5307
e-mail: admin@esnt.com

Mr. Paul V. Dean
Tetra Tech EM Inc.
1593 Springhill Road
Suite 300
Vienna VA 22182
USA
phone: 703/287/8806
fax: 703/287/8910
e-mail: deanp@prceim: or
(deanp@prcemi)

Mr. John A. Delashmit
U.S. Environmental Protection Agency
Region 7
726 Minnesota AVE
Kansas City KS 66101
USA
phone: 913/551/7821
fax: 913/551/7947
e-mail: delashmit.john@epamail.epa.gov

Mr. Peter W. Deming
Mueser Rutledge Consulting Engineers
708 Third AVE
New York NY 10017
USA
phone: 212/490-7110
fax: 212/953-5626
e-mail:

Mr. Narendra Desai
Aberdeen Proving Ground
U.S. Army
USAGAPG, DSIIE-ECRD, Bldg F4430
ATTN: STEAP-SH-ER
Aberdeen Proving Ground MD
21010-5423
USA
phone: 410/671/4569 or 3320
fax: 410/671/3010
e-mail:

Mr. Vincent B. Dick
Haley & Aldrich of New York
189 N Water ST
Rochester NY 14604
USA
phone: 716/327-5507
fax: 716/232-6768
e-mail: VBD@Haley Aldrich.com

Mr. Stephen D. Doss
BFI
28422 Frost RD
Livingstone LA 70754
USA
phone: 504/686-0122 ext.3001
fax: 504/686-0189
e-mail:

Mr. Jeff W. Douthitt
Lockheed Martin Energy Research
761 Veterans Avenue
Kevil KY 42053
USA
phone: 502/441/5088
fax: 502/441/5064
e-mail: douthittjw@ornl.gov

Mr. Eric H. Drescher
Batelle Memorial Institute
505 King Ave, RM 10-1-12
Columbus OH 43201
USA
phone: 614/424-3088
fax: 614/424-3667
e-mail: drescher@battelle.org

Dr. Stanislaw Dudka
Department of Crop and Soil Sciences
The University of Georgia
3111 Miller Plant Science BLDG
Athens GA 30602-7272
USA
phone: 706/542-2461
fax: 706/542-0914
e-mail: sdudka@uga.cc.uga.edu

Dr. Brian P. Dwyer
Sandia National Laboratories
MS 0719
Albuquerque NM 87185-0719
USA
phone: 505/845-9894
fax: 505/844-0543
e-mail: bpdwyer@sandia.gov

Mr. Stephen F. Dwyer
Sandia National Laboratories
Dept. 6621, MS-0719
Albuquerque NM 87185
USA
phone: 505/844-0595
fax: 505/844-0543
e-mail: sfdwyer@sandia.gov

Dr. Ali Ebadian
Hemispheric Center for Environ. Techn.
Florida International University
University Park
Center for Engineering and Applied
Science
Miami FL 33199
USA
phone: 305/348-3585
fax: 305/348-4176
e-mail:

Conference Participants

Mr. James C. Edwards
Inquip Associates, Inc.
1300 Old Chain Bridge Road
McLean VA 22101
USA
phone: 703/442-0143
fax: 703/442-0188
e-mail:

Mr. Neal S. Egan
MSE Technology Applications
P.O. Box 4078
Butte MT 59702
USA
phone: 406/494-7265
fax: 406/494/7230
e-mail: negan@buttenet.com

Mr. Frank J.J. Elskens
Bitumar N.V.
Haven 1025
Scheldeduk 30
2070 Zwundrecht BELGIUM
phone: 32/3/2505443
fax: 32/3/2505269
e-mail:

Dr. Dave A. Emilia
MSE Technology Applications, Inc.
P.O. Box 4078
Butte MT 59702
USA
phone: 406/494/7100
fax: 406/494/7230
e-mail:

Mr. Gary B. Emmanuel
Environmental Resources Management,
Inc.
855 Springdale Drive
Exton PA 19341
USA
phone: 610/524/3500
fax: 610/524/7796
e-mail:

Ms. Annette Esnault
Bachy
4, rue Henri Sainte-Claire Deville
Les Colonnades
92563 Rueil Malmaison Cedex FRANCE
phone: 33-1/4714-2600
fax: 33-1/4714-2626
e-mail:

Dr. Jeffrey C. Evans
Dept. of Civil Engineering
Bucknell University
Lewisburg PA 17837
USA
phone: 717/524-1371
fax: 717/534-1822
e-mail: evans@bucknell.edu

Mr. Lorne Everett
Geraghty & Miller
3700 State ST, STE 350
Santa Barbara CA 93105
USA
phone: 805/687-7559
fax: 805/687-0838
e-mail:

Mr. Tory Failmezger
Global Environ. & Technology
Foundation (GNET)
7010 Little River Turnpike
STE 300
Annandale VA 22003
USA
phone: 703/750-6401
fax: 703/750-6506
e-mail: victor.failmezger@gnet.org

Ms. Virginia Fairweather
Civil Engineering Magazine
345 E 47th ST
New York NY 10017-2398
USA
phone: 212/705-7463
fax: 212/705-7486
e-mail: vfairweather@asce.org

Dr. Hsai-Yang Fang
CEEST
University of Massachusetts Lowell
One University AVE
Lowell MA 01854-2881
USA
phone: 508/934-2285
fax: 508/934-3092
e-mail:

Mr. James E. Fanon
LMES/US. DOE/OST EM-50
12800 Middlebrook RD
Germantown MD 20874
USA
phone: 301/916-2805
fax: 301/916-8699
e-mail:

Mr. Richard K. Farnsworth
Lockheed Martin Idaho Technologies
Company
Idaho National Engineering Laboratory
P.O. Box 1625, MS-3710
2525 Fremont AVE
Idaho Falls ID 83415-3710
USA
phone: 208/526-6986
fax: 208/526-6802 or 5142
e-mail:

Mr. James M. Fenstermacher
Clean Harbors Environmental Services,
Inc.
1501 Washington Street
Braintree MA 02135
USA
phone: 617/849-1800 ext. 1127
fax: 617/794-1760
e-mail:

Ms. Danette R. Fettig
IFAI
345 Cedar ST, STE 800
St. Paul MN 55101
USA
phone: 612/222-2508 /DL=800/636-5042
fax: 612/222-8215
e-mail: ifaidan@aol.com

Dr. George M. Filz
Dept. of Civil Engineering
Virginia Tech
109 Patton Hall
Blacksburg VA 24061-0105
USA
phone: 540/231-7151
fax: 540/231-7532
e-mail: filz@vt.edu

Dr. Stefan Finsterle
Earth Sciences Division
Lawrence Berkeley National Laboratory
University of California
MS 90-1116
One Cyclotron RD
Berkeley CA 94720
USA
phone: 510/486-5205
fax: 510/486-5686
e-mail:

Mr. David C. Floyd
ENTACT, Inc.
1616 Corporate Court, STE 150
Irving TX 75038
USA
phone: 972/580-1323
fax: 972/550-7464
e-mail:

Conference Participants

Mr. R. M. Focht
EnviroMetal Technologies, Inc.
42 Arrow RD
Guelph Ontario N1K 1S6
CANADA
phone: 519/824-0432
fax: 519/763-2378
e-mail: eti@beak.com

Mr. Mark Fuhrmann
Brookhaven National Laboratory
BLDG 830
Upton NY 11973-5000
USA
phone: 516/344-2224
fax: 516/344-4486
e-mail: fuhrman1@bnl.gov

Mr. Glendon W. Gee
Battelle Pacific Northwest Laboratory
P.O. Box 999
Batelle-MS K9-33
Richland WA 99352
USA
phone: 509/372-6096
fax: 509/372-6089
e-mail: gw_gee@pnl.gov

Mr. Tad C. Fox
Battelle
505 King Avenue
Columbus OH 43201
USA
phone: 614/424/7577
fax: 614/424/3667
e-mail: foxtc@battelle.org

Mr. Allen J. Furth
Hayward Baker Inc.
1875 Mayfield Road
Odenton MD 21113
USA
phone: 410/551-1980
fax: 410/551-8206
e-mail:

Dr. Bruno Gemmi
Geotechnical Consultant
Via XXV Aprile n.2
43020 - Basilicagoiano - Parma ITALY
phone: 39-521/243464 or 39-336/766496
fax: 39-521/243454 or /686121
e-mail: gemmib@mbox.vol.it

Dr. Clyde W. Frank
Office of Science and Technology
U.S. Department of Energy (EM-50)
1000 Independence AV SW, 58-014
Washington DC 20585
USA

Ms. Alyssa Gall
SBP Technologies, Inc.
105 Gregory Square
Pensacola FL 32501
USA
phone: 904/470-0055
fax: 904/470-0058
e-mail:

Mr. John G. Gillroy
The Eicon Group, Inc.
142 Temple ST
New Haven CT 06510
USA
phone: 203/789-1260
fax: 203/789-8261
e-mail:

Mr. Carl R. Froede, Jr.
U.S. Environmental Protection Agency -
Region 4
100 Alabama ST SW
Atlanta GA 30303-3104
USA
phone: 404/562/8550
fax: 404/562/8628
e-mail:

Mr. David H. Garcia
Naval Facilities Engineering Service
Center
Code 411
1100 23rd AVE
Port Hueneme CA 93043
USA
phone: 805/982-1764
fax: 805/982-4304
e-mail: Dgarcia@NFESC.NAVY.MIL

Dr. Jean-Pierre Giroud
GeoSyntec Consultants
621 NW 53rd ST, STE 650
Boca Raton FL 33487-8220
USA
phone: 561/995-0900
fax: 561/995-0925
e-mail: JPGiroud@geosyntec.com

Dr. John S. Fruchter
Battelle, Pacific Northwest National
Laboratory
P.O. Box 999, MSIN K6-96
Richland WA 99352
USA
phone: 509/376-3937
fax: 509/372-1704
e-mail: js_fruchter@pnl.gov

Dr. Kevin P. Garon
DuPont Environmental
Barley Mill Plaza 27-2370
P.O. Box 80027
Wilmington DE 19880-0027
USA
phone: 302/992-6775
fax: 302/892-7637
e-mail: garonkp@csoc.dnet.dupont.com

Mr. Will Goldberg
MSE Technology Applications, Inc.
P.O. Box 4078
Butte MT 59701
USA
phone: 406/494/7330
fax: 406/494/7230
e-mail: goldberg@buttenet.com

Mr. Rene F. Fuentes
Groundwater Forum Member
U.S. Environmental Protection Agency -
Region 10
1200 - 6th AVE M/S (OEA-O95)
Seattle WA 98101
USA
phone: 206/553-1599
fax: 206/553-0119
e-mail: fuentes.rene@epamail.epa.gov

Ms. Penny M. Gaynor
Georgia Environmental Protection
Division
205 Butler ST, STE 1162
Atlanta GA 30334
USA
phone: 404/656/2833
fax: 404/656/9425
e-mail:

Ms. Martha L. Gonzalez
Naval Facilities Engineering Service
Center
1100 23rd AVE
Port Hueneme CA 93043-4370
USA
phone: 805/982-5270
fax: 805/982-4304
e-mail: mgonzal@nfesc.navy.mil1

Conference Participants

Mr. Herbert M. Gorrod
U.S. Environmental Protection Agency
Region 6
1445 Ross AVE
Dallas TX 75202
USA
phone: 214/665/6779
fax: 214/665/6680
e-mail:

Dr. Peter Grathwohl
Applied Geology, Geological Institute
University of Tuebingen
Sindelfinger Str. 57
72070 Tübingen GERMANY
phone: 49-7071/297-5429
fax: 49-7071/5059
e-mail: grathwohl@uni-tuebingen.oe

Mr. Laymon L. Gray
CHAERSE
Florida State University
2035 E Paul Dirac DR
226 HMB
Tallahassee FL 32310-3700
USA
phone: 904/644-5524
fax: 904/574-6704
e-mail:

Mr. Ronald J. Griffith
E.I. DuPont
Barley Mill Plaza 27/2292
P.O. Box 80027
Wilmington DE 9880-0027
USA
phone: 302/892-7451
fax: 302/892-7641
e-mail: griffirjea1.engg.uml.dupont.com

Mr. Darwin M. Grigg
Lockheed-Martin Idaho Technologies Co.
P.O. Box 1625
Idaho Falls ID 83401
USA
phone: 208/522-4338

Ms. Beth A. Gross
GeoSyntec Consultants
1004 E 43rd ST
Austin TX 78751-4407
USA
phone: 512/451-4003
fax: 512/451-9355
e-mail: bethg@geosyntec.com

Dr. Baohua Gu
Environmental Sciences Division
Oak Ridge National Laboratory
P.O. Box 2008, MS 6036
Oak Ridge TN 37831-6036
USA
phone: 423/574-7286
fax: 423/576-8543
e-mail: gub1@ornl.gov

Mr. John L. Guglielmetti
DuPont Engineering
Beech Street Engineering Center
101 Beech ST, P.O. Box 80840
Wilmington DE 19880-0840
USA
phone: 302/695-0066
fax: 302/695-0734
e-mail:
JOHN.L.GUGLIELMETTI@usa.dupont.c
om

Mr. Richard (Dick) Guilliams
EnviroWall
One W Loop S, STE 100
Houston TX 77027
USA
phone: 713/964-6727
fax: 713/622-5513
e-mail:

Dr. Neeraj Gupta
Battelle
505 King Avenue
Columbus OH 43201
USA
phone: 614/424/3820
fax: 614/424/3667
e-mail: gupta@battelle.org

Dr. John H. Guswa
HSI GeoTrans
6 Lancaster County RD
STE 4
Harvard MA 01451
USA
phone: 508/772-7557
fax: 508/772-6183
e-mail:

Mr. John J. Gysling
Delaware Dept. of Natural Resources
715 Grantham LN
New Castle DE 19720
USA
phone: 302/323-4540
fax: 302/323-4561
e-mail: jgysling@state.de.us

Mr. Laique Haider
DuPont Environmental
140 Cypress Station, STE 140
Houston TX 77086
USA
phone: 281/586-5652
fax: 281/586-5650
e-mail:

Dr. Nadia Leïla Hakem
Earth Sciences Division
Lawrence Berkeley National Laboratory
University of California
MS 70A-1150
One Cycolotron Rd
Berkeley CA 94720
USA
phone: 510/486-7701 or 7794
fax: 510/486-5799
e-mail:

Ms. Janice B. Hall
JPS Elastomerics Corp.
9 Sullivan RD
Holyoke MA 01040
USA
phone: 413/552-1031
fax: 413/552-1198
e-mail:

Dr. John H. Hammill
Canadian Metal Rolling Mills
950 Industrial RD
Cambridge Ontario N3H 4WI
CANADA
phone: 519/650-2222
fax: 519/650-2223
e-mail:

Mr. Bryan L. Harre
Naval Facilities Engineering Service
Center
NFESC Code 411
1100 23rd AVE
Port Hueneme CA 93043
USA
phone: 805/982-1795
fax: 805/982-4304
e-mail: bharre@nfesc.navy.mil

Ms. Andrea T. Hart
Western Environmental Technology
Office
MSE Technology Applications, Inc.
P.O. Box 4078
Butte MT 59702
USA
phone: 406/494-7410
fax: 406/494-7230
e-mail: ahart@buttenet.com

Conference Participants

Mr. Robert F. Hayden
Geo-Con, Inc.
4075 Monroeville Blvd.
Corp One, BLDG. II, Suite 400
Monroeville PA 15146
USA
phone: 412/856/7700
fax: 412/373/3357
e-mail:

Mr. Joseph J. Hayes
EMCON
1 Mill Street
Burlington VT 05401
USA
phone: 802/658/6884
fax: 802/658/5014
e-mail: burlingt@emconinc.com

Mr. John Heiser
Environmental & Waste Technology
Center
Brookhaven National Laboratory
P.O. Box 5000, BLDG 830
34 N Railroad
Upton NY 11973-5000
USA
phone: 516/344-4405
fax: 516/344-4486
e-mail: heiser@bnl.gov

Mr. Mike Heisler
PECO Energy Company
2301 Market Street S21-2
Philadelphia PA 19101-8699
USA
phone: 215/841/5178
fax: 215/841/4062
e-mail:

Mr. Richard L. Helferich
Cercona of America, Inc.
5911 Wolf Creek Pike
Dayton OH 45426
USA
phone: 937/854/9860
fax: 937/854/9861
e-mail: rhelferich@coax.net

Dr. Roy C. Herndon
CHAERSE
Florida State University
2035 E Paul Dirac DR
226 HMB
Tallahassee FL 32310-3700
USA
phone: 904/644-5524
fax: 904/574-6704
e-mail:

Dr. Gerry M. Heslin
Department of Civil Engineering
Virginia Polytechnic Institute
Blacksburg VA USA
phone: 540/231-4417 or 231-7151
fax: 540/231-7532
e-mail:

Ms. Alison A. Hess
U.S. Environmental Protection Agency
290 Broadway
New York NY 10007-1866
USA
phone: 212/637/3959
fax: 212/637/4284
e-mail: hess.alison@epamail.epa.gov

Mr. Steven R. Hirsh
U.S. Environmental Protection Agency -
Region 3
841 Chestnut BLDG
Philadelphia PA 19107
USA
phone: 215/566/3352
fax: 215/566/3051
e-mail: hirsh.steven@epamail.epa.gov

Mr. Richard Ho
U.S. Environmental Protection Agency -
Region 2
290 Broadway, 19th Floor
New York NY 10007
USA
phone: fax: e-mail:

Mr. Tri T. Hoang
Office of Radiation and Indoor Air
U.S. Environmental Protection Agency -
(6602J)
401 M ST SW
Washington DC 20460
USA
phone: 202/233-9713
fax: 202/233-9650
e-mail:

Dr. Karl A. Hoenke
Chevron Research and Technology Co.
1003 W Cutting BLVD
Richmond CA 94804
USA
phone: 510/242-5901
fax: 510/242-1380
e-mail: khoe@chevron.com

Mr. Gary E. Hokkanen
Geomatrix Consultants, Inc.
1000 Shelard Parkway, Suite 335
Minneapolis MN 55426
USA
phone: 612/544/4614
fax: 612/544/4874
e-mail: ghokkanen@geomatrix.com

Dr. Gwen Hooten
U.S. Environmental Protection Agency
999 18th ST
Dewer CO 80202
USA
phone: 303/312-6571
fax: e-mail:
hooten.gwen@epamail.epa.gov

Ms. Tao Hu
University of Toronto
Toronto Ontario CANADA

Dr. David W. Hubble
Department of Earth Sciences
University of Waterloo
617 Highpoint Avenue
Waterloo Ontario N21 473
CANADA
phone: 519/884/3868
fax: 519/746/0183
e-mail:
DWHUBBLE@CGRPC.watstar.uwaterloo
.ca

Dr. Dale D. Huff
Oak Ridge National Laboratory
P.O. Box 2008
Oak Ridge TN 37831-6400
USA
phone: 423/574-7859
fax: 423/574-7420
e-mail: ddh@oml.gov

Dr. Scott G. Huling
U.S. Environmental Protection Agency
NRMRL/SPRD
P.O. Box 1198
Ada OK 74820
USA
phone: 405/436/8611
fax: 405/436/8614
e-mail: @ad3100.ada.epa.gov

Conference Participants

Mr. Kevin L. Hylton
Rochester Gas and Electric Corporation
89 East AVE
Rochester NY 14649
USA
phone: 716/724-8428
fax: 716/724-8683
e-mail:

Mr. David S. Ingle
Pinellas Area Office
U.S. Department of Energy
Pinellas FL USA
phone: 813/541-8943
fax: 813/541-8370
e-mail:

Dr. Hilary I. Inyang
CEEST
Dept. of Civil & Environmental
Engineering
University of Massachusetts
One University AVE
North Campus RM E-114
Lowell MA 01854
USA
phone: 508/934-2285
fax: 508/934-3092
e-mail:

Mr. Bob Janosy
Battelle Memorial Institute
505 King AVE
Columbus OH 43201
USA
phone: 614/424-7160
fax: 614/424-3667
e-mail: janosyr@battelle.org

Mr. Chester L. Janowski
U.S. Environmental Protection Agency
JFK Federal BLDG, MC HBO
Boston MA 02203
USA
phone: 617/573/9623
fax: 617/573/9662
e-mail: janowski.chet@epamail.epa.gov

Mr. Wm. (Bill) G. Jaques
W.G. Jaques Company
2183 NW 86th Street
Des Moines IA 50322
USA
phone: 515-276-5466
fax: 515-270-8329
e-mail:

Mr. David L. Jaros
U.S. Army Corps of Engineers
12565 W Center RD
CEMRO-HX-G
Omaha NE 68144
USA
phone: 402/697-2668
fax: 402/697-2673
e-mail:
dave.l.jaros@mrdo1.usacp.army.mil

Mr. Brian H. Jasperse
Geo-Con, Inc.
4075 Monroeville BLVD.
Corp. One, BLDG II., Suite 400
Monroeville PA 15146
USA
phone: 412/856/7700
fax: 412/373/3357
e-mail:

Dr. Stephan Arthur Jefferis
Golder Associates (UK) Ltd.
54 Moorbridge Road
Maidenhead
Berkshire SL6 8BN England UK
phone: 44-1628/771-731 or 586206=DL
fax: 44-1628/770699
e-mail: sjefferis@golder.com

Mr. Richard H. Jensen
DuPont
Experimental Station 304
Wilmington DE 19880
USA
phone: 302/695-4685
fax: 302/695-4414
e-mail:
JensenRH@esvax.dnet.dupont.com

Mr. Bjorn K. Jensen
VKI Water Quality Institute
AGERN ALLE II
DK 2970 Horsholm DENMARK
phone: 45/42/865211
fax: 45/42/867273
e-mail: dkj@vki.dk

Mr. Alan T. Jines, P.E.
Idaho Operations Office
U.S. Department of Energy
850 Energy Drive
Idaho Falls ID 83401
USA
phone: 208/526-7524
fax: 208/526/0598
e-mail: jinesa@inel.gov

Dr. Terrence G. Johnson
Roy F. Weston, Inc./REAC
GSA Raritan Depot, 2890 Woodbridge
AVE
BLDG 209 Annex
Edison NJ 08837-3679
USA
phone: 908/321-4241 or 4200
fax: 908/494-4021
e-mail:
johnson.terrance@epamail.epa.gov

Mr. Harry R. Johnson
ARCTECH, Inc.
14100 Park Meadow DR
Chantilly VA 20151
USA
phone: 703/222-0280
fax: 703/222-0299
e-mail: humnsorb@arctech.com

Mr. Tracy R. Johnson
Comanco Environmental Corporation
7911 Professional Place
Tampa FL 33637
USA
phone: 813/988-8829
fax: 813/988-8779
e-mail:

Ms. Carla Johnson
Waterstone Consultants, Inc.
7698 Fairview Road
Boulder CO 80303
USA
phone: 303/499/6789
fax: 303/499/0123
e-mail: johnson@waterstoneinc.com

Dr. Donald O. Johnson
Energy Systems Division
Argonne National Laboratory
9700 S Cass AVE
BLDG 362
Argonne IL 60439-4815
USA
phone: 630/252-3392
fax: 630/252-7288
e-mail: don_johnson@gmgate.anl.gov

Conference Participants

Mr. Carey A. Johnston
Office of Radiation and Indoor Air
U.S. Environmental Protection Agency -
(6602J)
401 M ST SW
Washington DC 20460
USA
phone: 202/233-9341
fax: 202/233-9650
e-mail: Johnston.carey@epamail.epa.gov

Mr. Eugene B. Jones
CHAERSE
Florida State University
2035 E Paul Dirac DR
226 HMB
Tallahassee FL 32310-3700
USA
phone: 904/644-5524
fax: 904/574-6704
e-mail:

Ms. Robin Jowett
Waterloo Barrier Inc.
P.O. Box 385
Rockwood Ontario N0B 2K0
CANADA
phone: 519/856-1352
fax: 519/856-2503
e-mail:

Mr. Donald R. Justice
Horizontal Technologies, Inc.
4767 Pine Island RD NW
Matlacha FL 33993
USA
phone: 941/283-5640
fax: 941/283-2222
e-mail: info@horizontal.com

Ms. Leslie A. Karr
Naval Facilities Engineering Service
Center
NFESC Code 411
1100 23rd AVE
Port Huenerne CA 93043
USA
phone: 805/982-1618
fax: 805/982-4304
e-mail:

Dr. Michael G. Katona
Environics Directorate
Armstrong Laboratory
U.S. Air Force
Code AL/EQ-CN
139 Barnes DR, STE 2
Tyndall AFB FL 32403-5323
USA
phone: 904/283-6274
fax: 904/283-6286
e-mail:

Dr. Joseph L. Kauschinger
Ground Environmental Services
200 Berry Glen CT
Alpharetta GA 30202
USA
phone: 770/993/3538
fax: 770/992/8011
e-mail: kausch@ix.netcom.com

Dr. Abidin Kaya
CEEST
Dept. of Civil Engineering
University of Massachusetts Lowell
One University AVE
Lowell MA 01854-2881
USA
phone: 508/934-3185 or 2291 or 2280
fax: 508/934-3092
e-mail: kayaa@woods.uml.edu

Mr. Paul E. Kerch
Armstrong Laboratory, Environics
Directorate
AL/EQW
139 Barnes DR, STE 2
Tyndall AFB FL 32403-5323
USA
phone: 904/283-6259
fax: 904/283-6286
e-mail:

Mr. Berg Keshian
Roy P. Weston, Inc.
2567 B 3/4 Road
Grand Junction CO 81503
USA
phone: 970/248/7671
fax: 970/248/7676
e-mail:
BERG.KESHIAN@GJPOMAIL.DOEGJP
O.COM

Ms. Lisa Keteltas
Wade's Frac Tanks, Inc.
P.O. Drawer 399
Ellisville MS 39437
USA
phone: 601/649-1817
fax: 601/477-8290
e-mail:

Mr. Thomas J. Kewen
Kewen Environmental Limited
9 Bayberry ST
Stouffville Ontario L4A 7Z1
CANADA
phone: 905/640/9454
fax: 905/640/9455
e-mail: kewen@kewen.com

Mr. Faizur R. Khan
American Society of Civil Engineer
Rollins Environmental Services
2939 Kennesaw Drive
Missouri City TX 77459
USA
phone: 281/835/9373
fax: 281/478/2102
e-mail: ckhan@msn.com

Dr. A. Khandelwal
Department of Civil Engineering
SUNY at Buffalo
230 Jarvis Hall
Buffalo NY 14260
USA
phone: 716/645-2114 ext. 2336
fax: 716/645-3667
e-mail:

Dr. Milind V. Khire
GeoSyntec Consultants
621 NW 53rd ST, STE 650
Boca Raton FL 33487
USA
phone: 561/995-0900
fax: 561/995-0925
e-mail: Milind@juno.com

Mr. Lawrence D. Kimmel
U.S. Environmental Protection Agency
999 18th St. Suite 500
Denver CO 80202-2466
USA
phone: 303/312/6659
fax: 303/312/6067
e-mail:

Mr. Steven E. Kinser
U.S. Environmental Protection Agency -
Region 7
726 Minnesota AVE
Kansas City KS 66101
USA
phone: 913/551/7728
fax: 913/551/7063
e-mail: kinser.steven@epamail.epa.gov

Mr. Glenn R. Kistner
U.S. Environmental Protection Agency
75 Hawthorne ST
San Francisco CA 94105
USA
phone: 415/744/2210
fax: 415/744/1796
e-mail: kistner.glenn@epamail.epa.gov

Conference Participants

Dr. Peter Kjeldsen
Dept. of Environmental Science &
Engineering
Technical University of Denmark
Building 115
DK 2800 Lyngby DENMARK
phone: 45/45/251600
fax: 45/45/932850
e-mail: pk@imt.dtv.dk

Mr. Mark A. Koelling
Hayward Baker, Inc.
2701 California AVE SW, STE 230
Seattle WA 98116
USA
phone: 206/223-1732
fax: 206/223-1733
e-mail: hbisea@aa.net

Ms. Loreen K. Kollar
CHAERSE
Florida State University
2035 E Paul Dirac DR
226 HMB
Tallahassee FL 32310-3700
USA
phone: 904/644-5524
fax: 904/574-6704
e-mail:

Mr. Nic Korte
Environmental Technology Section
Oak Ridge National Laboratory
P.O. Box 2567
Grand Junction CO 81502
USA
phone: 970/248-6210
fax: 970/248-6147
e-mail: kortene@ornl.gov

Col. John D. Koutsandreas
Florida State University
13643 Glenhurst RD
Gaithersburg MD 20878
USA
phone: 301/963-4944 or 8668
fax: 301/903-7234
e-mail:

Mr. Stewart Krause
Wyo-Ben, Inc.
P.O. Box 1979
Billings MT 59103
USA
phone: 406/652-6351
fax: 406/656-0748
e-mail:

Dr. Hans-Jurgen Kretzschmar
DBI Gas- und Umwelttechnik GmbH
Halsbrüker Str. 34
D-09599 Freiberg GERMANY
phone: 49-3731/365-355
fax: 49-3731/365-432
e-mail:

Mr. Ronald K. Krieg
RKK Limited
404 Smokey Point BLVD, STE 303
Arlington WA 98223
USA
phone: 360/653-4844
fax: 360/653-7456
e-mail: rkk@cryocell.com

Mr. John W. Kubarewicz
ORO STCG
Oak Ridge National Laboratory
P.O. Box 2008
125 Broadway Avenue
Oak Ridge TN 37830
USA
phone: 423/220/4943
fax: 423/220/4848
e-mail: ukf@ornl.gov

Mr. Douglass J. Kuhns
Lockheed-Martin Idaho Technologies Co.
P.O. Box 1625, MS 3920
Idaho Falls ID 83415-3920
USA
phone: 208/526-8826
fax: 208/526-6852
e-mail: dkh@inel.gov

Mr. J. Michael Kuperberg
CHAERSE
Florida State University
2035 E Paul Dirac DR
226 HMB
Tallahassee FL 32310-3700
USA
phone: 904/644-5524
fax: 904/574-6704
e-mail:

Mr. Michael E. Lail
Avisco Inc.
6621 Wilbanks RD
Knoxville TN 37912
USA
phone: 423/689-6383
fax: 423/281/8848
e-mail:

Mr. Nicholas Lailas
Center for Remediation Technology &
Tools
U.S. Environmental Protection Agency
401 M ST SW
ORIA(6603J)
Washington DC 20460
USA
phone: 202/233-9371
fax: 202/233-9650
e-mail:

Prof. Dr. István Lakatos
Research Laboratory for Mining
Chemistry
Hungarian Academy of Sciences
PO Box 2.
H-3515 Miskolc-Egyetemváros
HUNGARY
phone: 36-46/367-211
fax: 36-46/363-349 or 369-415
e-mail:

Dr. Fayaz Lakhwala
SBP Technologies, Inc.
105 Gregory Square
Pensacola FL 32501
USA
phone: 904/470-0055
fax: 904/470-0058
e-mail: 75357.1355@compuserve.com

Ms. Susan J. Lampman
CPD
Florida State University
TC214
Tallahassee FL 32306-2027
USA
phone: 904/644-7539
fax: 904/644-2589
e-mail: slampman@mailer.fsu.edu

Mr. Richard C. Landis
Core Resources Section
DuPont Specialty Chemicals
Barley Mill Plaza 27/2264
P.O. Box 80027
Wilmington DE 19880-0027
USA
phone: 302/892-7452
fax: 302/892-7641
e-mail:
landisrc@engg-mail.lvs.dupont.com

Conference Participants

Mr. David E. Langseder
Dept. of Natural Resources and Environ.
Control
State of Delaware
715 Grantham LN
New Castle DE 19720
USA
phone: 302/323-4540
fax: 302/323-4561
e-mail: dlangseder@dnrec.state.de.us

Dr. Christine A. Langton
Westinghouse Savannah River Company
SRTC, BLDG 773-A
Aiken SC 29808
USA
phone: 803/725-5806
fax: 803/725-4704
e-mail: Christine.Langton@srs.gov

Dr. John W. Laundré
Department of Biological Sciences
Idaho State University
Campus Box 8007
Pocatello ID 83201
USA
phone: 208/236-3914 or 236-3765
fax: 208/236-4570
e-mail: launjohn@fs.isu.edu

Ms. Maureen E. Leavitt
SAIC
800 Oak Ridge TPKE
Oak Ridge TN 37831
USA
phone: 423/481-4614
fax: 423/481-8797
e-mail: leavittm@orjt1.saic.com

Dr. Kun-Chieh Lee
Union Carbide Corporation
P.O. Box 8361
S. Charleston WV USA
phone: 304/747-5221
fax: 304/747-3680
e-mail:

Mr. Nikolaj K.J. Lehmann
VKI, Water Quality Institute
Agern Allé II
2970 Hørsholm DENMARK
phone: 45-4286-5211
fax: 45-4286-7273
e-mail:

Mr. Paul H. Leonard
U.S. Environmental Protection Agency -
Region 3
841 Chestnut Street
Philadelphia PA 19107-4431
USA
phone: 215/566/3350
fax: 215/566/3001
e-mail: leonard.paul@epamail.epa.gov

Mr. Eric Lightner
Office of Science and Technology
(EM-53)
U.S. Department of Energy
Cloverleaqf 1182
19901 Germantown RD
Germantown MD 20874-1290
USA
phone: 301/903-7935
fax: 301/903-7457
e-mail:

Ms. Vicki Lloyd
U.S. Environmental Protection Agency
OAR / ORIA/ NAREL
540 S. Morris AVE
Montgomery AL 36115-2601
USA
phone: 334-270-3467
fax: 334/270-3454
e-mail:

Mr. John D. Long
Lockheed Martin Energy Systems, Inc.
P.O. Box 2008
BLDG 1053; MS 6338
Oak Ridge TN 37831-6338
USA
phone: 423/574-8656
fax: 423/576-2893
e-mail: L5g@ornl.gov

Mr. Rich K. Lowe
STS Consultants Ltd.
11425 W Lake Park DR
Milwaukee WI 53224
USA
phone: 414/359-3030
fax: 414/359-0822
e-mail:

Mr. William E. Lowry
Science & Engineering Associates, Inc.
1570 Pacheco, Suite D-1
Santa Fe NM 87505
USA
phone: 505/983/6698
fax: 505/983/5868
e-mail: blowry@seabase.com

Dr. Ralph D. Ludwig
Water Technology International Corp.
867 Lakeshore Road
P.O. Box 5068
Burlington Ontario L7R 467
CANADA
phone: 905/336/4720
fax: 905/336-8913
e-mail: ralph.ludwig@cciw.ca

Dr. Ronaldo Luna
Department of Civil & Environmental
Engineering
Tulane University
Civil Engineering BLDG, RM 214
New Orleans LA 70118
USA
phone: 504/862-3252
fax: 504/862-8941
e-mail: ronaldo.luna@tulane.edu

Dr. Peter R. Lundie
Envirotech (Scotland) Limited
Woodburn Road, Blackburn
Aberdeen ABR ORX SCOTLAND
phone: 44/1224/79019
fax: 44/1224/790660
e-mail:

Mr. Larry D. Lydick
National Seal Company
1245 Corporate BLVD
STE 300
Aurora IL 60504
USA
phone: 630/898-1161
fax: 630/898-6556
e-mail:

Mr. Ian D. MacFarlane
EA Engineering, Science, & Technology,
Inc.
15 Loveton Circle
Sparks MD 21152
USA
phone: 410/329/5145
fax: 410/771/4204
e-mail:
idm@eaeng.mhs.compuserve.com

Conference Participants

Dr. Patricia D. Mackenzie
Corporate Research and Development
Center
General Electric
1 Research Circle
BLDG K1, RM 5A47
Niskayuna NY 12309
USA
phone: 518/387-6831
fax: 518/387-5592
e-mail: mackenzie@macgw1.crd.ge.com

Ms. Marianne Madsen
Environment and Energy Division
Hedeselskabet
Ringstedvej
DK-4000 Roskilde DENMARK
phone: 445/46300310
fax: 445/46300311
e-mail:

Mr. Daniel W. Mageau
GeoEngineers, Inc.
8410-154th Avenue, N.E.
Redmond WA 98052
USA
phone: 206/861-6000
fax: 206/861-6050
e-mail:

Mr. Jeffrey S. Mahan
Geraghty & Miller, Inc.
16 Carmel DR
Annapolis MD 21401
USA
phone: 410/987-0032
fax: 410/987-4392
e-mail:

Mr. Thomas M. Malloy
MSE Technology Applications, Inc.
P.O. Box 4078
Butte MT 59702
USA
phone: 406/494/7202
fax: 406/494/7230
e-mail: tmmalloy@buttenet.com

Mr. Peter C. Maltese
Geo-Con, a Woodward-Clyde Company
4075 Monroeville BLVD
Corporate One, BLDG II, STE 400
Monroeville PA 15146
USA
phone: 412/856-7700
fax: 412/373/3357
e-mail:

Mr. Michael A. Malusis
Department of Civil Engineering
Colorado State University
Fort Collins CO 80523
USA
phone: 970/491-2559
fax: 970/491-3584
e-mail: mm788363@engr.colostate.edu

Mr. Kenneth R. Manchester
MSE Technical Applications
P.O. Box 4078
Butte MT 59702
USA
phone: 406/494-7397
fax: 406/494-7230
e-mail: kmanch@buttenet.com

Mr. Stephen Mangion
ORSI (8104)
U.S. Environmental Protection Agency
401 M ST SW
Washington DC 20037
USA
phone: 202/260-1084
fax: 202/260-0106
e-mail:
Mangion.Stephen@epamail.epa.gov

Mr. Chris R. Manz
Montgomery Watson
11925 W Lake Park DR
STE 200
Milwaukee WI 53224
USA
phone: 414/359-1144
fax: 414/359-1145
e-mail: chris.manz@us.mw.com

Mr. Donald L. Marcus
EMCON
3200 N San Fernando Blvd.
Burbank CA 91504
USA
phone: 818/841/1160
fax: 818/846/9280
e-mail: dmarcus@emconinc.com

Dr. Doyle Markham
Enviromental Science & Research
Foundation
P. O. Box 51838
Idaho Falls ID 83405
USA
phone: 208/525-7038
fax: 208/525-7036
e-mail: markhamd@env.esrf.isu.edu

Mr. Scott A. Marquess
U.S. Environmental Protection Agency -
Region 7
726 Minnesota AVE
Kansas City KS 66101
USA
phone: 913/551/7131
fax: 913/551/7063
e-mail:

Dr. Wayne J. Martin
Pacific Northwest National Laboratory
(PNNL)
P.O. Box 999 (K9-14)
Richland WA 99352
USA
phone: 509/372-4881
fax: 509/375-5963
e-mail: wj_martin@pnl.gov

Dr. Lisa A. Martinenghi
Martinenghi Engineering
Vicolo Dei Saroli #1
6944 Cureglia SWITZERLAND
phone: 41-91/967-3517
fax: 41-91/967-3519
e-mail: martinen@swissonline.ch

Dr. Mark R. Matsumoto
Bourns College of Engineering
UC Riverside
Riverside CA 92521
USA
phone: 909/787-5318
fax: 909/787-3188
e-mail: matsumot@engr.ucr.edu

Dr. Gretchen E. Matthern
Lockheed Martin Idaho Technologies Co.
Idaho National Engineering Laboratory
P.O. Box 1625, MS 3710
Idaho Falls ID 83415
USA
phone: 208/526-8747
fax: 208/526-6802
e-mail: gtn@inel.gov

Ms. Sharon E. Matthews
Hazardous Waste Section
U.S. Environmental Protection Agency -
Region 4
980 College Station RD
Athens GA 30605
USA
phone: 706/355-8608
fax: 706/355-8508/8509/8744
e-mail:

Conference Participants

Mr. James A. McBane
U.S. Army Corps of Engineers, Seattle District
4735 E. Marginal Way South
Seattle WA 98134-2385
USA
phone: 206/764/3712
fax: 206/764/6795
e-mail:

Ms. A. Lynn McCloskey
Western Environmental Technology Office
MSE Technology Applications, Inc.
P.O. Box 4078
Butte MT 59701
USA
phone: 406/494-7371
fax: 406/494-7230
e-mail: lmcclosk@buttenet.com

Mr. Richard G. McGregor
Water Technology International
P.O. Box 5068
867 Lakeshore RD
Burlington Ontario L7R 467
CANADA
phone: 905/336-6479
fax: 905/336-8912
e-mail: richard.mcgregor@cciw.ca

Mr. Frank McInturff
Environmental & Safety Designs, Inc.
2114 Airport Blvd.
Suite 1150
Pensacola FL 32504
USA
phone: 904/479-4595
fax: 904/479-9120
e-mail: fmcinturff@ensafe.com

Mr. Charles McLellan
Hancock Capitol
1407 Nashville Avenue
New Orleans LA 70115
USA
phone: 504/895-2325
fax: 504/895-3232
e-mail:

Mr. Richard W. McManus
SOUND Environmental Services, Inc.
600 E Sandy Lake RD, #124
Coppell TX 75019
USA
phone: 972/393-6965
fax: 972/304-0762
e-mail: c66635@aol.com

Mr. Scott McMullin
Savannah River Operations Office
U.S. Department of Energy
P.O. Box A, Road One
BLDG 703-46A
Aiken SC 29802
USA
phone: 803/725-9596
fax: 803/725-2123
e-mail: Scott.McMullin@srs.gov

Mr. John H. McNeilly
SAIC/CVR
P.O. Box 8500
8500 Cinder Bed Road, Suite 120
Newington VA 22122-8500
USA
phone: 703/550/0340
fax: 703/550/1986
e-mail:
johnm@div336.cvr.cpmspc.mail.sail.com

Dr. Tamás Meggyes
BAM
Federal Inst. for Materials Research and Testing
Dept. IV. Environ. Caompatibility of Materials
Unter den Eichen 87
D-12205 Berlin GERMANY
phone: 49-30/810 43289
fax: 49-30/81041737
e-mail:

Dr. Theodore O. Meiggs
FOREMOST Solutions
350 Indiana ST, STE 415
Golden CO 80401
USA
phone: 303/271-9114 or 278-7452(home)
fax: 303/278-0624
e-mail: profind@ecentral.com

Dr. Stefan Melchior
IGB Hamburg
Heinrich-Hertz-Str. 116
D-22083 Hamburg GERMANY
phone: 49-40/2270-0038 or home4200486
fax: 49-40/2270-0034
e-mail: 106033.566@compuserve.com

Mr. Robert W. Menzel
Radian International, LLC
2301 N Brazosport BLVD
BLDG DC-708
Freeport TX 77541
USA
phone: 409/238-9416
fax: 409/238-0922
e-mail:

Dr. James W. Mercer
GeoTrans, Inc.
46050 Manekin Plaza, STE 100
Sterling VA 20166
USA
phone: 703/444-7000
fax: 703/444-1685
e-mail: jim@geotrans.com

Mr. Marcelo P. Merino
The North American Coal Corporation
14785 Preston Road, Suite 1100
Dallas TX 75240-7891
USA
phone: 972/448-5478
fax: 972/387-1051
e-mail:

Mr. James L. Mersereau-Kempf
DOW Corning Corporation
P.O. Box 995 (MID 544)
Midland MI USA
phone: 517/496-5813
fax: 517/496-4175
e-mail:

Dr. Margarita Metka
Institute of Geological Researches
Blloku 'Vasil Shanto'
Tirana ALBANIA
phone: 355-42/28703
fax: 355-42/27903 or 27360
e-mail:

Mr. Dick R. Meyer
BMC
9433 HWY 23
Belle Chasse LA 70037
USA
phone: 504/398-0501

Dr. Carol J. Miller
Civil and Environmental Engineering
Wayne State University
2158 Engineering Building
5050 Anthony Wayne Drive
Detroit MI 48202
USA
phone: 313/577-3876
fax: 313/577-3881
e-mail: cmiller@ce.eng.wayne.edu

Conference Participants

Mr. A. David Miller
CDM Engineers & Constructors, Inc.
1331 17th ST
STE 1200
Denver CO 80202
USA
phone: 303/298/1311
fax: 303/298/9886
e-mail: millerad@com.com

Mr. Ross Miller
Lockheed Martin Energy Systems, Inc.
761 Veterans Avenue
Kevil KY 42053
USA
phone: 502/441/5085
fax: 502/441/5064
e-mail: g16@ornl.gov

Mr. Samuel P. Miller
USACE Waterways Experiment Station
3909 Halls Ferry Road
Vicksburg MS 39180
USA
phone: 601/634/3247
fax: 601/634/3453
e-mail:

Mr. Christopher A. Miron
Horizon Environmental Corp.
4595 Broadmoor SE, Suite 200
Grand Rapids MI 49512
USA
phone: 616/554/3210
fax: 616/554/3211
e-mail: camiron@horizonenv.com

Mr. Donald J. Moak
Resonant Sonic International
P.O. Box 4194
West Richland WA 99353
USA
phone: 509/377-3977
fax: 509/377-3980, 3799
e-mail: sonicdjm@earthlink.net

Mr. John E. Moerlins
CHAERSE
Florida State University
2035 E Paul Dirac DR
226 HMB
Tallahassee FL 32310-3700
USA
phone: 904/644-5524
fax: 904/574-6704
e-mail:

Dr. Horace K. Moo-Young, Jr.
Dept. of Civil and Environmental
Engineering
Fritz Engineering Laboratory
Lehigh University
13 E Packer Ave
Bethlehem PA 18015
USA
phone: 610/758-6851
fax: 610/758-6405
e-mail:

Mr. Harry M. Moore
Joyce Engineering Inc.
4808 Radford AVE
Richmond VA 23230
USA
phone: 804/355-4520
fax: 804/355-4282
e-mail:

Dr. Frank Dale Morgan
Earth Resources Laboratory
Dept. of Earth, Atmospheric & Planetary
Sciences
Massachusetts Institute of Technology
42 Carleton ST, BLDG E34-462
Cambridge MA 02142-1324
USA
phone: 617/253-7857 or 8027
fax: 617/253-6385
e-mail:

Dr. George J. Moridis
Earth Sciences Division
Lawrence Berkeley National Laboratory
University of California
MS 90-1116
One Cyclotron RD
Berkeley CA 94720
USA
phone: 510/486-5202 or 4746
fax: 510/486-5686
e-mail:

Ms. Nancy R. Morlock
U.S. Environmental Protection Agency -
Region 6
1445 Ross Avenue Mail Code 6PD-N
Dallas TX 75202
USA
phone: 214/665/6650
fax: 214/665/7263
e-mail: morlock.nancy@epamail.epa.gov

Dr. Ric Morris
Department of Civil and Mining
Engineering
University of Wollongong
Wollongong NSW 2522 AUSTRALIA
phone: 61-42/214642
fax: 61-42/213238
e-mail: rmorris@uow.edu.au

Mr. Stan J. Morrison
Roy Weston
P.O. Box 14000
2597 B3/4 RD
Grand Junction CO 81504
USA
phone: 970/248-6373
fax: 970/248-6040
e-mail:
stan.morrison.@gjpomail.doegjpo.com

Dr. Jim G. Mueller
SBP Technologies, Inc.
105 Gregory Square
Pensacola FL 32501
USA
phone: 904/470-0055
fax: 904/470-0058
e-mail: 75357.1357@compuserve.com

Mr. David R. Muhlbaier
Westinghouse Savannah River Company
Savannah River Site
Aiken SC 29803
USA
phone: 803/725-2607
fax: 803/725/2956
e-mail: david.muhlbaier@srs.gov

Dr. Ishwar Murarka
Land and Water Quality Studies Program
Environment Division
Electric Power Research Institute
P.O. Box 10412
Palo Alto CA 10412
USA
phone: 415/855-2478
fax: 415/855-1069
e-mail:

Dr. Lawrence C. Murdoch
Geological Sciences Department
Clemson University
340 Brackett Hall
Box 341908
Clemson SC 29634
USA
phone: 864-656-2597
fax: 864-656-1041
e-mail: lmurdoch@clemson.edu

Mr. Paul S. Mushovic
U.S. Environmental Protection Agency -
Region 8
999 18th St- Suite 500
Denver CO 80202-2466
USA
phone: 303/312/6662
fax: 303/312/6067
e-mail:

Conference Participants

Dr. David L. Naftz
U.S. Geological Survey
1745 W 1700 S
Salt Lake City UT 84104
USA
phone: 801/975-3389
fax: 801/975-3424
e-mail: dlnaftz@usgs.gov

Dr. Dominique Namy
Inquip Associates, Inc.
1300 Old Chain Bridge RD
P.O. Box 6277
McLean VA 22106
USA
phone: 703/442-0143
fax: 703/442-0188
e-mail: 103244.2012compuserve.com

Mr. Carl L. Nardin
U.S. Army Corps of Engineers
215 N Street
Omaha NE 68102-4978
USA
phone: 402/221-7774
fax: 402/221-7769
e-mail:
carl:l.nardin@mro01.usacc.army.mil

Dr. Alex A. Naudts
ECO Grouting Specialists Ltd.
73 Credit Road
Cheltenham Ontario LOP 1C0
CANADA
phone: 905/838-0150
fax: 905/838-3825
e-mail: ecogrout@passport.ca

Dr. Priscilla P. Nelson
G3S/CMS, Directorate for Engineering
National Science Foundation
4201 Wilson BLVD, Rm 545.17
Arlington VA 22230
USA
phone: 703/306-1361
fax: 703/306-0291
e-mail: pnelson@nsf.gov

Mr. Floyd Nichols
U.S. Environmental Protection Agency
999 18th ST
Denver CO 80202-2405
USA
phone: 303/312-6983
fax: 303/312-6067
e-mail: nichols.floyd@epamail.epa.gov

Mr. Bruce Nichols
Russell Reid
200 Smith ST
Keasbey NJ 08832-1159
USA
phone: 908/225-2238
fax: 908/417-0367
e-mail:

Mr. Peter J. Nicholson
Geo-Con
4075 Monroeville BLVD
Corporate One, BLDG II, STE 400
Monroeville PA 15146
USA
phone: 412/856-7700
fax: 412/373-3357
e-mail: pjnc@telerama.lm.com

Mr. Dave F. Nickelson
Lockheed Martin Idaho Technologies Co.
Idaho National Engineering Laboratory
P.O. Box 1625, MS 3710
Idaho Falls ID 83415
USA
phone: 208/526-9061
fax: 208/526-6802
e-mail: dfn@inel.gov

Dr. Kurt Ambo Nielsen
Krüger A/S
Gladsaxevej 363
2860 Soborg DENMARK
phone: 45/3969/0222
fax: 45/3167/4950
e-mail:

Ms. Mary A. North-Abbott
MSE Technology Applications
P.O. Box 4078
Butte MT 59702-4078
USA
phone: 406/494-7279
fax: 406/494-7230
e-mail: northabb@buttenet.com

Dr. John W. Nyhan
Environmental Science Group
Los Alamos National Laboratory
Mail Stop J-495
Los Alamos NM 87545
USA
phone: 505/667-3163
fax: 505/665-9196
e-mail: jwn@ees15.ianl.gov

Mr. Kent E. O'Brien
Geraghty & Miller, Inc.
1050 Marina Way S
Richmond CA 94804
USA
phone: 510/233-3200
fax: 510/233-3204
e-mail: kobrien@gmgw.com

Ms. Stephanie F. O'Hannesin
Institute for Groundwater Research
Department of Earth Sciences
University of Waterloo
200 University AVE W
Building BFG
Waterloo Ontario N2L 3G1
CANADA
phone: 519/885-1211 ext. 3159
fax: 519/746-0183
e-mail:

Mr. Donald L. Ochs
Regenesis
5 Erlington Drive
Cinnaminson NJ 08077
USA
phone: 609/786/2197
fax: 609/786/1758
e-mail:

Ms. Claire Olson
CPD
Florida State University
TC214
Tallahassee FL 32306-2027
USA
phone: 904/644-7544
fax: 904/644-2589
e-mail:

Mr. E. Timothy Oppelt
National Risk Management Laboratory
Office of Research and Development
U.S. Environmental Protection Agency
26 W Martin Luther King DR
Cincinnati OH 45268
USA
phone: 513/569-7418
fax: 513/569-7680
e-mail:

Mr. Howard M. Orlean
U.S. Environmental Protection Agency -
Region 10
1200 6th AVE : ECL 113
Seattle WA 98101
USA
phone: 206/553-6903
fax: 206/553-0124
e-mail: orlean.howard@epamail.epa.gov

Conference Participants

Dr. V. V. Oshchapovsky
Laboratory 'Photoplast'
Ukrainian Res. Inst. of Polygraphic
Industry
Vladimir Velikiy str., 4
290026 Lvov UKRAINE
phone: 380-322/63-51-33
fax: 380-322/63-20-09
e-mail:

Mr. Paul L. Osley
Chastain-Skillman, Inc.
4508 Oakfair BLVD, STE 101
Tampa FL 33610
USA
phone: 813/621-9229
fax: 813/626-9698
e-mail:

Dr. Yehia A. Osman
Department of Molecular Biology
University of Wyoming
P.O. BOX 3944
Laramie WY 82071-3944
USA
phone: 307/766-3300
fax: 307/766-3875
e-mail:

Mr. William K. Overbey
BDM International
1199 Van Voorhis Rd.
Morgantown WV 26505
USA
phone: 304/598/2666
fax: 304/598/2515
e-mail: woverbey@access.mountain.net
or woverbey@bdm.com

Dr. Angelus S. Owili-Eger
Conoco Inc.
P.O. Box 1267
Ponca City OK 74602-1267
USA
phone: 405/767/3384
fax: e-mail:

Mr. Andrew Palestini
U.S. Environmental Protection Agency -
Region 3
841 Chestnut ST
Philadelphia PA 19107
USA
phone: 215/566-3233
fax: 215/566-3001
e-mail: Palestini.andy@epa.gov

Mr. Philip A. Palmer
Corporate Remediation Group
DuPont Chemicals
Barley Mill Plaza 27/2280
P.O. Box 80027
Wilmington DE 19880-0027
USA
phone: 302/892-7456
fax: 302/892-7641
e-mail: palmerpa@csoc.dnet.dupont.com

Mr. Peter L. Palmer
Geraghty & Miller, Inc.
14497 N. Dale Mabry Hwy. Suite 115
Tampa FL 33618
USA
phone: 813/961/1921
fax: 813/264/1850
e-mail:

Ms. Sandra A. Parker
NASA-Johnson Space Center
Mail Code JJ12
Houston TX 77058
USA
phone: 281/483-3119
fax: 281/483-3048
e-mail: sparker@ja1.jsc.nasa.gov

Ms. Karen Pederson
First Commercial
28441 Rancho California RD
Temecula CA 92590
USA
phone: 909/695-1234

Dr. Louise Pellerin
Lawrence Berkeley National Laboratory
BLDG 90-2024, MS 90-1116
1 Cyclotron RD
Berkeley CA 94720
USA
phone: 510/486-5026
fax: 510/486-5686
e-mail: LPellerin@lbl.gov

Dr. Frank Pepe, Jr.
Geotechnical & Tunneling Division
Parsons Brinckerhoff Quade & Douglas
One Penn Plaza
New York NY 10119
USA
phone: 212/465-5215
fax: 212/465-5592
e-mail: Pepe@pbworld.com

Mr. Jean-Yves Perez
Woodward-Clyde Consultants
4582 S Ulster ST PKWY
Stanford Place 3, STE 600
Denver CO 80237
USA
phone: 303/740-2600
fax: 303/740-2650
e-mail: jyperez@owcc.com

Mr. William M. Perpich
STS Consultants Ltd.
1035 Kepler DR
Green Bay WI 54311
USA
phone: 414/468-1978
fax: 414/468-3312
e-mail:

Ms. Pat Perry-Werneiwski
Target Stores
2621 W Schaumburg RD
Schaumburg IL 60194
USA
phone: 847/798-0776
fax: 847-798-1314
e-mail:

Dr. Peter Persoff
Earth Sciences Division
Lawrence Berkeley National Laboratory
University of California
Mail Stop 90-1116
Berkeley CA 94720
USA
phone: 510/486-5931
fax: 510/486-5686
e-mail: persoff@lbl.gov

Mr. David M. Petrovski
U.S. Environmental Protection Agency -
Region 5
77 West Jackson, DRP-8J
Chicago IL 60604
USA
phone: 773/881-0997
fax: 773/353-4788
e-mail:

Mr. Steven J. Phillips
AGEC, Inc.
P.O. Box 1280
Richland WA 99352-1280
USA
phone: 509/943-2432
fax: 509/943-1084
e-mail: agec@oneworld.owt.com

Dr. Mel G. Piepho
Daniel B. Stephens & Associates, Inc.
1845 Terminal DR, STE 200
Richland WA 99352
USA
phone: 509/946-6627
fax: 509/946-6712
e-mail: stephens@oneworld.owt.com

Mr. Frederick G. Pohland
Department of CEE
University of Pittsburgh
1140 Benedum Hall
Pittsburgh PA 15261
USA
phone: 412/624-1880
fax: 412/624/0135
e-mail: pohland@civ.pitt.edu

Mr. Raymond J. Poletto
Mueser Rutledge Consulting Engineers
708 Third AVE
New York NY 10017
USA
phone: 212/490-7110
fax: 212/953-5626
e-mail: 103-644,501@compuserve.com

Mr. Will Pope
SBP Technologies, Inc.
105 Gregory Square
Pensacola FL 32501
USA
phone: 904/470-0055
fax: 904/470-0058
e-mail:

Mr. Robert M. Powell
Powell & Associates Science Services
8310 Lodge Haven
Las Vegas NV 89123
USA
phone: 702/260/9434
fax: 702/260/9435
e-mail: powell.associates@mci2000.com

Mr. John D. Powell
U.S. Geological Survey
414 National Center
Reston VA 20192
USA
phone: 703/648/4169
fax: 703/648/5722
e-mail: jdpowell@usgs.gov

Ms. Cynthia C. Powels
U.S. Army Garrison
Aberdeen Proving Ground
ATTN: STEAP-SH-ER
USAGAPG, DSHE-ECRD, BLDG E4430
Aberdeen Proving Ground MD
21010-5423
USA
phone: 410/671-4568/3320
fax: 410/671-3010
e-mail:

Dr. Robert W. Puls
R.S. Kerr Environmental Research
Laboratory
U.S. Environmental Protection Agency -
NRMRL
P.O. Box 1198
919 Kerr Research DR
Ada OK 74820
USA
phone: 405/436-8543
fax: 405/436-8703
e-mail:

Mr. John E. Quander
U.S. Environmental Protection Agency
OSWER/TIO
401 M ST SW
Washington DC 20460
USA
phone: 703/603/7198
fax: 703/603/7195
e-mail: quander.john@epamail.epa.gov

Dr. Alan J. Rabideau
Department of Civil Engineering
SUNY at Buffalo
230 Jarvis Hall
Buffalo NY 14260-4300
USA
phone: 716/645-2114 (x2327)
fax: 716/645-3667
e-mail: rabideau@eng.buffalo.edu

Mr. V. Rajaram
PRC Environmental Management, Inc.
1921 D Rohlwing RD
Rolling Meadows IL 60008
USA
phone: 847/255-4166
fax: 847/255-8528
e-mail: rajaram@prc emi.com

Mr. Andre M. Reboucas
Hidro Ambiente PC.S. S/C Ltda
R Arao Adler 22 Pq. Continental
Sao Paulo S. P.   CEP 05328 010
BRAZIL
phone: 55/11/8694500
fax: 55/11/8690483
e-mail: hidroamb@dialdata.com.br

Mr. Craig L. Reese
Parsons Infrastructure & Technology
Group, Inc.
P.O. Box 1625 MS 3954
Idaho Falls ID 83415-3954
USA
phone: 208/526-84??
fax: 208/526-8426
e-mail:

Mr. Charles V. Reeter
Naval Facilities Engineering Service
Center
1100 23rd AVE, Code ESC411
Port Hueneme CA 93043
USA
phone: 805/982-1808
fax: 805/982-4304
e-mail: creeter@nfesc.navy.mil

Mr. David K. Reichhardt
MSE Technology Applications
220 N Alaska St.
Butte MT 59701
USA
phone: 406/494-7195

Dr. Debra R. Reinhart
College of Engineering
University of Central Florida
P.O. Box 162993
Orlando FL 32816-2993
USA
phone: 407/823-2315
fax: 407/823-5483
e-mail: reinhart@ucf.edu

Mr. Ralph E. Remmert
Cargill Fertilizer, Inc.
U.S. HWY 60 W
Bartow FL 33830
USA
phone: 941-534-9610
fax: 941/534-9686
e-mail:

Mr. Chris W. Rhyne
U.S. Environmental Protection Agency
401 M St. SW (5303W)
Washington DC 20460
USA
phone: 703/308/8658
fax: 703/308/8609
e-mail: rhyne.chris@epamail.epa.gov

Conference Participants

Mr. Michael W. Ribordy
U.S. Environmental Protection Agency
77 W Jackson BLVD (DRE-8J)
Chicago IL 60604
USA
phone: 312/886-4592
fax: 312/353-4788
e-mail:

Mr. Wray Rohrman
U.S. Environmental Protection Agency
USA

Ms. Dawn A. Sawvel
GFR Magazine
345 Cedar St., STE 800
St. Paul MN 55101-1088
USA
phone: 612/222-2508
fax: 612/222-6966 or 8215
e-mail: gfr@ifai.com

Ms. Norberta Rimbach
Pollution Equipment News
8650 Babcock BLVD
Pittsburgh PA 15237-5821
USA
phone: 412/364-5366
fax: e-mail:

Mr. James R. Romer
EMCON, Inc.
1150 Knutson Road Suite 4
Medford OR 97504
USA
phone: 541/770/6977
fax: 541/770/7019
e-mail:

Dr. Hermann Schad
I.M.E.S. GmbH
Kocherhof 4
D-88239 Wangen GERMANY
phone: 49-7528/97130
fax: 49-7528/97131
e-mail: hermann.schad.imes@t-online.de

Mr. William A. Roach
U.S. Environmental Protection Agency
290 Broadway
New York NY 10007
USA
phone: 212/637-4335
fax: 212/637-3256
e-mail: roach.bill@epamail.epa.gov

Mr. J. C. Rondeau
Environmental Compliance
UGI Utilities, Inc.
P.O. Box 12677
Reading PA 19612-2677
USA
phone: 610/796-3532
fax: 610/796/3402
e-mail: jrondeau@redrose.net

Mr. Robert M. Schindler
Geo-Con, a Woodward-Clyde Company
4075 Monroeville BLVD
Corporate One, BLDG II, STE 400
Monroeville PA 15146
USA
phone: 412/856-7700
fax: 412/373-3357
e-mail:

Dr. Will D. Robertson
Department of Earth Sciences
Waterloo Centre for Groundwater
Research
University of Waterloo
Waterloo Ontario N2L 3G1
CANADA
phone: 519/885-1211 or 6800
fax: 519/746-7484
e-mail:

Mr. Mark S. Rurka
Harza Environmental Services, Inc.
233 S. Wacker Drive
Chicago IL 60606
USA
phone: 312/831/3822
fax: 312/831/3999
e-mail: mrurka@harza-es.com

Ms. Gail Schmednecht
Slurry Systems, Inc.
6515 E Melton RD
Gary IN 46403
USA
phone: 219/938-6667
fax: 219/938-3437
e-mail:

Mr. Tony Robinson
BDM Federal
Waste Policy Institute
227 Gateway DR, STE 223
Aiken SC 29803
USA
phone: 803/652-8020
fax: 803/652-8484
e-mail:

Dr. Philip E. Rushbrook
World Health Organization
European Centre for Environment and
Health
Nancy Project Office
O.M.S., 149 rue Gabriel Peri
F-54500 Vandoeuvre les Nancy FRANCE
phone: 33-383/158770 or 158774
fax: 33-383/158773
e-mail:

Mr. Fred C. Schmednecht
Slurry Systems, Inc.
6515 E Melton RD
Gary IN 46403
USA
phone: 219/938-6667
fax: 219/938-3437
e-mail: SSI@niia.net

Mr. Edward J. Rogan
Woodward Clyde International &
Geo-Con
2020 E. First St. Suite 400
Santa Ana CA 92705
USA
phone: 714/835/6886
fax: 714/667/7147
e-mail: ejrogan@wcc.com

Mr. Chris Ryan
Geo-Solutions Inc
201 Penn Center BLVD
STE 404
Pittsburgh PA 15235
USA
phone: 412/825-5164
fax: 412/825-5127
e-mail: cryan@concentric.net

Ms. Dana A. Schmednecht
Slurry Systems, Inc.
6515 E Melton RD
Gary IN 46403
USA
phone: 219/938-6667
fax: 219/938-3437
e-mail:

Conference Participants

Ms. Eleanor Schmednecht
Slurry Systems, Inc.
6515 E Melton RD
Gary IN 46403
USA
phone: 219/938-6667
fax: 219/938-3437
e-mail:

Mr. Richard T. Schmidt
Klohn-Crippen
Unit 7, 1351 C
Kelly Lake RD
Sudbury Ontario P3E 5P5
CANADA
phone: 705/522-1367

Mr. William L. Schmithorst
Parsons Engineering Science, Inc.
401 Harrison Oaks BLVD, STE 210
Cary NC 27513
USA
phone: 919/677-0080
fax: 919/677-0118
e-mail: Bill_Schmithorst@parsons.com

Ms. Karen E. Schmitt
University of Texas (now with Geosyntec)
2100 Main St. Suite 150
Huntington Beach CA 92647
USA
phone: 714/969-0800
fax: 714/969-0820
e-mail: kschmitt@GeoSyntec.com

Ms. Cindy G. Schreier
Geochemistry Group
SECOR International, Inc.
1787 Tribute RD, STE C
Sacramento CA 95815
USA
phone: 916/648-9160
fax: 916/648-8052
e-mail: cschreier@secor.com

Ms. Thea T. Schuhmacher
Levine•Fricke•Recon
1920 Main ST, STE 750
Irvine CA 92662
USA
phone: 714/955/1390
fax: 714/955-0683
e-mail:
Thea_Schuhmacher@LFI.ccmail.compus
erve.com

Dr. Dale S. Schultz
DuPont
Experimental Station, BLDG 304
P.O. Box 6101
Wilmington DE 19880-0304
USA
phone: 302-695-9956
fax: 302-695-4414
e-mail:
schultds@a1.esvax.umc.dupont.com

Mr. Gary Schwab
ENRID
2/7 Pitt Way
Myaree Western Australia 6194
AUSTRALIA
phone: 61-9/330 8282
fax: 61-9/3308283
e-mail:

Ms. Pamela J. Langston Scully
U.S. Environmental Protection Agency -
Region 4
100 Alabama ST
Atlanta GA 30341
USA
phone: 404/562-8935
fax: 404/562-8896
e-mail: scully.pam@epamail.epa.gov

Dr. Lily S. Sehayek
Dept. of Civil and Environmental
Engineering
Penn State Great Valley
30 East Swedesford RD
Malvern PA 19355-1443
USA
phone: 610/648-3373 (W) 687-2469 (H)
fax: 610/648-3377
e-mail:

Mr. R. Jeffrey Serne
Water and Land Resource Department
Pacific Northwest National Laboratory
(PNNL)
P.O. Box 999
Mail Stop K6-81
Richland WA 99352
USA
phone: 509/376-8429
fax: 509/376-5368
e-mail: rjserne@pnl.gov

Mr. Michael G. Serrato
Westinghouse Savannah River Company
Building 773-42A-217
Aiken SC 29808
USA
phone: 803/725/5200
fax: 803/725/7673
e-mail: michael.serrato@srs.gov

Mr. Jeffrey P. Sgambat
Geraghty & Miller, Inc.
1131 Benfield Boulevard, Suite A
Millersville MD 21140
USA
phone: 410/987/0032
fax: 410/987/4582
e-mail: jsgambat@gmgw.com

Dr. Charles D. Shackelford
Department of Civil Engineering
Colorado State University
Fort Collins CO 80523-1372
USA
phone: 970/491-5051
fax: 970/491-7727 or 3584
e-mail: shackel@lance.colostate.edu

Ms. Ellen M. Shannon
GSE Lining Technology Inc.
19103 Gundle RD
Houston TX 77073
USA
phone: 281/230-6708
fax: 281/230-6704
e-mail: ellens@gse.world.com

Mr. Peter G. Shaw
Lockheed Martin Idaho Technologies Co.
Idaho National Engineering Laboratory
P.O. Box 1625, MS-3710
Idaho Falls ID 83415
USA
phone: 208/526-5917
fax: 208/526-6802
e-mail: sgp@inel.gov

Mr. Ian D. Shaw
Draper Aden Associates
2206 South Main Street
Blacksburg VA 24060
USA
phone: 540/552/0444
fax: 540/552/0291
e-mail:

Dr. Birinder Shergill
Mantech Environmental
P.O. Box 1198
Ada OK 74820
USA
phone: 405/436/8707
fax: 405/436/8501
e-mail: shergill@ad3100.ada.epa.gov

Conference Participants

Dr. Malcolm D. Siegel
Geochemistry and Reactive Transport
WIPP Chemical and Disposal Room
Processes Dept.
Sandia National Laboratories
MS-1320
Albuquerque NM 87185-1320
USA
phone: 505/848-0631
fax: 505/848-0622
e-mail:

Mr. Anthony Silva
Kaiser Ventures, Inc.
3633 E Inland Empire BLVD
STE 850
Ontario CA 91764
USA
phone: 909/483-8507
fax: 909/944/6605
e-mail:

Dr. Timothy M. Sivavec
Corporate Research and Development
Center
General Electric
1 River RD
BLDG K1, RM 5A45
Schenectady NY 12301
USA
phone: 518/387-7677
fax: 518/387-5592
e-mail: sivavec@crd.ge.com

Mr. Kenneth Skahn
U.S. Environmental Protection Agency
401 M ST SW
MC=5204G
Washington DC 20460
USA
phone: 703/603-8801
fax: 703/603-9100
e-mail: skahn.ken@epamail.epa.gov

Dr. Brent E. Sleep
Department of Civil Engineering
University of Toronto
35 St. George ST
Toronto Ontario M5S LA4
CANADA
phone: 416/978-3005
fax: 416-978-3674
e-mail:

Mr. Chris Smith
Lockheed Martin Marietta Corp.
P.O. Box 2009
Y-12 Plant, MS 8247
Oak Ridge TN 37831-8247
USA
phone: 423/576-6526
fax: 423/576-3808
e-mail: smithcm@oml.gov

Ms. Ann Marie Smith
Lockheed Martin Idaho Technologies Co.
Idaho National Engineering Laboratory
P.O. Box 1625
Idaho Falls ID 83415-3765
USA
phone: 208/526-6877
fax: 208/526-0425
e-mail: aqs@inel.gov

Ms. Ann P. Smith
Groundwater Services, Inc.
5252 Westchester, STE 270
Houston TX 77005
USA
phone: 713/663-6600
fax: 713/663-6546
e-mail: apsmith@gsi-net.com

Mr. David J.A. Smyth
Department of Earth Sciences
University of Waterloo
200 University AVE W
Building BFG
Waterloo Ontario N2L 3G1
CANADA
phone: 519/888-4567 ext. 2899
fax: 519/746-5644
e-mail: dsmyth@sciborg.uwaterloo.ca

Ms. Glori Snow
American Compliance Technologies, Inc.
1875 W Main ST
Bartow FL 33830-7718
USA
phone: 941/533-2000
fax: 941/534-1133
e-mail:

Mr. Gary W. Snyder
Black & Veatch
The Curtis Center
601 Walnut ST, STE 850 W
Philadelphia PA 19106-3307
USA
phone: 215/928-2233 or 0700
fax: 215/928-1780
e-mail: snydergw@bv.com

Mr. John Soter
SBP Technologies, Inc.
105 Gregory Square
Pensacola FL 32501
USA
phone: fax: 904/470-0058
e-mail:

Mr. Robert L. Stamnes
U.S. Environmental Protection Agency -
Region 10
12015 - 11th NW
Seattle WA 98177
USA
phone: 206/553-1512
fax: 206/553-0119
e-mail: stamnes.robert@epamail.epa.gov

Dr. Robert C. Starr
Idaho National Engineering Laboratory
P.O. Box 1625
Idaho Falls ID 83415-2107
USA
phone: 208/526-5687
fax: 208/526-0875
e-mail: starr@inel.gov

Dr. Leonid R. Stavnitser
NIIOSP
2 Institutskaya St., 6
6 Moscow 109428 RUSSIA
phone: 7-095/1707012
fax: 7-095/1713701
e-mail:

Captain Jeffrey A. Stinson
Armstrong Laboratory
U.S. Air Force
Code AL/EQ-CN
139 Barnes DR, STE 2
Tyndall AFB FL 32403-5323
USA
phone: 904/283-6254
fax: 904/283-6064
e-mail:
jeff.stinson@ccmail.aleq.tyndall.af.mil

Mr. Bryan W. Stone
RETEC, Inc.
1011 SW Klickitat Way, STE 207
Seattle WA 98134
USA
phone: 206/624-9349
fax: 206/624-2839
e-mail: BStone@retecinc.com

Dr. John C. Stormont
Department of Civil Engineering
University of New Mexico
Albuquerque NM 87131
USA
phone: 505/277-6063
fax: 505/277-1988
e-mail: jcstorm@unm.edu

Conference Participants

Mr. Richard P. Stulgis
Haley & Aldrich, Inc.
Ten Harvey Road
Bedford NH 03110
USA
phone: 603/625/5353
fax: 603/624/8307
e-mail:

Ms. Jennifer Su
DuPont
510 1/2 W Lockhart ST
Sayre PA 18840
USA
phone: 717/268-3758
fax: 717/268-3977
e-mail: <dcl1::suj

Mr. Stanley M. Swartzel
USACE Waterways Experiment Station
3909 Halls Ferry Road
Vicksburg MS 39180
USA
phone: 601/634/3326
fax: 601/634/3453
e-mail: swartzs@ex1.wes.army.mil

Dr. Frank S. Szerdy
GeoMatrix Consultants, Inc.
100 Pine Street, 10th Floor
San Francisco CA 94131
USA
phone: 415/434/9400
fax: 415/434/1365
e-mail: fszerdy@geomatrix.com

Mr. Osamu Taki
SCC Technology, Inc.
P.O. Box 1297
Belmont CA 94002
USA
phone: 415/592-3435
fax: 415/637-1570
e-mail: taki@scc-tech.com

Mr. Gilbert R. Tallard
Liquid Earth Support, Inc.
128 Corlies AVE
Pelham NY 10803-1902
USA
phone: 914/738-4880
fax: 914/738-4804
e-mail: tliquid@ix.netcom.com

Ms. Edde M. Tallard
Liquid Earth Support Inc.
128 Corlies AVE
Pelham NY 10803
USA

Ms. Jeanne M. Tarvin
STS Consultants Ltd.
11425 W Lake Park DR
Milwaukee WI 53224
USA
phone: 414/359-3030
fax: 414/359-0822
e-mail:

Mr. Art Taylor
Wyo-Ben, Inc.
P.O. Box 1979
Billings MT 59103
USA
phone: 406/652-6351
fax: 406/656-0748
e-mail:

Dr. Paul Tedd
Building Research Establishment, Garston
Watford WD2 7JR England UK
phone: 44-1923/664849
fax: 44-1923/664085
e-mail: teddp@bre.co.uk

Mr. Wayne Ten Bruin
Inquip Associates, Inc.
STE 282
5824 Bee Ridge RD
Sarasota FL 34233
USA
phone: 941/378-9606
fax: 941/378-9505
e-mail:

Dr. George G. Teutsch
Geological Institute
University of Tübingen
Sigwartstr. 10
D-72827 Tuebingen GERMANY
phone: 49-7071/29-76468
fax: 49-7071/5059
e-mail: teutsch@uni-tuebingen.de

Mr. Richard W. Thomas
TRI/Environmental, Inc.
9063 Bee Cave RD
Austin TX 78733-6201
USA
phone: 512/263-2101 or 800/880-TEST
fax: 512/263-2558
e-mail: TRIRickT@aol.com

Ms. Alison Thomas
U.S. Air Force Armstrong Laboratory
AL/EQW-OL
139 Barnes DR, STE 2
Tyndall AFB FL 32403-5323
USA
phone: 904/283-6303
fax: 904/283-6064
e-mail:
alison_thomas@ccmail.aleq.tyndall.af.mil

Mr. Milind S. Thombre
1410 Chicago AVE, #407
Evanston IL 60201
USA
phone: 312/326-8513
e-mail: milind@unm.edu

Mr. Daniel Tiltges
Inquip Associates, Inc.
711 Burning Tree LN
Arlington Heights IL 60004
USA
phone: 708/398-8007
fax: 708/398-8034
e-mail:

Dr. Joachim Tolksdorff
Geological Institute
University of Tübingen
Sigwartstr. 10
D-72076 Tübingen GERMANY
phone: 49-7032/24989
fax: 49-7071/5059
e-mail:
joachim.tolksdorff@student.uni-tuebingen.de

Mr. Mark A. Topp
Comanco Environmental Corporation
7911 Professional Place
Tampa FL 33637
USA
phone: 813/988-8829
fax: 813/988-8779
e-mail:

Conference Participants

Mr. Dana H. Toups
Synthetic Industries
330 Meadowmeade LN
Lawrenceville GA 30243
USA
phone: 770/513-0066
fax: 770/513-6555
e-mail:

Mr. Jos A. Van De Keybus
Bitumar N.V.
Haven J025
Scheldedijk 30
2070 Zwijnorecht BELGIUM
phone: 32/3/2505443
fax: 32/3/2505968
e-mail:

Ms. Veerle M. L. Vercruysse
SOILS NV
Haven Ac25 Scheldeduk 30
2070 Zwundrecht BELGIUM
phone: 0032/3/250 55 11
fax: 0032/3/250 52 54
e-mail:

Ms. Terri A. Towers
K & M Engineering and Consulting
Corporation
2001 L St NW, Ste. 500
Washington DC 20036
USA
phone: 202/728/0390
fax: 202/872/9174
e-mail: ttowers@mailer.kmec.com

Ms. Terry D. Vandell
DuPont - Conoco
1000 S Pine
Ponca City OK 74602
USA
phone: 405/767-6561
fax: 405/767-3549
e-mail:

Dr.-Ing. B.V. S. Viswanadham
Geotechnical Engineering Division
Central Road Research Institute New
Delhi
P.O. CRRI
New Delhi INDIA
phone: fax: e-mail:
visnath@cscrri.ren.nic.in

Ms. Deborah L. Tremblay
U.S. Environmental Protection Agency
MC 5101
401 M ST SW
Washington DC 20460
USA
phone: 202/260-8302
fax: 202/260-5646
e-mail:
termblay.deborah@epamail.epa.gov

Ms. Luanne N. Vanderpool
U.S. Environmental Protection Agency
5SRT-4J
77 W Jackson BLVD
Chicago IL 60604
USA
phone: 312/353-9296
fax: 312/353-9281
e-mail:
vanderpool.luanne@epamail.epa.gov

Mr. Ben Viveen
Heidemij
P.O. Box 264
6800 AG Arnhem THE NETHERLANDS
phone: 31-26/377-8899
fax: 31-26/445-7549 or 3892845
e-mail:

Mr. M. J. (Fred) Tschirch
Steel Piling Inc.
302 Walnut Bend
Houston TX 77042
USA
phone: 770/661-3401

Dr. Aleksej N. Vasiliev
Inst. of Bioorganic Chemistry &
Petrochemistry
Academy of Sciences of Ukraine
P.O. Box 305
252034 Kiev UKRAINE
phone: 380-44/559-0595
fax: 380-44/543-5152
e-mail: users@oil.freenet.kiev.ua

Mr. John L. Vogan
Enviro Metal Technologies Inc.
42 Arrow Road
Guelph Ontario N1K156
CANADA
phone: 519/824/0432
fax: 519/763/2378
e-mail: jvogan@beak.com

Dr. John P. Turner
Dept. of Civil & Architectural Engineering
University of Wyoming
P.O. Box 3295 University Station
Laramie WY 82071-3295
USA
phone: 307/766-4265
fax: 307/766-2721 or 4444
e-mail: turner@uwyo.edu

Ms. Deborah A. Vaughn-Wrigth
U.S. Environmental Protection Agency -
Region 4
100 Alabama
Atlanta GA 30303
USA
phone: 404/562-8539

Mr. Richard H. Walden
Baltimore Gas and Electric Co.
1699 Leadenhall Street
Baltimore MD 21203
USA
phone: 410/291/4731
fax: 410/291/4994
e-mail: richard.h.walden@bge.com

Mr. John R. Tushek
Radian International LLC
316 Live Oak LN
Lake Jackson TX 77566
USA
phone: 409/238-1144
fax: 409/238/0922
e-mail:

Frank J. Vavra
U.S. Environmental Protection Agency
841 Chestnut BLDG
Philadelphia PA 19107
USA
phone: 215/566-3221
fax: 215/566-7549
e-mail: fvavra@epa.gov.com

Mr. Timothy Walsh
Foamseal Inc.
P.O. Box 455
Oxford MI 48371
USA
phone: 810/628-2587
fax: 810/628-7136
e-mail:

Conference Participants

Mr. Michael J. Walsh
W.E.S., Inc.
6389 Tower LN
Sarasota FL 34240
USA
phone: 941/371-7617
fax: 941/378-5218
e-mail:

Ms. Linda M. Ward
Geo-Con, a Woodward-Clyde Company
4075 Monroeville BLVD
Corporate One BLDG II, STE 400
Monroeville PA 15146
USA
phone: 412/856-7700
fax: 412/373-3357
e-mail:

Dr. Chris Waring
ANSTO Environment Division
Jucas Heights Research Laboratories
P.M.B. #1
Menai NSW 2234 AUSTRALIA
phone: 61-2/9717 9045
fax: 61-2/9717 9286
e-mail: Chris.Waring@ansto.gov.au

Mr. Scott D. Warner
Geomatrix Consultants, Inc.
100 Pine ST, Tenth Floor
San Francisco CA 94111
USA
phone: 415/434-9400
fax: 415/434-1865
e-mail: swarner@geomatrix.com

Mr. Robert G. Wasp
SBP Technologies, Inc.
106 Corporate Park DR
White Plains NY 10604
USA
phone: 914/694-2280
fax: 914/694-2286
e-mail:

Mr. David B. Watson
Environmental Sciences Division
Oak Ridge National Laboratory
P.O. Box 2008, BLDG 1509
MS 6400
Oak Ridge TN 37831-6400
USA
phone: 423/241-4749
fax: 423/574-7420
e-mail: watsondb@ornl.gov

Mr. Steven E. Way
U.S. Environmental Protection Agency
Region 8
(MC EPR-ER)
999 18th ST, STE 500
Denver CO 80202
USA
phone: 303/312-6808
fax: 303/312-6071
e-mail: way.steve@epamail.epa.gov

Mr. Stephen W. Webb
Sandia National Laboratories
P.O. Box 5800
MS-1324
Albuquerque NM 87185-1324
USA
phone: 505/848-0623
fax: 505/848-0605
e-mail: swwebb@nwer.sandia.gov

Ms. Susan D. Webster
U.S. Environmental Protection Agency
Region 6
(6SF-RA)
1445 Ross AVE
Dallas TX 75282
USA
phone: 214/665-6784
fax: 214/665-7447
e-mail: webster.susan@epamail.epa.gov

Ms. Nandra Weeks
GeoSyntec Consultants
621 NW 53rd ST, STE 650
Boca Raton FL 33487
USA
phone: 561/995-0900
fax: 561/995-0925
e-mail:

Mr. Brent Weesner
Lockheed Martin
P.O. Box 2908
Largo FL 34649
USA
phone: 813/545-6793

Mr. Charlie Weiland
ENTACT, Inc.
802 S Woodrow Wilson
Plant City FL 33567
USA
phone: 813/754-7004
fax: 813/754-7708
e-mail:

Ms. Melanie Welch
CPD
Florida State University
Tallahassee FL 32306-2027
USA
phone: 904/644-7559
fax: 904/644-3803
e-mail:

Mr. Joseph P. Welsh
Hayward Baker Inc.
1875 Mayfield RD
Odenton MD 21113
USA
phone: 410/551-8200
fax: 410/551-1900
e-mail:

Dr. Joyce M. Whang
DuPont CR&D - CPD
Jackson Laboratory J-24 BLDG
Chambers Works, Rt. 130
Deepwater NJ 08023
USA
phone: 609/540-4275
fax: 609/540-4944
e-mail:
whangjm@a1.jlcl01.umc.dupont.com

Mr. Stephen J. White
Corps of Engineers
12565 West Center Rd.
Omaha NE 68144
USA
phone: 402/697/2660
fax: 402/697/2673
e-mail: stephen.j.white@usace.army.mil

Mr. Andreas Wieners
HSP Hoesch Spundwand und Profil
GmbH
Alte Radstraße 27
D-44147 Dortmund GERMANY
phone: 49-231/844-6449 or 4102
fax: 49-231/844-6162 or 3200
e-mail:

Mr. Ronald G. Wilhelm
Office Radiation and Air
U.S. Environmental Protection Agency
ORIA (6603J)
401 M ST SW
Washington DC 20460
USA
phone: 202/233-9379
fax: 202/233-9650
e-mail:

Conference Participants

Mr. Charles M. Wilk
Portland Cement Association
5420 Old Orchard RD
Skokie IL 60077
USA
phone: 847/966-6200
fax: 847/966-8389
e-mail: charles_wilk@portcement.org

Dr. John A. Wilkens
DuPont Company
P.O. Box 80304   c/o D.L. Leo
Wilmington DE 19880-0304
USA
phone: 302/695-3143
fax: 302/695-4414
e-mail:
wilkenja@a1.esvax.umc.dupont.com

Mr. Richard E. Willey
U.S. Environmental Protection Agency -
Region 1
JFK Federal BLDG
Boston MA 02203
USA
phone: 617/573-9639
fax: 617/573-9662
e-mail:

Ms. Cecelia V. Williams
Environmental Restoration Technologies
Sandia National Laboratories
Department 6621, MS-0719
P.O. Box 5800
Albuquerque NM 87185-0719
USA
phone: 505/844-5722
fax: 505/844-0543
e-mail:

Mr. Nicolas J. Williams
P-Squared Technologies, Inc.
P.O. Box 22668
10938 Hardin Valley Road
Knoxville TN 37932
USA
phone: 423/691-3668
fax: 423/691-0611
e-mail: nicolas@p2t.com

Dr. Ryan D. Wilson
Department of Earth Sciences
University of Waterloo
200 University Avenue West
Waterloo Ontario N2L 3G1
CANADA
phone: 519/888-4567 ext. 5372
fax: 519/746-5644
e-mail: rdwilson@sciborg.uwaterloo.ca

Mr. Bob Windschaver
Subsurface Detection Investigations, Inc.
7381 - 114th AVE N
STE 405B
Largo FL 33773
USA
phone: 813/544-5020
fax: 813/544-5020
e-mail:

Dr. John C. Wirth
Sandtransisco
304 N Flagler AVE
Stuart FL 34994
USA
phone: 407/692-0221
fax: 407/287-4546
e-mail:

Ms. Kay Wischkaemper
U.S. Environmental Protection Agency -
Region 4
100 Alabama ST SW
Atlanta GA 30303-3104
USA
phone: 404/562-8641
fax: 404/562-8566
e-mail:
wischkaemper.kay@epamail.epa.gov

Mrs. Carol A. Witt-Smith
U.S. Environmental Protection Agency -
Region 5
DRP - 8J
77 W Jackson BLVD
Chicago IL 60604
USA
phone: 312/886-6146
fax: 312/353-4788
e-mail: witt-smith.carol@epamail.epa.gov

Dr. L. Anthony Wolfskill
Woodward-Clyde
4 Waterwood
Huntsville TX 77340
USA
phone: 409/891/5102
fax: 409/891/5103
e-mail:

Mr. Bernard Woolley
LaFarge Calcium Aluminates, Inc.
100 Ohio Street
Chesapeake VA 23324
USA
phone: 757/543/8832
fax: 757/545/8933
e-mail: lafarge@kainc.com

Mr. Mark Q. Wyllie
ICI Explosives
Ardeer Operating Services
Ardeer Site
Stevenston Ayrshire Scotland KA20 3LN
UK
phone: 44-1294/487479
fax: 44-1294-487280
e-mail:

Mr. Peter T. Yen
Bechtel Corporation
P.O. Box 193965
50 Beale St. (50/5/b103)
San Francisco CA 94105
USA
phone: 415/768-7438
fax: 415/768-4955
e-mail: pyen@bechtel.com

Mr. Douglas J. Yeskis
U.S. Environmental Protection Agency -
Region 5
Mail Code: SRT-4J
77 W Jackson BLVD
Chicago IL 60604
USA
phone: 312/886-0408
fax: 312/353-9281
e-mail: yeskis.douglas@epamail.epa.gov

Mr. Hiroshi Yoshida
Engineering Division
Chemical Grouting Company
Anzen Bldg., 1-6-4
Motoakasaka, Minato-ku
Tokyo 107 JAPAN
phone: 81-3/3475-0201
fax: 81-3/3475-1545
e-mail: grouthyo@pub.kajima.co.jp

Mr. Stephen J. Zarlinski
Kiber Environmental Services, Inc.
3786 Dekalb Technology PKWY NE
Atlanta GA 30340
USA

Mr. Stanley J. Zawistowski
U.S. Environmental Protection Agency -
Region 8
EPR-F
999 18th ST, STE 500
Denver CO 80202
USA
phone: 303/312-6255
fax: 303/312-6067
e-mail:

Conference Participants

Mr. Andrew P. Zdinak
Western Environmental Technology
Office
MSE Technology Applications, Inc.
P.O. Box 4078
Butte MT 59702
USA
phone: 406/494-7410
fax: 406/494-7230
e-mail:

Ms. Jo Ellen Zeiler
MSE Technology Applications, Inc.
P.O. Box 4078
Butte MT 59702
USA
phone: 406/723-8328

Ms. Yan Zhang
Department of Geology
University of Alabama
Tuscaloosa AL 35487
USA
phone: 205/348/5148
fax: 205/348/0818
e-mail:

Dr. Chunmiao Zheng
Department of Geology
University of Alabama
Box 870338
202 Bevill BLDG
Tuscaloosa AL 35487-0338
USA
phone: 205/348-0579 or 5095
fax: 205/348-0818 or 9268
e-mail: czheng@wgs.geo.ua.edu

Dr. Thomas F. Zimmie
Department of Civil Engineering
Rensselaer Polytechnic Institute
Troy NY 12180
USA
phone: 518/276-6939
fax: 518/276-4833
e-mail: zimmit@rpi.edu

Mr. Thomas C. Zwick
Batelle Memorial Institute
505 King Avenue
Columbus OH 43201
USA
phone: 614/424/6199
fax: 614/424/3667
e-mail:

Mr. Thomas de Beyer
FlowTex
Chausseestraße 1
06317 Amsdorf GERMANY
phone: 49-34601/40 168
fax: 49-34601/40 159
e-mail: thomas.de-beyer@romonta.de

Mr. Peter W. de Vries
Consultant & Project Manager
Bilderdgklaan 6
3818 WE Amersfoort THE
NETHERLANDS
phone: 31-33/4611729
fax: 31-33/4656067
e-mail:

Author Index

Author Index